

e-books download weblog:
<http://www.tooraj-sabzevari.blogfa.com/>
(water engineering weblog)

HANDBOOK OF HYDRAULIC FLUID TECHNOLOGY



edited by
GEORGE E. TOTTEN

HANDBOOK OF HYDRAULIC FLUID TECHNOLOGY

MECHANICAL ENGINEERING

A Series of Textbooks and Reference Books

Founding Editor

L. L. Faulkner

*Columbus Division, Battelle Memorial Institute
and Department of Mechanical Engineering
The Ohio State University
Columbus, Ohio*

1. *Spring Designer's Handbook*, Harold Carlson
2. *Computer-Aided Graphics and Design*, Daniel L. Ryan
3. *Lubrication Fundamentals*, J. George Wills
4. *Solar Engineering for Domestic Buildings*, William A. Himmelman
5. *Applied Engineering Mechanics: Statics and Dynamics*, G. Boothroyd and C. Poli
6. *Centrifugal Pump Clinic*, Igor J. Karassik
7. *Computer-Aided Kinetics for Machine Design*, Daniel L. Ryan
8. *Plastics Products Design Handbook, Part A: Materials and Components; Part B: Processes and Design for Processes*, edited by Edward Miller
9. *Turbomachinery: Basic Theory and Applications*, Earl Logan, Jr.
10. *Vibrations of Shells and Plates*, Werner Soedel
11. *Flat and Corrugated Diaphragm Design Handbook*, Mario Di Giovanni
12. *Practical Stress Analysis in Engineering Design*, Alexander Blake
13. *An Introduction to the Design and Behavior of Bolted Joints*, John H. Bickford
14. *Optimal Engineering Design: Principles and Applications*, James N. Siddall
15. *Spring Manufacturing Handbook*, Harold Carlson
16. *Industrial Noise Control: Fundamentals and Applications*, edited by Lewis H. Bell
17. *Gears and Their Vibration: A Basic Approach to Understanding Gear Noise*, J. Derek Smith
18. *Chains for Power Transmission and Material Handling: Design and Applications Handbook*, American Chain Association
19. *Corrosion and Corrosion Protection Handbook*, edited by Philip A. Schweitzer
20. *Gear Drive Systems: Design and Application*, Peter Lynwander
21. *Controlling In-Plant Airborne Contaminants: Systems Design and Calculations*, John D. Constance
22. *CAD/CAM Systems Planning and Implementation*, Charles S. Knox
23. *Probabilistic Engineering Design: Principles and Applications*, James N. Siddall
24. *Traction Drives: Selection and Application*, Frederick W. Heilich III and Eugene E. Shube
25. *Finite Element Methods: An Introduction*, Ronald L. Huston and Chris E. Passerello
26. *Mechanical Fastening of Plastics: An Engineering Handbook*, Brayton Lincoln, Kenneth J. Gomes, and James F. Braden
27. *Lubrication in Practice: Second Edition*, edited by W. S. Robertson
28. *Principles of Automated Drafting*, Daniel L. Ryan
29. *Practical Seal Design*, edited by Leonard J. Martini
30. *Engineering Documentation for CAD/CAM Applications*, Charles S. Knox
31. *Design Dimensioning with Computer Graphics Applications*, Jerome C. Lange
32. *Mechanism Analysis: Simplified Graphical and Analytical Techniques*, Lyndon O. Barton
33. *CAD/CAM Systems: Justification, Implementation, Productivity Measurement*, Edward J. Preston, George W. Crawford, and Mark E. Coticchia
34. *Steam Plant Calculations Manual*, V. Ganapathy
35. *Design Assurance for Engineers and Managers*, John A. Burgess
36. *Heat Transfer Fluids and Systems for Process and Energy Applications*, Jasbir Singh

37. *Potential Flows: Computer Graphic Solutions*, Robert H. Kirchhoff
38. *Computer-Aided Graphics and Design: Second Edition*, Daniel L. Ryan
39. *Electronically Controlled Proportional Valves: Selection and Application*, Michael J. Tonyan, edited by Tobi Goldoftas
40. *Pressure Gauge Handbook*, AMETEK, U.S. Gauge Division, edited by Philip W. Harland
41. *Fabric Filtration for Combustion Sources: Fundamentals and Basic Technology*, R. P. Donovan
42. *Design of Mechanical Joints*, Alexander Blake
43. *CAD/CAM Dictionary*, Edward J. Preston, George W. Crawford, and Mark E. Coticchia
44. *Machinery Adhesives for Locking, Retaining, and Sealing*, Girard S. Haviland
45. *Couplings and Joints: Design, Selection, and Application*, Jon R. Mancuso
46. *Shaft Alignment Handbook*, John Piotrowski
47. *BASIC Programs for Steam Plant Engineers: Boilers, Combustion, Fluid Flow, and Heat Transfer*, V. Ganapathy
48. *Solving Mechanical Design Problems with Computer Graphics*, Jerome C. Lange
49. *Plastics Gearing: Selection and Application*, Clifford E. Adams
50. *Clutches and Brakes: Design and Selection*, William C. Orthwein
51. *Transducers in Mechanical and Electronic Design*, Harry L. Trietley
52. *Metallurgical Applications of Shock-Wave and High-Strain-Rate Phenomena*, edited by Lawrence E. Murr, Karl P. Staudhammer, and Marc A. Meyers
53. *Magnesium Products Design*, Robert S. Busk
54. *How to Integrate CAD/CAM Systems: Management and Technology*, William D. Engelke
55. *Cam Design and Manufacture: Second Edition; with cam design software for the IBM PC and compatibles, disk included*, Preben W. Jensen
56. *Solid-State AC Motor Controls: Selection and Application*, Sylvester Campbell
57. *Fundamentals of Robotics*, David D. Ardayfio
58. *Belt Selection and Application for Engineers*, edited by Wallace D. Erickson
59. *Developing Three-Dimensional CAD Software with the IBM PC*, C. Stan Wei
60. *Organizing Data for CIM Applications*, Charles S. Knox, with contributions by Thomas C. Boos, Ross S. Culverhouse, and Paul F. Muchnicki
61. *Computer-Aided Simulation in Railway Dynamics*, by Rao V. Dukkipati and Joseph R. Amyot
62. *Fiber-Reinforced Composites: Materials, Manufacturing, and Design*, P. K. Mallick
63. *Photoelectric Sensors and Controls: Selection and Application*, Scott M. Juds
64. *Finite Element Analysis with Personal Computers*, Edward R. Champion, Jr., and J. Michael Ensminger
65. *Ultrasonics: Fundamentals, Technology, Applications: Second Edition, Revised and Expanded*, Dale Ensminger
66. *Applied Finite Element Modeling: Practical Problem Solving for Engineers*, Jeffrey M. Steele
67. *Measurement and Instrumentation in Engineering: Principles and Basic Laboratory Experiments*, Francis S. Tse and Ivan E. Morse
68. *Centrifugal Pump Clinic: Second Edition, Revised and Expanded*, Igor J. Karassik
69. *Practical Stress Analysis in Engineering Design: Second Edition, Revised and Expanded*, Alexander Blake
70. *An Introduction to the Design and Behavior of Bolted Joints: Second Edition, Revised and Expanded*, John H. Bickford
71. *High Vacuum Technology: A Practical Guide*, Marsbed H. Hablanian
72. *Pressure Sensors: Selection and Application*, Duane Tandeske
73. *Zinc Handbook: Properties, Processing, and Use in Design*, Frank Porter
74. *Thermal Fatigue of Metals*, Andrzej Weroniski and Tadeusz Hejwowski
75. *Classical and Modern Mechanisms for Engineers and Inventors*, Preben W. Jensen
76. *Handbook of Electronic Package Design*, edited by Michael Pecht
77. *Shock-Wave and High-Strain-Rate Phenomena in Materials*, edited by Marc A. Meyers, Lawrence E. Murr, and Karl P. Staudhammer
78. *Industrial Refrigeration: Principles, Design and Applications*, P. C. Koelet
79. *Applied Combustion*, Eugene L. Keating
80. *Engine Oils and Automotive Lubrication*, edited by Wilfried J. Bartz

81. *Mechanism Analysis: Simplified and Graphical Techniques, Second Edition, Revised and Expanded*, Lyndon O. Barton
82. *Fundamental Fluid Mechanics for the Practicing Engineer*, James W. Murdock
83. *Fiber-Reinforced Composites: Materials, Manufacturing, and Design, Second Edition, Revised and Expanded*, P. K. Mallick
84. *Numerical Methods for Engineering Applications*, Edward R. Champion, Jr.
85. *Turbomachinery: Basic Theory and Applications, Second Edition, Revised and Expanded*, Earl Logan, Jr.
86. *Vibrations of Shells and Plates: Second Edition, Revised and Expanded*, Werner Soedel
87. *Steam Plant Calculations Manual: Second Edition, Revised and Expanded*, V. Ganapathy
88. *Industrial Noise Control: Fundamentals and Applications, Second Edition, Revised and Expanded*, Lewis H. Bell and Douglas H. Bell
89. *Finite Elements: Their Design and Performance*, Richard H. MacNeal
90. *Mechanical Properties of Polymers and Composites: Second Edition, Revised and Expanded*, Lawrence E. Nielsen and Robert F. Landel
91. *Mechanical Wear Prediction and Prevention*, Raymond G. Bayer
92. *Mechanical Power Transmission Components*, edited by David W. South and Jon R. Mancuso
93. *Handbook of Turbomachinery*, edited by Earl Logan, Jr.
94. *Engineering Documentation Control Practices and Procedures*, Ray E. Monahan
95. *Refractory Linings: Thermomechanical Design and Applications*, Charles A. Schacht
96. *Geometric Dimensioning and Tolerancing: Applications and Techniques for Use in Design, Manufacturing, and Inspection*, James D. Meadows
97. *An Introduction to the Design and Behavior of Bolted Joints: Third Edition, Revised and Expanded*, John H. Bickford
98. *Shaft Alignment Handbook: Second Edition, Revised and Expanded*, John Piotrowski
99. *Computer-Aided Design of Polymer-Matrix Composite Structures*, edited by S. V. Hoa
100. *Friction Science and Technology*, Peter J. Blau
101. *Introduction to Plastics and Composites: Mechanical Properties and Engineering Applications*, Edward Miller
102. *Practical Fracture Mechanics in Design*, Alexander Blake
103. *Pump Characteristics and Applications*, Michael W. Volk
104. *Optical Principles and Technology for Engineers*, James E. Stewart
105. *Optimizing the Shape of Mechanical Elements and Structures*, A. A. Seireg and Jorge Rodriguez
106. *Kinematics and Dynamics of Machinery*, Vladimír Stejskal and Michael Valášek
107. *Shaft Seals for Dynamic Applications*, Les Horve
108. *Reliability-Based Mechanical Design*, edited by Thomas A. Cruse
109. *Mechanical Fastening, Joining, and Assembly*, James A. Speck
110. *Turbomachinery Fluid Dynamics and Heat Transfer*, edited by Chunill Hah
111. *High-Vacuum Technology: A Practical Guide, Second Edition, Revised and Expanded*, Marsbed H. Hablani
112. *Geometric Dimensioning and Tolerancing: Workbook and Answerbook*, James D. Meadows
113. *Handbook of Materials Selection for Engineering Applications*, edited by G. T. Murray
114. *Handbook of Thermoplastic Piping System Design*, Thomas Sixsmith and Reinhard Hanselka
115. *Practical Guide to Finite Elements: A Solid Mechanics Approach*, Steven M. Lepi
116. *Applied Computational Fluid Dynamics*, edited by Vijay K. Garg
117. *Fluid Sealing Technology*, Heinz K. Muller and Bernard S. Nau
118. *Friction and Lubrication in Mechanical Design*, A. A. Seireg
119. *Influence Functions and Matrices*, Yuri A. Melnikov
120. *Mechanical Analysis of Electronic Packaging Systems*, Stephen A. McKeown
121. *Couplings and Joints: Design, Selection, and Application, Second Edition, Revised and Expanded*, Jon R. Mancuso
122. *Thermodynamics: Processes and Applications*, Earl Logan, Jr.
123. *Gear Noise and Vibration*, J. Derek Smith
124. *Practical Fluid Mechanics for Engineering Applications*, John J. Bloomer

125. *Handbook of Hydraulic Fluid Technology*, edited by George E. Totten

Additional Volumes in Preparation

Heat Exchanger Design Handbook, T. Kuppan

Mechanical Engineering Software

Spring Design with an IBM PC, Al Dietrich

Mechanical Design Failure Analysis: With Failure Analysis System Software for the IBM PC, David G. Ullman

This page intentionally left blank

HANDBOOK OF HYDRAULIC FLUID TECHNOLOGY

edited by

GEORGE E. TOTTEN

*Union Carbide Corporation
Tarrytown, New York*



MARCEL DEKKER, INC.

NEW YORK • BASEL

ISBN: 0-8247-6022-0

This book is printed on acid-free paper.

Headquarters

Marcel Dekker, Inc.
270 Madison Avenue, New York, NY 10016
tel: 212-696-9000; fax: 212-685-4540

Eastern Hemisphere Distribution

Marcel Dekker AG
Hutgasse 4, Postfach 812, CH-4001 Basel, Switzerland
tel: 41-61-261-8482; fax: 41-61-261-8896

World Wide Web

<http://www.dekker.com>

The publisher offers discounts on this book when ordered in bulk quantities. For more information, write to Special Sales/Professional Marketing at the headquarters address above.

Copyright © 2000 by Marcel Dekker, Inc. All Rights Reserved.

Neither this book nor any part may be reproduced or transmitted in any form or by any means, electronic or mechanical, including photocopying, microfilming, and recording, or by any information storage and retrieval system, without permission in writing from the publisher.

Current printing (last digit):

10 9 8 7 6 5 4 3 2 1

PRINTED IN THE UNITED STATES OF AMERICA

Preface

One of the most frustrating practices of my career has been the search for information on hydraulic fluids, which includes information on fluid chemistry; physical properties; maintenance practices; and fluid, system, and component design. Although some information on petroleum oil hydraulic fluids can be found, there is much less information on fire-resistant, biodegradable, and other types of fluids. Unfortunately, with few exceptions, fluid coverage in hydraulic texts is typically limited to a single-chapter overview intended to cover all fluids. Therefore, it is often necessary to perform a literature search or a time-consuming manual search of my files. Some time ago it occurred to me that others must be encountering the same problem. There seemed to be a vital need for an extensive reference text on hydraulic fluids that would provide information in sufficient depth and breadth to be of use to the fluid formulator, hydraulic system designer, plant maintenance engineer, and others who serve the industry.

Currently, there are no books dedicated to hydraulic fluid chemistry. Most hydraulic fluid treatment is found in handbooks, which primarily focus on hydraulic system hardware, installation, and troubleshooting. Most of these books fit into one of two categories. One type of book deals with hydraulic equipment, with a single, simplified overview chapter covering all hydraulic fluids but with a focus on petroleum-derived fluids. The second type of book provides fluid coverage with minimal, if any, discussion of engineering properties of importance in a hydraulic system.

The purpose of the *Handbook of Hydraulic Fluid Technology* is to provide a comprehensive and rigorous overview of hydraulic fluid technology. The objective is not only to discuss fluid chemistry and physical properties in detail, but also to integrate both classic and current fundamental lubrication concepts with respect to various classes of hydraulic fluids. A further objective is to integrate fluid dynamics with respect to their operation in a hydraulic system in order to enable the reader to obtain a broader understanding of the total system. Hydraulic fluids are an important and vital component of the hydraulic system.

The 23 chapters of this book are grouped into three main parts: hardware, fluid properties and testing, and fluids.

HARDWARE

Chapter 1 provides the reader with an overview of basic hydraulic concepts, a description of the components, and an introduction to hydraulic system operation. In Chapter 2, the rolling element bearings and their lubrication are discussed. An extremely important facet of any well-designed hydraulic system is fluid filtration. Chapter 3 not only provides a detailed discussion of fluid filtration and particle contamination and quantification, but also discusses fluid filterability.

An understanding of the physical properties of a fluid is necessary to understand the performance of a hydraulic fluid as a fluid power medium. Chapter 4 features a thorough overview of the physical properties, and their evaluation and impact on hydraulic system operation, which includes: viscosity, viscosity-temperature and viscosity-pressure behavior, gas solubility, foaming, air entrainment, air release, and fluid compressibility and modulus.

FLUID PROPERTIES AND TESTING

Viscosity is the most important physical property exhibited by a hydraulic fluid. Chapter 5 presents an in-depth discussion of hydraulic fluid viscosity and classification. The hydraulic fluid must not only perform as a power transmission medium but also lubricate the system. Chapter 6 provides a thorough review of the fundamental concepts involved in lubricating a hydraulic system. In many applications, fluid fire resistance is one of the primary selection criteria. An overview of historically important fire-resistance testing procedures is provided in Chapter 7, with a discussion of currently changing testing protocol required for industry, national, and insurance company approvals. Ecological compatibility properties exhibited by a hydraulic fluid is currently one of the most intensive research areas of hydraulic fluid technology. An overview of the current testing requirements and strategies is given in Chapter 8.

One of the most inexpensive but least understood components of the hydraulic system is hydraulic seals. Chapter 9 provides a review of mechanical and elastomeric seal technology and seal compatibility testing. An often overlooked but vitally important area is adequate testing and evaluation of hydraulic fluid performance in a hydraulic system. There currently is no consensus on the best tests to perform and what they reveal. Chapter 10 reviews the state-of-the-art of bench and pump testing of hydraulic fluids. Vibrational analysis not only is an important plant maintenance tool but is also one of the most important diagnostic techniques for evaluating and

troubleshooting the operational characteristics of a hydraulic system. Chapter 11 provides an introductory overview of the use of vibrational analysis in fluid maintenance. No hydraulic system operates trouble-free forever. When problems occur, it is important to be able to identify both the problem and its cause. Chapter 12 provides a thorough discussion of hydraulic system failure analysis strategies.

FLUIDS

Although water hydraulics do not constitute a major fluid power application, they are coming under increasing scrutiny as eco-compatible alternatives to conventional hydraulic fluids. Chapter 13 offers an overview of this increasingly important technology.

The largest volume fluid power medium is petroleum oil. In Chapter 14, the reader is provided with a thorough overview of oil chemistry, properties, fluid maintenance, and change-out procedures. Chapter 15 reviews additive technology for petroleum oil hydraulic fluids.

There are various types of synthetic hydraulic fluids. Chapter 16 describes the more important synthetic fluids, with a focus on aerospace applications.

Chapters 17 to 20 describe fire-resistant hydraulic fluids. Emulsions, water-glycols, polyol esters, and phosphate esters are discussed individually and in depth in Chapters 17, 18, 19, and 20, respectively. This discussion includes fluid chemistry, physical properties, additive technology, maintenance, and hydraulic system conversion.

Vegetable oils are well-known lubricants that have been examined repeatedly over the years. Currently, there is an intensive effort to increase the utilization of various types of vegetable oils as an ecologically sound alternative to mineral oil hydraulic fluids. Chapter 21 provides a review of vegetable oil chemistry, recovery, and properties. The applicability of these fluids as hydraulic fluid basestocks is examined in detail.

Chapter 22 discusses electrorheological fluids, which are becoming increasingly interesting for use in specialized hydraulic applications.

In Chapter 23, various standardized fluid maintenance procedures are discussed and a summary of equivalent international testing standards is provided.

The preparation of a text of this scope was a tremendous task. I am deeply indebted to many colleagues for their assistance, without whom this text would not have been possible. Special thanks go to Dr. Stephen Lainer (University of Aachen), Prof. Atsushi Yamaguchi (Yokohama National University), Prof. Toshi Kazama (Muroran Institute of Technology), K. Mizuno (Kayaba Industrial Ltd.), and Jürgen Reichel (formerly with DMT, Essen, Germany).

Special thanks also goes to my wife, Alice, for her unending patience, and to Susan Meeker, who assisted in organizing and editing much of this material; to Glenn Webster, Roland J. Bishop, Jr., and Yinghua Sun, without whose help this text would never have been completed; and to Union Carbide Corporation for its support.

George E. Totten

Contents

<i>Preface</i>	<i>iii</i>
<i>Contributors</i>	<i>xi</i>

HARDWARE

1. Basic Hydraulic Pump and Circuit Design	1
<i>Richard K. Tessmann, Hans M. Melief, and Roland J. Bishop, Jr.</i>	
2. Bearing Selection and Lubrication	65
<i>Faruk Pavlovich</i>	
3. Fluid Cleanliness and Filtration	147
<i>Richard K. Tessmann and I. T. Hong</i>	
4. Physical Properties and Their Determination	195
<i>George E. Totten, Glenn M. Webster, and F. D. Yeaple</i>	

FLUID PROPERTIES AND TESTING

5. Fluid Viscosity and Viscosity Classification	305
<i>Bernard G. Kinker</i>	
6. Lubrication Fundamentals	339
<i>Lavern D. Wedeven and Kenneth C Ludema</i>	

7. Fire-Resistance Testing Procedures of Hydraulic Fluids	393
<i>Glenn M. Webster and George E. Totten</i>	
8. Ecological Compatibility	427
<i>Gary H. Kling, Dwayne E. Tharp, George E. Totten, and Glenn M. Webster</i>	
9. Seals and Seal Compatibility	469
<i>Ronald E. Zielinski</i>	
10. Bench and Pump Testing of Hydraulic Fluids	523
<i>Lin Xie, Roland J. Bishop, Jr., and George E. Totten</i>	
11. Vibrational Analysis for Fluid Power Systems	577
<i>Hugh R. Martin</i>	
12. Failure Analysis	601
<i>Steven Lemberger and George E. Totten</i>	
FLUIDS	
13. Water Hydraulics	675
<i>Kari T. Koskinen and Matti J. Vilenius</i>	
14. Mineral-Oil Hydraulic Fluids	711
<i>Paul McHugh, William D. Stofey, and George E. Totten</i>	
15. Lubricant Additives for Mineral-Oil-Based Hydraulic Fluids	795
<i>Stephen H. Roby, Elaine S. Yamaguchi, and P. R. Ryason</i>	
16. Polyalphaolefins and Other Synthetic Hydrocarbon Fluids	825
<i>Ronald L. Shubkin, Lois J. Gschwender, and Carl E. Snyder, Jr.</i>	
17. Emulsions	847
<i>Yinghua Sun and George E. Totten</i>	
18. Water-Glycol Hydraulic Fluids	917
<i>George E. Totten and Yinghua Sun</i>	
19. Polyol Ester Fluids	983
<i>Robert A. Gere and Thomas V. Hazelton</i>	
20. Phosphate Ester Hydraulic Fluids	1025
<i>W. D. Phillips</i>	
21. Vegetable-Based Hydraulic Oils	1095
<i>Lou A. T. Honary</i>	
22. Electro-rheological Fluids	1153
<i>Christian Wolff-Jesse</i>	
23. Standards for Hydraulic Fluid Testing	1185
<i>Paul Michael</i>	

Appendixes

1. <i>Temperature Conversion Table</i>	1209
2. <i>SI Unit Conversions</i>	1213
3. <i>Commonly Used Pressure Conversions; Fraction Notation</i>	1215
4. <i>Volume and Weight Equivalents</i>	1216
5. <i>Head and Pressure Equivalents</i>	1217
6. <i>Flow Equivalents</i>	1218
7. <i>Viscosity Conversion Charts</i>	1219
8. <i>Number of U.S. Gallons in Round and Rectangular Tanks</i>	1222
9. <i>Water Vapor Pressure Chart</i>	1225
10. <i>Physical Properties of Ethylene, Diethylene, and Propylene Glycol</i>	1226
11. <i>Common Wear Problems Related to Lubricants and Hydraulic Fluids</i>	1242

<i>Index</i>	1247
--------------	------

1

Basic Hydraulic Pump and Circuit Design

RICHARD K. TESSMANN

FES, Inc., Stillwater, Oklahoma

HANS M. MELIEF

The Rexroth Corporation, Bethlehem, Pennsylvania

ROLAND J. BISHOP, JR.

Union Carbide Corporation, Tarrytown, New York

1 INTRODUCTION

Hydraulics, according to Webster, is defined as “operated, moved, or effected by means of water.” In the 17th century, it was discovered that a fluid under pressure could be used to transmit power [1]. Blaise Pascal (1623–1662) observed that if a fluid in a closed container was subjected to a compressive force, the resulting pressure was transmitted throughout the system undiminished and equal in all directions [1].

Hydraulics is by far the simplest method to transmit energy to do work. It is considerably more precise in controlling energy and exhibits a broader adjustability range than either electrical or mechanical methods. To design and apply hydraulics efficiently, a clear understanding of energy, work, and power is necessary.

In this chapter, fundamentals of hydraulic pump operation and circuit design will be provided. This will include the following:

- Hydraulic principles
- Hydraulic system components
- Hydraulic pumps and motors
- System design considerations

2 DISCUSSION

2.1 Hydraulic Principles

Work is done when something is moved. Work is directly proportional to the amount of force applied over a given distance according to the following relation,

$$\text{Work (ft-lbs)} = \text{Distance (ft)} \times \text{Force (lbs)} \quad (1.1)$$

Power is defined as the rate of doing work and has the units of foot-pounds per second. A more common unit of measure is "horsepower (hp)." Horsepower is defined as the amount of weight in pounds that a horse could lift 1 ft in 1 s (Fig. 1.1) [1]. By experiment, it was found that the average horse could lift 550 lbs. 1 ft in 1 s; consequently,

$$1 \text{ hp} = \frac{550 \text{ ft-lbs}}{\text{s}} \quad (1.2)$$

Energy is the ability to do work. It may appear in various forms, such as mechanical, electrical, chemical, nuclear, acoustic, radiant, and thermal. In physics, the Law of Conservation of Mass and Energy states that neither mass nor energy can be created or destroyed, only converted from one to the other.

In a hydraulic system, energy input is called a "prime mover." Electric motors and internal combustion engines are examples of prime movers. Prime movers and hydraulic pumps do not create energy; they simply convert it to a form that can be utilized by a hydraulic system.

The pump is the heart of the hydraulic system. When the system performs improperly, the pump is usually the first component to be investigated. Many times, the pump is described in terms of its pressure limitations. However, the hydraulic pump is a flow generator, moving a volume of fluid from a low-pressure region to a higher-pressure region in a specific amount of time depending on the rotation speed.

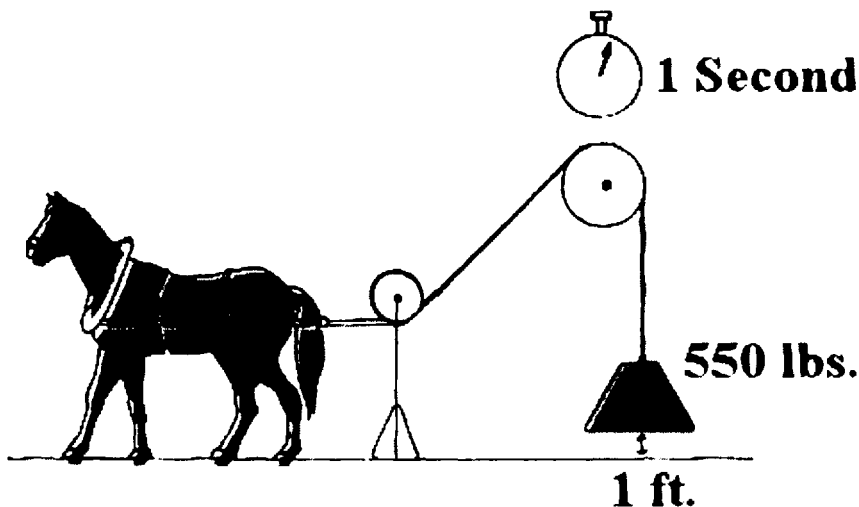


Figure 1.1 Illustration of the horsepower concept.

Therefore, the pump is properly described in terms of its displacement or the output flow rate expected from it.

All pumps used in a hydraulic system are of the positive displacement type. This means that there is an intentional flow path from the inlet to the outlet. Therefore, the pump will move fluid from the inlet or suction port to the outlet port at any pressure. However, if that pressure is beyond the pressure capability of the pump, failure will occur. The pressure which exists at the outlet port of the pump is a function of the load on the system. Therefore, hydraulic system designers will always place a pressure-limiting component (i.e., a relief valve) at the outlet port of a pump to prevent catastrophic failures from overpressurization.

Most pumps in hydraulic systems fall into one of three categories: vane pumps, gear pumps, or piston pumps (Sec. 2.2). The action of the hydraulic pump consists of moving or transferring fluid from the reservoir, where it is maintained at a low pressure and, consequently, a low-energy state [2]. From the reservoir, the pump moves the fluid to the hydraulic system where the pressure is much higher, and the fluid is at a much higher-energy state because of the work that must be done by the hydraulic system. The amount of energy or work imparted to the hydraulic system through the pump is a function of the amount of volume moved and the pressure at the discharge port of the pump:

$$\text{Work} \propto \text{Pressure} \times \text{Flow} \quad (1.3)$$

From an engineering standpoint, it is common to relate energy to force times distance:

$$\text{Work} \propto \text{Force} \times \text{Distance} \quad (1.4)$$

However, hydraulic pressure is force divided by area, and volume is area times distance:

$$\text{Pressure} = \frac{\text{Force}}{\text{Area}} \quad (1.5)$$

$$\text{Volume} = \text{Area} \times \text{Distance} \quad (1.6)$$

From these relationships, Eq. (1.7) shows that pressure times volume is equivalent to force times distance.

$$P \text{ (lbs/in.}^2\text{)} \times V \text{ (in.}^3\text{)} = F \text{ (lbs)} \times D \text{ (in.)} \quad (1.7)$$

The hydraulic pump is actually a “three-connection” component. One connection is at the discharge (outlet) port, the second is at the suction (inlet) port, and the third connection is to a motor or engine (Fig. 1.2) [1]. From this standpoint, the pump is a transformer. It takes the fluid in the reservoir, using the energy from the motor or engine, and transforms the fluid from a low-pressure level to a higher-pressure level. In fact, the hydraulic fluid is actually a main component of the hydraulic system, and as we will see throughout this book, has a major influence in the operation of the system. Hydraulic pumps are commonly driven at speeds from 1200 rpm to 3600 rpm or higher and maximum pressures may vary from <1000 psi (pounds per square inch) to >6000 psi. Tables 1.1 and 1.2 [1] show typical pressure and speed limitations for various types of pumps and motors.

In addition to pressure, there is also a temperature limitation imposed by the hydraulic fluid. This is caused by the decrease in viscosity as the fluid temperature

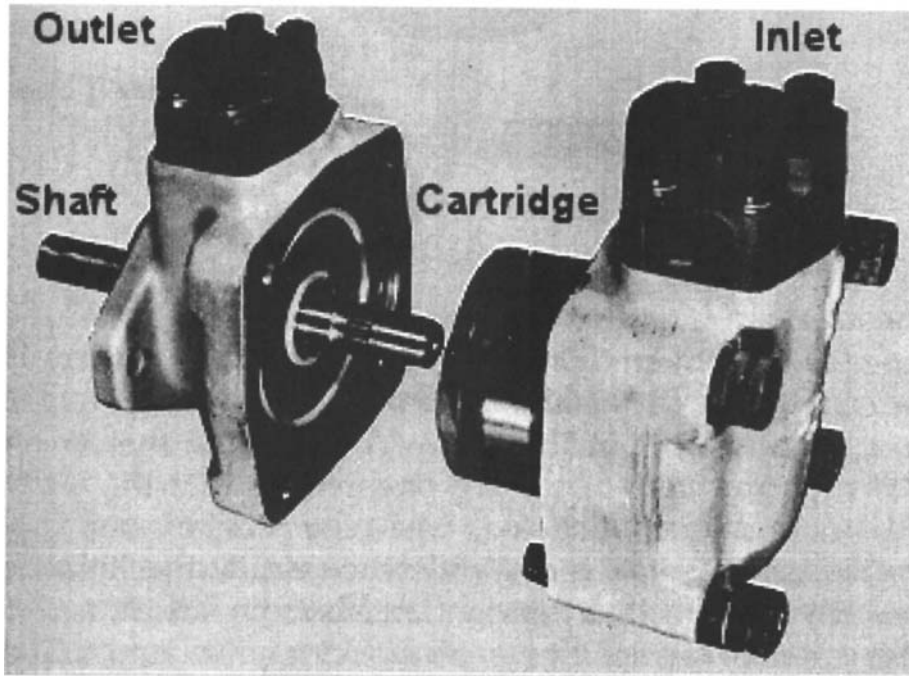


Figure 1.2 Illustration of pump connections.

increases. Generally, pump manufacturers set upper and lower viscosity limits on the hydraulic fluids used in their pumps. The upper viscosity limit determines the minimum temperature for pump start-up to prevent cavitation. Cavitation occurs when there is insufficient fluid flow into the pump inlet. During cavitation, the fluid will release any dissolved gases or volatile liquids. The gaseous bubbles produced will then travel into the high-pressure region of the pump where they will collapse under high pressure and may cause severe damage to the pump. Also, overheating of the pump bearings could result because of insufficient cooling as a result of inadequate flow.

Table 1.1 Typical Pump Performance Parameters for One Manufacturer

Hydraulic Pump Type	Flow	Maximum Pressure (psi)	Maximum Speed (rpm)	Total Efficiency (%)
External Gear	Fixed	3,600	500–5,000	85–90
Internal Gear	Fixed	3,000	900–1,800	90
Vane	Fixed	2,500	900–3,000	86
Vane	Variable	1,000–2,300	750–2,000	85
Radial Piston	Fixed	10,000	1,000–3,400	90
Axial Piston (bent axis)	Fixed	5,100–6,500	950–3,200	92
Axial Piston (bent axis)	Variable	5,800	500–4,100	92
Axial Piston (swash plate)	Variable	4,600–6,500	500–4,300	91

Table 1.2 Typical Motor Performance Parameters for One Manufacturer

Hydraulic Motor Type	Flow	Maximum Pressure (psi)	Maximum Speed (rpm)	Total Efficiency (%)
Gear	Fixed	3600	500–3000	85
Radial Piston	Fixed	6100–6500	1–500	91–92
Radial Piston	Variable	6100	1–500	92
Axial Piston (bent axis)	Fixed	5800–6500	50–6000	92
Axial Piston (bent axis)	Variable	6500	50–8000	92
Axial Piston (swash plate)	Variable	4600–5800	6–4900	91

The lower viscosity limit will establish the upper temperature limit of the fluid. If the upper temperature limit is exceeded, the viscosity will be insufficient to bear the high operating loads in the pump and, thus, lubrication failure will result in shortened pump life and/or catastrophic pump failure. Table 1.3 shows the effect of viscosity index on the pump operating temperatures for one major pump manufacturer [1].

Viscosity index is a measure of the viscosity change or resistance to flow of a liquid as the temperature is changed. A higher viscosity index produces a smaller viscosity change with temperature than a fluid having a lower viscosity index (see Chapter 4).

2.1.1 Torque and Pressure

The input parameters to the hydraulic pump from the prime mover are speed and torque. The input torque to the pump is proportional to the pressure differential between the inlet port and the discharge port:

$$\text{Torque}_{\text{input}} \propto (\text{Pressure}_{\text{outlet}} - \text{Pressure}_{\text{inlet}}) \times \text{Displacement} \quad (1.8)$$

The torque required to drive a positive displacement pump at constant pressure is [3–7]

$$T_a = T_t + T_v + T_f + T_c \quad (1.9)$$

where T_a is the actual torque required, T_t is the theoretical torque due to pressure differential and physical dimensions of the pump, T_v is the torque resulting from viscous shearing of the fluid, T_f is the torque resulting from internal friction, and T_c is the constant friction torque independent of both pressure and speed.

Table 1.3 A Pump Manufacturer's Viscosity Index and Temperature Guidelines

Temperature (°F)	Viscosity Index (50)	Viscosity Index (95)	Viscosity Index (150)
Minimum	18	5	0
Optimum	85–130	80–135	75–140
Maximum	155	160	175

Substituting the operational and dimensional parameters (using appropriate units) into Eq. (1.9) produces the following expression:

$$T_a = (P_1 - P_2)D_p + C_v D_p \mu N + C_f (P_1 - P_2)D_p + T_b \quad (1.10)$$

where P_1 is the pressure at the discharge port, P_2 is the pressure at the inlet port, D_p is the pump displacement, C_v is the viscous shear coefficient, μ is the fluid viscosity, N is the rotation speed of the pump shaft, C_f is the mechanical friction coefficient, and T_b is the breakaway torque.

Actual values of the parameters such as viscous shear coefficient, mechanical friction coefficient, and breakaway torque are determined experimentally. From Eq. (1.10), the required torque to drive a pump is primarily a function of the pressure drop across the pump ($P_1 - P_2$) and the displacement (D_p) of the pump.

2.1.2 Rotational Speed and Flow

The output flow of a hydraulic pump is described by

$$Q_a = Q_t - Q_l - Q_r \quad (1.11)$$

where Q_a is the delivery or actual flow rate of the pump, Q_t is the theoretical flow, Q_l is the leakage flow, and Q_r is the losses resulting from cavitation and aeration (usually neglected).

Substituting the operational (speed, flow, and pressure) and dimensional (pump displacement) parameters into Eq. (1.11) yields

$$Q_a = ND_p - \frac{C_l D_p (P_1 - P_2)}{\mu} \quad (1.12)$$

where Q_a is the delivery or actual flow rate of the pump and C_l is the leakage flow (slip) coefficient. From Eq. (1.12) it is apparent that pump delivery (Q_a) is primarily a function of the rotational speed (N) of the pump, and the losses are a function of the hydraulic load pressure ($P_1 - P_2$).

The leakage flow or slip that takes place in a positive displacement pump is caused by the flow through the small clearance spaces between the various internal parts of the pump in relative motion. These small leakage paths are often referred to as capillary passages. Most of these passages are characterized by two flat parallel plates with leakage flow occurring through the clearance space between the flat plates (Fig. 1.3) [1]. Therefore, the fundamental relationships for flow between flat plates are normally applied to the leakage flow in hydraulic pumps. However, to apply Eq. (1.12), it is necessary to obtain the value of the slip flow coefficient through experimental results [3,6].

2.1.3 Horsepower (Mechanical and Hydraulic)

Of interest to the designers and users of hydraulic systems is the power (Hp_{input}) required to drive the pump at the pressure developed by the load and the output power (Hp_{output}), which will be generated by the pump. The expression (using appropriate units) which describes the "mechanical" input horsepower required to drive the pump is

$$Hp_{\text{input}} = \frac{T_a N}{5252} \quad (1.13)$$

where Hp_{input} is the required input power (hp), T_a is the actual torque required (lb-

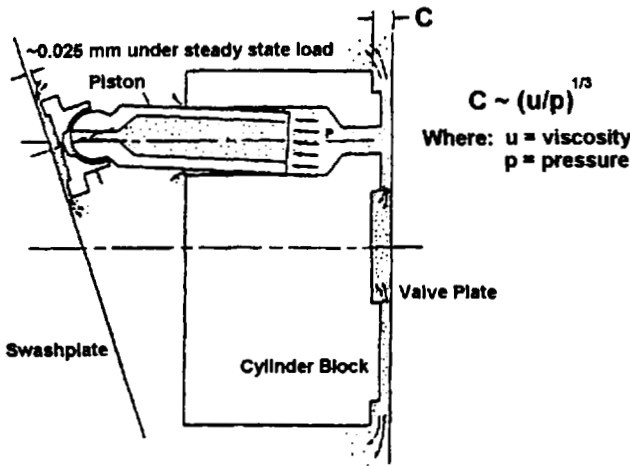


Figure 1.3 Illustration of the leakage path between two flat plates in a piston pump.

ft), and N is the rotational speed of the pump shaft (rpm). The “hydraulic” output horsepower of a hydraulic pump is described by the expression

$$Hp_{\text{output}} = \frac{PQ}{1714} \tag{1.14}$$

where Hp_{output} is the power output of the pump (hp), P is the pressure at the pump discharge port (psi), and Q is the delivery or actual flow output (gpm).

However, in the real world, $Hp_{\text{input}} > Hp_{\text{output}}$. This is always true because no pump or motor is 100% efficient. As will be shown in the next subsection, this is mainly due to internal mechanical friction and fluid leakage within the pump.

2.1.4 Pumping Efficiency

Hydraulic pumping efficiency or total efficiency (E_t) is a combination of two kinds of efficiencies: volumetric (E_v) and mechanical (E_m). Volumetric efficiency is given by

$$E_v = \frac{\text{Actual flow output}}{\text{Theoretical flow output}} \tag{1.15}$$

The second kind of efficiency is called the torque efficiency or the mechanical efficiency (E_m). The mechanical efficiency is described by

$$E_m = \frac{\text{Theoretical torque input}}{\text{Actual torque input}} \tag{1.16}$$

The overall or total efficiency (E_t) is defined by

$$E_t = E_v E_m \tag{1.17}$$

The total efficiency is also related to power consumption by

$$E_t = \frac{\text{Power output}}{\text{Power input}} \quad (1.18)$$

Substituting Eqs. (1.13) and (1.14) into Eq. (1.18) produces the following expression for the overall efficiency of a hydraulic pump:

$$E_t = \frac{0.326T_a N}{PQ} \quad (1.19)$$

Theoretical pump delivery is also determined from the dimensions of the pump. However, if the dimensions of the pump are not known, they are determined by pump testing. The overall efficiency of a pump may also be measured by testing. However, it is difficult to measure mechanical efficiency. This is because internal friction plays a major role and there is no easy way of measuring this parameter within a pump. Rearrangement of Eq. (1.17) gives the mechanical efficiency as the overall efficiency divided by the volumetric efficiency:

$$E_m = \frac{E_t}{E_v} \quad (1.20)$$

2.1.5 Hydraulic System Design

When designing a hydraulic system, the designer must first consider the load to be moved or controlled. Then, the size of the actuator is determined. The "actuator" is a component of a hydraulic system which causes work to be done, such as a hydraulic cylinder or motor. The actuator must be large enough to handle the load at a pressure within its design capability. Once the actuator size is determined, the speed at which the load must move will establish the flow rate of the system (gpm; gallons per minute):

For hydraulic cylinders,

$$\text{gpm} = \frac{AV}{231} \quad (1.21)$$

where A is the area (in.²) and V is the velocity (in./min)

For hydraulic motors,

$$\text{gpm} = \frac{(D)(\text{rpm})}{231} \quad (1.22)$$

where D is the displacement (in.³/rev.)

For example, calculate the hydraulic cylinder bore diameter (D) and flow (Q) required to lift a 10,000 lb load at a velocity of 120 in./min with a hydraulic load pressure not exceeding 3000 psi. Using the fundamental hydraulic expression,

$$\text{Force} = \text{Pressure} \times \text{Area} \quad (1.23)$$

Force is equal to 10,000 lbs and pressure is 3000 psi. The area of the head end of the cylinder is calculated by rearranging Eq. (1.23) and solving for the area:

$$\begin{aligned} \text{Area} &= \frac{\text{Force}}{\text{Pressure}} = \frac{10,000}{3,000} \\ &= 3.333 \text{ in.}^2 \\ &= \frac{\pi D^2}{4} \\ D &= 2.06 \text{ in.} \end{aligned} \quad (1.24)$$

Therefore, a double-acting single-rod cylinder with a cylinder bore of 2.25 or 2.5 in. may be used, depending on the requirements of the head side of the cylinder (Fig. 1.4) [1]. However, on the rod side, the area of the piston is reduced by the area of the rod. Because the effective area on the rod side of the cylinder is less than that on the head side, the cylinder would not be able to lift as large a load when retracting, because of pressure intensification at the rod end causing the system relief valve to open. For this reason, all single-rod cylinders exert greater force at the rod end when extending than retracting. On the other hand, a double-rod cylinder of equal rod diameters would exert an equal force in both directions (extending and retracting).

Once the size of the cylinder is selected, the designer must consider the speed requirements of the system. The speed at which the load must be moved is dependent on the pump flow rate. Of course, the velocity of the cylinder rod and the speed of the load must be the same. By using the equation

$$Q = \frac{VA}{231} \quad (1.25)$$

where Q is the flow rate into the cylinder (gpm), V is the velocity of the cylinder rod (in./min), and A is the cylinder area (in.²).

The flow rate (Q) needed to produce a specific velocity (V) can now be calculated by combining Eqs. (1.24) and (1.25); using a 2.5-in.-diameter cylinder as an example,

$$\begin{aligned} Q &= \frac{\pi D^2 V}{924} \\ &= \frac{(3.14)(2.5)^2(120)}{924} \\ &= 2.6 \text{ gpm} \end{aligned} \quad (1.26)$$

Once the pressure needed to support the load and flow to produce the specified load velocity is determined, the pump selection process and system design may begin.

There are several factors in pump selection and hydraulic system design that have not been addressed. For example, the service life required by the system must be decided along with the contamination level that must not be exceeded in the system. The piping sizes and the inlet conditions to the pump must be considered. The fluid to be used in the hydraulic system is an obvious consideration. These and other factors will be addressed in later sections of this chapter.

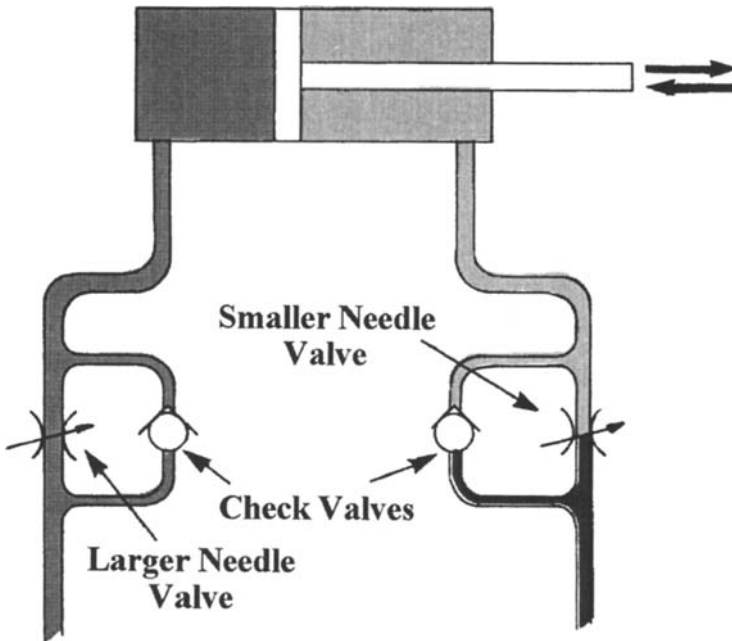


Figure 1.4 Illustration of a single-rod double-acting cylinder.

2.2 Hydraulic Pumps and Motors

There are three types of pumps used predominately in hydraulic systems: vane pumps, gear pumps, and piston pumps (Fig. 1.5) [1].

Although there are many design parameters that differ between a hydraulic pump and a hydraulic motor, the general description is fundamentally the same, but their uses are quite different. A pump is used to convert mechanical energy into hydraulic energy. The mechanical input is accomplished by using an electric motor or a gasoline or diesel engine. Hydraulic flow from the output of the pump is used to power a hydraulic circuit. On the other hand, a hydraulic motor is used to convert hydraulic energy back into mechanical energy. This is accomplished by connecting the output shaft of the hydraulic motor to a mechanical actuator, such as a gear box, pulley, or flywheel.

2.2.1 Vane Pumps

A typical design for the vane pump is shown in Fig. 1.6 [8]. The vane pump relies upon sliding vanes riding on a cam ring to increase and decrease the volume of the pumping chambers within the pump (Fig. 1.7). The sides of the vanes and rotor are sealed by side bushings. Although there are high-pressure vane pumps (>2500 psi), this type of pump is usually thought of as a low pressure pump (<2500 psi), see Table 1.1.

There are two vane pump designs. One is a balanced design, whereas the other is unbalanced. In the balanced design, there are opposing pairs of internal inlet and outlet ports which distribute the thrust force evenly around the shaft (Fig. 1.8) [8]. All modern vane pumps are of the balanced design. The vane pump is considered

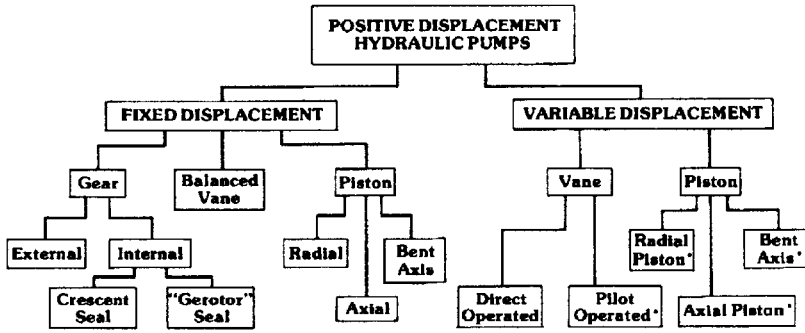


Figure 1.5 The family of hydraulic pumps.

one of the simplest of all positive displacement pumps and can be designed to produce variable displacement; that is, the output flow can be changed to suit the needs of the hydraulic system (Fig. 1.9) [8]. Fluid leakage in vane pumps occurs between the high- and low-pressure sides of the vanes and across the side bushings which results in decreased volumetric efficiency and, hence, reduced flow output. The unbalanced design suffers from shortened bearing life because of the unbalanced thrust force within the pump.

2.2.2 Gear Pumps

It is generally agreed that the gear pump is the most robust and rugged type of fluid power pump. Although there are many gear-type pumps, three are used predominately for hydraulic service. One is the external gear pump (Fig. 1.10) [8] and the other two are internal gear pumps of the “crescent” seal and “gerotor” seal type (Figs. 1.11 and 1.12, respectively) [8].

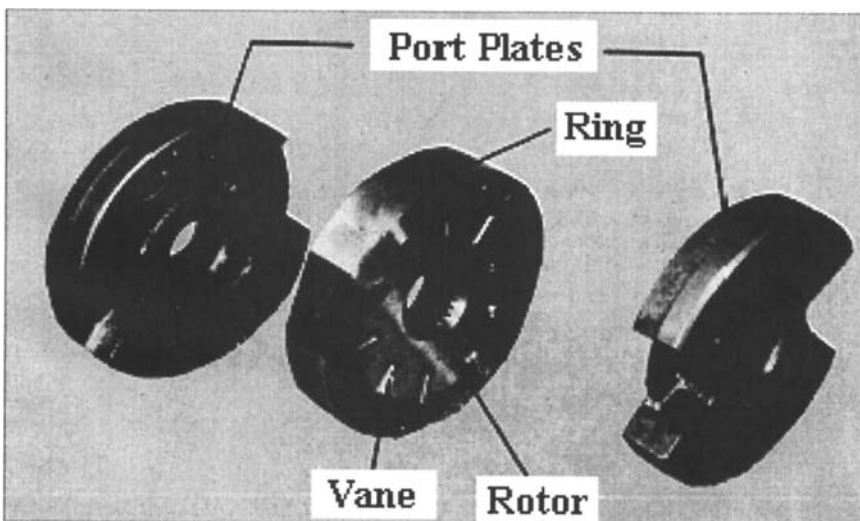


Figure 1.6 Illustration of a typical vane pump.

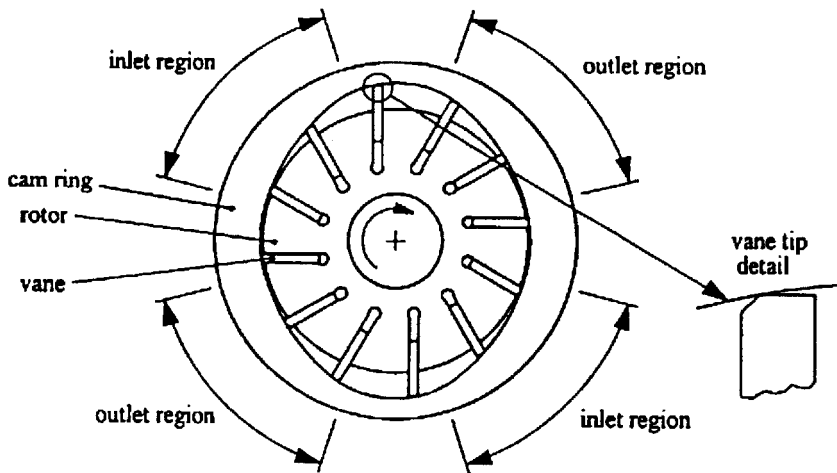


Figure 1.7 Illustration of cam ring and vanes in a vane pump.

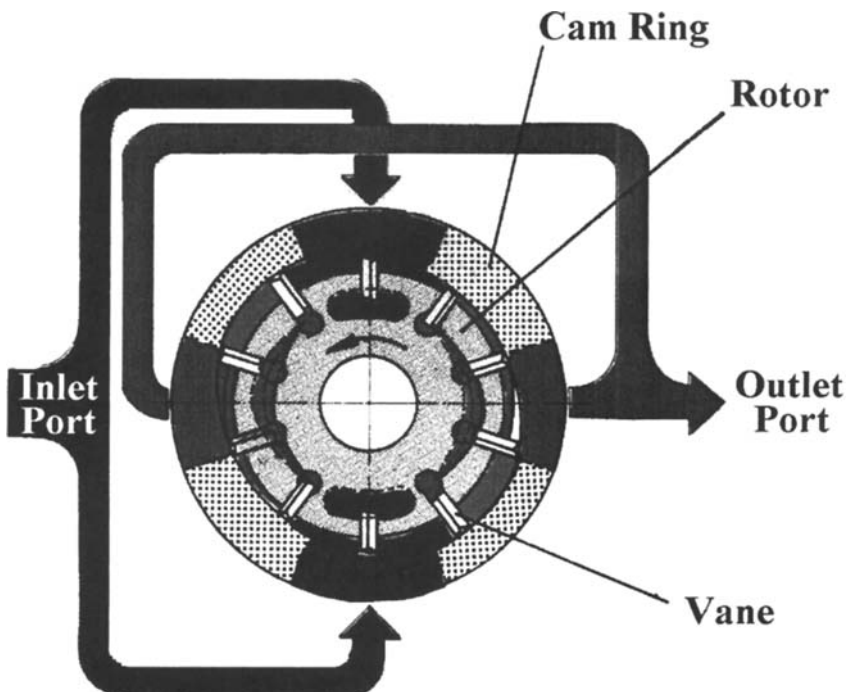


Figure 1.8 Illustration of a balanced-design vane pump.

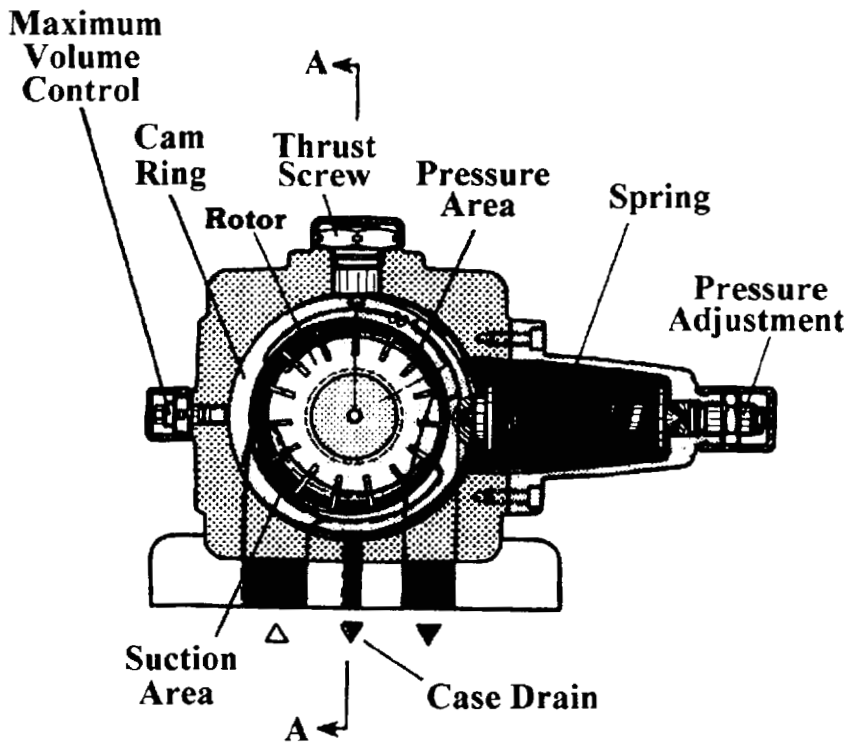


Figure 1.9 Illustration of a variable-displacement vane pump.

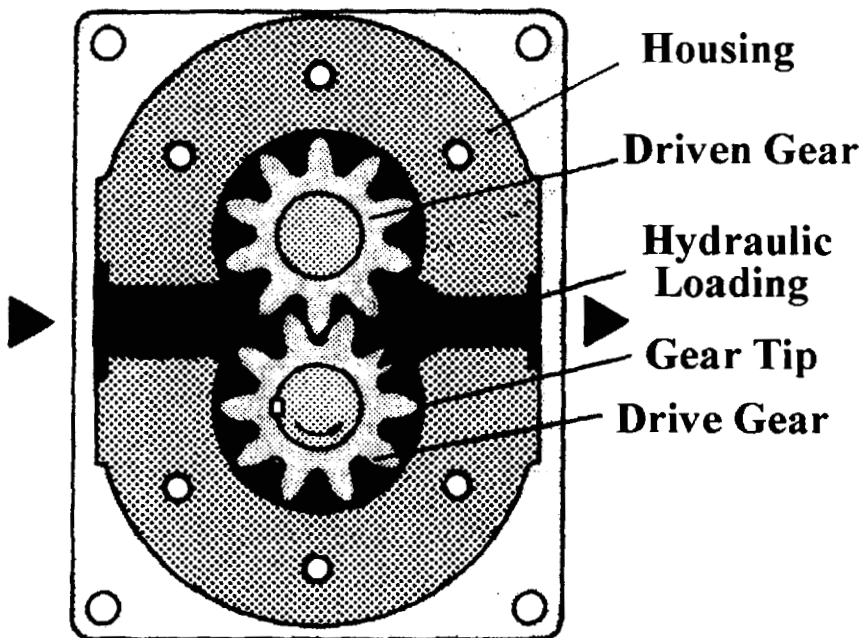


Figure 1.10 Illustration of an external gear pump.

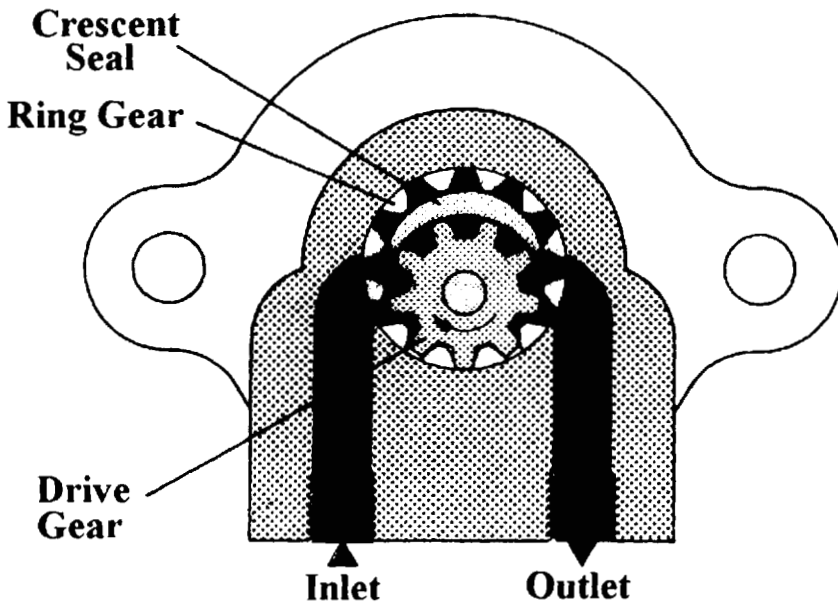


Figure 1.11 Illustration of an internal (crescent) gear pump.

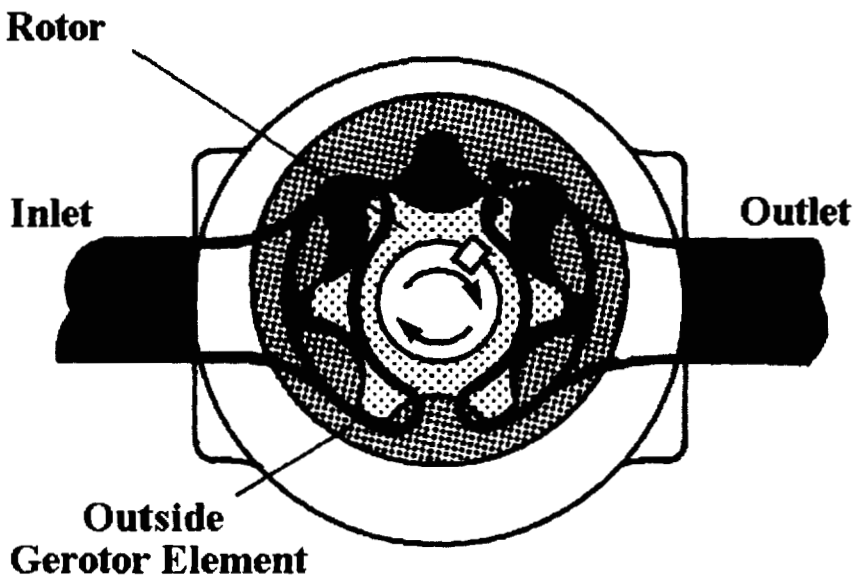


Figure 1.12 Illustration of an internal (gerotor) gear pump.

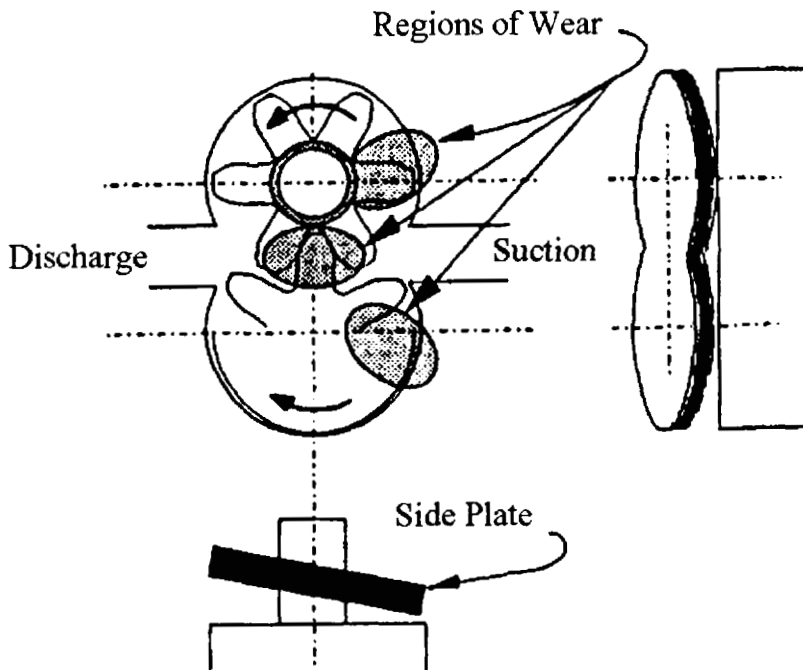


Figure 1.13 Illustration of the wear and leakage areas of the external gear pump.

The external gear pump is the most prevalent (Fig. 1.10) [8]. Note that there are two gears: a drive and a driven gear. The number of teeth, the pitch circle diameter, and the width of the gears are the dominant parameters which control the displacement. The gears are enclosed by the housing and a side plate. Fluid leakage in this type of pump occurs between the tips of the gears and across the side plate (Fig. 1.13) [8].

The crescent seal internal gear pump consists of a small internal gear and a larger ring gear (Fig. 1.11) [8]. The small internal gear is driven by the prime mover. The internal gear meshes with the ring gear and turns it in the same direction. The sealing of the high-pressure chamber from the pump's inlet is achieved by a crescent seal between the upper teeth of the internal small gear and the upper teeth of the ring gear. In the gerotor gear pump, the inner gerotor has one less tooth than the outer element (Fig. 1.12) [8]. The internal gear is driven by the prime mover and, in turn, drives the outer element in the same direction. There is no satisfactory gear pump design in which the displacement can be varied.

2.2.3 Piston Pumps

The piston pump is operated at the highest pressure of all of the pumps normally found in hydraulic applications. The piston pump is manufactured in the axial, bent-axis, and radial configurations. In addition, there are both fixed- and variable-displacement bent-axis configurations (Figs. 1.14 and 1.15, respectively) [8]. The axial design configuration predominates in hydraulic systems and will be the basis of the discussions here. A typical example of an axial fixed-displacement piston pump is

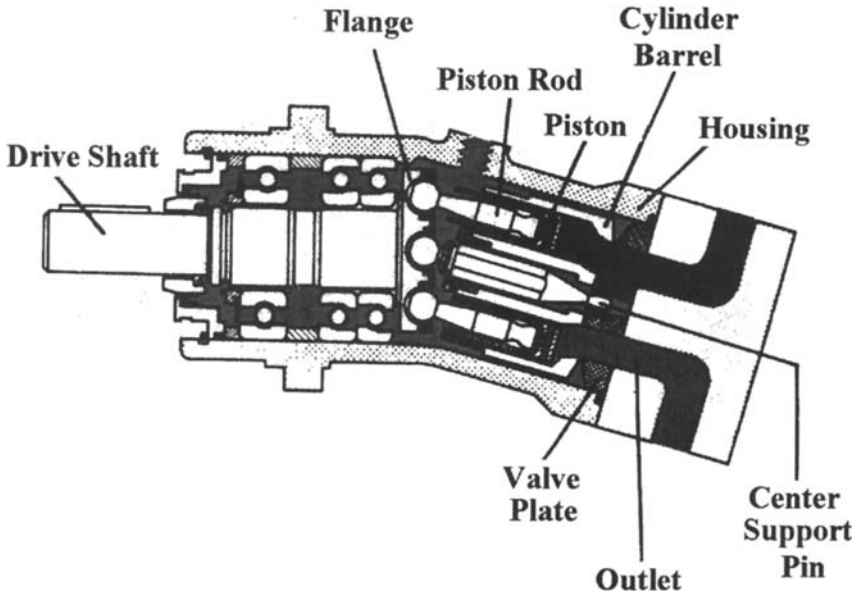


Figure 1.14 Illustration of a bent-axis fixed-displacement piston pump.

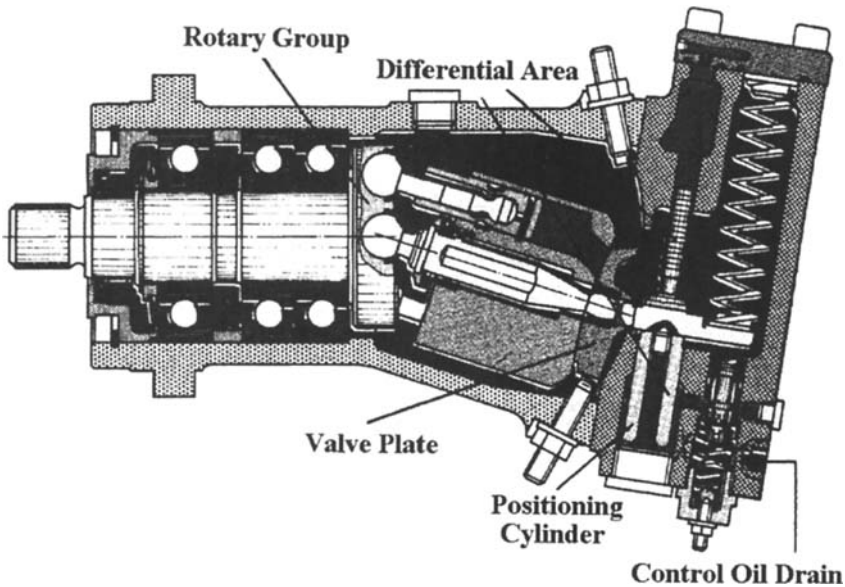


Figure 1.15 Illustration of a bent-axis variable-displacement piston pump.

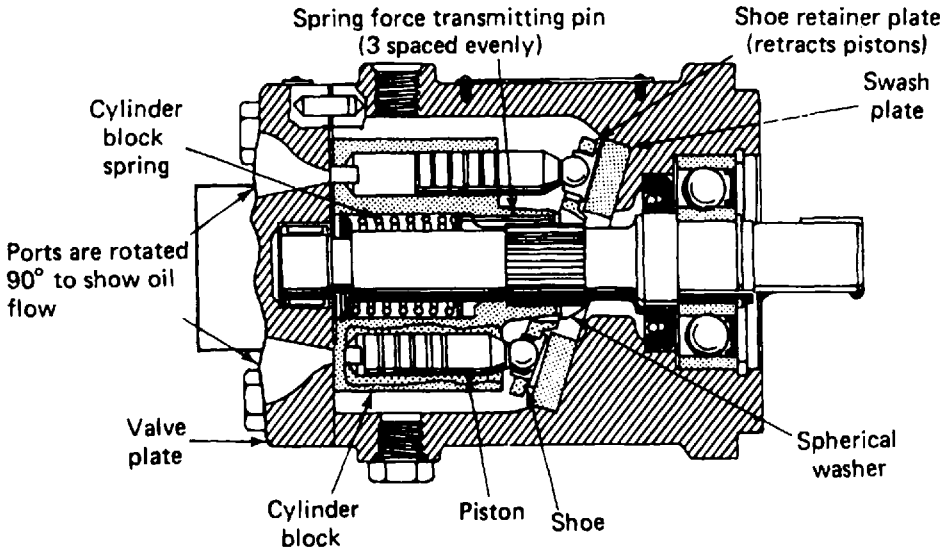


Figure 1.16 Illustration of an axial fixed-displacement piston pump.

shown in Fig. 1.16 [2] and a typical example of an axial variable-displacement piston pump is illustrated in Fig. 1.17 [2]. Variable-displacement piston pumps lend themselves to the incorporation of various valve mechanisms that will alter the performance of this pump; for example, it can be a pressure-compensated pump in one configuration, where the valve mechanism will alter the displacement of the pump to limit the outlet pressure to some preselected value. A pressure-compensated piston pump is illustrated in Fig. 1.17 [2].

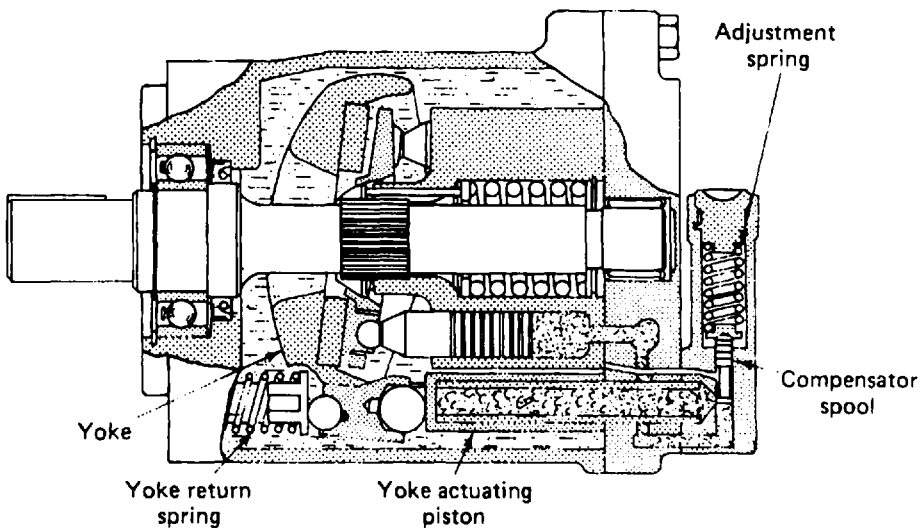


Figure 1.17 Illustration of an axial variable-displacement piston pump.

As seen in Figs. (1.16) and (1.17), the major components of a piston pump are the pistons, the piston or cylinder block, valve plate, piston shoes, swash plate, and the drive shaft. In operation, the shaft drives the piston block, which, in turn, rotates the pistons. The pistons are held against the swash plate by springs and a retainer plate. For the piston pump to produce a flow, the swash plate must be at some angle relative to the centerline of the shaft, which is also the axial center of rotation of the pistons. The pistons ride on the surface of the swash plate and the angle will force the pistons to move in and out of the piston or cylinder block. The greater the swash-plate angle, the larger the piston stroke and the greater the displacement of the pump. The dependence of pump displacement (V) on the swash-plate angle α is shown by the following equation and Fig. 1.18 [9]:

$$V = \frac{\pi d_k^2}{4} D_k (\tan \alpha) \quad (1.27)$$

where V is the pump displacement (in.^3), d_k is the piston bore diameter (in.), D_k is the piston bore circle diameter (in.), and α is the swash-plate angle (in degrees).

For an axial piston pump bent-axis design, the pump displacement (V) is described by the bent-axis angle α according to the following equation and Fig. 1.19 [9]:

$$V = \frac{\pi d_k^2}{4} (2r_h z) (\sin \alpha) \quad (1.28)$$

where r_h is the piston bore circle radius and z is the number of pistons.

The third kind of piston pump is the radial design (Fig. 1.20) [8]. In general, the radial piston pump has the highest continuous-pressure capability than any other type of pump (Table 1.1). Figure 1.21 [8] shows the basic configuration of a three-piston pump. The pistons are positioned radially to an eccentric drive shaft. Each

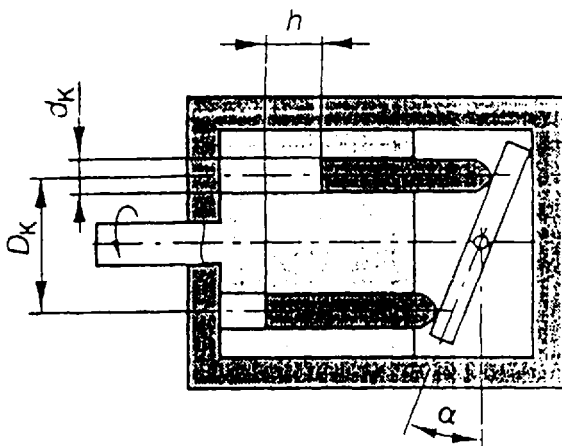


Figure 1.18 Sketch of an axial piston pump swash-plate design showing displacement angle α .

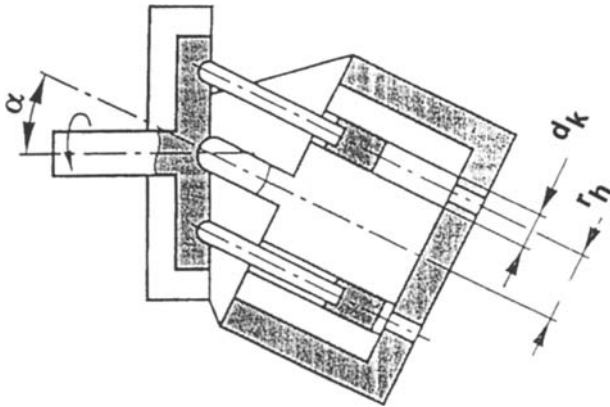


Figure 1.19 Sketch of an axial piston pump bent-axis design showing displacement angle α .

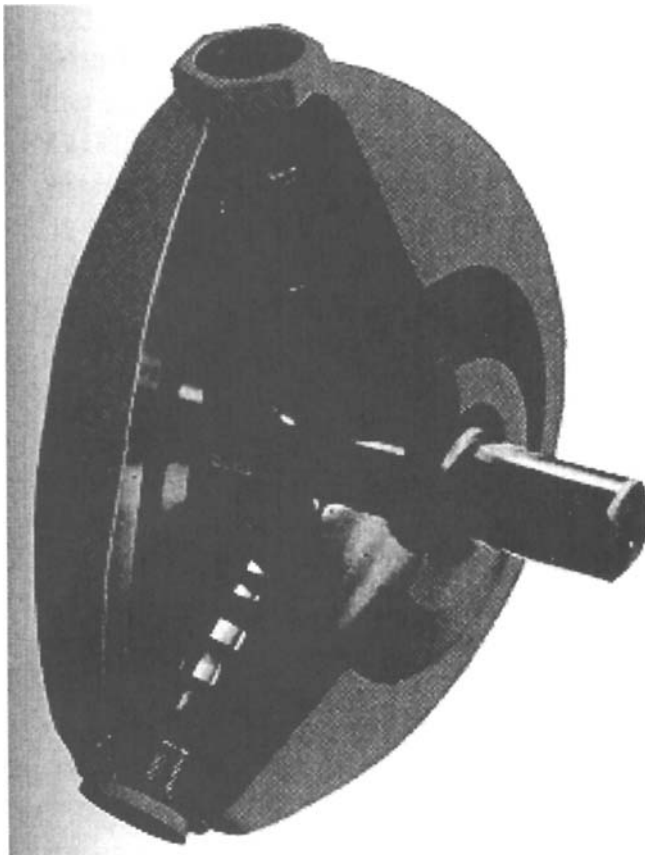


Figure 1.20 Cross-sectional view of a radial piston pump.

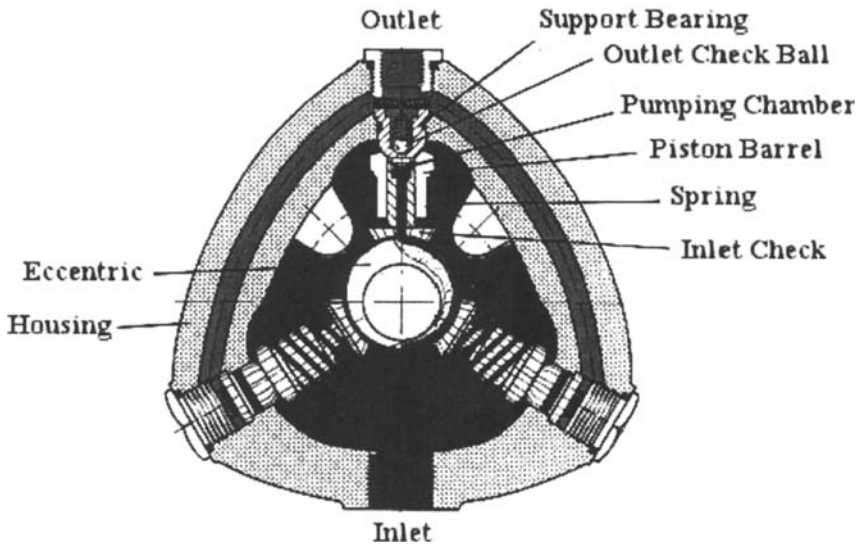


Figure 1.21 Illustration of the interior of a radial piston pump.

hollow piston consists of an inlet check valve, a spring, a piston barrel, a pumping chamber, an outlet check ball, and a support bearing.

As the drive shaft is rotated, the spring holds the base of the piston in contact with the eccentric cam shaft. The downward motion of the piston causes the volume to increase in the pumping chamber. This creates a reduced pressure that allows the inlet check valve to open, allowing oil to enter the pumping chamber. The oil enters the chamber by way of a groove machined into the cam-shaft circumference. Further rotation of the cam shaft causes the piston to move back into the cylinder barrel. The rapid rise in chamber pressure closes the inlet check valve. When the rising pressure equals the system pressure, the outlet check valve opens, allowing flow to exit the piston into the pressure port of the pump. The resulting flow is the sum of all the piston displacements. The number of pistons that a radial pump can have is only limited by the spatial restrictions imposed by the size of the pistons, housing, and cam shaft.

For a radial piston pump, the pump displacement (V) is defined by the piston bore (d_k) and the cam thrust (e) according to the following equation and Fig. 1.22 [9]:

$$V = \frac{d_k^2 \pi}{4} 2ez \quad (1.29)$$

where e , the cam thrust, is measured in inches.

Typical applications for radial pumps include cylinder jacking, crimping, and holding pressure on hydraulic presses. However, it should be noted that for extremely high-pressure applications, the displacements of radial pumps are usually not larger than 0.5 in.³/rev.; for example, at 1800 rpm, a 0.5-in.³/rev. displacement pump will only deliver ~3.9 gpm. Assuming an efficiency of 93% at a load pressure of 10,000 psi, the pump would require a 24-hp electric motor [Eqs. (1.14) and (1.18)].

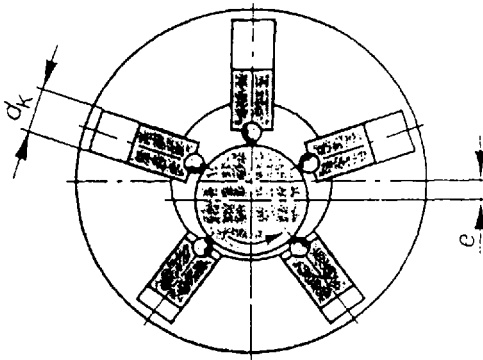


Figure 1.22 Sketch of a radial piston pump showing the parameters used to calculate displacement.

2.2.4 Sizing and Selection of Pumps

As was mentioned earlier, the sizing of the system pump actually begins with the load. The specification for a hydraulic system only deals with the movement of a load; therefore, the size of the pump must be calculated from this information. The pump is a flow generator which develops flow; pressure is a result of the pressure losses within the system and the pressure necessary to maintain the motion of the load. Hence, the first parameter in sizing a pump is to determine the required flow. Then, as was shown earlier, the pressure capability of the pump must be considered. The pressure necessary to deal with the load is determined by sizing the cylinder. Then, it is only necessary to add the system losses to the pressure to arrive at the pressure capability of the pump.

Once the size and pressure capability of the pump are known, the type of pump and the manufacturer must be selected. There are basically three types of pumps normally used. The main criterion that will play heavily in the selection of the pump is the type of control used. In an open-center system, which is not extremely high pressure, any of the three pump types can be used. In this case, price and personal opinions of the designer will prevail. However, if the system is to be a closed-center one with pressure or load compensation, the usual selection is the variable-displacement piston pump.

Open-Loop Circuit

The open-loop circuit is by far the most popular design. An example of an open-loop circuit is shown in Fig. 1.23 [8]. In this figure, an electric motor powers a variable-displacement pump which draws hydraulic fluid from the reservoir and pushes the fluid through a directional control valve. The fluid from the control valve can be directed to either side of a reversible hydraulic motor and then is sent back to the reservoir. Pumps used in open-loop applications can only pump fluid in one direction. In contrast to the reversible hydraulic motor, the pump's ports are not the same size—the inlet port is always larger than the outlet port. The advantage of an open-loop design is that, if necessary, a single pump can be used to operate several different actuator functions simultaneously. The main disadvantage is its large res-

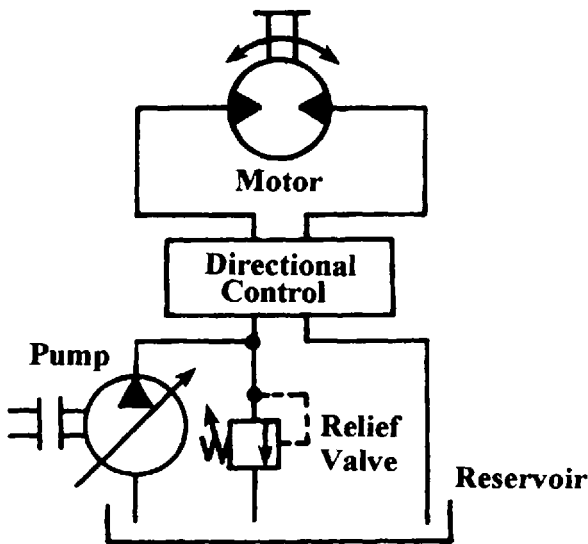


Figure 1.23 Illustration of an open-loop circuit.

ervoir size. Generally, the reservoir is sized to hold at least three times the volume of fluid that can be supplied by the pump in 1 min.

Closed-Loop Circuit

In contrast to the open-loop design, the closed circuit eliminates the need for a large storage reservoir. Figure 1.24 [8] shows an illustration of a closed-loop circuit. In this design, a reversible pump is used to drive a reversible hydraulic motor. The closed-loop design is always used in conjunction with a smaller “supercharge” circuit. The supercharge circuit consists of a small fixed-displacement pump (usually about 15% of the displacement of the main pump), a small fluid reservoir, filters, and a heat exchanger.

The supercharge circuit always works on the low-pressure side of the main loop. Its function is to pump freshly filtered fluid into the closed loop through check valves while bleeding-off a percentage of the hot fluid through a bleed valve. This hot fluid is then cooled by a heat exchanger and stored in a small reservoir before returning to the main system. The pressure in the supercharge circuit is limited to 100–300 psi by the supercharge relief valve. The pressure setting of this valve is determined by the requirements of the pump/motor combination and the operating conditions of the system. The cross-port relief valves on the motor are there only to protect the actuator from load-induced pressure spikes. They are not intended to function like those found in open-loop designs, which would cause severe overheating of the circuit due to insufficient fluid supply, inherent in a closed loop system, to carry away this extra heat. In closed-loop circuits, pressure, flow, and directional motor control are all achieved by controlling the variable-displacement pump.

The advantages of a closed-loop circuit is that high-horsepower systems are compact and efficient and require less hydraulic fluid storage. The high efficiency of this circuit is the result of the pump control being designed to supply only the fluid flow required by the actuator to operate at the load-induced pressure. The pump is

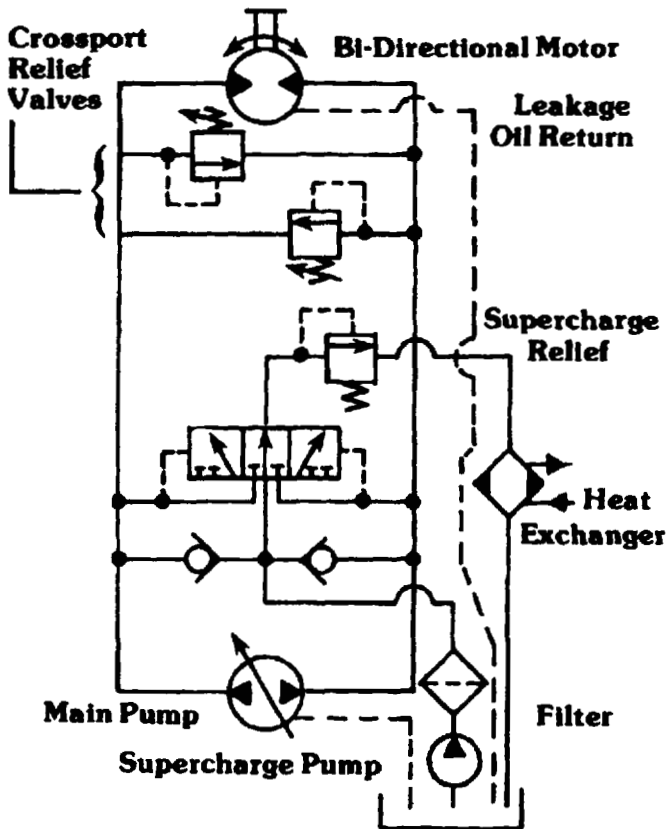


Figure 1.24 Illustration of a closed-loop circuit.

the heart of the system and controls the direction, acceleration, speed, and torque of the hydraulic motor, thus eliminating the need for pressure and flow control components.

A major disadvantage of a closed-loop circuit is that a single pump can only operate a single output function or actuator. In addition, this type of hydraulic circuit is generally used only with motor actuators.

Half-Closed-Loop Circuit

Figure 1.25 [8] is an illustration of a “half-closed”-loop circuit. This circuit is similar to the closed circuit except that it can be used with cylinder actuators having differential areas. As can be seen from the figure, during cylinder extension, the pump must generate a larger flow from its left-hand port than is being returned to its right-hand port from the cylinder. The extra fluid needed by the pump is supplied by its left-hand inlet check valve, which is an integral part of the pump.

When the pump control strokes the pump over the center, the flow from the pump is reversed and the cylinder begins to retract. During retraction, the differential area of the cylinder piston causes a larger flow than needed at the inlet of the pump. This excess flow is directed to the reservoir through the “unloading valve.” The

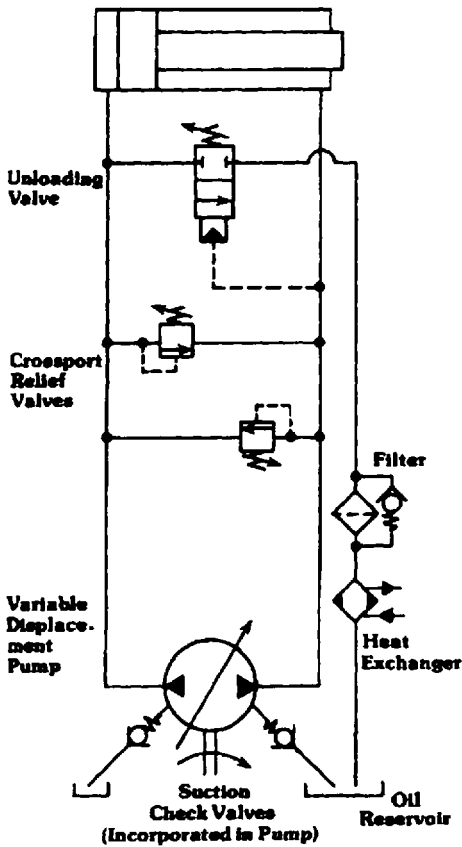


Figure 1.25 Illustration of a half-closed-loop circuit.

unloaded fluid is filtered and cooled prior to its return to the reservoir. In this way, a portion of the closed-loop fluid is filtered and cooled in an open-loop circuit each time the cylinder is cycled.

2.2.5 Contamination Considerations

Every hydraulic system will have particulate contamination entrained in the circulating fluid. These contaminant particles can enter the clearance space of every component, but more specifically, the hydraulic pump [10]. Contaminants will enter the system from reservoir breathers, seals, and so forth as well as from the wear of internal surfaces.

There are three ways of addressing the contamination problems in a hydraulic system. This can be accomplished by using return-line and reservoir breather filters. One way is to prevent particles from entering the system. Because the particles that enter the hydraulic system will cause wear on the internal surfaces of the components, the elimination of these particles will also reduce the production of wear debris. The second approach is to filter the particles that become entrained in the circulating fluid, and the third approach is to select components that effectively resist the contaminant attack.

In selecting the pump, none of these approaches are completely adequate. Due to the development of contaminant-sensitivity test procedures at the Fluid Power Research Center, formerly located at Oklahoma State University, it is now possible to evaluate the efficiency of seals [11,12] and breathers in preventing the entrance of particulate contamination as well as the removal efficiency of hydraulic filters [13,14]. In addition, contaminant sensitivity test procedures are available to evaluate the resistance or tolerance of a hydraulic component, such as a pump, to entrained particulate contaminants [15–17]. Therefore, knowing the ability of the seals and breathers to prevent the entrance of contamination and the effectiveness of the filter in removing that contaminant which does enter the system, a reasonable selection of the pump to produce the desired service life can be made.

Table 1.4 shows the level of cleanliness that can be achieved as a function of degree of filtration as it applies to various hydraulic components. This subject is covered in much greater detail in Chapter 3.

Preparation of Pipes and Fittings

When installing pipes and fittings on a hydraulic system, it is imperative that they be as clean as possible. The following steps are recommended to prepare metal pipes and fittings prior to installation [18]:

1. Ream inside and outside edges of pipe or tubing and clean with a wire brush to loosen and remove any particles.
2. Sandblast short pieces of pipe and tubing to remove any rust and scale. In the case of longer pieces or short pieces having complex shapes, they first should be cleaned of all grease and oil in a degreasing solvent and then pickled in a suitable solution until all rust and scale is removed.
3. After pickling, rinse all parts thoroughly in cold running water and then immerse parts in a tank containing neutralizing solution at the proper temperature and length of time as recommended by the manufacturer.
4. Rinse parts in hot water and place into another tank containing an antirust solution. If parts are not to be immediately installed, they should be left to air-dry with antirust solution remaining on them. If pipes are dry and will be stored, they should be capped to prevent dirt from entering. Before using any pickled part, it should be thoroughly flushed with a suitable degreasing solvent.
5. Cover all openings into the hydraulic system to prevent dirt and any foreign matter from entering the system.
6. Inspect all threaded fittings and remove any burrs or metal slivers.

Table 1.4 Filtration and Cleanliness Guidelines for Various Hydraulic Components

Filtration (μm)	Cleanliness (class)	Hydraulic Application
1–5	0–1	Servo valves
10	2–4	Piston pumps and motors, flow controls, relief valves
20–25	4–5	Gear and vane pumps
40	6	Infrequent duty cycle and noncritical components

7. Before filling or adding hydraulic fluid to the reservoir, make sure that the fluid is as specified and that it is clean.
8. When adding hydraulic fluid to the reservoir, use a fluid filtration cart to prefilter the fluid as it enters the reservoir. Never add fluid directly from the storage container or drum without filtering.

2.2.6 Pump Performance Characteristics

The performance of the pump is extremely important in the overall success of any hydraulic system. A pump exhibits mechanical-type losses as well as volumetric losses [19]. Mechanical losses are the result of the motion of the working element within the pump because of friction. As shown previously [Eq. (1.10)], the theoretical torque required to drive the pump is equal to the product of the pump displacement and the pressure differential across the pump. Obviously, the actual torque is greater than this theoretical value in order to make up for the mechanical losses within the pump. As stated earlier, the mechanical efficiency is the ratio of the theoretical torque to the actual torque [Eq. (1.16)].

The effectiveness of a pump in converting the mechanical input energy into output hydraulic energy must be measured by tests. Theoretically, at low pressures, the output flow of a positive displacement pump is equal to the product of the displacement and the shaft rotational speed as shown by

$$\text{Flow (gpm)} = \frac{\text{Displacement (in.}^3\text{/rev.)} \times \text{Speed (rpm)}}{231} \quad (1.30)$$

As the differential pressure across the pump increases, the flow through the clearances or leakage paths within the pump will increase to create slip flow, which will be subtracted from the output flow. Therefore, the volumetric efficiency is the ratio of the actual flow to the theoretical flow; this parameter reflects the magnitude of the volumetric losses [Eq. (1.15)].

Overall efficiency is equal to the volumetric efficiency multiplied by the mechanical efficiency [Eq. (1.17)]. Figure 1.26 illustrates the relationship among volumetric, mechanical, and overall efficiency of a hydraulic pump. To properly select a hydraulic pump for a given application, efficiency information is extremely important. These data must be acquired by the pump manufacturer by testing and are normally reported in a graph resembling that shown in Fig. 1.27. The upper curves in this figure show that at a given load pressure, the volumetric efficiency increases with speed. This is because all fluids have a property known as viscosity, and at greater and greater speeds, there is insufficient time available for the fluid to leak across to case or slip past clearances in the pump. Also, the lower curves indicate that at a given load pressure, the input power requirement increases as speed increases. This is the result of the increased flow output of the pump as rotational speed increases [Eqs. (1.12) and (1.13)]. It should be noted that these data are usually run at one temperature using one fluid. No viscosity or density effects are taken into consideration in these data. The cost penalty paid for poor efficiency can be significant. Therefore, care must be taken to evaluate the efficiency characteristics of the pump during the selection process.

The mechanical strength of the pump to survive the pressure duty cycle expected in the application is reflected by the proof- and burst-pressure information.

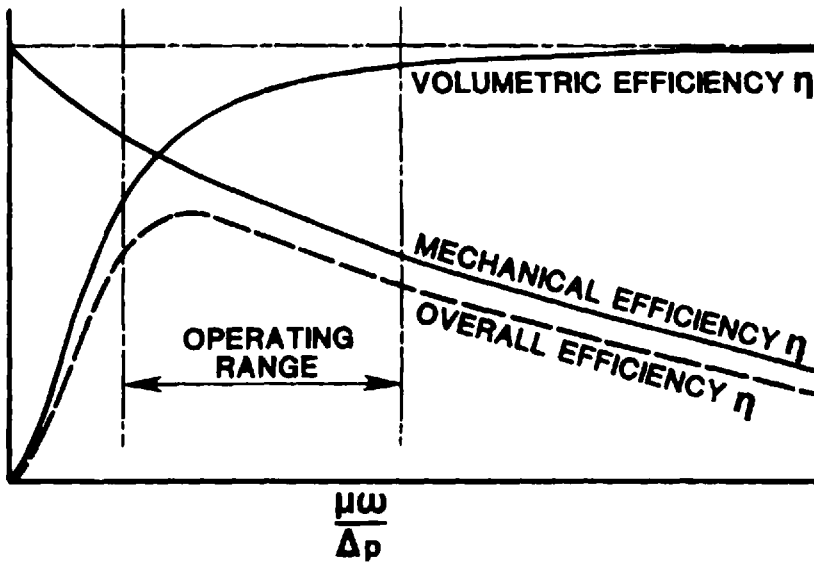


Figure 1.26 Typical hydraulic pump efficiency curves.

This information is obtained through failure tests conducted by the pump manufacturer. The proof pressure is normally 1.5 the rated pressure and the burst pressure is 2.5 times the rated pressure. The ability of the pump to operate for a sufficient time at the actual pressure duty cycle is determined by conducting endurance tests at conditions agreed upon by the industry.

2.2.7 Pump Inlet Condition

In theory, a positive displacement pump will produce flow in direct proportion to the shaft speed [Eq. (1.12)]. However, if the fluid cannot be supplied to the pumping chambers of the pump, this relationship will not hold and the pump is said to cavitate. The flow versus shaft speed for a typical hydraulic pump will be linear up to the point that fluid can no longer enter the pumping chambers of the pump as these chambers are opened and closed because of shaft rotation. When this occurs, the chambers will only partially fill and the outlet flow will reduce. Under these conditions, the pump will be starved for fluid. The speed that this starvation will occur depends on the viscosity and the density of the hydraulic fluid as well as the physical configuration of the pump inlet and the connecting lines. This phenomenon is illustrated in Fig. 1.28.

In considering the starvation of a positive displacement pump, there is normally very little that can be done with the configuration of the pump inlet by the system designer. Also, the fluid being used in the system is generally selected for reasons other than the pump inlet conditions, such as for high-temperature operation, fire resistance, or biodegradability. Therefore, it is necessary to size the inlet piping and position the pump relative to the reservoir such that the inlet pressure to the pump is positive. The pressure at the inlet to the pump is normally called the Net Positive Suction Head (NPSH) and may be calculated in terms of absolute pressure [20]. The

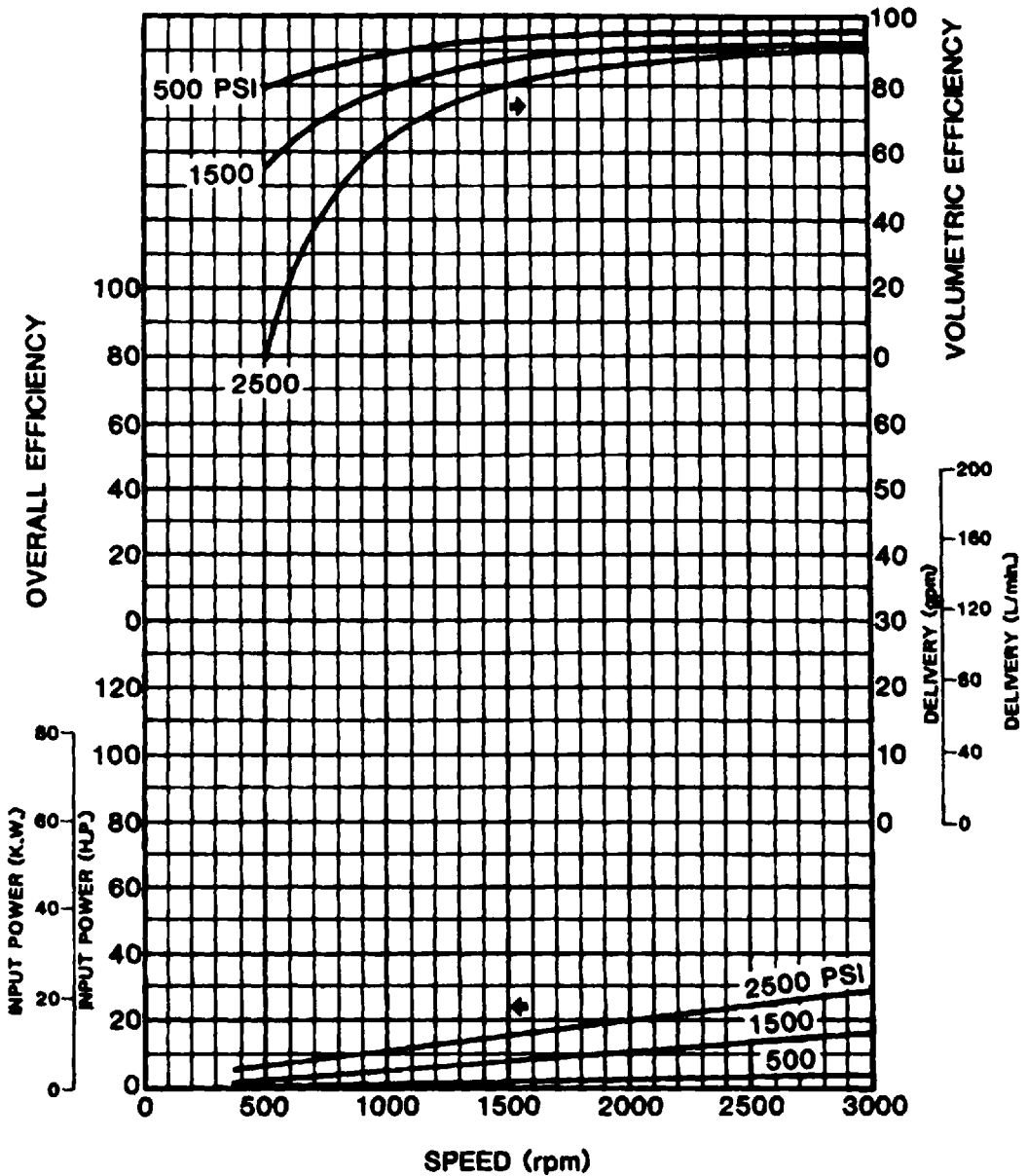


Figure 1.27 Typical performance data reported by a pump manufacturer.

entire system from the fluid level in the reservoir to the inlet port of the pump must be taken into account when determining the NPSH (Fig. 1.29) [20]. The primary factors in determining the NPSH are as follows:

- The atmospheric head or the atmospheric pressure at the particular location (H_a).

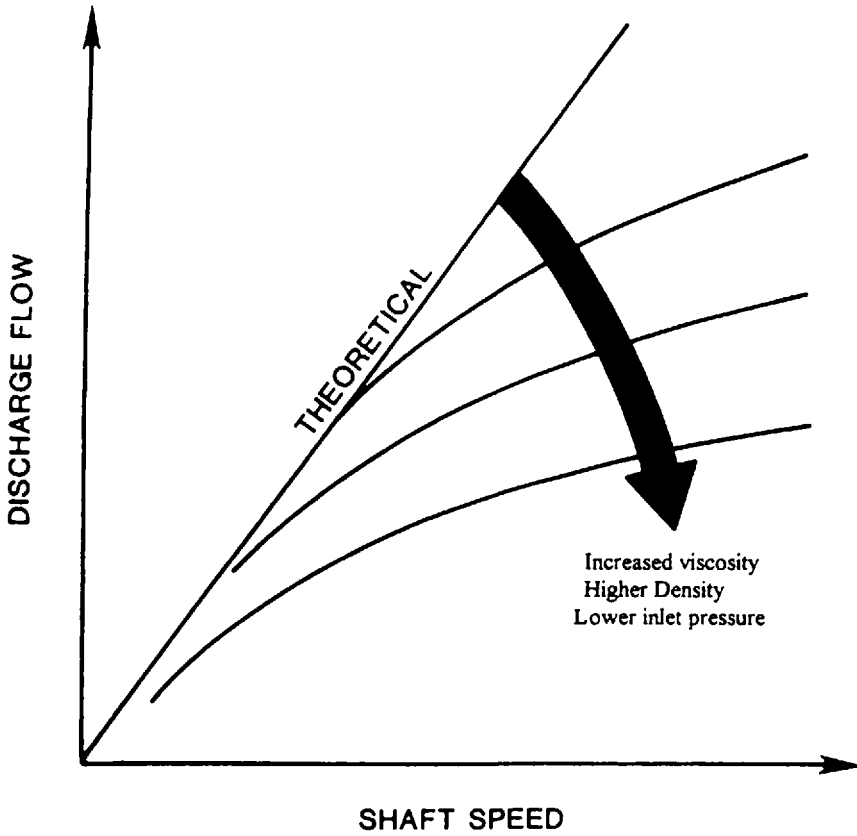


Figure 1.28 Discharge flow of a positive displacement pump as a function of shaft speed, fluid viscosity, and density.

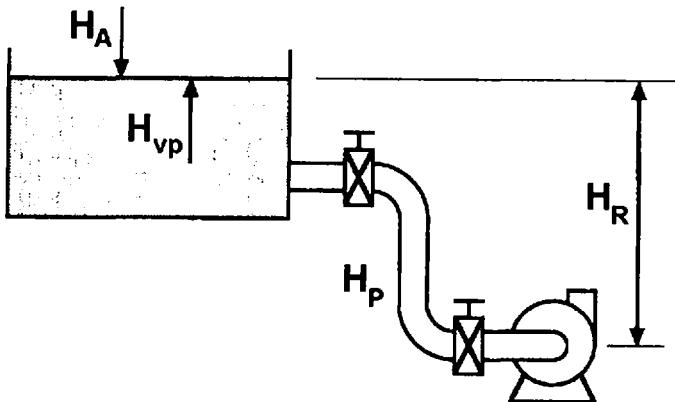


Figure 1.29 Illustration of the NPSH parameters.

- The friction head or the pressure needed to overcome the losses due to friction when the fluid is flowing through the pipe, fittings, valves, and area changes (H_f). Table 1.5 [21] shows data for various hose and pipe diameters.
- Static inlet head or the vertical distance from the centerline of the pump inlet to the free surface level in the reservoir (H_R).
- The vapor pressure of the fluid at the fluid temperature (H_{vp}).

The above parameters can be used to calculate the NPSH according to the equation,

$$\text{NPSH} = H_A + H_R - H_f - H_{vp} \quad (1.31)$$

It is interesting to note that the term H_{vp} , although negligible for mineral-oil-based hydraulic fluids, can be the most dominant term where volatile fluids are concerned, such as with water-based fire-resistant hydraulic fluids. Figure 1.30 shows a plot of water vapor pressure as a function of temperature [22].

There are equations for each of the factors involved in establishing the NPSH. However, numerous graphs and nomographs have reduced the burden of calculating the NPSH for a given pump and inlet condition. One such graph is given in Fig. 1.31. With this graph, one can determine the approximate NPSH at the pump inlet from the flow and speed of the pump. As an example, a pump having a displacement of 0.05 gpm running at 1800 rpm would, according to the nomograph, require a NPSH of ≈ 24 ft of oil pressure, or $0.35 \times 24 = 8.4$ psi (for mineral oil), to prevent cavitation. This graph provides information concerning the minimum NPSH and is fairly accurate for viscosities below about 200 SUS and specific gravities of about 0.9. Care should be taken when dealing with a fluid with a high specific gravity, such as many of the synthetic fluids (polyol esters, phosphate esters, etc.) and water-

Table 1.5 Pressure Drop ΔP (psi/ft) and Flow Rates (gpm) for Various Hose (H) and Pipe (P) Diameters at Typical Flow Velocities

Hose/pipe inner diameter (in.)	ΔP	ΔP	ΔP	ΔP	ΔP
	(gpm) 2 ft/s	(gpm) 4 ft/s	(gpm) 10 ft/s	(gpm) 15 ft/s	(gpm) 20 ft/s
0.500 H	0.176 (1.22)	0.352 (2.45)	0.880 (6.12)	1.32 (9.18)	2.92 (12.2)
0.750 H	0.0782 (2.75)	0.156 (5.51)	0.391 (13.8)	1.06 (20.7)	1.76 (27.5)
0.875 H	0.0575 (3.75)	0.115 (7.50)	0.432 (18.7)	0.878 (28.1)	1.45 (37.5)
1.00 H	0.0440 (4.90)	0.0880 (9.79)	0.365 (24.5)	0.743 (36.7)	1.23 (49.0)
2.00 H	0.0110 (19.6)	0.0220 (39.2)	0.154 (97.9)	0.312 (147)	0.517 (196)
3.00 H	0.00489 (44.1)	0.0186 (88.1)	0.0925 (220)	0.188 (330)	0.311 (441)
4.00 H	0.00275 (78.3)	0.0130 (157)	0.0646 (392)	0.131 (588)	0.217 (783)
0.493 P	0.181 (1.19)	0.362 (2.38)	0.905 (5.95)	1.36 (8.92)	2.97 (11.9)
0.742 P	0.0799 (2.70)	0.160 (5.39)	0.400 (13.5)	1.08 (20.2)	1.78 (27.0)
0.884 P	0.0563 (3.83)	0.113 (7.65)	0.426 (19.1)	0.867 (28.7)	1.43 (38.3)
1.049 P	0.0400 (5.39)	0.0800 (10.8)	0.344 (26.9)	0.700 (40.4)	1.16 (53.9)
2.067 P	0.0103 (20.9)	0.0206 (41.8)	0.147 (105)	0.300 (157)	0.496 (209)
3.068 P	0.00468 (46.1)	0.0181 (92.2)	0.0900 (230)	0.183 (346)	0.303 (461)
4.026 P	0.00272 (79.4)	0.0129 (159)	0.0641 (397)	0.130 (595)	0.215 (794)

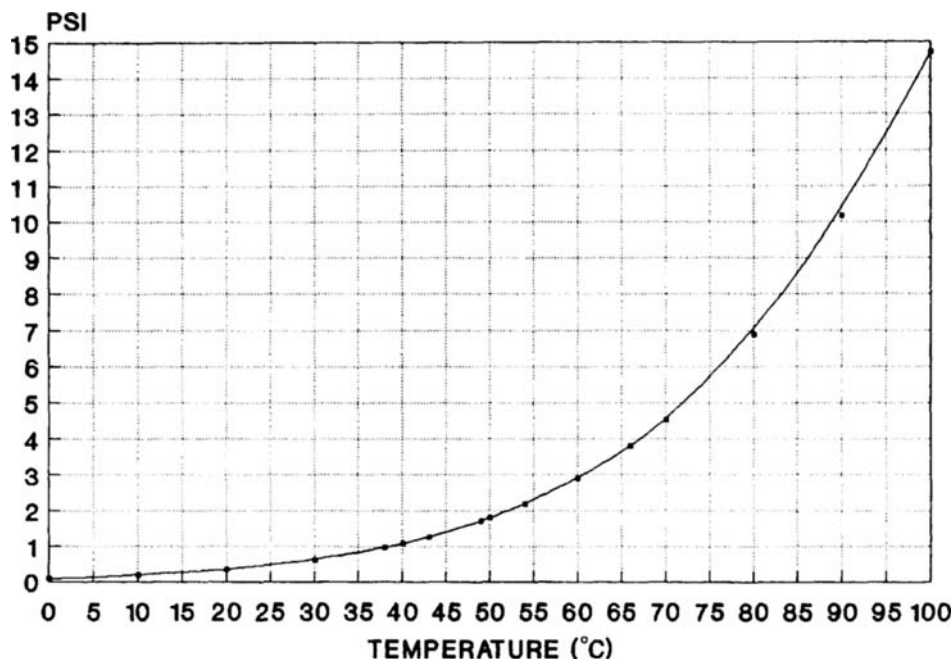


Figure 1.30 Water vapor pressure curve.

based fluids. In addition, complicated or exceptionally long inlet lines should be considered as special cases when determining the NPSH.

Friction head or the losses resulting from the pipe friction acting upon the fluid flowing through the pipe can be calculated using Darcy's equation:

$$\Delta P = \lambda \frac{L\rho Q^2}{2DA^2} \quad (1.32)$$

where ΔP is the pressure loss because of friction, λ is the friction factor, L is the length of pipe, ρ is the density of the fluid, Q is the flow through the pipe, D is the pipe diameter, and A is the cross-sectional area of the pipe.

The friction factor, λ , can be obtained from a modified Moody diagram, as shown in Fig. 1.32 [2]. It should be noted that the solid line on the left-hand side of the graph is for fully developed laminar flow, and the solid line on the right-hand side is for fully developed turbulent flow. The dashed lines show the changes that occur when the laminar flow is not fully developed and at very high Reynolds numbers. Equation (1.32) can be rewritten in terms of head loss as follows:

$$h = \frac{\Delta P}{\rho G} \quad (1.33)$$

where h is the head loss (ft) and G is the gravitational constant (ft/s^2).

The frictional losses can also be found using nomographs. The nomograph shown in Fig. 1.33 [2] can be used to find the pressure loss in a pipe because of friction under conditions of laminar flow. In the example in the figure, the fluid velocity is 2.0 m/s and the fluid viscosity is 30 cP. A straight line is drawn between

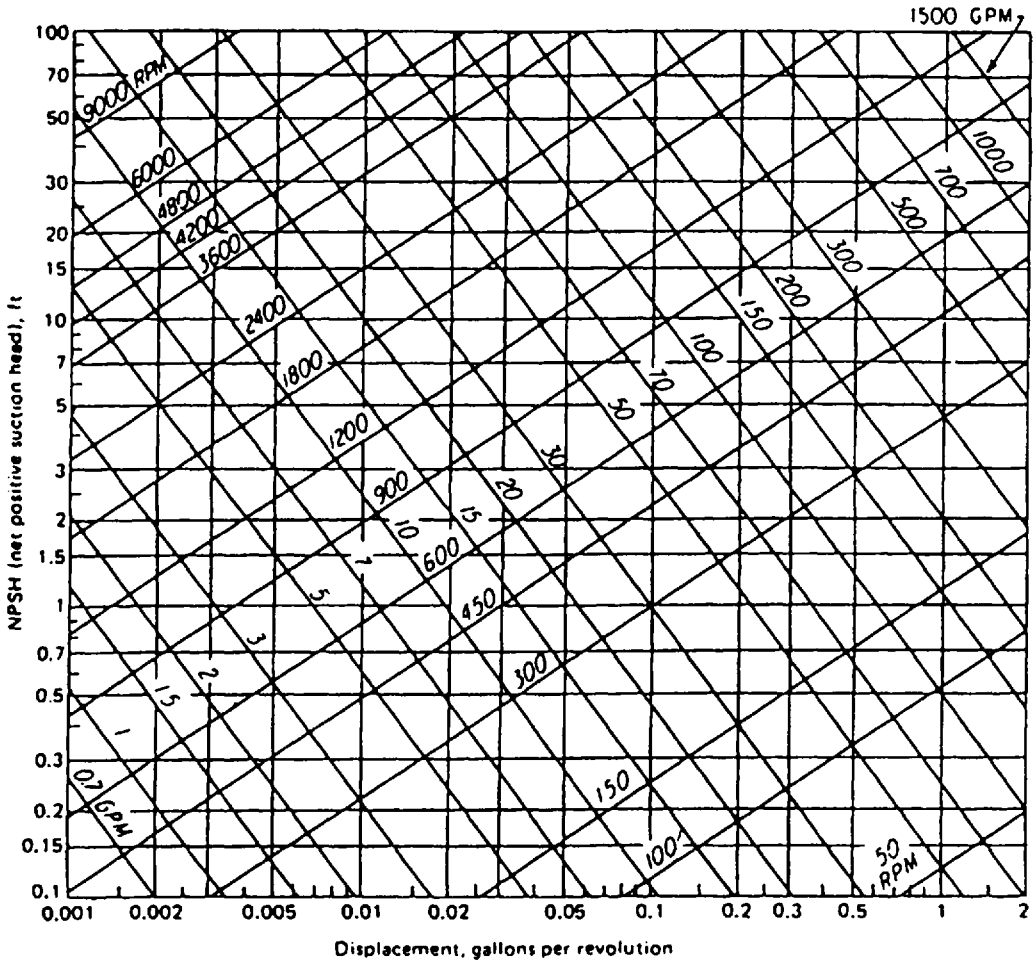


Figure 1.31 Minimum pump head pressure estimation nomograph.

these two points. The pipe diameter is 20 mm. By drawing a straight line between the pipe diameter of 20 mm through the intersection of the first line drawn with the turning line, one will find the pressure loss per foot of this pipe at these flow conditions to be approximately 0.06 bar/m. Then, multiply this number by the total length of the pipe to find the total pressure loss. The nomograph shown in Fig. 1.34 [2], for turbulent flow, is used in exactly the same way as that shown in Fig. 1.33 for laminar flow.

2.3 Hydraulic System Components

There are probably as many different hydraulic systems and component designs as there are designers. However, a fundamental hydraulic system consists of the following components and circuits in addition to the pumping component.

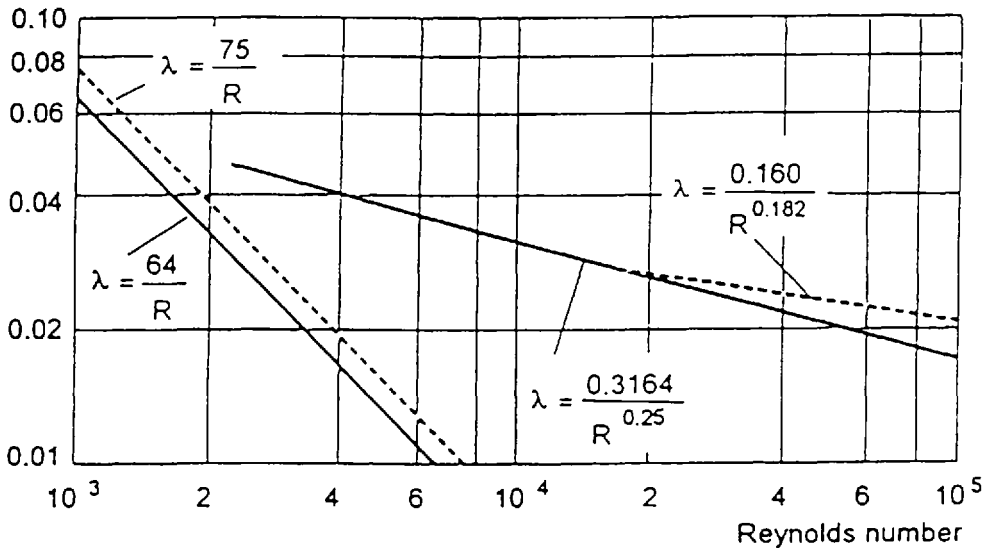
Friction factor λ 

Figure 1.32 Friction factor versus Reynolds number (Moody diagram).

- Flow control
- Pressure control
- Rotary and linear actuators
- Accumulators
- Piping and hose
- Reservoir

Each of these components have a unique mission in the operation of a hydraulic system.

2.3.1 Flow Control

Flow control in a hydraulic system is commonly used to control the rod velocity of linear actuators or the rotary speed of hydraulic motors. There are three ways to accomplish flow control. One is to vary the speed of a fixed-displacement pump; another is to regulate the displacement of a variable-displacement pump. The third way is with the use of flow control valves. Flow control valves may vary from a simple orifice to restrict the flow to a complex pressure-compensated flow control valve and to flow dividers.

Uncompensated Flow Control Needle Valves

The simplest uncompensated flow control is the fixed-area orifice. Normally, these orifices are used in conjunction with a check valve so that the fluid must pass through the orifice in one direction, but in the reverse direction the fluid may pass through the check, thus bypassing the orifice. Another design incorporates a variable-area orifice so that the effective area of the orifice can be increased or decreased (usually

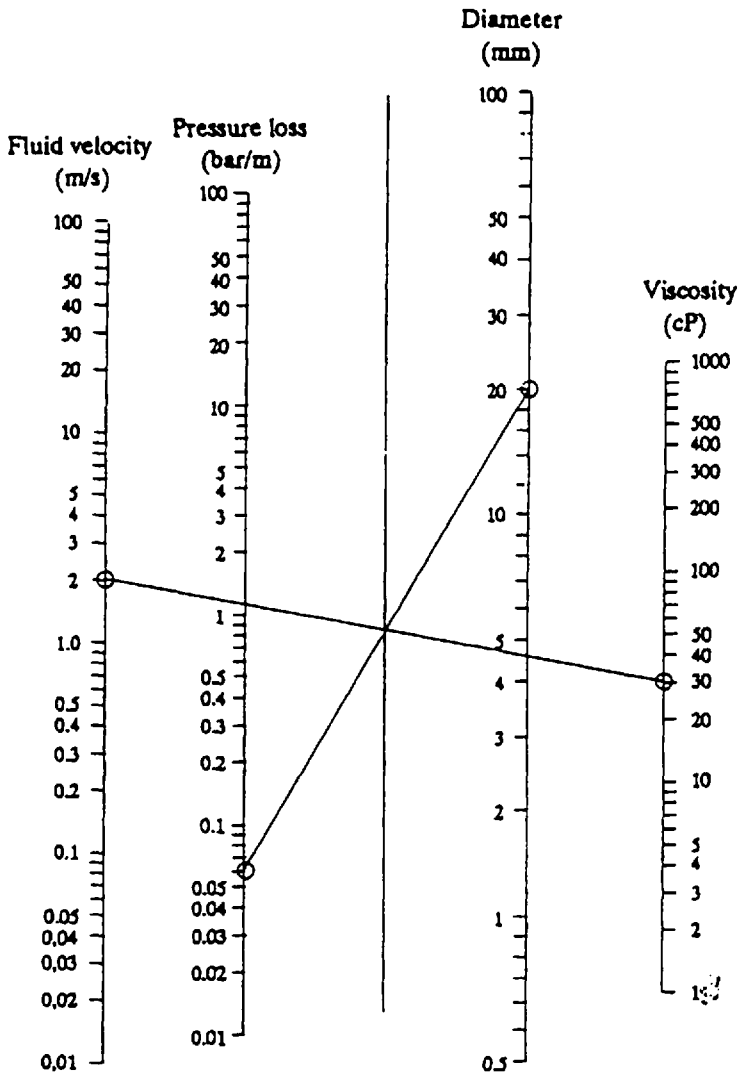


Figure 1.33 Pressure loss per unit pipe length for laminar flow.

manually). One style of the variable-area orifice with a reverse-flow check valve is shown in Fig. 1.35 [2]. These uncompensated flow control valves are used where exact flow control is not critical.

Flow through an orifice is proportional to the pressure drop across the orifice. Therefore, if the pressure differential increases, flow will also increase. To avoid this, a compensated flow control valve must be utilized.

Compensated Flow Control Needle Valves

A very simple compensated flow control valve is shown in Fig. 1.36 [2]. In this valve, the force opposed by the spring is a function of the pressure drop across the fixed orifice, not the pressure drop across the entire valve. As the pressure differential

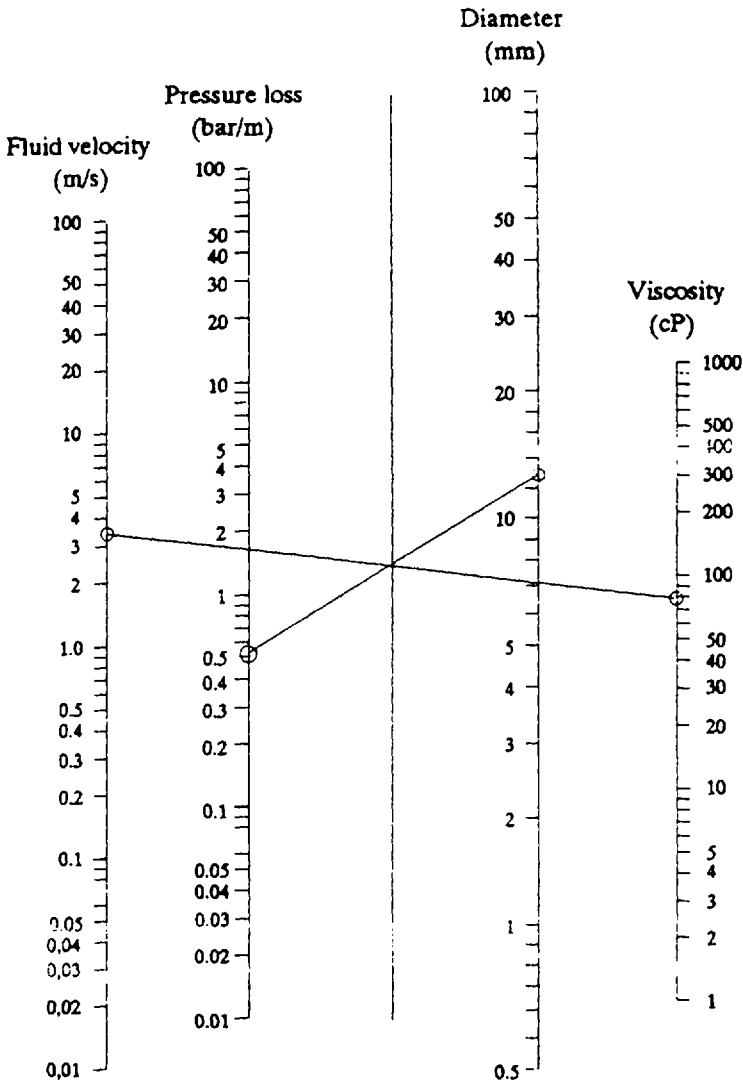


Figure 1.34 Pressure loss per unit pipe length for turbulent flow.

across the valve from the inlet to the outlet increases, flow will also attempt to increase. However, any increase in flow will be accompanied by a resulting increase in the pressure drop across the fixed orifice. When this pressure differential becomes larger than the spring preload, the valve spool will shift and the outlet port will be restricted. There are compensated flow control valves that are much more complex than the one shown; however, most operate the same because the pressure drop across the control orifice is held constant by utilizing a secondary variable orifice.

The following equations can be used to calculate the flow rate through a needle valve, or a series of valves, at a given system pressure. Refer to Fig. 1.37 [21] for the orifice coefficient (CD) values and circuit definitions.

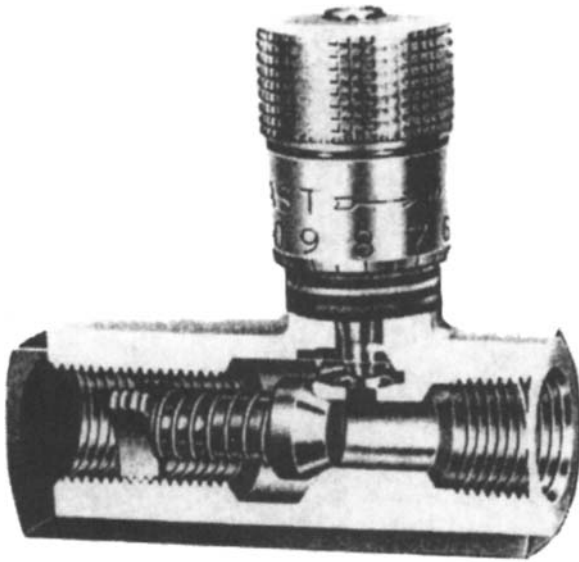


Figure 1.35 Illustration of an uncompensated flow control needle valve.

Parallel circuits:

$$Q = 29.81 \sqrt{\frac{\Delta P}{SG}} (CD_1 D_1^2 + CD_2 D_2^2 + \dots) \quad (1.34)$$

where Q is the flow rate (gpm), ΔP is the pressure drop (psig), SG is the specific gravity of fluid, CD is the orifice coefficient, and D is the orifice diameter (in.)

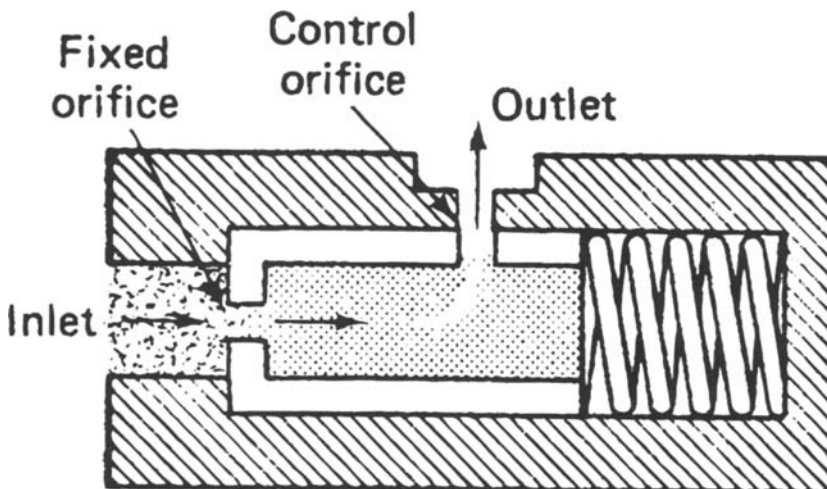
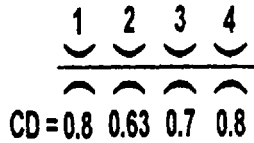
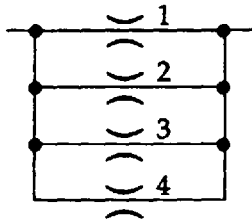
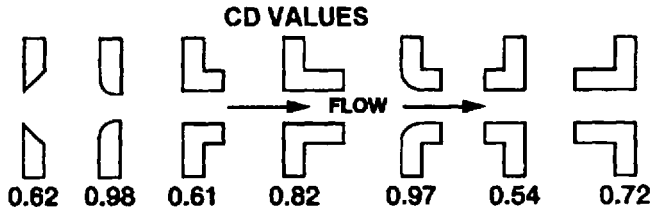
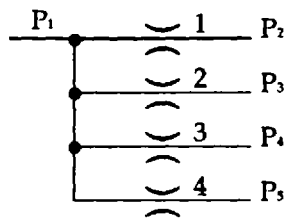
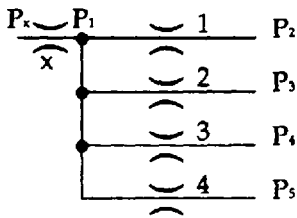


Figure 1.36 Illustration of a compensated flow control needle valve.



PARALLEL CIRCUIT

SERIES CIRCUIT



SERIES/PARALLEL CIRCUIT

PARTIAL PARALLEL CIRCUIT

Figure 1.37 CD values and circuit definitions for orifice calculations.

Series circuits:

$$Q = \sqrt{\frac{\Delta P(29.81)^2}{SG[(1/CD_1 D_1^2)^2 + (1/CD_2 D_2^2)^2 + \dots]}} \tag{1.35}$$

Series/parallel circuits:

$$Q_1 = 29.81 CD_1 D_1^2 \sqrt{\frac{\Delta P}{SG}} \tag{1.36}$$

Partial parallel circuits:

$$Q = \frac{29.81}{\sqrt{SG}} (CD_1 D_1^2 \sqrt{P_1 - P_2} + CD_2 D_2^2 \sqrt{P_1 - P_3} + \dots) \tag{1.37}$$

Flow Dividers

Flow dividers are a form of flow control valves. There are at least two types of flow dividers. One is called a priority flow divider; the other is a proportional flow divider. The priority type of flow control provides flow to a critical circuit at the expense of other circuits in the system. For example, many of the earth-moving machines are equipped with power steering. From a safety standpoint, the steering system is a very critical function.

Figure 1.38 [2] illustrates a priority flow divider. In operation, the flow will enter the priority flow divider from the right-hand end, as shown [2]. When the flow reaches a value such that the pressure drop across the fixed orifice produces a force larger than that provided by the spring, the spool will move to the left. This action will begin to close the priority outlet port and open the secondary outlet. When the flow is below the designed priority flow, the spool will be all the way to the right, the secondary will be closed, and the priority will be wide open. The proportional-type flow divider follows the same principle as the priority flow divider, except that two orifices are used and the spool is normally spring-loaded to a particular flow-split ratio.

2.3.2 Pressure Control

The primary pressure control valves are relief valves. There are direct-acting relief valves and pilot-operated relief valves. In addition, the pressure-reducing and the counterbalance valves fall under the pressure control category. There are a great many more valves that would fall into the pressure control category which will not be discussed here.

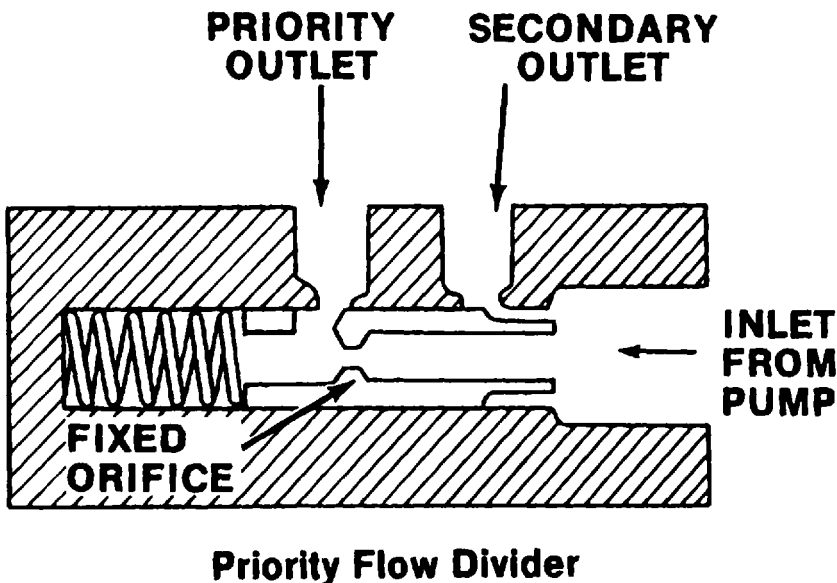


Figure 1.38 Illustration of a priority flow divider valve.

Pressure Relief Valves

There are two major kinds of pressure relief valves. One is described as a direct-acting valve and the other is pilot operated. The direct-acting relief valve is shown in Fig. 1.39 [2]. The model shown is actually adjustable, but not all direct-acting relief valves are externally adjustable. In operation, the flow enters from the bottom of the valve shown in Fig. 1.39. When the inlet pressure reaches the value such that the pressure times the exposed area of the ball is greater than the spring setting, the valve will begin to pass hydraulic fluid. Note that the spring must be compressed in order for the seat (ball) to move and provide greater flow area. Therefore, the pressure will increase as the flow through the valve increases. The pressure at which the valve first begins to open is called the cracking pressure; the pressure at rated flow is termed the full-flow pressure. In the case of the direct-acting relief valve, the difference between the cracking pressure and the full-flow pressure could be large. This difference is called the override pressure.

The pilot-operated relief valve is shown in Fig. 1.40 [2]. The pilot-operated pressure relief valve increases pressure sensitivity and reduces the pressure override normally found in relief valves using only the direct-acting force of the system

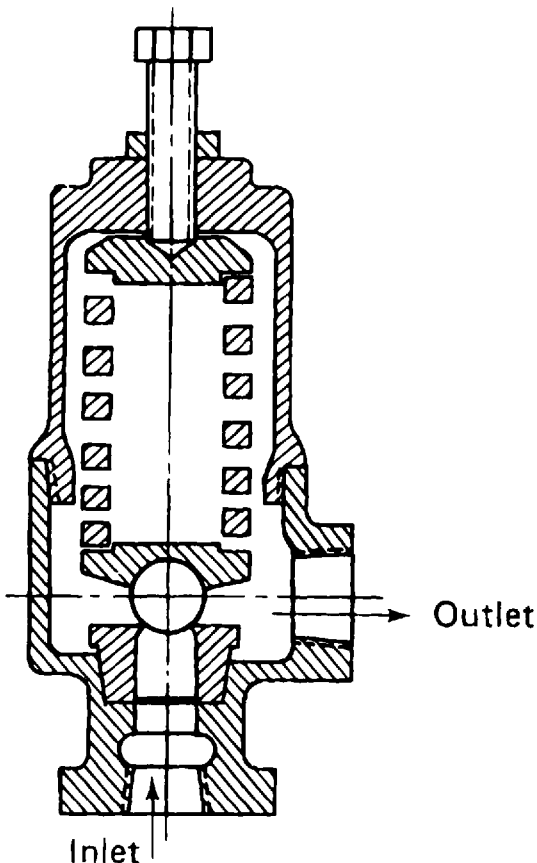


Figure 1.39 Illustration of a direct-acting relief valve.

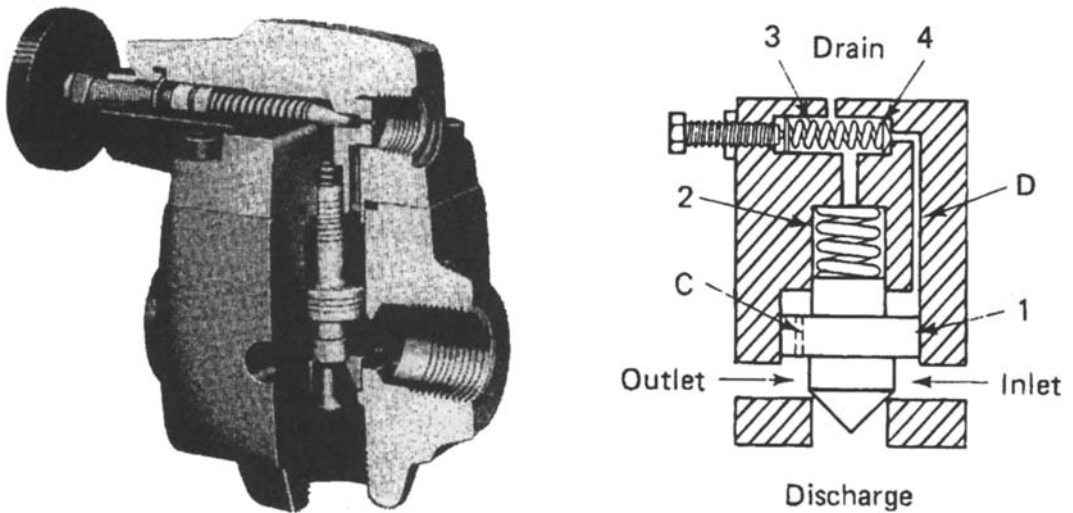


Figure 1.40 Illustration of a pilot-operated relief valve.

pressure against a spring element. In operation, the fluid pressure acts upon both sides of piston (1) because of the small orifice (C) through the piston and the piston is held in the closed position by the light-bias spring (2). When the pressure increases sufficiently to move the pilot poppet (4) from its seat, the fluid behind the piston will be directed to the low-pressure area, such as the return line. The resulting pressure imbalance on the piston will cause it to move in the direction of the lower pressure, compressing the spring and opening the discharge port. This action will effectively prevent any additional increase in pressure. The setting of the pilot-operated relief valve is adjusted by the preload of the poppet spring (3).

Pressure-Reducing Valves

Pressure-reducing valves are used to supply fluid to branch circuits at a pressure lower than that of the main system. Their main purpose is to step the pressure down to the requirements of the branch circuit by restricting the flow when the branch reaches some preset limit. The pressure-reducing valve is illustrated in Fig. 1.41 [2]. In operation, a pressure-reducing valve permits fluid to pass freely from port C to port D until the pressure at port D becomes high enough to overcome the force of the spring (2). At this point, the spool will move, obstructing flow to port D and thus regulating the downstream pressure. The direction of flow is irrelevant with a pressure-reducing valve, as the spool will close when the pressure at port D reaches the set value. If free reverse flow is required, a check valve must be used.

Counterbalance Valves

The normal use of counterbalance valves is to maintain back pressure on a vertically mounted cylinder to hold vertical loads such as encountered in hydraulic presses. A typical circuit using a counterbalance valve is shown in Fig. 1.42 [2]. Counterbalance valves can be operated by either a direct pilot or a remote pilot. As shown in Fig. 1.42, when a direct pilot is utilized, the pressure on the rod side of the cylinder must reach the valve setting before it will open and permit flow. When the valve is op-

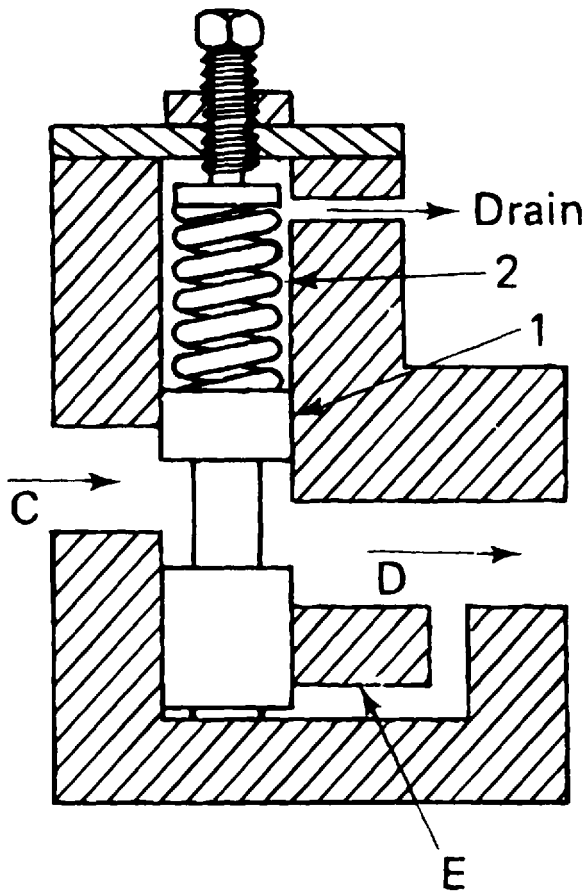


Figure 1.41 Illustration of a pressure-reducing valve.

erated by a remote pilot, this pilot line can be connected to the pump outlet. In this case, the valve will open when the inlet pressure to the cylinder reaches some value. There will be very little rod side pressure in this arrangement. Reverse flow will not pass through the counterbalance valve, as shown in Fig. 1.42. Therefore, a bypass check valve must be included to permit the cylinder to be raised.

2.3.3 Check Valves

Check valves are normally used to control the direction of fluid flow. However, their operation is similar to that of a direct-operated relief valve. Figure 1.43 [23] shows a simple check valve and a cross-sectional illustration of the parts. The valve consists of a seat, a poppet, and a spring. The valve remains closed against flow until the pressure at its inlet creates sufficient force to overcome the spring force. Once the poppet leaves its seat, hydraulic fluid is permitted to flow around and through the poppet to the valve outlet port. For this reason, a simple check valve can only allow flow in one direction. Like direct-operated relief valves, simple check valves have a cracking pressure. By changing the spring, cracking pressures between 5 and 75 psi can be obtained. For special applications, a “no-spring” version is also available.

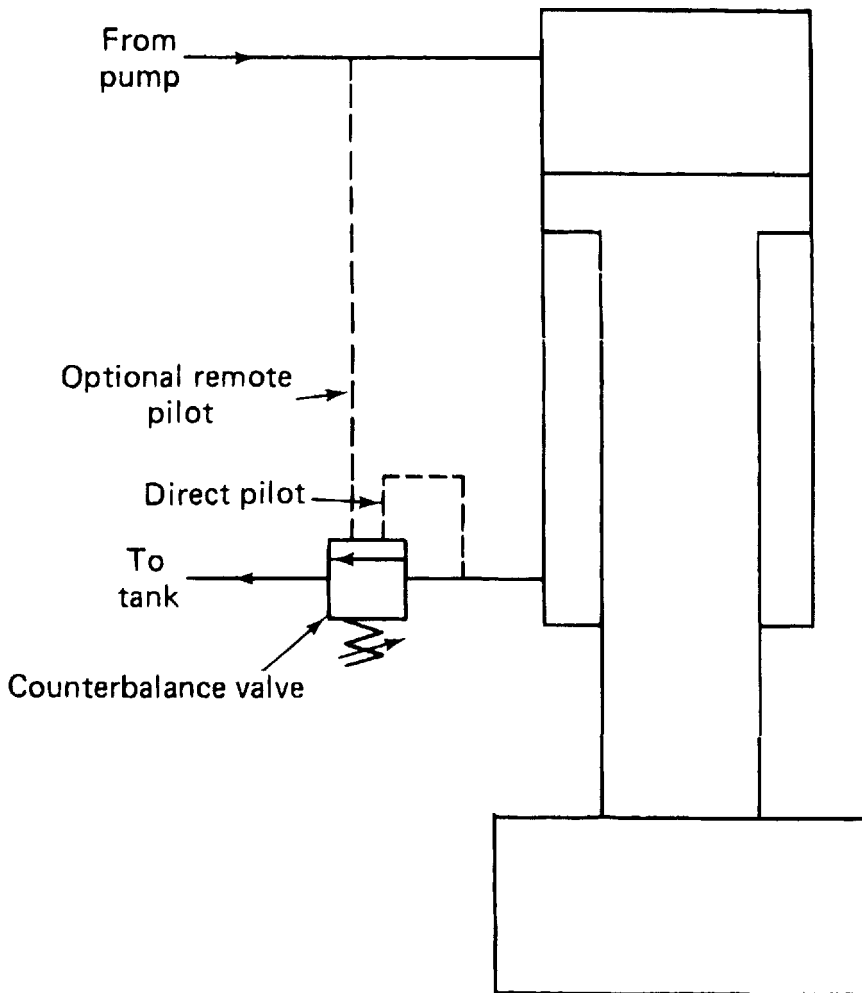


Figure 1.42 A typical counterbalance-valve hydraulic circuit.

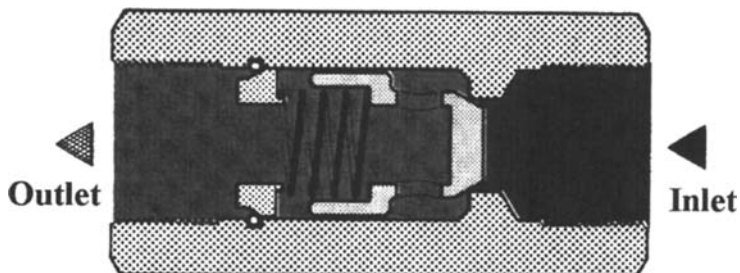


Figure 1.43 Illustration of a simple check valve.

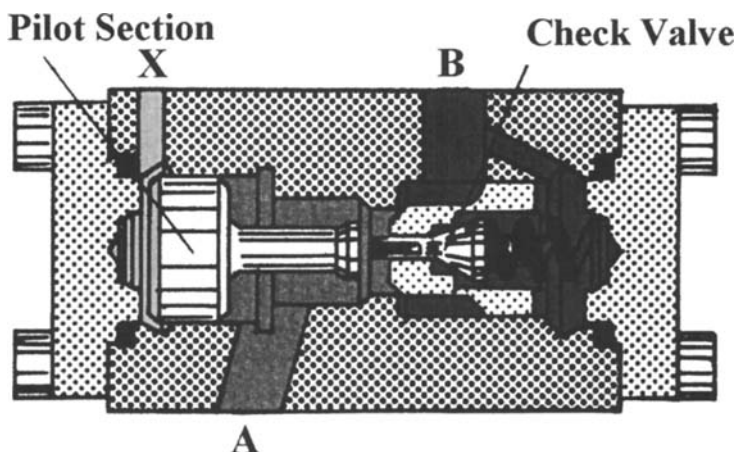


Figure 1.44 Illustration of a pilot-operated check valve.

For load holding and in decompression-type hydraulic press circuits, a pilot-operated check valve is used. It performs the same function as the simple check valve described above. However, in contrast to the simple check valve, a pilot-operated check valve can be piloted “open” when a reverse flow is required. Figure 1.44 [23] illustrates the components of a pilot-operated check valve. The valve has two distinct sections, the check-valve section and the pilot section. The check-valve section allows free fluid flow from port A to port B while preventing reverse flow from B to A without leakage. However, if a pilot pressure signal is supplied to port X, then a force is applied to the pilot piston, which forces the piston rod against the check-valve poppet. This force then unseats the poppet, allowing free flow of fluid from port B to port A.

2.3.4 Directional Control Valves

In typical hydraulic systems, there may be rotary or linear actuators present. These actuators normally have two ports. If oil is pumped into one of the ports while the other is connected to tank, the actuator will move in one direction. In order to reverse its direction of motion, the pump and tank connections must be reversed. The sliding-spool-type directional control valve has been found to be the best way to accomplish this change.

Figure 1.45 [24] shows an illustration of a sliding-spool-type directional control valve. The valve has a cylindrical shaft called a spool, which slides in a machined bore in the valve housing. The housing has ports to which the hydraulic pump, return line to tank, and lines for the actuator are connected. The number of ports designates the valve type. For example, a valve with four ports is referred to as a “4-way” valve; a valve with three port connections would be called a “3-way” valve. Furthermore, spool valves can be classified as “2-position” or “3-position” valves.

A 2-position valve can only be shifted fully left or fully right. A common use for such a valve would be in a cylinder application which only requires the cylinder to extend or retract to its fullest positions. Another application would be in hydraulic motors which only run in forward or reverse directions.

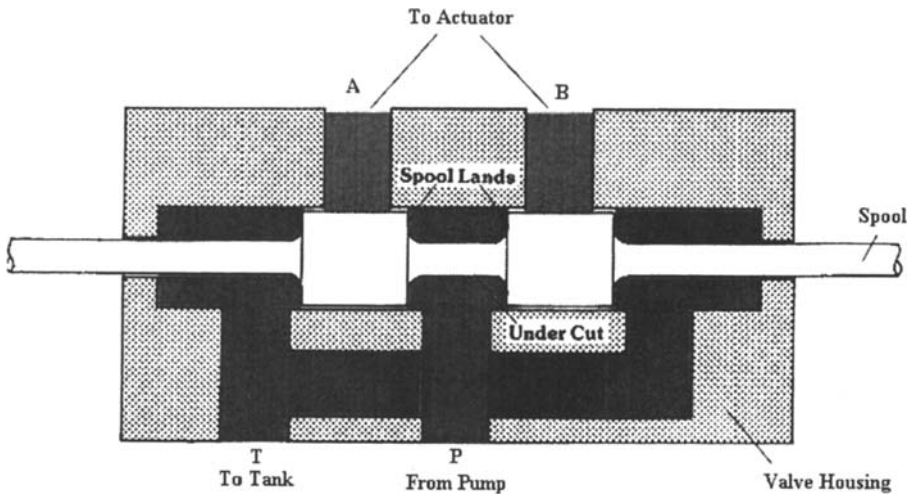


Figure 1.45 Illustration of a spool-type directional control valve.

A “3-position” valve is similar in operation to a “2-position” valve except that it can be stopped in a third or “neutral” position between ports A and B. While in the centered or neutral position, flow may or may not be possible, depending on the spool design of the center position. Figure 1.46 [24] shows some common “3-position” spool designs.

Most valve manufacturers test their valves for flow capacity and develop charts that plot valve flow rate versus pressure drop (ΔP). From these plots, a flow factor

TYPICAL FLOW PATHS AVAILABLE WITH 3 POSITION VALVE SPOOLS			
	Closed Center		Restricted Open Center
	Open Center		Regenerative End Closed Center
	Tandem Center		B Blocked P & A-T
	Float Center		P & B-T A Blocked
	Regenerative Center		P & B Blocked A-T
	Restricted Float Center		P & A Blocked B-T

Figure 1.46 Typical flow paths available for 3-position spool valves.

denoted CV can be determined for each valve. The CV factor then can be used to calculate the flow characteristics of the valve at other conditions; for example, a valve with a CV = 1 will flow 1 gpm at a 1-psig pressure drop using a 1.0 specific gravity (SG) fluid. Figure 1.47 [21] lists the circuit definitions used in the following equations. The CV factor is calculated by

$$CV = \frac{Q\sqrt{SG}}{\sqrt{\Delta P}} \tag{1.38}$$

Parallel circuits:

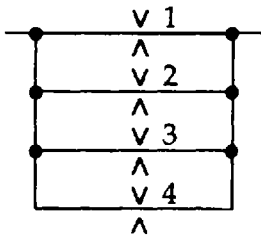
$$Q = (CV_1 + CV_2 + \dots) \sqrt{\frac{\Delta P}{SG}} \tag{1.39}$$

Series circuits:

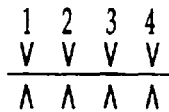
$$Q = \sqrt{\frac{\Delta P}{SG(1/CV_1^2 + 1/CV_2^2 + \dots)}} \tag{1.40}$$

Series/parallel circuits:

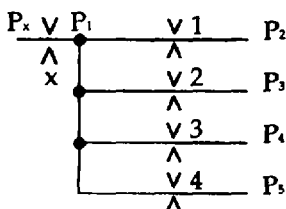
$$Q_i = CV_i \frac{\sqrt{P_i - P_1}}{\sqrt{SG}} \tag{1.41}$$



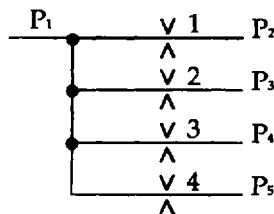
PARALLEL CIRCUIT



SERIES CIRCUIT



SERIES/PARALLEL CIRCUIT



PARTIAL PARALLEL CIRCUIT

Figure 1.47 Circuit definitions for valve flow CV factor calculations.

Partial parallel circuits:

$$Q = \frac{CV_2\sqrt{P_1 - P_2} + CV_3\sqrt{P_1 - P_3} + \dots}{\sqrt{SG}} \quad (1.42)$$

2.3.5 Rotary and Linear Actuators

Rotary motors and linear cylinders are used to convert the energy in the hydraulic circuit to either rotary torque and speed or linear force and velocity. Rotary actuators or motors can be gear, vane, or piston design and will operate very similar to a pump except that flow and pressure are inputs, and torque and rotation are outputs. These are normally referred to as continuous-rotation actuators. Another type of rotary actuator is the limited-rotation design and is sometimes called a rotary cylinder. In this design, the output shaft is limited, usually to less than 360° of rotation. By far, the most prevalent actuator found in hydraulic systems is the linear actuator or cylinder.

Cylinders are either single acting or double acting. Hydraulic cylinders are normally constructed of a barrel, piston assembly, piston rod, end caps, ports, and seals, as shown in Fig. 1.48 [7]. The piston provides the effective area against which the fluid pressure is applied and supports the piston end of the rod. The opposite end of the rod is attached to the load. The cylinder bore, end caps, ports, and seals maintain a fluid-tight chamber into which the fluid energy is connected. Whether the rod will extend or retract in a double-acting cylinder depends on which port fluid is directed. In a single-acting cylinder, there is only one port which when adequately pressurized will extend the rod. The single-acting cylinder depends on external forces such as weight and gravity to retract the rod.

Hydraulic cylinders are normally sized to accommodate the load requirements (Table 1.6) [21]; for example, if the load requirements are such that the cylinder must move a load of 20,000 lbs at a speed of 20 ft/min in the extend direction, this

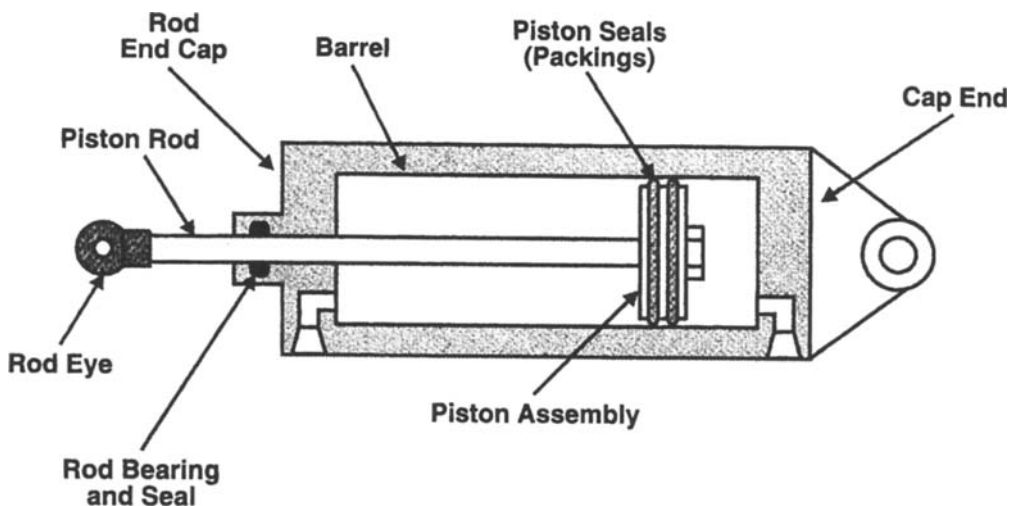


Figure 1.48 Components of a typical double-acting cylinder.

Table 1.6 Cylinder Size, Load, and Pressure Data

Bore diam. (in.) rod (2.5 in.)	Mode	Eff. area (in. ²)	d (lb) at 1000 (psi)	Load (lb) at 2000 (psi)	Load (lb) at 3000 (psi)	Load (lb) at 5000 (psi)
4	Pull	7.66	7,700	15,000	23,000	38,000
5	Pull	14.7	15,000	29,000	44,000	74,000
6	Pull	23.4	23,000	47,000	70,000	120,000
6	Push	28.3	28,000	56,000	85,000	140,000

information will determine the size of the cylinder, the necessary fluid pressure, and the input flow rate, as was shown in (Section 2.1.5).

2.3.6 Accumulators

The purpose of an accumulator in a hydraulic system is to store or provide fluid at a pressure to minimize short-duration pressure spikes or to reach a short-duration high-flow demand. Most accumulators used in hydraulic systems are the spring-loaded or the gas-charged type. The spring-loaded accumulator simply uses the spring force to load a piston. When the fluid pressure increases to a point above the preload force of the spring, fluid will enter the accumulator to be stored until the pressure reduces. The gas-charged accumulator can be either a piston type or a bladder type, as shown in Figs. 1.49 and 1.50, respectively [25]. In the gas-charged accumulator, an inert gas such as dried nitrogen is used as a precharge medium. In operation, this type of accumulator contains the relatively incompressible hydraulic fluid and the more readily compressible gas. When the hydraulic pressure exceeds the precharge pressure exerted by the gas, the gas will compress, allowing hydraulic fluid to enter the accumulator.

2.3.7 Components of a Hydraulic Circuit Diagram

The proper planning of any hydraulic system should start with a properly drawn hydraulic circuit, using ISO-1219-approved graphic symbols. Figures 1.46 [24], 1.51 [18], and 1.52 [18] show the most common symbols found in circuit diagrams. An example of a simple hydraulic circuit used by hydraulic fluid manufacturers is ASTM D-2882-83 "Standard Method for Indicating the Wear Characteristics of Petroleum and Non-Petroleum Hydraulic Fluids in a Constant Volume Vane Pump." This pump test is currently the only one that has ASTM status. Figure 1.53 is an illustration of the hydraulic circuit diagram for this test. The electric motor (1) supplies mechanical energy to a Vickers V-104 vane pump (2), which, in turn, converts mechanical energy into hydraulic energy. The pump outlet pressure is monitored by a pressure gauge (4). The relief valve (5) is adjusted to induce a load pressure of 2000 psi as measured by the pressure gauge (4). The outlet of the relief valve is at low pressure <20 psi. The fluid then passes through a filter (6), then through a flow meter (7), which measures the flow rate to be ~5–6 gpm (8 gpm at no load). The fluid then passes through a heat exchanger (8) and then into the reservoir (9). After the reservoir, the fluid passes through a 60-mesh filter (usually inside the reservoir at the outlet to the pump). A thermoregulator valve (13) is used to maintain a constant reservoir tem-

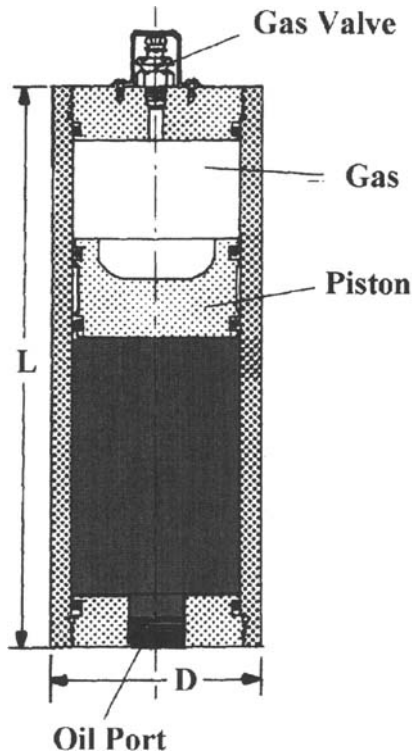


Figure 1.49 Illustration of a piston-type gas-charged accumulator.

perature (14) (set at 80°C for oil or 65°C for water-based fluids). Based on the known parameters of speed (1200 rpm), pressure (2000 psi), and flow (8 gpm, theoretical), other parameters, such as power, torque, and heat, can be readily calculated for this circuit as follows:

$$\text{Power}_{\text{input}} = \frac{(\text{gpm})(\text{psi})}{1714E_t} = \frac{(8.0)(2000)}{(1714)(1.0)} = 9.3 \text{ hp} \quad (1.43)$$

$$\text{Torque}_{\text{input}} = \frac{(\text{hp})(63,025)}{(\text{rpm})E_t} = \frac{(9.3)(63,025)}{(1200)(1.0)} = 490 \text{ in.-lbs} \quad (1.44)$$

$$\frac{\text{BTU}}{\text{h}} = 1.5(\text{gpm})(\text{psi}) = (1.5)(8.0)(2000) = 24,000 \quad (1.45)$$

It should be noted that these calculations have assumed the pump to be 100% efficient ($E_t = 1.0$). In the real world, this is never the case. Typically, vane pumps have $E_t < 0.9$. The effect of this would be to increase the power requirement of the pump to deliver the desired flow rate at a given load-induced pressure. However, from actual experience with this ASTM test, the Vickers V-104 pump delivers only ~5–6 gpm at 2000 psi. This is because the test requires running the pump at a 2000-psi-load pressure, which is 1000 psi higher than the designed maximum pressure for this pump. Therefore, the volumetric efficiency $E_v = \sim 6/8 = \sim 0.75$; assum-

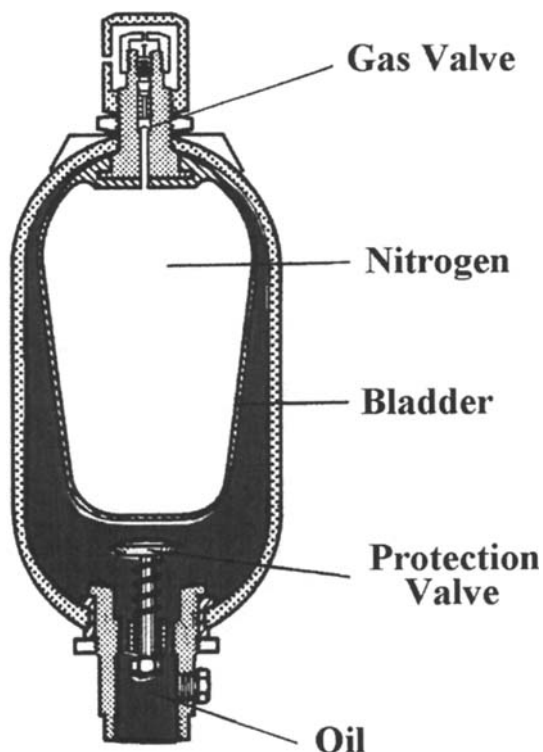


Figure 1.50 Illustration of a bladder-type gas-charged accumulator.

ing the mechanical efficiency $E_m = 0.9$, we have the total efficiency $E_t = (0.75)(0.9) = 0.68$ as a more reasonable value for the total efficiency of this pump at 2000 psi.

2.4 Basic Hydraulic System Design

2.4.1 Pipe and Hose Sizing

Whereas it is necessary to connect the various components in a hydraulic system with some kind of piping, such piping will produce flow resistance and therefore cause parasitic losses in the hydraulic system. To avoid as much loss as possible, the piping or hose must be sized properly. The internal diameter of the hose is extremely important because the fluid velocity at any given flow rate will depend on that diameter. In fact, the fluid velocity will equal the flow rate divided by the internal area of the pipe as follows:

$$V = \frac{0.3208Q}{A} \quad (1.46)$$

where V is the velocity (ft/s), Q is the flow rate (gpm), and A is the internal pipe area (in.^2).

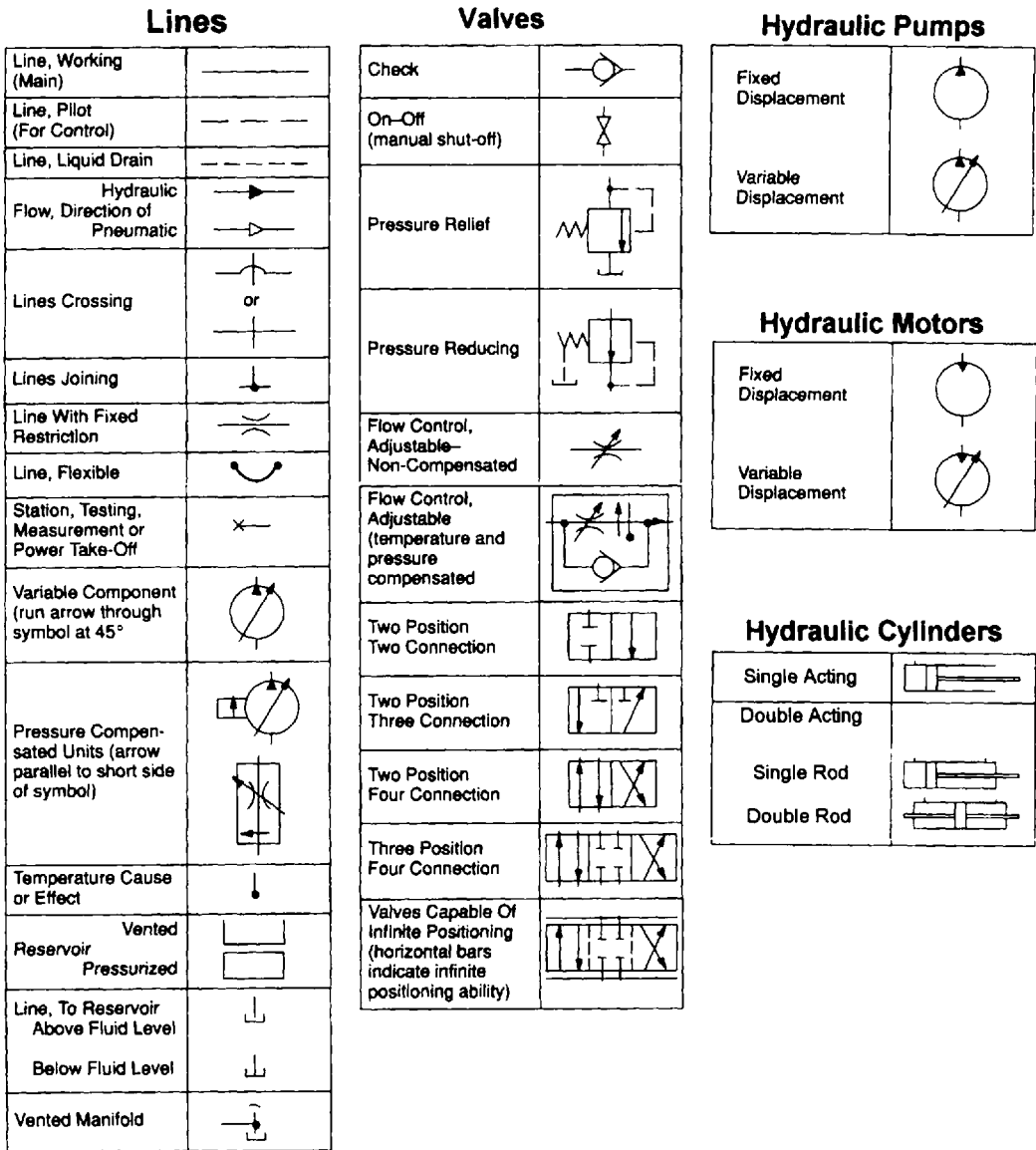


Figure 1.51 Basic hydraulic symbols—1.

The fluid velocities recommended for hydraulic systems are given in Table 1.7. Pressure-drop calculations for the piping or hose can be made using Eq. (1.32). Although most texts refer to the flow regime present in the pipe when making such calculations, the Moody diagram will take the flow regime into consideration, as it relies on the Reynolds number (N_r) which depends upon fluid velocity, fluid viscosity, and the inside diameter of the pipe as shown by the equation,



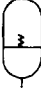
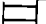
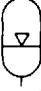

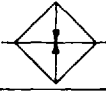

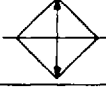

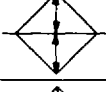
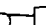
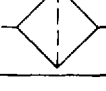

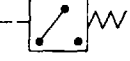


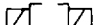



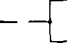


Miscellaneous Units		Operation Methods	
Electric Motor		Spring	
Accumulator, Spring Loaded		Manual	
Accumulator, Gas Charged		Push Button	
Heater		Push-Pull Lever	
Cooler		Pedal or Treadle	
Temperature Controller		Mechanical	
Filter, Strainer		Detent	
Pressure Switch		Pressure Compensated	
Pressure Indicator		Solenoid, Single Winding	
Temperature Indicator		Servo Control	
Component Enclosure		Pilot Pressure Remote Supply	
Direction of Shaft Rotation (assume arrow on near side of shaft)		Internal Supply	

Figure 1.52 Basic hydraulic symbols—2.

$$N_r = \frac{3162Q}{\mu d} \tag{1.47}$$

where N_r is the Reynolds number, μ is the viscosity (cSt), and d is the pipe inner diameter (in.).

Fittings and valves must be handled somewhat differently than straight runs of pipe. The easiest way to calculate the losses resulting from fittings and valves is to use the equivalent-length method to estimate the effect by treating it as if it were an

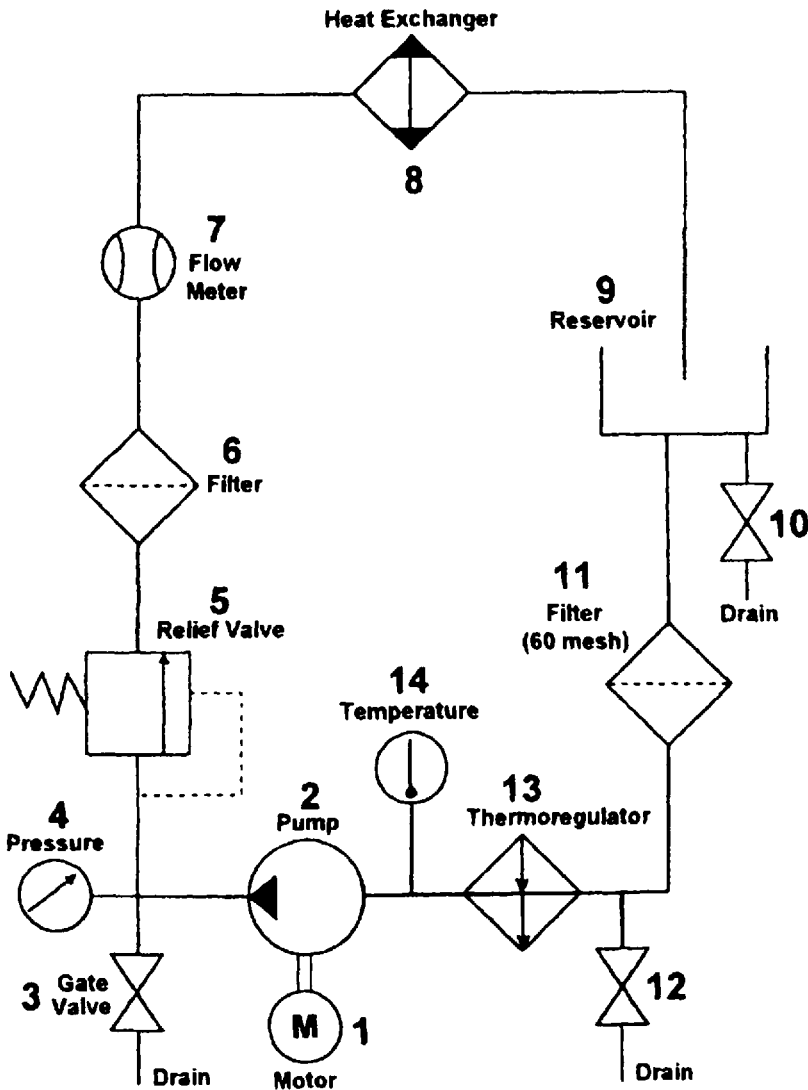


Figure 1.53 ASTM D-2882 pump test hydraulic circuit diagram.

additional length of pipe. Table 1.8 lists some common devices and their equivalent-length values, which are given as the length-to-diameter (L_e/D) ratios so that they can be used directly in the modification of the Darcy equation as follows:

$$h_f = \lambda \frac{L_e}{D} \frac{v^2}{2g} \quad (1.48)$$

where h_f is the equivalent length, λ is the friction factor, L_e/D is the equivalent-length values, v is the fluid velocity, and g is the gravitational constant.

The analytical methods presented here to calculate pressure losses in hydraulic piping and fittings is accurate but can be very time-consuming. A method that is less

Table 1.7 Recommended Hydraulic Circuit Flow Velocities

Suction line		Pressure line		Return line
Viscosity (SUS)	Velocity (ft/s)	Pressure (psi)	Velocity (ft/s)	velocity (ft/s)
700	2.0	365	8.2–10.0	5.5–15.0
465	2.5	725	11.5–13.0	5.5–15.0
230	4.0	1450	14.5–16.5	5.5–15.0
140	4.3	2900	16.5–20.0	5.5–15.0
140–700	4.3–2.0	<2900	20.0	5.5–15.0

accurate but provides a reasonable estimate of pressure losses in hydraulic systems involves the use of tables available from pipe manufacturers and in various handbooks concerning fluid flow (Table 1.5).

2.4.2 Reservoir Design

A typical design for an industrial reservoir is shown in Fig. 1.54 [7]. Several features can be seen in this figure. The overall dimensions should enclose a sufficient volume of oil to permit air bubbles and foam to escape during the resident time of the fluid in the reservoir. The depth must be adequate to assure that during peak pump demands, the oil level will not drop below the pump inlet level. The pump should be mounted below the reservoir so that a positive head pressure is available at all times. This is very critical when water-based hydraulic fluids are used, as these fluids can have a higher specific gravity as well as a much higher vapor pressure than mineral-oil-based fluids (Sec. 2.2.7). The reservoir should be sized to afford adequate fluid cooling. Baffles are provided to prevent channeling of the fluid from the return line to the inlet line. The bottom of the return line is usually cut at a 45° angle to assist in the redirection of the fluid away from the inlet. A cleanout plate is provide to promote cleaning and inspection. Sight gauges are normally used to monitor the fluid level. A breather system with a filter is provided to admit clean air and to maintain atmospheric pressure as fluid is pumped into and out of the reservoir. With water-based hydraulic fluids, a pressurized reservoir is recommended. Special breather caps

Table 1.8 Equivalent Length Values

Device	Equivalent length (L_e/D)
Check valve	150
90° Standard elbow	30
45° Standard elbow	16
Close return bend	50
Standard tee-run	20
Standard tee-branch	60

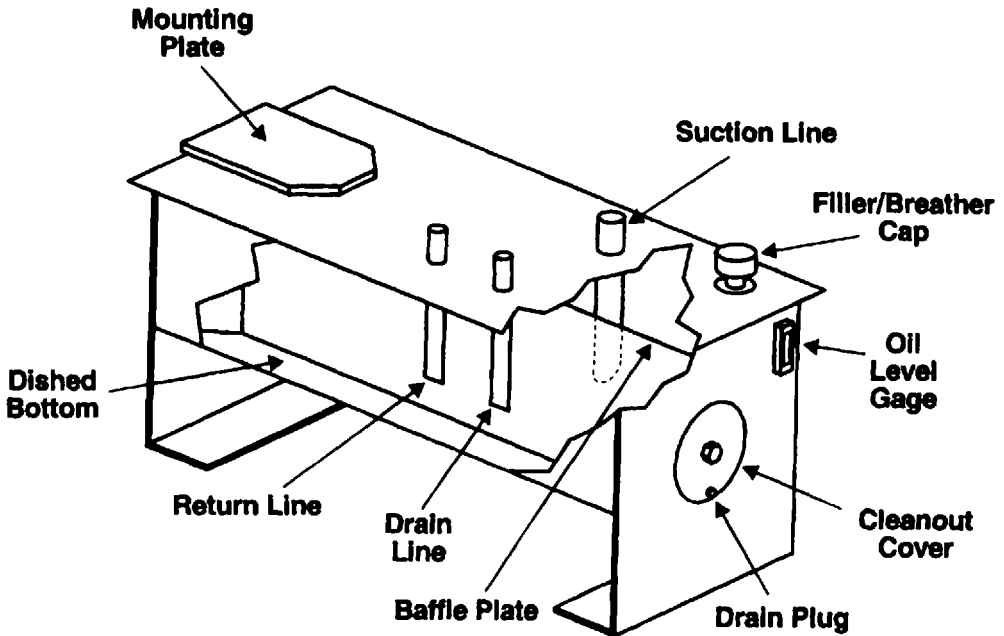


Figure 1.54 A typical design for an industrial reservoir.

can be purchased to vent between 1 and 15 psig. If one of these are used, make sure that it has a vacuum brake to vent at approximately -0.5 psig. (**Note:** Not all pressure caps have a vacuum brake.) This is important so that when the reservoir is cooling down, no appreciable vacuum develops in the reservoir tank. This feature will minimize pump cavitation upon start-up and also prevent a possible tank implosion.

2.4.3 Natural Frequency and Time Response

When designing any hydraulic system, especially when heavy masses are moved quickly, there is one very important design factor that needs to be considered. That factor is known as the “natural frequency” ($\bar{\omega}_0$) of the system. Knowledge of this frequency is important because it determines how fast one can accelerate a given load and, thus, its maximum achievable velocity.

From the physical laws of motion, the natural frequency of a hydraulic system can be found by taking the square root of the effective spring constant divided by the effective moving mass:

$$\omega_0 = \sqrt{\frac{C}{M}} \quad (1.49)$$

where $\bar{\omega}_0$ is the natural frequency, C is the effective spring constant, and M is the effective moving mass. This is a simple statement; however, determination of the effective spring constant and effective moving mass is not so simple. The effective spring constant not only includes the compressibility of the trapped hydraulic fluid

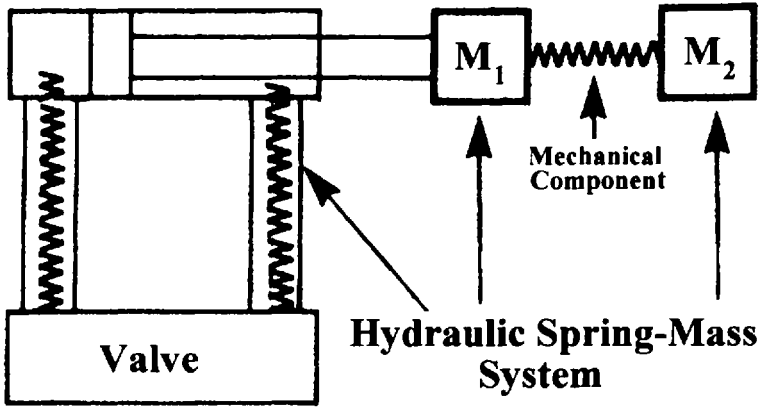


Figure 1.55 Illustration of the hydraulic spring-mass system.

between the valves and the actuators but also the movement of any hoses or piping, as well as structural vibrations. The effective mass of the system is the combination of all the moving loads, including the mass of the trapped fluid between the valves and actuators, as illustrated in Fig. 1.55 [26].

In the simplified case of a linear cylinder in a closed circuit (Fig. 1.56) [26], the natural frequency can be calculated using the following expression:

$$\omega_0 = \sqrt{\frac{A_b^2 \beta}{V_1 M} + \frac{A_e^2 \beta}{V_2 M}} \tag{1.50}$$

or

$$F_0 = \frac{\omega_0}{2\pi}$$

where ω_0 is the natural frequency (rad/s), A_b is the cylinder blind end area (in.²), A_e is the cylinder extending end area (in.²), β is the bulk modulus of fluid, V_1 is the cylinder blind end volume (in.³), V_2 is the cylinder extending end volume (in.³), M is the effective moving mass (lbs-s²/ft, slugs), and F_0 is the natural frequency (Hz). There are computer programs available which can be used to determine the frequency response of a hydraulic system by using the impulse method.

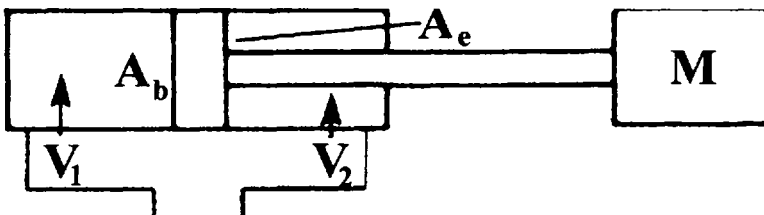


Figure 1.56 Illustration of the natural frequency parameters.

The time response of a hydraulic system is the synergistic result of the response times of all of the components used in the system [27]. Therefore, most component manufacturers will provide information relative to the responsiveness of their components. Unfortunately, the information derived from the component manufacturers is not consistent. The ability to understand and utilize the response information obtained from component manufacturers using a second-order system depends on the definition of several aspects of the response subject as follows:

- Delay time: the time required for the output to reach 50% of the steady output
- Rise time: the time required for the output to rise from 10% to 90% of the final output value
- Maximum overshoot: the time at which the maximum overshoot occurs
- Settling time: the time for the system to reach and stay within a stated plus-and-minus tolerance band around the steady-state output

A graph illustrating these parameters is presented in Fig. 1.57. Control technology can be used to evaluate the response of a complete hydraulic system if all of the component information is given in consistent and correct terms.

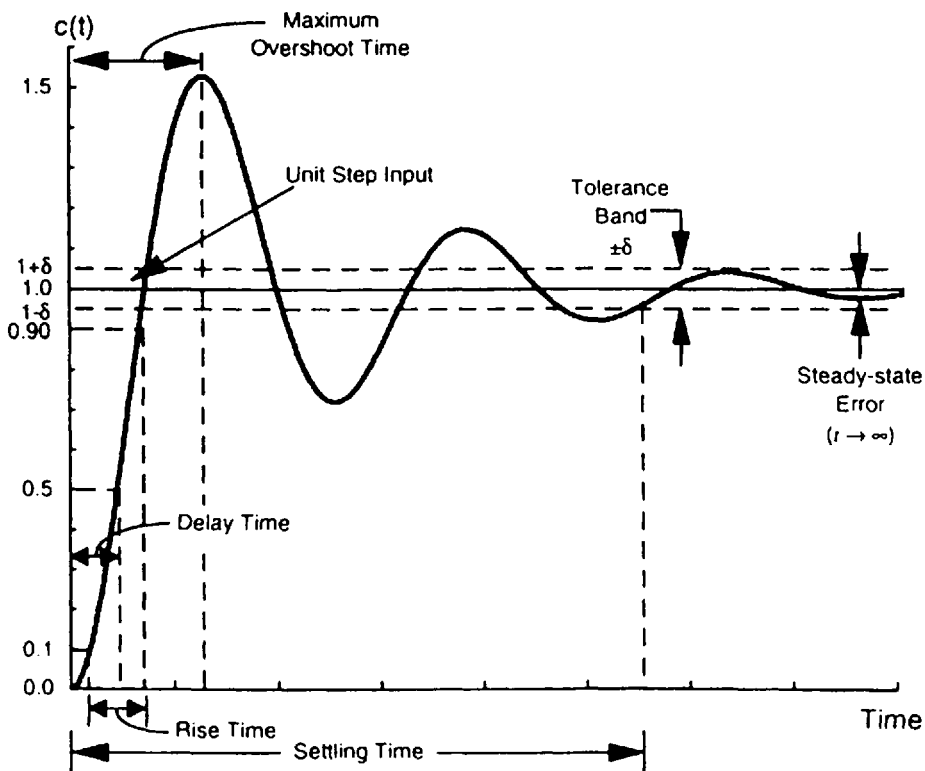


Figure 1.57 Step response of a second-order system.

Calculation of Natural Frequency, Acceleration, Maximum Velocity, Acceleration Pressure, and Flow Rate

For economic reasons, it is often desirable to operate a hydraulic system as fast as possible. This is especially true on automated assembly lines, where hydraulics are used to move parts.

As an example of a simple calculation, consider the following application, where one needs to determine the maximum speed and shortest cycle time to perform a repetitive task. By way of a single-rod hydraulic cylinder (1.5-in. bore, 1-in. rod), a proportional directional control valve is used to accelerate a 1000-lb load (M) to a constant velocity over a distance of 30 in. in 1 s and then decelerate the load to a stop. The load is then retracted in the same manner to start the cycle over again (Fig. 1.58) [26]. To solve this problem, the natural frequency must first be calculated so that the time to accelerate the load can be determined. Then, the maximum velocity, acceleration pressures, and required flow rates can be calculated for both the extending and retracting modes. The following information is given:

- $w = 1000$ lbs (load)
- $T_s = 1.0$ s (stroke time)
- $A_b = 1.76$ in.² (1.5 in. cylinder bore)
- $A_e = 0.98$ in.² (1.5-in.² bore area - 1-in. rod area)
- $S = 30$ in. (stroke distance)
- $\beta = 200,000$ lb/in.² (bulk modulus of oil)
- $L_1 = 46.50$ in. (cylinder blind-end pipe length)
- $L_2 = 38.75$ in. (cylinder rod-end pipe length)
- $D = 0.62$ in. (pipe inner diameter)

Pipe size = 0.75-in. outer diameter \times 0.065-in. wall

The first step is to calculate the pipe trapped volumes between the control valve and the cylinder blind-end inlet (V_3) and the rod-end inlet (V_4) in Fig. 1.58 [26] from the following equation:

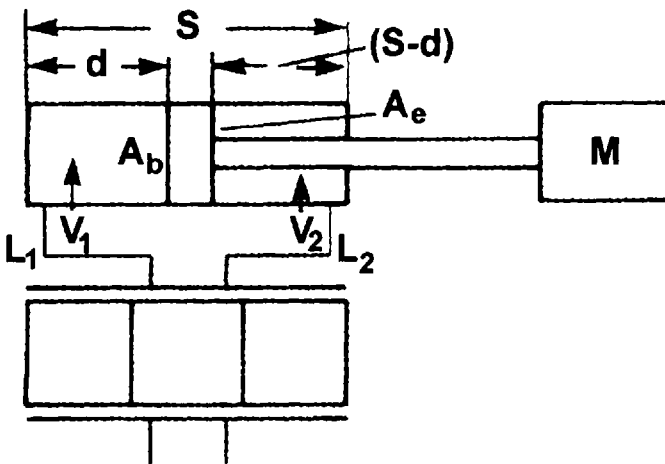


Figure 1.58 Illustration of a typical natural frequency calculation.

$$\begin{aligned}
 V_1 &= \frac{\pi D^3}{4} L_1 \\
 &= \frac{\pi(0.62)^3}{4} (46.5) \\
 &= 14.04 \text{ in.}^3 \\
 V_4 &= (0.30)(38.75) \\
 &= 11.7 \text{ in.}^3
 \end{aligned} \tag{1.51}$$

Next, calculate the dimension d , using the above values along with the given parameters, using the following expression:

$$\begin{aligned}
 d &= \left(\frac{A_r S + V_4}{\sqrt{A_r^3}} - \frac{V_1}{\sqrt{A_b^3}} \right) \left(\frac{1}{\sqrt{A_r}} + \frac{1}{\sqrt{A_b}} \right)^{-1} \\
 &= \left(\frac{(0.98)(30) + 11.7}{\sqrt{(0.98)^3}} - \frac{14.04}{\sqrt{(1.76)^3}} \right) \left(\frac{1}{\sqrt{0.98}} + \frac{1}{\sqrt{1.76}} \right)^{-1} \\
 &= 20.6 \text{ in.}
 \end{aligned} \tag{1.52}$$

Next, calculate the total trapped volume between the valve and cylinder blind end (V_1) and cylinder rod end (V_2), using the following relations:

$$\begin{aligned}
 V_1 &= V_1 + A_b d \\
 &= 14.04 + 1.76(20.6) \\
 &= 50.3 \text{ in.}^3 \\
 V_2 &= V_4 + A_r (S - d) \\
 &= 11.7 + 0.98(30 - 20.6) \\
 &= 20.9 \text{ in.}^3
 \end{aligned} \tag{1.53}$$

Convert the load to units of mass as follows:

$$M = \frac{W}{g} = \frac{1000}{386} = 2.59 \left(\frac{\text{lbs} \cdot \text{s}^2}{\text{in.}} \right) \tag{1.54}$$

where M is the effective moving mass (lbs \cdot s²/in., slugs), w is the load force (lbs), and g is the gravitational constant (in./s²). Then, substitute the known quantities into Eq. (1.50) to obtain the natural frequency ($\bar{\omega}_n$) of this system:

$$\begin{aligned}
 \bar{\omega}_n &= \sqrt{\frac{(1.76)^2(200,000)}{(50.3)(2.59)} + \frac{(0.98)^2(200,000)}{(20.9)(2.59)}} \\
 &= 91.1 \text{ rad/s}
 \end{aligned} \tag{1.55}$$

In calculating $\bar{\omega}_n$, we have not taken into consideration other factors that contribute to the spring constant of the system, namely hoses and other mechanical components. However, it has been shown over the years that a good approximation to determine the usable acceleration is to divide the calculated natural frequency by 3 [26]. This simplification avoids a much more complex mathematical analysis, which would have required variables which are difficult, if not impossible, to define. Therefore, the usable frequency ($\bar{\omega}$) can be estimated as

$$\omega = \frac{\omega_0}{3} = \frac{91.1}{3} = 30.4 \frac{\text{rad}}{\text{s}}$$

or

$$F = \frac{\omega}{2\pi} = \frac{30.4}{2\pi} = 4.8 \text{ Hz} \quad (1.56)$$

The acceleration time (T) or the time for one complete oscillation can now be calculated:

$$T = \frac{1}{\omega} = \frac{1}{30.4} = 0.033 \text{ s} \quad (1.57)$$

However, it has been determined that this period is too short for acceleration to stabilize using proportional valves. Generally, for stable acceleration, the time allowed must be a minimum of four to six times the time period for one oscillation [26]. Therefore, the acceleration stabilizing time (T_b) is calculated to be

$$T_b = 6T = 6(0.033) = 0.20 \text{ s} \quad (1.58)$$

From the stroke distance (S), the acceleration time (T_b) and the stroke time (T_s), the maximum velocity (V_{\max}), acceleration (A_{\max}), and the acceleration force (F_a) can be easily calculated from the following expressions:

$$V_{\max} = \frac{S}{T_s - T_b} = \frac{30}{1.0 - 0.2} = 37.5 \frac{\text{in.}}{\text{s}} \quad (1.59)$$

$$A_{\max} = \frac{V_{\max}}{T_b} = \frac{37.5}{0.20} = 188 \frac{\text{in.}}{\text{s}^2} \quad (1.60)$$

$$F_a = MA_{\max} = \frac{w}{g} A_{\max} = \left(\frac{1000}{386} \right) 188 = 487 \text{ lbs} \quad (1.61)$$

Before we can calculate the acceleration pressure at the blind end (P_b) and rod end (P_r) of the cylinder, the frictional force that the load imposes on the system needs to be determined. For this calculation, it is assumed that the coefficient of friction (μ) equals 0.58; we can then determine the force due to friction (F_μ) and the total force (F_t) as follows:

$$F_\mu = \mu w = (0.58)(1000) = 580 \text{ lbs} \quad (1.62)$$

$$F_t = F_\mu + F_a = 580 + 487 = 1067 \text{ lbs} \quad (1.63)$$

$$P_b = \frac{F_t}{A_b} = \frac{1067}{1.76} = 606 \text{ psi}$$

$$P_r = \frac{F_t}{A_r} = \frac{1067}{0.98} = 1089 \text{ psi} \quad (1.64)$$

One should note that for a single-rod cylinder, the rod-end pressure is always greater than the blind end, but only with double-rod cylinders having equal rod diameters will the pressure be the same at both ends.

Finally, the flow rate required at the blind end (Q_b) and rod end (Q_r) may be calculated as follows:

$$Q_b = \frac{V_{\max} A_b (60)}{231} = \frac{(37.5)(1.76)(60)}{231} = 17.1 \text{ gpm}$$

$$Q_c = \frac{V_{\max} A_c (60)}{231} = \frac{(37.5)(0.98)(60)}{231} = 9.6 \text{ gpm} \quad (1.65)$$

2.5 Hydraulic Fluid Considerations

2.5.1 Foaming

Most hydraulic fluids have an antifoaming agent as an additive. These additives have caused discussions among hydraulic system designers and users. Most of the additives used to control the foaming tendencies of hydraulic fluids accomplish this task by increasing the surface tension of the fluid. When the surface tension increases, the size of air or vapor bubbles which will coexist in the fluid become smaller and are therefore less likely to rise to the surface and cause a foaming situation. However, when the air is allowed to remain in the fluid, the compressibility of the fluid increases or, stated in another way, the bulk modulus of the fluid decreases. The suspension of air or vapor in the circulating fluid of a hydraulic system is a fault of the system; that is, a well-designed system will not permit air or vapor to become entrained in the fluid. Some expert designers of hydraulic systems have said that they would rather not have an antifoam agent present. Without the addition of the antifoaming agent, a system that is poorly designed will be readily apparent and can be fixed. Details on foaming, air entrainment, and air release are provided in Chapter 4.

2.5.2 Bulk Modulus

The bulk modulus of a fluid is a term used to describe the compressibility of the fluid. In fact, the bulk modulus is inversely proportional to the compressibility. The purpose of a hydraulic system is to raise the potential energy of the system by increasing the pressure of the fluid. This potential energy can then be converted into kinetic energy that will do useful work. However, a fluid with a low bulk modulus will be very compressible and the energy necessary to raise the pressure must also be sufficient to compress the fluid. Most hydraulic fluids have a very high bulk modulus in the pristine condition. However, when air is present, the effective bulk modulus will be low and the system fluid will need to absorb the heat generated when the compression takes place. Calculation procedures for bulk modulus and fluid compressibility is described in more detail in Chapter 4.

Fluid Compressibility and Cylinder Lunge

Fluid compressibility has a great effect on cylinder performance—especially when the fluid type is changed, such as changing from a mineral-oil- to a water-based or synthetic fluid. Hydraulic cylinders are especially sensitive to changes in bulk modulus. In critical operations, it is often necessary to extend the cylinder smoothly and at a very constant velocity. If the load changes, the compressibility of the hydraulic fluid will have a negative influence on the constant velocity. Also, any change in the volume (ΔV) of the fluid under compression will translate into a change in cylinder stroke (ΔS) defined as “lunge.” The following expressions can be used to calculate “lunge” (ΔS) and the resultant velocity change (Δv):

$$\Delta S = \frac{(V_p + AS)\Delta L}{A^2\beta} \tag{1.66}$$

$$\Delta v = \frac{(\Delta S)(60)}{\Delta\tau} \tag{1.67}$$

where ΔS is the lunge (in.), V_p is the volume in the pipe (in.³), A is the effective piston area (in.²), S is the Stroke (in.), ΔL is the load change (lbs), β is the bulk modulus of the fluid, Δv is the velocity change (in./min), and $\Delta\tau$ is the load change time (s).

We will now apply these equations to the meter-in (Fig. 1.59) [28] and the meter-out (Fig. 1.60) [28] circuits under the following conditions:

- $A_1 = 4.9 \text{ in.}^2$ (blind-end area)
- $A_2 = 2.5 \text{ in.}^2$ (rod-end area)
- $S = 24 \text{ in.}$ (stroke)
- $L_1 = 3000 \text{ lbs}$ (full load)
- $L_2 = 1000 \text{ lbs}$ (reduced load)
- $\Delta L = 2000 \text{ lbs}$ (load change, $L_1 - L_2$)

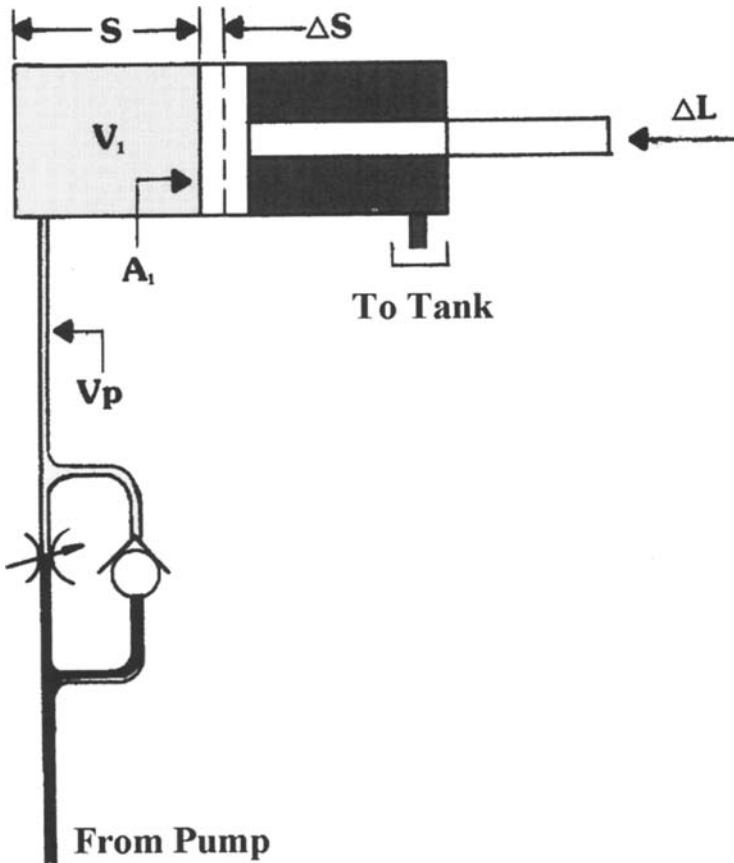


Figure 1.59 Illustration of a cylinder meter-in circuit.

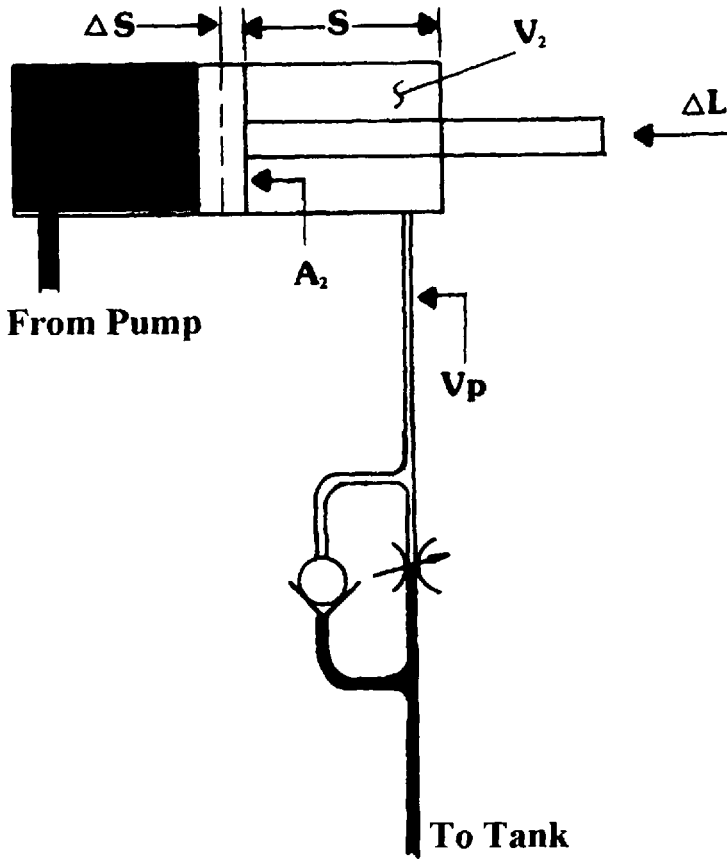


Figure 1.60 Illustration of a cylinder meter-out circuit.

$$\begin{aligned}\Delta\tau &= 1 \text{ s (load change time)} \\ V_p &= 36 \text{ in.}^3 \text{ (oil line volume)} \\ \beta &= 200,000 \text{ lb/in.}^2 \text{ (bulk modulus of oil)}\end{aligned}$$

For the meter-in mode (Fig. 1.59) using Eqs. (1.66) and (1.67), we calculate

$$\Delta S = \frac{[36 + (4.9)(24)](2000)}{(4.9)^2(200,000)} = 0.064 \text{ in.} \quad (1.68)$$

$$\Delta v = \frac{(0.064)(60)}{1} = 3.8 \frac{\text{in.}}{\text{min}} \quad (1.69)$$

For the meter-out mode (Fig. 1.60) using Eqs. (1.66) and (1.67), we calculate

$$\Delta S = \frac{[36 + (2.5)(24)](2000)}{(2.5)^2(200,000)} = 0.154 \text{ in.} \quad (1.70)$$

$$\Delta v = \frac{(0.154)(60)}{1} = 9.2 \frac{\text{in.}}{\text{min}} \quad (1.71)$$

As can be seen from the above examples, the degree of “lunge” is directly proportional to the load change and inversely proportional to the bulk modulus of the fluid. Also, the cylinder lunge is greater in the meter-out mode than in the meter-in mode. This is due to pressure intensification in the rod end of the cylinder as discussed earlier in this chapter (Section 2.1.5).

REFERENCES

1. T. C. Frankenfield, “Using Industrial Hydraulics,” Chapter 1, *Hydraulics & Pneumatics Magazine*, Cleveland, OH, 1990.
2. J. A. Sullivan, *Fluid Power Theory and Applications*, 2nd ed., 1982, Reston Publishing Company, Reston, VA.
3. J. F. Blackburn, G. Reethof, and J. L. Shearer, *Fluid Power Control*, 1960, The M.I.T. Press, Cambridge, MA.
4. W. E. Wilson, “Rotary-Pump Theory,” *Trans. ASME*, 1946, 68, pp. 371–384.
5. W. E. Wilson, “Clearance Design in Positive-Displacement Pumps,” *Mach. Design*, 1953, February, pp. 127–130.
6. E. C. Fitch and I. T. Hong, *Hydraulic Component Design and Selection*, 1997, BarDyne, Inc., Stillwater, OK.
7. F. D. Norvelle, *Fluid Power Technology*, 1995, West Publishing Company, New York.
8. T. C. Frankenfield, “Using Industrial Hydraulics,” Chapter 6, *Hydraulics & Pneumatics Magazine*, Cleveland, OH, 1990.
9. M. Rexroth, *Pump & Controls—Open Loop*, 1995, The Rexroth Training Center, Bethlehem Vocational Technical School, Bethlehem, PA.
10. E. C. Fitch, *Fluid Contamination Control*, 1988, FES Inc., Stillwater, OK.
11. R. K. Tessmann and J. M. Howsden, “Environmental Influence Upon Wiper Seal Performance,” *BFPR J.*, 1975, October, p. 75-5.
12. R. K. Tessmann and J. M. Howsden, “Service Life of Wiper Seals,” *BFPR J.*, 1976, October, p. 76-31.
13. E. C. Fitch and R. K. Tessmann, “Modeling the Performance of Filter Assemblies,” *BFPR J.*, 1973, October, p. 73-CC-12.
14. E. C. Fitch and R. K. Tessmann, “The Filter Selection Graph—A Basic Contamination Control Tool,” *BFPR J.*, 1974, October, p. 74-55.
15. M. L. Wolf, “Contaminant Particle Effects on Pumps as a Function of Size, Type and Concentration,” M.S. Thesis, FPRC/OSU, Stillwater, OK, 1965.
16. R. K. Tessmann, “Contaminant Wear in Hydraulic and Lubricating Systems,” *BFPR J.*, 1975, October, p. 75-4.
17. L. E. Bensch, “Verification of the Pump Contaminant Wear Theory,” *BFPR J.*, 1977, 11(2).
18. Vickers, Inc., *Hydraulic Hints & Troubleshooting Guide, No. 694*, 1996, Vickers, Inc., Troy, MI.
19. E. C. Fitch, *Fluid Power Engineering*, 1982, FES Inc., Stillwater, OK.
20. R. C. Mackay, “Pump Suction Conditions,” *Pumps Syst. Mag.*, 1993, May, p. 20.
21. *Lightning Reference Handbook*, 8th ed., 1994, Paul-Munroe Rucker, Inc.
22. *Handbook of Chemistry and Physics*, 49th ed., 1968–1969, The Chemical Rubber Co., Cleveland, OH, p. D109.
23. T. C. Frankenfield, “Using Industrial Hydraulics,” Chapter 4, *Hydraulics & Pneumatics Magazine*, Cleveland, OH, 1990.
24. T. C. Frankenfield, “Using Industrial Hydraulics,” Chapter 5, *Hydraulics & Pneumatics Magazine*, Cleveland, OH, 1990.

25. T. C. Frankenfield, "Using Industrial Hydraulics," Chapter 10, *Hydraulics & Pneumatics Magazine*, Cleveland, OH, 1990.
26. T. C. Frankenfield, "Using Industrial Hydraulics," Chapter 9, *Hydraulics & Pneumatics Magazine*, Cleveland, OH, 1990.
27. I. T. Hong and R. K. Tessmann, "What Time Do You Have?" in *Proceedings of the National Conference on Fluid Power, Vol. II*, 1996, National Fluid Power Association, pp. 23–25.
28. T. C. Frankenfield, "Using Industrial Hydraulics," Chapter 3, *Hydraulics & Pneumatics Magazine*, Cleveland, OH.

2

Bearing Selection and Lubrication

FARUK PAVLOVICH

*The College of New Jersey, Trenton, New Jersey, and University of Mostar,
Mostar, Bosnia and Herzegovina*

1 INTRODUCTION

The first practical studies to reduce resistance to motion date to ancient times. Figure 2.1 [1] illustrates the movement of heavy stone blocks during pyramid construction in ancient Egypt. This figure shows that basic empirical tribological science was applied as early as approximately 2400 B.C.

Two basic tribological principles are illustrated in Figure 2.1. The first principle is the preservation of the high resistance to sliding and the tribo-system is illustrated by the dry friction interface of the worker's feet to the ground, which results in the maximum friction force while pulling the load. The second principle is typified by the magnitude and shape of the load surface and modification of the friction properties of the ground interface with the introduction of a lubricant. This is a very basic representation of the first forms of sliding bearings.

The radial sliding bearing used for connecting the wheels and shaft illustrated in Fig. 2.2 [1] represents a more sophisticated modern tribo-system. The use of these bearings produce a significant decrease of friction by substitution of sliding friction by the rolling friction wheel-ground interface which produces a lower resistance to motion. The tribo-system is further modified by the introduction of a washer-bushing whose interfacial friction properties are dependent on the selection of the washer-bushing material pair, design, and lubricant selection.

One early application of rolling antifriction bearings, according to archeological evidence, was a thrust roller bearing used for the rotating potter's wheel illustrated in Fig. 2.3 [2]. Originally, the rolling element bearings and the raceway were constructed from hard wood. Later, bronze was used to construct the outside raceway.

Metal roller bearings were first manufactured at the end of the 18th century. Subsequently, both the bearing assembly and the production process were improved

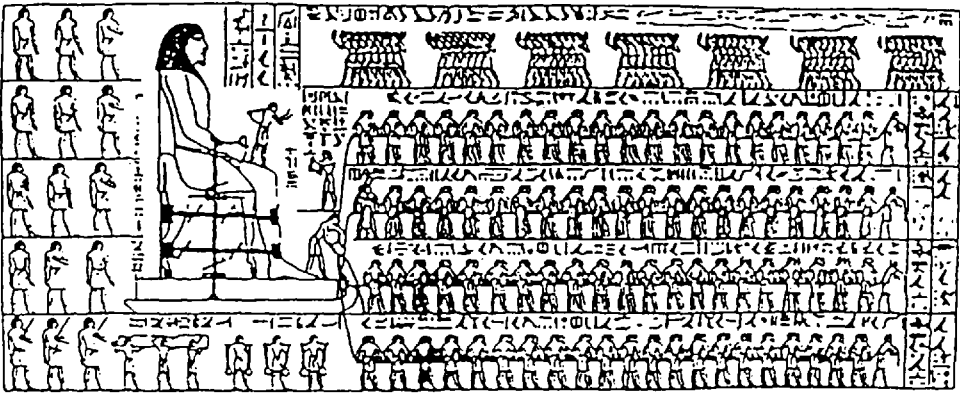


Figure 2.1 The transport of heavy stone blocks during pyramid construction in ancient Egypt.

and standardized. Currently, the focus of bearing technology research is to reduce friction energy losses and to significantly increase lifetimes. Additional objectives include broadening roller bearing load ranges, operating speeds and temperatures, applicability for use in aggressive environments, with and without application of lubricants, and use in high-vacuum applications.

2 APPLICATION OF ROLLER BEARINGS IN HYDRAULIC SYSTEMS

In addition to their ability to position rotating elements of mechanical systems with respect to each other, roller bearings are selected based on load, speed, and operating environment. Although the ability of a hydraulic fluid to provide adequate lubrication is currently important, research is in progress to develop rolling element bearings that are less sensitive to the lubricating properties of a hydraulic fluid. Bearing materials, such as ceramics, are being developed that may be used under conditions of poor lubrication and that will operate in high vacuum. Figure 2.4 [3,4] illustrates selected examples of pumps with the bedding positions of rolling element bearings used: centrifugal pump, propeller pump, gear pump with outside toothing, gear pump with inside toothing, winged pump, axial piston pump, and radial piston pump.

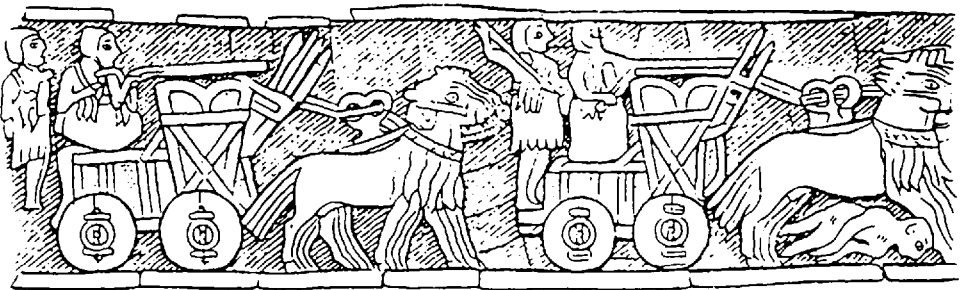


Figure 2.2 The first forms of radial sliding bearing.

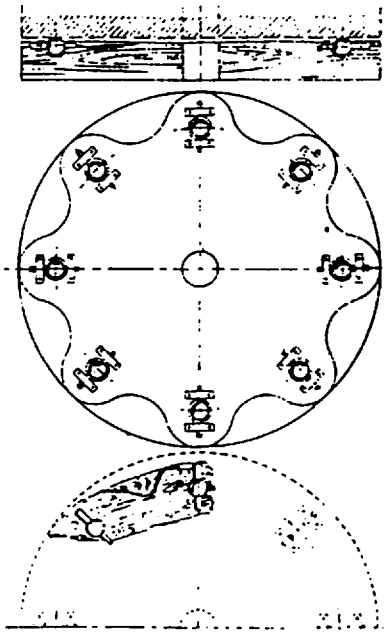


Figure 2.3 The thrust roller bearings used for rotating potters wheel.

3 TYPES OF ROLLER BEARINGS

Contemporary production of roller bearings is characterized by high diversification of bearing types and the broad range of materials facilitating their use to replace other bearings such as sliding hydrodynamic and hydrostatic bearings. Roller bearings are classified by the following: the direction of applied load: radial, axial and radi-axial; the shape of the rolling elements, including ball bearings, roller bearings, convex roller bearings, and needle bearings; position of contact—radial-contact bearings and angular-contact bearings; the material of construction—steel, ceramic, and hybrid bearings. The classification of bearings may also be done according to other characteristics, including number of raceways, high operation speeds, and area of application. In this section, the most frequently applied types of bearings and a brief description of their characteristics will be discussed.

3.1 Radial-Contact Roller Bearing

An example of a radial-contact roller bearing is illustrated in Figure 2.5 [5]. This bearing is designed for radial and radi-axial loads and high speeds. With increasing speed, the load capacity of the bearing-carrying capacity in the radial direction decreases. The bearing construction is rigid; therefore, it can sustain only minimum tilt of the support shaft without damage.

3.2 Single-Row Angular-Contact Roller Bearing

As opposed to radial-contact roller bearings (radial bearing) where the contact is perpendicular to the direction of the bearing axis, the contact points of the rolling

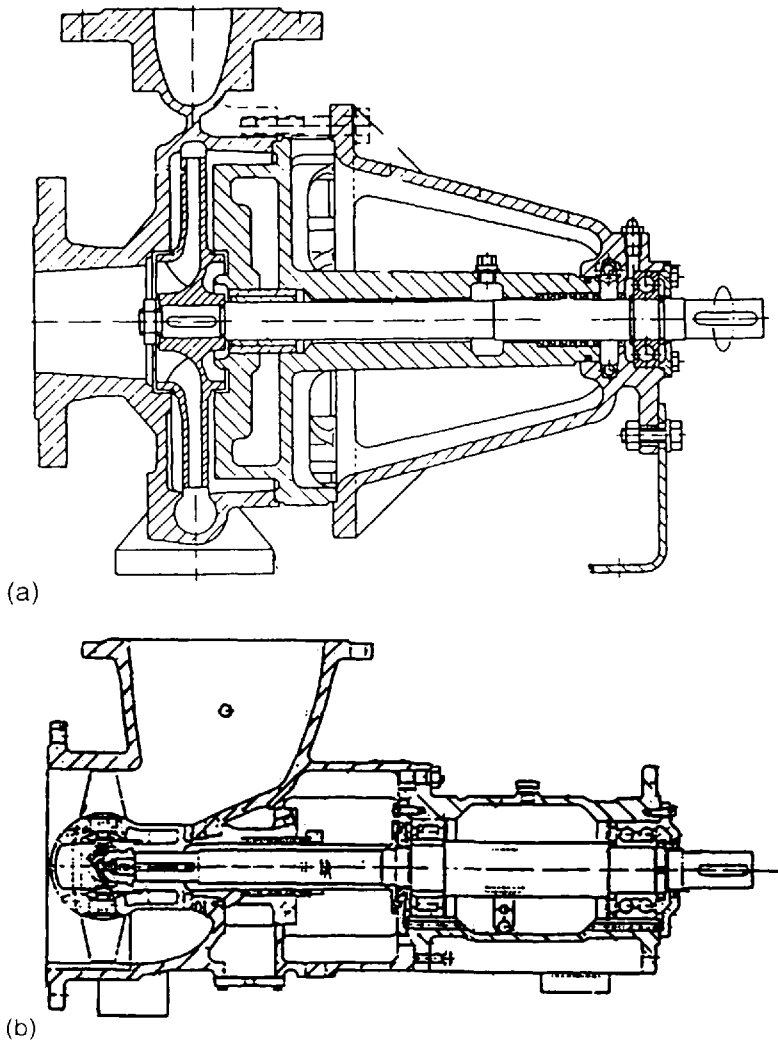
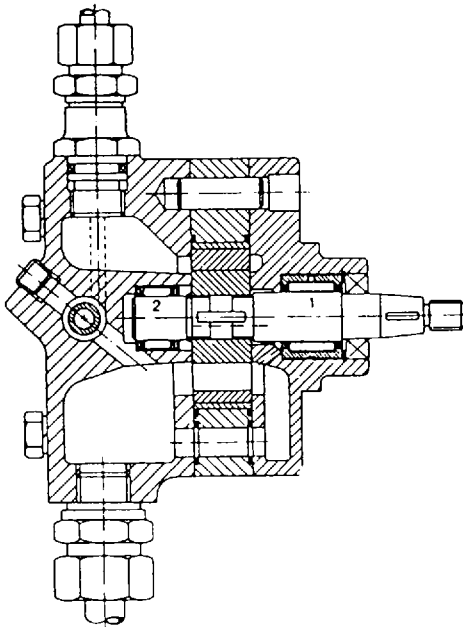
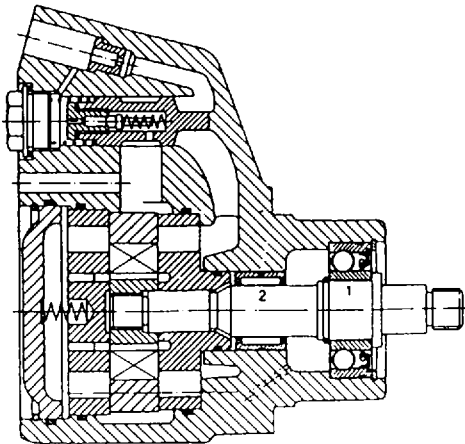


Figure 2.4 Types of pumps: (a) centrifugal pump; (b) propeller pump; (c) gear pump (with inside toothing); (d) winged pump; (e) axial piston pump; (f) radial piston pump.

elements for an angular-contact roller bearing with respect to the bearing raceways is tilted, not radial, as illustrated in Fig. 2.6. The tilted contact is capable of taking the axial load and axial force in the support in one direction only, even with pure radial loads. To eliminate the tendency of bearing raceway separation resulting from the action of load, this bearing is frequently installed as a pair. The angular-contact roller bearing is rigid, suitable for high operation speeds, and it has higher load-carrying capacity than the radial-contact bearing of the same size. This bearing type is used only for very rigid shafts or in pairs for supporting the load-carrying shaft on both ends.



(c)

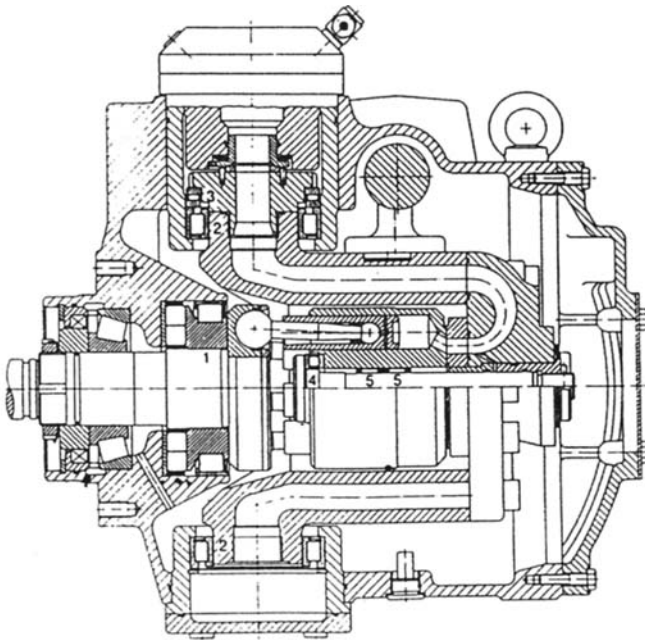


(d)

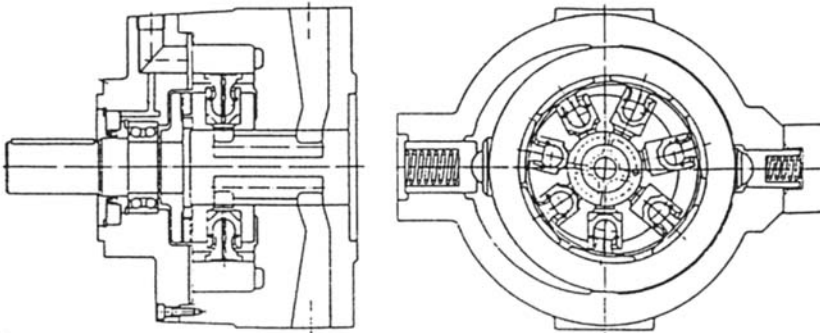
Figure 2.4 Continued

3.3 Double-Row Angular-Contact Roller Bearing

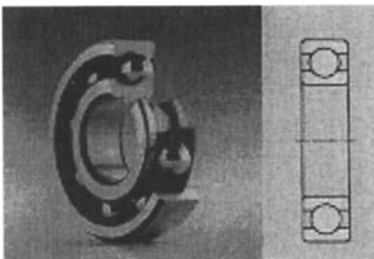
The double-row angular-contact roller bearing illustrated in Fig. 2.7 [5] looks like the double single-row angular-contact roller bearing and is designed to accept significant radial and two-sided axial loads. This bearing is characterized by high stiffness and it is most commonly applied for positioning very rigid shafts rotating at moderate speeds.



(e)



(f)

Figure 2.4 Continued**Figure 2.5** Radial-contact roller bearing.

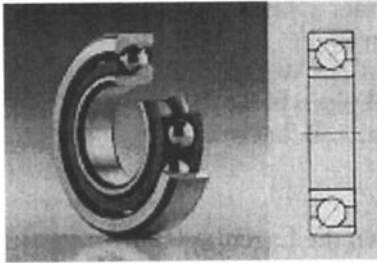


Figure 2.6 Single-row angular-contact roller bearing.

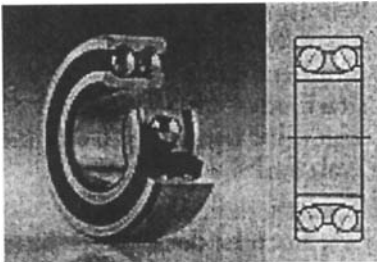


Figure 2.7 Double-row angular-contact roller bearing.

3.4 Double-Row Angular-Contact Aligning Roller Bearing

Double-row angular-contact aligning roller bearings, as illustrated in Fig. 2.8 [5], are capable of accepting both radial and moderate axial loads. Bearing alignment is achieved by the spherical shape of the outside raceway. These bearings are capable of high operating speeds and are used for shafts with a significant bedding tilt up to 4 in.

3.5 Single-Row Convex-Roller Aligning Bearing

Single-row convex roller aligning bearing, illustrated in Fig. 2.9 [5], exhibits a larger rolling element and raceway contact surface, providing a significantly larger load-carrying capacity than the roller bearings of the same dimensions. Bearing alignment of up to 4 in. of the shaft tilt in the bedding is ensured by the spherical shape of the

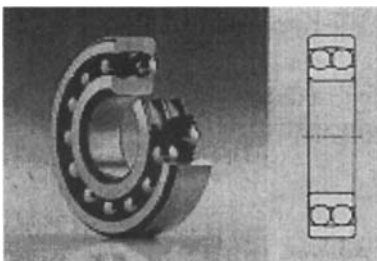


Figure 2.8 Double-row angular-contact aligning roller bearing.

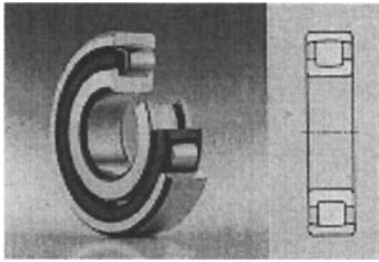


Figure 2.9 Single-row convex-roller aligning bearing.

outside raceway. The bearing is capable of sustaining high-impact loads and they are used at low operation speeds.

3.6 Double-Row Convex-Roller Aligning Bearing

The double-row convex-roller aligning bearing is self-aligning up to a tilt angle of 2° at lower loads and up to 0.5° at higher loads (Fig. 2.10) [5]. Bearing self-alignment is achieved by the spherical shape of the outside raceway. It is used for high loads, sustains significant impact loads, and used at low speeds.

3.7 Tapered Roller Bearing

An illustration of a tapered roller bearing is provided in Fig. 2.11 [5]. Tapered-roller-bearing raceways are cones whose generators cross at the same point on the bearing

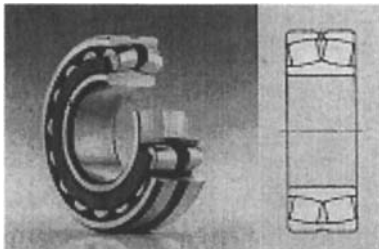


Figure 2.10 Double-row convex-roller aligning bearing.

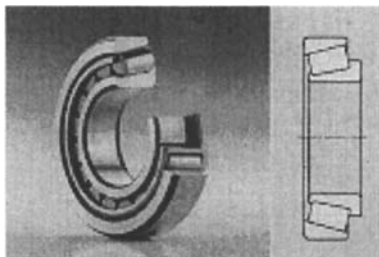


Figure 2.11 Tapered roller bearing.

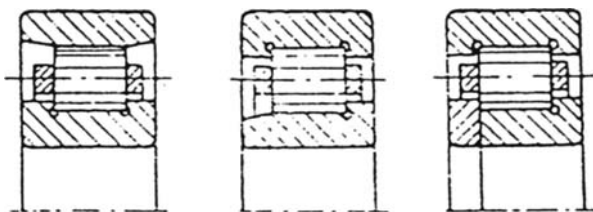


Figure 2.12 Different cylindrical radial roller bearing design.

axis. The rolling elements are also cones whose generators cross the bearing axis at the same point. The inside race has guiding ribs for the rolling elements and the outside race is positioned in the assembly by the axial force produced in use. The bearing is primarily used for transmitting axial loads but may also be used as a pure radial or radi-axial bearing. In comparison to the ball bearing of the same size, tapered roller bearings exhibit a higher load-carrying capacity, but it also produces higher noise. Tapered roller bearings are used at moderate speeds.

3.8 Cylindrical Radial Roller Bearing

Different cylindrical radial roller bearing designs are available as shown in Fig. 2.12. One example is illustrated in Fig. 2.13 [5]. This bearing is used only for radial loads. Because cylindrical roller bearings can accommodate axial displacement, no support shafts are required in the axial direction. These bearings are rigid, are used at high operating speeds, and are capable of sustaining high loads.

3.9 Needle Roller Bearings

The characteristic design feature of needle roller bearings, such as the bearing illustrated in Fig. 2.14 [6], is the shape of the rolling elements which are typically cylinders with a length-to-diameter ratio greater than 3. This type of bearing is characterized by the high load-carrying capacity with small dimensions. The small tolerance of the radial clearance enables the needle roller bearings to precisely guide the shaft. The needle bearing can only transmit radial loads, and it is used for moderately high angular speeds and oscillatory motion.

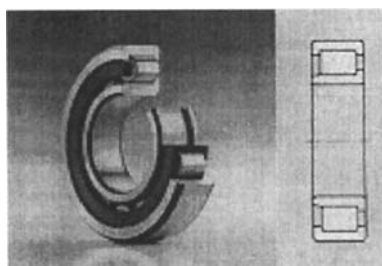


Figure 2.13 Cylindrical radial roller bearing.

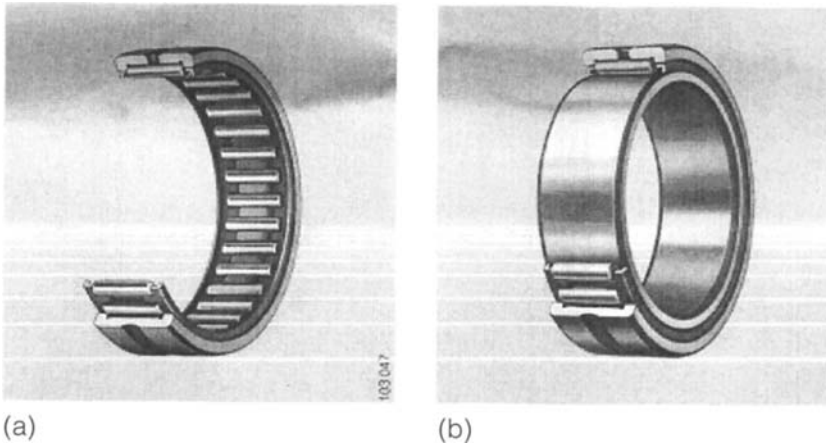


Figure 2.14 (a,b) Needle roller bearing.

3.10 Thrust Ball Bearing

Thrust ball bearings, illustrated in Fig. 2.15 [5], are exclusively applied for taking the axial loads. When used in combination with radial bearings, they can take significant radi-axial loads. Because of the centrifugal force action, which increases friction between balls and raceways, the rotational frequency is restricted to lower and moderate values.

3.11 Tapered Roller Thrust Aligning Bearing

Aligning of the tapered roller thrust aligning bearing is facilitated by the spherical construction of the raceways (Fig. 2.16) [5]. Besides high axial loads, tapered roller thrust aligning bearings can also accommodate moderate radial loads. Because of the significant hydrodynamic effect, these bearings may be used at high speeds.

4 ROLLER BEARING SELECTION

Application of theoretical and practical knowledge are required for roller bearing selection. Elasto-hydrodynamic (EHD) theory is used to predict the bearing lifetimes. The accuracy of such predictions is dependent on many factors, including steel purity, production quality, control of particulate contamination, and lubricant additives.

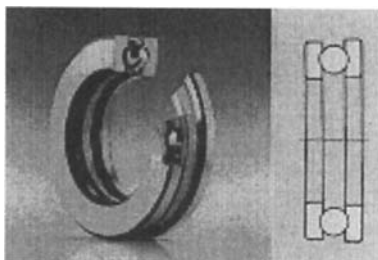


Figure 2.15 Thrust ball bearing.

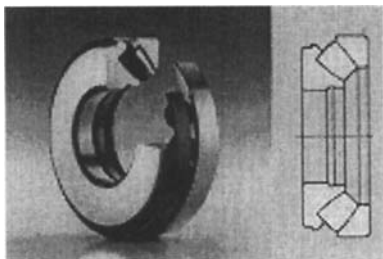


Figure 2.16 Tapered roller thrust aligning bearing.

4.1 Calculation of Minimum Thickness of the Oil Layer

The high specific loads deform the wear contact surfaces. Contact deformation may also be affected by fluid viscosity and temperature within the contact zone. Contact deformation is one of the criteria for elasto-hydrodynamic (EHD) lubrication. Figure 2.17 [7] illustrates the form and distribution of pressure in the lubricant layer during the EHD lubrication.

Lubrication within the EHD contact is characterized by three zones: input convergent region, Hertzian region, and output divergent region. Pressure distribution in the lubricant layer follows the Hertzian pressure in the material until the gap contracts. As a result of fluid-flow continuity immediately in front of the contraction, a very high-pressure spike is observed. In the Hertzian region, the lubricant is exposed to both high pressure and an elevated temperature which both act to affect fluid viscosity in an interrelated way. The fluid film within the gap determines the lubrication effectiveness. For calculation of the oil layer thickness, several procedures for varying complexity may be applied. Equations that quantitatively describe EHD lubrication will be provided here.

The minimum thickness of the lubricating film (h_{min}) under isothermal conditions is calculated by

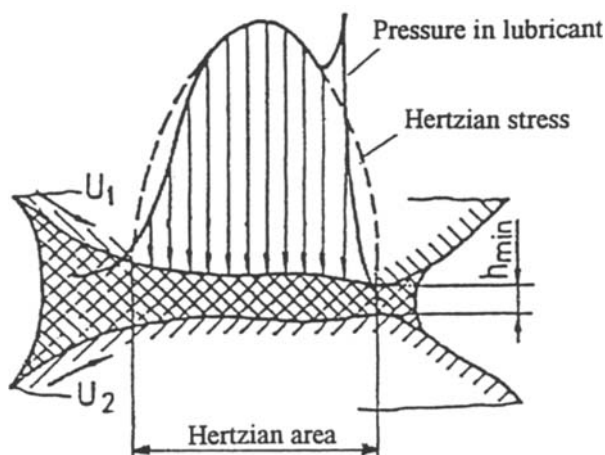


Figure 2.17 Distribution of pressure in the lubricant layer during the EHD lubrication.

$$h_{\min} = f(R, E, \eta_0, B, P)$$

where R is the radius of the reduced cylinder and is calculated by

$$R = R_1 R_2 (R_1 + R_2)^{-1}$$

The variables R_1 and R_2 are the radii of the coupled surface curvatures; E_c is the complex elasticity modulus, which is calculated by

$$E_c = 0.5[(1 - \mu^2 P_1)E_1^{-1} + (1 - \mu^2 P_2)E_2^{-1}]$$

where E_1 and E_2 are the elasticity moduli of the coupled materials, μ is the Poisson ratio. η is the dynamic viscosity of the lubricant, at atmospheric pressure and working temperature, and u_0 is the input velocity defined by

$$u_0 = 0.5(u_1 + u_2)$$

where u_1 and u_2 are the coupled surfaces velocities; B is the piezo viscosity coefficients, and P is the load.

By dimensional analysis, the ratio h/R is obtained as a function of the three dimensionless variables, usually denoted by G , U , and W :

$$\frac{h_{\min}}{R} = f(G, U, W)$$

The variable G is called the material parameter, U is the velocity parameter, and W is the load parameter.

For the line contacts, the equation for the dimensionless thickness of the oil layer has the form

$$\frac{h_{\min}}{R} = 2.65G^{0.54}U^{0.7}W^{-0.13}$$

in which the dimensionless variables have the form

$$G = BE_c$$

$$U = \eta u_0 E_c^{-1} R^{-1}$$

$$W = PE_c^{-1} l^{-1}$$

where l is the cylinder length.

For the point contact, if the contact surface is a circle, the dimensionless equation for film thickness is

$$\frac{h_{\min}}{R} = 1.83G^{0.49}U^{0.68}W^{-0.073}$$

where the values G and U are as defined above and W is defined as

$$W = PE_c^{-1} R^2$$

For the point contact, if the contact surface is an ellipse, the dimensionless equation is

$$h_{\min} = 3.63G^{0.49}U^{0.68}W^{-0.073}(1 - e^{-0.0688k})$$

where the value G is defined above and the values U and W are defined as

$$U = \eta u_0 E_s^{-1} R_a^{-1}$$

$$W = PE_s^{-1} R_a^2$$

$$R_a = R_{a1} R_{a2} (R_{a1} + R_{a2})^{-1}$$

$$R_b = R_{b1} R_{b2} (R_{b1} + R_{b2})^{-1}$$

where the notations for R_a and R_b correspond to Fig. 2.18 [7]. The variable k is called the ellipse parameter, and it represents the ratio $k = b/a$, where b and a are the ellipse axes' lengths.

The equation for determination of minimum oil film thickness for the isothermal conditions and line contact is

$$\frac{h_{min}}{R} = 2.65 G^{0.54} U^{0.7} W^{0.13}$$

For nonisothermal conditions, the dimensionless equation is

$$h_{min} = 2.65 B^{0.54} (\eta u_0)^{0.7} R^{0.43} l^{0.13} E_s^{-0.03} p^{-0.13} c$$

where c is the thermal correction factor.

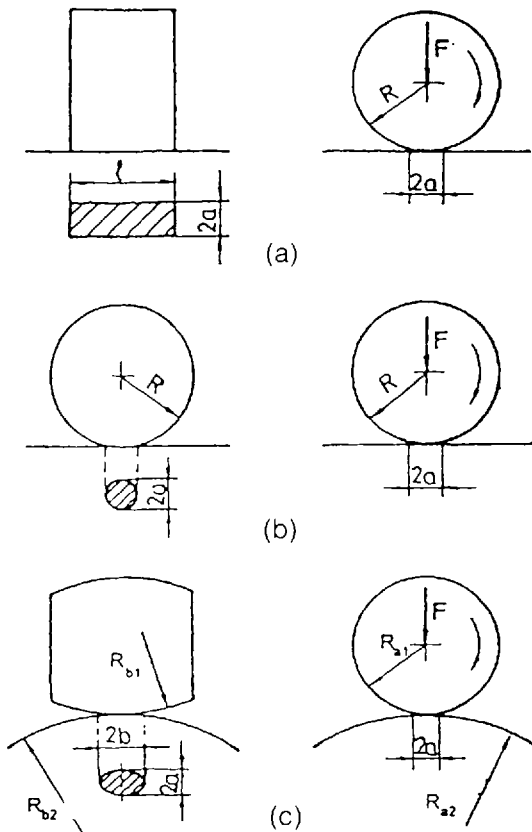


Figure 2.18 (a-c) Contact surface for different form of bearing elements.

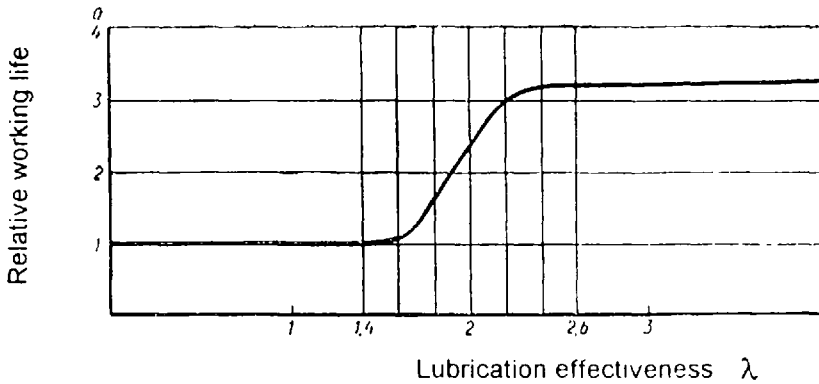


Figure 2.19 Relative working life as a function of lubrication effectiveness.

The lubrication effectiveness (λ) can be calculated from

$$\lambda = hR^{-1}$$

where h is the oil film thickness and R is the average value of the contact surfaces' roughness.

Figure 2.19 [8] illustrates the relative working life of a bearing as a function of λ . Bearing working life is directly proportional to the thickness of the lubricating film. For λ values greater than 4, bearings lifetimes are significantly longer than L , the nominal lifetime (L_{10}) of a bearing. The majority of bearings, however, operates under lubricating regimes characterized by a λ value between 1 and 3. When λ is less than 1, the bearing probably will not achieve the calculated working life because of wear contact surface destruction caused by adhesive wear and surface fatigue.

Fluid viscosity variation as a function of temperature is illustrated in Fig. 2.20 [7] and the dependence of mineral oil viscosity on pressure is illustrated in Fig. 2.21 [43].

4.2 Bearing Size

Roller bearings must be properly sized to assure proper bedding characteristics. Bearing sizing requirements are machine dependent. Variables affecting bearing selection include the following: the type of loads (static or dynamic, purely radial, axial, or radi-axial); low or high rotational speeds and accuracy, required noise level; and required bearings' lifetimes under conditions of good lubrication and so forth. Two selection procedures have been which are dependent on static and dynamic load rating.

4.3 Bearing Selection Based on Static Load Rating

The static load rating is defined as that load which, at the most critical point, will not cause plastic deformation larger than 0.0001 of the rolling element diameter; it is denoted by C . The relation between the plastic deformation and load was determined experimentally by the following expression for static bearing characteristics (f_s) interrelating static load rating (C_0) and static load (P_0):

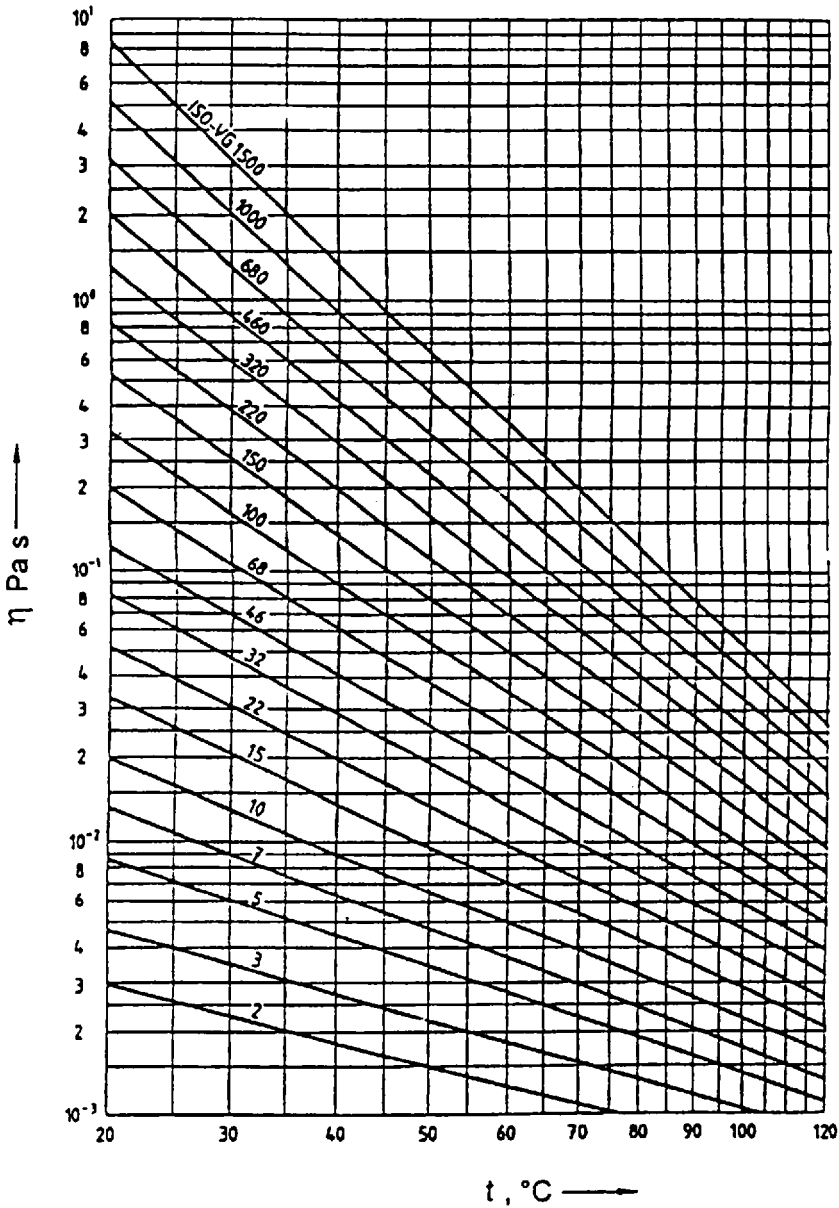


Figure 2.20 Fluid viscosity variation as a function of temperature.

$$f_s = \frac{C_0}{P_0}$$

The following classification scheme for f_s reflect the requirement to prevent plastic deformation:

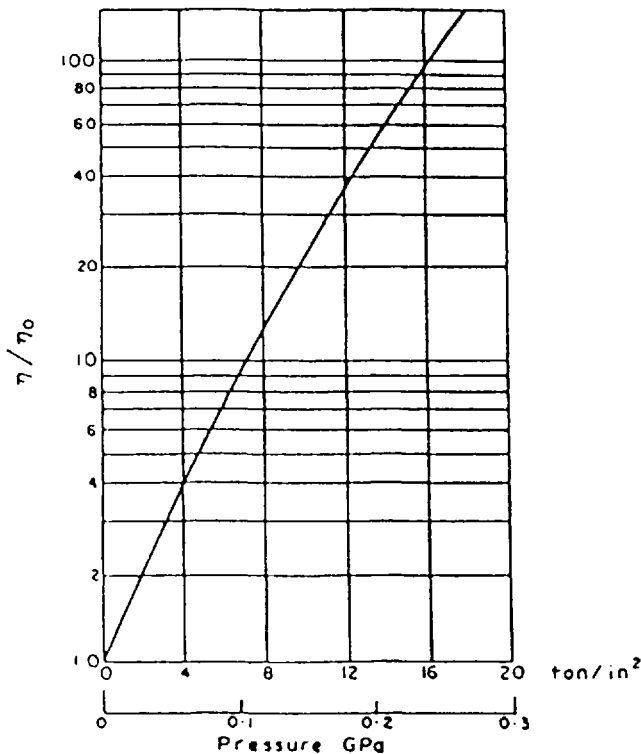


Figure 2.21 Mineral oil viscosity variation as a function of pressure.

$f_s = 1.5\text{--}2.5$ for high requirements

$f_s = 1.0\text{--}1.5$ for normal requirements

$f_s = 0.7\text{--}1.0$ for low requirements

The load C that corresponds to the static characteristics values of $f_s = 1$, at the most critical point of contact—the rolling element—raceway, a permanent deformation of 0.0001 of the rolling element diameter.

Standards ISO 76-1987 and DIN ISO 281 provide a standard criterion for definition of the static load. A maximum value was adopted for the calculated contact stress at the most critical point of contact, the rolling element on the raceway. The value of the contact stress (p) varies with the type of bearing:

- 4600 N/mm² for aligning ball bearings
- 4200 N/mm² for all other ball bearings
- 4000 N/mm² for all roller bearings

These data refer to standard bearings whose assembly components are constructed from steel of the same hardness.

4.3.1 Determination of the Equivalent Static Load

The static equivalent load is the calculated value of load; radial load for radial bearings and axial load for axial bearings, at the most loaded point between the

rolling element and raceway that causes the same effect as combined load. The expression for calculation of the static equivalent load (P_0) is

$$P_0 = X_0 F_r + Y_0 F_a$$

where P_0 is the static equivalent load (kN), F_r is the radial load (kN), F_a is the axial load (kN), X_0 is the radial load factor, and Y_0 is the axial load factor.

Values of axial and radial load factors for various bearing assembly designs are provided by the bearing manufacturer. If the calculated equivalent $P_0 < F_r$, then the radial force component is being neglected and the equivalent static load is assumed to be $P_0 = F_r$.

4.4 Bearing Choice Based on Dynamic Load Rating

The load rating for dynamically loaded bearings is dependent on material fatigue strength and pitting. The calculation procedures are described in various national and ISO standards. The most commonly used equation is

$$L_{10} = L = C^p P^{-p} \times 10^6 \text{ rpm}$$

where L_{10} is the rating life of 10^6 rpm, C is the dynamic load rating, P is the dynamic equivalent load, and p is the rating life power.

Dynamic load rating is defined as load of constant direction and intensity at which 90% of the tested bearings achieve 10^6 cycles (r) without the appearance of fatigue. Data on dynamic load rating are provided by the bearing manufacturer. The value of the rating life power varies with the type of bearing: $p = 3$ for ball bearings and $p = 3.33$ for cylindrical rolling elements bearings.

For a constant number of revolutions, the rating life in hours may be determined from

$$L_n 10 = L_n = \frac{(L \times 10^6)(n^{-1})}{60}$$

where $L_n 10$ is the rating life (required value), L is the rating life (tabular value), and n is the number of revolutions (min^{-1}).

The following equations are derived from the definition of dynamic load rating:

$$L_n = \frac{L 500(33.33)(60)n^{-1}}{60} h$$

or the more general equations,

$$L_n = C^p P^{-1} (33.33)n^{-1}$$

$$L_n^{1/p} 500^{-1/2} = (33.33)^{1/p} n^{-1/p} C P^{-1}$$

where $f_L = L_n^{1/p} 500^{-1/2}$ is the dynamic factor and $f_n = (33.33)^{1/p} n^{-1/p}$ is the number of revolutions factor; $f_L = 1$, at a rating life of 500(h) and $f_n = 1$, at the number of revolutions of 33.33 min^{-1} . Using these substitutions, the following equation is obtained:

$$f_L = f_n C P^{-1}$$

Values of f_L and f_n are available from the bearings' manufacturer for different types of machine and different rotational frequencies.

Determination of Dynamic Equivalent Load

The influence of the outside axial and radial forces acting on a bearing can be determined experimentally or the dynamic equivalent load (P) which represents the effect of axial and radial forces on expected lifetime of the bearing. This represents the same rating life as when it is exposed to a combined load. Dynamic equivalent load is calculated from

$$P = XF_r + YF_a$$

where P is the dynamic equivalent load (kN), F_r is the radial load (kN), F_a is the axial load (kN), X is the radial load factor, and Y is the axial load factor. These load factors vary with rolling element bearing design and construction and are available from the bearings' manufacturer.

For the axial bearings that are transmitting a radial force, the dynamic equivalent load is determined from

$$P = F_r$$

For needle bearings, the expression for determination the equivalent load is

$$P = F$$

where F is the radial outside load acting on the needle bearing.

Bearings Selection Based on the Modified Theory of Dynamic Load Rating

The relationship between the number of revolutions and the applied load was developed by Lundberg and Palmgren and has been the standard engineering practice for the prediction of rolling element bearing lifetime since 1947 [9]. However significant differences between calculated and determined lifetimes were observed. Some of the reasons for these differences include the effect of wear processes that accompany working surface coupling, the use of newer and better specification-grade steels, the effect contaminant particles and some wear products on initiation and development of bearing destruction, improved measures accuracy of surfaces finish, and development of methods for maintaining system cleanliness.

Alternative equations has been proposed for determining bearing life which include the influence of these significant parameters omitted in the Lundberg–Palmgren equation [5]:

$$L_{na} = a_1 a_2 a_3 L \text{ rpm}$$

$$L_{hna} = a_1 a_2 a_3 L_h \text{ h}$$

where L_{na} and L_{hna} are the bearing lifetimes determined by the modified theory, a_1 is the probability choice factor, a_2 is the material factor, a_3 is the working conditions factor, and L and L_h are the rating lives.

Contact surface fatigue obeys the Weibull's probabilities distribution. For rating lifetimes other than at 90% probability of failure, the appropriate factor is selected from Table 2.1 [5].

Instead of factors a_2 and a_3 , the complex factor of material and working conditions influences is introduced, obtained as a product $a_{2,31}$ and s , and $a_{23} = a_{2,31} s$ [5]. The factor a_{23} is calculated in several steps. The ratio of bearing load rating (C) and static equivalent load (P), f_s , is used along with the factor that is dependent on bearing type to determine K_1 (Fig. 2.22) [5].

Table 2.1 The Probability Factor a_1

Probability selection (%)	10	5	4	3	2	1
Life rating	L_{10}	L_5	L_4	L_3	L_2	L_1
Factor a_1	1	0.62	0.53	0.44	0.33	0.21

To determine K_2 , the ratio of “working” and “required” viscosity must be determined. The required viscosity is determined from the half-sum of the diameters of the outside and inside raceways, or their mean values, and working number of revolutions (Fig. 2.23) [5]. Working viscosity is determined based on the working temperature obtained from Fig. 2.24 [5]. The value of K_2 is determined from Fig. 2.25 [5], using the ratio of working to required viscosity and the value of $f_s = C_0/P_0$ for fluids not containing additives or for fluids containing additives whose influence on wear is untested. For fluids containing additives, which are used on the proper way, $K_2 = 0$.

The value of the factor a_{2311} is determined from Fig. 2.26 [5] and is dependent on the ratio of working to required viscosities and the factor K , which is the sum of factors K_1 and K_2 .

The lubricant purity factor s quantifies the influence of soiling on the rating life, depending on the degree of soiling V . Tables 2.2 and 2.3 [5] provide parameters suggested by international standard for the evaluation of the degree of lubricant soiling. The standard is based on experience about the influence of size and number of particles on initiation and development on the destruction process of the contact surfaces of rolling bearings:

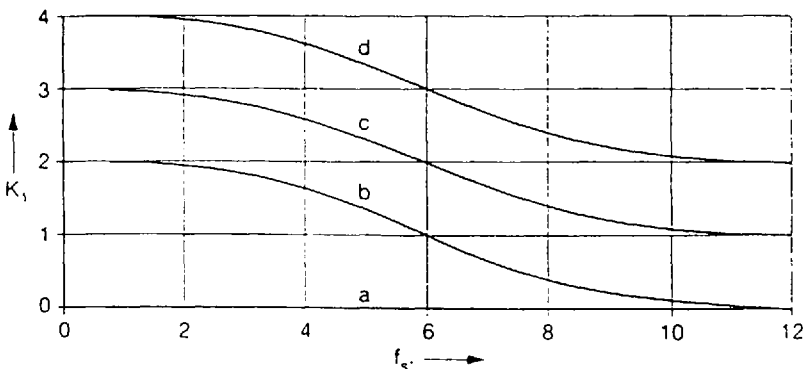


Figure 2.22 Determination of the K_1 factor: (a) ball bearings; (b) cylindrical radial roller bearings and tapered roller bearings; (c) radial and axial convex-roller bearings; (d) cylindrical roller bearings without separator.

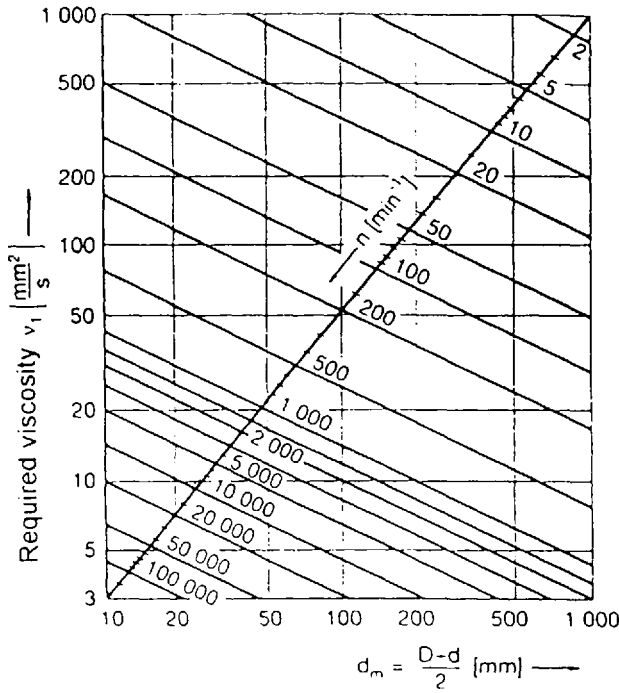


Figure 2.23 Required viscosity as a function of half-sum of diameters of the outside and inside raceways.

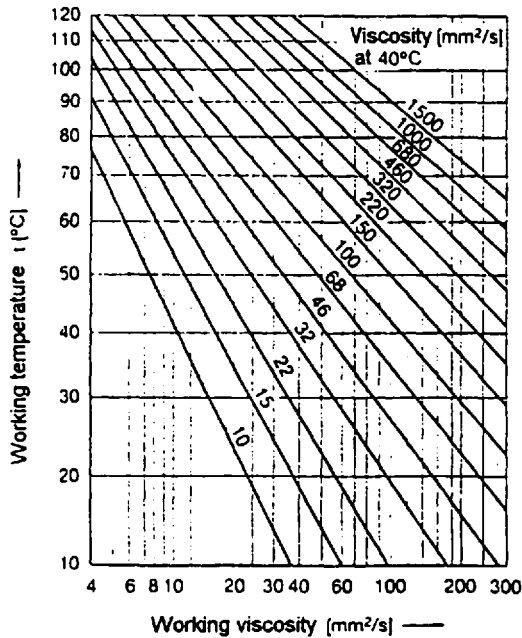


Figure 2.24 Working viscosity.

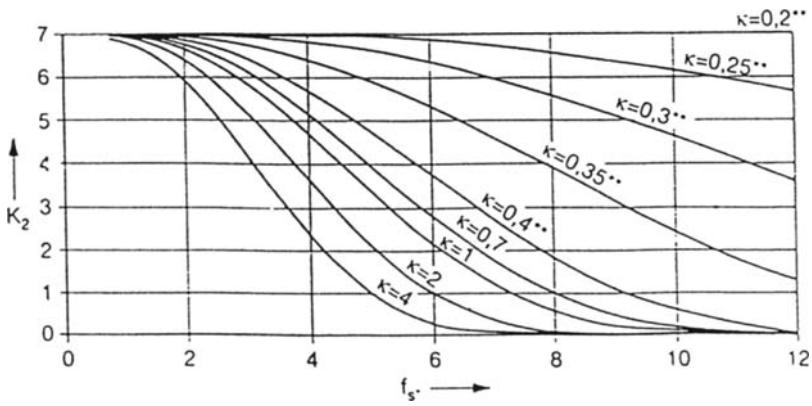


Figure 2.25 Determination of the K_2 factor.

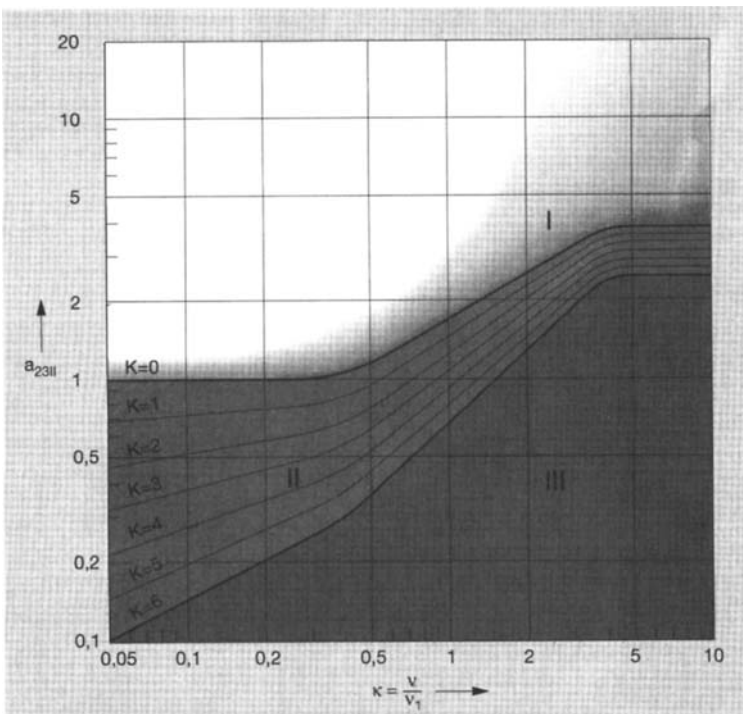


Figure 2.26 Determination of the a_{2311} factor.

Table 2.2 Approximate Value for a Purity Factor V

$(D - d)/2$ (mm)	V	Point contact:	Approximate	Line contact:	Approximate
		required purity level according to ISO 4406	effectiveness of filtration according to ISO 4572	required purity level according to ISO 4406	effectiveness of filtration according to ISO 4572
≤ 12.5	0.3	11/8	$\beta_3 \geq 200$	12/9	$\beta_3 \geq 200$
	0.5	12/9	$\beta_3 \geq 200$	13/10	$\beta_3 \geq 75$
	1	14/11	$\beta_6 \geq 75$	15/12	$\beta_6 \geq 75$
	2	15/12	$\beta_6 \geq 75$	16/13	$\beta_{12} \geq 75$
	3	16/13	$\beta_{12} \geq 75$	17/14	$\beta_{25} \geq 75$
>12.5 and <20	0.3	12/9	$\beta_3 \geq 200$	13/10	$\beta_3 \geq 75$
	0.5	13/10	$\beta_3 \geq 75$	14/11	$\beta_6 \geq 75$
	1	15/12	$\beta_6 \geq 75$	16/13	$\beta_{12} \geq 75$
	2	16/13	$\beta_{12} \geq 75$	17/14	$\beta_{25} \geq 75$
	3	18/14	$\beta_{25} \geq 75$	19/15	$\beta_{25} \geq 75$
>20 and <35	0.3	13/10	$\beta_3 \geq 75$	14/11	$\beta_6 \geq 75$
	0.5	14/11	$\beta_6 \geq 75$	15/12	$\beta_6 \geq 75$
	1	16/13	$\beta_{12} \geq 75$	17/14	$\beta_{12} \geq 75$
	2	17/14	$\beta_{25} \geq 75$	18/15	$\beta_{25} \geq 75$
	3	19/15	$\beta_{25} \geq 75$	20/16	$\beta_{125} \geq 75$
>35	0.3	14/11	$\beta_6 \geq 75$	14/11	$\beta_6 \geq 75$
	0.5	15/12	$\beta_6 \geq 75$	15/12	$\beta_{12} \geq 75$
	1	17/14	$\beta_{12} \geq 75$	18/14	$\beta_{25} \geq 75$
	2	18/15	$\beta_{25} \geq 75$	19/16	$\beta_{25} \geq 75$
	3	20/16	$\beta_{125} \geq 75$	21/17	$\beta_{25} \geq 75$

Table 2.3 Purity Class According to ISO 4406 (quotation)

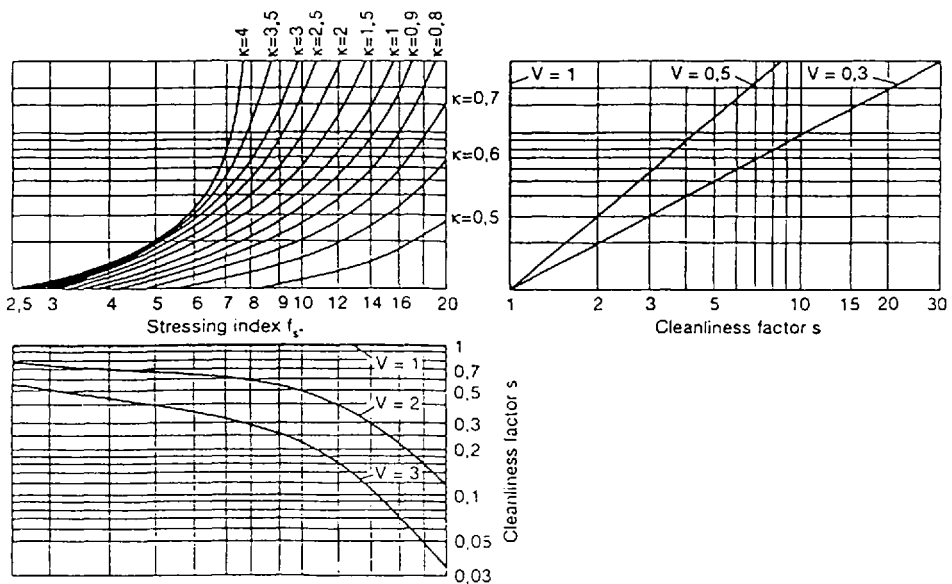
Number of particles per 100 mL				
Over 5 μm		Over 15 μm		Code
More than	Up to	More than	Up to	
500,000	1,000,000	64,000	130,000	12/17
250,000	500,000	32,000	64,000	19/16
130,000	250,000	16,000	32,000	18/15
64,000	130,000	8,000	16,000	17/14
32,000	64,000	4,000	8,000	16/13
16,000	32,000	2,000	4,000	15/12
8,000	16,000	1,000	2,000	14/11
4,000	8,000	500	1,000	13/10
2,000	4,000	250	500	12/9
1,000	2,000	130	250	11/8
1,000	2,000	64	130	11/7
500	1,000	32	64	10/6
250	500	32	64	9/6

- For the normal level of soiling $V = 1$, the purity factor takes the value $s = 1$.
- At realized increased and high purity, $V = 0.5$ and $V = 0.3$, respectively, depending on value of factor f_s and ratio of working to required viscosity (Fig. 2.27, top), factor s takes values of $s > 1$.
- At increased soiling, $V = 2$, and high soiling, $V = 3$, depending on the factor f_s , the purity factor takes values of $s < 1$ (Fig. 2.27, bottom).

The soiling factor V is dependent on bearing size, type of contact, and oil purity class [5]. When soiling occurs under high-load conditions, there is a stronger negative influence with decreasing contact surface area. As the size of rolling element bearings decreases, the sensitivity to soiling increases.

Using ceramic rollers with or without a coating and steel raceway with a modification of surface, hard and soft coating or both, special heat treatment can improve bearings life, particularly in extreme condition such as in high speed, poor lubrication, high temperature, high vacuum, ceramically active environments, presence of water, and other situations in which acceleration of wear is indicated [10–12].

The effects of fire-resistant fluids on bearing wear must be treated differently than mineral-oil-based hydraulic fluids [13]. For rolling element bearings lubrication with fire-resistant hydraulic fluids, the equation and Table 2.5 provided in Section 5.3 may be used. Bearing manufacturers often recommend hybrid and ceramic bearings for use with fire-resistant hydraulic fluids. The calculation procedures are iden-



Cleanliness factor s depending on V , stress level, expressed by f_s , and viscosity ratio κ

Figure 2.27 Cleanliness factor s depending on V , stress level, expressed by f_s , and the viscosity ratio.

tical as those used for steel bearings [5]. Under conditions of good lubrication, the absence of chemically active substances, and the absence of water and soiling, this approach is suitable because both steel and ceramic bearings have approximately equal working capacities. The working capacity of ceramic bearings with poor lubrication, the presence of soiling, high vacuum, and especially the presence of chemically active substances and water is several times higher than for steel.

5 COMMON WEAR MECHANISMS

Rolling element bearing wear varies with the loading history that will determine the mechanism of surface failure and wear. Proper analysis and identification of these failure mechanisms is critically important if future occurrences are to be avoided. Failure analysis procedures require consideration of bedding design for the bearing, type of bearing, material of construction, production procedures to increase contact surfaces' resistance to wear, manufacturing precision, determination of the contact surface topography, type of lubrication, lubricant, and system maintenance procedures.

With the exception of abrasive wear resulting from particular contamination, the most common failure mechanism of rolling element bearings is fatigue wear. Other types of wear, including adhesive, corrosive, and fretting, are less frequently encountered as the root cause of the bearing failure. However, they may occur as secondary wear processes.

5.1 Fatigue Wear

Fatigue wear is caused by cyclic action of contact stresses in surface layer. Figure 2.28 [14] shows the distribution of the contact stresses in the rough contact layer. As a result, complex stress states are present that are locally significantly and may exceed the yield stress after many repetitions, creating conditions for initiation of the fatigue crack.

Figure 2.29 [15] illustrates the distribution of normal and shear stresses under conditions of rolling without sliding. The primary shear stresses $\tau = 1/2(\sigma_x - \sigma_y)$ achieve their maximum value at a depth of $0.78a$, where a is the half-width of the Hertzian contact surface [15]. These shear stresses are the primary cause of initial crack creation, which, in the absence of other causes, appear in the zone of maximum stress.

When both rolling and sliding of contact surfaces occur, stress distribution is determined by the magnitude of friction force as shown in Fig. 2.30 [15]. Under these conditions, maximum shear stress, with increase of shear force, moves toward the surface, causing the fatigue crack to form closer to the surface.

Crack propagation is significantly influenced by physical, chemical, and metallurgical characteristics of the friction pair, as well as characteristics of the applied lubricant [16].

Observation of the macro and micro records of the surface layer of bearings exposed to high loads shows that a dark bandlike zone forms at a depth of 0.1–0.5 mm, preceding crack initiation. Upon enlargement, white spots are observed that are

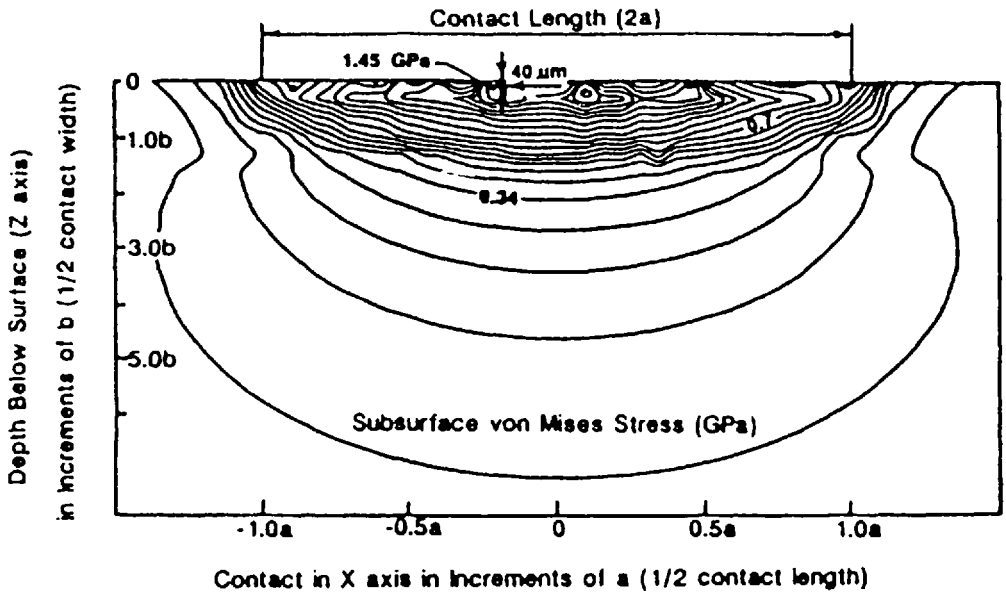


Figure 2.28 Contact stress in surface layer.

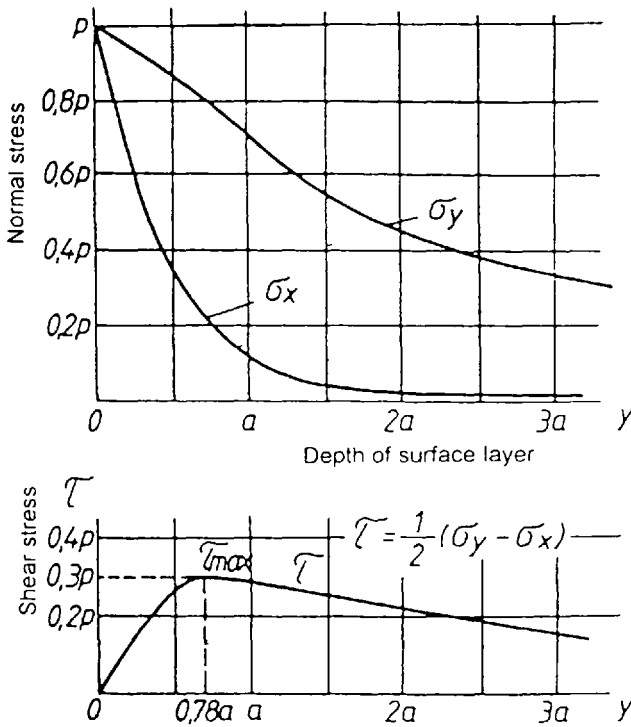


Figure 2.29 Distribution of normal and shear stresses under the condition of rolling without sliding.

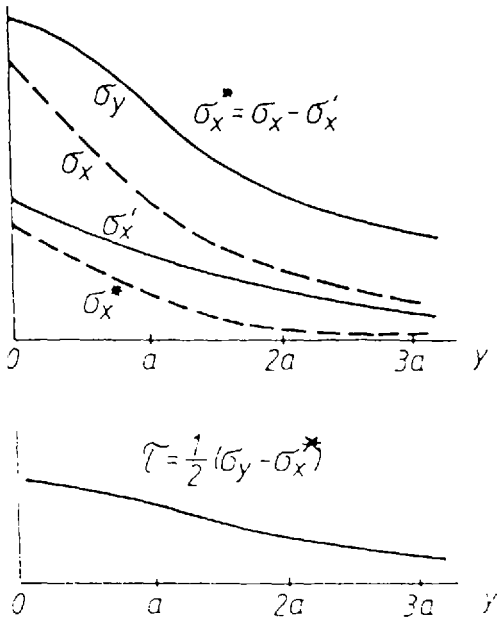


Figure 2.30 Distribution of stress under sliding and rolling conditions.

characterized by higher hardness and a cubic structure. Fatigue crack initiation occurs on the boundaries of these spots [16].

Figure 2.31 [17] illustrates typical changes of the material structure and also material properties, “white bands”, caused by repeated material stressing. This structural change is a decay of the martensite. Figure 2.32 [16] illustrates a microcrack in the initial failure phase.

The mechanism and speed of fatigue wear contact-surface failure of rolling element bearings depend on various factors, including magnitude of normal and shear stresses, significant influence of the surface-layer structure, load history, presence of the hard particles during the contact-surface coupling, corrosive activity of environment, lubricant base fluid, and composition [16,18–25].

5.2 Abrasive Wear

The presence of low levels of abrasive particles in the contact zone accelerates fatigue crack initiation’s decreasing resistance to fatigue wear [25–27]. In the presence of hard particles with intensive destruction processes occur at the contact surface resulting in rapid failure of the rolling element bearing.

Although the mechanism of material removal from the contact surfaces is basically identical, two types of abrasive wear have been reported: wear caused by impact of the abrasive particles on the surface, and wear caused by coupling of the contact surfaces by the abrasive particles.

The ratio of material surface hardness to abrasive particle hardness is directly related to the surface’s resistance to abrasive wear, as shown in Fig. 2.33 [7]. If particle hardness is lower than the hardness of the material working surface, the

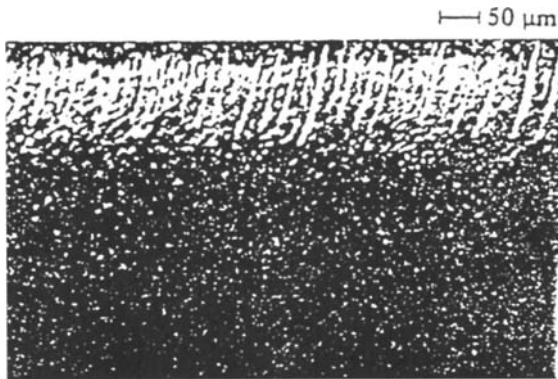


Figure 2.31 Typical material changes of fatigue specimens—white bands.



Figure 2.32 Microcracks in the initial failure phase (electron micrograph, two-stage surface replica, magnification 17,500 \times).

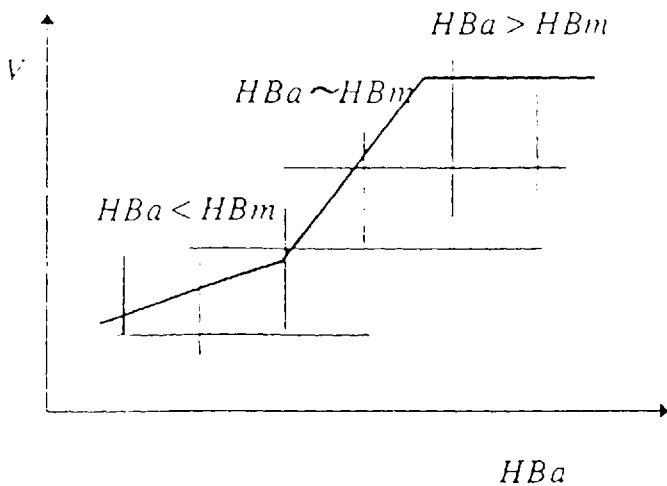


Figure 2.33 Volume of wear particles depending on the hardness of the surface and abrasive wear.

quantity of the wear product increases slowly with increase of the hardness of the abrasive particle. This type of wear is designated "light abrasive wear." When the hardness of the abrasive particle is approximately equal to the working surface hardness, greater quantities of wear products will result. If the hardness of the abrasive particle is greater than the working surface's hardness, no significant increase in wear products will be obtained. However, a significant increase friction will result. This is called "heavy wear."

In rolling element bearings, depending on the lubrication regime and hardness and size of the abrasive particles, light and heavy wear frequently occurs in combination with other types of wear. Generally, it is possible to control this type of wear by controlling the size and quantity of abrasive particles present in the lubricant. The intensity of wear as a function of the concentration of the introduced abrasive is shown in Fig. 2.34 [20]. The solid line represent a new bearing with a fresh abrasive, and the dashed line represents the same relationship when an old lubricant is with the new bearing. These data show that the intensity of wear is most intensive during the first few hours and that wear increases with each addition of the new abrasive. In Fig. 2.34 wear intensity is significantly smaller with a used lubricant. In Fig. 2.35 [26] is shown the relative bearing life depending on the kind of indented particles [26].

5.3 Adhesive Wear

When the lubricant film thickness is less than the height of surface roughness, direct contact occurs between the surface asperities when the bearing surfaces are in relative motion. High localized pressures are present at the wear contact points. When the surface asperities come into contact, strong intermolecular bonds between the two surfaces may be formed, as illustrated in Fig. 2.36. This may result in the formation of "microwelds." Because of tangential surface movement, existing bonds may be destroyed and new microwelds may be formed. This adhesive wear process is called

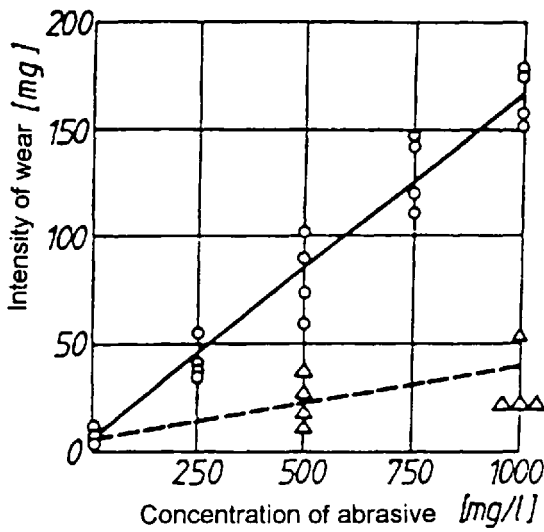


Figure 2.34 Intensity of wear as a function of concentration of the introduced abrasive; solid line represents new rolling bearing with fresh abrasive; dashed line represents new bearing with old lubricant.

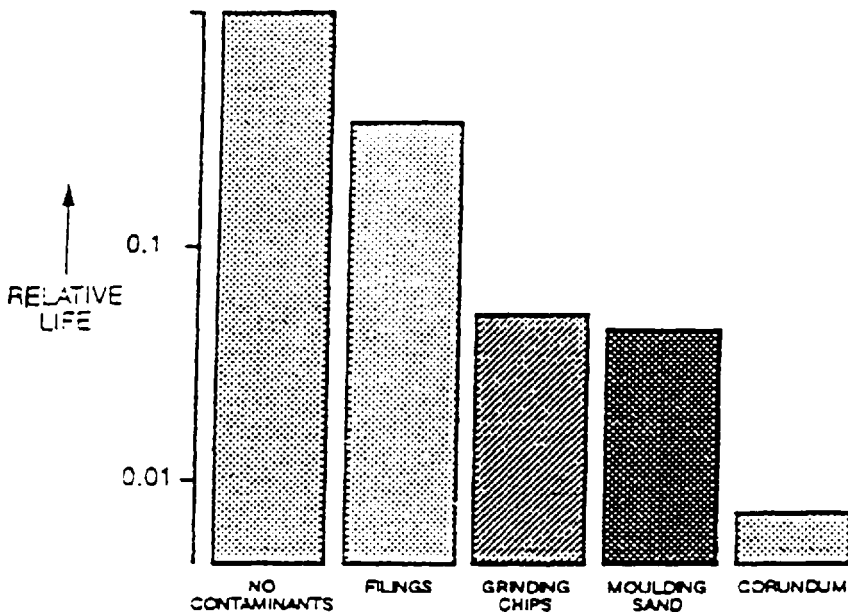


Figure 2.35 Relative bearing life depending on the kind of indented particles. (Reprinted with permission. SAE paper, Loesche T., Weingard M. *Quantifying and Reducing the Effect of Contamination on Rolling Bearing Fatigue*, c. 1995, Society of Automotive Engineers, Inc.)

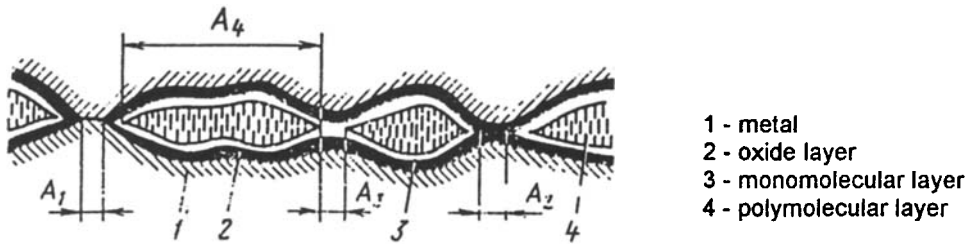


Figure 2.36 Model of contact surfaces under the condition of mixed lubrication. (1) metal; (2) oxide layer; (3) monomolecular layer; (4) polymolecular layer.

“scuffing” and is characterized by significant changes in surface topography (Fig. 2.88b [17]) and structure (Fig. 2.37 [17]) and by the formation of wear debris.

Rolling bearings subjected to high concentrated loads and significant raceway deformation with rolling elements characterized by a significant presence of inertial resistance to acceleration are frequently susceptible to adhesive wear. A change occurs in the perimeter velocity of the rolling element, and the angular velocity is significantly decreased with respect to the velocity of the forced rotation, as illustrated in Fig. 2.38 [17]. The reduction in surface velocity creates a situation of reduced elasto-hydrodynamic lubrication leading to surface asperity contact [17]. The resulting stresses at these asperity contacts is significantly higher than the yield point of the metal which leads to the formation of frictional bonds. The formation and subsequent breaking of frictional bonds results in the destruction of contact surfaces and adhesive wear. The presence of wear debris from this process at the wear contact coupling zone may initiate subsequent abrasive wear, depending on the hardness of the wear debris and the initiation of cracks and fatigue wear as a secondary process.

5.4 Corrosive Wear

Corrosive wear refers to surface destruction of steel, nickel, aluminum, and other metal surfaces by chemical or electrochemical attack. Surface corrosion produces

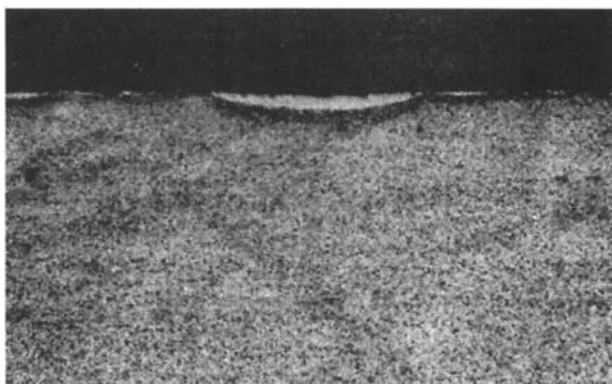


Figure 2.37 Cross section of damaged cylinder roller.

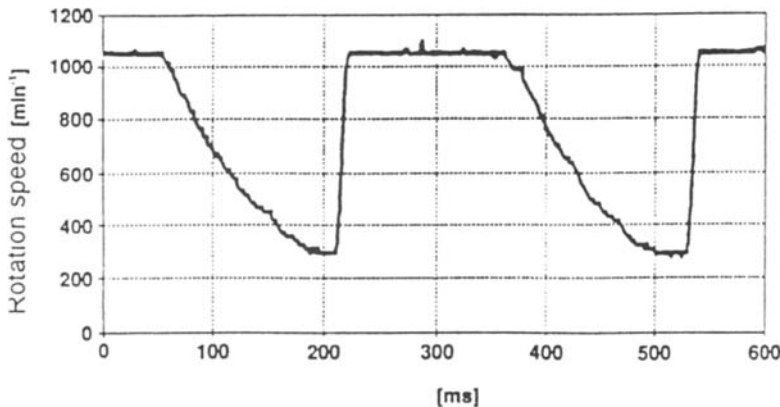


Figure 2.38 The change in surface velocity of the roller.

oxide coatings, passivating them to further attack. The type of surface passivation is dependent on the chemical characteristics of the corrosive environment and on the bearing material. For steel alloys, the oxide coating is typically paramagnetic iron oxide $\alpha\text{-Fe}_2\text{O}_3$, ferromagnetic iron oxide $\gamma\text{-Fe}_2\text{O}_3$, or magnetite Fe_3O_4 , which is typically formed in the presence of water, either in the form of humidity or may be present in the fluid. Magnetite may be transformed into rust ($\text{Fe}_2\text{O}_3 \cdot \text{H}_2\text{O}$). The oxide coating thickness and tribological characteristics are dependent on the quantity of the fluid.

The most frequently encountered forms of corrosive coating may be classified by its color and thickness; thin, relatively bright $<40\ \mu\text{m}$, gray and light brown $<500\ \mu\text{m}$, and thick and dark $>500\ \mu\text{m}$. Intensive contact loadings in the presence of unresisting oxide surface coatings destroys the passivating oxide layers, forcing the corrosion process deeper into the metal surface.

5.5 Fretting Corrosion

Fretting corrosion, illustrated in Fig. 2.39 [28], is most often encountered for machine elements constructed from non-corrosion-resistant materials that undergo small but repetitive movements (vibrations) and are exposed to corrosive environments. Surface destruction caused by fretting corrosion forms small micron-sized craters filled



Figure 2.39 Raceway damaged with fretting corrosion.

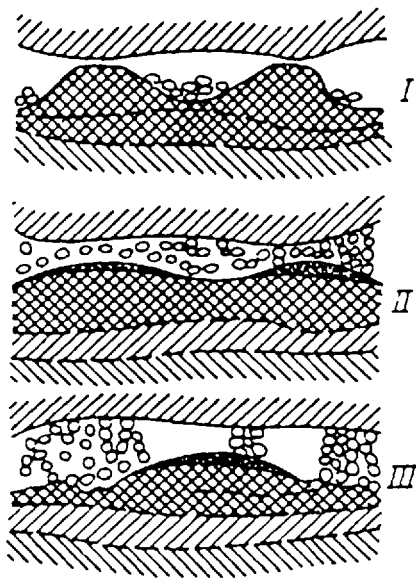


Figure 2.40 Typical phases in a fretting corrosion process.

with wear debris. The surfaces are characteristically covered with red Fe_2O_3 or dark Fe_3O_4 oxides or $\text{Fe}_2\text{O}_3 \cdot \text{H}_2\text{O}$ if humidity is present.

Figure 2.40 illustrates that fretting corrosion starts with hardening and cyclic plastic flow of the subsurface layer at the wear contact. This is caused by the vibration movement of the load. Surface asperities are plastically deformed where oxide layer destruction has occurred and intermolecular bonds develop. Mutual vibrational movement of the contact surfaces breaks these intermolecular bonds and, in the presence of the debris from fatigue material damage, creates conditions for contact-surface destruction. Initially, the wear debris consists of the metal oxide material.

The second phase of the fretting corrosion wear is characterized by formation of the corrosive environment which consists of wear debris, absorbed oxygen, and moisture (H_2O). A steady-state balance is established between the formation of wear products and their removal from the contact zone. Surface deformation activates the tribo-chemical reactions involved in the corrosion process. When the thin outer layer of surface oxides is destroyed, the work-hardened layer immediately below is subjected to the vibrational loads, leading to fatigue loads accelerated by the corrosion process.

Upon removal, the metal oxide debris acts as a catalyst accelerating the adsorption of oxygen and moisture. A reactive electrolytic environment is formed between the wear contact surfaces. Corrosive destruction progresses into the subsurface layer, creating corrosive fatigue damage, thus accelerating the wear process.

The investigation of the influence of the effect change on the angle of axle and the change in load showed that the angle of movement having a great effect on fretting wear is no more than 1 degree, but increases rapidly when the angle rate is greater (Fig. 2.41 [28]).

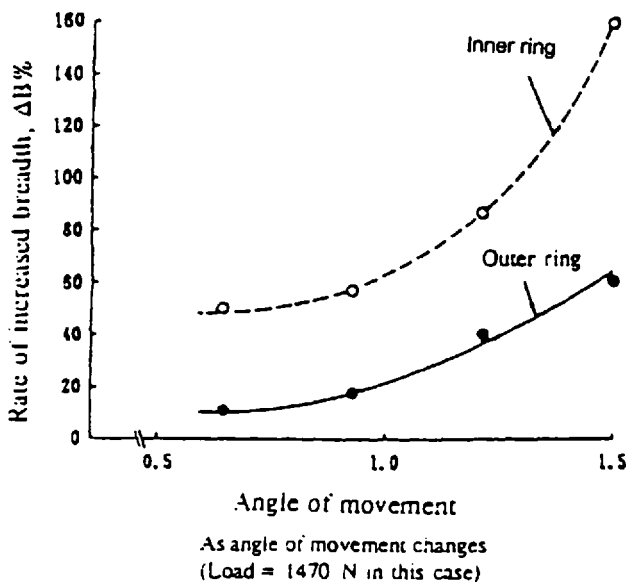


Figure 2.41 Influence of the angle of movement on the rate of increased breadth.

6 ENHANCEMENT OF ROLLER BEARING WEAR RESISTANCE

Roller bearings are typically subjected to various types of wear process throughout their lifetime, leading to a complex overall surface destruction process. The wear contact surface destruction process can be retarded by various measures, including wear surface material selection, process of producing these wear surfaces (heat treatment and surface roughness) of the bearings and raceways and resulting accuracy of the production process, protection of the bearing assembly against corrosive environments, lubricant selection, method of bearing lubrication, and system cleanliness.

6.1 Influence of Bearing Design on Wear

Bearing wear can be affected by the operating conditions and design. Bearing operating conditions can be affected by various factors, including selecting proper bearing type, assuring necessary accuracy of shafts and beddings, providing adequate shaft and bedding stiffness, protecting against the operating environment, lubrication system, and lubricant selection. Aspects of bearing design that affect wear include material pairs for the wear contact surface, size of the wear contact, weight of rolling elements, maximum friction reduction, load distribution, increasing working capacity, decreasing size, high speeds, autonomy, and reduction of system contamination. This discussion will be limited to the effects of bearing design on wear.

The best bearing designs should increase the wear contact surface area, provide homogeneous distribution of contact stresses, and organize spreading of deformations, as illustrated in Fig. 2.42 [29]. Usually, bearing design changes are made to modify the curvature of the rolling element and raceway contact with the inside and outside rings. Bearings with cylindrical and conical rolling elements exhibit line contact, and modification is performed to avoid peaks that appear at the end of

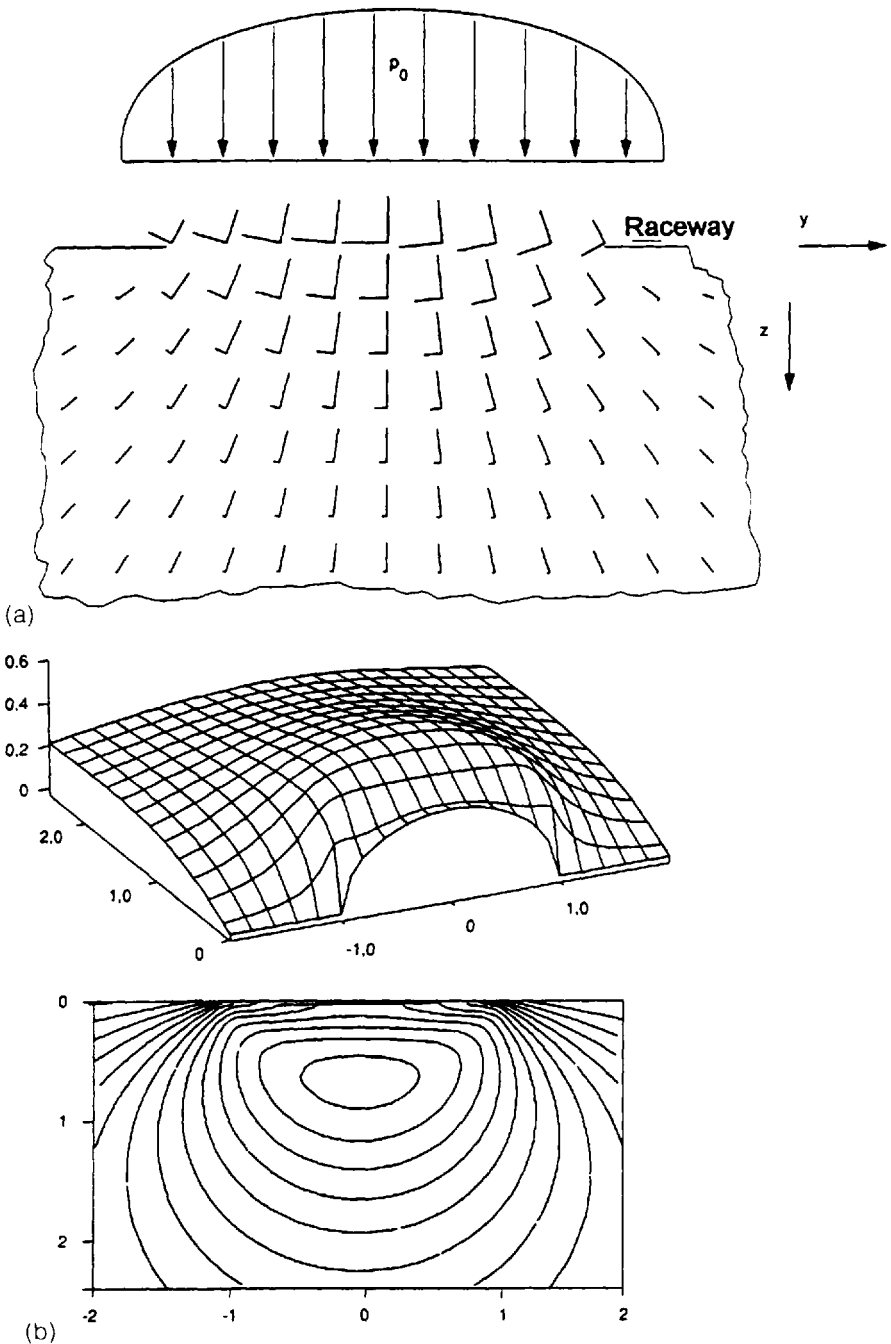
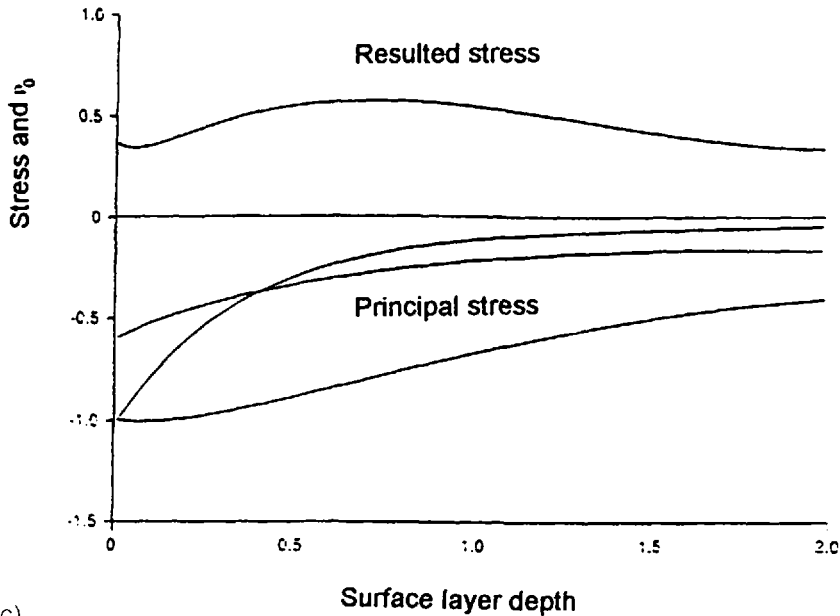


Figure 2.42 (a) Direction of deformation in a Hertzian contact; (b) distribution of stress in Hertzian contact; (c) distribution of principal and resulting stress under contact point.



(c)

Figure 2.42 Continued

contact, as illustrated in Fig. 2.43 [29]. Macrostress distribution improvement may be achieved by rounding the ends of cylindrical and conical rolling elements or by using raceways with a convex profile as illustrated in Fig. 2.44 [29]. In convex-roller bearings, the roller profile radius is smaller than the radius of raceway profile. Theoretically, the contact is treated as a rigid body and forms a point contact. Because

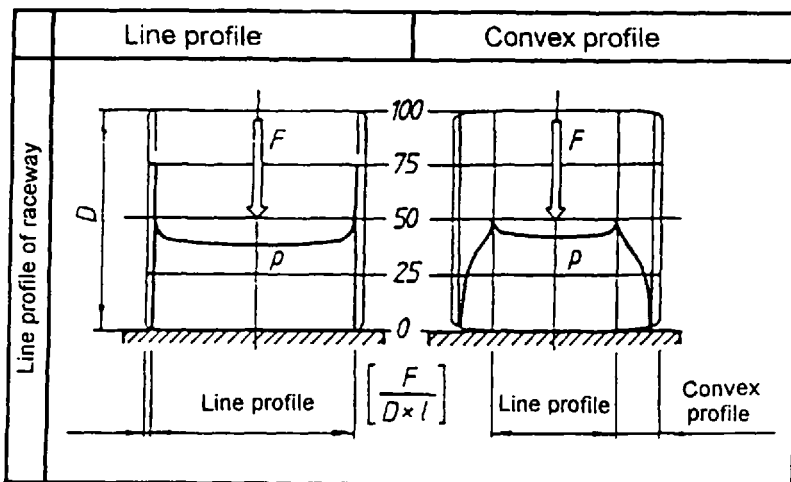


Figure 2.43 Distribution of pressure; convex profile of raceway; straight-line profile of roller; straight-line profile of raceway; and convex profile of roller.

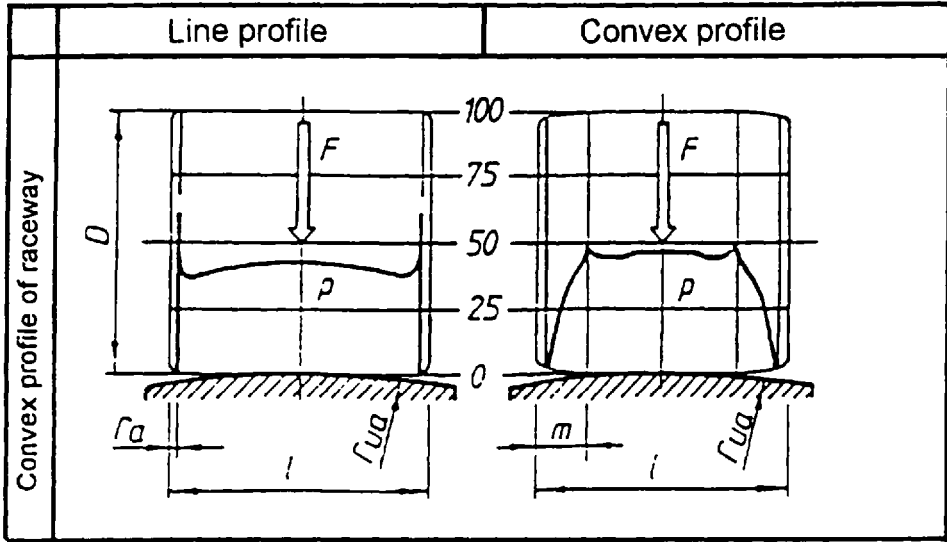


Figure 2.44 Distribution of pressure; straightline profile of raceway; straight-line profile of roller; convex profile of raceway; and convex profile of roller.

Real case $r_{ua} > r_{ka}$		Theoretical: $r_{ua} = r_{ka}$
$F \leq F_{gr}$ Very low load	$F > F_{gr}$ Low load	F General
Ellipse	Fragment of ellipse	Rectangle
Theoretical line contact		Line contact

Figure 2.45 The forms of contact area.

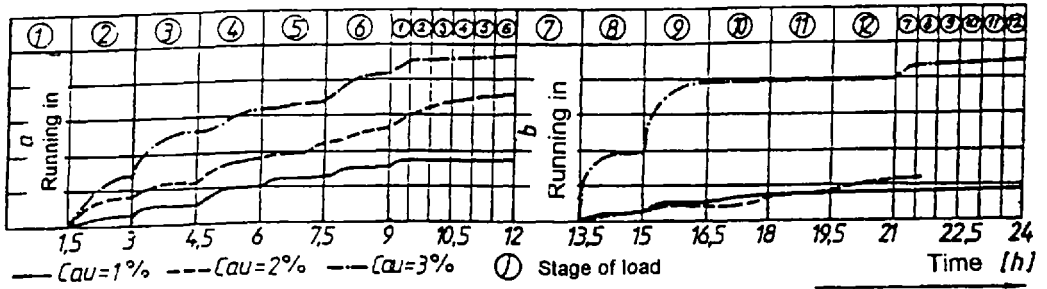


Figure 2.46 Dependence of rolling element and the raceways curvature on wear intensity.

the profile curvature of the contact surfaces is negligible at small loads, $F < F_n$, the surface contact forms an ellipse, as illustrated in Fig. 2.45 [29].

Figure 2.46 [30] illustrates the effect of rolling element and raceway curvature as expressed by the curvature parameters C_{ax} and C_{au} :

$$C_{ax} = (r_s - r_{ka})r_{ka}$$

$$C_{au} = (r_u - r_{ku})r_{ku}$$

These studies, which were conducted by measuring the radioactivity increase within the inside raceway, suggest mutual dependence of the ratios of coupled surface profiles and wear intensity.

Studies on the influence of different contact-surface profile curvatures in convex-roller bearings [30] suggest a positive influence of the small values of the curvature factor. $C_{au} < 1\%$, on wear reduction. At higher values of the curvature factor C , wear increases, which may be the result of contact-surface reduction and the corresponding increase in surface pressure within the contact zone. In addition, results of these studies suggest that wear debris in the contact zone can participate in the destruction of the roller-bearing surface.

Reduction in surface wear and an increase in efficiency ratio can be achieved by modification of the contact surface in the main load direction. Modification can also be performed on the face ribs and on the rolling element separators to reduce friction parasitic losses.

Figure 2.47 [31] illustrates the design of the rolling bearing with face contact over the conix and the convex front face. Investigations have shown that the friction losses in this case are less than losses of friction that occur during contact of flat front faces (Fig. 2.48) [31].

Decreasing parasitic friction losses in the bearing separator contact is most frequently accomplished using a material with a low friction coefficient (zinc-phosphate coatings, PTFE, MOVIC).

The coil separator illustrated in Fig. 2.49 [32] is elasto-hydrodynamically lubricated if there is sufficient fluid flow through the wear contact. This type of separator has performed well for low-speed applications such as gyroscopes.

One of the causes of vibration of the bearing is the shape error of bearing parts, such as the circularity of bearing track, cylindricity, eccentricity, paralellism, roughness of rotating surface, and the size variation of rolling elements per unit container. Roller bearings with a size accuracy of <0.1 mm are being used increasingly in high-

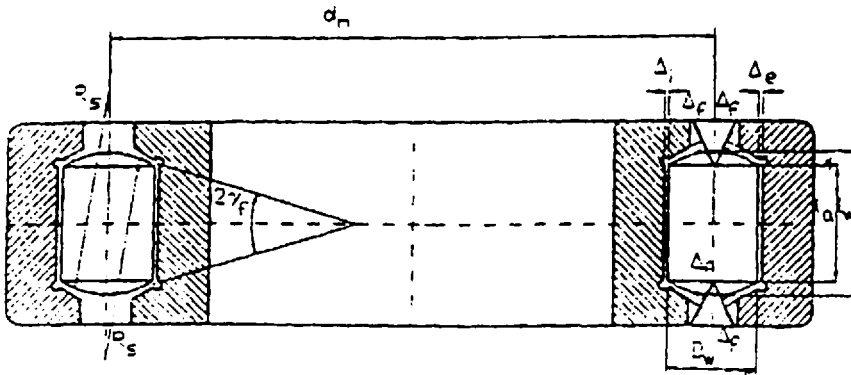


Figure 2.47 Internal geometry of NUP-type rolling bearing.

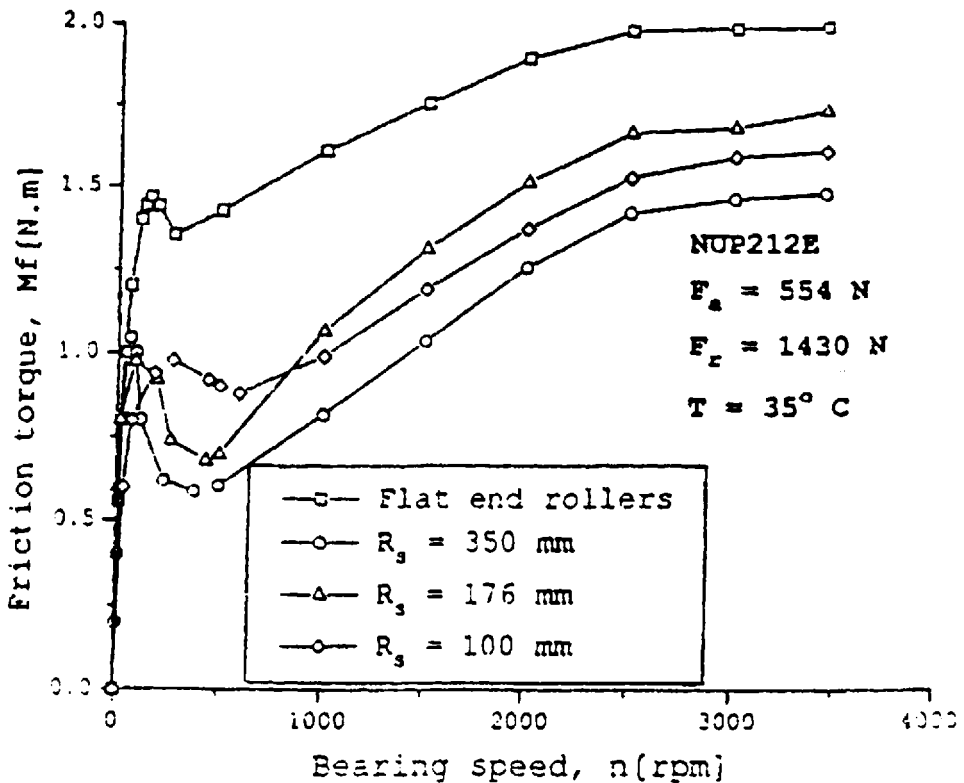


Figure 2.48 Dependence of friction torque and form of face contact.

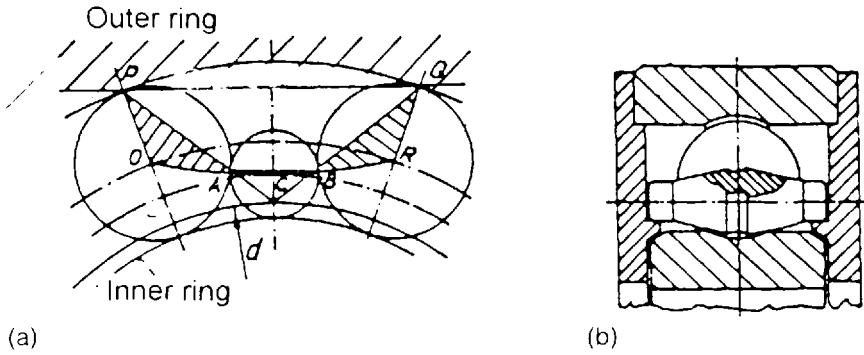


Figure 2.49 (a,b) Coil separator.

speed applications previously dominated by the use of slider bearings to decrease vibrations [33]. This is illustrated in Figure 2.50 [33] for the use of HDD spindle motors and bearings used in personal computers.

Low internal clearance typical for high-speed application requires the accurate control of bearing temperatures. Temperatures also govern the materials' propriety, lubricant properties, lubricant thermal stability, and overall thermal analysis of the bearing compartment. Subtrace cooling is used to help control the ring temperature gradient in aerospace applications (Figs. 2.51–2.53) [34,35].

Hybrid bearings restrain the buildup of heat generated by centrifugal force or gyro sliding of fast rotating balls, and research is progressing on oil–air lubrication that involves radically reducing the amount of lubricant to restrain heat generated by oil churning, and jet lubrication that involves the forced circulation of low-viscosity oil and the use of its coolant effects to restrain temperature rises which allows stable rotation up to a value of 2×10 [12].

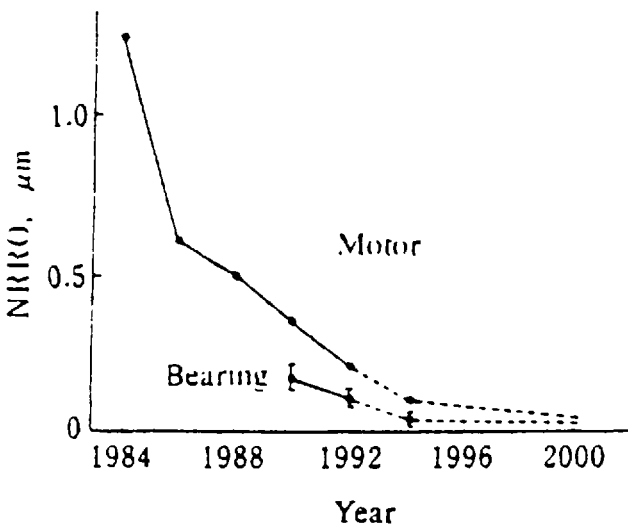


Figure 2.50 Trends in NRRO demand levels for HDD spindle motors and bearings.

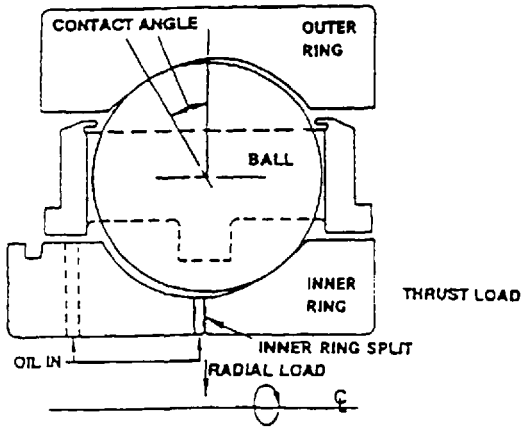


Figure 2.51 Subrace cooling; thrust bearing.

6.2 Material Selection

Steels are now produced with an oxygen content of <10 ppm, which has resulted in reduced the metal oxide content, which acts as initiation points for fatigue wear failure. This has enabled the control of size and number of intermediaries in existence per unit of area, providing optimal structure of the surface layer [33]. The availability of ultrahigh-purity steels has provided a greater than fivefold increase in the working capacity of rolling element bearings, as shown in Fig. 2.54 [33].

The most common bearing steel grade is AISI E52100, a high-carbon chromium steel. This steel alloy is produced in electric furnaces under vacuum to reduce the oxygen content, increasing the carrying capacity and reliability.

AISI 449 C steel is used when bearing materials with improved corrosion resistance are required. However, these steels exhibit lower carrying capacity at temperatures, $<100^{\circ}\text{C}$, with respect to E52100 [36].

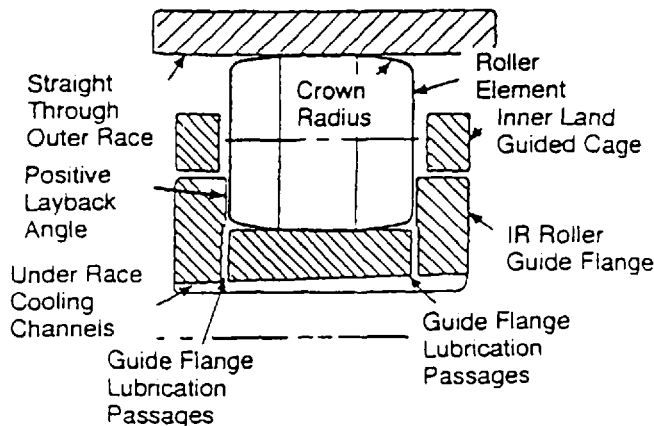


Figure 2.52 Subrace cooling; roller bearing.

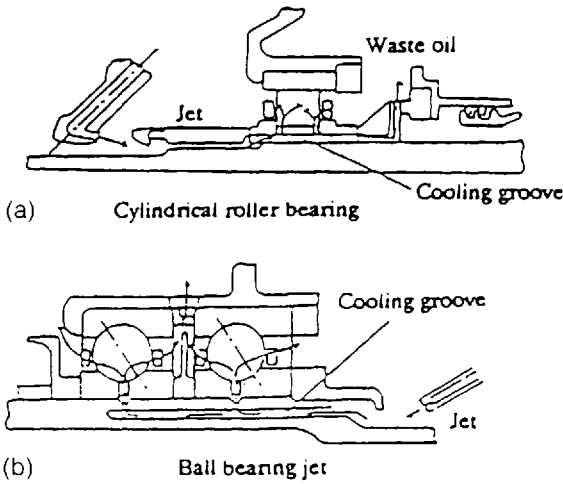


Figure 2.53 (a,b) Subtrace cooling; cooling increases.

For elevated temperature use, $>175^{\circ}\text{C}$, steel alloys containing molybdenum, tungsten, and vanadium alloying elements are used. These steels are capable of maintaining a hardness of 58 HRC at working temperatures as high as $315\text{--}480^{\circ}\text{C}$.

Halmo and M50 steels are used for working temperatures up to 310°C . For operation at extremely high temperatures (up to 427°C), T-1 and M-10 steels may be used. For working temperatures up to 492°C , AISI H-1 and H-2 steel alloys are used, and for temperatures up to 538°C , AISI WB-49 is used. Highly alloyed steels

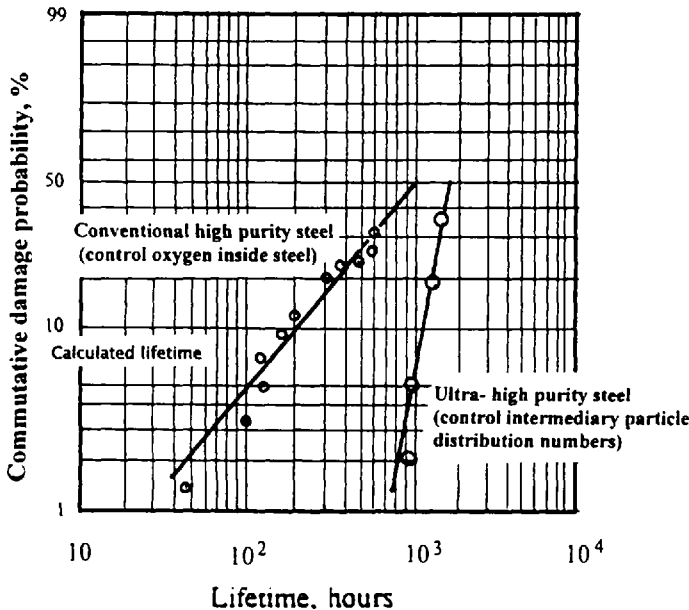


Figure 2.54 Extension of lifetime through increased purity of bearing steel.

that maintain high hardness at elevated temperatures typically exhibit lower resistance to contact surface destruction at working temperatures of $<65^{\circ}\text{C}$, as illustrated in Fig. 2.55 [36].

Figure 2.55a illustrates that the longest life is obtained for rolling elements of AISI EX-15. Halmo exhibits somewhat lower fatigue wear resistance, 78% of EX-15 wear resistance. The working life of H-1, M-10, M-50, T-1, and H-2 balls is less and the lowest fatigue wear at moderate working temperatures was obtained with AISI M-420 balls. It was found that the presence of carbide (Fe_3C) grains of larger sizes and larger number at temperatures $<100^{\circ}\text{C}$ initiates accelerated destruction of rolling bearings contact surfaces [36].

The presence of carbides is especially important for maintaining the required hardness at elevated temperatures. Chromium, molybdenum, and vanadium form carbides that maintain steel hardness at elevated temperatures. Although cobalt does not form carbides, it may affect carbide formation by other elements. The distribution, kind, size, form, and concentration of contained carbides determine the resistance to fatigue surface failure of bearing wear contact surfaces.

New alloys have been developed to extend the working temperature ranges of conventional carbon steels. Starting from Japanese steel JIS SUJ 2 ($\text{C}-1.0\%$, $\text{Si}-0.25\%$, $\text{Cr}-1.5\%$, $\text{Mo}-$, $\text{V}-$), a medium-heat-resistance bearing-steel, JIS KIJ 7 ($\text{C}-1.0\%$, $\text{Si}-1.0\%$, $\text{Mn}-0.5\%$ $<$ $\text{Cr}-2.0\%$, $\text{Mo}-0.5\%$), was developed; it is capable of maintaining hardness up to 250°C . Figure 2.56 [37] illustrates comparative test results for KIJ 751 and SUJ 251 steels at a working temperature of 250°C .

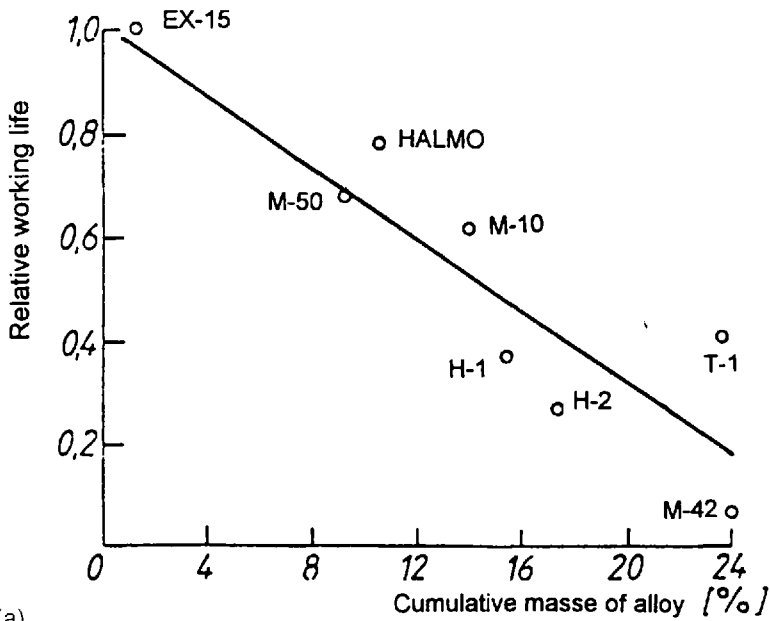
Increasing the requirements for high-speed operation, smaller sizes, friction reduction, reducing dependence on the friction reduction properties of the lubricant, increasing the resistance to aggressive environmental conditions such as corrosion and particulates, and increasing the reliability and working life of rolling element bearings has led to the development of new materials.

The required physical properties of contact layers are obtained by various surface heat-treatment practices. Heat-treatment practices include nitriding from a salt bath, nitrocarburizing and carburizing from atmospheres, and induction heat treatment; see Ref. 38.

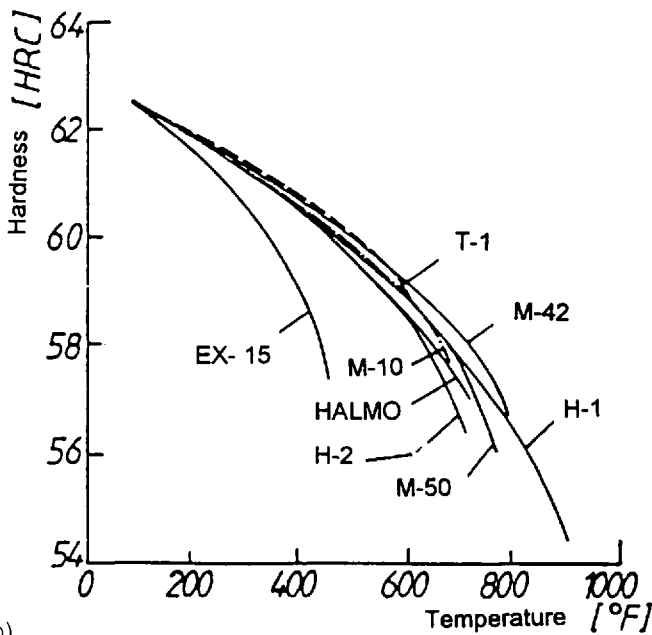
Ceramic materials are being used to significantly improve bearing lifetimes and reliability [10,39,40]. Ceramic materials were used partially for rolling elements of hybrid bearings and integrally for races and rolling elements of ceramic rolling bearings. The ceramic material used most extensively in bearing production is silicon nitride (Fig. 2.57) [40]. In Fig. 2.58 [41], a block diagram provides a comparison between the basic physical properties of steel and ceramic materials.

For achieving the high performances of ceramic materials, the procedure of hot isostatic pressing (HIP) illustrated in Fig. 2.59 [40] is used. Other technologies do not produce material structures that possess adequate physical properties necessary for roller bearing applications as shown in Fig. 2.60 [40].

The comparison of hybrid and steel bearings under conditions of elasto-hydrodynamic lubrication and with the use of filtration to remove particles larger than $0.5\ \mu\text{m}$ has been performed. Two load levels, $P = 2900\ \text{N}/\text{mm}^2$ and $P = 2400\ \text{N}/\text{mm}^2$, and a rotational speed of $n = 1200\ \text{rev}/\text{min}$ showed that hybrid bearings failed in less time than steel bearings at $P = 2900\ \text{N}/\text{mm}^2$. However, when evaluated at the lower load $P = 2500\ \text{N}/\text{mm}^2$, the hybrid bearings exhibited longer calculated lifetimes than steel M50 bearings, as shown in Fig. 2.61 [14].



(a)



(b)

Figure 2.55 (a) Dependence of relative life on concentration of steel alloys at temperatures <math><65^{\circ}\text{C}</math>; (b) dependence of hardness and temperatures of standard roller bearing steels.

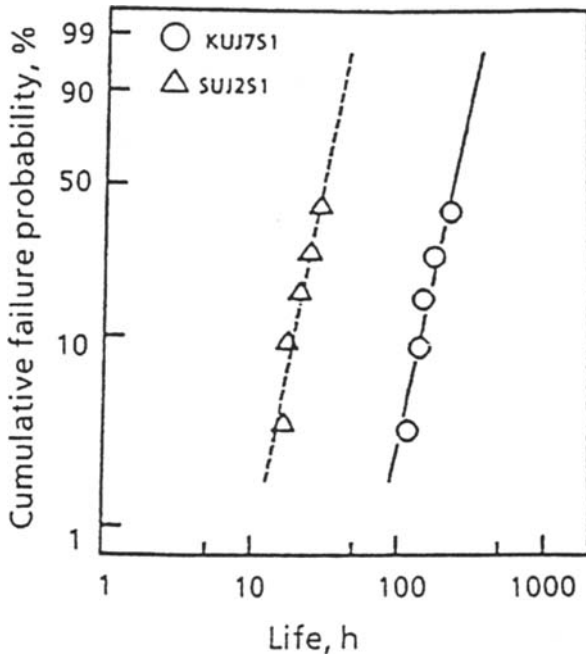


Figure 2.56 Comparative test results for KUJ 751 and SUJ 251 steels at temperature of 250°C.



Figure 2.57 Structure of silicon nitride ceramic sinter-HIP process.

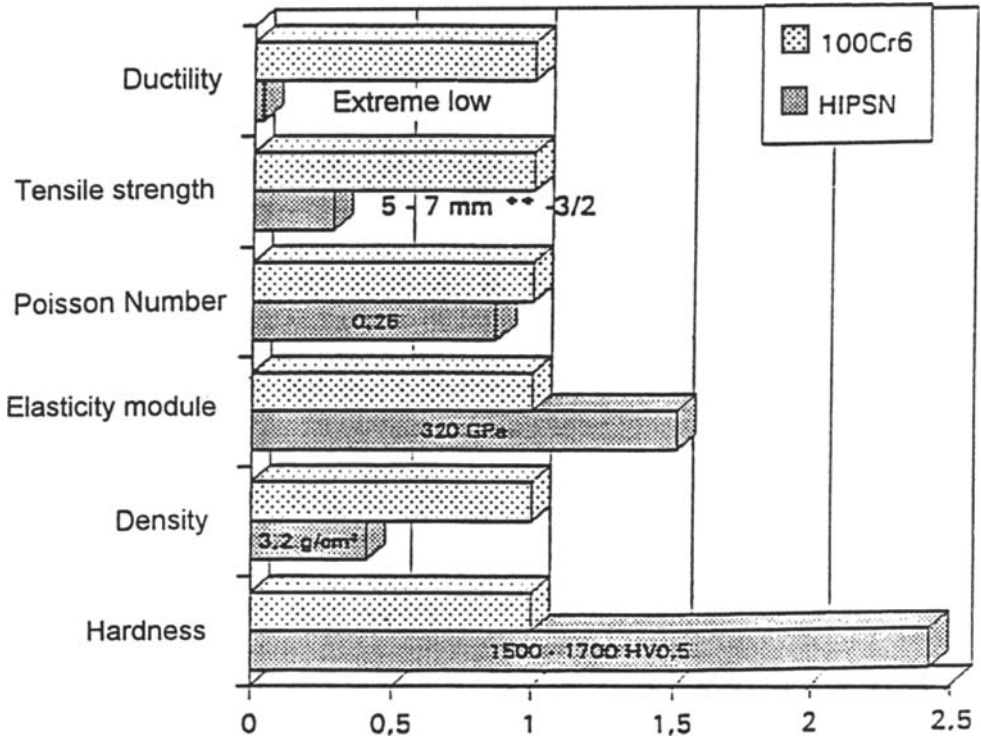


Figure 2.58 Comparison among basic physical properties of steel and ceramic materials.

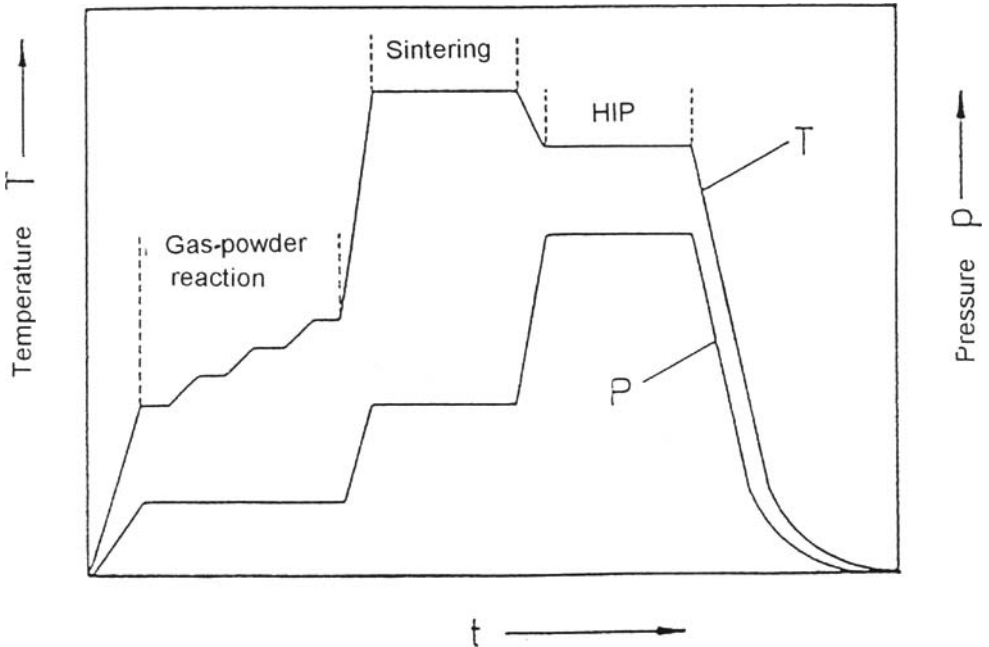


Figure 2.59 Hot isostatic pressing.

	Porosity %	Flexural loading resistance Nmm ⁻²	E-module kNmm ⁻²	Kic-value MNNm ^{-3/2}	Weibull-module
SSN	0-5	300-600	200-280	5-7	10-16
RBSN	15-20	100-300	70-200	2-4	10-16
HPSN	-	500-800	250-300	6-8	12-20
HIPSN	-	600-900	280-320	6-9	15-25

Figure 2.60 Basic physical properties for different Si₃N₄ qualities.

The effect of material selection to particulate contamination has also been illustrated [26]. Steel bearings built from M50, lubricated elasto-hydrodynamically, exhibited a lifetime that was 10 times the calculated value. However, hybrid bearings did not produce any increase in lifetime with filtration.

Figure 2.62 [26] illustrates the dependence of working temperature on the product Dn for the steel (line I) and hybrid bearings (line II).

Grease is often used to seal "lubricated for life" bearings. It was found that hybrid bearings exhibit a lifetime that was two to five times greater than a steel

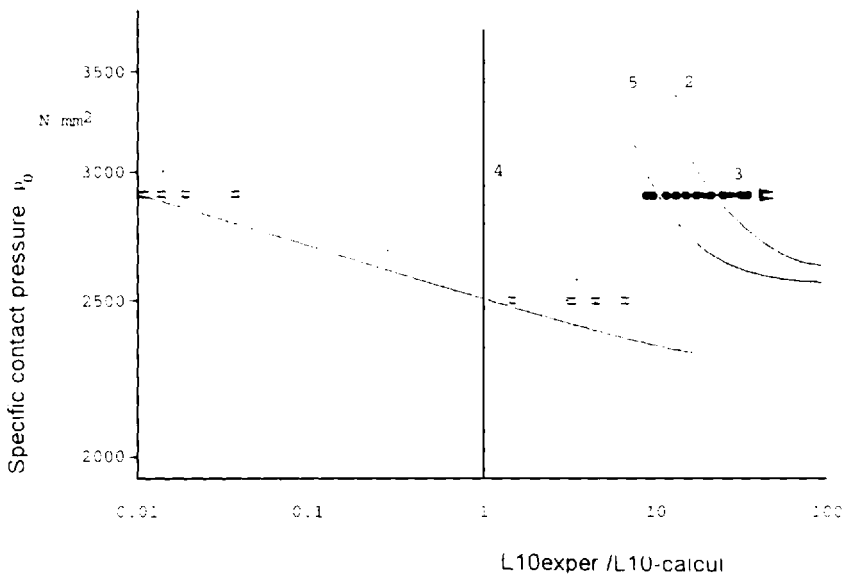


Figure 2.61 Comparison L10 of hybrid and steel bearing under condition of elasto-hydrodynamic lubrication. (1) Balls from ceramic with failure; (2) balls from steel; (3) balls from ceramic; (4) theoretical life rating; (5) inner raceway from steel.

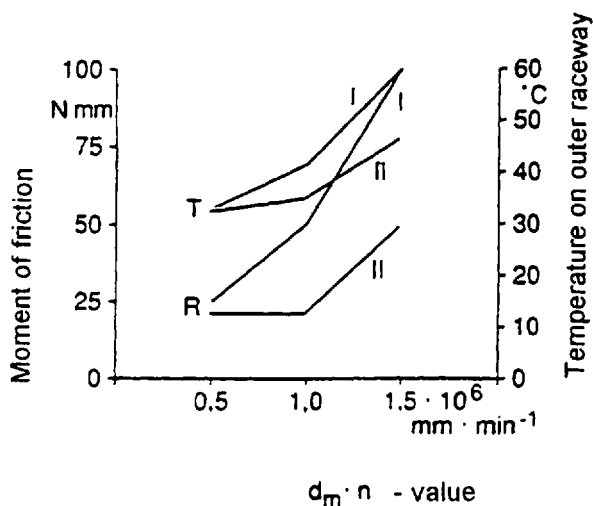


Figure 2.62 Dependence of working temperature and Dn value for steel (I) and ceramic (II) roller bearings. T = temperature; M = moment of friction.

bearing. This difference is even greater for nonlubricated bearings, with the hybrid bearing exhibiting a working lifetime five to seven times greater than that obtained for a steel bearing [39].

Ceramic bearings can be used at temperatures up to 1100°C with poor lubrication and under conditions that are corrosive to steel. In addition, ceramic bearings also exhibit a 40% reduction in friction and are approximately 60% lower in weight [42].

To improve the wear resistance, reduce friction, and improve corrosion resistance, coatings of various types may be applied to impart the desired property. Coating procedures include chemical and galvanization procedures, and coatings obtained by dipping, spraying, plasma vapor deposition (PVD), chemical vapor deposition (CVD), and ion implantation.

A porous Fe_3O_4 coating approximately 0.4 – 2.0 μm thick with a characteristic bright brown color is produced by burnishing procedure. This coating is suitable for working temperatures up to 400°C and is most frequently used for wear reduction.

Corrosion and wear resistance are improved under conditions of mixed lubrication by Zn phosphatizing. Good coating strength to the base material is typically obtained. The porous coating thickness is usually between 2 and 12 μm with a characteristic dark color and is suitable for working temperatures up to 300°C . Zinc phosphate coatings are typically used to improve corrosion resistance and the sliding properties of the cage.

Magnesium phosphatizing improves corrosion resistance and wear resistance under conditions of mixed friction. The coating color is brown, with noticeable porosity. The coating thickness is usually between 3 and 15 μm , and it is compatible with the base material.

Chemical nickel plating improves corrosive and wear resistance and the sliding properties of the base material. The metallic bright coating is thin, 15 – 20 μm , without porosity. The connection with the base material is very good, especially for rough

surfaces. The maximum working temperature is dependent on the base material and the applicability of the coating and is limited to 500°C.

Thin, hard chrome plating is used for repairing damaged working surfaces and for improving corrosion resistance. The connection with the base material is very good and the usual coating thickness is between 1 and 3 μm with a hardness of 1100 HV. Depending on the base material, temperatures up to 700°C may be used.

Zinc–nickel and zinc–iron coatings are applied mainly for improving corrosion resistance. They are deposited at a thickness of 3–10 or 1–7 μm , respectively. Depending on the type of the base material, they may be used at temperatures up to 250°C.

Galvanically deposited gold–silver coatings are used for improving wear resistance under dry lubrication. This coating exhibits a dark color and is approximately 5 μm thick. Corrosion resistance and working temperature are dependent on the base material. The maximum working temperature for the coating is 350°C.

Currently, the most frequently used coatings, titanium nitride, Me-I-C (Balinit c), and I-C coatings, are obtained by a PVD procedure. Titanium nitride (TiN) improves wear resistance and sliding properties and is deposited to thicknesses of 2–4.5 μm . The coating exhibits a bright golden color with hardness >2000 HV and it is well connected to the base material. A special PVD device is used to deposit TiN after cleaning. The process of material deposition is conducted from the plasma state to the desired surface or surfaces. The working piece temperature during the coating deposition phase is <500°C. The bright silver chrome–nitride Cr/CrN coating is used for improving wear resistance. It exhibits a hardness up to 1500 HV. It is deposited by a PVD process at temperatures lower than 500°C.

The bright black Me-I-C coating is deposited to thicknesses of 1–4 μm and it is very well connected to the base material. The coating hardness is about 1000 HV and is used for improving sliding properties and wear resistance. This coating is limited to working temperatures of about 300°C.

The I-C coatings are carbon coatings of amorphous dark color and they are deposited to thicknesses of 1–3 μm with a hardness of 3000–6000 HV. The connection with the base material is good. It is deposited at temperatures of 150–200°C. The coating improves the wear resistance and sliding properties of the base material.

The most frequently applied CVD coatings are titanium nitride and titanium carbide. The TiN coating exhibits a shiny golden color and a hardness >2000 HV and is deposited to thickness of 2–4.5 μm . The coating produced by the CVD procedure exhibits a very good connection to the base material. The coating deposition temperature is higher than 1000°C. The coating improves the base material wear resistance but worsens weldability.

Titanium carbide (TiC) coatings are applied by ion implantation and exhibit a shiny silver color and a hardness of 3500 HV and it is well connected to the base material. It is deposited to a thickness of 3 μm . The deposited coating worsens the surface quality of the base material and requires additional machining to ensure the required quality. The deposition temperature is over 1000°C. A film thickness of less than 0.5 μm improves the wear resistance of the base material. The appearance and surface structure remain identical to the initial ones. The maximum working temperature is determined by the base material. In combination with the PVD coating MoS, it is used for improving wear resistance and sliding characteristics of rolling elements of AISI 440C steel.

Ion-implanted CrN coatings are deposited to a thickness of less than 0.5 μm and are used to improve the wear resistance of the base material. The surface roughness is unchanged and the maximum working temperature is limited by the base material.

The most frequently used coatings applied by dipping and spraying are zinc and ceramic coatings. Ceramic coatings ($\text{Al}_2\text{O}_3 + \text{TiO}_2$) are metallic gray and are deposited to a thickness of about 250 μm . They exhibit a gray porous structure and are significantly harder, frequently over 1000 HV, than the base material. Their corrosive stability is excellent and they may be used at all normal working temperatures. The connection with the base material is good, but coated surfaces are additionally machined to achieve the desired surface quality. Ceramic coatings are used to isolate the influence of electric current. They are well suited for application to rolling bodies or the races.

The physical and chemical properties of PVD layers have an intermediate position between metals, and ceramic PVD layers are electrically conductive and have a metallic luster, but they do not build up alloys with other metals and they are sluggish in reaction with other materials [12].

In the past few years, full-coated bearings can be found in a new approach to combining ceramic balls with coated races to improve the behavior of a tribological system [12]. Because of their superior properties, four different kinds of coating have been selected for coating the races of the bearings: CrN, TiAlN, TiN + C, and WC + C. Figure 2.63 summarizes the properties of the different coatings [12].

6.3 Influence of Lubricant and Lubrication Systems

Elasto-hydrodynamic lubrication is dependent on many factors that include working surface geometry, elastic properties of the material, thermal conductivity, physical

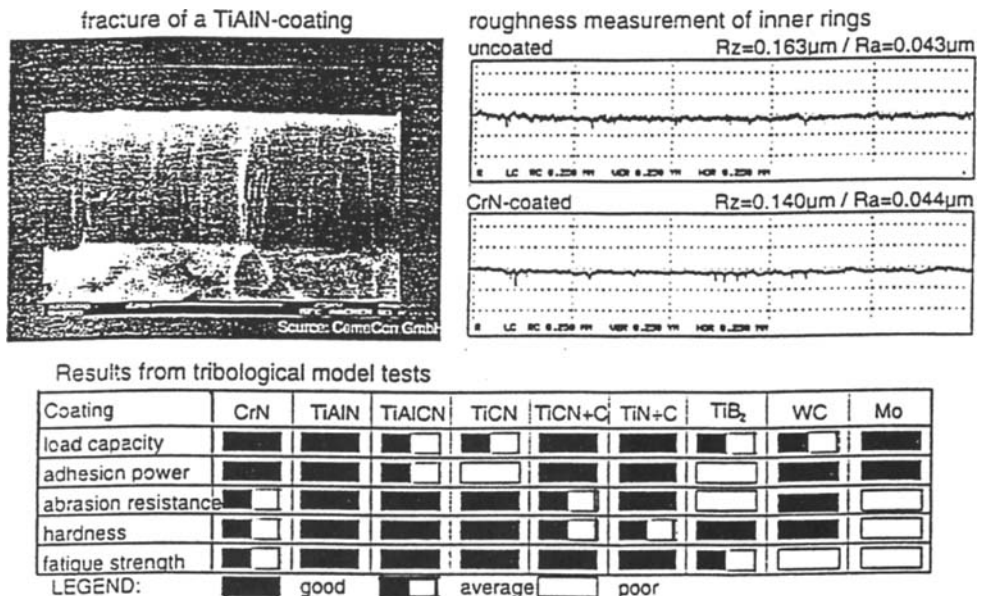


Figure 2.63 Comparison properties of coatings for roller bearings.

properties of the fluid, loads, speed, and the lubrication system. It has been shown that the use of bearings constructed from high-purity steel, high manufacturing accuracy, operating with a sufficient number of revolutions, with a fluid of adequate viscosity, with fluids free of contaminants, and under conditions of no contact deformation can exceed their life rating by up to 10 times. Under conditions of elasto-hydrodynamic lubrication, coupled surfaces are typically separated by an oil layer of 2–3 μm . Therefore, to assure no asperity contact between the working surfaces is to assure both manufacturing accuracy and the high quality of the surface finish.

To assure optimal bearing lifetimes, elimination of particles larger than the thickness of the oil layer is necessary. However, elasto-hydrodynamic lubrication rarely occurs under conditions of total absence of metal surface contact which occurs, for example, at the beginning of bearing rotation. Particles originating from wear debris and other sources, if their size is greater than the fluid film thickness, will increase the contact fatigue of the bearing surfaces. Elasto-hydrodynamic lubrication significantly reduces friction, therefore moving the point of the fatigue crack initiation deeper into the surface layer.

Figures 2.64 and 2.65 [43] illustrate the pressure distribution in the fluid film and stress distribution with material depth, respectively. Changes of pressure and the physical form of the fluid film as a function of physical properties of coupled cylindrical surfaces and the lubricant are shown in Figure 2.66 [43]: Curve a refers to rigid cylinders with a constant lubricant viscosity of lubricant; curve b refers to rigid cylinders and viscosity dependent on pressure; curve c refers to elastic cylinders and constant viscosity; curve d illustrates elastic cylinders and viscosity dependent on pressure.

Figure 2.67 [43] illustrates the variation of fluid pressure distribution and fluid film thickness as a function of material parameters. The pressure distribution and changes of the oil layer form as a function of rotational velocity is illustrated in Fig. 2.68 [42]. These data show that at constant load, the maximum pressure, minimum oil layer thickness, and oil layer gap are functions of the rotational velocity of the contact surface.

Figure 2.69 [43] illustrates the pressure distribution of nonidealized rough surfaces. Studies of the influence of surface roughness on the rough layer carrying

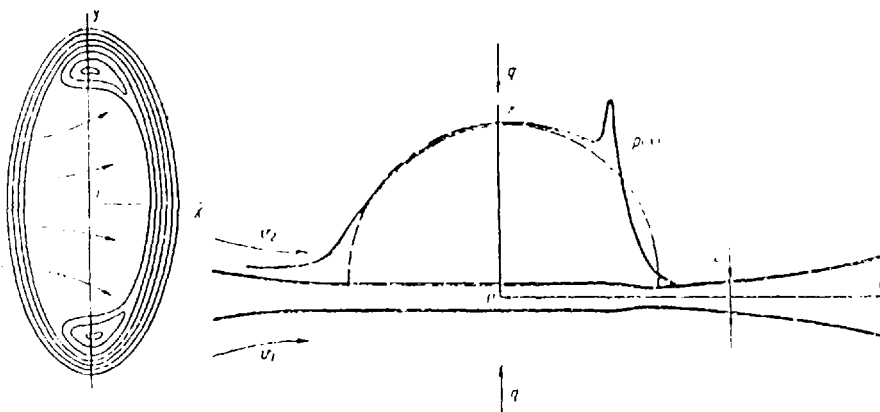


Figure 2.64 Pressure distribution in fluid film.

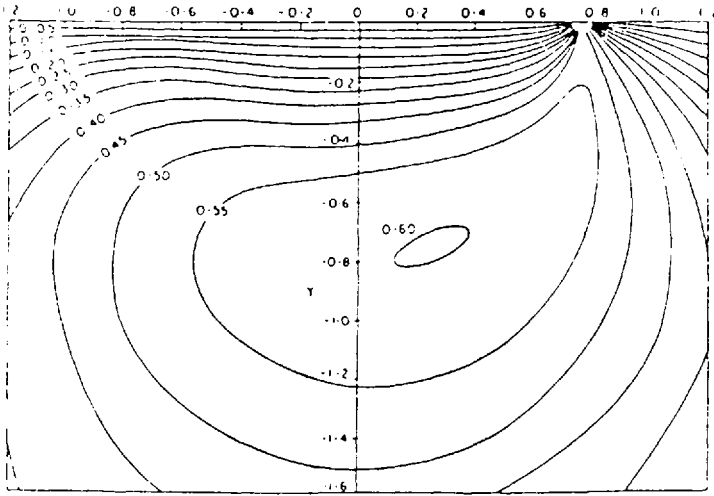


Figure 2.65 Stress distribution with material depth. $W = 3 \times 10^{-5}$; $G = 5000$; $U = 10^{-11}$.

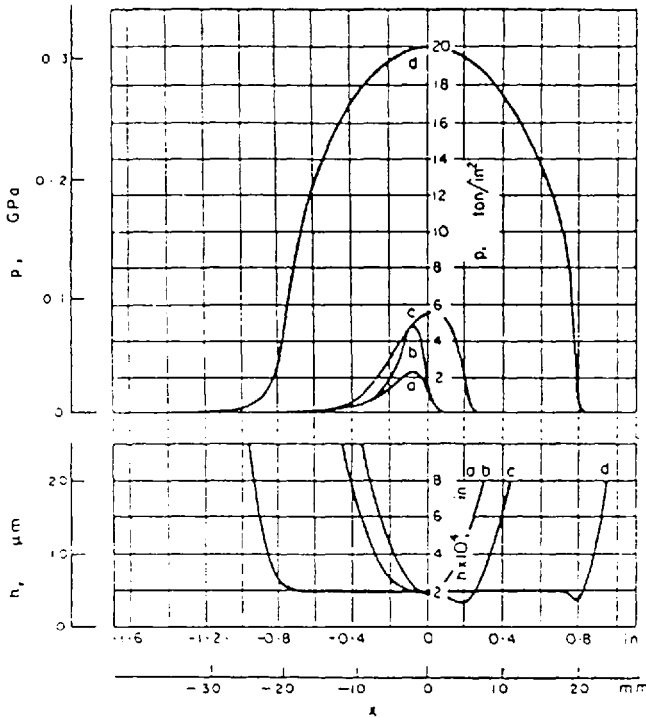


Figure 2.66 Change of pressure and physical form of the fluid film as a function of physical properties of coupled cylindrical surface.

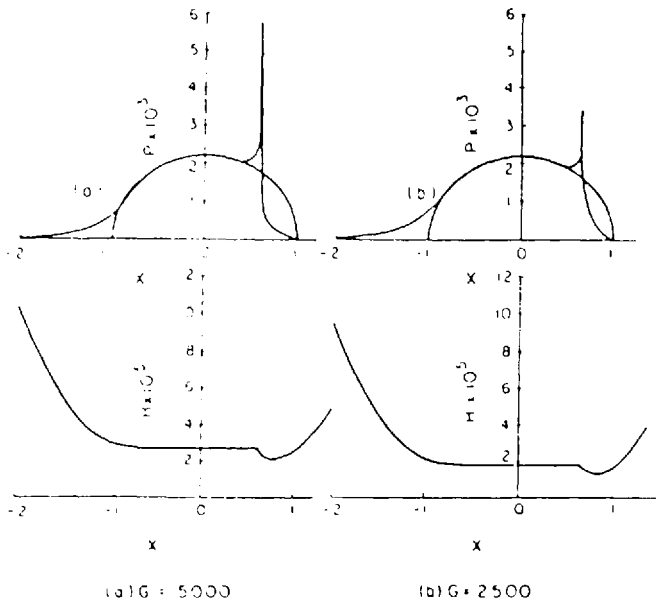


Figure 2.67 Variation of fluid pressure distribution and fluid film thickness as a function of material parameters. $W = 3 \times 10^{-5}$; $U = 10^{-11}$; $G = 5000$ for (a); $G = 2500$ for (b).

capacity showed that increased longitudinal roughness significantly reduces the carrying capacity of the oil layer [42].

The oil layer not only provides lubrication, which is pressure and speed dependent, but it also cools the wear contact. Figure 2.70 [43] depicts the temperature field within the elasto-hydrodynamic contact. The lubrication properties of the roller bearing at the moment that motion begins is characterized by direct contact of working surfaces, localized interruptions of fluid film, insufficient conditions to provide hydrodynamic lubrication, and the tribological characteristics determined by the interaction of very thin fluid film and the material surface. Lubrication (F_T) under these conditions is either mixed-film or boundary lubrication. Friction under these conditions is determined by

$$F_T = \alpha A_r \tau + (1 - \alpha) A_r \tau_x$$

where α is the contact coefficient of pure metals surfaces, A_r is the total real contact surface, τ is the material shear stress, and τ_x is the boundary layer shear stress.

The friction coefficient is

$$\mu = \alpha \mu_m + (1 - \alpha) \mu_x$$

where μ_m is the friction coefficient of the coupled surfaces and μ_x is the friction coefficient of the boundary layer.

Mixed friction occurs in bearings operating at high contact pressures and insufficient velocities required for elasto-hydrodynamic lubrication or a transient condition such as the moment when the bearing starts to move. It is critical to remove

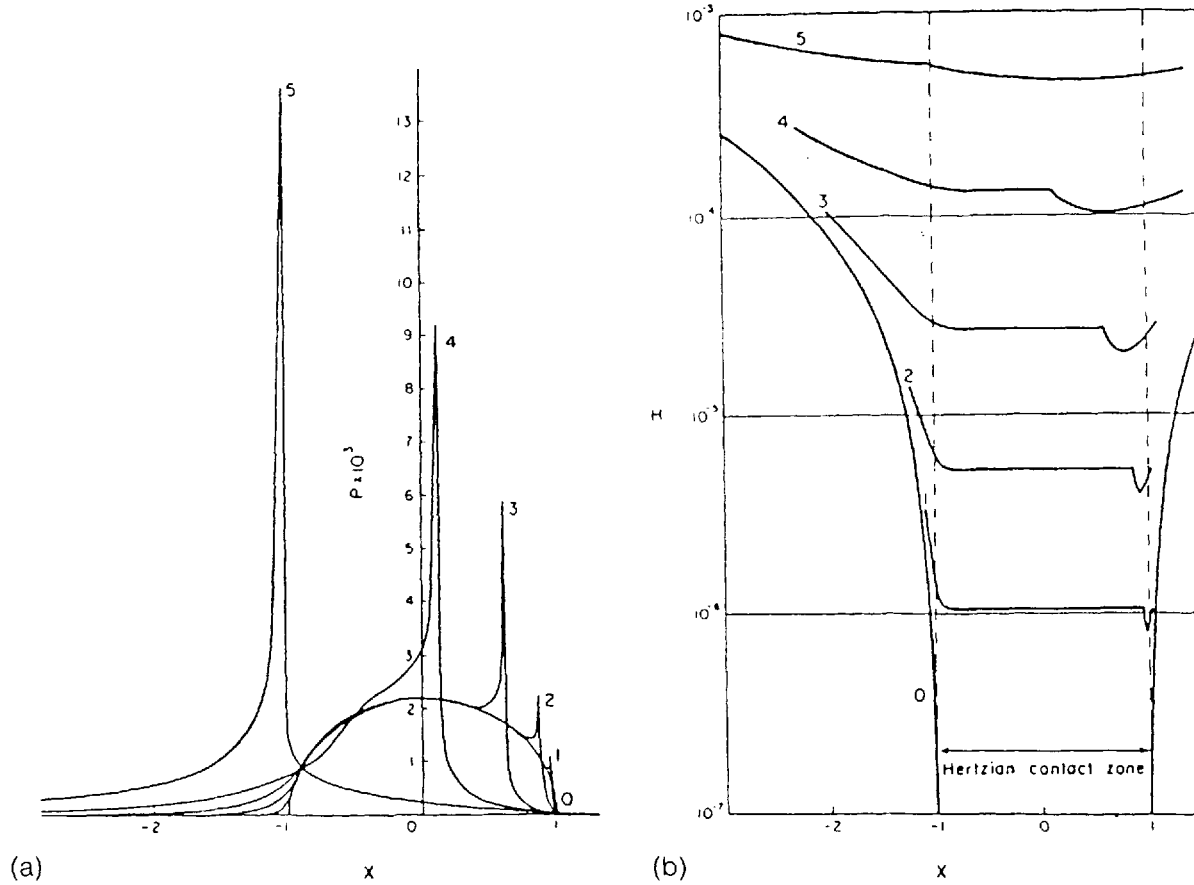


Figure 2.68 Pressure distribution (a) and change of the layer form (b) as a function of rotational velocity. $W = 3 \times 10^{-5}$; $G = 5000$; $U = 0$, dry contact (1); $U = 10^{-3}$ (1); $U = 10^{-12}$ (2); $U = 10^{-11}$ (3); $U = 10^{-10}$ (4); $U = 10^{-9}$ (5).

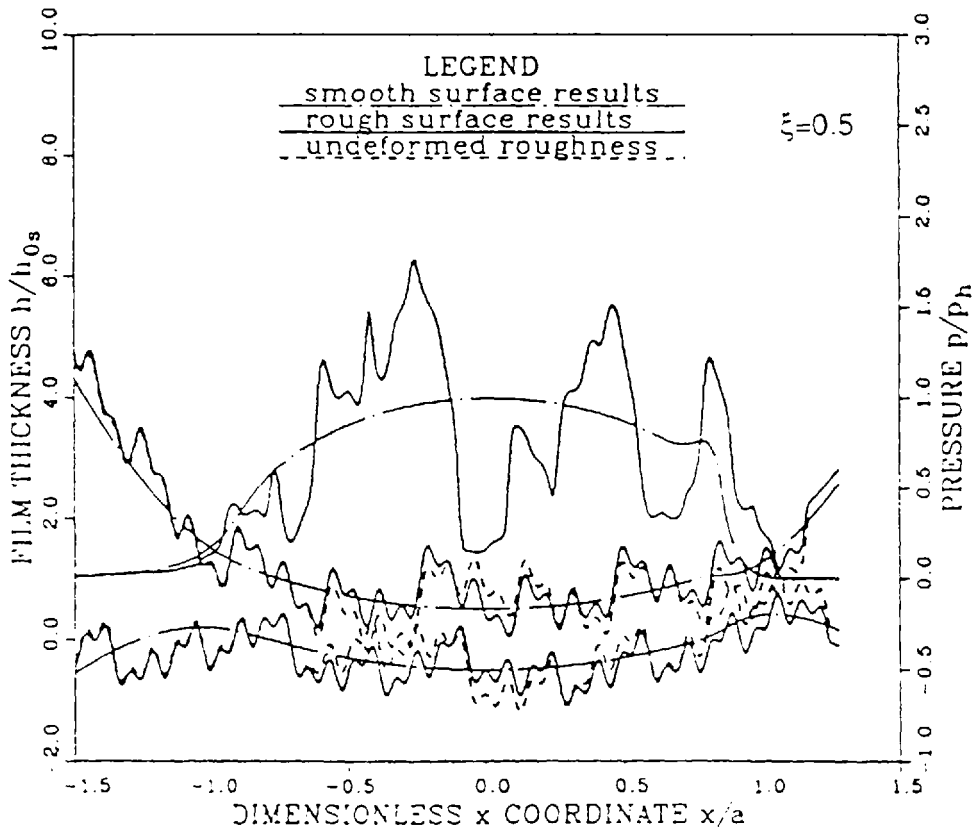


Figure 2.69 Pressure distribution of nonidealized surface.

particulate contamination when the bearing is in the mixed-film regime because some asperity contact already occurs as a result of the thin film in the wear contact. The effect of velocity on the coefficient of friction for boundary, mixed-film, and elasto-hydrodynamic lubrication is illustrated by the Stribeck diagram shown in Fig. 2.71.

Lubricants that must provide mixed-film and boundary lubrication contain additives that form the boundary layers that reduce the friction coefficient and prevent direct metal-to-metal contact. The boundary layer is formed on surfaces by atomic, molecular, and microparticle interactions. These additives are designated as friction modifiers, and antiwear and boundary lubricants for high pressure.

Although additives are necessary to provide adequate roller bearing lubrication, their effect is concentration dependent. Excessive, or inadequate, additive concentrations may enhance and accelerate fatigue wear. Figure 2.72 [44] illustrates the working life of roller bearings lubricated by oil, with and without EP (extreme pressure) additives. These data illustrate that the bearing working life is reduced by the use of nonoptimal EP additive concentrations [44].

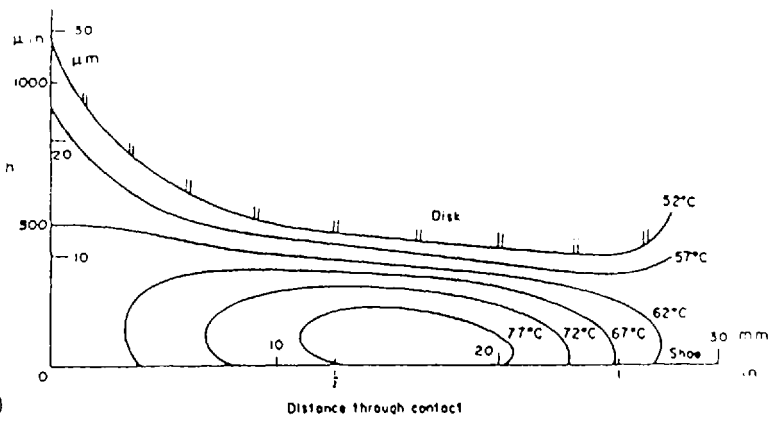
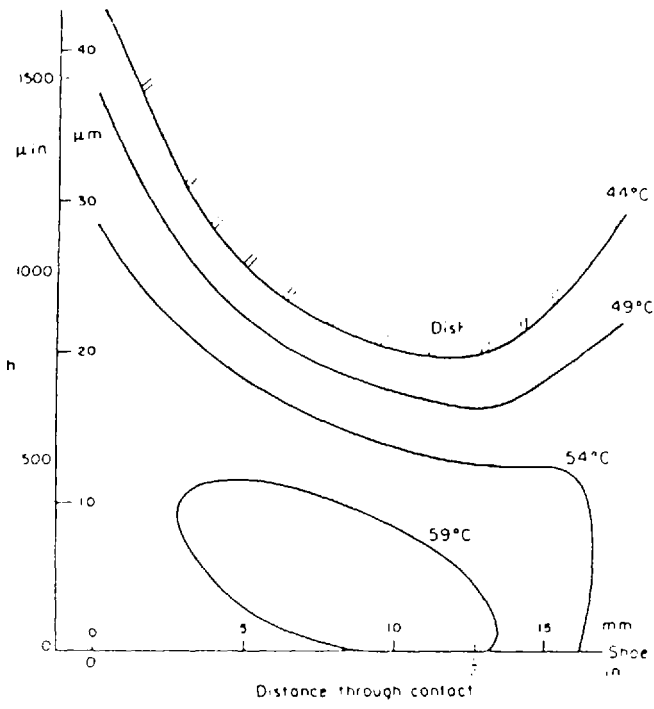


Figure 2.70 (a,b) Temperature field within the elasto-hydrodynamic contact.

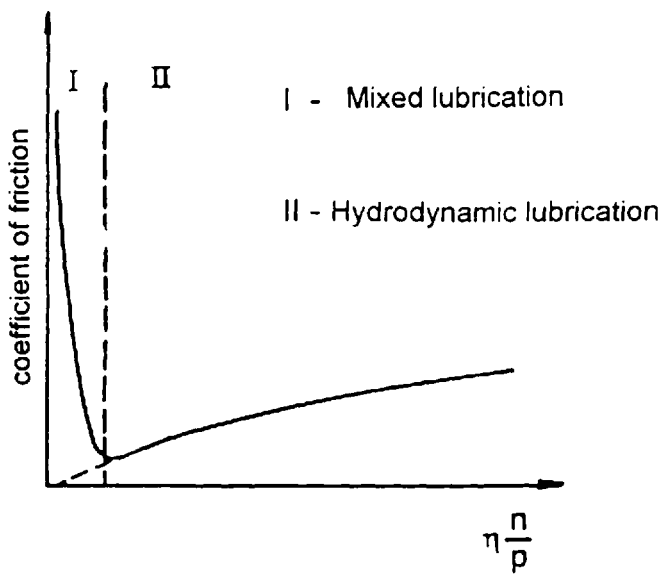
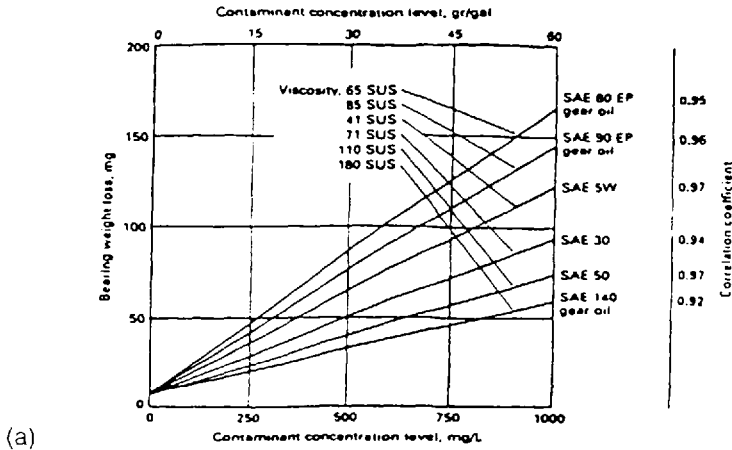


Figure 2.71 Stribeck diagram.

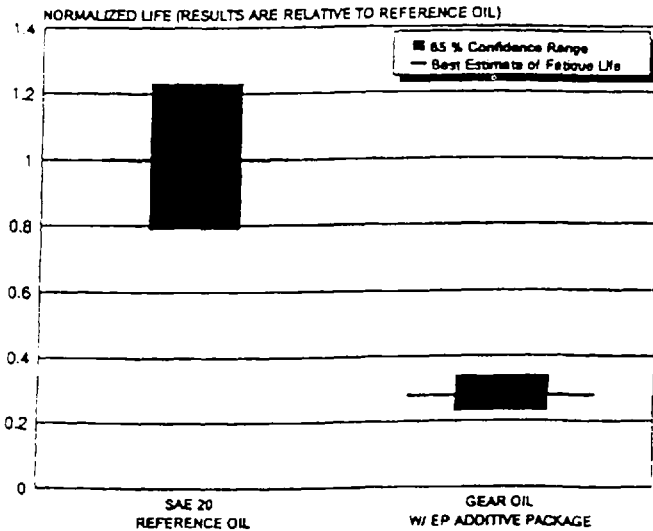
Mineral-oil-based fluids may contain low concentrations of water (500–600 ppm). However, water concentrations may be increased by adsorption of water from the air, particularly in humid environments. Studies using radioactive isotopes have shown that mineral oil–water contaminants may hydrogen-bond to metal surfaces [14]. Because water molecules are much smaller than the lubricant molecules, they diffuse to the tips of microcracks. Through chemical reaction, atomic hydrogen is produced which diffuses into the metal, causing hydrogen embrittlement of steel. Hydrogen embrittlement reduces fatigue strength. The structure of the surface layer of steel balls lubricated by oil with addition of water is shown in Fig. 2.73 [45]. Figure 2.74 [18] shows the effect of water concentration in lubricant on the working life of rolling bearings.

Various methods have been used to prevent the negative influence of water contamination in mineral oil, including hydrogen-bond complexation, hydrophobic layer isolation, and water isolation removal. For example, isopropylethanolamine (IPEA) has been used to negate the deleterious effects of water contamination in mineral oil. IPEA works by hydrogen-bonding the water, preventing cathodic reduction to hydrogen at the tips of the microcracks, thus preventing hydrogen embrittlement. This is illustrated in Table 2.4 [45].

Many industrial applications, such as mining, die casting, molten metal processing, and forging, require the use of various non-mineral-oil-derived hydraulic fluids. However, the use of these fluids with conventional bearing materials have resulted in a significant reduction in working life and reliability (Fig. 2.75) [46]. This has been particularly true with water-containing fluids. A correlation has been developed to predict the working life of roller bearings lubricated by mineral oil and fire-resistant hydraulic fluids [13]:



(a)



(b)

Figure 2.72 Working life of rolling bearing lubricated by oil with and without EP additives. (a) Bearing weight-loss comparisons to contaminant concentration levels for various lubricant viscosity grades. Note the increased wear for gear lubricants SAE80EP and SAE90EP, both with EP additives, as compared to the SAE140 gear oil not having EP additives. (b) Fatigue life performance comparison of a life test reference oil and a gear oil with similar viscosities. (Reprinted with permission. SAE paper, Nixon P. II., Zantopoulos II. *Observation of the Impact of Lubricant Additives on Fatigue Life Performance of Tapered Roller Bearings*, c. 1995 Society of Automotive Engineers, Inc.)

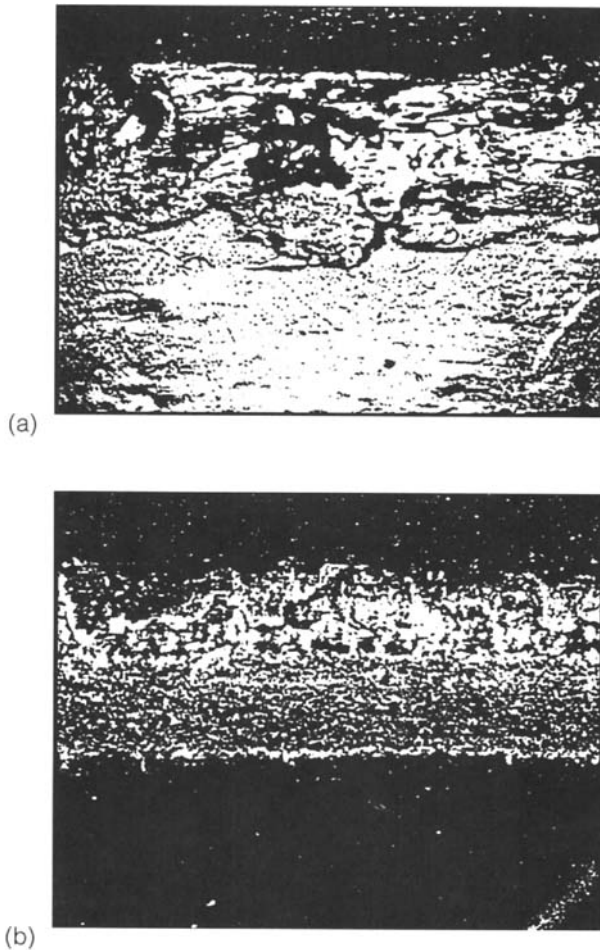


Figure 2.73 The structure of the surface layer of steel balls lubricated by oil with addition of water. (a) Continuous-type pitting failure produced by lubricant supersaturated with water ($\times 100$); (b) continuous-type pitting of a race experienced in practice when using lubricant contaminated with water.

$$F_L = L_{\text{oil}}^{1/3} L_{\text{fluid}}^{-1/3}$$

$$F_I = F L_{\text{fluid}}^{1/3} \cdot n^{1/3n}$$

where the values of coefficient (n) for various lubricants are provided in Table 2.5.

It has been reported that a water–glycol hydraulic fluid provided a bearing life of only approximately 10% of that obtained by a mineral-oil hydraulic fluid [22]. However, bearing lifetimes of up to 48% of that obtained by a mineral-oil hydraulic fluid was attainable with the use of a fatty acid additive. This same study showed that additives exhibited a significantly greater effect on the bearing life than increasing viscosity [22].

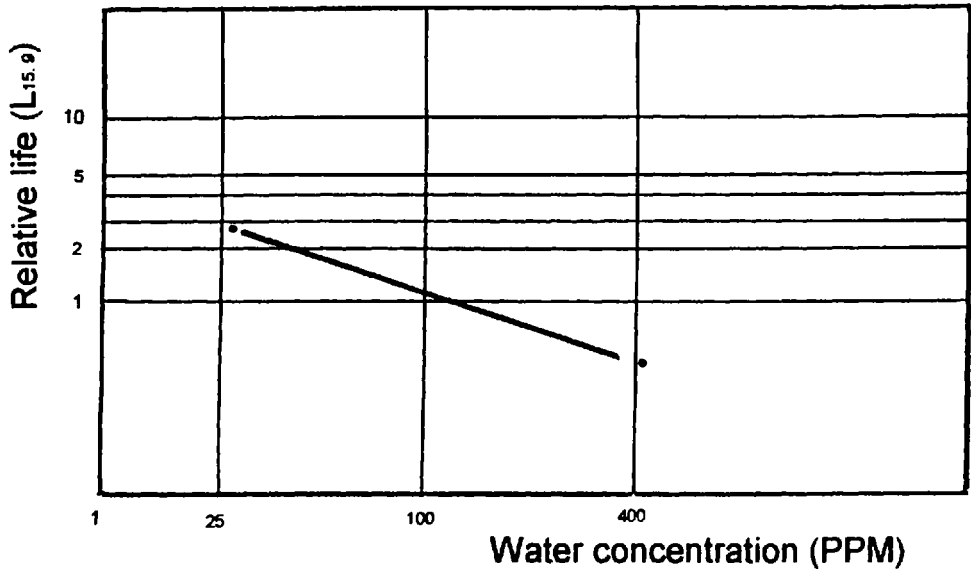


Figure 2.74 The effect of water concentration in lubricant on the working life of rolling bearings.

Lubricating greases are frequently used for approximately 80% of all bearings used in hydraulic, transportation, and other machine applications [47]. The primary lubricating characteristics of greases are as follows:

1. Lubricating greases are ductile, but not as liquid as lubricating oils, which reduces leakage in use.

Table 2.4 Effect of Additives*

Additive	Concentration (%)	Time of stressing (min)	Initial counting rate from fatigued track (c/min)	Mean pitting life corresponding to load (min)
None	—	20	33,400	26
Iso-amyl alcohol	3	40	49,500	34
Sarkosine derivative	2	20	37,000	22
Substituted imidazoline 'O'	2	20	24,000	59
Sarkosine derivative + substituted imidazoline 'O'	2	20	26,000	60
Substituted imidazoline 'O' + N-methyl glycine derivative	2			
Sarkosine derivative [†]	2	20	30,000	38

*Load, 600 Kg. Lubricant, NEL ref. oil + 3% tritiated water + additive.

[†]At a load of 500 Kg.

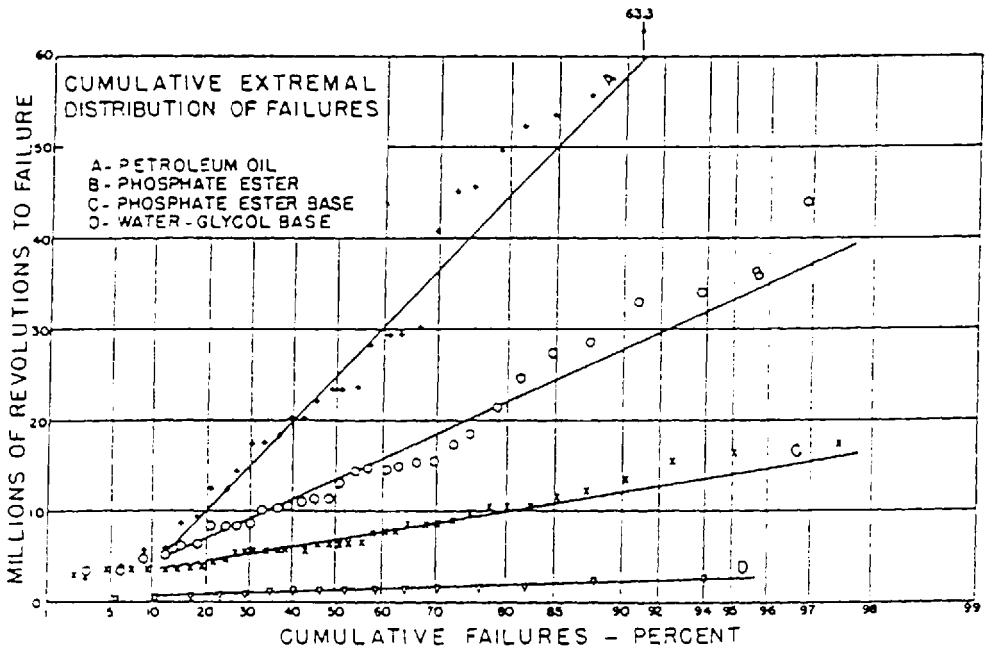


Figure 2.75 Effect of petroleum oil and combustion-resistant hydraulic fluid on the life of an angular-contact ball bearing.

Table 2.5 Lubricant Factors at 10% Failure Level

Fluid	Load		Life for 10% failures millions of revolutions	Lubricant factor
	kN	(lbf)		
Mineral oil	3.34	(750)	48.7	1
	2.45	(550)	123.0	1
Phosphate ester	3.34	(750)	13.7	1.53
	2.45	(550)	20.6	1.82
Water glycol solution	3.34	(750)	3.81	2.34
	2.45	(550)	5.34	2.84

Values of Lubricant Factors Based on Modal Life

Fluid	Lubricant factor
Water-glycol solution	2.6
Phosphate ester base	1.5
Phosphate ester	1.2

2. The load-carrying capacity of the lubricating film of a grease is significantly greater than an oil film with the same thickness.
3. The effect of lubricant loss on proper operation and working capacity of a grease is less than that of oil.
4. The reduced capillary activity of greases improves the resistance to those types of wear that are aggravated by capillary activity (pitting).
5. Greases can protect a system from particle ingress by blocking openings to the environment.

As with lubricating oils, lubricating greases are formulated with a combination of different additives. A schematic representation of the procedure for obtaining different types of grease is shown schematically in Fig. 2.76 [47]. Tables 2.6 and 2.7 [47] provide a summary of procedures and basic characteristics, respectively, for the most common types of grease. The most frequently used additives in lubricating greases manufacture are provided in Table 2.8 [47].

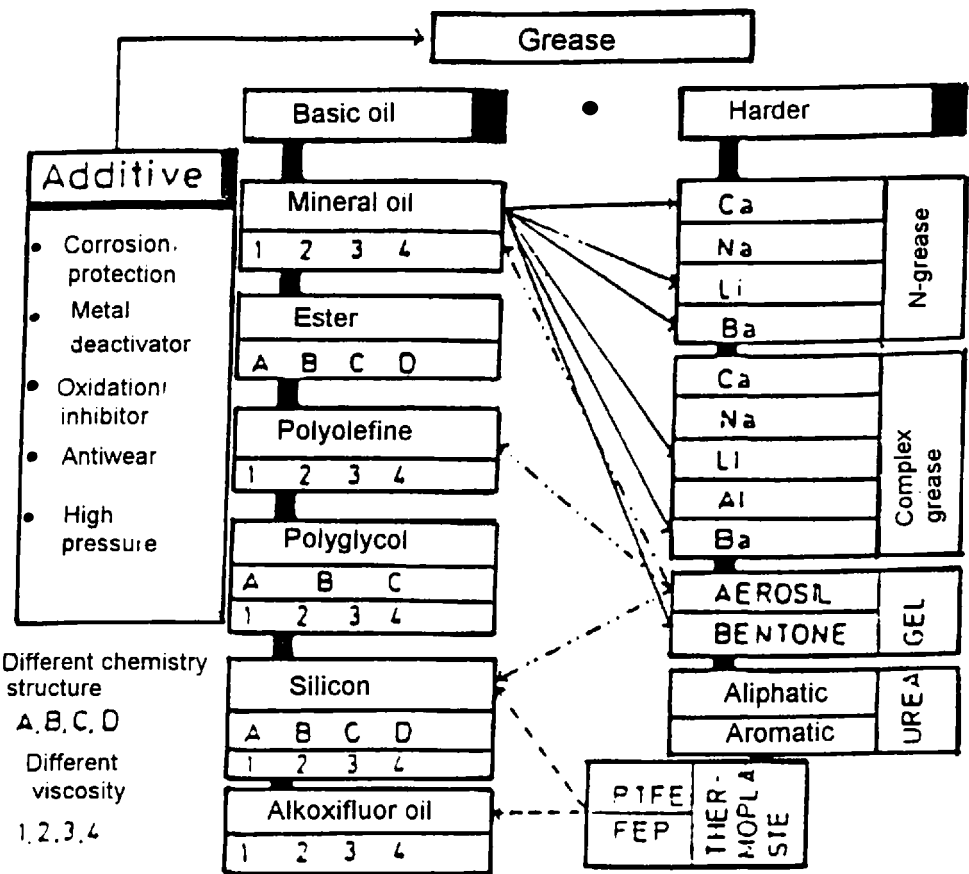


Figure 2.76 Procedure for obtaining different types of grease.

Table 2.6 Metal Soap Greases

Type of soap	Advantages	Disadvantages
Sodium	<ul style="list-style-type: none"> • Fibrous constitution, nonfluid character • Drooping point around 200°C • Low cost 	<ul style="list-style-type: none"> • Not water resistant • Application only up to 80–100°C • Low corrosion protection
Lithium	<ul style="list-style-type: none"> • Up to 80–90°C water resistant • Application to 120–145°C • Good corrosion protection • Drooping point around 190°C • Good working characteristics 	<ul style="list-style-type: none"> • Not resistant to steam
Aluminum	<ul style="list-style-type: none"> • Water resistant like sodium grease • Application up to 100°C 	<ul style="list-style-type: none"> • Hydropolysired under influence of water
Barium	<ul style="list-style-type: none"> • Water resistant • Application up to 100°C • Protection against corrosion • Low loss of oil 	<ul style="list-style-type: none"> • Difficult production • Expensive
Calcium	<ul style="list-style-type: none"> • Flexible on low temperature • Good water resistance • Often fibrous 	<ul style="list-style-type: none"> • Application only up to 60°C only • Drooping point around 100°C • Bad corrosion protection

7 ROLLER BEARINGS' WORKING SURFACES FAILURE

A survey of characteristic types of working surface damage of roller bearings will be reviewed here. Suggestions to prevent the occurrence of these failures will also be provided.

Lundberg and Palmgren showed that the end of the useful lifetime of a roller bearing was characterized by working surface fatigue wear as illustrated in Fig. 2.77 [48]. The initial phase of fatigue wear, illustrated in Fig. 2.78, is characterized by micropitting [48]. After the appearance of the initial phase of destruction, approximately 20–30% of the total working capacity remains (Fig. 2.79) [48]. Contact pressure strongly influences proper operation of the damaged bearing. Figure 2.80 [48] shows that the remaining working capacity at a Hertzian pressure of 2600 MPa is only 5% of the total working capacity. However, at a Hertzian pressure of 2000 MPa, the remaining working capacity is approximately 27%. The appearance of the working surfaces of the inside and outside raceways in the final phase of fatigue wear is shown in Fig. 2.81 [49].

Fatigue wear pitting, when it appears on diametrically opposite sides of raceways, indicates ring deformation under the working load as shown in Fig. 2.82 [49].

Bearing eccentricity causes inhomogeneous load distribution, localized increases in load that exceed the design limit of the bearing, and acceleration of fatigue crack development, as illustrated in Fig. 2.83 [50].

Table 2.7 Complex-Metal Soap Greases

Type of soap	Advantages	Disadvantages
Sodium K	<ul style="list-style-type: none"> • Stable up to 160–180°C • Drooping point over 220°C • Water resistant up to 90°C • Good corrosion protection 	<ul style="list-style-type: none"> • Not steam resistant
Lithium K	<ul style="list-style-type: none"> • Stable up to 150–160°C • Drooping point over 260°C • Very good stability against water 	<ul style="list-style-type: none"> • Critical additiving • Difficult production
Aluminum K	<ul style="list-style-type: none"> • Applicable up to 160°C • Drooping point over 260°C • Very good stability in water • Good pump effect • Fine structure • Not expensive 	<ul style="list-style-type: none"> • Not applicable with other grease • Soft under shear stress
Barium K	<ul style="list-style-type: none"> • Stable in water and steam • Stable under influence of alkali and acid environment • Applicable up to 150°, short term around 170°C • Drooping point over 260°C • Very good corrosion protection • Applicable under very high pressure 	<ul style="list-style-type: none"> • Difficult production • High soap demands • More expensive
Calcium K	<ul style="list-style-type: none"> • Water and steam resistant • Drooping point over 250°C • Good lubricant ability • Good corrosion protection • Very good press resistance • Good pump effect • Not expensive 	<ul style="list-style-type: none"> • Becomes harder under high temperature (Steep temperature-consistence-gradient) • Bad reversibility of consistency

Particle contamination in the coupling zone may cause different types of working surfaces damage which are dependent on the hardness of the particles. Fig. 2.84 [48] shows working surface damage caused by soft particles. Working surface damage caused by hard particles is shown in Fig. 2.85 [48]. The initial destruction caused by particle contamination significantly accelerates initiation and development of fatigue wear.

Figure 2.86 [48] shows craters caused by electric current flow. As with other causes of wear development, the craters and structural changes caused by electric current flow are a form of localized surface destruction which leads to accelerated destruction of working surfaces.

Adhesive wear of working surfaces illustrated in Fig. 2.87 [48] is caused by direct contact of metal surfaces in relative motion to each other with different perimeter velocities. This type of wear is frequently combined with or precedes fatigue or

Table 2.8 Additives

Material	Typical Bonding	Duty
EP additive	Carbon, chlorine, phosphor bond, off and on in combination with lead, graphite, or MoS ₂	Protects against adhesion wear
Wear-reducing additives	High molecular bonding like fatty acid oil, oxidized wax or lead soap, graphite, or MoS	Reduces wear under boundary and mixed lubrication conditions
Anticorrosion additive	Organic bonding, active sulfur, phosphor or particles as phosphite, metal salts, or tiophosphoric acid, sulfured wax or trepan	Protects of corrosion
Aging	Phenols, aromatic amines, sulfured phenols, zinc ditiophosphates	Protects from destruction caused by oxidation
Additions for improving surface-lubricant adhesion	Polyisobutilens, olefinpolymers, latex	Improves connection of lubricants with surface

**Figure 2.77** Fatigue wear.

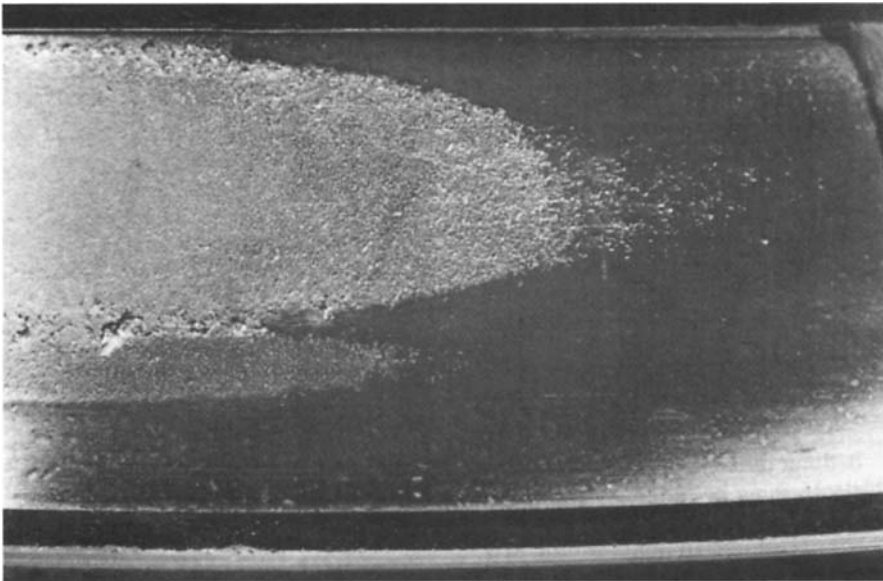


Figure 2.78 Micropitting.

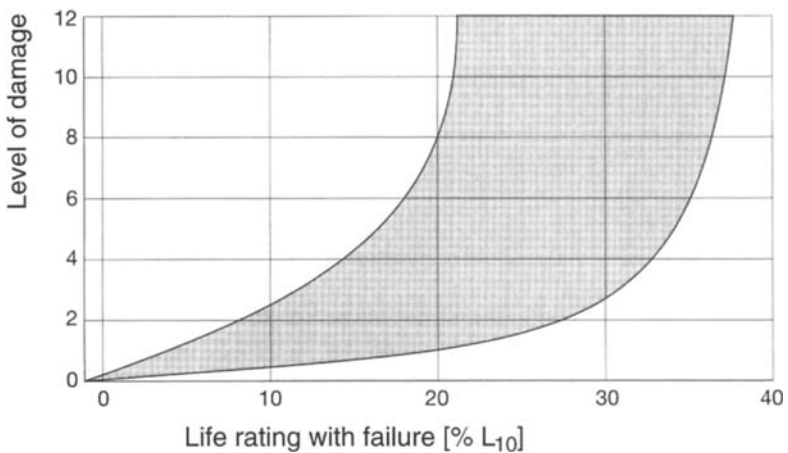


Figure 2.79 Intensity of failure in function of time.

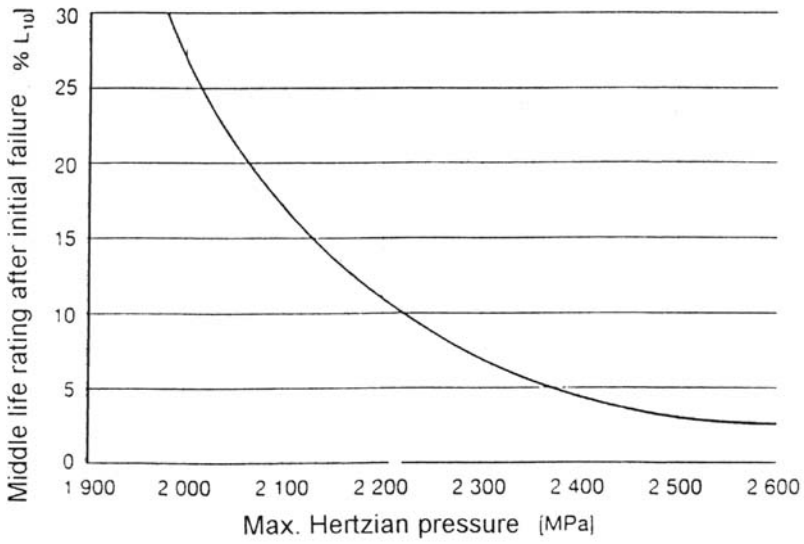


Figure 2.80 Influence of contact pressure on remaining working capacity.



Figure 2.81 The appearance of the working surface in the final phase of fatigue wear.

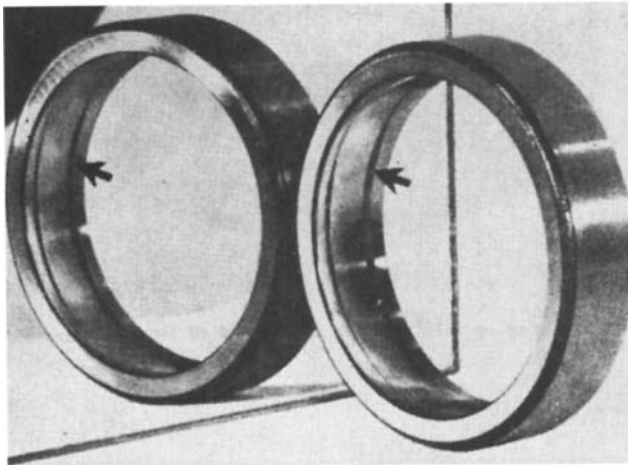


Figure 2.82 Pitting on opposite side of raceways.

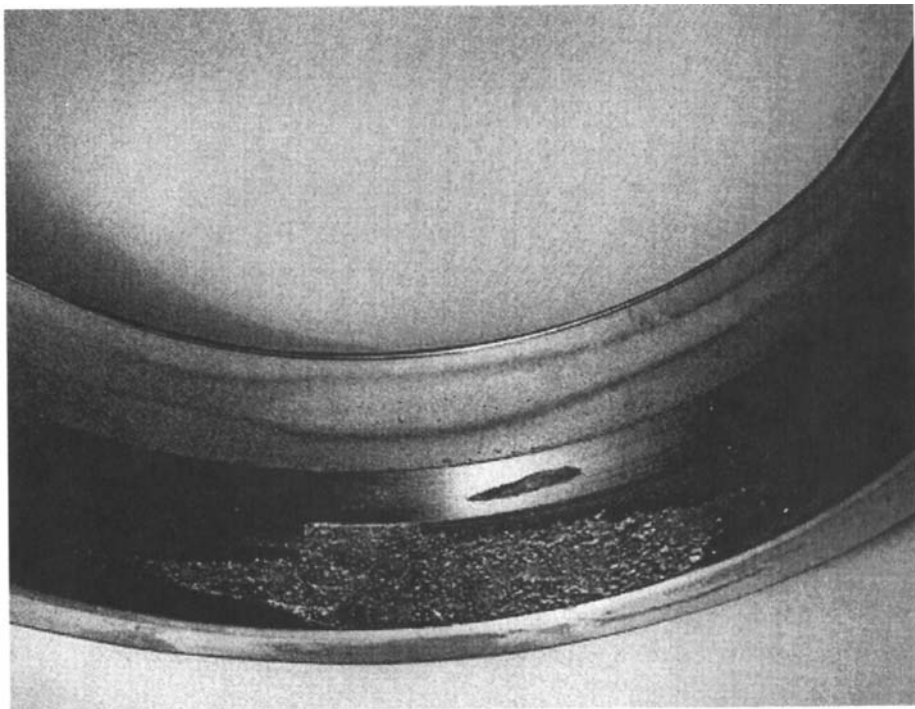


Figure 2.83 Fatigue wear caused inhomogeneous load distribution. (Reprinted with the permission of SKF.)

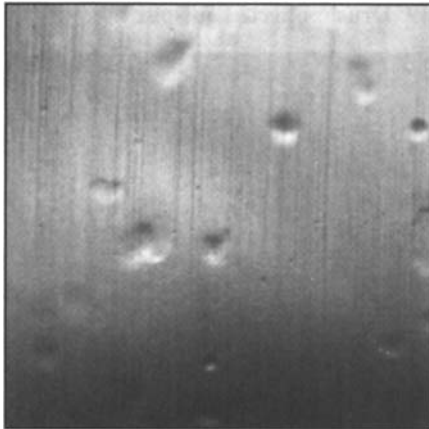
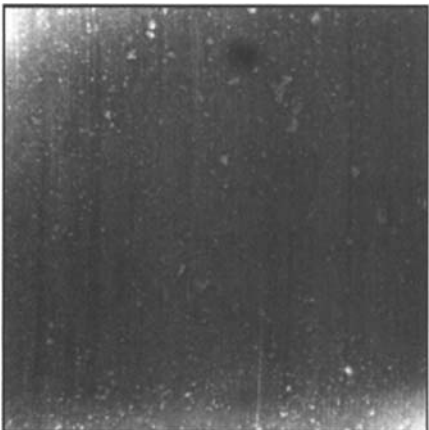
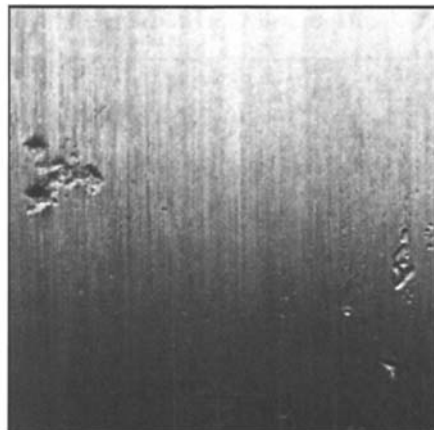


Figure 2.84 Working surface damages caused by soft particles.



(a)



(b)

Figure 2.85 (a,b) Working surface damages caused by hard particles.



Figure 2.86 The craters on working surface caused by electric current flow.

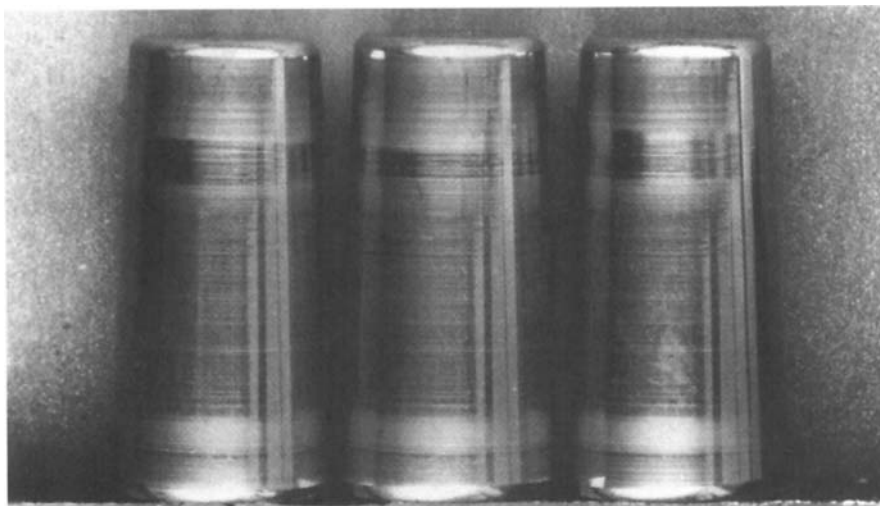
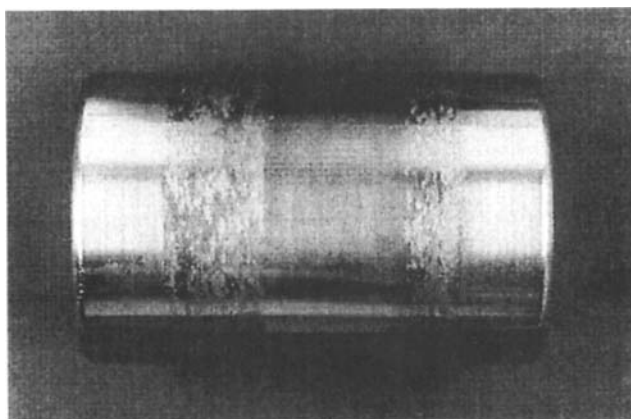
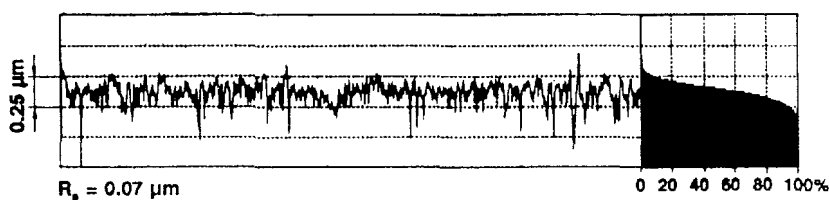


Figure 2.87 Adhesive wear of working surface.



(a)



(b)

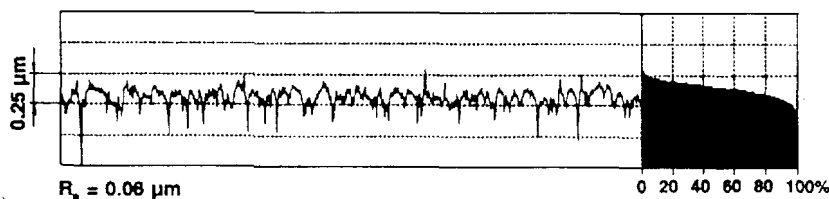


Figure 2.88 (a,b) Adhesive wear combined with abrasive and fatigue wear.

abrasive wear (Fig. 2.88) [48]. Material transfer from one working surface to another is observed in adhesive wear, as shown in Fig. 2.89 [17].

True brinelling occurs when loads exceed the elastic limit of the ring materials (Fig. 2.90) [49]. Brinell marks show as indentations in the raceways. Any static overload or severe impact can cause brinelling. Severe brinell marks can cause increasing vibration and, in connection with increasing vibrational load, can cause premature fatigue failure.

A small relative motion between balls and raceways that are subject to external vibration can cause elliptical wear marks in an axial direction with a bright finish and sharp demarcation at each ball position (Fig. 2.91) [49]. This form of wear is typical for nonturning bearing, where oil film cannot be formed to prevent raceway wear.

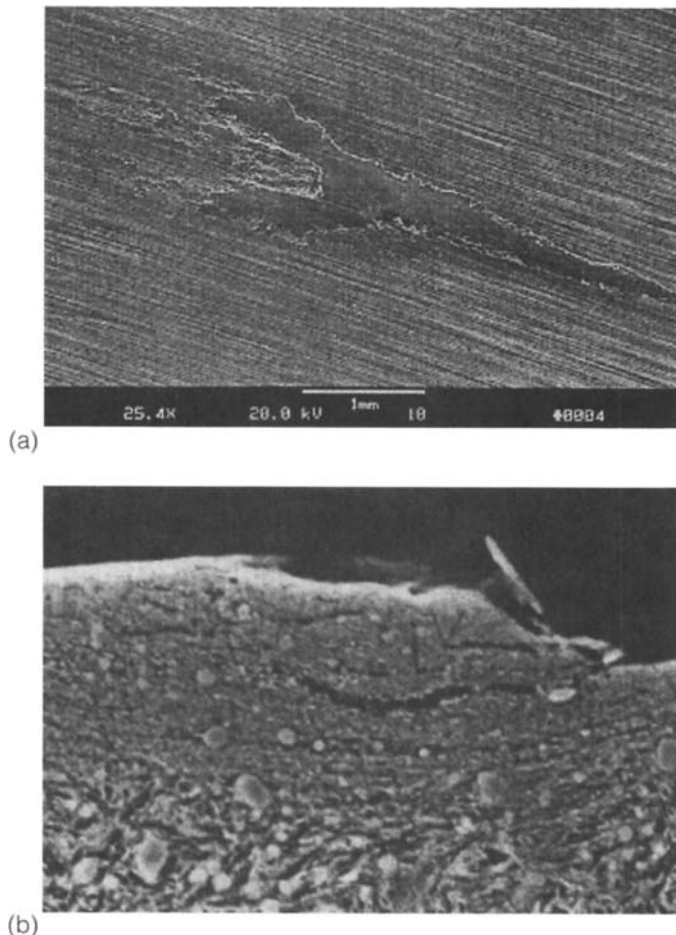


Figure 2.89 (a,b) Material transfer from one working surface to another.

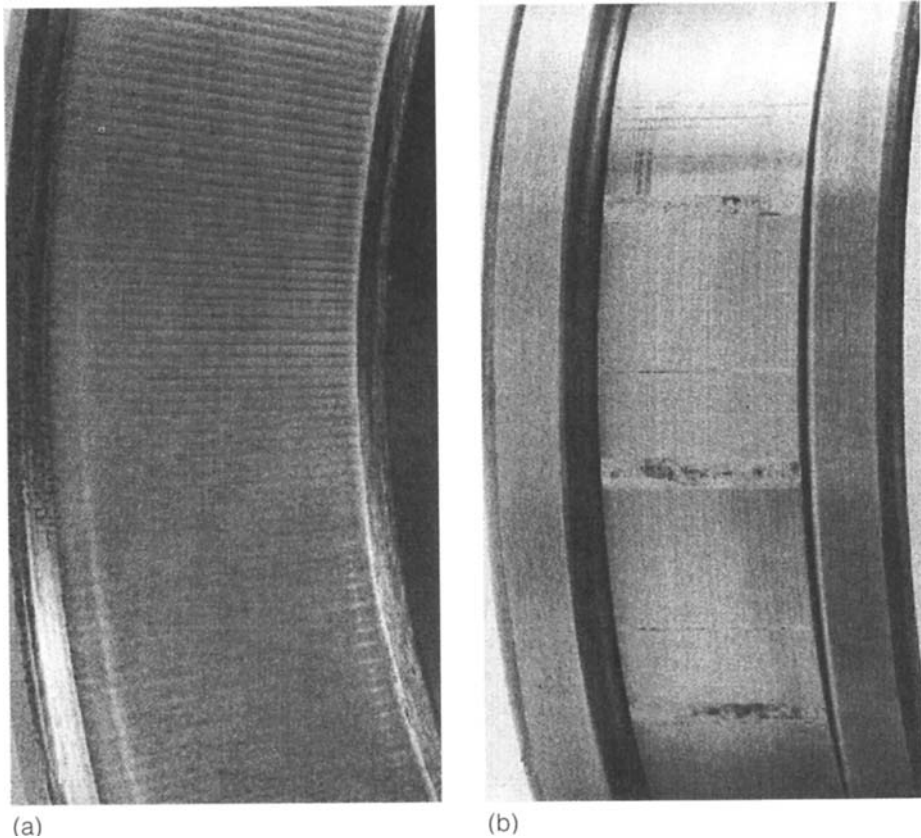


Figure 2.90 (a,b) The occurrence of true brinelling.

In addition to contributing to other wear processes, corrosive wear itself may cause major working surface destruction. Corrosive wear of roller bearings is caused by chemical and electrochemical processes and is most commonly encountered with *fixed, slowly moving, and normally operating* roller bearings. Roller bearing corrosion produces an oxide which appears as black–brown stains, as shown in Fig. 2.92 [49]. These coatings are destroyed or removed by system vibrations. After repetitive oxide formation and destruction, the process proceeds further into the material, leading to a reduction in bearing life. Figure 2.93 [49] illustrates the surface of a ball exposed to humidity and acid. Figure 2.94 [49] illustrates corrosive wear occurring on a raceway surface that was caused by humidity. The appearance of corrosive damage of rolling elements is illustrated in Fig. 2.95 [49].

Abrasive wear occurs from surface sliding because of the presence of particle contamination in the lubricant. Damage appears as narrow grooves in the direction of motion and is characterized by a change of color and surface topography (Fig. 2.96) [48]. As the process proceeds, wider grooves are observed in the direction of

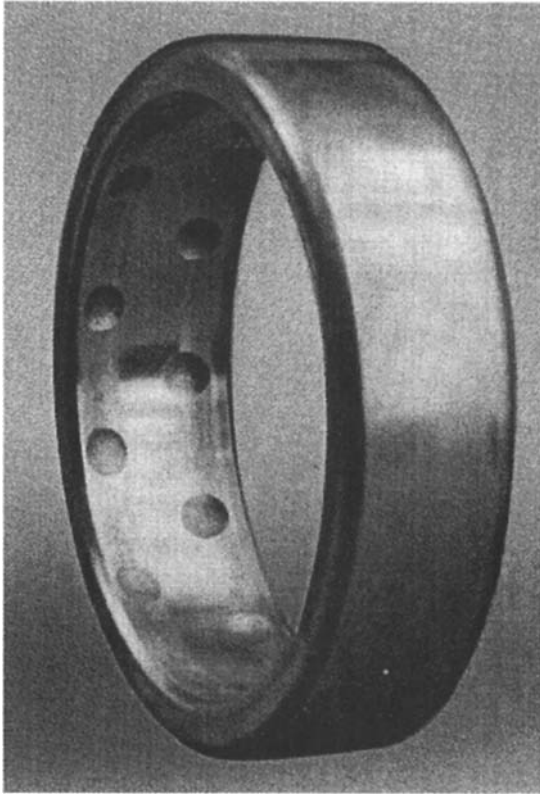


Figure 2.91 Elliptical wear marks caused by external vibration.

sliding; these grooves inhibit the formation of the lubricating film which accelerates working surface destruction as shown in Fig. 2.97 [48].

Besides destroying working surfaces in the direction of the primary load, particle contamination may also destroy the side surfaces of both rolling elements and raceways. Damage of the outside ring's surface is shown in Fig. 2.98 [48]. Damage of the roller's sides caused by hard particles in the contact zone is shown in Fig. 2.99 [48]. Figure 2.100 [48] shows the appearance of the side surface damage by abrasive wear.

Tribological wear may also occur on auxiliary elements of rolling bearings. Figure 2.101 [48] shows cage damage caused by particle contamination. Figure 2.102 [48] illustrates typical cage damage caused by rotational speed variation of the rolling element.

Bearing damage may be diagnosed even in the earliest stages by frequency-spectrum analysis. The frequency spectrum of a damaged and undamaged rolling bearing is shown in Fig. 2.103 [48].

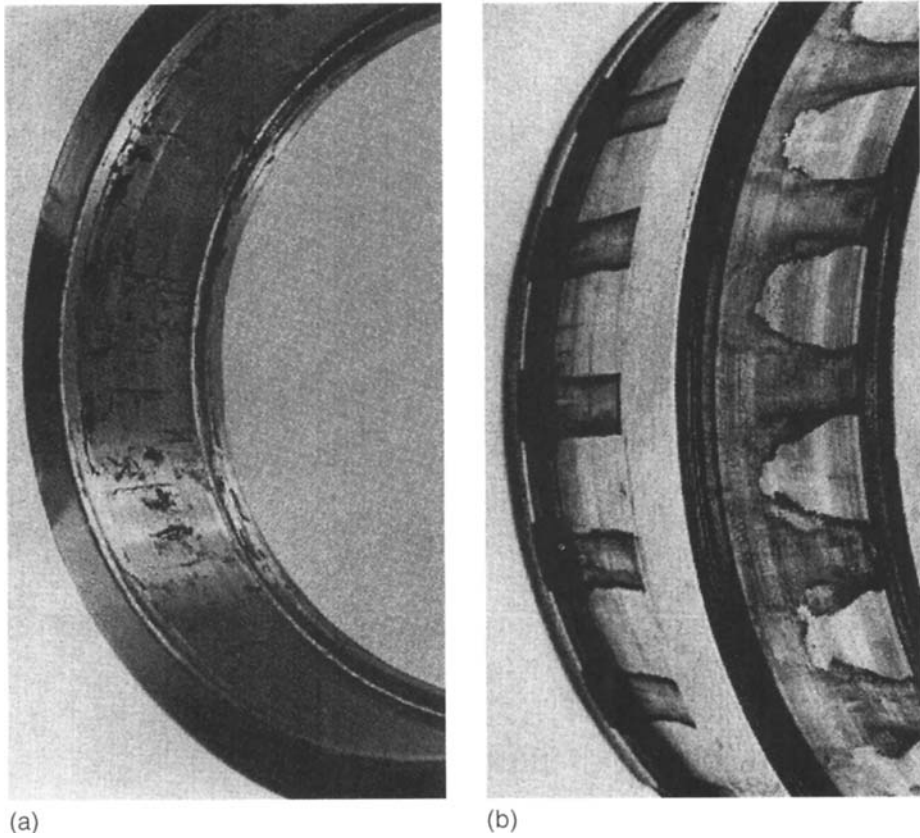


Figure 2.92 (a,b) Oxide caused by roller bearing corrosion.

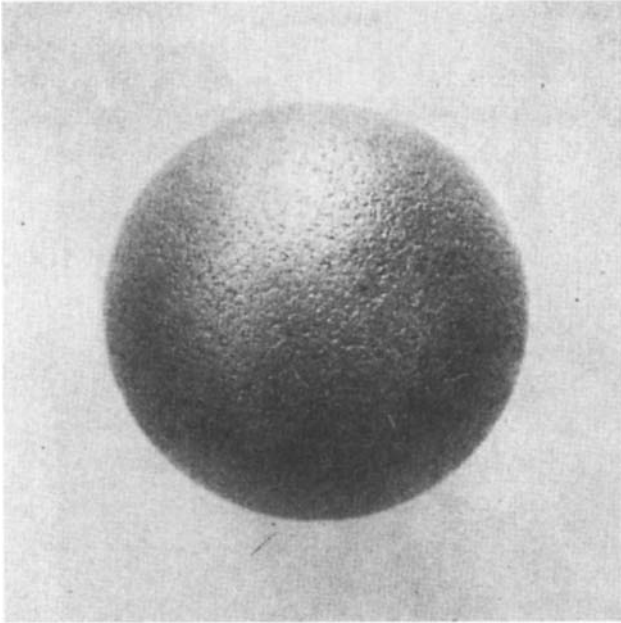


Figure 2.93 Surface of a ball exposed to humidity and acid.

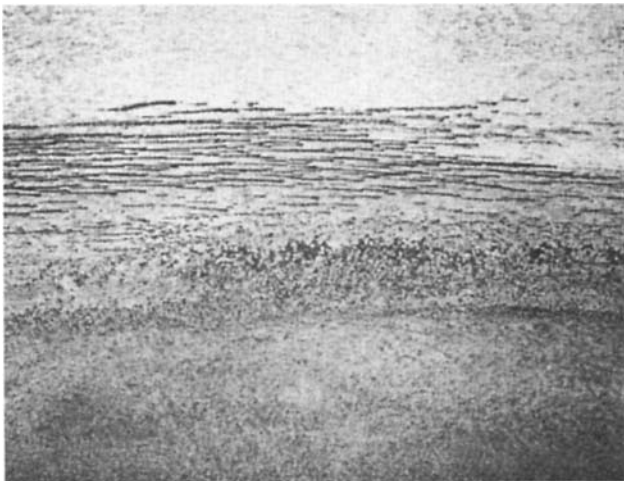


Figure 2.94 Corrosive wear on a raceway surface caused by humidity.

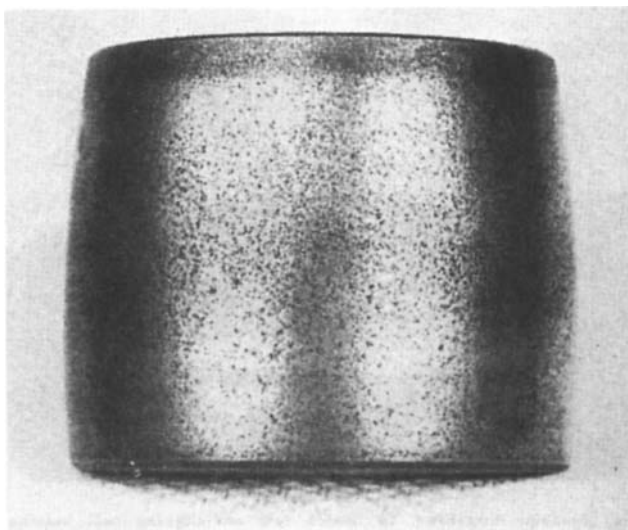


Figure 2.95 Corrosive damage of rolling elements.

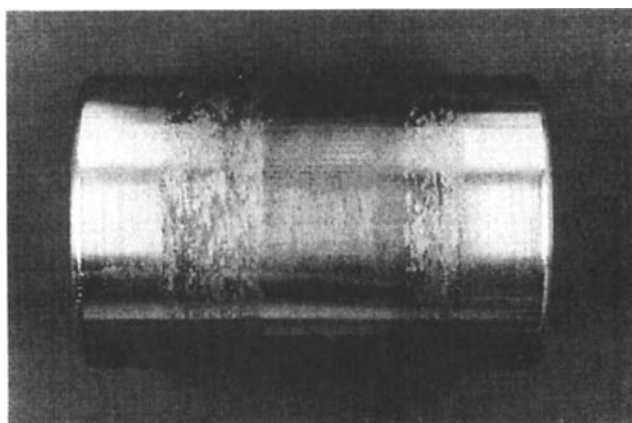


Figure 2.96 Damage caused by particle contamination in the lubricant.

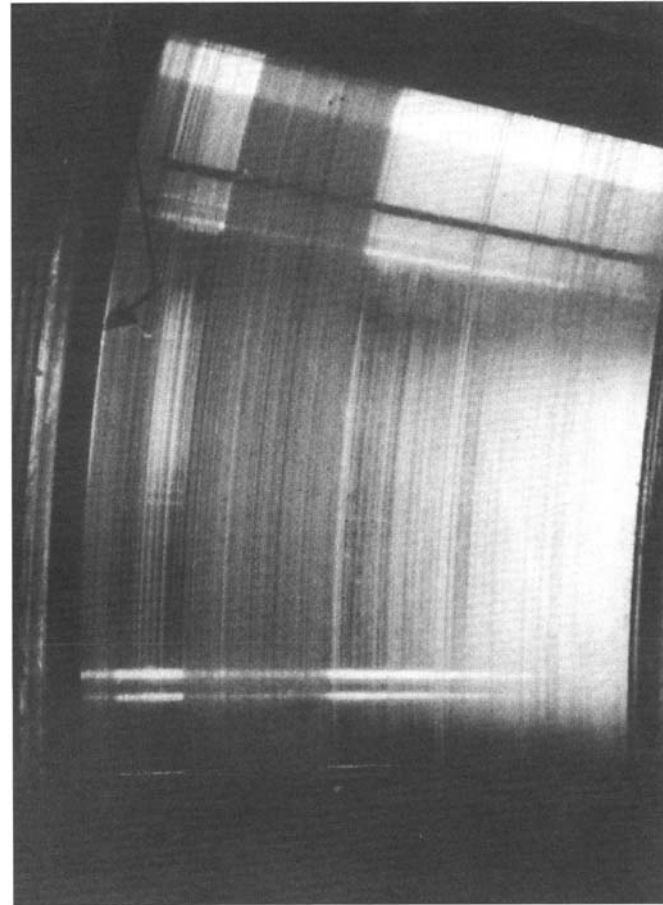
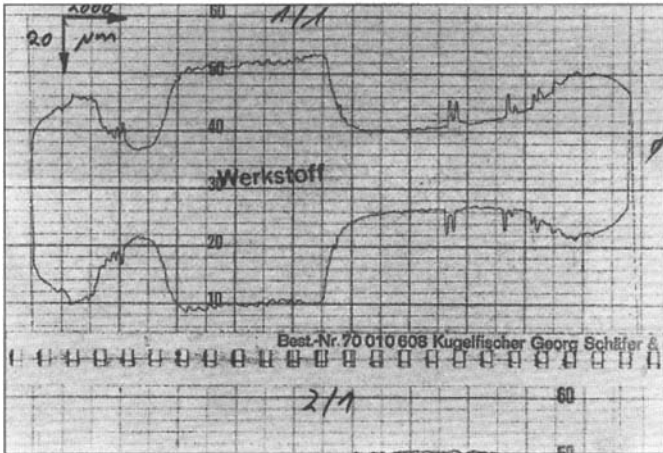
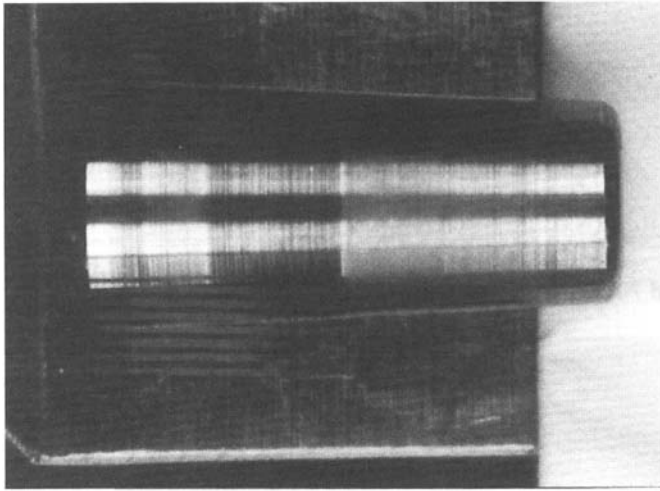


Figure 2.97 Further damage caused by particle contamination.

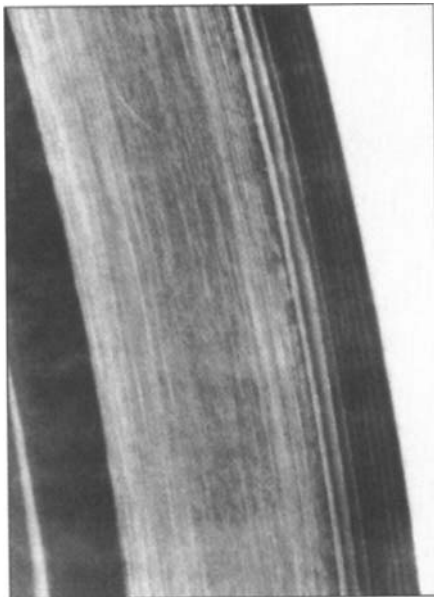


Figure 2.98 Outer ring damage caused by particle contamination.

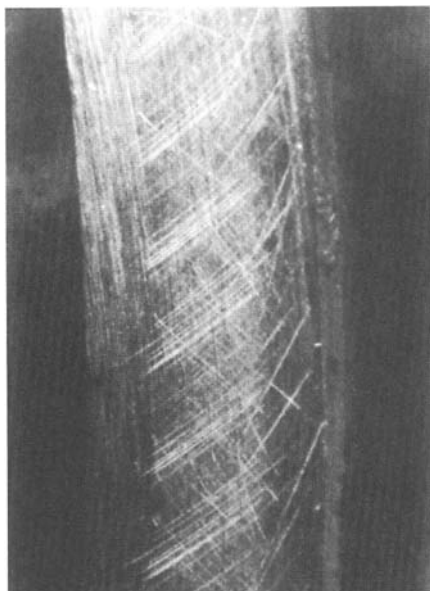


Figure 2.99 Damage to roller's sides caused by hard particles in the contact zone.

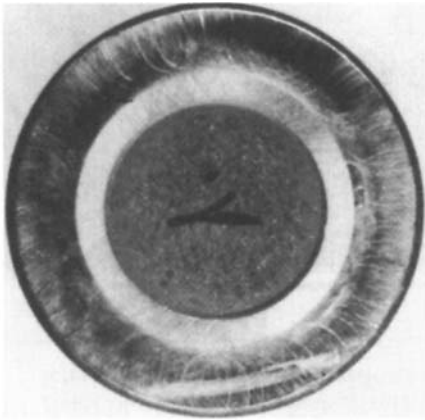


Figure 2.100 Side damage caused by abrasive wear.

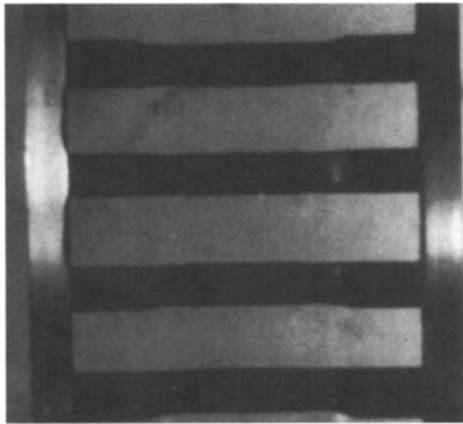


Figure 2.101 Tribological wear on auxiliary elements of rolling bearings.

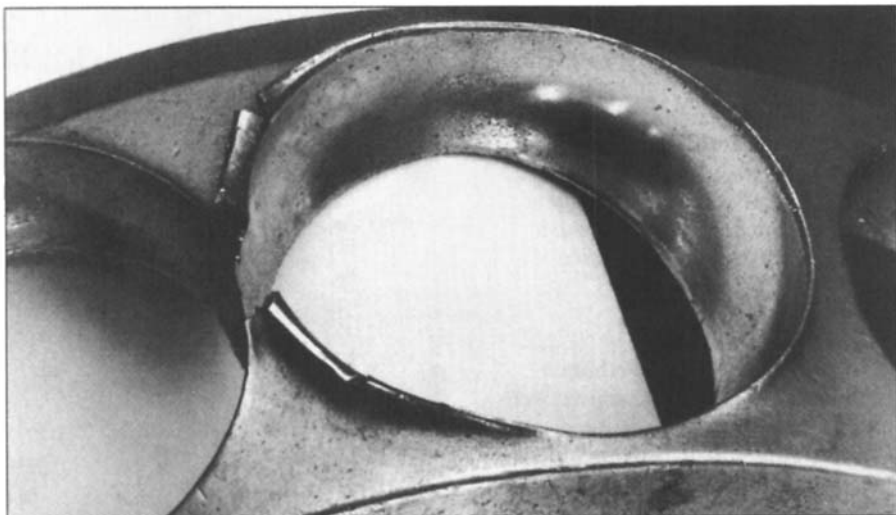


Figure 2.102 Cage damage caused by particle contamination.

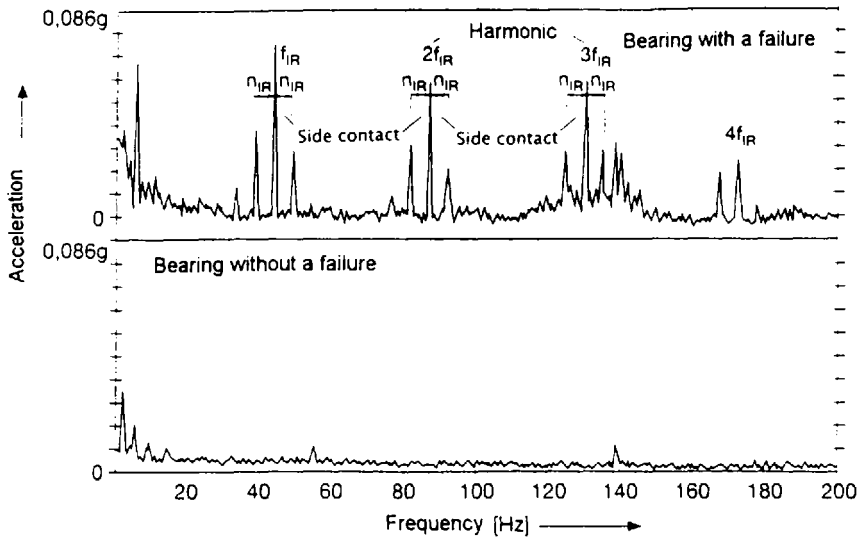


Figure 2.103 Frequency spectrum of damaged and undamaged rolling bearings.

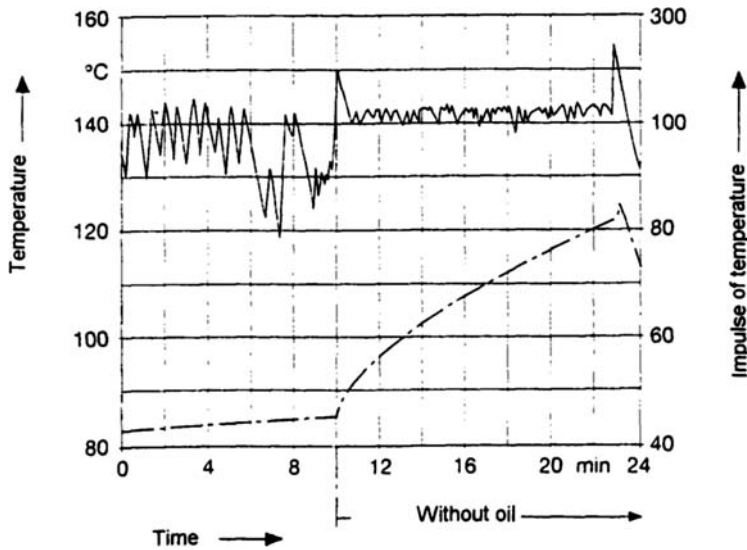


Figure 2.104 Recording of temperature variations with and without lubrication.

Damage caused by insufficient lubrication or lubricant loss may be readily detected by monitoring the bearings' operating temperature. Figure 2.104 [48] illustrates a recording of the temperature variations with and without lubrication.

REFERENCES

1. M. Hebde and A. B. Chechenadze, *Handbook of Tribotechnik, Mechanical Engineering*, 1989, VKL Warshave, Moscow.

2. J. Halling, *Principles of Tribology*, 1975, Macmilan, London.
3. FAG Kugelfischer, Publ.-Nr WL 00 200/4 DA.
4. INA, Examples of Use Rolling Bearings, by INA, 1996.
5. FAG Kugelfischer, Waelzlager, Katalog WL520/2 DB, Mai 1996, Schweinfurt.
6. INA, Katalog 306, by INA, 1995.
7. B. Ivkovich and A. Rac, *Tribology*, 1995, Yugoslavian Society of Tribology, Kragujevac.
8. I. V. Kragelsky and V. V. Alisina, *Friction Wear Lubrication, Handbook, Mechanical Engineering*, 1989, VKL Warshava, Moscow.
9. G. Lundberg and A. Palmgren, "Dynamic Capacity of Rolling Bearings," Acta Politechnica, Mechanical Engineering Series 2, Royal Swedish Academy of Engineering Sciences, No 3,7.
10. F. K. Shulz-Hausman and A. G. Leybold: Koeln, *Erfahrungen ueber Einsatz von Keramik-Kugellagern in Turbomolekular Pumpen*, 1992, VDI Tagung.
11. W. G. Keller, *Endbearbeitung Formqualitaet Einsatz*, 1992, Saphirwerk Industrieprodukte AG, CH Bruegg, VDI Tagung.
12. A. Sumacher, "Experimental Investigation of the Temperatures on Wear Behavior of Hybrid Bearings with Coated Races," 11th International Colloquium, Technische Akademie Esslingen, 1998.
13. R. Bietkowski, "Use of Fire Resistant Hydraulic Fluids," Colliery Guardian, 1971, May.
14. FAG Kugelfischer, *Forschung als Grundlage fuer Produkte der Zunkunft*, Publ. Nr. WL 40205 DA.
15. R. Tricot, "Influence des parametres metallurgiques sur les phenomenes de fatigue de contact enroulement glissements des roulements et engrenages," Rev. Met., 1976, 75(4).
16. F. T. Barwell and D. Scot, "Effect of Lubricant on Pitting Failure of Ball Bearings."
17. M. Wadewitz, "Ursachen der Ansmierungen in Waelz-Gleitkontakt," in *Konstruktionstechnik Maschinenelemente*, 1993, VDI Verlag.
18. R. E. Cantle, "The Effect of Water Lubricating Oil on Bearing Fatigue Life," Transl. ASLE, 1977, 20, 224–228.
19. H. V. Cordiano, E. P. Cochran, and R. J. Wolfe, "Effect of Combustion-Resistant Hydraulic Fluids on Ball-Bearing Fatigue Life."
20. D. Kolar, "Der Einfluss von Schmierstoffen auf Lebensdauer von Waelzlagern." *Smiierungstechnik*, 1983, 14(12).
21. W. E. Littman and R. L. Widner, "Propagation of Contact Fatigue from Surface and Subsurface Origins," Trans. ASME, 1966, September.
22. Y. Norio, O. Teruki, and S. Tokashi, "Improvement in Rolling Contact Fatigue Performance of Water–Glycol Hydraulic Fluids," Cosmo Research Institute, Japan.
23. F. G. Rounds, "Lubricant and Ball Steel Effects on Fatigue Life," ASME Paper 70-Lub-16.
24. J. Volkmuth, G. Whal, and F. Hengerer, "Auswirkungen der Abkuehlbedingungen beim Haeten auf die Mass- und Formaenderungen von Bauteilin, Htm 48, 1993.
25. H-K. Loroesh, "Research on Longer Life of Rolling Element Bearings," *Lubr. Eng.*, 1985, 41(1), pp. 37–45.
26. T. Loesche and M. Weingard, "Quantifying and Reducing the Effect of Contamination on Rolling Bearing Fatigue," International Off Life Highway & Powerplant Congress, Milwaukee, WI, 1995.
27. H. K. Loroesh, "The Life of the Rolling Bearing Under Varying Loads and Environmental Conditions," *Ball Roller Bearing Eng.*, 1981, 20.
28. Q. Li, M. Shima, T. Yamamoto, and J. Soto, "Thesis Study on Fretting Wear of Rolling Bearing," *Jpn. J Tribol.*, 1995, 40(12).
29. N. Kottrich and M. Albert, "Kontaktgeometrie und Leistung verougen der Waelzlager," *Machinewelt-Elektrotechn.*, 1984, 39(5).

30. B. Herkert, "Untersuchung ueber Verschleiss und Bewegungsverhalten Schnellaufender Waelzlager mit Hilfe von Radioisotopen, *Motortechn. Z.*, 1973, 33.
31. S. Cretu, G. Presaceru, I. Berecea, and N. Mitu, "The Effect of Rib Roller End Contact Geometry on Friction Torque in a Cylindrical Roller Bearings," 11th International Colloquium, Technische Akademie Esslingen, 1998.
32. S. Tanasijecivh, *Principles of Tribology Mechanical Parts*, 1989, Scientific Books, Belgrade.
33. T. Katsuya, "Rolling Elements Bearings," *Jpn. J. Tribol.*, 1996, 41(1).
34. A. Koichi, "Technology for Rolling Bearings Under High Speed Conditions," *Jpn. J. Tribol.*, 1992, 37(9).
35. R. M. Bransby, "Aerospace Bearing Life Rating Experience, Life Ratings for Modern Bearings," ASME/STLE Tribology Conference, San Francisco, 1996.
36. R. J. Parker and E. V. Zaretsky, "Rolling-Element Fatigue Lives of Troughhardened Bearings Materials," *Pap. ASME*, 1971, No 13.
37. A. Ohta and T. M. Johnst, "Medium Heat-Resistant Bearing Steel," International Off Life Highway & Powerplant Congress, Milwaukee, WI, 1995.
38. G. Totten, *Steel Heat Treatment Handbook*, Marcel Dekker, New York.
39. W. Hoering, "Hybridlager-Funktion und Einsatzmoeglichkeiten," 1992, VDI Tagung Keramische Waelzlagern, Duesseldorf.
40. SHM Werkstoffen Technologie, Pulversynthese, Aachen, VDI Tagung, 1992.
41. "Cerbear," Vollkeramiklager, Herzgenrath, VDI Tagung, 1992.
42. L. Chang, Jasson, and M. N. Webster, "A Study of Asperity Interaction in EHD Line Condition," *Tribol. Trans.*, 1993, 36.
43. D. Dowson and G. R. Higginson, *Elasto-Hydrodynamic Lubrication*, 1977, Pergamon Press Ltd., London.
44. P. H. Nixon and H. Zantopoulos, "Observation of the Impact of Lubricant Additives on Fatigue Life Performance of Tapered Roller Bearings," International Off Life Highway & Powerplant Congress, Milwaukee, WI, 1995.
45. L. Grunberg, D. T. Jamieson, and D. Scoot, "Hydrogen Penetration in Water-Accelerated Fatigue of Rolling Surface," *Phil Mag.*, 1993, 8(93).
46. H. V. Cordiano, E. P. Cochran, and R. J. Wolfe, "A Study of Combustion Resistant Hydraulic Fluids as Ball Bearing Lubricants," *Lubr. Eng.* 1956, July-August.
47. F. Munsch, "Schmierstoffe fuer Waelzlager," *Technische Miteilungen*, Munich, Oktober/November, 1986.
48. FAG Kugelfischer und Handel AG, Waelzlagerschaeden, Publ. Nr. WL 82 192/2 DA.
49. STLE, Interpreting Service Damage in Rolling Type Bearings, 1986.
50. SKF Waelzlagerschaeden und ihre Ursachen, Produktionformation 401, 1994.

BIBLIOGRAPHY

- Boehemer, H. J., *Einige grundlegende Betrachtung zur Waelzermuedug*, Forschung Grundlage fuer Produkte die Zunkuft, Publ. Nr. WL 40205 DA.
- Braendlein, K., "Reibung in Waelzlagern," *Antriebstechnik* 1979, 18(4).
- Carey, J. R., "The Practical Application of New Life Bearing Theory for the Design of Off-Highway Gearboxes," International Off Life Highway & Powerplant Congress, Milwaukee, WI, 1992.
- Danner, C. H., "Relating Lubricant Film Thickness to Contact Fatigue," Earthmoving Industry Conference, Peoria, IL, 1970.
- DIN ISO 281.
- Goldblatt, I. L., "Surface Fatigue Initiated By Fatty Acids," ASLE/ASME International Lubrication Conference, New York, 1972.

- Harris, T. D., "Load and Life Ratings for Modern Ball and Roller Bearings," ASME/STLE Tribology Conference, Orlando, FL, 1995.
- Harris T. D., and McCool, J. I., "On the Accuracy of Rolling Bearing Fatigue Life Prediction," ASME/STLE Tribology Conference, Orlando, FL, 1995.
- Hobbs, R. A., and Mullet, G. W., "Effects of Some Hydraulics Fluid Lubricants on the Fatigue Lives of Rolling Bearings," *Wear* 1996, 192, pp. 66–67.
- ISO 76 1987.
- Klainlein, E., *Schmierstoffe bei Mischreibung, Antriebstechnik*, 1991, 30(9).
- Kleinbreuer, W., *Verschleisserscheinungen an Fluegelzellenpumpen beim Einsatz von Schwerentflammbaren Druckfluessigkeiten, Oelhydraulik Pneumatik*, 1979, 23(2).
- Pearson, P. K., "Some Effects of Tensile Stressing on Rolling Contact Fatigue Initiation, International Off Highway & Powerplant Congress," 1996.
- Schatzberg, P., "Inhibition of Water-Accelerated Rolling-Contact Fatigue," ASME-ASLE Lubrication Conference, Cincinnati, OH, 1970.
- SKF, *Catalog 4000/IV T*, 1994.
- Timken, *Bearing Maintenance Manual for Transportation Applications*.
- Ventsel, E. S., Livada, G. F., and Ryaboshapka, V. M., "Study of Antifriction and Antiwear Properties of the Fire Resistant Hydraulic Fluid Promhydrol Treated with Hydrodynamic Dispersing Agent, *Trenie Friction Wear*, 1983, 4(4).

3

Fluid Cleanliness and Filtration

RICHARD K. TESSMANN

FES, Inc., Stillwater, Oklahoma

I. T. HONG

BarDyne, Inc., Stillwater, Oklahoma

1 INTRODUCTION

The life and reliability of all engineered systems has become of paramount importance. The cost of downtime and repair cannot be tolerated and therefore must be avoided or eliminated. Currently, the design life of most fluid systems is determined from a consideration of the stress levels to which the system components are subjected. Very little attention is given to the contamination level of the system fluid or to the tolerance that the system components exhibit to the presence of particulate contamination. Although fluid cleanliness and filtration are critical factors influencing the field life and reliability of hydraulic and lubrication systems, design engineers are without an adequate understanding of the nature of these parameters. The primary purpose of this chapter is to provide a broad understanding of the area that includes fluid cleanliness and filtration. This area is generally known as contamination control.

Contamination control is mandatory in maintaining the integrity of all power and motion systems. Without it, few, if any, systems could be expected to achieve their design goals, not to mention their expected field lives. Because fluid systems are the backbone of our industrial machinery, contamination control provides the keystone needed to achieve effective, reliable, and economical production of the necessities of our modern civilization. This critical technology is rapidly becoming accepted as an application science because its utilization is the key to the ultimate success of every engineered system.

Contamination control is a broad subject and applies to all types of engineered systems. It covers the planning, organizing, managing, and implementing of all aspects to determine and achieve a reasonable field life resulting from the presence of

contamination entrained in the system fluid. Some authors define contamination as any unwanted influence that can destroy the integrity of a system by causing an imbalance between the tolerance level of the system components and the contamination level of the system fluid. However, this definition is far too broad for adequate coverage in this chapter. Therefore, particulate contamination will be given primary consideration here. The more specific areas that comprise the contamination control technology can be summarized as follows:

1. **Identification:** This area includes the recognition and description of the various contaminants.
2. **Analysis:** This area includes the characterization and quantification of the contaminants.
3. **Exclusion:** This area includes the prevention of contamination from entering the circulating fluid of a hydraulic or lubrication system.
4. **Filtration:** This area includes the capture and retention of particulate contaminants that have already become entrained in the system fluid.
5. **Component tolerance:** This area includes the evaluation and improvement in the capability of a component to resist the attack of particulate contaminants.

The preceding summary should quickly lead the reader to the following axiom of the contamination control technology:

Any particulate contamination must be prevented from entering the fluid system. If we fail to accomplish the exclusion task, we must provide a method to remove that contamination which becomes entrained. If we fail at both of these tasks, then the component must be able to live for a sufficient length of time with the resulting contamination level.

2 PARTICULATE CONTAMINANT

Particulate contamination is discrete portions of material which exist as minute particles. Particulate contamination is very serious to all surfaces in relative motion within a system component as well as the integrity of the system fluid. Particulate contaminants found in operating fluid system come in all sizes and shapes and are normally described by their physical properties, structures, size, and size distribution. Of primary concern here, however, is where these contaminant particles normally come from and what effect they have on a fluid system.

2.1 Sources of Particulate Contamination

Particulate contaminants can enter the system fluid in one of three primary ways:

1. **Built-in contaminant**
2. **Ingressed contaminant**
3. **Generated contaminant**

A built-in contaminant is that contamination which is placed in the confines of the system during the fabrication process. For example, many times, oil rags are used to wipe off surfaces and hands. Lint and fibers associated with the rags themselves have often been found in the hydraulic and lubrication systems. Most of the time,

the reservoir used to store the excess oil of a fluid system is fabricated using a weldment. The process of welding the various seams of the reservoir will create slag and metal particles. These particles will become built-in contamination if some corrective action is not used.

Ingressed contamination is that material which enters the system fluid from the environment. Most fluid systems operate in a very dirty environment such as that encountered when dust is carried by the wind. The environmental dust and water, for that matter, will surround the system and can be sucked into the system during operation. The amount of particulate contamination entrained in the air surrounding a fluid system is illustrated in Fig. 3.1.

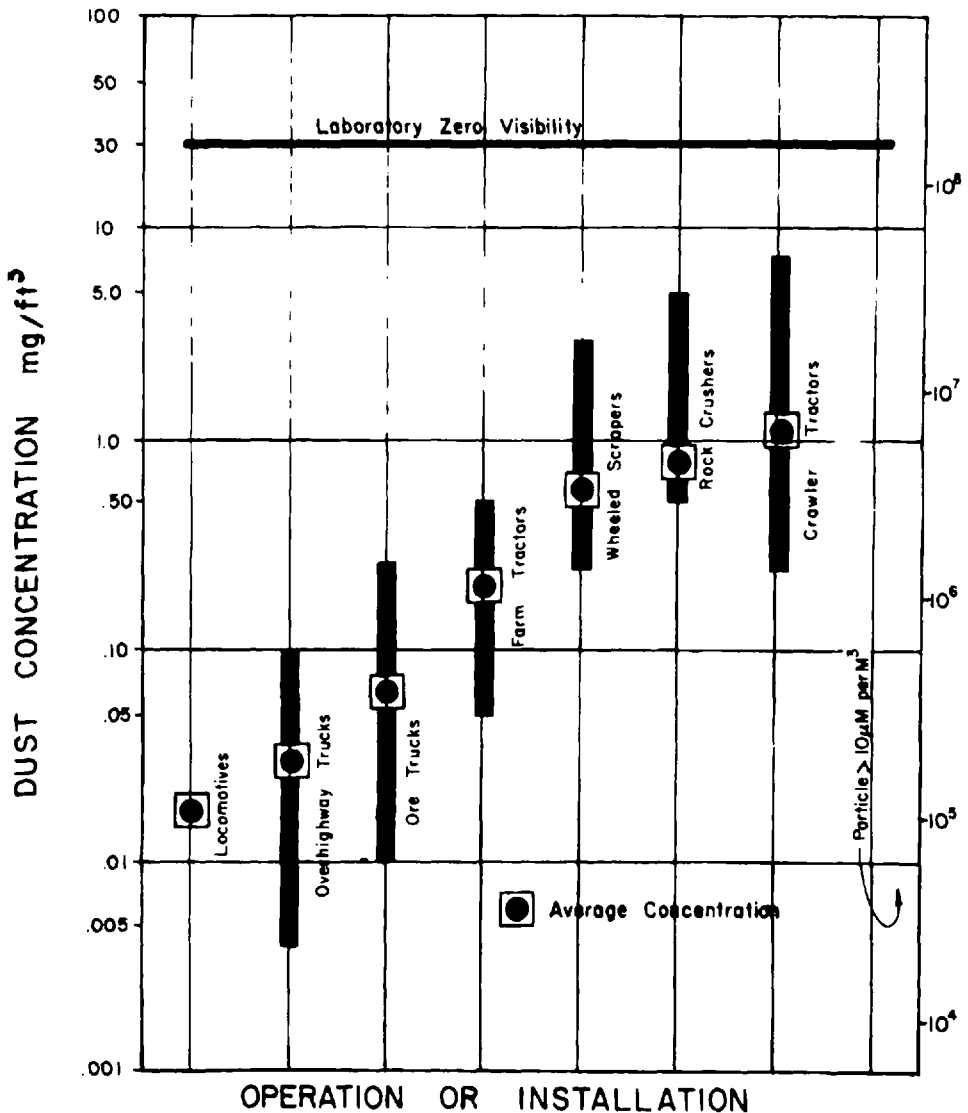


Figure 3.1 Concentration of environmental particulates.

As can be seen in Fig. 3.1, the concentration of dust particles in the air can be very high, especially when the surface is disturbed by the movement of a vehicle. The average dust concentration surrounding an over-the-highway truck is approximately 0.04 mg/ft^3 , whereas that of a crawler tractor operating in a earth-moving capacity is about 1.0 mg/ft^3 . The fluid systems will breathe (discharge air and suck in air) as they heat up and cool off. In addition, hydraulic systems breathe environment air when double-acting cylinders with single rods are operated; that is, the volume of fluid on one side of such a cylinder is larger than the other side owing to the area of the rod. When the double-acting, single-rod cylinder is extended, more fluid must enter the cylinder from the reservoir than will be returned to the reservoir by the rod end of the cylinder. Therefore, the volume of fluid in the reservoir will decrease. This decrease in volume will either create a vacuum in the reservoir or air must be drawn in to make up the volume. If the air is not properly filtered as it enters the reservoir, a large number of dust particles will ingress along with the air. These dust particles will become entrained in the circulating fluid, raising the contamination level of the fluid.

Generated contamination is caused by particles which are created when surfaces in relative motion wear. The wearing process will create wear debris in the form of particles composed of the materials comprising the surfaces in relative motion. There are many mechanisms and processes by which contamination can be generated within a fluid system and there are a great number of surfaces on which these mechanisms can occur. However, it would appear that this type of contaminant stems from one or more of the following:

1. Erosion
2. Cavitation
3. Fretting
4. Scoring
5. Broaching
6. Lapping
7. Abrasion
8. Corrosion
9. Oxidation
10. Others

Not to be overlooked is the contamination generated when the hydraulic fluid is doing double duty by acting as a general-purpose lubricant for gear trains, clutches, and other mechanical parts.

2.2 Effect of Contamination

The primary effect of particulate contamination is to accelerate the destruction of working surfaces in relative motion. However, contaminant particles can also become lodged in the clearances between moving parts and impede their movement or perhaps prevent the motion completely. The destruction of working surfaces by the influence of contaminant particles is called three-body abrasion as a process, and contaminant wear as a result; that is, scientists who study the various wear mechanisms usually call it surface destruction when contaminant particles are present in three-body abrasion. However, to the user of a fluid system, the only thing he is

aware of is the loss of performance of the system and the components. Therefore, contaminant wear is measured in terms of performance degradation and not in terms of dimensional changes as surfaces are destroyed. It has been estimated that up to 70% of the failures of fluid systems are effected by the presence of particulate contamination.

Motion failures resulting from entrained particles are commonly referred to as contaminant lock or particulate lock. Such a lock, or jam as it is sometimes called, can impeded the movement of internal parts or the flow of fluids; that is, contaminant particles can become wedged tightly between surfaces, preventing any relative motion, or they can accumulate in an annular space or orifice until the clearance or orifice area is completely blocked, preventing fluid flow. One situation encountered in some cases occurs when small particles accumulate in the clearance space between a spool and bore of a valve. These small particles can amass in sufficient numbers to fill at least part of the clearance space. When this happens, the spool will become stuck in the bore and the valve will cease to function. This phenomenon is called silting or silt lock because it is caused by silt-sized particles.

The degradation of system or component performance resulting from particulate contamination is generally called contaminant wear. There can be no doubt that the presence of contaminant particles will cause the destruction of internal surfaces within fluid components. Furthermore, this surface destruction is accompanied by a dimensional change in the surfaces. However, the performance of the component cannot be reliably predicted from knowledge of the dimensional changes to internal parts of the component. Therefore, many researchers and engineers utilize the concept of contaminant wear in estimating the deleterious effect of contamination. The degradation in performance of a fluid component as a function of particulate contamination is found by conducting a contaminant sensitivity test. In the evaluation, the component is subjected to various contamination environments and the degradation in performance is measured. More will be presented on contaminant sensitivity analysis later in this chapter.

2.3 Particle Size and Shape

The particles that become entrained in a fluid system are irregularly shaped. We need to be sure to understand that they are seldom, if ever, round. However, when scientists and engineers talk of contaminant particles, their size is usually described as so many micrometers in diameter. Of course this is not correct. Only a spherical particle can be correctly described by one dimension. In fact, particulate contaminants are normally measured by using their longest dimension, as shown in Fig. 3.2. Many times, this causes very large problems because many of the particle-sizing instruments in use today actually measure the projected diameter. It can be seen in Fig. 3.2 that there can be a large difference between the largest or longest dimension and the projected diameter. In order for particle-sizing technology to be placed on a common footing, automatic particle counters are normally calibrated to produce size dimensions relative to the longest dimension.

The shape of the particles making up the contaminants in a fluid system can only be described as irregular. Although contaminant particles exhibit features which reflect their origin, generating factors, and exposure, most attempts to quantify particulate contaminants according to some shape feature have not been successful. The

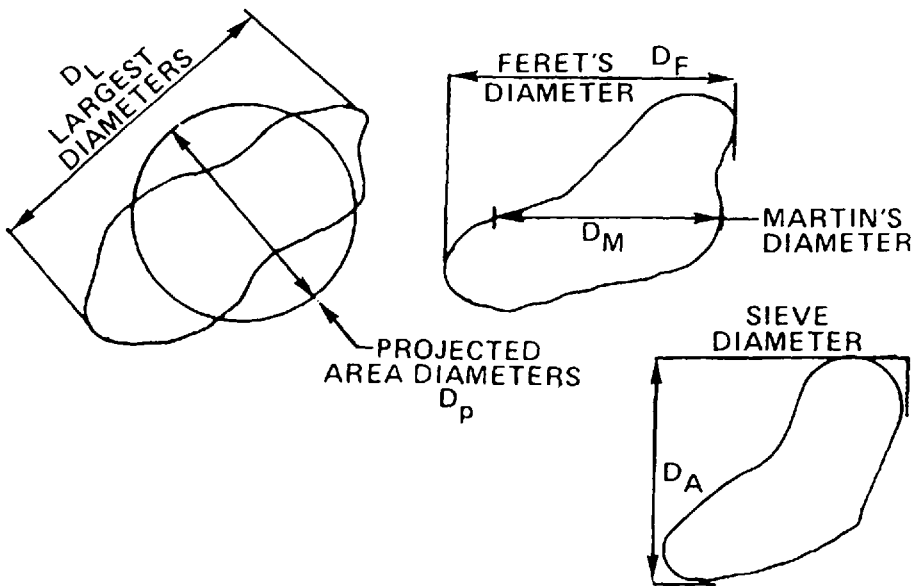


Figure 3.2 Particle size description.

one parameter that has offered some assistance in the contamination control technology is the shape factor, which utilizes one dimension to express the degree of irregularity of the particle. Shape factors are very significant in powder technology because the shape of particles influences their interaction with fluids, packing and entrainability among other things. In contamination control, particle shape can cause gross errors in size measurement. Hence, a shape factor must be taken into consideration to make statistical averaging independent of measurement.

From a contamination control standpoint, shape factors have at least three functions:

1. Conversion values for expressing actual particle size in terms of some equivalent size
2. Proportionality factors for particle size analysis
3. Transformation factors to express such terms as particle surface area, weight, and volume

The use of the longest dimension to describe the size of an irregularly shaped particle, even though it is imprecise, is common. Four well-known shape factors employed in this context are as follows:

- **Sphericity:** defined as the ratio of the surface area of a sphere having the same volume as the particle to its actual area
- **Circularity:** defined as the ratio of the perimeter of a circle having the same projected area as the particle to its actual perimeter
- **Flakiness:** defined as the ratio of breadth of the particle to its thickness
- **Elongation:** defined as the ratio of the length of the particle to its width

In most cases, the techniques for quantifying particle shape leave a lot to be desired. The necessary dimensions or values are difficult to obtain for an individual particle: for example, in order to determine the elongation factor, the length and width of a particle must both be measured.

Table 3.1 illustrates the average dimensions for some of the more common contaminant particles. As can be seen from this table, the diameter of a circle that has the same projected area as the contaminant particle is significantly less than the longest dimension of the actual particle. For comparison purposes, the circularity factor is shown in Table 3.1. The particle was considered rectangular in order to determine the actual particle perimeter. Because the width of the particles listed in Table 3.1 was normalized to 1, the elongation factor and the longest dimension are the same.

2.4 Test Contaminants

The contamination control technology relies heavily on the use of test contaminants, such as contaminants for calibrating particle-counting equipment, for evaluating filtration performance, and for measuring the contaminant sensitivity of system components. In order to produce test data which can be used for product development, performance comparison, and database type of analysis, it is very important that the contaminant used to generate the data is as consistent as possible.

For many years, the standard contaminant in the contamination control area was Air Cleaner Test Dust. This test dust was produced by the General Motors Corporation from the 1930s until very recently. At this point in time, General Motors is no longer producing test contaminants, but a replacement has not been agreed on by the various standards making bodies. Because Air Cleaner Test Dust was widely used in the past and a great deal of data being used today was generated using this standard contaminant, some description is needed here. In addition, some of the procedures, such as the particle-counter calibration procedure, still use AC Fine Test Dust from protected reserves.

Air Cleaner Test Dust was produced from natural Arizona road dust by the GM Phoenix Laboratory. From the raw dust, two grades or distributions of test contaminants were processed—AC Fine Test Dust (ACFTD) and AC Coarse Test Dust (ACCTD). The weight distributions of these two test contaminants is given in Table 3.2. It should be obvious from Table 3.2 that the difference between ACFTD and ACCTD can produce a significant variation in test data. The ACFTD is currently the basis of calibration procedures for Automatic Particle Counters as given by ISO 4402 international standard. The particle size distribution for ACFTD as shown in ISO 4402 is given in Table 3.3. This distribution is the “official” calibration contaminant currently used for automatic particle counters. Because this test dust is no longer in production, the supply will be exhausted at some point in the future. It is envisioned that a new “standard” test dust will be approved before that occurs.

Since General Motors has stopped production of Air Cleaner Test Dust, there are various other test contaminants currently available. These test dusts include silica-based material, spherical iron particles, iron oxide, pyron powders, various abrasives, aluminum oxide, and latex particles. However, care must be exercised when using these contaminants if it is necessary to compare test results with those obtained with other contaminants.

Table 3.1 Shape Factor Information for Environmental Contaminants

Particle identification	Relative Dimensions of Common Particles					
	Average width (<i>W</i>)	Average length (<i>L</i>)	Diameter of circle with projected area equal to $L \times W$	Perimeter of circle with projected area equal to $L \times W$	Circularity factor	Elongation factor
Limestone	1	1.95	1.58	4.96	0.84	1.95
AC Fine Test Dust	1	1.49	1.38	4.36	0.88	1.49
Aluminum oxide	1	1.48	1.37	4.30	0.87	1.48
Iron Powder	1	1.64	1.45	4.56	0.86	1.64
Quartz	1	1.65	1.45	4.56	0.86	1.65
Carborundum	1	1.65	1.45	4.56	0.86	1.65

Table 3.2 Weight Distribution of Air Cleaner Test Dust

Particle size increment	Fine grade	Coarse grade
0-5	39 ± 2%	12 ± 2%
5-10	18 ± 3%	12 ± 3%
10-20	16 ± 3%	14 ± 3%
20-40	18 ± 3%	23 ± 3%
40-80	9 ± 3%	30 ± 3%
80-200	—	9 ± 3%

Table 3.3 Particle Size Distribution of 1 mg/L Suspension of AC Fine Test Dust (per ISO 4402)

Diameter	No. part./mL > diameter	Diameter	No. part./mL > diameter	Diameter	No. part./mL > diameter	Diameter	No. part./mL > diameter
1.00	1751.943	26.00	11.758	51.00	1.1986	76.00	0.2534
2.00	1396.884	27.00	10.464	52.00	1.1151	77.00	0.2403
3.00	991.813	28.00	9.340	53.00	1.0386	78.00	0.2279
4.00	708.078	29.00	8.360	54.00	0.9682	79.00	0.2162
5.00	516.688	30.00	7.503	55.00	0.9035	80.00	0.2053
6.00	385.724	31.00	6.751	56.00	0.8439	81.00	0.1950
7.00	293.984	32.00	6.089	57.00	0.7890	82.00	0.1853
8.00	228.183	33.00	5.504	58.00	0.7383	83.00	0.1762
9.00	179.953	34.00	4.986	59.00	0.6914	84.00	0.1676
10.00	143.913	35.00	4.526	60.00	0.6481	85.00	0.1595
11.00	116.515	36.00	4.117	61.00	0.6079	86.00	0.1519
12.00	95.369	37.00	3.751	62.00	0.5707	87.00	0.1447
13.00	78.823	38.00	3.425	63.00	0.5362	88.00	0.1379
14.00	65.721	39.00	3.132	64.00	0.5042	89.00	0.1315
15.00	55.230	40.00	2.869	65.00	0.4744	90.00	0.1254
16.00	46.748	41.00	2.632	66.00	0.4467	91.00	0.1196
17.00	39.828	42.00	2.418	67.00	0.4209	92.00	0.1142
18.00	34.136	43.00	2.225	68.00	0.3968	93.00	0.1090
19.00	29.419	44.00	2.051	69.00	0.3744	94.00	0.1042
20.00	25.483	45.00	1.892	70.00	0.3535	95.00	0.0995
21.00	22.178	46.00	1.748	71.00	0.3339	96.00	0.0952
22.00	19.386	47.00	1.617	72.00	0.3156	97.00	0.0910
23.00	17.015	48.00	1.498	73.00	0.2985	98.00	0.0871
24.00	14.990	49.00	1.389	74.00	0.2825	99.00	0.0833
25.00	13.254	50.00	1.290	75.00	0.2675	100.00	0.0798

3 CONTAMINANT MEASUREMENTS

The measurement of particulate contamination entrained in a liquid is an important aspect of contamination control technology. The accuracy and credibility of particulate contaminant analysis depends on the controlling external influence, using proper methodology to collect samples, preparing samples correctly, and using accurate analysis methods.

3.1 Particle Size Distribution

From a contamination control standpoint, a particle size distribution is basically a statistical description of the particulate matter entrained in a liquid. Normally, it is given in terms of a plot of the number of particles per milliliter of liquid, whose longest dimension is greater than the size indicated on the abscissa versus the longest dimension. Particle size distributions found in operating hydraulic and lubrication systems are usually skewed and exhibit a log-normal form. Undoubtedly, the most familiar distribution function in general is the Gaussian or normal distribution, which exhibits a bell-shaped curve. However, contaminants found in operating systems seldom, if ever, exhibit the Normal or bell-shaped curve. A comparison of the log-normal and the normal distributions is shown in Fig. 3.3.

In contamination control, the cumulative particle size distribution is used almost universally. The exclusively used model for the cumulative particle size distribution is the log-normal model, which is commonly plotted on a graph where the vertical axis is to a log scale and the horizontal axis is log squared. This is normally referred to as the log-log squared graph or the Cole chart for the individual who first

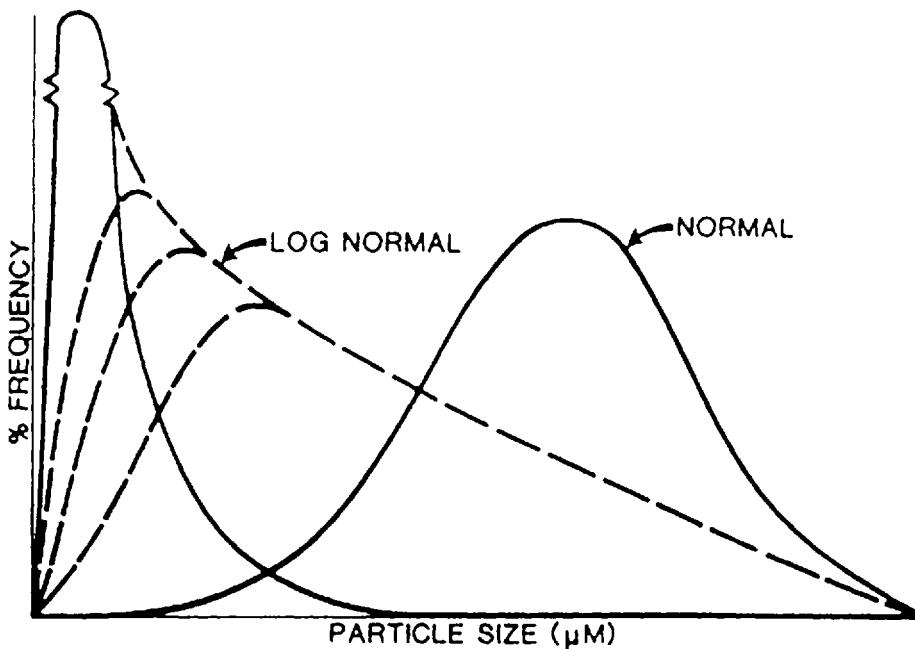


Figure 3.3 Comparison of normal and log-normal particle size distribution.

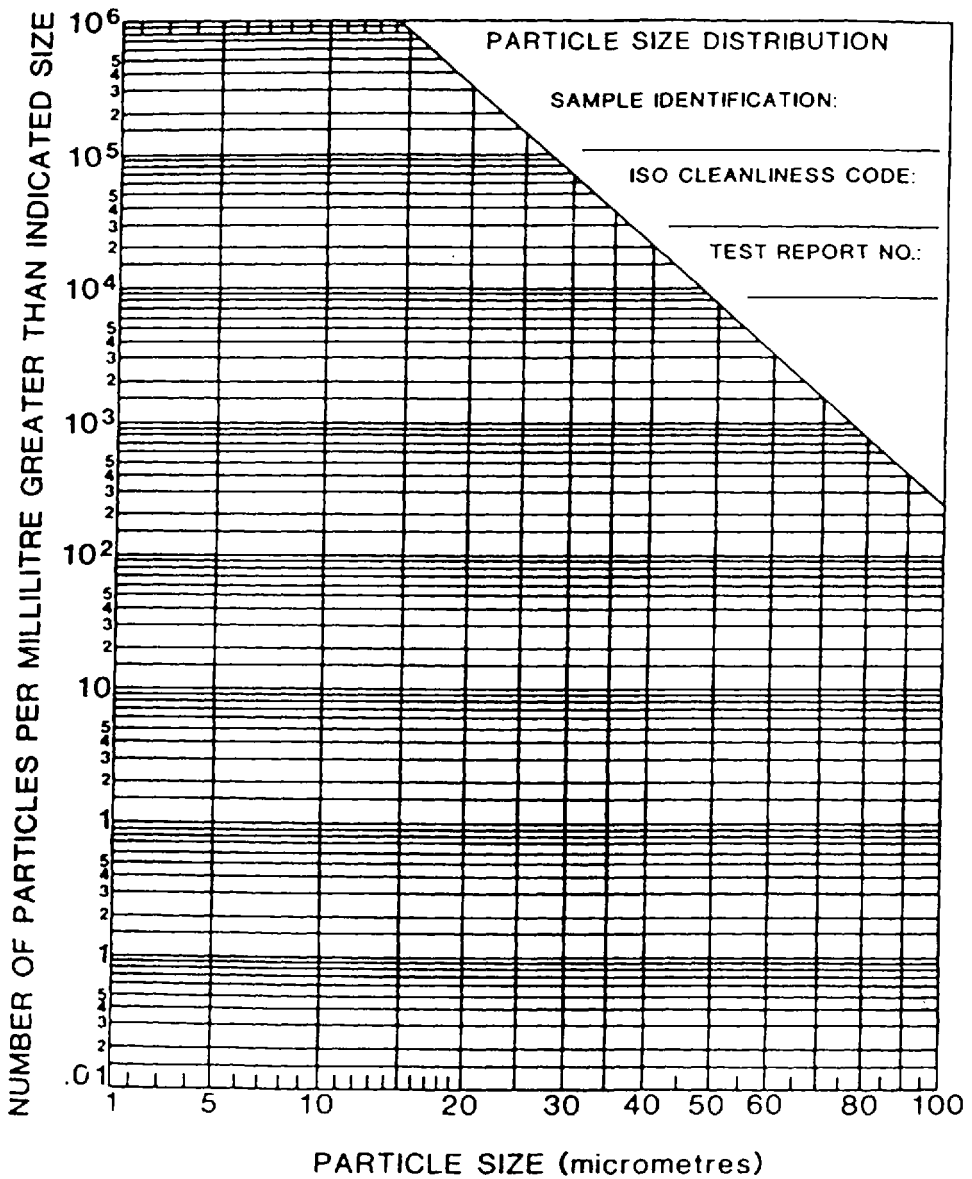


Figure 3.4 Log-log squared graph.

suggested the log-log squared model. Such a graph is shown in Fig. 3.4. The Cole chart is widely used for plotting cumulative particle size data in the contamination control technology.

3.2 Fluid Sampling Versus In-Line Analysis

In order to perform a contaminant analysis on the fluid of an operating system, it is necessary to evaluate the fluid itself. This means that either a representative sample

of the system fluid must be extracted from the system or the analysis must be made in-line. In either case, care must be taken to ensure that the fluid being sampled is indeed representative of that circulating in the system. In addition, it must be free of entrained air and water. Because of current limitations of the particle-counting equipment, in-line particle size analysis is normally confined to the laboratory. Therefore, field-type contaminant analysis relies on the extraction of fluid samples that can later be analyzed. Although several different analyses can be performed on a fluid sample, only particulate analysis will be considered here.

3.3 Sampling Hydraulic and Lubrication Systems

The credibility of particulate contaminant analysis depends on eliminating several aspects of the process. First, the extraction method has to eliminate the possibility of obtaining a nonrepresentative sample. In addition, the sample fluid must be collected in a clean sample container to prevent adding extra particles to the fluid. Another aspect involves the handling and preparation of samples prior to analysis. The final factor which can seriously affect the particulate contaminant analysis is the calibration of the particle-counting equipment.

3.3.1 Sample Container Cleanliness

The cleanliness level of sample containers, any processing fluid used in analysis, and the surfaces of the analysis equipment are all critical influences which will affect the validity of particulate contaminant analysis. The manner of cleaning the containers is not nearly as important as having complete confidence in the fact that they are indeed clean. The use of new bottles as fluid sample containers does not necessarily imply that there is little or no particulate contamination in the bottle. Even bottles described as surgically clean are not free of particulate contaminants. The term "surgically clean" means that there are no live microorganisms in the container; it does not mean that there are no particles. It must be kept in mind that particles which have a longest dimension of less than 40 μm cannot be seen with the naked eye. Therefore, the fact that there are not particles visible does not mean that the sample container is clean enough to be used for sampling purposes.

The effectiveness of a cleaning process used on any component depends not only on separating and dislodging particulate material but also on the cleanliness level of the rinsing fluid. Research has demonstrated that, under normal conditions, an ultrasonic bath with a power rating of at least 10 W/in.² of bath area is adequate to dislodge foreign material from most surfaces. In addition, the ultrasonic action will be more effective when detergents are added to the bath fluid. Detergents also provide a benefit in removing oil films that may be on the surfaces to be cleaned.

3.3.2 Sample Container Cleanliness Evaluation

The cleanliness level of a sample container must be evaluated by placing a superclean fluid in the container, vigorously agitating the container with the superclean fluid in it, and then determining the particle size distribution of the resulting fluid. It should be obvious that the evaluation of the sample is influenced not only by the matter remaining in the container after it has been processed through the cleaning procedure, but also on the cleanliness level of the superclean fluid and the accuracy of the counting technique used. Experiments have shown that it is practical to provide

superclean fluid that has a cleanliness level of less than one particle per milliliter greater than 5 μm. The operation and calibration of automatic particle counters are the subject of ISO Standard 4402, which will be discussed later in this chapter.

The qualification and control of the sample container cleaning method is established by ISO Standard 3722. The standard ignores the cleaning technique and concentrates on the ability of the procedure to produce clean or superclean sample containers. The flowchart shown in Fig. 3.5 illustrates the various aspects of the ISO qualification procedure. The procedure assumes that if a sufficient number of consecutive clean sample containers are produced by a given cleaning process and all of them meet a specified cleanliness level, then there is a high level of confidence that the process will continue to produce an acceptable container. The standard also relies on the premise that if samples from an outgoing stream of sample containers are selected at random, any failure to meet the acceptable cleanliness requirement will most likely reflect a change in the process which must be rectified.

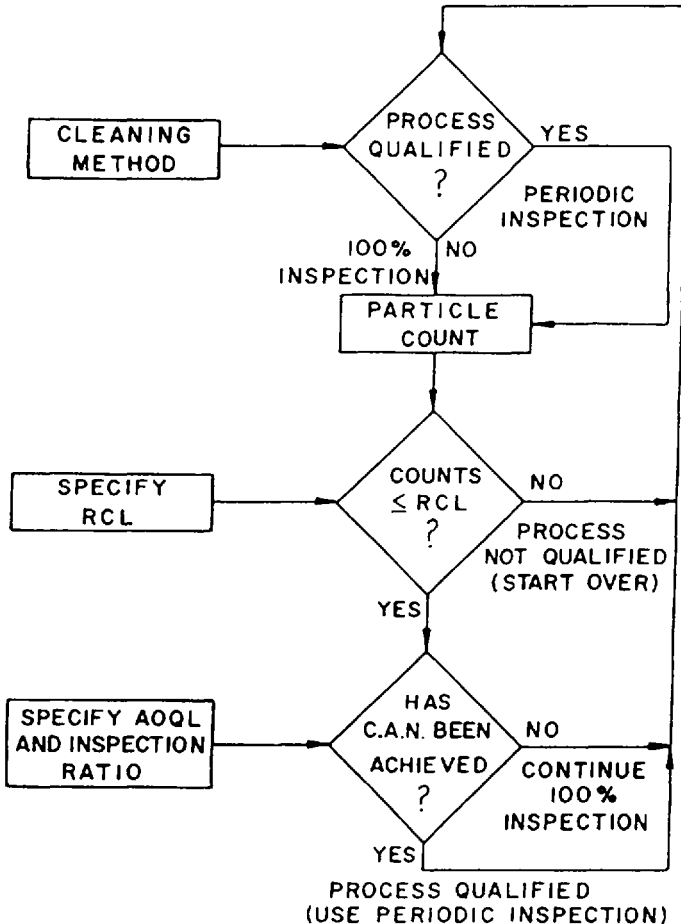


Figure 3.5 ISO sample container cleanliness qualification flow chart.

The flowchart indicates that 100% of the sample containers must be inspected until the cleaning procedure is qualified. Periodic inspection is permitted after the procedure is qualified. Because the cleanliness level of the sample container should depend on the contamination level of the fluid to be placed in the container, the Required Cleanliness Level (RCL) should be selected such that it is at least two orders of magnitude less than the anticipated fluid contamination level. In this manner, very little analysis error will occur because of the cleanliness of the sample container. There are two terms shown in Fig. 3.5 which need to be defined. However, an understanding of the ISO standard is not intended here. One term is Average Outgoing Quality Level (AOQL), which is an estimate of the percentage of containers that may not meet the criterion. For example, an AOQL of 1% suggests that there may be as many as 1% of the sample containers processed may not meet the cleanliness criterion. The second term is CAN, which stands for Consecutive Acceptance Number. This is the number of sample containers produced consecutively that must meet or exceed the cleanliness requirement before the cleaning process is qualified.

3.3.3 Sample Extraction

Fluid sampling can create a major source of error in particulate contaminant analysis. A great deal of effort has been expended in recent years to elevate sampling from an art to a science. The use of a sampling method that does not provide a representative sample for the system being evaluated can yield misleading and possibly dangerous results. There are two types of procedure for extracting useful samples—the static sampling method and the dynamic sampling technique. Static sampling, as the name suggests, draws fluid from a system at rest or when it is not operating. This method has the advantage of being easy to use; however, the fluid in a static system tends to develop a concentration and particle size gradient. Therefore, samples extracted at the high point in the system will exhibit a different contaminant analysis than a sample taken from a low point in a static system.

Dynamic sampling is far more prevalent in actual practice than static sampling. Dynamic samples are taken from the system while it is in operation. The basic types of dynamic sampling are laminar- and turbulent-flow sampling. The interest in laminar-flow sampling originated from sedimentation studies in open channels and has little value for particulate contaminant analysis. This can be more easily understood when it is realized that closed-conduit fluid systems, such as hydraulic and lubrication systems, seldom, if ever, operate in true laminar-flow conditions.

Turbulent-flow sampling is the optimal means of obtaining representative samples from a fluid system. As the name implies, a violent mixing action occurs across the full cross section of the conduit in a turbulent section of a hydraulic or lubrication system, which ensures uniform particulate distribution in the sampling field. The quality of a turbulent-flow sample does not depend on the sampling flow rate or the probe configuration, as long as the sample is extracted from a fully turbulent region of the system. ISO Standard 4021 is an accepted procedure for extracting samples from dynamic fluid lines. Figure 3.6 show an example of a generic sampling devise as called out in ISO 4021.

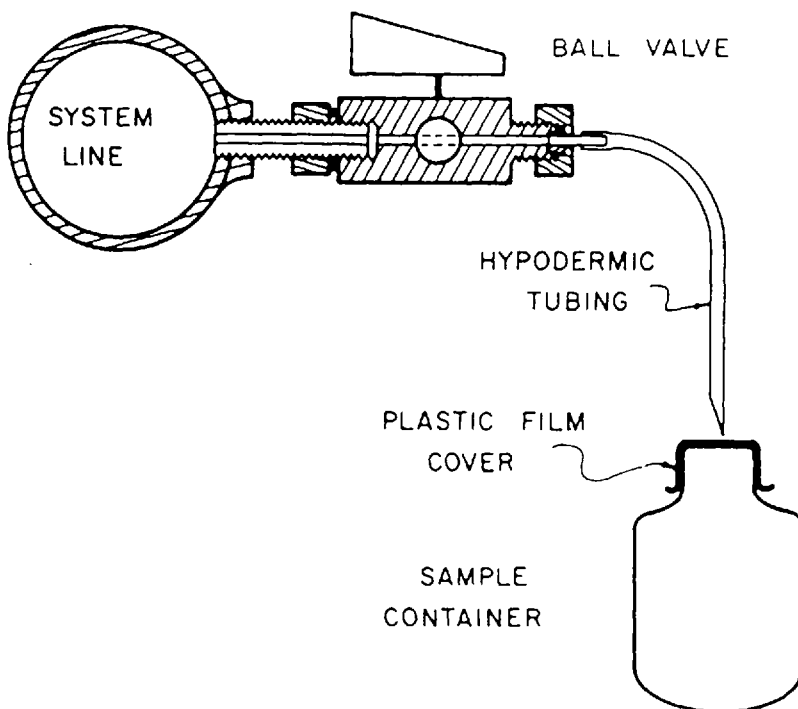


Figure 3.6 ISO turbulent-flow sampling method.

3.4 Sample Preparation

Because, many times, a sample may not be analyzed for several days after it is extracted, all samples should be prepared in such a manner that the settling which will occur when the sample remains inactive is eliminated. Therefore, sample preparation is concerned with the factors that can enhance the accuracy of the fluid analysis. Two of the primary factors which must be of special concern are particle dispersion and sample dilution.

3.4.1 Particle Dispersion

Most analysis methods require that particles be suspended and dispersed as discrete entities in the fluid so they can be assessed individually rather than as agglomerates. Poorly dispersed particles represent the largest single source of error in all size analysis methods that depend on the segregation of distinct particles. When agglomeration exists, particle size values are normally too large and the size distribution is too broad. Particles can usually be resuspended by violent agitation with a paint shaker for about 15 min, followed by a 30-s exposure in an ultrasonic bath. Sometimes, it is necessary to “heat soak” or apply heat to the sample before agitation. In every case, violent agitation with a paint shaker should precede the actual analysis procedure.

3.4.2 Sample Dilution

In all sizing and counting techniques, there is a limitation to the concentration of particles which can exist per unit volume of fluid without introducing a saturation error. This concentration limit can be avoided by diluting the sample prior to final preparation and analysis. If sample dilution is required, a minimum amount of dilution should be used to avoid unnecessary errors. Samples can be diluted in a single-step manner or serial dilution can be utilized. Single-step dilution, as the name implies, requires that the sample be diluted only one time. A serial dilution would repeat the dilution operation more than once to obtain the final dilution value. For example, if a sample is diluted 10 to 1 and then the resulting mixture is again diluted by 10 to 1, the final result is a dilution of 100 to 1 obtained in a series fashion.

When making dilutions, contaminated fluid should first be analyzed to determine an approximate dilution ratio. Then, clean dilution fluid should be used to flush the measuring equipment to ensure reliable subsequent measurements. Theoretically, the amount of dilution should make no difference as long as the counts decrease by the proper proportion. However, extreme care must be exercised when diluting highly concentrated samples because any measurement error is multiplied by the dilution factor. Dilute the sample until the particle count is just below the saturation limit of the counter. To check the reliability of a count, dilute further and recount the sample. The particle count should decrease by the same proportion as the dilution. If the counts do not decrease appropriately, further dilution is required. Once the proper dilution is reached, the original sample should be diluted using the one-step method to evaluate the errors made in the serial dilution. Either the one-step or the serial dilution technique is acceptable if executed with the proper amount of care.

3.5 Automatic Particle Counter Calibration

Without a doubt, automatic particle counters are the most widely used means of assessing fluid contamination levels in industry today. The success of these tools depend on the standards available with which to calibrate them. In the past, particle counter users depended on the counter manufacturers to calibrate and achieve repeatability. In the industry associated with hydraulic and lubrication systems, this ended with the adoption of ISO Standard 4402—a calibration procedure for automatic particle counters that use ACFTD as the calibration basis. The rationale for the calibration procedure is illustrated in Fig. 3.7. As can be seen from this flowchart, three items are needed:

1. AC Fine Test Dust
2. "Superclean" sample containers
3. An automatic particle counter with the manufacturer's operation manual

Two separate aspects are included in the calibration—a saturation procedure and a particle size calibration procedure.

The saturation procedure establishes the particle concentration level that the particle counter can accept without experiencing coincidence (two or more particles in the sensing zone simultaneously) or electronic timing problems. The counter is subjected to increasing concentrations levels until the count no longer increases lin-

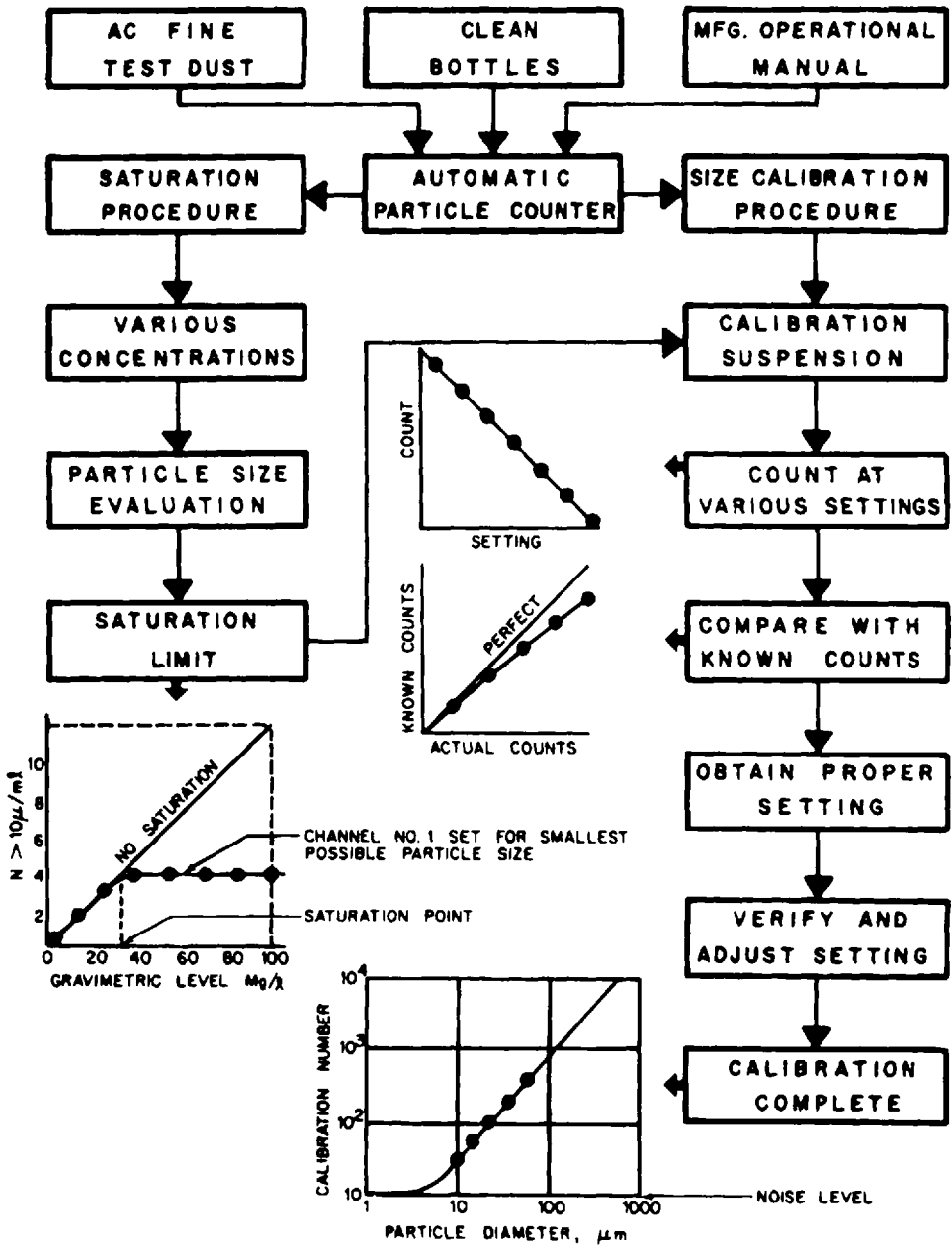


Figure 3.7 Automatic particle counter calibration flowchart.

early with the concentration. This concentration level is designated the saturation limit of the counter. The size calibration follows the saturation procedure and uses the established particle size distribution of ACFTD published in the standard. The counting threshold of the counter is adjusted until the resulting count agrees with the published particle count value.

3.6 Gravimetric Level Analysis

A second measurement method widely used in contamination control technology is the gravimetric analysis. The method was originally developed by the Society of Automotive Engineers (SAE/ARP-785) and is now ISO Standard 4405. In the technique, the analyst measures the dry weight of contaminant per unit volume of sample fluid. Then, the contamination level is reported in terms of milligrams of contaminant per liter of fluid. Particles are collected by filtering the sample fluid through two preweighed membranes placed one under the other. The top membrane retains the contaminant and the bottom membrane is for control purposes. After the sample has been filtered, the membranes are thoroughly rinsed with prefiltered solvent and the membranes are reweighed. The weight of the top membrane before and after filtering minus the weight change of the bottom membrane (the control membrane) represents the weight of the contaminant retained on the analysis or top membrane. The control membrane corrects the change in the membrane weight caused by such factors as the removal and/or absorption of plasticizers and other oil constituents.

Care must be exercised when interpreting gravimetric levels. It must be remembered that gravimetric levels do not relate to the particle size distribution of the system fluid. A gravimetric level composed of very small particles (silt-sized particles) will have an entirely different effect on the system components than the same gravimetric level composed of very large particles such as fatigue chunks and cutting wear debris.

3.7 Contaminant Cleanliness Levels

There are several ways of describing the cleanliness level of the fluid in hydraulic and lubrication systems. The cumulative particle size distribution and the gravimetric level are two examples of the various methods of expressing contaminant cleanliness levels. However, the most prevalent cleanliness levels callouts are those based on particle size distribution. In 1964, the National Aerospace Society adopted a cleanliness code which is still widely used today. Another cleanliness code was approved by the military in 1967 (MIL-STD-1246A) which essentially expanded the range of most of the existing codes. The main problem with all of these codes, which provided distinct particle size ranges or intervals, is that they were based on a constant slope for the particle size distribution curve. This presented a quandary in that not all particle size distributions have the same slope and, therefore, some interpretation was required.

The most useful and, therefore, the code that enjoys the most acceptance is the ISO Solid Contaminant Code. This code is based the premise that a step ratio of 2 for particle concentration is adequate to differentiate between significantly different systems and to allow for reasonable differences in measurements. Various particle concentration increments are identified by range numbers. To use the ISO code, a fluid is analyzed using counting equipment calibrated per ISO 4402 to determine the number of particles per unit volume greater than both 5 μm and 15 μm . The two results are assigned their appropriate range numbers, which can be determined from a tabular listing of the range numbers corresponding to particle concentration. However, the simplest and most direct method of assigning the code is by using a graph as shown in Fig. 3.8.

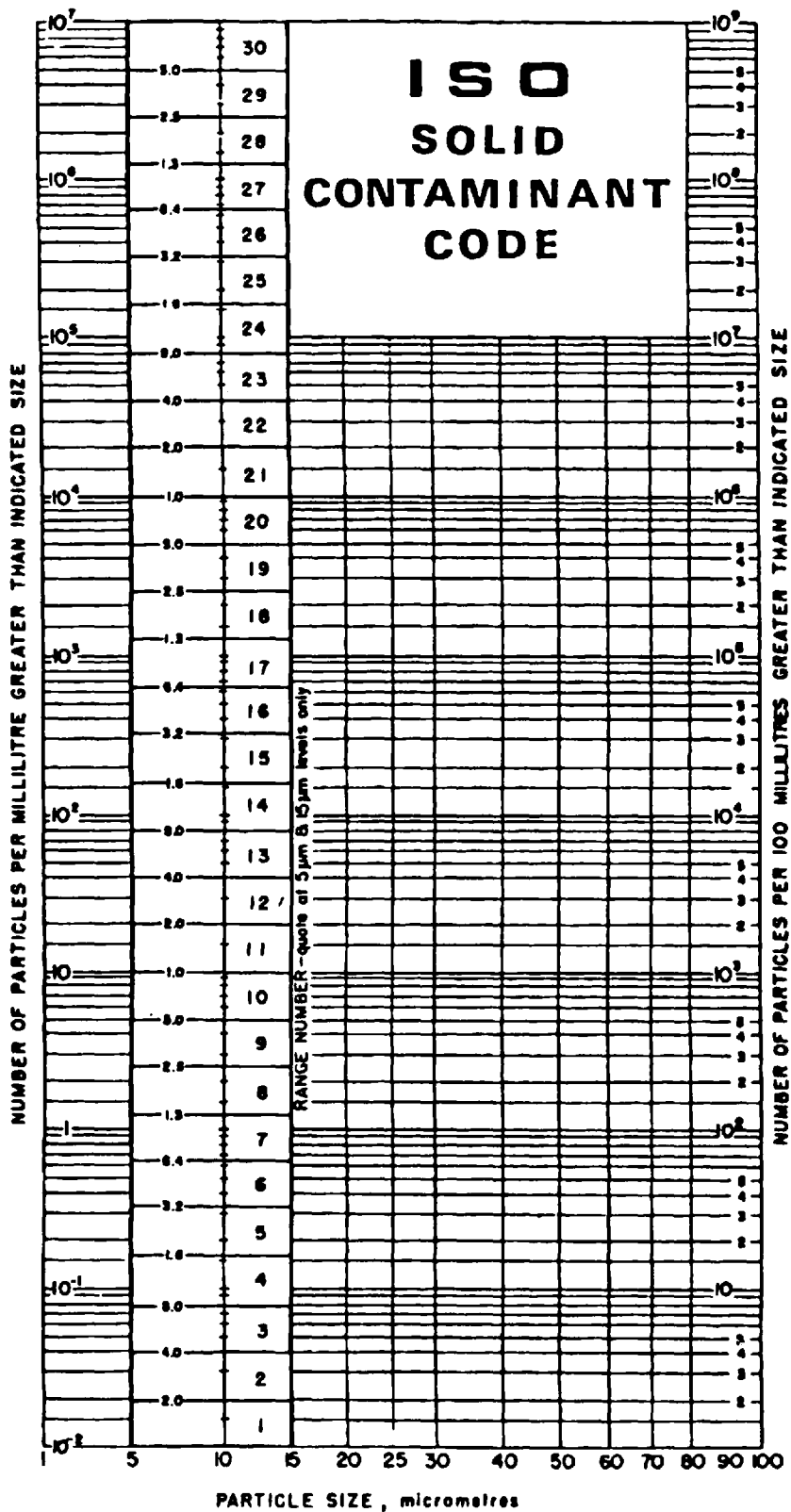


Figure 3.8 Graph for assigning ISO Solid Contaminant codes.

This graph allows a particle count which includes the counts for greater than 5 μm and greater than 15 μm to be plotted. The ISO code then would be the range of numbers where the distribution curve passed through the 5- and 15- μm lines. For example, a particle count of 50,000 particles/mL greater than 5 μm and 7000 particles/mL greater than 15 μm would have an ISO code of 23/20. Furthermore, a particle count of 1000 particles/mL greater than 5 μm and 100 particles/mL greater than 15 μm would have an ISO code of 17/14. It can be seen from Fig. 3.8 that the ISO Solid Contaminant Code is not based on a single slope of the particle size distribution curve and it covers the complete range of contaminant concentrations.

4 FILTRATION

The particulate contamination that ingresses a hydraulic or lubrication system must be removed or it will build up to a concentration that will be very detrimental to the system components. In the context here, the removal of contaminant particles from a fluid system is called filtration. Filtration methods are available that can be used to maintain an operating system at or below some contamination level.

4.1 Filtration Mechanics

An ideal filter is one which provides maximum resistance to the passage of entrained contaminants while offering minimum resistance to the flow of system fluid. Most of the filter media used to day consist of pores and capillary passages created by the structure of the medium. For example, many filters are composed of nonwoven fibrous material that forms a mat. When contaminated fluid passes through such material, a fraction of the particles in the fluid are captured and retained. Normally, the particles retained vary with the size of the particles, the separation capability of the medium, and the structural integrity of the filter. Particles mechanically trapped by the surface or by the pores within the medium are captured by a process called absorption. Therefore, absorption is a sieving or straining mechanism. Particles attracted and held by surface forces are removed by a process referred to as adsorption. Adsorption, hence, is created by electrostatic or van der Waals attractive forces, among others.

Filters are often referred to as "depth type" or "surface type." In this context, a surface-type filter is one in which the vast majority of the particles retained by the element are captured by the surface configuration of the medium. A typical example of a filter medium usually thought of as a surface type is a wire screen. A depth-type filter is one where the large particles will be captured on the surface, and smaller particles will enter the capillaries where they can be removed by pores or quiescent zones within the medium. This is undoubtedly a great oversimplification. The flow of particles, entrained in a fluid, through the passages of a fibrous medium is a complex phenomenon resulting from the transport, capture, and retention mechanisms involved. A further complication is created by the locations in a fiber matrix where the particles can be captured and by the probability that a particle will reach a potential capture site along with the probability that the particle will be retained once it is captured.

4.2 Filtration Performance

The performance of a filter is normally thought of in terms of three parameters—particle size efficiency, contaminant capacity, and pressure drop. Obviously, the particle size efficiency of a filter is determined by measuring the particle concentration upstream of the filter and downstream of the filter and performing the proper calculations. The contaminant capacity of a filter is found by measuring the amount of contaminant that can be exposed to the filter before the pressure drop becomes too large. The pressure drop is usually the clean element pressure differential and is related to the losses of the system. Both the particle size efficiency and the contaminant capacity are found by exposing the filter to some contaminant, using some specified test procedure. The particle size efficiency can be expressed for either a size interval or for a cumulative size range and often the values are not specifically identified. In addition, the contaminant used in determining the particle size efficiency is critical and seldom noted. These uncertainties led directly to a new expression for reporting filtration efficiency—the filtration ratio—which was introduced by the FPRC in 1970.

The filtration ratio (also known as the beta or alpha ratio) describes the capability of a filter to separate particles and only has a useful value when the specified conditions exist as follows:

1. Standard test dust: The beta ratio refers to the use of ACFTD; the Alpha Ratio is used with ACCTD.
2. Standard and qualified test system
3. Standard test conditions
 - Steady-state flow and temperature
 - Constant and measured ingress rate
 - Controlled fluid

These conditions were originally described in ISO Standard 4572, which is commonly referred to as the “Multipass Filtration Test.”

4.3 Filter Test Systems

In general, there are three different systems used to test filters for hydraulic and lubrication applications. These three test systems are described as follows:

- Single-pass system
- Multipass system
- Drawdown system

In a single-pass test system, contaminated fluid is pumped through the test filter and out to a separate reservoir, as in a fuel system where the fuel goes to an engine or a water system where the water is put through a sprinkler. In another version of the single-pass test system, a very high-efficiency filter is placed downstream of the test filter to catch the contaminant particles which escape the test filter. In the case of the multipass test system, the fluid is forced through the test filter and back to the test system reservoir. The fluid which returns to the test system reservoir is continually mixed with injected contaminant and reexposed to the test filter. Hence, the contaminant which escapes the test filter is recirculated through the test system in a multipass manner. A drawdown system is very similar to the multipass without the

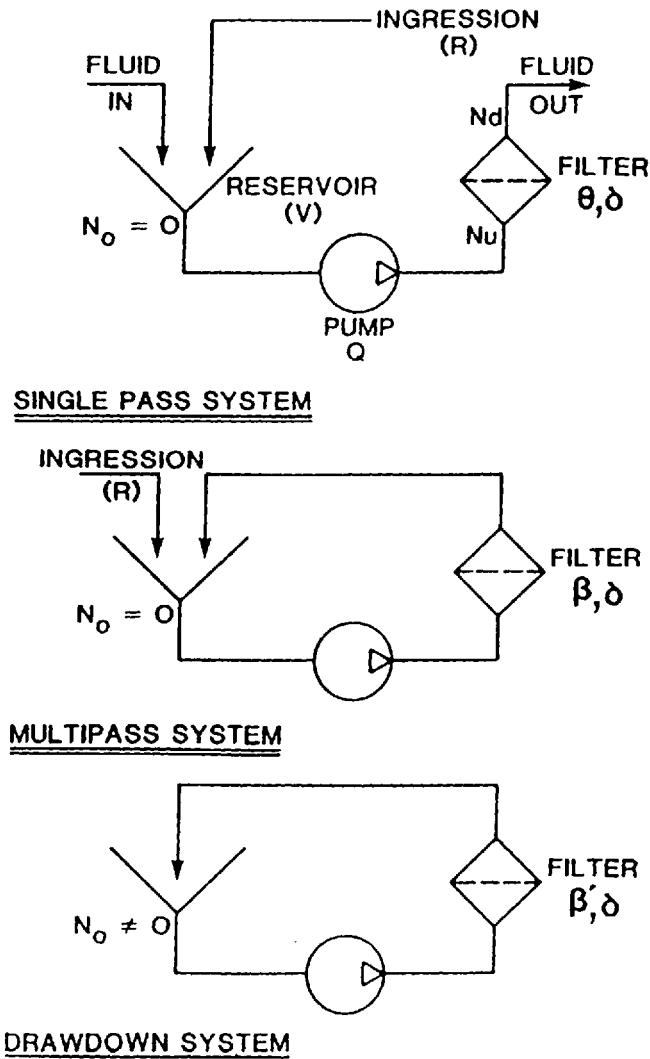


Figure 3.9 Examples of filter test systems.

continuous injection of contaminant; that is, a specified volume of fluid contaminated to a given contamination level is circulated through the test filter without the addition of more contaminant. Figure 3.9 shows a schematic for each type of filter test system.

4.4 Multipass Filtration Performance Tests

The multipass filter test system actually consists of two distinct circuits. One system is the filter test system and the other is the contaminant injection system. A schematic of the multipass test system is illustrated in Fig. 3.10. Both of these systems have reservoirs with conical bottoms and a return-line diffuser to aid in contaminant entrainment. In addition, both systems contain appropriate pumps, heat exchangers, and

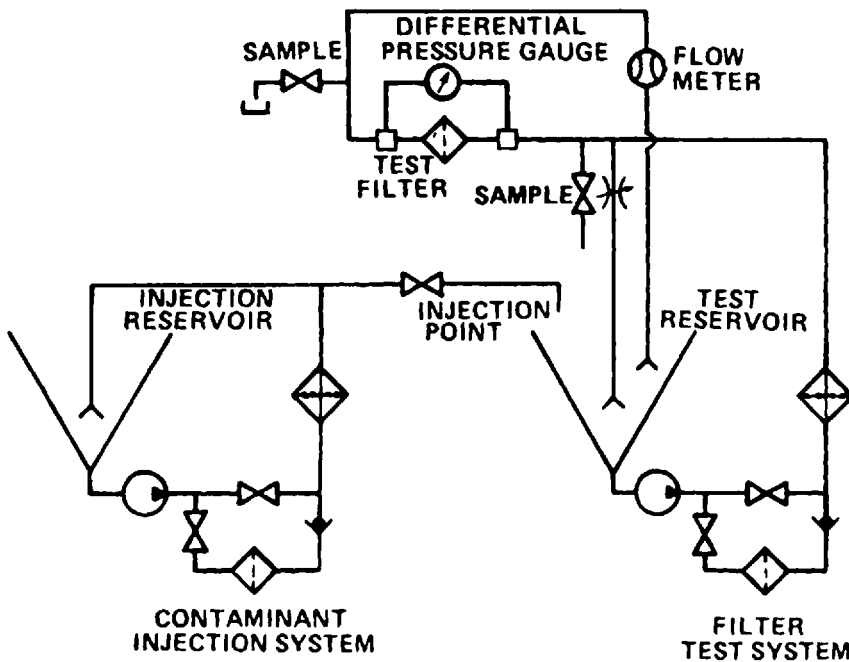


Figure 3.10 Schematic of multipass filter test system.

cleanup filter loops. In operation, a small stream is injected from the contaminant injection system to the main filter test system. The test facility must be qualified as specified in the ISO Standard 4572. The qualification procedure determines the capability of each of the multipass systems to maintain the contaminant in suspension throughout the expected duration of a filter test at the lowest flow rate to be used. The qualification not only reveals whether or not the facility can keep the particles in suspension but also shows if these particles are destroyed or more particles are added through wear of the system components.

A block diagram of the multipass test procedure is shown in Fig. 3.11. As can be seen in this figure, the procedure requires that the filter element to be tested first be subjected to a fabrication integrity as specified ISO Standard 2942. This is done to ensure that the element being tested does not have severe leaks resulting from manufacturing imperfections or handling damage. The operating conditions of the test must be established, such as flow, temperature, and so forth, and the injection system must be prepared so that there is sufficient contaminant to produce a 10-mg/mL base upstream gravimetric level at the prescribed injection flow rate. Then, the test element is subjected to a continuous flow and a continuous contaminant injection until a specified pressure drop is reached. The specified pressure differential is called the terminal pressure drop. Upstream and downstream samples are extracted at specified points in the loading curve based on the net pressure drop. The various pressure drop terms are illustrated graphically in Fig. 3.12.

Fluid samples are taken at 2 min after the injection has commenced and at 10%, 20%, 40%, and 80% of the net pressure drop. These samples are placed in clean sample containers which are certified per ISO Standard 3722 through a sam-

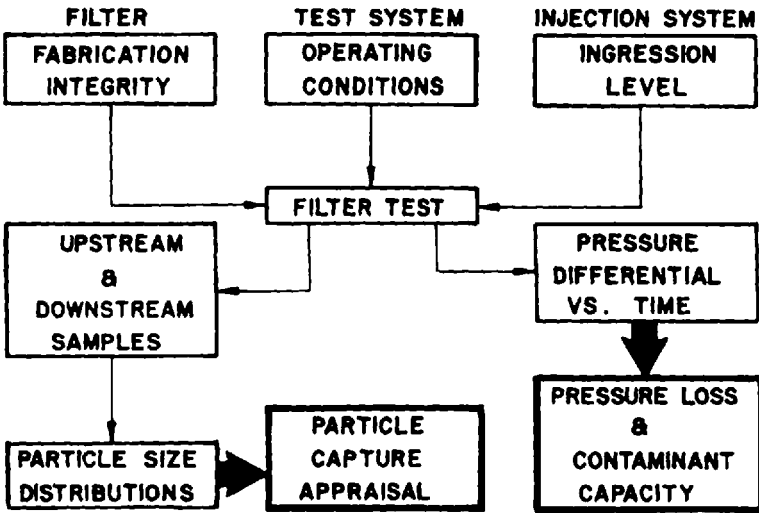


Figure 3.11 Block diagram of multipass filter test procedure.

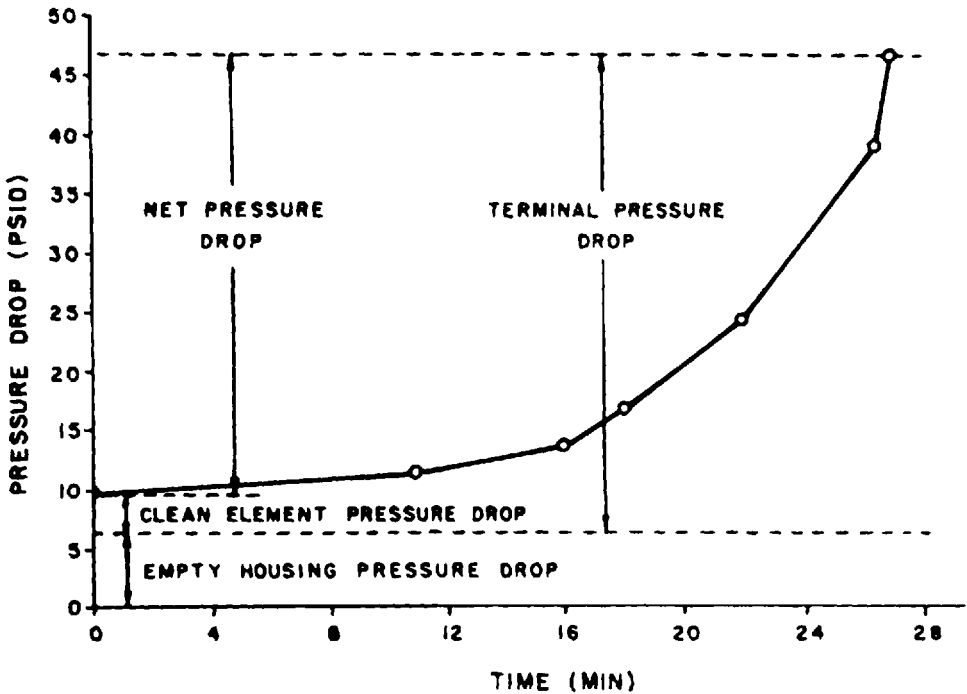


Figure 3.12 Graphical illustration of pressure drop terms.

pling procedure prescribed in ISO Standard 4021. In-line counting equipment and procedure can be used instead of sampling, provided it is properly qualified. Samples are analyzed by measuring the cumulative particle size distribution using particle-counting equipment calibrated per ISO Standard 4402. All data derived from the multipass test are recorded on a data sheet. Although there are several different data-sheet layouts which are used, the official test report sheet is shown in Fig. 3.13.

4.5 Multipass Data Interpretation

The multipass filter test produces several very important facts relative to the test element. The most obvious of these facts is the filtration ratio at each of the particle sizes counted throughout the test. It must be kept in mind that the multipass test requires steady-state conditions and, therefore, will not reveal the performance of the filter element under dynamic conditions. However, if a test element performs poorly under the steady-state conditions prescribed in the multipass test procedure, it is not apt to improve under dynamic conditions. A large value for the filtration ratio mean that the filter has captured and retained a large number of the particles from the influent. For example, a filtration ratio of 2 mean that one-half of the particles in the upstream fluid are captured, and a filtration ratio of 1 reveals that none of the particles in the influent were captured. When the test contaminant is ACFTD, the filtration ratio is indicated by the β and α is used for the filtration ratio when the test contaminant is ACCTD.

Experience has shown that many filters exhibit an increasing or decreasing filtration ratio during the multipass test. This is most likely due to changes in the structure of the fiber matrix as the filter loads up and pressure forces change. Therefore, at the conclusion of a multipass test, there will be a filtration ratio for each particle size evaluated at each service point, as shown in Fig. 3.13. Because the service points or pressure drop points where samples are extracted are also related to time, there are at least two methods of reducing the filtration ratios to a few meaningful values. Obviously, one could report the minimum value for the filtration ratio observed during the test at each particle size. However, if the assumption is made that the filter will perform in the field as it did in the test, then using the minimum filtration ratio does not fairly represent the performance of a filter element throughout its useful life. Therefore, a second designation is also used. This is the time-weighted-average filtration ratio. It is important to note that the development of the multipass test produced a mathematical relationship which described the particle concentration in the test system as a function of the test parameters and the performance of the test element. Although the mathematical derivation is beyond the scope of the material, it can be stated that the particle concentration in the system will resemble the solution to a first-order differential equation.

The results of the multipass test will also reveal information concerning the contaminant capacity of the test element. The total number of grams of test contaminant injected into the filter test system to reach the terminal pressure drop is designated as the apparent contaminant capacity, and because this value will be related to the kind of test contaminant used, the value must be qualified by stating the test contaminant. For example, if the test was conducted using ACFTD, then the capacity will be designated as the ACFTD capacity. Because the test filter will rarely, if ever, remove 100% of the contaminant subjected to it, there will be a difference between

FILTER ELEMENT MULTI-PASS TEST REPORT SHEET

FILTER FPRC NO. 60 TEST LOCATION FPRC-OSU DATE 6/27/72
 TEST FLOW 20.0 GPM BUBBLE POINT 7.0" H₂O INITIAL CLEANLINESS 8.0 Particles/MI > 10 μ M
 TERMINAL Δ P 40 PSID HOUSING Δ P 6.0 CLEAN ASSEMBLY Δ P 7.5 CLEAN ELEMENT Δ P 1.5

NET Δ P (<u>38.5</u>)	2 MIN.	5%	10%	20%	40%	80%	100%
Assembly Δ P	--	9.0	11.3	15.2	22.9	38.3	46.0
Time (min.)	--	15.9	20.3	27.5	29.7	32.0	32.5

Injection Fluid	Initial	Final	Average	BASE UPSTREAM LEVEL: <u>9.82</u> mg/litre
Injection Flow Rate (LPM)	0.520	0.490	0.505	FINAL GRAVIMETRIC LEVEL: <u>45.0</u> mg/litre
Gravimetric Level (mg/litre)	1482.2	1462.6	1472.4	ACFTD CAPACITY <u>24.2</u> g

PARTICLE DISTRIBUTION ANALYSIS (PARTICLES PER MILLILITRE)

SAMPLE	> 5 μ M	β_5	> 10 μ M	β_{10}	> 20 μ m	β_{20}	> 30 μ M	β_{30}	> 40 μ M	β_{40}
UP 2 MIN. DOWN	---		---		---		---		---	
UP 10.0% DOWN	---		1570.1 113.7	13.81	298.5 14.4	20.73	72.80 2.78	26.19	32.4 1.14	28.42
UP 20.0% DOWN	---		1637.8 129.2	12.68	303.3 5.0	60.66	71.08 0.96	74.04	31.08 0.44	70.64
UP 40.0% DOWN	---		1786.6 243.9	7.33	323.3 6.0	53.88	80.12 1.16	69.07	39.40 0.48	82.08
UP 80.0% DOWN	---		1842.7 521.9	3.53	316.9 17.8	17.80	75.84 3.78	20.06	35.04 1.66	21.11
MINIMUM β				3.53		17.80		20.06		21.11

Figure 3.13 ISO multipass filter test report sheet.

the amount of contaminant injected and the amount of contaminant retained by the filter. Because the conditions of the test are very carefully controlled, it is possible to estimate the amount of contaminant retained based on the test parameters and the apparent capacity.

The evaluation of the particle size separation performance of a filter using the multipass test procedure depends on the use of automatic particle counters and their accuracy. In order to produce accurate results, any automatic particle counter must be properly calibrated. In the case of automatic particle counters used in multipass testing, they must be calibrated per the ISO Particle Counter Calibration Method

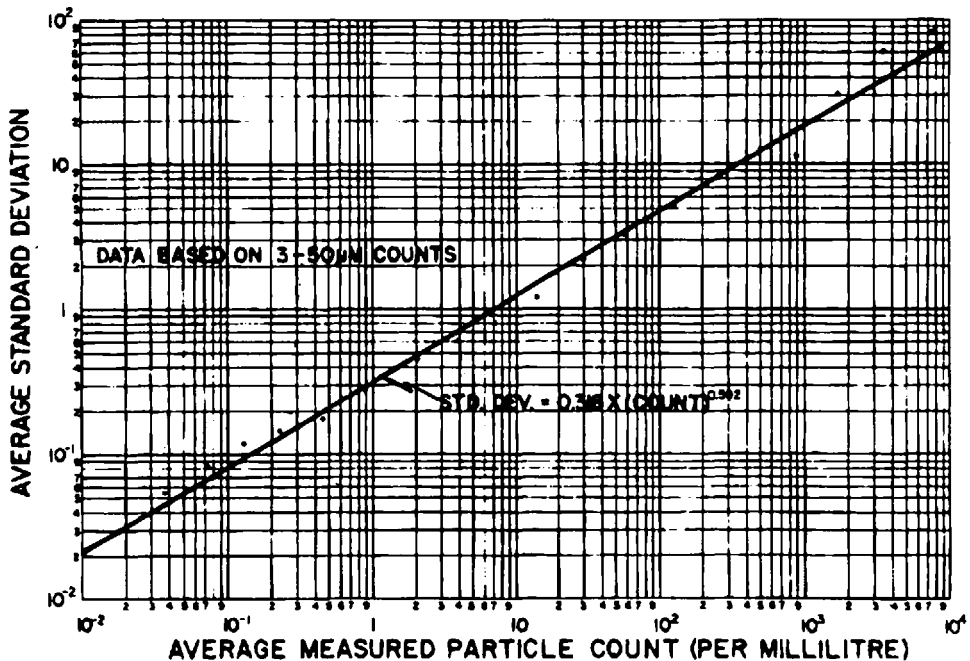


Figure 3.14 Accuracy assessment of automatic particle counters.

(ISO 4402) discussed earlier. An international “round-robin” survey relative to particle counter reproducibility was conducted to evaluate the accuracy of automatic particle counters. Based on the information obtained during this survey, the standard deviation versus particle count magnitudes was established as shown in Fig. 3.14. In addition, confidence intervals were calculated as shown in Fig. 3.15 to determine the limitations of accuracy for particle counters.

In order to apply the information on the accuracy of automatic particle counters to the results of a multipass filter test, assume that an upstream particle count of 2000 particles was obtained and the downstream count was 100. This means that the filtration ratio of the filter element at this particle size was 20. By examination of Fig. 3.15, it can be estimated that when a particle count of 2000 is obtained, one can be 95% confident that the actual count will be between approximately 1900 and 2100. Furthermore, the 95% confidence interval for a count of 100 is about 85–110. Therefore, based on the accuracy of the automatic particle counter, the 95% confidence interval for the filtration ratio would be approximately 17.3–24.7. The data show that accuracy.

4.6 Flow and Impulse Effects

Leakage through a filter element bypass valve, surges in the flow through the filter element, and impulses resulting from machine dynamics will all have significant influence on the performance of a filter element as measured by the multipass test. Most system designers depend on the filter element and housing manufacturer to ensure that the fluid which enters the filter housing is forced to go through the

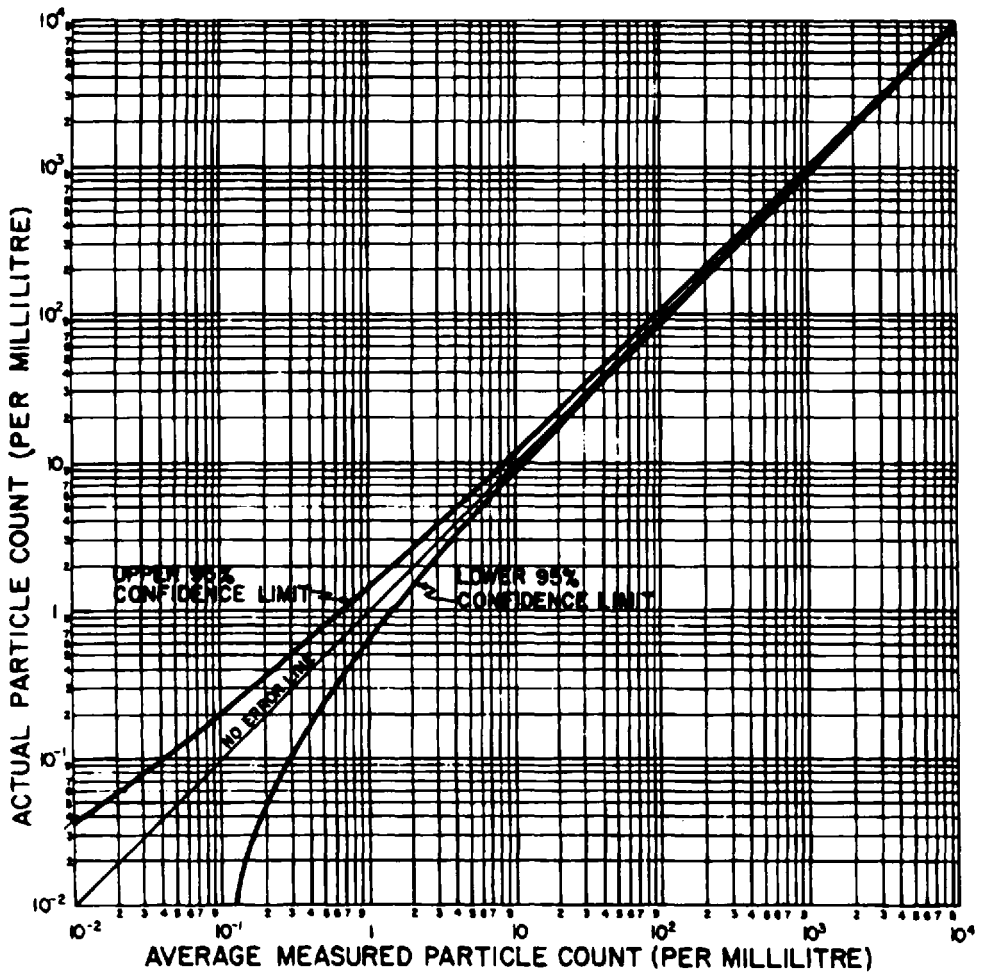


Figure 3.15 The 95% confidence intervals for automatic particle counters.

element. However, it is possible for fluid to bypass the element through several different passages. For example, most filter housings incorporate a bypass valve intended to protect the element from an excess pressure drop. An excessive pressure differential across an element could cause structural damage. Many of these bypass valves permit some fluid to leak through to the downstream side of the element. Many hydraulic and lubrication systems allow the flow to increase and decrease during a normal work cycle. For example, a hydraulic system with a pressure-compensated pump will produce large flow surges in typical operation. In addition, the flow through an engine lubrication filter is a function of engine speed. Therefore, as the engine speeds up or slows down, the flow through the filter element changes. Impulse, impact, and vibration are all imparted to the filter because of the structure of the machine on which the filter housing is mounted. For example, a tracked vehicle such as a dozer will cause very violent impulses not only to the filter housing but also to the operator himself.

Fluid can bypass a filter element for many reasons. Improperly sealed side seams and end caps on the filter element itself is one very real possibility. In addition, the element can rupture during operation or be damaged before installation, and the result will be high bypass flow. However, the two causes which are probably primary are a poor fit between the element and the housing, and a bypass valve which is poorly designed or stuck open due to silting. Particles which pass around the element will retain the upstream size distribution, as there is no modification by filtering. This bypass leakage alters the shape of the downstream particle distribution from that normally expected from a filtering action to something much flatter. As shown in Fig. 3.16, the expected particle size distribution downstream of a filter is very steep for a well-designed element. However, when a certain percentage of the flow is permitted to bypass then the downstream distribution will be a composite of the distribution imposed by the filter and the distribution of the upstream contaminant. These two distributions are added together before the fluid exits the housing. The large particles which ingress the system or are generated by the system components will have a very great effect on the performance characteristics of the filter when flow bypassing occurs.

Flow surges imposed on a filter element can have devastating effects on the wear rate exhibited by the system components. These surges cause the element to unload contaminant, which increases the overall contamination level of the system fluid. Several tests have been reported on the effect of cyclic flow during multipass testing. The results of some of these tests are shown in Figs. 3.17 and Fig. 3.18. Figure 3.17 reveals that a cyclic flow where the flow rate varied from a value of Q to one-half Q and back greatly reduced the effectiveness of the filter. However, when the flow was cycled from some value to zero and back there was even more effect. These data show that the change in filtration performance as a function of the magnitude of the flow cycle is certainly not linear. In studying Fig. 3.18, it can be observed that the performance of a “3- μm ” filter is significantly better than that of a “10- μm ” filter under steady flow conditions; however, under a cyclic flow environment, these two filters performed the same.

The effect of flow surges can be better appreciated by considering the overall influence on the contamination level of the system. If it is assumed that every time a filter is subjected to a surge that N particles are sloughed. If only one surge is subjected to the filter, these N particles will be recaptured by the filter when steady flow returns, and there will be little effect. However, if another surge occurs before the effects of the first surge can be eliminated, the overall influence is additive. As shown in Fig. 3.19, when a series of flow surges are imposed on a filter at some time interval T , then the particle concentration of the system fluid will increase in a manner inversely proportional to the time interval.

4.7 Partial and Dual-Flow Filtration

There are several different types of filter systems in use today—some are very advantage and some are detrimental. These filters are usually classified as follows:

- Full-flow filtration
- Partial- and dual-flow filtration
- Auxiliary filtration

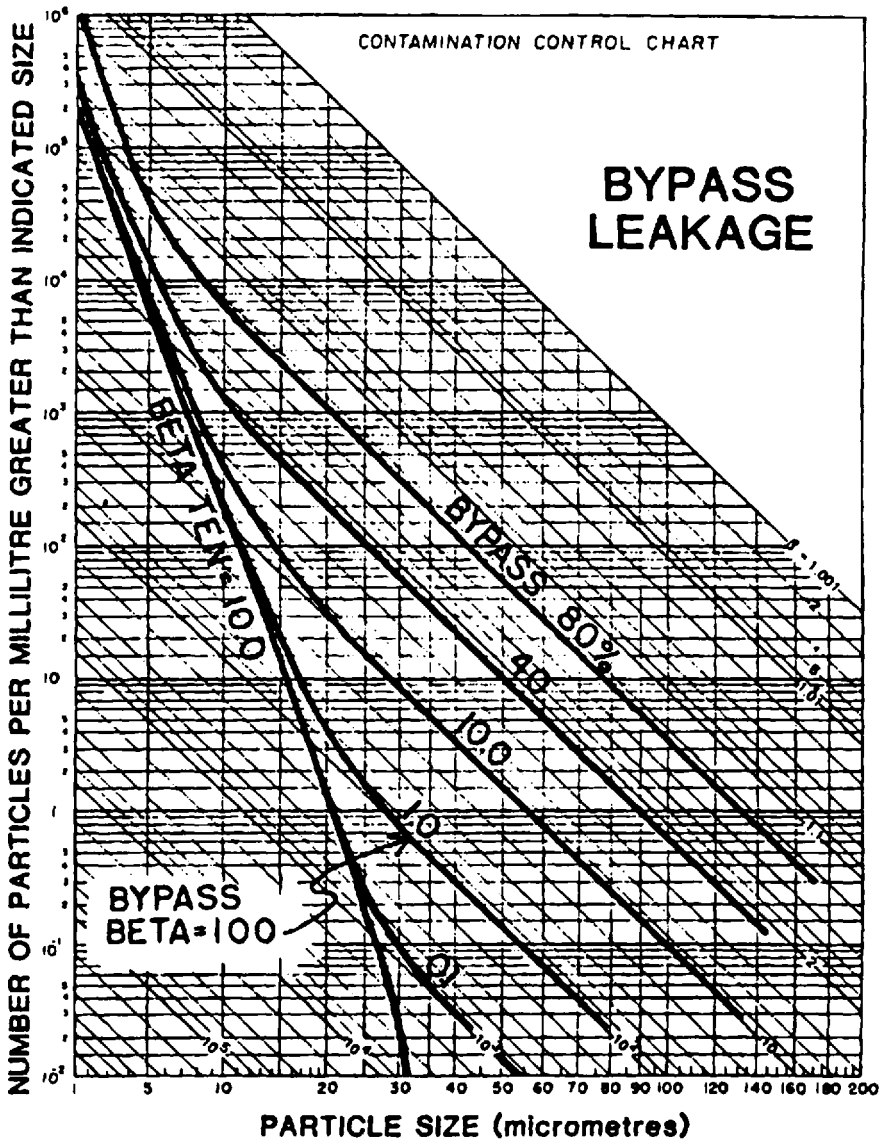


Figure 3.16 Effect of bypass leakage on filter downstream characteristics.

In a full-flow filtration system, the entire flow of the system passes through the filter. This is the most common type of filtration system used today. Full-flow filters are placed at various location in the system—suction line, pressure line, and return line. Partial-flow filtration is similar to the dual-flow filtration system in that the flow of the system is split into two paths. In the partial-flow filter system, some amount of the flow is allowed to bypass the filter in an unfiltered path, whereas in a dual-flow system, two filters are used instead of permitting an unfiltered flow path. The partial-flow system is illustrated schematically in Fig. 3.20 and a schematic of a dual-flow system is shown in Fig. 3.21.

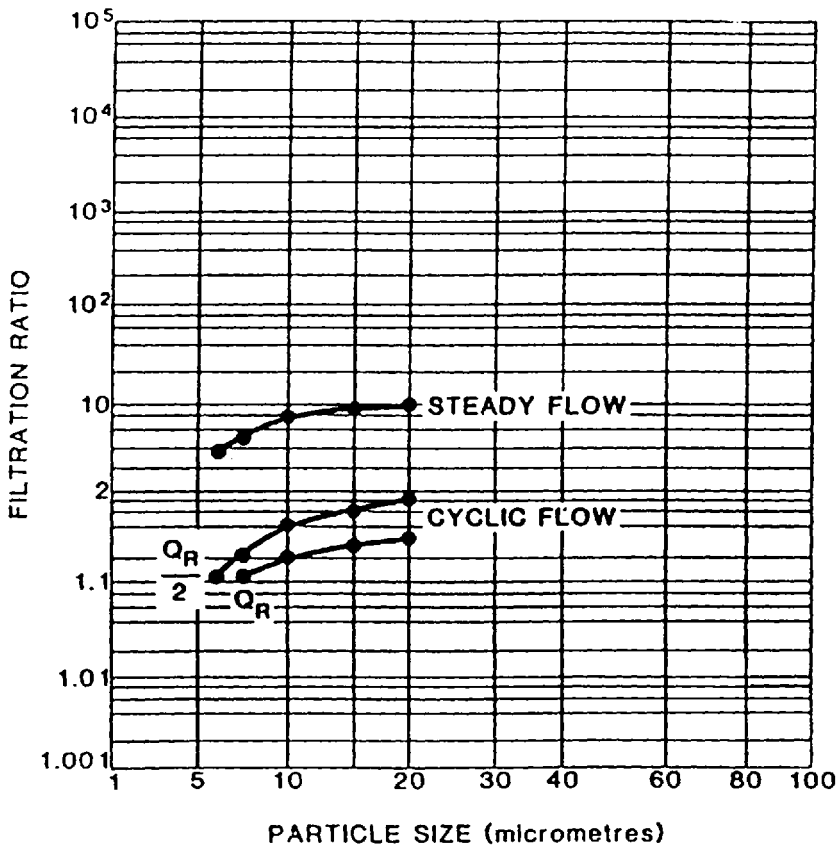


Figure 3.17 The effect of cycle flow versus steady flow on filtration ratio.

In a partial-flow filtration system, the bypass flow is normally controlled by a fixed-area orifice. However, the orifice is usually sized to permit the designated flow with the pressure drop exhibited by the filter when it is clean or has not been subjected to any contamination. This produces a problem which makes the partial-flow filtration system less than perfect. As the filter becomes loaded with contaminants, the pressure drop increases. Therefore, more flow will go to the unfiltered path and less will pass through the filter element. As this change of flow occurs, the apparent or effective filtration ratio will decrease until the point at which all of the fluid goes through the unfiltered passage; at that point, there will no filtration at all.

In dual-flow filtration, a portion of the flow normally passes through a fine filter while the remainder of the flow passes through a coarse filter. Dual-flow filtration does not yield a predictable performance. The problem lies in the fact that the proportion of the flow which passes through each filter constantly changes as the filters load up. Because a predictable filter performance is not possible and, therefore, a predictable system contamination level cannot be obtained, this type of filtration system should be used with great care.

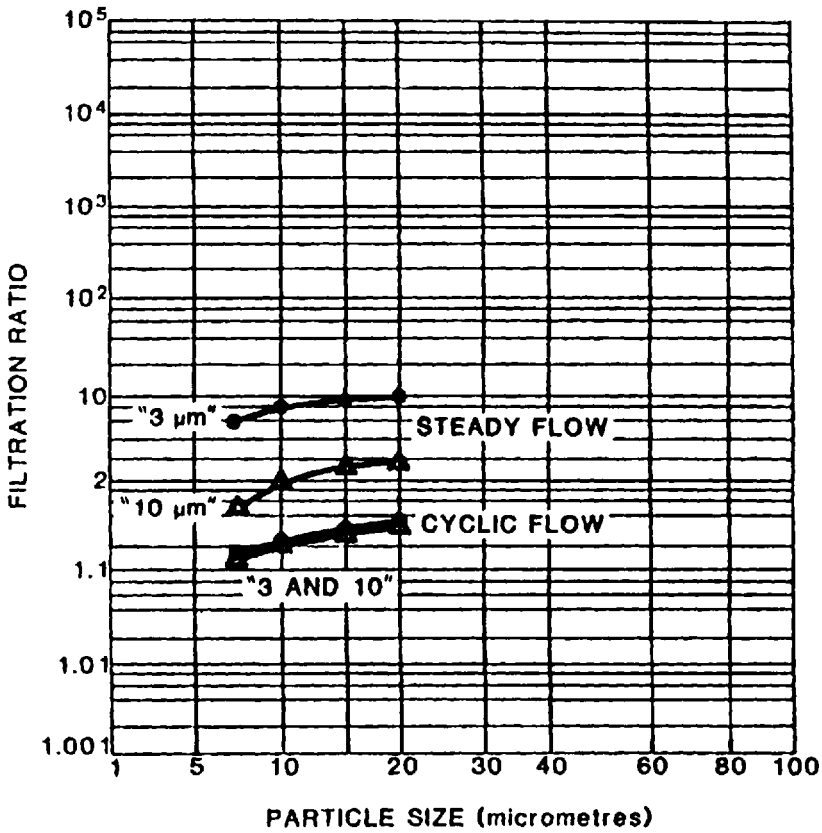


Figure 3.18 The effect of cyclic flow on 3- and 10-µm filters.

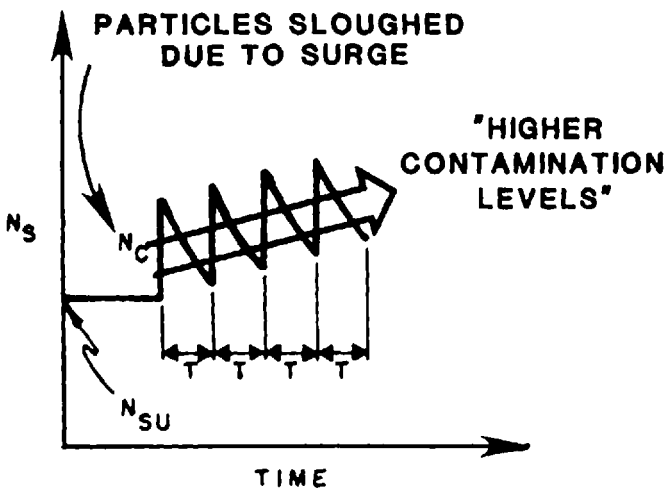


Figure 3.19 Effect of repeated flow surges on contamination level.

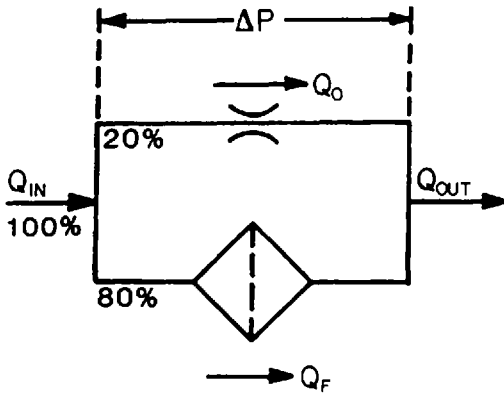


Figure 3.20 Schematic of a partial-flow filtration system.

4.8 Auxiliary Filtration Systems

Auxiliary filtration systems are often called off-line filtration. This type of filtering system offers an ideal location for the system filter because the filter is sheltered from the flow surges and disturbances that can create particle sloughing of the captured particles. A schematic of a simplified fluid system that includes an auxiliary filtering circuit is shown in Fig. 3.22. As can be seen in this figure, the system fluid is pumped from the reservoir through the off-line filter and back to the reservoir. Obviously, the contamination level maintained by the auxiliary filtration system is not only a function of the performance of the filter but also on the flow rate of the auxiliary circuit. Analysis indicates that the flow magnitude is an extremely important parameter in designing this type of system. The primary advantage of the off-line filtering circuit is that the filter element is not subjected to the flow changes normally encountered in the main system. In addition, many other fluid conditioning components such as heaters, coolers, dehydrators, and degassers can be incorporated into the auxiliary circuit much more effectively than in the main system.

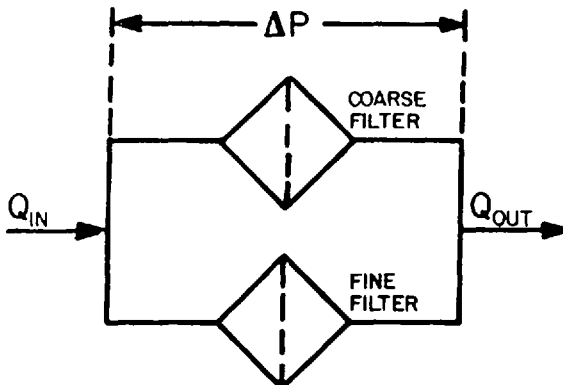


Figure 3.21 Schematic of a dual-flow filtration system.

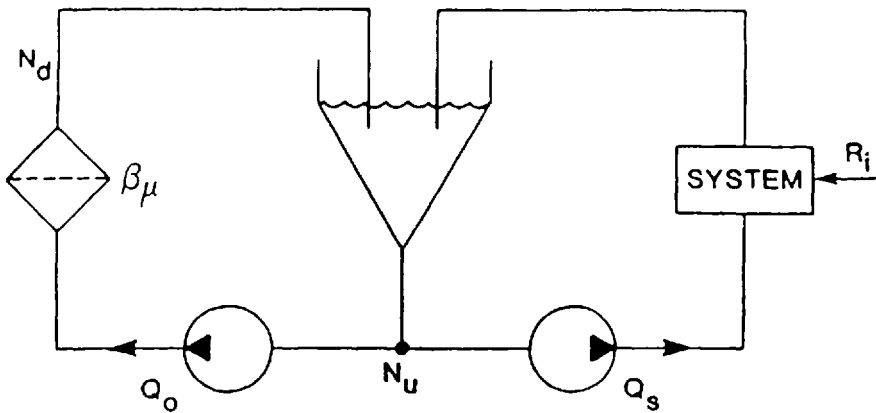


Figure 3.22 Simplified fluid system with auxiliary filter circuit.

5 COMPONENT CONTAMINANT TOLERANCE

Any discussion of contamination control could not be considered even close to complete without a section which, at least briefly, covers component contaminant sensitivity. An effective contamination control program cannot be established without first determining the contamination level with which the system can perform for a reasonable period of time. In order to discover this contamination level, component contaminant sensitivity tests are normally conducted. Contaminant sensitivity is generally expressed in terms of the degradation of some critical performance parameter as a function of contaminant exposure. Most tribologists are accustomed to thinking of wear in terms of material lost or dimensional changes. However, it is very difficult, if not impossible, to equate dimensional changes or material losses to a degradation of component or system performance. To the user of a hydraulic or lubrication system, the only thing that is of concern is the system performance. Therefore, the life of a system must be expressed as the amount of time the system can operate satisfactory. For example, in a hydraulic system, pump wear will result in a reduction in flow rate. When the flow decreases, all of the system functions will slow down. When a certain reduction in speed has occurred, the user will become unhappy. At that point, the system is effectively worn out. This section will discuss contaminant wear only briefly in an attempt to provide the reader with a little insight to the subject. The contaminant-related failure modes will be discussed along with the contaminant sensitivity testing. The results of the contaminant sensitivity test will be presented in terms of contaminant tolerance profiles and omega rating.

5.1 Contaminant-Related Failure Modes

A fluid system can fail for a number of reasons. One of the most prevalent causes for failure is excessive contamination in the system fluid. It has been estimated that approximately 70% of the failures in hydraulic systems are due to the presence of contamination. In considering particulate contamination, there are two predominate failure modes. In pumps, motors, and cylinders, for example, the contaminant-related failure mode is surface wear. However, although the internal surfaces of valves can wear, the predominate failure in these components is the result of a stoppage of

motion. Therefore, the primary contaminant-related failure modes in fluid system are contaminant wear and contaminant lock (motion failure is normally called contaminant lock).

5.2 Contaminant Lock

Motion failures result in some form of lock or jam and are characterized by the stopping of a given motion or function due to an interference mechanism. In addition, this type of failure can also result in a stoppage of flow, as when an orifice becomes plugged up. A frustrating characteristic of most contaminant lock failures is that there is little or no evidence of the presence of particulate contamination when the component is disassembled. The problem lies in the fact that when the component is disassembled, the offending particles will be moved, and as they would probably be much smaller than can be seen with the naked eye, there is no evidence of their presence. The three typical contaminant lock situations are shown schematically in Fig. 3.23. Contaminant particles can become jammed in several locations of the sliding spool valve. In addition, a large number of very small particles can settle out in the clearance between the bore and the spool. When this occurs, the force needed to actuate the spool will increase in proportion to the quantity of the silt-sized particles until the force becomes great enough to prevent spool motion entirely.

5.3 Contaminant Wear

Contaminant wear is characterized by performance degradation. Therefore, parts destroyed by contaminant wear are usually not replaced because they are broken but

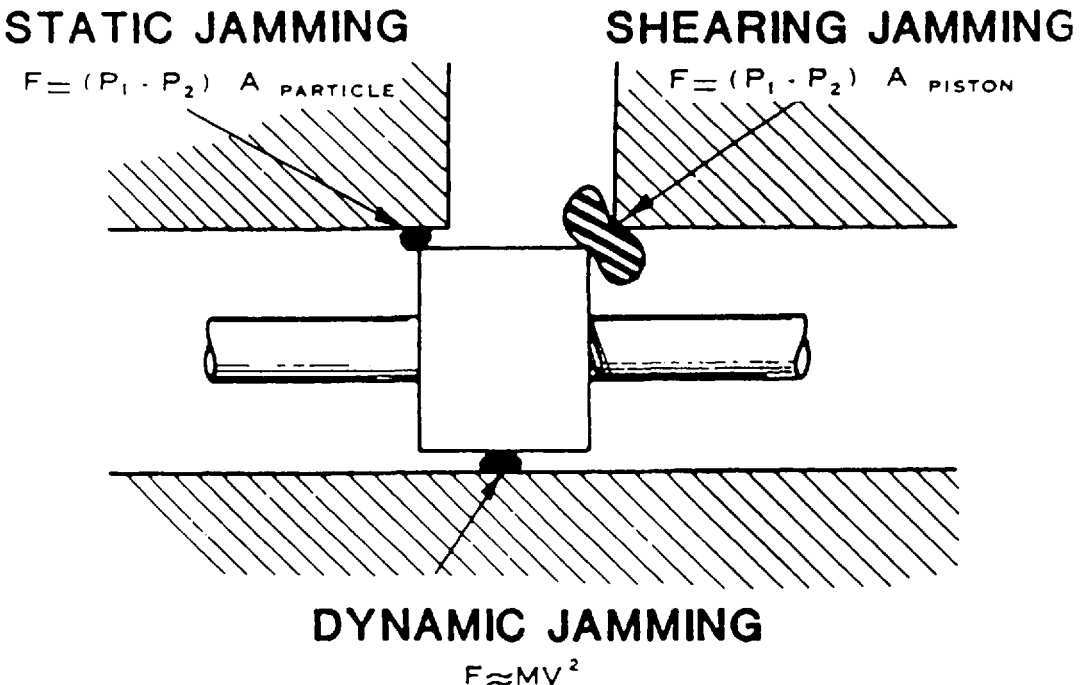


Figure 3.23 Three fundamental types of contaminant lock.

because they could no longer satisfy the performance requirements for which they were originally designed. Because contaminant wear results in the performance degradation of a system, a performance parameter that reflects the loss of material from critical surfaces and the wear debris in the fluid can be used to quantify and relate the severity of wear in a fluid system. The performance parameter which best reveals the amount of contaminant wear that has taken place in a component depends on the type of component being considered. For example, a fixed-displacement pump is a flow generator and, therefore, it would seem that flow would be the best parameter. However, if some thought is given to the steady performance model for a fixed-displacement pump, it would be soon be realized that the actual output flow of a pump is dependent on pressure; that is because the leakage flow is a function of pressure and the clearances within the pump. Contaminant wear will increase the clearances. Therefore, at low pressures, there will be very little change in flow rate as the contaminant wear increases the clearance paths. However, at high pressures, the loss of flow would be dramatic.

Variable-displacement pumps are somewhat different from fixed-displacement pumps in that they have a displacement-varying mechanisms. The most common of this type pump is the pressure-compensated pump in which the displacement is reduced when high pressures are exposed to the pump. In this case, there are normally two performance parameters used to assess contaminant wear. One of these parameters is the flow output at a high pressure that is somewhat below the compensator setting. For example, this parameter is usually the flow rate at two-thirds of the compensator setting. The second parameter is the actual standby pressure or the no-flow pressure. Each of the fluid components have one or more performance parameters which are sensitive to the wear of internal surfaces. The hydraulic motor normally relies on speed degradation at a fixed load or pressure differential. Cylinders use dynamic seal leakage, whereas valves are dependent on their intended purpose.

5.4 Contaminant Sensitivity Testing

Contaminant sensitivity is defined as the performance degradation of a fluid component in terms of contaminant exposure. Of course, the reason to know this information is to interpret it in terms of contaminant life. Contaminant life, in general, depends on three factors:

- The severity of the operating conditions such as pressure, speed, and temperature
- The contamination level of the circulating fluid
- The contaminant sensitivity of the system components

In order to assess contaminant sensitivity, it is necessary to perform a sensitivity test. The contaminant sensitivity test which was developed first and is of widespread use in the fluid industry is for a fixed-displacement pump. Therefore, the contaminant sensitivity test for a fixed-displacement pump will be used as an example to provide an overview of this area of contamination control technology.

All contaminant sensitivity tests rely on a qualified test system that allows the component to be exposed to increasing sizes of contaminant while the selected performance parameter is monitored. In the case of fixed-displacement pumps, the flow rate at a constant applied pressure is monitored to determine performance degrada-

tion. The qualification procedure certifies that the particular test is capable of exposing the pump to a designated contamination for an adequate length of time without permitting the contaminant to settle out.

A schematic of the test circuit needed for a contaminant sensitivity test on a fixed-displacement pump is shown in Fig. 3.24. The reservoir is required to have a conical bottom and the fluid entering the reservoir must be diffused below the surface of the fluid. These requirements are designed to prevent particulate contamination from settling during the test. Provisions are made to either pressurize the reservoir or use a charging pump to ensure adequate pressure at the pump inlet. The injection reservoir is constructed as shown in Fig. 3.24. The heat exchanger is either a one-pass or a two-pass unit and is mounted vertically with the fluid entering the bottom

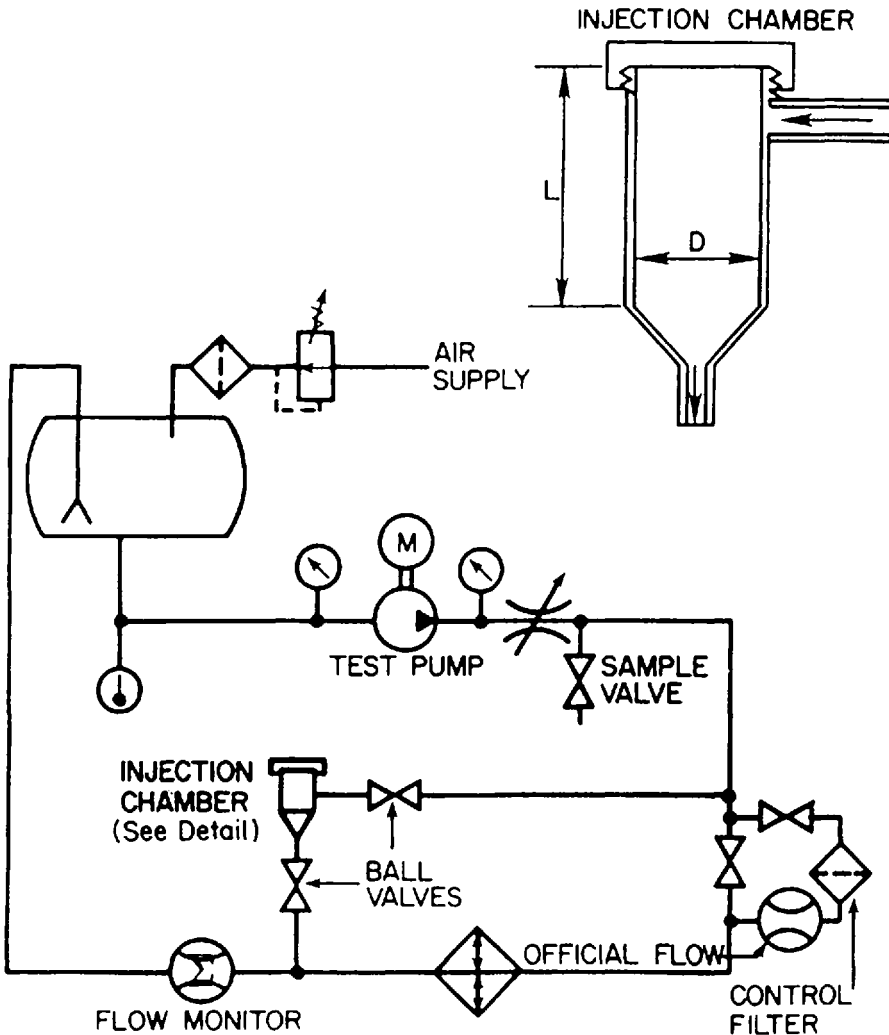


Figure 3.24 Schematic of contaminant sensitivity test system for a fixed displacement pump.

and circulating through the tube side. The load valve normally used is a simple needle-valve configuration.

The contaminant sensitivity assessment evaluation is conducted as indicated in the flowchart in Fig. 3.25. Research conducted on contaminant sensitivity testing showed that in order to obtain useful data on a wide spectrum of pumps and maintain reasonable wear rates, it was necessary to expose the pump to a gravimetric level of 300 mg/L for each size range. The size ranges needed for the test are 0–5, 0–10, 0–20, 0–30, 0–40, 0–50, 0–60, 0–70 and 0–80 μm . Experience has shown that many pumps are capable of being exposed to all of the size ranges at the specified 300 mg/L while sustaining very little damage. However, some pumps will exhibit excessive performance degradation after only the 0–30- μm exposure. It is not very useful to conduct the entire test without observing any degradation because it would be impossible to use this type of information as design criterion. Therefore, tests conducted at less than 300 mg/L would not produce useful information from the pumps with the least contaminant sensitivity.

During the test, with the pump operating at the rated condition prescribed by the manufacturer, the 0–5- μm slurry is injected and the pump is operated for 30 min at this exposure or until the flow remains constant for 10 min. Then, the fluid is circulated through the filter system until the contamination level is less than 10 mg/L. The injection and filtration process is continued through the size ranges until the flow rate decreases to less than 70% of the rated flow or until the 0–80- μm size range has been injected. The flow degradation ratio is found by dividing the final flow after each injection is filtered out by the rated flow. The flow degradation signature of the pump is obtained by plotting the flow degradation ratio versus the upper limit of the contaminant size range of the corresponding injection, as shown in Fig. 3.26. No additional interpretation procedure is required to recognize which pump shown in Fig. 3.26 has the best contaminant tolerance.

5.5 Interpretation of Contaminant Sensitivity Test Results

The flow degradation signature is essential in selecting a pump that is tolerant to the presence of particulate contamination. However, fluid systems can reach contamination levels that will destroy even the most tolerant pump. Therefore, a need exists to interpret the contaminant sensitivity test data in terms of pump life or pump contaminant life. Predicting the service life of a system and its individual components is an important feature of design mechanics. Classical machine design relies on stresses and strains to evaluate the endurance limit of component materials. From this information, the field life of a system is estimated. An early failure resulting from contaminant wear can occur even when the stresses and strains within the system are well below those anticipated during the design phase. Thus, the objective of contamination control is to ensure that the system life is shorter as a result of fatigue than contamination. The service life of a component or system because of particulate contamination is called the contaminant service life.

There have been two popular methods developed to interpret the results of a contaminant sensitivity test in terms of contaminant service life. A rigorous treatment of either of these techniques is beyond the scope of this material; however, a brief explanation of the two methods will be given. In chronological order, the contaminant tolerance profile was developed followed by the omega life. Both of these procedures

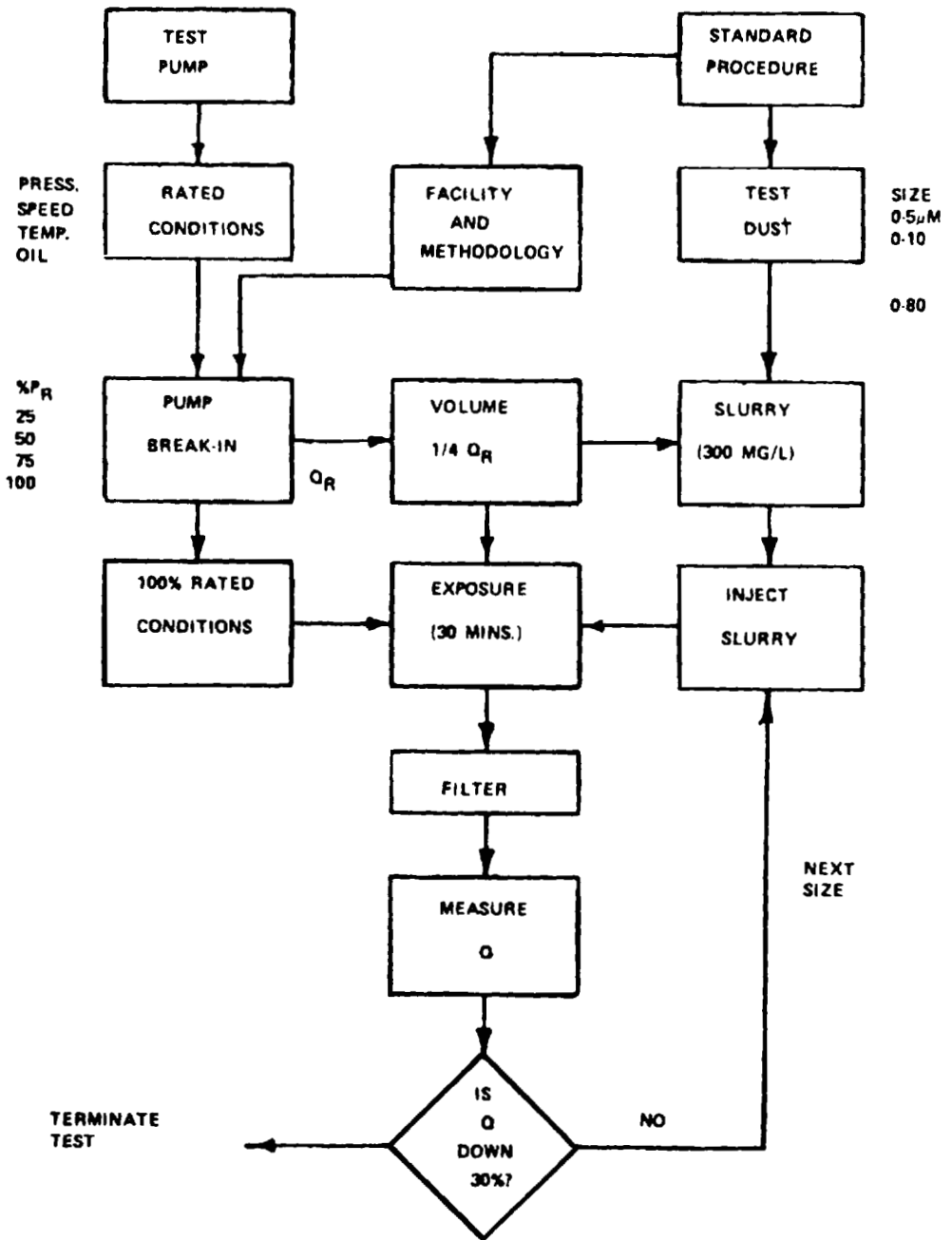


Figure 3.25 Flowchart of pump contaminant sensitivity test.

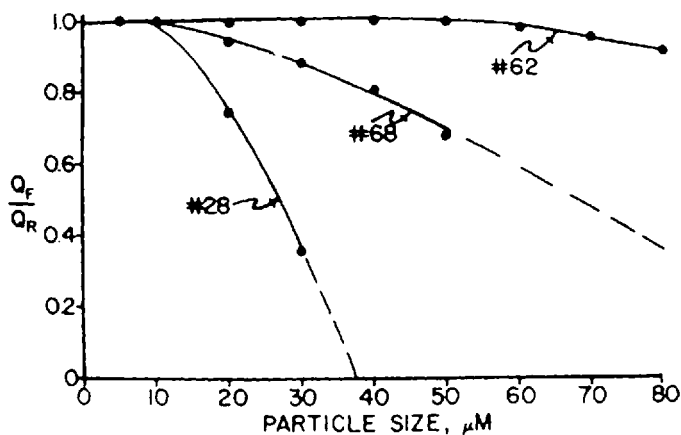


Figure 3.26 Flow degradation signatures of typical pumps.

are derived from the same base. The performance degradation observed in the contaminant sensitivity test is utilized to determine the contaminant sensitivity coefficients for the component at each particle size range. The contaminant exposure rate and the particle destruction rate are taken into account in evaluating the contaminant wear sensitivity coefficients. This is a fairly complex set of calculations because each particle size must be considered along with the effect of one size on the others. Once a complete set of sensitivity coefficients are available, they can be used to calculate the contaminant service life of the component operating at test conditions when the component is exposed to a given contamination level.

The contaminant tolerance profile describes the maximum particle size distribution level that can be continuously exposed to the pump without degrading its performance more than a designated amount during a specified period of time (say 1000 hs. for example). The tolerance profile is constructed by finding several different particle size distributions that produce the same contaminant life as determined from the contaminant sensitivity calculations. By definition, the contaminant tolerance profile is the locus of tangency points associated with particle size distribution lines that yield the same contaminant life. A partial construction of a profile is shown in Fig. 3.27. The profile is such that any contamination level with a particle size distribution which is tangent to the contaminant tolerance profile will provide a contaminant service life equal to the service life associated with that profile; for example, if a 1000-h contaminant tolerance profile is calculated for a given pump based on contaminant sensitivity test data, any particular size distribution which is tangent to, or falls below, that profile line will provide a contaminant service life 1000 h or greater for the component of.

The second method of interpreting the results of a contaminant sensitivity test is the omega rating concept. This method is actually an extension of the profile technique in that it requires the use of a contaminant tolerance profile calculated the same as described previously. However, in addition to the profile, the omega rating method also makes use of the Beta Ten Filtration Model. The Beta Ten model relies on the assumption that most filters used for decontaminating hydraulic and lubrication

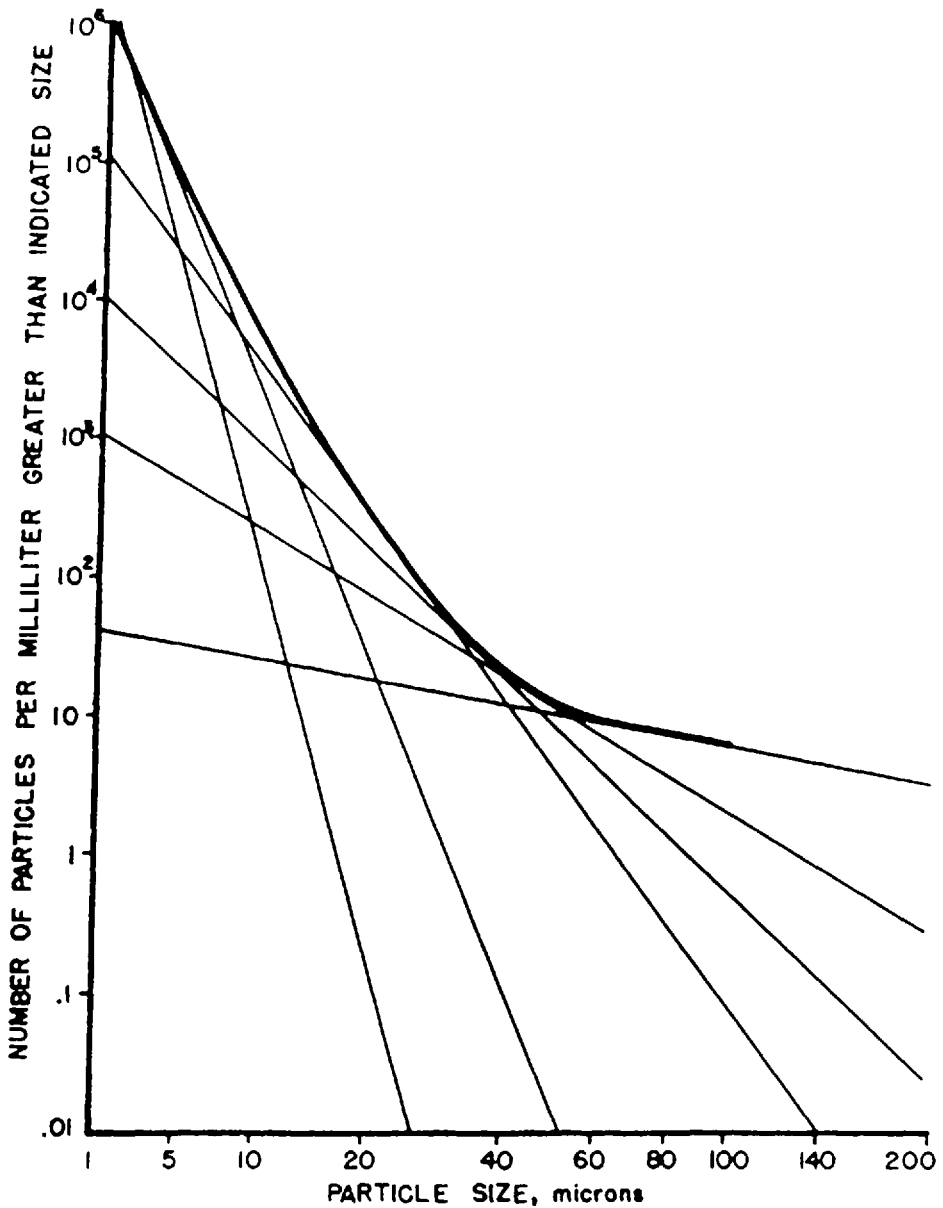


Figure 3.27 Contaminant tolerance profile.

tion systems obey the log-normal model. Using this model, the particle size distribution downstream of a filter can be calculated. Performing these calculation for an ingress rate of 10 mg/L and under the conditions of no element bypass, steady flow, and no vibration, the Beta Ten profiles can be plotted as shown in Fig. 3.28. As can be seen in Fig. 3.28, each of the filter profile lines are identified by the

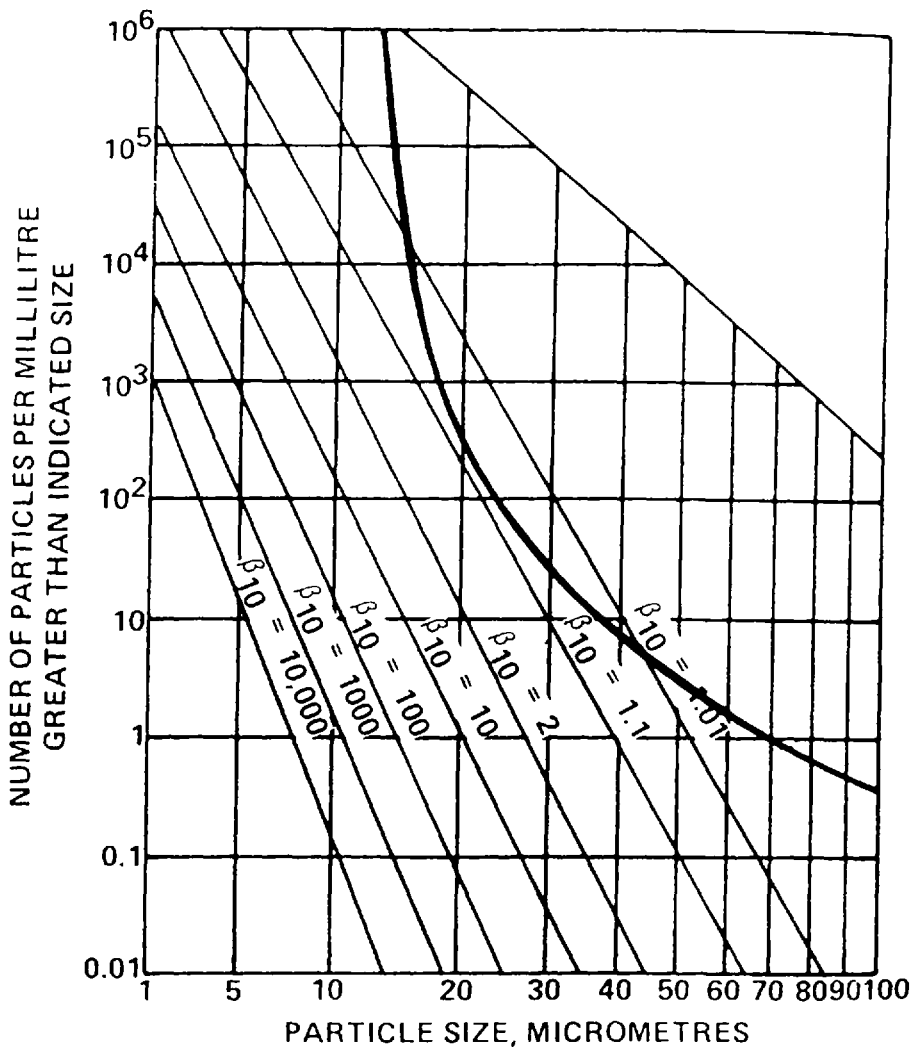


Figure 3.28 Omega rating concept.

filtration ratio (beta ratio) for particles greater than 10 μm as derived from the multipass filter test. In order to obtain an omega rating, the contaminant profile must be plotted on the log-log squared graph along with the Beta Ten profiles. The Beta Ten profile tangent to the contaminant tolerance profile defines the omega rating. Referring to Fig. 3.28, the Beta Ten profile tangent to the contaminant tolerance profile is identified by Beta Ten equal to approximately 1.08. Therefore, the omega rating for the pump which exhibited the contaminant tolerance profile shown in Fig. 3.28 would be 1.08. Of course, the preceding example does not take into account the actual operating conditions (pressure, temperature, fluid, etc.) and therefore can be used as a guide.

6 CONTAMINATION CONTROL METHODOLOGY

The contamination control to fluid systems is a much more complex task than the preceding sections would lead one to assume. Obviously, it involves the removal of particulate matter. However, if the particulate contamination were excluded from ever entering the system in the first place, there would be no need to remove it. In addition, if the system components were designed to live with extremely high contamination levels, again there would be little need to remove particulates. Another aspect of the contamination control task involves the fluid itself. The fluid manufacturers are researching additives to permit the system fluid to protect the components from attack by particulate contaminants. Finally, the duty-cycle severity and the penalty to be paid when a system fails will have a very great influence on the contamination control objectives. Therefore, in its total activity, contamination control is essentially a balance of many aspects.

6.1 Contamination Control Balance

The contamination control balance is shown schematically in Fig. 3.29. The ingress rate inherent in the system design operating in a given environment and the filtration provided work together to produce a contamination level in the system fluid. On the other side of the balance, the component contaminant sensitivity, the operational duty cycle, and the protection provided by the system fluid must be matched to the contamination level to produce an acceptable contaminant service life of the system. Fluid contamination control is practiced for only one purpose—to obtain an acceptable component contaminant service life and system reliability. This service life depends almost entirely on the two factor shown in Fig. 3.29—the contamination level of the system fluid and the contaminant tolerance of the system components.

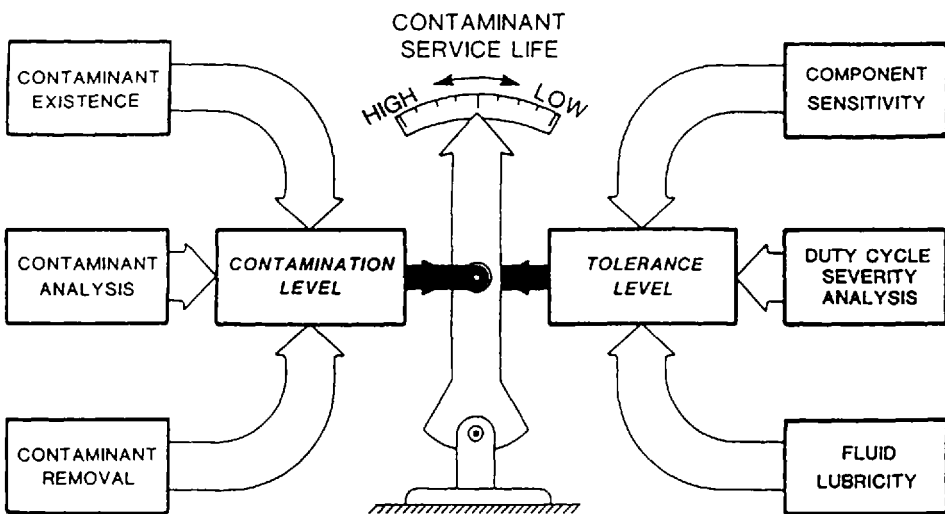


Figure 3.29 Contamination control balance.

6.2 Filter Performance Factors

There are many factors that must be considered in the filter selection process. However, before the filter selection activity can begin, some information about the components and system must be known or at least estimated. The contamination level the filter must maintain is determined by the most contaminant-sensitive component in the system. This is only logical because there may be only one filter. In cases where more than one filter is used, then the contaminant sensitivity of more than one component may be of importance. However, the actual contaminant tolerance level of the system is seldom a factor in the filter selection process. Instead, the system designer often relies on past experience and chooses a filter he has used successfully in the past. Whatever the selection criterion for the separation efficiency is, it must be the first consideration. Without adequate removal performance, an acceptable contamination level will be very difficult to maintain. The second parameter of the filter is contaminant capacity. If the filter cannot retain an adequate amount of particulate matter, it will become useless in a very short period of time. This leads to the use of a large number of elements or the filter will go into a bypass mode of operation and there might as well not be a filter in the system. The third filter performance factor is pressure drop. Because the filter will introduce some pressure loss in the system even when it is clean, this parasitic loss must be one of the considerations in filter selection.

Of course, there are filter factors other than performance factors that must be a part of the filter selection process. The construction of the housing and filter element must be such that there is adequate sealing of the element. If the seals allow fluid to bypass the element, the performance of the filter will be greatly reduced. In addition, if a bypass valve is used to protect the element during a cold start-up and other high-pressure-drop conditions, the construction of the bypass valve must be such that fluid is not inadvertently allowed to bypass the element. The compatibility of the filter element materials and the system fluid are a major consideration in filter element selection. In some cases, the system fluid can attack the element and degrade binders and adhesives. When this occurs, the element can essentially disintegrate and become additional contaminant material in the system.

It must always be remembered that fluid cleanliness and filtration can spell the difference between a successful system design and a failure. Fluid cleanliness cannot make a poorly designed system successful, but it can turn a good design into a catastrophe. Contamination control is not something that should be added to a system. It should be an integral part of the design process. The component should be selected to provide as much contaminant tolerance as can be found and afforded. This will reduce the work load of the filter. The fluid should be selected to provide protection for the components. Finally, the filter is selected to produce the contaminant environment in which these components will live for an adequate period of time.

BIBLIOGRAPHY

Introduction Section and Overall

Fitch, E. C., *Fluid Contamination Control*, 1988, FES, Inc., Stillwater, OK.

Particulate Contamination Section

- Bensch, L. E. and D. Kitzmiller, "Fundamental Properties of Test Contaminants," *BFPR J.* 1975.
- Fitch, E. C., "The Rod-Wiper Seal—The Real Culprit," *BFPR J.*, 1978, 11, pp. 153–157.
- Herdan, G., *Small Particle Statistics*, 1960, Butterworths, London.
- Inoue, R., "Log-Normal Transformation of AC Fine Test Dust Distributions," *BFPR J.*, 1979, 13(1), pp. 35–37.
- Iwanaga, M., "Particle Size Distribution of ACFTD—Experimental Investigation with Andreesen Pipette Apparatus," *BFPR J.*, 1980, 14(4), pp. 323–327.
- Iwanaga, M., "Particle Size Distribution of ACFTD—Part 2: Experimental Verification with Microscopic Counting," *BFPR J.*, 1981, 15(1), pp. 7–10.
- Iyengar, S. K. R., "Mathematical Description of Classified Contaminants," *BFPR J.*, 1972, pp. 259–286.
- Orr, C., *Particulate Technology*, 1966, The Macmillan Co., New York.

Contaminant Measurement Section

- Atkinson, R. H., "The Effect of Using Larger Pore Size Membranes for Gravimetric Analysis," *BFPR J.*, 1978, 12(1), pp. 29–34.
- Bensch, L. E., "International Survey of Automatic Particle Counter Calibration," *BFPR J.*, 1972, pp. 105–128.
- Bowman, B. and L. E. Bensch, "Accuracy of Dynamic Fluid Sampling Techniques," *BFPR J.*, 1979, 13(4), pp. 343–345.
- Carver, L. D., "Fluid Contamination Analysis by Light Blockage Counters," *BFPR J.*, 1982, 16(1), pp. 205–213.
- Day, M. J., "Calibration of Automatic Particle Counters," in *Contamination Control in Hydraulic Systems*, Institute of Mechanical Engineers, London, pp. 41–50.
- Fitch, E. C., "The New ISO Cleanliness Code—Let's Use It," *BFPR J.*, 1976.
- Frock, H. N., "Analysis of Particle Distributions Using Light Scattering Technique," *BFPR J.*, 16(1), pp. 229–232.
- Hunt, T. M. and D. G. Tilley, 1984, Techniques for Assessment of Contamination in Hydraulic Oils," in *Contamination Control in Hydraulic Systems*, 1984, Institute of Mechanical Engineers, London, pp. 57–63.
- Lieberman, A., "Fluid Contamination Analysis Using Particle Counters—Preliminary Preparation," *BFPR J.*, 1982, 16(1), pp. 215–221.
- Lieberman, A., "Fluid Contamination Analysis Using Particle Counters—In-Line Particle Counting," *BFPR J.*, 1982, 16(1), pp. 223–227.
- Moore, L. C., "Factors Involved in Obtaining Reliable Particle Counts," *BFPR J.*, 1974.
- Moore, L. C., "Comprehensive Guide for Measuring Fluid Contaminant with Liquid Automatic Particle Counters," *BFPR J.*, 1978, 12(2), pp. 159–162.
- Norvelle, F. D., "A Survey of Automatic Particle Counting Methods for Fluid Power Applications," *BFPR J.*, 1983, 17(2), pp. 295–302.
- Roberts, G. A., "Quality Control of Sample Container Cleanliness," *BFPR J.*, 1972, pp. 129–148.
- Roberts, G. A., "Particle Counting: An Analysis of the Problem of Calibration," *BFPR J.*, 1975.
- Sinvinske, H. D., *Contamination Control Handbook*, NASA—HASH-13245A, Report CR-61264, Sandia Laboratories, Albuquerque, NM, February 1969.
- West, G. C., "Conversion of Spherical Calibration to AC Fine Calibration," Application Note No. 3, HIAC, Division of Pacific Scientific Co., 1974.
- Wilson, P. J., *Solid Contaminant Profiles*, 1972, Association of Hydr. Equipment Manufacturers, London.

Filtration Section

- Bensch, L. E., "Influence of Cyclic Flow on Filtration Performance," *BFPR J.*, 1972, pp. 79–98.
- Bensch, L. E., "Surge Flow Effects on Filter Performance," *BFPR J.*, 1972.
- Bensch, L. E. and R. K. Tessmann, "Particle Counting Statistics," *BFPR J.*, 1975.
- Campbell, J. S. and M. Iwanaga, "Beta Rating Variation with Different Test Contaminants," *BFPR J.*, 1980, 14(1), pp. 87–93.
- Fitch, E. C. and R. K. Tessmann, "Modeling the Performance of Filter Assemblies," *BFPR J.*, 1973.
- Fitch, E. C. and R. K. Tessmann, "The Filter Selection Graph—A Basic Contamination Control Tool," *BFPR J.*, 1974.
- Iwanaga, M., "Filtration Ratio Vs. Contaminant Distribution," *BFPR J.*, 1978, 12(4), pp. 331–340.
- Reed, R. E., "Effects of Vibrations on Filtration," *BFPR Information Report*, No. 66-1, FPRC/OSU, Stillwater, OK, 1966, pp. 1–14.
- Rice, C. G., "Filtration Characteristics of Cellulose Filter Media," in *Contamination Control of Hydraulic Systems*, 1984, Institute of Mechanical Engineers, London, pp. 119–127.
- Saunders, D. H., "The Effect of Practical Operation Conditions on the Performance of Hydraulic Filters," *Contamination Control of Hydraulic Systems*, 1984, Institute of Mechanical Engineers, London, pp. 101–110.
- Steele, F. M., "Adsorbent Filter Media Application," *BFPR J.*, 1981, 15(3), pp. 307–314.
- Stuntz, R. M. and E. C. Fitch, "Filtration Physics Report," *BFPR J.*, 1971, pp. 1–147.
- Tessmann, R. K., "Filter Service Life Vs. Particle Size Distribution," *BFPR J.*, 1973.
- Tessmann, R. K., "Influence of Ingression Rates on Filter Performance," *BFPR J.*, 1973.
- Tessmann, R. K., "The Effect of Bypass Valve Leakage on Filter Performance," *BFPR J.*, 1975.
- Tessmann, R. K., "Effect of System Configuration on Filtration Performance," *BFPR J.*, 1975.
- Tessmann, R. K., "Optimizing Filter Selection by Considering All Three Performance Factors," *BFPR J.*, 1976.
- Verdegan, B. M., T. Jaroszczyk, and J. A. Stinson, "Interpretation of Filter Ratings for Lubrication Systems," *ASLE Paper No. 87-AM-2F-2*. ASLE, Anaheim, CA, May 1987, pp. 1–7.
- Xia, S. X., "The Effects of Flow Density on Filtration Performance," *BFPR J.*, 1982, 16(1), pp. 155–160.

Component Contaminant Tolerance Section

- Backe, W. and D. Winner, "Investigation of the Contamination Sensitivity of Hydraulic Pumps," in *Contamination Control of Hydraulic Systems*, 1984, Institute of Mechanical Engineers, London, pp. 129–134.
- Bensch, L. E., "Repeatability Assessment of the Hydraulic Pump Contaminant Sensitivity Testing," *BFPR J.*, 1978, 12(1).
- Bensch, L. E. and E. C. Fitch, "A New Theory for the Contaminant Sensitivity of Fluid Power Pumps," *BFPR J.*, 1972, pp. 99–158.
- Bensch, L. E. and E. C. Fitch, "Rod Seal Sensitivity to Contaminant Wear," *BFPR J.*, 1973.
- Bensch, L. E. and R. K. Tessmann, "Contaminant Sensitivity Characteristics of Pressure-Compensated Pumps," *BFPR J.*, 1973.
- Blackburn, J. F., J. L. Shearer, and G. Reethof, "The Effects of Dirt," in *Fluid Power Control*, 1960, John Wiley, New York.
- Bonner, W. T. and L. E. Bensch, "Hydraulic Motor Contaminant Sensitivity Testing," *BFPR J.*, 1974.
- Day, M. J. and R. M. Fairhurst, "Contamination Sensitivity of Hydraulic Pumps," in *Contamination Control of Hydraulic Systems*, 1984, Institute of Mechanical Engineers, London, pp. 135–141.

- Fitch, E. C., *Fluid Power Engineering*, 1982, FES, Inc., Stillwater, OK.
- Fitch, E. C., *Hydraulic Failure—Analysis and Prevention*, 1984, FES, Inc., Stillwater, OK.
- Fitzsimmons, B. and H. D. Clevenger, "Effect of Contaminated Lubricants Upon Tapered Roller Bearing Wear," *BFPR J.*, 1974.
- Harrison, H. L., "Reducing Servovalve Stiction," *Hydraulics Pneumatics*, March 1962, pp. 96–104.
- Hong, I. T., "Sliding Contact Wear Caused by Loose Abrasive Particles in Lubricant," *BFPR J.*, 1981, 15(2), pp. 153–162.
- Hong, I. T., and E. C. Fitch, "Wear of Gear Pump Under Abrasive Fluid Condition," *Proc. of NCFP*, 1985, NCFP, Chicago, pp. 1–7.
- Hong, I. T. and E. C. Fitch, "Tribological Effects of Obliteration on Sliding Valve Characteristics," *ASME-ASLE Tribology Conference Paper*, ASME, Pittsburgh, PA, 1986, pp. 1–23.
- Howell, G. W. and T. M. Weathers, *Aerospace Fluid Component Designer's Handbook*, Part 6.2.2-9, TRW Systems Group for Edwards AFB, Contract AF 94(611)-8385 and AF 94(611)-11316, March 1967.
- Inoue, R. and E. C. Fitch, "The Omega Pump Rating System," *BFPR J.*, 1978, 12(2).
- Kanijo, K., H. Kusama, and T. Sasada, "Hydraulic Lock on Spool Valve (Reports 1, 2, and 3)," *Bull. Tokyo Inst. Technol.*, 1970, pp. 45–89.
- Lobmeyer, R. J., M. A. Kelley, and R. J. Chapman, "Hydraulic Fluid Contaminant Sensitivity Test," *SAE Paper 770543*, SAE Earthmoving Industry Conference, Peoria, IL, April 1977.
- Mannam, J., "Hydraulic and Dirt Lock in Piston Type Control Valves," in *Hydraulic and Fluid Mechanics*, 1964, Pergamon Press, Oxford, pp. 15–31.
- Maroney, G. E. and E. C. Fitch, "Fundamental Method for Evaluating the Contaminant Tolerance of Fluid Power Control Valves," *BFPR J.*, 1972, pp. 159–182.
- Miller, D. G., "Erosive Wear Tests," *BFPR J.*, 1972, pp. 19–36.
- O'Conner, J. W., "Selection of Pumps and Filter Systems Based on Oil Contaminant Levels in an Agricultural Tractor," *SAE Paper 730798*, SAE Milwaukee Meeting, 1973.
- Perrotto, J. A., "Effect of Abrasive Contamination on Ball Bearing Performance," *ASLE Paper 79-AM-2B-3*, 1979.
- Phillips, J. F., "Theory on the Contaminant Sensitivity of Elastomeric Reciprocating Hydraulic Pressure Seals," *BFPR J.*, 1972, pp. 183–228.
- Schmitt, V. R., "Criteria for Contaminant Level in Flight Control Systems," *Paper 680190*, SAE, Phoenix, AZ, Oct. 1967, pp. 1–17.
- Scott, W., "Relationship Between Solid Particle Contaminant Size/Thickness of Oil Films in Hydraulic Systems," *Contamination Conference Paper C99/76IMEchE*, Bath, England, 1976, pp. 93–100.
- Tellier, G. F. and J. W. Lewellen, "Poppet and Seat Design Criteria for Contaminant-Particle Resistance," *Report AFRPL-TR-70-1*, Rocketdyne for Edwards AFB, April 1970.
- Tessmann, R. K., "Influence of Contaminant Characteristics Upon Pump Contaminant Sensitivity," *BFPR J.*, 1974.
- Tessmann, R. K., "Pump Contaminant Sensitivity Versus Operating Pressure," *BFPR J.*, 1974.
- Tessmann, R. K., "Contaminant Wear in Hydraulic and Lubricating Systems," *BFPR J.*, 1975.
- Tessmann, R. K., "Summary of FPRC Wear Mechanism Study," *BFPR J.*, 1977, 11(2).
- Tessmann, R. K., "A Ferrographic Wear Model for Hydraulic Pumps," *BFPR J.*, 1977, 11(3).
- Tessmann, R. K. and B. A. Foord, "Particle Size Distribution Effects on Servovalve Performance," *BFPR J.*, 1973.
- Tessmann, R. K. and B. A. Foord, "A Dynamic Approach to the Contaminant Sensitivity of Directional Control Valves," *BFPR J.*, 1973.
- Tessmann, R. K. and B. A. Foord, "Dynamic Contaminant Sensitivity of Pressure Control Valves," *BFPR J.*, 1973.

- Tessman, R. K., S. K. R. Iyengar, and E. C. Fitch, "Component Wear Report," *BFPR J.*, 1971, pp. 1–117.
- Wolf, M. L., "Contaminant Particle Effects on Pumps as a Function of Size, Type, and Concentration," M. S. Thesis, FPRC/OSU, Stillwater, OK, 1965.
- Yeaple, F., *Fluid Power Design Handbook*, 1984, Marcel Dekker, New York.

Filter Selection Methodology Section

- Glaeser, W. A., et al., "Application of Oil Analysis Techniques to the Diagnosis of Condition and Prediction of Failure," NTIS AD-770-461, MERDC Report by Battelle Laboratories, Columbus, OH, Nov. 1973.
- Fitch, E. C., "The Contamination Control Balance," *BFPR J.*, 1977, 11(1).
- Fitch, E. C., "Specifying Contamination Control Functions," *BFPR J.*, 1977, 11(1).
- Fitch, E. C., "A Perspective of Contamination Control Economics," *BFPR J.*, 1977, 11(1).
- Fitch, E. C., "What the User Should Know about the Assessment and Selection of Hydraulic Components," *BFPR J.*, 1980, 14(2), pp. 95–103.
- Fitch, E. C., R. K. Tessmann, and L. E. Bensch, "Contamination Control Report," *BFPR J.*, 1969, pp. 1–167.
- Fitch, E. C., R. K. Tessmann, and L. E. Bensch, "Contamination Control Report," *BFPR J.*, 1970, Supplement 70-1, pp. 1–155.
- Fitch, E. C., R. K. Tessmann, and L. E. Bensch, "Contamination Control Report," *BFPR J.*, 1971, pp. 1–309.
- Inoue, R., "Pump Selection Based on Life Cycle Cost," *BFPR J.*, 1977, 11(3), pp. 337–340.
- Norvelle, F. D., "Wear Monitoring and Prevention," *BFPR J.*, 1981, 15(2), pp. 121–130.
- Norvelle, F. D., "Designing for Contamination Control in Fluid Power Systems," *BFPR J.*, 1983, 17(2), pp. 289–294.
- Tessmann, R. K. and L. E. Bensch, "What's Ahead in Fluid Power Contamination Control," *BFPR J.*, 1976.

4

Physical Properties and Their Determination

GEORGE E. TOTTEN and GLENN M. WEBSTER

Union Carbide Corporation, Tarrytown, New York

F. D. YEAPLE†

TEF Engineering, Allendale, New Jersey

1 INTRODUCTION

The hydraulic fluid is a component of the hydraulic system. This component is used for power transmission. The most common fluids used in hydraulic application are shown in Table 4.1. Each of these fluids exhibits uniquely different physical properties and possess different advantages and limitations which are summarized in subsequent chapters.

Hydraulic system performance is affected by the physical properties of the fluid component, which include density, viscosity, air entrainment and air release, foaming, cavitation, and various electrical properties such as conductivity, resistivity, and permittivity. In this chapter, a review of these and other important physical properties will be provided. The role of these physical properties on fluid performance in hydraulic systems will also be discussed.

2 DISCUSSION

2.1 Viscosity

One of the most important fundamental physical properties of a hydraulic fluid is viscosity. Fluid viscosity, which is a measure of the “thickness” of the fluid, affects both operational characteristics of the hydraulic system and the lubrication properties exhibited by the fluid. (The effect of hydraulic fluid viscosity on lubrication will be discussed in Chapter 3.)

†Deceased.

Table 4.1 Illustrative Examples of Hydraulic Fluids Used in Industrial Applications

Petroleum oil
Polyol ester
Phosphate ester
Vegetable oil
Water-glycol
Water-in-oil emulsion
Chlorinated hydrocarbon
Synthetic hydrocarbon
Silicate ester
Silicone
Water

Minimum viscosity limits for hydraulic pumps are dependent on pump design. The maximum fluid viscosity that can be used, also known as “cold-start” viscosity, is dependent on [1]

1. Maximum viscosity that the pump will tolerate
2. Maximum viscosity creating a pressure drop in the suction line, which is dependent on pipe resistance, pipe bends, line strainers, and so forth and should equal the pump suction capacity
3. Maximum viscosity creating maximum acceptable pressure drops in long high-pressure lines

Zino used the five-zone viscosity selection chart shown in Fig. 4.1, which is derived from an ASTM D 341 log-log viscosity-temperature plot, to illustrate the critical dependence of hydraulic fluid viscosity on fluid temperature and system pressure [2]. Both temperature and viscosity must be considered if optimal hydraulic fluid performance is to be achieved.

In this section, hydraulic fluid temperature, pressure, and shear rates on viscosity will be discussed. Chapter 5 provides a general overview of fluid viscosity classification. Chapter 6 will discuss the effect of fluid viscosity on lubrication.

2.1.1 Hydraulic Pump Viscosity Limits

The effect of temperature and pressure on the pumpability of a fire-resistant emulsion is illustrated in Fig. 4.2, where it is apparent that there is an optimal range for the proper operation of a hydraulic pump [3]. This is also illustrated in Fig. 4.3, where it is shown that at very low temperatures, increased fluid viscosity leads to cavitation, and at excessively high temperatures, insufficient fluid viscosity results in pump slippage and poor efficiency [4]. Similar low-temperature effects on hydraulic pump operation have been reported by Stecki et al. [5].

Typical hydraulic fluid viscosity limits for vane, gear, and piston pumps are provided in Table 4.2 [1]. Similar recommendations have been provided for various vane, gear, and radial and axial piston pumps supplied by a number of specific manufactures [6]. Although these data illustrate the importance of viscosity on the

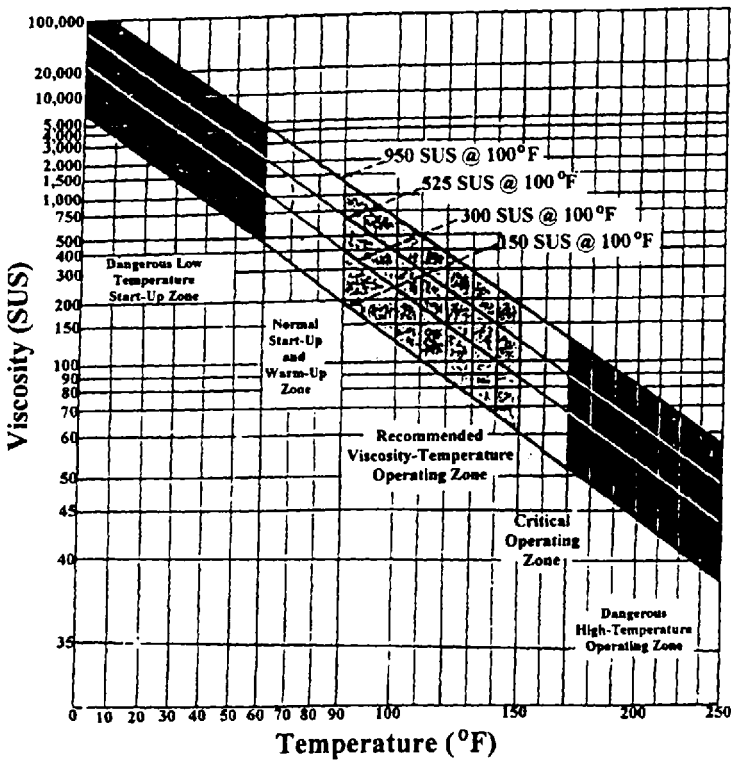


Figure 4.1 Five-zone chart for hydraulic fluid viscosity selection. (From Ref. 2.)

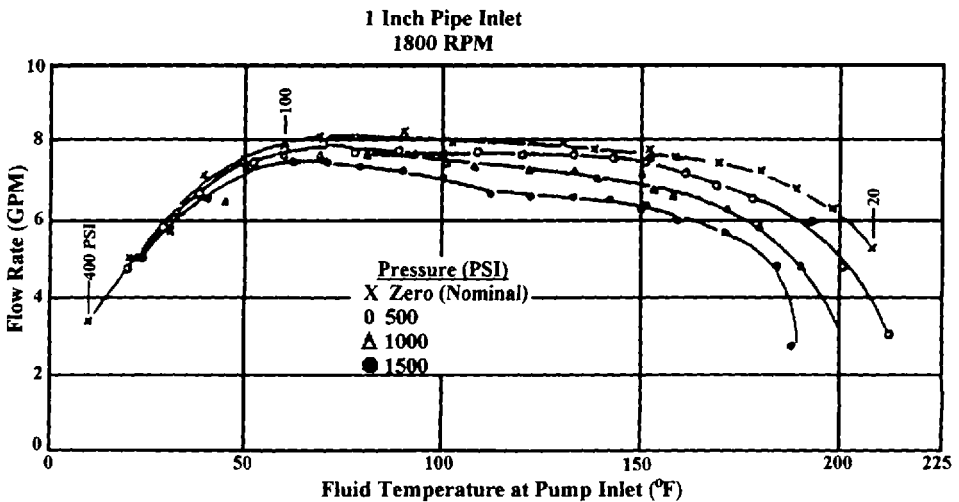


Figure 4.2 Effect of temperature and pressure on fluid pumpability. (From Ref. 3.)

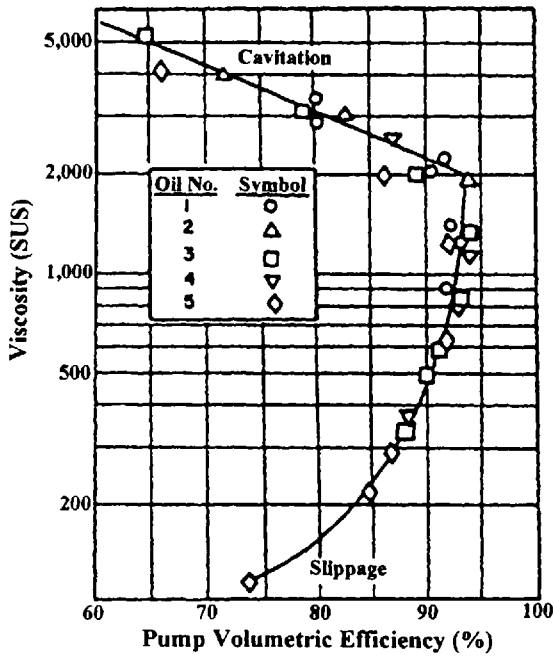


Figure 4.3 Effect of fluid viscosity on volumetric efficiency (vane pump with reservoir below the pump). (From Ref. 4.)

operation of a hydraulic system, specific viscosity limits for the pump and hydraulic circuit are dependent on the pump and hydraulic circuit in use.

2.1.2 Newtonian Viscosity

The "coefficient of viscosity" (η) for the fluid depicted in Fig. 4.4 [7] is linearly proportional to shear stress (τ) and shear rate (dv/dz):

$$\eta = \frac{\tau}{(dv/dz)}$$

The value dv/dz represents the change in fluid velocity with respect to change in position in the z direction [8].

Table 4.2 Typical Recommended Hydraulic Fluid Viscosity Ranges

Typical data	Vane	High-pressure gear pump		Unboosted piston	
		Plain bearings	Bearing	Sliding valves	Seated valves
Minimum viscosity (cS)	20	25	16	16	12
Optimum viscosity (cS)	25	25	20	30	20
Maximum viscosity (cS)	850	850	850	500	200
Suction capacity (in. Hg)	10	17	17	5	1

Source: Ref. 1.

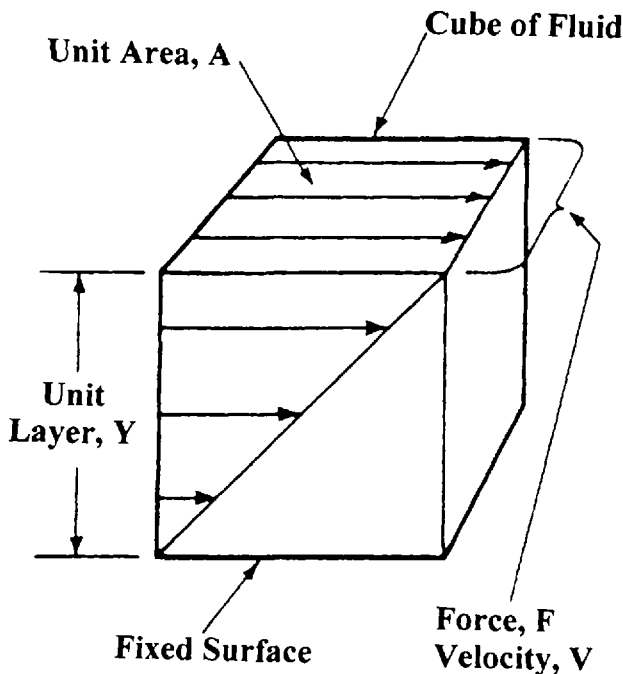


Figure 4.4 Visualization of absolute viscosity. (From Ref. 7.)

Newtonian/Non-Newtonian Behavior

Fluid viscosity is classified as Newtonian or non-Newtonian. As shown above, Newtonian fluid viscosity does not vary with shear rate [7]. Viscosities of non-Newtonian fluids do vary with shear rate, as illustrated in Fig. 4.5 [9]. Hydraulic fluids typically exhibit varying degrees of non-Newtonian viscosity behavior. At high shear rates, which are estimated to approach 10^6 s^{-1} in the inlet zone of the wear contact [10], even hydraulic fluids that normally exhibit Newtonian behavior at low shear rates may be non-Newtonian [11]. The fluid shown in Fig. 4.6 exhibits two Newtonian regions referred to as the “first” and “second” Newtonian regions [11]. The two Newtonian regions are connected by a non-Newtonian transition.

Non-Newtonian viscosity behavior is particularly important when considering the lubrication properties of a fluid. Aderin et al. have reported that non-Newtonian viscosity behavior at the Hertzian contact inlet region may account for significantly lower pressure–viscosity coefficients (see Chapter 3) than predicted from low-shear-viscosity measurements [12].

A general equation that has been used for non-Newtonian “power-law” fluids is the Ostwald–de Waele equation [8]:

$$\tau = \eta_0 \left(\frac{dv}{dz} \right)^n$$

where η_0 is the viscosity of the fluid at a reference low shear rate and n is the power-law exponent, which is 1 for Newtonian fluids and less than 1 for non-Newtonian fluids [13].

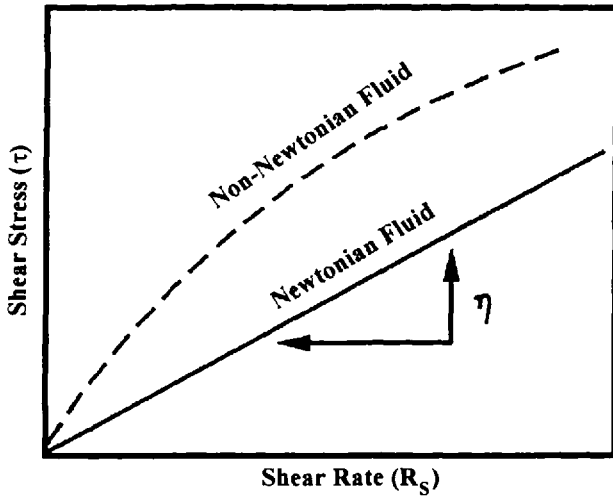


Figure 4.5 Illustration of shear-stress variation with shear rate for Newtonian and non-Newtonian fluids. (From Ref. 9.)

The power-law relationship may be modified to describe the two Newtonian and the non-Newtonian regions depicted in Fig. 4.7 [13]. One modification is the truncated power-law model where the three regions are simply connected as shown in Fig. 4.7 [13]. In this model, η_0 is the low shear viscosity in the first Newtonian region, η_* is the viscosity in the second Newtonian region, and the power law is

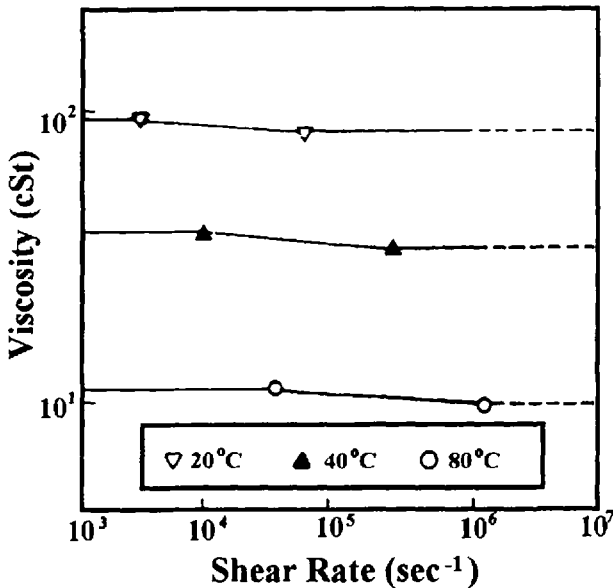


Figure 4.6 High-shear viscosity profile of a water-glycol hydraulic fluid. (From Ref. 11.)

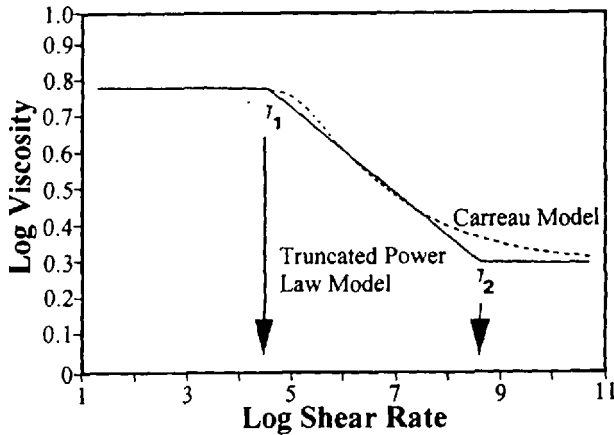


Figure 4.7 Illustration of the truncated power-law model and the Carreau model for non-Newtonian fluids. (From Ref. 13.)

used to describe the viscosity behavior during the transition from first to the second Newtonian regions.

One of the disadvantages of the truncated power-law model is the discontinuous first derivative. There are various alternative models that have been used to provide a continuous transition between the first and second Newtonian regions [14]. One alternative model to the truncated power-law model is the Carreau model [15]:

$$\frac{\eta - \eta_{\infty}}{\eta_0 - \eta_{\infty}} = \left[1 + \lambda \left(\frac{dv}{dz} \right) \right]^{(n-1)/2}$$

where η is a time constant and n is the power-law coefficient.

2.1.3 Viscosity–Temperature Relationship

Fluid viscosity varies with both temperature and pressure of the fluid as illustrated in Fig. 4.8 [7]. The temperature dependence of viscosity is described by Eyring and Ewell's equation [16,17]:

$$\eta = \frac{hN}{V} e^{\Delta E/RT}$$

where

- h = Planck's constant
- N = Avogadro's number
- V = molecular volume (molecular weight/density)
- ΔE = the activation energy for viscous flow
- R = the gas constant
- T = the absolute temperature (K).

Andrade's equation has been used as an alternative to Eyring and Ewell's equation:

$$\eta = Ae^{b/T}$$

where A and b are constants.

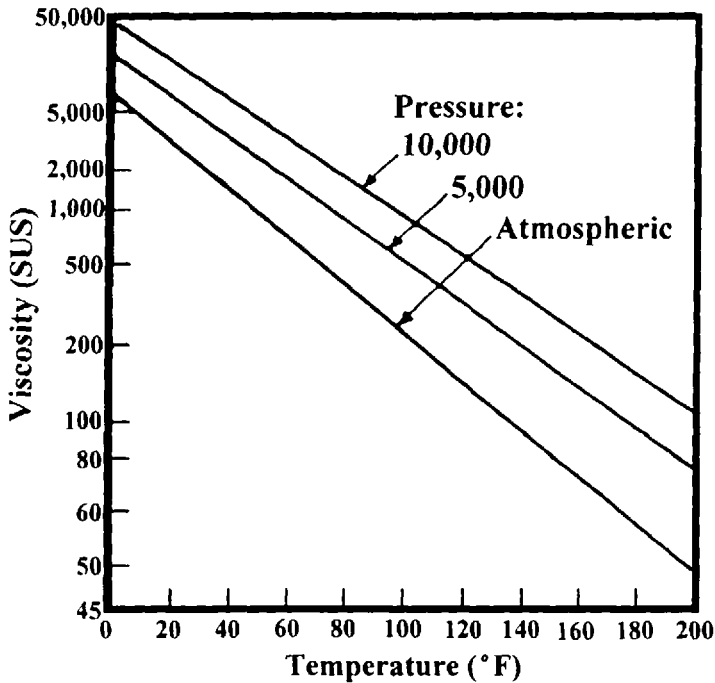


Figure 4.8 Viscosity versus pressure for a hydraulic oil. (From Ref. 7.)

Currently, one of the most commonly used equations to predict viscosity temperature relationships of mineral oils is the Walther equation [18,19]:

$$\log \log(\eta + c) = a - b \log T$$

where a and b are constants for a particular fluid and C varies with viscosity. This use of the equation is described in ASTM D 342-87 [20].

A more general treatment of the viscosity–temperature relationships is to curve-fit experimental viscosity–temperature data to the Vogel equation [12] and solve for a temperature–viscosity coefficient:

$$\eta = Ae^{B/(T-C)}$$

where A , B , and C are least-squares curve-fitting constants and T is the absolute temperature (K).

The temperature–viscosity coefficient can then be determined at any temperature from

$$\frac{d \ln \eta}{dT} = \frac{-B}{(T - C)^2}$$

2.1.4 Viscosity–Pressure Relationships

In addition to shear rate and temperature, the viscosity of hydraulic fluids may also be significantly affected by pressure, as shown in Fig. 4.8 [7]. This relationship is dependent on the chemical composition of the fluid, as shown for the paraffinic and naphthenic oils in Figs. 4.9 [21] and 4.10 [22].

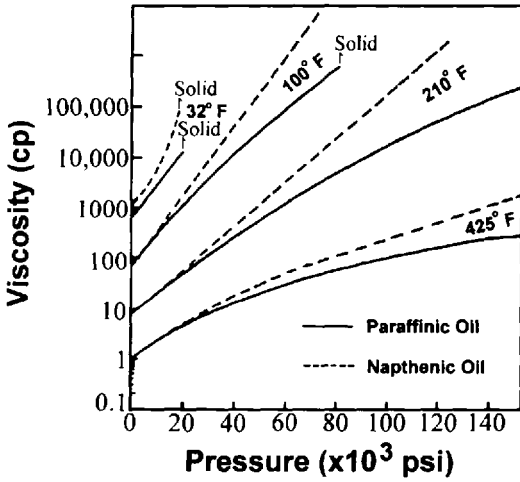


Figure 4.9 Viscosity–pressure relationships at different temperatures for paraffinic and naphthenic hydraulic oils. (From Ref. 21.)

The pressure–viscosity variation of naphthenic and paraffinic petroleum oils has been studied and a number of general observations were made [21]:

- Viscosity increases with increasing pressure.
- The increase of viscosity with pressure decreases with increasing temperature.

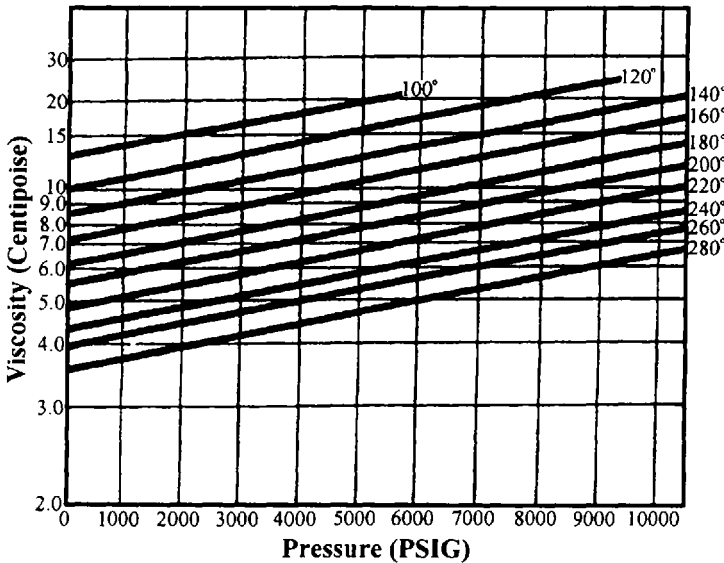


Figure 4.10 Viscosity–pressure relationship for Mil 5606 aerospace hydraulic fluid. (From Ref. 22.)

- At room temperature, the viscosity of most petroleum oils increases by approximately 2.3 when pressure is increased to 5000 psi.
- The same increases in pressure will exhibit a greater effect on viscosity at higher pressure.
- Increasing pressure will increase the viscosity index of naphthenic oil more than a paraffinic oil.

The effect of pressure on viscosity is modeled by the Barus equation [23]:

$$\eta_p = \eta_0 e^{\alpha P}$$

where η_p is the centipoise viscosity at pressure (P), η_0 is the viscosity at atmosphere pressure, P is the pressure, and α is the pressure–viscosity coefficient.

Unfortunately, as Jones et al. have shown, a linear graphical solution to the Barus equation by plotting $\ln \eta$ as a function of P is not obtained, except at low pressures (see Fig. 4.11) [24]. The slope of the tangent to $\log \eta$ as a function of P isotherm (α_{0T}) at atmospheric pressure is often used for the calculation of the pressure–viscosity coefficient used for elasto-hydrodynamic (EHD) lubrication analysis:

$$\alpha_{0T} \equiv \left. \frac{d \ln \eta}{dP} \right|_{T, P=1 \text{ atm}} = \left. \frac{1}{\eta} \frac{d\eta}{dP} \right|_{T, P=1 \text{ atm}}$$

However, α_{0T} , which is obtained by graphical differentiation, is dependent on a relatively few low-pressure data points which contribute substantially to overall error. An alternative solution which provides a more reliable viscosity–pressure response is to solve for α^* , as shown in Fig. 4.11 by graphically integrating [25]:

$$\alpha^* \equiv \left[\int_0^{P-x} \frac{\eta(T, P = 1 \text{ atm})}{\eta(P, T)} dP \right]^{-1} \Bigg|_T$$

The advantage of α^* is that all of the variations of viscosity with pressure over the entire pressure range are included in the calculation, as illustrated in Fig. 4.11 [24].

In many cases, the value of α is not available. One early attempt to predict α for petroleum oils at pressures up to 10,000 psi is reported by Fresco et al. [26]. Fresco's α -prediction chart is shown in Fig. 4.12 and is based on the viscosity–temperature properties of a fluid as represented by the “ASTM slope” [19].

The ASTM slope is the slope of the viscosity temperature line of the Walther equation, which is plotted as described in ASTM D 341. (This is not equivalent to the value B in the Walther equation.) In addition to determining the ASTM slope graphically, it can be calculated from [19]

$$\text{ASTM slope} = \frac{\log \log(\eta_1/\eta_2)}{\log(T_2/T_1)}$$

So and Klaus subsequently developed a single correlation which can be used for a broad range of fluids and fluid blends [27]. This correlation is based on the viscosity and density of the fluid at the temperature of interest. The viscosity–temperature behavior of the fluid utilizes the term m_0 , which is calculated from

$$m_0 = \frac{\text{ASTM slope}}{0.2}$$

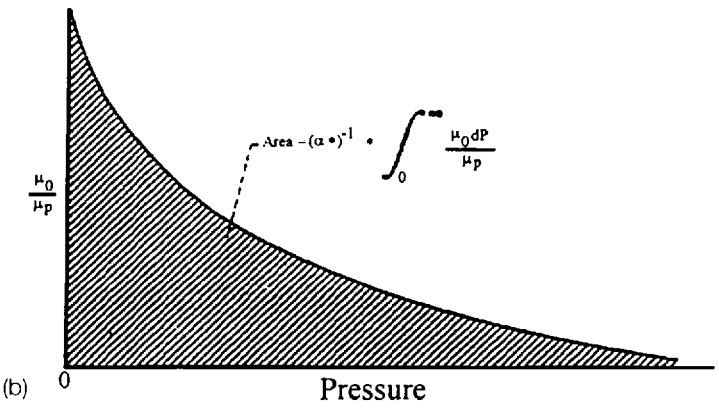
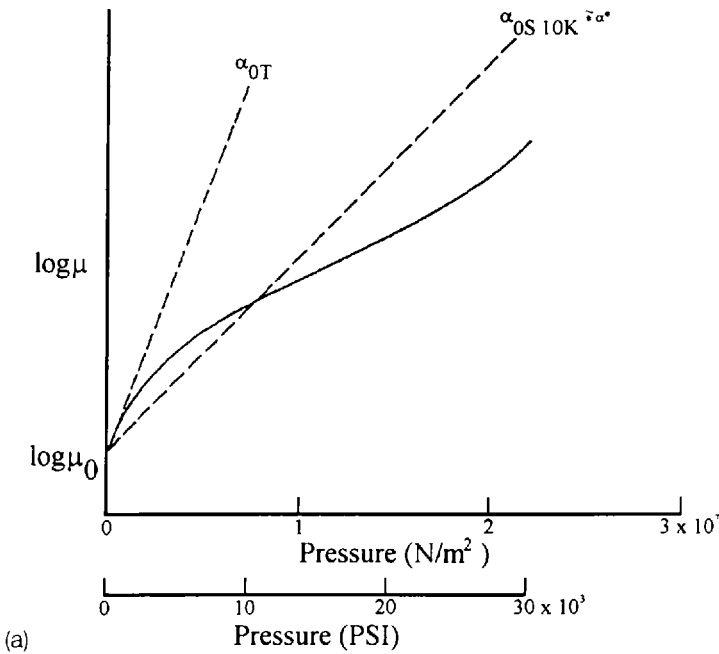


Figure 4.11 (a) Modeling viscosity–pressure behavior with α_{0T} and α^* . (b) Typical viscosity–pressure isotherm. (From Ref. 24.)

The So–Klaus correlation is [27,29]

$$\alpha = 1.030 + 3.509(\log \eta_0)^{3.0627} + 2.412 \times 10^{-4} m_0^{5.1903} (\log \eta_0)^{1.5976} - 3.387(\log \eta_0)^{3.0975} \rho^{0.1162}$$

where

- α = pressure–viscosity coefficient ($\text{kPa}^{-1} \times 10^5$) = $\partial(\log \eta) / \partial P$ at $P = 0$
- $\log \eta_0$ = base 10 logarithm of the atmospheric viscosity in centistokes at the temperature of interest
- ρ = atmospheric density in g/mL at the temperature of interest

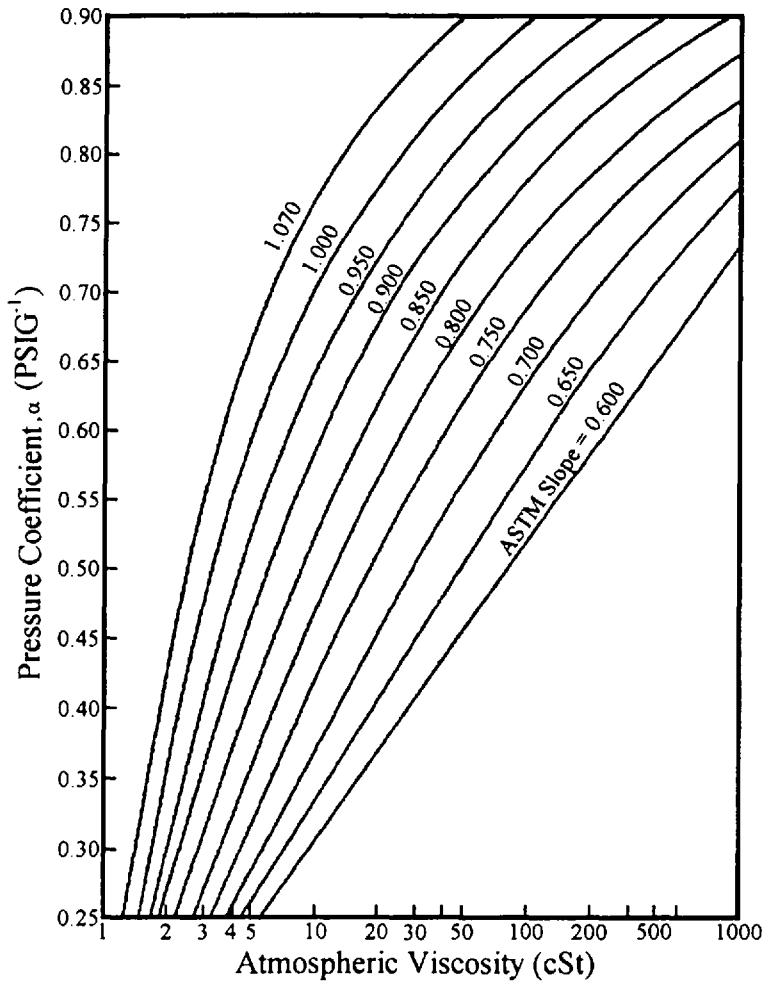


Figure 4.12 Nomogram for prediction of viscosity–pressure coefficient of mineral oil hydraulic fluid. (From Ref. 26.)

m_0 = the viscosity–temperature property based on atmospheric kinematic viscosities at 37.8°C (100°F) and 98.9°C (210°F) of the fluid of interest.

Wu et al. have developed a simplified equation for predicting α based on free-volume theory [28]:

$$\alpha = (0.1657 + 0.2332 \log \eta_0)m_0$$

where

α = the pressure–viscosity coefficient ($\text{kPa}^{-1} \times 10^5$)

m_0 = the viscosity–temperature property determined from the ASTM–Walther equation and is equal to ASTM slope/0.2

η_0 = the atmospheric kinematic viscosity at the temperature of interest (mm²/s)

Other methods used to predict the value of α are summarized in Table 4.3 [195].

The Appeldoorn equation has been proposed for the simultaneous calculation of the effects of both temperature and pressure on viscosity [28]

$$\log \left(\frac{\eta}{\eta_A} \right) = a \log(F/F_0) + \alpha P$$

Table 4.3 Various Methods Used in the Comparisons of the Effectiveness in Predicting the Pressure Effects on Viscosity

Developer	Correlation	Ref.
Kouzel	$\log \frac{\eta_r}{\eta_0} = \frac{P}{1000} (0.0239 + 0.01638 \eta_0^{0.278})$	188
Roelands et al.	For nonpolymer fluids $\log \frac{\eta_r}{\eta_0} = \left(\frac{P}{5000} \right) [(0.002C_A + 0.003C_A + 0.055) \log \eta_0 + 0.228]$ $\log(y - 0.890) = 0.00955(C_A + 1.5C_A) - 1.930$ For polymer fluids $\log(\log \eta_r + 1.200) = Z_B \log \left(1 + \frac{P}{28.400} \right) + \log(\log \eta_0 + 1.200)$ $Z_B = 0.6Z_{pr} + 0.4Z_{Hr}$	189
Fresco	$\log \frac{v}{v_0} = P\alpha'(10^{-4})$, $\alpha = \frac{560}{O_R}$, $\alpha' = A + B \log(V_0) + C(\log V_0)^2$ A, B, and C are function of ASTM slope	190
Kim	$\log \frac{v}{v_0} = P(\alpha' + \beta)(10^{-4})$ α' is calculated from Fresco's method $\beta = A' \log V_c + B'(\log V_c)^2$ A' and B' are a function of temperature; graphical method is also available	191
So and Klaus	$\log \left(\frac{\eta_r}{\eta_0} \right) = \alpha(98.1P)$ $s = 2.848 \times 10^{-4} m^{5.1903} [\log(V_0)]^{1.5976}$ $t = 3.999 [\log(V_0)]^{1.0975} p^{0.01162}$	192
Chu and Cameron	$\log \left(\frac{\eta_r}{\eta_0} \right) = 16 \log \left(1 + \frac{0.062(10^{-4})P \times 10^{-4}}{\eta_0^{0.062}} \right) + a = [0.183 + 0.2951 \log(\eta_0)]$ for naphthenics	193
Worster	$\log \left(\frac{\eta_r}{\eta_0} \right) = aP(10^{-4}) + a = [0.183 + 0.2951 \log(\eta_0)]$ for naphthenics	194
Johnston	$\alpha = \frac{\beta E}{\alpha, 2CRT^2}$	195
Shibada	$\alpha = 0.62044 v_0^{0.17615} m_0^{2.04746} p^{0.29292}$	196

Source: Ref. 195.

where

- η = the viscosity at temperature F , expressed in °F, and pressure P
- η_1 = a reference viscosity at atmospheric pressure and temperature F_0
- a = the viscosity–temperature (Appeldoorn) coefficient
- α = the pressure–viscosity coefficient.

Both temperature and pressure exhibit potentially large effects on viscosity and the simultaneous inclusion of both in viscosity calculations is desirable.

2.1.5 Shear Degradation

Many hydraulic fluids contain higher-molecular-weight viscosifiers or thickener additives that will degrade under the high-shear-rate conditions present in hydraulic pump applications. Molecular degradation due to high shear rates is called “mechanodegradation” [30–32].

High-molecular-weight additives such as viscosifiers and thickeners do not exist in solution in their chain-extended form as they are often drawn on paper. Instead, the hydrocarbon or polymeric portions of the molecules coil around each other, providing a relatively long-range order in solution that increases viscosity (thickening effect) with increasing concentration. The degree of intermolecular hydrocarbon or polymer chain entanglement increases with increasing molecular weight (chain length).

When mechanical energy (shear) is applied to thickened solution, for example, by circulation in a hydraulic pump circuit, a shear-induced thinning of the solution occurs. If this a reversible process; it is called non-Newtonian behavior, as discussed previously. However, if sufficient energy is applied, it may take less energy to break covalent C—C bonds in the entangled hydrocarbon or polymer chains (mechanodegradation) than to pull them apart (non-Newtonian shear thinning).

When C—C bond scission occurs, which is a nonreversible, permanent effect, the average molecular weight of the hydrocarbon or polymer is reduced. If there is a reduction in molecular weight, there will be corresponding reduction in solution viscosity. *Note:* it is important to realize that although other processes may produce molecular degradation, such as thermal and oxidative degradation, only shear degradation is a mechanodegradation process.

Hydraulic fluid shear stability has been studied using an Eaton hydraulic pump shear stability test conducted according to SAE 71R “Recommended Practices for Petroleum Fluid” [33]. The pump circuit used for this test is shown in Fig. 4.13 [33]. Figure 4.14 illustrates that varying degree of shear stability are possible with fluids of similar viscosity [34]. Fluid viscosity stability decreases with increasing pump rotational speed beyond a threshold value, as shown in Fig. 4.15 [34].

Figure 4.16 shows that fluid viscosity stability decreases with increasing pump pressure [34]. However, little effect of temperature on fluid viscosity shear stability was observed, as shown in Fig. 4.17 [34]. Similar viscosity stability tests have been conducted using a Vickers V104 vane pump [32].

Another viscosity shear stability test involves the use of a multiple-pass fuel-injection or diesel-injection nozzle system [35]. Currently, a Fuel Injection Shear Stability Test (FISST) described in ASTM D 3945-93 is used [36].

The FISST apparatus is illustrated in Fig. 4.18; it utilizes an American Bosch fuel-injection pump, fuel-injection nozzle, a fluid reservoir, and either the Deckel or

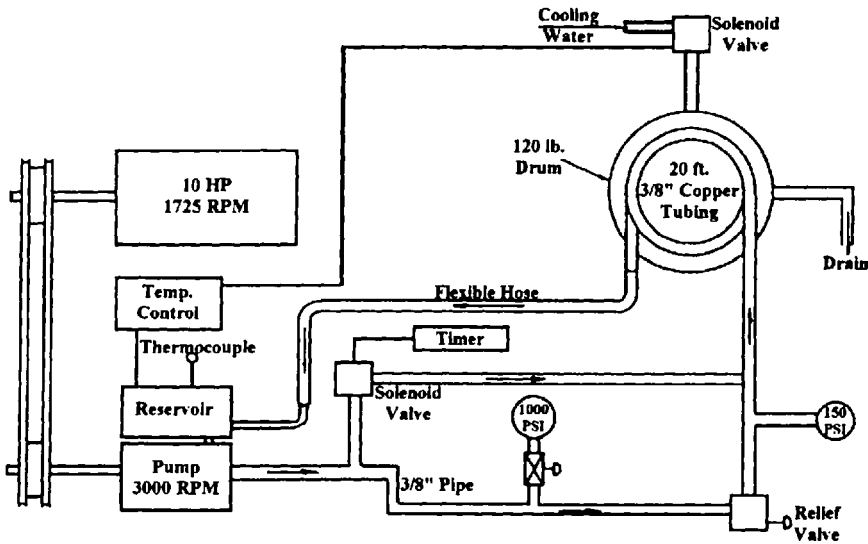


Figure 4.13 Schematic of hydraulic pump circuit for prediction of hydraulic fluid shear stability. (From Ref. 33.)

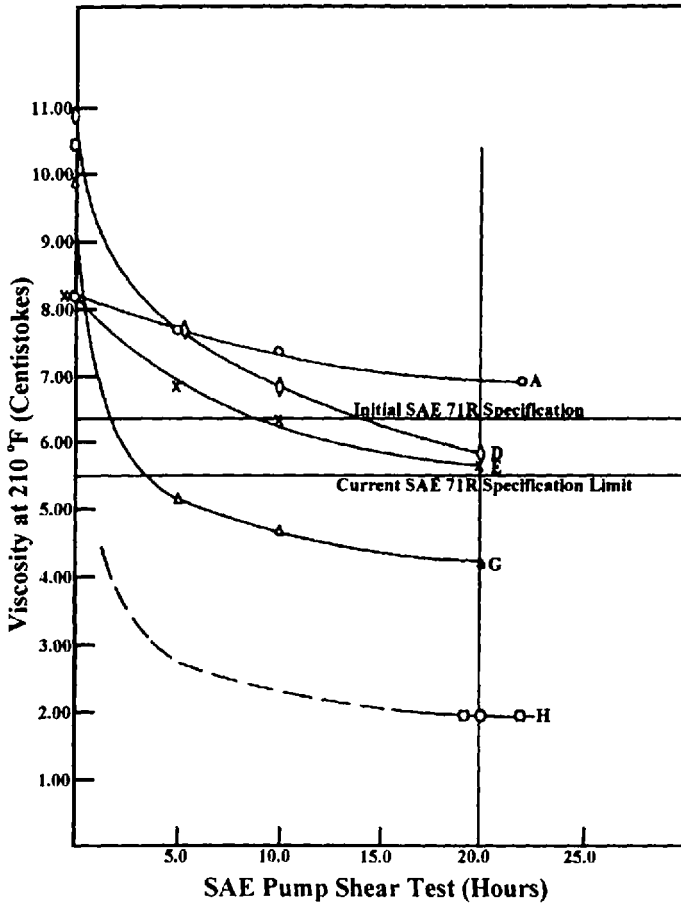


Figure 4.14 Illustration of viscosity-shear stability of various hydraulic fluids in the hydraulic pump test. (From Ref. 34.)

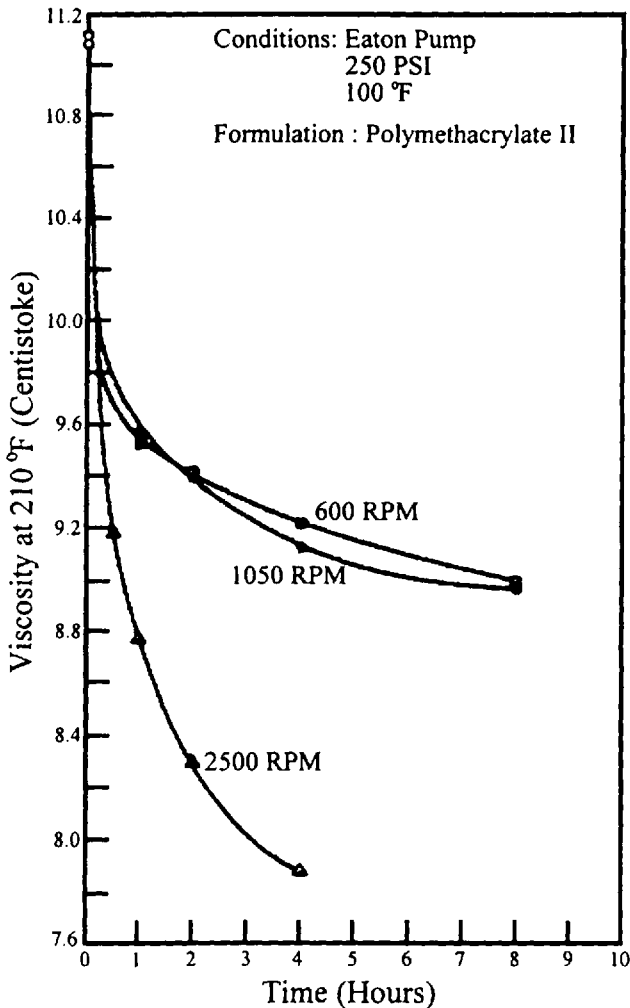


Figure 4.15 Effect of hydraulic pump motor rotational speed on shear stability. (From Ref. 34.)

a Pintel nozzle configuration, as illustrated in Fig. 4.19 [36]. Fluid shear stability is dependent on the type of nozzle selected, as shown in Fig. 4.20 [37].

Hydraulic fluid shear stability may also be modeled by a sonic shear stability test such as that discussed in ASTM D 2603 [33,38]. This test is conducted using a Raytheon Model DF-101 magnetostrictive oscillator rated at 200–250 W and 10 kilocycle. Potentially useful data have been obtained when the test is conducted at full power. An alternative test is this ultrasonic shear stability test [33].

2.2 Vapor Pressure

If the vapor pressure of a hydraulic fluid is too high, gas pockets may form in areas of low pressure, such as the inlet of the hydraulic pump. This will aggravate cavi-

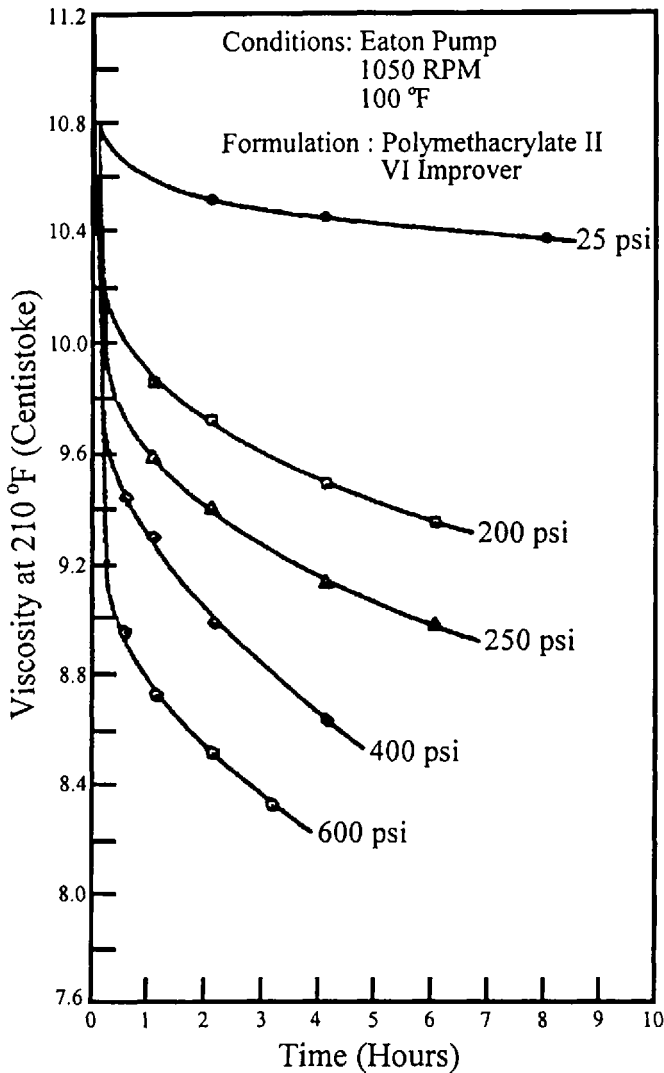


Figure 4.16 Effect of hydraulic pump pressure on shear stability. (From Ref. 34.)

tation. Fluid volatility also affects lubrication because hydrocarbon lubricants with higher volatility may result in higher wear [16].

Vapor pressure of hydraulic fluids is dictated by the most volatile components. For aqueous fluids, this would be water. For mineral oils, volatility is determined by the more volatile component of the oil. The chart shown in Fig. 4.21 may be used for determining the vapor pressure from the boiling point of the fluid [39].

For mineral oils exhibiting vapor pressures approaching 10^{-6} mm Hg, the Maxwell-Bonnell chart shown in Fig. 4.22 may be used [40]. Vapor pressure for

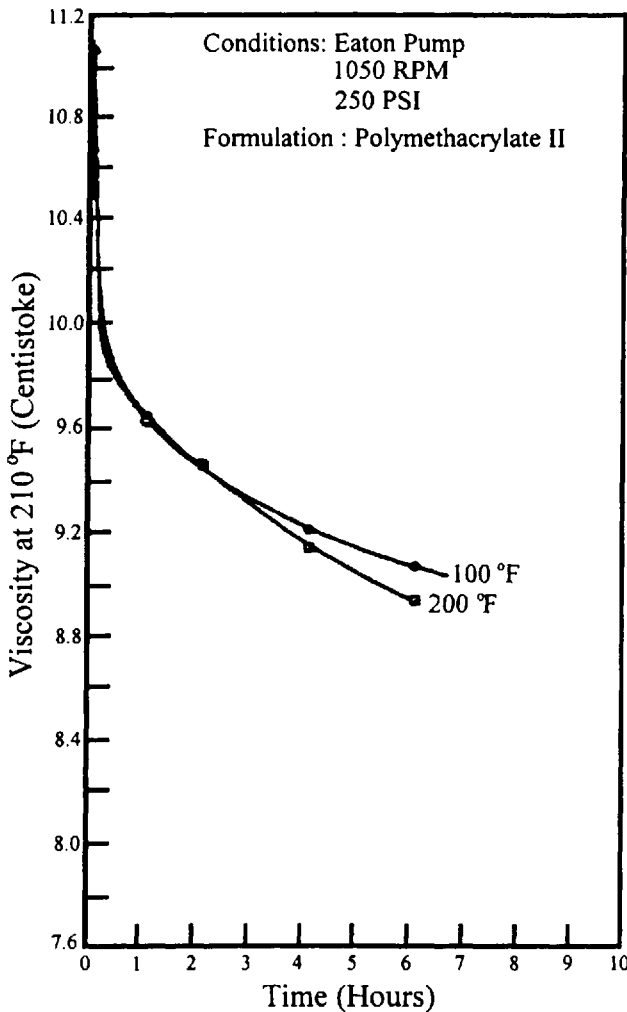


Figure 4.17 Effect of fluid temperature on shear stability. (From Ref. 34.)

low volatility synthetic oils should be appropriately corrected [41]. The variation of vapor pressure of various fluids with temperature is shown in Fig. 4.23 [7].

2.3 Gas Solubility

When a gas, such as air, comes into contact with a hydraulic fluid, a finite amount will become soluble in the fluid. Gas solubility is primarily dependent on the chemical composition of the fluid, concentration of the gas, and system pressure. Examples are provided in Fig. 4.24 [7].

The estimation of gas solubility is important when considering the effect of air entrainment on lubrication, cavitation, and potential foaming, especially on rapid depressurization [42]. In this section, the prediction of gas solubilization in various fluids will be discussed.

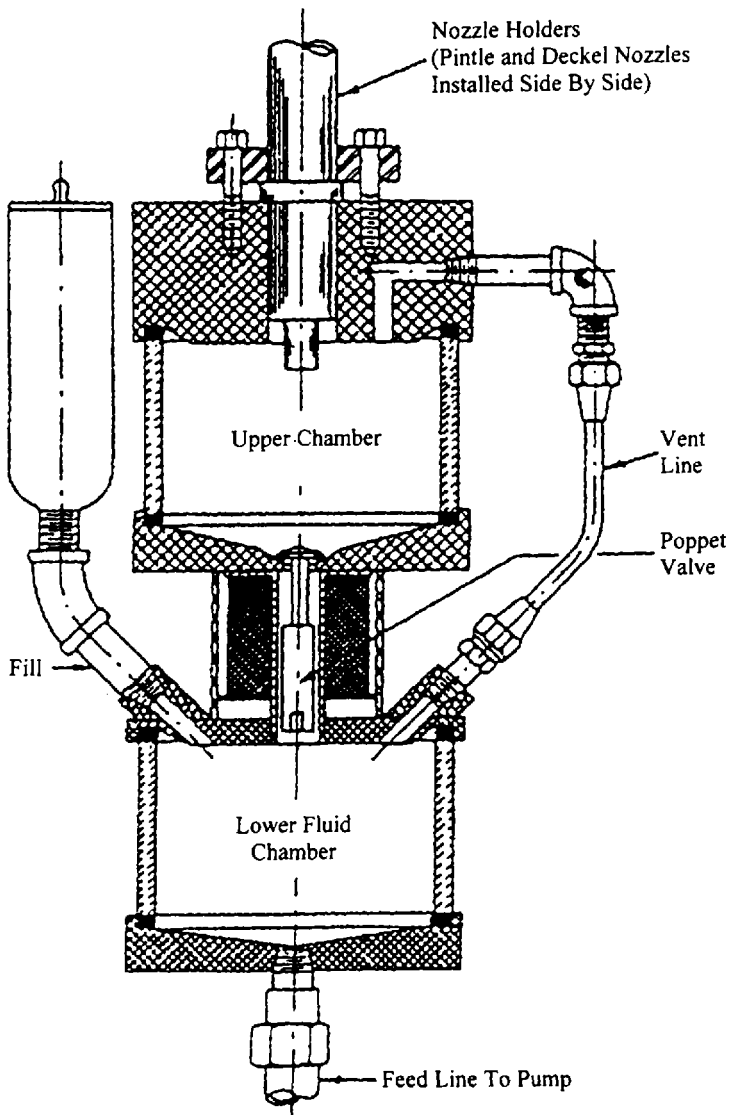


Figure 4.18 Automated fuel-injector shear stability tester. (From Ref. 36.)

The solubility of a dissolved gas in a fluid is quantitatively described by Henry's Law [43]:

$$K_t = \frac{P_g}{X_t}$$

where K_t is Henry's Law constant, P_g is the pressure of this gas, and X_t is the mole fraction of the dissolved gas in solution. This relationship indicates that the mole fraction of the dissolved gas will increase as the pressure of the gas increases. This is illustrated by the family of curves shown in Fig. 4.25 [44].

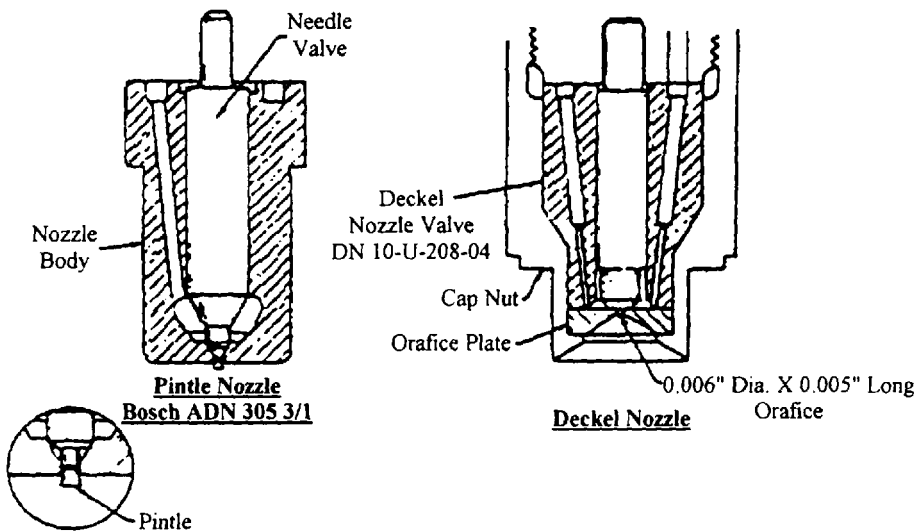


Figure 4.19 Nozzles for fuel-injection stability test machine. (From Ref. 36.)

One of the more common methods of describing gas solubility is by the Ostwald coefficient (L), where the solubility of a gas is expressed as volume of a gas (V_g) dissolved in a given volume of liquid (V_l) at equilibrium [43]:

$$L = \frac{V_g}{V_l}$$

The procedure for calculating the Ostwald coefficient (L_R) of a reference fluid (R) is provided in ASTM D 2779:

$$L_R = 0.300 \exp \left[\left(\frac{0.6399(700 - T)}{T} \right) \ln 3.333L_0 \right]$$

where L_0 is the Ostwald coefficient at 273°K and may be selected from Table 4.4. The Ostwald coefficient for the described fluid (L) is calculated from

$$L = 7.70L_R(980 - \rho)$$

where ρ is the density of the fluid (kg/L) at 288°K (59°F).

One of the disadvantages of ASTM D 2779 is that it is limited to use for petroleum oils. Beerbower has proposed an alternative model to calculate the Ostwald coefficient for a broader range of fluids [45]:

$$\ln L = [0.0395(\delta_1 - \delta_2)^2 - 2.66] \left(1 - \frac{273}{T} \right) - 0.303\delta_1 - 0.0241(17.60 - \delta_2)^2 + 5.731]$$

where L is the Ostwald coefficient, T is the absolute temperature in K, δ_1 is the solubility parameter of the fluid (in MPa)^{1/2} and is defined as

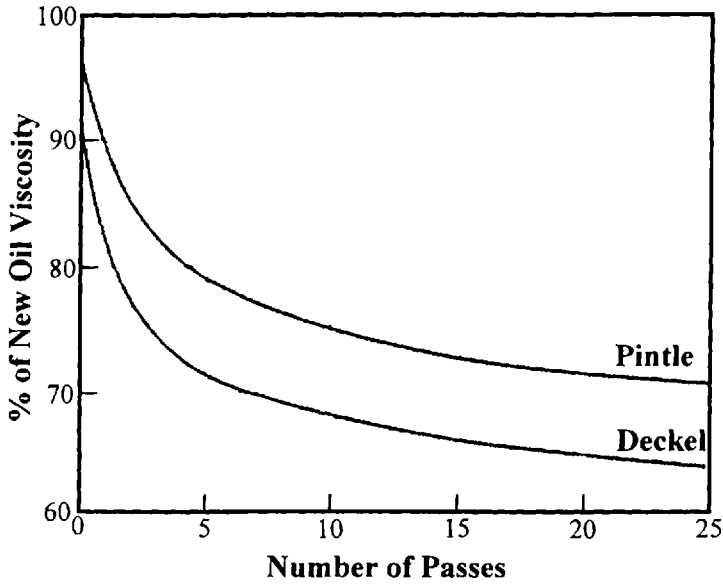


Figure 4.20 Effect of the number of cycles through the fuel-injection stability test machine on test severity. (From Ref. 37.)

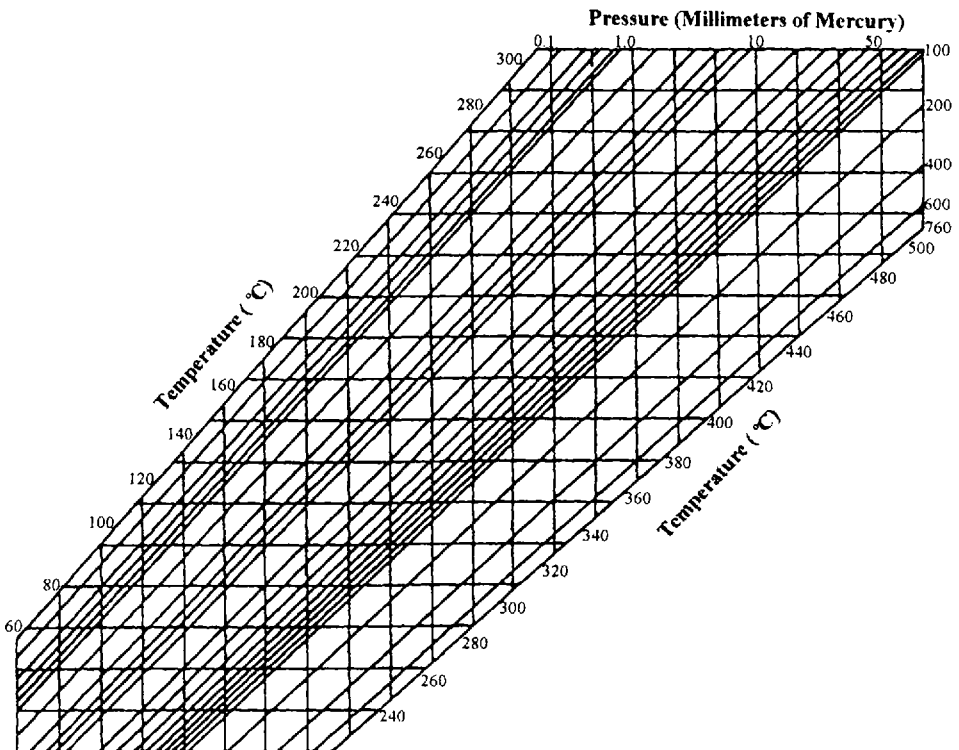


Figure 4.21 Hydrocarbon vapor pressure chart. (From Ref. 39.)

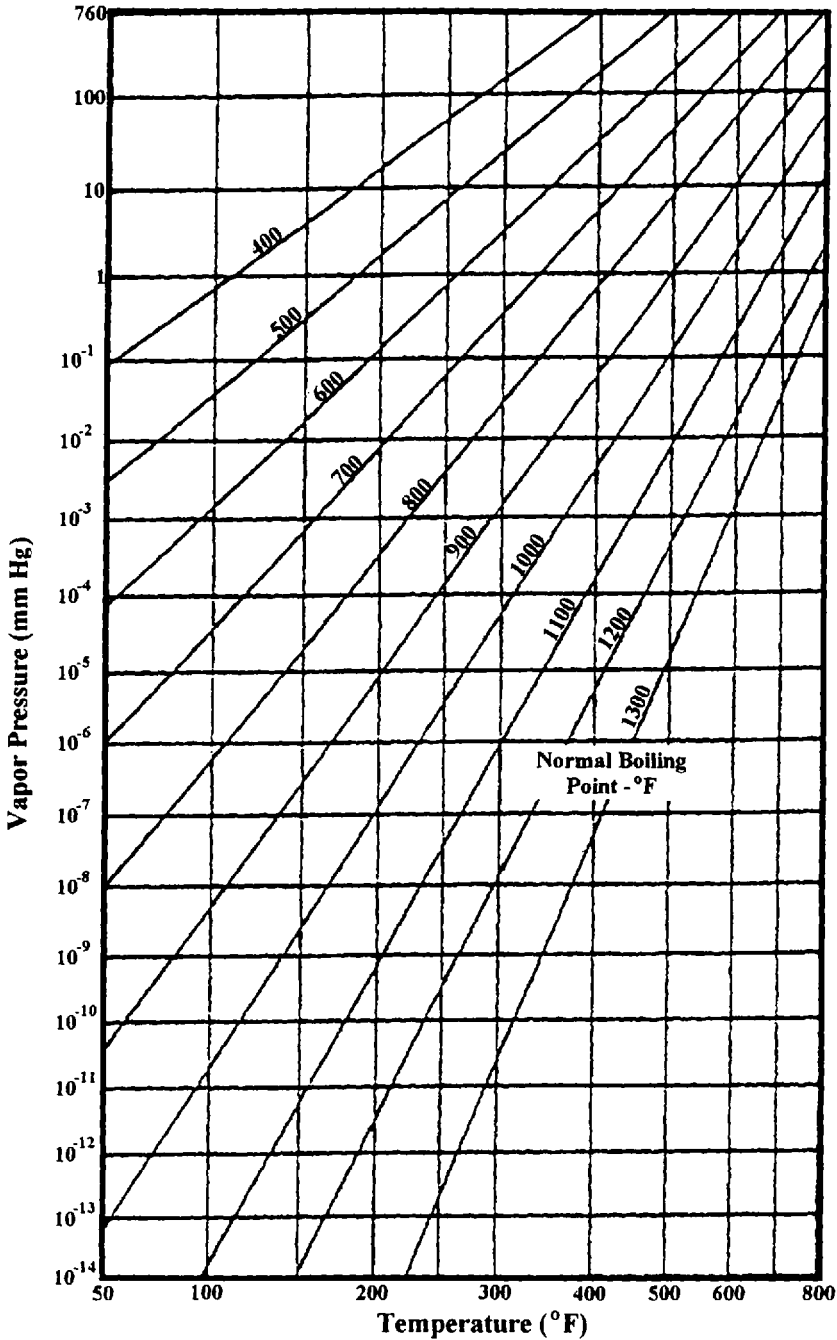


Figure 4.22 Maxwell-Bonnell chart for low vapor pressure. (From Ref. 40.)

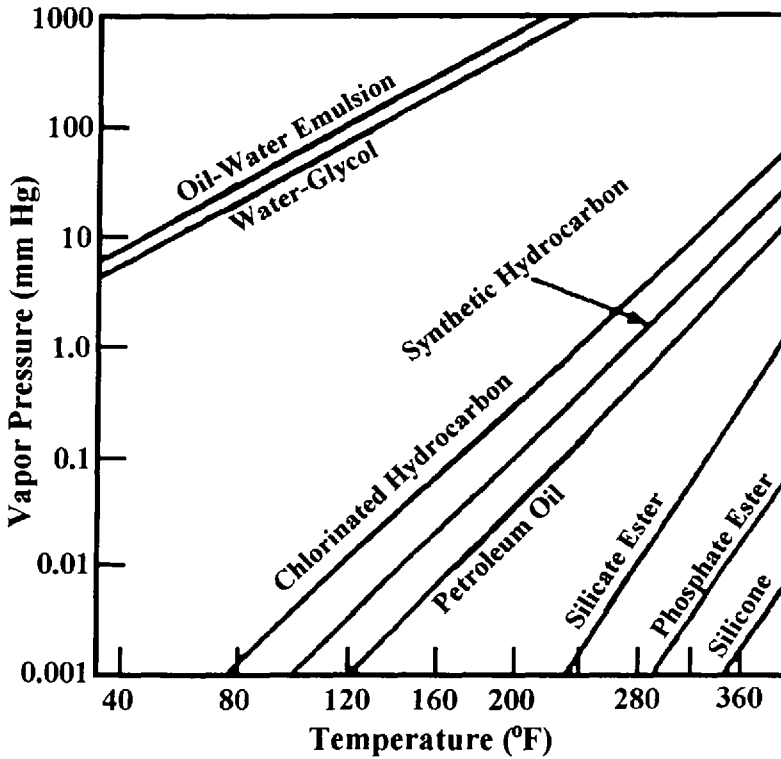


Figure 4.23 Typical vapor pressure values for different classes of hydraulic fluids. (From Ref. 7.)

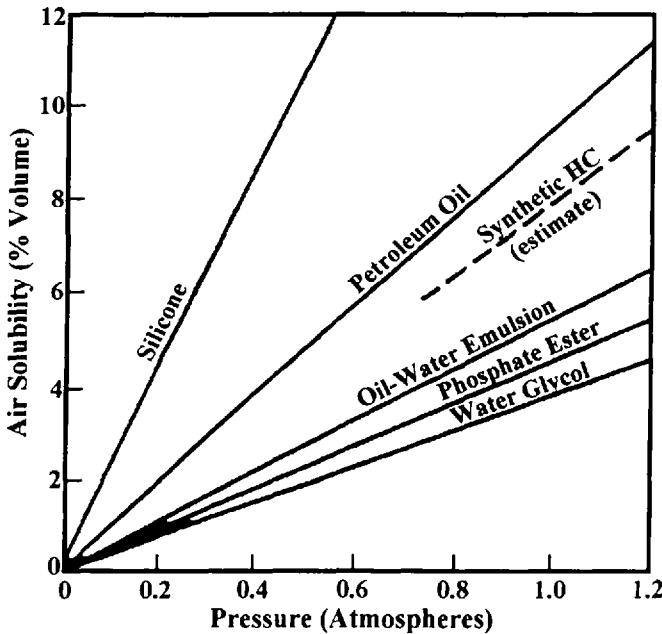


Figure 4.24 Air solubility in different hydraulic fluid types. (From Ref. 7.)

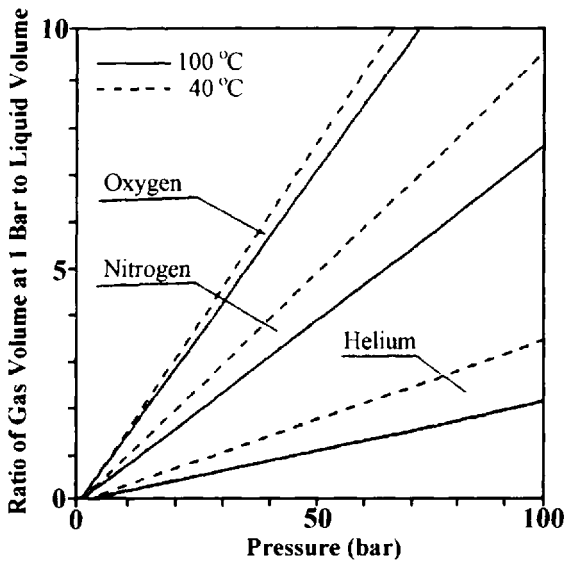


Figure 4.25 Gas dissolution in oil as a function of pressure and temperature. (From Ref. 44.)

Table 4.4 Gas Solubility Parameters

Gas	Ostwald coefficient (L) at 0°C ^a	Beerbower solubility parameter (δ_2) (MPa) ^{1/2}
Helium	0.012	3.35
Neon	0.018	3.87
Hydrogen	0.040	5.52
Nitrogen	0.069	6.04
Air	0.098	6.69
Carbon monoxide	0.12	7.47
Oxygen	0.16	7.75
Argon	0.18	7.77
Krypton	0.60	10.34
Carbon dioxide	1.45	14.81
Ammonia	1.7	—
Xenon	3.3	—
Hydrogen sulfide	5.0	—

^a L is applied only to petroleum fluids of 0.85 Kg/dm³ density, d , at 15°C. To correct for other densities; $L_c = 7.70 L (0.980 - d)$. See ASTM D 2779 for details.

$$\delta_1 = \left(\frac{\Delta H_v - RT}{V_l} \right)^{1/2}$$

where ΔH_v is the heat of vaporization and V_l is the volume of the fluid.

The solubility parameter (δ_1) may also be calculated from [45]

$$\delta_1 = 7.36 + 0.01203\rho$$

for densities up to 0.886 kg/m³ at 288 K (60°F). For higher-density fluids, the solubility parameter is calculated from the refractive index (n_D) at 298 K [45]:

$$\delta_1 = 8.63n_D^2 + 0.96$$

Value of δ_2 for the gas may be taken from Table 4.4.

Another common parameter that is used to describe gas solubility in a liquid is the Bunsen coefficient (α), which is the volume of a gas at 273 K (32°F) and 101.3 kPa (1 atm) dissolved by one volume of the liquid at a given temperature at 101.3 kPa (1 atm). The Bunsen coefficient may be calculated from ideal gas law [43]:

$$\alpha = \left(V_g \frac{273.15}{T} \frac{P}{760} \frac{1}{V_l} \right) \left(\frac{760}{P_g} \right)$$

where

P_g = the partial pressure of the gas

V_g = the volume of the gas absorbed at standard temperature and pressure

V_l = the volume of the absorbing solvent

T = the absolute temperature (K)

P = the total pressure.

The Bunsen coefficient may also be calculated according to ASTM D 3827:

$$\alpha = 2697 \frac{P - P_v L}{T}$$

where

P = the partial pressure of the gas (MPa)

P_v = the vapor pressure of the fluid (MPa)

T = the temperature (in K)

L = the Ostwald coefficient

Bunsen coefficients for a number of hydraulic fluids are provided in Table 4.5.

The variation of the Bunsen coefficients with pressure and temperature for various gases in a hydraulic oil is illustrated in Fig. 4.25 [44]. Interestingly, there is only minimal variation of the Bunsen coefficient for air in hydraulic oil with variation in temperature, as shown in Fig. 4.26 [46].

An example of the use of the Bunsen coefficient to predict air solubility in a mineral oil is provided by Fig. 4.27 [47]. In this example,

$$V_A = \alpha_{oil} V_{oil} \frac{P_2}{P_1}$$

where V_A is the volume of air (in cm³) at 760 mm Hg and 20°C, V_{oil} is the volume of oil (in cm³), α_{oil} is the Bunsen coefficient for mineral oil (~0.09), P_1 is the initial

Table 4.5 Bunsen Coefficients for Dissolved Air in Lubricating Oils

Fluids	Bunsen coefficient	Ref. ^a
Water	0.187	A
Mineral oil	0.07–0.09	A
Phosphate ester (HFD-R)	~0.09	A, B
Dicarboxylic ester	~0.09	A
Silicone oil	0.15–0.25	A
Polychlorinated biphenyls, (HFD-S)	~0.04	A
Oil-in-water emulsion (HFA)	~0.05	B
Water-glycol (HFC)	~0.04	B

^aReference A is W. Hamann, O. Menzel, and H. Schroeder, "Gase in Ölen—Grundlagen für Hydrauliken," *Fluid*, 1987, September, pp. 24–28; Reference B is D. Staack, "Gases in Hydraulic Oils," *Tribologie und Schmierunaptechnik*, 1987, 34(4), pp. 201–207. Reference B states that the Bunsen coefficient for air in a phosphoric and ester is ~0.05.

pressure in kPa/cm^3 , and P_2 is the final pressure (in kPa/cm^3). The example shows that the partial pressure of air of 1 kPa/cm^3 will result in 9 vol.% of air in the oil.

Another approach used to quantify gas solubility is the Hildebrand and Scott equation [48]:

$$\ln X_2 = -\ln P_2^\circ - \frac{V_2 \phi^2 (\alpha_1 - \alpha_2)^2}{RT}$$

where

X_2 = the mole fraction of gas in the fluid

P_2° = the vapor pressure of the gas at temperature T (absolute)

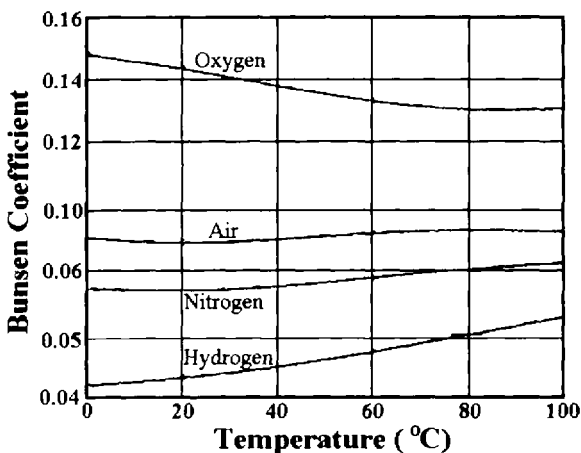


Figure 4.26 Variation of the Bunsen coefficient as a function of temperature for air, oxygen, nitrogen, and hydrogen. (From Ref. 46.)

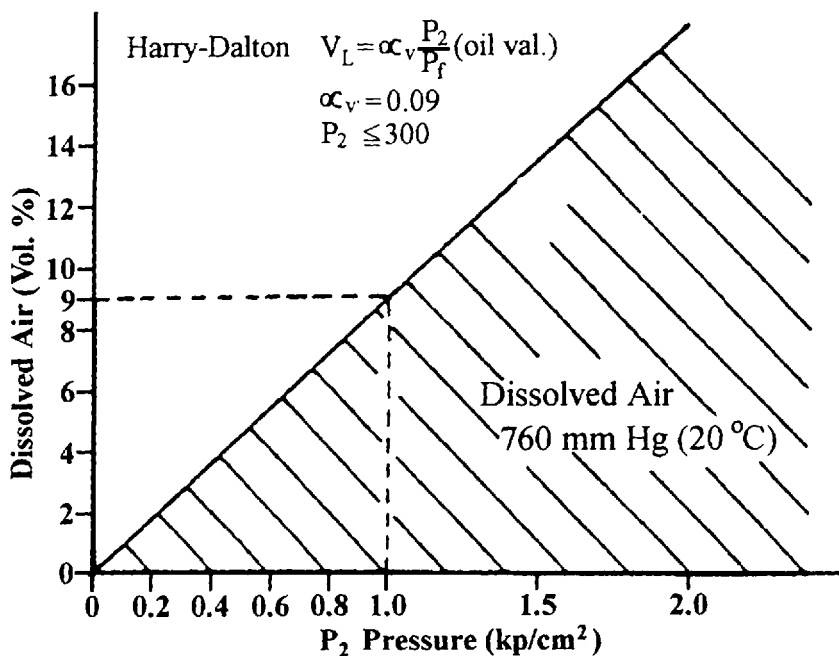


Figure 4.27 Illustration of the dependence of air dissolution on pressure. (From Ref. 47.)

- ϕ = the volume fraction of the gas
- X_2 = the partial molal volume of the gas
- α_1, α_2 = the solubility parameters of the fluid and gas, respectively.

The values for α may be taken from Table 4.6, Hildebrands' reference [48], or an extensive listing provided by Hoy [49].

2.3.1 Sources of Foaming and Air Entrainment

Excessive foaming and air entrainment may lead to numerous problems in a hydraulic system which include the following [50–54]:

- Spongy controls
- Loss of horsepower
- Reduction in bulk modulus
- Loss of system fluid
- Temperature effects
- Erosion and cavitation
- Noise
- Reduction in load bearing capacity of the lubricating film [55]

Increasing pump noise is one of the best indicators of fluid aeration problems. This is illustrated in Fig. 4.28 [56].

There are various sources of air entrainment which include the following [57]:

1. *Release of Dissolved Air.* All hydraulic fluids contain dissolved air which may be released when the pressure is rapidly decreased. This may occur

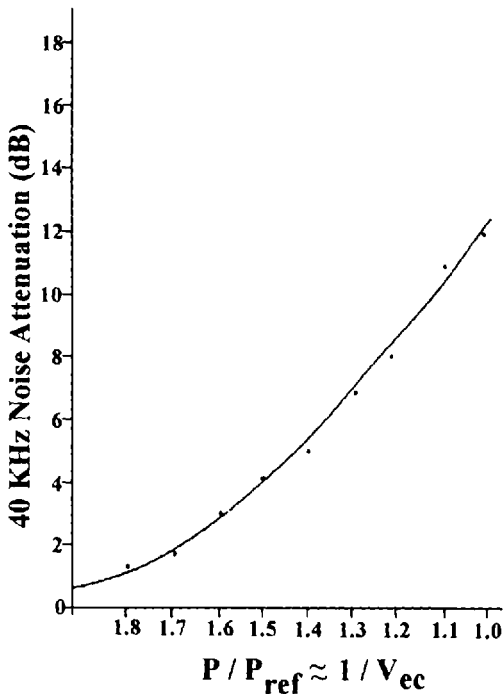


Figure 4.28 Hydraulic pump noise dependence on entrained air at the pump inlet. (From Ref. 56.)

at valves and orifices, the discharge side of the operating mechanism, and when the fluid returns to the reservoir.

2. *Mechanical Introduction.* Entrained air may be introduced at the vacuum side of hydraulic mechanisms or when there is leakage in the suction side of the pump.
3. *Improper Bleeding.* When initially filled, the hydraulic system will contain air in all forms (free, entrained, and dissolved). For proper operation, the hydraulic system should be properly bled for air removal.
4. *Improper Addition of Makeup Fluid.* Air may be entrained if additional fluid is added with splashing in the reservoir.
5. *Contamination.* A common source of increased air entrainment and foaming is fluid contamination by surface-active compounds. Alternatively, fluid contamination may cause precipitation of the antifoam or air-release agent, resulting in subsequent increases on air entrainment.

Improperly Designed Reservoirs

Hydraulic fluid air entrainment may be due to improperly designed fluid reservoirs [51,58,59]. Two commonly encountered errors in reservoir design are fluid return lines above the liquid level and insufficient immersion of the suction line, as shown in Fig. 4.29 [51]. Insufficient immersion of the return line causes splashing, increased foaming, and air entrainment. Insufficient immersion of the suction line causes surface vortexing, which will draw air into the fluid facilitating air entrainment.

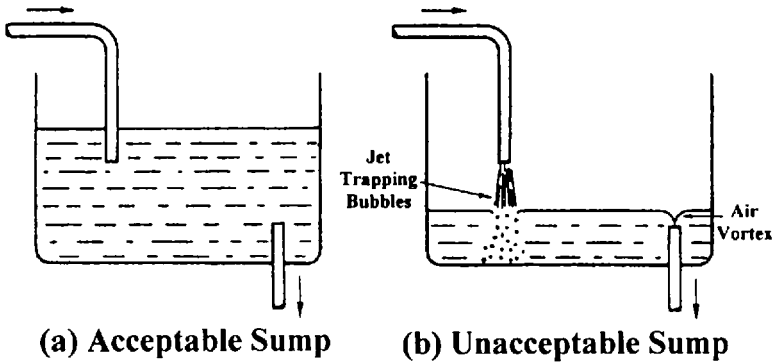


Figure 4.29 Illustration of the effect of reservoir design on air entrainment. (From Ref. 51.)

In some cases where it is difficult to remove air, a fine-wire gauze screen can be placed in the sump as shown in Fig. 4.30, which will “filter” all but the finest air bubbles in the system, preventing recirculation through the hydraulic system [51].

Air solubility decreases with decreasing pressure. One of the low-pressure points in the hydraulic system is at the inlet of the pump. Figure 4.31 illustrates how air bubbles form with decreasing pressure and then redissolve on the pressure side of the pump [51]. This is also illustrated for a gear pump in Fig. 4.32 [60]. To avoid pressure drops at the pump inlet, the pipe diameter from the reservoir should be maximized and the length of the line should be as short as possible. Similar pressure drops may be encountered at sharp bends, elbows, pinched or kinked flexible hose, and banjo joints.

One recommended reservoir design is illustrated in Fig. 4.33 [58]. Hallet recommended the following:

1. The main return line should be approximately 8 in. below the fluid surface.
2. The suction line should be located 6 in. from the bottom of the reservoir to minimize settled solid contaminants from entering the system.
3. A 3-in. air filter should be located at the top of the reservoir.

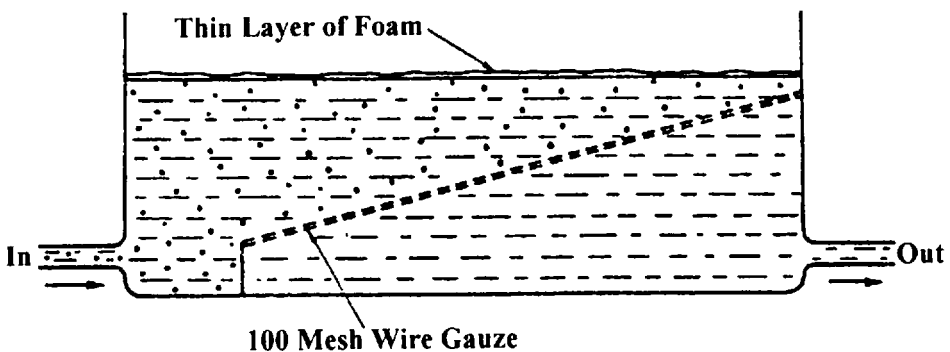


Figure 4.30 Illustration of the use of wire gauze to facilitate air-bubble removal from the reservoir. (From Ref. 51.)

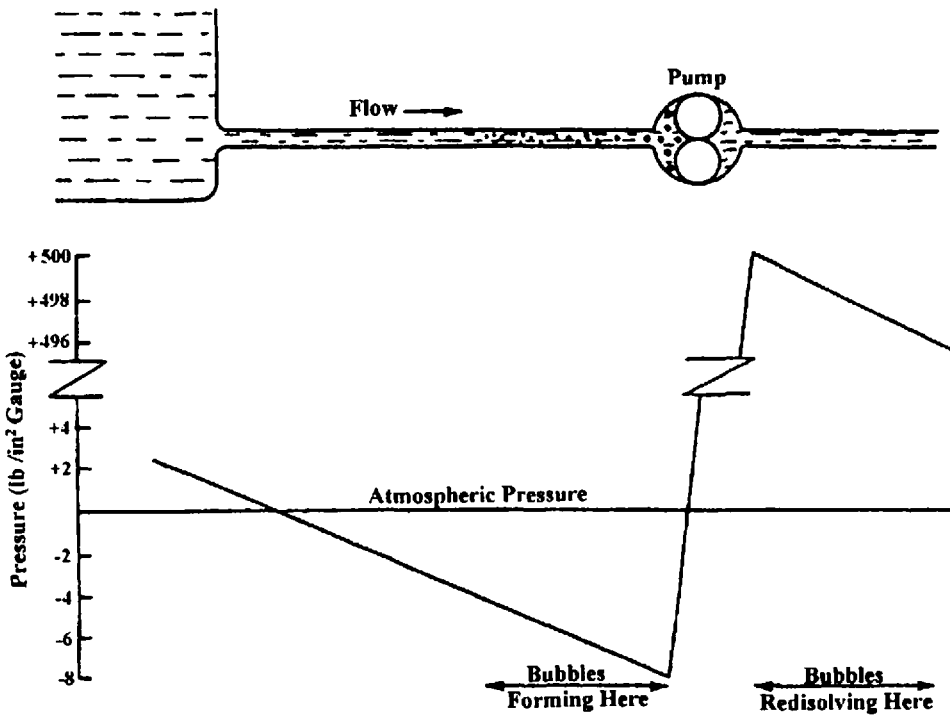


Figure 4.31 Suction-line pressure drop facilitation of air-bubble release from entrained air. (From Ref. 51.)

4. A float switch should be installed at the top of the tank to shut the system down if the oil level drops below the recommended working range.
5. A 4-in. suction fan should be installed at the top of the reservoir to prevent water condensation in cold weather by removing heated air.

If the reservoir is pressurized with compressed air or nitrogen, direct contact of the gas with the fluid should be minimized with the use of a perforated plate, as

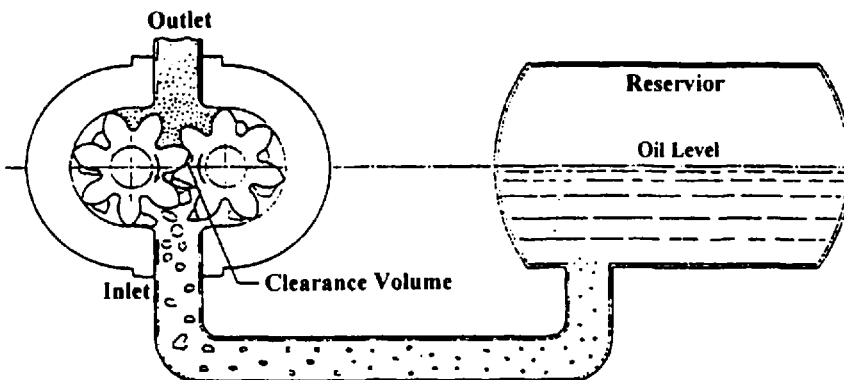


Figure 4.32 Illustration of air release at the inlet of a gear pump. (From Ref. 60.)

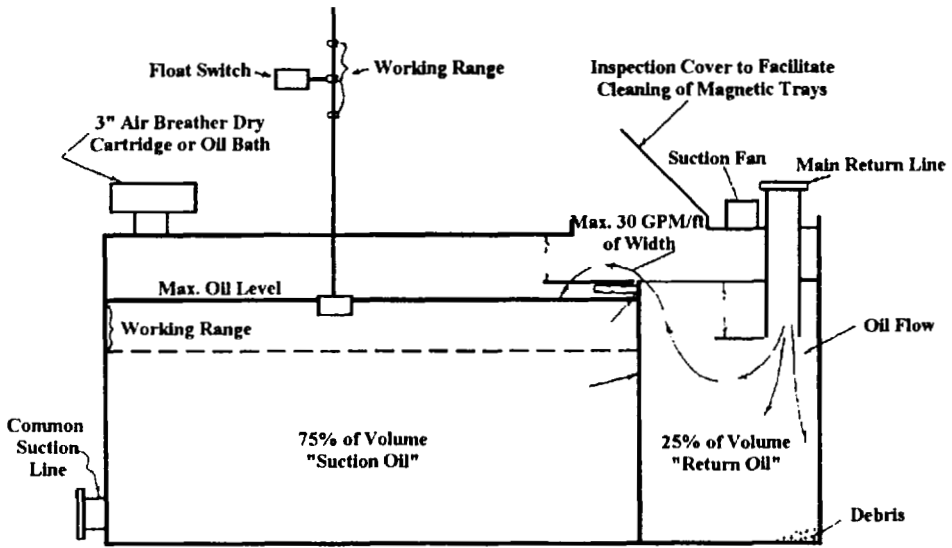


Figure 4.33 Dofasco 6000-gal reservoir design. (From Ref. 58.)

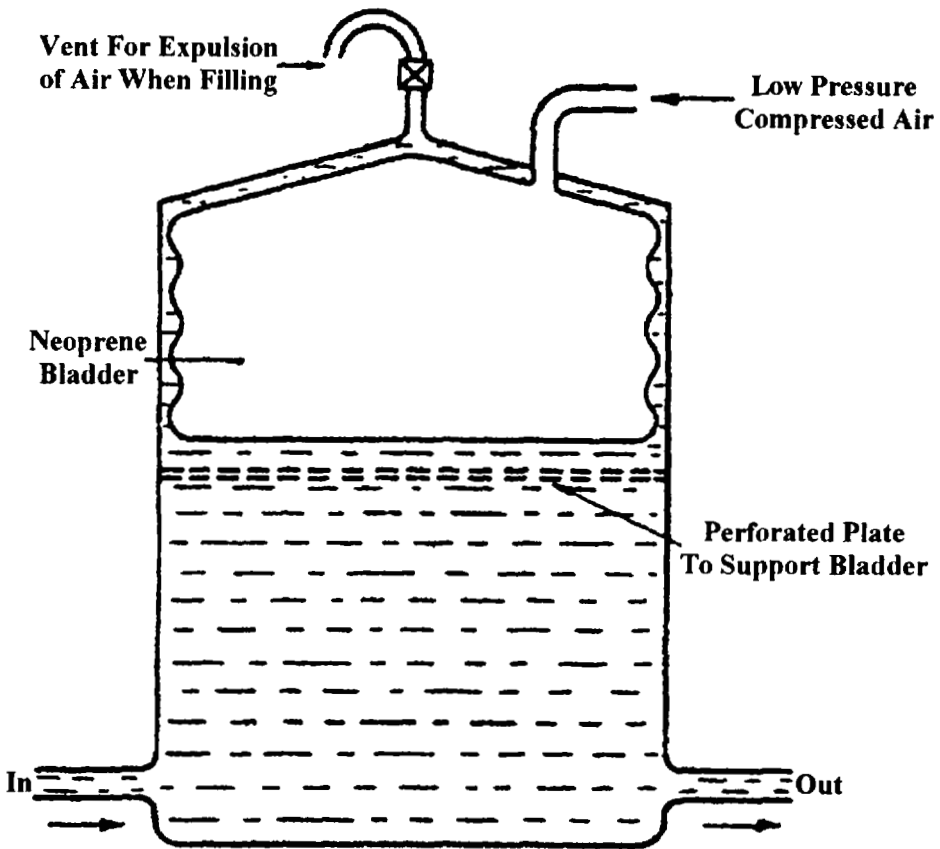


Figure 4.34 Procedure for hydraulic reservoir pressurization. (From Ref. 51.)

shown in Fig. 4.34 [51]. This will help prevent saturation of the hydraulic oil by the compressed gas. Another way of minimizing the potential saturation of the hydraulic fluid with a gas is to pressurize the reservoir hydraulically, as shown in Fig. 4.35 [51].

It may not be possible to design the pump reservoir and suction line as shown in Fig. 4.29 due to space limitation. In these cases, a possible alternative is to put the suction line inside of the reservoir, as shown in Fig. 4.36 [59]. A plug is placed at position A to break the siphon effect by the entry of air. An alternative design is provided by Fig. 4.37, which includes a suction screen chamber at the top of the reservoir.

Ingvast reported the use of a specially designed reservoir (see Fig. 4.38) that provides continuous degassing of a hydraulic fluid [61]. In addition to continuous

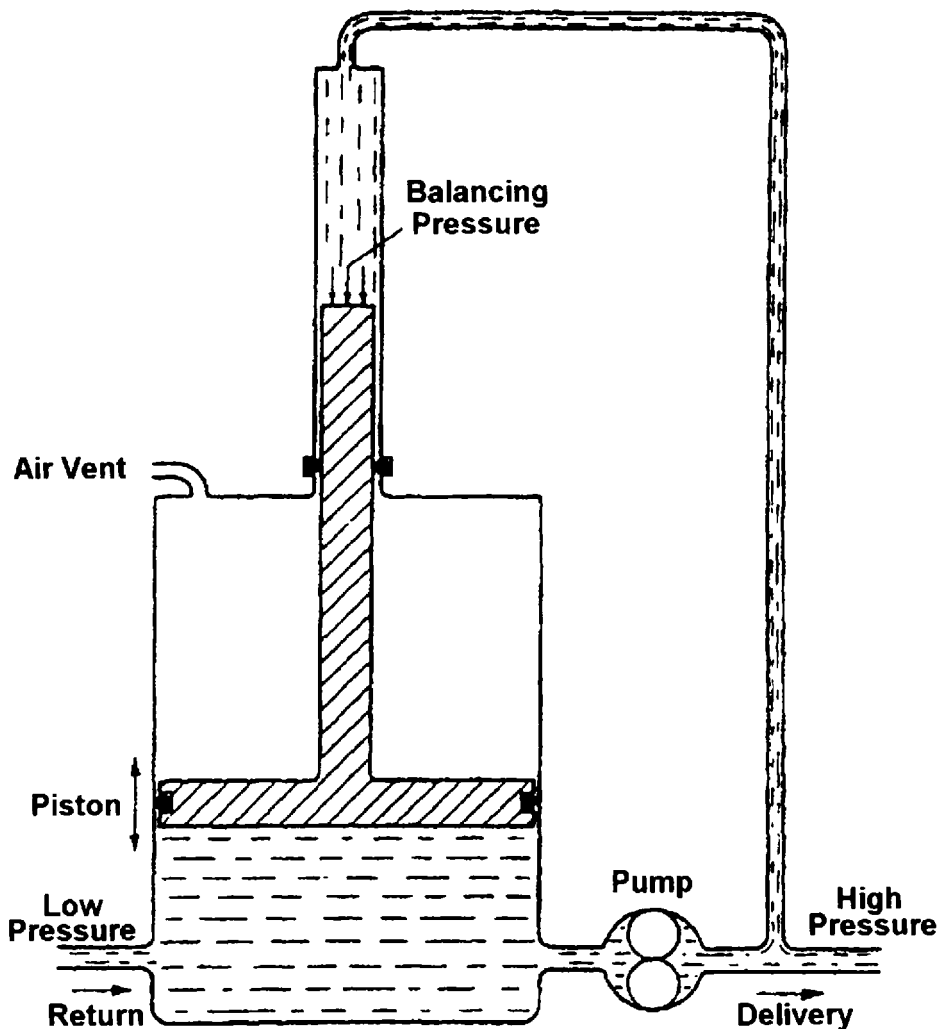


Figure 4.35 Reservoir pressurization using hydraulic pressure. (From Ref. 51.)

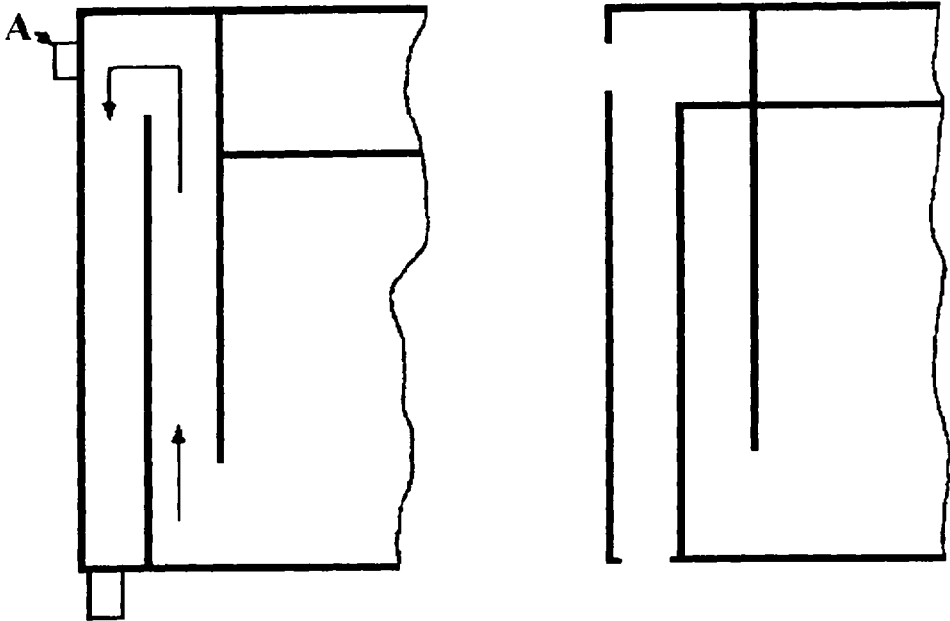


Figure 4.36 Illustration of pump suction-line placement inside of the reservoir. (From Ref. 59.)

degassing, it is also possible to continuously feed pressurized fluid to the pump inlet, thus minimizing the potential for both fluid air entrainment and cavitation.

Improper installation of air vents is another potentially significant source of air entrainment in a hydraulic system. Figure 4.39 illustrates that air pockets of entrapped air can be avoided by the use of properly designed air vents [62].

Foaming Versus Air Entrainment

When fluids are agitated or mixed in reservoirs and pumping through the hydraulic system they are in contact with a gas, usually air. Gases in a hydraulic fluid may be present in one or more of these possible forms: free air, entrained air, and dissolved air [53].

Free air refers to air trapped in a system, such as an air pocket in a hydraulic line, but not totally in contact with the fluid. Entrained air is air that is suspended, usually in the form of small bubbles, in the fluid. Dissolved air is in solution and is not free or entrained. It is estimated that petroleum oil hydraulic fluids may contain as much as 10% volume of dissolved air [52]. Although dissolved air is thought to have no significant effect while dissolved, processes that reduce air solubility such as decreasing pressure and increasing temperature will result in foaming or release of entrained air, both of which are deleterious processes [53].

The solubility of a gas in a fluid was treated quantitatively in the previous section. Problems of “free air” will be discussed in a subsequent section. In this section, the fundamental properties of the formation and elimination of air bubbles, either as foam or entrained air, is discussed. Although there is often a similarity drawn between foam and air entrainment, these are actually different processes and

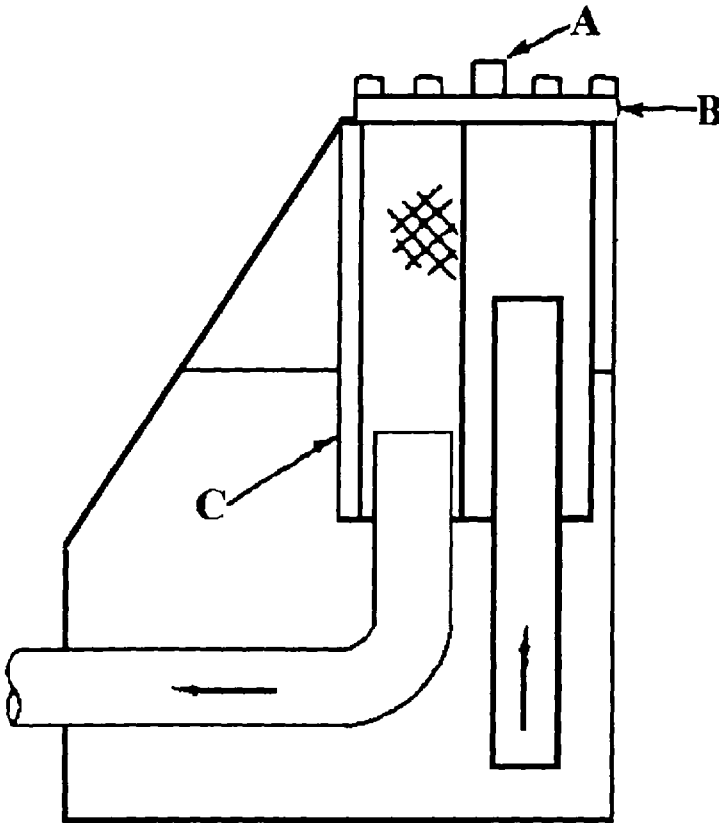


Figure 4.37 Illustration of a suction screen chamber. (From Ref. 59.)

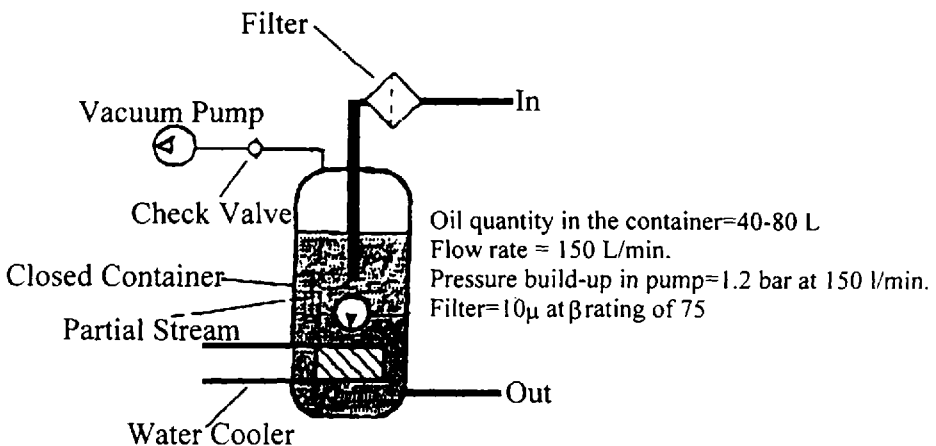


Figure 4.38 Facilitation of air release using a vacuum pump. (From Ref. 61.)

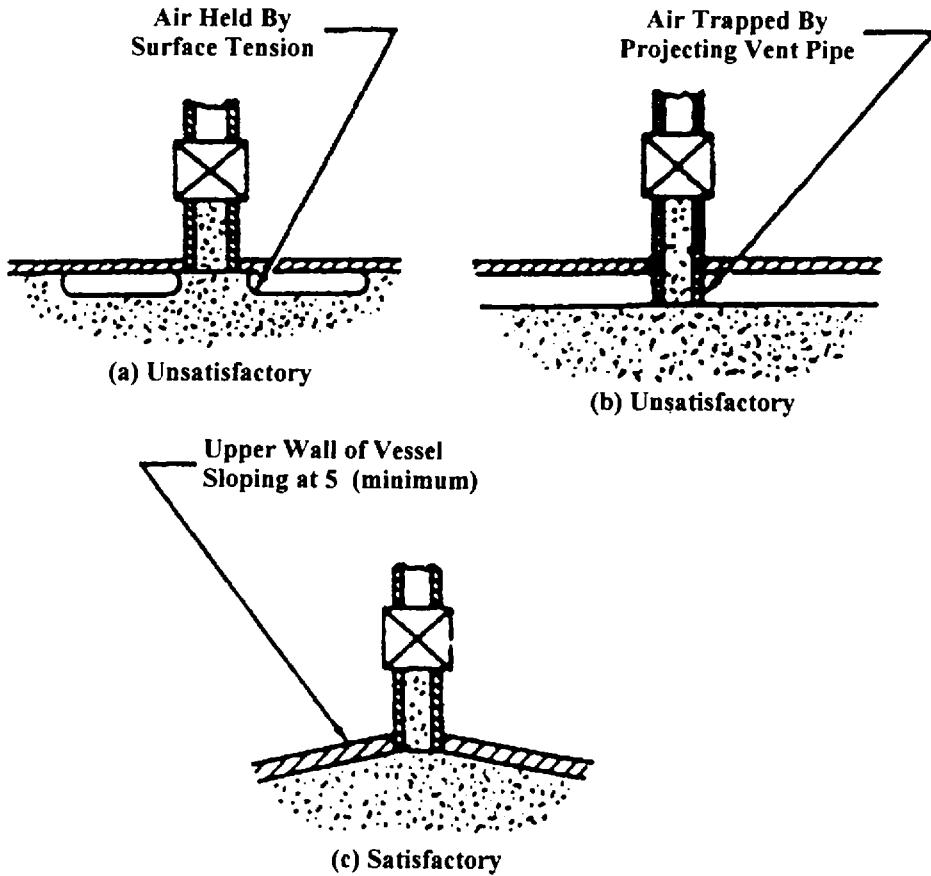


Figure 4.39 Air-vent designs that prevent air entrainment. (From Ref. 62.)

are associated with different problems. Air entrainment refers to the dispersion of individual air bubbles separated by a relatively thick fluid film in the hydraulic fluid. In foaming, air bubbles form a separate layer on the surface of the fluid and are separated by relatively thin fluid films, as illustrated in Fig. 4.40.

It should be noted that it is possible to have a high amount of unstable foam with relatively little air entrainment. Similarly, it is possible for air entrainment and high foam to coexist. The objective in fluid formulation is to reduce foaming and air entrainment.

Foaming

Foam is a dispersion of an entrapped gas in a liquid. To produce a stable foam, a surface-active component must be adsorbed into the gas-liquid interface, as shown in Fig. 4.41 [63]. This surface film prevents the coalescence of the air bubbles, thus stabilizing the film. Foam stability is dependent on the following [64]:

1. *Surface area.* Foam stability increases with increasing surface area, as shown in Fig. 4.42 [68]. Foam destabilization is dependent on bubble co-

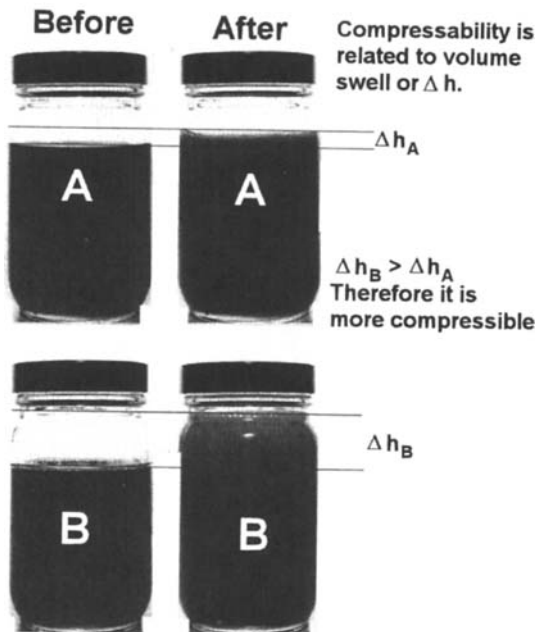


Figure 4.40 Illustration of foam and entrained air.

alescence. There is an energy balance of the Gibbs free energy (ΔG) of the system, which is quantitatively dependent on

$$\Delta G = \sigma \Delta A$$

where σ is the surface energy and ΔA is the changing surface area. In a foam, there is an increase in energy due to the surface area increase and a decrease in energy is due to the transfer of the profoamant (surfactant) molecules from the fluid to the gas–liquid interface [65].

2. *Surface tension.* Foam stability increases the surface tension decreases relative to the fluid film. More important is the way the surface tension changes with the surface area of the film, which follows the Gibbs relationship

$$E = 2A \frac{d\gamma}{dA}$$

where E is the surface elasticity, A is the surface area of the fluid film, and γ is the surface tension of the liquid film. Stable foams have a readily variable (elastic) surface films.

3. *Viscosity.* It is more difficult to form foams in higher viscosity fluids. However, once formed, these foams are more difficult to break. Table 4.6 and Fig. 4.43 shows that this is true up to approximately 100 mm²/s (cS). Above 100 mm²/s (cS), profoaming behavior decreases [66].

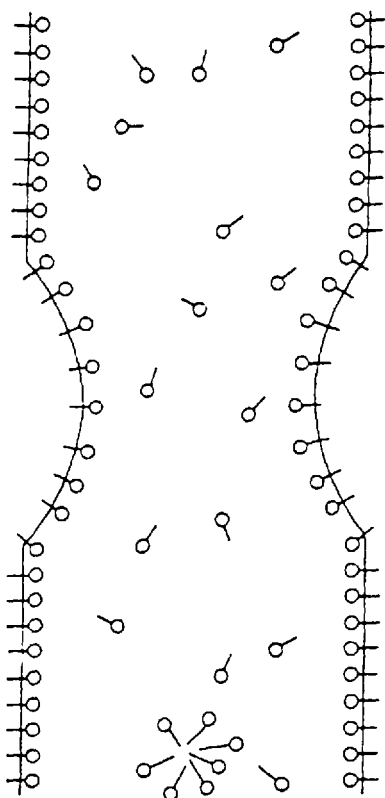


Figure 4.41 Mechanism of air-bubble stabilization by the Gibbs–Marangoni effect. (From Ref. 63.)

4. The temperature dependence of foam stability for various hydraulic fluids is shown in Fig. 4.44 [67]. Foam stability generally decreases with increasing temperature (decreasing viscosity).
5. *Contamination Concentration.* The magnitude and stability of foams formed in a fluid increase to a plateau point with increasing concentration of the profoaming contaminant.

The antifoam mechanism is shown in Fig. 4.45. The first step is introduction of the defoamant into the surface film that is stabilizing the foam. The defoamant then spreads throughout the surface film surrounding the air bubbles. As the defoamant spreads, a shearing force results, which causes a flow of the stabilizing film away from the gas–bubble interface, resulting in a thinning of the interfacial film which continues until the gas–bubble ruptures, releasing the gas inside of the bubble [68].

Antifoam compositions vary from single- to multiple-component systems. Single-component systems are typically water insoluble and surface active because they must displace the profoaming surfactant in the interfacial film stabilizing the gas bubbles. Examples of single-component systems include fatty acids and their glycerides/ethoxylates, polypropylene glycols, and higher alkylalcohols. Typically, this class of antifoams is used at concentrations of 0.1–0.4% [65].

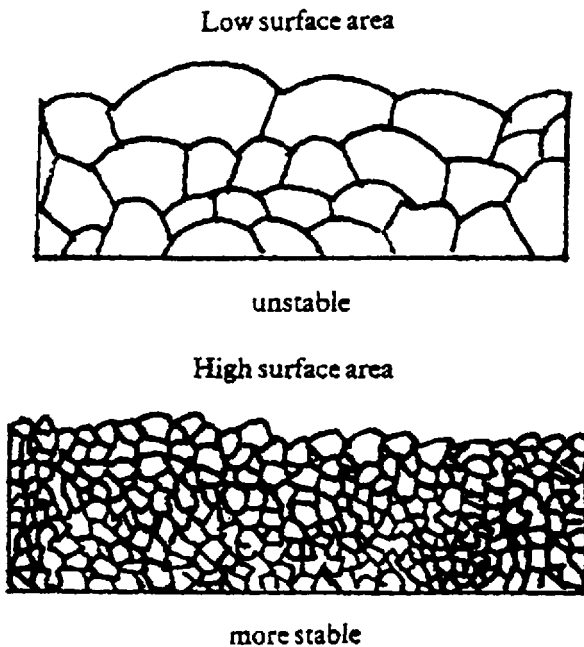


Figure 4.42 Relationship between bubble surface air and foam stability. (From Ref. 68.)

A multicomponent antifoam system typically contains a uniform dispersion of a mineral-oil-based material, hydrophobic silica, and a surfactant such as a fatty acid or alcohol ethoxylate composition in the fluid throughout the hydraulic system [65,69–72].

The rising velocity (U) and drag coefficients (C_d) of gas bubbles in a fluid can be calculated from Hadamard–Rybczynski equations [73]:

$$U = \frac{(\rho - \rho')gd^2}{6\eta} \frac{\eta + \eta'}{2\eta + 3\eta'}$$

$$C_d = \frac{8}{\text{Re}} \frac{2\eta + 3\eta'}{\eta + \eta'}$$

Table 4.6 Viscosity Dependence of Foaming Tendency of Mineral-Based Oils

Viscosity grade	Foaming tendency (mL) ^a			Air release ^b (50°/min)
	24°C	93.5°C	After	
VG 7	40/0	20/0	30/0	0
VG 22	100/0	20/0	110/0	0.5
VG 46	420/0	20/0	380/0	1.5
VG 460	200/0–	230/0	120/0	160.0

^aFoaming behavior was determined according to JIS K 2518.

^bAir release was determined according to ASTM D 3427.

Source: Ref. 66.

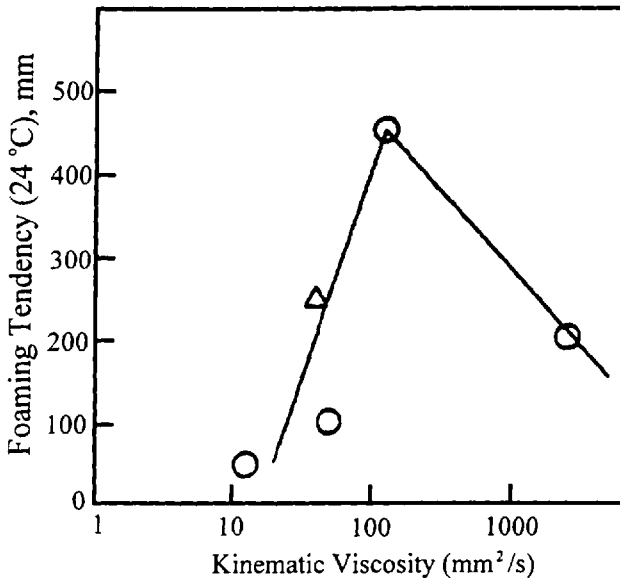
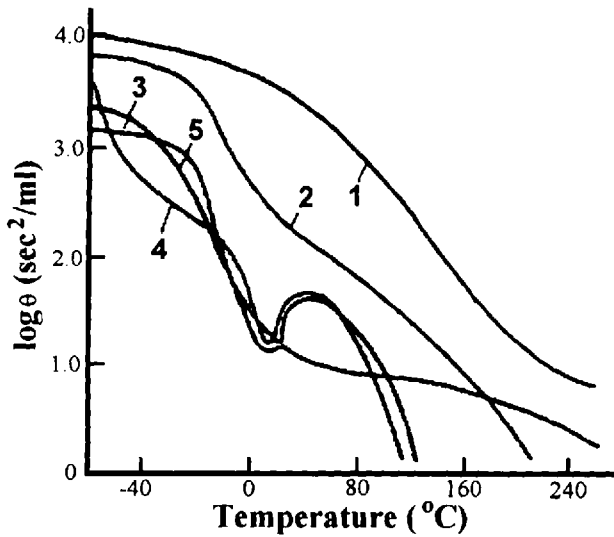


Figure 4.43 Effect of viscosity on foaming tendency. (From Ref. 66.)



COMPOSITION	Designation	Surface Tension (dyne/cm)
1. Polyalkylchlorarysiloxanes	PAKHS	21.7
2. Polyalkylsiloxanes 50% Dioctylsebacate 50%	PAS	28.4
3. Petroleum Fraction 200-300° C.+8% Butyl Ester of Polyvinyl Alcohol	NF	27.7
4. Alkylarylphosphates	AAF	34.1
5. Polyalkyl-gamma-Trifluoropropylsiloxanes	PAFS	18.8

Figure 4.44 Temperature dependence of foam stability of different fluids designated. (From Ref. 67.)

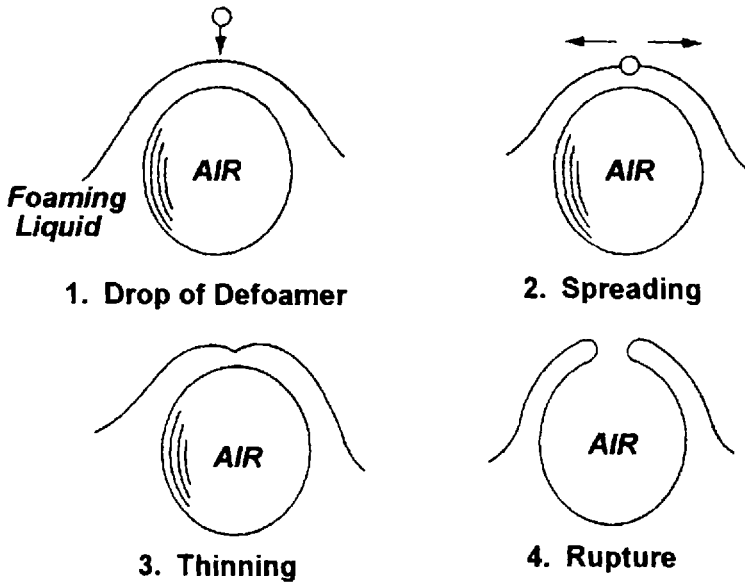


Figure 4.45 Mechanism of defoaming by foam-control agents. (From Ref. 65.)

where

ρ , η = the density and viscosity, respectively, of a fluid surrounding a spherical gas bubble

ρ' , η' = the density and viscosity, respectively, of the gas

d = the diameter of the bubble

g = the acceleration due to gravity

Re = the Reynolds number for the bubble, which may be calculated from

$$Re = \frac{Ud}{\eta/\rho}$$

For a gas bubble, $\rho \gg \rho'$ and $\eta \gg \eta'$; then, the well-known Stokes equations are derived, which state that the velocity of bubble movement is dependent on the density, viscosity, and diameter of the bubbles:

$$U = \frac{\rho g d^2}{12\eta}$$

$$C_d = \frac{16}{Re}$$

This model is represented by Fig. 4.46a. An alternative form of this equation is [74]

$$U = \frac{2r^2g}{9\eta}$$

where r is the radius of the gas bubble. The rate of ascent of the "naked" bubble is a function of diameter, as shown in Table 4.7 [74]. Typically, air bubbles range

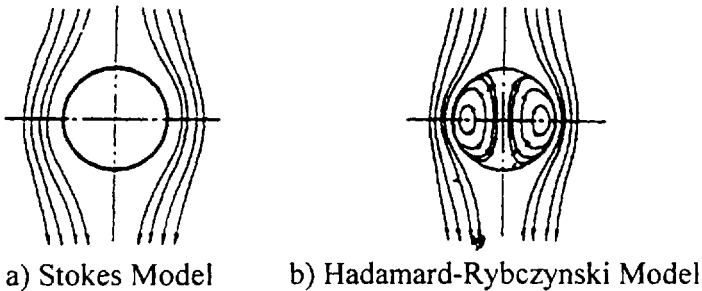


Figure 4.46 Comparison of the (a) Stokes and (b) Hadamard–Rybczynski models of fluid movement around an air bubble in solution. (From Ref. 73.)

from 10^{-7} to 10^{-3} m for a gas lyosol, 10^{-6} to 10^{-3} m for an aeroemulsion such as entrained air, and $>10^{-3}$ for coagulation for dispersed gas [75].

If a surface-active agent such as an antifoam composition is present, the stream lines around the bubble follow the Hadamard–Rybczynski model shown in Fig. 4.46b [73]. Slightly different forms of the Stokes equations should be used for this model:

$$U = \frac{\rho g d^2}{18\eta}$$

$$C_d = \frac{24}{Re}$$

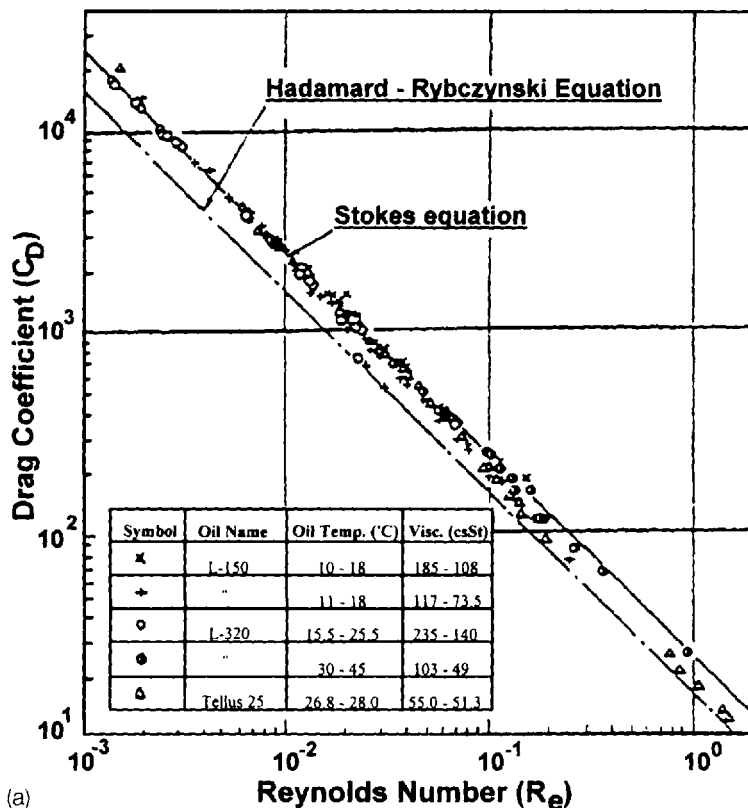
Drag coefficients of three different antiwear hydraulic oils as a function of varying Reynolds number are shown in Fig. 4.47a. Similar data for two fire-resistant hydraulic fluids—phosphate ester (SFR-C) and water–glycol fluid Iru 504—is provided in Fig. 4.47b. In both cases, the data correlate within the Stokes equation, which means that gas bubbles move as solid spheres in these fluids by the Stokes model [73].

Ida performed similar experiments with a silica-supported defoaming agent and a single-component higher-alcohol-type defoaming agent. His results showed that the silica-supported defoaming agent followed the Stokes model and the higher-alcohol defoaming agent (and other additives) followed the Hadamard–Rybczynski model [73].

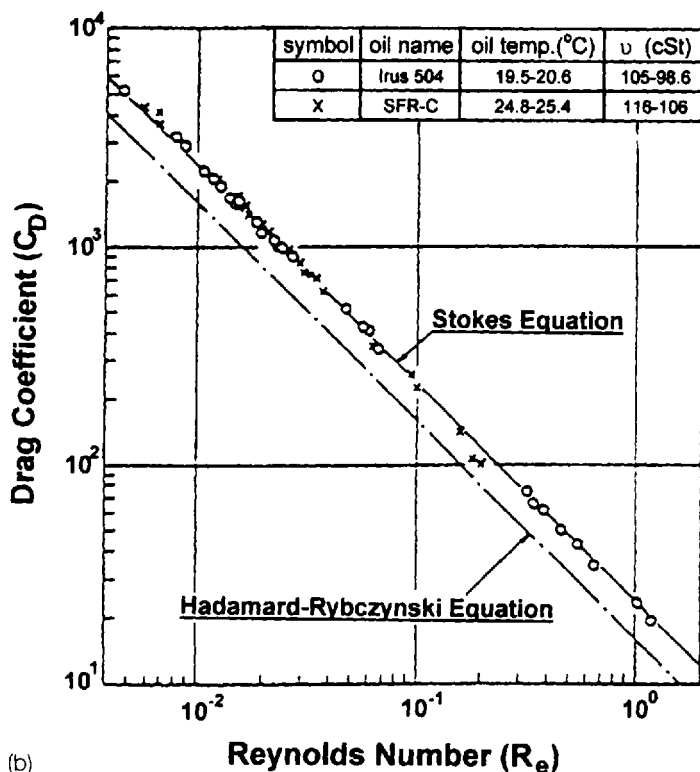
Table 4.7 Ascent Rates of Naked Bubbles

Bubble diameter (mm)	Terminal rates of ascent (mm/s)
1	11.00
10^{-1}	0.11
10^{-2}	0.0011
10^{-3}	0.000011

Source: Ref. 74.



(a)



(b)

Figure 4.47 Comparison of drag coefficients for (a) different petroleum oils and (b) fire-resistant fluids. (From Ref. 73.)

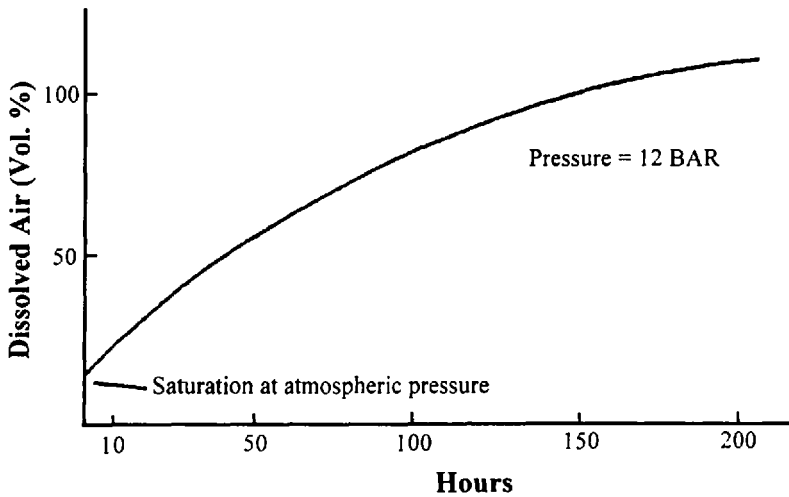


Figure 4.48 Dissolution rate of air in hydraulic oil under pressure. (From Ref. 78.)

Fowle studied the effect of a silicone antifoam on the air-release properties of a turbine oil [74]. Although these fluids initially exhibited both antifoaming and air-release properties, the air-release property was lost with increasing use time. Other work [76,77] has shown that although silicones exhibit excellent antifoam properties, at least initially, they do not exhibit superior air-release properties.

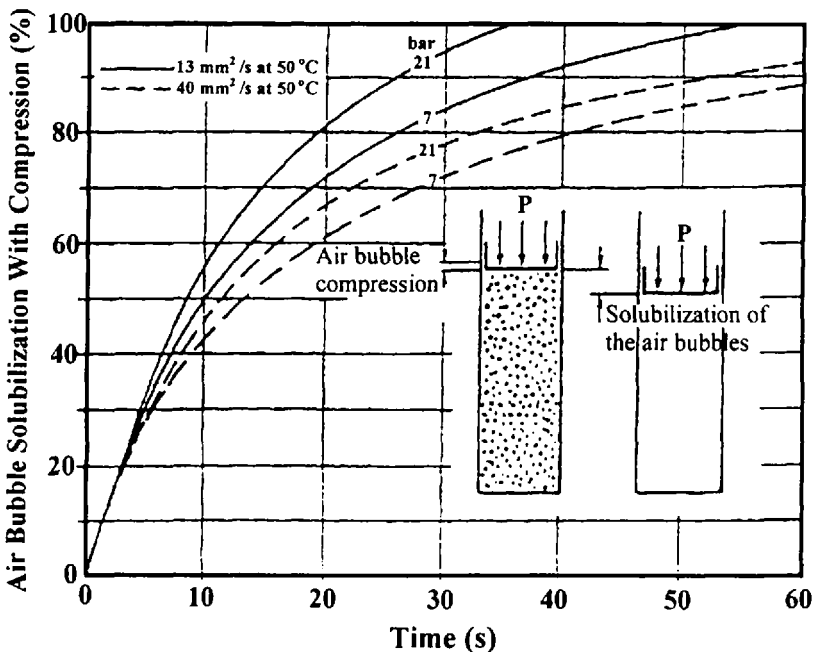


Figure 4.49 Effect of viscosity on air dissolution with compression. (From Ref. 79.)

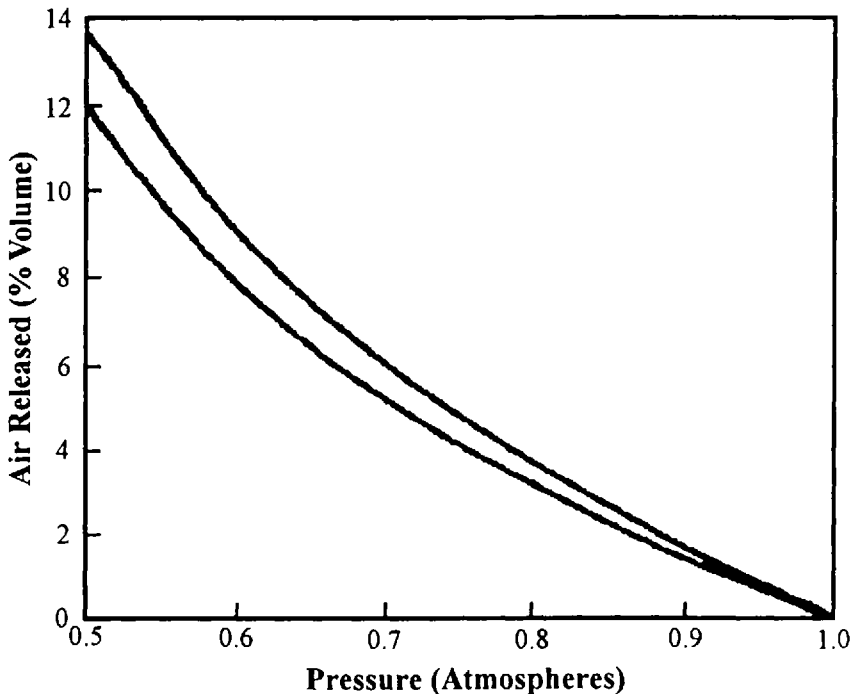


Figure 4.50 Air released from petroleum oil. (From Ref. 7.)

The dissolution of air in a fluid is a time-dependent diffusion process. Figure 4.48 shows the dissolution rate of air in a hydraulic oil with time at 12-bar pressures with no flow, which helps explain the relatively long diffusion times [78]. Figure 4.49 illustrates the solubilization of air bubbles with increasing pressure and fluid viscosity [79].

The reverse of this process is “air release.” Figure 4.50 shows that the release of air from a hydraulic fluid is enhanced by increasing temperature (lower viscosity) and *reduced* pressure [7]. Figure 4.51 illustrates the volume reduction of a hydraulic oil containing entrained air with respect to increasing pressure [78].

When an air-ignitable mixture is present inside of the air bubbles, ignition may occur from the temperature rise which occurs during compressing during a pressure cycle (see Fig. 4.52) [80]. This process requires only nanoseconds and the localized temperature may be as high as 1100°C. These high temperatures may subsequently lead to oil degradation [81]. This is called the “micro-diesel effect” and may cause localized hot spots and pressure spikes, which may subsequently lead to structural damage of the hydraulic pump [78].

Foam Tests

In this section, an overview of various laboratory tests that have been used to measure the foaming tendency of hydraulic and other industrial fluids will be discussed. The Tamura classification of these tests will be followed [82]. These test classifications include static tests, such as pouring, shaking, beating, rotational, and stirring, and dynamic tests, which include air injection and circulation. This discussion will be

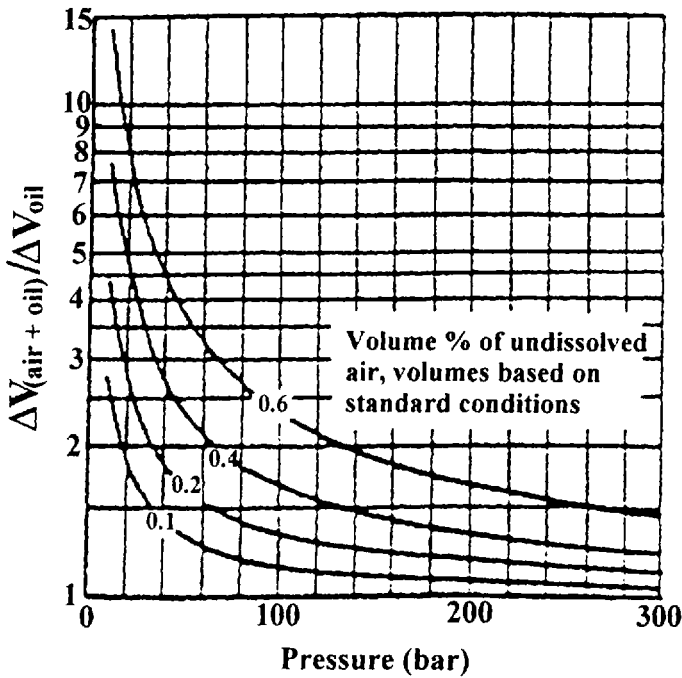


Figure 4.51 Volume reduction of H-L hydraulic oil (H-LP 36) permeated with air bubbles relative to bubble-free oil with increasing pressure. (From Ref. 78.)

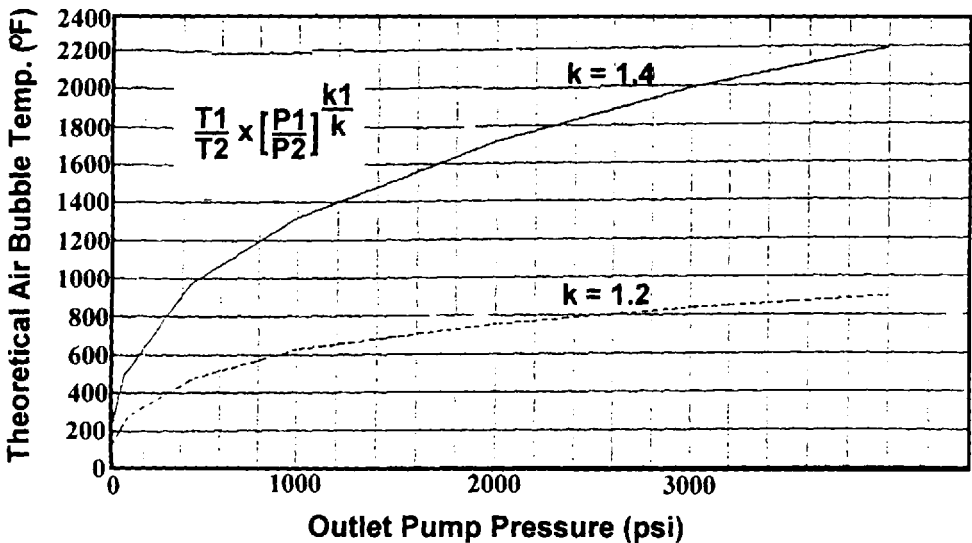


Figure 4.52 Theoretical bubble temperature increase with compression at atmospheric pressure. (From Ref. 80.)

followed by a description of pump tests that have been reported for measurement of the foaming tendency of hydraulic fluids.

STATIC TESTS

1. *Pouring tests.* One common test used to determine the foaming tendency of a fluid is the Ross–Miles method [83,100]. This test is conducted by allowing fluid to flow from a fixed height onto the surface of the same solutions using the test apparatus shown in Fig. 4.53a. The initial foam head and the foam head after 5 min is measured. These values provide a measure of foaming tendency and foam stability.
2. *Shake test.* Perhaps the simplest foam test, although not very reproducible, is the bottle shake test [85], where 200 mL of the fluid is placed in a 16-oz. wide-mouth, screw-top glass bottle and then shaken with an up-and-down motion. The initial foam height and after 5 min is recorded. The time required for the foam head to drop to 1 cm above the initial fluid level is recorded.

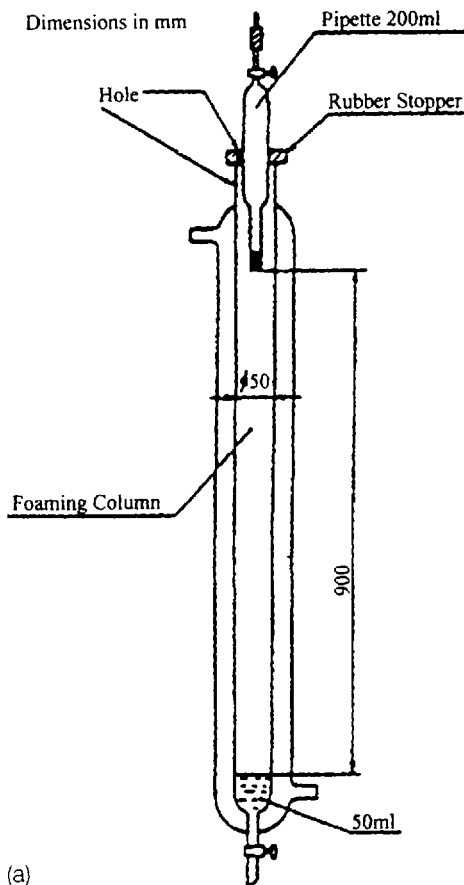
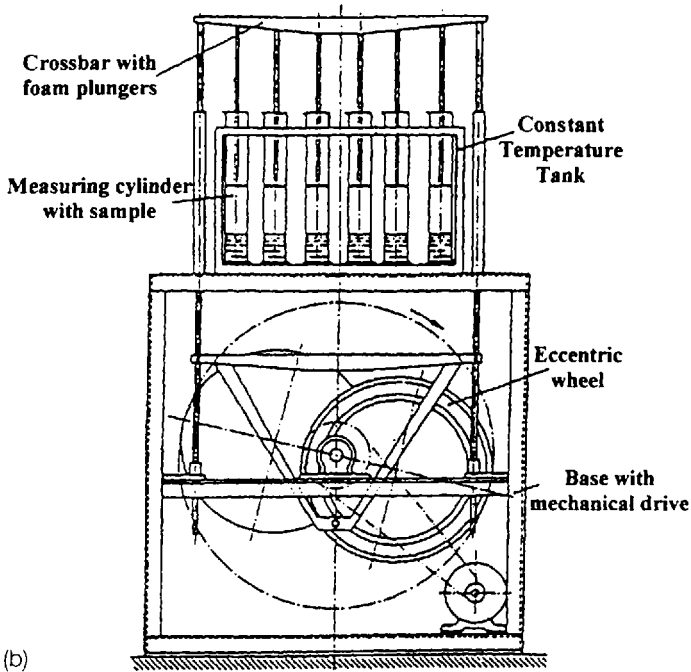
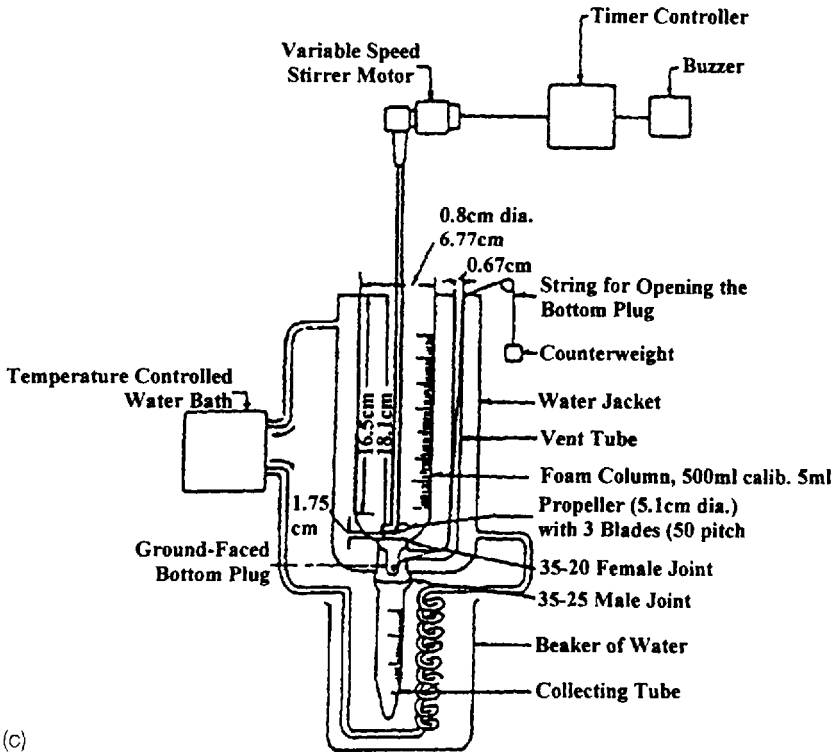


Figure 4.53 Measurement of foaming tendency: (a) Ross–Miles apparatus, (b) foam generation using plungers, and (c) Bhat and Harper apparatus. (From Ref. 82.)



(b)



(c)

Figure 4.53 Continued

3. *Beating method.* A standard volume (200 mL) of the fluid is placed in a 1-L cylinder and beaten 30 times in an up-and-down motion with a porous dish using the apparatus schematically illustrated in Fig. 4.53b [86]. The foam volume immediately after heating is recorded.
4. *Stirring method.* The ASTM D 3519 [87] test is used for (Waring blender) measurement of foaming of low-viscosity solutions under high-shear conditions. In this test, 200 mL of fluid is placed in a Waring blender and stirred at a high speed for 30 s and the initial foam height and foam height after 5 min is measured. The time for the foam head to drop to 1 cm above the initial fluid level is also measured. A variation of this test is the "Stirring Plate" method described in JIS K 2241 [88]. In this test, 60 mL of solution is placed in a 100-mL cylinder and stirred at 1500 rpm for 5 min. The foam volume 15 min after the stirring is stopped is measured. An example of this test apparatus is illustrated in Fig. 4.53c was reported by Bhat and Harper [89].

DYNAMIC TESTS

1. *Air-injection method.* Another common test to determine the foaming tendency of a hydraulic fluid is ASTM D 892 [90]. Air is injected at 94 mL/min through an 80 μM porous glass frit into 190 mL of test fluid contained in a 1-L graduated cylinder for 5 min, as illustrated in Fig. 4.54, at which time the foam height is measured. A simplified version of this test is used to measure the foaming properties of engine coolants is illustrated in Fig. 4.55a [82]. A similar version of this test using requested compressed gas flow was recently patented [91,92].
2. *Circulation method.* A French method [93] has been reported which involves continuously dropping the test fluid from a 750-mm height through

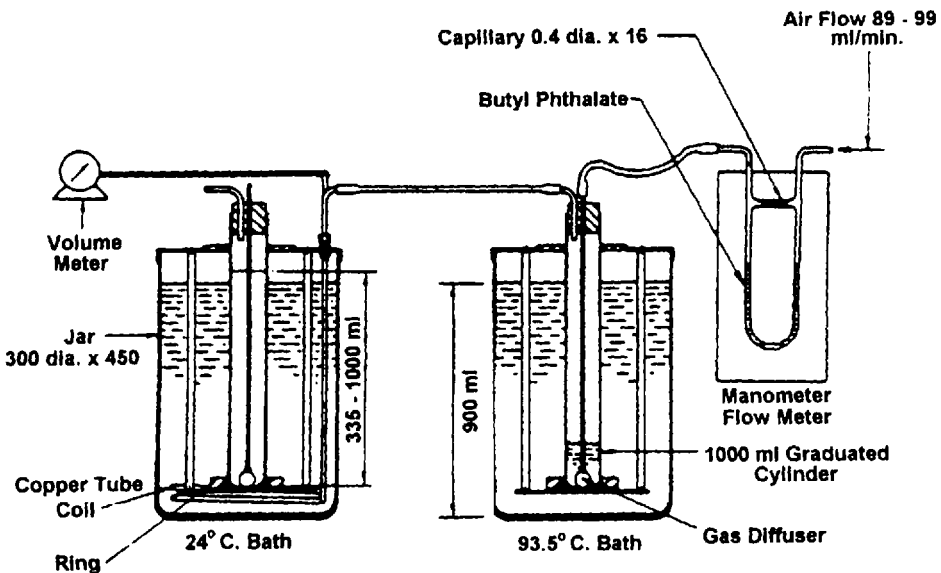


Figure 4.54 ASTM D 892 foam testing apparatus. (From Ref. 90.)

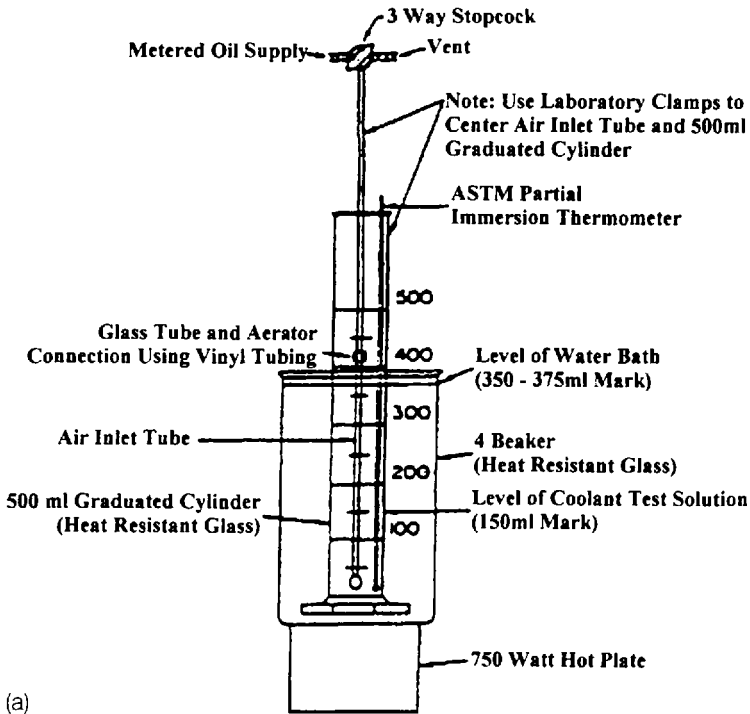


Figure 4.55 (a) Glassware foam test and (b) recycling and fall method. (From Ref. 82.)

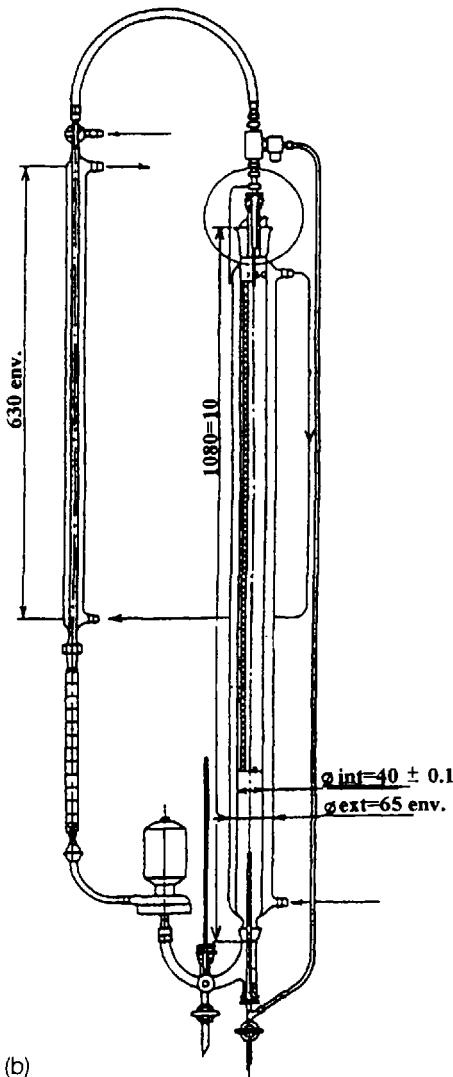
a nozzle placed in a 40-mm-diameter 1080-mm-high glass cylinder, as shown in Fig. 4.55b [82]. A pump is used to recirculate the fluid.

Air Entrainment—Experimental Procedures

Numerous experimental procedures have been reported to determine the propensity for a fluid to entrain air. Some procedures are based on relatively simple laboratory glassware apparatuses. Most often, proprietary experimental apparatuses which have been custom built for this specific purpose are used. An overview of experimental procedures that have been reported to study hydraulic fluid air entrainment will be provided here.

1. *“Bubbly” oil viscometer.* In order to study the effect of air-bubble entrainment on the viscosity of mineral-oil-based hydraulic fluids, Hayward developed the “bubbly” oil viscometer shown in Fig. 4.56a [94,95]. An aerator, illustrated in Fig. 4.56b, which is similar to a jet-type suction pump operating at 600 psi, is used to aerate the fluid [94]. Bubble content is controlled with the valve on the air suction line and oil pressure. Bubbly oil flows from the tank into a sump, from which it is returned to the aerator, forming a continuous circuit. The bubbles were separated by fitting the viscometer tank with a 60-mesh, 36-SWG wire gauze fitted at an angle of 30° in the sump.

Fluid flow through the viscometer tube in Fig. 4.56c was measured by placing a container of known volume beneath the jet at position A shown in Fig. 4.56a and measuring the time to fill the container with a stop watch [94].



(b)
Figure 4.55 Continued

Bubble content was determined by measuring the volume of the bubbles in the bubbly oil. Hayward found that bubbles imparted a relatively small increase in viscosity over the range of 30–170 cS at 30°C according to

$$\frac{\eta_b}{\eta_0} = 1 + 0.015\beta$$

where η_b is the viscosity of bubbly oil, η_0 is the viscosity of bubble-free oil, and β is the percentage of bubble content.

2. *Deutsche shell air-release test.* An air–oil emulsion is prepared using an aspirator usually fitted to water line to provide a vacuum source for fil-

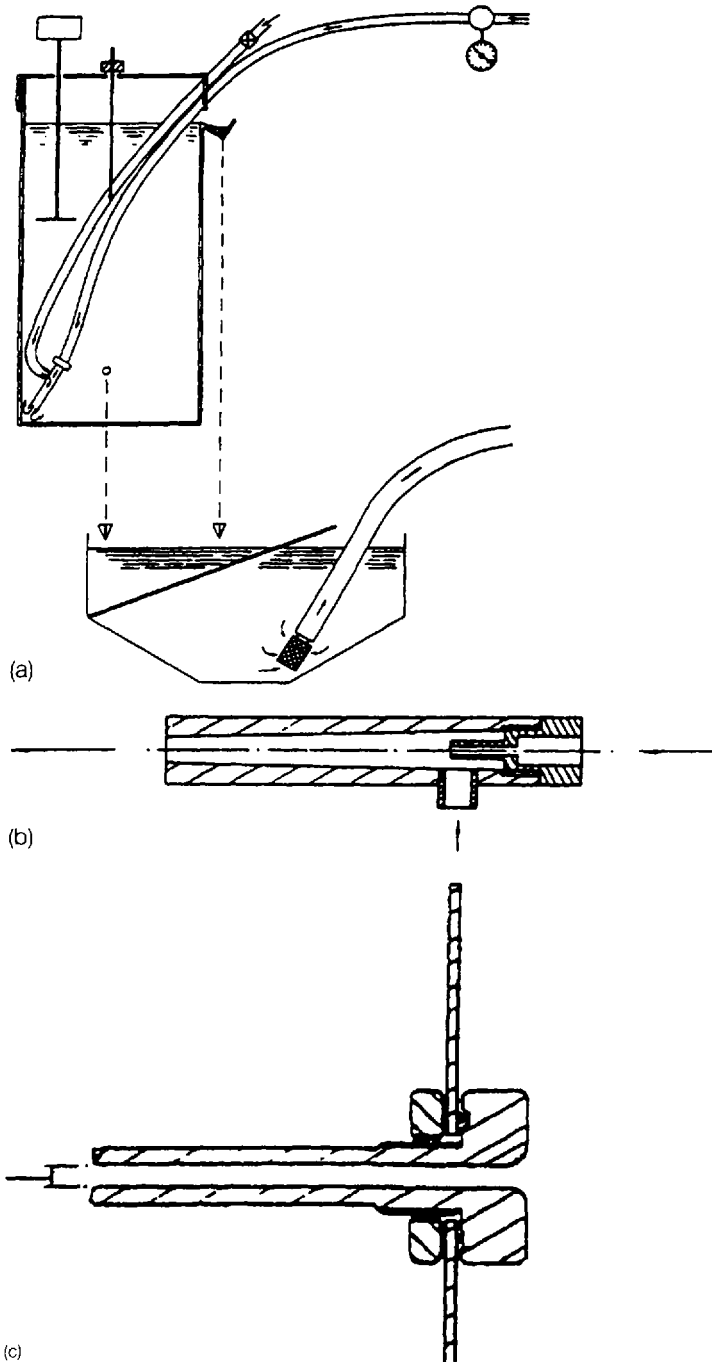


Figure 4.56 Hayward "bubbly" oil viscometer: (a) circulation system; (b) oil aerator; (c) viscometer tube. (From Ref. 94.)

tration [96]. Oil is fed through the entry, usually attached to the water line. The rate of air release from a 5% air–oil emulsion is determined graphically by plotting the change in density with time. Poor temperature control, which is vital, is one of the disadvantages of this procedure.

3. *Allgemeine Elek Tricitats—Gesellschaft (AEG) method.* This is basically a Waring blender test where 700 mL of the fluid at the test temperature (usually 50°C) is stirred at a “high” agitation rate approaching 20,000 rpm for 25 s. The fluid is then poured into a 1000-mL graduated cylinder and the rate of air-bubble loss is measured [96].
4. *Technischer ÜberwachungsVerein (TÜV) method.* This test method, DIN 51 381, involves the preparation of an air–water emulsion by introducing compressed air through a 2-mm capillary tube for 7 min using the apparatus illustrated in Fig. 4.57 [98].

The test temperature is usually 25°C, 50°C, or 75°C. Air release is determined by monitoring fluid density with time. The volume of dispersed air is calculated using

$$L = \frac{(\rho_0 - \rho_t) \times 100}{\rho_0 - \rho_L}$$

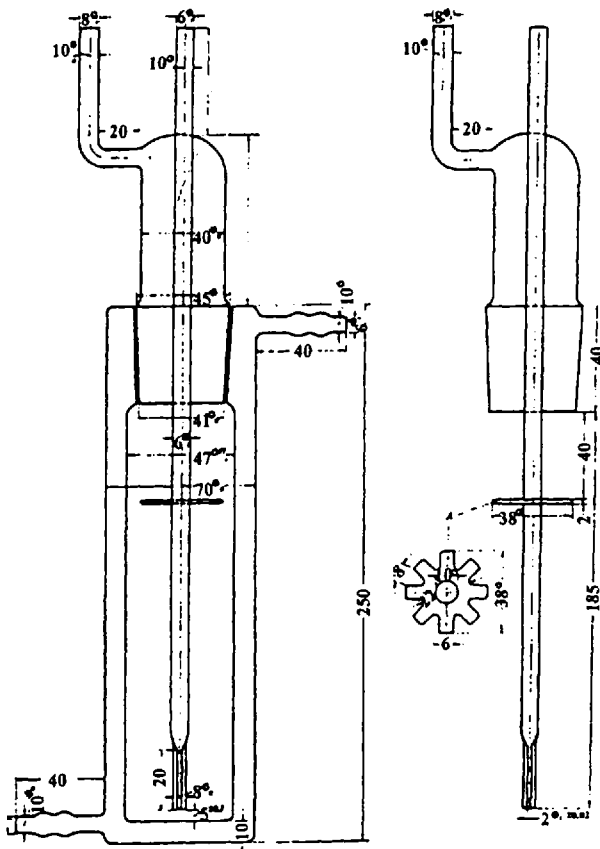


Figure 4.57 TÜV air-in-oil dispersion method. (From Ref. 98.)

where L is the volume % of dispersed air, ρ_p is the density (g/mL) of the bubble-free fluid, ρ_x is the density after time (x) (in min), and ρ_i is the density of air (in g/mL) at the test temperature.

5. *Rowland's air-entrainment method.* In this test, which is a variation of the AEG method discussed previously, 600 mL of the fluid at 100°F is mixed in a 1200-mL reservoir of a Waring blender at 9200 rpm for 10 s and then poured into a rectangular reservoir shown in Fig. 4.58a [99]. Because the amount of air is measured optionally, the sides of the reservoir are flatted to minimize error. The filled reservoir is immediately placed in a 100°F constant-temperature bath. The test cell is withdrawn periodically to measure bubble content by light absorption using the photocell shown in Fig. 4.58b and then replaced in the constant-temperature bath.
6. *Dynamic L.T.G. method.* The L.T.G. apparatus is shown in Fig. 4.59 [100]. This method is based on a circuit utilizing a gear pump. Air content may be varied from 5 to 20 L and the size of the reservoir may be varied. A "rest time" (TR) value is calculated from

$$TR_i = V_i/Q$$

where TR_i is the time of the oil in the settling tank (in s), Q is the volumetric capacity (L/s), and V_i is the volume of oil (L) in the tank being used.

The advantage of this method is that it not only measures air release but also the stability of the aerated fluid under operating conditions.

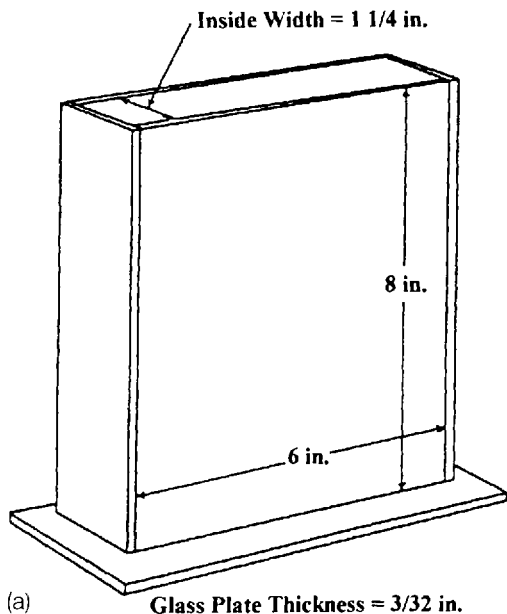


Figure 4.58 Measurement of bubble content by light transmission. (a) Glass measuring cell and (b) Light absorption measuring cell. (From Ref. 99.)

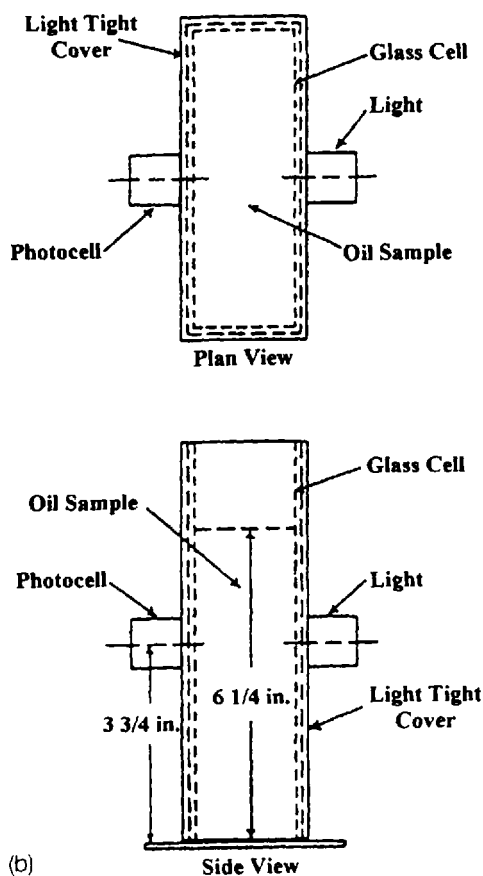


Figure 4.58 Continued

7. *Dead-weight apparatus.* The principle of measurement of bubble content for the dead-weight apparatus, which is shown in Fig. 4.60 is based on Henry's Law, where the solubility of a gas is proportional to the absolute pressure [101]. With sufficient compression, all of the gas bubbles will dissolve in the oil. The reduction in volume is a function of the bubble content.

This is one variation of the general class of piston-and-plunger methods, where a cylinder is filled to overflowing, a cap is then screwed on, a 15-lb. plunger is inserted, which creates a pressure of 300 psi [94]. The reduction in volume is proportional to the bubble content of the oil. Other variations of the general method have been reported by Magorien [53] and Liddell et al. [102]. An interesting variation of the system was reported, in which gas content of a water-glycol fire-resistant hydraulic fluid was measured using ram pressure and displacement curves while the fluid was in operation in an actual hydraulic circuit [103].

8. *Zander method.* Zander et al. have recently reported an apparatus (shown in Fig. 4.58) procedure capable of measuring relatively short air-release

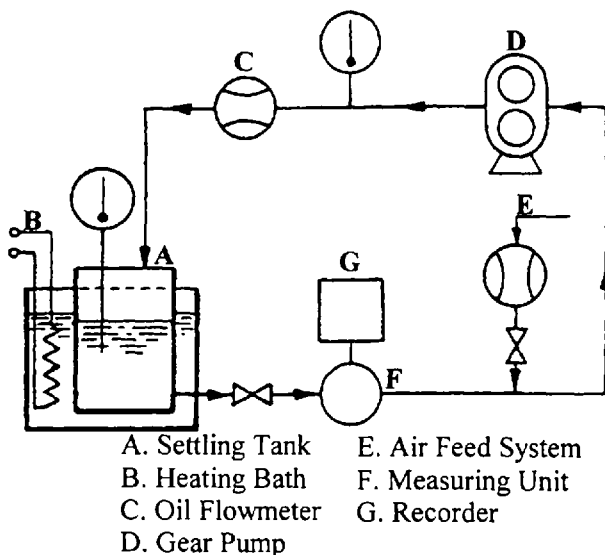


Figure 4.59 Schematic diagram for apparatus used for dynamic study of air entrainment: A—settling tank; B—heating bath; C—oil flowmeter; D—gear pump; E—air-feed system; F—measuring unit; G—recorder. (From Ref. 100.)

times [104]. This procedure is based on continuous measurement of the differential hydrostatic pressure between the points shown in Fig. 4.61 [104]. The volume fraction of air bubbles is calculated from the differential pressure divided by the fluid density and plotted as a function of time. This procedure is sensitive for air-release times less than 10 s.

9. *Hydrostatic balance.* A relatively simple procedure for the reproducible measurement of air-bubble volume is to apply Archimede's principle [101]. In this procedure, a heavy object of 10 spherical, of known volume (V) and weight (W), is immersed into the bubbly oil and the displaced fluid weight is measured (the volume will be equal to the volume of the object). The bubble content is calculated from

$$\text{Bubble content} = \frac{W_b - W_0}{W - W_0}$$

where

W_b = the apparent weight of an object when immersed in bubbly oil

W = apparent weight of an object when immersed in bubble-free oil

W_0 = the weight of the object.

10. *Sample bottle method.* The steel bottle shown in Fig. 4.62 is filled with bubble-free oil at atmospheric pressure and then the cap is immediately screwed on with the attached valve in the open position [105]. For either bubbly oil or bubble-free oil under pressure (or a vacuum) in a hydraulic system, the pressure-type sample bottle shown in Fig. 4.63 is used. The

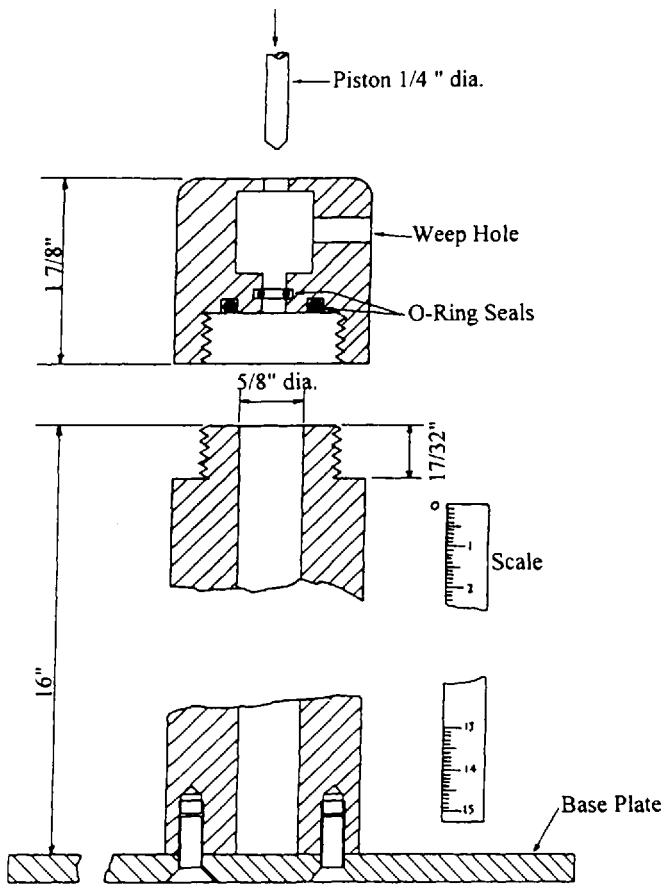


Figure 4.60 Dead-weight apparatus for measurement of air entrainment. (From Ref. 101.)

“bottles” are essentially $\frac{1}{8}$ -in. bare pipe with a $\frac{1}{8}$ -in. vacuum diaphragm valve at each end, capable of withstanding pressures up to 200 psi. After deaerating at 0.01–0.02 mm Hg and the gas content at standard temperature (273 K, 760 mm Hg), the volume of air content (1/1 by volume) is determined using

$$\text{Air content} = 35.92 \left(\frac{V_c}{V_b} \right) \frac{(P_2 - P_1)}{T}$$

where

V_c = the volume of the deaeration chamber (mL)

V_b = the volume of the sample bottle (mL)

P_2 = the final pressure of the deaeration chamber (mm Hg)

P_1 = the initial pressure of the deaeration chamber (mm Hg)

11. *Turbidity measurement.* Turbidity of hydraulic fluids varies with both the quantity and size of entrained air bubbles, as shown in Fig. 4.64 [106]. However, this figure also shows that turbidity measurements may possibly

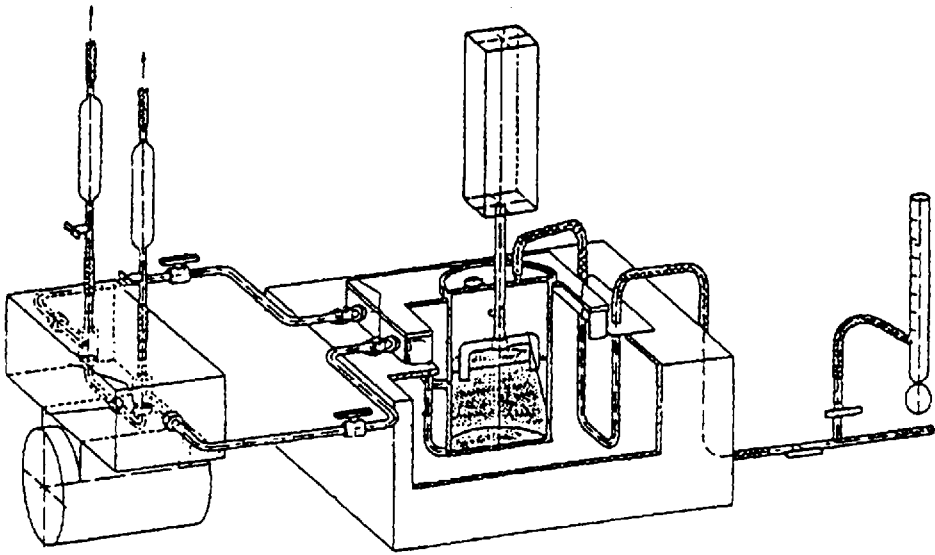


Figure 4.61 Measurement of entrained air by differential pressure. (From Ref. 104.)

yield erroneous results due to instrument sensitivity for very low levels of entrained air.

12. *In-line analysis of fluid aeration.* Tsuji and Katakura photographically examined and measured the effect of dissolved air on the changes of bubble size in a hydraulic system [107]. This study was performed using a measuring apparatus which was inserted in the hydraulic circuit, as shown in Fig. 4.65a. A schematic of the measuring apparatus is provided in Fig. 4.65b. In this work, deaerated oil was used and bubbles were injected into the system through a "bubble injection port." The characteristics of the injected bubble was then studied photographically.

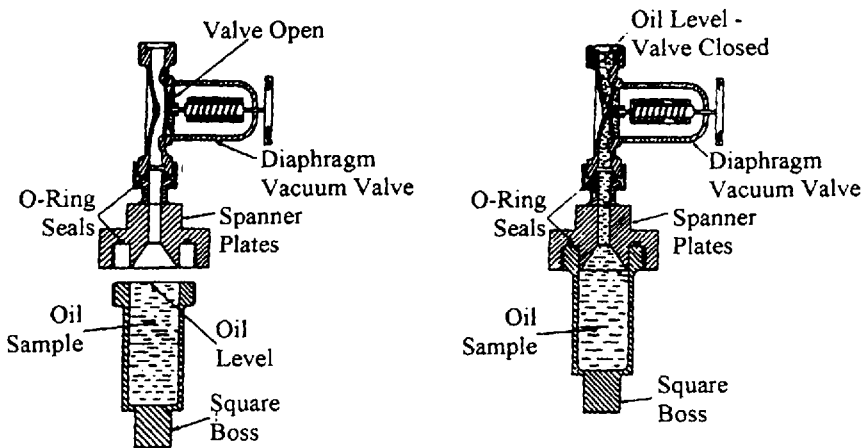


Figure 4.62 Open-type sample bottle. (From Ref. 105.)

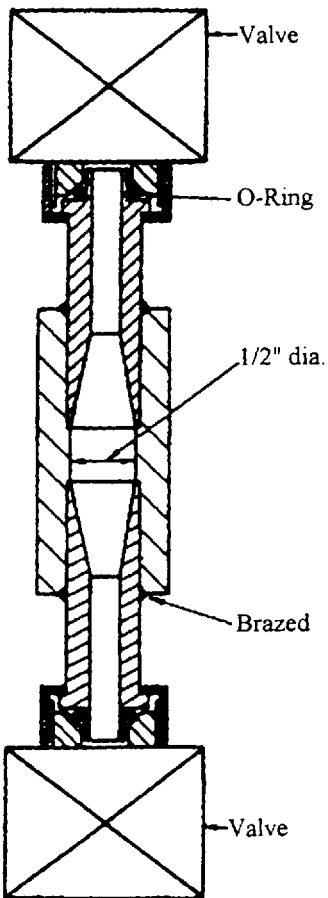


Figure 4.63 Pressure-type sample bottle. (From Ref. 105.)

In another study, Tsuji and Matsui quantitatively measured the bubble content of a hydraulic fluid during operation [108]. The experimental test circuit is shown in Fig. 4.66. Air is drawn into the hydraulic fluid by the suction with pressure of the pump and air content is controlled through with valve. Aerated fluid is sent to the measurement system by natural head. Bubbles in the fluid are photographed through a sight glass in the system shown in Fig. 4.66. The volume distribution of the bubbles in the fluid in the hydraulic circuit is shown in Fig. 4.67.

Air-Release Specifications

Barber and Perez have summarized the current national specifications for air release. These are summarized in Table 4.8 [76].

2.4 Compressibility and Bulk Modulus

When a hydraulic system is activated, the hydraulic fluid is compressed as shown in Fig. 4.68. Compression is defined as "volume percent decrease under adiabatic

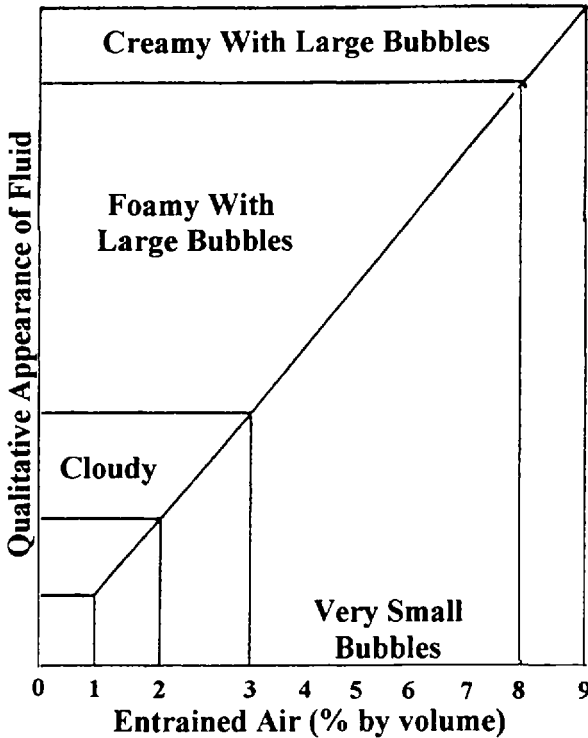


Figure 4.64 Quantification of entrained air by appearance. (From Ref. 106.)

conditions” [109]. (In adiabatic processes, it is assumed that there is no loss of heat due to compression.)

$$\text{Compressibility } (X) = \left(\frac{\Delta V}{V_0} \right) \Delta P$$

In the absence of specific technical data, it is often assumed that the compressibility of a petroleum oil is approximately 0.5% for each 100 psi pressure increase up to 4000 psi [110]. However, compressibility for representative fluids as a function of pressure is provided in Table 4.9 [111] and Fig. 4.69 [112].

Bulk modulus is defined as “the resistance to a decrease in volume when subjected to pressure” and is the inverse of compressibility [109]:

$$\text{Bulk modulus } (K) = -V_0 \left(\frac{\Delta P}{\Delta V} \right)$$

Although the bulk modulus of a fluid affects hydraulic system performance, it is especially important in servo valve operation. If the bulk modulus is too high, fluid is not sufficiently compressible and excessive fatigue failures of the valve housing may result.

The change in volume at a constant pressure is dependent on the type of compression process: isothermal compression with no change in temperature or adiabatic

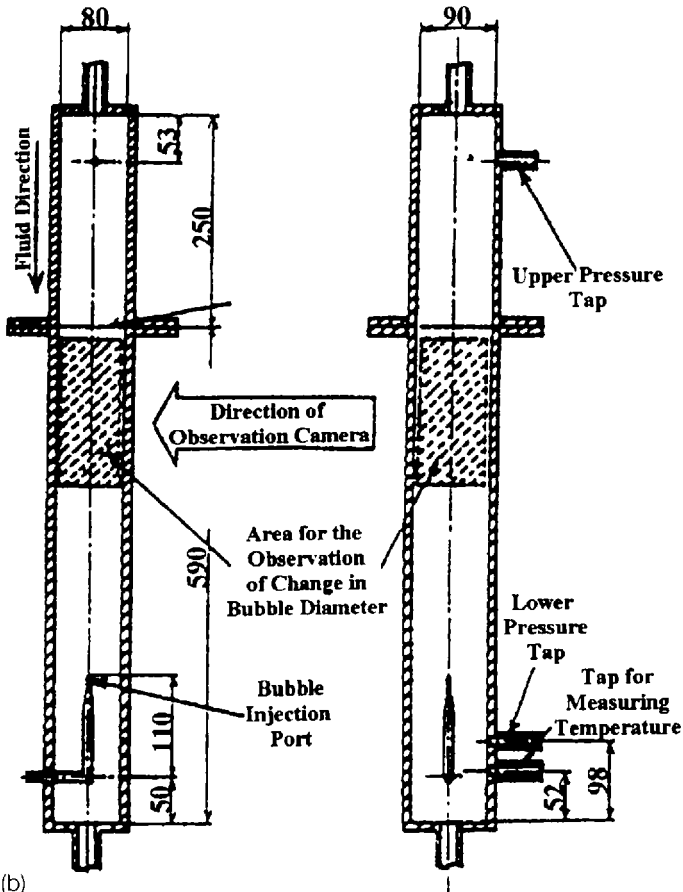
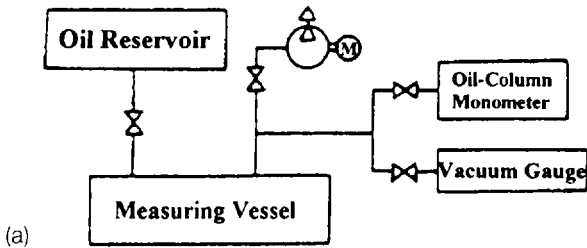
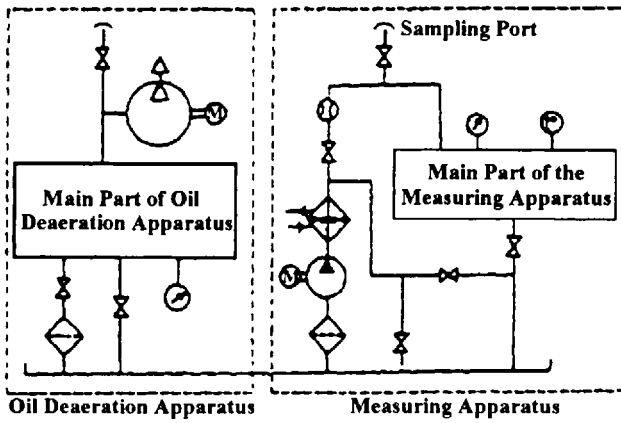
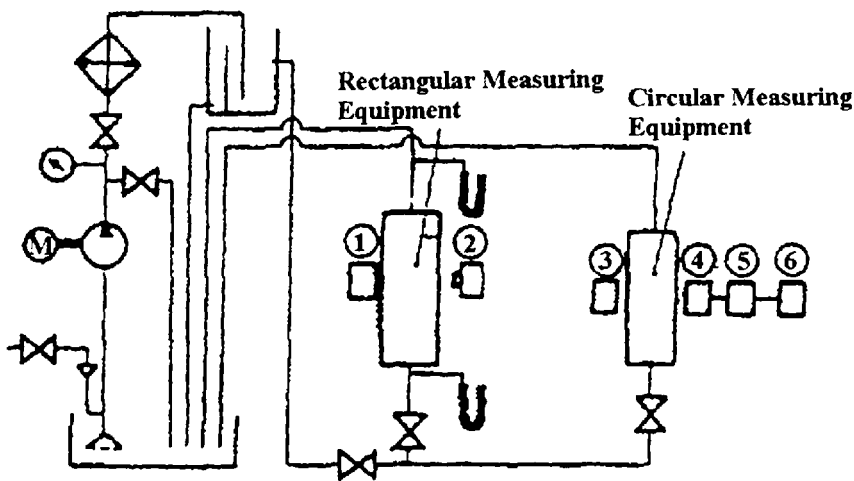


Figure 4.65 (a) Apparatus for measurement of air content of hydraulic oil; (b) observation cell of air-content measurement apparatus. (From Ref. 107.)



1. Light Source 4. Photo Cell
 2. Camera 5. D.C. Amp
 (a) 3. Light Source 6. Oscilloscope

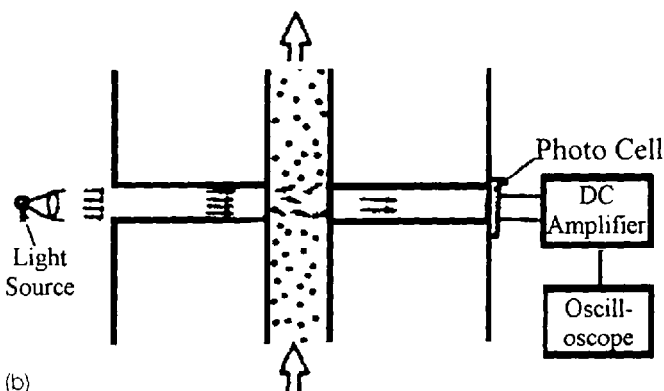


Figure 4.66 (a) Hydraulic circuit for measurement of air content: 1—light source; 2—camera; 3—light source; 4—photocell; 5—DC amp; 6—oscilloscope; (b) Optical cell for quantification of air-bubble content. (From Ref. 108.)

(isoentropic). Differences between isoentropic and isothermal compressibility are shown in Fig. 4.70 [112].

Hayward has reported the isoentropic compressibilities for selected fire-resistant fluids (Table 4.10). For mineral oils, the following expression for isoentropic mineral oil was given [113,114]:

$$\beta @ 20^{\circ}\text{C and } 10,000 \text{ lbs./in.}^2 = 3.5 - 0.2 \log \eta$$

where β is in $10^6 \text{ in.}^2/\text{lb.}$ and η is the kinematic viscosity at 22°C . The bulk modulus does not follow Hooke's Law because the relationship of pressure to specific volume ($\Delta V/V_0$) is not linear, as shown in Fig. 4.70 [112].

There are two general graphical solutions to determine the bulk modulus. One solution is the secant bulk modulus (K_{sc}), where a straight line is drawn between

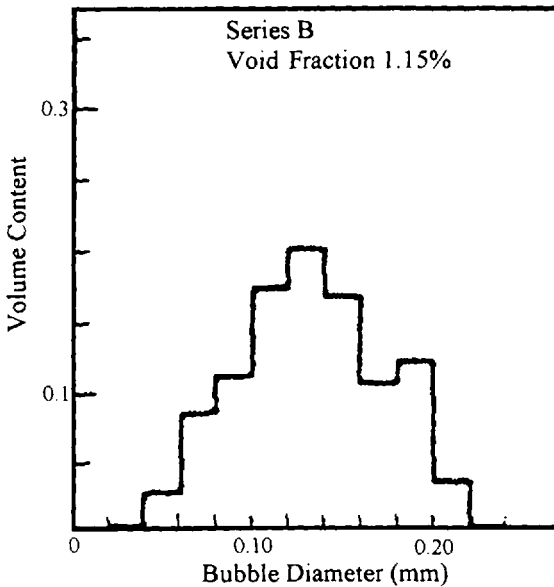


Figure 4.67 Bubble distribution in hydraulic oil. (From Ref. 108.)

Table 4.8 National Specifications for Air Release

Specification	Comment
DIN 51524 Parts 1, 2, and 3	For ISO VG grade, air release limit up to ISO VG 10, 22, and 32, 5 min maximum ISO VG 46 and 68, 10 min maximum ISO VG 100, 14 min maximum
Denson Hydraulic ATP-30283-A	Deaeration by AFNOR NFT 60-149 shall be 7 min maximum for any viscosity grade
Case Poclair SA	Deaeration by AFNOR NFT 60-149 shall be 7 min maximum for all grades. The test temperature varies according to the grade (PPF @ 30°C, PPTC @ 50°C, PPCC @ 70°C)
Svensk Standards ss 15 54 34	The air release requirement varies with the grade: SH15, 5 min maximum SH32 & 46, 10 min maximum SH68, 12 min maximum
AFNOR NF E 48-603	For the HM fluids, the requirement varies with ISO grade: up to ISO VG 32, 5 min maximum ISO VG 46, 7 min maximum ISO VG 68, 10 min maximum
ISO CD 11158	For up to ISO VG 32, 5 min maximum ISO VG 46 and 68 grades, 10 min maximum, and for ISO VG 100 and above, 14 min maximum

Source: Ref. 76.

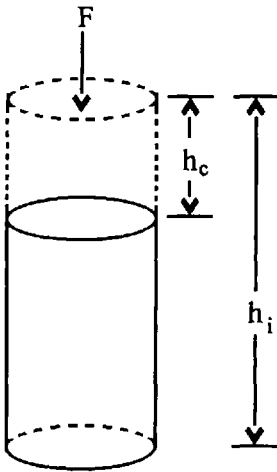


Figure 4.68 Illustration of fluid compressibility.

atmospheric pressure and the pressure of interest on the pressure-specific volume curve, as shown in Fig. 4.71 [112]:

$$K_{\text{sec}} = - \left(\frac{V_0}{\Delta V} \right) \Delta P \quad \text{at constant temperature}$$

The isothermal secant bulk modulus can be calculated for any fluid from density or viscosity as follows [1]:

From fluid kinematic viscosity:

$$K_{\text{sec}} = (1.30 + 0.15 \log \eta)[(\text{antilog } 0.0023)(20 - T)] \times 10^4 + 5.6P$$

From fluid density:

$$K_{\text{sec}} = [1.51 + 7(\rho - 0.86)][(\text{antilog } 0.0023)(20 - T)] \times 10^4 + 5.6P$$

where P is the pressure (in bars), T is the temperature (in °C), η is the kinematic viscosity at atmospheric pressure (in cS at 20°C), ρ is the density at 20°C and atmospheric pressure (in kg/L).

Table 4.9 Volume Reduction with Increasing Pressure for Common Hydraulic Fluids

Fluid	% Reduction in volume at 1000 psi	% Reduction in volume at 10,000 psi
Water	0.34	3.3
Water-in-oil	0.35	3.5
Water-glycol	0.26	2.6
Mineral oil	0.35	3.4
Phosphate ester	0.25	2.5
Chlorinated aromatic fluids	0.24	2.4
Silicone fluids	0.66	6.8

Source: Ref. 111.

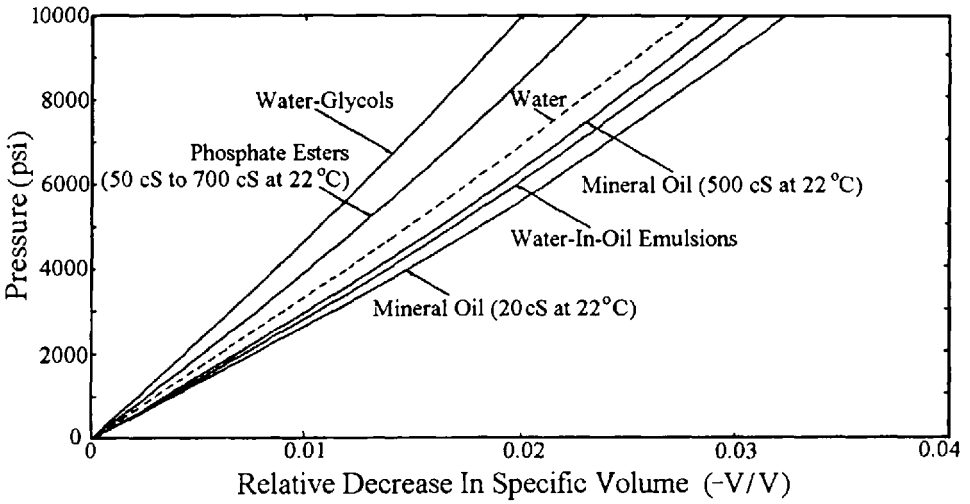


Figure 4.69 Relative decrease in specific volume ($-\Delta V/V_0$) for different hydraulic fluids. (From Ref. 112.)

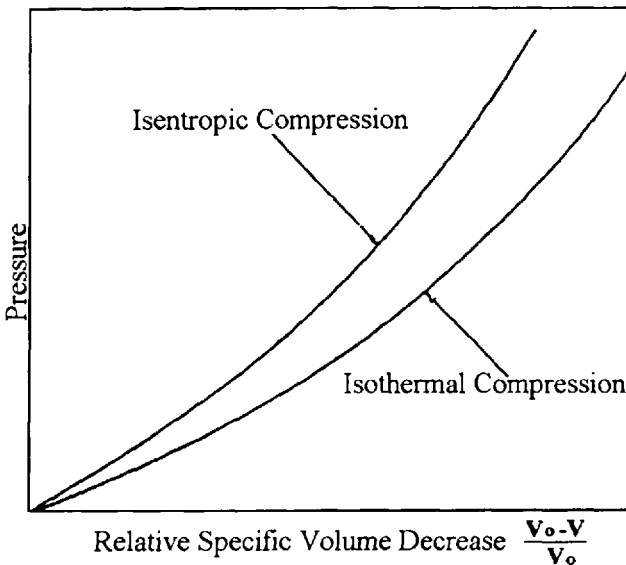


Figure 4.70 Illustration of the differences in specific volume ($(V_0 - V)/V_0$), for isentropic and isothermal compression. (From Ref. 112.)

Table 4.10 Compressibility Values for Various Formulation of Fire-Resistant Fluids

Fluid Description		Measured Values		
Type of fluid	Additives	Water content (wt.%)	Viscosity at 22°C (cS)	Isentropic secant compressibility at 10,000 lbs./in. ² and 20°C [(in. ² /lb.) × 10 ⁻⁶]
Water-glycol	Liquid-phase and vapor-phase corrosion inhibitors, metal deactivator, and lubricity improver	35-50	61.9	2.01
Water-glycol	Liquid-phase and vapor-phase corrosion inhibitors, metal deactivator, and lubricity improver	35-50	100	1.98
Diethylene glycol polyalkylene glycol mixture in water	Corrosion inhibitor and antiform	55	43.4	2.07
Water-glycol	Liquid-phase and vapor-phase corrosion inhibitor	50	91.7	2.05
Water-glycol	Liquid-phase and vapor-phase corrosion inhibitor	40	81.6	2.06
Water-glycol	Corrosion inhibitor antiwear and antioxidant	—	22.7	2.01
Water-glycol	Corrosion inhibitor antiwear and antioxidant	—	52.4	2.02
Water-glycol	Corrosion inhibitor antiwear and antioxidant	—	139	1.99
Water-glycol solution	Antirust	40	117	1.97
Water-in-oil emulsion	Emulsifier, corrosion inhibitor, antiwear and oxidation inhibitor	40	117	3.15
Water-in-oil emulsion	Emulsifier, antiwear, and antirust	43	77.7	3.00
Water-in-oil emulsion	Emulsifiers	37.5	1200	3.05
Water-in-oil emulsion	Emulsifier gum inhibitor, antirust and antiwear	40	222	3.09
Water-in-oil emulsion	Corrosion inhibitor and antiwear	—	145	3.08
Water-in-oil emulsion	Corrosion inhibitor and antiwear	—	182	3.07
Phosphate ester	Viscosity index improver, corrosion inhibitor, antioxidant, dye and other multipurpose additives	—	18.2	2.93
Phosphate ester (mixture of triaryl phosphates)	None	—	146	2.34
Phosphate ester	None	—	135	2.27
Phosphate ester	Antioxidant, copper deactivator, antirust, emulsifier and antiform	—	73.5	2.29
Phosphate ester	Viscosity index improver, antioxidant, copper deactivator, antirust, emulsifier, and antifoam	—	85.5	2.27
Phosphate ester	Antioxidant and antiform	—	142	2.34
Phosphate ester	Antiwear	—	342	2.33
Aryl phosphate	None	—	723	2.32
Aryl phosphate	None	—	149	2.36
Aryl phosphate	None	—	91.9	2.28
Aryl phosphate	None	—	82.5	2.28
Aryl phosphate	None	—	245	2.37
Mixed aryl alkyl phosphate ester	Viscosity index improver and traces of other additives	—	15.9	3.20
Mixed chlorinated diphenyl	Rust inhibitor, foam-control additive, and lubricity additive	—	182	2.27
Chlorinated polyphenyl	Viscosity index improver, antiwear, antifoam, and antirust	—	347	2.28
Sebacate diester	None	—	21.7	3.14
Adipate diester	None	—	22.6	3.28
Silicate ester	None	—	11.5	3.61
Chlorophenyl methyl polysiloxane	None	—	74.4	4.27

Source: Ref. 114.

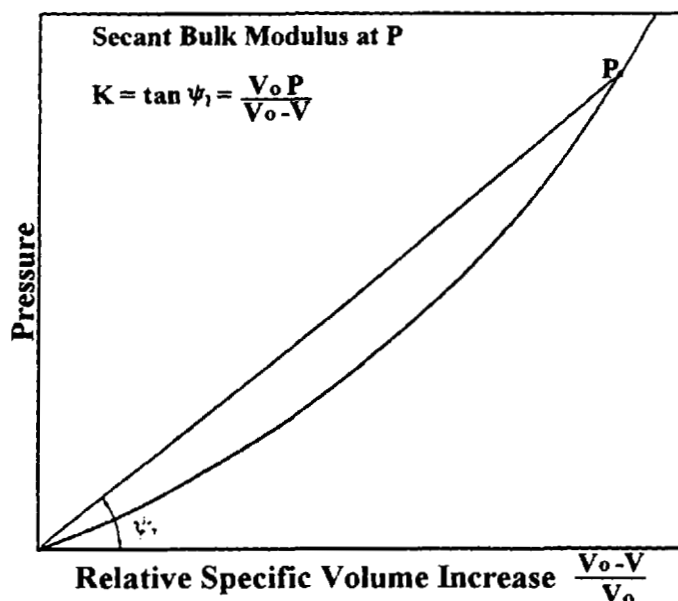


Figure 4.71 Illustration of the calculation of secant bulk modulus. (From Ref. 112.)

If sudden variations in pressure are encountered, as is typical in hydraulic systems, the use of the isentropic (dynamic) secant bulk modulus is preferred:

$$K_{\text{sec}} = - \left[\frac{V_0}{\Delta V} \right] \Delta P \quad \text{at constant entropy}$$

where V_0 is the specific volume at atmospheric pressure at constant entropy, ΔV is the difference in specific volume ($V_0 - V$) at pressure P .

The isentropic second bulk modulus may also be calculated from either fluid viscosity or density [9]. From fluid viscosity,

$$K_{\text{sec}} = (1.57 + 0.15 \log \eta)[(\text{antilog } 0.0024)(20 - T)] \times 10^4 + 5.6P$$

$$K_{\text{sec}} = [1.78 + 7(\rho - 0.86)][(\text{antilog } 0.0024)(20 - T)] \times 10^4 + 5.6P$$

The secant bulk modulus is dependent on both temperature, as shown in Fig. 4.72 [116] and Table 4.11 [115], and pressure, as shown in Fig. 4.73 [116]. The isothermal tangent bulk modulus is determined by drawing a line tangent to the pressure of interest on the pressure-specific volume curve, as shown in Fig. 4.74:

$$K_{\text{tan}} = -V \left(\frac{dP}{dV} \right) \quad \text{at constant temperature}$$

where V is the specific volume at pressure P .

The isentropic tangent bulk modulus may be calculated by multiplying the isothermal bulk modulus by the heat capacity ratio C_p/C_v . Typical values for mineral oils are provided in Table 4.12 [94].

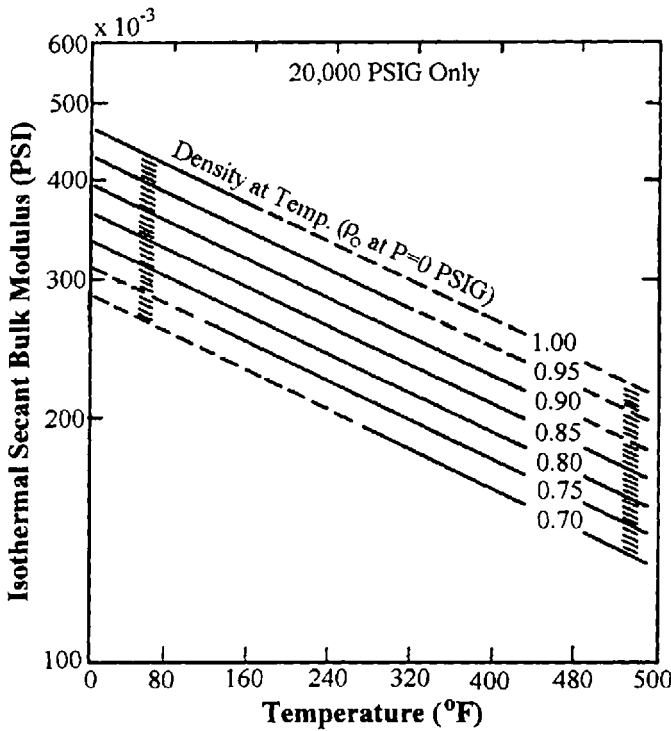


Figure 4.72 Secant bulk modulus versus temperature for petroleum oils. (From Ref. 116.)

All of the illustrative compressibility and bulk modulus data provided thus far has been for nonaerated fluids. However, as discussed previously, it is common for hydraulic fluids to undergo some aeration in use. Because air is more than 10,000 times as compressible as oil, aeration will significantly effect bulk modulus as shown in Fig. 4.75 [117]. The Hayward equation that describes the effect of air bubbles on secant bulk modulus is

$$\frac{K_{\text{fluid/air}}}{K_{\text{fluid}}} = \frac{V_f/V_a + 1}{V_f/V_a + KP_0/P^2}$$

Table 4.11 Variation of Bulk Modulus with Pressure and Temperature

Fluid type	Secant bulk modulus increase with pressure (0–5000 psig) (%)	
	100°F	400°F
Petroleum base	30	100
Phosphate ester	20	47

Source: Ref. 115.

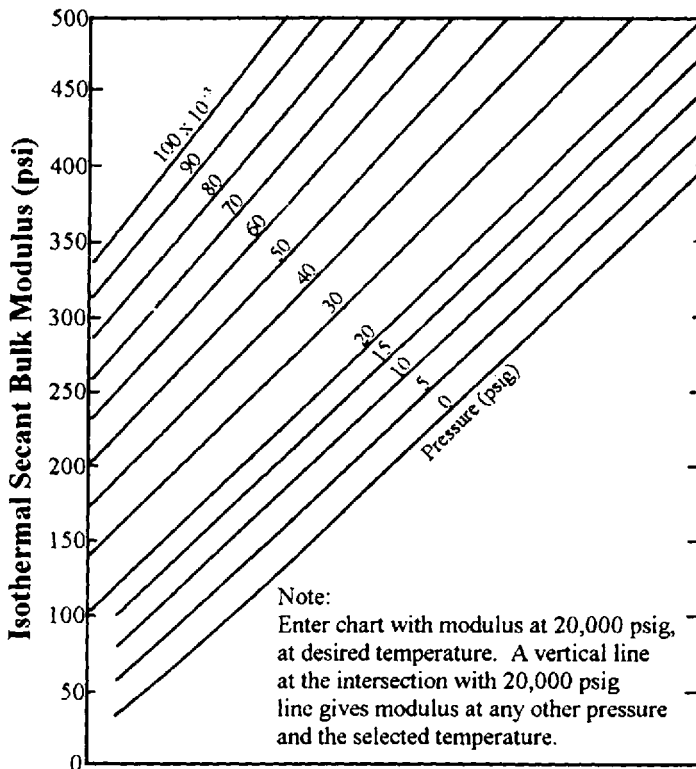


Figure 4.73 Secant bulk modulus versus pressure for petroleum oils. (From Ref. 116.)

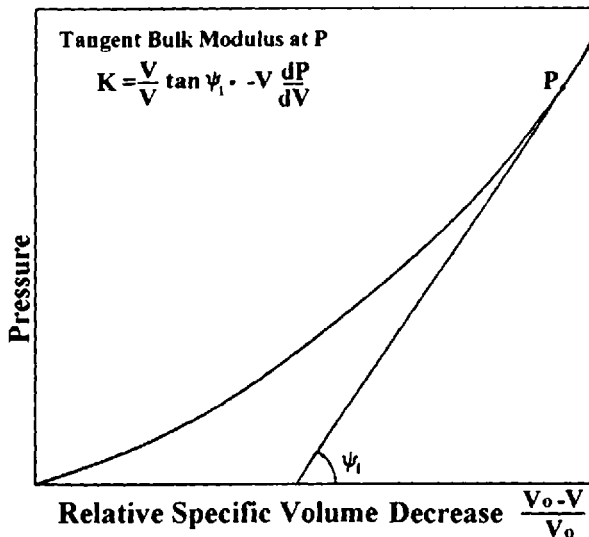


Figure 4.74 Illustration of the calculation of tangent bulk modulus. (From Ref. 112.)

Table 4.12 Typical C_p/C_v Ratios for Mineral Oils

Temperature (°C)	C_p/C_v (atmospheric pressure)	C_p/C_v (70 MPa)
10	1.175	1.15
60	1.166	1.14
120	1.155	1.13

Source: Ref. 94.

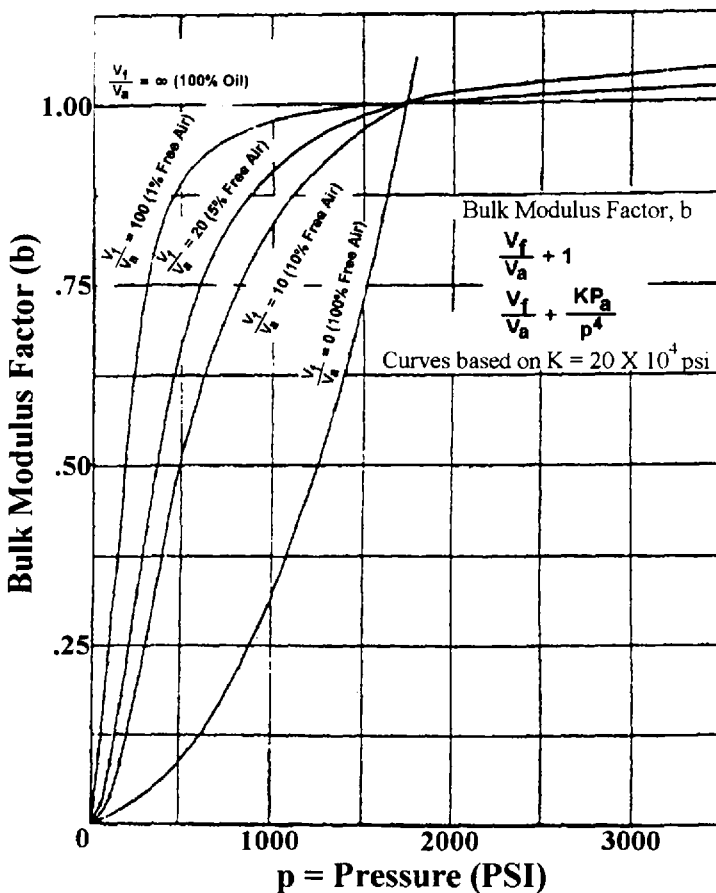


Figure 4.75 Bulk modulus factor–pressure curves for air–oil mixture. (From Ref. 117.)

where

V_t = the total volume at atmospheric pressure P_0

V_a = the air volume at atmospheric pressure P_0

P_0 = atmospheric pressure

P = the system pressure

K = the secant bulk modulus of the unaerated oil [94,118,119]

This equation should be used with caution due to the solubility of air in the fluid at higher pressures.

Hodges has provided nomograms to determine the secant and tangent bulk modulus of aerated fluids when the relative volume of the entrained air is known. The secant and tangent bulk modulus values are calculated from the value of ϕ taken from Figs. 4.76 and 4.77, respectively, and using the appropriate equation [9]:

Secant bulk modulus (aerated) = $K_{sec}\phi_{sec}$

Tangent bulk modulus (aerated) = $K_{tan}\phi_{tan}$

2.4.1 Prediction of Bulk Modulus

Because the modulus varies with temperature and pressure, it is of interest to be able calculate the value at a temperature or pressure other than the one available. Klaus

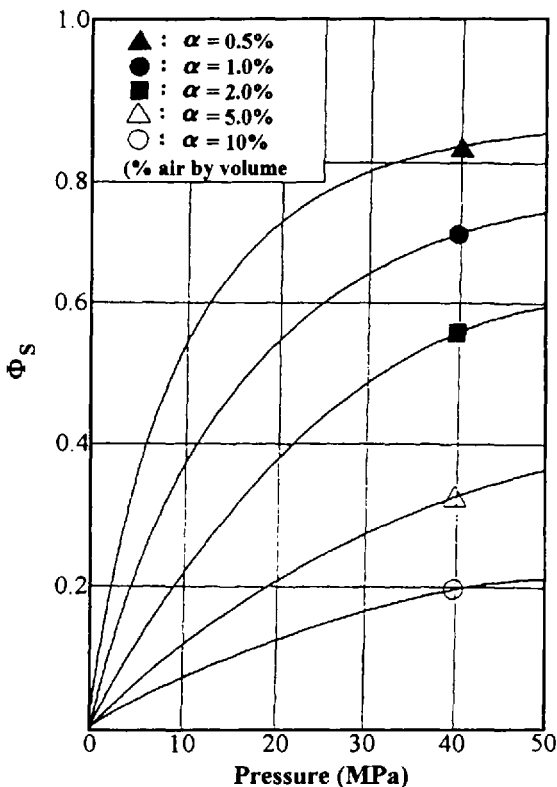


Figure 4.76 Correction coefficient for secant bulk modulus of any fluid containing undissolved air. (From Ref. 9.)

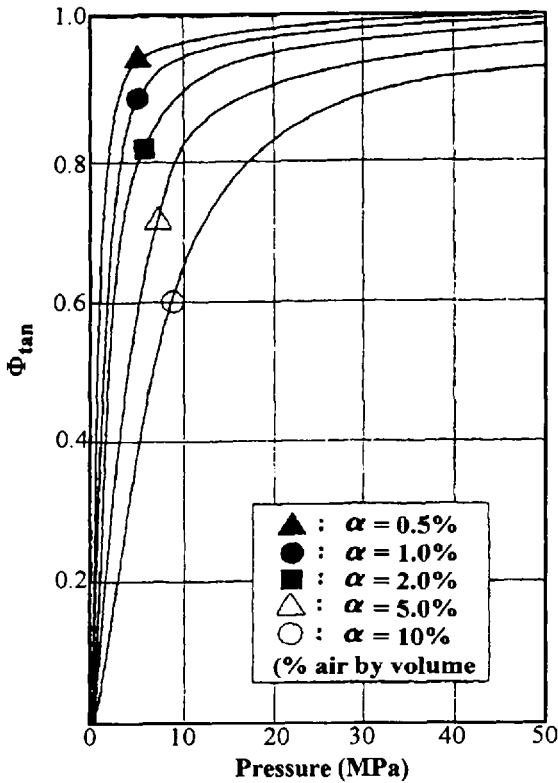


Figure 4.77 Correction coefficient for tangent bulk modulus of any fluid containing undissolved air. (From Ref. 9.)

and O'Brien have shown that the use of the following equations with Fig. 4.78 permits the calculation of secant bulk modulus at any temperature between 32°F and 425°F and pressure between 0 and 150,000 psig [120]:

$$K_{sec} = [(K_{sec})_0 + 5.30P]_T$$

where

K_{sec} = the isothermal secant bulk modulus at pressure P (psi) and temperature T (°F)

$(K_{sec})_0$ = the isothermal secant bulk modulus at 0 psig and temperature T

P = the pressure (psig)

$$\log \left(\frac{(K_{tan})_{T_1}}{(K_{tan})_{T_2}} \right) = [\beta(T_2 - T_1)]_P$$

where

$(K_{tan})_{T_1}$ = the isothermal secant bulk modulus at pressure P (psig) and temperature T_1 (°F)

$(K_{tan})_{T_2}$ = the secant isothermal bulk modulus at pressure P (psig) and temperature T_2 (°F)

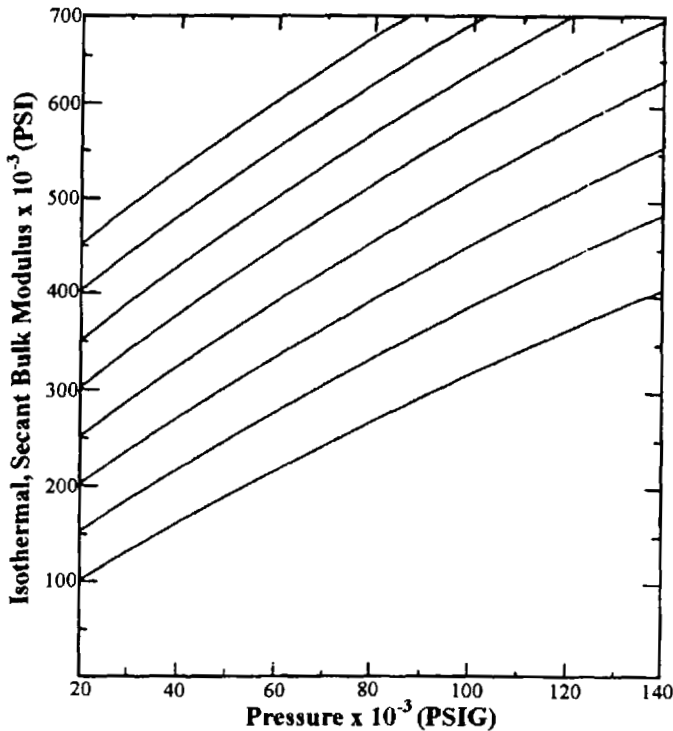


Figure 4.78 Generalized bulk modulus–pressure relationship (32–425°F). (From Ref. 120.)

The value of β is obtained from Fig. 4.79 [120].

Klaus also showed that the tangent bulk modulus and secant bulk modulus are interrelated by [120]

$$(K_{tan})_P = (K_{sec})_{2P}$$

Wright has provided a nomogram for the prediction of secant bulk modulus of a petroleum oil at different temperatures shown in Fig. 4.72 and pressures shown in Fig. 4.73 [121].

The bulk modulus varies with oil chemistry (paraffinic versus naphthenic), as shown in Fig. 4.80 [121].

2.4.2 Methods of Measurement

Various methods have been reported to determine the bulk modulus of fluids. These include a mercury piezometer, a single-liquid piezometer, metal bellows, and acoustic method, and a thermodynamic conversion method [113]. Goldman et al. have reported the use of a piston method using the apparatus shown in Fig. 4.81 [122].

A similar system has been developed by Hayward, where a load is applied through a rod entering the fluid being tested and the penetration of the rod is proportional to the compressibility of the fluid. A schematic of the instrument is shown in Fig. 4.82 [113].

Ultrasonic measurement of compressibility has also been applied using the apparatus similar to that shown in Fig. 4.83 [123,124].

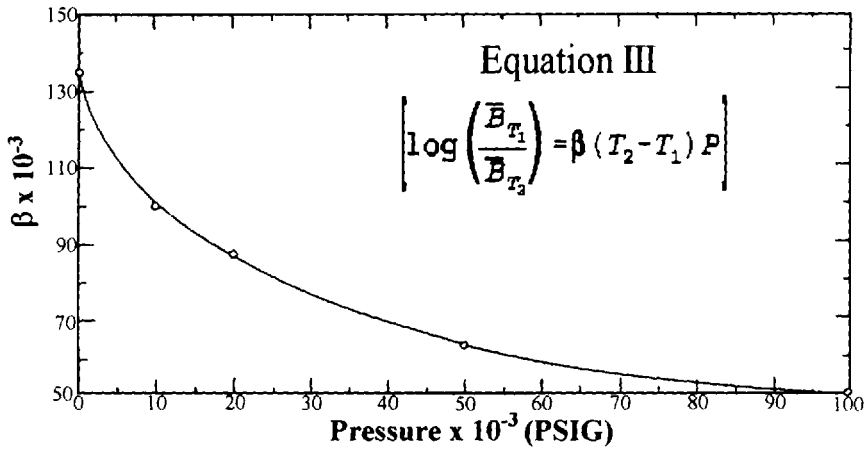


Figure 4.79 Effect of temperature and pressure on bulk modulus. (From Ref. 120.)

2.5 Cavitation

Cavitation is defined as “the dynamic process of gas cavity growth and collapse in a liquid” [125]. These cavities are due to the presence of dissolved gases or vaporizable liquids and they are formed when the pressure is less than the saturation

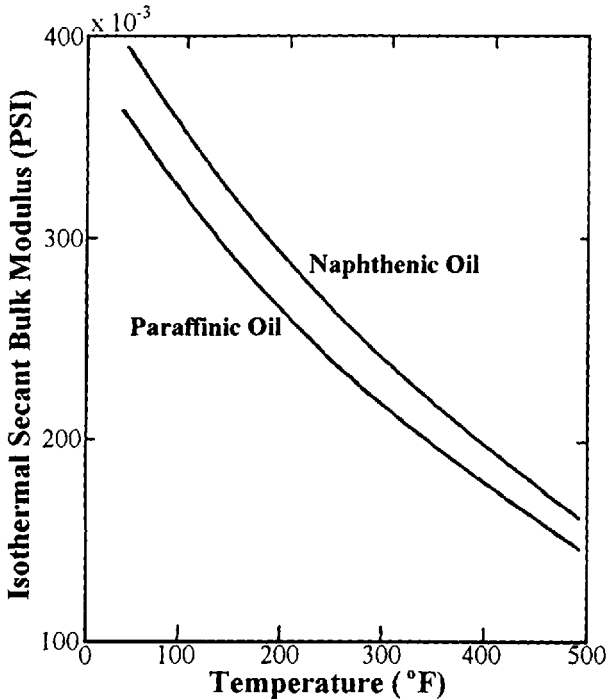


Figure 4.80 Effect of oil type and temperature on secant bulk modulus at 20,000 psig. (From Ref. 121.)

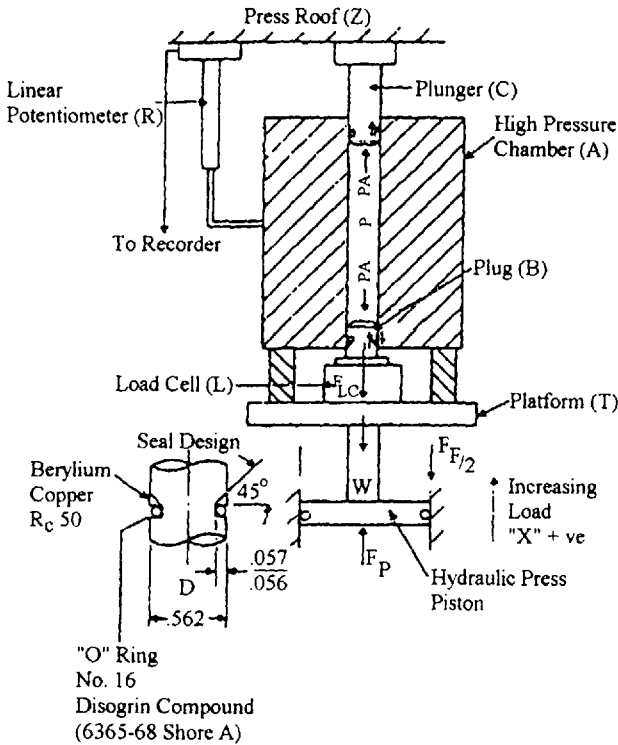


Figure 4.81 Apparatus for measurement of fluid compressibility. (From Ref. 122.)

pressure of the gas (gaseous cavitation) or the vapor pressure of liquid (vaporous cavitation) [126].

2.5.1 Gaseous Cavitation

According to Henry's Law, the solubility of a dissolved gas, such as dissolved (not entrained) air in a hydraulic fluid, is directly proportional to the pressure on the fluid. A decrease in pressure will decrease the solubility of the gas, releasing it from the solution in the form of bubbles. When the system is pressurized again, the gas will redissolve with the generation of heat. This process is called *gaseous cavitation*.

2.5.2 Vaporous Cavitation

If the pressure of a system is reduced below the vapor pressure of the fluid, vapor bubbles (cavities) will form. This is called *vaporous cavitation*. The vapor pressure of water, which is present in many fire-resistant fluids or as a contaminant in mineral oil, is shown in Fig. 4.84 [127]. The greater propensity for cavitation of water and water-containing fluids compared to mineral oil is due to the vapor pressure of water.

Of the two forms of cavitation, gaseous and vaporous, gaseous cavitation is most often encountered in hydraulic systems. However, even with relatively large amounts of entrained air, gaseous cavitation still may not occur, although hydraulic response times will be affected [128].

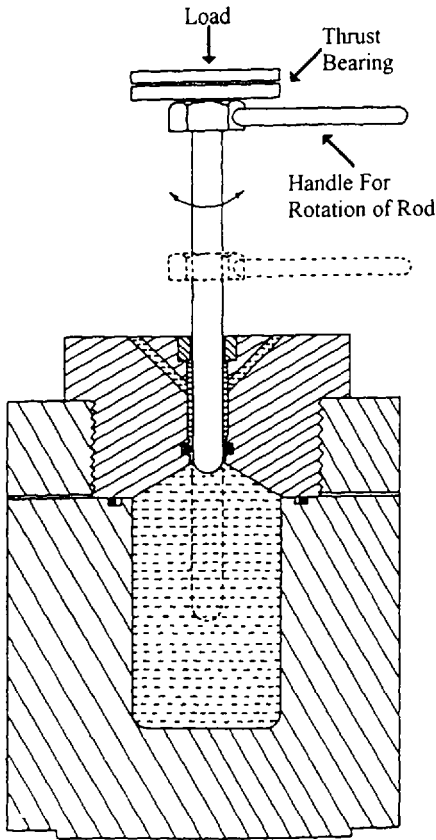


Figure 4.82 NEL bulk modulus tester. (From Ref. 113.)

2.5.3 Cavitation Numbers

Calculation of Cavitation Number

A common indicator of cavitation potential of a fluid at the cavitating surface is the cavitation number (K) [129,130]:

$$K = \frac{P_0 - P_v}{\frac{1}{2}\rho V_0^2}$$

where

- P_0 = the static pressure at the inlet
- P_v = the vapor pressure of the fluid
- V_0 = the velocity at the inlet
- ρ = the fluid density

The smaller the number, the greater the cavitation potential.

Hara et al. evaluated the effect of water content of a water–glycol and a water-in-oil (W/O) emulsion on the “critical” cavitation numbers (K_c) using an orifice in a hydraulic circuit test shown in Fig. 4.85 [131]. For this work, K_c is defined as

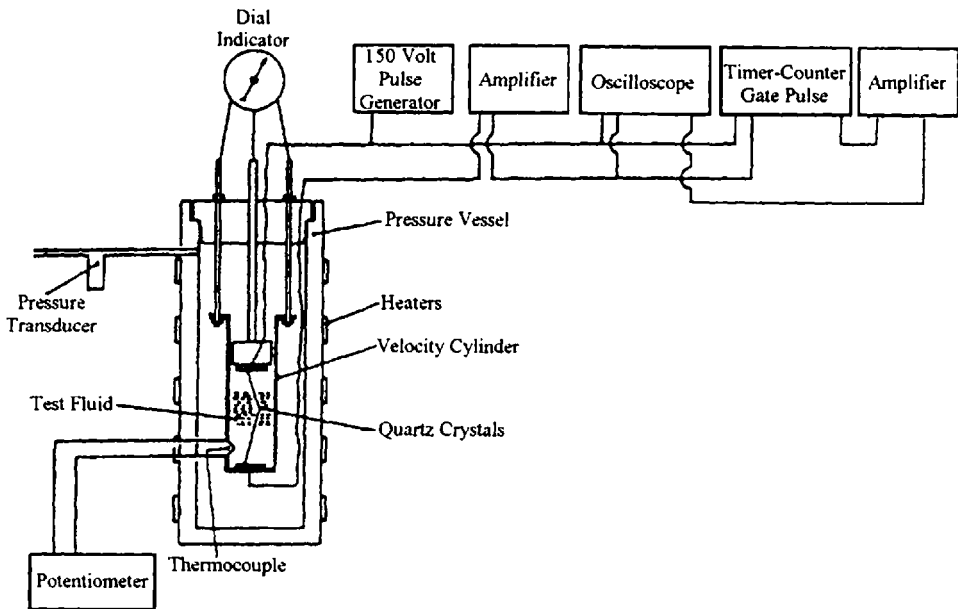


Figure 4.83 Ultrasonic velocity apparatus. (From Ref. 124.)

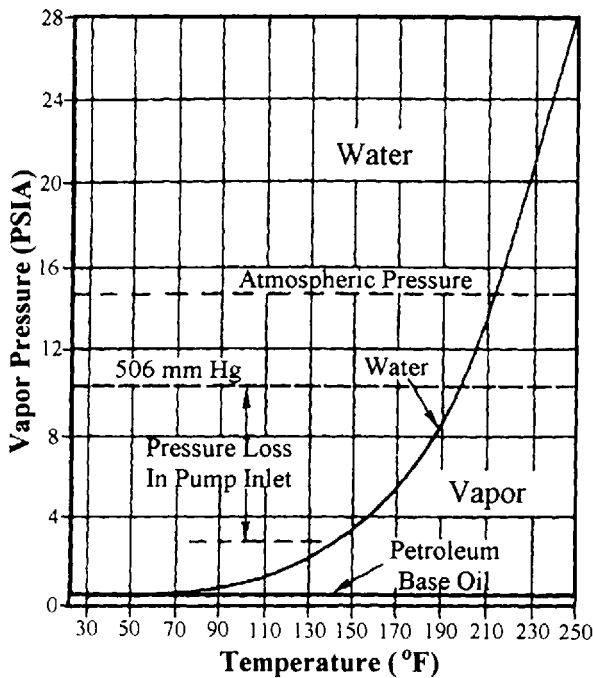


Figure 4.84 Vapor pressure of hydraulic fluids. (From Ref. 127.)

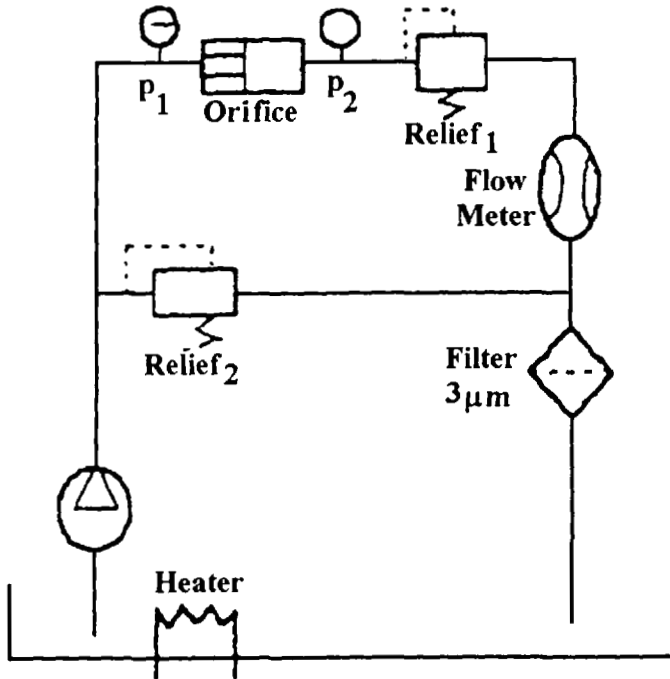


Figure 4.85 Hydraulic circuit for cavitation test. (From Ref. 131.)

$$K_c = \frac{P_2}{P_1 - P_2}$$

where P_1 is the orifice inlet pressure and P_2 is the orifice outlet pressure.

The results of this study showed that increasing water content produced a general increase in critical cavitation numbers with increasing Reynold's numbers for both the water-glycol and W/O emulsion fluids, as shown in Figs. 4.86 and 4.87, respectively [131].

2.5.4 Cavitation Equations

A dimensionless equation has been developed which provides an interrelationship between the type of pump and the required fluid velocity inside of the pump to assure no cavitation. This equation is [7]

$$\frac{Q_c}{Q_T} = 1 - \left(\frac{P_A}{\rho C V_p^2} \right) \left(\frac{P_i - P_v}{P_A} \right)$$

where

Q_c = the volume flow loss due to cavitation (ft^3/s)

Q_T = the total theoretical pump discharge flow rate (ft^3/s) calculated from $A_p V_p$
 $[A_p = \text{area (in ft)}$

$V_p = \text{velocity of piston, vane, or gear tooth (in ft/s)}$

$P_A = \text{atmospheric pressure (lbs./ft}^2\text{) (1 in. Hg = 70.7 lbs./ft}^2\text{)}$

$P_i = \text{the pump inlet pressure (lbs./ft}^2\text{)}$

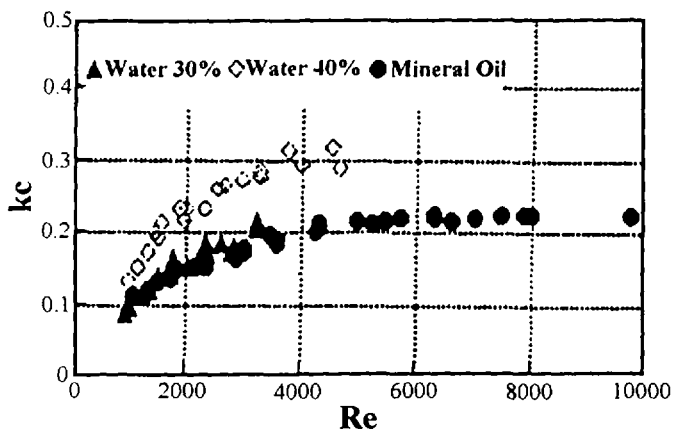


Figure 4.86 Effect of water content on cavitation of a water-glycol and a mineral-oil hydraulic fluid. (From Ref. 131.)

P_v = the vapor pressure of the fluid (lbs./ft²)

ρ = the fluid density (slugs/ft³)

C = the cavitation number, which is calculated from $(V_2 - V_1)/V_p$, where V_1 and V_2 are the velocity of the fluid in the pumping cavity at points 1 and 2, respectively (see Fig. 4.88)

The dimensionless term Q_i/Q_T indicates the loss of flow caused by cavitation, $(P_i - P_1)P_A$ is a measure of the static pressure available at in pump inlet to increase the fluid velocity, and $P_A/\rho CV_p^2$ is a coefficient that includes the effect of fluid density and flow rate. This equation was used to derive Figs. 4.89 and 4.90, which show the probability and nature of cavitation, respectively.

The dimensionless cavitation equation may be rewritten

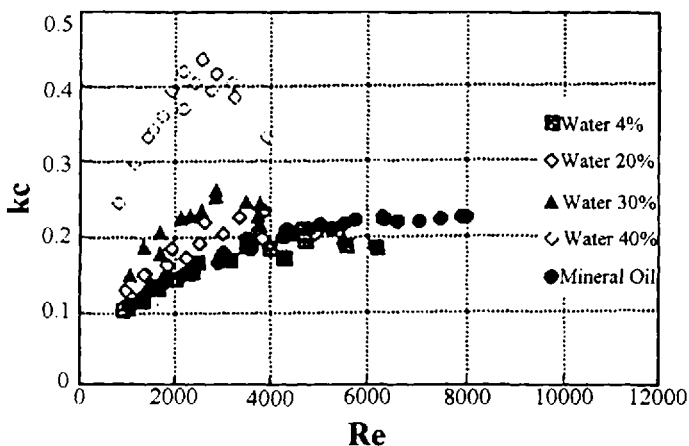


Figure 4.87 Effect of water content on a W/O emulsion and a mineral-oil hydraulic fluid. (From Ref. 131.)

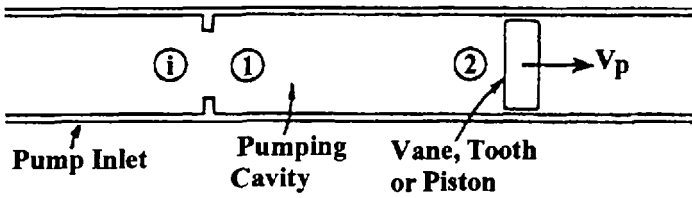


Figure 4.88 Schematic for derivation of the cavitation equation. (From Ref. 7.)

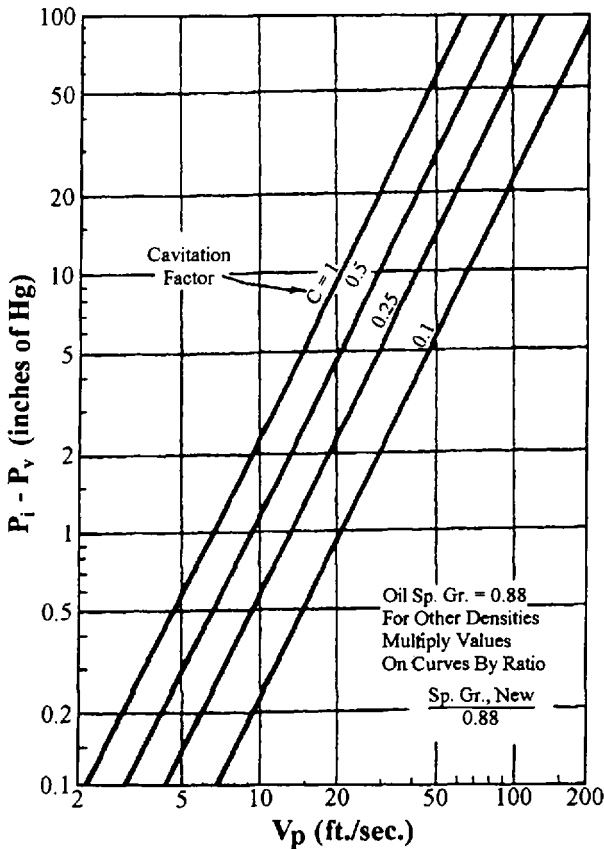


Figure 4.89 Probability of cavitation. This graph relates inlet pressure to pump velocity. The cavitation factor C is a measure of the acceleration required by the fluid to reach the velocity of the moving element. High values of C mean that the fluid is initially at a standstill and requires maximum acceleration. Low values of C mean the fluid has initial velocity that helps move the oil into the pumping cavity. The value of C is dependent on inlet design and pump type. Vanes in stator pumps typically may be as low as $C = 0.25$. Screw pumps may have $C = 0.3$. Spur gear and vane in rotor pumps will be no better than $C = 0.4$. Piston pumps may have $C < 0.7$. Any pump may approach $C = 1.0$ if the inlet design is not correct. (From Ref. 7.)

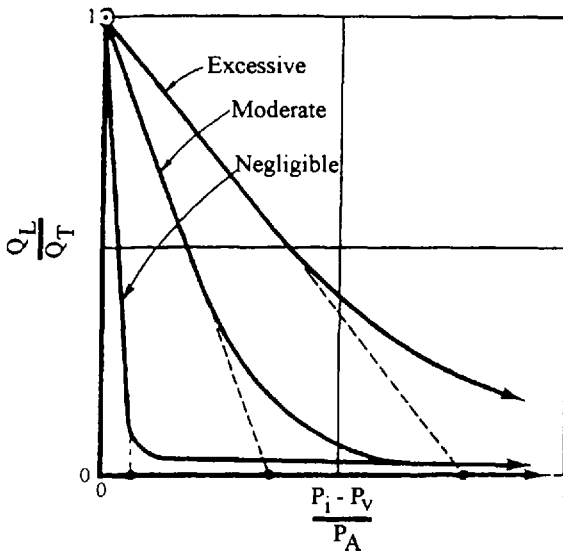


Figure 4.90 Nature of cavitation. Q_L/Q_T is a measure of the nature of cavitation and varies almost linearly with available net positive suction pressure in the region of severest cavitation. A hypothetical pump with zero cavitation corresponds to the curve on the extreme left, where any pressure is sufficient to give full flow. $Q_L/Q_T = 0$. Actual pumps will perform in the area indicated by the other three curves. These curves are for pure cavitation effects and do not include the effect of entrained air and slip. (From Ref. 7.)

$$Q_D = \frac{(P_i - P_v)A_p}{\rho CV_p}$$

where Q_D is the actual pump discharge flow volume (ft³/s) which is $Q_T - Q_2$.

The limitations to the use of these equations are as follows [7]:

1. A fluid that is cavitating may not completely flash to vapor. In this case, the pump will perform less than predicted because the back pressure is less. Conversely, fluid with vapor pressure (P_v) higher than the inlet pressure (P_i) can prevent pumping entirely and pressurization or cooling of the inlet may be required.
2. Air or gas entrainment may increase cavitation, particularly with large inlet pressure drops, because trapped air expands and occupies the pumping space. These equations assume that there is no entrained or dissolved air and that the theoretical vapor pressure is achieved.
3. Although temperature variation will affect vapor pressure, the slope of the curve Q_L/Q_T versus $(P_i - P_v)/P_A$ shown in Fig. 4.90 will remain the same. Any fluid at any temperature may be analyzed as long as there is a position suction head.
4. Viscosities up to 2000 (SUS) do not affect performance, but above that, cavitation increases. For fluid viscosities greater than 20,000 SUS, it may be necessary to pressurize the fluid.
5. Any one or all of these separate effects may produce a separate family of curves. For example, if the speed is increased but other factors remain the

same, cavitation may become “excessive” instead of “moderate.” However, inlet restriction or entrained air will give similar results. Therefore, careful analysis is necessary.

2.5.5 Gaseous and Vaporous Cavitation in Pumps and Orifices

Cavitation problems often occur when pressure losses in the suction line to the pump inlet are sufficient to reduce air solubility, producing an entrained air mixture. This mixture is then fed into the pump, resulting in gaseous cavitation. If the pressure drop is sufficient, vaporous cavitation may result.

One example of a potential vaporous cavitation problem is in a gear pump when gear teeth come out of mesh on the suction side, as shown in Fig. 4.91 [126]. Increasing void volume occurs due to the rotation of the gears. This volume must be filled through the orifice between the tip of the driving tooth and the face of the driven tooth. If there is insufficient fluid flow, vacuum cavities formed within the fluid may implode on the discharge side [126].

In cases where a fluid flows through an orifice, such as the constriction shown in Fig. 4.92, there must be a pressure drop at the constriction according to Bernoulli's theorem, which states

$$P_1 + \frac{1}{2}\rho V_1^2 = P_2 + \frac{1}{2}\rho V_2^2$$

where ρ is the fluid density, P_1 and P_2 , and V_1 and V_2 are the pressures (P) and flow rates (V), respectively, at points 1 and 2. To provide the necessary equality, the pressure at position 2 must be less than the pressure at position 1, as shown in Fig. 4.92, as the fluid velocity is greater at position 2 than position 1. This pressure decrease may be sufficient to cause vaporous cavitation. This situation may occur in orifices in a hydraulic system needle valves and gate valves such as in spool and poppet valves, as shown in Fig. 4.93a and 4.93b, respectively [126].

Hara also studied the effect of orifice shape on cavitation using the hydraulic circuit test illustrated in Fig. 4.85. The results of this work, summarized in Fig. 4.94, showed that sharp edges produce higher critical cavitation number (K_c) than rounded

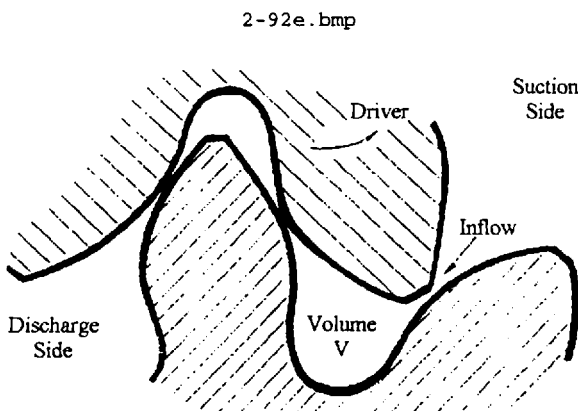


Figure 4.91 Suction mechanism of a gear pump. (From Ref. 126.)

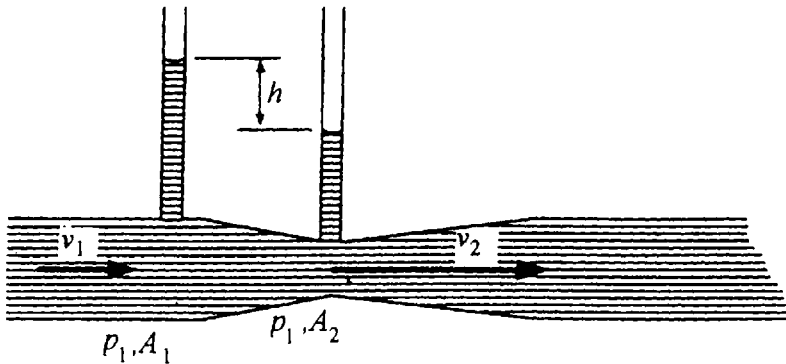


Figure 4.92 Illustration of a Venturi meter.

edges [131]. Hara has shown that cavitation pressure is not only dependent on fluid turbulence (R_c) but also on the internal surface friction [131].

Ying used flow numbers (f) to illustrate the effect of orifice shape on cavitation numbers (K) [132]. The equation for the cavitation number of a jet pumped through a long orifice where there is a constriction with a pressure difference across the constriction is [130]

$$K = \frac{P_d - P_v}{P_u - P_d}$$

where P_d is the downstream pressure, P_v is the vapor pressure of the fluid, and P_u is the upstream pressure. The equations for flow number are

$$f = \frac{2x}{\eta} \left(\frac{2(P_u - P_d)}{\rho} \right)^{0.5} = \frac{\text{Re}}{C_d}$$

$$f = \frac{2H \sin a}{\eta} \left(\frac{2(P_u - P_d)}{\rho} \right)$$

where

- a = the half-cone apex angle of the poppet valve
- x = the valve displacement relative to the sleeve
- H = the lift of a poppet valve
- C_d = the discharge coefficient
- ρ = the mass density
- η = the kinematic viscosity
- Re = the Reynolds number

These equations were used to calculate the cavitation number for hydraulic valve components. In hydraulic systems, the presence of cavitation is dependent on fluid flow or flow number (f). The critical value of K that produces cavitation is defined as the "incipient" cavitation number (K_i). Figure 4.95 illustrates the dependence of K_i on flow number and orifice shape [132]. Interestingly, the sensitivity of K_i to orifice shape decreases with increasing flow number. (When $K_i = 0$, cavitation will not occur.)

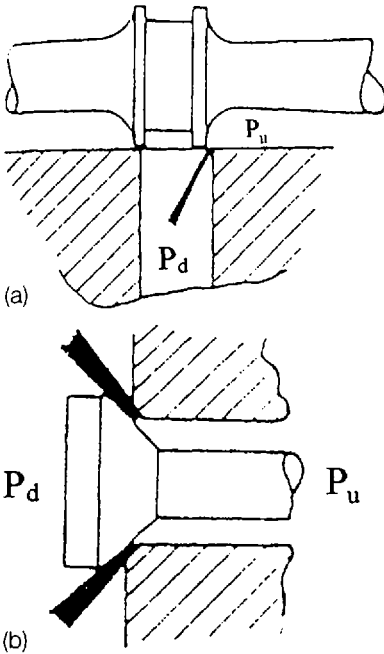


Figure 4.93 Typical orifices used in hydraulic systems: (a) spool valve and (b) poppet valve. (From Ref. 126.)

Figure 4.96 illustrates the dependence of the flow number on both fluid type and the dimension of valve opening [132]. This means that the O/W emulsion shown produces a significantly larger flow number than the other fluids evaluated and, therefore, will also exhibit a greater cavitation potential.

Figures 4.97a and 4.97b illustrate the dependence of cavitation in spool valves and poppet valves, respectively, on hydraulic fluid type using cavitation pressure (P_c).

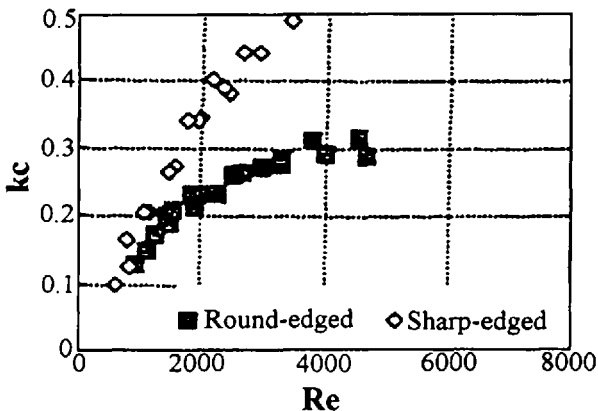


Figure 4.94 Influence of orifice shape on cavitation (water-glycol, 40% water). (From Ref. 131.)

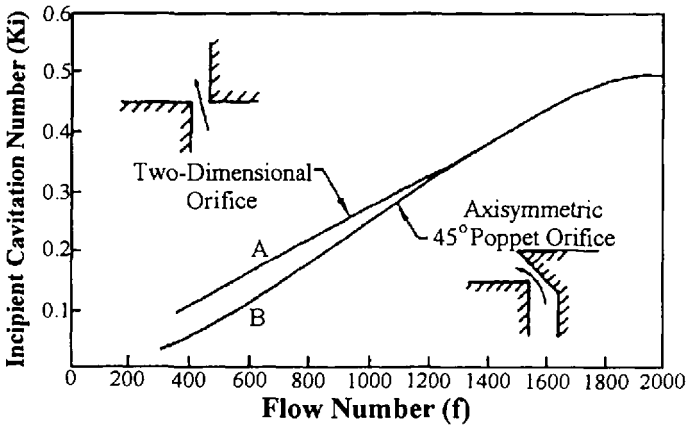


Figure 4.95 Cavitation number (K_i) versus flow number (f) for different orifices. (From Ref. 132.)

[132]. The cavitation pressure is the downstream pressure where cavitation occurs. The downstream pressure in these systems is equal to the pressure in the reservoir, which is often atmospheric pressure.

Cavitation should not occur because atmospheric pressure is greater than the vapor pressure. However, cavitation does occur due to the presence of “flash” pressure drops (jet cavitation), as shown in Fig. 4.98, which are caused by localized pressure drops in vortices which arise from turbulent mixing [126,133].

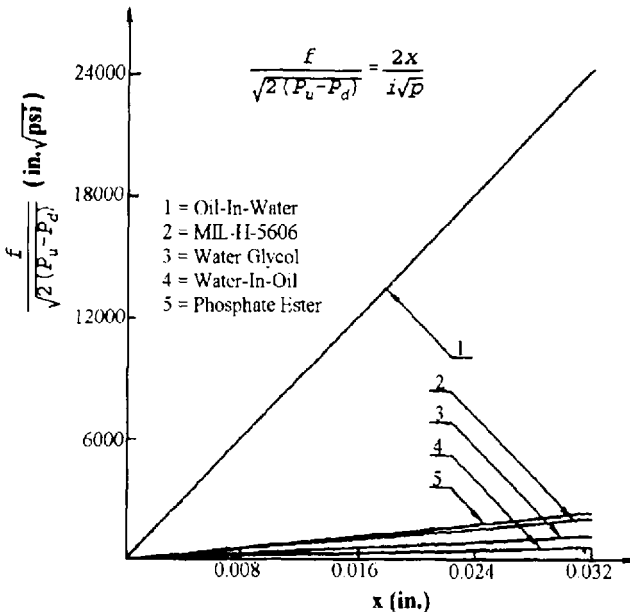


Figure 4.96 Flow number versus fluid types. (From Ref. 132.)

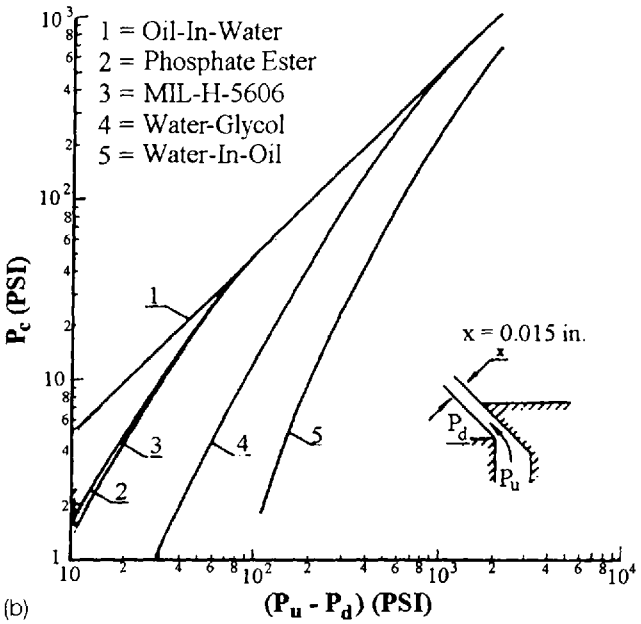
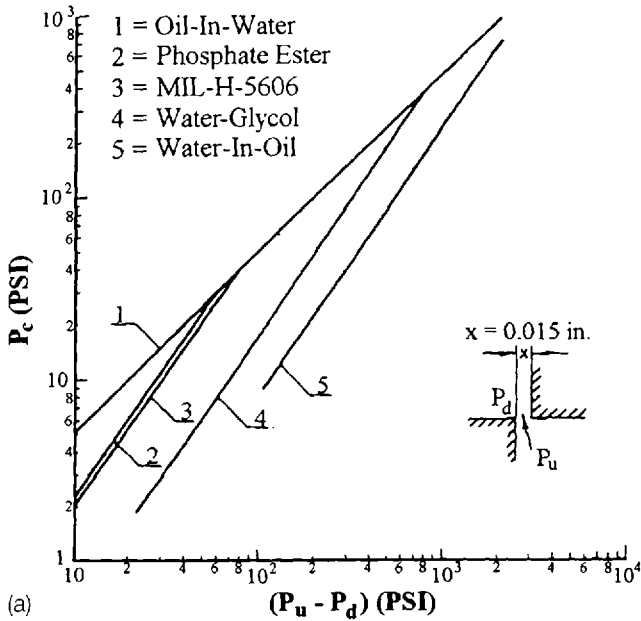


Figure 4.97 (a) Cavitation pressure versus fluid type for a spool valve; (b) cavitation pressure versus fluid type for poppet valves. (From Ref. 132.)

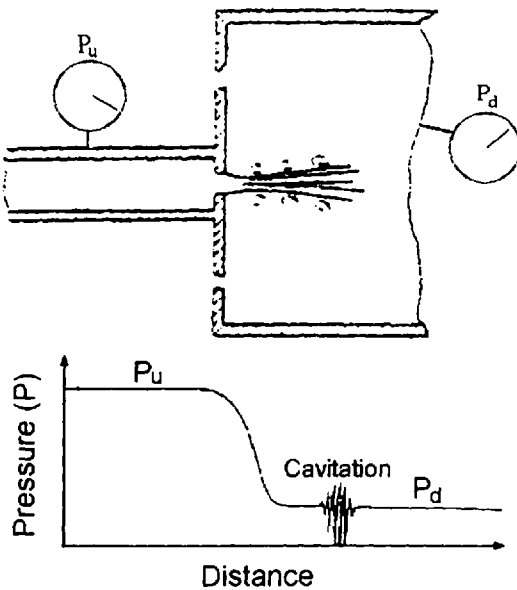


Figure 4.98 Cavitation in the mixing zone of a submerged jet. (From Ref. 126.)

2.5.6 Bubble-Collapse Mechanism

Figure 4.99 shows that bubbles begin to collapse with increasing pressure. Bubbles collapse nonsymmetrically, forming a liquid microjet which subsequently ruptures, forming a “water hammer” [134]. Kleinbreuer modeled the bubble collapse as a symmetrical process and the results are shown in Fig. 4.100 [135]. The wide range of bubble-collapse pressures have been reported up to >70 MPa and are summarized in Table 4.13 [136,137].

The impact force of the imploding bubble during cavitation is dependent on a number of factors such as the vacuum within the bubble at this time of collapse. For example, the bubble may be partially filled with either a gas (gaseous cavitation) or a liquid (vaporous cavitation), causing the implosion to be less intense [138]. Although cavitation damage is often associated with vaporous cavitation expected to occur when the hydraulic system pressure is equal or less than the vapor pressure of the fluid, this actually may not occur [139]. This is because cavitation failure is related to the tensile strength of the fluid, which is affected by contamination of the surface of the metal which will serve as sites to facilitate the bubble nucleation process, thus also facilitating cavitation [126,140].

Deshimaru studied the effect of the Reynolds number on the cavitation of fluids with or without additives [141]. The results of this study showed the following:

1. The cavitation number increases with turbulence at Reynolds number $[\text{Re} = d(2\Delta P/\rho)^{1/2}\eta^{-1}]$ values less than 8000. Higher Reynolds numbers produce slightly decreasing cavitation numbers.
2. Cavitation decreased with the addition of viscosity-modifying additives; this was attributed to the Thoms effect, the inhibition of cavitation by the

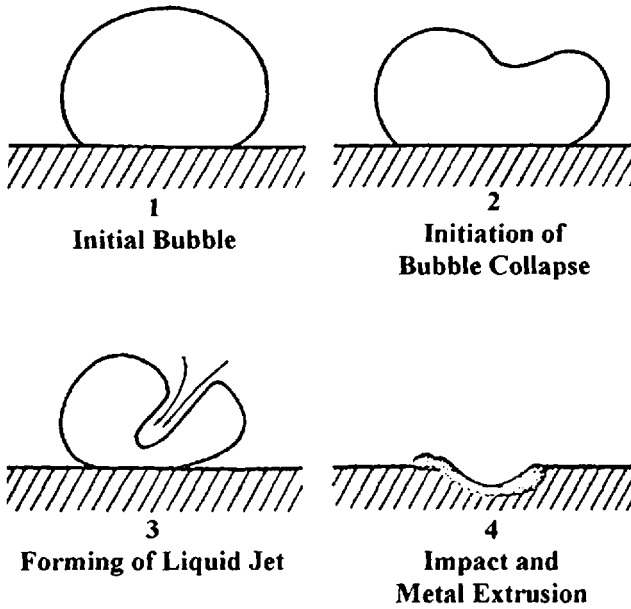


Figure 4.99 Mechanism of cavitation bubble collapse. (From Ref. 134.)

addition of viscosity-enhancing additives which promote more laminar flow, thus reducing the Reynolds numbers.

2.5.7 Material Effects

Cavitation erosion from bubble collapse occurs primarily by fatigue fracture due to repeated bubble implosions on the cavitating surface, if the implosions have sufficient

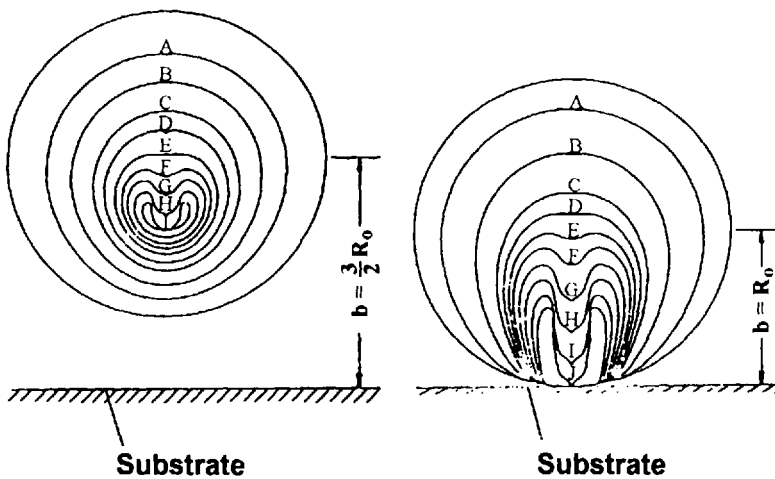


Figure 4.100 Theoretical bubble-rupture pattern during cavitation as bubble approaches a solid surface. (From Ref. 135.)

Table 4.13 Bubble-Collapse Pressures and Methods of Measurement

A. Bubble-Collapse Pressures					
	Investigators	Bubbles	Methods for calculation or measurement of collapse pressure	Results	Ref.
Theory	Rayleigh	Empty bubble	Spherical; incompressible	1260 atm at the stage of 1/20 of initial radius	175
	Hickling and Plesset	Gas bubble; initial gas pressure $P_c = 10^{-1}$ atm	Spherical; compressible	$<2 \times 10^4$ atm	176
	Ivany and Hammitt	Gas bubble; initial gas pressure $P_v = 10^{-1}$ atm $P_c = 10^{-4}$ atm	Spherical; compressible	6.77×10^4 atm 5.82×10^5 atm	177
	Plesset and Chapman	Vapor bubble	Based on microjet velocity	2×10^4 atm	178
	Experiment (single bubble)	Jones and Edwards	Spark-induced hemispherical bubble	Piezoelectric pressure-bar gauge	10^4 atm
Akamatsu and Fujikawa		H ₂ gas in water shock tube	Pressure gauge; holographic interferometry	Time duration: 2–3 μ s 10^4 – 10^5 atm	180
Tomita and Shima		Spark-induced bubble	Pressure transducer; photoelasticity	Several 10 MPa	181

B. Methods of Measurement

	Investigators	Apparatus to generate cavitation	Methods for measurement of collapse pressure	Results	Ref.
Experiment (cavitation cloud)	Sutton	Acoustic	Photoelasticity	Collapse time $2 \mu\text{s}$ $1.36 \times 10^4 \text{ atm}$	182
	Endo and Nishimura	Vibration	Observation of pit on steel surface	1.2–1.4 GPa	183
	Sanada et al.	Vibration	Holographic interferometry	>1 GPa	184
	Kato et al.	Hydrofoil Model propeller	Pressure-detecting film	Max. 50 MPa Max. 10 MPa	185
	Okabe et al.	Vibration	Same as above	Apparent impact pressure Max. 15 MPa	186
	Oba et al.	Jet-flow gate valve	Same as above	Erosive impact pressure >70 mPa	187

Table 4.14 Mechanical Properties of Various Materials

Steel JIS AISI	Tensile strength σ (MPa)	Modulus of elasticity (GPa)	Vickers Hardness (H_v)
S10C	420	204	130
S35C	615	204	180
S55C	706	204	240
HT80	853	204	300
Cu	196	122	98
Al	145	71	41

Source: Ref. 142.

impact force [142]. Therefore, the potential for cavitation is dependent on the material properties, especially tensile strength and the initial condition of the material surface [142,143] and, in some cases, material structure [144]. Some illustrative examples are provided in Table 4.14 [142].

Okada et al. have determined that impact loads of 9.1 N (aluminum) 9.7 N (copper), and 13.7 N (mild steel) are required to form a 4- μ m pit from a single implosion of a single bubble [145]. However, the bubble-collapse pressures will vary with the bubble size, shape, and location.

Talks and Moreton evaluated the volumetric cavitation erosion rates of different hydraulic fluids toward different steels using an ultrasonic cavitation erosion test; see Table 4.15 [146]. Their results, summarized in Table 4.16, illustrate that the general order of cavitation of different fire-resistant hydraulic fluids toward the different steels was water > W/O emulsion > water-glycol > invert emulsion > mineral oil. Although cavitation erosion rates were dependent on fluid properties, the erosion damage was only a function of the material properties [146].

Tsujino et al. in another ultrasonic laboratory study with a different group of hydraulic fluids found the order of erosion rates shown in Fig. 4.101 to be [147] water > HWBF > water-glycol > phosphate ester > mineral oil; HWBF denotes a high-water-base fluid. These data are consistent with the results predicted by Hara et al. from cavitation number calculations shown in Fig. 4.86 [131].

Typically, cavitation bubbles exist in a large "clouds." Figure 4.102 illustrates a cavity formed by cloud of bubbles from a HWBF. The actual eroded test specimen

Table 4.15 Volumetric Cavitation Erosion Rates for Different Hydraulic Fluids Toward Different Steels' Volumetric Erosion Rates (mm³/h)

Steel	Distilled water	W/O Emulsion	Water-glycol	Invert emulsion	Mineral oil
Mild steel	5.54	5.5	0.73	0.21	0.27
Stainless steel	1.47	1.2	0.34	0.05	0.02
Bearing steel	0.27	0.22	0.02	0.02	0.01

Note: Data based on an ultrasonic open-beaker laboratory test.

Source: Ref. 146.

Table 4.16 Cavitation Rating of Different Fluids

Cavitation rating	$Ce_{2(mg)}$	1 Straight mineral oil	2 Mineral oil with additives	3 Biodegradable hydraulic oils	4 Synthetic-base oil
Very low	4			BD 32	
Low	3	Tellus-68			Cassida-HF68
Medium low	2	Turbo-T68 Tonna-T220			
Medium high	1	Vitrea-150	Naturelle-HFE46 Naturelle-HFR32		Cassida-GL150 Cassida-HF46
High	0	Ondina-Vitrea-9	Omala-320 Tellus-32 Tellus-T32	Cassida-GL460 Cassida-HF32	Cassida-GL460 Cassida-HF32 Cassida-HF15

Source: Ref. 168.

is shown in Fig. 4.103 [148]. The varying distribution and shape of the eroded surfaces formed by different fluids was examined by scanning electron microscopy (SEM) and is illustrated in Fig. 4.104 [148]. Different studies have shown that every bubble in the cloud does not cause damage upon collapse. The damage frequency has been reported to vary between 1 in 16,000 [149] and 1 in 30,000 [150].

Cavitation bubbles may undergo multiple collapse and reformation processes. Knapp and Hollander have reported that a single bubble may undergo as many as seven collapse and reformation processes [151]. The breakage and reformation process will cease as the viscosity of the surrounding fluid dissipates the energy generated from bubble breakage.

Backe and Berger have reported that cavitation wear rate (mm^3/h) can be estimated from material properties [152]:

$$V_{\max} = 27252 \left(\frac{E^{0.562} R_{p0.2}^{0.618}}{\rho_w R_m^{1.071} W^{0.125} H^{1.971}} \right)$$

where

E (N/mm^2) = the elastic modulus of the material

$R_{p0.2}$ = the maximum yield strength at 0.2% elongation

R_m (N/mm^2) = tensile strength

W (N/mm^2) = the work to deform the test specimen for the tensile test (A_0L_0)

H = the Vickers hardness

ρ_w (g/cm^3) = the material density.

2.5.8 Test Methods

There have been a number of test procedures reported; they include spark-induced bubble formation and cavitation collapse [153], hydraulic cylinders [154,155], hydraulic circuits [131,156], and other devices. Although these tests, particularly the use of hydraulic circuitry, continue to be of interest, there are primarily two types

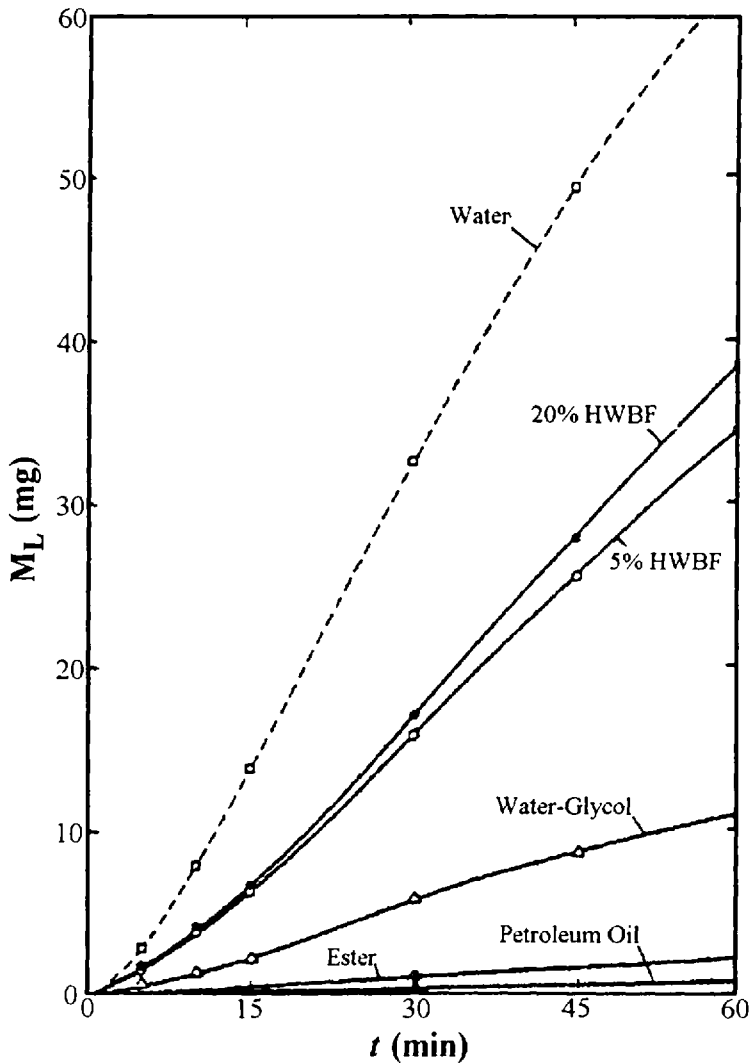


Figure 4.101 Propensity for cavitation damage for various hydraulic fluid types. (From Ref. 147.)

of laboratory screening test to determine the cavitation potential of fluids: submerged jets and ultrasonic vibratory apparatus.

Two common submerged-jet test configurations are in use. One is the configuration reported by Lichtarowicz and Kleinbreuer [157–163]. An illustration of the system reported by Lichtarowicz is provided in Fig. 4.105 [159] and the system reported by Kleinbreuer is illustrated in Fig. 4.106 [162].

The second most common type of test cell that is used for laboratory studies of cavitation is the ultrasonic vibratory test [164–167]. The ultrasonic vibrational cavitation test may be conducted in one of two possible configurations: the specimen or the fluid may be vibrated [166]; the test configuration of the ASTM G 32 test

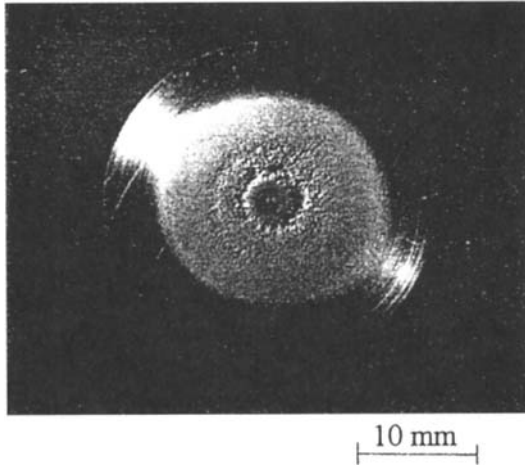


Figure 4.102 Illustration of a cavity formed by a cloud of bubbles from a high-water-base fluid. (From Ref. 148.)

procedure is shown in Fig. 4.107 [167]. A classification procedure has been proposed using a vibrational cavitation testing system based on the following criteria [168]:

- Cavitation threshold
- Cavitation power input
- Maximum cavitation erosion
- Slope of the cavitation erosion line

An illustration of the cavitation rating of different fluids is provided in Table 4.16 [168].

2.6 Density

Density not only influences flow rate and pressure drop, but it also affects the natural frequency of a hydraulic system. The natural frequency (f) is the square root of the density (ρ):

$$f_{\text{sys}} = \sqrt{\rho}$$

Some typical examples of density variation with temperature are provided in Fig. 4.108 [7]. Because fluid density will vary with the specific formulation, these values are best obtained from the fluid supplier.

Table 4.17 provides an approximation of the coefficient of expansion for mineral oil based fluids [16]. Similar data is available for other fluid classes.

2.7 Thermal Conductivity

The thermal conductivity of hydraulic fluids may be determined experimentally by various methods [169–173]. One relatively simple procedure is illustrated in Fig. 4.109 [169]. The thermal conductivity (k_L) is calculated using

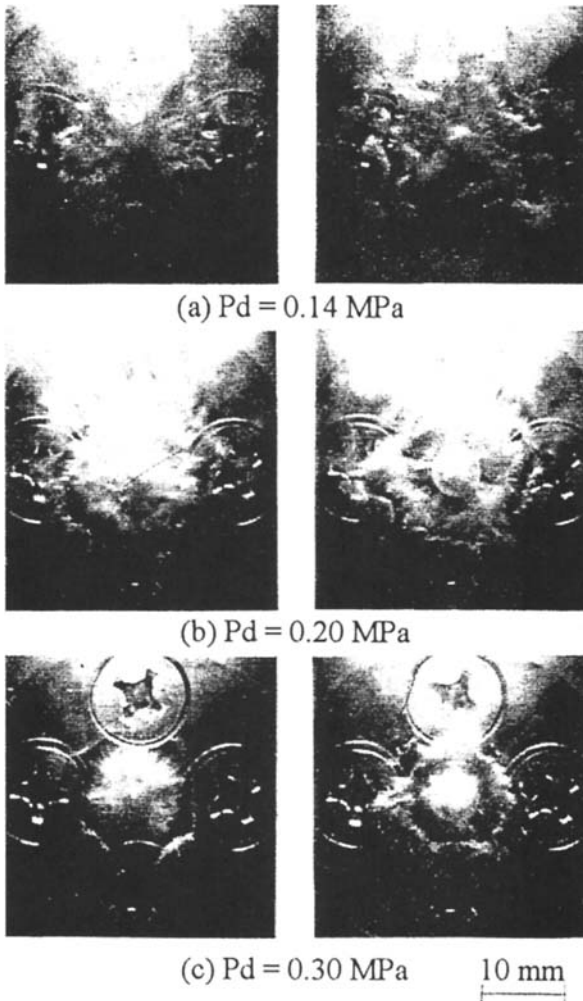


Figure 4.103 (a) Impinging cavity clouds for a HWBF; (b,c) resulting eroded test specimen. (Courtesy of A. Yamaguchi, Yokohama National University, Yokohama, Japan.)

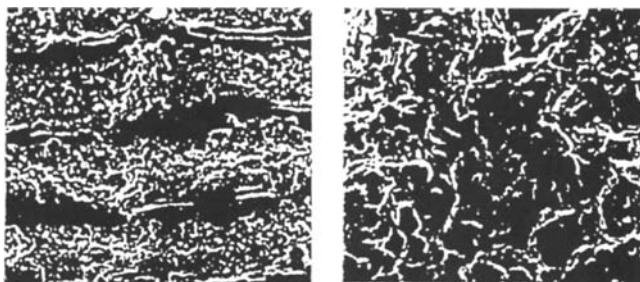
$$k_t = \frac{A}{m - B/\text{kg}} \quad J \text{ cm/s}^\circ\text{C}$$

where A and B are cell constants, kg is the mass of the fluid in the cell, m is the rate of change of cell resistance with power input, which is determined from least-squares analysis of the experimentally determined cell resistance (R) and power input (P):

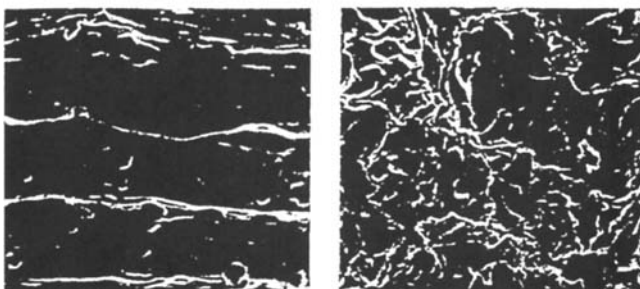
$$R = R_0 + mP$$

where R_0 is the resistance of the cell with zero current.

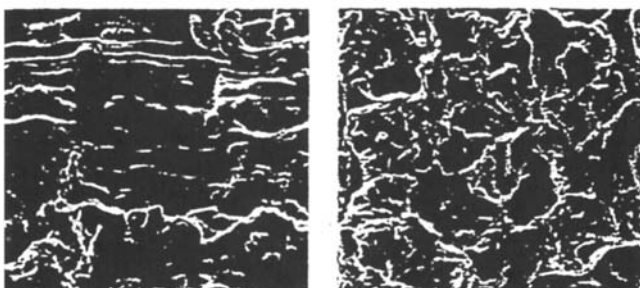
A typical range for thermal conductivity for mineral oil and synthetic hydrocarbon base oils is 0.14 W/m K at 0°C (273 K) and 0.11 W/m K at 400°C (673 K) [16].



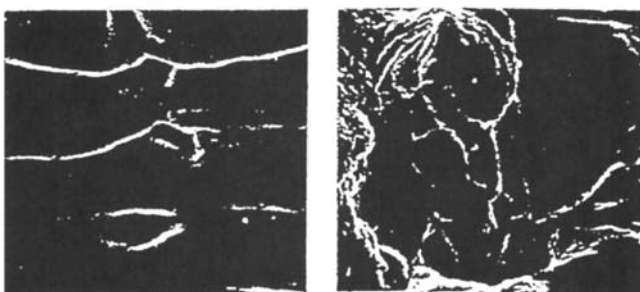
(a) S-95%, L=22.5 mm, 1.5 h



(b) E-B95%, L=20 mm, 0.5 h



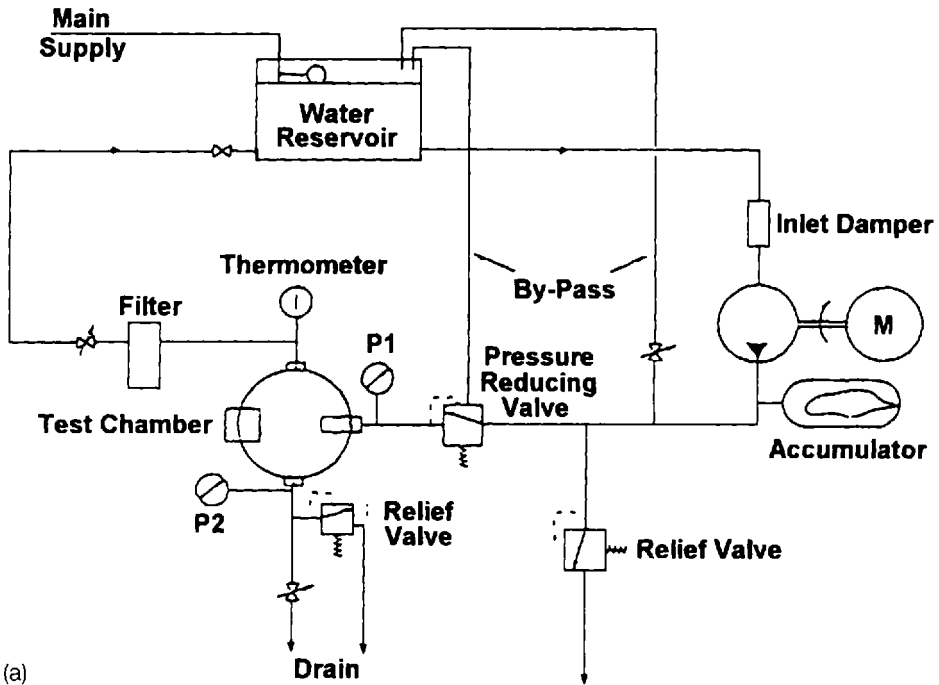
(c) Tap Water, L=22.5 mm, 1.5 h



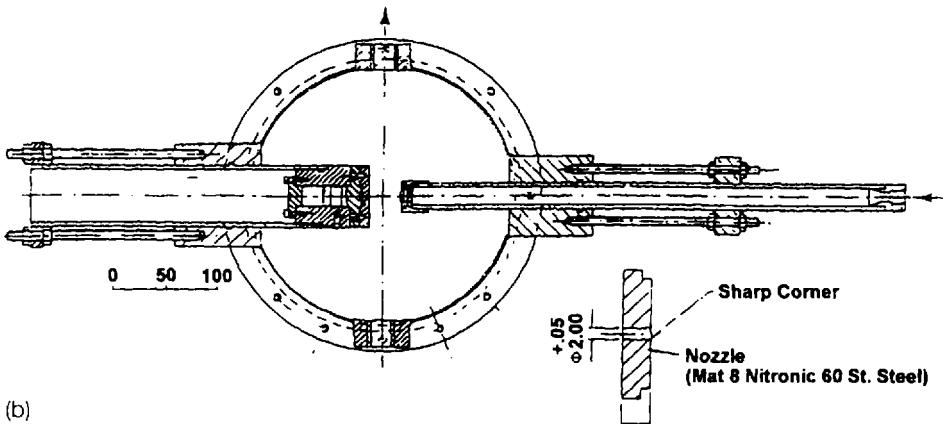
(d) Mineral Oil, L=20 mm, 5 h

50 μ m

Figure 4.104 SEM photographs of eroded surfaces. (Courtesy of A. Yamaguchi, Yokohama National University, Yokohama, Japan.)



(a)



(b)

Figure 4.105 (a) Momma-Lichtarowicz hydraulic circuit used for cavitation testing; (b) test chamber and nozzle. (From Ref. 159.)

2.8 Electrical Properties

2.8.1 Electrical Conductivity

The amount of electrical charge that passes any point in a conductor per unit time is the current. The current passing through an area of 1 cm^2 perpendicular to the direction of the current is current density ($j, \text{ A/cm}^2$); the current density is proportional to the potential gradient (dU/dx) and they are related by Ohm's Law:

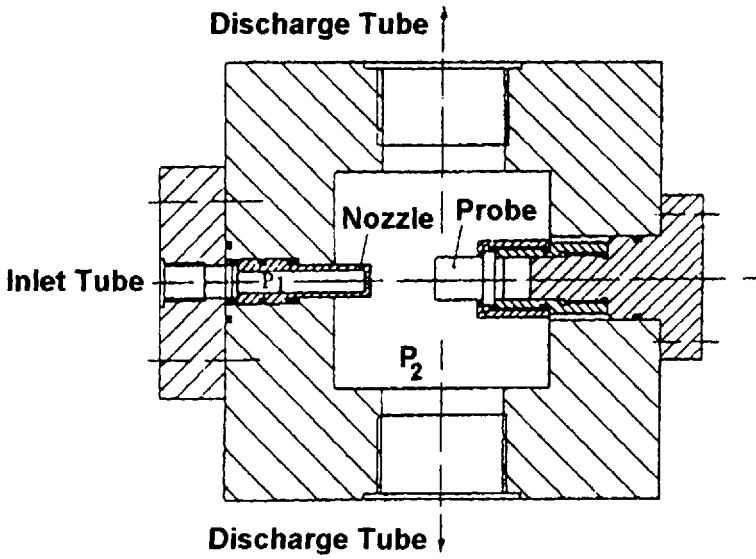


Figure 4.106 Aachen cavitation testing apparatus. (From Ref. 162.)

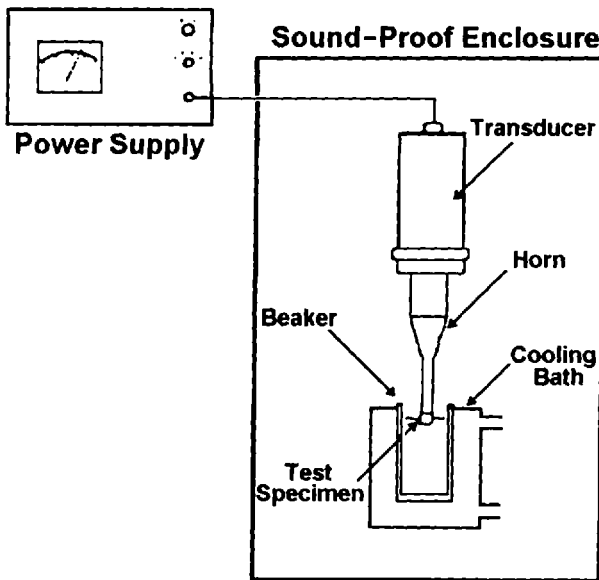


Figure 4.107 Schematic of ASTM G 32 vibratory cavitation erosion apparatus. (From Ref. 167.)

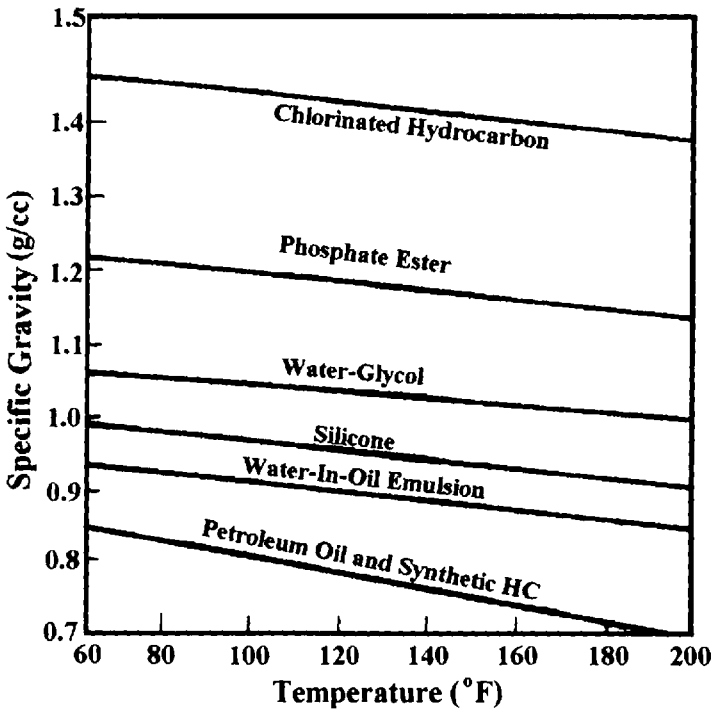


Figure 4.108 Densities of typical hydraulic fluids. (From Ref. 7.)

$$j = -\kappa \frac{\partial U}{\partial x}$$

The conductivity (κ) is the proportionality constant. The electrical field (E) is defined as

$$E = -\frac{\partial U}{\partial x}$$

Another expression for Ohm's Law is

Table 4.17 Coefficient of Expansion for Mineral-Oil Lubricant's Specific Gravity Coefficient of Expansion

Specific Gravity at 60°F (15.6°C)	Coefficient of Expansion per °C	Coefficient of Expansion per °F
1.076–0.967	0.00063	0.00035
0.966–0.850	0.00072	0.00040
0.849–0.776	0.00060	0.00050
0.775–0.742	0.00108	0.00060

Source: Ref. 16.

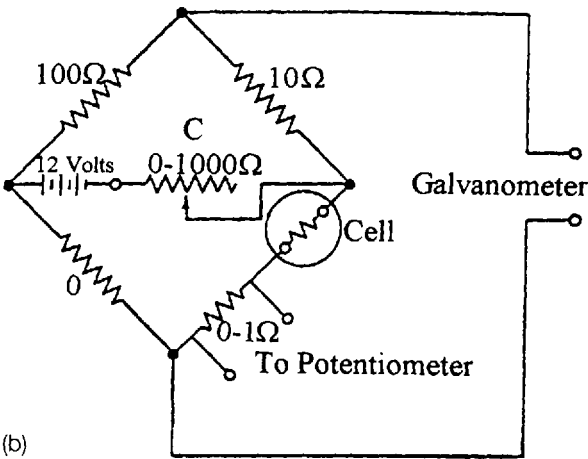
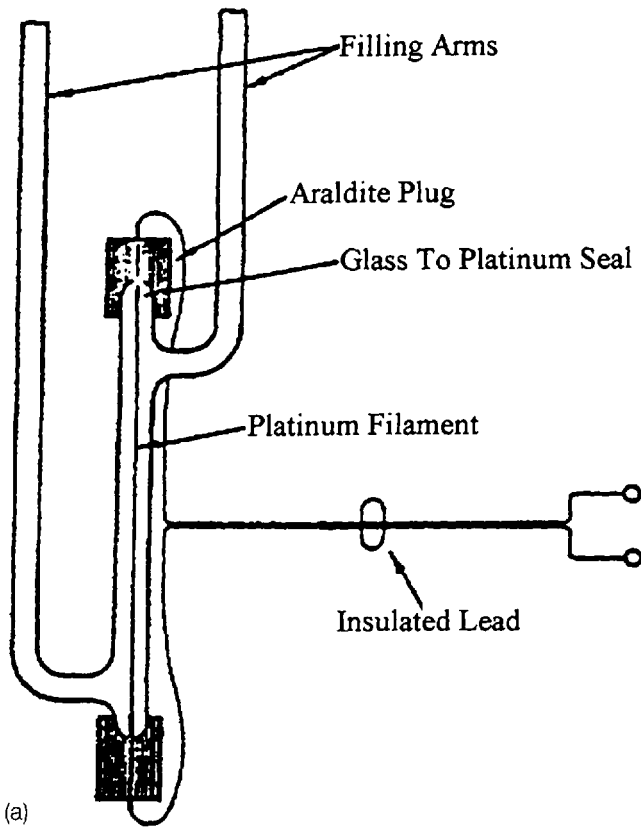


Figure 4.109 (a) Schematic of a cell used to measure thermal conductivity of fluids; (b) resistor test circuit diagram. (From Ref. 169.)

$$j = \kappa E$$

If the conductor has a length l' and a cross-sectional area of A , the electromagnetic force (EMF) (ε) across the ends is

$$\varepsilon = V_2 - V_1$$

$$E = \frac{V_2 - V_1}{l'} = \frac{\varepsilon}{l'}$$

The current carried by the conductor is related to the current density by

$$I = \frac{\kappa A E}{l'}$$

The conductance (L) is defined as

$$L = \frac{\kappa A}{l'}$$

The current is related to conductance by

$$I = L \varepsilon$$

The resistance (R) of the conductor is

$$R = \frac{1}{L} = \frac{l'}{\kappa A} = \frac{\rho l'}{A}$$

where ρ is the resistivity, which is the inverse of conductivity ($\rho = 1/\kappa$). Ohm's Law becomes

$$\varepsilon = IR$$

Fluid conductivity is measured using a conductivity cell, similar to that shown in Fig. 4.110. Two platinum electrodes, which are typically coated with platinum black, are sealed into the ends of the cell. The cell is filled with the fluid and the resistance is measured by placing the cell in one arm of a Wheatstone bridge. Typically, the frequency is 1000 cycles/s. The resistance of the cell (R) is

$$R = \rho \frac{l'}{A} = \left(\frac{1}{\kappa}\right) \left(\frac{l'}{A}\right)$$

The cell constant ($K = l'/A$) is determined by measuring the resistance (R), using a fluid of known conductivity (κ_s):

$$K = \frac{l'}{A} = \kappa_s R_s$$

The conductivity (κ) of an unknown fluid is calculated using

$$\kappa = \kappa_s \left(\frac{R_s}{R}\right)$$

It should be noted that fluid conductivity is dependent on temperature and composition.

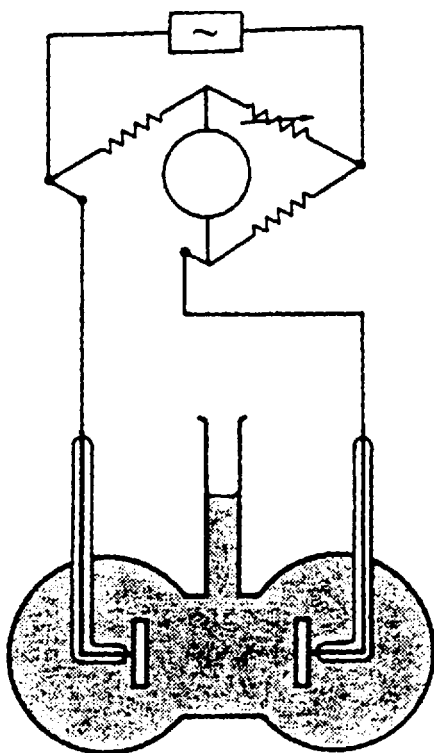


Figure 4.110 Test cell to measure fluid conductivity.

2.8.2 DC Resistivity

Direct current resistivity of an insulating material is the quotient of a DC electrical field strength and steady-state current within the material [174]. A DC test voltage is applied to the test fluid to provide an electrical stress of 250 V.

2.8.3 Volume Resistivity

Volume resistivities of an insulating material is the quotient of a DC electrical field strength and steady-state current within the material [174]. A DC test voltage is applied to a test fluid to provide an electrical stress of 250 V mm over 60 s. After the test, the current (I) and test voltage (V) is recorded. The resistivity (ρ) is calculated using

$$\rho = K \frac{I}{V}$$

where V is the test voltage (V), I is the test current (A), and K is the cell constant (m).

2.8.4 Relative Permittivity

The relative permittivity (ϵ_r) of a fluid is the ratio of the capacitance (C_r) of a capacitor in which the space between and around the electrodes is entirely filled with

the insulating fluid of interest, to the capacitance of the same cell in vacuum (IEC Std). The relative permittivity (ϵ_r) of a fluid is obtained from capacitance measurements of an unknown fluid and a known fluid and is calculated using

$$\epsilon_r = \frac{C_t}{C_a}$$

where C_t is the capacitance of the cell filled the test fluid and C_a is the capacitance of the cell filled with air as the dielectric.

REFERENCES

1. T. L. Jackson, "Viscosity Requirements of Mineral Oil in Hydraulic Systems," *Hydraulic Pneumatic Power Controls*, 1963, February, pp. 122–129.
2. A. J. Zino, "What to Look for in Hydraulic Oils III: Viscosity Index," *Am. Machinist*, 1947, December, pp. 112–124.
3. T. H. Randall, "The Pumpability of Fire Resistant Hydraulic Fluids," in *Natl. Conf. Fluid Power*, 1964, 18, pp. 87–94.
4. Anon., "Cold Weather Operation of Hydraulics," *Appl. Hydraulics*, 1956, February, pp. 67–68, 111.
5. J. S. Stecki, K. Szewczyk, and E. Lisowski, *Proc. SAE*, 1992, February, pp. 75–81.
6. A. J. Zino, "What to Look for in Hydraulic Oils II: Viscosity," *Am. Machinist*, 1947, November, pp. 112–116.
7. F. Yeaple, *Fluid Power Design Handbook*, 2nd ed., 1990, Marcel Dekker Inc., New York, Chap. 1, pp. 1–22.
8. J. Briant, J. Denis, and G. Parc, *Rheological Properties of Lubricants 1989*, Editions Technip, Paris, pp. 23–63.
9. P. K. B. Hodges, *Hydraulic Fluids*, 1996, John Wiley & Sons, New York, p. 43.
10. H. van Oene, "Discussion of Papers 73046 and 730487," *SAE Trans.*, 1973, 82, p. 1580.
11. G. E. Totten and G. M. Webster, "High Performance Thickened Water–Glycol Hydraulic Fluids," in *Proc. of the 46th Nat. Conf. on Fluid Power, March 23–24, 1994*, 1994, National Fluid Power Association, Milwaukee, WI, pp. 185–194.
12. M. Aderin, G. J. Johnston, H. A. Spikes, and G. Caporiccion, "The Elastohydrodynamic Properties of Some Advanced Non-Hydrocarbon-Based Lubricants," *Lubr. Eng.*, 1992, 48, pp. 633–638.
13. F. Gershick, "Non-Newtonian Fluid Dynamics in High Temperature High Shear Capillary Viscometers," in *Rheology and Tribology of Engine Oils SP-936*, 1992, SAE International, Warrendale, PA, pp. 75–86.
14. S. Bair, W. O. Winer, and F. Qureshi, "Lubricant Rheological Properties at High Pressure," *Lubr. Sci.*, 1993, 5, pp. 189–203.
15. J. P. Carreau, "Rheological Equations from Molecular Network Theories," Ph.D. Thesis, University of Wisconsin, pp. 196–198.
16. E. E. Klaus and E. J. Tewksbury, "Liquid Lubricants," in *CRC Handbook of Lubrication, Theory and Practice of Tribology—Vol. II: Theory and Design*, E. R. Booser, ed., 1986, CRC Press, Boca Raton, FL, pp. 229–254.
17. R. H. Ewell and H. J. Eyring, *Chem. Phys.*, 1937, 5, p. 726.
18. C. Walther, "The Viscosity–Temperature Diagram," *Petrol. Z.*, 1930, 26, p. 755.
19. E. Klaus and M. R. Fenske, "The Use of ASTM Slope for Predicting Viscosities," *ASTM Bull.*, 1956, 215, pp. TP143–TP150.
20. ASTM D 341-87, *Standard Viscosity–Temperature Charts for Liquid Petroleum Products*, 1987, American Society for Testing and Materials, Conshohocken, PA.

21. Anon., "Viscosity—II," *Lubrication*, 1961, 47, pp. 13–27.
22. P. Dransfield and C. James, "Measuring the Absolute Viscosity of Hydraulic Oils at High Pressure," 1969, February, pp. 83–84.
23. C. Barus, "Note on the Dependence of Viscosity on Pressure and Temperature," *Proc. Am. Acad. U.S.*, 1893, 19, p. 13.
24. W. R. Jones, R. L. Johnson, W. O. Winer, and D. M. Sanborn, "Pressure Viscosity Measurements for Several Lubricants to 5.5×10^8 Newtons Per Square Meter (8×10^4 PSI) and 149°C (300°F)," *ASLE Trans.*, 1974, 18(4), pp. 249–262.
25. C. H. A. Roelends, "Correlation Aspects of the Viscosity–Temperature–Pressure Relationship of Lubricating Oils," 1966, University Microfilm, Ann Arbor, MI.
26. G. P. Fresco, E. E. Klaus, and E. J. Tewksbury, *J. Lubr. Technol.*, 1969, July, pp. 451–458.
27. B. Y. C. So and E. F. Klaus, "Viscosity–Pressure Correlation of Liquids," *ASLE Trans.*, 1979, 23(4), pp. 409–421.
28. C. S. Wu, E. E. Klaus, and J. L. Duda, "Development of a Method for the Prediction of Pressure–Viscosity Coefficients of Lubricating Oils Based on Free-Volume Theory," *J. Tribol.*, 1989, pp. 121–128.
29. J. K. Appledoorn, *SAE J.*, 1963, 71, p. 108.
30. L. S. Zharkin, S. V. Sheberstov, N. V. Panfilovich, and L. I. Manevich, *Russ. Chem. Rev.*, 1989, 58(4), pp. 381–392.
31. J. Knight, "Mechanical Shear Degradation of Polymers in Solution, A Review," Royal Aircraft Establishment Technical Report 76073, June 1976.
32. T. D. Foster and E. R. Mueller, "Effect of Polymer Structure and Shear Stability of Polymer-Thickened Power Transfer Fluids," *ASTM Special Tech. Publ.*, 1965, 382, pp. 14–32.
33. R. P. Nejak and E. R. Dzuna, "Mechanical, Sonic, Ultrasonic and Radiation Studies of Polymer-Thickened Oil Shear Characteristics," in 1061 SAE International Congress and Exposition of Automotive Engineering, Detroit, MI, 1961.
34. R. L. Stambaugh and A. F. Preuss, "Laboratory Methods for Predicting the Viscosity Loss of Polymer-Thickened Hydraulic Fluids," SAE Technical Paper Series, Paper 680438, 1968.
35. I. R. H. Crail and A. L. Neville, "The Mechanical Shear Stability of Polymeric VI Improvers," *J. Inst. Petrol.*, 1969, 55(542), pp. 100–108.
36. ASTM D 3945-93, *Standard Test Method for Shear Stability of Polymer-Containing Fluids Using a Diesel Injector Nozzle*, American Society for Testing Materials, Conshohocken, PA.
37. M. D. Behrens, S. W. Rein, G. W. Roth, and H. T. Marshall, "An Automated Fuel Injection Shear Stability Tester," SAE Technical Paper Series, Paper 690158, 1969.
38. ASTM D 2603-91, *Test Methods for Sonic Shear Stability of Polymer Containing Oils*, 1991 American Society for Testing and Materials, Conshohocken, PA.
39. H. S. Myers, Jr., "Volatility Characteristics of High-Boiling Hydrocarbons," Ph.D. Thesis, Pennsylvania State University, 1952.
40. A. Beerbower and D. Zudkevich, "Predicting the Evaporation Behavior of Lubricants in the Space Environment," in *ACS Meeting No. 8, Div. of Petrol. Chem.*, American Chemical Society, 1963, pp. C-99–C-115.
41. J. B. Maxwell and L. S. Bonnell, *Ind. Eng. Chem.*, 1957, 49, p. 1187.
42. ASTM D 3827, *Standard Test Method for Estimation of Solubility of Gases in Petroleum and Other Organic Liquids*, American Society for Testing and Materials, Conshohocken, PA.
43. E. L. Wilkinson, "Measurement and Prediction of Gas Solubilities in Liquids," Ph.D. Thesis, The Pennsylvania State University, 1971.

44. P. Blok, *The Management of Oil Contamination*, Koppen and Lethem Anadrijzjftechniek B.V., Amsterdam, 1995, p. 44.
45. A. Beerbower, "Estimating the Solubility of Gases in Petroleum and Synthetic Lubricants," *ASLE Trans.*, 1980, 23(4), pp. 335–342.
46. W. Hamann, O. Menzel, and H. Schrooder, "Gase in Ölen—Grundlagen für Hydrauliken," *Fluid*, 1978, September, pp. 24–28.
47. E. Gulker, "Schaumbildung und deren Ursachen," *VDI-Berichte*, 1964, 1 85 I, p. 47–52.
48. J. H. Hildebrand and R. L. Scott, *The Solubility of Nonelectrolytes*, 1964 Dover Publications, New York.
49. K. L. Hoy, "New Values of the Solubility Parameters from Vapor Pressure Data." *J. Paint Technol.*, 1970, 42(541), pp. 76–118.
50. V. G. Magorien, "Effects of Air on Hydraulic Systems *Hydraulics & Pneumatics*," 1967, October, pp. 128–131.
51. A. T. J. Hayward, *How to Keep Air out of Hydraulic Circuits*, 1963. The National Engineering Laboratory, East Kilbridge, Glasgow.
52. Anon., "Air Entrainment and Foaming," *Fluid Power Int.*, 1974, January/February, pp. 43–49.
53. V. G. Magorien, "How Hydraulic Fluids Generate Air," *Hydraulics Pneumatics*, 1968, June, pp. 104–108.
54. W. D. Wood and W. C. Lindsay, "Dynamic Foam and Aeration Test Apparatus." Midwest Research Institute, Technical Report AFAPL-TR71-83, report prepared for the Air Force, June 1972.
55. K. Tonder, "Effect on Bearing Performance of a Bubbly Lubricant," in *Proc. JSLE/ASLE Lubrication Conf.*, Tokyo, 1975, pp. 213–221.
56. M. A. Honeyman and G. E. Maroney, "Air in Oil-Available Measurement Methods." *BFPR J.*, 11(3), pp. 275–281.
57. Anon., "Air Entrainment and Foaming," *Fluid Power Int.*, 1974, January/February, pp. 43–49.
58. B. Hallet, "Hydraulic Systems at a New High Speed Roll Mill," *Lub. Eng.*, 1968, 24(4), pp. 173–181.
59. A. A. Rood, "Hydraulic Reservoir Design and Filtration." *SAE Technical Paper Series*, Paper 902A, 1964.
60. R. B. Banks, "A Comparison Open-Center and Closed-Center Hydraulic Systems," in *Proc. of Natl. Conf. Ind. Hydraul.*, 1956, pp. 35–49.
61. H. Ingvast, "Deaeration of Hydraulic Oil Offers Many Effects," in *Third Scandinavian International Conference on Fluid Power*, 1993, Vol. 2, pp. 535–546.
62. A. T. J. Hayward, "How to Avoid Aeration in Hydraulic Circuits," *Hydraulic Pneumatics*, 1963, November, pp. 79–83.
63. J. Heidemeyer, "Des Schaumverhalten Wassergemischter Kuhischmierstoffe," *Schmiertechnik Tribol.*, 1978, 5, pp. 167–169.
64. L. J. Bowman, "Foam Control Agents—Technology and Application," *Spec. Chem.*, 1982, 2(4), pp. 4–10.
65. D. N. Willig, "Foam Control in Textile Systems," *Am. Dyestuff Rep.*, 1980, June, pp. 42–50.
66. M. Okada, "Anti-Foaming Properties of Lubricating Oils," *Ya Kagaku*, 1993, pp. 807–810.
67. V. N. Prigodorov and L. V. Gornets, "Foaming Properties of Hydraulic Fluids," *Chem. Technol. Fuels Oils*, 1970, 9–10, pp. 688–691.
68. L. J. Bowman, "Foam Control Agents—Technology and Application," *Spec. Chem.*, 1982, 2(4), pp. 5–9.

69. A. Beerbower and R. E. Barnum, "Studies on the Dispersion of Silicone Defoamant in Non-Aqueous Fluids," *Lubr. Eng.*, 1961, June, pp. 282–285.
70. F. E. Salb and F. K. Lea, "Foam and Aeration Characteristics of Commercial Aircraft Lubricants," *Lubr. Eng.*, 1975, 31(3), pp. 123–131.
71. R. D. Kakstra and P. Sosis, "Controlled Foam Laundry Formulation," *Tenside Deterg.*, 1972, 9(2), pp. 69–72.
72. G. K. Brower, "Current Status of Fuels and Lubricants from Construction Uses Viewpoint," SAE Technical Paper Series, Paper No. 775A, October 1963.
73. T. Ida, "Drag Coefficients of a Single Gas Bubble Rising in Hydraulic Fluids," *Yuutsu to Kukiatsu*, 1978, 9(4), pp. 261–269.
74. T. I. Fowle, "Aeration in Lubrication Oils," *Tribol. Int.*, 1981, 14, pp. 151–157.
75. U. J. Möller and U. Boor, *Lubricants in Action*, 1996, VDI Verlag, London.
76. A. R. Barber and R. J. Perez, "Air Release Properties of Hydraulic Fluids," NFPA Technical Paper Series, Paper 196-210, 1996.
77. T. Mang and H. Jünemann, "Evaluation of the Performance Characteristics of Mineral Oil-Based Hydraulic Fluids," *Erdöl Kohl-Erdgas—Petrochem Vereinigt Brennstoff-Chem.*, 1972, 25(8), pp. 459–464.
78. D. Staeck, "Gases in Hydraulic Oils," *Tribolog. Schmierungstechnik*, 1983, 34(4), pp. 201–207.
79. W. Hamann, "Gase in Ölen," *Fluid*, 1978, September, pp. 24–28.
80. E. H. Schanzlin, "Higher Speeds and Pressures for the Hydraulic Pump," in *Proc. Nat. Conf. Ind. Hydraul.*, 1956, pp. 35–48.
81. P. Blok, "The Management of Oil Contamination," 1994, Koppen & Lethem Aandrijftechniek B.V., Amsterdam, pp. 43–45.
82. T. Tamura, "Test Methods for Measuring Foaming and Antifoaming Properties of Liquids," *Yukagaku*, 1993, 42(10), pp. 737–745.
83. J. Ross and G. D. Miles, "An Apparatus for Comparison of Foaming Properties of Soaps and Detergents," *Oil Soap*, 1941, 18, p. 19.
84. ASTM D 1173, *Standard Test Method for Foaming Properties of Surface-Active Agents*, American Society for Testing Materials, Conshohocken, PA.
85. ASTM D 3601, *Standard Test Method for Foam in Aqueous Media (Bottle Test)*, American Society for Testing Materials, Conshohocken, PA.
86. DIN Standard 53902 Part I, "Prüfung von Tensiden und Textilhilfsmitteln Bestimmung des Schaum-ermögens LocI,scheibenSchlagverfahren," Normenausschuss Materialprüfung (NMP) Lm Deutsches Institut für Normung e.V.
87. ASTM D 3519, *Standard Test Method for Foam in Aqueous Media (Blender Test)*, American Society for Materials Testing, Conshohocken, PA.
88. JIS K 2241-86, *Cutting Fluid*.
89. G. R. Bhat and D. L. Harper, "Measurement of Foaming Properties of Surfactants and Surfactant Products," in *Surfactants in Solution* (K. L. Mihal, ed.), 1989, Plenum Press, New York, Vol. 10, pp. 381–399.
90. ASTM D 892-92, *Standard Test Method for Foaming Characteristics of Lubricating Oils*, American Society for Testing of Materials, Conshohocken, PA.
91. I. Saito, "Simple Method for Testing Foaming Tendency of Lubricating Oils," *Jpn. Patent*, JP 8-62206, August 18, 1994.
92. ASTM D 1881-96, *Standard Test Method for Foaming Tendencies of Engine Coolants in Glassware*, American Society for Testing and Materials, Conshohocken, PA.
93. AFNOR Draft T73-412.
94. A. T. J. Hayward, "Aeration in Hydraulic Systems—Its Assessment and Control," in *Proc. Inst. Mech. Eng. Conf. Oil Hydraulic Power and Control*, 1961, Institute of Mechanical Engineers, p. 216–224.

95. A. T. Hayward, "The Viscosity of Bubbly Oil," *J. Inst. Petrol.*, 1962, 48, pp. 156–164.
96. P. D. Claxton, "Aeration of Petroleum Based Steam Turbine Oils," *Tribology*, 1992, February, pp. 8–13.
97. V. H. W. Thoenes and K. Bauer, "Beitrag zur Bestimmung des Luft-abscheideverhaltens von Minerölen," *Erdöl Kohle Erdgas Petrochem.*, 1965, 21(9), pp. 543–546.
98. ISO/DIS 9120, *Petroleum-Type Steam Turbine and Other Oils—Determination of Air Release Properties—Impinger Method*, Draft International Standard, 1987, International Organization for Standardization.
99. H. H. Rowland, R. J. Patula, and L. B. Sargent, "The Evaluation of Air Entraining Tendency of Fluids," *J. Am. Soc. Lubr. Eng.*, 1973, November, pp. 491–497.
100. G. A. Volpato, A. G. Manzi, and S. Del Ross, "A New Method to Study Air Entrainment in Lubricating Oils," in *Proceedings First European Tribology Conference*, 1973, pp. 335–342.
101. A. T. J. Hayward, "Methods of Measuring the Bubble Content of Bubbly Oil," *NEL Fluids Note* 92, 1960.
102. R. E. Liddell, R. F. Rimmer, and R. E. H. Orr, "Design of Lubricating Oil System," *Proc. Inst. Mech. Eng.*, 1969, 184, pp. 41–52.
103. V. V. Tat'kov and L. Proizvodstvo, "Hydraulic Drive Performance in the Injection Mechanism of Pressure Diecasting Machines," *Sov. Cost. Techn.*, 1986, 6, pp. 43–46.
104. R. Zander, P. Rupprrath, G. M. Schneider, and E. Rohne, "New Laboratory Measurement Method for Evaluating Air Release Properties of Fluids—Part I," *Tribol. Schmirerungs Tech.*, 1995, 42(5), pp. 263–268.
105. A. T. J. Hayward, "Two New Instruments for Measuring the Air Content of Oil," *J. Inst. Petrol.*, 1961, 47(447), pp. 99–106.
106. M. A. Honeyman and G. E. Maroney, "Air in Oil—Available Measurement Methods," *BFPR J.*, 1978, 11(3), pp. 275–281.
107. S. Tsuji and H. Katakura, "A Fundamental Study of Aeration in Oil 2nd Report: The Effects of the Diffusion of Air on the Diameter Change of a Small Bubble Rising in a Hydraulic Oil," *Bull. JSME*, 1978, 21(1S6), pp. 1015–1021.
108. S. Tsuji and K. Matsui, "On the Measurement of Void Fraction in Hydraulic Fluid with Entrained Bubbles," *Bull. JSME*, 1978, 21(152), pp. 239–245.
109. M. J. Denherder, "Important Properties of Hydrostatic Transmission Fluids," *SAE Technical Paper Series*, Paper 650593, 1966.
110. Anon., "Hydraulic Fluids," *Machine Design*, 1995, June, p. 125.
111. Anon., "Hydraulic Fluids: Their Application and Selection," *Hydraulic Pneumatic Power Control*, 1963, August, pp. 572–584.
112. A. T. J. Hayward, "Compressibility Measurement on Hydraulic Fluids," *Hydraulic Pneumatic Power*, 1965, November, pp. 642–646.
113. A. T. J. Hayward, "The Compressibility of Hydraulic Fluids," *J. Inst. Petrol.*, 1965, 51, pp. 35–52.
114. A. T. J. Hayward, R. R. Martins, and J. Robertson, "Compressibility Measurements on Hydraulic Fluids Part II: Isoentropic Measurements on Thirty-Four Fire-Resistant Fluids at 20°C and Pressures up to 10,000 lb/in²," Report issued by the Department of Scientific and Industrial Research, National Engineering Laboratory, Glasgow, Scotland.
115. J. W. Noonan, "Ultrasonic Determination of the Bulk Modulus of Hydraulic Fluids," *Mater. Standards*, 1965, December, pp. 615–621.
116. W. A. Wright, "Prediction of Bulk Moduli and Pressure Volume–Temperature Data for Petroleum Oils," *ASLE Trans.*, 1967, 10, pp. 349–356.
117. D. Rendel and G. R. Allen, "Air in Hydraulic Transmission Systems," *Aircraft Eng.*, 1951, 23, pp. 337–346.

118. A. J. T. Hayward, "Air Entrainment and Compressibility of Hydraulic Fluids," *Mech. World*, 1961, October, p. 332.
119. A. J. T. Hayward, "How Air Bubbles Affect the Compressibility of Hydraulic Oil," *Hydraulic Power Transmission*, 1962, June, pp. 384–388, 419.
120. E. E. Klaus and J. A. O'Brien, "Precise Measurement and Prediction of Bulk-Modulus Values for Fluids and Lubricants," *J. Basic Eng., ASME Trans.*, 1964, 86(D-3), pp. 469–474.
121. W. A. Wright, "Prediction of Bulk Modulus and Pressure Volume-Temperature Data for Petroleum Oils," *ASLE Trans.*, 1967, 10, pp. 349–356. These data are the basis for an ANSI specification ANSI/B 93.63m-1964, *Hydraulic Fluid Power Petroleum Fluids—Prediction of Bulk Moduli*, National Fluid Power Association, Inc., Milwaukee, WI.
122. I. B. Goldman, N. Ahmect, P. S. Nlenkatesan, and J. S. Cartwright, "The Compressibility of Selected Fluids at Pressures up to 230,000 psi," *Lubr. Eng.*, 1971, October, pp. 334–341.
123. R. L. Peeler and T. Green, "Measurement of Bulk Modulus of Hydraulic Fluids," *ASTM Bull.*, 1959, January, pp. 51–57.
124. J. W. Noonan, "Ultrasonic Determination of the Bulk Modulus of Hydraulic Fluids," *Mater. Res. Stand.*, 1965, December, pp. 615–621.
125. G. Silva, "A Study of the Synergistic Effects of Pump Wear," Ph.D. Thesis, Oklahoma State University, Stillwater, 1987.
126. J. M. Hobbs and D. McCloy, "Cavitation Erosion in Oil Hydraulic Equipment," *Methods Mater.*, 1972, January, pp. 27–35.
127. Z. Y. Li, "Cavitation in Fluid Power Equipment Operating with Fire-Resistant Fluids," *FRH J.*, 1984, 4(2), pp. 191–199.
128. P. Radhakrishnan and S. Sundaram, "Effect of Entrained Air on Peak Pressures and Cavitation in a Linear Hydraulic System," *J. Inst. Eng. India—ME*, 1983, 63, pp. 213–219.
129. S. P. Hutton and J. Lobo Guerrero, "The Damage Capacity of Some Cavitating Flows," in *Proc. 5th Conf. on Fluid Machinery*, Budapest, 1975.
130. S. L. Coleman, V. D. Scott, B. McEnaney, B. Angell, and K. R. Stokes, "A Comparison of Tunnel and Jet Methods for Cavitation Erosion Testing," *Wear*, 1995, 194, pp. 73–81.
131. S. Hara, J. Deshimaru, and M. Kasai, "Study on Cavitation of Water Soluble Hydraulic Fluid," in *Proc. of the Int. Tribology Conf.*, Yokohama, 1995, Vol. 2, pp. 909–914.
132. G. L. Ying, "Cavitation and Cavitation Erosion of Spool and Poppet Valves in Fire Resistant Fluids," *FRH J.*, 1984, 5(1), pp. 61–68.
133. H. Rouse, "Cavitation in the Mixing Zone of a Submerged Jet," *La Houille Blanche*, 1953, 8(1), pp. 9–19.
134. R. E. Bose, "The Effect of Cavitation on Particulate Contamination Generation," Ph.D. Thesis, Oklahoma State University, Stillwater, 1966.
135. W. Kleinbreuer, "Untersuchung der Werkstoffzersetzung durch Kavitation in Olhydraulischen Systemen," Ph.D. Thesis, Rheinisch Westfälischen Technischen Hochschule Aachen, Aachen, Germany, 1997.
136. T. Okada and Y. Iwai, "Cavitation Erosion," *JSME Int. J.*, 1990, 33(2), pp. 128–135.
137. T. Okada, Y. Iwai, and K. Awazu, "Study of Cavitation Bubble Collapse Pressures and Erosion Part I: A Method for Measurement of Collapse Pressure," *Wear*, 1989, 133, pp. 219–232.
138. V. Riddel, P. Pacor, and J. K. Appeldoorn, "Cavitation Erosion and Rolling Contact Fatigue," *Wear*, 1974, 27, pp. 99–108.
139. V. A. Leshchenko and Yu. I. Gudilkin, "Cavitation in Self-Induced Vibration Conditions in Hydraulic Servo Systems," *Mach. Tooling*, 1967, 38(6), pp. 19–22.

140. P. H. Schweitzer and V. G. Szebehely, "Gas Evaluation in Liquids and Cavitation," *J. Appl. Phys.*, 1950, 21, pp. 1218–1224.
141. J. Deshimaru, "A Study of Cavitation on Oils: Effects of Base Oils and Polymers," *Jpn. J. Tribol.*, 1994, 36–40, pp. 531–542.
142. Y. Iwai, T. Okada, and S. Tanaka, "A Study of Cavitation Bubble Collapse Pressures and Erosion Part 2: Estimation of Erosion from the Distribution of Bubble Collapse Pressures," *Wear*, 1989, 133, pp. 233–243.
143. J. W. Tichler, J. B. van den Elsen, and A. W. J. de Gee, "Resistance Against Cavitation Erosion of 14 Chromium Steels," *J. Lubr. Technol. Trans. ASME*, 1970, April, pp. 220–227.
144. T. Okada, Y. Iwai, S. Hattori, and N. Tanimura, "Relation Between Impact Load and the Damage Produced by Cavitation Bubble Collapse," *Wear*, 1995, 184, pp. 231–239.
145. T. Okada, Y. Iwai, and K. Awazu, "Study of Cavitation Bubble Collapse Pressures and Erosion Part I: A Method for Measurement of Collapse Pressures," *Wear*, 1989, 133, pp. 219–232.
146. M. G. Talks and G. Moreton, "Cavitation Erosion of Fire-Resistant Hydraulic Fluids," in *Proc. ASME Symp. Cavitation Erosion Fluid Syst.*, 1981, pp. 139–152.
147. T. Tsujino, A. Shima, and Y. Oikawa, "Cavitation Damage and Generated Noise in High Water Base Fluids," *Nippon Kikai Gakkai Ronbunshu B-hen*, 1990, 56(532), pp. 3592–3596.
148. A. Yamaguchi and S. Shimiza, "Erosion Due to Impingement of Cavitating Jet," *Trans. ASME, J. Fluids Eng.*, 1987, 109(4), pp. 442–447.
149. R. T. Knapp, "Recent Investigations of the Mechanics of Cavitation and Cavitation Damage," *Trans. ASME*, 1955, October, p. 1045.
150. J. Robinson and F. G. Hammit, "Detailed Damage Characteristics in Cavitation Venturi," *Trans. ASME, J. Basic Eng.*, 1967, 89(1), p. 161.
151. R. T. Knapp and A. Hollander, "Laboratory Investigations of the Mechanism of Cavitation," *ASME*, 1948, 40, pp. 419–475.
152. W. Backe and J. Berger, "Kavitationerosion bei I-FA Flüssigkeiten," *Ölhydraulisch Pneumatik*, 1984, 28(5), pp. 288–296.
153. C. L. Kling and F. G. Hammit, "A Photographic Study of Spark Induced Cavitation Bubble Collapse," Report No. UMich 03371-4-T, University of Michigan, 1970.
154. A. Yamaguchi, "Cavitation in Hydraulic Fluids: Part I Inception in Shear Flow," *Fluidics Quart.*, 1980, 12(3), pp. 1–15.
155. A. Yamaguchi, "Cavitation in Hydraulic Fluids: Part 2—Delay Time for Stepwise Reduction in Pressure," *Fluidics Quart.*, 1980, 12(3), pp. 16–28.
156. J. Deshimaru, *Jpn. J. Tribol.*, 1994, 36(4), pp. 531–542.
157. A. Lichtarowicz, "Use of a Simple Cavitating Nozzle for Cavitation Erosion Testing and Cutting," *Nature (London), Phys. Sci.*, 1972, 239(91), pp. 63–64.
158. A. Lichtarowicz, "Cavitating Jet Apparatus for Cavitation Erosion Testing," in *Erosion: Prevention and Useful Application*, (W. F. Adlex, ed.), 1977 American Society for Testing and Materials, Conshohocken, PA, pp. 530–549.
159. A. Lichtarowicz, "Erosion Testing with a Cavitating Jet," in *Cavitation Erosion in Fluid System*, *Fluids Eng. Conf.*, 1981.
160. T. Momma and A. Lichtarowicz, "Some Experiences on Cavitation Damage Produced by a Submerged Jet," in *ASME/JSME Nuclear Engineering Conference*, 1993, Vol. 2, pp. 877–884.
161. T. Momma and A. Lichtarowicz, "A Study of Pressures and Erosion Produced by Collapsing Cavitation," *Wear*, 1995, 186–187, pp. 425–436.
162. W. Kleinbreuer, "Werkstoffzerstörung durch Kavitation in Ölhydraulischen Systemen, Industrie—Anzeiger," 1976, 98(61), p. 1096.

163. A. Yamaguchi and S. Shimizu, "Erosion Due to Impingement of Cavitation Jet," *Trans. ASME J. Fluid Eng.*, 1987, 109(4), p. 442.
164. W. J. Rheingans, "Accelerated-Cavitation Research," *Trans. ASME*, 1950, 72, pp. 705–724.
165. L. R. Jones and D. H. Edwards, "An Experimental Study of the Forces Generated by the Collapse of Transient Cavities in Water," *J. Fluid Mech.*, 1960, 7, pp. 596–609.
166. A. Sakamoto, H. Funaki, and M. Matsumura, "Influence of Galvanic Marco-Cell Corrosion on the Cavitation Erosion Durability Assessment of Metallic Materials—International Cavitation Erosion Test of Gdansk," *Wear*, 1995, 186–187, pp. 542–547.
167. ASTM G32-92, *Standard Test Method for Cavitation Erosion Using Vibratory Apparatus*, American Society for Testing and Materials, Conshohocken, PA.
168. Y. Meged, C. H. Venner, and W. E. ten Napel, "Classification of Lubricants According to Cavitation Criteria," *Wear*, 1995, 186–187, pp. 444–453.
169. D. T. Jamieson and J. S. Tudhope, "A Simple Device for Measuring the Thermal Conductivity of Liquids with Moderate Accuracy," *J. Inst. Petrol.*, 1964, 50(486), pp. 150–153.
170. O. B. Cecil and R. H. Munch, "Thermal Conductivity of Some Organic Liquids," *Ind. Eng. Chem.*, 1956, 48(3), pp. 437–440.
171. H. L. Mason, "Thermal Conductivity of Some Industrial Liquids from 0–100°C," *Trans. ASME*, 1954, July, pp. 817–821.
172. R. W. Powell and A. R. Challoner, "Thermal Conductivity Measurement on Oils," *J. Inst. Petrol.*, 1960, 46(440), pp. 267–271.
173. A. F. Schmidt and B. H. Spurlock, "The Thermal Conductivity of Fluids," *Trans. ASME*, 1954, July, pp. 823–830.
174. IEC Standard 247, *Measurement of Relative Permeativity, Dielectric Dissipation Factor and Resisting of Insulating Fluids*, International Electrotechnical Commission, Geneva.
175. Lord Rayleigh, "On the Pressure Developed in a Liquid during the Collapse of a Spherical Cavity," *Philos. Mag.*, 1914, 34, p. 94.
176. R. Hickling and M. S. Plesset, "Collapse and Rebound of a Spherical Bubble in Water," *Phys. Fluids*, 1964, 7(1), p. 7.
177. R. D. Ivany, and F. G. Hammitt, "Cavitation Bubble Collapse in Viscous Compressible Liquids—Numerical Analysis," *Trans. ASME, Ser. D*, 1965, 87, p. 977.
178. M. S. Plesset and R. B. Chapman, "Collapse of an Initially Spherical Vapour Cavity in the Neighborhood of a Solid Boundary," *J. Fluid Mech.*, 1971, 2, p. 283.
179. I. R. Jones and D. H. Edwards, "An Experimental Study of the Forces Generated by the Collapse of Transient Cavities in Water," *J. Fluid Mech.*, 1960, 7, p. 596.
180. S. Fujidawa and T. Akamatsu, "Experimental Investigations of Cavitation Bubble Collapse by a Water Shock Tube," *Bull. JSME*, 1978, 21(152), p. 233.
181. Y. Tomita and A. Shima, "Mechanisms of Impulsive Pressure Generation and Damage Pit Formation by Bubble Collapse," *J. Fluid Mech.*, 1986, 169, p. 535.
182. G. W. Sutton, "A Photoelastic Study of Strain Waves Caused by Cavitation," *Trans. ASME, J. Appl. Mech.*, 1957, 24(3), p. 340.
183. K. Endo and Y. Nishimura, "Fundamental Studies of Cavitation Erosion (in the Case of Low Cavitation Intensity)," *Bull. JSME*, 1973, 16(91), p. 22.
184. N. Sanada, K. Takayama, O. Onodera, and J. Ikeuchi, "Observation of Cavitation Induced Shock Waves in an Ultrasonic Vibratory Test," *Trans. Jpn. Soc. Mec. Eng.*, 1984, 50(458), p. 2275 (in Japanese).
185. H. Kato, M. Maeda, and Y. Nakashima, "A Comparison and Evaluation of Various Cavitation Erosion Test Methods," in *Proc. ASME Symp. on Cavitation Erosion Fluid Systems*, 1981, p. 83.
186. Y. Okabe, A. Kitajima, A. Koishikawa, and Y. Takeuchi, "Experimental Studies on Relationship Between Erosion Rate and Apparent Impact Pressure and Cavitation Monitoring System by Acoustic Detector," in *Proc. Int. Symp. on Cavitation*, 1986, p. 351.

187. R. Oba, K. Takayama, Y. Ito, H. Miyakura, S. Nozaki, T. Ishige, S. Sonoda, and K. Sakamoto, "Spatial Distribution of Cavitation Shock Pressure Around a Jet-flow Gate Valve," *Trans. Jpn. Soc. Mech. Eng.*, 1987, 53(487), p. 671.
188. B. Kouzel, Hydrocarbon Processing Petrol. Refiner, 1965, 443, p. 120.
189. C. J. A. Roelands and V. R. B. Druck, *Kleine der A3-4*, 1966, Groningen, Holland.
190. G. P. Fresco, M.S. Thesis, The Pennsylvania State University, University Park, PA, 1962.
191. H. W. Kim, Ph.D. Thesis, The Pennsylvania State University, University Park, PA, 1970.
192. B. Y. So and E. E. Klaus, *ASLE. Trans.*, 1980, 23(4), p. 409.
193. P. S. Y. Chu and A. Cameron, *J. Inst. Petrol.*, 1962, 48(461), p. 147.
194. R. C. Worster, "Discussion to Paper by A. E. Bringham," *Proc. Inst. Mech. Eng.*, 1951, 165, p. 269.
195. J. Shibada, *Nisseki Rebyu*, 1997, 39(2), pp. 46–56.

5

Fluid Viscosity and Viscosity Classification

BERNARD G. KINKER

Roh Max USA, Inc., Horsham, Pennsylvania

1 VISCOSITY

Viscosity is the most important property of a hydraulic fluid because it relates directly to hydrodynamic lubrication and power transmission. For adequate hydrodynamic lubrication, it is necessary to maintain a fluid film between moving surfaces under load. A lubricant of insufficient viscosity will fail to do this. For power transmission, a fluid of excessive viscosity will result in sluggish operation. The importance of viscosity is far more complex than described here, but these simple descriptions are a starting point for a discussion of viscosity and its relevance to hydraulic fluids.

1.1 Absolute Viscosity and Newton's Law

Viscosity is a fluid's resistance to flow. The viscosity of a fluid, either liquid or gas, describes opposition to a change in shape or to movement. A mathematical description was first developed by Sir Isaac Newton as a special case of his second law of motion:

$$\text{Shear stress} = (\text{Coefficient of viscosity})(\text{Shear rate}) \quad (5.1)$$

where the shear stress is the force per area and the shear rate is the velocity gradient. This leads to a description of viscosity as the force that must be overcome to cause a given fluid motion. Newton's viscosity law applies when laminar, or nonturbulent, flow occurs. Laminar flow can be imagined as numerous, discrete layers (lamina) of the fluid moving in the same direction, but the velocity of each layer will vary

depending on distance from a system boundary. The concept of velocity as a function of distance is known as the velocity gradient.

Fluid flow through a tube caused by an applied pressure, known as Poiseulle flow, is represented in Fig. 5.1. The arrows represent layers moving in streamlines between stationary, parallel walls. The layer closest to a wall is assumed to adhere to the wall and cause a frictional drag on the next layer, which is moving under the applied force. Successive layers experience gradually reduced frictional drag and flow at successively higher velocities. The central layer encounters the least friction from adjacent layers and, consequently, has the highest velocity. This change in velocity, from zero at the boundaries to the highest at the center, describes the term velocity gradient.

Another way to induce flow is to provide a tangential shearing force to one surface that moves with respect to a second surface (Couette flow). In Fig. 5.2, the upper, movable plate is being forced at a uniform velocity over a fluid film so as to exert a shearing force on the fluid. The bottom plate is stationary. Assuming adhesion, the fluid layer next to the moving surface experiences the same velocity as the moving plate, while the layer immediately next to the bottom surface is stationary. Moving up from the stationary layer, intervening layers experience gradually reduced drag and gradually higher velocities until arriving at the topmost layer, which moves in concert with the surface.

If the dimensions of the system in Fig. 5.2 are force = 1 N, velocity = 1 m/s, area of the moving plate = 1m², and the distance between the two plates is 1 m, then rearranging Eq. (5.1) and substituting

$$\text{Absolute viscosity} = \frac{\text{Force/Area}}{\text{Velocity/Distance}} = \frac{\text{N/m}^2}{\text{m/s/m}} = \frac{\text{Pa}}{\text{S}^{-1}} = \text{Pa} \cdot \text{s} \quad (5.2)$$

Newton's law describes absolute, or dynamic, viscosity which has the units of Pascal seconds. More commonly used units are the Poise (P), the cgs unit named after Jean

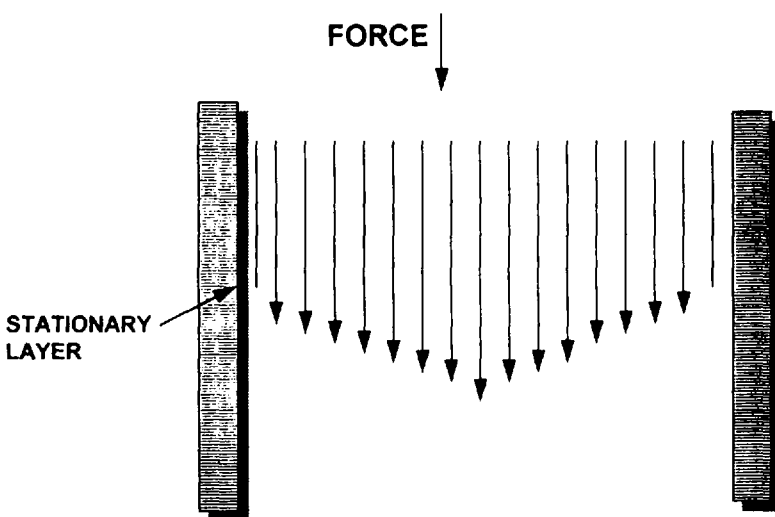


Figure 5.1 Schematic of streamline flow between two stationary boundaries.

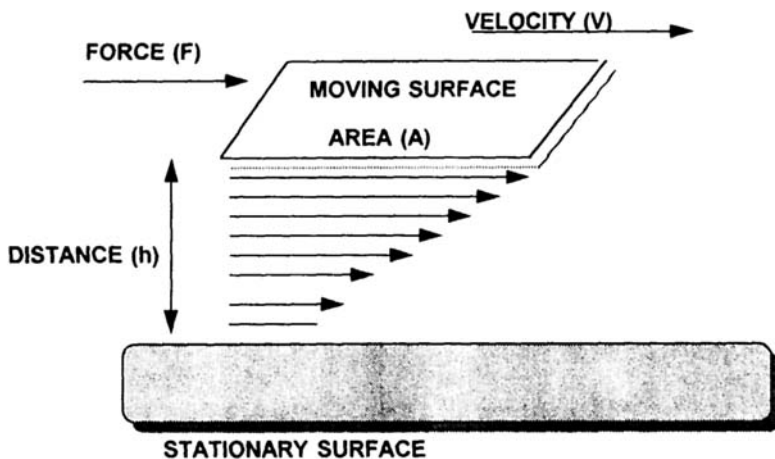


Figure 5.2 Schematic of streamline flow between moving and stationary surfaces.

Louis Marie Poiseuille, investigator of streamline flow, and the centipoise (cP); 1000 cP equals 10 P which equals 1 Pa·s. The usual symbol for viscosity is η .

Newtonian fluids, those that conform to Newton’s law, have a linear shear stress–shear rate relationship and the value of the slope is the coefficient of viscosity as shown in Fig. 5.3. By examining the shear stress–shear rate properties of the two fluids in Fig. 5.3, one can begin to gather a sense of the importance of viscosity in maintaining a fluid film between moving surfaces. A higher-viscosity fluid provides more resistance to flow out of a potential contact zone and generates a higher lifting force. By definition, Newtonian fluids have a constant viscosity over all values of shear rate; see Fig. 5.4. However, under certain conditions, not all fluids are Newtonian; important deviations relevant to lubricant behavior will be discussed in Section 5.

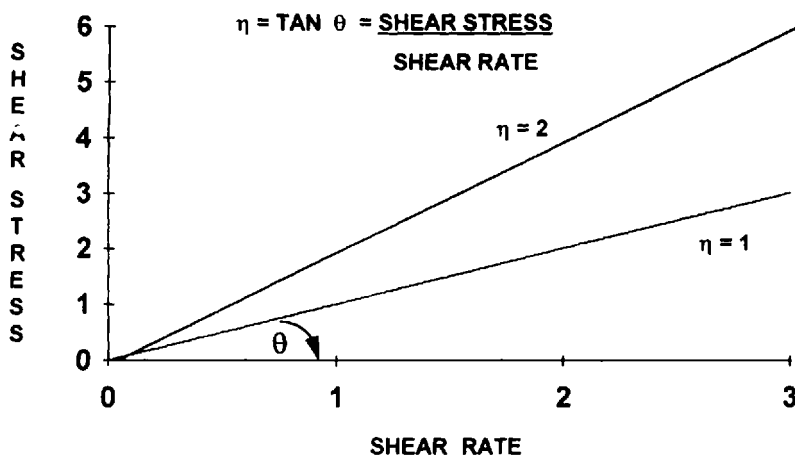


Figure 5.3 Newtonian liquids: relationship of shear rate versus shear stress.

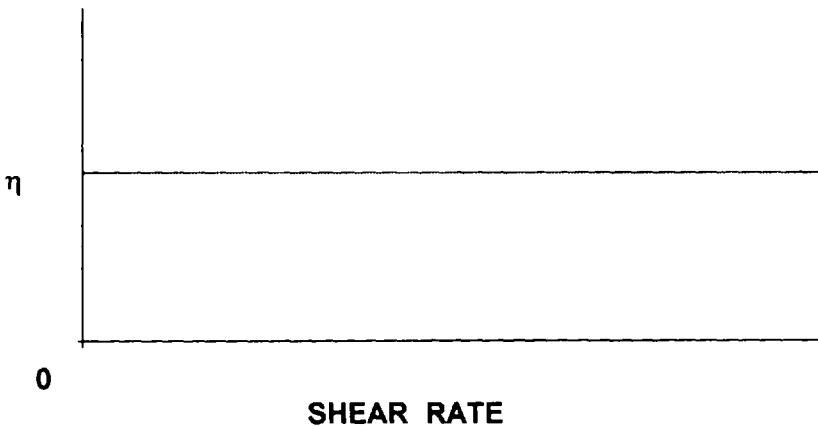


Figure 5.4 Newtonian liquids: constancy of viscosity with increasing shear rate.

Fluidity is the reciprocal of viscosity and conveys the meaning of ease of flow. Rearrangement of Eq. (5.1) yields

$$\begin{aligned} \text{Shear rate} &= (\text{Shear stress})(1/\text{Coefficient of viscosity}) \\ &= (\text{Shear stress})(\text{Fluidity}) \end{aligned} \quad (5.3)$$

When fluidity is high, the velocity gradient is large at constant shear stress.

1.2 Rheology and Kinematic Viscosity

Rheology, the study of flow, can be accomplished by a variety of techniques. The most common include measuring the time to flow through a capillary, measuring the force necessary to rotate a cylinder at a given angular velocity through a fluid, or measuring the time for a falling sphere to move through a fluid. Absolute viscosity is usually measured by the rotating cylinder technique. A more common technique, often used for lubricants, is to determine kinematic viscosity by passing a liquid through a capillary tube. Kinematic viscosity is calculated from Poiseuille's equation

$$\eta = \frac{P\pi r^4 t}{8Vl} \quad (5.4)$$

where t is the time for a volume V to flow through a capillary of radius r and length l under a pressure of P . However, the method is difficult to apply experimentally, so indirect measurements are usually made.

A very common, indirect procedure used to measure kinematic viscosity is ASTM D 445 (Kinematic Viscosity of Transparent and Opaque Liquids) [1]. The procedure utilizes a modified Ostwald viscometer, a U-shaped tube with a capillary near the bottom of one side of the U. When a liquid is higher on one side of the tube, the pressure that causes flow is proportional to the difference in height between the two levels, the density of the liquid, and the acceleration due to gravity. If the viscosity of one liquid is known, then time to flow between two reference points on the tube can be compared to the efflux time of an unknown liquid. Viscosity can be calculated by the simple equation

$$\frac{\eta_1}{\eta_2} = \frac{t_1}{t_2} \quad (5.5)$$

where the subscripts 1 and 2 represent values for the two liquids. Units of kinematic viscosity are normally reported as millimeters squared per second, commonly known as centistokes (cSt) (named for Stokes who investigated the motion of falling spheres in liquids). Because kinematic viscosity is measured only under gravity pressure, the shear rate is relatively low, about 100 s^{-1} . Kinematic viscosity should only be measured at temperatures above the cloud point, the temperature at which forming wax crystals begin to cause haze. Insoluble wax crystals can lead to serious errors in the measurement as the particles may interfere with flow through the capillary.

Kinematic viscosity is related to absolute viscosity by the density of the liquid

$$\text{Absolute viscosity} = (\text{Kinematic viscosity})(\text{Density}) \quad (5.6)$$

2 VISCOSITY–TEMPERATURE RELATIONSHIP

An ideal lubricant would be equiviscous at all temperatures in order to provide a constant degree of lubrication. However, viscosity is highly dependent on temperature. In the extreme, at hot temperatures, a fluid may no longer have sufficient viscosity to form a film of adequate strength between moving surfaces, whereas at cold temperatures, it may become too viscous to flow at all.

2.1 Effect of Temperature

The viscosity of a liquid decreases with increasing temperature; gases have the opposite relationship. An empirical relationship of viscosity to temperature for petroleum oils and hydrocarbons in general is given by the McCoull–Walther equation first described in 1921 [2] and the basis for ASTM D 341 (Viscosity–Temperature Charts for Liquid Petroleum Products):

$$\log \log(\eta + 0.7) = A - B \log T \quad (5.7)$$

where η is the kinematic viscosity, T is the absolute temperature, and both A and B are constants for a given liquid. The negative slope B indicates that higher temperatures result in lower viscosities, as shown for some selected liquids in Fig. 5.5. Taking the derivative of Eq. (5.7) yields the slope $B = (1/\eta)(\delta\eta/\delta T)$, usually referred to as the viscosity–temperature coefficient.

2.2 Viscosity Index

Apparent from Fig. 5.5 is that different liquids may have distinctly different viscosity–temperature relationships, as some lose far more viscosity than others when temperature increases. The extent of decreasing viscosity with increasing temperature is described by the viscosity index (VI), a dimensionless number calculated from measured viscosities using ASTM D 2270 (Calculating Viscosity Index from Kinematic Viscosity at 40 and 100°C). This arbitrary VI scale was originally devised by Dean and Davis [3]. The calculation of VI requires measurement of 100°C and 40°C kinematic viscosities at which are then compared to a reference scale. In the original scale, a Pennsylvania paraffinic oil which for the time had excellent viscosity–temperature properties was assigned a VI of 100. Another oil, a Texas

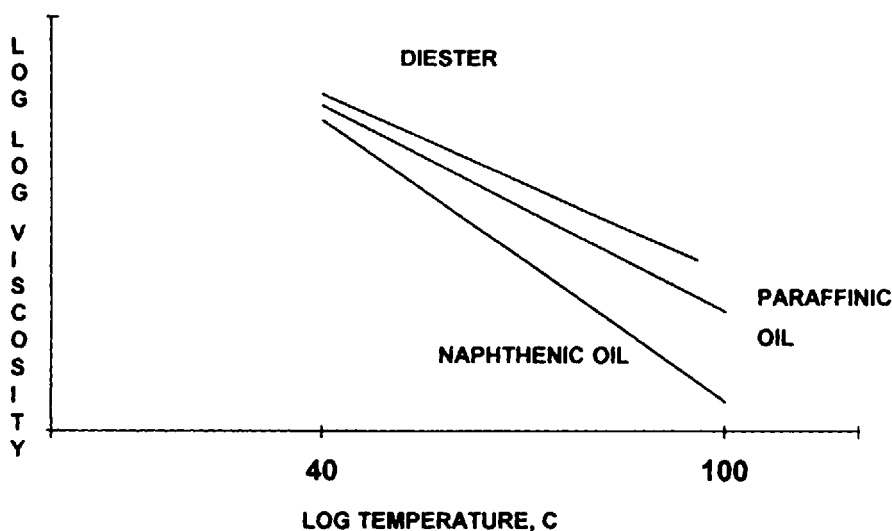


Figure 5.5 Viscosity–temperature properties of various liquids.

Gulf naphthenic oil with poor viscosity–temperature properties was assigned a VI of 0. VI is calculated by

$$\text{Viscosity index} = \left(\frac{L - U}{L - H} \right) \times 100 \quad (5.8)$$

where L is the kinematic viscosity at 40°C of a reference oil with VI = 0 and kinematic viscosity at 100°C equivalent to the oil being evaluated, H is the kinematic viscosity at 40°C of a reference oil with VI = 100 and kinematic viscosity at 100°C equivalent to the oil being evaluated, and U is kinematic viscosity at 40°C of the oil being evaluated. In practice, one rarely calculates VI; extensive tabulations are provided in ASTM DS 39B. For a given liquid, one can determine any viscosity between the reference temperatures with a knowledge of its VI and one reference viscosity.

High-VI lubricants tend to be preferred for applications that experience wide temperature variations, notably outdoor applications, because viscosity changes less with temperature. As shown in Fig. 5.6, for two oils with equivalent 40°C kinematic viscosities but different VIs, the higher-VI oil is more viscous as temperature increases and is less viscous at lower temperatures. The VI of a base oil can be enhanced by the use of polymeric additives known as viscosity index improvers (VI improvers), which are further described in Section 4.2. Oils containing VI Improvers are often known as multigrade oils or HV hydraulic fluids.

The viscosity index is often used as a quality indicator of lubricants. However, some caution must be used in interpreting VI beyond the reference temperature range and for multigrade oils. At sufficiently cold temperatures, below the cloud point of paraffinic oils, viscosity may be much higher than implied by VI because of the onset of wax crystallization, as shown in Fig. 5.7. Additionally, multigrade oils may be less viscous than implied by VI because of polymer shear thinning or shear

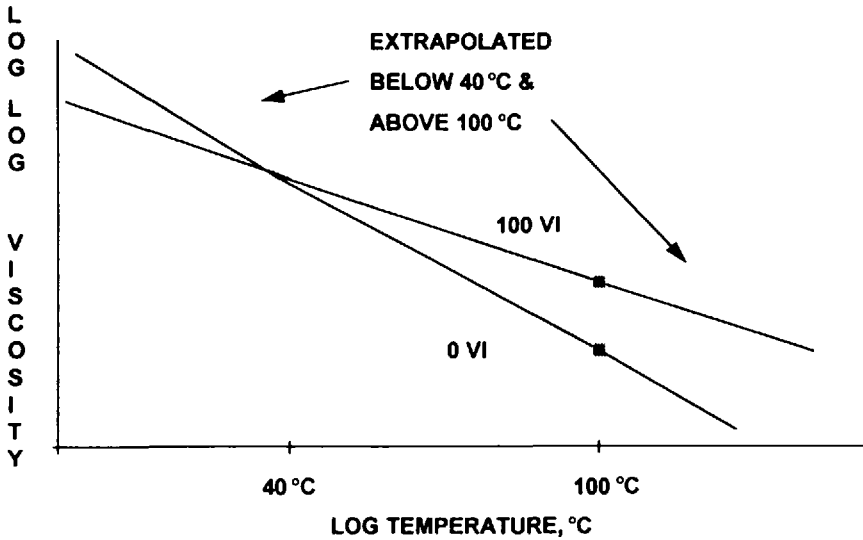


Figure 5.6 Viscosity–temperature properties of high- and low-viscosity-index liquids.

degradation in equipment operating at shear rates far higher than associated with determination of kinematic viscosity. Both cold temperature and shear-thinning effects will be discussed further in Section 5 on non-Newtonian behavior.

In addition to describing the viscosity–temperature behavior, VI may also be used to infer the chemical nature and quality of base oils. This should be apparent from the definition of VI, as high naphthenic and aromatic content oils have low VI values, whereas substantially paraffinic oils have higher VIs. In comparing the VIs

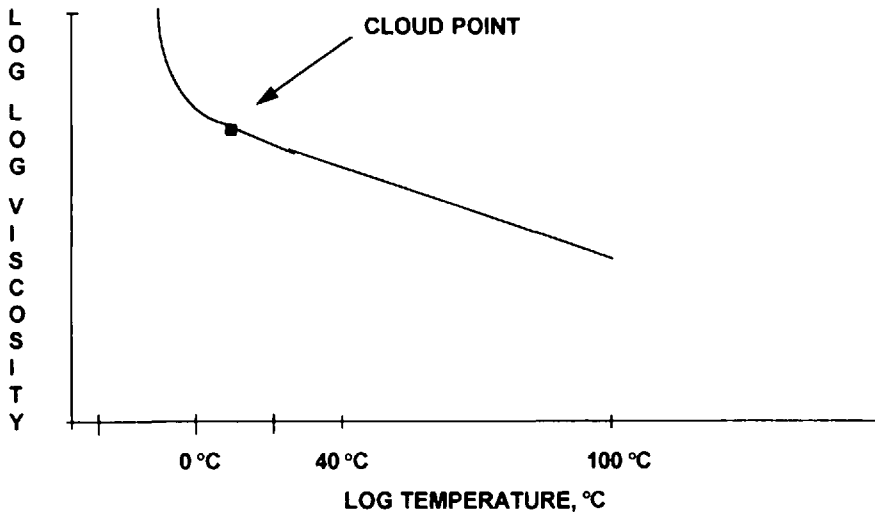


Figure 5.7 Effect of wax crystal formation on viscosity–temperature properties below the cloud point.

of two oils, one might assume that the higher-VI oil has a greater paraffin content and is, therefore, more oxidatively stable. However, caution must be used because VI does not impart knowledge of the distribution of naphthenic to aromatic molecules. Between two oils of unequal VI, it is possible that the higher-VI oil could have a higher concentration of undesirable, oxidatively unstable aromatic molecules.

3 VISCOSITY–PRESSURE RELATIONSHIP

Just as viscosity varies with temperature, it also varies with pressure, but in this case, viscosity increases with increasing pressure. This behavior is an important aspect of lubrication because a liquid is significantly more viscous or may even become an amorphous solid under sufficiently high loads. Peak Hertzian contact pressures are often in the 6.9×10^4 -kPa (100,000 psi) range, well above the solidification points of naphthenic [6.9×10^4 kPa (10,000 psi)] or paraffinic oils [1.4×10^4 kPa (20,000 psi)]. It is under such high-pressure conditions that elastohydrodynamic lubrication can occur, thus providing the film thickness necessary to maintain sufficient lubrication.

3.1 Effect of Pressure

High-pressure viscosity can be measured directly by various instruments: a falling-body high-pressure viscometer, a rolling-ball high-pressure viscometer, or a high-pressure capillary viscometer. In 1893, Barus [4] described an empirical isothermal viscosity–pressure relationship in which viscosity increases exponentially with pressure:

$$\eta_p = \eta_0 e^{\alpha p} \quad (5.9)$$

where η_p is the viscosity at pressure p , η_0 is the viscosity at atmospheric pressure, and α is the pressure–viscosity coefficient. It must be noted that viscosity–pressure properties do not vary uniformly; rather, α depends on the magnitude of pressure, the chemical nature of the liquid, and temperature.

3.2 Mathematic Relationships of Viscosity and Pressure

Viscosity–pressure relationships for liquids are normally expressed by the viscosity–pressure coefficient α in Eq. (5.9). A better sense of the nature of the coefficient comes from rearranging Eq. (5.9) to

$$\ln \left(\frac{\eta}{\eta_0} \right) = \alpha p \quad (5.10)$$

This indicates that the viscosity–pressure coefficient is the change in viscosity relative to the change in pressure. Higher values of α predict a more viscous liquid as pressure increases. For a change of pressure equal to $1/\alpha$, viscosity will change by a factor of 2.71.

Further defining α , the derivative of Eq. (5.10), $(1/\eta)(\delta\eta/\delta p)$, expresses the viscosity–pressure differential relative to viscosity at atmospheric pressure. Although Eq. (5.10) implies a linear relationship of $\ln(\text{viscosity})$ with pressure, this is seldom the case for most liquids except at low pressures. This is illustrated in Fig. 5.8, where a plot of isothermal viscosity–pressure properties indicates a decreasing slope (de-

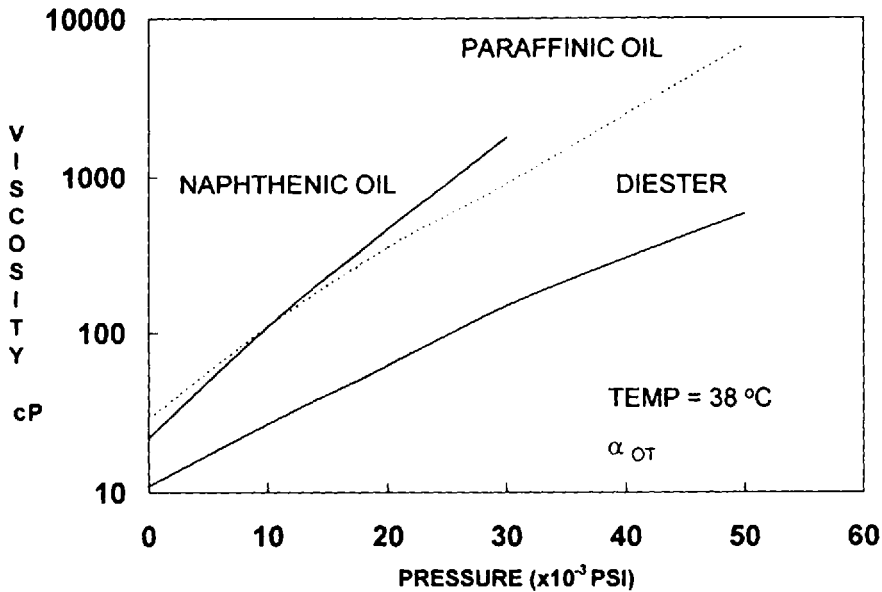


Figure 5.8 Viscosity–pressure properties of various liquids.

creasing viscosity–pressure coefficient) with increasing pressure [5]. For most liquids useful as lubricants or hydraulic fluids, the approximate range of the viscosity–pressure coefficient is $(1.5–5.0) \times 10^{-8} \text{ Pa}^{-1}$ [$(1–3) \times 10^{-4} \text{ psi}^{-1}$]. At pressures less than $2.8 \times 10^4 \text{ kPa}$ (4000 psi), the difference among viscosity–pressure coefficients of different fluids is relatively small, but at high pressures, the differences can be quite marked.

Because α is often a function of pressure, the methodology used to obtain its value must be stated. One well-known technique uses the value of the tangent, at atmospheric pressure, to a $\log(\text{viscosity})$ versus pressure plot. This form of the viscosity–pressure coefficient, termed α_{OT} , multiplied by atmospheric viscosity is often used to predict film thickness tendencies. Another technique is to evaluate the integral of $(\eta_0/\eta_p \delta p)^{-1}$ over the entire pressure range. This value is designated as α^* (reciprocal asymptotic isoviscous pressure) and is the least dependent on measurement procedures and errors.

An empirical relationship has been developed by Roelands [6] which smoothes viscosity–pressure data for a given liquid at a given temperature:

$$\log \eta_p + 1.200 = (\log \eta_0 + 1.200) \left(1 + \frac{P}{2000} \right)^z \tag{5.11}$$

where η is absolute viscosity in centipoise and P is gauge pressure in kilogram per square centimeter. A simplified form of Eq. (5.11) is

$$H = Zp + H_0 \tag{5.12}$$

where $H = \log(\log \eta_p + 1.200)$, $p = \log(1 + P/2000)$, $H_0 = \log(\log \eta_0 + 1.200)$, and Z , the slope of the relationship, is the pressure–viscosity index. A chart with axes proportional to H and p will linearize pressure–viscosity data for many fluids. The pressure–viscosity index and α_{OT} are related by

$$\log \alpha_{OT} = \log Z + (H_0 - 2.9388) \quad (5.13)$$

3.3 Factors Affecting Viscosity–Pressure Relationships

Viscosity–pressure properties vary greatly with the chemical nature of a liquid. Paraffinic and naphthenic oils, for example, behave differently under pressure, as shown in Fig. 5.8, where the naphthenic oil, relative to the paraffinic oil, has a greater viscosity increase with increasing pressure. One is reminded of the viscosity–temperature relationships of different chemical classes. The increase of naphthenic oil viscosity with pressure and the decrease with temperature are both greater than those for paraffinic oils. These behaviors lead to a general rule that when comparing two liquids of similar atmospheric viscosity but in different chemical classes, those with a lower viscosity index will have a higher value of α . Even within the same chemical class, higher-viscosity materials tend to have higher viscosity–pressure coefficients, as indicated by the data for naphthenic oils A and B in Table 5.1 [5].

Temperature also influences viscosity–pressure properties. Lower temperatures tend to give higher values of α and to produce larger differences of α within a chemical class. At sufficiently high temperatures, the differences become quite small, as shown by the 149°C data in Table 5.1. Viscosity–temperature and viscosity–pressure properties have been linked through an empirical equation [7] that relates viscosity–pressure coefficient to atmospheric viscosity and density at a given temperature and the viscosity–temperature property [the ASTM slope for Eq. (5.7) divided by 0.200]. It has also been shown that temperature and pressure effects on viscosity can be combined in a free-volume treatment (see Sec. 4.1 for a discussion of free volume) of viscosity [8].

The chemical nature, temperature, and pressure effects on viscosity are, indeed, quite complex, but they should become clearer after a more fundamental discussion of viscosity in the following section.

Table 5.1 Selected Viscosity–Pressure Coefficients

Fluid	$\alpha_{OT} \text{ (N/m}^2\text{)}^{-1}$			
	$\eta, 38^\circ\text{C (cP)}$	38°C	99°C	149°C
2 Ethylhexyl sebecate	11	1.39	1.19	
Paraffinic oil	29	2.18	1.78	
Naphthenic oil A	22	2.15	1.44	
Naphthenic oil A + VI Improver 1.21 ^a	60	1.83	1.24	
Naphthenic oil B 1.33	68	3.07	1.81	
Polybutene ($M_n = 409$)	90	3.18	2.22	

^aVI Improver = 4% PMA ($M_n = 560,000$)

4 MOLECULAR BASIS OF VISCOSITY

Viscosity is also identified with internal friction of a fluid, the friction generated by molecules as they move by each other during flow. How do molecules move during viscous flow? Why do some flow more slowly? Why do liquids become less viscous with increasing temperature, more viscous with pressure? Detailed scientific treatments have provided significant understanding of the physical chemistry and molecular movements during viscous flow. However, the theory is not so well advanced that accurate predictions can be made for liquids composed of complex molecules. Still, the principles help one comprehend the nature of viscosity and the behavior of different types of molecules during viscous flow.

4.1 Small Molecules

Base fluids contain molecules that fit into the category of small molecules. It should be recognized that most fluids contain mixtures of many different molecules, but flow properties still can be described by general theories of viscosity.

Lattice theory states that liquids consists of a matrix of molecules and vacancies or "holes" scattered throughout. During liquid viscous flow, the flow unit, which may be a group of molecules, a single molecule, or a segment of a molecule, "jumps" into an existing hole and thereby creates a new hole. Some source of energy is required for a molecule to jump over an energy barrier and into a hole. Under a shearing force, holes are filled so as to relieve the stress; thus, flow is in the direction away from the stress source. At higher temperatures, more energy is available and more jumps can be made per unit time, resulting in lower viscosity. At higher pressures, a fluid is compressed, resulting in smaller holes, so fewer jumps can be made, resulting in higher viscosity.

Energy of activation for viscous flow is related to the latent heat of vaporization of the molecule or molecular segment making the jump because the molecule must be removed from its surroundings. Activation energy for viscous flow tends to be about one-third to one-fourth of the heat of vaporization because the molecule remains in the liquid state and intermolecular forces are replaced. Eyring's equation [9,10] combines viscosity and energy-temperature terms

$$\eta = Ae^{\frac{\Delta G_v}{RT}} \quad (5.14)$$

where

R = gas constant

T = temperature

ΔG_v = standard free energy of activation for viscous flow (related to standard free energy of vaporization)

A = related to the molar volume of a given material

Several important viscosity relationships can be found in Eq. (5.14). The inverse relationship with temperature is clearly present in the exponential term and can be seen more clearly by differentiation of Eq. (5.14) at constant pressure:

$$\left(\frac{\delta(\ln \eta)}{\delta T} \right)_p = - \frac{\delta \Delta G_v}{RT^2} \quad (5.15)$$

The direct relationship of molecular weight, for a homologous chemical series, is in

ΔG , because higher molecular weight translates to higher heat of vaporization and thus higher viscosity. The validity of the viscosity–molecular weight relationship for linear paraffins [11] from pentane (C_5H_{12}) through hexadecane ($C_{16}H_{34}$) is shown in Fig. 5.9.

The constant A from Eq. (5.14) is defined by

$$A = \frac{hN_0}{MW/\rho} \quad (5.16)$$

where

- h = Planck's constant
- N_0 = Avagadro's number
- MW = molecular weight
- ρ = density
- MW/ ρ = molar volume (volume/mole)

The term A does not contain energy or temperature parameters but does incorporate molecular size. As the molecular weight increases, the value of A decreases, leading to the somewhat surprising consequence that viscosity is lower as molecular weight increases. A physical sense of this phenomenon is that a higher molecular weight yields a lower molar volume, thus fewer, although larger, molecules in a given volume. Accordingly, there would be more free volume or holes available for jumps. However, the exponential term by far dominates in Eq. (5.14), so that molecular weight, by its relationship to energy of activation, has a profound influence on increasing viscosity.

Further development of the theory [12] suggests that viscosity on a molecular scale can be related to the energy required for internal rotation of molecular linkages and the barriers to such rotation. If the energy barrier is high, then the molecule tends to be rigid and have a high-energy barrier for translational motion (flow into a hole) of the molecule or a molecular segment. Molecular structures can range from rigid to flexible. For example, in Table 5.2, the aromatic compound benzene is com-

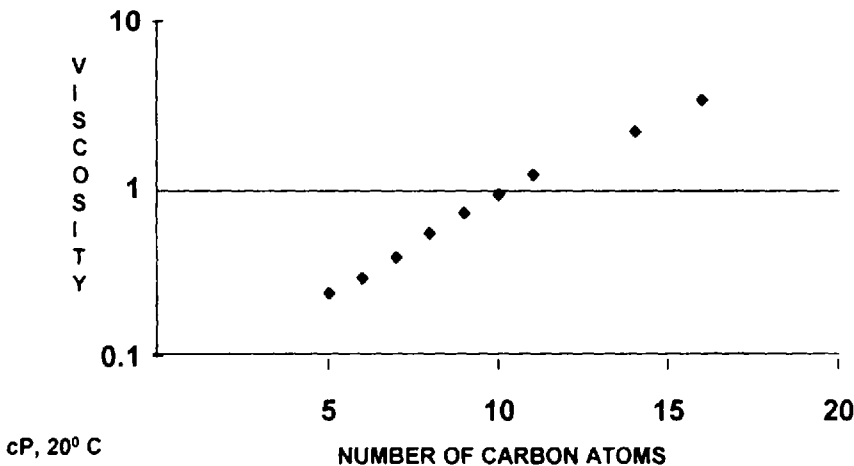


Figure 5.9 Effect of increasing molecular weight on viscosity of n -paraffins (cP) at 20°C.

Table 5.2 Molecular Structure Effects and Barriers to Internal Rotation on Molecular Flexibility

Compound	Structure effect	V_0 (kcal/mol of linkages) (barriers)	Flexibility ^a
n -C ₉ H ₂₀	Branching	2.8 (8)	2.1
(C ₂ H ₅) ₄ C		2.8 (4), 4.9 (4)	0.3
2,2,4,4-Tetramethylpentane		4.9 (8)	0.5
n -C ₁₃ H ₃₀	Double bonds	2.8 (13)	4.2
2,2,3,3,5,6,6-Heptamethylheptane		4.9 (all)	0.3
n -C ₆ H ₁₄		2.8 (5)	0.84
1-Hexene	Aromatic rings	2.8 (3), 2.0 (1)	0.85
1,5-Hexadiene		2.8 (2), 2.0 (2)	1.0
1,3,5-Hexatriene, cis		1.2 (2)	>1.7
Benzene, naphthalene	Naphthene rings	Infinite	0
Cyclopentane, cyclohexane, decalins		10 (1, 2) ^b	0.5
Diphenyl	Jointed rings	4.5 (1)	0.5
Dicyclohexyl		3.6 (1)	0.3
Tricyclopentylmethane	Crowding of rings on alkane	5 (all)	0.95
Tricyclohexylmethane		5 (all)	1.4
Tri(2-cyclohexylethyl)methane		3.6 (4), 2.8 (3)	5.1

^aExternal degrees of freedom including internal rotation, from density and vapor pressure data.

^bPseudorotation for cyclopentane and boat/chair transition for cyclohexane.

pletely rigid because the individual linkages cannot bend out-of-plane. Linear paraffins are flexible because rotation around the C—C linkage is possible, but a significant degree of branching in paraffins creates barriers to rotation, increasing the rigidity. Viscosity equations are similar to Eq. (5.14) but differ for rigid and flexible molecular structures:

$$\eta_{\text{rigid}} = Ae^{kE_0/5CRT} \quad (5.17)$$

$$\eta_{\text{flexible}} = A'e^{k'E_0/5CRT} \quad (5.18)$$

where

E_0 = standard energy of vaporization

k, k' = constants

C = flexibility

R = gas constant

T = temperature

$A, A' = (E_0/m)^{1/2}/v$

m = molecular mass

For rigid molecules, v is related to molecular surface area because a rigid surface must move in concert as the flow unit, and for flexible molecules, v is related to molecular cross-sectional thickness because a segment of the molecule may be the flow unit. The exponential energy term dominates and depends on the value of C

which is low for rigid molecules; therefore, viscosity is high. A physical sense is that rigid structures must move as a whole (complete rigidity) or in a highly coordinated state, whereas flexible molecules may experience segmental translations. The viscosity predictions for similar MW compounds are aromatic > naphthenic \cong highly branched paraffins > *n*-paraffins. Double bonds increase flexibility by allowing free rotation around the bond alpha (adjacent) to the double bond, thereby reducing viscosity.

The viscosity–temperature relationship clearly depends on activation energy but an additional element, density change associated with temperature change, needs to be considered. If ΔG , from Eq. (5.14) is replaced by the relationship $\Delta H_f - T\Delta S_f$, and density is transferred to the left-hand side of the equation, then differentiation at constant pressure yields

$$\left(\frac{\delta \ln(\eta/\rho)}{\delta T^{-1}} \right)_P = \frac{\Delta H}{R} \quad (5.19)$$

which indicates a viscosity–density relationship. As the temperature rises, the packing density of molecules will decrease, creating greater free volume or more holes. The relationship of viscosity to free volume is expressed as

$$\eta = Ae^{(B/V_f)} \quad (5.20)$$

where V_0 is the molal volume at 0°K and V_f is the free (unoccupied) volume that relates to the quantity and size of the holes in lattice theory. As the temperature rises, so does the free volume (as well as energy), with a corresponding reduction in viscosity of both rigid and flexible molecules. However, rigid molecules experience a greater loss of viscosity as translational motion into additional and larger holes becomes more favored. Rigid molecules are aromatic and naphthenic structures which tend to low viscosity index values.

The viscosity–pressure coefficient is also a function of free volume, molecular rigidity, and size of a flow unit participating in a jump. The viscosity–pressure relationship is approximated by

$$\ln \left(\frac{\eta}{\eta_0} \right) = \left(\frac{V_{\pi}}{RT} \right) P \quad (5.21)$$

where P is the pressure and V_{π} represents the size of holes per mole and is directly related to the viscosity–pressure coefficient at constant temperature. Clearly, pressure impacts free volume and the size of holes. Molecular rigidity considerations are the same as for viscosity–temperature, but with decreased hole size under higher pressure, the viscosity will increase.

4.2 Polymers in Solution

Polymeric additives known as viscosity index improvers (VI improvers) are used to increase both the viscosity and VI of base stocks. The VI improvers are widely used to formulate high-VI, or multigrade, fluids for use where excellent viscosity–temperature properties are required. One finds multigrade fluids used in automotive, off-highway, tractors, aircraft, and industrial equipment exposed to wide temperature ranges. To formulate a multigrade fluid, a low-viscosity base stock is thickened with a VI improver to a high-temperature viscosity target; ideally, the low-temperature

viscosity of the blend experiences only a relatively modest increase in viscosity (Fig. 5.10).

Because of molecular size and the possibility of chain entanglement, polymer flow is far more complex than that of small molecules, so the above viscosity treatments are far less precise. However, Eq. (5.9) still applies to describe viscosity properties of polymers. However, the heat of vaporization of the polymer is not the correct parameter to describe the activation energy of viscous flow [12]. It has been found that the ΔH_v of paraffins rises along with chain length to an asymptotic limit at about 30 carbons, suggesting that polymer segments of about 20–40 carbons may participate in translational motion in concert. This segment length is roughly similar to the size of base oil. Polymer flow appears to be controlled largely by the negative entropy of activation for viscous flow, perhaps due to the large molecular size. Similar negative entropies have been noted for small rigid molecules with the possible physical sense that insufficient space is available for translational motion; the exact meaning is obscure.

Polymer thickening of base stock is due to molecular size, which is immensely greater than that of the solvent or base stock in which it is dissolved. The long polymeric strand, the “backbone” of the polymer, is configured in a random coil shape. Coil size, or hydrodynamic volume, is proportional to polymer molecular weight, as a first approximation, but it is more exactly to the cube of the root mean square end-to-end distance of the polymer [13]. From a simplistic microscopic viewpoint, smaller, less viscous solvent molecules do not readily flow around or through the viscous, polymer coil [14]. Another viewpoint is that larger molecules more completely fill holes limiting the ability of other molecules or segments to participate in movement. The degree of viscosity increase depends on coil size, thus higher-molecular-weight polymers provide more thickening. The overall viscosity of a polymer-thickened solution is related to VI improver concentration and molecular weight through the following equation [15]:

$$\ln \eta = KM''_i c - k''(M''_i)^2 c^2 + \ln \eta_0 \tag{5.22}$$

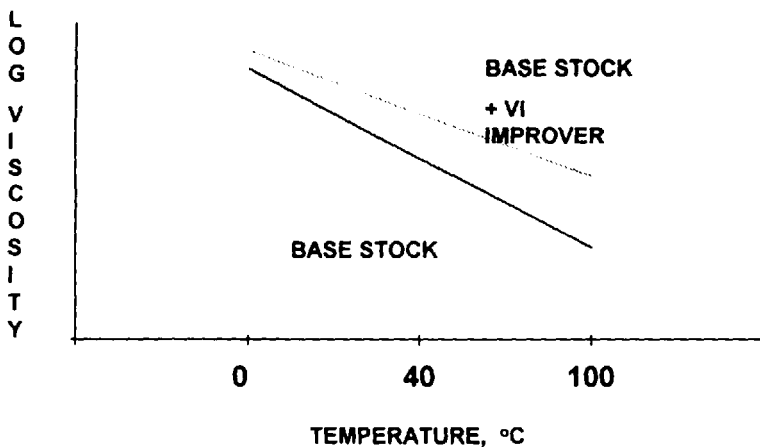


Figure 5.10 Thickening effect of viscosity index improver at high and low temperatures.

where

M_i = VI improver viscosity average molecular weight

c = VI improver concentration

η_0 = solvent viscosity

a = solubility of the specific polymer chemistry, solvent and temperature.

The VI lift shown in Fig. 5.10 seems anomalous because viscosity contribution is normally greater at lower rather than higher temperatures. The VI improver phenomenon is dependent on the chemical nature of the polymer, but those giving higher VI lifts function primarily by coil expansion with increasing temperature [16]. At lower temperatures, polymer solubility is relatively poor, resulting in a contracted, lower-volume coil. As the temperature increases, the solubility improves and, with better solvation, coils expand to a maximum size and donate greater viscosity. The process of coil expansion is entirely reversible, as coil contraction occurs with decreasing temperature (see Fig. 5.11). Polymer chemistry and molecular-weight effects have significant influence on coil expansion/contraction and, ultimately, VI lift. Polymers with polar chemical compositions (e.g., polymethacrylates and styrene polyester) undergo larger coil expansion/contraction because solubility in hydrocarbon solvents changes with temperature. In contrast, hydrocarbon polymers (e.g., olefin copolymers, polyisobutene, hydrogenated styrene–diene, and polyisoprene) are well solvated by hydrocarbon solvents at all temperatures so as to experience lesser degrees, sometimes none, of coil expansion/contraction [14]. These same chemical factors also relate to the value of the exponent a in Eq. (5.22). For a given chemistry, higher-molecular-weight polymers, being less soluble, impart higher VI lift than chemically equivalent lower-molecular-weight materials.

Commercial VI improvers are available in various chemical compositions and molecular weights ranging from about 20,000 to 800,000 Da. The higher-molecular-weight materials are the most efficient thickeners and provide the greatest VI lift but are also the most susceptible to shearing effects (see Section 5.3). Selection criteria should focus on the impact of the application on stability [17] as well as thickening efficiency and VI lift.

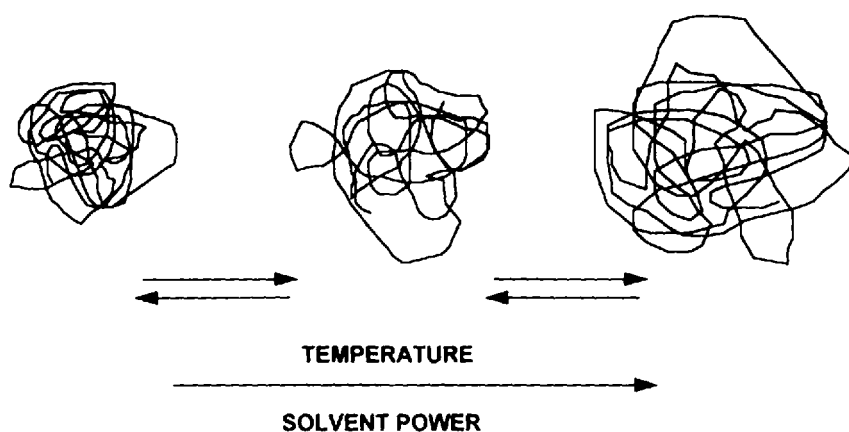


Figure 5.11 VI Improver coil expansion.

5 NON-NEWTONIAN BEHAVIOR

Under certain conditions, some liquids may not always obey Newton's viscosity law. "Non-Newtonian" behavior occurs when the viscosity changes depending on the value of shear stress or shear rate. Because viscosity may vary, it is often referred to as the apparent viscosity. There are several non-Newtonian behaviors, but lubricants generally fall into only two classes: Bingham fluids and pseudoplastic or shear-thinning fluids.

5.1 Bingham Fluids

Bingham fluids do not flow at low values of shear stress (force). They require the application of sufficient shear stress before flow is initiated; however, once flow begins, the liquid generally conforms to Newton's viscosity law if Eq. (5.1) is modified to include the yield stress (shear stress necessary to initiate flow):

$$(\text{Shear stress} - \text{Yield stress}) = \eta(\text{Shear rate}) \quad (5.23)$$

This behavior is represented in Fig. 5.12 when an adequate shearing force initiates fluid flow [18]. Bingham fluids contain a structure extending throughout the material that prevents flow at low values of shear stress because there is insufficient force to perturb the structure. Application of enough shear stress, relaxes or, in some cases, shatters, the structure so as to permit flow. For the case of a shattered structure, smaller elements may persist beyond the yield stress value, and increasing the shear stress may cause further destruction until only the smallest elements persist. The apparent viscosity decreases until stability is achieved at a shear stress, referred to as the upper Newtonian, high enough to complete the disintegration of the structure (Fig. 5.13).

5.2 Low-Temperature Rheology of Lubricants

Some hydraulic fluids act as Bingham fluids at cold temperatures. This behavior is most often associated with fluids based on paraffinic mineral oils containing small

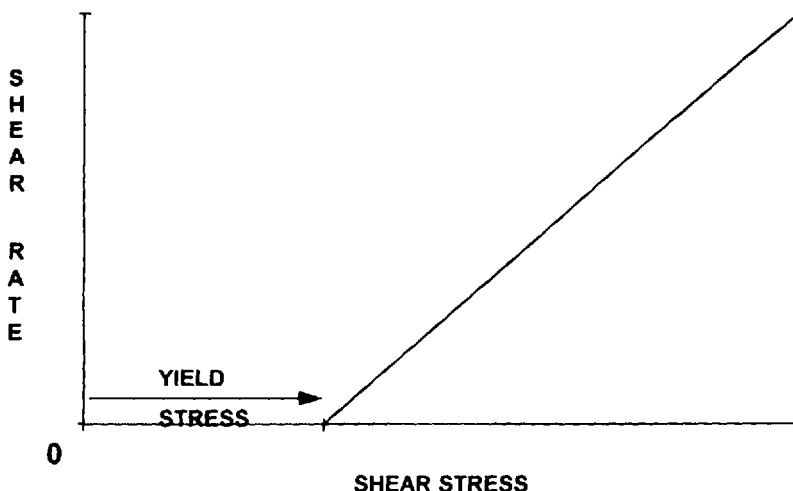


Figure 5.12 Bingham fluids: yield stress necessary to initiate flow.

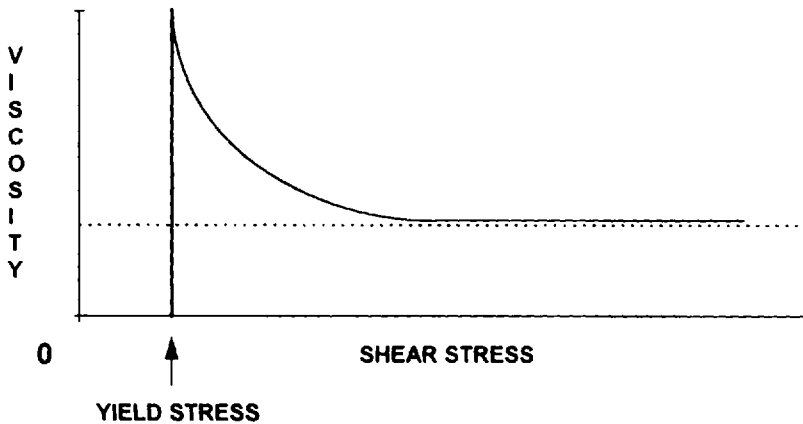


Figure 5.13 Bingham fluids: apparent viscosity and upper Newtonian region.

concentrations of naturally occurring waxes. At sufficiently low temperatures, these waxes begin to form crystals. The temperature at which an oil becomes visually hazy is known as the cloud point and is determined by ASTM D 2500 (Cloud Point of Petroleum Products). The crystallization process continues as wax solidifies in relatively flat plates that can eventually interlock with each other to form a three-dimensional network. The resulting wax matrix traps the remaining liquid and prevents flow even though the trapped liquid is still a vast preponderance of the total mass. This phenomenon is sometimes referred to as gelation of the oil. Two analogies come to mind: the entrapment of honey within a honeycomb and the entrapment of water in a sponge. In both cases, the liquid portion can be quite voluminous but cannot readily flow because of occlusion within the three-dimensional structure of the system.

Sufficient application of force, often simple shaking or stirring, can destroy the relatively weak wax structure, and flow is again possible. In hydraulic system reservoirs (and with other types of lubricants residing in static sumps) at cold ambient temperatures, there may not be sufficient force or suction to destroy wax structures and, in these cases, pump starvation can occur. Wax-impeded flow can severely restrict the low-temperature operating window of paraffinic oils and is of obvious concern for hydraulic fluids used during cold conditions.

Paraffinic oils are desirable lubricants because of good VI and oxidative stability properties, but they are susceptible to wax gelation. Gel problems can be alleviated by a small concentration of an additive type, known as "pour point depressant," which can dramatically delay the onset of gelation. These additives, usually low-molecular-weight polymers, contain linear hydrocarbon segments that are waxlike and function by cocrystallizing with waxy paraffins in oil. The additive's attachment to the wax crystal edge and large size hinder further growth in the plane. Additional growth is redirected, leading to crystal sizes and shapes other than the usual plates. Wax matrix formation is delayed and fluidity can be maintained. Gelation, or pour point, temperature can be improved substantially with proper treatment; a change from -12°C for untreated oil to -40°C for a well-treated oil is not

uncommon. However, the degree of improvement is highly dependent on the specific oil and its interaction with additive chemistry and additive concentration.

As previously discussed, wax crystallization phenomena restrict the usefulness of kinematic viscosity measurements and viscosity index applications below the cloud point. A more meaningful test to describe wax-impeded flow is ASTM D 97 (Pour Point of Petroleum Products). The measurement is made by placing a sample in a glass cylinder and cooling rapidly at a rate of approximately $0.6^{\circ}\text{C}/\text{min}$. Visual observations of flow are made at 3°C intervals after rotating the cylinder 90° . When perceptible flow can no longer be observed, this temperature plus 3°C gives the "pour point," the lowest observed temperature at which flow still occurred. The procedure, by virtue of a relatively large-diameter container and manual rotation, is accomplished at low shear rate ($\sim 10^{-1} \text{ sec}^{-1}$), which is important so as to not destroy wax structures which are the focus of the test. The ASTM Pour Point is a quick, convenient test well suited for screening wax gelation properties, but it has limited utility.

The ASTM Pour Point alone is inadequate to understand the cold-temperature rheology of a lubricant. There are two major limitations of the pour point test: its rapid cooling rate and its qualitative nature. Cooling rates can have great influence on wax crystallization and the resulting structure and strength of a gel matrix. ASTM D 97 employs a fairly rapid cooling rate that may not allow sufficient time for ultimate crystal growth and strength. For instance, vegetable oils used in environmentally acceptable hydraulic fluids often have acceptable ASTM pour points but can solidify at temperatures warmer than the "pour point temperature" upon extended storage time. Nor does the qualitative nature of ASTM D 97 provide a knowledge of fluid viscosity; it is only a determination of the temperature at which flow ceases. Even if wax is absent or under complete control, viscosity is still increasing significantly with decreasing temperature. Any liquid will eventually become so viscous that it can cause sluggish equipment operation or fail to be pumped because viscosity exceeds the pump's upper viscosity limit.

Because the pour point does not provide a high level of information, an additional rheological evaluation is often obtained to better predict a fluid's low-temperature operating window. The usual test for a hydraulic fluid is ASTM D 2983 (Low-Temperature Viscosity of Automotive Fluid Lubricants Measured by Brookfield Viscometer) usually referred to simply as "Brookfield viscosity." The procedure requires that a sample be placed in a glass tube and then shock-cooled by immersion in a cold air bath where it remains for 16–18 h at the desired test temperature. Still held at test temperature, a measurement is made with a Brookfield viscometer, which rotates a spindle at a low shear rate in the test fluid. The torque required to turn the spindle at constant angular velocity is measured and used to calculate viscosity. Low-shear-rate operation is important in order to measure any wax-gel-contributed viscosity. In fact, the procedure can be adapted to measure the yield stress in Eq. (5.18).

Because different cooling rates can exert a profound influence on low-temperature rheology, numerous other tests have been devised in order to predict lubricant viscosity and, ultimately, pumpability properties. These include Federal Standard 791b, Method 203 (Cycle C Stable Pour Point), ASTM D 2532 (Viscosity and Viscosity Change After Standing at Low Temperature of Aircraft Turbine Lubricants), ASTM D 3829 (Predicting the Borderline Pumping Temperature of Engine Oil), ASTM D 4684 (Determination of Yield Stress and Apparent Viscosity of Engine Oils at Low Temperature), ASTM D 5133 (Low Temperature, Low Shear Rate,

Viscosity/Temperature Dependence of Lubricating Oils Using a Temperature-Scanning Technique); Federal Standard 791, Method 3456 (Channel Point), JDQ73 Cold Soak, and JDQ74 Slow Cool. These low-temperature tests differ by cooling rate and/or techniques of measurement, but all are conducted at low shear rates to evaluate the potential influence of wax structure as it relates to viscosity. Individual tests are often cited in pertinent lubricant specifications.

Cold-temperature operation is of great importance for hydraulic fluids used out-of-doors. Knowledge of fluid low-temperature viscosity and equipment manufacturer's recommendation of maximum viscosity are important criteria for proper selection of a hydraulic fluid.

5.3 Pseudoplastic (Shear-Thinning) Fluids

Shear thinning is a non-Newtonian behavior usually associated with polymer-thickened liquids. At high shear rates, these fluids have lower viscosity than would be predicted from measurements conducted at low shear rate. When the shear rate rises above a critical level (Fig. 5.14), the apparent viscosity decreases and continues to do so with further increases of shear rate until a stable viscosity is again achieved [18]. The shear rate at which shear thinning of polymers begins varies with temperature, but this discussion will be limited to high temperature effects at $>40^{\circ}\text{C}$. Depending on equipment severity and polymer molecular weight, multigrade lubricants containing VI improvers can undergo shear thinning and experience both a temporary and a permanent loss of viscosity.

5.4 Polymer Viscosity-Loss Phenomena

5.4.1 Temporary Viscosity Loss

Individual polymer molecules of a VI improver are quite large but are not rigid. At a sufficiently high shear rates, typically 10^4 s^{-1} , a randomly coiled polymer molecule can distort and orient along the axis of flow. The polymer shape changes from a spherical coil to an elongated configuration which occupies a smaller hydrodynamic volume and, thus, contributes less viscosity. With further increases of shear rate,

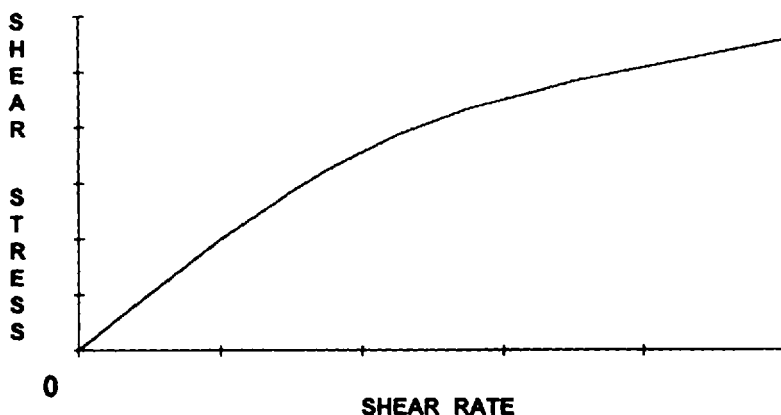


Figure 5.14 Shear-thinning behavior of a non-Newtonian fluid.

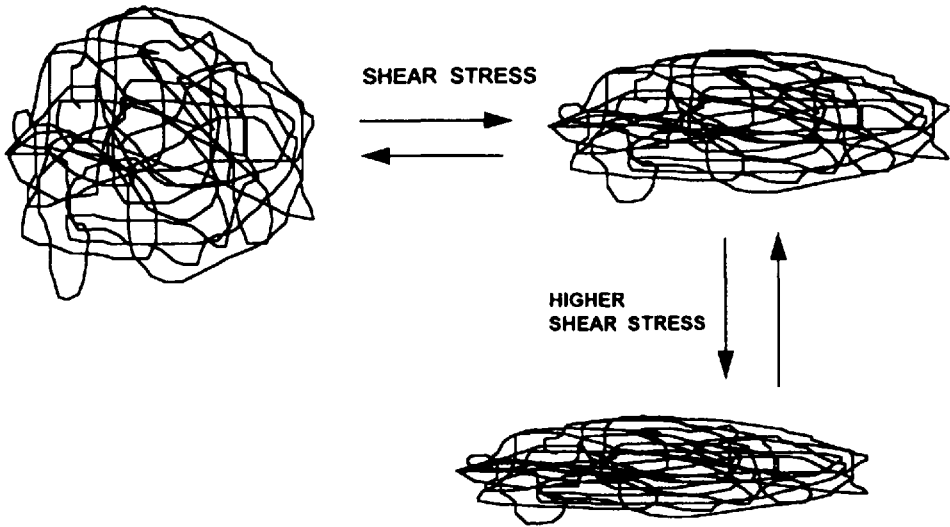


Figure 5.15 Schematic of polymer distortion under high shear stress.

molecules increasingly deform, leading to a corresponding greater loss of viscosity contribution. Eventually, maximum polymer distortion and loss of viscosity are reached at the second Newtonian region, and the viscosity becomes stable (Fig. 5.15). Shear thinning of lubricants is often referred to as “temporary loss of viscosity,” as the process is reversible upon removal of the high shear rate, unless, as discussed below, the shear stress is great enough to rupture polymer molecules. When the high shear stress is removed, distorted polymer molecules resume spherical, random coil shapes, reoccupy original hydrodynamic volumes, and, again, provide the original viscosity contribution as sketched in Fig. 5.16. The low-shear-rate, stable-viscosity

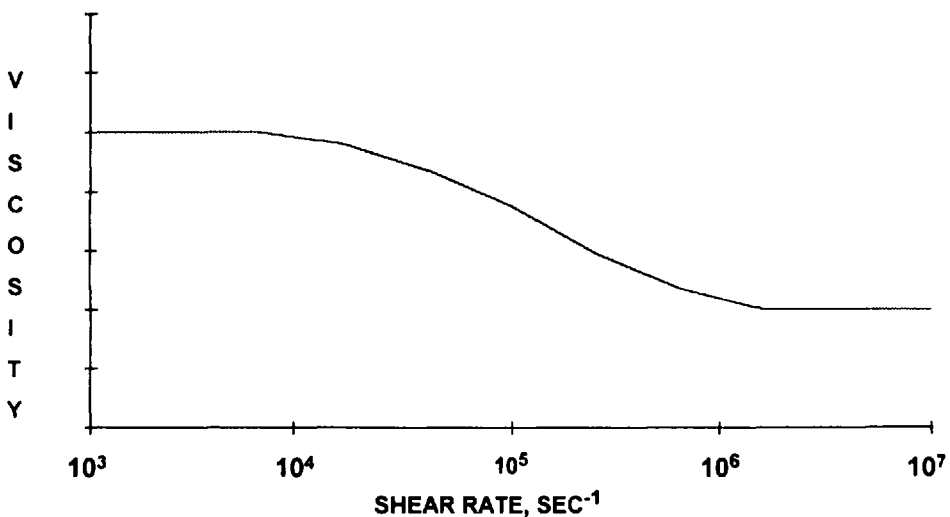


Figure 5.16 Shear thinning of apparent viscosity.

region of this graph is often referred to as the "First Newtonian," whereas the higher-shear-rate, stable-viscosity region is known as the "Second Newtonian," because viscosity in both regions obey Newton's law.

Shear thinning can occur in hydraulic system pumps and across pressure relief valves where shear rates can be on the order of 10^6 s^{-1} [19] and produce viscosities for multigrade fluids that are lower than predicted by low-shear-rate kinematic viscosity. Similarly, in engines, shear rates are on the order of 10^5 – 10^6 s^{-1} in main bearings and at the piston ring cylinder interface and at 10^6 – 10^7 s^{-1} in cams and followers. Because the effective, or "in-service," viscosity of multigrade fluids is lowered in these high-shear-rate regions, film thickness is also reduced. Thus, it is necessary to consider high-shear-rate viscosity as an important factor in lubrication or hydraulic systems.

The degree of temporary viscosity loss depends on both the level of shear stress and the molecular weight of the polymer. Higher-pressure hydraulic systems generate higher shear stresses so as to cause greater temporary viscosity losses in a given polymer-thickened fluid. Low-molecular-weight polymers, because of their small coil sizes, are less susceptible to elongation and, thus, to temporary viscosity losses. Depending on system severity, a polymer of a low enough molecular weight may experience relatively little shear thinning. Overall, severe operating conditions can be counterbalanced by multigraded fluids formulated with low-molecular-weight VI improvers.

Equipment shear stress must be sufficiently high to cause shear thinning of polymer-thickened oils. So too must laboratory techniques intended to measure shear thinning be energetic enough to cause the phenomenon. A variety of high-shear-rate rotational and high-pressure capillary techniques, usually operated at 10^6 s^{-1} , are available: ASTM D 4624 (Measuring Apparent Viscosity by Capillary Viscometer at High Temperature and High-Shear Rates), ASTM D 4683 (Measuring Viscosity at High Shear Rate and High Temperature by Tapered Bearing Simulator), and ASTM D 5481 (Measuring Apparent Viscosity at High Temperature and High Shear Rate by Multicell Capillary Viscometer). Some care must be taken when comparing results from different procedures because capillary viscometers give a marginally higher result compared to those from rotational devices [20]. The above methods are frequently used to evaluate and specify engine oils such as those described in Table 5.3, in which low-shear-rate kinematic and high-shear-rate viscosities are compared for VI improvers of different chemistries and molecular weights (or different shear stabilities). Although hydraulic fluid pumping efficiency has been related to high-shear-rate viscosity [17,21], other evaluation techniques are normally used. A more typical practice is to induce a permanent loss of viscosity by mechanical degradation and then measure kinematic viscosity.

5.4.2 Permanent Viscosity Loss

Very high-shear stresses, perhaps coupled with turbulent flow, can lead to extreme polymer coil distortion and concentrate enough vibrational energy to cause polymer rupture. Cavitation may also play a role by producing intense velocity gradients [22]. Polymer rupture occurs through cleavage of a carbon-carbon bond statistically near the middle of the polymer chain leading to two molecules each having approximately half of the molecular weight of the original molecule. Figure 5.17 represents molecular elongation and rupture concepts. The total hydrodynamic volume of the two

Table 5.3 High-Shear-Rate Viscosities

Fresh fluid	Kinematic viscosity (cSt)		High-shear-rate viscosity (cP) 150°C
	100°C	150°C	
A (base oil plus additive package)			
A plus VII 1 ^a	10.5	4.81	2.99
A plus VII 2 ^a	10.5	4.43	2.99
A plus VII 3 ^a	10.5	3.72	2.58
A plus VII 4 ^b	10.5	4.78	3.19
A plus VII 5 ^b	10.5	4.47	3.06
A plus VII 6 ^b	10.5	4.08	2.96

^aDifferent VI improver chemistries but of equivalent permanent shear stability (i.e., ASTM D 3945A SSI = 45).

^bDifferent VI improver chemistries but of equivalent permanent shear stability (i.e., ASTM D 3945A SSI = 25).

smaller molecules is less than that of the single starting molecule, resulting in a lower-viscosity contribution. Because bond scission is not reversible, the viscosity loss is permanent. The process is usually referred to as mechanical degradation of polymers.

Higher-molecular-weight polymers are more susceptible to distortion and mechanical degradation. Conversely, polymers of sufficiently low molecular weight may not undergo permanent shearing at all, depending on the severity of the application. Sheared polymer molecules are, of course, lower molecular weight than before shearing and, depending on the shear stress of the application, may not be susceptible to further degradation. Thus, the shearing process is self-limiting and viscosity becomes

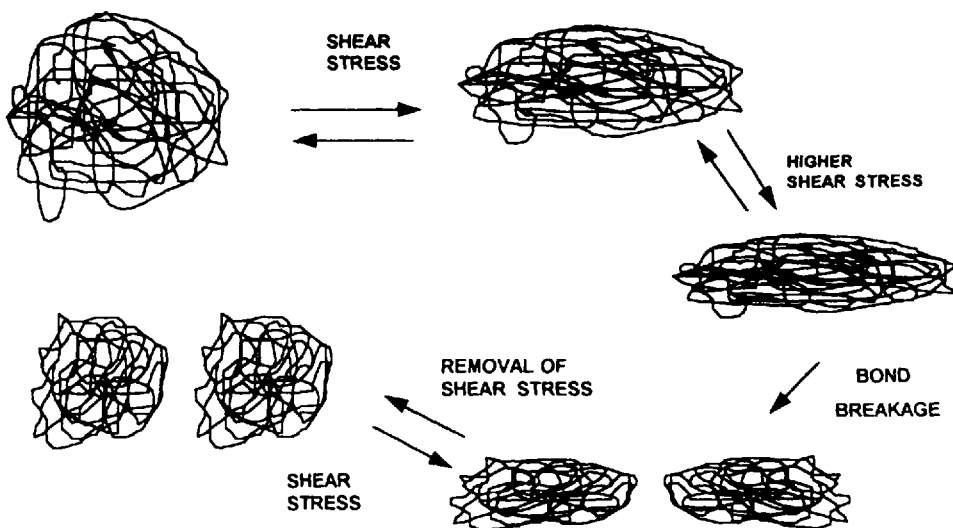


Figure 5.17 Schematic representation of polymer temporary and permanent shear thinning.

stable, as displayed in Fig. 5.18. It is also important to note that a VI improver characteristically contains a wide array of different molecular-weight species which have a Gaussian distribution around an average value. Therefore, not all of the molecules are as susceptible to shearing, and if the average molecular weight is appropriate for the application severity, only a minor portion are sheared. The degree of permanent viscosity loss, just as with temporary loss, is a function of equipment severity and polymer molecular weight.

Viscosity loss after mechanical degradation can be expressed mathematically as

$$\% \text{ Overall viscosity loss} = \left(\frac{\eta_i - \eta_s}{\eta_i} \right) \times 100 \quad (5.24)$$

where η_i is the viscosity before shear and η_s is the viscosity after shear. If the base-stock viscosity is known, a more meaningful calculation can provide a means to rank the shear stability of various VI improvers:

$$SSI = \left(\frac{\eta_i - \eta_s}{\eta_i - \eta_0} \right) \times 100 \quad (5.25)$$

where SSI is the shear stability index and η_0 is the viscosity of the base stock and other additives; the remaining terms are the same as in Eq. (5.19). The SSI is useful for VI improver ranking because it is an expression of viscosity lost due to polymer shearing relative to initial viscosity contributed by polymer. Caution must be used when comparing $SSIs$, as different test procedures can produce widely divergent shearing severity and results.

Various devices with sufficient energy to shear polymers—pumps, engines, ball mills, ultrasonic oscillators, high-speed stirring, gear sets, fuel injectors, and roller bearings—have been used to study mechanical degradation of polymer-thickened fluids in the laboratory. Although there is no standard, most hydraulic fluid shear stability work focuses on three procedures. ASTM D 2882 (Indicating the Wear Characteristics of Petroleum and Non-Petroleum Hydraulic Fluids in a Constant Vol-

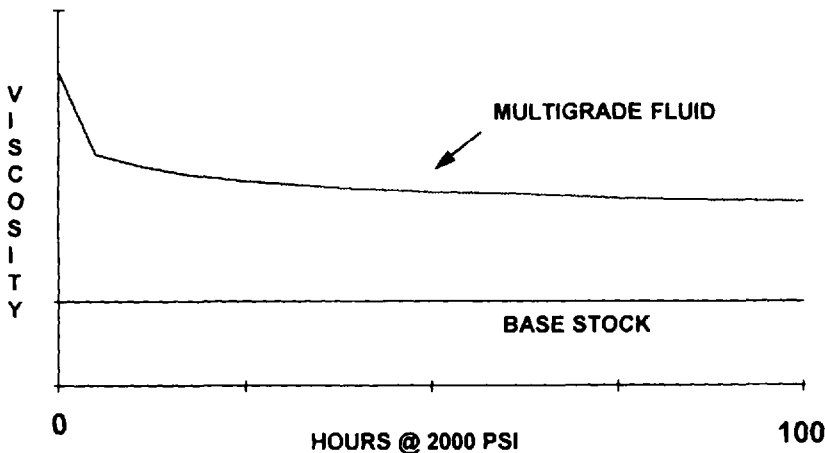


Figure 5.18 Permanent viscosity loss with time.

ume Vane Pump) was primarily used to measure wear performance but has often been used to evaluate shear stability. Equipment problems have forced recent workers to modify the test by substituting a more durable pump for the 100-h 13,800-kPa (2000-psi) operation. ASTM D 5621 (Sonic Shear Stability of Hydraulic Fluid) utilizes an ultrasonic oscillator that irradiates a small sample for 40 min. A similar test has long been used to specify military aircraft hydraulic fluids per MIL-H-5606. ASTM D 3945 (Shear Stability of Polymer-Containing Fluids Using a Diesel Injector Nozzle) uses a double-plunger European injector. The test was originally designed to evaluate engine oils and the procedure requires 30 passes of test fluid through the equipment; hydraulic fluids are often exposed to 250 passes because the VI improvers used in multigrade hydraulic fluids tend to be more shear stable than those used in engine oils. ASTM D 5275 utilizes Fuel Injector Shear Stability Test (FISST) equipment, where the injector is a single-plunger type and requires 20 passes through the injector. Despite the similarities of ASTM D 3945 and ASTM D 5275, results obtained on a given fluid in each procedure may differ. CEC L-45-T-93 Method C, a 20 hour test, is based on tapered roller bearing equipment and provides very high shearing. Severity of these methods can be ranked as TBR > pump > ultrasonic oscillator >> fuel injectors, but there is a reasonable degree of correlation among all three [21]. Care must be taken in interpreting results from the nonpump tests, as not only severity levels can differ but results can be biased relative to the chemistry of the polymeric VI improver. For instance, polymethacrylates are more severely sheared in the ultrasonic device than other VI improver chemistries.

5.4.3 Permanent and Temporary Viscosity-Loss Effects

Returning to the concept of shear thinning or molecular elongation, polymer-thickened fluids that have undergone permanent loss of viscosity can still undergo shear-thinning effects, albeit to a far lesser extent than an unsheared fluid. A schematic of this molecular concept is also present in Fig. 5.17. Permanently sheared, smaller molecules are less susceptible to elongation so that shear-thinning effects are far less pronounced. The high-shear-rate viscosity of a fluid mechanically degraded in a severe application is only marginally lower than its low-shear-rate viscosity as represented in Fig. 5.19 and is apparent from the data in Table 5.4 [19]. Thus, kinematic viscosity of appropriately degraded hydraulic fluids could be considered sufficient to evaluate in-service viscosity and has been shown to correlate well with vane pump flow rates [21].

6 VISCOSITY CONTROL AND IMPACT

In order to achieve the proper viscosity for a lubricant or hydraulic fluid, it is necessary to carefully select the base fluids and additives. The formulated oil must meet all important viscosity criteria whether at high or low temperature or at high or low shear rate.

6.1 Control

A hydraulic fluid is formulated to a desired viscosity by choice of base stock(s) and, if used, by VI improver and pour point depressant. To a first approximation, other additives do not contribute significantly to viscosity. The simplest case to formulate

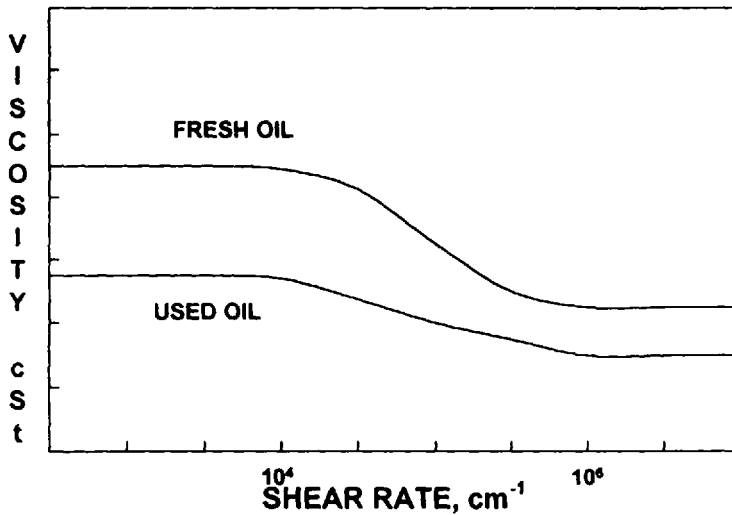


Figure 5.19 Combined permanent and temporary viscosity loss.

a fluid is to select a base stock meeting the requirements of the lubricant specification. However, if a base stock meeting the required viscosity is commercially available, one can mix a lower-viscosity base fluid with a higher-viscosity fluid in the proper ratio to achieve the target viscosity.

To prepare polymer-thickened multigrade fluids, a VI improver is added in sufficient quantity to thicken a low-viscosity liquid to the desired viscosity target. Temporary and/or permanent viscosity losses introduced by VI improvers can be accommodated by allowing for shearing effects and by choice of VI improver with suitable SSI. One may formulate a multigrade fluid to an initial viscosity such that sheared fluid will retain sufficient viscosity for the intended severity of application. The initial viscosity target is dictated in large part by the shear stability of the VI improver.

Table 5.4 Viscosities of Fluids at Pump Running Temperature

Fluid	Viscosity, 65.6°C (150°F)			
	Kinematic (cSt)		High-shear-rate at 10^6 s^{-1} (cP)	
	Fresh	100 h ^a	Fresh	100 H ^a
HSO-01	19.9	17.9	15.9	14.4
HSO-02	16.9	13.3	12.5	11.3
HSO-03	13.6	10.1	9.8	9.0
HSO-04	16.4	9.1	9.0	7.9
HSO-05	27.3	17.8	15.6	14.6
HSO-06	27.4	15.9	13.5	13.2

^aAfter 100 h in a 2000-psi vane pump circuit.

If paraffinic base oils are involved in the formulation, particularly lubricants intended for use at ambient temperatures, a pour point depressant is usually added to protect against wax gelation.

6.2 Impact

Hydrodynamic lubrication and power transmission principles have been more thoroughly discussed in previous chapters, but a very brief review may help to summarize the relationship to viscosity.

Hydrodynamic lubrication is defined as maintenance of a fluid film of sufficient thickness to prevent contact of two surfaces in relative motion to each other (e.g., the mating surfaces in a hydraulic system pump). At constant speed and load, film thickness depends on the presence of a fluid having minimum viscosity needed to maintain film strength. The shear stress–shear rate relationship of viscosity explains fluid resistance to leakage out of the zone between the two surfaces and a force to maintain separation. On the other hand, excessive viscosity is undesirable because energy must be expended to overcome the internal friction of the lubricant. During hydrodynamic lubrication, the coefficient of friction, f , depends on

$$f = \frac{k\eta V}{W} \quad (5.26)$$

where η is the dynamic viscosity, W is the load, and V is the sliding velocity. At constant load and velocity, increased friction results from higher than necessary viscosity. Selection of lubricant viscosity is a compromise between providing sufficient film strength at equipment operating conditions and temperature and minimizing friction from the lubricant.

At cold ambient temperatures, consideration must be given to low-temperature viscosity. A fluid should not be so viscous as to cause pump starvation, nor should it be prone to wax gelation at temperatures within the normal-operating-temperature window. Most pumps have maximum viscosity limits for start-up.

Hydraulic fluids are also power transmission fluids. Optimum system response occurs with low fluid viscosity, but some higher level of viscosity is required to seal or minimize internal leakage. A fluid of insufficient viscosity will suffer losses in pumping volume and efficiency because of leakage from the high-pressure side to the low-pressure side of pumps and valves.

Selection of hydraulic fluid viscosity is a careful balance of lubrication and power transmission requirements related to the specifics of the equipment, particularly the pump, and to the temperature range of use. OEMs provide viscosity recommendations for their equipment, often suggesting a maximum at start-up to avoid cavitation in the pump and a minimum at operating conditions to maintain lubrication and avoid high internal leakage.

7 VISCOSITY CLASSIFICATION

Lubricant applications can differ greatly in viscosity requirements. In order to aid end-user selection and to provide consistency, various viscosity classification systems have been devised. The classifications range from the simple ISO system to the more informative engine oil classification system.

7.1 ISO Viscosity Grades

Hydraulic fluid viscosity is classified according to ASTM D 2422 (Industrial Fluid Lubricants by Viscosity System) commonly referred to as ISO viscosity grades. The ISO system (Table 5.5) classifies fluids solely on kinematic viscosity measured at 40°C. The choice of 40°C as the reference temperature is a compromise between maximum operating and ambient temperatures. However, it is also convenient because it is a reference temperature used for determination of the viscosity index, a commonly reported property of hydraulic fluids. The system is an orderly mathematical construction of 18 ISO viscosity grades, usually written as ISO VG, starting at ISO VG 2 with a minimum viscosity of 1.98 mm²/s up to ISO VG 1500 with a maximum viscosity of 1650 mm²/s. Each grade is named by the whole number which is the rounded, midpoint viscosity of its associated range of viscosity. Each range is $\pm 10\%$ of the midpoint viscosity

The ISO viscosity grades are not continuous. Each ISO VG is approximately 50% more viscous than the next lower grade. These steps between grades coupled with individual grade ranges of only $\pm 10\%$ create a system with viscosity gaps between the grades. As a result, there are clear viscometric differences between grades, ensuring that moving from one grade to another brings with it a significant difference in viscosity. A disadvantage is that a fluid with a viscosity that does not fall into a ISO VG range cannot be formally classified.

The ISO viscosity classification is a simple, readily understood system. It does not imply any consideration of quality or performance other than to identify kinematic viscosity at 40°C. There have been recent attempts to provide a more elaborate

Table 5.5 ASTM D 2422 ISO Viscosity Grades

ISO VG	Kinematic viscosity, 40°C (mm ² /s)		
	Midpoint	Minimum	Maximum
2	2.20	1.98	2.42
3	3.20	2.88	3.52
5	4.60	4.14	5.06
7	6.80	6.12	7.48
10	10.0	9.00	11.0
15	15.0	13.5	16.5
22	22.0	19.8	24.2
32	32.0	28.8	35.2
46	46.0	41.4	50.6
68	68.0	61.2	74.8
100	100	90.0	110
150	150	135	165
220	220	198	242
320	320	288	353
460	460	414	506
680	680	612	748
1000	1000	900	1100
1500	1500	1350	1650

and informative classification system still based on ISO viscosity grades and nomenclature. This will be discussed further after a discussion of some other viscosity classification systems.

7.2 Gear Oil Classification

Industrial gear oils can be classified according to AGMA (American Gear Manufacturers Association) standards 250.04 for enclosed gears and 251.02 for open gears (Table 5.6). The AGMA classifications also rely on kinematic viscosity measured at 40°C, with two exceptions measured at 100°C because of their extremely viscous nature. The AGMA scale is referenced to the ISO VG scale for all grades that can be accommodated. The lowest is AGMA 1, equivalent to ISO VG 46, through AGMA 9, ISO VG 1500, and six more grades up to AGMA 15.

Gear oils used in transportation are classified according to SAE J306 JUL 98 [23], shown in Table 5.7. This system differs significantly from the previous two in that it incorporates two viscosity determinations, one at 100°C, rather than 40°C, and one at a cold temperature. Kinematic viscosity is the method of choice for the 100°C measurement. This higher reference temperature may be a better approximation of the most severe conditions experienced by the lubricant. In addition, the high temperature limit must be met after shear testing by CEC L-45-T-93 Method C (20 h). On the cold end of the scale, Brookfield viscosity is measured at a temperature suitable for the intended service of the lubricant. Viscosity determination under cold conditions is a major feature of SAE J306 JUL 98 in that these lubricants are intended for outdoor use and may experience service during cold conditions.

Table 5.6 AGMA Viscosity Classifications

AGMA Standard 250.04 enclosed gears			AGMA Standard 251.02 open gears			Viscosity (cSt), 40°C	
AGMA number R&O oil	AGMA number EP oils	ISO VG	AGMA number R&O oils	AGMA number EP oils	ISO VG	Min.	Max.
1	—	46	4	4 EP	150	135	165
2	2 EP	68	5	5 EP	220	198	242
3	3 EP	100	6	6 EP	320	288	352
4	4 EP	150	7	7 EP	460	414	506
5	5 EP	220	8	8 EP	680	612	748
6	6 EP	320	9	9 EP	1,500	1,350	1,650
7 Comp	7 EP	460	10	10 EP	—	2,880	3,520
8 Comp	8 EP	680	11	11 EP	—	4,140	5,060
8A Comp	8A EP	1,000	12	12 EP	—	6,120	7,480
			13	13 EP	—	25,600	38,400
						Viscosity (cSt), 100°C	
			14R	—	—	428.5	857.0
			15R	—	—	857.0	1,714

Table 5.7 Axle and Manual Transmission Lubricant Viscosity Classification SAE J306 JUL 98

SAE Viscosity grade	Maximum temperature for viscosity of 150,000 cP (°C)	Viscosity at 100°C (cSt)	
		Min.	Max.
70W	-55	4.1	—
75W	-40	4.1	—
80W	-26	7.0	—
85W	-12	11.0	—
80	—	7.0	<11.0
85	—	11.0	<13.5
90	—	13.5	<24.0
140	—	24.0	<41.0
250	—	41.0	—

The viscosity grade descriptions of SAE J306 JUL 98 are based on whole number designations, with higher numbers indicating higher viscosities. The lower numbered grades, those including the letter W (for winter), require a cold temperature measurement which varies by grade. The lower the SAE W grade, the lower the temperature of measurement and the better the ability to provide adequate lubrication under cold conditions. For example, a SAE 75W will be less viscous than a SAE 85W gear oil in cold-temperature service. An alternative way to look at this low-temperature classification is that if 150,000 cP is the maximum viscosity for sufficient flow and lubrication, then an SAE 75W oil will continue to provide operability as low as -40°C, whereas a SAE 85W oil will only operate down to -12°C. In practice, a user selects a grade suitable for prevailing conditions.

Other important aspects of SAE J306 JUL 98 are that it allows for a description of multigraded oils and that viscosity grades are continuous. At high temperature, W grades have only minimum requirements, so that an oil meeting the low-temperature requirements of a “W grade” but also meeting the high-temperature requirements of a higher SAE grade can be labeled as meeting both classifications. For instance, a SAE 75W-90 oil has the low-temperature properties of a SAE 75W and the high-temperature properties of a SAE 90. The continuity of viscosity from grade to grade allows any fluid to be classified.

7.3 Engine Oil Classification

Engine oils are classified according to SAE J300 APR 97 (Table 5.8). This classification system shares many of the features of the SAE gear oil classification: continuous viscosity descriptions (no gaps between the grades); W grades; cold-temperature requirements that vary by W grade; high-temperature requirements that approximate actual service conditions; and multigrading. Yet, the engine oil classification is more complex by including viscosity measurements under high shear rates at both cold ambient and hot operating temperatures.

SAE J300 APR 97 requires kinematic viscosity measurement at 100°C as well as a low-temperature measurement by Mini Rotary Viscometer—ASTM D 4684.

Table 5.8 Engine Oil Viscosity Classification SAE J300 APR 97

SAE Viscosity grade	Low-temperature (°C) cranking viscosity (cP), max.	Low-temperature (°C) pumping viscosity (cP), max. with no yield stress	Kinematic viscosity cSt at 100°C		High-temperature, high-shear viscosity (cP), 150°C, 106 s ⁻¹ , min.
			Min.	Max.	
0W	3,250 at -30	60,000 at -40	3.8	—	—
5W	3,500 at -25	60,000 at -35	3.8	—	—
10W	3,500 at -20	60,000 at -30	4.1	—	—
15W	3,500 at -15	60,000 at -25	5.6	—	—
20W	4,500 at -10	60,000 at -20	5.6	—	—
25W	6,000 at -5	60,000 at -15	9.3	—	—
20	—	—	5.6	<9.3	2.6
30	—	—	9.3	<12.5	2.9
40	—	—	12.5	<16.3	2.9
					(0W-40, 5W-40 & 10W-40)
40	—	—	12.5	<16.3	3.7
					(15W-40, 20W-40, 25W-40, 40)
50	—	—	16.3	<21.9	3.7
60	—	—	21.9	<26.1	3.7

The purpose of the low-temperature, low-shear-rate specification is to describe “pumpability,” an oil’s ability to be pumped from the sump under cold ambient conditions. Just as in SAE J306 for gear oils, the lower the numeric value of a “W grade,” the lower the temperature of measurement implying a lower operating window under cold conditions.

In addition to the above, high-shear-rate viscometric limits at both high and low temperatures are specified. These are cranking (ASTM D 5293 Cold Cranking Simulator) and high-shear-rate viscosity at 150°C and 10⁶ s⁻¹ (ASTM D 4863 or ASTM D 4741 or ASTM D 5481). These measurements are included to describe rheological performance under conditions present during low-temperature starting (cranking) and at the high-temperature, high-shear-rate operating conditions that occur in critical lubrication areas of engines such as bearings and piston rings. High-shear-rate measurements are of particular importance for multigraded oils containing VI improvers because under conditions of use, shear thinning can occur.

7.4 Hydraulic Fluid Classification

Returning to hydraulic fluid viscosity classification, ASTM D 6080 (Standard Practice for Defining the Viscosity Characteristics of Hydraulic Fluids) builds upon the current ISO VG classification in order to better describe rheological properties. An enhanced classification standard is needed because many workers view the current system (ISO 3448 and ASTM D 2422) as incomplete because it does not address the following:

- Cold-temperature requirements

- Multigraded (HV) oils
 - Description
 - Viscosity After Shearing
- Viscosity at operating temperature (viscosity index)
- Classification of fluids outside of ISO ranges

ASTM D 6080, a more comprehensive classification, builds on the ISO VG system because of its wide recognition. Retaining the current ISO VG definitions and nomenclature, hydraulic fluids can be labeled with the usual ISO VG information followed by a second tier of information indicating the following: cold-temperature grade; 40°C viscosity after shearing; and viscosity index after shearing. The second classification tier does not require viscosity to fall within the usual ISO ranges. This system is limited to ISO VG 5 through ISO VG 150, as these grades represent the great majority of hydraulic fluids. The classification system is voluntary, so a producer might label an ISO VG 32 fluid as

ISO 32
L22-32 (150)

where L22 is the low-temperature grade, 32 is the 40°C viscosity after shear, 150 is the viscosity index after shear.

The cold-temperature grade is an appropriate ISO number preceded by “L” (for low temperature) with measurement by a Brookfield viscometer (ASTM D 2983) and a limit of 750 cP maximum. This limit was chosen because it represents a relatively severe case for allowable viscosity at pump startup. Each ISO VG has an associated cold-temperature range based on extrapolation of current 40°C viscosity ranges, using 100 VI, down to the 750-cP limit. For instance, an ISO L22 has a temperature range of -15°C to -22.9°C ; additional grade descriptions can be found in Table 5.9.

Any fluid could be labeled with both low- and high-temperature grades, but the practice presents the possibility of clearly identifying multigraded oils. Oils containing VI improvers would be classified by 40°C kinematic viscosity after sonic shear (ASTM D 5621) for 40 min. Previous work has indicated good correlation of

Table 5.9 Hydraulic Fluid
Low-Temperature Grades

ISO VG	°C for Brookfield viscosity of 750 cP, max.
L10	-33 to -41.9
L15	-23 to -32.9
L22	-15 to -22.9
L32	-8 to -14.9
L46	-2 to -7.9
L68	4 to -1.9
L100	10 to 3.9
L150	16 to 9.9

this sonic shear procedure with mechanical shearing of multigraded oils in pump service [19].

A third classification element, viscosity index, is added in order to provide a basis for better understanding the viscosity of a fluid at operating temperatures encountered in equipment. A knowledge of viscosity index coupled with a 40°C viscosity can be used to calculate viscosity at any temperature from 40°C to 100°C. For oils containing VI improvers, the viscosity index would be reported after exposure to the sonic shear procedure described above.

The most controversial part of the proposal is that the 40°C viscosity reported in the second tier need not match a current ISO VG range. The main objection to this is the possibility that a multigrade oil could shear down to a viscosity outside of the original ISO VG. In response to this criticism, it has been argued that the sheared viscosity is actually reported, which would allow end users to discriminate among multigrade oils with the same nominal ISO VG. A positive aspect of reporting actual viscosity is that fluids that do not now fit into the current ISO ranges would have a basis for classification. For example, some vegetable oils cannot be classified in the current system; rapeseed (canola) oil has a typical viscosity of 38 mm²/s, which falls in the gap between ISO VG 32 and 46 and, thus, cannot be formally classified.

A similar classification system is being studied by the CEC for Europe. However, shear stability and low temperature test methodology may be different than ASTM D 6080.

REFERENCES

1. *Annual Book of ASTM Standards 1998, Vol. 5.01*, 1998, American Society for Testing and Materials, Philadelphia, PA, pp. 144–149.
2. N. McCoull and C. Walther, "Viscosity Temperature Chart," *Lubrication*, 1921, June.
3. E. W. Dean and G. H. B. Davis, "Viscosity Variations of Oils with Temperature," *Chem. Metall. Eng.*, 1929, 36, pp. 618–619.
4. C. Barus, "Isothermals, Ispiestics and Isometrics Relative to Viscosity," *Am. J. Sci.*, 1893, 45, pp. 87–99.
5. W. O. Winer, "The Mechanical Properties of Fluids in High Pressure Hydraulic Systems," In *National Conference on Fluid Power*, 1974, pp. 412–421.
6. C. Roelands, J. Vluger, and H. Waterman, "Correlational Aspects of the Viscosity–Temperature–Pressure Relationship of Lubricating Oils and in Correlation with Chemical Constitution," *Trans. ASME., J. Basic Eng.*, 1963, 11, pp. 601–619.
7. B. Y. C. So and E. E. Klaus, "Viscosity–Pressure Correlation of Liquids," *ASLE Trans.*, 1980, 23, pp. 409–421.
8. S. Yasutomi, S. Bair, and W. O. Winer, "An Application of a Free Volume Model to Lubricant Rheology I—Dependence of Viscosity on Temperature and Pressure," *J. Tribol.*, 1984, 106, pp. 291–303.
9. H. Eyring, *J. Chem. Phys.* 1936, 4, p. 283.
10. R. H. Powell and H. Eyring, *J. Chem. Phys.*, 1937, 5, p. 729.
11. R. C. Weast (ed.), *CRC Handbook of Chemistry and Physics*, 50th ed., 1969, Chemical Rubber Co., Cleveland, OH, pp. F37–F42.
12. A. Bondi, "Viscosity and Molecular Structure," in *Rheology Theory and Applications, Vol 4* (F. R. Eirich, ed.), 1967, Academic Press, New York, pp. 1–82.
13. F. W. Billmeyer, *Textbook of Polymer Science*, 1971, Wiley–Interscience, New York, p. 28.

14. A. Bondi, "Rheology of Lubrication and Lubricants," in *Rheology Theory and Applications, Vol 3* (F. R. Eirich, ed.), 1960, Academic Press, New York, pp. 444–478.
15. R. L. Stambaugh, "Viscosity Index Improvers and Thickeners," in *Chemistry and Technology of Lubricants* (R. M. Mortimer and S. T. Orszulik, ed.), 1992, Blackie Academic & Professional, London, pp. 124–159.
16. T. W. Selby, "The Non-Newtonian Characteristics of Lubricating Oils," *Trans. ASLE*, 1958, 1, pp. 68–81.
17. R. J. Kopko and R. L. Stambaugh, "Effect of VI improver on the In-Service Viscosity of Hydraulic Fluids," 1975, SAE Paper 750683.
18. R. S. Brodkey, *The Phenomena of Fluid Motions*, 1967, Addison-Wesley, Reading, MA, pp. 365–372.
19. R. L. Stambaugh and R. J. Kopko, "Behavior of Non-Newtonian Lubricants in High Shear Rate Applications," 1973, SAE Paper 730487.
20. F. Girshick, "Non-Newtonian Fluid Dynamics in High Temperature High Shear Capillary Viscosimeters," 1992, SAE Paper 922288.
21. R. L. Stambaugh, R. J. Kopko, and T. F. Roland, "Hydraulic Pump Performance—a Basis for Fluid Viscosity Classification," 1990, SAE Paper 901633.
22. A. Ram, "High-Shear Viscometry," in *Rheology Theory and Applications, Vol 4* (F. R. Eirich, ed.), 1967, Academic Press, New York, pp. 281–283.
23. *SAE Handbook 1999, Vol 3*, 1999, Society of Automotive Engineers, Warrendale, PA.

6

Lubrication Fundamentals

LAVERN D. WEDEVEN

Wedeven Associates, Inc., Edgmont, Pennsylvania

KENNETH C LUDEMA

University of Michigan, Ann Arbor, Michigan

1 INTRODUCTION

Hydraulics is associated with the transmission and control of forces and movement by means of a functional fluid. Hydraulic power is derived from a pump and transmitted to terminal elements such as rotary motors or linear cylinders. Although the primary demands on hydraulic fluid are associated with the power transmission, there are many secondary demands, which include corrosion protection, heat dissipation, environmental compatibility, and lubrication.

Advanced hydraulic systems place severe demands on hydraulic fluid. For the most part, lubricating attributes of a hydraulic fluid are not the primary considerations during selection of a hydraulic fluid. Yet, the performance and life of hydraulic components, especially the pump, are critically dependent on the lubricating quality of the fluid. Compared with other mechanical hardware that must be lubricated, hydraulic equipment is unique in that hydraulic fluids cover an enormous range of fluid types. The various fluid types include mineral oils, oil-in-water emulsions, various synthetic fluids, as well as nontypical fluids, which are highly environmentally acceptable. Additives, which have contributed significantly to wear protection, further expand the performance range of hydraulic fluids. Added to the broad scope of fluids is the complex nature of lubrication and wear mechanisms and their interactions with an enormous range of contacting materials in hydraulic equipment. Lubricants, and especially hydraulic fluids, have multidimensional lubricating characteristics. These characteristics are derived from both physical properties and chemical attributes of the fluid. Although physical properties and chemical attributes of fluids can be de-

scribed, their connection to lubrication performance and hydraulic equipment life is elusive.

Understanding and prediction of lubricating performance are the subjects of a field called tribology. Tribology is the science and technology of contacting surfaces in relative motion. Because of the complex nature of tribology within hydraulic systems, component design and fluid selection are accomplished with some degree of risk. Consequently, research and development rely heavily on testing. The use of pump tests for selection and development of hydraulic fluids provides limited reliability. Although bench tests may be more efficient to operate, and perhaps easier to understand, their results can sometimes be even more remote from predicting performance in service than pump tests.

Because of the complex state of affairs with respect to the lubricating characteristics of hydraulic fluids and how they play themselves out in hardware, this chapter presents a new approach by which lubricated contacts can be viewed. The new approach identifies key structural elements that control performance. It focuses on lubrication and failure mechanisms and their connection to various types of lubricated contacts within the hydraulic systems. What is important and, unfortunately, what is generally lacking is an understanding of how these mechanisms play themselves out in service. The approach taken in this chapter supports the concept of systematic tribology. Systematic tribology is the process of understanding and developing the structural elements of a lubricated contact system and its mechanisms of interaction in a systematic way.

Armed with an understanding of the mechanistic processes for lubrication and wear, a rationale can be developed for selection of fluids and their expected performance behavior. In addition, a fundamental understanding of lubrication and failure mechanisms is essential for failure diagnostics and the development of new technologies to enhance performance.

2 LUBRICATED CONTACTS IN HYDRAULIC SYSTEMS

Hydraulic fluids supply the lubricant to an enormous variety of load-bearing contacts constructed from a wide range of materials. Some of the most highly stressed and difficult-to-lubricate surfaces are found in hydraulic pumps, as shown in Figure 6.1. Under the rather harsh conditions of high pump pressure, high temperature, and contamination, the lubricating attributes of the hydraulic fluid must maintain the integrity of the contacting surfaces. Surface integrity is essential for pump life with respect to loss of clearances caused by wear, leakage, component alignment or position, friction, and torque. Because it is desirable to have hydraulic equipment small in size and light in weight, there is generally little margin for lubrication in many of the critical load-bearing contacts.

Some of the critical contacts in a piston pump shown in Figure 6.1 are the sliding contacts between the valve plate and cylinder block, piston and cylinder wall, piston and slipper socket, and slipper and swash plate. The critical areas in the gear pump shown in Figure 6.1 are near the tip and root of the gear teeth where high contact stresses accompany high sliding velocities. Other critical areas are associated with the highly stressed bearings supporting the rotating components. Pump life and durability is intimately associated with each lubricated contact system which consists of hydraulic fluid, materials or surface treatments, and design. The modes of dete-

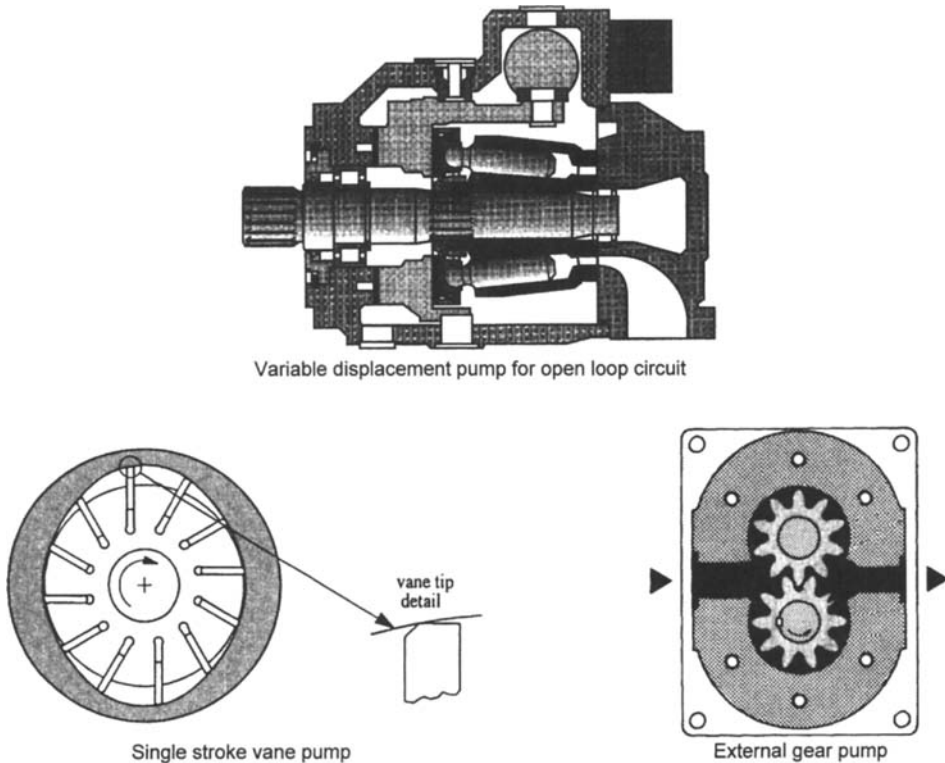


Figure 6.1 Types of hydraulic pumps and critical areas for lubrication.

rioration and failure analysis of these contacts are discussed in Chapter 8. The general mechanical features of the various contact systems are discussed in the next section.

3 BASIC MECHANICAL FEATURES OF LUBRICATED CONTACTS

To understand the tribology of hydraulic fluid-wetted parts, it is helpful to identify the types of contacts, their associated stress fields, and kinematics.

3.1 Types of Contacts

The geometry of contacting bodies creates the character of the contact with respect to stress and the mechanisms of lubrication. Conformal contacts, where contacting bodies conform to one another, distribute the load over relatively large areas. Conformal contacts, like piston or cylinder contacts, have clearance spaces that must be preserved. Concentrated contacts are nonconformal. They concentrate the load over small areas. The gear mesh in the gear pump of Figure 6.1 and the rolling element/raceway contacts in bearings are examples of concentrated contacts.

It is helpful to grasp the perspective of tribological contacts for their scale. The lubricated length of a conformal contact is generally less than a centimeter (10^{-2} m). The lubricated length of a concentrated contact is generally less than a millimeter

(10^{-3} m). These load-bearing areas are on a “macroscale” where they can be viewed with the unaided eye.

Within the world of macroscale contacts are “microscale” features which control tribology behavior. Surface roughness features (asperities) and the grain size of metals are on the order of microns (10^{-6} m). These microscopic features are critically linked to yet a lower scale of things that control lubrication and failure phenomena. Adsorbed films of molecular size that prevent adhesion between surfaces are on the order of nanometers (10^{-9} m). Here lies a fundamental difficulty within the tribology of hydraulic system hardware. Lubrication and failure mechanisms are controlled by microscale phenomena, but the parameters that control loads and motions of hydraulic system contacts are on the macroscale engineering level. To connect lubrication and failure mechanisms, which take place on a microscale, surface stresses and kinematics on the engineering level should be considered as input to a tribological contact system.

3.2 Kinematics and Dynamics of Lubricated Contacts

The relative motion of surfaces in contact invokes lubrication mechanisms as well as failure mechanisms. Kinematics is a description of these motions without reference to forces or mass, which cause these motions. The hydraulic pump hardware in Figure 6.1 encounters linear sliding, rotational sliding, reciprocating sliding, rolling with sliding, and near-pure rolling motions. Some of these motions are mechanically controlled and easily calculated, like the gear mesh in the gear pump. Other motions are indeterminate, like the rotational motions of the piston or slipper in the piston pump. These motions are controlled by friction forces acting on each body.

Dynamics treats the actions of forces on bodies in motion or at rest. Pressure forces and the rotating mass of pump components create dynamic forces that must be restrained by the contacting bodies. The durability of these contacts relies on other dynamic forces. However, these forces are generated between surfaces in contact. These forces are created by hydrodynamic or elastohydrodynamic (EHD) pressures generated by the kinematics of the contacts themselves. Since the kinematics of contacts is controlled by hardware operation, duty cycle in terms of motions and loads becomes an important consideration in tribological design and operating life.

3.3 Stress Fields

The dynamics of a tribological contact are composed of two major stress fields, illustrated in Figure 6.2. The load applied is distributed across the contact area as a normal stress. The strain within the contact gives rise to a tangential stress. The concepts of normal stress and tangential stress are valid for the entire macroscale contact as well as the microscale contacts within, which are created by interacting asperities between surfaces.

The normal stress of conformal contacts is typically in the range of megaPascals (MPa), $1,000,000$ N/m². The normal stress of concentrated contacts is typically in the range of gigaPascals (GPa), $1,000,000,000$ N/m². Concentrated contacts encounter significant elastic deformation. The elastic contact area and stress distribution can be calculated by using Hertzian theory [1].

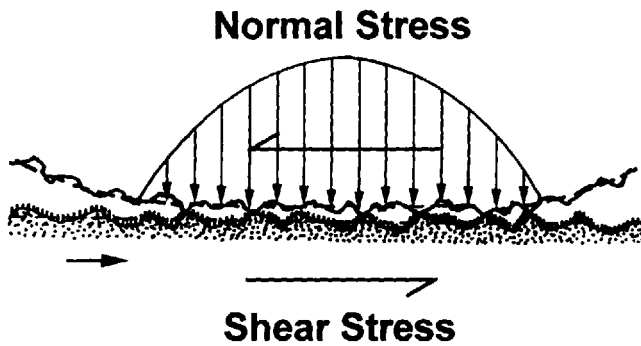


Figure 6.2 Two stress fields control the dynamics of a tribological contact.

Tangential stress is directly linked to the coefficient of friction, which is defined as the ratio of the tangential force to the normal force on the contact. Tangential stress may vary between 0.01 and 0.5 of the normal stress, depending on the degree of lubrication. The tangential stress, or coefficient of friction, of a contact can be the result of shearing an interposed material throughout the extent of the contact or it can be the summation of individual frictional events associated with interacting asperities between the surfaces. The friction of many of the contacts within hydraulic systems is mostly a combination of the two.

Because lubrication and failure mechanisms are frequently controlled by asperity-scale phenomena, it is important to remember that normal and tangential stresses at asperities may not be that different for conformal contacts as they are for highly stressed concentrated contacts. Asperity stresses depend on how the load is momentarily distributed among the surface features. Conformal contacts, with rough surfaces and a few contacting asperities, can have stresses similar to asperities found in concentrated contacts with smoother surfaces. Because concentrated contacts tend to have finer surface finishes than conformal contacts, this situation may be quite common. This means that asperity stresses for both conformal and concentrated contacts may be on the same order of magnitude, even if their “global” or overall pressure across the contact area is substantially different. The major difference between conformal and concentrated contacts is that the stress field of the latter penetrates deeper into the material. In addition, high global pressure for concentrated contacts can dramatically change hydraulic fluid viscosity, even before it is consumed by the contact.

Whether normal and tangential stresses are on a global scale or asperity scale, the objective of lubrication is to create or preserve interposing material that bears the normal stress and accommodates the tangential shear. This appears to be somewhat of a paradox since the interfacial film must then possess high compressive strength but low shear strength. The lubrication mechanisms described in Sections 6 and 8 reveal the dynamic power by which this can occur. Because it is difficult to link engineering parameters with microscale lubrication and failure mechanisms, it would seem that problem solving and technical developments of hydraulic systems should focus on capturing lubricating mechanisms and suppressing failure mechanisms.

4 APPROACH

Because engineering parameters are difficult to link to lubrication phenomena, this chapter deals with the mechanisms of lubrication and failure. The use of mechanisms allows the development of theory or models by which tribology performance of hydraulic fluids and hardware can be explained by the laws of mechanics, physics, and chemistry.

Lubrication and failure mechanisms are described within the context of a tribological system. A tribological system can be composed of four major structural elements: (1) hydrodynamic film, (2) surface film, (3) near-surface material, and (4) subsurface material. These structural elements create the operating environment for lubrication and failure mechanisms. They also establish the interconnections between the commercial suppliers of materials, fluids, and designs for hydraulic systems. Because one or two of the structural elements are dynamically generated, the mechanisms of hydrodynamic lubrication, EHD lubrication, and boundary lubrication are described along with typical material and hydraulic fluid properties. The interactions of lubrication mechanisms with failure mechanisms are described within the framework of a dynamic tribological system. The mechanism leading to failure processes of wear, scuffing, and surface fatigue are described and illustrated with performance maps based on engineering parameters. The material in this chapter introduces the concept of systematic tribology. Systematic tribology is the process of understanding and developing the structural elements of practical tribological contacts and their mechanisms of interaction in a systematic way.

5 STRUCTURAL ELEMENTS AND THE TRIBOSYSTEM

The performance of lubricated contacts is derived from the integrity of four general elements or regions, as shown in Figure 6.3. Each region performs certain functions with respect to lubrication and failure mechanisms. The success of lubrication depends on how well lubrication mechanisms handle the normal stress and the accommodation of tangential shear within these regions.

5.1 Hydrodynamic Film Region

The formation of an oil film between bodies in contact is a structural element that is dynamically generated. Its creation is a function of motion, which generates a pressure within a viscous fluid. Hydrodynamic films generated within conformal contacts may be tens of micrometers (μm) thick. Hydrodynamic or elastohydrodynamic (EHD) films generated in nonconforming contacts may be on the order of 1 μm thick. On a global scale, the EHD film is derived from the hydrodynamic pressure generated in the inlet region of the contact. On a local or asperity scale, hydrodynamic pressure is derived from the micro-EHD lubrication action associated with the local topographic features of the surfaces. These micro-EHD films are typically much less than 1 μm thick.

5.2 Surface Film Region

The surface film region contains the thin outer layers of the surface. They may consist of surface oxides, adsorbed films, and chemical reaction films derived from the lu-

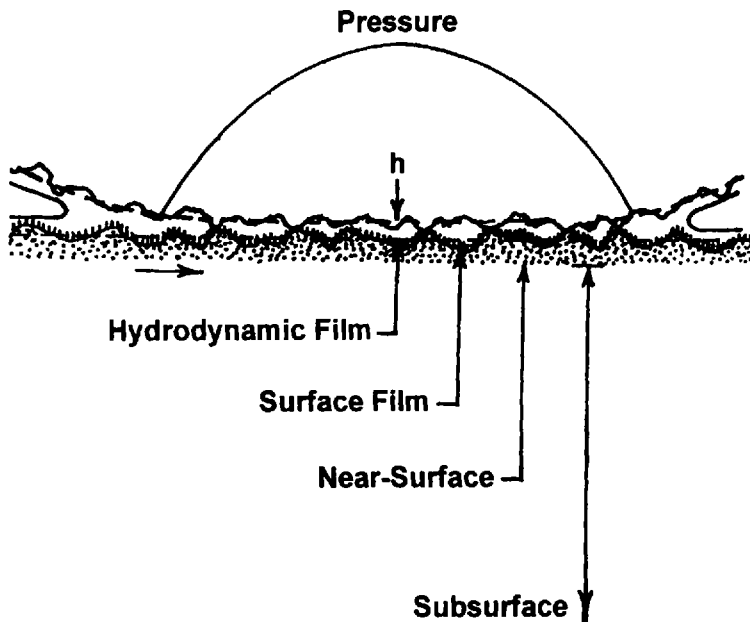


Figure 6.3 Structural elements of a tribosystem controlling lubrication and failure mechanisms.

bricant and its additives. These surface films are almost always less than $1\ \mu\text{m}$ thick. Although the surface film region is extremely thin, its formation by mechanisms of surface forces and chemical reactions has a profound effect on surface lubrication.

5.3 Near-Surface Region

The near-surface region contains the inner layers of the surface. This region may include a finely structured and highly worked or mechanically mixed layer. It may also include compacted wear debris or transferred material from a mating surface. The deformed layers, which are of a different microstructure than the material below them, may arise from surface preparation techniques such as grinding and honing. They may also be induced during operation, e.g., during run-in. Hardness and residual stress may vary significantly in this region. They may also be substantially different from the bulk material below. The near-surface region may be on the order of $50\ \mu\text{m}$ below the surface.

5.4 Subsurface Region

The subsurface region is particularly important for highly stressed concentrated contacts. The subsurface region can be on the order of 50 to 1000 microns below the surface. This region is not significantly affected by the mechanical processes that produce the surface or the asperity-induced changes that occur during operation. Its microstructure and hardness may still be different from the bulk material below it, and significant residual stresses may still be present. These stresses and microstructures, however, are the result of macroprocesses such as heat treatment, surface

hardening, and forging. For typical Hertzian contact pressures, and neglecting asperity pressures, the maximum shear stress is located within the subsurface region (see Figure 6.3). In other words, the detrimental global contact stresses are communicated to the subsurface region where subsurface-initiated fatigue commences.

These structural elements define the operating environment for lubrication and failure mechanisms. They also form the ingredients by which surface life and durability are determined. Because some of the structural elements are self generated within the contact, it is clear that the structural elements constitute a dynamic system. When we consider the practical construction of this dynamic system, we find the wide-ranging businesses of hydraulic technology intimately linked. The lubricated contact is a tribosystem where everything is joined together and operated in a dynamic fashion. This tribosystem is a melting pot of many commercial contributions that involve materials, surface treatments, hydraulic fluids, additives, equipment designs, and manufacturing.

The dynamics of this interdisciplinary tribosystem are described in Section 10. However, it can be said at the outset that the dynamics of practical systems are not adequately known. This state of affairs makes it difficult to solve problems and has resulted in disjointed efforts in developing hydraulic system technology. This is a common problem among nonintegrated businesses and disciplines that supply materials to the interdisciplinary field of tribology. Clearly the assembly of new tribology technology has not taken advantage of the potential synergism that can be obtained by constructing load-carrying materials, fluids, and designs as a system that operates on mechanisms.

6 HYDRODYNAMIC AND ELASTOHYDRODYNAMIC MECHANISMS

This section describes the fundamental mechanisms associated with self-generation of a fluid film between contacting surfaces in motion. Elastohydrodynamic (EHD) lubrication is a "miracle" mechanism that is able to separate surfaces under enormous stress on both a macroscale and microscale. The mechanism of EHD lubrication is essentially an extension of ordinary hydrodynamic lubrication, which was described by Osborne Reynolds in 1886 [1]. The concepts involved in hydrodynamic lubrication are fundamental to the understanding of EHD lubrication. These fundamental concepts are basic to hydraulic fluid properties and how they lubricate many of the load-bearing contacts in hydraulic systems.

6.1 Viscous Flow—Parallel Surfaces

First, consider the flow of fluid between two parallel surfaces as shown in Figure 6.4. The fluid molecules adjacent to the solid surfaces adsorb or stick to it. The adsorption of liquids onto solid surfaces is caused by fundamental atomic attraction. The formation of adsorbed material on solid surfaces is fundamental to the mechanism of boundary lubrication. The mechanism of adsorption is described in Section 8.2.

Because fluid molecules are attached to the bottom surface, they are forced to move with that surface at a velocity u . The molecules on the top surface remain stationary. The molecules of fluid in between are dragged along by the bottom surface. The velocity of the fluid at various positions within the film is shown by the

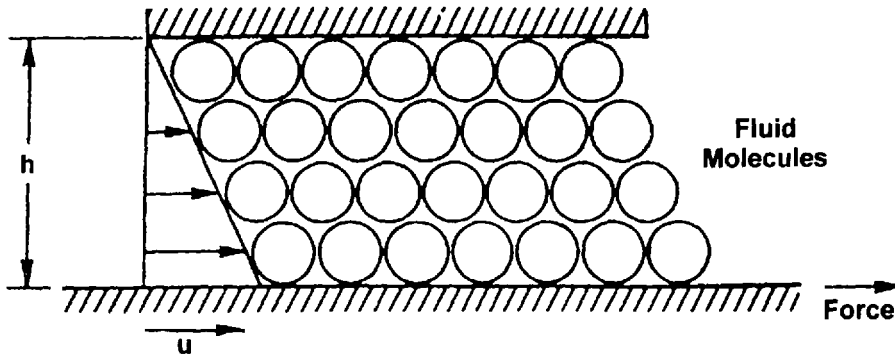


Figure 6.4 The flow of fluid between parallel surfaces in motion. Flow in cannot be larger than flow out.

arrows in Figure 6.4. Note that the velocity of the fluid increases linearly from the top surface to the bottom.

The engagement of molecules in a fluid and their relaxation under strain create an inherent resistance to flow, which is expressed in terms of its viscosity. Therefore, it requires a force to move the bottom surface relative to the top surface. The amount of shear force required is a function of the viscosity of the fluid. The force also depends on the rate at which the fluid molecules are being sheared. The rate of shear for the linear velocity distribution shown in Figure 6.4 is proportional to the surface velocity u and inversely proportional to the thickness of the film h . Therefore, an increase in u or a decrease in h will require a greater force to move the bottom surfaces. The shear force is parallel to the surfaces, and the relationship between shear force and shear rate is the definition of viscosity.

The situation of flow between parallel surfaces provides no lifting force, which is required for lubrication. On the other hand, if the surfaces were allowed to collapse, it would take a finite time for the fluid to squeeze out. This momentary lifting force of the fluid while the surfaces are normally approaching is called a hydrodynamic squeeze film. The hydrodynamic squeeze film is a useful concept to remember in connection with the mechanism of elastohydrodynamic lubrication.

6.2 Closing the Gap

Consider now the flow of fluid between two converging surfaces shown in Figure 6.5. The top surface, which is of finite length, is at an angle to the bottom one. The gap between the surfaces is thicker at the inlet than it is at the outlet. The fluid adjacent to the lower surface moves with a velocity u , and the fluid adjacent to the upper surface is stationary. The inlet region would like to uniformly drag in fluid with a velocity distribution that is linear. At the same time, the outlet region would like to drag out fluid with a linear velocity distribution. The amount of fluid coming in is represented by the area of the triangle at the inlet. The amount of fluid going out is represented by the area of the triangle at the outlet. Because the triangle in the inlet is bigger, we find that the inlet would like to take more fluid in than the outlet will allow out. This pumping of the fluid into a converging region creates a

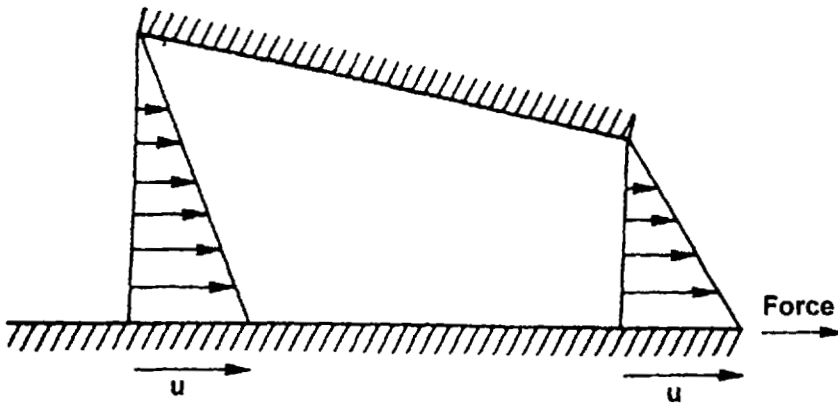


Figure 6.5 The flow of fluid between two converging surfaces in motion (hypothetical).

pressure between the surfaces as shown in Figure 6.6. The high pressure in the center forces the fluid to slow down in the inlet and makes the fluid go faster at the outlet so that the flow coming in will equal the flow going out.

The pressure generated by this pumping action creates a lifting force that separates the surfaces with a fluid film. The dynamically generated pressure is a hydrodynamic pressure. The mechanism by which this pressure separates surfaces under load is called hydrodynamic lubrication. The load that a bearing of the configuration represented in Figure 6.6 is able to carry is a function of the hydrodynamic pressure generated. If the viscosity of the fluid is increased, more work is required to slow the fluid down in the converging inlet space, and as a consequence a greater pressure is generated. Increasing the velocity u will also increase the hydrodynamic pressure.

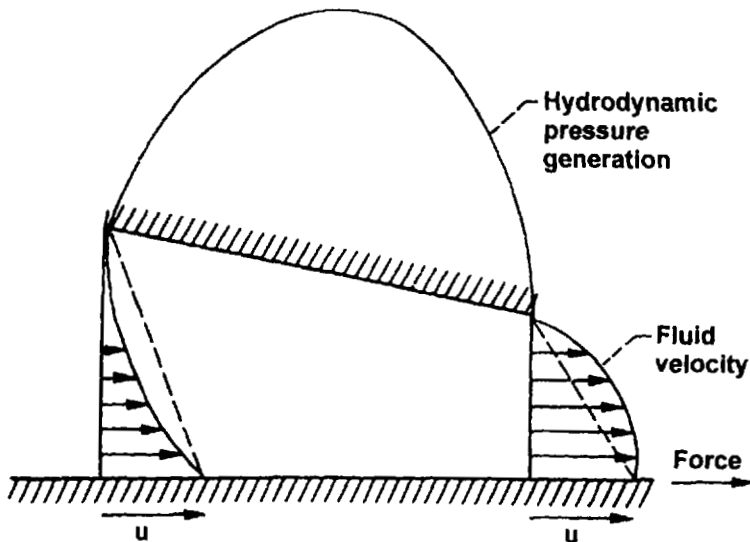


Figure 6.6 Hydrodynamic pressure generated between converging surfaces in motion.

If the surfaces pump fluid into the convergent space at a greater rate, a greater pressure is needed to slow the fluid down so that continuity of flow between the inlet and outlet is maintained.

There are three basic requirements for the generation of hydrodynamic pressure of the type shown in Figure 6.6: (1) the surfaces must be moving, (2) the surfaces must be converging, and (3) a viscous fluid must be between them.

The bearing shown in Figure 6.6 is a simple bearing. It is called a slider bearing or pad bearing. Several of these pads arranged in a circle make a thrust bearing of the type found in many machines.

Another common bearing that uses hydrodynamic film generation is the journal bearing shown in Figure 6.7. Here, the converging surfaces are formed by virtue of the fact that the journal is not concentric with the bearing housing. When the journal rotates, it drags fluid into the converging region, thus generating a pressure that separates the surfaces.

6.3 Properties in Hydrodynamic Lubrication

When the motion of the surfaces draws the fluid into a converging space, the viscous nature of the fluid resists this motion and generates an internal pressure that is able to resist the normal stress applied to the contact. The pressure generated is governed by the Reynolds equation:

$$\frac{dp}{dx} = 12\mu U \left[\frac{(h - h_0)}{h^3} \right] \quad (6.1)$$

The pressure gradient, dp/dx , is proportional to the viscosity μ , the surface speed U , and a geometry term $(h - h_0)/h^3$.

The pressure generated within a convergent space creates a hydrodynamic lubricant film. The thickness of lubricating films can be calculated by using equations derived from simplifying assumptions for certain types of contact geometry. All film

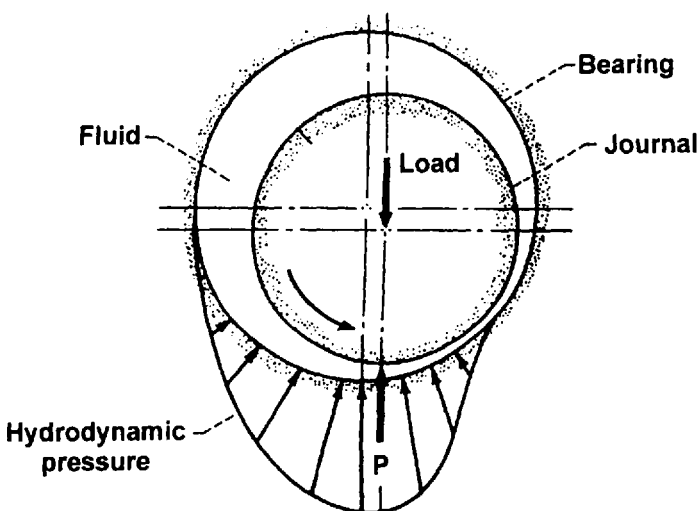


Figure 6.7 Hydrodynamic film generation in a journal bearing.

thickness equations show the important role of viscosity. The role of viscosity is easily seen in an equation for film thickness, assuming a contact of rigid cylinders and a viscosity independent of temperature or pressure [2].

$$\frac{h_0}{R} = 4.896 \frac{U\mu_0}{W} \quad (6.2)$$

where

- h_0 = film thickness on the line of centers
- R = equivalent radius of curvature
- U = one-half the sum of the surface speeds
- μ_0 = viscosity
- W = load

Because film thickness is directly related to viscosity, the level of viscosity can be selected for a given application to provide sufficient film thickness for complete surface separation. Because hydraulic system contacts seldom operate at constant speed, constant load, or constant temperature, fluid viscosity decisions must be made to select an appropriate level of viscosity for the entire range of conditions. In many cases, design decisions associated with geometry, surface finish, material, and normal stress are made to accommodate the use of typical hydraulic fluid properties.

The process of generating a hydrodynamic film between contacting surfaces consumes power and results in a temperature rise in the oil film. Both internal and external thermal effects can decrease the viscosity substantially. The rate of change of viscosity with temperature can be significant. The thermal effect on viscosity also varies with lubricant type (see fluid property data in other chapters).

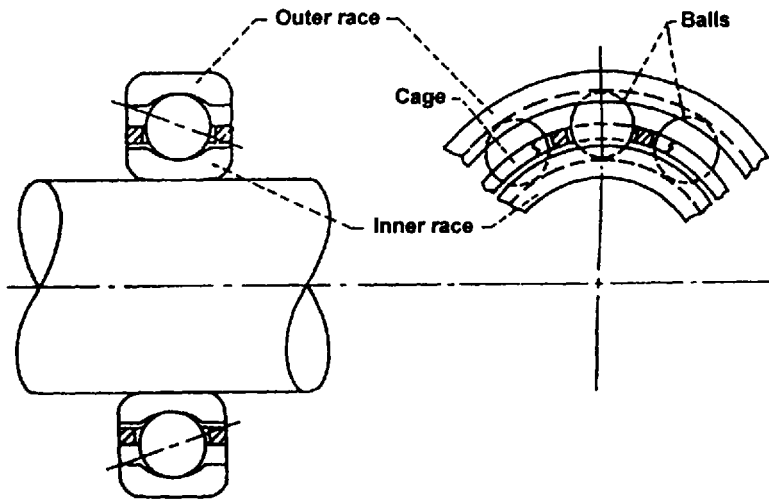
6.4 The Nonconformists

Hydrodynamic lubrication is characterized by conformal contacting surfaces where the normal stress is distributed over a relatively large area. The hydrodynamic mechanism is actively involved in the lubrication of piston/cylinder, slipper/swash plate, and many other sliding contacts. There are many hydraulic system contacts that are nonconforming where the load is concentrated on a small area. With concentrated contacts, the full burden of the load on a small area can cause considerable elastic deformation in and around the contact. Some examples of these nonconforming surfaces in hydraulic systems are rolling element bearings and gear teeth in gear pumps.

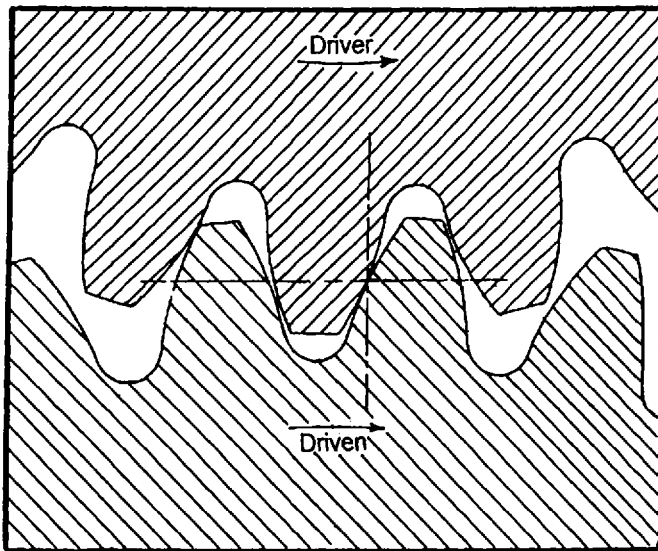
Figure 6.8 illustrates the nonconforming surfaces found in a ball bearing and gear mesh. The ball and race conform to some degree in one direction, but the side view of the bearing shows that curvatures of the ball and race have little degree of conformity. There was little belief up until the early 1950s that these nonconforming surfaces, with their extremely small area of contact, could be separated by an oil film. The lubrication of these nonconforming surfaces leads us to a remarkable and powerful film-generating mechanism called elastohydrodynamic lubrication.

6.5 Hertz—The Opposition

Let us first consider the contact condition between two nonconforming surfaces to see what the mechanism of elastohydrodynamic lubrication is up against. The contacting surfaces of bearings and gears may be represented by a sphere or cylinder



(a)



(b)

Figure 6.8 Nonconforming surfaces found in a (a) ball bearing and (b) gear mesh.

loaded against a flat surface as shown in Figure 6.9. The load, which presses the two bodies together, causes the surfaces to elastically deform and contact each other over a small but finite region of contact. This condition of elastic contact is named after Heinrich Hertz [1] who, in 1881, analyzed the contact between elastic bodies under conditions where the region of contact is much smaller than the radius of curvature. A close-up view of the intimate region of contact is shown in Figure 6.9. The load gives rise to a pressure, called the Hertzian pressure, which is distributed over a small region of contact, called the Hertzian region. The pressure has a parabolic distribution that is high in the middle and diminishes to zero at the edges of contact. Typical maximum Hertzian pressures found in bearing and gear contacts are very high, on the order of $1.5 \times 10^9 \text{ N/m}^2$. Note that this Hertzian pressure is an elastic pressure caused by the elastic deformation of the surfaces.

The Hertzian condition of contact is a dominating feature of EHD lubrication. It establishes the overall shape of the contacting surfaces. Thus, if we were to follow the journey of a fluid particle passing between the surfaces, it would first encounter a converging region, followed by a flat or parallel region, and finally it would be exposed to a diverging region. As stated above, one of the requirements for the generation of hydrodynamic pressure is that the surfaces must be converging. Therefore, we should expect all dynamic pressure-generating action to be in the converging region. The hydrodynamic pressure generated in this region has the task of separating the surfaces, which are forced together by the enormous pressure in the Hertzian region. When we consider that typical maximum Hertzian pressure may be on the order of 1.5 GPa, and that the usual hydrodynamic pressures generated in journal bearings are only on the order of 7 MPa, there doesn't seem to be much hope for the establishment of an oil film under these conditions.

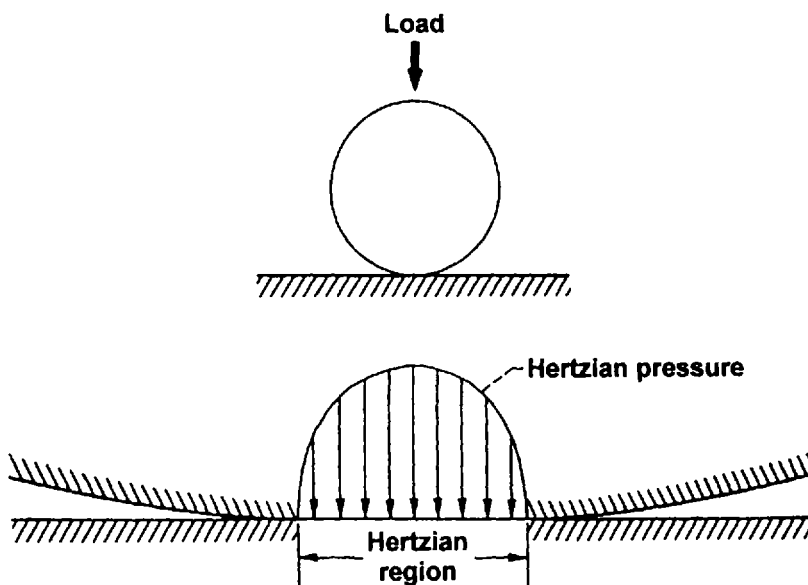


Figure 6.9 Hertzian pressure and deformation for nonconforming bodies in elastic contact.

6.6 Ankle Deep in Cheese

The power of elastohydrodynamics is derived from two important considerations, which together provide the teamwork necessary to separate the surfaces. The first is that typical EHD films are a great deal thinner (about 1,000 times thinner) than they are long. If, for example, the Hertzian region were the length of a football field and you were standing on the field, a typical EHD oil film would only be about ankle deep.

The second important consideration is the effect of pressure on the viscosity of the fluid. Figure 6.10 shows how the application of pressure influences the viscosity of a synthetic fluid at 38°C. The viscosity, which is given in centipoise (cp), is plotted on a logarithmic scale because it increases very rapidly with pressure. At atmospheric pressure, the viscosity is about 350 cp (approximately the same consistency as a typical motor oil). At $0.14 \times 10^9 \text{ N/m}^2$ the viscosity has increased by one order of magnitude to 3,500 cp. The fluid at this pressure has a consistency approaching that of molasses. At typical Hertzian pressures of $1.5 \times 10^9 \text{ N/m}^2$, the fluid viscosity can increase by several orders of magnitude so that its consistency may be more like butter or cheese.

The influence of pressure on viscosity is usually represented by a straight line, as shown in Figure 6.10, which has the equation

$$\mu = \mu_0 e^{\alpha p} \quad (6.3)$$

where μ is the viscosity at pressure p and μ_0 is the viscosity at atmospheric pressure. The exponent α is a property of the fluid called the pressure–viscosity coefficient. When α is large, the viscosity rises rapidly with pressure. When α is small, the viscosity rises more slowly with pressure.

6.7 Hydrodynamics versus Hertz

Figure 6.11 shows the flow of fluid in the convergent inlet region where hydrodynamic pressure is generated. It should be noted that this figure was drawn by using two conventions frequently used to graphically illustrate an EHD-lubricated concentrated contact. First, because typical EHD oil films are much thinner than they are long, the vertical dimensions are usually expanded about 1,000 times more than the horizontal dimensions. If this were not done, the thickness of a typical EHD oil film drawn to scale would be less than the thickness of the horizontal line shown in the Hertzian region of Figure 6.9. The second convention illustrates the contacting surfaces of machine elements with an equivalent sphere or cylinder on a flat surface with all the elastic deformation represented in the curved body.

The shape of the convergent region as shown in Figure 6.11 must be viewed with this in mind. The real shape of the convergent inlet region, where hydrodynamic pressure is generated, is actually long and narrow.

The surfaces shown in Figure 6.11 are in pure rolling, where each surface is moving with the same velocity, u . Each surface carries with it a certain quantity of fluid, which joins together at some location to fill the gap between the surfaces. Fluid adjacent to each surface is attached to it and travels with it. Because the surfaces are converging, the fluid in the interior of the film is forced to slow down and may even flow backward. Just as was previously explained, this slowing down of the fluid or pumping action of the surfaces to draw fluid into a converging region gen-

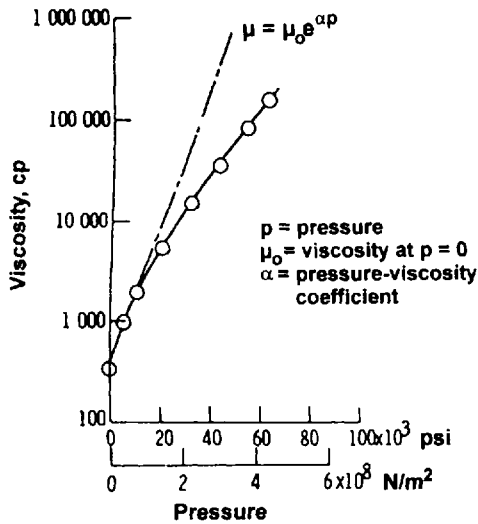
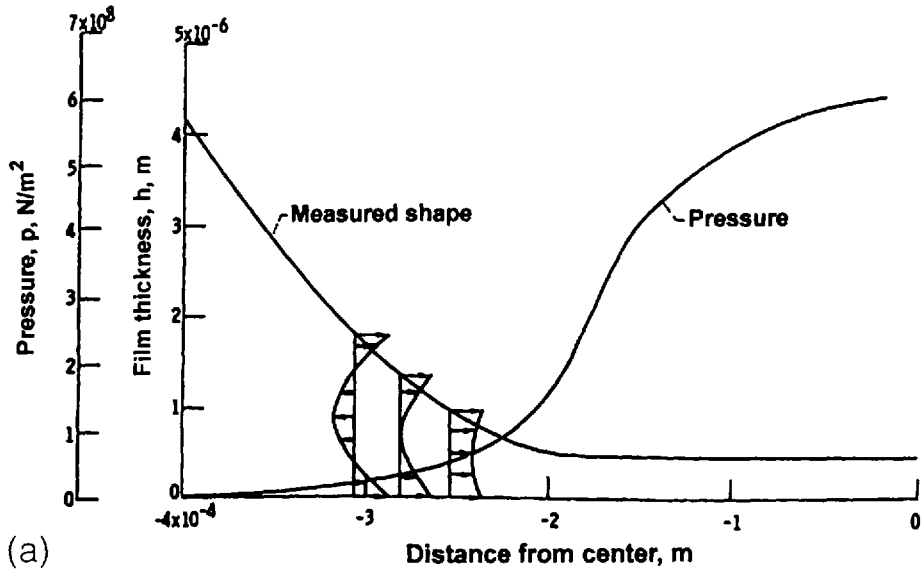


Figure 6.10 The effect of pressure on viscosity for a synthetic fluid at 38°C.

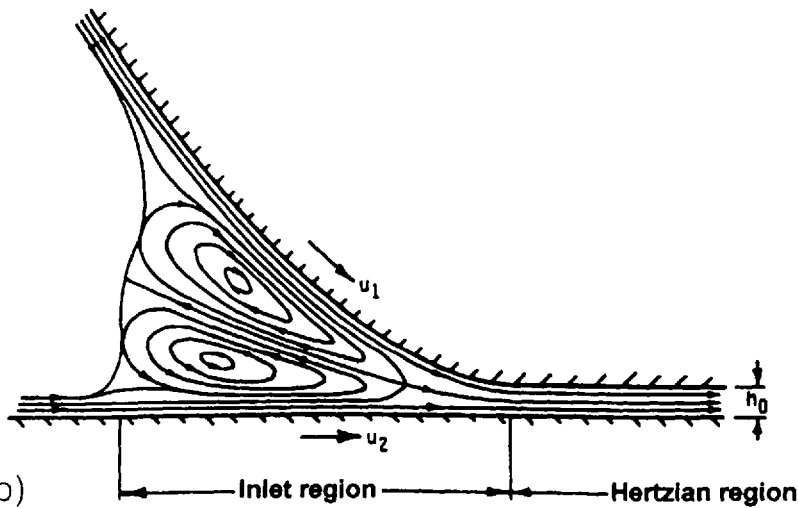
erates a hydrodynamic pressure. As the pressure rises in the inlet region, the viscosity rises with it. The higher viscosity produces even higher pressure. When the fluid reaches the leading edge of the Hertzian region, the viscosity of the fluid may have increased by an order of magnitude and the hydrodynamic pressure may have reached typical values of $0.15 \times 10^9 \text{ N/m}^2$. This hydrodynamic pressure must compete with the Hertzian pressure. While the hydrodynamic pressure is trying to separate the surfaces, the Hertzian pressure is trying to force them together.

The hydrodynamic pressure generated in the convergent inlet region is much lower than the maximum Hertzian pressure. Nevertheless, the hydrodynamic pressure is capable of separating the surfaces, and it does so in a very subtle way. It cannot compete with the Hertzian pressure in the center of the contact where the pressure is very high, but it can overcome the Hertzian pressure at the leading edge of the Hertzian region where the pressure is much lower. If it does this, and if it separates the surfaces at the leading edge of the Hertzian region, the hydrodynamic pressure will have achieved total surface separation. Total surface separation is achieved because of time (i.e., the dynamics of the moment). Once the fluid gets into the leading edge of the Hertzian region, it cannot escape because the viscosity becomes too high and the film is too thin. There will not be enough time for the Hertzian pressure to squeeze the fluid out because the motion of the surfaces passes the fluid through the Hertzian region very quickly (typically on the order of milliseconds).

The final pressure achieved along with the overall shape are shown in Figure 6.12. The final pressure and shape are very similar to the Hertzian pressure and shape except at the leading and trailing edges of the Hertzian region. The EHD pressure generated in the inlet region elastically deforms the surfaces to a greater extent than the original Hertzian shape. The EHD pressure near the exit region goes into a sudden perturbation with enormous pressure gradients. The sudden drop in pressure at the exit is associated with a drop in film thickness, which creates a fluid flow constriction. The local constriction at the trailing edge of the contact is a result of a require-



(a)



(b)

Figure 6.11 (a) Pressure and velocity distribution and (b) flow distribution in convergent inlet region.

ment to maintain continuity of flow. If there were no constriction, the sudden drop in pressure would force more fluid out than is coming in. Therefore, the surfaces deform in such a manner that they restrict the flow going out.

6.8 The Trinity

The conjunction zone of a typical EHD contact can be conveniently divided into three separate regions, as shown in Figure 6.12. Each region performs a unique function. The inlet region pumps the film up. The Hertzian region rides the film and

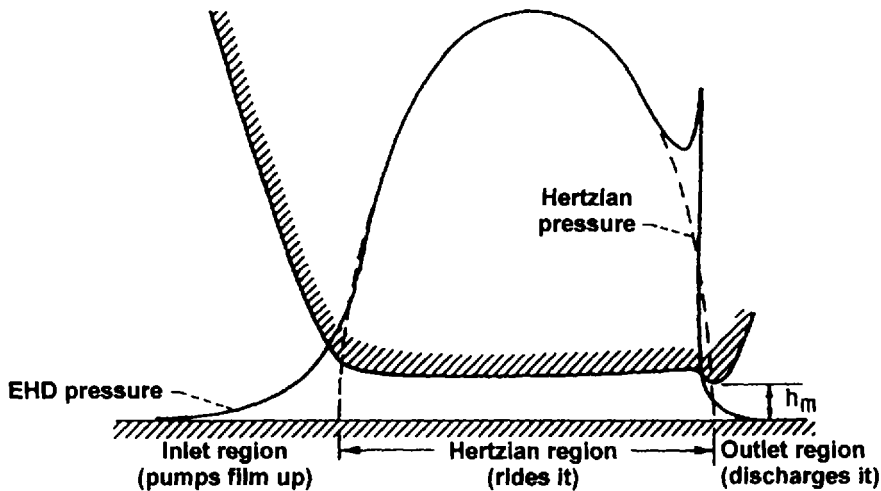


Figure 6.12 Typical pressure distribution and elastic deformation during EHD lubrication.

the outlet region discharges the film. The viscous character of the fluid changes drastically while passing through these regions, going from an easy flowing liquid to a pseudosolid and back to an easy flowing liquid within a matter of milliseconds.

The viscous properties of the fluid in each region are determined by the temperature, pressure, and shear conditions the fluid encounters or creates in each region. Because viscosity plays an important role in how these regions function, it is important to understand how the viscous character of the fluid is influenced by the environmental condition in these regions as it passes through.

For example, the film-forming capability of the hydrodynamic pressure generated in the inlet region is governed by the local viscosity throughout this region. Because the inlet region is extremely narrow, the viscosity of the fluid is controlled by the temperature of the solid surfaces. The variation of viscosity with pressure is usually accounted for by the α -parameter in Eq. (6.3). While the pressure-viscosity coefficient, α , as defined in Figure 6.10 departs from experiment at high pressures, its characterization of fluid behavior is sufficiently accurate over the pressure range generally encountered in the inlet region. The viscous properties of the fluid as governed by the pressure and temperature conditions in the inlet region influence the thickness of the fluid film, which is observed in the Hertzian region.

6.9 Stressed to the Limit

By the time the fluid has entered the Hertzian region, it has completed its task of pumping the film up. The viscous (or shear strength) character of the fluid in the Hertzian region now becomes important with respect to sliding friction (or traction). Because the fluid film in the Hertzian region has high viscosity, relative motion between the surfaces is resisted by tangential stress built up within the fluid in the Hertzian region. Because enormous pressures in the Hertzian region transform the fluid into a pseudosolid, the internal friction or traction of the fluid becomes governed by the shear strength of the solidified fluid instead of its viscosity. The tremendous

enhancement of viscosity with pressure is offset to some degree by frictional heating of the fluid in the Hertzian region as well as possible shear and time-dependent effects on fluid behavior. If the fluid in the Hertzian region is liquid like, frictional heating reduces its viscosity. If the fluid in the Hertzian region is solid like, frictional heating reduces the limiting shear stress of the fluid. In either case, sliding friction is reduced with temperature. Friction or traction coefficients of hydraulic fluids may range from 0.1 to 0.001. The level of traction is a function of the pressure and temperature in the Hertzian region. Because traction under high-pressure EHD conditions reflects the limiting shear strength of the fluid, traction coefficient is a function of the molecular structure of the fluid. Figure 6.13 shows EHD traction coefficients of four fluid types. The EHD traction measurements were conducted at a maximum Hertzian stress of 2.07 GPa and ambient temperature [3]. The traction data were taken over a range of rolling velocities, but with a constant sliding velocity (0.36 m/sec). With a constant sliding velocity and Hertzian stress, the frictional heating in the contact is the same for all rolling velocities. It is interesting that traction coefficient is almost independent of rolling velocity. From the discussion above, EHD film thickness should increase with surface entraining velocity. This means that traction coefficient under high-pressure EHD conditions is essentially independent of film thickness (or shear rate). The independence of traction with shear rate confirms that the fluid is shearing like a solid rather than a viscous liquid.

The fact that fluids under Hertzian pressure shear like solids has profound technological implications. If fluids remained viscous liquids (i.e., took on Newtonian behavior), the high shear rates typically found in EHD contacts would result in enormous friction coefficients. EHD lubricated contacts would then have to be op-

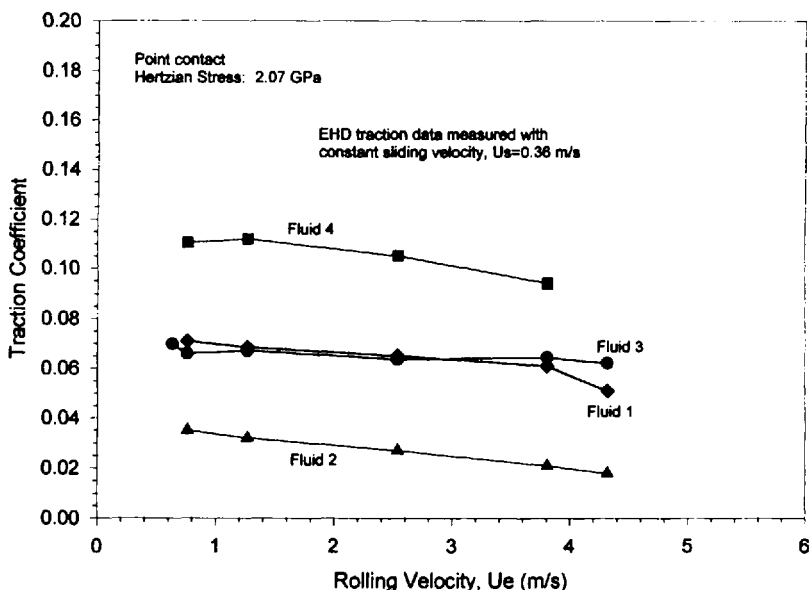


Figure 6.13 Traction coefficients of four fluids measured under high-pressure EHD conditions. Fluids 1 and 2 are model hydraulic fluids. Fluid 3 is a polyolester and Fluid 4 is a perfluoropolyalkyl ether.

erated at low shear rates or they would suffer meltdown by frictional heating. The transformation of the fluid to a pseudosolid limits frictional resistance caused by the limiting shear strength of the interposed material. Furthermore, as the shear rate and frictional heating in the contact increases, traction decreases. This is because the limiting shear strength of fluids, like ordinary solids, decreases with temperature.

6.10 Predicting Film Thickness

The practical importance of the mechanism of EHD lubrication lies in the thickness of the oil film between the surfaces. Its thickness is controlled by the operating conditions expressed in terms of various operating parameters such as surface velocity, load, and fluid viscosity.

The influence of these parameters on film thickness should be obvious if the basic concepts of EHD have been understood. For example, a change in any parameter, which causes a greater hydrodynamic pressure to be generated in the inlet region, will result in a larger film thickness. Thus, an increase in surface velocity or fluid viscosity will result in a larger film thickness.

An important feature of EHD lubrication is that the influence of load on film thickness is very small. This is not surprising if one considers that an increase in load merely increases the maximum Hertzian pressure and makes the Hertzian region larger. It does very little to the inlet region where the hydrodynamic pressure is generated.

The influence of various operating parameters on film thickness can be shown with an equation. Equation (6.4) has been derived from theory [4] for a line contact geometry presented by a cylinder on a plane as shown in Figure 6.9.

$$h_m = 2.65 \frac{(\mu_0 u)^{0.7} \alpha^{0.54} R^{0.43}}{E^{0.03} w^{0.13}} \quad (6.4)$$

where

h_m = film thickness at the rear constriction

μ_0 = viscosity at atmospheric pressure

α = pressure–viscosity coefficient as defined in Eq. (6.3)

u = velocity, defined as $u = \frac{1}{2}(u_1 + u_2)$ where u_1 and u_2 are the individual velocities of the moving surfaces

R = radius of equivalent cylinder

w = load per unit width

E = elastic modulus of equivalent cylinder (flat surface assumed completely rigid)

This equation shows that film thickness is most sensitive to the velocity (u), the lubricant properties (μ_0 and α) and the radius of curvature (R). An increase in any one of these parameters, which are in the numerator of Eq. (6.4), will result in a larger film thickness. The relationship between viscosity, μ_0 , and temperature is well known for hydraulic fluids and is covered in other chapters.

While the pressure–viscosity coefficient, α , is an essential fluid parameter for EHD film generation, its value is not frequently given for hydraulic fluids. Pressure–viscosity coefficients can be measured with high-pressure capillary viscometers. They can also be obtained from actual EHD film thickness measurements [3]. Pres-

sure–viscosity coefficient is a function of molecular structure. Because hydraulic fluids cover a wide variety of fluid types, their pressure–viscosity coefficients cover a wide range. The pressure–viscosity coefficients of four fluid types are plotted as a function of temperature in Figure 6.14. Fluids 1 and 2 are model hydraulic fluids. Fluid 3 is a polyolester and Fluid 4 is a perfluoropolyalkyl ether. Most mineral oils and some synthetic fluids have pressure–viscosity coefficients similar to Fluids 1 and 3. The data in Figure 6.14 show that pressure–viscosity coefficient decreases with temperature. This is particularly true for high-viscosity fluids. As a general rule, pressure–viscosity coefficient tends to increase with viscosity for a given fluid type.

The denominator in Eq. (6.4) has two parameters (E and w') which tend to decrease film thickness. However, neither the load w nor the elastic modulus E influence film thickness much because their exponents are very small (0.13 and 0.03). It is somewhat ironic that the lubrication mechanism that bears the name elasto-hydrodynamic shows film thickness to have little dependence on the elasticity of the materials. As long as the applied load causes elastic deformation similar to the Hertzian deformation, it does not matter if the elastic modulus is high like that of tungsten carbide or low like that of aluminum or brass. As previously discussed, the region of EHD pressure generation is the inlet region, the shape of which is only slightly affected by elastic modulus. However, if the elastic modulus is extremely low, like that of elastomeric seal materials, the pressure will not be sufficient to enhance the viscosity of the fluid. The mechanism of lubrication, while still elasto-hydrodynamic, cannot be described by Eq. (6.4) since it includes the pressure–viscosity coefficient α . Other equations that account for low elastic modulus materials can be used to calculate film thickness.

6.11 Experimental Verification of EHD Theory

For moderately hard materials, the theoretical prediction of film thickness as represented by Eq. (6.2) has been verified by experimental measurements. Because typical EHD films are extremely thin (generally less than 1 μm), film thickness measurements require special techniques.

One measurement technique that has been used is optical interferometry, which uses the wavelength of light as a unit of measure. Figure 6.15 shows a photomicrograph of light interference fringes that have formed between a steel ball rolling against a glass surface. The circular area is the Hertzian region. The fluid passes through the Hertzian region from left to right. A fluid cavitation pattern is clearly visible in the outlet region. The interference colors in the Hertzian region provide a contour map of the thickness of the oil film. The uniformity of color in the center of the contact indicates that the film is extremely parallel in the high-pressure region, i.e., the elastic shape is Hertzian. Some exceptions to the Hertzian shape are seen near the rear and sides of the contact region where the thinner films are observed. The thinner films at the sides of the EHD contact are the result of side leakage of the fluid immediately upstream in the inlet region. This side leakage inhibits the generation of hydrodynamic pressure and causes a thinner film to form in the portion of the Hertzian region immediately downstream. The thinner film at the rear of the EHD contact causes a restriction in flow immediately downstream of the high pressure in the center of the Hertzian region. This restriction is a necessary requirement to maintain continuity of flow, as previously discussed.

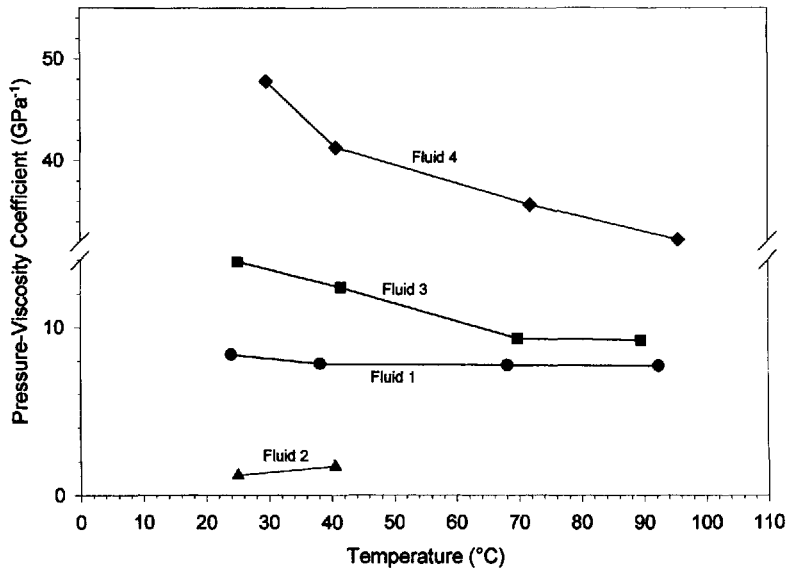


Figure 6.14 Pressure-viscosity coefficients of four fluid types. Fluids 1 and 2 are model hydraulic fluids. Fluid 3 is a polyolester and Fluid 4 is a perfluoropolyalkyl ether.

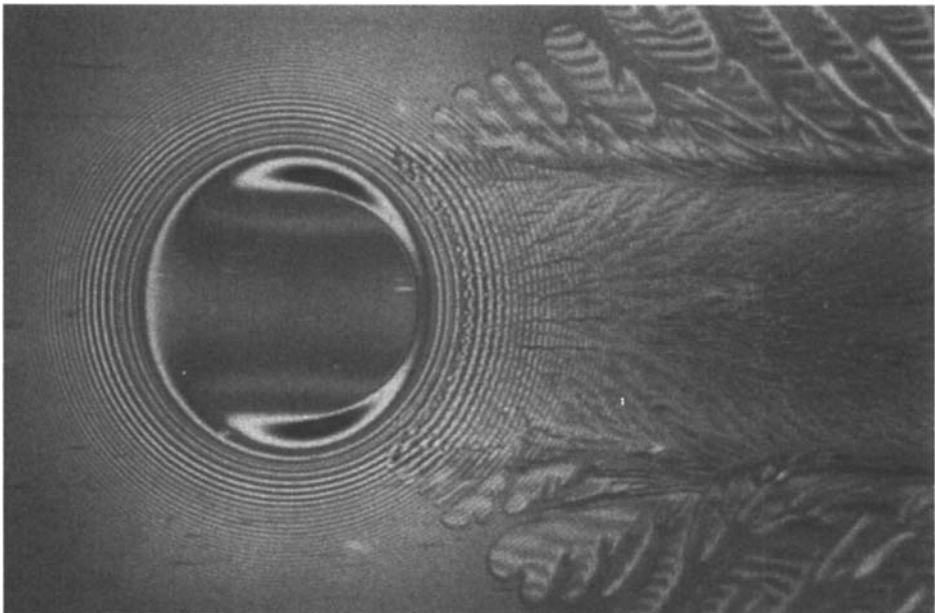


Figure 6.15 Photomicrograph of light interference fringes showing EHD film formed between a steel ball rolling against a transparent surface. Fluid passes through the Hertzian region from left to right.

6.12 Exit Region

After the fluid leaves the Hertzian region, it enters a diverging region. As the surfaces drag the fluid into the diverging space of the outlet region, the situation of fluid dynamics is opposite to that found in the inlet region. The outlet region attempts to generate a negative pressure. When subambient pressure is reached, dissolved gases in the fluid come out of solution and fill the space between the surfaces. This action ruptures the fluid film and terminates the hydrodynamic pressure. It is fortunate that fluids *out-gas* rather than respond by way of true cavitation. Although fluid cavitation can result in considerable damage to hydraulic system valves, the gentle cavitation that occurs at the termination of hydrodynamic pressure causes no trauma to the surfaces. The fluid merely “passes gas.”

6.13 Starvation

The oil film rupture in the exit region leaves thin residual ribs of lubricant downstream of the contact. Because most lubricated contacts repeatedly travel over the same track, there is a concern that the surfaces drawing fluid into the inlet region might not provide an adequate supply. Without some degree of external replenishment into the track, the inlet region can become *starved*. Experimental work on starvation [5] shows that a less than fully flooded inlet region decreases the EHD film thickness according to the degree of inlet starvation. Many lubricated contacts, like grease-lubricated bearings, run starved. So long as the EHD film thickness provides sufficient surface separation (or entrainment of chemistry), some degree of starvation can be tolerated. Fortunately, most highly stressed contacts in hydraulic equipment tend to be adequately supplied with fluid.

With regard to starvation, one should appreciate a little known fact that allows high-speed contacts to survive without starvation. The inlet flow field illustrated in Figure 6.11 shows that fluid entering the inlet region is recirculated. It “hangs around” awhile before it is consumed by the Hertzian region. The inlet region accumulates fluid and actually moves with the contact as it travels along the surface. This “inflight refueling” is one of several phenomena that make EHD lubrication a “miracle mechanism.”

6.14 Just a Tickle?

The thickness of EHD lubricating films found in lubricated contacts is frequently not much greater than the height of individual asperity features on the surfaces. If total surface separation can be achieved, the life of hydraulic pump contacts can be long, limited ultimately by fatigue of the metal surfaces. However, when total separation of the surface is not achieved, the load is partially supported by the EHD film and partially by local areas of asperity contact. These local areas are vulnerable sites for the initiation of surface wear and failure. The calculated thickness of the EHD film relative to the individual asperity height is an important criterion used in design. This is a first-order estimate of whether the intermittent contact between asperities is just a “tickle” or something more traumatic.

6.15 Micro-EHD

The power of the EHD mechanism, which has been described above with smooth surfaces, also carries its influence to the microworld of surface roughness features.

The realities of typical lubricated contacts are that EHD-generated films are on the same order of magnitude as the roughness heights of machine-finished surfaces. It is also interesting that typical “slopes” of surface roughness features are frequently on the same order of magnitude as the angle of convergence in the inlet region. As discussed above, the generation of a hydrodynamic pressure requires relative motion where a fluid is drawn into a convergent space. Therefore, undulations on the surface, which are of a scale less than the length of the inlet region or contact region, are subject to the same principles of EHD film generation as the global or bulk shape of contacting bodies. When these EHD principles become active on topographical features, it is called *micro-EHD* lubrication. Micro-EHD action can be superimposed on a high-pressure EHD lubricated contact as well as a low-pressure hydrodynamic contact. In the latter case, elastic deformation is confined to roughness features only and the effect of pressure on viscosity is confined to the neighborhood of the roughness features.

An example of micro-EHD lubrication at work is shown in Figure 6.16. Artificially produced undulations are seen traveling through an EHD contact region with a nominal EHD film thickness of $0.16\ \mu\text{m}$. The data points, which were obtained with light interference [6], give the actual shape of the undulations as these features go through the contact region under sliding motion. The dashed line shows the original geometry of the undulations, as measured with a stylus instrument. As these undulations move through the high-pressure and highly viscous Hertzian region, they create significant local EHD pressures at the converging sides of the undulations. The micro-EHD pressures are sufficient to cause a noticeable compression or flattening of the “peaks” to avoid local contact. At the same time, the micro-EHD action on the downstream or diverging side of the undulations tends to create a negative pressure. If cavitation does not occur, the “valleys” are relieved of pressure and they deform in a direction toward the mean plane of the surface. So, if topographical features are of an appropriate scale, micro-EHD action can momentarily

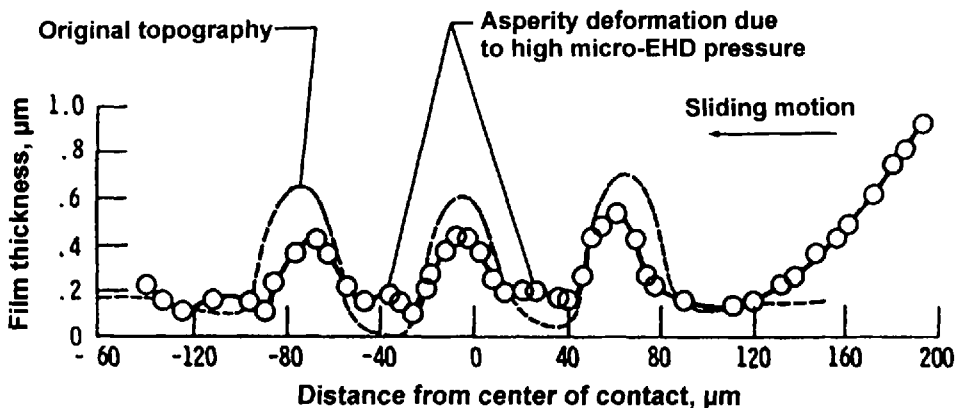


Figure 6.16 Micro-EHD pressures at roughness features with sliding motion “flatten” surface topography in Hertzian contact region.

flatten the roughness features. A severe encounter between surface roughness features may turn out to be only a tickle rather than a scratch.

6.16 Summary of EHD

Elastohydrodynamic lubrication deals with highly stressed surfaces that are elastically deformed by loads carried over small areas. The overall pressures and deformations are similar to the Hertzian conditions for dry contact. The dynamics of fluid entrained into the converging space upstream of the Hertzian contact generates pressure between the surfaces. The “macho” Hertzian pressure opposes this hydrodynamic pressure and, while the pressure of the battle builds up, the viscosity of the fluid increases. The enhancement of viscosity with pressure gives a tremendous boost to the generation of hydrodynamic pressure. Although the hydrodynamic pressure may still be much smaller than the maximum Hertzian pressure, it is sufficient to elastically deform and separate the surfaces at the leading edge of the Hertzian region. Once this is achieved, the fluid becomes captured by the contact. It cannot escape because its viscosity is too high, the gap between the surfaces in the Hertzian region is too thin, and the time is too short for it to “leak” out. Because Hertzian pressures are high, the momentarily captured fluid is transformed into a solidlike material. Friction is almost never more than 10% of the normal load. Because EHD films are generated upstream of the Hertzian contact, their thickness is almost independent of load. Their *load capacity* can easily exceed the plastic flow of metals.

The formation of hydrodynamic and EHD films has a profound effect on the life and durability of highly stressed hydraulic system components. Although the power of hydrodynamic and EHD mechanisms is somewhat amazing, it alone is not sufficient to preserve integrity of surfaces under all conditions of operation. These dynamic mechanisms create a structural element of the lubricated contact, which comes and goes with surface motion. The *attachment* of films, which do not require surface motion for their creation, is an equally important mechanism in the whole scheme of lubrication. The orchestration of surface films and dynamically generated films is the heart of lubrication practice.

Before we describe the mechanisms that create the structural element of *surface films*, the general features of surfaces and near-surface material should be understood. Surface films are part of the surface. In many cases, they are also part of the fluid. At the interface between surfaces, fluids can become “solid” and the solid surface can “flow” to accommodate stress or strain. Without some sort of modeling or understanding of the processes that go on between surface films and the surface, it is difficult to manage fluid chemistry, engineer surfaces, design contacting hardware, or solve problems.

7 THE SURFACE AND NEAR-SURFACE REGION

The near-surface region is a structural element that lubrication mechanisms attempt to preserve. The near-surface region, which includes surface topography, becomes the crime scene of almost all failure processes. These failure processes fall under general categories with descriptive terms, such as wear, scuffing, and surface fatigue. The near-surface region is a “constructed” element, as opposed to a dynamically generated element like hydrodynamic film. However, the near-surface region has

many dynamic features. The manufacture of a surface is not a benign process. Surfaces can acquire residual stresses, and they can possess “energy.” The material composition and microstructural features, which define the near-surface region of practical materials, cover an enormous scope and provide great opportunity. These opportunities will continue to grow with advancements in surface treatments and with developments in engineered surfaces. Whether the initial creation of contacting surfaces is high or low tech, an understanding of the characteristic features of the near-surface region is important for understanding its neighboring structural elements: the surface films and subsurface region.

7.1 Roughness, Asperities, and Substrates

All technological surfaces are rough or non-smooth on several arbitrarily defined dimensional scales. A nominally flat surface has “undulations” on the surface itself. This scale of roughness is often referred to as *waviness*. The next scale of roughness is the microscale, and this scale is referred to as *surface roughness*. Surface roughness with distinctive three-dimensional features may have *texture*. A third scale of roughness is the *nanoscale*, a scale not necessarily confirmed to be as important as the others in the lubrication of most technological surfaces. The microscale entities on surfaces that make up roughness are called *asperities*. The microscale is important because differences in surface roughness in this range strongly influence the functioning of heavily loaded, lubricated surfaces in relative motion.

Electronic surface tracer instruments yield a variety of surface parameters that describe height and spatial distribution of surface topography. Their numerical values in the microscale range, such as Ra (arithmetic average), are most commonly used. Computer and optical technology have fostered the development of optical topographic sensors, which enhance surface characterization in three dimensions.

Graphical traces from the old electronic instruments popularized the notion that asperities are jagged mountain peaks that are readily “broken off” when lateral forces are applied to them. This came about because the vertical scale on the trace was usually amplified at least 100 times more than the horizontal scale so that less paper was used to portray the important features of surfaces. Actually, asperities resemble rolling hills more than jagged mountain peaks, having slopes that average in the range of 1° to 5° or so. Asperity contact is better represented as occurring on very low slopes rather than the commonly drawn slopes of 30° or 45° .

7.2 Modeling Surfaces

The modeling of surfaces in contact requires some sort of numerical characterization of surface topography. The simplest notion of surface roughness is the sinusoidal ridge pattern, or perhaps the close-packed array of spheres. Actual roughness is much more complicated and quite difficult to express satisfactorily in numerical form. Roughness is thought of mostly in terms of asperity height, but distribution and shape of asperities are also important, and all of these attributes appear to be more random than regular across a surface. From a tribological perspective, peak height and slope of roughness features are important. Surfaces with a *plateau* texture are almost always desired over equally distributed *peaks* and *valleys*. Available instruments yield a host of ways to express surface roughness, most often statistical in nature. But few people, if any, can surely connect any single value or group of values

with surface performance. As with so many other topics in lubrication, the better course of action in using surface roughness–measuring instruments is to gain experience with only one or two surface roughness expressions (parameters) and to connect these with the functioning of the machine component of concern.

7.3 The Creation of Asperities

Asperities are usually taken as entities that simply “exist” on surfaces, but it is useful to consider how they are formed. Surfaces in mechanics are taken simply to be the boundary of a *semi-infinite* solid of no particular internal structure. Actually, metallic and ceramic solids are made up of atoms, and polymeric solids are made of identifiable arrays of atoms (i.e., molecules). Solids that are solidified (cast) from the molten state take on a surface topography (e.g., roughness, waviness) that is some combination of the surface features of the container (mold) plus the shape of surface grains as they attempt to grow in their natural crystallographic directions. Surfaces cut by tools or abrasive substances take shapes that result from the material being torn or fractured by the passing cutting edges. This leaves torn edges and “ironed” folds on the surfaces of ductile materials, which are severely cold-worked in the substrate. It leaves grooves and cracks on and in the surfaces of brittle materials. Surfaces influenced by corrosion assume shapes that result from having different grains corroding at different rates along different crystallographic directions.

7.4 Correcting Surface Deficiencies

Manufactured surfaces are certainly not perfect for their future encounters with mating partners in lubricated contacts. Because many processing steps are required to improve surface topography and near-surface integrity for their ultimate use, economic considerations play a large part in the final condition of the surface. As a practical matter, the contact just has to live with whatever surface quality it is given. To survive initial operation with less-than-perfect surfaces, chemical treatments such as phosphating are used.

Economic considerations also bring into play many low-cost materials that are surface hardened for improved durability. The diffusion of carbon (carburizing) or nitrogen (nitriding) into steel improves hardness and wear resistance. But hard iron nitrides, which appear as thin white layers at the surface when etched, can occur in nitrided steels. These *white layers* have low ductility and are easily fractured under stress.

If economic considerations permit, surfaces may be coated with hard or soft coatings. Silver coatings are used to provide “compliance” to the surface and improve heat transfer. Hard coatings, like titanium nitride (TiN) or thin dense chrome (TDC), are used for wear resistance and corrosion resistance. Diamond-like coatings (DLC) have the potential of making their way into use for wear resistance and low friction.

The near-surface region of lubricated contacts is enormously complex in terms of its topography, composition, and mechanical properties. To make matters worse, this structural element does not stand alone. Its neighboring structural element, the surface film region, is intimately connected to the near-surface region. The intimate connection is described in the following section.

8 SURFACE FILM REGION AND BOUNDARY LUBRICATION MECHANISMS

The structural element that we identify as the surface film region is a whisper in thickness, but mighty in influence. It is well known that surface films are important to the mechanism of boundary lubrication. These elusive films are the last defense mechanism to prevent adhesion and accommodate shear. These films may be in the form of oxides, adsorbed films from surfactants, and chemical reaction films from other additives. They can also be derived from bulk fluid or the surrounding atmosphere. The thin region of a surface film is illustrated in Figure 6.17.

8.1 Incompatible Assumptions about Surfaces: Mechanics versus Chemistry

In the mechanics of lubrication, a solid body ends at a plane and the next substance is a lubricant; the solid has its (bulk) properties, the lubricant has its (bulk) properties, and there is no interaction between them. Peculiarly, although successive layers of fluid between moving surfaces are sheared past one another, a common assumption in hydrodynamics is that the layer of fluid touching the solid surface does not “slip.” This is a most remarkable phenomenon. It is an essential feature of the mechanism of hydrodynamic lubrication, and it is the “engine” of boundary lubrication.

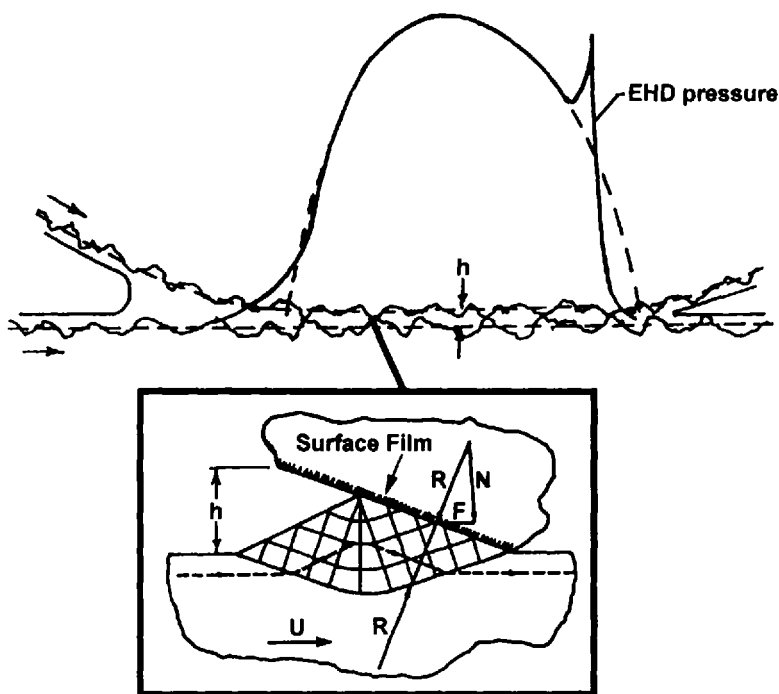


Figure 6.17 The surface film region.

There is, in fact, an interaction between a lubricant *in contact* with a solid. Solid surfaces are atoms with their outer “neighbors” removed from them. These outer atoms exist in a higher state of energy than when they were submerged in the solid. The increased energy is what was required to fracture the bonds that formed this new surface. In a tensile test, for example, this is most readily seen in the case of a perfectly brittle solid because no energy is expended in plastic deformation in the fracture region.

Simply stated, a surface atom in an elevated state of energy can be restored to its original energy state by returning neighbors of its own kind to its vicinity. However, if a neighbor of its own kind is not available, an atom of another kind will restore a fraction of the energy rise that occurred during fracture. The new neighbor becomes attached or adsorbed to the solid surface, with a strength of attachment roughly relative to the amount of energy released on adsorption. On introduction of shear, the strength of attachment may be sufficient to resist or impede large-scale slip between a fluid and solid surface.

8.2 Two Levels of Surface Energies in Adsorption

Surface interactions are actually surface *regions* of interactions. The outer layer of atoms in a surface is displaced from its equilibrium crystallographic lattice location. This displacement distorts the lattice array in the next layer, and so on, decreasingly into the next layers. *Surface energy* of a solid is the sum of the energy changes that occur in all affected layers of atoms into the solid substrate. In exactly the same way, all fluid molecules near the solid are altered in form and properties by the bonding energies in the region of interaction. The following paragraphs discuss the lubricating qualities of adsorbed substances. The discussion applies to all liquid and gaseous substances that approach a solid surface.

Some molecules adsorb to a solid surface with low energy, on the order of 0.2 kJ/mol of the adsorbate. There is no change in the chemical state of the attached molecules. Liquid molecules at the solid surface adjust their natural structure to the atomic structure of the solid. The range of adjustment extends with diminishing effect into the volume of attached molecules. The result is a significant increase in flow resistance or viscosity of the adsorbate. A large adjustment of physical properties occurs when gases adsorb to a solid. These gases build in several layers and pack so tightly on a solid surface that the adsorbed layer has properties similar to those of a liquid. These layers exist on all surfaces that are exposed to atmospheric gases, including water vapor. Their presence significantly affects sliding friction.

Some substances are chemically altered on adsorption to a solid. These chemical alterations are found to lower the surface energy by an amount in the range of 2.5 to 25 kJ/mol of the free adsorbate. This type of reaction is referred to as *chemical adsorption*. The adsorption of oxygen to all solids (except gold) results in the formation of oxides. Other reactive gases also form new compounds.

8.3 Adhesion

When two solid surfaces are brought close to one another within their normal atomic spacing of about 0.5 nm, they will adhere or bond together. No other action, rubbing, or heating is required. The strength of the bond varies widely. The ultimate bond strength is that in the substrate itself, but the relative lattice orientation of the two

surfaces can influence the strength of the bond to a great degree. In the case of metal, the atomic array or lattice pattern in the two surfaces need not align perfectly. They will create strong bonds, that is, the adhesion strength is high. In the case of ionic and covalent structures, as in most ceramic materials, adhesion strength is reduced to 2% or 3% of the substrate strength—provided the lattice patterns in the surfaces are out of alignment by only a degree or two.

However, if the solids cannot be brought to within 0.5 or even 2 nm of each other, they will not bond. Adsorbed films are usually thicker than these dimensions, and they prevent high adhesion. Physically adsorbed films can be displaced over time, but chemically adsorbed films are not likely to be displaced unless there is some sliding. Adhesion between solids is thus influenced by two factors: lattice alignment and *screening* by adsorbed substances. Two metals in close proximity can potentially produce the highest adhesion. But, compared with ceramic materials, they are more likely to have chemically adsorbed films which prevent adhesion. The bonding between polymeric surfaces is attributable to the weak van der Waals forces, which assure that only very weak adsorption occurs on these surfaces. Adhesion is important because the factors that influence adhesion also influence friction to a great extent.

8.4 The Lubricating (or Separating) Qualities of Adsorbed Substances

The scale of physical adsorption extends a distance into the adsorbed layer on the order of 5 to 10 nm in the case of simple fluid molecules. For long molecular chain fluids, the scale of influence extends to a micrometer. These long-chain molecules are often depicted as being attached to the solid surface by active end groups with long tails extending away from the solid. Whereas it is easy to refer to these scales of influence, it is much more difficult to develop sound models for the behavior of the altered fluid layers in practical systems. The properties of these fluid layers have not yet been measured. Quite simply, however, these films can be modeled as liquids with spatially increasing viscosity, to a high value approaching 1000 times the bulk viscosity in the first liquid “layer.” In this sense, these surface films cannot be defined in terms of thickness.

The effective scale of chemical adsorption is measured by the thickness of the new substance formed on the surface. This can range from nanometers (nm) to tens of micrometers (μm). The mechanical properties of the new film depend on what forms on the solid. In some instances, a long-chain molecular substance is formed (sometimes referred to as a polymer), and in other cases an ordered structure or solid is formed. Often a molecular substance forms on top of an ordered structure. The long-chain molecular substance could probably be characterized as a viscous substance, with the usual but not confirmed property of firm attachment to the solid surface. The solid would behave as a solid, but the strength of its attachment to the substrate also influences its lubricating function with imposed sliding. Many of the common solid substances that are formed, such as oxides and others materials, are brittle in bulk form. However, when they are present in the form of thin films, and particularly when they are under high three-dimensional compressive stresses, they become more likely to flow plastically.

8.5 Secret Compositions and Mysterious Properties

Despite the tremendous importance of surface films to boundary lubrication, the exact properties of adsorbed films are not well known. There is some value in speculating on these properties and incorporating reasonable properties into models and hypotheses for their lubricating qualities. There is far more work devoted to chemical composition of surface films than to their physical properties. The act of formulating fluids for the creation of surface films is an art more than a science. The process involves selecting chemistry, not physical properties or mechanisms. Therefore, composition and concentration reign in the storehouse of secret formulations.

Because surface film properties are mostly a mystery, technical progress is derived from an experience base gathered from the notions of field results or laboratory tests. Screening tests in the laboratory, as well as major qualification tests for the introduction of new fluid formulations into service, are more historical than rational. The difficulties of testing for performance attributes of new surface film formulations are partially attributable to the mysteries of surface films themselves. There is also a surprising lack of understanding of how the lubrication mechanisms actually play themselves out in service. A systematic approach to this is summarized in later sections. In the meantime, the fourth structural element of a lubricated contact, the *subsurface region*, is highlighted in Section 9.

9 SUBSURFACE REGION

The subsurface region, which may be on the order of 50 to 1000 μm below the surface, does not appear at first to be connected to lubrication mechanisms associated with hydrodynamic film generation or surface film formation. Although the subsurface region is remote from the tribological actions taking place at the surfaces, it still “feels” these actions by way of transmitted stress. The subsurface region is important with respect to failure mechanisms that result from plastic flow and fatigue. These failure mechanisms can have their initiating sites “subsurface.” The subsurface region is the foundation or “roadbed” of the tribosystem. Material properties in the subsurface region must be able to tolerate the transmitted stresses at the stress levels and stress cycles demanded by the duty cycle of the equipment.

9.1 Demands on Subsurface Region

The demands on the subsurface region are derived from the normal load, which gives rise to a pressure distributed over an area of “contact.” The subsurface region becomes an important element of the tribosystem when the applied pressure is high relative to the strength of the subsurface material. When the applied pressure is low compared with the strength of the subsurface region, the demands on the subsurface region are diminished. The stress field may then be confined to the near-surface region only.

Friction, which creates a tangential stress “at the surface,” can be thought of as a modifier to the stress field created by the normal load. The degree of modification on the normal stress field is directly related to the coefficient of friction.

If the load on a lubricated contact is being shared by asperities, or if surface motions generate micro-EHD pressures, the normal stress field is modified to yet another degree. The degree of asperity modification is influenced by asperity shape,

height distribution, the number of asperities sharing the load, and the elusive *asperity friction*. Asperity pressure and friction put a “ripple” on the pressure distribution across the area of contact. If the contact is finely divided among asperities, the subsurface region may not feel this ripple. If a few isolated asperities are at work, the subsurface region will be annoyed by the hammering upstairs.

This discussion shows that the depth of tribology technology in the surface to be concerned with is a function of the depth of the stress field below the surface. Although friction coefficient and asperity phenomena may complicate the picture, at least the size of the subsurface playing field can be identified so that the approach to problem solving and technical developments can be better focused.

9.2 Dimensions of Pressure and Stress Fields

Because the purpose of lubrication is to bear the stress and accommodate the strain in the contact, it is important to quantify the *dimensions* of the pressure and stress fields. The engineering dimension of the pressure of a conformal contact is simply the load divided by the area of contact. Design calculations for conformal contact are frequently based on the *projected* area of contact, although the actual area of contact may be significantly smaller. In addition, the *real* area of contact may be even smaller. Care must always be given to *edge effects* where the termination of one body does not coincide with its mating surface.

The pressure and stress fields of nonconforming bodies with elastic deformations are calculated from Hertzian theory [1]. The theory of Heinrich Hertz was motivated by his study of Newton’s optical interference fringes (such as those shown in Figure 6.15) and the problem of elastic deformation between two glass lenses in contact. His theory was worked out in 1880 during Christmas vacation when he was 23-years-old. From his theory, a combined elastic modulus E' can be defined as

$$\frac{1}{E'} = \left[\frac{(1 - \sigma_1^2)}{E_1} + \frac{(1 - \sigma_2^2)}{E_2} \right] \quad (6.5)$$

where σ_1 and E_1 are Poisson’s ratio and elastic modulus of body 1, and σ_2 and E_2 are Poisson’s ratio and elastic modulus of body 2.

9.3 Point Contact Dimensions

For a *point contact* where two spherical bodies are in elastic contact, a combined radius of curvature, R , is defined as

$$\frac{1}{R} = \frac{1}{R_1} + \frac{1}{R_2} \quad (6.6)$$

where R_1 and R_2 are the radii of curvatures of bodies 1 and 2 respectively.

In engineering practice, the normal load W is usually available, and it is used in Eq. (6.7) to calculate the radius, a , of contact and in Eq. (6.8) to calculate the maximum pressure, P_{\max} .

$$a = \left(\frac{3WR}{4E'} \right)^{1/3} \quad (6.7)$$

$$P_{\max} = \left(\frac{6WE'^2}{\pi^3 R^2} \right)^{1/3} \quad (6.8)$$

A characteristic of point contact elastic behavior is that the maximum pressure and Hertzian radius of contact are proportional to the cube root of the load.

Sometimes the maximum pressure is replaced with a *mean* pressure, which is $2/3 P_{\max}$. The pressure distribution over a point contact area is given by

$$P = P_{\max} \left[1 - \left(\frac{r}{a} \right)^2 \right]^{-1/2} \quad (6.9)$$

where P is the pressure at any radial point r within the contact. From Eq. (6.9), the pressure is maximum (P_{\max}) at the center of the contact, where $r = 0$. The pressure is zero at the edge of the contact, where $r = a$. The distribution of pressure produces a uniform normal displacement within the circular contact, that is, the contact is flat (the surfaces are parallel).

It is also of interest to calculate the total elastic deformation δ in the normal direction as a result of a normal load W .

$$\delta = \frac{a^2}{R} = \left(\frac{W^2}{16RE'^2} \right)^{1/3} \quad (6.10)$$

When the elastic deformation δ is calculated for typical EHD contacts, we find that the amount of elastic deformation is much greater than the thickness of the EHD film itself. This result is compatible with the notion that typical EHD lubricated contacts are Hertzian with respect to pressure and elastic shape.

9.4 Line Contact Dimensions

Line contacts are generated when one or more of the contacting bodies are cylindrical and the radii of curvature are generated around parallel axes. A line contact has a length L , a half-width of contact b , and a combined radius of curvature R . The characteristic line contacts can be calculated by using Eqs. (6.11) and (6.12).

$$b = \left(\frac{4WR}{\pi LE'} \right)^{1/2} \quad (6.11)$$

$$P_{\max} = \left(\frac{WE'}{\pi LR} \right)^{1/2} \quad (6.12)$$

A characteristic of line contact elastic behavior is that the maximum pressure and Hertzian half-width of contact are proportional to square root of the load. The pressure distribution for a line contact is given by

$$P = P_{\max} \left[1 - \left(\frac{x^2}{b^2} \right) \right]^{-1/2} \quad (6.13)$$

where x is a distance from the centerline of the contact.

9.5 Stresses Below the Surfaces

From the Hertzian pressures described above, it is possible to calculate the stresses in the contacting bodies. At the surface, the stress components are all compressive, except for the very edge of the contact where the stress is tensile for a point contact. This is the greatest tensile stress anywhere. This localized tensile stress is responsible for what are called *Hertzian stress cracks* in brittle materials.

A stress component of importance to fatigue is the *principal shear stress*, which has a value of approximately $0.3P_{\max}$. For point contact, the maximum shear stress is at a depth below the surface of about $0.48a$. For line contact, the maximum shear stress is located at about $0.78b$. The maximum shear stress of about $0.3P_{\max}$ is the greatest in the entire stress field, exceeding the shear stress at the edge of the contact. Therefore, plastic yielding is expected to initiate below the surface, rather than at the surface.

Surface friction modifies the stress field. As the coefficient of friction increases, the stress field becomes skewed, and the maximum shear stress moves closer to the surface. Asperities with *overpressure* (i.e., above Hertzian) create additional near-surface stresses. If surface friction is high enough, local asperity stress fields may join the subsurface stresses created by the Hertzian pressure. This condition may be critical. Surface-initiated cracks caused by asperity and other defects can then be driven deeper into the surface by the subsurface Hertzian stresses.

For Hertzian contacts, it is convenient to think of two major stress fields. The global stress field is created by the Hertzian pressure distribution, and the near-surface stress field is created by surface asperities, local depressions, debris, and other "defects" at the surfaces. Between these two stress fields one can also define a *quiescent zone*, which is located between the near-surface region and the subsurface region. The quiescent zone resides at a depth below the surface in which the local asperity and surface defect stresses are not significant and in which the stress field from the macroscopic Hertzian contact stress is not yet appreciable. This zone is quiescent from the point of view of stress and the accumulation of plastic flow and fatigue damage. The existence of the quiescent zone is important with regard to rolling contact fatigue. It inhibits the propagation of cracks between the stress field in the near-surface region and the stress field in the subsurface region.

9.6 The Core Region

Below the subsurface region is sometimes a *core material*, which is not really a structural element of the tribosystem. The core region is highlighted because materials, which must be selected for purposes other than tribological, are frequently surface modified to achieve desired qualities. There are many examples where it is desired to have properties of the core material different from the *case material*. To impart structural toughness, hydraulic pump gear teeth are usually case hardened to achieve wear and scuff resistance. The case may be hardened to a depth of approximately 1 mm, which is usually well below the subsurface region. The hardness of the core is controlled to achieve ductility for tooth strength. Although case-hardened materials generally provide good wear protection, they can lead to a catastrophic wear mode when the softer core material is exposed.

10 DYNAMICS OF A TRIBOSYSTEM

The preceding sections have described the structural elements of a tribosystem. The construction of the near-surface and subsurface regions must bear the applied stress. The generation of hydrodynamic films and the formation of surface films function to accommodate shear and control tangential friction forces. When the tribosystem is set into operation, the mechanistic processes within the structural elements begin.

There are many lubrication and failure pathways that can be taken. From the very start, some of the structural elements will never be the same again. If the structural elements are viewed as a dynamic system, it is possible to anticipate or explain some of these mechanistic pathways. The following sections describe some of the dynamic interactions likely to take place and their consequences in terms of failure processes.

10.1 Dynamics of Asperity Stresses During Initial Sliding

The most important interactions for the initiation of failure are those between the structural elements of the near-surface region and surface films. The controlling interactions are on a microscale and are associated with the dynamic interaction of asperities.

At the very start, many asperities on one surface encounter asperities on the opposite surface and transfer load from one to the other. New surfaces, which require some sort of “run-in,” transmit high pressure to the asperities approaching three times the yield strength of the softest of the two bodies. The surfaces are likely to have 90% of the normal load transferred through plastically deforming asperities. This makes it reasonably certain that most asperities are straining progressively during initial sliding.

In addition to the normal load, sliding introduces shear forces to the contacting asperities. This produces a result that cannot be predicted from the principles of elasticity. Shear forces, in addition to the normal load, influence the amount of plastic flow. When a shear force is applied, the contacting asperities tend to “collapse” inward, and the micro-area of contact increases. This behavior is associated with a *yield criterion* that is expressed in several equations, one of which is that of vonMises:

$$(\sigma_x - \sigma_y)^2 + (\sigma_y - \sigma_z)^2 + (\sigma_z - \sigma_x)^2 + 6(\tau_{xy}^2 + \tau_{yz}^2 + \tau_{zx}^2) = 2Y^2 \quad (6.14)$$

where σ is a normal stress, τ is a shear stress, and Y is the yield strength of a material in uniaxial tension. Taking only a single normal stress and a single shear stress, the equation could be simplified to $\sigma_x^2 + 3\tau_{xy}^2 = Y^2$. This result shows that when a shear stress is introduced, the normal stress on asperities is diminished, not by reducing the applied normal load but by increasing the area over which the load is carried.

10.2 Dynamics of Asperities During Continued Sliding

During initial sliding, the highest asperities experience severe deformation. After a few cycles these asperities will fail and produce loose particles in the interface. These entrapped particles can, in turn, inflict plastic deformation in other regions. If the “new” and exposed material created by plastic flow at the surface is not protected against adhesion, the surfaces will soon become unacceptable for further service unless the load is extremely light.

The protection of existing and newly created asperities is important with respect to adhesion and friction. This point is dramatically illustrated by experiments conducted in a vacuum. If the interaction of asperities is operating in the empty space of a vacuum, many asperities and loose particles may weld or bond together, effecting a pure state of adhesion. In air, which often contains water vapor in addition to oxygen, adhesion is inhibited considerably. Many soft metals slide together with no lubricant deliberately applied, but nonetheless are lubricated by oxides and physically

adsorbed gases on the surface. Some ceramic materials also acquire a surface layer by reaction with ambient gases, which act to inhibit adhesion.

The formation of these surface films is an essential event in the control of friction or shear force at the asperity site. The discussion in the previous section explains the role of shear force on the yielding of asperities to accommodate the normal load over a larger asperity area. There is a further and even more important effect of the shear force.

Values of the ratio of shear force to normal force that are below about 0.3 tend to "flatten" or reduce colliding asperities in height, whereas values of the ratio above 0.3 tend to "push" metal along and increase asperity height. This ratio of shear force to normal force is parallel to the notion of coefficient of friction, but in this case it is applied to asperity encounters. When the ratio of shear force to normal force is below 0.3, the sliding surface becomes smoother and, over time, fewer and fewer asperities will continue to plastically deform. However, although most asperities continue to deform elastically under load, some are likely to have high loads and high friction, and thus will plastically deform.

It is important to understand that the coefficient of friction at an asperity site may be quite different from the *global* friction coefficient measured across the entire contact. When the coefficient of friction on many asperities exceeds 0.3 by a good margin, the asperities will build up. The heights of asperities are built up by "pushing" metal in the sliding direction. The highest asperities will begin to carry a larger fraction of load, building up still more and remaining in this state over some distance of sliding. Temperatures in these asperities will increase, the metal softens, the adsorbed films become thinner or softer, and the coefficient of friction on such asperities will rise still more. This is a progression leading to gross loss of surface integrity as a growing number of asperities build up material in the same direction and at the same time.

Most manufactured surfaces for lubricated contacts are designed, perhaps unintentionally, to narrowly skirt disaster. They will be loaded to the point just short of failure. A small fraction of asperities on such surfaces is always progressing toward failure, but the loads upon them and the surface friction are momentarily relieved. If a sufficient supply of the *proper* chemical species is available to the surface during that short interval, a low-friction chemically adsorbed film will form to keep friction below 0.3 or so. The asperities in this sequence may be said to have "healed," and there is evidence that this takes place continuously on surfaces of many long-life lubricated contacts in service.

The availability of the *proper* chemical species is, incidentally, an uncommon occurrence across the wide range of industrial materials and lubricants. Low-cost iron-based materials with low total alloys operating in slightly acidic lubricants seem to form films of the right durability and at the right rate. Whereas low-alloy steels may be good candidate combinations for surface film formation, they are generally not the materials of choice for reasons associated with the requirement to accommodate high normal stresses in the near-surface and subsurface regions. In the whole scheme of things, hardness and strength are important trade-off attributes with surface film formation. Some of the worst candidates for surface film formation are stainless steels, where chrome oxides limit the access of surface film-forming chemical species.

10.3 Run-in and the Bifurcation

If the initial running of a lubricated contact is moderately well lubricated, the interacting asperities undergo plastic flow. As previously discussed, a friction coefficient at asperity encounters below about 0.3 is likely to “iron down” the most protruding asperities. Over time, the number of asperities that are subjected to plastic flow diminishes, and asperity friction is reduced. It is likely that most of these asperities will now be cycling in the elastic range of stress, although some will continue toward plastic failure.

Run-in is the conditioning of surface features, which initially stand proud above the average terrain of the original surface topography. Run-in of the type that seems to produce remarkably durable surfaces involves two interactive processes. *Topographical* run-in reduces asperity height and tends to create a “plateau” surface texture. *Chemical* run-in creates durable and perhaps low-friction surface films. Surfaces that are properly run-in are less vulnerable to overload, start/stop events, and momentary liquid lubricant interruption.

If the initial running of a contact is not properly lubricated, high asperity pressures and shear forces can lead the contact down a pathway of surface roughening. In many cases, only minor changes in operating conditions will determine whether the asperity events lead to run-in or complete loss of surface integrity. This elusive bifurcation is associated with many puzzling early component failures.

10.4 The Thermal Effect

Thermal conditions on a micro- and global scale drive the fires of interactions among the lubricant films, surface films, and the near-surface region. Surface temperature is an important ingredient in these interactions and a key link between lubrication and failure. Temperature significantly influences the viscous properties of the fluid that control the thickness of a hydrodynamic or EHD-generated lubricant film. It is also a major driving force in the formation of chemical reaction films. Temperature influences the rate of fluid degradation. It influences the strength of surface films as well as the flow properties of the material in the near-surface region. Consequently, it is not surprising that the “total” temperature in a contact is frequently used as a failure criterion for catastrophic failure event, such as scuffing.

From a simplistic point of view, the total temperature (T) is the sum of the bulk temperature (T_b) of the component and the “flash” temperature (T_f) associated with the instantaneous temperature rise derived from the friction in the lubricated contact. Flash temperature may arise from the traction of the lubricant film as well as from the energy dissipated at asperity encounters. The temperature rise at an asperity encounter may be derived from micro-EHD film generation, shear of surface films, adhesion between asperities, and deformation of the material in the near-surface region. The magnitude of T_f can be predicted if simplifying assumptions about the coefficient of friction and convection heat transfer are made.

10.5 Feeding the Frenzy

The survival of sliding surfaces in severe service is clearly dependent on the availability of a *protective film* in the vicinity of the asperities of sliding surfaces. This protective substance can be inserted into the tribosystem in its final form by at least

two methods. One method is to coat a surface before use with a substance; if it "lubricates," it will be called a solid lubricant. The solid lubricant is bonded to the surface and accommodates interfacial shear generally as a sacrificial film, which eventually wears away. Another method is to insert useful substances into a stream of liquid carrier and hope that enough of it gets to the right place to "lubricate."

A more common method of providing a protective film is to add a physically or chemically active substance into a liquid carrier. The active substance, or *additive*, adsorbs to the surface or reacts with the solid surface to create a new substance. The liquid carrier or fluid is itself a lubricant and serves to generate hydrodynamic or EHD films. The formulated fluid has inherent physical properties as represented by its temperature–viscosity, pressure–viscosity, and traction behavior. The formulated fluid also has chemical attributes that are derived from small concentrations of active ingredients as well as from the base fluid itself. It is important to understand that physical adsorption and chemical attributes for lubrication are realized in the lubricated contact. The chemically derived lubricating properties are not inherent in the fluid itself. They are developed as part of the tribosystem.

Additives or constituents of the base fluid having physical adsorption to the surface no doubt provide some effectiveness over limited range of pressure. Fundamental studies have been conducted by surface scientists in which a very thin film of some simple molecule, a solvent for example, is placed between flat mica sheets. Sliding resistance and film thickness are usually measured. There is clear evidence that the molecules of the first layer near the solid assume an ordered lattice arrangement of the solid, with decreasing order in succeeding layers of the liquid. This order enhances the near-surface viscosity for a limited range into the fluid. On sliding, the order becomes momentarily disrupted. It is likely the same order could be seen in commercial fluids in practical systems, but the practical effectiveness of adsorbed layers is not clear.

It seems quite clear that if the proper chemical reaction occurs between some constituent in the lubricant and a metal (or metal oxide) surface, the surface will endure much greater severity than without that constituent in the lubricant. Some of the products of the chemical reaction have been identified, but the physical properties of these products in commercial systems are not understood.

The actions of chemical attributes of fluids in the lubricated contact are sometimes referred to as *chemical boundary lubrication*. The chemical pathway by which the effective boundary lubricating films are formed is mostly a mystery. It appears that effective surface films require high "confinement" pressures and/or high shear rates. Although surface films are observed in areas where high pressures or temperatures do not exist, they are much less effective. A common notion is that high flash temperatures generated in the contact are the driving force behind the formation of effective surface films. The action of confinement pressures, which are generated at local sites by entrapped fluid under high shear, may play a more significant role than conventionally thought. This *tribochemical* action is no doubt accelerated by temperature rise at the surface. Along with the assistance of temperature, the catalytic actions of the near-surface or contaminant materials help to control chemical film formation.

Asperity encounters under severe operation are producers of chemical products which react and "combine" with the surface. Some chemical products may be lost to the system by dissolving into the fluid and being transported away. Some of the

chemical products generated during operation can have ample time to dissolve into the fluid after the equipment is shut down.

10.6 Always Vulnerable

A major point to understand is that the formation of an adequate chemical boundary film requires some sliding, during which time the surfaces are unprotected and vulnerable to failure by scuffing or galling. The rate of chemical reaction is thus important. Hydraulic fluid chemistry is carefully formulated to simultaneously avoid severe corrosive reactions at the surfaces and achieve chemical reactivity responsive enough for protection. If original surfaces put into service are adequately prepared, the formulated reactivity of the fluid should be sufficient during initial run-in as well as in repairing damage during operation. Operational damage may be caused by overload, by the entrapment and abrasive action of debris, and by moments of inadequate supply of reactive chemical species to the sites that need to be repaired. Although there is incomplete understanding of the formation of protective films, there is evidence that some plastic flow of asperities and flaking off of native metal oxide are necessary events in the formation of protective substances.

The dynamic interactions and "competition" between chemically active materials in the fluid and the surrounding environment of lubricated contacts present a significant difficulty for fluid formulation, testing, and performance prediction. The formation of surface films and their composition and "properties" are part of the tribosystem itself. There is little understanding of how these films play out in lubricating the near-surface region. There are also no engineering parameters that connect to the dynamic actions in the tribosystem. The adequacy of film regeneration depends on an adequate supply of the necessary chemical species in the liquid carrier, adequate flow of the carrier through the contact region, and adequate time in microscopic contact regions to allow completion of chemical reaction. The adequacy of lubrication depends on the thickness and mechanical properties of these films.

10.7 Functional Role of Lubrication: Stress Relief

Having taken an inside view of asperity encounters, the functional role of lubrication becomes clear. Lubrication action must relieve normal stress and tangential stress (friction) at asperity sites.

The easiest lubrication means for normal stress relief of asperities is the generation of hydrodynamic or EHD films. Although adequate hydrodynamic or EHD films can reduce asperity stresses to minimal values, the pressure of commerce usually results in a final manufactured design that is barely adequate. There will always be asperity encounters in essentially all practical contacts. The dynamic generation of films diminishes to nothing during starts and stops. It is hoped that at least partial surface separation is achieved during operation to ease the pain. This action moderates the pressure in the contact from high local pressures at asperity sites to minor pressure ripples along the expanse of the contact. The dynamic imposition of a fluid also creates an alternative means to accommodate shear. The degree of normal stress relief is, to a first approximation, a function of the hydrodynamic film thickness relative to the roughness heights of asperities. Remember also that when surfaces are in relative motion, micro-EHD-generated pressure at asperity sites can offset what is anticipated from the average film thickness generated. Hydrodynamic and

EHD films transform load support from the microscale to the global scale and, in the process, reduce the maximum pressure everywhere. The lubricated contact becomes relieved of its “headache” and is less vulnerable to failure.

It is important to understand the scale of dynamic pressure generation and surface stress fields. Pressure generation in conformal contacts is low (MPa range) and distributed over a relatively large area. Concentrated contacts form high-pressure (GPa range) EHD films that are concentrated in small Hertzian deformation regions. The stressed region for concentrated contacts is transmitted much deeper into the supporting materials than are conformal contacts. Even with fully separated surfaces, high subsurface stress for concentrated contacts is not relieved. But in both cases, the dynamic generation of a film relieves asperity stress.

The functional role of lubrication to relieve tangential stress (friction) at asperity sites is a more complex situation than normal stress relief. One can rationalize the notion that the dynamic imposition of a fluid creates an alternative substance to help accommodate shear in a field of asperity sites. Without a “full film,” the shear is now distributed in the contact between a fluid and surface film. This situation is commonly known as *mixed-film lubrication*, i.e., the lubrication is mixed between hydrodynamic, or EHD, mechanisms and the so-called boundary lubrication mechanisms.

We must now address the most common dynamic interaction between the two major structural elements of a lubricated contact found in practice: hydrodynamic, or EHD, films and surface films. The dynamics of this interaction have enormous implications for the success of lubrication and the prevention of failure. Hydrodynamic films provide the chemistry to enter the workplace. The chemistry that is carried by the fluid “conditions” the surfaces to allow the hydrodynamic, or EHD, mechanisms to flourish. If the dynamic condition for hydrodynamic film generation is limited, the transported chemistry steps in to help carry the load and bear the shear. The dynamics of this interaction is reflected in friction. Although the sources of this friction in the contact are important for survival, they can only be inferred from gross friction measurements and asperity damage that appear on the surfaces.

10.8 Mechanisms of Global Friction

Although friction is rarely measured in lubricated contacts of operating equipment, it is an important internal parameter that governs the generation of heat and the onset of failure. Friction can be measured on a global scale, encompassing everything in the contact. Friction reflects the state of the material being sheared in the contact. From experiments, we know that characteristic friction behavior also reflects *what* is being sheared. Monitoring friction coefficient is like monitoring the heartbeat of the contact.

Starting from the simplest form of friction, the shear force of a full hydrodynamic film is directly connected to its viscosity and shear rate. Shear rate varies with film thickness and the relative velocity between the surfaces. The friction coefficient of hydrodynamic films may be on the order of 0.01. One must be cognizant of the fact that the total viscous friction of high-speed or high-viscosity hydrodynamic films is greatly influenced by the viscous churning of the fluid upstream of the point of closest approach. The churning component hides the component of viscous friction in the area where additional friction forces may be coming from asperity encounters.

With high-viscous churning friction, asperity friction may be lost in the noise until catastrophic asperity friction is on its way.

As contact pressure increases, the viscosity of the fluid may increase as a result of the generated pressure. Viscous friction, then, is a function of pressure as well as temperature. As discussed above, fluids under Hertzian-like pressures in the range of GPa shear like pseudosolids with a shear limit. For most hydraulic fluids, the shear limit gives a maximum friction or traction coefficient of about 0.08 for mineral oils and most synthetic fluids. The shear limit of some types of hydraulic fluids gives a friction coefficient as low as 0.02. The shear limit decreases linearly with temperature so that EHD friction coefficient for high-temperature contacts may be on the order of 0.01. Note that high-pressure EHD friction coefficients on the low end (0.01) may actually be about the same as hydrodynamic friction coefficients. In addition, EHD friction coefficient on the high end (0.1) is approximately equal to the friction coefficient of surface films. Although friction coefficient is the heartbeat of the contact, it may only reflect the general health of the contact without saying much about exactly what is wrong or right. This is unfortunate, because surface failure is primarily attributable to events on the asperity scale, and the asperity scale friction can sometimes be hiding from detection. Nevertheless, friction measurements can be made which separate EHD friction, micro-EHD-generated tangential forces, and some sort of surface film or plastic flow friction. Notions of friction should be centered around the thickness of hydrodynamic films relative to asperity height and the pressure in these films. With respect to friction coefficients over the entire contact that can be tolerated without gross failure, the sliding velocity plays an important role. Low-speed sliding can generally tolerate high friction coefficients better than high-speed sliding.

10.9 Mechanisms of Asperity Friction

The friction or resistance to sliding of contacts is primarily attributable to events on a global scale, whereas surface failure is primarily attributable to events on the asperity scale. Asperity friction refers to resistance to sliding of one asperity "over" another. The summation of friction on all asperities in a contact system that survive for even a short time is not likely to exceed 2% or 3% of the overall friction of that contact. This is because the sum of asperity contact areas is usually only a small fraction of the total contact area between two mating surfaces. However, asperity friction profoundly affects the progression of surface failure by its combined influence on the formation of chemically adsorbed films and on the rate of progression toward failure of material in and around asperities.

The relatively small contribution of asperity friction to overall friction seems counterintuitive because the friction in failing systems usually increases considerably just before catastrophic failure. But surface failure has usually progressed toward system failure irreversibly by the time a friction increase is observed. Small *failing events* occur continuously, but in systems that survive, these failing sites do not expand or generate new failures downstream. Rather, they recover in time to continue to function during subsequent contact events.

Surface failure occurs when both normal and shear (frictional) stresses are applied that are of sufficient magnitude and number of cycles to cause movement of substrate material of solid films, either along or from the surface. The action begins

on and in asperities. Removal of material (wear) may occur, along with displacement of material. Both may alter surface roughness and, depending on the direction roughness takes, the surfaces may run-in or lose surface integrity.

When fluid films in lubricated contact become progressively thin, asperity encounters may start off as benign events, resulting in only small perturbations in pressure. With thinner overall films, one asperity would be expected to sweep out an area occupied by a passing asperity and, as they approach one another, the fluid between them becomes highly compressed and shears at a high rate. Asperity encounters with severe interference can progress in a variety of ways depending on the "energy" of encounter. At this point, it is convenient to consider the outcome of events depending on whether the encounter is a low frictional energy event or a high frictional energy event. Recall that frictional energy is the product of frictional force and shear rate.

10.9.1 Low Frictional Energy Events

Asperity encounters with low frictional energy include low plastic deformation rates at asperity sites. As hydrodynamic or micro-EHD films become thinner, their thickness approaches that of adsorbed films. Because of the influence of the surface forces from the substrate, any physically adsorbed films that are present may have effective viscosity greater than the bulk fluid. Chemically adsorbed films are likely to have an oxide attached to the solid and other products of chemical conversion adsorbed to the oxide. One can envision a process involving the behavior of a squeezed-down fluid film merging with adsorbed films. At some point, it may be possible that the adsorbed film is controlling asperity friction, and thus an interposed fluid film may not be necessary. The lack of interposed fluids is usually referred to as "dry sliding," but so-called dry surfaces in air are always covered with oxides (except gold) plus adsorbed liquids and gases. This explains why solids in long-term static contact do not weld or bond together.

Low asperity pressure and shear stress characterize low frictional energy events. They survive on weak physically adsorbed films or chemically adsorbed films from mild reactions.

10.9.2 High Frictional Energy Events

Asperity encounters with high frictional energy include high rates of plastic flow in asperities. The events described in the previous section are altered by high-energy input caused by high sliding velocities or high asperity pressure. The high shear rate in both the fluid and asperities heats the surrounding fluid, thereby reducing its viscosity, which results in thinner fluid films. It should be noted that for EHD contacts, heating of the fluid in a load-carrying region does not affect the EHD film thickness, which is determined in the inlet region. The local heating of the fluid affects the micro-EHD film thickness at the inlet of the asperity encounter. At the same time, adsorption strength of physically adsorbed substances diminishes when temperature rises, thereby reducing the effective viscosity in the adsorbed film.

Chemical adsorption is also influenced by temperature, depending on the availability of proper chemical species in the vicinity of the asperities. Higher temperature increases the rate of oxidation and the reaction rates leading to the formation of the polymeric substances on top of oxides. Although the latter reaction rates increase with temperature rise, the physical properties are diminished with temperature rise.

Thus, there is an optimum combination of the thickness of surface films and physical properties of these films for achieving minimum asperity friction.

High asperity pressure and shear stress characterize high frictional energy events. They survive only by chemical adsorption and reaction films, which are quick to respond to the severe demands of the moment. Although the temperature rise and plastic flow of high-energy encounters increase the rate of chemical reaction, the shear strength of the reaction films may decrease and chemical composition may be altered.

10.10 Failure Without Touching

Material failure in surfaces that are in sliding or even rolling can, and likely often do, take place without actual contact. Contact is in the sense of the atoms in opposing surfaces being subject to one another's force fields. This seems like a trivial distinction, but it is important when it comes to describing the sequence of events that leads to either successful lubrication or failure of systems on the scale of asperities. A common notion in engineering is that surfaces are either adequately lubricated or fail by adhesion. If this were completely true, debris would never fall from a sliding pair! Failed surfaces often show evidence of some severe sliding, which may look like adhesion has taken place, but these events usually occur in the last seconds of failure. These are not the initiating events.

Surface failure without contact may be seen to occur in cavitation erosion, which is common in hydraulic systems. Surface initiated rolling contact fatigue with micro-EHD films can easily be initiated without contact. This is a common occurrence on rolling contact surfaces damaged by debris dents. Cracks initiate near the shoulders of the dents, where high micro-EHD pressures are generated. Sufficient stress can be imposed on a solid by a liquid to easily plastically deform ductile materials and fracture brittle materials.

10.11 Failure Processes and Descriptive Terms

There are numerous failure processes emanating directly from asperity encounters and many other failure processes not directly related to asperity events. In essentially all cases, the source of failure initiation is confined to localized and microscale events. Failure processes are controlled by four basic mechanisms involving adhesion, plastic flow, fatigue, and chemical reaction. The user ultimately defines the success of lubrication and the failure of surfaces. Failed surfaces are characterized with descriptive terms, not always reflecting the failure process. Most wear and fatigue failure terms reflect only one of several failure processes along the pathway to the final surface condition, not to mention the initiating failure event. Although a host of surface deterioration and failure terms are in common use, they all seem to fall into three major categories: wear, scuffing, and fatigue.

10.11.1 Wear

Continued plastic flow of asperities can lead to loss of surface material by wear. Actually, the removal of material may occur by low cycle fatigue. It may not be necessary to completely eliminate all low cycle fatigue of asperity material to maintain satisfactory performance. However, it is necessary to keep the size and flow rate of loosened particles down. Low-rate wear particle generation, which may also be

called *mild wear*, tends to polish the surfaces and is therefore also called *polishing wear*. Polishing wear can be associated with a continual process of removal and reformation of chemically adsorbed species, like oxides. If chemical reactions occur, the reaction products may be removed by a sacrificial wear process to prevent adhesion. If the sacrificial wear process occurs at a high rate, the result may be called corrosive wear. At the other extreme, local adhesion, or adhesive wear, can occur if chemical reaction products are not present to accommodate shear at the interface.

Failure by wear is generally attributable to loss of engineering tolerance. The consequence for hydraulic systems is excessive leakage. The rate of wear on a surface can easily be accelerated by its own wear particles. Once bits of material loosen, they can migrate in the contact regions. Some may re-adhere, although not very firmly in most instances because the “active” surfaces on newly formed particles can become protected from adhesion by adsorbed films. Wear particles are usually hard and will form grooves when entrapped between softer surfaces. The hard particles will also remove chemically adsorbed films or chemical-reaction films (see Fig. 6.18). The availability of fluid to flush out wear debris particles and the access of channels through which loosened particles may escape from the system are essential to prevent accelerated wear.

10.11.2 Scuffing

Scuffing is a catastrophic form of wear derived from a high frictional energy event. Scuffing is driven by high sliding velocities. Scuffing initiated from high asperity pressures can result in a sudden and total loss of surface integrity and gross failure

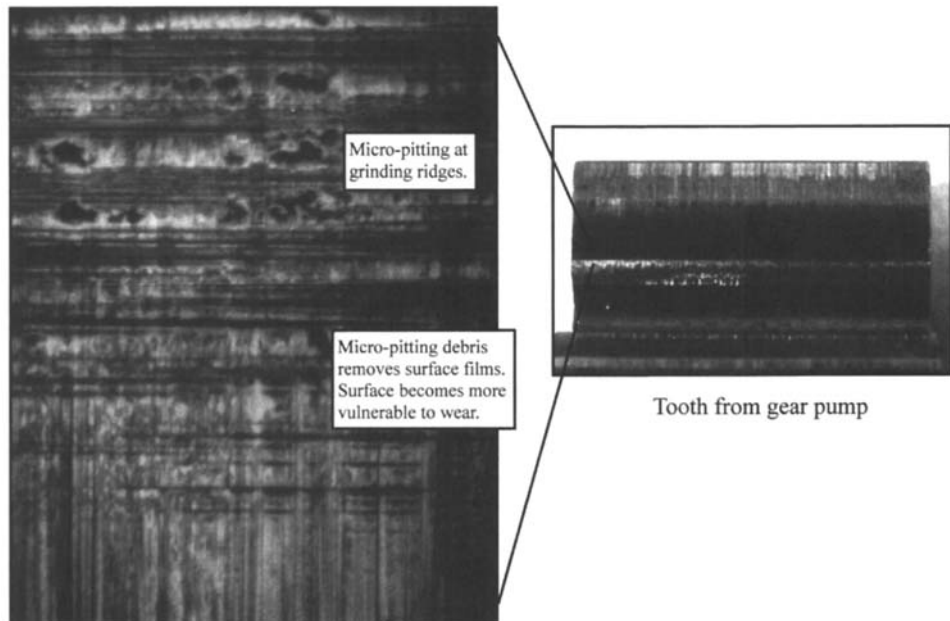


Figure 6.18 Entrapped micro-pitting debris removes surface films, causes wear grooves, and makes the surface vulnerable to scuffing.

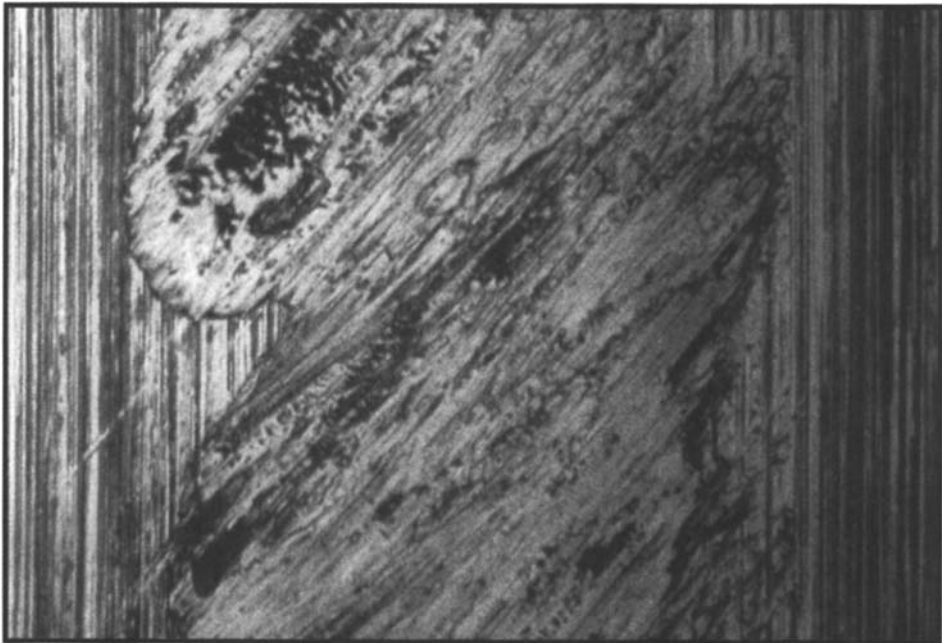


Figure 6.19 Scuffing is a high-energy event associated with a sudden and catastrophic loss of surface integrity.

of the near-surface region (see Fig. 6.19). When scuffing is initiated from low asperity pressures, the damage may be confined to the surface roughness features only. This is sometimes called *microscuffing*. Scuffing is also sometimes called *galling*, but galling seems to be used more frequently with unlubricated sliding.

10.11.3 Fatigue

Concentrated contacts with high Hertzian pressures or weak subsurface material can lead to crack initiation in the region of maximum subsurface shear stress. If cracks propagate under cyclic stresses to the surface, sections of subsurface and near-surface material are removed, which causes *spalling*. Spalling is a subsurface initiated failure caused by the Hertzian stress field, which can be influenced by frictional stress at the surface.

When the fatigue process initiates at or near the surface, the loss of small fatigue particles is called *pitting*. Pitting may initiate at asperity sites where local pressures are high. When pitting occurs on roughness features during or shortly after run-in, it is called *initial pitting*. After run-in and with marginal hydrodynamic or EHD film thickness, microcracks can form on the surface because of high surface friction. Microcracks are frequently formed in the presence of one-way sliding friction, where the near-surface material is strained or “ratcheted” in one direction (see Fig. 6.20). This progression to failure is equivalent to adding loads to a tensile specimen progressively until it fails. The details may not be important, but the result is that cracks grow and join others. The rate of progression in crack propagation increases logarithmically with applied stress, which is to say asperity cracking rates

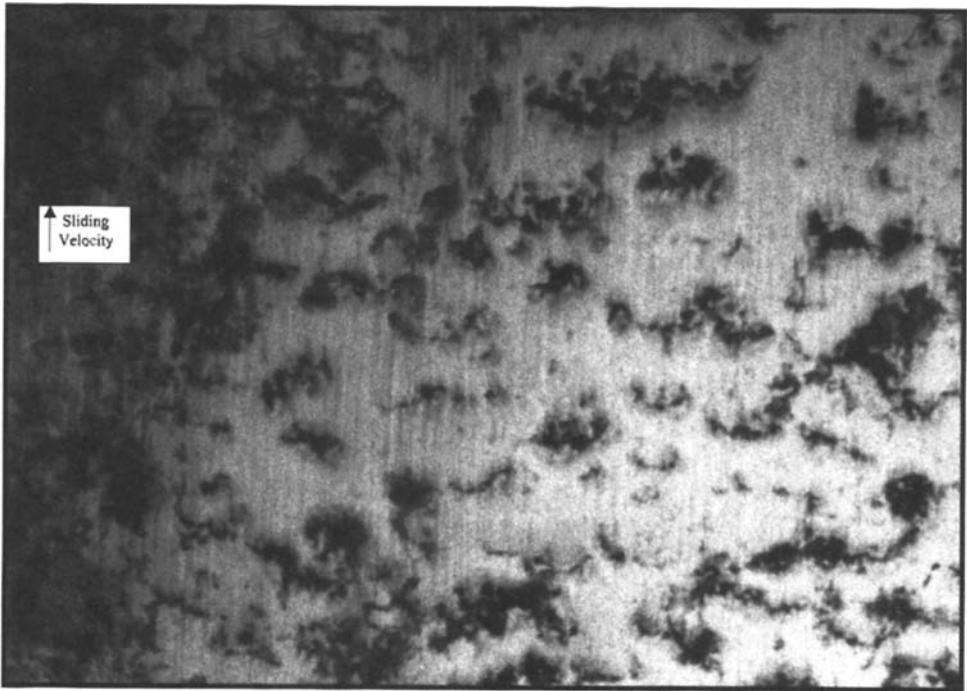


Figure 6.20 Microcracks on gear surface following many cycles of tangential and normal stress.

will increase logarithmically with applied load. Furthermore, acidic environments have been found to increase the rate of crack propagation in fatigue cycling.

Surface-initiated fatigue is complex and almost always influenced by wear. It can be both an interactive and competitive process. The wearing away of surface-roughness features during initial running reduces the propensity for pitting. Pitting can be initiated by at least three factors: (1) high asperity stress without high friction, (2) poor surface film and high friction at asperity sites, and (3) microcorrosion pits caused by reactive additives in the fluid.

11 SYSTEMATIC TRIBOLOGY

The previous sections show that most of the fundamental mechanisms of lubrication and surface failure deal with events on a microscale. The mechanisms involve four major structural elements that are dynamically linked in a tribosystem. The development of hydraulic systems requires the management of these mechanisms on engineering terms. Because hydraulic systems encompass a multitude of conformal and concentrated contacts composed of structural elements with numerous materials, the engineering task is unwieldy. When one considers the complexity of each lubricated contact in hydraulic systems, it is not surprising that fluid formulation, material development, and design sometimes turn out to be incompatible. The lack of correlation among fluid bench tests and their disconnect with field service is a testimony of the tribology nightmare.

The complexities of the situation can be overcome to a large degree by introducing the concept of *systematic tribology*. Systematic tribology is the process of understanding and developing the structural elements of practical tribological contacts and mechanisms of interaction in a systematic way. The challenge of fluid formulation, material development, and design is to “capture” mechanisms that control performance. The focus is on the creation of structural elements whose attributes are able to carry high normal stress and bear the severe tangential shear in the setting of a tribosystem. With this approach, external engineering parameters take on a new meaning, which gives a more rational connection to what is happening on a micro-scale.

11.1 Tribosystem Input and Output

The framework of thinking for systematic tribology is illustrated in Figure 6.21. The tribosystem is identified with its major structural elements:

- HF hydrodynamic film
- SF surface film
- NS near-surface region
- SS subsurface region

The tribosystem is driven by “input” parameters, which can be appropriately characterized as stress, kinematics, and environment. Stress is the normal stress applied to the contacting bodies. If available, it can also be the normal asperity stress. Kinematics defines the motions within the tribosystem, in particular, the sliding velocity and entraining velocity. The environment is defined by thermal and chemical conditions in and around the tribosystem. The chemical environment includes the surrounding gases and fluid-supplied chemistry that are introduced into the system.

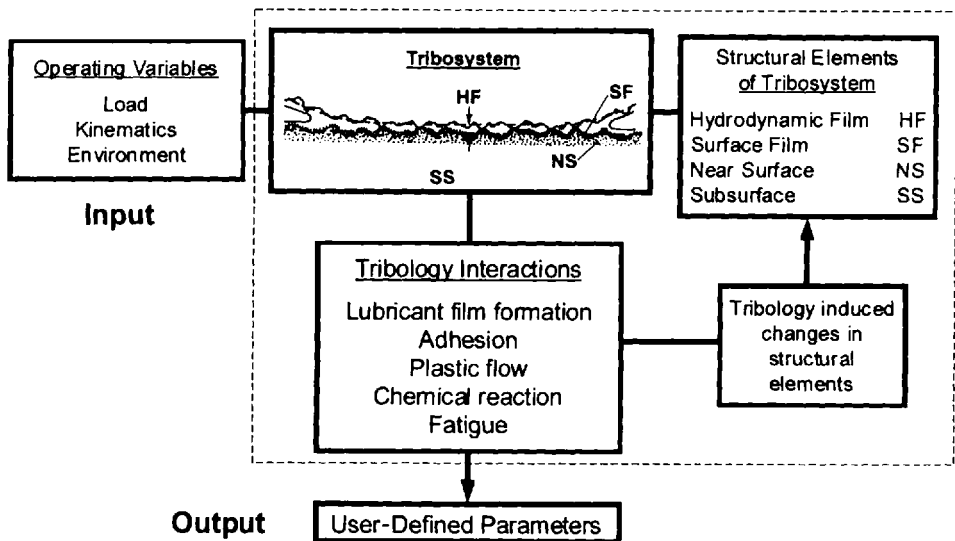


Figure 6.21 Dynamic interactions among the structural elements of a tribosystem in operation.

Once the tribosystem is put into operation, mechanistic processes like hydrodynamic film generation, adsorption, plastic flow, and fatigue are set into action. These mechanistic processes induce changes in the structural elements which in turn influence the mechanistic processes. This cycle of activity defines the dynamic interactions among the structural elements.

From an engineering perspective, the dynamic interactions among the structural elements can be considered a so-called black box. The black box is driven by input parameters defined in engineering parameters. The output parameters to the black box can also be defined in engineering terms. The output parameters are user defined. Depending on the functional demands of the lubricated contact required for service, they may vary considerably. Examples of output parameters are scuffing resistance for high load, wear resistance for low-speed reciprocating motion, abrasive wear resistance for debris-contaminated hydraulic fluids, or long-life pitting resistance.

The purpose of the tribosystem, as illustrated in Figure 6.21, is to connect engineering parameters with mechanistic processes. The internal working of the black box need to be exposed in understandable mechanistic processes, which relate directly to the construction of structural elements and how they perform in service. Without this understanding, fluid formulation and material development will continue to be conducted on a trial-and-error basis with bench tests having little correlation with service.

11.2 Connecting Engineering Parameters with Mechanistic Processes

Engineering parameters can be connected to both mechanistic processes and their interactions among the structural elements by considering the basic functions of lubrication. The structural elements must carry the load and bear the shear without losing surface integrity and ability to function. The task is to select engineering parameters that can be most appropriately linked to normal stress and tangential strain at asperity sites.

11.2.1 Entraining Velocity

Among all the tribological mechanisms, the generation of a hydrodynamic, or EHD, film is by far the most mature with respect to theory and predictability. Film thickness controls the degree of asperity encounter. The separation of surfaces, particularly with EHD-generated films, is highly precise and predictable. The film is remarkably "stiff" with respect to the elasticity of the surfaces and the applied load.

Film thickness is directly related to the fluid entraining motion of the surfaces. Because the kinematic motions of load-carrying components are generally known, the entraining velocity provides a useful engineering connection to fluid film-forming mechanisms. The entraining velocity, U_e is defined as

$$U_e = \frac{1}{2}(U_1 + U_2) \quad (6.15)$$

where U_1 and U_2 are the surface velocities of the contacting bodies at the point of contact. The entraining velocity is directly linked to the flow of fluid through the contact. For a "pure" sliding contact, the entraining velocity is equal to half the velocity of the moving surface. A contact with a combination of rolling and sliding has an entraining velocity that is half the sum of the surface velocities. Surface

velocities are vector quantities, which means that an entraining velocity for surfaces moving at an angle relative to one another can be calculated as a vector sum.

The engineering value of the entraining velocity results from how it controls the dynamic generation of a structural element (HF) of the tribosystem and how its thickness varies with the duty cycle of the equipment. Because the thickness of a hydrodynamic film determines the degree of engagement between asperities, the entraining velocity is directly linked to asperity-controlled mechanisms. Another engineering value of the entraining velocity and its connection to hydrodynamic, or EHD, film generation is that it is directly linked to the suppliers of base fluids. Fluid properties representing temperature–viscosity and pressure–viscosity characteristics are key ingredients for the construction of the dynamically generated HF element.

11.2.2 Sliding Velocity

The sliding velocity across the contact controls the shear between the contacting surfaces. The sliding velocity U_s is defined as

$$U_s = (U_1 - U_2) \quad (6.16)$$

Sliding velocity is also a vector quantity. The magnitude of sliding is a frequently known engineering parameter that can be connected to the duty cycle of the equipment. The sliding velocity, in conjunction with the entraining velocity, provides an engineering link to the degree of strain at asperity encounters. Another engineering value of sliding velocity is that for EHD contacts, the sliding velocity invokes traction behavior, which is a fundamental property of base fluids.

11.2.3 Normal Load and Pressure Distribution

The engineering parameters of entraining velocity and sliding velocity control the level of penetration during asperity encounters and their rate of shear. The all-important pressure at asperity sites is controlled by the distribution of pressure among asperities and the fluid film. The contribution of pressure distributed directly to asperities is an engineering unknown. The best that can be done is simply to address the normal load or pressure applied on a global scale.

The applied load is a frequently known or estimated engineering quantity. For concentrated contacts, the applied pressure is calculated from the load through Hertzian theory. For conformal contacts, the pressure may simply be calculated by assuming the load is distributed over a “projected” area. The pressure calculated is sometimes used to judge the lubrication severity of a contact through the use of a “PV” factor. The PV factor is the product of the pressure (P) and sliding velocity (V). Unfortunately, PV is not directly linked to mechanisms that control performance.

11.3 Mapping Dynamic Interactions with Entraining and Sliding Velocity

To demonstrate the engineering control afforded by entraining velocity and sliding velocity, hydraulic fluids have been mapped over a range of U_e and U_s [3]. Mapping is conducted with a single contact where the entraining velocity and sliding velocity are independently controlled. The mapping results for two hydraulic fluids are shown in Figures 6.22 and 6.23. The contacting surfaces are a steel ball running against a steel disc with surface roughness of 0.25 μm , Ra and 0.075 μm , Ra, respectively.

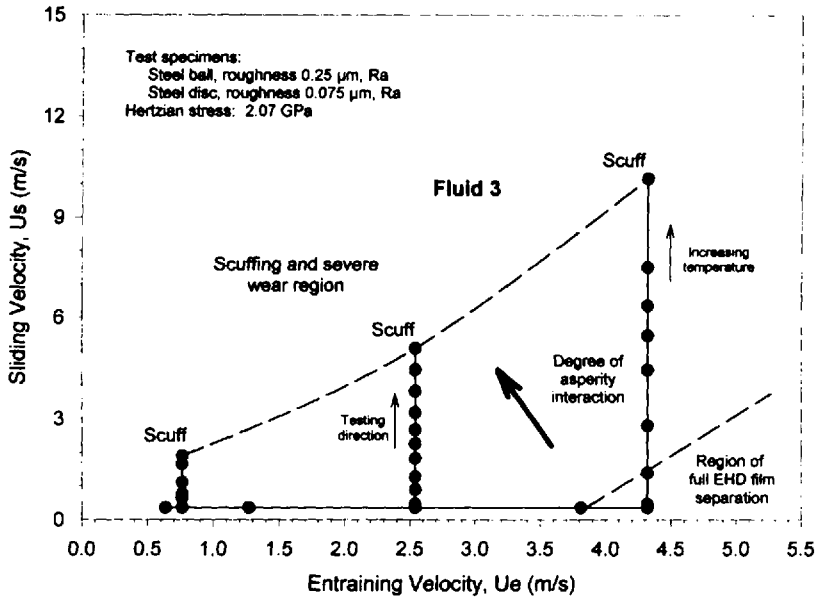


Figure 6.22 Performance mapping of a fluid using entraining velocity and sliding velocity to determine failure tolerance to degree of asperity encounter.

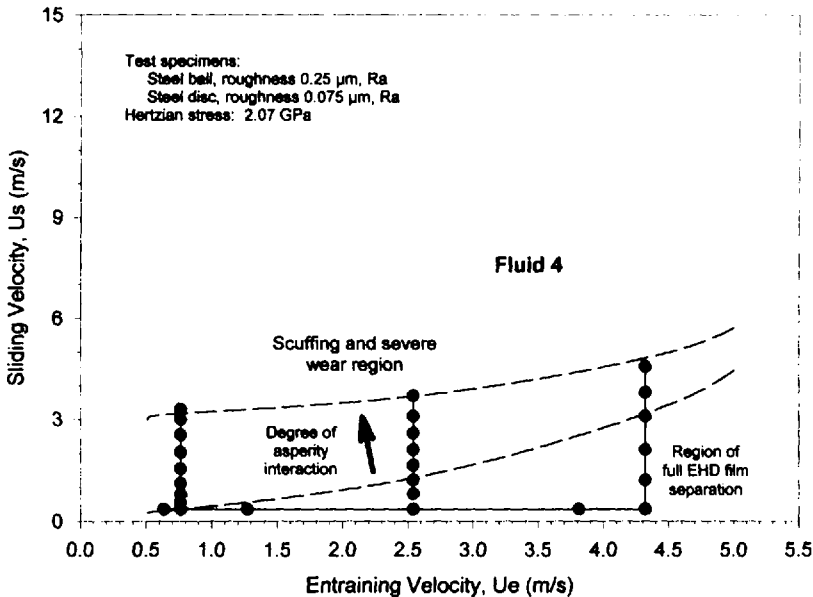


Figure 6.23 Performance mapping of a fluid using entraining velocity and sliding velocity to determine failure tolerance to degree of asperity encounter.

The applied load gives a Hertzian contact stress of 2.07 GPa. A series of tests is conducted for ten minutes, each over a range of entraining velocities and sliding velocities. New specimens are introduced for each test. Friction coefficient and surface temperatures are monitored to detect failure transitions.

High entraining velocities and low sliding velocities define a region of operation where shear is accommodated entirely by an EHD film (no asperity encounters). Lower entraining velocities and thinner EHD films relative to surface roughness reduce asperity height and create surface films (run-in). As sliding velocity increases, the surfaces eventually fail by scuffing. These experiments illustrate the dynamic generation of the structural elements for lubrication (HF and SF). The tests also evaluate the durability of the entire tribosystem. Failure is initiated at asperity sites, and the scuffing failure limit is clearly approached as the degree of asperity encounter increases.

The results in Figures 6.22 and 6.23 show that hydraulic fluids can have widely different lubrication performance because of the quality of the structural elements. Lubrication performance is derived from EHD films and surface films (elements of HF and SF). Fluid 2 shows much less EHD film-forming capability than fluid 3. However, fluid 2 is able to tolerate a much greater degree of asperity encounter than fluid 3.

These tests use engineering parameters to probe the individual structural elements of a tribosystem. The results have linkage to hydraulic gear pump lubrication and failure mechanisms. This linkage is made through the entraining velocities and sliding velocities that vary across a tooth face from its root to tip. The wide range of asperity shear above and below the pitch line gives rise to scuffing failure at the root or tip of the tooth along with pitting damage near the pitch line. Simulation of entraining and sliding velocities, along with other environmental conditions, allows replication of the same failure mechanisms found in service. If the appropriate failure mechanisms are simulated, fluid formulation and material developments can be orchestrated and efficiently tested to achieve predictable performance enhancement.

11.4 Mapping Failure Mechanisms in Engineering Terms

By considering dimensionless parameters with good engineering connection to real systems, the mapping of dynamic interactions of the structural elements, as described in the previous section, can be carried a little further. Because we need to have engineering connection to the asperity encounters, we can substitute the entraining velocity for the ratio of hydrodynamic of EHD film thickness (h) to surface roughness (σ). This is a more direct way to make an engineering link to asperity encounters. The roughness parameter, σ , reflects the combined roughness of the contacting pair. It is defined as

$$\sigma = (\sigma_1^2 + \sigma_2^2)^{1/2} \quad (6.17)$$

where σ_1 and σ_2 are the centerline average heights of body 1 and body 2. The ratio h/σ is known as the lambda (λ) ratio. The lambda ratio is commonly used to judge the quality of lubrication. Because surface roughness (σ) is characterized by average height departure from a mean plane and does not include three-dimensional texture, the lambda ratio has many difficulties. In addition, the truncation of asperities caused

by run-in is frequently ignored. Nevertheless, the ratio h/σ is a first-order parameter that serves a good purpose for now.

The sliding velocity used above reflects the shear between the surfaces. Another way to handle sliding, which is particularly appropriate when there is combined rolling and sliding, is to use the ratio of sliding velocity to entraining velocity (U/U_c). The ratio (U/U_c) is called the *slide-to-roll ratio*. With the definitions of U , and U_c given above, pure sliding, which has one surface stationary, gives a slide-to-roll ratio of 2. Pure rolling, where both surfaces are moving with equal (and collinear) velocities, the slide-to-roll ratio is 0.

From testing experience gathered over time, a number of life-limiting surface failure mechanisms can be mapped with the parameters for h/σ and slide-to-roll ratio (U/U_c). Such a map is illustrated in Figure 6.24. When a large portion of the duty cycle allows operation at high h/σ , asperity pressures are low and surface life is long. With high Hertzian stress or low fatigue-resistant materials, fatigue initiation is subsurface, and the surface ultimately fails by spalling or pitting. Relatively low h/σ , along with high sliding, can initiate asperity scuffing, which can transition into catastrophic scuffing. This phenomena is only observed at high surface speeds.

Low values of h/σ create high asperity pressure. When V/V_c is low, tangential stress on asperities is low, and asperity failure may teeter between asperity wear and fatigue (micropitting). Near-surface damage under low h/σ and low sliding, which is common to rolling element bearings, is frequently called surface distress or frosting. If higher sliding is present, asperities will tend to *wear* rather than fail by fatigue. Still higher sliding velocities can cause asperities to transition into scuffing or severe wear. Sometimes an intermediate region of microscuffing is present, when failure is confined to asperities only and the surface still has a chance to recover.

Operation at the extreme low end on h/σ only seems possible at low surface speeds without severe wear or scuffing. Surface durability is limited by wear, but wear may also be influenced by low cycle fatigue. The wear process tends to increase surface roughness.

11.5 The Consequence of Systematic Tribology

If asperity scale mechanisms can be linked to engineering parameters as illustrated above, the dynamic processes among the structural elements can be put on a more rational basis. The tribosystem becomes more understandable and is less of a black box. With better understanding, surface inspection of service hardware and failure analysis can now be much more revealing.

By using a systematic approach, actions taken to improve viscosity or pressure-viscosity properties of base fluids can be immediately evaluated with respect to failure modes mapped out. Additive enhancements can be evaluated for their impact on wear, scuffing, or fatigue processes. The performance gains with new materials or surface-engineering technologies can also be put into perspective. With a better correlation between testing failure modes and service failure modes, there is greater assurance that corrective actions taken will actually be realized in service.

If the structural elements of hydraulic system contacts are addressed as a tribological system, the introduction of new materials and fluid formulations can be accomplished with greater effectiveness. Systematic tribology helps to integrate the diverse technologies that are introduced into a tribosystem. Consideration of struc-

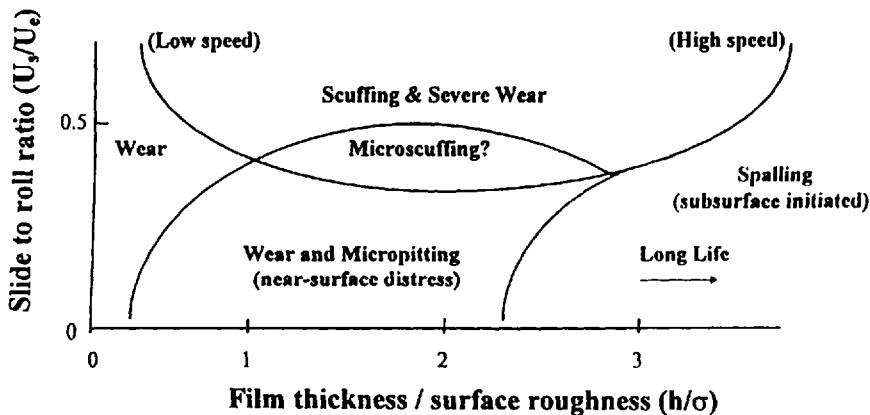


Figure 6.24 Postulated life-limiting failure modes controlled by engineering parameters.

tural elements identifies the connection between technical businesses that are normally disconnected. The hydrodynamic film element is associated with base stock suppliers. The surface-film element is associated with additive suppliers. The near-surface element is associated with heat treatment, coating, surface treatment, and surface finishing businesses. The subsurface element is associated with material suppliers. If design is focused more on capturing lubrication mechanisms and avoiding failure mechanisms, the potential outcome will be a synergistic construction of the technologies available. The consequence of systematic tribology is superior output from the tribosystem, even with greater input requirements. To do this requires practical engineering parameters, which reach down into asperity-scale events. This is clearly a work in progress.

REFERENCES

1. H. R. Hertz and J. R. Angew, Math (Crelle's j.) 1881, 92, pp. 156–171.
2. H. M. Martin, "The Lubrication of Gear Teeth," *Engineering*, 1916, 102, pp. 119–121.
3. L. D. Wedeven, G. E. Totten, and R. J. Bishop, "Testing Within the Continuum of Multiple Lubrication and Failure Mechanisms," ASTM STP 1310, *Tribology of Hydraulic Pump Testing* (G. E. Totten, G. H. Kling, and D. J. Smolenski, eds.) 1997, ASTM, West Conshohocken, PA, pp. 3–20.
4. D. Dowson, "Elastohydrodynamics," *Proc. Inst. Mech. Engr.*, 1967–1968, 182, part 3A, paper no. 10.
5. L. D. Wedeven, D. Evans, and A. Cameron, "Optical Analysis of Ball Bearing Starvation," *ASME Trans., J. Lubrication Technol., Series F*, 93(3), pp. 349–363.
6. C. Cusano and L. D. Wedeven, "Elastohydrodynamic Film Thickness Measurements of Artificially Produced Non-smooth Surfaces," *ASLE Trans.*, 1981, 24(1), pp. 1–14.

This page intentionally left blank

Fire-Resistance Testing Procedures of Hydraulic Fluids

GLENN M. WEBSTER AND GEORGE E. TOTTEN

Union Carbide Corporation, Tarrytown, New York

1 INTRODUCTION

Many test methods have been developed to reproducibly simulate industrial hydraulic fluid ignition hazards. In addition, fire hazards such as hydraulic system failure may also cause personal injury due to high-pressure, high-velocity fluid jets entering the body as the result of ruptured hoses, or parts of the system striking the body with great force [1]. Numerous factors must be modeled to adequately predict hydraulic fluid fire risk, including type of flame or source of ignition, amount of available energy relative to the amount of fluid, and physical state of the fluid [2]. The selection of appropriate tests to model fire resistance is usually mandated by either the government, insurance companies, or labor unions.

Hydraulic fluid fires have been disastrous with respect to loss of buildings, equipment, and, most importantly, human lives. Many of these fire losses have been detailed in the literature [3–7]. One article describes an incident in which workers were severely burned while working on a hydraulic line [8]. When the line burst, the fluid contacted an ignition source and caught fire, resulting in a death.

Fire is just one hazard that may be encountered while working with or near pressurized hydraulic equipment [1]. There have been reports of occurrences in which high-pressure, high-velocity fluid jets have entered the bodies of persons performing routine maintenance such as repairing a pinhole leak in a high-pressure hose. Several of these incidents have led to amputations and even deaths. This process of using high-pressure and high-velocity fluid has been utilized for administering inoculations and also as a precision cutting tool. Another hazard may be encountered when a section of a pressurized hydraulic system fails and strikes an individual with great force, causing injury or death. These examples illustrate the forces involved when employing high-pressure hydraulic systems.

In another 1956 example, a serious fire incident attributed to a hydraulic fluid occurred at the Marcinelle Mine in Belgium, at which time 261 men died [9]. It was later determined that 10 deaths were directly attributed to serious burns, but the other 251 died as a result of asphyxiation from the by-products evolved during the incineration of the hydraulic fluid. As a result of this disaster, ECSO countries, the National Coal Board, and the Ministry of Power in the United Kingdom initiated procedures to investigate the use of mineral oil hydraulic fluids underground. This study showed the following:

- Improperly designed or imperfections in hydraulic systems may substantially increase the temperature of the equipment and, subsequently, the temperature of the hydraulic fluid.
- Ignition of high-pressure fluid emissions due to equipment failure or line rupture has resulted in hydraulic fluid fires.
- Hydraulic fluid mists spraying from a high-pressure hose fracture could produce an electrostatic charge, causing fluid ignition.
- Underground fluid storage poses an increased fire risk and may serve as a fuel source during a fire.

A committee was subsequently formed by the National Coal Board and the Ministry of Power to produce a draft of testing requirements for fire-resistant fluids. The following criteria for defining a fire-resistant hydraulic fluid was proposed:

- The fluid shall demonstrate fire-resistance characteristics in compliance with adopted standards.
- The performance and longevity of hydraulic equipment will not be reduced below acceptable limits.
- Fire-resistant fluids shall not exhibit health hazards and will be environmentally acceptable.

The ASTM D.02 N.06 subcommittee was formed in 1966 to develop “improved” testing methods for hydraulic fluid applications. A 1966 ASTM symposium on hydraulic fluid flammability was held to examine fire-safety testing procedures in existence at that time for potential incorporation into national standards [10]. A second international symposium was recently held to update current international activities in this area [11].

In this chapter, an overview of the test procedures which have been reported to evaluate and quantify flammability properties of hydraulic fluids with respect to different types of ignition sources will be provided.

2 DISCUSSION

2.1 Fire Mechanisms

Fluid flammability is dependent on flammability mechanisms. Fire or combustion is an oxidation reaction consisting of three stages:

1. Initiation
2. Development
3. Termination

Numerous factors influence the duration and severity of these three stages [12]. Fire occurs in the vapor phase at the liquid surface and is dependent on the fuel availability, energy required to sustain the flame, and the presence of oxygen. The absence or removal of any one of these components will cause extinction of the fire.

Ease of ignition is a function of fluid vapor which is dictated by fluid viscosity and molecular weight and reactivity of the vapor with oxygen, which is dependent on chemical structure and thermal stability.

Reaction among the three components—fuel, energy, and oxygen—are required for fire generation and heat release. Heat may be accompanied by a cool (barely visible) flame or a hot (visible) flame.

The combustion reaction will continue after the initiation stage if the heat released is sufficient to provide the energy required to sustain the reaction of the fuel with oxygen. Therefore, heat release is an important variable in predicting fire potential. Continued fluid combustion is dependent on the rate of heat loss due to convection and radiation of heat through the air, and conduction through the liquid must be less than the sum of the rate of heat emitted by the ignition source and that available from the combustion process [12].

2.2 Ignition Sources

Hydraulic fluid ignition often occurs when a leak or break in the hydraulic system, usually operating at high pressures, results in a spray, stream, or mist of hydraulic fluid. The fluid may then ignite if it encounters an ignition source such as an electrical spark, flame, or hot surface [13].

The potential for a combustion of these various ignition sources must also be considered. For example, hot exhaust gases, hot metal surfaces, preexisting fire, or a spark may all potentially cause hydraulic fluid ignition [14].

A hydraulic leak or spill may wet a hot surface or form a pool, which may then be ignited by a nearby heat source. During ignition, a distillation process occurs which separates the hydraulic fluid into several components. One or more of these volatile components may be easily ignited by a spark or flame.

Porous or wicklike material such as pipe insulation, cardboard boxes, textiles, or even coal from mining operations may absorb hydraulic fluid. This fluid may slowly oxidize and form peroxide by-products which have the potential to undergo subsequent spontaneous combustion [13].

Table 7.1 summarizes several fire hazards to consider when selecting appropriate flammability test procedures [2]. Factors to consider when selecting a hydraulic fluid include the following [2]:

Table 7.1 Hydraulic Fluid Flammability Conditions

Source of ignition	Fluid condition	Environment
Flame	Pool or puddle	Air temperature
Spark	Spray-Stream or atomized	Air current
Hot metal surface	Vaporized	Equipment location
Electrical contact	Wicking	—

- Proximity of the fire hazard to the hydraulic equipment
- Availability of fire-resistant fluids
- Fluid properties
- Required equipment design changes

Various causes have been reported for naval fires and explosions of hydraulic fluid on shipboard systems. Potential causes of ignition include the following [15]:

1. Rapid compression or shock-wave ignition
2. Formation of carbon–oxygen complexes
3. Porous, oil-soaked medium present
4. Peroxide formation
5. Spontaneous ignition
6. Spray ignition
7. Electrostatic discharge

Because various sources of ignition may be present in a hydraulic application, it is important that the test method selected reasonably model the fire risk where the fluid will be used.

2.3 Fluid Classification

All fire-resistant fluids fall into two basic categories: those that derive their fire resistance from the presence of water and those that demonstrate fire-resistant qualities by their chemical composition or molecular structure [16].

The general designation for hydraulic fluids is HF [17]. Fire-resistant hydraulic fluids are further classified by composition according to ISO 6734/4 (Lubricants, industrial oils, and related products [Class L]—Classification—Part 4: Family H—Hydraulic systems) are shown in Table 7.2

Table 7.2 ISO Classification of Fire-Resistant Hydraulic Fluids

Fluid classification	Fluid description
HFAE	Oil-in-water emulsions, typically more than 80% water content
HFAS	Chemical solutions in water, typically more than 80% water content
HFB	Water-in-oil emulsions
HFC	Water–polymer solutions, typically less than 80% water
HFDR	Water-free synthetic fluids consisting of phosphate esters
HFDS	Water-free synthetic fluids consisting of chlorinated hydrocarbon
HFDT	Water-free synthetic fluids consisting of mixtures of HFDR and HFDS
HFDN	Water-free synthetic fluids of other compositions than HFD-R or HRD-S or HFD-T

Table 7.3 Factory Mutual Corporation Classification of Hydraulic Fluids

Group I	Water-glycol fluids with additives
Group II	Synthetic fluids including phosphate ester, polyol ester, and halogenated hydrocarbon fluids
Group III	Water-in-oil and oil-in-water emulsions

With respect to the FMRC HF classification scheme in Table 7.3, Group I fluids correspond to HFC, Group II fluids correspond to HFD(R,S,T,N), and Group III fluids correspond to HFAE, HFAS, and HFB, as summarized in Table 7.2.

Factory Mutual Research Corporation (FMRC) specifies three classifications for fire-resistant hydraulic fluids, which are shown in Table 7.3. Also shown are the general fluid properties, according to FMRC, that impart fire resistance [18].

2.4 Fire-Resistance Testing Strategies

One of the greatest concerns in fire-resistance testing is the selection of a procedure that adequately models the application of interest. Traditionally, most of tests conducted for modeling fluid flammability characteristics are the following [19]:

- Flash point
- Fire point
- Spontaneous ignition temperature

Two fundamental parameters should be considered when selecting a test to model an application [20]: ignition resistance and flame propagation. These two parameters model fluid ignition and the propensity of the fluid to continue to burn once ignited. The experimental strategy is twofold. First, the test should provide information regarding resistance to ignition. Second, if ignited, flame propagation must be considered.

Because each application has its own unique exposure, such as pool, spray, or mist, and ignition conditions, such as a hot metal surface or open flame, multiple tests are typically conducted [3].

The complexity of the thermal ignition process has led to the development of a variety of tests designed to model particular combustion mechanisms. These tests attempt to simulate flammability hazards encountered in industry with respect to exposed hot pipes, ventilated surfaces, surface material variations, and scale. Although there are many test procedures available, the testing, quantification, and interpretation of thermal ignition data are some of the most difficult problems in fire hazard evaluation [21].

2.5 Fluid Flammability Tests

2.5.1 Fluid Volatility Characterization

This section will summarize testing procedures normally required to model flammability potential due to fluid volatility.

Open-Cup Flash Point and Fire Point

The relative fire resistance of nonaqueous hydraulic fluids may be characterized by their flash and fire points. These procedures are described in ASTM D 92-90 (Standard Test Method for Flash and Fire Points by Cleveland Open Cup) [20–22]. Flash and fire points are determined by passing a flame over the surface of the fluid at constant time intervals during constant temperature rise. The flash point is the temperature at which the volatile vapors above the fluid surface ignite. The fire point is the temperature where the fluid itself ignites and burns for at least 5 s. These results are dependent on fluid chemistry and volatility primarily.

Increasing flash points and fire points are indicative of increasing fire resistance, particularly in applications where high-temperature fluid volatility is important, such as required in many aircraft applications. These tests are inappropriate for aqueous fire-resistant fluids because it is difficult to assess proper heat-up times. This leads to nonreproducible data because of variable evaporation rates. It is also difficult to directly relate the flash and fire point data to specific end-use fire-risk potential.

Oxygen Index

The oxygen index, as defined in ISO 4589, “is the minimum concentration of oxygen, by percentage volume in a mixture of oxygen and nitrogen, introduced at $23^{\circ}\text{C} \pm 2^{\circ}\text{C}$, that will just support combustion of a material under specified test conditions” [23]. The procedure for determining the oxygen index of a fluid is performed by placing a small quantity of test fluid into a glass cup positioned in a glass chimney, as shown in Fig. 7.1 [24]. An upwardly flowing mixture of oxygen and nitrogen is introduced and then ignited. The oxygen index is determined by the minimum amount of oxygen concentration required to sustain combustion for 60 s or more [25].

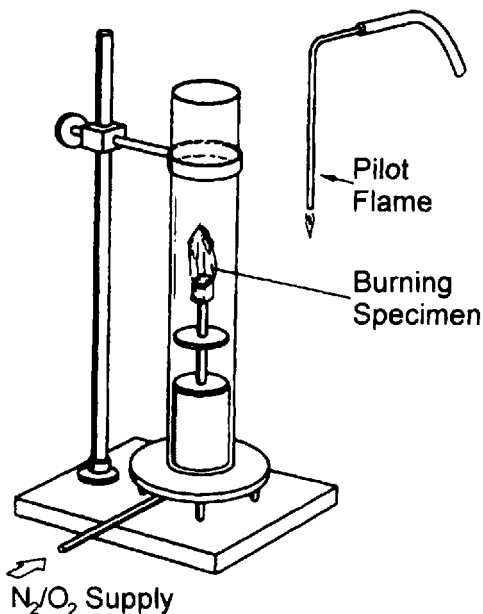


Figure 7.1 Apparatus for determining oxygen index.

Oxygen index determination is a simple and relatively inexpensive test to perform and appears promising as a quality control procedure, but it is not evident that this procedure offers any significant advantage over flash and fire points at this time [12]. Some illustrative examples of oxygen indices of various model compounds are provided in Table 7.4 [24].

It has been suggested that the measurement of the oxygen index is actually a measure of the “ease of flame extinction” and does not produce meaningful data with respect to fluid ignitability or flame propagation tendencies. This test also lacks sensitivity.

Autoignition Temperature

The autoignition temperature (AIT) is one of the most widely known thermal ignition test [21]. AIT is determined according to ASTM D 2155-66 (Standard Test Method for Autoignition Temperature of Liquid Petroleum Products), where a test fluid is

Table 7.4 Oxygen Indices for Selected Compounds

Trioctylphosphate	18.6
Ethylene glycol	14.8
Diethylene glycol	13.6
Trimethyl phosphate	23.7
Aroclor 1016	31.3
Aroclor 1221	20.5
Aroclor 5460	61.0
Castor oil	22.9
Dibutylsebacate	15.6
Ethylene glycol	14.8
Fyrquel 150 (Stauffer Chemical)	25.5
Fyrquel 20 (Stauffer Chemical)	25.9
Houghto Safe 1120 (EF Houghton Co.)	22.1
Houghto Safe P C F G 15	24.0
Hydraulic fluid MIL-H-83282	17.7
Hydraulic fluid MIL H 5606B	16.0
MIL-H-5606B hydraulic fluid	16.0
MIL-H-83282 hydraulic fluid fluorocarbon	17.7
Mineral oil USP	16.1
Mineral oil 5314A (Socony Molil Co.)	15.2
Olive oil	16.6
Paraffin oil, mineral oil (white, heavy)	16.4
SF96 (50)—GE Silicone fluid	21.4
SF96 (350)—GE Silicone fluid	27.3
SF1029—GE Silicone fluid	23.0
XF1050—GE Silicone fluid	13.3
Therminol 66	16.1
Trioctyl phosphate	18.6
Triphenyl phosphate	22.5
Tripropylene glycol	17.7
Vegetable oil	19.0

Source: Ref. 24.

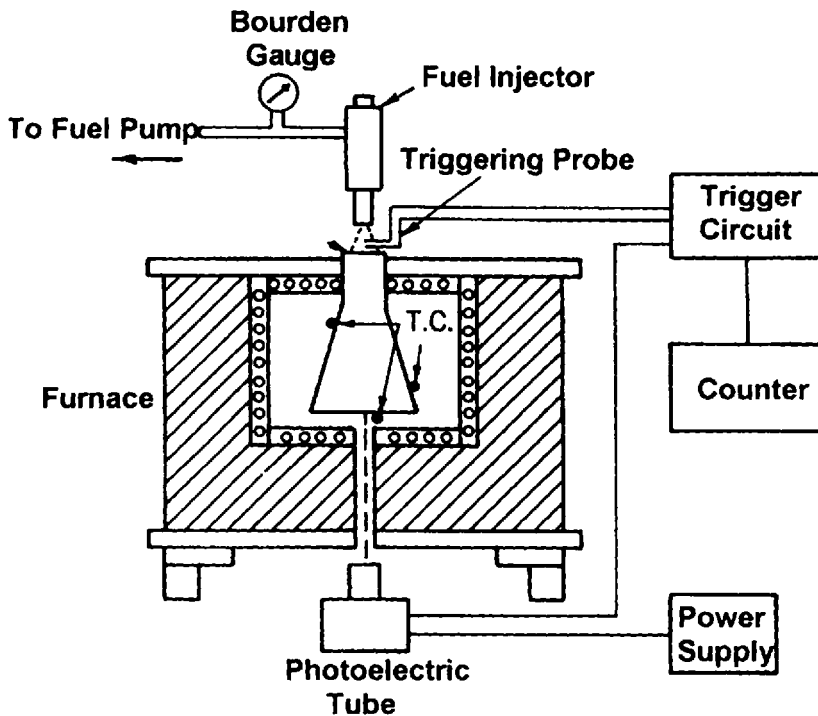


Figure 7.2 Apparatus for autoignition temperature (AIT) determination.

injected via a syringe onto the surface of an Erlenmeyer flask heated in an oven as shown in Figure 7.2 [20–30]. AIT measures the geometry-dependent spontaneous ignition temperature of a fluid in air at 1 atm of pressure. These measurements are difficult to relate to end-use applications [20]. MacDonald found that AIT varies with the size of the Erlenmeyer flask [31]. Table 7.5 shows AIT values for several common hydraulic fluids with corresponding fire and flash point data [12].

Table 7.5 Relative Autoignition Temperature and Open-Cup Flash/Fire Point Data of Common Hydraulic Fluids

Fluid	Autoignition temperature (°C)	Open-cup flash point (°C)	Open-cup fire point (°C)
ISO VG 10 mineral oil	320	166	180
ISO VG 46 triaryl phosphate	580	246	365
ISO VG 32 polyol ester	415	280	310
ISO VG 46 silicone fluid	470	300	340
ISO VG 7 Askarel (polychlorinated biphenyl)	>650	190	None

Rapid Compression

Ignition or explosion may occur when air in contact with a hydraulic fluid is rapidly heated by compression. Hydraulic fluid fires have occurred due to fluid ignition by rapid compression [32]. Because of this particular type of ignition hazard, tests have been developed to model the susceptibility of a hydraulic fluid to undergo compression ignition. A variety of compression-ignition tests are conducted by introducing air, at pressures comparable to those found in hydraulic systems, through a valve into a small-diameter pipe whose inner surface has been wetted with the test fluid [32].

A rapid-compression-ignition test has been developed by Faeth and White; it simulates a pipe containing high- and low-pressure air separated by a rapidly opening valve as illustrated in Fig. 7.3 [33]. When the valve is opened, pressure equalization occurs by pressure waves generated by opening the valve, as illustrated in Fig. 7.4 [33]. During this pressure equalization, a contact zone of rapidly changing temperature and density is formed which separates the expanded and cooled "upstream" gas from the compressed and heated "downstream" gas. This contact zone travels the length of the pipe, eventually compressing the "downstream" gas against the closed end of the pipe. It is in this region where pressure increases could potentially lower the spontaneous-ignition temperature (S.I.T) of a fluid, as illustrated in Fig. 7.5 [33]. Lowering the S.I.T in conjunction with the air-temperature increase ahead of the contact zone contributes to the fluid's potential for ignition.

This test has been performed using both 10- and 30-ft sections of pipe. The conclusions of these tests show that combustion is more difficult to obtain in the longer (30 ft) dead-ended sections where the rate of pressure increase is decreased due to the larger volume of the test section and the energy loss by convection and

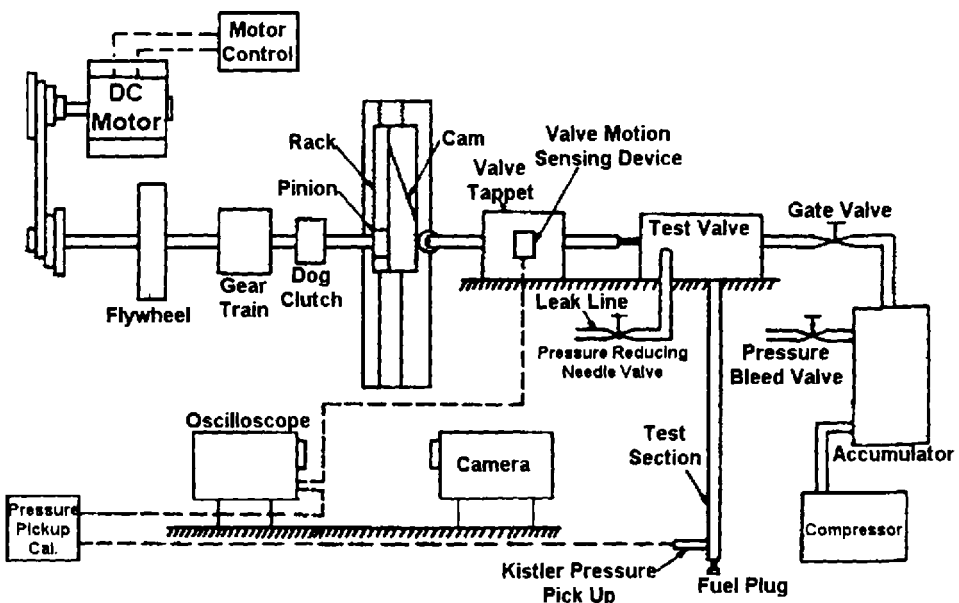


Figure 7.3 Illustration of the Faeth and White rapid-compression apparatus.

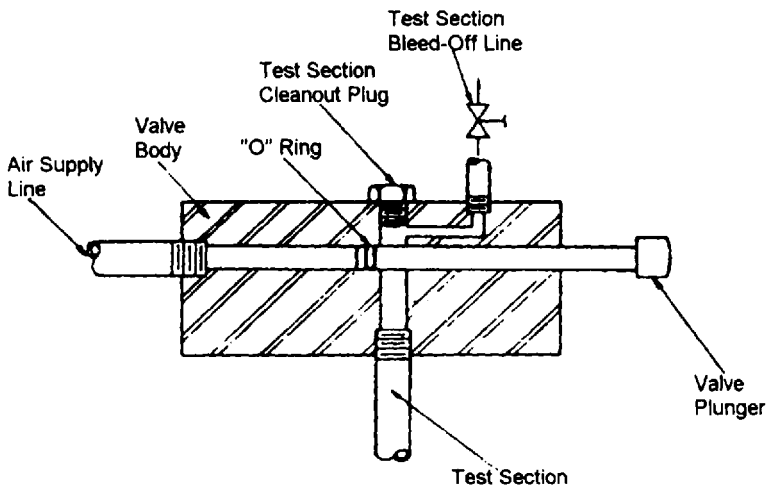


Figure 7.4 Illustration of the valve used for the rapid-compression test shown in Fig. 7.3.

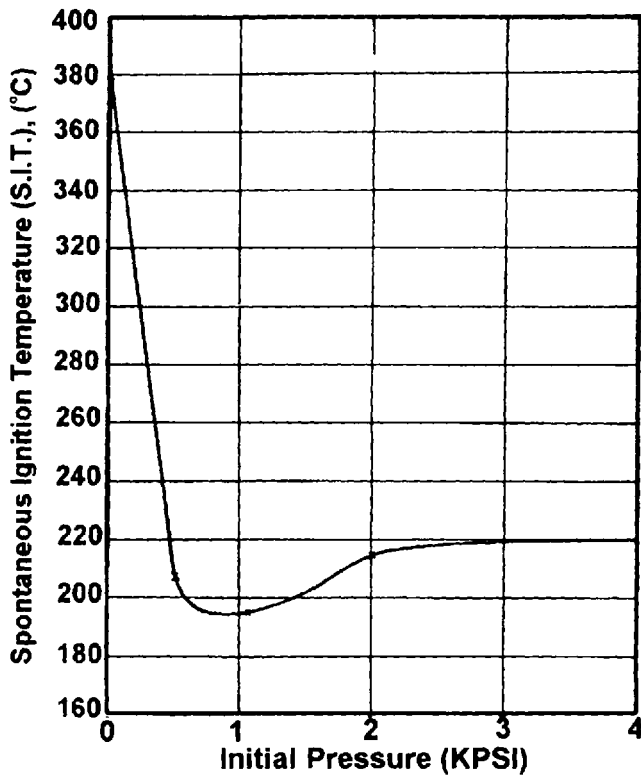


Figure 7.5 The effect of pressure on spontaneous-ignition temperature.

conduction through the pipe walls. This lowering of combustion potential can be attributed to the relatively low heat capacity of air, where a small amount of energy loss represents a relatively large decrease in temperature.

Another combustion test is "the combustion indicator test." This combustion test, which will not be reviewed in detail here, involves the determination of the compression ratio of the fluid in an engine where combustion occurs [34].

Shock-Tube Ignition Test

Although shock-tube tests have been used extensively in the study of gas-phase reactions, a limited amount of testing has been performed with gas-liquid reactions. A shock-tube apparatus [35] was used by Skinner to determine the ignition characteristics of different aerospace hydraulic fluids. Skinner's test results did not correlate well with conventional ignition-time data, indicating that the relative importance of drop breakup, evaporation, and convective and diffusive mixing with respect to chemical reactivity is poorly understood [36].

Gunfire Resistance

The gunfire resistance test (MIL-H-83282—Fire Resistant Hydraulic Fluid, Synthetic Hydrocarbon Base, Aircraft, Metric, NATO Code Number H-537) is a specialized ignition test for which the heat of ignition is provided by incendiary ammunition. Testing is performed by firing 50-caliber, armor-piercing incendiary ammunition into aluminum cans partially filled with the test fluid. Five shots are fired and the number of ignitions and severity of the fires are reported [37]. Results of a gunfire resistance test reported by Snyder and Krawetz are summarized in Table 7.6 [22].

An alternative procedure to the gunfire resistance test is performed to simulate a realistic flammability study of hydraulic fluids selected for use in aircraft weapons system. These fluid applications require full survivability studies against hostile gunfire and are simulated utilizing mock-up hydraulic systems functioning at actual weapon system operating pressures and fluid flow rates [37]. The ammunition used

Table 7.6 Flammability Characteristics of Current and Developmental Aerospace Hydraulic Fluids

Fluid	Spontaneous ignition temperature (°C)	Stream hot-manifold ignition temperature (°C)	Heat of combustion (kcal/kg)	Horizontal flame propagation rate (cm/s)	Gunfire resistance number of fires per 5 shots
MIL-H-5606	232	388	10,100	0.733	5
MIL-H-83282	354	322	9,800	0.212	1
Phosphate ester	524	760	7,100	0.00 ^a	0
Silicate ester	400	371	8,162	0.300	3
Silicone	409	477	5,411	0.218	0
Chlorofluorocarbon	630	927	1,328	0.00 ^b	0
Fluoroalkyl ether	669	927	989	0.00 ^b	0

^aSample self-extinguished (would not stay lighted) on asbestos wire.

^bSample could not be lighted on asbestos wire.

as the ignition source in these tests is chosen based on the threat that the hydraulic system may be subjected to under combat conditions.

2.5.2 Pool Fires

A pool fire may be defined as “a buoyant diffusion flame in which the fuel is configured horizontally” [38]. This includes not only flammable liquids but also solids and gasses. Although pool fires can form any geometric shape, controlled studies are usually performed on circular geometries characterized by the pool diameter and depth.

One method of determining the ignitability of a pool fire has been developed for the evaluation and comparison of less flammable insulating liquids [39]. This procedure is performed by igniting 4 gal of heptane in an open circular trough which surrounds 40 gal of the test fluid contained in an inner, concentric pan. Conductive and radiative heat-release rates of the pool fire at a “steady-state” condition are determined during the testing procedure.

Other flammability characteristics may be determined during pool fire testing and may include flash point, resistance to fire suppression, total heat-release rate, flame-spread rate, and heat radiation to surrounding areas. Factors affecting pool fires may also be introduced during testing and can include heated surfaces, the absence or presence of an enclosure, and variable ambient factors such as room temperature, wind, or ventilation.

As with other common bulk fluid flammability tests, it is difficult to compare water-containing fluids to non-water-containing fluids because of variable evaporation rates which produces nonreproducible data. Fluid ignition may occur after water evaporation; however, such data would not be representative of the original fluid condition.

2.5.3 Calorimetric Procedures

Heat of Combustion

Heat of combustion is not a measure of fluid flammability but a measure of the heat generated during combustion after ignition. This property is considered a significant factor in the determination of overall flammability characteristics [40]. Snyder and Krawetz [22] and Parts [26] have illustrated the correlation of heat of combustion with the fire resistance of a fluid. The heat of combustion may be determined according to ASTM D 240 (Standard Test Method for Heat of Combustion of Liquid Hydrocarbon Fuels by Bomb Calorimeter). Some illustrative examples for hydraulic fluids used in aerospace applications are shown in Table 7.6. As expected, fire resistance increases as the heat of combustion decreases. Marzani developed a “static bomb”-type reactor apparatus for evaluating the spontaneous-ignition temperature for fluids at elevated pressures [41].

Another method for measuring heat of combustion has been used by Monsanto to assess flammability characteristics of aircraft hydraulic fluids [42]. This method incorporates the heat of combustion of benzoic acid, which is combined with the sample being tested to attain a more complete combustion for those fluids that exhibit incomplete combustion tendencies. These test results are corrected for the quantity of benzoic acid added to the test fluid. The heat of combustion may be estimated from the summation of the bond strengths of the chemical compositions. The esti-

Table 7.7 Heat of Combustion Values for Commercial Hydraulic Fluids

Fluid type	Heat of combustion (kcal/g)
Mineral oil	10.7–11.0
Esters	8.5–9.6
Phosphate esters	7.6–7.7
Thickened water–glycol	2.6–3.5

mated heat of combustion values for some commercially available hydraulic fluids are shown in Table 7.7 [43].

Heating Time

Fire resistance of a fluid is reflected by the time required to heat a given volume of fluid to 90°C from ambient temperature and comparing the heating time to a petroleum oil hydraulic fluid and distilled water [28]. The experiment is conducted by heating a given volume of fluid in an insulated, stirred, 2-L stainless-steel beaker equipped with a 56-W immersion heater and a 76-mm immersion thermometer. Pollock et al. reported a heating time of 622 s for a hydrocarbon oil, 923 s for a water-in-oil emulsion, and 1815 s for distilled water. These differences in heating times are related to the heat capacity of the fluid [28].

Cone Calorimeter

Cone calorimeter tests have evolved from procedures developed to investigate the heat-release rates resulting from the combustion of solids such as building materials, plastics, and textiles. A standard cone calorimeter device has been described in ASTM E1354 (Standard Test Method for Heat and Visible Smoke Release Rates for Materials and Products Using an Oxygen Consumption Calorimeter) and in ISO 5660 and is illustrated in Fig. 7.6 [44]. The cone calorimeter is based on the principle of “oxygen consumption calorimetry,” where the net heat of combustion is directly related to the amount of oxygen consumed during combustion.

2.5.4 Evaporation (Wick) Tests

Evaporation, or wick, tests have been developed to identify the flammability characteristics of fluids which have impregnated porous or wicklike materials such as steam pipe lagging or foam insulation. The flammability hazard arises once the fluid has soaked into these porous materials, slowly oxidizing with increasing time. Fluids which, under normal conditions, are less likely to ignite may be easily ignited when retained by a wicklike material. The insulating properties of a porous material decrease the potential for heat loss and the fluid can sometimes self-heat and spontaneously ignite [13].

In industries, such as the mining industry, it is of interest to evaluate the fire-risk potential associated with hydraulic fluid leakage on absorbent material (e.g., coal) which would subsequently be exposed to an ignition source [20]. Tests used to model this risk are called “evaporation” or “wick” tests.

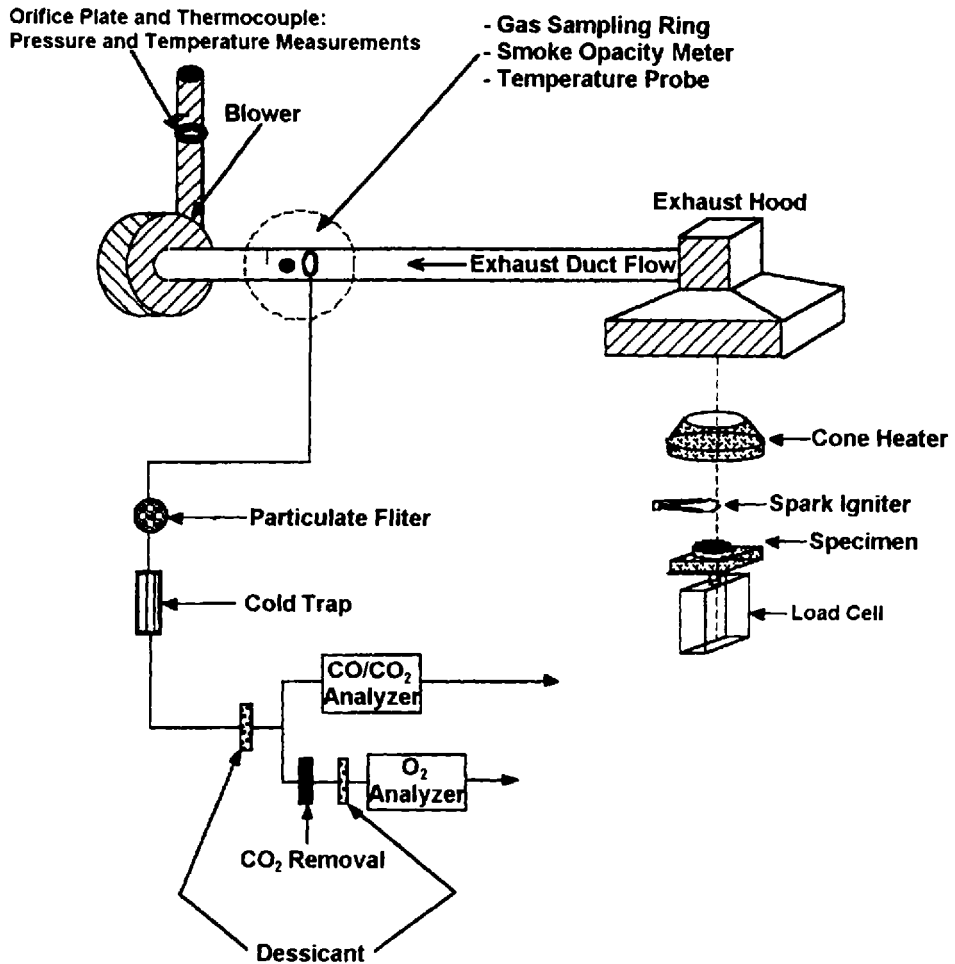


Figure 7.6 Illustration of the lowering of the spontaneous-ignition temperature (S.I.T) of a fluid.

There are primarily two evaporation tests. One test specifies an asbestos tape used as the wick. In view of the health hazards associated with the handling of asbestos, a ceramic fiber "tape" has replaced the asbestos in most current test procedures [45–47]. Alternatively, a pipe cleaner is used as the "wick" in some tests [20,48,49].

Ceramic Wick Test

The ceramic wick test is conducted by immersing one end of a piece of ceramic tape in the hydraulic fluid, as illustrated in Fig. 7.7. After equilibration, one end of the wick is ignited and the persistence of the flame after the removal of the ignition source is recorded. This is primarily a measure of the relative ease of hydraulic fluid flammability after saturation of a porous substrate such as pipe insulation, coal, and so forth.

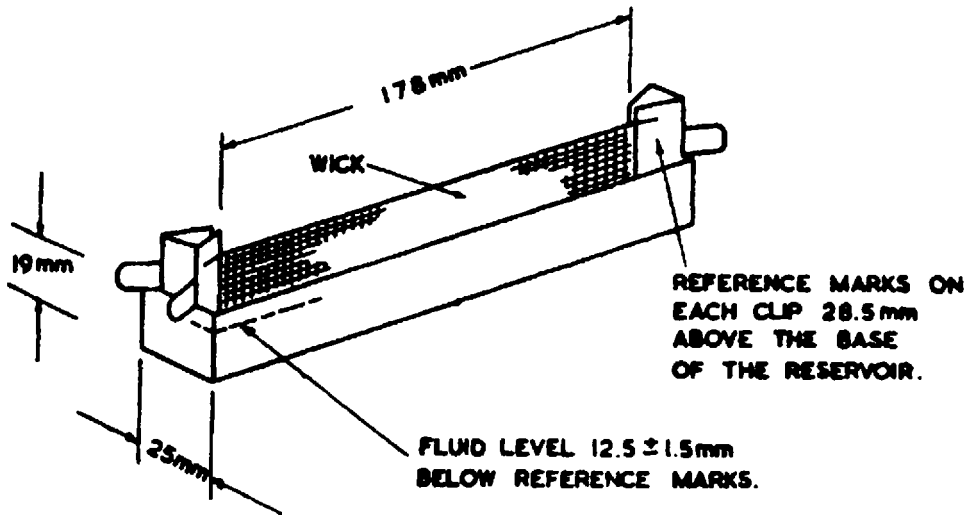


Figure 7.7 Illustration of the ceramic wick flammability test.

"Pipe Cleaner" Wick Test

The pipe cleaner wick test is conducted by soaking a pipe cleaner in the hydraulic fluid and then conditioning at 65°C (150°F) for 2 or 4 h in an oven. The conditioned pipe cleaner is then repeatedly passed through the flame of a Bunsen burner until ignition occurs, as illustrated in Fig. 7.8. The number of passes without ignition is recorded [27].

The water content of hydraulic fluids will affect the results of both of the wick tests described. This is illustrated in Fig. 7.9, which shows the relationship between

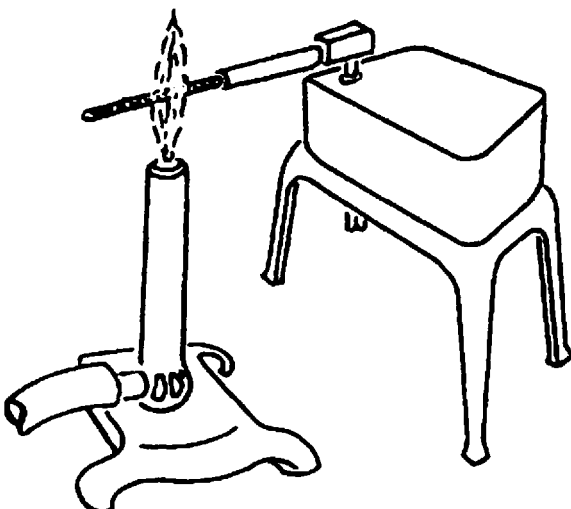


Figure 7.8 Illustration of the pipe cleaner flammability test.

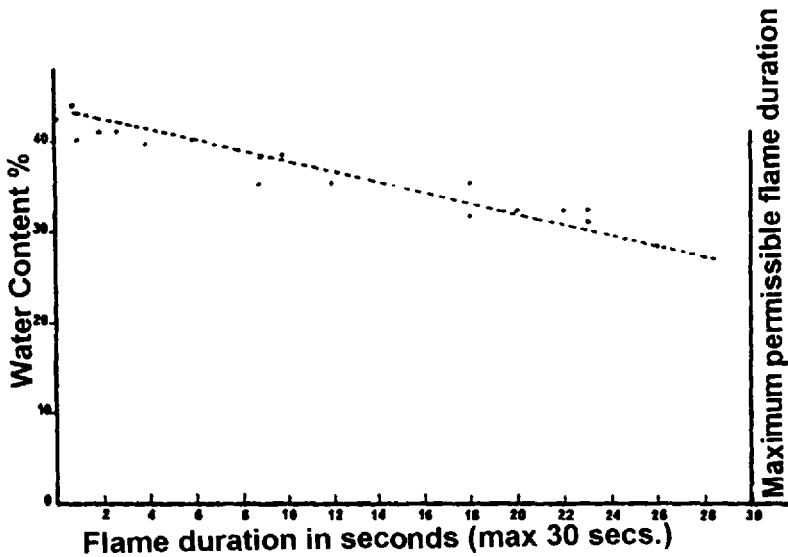


Figure 7.9 Illustration of the relationship between flame duration time and water content of a water-in-oil emulsion for the ceramic tape test.

flame duration time and the water content of a water-in-oil emulsion for the ceramic tape test [50].

Soaked-Cube Flammability Test

The soaked-cube flammability test models an exothermic reaction that may occur if a flammable fluid is absorbed into thermal insulation. The fluid is placed into a well that has been drilled into a 1 × 1 × 1-in. (25.4 × 25.4 × 25.4-mm) cube of asbestos-free calcium silicate insulation material [Johns-Manville-12 molded and block 2-in. (50.8-mm) pipe insulation] with a thermocouple mounted 1/8 in. (3.175 mm) below the bottom of the well, as illustrated in Fig. 7.10. The cube is placed into a furnace and the temperature is increased until an exothermic reaction occurs [51].

2.5.5 Flame Propagation

One of the greatest risks associated with petroleum-based hydraulic fluids upon ignition is flame propagation back to the ignition source [2]. Fire-resistant fluids are more difficult to ignite, and exhibit a reduced tendency for flame propagation. Therefore, it is not only important to measure the fire resistance but also flame propagation. Both properties are typically determined by the hot surface and the spray flammability tests, which will be discussed subsequently.

Linear Flame Propagation Test

Linear flame propagation measures the rate of flame travel on a ceramic fiber test sample presoaked with the hydraulic fluid (ASTM D 5306-92—Standard Method for Linear Flame Propagation Rate of Lubricating Oils and Hydraulic Fluids). Linear flame propagation rates are determined by placing a 500-mm ceramic string into the fluid to be tested for 60 s. The fluid-saturated ceramic string is then placed on the test apparatus, as shown in Fig. 7.11. Two differential thermocouples are attached to

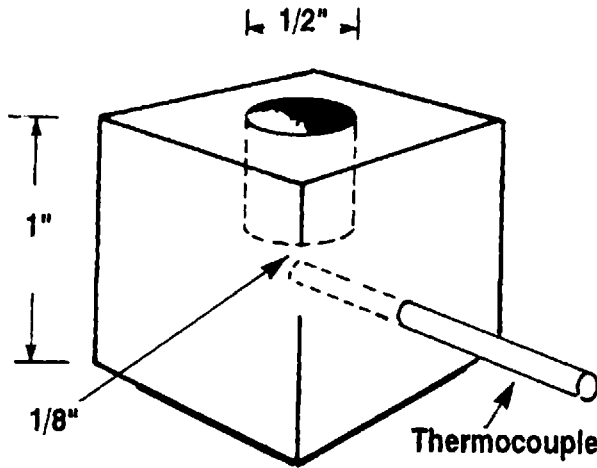


Figure 7.10 Schematic of the test specimen used for the soaked-cube flammability test.

the string 15.24 cm apart. One end of the string is ignited and the thermocouples are used to obtain the time required for the flame to propagate from one thermocouple position to the other. The linear flame propagation rate is reported in meters per second and is calculated as follows:

$$\text{Linear flame propagation rate} = \frac{dv}{p} \tag{7.1}$$

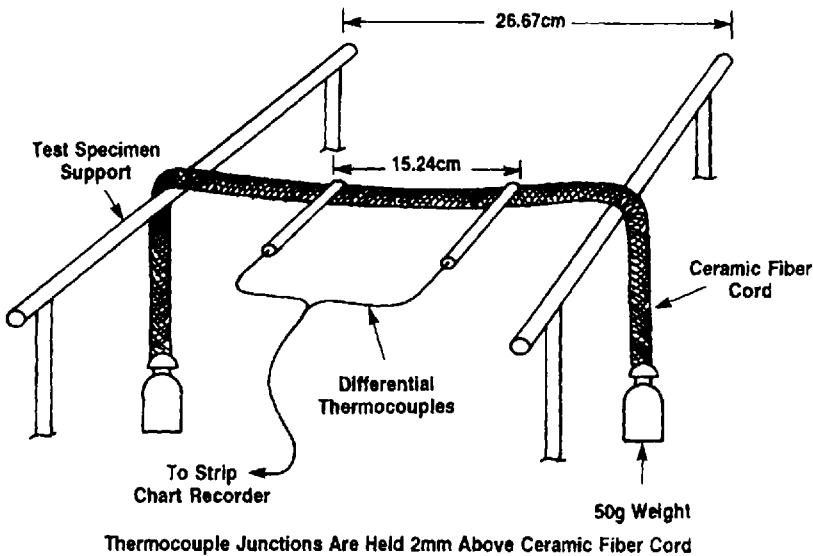


Figure 7.11 Apparatus to determine linear flame propagation rates.

where

d = distance between thermocouples (in mm)

v = chart speed (in mm/s)

p = distance measured peak to peak between thermal effects.

Linear flame propagation rates are dependent on relative flammability or ignitability of the fluid and do not relate to flammability properties of materials under actual fire-risk conditions. The linear flame propagation test is well suited for polyol esters and phosphate esters. This test is not utilized for volatile water-containing hydraulic fluids such as water–glycols, invert emulsions, and high-water-content hydraulic fluids.

2.5.6 Hot-Surface Ignition Tests

The purpose of modeling the ignition of a fluid when contacted with a hot surface is to determine if a hydraulic fluid would ignite and burn if it were sprayed on a hot surface, such as the manifold of earth-moving equipment or a pool of molten metal.

“Monsanto” Molten Metal Test

Monsanto developed a test to evaluate burning and flame propagation that may occur when a hydraulic fluid is sprayed on molten metal, either zinc at 800°F (427°C) or aluminum at 1200°F (649°C) [20,52]. Fluids may be poured, sprayed, or added dropwise to the molten metal (the mode and rate of addition are not specified). Burning rates and flame propagation to adjacent fluid-wetted areas is determined. This test may be performed with or without an external ignition source. An illustration of the Monsanto molten metal test is presented in Fig. 7.12a. The European version of the molten metal test involves pouring of the hydraulic fluid on to the molten metal, as illustrated in Fig. 7.12b [53]. In both tests, although visual differences between the various fire-resistant hydraulic fluids were observed, reproducibility of these tests is poor [53].

“Houghton” Hot-Surface Ignition Test

Houghton International has developed a hot-surface ignition test. This test is performed by introducing a sample onto the hot surface and recording the elapsed time, in seconds, before ignition and the temperature at which ignition occurs [68]. Illustrations of the differentiation of various classes of hydraulic fluids are shown in Fig. 7.13.

Hot-Manifold Test

In hydraulic systems, one of the primary concerns is the potential fire risk that may occur if a line ruptures near a heat source. One of the major tests used to model this situation is the hot-manifold test [20,26,54,55]. The hot-manifold test models the situation where hydraulic fluid may leak dropwise, or as a stream, directly onto a hot surface. In this test, 10 mL of the hydraulic fluid is applied dropwise onto the surface of a heated stainless-steel manifold (tube) at 1300°F (704°C), as illustrated in Fig. 7.14. The flashing or burning of the fluid upon contact with the hot tube and flame propagation to the fluid residues that are collected in the bottom of the enclosure is observed. This test was originally of particular interest to the aviation industry [22].

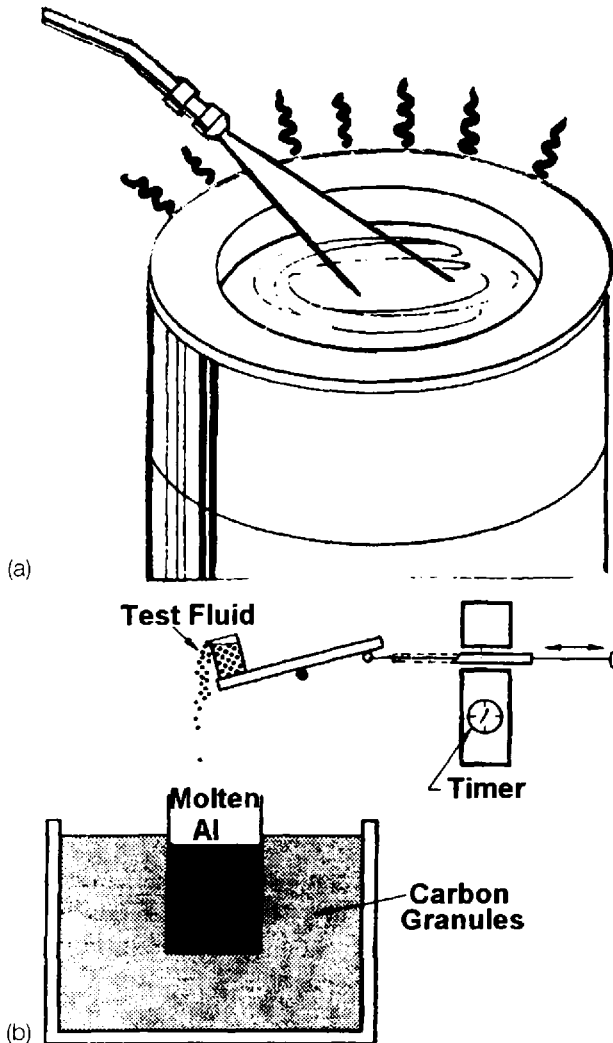


Figure 7.12 (a) Monsanto molten metal fire resistance test; (b) European version of the molten metal fire resistance test.

Factory Mutual Hot-Channel Ignition Test

When a hydraulic hose ruptures, it is more likely to form a spray, which may then contact a hot surface. This condition is modeled by a “hot-channel ignition” test [56,57] shown in Fig. 7.15. Factory Mutual Corporation has developed a test for the determination of fluid response upon contact with a heated surface [49].

In this test, the hydraulic fluid is sprayed onto a steel surface 7 in. (17.78 cm) wide and 27 in. (68.58 cm) long inclined at a 30° angle. The hot channel is heated by propane burners from below, to a minimum temperature of 1300°F (704°C). The burners are turned off prior to spray application of the fluid onto the hot surface. The fluid is sprayed from a distance of 6 in. (15.24 cm) from the hot surface for 60

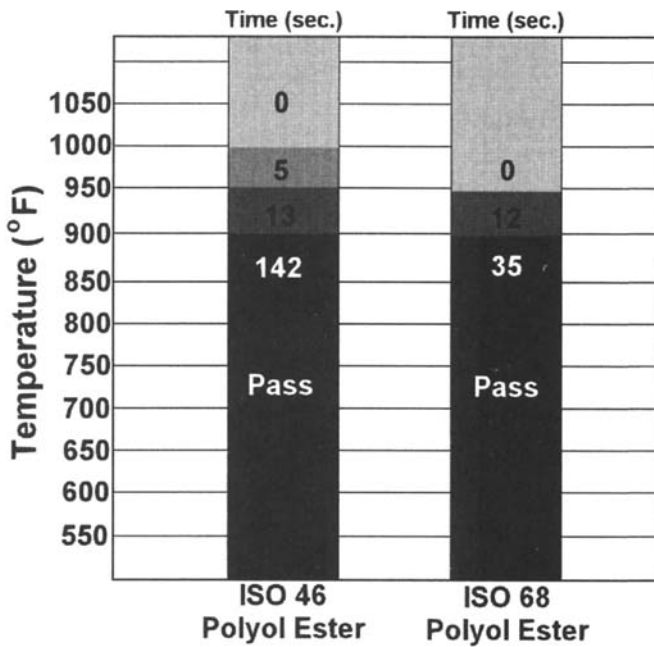


Figure 7.13 Illustrations of the differentiation of various classes of hydraulic fluids as determined by the Houghton Hot-Surface Ignition Test.

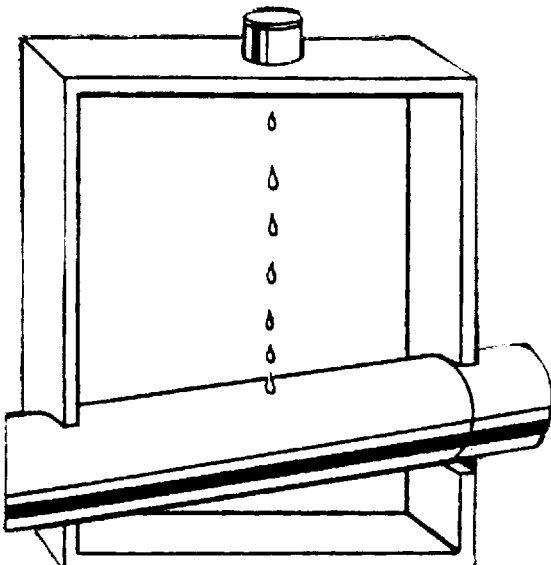


Figure 7.14 Hot-manifold test according to AMS-3150C.

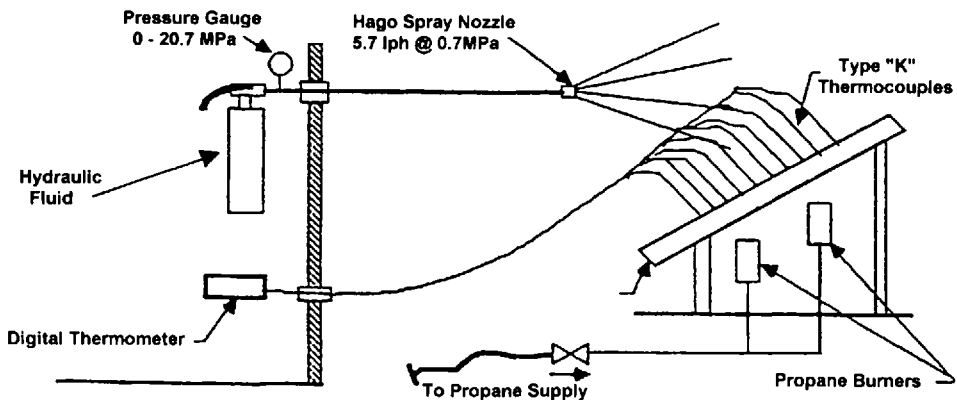


Figure 7.15 Illustration of the FMRC Hot-Channel Ignition Test apparatus.

s. To “pass” this test, the flame must not propagate and must not follow the spray source. Although this is an excellent end-use test, it is very difficult to quantify and is reported on a pass/fail basis.

Recently, it was shown that although polyol esters, phosphate esters, and water-glycols all pass the Factory Mutual Hot-Channel Ignition test, they all exhibit substantially different flammability properties, which are not indicated by the “pass” notation [58]. This is illustrated in Fig. 7.16. Interestingly, the fire-resistant properties of these fluids were similar to those obtained by the molten metal test [53].

One variant of these tests is to conduct them in a wind tunnel as described by Goodall and Ingle [55]. This work was conducted to model aerospace applications. The result showed that the risk of fire was dependent on the temperature of the critical volume of the fluid, the volume at which spontaneous ignition of the fluid will occur, and was not dependent on the hot-surface temperature.

2.5.7 Spray Ignition Flammability Tests

Low-Pressure Spray Flammability Tests

Perhaps the most common test to model potential fire risk of a hydraulic line break is the spray flammability test. A variation of this test is incorporated in national standards in the United Kingdom, France, and Canada, and is also being incorporated into ISO Specifications [17,45,46,59]. Although this test has been accepted as a standard, there are some deficiencies, such as the pass/fail ranking and the lack of repeatability when performed at different laboratories using similar test rigs. Although there is no national spray flammability test in the United States, a commonly encountered insurance industry standard is the Factory Mutual Research Corporation spray flammability test [56,57].

The ALCOA Low-Pressure Spray Flammability Test

ALCOA developed a relatively low-pressure spray flammability test which is described in Ref. 60. The low-pressure spray source is a Binks Thor No. 7 paint spray gun (1.8 cm orifice and pressurized to 0.28 MPa with air) [20,60]. The hydraulic fluid is sprayed over an ignition source such as oil-soaked rags, as illustrated in Fig. 7.17 [58], and the flame characteristics of the flame is visually recorded [20].

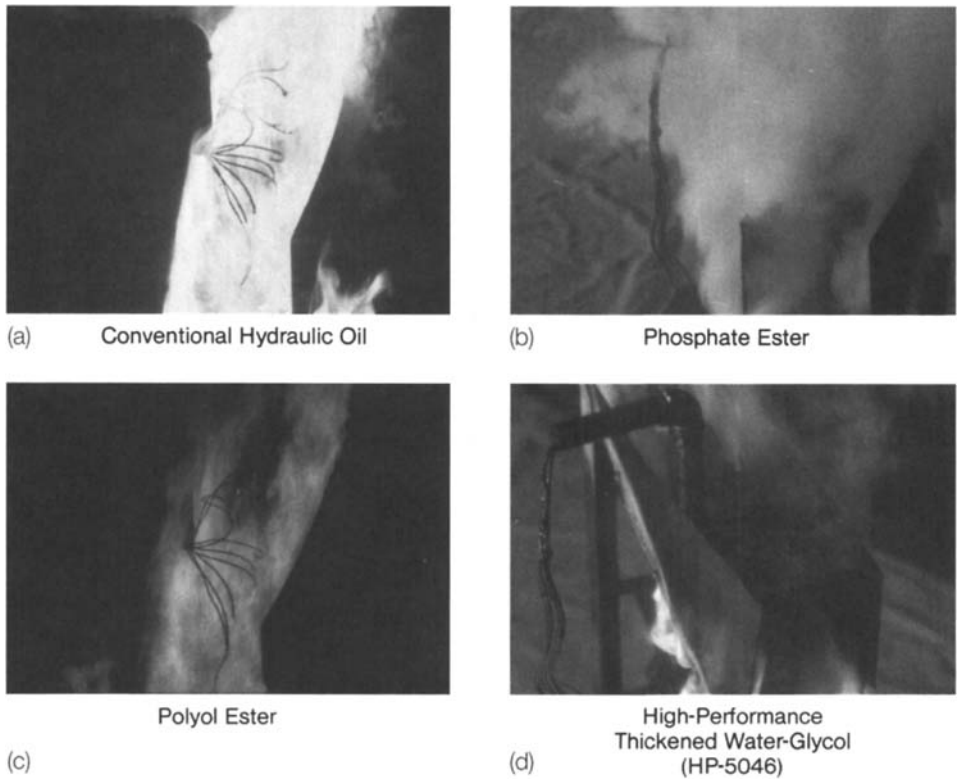


Figure 7.16 Hot-Channel Ignition Test fire-resistance properties for (a) mineral oil, (b) phosphate ester, (c) polyol ester, and (d) water-glycol hydraulic fluids.

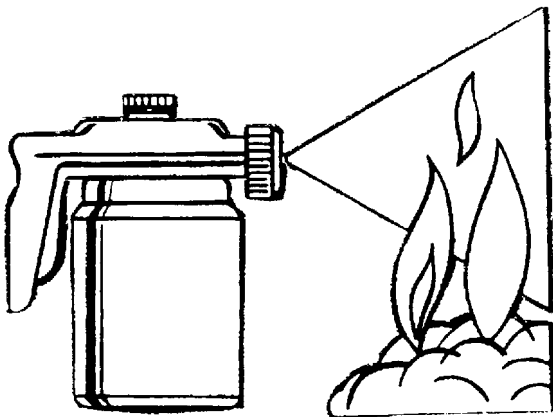


Figure 7.17 Low-pressure Binks No. 7 spray gun flammability test.

A number of high-pressure spray flammability tests are used throughout the world today. The most common tests are summarized in Table 7.8, which includes the source of ignition, fluid test temperature, spray pressure, nozzle description, pass/fail criteria, and references for the tests.

High-Pressure Spray Flammability Tests

THE FACTORY MUTUAL SPRAY IGNITION FLAMMABILITY TEST. The most commonly encountered test in the United States is the Factory Mutual Spray Ignition Flammability Test [56]. The test is performed by rotating a propane torch at 8 rpm in a mist of the hydraulic fluid preheated to 40°C, which is sprayed through a nozzle at 6.9 MPa. If the fluid ignites, the time is recorded, and if the fluid continues to burn 5 s after the removal of the flame, the fluid is considered to “fail” this test. An illustration of the FMRC spray flammability test apparatus is shown in Fig. 7.18.

Except for mineral-oil hydraulic fluids, all of the fire-resistant hydraulic fluids shown in Fig. 7.19 exhibit very different flammability properties, although all are rated as a “pass” in the current Factory Mutual Research Corporation spray flammability test [56]. Therefore, there has been an ongoing effort to identify a spray test to better differentiate hydraulic fluid flammability.

One of the most commonly used fluid flammability testing procedures utilizes a combination of hot-channel and spray flammability tests as specified by the Factory Mutual Research Corporation [56]. To pass the Factory Mutual spray flammability test, the resulting flaming fluid need only be self-extinguished within 5 s [56].

2.5.8 New Spray Flammability Test Developments

Two groups have recently reported test procedures that provide this quantification. Factory Mutual Research Corporation has developed the “spray flammability parameter” test. Another group located at the University of Manchester in England developed the “stabilized flame release test,” also known as the “Buxton test.” Both tests will be reviewed briefly here.

The Factory Mutual Spray Flammability Parameter Test

This test is conducted by spraying the fluid vertically upward from an 80° hollow cone nozzle having an exit as shown in Fig. 7.20. A “spray flammability parameter” (SFP) is calculated and is related to the critical heat flux required for fluid ignition and the chemical heat-release rate of the burning process. This is shown by Eq. (7.2) [57,61,62]:

$$\text{SFP} = \frac{4Q'_{\text{ch}}}{\pi d_x q_{\text{cr}}''} \quad (7.2)$$

where Q'_{ch} is the chemical heat-release rate expressed in kilowatts q_{cr}'' is the critical heat flux for ignition below which ignition is not possible, expressed in kilowatts per square meter, and d_x is the equivalent diameter of the nozzle, expressed in meters [nozzle exit diameter multiplied by the square root of the ratio of the fluid density at the least temperature to the ambient air densities (kg/m^3)].

Table 7.8 Summary of Existing Spray Flammability Test Methods

Test authority	Ignition source	Fluid temp. (°C)	Pressure and source [MPa (psig)]	Fluid spray nozzle	Orifice diameter	Rated flow	Distance from ignition [m (in.)]	Failure criterion or results reported as
MSHA	1. Electric spark 2. Propane torch 3. Flaming trough	65 ± 5	1.034 (150) (N ₂ cylinder)	90-m spray	0.635 (0.025)	3.28 gph	0.45 (17.7)	Flame not to exceed 6 sec. at 18 in.
Naval Research	Electric spark	Ambient 15.5–26.6	0.17 (25) (N ₂ /2 and O ₂)	Poasche Model ML-8	—	158 gph	—	Spray Flammability Limit (Minimum %O ₂)
AFNOR	A type REX No. 1 Charledave torch size 750 tip	65 ± 5	7 ± 0.3 (1015) (N ₂ cylinder)		1.6–0.4 with screen (0.063–0.016)	—	1.20 m (47.2)	1 = no ignition 2 = ignites but does not reach screen 3 = ignites and reached screen
Factory Mutual	Rotating propane torch	40	6.9 (1000) (N ₂ cylinder)	80-m hollow cone	—	1.50 gph	0.152 and 0.457 (6 and 18)	Flame not to exceed 5 s in 10 trials at 6 and 18 in.

NBS/CFR	Kerosene soaked cotton cheesecloth	65	1.034 (150) (N ₂ cylinder)	90-m spray Binks Model F-12-15	0.64 mm (0.025)	3.28 gph	0.68 (26.7)	Rated by temperature rise 204-296 mC considered high heat potential
British Coal Board	Oxyacetylene torch with No. 10 nozzle	Water-containing —65 All others 85	6.89 (1000) (N ₂ cylinder)	80-m hollow cone Monarch Manufacturing type F80	—	2.5 gph	rVaries	Length of spray and duration of flame
“New” Factory Mutual	15kW, 0.14-m-diameter propane-air ring burner	60	6.9, 5.2, 3.5, 1.7 (1000, 754, 507, 246)	80-m hollow cone	0.38 (0.015)	1.5 gph	Sprayed through ring burner	Spray flammability parameter
Buxton East of Stabilization	Vertical propane flame	13-20	90 mL/min	Spraying Systems Co. twin fluid atomizer nozzle type 1/4 JBC-12A	—	—	0.0425 (1.673)	Ignitability, flame length, smoke emissions

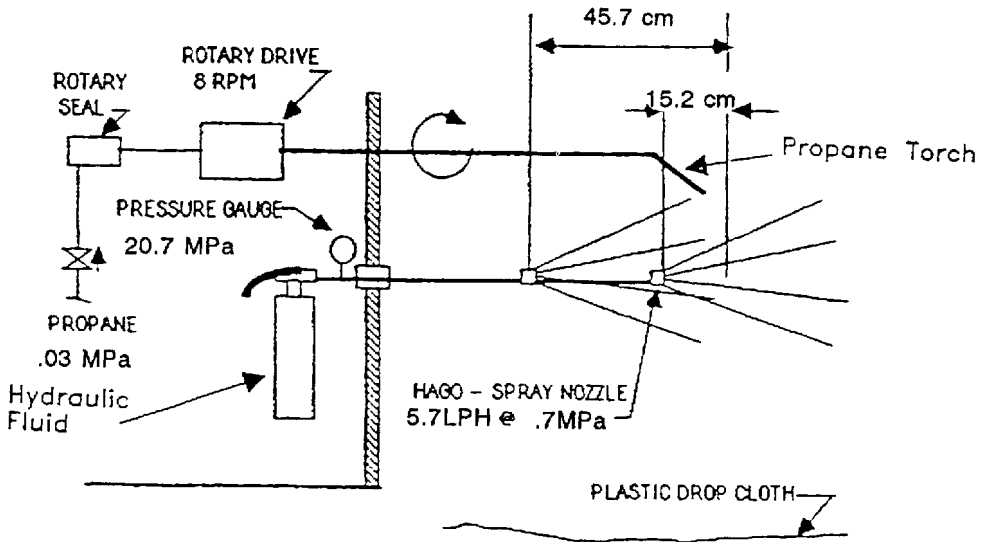
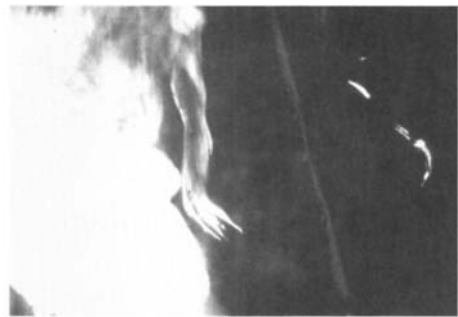


Figure 7.18 Illustration of the FMRC spray flammability test.



(a) Conventional Hydraulic Oil

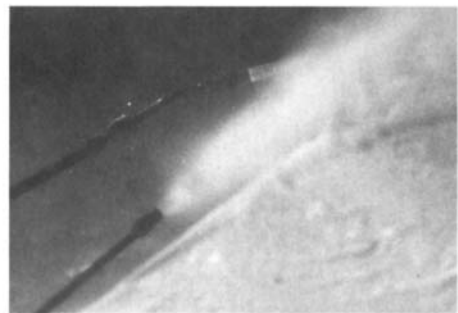


(b) Phosphate Ester



Polyol Ester

(c)



High-Performance
Thickened Water-Glycol
(HP-5046)

(d)

Figure 7.19 Spray flammability properties of (a) mineral oil, (b) phosphate ester, (c) polyol ester, and (d) water-glycol hydraulic fluids.

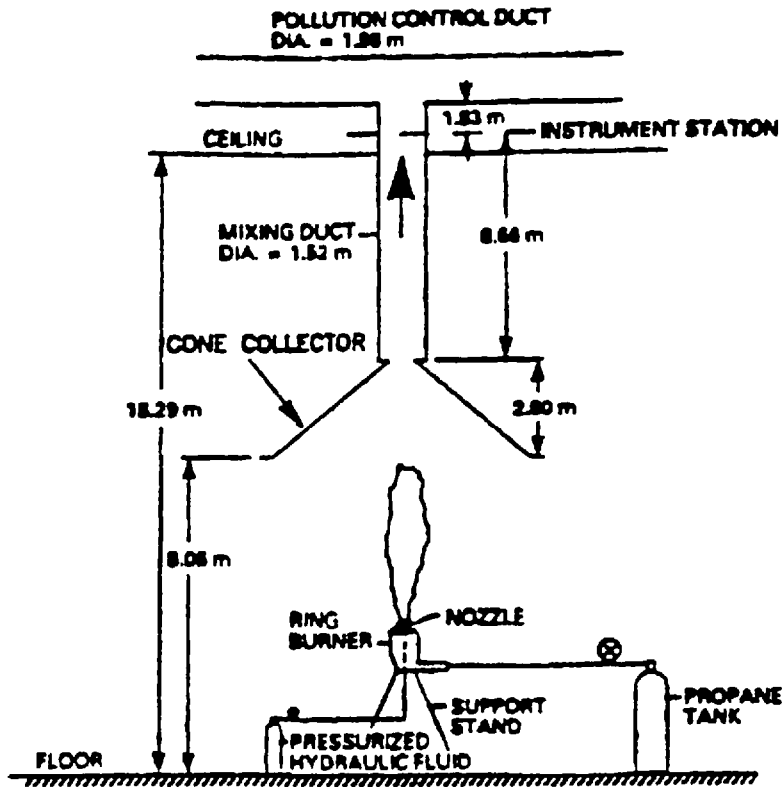


Figure 7.20 FMRC experimental apparatus for determination of the spray flammability parameter.

\bar{q}_{cr}'' may be related to the fire point temperature, T_{fire} ($^{\circ}\text{K}$), of the fluid as follows:

$$q_{cr}'' = \alpha \sigma T_{fire}^4 \quad (7.3)$$

where α is the fluid surface absorptivity, assumed to be unity, and σ is the Stefan–Boltzmann constant ($5.67 \times 10^{-11} \text{ kW/m}^2 \text{ K}^4$).

The successful use of the SFP to characterize and differentiate the potential fire risk of various hydraulic fluids is shown in Fig. 7.21. This test is currently being developed into an ASTM test procedure.

Recent work by Yule and Moodie has been performed using the twin-fluid spray apparatus shown in Fig. 7.22 [63]. A horizontal combustion chamber is utilized. Fluids were ranked by exhaust temperature, flame length, and particulate emissions. The fundamental ranking parameters were the exhaust temperature and “ignitability,” which were used to account for both ease of ignition and flame stabilization. Figure 7.23 illustrates Yule and Moodie’s correlation between heat of combustion and ignitability [63].

The “Buxton Test” or Stabilized Heat-Release Spray Test

This test will be required by EEC countries as the preferred fire-resistance testing method to determine the relative fire resistance of a fluid [64]. The test apparatus is

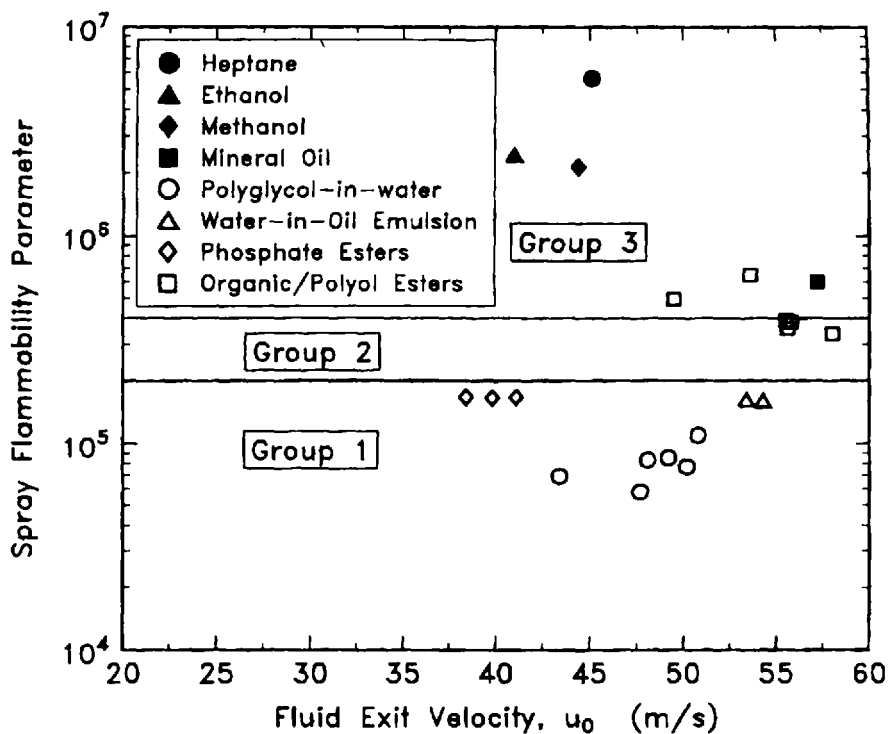


Figure 7.21 SFP characterization of various types of hydraulic fluids.

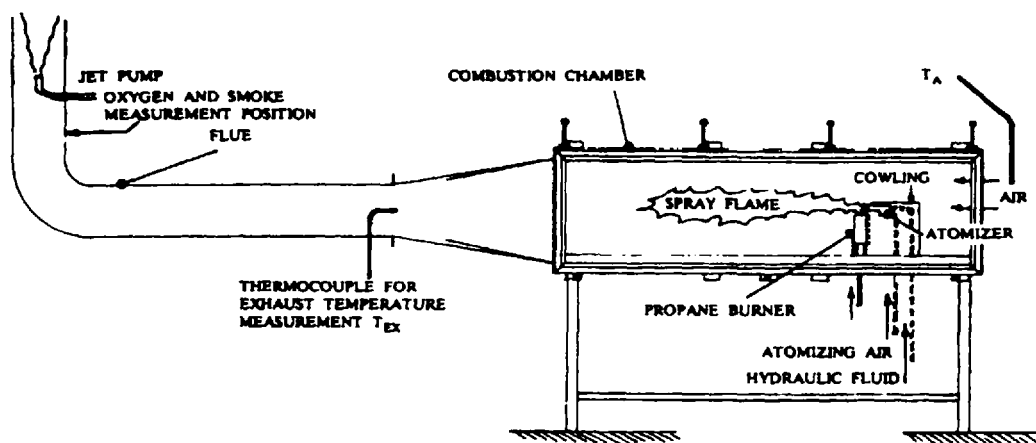


Figure 7.22 Yule and Moodie twin-fluid spray flammability apparatus ("Buxton test").

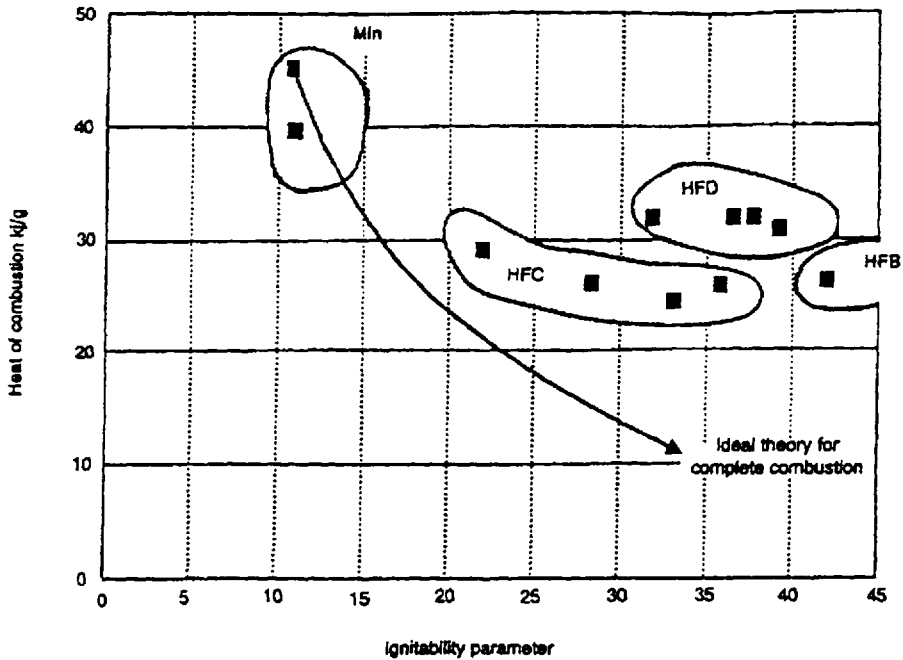


Figure 7.23 Correlation between heat of combustion and ignitability.

the same used for Yule and Moodie’s work and is shown schematically in Fig. 7.22. In the Buxton test, the relative fire resistance of a fluid is reflected by the RI index (Relative Ignitability index) which is determined from the exhaust temperatures of the hydraulic fluid during combustion. Figure 7.24 illustrates the RI index obtained for various hydraulic fluids and also illustrates interlaboratory reproducibility. The two laboratories shown are DMT (Gesellschaft für Forschung und Prüfung mbH) and HSE (Health Safety Executive in Buxton, UK). A third laboratory has recently obtained this test equipment which is constructed at the HSE in Buxton, UK [65].

In general, the RI index reflects the expected fire resistance indicated by Figure 7.24. It also illustrates excellent interlaboratory reproducibility. However, it is important to note that interlaboratory reproducibility can only be shown after appropriate calibration procedures have been applied [65]. This is done by developing a linear regression calibration equation, as illustrated in Fig. 7.25. The data obtained by the HSE laboratory are taken as the reference.

Holmstedt and Persson reported a procedure which multiparametrically ranked the relative fire risk of a hydraulic fluid using heat-release rates, heat of combustion, combustion efficiency, generation of carbon monoxide (CO), and smoke [66].

3 CONCLUSIONS

The fire-resistance properties of a hydraulic fluid cannot be adequately defined by a single test because there are often multiple potential sources for fluid flammability in a single industrial application. For example, spray ignition may occur from a spark or flame source or it may be ignited by spraying on a hot surface. Unfortunately,

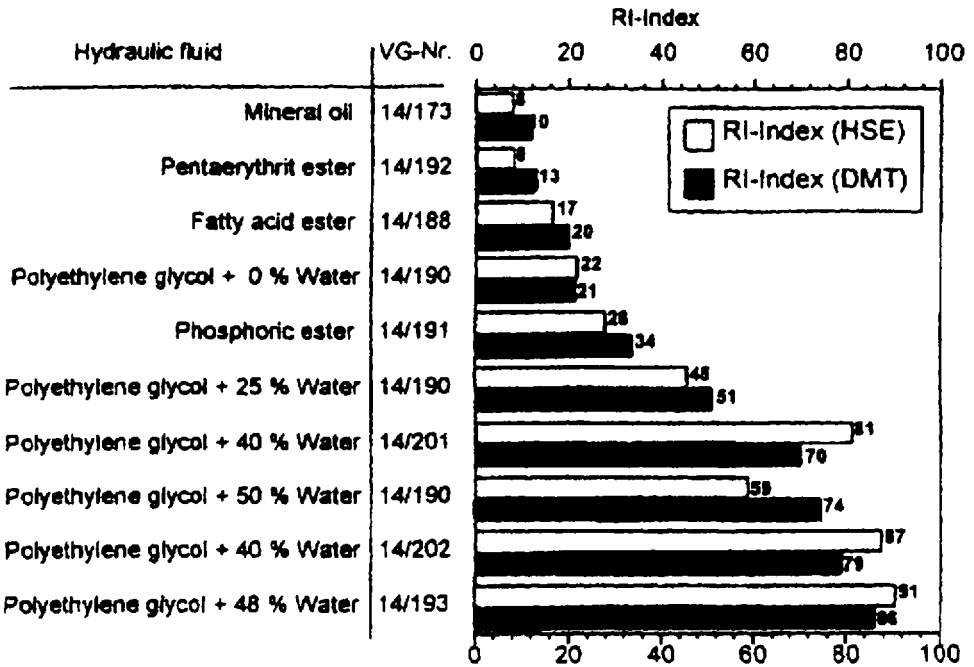


Figure 7.24 Comparison of the RI indices of various hydraulic fluids produced by two laboratories.

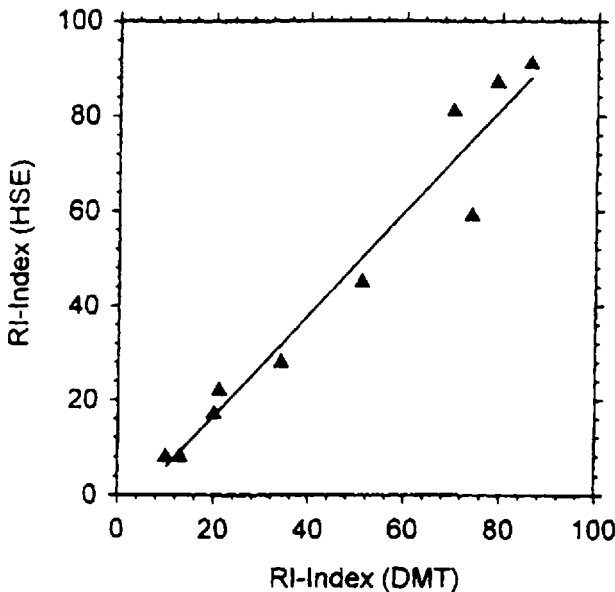


Figure 7.25 Correlation of RI index values obtained by DMT and HSE.

spontaneous ignition of a fluid-soaked lagging may occur in air, or ignition may occur from prolonged heating of a fluid resulting in a decrease of the autoignition temperature or flash point.

Because it is difficult to model the fire potential of an industrial process by one or even two tests, it is prudent to conduct a number of relevant fire-resistance tests to select the hydraulic fluid with the lowest overall risk. One approach is to require that the spray flammability and the stabilized heat-release method, or an equivalent test such as the Factory Mutual spray flammability parameter test, be conducted on every fluid. In addition to these tests, a number of optional standardized, application-specific tests should be performed taking into account the potential flammability hazards associated with the particular application of interest. Some of these tests include the following [67]:

- Autogeneous ignition temperature
- High-pressure spray
- Manifold ignition test
- Evaporative flammability
- Molten metal or salt
- Ignition on CFR motor
- Flame propagation
- Soaked lagging
- High-pressure spray with screen
- Wick test

Guidance for test selection is available from various insurance underwriters, government agencies, and also independent laboratories.

The information provided in this chapter will assist the user in making informed decisions regarding the selection of hydraulic fluids which exhibit adequate fire-resistance properties for the application of interest.

REFERENCES

1. Anon., *Wall Street Journal*, Dec. 12, 1995, p. B1.
2. R. E. Hatton and L. R. Stark, "Fire-Resistant Hydraulic Fluids—A Guide To Selection And Application," *Chem. Age India*, 1977, 28(9), pp. 765–772.
3. J. Mathe, "Fire-Resistant Hydraulic Fluids for the Plastics Industry," *SPE J.*, 1967, pp. 17–20.
4. J. M. Sullivan, "Wanted: Cheap, Safe, Enviro-Friendly Fluids," *Lubr. World*, 1992, September, pp. 49–53.
5. D. F. White, "The Unintentional Ignition of Hydraulic Fluids Inside High Pressure Pneumatic Systems," *ASNE. J.*, 1960, August, pp. 405–413.
6. S. P. Polack, "Progress in Developing Fire-Resistant Hydraulic Fluids," *Iron Steel Eng.*, 1958, August, pp. 87–92.
7. R. Davis, "Fire-Resistant Hydraulic Fluids," *Quart. J. NFPA*, 1959, July, pp. 44–49.
8. M. B. Myers, "Fire-Resistant Hydraulic Fluids—Their Application in British Mines," *Colliery Guardian*, 1977, October.
9. J. Clark Leis, "High Pressure Hydraulic Hazards," *Iron Steel Eng.*, 1963, 40(7), pp.109–112.
10. C. L. Early and R. E. Hatton, "Industrial and ASTM Fluid Fire-Test Programs," in *Fire Resistance of Hydraulic Fluids*, 1966, American Society for Testing and Materials, Philadelphia, PA, pp. 105–134.

11. G. E. Totten and J. Reichel (eds.), *Fire Resistance of Industrial Fluids*, 1996, American Society of Testing and Materials, Philadelphia, PA.
12. W. D. Philips, "Fire Resistance Tests for Fluids and Lubricants—Their Limitations and Misapplication," in *Fire Resistance of Industrial Fluids*, 1996, American Society of Testing and Materials, Philadelphia, PA, pp. 78–101.
13. J. P. Bai, "Fire Protection Gained from Synthetic Fluids," *FRH J.*, 1984, 4(2), pp. 139–145.
14. Anon., "Determination of Ignition Characteristics of Hydraulic Fluids Under Simulated Flight and Crash Conditions," U.S. Civil Aeronautics Administration, Tech. Development Report No. 64, 1947.
15. C. L. Brown and H. Halliwell, "Fire Resistance Fluid Development," SAE Technical Paper Series, Paper 656B, 1963.
16. A. J. Harrison, "Fire-Resistant Hydraulic Fluids—Their Development and Use in the Mining Industry," in *Potash Technology: Mining Processing, Maintenance, Transportation, Occupational Health and Safety, Environment* (Proc. 1st Int. Potash Technol. Conf.), pp. 459–465, 1983.
17. Commission of the European Communities, Safety and Health Commission for the Mining and Extractive Industries, Working Party Rescue Arrangements, Fires and Underground Combustion, Committee of Experts on Fire-resistant Fluids, Sixth Report on Specifications and Testing Conditions Relation to Fire-Resistant Hydraulic Fluids Used for Power Transmission (Hydrostatic and Hydrokinetic) in Mines, Doc. 2786/8/81 E, Luxembourg, 1983.
18. Factory Mutual Research Corp., *Approval Standard: Less Hazardous Hydraulic Fluid*, 1975, Factory Mutual Research Corporation, Norwood, MA.
19. M. V. Sullivan, J. K. Wolfe, and W. A. Zisman, "Flammability of the Higher Boiling Liquids and Their Mists," *Ind. Eng. Chem.*, 1947, 39, pp. 1607–1614.
20. D. F. Smith, *Hydraulics Pneumatics*, 1970, June, p. 77.
21. C. E. Snyder and H. Schwenker, "Materials on The Move," in *6th National Sampe Tech. Conf.*, 1974, p. 428.
22. C. E. Snyder and A. E. Krawetz, *J. Soc. Lubr. Eng.*, 1981, December, p. 705.
23. ISO 4589: "Plastics-Determination of Flammability By Oxygen Index," 1984.
24. G. L. Nelson, "Ease of Extinction—An Alternative Approach to Liquid Flammability," in *Fire Resistance of Industrial Fluids*, 1996, American Society of Testing and Materials, Philadelphia, PA, pp. 174–188.
25. IEC Standard No. 1144, "Test Method for the Determination of Oxygen Index of Insulating Fluids."
26. L. Parts, "Assessment of Flammability of Aircraft Hydraulic Fluids," Technical Report, AFAPL-TR-79-2055, 1978.
27. J. J. Loftus, "An Assessment of Three Different Fire-Resistant Tests For Hydraulic Fluids," Report NBSIR 81-2395, 1981.
28. S. P. Pollack, A. F. Smith, and H. F. Barthe, *Recent Developments in Fire-Resistant Hydraulic Fluids for Underground Use*, IC Bureau of Mines Circular 8043, 1961.
29. DIN 51,794, "Determination of Ignition Temperature," 1978.
30. S. P. Pollack, "Bureau of Mines Evaluates Fire Resistance of Hydraulic Fluids," *Iron Steel Eng.*, 1964, 4(8), pp. 105–110.
31. J. A. Macdonald, "Assessment of the Flammability of Aircraft Fluids," in *Fire Resistance of Hydraulic Fluids*, 1966, American Society of Testing and Materials, Philadelphia, PA, pp. 44–52.
32. *Fire Resistant Hydraulic Fluids in Enclosed Marine Environments*, 1979, (U.S.) National Materials Advisory Board (NRC), Washington, DC.
33. G. M. Faeth and D. F. White, "Ignition of Hydraulic Fluids by Rapid Compression," *ASNE J.*, 1961, August, pp. 467–475.

34. MIL-H-19457D, "Military Specification—Hydraulic Fluid, Fire resistant, Non-Neurotoxic," 1981.
35. G. B. Skinner and R. A. Ruehrwein, *J. Phys. Chem.*, 1959, 63, pp. 1736–1742.
36. G. B. Skinner, "Shock Tube Evaluation of Hydraulic Fluids," *J. Am. Chem. Soc.*, Div. Fuel Chem., 1964, 8(2), pp. 166–170.
37. C. E. Snyder and L. J. Gschwender, "Fire Resistant Hydraulic Fluids and Fire Resistance Test Methods Used by the Air Force," in *Fire Resistance of Industrial Fluids*, 1996, American Society of Testing and Materials, Philadelphia, PA, pp. 72–77.
38. A. Hamins, T. Kashiwagi, and R. Buch, "Characteristics of Pool Fire Burning," in *Fire Resistance of Industrial Fluids*, 1996, American Society of Testing and Materials, Philadelphia, PA, pp. 15–41.
39. Factory Mutual Standard, "Less flammable transformer fluids—Class 6933."
40. "Flammability of Aircraft Hydraulic Fluids—A Bibliography," CRC Report No. 545, Coordinating Research Council, Inc., Atlanta, GA, 1986.
41. J. A. Marzani, "An Apparatus for Studying the Fire Resistance of Hydraulic Fluids at Elevated Temperatures," in *Fire Resistance of Hydraulic Fluids*, 1966, American Society for Testing and Materials, Philadelphia, PA, pp. 3–18.
42. L. Parts, "Assessment of the Flammability of Aircraft Hydraulic Fluids," Technical Report AFAPL-TR-79-2055, Monsanto Research Corporation, Dayton, OH, 1979.
43. N. A. Clinton, "Relationship of Chemical Composition to Fire Resistance in Hydraulic Fluids," presented orally at the 50th STLE Annual Meeting, 1995.
44. A. F. Grand, and J. O. Trevino, "Flammability Screening and Fire Hazard of Industrial Fluids Using the Cone Calorimeter," in *Fire Resistance of Industrial Fluids*, 1996, American Society of Testing and Materials, Philadelphia, PA, pp. 157–173.
45. *Fire Resistant Fluids for Use in Machinery and Hydraulic Equipment*, 1981, National Coal Board, London (NCB Specification No. 570/1981).
46. CAN/CSA- M423-M87, "Fire Resistant Hydraulic Fluids," Canadian National Standard.
47. "Wick Test," CETOP Provisional Recommendation RP-66H, 1974-05-31.
48. "Effect of Evaporation on Flammability," CETOP Provisional Recommendation RP-64H, 1974-05-31.
49. CFR Part 35, "Fire Resistant Fluids" (U.S. Mine Safety and Health Administration).
50. M. B. Meyers, "Fire Resistant Hydraulic Fluids—Their Use in British Mines," *Colliery Guardian*, 1977, October, pp. 796–808.
51. Personal communication from Mr. R. J. Windgassen (Amoco Oil) to Mr. W. E. F. Lewis (Union Carbide Corporation) on July 16, 1986 concerning a new ASTM D.02N.06 working group for the development of "The Soaked Cube Flammability Test," chaired by J. Anzenberger (Stauffer Chemical Company).
52. C. H. Faulkner, personal communication, July 14, 1985.
53. F. D. Norvelle, "A Discussion of Fluid Flammability Tests—Part 2: Molten Metal Tests," *FRH J.*, 1985, Volume 4(2), pp. 133–138.
54. "Manifold Ignition Test," CETOP Provisional Recommendation RP-65H, 1974-05-31.
55. D. G. Goodall and R. Ingle, "The Ignition of Flammable Fluids by Hot Surfaces," in *Fire Resistance of Hydraulic Fluids*, 1966, American Society of Testing and Materials, Philadelphia, PA, pp. 66–104.
56. Factory Mutual Research Corp., *Approval Standard: Less Hazardous Hydraulic Fluid*, 1975, Factory Mutual Research Corporation, Norwood, MA.
57. M. Khan, "Spray Flammability of Hydraulic Fluids and Development of a Test Method," Technical Report FMRC J.1. 0T0W3.RC, Factory Mutual Corporation, Norwood, MA, 1991.
58. G. E. Totten, "Thickened Water–Glycol Hydraulic Fluids for Use at High Pressures," SAE Technical Paper Series, Paper 921738, 1992.

59. "Hydraulic Transmission Fluids: Determination of the Ignitability of Fire-Resistant Fluids Under High Pressure with a Jet spray on a Screen," Report AFNOR NF E 48-618, 1973.
60. H. H. Rowand and L. B. Sargent, "A Simplified Spray-Flammability Test for Hydraulic Fluids," in *Fire Resistant Hydraulic Fluids*, 1966, American Society for Testing of Materials, Philadelphia, PA, pp. 28–43.
61. M. M. Khan and A. Tewarson, *Fire Technol.*, 1991, November, p. 321.
62. M. M. Kahn and A. V. Brandao, "Method of Testing the Spray Flammability of Hydraulic Fluids," SAE Technical Paper Series, Paper 921737, 1992.
63. A. J. Yule and K. Moodie, *Fire Safety J.*, 1992, 18, p. 273.
64. "Specification and Testing Conditions Relating Fire-Resistant Hydraulic Fluids for Power Transmission (Hydrostatic and Hydrokinetic)," 7th Luxembourg Report, March 3, 1994, Doc. No. 4746/10/91, Safety and Health Commission for Mining and Other Extractive Industries. L-2920 Luxembourg, Commission of the European Economic Communities DG V/E/4.
65. K. Holke, "Testing and Evaluation of Fire-Resistant Hydraulic Fluids Using the Stabilized Heat Release Spray Test," in *Fire Resistance of Industrial Fluids*, 1996, American Society of Testing and Materials, Philadelphia, PA, pp. 157–173.
66. G. Holmstedt and H. Persson, in *Fire Safety Science—Proceedings of the First International Symposium*, 1985, p. 869.
67. "Schedule of Fire Resistant Tests for Fire Resistant Fluids," CETOP Provisional Recommendation RP 55 H, 1974-01-04, British Fluid Power Association, Oxfordshire, United Kingdom.
68. C. H. Faulkner, G. E. Totten, and G. M. Webster, "Fire Resistance Testing: A Technology Overview and Update," in *Proceedings of the 47th National Conference on Fluid Power*, 1996, Vol. 1, pp. 75–81.

Ecological Compatibility

GARY H. KLING and DWAYNE E. THARP

Caterpillar, Inc., Peoria, Illinois

GEORGE E. TOTTEN and GLENN M. WEBSTER

Union Carbide Corporation, Tarrytown, New York

1 INTRODUCTION

Although mineral oils have traditionally been the most commonly used hydraulic fluids in the fluid power industry, they are being subjected to ever-increasing controls, particularly because of the increasingly stringent governmental regulations regarding the impact of hydraulic fluid spill and fluid leakage on the environment [1]. Improper disposal, even if it is incidental, may be the source of large penalties or even litigation [2].

European studies have identified hydraulic fluid leakage as one of the primary sources of groundwater contamination [3]. This has been followed by a worldwide effort to identify hydraulic fluids that will exhibit reduced environmental and toxicological impact upon incidental contact with the environment [4,5]. (*Note:* The term "environmental impact" includes biodegradation and persistence, as well as toxicity.) Additional impetus for the use of biodegradable lubricants has been provided by the use of national environmental labeling criteria. Figure 8.1 illustrates various examples of ecolabels [6].

There are a number of national environmental standards and labeling procedures being developed. The most well known are summarized in Table 8.1 [7]. One of the first and most stringent environmental labeling procedures is the German "Blue Angel" label [8]. The philosophy of this labeling procedure is to avoid consumer products, including hydraulic fluids, that are hazardous to the environment. Although the Blue Angel labeling requirements have not been finalized, an approved hydraulic fluid will require greater than 80% biodegradability in 21 days by the CEC-L-33-A-93 test or greater than 70% biodegradation by the Modified Sturm Test.

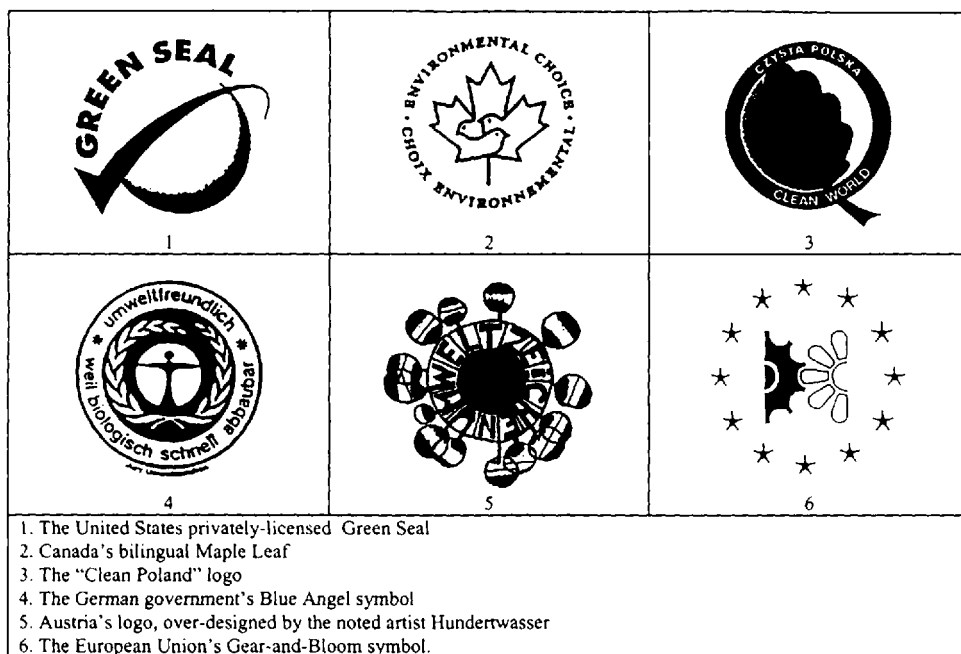


Figure 8.1 Illustration of different classes of molecular structures present in mineral oil. (From Ref. 6.)

Details of these testing procedures will be provided later in this chapter. All components must be nonpolluting and conform to Water Hazard Class 0 or 1 [9]. The components of this coding procedure are as follows [3]:

CEC	Coordinating European Council.
L	Lubricants testing.
33	These two digits refer to the order of the procedure
T or A	T indicates "tentative" procedures. Correlation programs have been completed. "A" indicates "accepted."

Table 8.1 Environmental Criteria for Various Ecolabeling Schemes

Country	Scheme	Environmental criteria
Germany	Blue Angel	Biod-Ecotox
Canada	Environmental Choice	Recycling
Japan	Eco-Mark	Biod-Ecotox
France	N-F Environment	Biod-Ecotox
Scandinavia	White Swan	Biod-Ecotox
United States	Green Seal and Green Cross (privately run schemes)	Recycling
India	Ecomark	Biod-Ecotox

Source: Ref. 7.

93 Indicates the year in which the procedure was agreed upon and accorded status by the Council.

Figure 8.2 shows the structure of the CEC European Industry Organization, which is composed of the following:

- ATIEL Concerned with technical matter related to the lubricating oil industry in Europe
- ATC Concerned with lubricant testing
- CCMC Operates on a wide front of matters and is particularly interested in the uniformity in technical regulations

Another program currently in development is the Environmental Choice Program of Canada [9]. This program was initially developed to provide guidance for the disposal or reclamation of used industrial oil, as indicated in Table 8.1 [10]. Interestingly, the term “EcoLogo” is used and not the term “environmentally friendly” because it was not intended to suggest that products with the EcoLogo were perfectly harmless to the environment. Very few products have **no** impact on the environment [10]. However, the Canadian Environmental Choice program is being used to provide a criteria for the “environmental friendliness” of industrial oils such as chain saw lubricants, hydraulic fluids, and others. *Note: The term “environmentally friendly” is used to denote those materials which exhibit little “environmental impact.”*

In the United States, work is underway by the ASTM D.02 N.03 Subcommittee to establish a standard for the classification of environmentally friendly hydraulic fluids. However, instead of “environmentally friendly,” these fluids will be classified as “eco-evaluated” (EE) [9,11]. Also, the ASTM D.02 N.03 Subcommittee is working to establish standards for the classification and testing of eco-evaluated fluids.

In addition to base stock, a hydraulic fluid typically contains additives. The additives are used to enhance the fluid properties, which include antioxidant, anti-wear, reduced foaming, and improved air-release properties. The presence of these

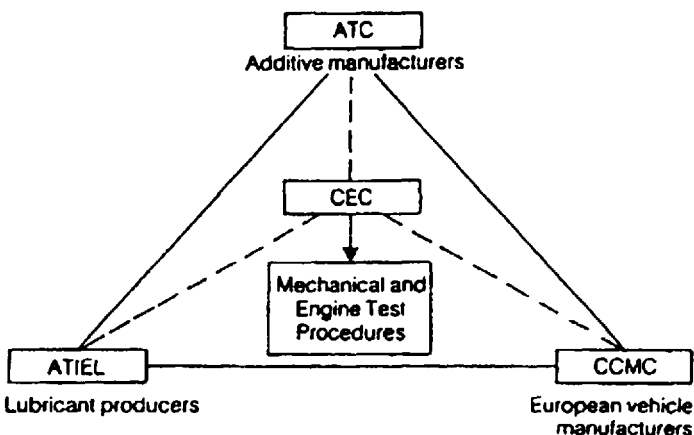


Figure 8.2 Structure of CEC European Industry Organization.

additives affect hydraulic fluid biodegradation and toxicological properties [12–15]. Therefore, additive selection is of paramount importance [16].

Thus far, the most commonly cited base stocks used for the formulation of “environmentally friendly” hydraulic fluids are either vegetable oils or synthetic esters [7,9,17]. The most common vegetable oils that have been identified for hydraulic fluid formulations are based on soybean oil [18–20], rapeseed oil [21], and high oleic sunflower oil [22]. Canola oil is also used. The amount of unsaturation in a vegetable oil is climate dependent [22]. For example, rapeseed grown in colder northern climates contains less unsaturation (canola oil) than when grown in warmer southern climates. This is important because the level of unsaturation affects physical properties and especially oxidative stability. For this reason, canola oil is one of the preferred vegetable oils for hydraulic fluid formulation [22].

Work by Rhee et al. have shown that synthetic esters exhibit a number of advantages over vegetable oils, such as a broader pour point temperature range, typically -40°C to 150°C versus vegetable-oil-derived fluids, which typically exhibit a temperature range of -10°C to 90°C [23]. This limited range of operational temperatures for vegetable oils may render them unsuitable for some cold-weather applications. Other workers have reported that in addition to a broader operational temperature range, synthetic esters provide substantial improvement in thermal/oxidative stability relative to vegetable-oil-based fluids [24,25].

The use of various vegetable-oil-derived hydraulic fluids has been published [21,26–29]. Typically, either vane or piston pumps were used for performance testing. Although the antiwear results were generally good, these tests showed that vegetable oils exhibit poorer oxidative stability than mineral-oil-based hydraulic fluids. In view of the significant market pressures for the availability of “environmentally friendly” hydraulic fluids, most hydraulic pump manufacturers and many equipment suppliers have developed guidelines for the selection and use of these fluids [30–34]. Because of the variability of the performance of vegetable-oil-based hydraulic fluids that are currently available, some manufacturers appear to have developed their own privately labeled fluids to provide greater quality assurance [33].

Because of their favorable low-temperature properties (pour point of -63°C), water solubility, and fire resistance, water-glycol hydraulic fluid compositions provide a potential alternative to vegetable oils and synthetic esters as biodegradable hydraulic fluids [35,36]. Unfortunately, although there are numerous references describing various biodegradability properties of vegetable oils and synthetic esters, there are considerably fewer references for the biodegradability properties of water-glycols using OECD GLP Principles (OECD, 1992a) [37]. In some cases, it is not clear how the reported data was obtained or if it was previously published in other sources.

This chapter will provide a selected overview of biodegradation and toxicity data published to date for different classes of hydraulic fluids. The general subject of biodegradation and testing procedure will be discussed. Selected examples of published comparative test data will be provided.

2 DISCUSSION

2.1 Biodegradable Fluids

A tabulation of various vegetable-based and synthetic ester-based hydraulic fluids available in the United States is provided in Table 8.2 [23]. An international listing

is provided in Table 8.3 [38]. In the biodegradable hydraulic fluid marketplace, rape-seed-oil-based hydraulic fluid compositions may be referred to as "European fluids," and canola-oil-based hydraulic fluids may be referred to as "Canadian fluids" [19,20,26,39,40]. There is a movement underway to make soybean-oil-based fluids the preferred American biodegradable vegetable-oil-based fluid composition [40].

Another class of hydraulic fluids to be discussed here is water-glycol fluids, also known as hydrolubes [41-43]. Water-glycol hydraulic fluids are part of a larger class of fire-resistant fluids. Additional fluids classified as "fire-resistant" include invert emulsions, polyol esters, and phosphate esters. Whereas polyol esters and phosphate esters derive their fire-resistance properties by either, chemical structure or additives, or both, water-glycols and other water-containing fluids derive their fire-resistance properties from the presence of water, also known as a "snuffer," in the fluid formulation.

A summary of the functions of the various components of a "typical" water-glycol hydraulic fluid is provided in Table 8.4. In addition to the components shown, other additives may be used as needed, such as dyes for leak detection, antifoam, air release agents, and so forth.

2.2 Biodegradation

In this section, the meaning of biodegradability will be discussed. An overview of test methods used to determine biodegradability will be provided. This discussion will be followed by an overview of published data on biodegradable hydraulic fluids.

2.2.1 Biological Degradation

There are various national standards currently being developed to define "biodegradability" and how it should be experimentally determined [44-47]. There are two general classifications that are often used to define biodegradability. One classification is based on the ultimate fate of the material after biodegradation. The other classification is based on the biodegradation rate. Recently, Wilkinson offered the following definitions and excerpts will be directly quoted from Ref. 47.

Rate Definitions

PRIMARY BIODEGRADATION. This is a measure of the conversion by biological systems of the original organic material into different products from the starting materials. This is not a measure of the biological impact of the substance but merely of the efficacy of the first step in what may be a long series of steps. In some cases, nontoxic substances which exhibit facile primary biodegradability can biodegrade into environmentally toxic materials.

ULTIMATE BIODEGRADATION. This is often referred to as "mineralization" and is the complete conversion by biological systems of the original organic material into carbon dioxide, water, and microbial biomass (and any inorganic ions, if present). (*Note:* Unfortunately, OECD methods and classifications do not recognize biomass incorporation.)

Rate Definitions

READY BIODEGRADATION. Substances which are classified as "readily biodegradable" exhibit greater than a certain fixed percentage conversion in a standard test (see Table 8.5) [48]. This is usually measuring a parameter related to the degree of "ultimate biodegradation."

Table 8.2 Domestic "Environmentally Acceptable" Hydraulic Fluids

Product name	Base stock	Description	Company name	Address
EL 146	Seed oil + mineral oil	Readily biodegradable and nontoxic ISO 46 hydraulic oil for use in heavy-duty hydraulic systems	EarthRight Technologies	33307 Curtis Blvd. Eastlake, OH 44095
Plantohyd 40	Rapeseed + sulfurized fatty vegetable oil	Universal, multigrade hydraulic oil for agricultural, forestry, and construction machinery	Fuchs Metal Lubricants Company	Metal Lubricants Co. 17050 Lathrop Ave. Harvey, IL 60426
Functional 9403071	Rapeseed	Biodegradable, corrosion-inhibited, antiwear hydraulic oils for mobile, industrial, and marine hydraulic systems	Greenoco Functional Products, Inc.	Functional Products, Inc. 24000 Mercantile Rd, Unit 5 Cleveland, OH 44122
Greenwood Hydraulic Fluids	Vegetable; rapeseed	Biodegradable, corrosion-inhibited, antiwear hydraulic oils for mobile, industrial, and marine hydraulic systems	Greenoco Inc.	The Green Oil Company P.O. Box 577 Blue Bell, PA 19422
HYD271, 272	Vegetable; canola	Biodegradable, antiwear, corrosion-inhibited, and oxidation-inhibited hydraulic oils for industrial hydraulic systems	International Lubricants, Inc	7930 Occidental South Seattle, WA 98108
Mobil EAL 244H	Vegetable; rapeseed	Biodegradable, antiwear, corrosion-protective hydraulic oil for moderate or severe operating conditions	Mobil Oil	3225 Gallows Rd., RM 5W806 Fairfax, VA 22037-0001
Mobil Xrl 1711-78	Synthetic ester	Antiwear, corrosion-protective hydraulic oil	Mobil Oil	3225 Gallows Rd., RM 5W806 Fairfax, VA 22037-0001
Quintolubric 822-220, 330, 450	Polyol ester	Fire-resistant hydraulic fluid to replace phosphate esters	Quaker Chemical Corp.	Conshohocken, PA 19428-0809

HVO-46 Hydraulic Vegetable Oil	Vegetable	For hydraulic systems that require both antiwear and rust and oxidation properties	Renewable Lubricants, Inc.	476 Griggy Rd., P.O. Box 474 Hartville, OH 44632
Royco 3100, 3046, RTJ27, RTJ41	Polyol ester	Biodegradable, antiwear hydraulic fluids	Royal Lubricants	P.O. Box 518, Merry Lane East Hanover, NJ 07936
OS 107086	Sunflower oil	Based on Sunyl PF 311; sunflower oil with alkylated phenol	SVO Specialty Products, Inc	35585-B Curtis Blvd. Eastlake, OH 44095
OS 106575	Sunflower oil	Based on Sunyl PF 311; sunflower oil with alkylated phenol	SVO Specialty Products, Inc	35585-B Curtis Blvd. Eastlake, OH 44095
Biostar Hydraulic 46, Code 1616	Rapeseed; ethyl hexyl oleate, C18 fatty acids	Environmentally friendly, zinc-free, antiwear oil for high-pressure hydraulic equipment	Texaco	Texaco Lubricants Co. N.A. P.O. Box 4427 Houston, TX 77210-4427
Synstar Hydraulic 46, Code 2073	Trimethyl-propane (TMP) and Penta-erythritol ester blend, BHT	Environmentally friendly, zinc-free, antiwear oil for high-pressure hydraulic equipment	Texaco	Texaco Lubricants Co. N.A. P.O. Box 4427 Houston, TX 77210-4427
Terra-Lube ECO 2000	Natural esters, triglycerides	Biodegradable and nontoxic natural-ester-based universal hydraulic fluid designed for use in all equipment	CoChem Inc	7555 Bessemer Ave. Cleveland, OH 44127
Calgene Q1093, 1094, 1095	Rapeseed, canola oil	Vegetable-oil-based VI Index, wear and oxidation additives	Calgene Chemical, Inc	7247 N. Central Park Ave. Skokie, IL 60076-4093
Clark Cone oil	Cone oil	Environmentally friendly product	CoChem, Inc	7555 Bessemer Ave. Cleveland, OH 44127

Note: The term "environmentally acceptable" (or "environmentally friendly") is not a well-defined term. There is no universally accepted criterion for "environmental acceptability" at the present time, although various national standards are in the process of being written. Therefore, the term "environmentally acceptable" is essentially a marketing term with little or no technical support. In fact, often "environmentally acceptable" is used synonymously with "vegetable oil."

Source: Ref. 23.

Table 8.3 Environmentally Acceptable Hydraulic Fluid HETG, HEPG, and HEE for Axial Piston Units

Type of fluid	Vegetable-oil-based hydraulic fluids, HETG				Synthetic hydraulic fluids based on polyglycol, HEPG			Synthetic hydraulic fluids based on esters, HEE			
ISO viscosity class	VG 22	VG 32	VG 46	VG 68	VG 22	VG 32	VG 46	VG 22	VG 32	VG 46	VG 68
ARAL							BAF-46 Vitam			EHF-46 Vitam	
ASEOL						Aqua VG 32	Aqua VG 46	Terra 15		Terra 46	Terra 68
AGIP										Agip Amica S 46	Agip Amica S 68
AUTOL			Autol Bio HVI 46								
AVIA		Avilub Hydraulic Bio 32	Avilub' Hydraulic Bio 46		Avia Hydrosynth 22	Avia' Ndyrosynth 32	Avia Nydrosynth 46			Avia Syntofluid 46'	Avia Syntofluid 68
BEICHEM		Bio-Hydraulik-öl 32			Hydrostar UWF 22	Hydrostar UWF 32	Hydrostar UWF 46		Hydrostar TMP 32	Hydrostar TMP 46	Hydrostar TMP 68
BINOL			Hydrap 46								
Biosttar Kellersberg			Biostar								
BLASER										Blasol LP8905	
BP			Bartran Biohyd 46				Biohyd PEG 46			Biohyd 46 SE'	Biohyd 68 SE
BRENNTAG			Hydraulic V 32		Hydraulic TR 22	Hydraulic TR 32'	Hydraulic TR 46				
BUCHER & Cie			Oekohydro 3268						Oekosynt 2246		
MOTOREX											
CASTROL	Biotec Alpin 22	Biotec HVX									
DEA		Econa R 32				Econa PG 32	Econa PG 46			Econa E 46	
DELTIN			Deltinol Bio-Hydraulik-öl HVI 46								
ELF										Hydroelf Bio 46	
ESSO		Hydraulik-öl PFL				Hydraulik-öl PGK 32'	Hydraulik-öl PGK 46			EGL 45947	
FINA		Biohydran RS 38					Hydrauliköl D3031.46		Biohydran TMP 32	Biohydran TMP 46	Biohydran TMP 68

FINKE		Aviaticon HV-BD 36							
FUCHS		Plantohyd N 32	Plantohyd N 46	Plantohyd N 68		Renodiol PGE 46	Plantohyd S 32	Plantohyd S 46	Plantohyd S 68
GLOBOIL							BHF 32	BHF 46	BHF 68
HOUGHTON		Trigolubric 32				Syntolubric 46			
KENDAL (Demmler & Co. Schweiz)								Synth. Natura 46HV	
KOMPRESSOL Kuwait Petroleum Q8		UW 500/32	UW 500/46			Biovis			
MOBIL		EAL 224H				Biofluid HLP 32*		Holbein 32	Holbein 46
MOLYDUVAL									
OMV	Biohyd M 15	Biohyd M 32	Biohyd M 46	Biohyd M 68			Biohyd MS 15	Chemlube 5126 Biohyd MT 32, MS 32	Biohyd MT 46 MS 46 Bio Synth. HYD 46
OEST		Bio- Hydraulik-öl HVI 34							
PANOLIN Schweitz							HLP Synth. 15	HLP Synth. 32	HLP Synth 46
QUAKER CHEMICAL				Quintolubric Greensave N 30					Quintolubric Greensave 46 Esterhyd HE 46
RAISON TEHTAAT. Finland TEBIOL. BRD New Process Schweiz		Florahyd RT-HVI 32							
SHELL		Naturelle HF-R-32*			Fluid BD 22	Fluid BD 32*	Fluid BD 46		Naturelle HF-E 46
									Naturelle HF-E 68

Table 8.3 Continued

Type of fluid ISO viscosity class Maker	Vegetable-oil-based hydraulic fluids, HETG				Synthetic hydraulic fluids based on polyglycol, HEPG			Synthetic hydraulic fluids based on esters, HEE			
	VG 22	VG 32	VG 46	VG 68	VG 22	VG 32	VG 46	VG 22	VG 32	VG 46	VG 68
SOLLNER		Connexol HD 32-68									
STRUB & CO Schmiertechnik CH-Reiden								Hydrosint HLP ISO 32	Hydrosint HLP ISO 46	Hydrosint HLP ISO 68	
TOTAL									Equivis Bio 46	Equivis Bio 68	
VALVOLINE			Ultraplant 40								
WENZEL & WEIDMANN		Ukabiol HY 32	Ukabiol HY 46			Ukadol 32 NG	Ukadol 46 NG'			Ukabiol HE 46	
WESTFALLEN AG		Bio Forbex R 32	Bio Forbex R 46							Bio-Forbex E-46	
WINTERSHALL		Wiolgan HR 32									
WISURA			Hydroma UWF 46								
YORK Ginouves										LT 777 Bio	
ZELLER & GMELIN			Biovinol HTG 46								

Note: The term "environmentally acceptable" (or "environmentally friendly") is not a well-defined term. There is no universally accepted criterion for "environmental acceptability" at the present time although various national standards are in the process of being written. Therefore, the term "environmentally acceptable" is essentially a marketing term with little or no technical support. In fact, often "environmentally acceptable" is used synonymously with "vegetable oil."

*Tested by Hydromatik (this does not imply that such tests were exhaustive or that a recommendation of such fluids is implied). All rights reserved, subject to revision.

Source: Ref. 38.

Table 8.4 Components of a "Typical" Water-Glycol Hydraulic Fluid

Component	Purpose
Water	Fire protection
Glycol	Freeze-point reduction and some thickening
Thickener	Thicken the formulation and to provide adequate film viscosity at the wear contact
Antiwear additives	Provide mixed film and some boundary lubrication
Corrosion inhibitors	Vapor and liquid corrosion protection

INHERENT BIODEGRADATION. This is the potential to eventually biodegrade, although at a rate lower than required for classification as "readily biodegradable."

The OECD procedure also incorporates a "10-day window," which requires "that the percent theoretical CO₂ must reach 60% within 10 days after reaching the 10% level" [11] if the fluid is to be classified as biodegradable. This requirement applies for all of the OECD 301 methods (A–E) shown in Table 8.5.

The OECD is currently reevaluating this "10-day window" criterion for the following reasons:

Table 8.5 Standard Biodegradability Tests

Method	Time (days)	Factor measured	Criterion
Ready biodegradability			
Modified AFNOR (OECD 301 A)	28	Loss of dissolved organic carbon	>70% ^a
Modified Sturm (OECD 301 B)	28	Production of carbon dioxide	>60% ^a
Modified MITI(1) (OECD 301 C)	28	Oxygen demand	>60% ^a
Closed bottle (OECD 301 D)	28	Oxygen demand	>60% ^a
Modified OECD screening test (OECD 301 E)	28	Loss of dissolved organic carbon	>70% ^a
Inherent biodegradability			
Modified Semicontinuous Activated Sludge (SCAS) (OECD 302 A)	>28	Loss of dissolved organic carbon	>20% ^b
Zahn–Wellens (OECD 302 B)	28	Loss of dissolved organic carbon	>20% ^b
Primary biodegradability			
CEC-L-33-T-82	21	Loss of hydrocarbon infrared bands	>67% ^c >80% ^d

^aFor classification as readily biodegradable.

^bFor classification as inherently biodegradable.

^cICOMIA standard.

^dGerman Blue Angel requirement for biodegradable hydraulic fluids.

Source: Ref. 48.

1. This requirement is of questionable applicability to substances that are poorly water soluble [11].
2. Inherently biodegradable substrates may produce a time lag in the degradation process but still undergo ultimate biodegradation [49]. Therefore, this requirement appears to be unduly restrictive.

The experimental strategies for the various tests listed in Table 8.5 involve the measurement of (1) the amount of the original carbon consumed, (b) the consumption of oxygen used in the degradation test, or (c) the evolution of carbon dioxide at the end of the biological degradation process. This is illustrated in Fig. 8.3 [50].

Of the tests for “ready biodegradability” shown in Table 8.5, those most frequently used include OECD 301A, 301B, and 301E [49]. The use criteria test for these tests are as follows [49]:

1. OECD 301A—AFNOR Test. This test is used for water-soluble compounds that are relatively nonvolatile and noninhibiting to bacteria at 40 mg/L dissolved organic carbon (DOC). The DOC of the test material is the sole source of COC for the aerobic microorganisms. The test criteria is based on loss of DOC after 28 days.
2. OECD 301B—Modified Sturm Test. This test is applicable for both water-soluble and water-insoluble compounds. Biodegradation is based on the yield of carbon dioxide produced over the 28-day duration of the test.
3. OECD 301E—OECD Screening Test. This test is designed for water-soluble, nonvolatile, and noninhibitory compounds (5–40 mg/L DOC). This test also monitors the change in DOC with respect to time and is similar to OECD 301A.

OECD 301B is often used to determine the biodegradability of hydraulic fluids for the following reasons [49]:

- The method allows for determination of biodegradability at the lowest concentration possible.
- The method is useful for both water-soluble and water-insoluble compounds.

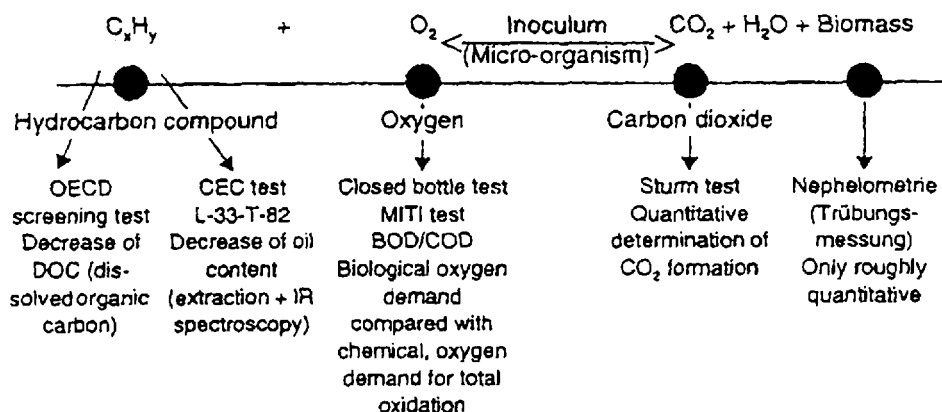


Figure 8.3 Test strategies for determining and quantifying biodegradation. (From Ref. 50.)

- Because titrations are used, the method is relatively simple and inexpensive to perform.

One of the difficulties in conducting these aqueous tests is the insolubility of hydraulic fluids, with the exception of the water-containing fluids such as a water-glycol hydraulic fluid. Girling reviewed the following procedures used to enhance oil solubility: vigorous shaking, blending (Waring blender), homogenizing, ultrasonification, and chemical dispersion [51]. The factors which are known to influence the composition of the aqueous test media include the following [51]:

- The bulk properties: viscosity, interfacial tension, and so on of the OBP (oil-based products)
- The mixing environment
- Properties of the aqueous phase such as pH, water temperature, hardness, and salinity
- Physical and chemical properties of the OBP constituents
- The OBP/water ratio

These difficulties skew BOD data in favor of water-insoluble fluids because the percentage of biodegraded substrate will increase as the solubility of the substrate decreases, assuming the degradation rate remains unchanged. One way that this can be envisioned is by examining the effect of oil-film thickness on biodegradability rate, which would presumably increase with increasing concentration and which should then result in lower degradation half-times. This was observed by Völtz et al. as illustrated in Fig. 8.4 [50]. Völtz et al. also showed that the type and concentration of microorganisms that may be present in the aquatic environment will also significantly affect biodegradation rates, as illustrated in Fig. 8.5 [50].

Biodegradation rates are often conducted by a number of possible tests as indicated in Table 8.5. Two of the most commonly encountered tests are the CEC-L-33-A-94 test and the modified Sturm shake flask test [11]. Table 8.6 provides a correlation of the two tests with respect to the vegetable oil and synthetic ester shown

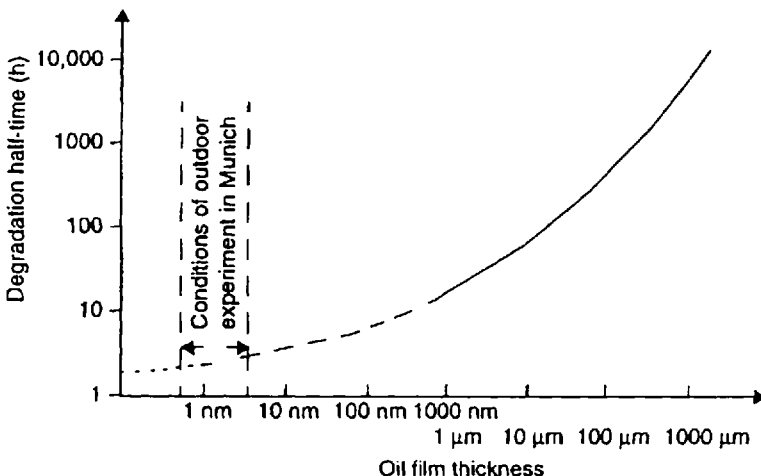


Figure 8.4 Dependence of oil-film thickness on biodegradation rate. (From Ref. 50.)

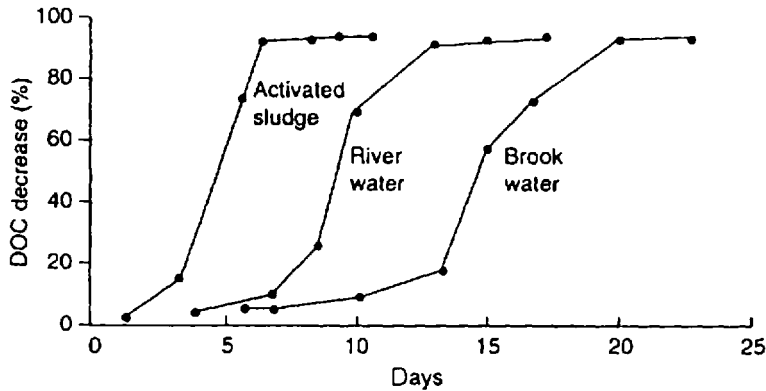


Figure 8.5 The effect of microflora on biodegradation rates. (From Ref. 50.)

[29]. These data are interesting because they illustrate the similarity and differences between the two commonly encountered testing methods. The following comments are offered with respect to these results:

- The CEC-L-33-A-94 method is used to determine primary biodegradation. (See Table 8.5.) Primary biodegradation refers to the first stage of degradation and corresponds to the initial changes in the molecular composition of the lubricant upon degradation. This is a useful screening test to assess the potential for degradation.
- The Modified Sturm Test is used to assess ultimate biodegradability. It is assumed that the lubricant components have completely “mineralized.”
- The data in Table 8.6 are interesting in that they show that primary degradation is always greater than the values for ultimate degradation [29]. Thus, it is possible for a substrate that only partially degrades to exhibit a high percentage of degradation in the primary biodegradability test. This helps to explain the relatively poor correlation between the two tests shown in Fig. 8.6 [47].

Table 8.6 Biodegradability of Selected Hydraulic Fluids

Product base stock	Biodegradability	
	Shake flask ^a	CEC test ^b
Mineral oil	42–48	N.T. ^c
Vegetable oil	72–80	>90
Polyglycol	6–38	N.T. ^c
Synthetic ester	55–84	>90

^aCO₂ evolution — EPA Method 560/6-82-003.

^bCEC Method CEC-L-T-82.

^cNot tested.

Source: Ref. 29.

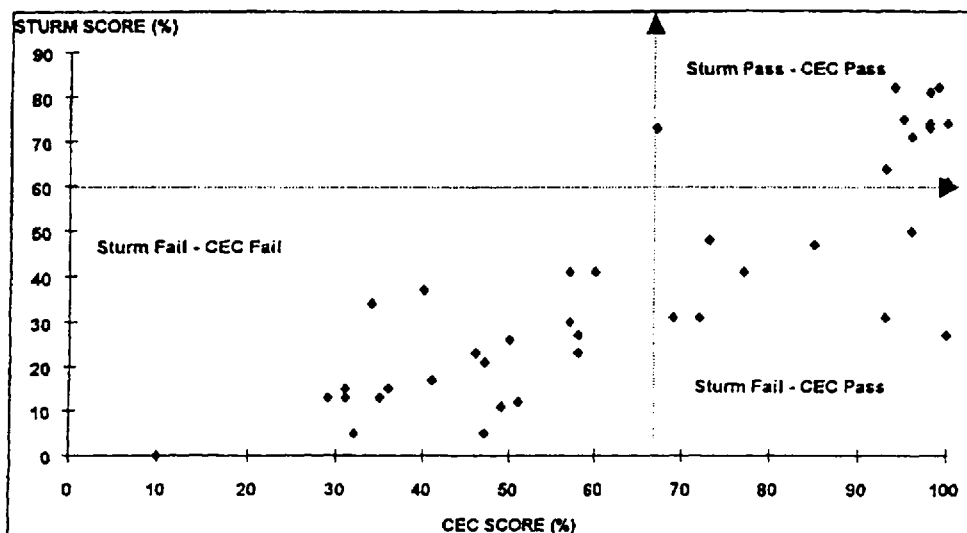


Figure 8.6 Comparison of CEC and Sturm test results. (From Ref. 47.)

- These data explain the occasional confusion that occurs in the marketplace if data from dissimilar test procedures are compared.

2.2.2 Published Biodegradation and Toxicity Data

Aquatic Biodegradability

Biodegradability, using the CEC-L-33-A-94 test procedure, of various mineral-oil base stocks was reported by Singh and selected examples are shown in Table 8.7. These data show that mineral-oil biodegradability is composition dependent. These data indicate that if aromatic, aliphatic, and heterocyclic derivatives are minimized and the saturation level is increased, mineral-oil-derived compositions may be produced with biodegradability properties that rival vegetable oil and polyol esters, the

Table 8.7 Biodegradability of Selected Fluids Using the CEC-L-33-A-94 Test Procedure

Fluid	% Biodegradability
LVI VG 100	35
Parafinic VG 100	60
Hydrotreated HVI VG 100	30
Naphthenic VG 100	47
Formulated predominantly mineral oil (R&O)	77
Hydrocracked very high VI	80
Formulated vegetable oil	95
Synthetic polyol ester	95

Source: Ref. 52.

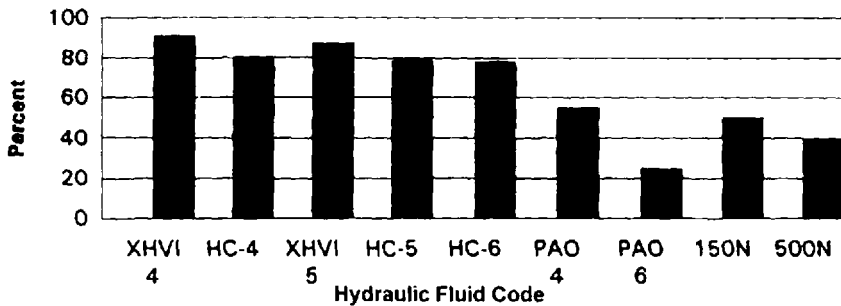


Figure 8.7 Effect of mineral-oil composition on biodegradability. Numbers following the designations are viscosities (cSt at 100°C) and those of solvent neutrals are SUS at 100°F. VHVI = high-VI oils; XHVI = shell wax isomerized base oils; HC = hydrocracked synthetics; PAO = polyalphaolefin; N = solvent-refined neutral oils. (From Ref. 53.)

closest functional competitors. As expected, vegetable oil and polyol ester based fluids exhibited considerably higher biodegradation rates [52].

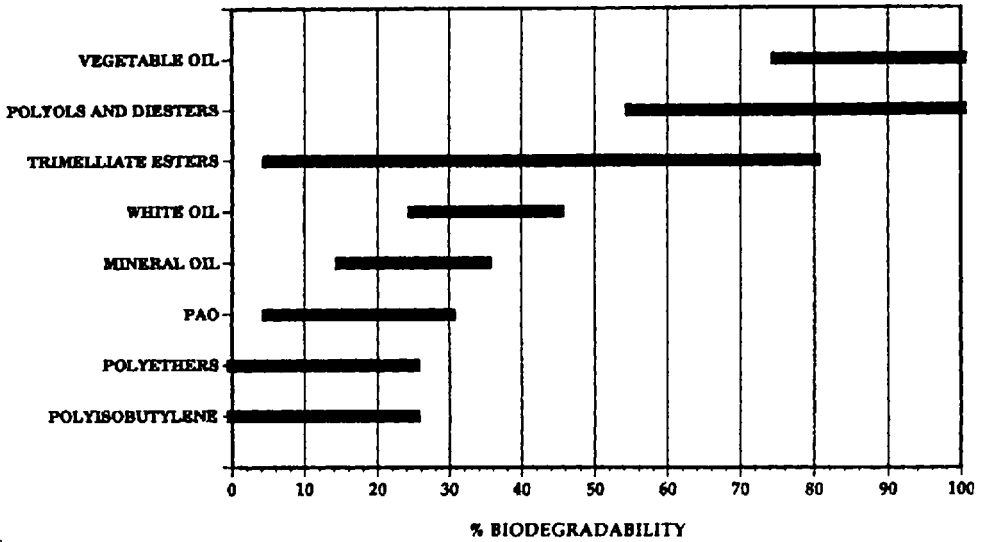
In a different study, Kiovsy using the updated procedure CEC-L-33-A-94 also examined the effect of mineral-oil base stock on biodegradability [53]. The results in Fig. 8.7 show that hydrocracking produced relatively good biodegradation rates, approximately 80%.

Naegely has provided a comparison of the biodegradability of white oils with typical ranges for vegetable oils, polyol esters, and diesters, which is summarized in Fig. 8.8a [22]. The values for polyethers (which are anhydrous) are significantly less than those published by Völtz, as shown in Fig. 8.8b [50], which are less than those reported by Henke (shown in Fig. 8.8c) [54]. (The mineral-oil hydrotreating procedure (see Section 1.e.) refers to catalytic hydrogenation.) All of the data were obtained by the CEC-L-33-A-94 biodegradability test. Figure 8.9 illustrates the variation in the limits required by different European specifications using the same CEC biodegradability test procedure to define “rapidly” biodegradable fluids [7].

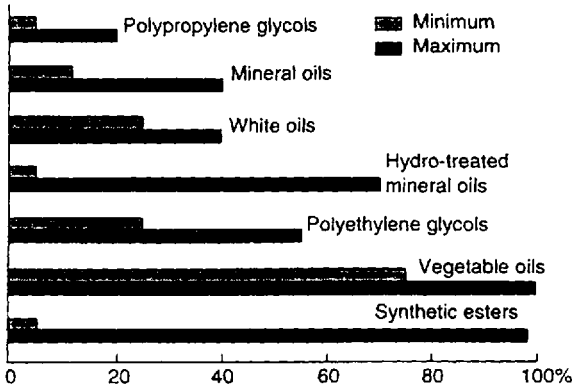
The rate of biodegradation of a mineral oil and a rapeseed oil, with respect to time, using the CEC test procedure is compared in Fig. 8.10 [3]. Clearly, the vegetable oil undergoes most of its bio-oxidation within 10 days. These are interesting data and indicate the potential impact of the so-called “10-day window” that was discussed earlier on the classification of hydraulic fluid biodegradability. Vegetable oils, as a class, undergo a relatively rapid initial biodegradation.

Aquatic Toxicity

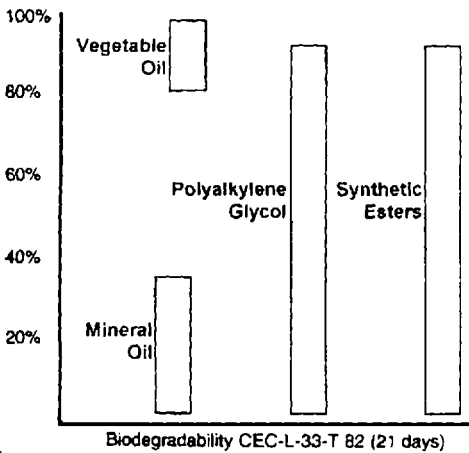
Toxicity (ecotoxicity) is defined as the “propensity” of the substance to produce adverse biochemical and physiological effects in a living organism. “It incorporates both acute and chronic effect but does not include physical effects. . . . An acute effect is one which occurs after a short exposure to the test substance, short being some time period which does not constitute a large fraction of the life span of the organism. A chronic effect is one which occurs after a long contact with the test substance” [46]. An example of a “physical effect” is the deprivation of a living organism of oxygen.



(a)



(b)



(c)

Figure 8.8 (a) Naegely biodegradation test data. (From Ref. 22.) (b) Völtz test data. (From Ref. 50.) (c) Henke test data. (From Ref. 54.)

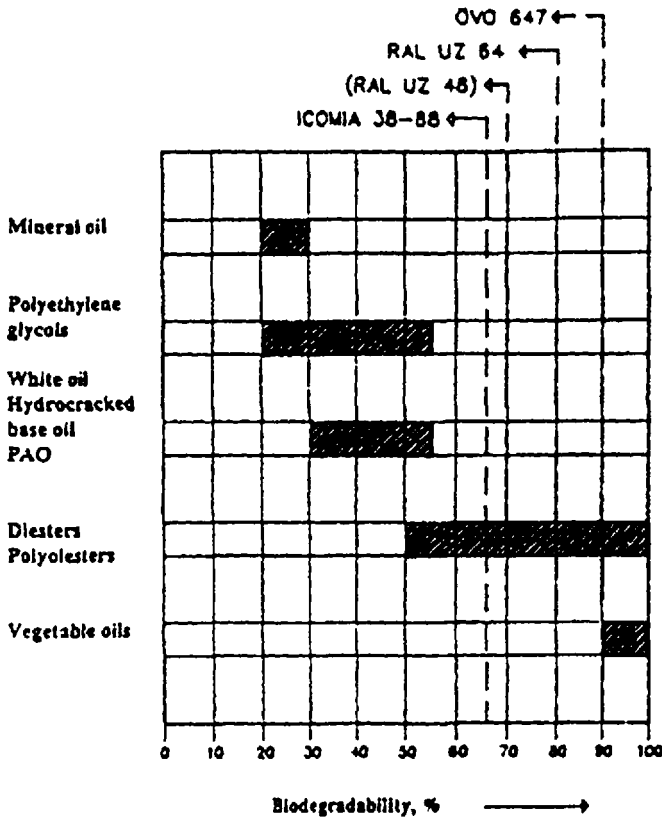


Figure 8.9 Illustration of differing biodegradation European regulations. OVO = Austrian law, 1.5. 1992; RAL = German authority for labeling; ICOMIA = International Council of Marine Industry Associates. (From Ref. 7.)

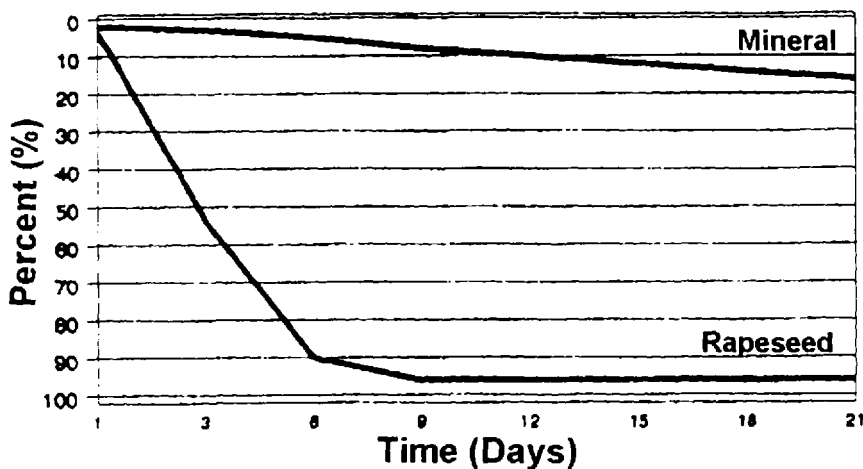


Figure 8.10 Comparison of the biodegradation rates of a mineral-oil and rapeseed-oil hydraulic fluid. (From Ref. 3.)

Toxicity is a complex subject to address adequately because different organisms react differently to the same substance. Toxicity is usually expressed in the following terms [46]:

LCXX: The “lethal concentration” to cause the death of XX% of the test organisms.

ICXX: The “inhibition concentration” for some inhibitory effect to occur in XX% of the test organisms.

ECXX: The “effect concentration” for some environmental effect such as growth or deformity to occur in XX% of the test organisms.

Comparative toxicity data on various biodegradable hydraulic fluids have been reported by Cheng et al. [29]. (Only base stocks were evaluated.) These data are summarized in Table 8.8 [29]. Rainbow trout were used for the study under mechanical dispersion conditions to facilitate an oil–water dispersion (as the oils evaluated were water insoluble). In general, none of the base stocks were determined to be toxic in this test.

Soil Biodegradability and Toxicity

Another area in which there is relatively little biodegradation data for all classes of hydraulic fluids is the fate and effects of biological degradation processes in soil [55]. Recently determined results of biodegradation of the hydrolube in soil will be reported here.

Currently, there are no international standards describing in-soil biodegradation testing procedures for hydraulic fluids. Also, there are relatively few soil biodegradation test results compared to aquatic biodegradation for the same series of hydraulic fluids. The objective here is to provide an overview of different soil biodegradation results published to date.

Völtz et al. described the Hamburg University Test, which measures CO₂ production (mmole CO₂/100 g soil) after 7 days with 4% oil. The data in Fig. 8.13 compares the biological rate of a conventional 15W-40 mineral oil and an “Eco-technology” 5W-40 fresh oil, which is based on a mixture of an ester and hydrocracked base stock [50]. As expected, the Eco-technology base-stock-derived oil degraded fastest.

Figure 8.11 illustrates the biodegradation rate of a series of mineral oils, synthetic esters, and a vegetable oil (sunflower cooking oil). Biodegradation rates were determined by determining the loss of the original fluids in soil [56]. The vegetable

Table 8.8 Comparative Toxicity of Selected Hydraulic Fluids

Product base stock	Trout LC ₅₀
Mineral oil	389–>5000
Vegetable oil	633–>5000
Polyglycol	80–>5000
Synthetic ester	>5000

Source: Ref. 29.

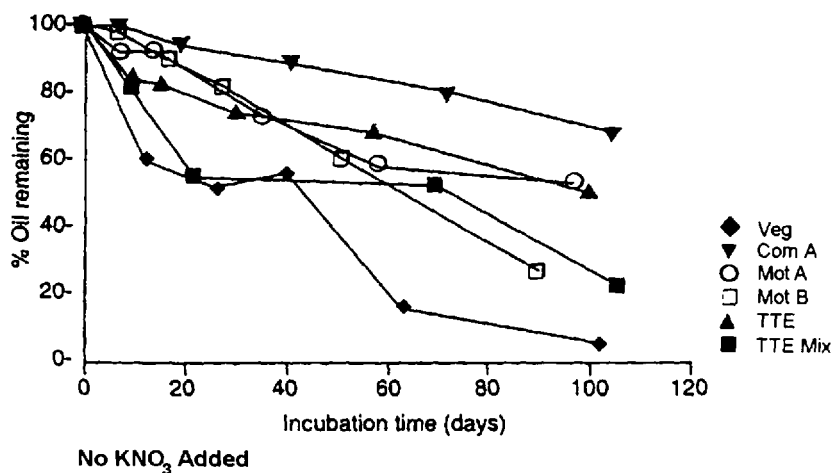


Figure 8.11 Biodegradation rates of various oils in soil. See Fig. 8.12 for explanation of oils. (From Ref. 50.)

oil was the most rapidly degraded fluid in the series. In general, natural fats and oils were not persistent in the environment.

To enhance the soil degradation rates, a nutrient (KNO_3) was added to the soil in one set of experiments (see Fig. 8.12). These data show the following:

- The vegetable oil exhibited the fastest degradation rate.
- The TTE mix, a formulated synthetic ester containing mineral spirits (see Fig. 8.12 caption) exhibited the second fastest biodegradation rate. The commercial mineral oil (Com A) was the most persistent.

In summary, these results showed that although synthetic esters biodegrade faster in soil studies than mineral oil, they are still more persistent than a vegetable oil.

Haigh described the use of a 1-m^2 section of an agricultural field [55]. Oil was added at concentrations varying from 0.25 to 5.0 L/m^2 of soil through an inverted test tube to a depth of 6 cm . Spring wheat, Broom variety, was planted. Seed germination (%) and growth rate (mm/day) was determined.

In another Haigh study [56], which was conducted on the lubricants shown in Table 8.9, the following observations were confirmed:

- The synthetic ester did not biodegrade as extensively as the vegetable oil. However, although the vegetable oil biodegraded rapidly, it took more than 1 year for the extractable residues to decrease to levels comparable to the naturally occurring lipids present in the soil.
- The mineral-oil-based fluids biodegraded less rapidly than synthetic esters. As with the other fluids, the biodegradation rate increased with soil temperature.
- Crop damage was not necessarily related to the level of the oil residues. For example, the dibasic esters, although biodegrading rapidly, caused complete inhibition of seed germination.

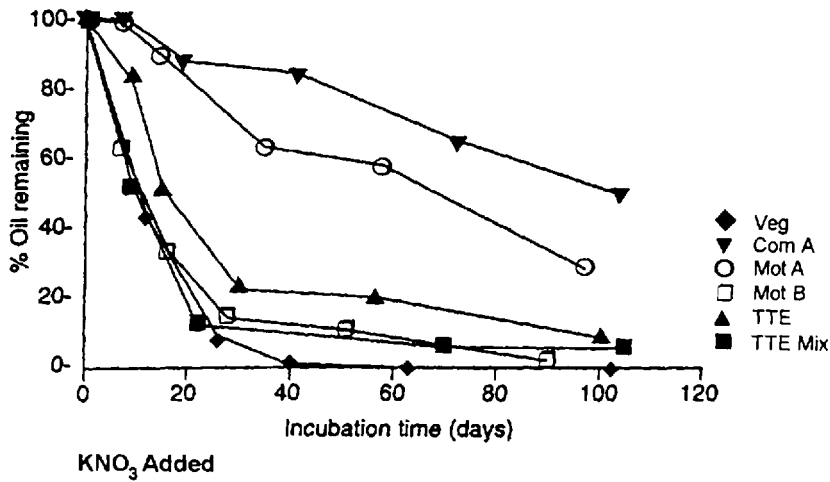


Figure 8.12 Illustration of biodegradation rate of 1% of the following: TTE—a commercial mixture by weight, isostearic acid ester of trimethylolpropane; TTE mix—a mixture of 60% TTE, 20% white spirit, and 20% of a substituted imidazoline additive; Mot A—dibasic acid esters of dodecanoic acid; Mot B—analogue to Mot A except using a longer-chain acid; Com A—a highly refined formulated motorcycle mineral-oil lubricant; Veg—“pure” sunflower cooking oil. To the soil samples were added: (a) 2 mL of distilled water and (b) 2 mL of KNO_3 (14 mg NO_3-N). The samples were incubated at 25°C and moisture levels maintained by distilled water addition.

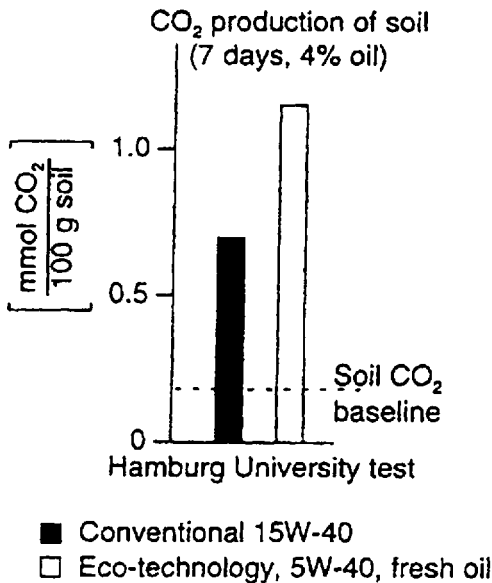


Figure 8.13 Comparative biodegradation test results.

Table 8.9 Plant Yields of Spring Wheat Treated with Different Lubricating Oils

Fluid	Ave. germination rate ^a	Ave. yield (g/plant)	Ave. growth rate (mm/day)
Trimethylolpropane triisostearate (TTE)	83.5	95.0	99.9
TTE + substituted imidazoline (TTE + additive)	74.0	95.0	99.9
TTE + white spirit (20%) + 20% substituted imidazoline (TTE mix)	63.0	NS ^b	99.9
“Pure” sunflower cooking lubricant (Veg)	81.5	99.9	99.9
Highly refined mineral-oil motorcycle lubricant (Com A)	80.0	90.0	NS ^b
Highly refined mineral-oil automotive lubricant (Com B)	70.0	95.0	
White spirits	63.5	99.9	99.9
Dibasic acid C-12 ester (Mot A)	0.0	Complete inhibition of germination	
Dibasic acid C-12 with a longer-chain ester (Mot B)	0.0	Complete inhibition of germination	

^aThe control for untreated soil was 88.5% germination.

^bNS = not significant.

Source: Ref. 56.

- The white spirit and vegetable oil permitted seed germination but significantly inhibited both growth rate and yield.

There are a number of mechanisms by which an oil can retard plant growth. These include the following [57]:

1. Oils may coat the seeds, thus creating a physical barrier inhibiting germination.
2. Growth inhibition may occur by root suffocation or by oxygen depletion of the soil by the oil biodegradation process.
3. Poor growth may also be due to reduced water uptake by the plants and/or immobilization of nitrogen and phosphorus in the soil.
4. In general, the smaller the molecule, the more toxic the behavior due to increased ease of penetration onto the plant tissue.

The results of Haigh's work [55,56] showed that, as expected, synthetic esters are degraded more rapidly than mineral oil but not as rapidly as vegetable-oil-derived lubricant. In general, even vegetable oil requires ≥ 1 year for extractable residues to decrease to levels comparable to the natural lipids present in the soil. The effects of these oils on growth rates varied from small reductions to complete inhibition. The degree of inhibition was not related to the persistence of the oil residues. This means that it is important to monitor both biodegradation and toxicity.

2.2.3 Biodegradability and Toxicity Data for a Water–Glycol Hydraulic Fluid

Extensive biodegradability and toxicity data for one water–glycol hydraulic fluid formulation has been reported [36]. This fluid exhibited 80% biodegradation after 28 days, according to the OECD Modified Sturm test protocol 301B shown in Table 8.10 [36].

Mammalian acute toxicity and irritancy of this fluid was also determined. The acute oral LD_{50} for rats was determined to be >20.0 g/kg. Dermal irritation determined on rabbits exhibited a Draize score of 0, which means it is not a skin irritant according to this test.

Toxicity toward aquatic and terrestrial organisms was determined. The aquatic organisms that were tested included fish, invertebrates, and algae. The terrestrial organisms included plants (radish) and invertebrates (earthworms). As the results in Tables 8.11 and 8.12 indicate, this water–glycol fluid was practically nontoxic to the aquatic organisms evaluated. For reference, the aquatic toxicity reference scale is shown in Table 8.13.

Table 8.10 Biodegradability and Mammalian Toxicity and Irritancy Data for a High-Performance Water-Glycol Hydraulic Fluid^a

Test	Result
OECD 301B—Modified Sturm test	80% in 28 days
Acute oral LD_{50} —rats	>20.0 g/kg
Dermal irritation—rabbits	Draize score of 0

^aUCON Hydrolube HP-5046 (Union Carbide Corporation, Danbury, CT.).

Source: Ref. 36.

Table 8.11 Ecotoxicity Toward Aquatic Organisms for a High-Performance Water-Glycol Hydraulic Fluid^a

Test	Test type	Endpoints LC50/IC50
Rainbow trout	Survival acute/96 h	LC50—10,607 $\mu\text{L/L}$
<i>Daphnia magna</i>	Survival acute/96 h	LC50—10,607 $\mu\text{L/L}$
<i>Selenastrum capricornutum</i>	Growth chronic/96 h	IC50—467 $\mu\text{L/L}$

^aUCON Hydrolube HP-5046 (Union Carbide Corporation, Danbury, CT.).

Source: Ref. 36.

A hazard evaluation model was developed to determine the toxicity and exposure levels if an accidental spill were to occur. The assumptions used for this model are summarized in Table 8.14. The results of this evaluation showed the following [58]:

- Terrestrial Environment—small boreal mammals. The model provided an estimated dose for red squirrels of 2690–11,920 mg/kg/day and the acute oral LD₅₀ for rats was determined to be >20 g/kg. These data indicate that there is no significant hazard for a single event under the conditions modeled (see Table 8.5).
- Terrestrial Environment—invertebrates. The model estimated the concentration of the high-performance hydrolube in the soil to be 3400 mg/kg soil. The LC₅₀ for earthworm survival is 26,574 mg/kg soil, the LC₅₀ for seedling emergence is 6388 mg/kg soil, and the LC₅₀ for seedling growth is 493 mg/kg soil. These results indicate that there is no significant hazard for invertebrates and plants.
- Aquatic Environment. The estimated concentration of the high-performance hydrolube in water is 0.16 $\mu\text{L/L}$. The LC₅₀ for rainbow trout survival is 10,607 $\mu\text{L/L}$, the LC₅₀ for *Daphnia magna* survival is 10,607 $\mu\text{L/L}$, and the IC₅₀ for *Selenastrum capricornutum* growth is 467 $\mu\text{L/L}$. On the basis of this model, there is no significant hazard for fish, invertebrates, or algae.

2.3 Current Specification Status

Cheng et al. first proposed the following biodegradability criteria to determine if a lubricant would be acceptable for use in environmentally sensitive areas at the 1991 SAE Earth Moving Conference [29]:

Table 8.12 Ecotoxicity Toward Terrestrial Organisms for a High-Performance Water-Glycol Hydraulic Fluid^a

Test	Test type	Endpoints LC50
Radish seedling	Emergence chronic/21 days	6,388 mg/kg soil
	Growth chronic/21 days	493 mg/kg soil
Earthworm	Survival chronic/14 days	26,574 mg/kg soil

^aUCON Hydrolube HP-5046 (Union Carbide Corporation, Danbury, CT.).

Source: Ref. 36.

Table 8.13 Aquatic Toxicity Classification Scale

Classification	LC50 (mg/L or ppm)
Super toxic	>0.01
Extremely toxic	0.01–0.1
Highly toxic	>0.1–1.0
Moderately toxic	>1.0–10.0
Slightly toxic	>10–100
Practically nontoxic	>100–1000
Relatively harmless	>1000

Source: U.S. Fish and Wildlife Service Research Information Bulletin 84-78, 1984.

- > 60% Conversion to CO₂ in 28 days
- Aquatic toxicity for rainbow trout of >1000 ppm

There are a number of national standards under development that currently have various levels of international acceptance. These will be reviewed briefly in the next subsection.

2.3.1 Ecolabel Testing Requirements

The testing requirements for three ecolabels will be discussed here. They include German Blue Angel, Canadian EcoLogo, and the method currently being developed by ASTM in the United States to define Eco-evaluated (EE) fluids. In addition, the Caterpillar BF-1 specification [34] will be discussed. These procedures will be discussed here in order.

German Blue Angel

The current German Blue Angel testing requirements are summarized in Table 8.15. The objective is that the claim for reduced environmental impact should be supported by test data. The Blue Angel procedure developed in Germany incorporates a water hazard classification system which requires measurement of mammalian, fish, and

Table 8.14 Hazard Evaluation Assumptions

Total area of forest impacted by spill	200 m ²
Depth of soil impacted	0.1 m
Total volume of HP-5046 released during spill	100 L
Loss of HP-5046 in environment due to biodegradation	0%
Weathering rate of HP-5046 on vegetation (s ⁻¹)	5.73×10^{-7}
Vegetation yield (kg plant/m ²)	2.8 (value for grass, wet weight)
Density of HP-5046	1.09 mg/ μ L
Solid loads in water of Canadian forested regions	50 mg/L
Soil ingestion (small animals)	13% of food ingestion food ingestion = 0.0124 kg/day
Red squirrel body weight	145–260 g

Table 8.15 Summary of German Blue Angel Criteria

- The product shall meet all relevant technical specifications.
- Every component, including additives, must be Water Hazard Class 0 or 1. (See Table 8.21.)
- The product must be free of organic chlorine, nitrite-containing compounds and metals (with the exception of calcium up to 100 ppm). No definition of "free" (in terms of an upper concentration limit) is given.
- Readily biodegradable components can be incorporated in the product in any concentration but must collectively account for at least 93% of the product composition. Such components are defined in terms of one of the following tests and pass levels:

Test	Pass level
Modified AFNOR	70%
Modified OECD Screening Test	70%
Modified Sturm	70%
Modified MITI (1)	70%
Closed Bottle	70%
CEC-L-33-A-93 (poorly soluble components only)	80%

- Total concentration of "inherently" biodegradable components cannot exceed 5%. Such components are defined in terms of any one of the following tests and pass levels:

Test	Pass level
Modified SCAS	20%
Modified MITI (2)	20%
Zahn-Wellens	20%

- Total concentration of nonbiodegradable components (i.e., components that fail to achieve the pass levels in the tests for "inherent" biodegradability) cannot exceed 2%.
- All "inherently" biodegradable and nonbiodegradable components must satisfy the following ecotoxicological criteria:
- They must be nontoxic to aquatic organisms:

Potential for Bioaccumulation	No	Yes
OECD 202 Part 1 (Daphnia) EC_{50}/LC_{50}	≥ 1 mg/L	≥ 100 mg/L
OECD 203 (fish) EC_{50}/LC_{50}	≥ 1 mg/L	≥ 100 mg/L
OECD 203 (fish) NEC	≥ 0.01 mg/L	≥ 1 mg/L

- They must be nontoxic to higher plants:
- In addition to the above, all nonbiodegradable components must be nontoxic to bacteria:
- All nonbiodegradable polymer components must be insoluble in water:

(solubility ≥ 1 mg/L)

Table 8.16 German Water Hazard Classification System

Acute Oral Mammalian Toxicity (AOMT)

Measured as an LD₅₀ for laboratory animals. The LD₅₀ is used to determine a "Water Endangering Number" (WEN) using the following scale:

LD ₅₀ (mg/kg)	WEN (AOMT)
<25	7
25–200	5
200–2000	3
>2000	1

Acute Bacterial Toxicity (ABT)

Measure as a "no-effect" concentration (NEC). The WEN (ABT) is determined from

$$WEN(ABT) = -\log(NEC \text{ in ppm}/10^6 \text{ ppm})$$

Acute Fish Toxicity (AFT)

Measured as a WEC. The WEN (AFT) is determined from

$$WEN(AFT) = -\log(NEC \text{ in ppm}/10^6 \text{ ppm})$$

Water Endangering Number (WEN)

The overall WEN is calculated from

$$\text{Overall WEN} = \frac{1}{3}[WEN(AOMT) + WEN(ABT) + WEN(AFT)]$$

WGK Number

The Water Hazard Classification is then determined from

WEN	WGK number	Classification
0–1.9	0	Not hazardous to water
2–3.9	1	Slightly hazardous to water
4–5.9	2	Moderately hazardous to water
>6	3	Highly hazardous to water

"Readily" biodegradable substances are assigned to the next lower Water Hazard Class. (Rapeseed oils and polyethylene glycols are WGK 0.)

Source: Ref. 48.

bacterial toxicity [48]. The Blue Angel requirement is dependent on the water hazard classification (WGK) number which is summarized in Table 8.16 [48].

Canadian EcoLogo Testing Requirements

The Canadian EcoLogo is the most commonly encountered national environmental standard for hydraulic fluid use in North America [59]. The acceptance criteria to receive this label is summarized in Table 8.17.

ASTM "Eco-evaluated" Testing Criteria

The ASTM D.02N.03 Subcommittee is developing a testing criterion to evaluate the potential impact of the use of unused hydraulic fluids on the environment. Table 8.18 summarizes the current major classification designations [59]. Because the standard is under development, the complete selection of required test methods is not

Table 8.17 Environmental Choice Ecologo-Product-Specific Requirements

-
1. Demonstrate (a) or (b) below:
 - (a) Have a C_{50} or an EC_{50} not lower than 1000 mg/L when the OWD (fish) and the WAFs (*Daphnia* and algae) prepared from the whole formulation are tested according to
 - Biological Test Method: Acute Lethality Test Using Rainbow Trout, Report EPS1/RM/9, July 1990, Environment Canada, and, Biological Test Method: Acute Lethality Test Using *Daphia* Spp., Report EPS 1/RM/11 July 1990, Environment Canada and Biological Test Method: Growth Inhibition Test Using the Freshwater Algae *Selenastrum Capricornutum*, Report EPS 1/RM/25 November 1992, Environment Canada; or
 - Test acceptable to the ECP (Environmental Choice Program).
 - (b) Have a EC_{50} or LC_{50} not lower than 2500 ppm when the whole formulation is tested according to Microtox[®] test.
 2. Be biodegradable according to CEC-L-33-T82.
 3. Not contain more than 5% (w/w) additives.
 4. Not contain more than 3% (w/w) of an additive that is not proven to be biodegradable.
 5. Not contain more than 0.1% petroleum oil or additives containing petroleum oil.
 6. Not contain:
 - (a) organic chlorine or nitrite compounds
 - (b) lead, zinc, chromium, magnesium, or vanadium.
 7. Not have to be labeled according to Class D, "Poisonous and Infectious Material," or set out in the "Controlled Products Regulation of the Hazardous Products Set."
 8. Be packaged in a container which bears a label indicating both the pour point as determined by ASTM D97 "Standard Test for Pour Point of Petroleum Oils" and the low-temperature fluidity performance.
 9. Yield negative results when tested against ASTM D665 "Standard Test Method for Rust Preventing Characteristics of Inhibited Mineral Oil in the Presence of Water."
 10. Not have a flash point lower than 200°Cm if ISO grade VG 32 and higher, and not lower than 190°Cm if ISO grade VG 15-22 when measured according to ASTM Test Method D92 "Standard Test Method for Flash and Fire Points by Cleveland Open Cup," D 93 Standard Test Method for Flash Point by Pensky-Martens Closed Tester," or D 56 "Standard Test Method for Flash Points by TAG Closed Tester."
 11. Be proven to have good oxidation stability when tested according to ASTM D 525 "Standard Test Method for Oxidation Stability of Gasoline (Induction Period Method), or modified according to U.S. Patent 4,783,274 (1983) Hydraulic Fluids, K.V. Jokinson et al., the pressure drag is not greater than 35 psi.
 12. Demonstrate a low tendency for foaming according to ASTM Test D-892.
-

yet firmly established. Nevertheless, the most current test methods under consideration are reported here. Fluids are designated as Pw_1 , Pw_2 , and so forth according to their performance in specified tests.

The current test method under development will only focus on environmental persistence (Category P) and acute ecotoxicity (Category T) of hydraulic fluids. As only test methods for determination of aerobic freshwater have been developed to date [60], this new standard will be limited to the evaluation of unused hydraulic fluids in aerobic fresh water (Pw). The proposed classification system is provided in Table 8.19. The test methods are summarized in Table 8.20.

Table 8.18 Classification Designations of ASTM “Eco-evaluated” Fluids

Environmental component	Categories of environmental impact		
	Environmental persistence	Exotoxicity	Bioaccumulation
Freshwater	Pw	Tw	Bw
Marine	Pm	Tm	Bm
Soil	Ps	Tx	Bs
Anaerobic	Pa	Ta	Ba

Source: Ref. 59.

The proposed classification of “ecotoxicity” properties of hydraulic fluids is summarized in Table 8.21 and the proposed uses for ecotoxicity are provided in Table 8.22.

Caterpillar BF-1 Specification

NEED FOR COMPREHENSIVE PERFORMANCE REQUIREMENTS. In the third quarter of 1991, Caterpillar released its first recommendations for the use of biodegradable hydraulic oils specifically for Caterpillar hydraulic systems. At that time, veg-

Table 8.19 Environmental Persistence Classification—Aerobic Freshwater

A. For Hydraulic Fluids Containing Less than 10 wt% O₂		
Persistence designation	Ultimate biodegradation test results	
	% Theoretical CO ₂	% Theoretical O ₂
Pw 1	≥60% in 28 days	≥67% in 28 days
Pw 2	≥60% in 84 days	≥67% in 84 days
Pw 3	≥40% in 84 days	≥45% in 84 days
Pw 4	<40% in 84 days	<45% in 84 days
B. For Hydraulic Fluids Containing 10 wt% or More O₂		
Persistence designation	Ultimate biodegradation test results	
	% theoretical CO ₂ or theoretical O ₂	
Pw 1	≥60% in 28 days	
Pw 2	≥60% in 84 days	
Pw 3	≥40% in 84 days	
Pw 4	<40% in 84 days	
C. For All Hydraulic Fluids		
Persistence designation	Primary biodegradation test results	
	% loss of starting material	
Pw-C	≥80% in 21 days	
Pw 4	<80% in 21 days	

Table 8.20 Tests of Biodegradability in Aerobic Aquatic Environments

Test title	Measurement	Sponsoring organization
D 5864. Test Method for Determining the Aerobic Aquatic Biodegradation of Lubricants	% Theoretical CO ₂	ASTM
9429:1990, Technical Corrigendum 1, Water Quality —Evaluation in an aqueous medium of the "ultimate biodegradability of organic compounds" —Method by analysis of released carbon dioxide	% Theoretical CO ₂	ISO
301 B, CO ₂ Evolution Test (Modified Sturm Test)	% Theoretical CO ₂	OECD
301 C, Modified MITI Test (1)	% Theoretical O ₂	OECD
301 F, The Monometric Respirometry Test	% Theoretical O ₂	OECD
Aerobic Aquatic Biodegradation Test	% Theoretical CO ₂	US EPA
C:4-C: Carbon dioxide(CO ₂) evolution	% Theoretical CO ₂	EU
C:4-D: Monometric Respirometry ^a	% Theoretical O ₂	EU
Primary Biodegradation Tests	% Loss of	CEC
L-33-A-93. Biodegradability of Two Stroke Cycle Outboard Engine Oils in Water (Formerly L-33-T-82)	extractable CH ₂ groups	

^aIndicated OECD equivalent.

etable oils, particularly those extracted from rapeseed, were widely used and generally available. Over time, customers required a fluid that exceeded the capabilities of conventional rapeseed-based oils. Increased demands on the hydraulic system and on the fluid require biodegradable hydraulic fluids demonstrating better oxidation resistance. In applications where better oxidation stability of the oil was required, it became necessary to use synthetic ester-based hydraulic fluids.

A survey of the available industry standards revealed no existing industry performance category for high-performance biodegradable hydraulic fluids meeting Caterpillar system needs. With the advent of higher-performing components in hydraulic systems, hydraulic fluids capable of better lubricity, higher-temperature stability, and

Table 8.21 Acute Ecotoxicity Classification

Ecotoxicity in soil designation	Ecotoxicity in water designation	Loading rate (wppm), LL ₅₀ , IL ₅₀ , or EL ₅₀
Ts 1	Tw 1	>1000
Ts 2	Tw 2	1000–100
Ts 3	Tw 3	100–10
Ts 4	Tw 4	<10

Table 8.22 Test for Ecotoxicity

Test title	Sponsoring organization
Soil Invertebrates	
A.8.5 Earthworm Survival (<i>Eisenea foetida</i>)	US EPA
207 Earthworm Acute Toxicity Test	OECD
Soil Plants	
A.8.7 Lettuce Root Elongation (<i>Lactuca sativa</i>)	US EPA
A.8.6 Lettuce seed germination (<i>Lactuca sativa</i>)	US EPA
208, Terrestrial Plants Growth Test	OECD
797.2750 of TSCA, Seed germination/root elongation toxicity test	US EPA
797.2800 of TSCA, Early seedling growth toxicity test	US EPA
Water Plants	
Section 797.1050 of TSCA, Algae acute toxicity	US EPA
Section 797.1060 of TSCA, Freshwater algae acute toxicity	US EPA
Section 797.1075 of TSCA, Freshwater & marine acute toxicity test	US EPA
C.3 Algae inhibition test	EU
Biological Test Method: Growth inhibition test using freshwater algae (<i>Selenastium capricornutum</i>)	
201, Algae Growth Inhibition Test	OECD
A.8.4 Algae growth (<i>Selenastium Capricornutum</i>)	US EPA
Water: Invertebrates	
20.2 <i>Daphnia</i> sp. Acute Immobilization Test and Reproduction Test	DECD
Biological test method: Acute lethality test using <i>Daphnia</i> spp.	Canada
C.2 Acute toxicity for <i>Daphnia</i>	EU
A.8.2 <i>Daphnia pubex</i> and <i>Daphnia magna</i> Survival	US EPA
797.1300 of TSCA, <i>Daphnia</i> acute toxicity test	ASTM
E 1440, Acute Toxicity Test Rotifer Brachions	ASTM
MENVIQ.92.03/800-D.Mag. 1.1 Determination de la toxicite lethal CL 500-48h (<i>Daphnia magna</i>)	Quebec
Water: Vertebrates	
203, Fish, Acute Toxicity Test	OECD
797.1400 of TSCA, Fish, Acute Toxicity Test	US EPA
797.1400 of TSCA, Fish, Acute Toxicity Test*	US EPA
C.1. Acute Toxicity for fish*	EU
Biological Test Method: Acute Lethality Test Rainbow Trout	Canada
Biological Test Method: Referenced method for determining acute lethality of effluents to rainbow trout	Canada
A.8.3 Fathead Minnow Survival	US EPA

*Denotes an OECD equivalent test.

better oxidation stability became necessary. Although such products are now commercially available, there is a wide range of performance characteristics even among these new products. For this reason, Caterpillar published a comprehensive set of hydraulic fluid requirements for a high-performance biodegradable hydraulic fluid, known as BF-1, Biodegradable Hydraulic Fluid Requirements, which are shown in Table 8.23.

Table 8.23 BF-1, High-Performance Biodegradable Oil Requirements for New Fluid Chemical and Physical Properties

Measured property	Standard test procedure	Required value	
Fluid cleanliness	ISO 4406	15/13 maximum	
Homogeneity	Caterpillar Procedure	Max. 0.01 Vol% sedimentation	
Fluid compatibility	Caterpillar Procedure	No sedimentation	
Foaming characteristics	ASTM D892	Sequence I—25/0	
		Sequence II—50/0	
		Sequence III—25/0	
Foaming characteristics (with 0.1% water added)	ASTM D892 (modified)	Sequence I—25/0	
		Sequence II—50/0	
		Sequence III—25/0	
Humidity corrosion	Caterpillar Procedure	Minimum of 200 h to failure	
Copper strip corrosion	ASTM D1401	1: a minimum rating	
Low-temperature storage	Caterpillar Procedure	No precipitation after 168 h at -25°C	
Demulsibility	ASTM D1401	Minimum of 37 mL of water separated in 20 min	
Iodine number	AOCS Da 15-48 (WIJS Method)	Report values	
Flash point	ASTM D92	Minimum 200°C	
Pour point	ASTM D97	Maximum -35°C	
Water content	ASTM D1744	Maximum of 0.1 vol%	
Oxidation stability	ASTM D943 (modified—no water added)	Report values	
Viscosity	ASTM D445	Temperature (°C)	Kinematic viscosity (cSt)
		0	780 max.
		40	41.4 min.
		40	50.6 max.
		100	6.1 min.
Viscosity index	ASTM D2270	150 min	
Vane pump	Vickers 35VQ25	Vane weight loss: 15 mg, maximum	
		Ring weight loss: 75 mg, maximum	
FZG Rating	ASTM D5182	Minimum 11 stages	
Four-ball wear	ASTM D4172	0.40 mm, maximum scar	
Biodegradability	EPA 560/6-82-003	Minimum 60% (weight) biodegraded to carbon dioxide in 28 days	
Toxicity, water hazard	German Classification	WGK 0	
Toxicity, fish	OECD 203	I.C. ₅₀ >1000 ppm	
Friction properties	Caterpillar Procedure	See BF-1 requirements	

BF-1 REQUIREMENTS. The performance properties of VDMA 24,568 were used as a starting point for developing the high-performance biodegradable hydraulic fluid requirement [61]. Because the scope of the VDMA 24,568 document covered the minimum requirements for all hydraulic fluids and not specifically for a high-performance product, Caterpillar selected test procedures and performance levels that differed from the VDMA requirement. Reaction from the survey participants indicated that several test procedures in the VMDA requirement proved to be adequate for evaluating vegetable-based biodegradable hydraulic oils but did not provide a good yardstick for comparing the properties of all available biodegradable hydraulic fluids. Better test methods were required. For example, a new test procedure covering fluid performance at low temperature was needed because the existing procedures were not adequate.

The performance parameters listed in VDMA 24,568 are viscosity, pour point, flash point, insolubles, water content, a steel corrosion test, a copper corrosion test, oxidation stability, elastomer compatibility, air release, foaming, demulsification, FZG load test, vane pump test, density, ash content, and neutralization value (TAN). Although these tests gave a good first look at the performance of a hydraulic fluid, additional requirements, including some Caterpillar procedures, were added for a more complete representation of fluid performance. These included test procedures for homogeneity, fluid compatibility, foaming characteristics, humidity corrosion, elastomer compatibility, and frictional properties. These test methods will be described below.

In addition, this document also contains requirements for the cleanliness of new fluid, compatibility between fluids, the foaming characteristics of the oil when a small quantity of water is present, low-temperature storage requirements, the iodine number, demulsibility of water, viscosity index, four-ball wear, static and dynamic friction properties, and, most importantly, requirements for biodegradability and toxicity. With the exception of the iodine number, biodegradability, and toxicity, knowledge of these additional requirements is important in mobile hydraulic systems. Together, these tests are intended to ensure that a fluid described by BF-1 would provide high system performance and be truly biodegradable with low toxicity.

The measured chemical and physical properties, test method, and requirements as published in the first edition of BF-1 are listed in Table 8.23. The elastomer compatibility properties and limits are listed in Table 8.24. The specific values chosen for each of the requirements were obtained either through the recommendations of the reviewers of BF-1 or through testing high-performance fluids at the Caterpillar laboratories. As with all work, lessons were learned through the evaluation process. Further explanation of the values chosen, some of the problems encountered when developing the requirements, and lessons learned on the tests will be discussed below.

Fluid Cleanliness. Caterpillar chose ISO 15/13 cleanliness as the minimum cleanliness requirement for oil that is to be used for factory filling of Caterpillar machines. This requirement is intended to be applied only to new oil, not to oil that has been or is currently being used in a Caterpillar hydraulic system.

Homogeneity. A test method was developed to evaluate the compatibility of additives with the high-performance biodegradable fluid. This method is specified to measure the homogeneity of the formulated oil and to determine how well the additives will remain in solution under variable-temperature conditions. The test method requires that the fluid must be cooled to -32°C for 24 h, warmed to room

temperature, and then centrifuged at $100,000 \text{ m/s}^2$. The presence of any sedimentation must be reported and the volume of the sedimentation must not exceed 0.01 vol% of the total fluid volume.

Fluid Compatibility. Customers owning and using Caterpillar machines may choose to convert their current equipment to use environmentally friendly oils. To do this, they must drain the system of its hydraulic fluid and replace it with new biodegradable oils. Unfortunately, the draining process does not completely eliminate all of the old oil from the system. No matter how carefully the oil is changed, residual oil will remain in the system. Because of this, mixing of chemically different types of oil will occur. For this reason, it is important that the oils that become mixed are compatible.

To avoid problems with additive dropout and immiscibility between fluids, Caterpillar has required that any fluid evaluated against the BF-1 requirements should be tested for compatibility with a mineral oil, a vegetable oil, and a synthetic ester. This is done by mixing 50 mL of the test fluid with 50 mL of each of the above-mentioned fluids. The mixture should be heated to 204°C and cooled to room temperature. The cooled fluid should be centrifuged at $100,000 \text{ m/s}^2$ for 30 min. A fluid that successfully passes this requirement will not show any sedimentation or precipitation following centrifuging.

Foaming Characteristics. During thermal cycling, hydraulic systems are designed to draw in air to replace the lost volume previously occupied by the fluid. If the air being drawn into the system is humid, the hydraulic oil may become contaminated with water, which may act to help stabilize the formation of foam. Obviously, the presence of foam will make the system respond slowly or not at all, causing system malfunction and poor performance of the equipment. For this reason, Caterpillar requires that the fluid be evaluated for its foaming tendency by ASTM D892 dry and with 0.1% water added.

Humidity Corrosion. Because water may be introduced into a hydraulic system over time, it is important to evaluate how well the fluid protects the hydraulic components from water corrosion. The test method used to evaluate this ability is a Caterpillar "in-house" procedure. Carbon-steel rods are prepared by cleaning any residual oils and dirt from their surface. Removing the thick oxide layers exposes a clean surface by abrasion. The clean rod is then immersed in the test fluid and subsequently suspended above a water bath that is being held at $32 \pm 1^\circ\text{C}$. Fluids that prevent pitting to a level of six or more spots per 2.54 cm (linear inch) for more than 200 h have passed the test.

Low-Temperature Storage. Prior experience with rapeseed-based (HETG) hydraulic fluids indicated that the low-temperature properties of the fluids were time dependent. A fluid in the machine exposed to low temperatures for short periods of time (up to 12 h) would likely flow at machine start-up. However, extended cold-temperature exposure times would result in fluid gelling, causing resistance to flow and ultimately pump damage due to lack of lubrication at start-up.

The test method for low-temperature storage requires that before testing, the fluid should be heated to remove any trapped air. The fluid is then cooled to -25°C and held at that temperature for a full week. The fluid should be examined every 24 h to determine its fluidity and to ensure that no precipitation has occurred. The fluid has passed this test if it has remained fluid for 168 h and has not had any solid

precipitation over the same period. This procedure was developed by an ASTM committee and has been adapted to meet Caterpillar's requirements.

Iodine Number. The degree of unsaturation present within a molecule will indicate how well a base fluid is capable of resisting oxidation and how well the fluid will flow at low temperatures. A measure of the iodine number for the fluid will provide information on the degree of unsaturation within the molecules. This requirement was added in order to help evaluate the fluid's ability to resist oxidation and estimate its low-temperature properties.

Water Content. It is a well-known fact that the presence of water in ester-based fluids may be detrimental to the chemical stability of the fluid. At high temperature and in the presence of water, esters can revert back to an alcohol and an acid. However, field evaluations on different ester-based fluids have indicated that the critical concentration of water is higher than the water level measured in the machines. Because of this, Caterpillar does not believe it is necessary to include a test for hydrolytic stability in their BF-1 requirements.

Although hydrolysis of the fluid does not appear to be a problem in hydraulic systems, it is important to keep the amount of water to a minimum. The presence of water in a hydraulic system may cause corrosion on the mechanical components as well as foaming. Several hydraulic component manufacturers have determined that fluids having water content around 0.1% may cause damage to mechanical hydraulic components. Because of this, Caterpillar requires that new fluids meeting BF-1 have less than 0.1% water content.

Elastomer Compatibility. To avoid sealing problems, elastomers commonly used in hydraulic systems should be compatible with the fluid. BF-1 requires that the compatibility between hydrogenated nitrile (HNBR), nitrile (NBR), fluorocarbon rubber (FKM), urethane (AU), and chloroprene, and the hydraulic fluid be evaluated by measuring the hardness, volume change, loss in tensile strength, loss in elongation, and residual elongation in the elastomers. The BF-1 requirements are shown in Table 8.24.

Oxidation Stability. DIN 51554-3, better known as the Baader Oxidation Test, was chosen as the standard test by the VDMA in its requirement. At the time its requirement was being developed, this test was considered to be one of the best oxidation tests available for biodegradable fluids. Although the Baader test had been applied to vegetable-oil-based hydraulic fluids, it could not distinguish performance levels among synthetic esters.

Oxidation tests similar to the ASTM D943 (TOST) test were considered "state-of-the-art" for mineral oils, but they were not capable of discriminating between biodegradable oils. The primary reason was that the TOST test required the addition of water to accelerate the degradation process. Biodegradable hydraulic fluids will oxidize by a reaction similar to mineral oils, but the presence of water at elevated temperatures will cause the ester-based oils to hydrolyze. The TOST test measures the acid content of the fluid. Because both oxidation and hydrolysis contribute to the acid content, this test does not provide a valid measure for oxidation alone.

One solution to the problem was to perform the TOST oxidation test without any added water ("dry" TOST). This would eliminate the hydrolysis problem experienced with ester-based oils. To determine if this approach was sound, a well-known oil company formulated three different synthetic ester-based hydraulic fluids having known differences in their oxidation stability. Their laboratory performed the

Table 8.24 BF-1, High-Performance Biodegradable Oil Requirements for New Fluid Elastomer Compatibility

Compound	Test temp (°C)	Shore hardness change (PTS)	Relative volume change (%)	Loss in tensile strength (% max.)	Loss in elongation (% max.)	Residual elongation (% min.)
HNBR	100	+10/-15	-3/+20	50	50	80
NBR	100	+10/-15	-3/+20	50	50	80
FKM	100	+10/-15	-3/+20	50	50	80
AU	80	+10/-15	-3/+20	50	50	80

Note: Values are valid as of 1 January 1998.

Baader test and the TOST test with water on a rapeseed fluid and the two least stable synthetic ester fluids and the “dry” TOST test on all four fluids. The data obtained by that laboratory are listed in Table 8.25.

The fluids were designed to demonstrate a wider performance gap than measured by the Baader test. Note that the viscosity and acid value increases obtained by the Baader test on the rapeseed fluid was expected. The data obtained for the synthetic esters indicated that little oxidation occurred. The only conclusion was that the Baader test was not capable of adequately distinguishing between ester fluids that demonstrate differences in their oxidation stability. The data obtained on the fluids using the regular D943 TOST test are also given. Note that the TOST test does not clearly indicate whether the two synthetic esters exhibit different oxidation stabilities.

Further testing with a modified TOST test provided the results represented in Fig. 8.14. The data show the change in the acid value over time. These results indicate that the “dry” TOST test produces data that discriminate and are consistent with the known oxidation stability of the four oils. Caterpillar has chosen to require that the “dry” TOST test be performed in the BF-1 requirement.

The information obtained from the above-described oxidation test evaluation has been shared with many groups that have been working on biodegradable hydraulic fluid specifications. The VDMA and ISO both responded by further evaluation of the “dry” TOST procedure. Also, the ASTM is investigating other candidate test procedures.

Viscosity. The initial release of BF-1 required only ISO viscosity grade 46 because it covers the best set of viscometric properties over a wide temperature range. The addition of requirements for fluids with ISO viscosity grade 32 is being considered, but further testing for its low-temperature storage, oxidation, and elastomer compatibility properties are required.

Table 8.25 Comparison of Oxidative Performance of Biodegradable Oils in Baader, TOST, and Dry TOST Tests

	Fluid A rapeseed	Fluid B synthetic ester	Fluid C synthetic ester
Baader Test			
Based on DIN 51554, Part 3			
Acid value change	+1.8 ^a	-0.3 ^b	0.1 ^c
Viscosity increase at 40°C	24%	-0.20%	0.40%
ASTM D942, TOST test			
Hours to acid value of 2 mg KOH/g	72	79	95
ASTM D942, TOST Test			
Modified, no water			
Hours to acid value of 2 mg KOH/g	<50	168	1260

^a72 h at 95°C.

^b72 h at 110°C.

^c100 h at 120°C.

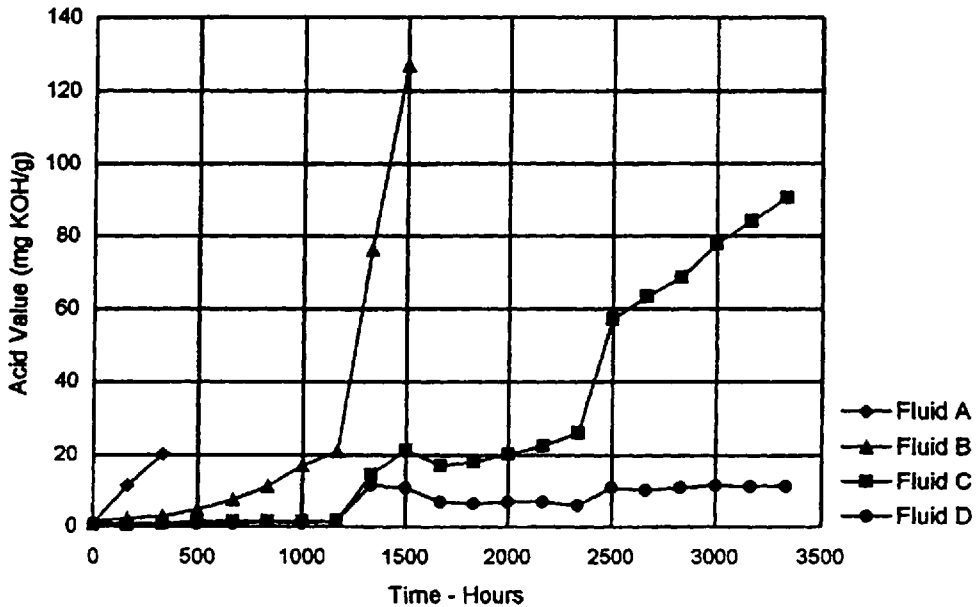


Figure 8.14 Oxidative stability of biodegradable hydraulic fluid: ASTM D943 — “Dry” TOST (no water added).

Friction and Wear Testing. An understanding of the friction and wear characteristics of a fluid is necessary to ensure that the lifetime of the hydraulic components is maximized. Caterpillar has extensive experience in evaluating these properties. Some hydraulic systems have been designed to use the fluids in multiple roles. It is not uncommon to find a machine that uses its hydraulic fluid in power-transmission compartments or in braking applications. To avoid performance problems, it is necessary to know the function properties of the fluid and to design machines to compensate for differences in friction coefficients demonstrated by environmentally friendly fluids. Caterpillar has developed a standard test method and its associated machinery to evaluate the frictional properties of all hydraulic fluids. Further information may be found in BF-1.

The specific wear tests (vane pump, FZG, and four-ball wear) have been specified on the basis of earlier work performed on antiwear hydraulic fluids at Caterpillar. It was important to understand the extreme pressure characteristics of the fluid by performing a FZG gear test, the lower-pressure wear-prevention properties of fluids by the four-ball wear test, and, finally, how the fluid will perform when it has been evaluated in a laboratory-scale component test. Each test provides a piece of the information necessary to adequately describe the wear-prevention characteristics of the fluids.

Environmental Testing. BF-1 includes standard requirements for determining the environmental impact that a high-performance biodegradable fluid will have on the environment. The biodegradability and the toxicity of the fluid must be known to determine its affect on the environment. The levels of the biodegradability and toxicity requirements were selected to best represent the current attitude of the community.

The test methods required by BF-1 were selected on the basis of their applicability. It was believed that the CEC methods for biodegradability did not define biodegradability well enough and, therefore, the US EPA methods had better application. The German Water Hazard Classification (WGK rating) provides an excellent method for determining the overall toxicity of a substance to water-dwelling creatures. Including this parameter is very important. Additionally, it was determined that setting a limit for fish toxicity was necessary.

The BF-1 requirement is intended to give guidelines for the physical and chemical performance of a high-performance biodegradable fluid for use in mobile hydraulic systems. This set of requirements is believed to be comprehensive and includes pertinent information about the system requirements for a biodegradable fluid. This does not mean that the BF-1 document is final. A substantial amount of additional refinement must be done to ensure that the requirements outlined in BF-1 adequately represent the needs of mobile-product hydraulic systems.

3 CONCLUSIONS

Although mineral-oil-based hydraulic fluids exhibit some of the best overall properties, they have two significant deficiencies; fire resistance and biodegradability which may preclude their continued use in many applications. While there is little that can be done about the poor fire resistance of mineral oils, except engineering or hardware modifications, biodegradability may be improved. In general, hydrogen reduction or removal of aromatic compounds and increasing the overall paraffinic composition will improve aquatic biodegradability, but not to vegetable oil or synthetic ester levels. However, even highly refined mineral oil compositions are among the most persistent in soil biodegradability tests.

Two biodegradable alternatives to mineral-oil-based hydraulic fluids are vegetable oils and synthetic esters. They are more biodegradable than mineral oil. Of the two base stocks, vegetable oils are somewhat more biodegradable, although that depends somewhat on molecular structure. In soil tests, vegetable oils are clearly more biodegradable. One vegetable oil, sunflower oil, although biodegradable, exhibited significant toxicity to seedling growth and yield.

Polyol esters, usually those based on trioleate esters of trimethylolpropane, exhibit excellent thermal stability relative to vegetable oils. Formulated fluids, although exhibiting excellent biodegradability, exhibit relatively poor soil biodegradability, a notable disadvantage in addition to their relatively higher cost.

Another class of synthetic fluids is the diesters. Like the polyol esters, all diester-based hydraulic fluids demonstrate excellent thermal stabilities when compared with vegetable oils and exhibit a range of oxidative stabilities. In diester fluids, the degree of oxidation stability is related to the amount of unsaturation on the fatty acid chain. The more saturated the fluid, the greater the oxidative stability. Therefore, a diester hydraulic fluid with good thermal and oxidative stabilities would be one that has very few or no double bonds in its fatty acid side chains. Although diesters are not as biodegradable as vegetable oils, they demonstrate good to excellent biodegradability. The rate at which diester-based fluids degrade varies widely depending on the length and number of branches of the fatty acid side chain.

It was shown that water-glycol hydraulic fluids offer an excellent alternative to vegetable oils, as they provide *both* excellent fire resistance and biodegradability.

In addition to potentially exhibiting excellent biodegradability properties, water-glycol hydraulic fluids are also relatively nontoxic.

REFERENCES

1. N. Jones, "Managing Used Oil," *Lubes Greases*, 1996, 2(6), pp. 20–23.
2. M. M. Mustokoff and J. E. Baylinson, "No Case Is Too Small," *Hydraulics Pneumatics*, 1995, February, pp. 35–37.
3. H. F. Eichenberger, "Biodegradable Hydraulic Lubricant—An Overview of Current Developments in Central Europe," SAE Technical Paper Series, Paper 910962, 1991.
4. J. Meni, "Selection of an Environmentally Friendly Hydraulic Fluid for Use in Turf Equipment," SAE Technical Paper Series, Paper 941759, 1994.
5. S. Ohkawa, "Rough Road Ahead for Construction Machinery Lubes," *Lubes Greases*, 1995, 1(2), pp. 20–23.
6. L. Tocci, "Mother Nature on Lubes: No Simple Choices," *Lubes Greases*, 1995, 1(5), pp. 16–19.
7. T. Mang, "Environmentally Friendly Biodegradable Lube Base Oils—Technical and Environmental Trends in the European Market," in *Adv. Prod. Appl. Lube Base Stocks, Proc. Int. Symp.*, 1994, pp. 66–80.
8. H. Fischer, "Environmental Labeling in German Award Criteria for Hydraulic Fluids," SAE Technical Paper Series, Paper 941078, 1994.
9. J. Y. Chien, "The Dirt on Environmentally Friendly Fluids," *Hydraulic Pneumatics*, 1995, May, pp. 47–48.
10. *Environmental Choice*, Brochure available from Environmental Choice, Environment Canada, Ottawa, Ontario, K1A 0H3.
11. ASTM D 6006-96, "Standard Guide for Assisting Biodegradability of Hydraulic Fluids," *Annual Book of ASTM Standards, Vol. 05.03*, American Society for Testing and Materials, Conshohocken, PA, pp. 1290–1294.
12. D. G. Clark, "The Toxicology of Some Typical Lubricating Oil Additives," *Erdol Kohle*, 1978, 31(12), p. 584.
13. R. K. Hewstone, "Environmental Health Aspects of Additives for the Petroleum Industry," *Regul. Technol. Pharmacol.*, 1985, 5, pp. 284–294.
14. C. M. Cisson, G. A. Rausina, and P. M. Stonebraker, "Human Health and Environmental Hazard Characterization of Lubricating Oil Additives," *Lubr. Sci.*, 1996, 8(2), pp. 145–177.
15. R. J. C. Biggin, "Additives for Lubricants with Improved Environmental Compatibility," in *Adv. Prod. Appl. Lube Base Stocks, Prod. Int. Symp.*, 1994.
16. C. Busch and W. Backè, "Development and Investigation in Biodegradable Hydraulic Fluids," SAE Technical Paper Series, Paper 932450, 1993.
17. H. Hydrick, "Synthetic vs. Vegetable," *Lubr. World*, 1995, May, pp. 25–26.
18. R. A. Padavich and L. Honary, "A Market Research and Analysis Report on Vegetable-Based Industrial Lubricants," SAE Technical Paper Series, Paper 952077, 1995.
19. L. A. T. Honary, "Potential Utilization of Soybean Oil as an Industrial Hydraulic Oil," SAE Technical Paper Series, Paper 941760, 1994.
20. L. A. T. Honary, "An Investigation of the Use of Soybean Oil in Hydraulic Systems," *Bioresource Technol.*, 1996, 56, pp. 41–47.
21. S. D. Scott, "Biodegradable Fluids for Axial Piston Pumps & Motors—Application Considerations," SAE Technical Paper Series, Paper 910963, 1991.
22. P. C. Naegly, "Environmentally Acceptable Lubricants," in *Seed Oils for the Future*, S. L. MacKenzie and D. C. Taylor, eds., 1992, pp. 14–25.
23. In-Sik Rhee, C. Velez, and K. Von Bernewitz, "Evaluation of Environmentally Acceptable Hydraulic Fluids," TARDEC Technical Report No. 13640, U.S. Army Tank-Au-

- tomotive Command Research, Development and Engineering Center, Warren, MI, March 1995.
24. I. Legisa, M. Picek, and K. Nahal, "Some Experiences with Biodegradable Lubricants," *J. Synth. Lubr.*, 1997, 13(4), pp. 347–360.
 25. Anon. "Hydraulic Fluids Are Getting More Friendly," *Fluid Power*, 1992, No. 7, pp. 68–73.
 26. L. Honary, "Performance of Selected Vegetable Oils in ASTM Hydraulic Tests," SAE Technical Paper Series, Paper 952075, 1995.
 27. S. Ohkawa, A. Konishi, H. Hatano, K. Ishihama, K. Tanaka, and M. Iwamura, "Oxidation and Corrosion Characteristics of Vegetable-Base Biodegradable Hydraulic Oils," SAE Technical Paper Series, Paper 951038, 1995.
 28. V. M. Cheng, A. Galiano-Roth, T. Marougy, and J. Berezinski, "Vegetable-Based Hydraulic Oil Performance in Piston Pumps," SAE Technical Paper Series, Paper 941079, 1994.
 29. V. M. Cheng, A. A. Wessol, P. Baudouin, M. T. BenKinney, and M. J. Novick, "Biodegradable and Non-Toxic Hydraulic Oils," SAE Technical Paper Series, Paper 910964, 1991.
 30. J. Reichel, "Biologically Quickly Degradable Hydraulic Fluids," Sauer Sundstrand Technical Application Information ATI 9101 (Status 03/91).
 31. "Environmentally Compatible Fluids for Hydraulic Components," Mannesmann Rexroth, Technical Bulletin No. 03 145/05.91.
 32. "Guide to Alternative Fluids," Vickers Technical Bulletin No. 579, 11/92.
 33. "Cat Biodegradable Hydraulic Oil," Caterpillar (BIO HYDO) Product Data Sheet, No. PEHP1021.
 34. K. D. Erdman, G. H. Kling, and D. E. Tharp, "High Performance Biodegradable Fluid Requirements for Mobile Hydraulic Systems," SAE Technical Paper Series, Paper 981518, 1998.
 35. D. Thiel, "Experiences with Sealing Materials, Hydraulic and Lubricating Oils and Biologically Decomposable Hydraulic Fluids," *Gepgyartastechnologia*, 1993, 33(9–10), pp. 433–441.
 36. G. E. Totten, J. Cerf, R. J. Bishop, and G. M. Webster, "Recent Results of Biodegradability and Toxicology of Water–Glycol Hydraulic Fluids," SAE Technical Paper Series, Paper 972789, 1997.
 37. "Environmentally Acceptable Hydraulic Fluids HETG, HEPG, HEE for Axial Piston Units," Brochure No. RE 90221/02.92 available from Mannesmann Rexroth, Hydro-matik GmbH, Elchingen, Germany.
 38. OECD standards and methods are available from the Organization for Economic Cooperation and Development, Paris.
 39. L. A. T. Honary, "Soy-Based Hydraulic Oil: A Step Closer," *Off-Highway Eng.*, 1995, April, pp. 15–18.
 40. L. A. T. Honary, director of the ABIL (Ag-Based Industrial Lubricants) program at the University of Northern Iowa, Waverly, personal communication.
 41. F. H. Roberts and H. R. Fife, U.S. Patent 2,425,755 (1947).
 42. W. E. F. Lewis, U.S. Patent 4,855,070 (1989).
 43. G. E. Totten and G. M. Webster, "High Performance Thickened Water–Glycol Hydraulic Fluids," in *Proc. of the 46th National Conference on Fluid Power*, 1994, pp. 185–193.
 44. F. A. Litt, "Standards for Environmentally-Friendly Hydraulic Fluids," in *National Fluid Power Conference*, 1996.
 45. D. I. Hoel, "Lubricant Development Meets Biology," *ASTM Standardization News*, 1994, June, pp. 42–45.
 46. D. L. Hooper and D. I. Hoel, "Lubricants, the Environment and ASTM D02," SAE Technical Paper Series, Paper 961727, 1996.

47. J. Wilkinson, "Biodegradable Oils—Design, Performance, Environmental Benefits and Applicability," SAE Technical Paper Series, Paper 941077, 1994.
48. J. Baggott, "Biodegradable Lubricants," in Institute of Petroleum Symposium: Life Cycle Analysis and Eco-Assessment in the Oil Industry, 1992.
49. G. Gilron (Beak Internation, Brompton, Ontario) "Review of Draft ISO Standard Criteria for Toxicity and Biodegradability for Ecologically Acceptable Water Glycol Hydraulic Fluids," Letter to J. Cerf (UCC-Canada), 1996.
50. M. Völtz, N. C. Yates, and E. Gegner, "Biodegradability of Lubricant Base Stocks and Fully Formulated Products," *J. Synth. Lubr.*, 1995, 12(3), pp. 215–230.
51. A. E. Girling, "Preparation of Aqueous Media for Aquatic Toxicity Testing of Oils and Oil-Based Products: A Review of the Published Literature," *Chemosphere*, 1989, 19(10/11), pp. 1635–1641.
52. M. P. Singh, V. K. Chhatwal, B. S. Rawat, M. I. S. Sastry, S. P. Srivastava, and A. K. Bhatnagar, "Environmentally Friendly Base Fluids for Lubricants," in *Adv. Prod. Appl. Lube Base Stocks, Proc. Int. Symp.*, H. Singh, P. Rao and T. S. R. Tata, eds., 1994, McGraw-Hill, New Delhi, pp. 362–370.
53. T. E. Kivovsky, T. Murr, and M. Voeltz, "Biodegradable Hydraulic Fluids and Related Lubricants," SAE Technical Paper Series, Paper 942287, 1994.
54. R. Henke, "Increased Use of 'ECOFLUIDS' May Put a Veggie in Your Hydraulic Reservoir," *Diesel Progr., Engines Drives*, 1994, September, pp. 7–9.
55. S. D. Haigh, "Fate and Effects of Synthetic Lubricants in Soil: Biodegradation and Effect on Crops in Field Studies," *Sci. Total Environ.*, 1995, 168, pp. 71–83.
56. S. D. Haigh, "Determination of Synthetic Lubricant Concentrations in Soil During Laboratory-Based Biodegradation," *J. Synth. Lubric.*, 1994, 11(2), pp. 83–93.
57. E. Zhou, A. Shanahan, W. Mammel, and R. L. Crawford, "Biodegradability Study of High-Erucic-Acid-Rapeseed-Oil-Based Lubricant Additives," in *Monitoring and Verification of Bioremediation*, R. E. Hinchoe, G. S. Douglas, and S. K. Ong, eds., Battella Press, 1995, pp. 97–103.
58. G. Gilron (Beak Internation, Brompton, Ontario), UCON® Hydrolube HP-5046 Ready Biodegradability Criteria," Letter to J. Cerf (UCC-Canada), 1997.
59. ASTM D 6046-97, "Standard Classification of Hydraulic Fluids for Environmental Impact," American Society for Testing and Materials, West Conshohocken, PA.
60. ASTM D 5864-95, "Standard Test Method for Determining Aerobic Aquatic Biodegradation of Lubricants or Their Components," *Annual Book of ASTM Standards, Vol. 05.03*, American Society for Testing and Materials, Conshohocken, PA, pp. 1135–1141.
61. VDMA 24,568, "VDMA Harmonization Sheet, Fluid Power, Rapidly Biologically Degradable Hydraulic Fluids, Minimum Technical Requirements," March 1994.

9

Seals and Seal Compatibility

RONALD E. ZIELINSKI

PolyMod Technologies Inc., Fort Wayne, Indiana

1 INTRODUCTION

The majority of seals used in industrial applications are either “elastomer contact” or “elastomer energized.” Elastomer contact seals are those that rely solely on elastomer contact for sealing. Elastomer energized seals are those that use the elastomer to force a plastic seal element against one of the faces that must be sealed. Because both types of seals utilize an elastomer as an essential part of the seal, the choice of a proper elastomeric material and verification of its compatibility with the system’s fluids is essential for sealing performance. Therefore, the first topic to be discussed is elastomer materials and fluid compatibility.

The discussion on elastomer contact seals will focus on the O-ring as the principal elastomer seal. The O-ring was chosen because it is still the most widely used elastomer seal configuration. Specialty seal configurations are derived from the O-ring. These configurations were driven by attempts to improve the seal geometry by addressing O-ring geometry deficiencies. Elastomer energized seals will be discussed because the O-ring is the principal energizer.

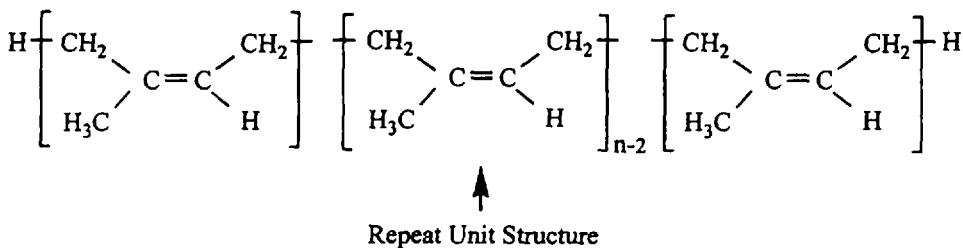
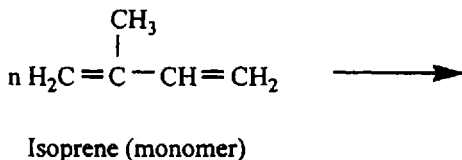
Additional subjects to be discussed in this chapter include lip or pressure-energized seals, oil seals, and mechanical seals. Basic principles of seal technology will be provided to facilitate optimum selection seal.

2 SEAL CHEMISTRY

In this section, a brief primer on seal chemistry and terminology will be provided to facilitate understanding of the following discussion by the nonchemist.

Elastomeric seal materials are derived from either natural or synthetic polymers. A *polymer* (or *macromolecule*) is a large molecule that is built up by the repetition

of smaller molecules or *repeat units*. For example, natural rubber, *cis*-polyisoprene, is synthesized in nature from the *monomer* isoprene (1,3-butadiene).



cis-Polyisoprene - Natural Rubber

Most, but not all, polymers used for seal manufacture have >10,000 repeat units.

One method of characterizing polymers is by the *sequence* that the monomer units are connected together. If the polymer is composed by only one monomer (A), it is classified as a *homopolymer*.



Homopolymer

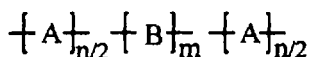
If the polymer is composed of two or more monomers, it is called a *copolymer*. Copolymers can be further classified according to the sequence of the constituent monomers. For a copolymer composed of monomers A and B, these classifications include the following:

Random: The placement of monomers A and B occur randomly within the polymer chain; for example,



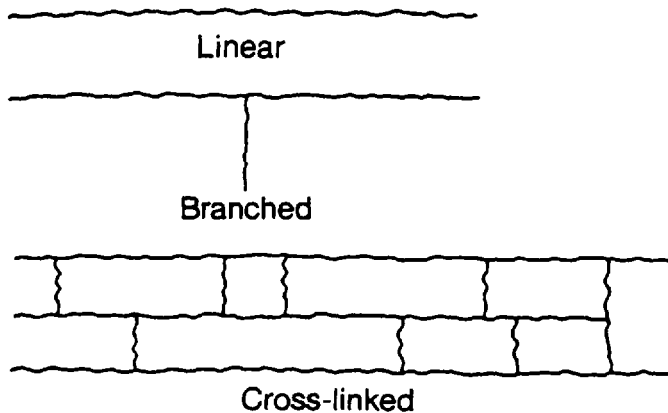
Random Copolymer

Block: The monomer units A and B occur together in the polymer; for example,



Block Copolymer

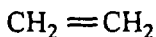
Polymer properties are dependent on polymer structure. Polymers may exist in a number of *configurations*. The most common are *linear*, *branched*, and *cross-linked*. Cross-linked polymers are synthesized by introducing chemical linkages between linear or branched polymers to form a three-dimensional *network* structure.



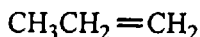
Rubbers or elastomers are high-molecular-weight linear polymers ($M_n > 1,000,000$) that have been minimally cross-linked to eliminate flow. Elastomers typically exhibit long-range reversible extensibility, often $\geq 600\%$ extension, under relatively small applied stress.

Polymers used for seal materials include *natural* polymers such as *cis*-polyisoprene (natural rubber) or *synthetic* polymers, those produced industrially. With the exception of natural rubber, most seal materials are derived from synthetic polymers.

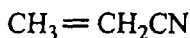
Some of the monomers used to synthesize polymers used for seals include the following:



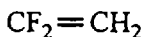
Ethylene



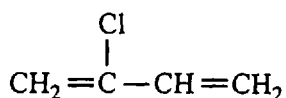
Propylene



Acrylonitrile



Vinylidene Fluoride



Chloroprene

3 ELASTOMER COMPOUNDS

Elastomer materials used for hydraulic applications include natural rubber, poly(*cis*-1,4-isoprene), or synthetic polymers compounded (mixed) with several different ingredients to facilitate ease of molding and to impart desirable properties in the molded seal [1].

An elastomer compound typically consists of the following types of ingredients:

Elastomer	Activator
Processing aid	Antidegradant
Vulcanizing agent	Filler
Accelerator	Plasticizer

Elastomer polymers possess some common characteristics. They are elastic, flexible, impermeable to air and water, and tough. However, each elastomer exhibits properties unique to its polymer structure and it is these properties that influence the selection of an elastomer for a specific application.

Processing aids are added to the elastomer compound to aid in mixing and molding the compound. Low-molecular-weight polyethylene can be added to serve as a release agent to facilitate removal of molded parts from the mold. It can also serve as a lubricant to reduce the inherently high friction of the elastomer part. In the molded part, the polyethylene would migrate to the surface and form a lubricating layer between the elastomer and the surface against which it is sealing. Paraffin wax and petroleum hydrocarbons serve the same purpose. Aliphatic–naphthenic–aromatic resins can be added to aid in homogenizing the elastomer compound during mixing.

Vulcanizing agents are necessary additives to thermoset elastomers. They cause the chemical reactions which result in cross-linking of the elastomer. The chemical cross-linking changes the elastomer compound from a soft, tacky material to one that is thermally stable and has a defined set of physical properties: tensile strength, resilience, and elongation.

Accelerators are added to reduce the curing cycle. Most accelerators are organic substances that contain nitrogen and sulfur. The most widely used ones are thiazoles such as benzothiazyl disulfides.

Activators are used to activate the accelerator and improve its efficiency. Zinc oxide and stearic acid are added with sulfur and organic accelerators to ensure good cross-linking efficiency.

Antidegradants are added to slow down the aging process in molded parts. The antidegradants act as sacrificial ingredients to slow down the attack on the molded elastomer which can result from exposure to oxygen, ozone, heat, light, and metal catalysts. One of the best antidegradants is *para*-phenylene-diamines. Waxes are often used in conjunction with antidegradants. The waxes migrate to the surface of the molded part and form a coating, which protects the part from ozone attack.

Fillers are normally used to reinforce or modify the physical properties of the molded elastomer. A reinforcing filler, usually carbon black or a fine-particle mineral pigment such as fumed silica, is used to enhance hardness, tensile strength, and abrasion resistance. Carbon blacks are the best reinforcing fillers. Non-carbon-black fillers are typically used to impart heat resistance. Many oil seals are mineral filled to resist heat buildup at the sealing lip. Fillers may also be used as extenders. Calcium

carbonate and talc may be added to the compound to reduce cost and improve processing.

Plasticizers are added to aid in mixing the compound or to provide flexibility in the molded part at low temperature. Ester plasticizers, such as dioctyl phthalate, provide for good low-temperature flexibility. The wrong choice of plasticizer may adversely affect performance. The plasticizer may leach out of the part when it is exposed to the hydraulic fluid which substitutes for the plasticizer, causing high elastomeric volume swell. When plasticizers are removed from the elastomer, a significant change in the elastomer's physical properties may occur and the elastomer may become tacky. This can adversely affect the elastomer's performance.

4 MOLDING

Once the ingredients are mixed into the elastomer compound, the fully formulated elastomer is molded into a finished part. There are three primary types of molding processes [1]: compression molding, transfer molding, and injection molding.

Compression molding consists of placing a precut blank, a "preform," into a two-piece mold that is then closed. Pressure is applied to allow the preform to fill the mold cavity. The excess material flows out of the mold cavity into flash grooves. The mold remains under pressure at an elevated temperature for a specified time to allow vulcanization to occur. The pressure is then released and the mold is opened to remove the finished elastomer part. A typical compression mold is shown in Fig. 9.1.

Transfer molding, illustrated in Fig. 9.2, forces the uncured elastomer from the pot into the mold cavity as pressure is applied to the mold. Although transfer molds are more costly than compression molds, the transfer process exhibits shorter cure times because higher molding pressures result in better heat transfer.

In injection molding (Fig. 9.3), the elastomer stock is temperature controlled as it is forced into the mold. This results in lower vulcanization times. Injection molds are expensive, but for high-volume parts, reduction in cycle time is an economic advantage.

In molding operations, curing or vulcanization is the most important process. The curing process converts the elastomer material from a shapeless plastic material into a strong elastic product with a definite geometric shape with desired engineering properties. In the curing process, randomly oriented polymer chains are cross-linked to produce the desired physical properties. Characteristically, a cross-linked elastomer will recover quickly and forcibly [2]. During the vulcanization process, the elasto-

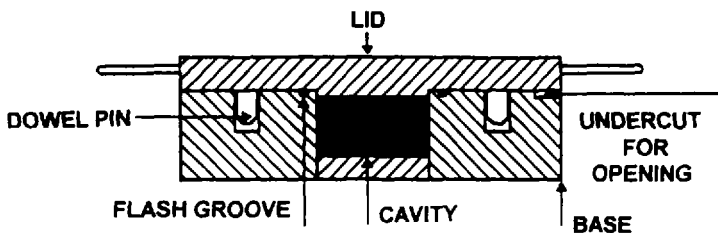


Figure 9.1 Illustration of a compression mold.

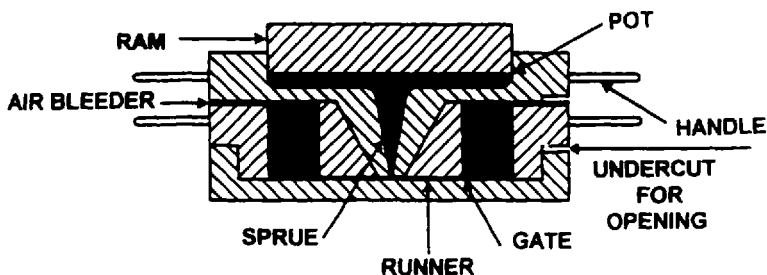
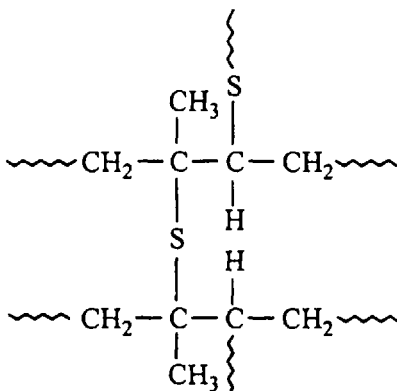


Figure 9.2 Illustration of a transfer mold.

meric polymer develops improved resistance to degradation by heat, light, and chemical aging.

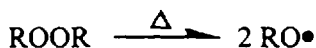
The most common curing system is sulfur [3]. When sulfur is used as a curative, sulfur atoms form a bond between carbon atoms on adjacent polymer chains. This bond effectively cross-links the molecules:



Sulfur Cross-Linked Natural Rubber

It is possible to have multiple bonds, such as $-\text{C}-\text{S}-\text{S}-\text{S}-\text{C}-$, when sulfur is used as the vulcanization agent. Sulfur donors, such as thiuram disulfide and dithiodimorphaline, are also used. These materials make sulfur atoms available for the curing process but limit the amount of sulfur atoms available, thus bonds are shorter. Sulfur bonds achieved with sulfur donor cures have only one or two sulfur atoms and are more stable than longer-chain sulfur bonds (Table 9.1).

A nonsulfur cure is required for saturated rubber because it contains no carbon double bonds to accommodate sulfur-bonding [3]. Peroxide curatives promote the formation of radicals to form the carbon-to-carbon bonds on adjacent polymer chains. The peroxide undergoes thermal decomposition to produce oxyradicals:



Peroxide

oxy radicals

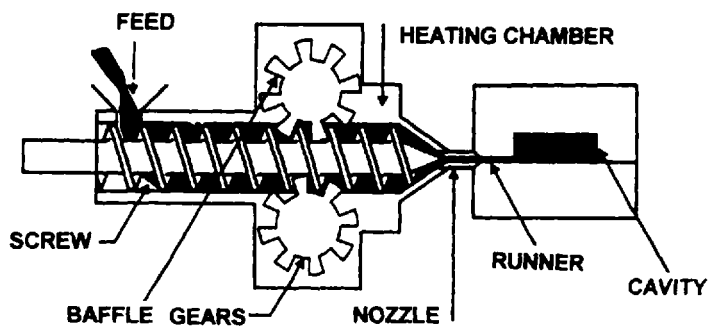
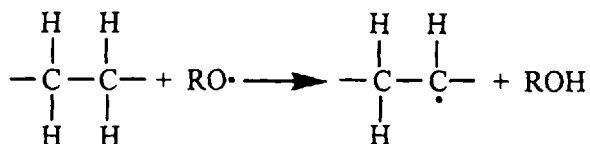


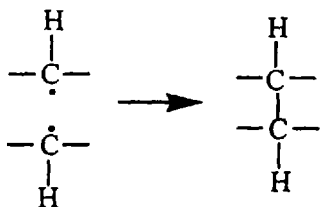
Figure 9.3 Illustration of rubber injection molding.

The radical interaction abstracts peroxide "oxy radicals" hydrogen atoms from the polymer chain. This results in a free-radical site on the polymer chain:



Free Radical Formation

Two free-radical sites then couple to form a C—C cross-link:



Other cure systems also work in this manner. Carbon-to-carbon vulcanization is relatively stable as shown in Table 9.1

Table 9.1 Vulcanization Bond Strength

Bond	Disassociation energy (kcal/mol)
—C—C—	80
—C—S—C—	74
—C—S—S—C—	74
—C—S—S—S—C—	54
—C—S—S—S—S—C—	34

The thermal stability of the peroxide —C—C bond is equivalent to any of the carbon-carbon bonds in the polymer backbone. Peroxide cross-links are stable to oxidation, whereas sulfur cross-links may oxidize and result in cross-link rupture. Peroxide-cured elastomers generally have better compression set resistance and better low-temperature flexibility. On the other hand, sulfur-cured elastomers generally have the better abrasion resistance and tear strength.

Some curatives may remain unreacted in the elastomer after processing [4]. This can cause further curing when the elastomer is in service, which results in significant property changes.

The choice of vulcanization or curing agent is influenced by elastomer selection. Sulfur or sulfur-donor cure systems are used with natural rubber, isoprene, butyl, ethylene propylene, and nitrile elastomers. Peroxide cure systems are used with urethane, silicone, nitrile, ethylene propylene, and fluorocarbon elastomers. Organic amines are used with fluorocarbon, epichlorohydrin, and ethylene-acrylic elastomers. Metallic oxides are used with chloroprene and chlorosulfonated polyethylene elastomers.

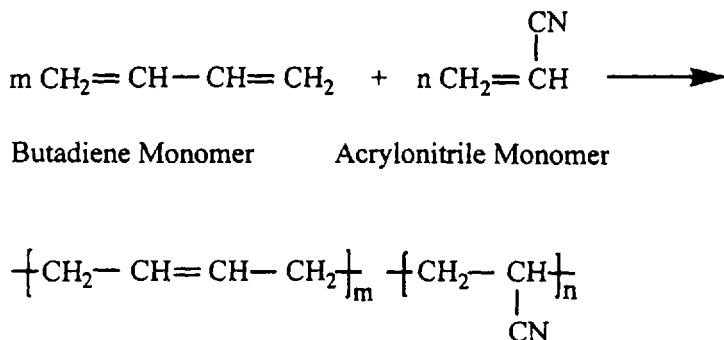
5 ELASTOMER SEAL MATERIALS

There are numerous elastomer seal materials [5]. However, nitrile (NBR), fluorocarbon (FKM), ethylene propylene (EPR, EPDM), chloroprene (CR), and urethane (AU, EU) are the most commonly used materials for industrial applications. The designations for the various elastomers, such as NBR, EPDM, and so forth, were developed in 1955 and are detailed in Ref. 5.

5.1 Nitrile

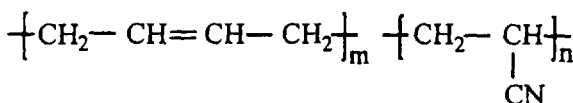
Nitrile seals are the most widely used industrial elastomeric seals because of their use temperature of -65°F (-54°C) to 250°F (121°C) and their oil and fuel resistance [6]. The actual temperature range and degree of chemical resistance for particular seals are dependent on the seal's polymer composition.

Nitrile elastomers are emulsion copolymers of butadiene and acrylonitrile:



Butadiene Monomer

Acrylonitrile Monomer



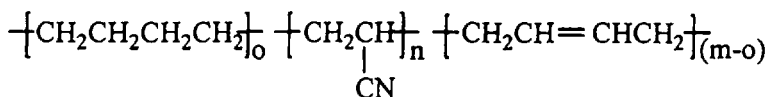
Random Copolymer

The ratio of these two monomers defines seal performance. NBR is polar because of the presence of the "polar" monomer acrylonitrile (ACN). Acrylonitrile functionality imparts fuel and oil resistance. Acrylonitrile content may vary from 20% to

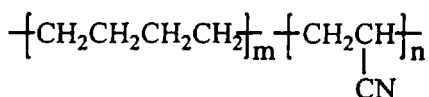
50%. High levels of ACN content provide increased strength, decreased gas permeability, and lower volume swell when exposed to fluids. These benefits are obtained at the expense of low-temperature resilience. Low ACN content results in better low-temperature characteristics and higher volume swell [6], as shown in Table 9.2. As there is unsaturation in the butadiene, NBR is also susceptible to oxygen and ozone attack and consequent degradation.

In addition to conventional nitrile elastomers, carboxylated nitrile (XNBR) and highly saturated nitrile (HNBR) may also be used. Carboxylated nitrile contains carboxyl groups (COOH) distributed in the rubber molecule. This structure change results in an elastomer with much better abrasion resistance than conventional nitrile elastomers [6] at the expense of compression set resistance. Compatibility problems with gasoline and high-swell, petroleum-based hydraulic fluids are observed. However, reducing abrasive wear and prolonging seal life is sometimes a very important consideration in reducing costly downtime between seal replacements.

Nitrile rubber contains unsaturated double bonds, as shown previously. Highly saturated nitrile has pendant ethyl groups. Highly saturated nitrile offers improved aging resistance and high-temperature resistance (300°F). HNBR is prepared by grinding the base NBR polymer, dissolving it in a suitable solvent, and selectively hydrogenating the NBR polymer under pressure with a suitable catalyst. The solvent and catalyst are then recovered after the formation of HNBR [7]. HNBR may be partially or fully saturated:



Partially Hydrogenated



Fully Hydrogenated

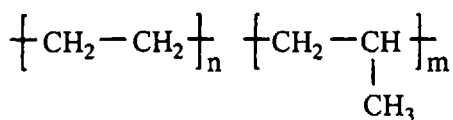
Table 9.2 Effect of ACN Content on Nitrile Elastomers

	ACN Content				
	20%	28%	33%	40%	50%
Tensile strength (psi)	2500	2800	2800	3100	2200
Compression set (%), 70 h at 212°F (100°C)	25	27	27	32	40
Low-temp. brittleness, ASTM D 746	-71°F -57°C	-57°F -49°C	-43°F -42°C	-15°F -26°C	+5°F -15°C
Volume change—Fuel B, 4 weeks at room temp.	85%	52%	41%	27%	23%
Volume change—ASTM No. 3 oil, 70 h at 212°F (100°C)	61%	32%	21%	10%	7%

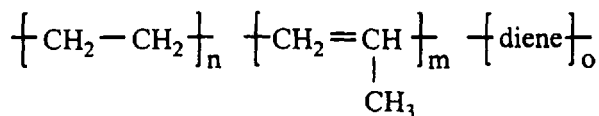
Hydrogenation of medium- and low-ACN NBR reduces low-temperature resilience. HNBR exhibits equivalent oil, fuel, and solvent resistance and better water, ozone, and oil-additive resistance than conventional NBR. HNBR may be used as an alternative to fluorocarbon elastomers because of its high-temperature capability; however, fluid compatibility must be verified throughout the operating temperature range. Lower-temperature and short-term test results are poor models for comparison of elastomer compatibility because they do not adequately reflect the operational environment. Consequently, lower-priced alternatives may not be the most cost-effective solution for long-term use.

5.2 Ethylene Propylene

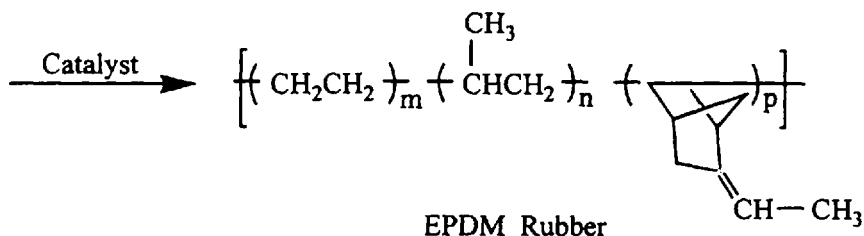
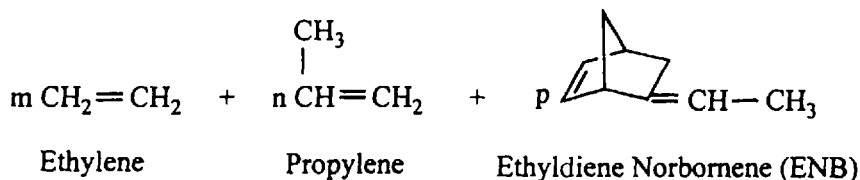
Two types of ethylene propylene (EP) polymers are used: ethylene propylene rubber (EPR), a random copolymer of ethylene and propylene monomers,



and ethylene propylene diene (EPDM),



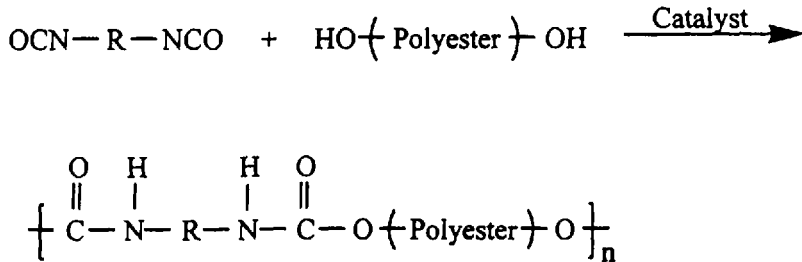
The diene is the principal variant in this polymer. The ethylene propylene diene usually combines ethylene and propylene monomers with a comonomer such as 1,2 butadiene or ethyldiene norbornene (ENB).



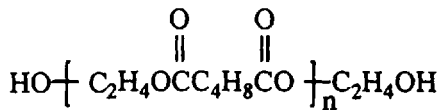
A postcure converts the diene into a phenol complex, which is a stabilizer. Other dienes that are used include 1,4 hexadiene and dicyclopentadiene. EP and EPDM elastomers have a useful temperature range of -67°F to 302°F . They possess poor solvent and petroleum oil resistance.

5.3 Urethane

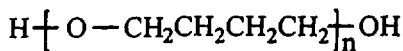
Polyurethanes are either ether-based (EU) or ester-based (AU) [8]:



A common polyester is polyethylene adipate:



A common polyether is polytetramethylene glycol:

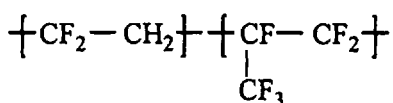


The most common diisocyanates are 2,4- and 2,6-toluene diisocyanate (TDI) and 4,4'-diphenylmethane diisocyanate (MDI).

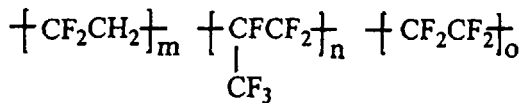
These elastomers are becoming more popular due to their excellent abrasion resistance in dynamic seal applications. Their principal limitation has been their high-temperature capability. Conventional urethanes exhibit fluid compatibility characteristics equivalent to that of nitrile up to temperatures of 158°F, although they are sometimes rated for service up to 212°F. As operating temperatures increase, frictional heating of the seal causes softening, a loss of physical properties, and accelerated compatibility problems because the higher temperatures accelerate chemical reactions. Water and high humidity may damage urethane elastomers by hydrolyzing the ester, such as —COOC, in the polymer. Polyether-based materials are, by nature, more hydrolytically stable than polyester-based materials [8]. New grades of polyurethanes are being introduced that provide dry heat resistance capability up to 250°F. However, it is essential that fluid compatibility and physical property retention also be confirmed by testing at the higher temperatures before these materials be considered for use as seals above 158°F.

5.4 Fluorocarbon

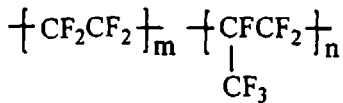
Fluorocarbon elastomer (FKM) is a class of polymers that are principally copolymers of vinylidene and hexafluoropropylene:



or terpolymers of vinylidene, hexafluoropropylene and tetrafluoroethylene:



An exception to this is tetrafluoroethylene/hexafluoropropylene:



These materials can be effective seals over the temperature range of -40°F to 437°F . The actual temperature range for a specific compound, however, is dependent on polymer type and fluorine content of the polymer. By varying the ratio of the three monomers, fluorocarbon elastomers with 65–70% fluorine content can be produced. The fluorine content of the polymer backbone affects chemical resistance and low-temperature capability, as is illustrated in Table 9.3. In this table [9], T_g is the glass transition temperature. This is the temperature at which an elastomer loses its elasticity and becomes glassy and brittle [10].

Fluorocarbon elastomers can be used with petroleum fluids, diester lubricants, silicone fluids, halogenated hydrocarbons, and some acids. They cannot be used with phosphate esters, amines, ketones, hot water, steam, and brake fluids. However, tetrafluoroethylene/hexafluoropropylene elastomers are being used successfully with newer brake fluids. Fluorocarbon elastomers are relatively high cost and are normally used where high temperature and longer term compatibility requirements are essential.

6 SEAL COMPATIBILITY

6.1 Empirical Prediction of Elastomer Compatibility

The compatibility of an elastomer with hydraulic fluid is a critical factor in system performance. Although considerable effort has been expended in the attempt to empirically predict seal compatibility, these efforts have not been successful to date. One reason is the inability to accurately model the broad range of environmental conditions and chemical interactions encountered in an actual hydraulic system. Another reason is the inability to adequately define the term ‘‘compatibility.’’

A compatible elastomer is one that will function as an effective seal in an actual hydraulic system for an effective period of time. The property changes ex-

Table 9.3 Effect of Fluorine Concentration in the Polymer on Its Low-Temperature and Chemical-Resistance Characteristics

Property	65% Fluorine	67% Fluorine	69% Fluorine
T_g [$^\circ\text{F}$ ($^\circ\text{C}$)]	(-22)	(-19)	(-9)
Volume swell in Methanol (%) (room temp., 7 days)	120	25	2

perienced by the elastomer exposed to the system's fluid and environment should not prematurely affect its ability to function as a seal.

The empirical approach principally addresses the chemical interaction between the elastomer and the fluid base stock only. This will identify elastomers which are obviously incompatible with the fluid base stock, but it does not address subtle chemical reactions due to the presence of additives nor does it address the thermal effects that occur in actual systems. Several of the empirical approaches to identifying large variation in seal incompatibility will be provided here.

Fluid interaction with elastomeric polymers has been addressed by Hertz [11]. Most elastomers approximate supercondensed gases because they are long-chain polymers: C_2 (alkene and vinyl) and C_4 (diene) structures. Hertz stated, "The C_2 monomers range from ethene ($CH_2=CH_2$) to ethenyl ($CH_2=CH-$) or vinyl ethylene ($-CH=CH-$) or vinylene, or ethenylidene ($CH_2=C$) or vinylidene. C_4 examples are conjugated dienes, specifically butadiene, 2-methyl-1,3-butadiene (chloroprene)." Because elastomer densities approach those of comparable liquids, the solubility concept of "like dissolves like" is the initial basis for discussing elastomer-liquid compatibility.

Although this simplistic approach initially seems to have merit, Hildebrand and Scott [12] explained that the problem is more complex. They concluded that the heat of vaporization (ΔH_v) minus the volume work (RT) is the estimate of energy necessary to maintain the liquid state. Dividing this value by molar volume (V) corrects for density and the square root of this result is the solubility parameter (δ):

$$\delta = \left(\frac{(\Delta H_v - RT)}{V} \right)^{1/2}$$

This approach is inadequate except for vapors that obey the ideal-gas law or nonpolar fluids (nonelectrolytes).

Barton [13] attempted to address polar (aqueous and nonaqueous electrolytes) fluids by assuming that they have three intermolecular forces: dispersion, hydrogen-bonding, and dipole moment. Hansen and Beerbower [14] tried to clarify Barton's concept but were unable to adequately address solubility problems with solvent mixtures. The modification that was proposed,

$$\delta = \delta_d^2 + \delta_p^2 + \delta_h^2$$

would result in only positive or endothermic values for the solubility parameter. A mixture that is exothermic upon mixing is not addressed by this approach because the solubility parameter would be negative. Therefore, this approach was incapable of accurately predicting nonideal fluid-elastomer interactions.

Jensen [15] noted that most solubility parameter concepts use the historic "similarity matching" of properties rather than the more appropriate "complementary matching" of properties and, consequently, do not address real situations in which elastomers and fluids have complementary properties.

Although considerable effort has been expended in the attempt to adequately predict seal compatibility, these have ignored the broad range of conditions encountered in a hydraulic system. The empirical approach falls short of adequately predicting seal-fluid compatibility in a hydraulic system. The solubility parameter concept is not valid for solvent-solute conditions which are not in thermodynamic equilibrium.

Beerbower and Dickey [16] developed the “swell criterion,” which states that if an elastomer swells 25% or less in a fluid, it is compatible based on these solubility premises. However, this does not address true chemical compatibility, which involves chemical reactions, such as oxidation, not just the physical absorption of fluid. For example, if an elastomer swelled 25% and had no significant physical property degradation, it would be considered noncompatible, even though it would perform well as a seal. Thus, the fundamental difficulty with solubility theories is the assumption that no chemical reactions occur between the elastomer and fluid [17]. This is a greater deficiency when considering their failure to account for the potential effects that can occur because of the high pressures and temperatures encountered in a hydraulic system. Many compatibility listings [18] use room-temperature, volume-swell data to define compatibility. The user of these charts must determine how the data were generated and carefully assess the relevancy of that data to his situation.

Unfortunately, there is no universally accepted empirical method for assessing compatibility because elastomers and fluids are not simple two-component systems. Elastomeric polymers are normally multicomponent polymers containing other organic materials. Fluids are also complex, containing not only base stocks but also performance additives. Additives may interact with the polymers to affect compatibility. This is why compatibility tests should be run with elastomers and actual fluids used in the system.

6.2 Elastomer Compatibility Tests

Standard elastomer compatibility tests normally involve measuring the physical properties of an elastomer sample prior to testing to obtain tensile strength, elongation, and hardness. Another sample is then soaked for a short period of time in a standard test fluid and then removed and tested for volume swell and physical properties. If the volume swell and physical properties fall within a specified range, then the elastomer is considered compatible. Although the test procedure is straightforward, the problem is to properly select test fluids, test times, and property change limits to adequately define compatibility for the system being modeled. Standard test fluids do not contain performance additives of a fully formulated fluid and these additives may exhibit a deleterious effect on the elastomer.

There is normally no rigorously determined technical basis for the property change limits that have been established. For example, some specifications permit the volume swell to range from a negative number (−8%) to a positive number (20%), whereas others allow a range of 0–40% and still others a range of 0.5–15% [19–22]. Unfortunately, there is no adequate guidance in the literature defining meaningful volume-swell ranges. These specifications were typically created using test results from the first elastomer to work in an application. They ignore the questions: Was this the best elastomer for the application? What properties really affected performance? If some of the limits were changed, would the result be a better seal? Are the correct properties to accurately assess compatibility being monitored?

Elastomer compatibility tests are normally short term, 24-, 48-, and 72-h tests. Fluid tests such as ASTM D 943 [23] are normally 700+-h tests. If the elastomer degrades in the short-term test, then it is obviously incompatible. If it does not, then compatibility cannot be assumed unless the service life is 72 h or less. Elastomers

are principally organic materials and, therefore, undergo aging. An example of misleading information from short-term tests is shown in Fig. 9.4. At 24 h, the change in Young's modulus for both elastomer specimens was approximately the same. As the tests continued, the difference in chemical aging of the elastomers is dramatic. It took much longer for one elastomer to become saturated before chemical aging began. In both of these cases, a short-term test would have been very misleading.

Many companies rely on ASTM D 2000 line callouts [24] to specify their elastomers. This standard was developed to classify elastomers into general classes using standard tests and a documented range of values for the properties that are being monitored. Each of the line callouts represents the fact that this elastomer was tested to a particular set of test conditions and the test results were within the limits established for that test. An example of a line callout would be M2BG614B14EO16. Referencing ASTM D 2000, this call out can be translated as follows:

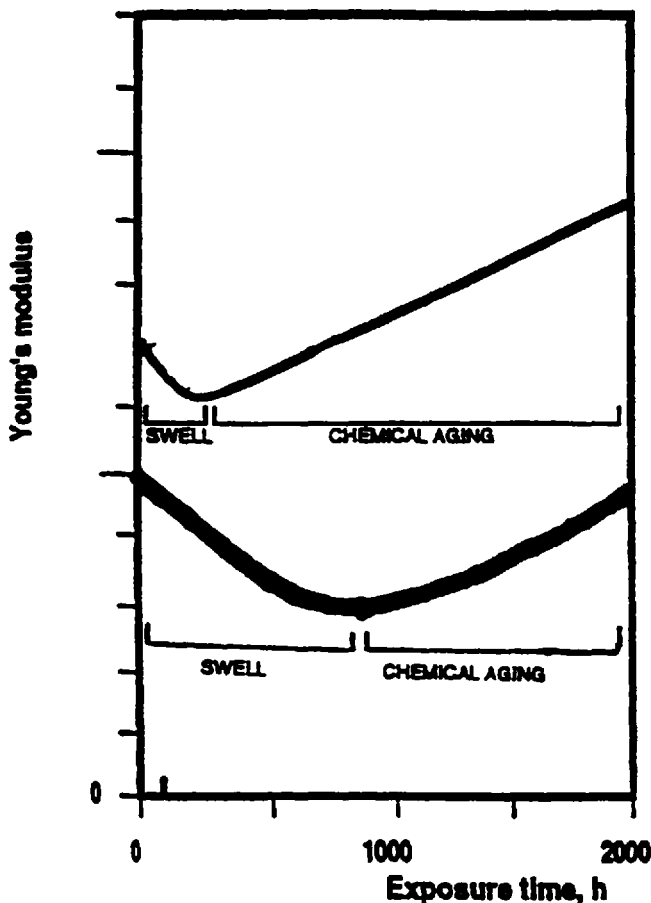


Figure 9.4 A comparison of the change in Young's modulus for two different elastomer compounds as a function of time.

M	Metric units; 2 = grade (medium- to low-ACN content)
BG	NBR heat-aged for 70 h at 100°C (212°F): in air, to result in a maximum change in elongation of -50%, a change in tensile strength of no more than $\pm 30\%$, a change in hardness of no more than ± 15 points; in ASTM oil No. 3, to result in a 40% maximum volume swell
6	Hardness (60 ± 5 Shore A); 14 = 14 MPa (2031 psi) tensile strength, minimum value
B14	Compression set test required on sheet sample for 22 h at 100°C (212°F)
EO14	Fluid resistance test required in ASTM Reference Fuel A for 70 h at 100°C (212°F).

The above information categorizes a nitrile elastomer based on a series of standard tests performed in standard test fluids. The property values listed are for sheet material, not seals. The standard test fluids are reference fluids, such as ASTM Reference Fuel A, not fully formulated hydraulic fluids. The tests are short term, no longer than 70 h. The specified limits are based on the maximum limits at which an elastomer could be considered nonfunctional. ASTM stresses that these line callouts are not to be used to establish compatibility or performance acceptability.

Line callouts are general classification methods and not specification requirements. Another example would be the line callout for the ASTM No. 3 Oil Test Requirement. This test is a 70-h test at 212°F. The acceptable limits are as follows: hardness change of -10 to +5; tensile strength change of -45%, maximum; elongation change of -45%, maximum; volume change of 0% to 25%. One elastomer has a hardness change of -1, a tensile strength change of -6%, an elongation change of -3%, and a volume change of 4%. Another elastomer has a hardness change of -9, a tensile strength change of -42%, an elongation change of -37%, and a volume change of 24%. Both of these elastomers qualify for the same ASTM line callout even though they are significantly different and, almost certainly, would not perform the same in service. Table 9.4 presents an ASTM line callout and test data for two elastomers that meet the callouts. Elastomer A performed well in actual dynamic service in a Naphthenic Mid VI fluid, whereas Elastomer B failed shortly after being installed. When the failed elastomer was removed the the seal gland, the O-ring was swollen into a rectangular shape which fully occupied the gland volume. The O-ring was very soft and abraded. This example illustrates that ASTM line callouts do not accurately assess seal compatibility.

6.3 Guidelines

Basic guidelines that may be used to facilitate the search for suitable elastomers involve short-term testing of the actual elastomer in standard test fluids. From these test results, it is possible to categorize a general compatibility table. Table 9.5 [25,26] presents general compatibility guidelines for initial selection of the elastomer polymer for the sealing application.

After the elastomer polymer has been selected, specific application problems are then addressed. This is done by reviewing system requirements and properties of elastomers that affect sealability. Elastomers are both engineered materials and organic polymers; therefore, their engineering and age-resistance properties are im-

Table 9.4 Evaluation of Compounds A and B to ASTM D 2000 M2BG714B14EA14EF11EF21EO14EO34

Properties	Specification	Compound A	Compound B
Original			
Hardness (A)	65–75	70	69
Tensile (psi)	2031 (min.)	2220	2050
Elongation (%)	250 (min.)	300	375
Air Aging, 70 h at 100°C			
Hardness change	+15 to -15	+5	+11
Tensile change (%)	+30 to -30	+8	+21
Elongation change (%)	-50 (max.)	-10	-24
Comp. set, 22 h at 100°C, % of original	25 (max.)	12	19
Water Immersion, 70 h			
Hardness change	+10 to -10	-2	-5
Volume change (%)	+15 to -15	+3	+6
Fuel A, 70 h at 23°C			
Hardness change	-10 to +10	0	+5
Tensile change (%)	-25 (max.)	-16	-22
Elongation change (%)	-25 (max.)	-10	-17
Volume change (%)	-5 to +10	0	-4
Fuel B, 70 h at 23°C			
Hardness change	0 to -30	-6	-12
Tensile change (%)	-60 (max.)	-23	-40
Elongation change (%)	-60 (max.)	-18	-32
Volume change (%)	0 to +40	+17	+27
ASTM No. 1, 70 h at 100°C			
Hardness change	-5 to +10	+2	-3
Tensile change (%)	-25 (max.)	-10	-19
Elongation change (%)	-45 (max.)	-8	+5
Volume change (%)	-10 to +5	-4	+4
ASTM No. 3, 70 h at 23°C			
Hardness change	-10 to +5	-6	-9
Tensile change (%)	-45 (max.)	-10	-23
Elongation change (%)	-45 (max.)	-5	-18
Volume change (%)	0 to +25	+15	+22

portant. The engineering moduli—shear and Young's—elastic recovery, and the chemical degradation of the elastomer are important in assessing compatibility. Engineering moduli address seal stiffness and effectiveness in shearing the fluid film and keeping the fluid in the system.

Peacock [27] presents a good explanation of the value of shear modulus in elastomer assessment. Unless there is immediate deterioration of the elastomer, these properties must be evaluated in long-term static soak tests followed by functional tests. They should also be performed in the actual hydraulic fluid at the operating temperature of interest. Testing time should be sufficient for fluid saturation of the elastomer and chemical reactions to occur; this can be as long as 500–1000 h.

Table 9.5 General Elastomer Compatibility

Polymer	Continuous service temp. (°F)	Service temp. limits (°F)	Compatible fluids	Noncompatible fluids
NBR-1 ^a	-20 to +210	-20 to +240	Aliphatic hydrocarbons, mineral oils and greases, oil-in-water and water-in-oil emulsions, water-glycol, ethylene glycol, soybean oil, sunflower oil, corn oil	Phosphate esters, aromatic hydrocarbons, halogenated solvents, esters
NBR-2	-40 to +195	-40 to +230	Aliphatic hydrocarbons, mineral oils and greases, oil-in-water and water-in-oil emulsions, water-glycol, ethylene glycol, soybean oil, sunflower oil, corn oil	Phosphate esters, aromatic hydrocarbons, halogenated solvents, esters
NBR-3	-60 to +195	-40 to +230	Aliphatic hydrocarbons, mineral oils and greases, oil-in-water and water-in-oil emulsions, water-glycol, ethylene glycol, soybean oil, sunflower oil, corn oil	Phosphate esters, aromatic hydrocarbons, halogenated solvents, esters
EPDM	-60 to +240	-60 to +300	Phosphate esters, air, acids, bases, water-glycol, steam, water, rapeseed oil, silicon fluids and greases	Hydrocarbons, halogenated hydrocarbons
FKM	-40 ^b to +390	-40 ^b to 480	Aliphatic and aromatic hydrocarbons, mineral oils and greases, halogenated hydrocarbons, polyglycol, diesters, silicone fluids	Phosphate esters, hot water, steam
HNBR	-20 to +265	-29 to +300	Mineral oils and greases, aliphatic hydrocarbons, air, steam, water-in-oil and oil-in-water emulsions, glycol	Aromatic hydrocarbons, acids, halogenated solvents

^aNBR compounds are listed in order of aliphatic hydrocarbon compatibility with NBR-1 being the best.

^bThis is the low temperature limit for the low temperature grade. -20°F is the acceptable limit for the other grades.

Elastomer seals of the actual size that will be used in the hydraulic system should be the test specimens.

To illustrate this point, soak tests were performed on two different size EPDM O-rings. The first O-ring (2-214) had a cross section of 0.139 in. and an inside diameter of 0.984 in. The second O-ring (2-316) had a cross section of 0.210 in. and an inside diameter of 0.850 in. The first test involved soaking the O-rings at 225°F in phosphate ester fluid and measuring the time to saturation. The 2-214 O-ring reached 99% saturation in 19 h, whereas it took 42 h for the 2-316 O-ring to reach 99% saturation. The second test was performed in the same fluid at 185°F and it took 36 h for the 2-214 O-ring to reach 99% saturation. Testing times of 79 h for the 2-316 O-ring to reach 99% saturation were required. If a compatibility test was performed at 185°F for 70 h, the 2-316 O-ring would not be saturated and chemical interaction would not be accurately evaluated.

Elastomers are organic materials. Compatibility involving chemical processes cannot be fully evaluated until the specific elastomer being evaluated is saturated with the actual fluid of use in an equilibrium condition. This can take several days or longer depending on the polymer, the specific compound formulation, the test temperature, and the service fluid. The test temperature needs to be the service temperature in order to accurately fix the chemical system. The test time needs to be a certain period of time beyond saturation to allow chemical reactions to occur in the elastomer matrix. This should be 1000 h to be sure that saturation has occurred and chemical reactions have been allowed to continue for a sufficient period of time to represent service time periods. Actual service fluid–elastomer interaction needs to be assessed because of subtleties in compositions.

7 PHYSICAL PROPERTIES

Elastomer seals must resist chemical degradation and maintain their engineering properties over their service lifetime. Typically, a stress–strain curve is obtained each time a tensile test is performed. Three parameters [28] are reported from the data: tensile strength, which is the stress at the strain point that the elastomer breaks; it is recorded as the ultimate elongation—how far it stretched before it broke. Another value that is often recorded is the “modulus at XXX% elongation.” This is the stress at the particular strain point. Stress is the force acting across a unit area to resist separation (tensile), compression (compressive), or shearing (shear). Strain is the change in length of a material in the direction of force per unit undistorted length. Thus, in tensile, as a load is applied to pull the sample apart, strain results as the sample is stretched. A typical stress–strain curve is shown in Fig. 9.5. Young’s modulus is the ratio of the stress applied to the elastic strain that results. Because a force is moving through a distance, integrating under the stress–strain curve would yield the value of work that is being done. In any engineered material, Young’s modulus is a key parameter. Young’s modulus (E) and shear modulus (G) are engineering values, and for an isotropic solid such as rubber,

$$E = 3G$$

The shear modulus for an unfilled elastomer is defined as [29]

$$G = \frac{\rho RT}{M_c}$$

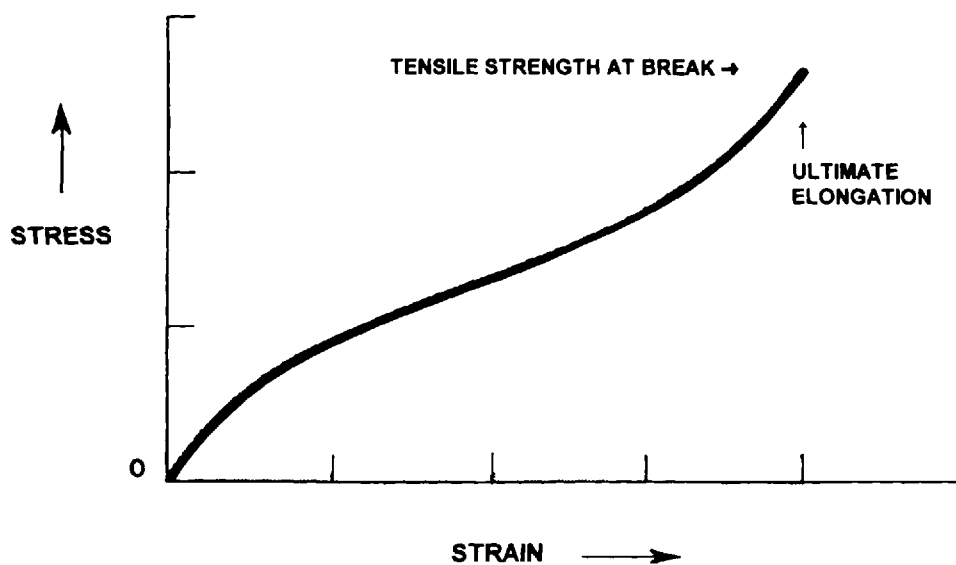


Figure 9.5 A typical stress–strain curve for an elastomeric O-ring.

where ρ is the density, R is the universal gas constant, T is the temperature (in K), and M_c is the molecular weight between cross-links. M_c is the variable that reflects the chemical changes that would occur during the aging process and, to a degree, the changes can be monitored in real time by monitoring the value of G before, after, and during the aging process. Work is a product of shear modulus times an extension ratio δ . The extension ratio is a nonlinear function: $\delta = 1 + \text{elongation}$. Work can be determined by integrating the area under a stress–strain curve. A finite value of work will give an accurate representation of the changes that are occurring during the aging process. This can be called the work function [27] and can be determined by integrating the area under the stress–strain curve from 0% to 20% elongation. Thus, the work function can be used to assess elastomer aging and the loss of engineering performance.

The elements that should be in a test program include the following: tests should be conducted at the expected maximum operating temperature in the actual operational fluid for a sufficient amount of time to allow elastomer saturation and chemical reactions to occur. Only after saturation can chemical compatibility be assessed. The actual operational fluid is required because assumptions based on test results using standard test fluids without performance additives present can be misleading. In the studies conducted to date, it appears that 500 h is a minimal test time and tests should be conducted to 1000 h for a full assessment. This will also indicate the elastomer's compatibility over a meaningful service period. It also appears that a change of greater than 20% in the starting value of the work function has a deleterious effect on elastomer engineering performance as a seal [30]. The elastomer test specimens should be O-rings of the appropriate cross sections to be used in the system in order to adequately assess actual operational situations.

In addition to the chemical or aging changes of elastomers, volume changes must be considered. Elastomers can swell with the uptake of fluid or they can shrink

with the depletion or withdrawal of components in the elastomer compound. Most seal glands are designed to accommodate 15% volume swell of the elastomer [31,32]. If elastomer swelling beyond 15% occurs, the seal not only fully occupies the gland volume but also flows out of the gland. Excessive swelling leads to softening and abrasion, loss of resilience, extrusion and nibbling of the seal as it flows out of the gland, and, consequently, seal failure. Elastomer seal shrinkage leads to hardening and a reduction in seal force, which results in seal failure. Shrinkage may occur when a system is idle and the seal is allowed to “dry out.” If the seal has taken a set during operation and then dries out, it may not function when the system is restarted. If a seal shrinks away from a mating surface and has taken a set or hardened on the surface, when it swells again on exposure to fluid, it might not mate correctly against the surface it is supposed to seal. This results in leakage.

Volume swell and volume shrinkage should also be assessed. Actual volume swell in a gland is normally considered to be approximately 50% of the value obtained in a free-volume-swell test, where the elastomer is soaked in the free state in fluid. Thus, values of free volume swell of less than 25% are considered acceptable. Allowing for variability and margin of error, a material that exhibits a maximum of 20% free volume swell would be required. Some volume swell is beneficial because it compensates for compression set. Compression set is the tendency of seal materials to return only part way to their free state after being compressed; this reduces the sealing force. If an elastomer shrinks in service, the sealing force is reduced and shrinkage combined with compression set always leads to leakage. Therefore, no shrinkage should be allowed.

Also, as the elastomer reswells, its surface conformance changes, resulting in wear and leakage. After a soak test, the seal should be allowed to dry out for a 24-h period, and if shrinkage is $\geq 4\%$ from the swelled value, there is a high potential for seal leakage.

In summary, the factors for elastomer seal compatibility are as follows:

- Fluid dissolves into the sealing surface and then diffuses into the interior.
- An equilibrium fluid concentration occurs.
- Fluid in the elastomer interacts physically and chemically.
- The elastomer ages through local fracturing of bonds, oxidation, and other chemical reactions.

The compatibility program should address seal volume change, chemical reactions that occur in the seal after fluid saturation, and changes in Young's modulus, and should be conducted in the actual fluid for a sufficient amount of time to assess changes. The test time should be no less than 500 h and the test temperature should be the actual maximum temperature the seal will see in service.

8 SEAL COMPATIBILITY TEST PROCEDURE

A seal compatibility test procedure that may be easily performed will be provided here. Mechanical test equipment and laboratory ovens are required. The results will assist in evaluating optimal elastomers for a specific application.

The test fluid should be the actual system fluid and the test temperature should be the maximum seal exposure temperature. Test samples should be analyzed at 24, 70, 100, 250, 500, and 1000 h to assess the compatibility of the seal over the min-

imum service life of the fluid. The test is concluded when the property changes exceed the established limits. The test samples should approximate the cross section of the actual seal used so that the saturation effect is properly considered. The test samples should be either 2-021, -120, -214, or -320 O-rings per AS568 [33], which is the specification that identifies the actual sizes of O-rings. These have an approximate inside diameter of 1 in. and represent the most popular cross sections of seals used in industrial systems. The test specimen need to be molded from the same compound as the actual seal.

The following tests should be performed on the O-rings:

1. Hardness change
2. Volume swell
3. Tensile strength change
4. Elongation change
5. Work function change

8.1 Hardness Change

Measure the hardness per ASTM D 1414 [34] Section 16 using a micro hardness tester and record the mean value. Measurements are to be taken before and after exposure to fluid. The hardness change is calculated as

$$\Delta H = H_1 - H_2$$

where ΔH is the hardness change, H_1 is the hardness before fluid exposure, and H_2 is the hardness after fluid exposure.

The units are given as Shore A points. The Shore hardness scale was developed for elastomers and has no correlation to other hardness scales, although it does overlap a portion of the IRHD scale [35], which is used in ISO specifications and does have a relationship to Young's modulus.

8.2 Volume Swell

Apparatus: A quart glass canning jar with a standard two-piece lid to prevent liquid and vapor from escaping.

Heating Device: A forced-air oven. The temperature shall be maintained within $\pm 1^\circ\text{C}$ (1.8°F).

Test Specimen: The test specimen shall consist of an entire O-ring. The same specimen may be used for all tests with hardness and volume determinations made prior to stress-strain tests.

Procedure

1. Weigh each test specimen in air, M_1 , to the nearest 1 mg and then weigh each specimen immersed in water, M_2 , at room temperature. It is important that all air bubbles clinging to the test specimen be removed before reading the weight in water. Blot the specimen dry on a lint-free paper towel.
2. Suspend the specimens in the glass jar by the use of corrosion-resistant wire. Separate the specimens by the use of glass beads or corrosion-resistant washers or by bending small loops in the wire.
3. Suspend the specimen vertically so that 1 in. of test fluid is between the lower extremity of the specimen and the bottom of the apparatus. Add

enough test fluid to cover the specimen to a depth of 1 in. over the upper extremity of the specimen.

4. Place the test apparatus in the oven at the test temperature for the appropriate test time. At the end of the immersion period, remove the specimen from the apparatus. Cool the specimen to room temperature by immersing it in a fresh amount of the test fluid for 45 min.
5. At the end of the cooling period, remove the specimen from the fluid and blot dry. Weigh each test specimen in air, M_3 , and then weigh each specimen immersed in water, M_4 .
6. The change in volume is calculated as

$$\Delta V(\%) = \frac{(M_3 - M_4) - (M_1 - M_2)}{M_1 - M_2} \times 100$$

where

M_1 = initial mass of specimen in air (g)

M_2 = initial mass of specimen in water (g)

M_3 = mass of specimen in air after immersion (g)

M_4 = mass of specimen in water after immersion (g)

8.3 Shrinkage

Apparatus: A screen or oven rack that allows a circulation around the test specimen.

Heating Device: A forced-air oven capable of maintaining the temperature at $23 \pm 1^\circ\text{C}$ ($73.4 \pm 1.8^\circ\text{F}$).

Test Specimen: The test specimen shall consist on an entire O-ring. The same specimen that was used for the volume-swell test may be used provided that this specimen was not used for the stress-strain tests.

Procedure

1. Place the test specimen from the volume-swell test on the oven rack and maintain the oven at the test temperature for 22 ± 0.25 h. At the end of the required period, remove the specimen from the oven and allow it to air cool.
2. Weigh each test specimen in air, M_5 , and then weigh each specimen immersed in water, M_6 .
3. The change in volume or shrinkage is calculated as

$$\Delta V(\%) = \frac{(M_5 - M_6) - (M_1 - M_2)}{M_1 - M_2} \times 100$$

where

M_3 = initial mass of volume-swell specimen in air (g)

M_4 = initial mass of volume-swell specimen in water (g)

M_5 = mass of specimen in air after drying out (g)

M_6 = mass of specimen in water after drying out (g)

8.4 Tensile Strength Change

Testing Machine: The testing machine shall conform to the requirements specified in Section 3 of ASTM D 412 [36] with the exception of grips. Grips for testing O-rings shall consist of ball-bearing spools at least 0.35 in. in diameter and be capable of being brought within 0.75 in. center-to-center distance at closest approach. (These grips should be readily available from the manufacturer of the testing machine.) Stresses within the specimen shall be minimized by rotating one spool of the grips or by lubricating the contact surface of the spools with castor oil.

Test Specimen: The test specimen shall consist of an entire O-ring.

Procedure

1. Bring the grips close enough together so the specimen can be installed without stretching. Separate the grips to remove any slack in the specimen. Care should be taken that no load is placed on the specimen.
2. Pull the specimen at a rate of 20 in./min. Record the breaking force value, F , at the time of rupture.

Calculations

Tensile strength

$$T = \frac{F}{A}$$

where

T = tensile strength (psi)

F = breaking force (lb.)

A = twice the cross-sectional area calculated from axial thickness, W (in.²), as follows:

$$A = \frac{\pi W^2}{2} = 1.57W^2$$

Tensile strength change

$$\Delta T = \frac{T_2 - T_1}{T_1} \times 100$$

where

ΔT = tensile strength change (%)

T_2 = tensile strength after immersion

T_1 = tensile strength prior to immersion

8.5 Elongation Change

Testing Machine: Same as for tensile strength change.

Test Specimen: Same as for tensile strength change.

Procedure: Same as for tensile strength change, except record the center-to-center distance between the spools at rupture to the nearest 0.1 in. and record the value for D .

Calculations

Ultimate elongation

$$E(\%) = \frac{2D + G - C}{C} \times 100$$

where

D = distance between centers of the spool grips at the time of rupture of the specimen

G = circumference of one spool (spool diameter \times 3.14)

C = inside circumference of the specimen (inside diameter \times 3.14)

Change in elongation

$$\Delta E(\%) = \frac{E_2 - E_1}{E_1} \times 100$$

where

E_2 = elongation after immersion

E_1 = elongation prior to immersion

8.6 Work Function Modulus Change

Testing Machine: Same as for tensile strength change.

Procedure: Same as for tensile strength change.

Calculations: Calculate the work function (WF) as the energy per unit volume at 20% elongation. This value is determined as the area under the stress-strain curve from 0–20% strain.

Change in work function

$$\Delta WF = \frac{WF_2 - WF_1}{WF_1} \times 100$$

where

ΔWF = change in work function (%)

WF_2 = work function after immersion (psi)

WF_1 = work function prior to immersion (psi)

During the course of the program, the test results should be plotted as a function of time to detect any radical property changes or definitive trends. For a critical seal application, property changes limits as detailed below should be monitored. These limits have been established in the ASTM [30] and NFPA [37] compatibility programs and will indicate good chemical compatibility. The Compatibility test limits are as follows:

Hardness change: ± 8 pts

Volume swell: 0 to +15%

Shrinkage after swell test: -4%, maximum

Tensile strength change: $\pm 20\%$

Elongation change: $\pm 20\%$

Work function change: $\pm 12\%$

If all the changes are within these limits, the elastomer should be considered compatible.

Once a seal material is found to be compatible, all seals for that system should be ordered by specific compound and not by ASTM D 2000 Line Call Out or generic polymer designation. Carefully selecting the initial seal avoids problems later.

To illustrate the property changes that can be experienced in a compatibility test, a 2-120 NBR O-ring set was submitted to the compatibility test program. The O-rings were tested in a naphthenic fluid at 100°C. The average test results for the samples are shown in Table 9.6.

An examination of the complete test results shows several interesting points. The work function value exceeded 12% after just 24 h, even though saturation did not occur until approximately 500 h, as indicated by the volume swell reaching a maximum. The lower the test temperature, the longer the time to saturation. This is why short-term tests at low temperatures are meaningless. Work function data also showed a reaction trend with the value starting off as a significant negative change, gradually getting positive until the significant positive change at 1000 h. This indicated that the chemical reaction, once begun, continued. If the work function was not monitored, the tensile and elongation data would have not indicated incompatibility until the 500-h test; thus, any short-term test would have indicated full compatibility. If only hardness change and volume change were monitored, there would have been no indication of incompatibility. This test sequence illustrates the problem of relying solely on volume-swell and hardness changes as compatibility indicators.

9 SEALS

9.1 Introduction

A seal is used between two surfaces to maintain a pressure drop from a positive fluid (liquid or gas) pressure area to a relatively lower fluid pressure area for a specific amount of time [38]. A seal's effectiveness is measured in terms of leakage. Thus, a zero leak seal is one that theoretically allows no leakage across its interface or sealing contact surface.

The earliest seals were nothing more than stuffing boxes packed with waxed string or cord, leather strips, pieces of rubber, cotton, wool, or even paper (Fig. 9.6).

Table 9.6 Compatibility Test Results for a 2-120 NBR O-Ring

Test time (h)	Tensile change (%)	Elongation change (%)	Work function change (%)	Hardness change (pts.)	Volume change (%)
0	0	0	0	0	0
24	+7.5	+2.9	-24.1	-1	+3.61
100	+4.3	-1.3	-12.4	-1	+4.16
250	-13.3	-17.0	-7.0	+1	+4.21
500	-63.9	-54.1	+0.5	+3	+4.7
1000	-73.0	-79.3	+126.0	+8	+2.78

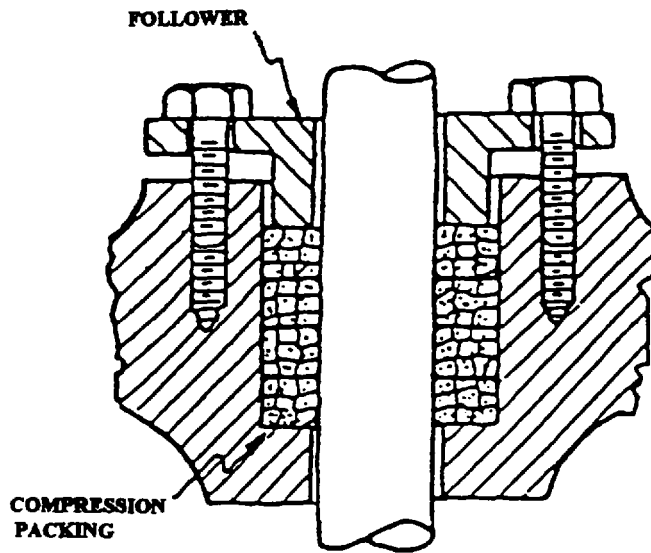


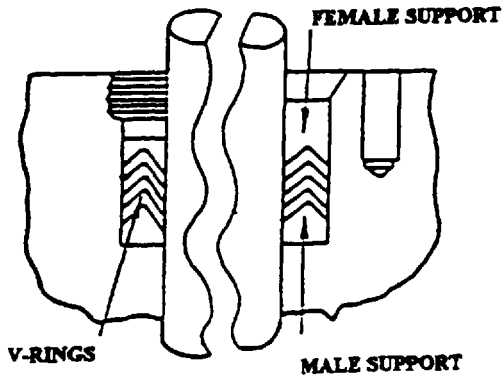
Figure 9.6 An illustration of a stuffing-box sealing arrangement.

If leakage was observed, more material was stuffed in until the leakage stopped or became acceptable. These sealing methods were acceptable because the inefficiency of the seal was a small contributor to the overall inefficiency of the equipment being used.

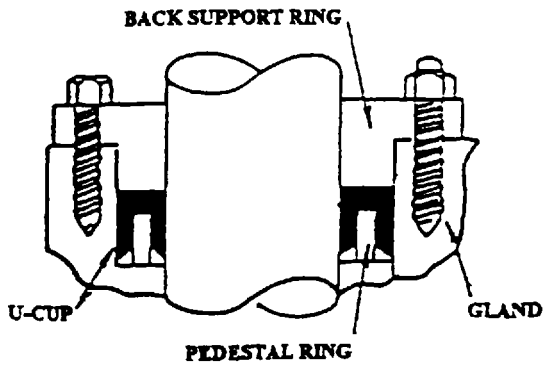
The first advance in sealing technology was the development of V-Rings (Chevron Rings) and U-Cups (Figure 9.7). These seals are reasonably effective but require hardware modifications, which may be complex. Another disadvantage is that these seals are unidirectional because they are pressure-activated. Thus, two seals are needed to seal in both directions. As pressure is increased, more V-seals must be added. Thus, three or more V-seals can be required to seal system pressures in excess of 2000 psi. U-Cups have a pressure limitation of 1500 psi.

The next advance in sealing technology was the O-ring (Fig. 9.8). The O-ring was patented in the 19th century. The original application called for use of the O-ring in a very long groove. The O-ring was intended to roll during the motion of the parts and thus act like a wiper and seal barrier. Around 1940, an elastomeric O-ring was developed. The sizes of the O-rings were then standardized for universal use [19,33,39–42]. The simple design allowed the O-ring to be used both as a static and dynamic seal. Because it was a compression seal, it was also a bidirectional seal in that it was elastic and distorted with pressure and acted as an effective barrier to prevent leakage.

During the Second World War, the O-ring became the seal of choice because the war effort forced the simplification and standardization of hydraulic components. During this time, many new applications were developed for O-rings because of their simplicity and effectiveness in sealing.



(a)



(b)

Figure 9.7 (a) Illustration of chevron V-rings used as a static seal. (b) Illustration of a U-cup used as static seal.

9.2 Seal Types

9.2.1 Static

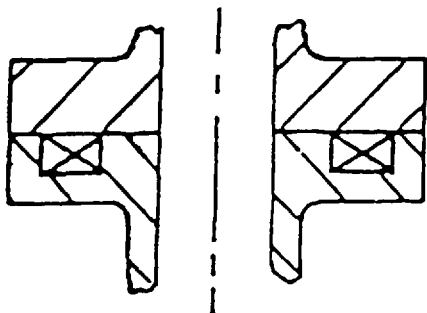
A static seal is one that maintains a pressure drop across two stationary surfaces. Although the surfaces are considered stationary in theory, in fact none are stationary



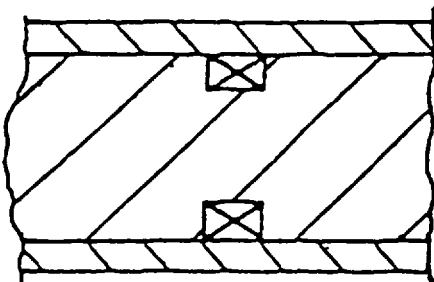
Figure 9.8 An O-ring profile.

due to vibration, seal set, and so forth. Static seals are sometimes referred to as joints or gaskets because they are predominantly face seals in that they seal in a plane located at right angles to the centerline of the seal (Fig. 9.9). The requirements for static seals are considered not as rigorous as for dynamic seals: Groove finish can be rougher; higher squeeze is also used, as friction is not a factor. Static seal geometries include O-rings, square rings (lathe cuts), D-rings, X-rings, T-seals, and cap seals (Fig. 9.10). Many other geometries are used. For large static seals, there is a tendency to use extruded cord stock. This stock is cut to size and bonded together to form a ring. The profile can vary. This lowers cost because a static seal is not a high-performance seal. This can be done; however, extruded material does not have the same physical properties as molded seals. Extruded material has lower physical properties than molded material because it is processed differently. The resulting lower density, strength, resistance to compression set, and different compatibility behavior can adversely affect sealability. If extruded stock is to be used, it should be tested in the fluid of use at the temperature of operation to verify that it will perform satisfactory service. Compression set and low-temperature elasticity should also be verified.

The most common causes of static seal leakage are installation damage, extrusion, sealing finish, overfill, splice, and use of the wrong seal material [38]. Installation damage can occur to any seal and care has to be exhibited on installation to



(a)



(b)

Figure 9.9 (a) Illustration of the seal gland location for a static face seal application. (b) Illustration of the seal gland location for a static rotary seal application.

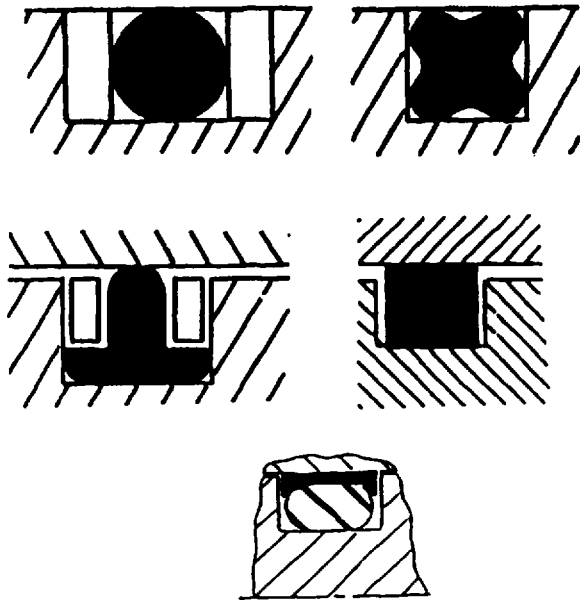


Figure 9.10 Illustration of the various static seal types.

ensure that the seal is installed correctly and is not cut, twisted, or pinched during installation. After the seal is installed, correct installation should be verified before the hardware is assembled. This caution saves time and money.

Extrusion, or the tendency of the seal material to flow out of the seal gland, is normally associated with dynamic seals. A static seal is also dynamic because relative movement occurs between hardware components, and pressure pulsations can force the static elastomeric seal into the clearance between the sealing faces. To avoid this, the gap between the sealing faces is minimized. A harder elastomer should be used as the static seal; caps and backup rings can also be used. As pressure is increased, backup rings should be considered. Again, the initial incremental cost is low when measured against downtime costs.

Sealing finishes should not exceed 64 micro inches RMS (root mean square), which is an expression of an effective average depth of the surface irregularities, and preferably should be 32 micro inches RMS or better [38]. An elastomer seal must conform to the surfaces it is sealing, and if the sealing surface is very rough, conformance will not occur and leakage will result. If cap seals are used, harder cap material cannot conform to real rough finishes with radical peak-to-valley ratios (the ratio of the highest point on a surface to the lowest point).

Overfill is also a problem. The elastomer fills only a portion of the seal groove. As a result of swell upon exposure to fluid, the elastomer expands into the void area of the groove. If the groove becomes overoccupied, the elastomer is forced into the gap between the sealing surfaces where cutting and nibbling can occur. Fluid exposure results in elastomer swell and softening and this can accelerate seal failure. Initial occupancy of the gland should not exceed 85%.

For extremely large-sized seals used in static applications, it is economical to use extruded rubber stock cut to size and bonded together at the splices to form a

seal ring. However, splice failures frequently occur [43]. Often, no attention is paid to the splice. There are many different ways to splice elastomeric materials, and the splice geometry, bonding technique, and bond strength must be addressed so that the seal withstands operational conditions. Leakage and operational safety require that care be exercised in choosing spliced seals. The specific application and system requirements can be discussed with the seal supplier.

A compatibility test such as that described above is a wise investment if, indeed, optimum performance and *zero leak* are requirements. By verifying the bond strength of the splice on a test sample before and after exposure to the operational temperature and fluid, it can be verified that the correct seal has been chosen for the application. This test also serves to characterize the compatibility of the elastomer material.

Although the O-ring has been the most popular shape for static seals, some engineers suggest that square rings are more effective static seals because they permit a wider seal contact area and more insurance for zero leak [44]. The square ring was initially proposed as a dynamic seal to overcome the tendency of an O-ring to roll and twist. Because of its geometry, the square ring creates a wider footprint, and in dynamic situations with identical squeeze, higher friction results. This is not the case in static sealing conditions where friction is not an important factor. In static systems, the O-ring is still the most popular seal shape, especially because it is easier to extrude and bond a circular shape. The square ring, however, can offer some advantages if it is prepared from a good elastomeric material and it is proven to be compatible in long-term tests. The square ring also should be more extrusion resistant because of its geometry.

For square rings or O-rings in face seal applications, the groove should be designed to assure seal contact with the low-pressure side of the groove assembly. For internal pressure applications, the seal groove and the outside diameter of the seal are matched. When pressure is external, the gland should be designed to support the seal on the inside diameter.

Design charts for static O-rings are presented in Tables 9.7 and 9.8 [38]. In these tables, there is a term called "squeeze." This is the amount of distortion put on a seal when it is installed in the system. Squeeze is necessary to allow the seal to maintain a positive seal force. The seal is actually distorted that amount when it is installed between the sealing members. Other elastomer seals generally use the same guidelines.

9.2.2 Dynamic Seals

A dynamic seal is one that is used to maintain the pressure drop across two surfaces moving relative to one another. Dynamic seals can be further categorized as I.D. or rod seals and O.D. or piston seals (Fig. 9.11). These are traditionally reciprocating seals. Dynamic seals can also be rotary seals when they prevent leakage between one surface which has angular movement relative to the other surface (Fig. 9.12) [38].

Seal effectiveness is measured using several requirements. Good seals should have the following characteristics:

Integrity: Must not leak

Reliability: Must ensure system integrity for a desired period of time

Table 9.7 Static O-Ring Guidelines; Design Chart for O-Ring Face Seal Gland

O-ring size	Cross-section (<i>W</i>)		Gland depth (<i>L</i>)	Squeeze		Groove width (<i>G</i>)		Groove radius (<i>R</i>)
	Nominal	Actual		Actual	%	Liquids	Vacuum and gases	
004–050	1/16	0.070 ± 0.003	0.050–0.054	0.013–0.023	19–32	0.101–0.107	0.083–0.088	0.005–0.015
102–178	3/32	0.103 ± 0.003	0.074–0.080	0.020–0.032	20–30	0.136–0.142	0.118–0.123	0.005–0.015
201–284	1/8	0.139 ± 0.004	0.101–0.107	0.028–0.042	20–30	0.177–0.187	0.157–0.163	0.010–0.025
309–395	3/16	0.210 ± 0.005	0.152–0.162	0.043–0.063	21–30	0.270–0.290	0.236–0.241	0.020–0.035
425–475	1/4	0.275 ± 0.006	0.201–0.211	0.058–0.080	21–29	0.342–0.362	0.305–0.310	0.020–0.035
Special	3/8	0.375 ± 0.007	0.276–0.286	0.082–0.108	22–28	0.475–0.485	0.419–0.424	0.030–0.045
Special	1/2	0.500 ± 0.008	0.370–0.380	0.112–0.138	22–27	0.638–0.645	0.560–0.565	0.030–0.045

Note: These dimensions are intended primarily for face-type seals and low-temperature applications.

Table 9.8 Static O-Ring Guidelines; Design Chart for Industrial O-Ring Static Seal Gland

O-Ring size	Cross section		Gland depth ^a	Squeeze ^b		Diametral clearance (E) ^c	Groove width			Groove radius (R)	Eccentricity max. ^d
	Nominal	Actual		Actual	%		No backup rings	One backup ring	Two backup rings		
004-050	1/16	0.070 ± 0.003	0.050-0.052	0.015-0.223	22-32	0.002-0.005	0.093-0.098	0.138-0.143	0.205-0.210	0.005-0.015	0.002
102-178	3/32	0.103 ± 0.003	0.081-0.083	0.017-0.025	17-24	0.002-0.005	0.140-0.145	0.171-0.176	0.238-0.243	0.005-0.015	0.002
201-284	1/8	0.139 ± 0.004	0.111-0.113	0.022-0.032	16-23	0.003-0.006	0.187-0.192	0.208-0.213	0.275-0.280	0.010-0.025	0.003
309-395	3/16	0.210 ± 0.005	0.170-0.173	0.032-0.045	15-21	0.003-0.006	0.281-0.286	0.311-0.316	0.410-0.415	0.020-0.035	0.004
425-475	1/4	0.275 ± 0.006	0.226-0.229	0.040-0.055	15-20	0.004-0.007	0.375-0.380	0.408-0.413	0.538-0.543	0.020-0.035	0.005

^aFor ease of assembly when backup rings are used, gland depth may be increased up to 5%.

^bClearance gap must be held to a minimum consistent with design requirements for temperature-range variation.

^cReduce maximum diametral clearance 50% when using silicone or fluorosilicone O-rings.

^dTotal indicator reading between groove and adjacent bearing surface.

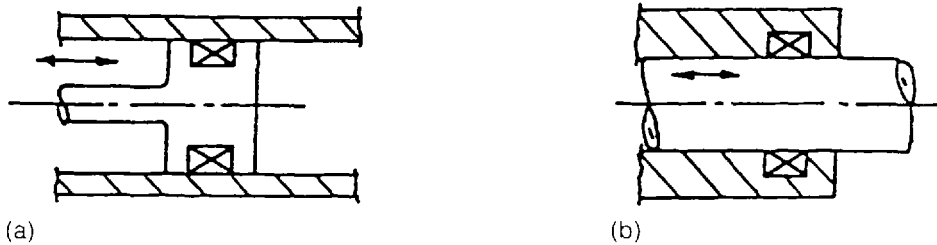


Figure 9.11 Illustration of the seal gland locations for (a) dynamic piston and (b) rod seal applications.

Long life: Must minimize downtime for change outs

Ease of Installation: Must be easy to install and replace

Compatibility—Must be compatible with the fluid it seals throughout the operational range of pressures and temperatures

Currently, the majority of seals contain elastomer components. This is true because elastomers are still very effective in maintaining system integrity. Whether the seal is an elastomer, such as an O-ring, square ring, U-cup, and so forth, or a slipper seal which has a plastic component energized (squeezed against the surface to be sealed) by an elastomer, the elastomer is an essential component of the majority of seals used in today's systems.

Seals can be further categorized as "squeeze-type" or "pressure-activated" (lip-type) seals (Fig. 9.13). The squeeze-type seals are principally elastomeric seals of various geometries. The most common squeeze-type seal is the O-ring. This is because it is readily available in a wide range of sizes and materials; it is a low-cost seal easily installed and, most importantly, it is a very effective seal. In general, O-rings can be used to effectively seal up to 1500 psi by imparting 15–30% squeeze on the ring. Sealing above 1500 psi is possible with the use of 80–90 Shore A elastomeric materials and reduced clearance gaps or the use of backup rings [38]. The clearance gap is the maximum difference between the dimensions of the hardware components. For a piston application, this would be the maximum difference between the piston diameter and the bore diameter. For a rod application, this would be the maximum difference between the rod diameter and the bore diameter. Table

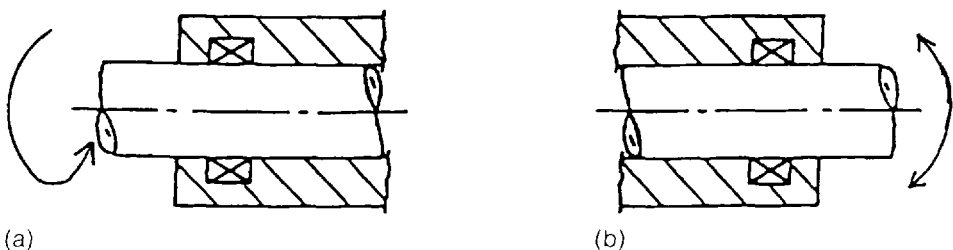


Figure 9.12 Illustration of the seal gland locations for (a) rotary and (b) oscillatory seal applications.

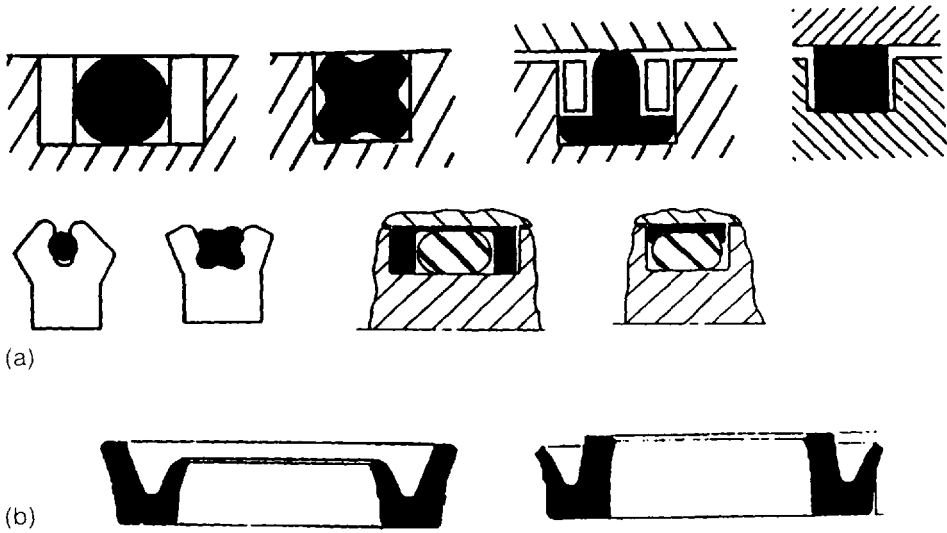


Figure 9.13 Illustrations of (a) the various squeeze- (compression) type dynamic seals and (b) typical lip (pressure-activated) seals.

9.9 lists the recommended clearance gaps for elastomer seals with different hardnesses. These gaps can be widened when backup rings are used with the elastomer. The backup rings function as elastomer protection, blocking the flow of the elastomer into the gap where the elastomer can be torn and nibbled. Backup rings should be used when system pressure exceeds 1500 psi.

An elastomer can act as if it remembers the original shape it was molded into and can return to this shape for relatively long periods of time while undergoing deformation due to pressure (memory effect). In low-pressure situations, an elastomer squeezed into a gland has a tendency to maintain its original shape and this creates the seal. In high-pressure situations, the elastomer is deformed against one side of the gland, but it maintains a sealing force against the surface it is sealing. This force is equal to the force deforming it [38].

Table 9.9 Recommended Clearance Gap Between Hardware Components for Different Hardness Elastomer Seals at Different Pressures

Pressure (psi)	Elastomer Shore Hardness			
	60A	70A	80A	90A
5000	X	X	0.0004 in.	0.002 in.
3000	X	0.0002 in.	0.002 in.	0.008 in.
2000	X	0.0015 in.	0.0055 in.	0.010 in.
1000	0.002 in.	0.007 in.	0.012 in.	0.018 in.
500	0.010 in.	0.015 in.	0.020 in.	0.025 in.
100	0.030 in.	0.033 in.	0.035 in.	0.036 in.

If an elastomer is treated as an incompressible fluid, its viscosity is directly correlatable to its hardness. Thus, an 80 Shore A elastomer would have a higher viscosity than a 70 Shore A material and would exhibit a higher compressive force. Compressive force relates directly to the sealing force that an elastomer exhibits. Compression modulus is the ratio of compressive stress to compressive strain [45]. This is simply compressive force versus deflection.

Squeeze-Type Seals

The O-ring is a toroidal shaped ring (Fig. 9.8). Most O-rings are molded from elastomeric materials to always be consistent in size and tolerance. The O-ring is installed in a groove designed to accommodate it and to allow firm contact with both the inner and outer walls of the groove. Thus, it is squeezed out of round when confined in the groove. As pressure is applied, the ring deforms against the surface to be sealed. As pressure is increased, the tighter the seal becomes (Fig. 9.14).

The O-ring is pressure responsive and seals at high pressures despite minor wear or cuts in the seal or somewhat irregular sealing surfaces. The O-ring is easily installed in one piece glands, thus simplifying engineering designs. The O-ring makes an excellent static seal but has some limitations as a dynamic seal. In high-pressure applications, O-rings have a tendency to roll because of their high friction. This can limit the life of the O-ring. This effect can be minimized by lowering the frictional characteristics of the elastomer using internal lubes or newly developed polymer modification techniques that reduce the friction of the elastomer to the range of PTFE. Friction reduction of the O-ring by minimizing squeeze is not recommended. The sealing force is changed and it is a short-term solution that will produce premature leakage.

O-rings at a high pressure exhibit a tendency to flow into the space between the hardware elements. This extrusion can lead to nibbling or cutting of the O-ring, resulting in premature failure. To protect the O-ring from this effect, an antiextrusion device usually called a backup ring is used [46–50]. The sole purpose of the backup ring is to maintain zero diametrical clearance, preventing extrusion of the O-ring.

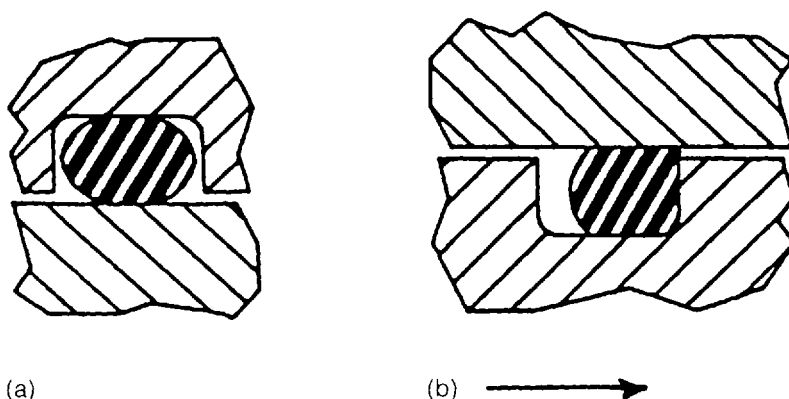


Figure 9.14 Illustration of an O-ring's location in the seal gland at (a) zero pressure and when (b) high pressure is applied, forcing the O-ring against the gland wall to seal the gap between the hardware components.

An O-ring with a low friction elastomer and backup rings can be a very effective dynamic seal (Fig. 9.15).

Because the O-ring was developed and became the primary seal in hydraulic and pneumatic systems, other compression-type seals have been designed primarily to accommodate the perceived shortcomings of the O-ring. These include T-seals, X-rings, D-rings, and many proprietary shapes. However, the O-ring has been a key element in the advancement of highly efficient fluid power systems.

The “rules of thumb” for dynamic elastomer seals are the same regardless of geometric shape. These include the following:

- Choose a seal material that provides reliable, functional service at the system’s maximum system temperature for at least 1000 h.
- Determine the low-temperature seal capability from its T_c and TR_{10} values. Under normal circumstances, the seal should be effective up to 15°F below the TR_{10} value.
- Squeeze less than 5% and greater than 25% can result in enhanced compression set and leakage.

During installation, the elastomer seal should not be stretched beyond 100%. If stretch exceeds 20% during installation, the seal should be allowed to fully recover before final assembly of the hardware. Installed stretch of a dynamic seal should not exceed 5%. Seals deteriorate under excessive stretch. EPDM, FKM, CR and urethane elastomers are the best for high stretch. NBR elastomers are the worst. Excessive stretching leads to the Joule effect [28] and may result in seal leakage. The Joule or Gow–Joule effect can be demonstrated with a thick rubber band and a match. Stretch the rubber band between your fingers and bring the match close to the rubber band. The rubber band might be expected to stretch further. However, the opposite occurs. When a piston seal is stretched excessively, it heats up due to friction and system temperature, pulls away from the bore, and tightens its grip on the piston. The sealing force on the bore is reduced and leakage occurs. In a rod situation, the seal would tighten on the rod and pull away from the base of the groove.

If the stretch is greater than 2–3%, the cross section of the seal is reduced. This is sometimes ignored because significant stretch is thought to produce a better

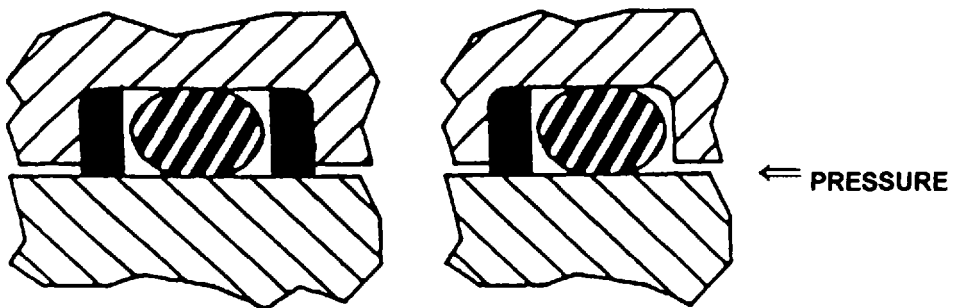


Figure 9.15 Illustration of the use of backup rings with elastomer seals. Two backup rings are used when the pressure is reversible and one backup ring is used when the pressure is always unidirectional; this backup ring is positioned at the downstream side of the pressure direction.

seal based on the belief that stretch exhibits more sealing force on the two sealing elements. What is ignored is the Gow–Joule effect and the fact that the seal cross section is reduced approximately 50% of the diametral stretch. Thus, a seal that is stretched 16% suffers an approximate 8% reduction in cross section.

Differential pressure must be greater than 50 psi to distort a seal beyond installation squeeze.

Dynamic seals are normally designed for a maximum of 85% gland occupancy [51–55]; thus, seal swell is an important factor. A seal that swells excessively can soften and abrade. It can leave the gland, and tearing and extrusion can result. An overoccupied gland can change seal force and system frictional characteristics.

Seals can shrink due to incompatibility and dry out. This can also lead to leakage on start-up and during operation. Seal shrinkage of 4% or more can lead to leakage.

Seal friction is not normally considered in system design because in a standard operating system, the seal eventually rides on an oil film which lubricates the seal and reduces friction. However, short strokes, long extent strokes after long downtimes, eccentricity, and wear prevent a uniform oil layer to fully develop. In these cases, low-friction elastomers offer performance benefits. The additional costs are minimal when considered against the downtime costs due to seal leakage. In a zero leak system, low friction elastomeric seals and scheduled preventive maintenance are necessities.

The following guidelines should be followed to reduce dynamic friction [38]:

- Surface finish of the bore or rod should be better than 16 RMS
- Increase the speed of moving parts
- Decrease seal cross section and hardness
- Decrease the environmental temperatures for pistons and increase it for rods
- Use reduced friction elastomers

When considering reduced-friction elastomers, make sure the following are considered: Additives that are used to reduce friction affect the seal's properties and compatibility; make sure the new seal is compatible. These additives can also contaminate systems. Surface treatments such as chlorination and ion etching are surface treatments which quickly wear away and friction returns. Greases used for installation are washed away, increasing friction. Greases sometimes harden the elastomer when the system heats up. Polymer modified elastomers have a polymer modification inherent in the seal that does not leach out nor is it a surface coating. Good hardware design and the proper choice of seal material and design are important to reduce system friction.

Cap seals are also used to reduce friction [56,57]. A cap seal is typically an elastomer-energized PTFE shape (Fig. 9.16). Although this seal design reduces break away or static friction, it results in higher running friction. It has been felt that the cap seal was the only way to reduce seal friction without compromising hardware design. The cap seal, however, is not a zero leak seal if it is functioning correctly. The cap seal would have limited life in a system if it were not for the oil layer on which the cap eventually rides. As the cap wears, leakage can occur and this is why a cap seal is sometimes used in tandem with an elastomer contact seal. The cap seal is a buffer seal that reduces pressure and the elastomer seal is the primary seal which sees pressures below the system pressure. In this way, the elastomer seal becomes

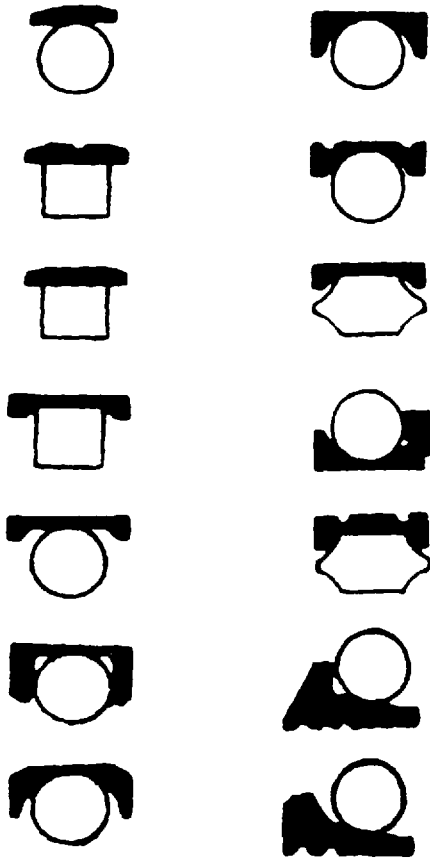


Figure 9.16 Illustration of typical cap seal geometries. These are called cap seals because the cap, which is a plastic element, usually a PTFE material, is energized (or forced against the sealing surface) by an elastomer which, because of its elastomeric nature, can be called an energizer because it exerts a sealing force on the cap.

an effective zero leak seal because it only seals what gets by the buffer seal. Pressure buildup between the seals is addressed in the hardware and/or cap design. The primary seal in this system must have low friction to minimize wear, heat buildup, and hysteresis. A polymer-modified elastomer with its inherent low-friction properties is often used in this position for optimum performance.

Guidelines for designing a sealing system may be summarized into two basic categories: industrial and military. The industrial guidelines are subdivided into static and dynamic, whereas the military guidelines use one design guide to cover both static and dynamic applications. The industrial guidelines result in more stretch and squeeze of the seal, whereas the military guidelines utilize less stretch and squeeze. For static applications, the industrial guidelines are preferred. For dynamic applications, the military guidelines are preferred. Use of military guidelines helps in reducing dynamic friction. These guidelines are presented in Table 9.10.

Table 9.10 Dynamic O-Rings Guidelines; Military Gland Design and O-Ring Selection

O-ring size, 568A series	O-Ring cross section (<i>W</i>)	Gland depth (<i>L</i>)	Squeeze		Diametrical Clearance Max. (<i>D</i>)	Groove width (<i>G</i>) +0.010/ -0.000			Groove radius (<i>R</i>)	Eccentricity max.
			Inches	%		No backup ring	One backup ring	Two backup rings		
001	0.040 ± 0.003	0.031–0.032	0.005–0.012	13.5–28	0.004	0.063			0.005–0.015	0.002
002	0.050 ± 0.003	0.040–0.041	0.006–0.013	13–24.5	0.004	0.073			0.005–0.015	0.002
003	0.060 ± 0.003	0.048–0.049	0.008–0.015	14–24	0.004	0.083			0.005–0.015	0.002
004	0.070 ± 0.003	0.057–0.058	0.009–0.016	13.5–22	0.004	0.094	0.149	0.207	0.005–0.015	0.002
005	0.070 ± 0.003	0.565–0.0575	0.0095–0.0165	14–23	0.004	0.094	0.149	0.207	0.005–0.015	0.002
006–012	0.070 ± 0.003	0.056–0.057	0.010–0.017	15–23	0.004	0.094	0.149	0.207	0.005–0.015	0.002
013–050	0.070 ± 0.003	0.056–0.058	0.009–0.017	13.5–23	0.005	0.094	0.149	0.207	0.005–0.015	0.002
110–129	0.103 ± 0.003	0.089–0.091	0.010–0.017	10–16	0.005	0.141	0.183	0.245	0.005–0.015	0.002
130–178	0.103 ± 0.003	0.089–0.091	0.010–0.017	10–16	0.006	0.141	0.183	0.245	0.005–0.015	0.002
210–284	0.139 ± 0.004	0.1215–0.1235	0.0115–0.0215	8.5–15	0.006	0.188	0.225	0.304	0.010–0.025	0.003
325–395	0.210 ± 0.005	0.186–0.188	0.017–0.029	8.3–13.5	0.007	0.281	0.334	0.424	0.020–0.030	0.004
425–475	0.275 ± 0.006	0.2385–0.2415	0.028–0.425	10.5–15	0.010	0.375	0.440	0.579	0.020–0.030	0.005

When using cap seals, remember that the squeeze on the elastomer is increased by the thickness of the cap, so make sure that for the particular application that the squeeze does not exceed 25%.

Although the above information addresses O-rings specifically, it is also true for all elastomer contact seals. Whether an O-ring or other geometric design is being used, these basic guidelines still apply and it is important to review them with the seal supplier during the design phase. Quite often during system design, the sealing system is considered as an afterthought and this is when problems arise. Seals might be the least expensive component in the hardware; however, they are engineered components of the system and require design attention. Seal material selection and design should be supported by valid technical data. Do not accept seal substitutes until it can be verified that their performance is equivalent or better.

Lip Seals

Lip seals are also used in hydraulic systems. These seals are appropriate for systems that are low speed and operate at low pressure. At higher pressures, they produce increasing friction and accelerated wear [38]. They are pressure activated in the sense that they have low squeeze to begin with, and when exposed to pressure, their lips spread to effect a wider sealing face [38]. Lip seals have to be aligned with their lips facing the pressure direction because they are pressure activated. In the case of systems that operate with pressure reversal, two seals must be used. Lip seals also require special glands [58]. This means that lip seals cannot be retrofitted with a standard squeeze-type seal. This is a definite disadvantage when compared to squeeze-type seals, as most squeeze-type seals can be interchanged in the same gland.

Lip seals can be used up to 800 psi without backup rings. Above 800 psi, backup rings should be used. Some designers consider 1500 psi as the maximum service pressure for lip seals; however, the seals with backup rings have operated at 2500 psi without problems [38]. Because of their light initial squeeze and the way they function, lip seals require a surface finish of 8–16 RMS.

Lip seals vary in lip design and configuration (Fig. 9.17). Lips can be rounded or flat. The seals can be symmetrical or asymmetrical. Depending on the manufac-

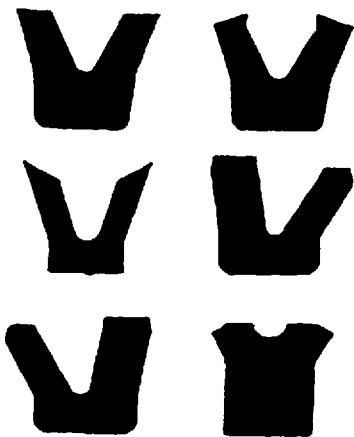


Figure 9.17 Illustration of typical profiles of lip seals.

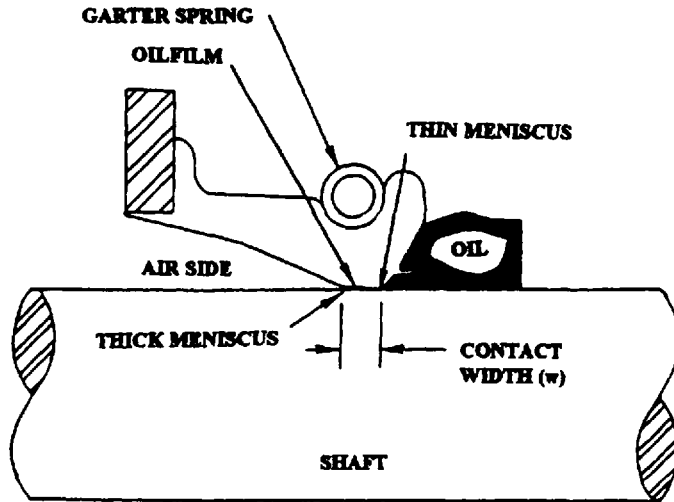


Figure 9.18 Illustration of the principle of operation of a radial lip seal.

turer, a case can be made for each of the configurations and geometry. Lip seals are available in the common polymers as are squeeze-type seals.

9.2.3 Radial Lip Seals

Radial lip seals [59,60] are primarily designed for rotary applications [43,61]. Figure 9.18 illustrates how they operate. Essentially, they act like bearings [62]. An oil film is generated between the lip and shaft. If the oil film thickness is minimal, the meniscus formed at the air side of the interface will not break and leakage will be avoided [43].

An important rule regarding radial lip seals is that they are essentially low-pressure seals [43,63]. Conventional radial lip seals operate between 5 and 10 psi [43,64]. Special seals are available that will operate up to 100 psi. These special seals have broader lips and must operate at slower speeds. Figure 9.19 illustrates how the lip is deformed as pressure is increased. Figure 9.20 shows the influence of pressure on seal life [43,65].

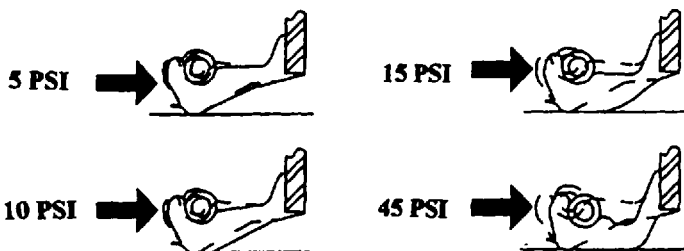


Figure 9.19 Illustration of how the radial seal lip deforms as a function of pressure: The greater the deformation, the greater the seal wear and, consequently, the shorter the seal life.

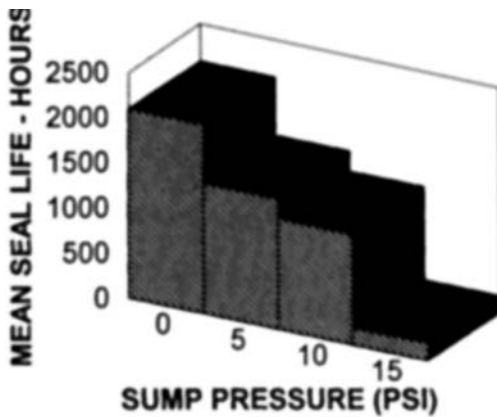


Figure 9.20 Illustration of how sump pressure affects the mean life of radial lip seals.

Normally, a manufacturer will provide peripheral speed limits for his seals, and any rubbing speed up to these limits is acceptable. This speed is typically on the order of 3500 ft/min. From this limitation, it is obvious that shaft size needs to be considered. For shaft sizes under 1.25 in. in diameter, standard seals will work up to 7000–8000 revolutions per minute. For shaft sizes between 2.5 and 3 in. in diameter, the revolutions per minute are reduced to 3000 to 4000. Figure 9.21 shows the effect of shaft speed on seal life [43].

Seal life can be affected by other factors: Shaft size (the smaller the shaft, the longer the seal life), oil viscosity (as oil ages and viscosity changes, seal life is reduced), and fluid additives (seal lips run hot, facilitating fluid additive reaction with the elastomer, causing hardening or softening, and, consequently, affecting seal balance which results in leakage). Friction and heat can result in compatibility problems resulting in hardening and cracking of the seal lip, which leads to seal leakage [43].

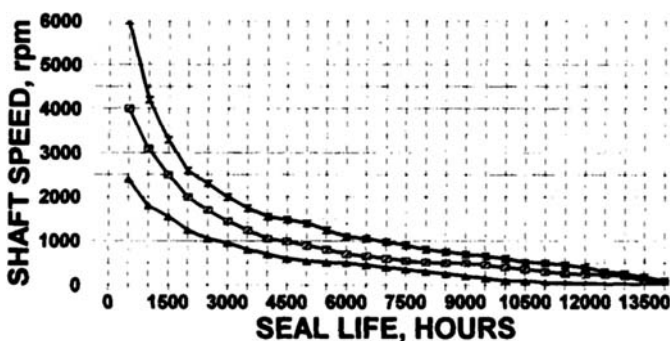


Figure 9.21 Illustration of how shaft speed affects the life of nitrile radial lip seals of various sizes. Higher speed means shorter life; radial lip seals for larger shafts inherently have a shorter life than radial lip seals for smaller shafts. ▲: 3-in.-diameter shaft; X: 0.5-in.-diameter shaft; ■: 1.75-in.-diameter shaft.

Corrosion of the shaft affects seal performance. Nicking, cutting, and pitting of the shaft can affect the nature of the oil film or cause mechanical leak paths, which affect the ability of the seal to work effectively [66]. Case leakage and excessive eccentricity can also affect sealability.

The frictional nature of the elastomer seal lip can radically affect the seal's performance. High friction results in stick-slip, frictional heat buildup, excessive lip wear, hardening of the lip, and elastomer degradation—all of which adversely affect the seal's performance.

Wave seals, helix seals, and other design modifications allow more oil at the lip-shaft interface and, therefore, effect lower friction. This is true during operation. However, the friction and wear problems begin at start-up. It takes time for the oil film to develop, and during this time, the seal lip is running on a dry shaft, generating frictional heat. Some of the newer seal designs minimize the time for the oil film to develop, but they do not eliminate dry start-up. To minimize dry start-up effects, low-friction elastomers should be used. This is an area where polymer modified materials have an advantage. They do not adversely affect the properties of the elastomer lip and provide low friction until the oil film develops. They also serve to minimize or eliminate stick-slip.

Some seals also include wiper lips (Fig. 9.22). These lips are designed to keep the shaft free from dust and dirt that can work its way under the seal and cause leakage.

When using radial lip seals, the following cautions should be employed [43,67,68]:

1. Verify the seal quality prior to installation.
2. Verify that there is no shaft damage that will result in mechanical leakage or change the properties of the oil film.

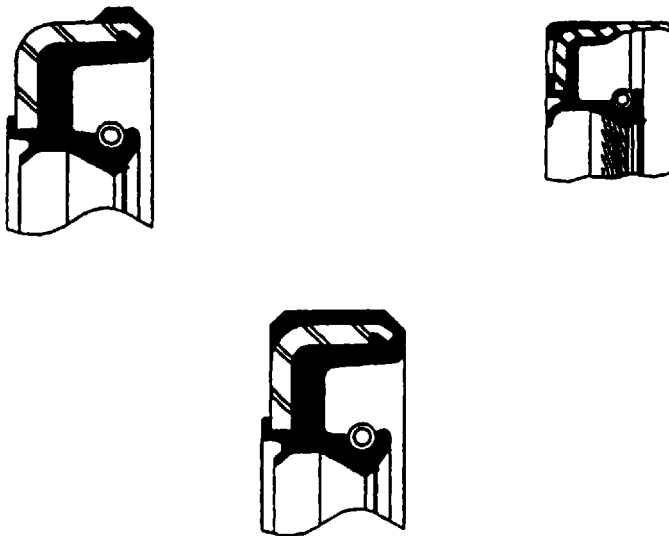


Figure 9.22 Illustration of typical seal lip geometries of radial lip seals with a wiper lip designed to keep external contamination out of the system.

3. Maintain clean oil in the system.
4. Dirty oil affects the viscosity and adversely changes the properties of the oil film.
5. Abrasive debris may result in seal lip abrasion and cutting.
6. Choose the correct elastomer for the application. Incompatibility can affect the thin seal lip more dramatically in this type of seal. It is extremely important to verify the compatibility of the elastomer in the fluid of use at the maximum lip temperature.
7. Remember that the thermal expansion of an elastomer is an order of magnitude greater than that for most metals, and as the elastomer expands, the nature of the lip changes.
8. Properly handle and install the seal.

If seal failure occurs, it is important that a detailed failure analysis is performed so that there is sufficient information available to address the failure and correct it [43]. A failure analysis check list follows. It should be used to accumulate sufficient information to review and analyze so that future failures can be avoided. By following the check list, information is accumulated at the time of failure and not trusted to memory to be recalled at a later time. Similar check lists can be used for all seal failures. This would aid in failure analysis.

Radial Lip Seal Failure Analysis Checklist

1. Note the condition of the system prior to removal

Amount of leakage: Slight Heavy Damp
 Condition of the area: Dirty Clean Dusty
 Leakage observed at: Area between lip & shaft Between seal elements
 Between O.D. & bore At retainer gasket
 Between wear sleeve & shaft At retainer bolt holes

2. After wiping the area clean, inspect for the following:

Nicks on bore chamfer Seal installed improperly
 Shaft to bore misalignment Seal cocked in bore
 Seal loose in bore Seal case deformed
 Paint spray or other deposits on seal

Other _____

3. If shaft can be rotated, observe for

Excessive end play Excessive run out

4. If you could not determine the seal leak, dust the area with talcum powder and operate the system for approximately 15–20 min and see if the location of the leak can be determined.

Location _____

5. Mark the seal so you know how it was positioned and retain an oil sample for cleanliness and viscosity determination.

6. Inspect the hardware upon seal removal for

Shaft: Clean Discolored Corroded Damaged
 Rough bore surface Deposits or coke on shaft
 Flaws or pits in bore

7. Seal observations:

Primary lip Soft Normal Hardened Damaged
 Lip wear: Excessive Eccentric Normal None
 Seal O.D.: Damaged Axial scratches or scores Normal
 Spring: In place Missing Separated Corroded

The effects of leakage are accumulative. When a few drops of leakage appear, sometimes they are ignored because after all: "It's just a few drops." Table 9.11 shows what a few drops really mean. Considering that there are 45 gal per barrel, a few drops of leakage affects the overall operating cost. Once a leak starts, it never gets smaller. Making sure that operations start with the correct seal and a leak-free system is important, as downtime costs to change out the seal can be high.

Radial lip seals may also be used in reciprocating systems. In this case, selected seals must be designed for this use. Normally, these seals have thicker lips and will work in systems where the surface speed is limited to 40 ft/min.

O-rings can also be used as a rotating shaft seals [38]. O-rings will give satisfactory performance up to speeds of 1500 ft/min. To use an O-ring in a rotary application, the following guidelines need to be employed:

- The O-ring should be located in a groove in the mating member.
- The O-ring should be located as close to the lubricating fluid as possible.
- There should be little to no stretch on the O-ring.
- The O-ring should be used only as a seal and not as a load-bearing device.
- The concentricity should be better than 0.005 in.
- The smallest possible cross-section O-ring should be used.

Design guidelines for O-rings in rotary applications are listed in Table 9.12.

9.2.4 Mechanical Face Seals

Mechanical face seals are used to prevent leakage in rotating shaft applications that exceed the capabilities of radial lip shaft seals and packings [43]. The seals have no

Table 9.11 Oil Volume Lost by Leakage

Leakage rate	Loss per day (gal)	Loss per week (gal)	Loss per month (gal)
1 drop/10 s	0.09	0.66	2.7
1 drop/5 s	0.19	1.32	5.6
1 drop/s	1.05	7.32	31.5
3 drops/s	3.15	22	94
5 drops/s	5.25	36.6	157.5
Drips	20.0	140	420

Table 9.12 O-Ring Design Data for Rotary Applications; Groove Dimensions

Cross-section		Maximum rubbing speed (ft/min)	Gland depth	Diametral clearance (<i>E</i>) ^a	Groove width	Groove radius (<i>R</i>)	Eccentricity max. ^b	Bearing length minimum
Nominal	Actual							
1/16	0.070 ± 0.003	1500	0.065–0.067	0.012–0.016	0.075–0.079	0.005–0.015	0.002	0.700
3/32	0.103 ± 0.003	600	0.097–0.099	0.012–0.016	0.108–0.112	0.005–0.015	0.002	1.030
1/8	0.139 ± 0.004	400	0.133–0.135	0.016–0.020	0.144–0.148	0.010–0.025	0.003	1.390

^aFor maximum working pressure of 500–750 psi; for higher pressures, clearances would be reduced.

^bTotal indicator reading between the groove O.D., and shaft and adjacent bearing surface.

universal standards because designs and applications vary significantly. Four typical seal configurations are shown in Fig. 9.23. The seals tend to be customized for the specific application and differ widely based on specific application. They have significant advantages over radial shaft seals: They can handle all types of fluids—acids, salts, some abrasive media, and so on. They function in slightly misaligned and nonconcentric situations. They work with bidirectional shaft rotation, high pressure, temperature, and speed excursions. The condition of the shaft is not as critical for their performance and they normally have long operating lives.

However, mechanical face seals require more space and unique configurations. The seal must be optimized for the specific applications, and because they replace an existing seal with a new design, hardware modifications are normally required. Mechanical face seals cannot handle axial end play. The sealing faces must be finished smooth ($0.08\text{--}0.4\ \mu\text{m}$) and can easily be damaged [43]. They cost significantly more initially because they are highly specialized and require hardware modifications.

The performance of mechanical face seals is dependent on geometric, hydrodynamic, and thermal effects [38]. All of these factors interact and make mechanical face seal designs complex. The geometric factors include face deformation, shaft

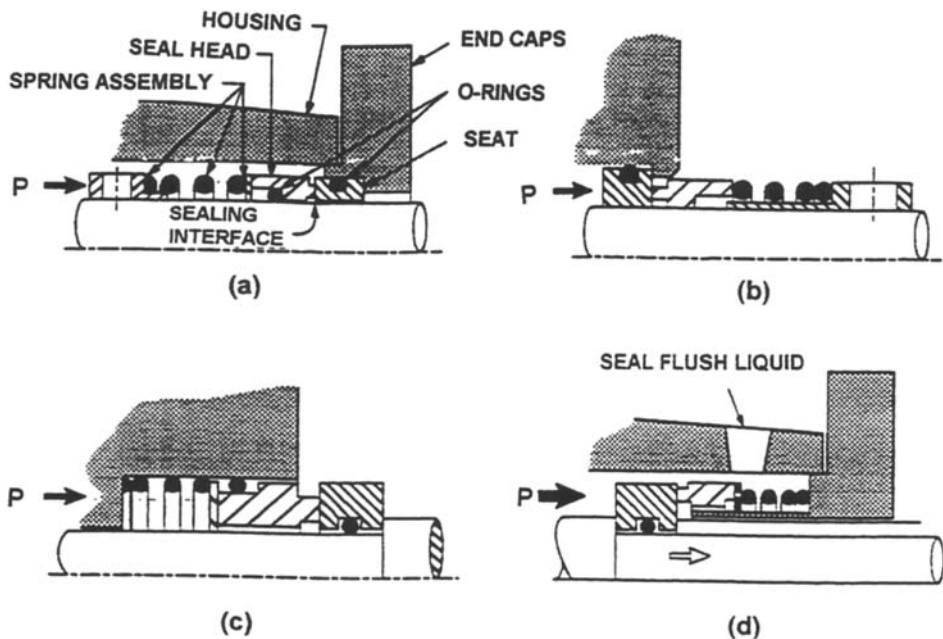


Figure 9.23 Illustrations of typical mechanical seal configurations. (a) Rotating seal head pressure on the outside diameter of the faces; (b) rotating externally mounted seal head pressure on the inside diameter of the faces; (c) stationary internally mounted seal head pressure on the inside diameter of the faces; (d) stationary externally mounted seal head pressure on the outside diameter of the faces.

eccentricity, misalignment, and vibration. Hydrodynamic effects concern the fluid to be sealed and include viscosity, lubricity, and surface tension. Thermal effects include vapor pressure and the sealing face heat buildup due to friction and thermal conductivity.

Mechanical face seals are not zero leak seals. For a 2-in. seal operating at 3000 rpm, typical leakage is 0.1–10 cm³/h. When volatile fluids are sealed, liquid-phase leakage may appear to be zero, but vapor-phase leakage on the order of 0.1–10 g/h is possible. Vapor-phase leakage may also occur when the seal is stationary. A first approximation of leakage can be estimated by

$$L(\text{cm}^3/\text{h}) = 2 \times 10^{-4} \eta^{0.5} \left(\frac{N}{P} \right)^{1.5} D_o p b^2$$

where

η = absolute viscosity of the liquid being sealed (N·s/m²)

N = rotational speed (rpm)

P = closing force per unit area of interface (MPa)

D_o = outside diameter of seal interface (mm)

p = sealed pressure differential (MPa)

b = interface radial width (mm)

Mechanical face seals are best specified by working with the seal manufacturer and it is critical that during the specification process, all system parameters and requirements are reviewed. Key requirements that the mechanical face seal should meet are specific to the application [38,43]. These are listed below and it is important that the seal manufacturer demonstrate how these requirements are to be met for the seal being recommended for the application.

For *water and fuel applications*, low shaft erosion, high-temperature operational capability, and abrasion resistance are key seal requirements. For *slurries*, the seal should be abrasion resistant. For *food and medical applications*, the seal must include all approved materials. The seal needs to be abrasion resistant. It should have a profile that eliminates trapping of material and it should be capable of withstanding multiple system sterilizations.

For mildly corrosive fluids and refrigerants, the seal needs to have low shaft erosion; it must have corrosion resistant materials and be abrasion resistant. It must have demonstrated low leakage. For highly corrosive fluids, it should meet the same requirements for seals used with mildly corrosive fluids and, in addition, have predictable life so that preventive maintenance can be performed prior to seal failure.

For hydrocarbons, seal requirements are dictated by the operation temperature of the system. For hot systems, the seal should have low shaft erosion, abrasion resistance, and low leakage, and be capable of high-temperature operation. For lower-temperature systems, the seal must have low leakage and be capable of sealing high pressures at low temperature.

For gas compressors, the seal must be capable of operating at high temperature and pressure with low leakage. It must also accommodate high shaft speeds.

Although most of the discussion on seal requirements, design, and performance are specific to the application, there are some basic properties of the seal face:

Hardness of seal face materials is expressed in values on the Moh scale [43].

Hardness for a seal face material is a measure of the material's resistance to scratching. The Moh scale ranges from 1 for talc to 10 for diamond. For a mechanical face seal to function properly, the wear plates should have a higher hardness than the mating seal face. The wear plate should also have a higher hardness than any particulate matter suspended or found in the fluid.

Stiffness in the seal face resists distortion caused by pressure gradients, thermal gradients, and speed distortion. In some applications, low stiffness is desirable to allow the seal to conform to the mating surface. Stiffness can be a function of both material selection and design. Stiffness is reflected by the elastic modulus of the material.

Tensile strength is important in calculating hoop stress, which is the result of internal hydraulic pressure. A seal face must have sufficient tensile strength to withstand the hoop stresses present in the system. Seal design can accommodate a lower-tensile-strength material, but it is important that this is demonstrated prior to seal selection.

A *low coefficient of thermal expansion* is required to resist the risk of failure by thermal shock. This is very important when the elastic modulus is high and the tensile strength and thermal conductivity are low.

Thermal conductivity controls the temperature gradient from localized hot spots. If the thermal conductivity is low, spalling, heat checking, and seal failure can result.

A *high-density sealing face* increases the mass of the rotating parts and can make it difficult to obtain dynamic balance of the seal assembly.

Temperature limitation and *chemical compatibility* are obvious requirements. The sealing face material must be capable of operating in the required temperature range without a drastic change of properties. If there is system incompatibility, seal failure is the result.

Finally, the *seal face must exhibit low wear*. Unfortunately, seal face wear data are not always true indicators of seal wear because of the influence of the actual operating conditions and environment. Laboratory-controlled wear tests on the seal face materials often underestimate the actual seal face wear in an actual service.

As with all other seals, mechanical face seals do have finite life and it is important to analyze the seal failure to make changes or to at least assess predicted life to avoid unanticipated system shutdowns. If premature leakage occurs, this could be the result of improper seal selection, use, or installation. It could also be the result of incorrect material usage. If a seal fails due to leakage, it is important to note the conditions prior to failure and the condition of the hardware, fluid, and seal on disassembly. This information is important for determining the cause of failure and implement corrective action. The items that need to be observed and noted include the following: Does the seal leak steadily whether the shaft is rotating or stationary? Is there steady leakage at low pressure and no leakage at high pressure? Is there steady leakage when the shaft is rotating but little to no leakage when the shaft is stationary? Is there visible seal damage? If there are elastomers present, what are their condition? Is there hardware damage? Did the seal appear to be installed correctly?

10 SUMMARY

The subject of seals is often ignored when a system is being designed. This is true more often than not because the seals represent the lowest cost items of the system. They are the afterthought: as long as it is black and round, it should work. A recent ad showed a picture of a \$600,000 O-ring. It had failed prematurely and the resulting cost in system damage, downtime, lost revenue, and lost customers totaled this value. Although this might have been an exaggeration, the message should be clear. As much care and effort should be put into finding the optimum seal for a system as goes into the rest of system design. A system is only as good as the seals used to make it work. *Cost-effective* is a very important term that seems to be ignored in today's hectic environment. Care should be taken in selecting and maintaining the best seals for the system to avoid the \$600,000 O-ring.

REFERENCES

1. M. Morton, ed., *Rubber Technology*, 3rd ed., 1987. Van Nostrand Reinhold: New York.
2. ASTM D 1566, "Standard Terminology Relating to Rubber," American Society for Testing and Materials, Philadelphia, PA.
3. M. A. Fath, "Vulcanization of Elastomers," *Rubber World*, 1993, October, pp. 22–25.
4. B. M. Boyum and J. E. Rhoads, "Elastomer Shelf Life: Aged Junk or Jewels," *IEEE Trans. Energy Convers.*, 1989, 4(2), pp. 197–203.
5. ASTM D 1418, "Standard Practices for Rubber and Rubber Lattices—Nomenclature," American Society for Testing and Materials, Philadelphia, PA.
6. R. O. Babbit, ed., *Vanderbilt Handbook*, 1978, R. T. Vanderbilt Co.: Norwalk, CT.
7. J. Thoermer, J. Mirzo, Z. Szentivanyi, W. Obrecht, and E. Rohde, *Effect of Cross Linking System on the Processing Behavior and Performance Profile of Hydrogenated Rubber (HNBR)*, 1988, Miles Inc.: Akron, OH.
8. C. Hepburn, *Polyurethane Elastomers*, 1982, Applied Science Publishers: London.
9. A. T. Worm and R. A. Brullo, "A High Fluorine-Containing Tetrapolymer for Harsh Chemical Environments," Rubber Division, ACS Meeting, 1983.
10. R. J. Schaefer, "Dynamic Properties of Rubber," *Rubber World*, 1994, September, pp. 17–18.
11. D. L. Hertz, *Chemtech*, 1990, September, pp. 574–576.
12. J. H. Hildebrand and R. L. Scott, *Solubility of Nonelectrolytes*, 3rd ed., 1949. Rheinhold Publishing: New York.
13. A. F. M. Barton, *Handbook of Solubility Parameters and Other Cohesion Parameters*, 1983, CRC press Inc.: Boca Raton, FL.
14. C. Hansen and A. Beerbower, *Kirk Othmer Encyclopedia in Chemical Technology*, A. Standey, ed., *Supplementary Vol.*, 2nd ed., 1971, Wiley-Interscience: New York.
15. W. B. Jensen, *Surface and Colloid Science in Computer Technology*, K. L. Mittal, ed., 1987, Plenum Press: New York, pp. 27–59.
16. A. Beerbower and J. R. Dickey, *Am. Soc. Lubric. Eng. Trans.*, 1969, January, p. 12.
17. J. Eleftherakis, "A New Method of Determining Hydraulic Fluid/Elastomer Compatibility," 40th Annual Earthmoving Industry Conference, 1989.
18. K. M. Pruet, *Chemical Resistance Guide for Elastomers*, 1988, Compass Publications: La Mesa, CA.
19. J-120a "Rubber Rings for Automotive Applications," Society of Automotive Engineers, Warrendale, PA, 1968.
20. AMS 7270J, "Rings. Sealing, Butadiene-Acrylonitrile (NBR) Rubber Fuel Resistant 65-75," Society of Automotive Engineers, Warrendale, PA.

21. MIL-P-25732C, "Packing, Preformed, Petroleum Hydraulic Fluid Resistant, Limited Service at 275°F (132°C)," Naval Publications and Forms Center, Philadelphia, PA.
22. MIL-R-7362C, "Rubber, Synthetic, Solid, Sheet and Fabricated Parts, Synthetic Oil Resistant," Naval Publications and Forms Center, Philadelphia, PA.
23. ASTM D 943, "Standard Test Method for Oxidation Characteristics of Inhibited Mineral Oils," American Society for Testing and Materials, Philadelphia, PA.
24. ASTM D 2000, "Classification System for Rubber Products in Automotive Applications," American Society for Testing and Materials, Philadelphia, PA.
25. ISO/CD 15272-4, "Fluid Systems—Sealing Devices—Metric O-Rings for Industrial Applications Part 4: Recommended Elastomeric Materials," National Fluid Power Association, Milwaukee, WI.
26. NF T 47-503, "Rubber O-Rings—Material Requirements for the Common O-Ring Types," French Commission of Normalization, 1996.
27. C. R. Peacock, "Quality Control Testing of Rubber Shear Modulus," *Elastomerics*, 1992, 42, pp. 42–45.
28. *The Language of Rubber*, 1957, E. I. du Pont de Nemours & Co. (Inc.): Wilmington, DE.
29. A. N. Gent, ed., *Engineering with Rubber—How to Design Rubber Components*, 1992, Oxford University Press: New York.
30. M. Seabury, "Compatibility of Elastomer Seals and Industrial Hydraulic Fluids," in ASTM D02 Meeting, 1995.
31. MIL-G-5514, Rev G, "Gland Design; Packing; Hydraulics, General Requirements for," Naval Publications and Forms Center, Philadelphia, PA.
32. AS-4716, "Aerospace standard, Gland design, O-Ring and Other Elastomeric seals," Society of Automotive Engineers, Warrendale, PA.
33. AS-568A, "Aerospace Size Standards for O-rings," Society of Automotive Engineers, Warrendale, PA.
34. ASTM D 1414, "Test Methods for Rubber O-Rings," American Society for Testing and Materials, Philadelphia, PA.
35. ASTM D 1415, "Test Methods for Rubber Property—International Hardness," American Society for Testing and Materials, Philadelphia, PA.
36. ASTM D 412, "Test Methods for Vulcanized Rubber and Thermoplastic Rubbers and Thermoplastic Elastomers—Tension," American Society for Testing and Materials, Philadelphia, PA.
37. D. Vander Laan, "Compatibility of Elastomer Seals and Industrial Hydraulic Fluids," in National Fluid Power Association Meeting, 1996.
38. *Seals and Sealing Handbook*, 1986, DuPont de Nemours International S. A., Geneva.
39. J-515, "Hydraulic O-Ring," Society of Automotive Engineers, Warrendale, PA.
40. MA 2010, "Packing, Preformed—O-Ring Seal Standard Sizes & Size Codes, Metric," Society of Automotive Engineers, Warrendale, PA.
41. ISO 3601-1, "Fluid systems—Sealing Devices—O-Rings—Part 1: Inside Diameters, Cross Sections, Tolerances and Size Identification," National Fluid Power Association, Milwaukee, WI.
42. ANSI/B93.35M, "Cavity Dimensions for Fluid Power Exclusion Devices (Inch Series)," American National Standards Institute, New York.
43. R. V. Brink, editor, *Handbook of Fluid Sealing*, 1993, McGraw-Hill: New York.
44. *O+P Round Table: Leakages - Are They Inevitable?*, Germany, 1996.
45. L. P. Smith, *The Language of Rubber*, 1993, Butterworth-Heinemann Ltd.: Oxford.
46. MIL-R-8791/1, "Retainer, Packing, Hydraulic and Pneumatic Polytetrafluoroethylene Resin (Single Turn)," Naval Publications and Forms Center, Philadelphia, PA.
47. MS-27595D, VN, "Retainer, Packing Back-up, Continuous Ring, PTFE," Naval Publications and Forms Center, Philadelphia, PA.

48. MS-28782D, VN, "Retainer, Packing Back-up, Teflon," Naval Publications and Forms Center, Philadelphia, PA.
49. MS-28783E, Notice 1, "Ring, Gasket, Back-up Teflon," Naval Publications and Forms Center, Philadelphia, PA.
50. ARP-1802A, "Selection and Application of Polytetrafluoroethylene (PTFE or TFE) Backup Rings for Hydraulic and Pneumatic Fluid Power Applications," Society of Automotive Engineers, Warrendale, PA.
51. ANSI/B93.76M, "Hydraulic Fluid Power—Cylinder Rod and Piston Seals for Reciprocating Applications—Dimensions and Tolerances of Housing," American National Standards Institute, New York.
52. ANSI/B93.93M, "Hydraulic Fluid Power—Cylinders—Piston Seal Housings Incorporating Bearing Rings—Dimensions and Tolerances," American National Standards Institute, New York.
53. ARP-1232A, "Gland Design, Elastomeric O-Ring Seals, Static Radial," Society of Automotive Engineers, Warrendale, PA.
54. ARP-1233, "Gland Design, Elastomeric O-Ring Seals, Dynamic Radial, 1500 psi Max," Society of Automotive Engineers, Warrendale, PA.
55. ARP-1234A, "Gland Design, Elastomeric O-Ring Seals, Static Axial, Without Back-up Rings," Society of Automotive Engineers, Warrendale, PA.
56. AIR-1244, "Selecting Slipper Seals for Hydraulic-Pneumatic Fluid Power Applications," Society of Automotive Engineers, Warrendale, PA.
57. AIR-1243, "Anti-Blow-By Design Practice for Cap Strip Seals," Society of Automotive Engineers, Warrendale, PA.
58. *Hydraulic Seals, Engineering Manual and Catalog*, 1988, Disogrin Industries, Manchester, NH.
59. J-111, "Seals—Terminology of Radial Lip," Society of Automotive Engineers, Warrendale, PA.
60. ISO 6194-2, "Rotary Shaft Lip Type Seals—Part 2: Vocabulary," National Fluid Power Association, Milwaukee, WI.
61. OS-4, "Technical Bulletin: Application Guide for Radial Lip Type Shaft Seals," Rubber Manufacturers Association, Washington, DC.
62. E. Jagger, "Rotary Shaft Seals—The Sealing Mechanism of Synthetic Rubber Seals Running at Atmospheric Pressure," in *Proceedings of the Institute of Mechanical Engineers*, 1957.
63. OS-6, "Radial Lip Seals, Shaft Seals, Radial Force Measurement," Rubber Manufacturers Association, Washington, DC.
64. J-110, "Seals—Testing of Radial Lip," Society of Automotive Engineers, Warrendale, PA.
65. OSU-HS-1, "Method for Determining the Pressure Sealing Capabilities of a reciprocating Hydraulic Seal," Fluid Power Research Center, Oklahoma State University, Stillwater, OK, 1972.
66. OS-1, "Handbook: Shaft Finishing Techniques for Rotating Shaft Seals," Rubber Manufacturers Association, Washington, DC.
67. OS-7, "Technical Bulletin: Storage and Handling Guide for Radial Lip Type Shaft Seal," Rubber Manufacturers Association, Washington, DC.
68. OS-16, "Recommended Methods for Assuring Quality of Radial Lip Seal Characteristics," Rubber Manufacturers Association, Washington, DC.

BIBLIOGRAPHY

- ANSI/B93.98M, "Rotary Shaft Lip Seals—Nominal Dimensions and Tolerances," American National Standards Institute, New York.

- ANSI/B93.58M, "Fluid Systems—O-Rings—Inside Diameters, Cross-Sections, Tolerances and Size Identification," American National Standards Institute, New York.
- ANSI/B93.62M, "Method of Testing, Measuring and Reporting Test Results for Reciprocating Dynamic Hydraulic Fluid Power Sealing Devices," American National Standards Institute, New York.
- ANSI/B93.111M, "Fluid Power Systems and Components—Cylinders—Housings for Rod Wiper Rings in Reciprocating Applications—Dimensions and Tolerances," American National Standards Institute, New York.
- T3.19.25-1995, "Information Report—Fluid Power Systems—Sealing Devices—Storage, Handling and Installation of Elastomeric Seals and Exclusion Devices," National Fluid Power Association, Milwaukee, WI.
- MIL-P-19918 (1), "Packing V Ring," Naval Publications and Forms Center, Philadelphia, PA.
- OS-5, "Technical Bulletin: Garter Springs for Radial Lip Seals," Rubber Manufacturers Association, Washington, DC.
- OS-8, "Handbook: Visual Variations Guide for Rotating Shaft Seals," Rubber Manufacturers Association, Washington, DC.
- OR-1, "Handbook: O-Ring Inspection Guide: Surface Imperfections Control," Rubber Manufacturers Association, Washington, DC.
- OR-2, "Technical Bulletin: Compression Set and Its Relationship to O-Ring Performance," Rubber Manufacturers Association, Washington, DC.
- OR-6, "Technical Bulletin: O-Ring Standard Dimensional Measurement Practices," Rubber Manufacturers Association, Washington, DC.
- OR-7, "Technical Bulletin: Test Methods for O-Ring Compression Set in Fluids," Rubber Manufacturers Association, Washington, DC.
- AIR-1707, "Patterns of O-Ring Failures," Society of Automotive Engineers, Warrendale, PA.
- AS-708A, "Top Visual Quality (TVQ) O-Ring Packings and Gaskets, Surface Inspection Guide and Acceptance Standards," Society of Automotive Engineers, Warrendale, PA.
- A. K. Bhowmick, ed., *Rubber Products Manufacturing Technology*, 1994, Marcel Dekker, Inc.: New York.
- R. S. Fein, "Boundary Lubrication," *Lubrication*, 1971, 57(1), pp. 3–12.
- P. E. Johnston, "Using the Frictional Torque of Rotary Shaft Seals to Estimate the Film Parameters and the Elastomer Surface Characteristics," in *8th International Conference of Fluid Sealing (BHRA)*, 1978.
- O-Ring Handbook ORD5700*, 1991, Parker Seal Company, Lexington, KY.

10

Bench and Pump Testing of Hydraulic Fluids

LIN XIE

Solid Works Corporation, Concord, Massachusetts

ROLAND J. BISHOP, JR. and GEORGE E. TOTTEN

Union Carbide Corporation, Tarrytown, New York

1 INTRODUCTION

One method of evaluating lubrication properties of a hydraulic fluid is to perform a test in the hydraulic pump (or motor) of interest. However, this is clearly impractical in view of the numerous pump manufacturers and models available. This issue may be further complicated because various types of pumps may be configured differently or manufactured with different materials, depending on the pump manufacturer. This problem could be greatly simplified with the use of one or at least a limited number of “standard” hydraulic pump tests.

One standard test, ASTM D-2882 [1], has been developed for this use. This test is conducted for 100 h with a Sperry–Vickers V-104 vane pump with a 5-gal (19.9-L) reservoir at 65°C, 13.8 MPa (2000 psi), and 1200 rpm, using an 8-gal/min (30.3-L/min) cartridge. The German specification, DIN 51389, is the same except that the test is conducted for 250 h, 50°C, 10.3 MPa (1500 psi), and 1500 rpm. Recently, the American automotive industry has issued a hydraulic fluid testing specification also incorporating the Sperry–Vickers V-104 vane pump [2].

Although the Sperry–Vickers V-104 vane pump has wide acceptance and has served the industry well, it does possess a number of disadvantages, such as relatively high cost per test and a test duration that is sufficiently long to preclude its use for such applications as quality control testing and general fluid development, as well as used fluid performance troubleshooting. Therefore, it would be desirable to develop a faster, lower-cost “bench test” as a viable alternative to routine pump testing.

In Section 2.1 of this chapter, the “bench-test” performance results using a number of ASTM test procedures to comparatively evaluate the lubrication performance of a number of experimental hydraulic fluids relative to the results obtained for the same fluids using ASTM D-2882 will be reported. A summary of custom-designed bench tests that have been reported to successfully model V-104 vane-pump antiwear results will be discussed. This will be followed by a discussion of the evaluation of expected lubrication performance based on fundamental lubrication concepts. Finally, general recommendations will be offered for consideration for future hydraulic fluid “bench-test” development.

Silva published a thorough review of the wear mechanisms in hydraulic pump operation [3]. The role of cavitation, adhesion, corrosion, and abrasion wear was described. Also discussed was the role of fluid viscosity and the speed and loading at the wear contact as modeled by the classic Stribeck curve illustrated in Fig. 10.1. However, discriminating methods of experimental modeling of pump wear were not discussed.

There are numerous references to the use of hydraulic pump tests to evaluate component durability [4,5] or to evaluate some aspect of component design features on either the efficiency or mechanism of energy transfer. However, there are fewer references on the development and use of hydraulic pumps as “tribological tests” to evaluate fluid lubrication wear.

There have been some references describing the impact of fundamental lubrication properties of hydraulic fluids, such as film thickness, on pump wear using the hydraulic pump as a tribological test [6]. However, there are a number of problems with such testing procedures which include pump cost, energy, and components, relatively long testing times, relatively poor manufacturing precision of some of the components for use in reproducible tribological testing, and volumes of fluid required and subsequent disposal. Therefore, there has been a long-standing effort to develop “bench-test” alternatives to evaluate hydraulic fluid lubricity [7].

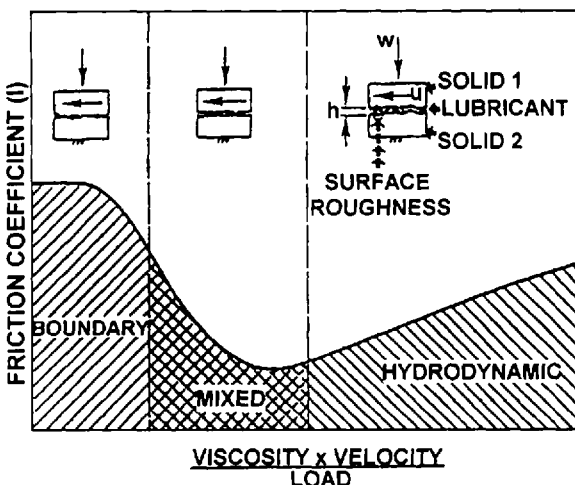


Figure 10.1 Illustration of the effect of wear contact loading and speed, and fluid viscosity on wear (Stribeck curve).

Because standardized bench tests have been generally shown to be unreliable [8–15], pump lubrication often must be examined using hydraulic pumps with a range of test conditions and appropriate material pairs [13]. Section 2.2 of this chapter will provide an overview of various pump testing procedures that have been used to study hydraulic fluid lubrication. This discussion will include vane-, piston-, and gear-pump testing procedures and also a summary of evaluation criteria will be provided.

2 DISCUSSION

2.1 Part I: Bench-Test Correlation [16]

2.1.1 ASTM D-2882 Test Results

The pump tests were conducted according to ASTM D-2882 [1] with the following modifications:

- A 1-gal reservoir was used. (ASTM D-2882 calls for a 5-gal reservoir.)
- Instead of solvent flushing, as required by ASTM D-2882, the pump was dismantled; the heat exchanger and recirculation hoses were removed and cleaned individually and thoroughly to eliminate any possibility of system contamination.

Five experimental fluids representing a wide range of wear, but not pump failure, were evaluated. Where sufficient quantities of fluid were available, the pump tests were run in duplicate. The results obtained are shown in Table 10.1. The fluids selected show four to five orders of magnitude difference in wear rates and the results are reasonably reproducible.

2.1.2 Shell 4-Ball Test Results

Various forms of the Shell 4-ball test are frequently encountered in fluid lubrication tests. Performance criteria as purchasing specifications for hydraulic fluids and for wear characterization of new and used fluids.

The Shell 4-ball test is conducted by mounting four balls; three balls are fixed in the bottom assembly and the top ball is rotated at a constant rpm speed. These and the applied load are shown in Fig. 10.2. This test was conducted according to ASTM D-4172 [17] with an applied load of 40 kg (88 lbs.) and a rotational speed

Table 10.1 ASTM D-2882 Pump Test Results

Fluid ID	Wear rate (mg/h) ^a		
	Trial 1	Trial 2	Average
1	2.2	1.1	1.65
2	0.16	0.06	0.11
3	0.10	0.50	0.30
4	23.0	18.6	20.8

^aThe wear rates were calculated by dividing the total wear of the vanes and the ring (mg) by 100 (h) to give mg/h.

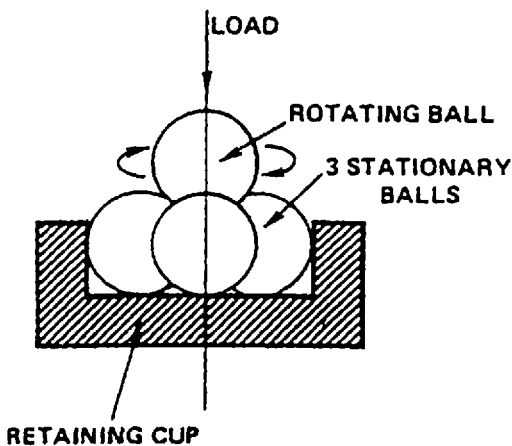


Figure 10.2 Illustration of the four-ball test configuration.

of 1200 rpm. The test was conducted for 1 h and the wear scar was measured. Typically, the temperature range for this test was 23–47°C, as there is no way to control the reservoir temperature on this test rig.

The test results, which are summarized in Table 10.2, showed that although the wear scar was generally reproducible, there was essentially no correlation with the ASTM D-2882 pump test results.

The Shell 4-ball test and a test modification where the bottom three balls were replaced with rollers has been used to characterize polyol ester, phosphate ester, and water–glycol hydraulic fluids [18]. This work showed that these tests gave erratic results, especially for water–glycol hydraulic fluids.

Perez et al. [19–21] developed a “sequential” four-ball test which was reported to provide an excellent correlation with the Sperry–Vickers 35VQ vane pump test [22] for mineral oil, phosphate ester, and water–glycol hydraulic fluids. This test was also used to compare new and used hydraulic fluids [23].

Table 10.2 ASTM D-2882 Correlation with the Shell 4-Ball Wear Scar Results (ASTM D-4172)

Fluid ID	Wear scar (mm)			D-2882 Wear (mg/h)
	Trial 1	Trial 2	Average	
1	0.73	0.79	0.76	1.65
2	0.58	0.58	0.58	0.11
3	0.78	0.71	0.74	0.30
4	0.72	—	0.72	20.8
5	0.51	0.47	0.49	0.01

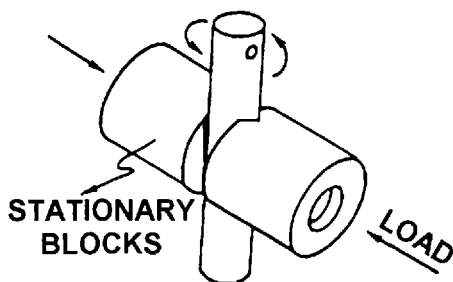


Figure 10.3 Illustration of the Falex pin-on-V-block test configuration.

2.1.3 Falex Pin-on-V-Block Test

Another widely used lubrication antiwear evaluation is the Falex pin-on-V-block test. The test configuration is illustrated in Fig. 10.3. The work discussed here was conducted according to ASTM D-2670 [24].

Wear may be recorded as the number of teeth on the instrument ratchet mechanism advanced over the duration of the test, weight loss, or wear scar. For this work, the number of teeth advanced was evaluated. The results are shown in Table 10.3. (The weight-loss data will be described subsequently.)

One of the greatest disadvantages of these bench tests is that it is not possible to control the reservoir temperature [25]. To evaluate the effect of temperature, this test was conducted with an experimental apparatus equipped with a reservoir temperature control [16]. The use of fluid reservoir temperature gave essentially the same results as described above and did not provide better correlation with the ASTM D-2882 test results [16].

The Falex antiwear test using the pin-on-V-block test configuration was modified to provide a conforming journal contact as shown in Fig. 10.4 [26,27]. Along with the journal contact with a conforming surface, the test system was modified to provide reservoir temperature control and filtration. This system was designated the "gamma-Falex" test and has been reported to successfully model the ASTM D-2882 test when used for water-containing hydraulic fluids (e.g., water-glycol and high-water-base fluids) [25,26,28,29].

Table 10.3 Falex Wear Pin-on-V-Block Test Correlation With ASTM D-2882

Fluid ID	Unheated No. of teeth	Weight loss (mg)	D-2882 Wear rate (mg/h)
1	18, 9 (13.5)	0.0251	1.63
2	24, 30 (27)	0.045	0.11
3	43, 56 (49.5)	0.0601	0.30
4	122		20.8

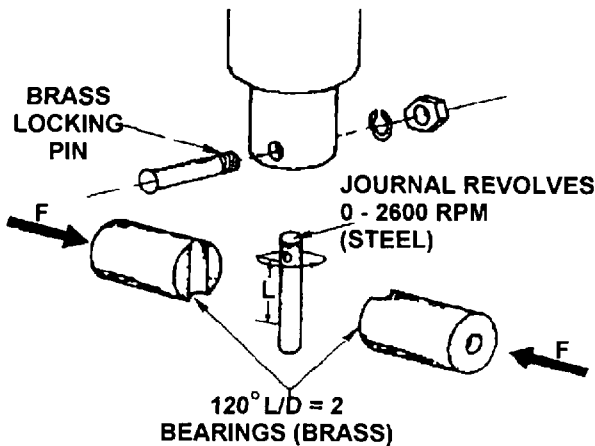


Figure 10.4 Illustration of the wear contact configuration for the gamma-Falex test.

2.1.4 Correlation of SRV Test Results with ASTM D-2882

Another test with a wide variety of possible wear contact configurations is the SRV test. This test was conducted with the ball-on-disk test configuration shown in Fig. 10.5 [30]. The test was conducted at 50°C. The break-in load was 50 N and the test load was 200 N at 50 Hz with a 1.00-mm stroke. The data reported for this test were wear scar (length and width) and the coefficient of friction (maximum and minimum). The results obtained from this study are summarized in Table 10.4. As with the previous studies, no correlation with ASTM D-2882 pump wear was observed.

2.1.5 Timken Test Correlation with ASTM D-2882

The Timken wear test utilizes a block-on-ring wear contact, as illustrated in Fig. 10.6. This test was conducted according to ASTM D-2782 [31] using four of the hydraulic fluids shown in Table 10.1. The fluids used for this work were selected to represent fluids with similar composition but significantly different ASTM D-2882 wear rates. The wear test comparison is provided in Table 10.5, which shows essentially no correlation.

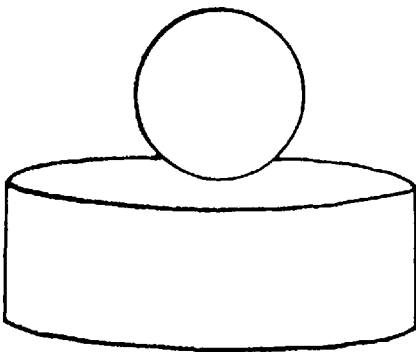


Figure 10.5 Illustration of the ball-on-disk test configuration used for the SRV test.

Table 10.4 SRV Ball-on-Disk Antiwear Test Comparison with ASTM D-2882 Results

Fluid ID	Ball wear scar (mm)		Coeff. of friction		ASTM D-2882 (mg/h)
	Min.	Max.	Min.	Max.	
1	0.65	0.60	0.09	0.115	1.64
2	0.50	0.45	0.06	0.475	0.11
3	0.60	0.55	0.09	0.13	0.30
4	0.75	0.95	0.095	0.130	0.18
5	0.70	0.65	0.096	0.175	20.8
6	0.80	0.80	0.095	0.485	0.008

2.1.6 Cyclic Contact Stress Test Correlation with ASTM D-2882

One common feature of all the bench tests reported thus far is that the geometry of the wear contact is different from the vane-on-ring wear that is actually being measured. One test that has been introduced recently by Falex Corporation is the "Cyclic Contact Stress Test" which actually has a 3-vane-on-disk wear contact, as shown in Fig. 10.7.

The cyclic contact stress test is conducted at a lubricant flow rate of 19 L/min (5 gal/min), 65°C, and 1500 rpm. The load is increased by 45 kg (100 lbs.) every 2 min until a total test load of 360 kg (800 lbs.) is achieved. If the test fails before the maximum load of 360 kg (800 lbs.), the last load to pass the test is recorded. The average torque and coefficient of friction is also reported. The data obtained for the fluids evaluated by this test are summarized in Table 10.6. No simple correlation with ASTM D-2882 wear was observed.

Of the various tests conducted thus far, this test most closely models the ASTM D-2882 wear contact. However, it produced one of the poorest correlations. One possible explanation is that the contact pressure and speed of the bench test may be significantly different from that actually encountered in the pump. Also, better fluid temperature control would be desirable. Therefore, this test is in the process of being

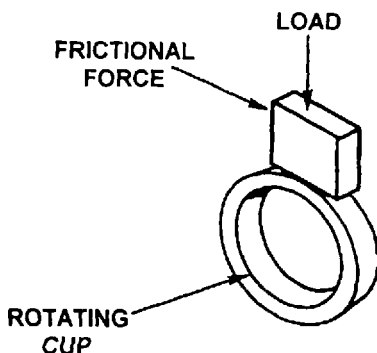
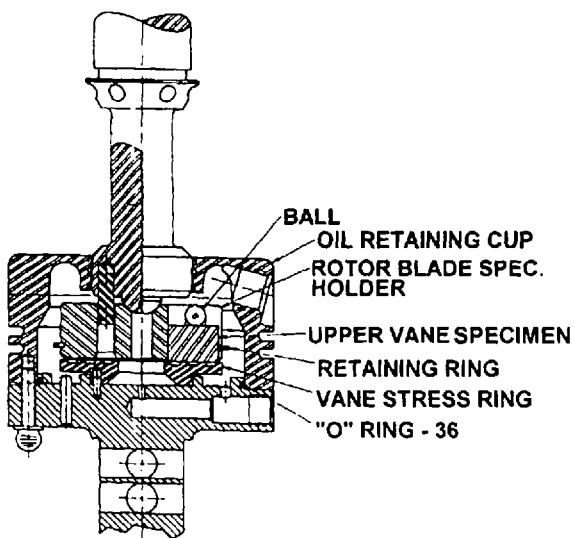


Figure 10.6 Illustration of the block-on-ring wear contact of the Timken wear test.

Table 10.5 Comparison of Timken Wear Test Results with ASTM D-2882

Fluid ID	Timken wear OK load	Test (kg) failure load	D-2882 Wear rate (mg/h)
1	18	21	1.65
2	18	21	0.11
3	15	18	0.30
4	15	18	20.8

**Figure 10.7** Illustration of the 3-vane-on-disk wear contact used for the "cyclic contact stress test."**Table 10.6** Cyclic Contact Stress Test Correlation with ASTM D-2882 Results

Fluid ID	Load (lbs.)	Torque (lb.-in.)	Coeff. of friction	D-2882 (mg/h)
1	700	31.1	0.070	1.65
2	600	27.6	0.068	0.11
3	700	28.4	0.064	0.30
4	700	32.2	0.073	0.008

repeated under wear conditions more closely approximating the condition encountered in the V-104 vane pump.

Jung et al. used a hydraulically operated vane-on-disk test apparatus to study the wear mechanism and lubrication of a vane on a cam ring [32]. The results of this study showed that the vane tip operated in a transition between hydrodynamic to mixed-film lubrication.

2.1.7 FZG Gear Test [33,34]

Reichel has reported the use of an FZG gear test to compare the antiwear performance of a hydraulic oil and vegetable oil with and without the addition of antiwear additives [34,35]. The test configuration of the FZG gear apparatus is illustrated in Fig. 10.8. It is used to measure wear with increasing increments of load. The results of this work, shown in Fig. 10.9 [34], exhibited the expected differences in the antiwear properties of these fluids. However, direct correlations with pump wear was not provided nor was the ability of the FZG gear test to discriminate between small differences in antiwear properties demonstrated.

2.1.8 Custom Bench Tests

Although it would be desirable to conduct bench tests as alternatives to hydraulic pump testing, with few exceptions these tests have provided poor correlation with pump lubrication. For example, Renard and Dalibert found no correlation between either the Shell 4-ball (ASTM D-2596-87 [36]) or "extreme pressure" (ASTM D-2783 [37]) tests and wear results obtained with a Sperry-Vickers V-104 vane pump test (ASTM D-2882) [1]. Knight reported, "... Regrettably the data from these tests not only failed to give quantitative correlation with data determined from machines, but even the ranking between different fluids failed to agree..." [9]. More recently, Lapotko et al. reported that 4-ball test results "... may deviate considerably from

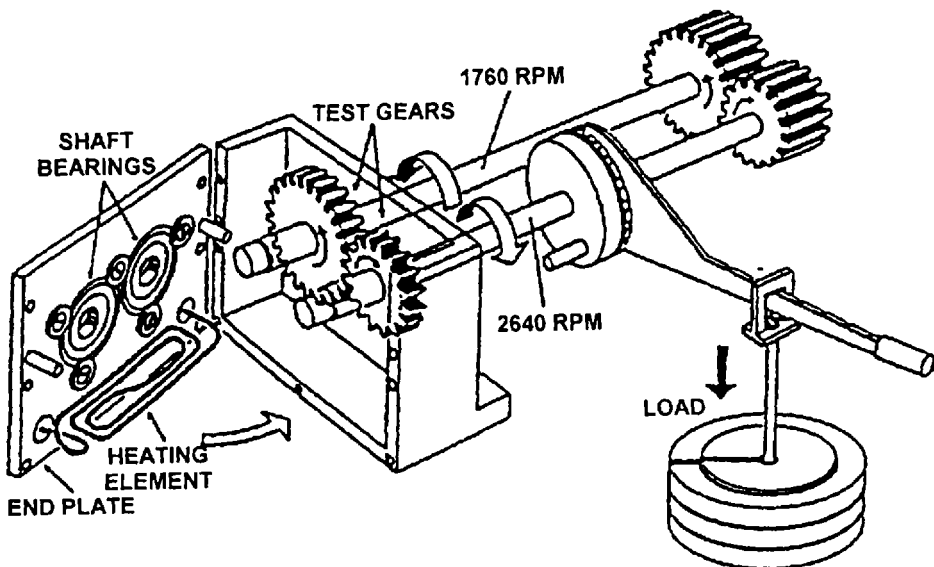


Figure 10.8 Schematic illustration of the FZG gear test machine.

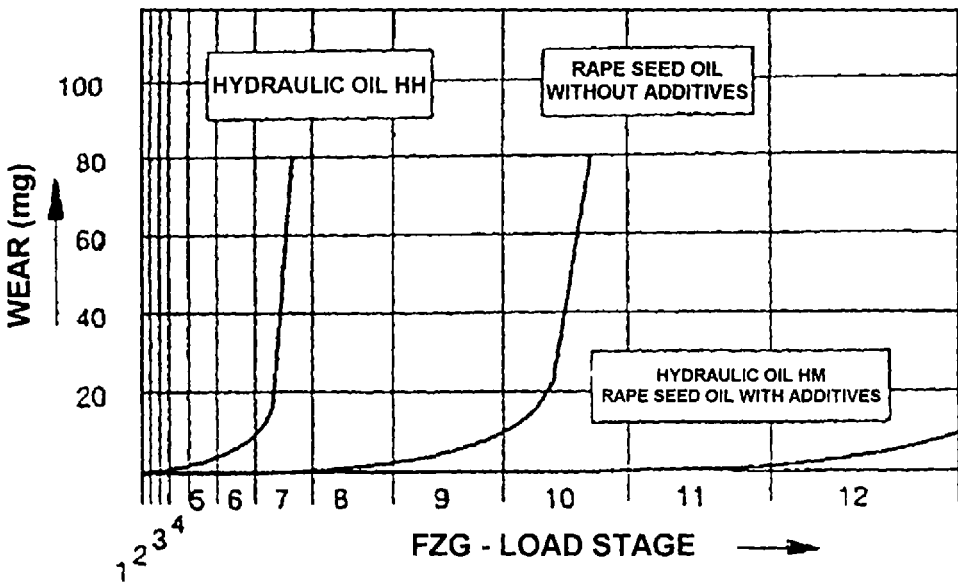


Figure 10.9 Evaluation of the antiwear properties of a rapidly biodegradable hydraulic fluid using the FZG gear test.

the data obtained in actual service . . .” [10]. Urata also found no correlation between 4-ball wear and the V-104C pump wear results for a series of high-water-base hydraulic fluids [38].

These problems were confirmed in the above discussion in which the inability of “standard” bench tests to model the ASTM D-2882 Vickers V-104 hydraulic vane pump wear was described. However, in some cases, bench tests have been either specially modified or even custom designed to model wear of a specific contact within a pump. Selected examples will be provided in the following discussion.

University of Aachen Sliding Wear Bench Test

A custom-designed bench test was reported by Jacobs et al. which was used to examine sliding wear occurring in hydraulic pumps with different material pairs [39]. This machine is schematically illustrated in Fig. 10.10. The wear contact is a rotating disk.

University of Leeds Testing Machine

Priest et al. have also reported a bench test that is custom designed as illustrated in Fig. 10.11 to model the sliding wear contact in the V-104 vane pump [40]. A schematic comparison of the wear contacts in the bench and V-104 vane pump tests is illustrated in Figs. 10.12 and 10.13, respectively. Excellent correlation between the bench and vane pump tests has been reported [40].

Cameron–Plint Wear Test Apparatus

The effect of metallurgy on sliding wear using various hydraulic fluids for aerospace applications has been performed using the Cameron–Plint wear testing apparatus

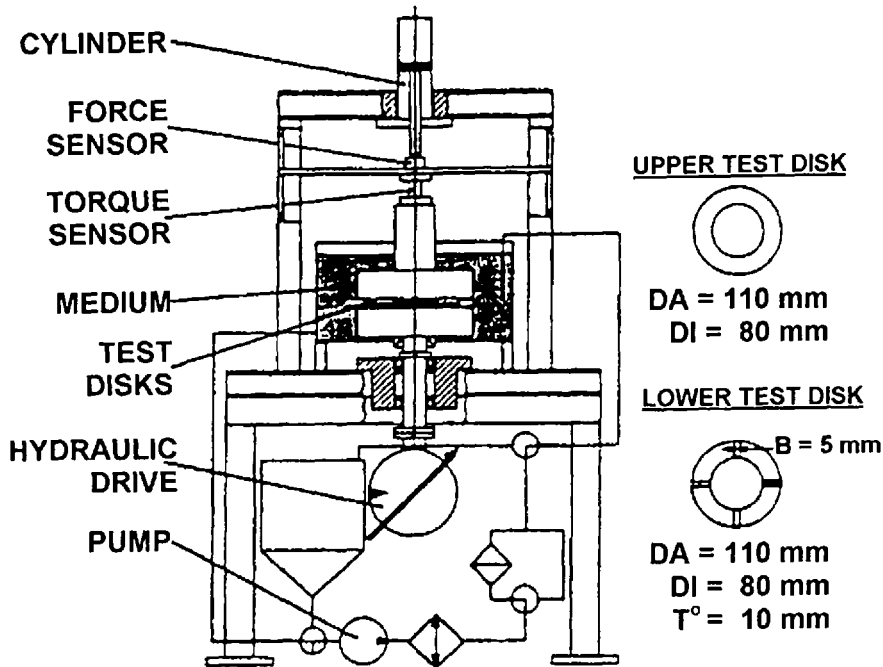


Figure 10.10 Aachen mixed-friction sliding wear machine.

shown in Fig. 10.14 [41]. In this test, the sliding motion of an upper cylinder on a lower plate surface is controlled by a variable-speed motor.

Unisteel Rolling Fatigue Machine

Another bench test that has been used to model hydraulic fluid wear is the Unisteel rolling fatigue machine shown in Fig. 10.15. In this test, a flat ring forms the upper

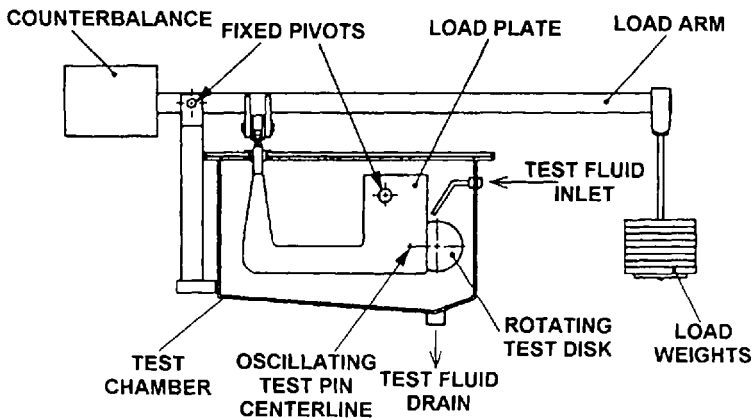


Figure 10.11 University of Leeds test machine.

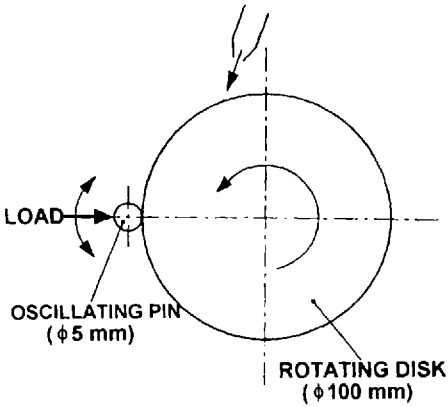


Figure 10.12 Wear contact for the University of Leeds test machine.

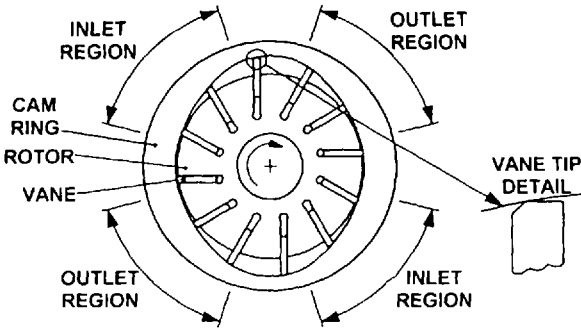


Figure 10.13 Wear contact for Vickers V-104 vane pump.

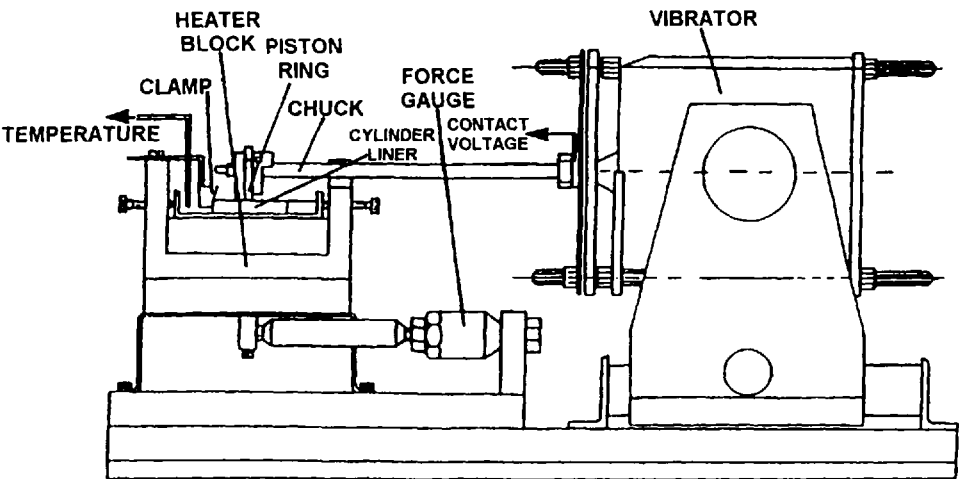


Figure 10.14 Cameron-Plint wear test machine.

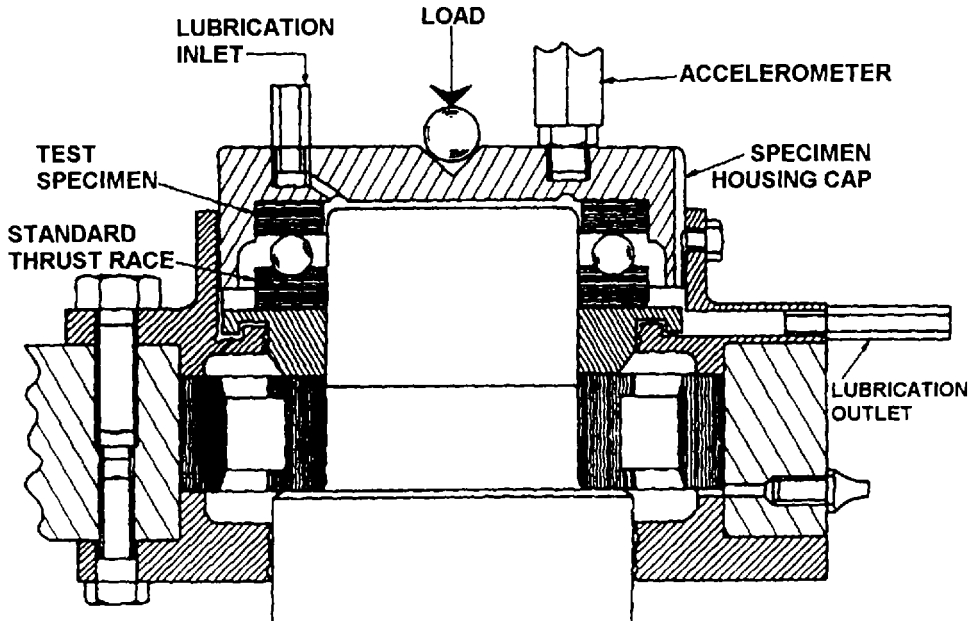


Figure 10.15 Unisteel rolling fatigue machine.

part of a thrust bearing which contains the cage, half the balls, and one race from a production thrust bearing assembly [42].

Modified Amsler Disk Machine

The potential for yellow metal wear that may occur with bronze or brass slippers may be evaluated using a modified Amsler disk machine. The modification, shown in Fig. 10.16, entails the replacement of one of the original disks in the machine by a phosphor-bronze or high-tensile-brass block. The block is spring-loaded to the

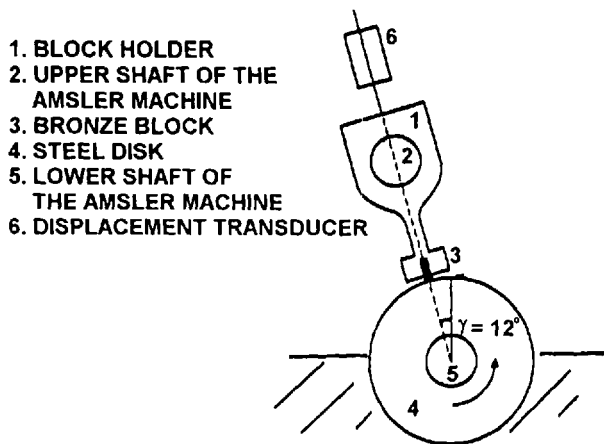


Figure 10.16 The setup of the Amsler rig.

disk surface. Wear is continuously recorded using an inductive displacement transducer. Excellent correlation with piston-pump, slipper-pad wear was obtained as shown in Fig. 10.17 [43].

2.1.9 Hydraulic Fluid Evaluation Using Fundamental Lubrication Parameters

Stribeck–Hersey Curve

Hydraulic fluid lubrication may occur by one of at least four wear mechanisms: hydrodynamic, elasto-hydrodynamic (EHD), mixed-film, and boundary lubrication. The particular mechanism encountered is dependent on the film viscosity, velocity, and applied load as illustrated in Fig. 10.1 [3]. Hydrodynamic lubrication is characterized by relatively thick films, typically >300 nm, which are substantially thicker than the asperity contacts of the wear surface. EHD lubrication is characterized by thin-film lubrication. Although the lubrication films are only ~ 30 nm thick, they are greater than the asperity contacts. Film thicknesses for boundary lubrication, typically approximately 3 nm, are less than the height of the asperity contacts. Mixed-film lubrication occurs at the transition from EHD to boundary lubrication.

Ideally, hydraulic pumps operate in the hydrodynamic lubrication regime [3]. Under these conditions, the lubricating capability of the fluid is primarily dependent on the fluid film viscosity. However, it is not possible to assure hydrodynamic lu-

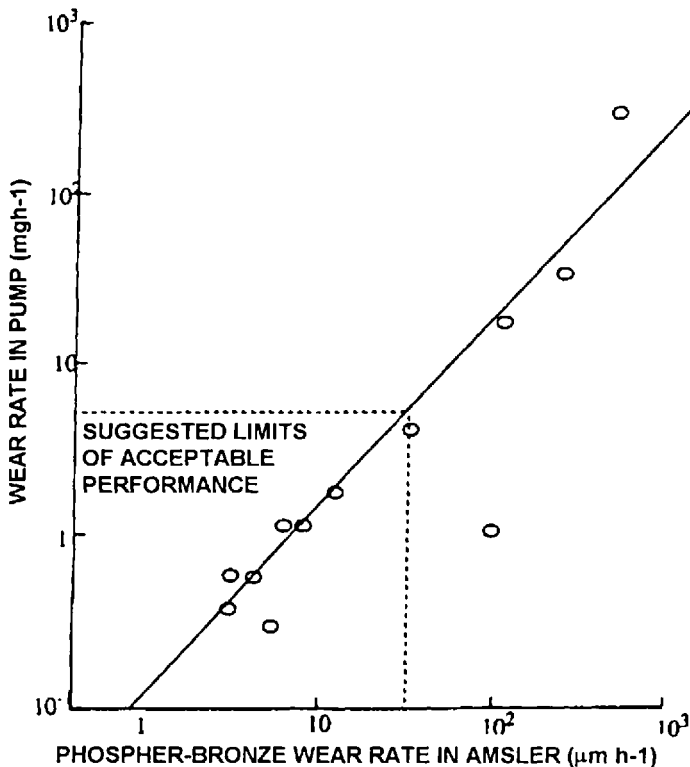


Figure 10.17 Correlation between the results of pump and Amsler tests.

brication under all operating conditions. For example, start-up conditions, oscillating motion, and so forth can create contact speeds insufficient to support hydrodynamic lubrication. Thus, a hydraulic fluid must exhibit some antiwear characteristics.

Performance Map Characterization

It is possible to construct "performance maps" to identify EHD, mixed-film, and boundary lubrication properties of a hydraulic fluid [14,44,45]. A typical performance map is illustrated in Fig. 10.18.

As Fig. 10.18 shows, performance maps are constructed in terms of rolling speeds (R) and sliding speeds (S). This is important because the generation of an EHD film is primarily a function of the entraining velocity (R) in the inlet region of the Hertzian contact (see Chapter 3). In this region, lubricating film generation is primarily a function of the physical properties (viscosity, pressure viscosity coefficient, etc.) of the hydraulic fluid. The sliding speed (S) determines the shear strain within the high-pressure Hertzian contact region. This region is important with respect to heat generation, surface film formation, wear, and scuffing within the tribocontact (see Chapter 6). The magnitude of the degree of surface interaction achieved, as a result of thin EHD films, influences the chemical properties of the fluid (e.g., adsorbed films, chemical reaction films, tribochemical reactions, and thermal/oxidative stability).

A correlation between the Ryder gear test, Shell 4-ball antiwear test, and their predictive placement on a performance map has been made [14]. As Fig. 10.19 shows, the lubrication results of the test represent just one point on the overall performance map and perhaps this point may be outside of the *range* required for the various lubricated surfaces in a particular hydraulic pump design. In fact, this is

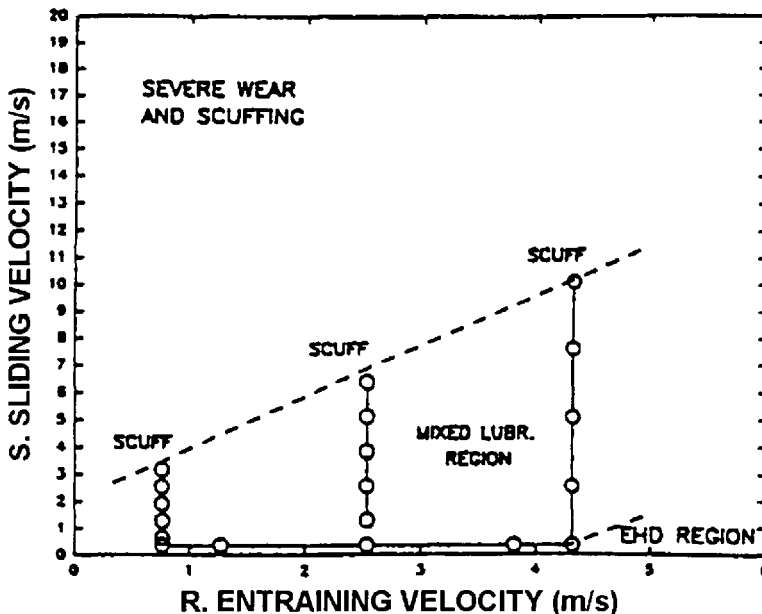


Figure 10.18 Illustration of a typical performance map for a hydraulic fluid.

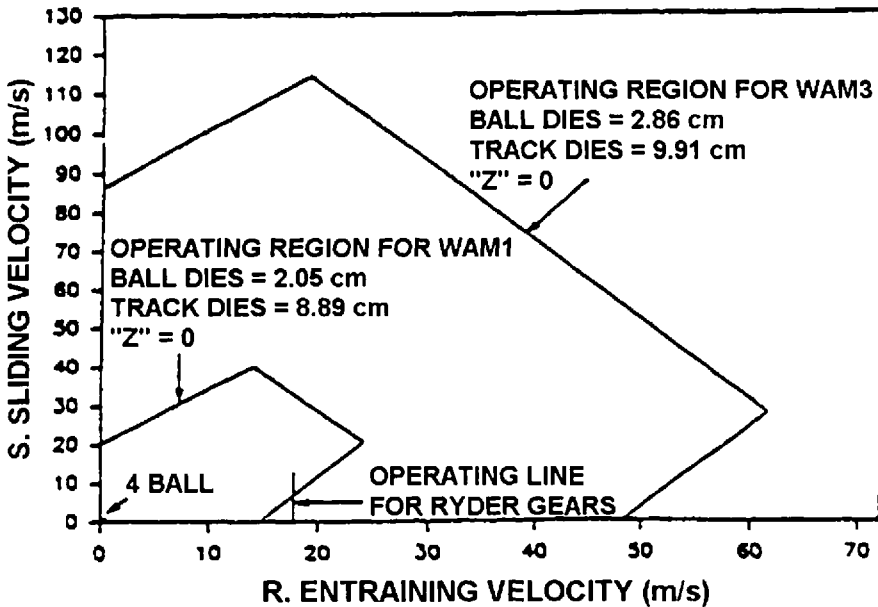


Figure 10.19 Map of entraining velocity (R) and sliding velocity (S).

a deficiency of conducting bench tests relative to the varying lubrication requirements in a machine, such as a hydraulic pump.

Wear Contact Geometry

The contact geometry of a tribocontact should also be considered. There are typically three characteristic types. These are point contact (such as ball-on-disk), line contact (such as a roller-on-disk), and an area contact (such as a flat surface-on-disk). All of these represent uniquely different lubrication problems and, ideally, the contact geometry of the tribocontact should reasonably model the actual system being studied [46]. The common tribocontact surface geometries are shown in Fig. 10.20 [47].

It is recommended that the contact geometry of the bench test selected reasonably model the actual system [47,48]. Recently, Voitik has recommended the use of "tribological aspect numbers (TAN)" to quantitatively and systematically characterize a wear contact [49].

There are four characteristics to be determined in the calculation of a TAN [40]:

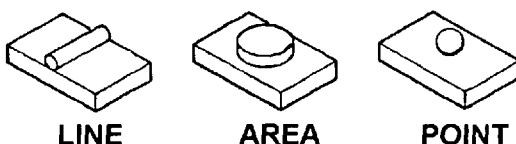


Figure 10.20 Tribocontact surface-geometry classification.

**TRIBOLOGICAL ASPECT NUMBERS
CONTACT VELOCITY CHARACTERISTICS**

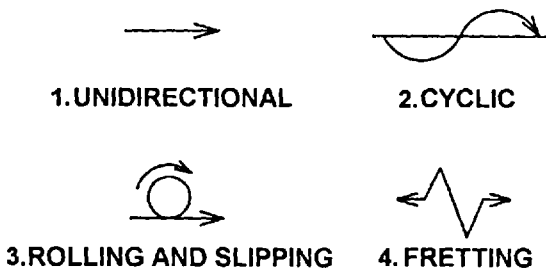


Figure 10.21 Contact-velocity characteristics for TAN calculation.

1. Contact velocity
2. Contact area
3. Contact pressure
4. Entry angle

CONTACT-VELOCITY CHARACTERIZATION. There are four contact-velocity characteristics which are illustrated in Fig. 10.21: (1) unidirectional, (2) cyclic, (3) roll/slip, and (4) fretting. The first digit of the TAN number is selected from 1 to 4.

CONTACT-AREA CHARACTERIZATION. The second digit of the TAN represents the contact-area characteristic and is selected from one of the eight possible values illustrated in Fig. 10.22: (1) point to point, (2) line to line, (3) point to area (circle), (4) line to area (rectangle), (5) area to area, (6) smaller area to larger area, (7) open fixed area, and (8) open variable area.

CONTACT-PRESSURE CHARACTERISTIC. The third digit of the TAN number is selected from one of the three contact-pressure designations shown in Fig. 10.23: (1) unidirectional, (2) high frequency, and (3) cyclic loading.

**TRIBOLOGICAL ASPECT NUMBERS
CONTACT AREA CHARACTERISTICS**

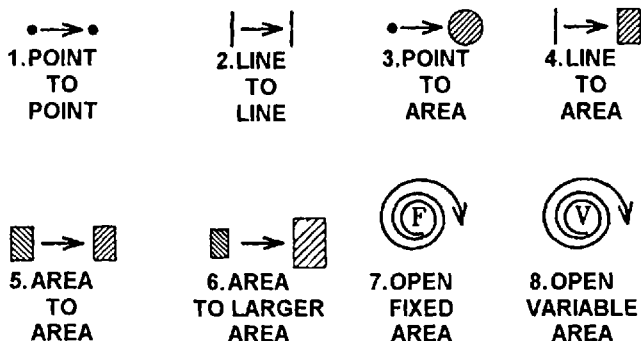


Figure 10.22 Contact-area characteristics for TAN calculation.

TRIBOLOGICAL ASPECT NUMBERS
CONTACT PRESSURE CHARACTERISTICS

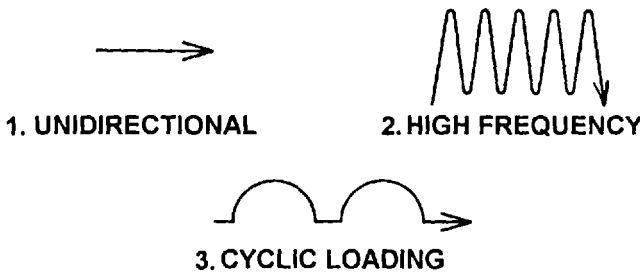


Figure 10.23 Contact-pressure characteristics for TAN calculation.

INTERFACIAL ENTRY ANGLE. Nine characteristic entry angles have been characterized between 0° and 90° and are shown in Fig. 10.24. These values reflect hydrodynamics, plowing, starvation, debris entry, thermal conductivity, and other effects on tribological wear.

Values reported by Voitik for some of the bench tests reported here are summarized in Table 10.7 [49]. None of the test configurations exhibit the same TAN as the vane-on-disk, which models the vane-on-ring of the vane pump. Also, different TANs would be expected for bearing lubrication (e.g., cylinder in bore) encountered in other pump designs.

Table 10.8 summarizes various TANs for different wear contacts that may be encountered in hydraulic components. The wear surfaces (1–19) from Table 10.8 are illustrated in Fig. 10.25 (1–14), Fig. 10.26a (15–17), and Fig. 10.26b (18 and 19).

2.1.10 Bench-Test Considerations

In addition to modeling the actual wear mechanism in the hydraulic pump, a successful bench test should do the following [47]:

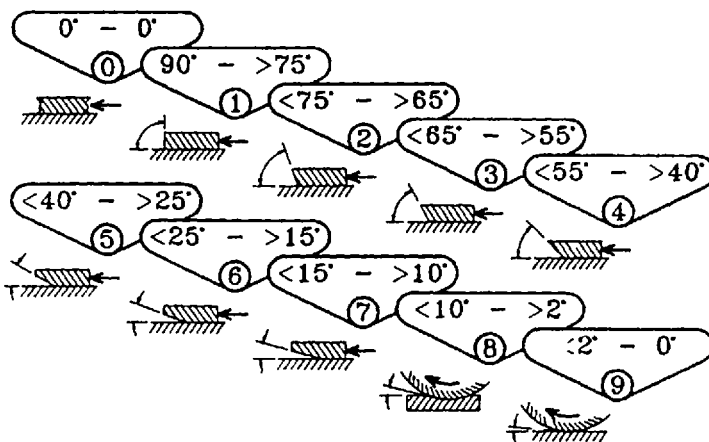


Figure 10.24 Interfacial entry angles for TAN calculation.

Table 10.7 Comparison of Tribological Aspect Numbers of Various Bench-Test Configurations

TAN	Contact geometry
1418	Timken
1317	Shell 4-Ball
1419	Vane-on-Disk
1519	Pin-on-Disk
1318	Ball-on-Disk
3229	FZG Test

- Reproduce the wear mechanisms in the application of interest
- Reproduce the temperature level of the material during normal wear

Accelerated tests may rate lubricants in the correct order (which did not occur in the work described earlier in this chapter); however, the magnitude of the difference between the fluids studied may not be proportional with actual field experience [48].

If a bench test is to model field experience, it should do the following [48]:

Table 10.8 Wear Aspects of Significant Parts and Subassemblies

Item no.	Description	Material	TAN no.			
			A	B	C	D
01	Cylinder barrel bushing	Brass	3	4	2	9
02	Cylinder control surface	Brass	2	7	2	1
03	Valve plate	Nitrided steel	2	7	2	1
04	Piston	Nitrided steel	3	4	3	8
05	Slipper shoe	Brass	3	6	3	1
06	Swash plate	Nod. cast iron GGG-60	2	5	3	1
07	Sliding plate	Nitrided steel	2	5	3	1
08	Saddle bearings	Brass	2	5	3	1
09	Retainer ball	Nitrided steel	2	4	3	9
10	Retainer plate	Tool steel	2	4	3	9
11	Drive shaft	Steel, induction hardened	2	5	3	0
12	Cylinder roller bearing	Steel, hardened	2	4	3	9
13	Shaft seal	FKM/PTFE	2	4	3	1
14	Seals	BUNA-N/FKM	2	6	3	0
15	Control piston	Tool steel, induction hardened	2	5	3	1
16	Piston housing	Cast iron GGG-40	2	5	3	1
17	Slide stone	Steel, hardened	2	5	3	1
18	Control-valve housing	Cast iron GGG-40	3	5	2	8
19	Control-valve spool	Tool steel	3	5	2	8

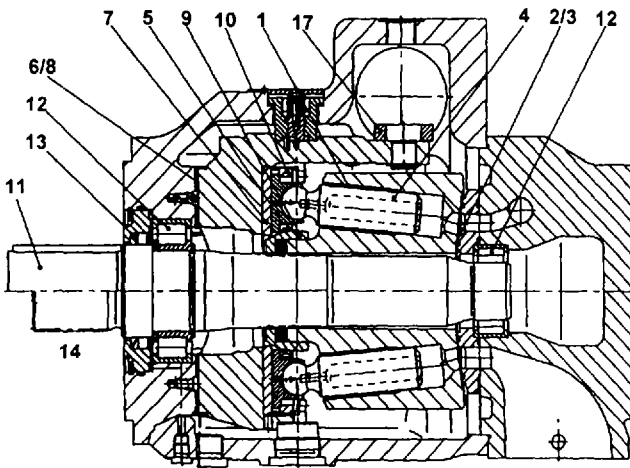


Figure 10.25 Wear surface TANs for the axial piston pump. See Table 10.8 for part labels.

- Provide reasonable reproducibility.
- The results obtained must have some degree of correlation with results observed in actual service.

Although the bench tests discussed here were reasonably reproducible, they provided poor, if any, correlation with hydraulic pump results. By this criteria, none of the tests evaluated were suitable models of hydraulic performance.

It is also important to recognize the various forms of wear that may occur in pump operation. Some of these include the following [3]:

- Abrasive wear
- Adhesive wear
- Cavitation wear
- Corrosion wear

With bench testing of hydraulic fluids under atmospheric pressure, it is difficult to model exactly the fluid pressure conditions encountered in hydraulic pumps. Thus, potential for wear by cavitation may not be observed. Similarly, corrosive processes or rolling contact fatigue often take many hours, days, or even months to occur in actual operation. They simply will not have time to occur under the accelerated conditions of the bench test. Furthermore, the promotion of the accelerated wear conditions may actually be accompanied by a change in the wear mechanism; for example, from abrasive to adhesive failure.

Recently, Mizuhara and Tsuya studied the ability of a block-on-ring test (ASTM D 2714-68 [50]) to model three different hydraulic pump (vane, gear, and piston) tests. The hydraulic fluids studied were antiwear oil, water-glycol, oil-in-water emulsion, water-in-oil emulsion, phosphate ester, and polyol ester. The conclusions from this study were as follows [13]:

- It was necessary to evaluate the fluids under a wide range of conditions.
- Load-carrying capacity has nothing to do with the antiwear properties.
- Accelerated tests usually provide the wrong results.
- Materials for the actual test pieces must be similar to the actual machine.

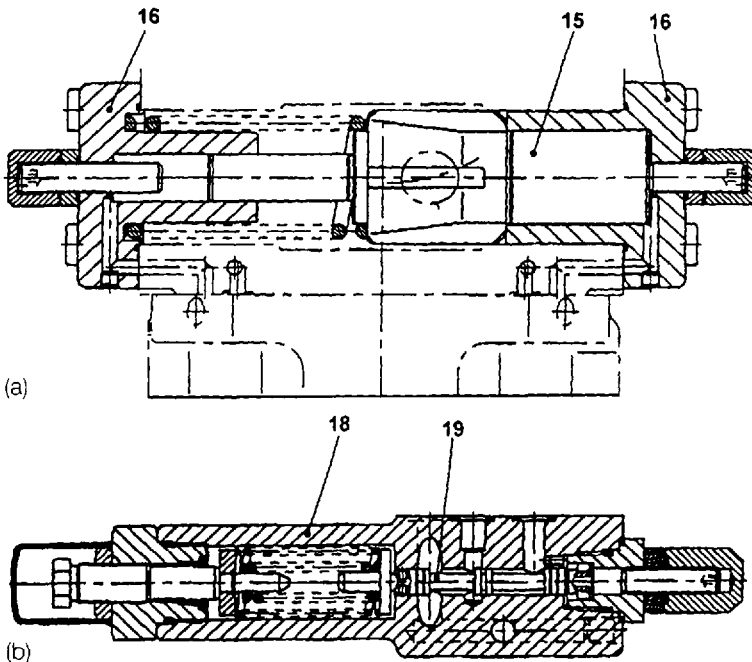


Figure 10.26 TAN characterization of valve wear surfaces. See Table 10.8 for part labels.

- To successfully evaluate the wear characteristics of hydraulic fluids, a wear test in a hydraulic pump must be conducted.

The following test strategy was recommended for the use of laboratory wear-testing machines:

1. Rank hydraulic fluids according to hydraulic pump tests.
2. Evaluate hydraulic fluids in a wear-testing machine under a wide variety of test conditions and material pairs.
3. Determine the testing condition that provides the proper fluid ranking according to hydraulic pump tests.
4. If the proper testing conditions are not found, expand the test variables.
5. Repeat procedure 3; if inadequate correlations are obtained, change the wear-testing apparatus.

These conclusions, while cumbersome, are reasonable in view of the tribological principles reviewed earlier.

Ludema has stated that “the best approach to wear modeling is to develop an organized way to accumulate empirical results from tests that simulate practical systems and build models from those data” [51]. Clearly, if such a database were available, it would greatly facilitate correlation of standard wear test results to those obtained with hydraulic pumps under widely varying wear conditions.

2.2 Part II: Lubrication Characterization by Pump Testing

2.2.1 Pump-Failure Modes

There are numerous reasons for conducting laboratory hydraulic pump tests. These include [15]:

1. To compare the differences in equipment performance
2. To obtain controlled performance experience with new fluids
3. To troubleshoot field performance problems
4. To obtain comparative lubrication data on various hydraulic fluid types and manufacturers.

Pump failures are typically accompanied by increased noise and loss of volumetric efficiency. During the course of conducting pump tests, as a minimum, observations must be made to determine the cause of pump performance loss or failure. Preferably, more quantitative wear determinations coupled with photographic record-keeping and a continuous analysis of pump operation should be performed. A summary of some common failure modes for gear pumps, axial piston pumps, and vane pumps are provided in Table 10.9 [15,52,53] and Chapter 12.

2.2.2 Fluid-Specific Properties

In addition to pump testing, and preferably prior to it, a number of fluid-specific properties should be determined. These include metal and nonmetal compatibility. For example, vapor, liquid, and dry film corrosion properties should be performed [53]. Copper and other soft-metal corrosion should also be determined [54,55]. Propensity for sludge formation, viscosity and viscosity stability, pH, and wettability are other important variables. Feicht has recommended that because of compressibility differences among hydraulic fluids, valve-housing stability be examined. Nonmetal or seal compatibility is vitally important [55].

2.2.3 Vane-Pump Testing

The output pressure of a vane pump is directed to the back of the vanes which hold them against the ring. The leading edge of the vane forms a *line contact* with the ring and the rotation of the vane against the ring generates a *sliding motion* as shown in Fig. 10.27. The challenge is to maintain adequate lubrication between the vane tip and the cam ring with increasing pressures and rotational speeds [6].

Ueno et al. have used the vane pump as a tribological test stand to study the effects of pump delivery pressure, rotational speed, eccentricity, and hardness of the cam ring, vane-tip curvature, and the length of action range of vane equilibrium force during rotation on the total wear of the vanes and ring [6,56]. Their results showed that the wear rate simply cannot be estimated from the friction work due to these factors. However, the occurrence of severe wear is proportional to $P_H V$ where, P_H is the maximum Hertzian contact stress and V is the sliding velocity.

Table 10.9 Common Pump-Failure Modes

Pump type	Failure mode
Gear	Roller-bearing fatigue, gear-tooth surface pitting and fatigue, seal-plate scoring and seizure.
Piston (axial)	Roller-bearing fatigue, valve-plate scoring and erosion, slipper-pad failures, piston and cylinder wear, cavitation
Vane	Severe vane and ring, port plate, bearing, and cavitation wear.

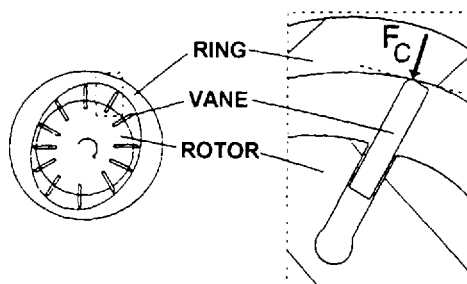


Figure 10.27 Illustration of the sliding line contact with vane-on-ring.

Hemeon reported the application of a “yardstick formula” to quantitatively analyze and report vane-pump wear. The critical part of the analysis was weight loss of the ring, as dimensional changes due to wear will significantly affect volumetric efficiency and lead to noise and pulsation [57]. The yardstick formula is

$$Y = K(1.482)(mep)(gpm) \quad (10.1)$$

where

Y = duty load on the pump in BTU/h.

K = a constant to correct for air entrainment, degraded or contaminated oil, and fluid turbulence

mep = mean effective pressure

gpm = flow in gallons per minute

Although K may be as high as 1.4, a value of 1.03 is typical. The conversion constant 1.482 permits the use of pressures in pounds per square inch and weight loss in grams. Interestingly, in order to obtain reproducible and reliable weight-loss data, it was reported that the ring had to be washed and baked at 200°F for 24 h because the porous metal adsorbed the solvent and gave incorrect weight data.

Bosch (Racine fluid power) also utilized a cycled-pressure, vane-pump test. The pressure–time sequence and test circuit is illustrated in Fig. 10.28 [58]. This is reported to be a more representative test because it better incorporates pressure spikes that will invariably occur in a hydraulic system during circuit activation and deactivation. At the conclusion of the test, the weight loss of the ring, vanes, port and cover plate, and body and cover bearings were measured. The ring and bearings were inspected for unusual wear patterns and for evidence of corrosion, rusting, and pitting.

Lapotko et al. have reported an alternative vane-pump test designated as the “MP-1 test” [10,59]. A schematic of the MP-1 vane pump is shown in Fig. 10.29. Although the MP-1 may be run at pressures up to 10 MPa (1450 psi), the reported test pressure is 7 MPa, with a total fluid volume of 0.7 L. In addition to lower volume, the MP-1 test is conducted for only 50 h (and in some cases, for only 10 h). The wear rate is based on the weight loss of the vanes only after the test is completed. In view of the relatively small size, this test comes as close to a “bench hydraulic pump test” as has been reported to date.

The Vickers V-104 vane pump shown in Fig. 10.30 and the test circuit in Fig. 10.31 continue to be the most commonly utilized hydraulic fluid pump test [60].

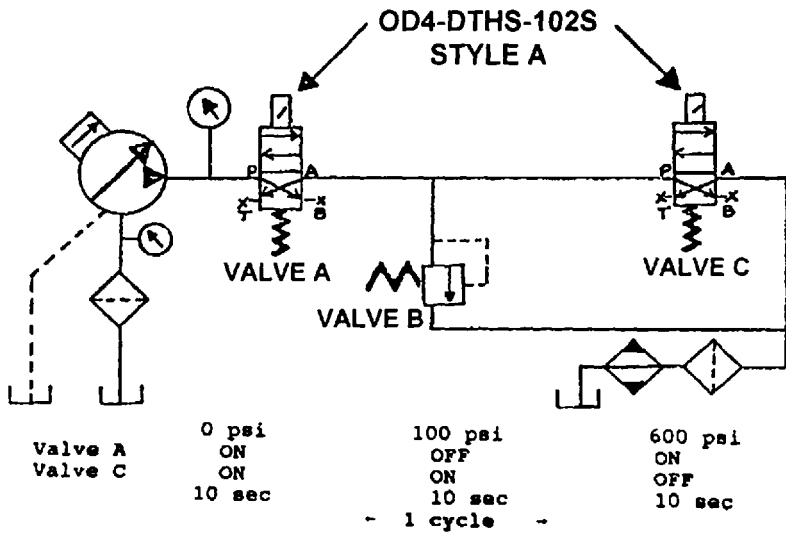


Figure 10.28 Test circuit for Racine cycled-pressure, vane-pump test utilizing a 7.5-hp electric motor, SV-10 vane pump, and a 20-gal reservoir.

There are at least three national standards based on the use of this pump: ASTM D-2882, DIN 51389, and BS 5096 (IP 281/77). A comparison of the test conditions is provided in Table 10.10. The total weight loss of the vanes plus ring at the conclusion of the test is the quantitative value of wear.

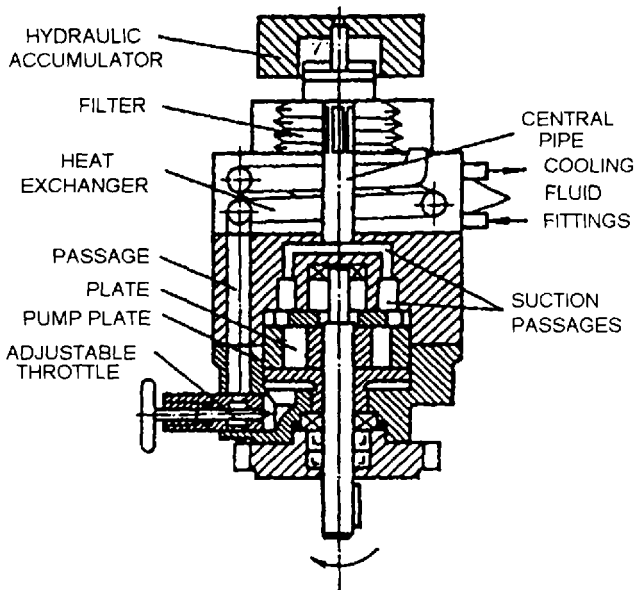


Figure 10.29 Schematic illustration of the Russian MP-1 vane pump.

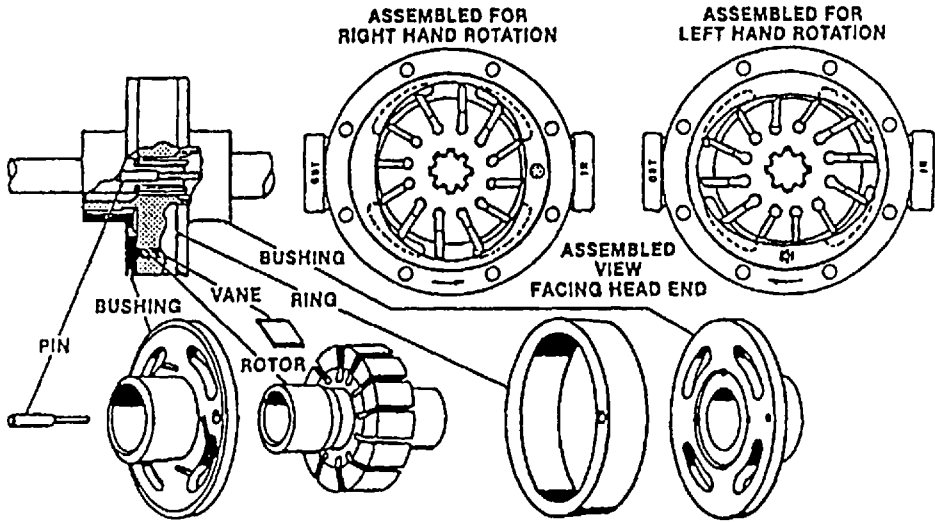


Figure 10.30 Illustration of the Sperry-Vickers V-104 vane pump.

Although the Vickers V104C vane pump in any of its various forms (ASTM D2882, DIN 51389, and IP 281/77) has served the industry reasonably well in its ability to characterize antiwear properties of hydraulic fluids, it is notorious for providing poor interlaboratory reproducibility. Another common problem is rotor breakage during the test.

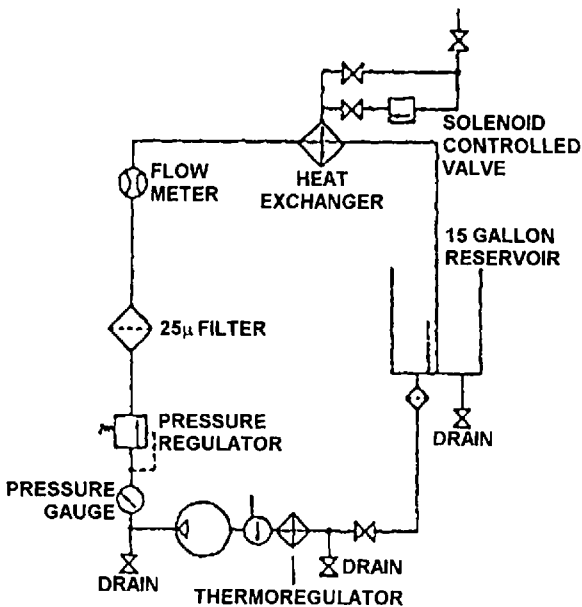


Figure 10.31 Test circuit for the Vickers V-104 vane-pump test.

Table 10.10 Comparison of Sperry–Vickers V-104 Vane-Pump Testing Procedures

Test parameter	ASTM D-2882	DIN 51389	BS 5096 IP 281/77
Pressure	14 MPa 2000 psi	10 MPa 1500 psi	14 MPa ^a 2088 psi 11 MPa ^b 1540 psi
Rev./min	1200	1500	1500
Time (h)	100	250	250
Fluid volume (L)	56.8	56.8	55–70
Fluid temperature	150°F		

^aFor mineral-oil-type fluids.

^bFor HFA, HFB, and HFC fluids.

^cThe temperature is selected to give 46 cSt viscosity.

Recently, Gent conducted a study to identify the greatest sources in testing variation [61]. These were found to include the following:

1. Parts preparation. This was identified as the single most important factor in obtaining a successful test run.
2. Rotor failure. Failure occurred regardless of inspection or testing procedure.
3. ASTM D2882 advises using 10 in.-lb. increments up to 100–140 in.-lb. Feeler gauges and shim stock should be used to ensure that the head is not cocked, resulting in seating against the pump cartridge.
4. Bushing failure. Bushing failures can be essentially eliminated by proper parts preparation, maintenance of proper clearances in the cartridge, and use of proper torquing techniques.
5. Wear results. Variations in material chemistry and geometry may effect wear results.
6. Rotor reuse. It is common practice to reuse the rotor until breakage.
7. Pump maintenance. According to ASTM D2882, seals must be replaced after each test and the shaft and bearing must be replaced after five tests.
8. Fluid volume, reservoir shape, and baffling vary significantly among laboratories.
9. Filtration. Although ASTM D2882 requires 20- μ m filtration, most laboratories use 10- μ m filtration.
10. Test conditions. Many laboratories have reduced the pump pressure.
11. Flushing. No laboratory is using the flushing required by ASTM D-2882.

Reference 62 has provided additional recommendations to obtain improved intralaboratory reproducibility. In addition to those variables identified by Gent, the following were recommended:

1. The ring and vanes should be inspected for machining irregularities and precision. Machining and scoring marks are unacceptable.

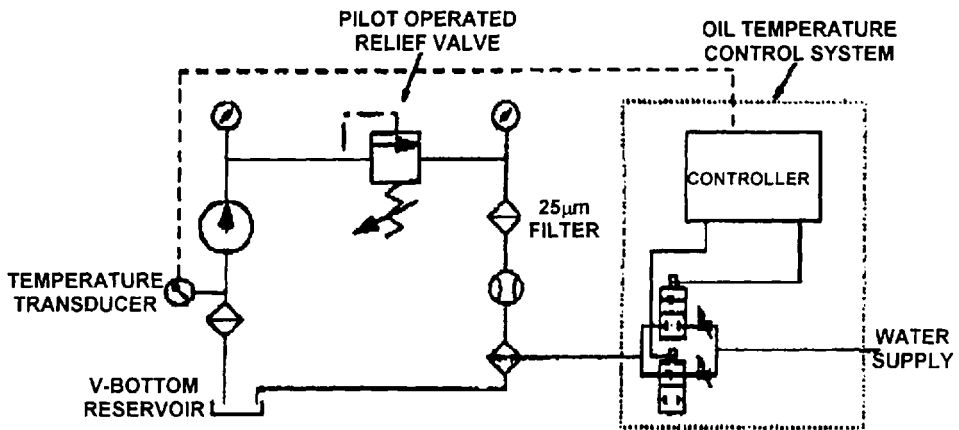


Figure 10.32 Low-volume hydraulic and temperature-control system schematic.

2. The system pressure gauge should be recalibrated before and after every run.
3. Fluid composition such as water and reserve alkalinity for aqueous fluids must be monitored and controlled.
4. To minimize the potential for system contamination, which may have disastrous consequences, the hydraulic system must be dismantled, scrubbed, and water washed followed by solvent cleaning (use clean solvent) after every run.
5. Water-compatible filters, preferably 3–5- μm fiberglass should be used for water-containing fluids.
6. System temperature variation should be controlled to $\pm 1^\circ\text{C}$.
7. It is insufficient to only use weight loss for the vanes and ring. The complete system, including end plates and bearings, must be inspected and observations recorded, preferably photographically.

A 100-h low-volume hydraulic pump test that utilizes only 1.3 L (0.35 gal) of fluid has been reported by Glancey et al. [63]. This test utilizes a Vickers V10-1P3P1A20 vane pump with a $9.84\text{-cm}^3/\text{rev}$. displacement. The hydraulic circuit is shown in Fig. 10.32 [63]. A comparison of the test conditions is shown in Table 10.11.

Table 10.11 Comparison of Test Conditions for Low-Volume Vickers V-10 Vane-Pump Test with ASTM D2882 (Vickers V-104C Vane Pump)

Operating parameter	ASTM (D2882)	Low-volume system
Pump outlet pressure (MPa)	13.8 ± 0.28	13.79 or 17.18 ± 0.03
(psi)	2000 ± 40	2000 or 2500 ± 4
Fluid temp. ($^\circ\text{C}$)	65.6 ± 3	65.5 ± 1.5
Pump speed (rpm)	1200 ± 60	1200 ± 40

Table 10.12 Comparison of the Test Conditions of the Sperry–Vickers V-104 and 20VQ5 Pumps

Parameter	V-104	20VQ5
Vane load (lbs./1000 psi)	47	25
Max. pressure (psi)	1000	3000
Max. speed (rpm)	1500	2700
End plates (bronze)	Cast	Sintered

A regression equation was developed to interrelate wear obtained when tested according to ASTM D2882 and when tested using the low-volume V-10 vane-pump test [63]:

$$Y = -4.45 + 1.76X$$

where Y is the equivalent wear for the ASTM D2882 test (mg) and X is the wear (mg) from the low-volume test system.

Recently, there has been interest in the replacement of the older Vickers V-104 pump with the newer Vickers 20VQ5 vane pump. However, it is important to acknowledge that the tribological conditions are significantly different for both pumps. A comparison of the recommended test conditions are summarized in Table 10.12. In addition, it is also important to recognize that the vane design is fundamentally different for the two pumps. The 20VQ5 pump has an “intravane” configuration, whereas the V-104 pump has a single-vane arrangement. These vane arrangements and the configuration of the vane cartridge in the two pumps are compared in Figs. 10.33–10.35.

In addition, to the physical differences in these pumps, it should also be noted that under the recommended test conditions, the current V-104 pump is being operated at 2000 psi for the ASTM D2882 test protocol, which is outside of the recommended pressure limit of 1000 psi for the pump. The recommended pressure for the test using the 20VQ5 pump is 3000 psi, which is also the recommended pressure

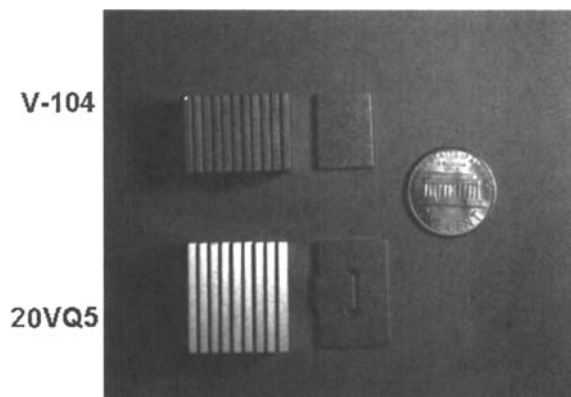


Figure 10.33 Comparison of the vanes in the Vickers V-104 and 20VQ5 pumps.

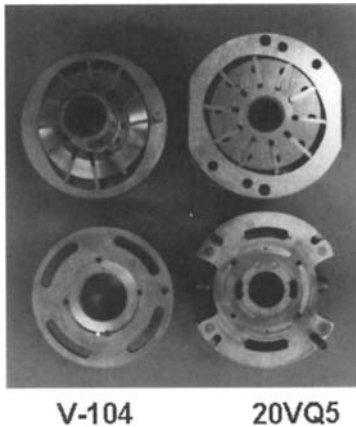


Figure 10.34 The internal view of the Vickers V-104 and 1 20VQ5 pumps.

limit of the pump [64]. This is particularly important because every pump has its own characteristic wear regions as a function of speed and load [65]. Almost certainly, under these conditions, the V-104 pump would have a significantly greater hydraulic film-load requirement to provide adequate lubrication than would the 20VQ5 pump. This is especially true in view of the different vane designs of the two pumps. Therefore, it is not likely that there is a direct wear correlation between the two pumps.

Experimental water–glycol hydraulic fluids were selected that would provide significant differences in vane pump total wear (vanes plus ring) after completion of the test. Table 10.13 shows the operating parameters used for the V-104 and 20VQ5 pumps in this study.

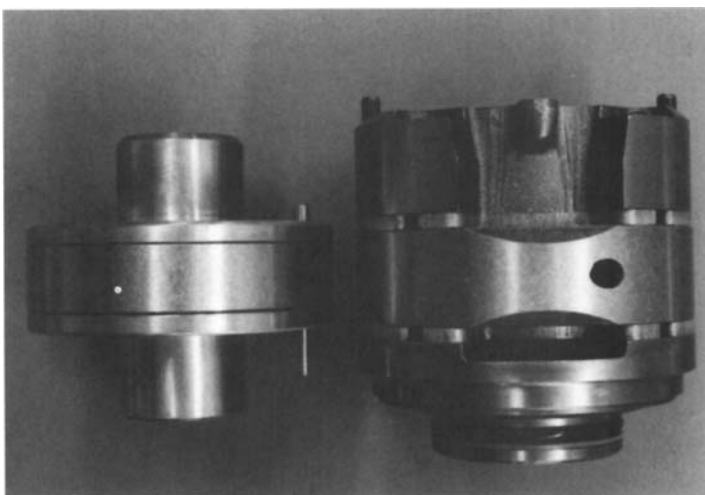


Figure 10.35 Comparison of the assembled cartridges of the Vickers V-104 (left) and 20VQ5 (right) pumps.

A comparison of the wear results obtained for these fluids using a variety of test conditions is provided in Table 10.14. The results show the following:

- The worst formulations tested in the V-104 pump, fluids B and E, gave very low wear in the 20VQ5 pump.
- Generally for a given fluid, the 20VQ5 pump gives lower wear than the V-104 pump.

Figure 10.36 provides a graphical comparison of the wear data obtained with the V-104 pump using a “modified” ASTM D-2882 protocol (2000 psi, 1200 rpm, 1-gal reservoir) with that obtained using the 20VQ5 pump at 3000 psi and 1200 rpm [66]. These data illustrate that the 20VQ5 pump, at least under the recommended test conditions, provides insufficient discrimination of the lubrication properties of fluids.

In another test, a fluid formulation was tested at two different speeds (1200 and 2400 rpm) using the 20VQ5 pump. Although the fluid exhibited very low total wear of the vanes plus ring, fluid B exhibited dramatic cavitation of the bushing at 2400 rpm, as shown in Fig. 10.37. This is also important because neither the ASTM D-2882 nor the proposed 20VQ5-pump-testing protocols requires the reporting of any wear except on the vanes and ring.

A test has been developed using a Chinese-built YB-6 dual-function vane pump operating under ASTM D-2882 testing conditions [67]. In addition to measuring the total wear of the cam ring and vanes, the temperature rise, noise level, and volumetric efficiency were measured.

One of the deficiencies of all of the previously described vane-pump tests is that they are either conducted at relatively low pressure or rotational speed (rpm), compared to vane pumps in industrial use. Although not a national standard, the Vickers 35VQ pump test is often acknowledged to provide a more rigorous and, in some cases, a more realistic accelerated industrial-pump wear test (20.7 MPa, 3000 psi, 2400 rpm) [67–73,97]. A schematic of this test is provided in Fig. 10.38 [86]. The maximum weight loss of the vanes for each of the test cartridges must not exceed 15 mg and the total weight loss of the ring for each cartridge must not exceed 75 mg for the three cartridges used. If the weight loss of any of the cartridges exceeds these values, two more tests with new cartridges must be run. A comparison of the test conditions for the V104C, 20VQ5, and 35VQ25 pump tests is provided in Table 10.15 [68].

Table 10.13 Comparison of Pump Operating Parameters

Parameter	Vickers V-104 vane pump		Vickers 20VQ5 vane pump		
Flow (gpm)	8	10	5	10	11.3
Pressure (psi)	2000	1500	3000	3000	3000
Speed (rpm)	1200	1500	1200	2400	2700*
Power (hp)	9.3	8.8	8.8	17.5	19.7
Torque (in.-lbs.)	490	370	460	460	460

*Maximum rated speed at 3000 psi using a 5-gpm cartridge.

Table 10.14 Results of Pump Tests

Fluid	Flow (gpm)	Pressure (psi)	Speed (rpm)	Ring/vane wt. loss (total wear)*	End-plate wt. loss (total wear)*	V-104 pump	20VQ5P pump
A	8.2	2000	1200	21		X	
	10.3	1500	1500	31	23	X	
	5.7	3000	1200	13			X
	12.8	3000	2700	34			X
B	8.2	2000	1200	205	7	X	
	10.3	1500	1500	199	38	X	
	5.7	3000	1200	12	60		X
	11.4	3000	2400	10	482		X
C	8.2	2000	1200	22	20	X	
	10.3	1500	1500	116	14	X	
	5.7	3000	1200	18	40		X
	8.7	3000	1200	37	25		X
	11.4	3000	2400	7.3	130		X
	11.4	3000	2400	16	168		X
D	8.2	2000	1200	37		X	
	5.7	3000	1200	57			X
E	8.2	2000	1200	5110		X	
	5.7	3000	1200	16			X
F	8.2	2000	1200	83		X	
	5.7	3000	1200	93			X
G	8.2	2000	1200	40		X	
	5.7	3000	1200	9.5			X
H	8.2	2000	1200	34		X	
	5.7	3000	1200	20			X
I	8.2	2000	1200	25		X	
	5.7	3000	1200	22			X

*These weights were determined after 100 hours under the conditions shown.

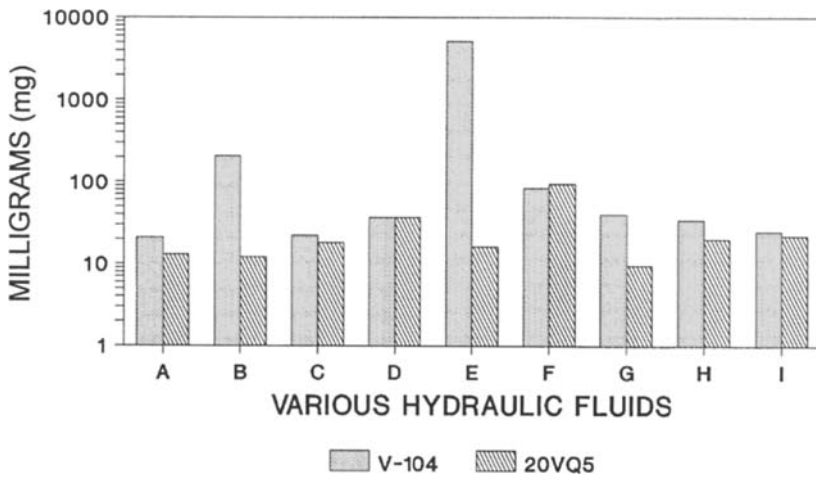


Figure 10.36 Chart of ring plus vane wear (in milligrams) from V-104 and 20VQ5 pumps running at 1200 rev/min with nine fluids at pressures of 2000 and 3000 psi for the V-104 and 20VQ5 pumps, respectively.



Figure 10.37 Comparison of 20VQ5 bushing wear (by cavitation) obtained at two speeds (A) 1200 rev/min and (B) 2400 rev/min at 3000 psi using a fluid that exhibited very low wear on the ring and vanes (12 and 10 mg total wear, respectively after 100 h).

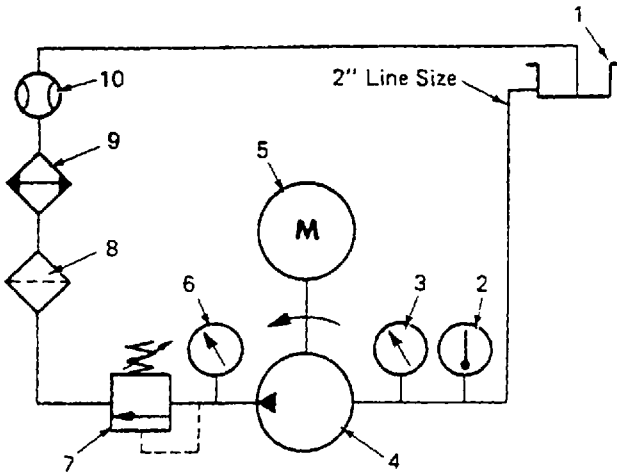


Figure 10.38 Schematic of the Vickers 35VQ test stand. 1—Reservoir (50 gal min.; elevated above centerline to provide gravity feed); 2—temperature gauge or thermocouple; 3—inlet pressure valve; 4—pump (35 VQ25A-11*20; cartridge kit P/N 413421); 5—electric motor (125 hp); 6—outlet pressure gauge; 7—pressure relief valve; 8—filter (10 μ m nominal); 9—cooler; 10—flow meter.

Hagglunds–Denison has also developed a two-part recommended pump-testing protocol HFO (Denison Hydraulics, Marysville, OH). Although this test is used widely in the hydraulics industry, it is not a national standard test. The HFO procedure is composed of two parts: a vane-pump test and a piston-pump test. Only the vane-pump test will be discussed at this time.

The test circuit for the Hagglunds–Denison vane-pump wear test is based on their T5D-042 vane pump, which is located in a “bootstrap” circuit with the Denison series 46 piston pump. The T5D vane-pump test circuit is shown in Fig. 10.39. The vane pump is operated at 2400 rpm and 2500 psi and is driven by a 136-hp electric motor. At the conclusion of the test, the procedure requires that the following be recorded:

- Cam–rotor and cam–vane clearance
- Vane-and-slot clearance for all vanes.
- Tracings of lip contours of vanes 1, 4, and 8.

Table 10.15 Comparison of Pump Test Conditions

Pump	Rotational speed (rpm)	Surface (m/s)
V104C	1200	4.2
20VQ5	1200	3.9
35VQ25	2400	11.4

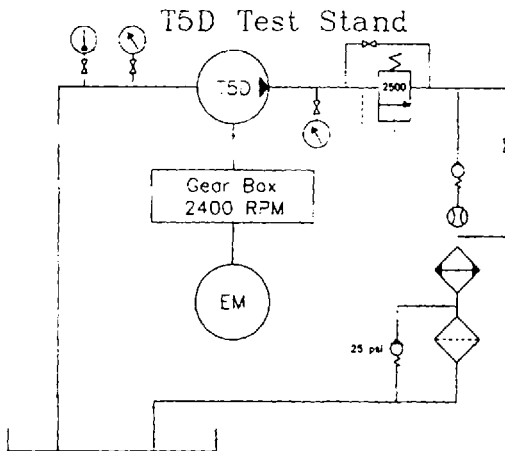


Figure 10.39 Hagglunds–Denison T5D vane-pump hydraulic test circuit.

- Visual appearance of cam-ring interior surface.
- Visual appearance of both plate surfaces that are against the rotating pumping elements.

Hagglunds–Denison has also developed a SK-30320 vane-pump test to evaluate vegetable oil durability. This test is also based on the Hagglunds–Denison T5D-042 vane pump and is a 600-h, cycled-pressure test (300 h under “dry” conditions and then 300 h after the addition of 1% water). The pressure cycles from 10 to 240 bars each second and the fluid temperature is 70°C.

Most of the references described above utilize a gravimetric determination of wear by either measuring the weight loss of the vanes, ring, or both. However, some hydraulic fluids exhibit non-Newtonian viscosity behavior leading to internal leakage and loss of power-transmission efficiency. These problems can be detected by experimental determination of pumping efficiency by flow-rate measurement [74].

2.2.4 Piston-Pump Testing

There are numerous wear surfaces in a piston pump. In addition to sliding wear, such as pistons in cylinders, there is mixed rolling and sliding, which would occur with rolling element bearings, rolling contact fatigue, which also may occur with rolling element bearing, and corrosion and cavitation wear, which might occur on the swash plate and other positions within the hydraulic pump. The relative amount of wear that would occur would also be critically dependent on the material pairs used for construction of the wear contacts. In view of the wide range of materials used for the construction and design of piston pumps, this is one reason why most of the “standard” pump tests developed to date have been vane-pump tests.

The objective of piston-pump design is to minimize energy consumption while optimizing hydrodynamic lubrication to minimize wear and internal leakage. The performance parameters are fluid flow, speed, torque, pressure, viscosity, and inlet pressure. To minimize friction and internal leakage, wear contact loading (pressure), speed, and viscosity must be optimized as shown in Fig. 10.1 [3]. In a piston pump,

the piston clearances may vary with eccentricity due to load and fluid viscosity. This may produce a change in the lubrication mechanism (e.g., hydrodynamic to boundary), resulting in increased wear and friction.

One piston-pump test commonly used in the hydraulic fluid industry is the Sundstrand Water Stability Test Procedure [75]. The test circuit containing a Sundstrand Series 22 axial piston pump is shown in Fig. 10.40. The test conditions are as follows:

Input speed:	3000–3200 rpm
Load pressure:	5000 psi
Charge pressure:	180–220 psi
Case pressure:	40 psi max.
Stroke:	1/2 of full
Reservoir temperature:	150 ± 10°F
Loop temperature:	180 ± 10°F
Maximum inlet vacuum:	5 in. Hg

The objective of this test is to determine the effect of water contamination on mineral-oil hydraulic fluid performance. The duration of the test is 225 h. In addition to disassembly and inspection for wear, corrosion, and cavitation, the test criterion is “flow degradation.” Flow degradation of 10% is considered a failure.

A cyclic loading variation of this test was recently reported to evaluate the performance of a water–glycol hydraulic fluid under these relatively high-loading conditions [76,77]. In this test, a Sundstrand swash-plate, axial piston pump which was driven by a Sundstrand Series 20 swash-plate piston motor at 890 rpm was tested at 3175 rpm. The load was supplied by a Vickers vane pump at 975 rpm. The test sequence is summarized in Table 10.16. The rotating components are visually inspected for wear.

The test circuit for the piston-pump portion of the Haggblunds–Denison HFO piston pump is illustrated in Fig. 10.41. This test, which utilizes a Dennison P46 piston pump, was developed to evaluate the multimetal compatibility of a fluid and its corrosiveness against soft metals in a severe hydraulic environment. This test is conducted for 100 h and then the pump components are visually inspected for wear, corrosion, and cavitation at the conclusion of the test.

Another piston-pump test has recently been proposed by The Rexroth Corporation [78]. The test circuit is provided in Fig. 10.42 and is based on a Breuningham A4VSO swash-plate, axial piston pump. The objective of this test is to better discriminate and classify hydraulic and wear performance of a hydraulic fluid. It is proposed that this would be done by prescribing performance levels to be achieved. Establishment of these performance levels has not been developed as of this time.

A less well-known cycled-pressure, piston-pump test is the Vickers AA 65560-1SC-4 piston pump test [79]. Previous work showed that if there is no cavitation resulting from inlet starvation and if the hydraulic fluid is clean, then there are four principle modes of failures: (1) spalling of the yoke and spindle-bearing group, (2) fatigue failure of the control piston assembly, (3) rotating group assembly failure due to worn front and tail drive bearings, and (4) static and dynamic O-ring failures. In a sense, piston-pump tests are excellent bearing and cavitation tests.

Janko used high-speed piston-pump tests conducted for 1250 h to supplement successful preliminary vane-pump testing [80]. This test was conducted at constant

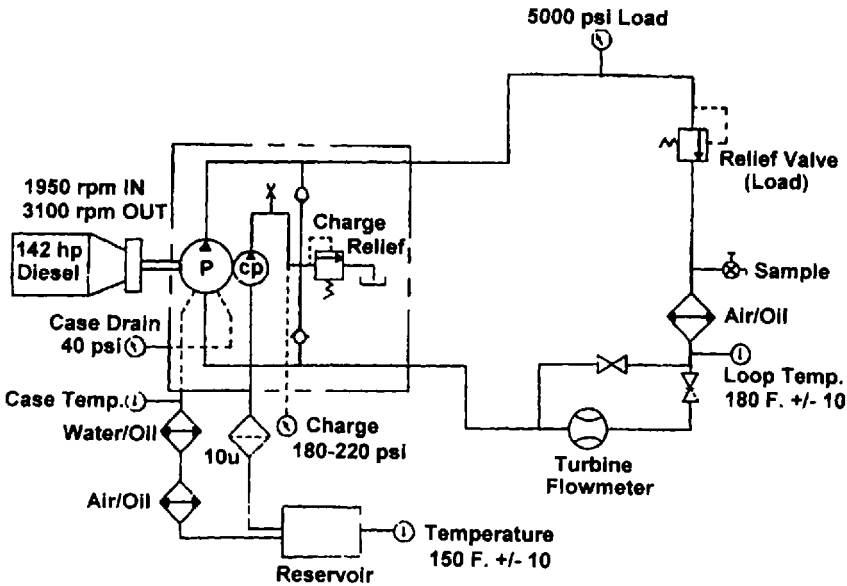


Figure 10.40 Schematic of the Sundstrand water stability test circuit.

140 bars pressure for 1000 h and then completed by cycling the pressure between 70 and 140 bars at 0.1 Hz. The pump was disassembled every 250 h and visually inspected. The stressed components, including the pistons, piston slippers, cylinder barrel, and reversing plate, were inspected and measured for wear. In addition, it was learned that the hydraulic fluids being studied caused such severe bearing wear that they had to be replaced every 250–500 h. The same fluids produced severe wear on the drive shaft with spline ring and thrust pins. These results show the value of piston-pump testing to significantly increase the wear stress of hydraulic fluids.

Edghill and Rubbery studied the correlation of laboratory testing with the type and frequency of field failures [79]. Their analysis showed that the most critical areas for failure are as follows:

Table 10.16 The 500-h Cycled-Pressure Sundstrand Pump Test

Duration ^a (s)	Vickers (MPa)	Sundstrand (MPa)
130	1.17	21.37
325	0.72	17.24
60	2.07	31.03
85	0.72	17.24

^aThe total time per cycle is 600 s.

P46 Test Stand

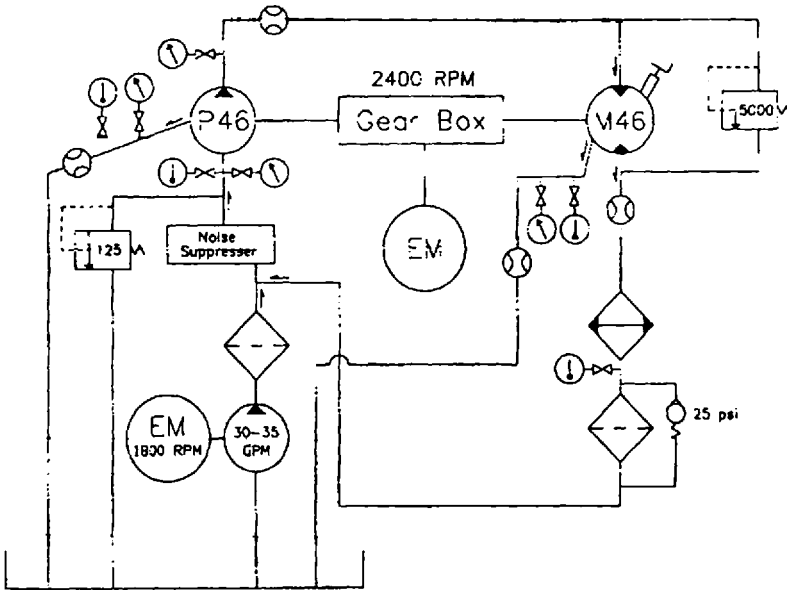


Figure 10.41 Schematic of the Denison P46 piston-pump test portion of the Hagglands-Denison HFO protocol.

For strength

1. Piston necks
2. Shafts
3. Body kidney ports

For bearing surfaces

1. Slipper-cam plate interface
2. Piston skirt-cylinder bore
3. Cam-plate trunion liners

Recently, Ohkawa et al. developed a piston pump test to evaluate biodegradable vegetable oil derived hydraulic fluids [80]. This test stand (see Fig. 10.43) utilized a Komatsu HPV35+35 twin-piston pump under the following cycled-pressure test conditions (Fig. 10.44):

Pressure:	10–420 kg/cm ² (140–6000 psi)
Oil Flow:	16 gal (at 140 psi), 5 gal (at 6,000 psi)
Speed:	2100 rpm
Temperature:	80°C
Tank Volume:	16 gal
Duration:	500 h

The test criteria included pump efficiency change, wear and surface roughness, formation of lacquer and varnish, and hydraulic-oil deterioration.

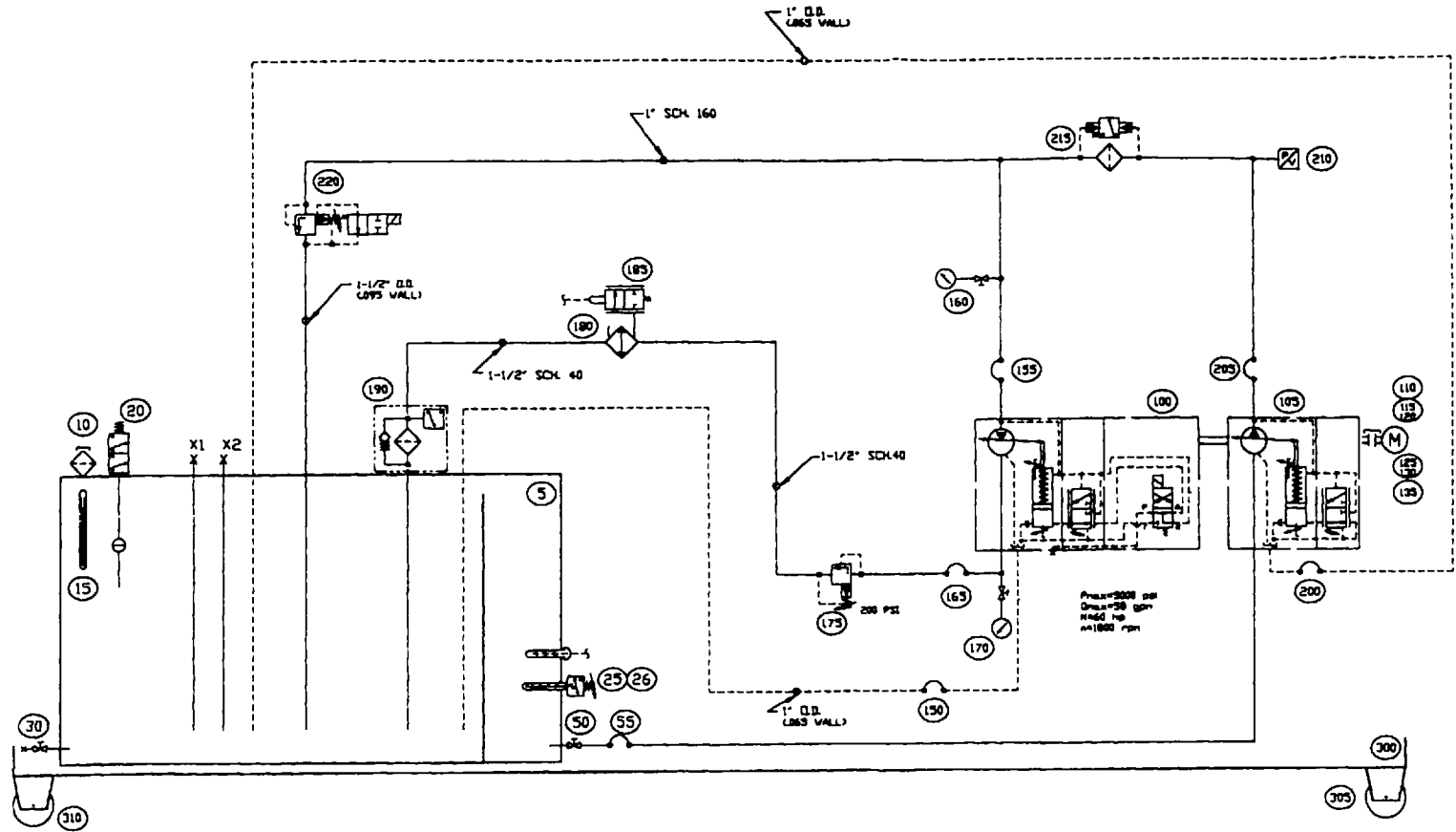


Figure 10.42 Schematic of the proposed Rexroth piston-pump test.

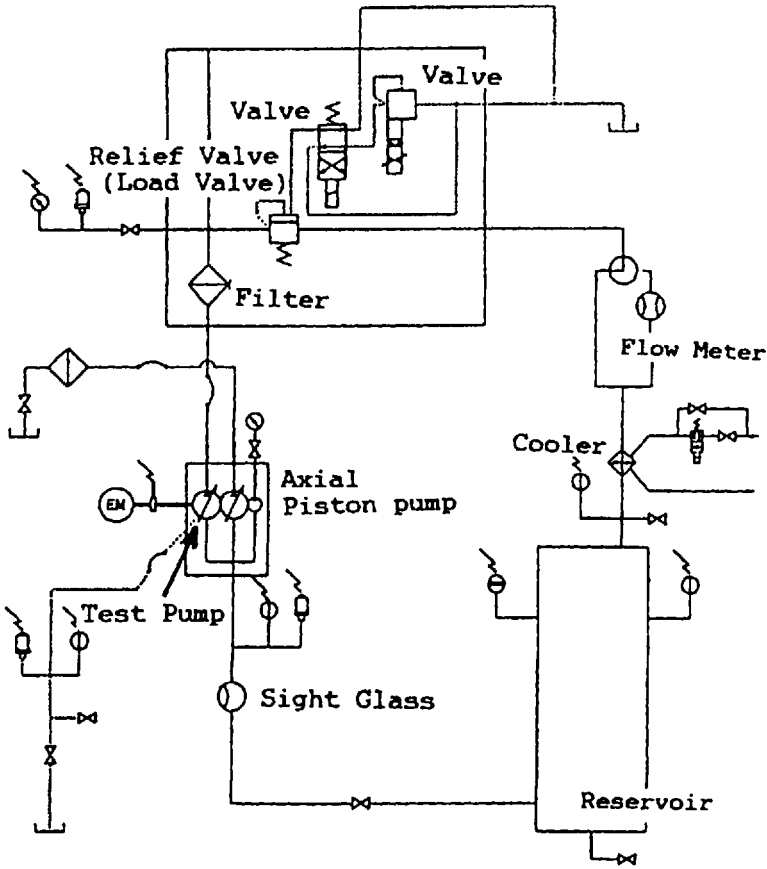


Figure 10.43 Komatsu HPV35+35 piston-pump test stand circuit.

Some piston pumps are used in a very broad-range temperature environment (-46°C to 204°C). There are two tests that have been reported for these applications. Hopkins and Benzing utilized the test circuit shown in Fig. 10.45, which uses a Manton Gaulin Model 500 HP-KL6-3PA, three-piston pump [81]. The modifications used for this pump did not facilitate the analysis of pump wear surfaces. Instead, the

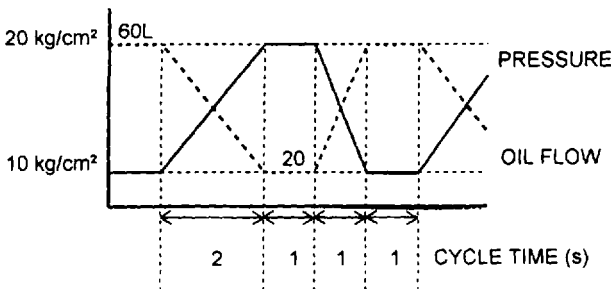


Figure 10.44 Summary of Komatsu test conditions.

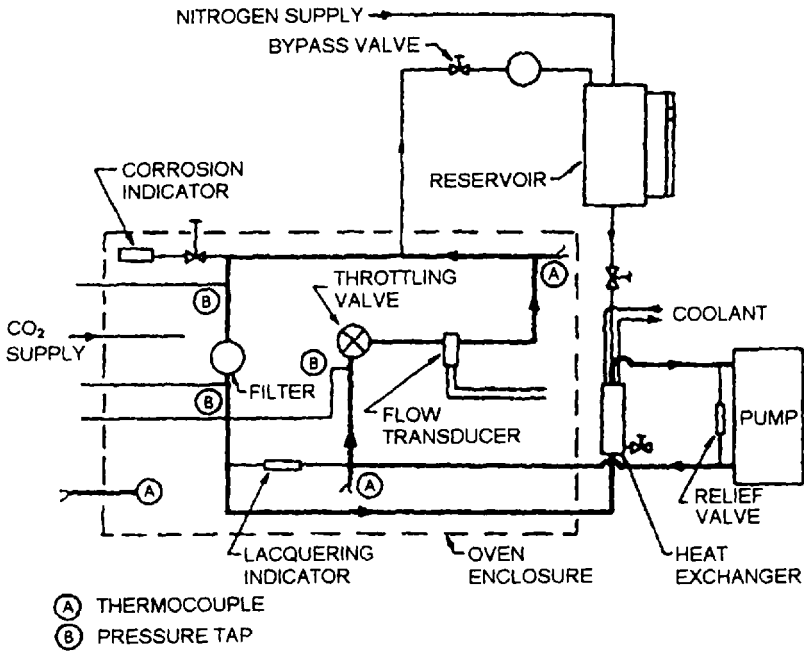


Figure 10.45 Hopkins-Benzing high-temperature modified Manton Gaulin piston-pump test circuit.

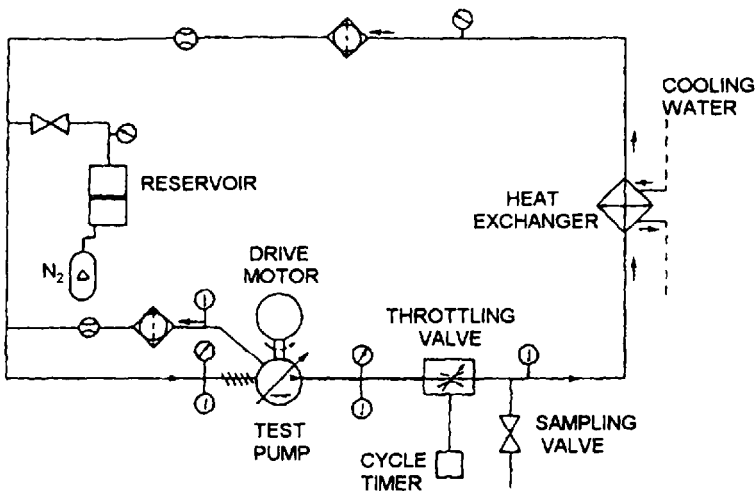


Figure 10.46 Gschwender piston-pump test stand.

tests, which were conducted at 3000 psi, 550°F for 100 h were designed to evaluate fluid degradation, corrosion, lacquering, and sludging tendencies.

Gschwender et al. used a test circuit utilizing a Vickers model PV3-075-15 pump to evaluate the wear of high-temperature (122°C/250°F) poly(alpha-olefin)-based hydraulic fluids [82]. The test circuit is illustrated in Fig. 10.46. The tests were conducted at 20.4 MPa (2960 psi) and 5400 psi with the throttle valve closed and 5000 psi with the throttle valve open.

2.2.5 Gear-Pump Testing

In the above discussion regarding vane pumps, it was observed that the primary mode of wear, although certainly not the only one, was sliding wear of the vanes on the ring. For piston-pump testing, failure analysis was more complex because there were numerous surfaces that must be inspected. Sliding with hydrodynamic wear was still the primary component. However, although sliding wear is still important in gear pumps, the wear mechanisms are even more variable. For example, in open gears, hydrodynamic, EHD, mixed-EHD, and boundary lubrication mechanisms may all occur simultaneously, depending on the position and speed of the gear, as seen in Fig. 10.47 [83].

Frith and Scott performed a detailed theoretical analysis of gear-pump wear. They noted that the primary areas of wear are the side plate near the suction port, the gear meshing zone, the gear tips, and casing, especially near the suction port [84]. In addition, the imbalance of pressure across the pump may cause the gear shaft to deflect toward the inlet, creating a reduction in gear-tip clearance at the inlet. Also, a hydrodynamic wedge between the gear ends and the side plate, in combination with the pressure behind the plate, tends to force the side plate against the gears in the inlet region, as shown in Fig. 10.48. All of these conditions may affect the efficiency of gear-pump operation. Interestingly, there have been relatively few reports of hydraulic fluid lubrication in a gear pump and there are no industry-standard gear-pump lubrication tests.

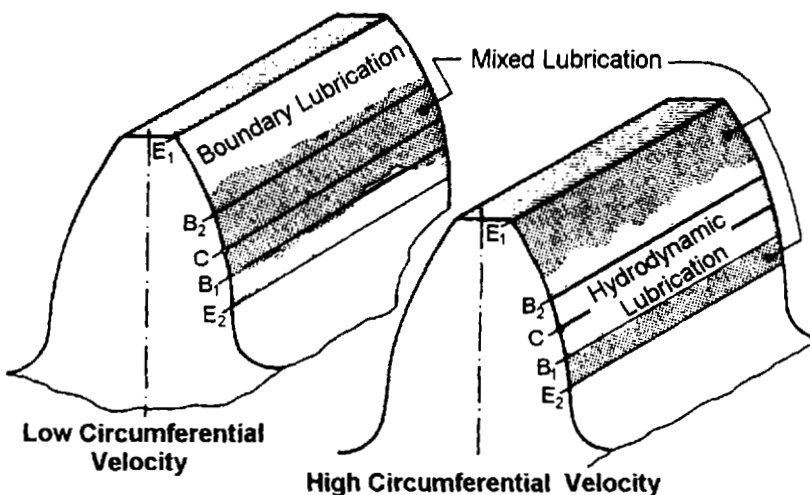


Figure 10.47 Lubrication mechanisms on the gear tooth as a function of speed.

One study that has been reported was conducted by Knight, who used the multiple-gear-pump test stand shown in Fig. 10.49 [85]. Seven Hamworthy Hydraulics Ltd. Type PA 2113 gear pumps were run at 14.3 MPa (2075 psi). The test is run until pump failure, usually due to needle-bearing fatigue. The condition of the roller bearings was monitored at least once every 24 h.

In another study, a cycled load over 500,000 cycles from zero to the maximum rated pressure, speed, and temperature for the pump and the fluid was recommended [86]. In addition to the cycled loading test, an endurance test (maximum pressure, speed, and temperature for the fluid for 250 h, “proof” test where the pump is operated under extreme conditions at relatively short periods of time (e.g., 5 h) and an initial run-in test. Toogood stated that although degradation in performance would occur under extreme conditions, it was not clear if the damage was greatest under constant-pressure or cycled-pressure conditions [87].

Wanke conducted a study of the effects of fluid cleanliness with a multiple-gear-pump test stand shown in Fig. 10.50 [88]. Two test sequences were used. One was a cycled-pressure test (1 cycle/10 s). The other sequence was an endurance test. As a result of this work, it was recommended that although flow was an adequate measure of the pump’s integrity, monitoring the torque throughout the test would provide greater insight into overall pump integrity during the test.

2.2.6 Evaluation of Pump-Lubrication Results

The most commonly used analytical methods to monitor hydraulic pump operation have been reviewed in detail [89]. These methods include flow analysis, volumetric and overall efficiency, cavitation pressure, minimum inlet pressure, and others. Johnson has provided a detailed review of pump-testing methods to monitor pump durability and hydraulic operation [90].

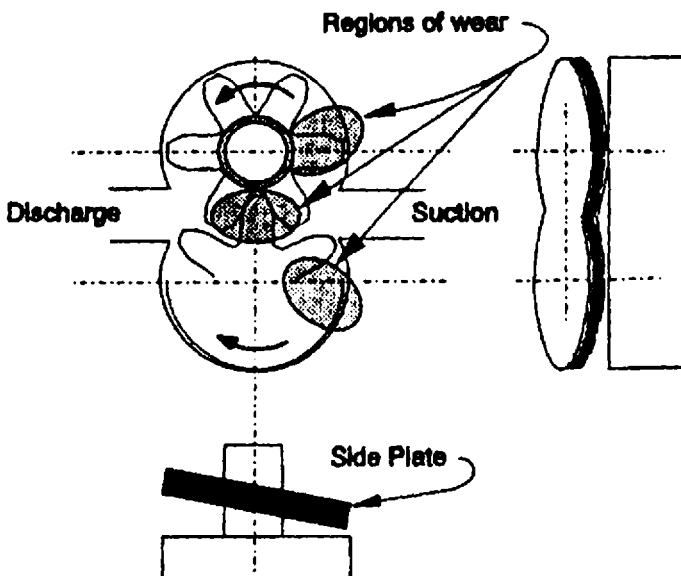


Figure 10.48 Side-plate action in a gear pump.

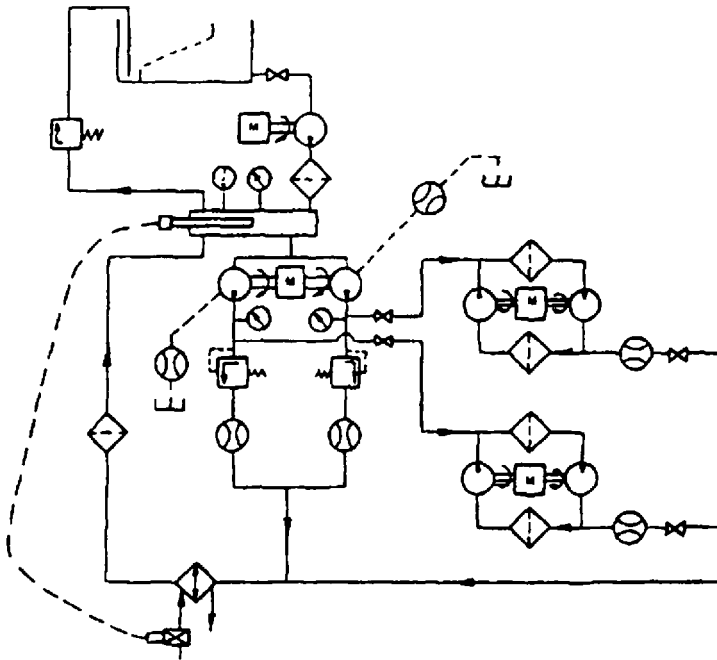


Figure 10.49 Gear-pump test circuit used at the British National Coal Board.

Hunt has viewed pump-lubrication analysis from the standpoint of failure correlation. For example, hydraulic pumps are periodically inspected throughout the test for the following:

- Cavitation of port plate
- Bearing wear and breakup
- Piston slipper pad wear and blockage
- Blockage of control devices
- Piston and cylinder wear
- Case seal defects
- Gear teeth wear or fracture

In addition to inspection, temperatures, pressures, and flow throughout the test should be monitored, as they are indicative of friction generation and fluid contamination. Also, wear analysis and vibration analysis as continuous monitors of wear should be performed [91–93]. Common vibrational and acoustical monitoring procedures and interpretive methods have been reviewed previously [94,95].

2.2.7 A “Universal” Hydraulic-Pump Test Stand as a Tribological Test

Currently, Feldmann et al. [96] are in the process of developing a “universal” hydraulic-pump test stand that will provide a means of characterizing the expected wear at various wear contacts within the hydraulic system. This test, although still in development, will be based on tribological analysis. Wear contacts for a vane pump and an axial piston pump are illustrated in Fig. 10.51. Wear contact geometries

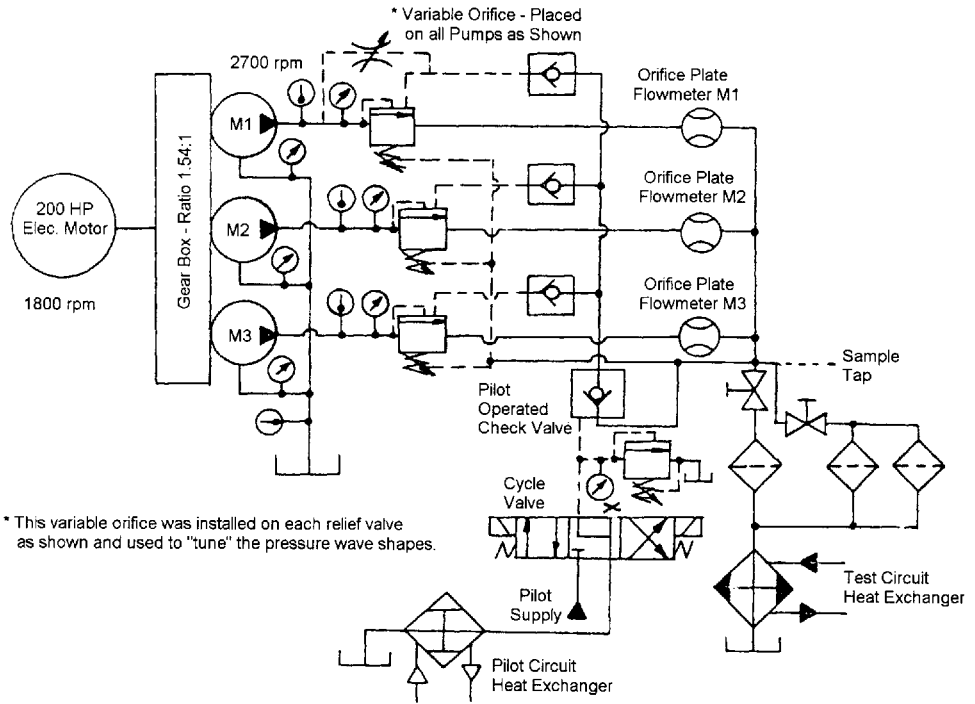


Figure 10.50 Wanke gear-pump test stand.

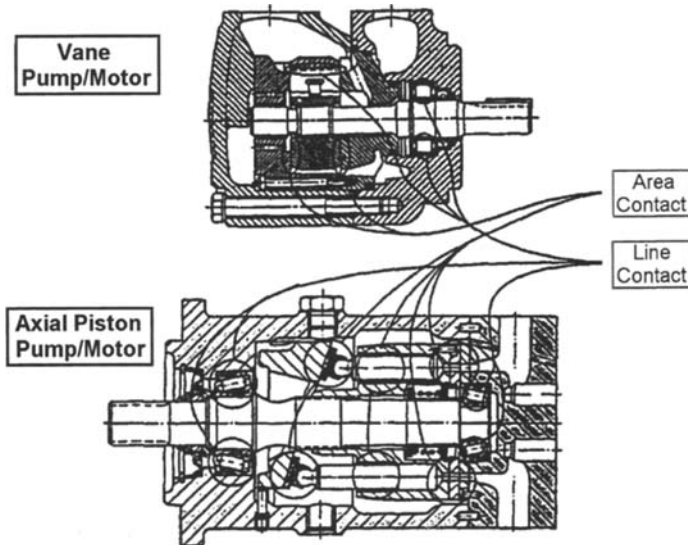


Figure 10.51 Characterization of wear surfaces in a piston pump.

Table 10.17 Tribological Stresses

	Type of motion			Contact geometry			Operational sequence of motions		Other tribologically relevant parameters				
	Rolling	Sliding	Impacting	Point contact	Line contact	Area contact	Continuous	Oscillating	Pressure difference	Dynamic normal force	Asymmetric load	Superimposed motion	Variability
Vane pumps/motors													
Vane–ring	(E)		(E)		(E)		(E)	(E)	Yes	Yes	No	No	Yes
Vane–slot		(E)			(E)			(E)	Yes	Yes	No	No	No
Vane–sides		(E)				(E)	(E)		Yes	No	No	Yes	No
Gear pumps/motors													
Gear wheel–sides		(E)				(E)	(E)		Yes	No	No	No	No
Gear wheel work	(E)				(E)			(E)	No	Yes	No	No	Yes
Piston pumps/motors													
Piston pin bushing (A/R)		(E)				(E)		(E)	Yes	Yes	Yes	Yes	No
Sliding block–plate (A)		(E)				(E)	(E)		Yes	Yes	No	Yes	Yes
Sliding block–plate (R)		(E)				(E)	(E)		Yes	Yes	No	No	Yes
Sliding block–piston head (A)		(E)				(E)			No	Yes	No		Yes
Sliding block–piston head (R)		(E)				(E)			No	Yes	No		Yes

Table 10.17 Continued

	Type of motion			Contact geometry			Operational sequence of motions		Other tribologically relevant parameters				
	Rolling	Sliding	Impacting	Point contact	Line contact	Area contact	Continuous	Oscillating	Pressure difference	Dynamic normal force	Asymmetric load	Superimposed motion	Variability
Valve plate – piston barrel (A)		(E)				(E)	(E)		Yes	No	Yes	No	Yes
Support for captive C-ring (A)	(E)				(E)			(E)	No	No	No	No	Yes
Axial distributor (R)		(E)				(E)	(E)		No	No	Yes	No	No
Rotary slide valve		(E)				(E)	(E)		No	No	No	No	Yes
Retainer plate – guide ball (A)		(E)			(E)			(E)	No	No	No	No	Yes
Sliding block – retainer plate (A)		(E)				(E)	(E)		No	No	No	No	Yes
Cylinders													
Piston – cylinder tube		(E)				(E)		(E)	Yes	No	No	No	No
Rod seal		(E)				(E)		(E)	Yes	No	No	No	Yes
Others													
Roller bearings	(E)				(E)		(E)		No	No	No	No	No
Shaft – radial shaft sealing ring		(E)			(E)		(E)		Yes	No	No	No	Yes
Serrated shaft				(E)		(E)	(E)		No	No	No	No	Yes
Plain bearing		(E)				(E)	(E)		Yes	No	No	No	Yes

Note: (A): axial piston machine; (R): radial piston machine; (E): extremely important with respect to failure behavior.

Table 10.18 Tribological Stresses in Axial Piston Machines (Test Runs in the Working Range with Synthetic Esters)

Pairings	Sliding wear	Rolling wear	Grain slip wear	Erosive wear	Cavitation	Wear by impact	Vibration wear	Additional observation	Wear behavior relative to mineral oil
Piston pin bushing	(W)		(W)	(W)	(W)				
Sliding block – plate	(C)		(C)	(W)	(W)			Erosion or cavitation not significant	Comparable
Sliding block – piston head	(W)		(W)	(C)	(C)				
Valve plate – piston barrel	(C)							In some case, discoloration and transfer of material	Comparable or better
Retainer plate – holding-down clamp for the plate	(W)		(W)						
Sliding block – retainer plate	(C)							Dug in up to 25 μm deep	Worse
Shaft – radial shaft sealing ring	(C)							Track worn in (up to 24 μm) leakage	Worse
Plain bearing	(C)		(C)	(W)	(W)			In some cases, PTFE layer worn away	Comparable
Roller bearing	(W)	(C)						Tracks, pitting, pressure marks	Comparable or worse
Serrated/polygonal shaft						(W)	(C)	Pitting development, removal of material	Worse

(W): pairings where wear is expected; (C): pairing with conspicuous wear.

and characteristic wear mechanisms have also been classified as shown in Tables 10.17 and 10.18, respectively.

3 CONCLUSIONS

An unsuccessful attempt was made to correlate the wear test results of various bench tests commonly employed for hydraulic fluid selection and troubleshooting performance of used fluids with ASTM D-2882, a Sperry–Vickers vane pump test. The bench tests included Shell 4-ball, pin-on-V-block, SRV ball-on-disk, Timken ASTM D-2782, and a recently developed cyclic contact stress test. In no case did the bench tests successfully predict the wear-rate rankings of the ASTM D-2882 test, nor were they consistent with each other. Analysis of the problem using fundamental principles of lubrication suggest that the poor correlations are probably reasonable because the actual loading, rolling and sliding speeds, contact geometry, and materials were not adequately considered. Therefore, if bench tests are to be used, they should be custom designed to model the pump-wear contact of interest and correlation between the bench test and hydraulic pump wear must be established.

An overview of selected vane-, piston-, and gear-pump testing circuits and procedures from the viewpoint of tribological testing have been provided here. With the exception of the various tests based on the Vickers V-104 vane pump and perhaps the Haggblunds–Denison HFO piston-pump test, none of the pump tests described here have achieved broad industry acceptance. Most of the tests are pass/fail tests based either on inspection for cavitation and wear, fluid flow leakage, or weight loss of critical rotating components. Most of these tests do not employ continuous monitoring of hydraulic efficiencies and pressures, torque, vibrational analysis, and so forth. Therefore, although it may be desirable to either use or modify some of the tests reported here in the development of national standards, they should all be updated to reflect current engineering practice and possibilities to better model the tribological performance of the pump during use with a particular hydraulic fluid.

REFERENCES

1. ASTM D2882-83, "Standard Method for Indicating the Wear Characteristics of Petroleum and Non-Petroleum Hydraulic Fluids in a Constant Volume Vane Pump," American Society for Testing and Materials, Conshohocken, PA.
2. J. Steiger, "AAMA 524 Part 2: Anti-Wear Hydraulic Oils," American Automobile Manufacturers Association, 1995.
3. S. Silva, "Wear Generation in Hydraulic Pumps," SAE Trans., 1990, 99, pp. 635–652.
4. R. Blanchard and L. R. Hulls, "Automated Test Facility for Aircraft Hydraulic Pumps and Motors," RCA Eng., 1975, 20(6), pp. 36–39.
5. A. Hibi, T. Ichikawa, and M. Yamamura, "Experimental Investigation on Torque Performance of Gear Motor in Low Speed Range," Bull. JSME, 1976, 19, pp. 179–186.
6. H. Ueno and K. Tanaka, "Wear in a Vane Pump," Junkatsu (J. Jpn. Soc. Lubr. Eng.), 1988, 33, pp. 425–430.
7. W. M. Shrey, "Evaluation of Fluids by Hydraulic Pump Tests," Lubr. Eng., 1959, 15, pp. 64–67.
8. R. Renard and A. Dalibert, "On the Evaluation of Mechanical Properties of Hydraulic Oils," J. Inst. Petrol., 1969, 55, pp. 110–116.

9. G. C. Knight, "The Assessment of the Suitability of Hydrostatic Pumps and Motors for Use With Fire-Resistant Fluids," in *Rolling Contact Fatigue: Perform. Test. Lubr., Pap. Int. Symp.*, R. Tourret and E. P. Wright, eds., 1977, pp. 193–215.
10. O. P. Lapotko, V. M. Shkol'nikov, Sh. K. Bogdanov, N. G. Zagorodni, and V. V. Arsenov, "Evaluation of Antiwear Properties of Hydraulic Fluids in Pump," *Chem. Tech. Fuels and Oils*, 1981, 17, pp. 231–234.
11. R. K. Tessmann and I. T. Hong, "An Effective Bench Test for Hydraulic Fluid Selection," *SAE Technical Paper Series*, Paper 932438, 1993.
12. J. M. Perez, R. C. Hanson, and E. E. Klaus, "Comparative Evaluation of Several Hydraulic Fluids in Operational Equipment, A Full-Scale Pump Stand Test and the Four-Ball Wear Tester. Part II. Phosphate Esters, Glycols and Mineral Oils," *Lubr. Eng.*, 1990, 46, pp. 249–255.
13. K. Mizuhara and Y. Tsuya, "Investigation for a Method for Evaluating Fire-Resistant Hydraulic Fluids by Means of an Oil-Testing-Machine," in *Proc. of the JSLE Int. Tribol. Conf.*, 1985, pp. 853–858.
14. L. D. Wedeven, G. E. Totten, and R. J. Bishop, Jr., "Performance Map Characterization of Hydraulic Fluids," *SAE Technical Paper Series*, Paper 941752, 1994.
15. A. Platt and E. S. Kelley, "Life Testing of Hydraulic Pumps and Motors on Fire Resistant Fluids," in *Proc. of the 1st Fluid Power Symposium*, The British Hydromechanics Research Association, 1969, paper SP 982.
16. G. E. Totten, R. J. Bishop, Jr., and G. H. Kling, "Evaluation of Hydraulic Fluid Performance: Correlation of Water–Glycol Fluid Performance by ASTM D2882 Vane Pump and Various Bench Tests," *SAE Technical Paper Series*, Paper 952156, 1995.
17. ASTM D4172-88, "Standard Method for Wear Preventative Characteristics of Lubricating Fluids (Four-Ball Method)," American Society for Testing and Materials, Conshohocken, PA.
18. J. Korycki and B. Wislicki, "Criteria the Lubricating Properties of Synthetic Fluids," in *Proc. Conf. Synth. Lubr.*, A. Zakar, ed., 1989, pp. 213–219.
19. J. M. Perez, R. C. Hanson, and E. E. Klaus, "Comparative Evaluation of Several Hydraulic Fluids in Operational Equipment, A Full-Scale Pump Stand Test and the Four-Ball Wear Tester: Part II—Phosphate Esters, Glycols, and Mineral Oils," *Lubr. Eng.*, 1990, 46, pp. 249–255.
20. E. E. Klaus and J. M. Perez, "Comparative Evaluation of Several Hydraulic Fluids in Operational Equipment, a Full-Scale Pump Test Stand, and the Four-Ball Wear Tester," *SAE Technical Paper Series*, Paper 831680, 1983.
21. J. M. Perez, "A Review of Four-Ball Methods for the Evaluation of Lubricants," in *Tribology of Hydraulic Pump Testing ASTM STP 1310*, G. E. Totten, G. H. Kling, and D. J. Smolenski, eds., 1996, American Society of Testing and Materials; Conshohocken, PA, pp. 361–371.
22. "Pump Test Procedure for Evaluation of Antiwear Hydraulic Fluids for Mobile Systems," Form M-2952-S, Vickers Incorporated, Troy, Michigan.
23. J. M. Perez, E. E. Klaus, and R. C. Hansen, "Comparative Evaluation of Several Hydraulic Fluids in Operational Equipment, a Full-Scale Pump Stand Test and the Four-Ball Wear Tester—Part III: New and Used Hydraulic Fluids," *Lubr. Eng.*, 1996, 52, pp. 416–422.
24. ASTM D2670-81, "Standard Method for Measuring Properties of Fluid Lubricants (Falex Pin and V-Block Method)," American Society for Testing and Materials, Conshohocken, PA.
25. R. Inoue, "Antiwear Characteristics of Fire Resistant Fluids—Results of the Gamma Falex Tests," *FRH J.*, 1982, 3, pp. 45–49.
26. J. Chu and R. K. Tessman, "Antiwear Properties of Fire-Resistant Fluids," *FRH J.*, 1980, 1, pp. 15–20.

27. J. G. Eleftherakis and R. P. Webb, "Correlation of Lubrication Characteristics to Pump Wear Using a Bench Top Surface Contact Test Method," in *Tribology of Hydraulic Pump Testing ASTM STP 1310*, G. E. Totten, G. H. Kling, and D. J. Smolenski, 1996, American Society for Testing and Materials; Conshohocken, PA, pp. 338–348.
28. R. Inoue, "Surface Contact Wear—Part 2: Repeatability of the Gamma Falex Test," *BFPR J.*, 1983, 16, pp. 445–453.
29. R. K. Tessman and T. Hong, SAE Technical Paper Series, Paper 932438, 1993.
30. ASTM D4995-95, "Standard Method for Evaluating Wear Characteristics of Tractor Hydraulic Fluids," American Society for Testing and Materials, Conshohocken, PA.
31. ASTM D2782-77, "Standard Method for Measurement of Extreme-Pressure Properties of Lubricating Fluids (Timken Method)," American Society for Testing and Materials, Conshohocken, PA.
32. S.-H. Jung, U.-S. Bak, S.-H. Oh, H.-C. Chae, and J.-Y. Jung, "An Experimental Study on the Friction Characteristics of Oil Hydraulic Vane Pump," in *Proc. of the Int. Tribology Conf.*, 1995, pp. 1621–1625.
33. ASTM 5707-97, "Standard Method for Measuring Friction and Wear Properties of Lubricating Grease Using a High-Frequency Linear-Oscillator (SRV) Test Machine," American Society for Testing and Materials, Conshohocken, PA.
34. J. Reichel, "Mechanical Testing of Hydraulic Fluids," in *Industrial and Automotive Lubrication*, 11th Int. Colloquium at Technische Akademie Esslingen, 1998, Vol. III, pp. 1825–1836.
35. DIN 51,354-2, "Prüfung von Schmierstoffen FZG-Zahnrad-Verspannungs-Prüfmaschine," Deutsches Institute für Normung. V., Berlin, 1992.
36. ASTM D2596-87, "Standard Test Method for Measurement of Extreme-Pressure Properties of Lubricating Grease (Four-Ball Method)," American Society for Testing and Materials, Conshohocken, PA.
37. ASTM D2783-82, "Standard Method for Measurement of Extreme-Pressure Properties of Lubricating Fluids (Four-Ball Method)," American Society for Testing and Materials, Conshohocken, PA.
38. E. Y. Urata, Y. Iwaizumi, and K. Iwamoto, "Assessment of the Antiwear Properties of High-Water-Content Fluids Using a Vickers V104C Vane Pump," *Yuatsu to Kukiatsu*, 1986, 17(7), pp. 543–553.
39. G. Jacobs, W. Backe, C. Busch, and R. Kett, "A Survey on Actual Research Work in the Field of Fluid Power," in *1995 STLE National Meeting*, 1995.
40. M. Priest, C. N. March, and P. V. Cox, "A New Test Method for Determining the Antiwear Properties of Hydraulic Fluids," in *Tribology of Hydraulic Pump Testing, ASTM STP 1310*, G. E. Totten, G. H. Kling, and D. M. Smolenski, eds., 1995, American Society for Testing and Materials; Conshohocken, PA.
41. P. I. Lacey, D. W. Naegeli, and B. R. Wright, "Tribological Properties of Fire-Resistant, Non-Flammable and Petroleum-Based Hydraulic Fluids," in *Tribology of Hydraulic Pump Testing, ASTM STP 1310*, G. E. Totten, G. H. Kling, and D. M. Smolenski, eds., 1995, American Society for Testing and Materials; Philadelphia, PA.
42. P. Kenny and E. D. Yardley, "The Use of Unisteel Rolling Fatigue Machines to Compare the Lubricating Properties of Fire-Resistant Fluids," *Wear*, 1972, 20, pp. 105–121.
43. K. J. Young, "Hydraulic Fluid Wear Test Design and Development," in *Tribology of Hydraulic Pump Testing ASTM STP 1310*, G. E. Totten, G. H. Kling, D. M. Smolenski, eds., 1995, American Society for Testing and Materials, Conshohocken, PA, pp. 156–164.
44. L. Wedeven, G. E. Totten, and R. J. Bishop, Jr., SAE Technical Paper Series, Paper 941752, 1994.
45. L. D. Wedeven, G. E. Totten, and R. J. Bishop, Jr., Performance Map and Film Thickness Characterization of Hydraulic Fluids," SAE Technical Paper Series, Paper 952091, 1995.

46. M. Maamouri, J. F. Masson, and N. J. Marchand, "A Novel System to Study Wear, Friction and Lubricants," *J. Mater. Eng. Perf.*, 1994, 3, pp. 527–539.
47. S. Hogmark and S. Jacobson, "Hints and Guidelines for Tribotesting and Evaluation," *Lubr. Eng.*, 1992, 48, pp. 569–579.
48. G. H. Robinson, R. F. Thomson, and F. J. Webbere, "The Use of Bench Wear Tests in Materials Development," *SAE Trans.*, 1959, 67, pp. 569–579.
49. R. M. Voitik, "Realizing Bench Test Solutions to Field Tribology Problems Utilizing Tribological Aspect Numbers," in *Tribology—Wear Test Selection for Design and Application*, A. W. Ruff and R. G. Bayer, eds., 1993, American Society for Testing and Materials; Conshohocken, PA, ASTM STP 1199, pp. 45–59.
50. ASTM D2714-68. "Standard Method for Calibration and Operation of the Alpha Model LFW-1 Friction and Wear Testing Machine," American Society for Testing and Materials, Conshohocken, PA.
51. K. C. Ludema, "Cultural Impediments for Practical Wear Modeling of Wear Rates," in *Tribological Modeling for Mechanical Designers*, K. C. Ludema and R. G. Mayer, eds., 1991, American Society for Testing and Materials; Conshohocken, PA, ASTM STP 1105, pp. 180–185.
52. A. B. Turski, "Studies of Engineering Properties of Fire Resistant Hydraulic Fluids for Underground Use," *Mining Miner. Eng.*, 1969, February, pp. 50–59.
53. G. C. Knight, "Experience with the Testing and Application of Fire-Resistant FLuids in the National Coal Board," *SAE Technical Paper Series*, Paper 810962, 1981.
54. T. Horiuchi, "Hydraulic Fluids and Trends in Oil Pumps and Motors," *Nisseki Rev.*, 1979, 21(3), pp. 151–158.
55. F. Feicht, "Factors Influencing Service Life and Failure of Hydraulic Components," *Oilhydraulik Pneumatic*, 1975, 20(12), pp. 804–806.
56. H. Ueno, K. Tanaka, and A. Okajima, "Wear in the Vanes and Cam Ring of a Vane Pump," *Nippon Kikai Gakkai Ronbunsho Bhen*, 1985, 52(480), pp. 2990–2997.
57. J. R. Hemeon, "How to Evaluate Performance of a Hydraulic Fluid," *Appl. Hydraulics*, 1995, August, pp. 43–44.
58. Paul Schacht verbal communication regarding this procedure as the standard cycled pressure vane pump test recommended by (Robert Bosch) Racine Fluid Power, Racine, WI.
59. V. V. Arsenov, L. O. Sedova, O. P. Lapotko, L. V. Zaretskaya, V. I. Kel'bas, and V. M. Ryaboshapka, "Method for Investigating the Antiwear Properties of the Water–Glycol Liquids," *Vestnik Mashinostroeniya*, 1988, 68, pp. 32–33.
60. H. W. Thoenes, K. Bauer, and P. Herman, "Testing the Antiwear Characteristics of Hydraulic Fluids: Experience with Test Rigs Using a Vickers Pump," in *Performance Testing of Hydraulic Fluids*, R. Turret and E. P. Wright, eds., 1978, Heyden and Son Ltd.; London.
61. G. M. Gent, "Review of ASTM D 2882 and Current Possibilities," in *Tribology of Hydraulic Pump Testing*, G. E. Totten, G. H. Kling and D. J. Smolenski, eds., 1996 American Society for Testing and Materials; Conshohocken, PA, pp. 96–105.
62. G. E. Totten, R. J. Bishop, Jr., and G. M. Webster, "Water–Glycol Hydraulic Fluid Evaluation by ASTM D2882: Significant Contributors to Erroneous and Non-Reproducible Results," *SAE Technical Paper Series*, Paper 961740, 1996.
63. J. L. Glancey, E. R. Benson, and S. Knowlton, "A Low Volume Fluid Power Test for the Evaluation of Genetically Modified Vegetable Oils as Industrial Fluids," in 1998 SAE Off-Highway Conference.
64. Vickers Inc., "Vane Pump & Motor Design Guide for Mobile Equipment," Bulletin No. 353, revised 11-1-92, pp.10.
65. T. Runhua and Y. Caiyun, "The Vane Profile Improvement for a Variable Displacement Vane Pump," in *Proceedings of the International Fluid Power Applications Conference*, 1992, National Fluid Power Assoc., Milwaukee, WI.

66. R. J. Bishop, Jr. and G. E. Totten, "Comparison of Water-Glycol Hydraulic Fluids Using Vickers V-104 and 20VQ Vane Pumps," *Tribology of Hydraulic Pump Testing ASTM STP 1310*, 1995, G. E. Totten, G. H. Kling, and D. M. Smolenski, eds., American Society for Testing and Materials; Philadelphia, PA.
67. L. Gengcheng and M. Huanmou, "Test Stand Testing of Water-Glycol-Based, Non-Flammable Hydraulic Fluids," *Runhua Yu Mifeng*, 1985, 3, pp. 23-28.
68. H. T. Johnson and T. I. Lewis, "Vickers' 35VQ25 Pump Test," in *Tribology of Hydraulic Pump Testing*, G. E. Totten, G. H. Kling and D. J. Smolenski, eds., 1996 American Society for Testing and Materials; Conshohocken, PA, pp. 129-139.
69. E. H. Broszeit, H. Steindorf, and A. Kunz, "Testing of Hydraulic Fluids with Cell Vane Pumps," *Tribol. Schmierungstechnik*, 1990, 37(4), pp. 202-209.
70. A. J. Kunz and E. Broszeit, "Comparison of Vane Pump Tests Using Different Vane Pumps," in *Tribology of Hydraulic Pump Testing*, G. E. Totten, G. H. Kling, and D. J. Smolenski, eds., 1996, American Society for Testing and Materials; Conshohocken, PA, pp. 140-155.
71. A. Kunz, R. Gellrich, G. Beckmann, and E. Broszeit, "Theoretical and Practical Aspects of the Wear of Vane Pumps, Part B: Analysis of Wear Behaviour in the Vickers Vane Pump Test," *Wear*, 1995, 181-183, pp. 868-875.
72. J. F. Maxwell, S. E. Schwartz, and D. J. Viel, "Flow Characteristics of Hydraulic Fluids of Different Viscosities II. Flow in Pumps: Internal Leakage and Loss of Efficiency," ASLE Prepr. No. 80-AM-713-2, 1980.
73. "Sundstrand Water Stability Test," Sundstrand Bulletin 9658. (The test Protocol described was conducted by Southwest Research Institute in San Antonio, TX.)
74. G. E. Totten and G. M. Webster, "High Performance Water-Glycol Hydraulic Fluids," in Proc. of the 46th Natl. Conf. on Fluid Power, 1994, pp. 185-194.
75. S. Lefebvre, "Evaluation of High Performance Water/Glycol Hydraulic Fluid in High Pressure Test Stand and Field Trial," in STLE Annual Conference, 1993.
76. H. M. Melief, "Proposed Hydraulic Pump Testing for Hydraulic Fluid Qualification," in *Tribology of Hydraulic Pump Testing ASTM STP 1310*, G. E. Totten, G. H. Kling, and D. J. Smolenski, eds., 1995, American Society for Testing and Materials; Conshohocken, PA, pp. 200-207.
77. "Conduct Test-To-Failure on Hydraulic Pumps," Vickers AA-65560-1SC-4), NTIS No. AD 602244, 1963.
78. K. Janko, "A Practical Investigation of Wear in Piston Pumps Operated with HFA Fluids with Different Additives," *J. Synth. Lubr.*, 1987, 4, pp. 99-114.
79. C. M. Edghill and A. M. Rubbery, "Hydraulic Pumps and Motors—Development Testing: Its Relationship With Field Failures," in First European Fluid Power Conference, 1973, Paper No. 31.
80. S. Ohkawa, A. Konishi, H. Hatano, K. Ishihama, K. Tanaka, and M. Iwamura, "Oxidation and Corrosion Characteristics of Vegetable-Base Biodegradable Hydraulic Oils," SAE Technical Paper Series, Paper 951038, 1995.
81. V. Hopkins, and R. J. Benzing, "Dynamic Evaluation of High Temperature Hydraulic Fluids," *Ind. Eng. Chem. Prod. Res. Dev.*, 1963, 2, pp. 77-78.
82. L. J. Gschwender, C. E. Snyder, Jr., and S. K. Sharma, "Pump Evaluation of Hydrogenated Polyalphaolefin Candidates for a -54°C to 135°C Fire-Resistant Air Force Aircraft Hydraulic Fluid," *Lubr. Eng.*, 1987, 44, pp. 324-329.
83. C. G. Paton, W. B. Maciejewski, and R. E. Melley, "Test Methods for Open Gear Lubricants," *Lubr. Eng.*, 1990, 46, pp. 318-326.
84. R. H. Frith and W. Scott, "Wear in External Gear Pumps: A Simplified Model," *Wear*, 1994, 172, pp. 121-126.
85. G. C. Knight, "Experience with the Testing and Application of Fire-Resistant Fluids in the National Coal Board," *Trans. SAE*, 1981, 90, pp. 2958-2969.

86. "Pump Test Procedure for Evaluation of Antiwear Fluids for Mobil Systems," Vicker's Form No. M-2952-S.
87. G. J. Toogood, "The Testing of Hydraulic Pumps and Motors," in Proc. Natl. Conf. Fluid Power, 37th, 1981, National Fluid Power Association, Milwaukee, WI, Vol. 35, pp. 245–252.
88. T. Wanke, "A Comparative Study of Accelerated Life Tests Methods on Hydraulic Fluid Power Gear Pumps," in Proc. Natl. Conf. Fluid Power, 37th, 1985, Vol. 35, pp. 231–243.
89. American National Standard, "Hydraulic Fluid Power—Positive Displacement Pumps—Method of Testing and Presenting Basic Performance Data," ANSI/B93.27-1973.
90. K. L. Johnson, "Testing Methods for Hydraulic Pumps and Motors," in Proc. Natl. Conf. Fluid Power, 30th, 1974, Vol. 28, pp. 331–370.
91. T. M. Hunt, "Diagnostics in Fluid Power Systems—A Review," Tech. Diagnost., 1981, November, pp. 89–99.
92. T. M. Bashta and I. M. Babynin, "Determining the Operating Characteristics of Pumps," Sov. Eng. Res., 1983, 3(5), pp. 3–5.
93. G. A. Avrunin and G. N. Bakakin, "On Choosing the Conditions for Diagnosis of the Technical State of Hydraulic Motors," Sov. Eng. Res., 1989, 9(10), pp. 37–39.
94. G. E. Maroney and E. Fitch, in 3rd International Fluid Power Symposium, 1973, pp. C5-81–C5-96.
95. M. Dowdican, G. Silva, and R. L. Lowery, Oklahoma State Univ.—Fluid Power Research Center, Report No. OSU-FPRC-A5/84, 1984. (Reports currently available from FES, Inc., Stillwater, OK.)
96. Feldmann, J. Hinrichs, M. Kessler, and J. Nottrodt, "Ermittlung der Anwendungseigenschaften von Biologisch Schnell Abbaubaren Hydraulikflüssigkeiten durch Labortests," in Industrial and Automotive Lubrication, 11th Int. Colloquium at Technische Akademie Esslingen, 1998, Vol. I, pp. 271–280.
97. R. Gellrich, A. Kunz, G. Beckmann, and E. Broszeit, "Theoretical and Practical Aspects of the Wear of Vane Pumps, Part A: Adaptation of a Model for Predictive Wear Calculation," Wear, 1995, 181–183, pp. 862–867.

This page intentionally left blank

Vibrational Analysis for Fluid Power Systems

HUGH R. MARTIN

University of Waterloo, Waterloo, Ontario, Canada

1 INTRODUCTION

A wide range of manufacturing and processing equipment employs fluid power as a means of transporting energy to the work area. The fundamental operation of components within such a system generates vibrational energy that can result in unacceptable levels of noise and vibration. Often, this can be an indicator that the components inside the machine are starting to break down as a result of wear or the development of damage. In order to detect and analyze such problems, the following are important:

1. To have a good understanding of the processes involved
2. To know how to collect and analyze the resultant data
3. To know how to ensure that the data are clean of spurious information
4. To understand how to draw meaningful information from these results

It is the interaction between surfaces moving relative to each other that is a major cause of introducing vibrational energy into the surrounding structure. This, in turn, can generate further vibrations by exciting passive resonant frequencies within the structure itself. If the transfer of energy is at a sufficiently high amplitude level, then a sensor placed on the external surface of the component can detect useful information relating to the behavior and running condition of the machine.

In general, failure of surfaces in contact, such as bearings or gears, can result from several different activities, such as the following:

1. Pitting, which occurs at points of maximum Hertzian stress.

2. Scuffing, which is related to failure of lubricating films, caused by overheating. This is often the result of friction problems as a result of alternating welding and tearing of asperities in the surface structure.
3. Plastic flow, due to cold-working of the surfaces in contact.
4. Wear, which, unlike other types of surface damage, is not a local failure but is spread over large areas.

Any of these actions will produce distinct vibrational patterns. However, this information, when received at the sensor, will also contain energy from other sources such as structural resonances and externally generated noise. Signal processing provides the tools to extract the relevant information.

There is also a direct relationship between vibration and radiated noise. The propagation of sound, like vibration, is a dynamic process. In the former case, it is due to the fluctuations of pressure about a mean atmospheric-pressure level, which travel at the speed of sound for the media. Noise starts, for example, as the mechanical vibration of a surface, which then connects to the surrounding air to generate pressure disturbances. For simple plane waves, it can be shown that the pressure is proportional to surface velocity; the constant of proportionality is called the acoustic impedance (ρc). Hence, it is possible to use sound as a diagnostic tool to track the condition of equipment.

2 BASICS DEFINITIONS [1]

The propagation of both sound and vibration signals are dynamic events, measured in the one case as fluctuations of pressure in the atmosphere and the other as fluctuations of stress in the material. The only real difference is the speed at which the energy propagates; for example, in air at 343 m/s and in steel at 5000 m/s. The simplest signal in the time domain is the pure tone, which is described mathematically by

$$v(t) = v_{\max} \sin(\omega t)$$

where $\omega = 2\pi f$. In taking measurements with equipment, it is important to understand what the readout display is showing. It could be showing peak, that is max value, peak to peak or it could be showing root mean square (rms) value:

$$v_{\text{rms}} = \frac{v_{\max}}{\sqrt{2}}$$

These are all related to the average value, provided the signal is deterministic. Note that for a pure sine wave, the average value will be zero:

$$v_{\text{av}} = 0.9v_{\text{rms}} = 0.637v_{\text{pk}}$$

These are all just simple ways of obtaining some information about the signal; the peak value is obvious, the average value gives a measure of the offset of DC level, and the square of the signal gives a direct measure of the power content. For symmetrical signals about the positive and negative directions, the rms value is used instead of the average value. In the case of more complex signals with sharp rise times, these values are not accurate and a shape factor needs to be introduced:

Form factor

$$F_f = \frac{v_{rms}}{v_{av}}$$

Crest factor

$$F_c = \frac{v_{rms}}{v_{pk}}$$

Most measurements are expressed in terms of decibels. This nondimensional scale allows a wide of magnitude values in the data to be compressed into a reasonable size for plotting. In the case of frequency plots, the x axis is often a log scale, whereas decibels are on a linear scaled y axis.

The “bel” was developed for electronic power measurements, especially in relationship to audio applications. The ratio between two power values is

$$\frac{W_1}{W_2} = n$$

where n is a ratio. Taking logarithms of both sides,

$$\log_{10} \left(\frac{W_1}{W_2} \right) = \log_{10} n$$

or

$$\log_{10} W_1 - \log_{10} W_2 = \log_{10} n$$

If $n = 10$, then

$$\log_{10} W_1 - \log_{10} W_2 = 1.0$$

and this difference is defined as “1 bel.” To obtain a smaller unit, the decibel equal to one-tenth of a “bel” was introduced. Because 1 bel = 10 decibels (dB), the above equation can be multiplied by 10 to give

$$10 \log_{10} W_1 - 10 \log_{10} W_2 = 10 \log_{10} n$$

if $n = 10$,

$$10 \log_{10} W_1 - 10 \log_{10} W_2 = 10$$

The difference is now said to be 10 dB (or 1 bel).

However, power ratios are not useful means of expressing level. It is well known that in electrical terms, power is the product of voltage and current; hence,

$$W = Vi, \quad V = Ri; \quad \text{then } W = \frac{V^2}{R}$$

If R is common to two power measurements, then

$$10 \log_{10} \left(\frac{W_1}{W_2} \right) = 10 \log_{10} \left(\frac{V_1}{V_2} \right)^2 = 20 \log_{10} \left(\frac{V_1}{V_2} \right)$$

Because the decibel is a nondimensional ratio, the denominator is usually a reference value; for example, in acoustics the reference pressure is 2×10^{-5} Pa, and the

MECHANICAL ENGINEERING

A Series of Textbooks and Reference Books

Founding Editor

L. L. Faulkner

*Columbus Division, Battelle Memorial Institute
and Department of Mechanical Engineering
The Ohio State University
Columbus, Ohio*

1. *Spring Designer's Handbook*, Harold Carlson
2. *Computer-Aided Graphics and Design*, Daniel L. Ryan
3. *Lubrication Fundamentals*, J. George Wills
4. *Solar Engineering for Domestic Buildings*, William A. Himmelman
5. *Applied Engineering Mechanics: Statics and Dynamics*, G. Boothroyd and C. Poli
6. *Centrifugal Pump Clinic*, Igor J. Karassik
7. *Computer-Aided Kinetics for Machine Design*, Daniel L. Ryan
8. *Plastics Products Design Handbook, Part A: Materials and Components; Part B: Processes and Design for Processes*, edited by Edward Miller
9. *Turbomachinery: Basic Theory and Applications*, Earl Logan, Jr.
10. *Vibrations of Shells and Plates*, Werner Soedel
11. *Flat and Corrugated Diaphragm Design Handbook*, Mario Di Giovanni
12. *Practical Stress Analysis in Engineering Design*, Alexander Blake
13. *An Introduction to the Design and Behavior of Bolted Joints*, John H. Bickford
14. *Optimal Engineering Design: Principles and Applications*, James N. Siddall
15. *Spring Manufacturing Handbook*, Harold Carlson
16. *Industrial Noise Control: Fundamentals and Applications*, edited by Lewis H. Bell
17. *Gears and Their Vibration: A Basic Approach to Understanding Gear Noise*, J. Derek Smith
18. *Chains for Power Transmission and Material Handling: Design and Applications Handbook*, American Chain Association
19. *Corrosion and Corrosion Protection Handbook*, edited by Philip A. Schweitzer
20. *Gear Drive Systems: Design and Application*, Peter Lynwander
21. *Controlling In-Plant Airborne Contaminants: Systems Design and Calculations*, John D. Constance
22. *CAD/CAM Systems Planning and Implementation*, Charles S. Knox
23. *Probabilistic Engineering Design: Principles and Applications*, James N. Siddall
24. *Traction Drives: Selection and Application*, Frederick W. Heilich III and Eugene E. Shube
25. *Finite Element Methods: An Introduction*, Ronald L. Huston and Chris E. Passerello
26. *Mechanical Fastening of Plastics: An Engineering Handbook*, Brayton Lincoln, Kenneth J. Gomes, and James F. Braden
27. *Lubrication in Practice: Second Edition*, edited by W. S. Robertson
28. *Principles of Automated Drafting*, Daniel L. Ryan
29. *Practical Seal Design*, edited by Leonard J. Martini
30. *Engineering Documentation for CAD/CAM Applications*, Charles S. Knox
31. *Design Dimensioning with Computer Graphics Applications*, Jerome C. Lange
32. *Mechanism Analysis: Simplified Graphical and Analytical Techniques*, Lyndon O. Barton
33. *CAD/CAM Systems: Justification, Implementation, Productivity Measurement*, Edward J. Preston, George W. Crawford, and Mark E. Cotichchia
34. *Steam Plant Calculations Manual, V. Ganapathy*
35. *Design Assurance for Engineers and Managers*, John A. Burgess
36. *Heat Transfer Fluids and Systems for Process and Energy Applications*, Jasbir Singh

where the Fourier coefficients are given by

$$a_k = \frac{2}{T} \int_0^T f(t) \cos(k\omega_0 t), \quad k \neq 0$$

$$b_k = \frac{2}{T} \int_0^T f(t) \sin(k\omega_0 t) \quad k \neq 0$$

$$\frac{a_0}{2} = \frac{1}{T} \int_0^T f(t) dt$$

where T is the time to record a block of data, for the periodic signal $2\pi/\omega_0$, and ω_0 is the fundamental frequency.

2. Combined real form: Another way of expressing the Fourier series is in a form that requires a single coefficient representing a spectral line at each frequency calculated. Any signal of the form

$$f(t) = a \cos \omega_0 t + b \sin \omega_0 t$$

can be expressed in the form

$$f(t) = C \cos(\omega_0 t + \phi)$$

provided that a and b depend on C and ϕ ,

$$C = \sqrt{a^2 + b^2}$$

and

$$\phi = -\tan^{-1} \left(\frac{b}{a} \right)$$

Then, the Fourier series, Fig. 11.1, can be expressed in the form

$$f(t) = C_0 + \sum_{k=1}^{\infty} C_k \cos(k\omega_0 t + \phi_k) \tag{11.2}$$

where $C_0 = a_0/2$; C_k is the amplitude of excitation at frequency $k\omega_0$, and

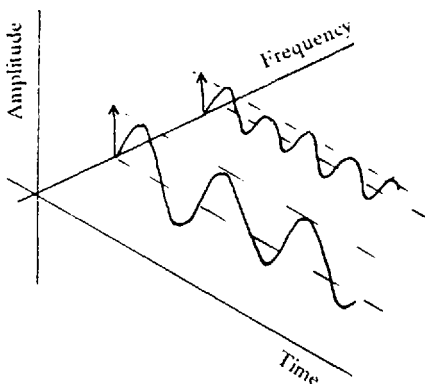


Figure 11.1 Relationship between Time and Frequency domains.

ϕ_k is the phase angle between the fundamental and its harmonics at frequency $k\omega_0$.

3. **Complex form:** The complex form expresses the series in terms of exponential and is therefore more mathematically compact. Because

$$\begin{aligned}\cos(k\omega_0 t) &= \frac{1}{2}(e^{jk\omega_0 t} + e^{-jk\omega_0 t}) \\ \sin(k\omega_0 t) &= \frac{1}{2}j(e^{jk\omega_0 t} - e^{-jk\omega_0 t})\end{aligned}$$

From Eq. (11.1),

$$f(t) = \frac{a_0}{2} + \sum_{k=1}^{\infty} \frac{1}{2} (a_k - jb_k)e^{jk\omega_0 t} + \sum_{k=1}^{\infty} \frac{1}{2} (a_k + jb_k)e^{-jk\omega_0 t}$$

which can be reduced to

$$f(t) = \sum_{k=-\infty}^{\infty} \frac{1}{2} (a_k - jb_k)e^{jk\omega_0 t}$$

Now, let

$$\begin{aligned}C_k &= \frac{1}{2}(a_k - jb_k) \\ &= \frac{1}{2} \left(\frac{2}{T} \int_0^T f(t) \cos(k\omega_0 t) dt - \frac{2j}{T} \int_0^T f(t) \sin(k\omega_0 t) dt \right) \\ &= \frac{1}{T} \int_0^T f(t) e^{-jk\omega_0 t} dt\end{aligned}\tag{11.3}$$

which represents the complex coefficients of the Fourier series.

Hence, the Fourier series breaks a deterministic waveform down into frequency- and amplitude-weighted components of a fundamental sine or cosine waveform. However, the series method of analysis has two major disadvantages:

1. It assumes that for absolute accuracy, the time function is of infinite duration, whereas, in practice, a signal is often of limited duration or a transient of short duration.
2. It assumes that a signal is periodic, whereas in reality, data are often nonperiodic.

It is possible in most cases to reduce these problems by introducing the Fourier integral. It was shown earlier that the Fourier series broke down a waveform into a set of coefficients, a_k and b_k , spaced at

$$\Delta\omega = \frac{2\pi}{T}$$

As T , the sample time, becomes larger, then the spacings between the spectral lines become smaller until a stage is reached where the Fourier coefficients become so tightly packed that they are essentially continuous. Under these conditions, The Fourier series becomes the Fourier integral and the Fourier coefficients become a continuous function of frequency called the Fourier transform. In this case, it can be shown that

$$F(\omega) = \frac{1}{2\pi} \int_{-\infty}^{\infty} f(t)e^{-j\omega t} dt$$

The inverse Fourier transform is then

$$f(t) = \int_{-\infty}^{\infty} F(\omega)e^{j\omega t} d\omega$$

Modern spectral analysis is carried out using digital processing. The analog (continuous) signal taken from a sensor is digitized through an analog-to-digital convertor, so that the time signal is processed in discrete lumps. Although the Fourier integral is the "ideal" transform, it is not practical to use because it requires knowledge of the total time signal.

The discrete Fourier transform (DFT) processes times signals in blocks of data. Because the transform form acts on discrete data, the integral in the equation can be replaced by a summation in terms of the coefficients C_k . Hence, Eq. (11.3) can be rewritten as

$$C_k = \frac{1}{T} \sum_{r=0}^{r=N-1} x_r \exp \left[-j \left(\frac{2\pi k}{T} \right) (r \Delta t) \right] \Delta t \tag{11.4}$$

The continuous signal is divided up into r amplitude measurements in the range 0 to r , as shown in Fig. 11.2.

If N is the number of time-domain data points, then $r = 0$ is the start and $r = N - 1$ is the last amplitude measurement used. Because all discrete transforms act on discrete data and the integral is replaced by a summation, there is a limit to the highest frequency that can be handled:

$$f_{\max} = \frac{1}{2\Delta t} = \frac{N}{2T} \tag{11.5}$$

where N is the number of time-domain data points to be recorded during the sample time.

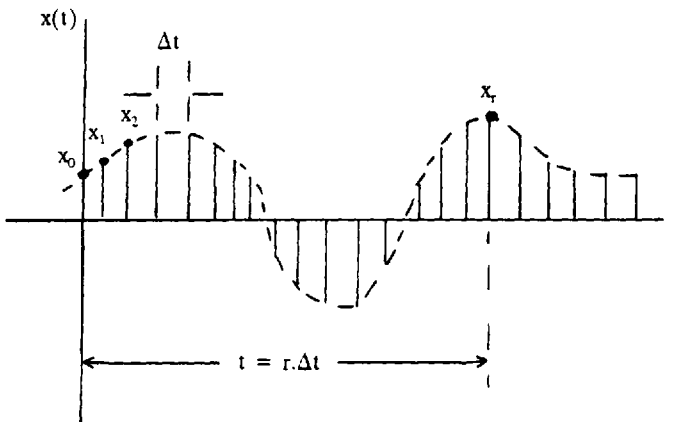


Figure 11.2 A continuous signal divided into equally spaced samples.

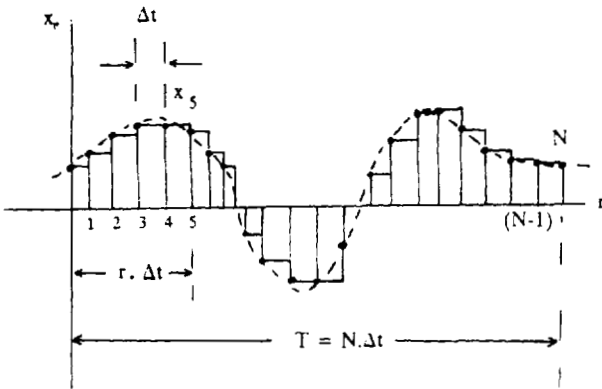


Figure 11.3 A digitally sampled signal.

For the function plotted in Fig. 11.3, regularly spaced sample values are shown such that the value of the amplitude at r is x_r , at time t from the start of the sampling period. Because $\Delta t = T/N$, Eq. (11.4) can be rewritten

$$C_k = \frac{1}{N} \sum_{r=0}^{N-1} x_r e^{-j(2\pi k r/N)} \quad (11.6)$$

which may be regarded as an approximation for calculating the coefficients of the Fourier series, where C_k represents the spectral lines corresponding to frequencies

$$\omega_k = \frac{2\pi k}{T} = \frac{2\pi k}{N\Delta t}$$

The inverse discrete Fourier transform is therefore

$$x_r = \sum_{k=0}^{N-1} C_k e^{j(2\pi k r/N)} \quad (11.7)$$

The fast Fourier transform (FFT) is an algorithm based on the DFT, but obtaining the results with a greatly reduced number of arithmetical operations [4].

4 WAVEFORM SAMPLING

There are a number of reasons for quantizing a continuous signal; for example, to convert it into a form to suit digital processing or because the signal is nonperiodic and cannot be handled by the Fourier integral. For the sine wave shown in Fig. 11.4, there are 18 intervals (Δt) in the record period taken, whereas the actual signal period for 1 cycle has 12 intervals within the period $2\pi/\omega$. If n_d is the number of intervals in the data set, then the time interval Δt is equal to the time taken to store one block divided by n_d . If the block time equals the periodic time of a deterministic signal, then

$$\Delta t = \frac{2\pi/\omega}{n_d} = \frac{1}{fn_d}$$

where the intervals range from $r = 0$ to $r = n_d$. In this case, the amplitude at any time $t = r \cdot \Delta t$ is

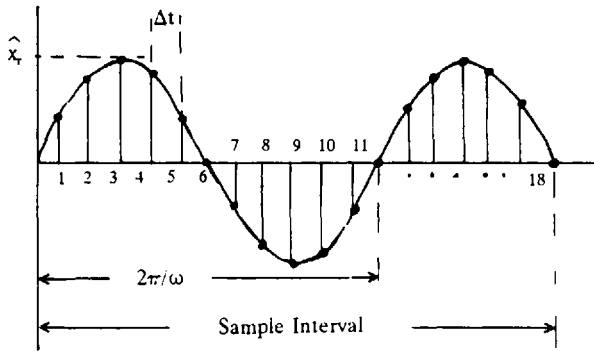


Figure 11.4 Signal sampling.

$$x_r = x_{\max} \frac{(2\pi r)}{n_d}$$

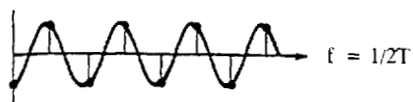
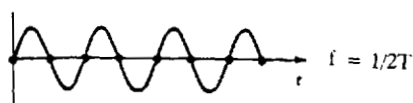
Because many signals encountered are not periodic, but are, for example, transient- or random-type signals, the choice of sample rate is more difficult. A sensor produces an analog signal, which is continuous, but the computer processing the data requires the signal to be sampled at equal time intervals and digitized. Random signals cannot be analyzed exactly, unless the sampling time is infinitely long. Finite sampling times applied to such signals will introduce errors and it becomes a decision process as to what level of error is acceptable. The FFT requires that the number of points should be a power of 2. Hence, to reproduce the original signal, there are now only a finite number of points available. On the other hand, the more sample points taken, the better the resolution obtained, but this can quickly fill up the hard-disk space available. The prevention of aliasing is the most commonly used basis for choosing a suitable sampling rate. Shannon's theorem states that in order for a true picture of the spectrum to be presented in the frequency domain, the sampling rate should be greater than twice the highest frequency of interest. In practice, it is usual to set the sampling rate at

$$f_s = 2.56f_{\max} \quad (11.8)$$

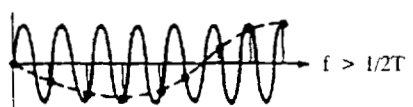
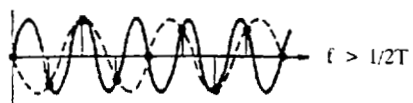
this value satisfies computing requirements.

If aliasing is not prevented, then "ghost" peaks occur in the spectrum, representing results that do not exist. For example, Fig. 11.5a shows a case in which the sampling frequency is exactly twice the frequency of interest, resulting in no data reproduced. Even if the sampled points are shifted in time, the correct amplitude for the original signal cannot be exactly described. Figure 11.5b demonstrates the result of using a sampling rate that is too low in relationship to the highest frequency of interest. The sampled points allow other nonexistent wave shapes to be reproduced, which, in turn, result in nonexistent spectral lines. Aliasing can be avoided by filtering the signal in the time domain to a specific bandwidth consistent with the sampling rate available from the A/D converter.

A second practical problem relates to the FFT algorithm assuming that the collected data block from the sensor is continuous in time. See Fig. 11.6a. In the case of a sine wave for example, there is no problem with the phenomenon of

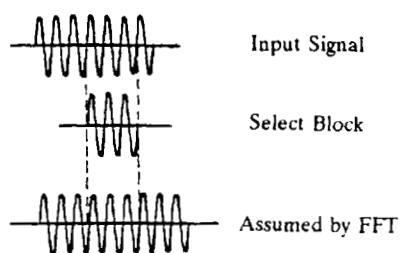


(a)

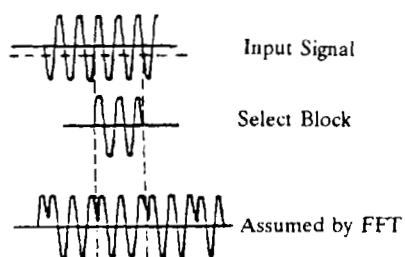


(b)

Figure 11.5 Examples of aliasing.



(a)



(b)

Figure 11.6 Causes of leakage.

leakage, provided that an integer number of cycles fits into the data block, with the amplitude zero at $t = 0$. If the input data fail to meet this requirement, then the FFT assumes a distorted waveform, similar to that shown in Fig. 11.6b. When the data are transformed into the spectral domain, the distribution is not clean (see Fig. 11.7a), but it is smeared over the spectrum, as shown in Fig. 11.7b. This can result in small signal peaks being masked if they are near significant spectral components.

The normal method of overcoming this effect is to apply window filtering. Examination of Fig. 11.7b shows that the problem occurs at the edges of the time block. If the FFT could ignore this area and concentrate on the middle portion, then the smearing effect could be reduced. This is achieved by multiplying the time block by a function that is zero at the start and finish of the block and unity through the middle portion. A popular window used for this purpose is the Hanning window. Its effect is shown in Fig. 11.8. For example,

- Highest frequency of interest = 5000 Hz
- Number of samples (power of 2) = 1024
- Recommended sampling rate, $f_s = 2.56f_{\max} = 12,800$ Hz

therefore

- Time between samples, $t = 1/f_s = 0.78 \times 10^{-4}$ s
- Spectral resolution, $f = 1/(Nt) = 12.5$ Hz
- Number of spectral components (lines), $f_{\max}/f = 400$

For $N = 1024$ samples of the time signal,

- Number of operations using straight DFT, $N^2 = 1,048,576$
- Number of operations using FFT, $N \log_2 N = 10,240$

In many practical situations, data collection has to be carried out in a noisy environment, which means that the signal to be analyzed is contaminated by unwanted signals from outside sources. In many cases, this “noise” is broadband and if the signal has a near-zero mean value, then the signal-to-noise ratio can be improved by averaging several blocks of data, collected initially. The signal-averaging approach

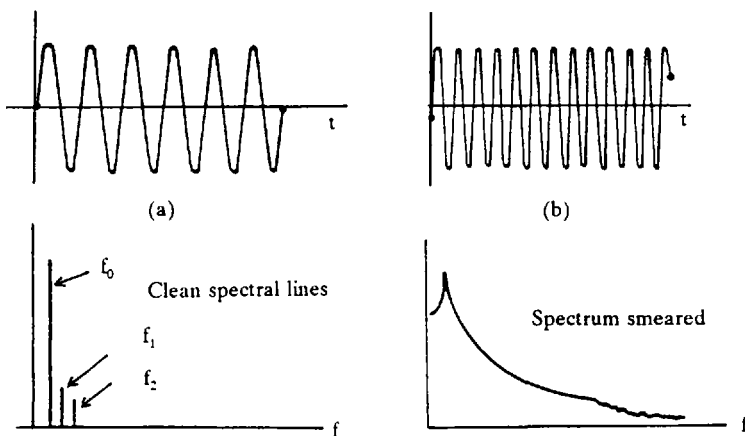


Figure 11.7 (a, b) Results of leakage of the frequency domain.

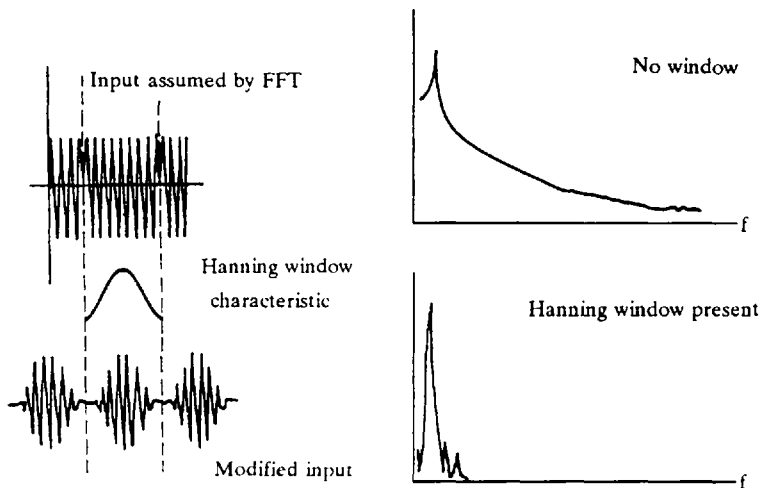


Figure 11.8 Application of windows.

is most effective when a deterministic signal is buried in random noise. It can be applied to the raw time data or the resultant spectrum of each block. Random signals cannot be analyzed exactly, unless the sampling time is infinitely long. Finite sampling times applied to random signals will introduce errors and it becomes a decision process as to what level of error is acceptable.

5 INSTRUMENTATION

In recent years, with the introduction of the microcomputer, the flexibility of instrumentation systems for vibration and noise analysis has improved dramatically. Most signals for analysis will result from a transducer of some sort and will be in the form of an analog voltage. The data from such signals may even have been transported from the source to the analyzer by means of a tape recorder. These signals are then displayed in various ways, the most useful being the spectral distribution as a result of Fourier analysis. A signal is a variation of a significant physical quantity with time and can fall into many classifications. Deterministic signals can be defined mathematically and are normally sinusoidal or transient (e.g., gear meshing or machine impact). Random signals are usually stationary, such as fluid flowing in a pipe, but can also be nonstationary, as exhibited in traffic flow. Such signals have to be assessed on a statistical basis.

Even the most basic signal is affected when propagated through a system. These resultant distortions and amplitude reductions are often used to find out information about the machine under investigation. Although the Fourier approach will convert the time-domain data into a spectral distribution, it is often convenient to look in more detail at a specific part of this display, or even to get rid of sections. This is the role of filters, which can be either in the form of hardware or as imbedded algorithms in the analysis code.

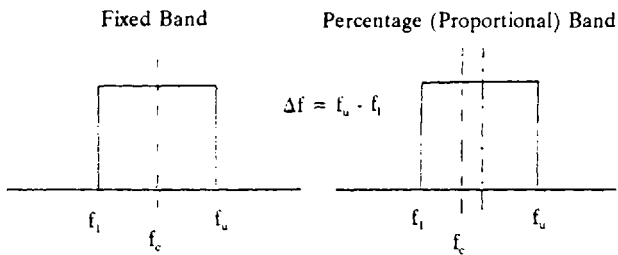


Figure 11.9 Idealized fixed and percentage band filters.

5.1 Filters

Filters can be fixed, in which the bandwidth is independent of the center frequency, or proportional, in which the bandwidth is some constant percentage of the center frequency. The point of this is that the latter can provide a general feel for the distribution of the signal over the whole spectrum, whereas the former can be used to obtain much more detail about particular areas of interest.

A highly idealized fixed band filter is shown in Fig. 11.9, left, where f_c is the center frequency and f is the bandwidth centered symmetrically about this value. Hence, all frequencies within f are not attenuated, but any other frequencies outside f are totally rejected.

In the case of the percentage band filter, Fig. 11.9, right, the center frequency f_c is the geometric mean of the upper and lower cutoff frequencies such that

$$f_c = \sqrt{f_l f_u} \quad (11.9)$$

Various constant-percentage band filters are available, the most used being 1/1 octave and 1/3 octave.

The standard octave band center frequencies are shown in Table 11.2. Note how this filter window gets wider with increasing center frequency and that the bandwidth $f_l = 70\%$ of f_c . Note that a 1/1 hardware filter of this type consists of 11 separate filters, usually manually switched. On the other hand, a 1/3 octave unit will

Table 11.2 Standard Octave Band Center Frequencies (Hz)

f_l	f_c	f_u	Δf
31.5	22	44	22
63	44	88	44
125	88	177	88
250	177	355	177
500	355	710	355
1,000	710	1,420	710
2,000	1,420	2,840	1,420
4,000	2,840	5,680	2,840
8,000	5,680	11,360	5,680
10,000	11,360	22,720	11,360
31,500	22,720	45,440	22,720

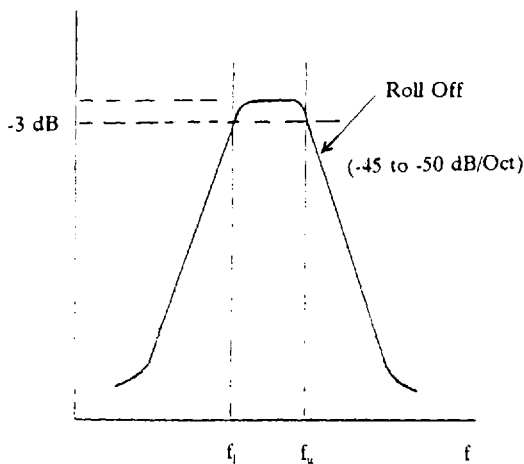


Figure 11.10 Practical filter shape.

have 33 separate filters, which provides a lot more detail. The frequency range of interest for most industrial machinery applications is 63–8000 Hz.

A practical filter shape is shown in Fig. 11.10, where f_u and f_l are identified at the -3 -dB attenuation level. The other important feature defining the quality of a filter is the roll-off rate of the skirts; that is, the rate of attenuation for each side of the band pass. A rate of 45–50 dB/octave would define a good filter.

5.2 Sensors

The purpose of a sensor or transducer is to convert a physical measurement into an electrical signal convenient for further processing. It is important that the sensor does not distort the signal with noise or spurious voltages and that it has sufficient dynamic bandwidth with no resonance in the working range desired. The bandwidth of operation is determined by the resonant frequency of the sensor, because beyond that point, the signal is severely attenuated. Impedance matching between the sensor and other equipment is also a critical factor to consider. The conversion mechanism of such sensors as accelerometers and microphones must be very sensitive, as the forces involved are usually very small.

Accelerometers [5] used in the measurement of vibration are commercially available and are based on many different principles of operation. These can be electromagnetic, electrodynamic, capacitive, strain-gauge, and piezoelectric techniques. The latter is the most rugged and, therefore, most popular for industrial measurements. It is self-generating, small in size, and can be designed to be free of resonances over a wide frequency range and to have good stability. Sensitivity is normally expressed in mV/g , where g is taken as 9.81 m/s^2 with typical values in the range 1 mV/g to 1 V/g . The sensitivity is also expressed in terms of charge (pC/g). This is appropriate when the sensor is connected to a charge amplifier.

It should be realized that an accelerometer is normally a piezoelectric crystal which develops a charge between its faces when mechanically distorted. This charge leaks away, as the crystal is effectively a capacitance. On the other hand, it has the

Table 11.3 Performance Data for a General-Purpose Accelerometer and One Used in Seismic Studies

Characteristics	General	Seismic
Weight (g)	30	500
Sensitivity (pC/g)	48	10,000
Sensitivity (mV/g)	40	10,000
Capacity (inc Cable pf)	1,200	1,000
Mounted Resonance (kHz)	22	5
Flat response (kHz)	7	1
Max. shock (g)	5,000	100

unique property of being mechanically distorted if a charge is presented across its faces. The output, being a charge, will not support any power drain and so must be interfaced to a very high input impedance at the conditioning amplifier. These interface units can be in the form of either voltage or charge conditioning amplifiers, but not ordinary operational amplifiers. The advantage of the former is that the response is uniform down to a few Hertz; however, the leads between the amplifier and the accelerometer must be kept as short as possible. If the low-frequency response is not an issue, then the charge version of the amplifier is commonly used. In this case, the lead length is not a problem.

Typical performance data for a general-purpose accelerometer and one used in seismic studies are shown in Table 11.3. Although the latter is much heavier than the general-purpose sensor, it has much better sensitivity. On the other hand, the smaller the accelerometer, the wider the frequency response characteristics, but the reduced sensitivity means that care must be taken to reduce electrical noise. Care must also be taken when mounting an accelerometer. If possible, it should be rigidly attached to the structure with a stud; other methods will reduce the bandwidth, the worst case being hand-held.

Closely related to vibration measurements is the use of noise as an analysis tool. For airborne-sound measurements, the three most widely used microphones are piezoelectric, moving coil, and condenser, the latter being the most popular [6]. Their characteristics are shown in Table 11.4. The condenser microphone has a high acoustical impedance and can be fitted to a probe, where sound-pressure measurements are at positions which are inaccessible. Similar to accelerometers, the smaller the microphone the wider the working frequency response, but the poorer the sensitivity.

Table 11.4 Characteristics of Three Types of Microphones

Characteristics	Piezoelectric	Moving coil	Condenser
Frequency response	10 kHz	Limited	100 kHz
Impedance (electrical)	0.8 M Ω at 100 Hz	75 Ω	Very high
Impedance (acoustic)	Moderate	Low	High
Noise level	Moderate	Low	Low
Transient response	Moderate	Moderate	Good

The moving-coil microphone is not really suitable for taking measurements, because it has a poor frequency response; so the choice lies between the other two. The condenser microphone is usually preferred. Where the frequency range of interest extends up to 10 kHz, it is advisable to restrict the microphone diameter to $\frac{1}{2}$ in. to avoid corrections as a result of diffractions effects. The low-frequency limit will be around 10 Hz.

The larger the numerical value of the sensitivity, the easier it is to take measurements, but this will also mean a limited frequency response. For impact-type noise, a wide bandwidth is needed, as a large number of harmonic components are needed to reproduce the event.

6 EXAMPLES OF DATA PLOTS

Figure 11.11 shows an example of the raw time-domain data collected from a gear casing using an externally mounted accelerometer [7]. In this particular example, the gears have 15 teeth each, so that when driven at 1221 rpm, the tooth meshing frequency is

$$\begin{aligned} \text{Meshing frequency} &= \frac{(\text{Shaft speed})(\text{Number of teeth})}{60} \\ &= \frac{(1221)(15)}{60} = 305.25 \text{ Hz} \end{aligned}$$

The plot show that the time for one revolution as $60/1221 = 0.04914$ s, and because

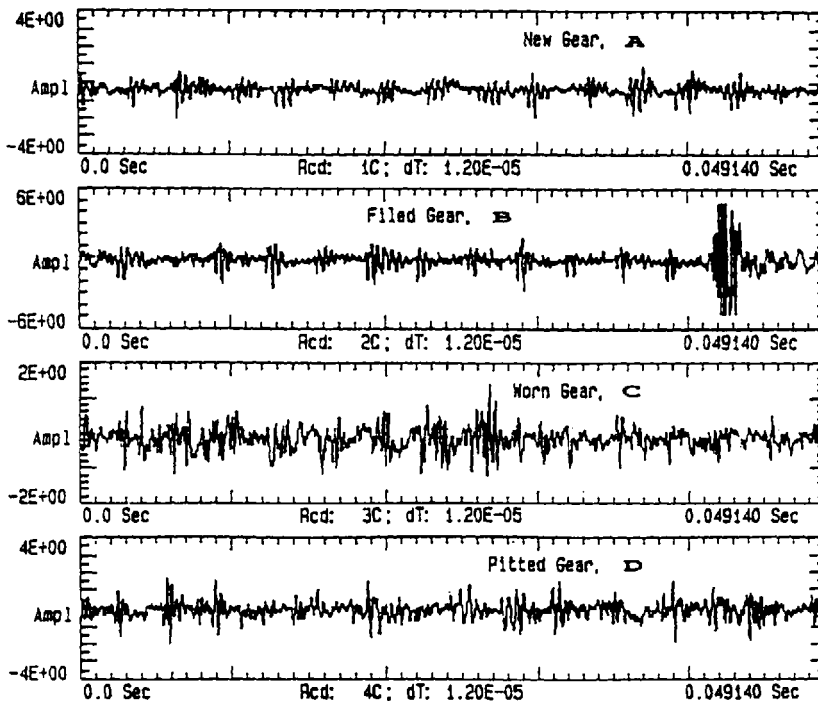


Figure 11.11 Examples of gear damage.

there are 4096 points taken in the collection of this block of data, the sample time $t = T/N = 1.1997 \times 10^{-5}$ s. Because $T = N/(2.56f_{\max})$, $f_{\max} = 32,560$ Hz, and the sampling frequency f_s must be $2.56f_{\max} = 83,353$ Hz.

In alphabetical order, the meaning of each plot in Fig. 11.11 is as follows: plot A shows the result from a set of gears in good running condition; plot B is the result corresponding to one tooth of the drive gear being filed to approximately $100 \mu\text{m}$ depth; plot C is the worn condition obtained by running a set of gears for 20 h under load, with no lubrication; plot D is the result of the gears placed in a solution of CuCl_2 for 18 h. This resulted in fairly uniform pitting, ranging in depth between 100 and 200 m. Although it is clear there are pattern differences between each of these time plots, they do not present much detailed information. This comparison is highlighted in Fig. 11.12, which shows both the time and spectral distributions for a gear set in good condition [6]. The dominant spectral line is at 2135 Hz, which corresponds to seven times the tooth meshing frequency of 305 Hz. Such higher-frequency harmonics should be much smaller in amplitude, so there must be another event superimposed. Figure 11.13 shows where the problem lies.

An impact test on the structure holding the gear box shows a passive structural resonance at 2500 Hz, so taking into account the bandwidth of the measurement window, this is close enough to cause the problem. None of this information can be readily detected from the time-domain plot of Fig. 11.11.

Another example of the use of spectral analysis is shown in Fig. 11.14, where a set of gears in good condition are compared to an identical set which has a crack

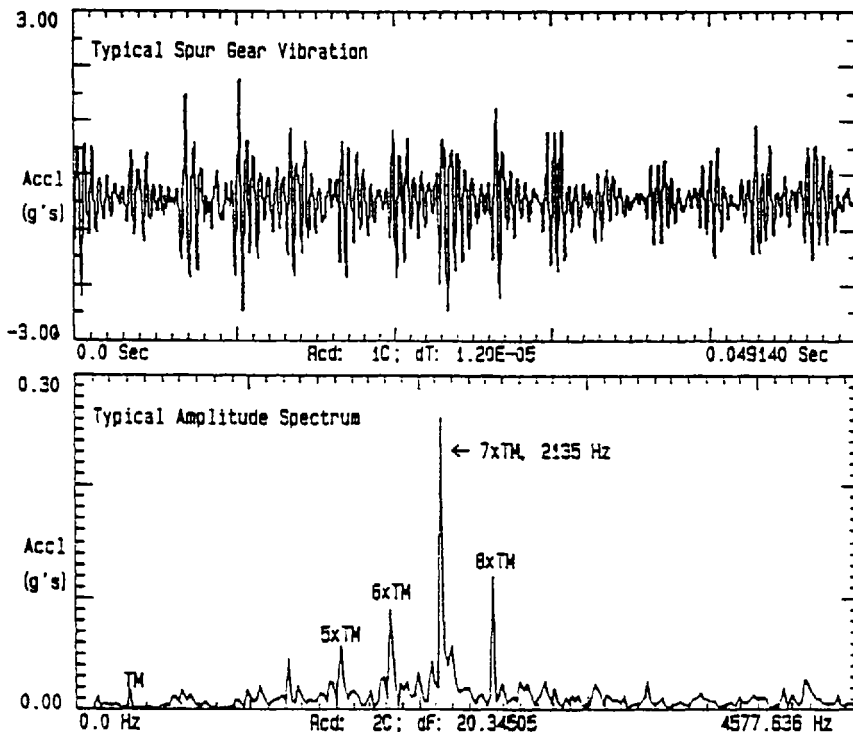


Figure 11.12 Time and frequency plots of gear vibration.

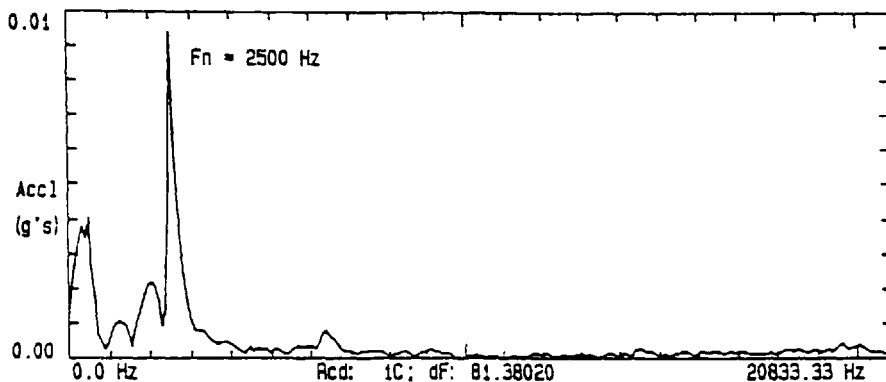


Figure 11.13 Structural impact test.

at the root of one gear tooth. The top plot shows the tooth-meshing frequency of 300 Hz and the first two harmonics. The second plot shows the changes due to a cracked tooth, which is usually associated with side bands developing on each side of the harmonics. These are at \pm the shaft speed; in this case, that would be $1221/60 = 20.35$ Hz. However, these are usually only detected by zooming in on this part of the spectrum. In this plot, the peak at 540 Hz is more likely to be a resonance.

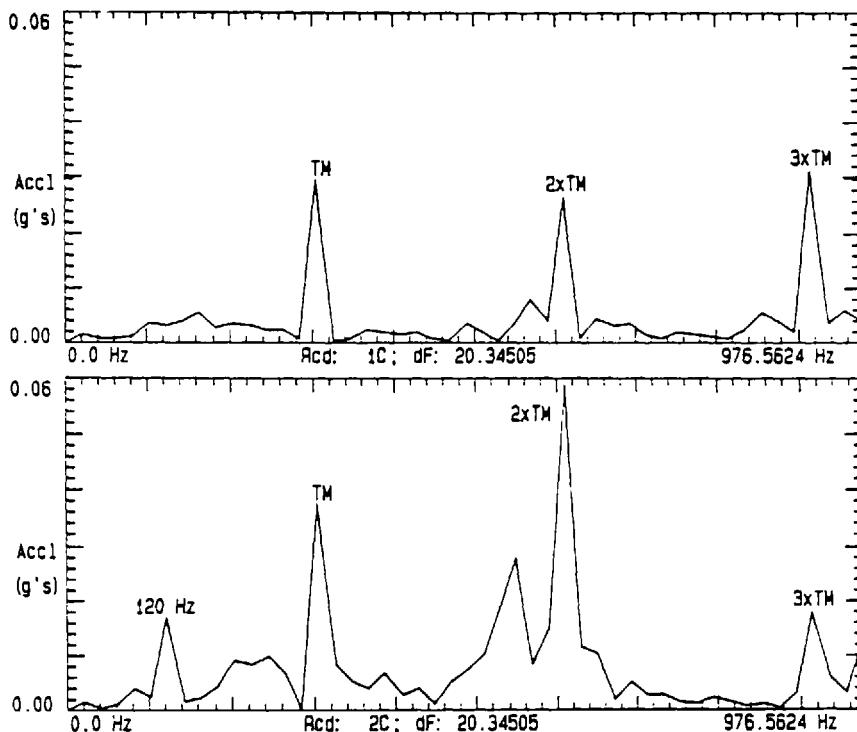


Figure 11.14 Gear without and with a tooth crack.

Both the fundamental and second harmonic have increased in amplitude. Note also the second harmonic of the line frequency 2×60 Hz also appears.

Figure 11.15 shows data taken from an accelerometer attached to the end plate of a nine-piston pump, using a 30-Hz fixed-bandwidth filter. In this case, the shaft speed is 1750 rpm, giving a fundamental pumping frequency of 252 Hz. Much more information is available with the better resolution, and it is seen that a lot of harmonics are contributing to the end-plate vibration, which, in turn, results in radiated noise.

It was pointed out earlier that there was a relationship between the noise radiated and the vibration of a structure through the acoustic impedance. This is demonstrated in Fig. 11.16, where the octave-band sound-pressure level is compared with the casing acceleration and velocity of a vane pump. The three curves have been separated for ease of viewing. In its simplest, $p = (\rho c)v$ assumes an infinitely large flat-plate model so that the acoustic impedance is real. At the other extreme, a spherical radiator exhibits a complex impedance given by

$$p = \rho c \left(\frac{k^2 a_r^2}{1 + k^2 a_r^2} + j \frac{ka_r}{1 + k^2 a_r^2} \right) v$$

where k is the wave number and a , is the radius of the sphere. It is seen that as a , becomes larger, this relationship approaches the flat-plate form. In practice, machines are represented somewhere between these two extremes, but the complex aspect introduces phase shifting that affects the resultant spectrum.

The sources of noise can often be pinpointed on the spectrum; for example, Fig. 11.17 (lower plot) shows the noise radiated as a result of flow being dumped

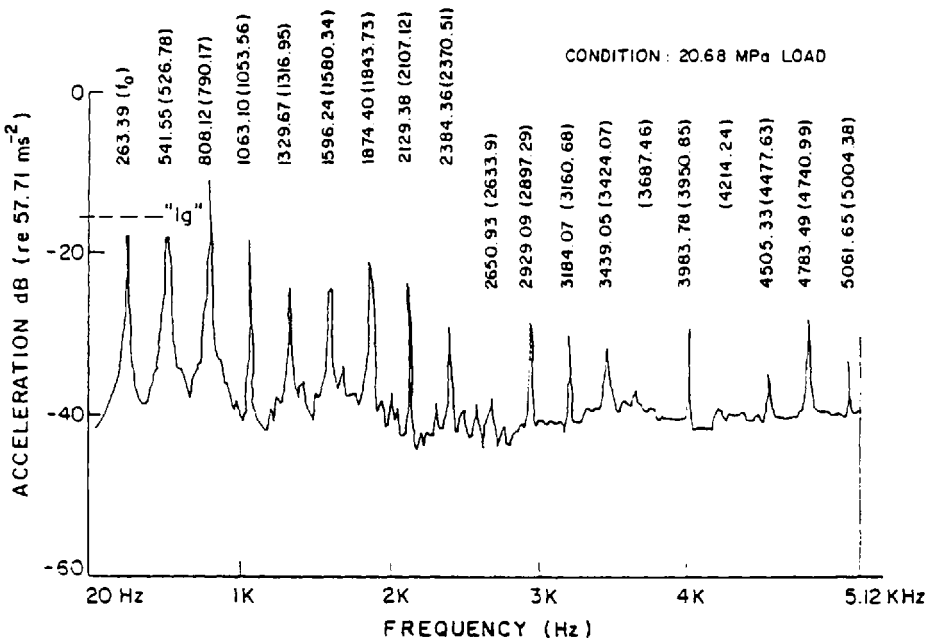


Figure 11.15 Fixed band filter analysis of pump end plate.

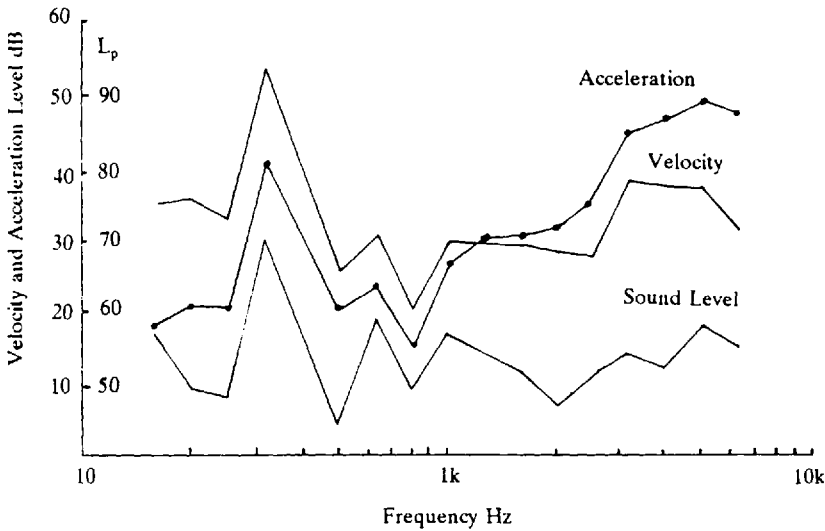


Figure 11.16 Correlation among acceleration, velocity, and sound level.

via a discharge valve to a tank, from a pump set. The load valve is open so that the loading on the system is light. In the upper plot of Fig. 11.17, the discharge valve is operating, directing flow to the circuit and resulting in significant amounts of energy being introduced at frequencies about 600 Hz, but not significantly around the pumping frequency. The contribution from the discharge valve is seen to be essentially broadband energy related to turbulent flow through the discharge valve. On the other hand, Fig. 11.18 shows a different sound pattern when load is applied

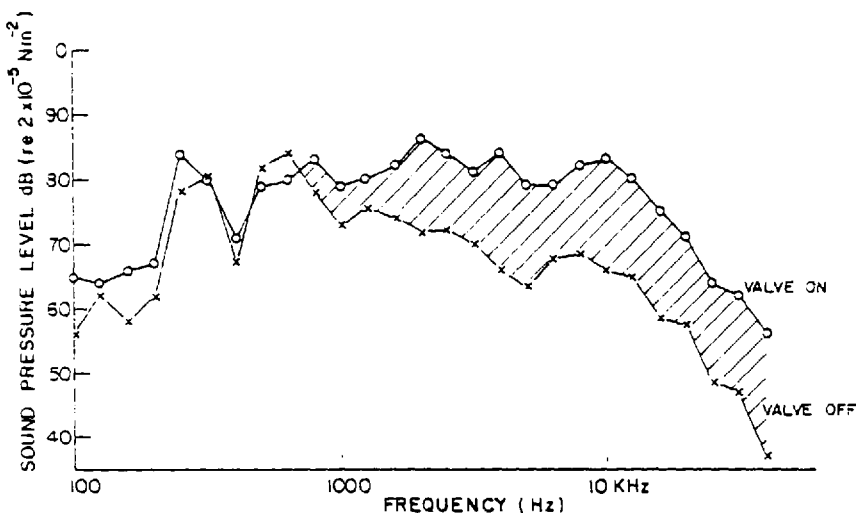


Figure 11.17 Effect of a solenoid discharge valve.

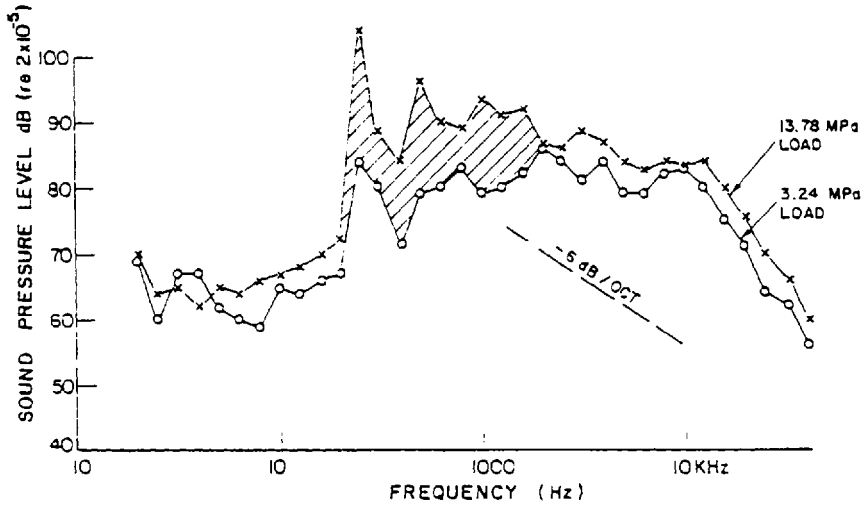


Figure 11.18 Effect of hydraulic load on a pump.

to the output end of the circuit. The major effect is seen at the fundamental pumping frequency, where there is a dramatic rise in sound-pressure level.

Cavitation in fluid power systems is the result of imploding voids in the fluid. This occurs when the local velocity of flow becomes high, say through an orifice, causing the local pressure to drop to the vapor pressure of the oil. When these implosions occur, broadband random noise is radiated at significant levels; an example of this is shown in Fig. 11.19.

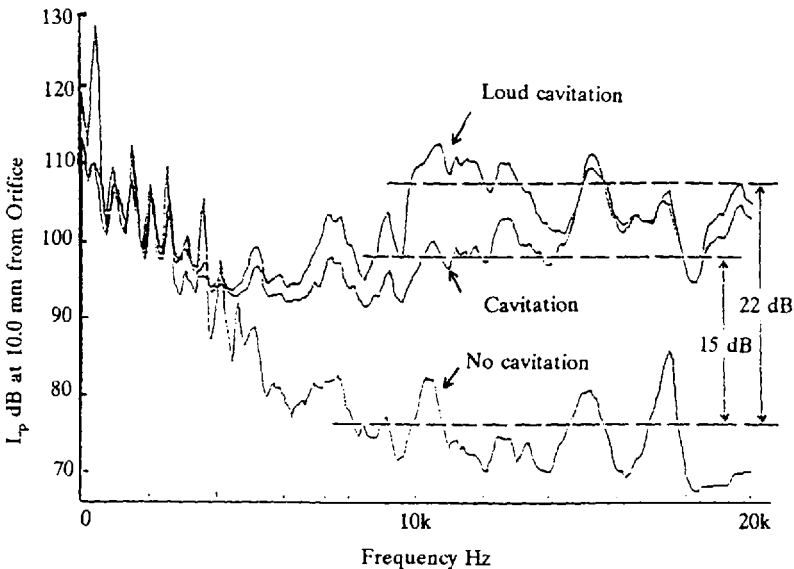


Figure 11.19 Noise spectrum of a cavitating orifice.

Vibration and the resultant radiated noise can be used as an effective tool for the detection of the condition of moving parts with a machine. The relatively recent developments in sensor technology, low-cost computers, and user-friendly software have allowed more quantitative methods to be developed. By far the most used signal processing method is based on the fast Fourier transform, which allows a spectral distribution to be viewed. This is much more informative than the raw time-domain signal, because the energy is now distributed through a range of frequencies. However, the use of digital processing is not without its own limitations, and it is important for the user to have a good understanding of the processing involved, so as to avoid incorrect interpretation of the data.

NOMENCLATURE

a, a_0	Acceleration (m/s^2)
a_k, b_k	Fourier coefficients
c	Velocity of sound (m/s)
C_k	Coefficient representing the k th spectral line
d, d_0	Displacement (m)
f	Frequency (Hz)
$f(t)$	Variation of voltage with time (V)
f_c	Center frequency (Hz)
f_u, f_l	Upper and lower frequency limits (Hz)
f_s	Sampling rate (Hz)
f_{max}	Maximum frequency of interest (Hz)
f	Frequency difference or bandwidth (Hz)
F	Form factor or force ($-, \text{N}$)
$F(\omega)$	Result of forward Fourier transform
i	Current (mA)
N	Number of samples
p, p_0	Pressure (Pa)
r	Index
R	Resistance (Ω)
t	Time (s)
t	Time between samples (s)
T	Time to record a block of data or sample time (s)
W, W_0	Power (W)
V, V_0	Voltage (V)
v, v_0	Velocity (m/s)
$v(t)$	Variation of voltage with time (V)
x_r	Sampled amplitude of a signal
ϕ_k	Phase angle of k th harmonic (radian)
ρ	Density (kg/m^3)
ω	Frequency (radians/ s)

ACKNOWLEDGMENTS

The author would like to acknowledge the contributions to the research made by his graduate students, and especially to A. Sakuta, F. Honavar, and D. Oguamanam. The

financial support provided by the Natural Sciences and Engineering Research Council of Canada and the Manufacturing Research Corporation of Ontario is also acknowledged.

REFERENCES

1. L. L. Faulkner, ed., *Handbook of Industrial Noise Control*, 1976, Industrial Press; New York.
2. D. Reynolds, *Engineering Principles of Acoustics*, 1981, Allyn and Bacon; Boston.
3. I. P. Castro, *An Introduction to Digital Analysis of Stationary Signals*, 1989, Adam Hilger/ESM.
4. A. V. Oppenheim and R. W. Schaffer, *Digital Signal Processing*, 1975, Prentice-Hall; Englewood Cliffs, NJ.
5. *The Theory and Application Handbook for Piezoelectric Accelerometers*, 1978, Bruel and Kjaer.
6. L. Beranek, *Noise and Vibration Control*, 1971, McGraw-Hill; New York.
7. H. R. Martin, "Gear Pump Condition Monitoring," in Proc. 45th Natl. Conf. on Fluid Power, 1992.
8. H. R. Martin, "Noise, Radiation from Hydraulic Circuits," in ASME Design Conf., 1978, Paper 78-DE-23.
9. E. Williams and H. R. Martin, "Noise Characteristics of a Cavitating Orifice under Reattached Flow Conditions," in Proc. 34th Natl. Conf. on Fluid Power, 1978.

BIBLIOGRAPHY

- Collacott, R. A., *Mechanical Fault Diagnosis*, 1977, Chapman & Hall; New York.
- Lyons, R. H., *Machinery Noise and Diagnostics*, 1987, Butterworths; Boston.
- Martin, H. R., *The Design of Hydraulic Components and Systems*, 1995, Ellis Horwood/Prentice-Hall; Englewood Cliffs, NJ.
- McCloy, D., and H. R. Martin, *Control of Fluid Power, Analysis and Design*, 1980, Ellis Horwood/Wiley; New York.
- Mitchell, J. S., *Machinery Analysis and Monitoring*, 1981, Penwell Books.
- Norton, M. P., *Fundamentals of Noise and Vibration Analysis for Engineers*, 1981, Cambridge University Press; Cambridge.
- Skaistis, S., *Noise Control of Hydraulic Machinery*, 1988, Marcel Dekker, Inc., New York.

This page intentionally left blank

12

Failure Analysis

STEVEN LEMBERGER

John Crane N.A., Morton Grove, Illinois

GEORGE E. TOTTE

Union Carbide Corporation, Tarrytown, New York

1 INTRODUCTION

In the past 25 years, hydraulic applications have greatly improved. Machines have become more powerful, faster, and more versatile through the use of hydraulic drives and controls. Heavier loads and faster cycles require hydraulic systems to have pumps with larger capacities and higher pressure ratings. Higher-pressure pumps create greater stresses on system components. Therefore, hydraulic pump maintenance is becoming increasingly critical to reduce failure rates and extend service life.

The most common cause of hydraulic pump failure is improper pump use. Root-cause analysis of pump failures has shown that 80% of the failures were caused by improper operation and maintenance. The most common sources of failures are shown in Table 12.1.

A detailed discussion of hydraulic pumps, components, and circuitry is provided in Chapter 1. The importance of fluid properties on properties such as viscosity, foaming, and cavitation is provided in Chapter 4. Fundamental lubrication principles are provided in Chapter 6. In this chapter, an overview of hydraulic pump wear surfaces and lubrication will be provided. Hydraulic pump wear and failure mechanisms will be discussed in detail and a root-cause analysis procedure will be introduced. Examples of various examples of hydraulic pump component failure and their root causes will be discussed.

Table 12.1 Most Common Sources of Hydraulic Pump Failures

Source	Failure frequency (%)
Design	2
Manufacture	6
Installation	12
Operation and maintenance	80

2 DISCUSSION

2.1 Hydraulic Pump Lubrication

One source of hydraulic pump failure is improper lubrication. The effect of fluid-film lubrication, material strength, heat balance of fluid film and rolling element bearing lifetimes, and cavitation on the limits of operation of a hydraulic pump is illustrated in Fig. 12.1 [1]. Illustrative examples of fluid-film lubrication of hydraulic pump components will be provided here.

Many components within piston and vane pumps are in pure sliding contact. (The rolling component is negligible.) Sliding surfaces in a piston pump include valve plate and cylinder block, piston and cylinder wall, and slipper and swash plate surfaces, which are illustrated in Fig. 12.2 [1]. The sliding contact within a vane pump is the vane on cam-ring surface illustrated in Fig. 12.3 [2].

Sliding wear at the valve plate–cylinder block surface will affect the performance of both swash-plate and bent-axis piston pumps. Wear at this interface may facilitate case leakage, which will increase with decreasing fluid viscosity [1].

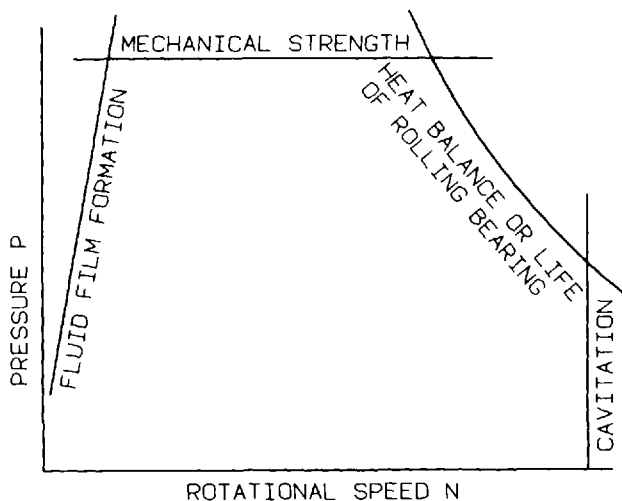


Figure 12.1 Hydraulic pump and motor operation limits. (Courtesy of A. Yamaguchi, Yokohama National University.)

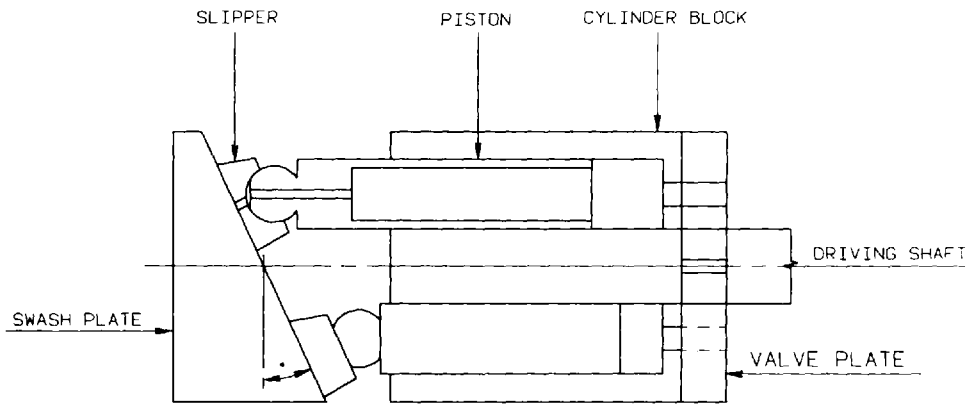


Figure 12.2 Sliding contacts of a swash plate piston pump. (Courtesy of A. Yamaguchi, Yokohama National University.)

The slipper–swash plate wear contact will significantly impact pump performance. Figure 12.2 shows that the slipper–piston contact may be treated as spherical bearing. Due to the small size, this contact operates in the mixed-film lubrication regime [1].

The force acting on the cylinder block is supported by the shaft and fluid-film pressure acting on the valve plate with a hydrodynamic pad is illustrated in Fig. 12.4 [1]. A journal bearing may also be used to support the force, as shown in Fig. 12.5 [1]. The total fluid-film pressure acting on the sliding valve plate–cylinder block surface illustrated in Fig. 12.6 is composed of hydrostatic effect, wedge–film effect, and a squeeze-film effect [1]. Loading of the valve plate and cylinder block is primarily determined by the pressure of the high-pressure side of the pump. It has been shown that fluid-film thickness is relatively stable at rotational speeds up to 10^5 rpm [1].

The piston and cylinder wall are also in sliding contact. For many swash-plate piston pumps, metal–metal contact is difficult to avoid because of the high lateral forces acting on the pistons [1]. Lubrication at these surfaces is enhanced by de-

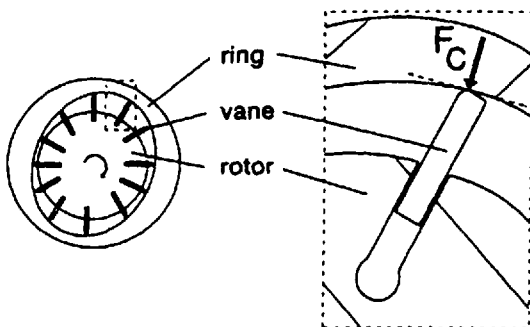


Figure 12.3 Vane-on-ring sliding line contact.

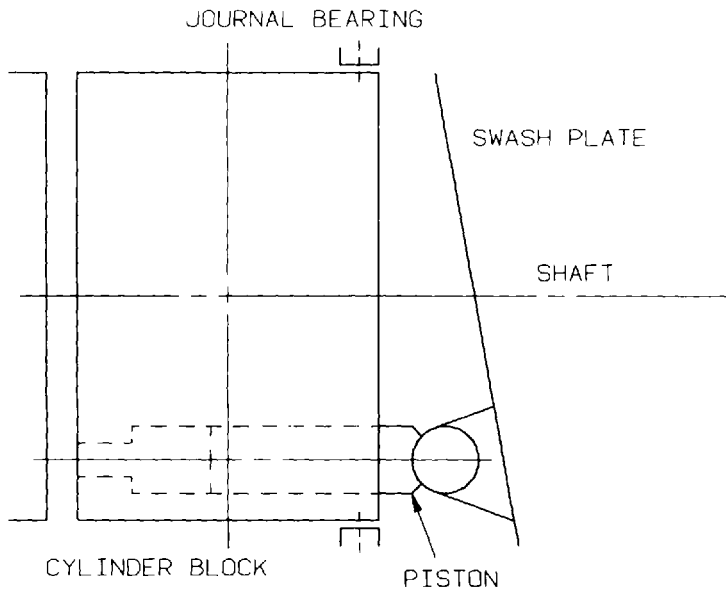


Figure 12.4 Force acting on a cylinder block. (Courtesy of A. Yamaguchi, Yokohama National University.)

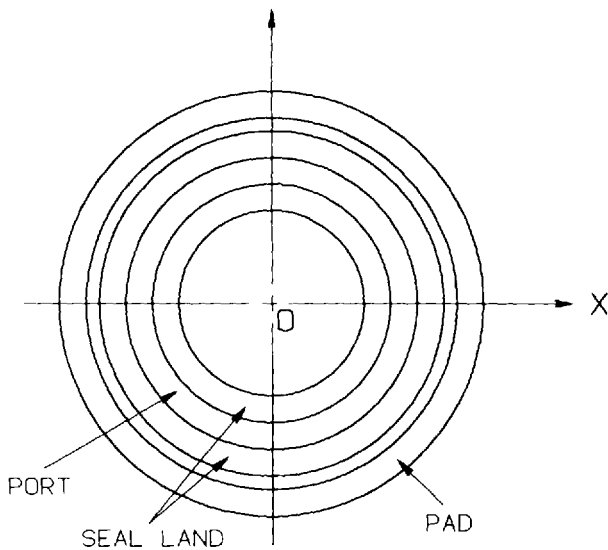


Figure 12.5 Valve plate with hydrodynamic pad. (Courtesy of A. Yamaguchi, Yokohama National University.)

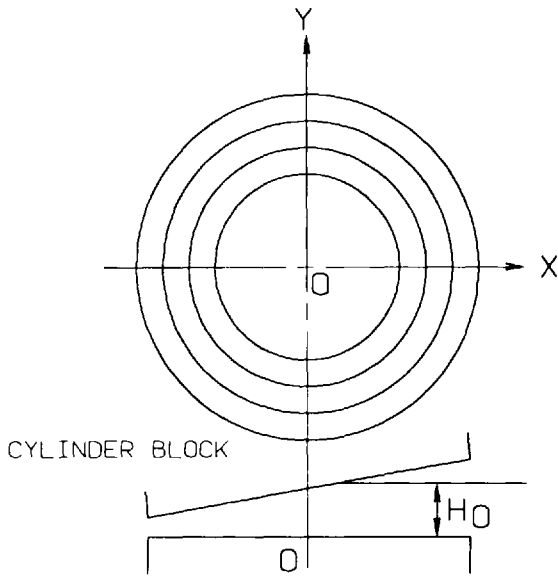


Figure 12.6 Fluid-film formation between valve plate and cylinder block. (Courtesy of A. Yamaguchi, Yokohama National University.)

signing for enhanced hydrostatic lubrication and by varying the piston shape and size.

An example of a bushing that may be used in high-pressure gear pumps is illustrated in Fig. 12.7 [3]. It has been shown that these bearings are lubricated hydrodynamically due to hydrostatic pressure generation arising from gear tilt and nonflatness of the ends of the gear teeth and bushing surface [3].

The limits of lubrication of a representative bearing surface has been modeled and the results are illustrated in Fig. 12.8 [1]. Metal-metal contact during the pump delivery stroke is represented by the shaded area No. 1. The suction to delivery stroke, which is the fluid-trapping period, is represented by the shaded area No. 2.

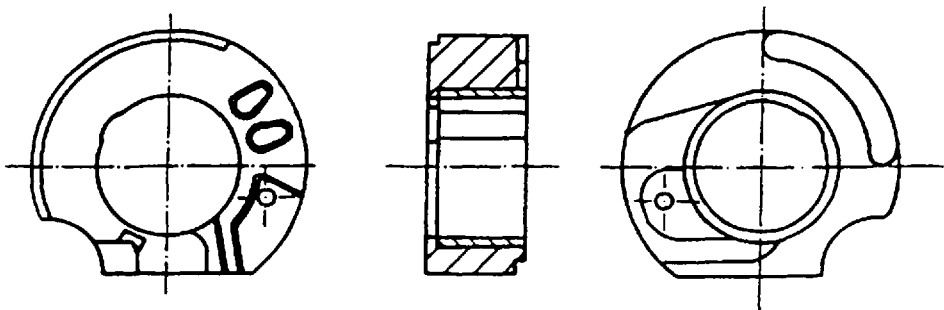


Figure 12.7 Schematic of a bushing-type bearing.

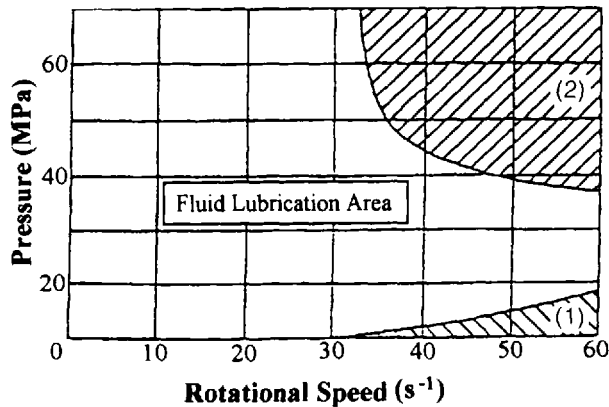


Figure 12.8 Fluid lubrication in a slipper bearing: (1) metal–metal contact during the pump delivery stroke and (2) suction to delivery stroke. (Courtesy of A. Yamaguchi, Yokohama National University.)

These examples show that hydraulic pump lubrication and performance is dependent on preventing pump and component damage and maintaining design clearances. Anything that produces a change in these clearances, such as lubrication failure and wear, may dramatically affect hydraulic pump performance.

2.2 Hydraulic Pump Failure

2.2.1 Causes of Hydraulic Pump Failure

The pump is the “heart” of any hydraulic system. It is unusual for pump failures to be caused by manufacturing defects. Pump failures are usually a symptom of another problem in the system. Preventing recurring failures requires determination of the failure mechanism and performance of preventive maintenance procedures to reduce the probability of future reoccurrence.

Typically, 85–95% of pump failures can be attributed to one or more of the following causes [4]:

- Foaming and aeration
- Cavitation
- Contamination
- Fluid oxidation
- Overpressurization
- Improper viscosity

Foaming and Aeration

Although some fluid foaming is to be expected, excessive foaming may lead to the introduction of foam into the pump inlet leading to air-entrainment problems such as poor fluid compressibility and sluggish hydraulic response. Cavitation may also result. Foaming is caused by the following [5,6]:

1. **Improper Location of the Return Discharge Line.** Hydraulic systems should discharge the returning fluid below the oil surface in the reservoir to minimize foaming. Alternatively, the return line may discharge fluid onto an inclined plane or over a screen. Time is needed for the fluid to release entrained air to the surface before reentry into the system. Therefore, returning fluid should not be discharged directly to the reservoir outlet. If this occurs, baffles are needed to prevent direct discharge to the outlet.
2. **Improperly Sized Reservoir.** If the reservoir is too small or deep relative to surface area, there may be insufficient time to permit release of the entrained air before the fluid reenters the system.
3. **Rapid Pressure Release.** Rapid pressure release may result in the insolubilization of air, which was soluble under the higher-pressure conditions, resulting in an entrained-air condition and increased foaming. Rapid pressure releases may be caused by sharp changes in pipe sizes or excessive vacuum on the discharge side of the pump inlet, discharge of metering valves and orifices to the reservoir, and a large pressure drop in the inlet line from the pressurized reservoir.

In some cases, a negative suction head must be eliminated. The use of a supercharging (booster) pump may be required to pressurize the inlet.

To minimize the potential for rapid pressure release and other inlet flow problems, abrupt changes in pipe sizes should be eliminated if possible. Piping recommendations include the following [7,8]: (1) suction lift should be 24 in. maximum, (2) not more than two elbows in addition to a filter should be used in the suction line whose maximum length should not exceed 36 in., and (3) match the line size to the pump port size, if possible.

4. **Insufficient Fluid in the Reservoir.** If the oil level in the reservoir is too low, there may not be enough time for air release before reentry of the fluid into the system. In addition, this condition may lead to vortexing at the suction inlet, causing increased air entrainment of the oil.
5. **Hydraulic System Leaks.** Air may be drawn into the hydraulic fluid at packings or suction-line connections and from gas leaks from the accumulator. As the fluid is returned to the reservoir, excessive foaming will result. The suction-line strainer may also act as an air trap.
6. **Moving Parts.** Crankshafts, gear teeth, and couplings, either too deep or shallow, may beat air into the hydraulic fluid that must be released upon return to the reservoir.
7. **Fluid Viscosity.** As shown in Chapter 4, higher-viscosity fluids may exhibit greater foam stability, although lower foaming tendency. The use of higher temperatures, or lower fluid viscosity if it is still within the manufacturers operating requirement, may minimize foam stability and facilitate air release.
8. **Oil Oxidation.** In addition to increasing viscosity, some oxidation by-products may stabilize foam.
9. **Contamination.** A common cause of foaming is fluid contamination. Finely divided rust and scale may increase the foaming tendency. Detergent additives in mineral-oil hydraulic fluids may stabilize foaming with water contamination. Contamination with other fluids may also cause foaming.

Aeration and Air Entrainment

In addition to the sources of foaming discussed above, air ingress into the system may cause air entrainment. These include the following [5]:

1. **Soluble Air.** Air is soluble in hydraulic fluid and air solubility increases with increasing temperature and pressure. (See Chapter 4.)
2. **Mechanical Introduction.** Air ingress into the system may occur where negative pressure exists.
3. **Improper System Bleeding.** Increased air entrainment may occur if the hydraulic system is not bled properly to release trapped air. Trapped air may occur during system filling, and vacuum filling may be necessary.
4. **Improper Fluid Addition.** Makeup fluid poured into the reservoir causing splashing or increased agitation may entrap air in the fluid.

In some cases, the only solution to air-entrainment problems is to use a deaerator, where air is removed from a bypass stream under vacuum [9].

Cavitation

Cavitation may occur if the hydraulic fluid is too cold or the fluid viscosity is excessively high. This will lead to the formation of voids within the fluid caused by oil starvation on the suction side of the pump. In addition to excessive fluid voids, cavitation may also be due to insufficient pumping capacity and restricted passages in the piping and strainers. Overall flow resistance should not create a net inlet vacuum in excess of 5–10 in. Hg maximum [10]. Additional potential sources of cavitation include excessive pump-shaft speeds, fluid-specific gravity higher than system design accommodation, high altitude, boost or makeup pressure too low, and no baffle plate in the reservoir.

Fluid viscosity at the onset of cavitation may be calculated by the following [10]:

1. Adding or subtracting the head or lift to the pump suction capacity.
2. Express the bends, elbows, strainers, and valves of the suction system as equivalent length of straight intake pipe and add this length to the suction pipe in feet.
3. Calculate the oil viscosity causing the maximum depression at the pump inlet (onset of cavitation) from

$$\text{Viscosity (cS)} = \frac{843ad^2}{bV} \left(\frac{0.87}{\text{SPG}} \right)$$

where

a = the pump suction capacity (in in. Hg)

b = the equivalent length of suction system (in ft)

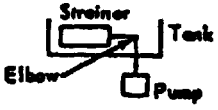

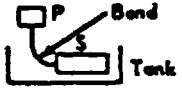
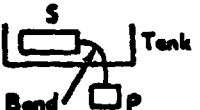
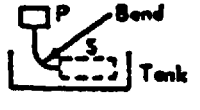
d = the diameter of the suction pipe (in in.)

V = the fluid velocity (in ft/s)

SPG = the specific gravity of the hydraulic fluid

A number of calculation examples are provided in Table 12.2 [10].

Table 12.2 Illustrative Maximum Fluid Calculations

		Examples									
		1		2		3		4		5	
											
Flow rate	2 ft/s	2 ft/s	4 ft/s	4 ft/s	2 ft/s	2 ft/s	2 ft/s	2 ft/s	2 ft/s	2 ft/s	
Pipe size	1 in. diameter	1 in. diameter	2 in. diameter	2 in. diameter	1 1/2 in. diameter	2 in. diameter	2 in. diameter	2 in. diameter	2 in. diameter	2 in. diameter	
		Mineral oil		Mineral oil		Mineral oil		Synthetic fluid		Emulsion fluid	
(a)											
Head (+)	1 ft	+ 0.78	1 ft	-0.78	2 ft	$2 \times 0.78 = 1.56$	2 ft	$2 \times 1.02 = +2.04$	1 ft	$1 \times 0.81 = -0.81$	
Lift (-)											
Pump suction	10 in. Hg	$\frac{10.00}{10.78}$ in. Hg	10 in. Hg	$\frac{10.00}{9.22}$ in. Hg	10 in. Hg	$\frac{10.00}{8.44}$ in. Hg	5 in. Hg	$\frac{5}{7.04}$ in. Hg	1.5 in. Hg	$\frac{1.5}{0.69}$ in. Hg	
(b)											
		Equivalent length of pipe (ft)		Equivalent length of pipe (ft)		Equivalent length of pipe (ft)		Equivalent length of pipe (ft)		Equivalent length of pipe (ft)	
Pipe length	1 ft	1	1 ft	1	5 ft	5	4 ft	4	2 ft	2	
Bead	—	—	—	—	—	—	1	1 1/2	1	—	
Elbow	1	$3 \times 1 = 3$	1	$3 \times 1 = 3$	1	$1 \times 2 = 2$	1	—	—	$1 \times 2 = 2$	
Strainer	1	S $\frac{3.3}{ft 7.3}$	1	S $\frac{3.3}{ft 7.3}$	1	S $\frac{6.6}{ft 13.6}$	1	S $\frac{3.7}{ft 9.2}$	—	a $\frac{a}{ft 4}$	
Maximum viscosity (approx.) ^b	$\frac{843ad^2}{bV}$	$\frac{843 \times 10.78 \times 1}{7.3 \times 2} = 620$ cS	$\frac{843 \times 9.22 \times 1}{7.3 \times 2} = 500$ CS	$\frac{843 \times 8.44 \times 4}{13.6 \times 4} = 520$ cS	$\frac{843 \times 7.04 \times 2.25 \times 0.87}{9.2 \times 4 \times 1.15} = 275$ cS	$\frac{843 \times 0.69 \times 4 \times 0.87}{4 \times 2 \times 0.92} = 275$ cS					

^aStrainers not usually fitted owing to the low pump suction value permitted. Where fitted, a strainer with four times normal capacity would be employed. In this case, the result = 150 cS (approx.).

^b $843ad^2/bV$ is derived from Fanning's equation for fluids with a centistoke viscosity greater than $3.7dV$, where d is the diameter in inches and V is the velocity in feet, and where flow is streamline having Reynolds numbers less than 2100.

Table 12.3 Equivalent Linear Length Factors

Component	Equivalent length of pipe (ft)
Elbow	3 × diameter (in.)
Bend	1 × diameter (in.)
Gate valve (open)	0.5 × diameter (in.)
Wire strainer (gap of 0.005–0.008 and aperture area of 2 in. ² /gal flow/min) ^a	$\frac{6.6d^2}{V}$ (ft)

^aAdjust for other aperture areas: area × value = 13.2.

The above equation is derived from Fanning's equation for fluids with a viscosity in centistokes greater than 3.6 V and for fluids with a Reynolds number less than 2100.*

The equivalent length of pipe (in ft) for elbows, bends, gate valves, and strainers may be calculated from Table 12.3 [10].

Procedures to identify sources of cavitation include the following:

1. Check the manufacturers recommendation for start-up and operating viscosities of the fluids. These recommendations are pump- and manufacturer-specific.
2. Check the inlet inside diameter and inlet flow velocity.
3. Check the size of the inlet strainer. The capacity of the inlet strainer should be at least two times the pump volume. (See subsection on Fluid Oxidation.)
4. Be sure that the inlet strainer has been cleaned properly. (See subsection on Fluid Oxidation.)

One of the most common causes of hydraulic pump cavitation is improper pump inlet designs that do not provide the necessary NPSH_λ (Net Positive Suction Head available) for the fluid being used. The available NPSH at the pump inlet for a simple system may be calculated from the following equation (also see Fig. 12.9) [12]:

$$\text{NPSH}_\lambda = H_a + H_s - H_{v_p} - H_f$$

*Fanning's equation, also known as the Darcy–Weisbach equation, is used to calculate friction loss in fluid flow through a pipe and is written as

$$h_f = f \left(\frac{L}{D} \right) \left(\frac{V^2}{2g} \right)$$

where h_f is the friction loss (in ft) of fluid, L is the length of pipe (ft), D is the average inside diameter of the pipe (ft), V is the average velocity (ft/s), g is the gravitational constant (32.174 ft/s²), and f is the friction factor (see Appendices at back of book) [11].

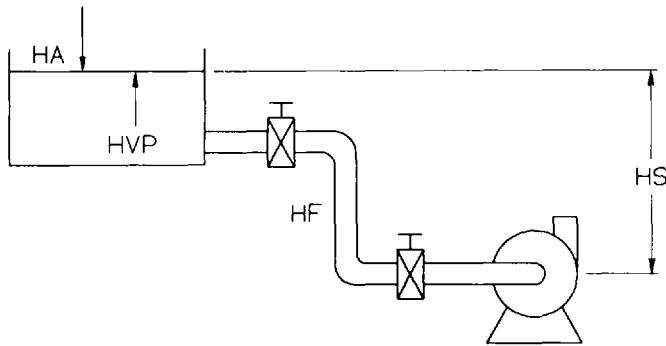


Figure 12.9 Illustration of contributing head pressures acting on a hydraulic pump inlet in a simple hydraulic circuit.

where

H_a = head pressure acting on the fluid surface in the tank. If the system is not pressurized, this will be atmospheric pressure.

H_s = head pressure between the surface of the fluid and centerline of the pump inlet. It is very important to note that this value will be negative if the fluid surface is below the pump inlet.

H_{VP} = vapor pressure of the fluid at the fluid temperature expressed as feet of head.

H_f = friction loss in the suction piping.

Alternatively, the following equation can also be used [54]:

$$NPSH_A = H_a + H_k + \frac{V^2}{2g} - H_{VP}$$

where

H_a = atmospheric pressure in feet of head

H_k = gauge pressure at the suction flange in feet of head.

$V^2/2g$ = velocity head at the point of measurement (in. Hg). This adjustment is required because gauge pressures do not typically include velocity head.

Cavitation damage is exemplified by the formation of pitting, holes, and craters on the wear surface. This is shown in Fig. 12.10.

Contamination

Any foreign material in a hydraulic fluid that exhibits a harmful effect is a fluid contaminant. Contaminants may be solid particles, liquids, or gases. Most solid contaminants cause an abrasive action, increasing the dimensions between the components. Solid contamination is discussed in detail in Chapter 3. Table 12.4 provides a summary of major contaminant types and possible damage that they may cause [13].

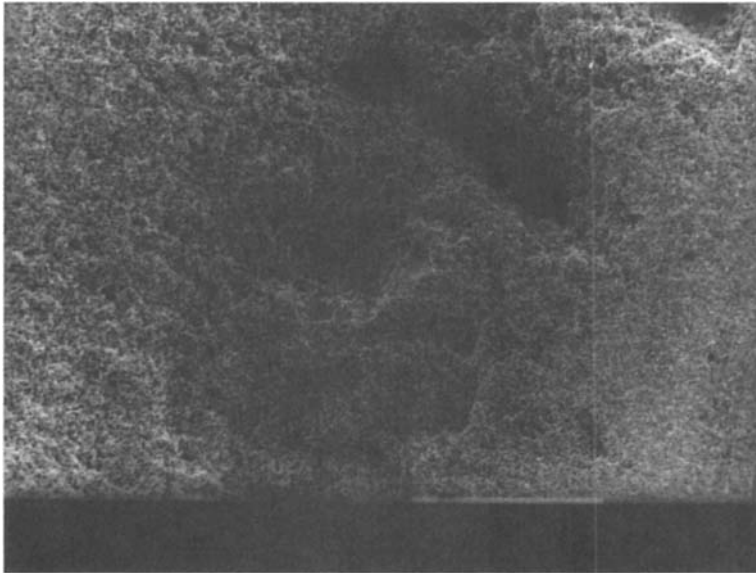


Figure 12.10 Surface damage, pitting, and cratering due to cavitation. (Courtesy of IFAS, Aachen, Germany.)

Table 12.4 Common Fluid Contaminants and Possible Damage

Contaminant	Damage
Ingested dirt	Solids interfere with oil-film formation. Hard particle abrasion. Fine particles cause polishing wear. Fatigue failure in rolling element bearings due to dents from particles.
Water	Produces nonuniform fluid film formation. Causes rust. Catalyzes oxidative oil degradation.
Manufacturing debris	Metal chips penetrate oil film and initiate scuffing.
Chemicals	Causes corrosion and oil degradation.
Wear debris	Wear debris accumulation promotes oil degradation. Destroys surface of babbitt bearings.
Wrong oil	If viscosity is too low, oil film is too thin. If viscosity is too high, pump efficiency decreases. ^a If additives are too chemically active, corrosion and polishing will result. If additives are not sufficiently chemically active, risk of scuffing increases.

^aEfficiency increases with increasing viscosity due to reduced internal leakage. Excessive fluid viscosities produce cavitation.

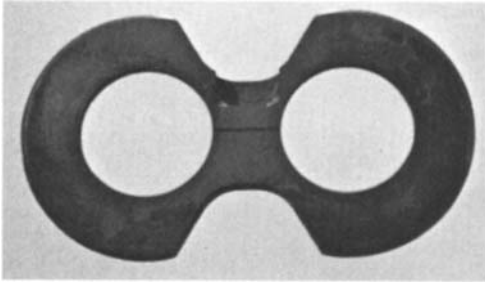


Figure 12.11 Pressure plate is black due to excessive heat caused by high (>300°F) oil temperature. This plate cannot be reused. (Courtesy of Dana Corp.)

Fluid Oxidation

It is normal for fluids to form acids and sludges due to oxidation over their lifetime. This is accelerated with extended operation at high temperature and thermal cycling [14]. Although operating temperatures of mineral-oil hydraulic fluids will vary with the application, there are some guidelines: Typically, the maximum operating temperature at atmospheric pressure is 150°F (65°C), operating temperatures of 180–200°F (82–93°C) are possible, but the fluid must be changed two to three times as often, and operation at temperatures at 250°F (121°C) causes relatively rapid fluid decomposition. Fluid lifetimes, perhaps as short as 24 h, will result [14].

In addition to heat-exchanger failure, excessive heating of hydraulic fluids may be due to a sticking valve or relief valve set too low. If the sticking valve does not return to the neutral position, the system energy goes to heat and not work, thus overheating the fluid. If the relief valve is set too low, a portion of the fluid will be dumped across the relief valve with each cycle, causing both overheating and slow operation [15]. The effect of high-temperature excursions on hydraulic equipment is illustrated in Figs. 12.11 [16], 12.12 [16], 12.13 [17], and 12.14.

One of the most common sources of hydraulic system problems is the deposition of oil oxidation by-products [18,19]. It has been shown that suction strainer clogging by resinous oil oxidation by-products led to cavitation and at least 50% reduction in hydraulic pump lifetime [19]. The resinous by-products form an insulation coating on the strainer mesh as shown in Fig. 12.15 [19]. This will lead to a

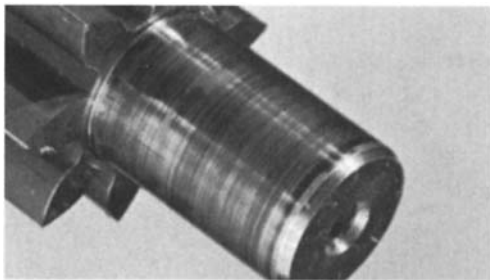


Figure 12.12 Black coloration of gear and shaft due to excessive overheating of the oil (>300°F). This part is not usable. (Courtesy of Dana Corp.)

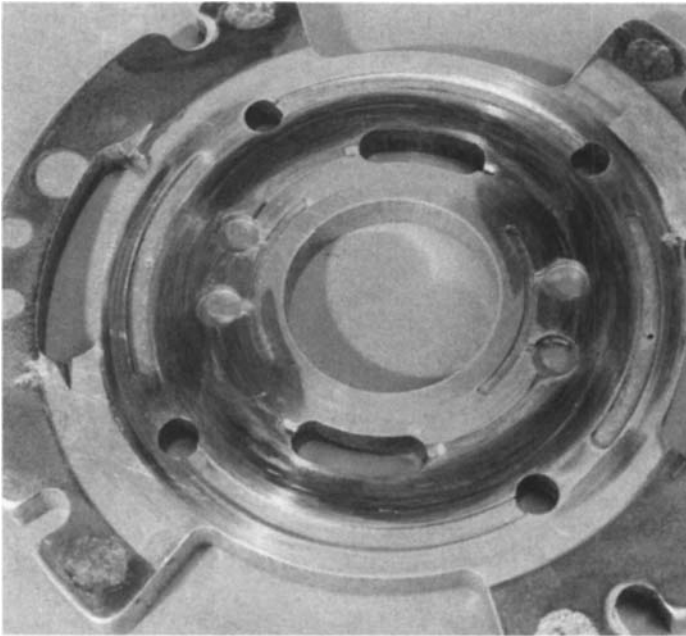


Figure 12.13 Flex plate discoloration from excessive heat. Some erosion damage is also observable. (Courtesy of Vickers, Inc., Troy, Inc.)



Figure 12.14 Rotor, vanes, and bushing covered with fluid oxidation deposits. (Courtesy of DMT-Gesellschaft für Forschung and Prüfung mbH, Essen, Germany.)

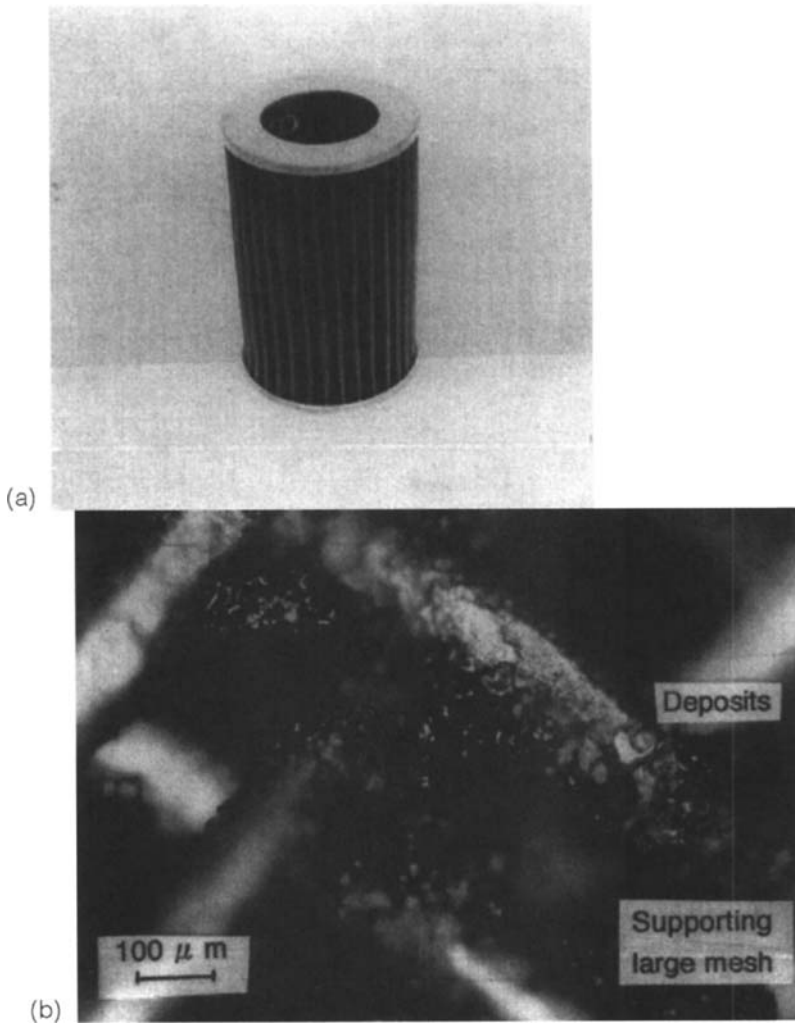


Figure 12.15 (a) Clogged inlet strainer. (Courtesy of A. Sasaki, Kleentek, Inc.) (b) Illustration of sludge buildup on a strainer. (Courtesy of A. Sasaki, Kleentek Inc.)

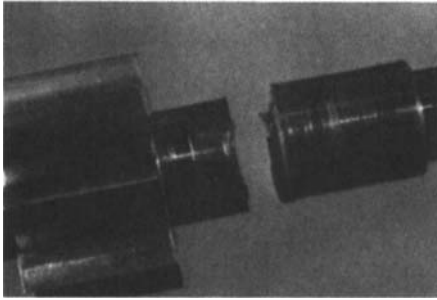


Figure 12.16 Shaft breakage due to relief valve failure or by repeated excessive pressure surges. (Courtesy of Danfoss Fluid Power, Inc.)

buildup of static electricity and a spark discharge on full-flow filters (strainers), causing further oil breakdown [13]. This subsequently led to pump failure by cavitation due to reduced flow rate. As a result of this study, it is recommended that suction filters and strainers be avoided in hydraulic systems [19].

Electrical discharge in mineral-oil hydraulic fluids has been reported previously and it was proposed that this is due to high fluid frictional effects and the length of the spark increased with fluid flow rate [20].

Overpressurization

A hydraulic pump should not be subjected to operating pressures greater than those for which the pump was designed. Overpressurization creates forces against various internal components and may cause premature failure.

Overpressurization may also be caused by component failure. There are two possible causes for overpressurization [15]: (1) relief-valve failure, causing an extreme pressure surge and component failure, as illustrated in Fig. 12.16 [15] and (2) if the relief-valve setting is too high, repeated pressure breaks may result.

Viscosity

Viscosity is a measure of a fluid's internal friction or its resistance to flow. The use of higher than recommended fluid viscosity (or cold oil) may cause pump cavitation, increased pressure drop throughout the circuit, higher oil temperatures, sluggish hydraulic operation, or lower mechanical efficiency [21]. If the fluid viscosity is too low, increased oil leakage, inability to hold pressure, lack of positive hydraulic control, or lower volumetric pump efficiency due to increased internal leakage and an accompanying increase in heat may result [21]. Therefore, the use of the appropriate fluid with the recommended viscosity at the operating temperature must be used. A summary of common hydraulic operation problems and solutions is provided in Table 12.5 [22].

2.3 Wear Mechanisms

To conduct successful failure analysis, it is first necessary to understand and recognize common wear mechanisms upon inspection. The objective of this section is to discuss commonly encountered wear processes, including (1) abrasive wear, (2) adhesive wear, (3) erosive wear, (4) cavitation wear, (5) corrosive wear, (6) contact stress fatigue wear, and (7) other forms of wear.

Table 12.5 Trouble Shooting Chart

Cause	What to do
Noisy Pump	
Air leaking into system	Be sure the oil reservoir is filled to normal level and that oil intake is below surface of oil. Check pump packing, pipe and tubing connections, and all other points where air might leak into system. One good way to check a point on the intake side suspected of leakage is to pour oil over it; if the pump noise stops, you have found the leak.
Air bubble in intake oil	If oil level is low or return line to reservoir is installed above oil level, air bubbles will form in oil in reservoir. Check oil level and return-line position.
Cavitation (the formation of vacuum in a pump when it does not get enough oil)	Check for clogged or restricted intake line, plugged air vent in reservoir. Check strainers in intake line. Oil viscosity may be too high. Check recommendations.
Loose or worn pump parts	Check manufacture's maintenance instructions first; Tightening every nut in sight may not be the way to stop leakage. Look for worn gaskets and packings; replace if necessary. There is usually no way to compensate for wear in a part; it is always better to replace it. Oil may be of improper grade or quality; Check recommendations. Parts may be stuck by metallic chips, bits of lint, etc. If so, disassemble and clean thoroughly. Avoid the use of files, emery cloth, steel hammers, etc. on machined surfaces.
Stuck pump vanes, valves, pistons, etc.	Products of oil deterioration such as gums, sludges, varnishes, and lacquers may be the cause of sticking. Use solvent to clean parts and dry thoroughly before reassembling. If parts are stuck by corrosion or rust, they will probably have to be replaced. Be sure oil has sufficient resistance to deterioration and provides adequate protection against rusting and corrosion.
Filter or strainer too dirty; filter too small	Filter and strainers must be kept clean enough to permit adequate flow. Check filter capacity. Be sure that original filter has not been replaced by one of smaller capacity. Use oil of quality high enough to prevent rapid sludge formation.
Pump running too fast	Determine recommended speed. Check pulley and gear sizes. Make sure that no one has installed replacement motor with other than recommended speed.
Pump out of line with driving motor	Check alignment. Misalignment may be caused by temperature variation.
Leakage Around Pump	
Worn packing	Tighten packing gland or replace packing. Trouble may be caused by abrasives in oil. If you suspect this sort of trouble, make a thorough check of points where abrasives may enter system.

Table 12.5 Continued

Cause	What to do
Head of oil on suction line	Usually it is better to have no pressure on the suction side of the pump, although it may be necessary. With more than slight head, leakage may result. If head is not required and components can be rearranged, do so. Otherwise, do not worry about the leakage. Just wipe off the pump periodically and, if feasible, install a drip pan. Do not let oil leak onto floor!
Overheating	
Oil viscosity too high	Check oil recommendations. If you are not sure of the viscosity of oil in system, it may be worth your while to drain the system and install oil of proper viscosity. Unusual temperature conditions may cause oil of proper viscosity for "working temperature" to thicken too much on way to pump. In this case, use of oil with a higher viscosity index may cure trouble.
Internal leakage too high	Check for wear and loose packings. Oil viscosity may be too low. Check recommendations. Under unusual working conditions, temperature may go high enough to reduce viscosity of recommended oil too much. Proceed with caution if you are tempted to try a higher viscosity oil.
Excessive discharge pressure	If oil viscosity is found to be OK, trouble may be caused by a high setting of relief valve. If so, reset.
Poorly fitted pump parts	Poorly fitted parts may cause undue friction. Look for signs of excessive friction; be sure all parts are in alignment. On any machine equipped with an oil cooler, it is probably that high temperatures are expected. If temperatures run high normally, they will go even higher if oil cooler passages are clogged.
Oil cooler clogged	If you find a clogged cooler, try blowing it out with compressed air. If this will not work, try solvents.
Low oil	If the oil supply is low, less oil will be available to carry away just as much heat. This will cause a rise in oil temperature, especially in machines without oil coolers. Be sure oil is up to level.
Pump Not Pumping	
Pump shaft turning in wrong direction	Shut down immediately. Some types of pumps can turn in either direction without causing damage; others are designed to turn in one direction only. Check belts, pulleys, gears, motor connections. Reversed leads on three-phase motor are most common cause of wrong rotation.
Intake clogged	Check line from reservoir to pump. Be sure filters and strainers are not clogged.
Low oil level	Be sure oil is up to recommended level in reservoir. Intake line must be below level of oil.

Table 12.5 Continued

Cause	What to do
Air leak in intake	If any air at all is going through pump, it will probably be quite noisy. Pour oil over points suspected of leakage: if noise stops, you have found the leak.
Pump shaft speed too low	Some pumps will deliver oil over a wide range of speeds; others must turn at recommended speed to give appreciable flow. Find out first the speed recommended by the manufacturer; then, with a speed counter if possible; check the speed of the pump. If speed is too low, look for trouble in driving motor.
Oil too heavy	If oil too heavy, some types of pumps cannot pick up prime. You can make a very rough check of viscosity by first getting some oil that is known to have the right viscosity. Then, with both oils at the same temperature, pour a quart of each oil through a small funnel. The heavier oil will take a noticeably longer time to run through. Oil that is too heavy can do great harm to hydraulic systems. Drain and refill with oil of the right viscosity.
Mechanical trouble (broken shaft, loose coupling, etc.)	Mechanical trouble is often accompanied by a noise that you can locate very easily. If you find it necessary to disassemble, follow the manufacturer's recommendations to the letter.
Low Pressure in System	
Relief valve setting too low	If relief-valve setting is too low, oil may flow from pump through relief valve and back to the oil reservoir without reaching point of use. To check relief setting, block discharge line beyond relief valve and check line pressure with pressure gauge.
Relief valve stuck open	Look for dirt or sludge in valve. If valve is dirty, disassemble and clean. Stuck valve may be indication that system contains dirty or deteriorated oil. Be sure, therefore, that oil has high enough resistance to deterioration.
Leak in system	Check whole system for leaks. Serious leaks in the open are easy to detect, but leaks often occur in concealed piping. One routine in leak testing is to install a pressure gauge in the discharge line near pump and then lock off the circuit progressively. When the gauge pressure drops with gauge installed at a given point, leak is between this point and check point just before it.
Broken, worn, or stuck pump parts	Install pressure gauge and block system just beyond relief valve. If no appreciable pressure is developed and relief valve is OK, look for mechanical trouble in pump. Replace worn and broken parts.
Incorrect control valve setting; oil "short-circuited" to reservoir	If open-center directional control valves are unintentionally set at neutral position, oil will return to reservoir without meeting any appreciable resistance and very little pressure will be developed. Scored control-valve pistons and cylinders can cause this trouble. Replace worn parts.

Table 12.5 Continued

Cause	What to do
Erratic Action Valves, pistons, etc., sticking or binding	First, check suspected part for mechanical deficiencies such as misalignment of a shaft, worn bearings, etc., then look for signs of dirt, oil sludge, varnishes, and lacquers caused by oil deterioration. You can make up for mechanical deficiencies by replacing worn parts, but do not forget that these deficiencies are often caused by the use of the wrong oil.
Sluggishness when a machine is first started	Sluggishness is often caused by oil that is too thick at starting temperatures. If you can put up with this for a few minutes, oil may thin out enough to give satisfactory operation. But if oil thins out or if surrounding temperature remains relatively low, you may have to switch to oil with lower pour point, lighter viscosity, or, perhaps, higher viscosity index. Under severe conditions, immersion heaters are sometimes used.

2.3.1 Abrasive Wear

Abrasive wear refers to the cutting of a metal by hard particles or a rough surface by a ploughing or microcutting mechanism [13,23]. When abrasion wear is caused by a hard particle between two surfaces, it is termed three-body wear, which is depicted in Fig. 12.17 [24]. Hard particles causing three-body wear may be introduced into the system from the component manufacturing process, generated inter-

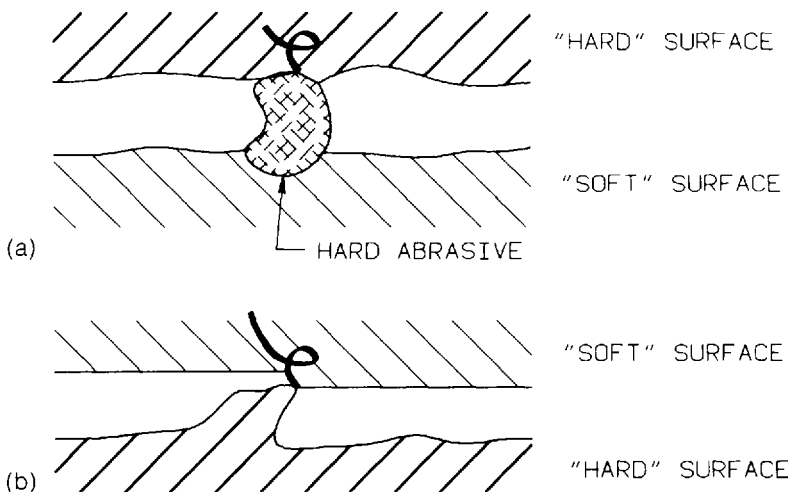


Figure 12.17 Abrasive wear: (A) three-body wear; (B) two-body wear.

nally as wear debris, ingested through a breather or seals, or it may be added as a contaminant in the fluid upon addition to the system [25].

Abrasive wear is dependent on particle size distribution, shape, toughness, and hardness [24]. The mechanism illustrated by Fig. 12.18 [24] shows that hard particles penetrate and become embedded into one of the wear surfaces. The embedded particle, tilted at angle (ϕ), then cuts the opposite surface. The energy from the micro-cutting action causes plastic deformation and the formation of parallel furrows and ridges in the direction of surface movement [13]. A surface that has undergone abrasive wear is illustrated in Fig. 12.19. Severe gear-tooth abrasion is illustrated in Fig. 12.20 [26]. Additional examples of three-body wear are presented in Figs. 12.21–12.25.

Two-body wear, shown in Fig. 12.17B, is caused by a harder surface with asperity dimensions sufficiently large to penetrate the lubricating oil film causing a ploughing or microcutting action on the other softer surface, which is in relative motion. This is depicted in Fig. 12.26 [24]. This form of wear is also known as cutting, ploughing, gouging, lapping, grinding, or broaching wear [24].

Abrasive wear may be minimized by the following [25]:

1. Removing potential residual manufacturing debris by proper draining and flushing procedures before starting
2. Using wear-resistant materials of construction
3. Minimizing ingested particles by the use of proper breather filters and by keeping the system tight

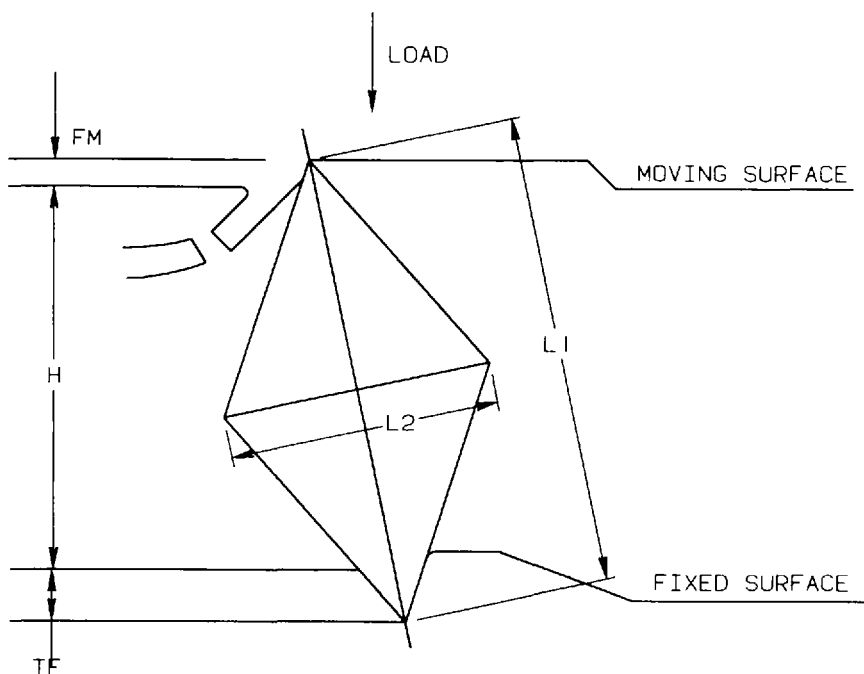


Figure 12.18 Three-body wear model.

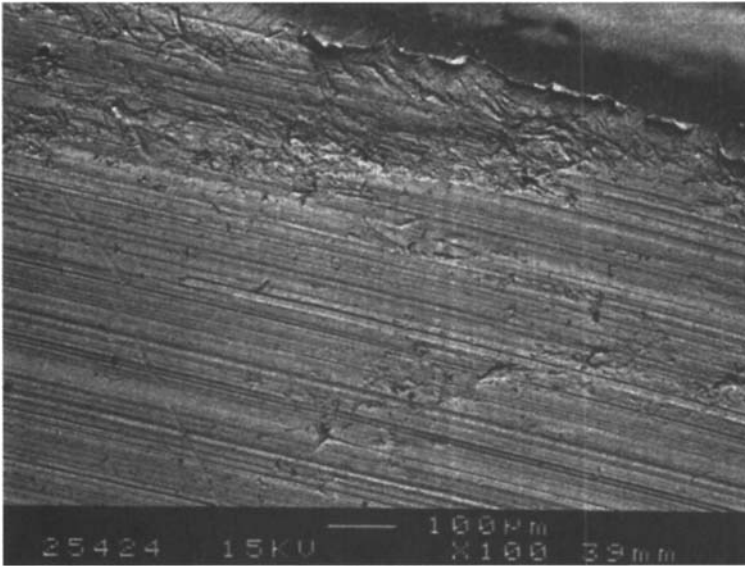


Figure 12.19 Illustration of abrasion surface wear. (Courtesy of IFAS, Aachen, Germany.)

4. Using fine filtration to minimize particulate contamination of the hydraulic fluid
4. Performing proper fluid maintenance and periodic fluid analysis

2.3.2 Adhesive Wear

Adhesive wear, as depicted in Fig. 12.27, occurs when surface asperities come into sliding contact under a load. If sufficient heat is generated, microwelding of the asperity with subsequent shearing and material transfer of the contact will be observed, as illustrated in Fig. 12.28. This process will continue until larger surfaces are in contact and macrowelding or seizure occurs. Generation of adhesive wear

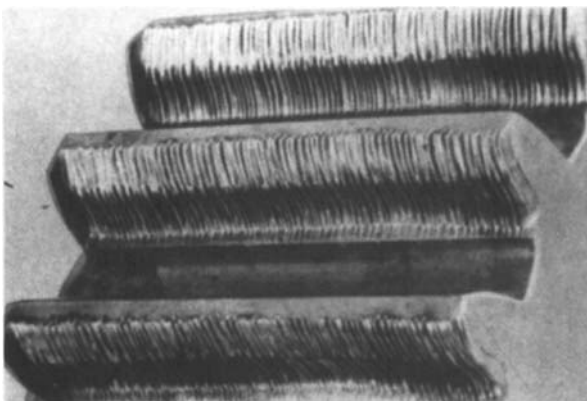


Figure 12.20 Extreme abrasion wear. (Courtesy of American Gear Manufacturers Association.)

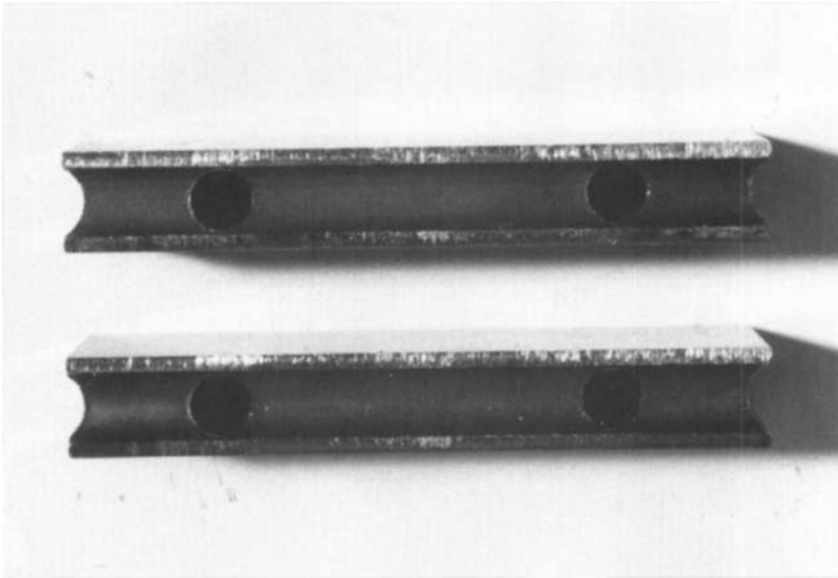


Figure 12.21 Vane-tip wear due to particle ingress through breather pipe. No air filter was used. (Courtesy of Denison Hydraulics Inc., Marysville, OH.)

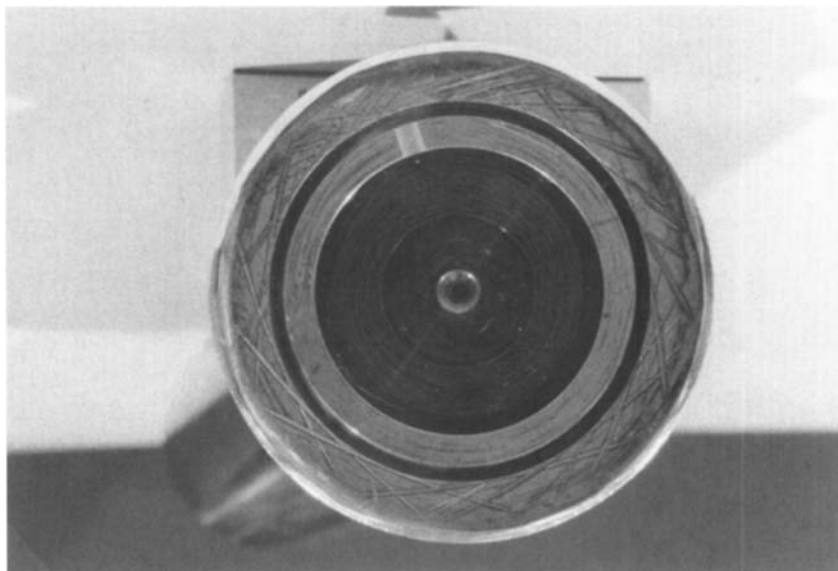


Figure 12.22 Scratch marks on the face of a piston shoe due to fluid particle contamination. (Courtesy of Denison Hydraulics Inc., Marysville, OH.)

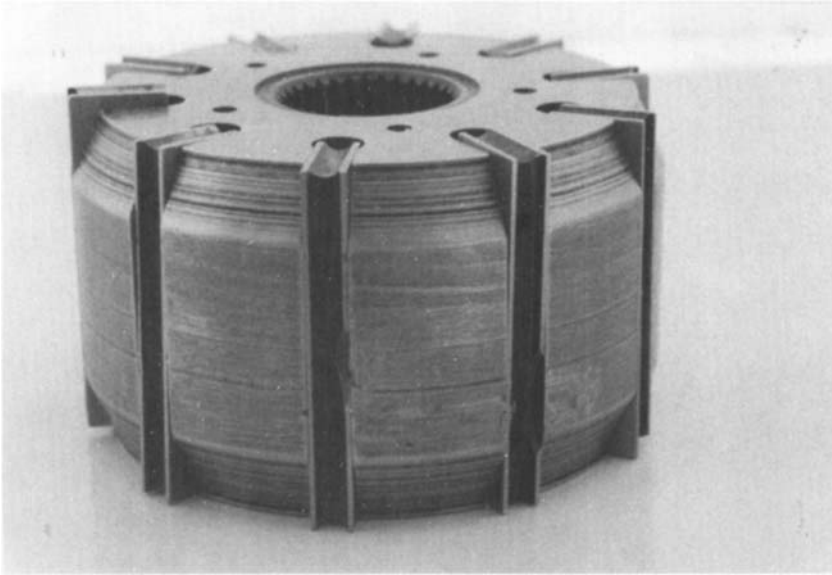


Figure 12.23 Vane-rotor assembly damage due to large-particle contamination. Only one-half of fluid flow was being filtered. The filter had a rating of $\beta_{20} = 5$, which was plugged due to water contamination. (Courtesy of Denison Hydraulics Inc., Marysville, OH.)

debris may then cause abrasion wear. Therefore, it is possible for both wear processes to occur together. If the temperature is sufficiently high, metal flow and “smearing” will be observed. If the part is constructed from steel, tempering colors may be observed, and if the temperature of the total part is high enough, plastic deformation and fracture may result, as illustrated in Fig. 12.29 [23].

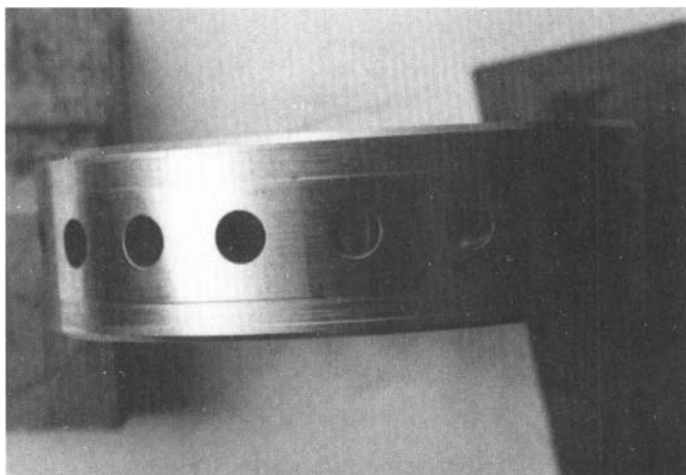


Figure 12.24 Internal wear contact surface with abrasive damage due to hard-particle contamination. (Courtesy of Kayaba Industry Co., Tokyo, Japan.)

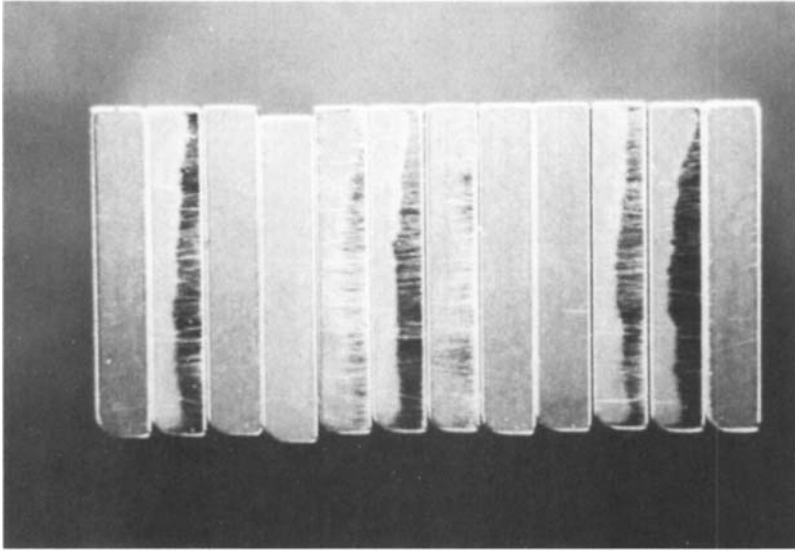


Figure 12.25 Fine-particle abrasive wear on the vane tips is due to surface varnish formation from the oil. (Courtesy of Quaker Chemical Corporation, Conshohocken, PA.)

Adhesive wear is dependent on the following [27]:

1. Surface characteristics, including hardness, shear strength, roughness, surface “waviness,” geometry, elastic modulus, tensile strength, ductility, melting temperature, and interfacial metal compatibility
2. Normal loading and tangential sliding force
3. Lubrication conditions, including presence of oxide films, extreme pressure lubricants, oil films, and contaminants

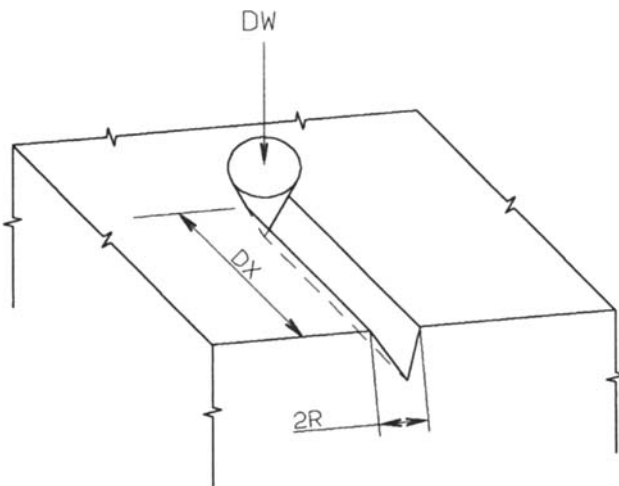


Figure 12.26 Model of two-body wear process.

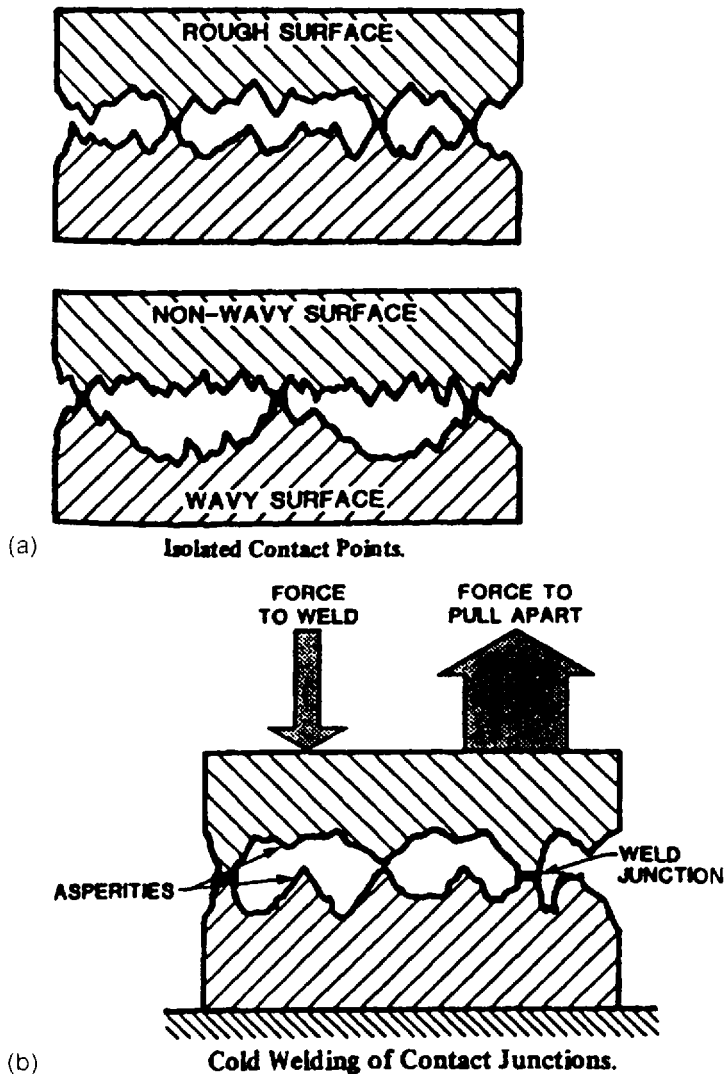


Figure 12.27 Illustration of (a) surface asperity contacts and (b) adhesive wear.

4. Environmental properties such as dust, salt, fog, water, temperature, and chemicals

Fitch has provided the following “Six Laws of Adhesive Wear” [27]:

1. The area of contact between the two surfaces is directly proportional to the applied normal load and inversely proportional to the indentation (Brinell) hardness of the softer material.
2. The volume of material worn away when one of the surfaces slides over the other is proportional to the true area of contact, the total sliding distance, and the wear coefficient of the material pair. Wear coefficients are provided in Table 12.6 [27].

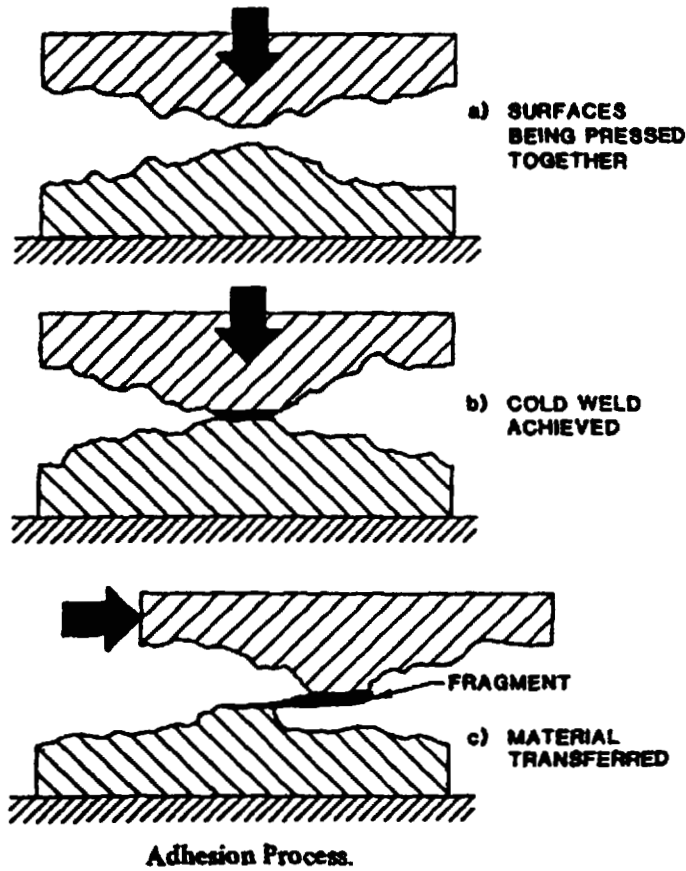


Figure 12.28 Model of adhesive wear process.

3. The average wear depth is obtained by dividing the volume of material wear by the nominal area of contact.
4. For surfaces of different materials, the ratio of wear depth of the harder material equals the square of the ratio of the yield strengths of the softer material to the harder material.
5. The wear coefficient remains constant as long as the pressure does not exceed one-third the material hardness. As long as the wear coefficient is constant, wear will vary linearly with the distance traveled and the wear rate will be constant. At pressures in excess of one-third the hardness, the wear coefficient begins to increase and the wear increases nonlinearly and rapidly.
6. The values of wear coefficients are determined by the material pairs used and are established experimentally. The values are affected by oxide layers, surface contamination, surface finish, and experimental conditions.

Adhesive wear may be reduced by increasing material hardness, surface hardening, avoiding metallurgically similar material pairs, avoiding highly soluble materials,

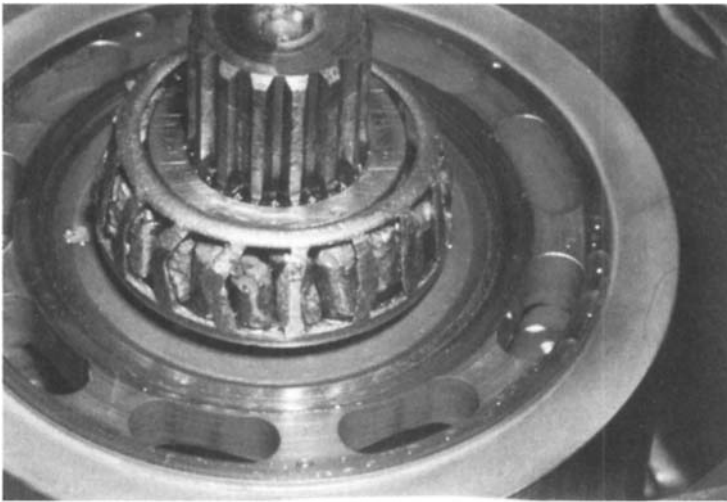


Figure 12.29 Damaged roller bearing from an axial piston pump with plastically deformed roller due to poor lubrication and adhesive wear. (Courtesy of DMT-Gesellschaft für Forschung und Prüfung mbH, Essen, Germany.)

using welding-resistant materials, and providing a soft layer containing compounds of sulfur and phosphorus [27].

Adhesive wear may occur in areas where the friction contacts are greatest due to tight fits, misalignment, high loading, poor lubrication, and high temperature [28]. Examples of adhesive wear are provided in Figs. 12.30 (cam ring) [29], 12.31 (bearing area of gear shaft) [28], 12.32 (piston) [29], 12.33 (bearing surfaces) [30], 12.34 (piston-shoe metal transfer), and 12.35 (piston-shoe/tin-brass layer adhesive failure).

Polishing

Polishing wear may occur by one of two mechanisms. One mechanism is chemical and occurs when the EP additives that are present in the hydraulic oil are too aggressive, leaving a bright, mirrorlike surface [25]. This is undesirable because the polished surface is less resistant to wear.

Alternatively, polishing wear may occur during component break-in when surface asperity adhesive wear occurs until a very fine, smooth surface results [26,31]. This is caused by insufficient electro-hydrodynamic (EHD) lubrication to prevent such asperity contact. Polishing wear can be minimized or avoided with the use of a high-viscosity lubricant or reduced operating temperature. Polishing wear for the drive and gear teeth of a properly operating pump is illustrated in Fig. 12.36 [16].

2.3.3 Erosion Wear

Moving particle surface impingement erosion wear (erosion wear), as illustrated in Fig. 12.37 [32], may result in scratching, surface indentation, chipping, and gouging, as shown in Fig. 12.38. Mechanistically, erosion wear is a combination of two processes: surface fatigue and abrasive cutting [32].

Figure 12.39 illustrates that erosion wear is an exponential process including an initiation time, acceleration, and a period of maximum rate loss [32]. The param-

Table 12.6 Approximate Wear Coefficients

Material A	Material B	Wear coefficient $\times 10^4$
Cu	Pb	0.03
Ni	Pb	0.07
Fe	Ag	0.23
Ni	Ag	0.23
Al	Pb	0.47
Ag	Pb	0.84
Mg	Pb	0.87
Zn	Pb	0.87
Ag	Ag	1.14
Al	Zn	1.31
Al	Ni	1.58
Al	Cu	1.61
Al	Ag	1.78
Al	Fe	2.02
Fe	Zn	2.82
Ag	Zn	2.82
Ni	Zn	3.70
Zn	Zn	3.90
Mg	Al	5.24
Zn	Cu	6.21
Fe	Cu	6.41
Ag	Cu	6.65
Pb	Pb	8.00
Ni	Mg	9.60
Zn	Mg	9.76
Al	Al	10.00
Cu	Mg	10.25
Ag	Mg	10.90
Mg	Mg	12.25
Fe	Mg	12.92
Fe	Ni	20.00
Fe	Fe	26.00
Cu	Ni	27.20
Cu	Cu	42.30
Ni	Ni	95.90

eters that affect erosion wear include fluid-flow velocity, particle and fluid density, drag coefficient, Reynolds number, and particle size. In general, if particles are $\leq 100 \mu\text{m}$, erosion wear rate increases with particle size. If the particles are $> 100 \mu\text{m}$, wear volume by erosion is independent of particle size [32].

Erosion wear occurs where there is a change in fluid-flow direction such as in orifices, line restrictions, turns in fluid passageways, and the leading edge of rotating parts [28]. An illustration of erosion wear is provided in Fig. 12.40, in which erosion wear above and below a piston bore is illustrated [30]. (It should be noted that the erosion is greater at the top of the bore.)

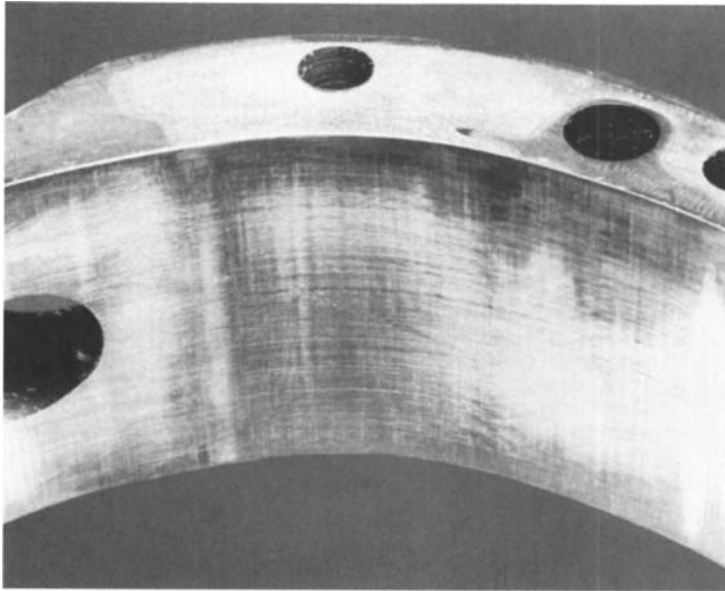


Figure 12.30 Cam-ring smearing damage and discoloration. (Courtesy of Caterpillar Inc., Peoria, IL.)

2.3.4 Cavitation Wear

Cavitation arises when there is a sudden collapse (implosion) of a gas bubble entrained in the hydraulic fluid; it is illustrated in Chapter 2 (Fig. 2.99). The bubble implosion process forms a high-velocity microjet capable of high-impact energy. The implosion process and subsequent microjet surface action is often called the “water

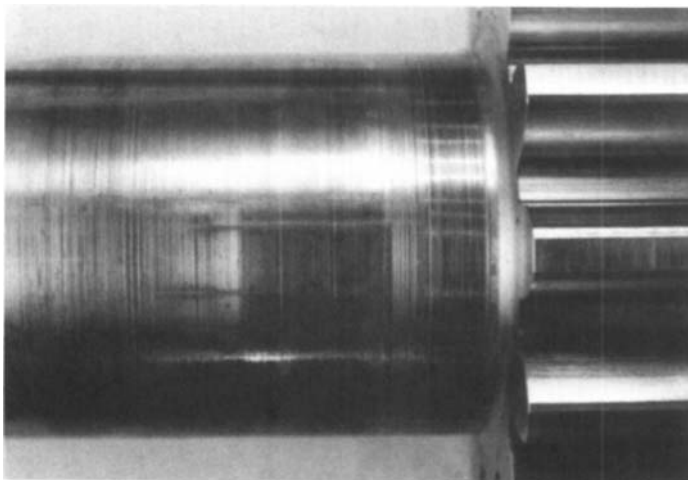


Figure 12.31 Gear shaft with subsequent cracking due to heat from adhesive wear process. (Courtesy of Kayaba Industry Co., Tokyo, Japan.)



Figure 12.32 This hydraulic pump piston has undergone polishing due to smearing. (Courtesy of Caterpillar Inc., Peoria, IL.)

hammer'' effect. Cavitation occurs when there are excessive gas bubbles, high loading, or abrupt surface contour changes. The mechanism of the cavitation process was explained in detail in Chapter 2.

After repeated bubble implosions, material fatigue damage results in surface damage with the formation of pitting and larger holes as shown in Fig. 12.41. The propensity for cavitation is dependent on material properties. A general ranking of various properties with respect to the potential for cavitation damage is shown in Fig. 12.42 [33]. Hobb's has reported a correlation of cavitation damage with "ultimate resilience" which was defined as [34]

$$\text{Ultimate Resilience} = \frac{0.5(\text{Tensile strength})^2}{\text{Elastic modulus}}$$

Various examples of cavitation damage are provided in Figs. 12.43–12.57.

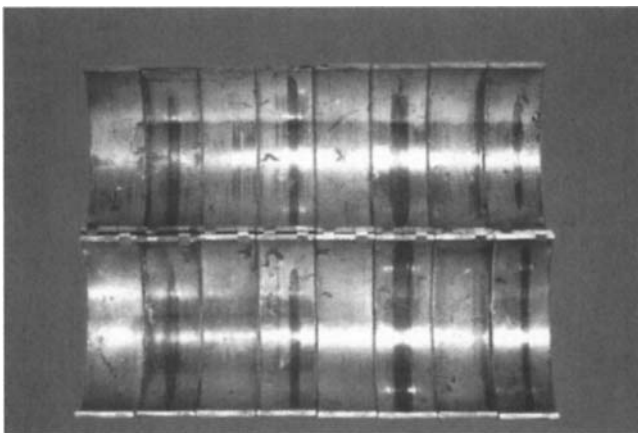


Figure 12.33 Polishing of lead-tin bearing surfaces due to smearing caused by poor lubrication. (Courtesy of Caterpillar Inc., Peoria, IL.)

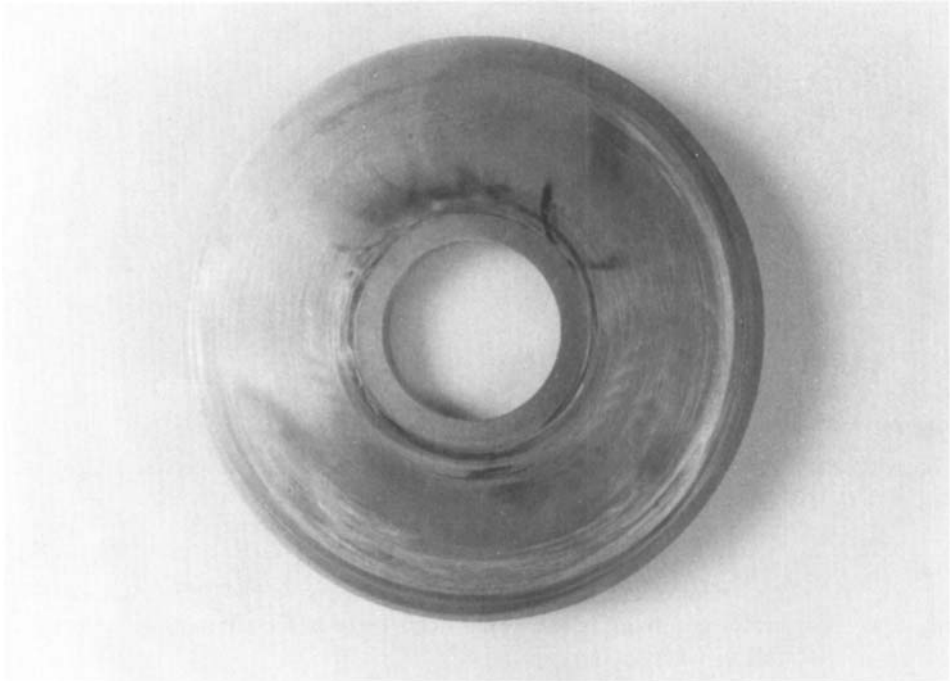


Figure 12.34 Yellow metal transfer from piston shoes to swash plate. (Courtesy of Southwest Research Institute, San Antonio, TX.)

2.3.5 Corrosive Wear

Corrosion wear is surface damage related to electrochemical attack of the metal component. Corrosion may be classified as follows:

1. Crevice or cell corrosion occurs when the tendency for corrosion is greater in cracks or crevices.
2. Dezincification occurs when brass is used. Zinc, an alloying element in brass, dissolves preferentially as a soluble salt. Brasses with greater than 15% zinc are most susceptible to dezincification, particularly in a saltwater environment.
3. Stray electrical currents from motors or generators may come into contact with fabricated metal sections or hydraulic components, accelerating electrochemical attack.
4. Pitting is caused by contact with extreme temperature or acids. This will result in localized oxidative breakdown of the material. The corroded area is anodic and loses metal locally to the cathodic area, causing pitting. Severe abrasive wear damage due to oxidative pitting is illustrated in Fig. 12.58.
5. Fatigue stresses caused by internal or external pressures such as a nut on a bolt may occur in a metal. This will create a pathway within the material that will corrode more rapidly. If the stresses are cyclic, accelerated corrosion or corrosion fatigue may result.

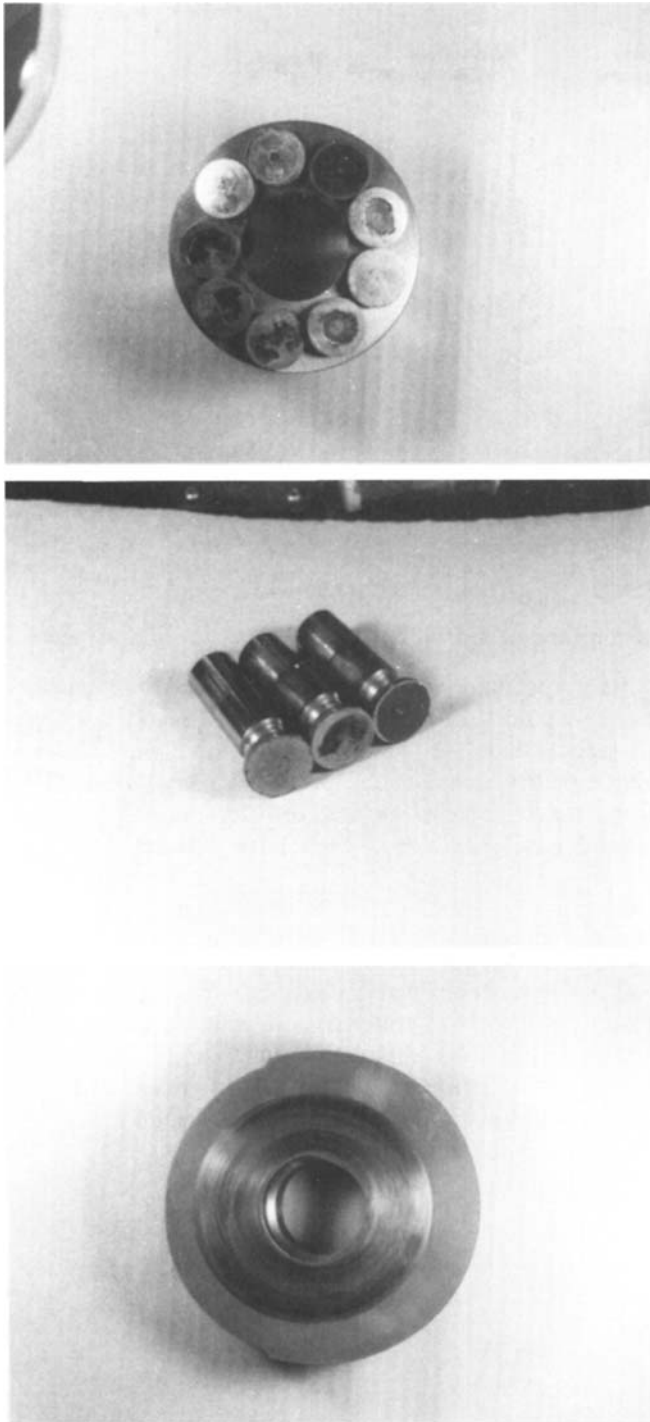


Figure 12.35 Illustration of adhesive failure of carbon-steel piston shoes which have a sliding surface with a layer of sintered tin-brass. The pockets on the shoe surface are present to facilitate hydrostatic lifting. The pockets have disappeared due to excessive wear and the sintered tin-brass has transferred to the surface of the swash plate. Failure was due to inadequate adhesive strength of the tin-brass coating on the side of the steel pistons. (Courtesy of Kayaba, Industry Co., Tokyo, Japan.)

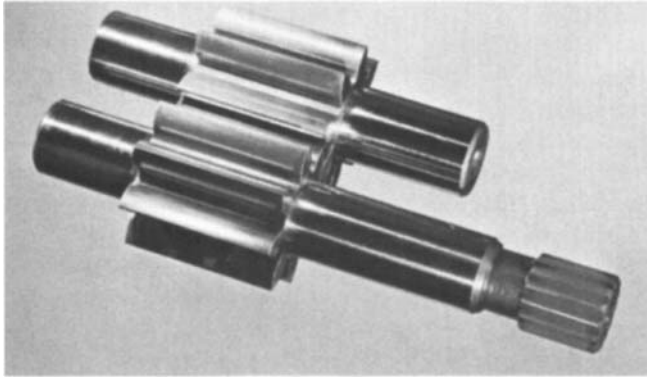


Figure 12.36 Illustration of polishing of the loaded side of gear teeth. Some pitting will occur in the root of the gear teeth after extended operation. High gloss of the journals indicate a properly operating pump. (Courtesy of Caterpillar, Inc., Peoria, IL.)

6. Intergranular corrosion may occur within grain boundaries of the metal.

One result of corrosion is the formation of metal oxides, which have characteristic colors [28]. Ferrous alloys or steel often form reddish-brown oxides. Copper or brass forms bluish-green oxides. Oxides of aluminum are gray. Figure 12.59 illustrates the characteristic nature of the porous nature of an oxide coating on steel. Figure 12.60 illustrates a combination of bronze surface corrosion due to water contamination and additive hydrolysis and cavitation. Figure 12.61 illustrates abrasive wear failure when the root cause is corrosion.

Common causes of metal corrosion include the following [35]:

1. Water from humid air ingress and subsequent condensation, liquid water from spray or splash contamination, water ingress from defective enclosure and cooling coil leakage, and water-contaminated lubricant
2. Lubricant chemistry: poor lubricant formulation using aggressive EP additives, presence of acids from decomposition or exposure to active metals, and lubricant and system incompatibility such as yellow metal attack
3. Corrosive chemical vapors in the atmosphere

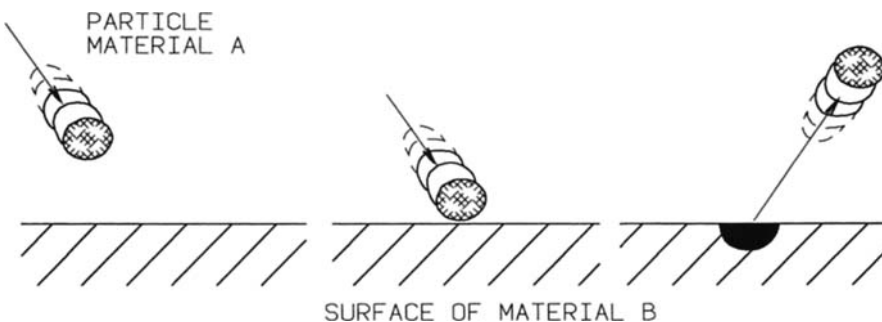


Figure 12.37 Model of erosive wear.

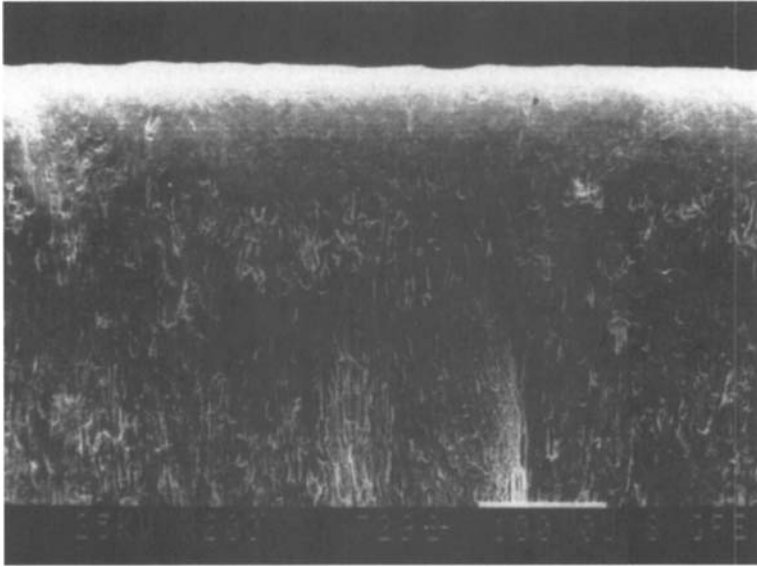


Figure 12.38 Illustration of erosion surface wear. (Courtesy of IFAS, Aachen, Germany.)

4. Corrosive processing chemicals such as coolants and cleaning fluids
5. Galvanic couple formation between metals with different electrochemical potential such as yellow metal separators in martensitic steel roller bearings, stainless-steel surfaces contaminated with martensitic steel, and aluminum alloy components with unprotected surfaces in contact with steel and in the presence of an electrolyte which is any ion-conductive fluid

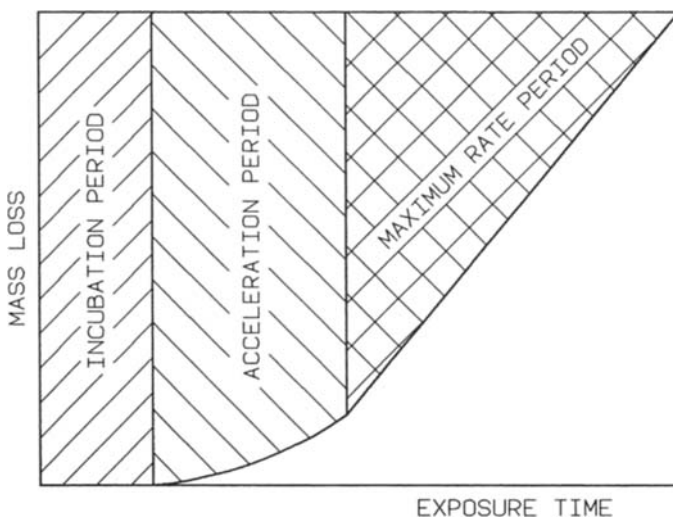


Figure 12.39 Mass removal kinetics of erosive wear process.

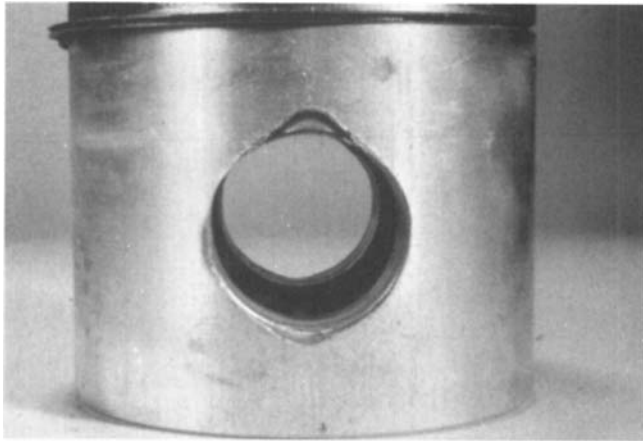


Figure 12.40 Illustration of erosive wear on a cylinder piston. (Courtesy of Caterpillar Inc., Peoria, IL.)

Corrosion may be avoided by using appropriate design methodology. Some guidelines for proper design include the following [36]:

1. Avoid galvanic couples by insulating dissimilar metals or increase electrical resistance. This may be accomplished by using more noble metals or metals close to the metal of interest in the galvanic series shown in Fig. 12.62 [37].
2. Avoid small anodic areas (the more active metal is the anode) relative to the cathode (the less active metal), such as fasteners, by using alloys that are cathodic with respect to the main structure
3. Avoid concentration cells by welding to eliminate crevices and by using fluorocarbon gaskets between contact surfaces



Figure 12.41 Illustration of cavitation surface damage. (Courtesy of IFAS, Aachen, Germany.)

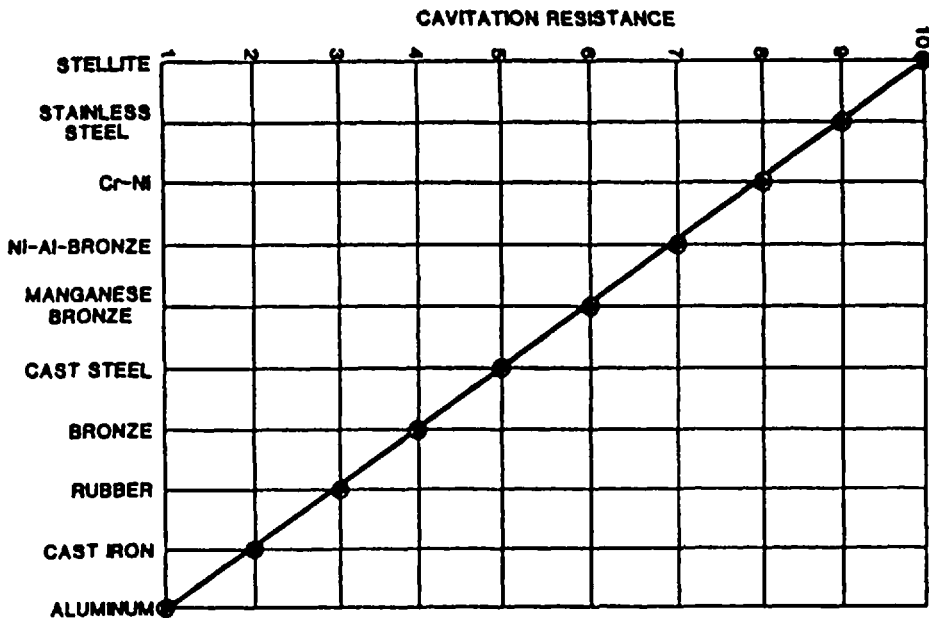


Figure 12.42 Cavitation resistance of various materials. (Courtesy of IFAS, Aachen, Germany.)

4. Protect from corrosive environments by providing a drop skirt or design to eliminate collection of contaminants by geometry or capillarity; allow adequate drainage to prevent collection of corrosive solutions
5. Avoid sections with high tensile stress
6. Use protective coatings where possible

Galvanic Corrosion

Galvanic corrosion is recognizable by the appearance of increased corrosion near the junction of dissimilar metals [38]. This is caused by electrochemical transfer of one metal to another. The propensity for galvanic corrosion is dependent on the position of the two metals in the galvanic series shown in Fig. 12.62 [37]. Any metal will have a greater tendency to corrode when it is in contact with another metal in a lower position in the series in the presence of an electrolyte. The farther apart the two metals in the series, the greater the potential for galvanic attack. The example provided in Fig. 12.62 was developed for steel rivets in copper plates in seawater. Electrons flow from steel to copper, resulting in a deposit of iron oxide on copper.

Galvanic corrosion may be minimized by the following:

1. Use the same or similar metals, especially if an electrolyte is present.
2. Avoid combining dissimilar metals where the area of the less noble metal is relatively small.
3. Use a dielectric material, paint, or coating to separate dissimilar materials where possible.
4. If a pair of dissimilar metals must be used, couple them to a piece of less noble metal, often zinc, which may be used for sacrificial corrosion [28].

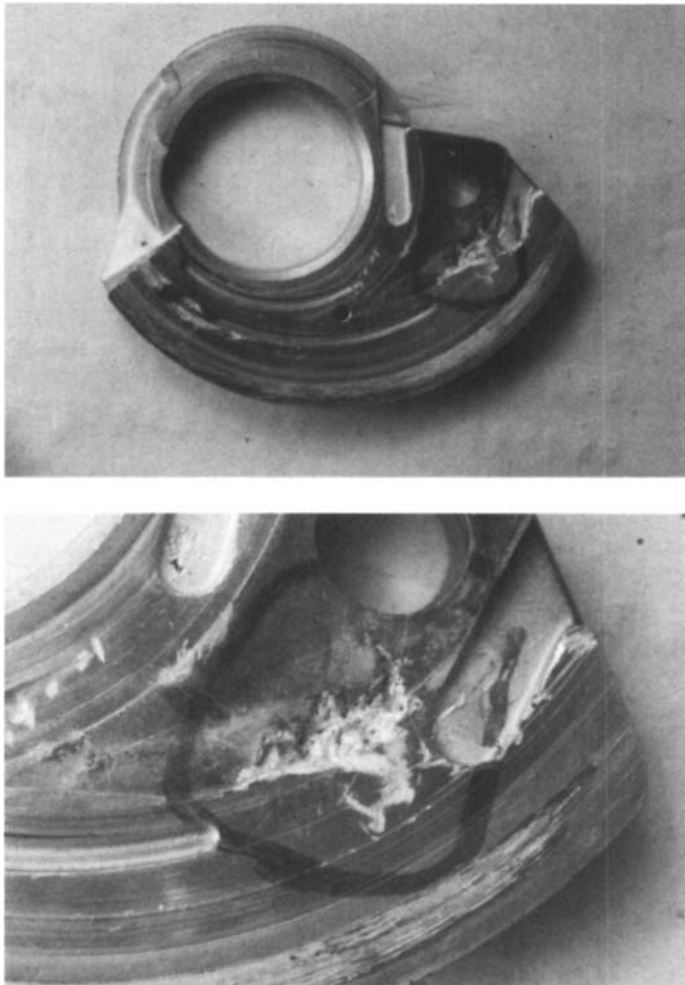


Figure 12.43 Hydraulic pump cavitation damage. (Courtesy of Kayaba Industry Co., Tokyo, Japan.)

Electrochemical Erosion (Pitting Corrosion)

Electrochemical erosion (pitting corrosion) may be encountered with the use of fire-resistant phosphate ester hydraulic fluids with components with small orifices [39] such as spool valves [40]. This erosion occurs most rapidly when the valves are in the closed position, with the formation of a large pressure drop across the orifice by the edge of the slide and port in the sleeve [41]. This erosion is primarily a function of chloride ion contamination and electrical resistance [40].

Beck et al. [42,43] reported that the mechanism of electrochemical erosion was driven by electrical currents that arose from the electrical double layer formed at the fluid interface, as shown in Fig. 12.63 [44]. A streaming current (I) is formed when fluid flow parallel to the double layer–metal interface causes movement of the free charge, typically from chloride anions. The sum of the total charges at the fluid–

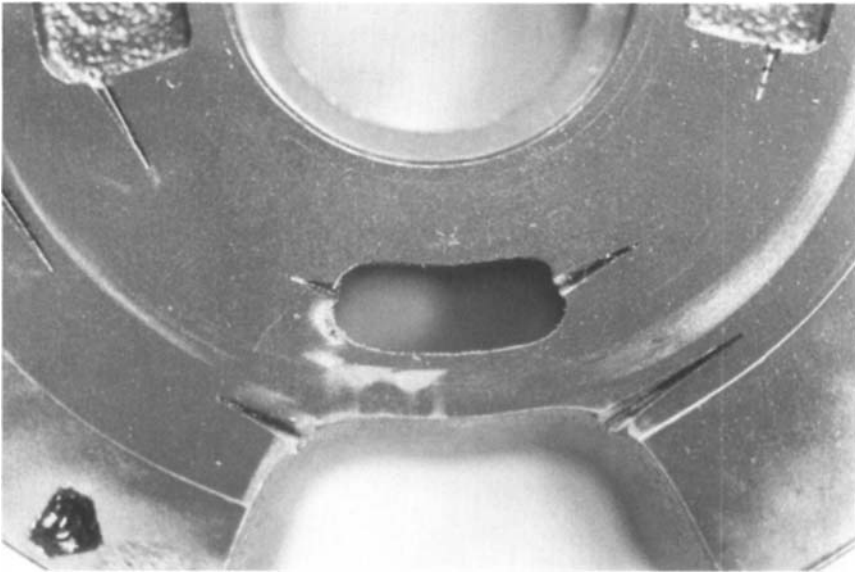


Figure 12.44 Cavitation damage of the port plate of a vane pump due to insufficient release of entrained air in the fluid. This pump was operated at very fast pressure cycles. The pump was equipped with a flooded inlet and an inlet strainer. (Courtesy of Denison Hydraulics Inc., Marysville, OH.)

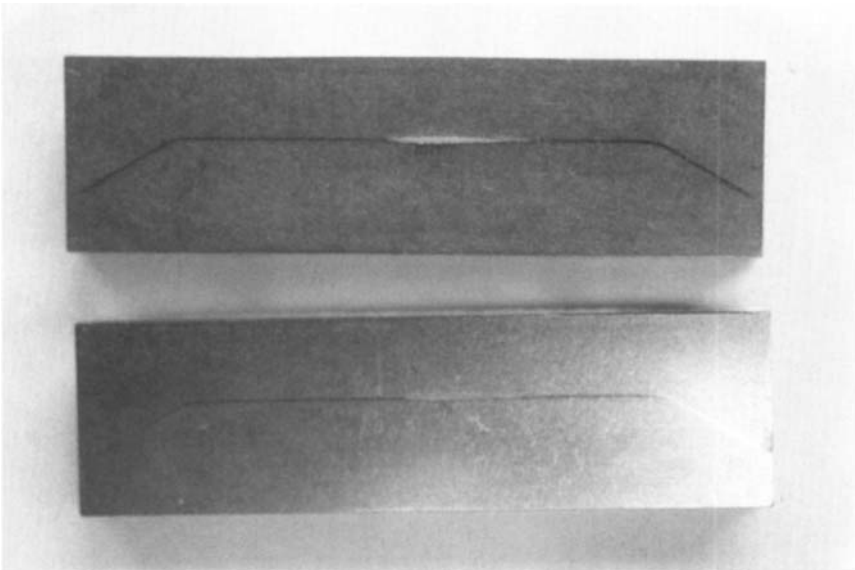


Figure 12.45 Two vanes exhibiting cavitation damage taken from the same pump as the port plate shown in Fig. 12.44. The vanes exhibited cavitation in an area matching the port plate damage. Thus, cavitation not only occurs on the surface of one port but on different ports from the same area. (Courtesy of Denison Hydraulics Inc., Marysville, OH.)

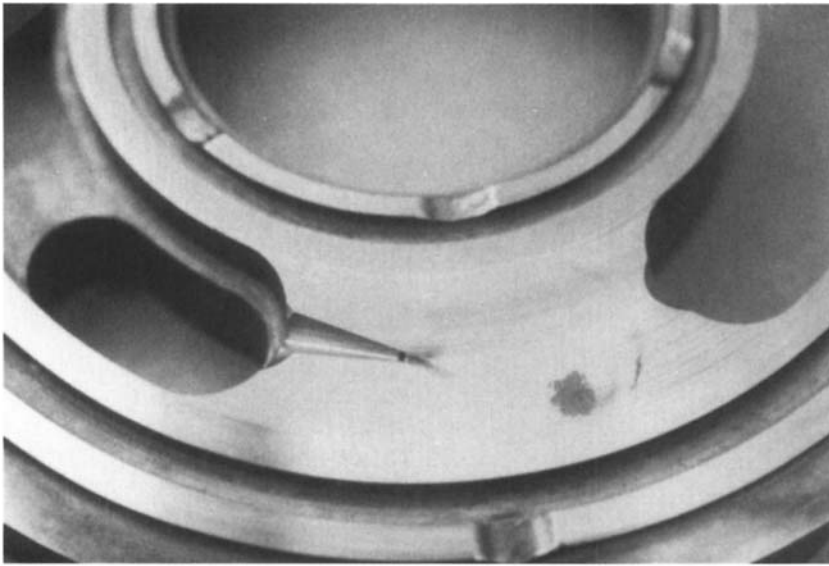


Figure 12.46 Localized cavitation damage of the end plates of a piston pump.

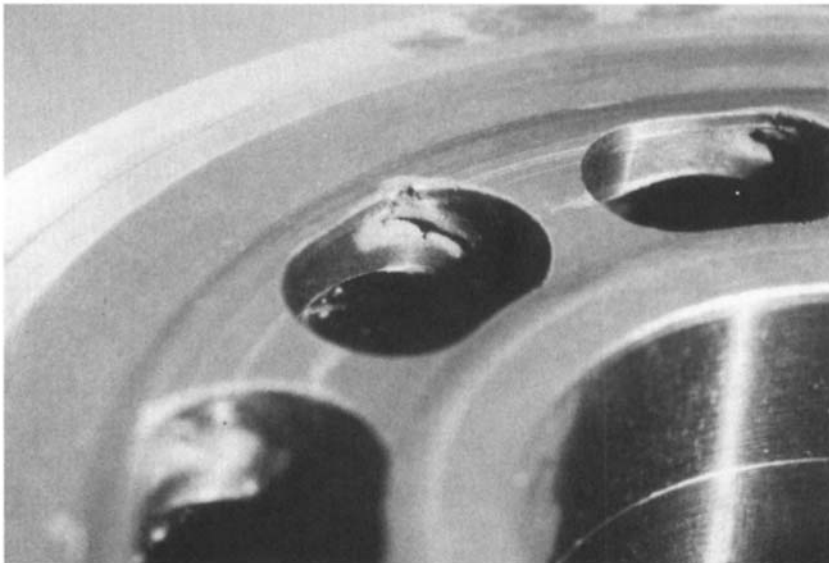


Figure 12.47 Cavitation damage of the control plate of a piston pump.

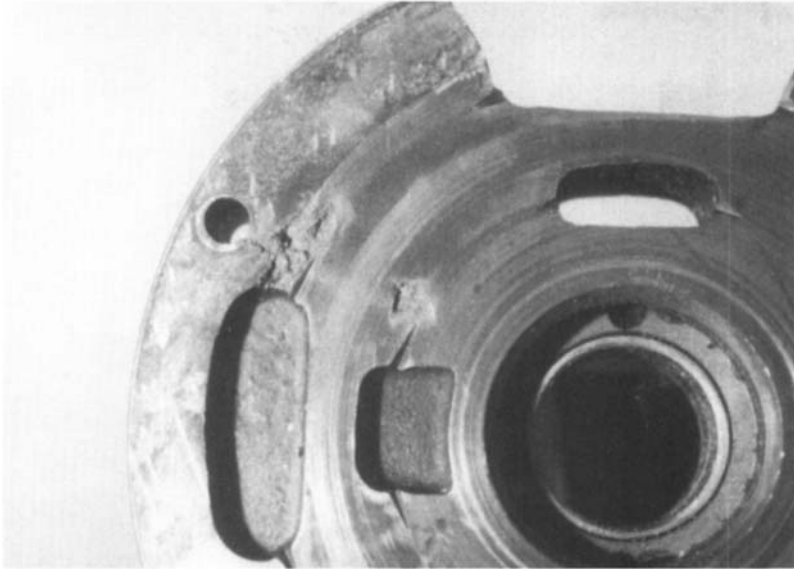


Figure 12.48 Cavitation damage of a piston-pump port plate. (Courtesy of Kayaba Industry Co., Tokyo, Japan.)

metal interface must be zero. Therefore, as additional current is formed from the streaming potential, additional current for electrical neutrality usually is provided by the metal, because the fluid exhibits low conductivity, and is designated as wall current (I_w). This process leads to the corrosion observed:



The wall current, assuming no current is provided by the fluid, may be calculated from: [44]

$$I_w = \frac{1.17\varepsilon\xi\nu}{x^3} \left(\frac{Q}{V} \right)^{3/2}$$

where

ε = fluid permittivity (F/m)

ξ = the potential difference (V) between the electrical double layer–metal interface and the fluid outside of the double layer (zeta potential)

ν = the fluid viscosity (m^2/s)

Q = the laminar flow rate (in m^3/s)

x = the distance from the metering edge (m) [45]

The total current normal to the metal surface (I_N) per unit length of the orifice is [44]

$$I_N = \frac{0.585\varepsilon\xi\nu}{g^2} \left(\frac{Q}{V} \right)^{3/2}$$

where g is the gap size.

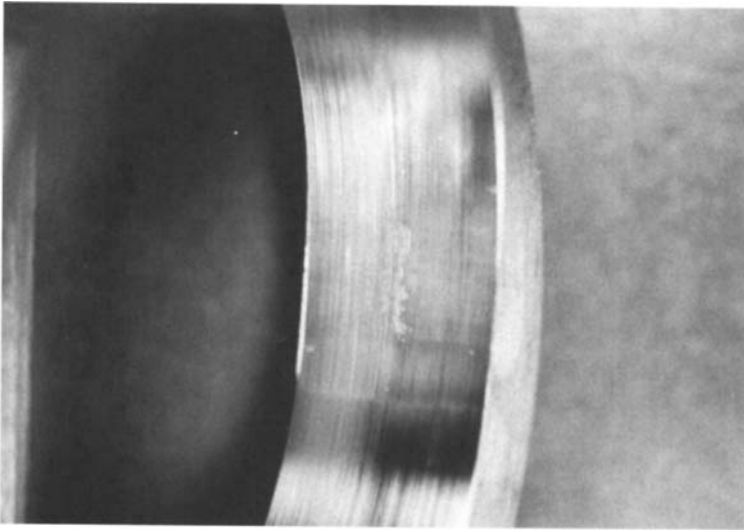


Figure 12.49 Cavitation damage on the inside of a cam ring with accompanying discoloration due to overheating. (Courtesy of Quaker Chemical Company, Conshohocken, PA.)

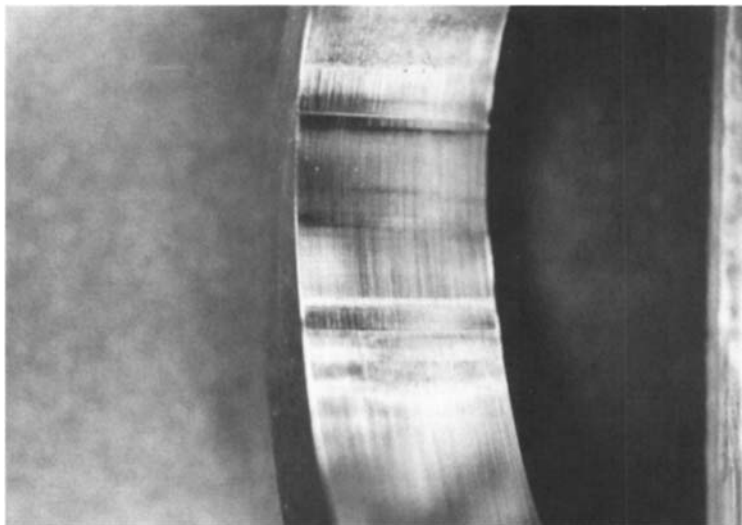


Figure 12.50 Vanes may exhibit a “chattering” noise upon contact with the cam ring with fluid aeration and poor air release. The rippling effect observed here is due to vane chatter. Some discoloration due to overheating is also visible. (Courtesy of Quaker Chemical Company, Conshohocken, PA.)

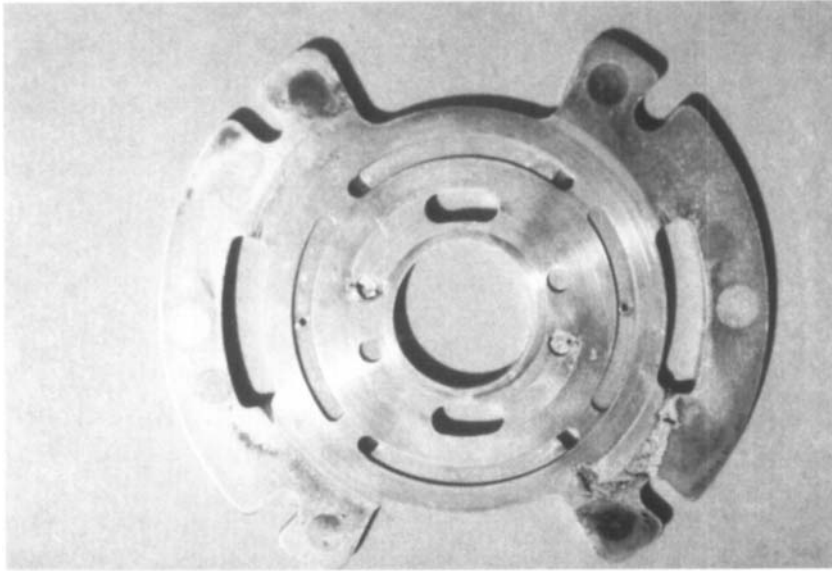


Figure 12.51 Cavitation damage of an end plate from a Vickers V-104 vane pump.

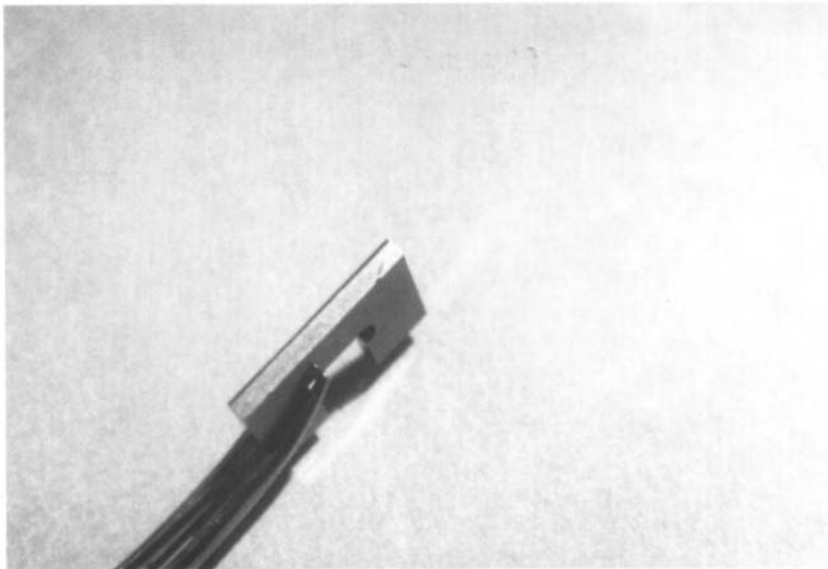


Figure 12.52 Cavitation damage of a vane from same pump side plate as shown in Fig. 12.51.

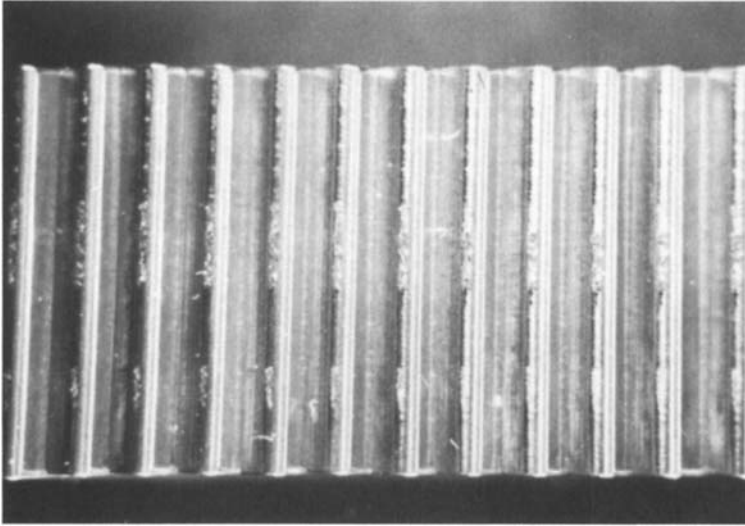


Figure 12.53 Vane-tip cavitation with some discoloration due to overheating. (Courtesy of Quaker Chemical Company, Conshohocken, PA.)

Inspection of these equations shows that the current is greatest with the following [40]:

1. Small gaps or orifices.
2. High fluid velocity. The flow rate across the metering edge for an ISO VG 46 phosphate ester at 70 bars pressure is estimated to be 120 mph. Wall

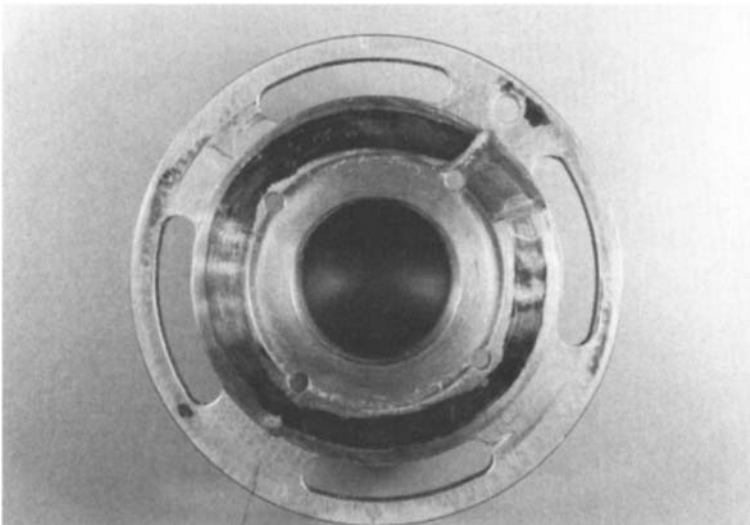


Figure 12.54 Although cavitation damage is observed on the flex plate of a vane pump, the major problem is inadequate lubrication due to severely acrated oil. Adhesive smearing and heat discoloration are also visible.

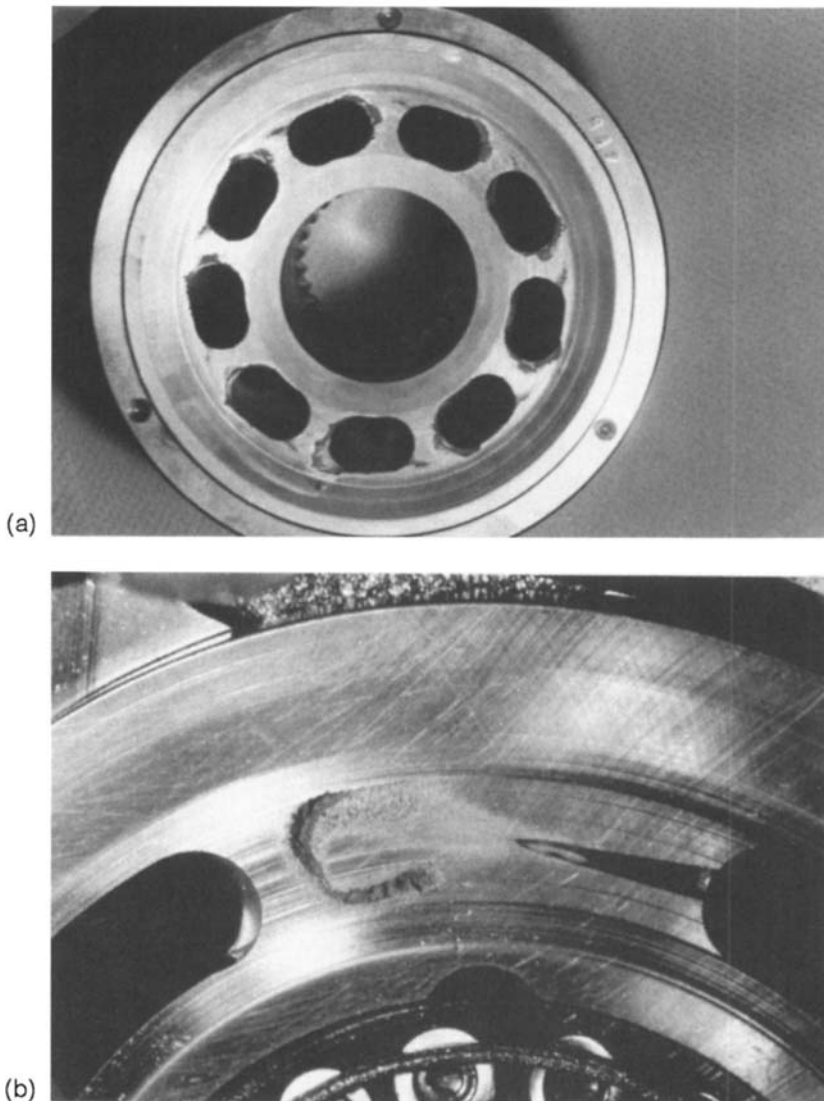


Figure 12.55 Cavitation erosion damage with subsequent fatigue for (a) a bronze control plate and (b) a bronze cylinder from axial piston pump (brass). Note that the highest pressure is on the suction side. As the pressure increases, bubbles of entrained air implode, eroding the material. The erosion is concentrated on the outer edge of the slots because the circumferential speed is slightly greater at this point. As the radius increases, the circumferential speed will also increase. (Courtesy of DMT-Gesellschaft für Forschung und Prüfung mbH, Essen, Germany.)

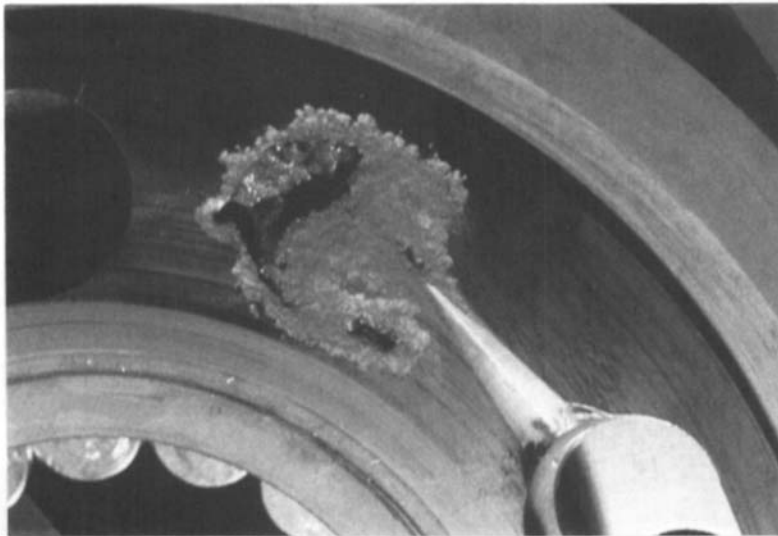
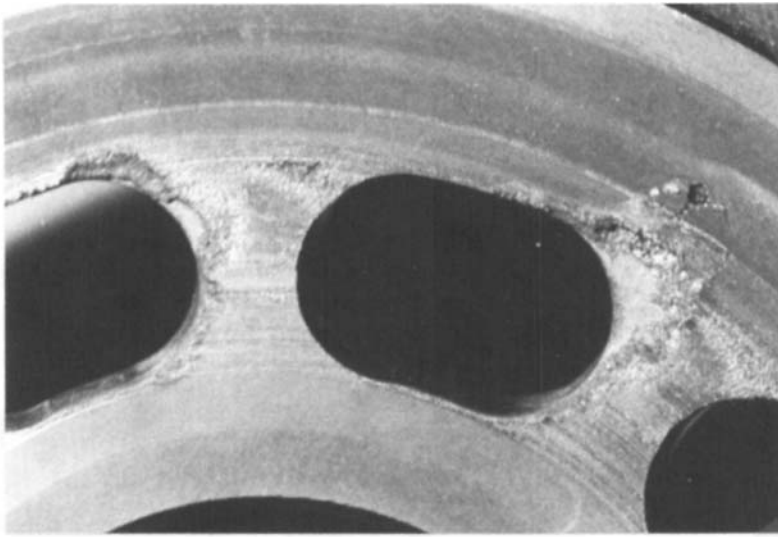


Figure 12.56 Cavitation erosion damage with subsequent fatigue for (a) a steel control plate and (b) a bronze cylinder plate. Note that the steel control plate exhibits much greater cratering than the bronze control plate shown in Fig. 12.55. The reason for the greater damage was that the steel control plate was used in a pump under higher pressure. (Courtesy of DMT-Gesellschaft für Forschung and Prüfung mbH, Essen, Germany.)

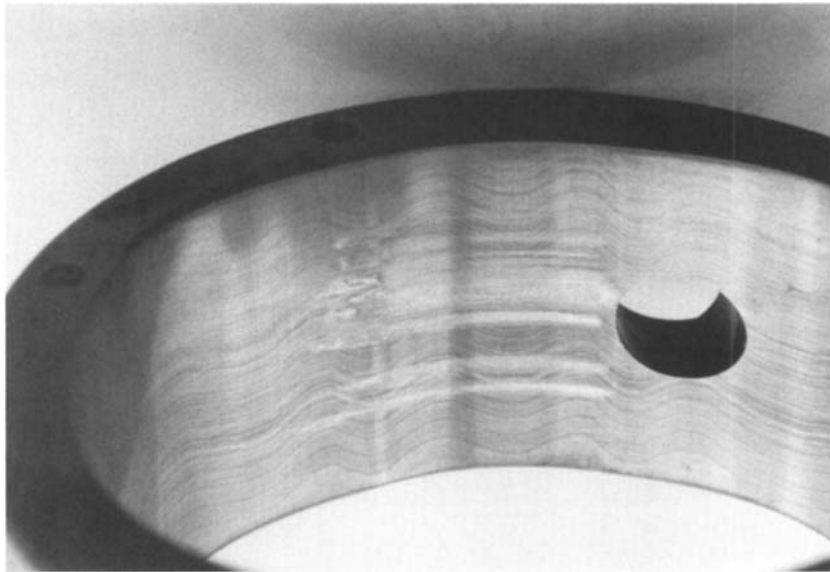


Figure 12.57 This cam ring exhibits two modes of wear: cavitation and adhesive smearing. The wavy marks are the original grinding marks. The root cause of failure was loss of antiwear additives in the hydraulic oil. (Courtesy of Denison Hydraulics Inc., Marysville, OH.)

current is proportional to the pressure drop (ΔP):

$$I_w \propto \frac{\Delta P^3}{4}$$

3. High fluid permittivity. Fluids with a permittivity of $(2-5) \times 10^{-11}$ F/m exhibit no damage. Permittivities of $(12-15) \times 10^{-11}$ F/m produce significant erosion damage [40]. New phosphate ester fluids typically exhibit permittivities of $(7-8) \times 10^{-11}$ F/m [40].
4. High zeta potential. Although commercially available phosphate ester fluids exhibit zeta potentials of 25–150 mV [41], treatment with Fuller's earth may reduce the zeta potential to 0.5 mV. Fuller's earth treatment increases the electrical resistivity from 4×10^9 to $14 \times 10^9 \Omega \cdot \text{cm}$ [40].

Electrochemical erosion may be reduced by reducing the conductivity of the fluid. Nelson and Waterman [45] have reported that fluids exhibiting conductivities of 3×10^{-7} to 5×10^{-8} mho/cm will produce electrochemical erosion. In this case, the neutralizing current is supplied by the metal. However, fluids exhibiting higher conductivities ($>3 \times 10^{-7}$) do not exhibit electrochemical erosion. In this case, the neutralizing current is supplied by the fluid [45]. Table 12.7 provides a summary of reported methods for reducing electrochemical erosion [40].

2.3.6 Contact-Stress Fatigue Wear

Contact-surface fatigue is favored by small contact areas, high loadings, and repeated flexing action under cyclic rolling or reciprocal sliding loads, although each occurs

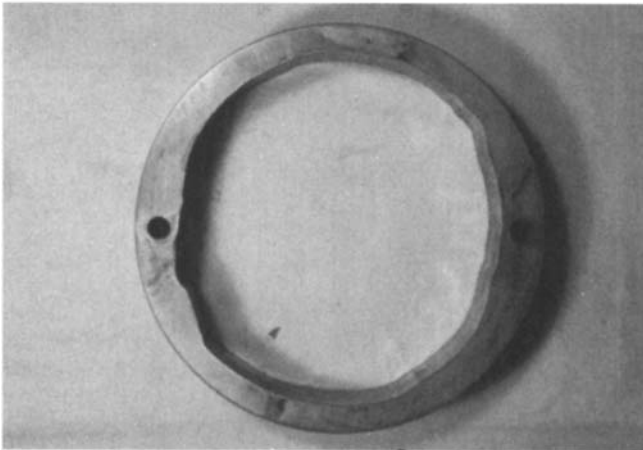
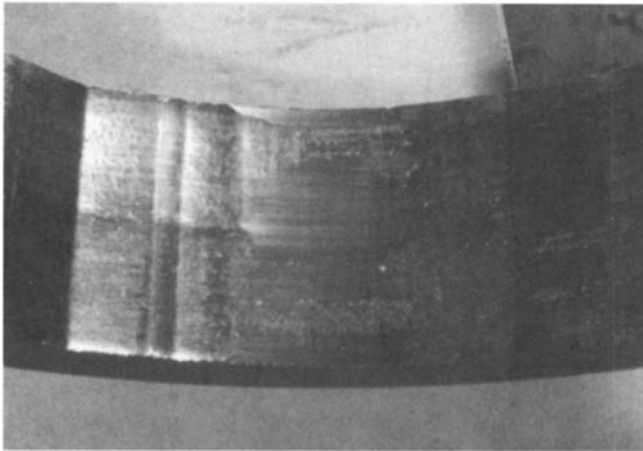


Figure 12.58 Fluid contamination led to the generation of surface pitting and formation of debris which caused severe wear damage. (Courtesy of Kayaba Industry Co., Tokyo, Japan.)

under different conditions, as illustrated in Fig. 12.64 [46]. The applied stresses are less than the material yield stress, and the process is often accompanied by frictional heat and plastic flow. Subsurface structural changes are also observed metallographically. Contact-stress fatigue wear processes are distinguishable from abrasion, adhesion, and corrosion, as shown in Table 12.8 [47].

Reciprocal sliding action produces a cyclic shear load. Cracking initiates at the surface and progresses into the subsurface zones [30] and is characterized by pitting as illustrated in Fig. 12.65 [26].

Rolling action compresses the surface and cracks initiate below the surface at points of maximum Hertzian stresses, as shown in Fig. 12.66 [48] (or deformation). For many materials, maximum shear stress occurs at a 0.01-mm depth below the surface [48]. Traditionally, it was believed that crack initiation almost invariably occurs at subsurface nonmetallic inclusion sites or grain boundaries or at surface

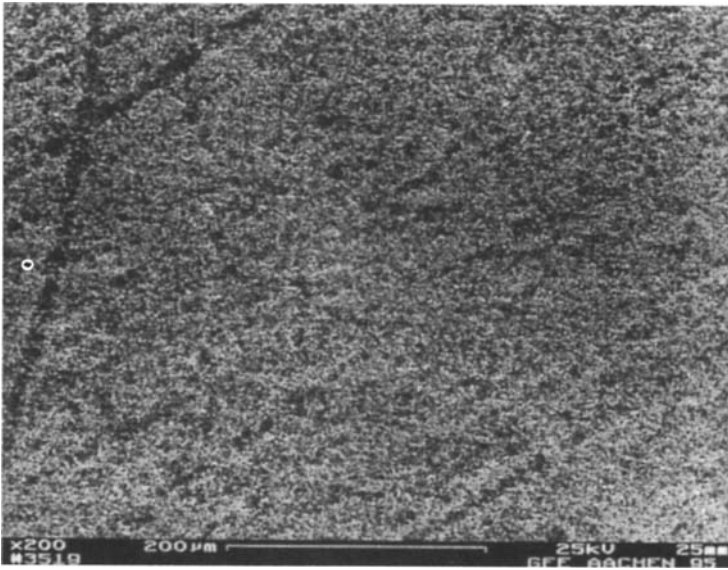


Figure 12.59 Illustration of porous nature of corroded surfaces. (Courtesy of IFAS, Aachen, Germany.)

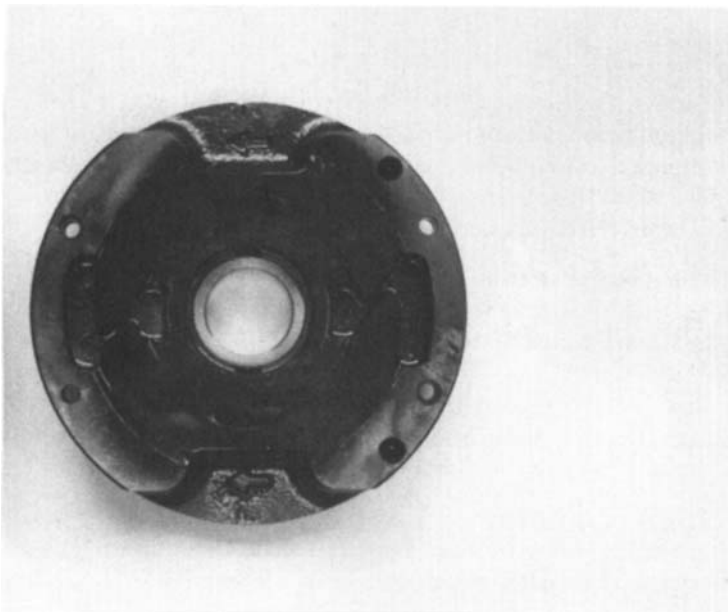


Figure 12.60 Bronze port plate discoloration due to fluid contamination by water with subsequent additive hydrolysis. Cavitation damage is also observed. (Courtesy of Denison Hydraulics Co., Marysville, OH.)

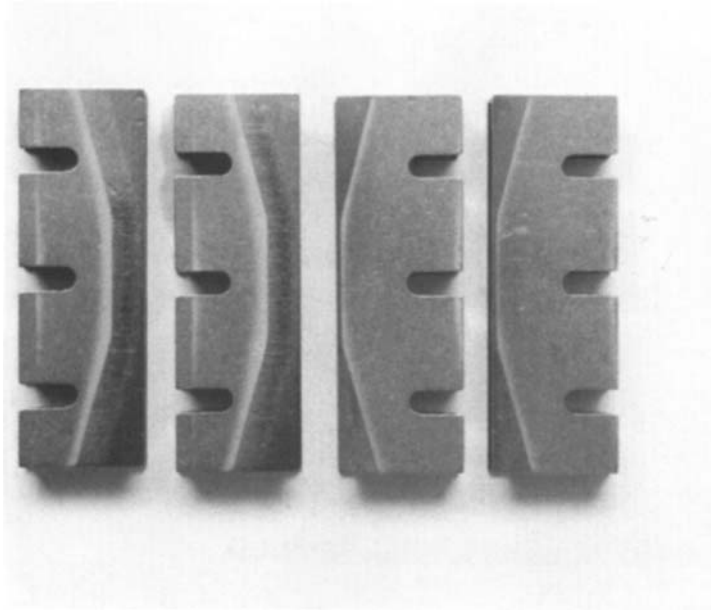


Figure 12.61 Vanes taken from a vane pump using a water-contaminated phosphate ester fluid. Water contamination causes corrosion and corresponding formation of metal oxides that produced the observed abrasive wear. The coarse abrasive debris plugged the system filter. Fine debris caused surface abrasion of the vanes. The two vanes on the left show the back side of the vanes and the two vanes on the right show coloration due to varnish deposits from the fluid. (Courtesy of Denison Hydraulics Co., Marysville, OH.)

stress risers such as a keyway, as illustrated in Fig. 12.67 [46]. However, it has also been shown that cracking may initiate from surface work hardening to about $20\ \mu\text{m}$, with accompanying formation of tempered martensite [46]. Fatigue failure modes are summarized in Table 12.9 [23,49].

Surface fatigue is typically manifested by the following [50]:

1. Pitting. Pit sizes may vary from small (0.4–0.5 mm) to much larger destructive holes that often occur in the negative sliding condition. Surface pitting due to surface contact fatigue are shown in Fig. 12.65 [26].
2. Spalling. Surface “spalls” may be much larger, shallower and more irregular shapes than pits, as illustrated in Fig. 12.68 [26].
3. Case Crushing. This is a subsurface fatigue failure that occurs just below the hardened case [26] with longitudinal cracks ending on the surface, as shown in Fig. 12.69 [26].

Design factors that effect surface contact fatigue include EHD film thickness, surface roughness, surface loading, sliding velocity, lubricant additives [51,52], and material properties [48].

The fatigue life of roller bearings has been related to the lambda ratio (specific film thickness ratio), as shown in Table 12.10. The value lambda is calculated from [53]

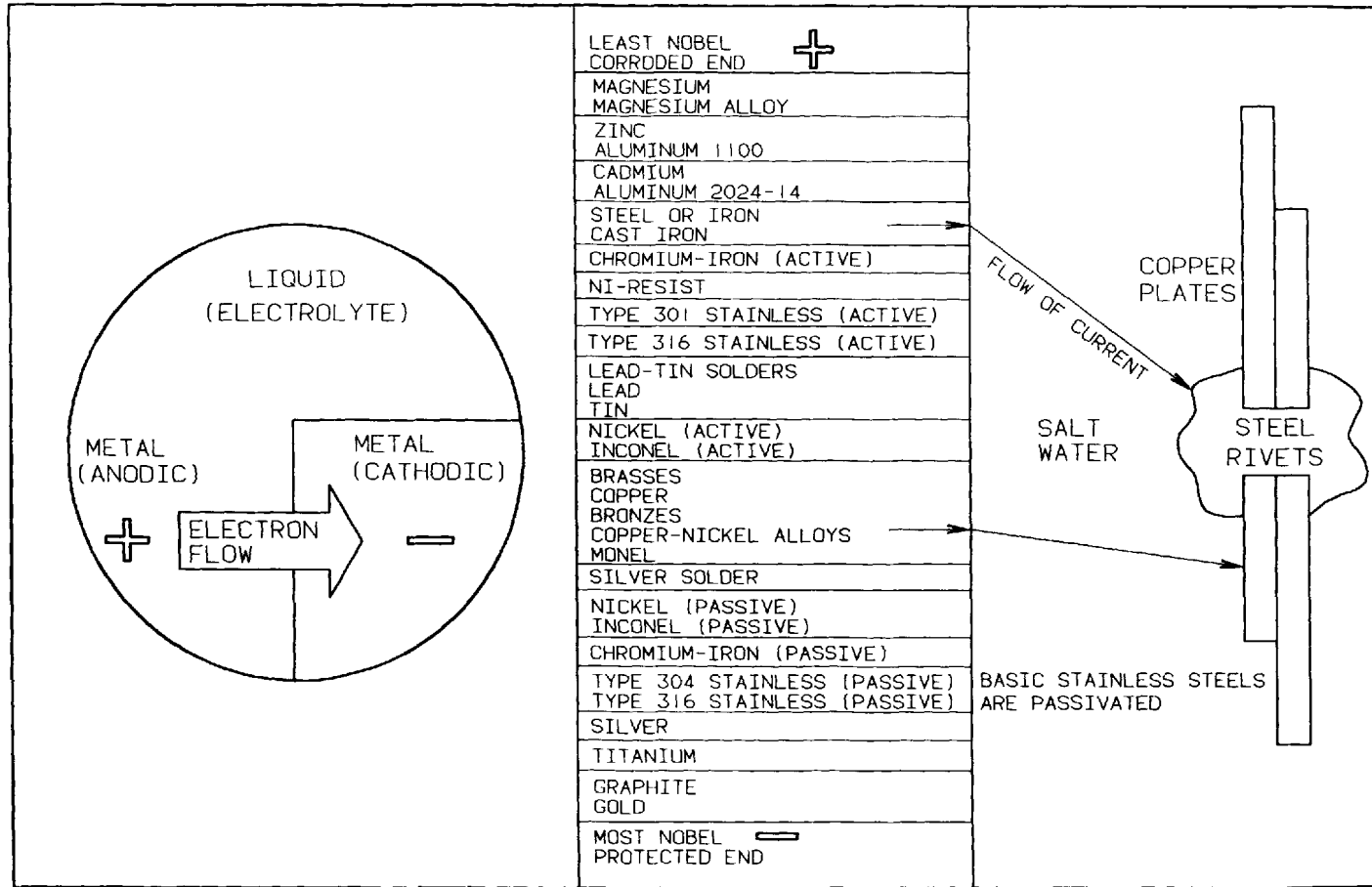


Figure 12.62 Illustration of galvanic corrosion and the galvanic series.

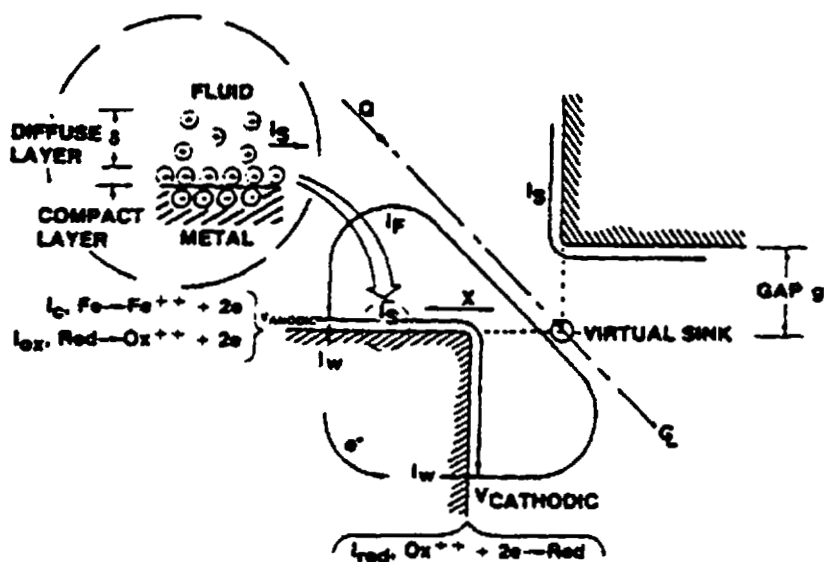


Figure 12.63 Generation of electrokinetic streaming current: streaming currents, wall currents, and fluid current flows.

$$\Lambda = \frac{h_0}{\sigma}$$

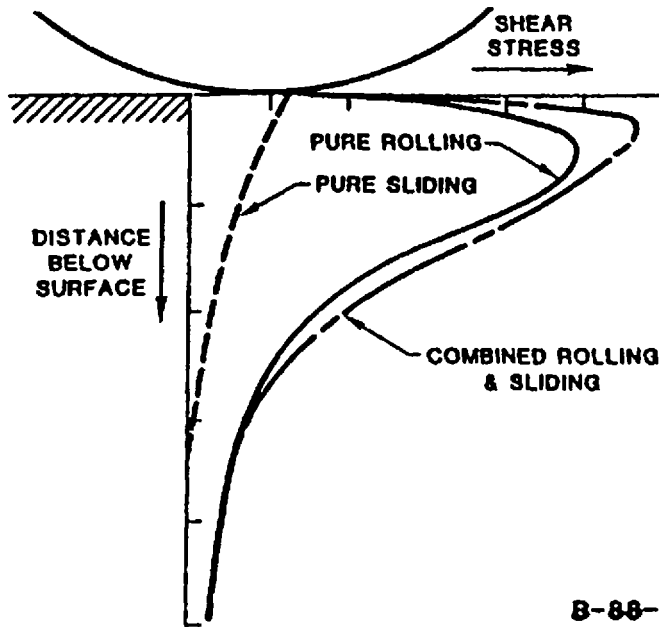
where h_0 is central EHD film thickness and σ is defined as

$$\sigma = (\sigma_1^2)^{1/2}$$

where σ_1 and σ_2 are the root-mean-square (rms) surface finishes of contact surfaces 1 and 2, respectively. For many bearings, this value can be assumed to be $0.12 \mu\text{m}$. For very large industrial bearings, σ can be assumed to be $0.65 \mu\text{m}$ [53].

Table 12.7 Methods to Minimize Electrochemical Valve Erosion

System design	Fluid type/maintenance
Reduce flow rates or pressure drop across the valves	Use Fuller's earth treatment to reduce fluid acidity and increase resistivity
Minimize thermal stress on the fluid	Avoid contamination by halogenated solvents
Use corrosion-resistant steel	Use additives to reduce the zeta potential
Use zero or overlap designs for the servo valve	Use fluids of good thermal, oxidative, and hydrolytic stability
Minimize water contamination and maintain slight vacuum over the fluid in the tank	



B-88-28

Figure 12.64 Model of shear stresses formed by rolling, sliding, and a combination of both processes.

Table 12.8 Differentiation of Surface Contact Fatigue from Other Wear Processes (Abrasion, Adhesion, and Corrosion)

Mechanism	Surface-contact fatigue	Other wear mechanisms
Nature of contact	Counter formal	Conformal
Stress system	Hertzian and alternating	Dispersed and continuous
Lubrication and oil film	Partial to full EHD	Partial hydrodynamic to starvation
Relative motion to mating surface	Usually rolling	Usually sliding
Wear process	Crack initiation and propagation or material subsidence	Material adhesion, ploughing, corrosion, etc
Wear particle characteristics	Lamina, sphere, and spall particles	Normal/severe sliding wear particles, cutting, wear particles, etc.

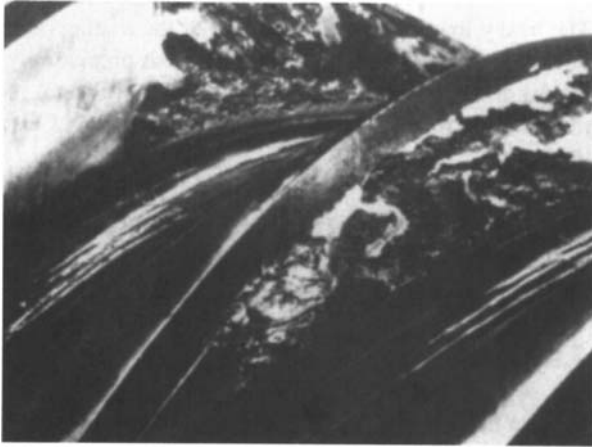


Figure 12.65 Destructive pitting due to surface-contact fatigue. (Courtesy of American Gear Manufacturers Association.)

An alternative to lambda, often designated as Λ_{exp} , is to use a corrected Λ_{adj} value, which is calculated from

$$\Lambda = \left(\frac{h}{\sigma} \right) k_h$$

where k_h is the EHD film correction factor, which may be determined from Fig. 12.70 [53]. For a roller bearing, the value of the lubricant flow number GU in Fig. 12.70 is calculated from [53]

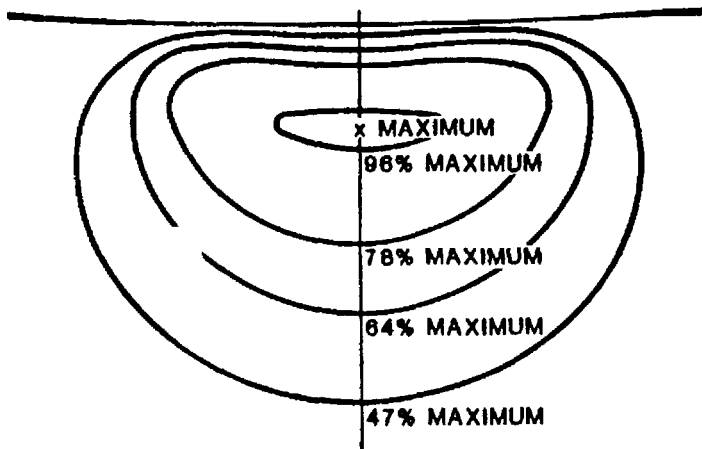


Figure 12.66 Location of maximum shear stress locations in a Hertzian contact.

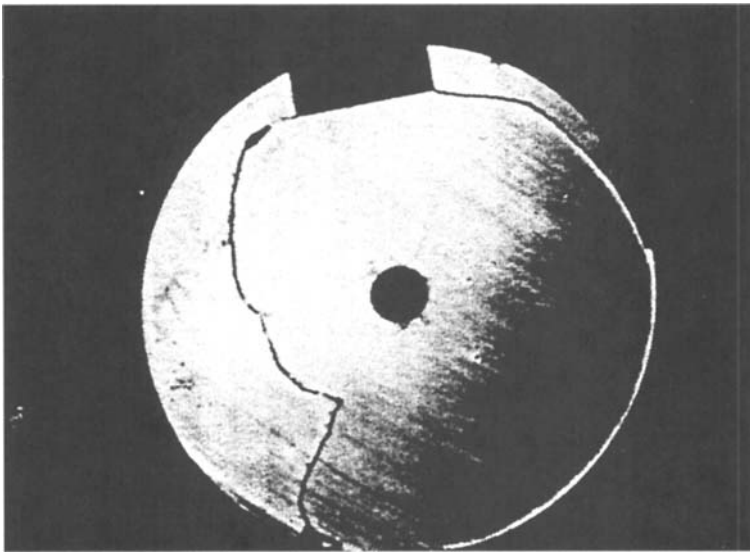


Figure 12.67 Fatigue cracking that was initiated by the keyway which acted as a stress riser. [Courtesy of Society of Tribologists and Lubrication Engineers (STLE).]

$$GU = k_G \alpha Z_0 N \left(\frac{OD + ID}{OD - ID} \right)$$

where α is in.²-lb. force and k_G is 1.52×10^{-10} min/cP [P is equivalent bearing load (in N), lbf/100].

Townsend and Shimski used correlated lambda (Λ) with gear surface fatigue life as shown in Fig. 12.71 [51].

Table 12.9 Surface Fatigue Failure Modes

Mode	Characteristics
Wear-type failures	Surface removal 1. Removal of loose wear particles 2. Chemical or electrical surface removal
Plastic flow	Cumulative surface material transfer "smearing" Loss of contact geometry due to cold flow Material softening due to overheating
Contact fatigue	Pitting or spalling Surface distress (cracks)
Bulk failures	Overload cracking Overheat cracking Bulk fatigue Permanent dimensional changes Fretting of fit surfaces

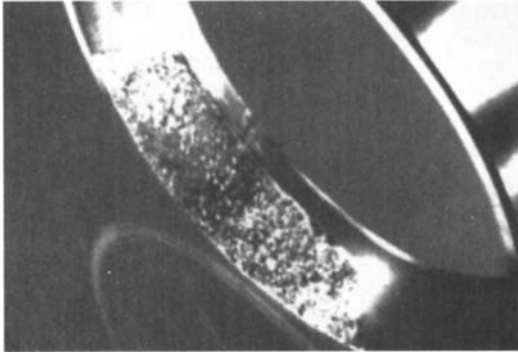


Figure 12.68 Bearing race damage by spalling. (Courtesy of Caterpillar Inc., Peoria, IL.)

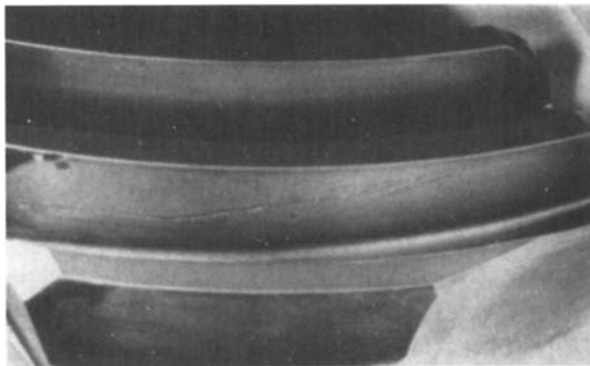


Figure 12.69 Illustration of case crushing of a carburized bevel gear. (Courtesy of American Gear Manufacturers Association.)

Table 12.10 Correlation of Lambda (Λ) and Fatigue Cracking of Roller Bearings

A value	Wear observation
<1	Surface smearing or deformation
1–1.5	Surface distress accompanied by surface pitting
1.5–3	Surface glazing accompanied by subsurface failure
≥ 3	Minimal wear, long life, eventual subsurface contact fatigue failure

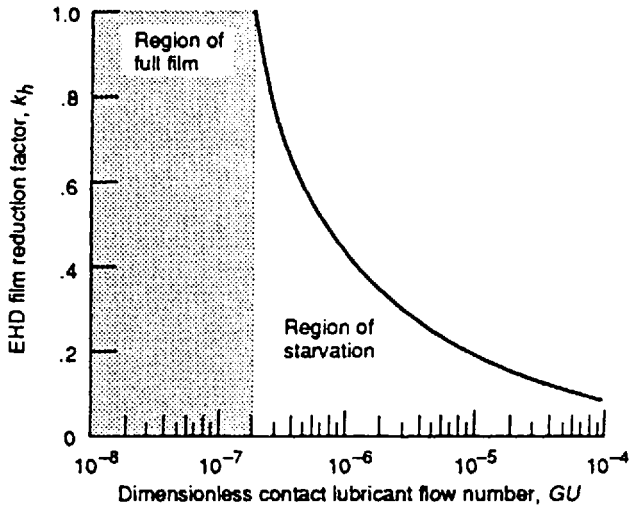


Figure 12.70 Elasto-hydrodynamic film reduction factor as a function of contact lubricant flow number. [Courtesy of Society of Tribologists and Lubrication Engineers (STLE).]

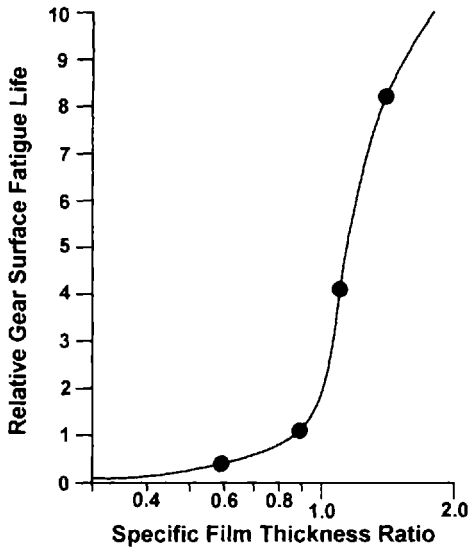


Figure 12.71 Relative gear fatigue life as a function of specific film thickness ratio.

Table 12.11 Correlation of Modified Lambda and Contact Fatigue Failure

λ_m Ratio	Initiation of contact fatigue	Material influence	Surface roughness influence	Geometry influence
>3.0	Subsurface fatigue inclusion ^a	Important	Minor	Important
3–1.0	Subsurface/near surface mostly inclusion	Important	“Sharp”/High Asperities	Important
1.0–0.3	Some inclusion; some surface related	Somewhat important	Important	Somewhat important
<0.3	Surface related ^b	Minor	Important	Less important
Any ratio	Localized stress risers	Mixed	Mixed	Mixed
	PSO ^c —dents, grooves, and surface inclusions	Minor	Somewhat important	Minor
	GSG ^d —edge fatigue misalignment	Somewhat important	Minor	Somewhat important

^aFatigue originates at nonmetallic inclusion in the maximum shear zone below the surface for both bearings and gears.

^bCalled peeling or micropitting for bearings; spalling for gears.

^cPSO (point surface origin): fan-shaped spall propagation starting in the surface.

^dGSC (geometric stress concentration) starting at end of line contact.

Moyer has reported that the use of a modified lambda ratio (λ_m) provides a better correlation for contact fatigue wear that may occur for both gears and roller bearings, which is calculated from [23]

$$\lambda_m = h \left(\frac{L}{2b} \right)^{1/2}$$

where L is the large end wavelength used to measure surface roughness and is usually equal to 0.8 mm (0.030 in.) and $2b$ is the width of the contact in the direction of motion. A correlation of λ_m and contact fatigue wear for both gears and bearings is provided in Table 12.11 [23].

Hardened and unhardened steels behave differently when exposed to contact-surface fatigue. Plastic flow may arise in the surface layers of unhardened steels which will not occur in hardened steels. For example, unhardened spur gears may exhibit pitting along the pitch line at the point of highest contact stress. Hardened gears, on the other hand, undergo pitting along the pitch line where traction forces are highest [48]. When traction occurs along the pitch line for hardened steels, the following is true [48]:

1. Surface fatigue is less at low slide-to-roll ratios than when pure rolling occurs.
2. More cracks propagate on the lower peripheral speed surface than at the edge.
3. Performance is sensitive to steel composition, heat treatment, and lubricant composition. There have been reports that surface contact fatigue is significantly reduced by the addition of certain additives [51,52].
4. Surface-nucleated cracks produce earlier failures than subsurface cracks.
5. Surface-nucleated cracks tend to be located in asperity peaks.
6. Surface-nucleated failures are sensitive to surface temperature and therefore to EP reactions in the lubricant.

In summary, (1) fatigue cracks are caused by repetitive stress fluctuations, (2) failure times decrease with increasing stresses, (3) fatigue cracks occur at stresses less than the material yield stress, and (4) there is a finite time between the origination of the crack and final failure [46]. Various examples of fatigue failure are illustrated in Figs. 12.72 through 12.76.

2.3.7 Other Forms of Wear

Brinelling

TRUE BRINELLING. If the applied load exceeds the elastic limit of the material, elliptical “brinell marks” or brinelling will be observed as illustrated in Fig. 12.77 [54]. Brinelling may occur when a hammer is used to install or remove a rolling element bearing assembly or when it is dropped [55]. Brinelling is due to impact deformation, not wear.

FALSE BRINELLING. Elliptical wear patterns in the axial direction at each roller or ball position in the rolling element assembly, as illustrated in Fig. 12.78 [55], is called “false brinelling.” The elliptical pattern is often surrounded by debris. False brinelling is caused by vibration-induced wear.

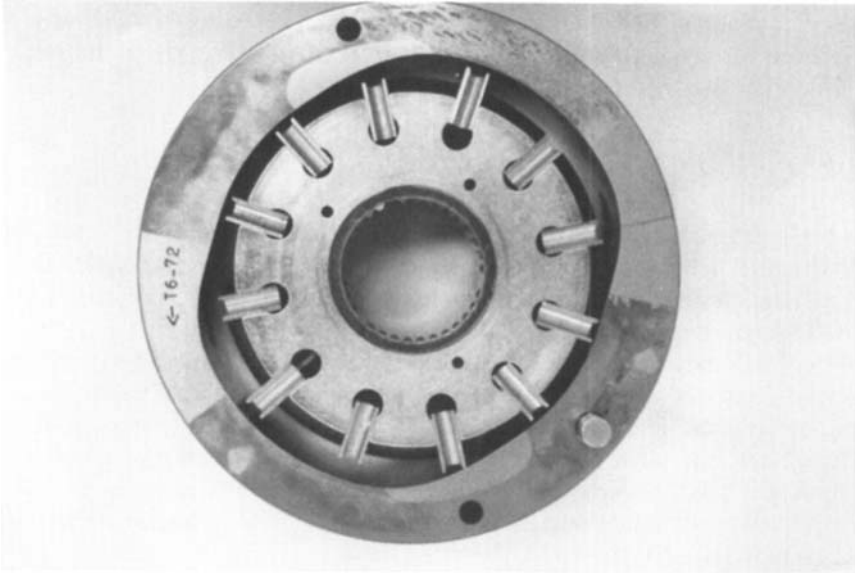


Figure 12.72 Fatigue fracture at the weakest point was due to excessive fluid aeration, which was caused by flow turbulence occurring during fast pressure changes. The resulting aerated fluid possessed poor compressibility, creating pressure spikes that exceeded the design limits of the cam-ring material. (Courtesy of Denison Hydraulics, Marysville, OH.)

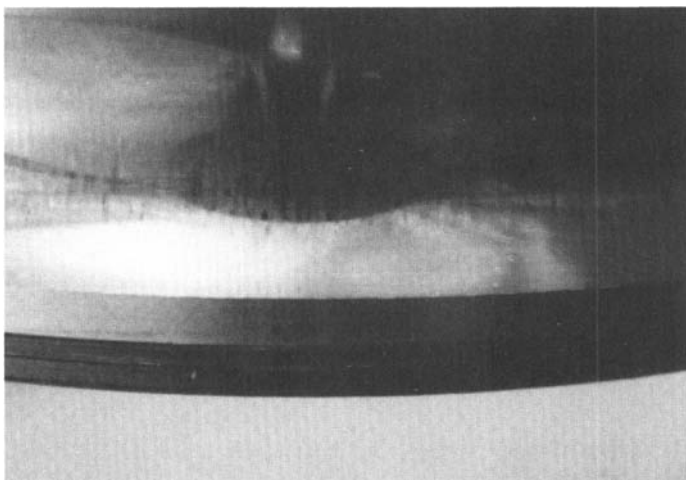


Figure 12.73 Fatigue crack on hydraulic pump flange caused by hammering impact during installation. (Courtesy of Kayaba Industry Co., Tokyo, Japan.)

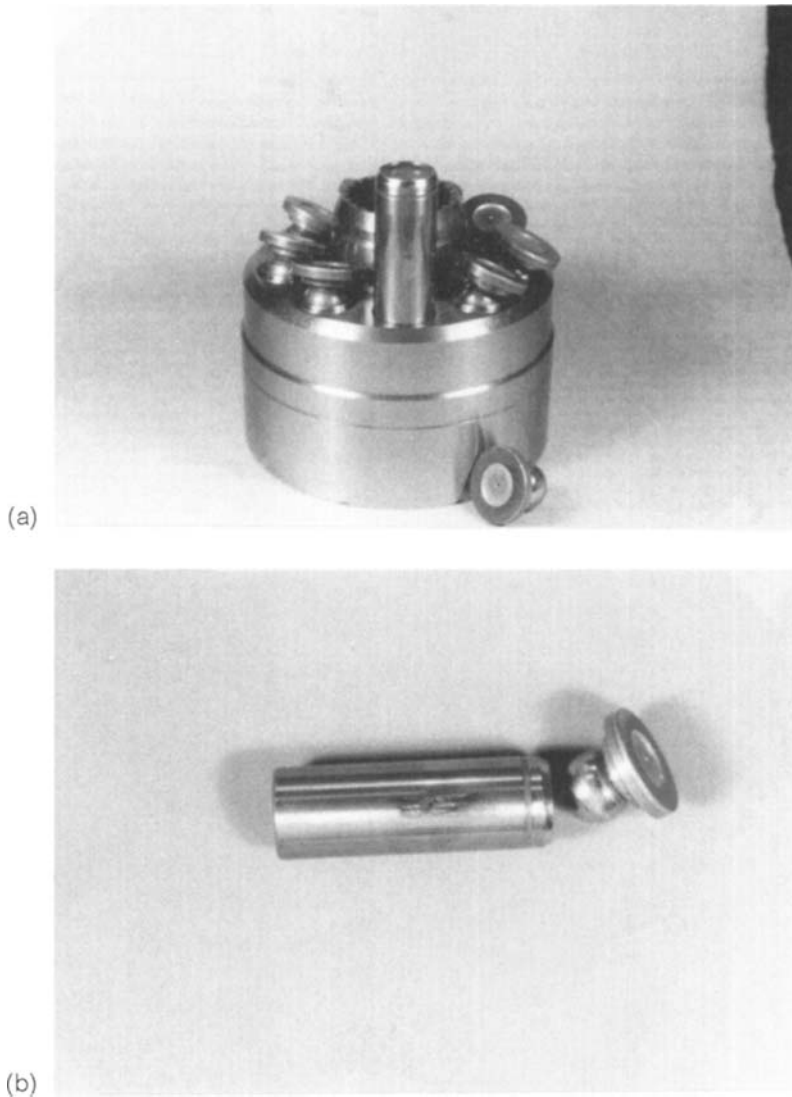
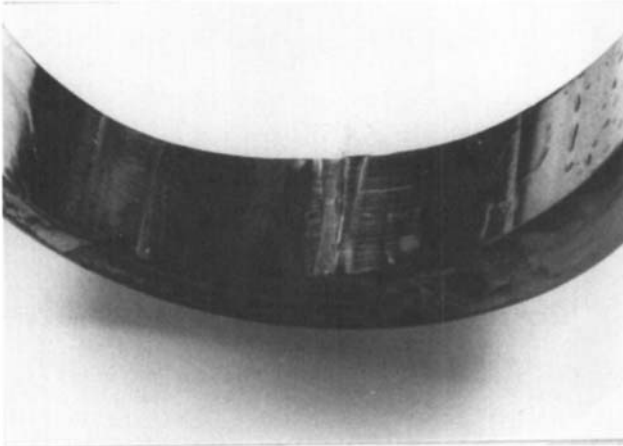
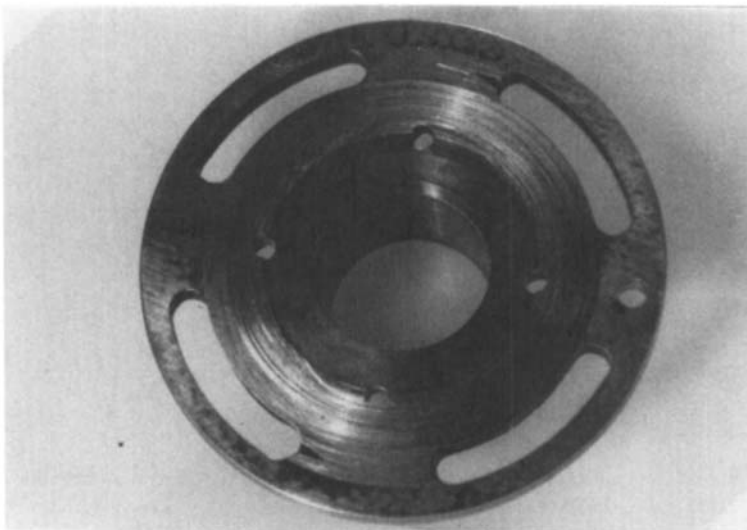


Figure 12.74 Surface fatigue of a piston from a swash-plate piston motor due to poor lubrication. In this case, the motor was tested without loading by increasing the rotational speed. Seizure occurred at 8000 rpm between the piston and the cylinder block. The piston was locked in the bore and the shoe was pulled off by the retainer plate. The failure was due to insufficient lubrication due to the high sliding speeds and increasing centrifugal force. (Courtesy of Keyaba Industry Co., Tokyo, Japan.)

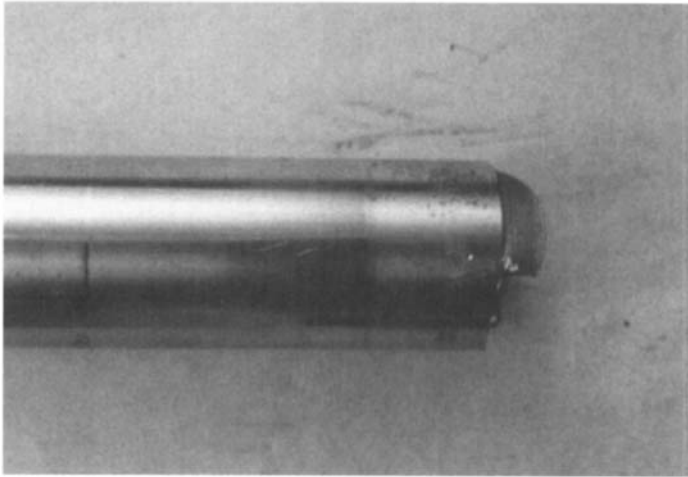


(a)

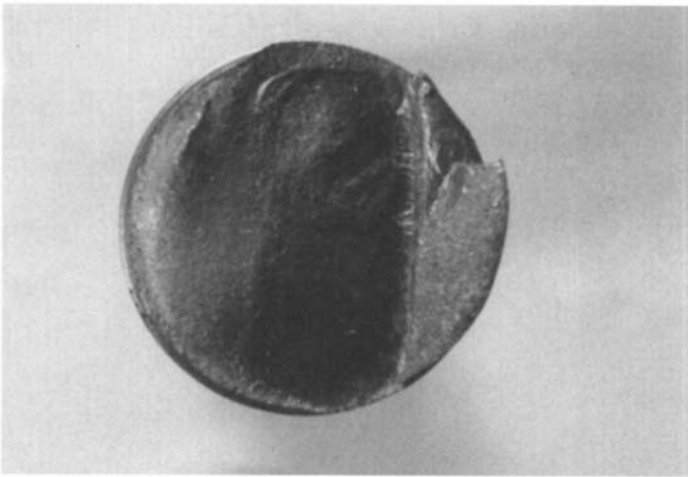


(b)

Figure 12.75 The cam-ring (a) and bushing (b) failure was due to several wear mechanisms, including abrasion, cavitation, erosion, corrosion, and fatigue. Rippling was due to uneven pressure on the vanes (see Fig. 12.50), producing a chattering effect from aerated fluid. Severe cavitation erosion produced debris and three-body abrasion wear. The abrasion process overheated the parts causing fatigue failure. (Courtesy of DMT—Gesellschaft für Forschung und Prüfung mbH, Essen, Germany.)



(a)



(b)

Figure 12.76 Fatigue failure due to nonuniform hardening of the hydraulic pump shaft. (Courtesy of Kayaba Industry Co., Tokyo, Japan.)

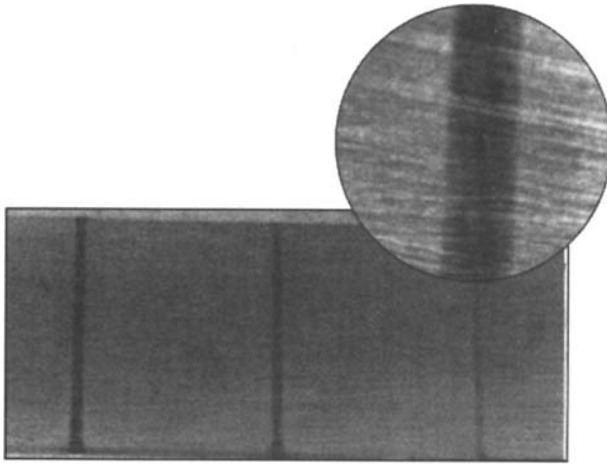


Figure 12.77 Brinelling impact damage to a bearing race. (Courtesy of The Timken Company, Canton, OH.)

Fretting Corrosion

Fretting corrosion occurs when the tips of the asperities of adjacent moving surfaces come into contact and microwelding occurs. Continued surface movement causes the tips of the microwelded asperities to pull off, producing a pitting effect. The heat of the microwelding process enhances oxidation of the fresh metal surfaces. If water is present, corrosion will result. Fretting corrosion, as illustrated in Figs. 12.79 and

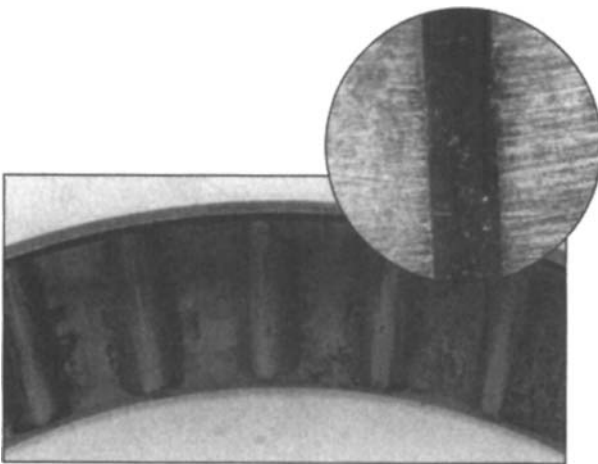


Figure 12.78 False brinelling of a bearing due to wear. Note the oxide deposits surrounding the wear damage. (Courtesy of The Timken Company, Canton, OH.)



Figure 12.79 Fretting corrosion on the outer surface of a rolling element bearing. (Courtesy of Caterpillar, Inc., Peoria, IL.)

12.80 [56], may occur on the surfaces of moving tightly fitted assemblies such as roller bearings [28].

Electrical Currents

A burning or arcing effect may be observed when electrical current contacts a component surface such as a bearing race. This may occur during a process such as welding or during long-term contact with lower currents. Either a “fluting” effect or “pitting” as illustrated in Figs. 12.81 and 12.82, respectively, may be observed [54]. Therefore, it is essential that equipment be properly grounded.

Miscellaneous Failures

In addition to those failures shown previously, there are a number of other possible causes. Some of the more commonly encountered sources include a poor or loose fitting, misalignment, and heat treatment. Examples of these failure modes are provided in Figs. 12.83, 12.84, and 12.85, respectively. A tabulated summary of various failure mechanisms and their characteristics that may be encountered in hydraulic pump failure analysis, see Appendix 11 [57].

2.4 Failure Analysis

Each of the failure mechanisms described in the previous sections exhibits their own distinctive type of damage. In order to properly troubleshoot, correct, and maintain hydraulic equipment, it is important to recognize and understand these different failure modes. The process by which this is done is called “failure analysis.” The objective is to determine the “root cause” of the problem by hardware inspection. In this section, a process by which this identification can be made will be described.

2.4.1 System Overview and Disassembly

The first step in this process is to perform a survey of the use of hydraulic pump or system component of interest. The initial steps of this process are as follows:

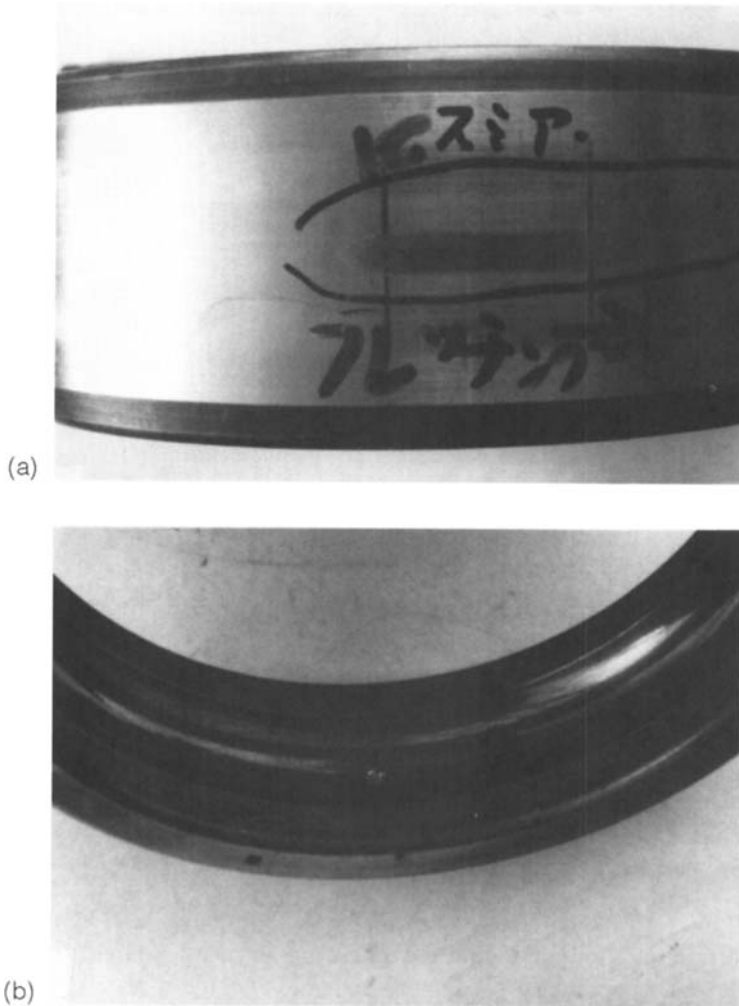


Figure 12.80 Axial movement during stopping produced temperatures in excess of 700°C causing nonuniform distribution of the lubricating grease leading to fretting damage and localized smearing. (Courtesy of Kayaba Industry Co., Tokyo, Japan.)

1. Know the equipment where the pump was used.
2. Know how the new part looks so that changes can be readily identified.
3. Observe how the external part of the pump looked before disassembly. Photograph it, if possible.
4. Carefully disassemble the pump and make written notes during the disassembly process. Photograph these steps, if possible.
5. Thoroughly examine the internal parts making written notes of any observations.
6. Identify the probable cause.
7. Communicate with the customer.

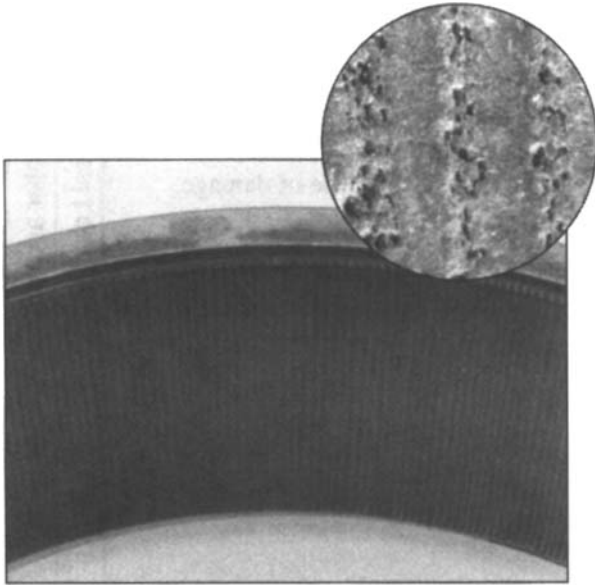


Figure 12.81 Fluting damage of a bearing race caused by exposure to electric current. (Courtesy of The Timken Company, Canton, OH.)

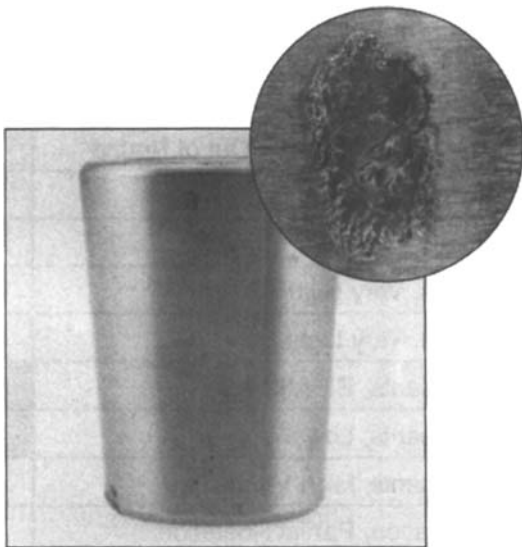


Figure 12.82 Pitting damage of a rolling element caused by exposure to electric current. (Courtesy of The Timken Company, Canton, OH.)

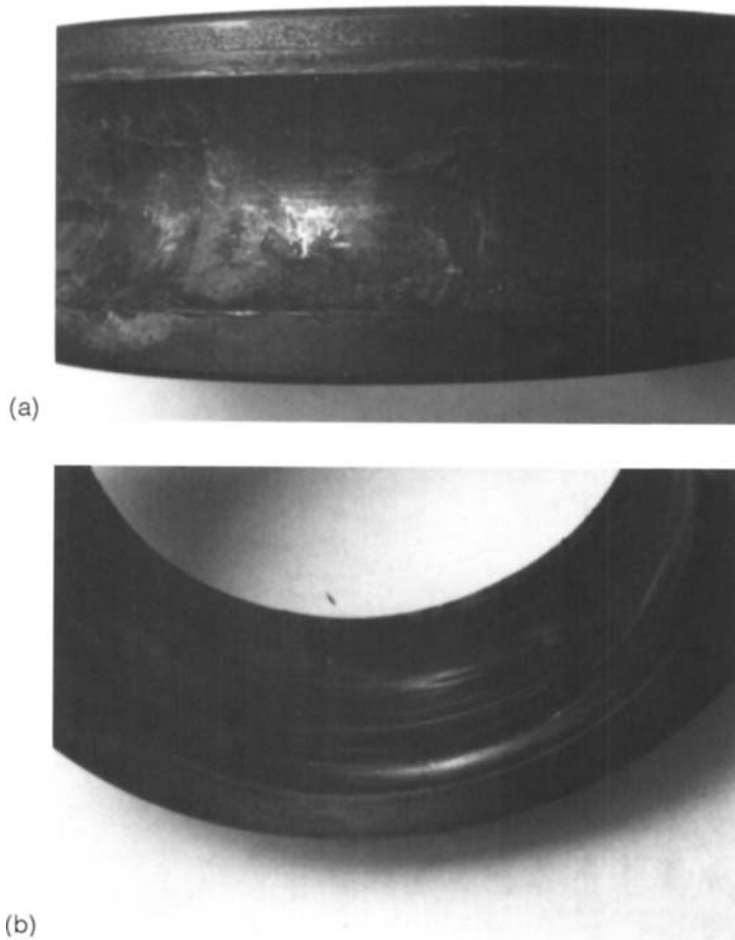


Figure 12.83 Bearing track damage caused by loose-fitting shaft resulting in a temperature rise to $>700^{\circ}\text{C}$ and creep. (Courtesy of Kayaba Industry Co., Tokyo, Japan.)

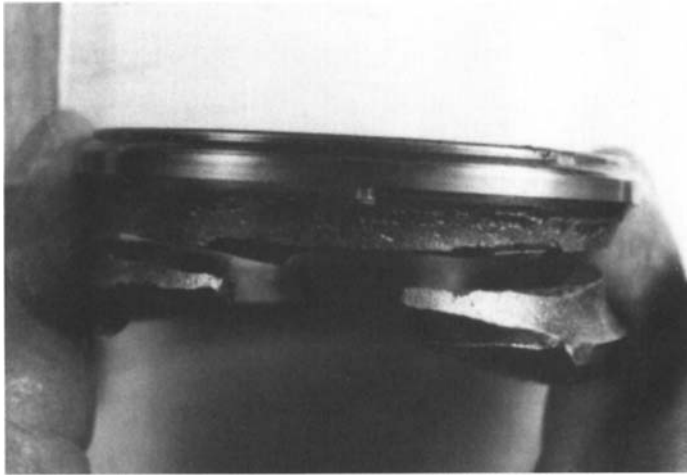


Figure 12.84 Bearing misalignment resulting in very short lifetimes. (Courtesy of Kayaba Industry Co., Tokyo, Japan.)

2.4.2 Determination of Probable Cause (Root-Cause Analysis)

The next step of this process is very similar to the root cause analysis of roller bearings reported previously by Washo [58].

There are three primary steps in root-cause analysis [58]:

1. Establish the symptom. For example, what led to the problem: noise, vibration, high temperature, sluggish response, high friction, and so forth.
2. Determine general failure cause including abrasion, adhesion, corrosion, surface contact fatigue, and overheating.

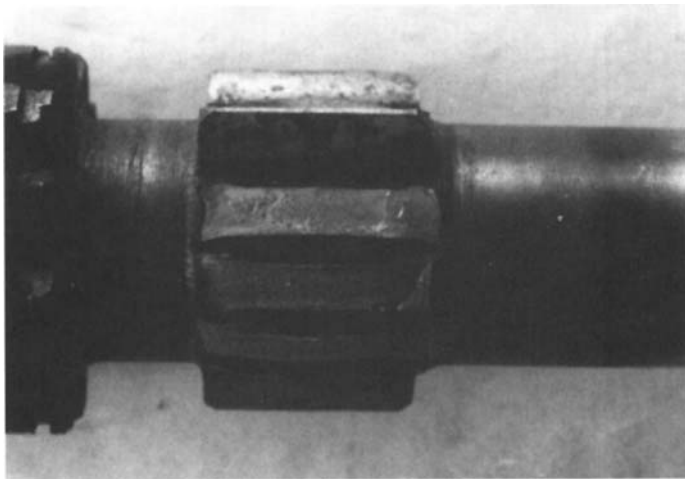


Figure 12.85 Gear shaft for reducing gear box with a quench crack after induction hardening. (Courtesy of Kayaba Industry Co., Tokyo, Japan.)

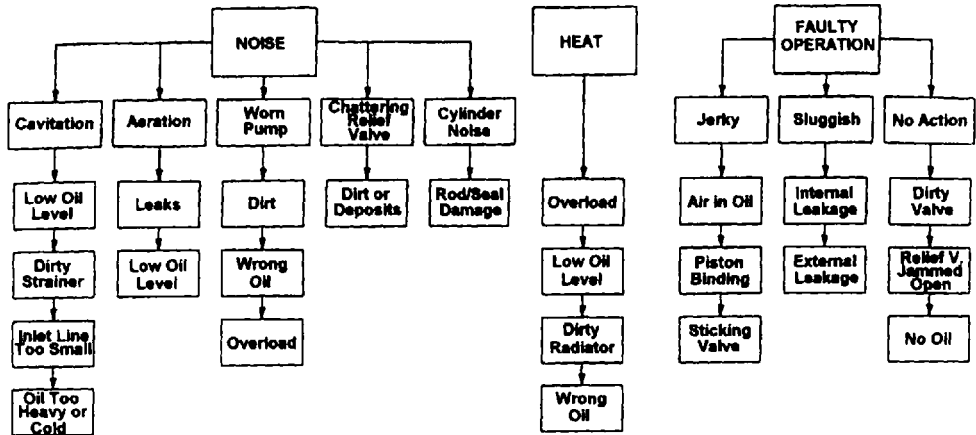


Figure 12.86 Mobil hydraulic system troubleshooting flowchart. (Courtesy of D. Scheetz, Mobil Oil Company, Aurora, IL.)

3. Determine the root cause by identifying the wear failure mode using reference figures from various sources such as the manufacturer, those provided here, and previous experience.

Figure 12.86 provides a helpful troubleshooting overview of the possible failure modes that should be considered in root-cause analysis [59].

ACKNOWLEDGMENT

Sincere appreciation to Mr. Larans Kambool for his assistance with the preparation of the figures shown herein.

REFERENCES

1. A. Yamaguchi, "Tribology of Hydraulic Pumps," in *Tribology of Hydraulic Pump Testing*, G. E. Totten, G. H. Kling, and D. J. Smolenski, eds., 1996, American Society for Testing and Materials; Conshohocken, PA, pp. 49–61.
2. G. E. Totten and R. J. Bishop, "Evaluation of Vickers V-104 and 20VQ5 Vane Pumps for ASTM D-2882 Wear Tests Using Water-Glycol Hydraulic Fluids," in *Tribology of Hydraulic Pump Testing*, G. E. Totten, G. H. Kling, and D. J. Smolenski, eds., 1996, American Society for Testing and Materials; Conshohocken, PA, pp. 118–128.
3. E. Koc, A. O. Kurban, and C. J. Hooke, "An Analysis of the Lubrication Mechanisms of the Bush-Type Bearings in High-Pressure Pumps," *Tribol. Int.*, 1997, 30(8), pp. 553–560.
4. Vickers, Inc., *Pump Failure Analysis*, Vickers, Incorporated; Troy, MI.
5. Mobile Oil, *Foaming and Air Entrainment in Lubrication and Hydraulic Systems*, 1971, Mobil Oil Co., Ltd.; London.
6. T. I. Fowle, "Problems in the Lubrication Systems of Turbomachinery," *Proc. Inst. Mech. Eng.*, 1972, 186, pp. 705–716.
7. B. Rosean, *A Study to Assure Proper Pump Environment When Using Fire Resistant Fluids and Effect of Piping and Filters in Suction Lines*, The Rosean Filter Company; Hazel Park, MI.

8. Rosean Filter Co., *Piping Recommendations*, The Rosean Filter Company; Hazel Park, MI.
9. H. Ingvast, "Deaeration of Hydraulic Oil offers Many Effects," in *Third Scandinavian Int. Conf. on Fluid Power*, 1993, Vol. 2, pp. 535–546.
10. T. L. Jackson, *An Introduction to Industrial Hydraulic Oils*, 1965, Fluid Power International; pp. 17–23.
11. C. C. Heald, *Cameron Hydraulic Data*, 18th ed., 1994, Ingersoll-Dresser Pumps; Liberty Corner, NJ, p. 3-3.
12. R. C. Mackay, "Pump Suction Conditions," *Pumps Syst. Mag.*, 1993, May, pp. 20–24.
13. D. Godfrey, "Gear Wear Caused by Contaminated Oils," *Gear Tech.*, 1996, September/October, pp. 45–49.
14. T. D. Newingham, "Selecting the Best Hydraulic Fluid," *Power Transmiss. Design*, 1986, October, pp. 27–31.
15. Danfoss Fluid Power, *Failure Analysis—Hydraulic Gear Pumps*, Danfoss Fluid Power; Racine, WI.
16. Caterpillar Inc., *Diagnosing Tyrone Gear Pump Failures*, Caterpillar Brochure Number Caterpillar Inc.; Peoria, IL.
17. Vickers Inc., *Pump Failure Analysis*, Vickers, Incorporated, Troy, MI.
18. A. Sasaki, "A Study of Hydraulic Valve Problems," *Lubr. Eng.*, 1989, 45(3), pp. 140–146.
19. A. Sasaki, "A Review of Contamination Related Hydraulic Pump Problems in Japanese Injection Molding, Extrusion, and Rubber Molding Industries," in *Tribology of Hydraulic Pump Testing*, G. E. Totten, G. H. Kling, and D. J. Smolenski, eds., 1996, American Society for Testing and Materials; Conshohocken, PA, pp. 277–287.
20. W. L. Green, "Lightning in Hydraulic Oil," *Fluid Power Int.*, 1968, December, pp. 51–52.
21. A. J. Zino, "What to Look for in Hydraulic Fluids," *Iron Steel Eng.*, 1951, September, pp. 119–123.
22. H. E. Tiffany, "Trouble-Shooting Hydraulic Systems," in *Hydraulics*, W. E. Wambach Jr., ed., 1983, American Society of Lubrication Engineers; Park Ridge, IL, pp. 45–49.
23. C. A. Moyer, "Comparing Surface Failure Modes in Bearings and Gears: Appearances versus Mechanisms," *A. Gear Manf. Assn., Technical Paper 91 FTM 6*, 1991.
24. E. C. Fitch, I. T. Hong, and J. L. Xuan, "Abrasion Wear," *BFPR J.*, 1988, 21, pp. 9–29.
25. R. Erichello, "Lubrication of Gears—Part 2," *Lubric. Eng.*, 1990, 46(2), pp. 117–121.
26. National Standard—Nomenclature of Gear Tooth Failures, ANSI/AGMA 110.04—1980, AGMA; Alexandria, VA, 1980.
27. E. C. Fitch, I. T. Hong, and J. L. Xuan, "Adhesion Wear," *BFPR J.*, 1988, 21, pp. 31–45.
28. Caterpillar Inc., *Fundamentals of Applied Failure Analysis, Module 4: Analyzing Wear*, Caterpillar Inc.; Peoria, IL.
29. Caterpillar Inc., *Hydraulic Pumps and Motors: Applied Failure Analysis*, Caterpillar Inc.; Peoria, IL.
30. Caterpillar Inc., *Principles of Wear: Applied Failure Analysis*, Caterpillar Inc.; Peoria, IL.
31. L. Faure, "Different Types of Wear—How to Classify?" *Am. Gear Manf. Assn., Technical Paper 90 FTM 4* (1990).
32. E. C. Fitch, I. T. Hong, and J. L. Xuan, "Adhesion Wear," *BFPR J.*, 1988, 21, pp. 93–106.
33. E. C. Fitch, I. T. Hong, and J. L. Xuan, "Cavitation Wear," *BFPR J.*, 1988, 21, pp. 107–118.

34. J. M. Hobbs, "Experience With a 20-KC Cavitation Erosion Test," in *Erosion by Cavitation or Impingement*, 1967, American Society for Materials Testing; Philadelphia, PA, pp. 159. The propensity for cavitation is dependent on material properties. A general ranking of various with respect to the potential for cavitation damage is shown in Fig. 12.14.
35. T. E. Tallian, *Failure Atlas for Hertz Contact Machine Elements*, 1992, American Society of Mechanical Engineers, New York.
36. E. C. Fitch, I. T. Hong, and J. L. Xuan, "Corrosion Wear," *BFPR J.*, 1988, 21, pp. 119–128.
37. J. R. Scully, "Electrochemical," in *Corrosion Tests and Standards: Application and Interpretation*, R. Baboian, ed., 1995, American Society for Testing and Materials; Conshohocken, PA, pp. 75–90.
38. M. Henthorn, "Fundamentals of Corrosion: Part I," *Chem. Eng.*, 1971, May, pp. 127–132.
39. C. E. Snyder, G. J. Morris, L. J. Gschwender, and W. B. Campbell, "Investigation of Airforce Mil-H-5606 Hydraulic System Malfunctions Induced by Chlorinated Solvent Contamination," *Lubr. Eng.*, 1981, 37(8), pp. 457–461.
40. W. D. Phillips, "The Electrochemical Erosion of Servo Valves by Phosphate Ester Fire-Resistant Hydraulic Fluids," *Lubr. Eng.*, 1988, 44(9), pp. 758–767.
41. T. R. Beck, "Wear by Generation of Electrokinetic Streaming Currents," *ASLE Trans.*, 1983, 26(2), pp. 144–150.
42. T. R. Beck, D. W. Mahaffey, and J. H. Olsen, "Wear of Small Orifices by Streaming Current Driven Corrosion," *ASME Trans., J. Basic. Eng.*, 1970, 92, pp. 782–791.
43. T. R. Beck, D. W. Mahaffey, and J. H. Olsen, "Pitting and Deposits with an Organic Fluid by Electrolysis and Fluid Flow," *J. Electrochem. Soc.*, 1972, 119(2), pp. 155–160.
44. T. R. Beck, J. F. Curulla, B. C. Hainline, A. Lauba, and D. C. Sullivan, "Effect of Mixed Phosphate Ester Fluids on Aircraft Hydraulic Servovalve Erosion," *SAE Technical Paper Series, Paper 801100*, 1980.
45. W. G. Nelson and A. W. Waterman, "Advances in Commercial Airplane Hydraulic Fluids," in Meeting No. 76, SAE Committee A-6, 1974.
46. N. W. Sachs, "Metal Fatigue," *Lubr. Eng.*, 1991, 47(12), pp. 977–981.
47. X. Z. Jin and N. Z. Kang, "A Study on Rolling Bearing Contact Fatigue Failure by Macro-Observation and Micro-Analysis," *Proc. of Int. Conf. on Wear of Materials, 1989, Denver, CO*, K. Ludema, ed., 1989, American Society of Mechanical Engineers; New York, Vol. 1, pp. 205–213.
48. E. C. Fitch, I. T. Hong, and J. L. Xuan, "Surface Fatigue Wear," *BFPR J.*, 1988, 21, pp. 47–62.
49. T. E. Tallian, "On Competing Failure Modes in Rolling Contact," *ASLE Trans.*, 1967, 10, pp. 418–439.
50. Caterpillar, Inc., *Diagnosing Hydraulic Pump Failures*, Caterpillar Inc.; Peoria, IL.
51. D. P. Townsend and J. Shimski, "EHL Film Thickness, Additives and Gear Surface Fatigue," *Gear Tech.*, 1995, May/June, pp. 26–31.
52. K. D. MacKenzie, "Why Bearings Fail," *Lubric. Eng.*, 1978, January, pp. 15–17.
53. E. V. Zaretsky, *STLE Life Factors for Roller Bearings*, 1992, Society of Tribologists and Lubrication Engineers; Park Ridge, IL, pp. 199–201.
54. The Timken Co., *Bearing Maintenance Manual for Transportation Applications*, The Timken Company; Canton, OH.
55. The Barden Corp., *Bearing Failure Causes and Cures*, The Barden Corporation; Danbury, CT.
56. Caterpillar Inc., *Anti-friction Bearings: Applied Failure Analysis*, Caterpillar Inc.; Peoria, IL.

57. D. Godfrey, "Recognition and Solution of Some Common Wear Problems Related to Lubricants and Hydraulic Fluids," in *Starting from Scratch—Tribology Basics*, F. Litt, ed., Society of Lubrication Engineers, Park Ridge, IL, pp. 11–14.
58. M. W. Washo, "A Quick Method of Determining Root Cause and Corrective Actions of Failed Ball Bearing," *Lubr. Eng.*, 1996, 52(3), pp. 206–213.
59. Mobil Oil Company, *Ailing Hydraulic Systems Have Three Common Symptoms*, Mr. David Scheetz, Mobil Oil Company, Aurora, IL.

This page intentionally left blank

Water Hydraulics

KARI T. KOSKINEN and MATTI J. VILENIUS

*Institute of Hydraulics and Automation, Tampere University of Technology,
Tampere, Finland*

1 INTRODUCTION

Although the first water hydraulic applications were known from 400–500 B.C., the first modern applications occurred at the end of 18th century, as illustrated in Fig. 13.1. Since that first application over 100 years ago, all hydraulic systems have used water as a pressure medium. In the early 20th century, the use of hydraulics increased greatly when pressure-medium-lubricated pumps and motors and oil-resistant seal materials were developed.

In recent years, water hydraulic applications have increased and continues to increase. One reason for this growth is the increasing importance of the environmental aspects of hydraulic fluids throughout the world. Water as a pressure medium offers many other benefits compared to oil, including easy maintenance, good availability, low cost, nonflammability, and so forth. One other springboard for the development of water hydraulics has been the recent development in material technology. Many new materials have been developed that provide longer life expectancies with water without corrosion and erosion.

Applications in water hydraulics have traditionally been in mining, steel, aluminum, automotive industries, and water-treatment plants. Examples of new application areas include rescue equipment, food industry, pulp and paper industries, and land and marine diesel engines. Exotic new applications being developed include municipal engineering and fusion reactor remote-handling equipment. The most recent research area is low-pressure water hydraulics.

2 WATER AS A PRESSURE MEDIUM IN FLUID POWER SYSTEMS [1,2]

2.1 Water Hydraulic Fluids

When water hydraulic applications are discussed, they typically include tap-water hydraulic replacements for current HFA-fluid or HFC-fluid applications. Seawater is

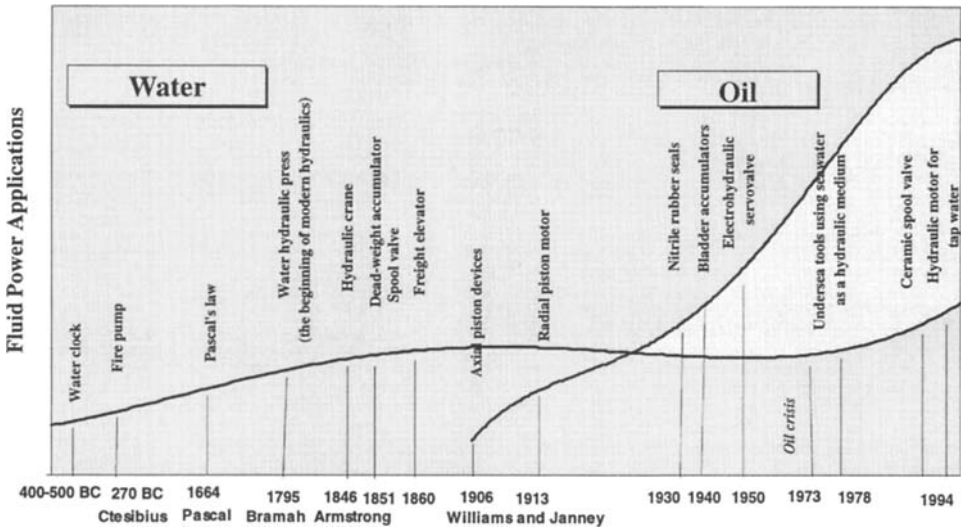


Figure 13.1 History of fluid power technology. (From Ref. 1.)

not commonly used except in special offshore applications. HFA fluids typically contains 95% water and 5% concentrate. The concentrate normally includes emulsification additives and wear inhibitors. HFA fluids are also sometimes called HWCF or HWBF fluids. HFC fluids consist of approximately 40% water and 60% of a glycol, additives, and a thickener. The use of HFC fluids has decreased in recent years. One reason might be cost. HFB fluids have been used, but their use has also decreased.

Tap water is, of course, the genuine form of water hydraulic fluid. It is inexpensive, nontoxic, and nonflammable and has very good availability. Water is clean, so storage and disposal is inexpensive and simple. The problems with water are in regard to component materials, which must be resistant to corrosion, erosion, cavitation, and so forth. Because the objective is that almost all water hydraulic systems are typically tap-water systems, this article will concentrate on such systems.

Water is a very efficient pressure transmitter in a hydraulic system. Due to low compressibility and viscosity, a water hydraulic system contains more energy relative to an equivalent oil hydraulic system. Therefore, the dynamics are faster than in oil hydraulic systems. On the other hand, poorer lubrication and additional seals increase Coulomb friction, worsening the dynamic properties.

2.2.1 Physical Properties of Water

The properties of water differ considerably from those of mineral oil. The viscosity, density, and bulk modulus of water and typical mineral oil have been determined. A typical mineral oil is ISO VG 32 (ESSO Univis 32). In Fig. 13.2, the temperature dependency of the properties of water and typical mineral oil are shown. The change in density of mineral oil may be calculated from an empirical formula:

$$\rho_t = \rho_{15^\circ\text{C}} \frac{1}{1 + \bar{\gamma}(t - 15)} \quad (13.1)$$

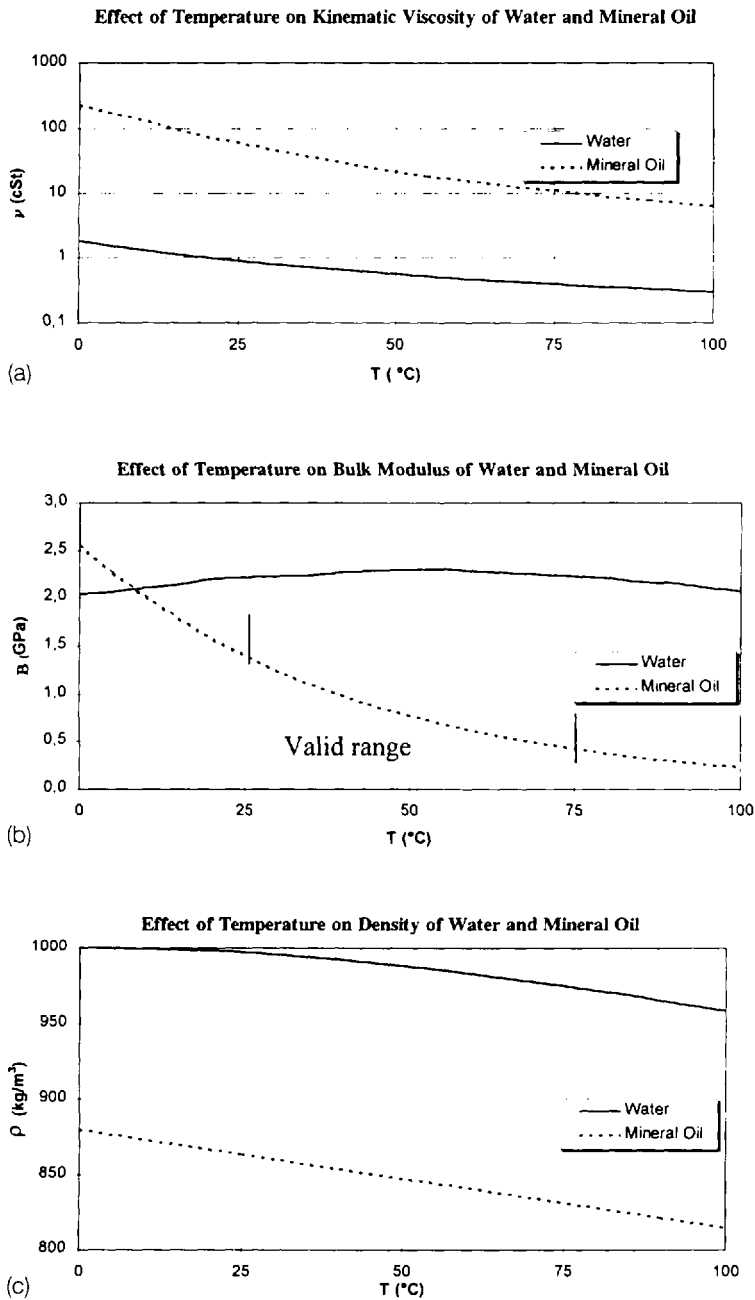


Figure 13.2 The effect of temperature on viscosity, density, and bulk modulus of water and typical mineral oil.

where the thermal volume coefficient is

$$\bar{\gamma} = \frac{\Delta V_p}{V_0} \frac{1}{\Delta t_p} \quad (13.2)$$

The value $\bar{\gamma} \approx 65 \times 10^{-5} \text{ L}^\circ\text{C}$ is generally accepted for mineral oils. The change of bulk modulus of mineral oil can be calculated from the following empirical formula:

$$\beta = 1000 \left[1.78 + 7 \left(\frac{\rho_0}{1000} - 0.86 \right) e^{10(0.0025(20 - T))} \right] \quad (13.3)$$

where ρ_0 is the density of mineral oil at $T = 20^\circ\text{C}$. Equation (13.3) is valid when $20^\circ\text{C} < T < 70^\circ\text{C}$. The pressure dependency of water and of a typical mineral oil are shown in Fig. 13.3. The viscosity change of mineral oil can be calculated from the following empirical formula:

$$\nu_p = \nu_{p_0} e^{0.0017(p_p - p_0)} \quad (13.4)$$

The bulk modulus of water can be calculated from the change of relative density:

$$\beta_p = \frac{\rho_p}{\rho_0} \beta_0 \quad (13.5)$$

The density change of mineral oil can be calculated from empirical formula

$$\rho_p = \rho_{p0} \left(\frac{1}{1 - 65 \times 10^{-11} p(10000)} \right) \quad (13.6)$$

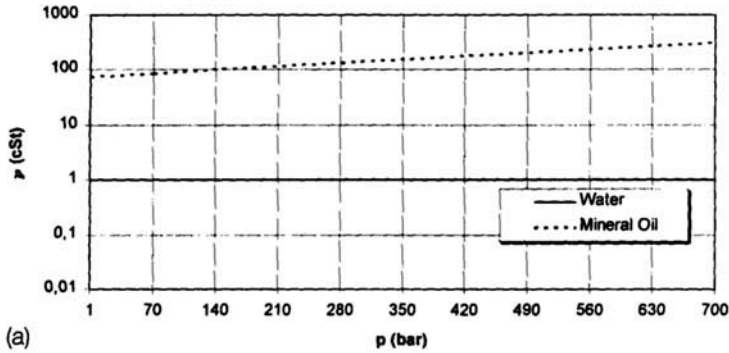
It can be seen that the kinematic viscosity decreases with increasing temperature for both water and mineral oil. However, the decrease of the kinematic viscosity of mineral oil is much greater than water over the entire temperature range. For example at 40°C , the kinematic viscosity of water is approximately 0.7 cSt and the kinematic viscosity of mineral oil is approximately 32 cSt. The ratio is approximately 1:46.

The variation of bulk modulus is also greater for mineral oil than water. The bulk modulus of water is almost constant between 0°C and 100°C . On the other hand, the bulk modulus of mineral oil decreases quite strongly with temperature rise. Both bulk moduli are almost the same at 15°C , but at 50°C , the difference is about 1.4 GPa.

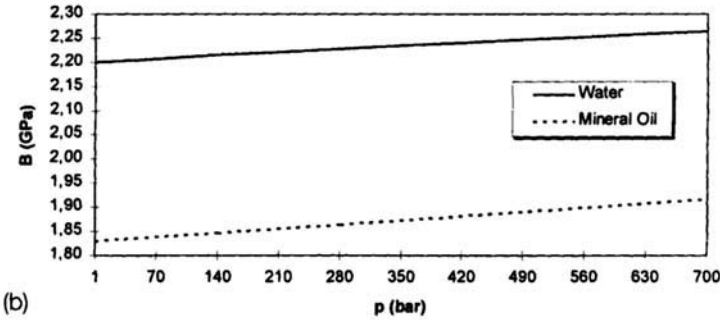
The effect of temperature on the densities of water and mineral oil is almost the same. The density of water is about 150 kg/m^3 greater than the density of mineral oil across the entire temperature range.

The effect of pressure on the kinematic viscosity, the bulk modulus and density of water and of a typical mineral oil is presented in Fig. 13.3. The pressure range selected is from 1 bar to 700 bars because most normal water hydraulic systems use pressures in this range. The temperature is 20°C . Figure 13.3 shows that the kinematic viscosity of water is not affected by system pressure. However, the kinematic viscosity of mineral oil increases with the system pressure. This is a great benefit for water, especially in the high-pressure applications. The effect of pressure on the bulk moduli of water and mineral oil is about the same. They both increase with pressure, but the increase of water bulk modulus is slightly smaller. Also, the effect of pressure on the density of water is slightly less than with mineral oil.

Effect of Pressure on Kinematic Viscosity of Water and Mineral Oil
in $T = 20\text{ }^\circ\text{C}$



Effect of Pressure on Bulk Modulus of Water and Mineral Oil
in $T = 20\text{ }^\circ\text{C}$



Effect of Pressure on Density of Water and Mineral Oil
in $T = 20\text{ }^\circ\text{C}$

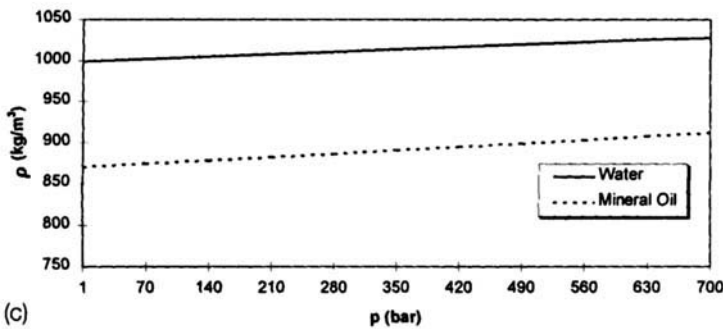


Figure 13.3 The effect of pressure on viscosity, density, and bulk modulus of water and typical mineral oil.

The change of vapor pressure of water and mineral oil with temperature is shown in Fig. 13.4. This data shows that the vapor pressure of water changes strongly with increasing temperature. At the same temperatures, the vapor pressure of mineral oil is nearly constant. This illustrates the cavitation sensitiveness of water compared mineral oil. The thermal conductivity of a fluid essentially affects the heat balance of a hydraulic system. The advantage of water relative to mineral oil is illustrated in Fig. 13.4. The thermal conductivity of water is about five to six times greater than the thermal conductivity of oil. In addition, the thermal conductivity of water increases slightly with increasing temperature.

The solubility of air in a fluid affects its compressibility, which may, in some cases, be significant for system operation. The lower solubility of air in water relative to mineral oil as a function of pressure is illustrated in Fig. 13.4.

From Figs. 13.2–13.4, it is clear that water and mineral oil exhibit significantly different physical properties. These differences affect to the system performance in different ways depending on the application and operation conditions. In this context, it is also worth considering that water does not exhibit the same properties because the hardness of water can vary in calcium and magnesium content. Water acidity may also vary, and the bacteria level in water may also affect hydraulic system performance.

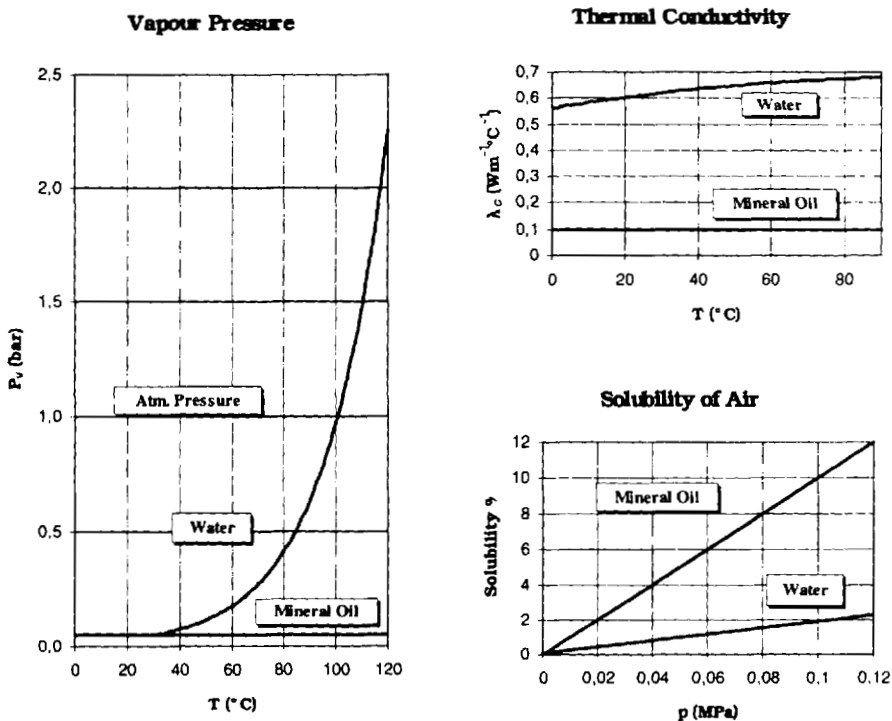


Figure 13.4 Vapor pressure, thermal conductivity, and solubility of air of water and mineral oil.

2.1.2 Chemical Properties of Water

The chemical properties of water vary with the source and geographically. The European Union has given the directive Water Quality Standards in EU, 80/778/EEC, where the requirements for drinking water are described. Some component manufacturers have based their component application limits on the chemical properties of water provided in this directive. In the following discussion, the most significant chemical parameters of water used as a pressure medium are listed:

- Hydrogen-ion concentration
- Chloride content
- Hardness
- Bacteria and other microbiological organisms
- Solid-particle content

All these values should be measured to ensure the quality of water. However, in practice, the measurement of all of these values may be expensive and time-consuming. Monitoring the water quality should be continuous, which is difficult to arrange in many applications. Good and simple measurement and monitoring methods providing reliable information on the quality of the water but still easy to apply to all systems, must be developed. In addition, general methods for cleaning the system must be developed. Because the requirements may be component dependent, this will increase the difficulty of identifying generally acceptable purification methods.

2.2 Steady-State Pipe Flow

The steady-state pipe flow is the simplest parameter to identify differences between water and mineral oil as a hydraulic fluid. A smooth-surface pipe, 1 m long and 10 mm in diameter, is illustrated in Fig. 13.5. When we use the values presented in Table 13.1 for the physical properties of water and mineral oil, the Reynolds number and pressure drop curves for water and typical mineral oil illustrated in Figs. 13.6–13.8 are obtained.

Flow in a pipe changes gradually from laminar to turbulent across a transition region. This region contains the critical Reynolds number Re_{cr} . Normally Re_{cr} can be assumed to be in the range 1500–2500. The Reynolds number can be calculated from

$$Re = \frac{vd_h}{\nu} \quad (13.7)$$

where d_h is the hydraulic diameter

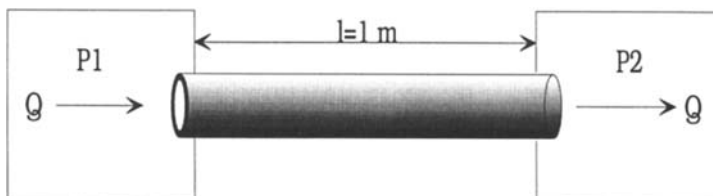


Figure 13.5 Smooth-surface pipe.

Table 13.1 Densities and Viscosities

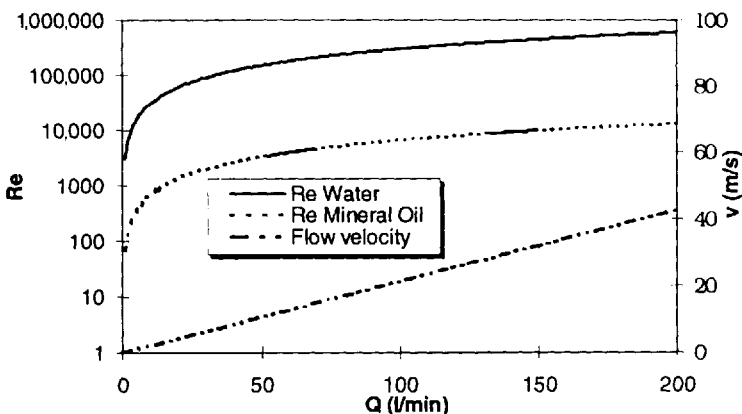
Water ($T = 40^{\circ}\text{C}$)
Density = 992 kg/m ³
Viscosity = 0.7 cSt
Mineral Oil ($T = 40^{\circ}\text{C}$)
Density = 870 kg/m ³
Viscosity = 32 cSt

$$d_h = \frac{4A}{P} \quad (13.8)$$

For a pipe, the hydraulic diameter $d_h = d$. The flow velocity in a pipe can be calculated from

$$v = \frac{Q}{A} = \frac{4Q}{\pi d^2} \quad (13.9)$$

From Fig. 13.6, we can observe that the Reynolds numbers of water and mineral oil have totally different magnitudes. The Reynolds number of water is about 50 times greater than the Reynolds number of mineral oil across the whole of the flow range presented. That means that the flow of water is in practice always fully turbulent, because the transition area from laminar to turbulent is somewhere between the values 0 L/min and 1 L/min. The Reynolds number of mineral oil is with small flows laminar and the transition area from laminar to turbulent flow is somewhere between the values 30 L/min and 60 L/min. The flow velocity curve is also presented in Fig. 13.6 on the right-hand-side Y axis. By studying the Reynolds numbers and flow velocity, it is evident that the water hydraulic system has greater internal flow energy, even with the same flow velocity, compared to mineral-oil flow. How that shows in

**Figure 13.6** Reynolds numbers and flow velocity in a smooth pipe.

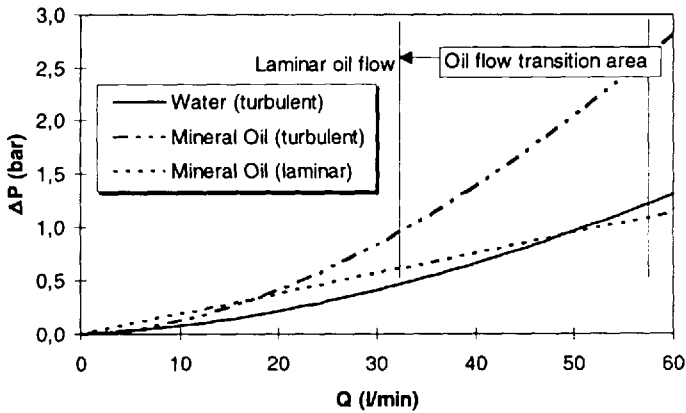


Figure 13.7 Mineral-oil pipe flow transition area.

pressure drop in the pipe is examined in Fig. 13.7, where the pressure drop of laminar and turbulent mineral oil and turbulent water flow is presented for lower flows.

Figure 13.7 shows that pressure drop in pipe flow is always smaller with water than with mineral oil, even the case when the mineral oil flow is laminar. The difference is not large with smaller flows, but as the flow increases, the two curves diverge even further. The transition area for mineral oil is also presented in Fig. 13.7. This occurs between 30 L/min and 60 L/min, when the limit values 2000 and 4000 as Reynolds numbers are used. Therefore, when modeling and simulating systems where the flows are in the right area and the small pressure drops in pipe flow are significant, the location of transition area must be taken account. In Fig. 13.8, the pressure drop in turbulent flow with water and mineral oil is provided for flow rates up to 200 L/min. These data show that the benefits of using water are greater with larger flows.

The effect of the roughness of the pipe surface is presented in Fig. 13.9. The relative roughness R_u is on the X axis and the loss head coefficient l is presented on

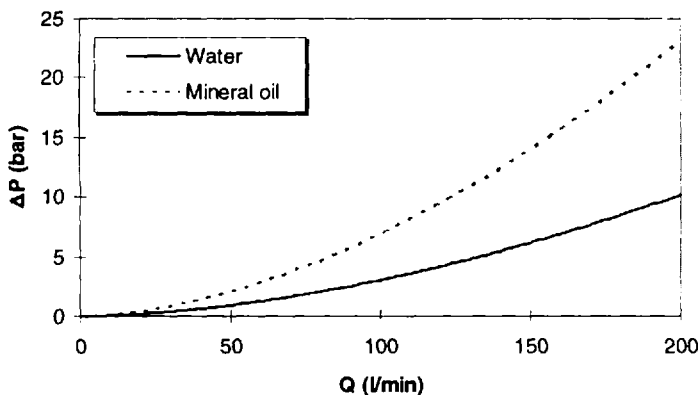


Figure 13.8 Pressure drop in turbulent pipe flow.

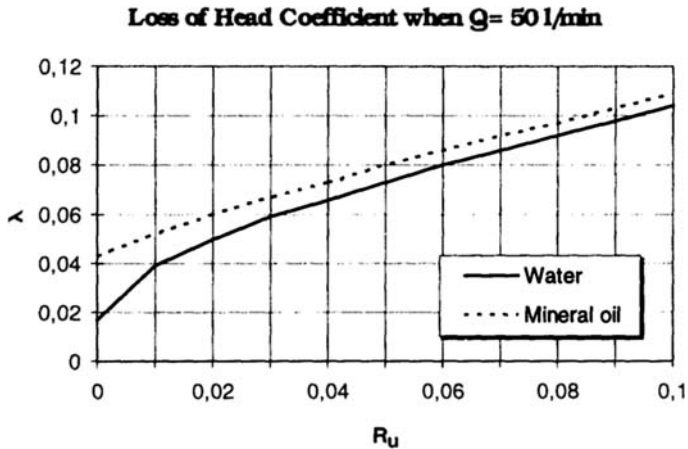


Figure 13.9 The effect of pipe surface roughness on loss of head coefficient.

the Y axis. Figure 13.9 shows a completely smooth pipe with very small relative roughness; the difference in loss of head coefficients increases with increasing relative roughness. The difference decreases with increasing roughness. For small roughness values, the use of water instead of oil is more efficient than in very rough pipes.

2.3 Leakage Flow

Low-viscosity leakage is a greater problem in water hydraulic components than in oil hydraulic components. Leakage flow is significant, for example, in displacement pumps and control valves. In control valves, clearances are normally between 1 and 100 μm . Laminar leakage flow in an annular clearance is usually calculated from

$$Q = \frac{[1 + 1.5(\epsilon/h)]\pi Dh^3}{12\rho\nu L} \Delta p \quad (13.10)$$

The annular clearance between the piston and cylinder is illustrated in Figure 13.10. Also illustrated in Fig. 13.10 is the leakage flow of water and mineral oil as a function of clearance width. Both flows have been assumed to be laminar. The leakage flow with water is much greater than with mineral oil. For the same leakage flow (e.g., 10 mL/min), the clearance may be about 20 μm with oil but only 5 μm with water. The difference increases with increasing clearances.

On the other hand, some differences between laminar theory and practice may be observed. The flow–pressure curves and Reynolds number curve of a fully eccentric piston in an annular clearance is presented in Fig. 13.11. The measured and calculated curves are similar for small pressure differences (low Reynolds numbers), but the difference between measured and calculated curves increases with increasing flows. (The measurements, in this case, were conducted with seawater.) The reason for this behavior is that the flow is turbulent with larger Reynolds numbers. The accuracy of the flow model can be improved by accounting for the annulus inflow and outflow effects.

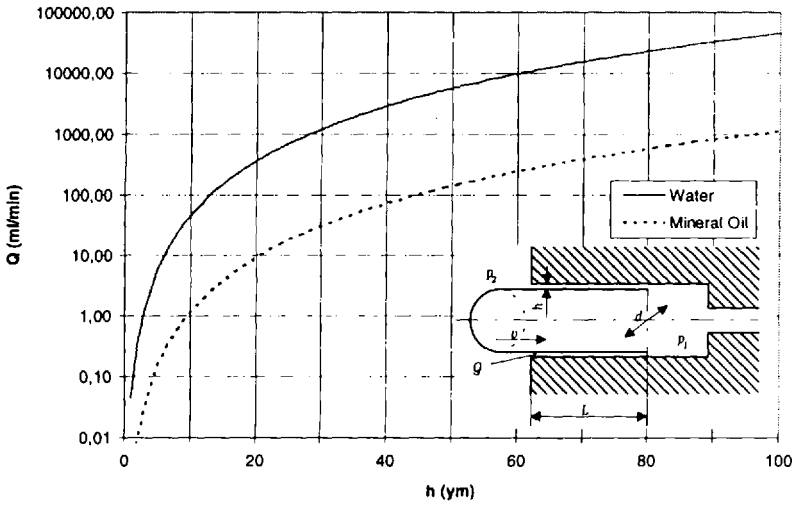


Figure 13.10 Laminar leakage flow in annular clearance.

Pressure losses within an annulus are composed of pressures on both ends and in the annular duct as illustrated in Fig. 13.12. The pressure loss within the annulus can be derived according to laminar or turbulent flow. For laminar flow,

$$\Delta p = \zeta \rho \frac{v^2}{2} \tag{13.11}$$

For calculating pressure loss due to sudden change of the flow cross-section area, flow model 1 may be derived; it is presented in Eqs. (13.12)–(13.14):

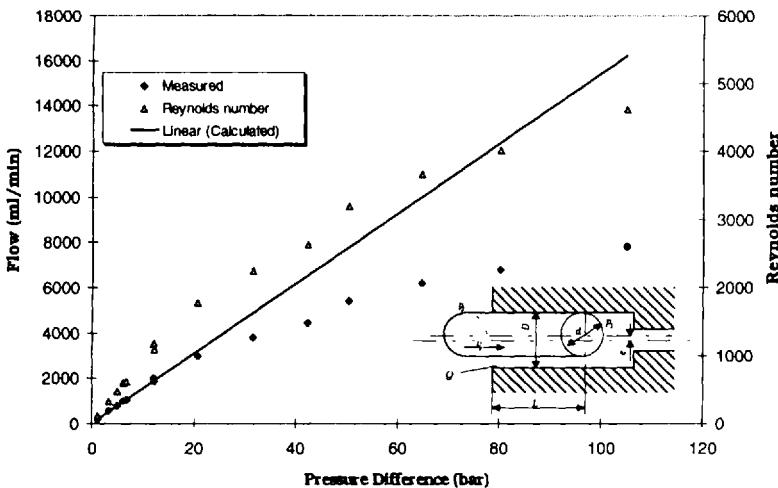


Figure 13.11 Leakage flow in totally eccentric annular clearance with seawater.

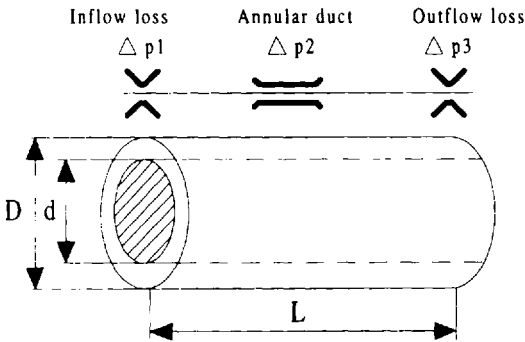


Figure 13.12 Pressure losses in an annular duct.

$$Q = \frac{k_2}{2} \left[\sqrt{\left(\frac{k_2}{k_1}\right)^2 + 4\Delta p} - \frac{k_2}{k_1} \right] \quad (13.12)$$

$$k_1 = \frac{[1 + 1.5(\epsilon/h)] \pi Dh^3}{12\rho\nu L} \quad (13.13)$$

$$k_2 = \frac{1}{\zeta} \pi Dh \sqrt{\frac{2}{\rho}} \quad (13.14)$$

Pressure-loss coefficients for different cases have been presented in Ref. 3. The coefficient for sharp-edged inflow is 0.5 and the coefficient for outflow is 1.0. These can be combined to one pressure-loss coefficient $\zeta = 1.5$.

For turbulent flow of a Newtonian fluid, the annulus is considered as a pipe with diameter $2h$. Pressure loss in a pipe can be solved using

$$\Delta p = \xi \rho \frac{v^2 L}{2 d_h} \quad (13.15)$$

The friction factor ξ is a function of the Reynolds number and the relative surface roughness. For a smooth surface, empirical friction equations have been reported. Reference 4 provides a method for the determination of friction factor for an annulus with fine clearance. The equation is valid in the range $2 \times 10^3 \leq Re \leq 2 \times 10^4$. The influence of piston eccentricity has also been studied and can be calculated from

$$\xi = \frac{0.316}{Re^{0.21}} \frac{1}{1 + 0.2(\epsilon/h)} \quad (13.16)$$

For turbulent flow, flow model 2 may be derived by combining Eqs. (13.11), (13.15), and (13.16):

$$Q = A \sqrt{\frac{2\Delta p}{\rho} \left(\frac{d_h}{\xi L} + \frac{1}{\xi^2} \right)} \quad (13.17)$$

$$\xi = \frac{0.316}{Re^{0.21}} \frac{1}{1 + 0.2(\epsilon/h)} \quad (13.18)$$

The accuracy of flow models 1 and 2 are verifiable with laboratory measurements. The measurement and verification results are presented in Ref. 5. The results show that the effect of inflow and outflow is very important in a short annulus. The radial elasticity of the housing has to be taken account when considering small clearances. The conventional laminar pipe model for flow in an annulus is valid for short ducts when the Reynolds number is less than 1000. When the Reynolds number is >1000 , flow is clearly turbulent.

Flow model 2 is a combination of a turbulent entrance loss and a turbulent pipe loss model. It is valid for a high Reynolds number flow only because flow is laminar with a low Reynolds number. Modeling accuracy could be improved if the relative surface roughness were accurately known, which is not usually the case.

Flow model 1 is a combination of a turbulent entrance loss and a laminar pipe flow model. It provides the same result as the conventional pipe model for low-Reynolds-number flow and with satisfactory accuracy at high-Reynolds-number flow. Therefore, flow model 1 is suitable for modeling annular clearances with various Newtonian fluids.

From these relationships, it is concluded that clearances must be smaller to achieve good efficiency in water hydraulic systems. The smaller clearances are more expensive to manufacture and increases the cost of water hydraulic components. However, the leakage flow in small clearances with water may also be turbulent with large pressure differences and in that case, the actual leakage flow is smaller than predicted by the laminar leakage flow equation. That must be considered when studying, for example, water hydraulic valves and pumps.

2.4 Pressure Transients

Pressure transients can complicate the performance of a hydraulic system. Due to pressure transients, the system pressure rises momentarily far above the normal operation pressure, which may result in component damage. Pressure transients originate from a sudden change in flow velocity. A sudden valve opening and closing and sudden actuator stops generally cause pressure transients. In water hydraulics, the importance of pressure transients is emphasized because the greater density and the greater bulk modulus compared to mineral oil means the fluid is less compressive and the resulting velocity change results in a stronger pressure rise.

The results of computer simulation of hydraulic system pressure transients are illustrated in Fig. 13.13. The symmetrical cylinder is controlled by a 4/3 valve. When the cylinder piston moves to the right in the central position, the valve spool is changed from position 1 to the central position, at which point, pressure transients occur in cylinder chambers. When the system is simulated using the same components and parameters with water and mineral oil, the effect of the fluid on the pressure transients can be approximated. The valve spool is controlled as shown in Fig. 13.13. The pump output flow is modeled with a constant value. The pressure relief valve is modeled with the first-order model, but its behavior is not shown because only cylinder pressures are examined.

In Fig. 13.14, the pressures of the cylinder chambers PA and PB with water and oil are presented. When the piston moves to the right, the pressure in PA is greater with water because of smaller flow resistance. In addition, pressure vibration in a water system exhibits a larger amplitude and frequency than in an oil system.

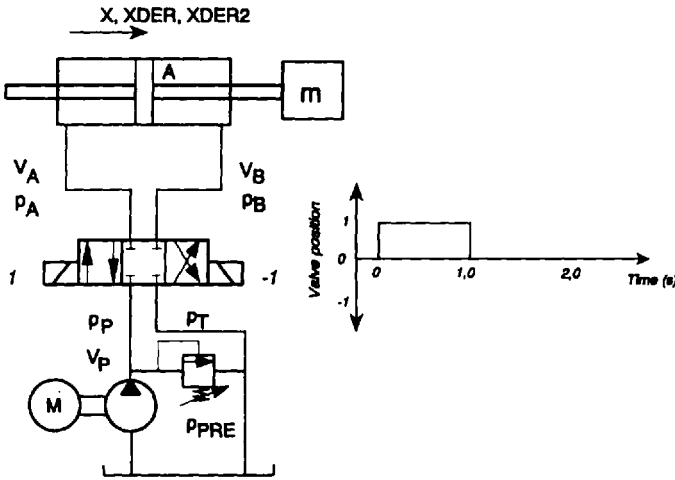


Figure 13.13 Simple hydraulic cylinder control system.

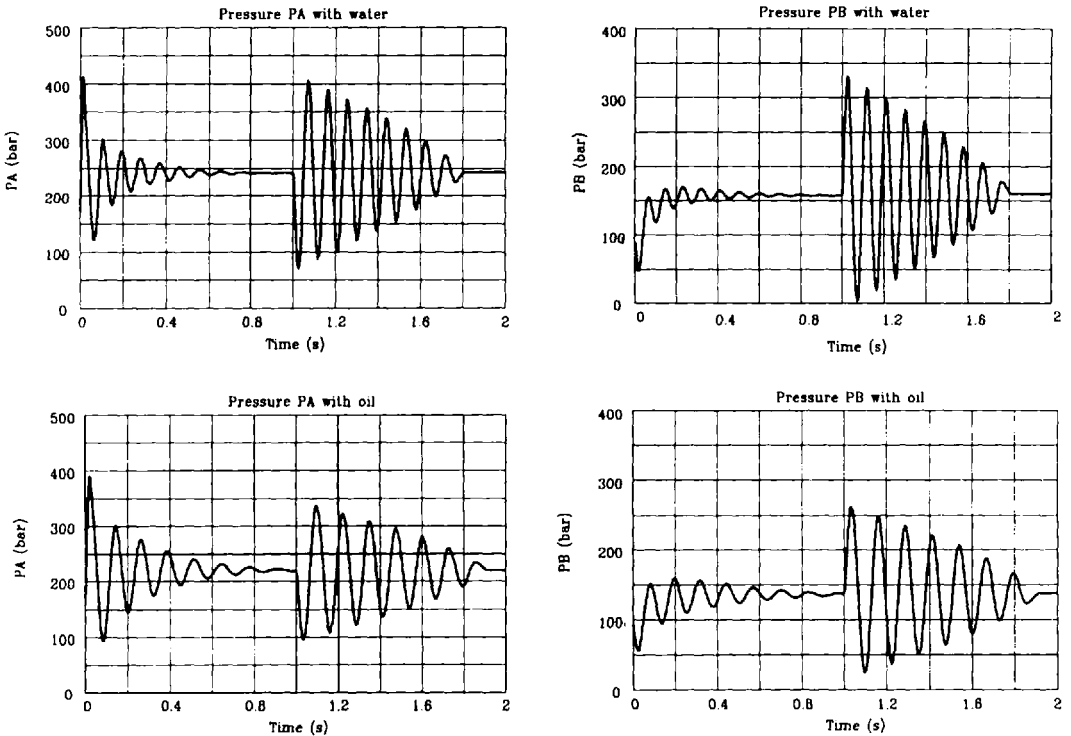


Figure 13.14 Simulated cylinder chamber pressures with water and oil.

Vibration is dampened slightly faster in the water system because of the larger internal leakage in cylinder. For the water system, the pressure in PB falls almost to zero instantly, whereas in the oil system, the minimum is at about 25 bars. This is one example of the cavitation sensitivity of a water hydraulic system, which may also result from excessive pressure transients.

It can be concluded that pressure transients and vibrations exhibit different behaviors in water hydraulic systems compared to oil hydraulic systems. However, the pressure transients are not an insuperable problem in water hydraulics. The generation of pressure transients can be avoided or minimized by proper design of components and systems, as illustrated in Fig. 13.14.

2.5 Cavitation and Erosion

One of the most difficult phenomenon to research in hydraulic systems is cavitation. The role of cavitation in water hydraulic systems is much more significant than in oil systems. Cavitation may occur in pumps, valves, and actuators.

Cavitation may be either gaseous cavitation or vaporous cavitation. Gaseous cavitation is caused by the rapid reduction of pressure, resulting in the release of dissolved air or gas. However, gaseous cavitation is less likely to occur in water hydraulics because the density and bulk modulus of water are greater than with oil. Also, the amount of dissolved air in water is less than in oil at the same pressure. However, vaporous cavitation is far more likely to occur in water hydraulics than in oil hydraulics. Vaporous cavitation occurs when the pressure instantly drops to the fluid's vapor pressure. At this point, cavities will develop, and as they move downstream into a higher-pressure regime, they collapse, producing noise and vibration. Because the vapor pressure of water is higher than the vapor pressure of mineral oil, especially at higher temperatures, it is obvious that water is more susceptible to cavitation than mineral oil.

When considering, for example, a simple orifice, cavitation may occur downstream of the restrictor due to the high velocity of the fluid just after the restrictor. The flow through the orifice with water is greater than with oil when the pressure difference over the orifice is the same. That means that the flow velocity is higher with water just after the orifice. The nondimensional cavitation index K for control valves gives the sensitivity of cavitation. K is defined as

$$K = \frac{P_1 - P_3}{P_1 - P_v} \quad (13.19)$$

where

P_1 = the supply pressure

P_3 = the system back pressure

P_v = the vapor pressure of the fluid

From this equation, it is evident that system back pressure dominates the cavitation index. When comparing water and mineral oil, it can be concluded that the term P_v is greater with water than with oil, especially at higher temperatures, and the critical value K_c is greater with water at the same pressure difference. In Fig. 13.15, the typical relationship between cavitation index and fluidborne noise is shown.

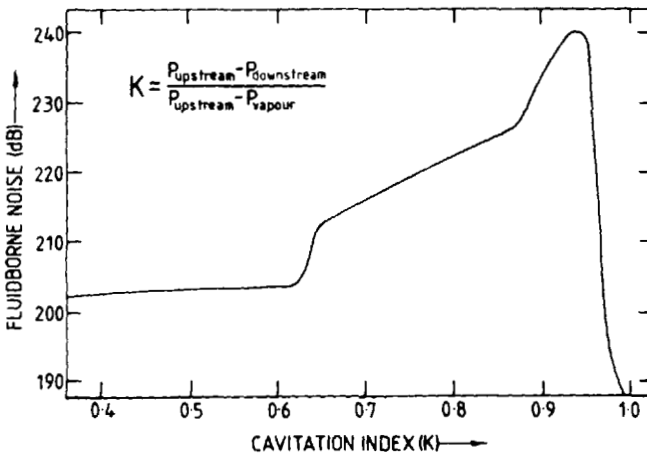


Figure 13.15 Typical relationship between cavitation index and fluidborne noise.

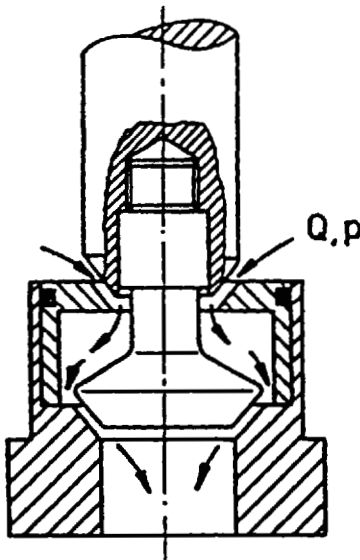


Figure 13.16 Cavitation reduction with double-seat construction in a poppet valve.

Erosion caused by cavitation is strongly dependent on the materials and the design of components. One possibility for the reduction of cavitation is with the use of cascading restrictors. Then, the pressure drop across one restrictor is reduced and the cavitation index stays low. This method is commonly used for valves for use in the water hydraulic system. One example is the poppet valve shown in Fig. 13.16.

3 WATER HYDRAULIC COMPONENTS

3.1 Pumps

New materials and design innovations have recently increased the types of water hydraulic pump available. Axial and radial piston pumps, and the more traditional

plunger-, centrifugal-, and piston-type pumps are currently available. A water hydraulic axial piston pump is shown in Fig. 13.17. Axial piston pumps are the newest pumps in the market. There are many newly developed materials used in these pumps, including reinforced plastics, overmolded stainless steel, and special seals. These pumps are normally designed for hydraulic systems with a maximum pressure of 140 bars. All parts of these pumps are water lubricated, which means that no oil is used inside the pump.

A water hydraulic triplex-piston pump is illustrated in Fig. 13.18. These pumps have been used for many years in mining and steel industries for high-pressure generation in various applications. The three pistons are driven by an oil-lubricated crankshaft mechanism. The oil side and water sides are totally separated from each other to prevent fluids mixing. In the water side, all of the parts are made of corrosion-resistant materials such as stainless steel or industrial ceramics. The pumping unit is a normal piston with suction and pressure valves. The valves are usually seat valves. The typical flow rate for this kind of pump is up to 700 L/min and pressures are up to 800 bars.

One possibility of producing high-pressure water is to use a pressure intensifier such as that illustrated in Fig. 13.19. The pump unit is driven by oil pressure, which is supplied to the center part of the intensifier. The water pistons are located in both ends and water is pumped in every stroke. When one end is pumping, the other end is priming. The change of direction is automatically controlled by the oil valve, which is integrated to the oil piston.

When using a pressure intensifier, oil hydraulic power is needed. In some applications, this might lead to problems and higher costs, but there are also many applications, where oil hydraulic power is already present for other reasons. Then, the pressure intensifier may be economically acceptable. Pressure intensifiers have been traditionally used in water jet cutting systems, where pressures may be as high

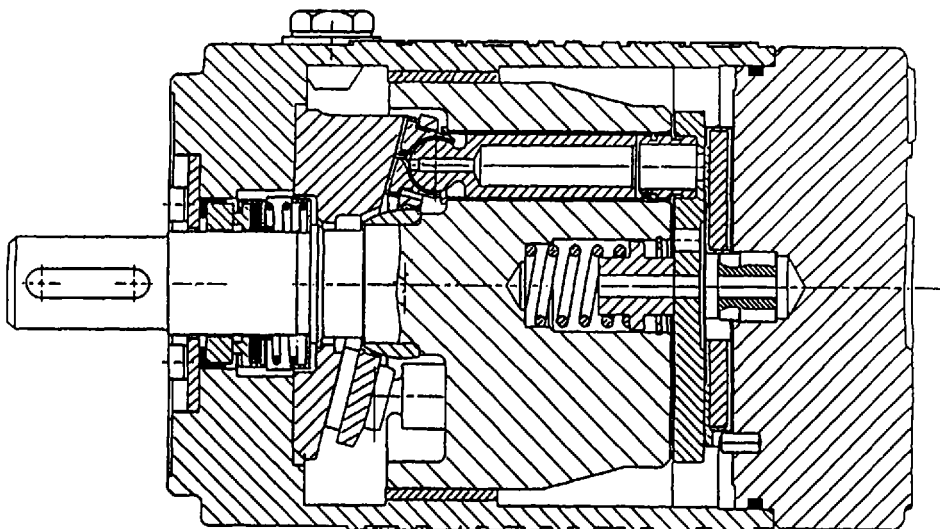


Figure 13.17 Water hydraulic axial piston pump (Danfoss). (From Ref. 6.)

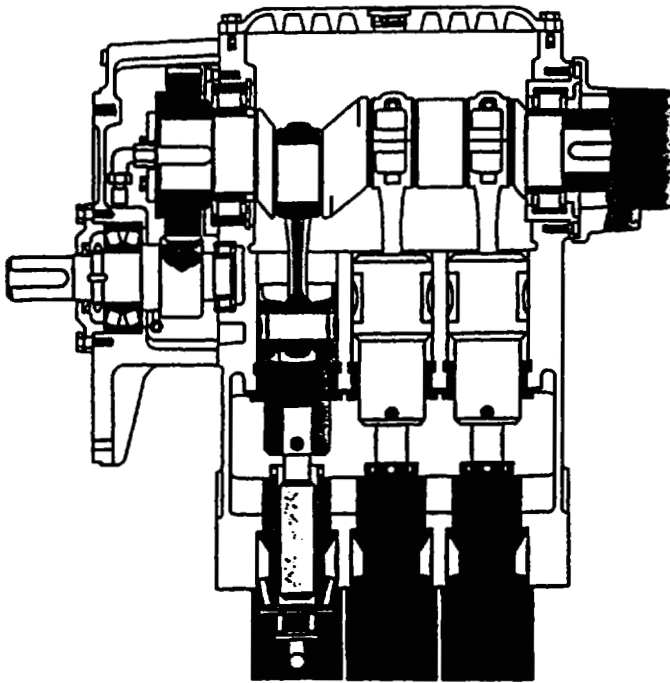


Figure 13.18 Water hydraulic triplex pump (Hauhinco). (From Ref. 6.)

as 4000 bars. The intensifier shown in Fig. 13.19 is typically designed for 200–800 bars.

In low-pressure applications, where the pressure is between 10 and 50 bars, a centrifugal pump is a potential alternative. Centrifugal pumps are simple and reliable, and with multistage pumps, 30 bars can be easily achieved. The centrifugal pump also simplifies the hydraulic circuit because no pressure relief valve is needed. The

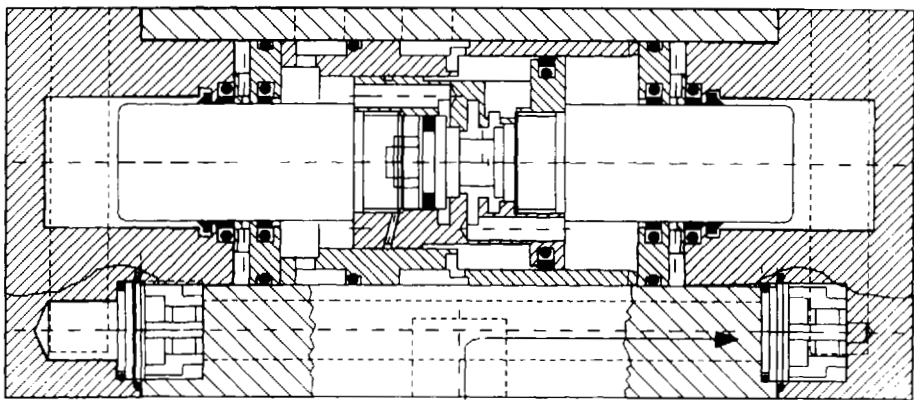


Figure 13.19 Water hydraulic pressure intensifier (Dynaset). (From Ref. 7.)

pump cannot increase the pressure over its capability. However, low-pressure water hydraulics is still a relatively new idea and there are not many examples of the use of centrifugal pumps in water hydraulic systems.

3.2 Control Valves [8]

3.2.1 On–Off Valves

On–off valves are the simplest control valves that can be used in cylinder position control. There are a few different on-off valves suitable for tap water available in the market. Traditionally, ball seat valves have been used with smaller flows and piloted seat valves have been used in larger flow systems. Spool valves have not been used for tap water until recently, when the ceramic spool valve was introduced.

One new on–off valve for tap water use is shown in Fig. 13.20. The valve is an electrically activated valve which includes built-in pressure peak dampening. The maximum pressure is 140 bars and the maximum flow is either 30 or 60 L/min. The valve opening time with maximum pressure is 70 ms and the closing time is about 350 ms. On–off valves can be used for the positioning of a water hydraulic cylinder with a sophisticated control system.

3.2.2 Flow-Control Valves

The easiest way to control cylinder speed is to use flow-control valves. The speed of a hydraulic cylinder can be controlled easily with a pressure-compensated flow control valve. Especially in applications where the speed is the same in every working cycle, the correct flow can be adjusted beforehand for both directions. The direction control can be handled with separate arrangements, such as on–off valves. However, there are only a limited number of pressure-compensated flow-control valves suitable for use with tap water. One example is provided in Fig. 13.21.

3.2.3 Proportional Valves

Ball seat valves, as shown in Fig. 13.22, are quite commonly used as proportional tap-water valves. Ball seat valves have the advantage of small leakage and reliable operation. The manufacturing is also relatively easy because the parts can be designed to be very simple and advanced materials can be used. The balls, for example, may be constructed from stainless steel or industrial ceramics. Ball seat valves are available both as 2/2-way and 3/2-way versions. In the position servo system, the 4/3 function can be established with two pieces of 3/2 valves or four pieces of 2/2 valves.

The ceramic spool valve illustrated in Fig. 13.23 is the newest development in water hydraulic proportional valves. There are few spool valves available that can be used with tap water, although spool valves possess many advantages compared to other valve types. When used with water, the main problems in spool valves are high-leakage, high-flow forces, cavitation, and erosion caused by the high flow velocity. The spool and the housing sleeve is constructed from industrial ceramics and the outer housing is made of stainless steel. To achieve high pressures, low leakage rates, long lifetimes, and very fine manufacturing tolerances are necessary. These are also different design criteria and manufacturing technology requirements for ceramic materials compared to steel valves.

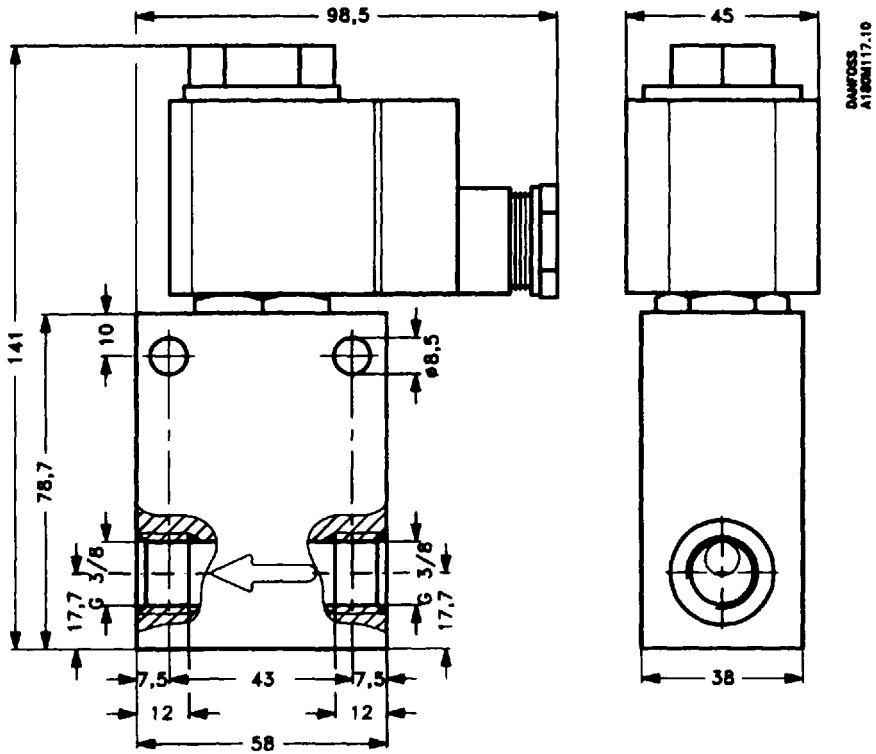


Figure 13.20 Electrically operated on-off valve (Danfoss).

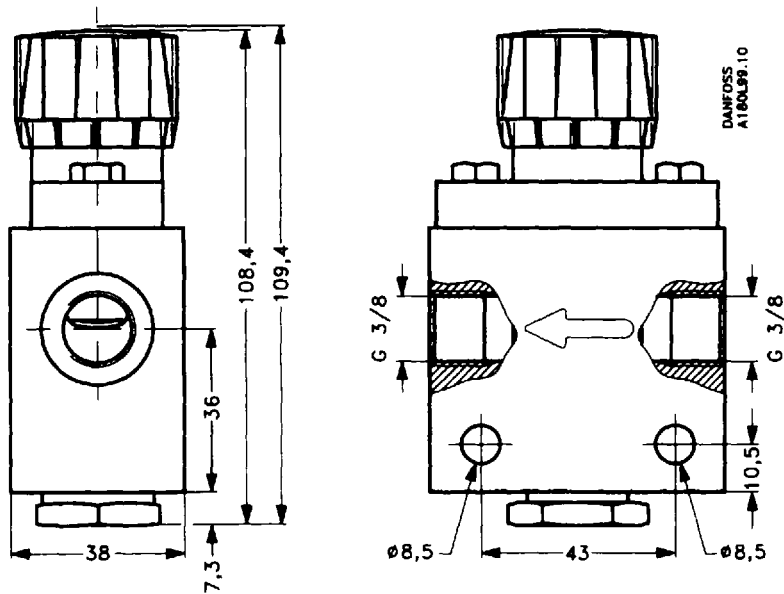


Figure 13.21 Manually operated flow-control valve (Danfoss).

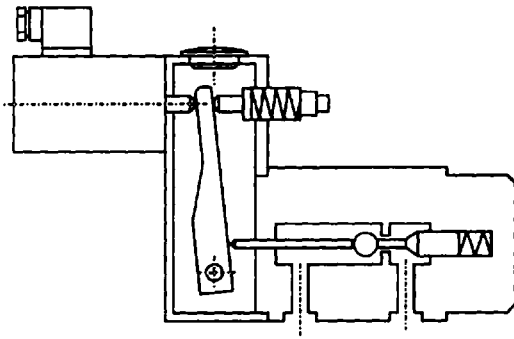


Figure 13.22 Proportional ball seat valve (Hauhinco).

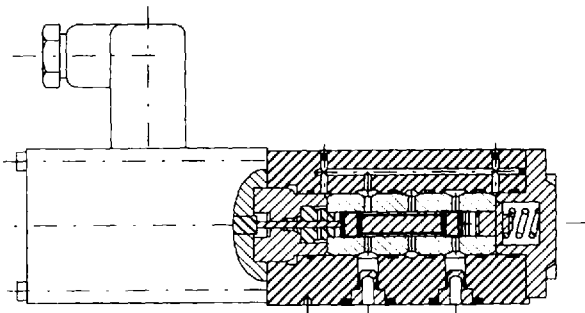


Figure 13.23 Proportional ceramic spool valve (Hauhinco).

3.2.4 Servo Valves

There are no commercially available servo valves especially designed for tap water currently available. Some manufacturers have stainless-steel versions of their normal oil hydraulic servo valves. The characteristics of these valves are guaranteed for HFA fluids, but are not necessary for tap water. Although these valves operate properly with tap water, their lifetimes are unknown because there is relatively little applications experience. The Ultra Hydraulics 4658 servo valve is illustrated in Fig. 13.24. According to the manufacturer, the stainless-steel version of the valve has been successfully tested with water, water–glycol, and HFA fluids. In TUT/IHA, 4658 servo valve performance is being tested in a servo system with success, but the durability test will be carried out in the future. The hysteresis of the valve is $<3\%$ and the threshold is $<0.5\%$. Null leakage of the valve at 140 bars supply pressure is 1.6 L/min. The opening and closing times from 0% to 100% at 210 bars are about 8 ms. These values have been measured with hydraulic oil. The characteristics with tap water are obviously slightly different, but these values are not yet available. This must be considered when designing a water hydraulic servo system. The Moog Sea Water Servo Valve shown in Fig. 13.25 is the only servo valve found to be originally designed to be used with water—in this case, seawater. The valve is a prototype valve, which is developed from standard Moog 26 servo valve. The valve has successfully tested with seawater, but it has not been put into the production yet.

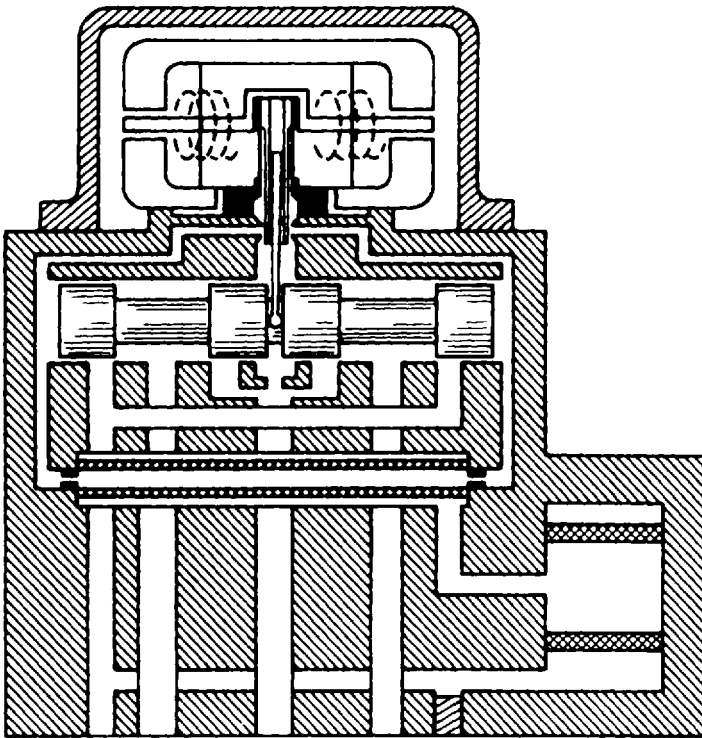


Figure 13.24 Stainless-steel servo valve (Ultra).

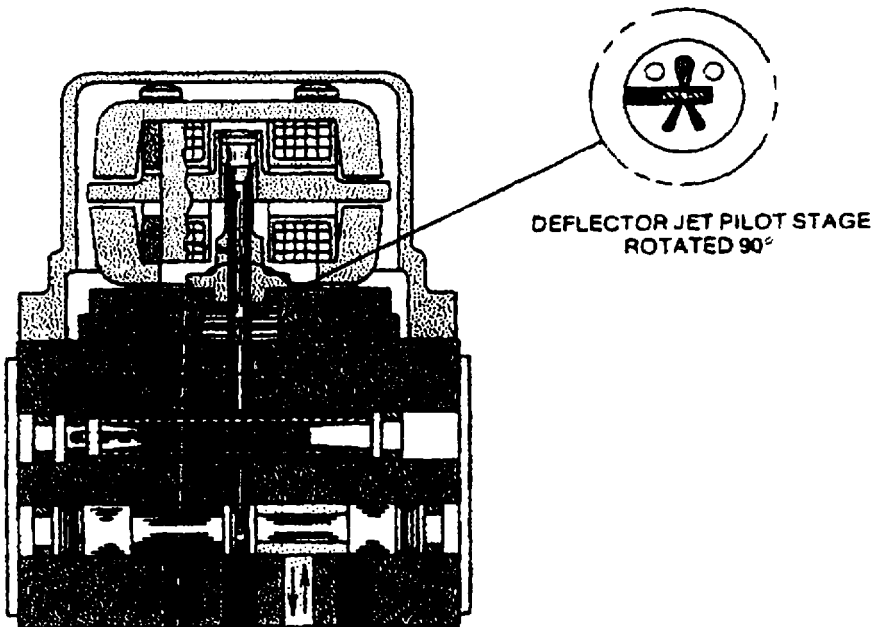


Figure 13.25 Seawater servo valve (Moog).

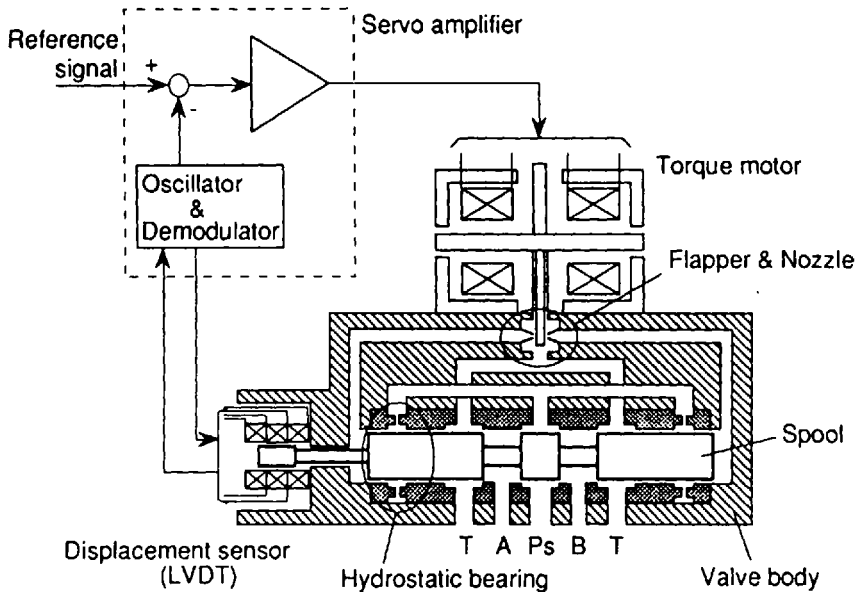


Figure 13.26 Water hydraulic servo valve (Ebara). (From Ref. 9.)

At present, there is only one manufacturer which provides servo valves originally designed for water use. These valves utilize a hydrostatic spool support on a servo valve spool (Fig. 13.26). Using this arrangement, the friction forces have been minimized and good linearity has been achieved.

3.3 Actuators

3.3.1 Cylinders

The variety of reliable water hydraulic cylinders is still quite limited. There are primarily two factors critical in manufacturing a water hydraulic cylinder: materials and seals. The materials have to be able to work with water, which is not the best possible lubrication fluid. Different types of stainless steel are most commonly used in the piston, rod, and cylinder tube. Ceramic materials and different surface coatings may also be used.

Materials selection for piston and piston-rod seals are also important when designing a water hydraulic cylinder. The seals must exhibit low-friction characteristics or the seal friction of the cylinder will be too high for high-accuracy applications. Excessive friction generates heat and increased wear reduces the lifetime of the cylinder. Normal materials used for these seals are Perbunan, PTFE, and PEEK.

The use pressure significantly affects the construction of the cylinder. The present commercial cylinders are designed primarily for 70–160-bar pressures. Higher-pressure cylinders, up to 310 bars, are custom constructed in most cases. When using lower pressures (10–50 bars), the cylinder construction is simplified and more plastic materials may be used. This will significantly affect the component cost. One example of a water hydraulic cylinder is illustrated in Fig. 13.27.

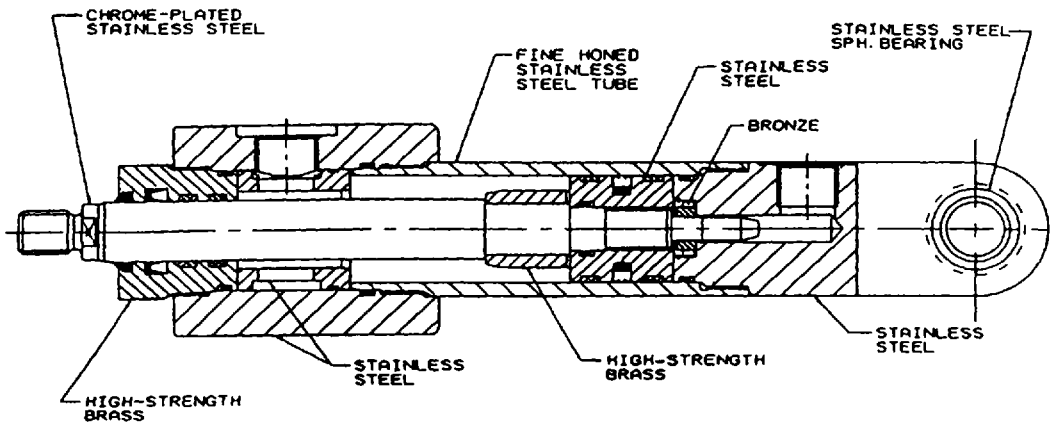


Figure 13.27 Water hydraulic cylinder (Parker Hannifin). (From Ref. 6.)

3.3.2 Motors

The use of tap water for hydraulic motors is still quite rare. Although some axial-piston-type motors have recently become available, there are only a limited number of choices with respect to size and operational parameters. Some motors are specifically designed to use tap water to lubricate moving parts. To minimize leakage against the inherent low viscosity of water, small clearances between moving parts and longer leakage paths are incorporated.

In Fig. 13.28, a recent design of an axial-piston motor is illustrated. The motor has been developed for tap water and seawater use. That means that the materials used are very carefully selected, because seawater is much more corrosive than tap water. The maximum pressure of the motor is 210 bars.

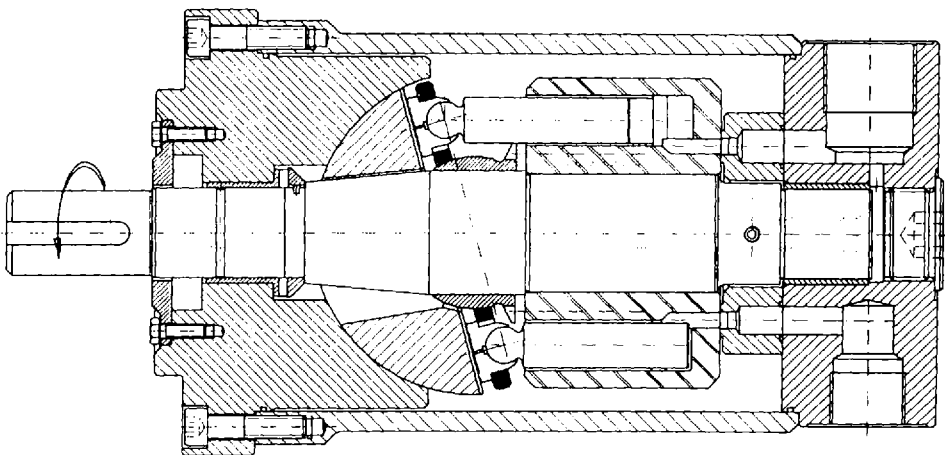


Figure 13.28 Water hydraulic axial-piston motor (Hytar).

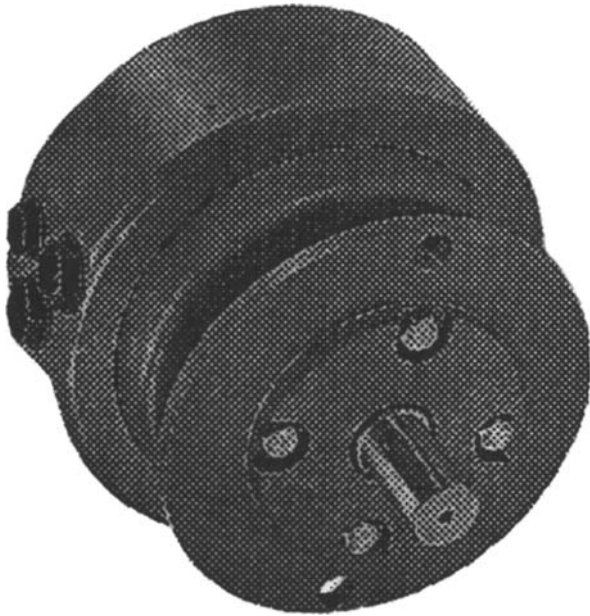


Figure 13.29 Water hydraulic vane motor (Danfoss). (From Ref. 10.)

The most recent water hydraulic motor development is the vane motor shown in Fig. 13.29. The motor is designed for maximum 50 bar pressure and the speed is between 10–200 rpm. The motor is bi-directional and the total efficiency is about 80%.

4 WATER HYDRAULIC APPLICATIONS

4.1 Water Injection in Large Diesel Engines [11]

In large diesel engines, high-pressure water is direct injected into the combustion chamber to reduce nitrogen oxides (NO_x). This is necessary because NO_x is the main pollutant coming from the diesel engines. Recently, both the international and local legislations have become more restrictive with respect to No_x emissions.

The principle of the injection system is shown in Fig. 13.30. High-pressure water is supplied by the power pack and injected via a separate needle to the combustion chamber. The pressure level is in the range 250–400 bars. The injection timing and duration is controlled by a separate rail valve, which controls the needle.

Under laboratory conditions, the water-injection system was tested and measured. The schematic of the hydraulic test system is presented in Fig. 13.31. Water pressure was generated by a water hydraulic power pack. The pressure level is about 400 bars. The seal oil pressure was generated by a small oil hydraulic power pack. Seal oil was used between the water part and oil part to prohibit mixing of the fluids. The control oil pressure was generated by a small oil hydraulic power pack with a pump. The orifice in the water line simulated the flow fuse in test measurements. The actual flow-fuse design parameters were obtained from the flow characteristics in the orifice. The electronic rail valve used was a fast-switching rail valve. The

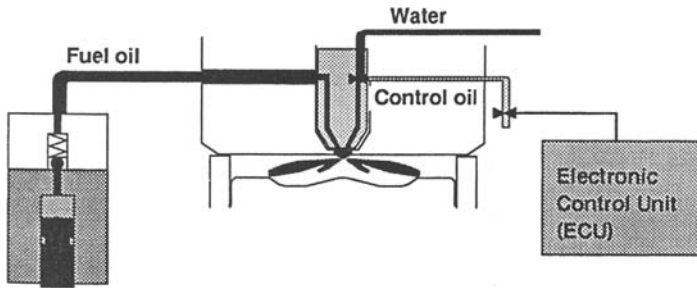


Figure 13.30 Water injection to the combustion chamber.

pressures from the both sides of the orifice were measured and, in addition, the control-oil pressure, seal-oil pressure, and water-injection pressure was measured. The needle lift was also measured.

The system was measured with many different variations of the accumulator pipe. The effect of the accumulator pipe between the orifice and injector was discovered to be essential for injection characteristics. The pressure drop in the accumulator pipe during the injection depends on the volume, shape, and material of the pipe. Also, the pressure pulsation occurring during the injection can be strongly affected by the design of the accumulator pipe.

The test system operation was also computer simulated. The model takes into account the dynamic behavior of the accumulator pipe without acoustic characteristics. In Fig. 13.32, the simulated and measured orifice flows and accumulator pipe pressures during the injection are shown. The flow through the orifice is about 20 L/min and the pressure drop during the injection is about 100 bars. The simulated

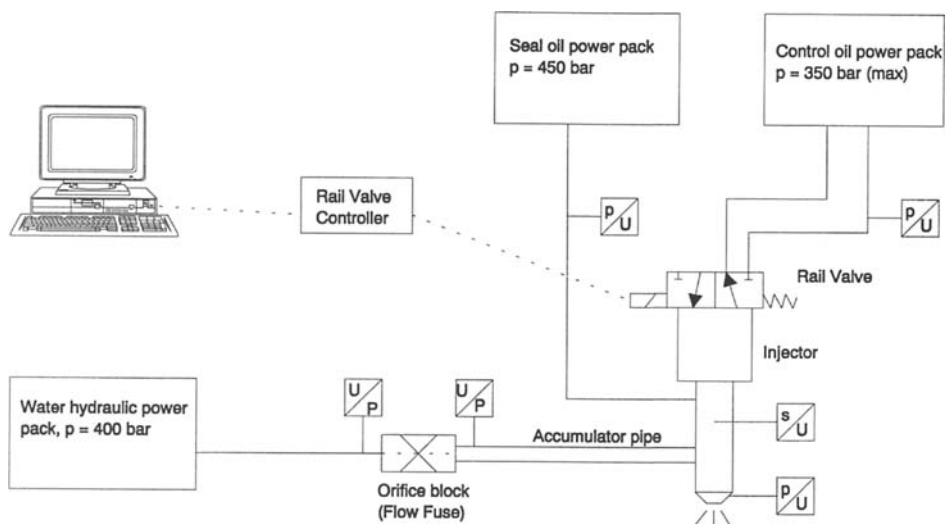


Figure 13.31 Schematic of the water-injection test system.

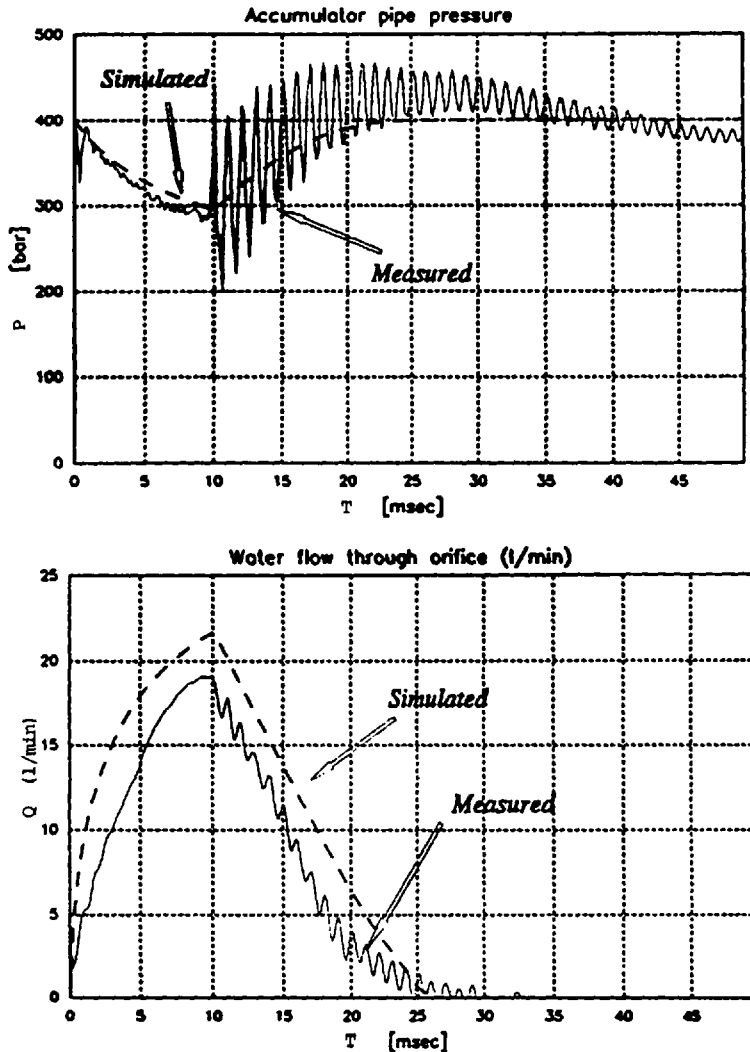


Figure 13.32 The accumulator pipe pressure and the orifice block flow of the test system.

curves correlate quite well with the measured curves if the acoustic pressure ripples are included.

In the high-pressure line before the injector, there is a flow fuse, which is a safety component that prevents water overflow to the diesel-engine combustion cylinder. The overflow is possible only in some kind of malfunction; for example, in the case of a needle sticking in the open position. In this situation, the flow fuse prevents the filling of the combustion chamber with water, which could cause failure. Normally, flow fuses are switch type, which receive the closing and opening signals from pressure difference over the fuse. The pressure difference corresponds to a certain flow rate through the flow fuse. Switch-type flow fuses exhibit stability problems and they are often very sensitive to pressure transients in the system.

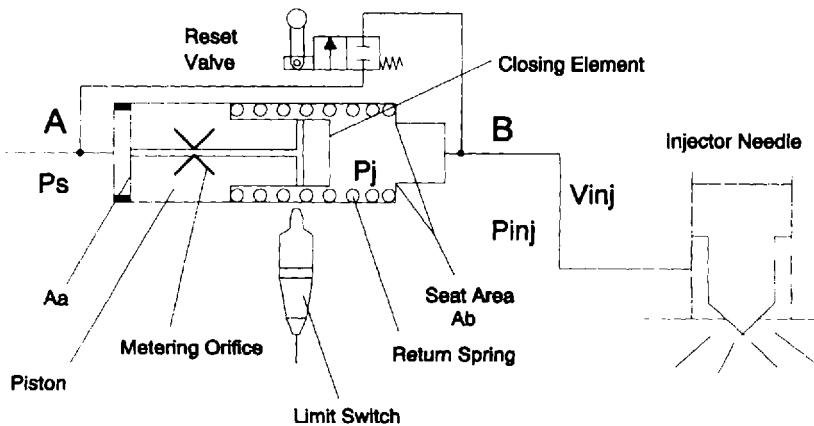


Figure 13.33 Schematic of the active-type flow fuse.

An active-type flow fuse (AFF) operates by a different principle than the switch type. The prototype of the AFF developed by IHA is provided in Fig. 13.33. AFF operates by a displacement principle. This means that in every injection, the piston moves and displaces a certain amount of water to the injector. In normal injection operation, the injected flow consists of the flow through the metering orifice and the flow displaced by the piston. The operation of the flow fuse is active because the displacement piston moves actively in every injection. When the injector needle stays open, the flow demand in the injector increases and the pressure P_{inj} decreases. In this situation, the piston moves the whole stroke and the closing element closes the fuse. The closing can be observed by the electrical switch. When the fuse closes, it also stays closed because the pressure forces are keeping the piston in its close position until the reset valve is opened.

One problem in direct water injection of a diesel engine is the pressure pulsation that occurs in the injector and pipe during the injection. The active-type flow fuse reduces the pressure pulsation because it displaces a specific amount of fluid in every injection. AFF efficiently reduces high-frequency vibrations and the supply pressure drop decreases. Therefore, the active-type flow fuse increases the injection volume and smaller piping dimensions can be used, which is an important factor in diesel-engine design.

From the simulation shown in Fig. 13.34, it is apparent that the pressure P_{inj} in volume V_{inj} is decreasing by about 30 bars and the flow-fuse piston is moving about 5 mm. The maximum stroke of the flow fuse is 10 mm. The pressure drop without the flow fuse was about 100 bars. The effect of the flow fuse on pressure ripple damping can also be shown in Fig. 13.34.

The situation when the needle is sticking in the open position is illustrated in Fig. 13.35. The pressure decreases until the flow-fuse piston reaches the other end and the flow fuse is closed and does not reopen until the reset valve is opened.

4.2 Water Hydraulic Pipe Crawler

The water hydraulic pipe crawler illustrated in Fig. 13.36 is a novel robot been developed for cutting roots from sewer pipes. Roots of trees and plants block sewer

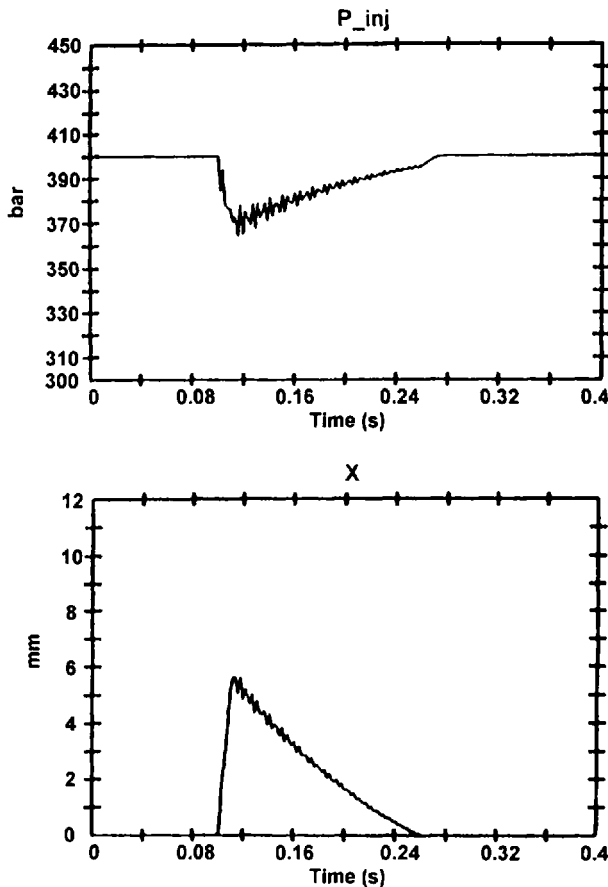


Figure 13.34 The pressure P_{inj} and the movement of the flow-fuse piston in normal injection.

pipes and without a pipe robot, the only repair possibility is to dig up the pipe. This is, of course, expensive. The crawler offers a less expensive and much quicker alternative for the job. Important characteristics for the crawler are environmentally friendly operation and reliability. The first crawler utilized a bio-oil as a power transmission medium; however, the newest version uses pure tap water.

The reliability is a result of the mechanical construction of the crawler. The crawler consists of five major components:

- Body with integrated traction control cylinder and gear box
- Water hydraulic motor
- Gear reducer
- Three drive chains
- Cutting-end mechanism

The water hydraulic motor rotates the cutting end via a gear reducer. The same power is also used to drive the three drive chains for traction. The integrated traction control

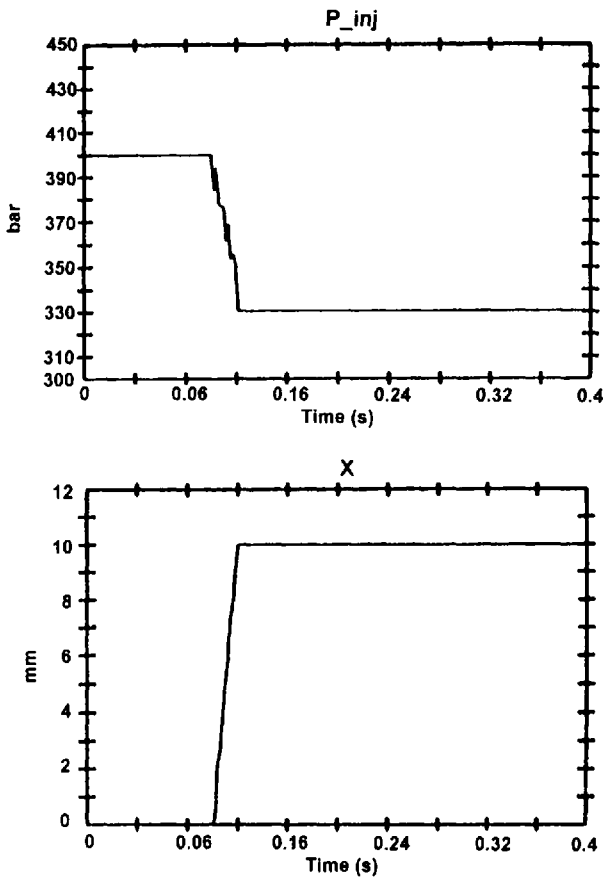


Figure 13.35 The pressure P_{inj} and the movement of the flow-fuse piston when the needle is stuck in the open position.

cylinder presses the drive chains against the pipe wall so that the crawler centers itself automatically in the pipe, as shown in Fig. 13.37.

Driving with forward traction is allowed when cutting, but reverse movement must be done manually or with a hose-reel hydraulic motor. The cutting end is able to rotate in both directions. A very important factor for the reliable operation of the crawler is the cutting-end mechanism, which is opened by centrifugal force. That means that when rotating, the cutting end contracts and sticking is avoided. Also, the spring-loaded traction-control cylinder contracts the drive chains and the crawler is easy to pull out from the pipe. The pipe crawler is also able to travel through overlapped joints because of the flexible traction control mechanism; this is shown in Fig. 13.38.

The technical values of the water hydraulic pipe crawler are as follows:

- Pipe size: 232–310 mm
- Maximum operation pressure: 140 bars
- Maximum water flow: 20 L/min

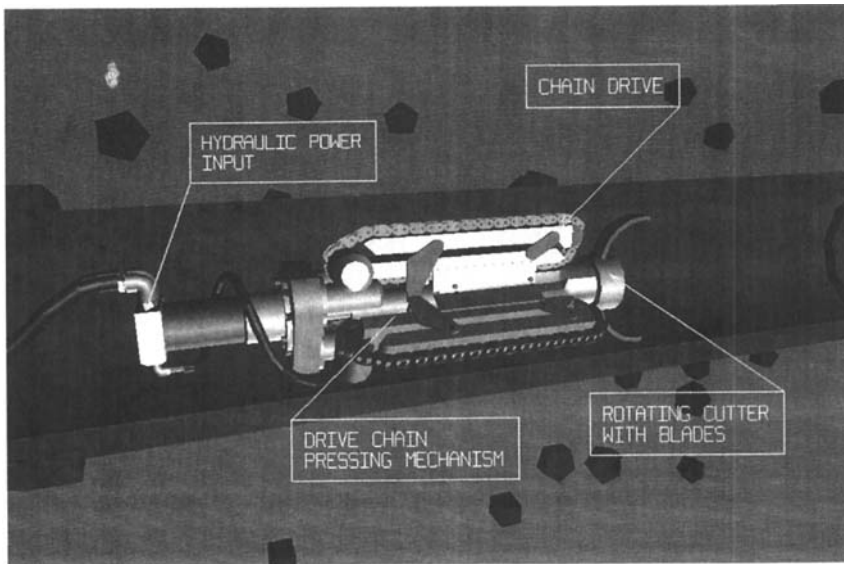


Figure 13.36 Water hydraulic pipe crawler.

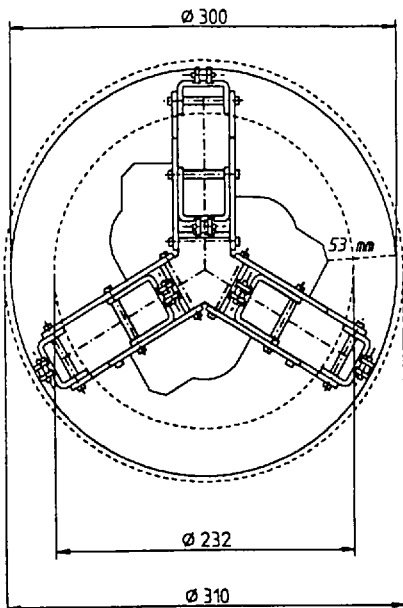


Figure 13.37 Illustration of automatically centered crawler within the pipe.

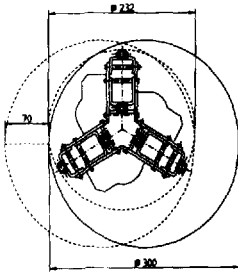


Figure 13.38 Pipeline joint overlapped.

- Maximum rotation speed of the cutting end: 700 rev./min
- Maximum torque with 110 bars: 35 N m
- Weight: 31 kg
- Length: 79 cm
- Hose length: 100 m

The water hydraulic system of the crawler consists of a hydraulic pump, hydraulic control valves, a hydraulic motor, and a hydraulic cylinder. All the water hydraulic components used are commercial components except the traction control cylinder and shuttle valve. The hydraulic control valves are illustrated in Fig. 13.39. Direction control valve DCV1 is acting as a bypass valve when the crawler is in the rest position. The operation pressures are adjusted by pressure relief valves PRV1 and

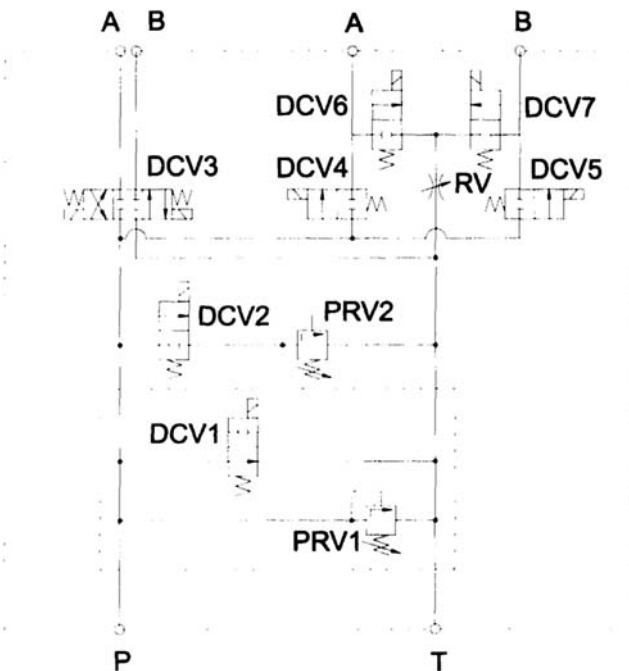


Figure 13.39 The hydraulic control valves of the crawler.

PRV2. PRV1 represents 100 bars and PRV2 represents 70 bars of operation pressure. Different operation pressures are controlled via direction control valves DCV1 and ACV2. Valve DCV3 is a control valve for a hydraulically operated hose reel. The direction control valves DCV4, DCV5, DCV6, and DCV7 are for the operation of the crawler. The restricting valve RV is building back pressure for the crawler's hydraulic motor. When controlling the resisting pressure, the pressing force of the drive chains can be adjusted. The pressure for the traction control cylinder is taken through the shuttle valve SV presented in Fig. 13.40. As there were no suitable commercially cylinder and shuttle valves, they were custom designed and manufactured.

In the development phase, the water hydraulic pipe crawler was tested and measured carefully under laboratory conditions. Also, the behavior of the custom-made components were tested separately. The operation was found to be very good and now the crawler is a commercial product of a Finnish company. There are also many possibilities for widening the application areas of the crawler, such as power plants and gas pipes as an inspection robot, cleaning of pipes in oil refinery, water supply network inspection, and so forth. In the future, the possibility of utilizing the pressure media in a pipe as an energy source of the crawler will be examined.

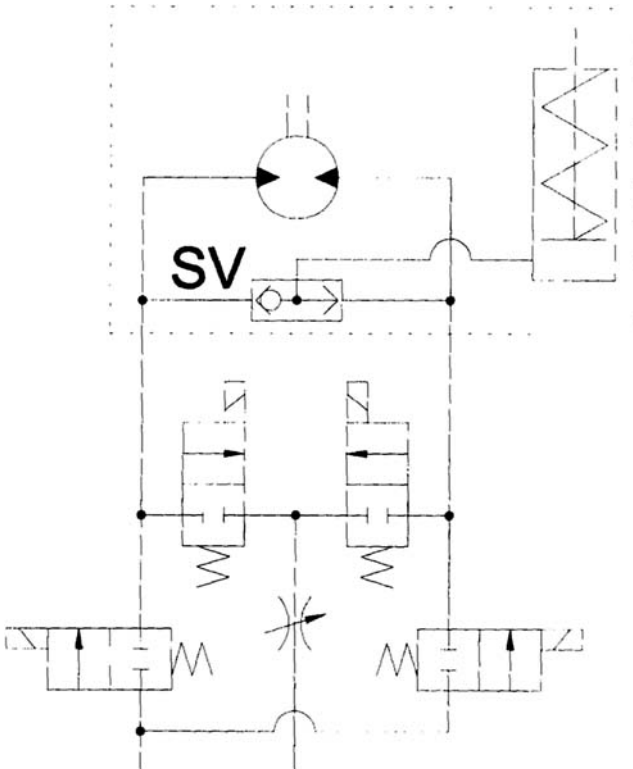


Figure 13.40 The operation of the traction control cylinder.

4.3 Water-Jet Cutting in the Paper Industry

Another new development for water hydraulics is a water-jet cutting system for paper machinery. The edge of the paper reel is usually trimmed by conventional mechanical knives. The problem is that because the knives wear, they must be changed frequently. An alternative is to use water-jet cutting. Using a high pressure (800–1000 bars), the edge can be trimmed quite sharply and without wearing parts. The system is presented in Fig. 13.41.

The critical part in the system is the pump producing the water hydraulic power. The lifetime and reliability must be very good because the system operates 24 h/day and service is allowed once a year. This provides high demands for the design and materials of the pump. A Dynaset pressure converter (Fig. 13.42) is now used as a pressure source [7]. The converter has a simple design, which makes it quite reliable. The converter is driven by oil pressure and the pressure ratio is about 4.

5 SUMMARY

Water is a very efficient pressure transmitter in a hydraulic system. Due to low compressibility and viscosity, a water hydraulic system contains more intrinsic energy than the same sized oil system. Thus, the dynamic properties of water systems in principle are faster than in oil hydraulic systems. For example, a servo system using tap water as a pressure medium is theoretically a faster system than an oil servo system, if only fluid compressibility is considered. However, the compressibility of component structures are also a major factor in the efficient bulk modulus of the servo system and, therefore, the actual difference is smaller. On the other hand, poorer lubrication and possible extra seals can make the coulomb friction higher, making dynamic properties worse. Internal leakage in the components also increases damping in the system, and cavitation and erosion have a more significant meaning in water hydraulics than in oil systems. In the future when component variety and quality improves along with developing design, material technology, and

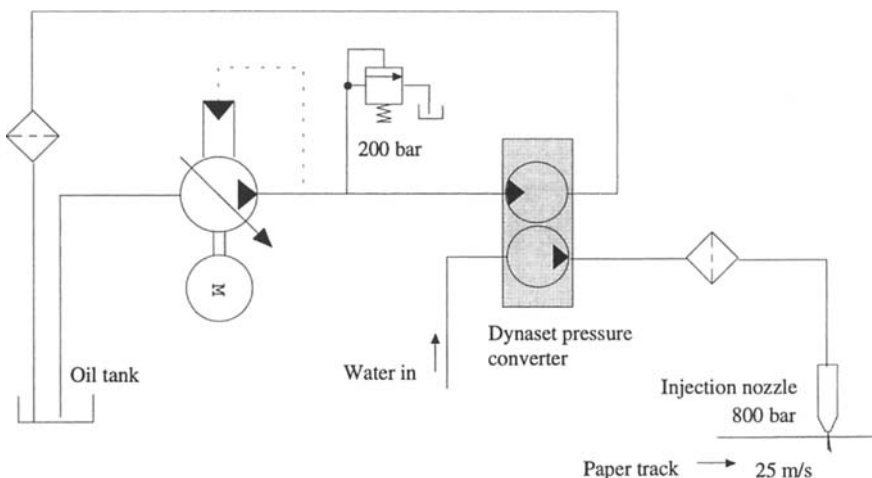


Figure 13.41 The operation of the water-jet cutting system.

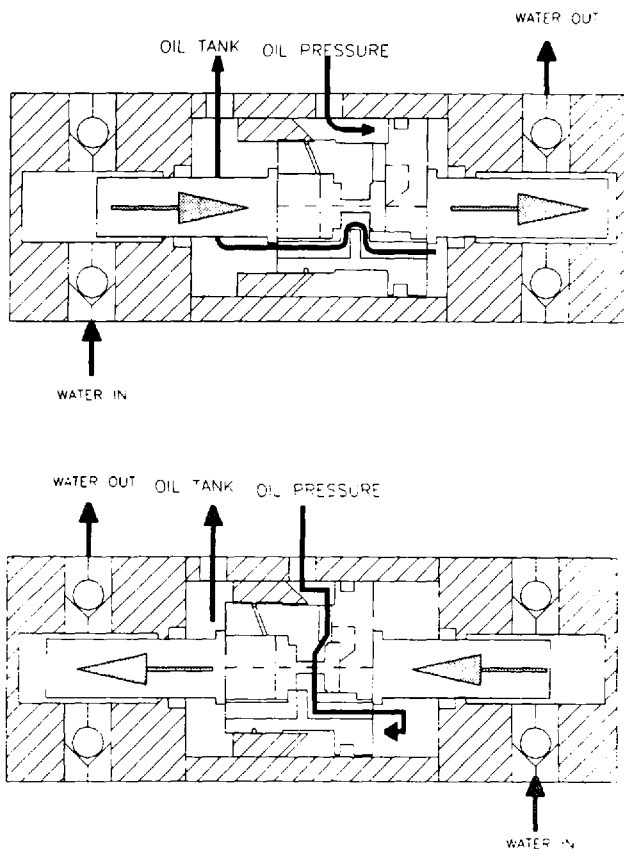


Figure 13.42 The operation of the Dynaset pressure converter. (From Ref. 7.)

control technology, the benefits of water as pressure a medium will be far better utilized in industrial applications.

The general component variety in water hydraulics is still quite poor compared to oil hydraulics and pneumatics. Due to the more difficult design, more expensive materials, and small production series, the price level of water hydraulic components is today quite high. This, of course, affects the willingness to apply water hydraulic technology in mechanical engineering. However, the market of water hydraulics is expanding slowly and the development of new, more intelligent but inexpensive components will probably accelerate the trend. Also, the introduction of low-pressure hydraulics in the market will open many new application areas for water hydraulics. Therefore, in the future, water hydraulics will offer an environmentally friendly, complementary alternative for the traditional power transmission methods: electrical drives, oil hydraulics, and pneumatics.

REFERENCES

1. K. Koskinen, "Proposals for Improving the Characteristics of Water Hydraulic Proportional Valves Using Simulation and Measurement," dissertation, Tampere University of Technology, 1996.

2. K. T. Koskinen and M. J. Vilenius, "Water as a Pressure Medium in Fluid Power Systems," in IFAC Workshop on Trends in Hydraulic and Pneumatic Components and Systems, 1994.
3. D. S. Miller, *Internal Flow Systems*, 1990 BHRA; Cranfield, Bedford, U.K.
4. N. L. Tao and W. F. Donovan, "Through-Flow in Concentric and Eccentric Annuli of Fine Clearance With and Without Relative Motion of the Boundaries," *Trans. ASME*, 1955, 77.
5. A. Ellman, K. T. Koskinen, and M. J. Vilenius, "Model for Steady State Flow in Circular Annulus. Automotive and Agricultural Applications of Fluid Power," in 1995 ASME Winter Annual Meeting, 1995.
6. E. Trostman, *Water Hydraulics Control Technology*, 1996, Marcel Dekker, New York.
7. R. Karppinen, "Dynaset HPW-Pressure Converter," in Fluid Power Theme Days in IHA, Water Hydraulics, 1997.
8. K. Koskinen, E. Mäkinen, M. Vilenius, and T. Virvalo, "Position Control of a Water Hydraulic Cylinder," in Araki, K. (ed). *Proceedings of the Third JHPS International Symposium on Fluid Power*, Yokohama '96, K. Araki, ed., 1996, pp. 43–48.
9. E. Urata, S. Miyakawa, and C. Yamashina, "Hydrostatic Support of Spool for Water Hydraulic Servovalves," in *The Fourth Scandinavian International Conference on Fluid Power*, 1995.
10. A. Adelstorp, "New Motor and Valves for Water Hydraulics," in Fluid Power Theme Days in IHA, Water Hydraulics, 1997.
11. D. C. Jay, O. A. Rantanen, and K. Koskinen, "Diesel engine—Combustion Control with High Pressure Water Injection," in *Proceedings of the Fourth Scandinavian International Conference on Fluid Power*, 1995, pp. 872–884.

Mineral-Oil Hydraulic Fluids

PAUL McHUGH

CITGO Petroleum Corporation, Tulsa, Oklahoma

WILLIAM D. STOFEY

American Ultra Specialties, Inc., Hudson, Ohio

GEORGE E. TOTTEN

Union Carbide Corporation, Tarrytown, New York

1 INTRODUCTION

Mineral-oil hydraulic fluids as a class are the most common hydraulic fluid used in the fluid power industry. In addition to their traditional use in fluid power systems, additional contributors to their dominant market position include low cost, availability, good viscosity and viscosity–pressure properties, excellent lubricity, suitability for high-temperature use, and metal and seal compatibility, and they do not promote corrosion. Disadvantages of the use of mineral-oil hydraulic fluids include flammability characteristics, potential biodegradability, and ecotoxicity problems where there is danger of leakage into underground aquifers, potential leakage into metalworking formulations, and generally poor viscosity–temperature properties when used over a broad temperature range [1].

In this chapter, the production, formulation, and properties of mineral-oil hydraulic fluids will be discussed. Specific subjects that will be addressed are mineral-oil composition and refining, hydraulic-oil classification, physical properties, chemical properties, an overview of additive chemistry, performance testing, biodegradability, compatibility, oxidative stability, and recycling.

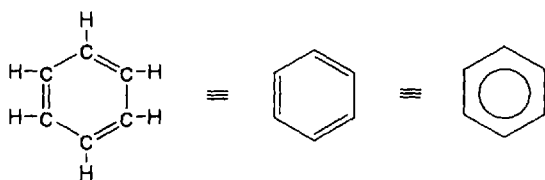
2 DISCUSSION

2.1 Petroleum-Oil Composition

Crude petroleum oil is a complex mixture of hundreds of compounds, including solids, liquids, and gases separated by refining. Solid components include petroleum

coke, asphalt bitumen, and inorganics. Liquids of increasing viscosity vary from gasoline, kerosene (paraffin oil), diesel oil, engine crankcase oil, light and heavy machine oil, and cylinder oils. Also included are methane, ethane, propane, and butane, the major components of natural gas, which are gases at room temperature [2].

Crude oils are classified as paraffinic, naphthenic, intermediate (mixed), or asphaltic as shown in Table 14.1 [2]. Paraffinic fractions are saturated linear or branched alkanes. Naphthenic fractions contain cyclic alkane (alicyclic) structures. Generic examples of typical chemical structures of these classes are illustrated in Fig. 14.1 [3,4]. Also included in Fig. 14.1 are aromatic (polyunsaturated cyclic) chemical structures, which are derived from benzene.



Aromatic components exhibit a greater tendency to form sludge and varnish than do paraffinic or naphthenic derivatives [5].

Paraffinic base oils contain 45–60% paraffinic compounds. Naphthenic base oils contain 65–75% of naphthenic compounds and aromatic base oils contain 20–25% aromatic compounds [3].

The relationship between molecular carbon content and density for paraffinic, naphthenic, and aromatic and density is summarized in Table 14.2 [2].

Aromatic asphaltic materials are classified as resins, asphaltines, or carbenes depending on their solubility [2]:

- Resins—pentane or heptane soluble
- Asphaltenes—pentane or heptane insoluble, benzene soluble
- Carbenes—benzene insoluble, carbon disulfide soluble

In addition to paraffinic, naphthenic, and aromatic derivatives, petroleum oils also contain heterocyclic (cyclic derivatives of nitrogen, sulfur, and oxygen) and other polar compounds such as carboxylic acids, usually saturated aliphatic or cycloaliphatic (naphthenic) acids, and aldehydes. Selected examples of polar derivatives that may be found in petroleum oils are illustrated in Fig. 14.2 [2–4]. Traces of phenolic and furan derivatives may also be present. A summary of the overall effect of these different derivatives on physical and chemical properties is provided in Table 14.3 [3].

Yoshida et al. have shown that the pro-oxidant effect of nitrogen heterocyclic compounds is a function of the basicity of the nitrogen in the compound. Generally, only the more basic nitrogen heterocyclic compounds, pyridine and quinoline derivatives, exhibit a pro-oxidant effect and this effect is accelerated in the presence of copper. The proposed mechanism involved a “ligand effect” through complexation with alkyl hydroperoxides [6].

The chemical composition of a petroleum base oil may be calculated from physical properties [refractive index (n_D^{20}) at 20°C, density at 20°C (d_4^{20}), percentage

Table 14.1 Crude Oil Content and Suitability

Crude type	Solvent neutral base oil	Base oil	Specialty oil	Wax content	S and N content ^a	Asphalt	API gravity ^b
Paraffinic base	Yes	Yes	No	Yes	Low	No	>40
Naphthenic base	No	Yes	Yes	No	Low	No	<33
Mixed base	No	Yes	No	Yes	Low	Yes	33–40
Asphaltic base	No	Yes	No	No	High	Yes	—

^aS is sulfur and N is nitrogen.

^bAPI gravity is scale in degrees adopted by the American Petroleum Institute where $^{\circ}\text{API} = [141.5/\text{specific gravity}] - 131.5$.


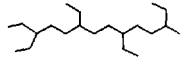
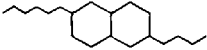
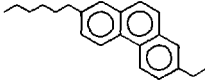
<u>Nomenclature</u>	<u>Structure</u>	<u>Viscosity Index</u>	<u>Pour Point</u>
n-Paraffins		Very high	High
iso-Paraffins		High	Low
Naphthenes		Moderate	Low
Aromatics		Low	Low

Figure 14.1 Typical organic structures present in a mineral oil.

sulfur concentration (S), and average molecular weight (M)] by ASTM D 3238, which describes the “ n - d - M Method” [7]. After determining these physical properties, the computations to be performed are as follows:

Step 1. Calculate the factors v and w

$$v = 2.51(n_D^{20} - 1.4750) - (d_4^{20} - 0.8510)$$

$$w = (d_4^{20} - 0.8510) - 1.1(n_D^{20} - 1.4750)$$

Step 2. Calculate percent aromatic carbon (C_A)

If v is positive:

$$\% C_A = 430v + \frac{3660}{M}$$

if v is negative:

$$\% C_A = 670v + \frac{3660}{M}$$

Step 3. Calculate percent total aromatic + naphthenic carbon (C_R)

If w is positive:

Table 14.2 Relationship Between Molecular Carbon Type and Density

Base oil type	Paraffinic carbon	Naphthenic carbon	Aromatic carbon	Density (kg/L)
Paraffinic	65–70	25–30	3–8	0.800–0.812
Naphthenic	50–60	30–40	8–13	0.834–0.844
Mixed	48–57	24–33	17–22	0.850–0.872
Aromatic	21–35	20–30	40–50	0.943–1.005

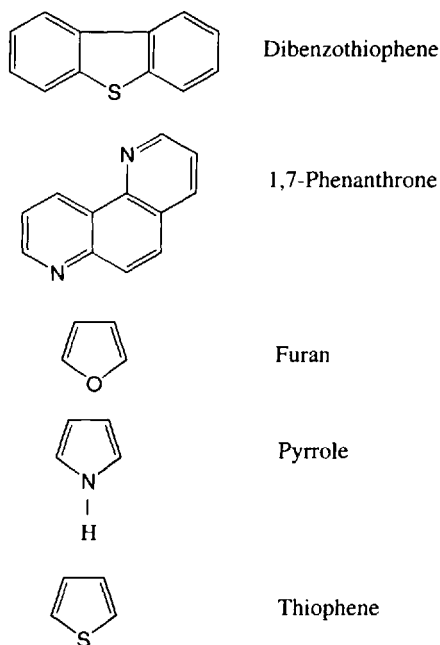


Figure 14.2 Illustration of heterocyclic derivatives typically present in a mineral oil.

$$\% C_R = 820w - 3S + \frac{10,000}{M}$$

If w is negative:

$$\% C_R = 1440w - 3S + \frac{10,600}{M}$$

Step 4. Calculate percent naphthenic carbon (C_N) and paraffinic carbon (C_P)

$$\% C_N = \% C_R - \% C_A$$

$$\% C_P = 100 - \% C_R$$

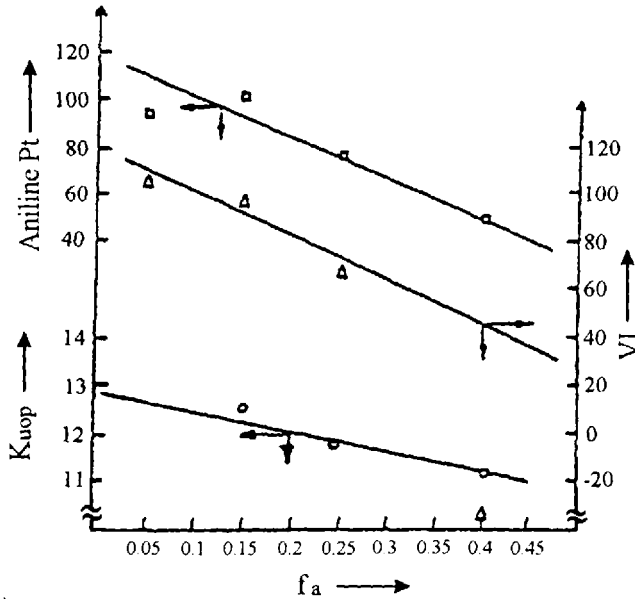
Figures 14.3a–14.3c illustrate the effect of C_A , C_R , and C_N on the viscosity index, aniline point, and volatility (K_{UOP}), respectively [8,9]. This work has shown that base-oil properties may be estimated from aromaticity, as aromaticity is primarily dependent on the degree of refining [8,10].

Two parameters that are important relate to polar compound composition and are reflective of base-oil quality are sulfur content and aniline point. The sulfur-containing polar compounds may exhibit significant antioxidant activity. Base oils containing low sulfur contents may require the addition of additional antioxidants.

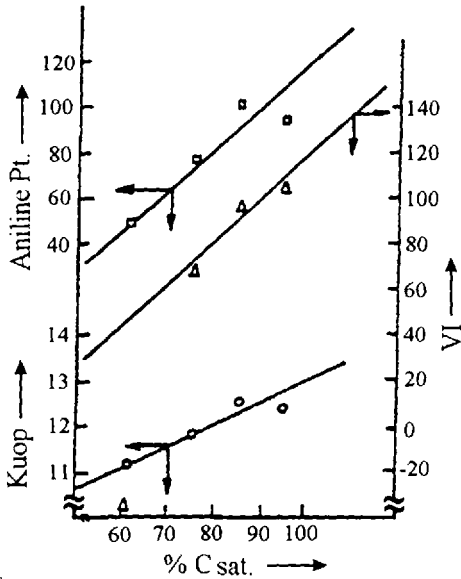
The aniline point is determined by mixing the base oil with the polar solvent aniline. The mixture is then heated until a homogenous solution is obtained, at which point the solution is cooled. The temperature at which the base oil separates from the solution is the aniline point. Increasing the paraffinic/naphthenic content increases the aniline point [3].

Table 14.3 Effect of Composition on Base Stock Properties

Chemical component	Viscosity index	Pour point (high/low)	Oxidative stability	Response to antioxidants	Volatility (high = poor, low = good)
<i>n</i> -Alkane	Very high	High	Good	Good	Good
iso-Alkane	High	Low	Good	Good	Good/average
Naphthene	Low	Low	Average	Good	Average
Aromatic	Low	Low	Average/poor	Some poor	Poor
Polar compounds	Low	Low	S is antioxidant; N and O are pro-oxidant	Poor	Poor



(a)

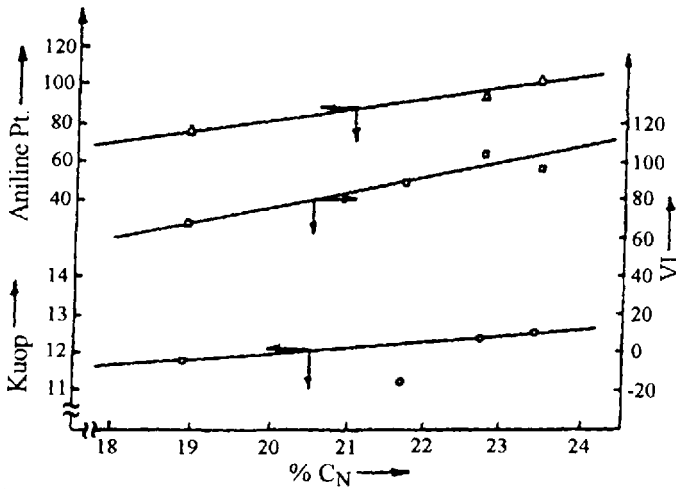


(b)

Figure 14.3 Effect of (a) aromatic, (b) naphthenic, and (c) paraffinic carbon content on viscosity index, aniline point, and volatility of a mineral oil.

2.2 Petroleum Refining Processes

Crude petroleum must be refined before it is used for lubricant formulation. In this section, distillation, deasphalting, solvent extraction, dewaxing, hydrofinishing, and hydrocracking processes will be introduced. Table 14.4 provides a general overview



(c)

Figure 14.3 Continued.**Table 14.4** Usual Effect of Processes on Base-Oil Composition and Properties

	Deasphalting	Refining	Dewaxing	Finishing
Constituent				
Asphaltenes	*	*	+	*
Resins	*	*	+	*
Aromatics	*	*	+	V
Naphthenes	+	V	+	V
Paraffins	+	V	*	+
Wax content	+	V	*	N
Nitrogen	*	*	+	*
Sulfur	*	*	+	*
Properties				
Specific gravity	*	*	+	V
Flash point	*	*	+	V
Viscosity	*	*	+	V
Viscosity index	+	+	+	V
Pour point	+	*	*	V
Color	*	*	*	*
Stability	+	+	V	+
Additive response	+	+	V	+

Note: * -- decreases; + -- increases; V -- variable; N -- no change.

of the impact of deasphalting, refining, dewaxing, and finishing processing on composition and physical properties [11].

2.2.1 Distillation

Distillation of crude oil is conducted in different steps (see Fig. 14.4) [4]. The first step is to remove inorganic salts. Then, after heating to approximately 350°C under pressure, an atmospheric distillation is conducted, at which point the most volatile components are fractionated in the distillation column. Typically, fractions including C1 to C4 hydrocarbons, gasoline, naphtha, and kerosene are removed at this point [2].

The next step is a vacuum distillation process conducted at 10–40 mm Hg or 20–100 mm Hg in combination with steam up to 450°C. The fractions removed by vacuum distillation include light, medium, and heavy neutral lubrication-oil fractions.

2.2.2 Deasphalting

A high-viscosity base oil may be removed from the residue remaining after distillation by a deasphalting process. A volatile, low-molecular-weight hydrocarbon, such as liquefied propane, is used to dissolve the bright stock, leaving an asphaltic residue (bitumen) behind.

2.2.3 Solvent Extraction

To improve physical properties, such as viscosity index and oxidative stability, solvent extraction is used to reduce the aromatic content of the base stock obtained after distillation, as shown in Fig. 14.5 [2]. Some naphthenic derivatives and other undesirable materials are also removed. Solvents used for the extraction process are miscible with aromatic derivatives and include phenol, furfural, and *N*-methylpyr-

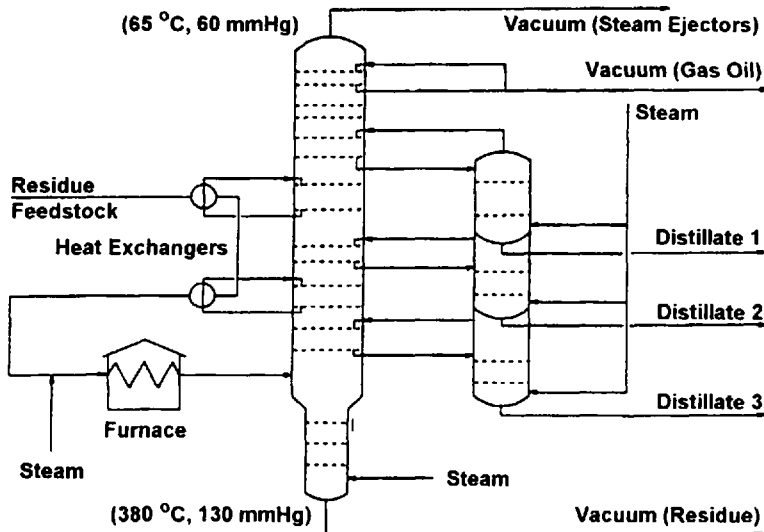


Figure 14.4 Vacuum distillation unit for lubrication oils.

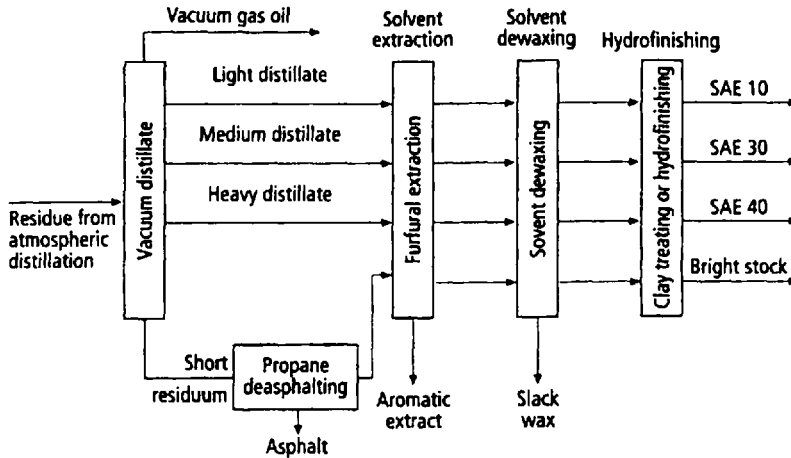


Figure 14.5 Simplified flowchart for solvent-refining process.

rolidone (NMP). Of these, furfural has traditionally been the more commonly used solvent [12].

2.2.4 Clay Treatment

Base-oil color and thermal stability can be improved by treatment with clay (or Fuller's earth) to remove polar compounds by adsorption [2].

2.2.5 Solvent Dewaxing

Cold-flow properties of paraffinic base oils may be improved by removal of waxy fractions in the oil. This is accomplished by the addition of a mixture of methyl ethyl ketone (or methyl isobutyl ketone) and toluene solvent, chilling, then removal of the insoluble waxes by filtration of the chilled mixture, and subsequent removal of the solvent from the remaining base oil [12].

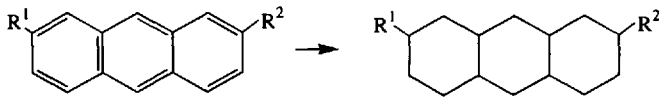
2.2.6 Hydrofinishing (Hy-Finishing)

The remaining polar compounds and further reduction in aromatic content of base oils may be accomplished by catalytic hydrogenation at an elevated temperature. This will produce a base stock with improved color and oxidative stability. Hydrofinishing has largely replaced clay treatment in most modern refineries [2], although in some refining processes, both hydrofinishing and clay treatment are performed [12].

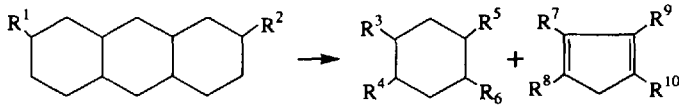
2.2.7 Hydrocracking

Hydrocracking is the most severe part of the base-oil refining process. Hydrocracking is conducted by heating a base oil/hydrogen mixture to 370°C at 20 MPa pressure and passing the mixture over a catalyst bed [2]. The exothermic hydrogenation reactions are cooled by hydrogen. Examples of hydrocracking reactions are provided in Fig. 14.6.

1. Aromatic Saturation



2. Ring Opening



3. n-Paraffin to iso-Paraffin Isomerzate



Other Reactions:

- a. Cracking
- b. Desulfurization
- c. Denitrogenation

Figure 14.6 Illustrative hydrocracking reactions.

During hydrocracking, large condensed aromatics are converted into more desirable hydroaromatics, the occurrence of cracking/dealkylation during hydrogenation leads to the formation of various carbonyl-containing compound, and significant denitrogenation and desulfurization results [13].

There is increasing interest in the use of hydrocracked base stocks in view of their improved viscosity, thermal stability, and biodegradability properties [14].

2.2.8 Commonly Used Terms in Petroleum for Petroleum Oils

The following definitions were taken from Ref. 2

Base stock or base oil. Oil produced in the refining process, before blending and without additives.

Bright stock. Fully refined and dewaxed, very high-viscosity lubricating oil produced from the residue (bottoms) of the vacuum-distillation column.

Cracking. Breaking down of large oil molecules into smaller, lower-viscosity, lower-boiling-point molecules. At the same time, some of the more reactive molecules combine (polymerize) to give even larger molecules, forming tar and coke.

Cylinder stock. The residue remaining after the lighter portions of the crude oil have been removed by evaporation.

Distillate. Product of oil distillation collected by vapor condensation.

Finishing. Chemical, solvent, and hydrogen refining processes for removing undesirable components and improving quality, stability, and appearance of the base oil.

Fraction or cut. The portion of a crude oil with a certain boiling-temperature range separated out in the distillation process, also applied to the part separated by precipitation, crystallization, and so forth.

Lubricating base oil. A range of hydrocarbons derived from atmospheric distillation of petroleum. They have high boiling points between 350° and 500°C, typically 25–35 carbon atoms per molecule and molecular weights between 400 and 550 (bright stocks 750). Corresponding viscosities would be 30 and 95 cSt (bright stock 400) at 40°C. A typical base oil would be composed of 70% paraffinic, 25% naphthenic, and less than 5% aromatic hydrocarbons. There would be traces of organosulfur, organonitrogen compounds, and oxygen compounds in the form of carboxylic acids.

Middle distillates. Boiling fractions from vegetable, animal, or synthetic oils.

Petrolatum (petroleum jelly). A mixture of oil and microcrystalline wax obtained from petroleum residue by propane precipitation. When purified into white petrolatum, the product is known as Vaseline® and is used in ointments and cosmetics.

Solvent neutral oil. Vacuum-distilled paraffinic base oil refined by solvent extraction containing no free acidity and has been dewaxed and finished ready for use in blending. Referred to as neutrals or SNO 40, 100, 150, 320, 850, and so forth, where the number refers to SUS (Saybolt Universal Seconds at 37.8°C). SNO 150 oils have viscosities of approximately 33 cS and SNO 850 approximately 190 cS at 40°C.

Wax. High-molecular-weight hydrocarbons that separate from oil when the temperature is lowered below the pour point. Paraffinic waxes are crystalline (see Fig. 14.7) [145], long, straight-chain, normal paraffins with 20–35 carbon atoms per molecule, molecular weights of 300–500, and melting points between 40°C and 70°C. Microcrystalline waxes with 35–75 carbon atoms per molecule and average molecular weights of 600–1000 are primarily branched-chain iso-paraffins with some naphthenic hydrocarbons. Melting points are between 55°C and 95°C [145]. Wax is the material in an asphaltene–resin-free oil which is insoluble in the solvent methyl ethyl ketone (MEK).

2.3 Oil Analysis and Characterization Procedures

There are a number of references concerning standardized testing procedures used to characterize petroleum products [15,16]. A detailed description of these procedures is beyond the scope of this text. There are also numerous references on newer analytical techniques that are being employed to both characterize specific chemical composition as well as the more traditional approach of characterizing paraffinic, naphthenic and aromatic content of the oil. Much of this work is focused on the correlation of base oil composition with various physical and chemical properties through the use of multiple regression equations. Selected examples will now be provided.

2.3.1 Nuclear Magnetic Resonance Spectroscopy

Both ¹HMR (proton magnetic resonance) and ¹³CMR (carbon magnetic resonance) spectroscopy have been used to examine structure–performance relationships of petroleum-oil base stocks [8,13,17]. Although most of this work has focused on the

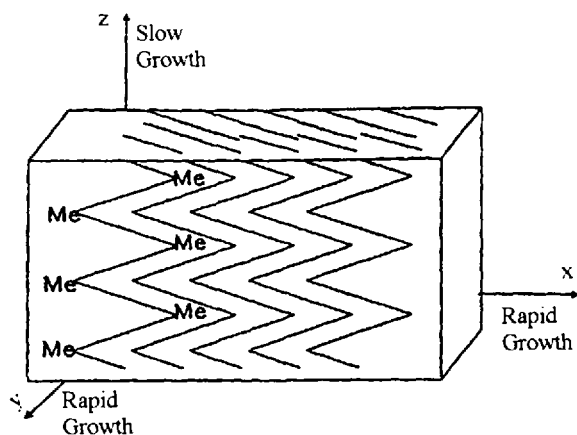


Figure 14.7 Wax crystal-growth pattern (Me = methyl group).

use of nuclear magnetic resonance (NMR) techniques to generically classify the paraffinic, naphthenic, and aromatic contents of oil for subsequent physical property studies, some work has been conducted to elucidate various chemical moieties in these very complex mixtures.

2.3.2 Fourier Transform Infrared Spectroscopy

Fourier transform infrared (FTIR) spectroscopy may also be used to assist in the relatively rapid characterization, compared to ^{13}C MR spectroscopy, of the aromatic content of a petroleum base oil [8]. Singh and Swaroop used FTIR to analyze the relative impact of aromatic carbon content on base-stock oxidative stability [18].

2.3.3 Thin-Layer Chromatography

Thin layer chromatography (TLC) using a flame-ionization detector (TLC-FID) has been used to quantitatively determine the ratios of paraffinic, naphthenic, aromatic, and polar components in a base oil [19]. It was proposed that this procedure was superior to the open-column gel chromatographic procedure of ASTM D 2007 [20].

2.3.4 Gel-Permeation Chromatography

Gel-permeation chromatography (GPC) analysis using a diode-array detector and a RI (differential refractance) detector was conducted which permitted fractionation, identification, and quantitative characterization of aromatic functionality in a petroleum oil [21].

2.3.5 Combination of Chromatography and Spectral Methods

Recent reports have described the successful use of the use of NMR or FTIR as a detector to structurally identify the eluents obtained by chromatographic analysis such as high-pressure liquid chromatography (HPLC) and NMR [22], and HPLC and mass spectrometry [23]. These analytical procedures provide a much finer discrimination of the chemical structures present in a petroleum base oil and/or structure-performance interdependence with respect to additive interactions and so forth.

3 HYDRAULIC OIL CLASSIFICATION

3.1 Classification by Oil Type

Mineral-oil base stocks used for hydraulic fluid formulation are either naphthenic or paraffinic [24]. Mixed-base fluids are also available [25]. Naphthenic base stocks contain a high percentage of ring-containing cycloaliphatic compounds. Typically, these fluids exhibit relatively low viscosity indices and, therefore, are not useful for applications where wide use-temperatures will be encountered. These oils exhibit relatively low pour points. Generally, their maximum use-temperature is 150°C. These fluids are available in a full range of viscosities, exhibit good demulsifiability characteristics, and are resistant to foaming [24].

Paraffinic oils contain a high percentage of straight- and branched-chain aliphatic compounds. These fluids exhibit higher viscosity indices than naphthenic oils and, therefore, are more suitable for use at higher temperature. These oils exhibit somewhat higher pour points than naphthenic oils. When adequately stabilized, paraffinic hydraulic fluids may be used continuously at temperatures up to 140°C [24].

Mixed-base oils, also referred to as intermediate-viscosity-index oils, which are blends of naphthenic and paraffinic base stocks are also available. They may be used at either high or low temperatures, although they do not exhibit the best features of either of their component oils [25].

3.2 Classification Based on Additives

Hydraulic oils may also be classified based on the additive protection that they offer [25]. These include rust and oxidation (R&O), antiwear (AW), extreme pressure (EP), antileak, ashless, and industrial detergent oils.

R&O hydraulic oils may be formulated with naphthenic, paraffinic, or mixed-base oils. Additives are added to provide rust and antioxidant protection.

Antiwear oils may be formulated with naphthenic, paraffinic, or mixed-base oils. They may also contain R&O inhibitors. They will contain an antiwear additive such as ZDDP (zinc dialkyldithiophosphate), which provides additional antiwear protection for metal parts in the hydraulic system.

Extreme-pressure (EP) fluids are formulated to provide lubrication to both the hydraulic system components and the machine–tool ways to prevent stick–slip operation. Typically, these fluids only offer antirust protection without antileak, antioxidant, or viscosity-index (VI) improvers [25].

Antileak oils are used to reduce fluid leakage by assuring seal pliability. Although these oils may be suitable for low-temperature start-up, they are not generally suitable for high-temperature use.

Industrial detergent oils are used in mobile equipment and robotic applications which are subjected to a dirty environment. These fluids are typically formulated to provide R&O protection, to exhibit a high viscosity index, and to be suitable for use over a broad range of temperatures.

Ashless hydraulic oils are typically formulated without a zinc-containing additive and do contain phosphorus-, nitrogen-, and sulfur-containing additives for antiwear performance. This is an emerging area of hydraulic fluid technology.

A comparison of the advantages and disadvantages of these oils is provided in Table 14.5 [25].

Table 14.5 Selection Chart for Hydraulic Oils and Fluids

System requirements	Straight naphthenic	Straight paraffinic	R&O quality + antiwear, paraffinic	R&O less-than-turbine quality, paraffinic base	R&O less-than-turbine quality, paraffinic base	R&O + antiwear detergent, paraffinic base	Antileak, naphthenic base	Antileak & antiwear, naphthenic base	R&O quality + antiwear naphthenic base	Combination way lube & hydraulic oil
Normal service life			X	X		X	X	X		
Long service life			X	X	X	X	X	X	X	X
Antirust and corrosion			X	X	X	X	X	X	X	
Exceptional antiwear			X			X		X		
Antifoam properties	X	X	X	X	X	X	X	X	X	X
High-temperature operation			X	X		X				
Low-temperature start-up	X									
Continuous contamination, extraneous materials	X					X				
Continuous contamination, cutting fluids, with frequent changes	X									
Moderate leakage		X					X	X	X	
Excessive leakage	X						X	X		
Tight system, little or no makeup			X	X	X	X			X	
Active filter use	X	X								X
Inactive filter use	X	X	X	X	X	X	X	X	X	X
Way lubrication by hydraulic oil									X	
High degree of water separation	X	X	X	X						
Hydraulic system cleaner						X				

*Will handle noncritical way lubricant.

3.3 Classification Based on Viscosity

Hydraulic fluids may also be classified according to ASTM D 2422 "Viscosity System for Industrial Fluid Lubricants" [2,26]. The viscosity classification system is provided in Table 14.6. This classification system only provides information on the viscosity at 40°C. Viscosities at other temperatures are dependent on the viscosity-index properties of the fluid.

3.4 ISO 6743/4 Mineral Oil Classification System

Mineral oils may also be classified according to an ISO system which is based on the properties exhibited by the fluid [27,28]. The ISO classification categories are provided in Table 14.7.

3.5 Brief Historical Overview and System Requirements

Table 14.8 provides a time line for critical developments in hydraulic fluid technology since 1920 [29]. Although past problems have been successfully addressed, from this table, it is evident that fluid formulation and performance continue to provide significant challenges for the hydraulic fluid industry.

4 PHYSICAL PROPERTIES

Knowledge of the physical properties of a hydraulic system is important in the design and operation of a hydraulic system. These properties include viscosity, viscosity

Table 14.6 ASTM D 2422 Viscosity Classification System

ISO viscosity grade	Kinematic viscosity limits [cSt (mm ² /s)] at 40°C		
	Midpoint	Minimum	Maximum
ISO VG 2	2.2	1.98	2.42
ISO VG 3	3.2	2.88	3.52
ISO VG 5	4.6	4.14	5.06
ISO VG 7	6.8	6.12	7.48
ISO VG 10	10	9	11
ISO VG 15	15	13.2	16.5
ISO VG 22	22	19.8	24.2
ISO VG 32	32	28.8	35.2
ISO VG 46	46	41.4	50.6
ISO VG 68	68	61.2	74.8
ISO VG 100	100	90	110
ISO VG 150	150	135	165
ISO VG 220	220	198	242
ISO VG 320	320	288	352
ISO VG 460	460	414	506
ISO VG 680	680	612	748
ISO VG 1000	1000	900	1100
ISO VG 1500	1500	1350	1650

Note: If 40°C is not the temperature used when measuring the viscosity (as is sometimes the case with very viscous fluids), then the related viscosity at 40°C shall be established using ASTM D 341.

Table 14.7 ISO 6743/4 Mineral Oil Classification System

Category	Composition typical properties	Applications operating temperatures
HH	Noninhibited refined mineral oils	-10°C to 90°C
HL	Refined mineral oils with improved antirust and antioxidant properties	-10°C to 90°C
HM	Oils of HL type with improved antiwear properties	General hydraulic systems which include highly loaded components -20°C to 90°C
HR	Oils of HL type with improved viscosity/temperature properties	-35°C to 120°C
HV	Oils of HM type with improved viscosity/temperature properties	Mobile applications, -35°C to 120°C
HS	Synthetic fluids with no specific fire-resistant properties	-35°C to 120°C

index, pour point, compressibility, gas solubility, and foaming, in addition to various thermal and electrical properties [2,30]. In this section, the specific importance of these physical properties will be described.

4.1 Viscosity

Viscosity is the single most important physical property exhibited by a hydraulic fluid. If the hydraulic fluid viscosity is too high, the following can occur: (1) the internal friction will increase, which will increase the flow resistance through the clearances in the pump and valves; (2) the system temperature will increase; (3) the system operation will become sluggish; (4) there will be an increased pressure drop in the system; (5) power consumption will increase. If the fluid viscosity is too low, the following can occur: (1) the internal and external leakage will increase; (2) pump

Table 14.8 History of Hydraulic Fluids

Years	Type of hydraulic fluid	Remarks
1920	Water based	Restricted working temperature, rust/corrosion problems
1920	Plain mineral oils	Gum formation, acidity buildup resulting in corrosion
1940	R&O oils	Wear problems with vane pumps of sophisticated design, output of 1000 psi
1950	Motor-oil based	Excellent wear protection, poor demulsibility
1960	Conventional ZDDP-based oils	High wear of bronze piston shoes
1970	Thermally stable ZDDP-based oils	Meeting all international specifications
Latest trends	Ashless (S-P-N)-based oils	Work continuing

slippage will increase reducing efficiency and increasing temperature; (3) the wear rate will increase, (4) a loss of pressure will occur; (5) there will be a loss of pressure control [31].

The maximum fluid viscosity for proper pump operation is dictated by the hydraulic pump design and is therefore manufacturer-specific. Some general guidelines are provided in Table 14.9. Pump manufacturers publish minimum and maximum specifications for their pumps [32–34]. These specifications typically include minimum, optimum, maximum, and maximum start-up viscosity [32]. An illustration of a viscosity-recommended viscosity–temperature chart for a hydraulic oil is provided in Fig. 14.8 [32].

4.2 Viscosity Index

The viscosity will vary with temperature and that variation is dependent on oil composition, which was illustrated in Chapter 4 (Fig. 4.9) for paraffinic and naphthenic oils. The magnitude of viscosity–temperature variation is quantified by the use of a single number—VI or viscosity index. The calculation of VI from viscosity–temperature data is illustrated in Chapter 5. The lower the VI, the greater the variation of viscosity with temperature. Most pump manufacturers recommend that the VI of a hydraulic oil be at least 78, or greater [33,34]. The VI value of an oil is especially important because it determines the temperature range over which the oil may be used.

4.3 Viscosity–Pressure Behavior

A general property of fluids is that they exhibit an increase in viscosity with increasing pressure and the viscosity increase will be greater at higher pressures than lower pressures [31]. In addition, the viscosity increase with pressure will be greater for naphthenic oils than paraffinic oils (see Fig. 4.9). The effect of increasing pressure increases as the fluid viscosity increases, and fluid pressure increases will also increase the VI index of the oil [31]. Although the fluid viscosity increases with increasing temperature, this effect is usually not significant up to system pressures of 2000 psi [24].

Table 14.9 Recommended Maximum Inlet Viscosities for Different Types of Hydraulic Pumps^a

Pump type	Maximum inlet viscosity (mm ² /s, cS)
Gear pumps	2000
Piston pumps	1000
Vane pumps	500–700

^aThese are only general recommendations. They will vary with specific pump design and the manufacturer of the pump.

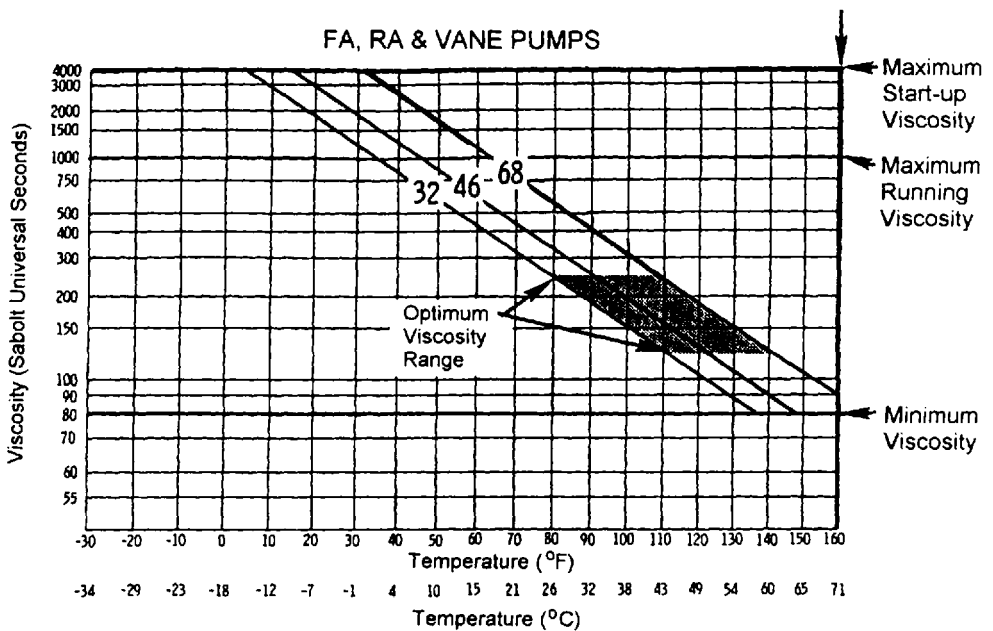


Figure 14.8 Vane-pump viscosity recommendation chart for Racine FA, RA, and K vane pumps.

4.4 Compressibility and Bulk Modulus

Fluid compressibility (bar^{-1}) is defined by

$$\beta = -\frac{1}{V} \left(\frac{dV}{dP} \right)$$

where

β = the fluid compressibility

V = the initial volume

P = fluid pressure

Another term, compressibility module (M) or bulk modulus, is occasionally used [30]:

$$M = \frac{1}{\beta}$$

where M is reported in pressure units of bar. The effect of pressure and temperature on relative volume of a mineral oil (D.T.D. 585) is illustrated in Fig. 14.9 [35]. Comparison of isentropic and isothermal bulk moduli as a function of temperature is illustrated in Fig. 14.10.

4.5 Estimation of Relative Cavitation Potential from Rho-C Values

One method that has been used to estimate the potential for cavitation is the “rho-c value” or “acoustical impedance.” The isentropic bulk modulus (M_i) is related to the velocity of sound (c) through the fluid and density (ρ) by

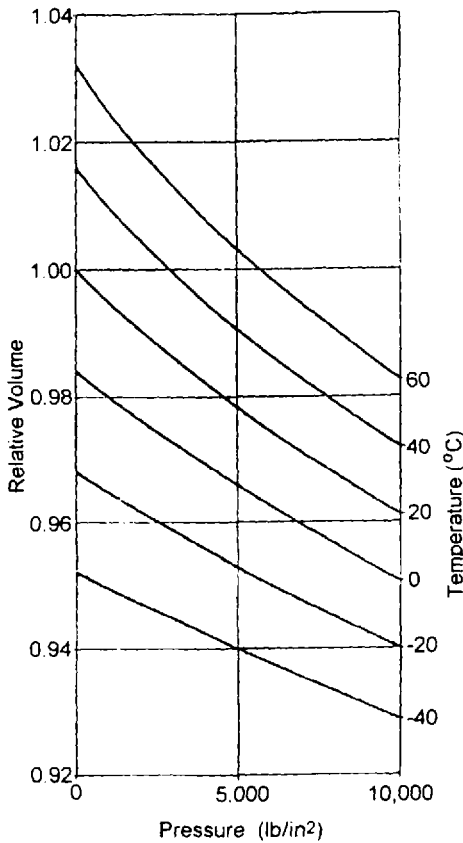


Figure 14.9 Effect of temperature and pressure on relative volume.

$$M_t = \rho c^2$$

Generally, the potential for a fluid to cavitate increases with the rho-c value [30,36]. Figure 14.11 illustrates the effect of pressure and temperature on sound velocity in a hydraulic fluid [30].

4.6 Gas Solubility

The amount of dissolved gas in a fluid is related to the fluid pressure (P) and the solubility (Bunsen) coefficient (α) of the gas by

$$V_{\text{gas}} = V_{\text{liquid}} \alpha P$$

Table 14.10 provides Bunsen coefficients for a mineral oil at 0°C, 50°C, and 100°C [30]. Details of the use of Bunsen coefficients and other calculation procedures to determine gas solubility are provided in Chapter 4.

4.7 Foaming

Foaming, as illustrated in Fig. 14.12, may arise from various sources, including fluid contamination, poor reservoir design, and the formation of metallic soaps such as

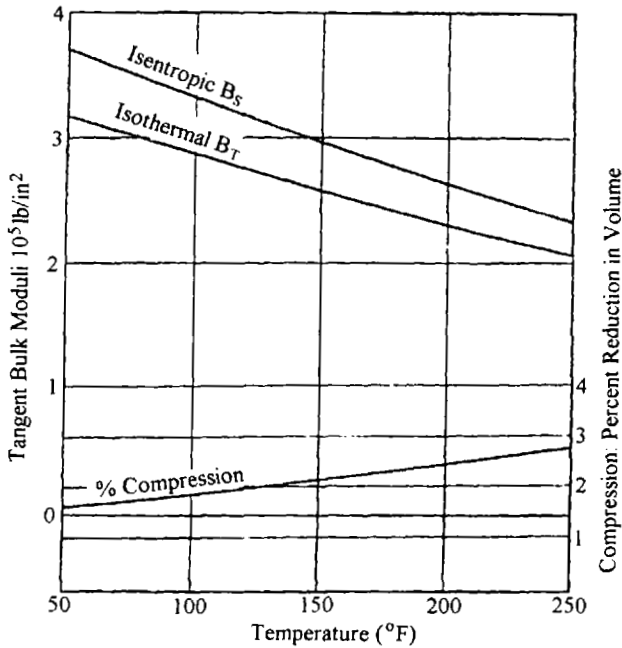


Figure 14.10 Isoentropic and isothermal tangent bulk modulus for a typical Shell Tellus oil at 5000 psi.

might be formed from the corrosive reaction of additives in the fluid with lead coatings [35]. The propensity for foaming is measured according to ASTM D 892 [37]. In this test, air is injected into the hydraulic fluid at a constant temperature through a gas-diffusion stone at a constant rate, as illustrated in Fig. 14.13. The foam height is measured immediately at the conclusion of the fluid aeration period and

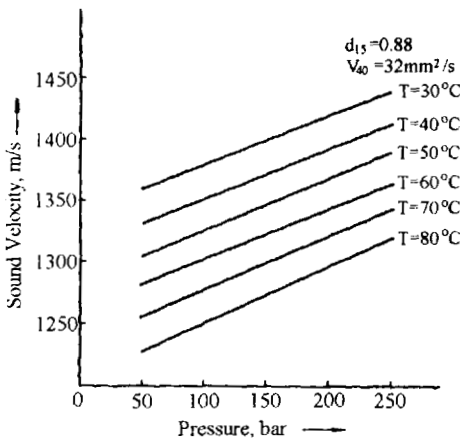


Figure 14.11 Sound velocity as a function of temperature and pressure (ISO 32 mineral oil).

Table 14.10 Bunsen Coefficients for Different Gases in Mineral Oil as a Function of Temperature

Gas	Bunsen coefficient ^a (α)		
	0°C	50°C	100°C
Air	0.092	0.091	0.091
Oxygen	0.150	0.137	0.130
Nitrogen	0.081	0.088	0.090
Hydrogen	0.047	0.053	0.067
Carbon dioxide	1.000	—	—

^aHigher values of α are obtained with low-viscosity fluids.

again after 10 min of standing unagitated. The foam retention characteristics, measured in millimeters, are proportional to the propensity for foaming.

4.8 Air Entrainment

When the concentration of air exceeds the saturation level, the gaseous bubbles are suspended in the hydraulic fluid. Air entrainment must be minimized for proper fluid performance in the hydraulic pump. Air entrainment properties of a hydraulic fluid may be determined according to ASTM D 3427 [147]. In this test, air is blown into the fluid through a gas inlet at the bottom of a glass vessel at a constant flow rate

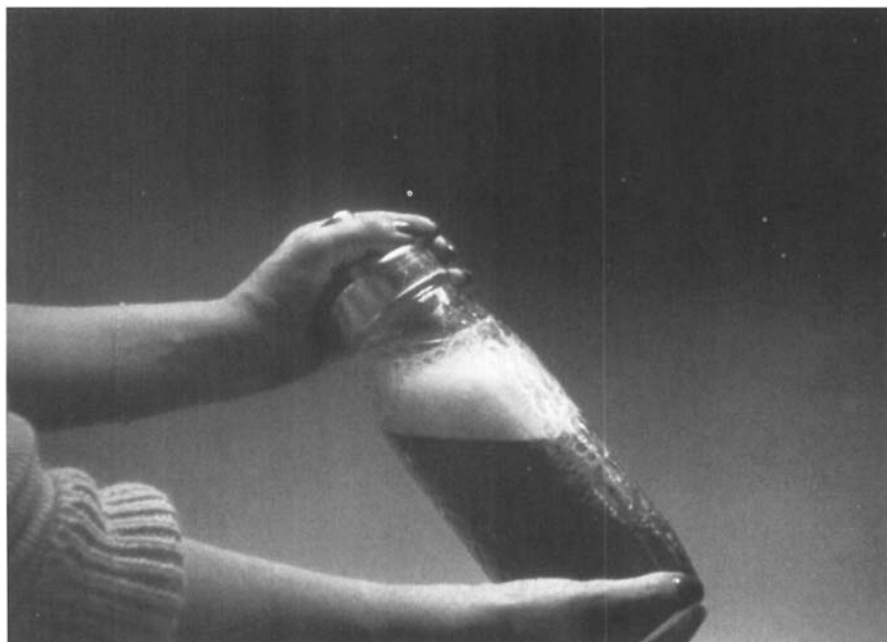


Figure 14.12 Hydraulic oil foam formation. (Courtesy of CITGO Petroleum Oil Company.)

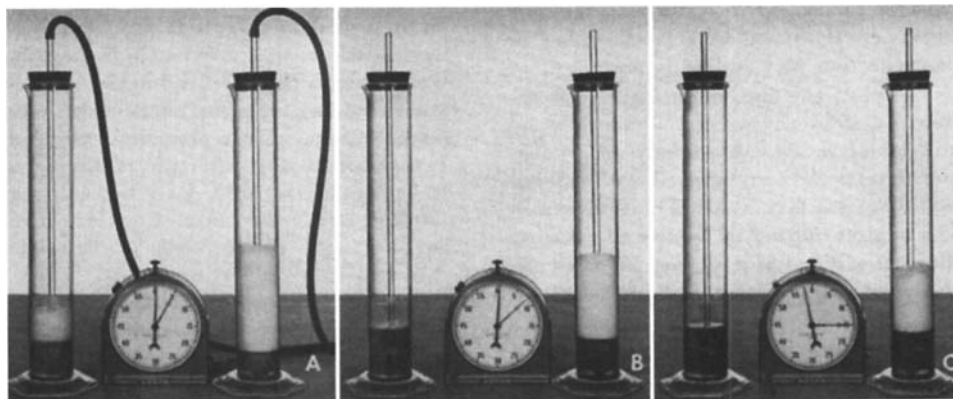


Figure 14.13 Illustration of ASTM D 892 foam stability test to measure foam formation, stability and effectiveness of antifoam addition. (Courtesy of Texaco Inc.)

and fluid temperature for 7 min. The change in fluid density relative to the starting fluid condition is recorded until the total volume of entrained air is equal to 0.20% of the original volume. The time required to obtain this volume is the “gas-separation time.”

4.9 Density

Fluid density at a given pressure (ρ_p) is determined from [30]

$$\rho_p = \frac{\rho}{100 - \Delta V_p}$$

where ρ is the density at atmospheric conditions and ΔV_p is the volumetric change with increasing pressure (P).

The density of mineral oils may also be represented as °API which is defined as [38]

$$\text{Degrees API} = \frac{141.5}{\text{Sp. Gr. @ } 15.6/15.6^\circ\text{C}(60/60^\circ\text{F})} - 131.5$$

where Sp. Gr. is the Specific gravity of the fluid.

4.10 Pour Point

The pour point is the lowest temperature at which the fluid will flow [2]. Pour points are important for mobile equipment operations where the equipment must be started after sitting outside in cold weather. The oil used in such operations must have a pour point below the lowest start-up temperature anticipated. However, pour points must be considered with the fluid viscosity at these temperatures and with the pump manufacturer’s highest recommended start-up viscosity [39].

Pour points may be determined by various standard procedures, both manually and automatically, including oil fluidity [40], automatic tilting method [41], auto-pulsing method [42], and the rotational method [43].

4.11 Thermal Expansion

Because oil may expand and create a potential overflow condition, it is necessary to account for the thermal expansion that may occur when designing a hydraulic system. Thermal expansion is expressed as the coefficient of thermal expansion, which is ratio of volume change after heating to the initial volume after heating 1°C . It is expressed as $^{\circ}\text{C}^{-1}$. The coefficient of thermal expansion for a mineral-oil hydraulic fluid is approximately $6.4 \times 10^{-4}^{\circ}\text{C}^{-1}$ [38]. A procedure for obtaining more accurate values for thermal expansion is provided by ASTM D 1250 [44].

Figure 14.9 illustrates the change in relative volume of a mineral-oil hydraulic fluid as a function of temperature and pressure. Figure 14.14 provides an estimate of the effect of pressure on the coefficient of thermal expansion [35].

4.12 Thermal Conductivity

Thermal conductivity is the rate of heat transfer through the hydraulic oil. Heat-transfer rates increase with thermal conductivity. The thermal conductivity for most mineral oils is approximately $0.1 \text{ W m}^{-1} ^{\circ}\text{C}^{-1}$ [38].

4.13 Heat Capacity and Specific Heat

Heat capacity is the amount of heat required to raise the temperature of a given mass one degree of temperature ($^{\circ}\text{C}$ or $^{\circ}\text{F}$). The units of heat capacity are $\text{J kg}^{-1} ^{\circ}\text{C}^{-1}$. The specific heat of oil is the ratio of heat capacity of oil to that of water at 15°C ($1 \text{ J kg}^{-1} ^{\circ}\text{C}^{-1}$). The values of heat capacity and specific heat are numerically equal. Values for mineral oil hydraulic fluids have been reported to be approximately 0.444–0.456 [35].

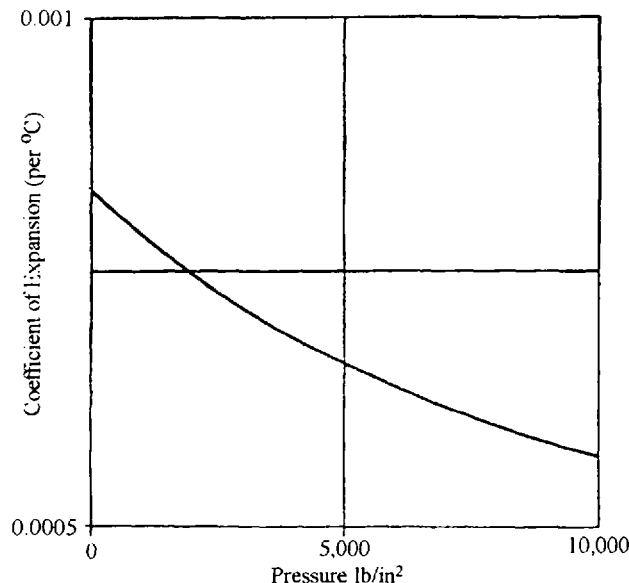


Figure 14.14 Effect of pressure on the coefficient of thermal expansion of D.T.D. 585.

4.14 Electrical Conductivity/Dielectric Strength

Electrical conductivity is the amount of electricity per unit area transferred through the oil at a given voltage [45]. The unit of electrical conductivity is mho/cm. The unit mho is the reciprocal of resistance ($1/\text{ohm} = \text{mho}$). A clean, dry mineral oil typically exhibits an electrical conductivity of 10^{-14} mho/cm. Dielectric constants for a mineral oil have been reported to be 2.25 at 50°C, 2.21 at 75°C, and 2.17 at 100°C [35].

4.15 Flash Points and Fire Point

The flash point is defined as “the temperature to which a fluid must be heated to give off sufficient vapor to momentarily form a flammable mixture with air when a small flame is supplied under specified conditions” [46]. An open-cup flash-point test is conducted in the open air [47]. A closed-cup flash-point test is conducted in a closed vessel [48]. The fire point is defined as the lowest temperature at which the fluid will sustain burning for 5 s in the ASTM D 92 test [48].

Although flash points and fire points do not affect the operation of the hydraulic fluid in a system, these values should be considered in system design safety, especially if there is the possibility of hot spots in the system where the fluid temperature may exceed the flash point or fire point of the fluid [46,49,146]. Alternatively, a situation may occur where an air pocket may develop when a source of ignition is present, such as air accumulation in the housing of a pump seal where the resulting air lock may cause oil starvation and a localized temperature rise which may create a condition sufficient for an explosion to occur [36].

4.16 Seal Compatibility

The potential for a mineral oil to cause swelling or shrinkage of a seal is important if optimal seal strength is to be maintained and system leakage is to be minimized. One of the oldest methods of estimating hydraulic seal compatibility is the aniline point of the fluid. Generally, low-aniline points cause the highest swelling with neoprene and BUNA-N nitrile rubber, as shown in Fig. 14.15 [36,50]. Although generally true, it has not been possible to calibrate the aniline point of an oil to predict the swelling of various elastomeric seal composition with respect to different base oils and additive combinations [51]. Seal materials most prone to encounter problems with mineral-oil hydraulic fluids are usually made from natural rubber. Neoprene and nitrile seals, however, are generally acceptable for use with mineral-oil hydraulic fluids [52].

Another method that was used was the American Hydraulic Equipment Manufacturers (AHEM) Seal Compatibility Index (SCI) [51]. This method involves the use of a standard nitrile rubber (AHEM, Standard Nitrile Rubber No. 1) and measuring the volume uptake of the hydraulic fluid at equilibrium. The test specimens may be O-rings (1 ± 0.01 in., 25 ± 0.25 mm) or squares (0.060 ± 0.006 in. or 1.5 ± 0.15 mm) [51]. The specimens are immersed into the test oil in a jar and placed in an oven at $100^\circ\text{C} \pm 2^\circ\text{C}$ for 24 h after the initial inner diameter (ID) is measured (D_1). After cooling in cold oil, excess oil is removed and the ID of the ring is measured (D_2) using a tapered gauge. The AHEM SCI is the percentage of volume

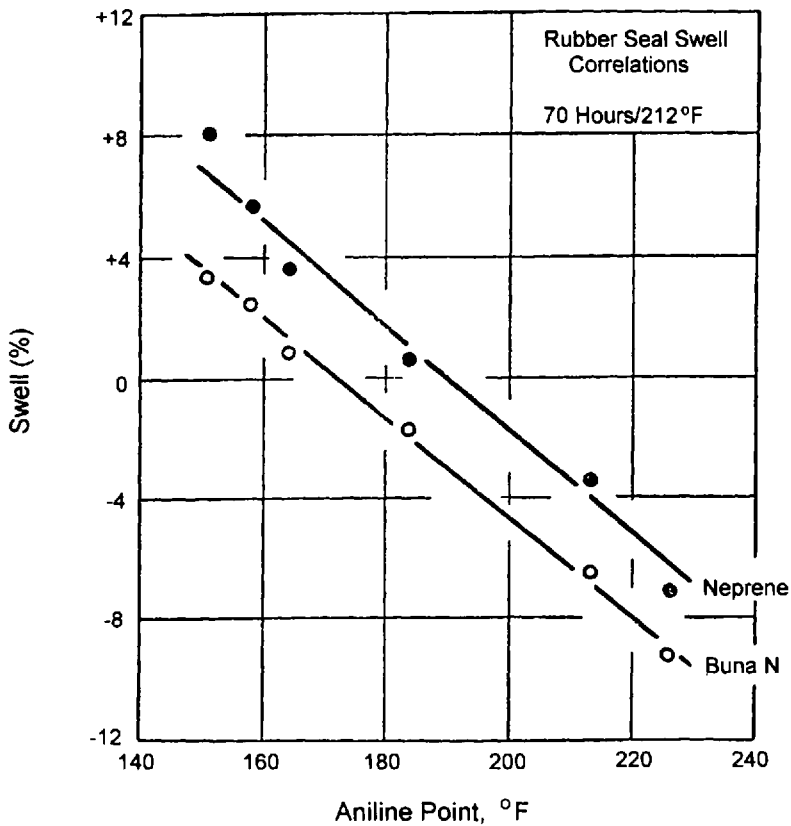


Figure 14.15 Correlation of volumn swell and aniline point for neoprene and BUNA-N rubber.

swelling, to the nearest whole number, obtained from linear swelling (S_D) and the standard conversion values in Table 14.11 [51]:

$$S_D = \frac{D_2 - D_1}{D_1} \times 100$$

The SCI values range from 0 to 50, as shown in Table 14.11.

The use of SCI values, although an interesting concept, has not gained acceptance in the industry. Currently, the testing methodology recommended in Chapter 9 is being considered as a standard test by ASTM.

4.17 Demulsibility

Water contamination of hydraulic fluids may occur when there is a difference in the hydraulic fluid in the reservoir and the humid atmosphere above the fluid, constant air leakage into the circuit, or seepage of the heat-exchanger coolant into the hydraulic fluid [53]. The contaminated oil may then form an emulsion with the water contaminant due to the churning action of the fluid mixture in the system, which is

Table 14.11 Conversion to Linear Swell to Seal Compatibility Index

SD %	$D_2 - D_1$ (in.)	SCI	SD %	$D_2 - D_1$ (in.)	SCI
0.2	0.002	0.6	8	0.08	26
0.4	0.004	1.2	8.2	0.08	26.7
0.6	0.006	1.8	8.4	0.08	27.4
0.8	0.008	2.4	8.6	0.08	28.1
1	0.01	3	8.8	0.08	28.8
1.2	0.012	3.6	9	0.09	29.5
1.4	0.014	4.3	9.2	0.09	30.3
1.6	0.016	4.9	9.4	0.09	31
1.8	0.018	5.5	9.6	0.09	31.7
2	0.02	6.1	9.8	0.09	32.4
2.2	0.022	6.8	10	0.1	33.1
2.4	0.024	7.4	10.2	0.1	33.8
2.6	0.026	8	10.4	0.1	34.6
2.8	0.028	8.6	10.6	0.11	35.3
3	0.03	9.3	10.8	0.11	36.1
3.2	0.032	9.9	11	0.11	36.8
3.4	0.034	10.6	11.2	0.11	37.5
3.6	0.036	11.2	11.4	0.11	38.3
3.8	0.038	11.8	11.6	0.12	39
4	0.04	12.5	11.8	0.12	39.8
4.2	0.042	13.2	12	0.12	40.5
4.4	0.044	13.8	12.2	0.12	41.3
4.6	0.046	14.4	12.4	0.12	42.1
4.8	0.048	15.1	12.6	0.13	42.8
5	0.05	15.8	12.8	0.13	43.5
5.2	0.05	16.4	13	0.13	44.3
5.4	0.05	17.1	13.2	0.13	45.1
5.6	0.05	17.8	13.4	0.13	45.8
5.8	0.05	18.4	13.6	0.14	46.6
6	0.06	19.1	13.8	0.14	47.4
6.2	0.06	19.8	14	0.14	48.2
6.4	0.06	20.5	14.2	0.14	49
6.6	0.06	21.2	14.4	0.14	49.7
6.8	0.06	21.8	14.6	0.15	50.5
7	0.07	22.5	14.8	0.15	51.3
7.2	0.07	23.2	15	0.15	52.1
7.4	0.07	23.9			
7.6	0.07	24.6			
7.8	0.07	25.3			

a high shear process [1]. Water-contaminated hydraulic systems may lead to numerous potential problems such as formation of “thin and watery” or “thick and pasty” fluids, promotion of dirt and dust contamination, improper functioning valves, increase wear and corrosion, oil oxidation, additive depletion, foaming, and filter plugging [1,53]. Therefore, water contamination should be avoided, or if it occurs, the water contaminant must be removed from the hydraulic oil as soon as possible!

Although highly refined mineral oil is hydrophobic, additives and oil-oxidation by-products such as acids may promote the emulsification of water in the fluid. An early test of water contamination from oil oxidation was to measure the surface tension of the fluid. As the fluid ages and oxidation occurs, surface tension of the fluid decreases, as illustrated in Fig. 14.16 [53]. Oil replacement is recommended when the surface tension is ≤ 15 dyn/cm.

Currently, the ability to separate water from a hydraulic oil is determined by ASTM D 1401 [54,55]. Water-separation ability is determined by mixing 40 mL of distilled water and 40 mL in the oil in a 100-mL graduated cylinder at 54°C as illustrated in Fig. 14.17. The time for complete separation is measured. Typically, oils that exhibit separation times of ≤ 30 min are suitable for continued use [1]. Factors that affect the accuracy of the test include cleanliness of the test equipment, speed and position of the stirrer, bath temperature, test duration, and stray vibrations [55].

4.18 Filterability

Some hydraulic oils are formulated to contain additives, such as viscosity modifiers [56], which exist as very small particles in the fluid. Although these particles may not be visible to the naked eye, they may be removed by high-efficiency, fine (3 μm) filtration [57]. These fine particles will actually cause plugging of the filters. Therefore, it is desirable to evaluate the “filterability” of a hydraulic fluid as both a measure of potential filter plugging and additive removal.

Evaluation of fluid filterability may be performed using the “Pall Filterability Test” [56,58,59] which involves the use of a pump stand where the time it takes for the fluid to pass through a filter under a partial vacuum is determined. An alternative test under evaluation is to pass the fluid through a membrane instead of a filter on a pump [56].

5 CORROSION PROPERTIES

5.1 Rusting or Corrosion

Although the terms “rusting” and “corrosion” are often used interchangeably, they are fundamentally different processes with different fluid-formulation challenges [60]. Rusting is caused by the reaction of water and air with a ferrous surface in the hydraulic system [61]. Corrosion is caused by the reaction of organic acids in the presence of peroxides, both originating from oxidation of the hydraulic oil [49]. Rusting results in the buildup of a film due to the formation of iron oxides [61], typically accompanied by an increase in weight, and corrosion results in a weight loss and surface pitting [49,61].

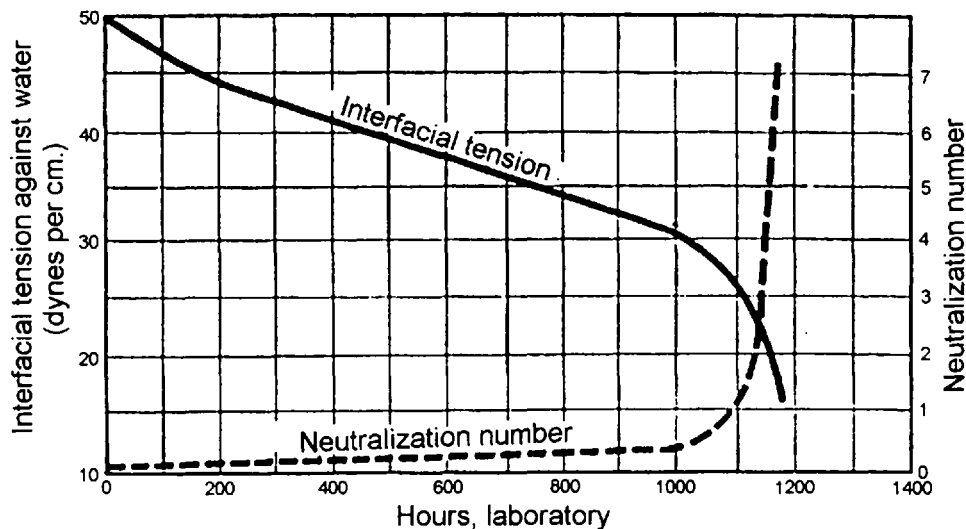


Figure 14.16 Effect of oil oxidation on surface (interfacial) tension.

Rusting is encountered in systems that are contaminated with water and air ingress, resulting in foaming [61]. Water may condense in cooling oil in the reservoir during shutdowns. Rusting may occur in the vapor space above the fluid level in the reservoir or in piping. This may lead to flaking of the rust into the fluid. This effect may be minimized by coating the reservoir with an oil-compatible preservative paint [60]. In addition to causing abrasive wear, the presence of rust particles in the oil may plug passages or damage valves [39,62]. Rust may also catalyze oil oxidation [62].

Highly refined mineral oils exhibit poor rust-preventative characteristics. However, the use of a rust inhibitor is an effective preventative. There are two types of rust preventatives. An inhibitor is added to protect ferrous metal surfaces from rusting when in contact with water when submerged in the oil; it is "rust inhibited." Rust-inhibited fluids do not prevent rusting when the ferrous surface is covered with a thin film of oil or when exposed to air, such as in the head space above the oil in the reservoir. Rust protection in this situation requires a "rust preventative" [57]. Rust preventatives typically provide rust inhibition also.

Corrosion occurs in systems that have undergone significant oil oxidation which would typically be enhanced if there are hot spots in the system. Highly refined mineral oils that contain an oxidation inhibitor typically do not exhibit corrosion problems [49,62]. Typically, protection against both corrosion and rusting require the use of two inhibitors [61].

5.2 Chemical Corrosion

Chemical corrosion may occur when the hydraulic oil is contaminated with halocarbons such as trichloroethane. When this occurs, components with small orifices, such as hydraulic actuators, may fail due to corrosion and deposit formation [63].

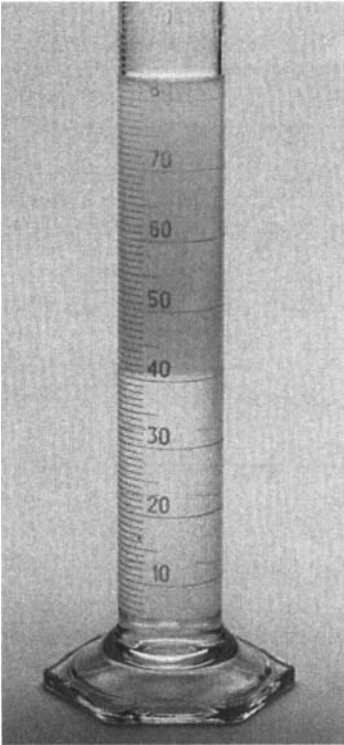


Figure 14.17 Illustration of ASTM D 1401 oil demulsibility test. (Courtesy of The Lubrizol Corporation.)

When subjected to water contamination, heat, and pressure, the presence of as little as 0.02% of the halocarbon may hydrolyze in the hydraulic oil to yield hydrochloric acid, which will then attack and etch the metal surface forming iron chloride (FeCl_3). Iron chloride, along with the water contaminant in the oil, will catalyze the oxidative degradation of the oil, forming weak organic acids, sludge, and varnish, which will form a brown, sticky residue on the metal surface.

5.3 Testing for Corrosion and Rusting

Copper corrosion properties of a mineral-oil hydraulic fluids are usually tested according to ASTM D 130 [64]. The rust-inhibiting properties is usually evaluated using ASTM D 665 [65]. Although the use of other tests such as “The Fog Cabinet,” solubility and colloidal stability test, and the static water drop corrosion test have been reported [66], only ASTM D 130 and ASTM D 665 will be discussed here, as they are the tests most commonly utilized for mineral-oil qualification [46].

5.3.1 ASTM Rust-Preventing Characteristics Test

ASTM D 665 is used to evaluate the ability of a mineral-oil hydraulic fluid to inhibit rusting of ferrous surfaces if the hydraulic oil were to become contaminated with water. There are two variations of this procedure, A and B. Procedure A involves stirring 300 mL of the hydraulic oil with 30 mL of distilled water at 60°C (140°F) for 24 h with a cylindrical steel rod immersed in the oil, as shown in Figs. 14.18 and 14.19. After the test is completed, the steel rod is inspected for the presence of rust. Procedure B is identical to Procedure A except that synthetic seawater is used instead of distilled water. Some of the test variables that must be controlled include the pH of the water, the type and age, in addition to grinding and drying of the steel

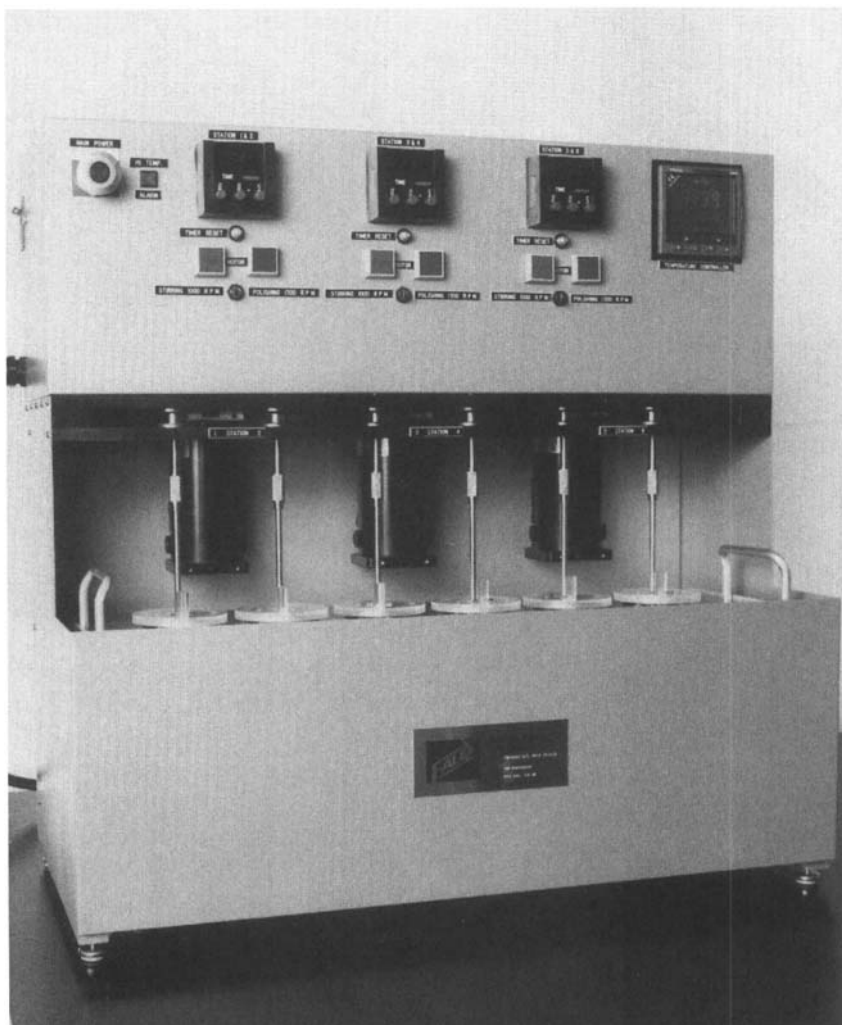
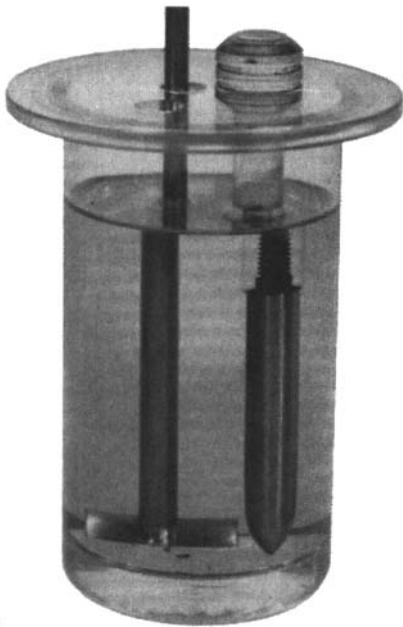
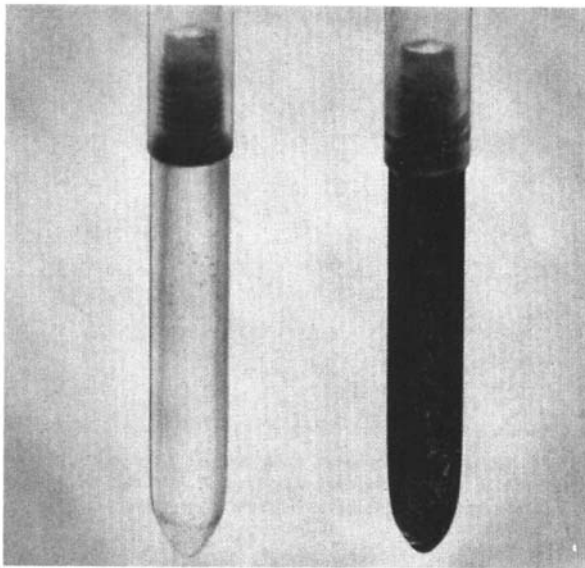


Figure 14.18 Illustration of the ASTM Oil Rust Test apparatus. (Courtesy of Falex Corporation.)



(a)



(b)

Figure 4.19 (a) Illustration of the oil-rust testing cell showing agitator and steel rod; (b) comparison of a good and bad rust testing result. (Courtesy of Texaco, Inc.)

rod (spindle), fitting of the rod in the plastic stem, stirring quality and magnitude, bath temperature, and, possibly, laboratory temperature and humidity [55].

5.3.2 Copper Corrosion by the Copper Strip Tarnish Test

ASTM D 130 has been recommended for evaluation of the potential of an oil to corrode copper [46]. This test is conducted by immersing a polished copper strip into 30 mL of the hydraulic oil in a 25 × 150-mm test tube which is then placed in a stainless-steel test bomb. After sealing, the test tube–bomb assembly is heated in a constant-temperature bath at 100°C for 2 h. The test tube is then removed from the bomb after cooling in cold water and the copper strip is removed and the degree of corrosion is determined by comparison to ASTM Copper Strip Corrosion Standards available from ASTM* and illustrated in Fig. 14.20. Provisions are made in the test procedure for higher test temperatures if more rigorous conditions are desired.

6 OXIDATION STABILITY

Oxidation stability refers to the “ability of an oil to resist polymerization and thermal decomposition in the presence of air, water, heat and dissimilar materials” [49]. Additional variables affecting oil-oxidation rates include ambient temperatures, atmospheric conditions, contamination, oil viscosity, type of pump, pump pressures, and pressure cycling [60,146].

Oil-decomposition products are either soluble or insoluble. Soluble oil-degradation products generally thicken the oil [67]. Insoluble products for sludge deposits in the oil which will lead to filter clogging, sticking of valves and pistons, and even hydraulic lock [68–70], increased wear, and corrosion [67]. Oil degradation by-products (water) and wear and corrosion debris (copper and iron) may catalyze the overall oxidative degradation process. This is illustrated in Table 14.12 which shows that if properly inhibited, water or the metal (copper or iron) alone had a minimal effect in accelerating degradation. However, when both water and the metal are present, the oil degradation rate was 10 (iron)-fold to 30 (copper)-fold greater [71].

Oxidative stability is a function of the base stock selected. For example, paraffinic oils exhibit better oxidative stability than naphthenic oils, but they exhibit poorer “solvency”—poorer ability to dissolve additives [72]. The presence of alkylaromatic derivatives and some polar components further increase the susceptibility of a petroleum oil to oxidation, and others exhibit a stabilizing effect [73]. Temperature exhibits the greatest impact on oxidative stability. On the basis of temperature–viscosity performance, optimum fluid temperature ranges are often between 90 and 160°F [49]. Generally, below oil temperatures of 135°F, oil-oxidation rates are relatively slow. However, above 145°C, the oxidation rate doubles for each 10°C rise in temperature [67,74]. Some of the greatest thermal stress on the fluid may occur in valves where the fluid is forced through small orifices at high velocities. This will produce localized thermal excursions due to fluid friction [60]. It has been shown that even at oil temperatures as low as 100°F, the presence of varnish deposits on valves have indicated the presence of localized temperatures in excess of 200°F [60].

*The ASTM Copper Strip Corrosion Standards may be obtained from ASTM Headquarters, 100 Barr Harbor Drive, West Conshohocken, PA 19428.



Figure 14.20 Illustration of the ASTM Copper Strip corrosion Standards. (Courtesy of Koehler Instruments Inc.)

Table 14.12 Effect of Water and Catalysts on Oil Oxidation

Catalyst	Water	Hours	Final TAN
None	No	3500	0.17
None	Yes	3500	0.9
Iron	No	3500	0.65
Iron	Yes	400	8.1
Copper	No	3000	0.89
Copper	Yes	100	11.2

Note: Tests were run at 200°F on a 150 SUS (at 100°F) turbine-grade oil according to ASTM D 943 test procedure.

Foaming and air entrainment will increase oxygen contact with the fluid and accelerate oxidative degradation, especially at high temperatures. Oxidative degradation rates are dependent on the amount of dissolved and entrained air that is present in the fluid. Dissolved gas will be released from the fluid as it flows through orifices within the system. Downstream pressure will redissolve the air, which will be accompanied by high localized temperatures because the time interval is too short for the bubbles to redissolve before compression. This may facilitate the oxidation process [57]. For example, Table 14.13 presents that bubble compression temperatures, starting from an inlet temperature of 100°F, may be as high as 2100°F for a pump pressure of 3000 psi. In fact, in addition to oxidative degradation, thermal cracking and nitration of the oil is also possible [75].

Backé and Lipphardt studied the effect of entrained air on mineral-oil oxidation. One of the variables that was examined was the effect of entrained air on the amount of oxidation as measured from the change in neutralization number and running time. Figure 14.21 shows that there is an initial oxidation rate that is controlled by the amount of air dissolved in the oil [76]. As the concentration of entrained air increases, the number of undissolved air bubbles increases and the rate of increase in neutralization number (oxidation) increases because larger amounts of oxygen necessary for the oxidation reaction can be supplied faster [76]. In a hydraulic system, the high temperatures produced by compression of the air bubbles will facilitate oil oxidation at the air bubble–oil interface, thus accelerating the overall oil-oxidation process. This process is retarded when a nitrogen atmosphere is provided or if antioxidants are used.

Backé and Lipphardt also showed that if the conditions including pressure, rate of pressure increase, and bubble size, ignition at the air bubble–oil interface will occur. This is called the “microdiesel effect” [76]. The conditions required for the microdiesel effect to occur are illustrated in Fig. 14.22 [76]. By calculation, it was found that for ignition to occur, the temperature on the bubble surface was typically 340–360°C (when starting from 25°C and compressed at 150,000 bars/s), which corresponded to the “ignition temperature” of the oil when measured by DIN 51,794.

Robertson and Allen performed a detailed analysis of the potential for hydraulic system variables such as reservoir size, pump type, and so forth to promote oil oxidation, thermal cracking, and nitration; their conclusions were as follows [75]:

Table 14.13 Gas Bubble
Compression Temperature Variation
with Pump Pressure

Pump pressure (psi)	Air bubble temp. ^a (°F)
1000	1410
2000	1820
3000	2100

^aCalculations based on 100°F inlet temperature.

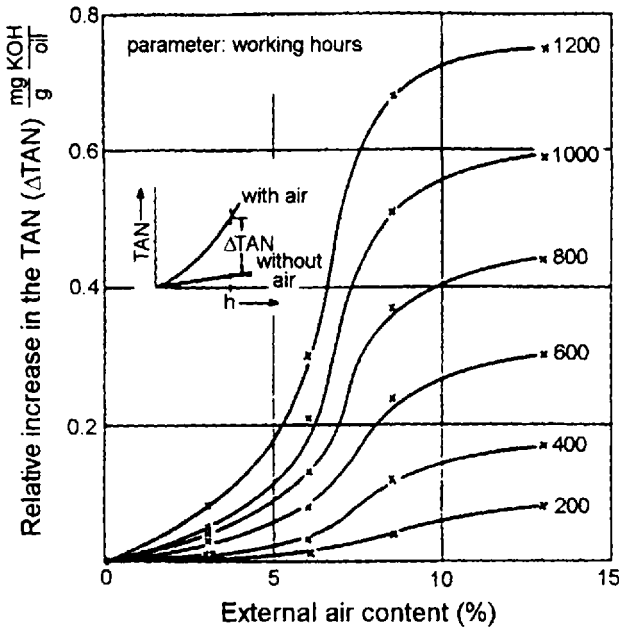


Figure 14.21 Relative increase in neutralization number with increasing air content.

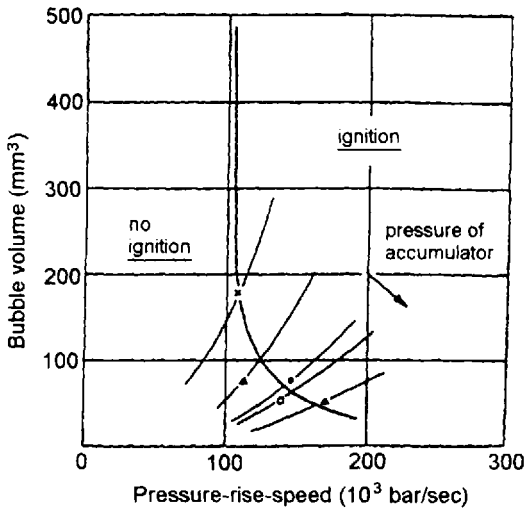


Figure 14.22 Backé and Lipphardt limiting curve for ignition during the compression of single air bubbles in petroleum oil.

1. Fluid aeration was the major factor contributing to accelerated oil-degradation processes. Constant-volume hydraulic pump systems with short residence times were the most prone to exhibit oil degradation and servo-valve problems.
2. It was shown that these problems could be modeled in the laboratory and were correlated to fluid air entrainment.
3. It is unlikely that laboratory bench tests for oxidation or thermal stability can completely assess the capabilities and limitations of a hydraulic fluid in the pump.
4. To minimize potential oxidative degradation, thermal cracking, and nitration problems with respect to hydraulic pump and servo-valve performance, the following are recommended:
 - (a) Use variable volume pumps if possible.
 - (b) Assure that the reservoir volume is at least 2½ times the pump capacity. (This is especially important for constant-volume pumps.)
 - (c) Design reservoir and return lines to keep turbulence at a minimum and allow for oil deaeration.
 - (d) Ensure that bulk oil temperature is maintained below 120°F.
 - (e) Avoid the use of copper tubing.

Clearly, it is important that optimal separation of the entrained air be promoted, usually by the addition of an air-release additive [61].

6.1 Oil Oxidative Degradation Processes

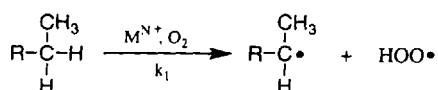
The oxidative degradation reaction mechanisms for petroleum oils will be reviewed here. These will include a discussion of (1) oxidative degradation processes below 120°C, (2) metal-catalyzed reactions, and (3) by-products of oxidative degradation. This discussion is based on detailed reviews on these subjects available in Refs. 77 and 78.

6.1.1 Hydrocarbon Oxidation Below 120°C

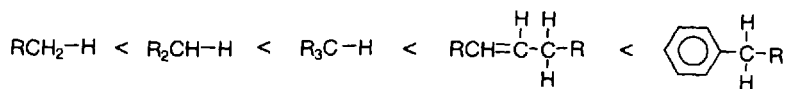
The hydrocarbon degradation mechanism occurs in four steps:

1. Chain initiation
2. Chain propagation
3. Chain branching
4. Chain termination

The first step, chain initiation, occurs when the oxygen partial pressure is greater than 50 torr. This is the slow or rate-determining step and is catalyzed by trace concentrations of transition metals:



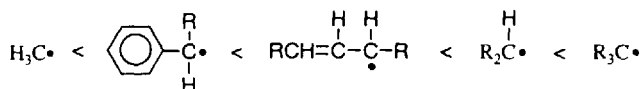
where R is an alkyl substituent and M^{n+} is a transition metal such as Fe, Cr, and Cu. The rate of hydrogen radical abstraction follows the order:



The second step of the reaction is the irreversible reaction of the alkyl radical formed in Step 1 to form a peroxy radical:



The rate of reaction of the alkyl radical with oxygen follows the order:



Alkyl radical reactivity increases with increasing alkyl substitution on the carbon where the hydrogen abstraction occurred. This is why branched hydrocarbons are more susceptible to oxidation than unbranched *n*-paraffinic hydrocarbons.

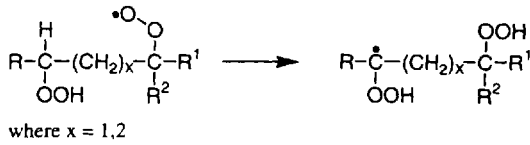
The chain propagation reaction continues with the abstraction of a hydrogen radical by the peroxy radical to form a hydroperoxide:



The relative rate of hydrogen abstraction by a peroxy radical is [78]

	$\begin{matrix} H \\ \\ R-C-H \\ \\ H \end{matrix}$	$\begin{matrix} R \\ \\ R-C-H \\ \\ H \end{matrix}$	$\begin{matrix} R \\ \\ R-C-H \\ \\ R \end{matrix}$
	primary	secondary	tertiary
Rel. Rate % H• Abstraction	1	30	300

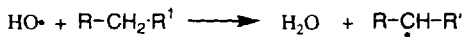
There are numerous possibilities of intramolecular hydrogen abstraction which will not be discussed here. One possible intermediate from multiple intramolecular abstraction processes is [78]



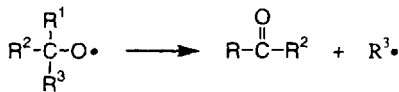
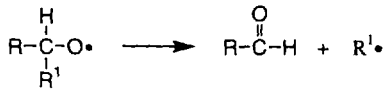
Hydroperoxides may undergo homolytic cleavage to yield an alkoxy and a hydroxy radical:



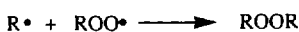
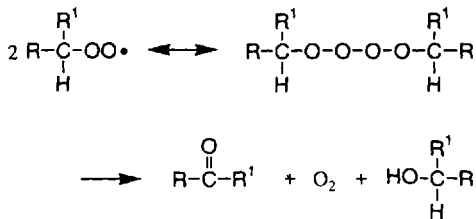
The third step of this process is chain branching:



Secondary and tertiary alkoxy radicals preferentially form aldehydes and ketones:

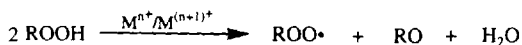


The final step of the process is chain termination. There are numerous possible radical combinations that will lead to termination of the oxidation process. These include



6.1.2 Metal-Catalyzed Reactions

Transition metals (0.1–50 ppm) capable of a one-electron transfer process will act as a catalyst for hydrocarbon oxidation [78]. However, to be catalytically active, they must be in the form of a metal soap which results from the formation of iron oxide with organic acids. Homolytic peroxide decomposition is catalyzed by metal soaps:



In summary, these free-radical oil-degradation processes, and others not shown, are strongly affected by temperature and are catalyzed by metal soaps. They explain the formation of volatile by-products, increasing oil viscosity with use, and the formation of sludge and other condensation by-products. Figure 14.23 summarizes these processes [78].

6.1.3 By-products of Oxidative Degradation

Oil-degradation by-products are not only specific to the composition of the base oil, and therefore its source, but the specific by-products formed will vary with the degradation conditions. However, for illustrative purposes, Table 14.14 provides a summary of those by-products identified from an oxidative degradation study of a Middle Eastern oil [77].

6.2 Fluid-Oxidation Testing Procedures

The amount of fluid oxidation or remaining useful life of an oil may be determined or at least estimated by laboratory analysis. The most commonly encountered oxidation tests used for petroleum hydraulic fluid characterization are neutralization number, TOST (Test for Oxidative Stability of Steam Turbine Oils) and RBOT (Rotary Bomb Oxidation Tests). The results of these tests are expressed as a titer (mg KOH/g oil), time required to achieve a predetermined amount of oxygen consumed, or amount of antioxidant depletion [72]. Although these tests will be discussed here, additional tests that have been utilized for either hydraulic fluid characterization or base oil oxidation studies will also be provided.

6.2.1 Neutralization Number

The neutralization number or total acid number (TAN) may be determined potentiometrically (ASTM D 664) [148] or colorimetrically (ASTM D 974) [149] and is expressed as “mg of potassium hydroxide required to neutralize the acid component in 1 gram of oil” [150].

An illustration of the variation of TAN with time in use for a hydraulic oil is provided in Fig. 14.16 [53]. Typically, the TAN number will increase slowly with time until it reaches a critical point where there is an exponential increase. This point

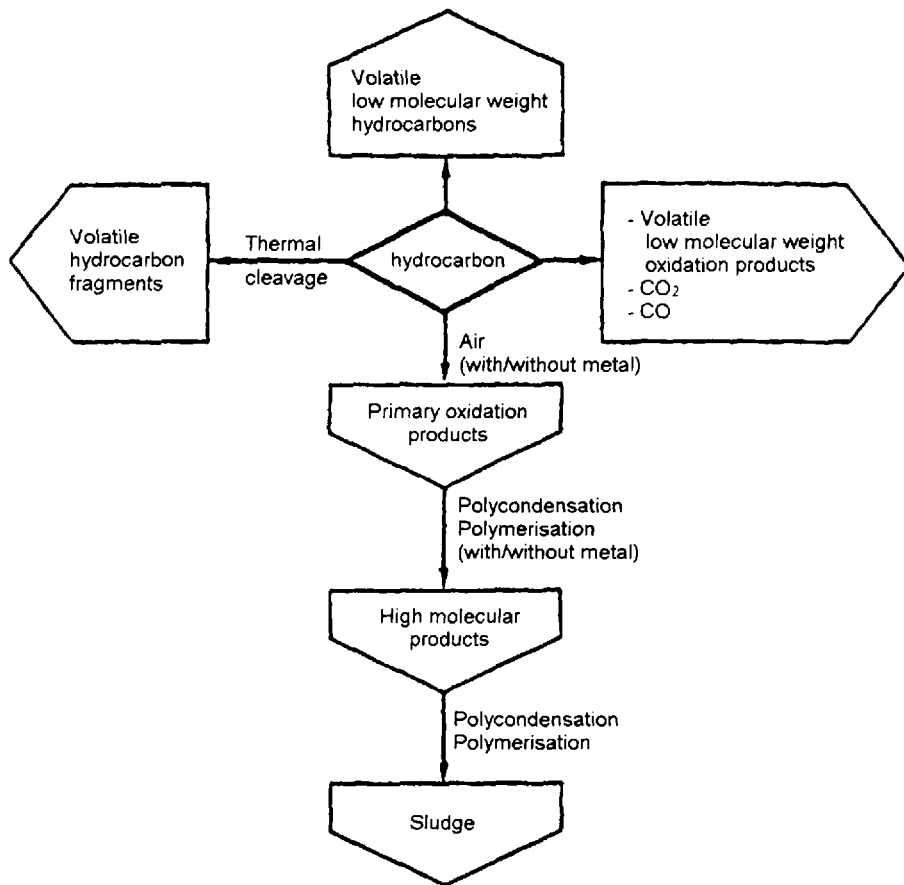


Figure 14.23 Rasberger model of lubricant degradation under high-temperature conditions.

Table 14.14 Oxidative Degradation By-products Obtained from a Middle Eastern Oil

By-product type	Identity
Water	Water
Acids	Formic, acetic
Alcohols	Ethanol, isopropanol, 1-propanol, 2-butanol, 1-pentanol, hexanol, 2-methyl propanol
Aldehydes	Acetaldehyde, butanal, 2-butanal, 2-pentanal, hexanal, 2-butanal, 2-pentanal
Ketones	Acetone, 2-butanone, 2-pentanone, 3-penten-2-one, 4-methyl-2-pentanone, cyclopentanone, 2-hexanone, 3-methylcyclohexanone, hexane-2,5-dione
Esters	Methyl acetate, ethyl acetate
Lactones	Dihydro-2-furanone, 2-cyclohexene-2-one, 5-methyl dihydro-2-furanone
Ethers	Tetrahydrofuran, 2-methyl-dihydrofuran, dimethyldihydrofuran, 2-formylfuran
Aromatics	C-9 aromatics

is dependent on the oil, hydraulic system, and use conditions. This characteristic exponential increase in TAN is the onset of a dangerous use condition. Typically, it is recommended that the maximum allowable TAN be 2.0 [61].

Mang and Jünnemann have reported that the use of TAN values to monitor fluid oxidation is the subject to misinterpretation and have recommended that this test only be used with oils of similar structure [79]. The reasoning provided was that TANs are affected by both oxidation of the base oil and by the reaction mechanism of the additives.

6.2.2 Test for Oxidative Stability of Steam Turbine Oils

Oxidative stability has been defined as “the ability of a fluid formulation to resist reaction with oxygen under a given set of environmental conditions including temperature and material of construction” [80]. ASTM D 943 [81], Test for Oxidative Stability of Steam Turbine Oils (TOST), is an accelerated oxidative stability test used to compare the ability of a fresh oil to resist oxidation. The oxidation process is catalyzed using a mixture of copper, iron, and water. TOST is conducted by bubbling oxygen (3 L/h) through 300 mL of oil and 60 mL of water at 95°C in the presence of the iron–copper catalyst until a TAN value of 2 mg KOH/g oil is obtained. The ASTM D 943 TOST apparatus is illustrated in Fig. 14.24. The test results are reported in hours. Although ASTM D 943 may be too severe for hydraulic oils operating at lower reservoir temperatures, it does provide a useful comparison between the relative inhibitory properties offered for hydraulic fluids containing different inhibitor additive packages, as illustrated in Fig. 14.25 [60].

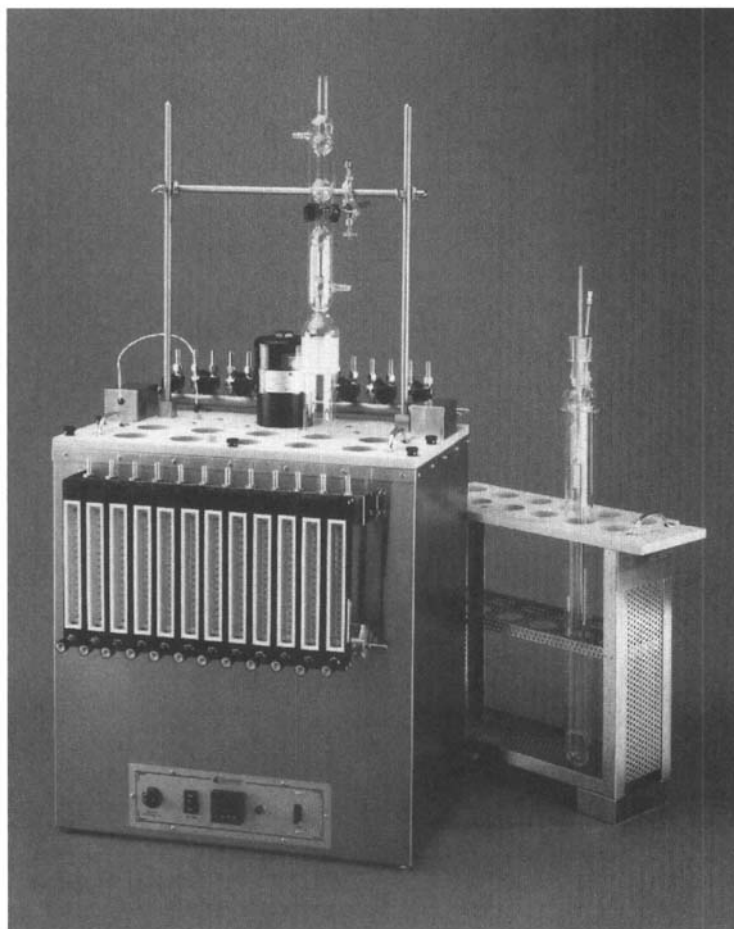
With the most recent version of DIN 51,587, the German standard for TOST, TAN characterization up to 2 mg KOH/g oil is not allowed due to potential additive interference. Mang and Jünnemann have suggested an alternative infrared analysis technique, which is discussed in Section 6.2.5. An illustrative comparison of TOST results for a series of hydraulic oils is provided in Fig. 14.26 [74].

TOST was used to evaluate the base-oil components that aggravate color generation during use [82]. After chromatographic identification of the by-products of the base oils evaluated in this oxidation test, it was found that the greatest contributors to color generation were by-products formed by acid-catalyzed oligomerization of aromatic sulfur compounds and other base-stock components high in aromatic carbon. Color may be reduced by the elimination of strong acids which may act as catalysts for these oligomerization reactions. The results of this work is summarized in Table 14.15 [82].

6.2.3 Rotary Bomb Oxidation Test

Oxygen tolerance is another very important property for a hydraulic fluid. Oxygen tolerance has been defined as “the amount of oxygen that can be reacted with a test fluid under a given set of environmental conditions including temperature and materials of construction without causing dirtiness or property changes in the fluid” [80]. Oxygen tolerance is determined using the Rotary Bomb Oxidation Test (RBOT) (ASTM 2272) [83].

The RBOT is conducted by heating 50 g of a fresh or used oil, 5 mL of water, and a copper catalyst coil in a steel bomb which is pressurized with 620 kPa (90 psi) of oxygen. The bomb is then heated in a constant temperature bath at 150°C while rotating at 100 rpm at a 30° angle from horizontal. The test is completed after



(a)

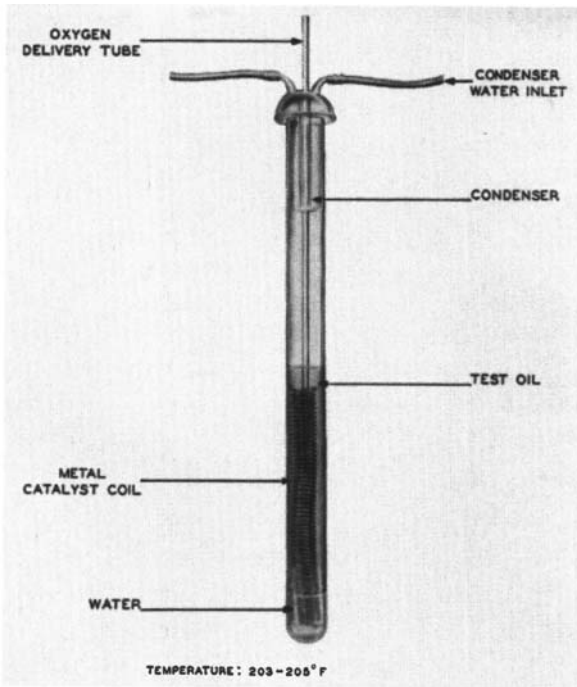
Figure 14.24 Illustrations (a and b) of the ASTM TOST apparatus. (Courtesy of Koehler Instruments Inc.)

a pressure drop of more than 175 kPa (25.4 psi) below the maximum pressure, and the time to obtain this pressure drop, indicating the onset of oxidation, is recorded. The pressure–time plot of two test runs is illustrated in Fig. 14.27 [83].

6.2.4 Hot-Panel Coking Test

One of the earliest tests conducted to determine the tendency of an oil to form lacquer deposits at elevated temperatures was the hot-panel coking test [84]. Although this test has been used primarily to evaluate engine oils, it may be useful for evaluating hydraulic fluids because maintenance of fine tolerances are critical to the proper operation of a hydraulic system [55].

In the hot-panel coking test, oil is splashed from a reservoir onto a heated aluminum test panel that covers the reservoir. The test apparatus is illustrated in Fig. 14.28. The data obtained include weight of deposits on the panel, change in TAN and oil viscosity, and the weight of insolubles in the oil in the reservoir.



(b)

Figure 14.24 Continued.

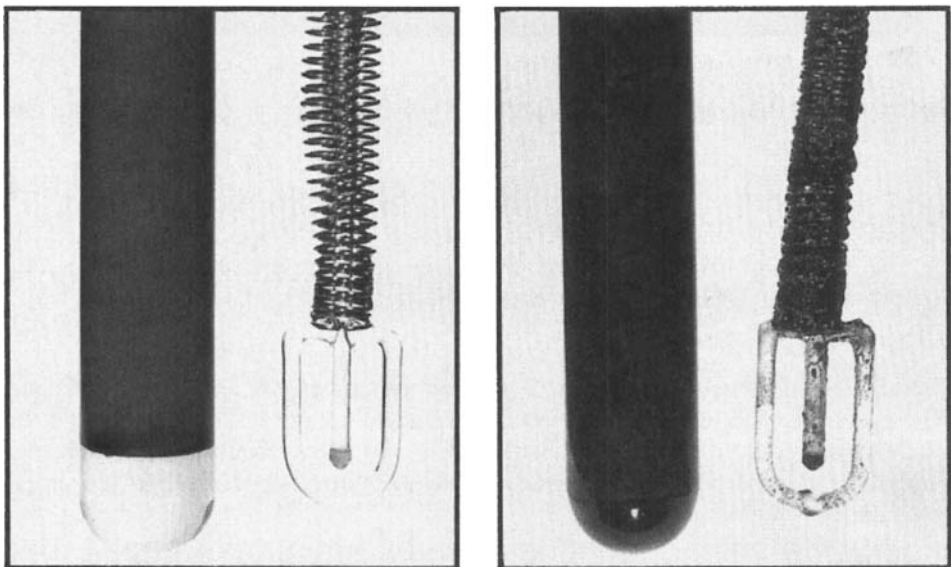


Figure 14.25 Comparison of oils possessing excellent (left) and poor (right) oxidative stability after testing according to ASTM D 943. (Courtesy of The Lubrizol Corporation.)

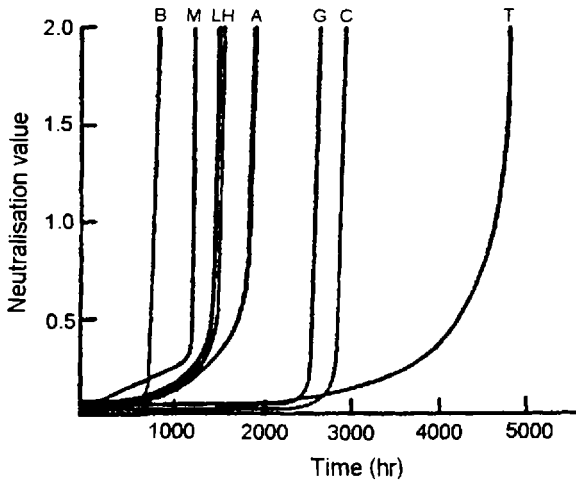


Figure 14.26 Comparison of TOST results for various petroleum oil hydraulic fluids. Note the varying induction times for oxidation to occur.

6.2.5 Infrared Spectroscopy

Mang and Jünemann described the use of infrared (IR) spectroscopy as a preferred alternative to TAN to analyze the oxidation resistance of HL and HL-P hydraulic oils. (See Table 14.7 for ISO hydraulic oil nomenclature.) Hydraulic oils were aged according to a TOST (DIN 51,387) and a comparative IR absorbance of the C=O stretching vibrations at 1710 cm^{-1} , as shown in Fig. 14.29, was used to estimate the degree of oxidation of the oil, even in the presence of additives [79].

Infrared analysis has also been used to identify and quantify the following [85].

- Metal carboxylate salts— 1600 and 1400 cm^{-1}
- Carboxylic acids— 1710 cm^{-1}
- Metal sulfates— 1100 and 1600 cm^{-1}
- Esters— 1270 and 1735 cm^{-1}

6.2.6 Cincinnati Milicron Test

The Cincinnati Milicron Thermal Stability Test Procedure is conducted by heating 200 mL of an antiwear hydraulic oil at 135°C in the presence of copper and steel

Table 14.15 Correlation of Base-Stock Aromatic Composition and Color Generation During Oxidation

Lube	N (ppm)	S (ppm)	Wt.% aromatics	ASTM color after oven treatment
A	27	6200	26 ^a	>8
B	1	92	4	5.5
C	<0.2	1	1	2.5

^aThis was an 84/12.5/3.5 mixture of mono/di/tri-nuclear aromatics structures as determined by mass spectral analysis.

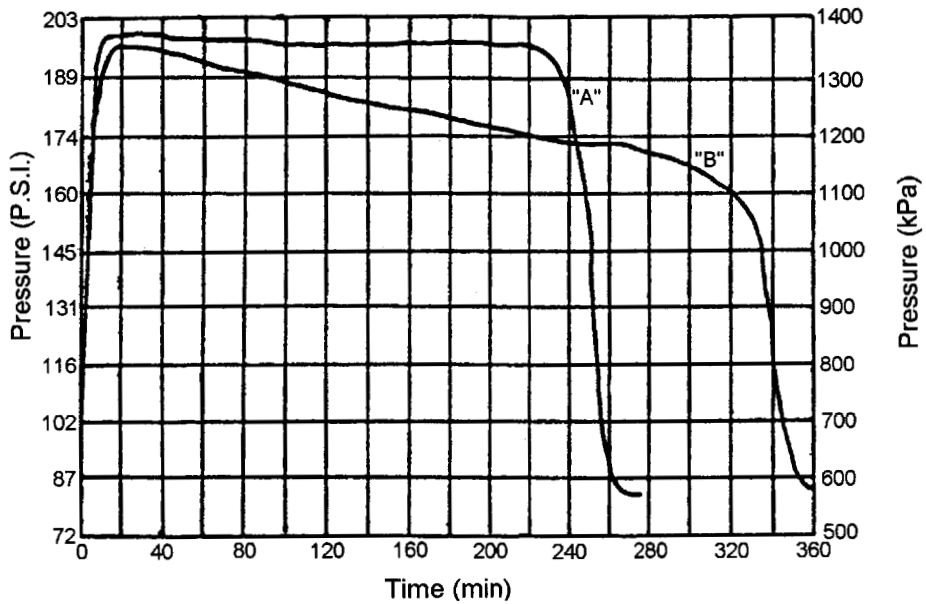


Figure 14.27 Pressure versus time plots for two RBOT runs.

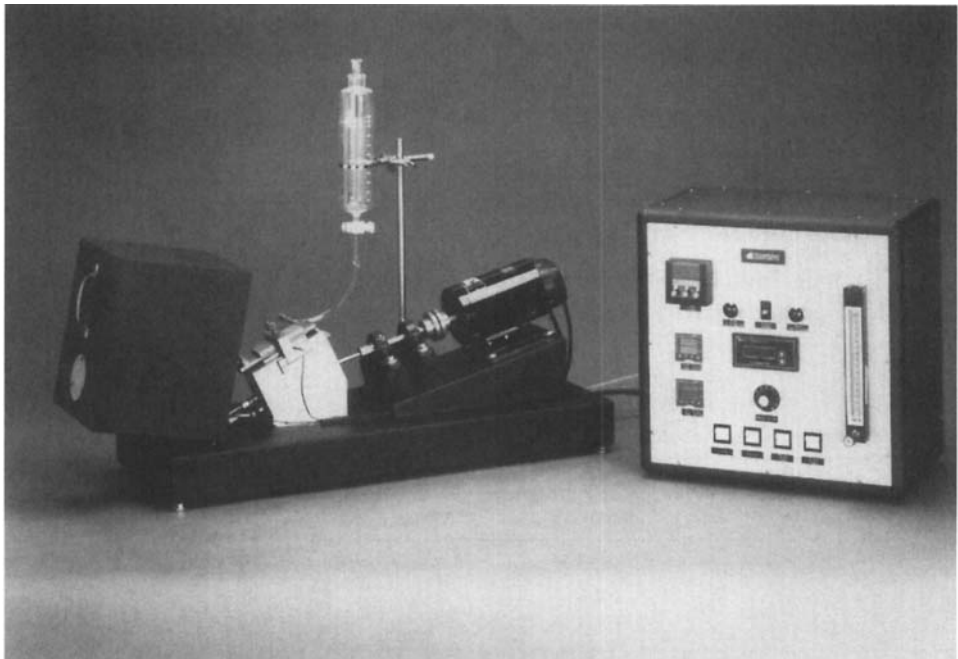


Figure 14.28 Hot-panel coking test apparatus. (Courtesy of Koehler Instruments Inc.)

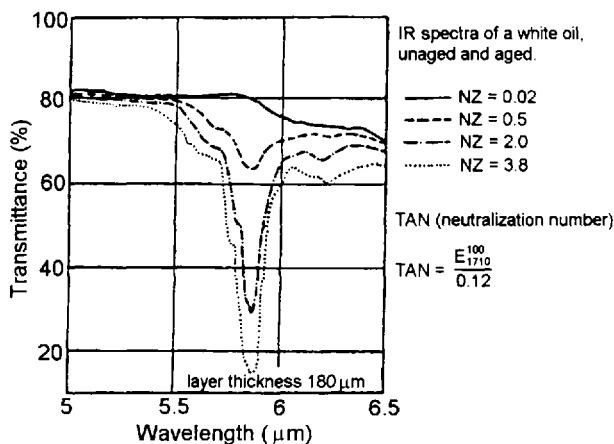


Figure 14.29 Aging of mineral oils according to DIN 51,587 (TOST) using IR spectroscopic comparison.

rods (multimetal compatibility) in a 250-mL beaker heated in an aluminum block [29]. Upon completion of the test, the used oils are observed for color change, filtered, and submitted for elemental analysis. Figure 14.30 provides a comparison of good and poor multimetal compatibility. The test is suitable for distinguishing oil additive performance. *Note:* There are three specifications for this test: P-68, P-69, and P-70. Tests are all conducted in the same manner; the different specifications refer to different fluid viscosities at 40°C (104°F). The P-68 test is for 32 cS fluids, P-69 is for 68 cS fluids and P-70 for 46 cS fluids.

6.2.7 Differential Scanning Calorimetry

Differential scanning calorimetry (DSC) analysis has been used to study the relative oxidative stability of different classes of hydrocarbon structures [73]. This was performed by oxidizing the base oils according to IP-48 [85] over 48 h at 120°C in a glass reactor, using an activated copper catalyst and varying levels of ZDDP as an antioxidant. Dry oxygen (1 L/h) was passed into the oil. DSC studies were performed on 5-mg samples heated at preprogrammed rates of 5, 10, and 20°C/min at a constant pressure of 100 psi. The characteristic temperature at the onset of degradation and the temperature at the maximum rate of degradation was determined [86]. A plot of the variation of onset times as a function of heating rate is provided in Fig. 14.31 and that with the oil structure is provided in Fig. 14.32 [73].

6.2.8 Penn State Micro-Oxidation Test

The Penn State Micro-Oxidation (PMSO) test is a thin-film oxidation test which can be calibrated to model various application conditions by varying testing conditions such as temperature [87]. The PMSO test apparatus, illustrated in Fig. 14.33, utilizes a glass reactor, 13 cm high × 2.5 cm inside diameter with a 24/40 ground-glass joint. A low-carbon steel, 19.1 mm (outer diameter) × 7 mm thick with a 1-mm rim edge sample container is machined, polished, and washed in tetrahydrofuran. A 40-μL sample, which forms approximately a 160-μm-thick film, is placed on the coupon and weighed. The “reactor” is placed in an aluminum block heater at 225°C (see

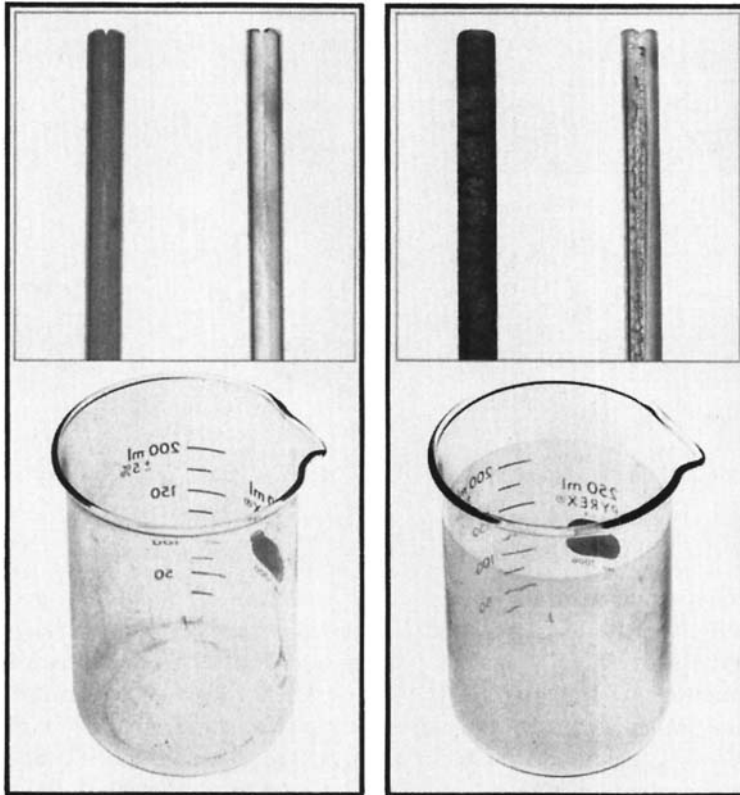


Figure 14.30 Illustration of good (left) and bad (right) multimetal compatibility according to the Cincinnati Milacron thermal stability test. (Courtesy of The Lubrizol Corporation.)

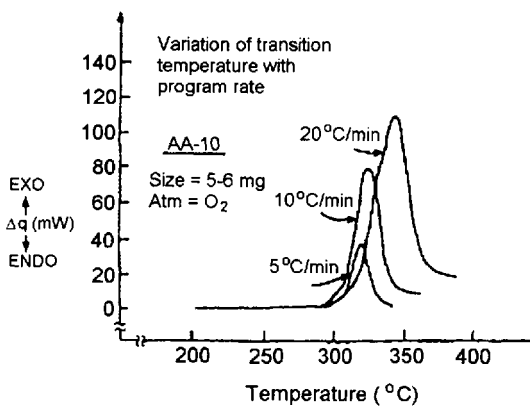


Figure 14.31 Illustration of DSC characterization of the oxidative stability of a petroleum oil.

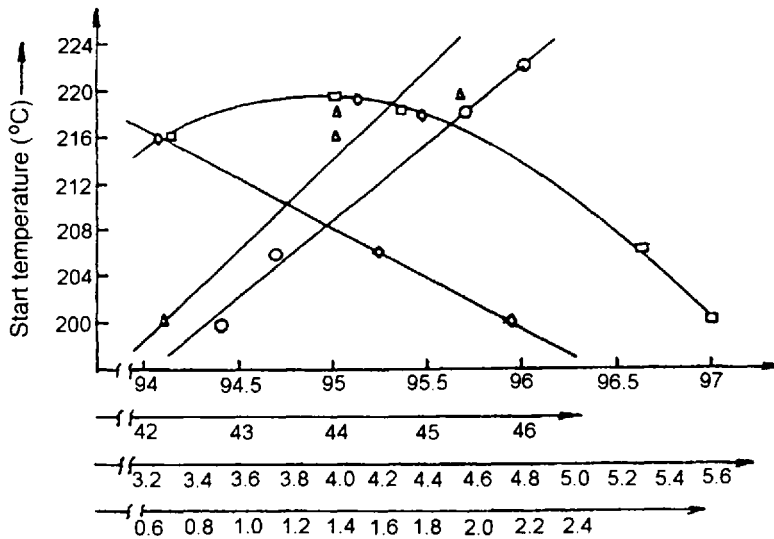


Figure 14.32 Comparison of the start of oxidative degradation by DSC measurement as a function of base-oil composition.

Fig. 16.33b). The system is flushed with nitrogen ($20 \text{ cm}^3/\text{min}$) for 30 min, then air ($20 \text{ cm}^3/\text{min}$) for 10 min. The test coupon was inserted into the preheated and purged "reactor" and the test was conducted with $20 \text{ cm}^3/\text{min}$ of air purge. At the conclusion of the test, the weight loss due to evaporation was determined gravimetrically and the residue is characterized chromatographically. A "typical" result is shown in Fig. 14.34.

6.2.9 IFP OXYTEST

A schematic of the IFP OXYTEST is shown in Fig. 14.35 [77]. The test measures oxygen uptake throughout the oxidation process to provide oxygen consumption data as a function of time. Other variables that are determined include induction period and the point of maximum uptake. An additional feature of this test is that the gaseous by-products are collected in a cold trap for subsequent identification.

6.2.10 Thin-Film Oxygen Uptake Test

The Thin-Film Oxygen Uptake Test (TFOUT), ASTM D 4742 [88], measures the oxidative stability of 1–2 g of fluid spread over a glass coupon in a rotating bomb under pure oxygen. The oxygen pressure is measured continuously and the induction period, the time required before oxygen pressure starts to drop, is recorded. The ASTM TFOUT is conducted in the presence of a soluble metal catalyst and water.

7 ADDITIVES

Most modern hydraulic fluids contain additives to enhance low-temperature properties (pour-point depressants), modify viscosity–temperature properties (VI improvers), oxidative stability, and rust and corrosion resistance. Current emphasis on hydraulic system design for mobile equipment is on smaller reservoirs and higher

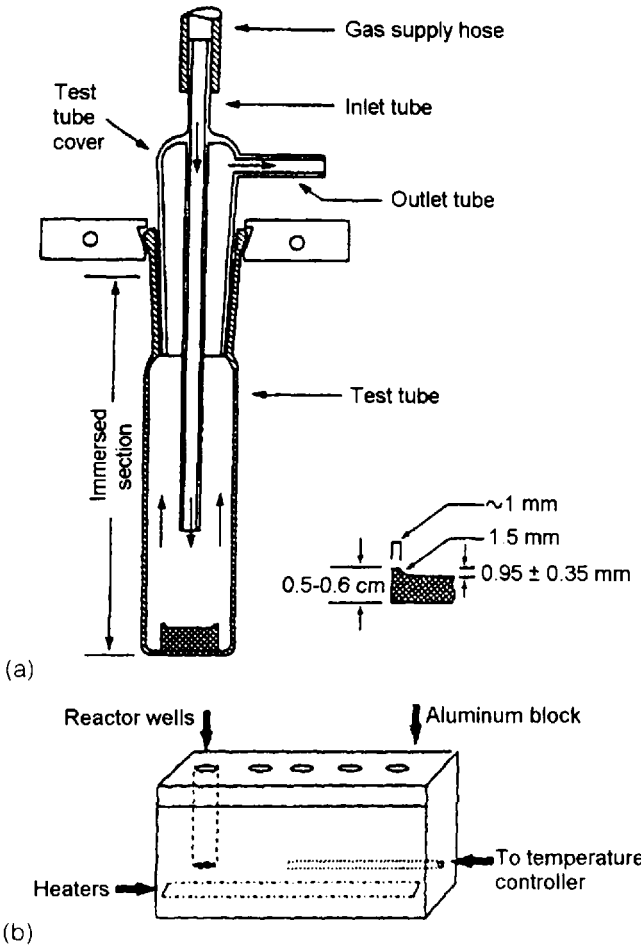


Figure 14.33 Illustration of the PSMO test apparatus: (a) test cell; (b) heating block.

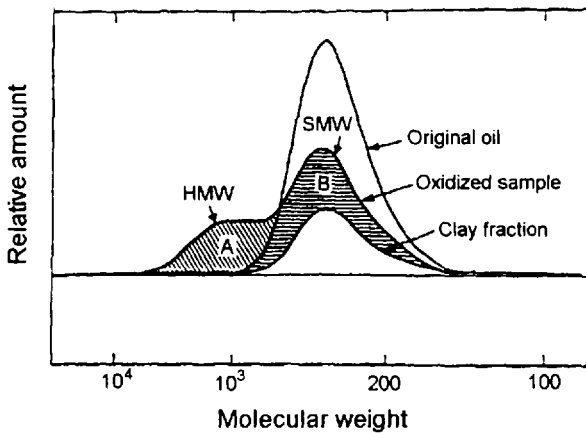


Figure 14.34 Typical PSMO test result.

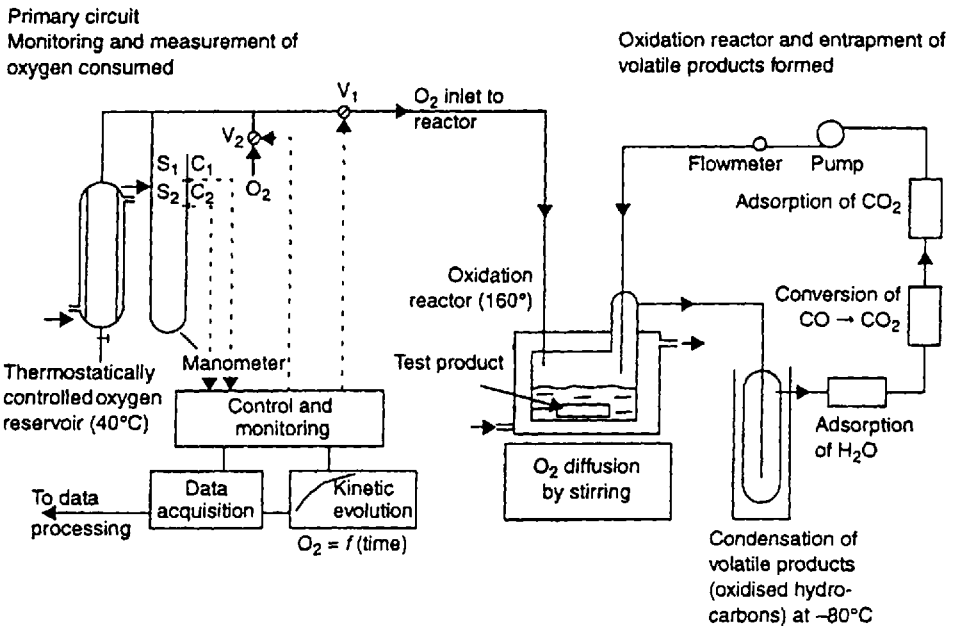


Figure 14.35 Schematic of IFP OXYTEST apparatus. V_1 : O_2 inlet valve to reactor; V_2 : O_2 inlet valve to measurement circuit; C_1/S_1 : control of primary circuit closure and reactor opening; C_2/S_2 : control of primary circuit opening and reactor closure.

pressures. Hydraulic designs to accomplish this significantly increases the severity of the operating conditions of the hydraulic oil because mechanical energy is converted to thermal energy which must be dissipated by the oil. In some cases, these conditions may result in a temperature rise that approaches the decomposition limits of some of the oil components or of additives such as ZDDP (zinc dialkyldithiophosphate). Additive degradation by-products may then attack component surfaces such as copper alloys, which may then lead to failure [89]. Therefore, hydraulic fluid additive technology is a critically important consideration in proper fluid selection and use.

Hydraulic fluid additive chemistry, including typical structures and performance mechanisms, is discussed in Chapter 15 and such detail will not be provided here. In this section, an overview of base-oil effects on additive performance, additive classification and function, history and use of ZDDP additives in antiwear hydraulic fluid formulation, and ashless fluid technology, and a brief discussion on additive analysis will be discussed.

7.1 Base-Oil Effects

Base-oil composition exhibits some of the greatest contributions to physical properties, such as viscosity–temperature, pour point, and oxidative stability [90–92]. For example, oxidation characteristics of a base oil are dependent on the base oil itself, antioxidant additives such as hindered phenols, alkylated aromatic amines, or various synergistic combinations of both, and interactions between the base oil and the antioxidant additives [90].

Paraffinic components of the base oil may improve the synergism between antioxidants, thus improving oxidative stability, but they aggravate antiwear and detergency properties of the oil [92]. Naphthenic and aromatic base-oil components improve antiwear and detergency properties by improving solubility of additives, such as ZDDP, in the oil. Multiple linear-regression equations have been developed to predict these effects based on oil composition [92].

Base-oil composition is dependent on the refining process used. Earlier in this chapter, it was shown that processes such as solvent refining, hydrocracking, and hydrotreating will reduce the concentration of sulfur-, nitrogen-, and aromatic-containing components which will exhibit substantial improvements in the base oil [93]. The amount of reduction of these components is dependent on the refining process. The additive solubility problems in base oils containing increased paraffinic content is typically addressed by additive modification [93].

Additive response may vary with the type and amount of oil-degradation by-products present during use. This has been shown to be particularly notable with the presence of aldehyde-degradation by-products which substantially reduced antioxidant properties of ZDDP, 2,6-di(*t*-butyl)-4-methylphenol, and *N*-phenyl-1-naphthylamine [94]. Carboxylic acids, ethers, alcohols, and ketones also exhibited a negative effect, but much less notable, on the antioxidant properties of these additives. Interestingly, ester-containing by-products exhibited almost no effect [94].

7.2 Additive Classification and Function

Although one of the primary functions of the hydraulic fluid is to act as an energy-transfer medium, it is also important to realize that the fluid must also provide adequate lubrication of the moving surfaces in the hydraulic system. Additives are used to provide and enhance the performance of the hydraulic oil, including viscosity-temperature properties, antiwear properties, rust inhibition, antioxidant performance, gum solvency (to assist in maintaining a clean system by solvating "sticky" degradation by-products which cause sticking and hesitation of hydraulic system components), and antifoaming/air-release properties [95]. The performance characteristics of a petroleum-oil hydraulic fluid is dependent on both the base-oil composition and the additives used [96]. Table 14.16 provides a summary of the various types of additives, with respect to function and chemical type, that may be used in hydraulic oil formulation and also the types [96,97].

7.2.1 "Oiliness" Additive Properties

One of the additive classification terms from Table 14.16, "oiliness," is seldom encountered in the industry today. Oiliness has been defined as "that chemical feature of an oil which permits it to wet metallic surfaces and establish a minimum coefficient of friction between two rubbing surfaces under condition of boundary friction" [98]. Film strength is a property of a lubricant that "enables it to maintain protective films on the rubbing surfaces under conditions of boundary lubrication . . ." [99]. These terms are not rigorously correct and do not properly define the required lubrication requirements for different wear surfaces in a hydraulic pump.

Papay has addressed this problem and has provided proper definitions for "friction modification," "antiwear," and "extreme pressure," which can all be distinctively and correctly defined [100]. Boundary lubrication refers to the use of an ad-

Table 14.16 Function and Chemical Type of Additives Used for Hydraulic Fluid Formulation

Additive	Purpose	Function	Typical compounds
Oxidation inhibitors	Prevent varnish and sludge formation; extend fluid life 10–100 times	Terminates oil oxidation by the formation of inactive compounds or by oxygen scavenging	Organic compounds containing sulfur, phosphorus, or nitrogen such as zinc dithiophosphates, organic sulfides, thiophosphates, hindered phenols, and alkylated aromatic amines
Viscosity index improver	Lower the rate of change of viscosity with temperature; Ix VI improver	Because of the solubility differences, viscosity is increased more at high temperature than at low temperatures	Polymerized olefins for iso-olefins, butylene polymers, alkylated styrene polymers, polymethacrylate
Pour-point depressant	Lower the pour-point temperature	Modification of wax crystals to prevent growth with accompanying solidification at low temperatures	Alkylated naphthylene or phenols and their polymers, methacrylate polymers
Antifoamant	Prevent formation of stable foam and entrained air which may increase compressability	Change interfacial tension to permit bubble coalescence into larger bubbles which separate faster	Silicone polymers, organic polymers (acrylate esters)
Antiwear agent	Reduce wear	Forms a film on metallic-contacting surfaces	Organic phosphates and phosphites, zinc dithiophosphate
Extreme-pressure (EP) additive	Prevent galling, scoring, and seizure	Formation of low-shear films on metal surfaces at point of contact	Sulfur-, chlorine-, phosphorus-containing materials
Rust inhibitor	Prevent or reduce rusting	Preferential adsorption of polar, surface-active materials: neutralize corrosive acids	Sulfonates, amines, fatty oils, oxidized wax, and halogenated ferivatives of some fatty acids
Corrosion inhibitor	Prevent corrosive attack on alloys or other metallic surfaces	Inhibits formation of acidic bodies or forms a protective film over metallic parts	Organic compounds containing sulfur, phosphorus, or nitrogen such as phosphites, metal salts of thiophosphoric acid, and terpenes
Detergent	Keep surfaces free of deposits	Chemical reaction with sludge and varnish precursors to neutralize them and keep them soluble	Metallo-organic compounds of barium, calcium and magnesium phenolates, phosphates, and sulfonates
Dispersant	Keep insoluble contaminants dispersed	Contaminants are bonded by polar attraction to dispersant molecules, preventing agglomeration and kept in suspension due to solubility of dispersant	Polymeric alkylthiophosphonates and alkylsuccinamides
Oiliness agent (boundary lubrication additive)	Reduce friction under near-boundary conditions	Adherence of polar materials to metal surfaces	High-molecular-weight compounds such as fatty oils, oxides, waxes, or lead soaps

ditive, "friction modifier" which is chemisorbed, to prevent converging surfaces from undergoing asperity contact [151]. An example of a friction-modifying additive is a fatty acid such as stearic acid. Figure 14.36 illustrates a closely packed array of stearic acid molecules formed on a surface by chemisorption [100]. Coefficients of friction of friction-modified films are typically approximately 0.01–0.02, relative to an unlubricated surface of 0.5. For reference, the coefficients of friction of fluid films, hydrodynamic lubrication, are typically 0.001–0.006.

Antiwear (AW)/extreme pressure (EP) additives, such as ZDDP, function by a different mechanism. AW/EP additives form semiplastic films that are difficult to remove by the shearing forces present with very close surface asperity contact. The coefficient of friction for an AW/EP film is approximately 0.1–0.2 [151].

Although hydraulic pumps are designed to be operated hydrodynamically, it has been shown that hydraulic pumps operate under conditions of mixed-film (EP) [101] or boundary lubrication [102] during some mode of their operation. Moving surfaces within a hydraulic pump that are most susceptible to boundary or mixed-film lubrication include (1) the interface between the leading edge of the vanes and the cam ring of a vane pump, (2) the line contact between the mating gear teeth of

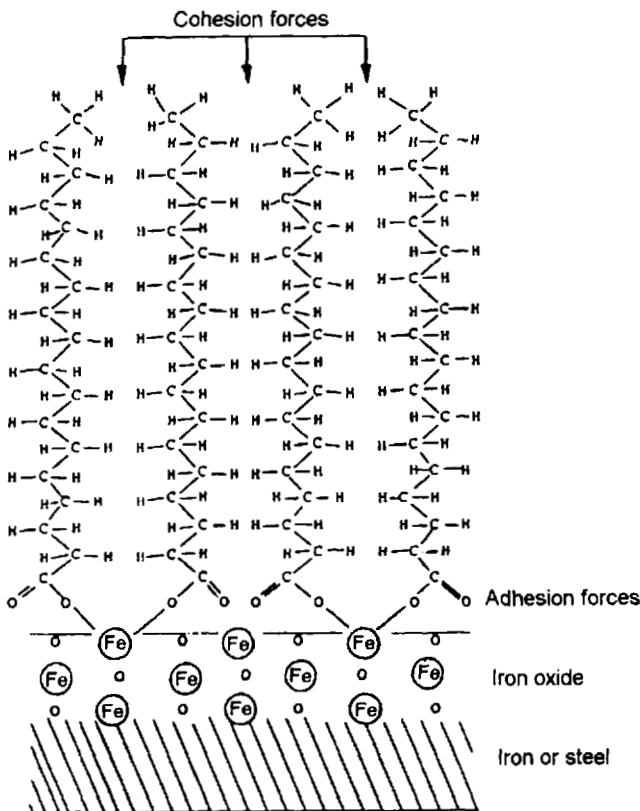


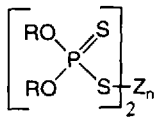
Figure 14.36 Illustration of chemisorption of stearic acid on iron–iron oxide surfaces.

a gear pump, (3) the interface between the connecting rod and piston of certain types of piston pump, (4) the interface between the piston and swash plate of other types of axial piston pump, and (5) the interface between rotary valve plates and housings [98]. The lubrication of these controlled clearances demands the use of a lubricant that provides effective EP and boundary lubrication along the proper surface finish. In addition, the selection of the additive package to provide the required lubrication effect is dependent on the surface being lubricated (material pair) and the oil [103].

7.3 ZDDP Additives

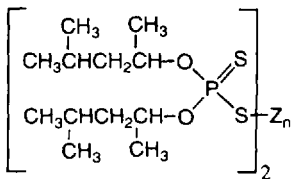
An antiwear additive is required to provide the necessary lubrication demanded by highly loaded wear contacts. Under these conditions, the protective oil film that is formed between the moving surfaces is penetrated by surface aspirates coming into contact with each other. Antiwear (AW) additives react with the metal asperities to form solid films which reduce wear at the contacting surface [104]. As the moving surfaces come into even closer contact, extreme-pressure (EP) additives react with the metal surface by a mechanism whereby the heteroatom (S or P) present in the EP additive is actually extruded into the metal surface, forming a softer metal-heteroatom surface coating which inhibits adhesive failure (microwelding of the surface aspirates as they come into contact with each other). The primary difference between AW and EP lubrication is the interfacial temperatures present within the wear contact [104].

One of the most common AW additives used in hydraulic oil formulation is ZDDP.

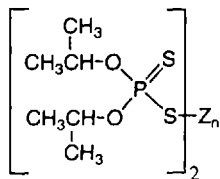


ZDDP
(Zinc Dialkyl Dithiophosphate)

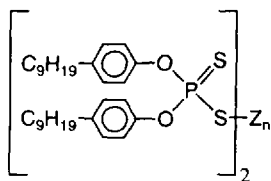
Some illustrative examples of ZDDP used as AW additives include [104]



Zinc di-4-methylpentyl-dithiophate



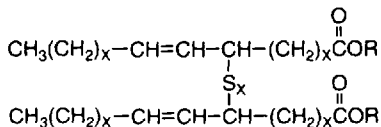
Zinc di-iso-propyl-dithiophate



Zinc di-nonylphenyl-propyl-dithiophate

It has been shown that ZDDP compositions decomposed and reacted with metal surfaces to form films containing zinc, phosphorus, and sulfur. The rate of formation and thickness of the films was a function of the fluid temperature, additive concentration and interaction, base-oil composition, atmosphere, and time [104]. In addition, decreasing thermal stability of the ZDDP resulted in increased the load-bearing capacity.

Generally, the structures exhibiting the best AW activity exhibit the worst EP performance. Thus, different additives must be used such as a sulfurized fatty ester and others, if effective EP activity is desired.



Sulfurized fatty ester

Antiwear oils were originally developed for vane pumps which operate at high speed and high pressure. R&O (rust and oxidation inhibited) oils were generally used with piston pumps which typically utilized a yellow metal for the shoes which rode against a steel or ferrous plate [105]. Unfortunately, the antiwear additive ZDDP, which was commonly used for formulating AW oils, was susceptible to hydrolysis, and the hydrolysis by-products would attack the yellow metals in piston pumps, precluding the use of a single oil for the two pumps.

The Lubrizol Corporation has illustrated the effect of varying the alcohol substituent (RO) on the ZDDP molecule on various performance properties, including hydrolytic stability, as shown in Table 14.17 [106]. Additives such as detergents and dispersants will also affect ZDDP performance [107].

7.4 Ashless Fluid Technology

Currently, there is a great deal of interest in the development and use of a nonmetal-containing additive, such as ZDDP, containing hydraulic fluids [97,100]. These additives are called "ashless additives." These fluids typically contain sulfur- and phosphorus-containing additives. Recent work has shown that hydraulic fluids formulated with ashless additives exhibit performance properties that are superior to ZDDP-formulated fluids, especially with respect to oxidative stability, protection of yellow metals, antiwear, and longer lifetimes. Ashless additive technology offers a significant advantage over conventional ZDDP additive technology with respect to increasing potential environmental and toxicological concerns with fluid leakage and disposal [108,109,117]. Fluid development in this area is continuing.

Table 14.17 Effect of ZDDP Structure on Thermal Performance

Zinc type	Antiwear	Extreme pressure	Antioxidant	Hydrolytic stability	Corrosion of soft metals	Thermal stability
Primary	Good	Good	Good	Best	Low to moderate	Good
Secondary	Best	Best	Good to excellent	Average	Moderate	Poor to average
Aryl	Poor	Poor	Poor	Poor	Moderate	Best

7.5 Additive Analysis

Although there are various methods for analyzing changes in additive concentration during use, one of the most common methods is infrared spectroscopy [110]. These methods are based on the infrared absorbency properties of the additives being utilized. Infrared absorbance follows Beer's law, which states

$$A = abc$$

where

A = the absorbency

a = the absorptivity, which is dependent on the molecular structure

b = the path length of light through the sample in the spectrometer

c = the concentration

Newer infrared spectrometers have subroutines which permit the simultaneous analysis of various additives based on the solution of simultaneous Beer's-law equations for each additive. Of course, the additive must be infrared active for this method to be used.

8 DETERMINATION OF LUBRICATION PERFORMANCE

One of the most common bench tests that has been traditionally employed to evaluate the antiwear properties of hydraulic fluids is the 4-ball test. Figure 14.37 illustrates the use of a 4-ball test to evaluate the effect of dissolved oxygen on wear behavior

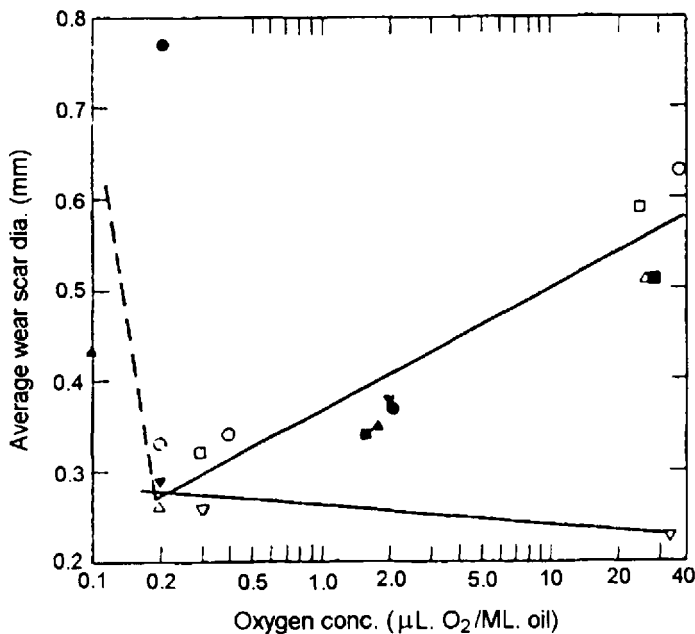


Figure 14.37 Effect of dissolved oxygen on wear exhibited by a mineral oil in a 4-ball wear scar test.

of mineral oil [111]. Although the 4-ball test (ASTM D 2783) has been proposed as a performance specification [46], none of the various attempts that have been made to correlate standard 4-ball wear with pump wear obtained with ASTM D 2882, which utilizes a Vickers V-104 vane pump, have been successful [112,113]. In fact, the only correlation data that have been published were performed at various test loads [114]. Poor correlation or no correlation was obtained; however, the best correlation was obtained with a 30-kg load as shown in Fig. 14.38 [114].

Tessmann et al. have developed a modified Falex pin-and-V-block test, which was designated as the “gamma wear test,” which reportedly does correlate with ASTM D 2882 [142]. However, this test has not gained industry acceptance to date. Additional, experimental potential bench-testing options are provided in Chapter 6.

In view of the general failure of bench performance tests to model pump wear, various pump tests have been developed [113,115]. As indicated previously, the most commonly encountered test is based on the Vickers V-104 vane pump. Figure 14.39

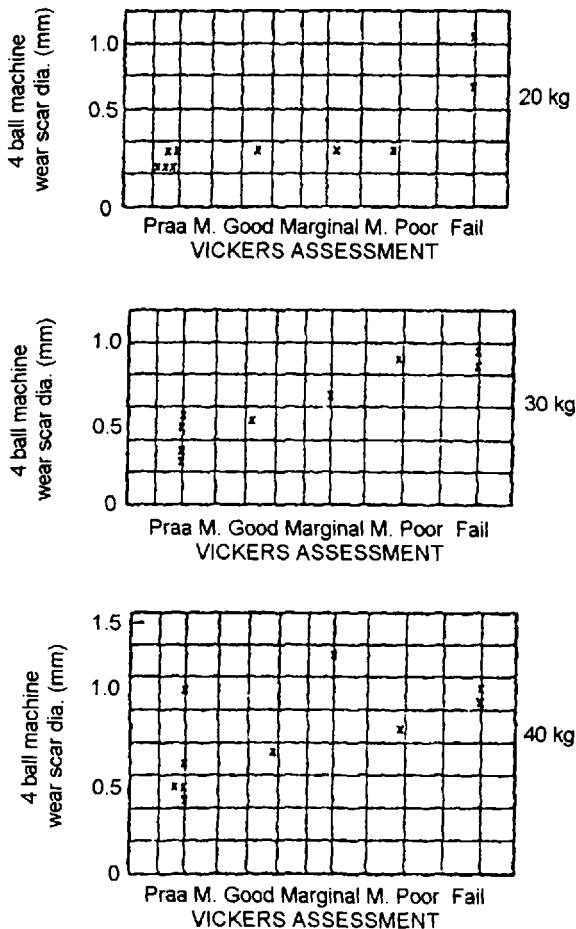


Figure 14.38 Attempted correlation of 4-ball machine wear and Vickers V-104 vane-pump wear.

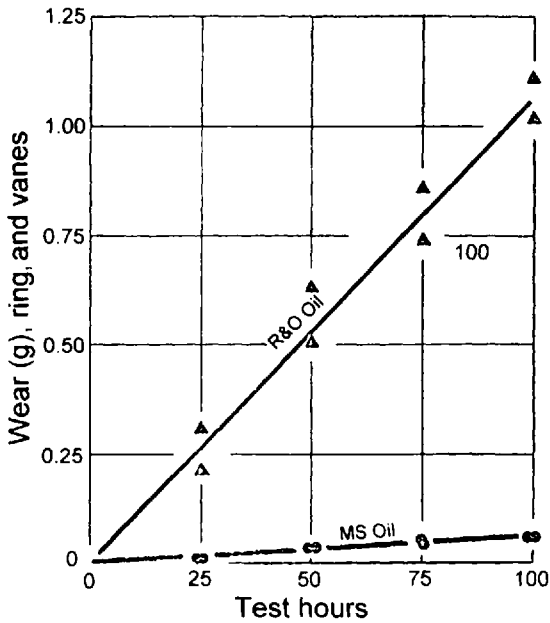


Figure 14.39 Comparison of R&O and antiwear oil performance using a Vickers V-104 vane-pump test (ASTM D 2882).

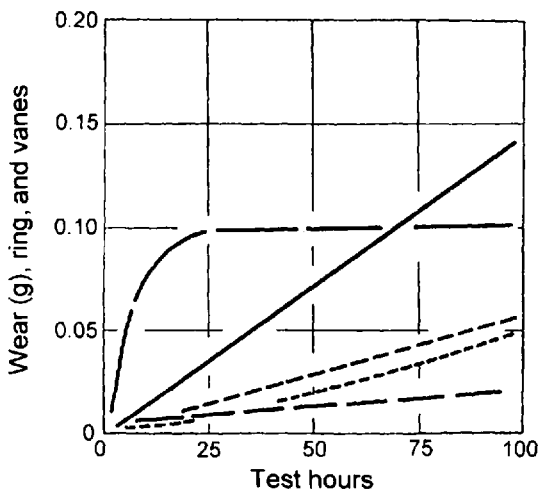


Figure 14.40 Comparison of antiwear performance of various mineral-oil hydraulic fluids using a Vickers V-104 vane-pump test (ASTM D 2882).

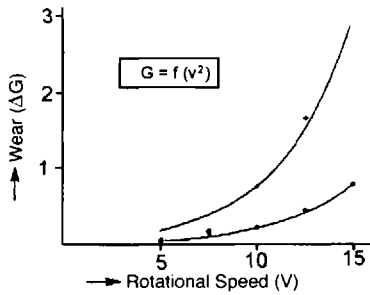


Figure 14.41 Dependence of Vickers V-104 vane pump test results on pump rotational speed.

illustrates the difference in ASTM D 2882 wear test results between a R&O oil and an antiwear oil [50]. Figure 14.40 illustrates typical differences in wear results obtained by different antiwear oils [50]. Langosch reported that V-104 vane-pump wear (ΔG) is exponentially dependent on the rotational speed (v) as shown in Fig. 14.41 [116]:

$$\Delta G = fv^2$$

Interestingly, there have been various proposals to couple a bench wear and V-104 vane-pump test requirements. Table 14.18 provides one illustration of such a proposed performance requirement [116].

Although the Vickers V-104 vane pump does permit differentiation of pump wear and thus provides a first-stage screening test, it is not a good indicator of expected pumpwear under more rigorous operating conditions such as higher pressure. Table 14.19 provides the requirements of four common pump performance tests and the required “pass” criteria [117]. Table 14.20 provides a recent recommendation for overall hydraulic fluid testing requirements which includes physical properties, rust and corrosion testing, oxidative stability, and pump lubrication performance [117].

In addition to the pump wear tests shown in Tables 14.19 and 14.20, additional tests have been developed to evaluate the effect of potential additive hydrolysis on yellow metal wear. One such test has been developed by Denison and is designated

Table 14.18 Hydraulic Fluid Wear Classification Tests

Hydraulic oil classification	V-104 vane-pump total wear (mg)	4-Ball test, 40-kg load, wear scar (mm)	Timken test 15 lbs., 1 h, wear scar (mm)	FZG Test A/8.3/90 number of stages passed
HLP I	<50	<0.6	<0.8	M10
HLP II	<250	<1.0	<1.2	M10
HL	<1000	<1.3	<2.0	M6
H	>1000	>1.3	>2.0	<6

Table 14.19 Criteria for Common Pump Performance Tests

Test	Denison HF-0	Denison HF-2	Vickers M-2950-S	DIN 51524 Part 2
Viscosity index	90 min	90 min		
Viscosity (cSt) at 40°C	a	a		a
Rust test (IP L35/ASTM D665)				
Method A	Pass	Pass	Pass	Pass
Method B	Pass	Pass	Pass	
Foam test (IP/ASTM D892)				
Seq I (stability/tendency)	No foam after 10 min	No foam after 10 min		150/0 max.
Seq II (stability/tendency)	No foam after 10 min	No foam after 10 min		75/0 max.
Seq III (stability/tendency)	No foam after 10 min	No foam after 10 min		150/0 max.
Air Release (IP 313), min.	No foam after 10 min	No foam after 10 min		5 max. for 32 grade
Demulsibility (ASTM D1401), min.			Report	40 max. for 32 grade
Oxidation at 1000 h (ASTM D4610)				
Neutralization value (mg KOH/g)	2.0 max.	2.0 max.	Report	2.0 max.
Insoluble sludge (mg)	200 max.	400 max.		
Thermal Stability Test (135°C, 168 h, Cu + Fe Rod)				
Sludge (mg)	100 max			

	Hydrolytic stability (ASTM D2619)		
Cu specimen weight loss (mg/cm ²)	0.20 max.	0.50 max.	
Acidity of water layer (mg)	4	6	
	Filterability test (TP 02100)		
(A) Max. filtration time without water (s)	600		
(B) Max. filtration time with 2% water (s)	2 × A		
	FZG test load stage (IP334)		
Fail			10 min.
	Pump tests		
ASTM D2882			
Ring wt. loss (mg)			120 max
Vane wt. loss (mg)			30 max
Vickers 35VQ25			Pass
Vane pump test (Denison T5D)	Pass	Pass	
Piston pump test (Denison P46)	Pass		

*Viscosity sufficient for application.

Table 14.20 Hydraulic Fluid State-of-the-Art Performance Plus Enhanced Load-Carrying Capabilities

	Specification or procedure	Typical fluid performance
Pump Performance		
Denison T5D vane	HF-0	Approved
Denison T-46 piston	HF-0	Approved
Vickers 35VQ-25 pump	M-2950-S	Pass
V-104C ring & vane wt. loss, mg @ 250 h	ASTM D2282	9.0
Racine, vane	S series variable	Approved
Oxidation and Corrosion		
Turbine oil oxidation, hours to 2.0 NNA	ASTM D943	2856 (17 weeks)
Sludge & metal corrosion	ASTM D4610 (1000 h)	
	HF-2	HF-0
NNA	2.0 max	2.0 max
Insoluble sludge (mg)	400 max.	200 max. 0.64
Total copper (mg)	200 max.	50 max. 85.2
Total iron (mg)	100 max.	50 max. 46.5
Hydrolytic stability		1.9
Copper wt. loss (mg/cm ²)	0.5 max.	0.2 max.
Copper appearance	ASTM D130	1B 0.14
Acidity of water layer (mg KOH)	6.0 max.	4.0 max.
Cincinnati Milacron thermal stability (168 h, 275°F (135°C), copper-steel cat.)		Basic
Sludge (mg/100 mL)	25 max.	7.8
Condition of copper rod, appearance (CM color class)	5 max.	2
Condition of steel rod, appearance (CM color class)	5 max.	2
Assessment		Approved
Turbine oil rust		
A—Distilled water	ASTM D665	Pass
B—Syn. seawater		Pass
Miscellaneous		
Turbine oil demulsibility 135°F, 54.4°C, mL: oil-water cuff (min)	ASTM D1401	40-40-0 (15)
Denison filterability, 1.2- μ m filter	HF-O	
A—No water (s)	600 max.	166
B—2% water (s)	2 \times A max.	219
Foam (tendency-stability)	ASTM D892	
Sequence I		0-0
Sequence II		20-0
Sequence III		0-0
FZG (failure load stage)	DIN 51534 Part 2	13/12

the "T6C test" [105,115]. This test is based on the Denison T6C vane pump and is conducted for 300 h "dry" and then 300 h "wet," which is accomplished by the addition of 1% water to the hydraulic oil. The test is conducted under 250 bars variable pressure for both dry and wet stages. The test temperature is 85°C. A 6- μm filter is used to determine if hydrolysis by-products cause filter plugging.

9 FLUID MAINTENANCE PROCEDURES

Periodic analysis of used hydraulic oils is a necessary part of any plant maintenance program in order to assure optimal performance with minimal downtime. There are two primary reasons for conducting an oil-analysis program (1) to determine if the oil quality is acceptable for continued use and (2) to assist in determining the root cause of a problem with the hydraulic system or one of its components [118].

Various factors may affect the useful lifetime of a hydraulic oil. Some of the most common factors are summarized in Table 14.21 [118]. Of those factors cited, the most common factor is excessive operating temperatures or system hot spots [118–121]. Optimal hydraulic oil temperature is 130–140°F (55–60°C). Excessive operating temperatures will result in significant reduction in the operating lifetime of the oil from years to hours. Therefore, a well-maintained hydraulic system is essential for minimizing downtime and equipment loss and malfunction. Periodic fluid analysis is an integral part of the maintenance program.

In this section, a series of recommended tests that should be performed periodically on a used hydraulic oil and their meaning will be outlined. This discussion will be supplemented with additional tests that may be conducted to gain further insight into fluid performance or system failure.

Table 14.21 Major Factors Influencing Useful Hydraulic Oil Lifetime

Problem	Fluid response
Excessive operating temperature and system hot spots	Viscosity increase due to fluid degradation accompanied by presence of acidic by-products that promote corrosion. Sludge and varnish is also formed, which reduces heat transfer and causes actuator malfunction
Contaminants	
Water	Catalyzes fluid oxidation, promotes rusting, and may lead to emulsification of the fluid which will lead to a reduction of lubrication effectiveness.
Airborne dirt and debris	Increase wear due to abrasion
Metalworking fluids	May promote sludging or corrosion.
Foaming and aeration	Causes poor lubrication and sluggish hydraulic system response.
Wear metals	Promotes fluid oxidation, causes abrasive wear, and may stabilize the potential formation of oil-water emulsions form by water contaminants.

9.1 Fluid Sampling

Fluid sampling should be taken from an operating system at operating temperature. The sample should be taken from the middle of the reservoir using a hand pump such as a large syringe (50 cc) with tubing of sufficient length attached. Routine sampling should not be taken from drains, low spots, or after the system is shut down for more than 2 h [122]. If a sample is taken from the pressure line, at least 1 quart of fluid should be removed before the sample is taken. Do not close the opening until the sample is taken. It is critical that all sampling equipment and bottles be scrupulously cleaned [122].

The necessary fluid sampling frequency will vary with the system operating conditions and the fluid. To determine the appropriate frequency, sampling could be weekly initially and the frequency decreased to an appropriate level based on the test results. Also, routine testing such as fluid cleanliness, water content, and viscosity could be more frequent and detailed analyses performed at less frequent intervals or as needed [122].

9.2 Basic Fluid-Analysis Tests

The basic tests that are conducted on used hydraulic oils are clarity, color, odor, water, viscosity, specific gravity, neutralization number or differential infrared analysis, sediment, ash, elemental analysis, and foaming/air entrainment [118].

9.2.1 Clarity, Color, and Odor

Fluid clarity is the first observation that is made in hydraulic fluid sampling. Uncontaminated or thermally abused fluid should be clear. Haziness or cloudiness is indicative of contamination, often by water or a water-containing source.

Color is perhaps the second observation. A sudden change in fluid darkness is indicative of oil oxidation, as illustrated in Fig. 14.42. This is typically accompanied by a rancid or pungent odor (burned fluid odor) and an opaque appearance due to water contamination and possibly also due to sediment, sludge, and so forth [118,119]. If fluid potential oxidation is evident, the TAN should be determined on the fluid.

Other sources of odor may be contaminants such as flushing fluids or a strong sulfur odor which may arise from contamination by other fluids such as flushing fluids [118].

9.2.2 Water

Hydraulic oils may absorb significant quantities of water through the reservoir breather pipe and also from other sources. As illustrated in Fig. 14.43, one of the determining factors for the amount of water absorbed is the base-oil composition [143]. Water contamination of a hydraulic oil may cause corrosion, enhance bearing wear, catalyze fluid oxidation resulting in reduced lifetime by as much as 70%, and affect component operation [123]. One common source of water contamination is ingress through the breather pipe in the reservoir. Generally, water concentrations should not exceed 200–300 ppm [123]. The effect of water concentration on fluid clarity is illustrated in Fig. 14.44.

There are a number of tests for the presence of water in a hydraulic oil. These include the following:

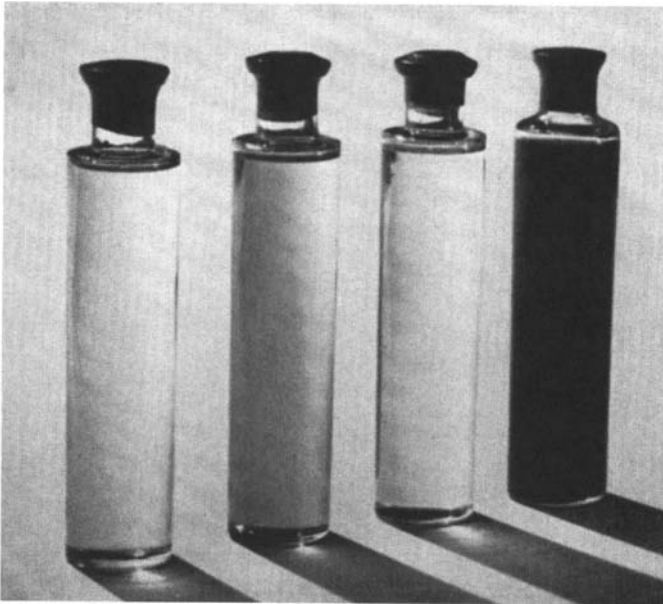


Figure 14.42 Comparison of color and TAN of new and oxidized oils from ASTM TOST. From the left: New inhibited hydraulic oil, same oil after 1000-h TOST test (TAN is approximately 0.1), new straight mineral oil, and same oil after a 100-h TOST (TAN is > 2.0 , the maximum allowable value). (Courtesy of Texaco, Inc.)

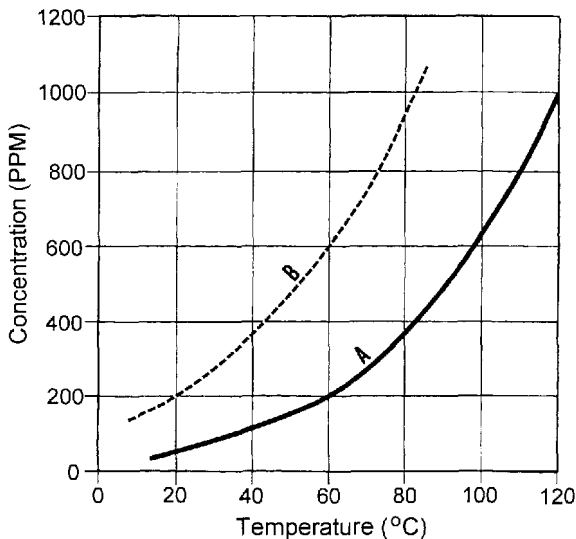


Figure 14.43 Effect of base-oil composition and temperature on maximum water solubility concentration. Curve A is a transformer oil and curve B is a high aromatic content oil.

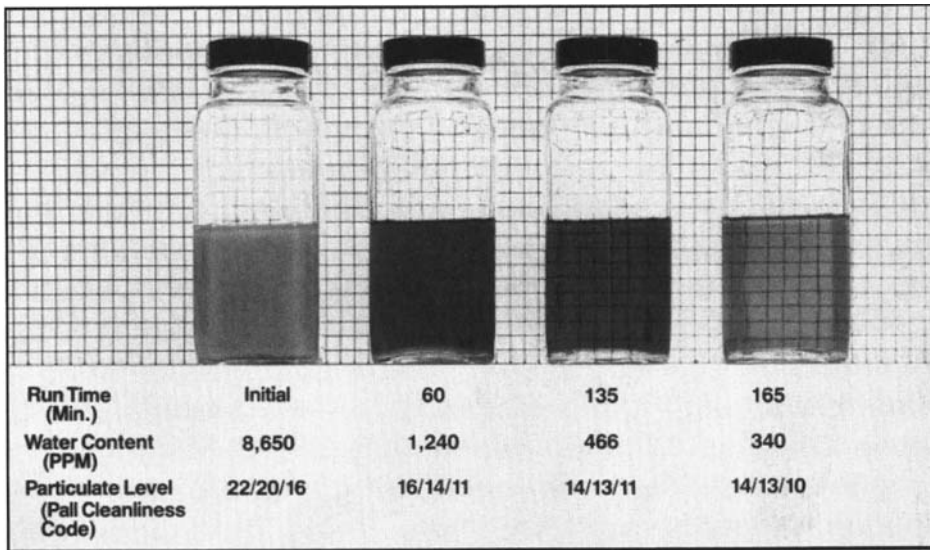


Figure 14.44 Illustration of hydraulic fluid clarity and water concentration. Also illustrated is the effectiveness of the use of an oil purifier in reducing water and solids contamination. (Courtesy of Pall Industrial Hydraulics Company.)

- **Crackle test.** This is a qualitative test for the presence of water that may be performed tankside. The crackle test is conducted by placing the fluid on a hot plate or even in a small piece of aluminum foil which is heated with a match using appropriate eye and face protection, as the fluid will make a “crackling” sound and spatter if it contains water [118].
- **Distillation method.** A sample of hydraulic fluid is heated with a solvent such as toluene or xylene in a round-bottomed flask equipped with a Dean–Stark trap and condenser as described in ASTM D 95 [124]. The mixture is heated until condensation of water into the trap ceases. The volume percentage of water in the oil is then calculated.
- **Karl Fischer method.** This test is conducted according to ASTM D 1744 and is suitable for water concentrations of 50–1000 ppm [125].
- **Centrifugation.** This test may be performed according to ASTM D 1796 if the hydraulic oil is hazy or cloudy [126]. It is performed by centrifuging a sample of the used oil at 6000 rpm to clarify the oil. After centrifuging, the clarified oil is at the top, metallic contaminants at the bottom, carbonaceous materials are above the metal contaminants, and the water, if present, forms an intermediate layer [118].

9.2.3 Viscosity

Fluid viscosity may be determined by ASTM D 445 [kinematic viscosity in centistokes (cS)] or in Saybolt Universal Seconds (SUS) according to ASTM D 2161 [128]. Viscosity may also be readily determined in the field using an instrument such as that shown in Fig. 16.45.

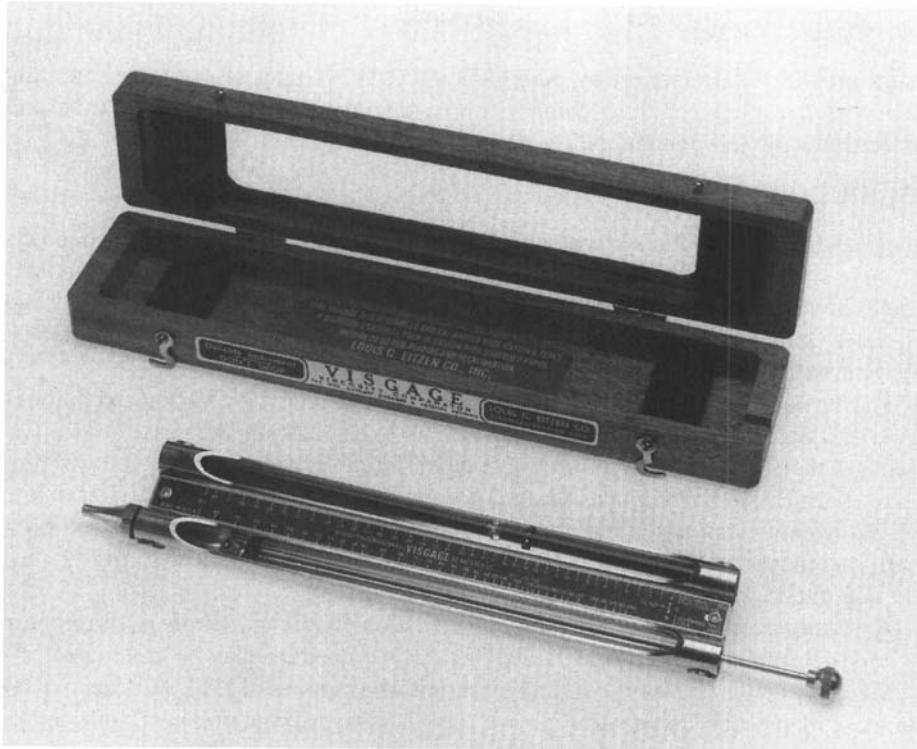


Figure 14.45 Illustration of the Kleentek patch test to quantify the presence of oil oxidation by-products. (Courtesy of Kleentek—A CLARCOR Company.)

Low viscosity values usually indicate contamination with a lower-viscosity oil, solvent contamination, or additive deterioration [122]. Higher viscosity values indicate oxidative degradation, contamination by a higher-viscosity oil, or water contamination [122]. If oxidative degradation had occurred to a sufficient extent to lead to increased viscosity, a corresponding increase in TAN (total acid number) should be observed [118]. It is essential that the fluid viscosity be maintained within the hydraulic pump manufacturer's limits.

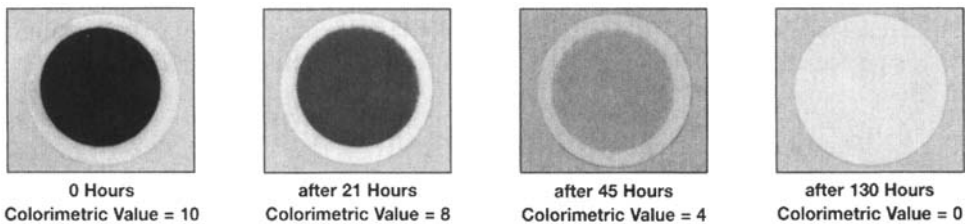


Figure 14.46 Illustration of a viscosity measurement gauge suitable for tankside use. (Courtesy of Visgauge Inc.)

9.2.4 Specific Gravity

Specific gravity determination by ASTM D 4052 [129] may also be an important indicator of variations in fluid composition which may occur with oxidative and other degradation and contamination processes [121].

9.2.5 Oil Degradation

Oil degradation by-products may cause rusting or the “gummy” sludge deposits may cause sticking and malfunctioning of hydraulic actuators [119,120]. Oil oxidation may be detected by more traditional testing methods such as TOST, RBOT, and TAN. These procedures were discussed in Sections 6.2.1, 6.2.2, and 6.2.3, respectively, and will not be detailed here.

The presence of oil-oxidation products may be detected by various techniques such as the patch test illustrated in Fig. 14.46 [120,122]. In this case, the oil is diluted and then filtered through a 0.8- μm patch filter. A predominantly yellow color indicates varnishlike by-products. Gray color residues indicate dust and other debris [120]. Whirlpool corporation has reported the use of a colorimetric test based on a spectrophotometric analytical procedure which provides a numerical rating (1–10) of the amount of oxidation by-products present [120].

An alternative to these tests for the detection of oil oxidation is differential infrared spectrometry [118,124,130]. This analysis procedure may be conducted off-line [118,131] or on-line as a continuous monitoring process [131]. Differential refractance will provide information on oil type, additives, contaminants, and degradation by-products [118].

9.2.6 Ash

Analysis of used hydraulic fluids for ash content may be helpful in determining additive depletion (for zinc-containing antiwear oils) or the presence of wear metals, dirt, coolants, and other contaminants [118]. ASTM D 482 [132] is used for determining the ash content of R&O hydraulic oils that do not contain ash-forming additives [118]. ASTM D 874 [133] is used to determine the ash content of antiwear hydraulic oils formulated with ash-containing additives.

9.2.7 Elemental Analysis

The ash residue obtained from ASTM D 482 or ASTM D 874 may be further analyzed for elemental content using emission, atomic absorption (AA), or induction-coupled plasma (ICP) spectroscopy. The elemental content may provide insight into the source of the ash-containing residue as shown in Table 14.22 [118].

X-ray diffraction may be used to assist in identifying the source of crystalline solid residues that may be present in a hydraulic fluid. A selected listing of crystalline solids potentially identifiable by x-ray diffraction was presented previously by Young and is given in Table 14.23.

9.2.8 Foaming/Air Release

Hydraulic oils that are either contaminated or that have undergone oxidation are more susceptible to foaming and air entrainment. Foaming and air entrainment not only lead to “spongy” hydraulic control due to increased fluid compressibility but also to increased susceptibility to sludge and varnish formation due to accelerated

Table 14.22 Sources of Possible Mineral Elements That May Be Present in Ash Residue of Hydraulic Fluids

Element	Sources
Aluminum, silicon	Dust and airborne dirt
Boron, potassium, sodium	Coolant inhibitor residues
Calcium, magnesium	Hard water
Calcium, sodium	Salt water (brine)
Chromium, copper, iron, zinc, lead, tin	Wear, corrosion, or assembly debris
Barium, calcium, magnesium, phosphorus, zinc	Engine-oil additives

oxidation rates, as discussed in Section 6. Description of tests for foaming and air entrainment were provided earlier in Sections 4.7 and 4.8, respectively, and will not be discussed further here.

9.3 Fluid Cleanliness

It is generally accepted that control of fluid cleanliness is vitally important for the proper operation and maintenance of hydraulic systems [119,134]. One form of analysis of fluid cleanliness is particle counting. Particle-counting procedures for determining fluid cleanliness are described in detail in Chapter 12. However, a diagnostic procedure is to determine the source of the particles. Spectrophotometric

Table 14.23 Compounds Identifiable by Elemental Composition and X-Ray Diffraction Spectroscopy

Element	Chemical formula	Examples
Chromium	Cr	Wear metal
Copper	Cu	Wear metal or corrosion
Copper oxides	CuO and Cu ₂ O	Wear metal or corrosion
Iron	Fe	Wear metal
Iron oxide	FeO (Wustite)	Fretting corrosion at high temperature
Iron oxide	α Fe ₂ O ₃ (Hematite)	Fretting corrosion
Iron oxide	Fe ₃ O ₄ (Magnetite)	Corrosion of iron with limited supply of oxygen (under oil layer)
Iron oxide hydrate	γ Fe ₂ O ₃ · H ₂ O (Lepidocrocite)	Light surface rusting
Iron oxide hydrate	α Fe ₂ O ₃ · H ₂ O (goethite)	Bulk or heavy rusting
Iron oxide hydrate	β Fe ₂ O ₃ · H ₂ O (beta iron oxide hydrate)	Halide corrosion or paint pigment residue
Silicon dioxide	SiO ₂	
Sodium chloride	NaCl (salt)	
Tin	Sn	
Tin oxides	SnO and SnO ₂	

procedures may be used as described in Section 9.2.7 or ferrographic analysis may be used. Analytical ferrography may be used to identify the source of larger particulate debris in a hydraulic fluid. Figure 14.47 provides a comparison of the differences in the sizes of particles analyzed by these different procedures [130].

10 SYSTEM FLUID REPLACEMENT

During use, there is a buildup of oil-oxidation films and deposits in the hydraulic system. It is therefore necessary to clean the system and replace the hydraulic oil periodically. If the deposits are films or light emulsion coatings on the metal surfaces, the system can usually be cleaned by flushing [135]; however, if there is a substantial buildup of these deposits, manual cleaning of the dismantled system is often necessary.

10.1 Flushing Fluid

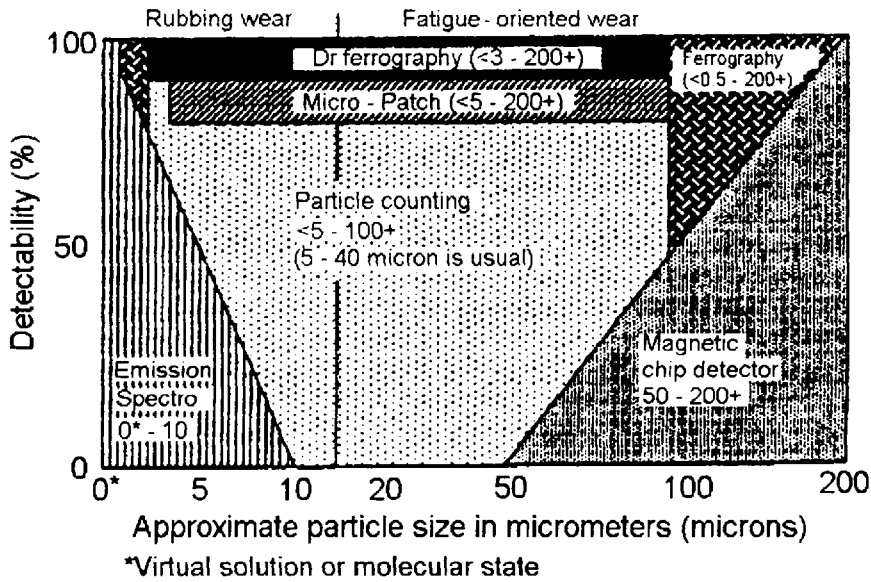
The flushing fluid should have the following qualities [135]:

- Possess a viscosity high enough, typically 70–110 SUS at 100°F, to lubricate moving parts and to keep solid contaminants suspended. The flushing fluid may be the system operating fluid or a special flushing fluid.
- Exhibit sufficient solvency to remove oily deposits. Usually naphthenic oils are better in this regards. It is not recommended that “gum or varnish solvents” be used.
- Contain rust and oxidation inhibition in order to maintain these properties when blended with the final charge of hydraulic oil.
- Solvents and chemical cleaners are not recommended; for example, halogenated petroleum solvents, caustic compounds, and so forth must not be used [136].
- Steam cleaning is not recommended. It is not possible to remove all traces of water and system rusting and oil contamination will result.
- The flushing fluid must be compatible with all components of the hydraulic system, including seals, hoses, components, rust-preventative paints, and preservatives in pipes or tubes that are normally not removed.

10.2 Flushing Procedure [136]

The following procedure was excerpted from ASTM D 4174. The reader is encouraged to obtain and follow this, or an equivalent standard, prior to flushing his hydraulic system.

- Prior to flushing, all accessible areas of the system should be inspected.
- Do not flush through valves; use bypasses. All leads to cylinders and motors should be blanked off using jumpers.
- External pumps must be used, if necessary, to assure turbulent flow (Reynolds numbers > 20,000) through the system. Fluid flow should be at least three times the normal flow velocity.
- Temporary humidity control devices that have been placed in the system before flushing should be removed.



	IDENTIFICATION				Interference		
	Wear metals	Size	Shape	Abrasives	Other	Water	Opacity
Emission spectro	Excellent	Poor	No	V.Good	Additives coolant	Minimal	Minimal
Particle counting	Poor	Excell	No	Poor	----	Bad	Bad
Ferroggraphy	Fair	V.Good	Excell	V.Good	Fibers heat	Minimal	Minimal
Direct reading ferroggraphy	Iron	Fair	No	No	----	Minimal	Minimal
Micro - Patch	Fair	Fair	Good	Good	Fibers rust	Minimal	Minor

Figure 14.47 Graphic illustration of estimated particle size operating range for various particulate characterization methods. (Courtesy of Lubricant Consultants, Inc.)

- Solid contamination in the lines can be loosened by hammering and vibration.
- The fluid used for flushing should be preheated to 140–180°F (60–80°C) prior to the flushing operation.
- Flushing times may vary from 12 h to several days. The flow capacity should be 10–20% of the total volume of the fluid during flushing.
- System pump discharge pressures should be reduced during flushing by lowering relief valve or compensator pressures.
- When flushing is completed, the flushing fluid should be completely drained from the system, coolers, and strainers.
- After flushing, the system is charged with operating fluid. If significant quantities of the flushing fluid remain, the system should be flushed again with the operating fluid. All fluids entering the hydraulic system should be prefiltered to at least 3–10 μm absolute.

11 HYDRAULIC FLUID RECYCLING AND RECLAMATION

There is increasing interest in extending the lifetime of hydraulic oils. The reasons for this interest include reduced environmental liability, reduced disposal costs, saving in oil purchases, relatively low cost of reclamation, and excellent quality control procedures available [137]. The four primary processes for reclaiming used hydraulic oil include (1) recovery as fuel, (2) re-refining, (3) oil laundering, and (4) reconditioning on-site [138]. Brief overviews of these processes will be provided here.

11.1 Recovery as Fuel

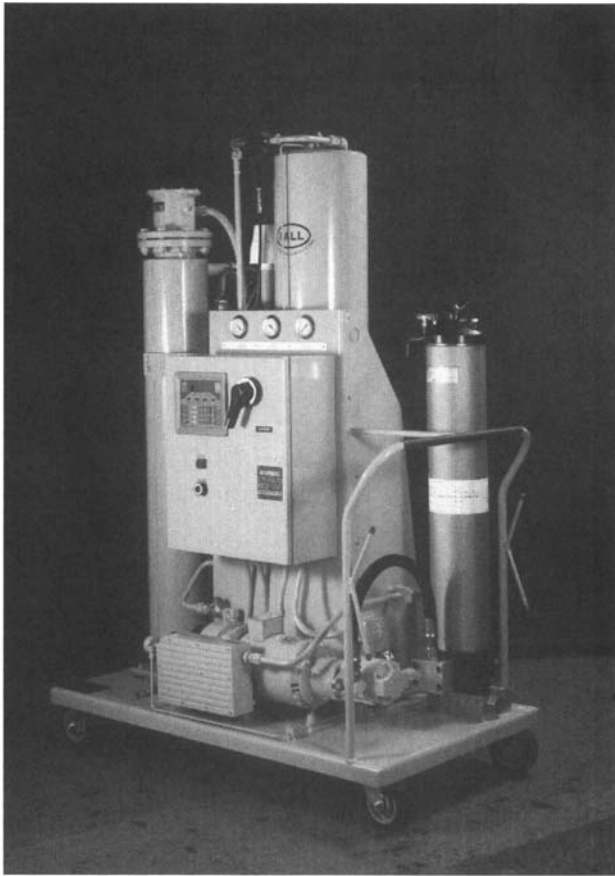
Recovery and use as a fuel source is perhaps the most common reclamation procedure in the industry at the present time [138]. This procedure involves emulsification and solids removal by filtration. The oil is then blended to the desired viscosity and used as fuel. This process, although still widely practiced, is coming under increasing scrutiny because of potential toxic emissions problems [138].

11.2 Re-refining

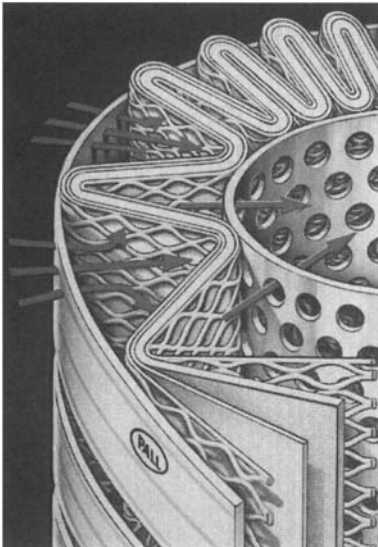
Re-refining of used hydraulic oil refers to treatment by one of a number of processes to remove contaminants such as dust, moisture, combustion by-products, corrosion products, and metal wear debris [139]. One common re-refining process involves vacuum dehydration of the used oil at 650 mm Hg and 150°C. The oil is cooled to approximately 40°C and then treated with sulfuric acid to facilitate sludge separation and removal. After the sludge is removed, approximately 6% of clay is added to form a clay-oil slurry. After heating at 300°C for 2–3 h, the vapors are condensed and the hot slurry is filtered. The re-refined oil is then treated with additives at 40–60°C before reuse [139]. This process, however, is only applicable for large-volume reclamation; due to environmental concerns, it is not normally used. Re-refining is more commonly done by vacuum distillation followed by severe hydrotreating. Large volumes of oils are processed by this method and are used as base stock for many hydraulic oils.

11.3 Oil Laundering

Oil laundering refers to recovery and cleaning of bulk loads of hydraulic oil and then returning them to the same company for reuse [138,140]. In this process, water vapor, solids, and oil-oxidation by-products must be removed. Various processes may be used in oil reclamation, typically classified as mechanical separation, chemical separation, and electrostatic filtration [141]. Mechanical separation methods of dirt and debris removal most commonly include filtration and centrifugation, which is most applicable for large-volume processing. Water vapor is removed by various processes, including distillation or vacuum dehydration [142,143]. A combination process illustrated in Fig. 14.48 may also be used. Chemical separation processes include the use of adsorption and filtration of acidic oxidation by-products or chemical conversion to less harmful components by chemical reduction. Electrostatic filtration is used to remove charged oil-soluble oxidation by-products.



(a)



(b)

Figure 14.48 Illustration of a stationary (a) and portable (b) Pall oil purifier for removal of water, dirt, and air contaminants from a hydraulic oil. The system operates under low (24 in. Hg) vacuum and employs a spinning disk (c) which facilitates contaminant separation by increasing surface area of the oil by formation of oil droplets during the separation process. (Courtesy of Pall Industrial Hydraulics Inc.)

Table 14.24 New Hydraulic Oil Specification and Typical Results from Recycling Trials in the Cold Mill

Test	Reference	Specification	Waste oil	Reclaimed oil
Particle count	ISO 4406	16/13 (Report)	Too contaminated	16.13
Appearance	Visual	Clear and bright	Black and hazy	Clear and bright
Water (ppm)	Karl Fischer	100 max.	214.000	62.000
Viscosity (cSt @ 40°C)	ASTM D445	41.4–50.6	46.700	44.000
Flash point (°C)	ASTM D92	204 min.	Not tested ^a	209.000
Total acid no.	ASTM D974	1.0 max.	0.290	0.500
Demulsibility @ 54°C	ASTM D1401	37 mL in 30 min	Not tested ^a	37 mL in 30 min
Zinc (%)	ICP	0.04–0.06	0.029	0.050
Phosphorus (%)	ICP	0.04 min.	0.029	0.046
Sulfur (%)	ICP	0.15 max.	0.15	0.15
Copper corrosion 3 h @ 100°C	ASTM D130	1B max.	Not tested ^a	1a
Foam sequence 2	ASTM D892	100/0 max.	Not tested ^a	75/0
Foam sequence 3	ASTM D892	150/0 max.	Not tested ^a	100/0

^aThese tests are not normally conducted on waste oil, but should the sulfur content be greatly off-spec, the oil recycler may, at his discretion, choose to do so.

COLD MILL WASTE HYDRAULIC OIL RECYCLING PROCESS FLOW DIAGRAM

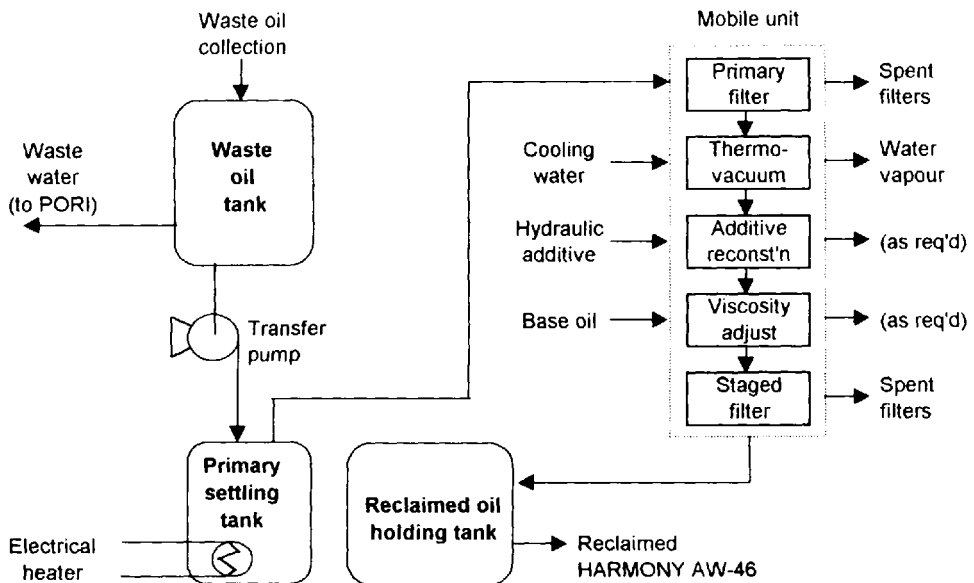


Figure 14.49 Schematic of a waste hydraulic oil reclamation process.

11.4 On-Site Reclamation

Oil may also be reconditioned on-site [137,138,144]. This is usually performed using processes such as vacuum dehydration, filtration, and adsorption methods [137,144]. Table 14.24 illustrates the successful recondition of used hydraulic oil following the process illustrated in Fig. 14.49 [137]. Although this is a relatively large on-site recondition process, it does provide an example of a successful process.

REFERENCES

1. F. J. Villforth, ed., "Hydraulics," *Lubrication*, 1996, 82(1), pp. 18–24.
2. Anon., "Product Review: Oil Refining and Lubricant Base Stocks," *Ind. Lubr. Tribol.*, 1997, 49(4), pp. 181–188.
3. G. H. Hoo and E. Lewis, "Base Oil Effects on Additives Used to Formulate Lubricants," in *Adv. Prod. Appl. Lube. Base Stocks, Proc. Int. Symp.*, H. Singh, P. Rao, and T. S. R. Tata, eds., 1994, McGraw-Hill; New Delhi, pp. 326–333.
4. R. J. Prince, "Base Oils From Petroleum," in *Chem. Technol. Lubr.*, R. M. Mortier and S. T. Orszulik, eds., 1992, Blackie; Glasgow, pp. 1–31.
5. H. Singh, "Characterization of Lube Oil Base Stock—Approach and Significance," in *Adv. Prod. Appl. Lube. Base Stocks, Proc. Int. Symp.*, H. Singh, P. Rao, and T. S. R. Tata, eds., 1994, McGraw-Hill; New Delhi, pp. 303–310.
6. T. Yoshida, H. Watanabe, and J. Igarashi, "Pro-oxidant Properties of Basic Nitrogen Components in Base Oil," in *Proc. of 11th Int. Colloquium Industrial and Automotive Lubrication—Vol. 1*, W. J. Bartz, ed., 1998, Technische Akademie Esslingen; Esslingen, pp. 433–444.

7. ASTM D 3238-90, "Standard Test Method for Calculation of Carbon Distribution and Structural Group Analysis of Petroleum Oils by the n-d-M Method," American Society for Testing and Materials, Conshohocken, PA.
8. A. Adhvaryu and I. D. Singh, "FT-NMR and FTIR Applications in Lubricant Distillates and Base Stocks Characterization," *Tribotest J.*, 1996, 3(1), pp. 89-95.
9. H. Singh, A. Adhvaryu, I. D. Singh, and G. S. Chaudhary, "NMR Based Characterization of Lubricant Base Oils," in *Symp. on Worldwide Perspectives on the Manf., Charac., and Appl. of Lubricant Base Oils*, Div. of Pet. Chem. Inc., 213th Nat. Meet. of Am. Chem. Soc., 1997, pp. 255-258.
10. H. Singh and I. D. Singh, "Use of Aromaticity to Estimate Base Oil Properties," *Adv. Prod. Appl. Lube Base Stocks, Proc. Int. Symp.*, H. Singh, P. Rao, and T. S. R. Tata, eds., 1994, McGraw-Hill; New Delhi, pp. 288-294.
11. A. K. Bhatnagar, "Base Oil Composition and Lubricant Performance," in *Adv. Prod. Appl. Lube Base Stocks, Proc. Int. Symp.*, H. Singh, P. Rao, and T. S. R. Tata, eds., 1994, McGraw-Hill; New Delhi, pp. 402-417.
12. M. Al-Banwan, "Base Stocks Properties/Characteristics, Additive Response and Their Interrelationship," in *Adv. Prod. Appl. Lube Base Stocks, Proc. Int. Symp.*, H. Singh, P. Rao, and T. S. R. Tata, eds., 1994, McGraw-Hill; New Delhi, pp. 303-310.
13. H. Singh, A. Adhvaryu, D. Singh, and G. S. Chaudhary, "Influence of Refining on Base Oil Composition," in *Symp. on Worldwide Perspectives on the Manf., Charac., and Appl. of Lubricant Base Oils*, Div. of Pet. Chem. Inc., 213th Nat. Meet. of Am. Chem. Soc., 1997, pp. 259-261.
14. E. Metro, "Fuchs Study Sees Trends Toward Hydrocracked Base Oil Manufacturing Within 5 Years," *Fuels Lubes Int.*, 1998, 4(3), p. 7.
15. G. V. Dyroff, ed., *ASTM Manual on Significance of Tests for Petroleum Products*, 6th ed., 1993, American Society for Testing and Materials; Conshohocken, PA.
16. A. W. Drews, ed., *ASTM Manual on Hydrocarbon Analysis*, 5th ed., American Society for Testing and Materials, Conshohocken, PA.
17. A. S. Sarpal, G. S. Kapur, S. Mukherjee, and S. K. Jain, "Characterization by ^{13}C NMR Spectroscopy of Base Oils Produced by Different Processes," *Fuel*, 1997, 76(10), pp. 931-937.
18. H. Singh and S. Swaroop, "Oxidation Behavior of Base Oils and their Constituting Hydrocarbon Types," in *Symp. on Worldwide Perspectives on the Manf., Charac., and Appl. of Lubricant Base Oils*, Div. of Pet. Chem. Inc., 213th Nat. Meet. of Am. Chem. Soc., 1997, pp. 218-220.
19. B. N. Barman, "Bias in the IP 346 Method for Polycyclic Aromatics in Base Oils and in ASTM D 2007 Method for Hydrocarbon Type Determination," in *Symp. on Worldwide Perspectives on the Manf., Charac., and Appl. of Lubricant Base Oils*, Div. of Pet. Chem. Inc., 213th Nat. Meet. of Am. Chem. Soc., 1997, p. 263.
20. "Standard Test Method for Characteristic Groups in Rubber Extender and Processing Oils and Other Petroleum Derived Oils by the Clay-Gel Absorption Chromatographic Method," American Society for Testing and Materials, Conshohocken, PA.
21. N. Varotsis and N. Pasadakis, "Rapid Quantitative Determination of Aromatic Groups in Lubricant Oils Using Gel Permeation Chromatography," *Ind. Res. Chem. Res.*, 1997, 36, pp. 5516-5519.
22. P. Daucik, T. Jakubik, N. Pronayova, and B. Zuki, "Structure of Oils According to Type and Group Analysis of Oils by the Combination of Chromatographic and Spectral Methods," *Mech. Eng.* 80 (Eng. Oils and Auto Lub.), 1993, pp. 48-58.
23. S. S. V. Ramakumar, N. Aggarwal, A. Madhusudhana Rao, S. P. Srivastava, and A. K. Bhatnagar, "Effect of Base Oil Composition on the Course of Additive-Additive Interactions," *Adv. Prod. Appl. Lube Base Stocks, Proc. Int. Symp.*, H. Singh, P. Rao, and T. S. R. Tata, eds., 1994, McGraw-Hill; New Delhi, pp. 334-340.

24. P. A. Maas, "Selecting Hydraulic Fluids," *Plant. Eng.*, 1973, October, pp. 122–125.
25. H. E. Tiffany, "How Additives Improve Hydraulic Fluids," *Machine Design*, 1973, December 27, pp. 48–51.
26. ASTM D 2422-86, "Standard Classification of Industrial Fluids Lubricants by Viscosity System," American Society for Testing and Materials, Conshohocken, PA.
27. International Standard ISO 6743/4, "Lubricants, Industrial Oils and Related Products (Class L)—Classification Part 4: Family H (Hydraulic Systems), First Edition, 1982.
28. J. Reichel, "Pump Testing Strategies and Associated Tribological Considerations—Vane Pump Testing Methods ASTM D 2882, IP281, and DIN 51389," in *Tribology of Hydraulic Pump Testing*, G. E. Totten, G. H. Kling, and D. J. Smolenski, eds., 1996, American Society for Testing and Materials, Conshohocken, PA, pp. 85–95.
29. D. Saxena, R. T. Mookerjee, S. P. Srivastava, and A. K. Bhatnagar, "An Accelerated Aging Test for Anti wear Hydraulic Oils," *Lubr. Eng.*, 49(10), pp. 801–809.
30. D. Klamann, "11.9 Hydraulic Fluids," in *Lubricants and Related Products—Synthesis, Properties, Applications, International Standards*, 1984, Verlag Chemie; Weinheim, pp. 307–323.
31. Anon., "Industrial Hydraulic Oils," *Lubrication*, 1956, 42(7), pp. 89–100.
32. Racine Hydraulics & Machinery, Inc., *Petroleum Hydraulic Fluids Recommendations*, Racine Hydraulics & Machinery, Inc.; Racine, WI.
33. Vickers Inc., *Hydraulic Fluid Recommendations for Industrial Machinery Hydraulic Systems*, Vickers Inc., Rochester Hills, MI.
34. Oilgear Co., *Oil Recommendations*, The Oilgear Company, Milwaukee, WI.
35. A. E. Bingham, "Some Problems of Fluids for Hydraulic Power Transmission," *Inst. Mech. Eng.—War Emergency Proc.*, 1951, 165(69), 254–277.
36. A. C. Smith, "Some Notes on the Data on Hydraulic Oil Properties Required by Systems Designers," *Sci. Lubr.*, 1965, February, pp. 63–69.
37. ASTM D 892-74, "Standard Test Method for Foaming Characteristics of Lubricating Oils," American Society for Testing and Materials, Conshohocken, PA.
38. D. G. Godfrey and W. R. Herguth, "Physical and Chemical Properties of Industrial Mineral Oils Affecting Lubrication—Part 2," *Lubr. Eng.*, 1995, 51(6), pp. 493–496.
39. M. E. Wege, "Hydraulic Fluid Requirements—Construction Equipment," SAE Technical Paper Series, Paper 710723, 1971.
40. ASTM D 97-87, "Standard Test Method for Pour Point Determination of Petroleum Oils," American Society for Testing and Materials, Conshohocken, PA.
41. ASTM D 5949-96, "Standard Test Method for Pour Point of Petroleum Products (Automatic Tilt Method)," American Society for Testing and Materials, Conshohocken, PA.
42. ASTM D 5950-96, "Standard Test Method for Pour Point of Petroleum Products (Automatic Pressure Pulsing Method)," American Society for Testing and Materials, Conshohocken, PA.
43. ASTM D 5985-96, "Standard Test Method for Pour Point of Petroleum Products (Rotational Method)," American Society for Testing and Materials, Conshohocken, PA.
44. ASTM D 1250-80, "Standard Guide for Petroleum Measurement Tables," American Society for Testing and Materials, Conshohocken, PA.
45. D. G. Godfrey and W. R. Herguth, "Physical and Chemical Properties of Industrial Mineral Oils Affecting Lubrication—Part 3," *Lubr. Eng.*, 1995, 51(10), pp. 825–828.
46. A. A. Mently, "Basic Properties of Fluids for Hydrostatic Transmissions," 1979, September, pp. 93–96.
47. ASTM D 92-85, "Standard Test Method for Flash and Fire Points by Cleveland Open Cup," American Society for Testing and Materials, Conshohocken, PA.
48. ASTM D 93-85, "Standard Test Methods for Flash Point by Pensky-Martens Closed Tester," American Society for Testing and Materials, Conshohocken, PA.

49. A. J. Zino, "What to Look for in Hydraulic Fluids—I," *Machinist*, 1947, November 6, pp. 93–96.
50. J. Q. Griffith, W. H. Reiland, and E. S. Williams, "Laboratory and Field Performance of Wear Resistant Antileak Hydraulic Oils," *National Fuels and Lubricants Meeting*, 1969, Paper F&L-69-64.
51. Association of Hydraulic Equipment Manufacturers (AHEM) Working Party Report, "Proposed Method of Classifying Mineral Oils by Seal Compatibility Index," *J. Inst. Petrol.*, 1968, 54(530), pp. 36–43.
52. EXXON Co., *Industrial Hydraulic Fluids*, Lubetext DG-2C, EXXON Company, U.S.A., Houston, TX.
53. A. J. Zino, "What to Look for in Hydraulic Oils—IV Demulsibility," *Am. Machinist*, 1947, December 18, pp. 94–95.
54. ASTM D 1401-84, "Standard Test Method for Water Separability of Petroleum Oils and Synthetic Fluids," American Society for Testing and Materials, Conshohocken, PA.
55. A. G. Papay and C. S. Harstick, "Petroleum-Based Industrial Oils—Present and Future Developments," *Lubr. Eng.*, 1975, 31, January, pp. 6–15.
56. H. Hydrick, "Hydraulic Systems Benefit from Filtering Standard," *Lubr. World*, 1995, 5(6), pp. 19–20.
57. R. L. Leslie, "Hydraulic Fluids for Extreme Service," *Machine Design*, 1972, January 13, pp. 114–117.
58. Pall FIT-PMO Rev. 4, "Pall Filterability Index Test for Paper Machine Oils," Pall Corporation, Glen Cove, NY.
59. S. Antika, W. Y. Wang, and T. G. Dietz, "Development of Advanced Paper Machine Lubricant," *TAPPI J.*, 1998, 81(4), pp. 62–74.
60. F. Ross, "Why *Treated* Hydraulic Oils," *Appl. Hydraul.*, 1950, April, pp. 21–23, 42, 52.
61. R. H. Dipple, "Hydraulic Oils—Their Physical Properties and Maintenance," *Hydraul. Power Transmiss.*, 1962, April, pp. 240–242.
62. A. C. Smith, "Selection of Oils for Industrial Hydraulic Systems," *Sci. Lubr.*, 1951, July, pp. 20–26.
63. R. J. Cappell, "Failure Analysis of Hydraulic Actuators—Break-down of Trichloroethane Used as Cleaning Agent Releases Chlorides," *Mater. Protect.*, 1962, December, pp. 30–31, 33–34, 36.
64. ASTM D 130-83, "Standard Method for Detection of Copper Corrosion from Petroleum Products by the Copper Strip Tarnish Test," American Society for Testing and Materials, Conshohocken, PA.
65. ASTM D 665-83, "Standard Test Method for Rust-Preventing Characteristics of Inhibited Mineral Oil in the Presence of Water," American Society for Testing and Materials, Conshohocken, PA.
66. H. R. Baker, D. T. Jones, and W. A. Zisman, "Polar-Type Rust Inhibitors: Methods of Testing the Rust-Inhibition Properties of Polar Compounds in Oils," *Ind. Eng. Chem.*, 1949, 41, pp. 137–140.
67. C. Jones, "Properties of Hydraulic Fluids," *Mechan. World Eng. Rec.*, 1964, January, pp. 3–5.
68. A. Sasaki, T. Tobisu, S. Uchiyama, and M. Kawasaki, "GPC Analysis of Oil Insoluble Oxidation Products of Mineral Oil," *Lubr. Eng.*, 1991, 47(7), pp. 525–527.
69. A. Sasaki, T. Tobisu, S. Uchiyama, and M. Kawasaki, "Evaluation of Molecular Weight and Solubility in Oil of Two Different Types of Oils," *Lubr. Eng.*, 1991, 47(10), pp. 809–813.
70. A. Sasaki and T. Yamamoto, "A Review of Studies of Hydraulic Lock," *Lubr. Eng.*, 1993, 49(8), pp. 585–593.

71. J. A. Farris, "Extending Hydraulic Fluid Life by Water and Silt Removal," Field Service Report 52, Industrial Hydraulics Division, Pall Corporation, Glen Cove, N.Y.
72. D. Godfrey and W. R. Herguth, "Physical and Chemical Properties of Industrial Mineral Oils Affecting Lubrication—Part 4," *Lubr. Eng.*, 1995, 51(12), pp. 977–979.
73. A. Adhvaryu, D. C. Pandey, and L. D. Singh, "Effect of Composition on the Degradation Behavior of Base Oil," in *Symp. on Worldwide Perspectives on the Manf., Charac., and Appl. of Lubricant Base Oils*, Div. of Pet. Chem. Inc., 213th Nat. Meet. of Am. Chem. Soc., 1997, pp. 225–228.
74. S. F. Chisholm, "Petroleum Hydraulic Fluids," *Sci. Lubri.*, 1960, May, pp. 35–38.
75. R. S. Robertson and J. M. Allen, "Study of Oil Performance in Numerically Controlled Hydraulic Systems," in *Proc. Natl. Conf. Fluid Power*, Annual Meeting 30th, 1974, Vol. 28, pp. 435–454.
76. W. Backé and P. Lipphardt, "Influence of Dispersed Air on the Pressure Medium," in *Proc. Contamination in Fluid Power Systems*, 1977, C97/76, pp. 77–84.
77. X. Malleville, D. Faure, A. Legros, and J. C. Hipeaux, "Oxidation of Mineral Base Oils of Petroleum Origin: The Relationship Between Chemical Composition, Thickening, and Composition of Degradation By-Products," *Lubr. Sci.*, 1996, 9(1), pp. 3–60.
78. M. Rasberger, "Oxidative Degradation and Stabilization of Mineral Oil Based Lubricants," in *Chemistry & Technology of Lubricants*, R. M. Mortier and S. T. Orszulik, eds., 1992, Blackie Academic & Professional; Boston, pp. 83–123.
79. T. Mang and H. Jünemann, "Evaluation of the Performance Characteristics of Mineral Oil-Based Hydraulic Fluids," *Erdöl kohle-Erdgas-Petrochem. verneigt Brennstoff-Chemie*, 1972, 25(8), pp. 459–464.
80. E. E. Klaus, "To Make Improved Hydraulic Fluids," *Hydrocarbon Process.*, 1966, 45(6), pp. 167–170.
81. ASTM D 943-81, "Standard Test Method for Oxidation Characteristics of Inhibited Mineral Oils," American Society for Testing and Materials, Conshohocken, PA.
82. M. E. Landis and W. R. Murphy, "Analysis of Lubricant Components Associated with Oxidative Color Degradation," *Lubr. Eng.*, 1991, 47(7), pp. 595–598.
83. ASTM D 2272-85, "Standard Test Method for Oxidative Stability of Steam Turbine Oils by Rotating Bomb," American Society for Testing and Materials, Conshohocken, PA.
84. F. G. Rounds, "Coking Tendencies of Lubricating Oils," SAE National Fuels and Lubricants Meeting, 1957.
85. H. Watanabe and C. Kobayashi, "Degradation of Turbine Oils—Japanese Turbine Lubrication Practices and Problems," *Lubr. Eng.*, 1978, 38(8), pp. 421–428.
86. E. Gimzewski, "The Relationship Between Oxidation Induction Temperatures and Times for Petroleum Products," *Thermochin. Acta*, 1992, 198, pp. 133–140.
87. P. A. Gabilondo, J. M. Perez, and W. A. Lloyd, "Development of a Microreactor Bench Test for Lubricant Evaluation," in *Symp. on Worldwide Perspectives on the Manf., Charac., and Appl. of Lubricant Base Oils*, Div. of Pet. Chem. Inc., 213th Nat. Meet. of Am. Chem. Soc., 1997, pp. 278–280.
88. ASTM D 4742-96, "Standard Test Method for Oxidation Stability of Gasoline Automotive Engine Oils by Thin-Film Oxygen Uptake (TFOUT)," American Society for Testing and Materials, Conshohocken, PA.
89. Anon., "Hydraulic Fluid: Making the Choice," *Eng. Mater. Design*, 1988, July–August, pp. 37–38.
90. B. C. Roell and C. L. Cerda De Groote, "Turbine and Hydraulic Fluids," in *Proceedings of 11th International Colloquium on Industrial and Automotive Lubrication—Vol. 3*, W. J. Bartz, ed., 1998, Technische Akademie Esslingen; Esslingen, 1998, pp. 1811–1816.

91. H. Zhou, K. Li, X. Wang, Y. Xu, and F. Shen, "Pattern Recognition Studies on the Influence of Chemical Composition on Some Properties of Lubricating Base Oils," in Proc. Int. Conf. Pet. Refin. Petrochem. Process., 1991, pp. 387–392.
92. S. S. V. Ramakumar, N. Affarwal, A. Madhusudhana Rao, S. P. Srivastava, and A. K. Bhatnagar, "Effect of Base Oil Composition on the Course of Additive–Additive Interactions," in Adv. Prod. Appl. Lube Base Stocks, Proc. Int. Symposium, H. Singh, P. Rao, and T. S. R. Tata, eds., 1994, McGraw-Hill; New Delhi, pp. 334–341.
93. A. S. Galiano-Roth and N. M. Page, "Effect of Hydroprocessing on Lubricant Base Stock Composition and Product Performance," *Lubr. Eng.*, 1994, 50(8), pp. 659–664.
94. I. Minami, "Influence of Aldehydes in Make-Up Oils on Antioxidation Properties," *Lubr. Sci.*, 1995, 7(4), pp. 319–331.
95. B. B. Flick, "Which Characteristics for Hydraulic Fluid?," *Product Eng.*, 1953, August, pp. 149–153.
96. T. D. Newingham, "What You Should Know About Hydraulic Fluid Additives," *Hydraul. Pneumatics*, 1986, November, p. 62.
97. J. Chu and R. K. Tessmann, "Additives Packages for Hydraulic Fluids," *BFPR J.*, 1979, 12(2), pp. 111–117.
98. A. J. Zino, "What to Look for in Hydraulic Oils. VI—Lubricating Value," *Am. Machinist*, 1948, January 15, pp. 97–100.
99. A. G. Bergstrom and R. Q. Sharp, "Give Life to Hydraulic Systems," *Machine Design*, 1950, January, pp. 80–86, 154, 156.
100. A. G. Papay, "Advances in Hydraulic Oil Additives Technology," SAE Technical Paper Series, Paper 760573, 1976.
101. S.-H. Jung, U.-S. Bak, S.-H. Oh, H.-C. Chae, and J.-Y. Jung, "An Experimental Study on the Friction Characteristics of an Oil Hydraulic Vane Pump," in Proceedings of International Tribology Conference—1995, Vol. III, pp. 1621–1625.
102. R. L. Leslie, "Views on Oils for Hydraulic Service," in National Fuels and Lubricants Session, National Petroleum Refiners Assoc., 1965, Paper 65-34L.
103. Anon., "The Graphoid Surface—An Aid to Oiliness," *Sci. Lubr.*, 1951, July, pp. 25–26.
104. E. S. Forbes, "Antiwear and Extreme Pressure Additives for Lubricants," *Tribology*, 1970, August, pp. 145–152.
105. B. J. Lloyd, "Water, Water Everywhere," *Lubes-N-Greases*, 1997, 3(11), pp. 44–53.
106. Lubrizol Corp., *Industrial Lubricants At-a-Glance*, 1989, Lubrizol Corporation; Wickliffe, OH, Vol. 2, No. 2.
107. J. Jin and C-Z Zhao, "Applied Research of Detergents and Dispersants in Antiwear Hydraulic Oil," in *Proceedings of 11th International Colloquium on Industrial and Automotive Lubrication—Vol. 3*, W. J. Bartz, ed., 1998, Technische Akademie Esslingen; Esslingen, pp. 1837–1845.
108. C. I. Betton, "Lubricants and Their Environmental Impact," in *Chemistry and Technology of Lubricants—2nd ed.*, R. M. Mortier and S. T. Orszulik, 1997, Blackie Academic & Professional; London, UK, pp. 349–370.
109. Anon., "Hydraulic Fluids—Performance Criteria," *Fluid Air Technol.*, 1995, February/March, pp. 28–30.
110. W. D. McHendry and O. J. Littig, "Application of Infrared Spectrometric Techniques on the Quantitative Analysis of Hydraulic Fluids," *ASLE Trans.*, 1969, 13, pp. 99–104.
111. E. E. Klaus, E. J. Tewksbury, and M. R. Fenske, "High-Temperature Hydraulic Fluids from Petroleum," *I&EC Product Res. Devel.*, 1963, 2(4), pp. 332–338.
112. ASTM D 2882-83, "Standard Method for Indicating the Wear Characteristics of a Petroleum and Non-Petroleum Hydraulic Fluids in a Constant Volume Vane Pump," American Society for Testing and Materials, Conshohocken, PA.

113. G. E. Totten, R. J. Bishop, Jr., R. L. McDaniels, and G. H. Kling, "Evaluation of Hydraulic Fluid Performance Correlation of Water-Glycol Hydraulic Fluid Performance by ASTM D-2882 Vane Pump and Various Bench Tests," SAE Technical Paper Series, Paper 952156, 1995.
114. A. Maccleod, "Developments in Hydraulic Oils," *Ind. Lubr.*, 1968, January, pp. 11–19.
115. R. J. Bishop and G. E. Totten, "Tribological Testing with Hydraulic Pumps: A Review and Critique," in *Tribology of Hydraulic Pump Testing—ASTM STP 1310*, G. E. Totten, G. H. Kling, and D. M. Smolenski, eds., 1995, American Society for Testing and Materials; Conshohocken, PA, pp. 65–84.
116. O. Langosch, "Berechnen und Testen des Konstruktionselementes Hydrauliköl," *Ölhydraulik Pneumatik*, 1972, 16(12), pp. 498–501.
117. K. B. Grover and R. J. Perez, "The Evolution of Petroleum Based Hydraulic Fluids," *Lubr. Eng.*, 1990, 46(1), pp. 15–20.
118. C. H. Young, "Used Hydraulic Oil Analysis," *Lubrication*, 1977, 63(4), pp. 37–48.
119. Anon., "Proactive Hydraulic Oil Maintenance," *Maintenance Technol.*, 1994, March, pp. 39–40.
120. J. Ogando, "A New Way to Look at Hydraulic Oil Cleanliness," *Plast. Technol.*, 1993, 39(13), December, p. 42.
121. Anon., "Oil Maintenance in Today's Environment," *Fluid Air Technol.*, 1994, January/February, pp. 32–37.
122. J. P. Duncan, "How to Field-Evaluate Used Hydraulic Fluids," *Hydraul. Pneumatics*, 1973, November, pp. 99–101.
123. Anon., "Is There Water in Your Oil," *Fluid Air Technol.*, 1994, April/May, pp. 50–51.
124. ASTM D 95, "Standard Test Method for Water in Petroleum Products and Bituminous Materials by Distillation," American Society for Testing and Materials, Conshohocken, PA.
125. ASTM D 1744-83, "Standard Test Method for Water in Liquid Petroleum Products by Karl Fischer Reagent," American Society for Testing and Materials, Conshohocken, PA.
126. ASTM D 1796-83, "Standard Test Method for Water and Sediment in Fuel Oils by the Centrifuge Method," American Society for Testing and Materials, Conshohocken, PA.
127. ASTM 445-71, "Standard Test Method for Kinematic Viscosity of Transparent and Opaque Liquids (and the Calculation of Dynamic Viscosity)," American Society for Testing and Materials, Conshohocken, PA.
128. ASTM D 2161-87, "Standard Test Method for Conversion of Kinematic Viscosity to Saybolt Universal Viscosity or to Saybolt Furol Viscosity," American Society for Testing and Materials, Conshohocken, PA.
129. ASTM D 4052-91, "Standard Test Method for Density and Relative Density of Liquids by Digital Density Meter," American Society for Testing and Materials, Conshohocken, PA.
130. J. Poley, "Oil Analysis for Monitoring Hydraulic Systems, A Step-Stage Approach," STLE Preprint No. 89-AM-1E-1, 1989.
131. J. Dong, F. R. Van De Voort, A. A. Ismail, and D. Pinchuk, "A Continuous Oil Analysis and Treatment (COAT) System for the Monitoring of Oil Quality and Performance of Additives," *Lubr. Eng.*, 1997, 53(10), pp. 13–18.
132. ASTM D 482-87, "Standard Test Method for Ash from Petroleum Products," American Society for Testing and Materials, Conshohocken, PA.
133. ASTM D 874-82, "Standard Test Method for Sulfated Ash from Lubricating Oils and Additives," American Society for Testing and Materials, Conshohocken, PA.

134. V. Srimongkokul, "Why a Proactive Maintenance Program for Hydraulic Oil Is Part of Statistical Quality Control," *Lubr. Eng.*, 1997, 53(4), pp. 10–14.
135. Anon., "Keep Hydraulic Oils Clean," *Lubrication*, 1956, 42(8), pp. 101–108.
136. ASTM D 4174-82, "Standard Practice for Cleaning, Flushing, and Purification of Petroleum Fluid Hydraulic Systems," American Society for Testing and Materials, Conshohocken, PA.
137. R. E. Bowering, C. T. Davis, and D. P. Braniff, "Managing and Recycling Hydraulic and Process Oils at a Cold Mill," *Lubr. Eng.*, 1997, 53(7), pp. 12–17.
138. B. Wilson, "Used Oil Reclamation Processes," *Ind. Lubr. Tribol.*, 1997, 49(4), pp. 178–180.
139. G. S. Dang, "Rerefining of Used Oils—A Review of Commercial Processes," *Tribotest J.*, 1997, 3(4), pp. 445–457.
140. D. J. Neadle, "Lubricants Recycling," *Ind. Lubr. Tribol.*, 1994, 46(4), pp. 5–7.
141. W. Stofey and M. Horgan, "Reclaiming Hydraulic Oil Eliminates Oil Disposal Problems," *Hydraul. Pneumatics*, 1993, December, pp. 36–37, 76.
142. R. K. Tessmann, I. T. Hong, and E. C. Fitch, *Lubr. Eng.*, 1993, 49(9), pp. 666–670.
143. L. B. Baranowski, "Degasification and Dehydration of Hydraulic Systems," 23rd National Conference on Fluid Power, 1967.
144. S. Siegel and C. Skidd, "Case Studies Utilizing Mobile On-Site Recycling of Industrial Oils for Immediate Reapplication," *Lubr. Eng.*, 1995, 51(9), pp. 767–770.
145. J. F. Gzauskas, F. P. Abbott, and N. R. Baumgartner, "Characteristics of Wax Extracted from Lubricant Basestocks," *Lubri. Eng.*, 1994, 50(4), pp. 326–336.
146. C. W. Hughs, "Designing to Accommodate High Temperature in Hydraulic Systems," *Machine Design*, 1968, December 19, pp. 134–138.
147. ASTM D 3427-86, "Standard Test Method for Gas Bubble Separation Time of Petroleum Oils," American Society for Testing and Materials, Conshohocken, PA.
148. ASTM D 664-87, "Standard Test Method for Acid Number of Petroleum Products by Potentiometric Titration," American Society for Testing and Materials, Conshohocken, PA.
149. ASTM D 974-87, "Standard Method for Acid and Base Number by Color-Indicator Titration," American Society for Testing and Materials, Conshohocken, PA.
150. D. Godfrey and W. R. Herguth, "Physical and Chemical Properties of Industrial Mineral Oils Affecting Lubrication—Part 5," *Lubr. Eng.*, 1995, 52(2), pp. 145–148.
151. A. G. Papay, "Oil-Soluble Friction Reducers—Theory and Application," *Lubr. Eng.*, 1983, 39(7), pp. 419–426.

Lubricant Additives for Mineral-Oil–Based Hydraulic Fluids

STEPHEN H. ROBY

Chevron Products Company, Chevron Corporation, Richmond, California

ELAINE S. YAMAGUCHI

Chevron Chemical Company, Oronite Global Technology, Richmond, California

P. R. RYASON

Tamalpais Tribology, Fairfax, California

1 INTRODUCTION

The primary function of an oil in a hydraulic system is to serve as the working fluid. As such, only one property of the oil is important in determining the response and control characteristics of the hydraulic system: the bulk modulus [1]. Methods of determining the bulk moduli of liquids are well known [2,3]. Response characteristics of hydraulic systems are well understood and have been discussed at length [2]. However, providing a value for the bulk modulus does not suffice to specify a hydraulic oil.

Hydraulic oil functions not only as the working fluid but also as the lubricant for the mechanical parts of the hydraulic system. Thus, in addition to the bulk modulus, lubrication properties must also be specified for a hydraulic oil. Hydraulic systems typically include pumps, valves, pistons sliding in cylinders, bearings, filters, and both moving and stationary seals. Not uncommonly, more than one metal is used in a hydraulic system.

Lubricants, wherever used, serve several functions. Most importantly, they must adequately lubricate the mechanical device in which they are used. Additionally, lubricants control contaminant formation, protect metal surfaces, and transfer heat. The performance characteristics of a premium mineral hydraulic oil are shown in Table 15.1. Virtually any liquid may serve as the base fluid for a hydraulic lubricant.

Table 15.1 Examples of Hydraulic Lubricant Test Procedures and Requirements

	Denison HF-0	U.S. Steel 126/127	U.S. Navy MIL-H-24450	Cincinnati Milacron P-68	Vickers M-2952-S/ I-286-S
Hydrolytic stability	X		X		X
Thermal stability	X		X	X	X
Oxidation stability	X	X	X		X
Water separability		X	X		X
Rust protection	A/B ^a	A ^a	B ^a	A	A/B
Wear protection					
Vickers 35VQ25					X
ASTM D2882		X	X	X	X
Denison pump tests	X				
4-Ball wear		X			
Filterability	X				

^aA = distilled water; B = synthetic seawater.

Additives are used to modify physical properties of the oil, to reduce friction and wear, to control contaminant formation, and to extend the life of the lubricant. This chapter will discuss various types of the most common additives for mineral-oil-based hydraulic fluids. The discussion will exclude tractor hydraulic fluids, which must also lubricate gears, clutches, and wet brakes, and so require more and substantially different compounding from simple antiwear hydraulic oils.

2 DISCUSSION

2.1 Lubricant Functions

2.1.1 Reduction of Friction and Wear

By definition, a lubricant is a material interposed between two surfaces that are in relative motion to reduce friction and wear. Although not explicitly stated in this definition, a force is exerted on the surfaces perpendicular to the direction of motion. As a result, the lubricant layer is under pressure. Although lubricants may be gases, liquids, or solids, for most industrial hydraulic applications, a liquid, most often a mineral oil, is used.

Oil-lubricated contacts may operate in any of three lubrication regimes known as hydrodynamic, elastohydrodynamic, and boundary lubrication. An overview will be provided here. These lubrication regimes will be discussed in more detail in Chapter 6.

In hydrodynamic lubrication [4], contacts are most often conformal, loads are relatively light, and the surfaces are completely separated by an oil film. Common examples are rotating journal bearings and pistons sliding in cylinders at the mid-stroke position. The oil film that supports the load is sustained by the motion of the moving part.

In elastohydrodynamic lubrication [5], contacts are nonconformal, contact areas are small, and pressures are high. Common examples are rolling element bearings,

gears, and engine valve trains. However, the contacting surfaces are separated by an oil film. The pressures are sufficiently high that the contacting surfaces are elastically deformed. Oil-film thicknesses in elasto-hydrodynamic lubrication are much thinner than oil films in hydrodynamic lubrication (about 1/1000 times as thick).

At still higher loads, the oil film is squeezed out of the contact, and metal-metal contact would occur without a boundary lubrication additive [6]. Boundary lubricants are materials added to an oil that absorb on the surface of the contact and react with the material of the contact to form solid or semisolid films that prevent metal-metal contact (see Subsections of Section 2.3.1). Such films are thinner than the oil films formed in elasto-hydrodynamic lubrication.

In practice, surfaces are neither perfectly smooth nor perfectly aligned, and mixed lubrication occurs, usually a combination of elasto-hydrodynamic lubrication and boundary lubrication. Even in a system designed to operate in the elasto-hydrodynamic regime, asperities come into contact. Provided that the lubricant contains a boundary lubrication additive, asperity-asperity contacts develop boundary lubricant films, and high friction and unacceptable wear do not occur. Lubricating fluids formulated with the appropriate additives will ensure that machinery will be long-lived and economically viable.

Considerable reduction in friction and wear is achieved by lubricants. For unlubricated sliding metal contacts, coefficients of friction are in range of 0.5–0.7 [7]. Surfaces separated by oil films in hydrodynamic lubrication have coefficients of friction in the neighborhood of 0.001–0.01 [8]. Under elasto-hydrodynamic conditions for pure rolling contact, coefficients of friction are in the range of 0.0005–0.003 [8]. Boundary lubricant films provide coefficients of friction in the range of 0.02–0.3 [8]. Under mixed-lubrication conditions, coefficients of friction may range from 0.02 to 0.10 [9], depending on conditions of load, speed, and temperature. Lubricants reduce wear by 1000- to 10,000-fold [7].

Hydrodynamic, elasto-hydrodynamic, and boundary lubrication regimes are all found in hydraulic systems. Table 15.2 presents selected data comparing lubricant-film thicknesses in hydraulic pumps and commonly encountered contacts. Although the normal pressures are relatively low, a sliding seal-cylinder contact operates in the elasto-hydrodynamic regime because of the relatively small elastic modulus of

Table 15.2 Comparison of Lubricant Film Thicknesses in Hydraulic System Components and Other Contacts

Components	Lubrication regimes	Film thickness (μm)
Journal bearings	Hydrodynamic	0.5–100
Piston pump: piston bore	Hydrodynamic	5–40
Rolling element bearings	Elasto-hydrodynamic	0.1–1
Gears	Mixed (elasto-hydrodynamic and boundary)	0.1–1
Vane pump: vane side	Hydrodynamic	5–13
Vane pump: vane tip	Mixed (elasto-hydrodynamic and boundary)	0.5–1

Source: Adapted from Ref. 10.

the O-ring seal. Thus, merely to accommodate the lubrication requirements of a hydraulic system (not considering the other functions a lubricant must serve), a hydraulic oil must be properly formulated to function optimally in all the lubrication regimes.

Among the boundary lubricants, distinctions are made among friction modifiers, antiwear agents, and extreme pressure agents. Generally speaking, this order is also the order of decreasing chemical reactivity. Increasing load or lowering sliding speeds results in higher temperatures in the contact and, correspondingly, films will be formed under these more severe conditions by the less reactive additives [11]. Choice of an antiwear agent may depend on the metals used in the hydraulic system. For example, if both copper alloy and steel components are present, then an antiwear agent such as zinc dialkyldithiophosphate (ZDDP) may protect the ferrous alloy but may corrode the copper-based component [12]. Sliding silver-iron contacts require a lubricant free of ZDDP [13]. Antiwear agents and their uses will be discussed in a Subsection of Section 2.3.1.

2.1.2 Contaminant Control

Contaminants pose serious threats to the useful life of a hydraulic system. Oil-insoluble particles may clog valves and prevent action [14,15]. Sludge and varnish deposits interrupt the efficient transfer of heat away from the lubricated system by coating metal surfaces and slowing the transfer of heat from the oil to the environment. Oil-suspended sludge also thickens the lubricant, increases the viscosity, and makes efficient oil circulation more difficult, further slowing heat transfer. Dirt and wear debris can be extremely abrasive, damaging moving parts and increasing the machined tolerances, hence reducing the efficiency of the hydraulic system. Hydraulic fluids are formulated with a number of chemical additives designed to reduce wear, control oxidation, and suspend sludge and varnish. These additives are slowly consumed during system operation. If additives are depleted, wear, oxidation, and deposit formation can proceed very quickly. Hydraulic fluids must be carefully monitored to ensure that sufficient additive remains to protect the lubricant and are replaced before excessive wear and oxidation can occur to damage the machinery.

Higbee [16] suggests that for hydraulic equipment “70 to 90% of equipment wear and failure is attributable to contamination.” Although the properly formulated lubricant can minimize wear rates and deposit formation, modern hydraulic systems include filters to remove particulate debris and suspended insolubles that would otherwise damage, clog, or jam key components [10]. Mills and Davis [12] and Needelman [10] have demonstrated the effects of external contamination and filter malfunction on increasing wear in hydraulic systems: proper maintenance of hydraulic systems including the lubricant or working fluid; the system components including valves, servos, and pumps; and the filtration system, which is critical to optimum performance [16]. Chapter 3 offers suggestions for hydraulic system filtration practices. References 10 and 16 contain discussions on filtration theory plus filter design and testing.

Wear debris and oil-derived oxidation products are the most common contaminants generated within a hydraulic system. Wear is controlled by additives that include antiwear, extreme pressure, and friction-modifying agents. Oil-derived oxidation products can be controlled in several ways. First, oxidation inhibitors are added to an oil to slow oxidation rates and minimize insolubles formation. Second,

dispersants can be used to suspend oxidized material in the oil and to prevent it from separating from the continuous oil phase. Finally, detergents can be added that can remove deposits from surfaces and solubilize them in the oil phase. These additives and their functions will be more fully discussed in Section 2.3.

2.2 Lubricant Base Stocks

Most hydrocarbon-type lubricants are formulated from refined mineral oil [19]. Refined mineral oil results from distilling, dewaxing, and, frequently, hydrotreating crude oil fractions to improve oxidation stability, wax content, and fluidity. Mineral-oil base stocks are usually the most cost-effective approach. Mineral-oil refining processes are discussed in Chapter 14.

Other lubricant base stocks, commonly called synthetic base stocks, are designed to have specific desirable chemical and physical properties [20]. Synthetic base stocks may be used when low-temperature properties, oxidation resistance, or thermal stability are critical to performance. Common synthetic base stocks include the following types:

- Alkylated aromatics
- Olefin oligomers (e.g., polyalphaolefins or PAOs, and polybutylenes)
- Esters (see Chapter 19)
- Polyglycols (see Chapter 18)
- Phosphate esters (see Chapter 20)

Other, less common types of hydraulic fluid base stocks for very special applications include the following:

- Silicones
- Silicate esters
- Polyphenyl ethers

These special-purpose fluids are discussed in Chapter 16.

Synthetic base stocks range in cost from 2 to 100 times that of conventional mineral oil.

Water-based hydraulic fluids are increasingly common, having first been introduced in 1947 following onboard fire problems in World War II [21]. These fluids are generally oil-in-water or water-in-oil emulsions and are used when fire hazards are high [22]. These fluids exhibit the following order of fire resistance: water-glycol > phosphate ester > polyol ester > mineral oil [22]. Water-based hydraulic fluids are discussed in Chapter 17.

Biodegradable hydraulic fluids represent a small portion of the market. Examples of biodegradable hydraulic base fluids include polyglycerols, vegetable oils, polyolesters, and diesters. The fatty acid content of a vegetable oil may include palmitic, steric, oleic, and linoleic acid and others [23]. Biodegradable hydraulic fluids are discussed in Chapter 21.

2.3 Lubricant Additives [24–29]

2.3.1 General Function

An additive is a material that provides or enhances a desirable property of the lubricant, such as oxidation stability or low-temperature fluidity [26]. Frequently, ad-

ditives are multipurpose, meeting several requirements of a lubricant simultaneously. Classes of the most common mineral-oil additives and their functions are shown in Table 15.3. (References 24–29 will give the interested reader a more detailed account of additive mechanisms, syntheses, and the historical development of this industry.) Specific additive structures and functions will be addressed in the following sections.

A typical mineral-oil-based hydraulic oil may contain detergent, antioxidant, antiwear, rust inhibitor, corrosion inhibitor, metal deactivator, dispersant, viscosity improver, pour point depressant, demulsifier, and antifoam additives [13,26]. Frequently, more than one type of a specific additive may be used to attain the required performance across a range of operating conditions. For example, two or more types of antioxidants may be included in a formulation: a peroxide decomposer to inhibit the onset of an oxidation chain reaction and a more specific radical trap to safely eliminate reactive species that do form. Illustrative compositions of two fully formulated mineral-oil-based antiwear hydraulic fluids are shown in Table 15.4

Rust and oxidation (R&O) oils form a separate class of hydraulic fluids formulated to provide rust and oxidation protection and foam suppression in light-duty

Table 15.3 Additive Types and Functions

Lubricant function	Additive type	Additive purpose
Heat transfer	Antioxidants	Prevent oil thickening due to oxidative processes
	Viscosity improvers	Reduce viscosity loss at higher temperatures
Contaminant control	Dispersants and detergents	Solubilize oxidation products and neutralize acidic oxidation products
	Antiwear agents	Reduce wear rates to control wear debris
	Antirust agents	Prevent oxidation of ferrous metals to control corrosion debris
	Antioxidants	Slow oxidation processes to prevent accumulation of oil-insoluble products
	Corrosion inhibitors	Prevent oxidation of nonferrous metals to control corrosion debris
Friction and wear control	Demulsifiers	Promote rapid separation of bulk water from oil
	Antiwear agents	Reduce wear rates
	Extreme-pressure agents	Reduce wear rates and prevent seizure
	Viscosity improvers	Reduce viscosity loss at higher temperatures to maintain hydrodynamic lubrication
	Pour point depressants	Prevent low-temperature thickening from wax in mineral oil
	Antifoam agents	Prevent foaming and maintain pumpability of lubricant
	Friction modifiers	Reduce wear rates and friction coefficients

Table 15.4 Hydraulic Fluid Composition

Formulation A	Formulation B	Function	% Weight treatment
Zinc dialkyldithiophosphate	Zinc dialkyldithiophosphate	Antiwear, antioxidant	0.50
Neutral calcium sulfonate	Neutral calcium sulfonate	Rust inhibitor	0.05
Low–molecular-weight polymethacrylate	Low–molecular-weight polymethacrylate	Pour point depressant	0.20
Triazole	Triazole	Metal deactivator	0.003
Detergent/dispersant	Detergent/dispersant	ZDDP stabilizer	0.10
	Hindered phenol	Antioxidant	0.20
	Ethoxylated alcohol	Demulsifier	0.01
	Poly(acrylate)	Foam inhibitor	0.01
	High–molecular-weight polymethacrylate	Viscosity index improver	2–10

hydraulic systems. R&O oils contain no antiwear additives and are not recommended for heavy-duty systems [13].

Lubricant additives may be divided into two groups. One group serves to prolong the service life of the lubricant and to enhance certain physical properties of the lubricant not directly related to the lubricant function. The other group contributes directly to lubrication functions. Examples of the first group are additives such as antioxidants, detergents, dispersants, pour point depressants, and antifoam agents. Viscosity improvers, friction modifiers, antiwear additives, and extreme-pressure (EP) additives exemplify the second group. In both groups, some of the additives are consumed in service and some are not. Oxidation inhibitors, for example, act by reacting with oxidation intermediates, thus reducing the rate of oil oxidation and lengthening the service life of the oil. Dispersants bind with oxidation products and polar contaminants, suspending these materials in the oil and preventing sludge formation. Although not destroyed, the bound dispersant becomes unavailable to bind with additional polar material. Detergents also bind polar materials and suspend them in the oil. Detergents are strongly attracted to surfaces and may displace polar materials already bound to a metal surface. Like dispersants, detergents help maintain the cleanliness of internal parts of the hydraulic system.

In an operating journal bearing, the oil film is mechanically sheared between the stationary bearing shell and the rotating journal. Viscosity index (VI) improvers are of sufficiently high molecular weight that part of a single molecule may be in a layer of oil that is moving rapidly and another portion of the same molecule in an adjacent layer that is moving more slowly. Drag of the oil on the polymer molecule varies by position on the VI improver molecule. As a result, the polymer's chemical bonds are broken by the mechanical shearing stress imposed by the lubricant flow. Breaking the VI's chemical bonds results in lower-molecular-weight fragments that are less effective in maintaining the viscosity of the oil. The lower thickening power of the polymer arising from mechanical degradation is often termed permanent shear loss. Thus, VI improvers have a finite service life. Pour point depressants are also often polymeric materials, but of lower molecular weight than VI improvers. Thus they are less subject to mechanical shear degradation.

Antifoam agents may also be polymeric materials of lower molecular weight than VI improvers. Although both pour point depressants and antifoam agents are normally considered to be relatively chemically inert, they may be adsorbed on oil filters and, thus, removed from the lubricant.

Friction modifiers, antiwear additives, and EP additives are strongly attracted to surfaces and adsorb on metal surfaces to some extent. Once adsorbed, they react with the surface, and in the case of antiwear and EP additives, they react with the surface to form antiwear and EP films. These additives are thereby removed from the oil during use, slowly, but steadily, as will be discussed in Subsections of Section 2.3.1.

Some members of both groups of additives function in the bulk oil, and some members function on the internal surfaces of the hydraulic system. Antioxidant, VI improvers, and pour point depressants exert their effects in the bulk oil. Antiwear additives and EP additives act on the contacting metal surfaces. Detergents solubilize polar materials both in the bulk oil and at the metal surfaces. Antifoam agents work at the oil-air interface.

All additives interact with one another to a greater or lesser extent. Generally, those that function principally in the bulk oil interact with each other to a smaller extent than those that function on the surface. In particular, the interaction of detergents and antiwear agents may lessen the effectiveness of the antiwear agent. A very important part of the formulator's task is to select combinations of additives that result in an oil that meets the specifications, passes the required laboratory tests, and performs well in the field. Even so, a properly balanced formulation undergoes changes in service and must be replenished with fresh oil.

Chemical additives may also be classified by where they function. For example, antiwear agents must migrate to wear sites, adsorb on the wear sites, and then react to produce the films necessary to maintain low wear rates in the mixed or boundary lubrication regimes. To do this, antiwear agents must be soluble in the carrier fluid but also have some affinity for the wear surface [30]. Too much solubility in the carrier and the antiwear agent will not adsorb sufficiently. This affinity for the wear sites is termed surface activity. The surface activity of the various chemical additives must be carefully balanced to optimize performance. Table 15.5 summarizes the type of activity of some common mineral-oil lubricant additives.

Besides performance requirements, lubricants must meet a variety of other qualifications. Compatibility with other lubricants is a major consideration for many applications because complete flushing of the system is often impossible. Customers frequently specify the color of the fully formulated oil because color changes are used to indicate the end of the useful lubricant life. Odor and toxicity are primary considerations in environments where people may be exposed to the lubricant. Finally, economics is a consideration. If a lubricant is overformulated for a given application, it may be too costly for a customer to use.

Dispersants [28,39]

Dispersants are designed to control contamination and deposit formation. Dispersants are made of an oil-soluble hydrocarbon tail attached to a polar head. Like the base oil itself, the oil-soluble hydrocarbon tail is composed of carbon and hydrogen only and is therefore nonpolar. The dispersant's polar head group is usually composed of carbon, hydrogen, nitrogen, and oxygen.

Sludge precursors are quite polar and are composed of oxidized oil, decomposed additives, and other debris. Sludge and sludge precursors are oil insoluble

Table 15.5 Surface Activity of Some Common Classes of Lubricant Additives

Additive type	Surface active	Bulk solution active	Refs.
Dispersants	X	X	31–35
Detergents	X	X	36, 37
Antiwear agents	X		36
Antioxidants		X	29
Corrosion inhibitors	X		38
Viscosity modifiers		X	28
Pour point depressants		X	26, 27
Foam inhibitors		X	26, 27
Friction modifiers	X		26, 27

because their high oxygen and nitrogen content makes them very polar, hence dissimilar to the nonpolar oil. The dispersant's very long nonpolar, hydrocarbon tail ensures that the dispersant molecule and the highly polar sludge it interacts with are soluble in the oil phase. A stylized description of the interaction of a dispersant with a polar contaminant particle is shown in Fig. 15.1.

Dispersants are typically neutral or slightly basic. The polar end of the molecule is most often an ester or amine group. The most common dispersants are based on either succinimide, succinate ester, or Mannich functional groups with a poly (isobutylene) tail. They function by interaction with the acidic products of oxidation, in the oil phase, and solubilizing them into the bulk solution.

Most dispersants have a hydrocarbon tail consisting of 50–200 carbon atoms and a polar head group consisting of various combinations of carbon plus oxygen and/or nitrogen. The (usually) basic polar head group of the dispersant attaches itself to the acidic sludge or varnish molecules present in the used oil. Several studies have shown the importance of the dispersant's nonpolar tail in preventing the growth of sludge molecules and preventing agglomeration of particles [31–33]. Forbes and Neustadter [34] have studied the effects of various polar head groups and poly

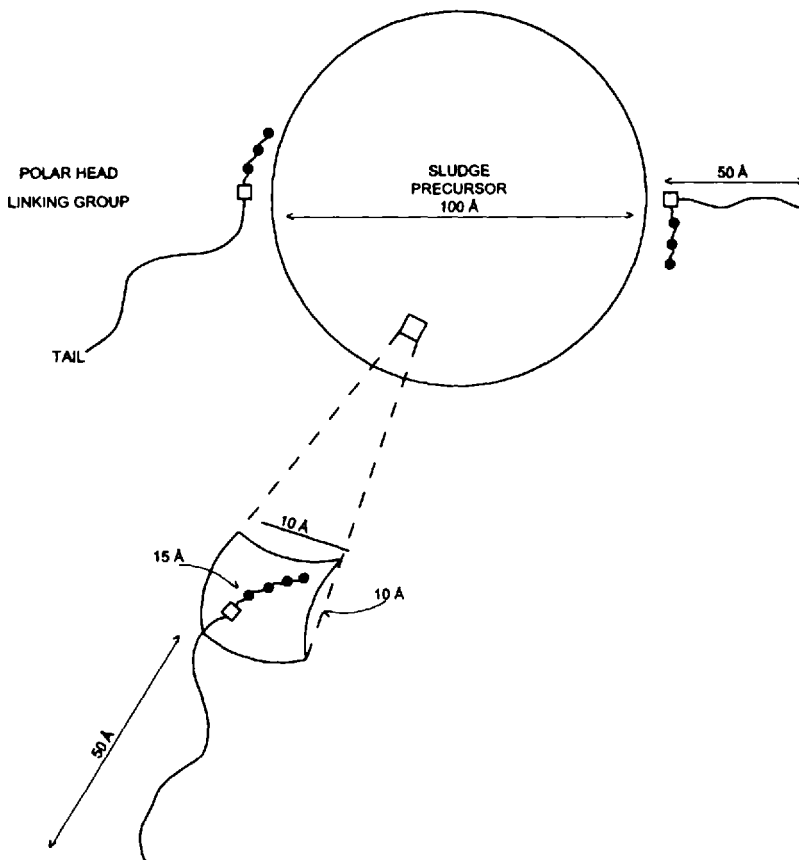


Figure 15.1 Schematic dispersancy mechanism.

Table 15.6 Dispersant Components

Oil-solubilizing tail	Linking group	Polar group
Polyisobutylene, or polypropylene	None, succinoyl, or phenol	Polyamine, or polyol

(isobutylene) alkyl groups on the dispersing ability of succinimide-type compounds. He found that succinimide-type dispersants stabilize sludge through a steric mechanism, the long nonpolar alkyl tails acting to keep suspended sludge separate. Endo and Inoue [35] have also studied sludge dispersancy and found that higher total base number (TBN) and longer alkyl chain length improved the dispersing ability of succinimide dispersants. The fundamental chemical components of commercially important dispersants are summarized in Table 15.6.

Detergents [25,28,39]

Detergents and dispersants have a complementary function. Detergents are designed to control contamination, but more specifically to neutralize acidic by-products of oxidation and to inhibit rust formation. Detergents are composed of an oil-soluble hydrocarbon tail of between C₁₈ and C₂₀, or higher, attached to a very polar group. The polar functionality is most often a sulfonate, a phenate, or a salicylate group.

Some detergents are overbased; that is, they contain a high proportion of a carbonate salt. In hydraulic lubricants, the overbased detergent is usually a phenate or salicylate. Overbasing is accomplished by slowly adding a metal oxide to an appropriate acid, then bubbling carbon dioxide through the mixture [46]. As the reaction proceeds, colloidal dispersions of the alkaline earth carbonates form as small particles stabilized by the detergent. In a lubricating oil, the carbonate is slowly depleted as the detergent neutralizes acids. The carbonate is most often a calcium, magnesium, or sodium salt. Preparation of an overbased sulfonate detergent is shown in Fig. 15.2. Detergent basicity is measured by TBN, a number equivalent to the milligrams of potassium hydroxide (a very powerful alkali) per gram of oil. The higher the TBN of the oil, the more acid can be neutralized before the basic component is depleted (Table 15.7).

Detergents function at surfaces and in solution to solubilize polar materials. Detergents are quite surface active and can compete for surface sites with antiwear agents. This was recently shown in a series of electrical contact resistance studies using combinations of detergents and zinc dialkyldithiophosphates in an iron–iron tribocouple. Specifically, this study showed that the rate of antiwear film formation by ZDDP was slowed more by phenates than by sulfonates [36]. Apparently, the overall rate of film formation for the ZDDP + sulfonates was greater than that of ZDDP + phenates; that is, despite the inherent film-removal processes in the experiment, the ZDDP + sulfonate combination was able to establish an insulating film

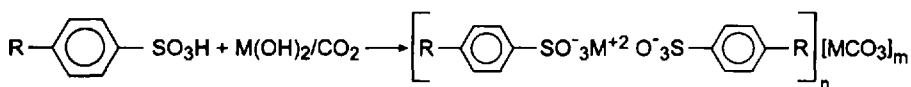
**Figure 15.2** Preparation of overbased sulfonate detergent.

Table 15.7 Detergent Comparison

High-base-number detergent	Low-base-number detergent
150–400 TBN*	0–80 TBN
High-base content	Low-base content
Lower detergency	High detergency
Low cost (on metal-content basis)	High cost (on metal-content basis)

*TBN equals total base number, defined as milligrams of KOH per gram of oil.

faster than the ZDDP + phenate combination. Fox et al. [41] has studied the solubilizing mechanism of detergents in nonpolar media and has described the interaction of detergents with other common lubricant additives. Papke [37] has explored the solubilization of low-molecular-weight acids by sulfonate detergents. He found that the neutralized acid salts are held in solution by micelle formation with the detergents, even after complete depletion of the detergent TBN.

Detergents are most often based on sulfonate, phenate, salicylate, or phosphonate substrates. Neutral dinonyl naphthalene is a popular sulfonate substrate used for rust inhibition or demulsification in hydraulic lubricants. Some characteristics of detergents are given in Table 15.7.

Antiwear Agents [42]

Antiwear agents are designed to adsorb onto and react with wear surfaces to reduce friction and wear rates under mixed-lubrication and boundary lubrication conditions. A schematic illustration of the formation of an antiwear film is shown in Fig. 15.3. An asperity-to-asperity contact collision is depicted, in which metal-to-metal contact is occurring. Both surfaces are immersed in an oil containing ZDDP. (The typical

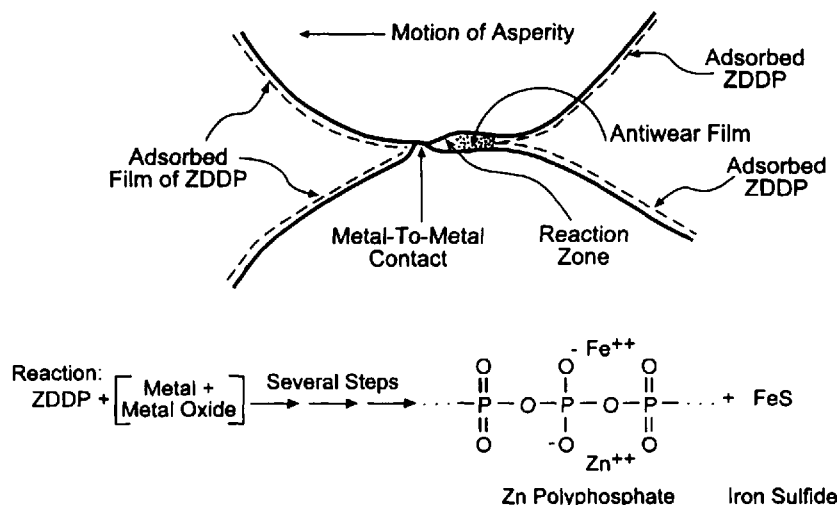


Figure 15.3 Schematic of antiwear film formation in an asperity collision (metal-to-metal contact).

concentration of ZDDP in a hydraulic fluid is around 0.5% by weight.) As a consequence, both surfaces bear a film of adsorbed ZDDP. Upon collision, the temperature rises to approximately 120–157°C and the adsorbed ZDDP reacts with the metal surface to form polyphosphates admixed with metal sulfides [43]. The specific reaction pathway has not been elucidated. Nascent metal resulting from the collision of asperities rapidly adsorbs ZDDP from the surrounding lubricant, and subsequent collisions may generate more antiwear film if the temperatures are sufficiently high to promote the reactions. The antiwear film is more easily sheared than is the metal, but it is sufficiently strong to resist flow under load and, thus, remains interposed between the metal surfaces and serves as an efficient lubricant under high-load conditions. For hydraulic fluids, the need for these additives is critical in the vane pump [44]. However, the surface activity of the antiwear or extreme pressure agents must be carefully balanced against that of the detergents: if the antiwear agents are insufficiently surface active (or too soluble in the lubricant) or the detergents are too surface active, the antiwear function may be insufficient.

Surface activity is quantitatively described by the adsorption isotherm. Adsorption isotherms are curves showing the amount of a surface-active agent adsorbed on a surface for a given concentration of that agent dissolved in the fluid (in this case, mineral oil) in contact with the surface. The relationship is for equilibrium conditions. Determination of adsorption isotherms is tedious. Different oils or surfaces result in different isotherms for a given surface-active agent. Furthermore, the question of impurities dominating the result is a serious issue. A detailed discussion of adsorption isotherms is outside the scope of this chapter.

Measuring the adsorption isotherms for all possible combinations of surface-active agents, base oils, and metal surfaces would be an enormously impractical task. Detailed studies of adsorption isotherms are confined to selected specific combinations. For example, Tamura has studied the adsorption of calcium sulfonate detergent, barium sulfonate detergent, and ZDDP on metal surfaces [45,46]. Baldwin attempted to relate wear to the predicted ability to adsorb on a metal surface [47]. He found that the polarity of the adsorbed species and the sulfur content, even if unreactive sulfur, were key factors in reducing wear. He also found that the steric hindrance of the alkyl group could reduce adsorption, hence wear resistance. Jahanmir developed a simple model to relate the friction coefficient to adsorption parameters and explained the correlation in terms of the adsorbed molecule's structure [48]. In a subsequent article [49], he expanded his study to include the effects of an increasingly polar end group through the use of model compounds. See References 50 and 51 for further examples of ZDDP adsorption isotherms. In practice, experience provides examples of antiwear agent–detergent combinations effective in various classes of base oils and kinds of service. From these examples, reasonable candidate formulations can be specified, tested, and modified as required to satisfy new needs arising from equipment modifications or base-oil changes. The effect of antiwear agents is illustrated in Table 15.8 for a hydraulic oil application [13].

Antiwear agents are activated by the higher temperatures and pressures found in the contact area between sliding surfaces. During mixed or boundary lubrication, asperities of the surfaces come into intermittent contact. The friction-generated temperatures cause the adsorbed antiwear or extreme-pressure agents to react with the metal surfaces and produce a chemically bonded film. As an example of the temperatures and pressures necessary to activate antiwear agents, consider ZDDP in an

Table 15.8 Comparison of Hydraulic Oils in Wear Tests

Test	Procedure	R&O	Fluid-type TCP antiwear agent	ZDDP antiwear agent
Vane pump wear 100 h, mg weight loss	ASTM D2882	691	240	19
FZG (load stage fail)	U.S. Steel DIN 51354, Part 2	6	8	12
Ryder gear, <i>N</i>	ASTM D1947	8,896	9,408	13,789
4-Ball wear, scar diameter (mm)	ASTM 4172			
20-kg load		0.60	0.30	0.30
40-kg load		Score	Score	0.39

Source: Ref. 13.

automotive engine oil application. Camshaft lubrication is critical to ensure proper functioning of the engine. Camshaft surface temperatures in a Ford in-line four-cylinder 2.3-L overhead camshaft engine and an Oldsmobile V-8 5.7-L engine were determined to be approximately 200°C. Not surprisingly, similar ZDDP structure-reactivity effects are observed in the two engines; that is, secondary ZDDP performs better than primary ZDDP or an aryl ZDDP [52].

Although the exact nature of the antiwear film has not been determined for all hydraulic pump tribocouples (brass against iron, for instance), work has shown conclusively that in iron-iron tribocouples, zinc dialkyldithiophosphate (ZDDP), the most common antiwear additive used in these hydrocarbon based lubricants, is adsorbed on metal (ferrous) surfaces [50,53], among others [51]. The adsorbed ZDDP forms antiwear films on rubbing, whose structure consists of polyphosphate films as determined by different spectroscopic techniques [54–56]. Interestingly, the length of the polyphosphate chain is dependent on the ZDDP structure, with the neutral ZDDP structure forming a longer polyphosphate chain than the corresponding basic ZDDP structure (see Fig. 15.3) [55]. This film prevents direct metal-to-metal contact, albeit with a relatively high coefficient of friction of about 0.13, typical of an antiwear film. Table 15.9 summarizes the strengths and weaknesses of various commercially important ZDDPs.

A possible mechanism of antiwear film formation based on the oxidative decomposition of ZDDP has been proposed by Willermet and co-workers [57]. Based on extensive surface analytical studies, they suggest that it is the antioxidant reactions of the ZDDP products that lead to polyphosphate film formation. They also suggest that overbased detergents can interfere with the polyphosphate chain growth and, hence, inhibit antiwear protection.

In these cited studies, the films were not significantly depleted; however, under severe conditions, less robust ZDDP films will not hold up to environmental factors [58]. Hydraulic fluids do not experience such harsh conditions, resulting in lower overall requirements for ZDDP. The preparation and solid-state structure of ZDDP, the most common antiwear additive in hydrocarbon based lubricants, is shown in

Table 15.9 Zinc Dialkyldithiophosphate Study

ZDDP type	Secondary alkyl	Primary alkyl (type 1)	Primary alkyl (type 2)	Alkyl aryl
Oxidation inhibition	Excellent	Excellent	Excellent	Excellent
EP/wear protection	Excellent	Excellent	Excellent	Good/fair
Thermal stability	Fair	Good	Good/excellent	Good
Hydrolytic stability	Excellent	Excellent	Excellent	Good

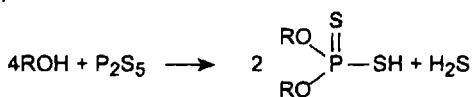
Source: Ref. 26.

Fig. 15.4. There are two structures termed neutral and basic ZDDP that comprise the commercial products.

Extreme-Pressure Agents [42]

Extreme-pressure (EP) agents generally require more strenuous reaction conditions (i.e., higher surface temperatures) to produce EP films. The EP films prevent direct metal-to-metal contact as in the case of the antiwear films, thus reducing wear and preventing seizure. Detailed surface studies have been done for some EP agents [42,59]. EP film formation is analogous to antiwear film formation. Adsorbed EP agent enters the contact zone, and under the high sliding temperatures and pressures, it is converted to an EP film (Fig. 15.4). Sulfur-containing EP additives require temperatures in the range of 490°C to react with iron and form a lubricious iron sulfide layer [60]. Other common EP agents contain chlorine that react with ferrous alloys to produce an iron chloride film [59]. Figure 15.5 illustrates the progressively higher load-carrying abilities of mineral-oil, mild antiwear, mild EP, and strong EP agents.

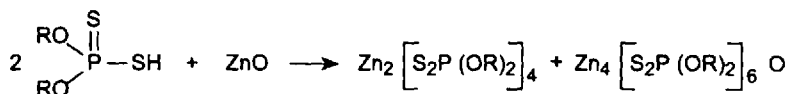
• Acid Reaction



R = C₃₋₁₀ Alkyl Alcohol
plus
Phosphorus Pentasulfide

Dithiophosphoric
Acid

• Neutralization Reaction



Dithiophosphoric
Acid

Zinc Oxide

Neutral Zinc
Dithiophosphate

Basic Zinc
Dithiophosphate (ZDDP)

Figure 15.4 Zinc dialkyldithiophosphate production.

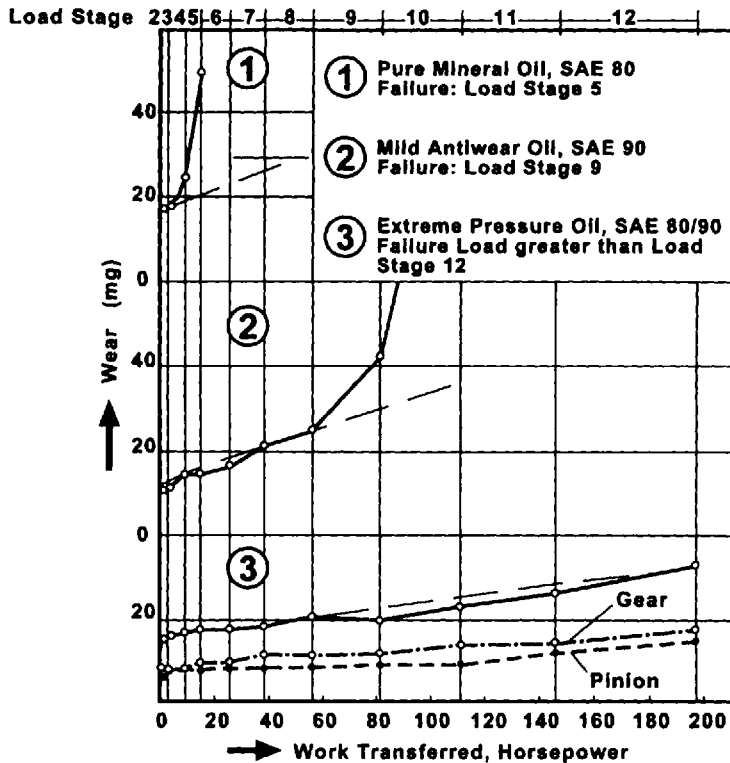


Figure 15.5 Load-carrying abilities of antiwear and EP agents. (Adapted from G. Niemann and H. Rettig, "Eigenschaften von Schmierstoffen für Zahnräder," *Erdöl Kohle-Erdgas-Petrochem.*, 1966, 19, 809–817).

Whereas antiwear films are effective in sustaining loads that result in pressures in the range 100,000–350,000 psi, EP films must sustain loads in the range 200,000–500,000 psi. There is not a sharp distinction between antiwear and EP ranges. A complete description of the formation and action of antiwear and EP films thus encompasses topics from adsorption isotherms and solid–solid reactions to the detailed mechanical properties of thin films. Most of this information is unavailable. Therefore, the selection of an appropriate EP agent is largely empirical.

Common EP agents for hydraulic system applications include sulfurized olefins, sulfurized fats, and thiophosphate esters.

Care needs to be exercised in recognizing that certain hydraulic fluids can attack bronze surfaces, especially those formulations containing thermally unstable ZDDPs. Indeed, as the severity of pump operations has increased over the years, two distinct additive systems have developed: one based on sulfur–phosphorus chemistry (ashless, i.e., metal-free), and the other on stabilized ZDDP. Both approaches aim to provide the user with the option of using a single fluid for both piston and vane pumps. Stabilizers commonly used include highly basic detergents, such as a high-TBN calcium phenate, or basic dispersants. It is hypothesized that such stabilizers, when added, improve the thermal stability of the ZDDP, but the exact mechanism is not worked out [61].

Oxidation Inhibitors [29]

Oxidation of a lubricant occurs whenever air is present in a lubricated system, resulting in thickening and degradation of the lubricant. Higher temperatures generated by frictional heating or compression processes accelerate oxidation. Oxidation is self-accelerating (e.g., autocatalytic): if not controlled by the addition of the appropriate type and amount of oxidation inhibitors, the rate of oxidation will continuously increase, and the lubricant will rapidly thicken and form acids plus oil-insoluble materials. Deposits may plug valves and damage oil-delivery systems.

Oxidation of lubricants eventually forms sludge. As the oxidation reactions progress, the suspended sludge thickens the oil. As discussed earlier in this chapter, these oxidation by-products impede efficient lubrication and can actually damage the lubricated equipment. Prevention or retardation of lubricant oxidation has been the subject of much research, which was recently summarized by Rasberger [62].

Klaus et al. [63,64], Lahijani and Lockwood [65], and Colclough [66] have modeled sludge formation. Their studies have investigated both the inhibition of oxidation by various common antioxidants and the catalysis of oxidation by soluble metals. These studies of soluble metal-induced oxidation catalysis emphasize the necessity to strictly control wear and corrosion processes in a lubricated system.

Hydrocarbon oxidation proceeds by a complex free-radical mechanism. In the early stages of the oxidation, an oxygen molecule abstracts a hydrogen atom from a hydrocarbon molecule. This results in the formation of a chemically reactive alkyl free radical (an unpaired electron on a carbon atom) and a hydroperoxy radical (the oxygen molecule with a hydrogen attached). The alkyl radical can react with another oxygen molecule in a fast step to yield an alkyl peroxy radical.

The alkyl peroxy and hydroperoxy radicals then abstract hydrogens from other hydrocarbon molecules (note that the concentration of hydrocarbons in the lubricant is very high relative to that of the peroxy radicals or oxygen molecules). The resulting hydroperoxides can cleave to form two free radicals from each hydroperoxide molecule, thus accelerating the reaction. If left unchecked, this chain reaction rapidly accelerates. Metal ions, particularly iron and copper ions, catalyze the oxidation processes by a complex sequence of reactions. A simplified reaction scheme is shown in Fig. 15.6. Metal-catalyzed oxidation mechanisms are more complex and are outside the scope of this chapter.

As the reaction progresses, the oxidized hydrocarbon molecules will begin to link together into increasingly polar, polymerlike chains. These polymerlike materials are sludge and varnish precursors that thicken the oil much as a viscosity index improver might. Eventually, the sludge precursors become too large and too polar to remain soluble in the oil and precipitate out of solution.

Oxidation inhibitors are added to lubricants to slow the rate of oxidation. The most common oxidation inhibitors are radical scavengers and hydroperoxide decomposers. Most lubricants usually contain a mixture of both types of oxidation inhibitor.

Radical scavengers work by reacting with peroxy radicals. In general, one radical scavenger can sequester two peroxy radicals before the inhibitor itself is consumed. The most common radical scavengers include phenolic and amine antioxidants.

Hydroperoxide decomposers react with the hydroperoxide or dialkyl peroxides to form nonradical products. The most common hydroperoxide decomposers include organosulfur compounds, zinc dialkyldithiophosphate (ZDDP), zinc dialkyldithio-

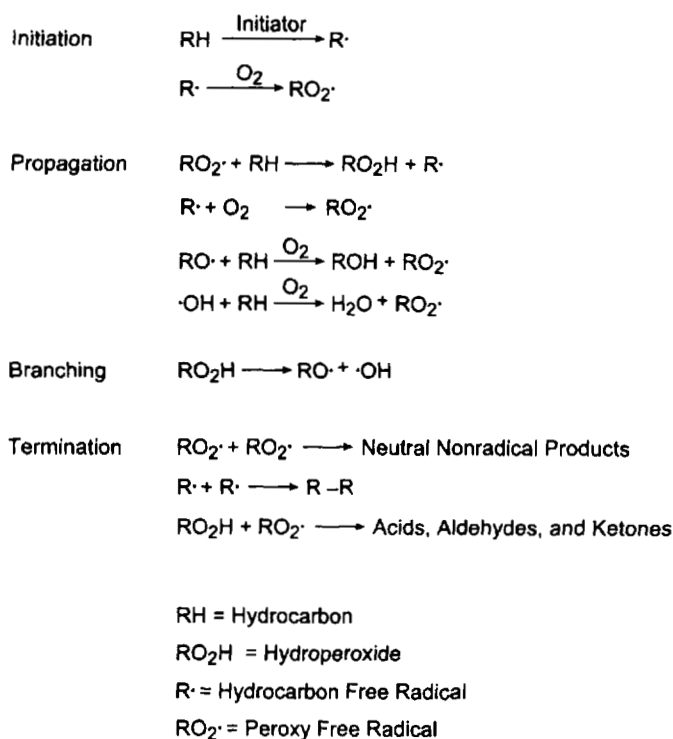


Figure 15.6 Simplified oxidation mechanism of hydrocarbons.

carbamate (ZDTC), organophosphates, organomolybdenum compounds, and over-based phenates or salicylates. The key species causing oxidation of lubricants and the appropriate antioxidants to control them are listed in Table 15.10. Structures of commercially important examples are given in Fig. 15.7. Because the various types of oxidation inhibitors function quite differently, combinations of inhibitors are used for optimum results, as exemplified by Formulation B in Table 15.4. In this formulation, the ZDDP serves as an antiwear agent and as a peroxide-decomposing

Table 15.10 Oxidation Intermediates and Appropriate Antioxidant Types

Reactive species	Mechanism of oxidation control
RO ₂ (alkyl peroxy radical)	Chain breaking Hindered phenolics Aromatic amines ZDDP Copper salts
ROOH (alkyl hydroperoxide)	Peroxide decomposition to nonradical products ZDDP Sulfur components

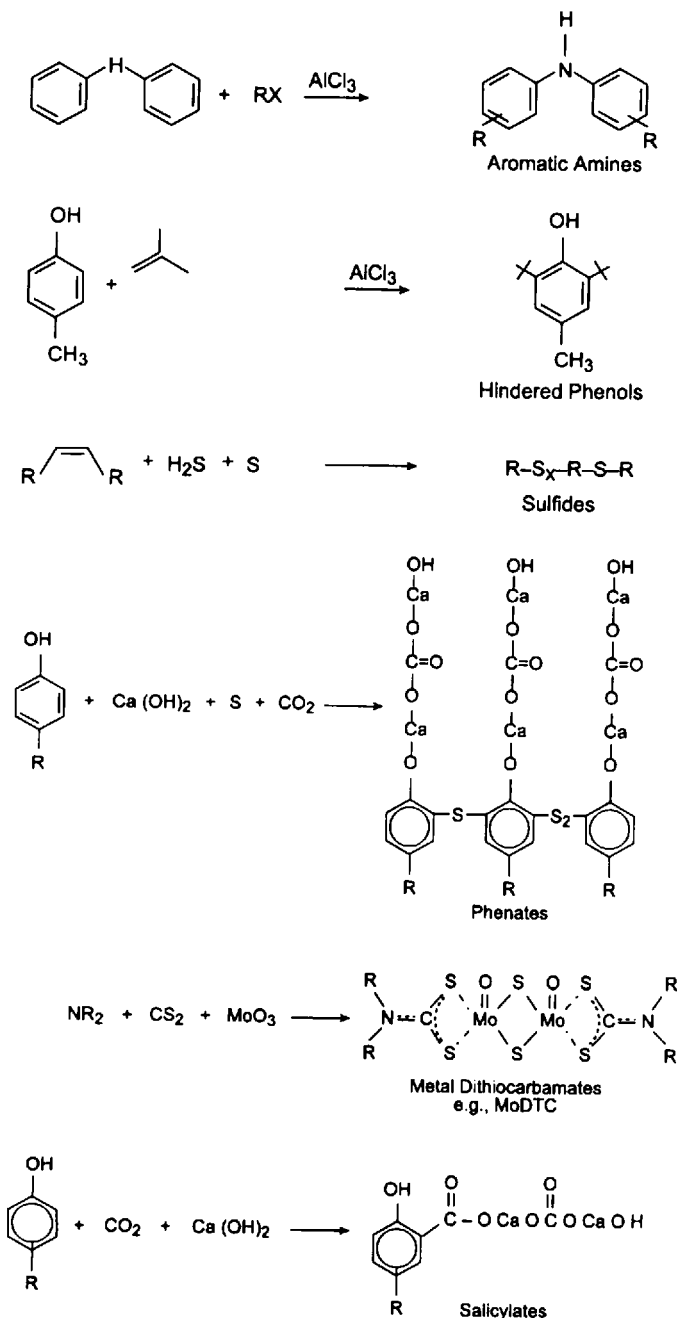


Figure 15.7 Some classes of oxidation inhibitors.

antioxidant. The other antioxidant in Formulation B is a hindered phenol, a chain-breaking antioxidant.

Aromatic amines are effective at high temperatures but offer little protection at low temperatures. Alkylated phenols function well at low temperatures, but some are volatile at higher temperature. Hard and fast rules for the selection of antioxidants singly or in combination cannot be given. Every base-oil blend will be different.

Rust and Corrosion Inhibitors [26]

Corrosion inhibitors adsorb on the metal surfaces, blocking the surfaces from acids, water, or other potentially corrosive substances. Because corrosion inhibitors are surface active with limited solubility in hydrocarbon solution, they compete with detergents, dispersants, and antiwear agents for metal surfaces.

Rust or ferrous corrosion inhibitors are generally low-molecular-weight alkyl amines or acids. Metal deactivators or nonferrous corrosion inhibitors are usually sulfur, nitrogen, or sulfur- and nitrogen-containing heterocyclic carbon rings. A rust or corrosion inhibitor acts by adsorbing onto the metal or metal oxide surface and blocking the surface from corrosion-producing acids. Hamblin et al. have prepared a discussion of corrosion inhibitors, corrosion-inhibition mechanisms, and corrosion tests [38].

Typical hydraulic oil rust inhibitors include barium or calcium sulfonates, alkyl succinic acid, substituted imidazolines, and substituted oxazolines. Metal deactivators include triazoles, benzotriazoles, and mercaptothiadiazoles.

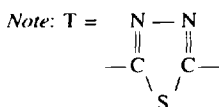
An interesting study of the mechanism of copper-corrosion inhibition by mercaptothiadiazole derivatives has been carried out by Luo and co-workers [67]. They reacted several mercaptothiadiazole bisdisulfide derivatives shown in Table 15.11 with active sulfur to give trissulfides as determined by Raman spectroscopy and mass spectroscopy. The thiadiazole bisdisulfides were shown to inhibit copper corrosion by scavenging the active sulfur and forming a protective film containing the thiadiazole ring on the copper surface.

Viscosity Index Improvers [27]

Viscosity index improvers (VII) or viscosity modifiers (VM) are polymeric materials of molecular weights between 50,000 and 1,000,000 that increase the resistance to flow, or viscosity, of a lubricant. They are designed to thicken oil more at high

Table 15.11 Dimercaptothiadiazole Derivatives

Compound	Structure
R ₁	CH ₃ (CH ₂) ₄ (CH ₃) ₂ CSS-T-SSC(CH ₃) ₂ (CH ₂) ₄ CH ₃
R ₂	CH ₃ (CH ₂) ₁₀ CH ₂ SS-T-SSCH ₂ (CH ₂) ₁₀ CH ₃
R ₁	CH ₃ (CH ₂) ₈ (CH ₃) ₂ CSS-T-SSC(CH ₃) ₂ (CH ₂) ₈ (CH ₃)
R ₄	CH ₃ (CH ₂) ₁₂ CH ₂ S-T-SCH ₂ (CH ₂) ₁₂ CH ₃



Source: Ref. 67.

Additives for Mineral-Oil–Based Hydraulic Fluids

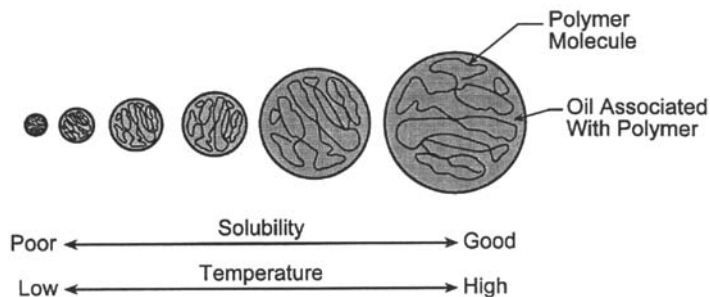


Figure 15.8 Viscosity improvers and the mechanism of thickening.

temperatures than at low temperatures (Fig. 15.8). Viscosity modifiers function by gradually uncoiling in solution as the temperature of the lubricant increases. The large volume occupied by the polymer blocks easy flow of the lubricant and increases the viscosity. If the polymer chain is damaged or broken by oxidation or by shear, the uncoiled polymer occupies less volume and is less effective at impeding oil flow. Therefore, the viscosity of the oil solution decreases. Common types of viscosity index improvers are shown in Table 15.12.

Hydraulic fluid viscosity modifiers are one route to a high-viscosity-index lubricant; the proper choice of base stock is another. Hydraulic VIIs have varying shear stability, so the polymer chosen must be carefully matched to the application. Hydraulic VIIs have generally good low-temperature properties but must be matched to the base stock. Other desirable properties include filterability to avoid clogging hydraulic mechanisms and filters, easy demulsification, good foam performance, and adequate viscosity at high temperature. Hydraulic lubricant specifications are summarized in Table 15.1. As of this writing, there are no shear stability requirements for hydraulic fluids; however, Fig. 15.9 clearly shows that different applications require viscosity-modifying polymers with a range of shear stability. Chapter 9 provides more discussion of viscosity index improvers' structural relationship to oil thickening.

Table 15.12 Viscosity Index Improver Types

General class	Dispersant type available	Monomers used
Hydrocarbon Type		
PIB (Polyisobutylene)	No	Isobutylene
OCP (Olefin copolymer)	Yes	Ethylene and propylene
SB or SI (Olefin copolymers)	No	Styrene with butadiene or isoprene
Ester Type		
Styrene ester	Yes	Styrene and maleic ester
Polymethacrylate	Yes	Methacrylic acid and alcohol

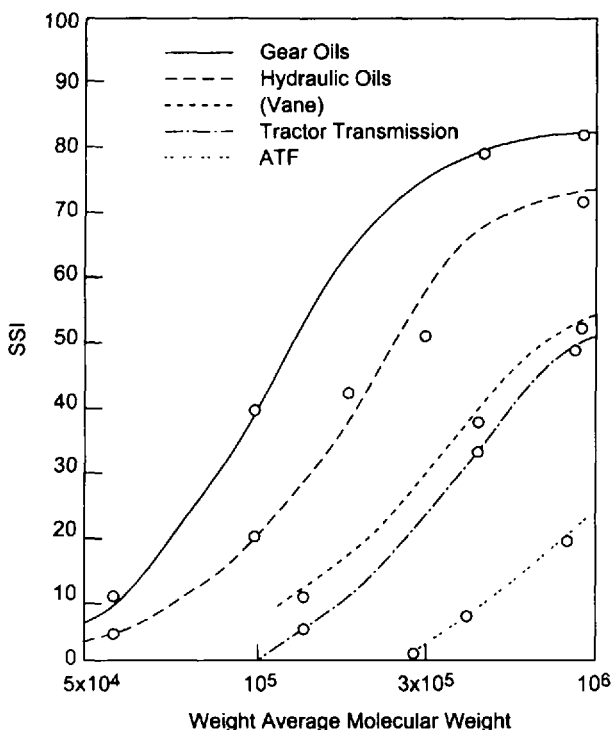


Figure 15.9 Relationship of molecular weight to SSI for various applications. (For details, see the brochure "Acryloid Hydraulic Fluid Viscosity Index Improvers," from RohMax Additives GmbH, Philadelphia, 1995.

Pour Point Depressants [27]

The pour point of an oil is the lowest temperature at which the oil will flow. Mineral oils contain waxes that precipitate from solution at temperatures around 0°C as crystals, forming a substantial network. If wax is allowed to form unimpeded, many mineral oils will become highly viscous or even solids at low temperatures. If the lubricating oil becomes too viscous, mobile hydraulic systems may not function because the oil cannot be pumped efficiently. In the worst case, equipment may fail from oil starvation.

Pour point depressants (PPD) are materials that cocrystallize with or adsorb onto waxes, preventing growth and limiting network growth. The most common types of PPDs are polymethacrylate polymers, styrene esters, poly(vinyl acetate) or alkylfumarates, alkyl naphthalenes, coupled alkylphenols, and poly(ethylene/vinyl acetates). The typical response of a base oil to a pour point depressant is shown in Fig. 15.10.

To understand the shape of the curve shown in Fig. 15.10, it is important to recall that the pour point depressant (PPD) itself is a waxy material and that care is necessary in adding the proper type and amount of PPD for the best response. In Fig. 15.10, the selected PPD has a large effect on the ASTM D97 at low concentrations. At higher concentrations, the same PPD has lesser effect and, at high concentrations, can promote wax formation in the oil [68].

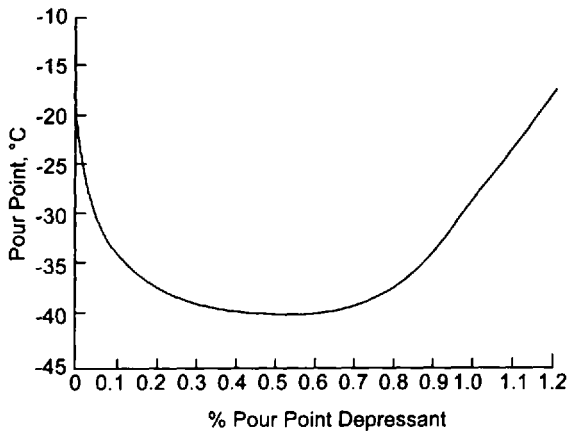


Figure 15.10 Effect of treat rate on ASTM D 97 pour point.

Common tests used to assess low-temperature properties of mineral-oil–based lubricants are given in Table 15.13.

Foam Inhibitors

Foams are often formed when a liquid is mechanically agitated in the presence of a gas. For hydraulic systems, that gas is usually air. Much more compressible than a liquid, a foam is undesirable in a hydraulic system, for it decreases pumping efficiency and increases system response times. Commonly, foam inhibitors are used to reduce or to eliminate the tendency of a lubricant to foam. For nonaqueous systems, certain requirements are agreed upon as essential for an effective foam inhibitor [69]. These include the following:

- Insolubility in the lubricant under use conditions
- A surface tension lower than that of the lubricant
- Dispersability in the lubricant
- Chemical inertness under use conditions to assure its continued presence

Table 15.13 Standard Tests for Determining the Low-Temperature Properties of Mineral-Oil–Based Lubricants

Test procedure	Title
ASTM D 97	Pour Point
SAE J300, Appendix B, or FTM 791b, Method 203, Cycle 3	Stable Pour Point
ASTM D 3829	Borderline Pumping Temperature
ASTM D 4684	Pumping Viscosity
ASTM D 2983	Brookfield Viscosity
ASTM D 5133	Scanning Brookfield Viscosity
Modified ASTM D 5133	Gelation Index
JDQ 73	John Deere Cold Soak
JDQ 74	John Deere Slow Cool

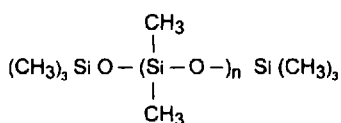
Typical foam inhibitors used in mineral oils are shown in Fig. 15.11.

Siloxane foam inhibitors in hydraulic oils are typically present in the range of 1–10 ppm [70]. To be effective, they must be highly dispersed in droplet form with a droplet diameter between 0.001 and 1.0 μm , preferably submicron size [71]. The polyacrylates are effective at concentrations less than 0.06% [72]. Dispersions of foam inhibitors in oil-soluble carriers are available. The neat foam inhibitors are also available but must be dispersed in the lubricant to be effective. Thorough mixing of the dispersed foam inhibitor with the lubricant is essential.

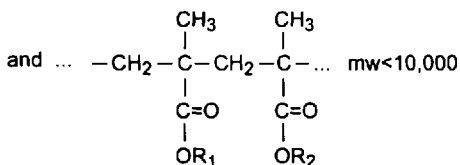
The exact mechanisms by which foam inhibitors function are in dispute (see Ref. 71). It has been hypothesized that droplets of foam inhibitor (insoluble in the oil) are surface active and spread over the surfaces of films of oil in foam bubbles, and that the duplex films so formed have lower stability than the oil film itself, resulting in enhanced oil-film rupture. However, it has been shown that nonspreading antifoam agents are also effective [71]. Spreading of an antifoam agent film on an oil film to form a duplex film alters the surface tension properties of the oil film. There is no agreement on how the surface tension changes are related to foam stability [71].

Agitation of a liquid in the presence of a gas may result not only in foaming but also entrainment of the gas in the liquid. Entrained air is undesirable in hydraulic system liquids [73]. Entrained air differs from foam in that the air bubbles are small and separated from each other by relatively thick layers of oil. Oil containing air bubbles is more compressible than oil alone, with resulting decreases in pumping efficiency and increases in system response times. Air-release times (or more generally, gas-bubble-release times) are therefore important. Air-release time is defined as “the time taken for the volume of dispersed air in the oil to reduce to 0.2%” [74]. Various procedures have been adopted to determine air-release-time values, all using the same apparatus [75].

The significance of air-release-time values of additives in hydraulic oils is that additives (and the base oils themselves) affect air-release times [75]. In particular,



polydimethylsiloxanes (60,000 cp, 30,000 cp, 12,500 cp) [66]



R₁- Alkyl Group With 1 to 18 C Atoms; R₂- Alkyl Group With 3 to 7 C Atoms
polyacrylates [67]

Figure 15.11 Chemical structures of common foam inhibitors for mineral-oil-based lubricants.

antifoam agents may *increase* air-release times [75]. Adding more antifoam agent than needed may adversely affect oil performance. Foam stability and dispersed air bubble size are strongly affected by small concentrations of surface active materials in the oil. Changes in hydraulic oil foaming tendencies during service may result from contamination.

In practice, foam-inhibitor selection proceeds by testing candidate formulations in foaming tendency (ASTM D892-92) and gas bubble separation time (ASTM D3427-93) tests. Selection of the foam inhibitor is usually the last step in formulation development. Examples of passing limits are provided in the AAMA Hydraulic Standard [76] and in Ref. 75.

Demulsifiers

Demulsifiers are used to cause rapid separation of water from oil. Water in hydraulic fluids can cause rust, cavitation, deterioration of the fatigue life of components, an increase in the oxidation rate of the hydrocarbon carrier, and formation of emulsions or sludge. Both ZDDPs and detergents, particularly overbased detergents, are hydrolyzed by water. Not only does this hydrolysis deplete these additives, but the products of hydrolysis are typically voluminous hydrous oxides. For example, hydrated calcium hydroxide (an oil-insoluble inorganic salt derived from the detergent) could block filters if present in sufficient quantities. If used at improper levels, demulsifiers can promote emulsification and antagonize the problems caused by water. Typical mineral-oil–based hydraulic fluid demulsifiers include polyethylene glycols, metal salts of dinonyl naphthalene sulfonates, and polyoxy-alkylated phenols.

Friction Modifiers [77]

Friction modifiers are used to reduce friction and wear between surfaces when mild sliding occurs. The best of these materials consist of a long, linear hydrocarbon chain and a small polar functional group. One example is oleic acid, an 18-carbon carboxylic acid. Friction modifiers function by adsorbing onto a metal surface in a regular assembly and producing a low-friction, boundary film that is easily sheared, preventing metal-to-metal contact, but only under a light load. Hydraulic fluid friction modifiers are generally sulfurized fats, but other common types include fatty amines, fatty acids, fatty amides, and fatty phosphates.

As with most lubricant additives, friction modifiers cannot be used indiscriminately under all operating conditions without encountering problems [78]. Hercamp [79] has reported rapid corrosion of copper-alloy bearings in some heavy-duty diesel engines due to the presence of a molybdenum-containing friction modifier. Hu et al. [80] have studied the corrosion of copper by stearic acid, an oft-suggested antiwear/friction-modifying agent. They found that stearic acid in hydrocarbon solution adsorbs strongly on copper surfaces and forms copper stearate but can become corrosive at temperature above 140°C.

As is usual in the development of many lubricants, including hydraulic oils, the selection of a friction modifier or antiwear agent for a formulation is an empirical process. The formulator, calling upon accumulated experience, tests a number of possible additive combinations (candidate oils) in appropriate bench tests, known to provide insight into actual field performance. Based on the results, a new round of candidate oils is blended, and the screening tests repeated. Finally, with all the results known, a few candidate oils are subjected to the full array of tests shown in Table

15.1. Hopefully, one of the candidates proves to be satisfactory. If not, more modifications must be made to the most promising formulation, and the battery of tests repeated. Adequate performance in bench tests does not guarantee that the oil will be a success under actual field conditions. Lubricants must be subjected to field testing, a process that can literally take years to complete, depending on the application.

ACKNOWLEDGMENTS

Helpful discussions with Julio Quintero of Chevron Global Lubricants and S. H. Brown of Oronite Global Technology are gratefully acknowledged.

REFERENCES

1. E. E. Lewis and H. Stern, "Design of Hydraulic Control Systems," 1962, McGraw-Hill; New York, pp. 185–189.
2. E. E. Klaus and J. A. O'Brien, "Precise Measurement and Prediction of Bulk-Modulus Values for Fluids and Lubricants," *ASME J. Basic Eng.*, 1964, 86, pp. 469–474.
3. R. L. Peeler and J. Green, "Measurement of Bulk Modulus of Hydraulic Fluids," *ASTM Bull.*, 1959, 235, p. 51.
4. A. Cameron ed., *The Principles of Lubrication*, 1st ed., 1966, John Wiley & Sons; New York, pp. 3–14 and 49–79.
5. A. Cameron ed., *The Principles of Lubricants*, 1st ed., John Wiley & Sons; New York, pp. 187–212.
6. G. R. Rowe, in *The Principles of Lubricants*, A. Cameron, ed., 1966, John Wiley & Sons; New York, pp. 450–467.
7. E. Rabinowicz, *Friction and Wear of Materials*, 2nd ed., 1995, John Wiley & Sons; New York, pp. 118 and 166.
8. W. A. Glaeser, R. C. Erickson, K. F. Dufrane, and J. W. Kannel, "Tribology: The Science of Combating Wear, Part II," *Lubr. Eng.*, 1992, 48(12), pp. 949–952.
9. W. A. Glaeser, R. C. Erickson, K. F. Dufrane, and J. W. Kannel, "Tribology: The Science of Combating Wear," *Lubr. Eng.*, 1992, 48(11), pp. 867–873.
10. W. M. Needelman, "Filtration for Wear Control," in *The Wear Control Handbook*, M. B. Peterson and W. O. Winer, eds., 1980, American Society of Mechanical Engineers; New York, pp. 507–582.
11. C. N. Rowe, in *Handbook of Wear Control*, M. B. Peterson and W. O. Winer, eds., 1980, American Society of Mechanical Engineers; New York, pp. 143–160.
12. A. Bos, "The Effect of Zinc Di-*N*-Butyl Dithiophosphate on Bronze Wear in a Lubricated Bronze-on-Steel Contact," *Wear*, (1978), 49(5), pp. 359–372.
13. K. B. Grover and R. J. Perez, "The Evolution of Petroleum Based Hydraulic Fluids," *Lubr. Eng.* 1990, 46(1), pp. 15–20.
14. A. Sasaki, M. Kawasaki, T. Sakai, H. Kojima, and S. Takayama, "A Study of Hydraulic Valve Problems," *Lubr. Eng.*, 1989, 45(3), pp. 140–146.
15. A. Sasaki, M. Sasaoka, T. Tobisu, S. Uchiyama, and T. Sakai, "The Use of Electrostatic Liquid Cleaning for Contaminant Control of Hydraulic Oil," *Lubr. Eng.*, 1988, 44(3), pp. 251–256.
16. T. B. Higbee, "Trends in Filter Technology and Application," *STLE 50th Annual Meeting*, 1995, Preprint Number 95-AM-3D-1.
17. G. H. Mills and F. A. Davis, "A Ferrographic Case Study Applied to Hydraulic Systems," *Wear*, 1983, 90(1), pp. 101–106.

18. B. M. Verdegan, T. Jaroszczyk, and J. A. Stinson, "Interpretation of Filter Ratings for Lubrication Systems," *Lubr. Eng.*, 1988, 44(5), pp. 424–430.
19. D. Klamann, *Lubricants and Related Products*, 1984, Verlag Chemie, Weinheim, pp. 51–83.
20. D. Klamann, *Lubricants and Related Products*, 1984, Verlag Chemie; Weinheim, pp. 96–153.
21. G. E. Totten and R. J. Bishop, "Historical Overview of the Development of Water-Glycol Hydraulic Fluids," SAE International Off-Highway and Power Plant Congress, 1995, SAE Paper 952076.
22. V. W. Castleton, "Practical Considerations for Fire-Resistant Fluids," *Lubr. Eng.*, 1998, 54(2), pp. 11–17.
23. A. Fessenbecker, I. Roehrs, and P. Pagnoglou, "Additives for Environmentally Acceptable Lubricants," *NLGI Spokesman*, 1996, 60(6), pp. 9–25.
24. R. W. Watson and T. F. McDonnell, Jr., "Additives—The Right Stuff for Automotive Engine Oils," SAE Technical Paper 841208, 1984.
25. S. Q. A. Rizvi, "Lubricant Additives," *Petrol. Coal*, 1996, 38(3), pp. 15–24.
26. S. Q. A. Rizvi, "Additives—Chemistry and Testing," in *Tribology Data Handbook*, 1997, CRC Press; Boca Raton, FL, pp. 117–137.
27. C. Kajdas, "Engine Oil Additives: A General Review," in *Engine Oils and Automotive Lubrication*, W. J. Bartz, Ed., Expert Verlag GmbH, Inc., Ehningen, Germany, (1993), pp. 149–175.
28. T. V. Liston, "Engine Oil Additives—What They Are and How They Function," *Lubrication Engineering*, 1992, 48(5), pp. 389–397.
29. G. J. Schilling and G. S. Bright, "Fuel and Lubricant Additives—II, Lubricant Additives," *Lubrication*, 1977, 63(2), pp. 13–24.
30. R. S. Fein, "Boundary Lubrication," *Lubrication Engineering*, 1991, 47(12), pp. 1005–1008.
31. R. J. Pugh, T. Matsunaga, and F. M. Fowkes, "The Dispersibility and Stability of Carbon Black in Media of Low Dielectric Constant. 1. Electrostatic and Steric Contribution to Colloidal Stability," *Colloids and Surfaces*, 1983, 7, pp. 183–207.
32. R. J. Pugh and F. M. Fowkes, "The Dispersibility and Stability of Carbon Black in Media of Low Dielectric Constant. 2. Sedimentation Volume of Concentrated Dispersions, Adsorption and Surface Calorimetry Studies," *Colloids and Surfaces*, 1984, 9, pp. 33–46.
33. R. J. Pugh and F. M. Fowkes, "The Dispersibility and Stability of Coal Particles in Hydrocarbon Media with a Polyisobutylene Succinamide Dispersing Agent," *Colloids and Surfaces*, 1984, 11, pp. 423–427.
34. E. S. Forbes and E. L. Neustadter, "The mechanism of action of polyisobutenyl succinimide lubricating oil additives," *Tribology*, 1972, 5(2), pp. 72–77.
35. K. Endo and K. Inoue, "Effects of the Structure on Various Performances of Polyisobutenylsuccinimides," *Mech. Eng.*, 1993, 80, pp. 242–252.
36. E. S. Yamaguchi, P. R. Ryason, S. W. Yeh, and T. P. Hansen, "Boundary Film Formation by ZnDTPs and Detergents Using ECR," *World Tribology Congress 1997*, Preprint 97-WTC-17.
37. B. L. Papke, "Neutralization of Basic Oil-Soluble Calcium Sulfonates by Carboxylic Acids," *Tribol. Trans.*, 1988, 31(4), pp. 420–426.
38. P. C. Hamblin, U. Kristen, and D. Chasan, "Ashless Antioxidants, Copper Deactivators, and Corrosion Inhibitors: Their Use in Lubricating Oils," *Lubr. Sci.*, 1990, 2(4), pp. 287–318.
39. N. K. Myshkin, C. K. Kim, and M. I. Petrokovets, *Introduction to Tribology*, 1997, Cheong Moon Gak, Seoul, pp. 1–32 and 204–220.

40. C. Belle, R. Gallo, F. Jacquet, P. Hoornaert, and J. P. Roman, "The Overbasing of Detergent Additives: The Behaviour of Promoters and Determination of Factors Controlling the Overbasing Reaction," *Lubr. Sci.*, 1992, 5(1), pp. 11–31.
41. M. F. Fox, Z. Pawlak, and D. J. Picken, "Inverse Micelles and Solubilization of Proton Donors in Hydrocarbon Formulations," *Tribol. Int.*, 1991, 24(6), pp. 341–349.
42. A. G. Papay, "Antiwear and Extreme Pressure Additives in Lubricants," *Technische Akademie Esslingen 10th International "Tribology—Solving Friction and Wear Problems" Colloquium*, 1996, Vol. 2, pp. 1093–1099.
43. F. G. Rounds, "Some Environmental Factors Affecting Surface Coating Formation with Lubricating Oil Additives," *ASLE Trans.*, 1966, 9, pp. 88–100.
44. W. A. Glaeser, R. C. Erickson, K. F. Dufrane, and J. W. Kannel, "Tribology: The Science of Combating Wear, Part IX," *Lubr. Eng.*, 1994, 50(10), pp. 785–787.
45. K. Tamura, "Adsorption of Lubricating Oil Additives by Surface Analysis," *Junkatsu*, 1983, pp. 838–844.
46. K. Tamura, "Adsorption of Dinonylnaphthalene Sulfonates on Carbon Black in the Presence of Polar Compounds," *Sekiyu Gakkaishi*, 1982, 25(5), pp. 306–314.
47. B. A. Baldwin, "The Effect of Adsorption and Molecular Structure of Antiwear Additives on Wear Mitigation," *ASLE Trans.*, 1985, 28(3), pp. 381–388.
48. S. Jahanmir and M. Beltzer, "An Adsorption Model for Friction in Boundary Lubrication," *ASLE Trans.*, 1986, 29(3), pp. 423–430.
49. S. Jahanmir and M. Beltzer, "Effect of Additive Molecular Structure on Friction Coefficient and Adsorption," *J. Tribol.*, 1986, 108, pp. 109–116.
50. S. Plaza, "The Adsorption of Zinc Diisobutyl Dithiophosphates on Iron and Iron Oxide Powders," *ASLE Trans.*, 1987, 30(2), pp. 233–240.
51. S. Plaza and L. Margielewski, "The Adsorption of the Zinc Dithiophosphates and Bis-(Diisobutoxyphosphinothioyl) Disulfide on Carbon Black from *n*-Hexadecane Solutions," *Tribol. Trans.*, 1993, 36(2), pp. 207–212.
52. J. A. Mc Geehan, J. P. Graham, and E. S. Yamaguchi, "Camshaft Surface Temperatures in Fired-Gasoline Engines," *SAE International Fuels and Lubricants Meeting and Exposition*, 1990; published as SAE Technical Paper 902162.
53. B. Dacre and C. H. Bovington, "The Effect of Metal Composition on the Adsorption of Zinc Di-Isopropylidithiophosphate," *ASLE Trans.*, 1983, 26(3), pp. 333–343.
54. Z. Yin, M. Kasrai, G. M. Bancroft, K. F. Laycock, and K. H. Tan, "Chemical Characterization of Antiwear Films Generated on Steel by Zinc Dialkyl Dithiophosphate Using X-Ray Absorption Spectroscopy," *Tribol. Int.*, 1993, 26(4), pp. 383–387.
55. M. Fuller, Z. Yin, M. Kasrai, G. M. Bancroft, E. S. Yamaguchi, P. R. Ryason, P. A. Willermet, and K. H. Tan, "Chemical Characterization of Tribochemical and Thermal Films Generated From Neutral and Basic ZDDPs Using X-Ray Absorption Spectroscopy," *Tribol. Int.*, 1997, 30(4), pp. 305–315.
56. P. A. Willermet, R. O. Carter III, and E. N. Boulous, "Lubricant-Derived Tribochemical Films—An Infrared Spectroscopic Study," *Tribol. Int.*, 1992, 25(6), pp. 371–380.
57. P. A. Willermet, D. P. Dailey, R. O. Carter III, P. J. Schmitz, and W. Zhu, "Mechanism of Formation of Antiwear Films from Zinc Dialkylidithiophosphates," *Tribol. Int.*, 1995, 28(3), pp. 177–187.
58. J. A. Mc Geehan and E. S. Yamaguchi, "Gasoline Engine Camshaft Wear: The Culprit Is Blowby," *SAE Technical Paper 892112*, 1989.
59. J. Lara, P. V. Kotvis, and W. T. Tysoe, "The Surface Chemistry of Chlorinated Hydrocarbon Extreme-Pressure Lubricant Additives," *Tribol. Lett.*, 1997, 3(4), pp. 303–310.
60. T. Sakurai and K. Sato, "Study of Corrosivity and Correlation Between Chemical Reactivity and Load-Carrying Capacity of Oils Containing Extreme Pressure Agent," *ASLE Trans.*, 1966, 9, pp. 77–87.

61. D. Saxena, R. T. Mookken, S. P. Srivastava, and A. K. Bhatnagar, "An Accelerated Aging Test for Antiwear Hydraulic Oils," *Lubr. Eng.*, 1993, 49(10), pp. 801–809.
62. M. Rasberger, "Oxidative Degradation and Stabilization of Mineral Oil Based Lubricants," in *Chemistry and Technology of Lubricants*, 1997, pp. 98–143.
63. E. E. Klaus, V. Krishnamachar, and H. Dang, "Evaluation of Basestock and Formulated Lubes Using the Penn State Microoxidation Test," in *Proceedings on Measurements and Standards for Recycled Oil/Systems for Performance and Durability*, National Bureau of Standards Special Publication 584, Gaithersburg, MD, 1979.
64. E. E. Klaus, J. L. Duda, and J. C. Wang, "Study of Copper Salts as High-Temperature Oxidation Inhibitors," STLE/ASME Tribology Conference, 1991, STLE Preprint 91-TC-5D-3.
65. J. Lahijani and F. E. Lockwood, "The Influence of Metals on Sludge Formation," ASME/ASLE Lubrication Conference, 1980, ASLE Preprint 80-LC-1C-4.
66. T. Colclough, "Role of Additives and Transition Metals in Lubricating Oil Oxidation," *Ind. Eng. Chem. Res.*, 1987, 26, pp. 1888–1895.
67. Y.-H. Luo, B.-Y. Zhong, and J.-C. Zhang, "The Mechanism of Copper-Corrosion Inhibition by Thiadiazole Derivatives," *Lubr. Eng.*, 1995, 51(4), pp. 293–296.
68. RohMax Additives GmbH, "Pour Point Depressants," Technical Report RM-96-12-02, 1996, RohMax Additives GmbH, Philadelphia, pp. 1–12.
69. I. C. Callaghan, in *Defoaming Theory and Applications*, P. R. Garrett, ed., 1993, Marcel Dekker, Inc.; New York, pp. 146–147.
70. P. G. Pape, *J. Petrol. Tech.*, 1983, 35, pp. 1197–1204.
71. P. R. Garrett, in *Defoaming Theory and Applications*, P. R. Garrett, ed., 1993, Marcel Dekker, Inc.; New York, pp. 19–30.
72. J. E. Fields, U.S. Patent 3166508 (January 19, 1965).
73. G. E. Totten, Y. H. Sun, and R. J. Bishop, "Hydraulic Fluids: Foaming, Air Entrainment and Air Release—A Review," SAE Technical Paper 972789, 1997.
74. ASTM D3427093.
75. A. R. Barber and R. J. Perez, "Air Release Properties of Hydraulic Fluids," NFPA Technical Paper Series 196-2, 10 April 1996.
76. *AAMA Hydraulic Fluid Standard*, 1995, American Automobile Manufacturers Association.
77. A. G. Papay and M. T. Devlin, "Friction and Friction Modifiers in Lubricants," Technische Akademie Esslingen 10th International "Tribology—Solving Friction and Wear Problems," Colloquium, 1996, Vol. 2, pp. 1073–1078.
78. M. Tohyama and T. Ohmori, "Influence of Lubricating Oil Viscosity and Friction Modifier on Engine Parts Wear," *Toraiborojisuto*, 1997, 42(11), pp. 841–846.
79. R. D. Hercamp, "Reduced Durability Due to a Friction Modifier in Heavy Duty Diesel Lubricants," SAE Technical Paper 851260, 1985.
80. Z. Hu, S. M. Hsu and P. S. Wang, "Tribocchemical and Thermochemical Reactions of Stearic Acid on Copper Surfaces Studied by Infrared Microspectroscopy," STLE Preprint 91-AM-3B-1, 1991.

This page intentionally left blank

Polyalphaolefins and Other Synthetic Hydrocarbon Fluids

RONALD L. SHUBKIN

Albemarle Corporation, Baton Rouge, Louisiana

LOIS J. GSCHWENDER and CARL E. SNYDER, JR.

U.S. Air Force, Wright-Patterson Air Force Base, Ohio

1 INTRODUCTION

Synthetic hydrocarbon fluids are fluid compounds or mixtures of compounds that are characterized as having specific molecular compositions containing only carbon and hydrogen atoms. Synthetic hydrocarbons may be distinguished from highly refined mineral oils because they are manufactured from specific raw materials by known chemical transformations. Mineral oils, on the other hand, are produced from petroleum base stocks by a variety of refining processes which may include cracking, extraction, dewaxing, distillation, isomerization, hydrocracking, and hydrorefining [1].

Although many synthetic hydrocarbon fluids have physical and chemical properties that are superior to those of equiviscous petroleum-based mineral oils, they also tend to be totally miscible in mineral oils and compatible with systems designed for mineral oils. This characteristic sets synthetic hydrocarbons apart from many other classes of synthetic fluids in that they may often be used to replace mineral oils (fully or partially) without the need to retrofit equipment.

There are five families of fluids classified as synthetic hydrocarbons:

1. Polyalphaolefin (PAO) Fluids. First and foremost in commercial importance among the synthetic hydrocarbons are the polyalphaolefin (PAO) fluids [2]. These fluids are enjoying a rapidly growing market for a wide variety of applications, including hydraulics.

2. Alkyl Aromatic (AA) Fluids. Second in importance are a class of fluids manufactured by attaching hydrocarbon chains (alkyl groups) to aromatic rings [3]. Alkyl aromatic (AA) fluids gained a degree of prominence in the 1970s during the building of the Alyeska pipeline in Alaska. Although still an important class of commercial fluids, AAs have not undergone the rapid growth of the PAO fluids.
3. Silahydrocarbon (SiHC) Fluids. Silahydrocarbon (SiHC) fluids are not hydrocarbons in the strict sense of the word, but are often classified as such because their chemical and physical properties are so similar to hydrocarbon fluids [4]. SiHCs have never been manufactured on a commercial scale, but their superior performance, especially in aeronautic hydraulic fluid applications, makes it worthwhile to include them in this chapter.
4. Polybutene (PB or PIB) Fluids. Polybutenes fluids are important commercially [5], but they are not used in hydraulic applications and will not be discussed in this chapter.
5. Cycloaliphatic Fluids. Cycloaliphatic fluids are the fifth class of hydrocarbon fluids [6]. A wide variety of cycloaliphatic fluids have been synthesized and evaluated, and many have excellent properties. Only one, however, has been commercialized, and that low-volume application is as a bearing lubricant in spacecraft. Cycloaliphatic fluids will not be further considered in this chapter.

2 HISTORY

Synthetic hydrocarbon compounds were being developed and patented for use as lubricating fluids as early as 1928 in Germany [7,8] and in the United States [9,10]. The first attempt to commercialize a synthetic hydrocarbon oil was made by Standard Oil Company of Indiana in 1929. The project was unsuccessful because of a lack of demand.

The onset of World War II and the subsequent shortages of petroleum feedstocks in Germany, France, and Japan revitalized interest in synthetic lubricants. Moreover, the German disaster at the Battle of Stalingrad in 1942 demonstrated the inadequacy of then current petroleum products to perform satisfactorily in extremely cold weather. During the winter of 1942, the lubricants used in tanks, aircraft, and other military vehicles gelled, and the engines used in the vehicles could not be started. An intense German research effort to find alternative lubricants followed the Stalingrad debacle and led to the first manufacture of synthetic products derived by olefin polymerization.

Alkylaromatic fluids were also produced in Germany during World War II, and they later became important as low-temperature lubricants during the Alaskan oil explorations in the 1960s and the building of the Alyeska pipeline in the 1970s. A dialkylbenzene product was used as an engine crankcase oil and as a hydraulic fluid.

During the Southeast Asia war in the 1960s, the need was recognized for a less flammable hydraulic fluid for military aircraft [11]. Although commercial aircraft had switched to hydraulic fluids based on phosphate esters, the military felt it was necessary to develop a fluid that was completely compatible with mineral-oil-based MIL-H-5606 [12] and which would require no retrofit of equipment. A PAO-based fluid was developed at the Wright Materials Laboratory, Wright-Patterson Air Force

Base, which was eventually designated as MIL-H-83282 [13]. MIL-H-83282 replaced MIL-H-5606 in most Air Force applications except those requiring operation at very low temperatures. More recently, MIL-H-87257 [14], also PAO based, has been approved for low-temperature hydraulic applications.

As in the case of PAO fluids, the U.S. Air Force Materials Laboratory, starting in the 1950s, played a pivotal role in the development of silahydrocarbon fluids [15–17]. Again, the driving force for this program was the recognition by the Air Force that fluids operating in high-temperature/high-load environments would be required in the high-performance military weapons systems under development.

3 POLYALPHAOLEFIN FLUIDS

Polyalphaolefin fluids are gaining rapid acceptance as high-performance lubricants and functional fluids because they have certain inherent, and highly desirable, characteristics relative to mineral oils. Among these favorable properties are the following:

- A wide operational temperature range
- Good viscometrics (high viscosity index)
- Thermal stability
- Excellent response to conventional antioxidants
- Hydrolytic stability
- Shear stability
- Low corrosivity
- Compatibility with mineral oils
- Compatibility with various materials of construction
- Low toxicity
- Good to moderate relative biodegradability
- Low deposit formation
- Ability to be “tailored” to specific end-use application requirements

3.1 Historical Development

In 1931, Standard Oil, in an article by Sullivan et al. [18] disclosed a process for the polymerization of olefins to form liquid products. These workers employed cationic polymerization catalysts such as AlCl_3 to polymerize olefin mixtures obtained from the thermal cracking of wax. At about the same time that the work at Standard Oil was being carried out, Zorn of I.G. Farben Industries independently discovered the same process [19].

The first use of a linear α -olefin to synthesize an oil was disclosed by Montgomery et al. in a patent issued to Gulf Oil Company in 1951 [20]. AlCl_3 was used in these experiments as it was in the earlier work with olefins from cracked wax.

The use of free-radical initiators as α -olefin oligomerization catalysts was first patented by Garwood of Socony-Mobil in 1960 [21]. Coordination complex catalysts, such as the ethylaluminum sesquichloride–titanium tetrachloride system, were disclosed in a patent issued to Southern et al. at Shell Research in 1961 [22].

The fluids produced by the various catalyst systems described above contained oligomers with a wide range of molecular weights. The compositions and internal structures of these fluids resulted in viscosity–temperature characteristics that gave

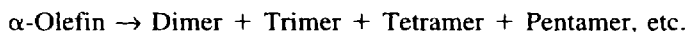
them no particular advantage over the readily available and significantly less expensive mineral oils of the day.

A patent describing the use of boron trifluoride (BF_3) as a catalyst for the oligomerization of linear α -olefins to make fluids suitable for use in lubricating oils was issued to Hamilton et al. of Socony Mobil in 1964 [23]. This patent describes a variety of oligomerization catalysts and gives only one example of the use of BF_3 . There is no mention in the patent regarding the unique properties of the product prepared using the BF_3 catalyst. In 1968, Brennan, also at Socony Mobil, patented a process for the oligomerization of α -olefins using a BF_3 catalyst system [24]. Prior to that time, BF_3 catalysis had given irreproducible results. Brennan showed that the reaction could be controlled if two streams of olefins were mixed in the reactor. The first stream contained the olefin plus a $\text{BF}_3 \cdot \text{ROH}$ complex, where ROH is an alcohol. The second stream contained the olefin saturated with gaseous BF_3 . Of particular interest was the fact that this catalyst system produced a product consisting of a mixture of oligomers that was markedly peaked at the trimer. There was no mention of a lubricating oil application in this patent.

Shubkin of the Chemicals Group of Ethyl Corporation (spun off as Albemarle Corporation on March 1, 1994) showed that H_2O [25], as well as other protic cocatalysts such as alcohols and carboxylic acids [26], could be used in conjunction with BF_3 to produce oligomers of uniform quality. The experimental technique employed a molar excess of BF_3 in relation to the cocatalyst. The excess was achieved by sparging the reaction medium with BF_3 gas throughout the course of the reaction or by conducting the reaction under a slight pressure of BF_3 . These studies showed that the oligomerization products exhibited pour points that were well below those anticipated for such compounds, even when dimeric products were allowed to remain in the final mixture. Until then, the molecular structure of the dimer was believed to consist of a straight carbon chain containing a single methyl group near the middle. Such branched structures were known to exhibit relatively high pour points. These patents were the first to address the unique qualities, and thus the potential importance as synthetic lubricants, of PAOs derived from $\text{BF}_3 \cdot \text{ROH}$ catalyst systems. Shubkin et al. later showed that the unique low-temperature properties could be attributed to a high degree of branching in the molecular structure [27].

3.2 Manufacture

Polyalphaolefins are manufactured by a two-step process from linear α -olefins, which are themselves manufactured from ethylene. The first synthesis step entails oligomerization, which simply means a polymerization to relatively low-molecular-weight products:



For the production of low viscosity (2–10 cSt), PAOs, the catalyst for the oligomerization reaction is usually boron trifluoride. (Note: PAOs are commonly classified by their approximate kinematic viscosity at 100°C. That convention will be used throughout this chapter. Thus, a fluid referred to as PAO 4 has a viscosity at 100°C of ~ 4 cSt.) The BF_3 catalyst is used in conjunction with a protic cocatalyst such as water, an alcohol, or a weak carboxylic acid. The $\text{BF}_3 \cdot \text{ROH}$ catalyst system is unique because of its ability to form highly branched products with the oligomer

distribution peaking at the trimer. Figure 16.1 shows a gas chromatography (GC) trace indicating the oligomer distribution of a typical reaction product from 1-decene and $\text{BF}_3 \cdot \text{C}_4\text{H}_9\text{OH}$ as the catalyst system [26]. Higher-viscosity (40 and 100 cSt) PAO fluids are manufactured using alkylaluminum catalysts in conjunction with an organic halide [28] or by the use of AlCl_3 .

The second step in the manufacturing process entails hydrogenation of the unsaturated oligomer. The reaction is carried out over a metal catalyst such as nickel or palladium. Hydrogenation gives the final product enhanced chemical inertness and added oxidative stability. Distillation, either before or after hydrogenation, is usually employed to separate the total product into different viscosity grades.

One of the distinct advantages in the manufacture of PAO fluids is that they can be “tailor-made” to fit the requirements of the end-use application [29]. This customizing is done by manipulation of the reaction variables which include the following:

- Temperature
- Time
- Pressure
- Cocatalyst type
- Cocatalyst concentration
- Distillation of final product
- Chain length of olefin raw material

Today, the commercial PAO market is dominated by decene-derived material because these products have the broadest temperature range of desirable properties. Manipulation of the first six variables (see above) are the common practice for manufacturing the usual grades of PAO (PAO 2, PAO 4, PAO 6, PAO 8, and PAO 10).

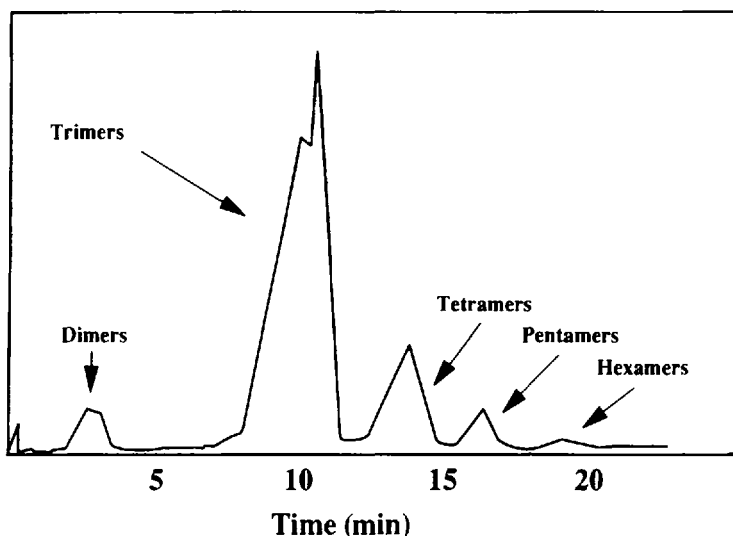


Figure 16.1 Gas chromatography trace of total product from the oligomerization of 1-decene using a $\text{BF}_3 \cdot \text{ROH}$ catalyst.

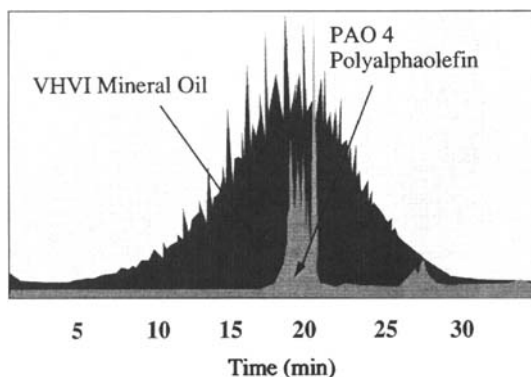


Figure 16.2 Gas chromatography comparison of PAO 4 and a VHVI mineral oil.

Some PAO fluids manufactured from other olefin streams (mainly 1-octene and 1-dodecene) are being offered to fill the needs of certain niche markets.

Figure 16.2 compares the gas chromatography (GC) trace of a commercial 4.0-cSt PAO (PAO 4) with that of a hydrotreated VHVI (very high-viscosity index) mineral-oil base stock having the same approximate viscosity at 100°C. The trace from the mineral oil shows that it consists of a broad range of different kinds of molecules. Included in the mineral oil are low-molecular-weight material that adversely affect volatility and high-molecular-weight components which adversely affect low-temperature properties. By comparison, the PAO 4 is primarily decene trimer, with small amounts of decene tetramer and pentamer present.

The fine structure in the trace on Fig. 16.2 is attributable to isomers of the different oligomers. (Note: Oligomers are low-molecular-weight polymers such as dimers, trimers, and so forth. Isomers are molecules with identical formulas and molecular weights, but with different skeletal structures.) A knowledge of reaction variables can be used to control the relative abundance of the various isomers and provides the producer another method to influence the physical properties of the final product [30].

3.3 Physical Properties

Table 16.1 lists the physical properties of various grades of PAO base fluids. These products are produced from decene, and the differences in properties illustrate what can be accomplished by manipulation of the reaction parameters. Some of these products are coproduced and separated by distillation. The properties are typical of what is currently available and do not represent the specifications of any particular producer. It should be noted that the data represent typical values collected over time. Because of this, the listed viscosity index (VI), which is calculated from the kinematic viscosities (KV) at 40°C and 100°C by a very complex relationship, is not the same as would be calculated from the viscosities shown.

Table 16.2 is a brief listing of the physical properties of PAO fluids prepared from different olefin raw materials. Each of these fluids was prepared in the laboratory using the same recipe, which included distilling off the dimer product and

Table 16.1 Typical Physical Properties of Commercial PAO Fluids

	PAO 2	PAO 4	PAO 6	PAO 8	PAO 10	PAO 40	PAO 100
KV at 100°C (cSt)	1.80	3.90	5.90	7.80	9.60	40.0	100
KV at 40°C (cSt)	5.54	16.8	31.0	45.8	62.9	395	1,250
KV at -40°C (cSt)	310	2,460	7,890	18,160	32,650	—	—
Viscosity index ^a	—	129	138	140	134	151	168
Pour point (°C)	<-63	-70	-68	-63	-53	-34	-20
Flash point (°C) ^b	>155	215	235	252	264	272	288
NOACK (% loss) ^c	99	12	7.0	3.0	2.0	0.8	0.6

^aVI is the average of samples. It is not calculated from viscosities given.

^bCleveland Open Cup, ASTM D92.

^cVolatility at 250°C, 1.0 h, DIN51581.

hydrogenating the final fluid [31]. None of the fluids in Table 16.2 are offered commercially.

Table 16.3 compares the physical properties of a commercial 4.0-cSt PAO with those of two 100N (neutral) mineral oils, a 100NLP (low pour) mineral oil, and a hydrotreated VHVI mineral oil. The PAO shows markedly better properties at both high and low temperatures. At high temperatures, the PAO has lower volatility and a correspondingly higher flash point. Low volatility is an important property in order for a fluid to “stay in grade” (i.e., retain original viscosity) during its working life. At the low end of the temperature scale, the differences are equally dramatic. The pour point of the PAO is less than -65°C, and pour points for the three 100N mineral oils and the VHVI oil are -15°C, -12°C, -15°C, and -27°C, respectively.

Table 16.4 compares a commercial 6.0-cSt PAO with a 160HT (hydro-treated) mineral oil, a 240N oil, a 200SN (solvent neutral) mineral oil, and a UHVI (ultrahigh-viscosity index) fluid. The broader temperature range of the PAO is again apparent. Table 16.5 makes similar comparisons for 8.0-cSt fluids.

Table 16.2 Physical Properties of PAO Fluids from Various Olefins

	C8 ^a	C10 ^a	C12 ^a	C14 ^a
KV at 100°C (cSt)	2.77	4.10	5.70	7.59
KV at 40°C (cSt)	11.2	18.7	27.8	41.3
KV at -18°C (cSt)	195	409	703	1150
Viscosity index	82	121	152	154
Pour point (°C)	<-65	<-65	-45	-18
Flash point (°C) ^b	190	228	256	272
NOACK volatility (%) ^c	55.7	11.5	3.5	2.3

^aNot a commercial product.

^bCleveland Open Cup, ASTM D 92.

^cVolatility at 250°C, 1.0 h, DIN 51581.

Table 16.3 PAO 4 Compared to Equiviscous Mineral Oils

	PAO	100N	100N	100NLP	VHVI
KV at 100°C (cSt)	3.90	3.81	4.06	4.02	3.75
KV at 40° C (cSt)	16.8	18.6	20.2	20.1	16.2
KV at -40°C (cSt)	2460	Solid	Solid	Solid	Solid
Viscosity index	137	89	98	94	121
Pour point (°C)	-70	-15	-12	-15	-27
Flash point (°C) ^a	215	200	212	197	206
NOACK (% loss) ^b	12.0	37.2	30.0	29.5	22.2

^aCleveland Open Cup, ASTM D 92.

^bVolatility at 250°C, 1.0 h, DIN 51581.

Table 16.4 PAO 6 Compared to Equiviscous Mineral Oils

	PAO	160HT	240N	200SN	UHV1
KV at 100°C (cSt)	5.90	5.77	6.96	6.31	5.49
KV at 40°C (cSt)	31.0	33.1	47.4	40.8	25.9
KV at -40°C (cSt)	7890	Solid	Solid	Solid	Solid
Viscosity index	135	116	103	102	156
Pour point (°C)	-68	-15	-12	-6	-9
Flash point (°C) ^a	235	220	235	212	226
NOACK (% loss) ^b	7.0	16.6	10.3	18.8	14.3

^aCleveland Open Cup, ASTM D 92.

^bVolatility at 250°C, 1.0 h, DIN 51581.

Table 16.5 PAO 8 Compared to Equiviscous Mineral Oils

	PAO	325SN	325N
KV at 100°C (cSt)	7.80	8.30	8.20
KV at 40°C (cSt)	45.8	63.7	58.0
KV at -40°C (cSt)	18,160	Solid	Solid
Viscosity index	136	99	110
Pour point (°C)	-63	-12	-12
Flash point (°C) ^a	252	236	250
NOACK (% loss) ^b	3.0	7.2	5.1

^aCleveland Open Cup, ASTM D 92.

^bVolatility at 250°C, 1.0 h, DIN 51581.

3.4 Environmental Impact

The use of environmentally friendly fluids has become an important issue in a number of hydraulic fluid applications. Particularly important are those applications where there is a potential for large-scale contamination of either soil or water by the accidental rupture of hydraulic lines. Off-road construction and mining are examples where very large hydraulic machinery are used. Contamination by oil spills can result in serious long-term damage to the environment.

Polyalphaolefin fluids are exceptional in their low toxicity. They have Food and Drug Administration approval for both indirect and incidental food contact, and they are used in a number of personal-care products. In addition, PAO fluids do not bioaccumulate and, depending on viscosity, biodegrade readily [32]. These characteristics, combined with excellent viscometrics and lubricity, have made low-viscosity PAO fluids a significant player in off-shore drilling mud formulations. Figure 16.3 shows the biodegradability by the CEC-L-33-A-94 test. The range of results shown on the graph indicates the range of data obtained from three independent laboratories on multiple samples over a period of time. PAO 2 and PAO 4 show very good biodegradability under these test conditions, but the higher-viscosity fluids do not.

Demonstration formulations have indicated that high-performance, biodegradable hydraulic fluids can be prepared using PAO 2, a styrene/isoprene comonomer viscosity index improver (8.0–18.5%), an ashless antiwear agent (1.0%), and an ester (10%). Three grades were formulated: ISO 15, ISO 32, and ISO 46. Biodegradability

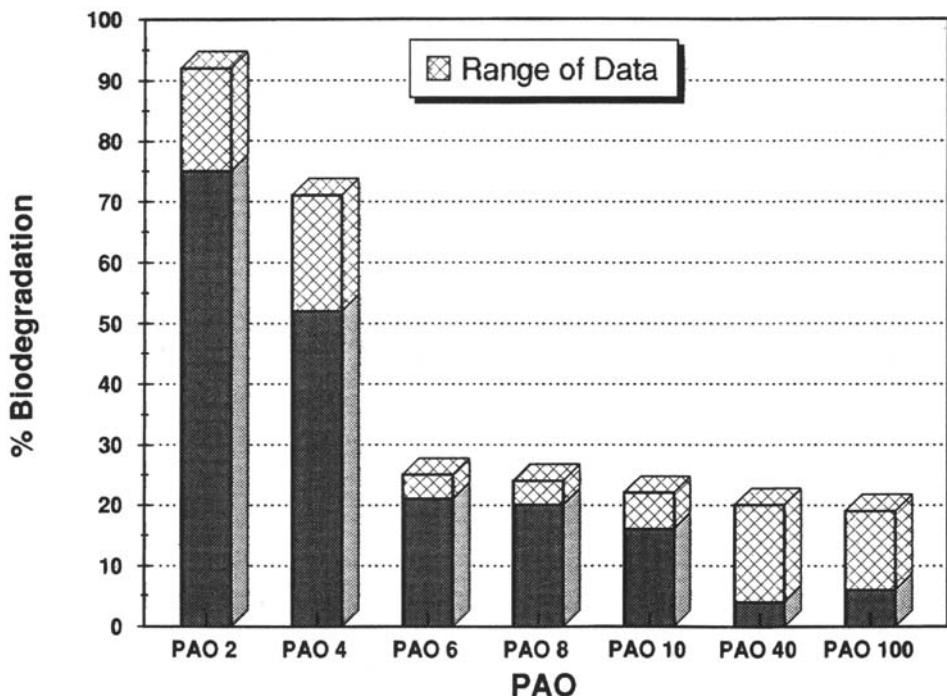


Figure 16.3 Biodegradability of PAO fluids by the CEC-L33-A94 test.

by the CEC-L-33-A-94 test ranged from 76% to 79% for the fully formulated fluids. Excellent performance was found in the Turbine Oil Stability Test (TOST), the Kurt Orbahn Shear Stability Test, and the FZG Anti-Wear Gear Test. Finally, unlike many ester-based fluids, the PAO is hydrolytically stable [33].

4 ALKYLATED AROMATIC FLUIDS

The class of fluids commonly referred to as alkylated aromatics (AAs) includes several different, but related, chemical types. The class may conveniently be broken down into three categories or subclasses, which are the alkylbenzenes, the alkyl-naphthalenes, and the alkylated multiring aromatics other than naphthalenes [3].

Alkylated aromatic fluid first gained prominence because of the following qualities:

- Exceptionally good low-temperature performance
- Excellent thermal stability
- Excellent oxidative stability
- Hydrolytic stability
- Miscibility with mineral oils
- Ability to solubilize additives
- Seal compatibility

4.1 Historical Development

The early development of AA fluids for use as functional fluids dates back to 1928–1936 [7–10]. The first commercial production of AA fluids for use as lubricants appears to have been at the Chemische Werke Rheinpreussen, where alkynaphthalene oils were produced on a 7.2 MM lb./year scale from 1942 to 1946 [34]. These products were made by the alkylation of naphthalene with chlorinated aliphatic hydrocarbons in the presence of aluminum chloride catalysts.

In the period following World War II, relatively low-cost dialkylbenzenes became available as by-products of the manufacture of sodium alkylbenzenesulfonate detergents. In the 1950s, these were branched-chain alkylbenzenes made by the alkylation of benzene with propylene oligomers (trimers to pentamers). In the 1960s, the detergent industry turned to longer, linear alkyl chains, and the types of dialkylbenzene available for functional fluid use changed accordingly.

In the 1980s, AA fluids began to lose ground to PAO fluids, which were found to be more cost-effective and less toxic and to operate over a wider temperature range in many applications. Nevertheless, a good deal of research has been published on improved products and processes in recent years, and AA fluids remain the product of choice for a variety of applications. Unimolecular 1,3,5-tri-*n*-alkyl substituted alkyl benzenes were found to uniquely possess exceptional thermal stability, acceptable oxidative stability, and adequate low-temperature viscosities to provide acceptable temperature range capability for military applications. However, commercially feasible synthetic routes have not yet been developed to produce the 1,3,5-tri-*n*-alkyl substituted alkyl benzenes [35].

4.2 Manufacture

In general, the manufacture of alkyl aromatic fluids may be described as the alkylation of aromatic compounds with haloalkanes, alcohols or olefins in the presence of a Lewis or Bronsted acid catalyst. The nature of the resulting fluid, however, is very dependent on the type of aromatic nucleus, the nature of the alkylating agent, the degree of alkylation, the position of the alkyl groups on the aromatic ring, the position of the aromatic ring on the alkyl chain and the mixture of molecules in the final product. The degree of alkylation and the molecular structure are, in turn, determined by the type of catalyst and the reaction conditions.

As mentioned earlier, branched-chain alkyl benzenes are the by-product of detergent manufacture. Excess benzene is alkylated with propylene tetramer at 20–50°C in the presence of hydrofluoric acid or aluminum chloride as the catalyst. The monoalkylate is obtained in about 75% yield and is used as a precursor for the sulfonated detergent [36]. The remaining 25% is available as lubricant base stock.

Dialkyl benzenes incorporating linear alkyl chains are also by-products of detergent manufacture [37]. A C₁₀ to C₁₄ paraffin feed is chlorinated and then used to alkylate benzene. A variety of products are formed in this process, including the monoalkyl benzenes, the dialkyl benzenes, diphenylalkanes, tetralin, and indane derivatives. The benzene ring is not attached to the linear alkyl chain at the chain's terminal carbon atom. Rather, it is attached randomly to carbon atoms located along the chain. The process can be tailored to give relatively less or more dialkylbenzenes for the lube base-stock market.

An alternative process for the manufacture of dialkylbenzenes is by alkylation of the benzene with linear olefins. A great deal of progress has been made in recent years in accomplishing this reaction over solid catalysts [38].

A great many patents and papers have been published on alternative methods for the production of AA fluids. A good review of the literature from the mid-1970s to 1990 is available and recommended for those interested in more detail [3].

4.3 Physical Properties

The physical properties of AA fluids vary widely, depending on structure and purity. In 1969, Conoco began production of a series of formulated products based on a dialkyl benzene base stock which was designated DN-600 Stock. From this material, Conoco produced CN-600 Synthetic Motor Oil, DN-600 Antiwear Hydraulic Oil, DN-600 Gear Oil, and Polar Start DN-600 SRI Grease.

Table 16.6 shows the specifications and composition for Conoco's DN-600 Base Stock and Table 16.7 gives the specifications for DN-600 Antiwear Hydraulic Fluid.

In 1981, Conoco was acquired by Du Pont, and the alkylbenzene business was spun off to Vista Chemical. Vista was acquired by RWE-DWE Co. of Germany in 1991 [39]. Table 16.8 gives typical values for the Vista dialkylbenzene (DAB) base oil.

4.4 Environmental Impact

The toxicity of aromatic compounds varies, depending on structure. In general, however they cannot compete in applications where extremely low toxicity is important.

Table 16.6 Conoco DN-600 Base-Oil Properties and Specifications

	Specification	Test method
Specific gravity	0.8628–0.8576	ASTM D-2422
Gravity (°API)	32.5–33.5	ASTM D-287
Lbs./gal, Typical	7.16	
Flash point (COC) (°C)	≥224	ASTM D-92
Pour point (°C)	≤−65	ASTM D-97
KV at 100°C (cSt)	≥4.9	ASTM D-445
KV at 40°C (cSt)	26–27 typical	
KV at −40°C (cSt)	≤9500	ASTM D-2602
VI	100	ASTM D-2270
Composition (wt %)		
Monoalkylbenzenes	≤1.5	
Diphenylalkanes	≤12.5	
Dialkylbenzenes	≥80.0	
Polyalkylbenzenes	≤6.0	
Chlorine	≤0.01	

Source: Data from Ref. 3.

Table 16.7 Conoco DN-600 Antiwear Hydraulic Oil

	Specification	Typical
Gravity (°API)	31	
Flash point (°F)	≥300	325
KV at −40°C (cSt)	≤3000	2600
KV at 100°C (cSt)		3.3
VI		160
Pour point (°F)	≤−70	−80
ASTM rust, A&B	Pass	
Foam test	Pass	
Vickers vane pump	Pass	

Source: Data from Ref. 3.

Table 16.8 Comparison of Dialkylbenzene to Mineral Oils

	DAB	Paraffinic	Naphthenic
KV at 250°F	2.42	2.40	2.05
KV at 210°F	5.10	5.10	5.10
KV at 100°F	29.7	32.9	45.1
KV at 0°F	910	No flow	No flow
KV at −40°F	9540	No flow	No flow
Pour point (°F)	−70	0	−30

Source: Data from Ref. 3.

The same may be said for biodegradability, where micro-organisms normally found in soil or water cannot digest the aromatic ring.

5 SILAHYDROCARBON FLUIDS

Silahydrocarbons (SiHCs), or tetraalkylsilanes, may be characterized as having a central silicon atom to which four hydrocarbon chains are attached. The silicon atom provides a thermally more stable center than would a smaller, isovalent carbon atom. The resultant SiHC molecule has lower-temperature fluidity that is associated with hydrocarbon branching combined with higher thermal stability than would be anticipated from hydrocarbon branching on a carbon atom. Although SiHC fluids have never been produced on a commercial scale, they have been extensively studied by the U.S. Air Force for aerospace hydraulic fluid applications.

5.1 Historical Development

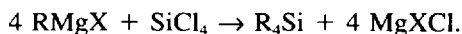
The first syntheses of tetraalkylsilane molecules were reported more than 130 years ago by the distinguished chemists Charles Friedel and James Mason Crafts [40,41]. There appears to have been little practical interest in these chemically inert curiosities until the U.S. Air Force Materials Laboratories (Wright-Patterson Air Force Base, OH) began to take an interest in the 1950s [15–17]. Researchers at Wright-Patterson first coined the term “silahydrocarbons” to reflect the similarity in behavior between these compounds and branched, aliphatic hydrocarbons of similar molecular weight [42].

The interest by the Air Force in the development of SiHC fluids was largely the same as their interest in PAO fluids. There was a general recognition that new high-performance aircraft would require lubricants and fluids capable of operating in a high-temperature/wide-liquid-range environment. Specifically, the Air Force was interested in developing a hydraulic fluid for a –54°C to 315°C missile application. Later, the Air Force was interested in developing a hydraulic fluid incorporating the low-temperature requirements of MIL-H-5606 (mineral-oil based) and the high-temperature requirements of MIL-H-83282 (PAO based). By the late 1970s, the Air Force had developed SiHC-based formulated fluids which very nearly met the target properties [42,43]. The particular tetraalkylsilane that allowed the properties of both applications to be met was a random mixture of compounds containing a 50 : 50 composition of octyl (C₈H₁₇-) and decyl (C₁₀H₂₁-) groups on the silicon.

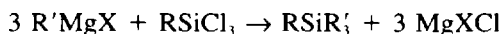
5.2 Synthesis

A variety of synthetic routes have been developed for their preparation.

The earliest preparation of SiHCs by Friedel and Crafts employed the reaction of an alkyl magnesium halide (Grignard reagent) with silicon tetrachloride [40,41]:



In 1946, Gilman and Clark studied the reaction of Grignard reagents with alkyl trichlorosilanes [44]:

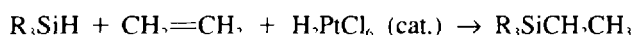
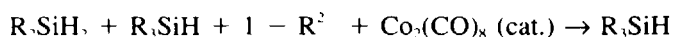
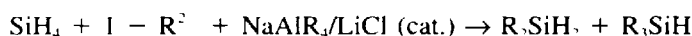


The Air Force developed a route based on the reaction of mixed alkyl mag-

nesium halides or mixed alkyl lithium reagents with tetrachlorosilane or methyltrichlorosilane [45]. The development of these SiHCs with mixed alkyl groups was important in obtaining low melting points.

Similar preparations based on the use of alkyl lithium, alkyl zinc, and alkyl aluminum compounds have been reported. A more detailed discussion with references may be found in Ref. 4.

A different approach to the preparation of silahydrocarbon fluids is the catalyzed hydrosilation of alkenes with alkylsilanes. This was first demonstrated by Austin et al., who studied the photocatalyzed addition of alkenes to trialkylsilanes in the presence of trinuclear metal carbonyl catalyst precursors [46]. Onopchenko and Saborin at Gulf Research and Development (now part of Chevron) later used platinum-based catalysts for hydrosilation [47,48]. Finally, researchers at Ethyl Corporation (now Albemarle Corporation) developed a route to ethyltrialkylsilanes starting from silane itself [49,50]:



5.3 Physical Properties

The physical properties of SiHC fluids show that they are suitable for applications over a wide temperature range. The properties depend, of course, on the four alkyl groups attached to the central silicon atom. Because there are no commercially available SiHC fluids, Table 16.9 is a listing of properties for laboratory-produced fluids [51]. Table 16.9 lists only methyltrialkylsilanes, $\text{CH}_3\text{SiRR}'\text{R}''$, where R, R', and R'' are linear alkyl chains that may be the same carbon number or a mixture of two carbon numbers as indicated. It may be noted from the data in the table that SiHCs have, in general, high VIs, low pour points, high flash points, and good thermal and oxidative stability.

Table 16.9 Physical Properties of Methyltrialkylsilane Fluids

	Carbon nos. of alkyl groups			
	C6/C8	C8/C10	C10	C12/C14
KV at -54°C (cSt)	906	2550	Solid	Solid
KV at -40°C (cSt)	256	627	1020	Solid
KV at 40°C (cSt)	5.84	9.84	12.7	25.1
KV at 100°C (cSt)	1.92	2.82	3.41	5.82
Viscosity index	Undefined	139	151	186
Pour point (°C)	<-65	<-65	-54	-9
Oxidation onset (°C)	197.6	197.7	198.0	197.8
Flash point (COC) (°C)	186	214	234	274
Fire point (COC) (°C)	188	232	254	>283

Note: Fluids are laboratory samples, not commercial fluids.

5.4 Environmental Impact

Silhydrocarbons, like PAO, have very low toxicity. Oral and dermal LD₅₀ values for octyl/decyl silhydrocarbons have been reported to be >5.0 g/kg and > 2.0 g/kg, respectively, and the inhalation LC₅₀ was >4.8 mg/L [52]. Little or no information is available on the biodegradability of SiHC compounds, but they would be expected to biodegrade in a fashion similar to PAO fluids—with better biodegradability for the lower-viscosity products.

6 APPLICATIONS

6.1 Background

The major outlet for synthetic hydrocarbon hydraulic oils as fire-resistant fluids has been in U.S. military hydraulic applications. Since the 1940s, aircraft used mineral oil for hydraulic fluid, but the industry was plagued from the beginning with fire hazards. The mineral oils were required to operate in extreme cold conditions, which require a relatively low-flash-point oil. In the 1950s, the commercial aircraft switched to fire-resistant phosphate ester hydraulic fluids, but the U.S. military remained with mineral oils mainly because of high- and low-temperature operational requirements and the reluctance to switch seals, paints, and other materials to phosphate ester-compatible materials.

For many years, MIL-H-5606 hydraulic fluid was the military standard hydraulic fluid for aircraft and MIL-H-6083 [53], the rust-inhibited version, was the standard tank hydraulic fluid. Table 16.10 shows comparative properties of military hydraulic fluids. These fluids were comprised of a very low-molecular-weight base fluid, in order to meet -54°C (-65°F) low-temperature operational requirements. These base fluids were thickened with approximately 17% viscosity index improver, typically a poly(methy methacrylate), allowing the fluid to meet 135°C (275°F) high-temperature viscosity requirements for a Type II MIL-H-5440 military hydraulic system. The inherent danger of this fluid is obvious in that the flash point of this oil is 100°C (212°F), by the Cleveland Open Cup method [54], well below the upper operational temperature for the aircraft of 135°C (275°F). For the Air Force alone, noncombat fire damage was costing over a \$20 million per year.

6.2 Polyalphaolefins

In the 1960s, both the Air Force and the Navy embarked on research programs to develop fire-resistant hydraulic fluids as drop-in replacements for MIL-H-5606, the standard mineral-oil-based DoD hydraulic fluid. This was a very difficult task because the replacement fluid had to be completely compatible with MIL-H-5606 as well as all of the other hydraulic system materials. The replacement fluid also had to provide equivalent hydraulic system performance. The Navy developed extensively fluids called MS5 and MS6, which were chlorophenylsilicone based [55]. These fluids were exceptionally fire resistant but did not have sufficient bulk modulus for the flight controls of operational aircraft. In F-4 iron bird testing with MS-6, the hydraulic controls experienced excessive flutter and the fluids were deemed unsafe for use in existing aircraft. No further development was performed with these fluids. The Air Force program led to the development of MIL-H-83282, based on the newly

Table 16.10 Selected Typical Physical Properties of Military Hydraulic Fluids

Property	MIL-H-5606	MIL-H-83282	MIL-H-6083	MIL-H-46170	MIL-H-87257	MIL-H-27601	Army SHF ^a
Kinematic viscosity							
(mm/s), ASTM D445							
at -54°C	2,450	20,000	3,480	25,000	2,480	20,000	3,450
-40°C	490	2,140	800	2,500	520	3,950	650
38°C	14.2	14.2	13.2	19.3	9.0	14.0	9.0
99°C	5.1	3.6	5.0	3.5	2.6	3.5	2.5
Pour point (°C)							
ASTM D97	<-59	<-59	<-59	<-54	<-59	<-40	<-60
Elastomer compatibility							
NBR-L ^b Rubber Swell							
(vol %), ASTM D4289	24	18	23	21	20	N/A ^c	22

^aSHF = single hydraulic fluid.

^bNBR-L is the designation for Buna N rubber.

^cN/A indicates that there is no elastomer compatibility requirement for this hydraulic fluid.

emerging commercialization of polyalphaolefins [56]. The U.S. Army developed a rust-inhibited version, MIL-H-46170, for ground vehicle applications [57]. Table 16.11 shows the comparative flammability properties of MIL-H-5606 and MIL-H-83282 and other DoD hydraulic fluids. MIL-H-83282 has a Cleveland Open Cup flash point of 224°C (435°F), well above the upper use temperature of 135°C (275°F). Considerable controversy over the flammability tests and their interpretation delayed the use of MIL-H-83282 in the Navy until 1976, in the Army until 1977, and in the Air Force until 1980. Even then, the Air Force did not convert all of their aircraft for many years based on the higher viscosity of MIL-H-83282 at low temperature, versus MIL-H-5606. [Even today, in extreme cold climates, MIL-H-5606 and MIL-H-6083 are used because they are -54°C (-65°F) lower-temperature-use fluids compared to MIL-H-83282 and MIL-H-46170, which are a -40°C (-40°F) low-temperature-use fluids.] Significant decrease in Air Force fire damage, from an average of \$20 million per year to an average of approximately \$600,000 per year, even with some of the aircraft still using MIL-H-5606, has borne out the predictions for savings with MIL-H-83282.

MIL-H-83282 is composed of 4-cSt PAO hydrogenated decene trimer with approximately 30% diester as a rubber swell agent. Smaller amounts of other performance-improving additives are used as required.

As mentioned earlier, some aircraft and tanks did not convert to MIL-H-83282 or to the rust-inhibited counterpart, MIL-H-46170, used in most U.S. Army tank applications. In response to the need for a low-temperature version of a fire-resistant fluid, the Air Force developed MIL-H-87257 hydraulic fluid in the 1980s [43,58]. As of this writing, MIL-H-87257 has successfully completed flight tests in a KC-135 and further testing is scheduled. MIL-H-87257 hydraulic fluid is composed of a blend of 2-cSt PAO and 4-cSt PAO along with the needed rubber swell ester and other additives. The low-temperature viscosity requirement in the military specification is less than or equal to 2500 cSt at -54°C (-65°F).

The U.S. Army embarked on development of a low-temperature fire-resistant hydraulic fluid for tank use based on somewhat different flammability and low-temperature limits and also containing the required rust inhibition for tank and other ground vehicle applications. This fluid, like MIL-H-87257, is also based on a blend of PAO hydrogenated decene dimer and trimer blends, but formulated with a rust inhibitor in addition to the other performance-improving additives. The intent of the development of this new fluid is to replace both MIL-H-6083 and MIL-H-46170 with one hydraulic fluid for logistic reasons. It is therefore called the Army single hydraulic fluid (SHF). This new fluid is currently in field tests [59,60].

Another military hydraulic fluid based on PAOs is MIL-H-27601B [61]. This fluid specification in previous versions was based on a highly refined, deep dewaxed paraffinic mineral oil and the fluid was only used in the once classified SR-71 aircraft. A PAO was developed by the Air Force as a no-retrofit, direct drop-in replacement for the mineral oil but has yet to be fielded because the aircraft was decommissioned. MIL-H-27601B is based on the 4-cSt PAO with some performance-improving additives, but with no rubber swell ester. Because of the imposed mission of the SR-71, the MIL-H-27601 temperature range was -40°C (-40°F) to 288°C (550°F). At that high upper temperature, no elastomeric seals were used in the aircraft, so no rubber swell ester was needed nor could it be used at that upper temperature. With the military emphasis on higher temperatures and increased performance, MIL-H-

Table 16.11 Flammability Properties of Military Hydraulic Fluids

Property	MIL-H-5606	MIL-H-83282	MIL-H-6083	MIL-H-46170	MIL-H-87257	MIL-H-27601	Army SHF ^a
Use temperature (°C)	−54 to 135	−40 to 200	−54 to 110	−40 to 135	−54 to 135	−40 to 290	−54 to 135
Flash point, D92 (°C)	102	224	126	220	166	224	182
AIT E659 (°C)	235	365	243	363	235	365	356
Linear flame propagation rate, D5306 (cm/s)	0.73	0.20	0.95	0.23	0.30	0.20	0.25

^aSHF = single hydraulic fluid.

27601 and other high-temperature hydraulic fluids continue to be considered for future applications [62].

6.3 Alkylaromatics and Silahydrocarbons

Both alkylaromatics [35] and silahydrocarbons [46,47,49], as previously described, have been investigated by the Air Force as high-temperature, fire-resistant hydraulic fluids in the past. The silahydrocarbon was extensively developed as a -54°C (-65°F) to 316°C (600°F) Advanced Strategic Air Launched Missile fluid, but the missile was never fielded because of demilitarization agreements between the United States and the Soviet Union in the 1970s.

Silahydrocarbon-based candidates were considered for both the MIL-H-87257 and the MIL-H-27601B applications and showed superior properties to the PAO-based replacements [61], but they could not compete with the PAO in cost, commercial availability, and use history. In addition to the excellent thermal stability exhibited by the *n*-alkyl-substituted silahydrocarbons, they also demonstrate excellent viscosity indices. If either alkylated aromatics or silahydrocarbons are used in the near future, it will likely be in a niche application where PAOs are unacceptable for some reason. However, as requirements become increasingly stringent, silahydrocarbons would be a natural candidate replacement base stock for the PAOs when the PAOs can no longer meet the requirements.

REFERENCES

1. A. Sequeira, Jr., *Lubricant Base Oil and Wax Processing*, 1994, Marcel Dekker; New York.
2. R. L. Shubkin, "Polyalphaolefins," in *Synthetic Lubricants and High-Performance Functional Fluids*, R. L. Shubkin, ed., 1993, Marcel Dekker; New York, pp. 1–40.
3. H. Dressler, "Alkylated Aromatics," in *Synthetic Lubricants and High-Performance Functional Fluids*, R. L. Shubkin, ed., 1993, Marcel Dekker; New York, pp. 125–144.
4. F. A. Pettigrew and G. E. Nelson, "Silahydrocarbons," in *Synthetic Lubricants and High-Performance Functional Fluids*, R. L. Shubkin, ed., 1993, Marcel Dekker; New York, pp. 205–214.
5. J. D. Fotheringham, "Polybutenes," in *Synthetic Lubricants and High-Performance Functional Fluids*, R. L. Shubkin, ed., 1993, Marcel Dekker; New York, pp. 271–318.
6. C. G. Venier and E. W. Casserly, "Cycloaliphatics," in *Synthetic Lubricants and High-Performance Functional Fluids*, R. L. Shubkin, ed., 1993, Marcel Dekker; New York, pp. 241–269.
7. British Patent 323,100 (December 3, 1928), to IG Farbenindustrie A.G.
8. H. Zorn, M. Mueller-Cunradi, and W. Rosinski, German Patent 565,249 (March 26, 1930), to IG Farbenindustrie A.G.
9. G. H. B. Davis, U.S. Patent 1,815,072 (July 14, 1931), to Standard Oil Development Company.
10. F. H. McLaren, U.S. Patent 2,030,832 (February 11, 1936), to Standard Oil Company in Indiana. Synthetic Lubricating Oils.
11. C. E. Snyder, Jr. and L. J. Gschwender, "Aerospace," in *Synthetic Lubricants and High-Performance Functional Fluids*, R. L. Shubkin, ed., 1993, Marcel Dekker; New York, pp. 525–532.
12. MIL-H-5606G Military Specification (1994), Hydraulic fluid, petroleum base, Aircraft missile and ordinance, NATO code number H-515.

13. MIL-PRF-83282D Military Specification (1997), Hydraulic fluid, fire resistant, synthetic base, aircraft metric, NATO code number H-537.
14. MIL-PRF-87257A Military Specification (1997), Hydraulic fluid, fire resistant; low temperature, synthetic hydrocarbon base, aircraft and missile, metric, NATO code number H-538.
15. H. Rosenberg, J. D. Groves, and C. Tamborski, *J. Org. Chem.*, 1960, 25, p. 243.
16. C. Tamborski and H. Rosenberg, *J. Org. Chem.*, 1960, 25, p. 246.
17. G. Baum and C. Tamborski, *J. Chem Eng. Data*, 1961, 6, p. 142.
18. F. W. Sullivan, Jr., V. Vorhees, A. W. Neeley, and R. V. Shankland, *Ind. Eng. Chem.*, 1931, 23, p. 604.
19. J. B. Boylan, "Synthetic Basestocks for Use in Greases," *NLGI Spokesman*, 1987, 51(5), pp. 188–195.
20. C. W. Montgomery, W. I. Gilbert, and R. E. Kline, U.S. Patent 2,559,984 (1951), to Gulf Oil Co.
21. W. E. Garwood, U.S. Patent 2,937,129 (1960), to Socony Mobil Oil Company.
22. D. Southern, C. B. Milne, J. C. Moseley, K. I. Beynon, and T. G. Evans, British Patent 873,064 (1961), to Shell Research.
23. L. A. Hamilton, Pittman, and F. M. Seger, U.S. Patent 3,149,178 (1964), to Socony Mobil Oil Company.
24. J. A. Brennan, U.S. Patent 3,382,291 (1968), to Socony Mobil Oil Company.
25. R. L. Shubkin, U.S. Patent 3,763,244 (1973), to Ethyl Corp.
26. R. L. Shubkin, U.S. Patent 3,780,128 (1973), to Ethyl Corp.
27. R. L. Shubkin, M. S. Baylerian, and A. R. Maler, "Olefin Oligomers: Structure and Mechanism of Formation," Symposium on Chemistry of Lubricants and Additives, Div. of Petroleum Chemistry, ACS, 1979; also published in *Ind. Eng. Chem., Product Res. Dev.*, 1980, 19, p. 15.
28. F. C. Loveless, U.S. Patent 4,469,910 (1984), to Uniroyal, Inc.
29. R. L. Shubkin and M. E. Kerkemeyer, "Tailor Making PAOs," 7th International Colloquium on Automotive Lubrication, 1990; also *J. Synth. Lubr.*, 1991, 8(2), pp. 115–134.
30. K. J. Theriot and R. L. Shubkin, "A Polyalphaolefin with Exceptional Low Temperature Properties," 8th International Colloquium, TRIBOLOGY 2000, 1990; also *J. Synth. Lubr.*, 1993, 10(2), pp. 133–142.
31. G. Kumar and R. L. Shubkin, "New Polyalphaolefin Fluids for Specialty Applications," 47th Annual Meeting of the Society of Tribologists and Lubrication Engineers, 1992; also *Lubr. Eng.*, 1993, 49(9), pp. 723–725.
32. J. F. Carpenter, "Assesment of Environmental Impact of PAOs," STLE Annual Meeting, 1993.
33. Unpublished data, Albermarle Corporation.
34. H. Koelbel, "Synthesis of Lubricants via the Alkylation of Naphthalene." *Erdoel Kohle*, 1948, 1, pp. 308–318.
35. L. J. Gschwender, C. E. Snyder, and G. Driscoll, "Alkyl Benzenes—Candidate High-Temperature Hydraulic Fluids," *Lubr. Eng.*, 1990, p. 377.
36. K. Kosswig, "Tenside," in *Ullmann's Encyclopedia of Technical Chemistry*, 4th ed., 1982, Verlag Chemie; Weinheim, Vol. 22, p. 455.
37. S. Tokoaka, SRI-PEP (Process Economics Program) Report No. 59A Supplement, Aliphatic Surfactants, Menlo Park, 1974.
38. *Oil Gas J.*, 1990, July 16, p. 48.
39. *Chem. Week*, 1991, January 16, p. 48.
40. C. Friedel and J. M. Crafts, *Ann. Chem.*, 1863, 127, p. 28.
41. C. Friedel and J. M. Crafts, *Ann. Chem.*, 1870, 259, p. 334.

42. C. E. Snyder Jr., L. J. Gschwender, C. Tamborski, G. J. Chen, and D. R. Anderson, "Synthesis and Characterization of Silahydrocarbon—A Class of Thermally Stable Wide Liquid Range Functional Fluids," *ASLE Trans.*, 1982, 25(3), pp. 299–308.
43. L. J. Gschwender, C. E. Snyder, Jr., and G. W. Fultz, "Development of a -54° to 135°C Synthetic Hydrocarbon-based, Fire-Resistant Hydraulic Fluid," *Lubr. Eng.*, 1986, pp. 485–490.
44. H. Gilman and R. N. Clark, *J. Am. Chem. Soc.*, 1946, 68, p. 1675.
45. C. Tamborski and C. E. Snyder, Jr., U.S. Patent 4,367,343 (1983), to the United States of America.
46. R. G. Austin, R. S. Paonessa, P. J. Giordano, and M. S. Wrighton, U.S. NTIS, AD Report, 1977. Available from Gov. Rep. Announce. Index (U.S.), 1977, 77(25), 92 74-1. *Chem. Abstr.*, 88(20), p. 144251x.
47. A. Onopchenko and E. T. Sabourin, U.S. Patent 4,578,497 (1986), to Gulf Research and Development Co.
48. E. T. Sabourin and A. Onopchenko, *Bull. Chem. Soc. Jpn.*, 1989, 62, p. 3691.
49. F. A. Pettigrew, L. Plonsker, G. E. Nelson, A. J. Malcolm, and C. R. Everly, Society of Tribologists and Lubrication Engineers, 1989.
50. A. J. Malcolm, C. R. Everly, and G. E. Nelson, U.S. Patent 4,670,574 (1987), to Ethyl Corporation.
51. Unpublished data, Albermarle Corporation.
52. E. R. Kinkead, S. K. Bunker, R. E. Wolfe, and C. R. Doarn, Harry G. Armstrong Medical Research Laboratory Report, AAMRL-TR-89-026, 1989. (Available from DODSSP, Subscription Services Desk, Building 4D, 700 Robbins Avenue, Philadelphia, PA.)
53. MIL-H-6083 Military Specification (1986), Hydraulic fluid, petroleum base, for preservation and operation.
54. ASTM D 92, Flash and Fire Points by Cleveland Open Cup.
55. J. N. DeMarchi and R. N. Haning, NADC-79120-60, 1981. (Available from DODSSP, Subscription Services Desk, Building 4D, 700 Robbins Avenue, Philadelphia PA.)
56. B. A. Loving, R. L. Adamczak, and H. Schwenker, AFML-TR-71-5, 1971. (Available from DODSSP, Subscription Services Desk, Building 4D, 700 Robbins Avenue, Philadelphia PA.)
57. MIL-H-46170 Military Specification (1988), Hydraulic fluid, rust inhibited, fire resistant synthetic hydrocarbon base.
58. L. J. Gschwender, C. E. Snyder Jr., and S. K. Sharma, "Pump Evaluation of Hydrogenated Polyalphaolefin Candidates for a -54°C to 135°C Fire-Resistant Air Force Aircraft Hydraulic Fluid," *Lubr. Eng.*, 1988, 44, p. 324.
59. E. M. Purdy, Technical Report, USA-BRDEC-TR//2540, 1993. (Available from DODSSP, Subscription Services Desk, Building 4D, 700 Robbins Avenue, Philadelphia PA 19111-5094.)
60. E. M. Purdy and D. M. Rutkowski, Technical Report, USA-TARDEC-TR-13620, 1994. (Available from DODSSP, Subscription Services Desk, Building 4D, 700 Robbins Avenue, Philadelphia, PA.)
61. MIL-H-27601B Military Specification. (1993), Hydraulic fluid, fire resistant, hydrogenated polyalphaolefin base, high temperature, flight vehicle, metric.
62. L. J. Gschwender and C. E. Snyder, Jr., "High Temperature Hydraulic Fluids," *J. Synth. Lubr.*, 1992, 9, p. 115–125.

This page intentionally left blank

Emulsions

YINGHUA SUN and GEORGE E. TOTTE

Union Carbide Corporation, Tarrytown, New York

1 INTRODUCTION

Although petroleum-oil hydraulic fluids provide outstanding performance, there are a number of application areas in which their high fire-risk potential with respect to equipment damage and loss of lives precludes their use. For example, in a 1956 underground mine fire in Marcinelle, Belgium, 267 miners lost their lives [1]. This fire was caused by damage to a hydraulic line containing mineral oil in the mine shaft. When the mineral-oil spray contacted a nearby electrical cable, an electric arc ignited the oil. As a result of this and other disastrous fires, government regulations in Europe, the United States, and other countries mandated that fire-resistant fluids be used.

Fire resistance is imparted to hydraulic fluids in one of two ways. One method is in a fluid molecular structure which would include fluids such as phosphate esters. The second common method of imparting fire resistance is by the use of water in the hydraulic fluid formulation. In this case, water has been called a "snuffer" [2] and water-containing fluids have been called "snuffer fluids" [3]. Water may be emulsified in oil (water-in-oil or w/o emulsions) or oil may be emulsified in water (oil-in-water or o/w emulsions) to provide fire-resistant emulsion-oil hydraulic fluids. In addition, water may be freely soluble when water-soluble components are used or it may be part of a microemulsion.

Since the 1956 Marcinelle fire, various water-containing emulsions have been among the most common types of fire-resistant fluids used in the coal mining industry [4–7]. Other industries that utilize emulsion hydraulic fluids include zinc and aluminum die casting [5], plastic injection molding [5], steel rolling [8], and continuous steel casting [9].

In this chapter, the formulation, properties, and use of emulsion hydraulic fluids will be discussed. This discussion will include the following:

- Fluid classification
- Fluid chemistry/formulation
- Fluid properties
- Fluid maintenance
- Fluid conversion

2 DISCUSSION

2.1 Fluid Classification

Emulsion hydraulic fluids are part of a larger ISO classification of fire-resistant fluids summarized in Table 20.1 (see Chapter 20) which include HFA, HFB, HFC, and HFD fluids [10,11]. The fluids designated as HFC (water–glycol hydraulic fluids) were discussed in detail in Chapter 18 and HFD fluids, polyol esters and phosphate esters were discussed in Chapters 19 and 20, respectively. Fluids classified as HFA and HFB will be discussed in detail in this chapter.

2.1.1 HFA Fire-Resistant Hydraulic Fluids

There are two subclassifications of HFA fluids. One is HFA-E, which is an emulsion (E) typically formed on-site by the user by mixing 1–5% oil and additives into water (95%) [11,12]. These fluids are often called “soluble oils” where water is the continuous phase. The oil is solubilized into water by a comicellization process depicted in Figs. 17.1a and 17.1b. A surfactant possesses a polar (either ionic or water-soluble polyether) and a nonpolar (often hydrocarbon) end. One method of hydraulic emulsion formation is to add the surfactant to the oil which upon dilution with water, the nonpolar end will penetrate into the nonpolar oil droplet, producing a water-soluble polyether or ionic functionalized surface as illustrated in Fig. 17.1a [13]. The functionalized droplet (comicelle) will be water dispersible (emulsion) or soluble (microemulsion). The amount of the “soluble” oil used will vary with the type of oil, fluid power application, and water hardness (in terms of calcium carbonate and chlorides) [4]. These fluids may exhibit viscosities as low as 1 cps. Fluid viscosity is increased by substantially decreasing water content [14].

The second subclassification of HFA-S is an emulsion or microemulsion of up to 20% of a synthetic polymer (S), additives, and water (>80%). These fluids are also known as high-water-base fluids (HWBF) [14]. Thickened or “viscous” versions of these fluids (VHWBF) are also available which contain approximately 6% of a synthetic polymer thickener, 4% additives, and up to 90% water [9,14]. The polymeric thickeners used typically employ an associative thickening mechanism dependent on surfactantlike hydrophobic interactions between either terminal or pendant hydrocarbon functional groups on the water-soluble polymer with itself as illustrated in Fig. 17.2 [14] or with an emulsifier. The polymer–polymer or polymer–surfactant complex behaves as a much larger molecule which exhibits a significant increase in thickening efficiency. These associative complexes may be large and opaque (emulsions) or small and clear (microemulsions). Some polymers used for HFA-S formulations are water soluble and do not employ associative thickening mechanisms. Solutions formed with these polymers are clear.

Therefore, HFA hydraulic fluids may be formulated as true solutions microemulsions (transparent appearance) and macroemulsions (opaque or white appear-

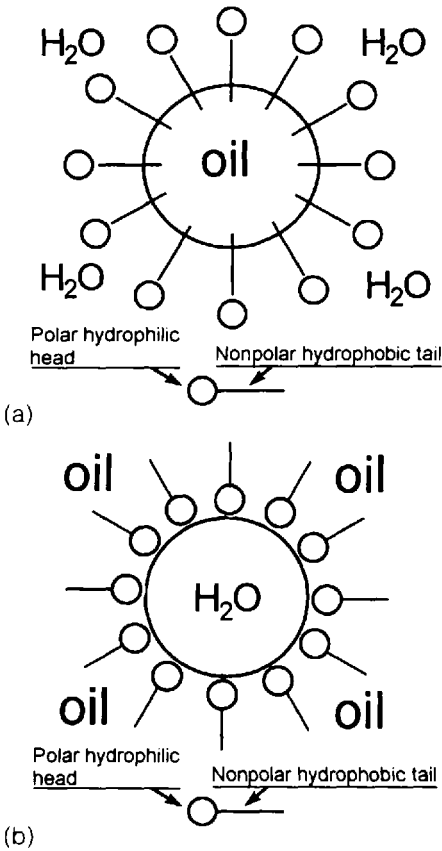


Figure 17.1 (a) Micelle-solubilized oil droplet with surfactant hydrophobe interpenetration into a hydrocarbon oil droplet and water solubilization by interaction of the water with the polar head of the surfactant. (b) Illustration of a “reverse micelle,” where water is solubilized in oil by adsorption of the polar head of the surfactant with the water droplet surface and oil solubilization is achieved by interaction of the hydrophobic tail of the surfactant with the oil.

ance) [11]. (Spikes reports macroemulsion particle sizes of 0.5–10 μm for these fluids [15].) Table 17.1 provides a summary of emulsion particle size and appearance [25].

In general, HFA macroemulsions may not be thermally stable and they may exhibit relatively poor antiwear properties in the hydraulic pump [11,16]. However, HFA microemulsions may exhibit improved thermal and viscosity stability relative to the macroemulsions in use [11].

2.1.2 HFB Fire-Resistant Hydraulic Fluids

HFB fluids are formulated by emulsifying 35–40% water into the oil, which is the continuous phase [12], as opposed to soluble oils (HFA-E). HFB emulsions are designated as “invert” emulsions. These fluids are supplied in ready-to-use form and are not mixed by the user on-site [15]. The colloidal particle size has been reported to be 3–8 μm [4].

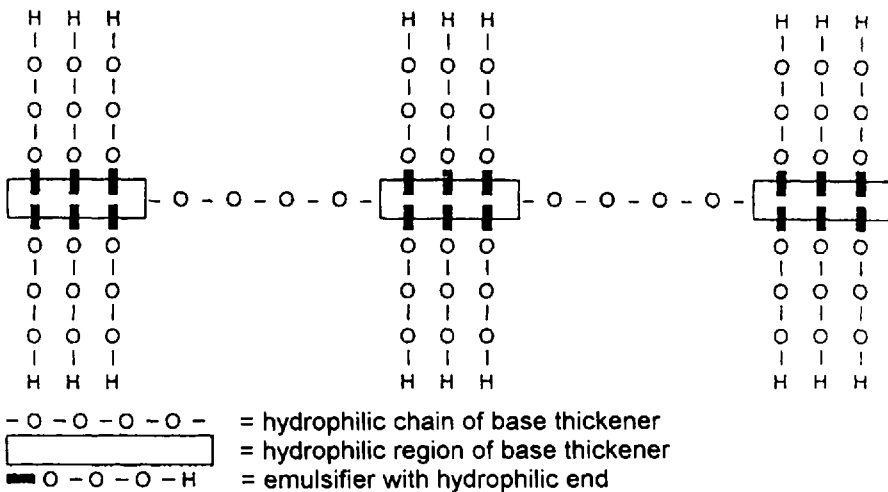


Figure 17.2 Illustration of an emulsifier with a thickener. The interaction occurs through interaction of the hydrophobic portion of the surfactant emulsifier with hydrophobic regions of the polymeric thickener. This interaction produces an “associative thickening” effect.

2.2 Fluid Formulation

An HFA-E or HFB emulsion hydraulic fluid is typically composed of mineral oil, surfactant, water, and additives. The surfactant that is selected is dependent on whether the final fluid will be an HFA-E or HFB. HFA-S fluids typically contain components similar to an HFA-E fluid with the exception that the mineral oil is replaced by a synthetic polymer. The additive package is selected to provide the desired emulsification, corrosion protection, antifoam, dyes for leak detection, and antiwear protection. A list of additive performance requirements is provided in Table 17.2 [9,10].

Because the lubrication mechanisms are different for aqueous fluids, including emulsions such as HFA and HFB hydraulic fluids, some of the additives utilized are different than those used for mineral oils [9,17]. Additives that may be used in the formulation of HFA and HFB fluids may include alkyl sulphonates, fatty esters and carboxylates, alkylated phenolic derivatives, and nonionic surface-active polymers for use as emulsifiers. Silicone polymers have been used as antifoam additives [18,19]. Antiwear properties have been provided by sulfurized sperm oil, metal di-

Table 17.1 Effect of Dispersed Phase Size on Emulsion Appearance

Particle size (μm)	Appearance
Greater than 1 μm	Milky white
1.0 to 0.1 μm	Blue-white emulsion
0.1 to 0.05 μm	Grey semitransparent
Less than 0.05 μm	Transparent

Table 17.2 Development of an Advanced Emulsion HFA Hydraulic Fluid

Performance requirement	Solution to problem
Emulsion stability	Emulsifier chemistry
High volumetric	Viscosity $>1 \text{ mm}^2\text{s}^{-1}$
Shear stability	Emulsifier and polymer chemistry
Corrosion protection	Compatible corrosion inhibitor
Wear protection	Chemistry of base oil, emulsifier, antipitter, antiwear, and polymer
Seal compatibility/wear	Emulsion in preference to solution
Low foaming	Compatible antifoam
Bacterial resistance	High pH, stable emulsion*

*Availability of compatible biocides for use if required.

thiocarbamates, metal dithiophosphates, polychloronaphtha alkyl xanthates, dibenzyl sulfides, or other derivatives [19]. Possible antioxidants include di-tertiarybutyl-para-cresol and phenyl-alpha-naphthylamine. Corrosion inhibitors, typically amine salts of acids and yellow metal passivators such as 2-mercaptobenzothiazole are also used [18,19]. An illustrative additive formulation and recommended concentration ranges that may be used in fluid formulation is provided in Table 17.3 [11].

2.3 Emulsification Technology

2.3.1 Surfactants

Surfactants are surface-active molecules or polymers that typically exhibit a water-loving end (hydrophilic) and a water-disliking end (lipophilic). Figure 17.1 schematically illustrates the use of a surfactant to solubilize oil in water or water in oil.

Table 17.3 Selected Additives for Improving Physical, Chemical, Rheological, and Tribological Properties of Hydraulic Fluids

Additive name	Functional application	Recommended concentration ranges (wt.%)
Alkylbenzotriazole	Copper passivator	0.1–1.0
Ethoxylated ethanolamide	Corrosion inhibitor	0.1–1.0
Polyalkylmethacrylate	Pour-point depressant and viscosity index improver	1.0–2.0
Tetraethylene glycol	Antifoam and pour-point depressant	0.1–1.0
ZDDP*	Antiwear agent	0.1–1.0
Nitroalkylmorpholine derivative**	Biocide	0.001–2.0
1-Phenyldodecane	Antiswelling agent	0.001–0.2

*For chemical formula.

**This additive consists of a mixture of 4-(2-nitrobutyl)morpholine and 4,4'-(2-ethyl-2-nitrotrimethylene)-dimorpholine.

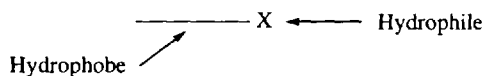
Illustrative surface-active (surfactant) molecules are depicted in Fig. 17.3. These include stearic acid which has a heptadecyl, $\text{CH}_3(\text{CH}_2)_{16}-$, a lipophilic end (hydrophobe), and a polar carboxyl, COOH , lyophilic end (hydrophile). Another example is sodium oleate, where the hydrophobe (water-disliking end) is $\text{CH}_3(\text{CH}_2)_4\text{CH}=\text{CHCH}_2\text{CH}=\text{CH}(\text{CH}_2)_7-$, and the hydrophile (water-loving end) is the sodium salt of the carboxylic acid COONa . Both are examples of ionic surfactants.

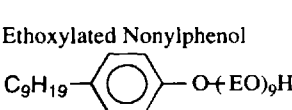
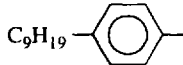
Examples of nonionic surfactants in Fig. 17.3 are ethoxylated oleyl alcohol where the oleyl group is the hydrophobe and the poly(ethoxy), $-(\text{CH}_2\text{CH}_2\text{O})_n-$, is the hydrophile. The larger the value of n , the more hydrophylic the poly(ethoxy) functionality. The other example shown is ethoxylated nonylphenol, where the hydrophobe is the nonylphenyl group and the poly(ethoxy) group is the hydrophile.

When a surfactant is first added to solvent (in this case, water), it exists as a random, unordered solution. As the surfactant concentration increases, a monolayer of oriented surfactant molecules is formed such as shown in Fig. 17.4. At this point, the critical micelle concentration, the surfactant molecules aggregate to form micelles. Experimental work has been done to characterize the surface coverage of water by stearic acid, as shown in Fig. 17.5 [20].

Surfactant HLB Characterization

The numerical expression of the balance and strength of the hydrophilic (water loving or polar) and the lipophilic (oil loving or nonpolar) groups of a surfactant is the



<u>Molecule</u>	<u>Hydrophobe</u>	<u>Hydrophile (X)</u>
Stearic Acid	Heptadecyl $(\text{CH}_3(\text{CH}_2)_{16}-)$	$-\text{COOH}$
Sodium Oleate	Oleyl $(\text{CH}_3(\text{CH}_2)_4=\text{CHCH}_2\text{CH}=\text{CH}(\text{CH}_2)_7-$ $(\text{C}_{18}:1)$	$-\text{COONa}$
$\text{C}_{18}:1(\text{EO})_2\text{H}$ Ethoxylated Oleyl Alcohols	$(\text{C}_{18}:1)$ ↓	$\text{O}-(\text{EO})_2\text{H}$ ↓
$\text{C}_{18}:1(\text{EO})_{20}\text{H}$	$(\text{C}_{18}:1)$	$\text{O}-(\text{EO})_{20}\text{H}$
Ethoxylated Nonylphenol C_9H_{19} 	C_9H_{19} 	$\text{O}-(\text{EO})_9\text{H}$

Where: EO is ethyleneoxy: $(\text{CH}_2\text{CH}_2\text{O})-$

Figure 17.3 Illustration of the hydrophobic and hydrophilic portions of commonly encountered surfactants.

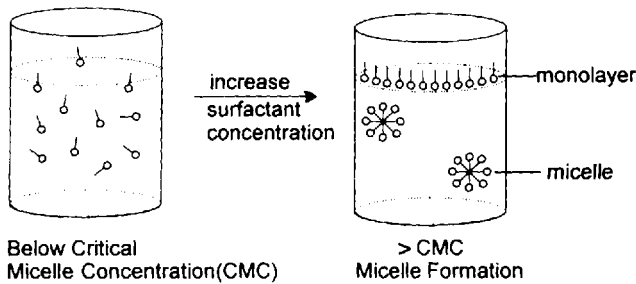
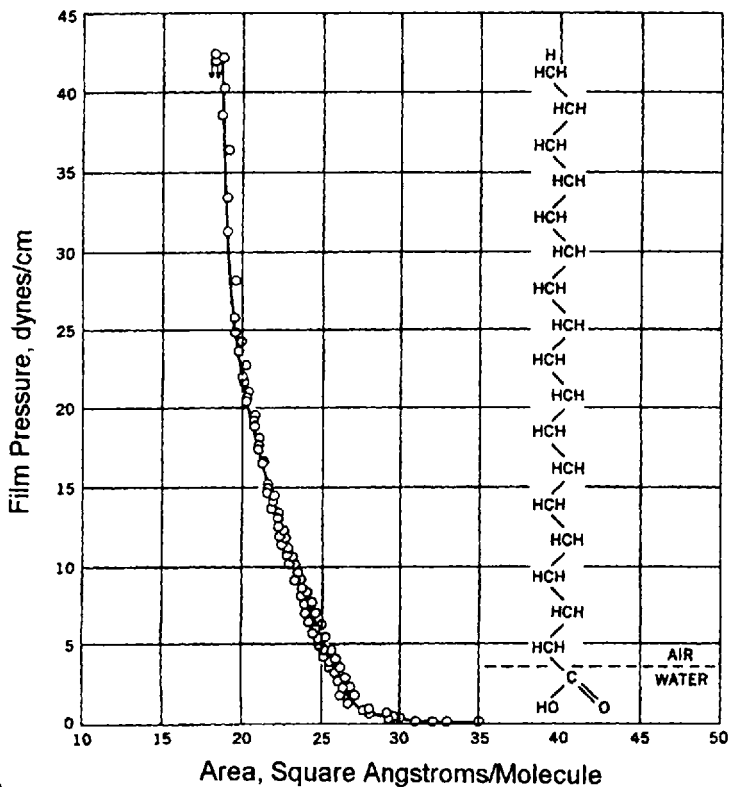


Figure 17.4 Micelle formation occurs only above a characteristic point called the critical micelle concentration.

HLB (hydrophile–lipophile balance) value of a surfactant. HLB values below 9.0 indicate that the surfactant is lipophilic in character. Hydrophilic surfactants exhibit HLB values >11.0. HLB values in the range 9–11 are considered intermediate between hydrophobic and hydrophilic.



(a)

Figure 17.5 (a) Film pressure–area isotherm and molecular orientation of stearic acid. (b) The dimensions of a monomolecular surface film of stearic acid on water.

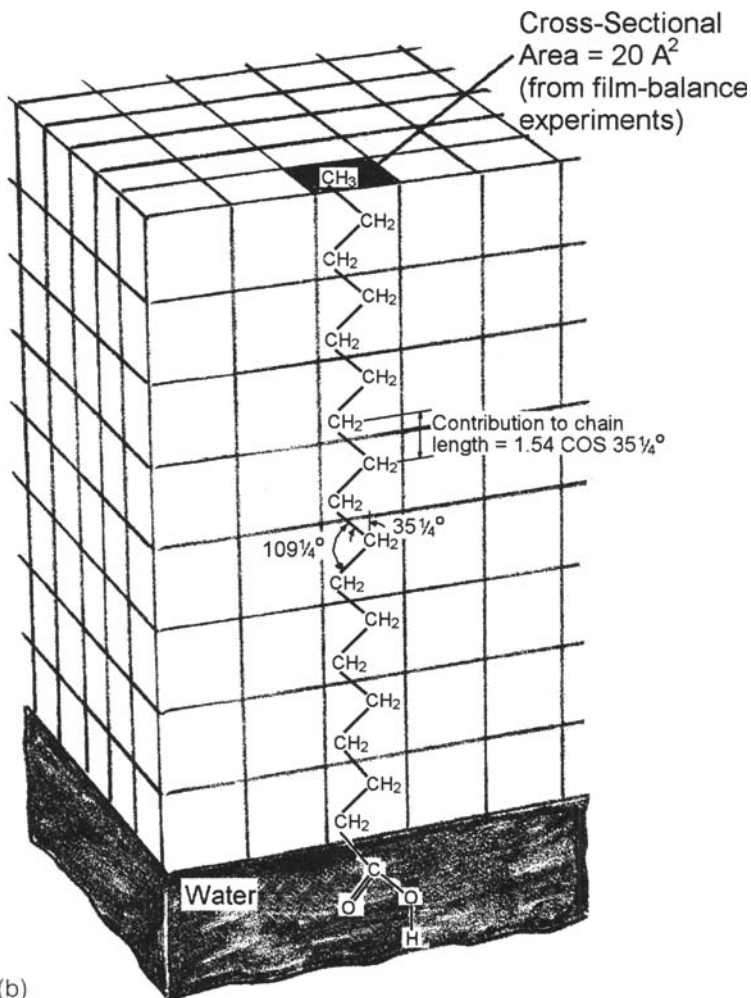


Figure 17.5 Continued.

A wide range of HLB values may be obtained by blending emulsifiers. The HLB value of a blend may be calculated by multiplying the fraction of the emulsifier in the blend times its HLB value. For example, if an emulsifier blend contains 70% of Emulsifier A with an HLB of 15.0 and 30% of Emulsifier B with an HLB of 4.3, the HLB of the blend will be

$$\text{Emulsifier A} \quad 0.7 \times 15.0 = 10.5$$

$$\text{Emulsifier B} \quad 0.3 \times 4.3 = 1.3$$

$$\text{HLB of the blend} = 11.8$$

The ability of an emulsifier to form an oil-in-water (O/W) or a water-in-oil (W/O) emulsion is dependent on the HLB value of the emulsifier system, as shown in Table 17.4 [21]. For example, to prepare an O/W emulsion, a water-soluble emul-

Table 17.4 Classification of Emulsifiers According to HLB Values

Range of HLB values	Application
3.5–6	W/O emulsifier
7–9	Wetting agent
8–18	O/W emulsifier
13–15	Detergent
15–18	Solubilizing agent

sifier (HLB 8–18) will be selected. Conversely, to prepare a W/O emulsion, an oil-soluble emulsifier (HLB 4–6) will be selected. The proper selection of the HLB value will affect the character of the dispersion as shown in Table 17.5 [22]. Also, it must be noted that HLB values do not reflect the stability of the emulsion, only the ability to form it [23].

It should be noted that HLB values of different chemical structures should not be used to compare the emulsification ability of one class of emulsifiers with respect to another. Instead, only the HLB values of similar structures should be directly compared [23].

Calculation of HLB Values

There are various methods for calculation of HLB values. One method is to calculate the HLB value from the chemical structure by summing a group's contributing number [21]: $HLB = \Sigma(\text{hydrophilic numbers}) - m$ (group number per $-\text{CH}_2-$ group) + 7. Table 17.6 provides a summary of illustrative HLB group numbers. A comparison of the HLB values calculated by this methods versus experimentally determined values is provided in Table 17.7.

In many cases, however, the chemical name of the emulsifier is only representative of the structure, which is actually a blend. This is true of many emulsifiers derived from natural products. In such cases, if possible, it is preferable to determine the HLB value experimentally. For polyol fatty acid esters, the HLB value can be calculated from [23]

$$HLB = 20 \left(1 - \frac{S}{A} \right) \quad (17.1)$$

where S is the saponification number of the ester and A is the acid number of the recovered ester.

Table 17.5 The Effect of HLB Rating of an Emulsifier on the Emulsion Produced

HLB range	Form of solution/dispersion
1–4	No dispersion in water
9–10	Stable milky dispersion
>13	A clear solution

Table 17.6 HLB Group Numbers

Hydrophilic groups	Group number
—SO ₃ ⁻ Na ⁺	38.7
—COO ⁻ K ⁺	21.1
—COO ⁻ Na ⁺	19.1
Sulphonate	about 11
Ester (sorbitan ring)	6.8
Ester (free)	2.4
—COOH	2.1
Hydroxyl (free)	1.9
—O—	1.3
Hydroxyl (sorbitan ring)	0.5
Lipophilic groups	
—CH—	0.475
—CH ₂ —	0.475
—CH ₃ —	0.475
—CH—	0.475
Derived group	
—(CH ₂ —CH ₂ —O)—	0.33

If the emulsifier is a fatty ester of a polyol, the following equation may be used to calculate HLB [23]:

$$\text{HLB} = \frac{E + P}{5} \quad (17.2)$$

where E is the weight percent of oxyethylene content and P is the weight percent of the polyol. The total value of the hydrophilic component is $E + P$.

In the case of nonionic emulsifiers containing a polyethyleneoxy as the hydrophilic nonionic moiety, such as polyoxyethylene stearate, the HLB value can be calculated from [23]

$$\text{HLB} = \frac{E}{5} \quad (17.3)$$

2.3.2 Emulsification

Emulsions are dispersions of one liquid that is insoluble in the other. An emulsion is composed of an internal phase, external phase, and an interphase. For an HFA hydraulic fluid, the internal phase is oil, the external phase is the continuous phase (in this case, water), and the interphase is the surfactant which interacts with both the internal and external phases. The efficiency of the stabilizing action is dependent on the hydrophile–lipophile balance [24].

Figure 17.1a illustrates the interaction of surfactant molecules with a dispersion of oil droplets in water. The dispersing process for HFA fluids (oil-in-water) involves

Table 17.7 Comparison of the HLB Values Calculated by This Method Versus Experimentally Determined Values

Surface active agent	HLB from expt.	HLB from group numbers
Na lauryl sulphate	40	(40)
K oleate	20	(20)
Na oleate	18	(18)
Tween 80 (sorbitan "mono-oleate" + 20 (CH ₂ —CH ₂ —O) groups)	15	16.5
Alkyl aryl sulphonate	11.7	—
Tween 81 (sorbitan "mono-oleate" + 6 (CH ₂ —CH ₂ —O) groups)	10	11.9
Sorbitan monolaurate	8.6	8.5
Methanol	—	8.3
Ethanol	7.9	7.9
n-Propanol	—	7.4
n-Butanol	7.0	7.0
Sorbitan monpalmitate	6.7	6.6
Sorbitan monostearate	5.9	5.7
Span 80 (sorbitan "mono-oleate")	4.3?	5.7
Propyleneglycol monolaurate	4.5	4.6
Glycerol monostearate	3.8	3.7
Propylene glycol monostearate	3.4	1.8
Sorbitan tristearate	2.1	2.1
Cetyl alcohol	1	1.3
Oleic acid	1	(1)
Sorbitan tetrastearate	~0.5	0.3

stirring the oil–water mixture sufficiently fast to break up the larger oil droplets into smaller droplets, thus increasing the surface area and improving the potential for emulsification or microemulsification. If the water is the continuous phase, as shown in Fig. 17.1a, the hydrophobic region of the surfactant molecule will adsorb on the oil droplet surface, creating a surface which is either polar or functionalized by a water-soluble polyether (polyethylene oxide) functionality. Once the oil droplet surface is functionalized in this way, it may form a stable dispersion (emulsion) in water.

The emulsification process for HFB fluids (water-in-oil) is reversed. As shown in Fig. 17.1b, the oil is the continuous phase. The surfactant molecule adsorbs at the water–oil interface such that the polar end adsorbs on the water droplet surface and the hydrophobic end extends into the oil phase. In this way, the surface of the water droplet is made hydrophobic, making a stable dispersion (invert emulsion) of the water in the oil.

Phase Diagram Characterization of O/W Microemulsions

Although HFB hydraulic fluids are typically macroemulsions, there has been some interest in developing microemulsion HFB fluids because they would be less susceptible to the very large viscosity variations that may be encountered with macro-

emulsions [11]. Garti et al. performed a systematic investigation of the effect of emulsifier type on the phase diagrams of water-in-oil mixtures of emulsifier/paraffinic mineral oil and distilled water [11]. The paraffinic mineral oil contained approximately 70% paraffinic oil fractions and 30% of a mixture of naphthenic and aromatic fractions. Two ethoxylated oleyl alcohol derivatives were used as emulsifiers. One derivative contained two ethoxyethyl groups (EO), which had an HLB of 4.9 and was designated as $C_{18:1}(EO)_2$. The other derivative contained an average of 20 mol of ethoxyethyl groups, which had an HLB of 15.3 and was designated as $C_{18:1}(EO)_{20}$. A third emulsifier was prepared by blending these two oleyl ethoxylates at a ratio of 58 $C_{18:1}(EO)_2$ /42 $C_{18:1}(EO)_{20}$ by weight to form an emulsifier with an HLB of 10.9. This HLB value was selected because it is the required value to form a microemulsion for this paraffinic oil. The three-component phase diagrams that were produced are shown in Figs. 17.6a–17.6d [11].

Figure 17.6a illustrates the three-component phase diagram formed with $C_{18:1}(EO)_2$ /mineral oil/water. The L_2 phase is a microemulsion of reverse micelles swollen with water in the core. (A reverse micelle refers to the surfactant micellar aggregate that is formed with the polar portion of the surfactant in the core and the hydrocarbon portion is extending into the oil.) Only minor amounts of water are solubilized in the L_2 region. The remainder of the diagram is a two-phase water–oil mixture because the surfactant was unable to form micelles in higher water concentrations by normal micellization due to its low HLB number (hydrophobicity).

Figure 17.6b illustrates the three-component phase diagram formed when $C_{18:1}(EO)_{20}$ is used as the emulsifier [11]. The L_2 microemulsion region is slightly larger and contained approximately 10% water. There is also a very large liquid-crystalline region with a hexagonal structure indicated by E.

The three-component diagram indicated shown in Fig. 17.6c [11]. The L_2 phase is larger than that obtained for Fig. 17.6a or 17.6b, indicating a synergy obtained by blending the two emulsifiers, and it contains approximately 22% water. There is also a small L_1 phase which consists of normal micelles with small amounts of oil that is solubilized. In between, L_1 and L_2 is a lamellar liquid-crystalline region indicated by region D. The lamellar liquid-crystalline phase is due to geometrical restrictions of the hydrophilic portion of the emulsifier.

To be commercially interesting, the microemulsion must contain at least 35% water to provide the minimum fire resistance. Therefore, Garti et al. prepared a four-component mixture by replacing the paraffinic oil with a 1/1 blend of pentanol and the paraffinic mineral oil. The phase diagram obtained is shown in Fig. 17.6a [11]. In this case, a very large L_2 region was obtained, which contained approximately 35% water. To form this component, nearly 27.3% of the emulsifier blend was required.

2.3.3 Emulsion Theory

In this section, a selected overview of various theoretical principles that will provide a greater fundamental understanding of emulsion technology will be provided.

The Einstein Equation and Volume Concentration in the Dispersed Phase

Emulsion viscosity (η) may be quantitatively expressed by the Einstein equation

$$\eta = \eta_0(\varphi + K) \quad (17.4)$$

where η is the emulsion viscosity, η_0 is the external-phase viscosity, φ is the phase–

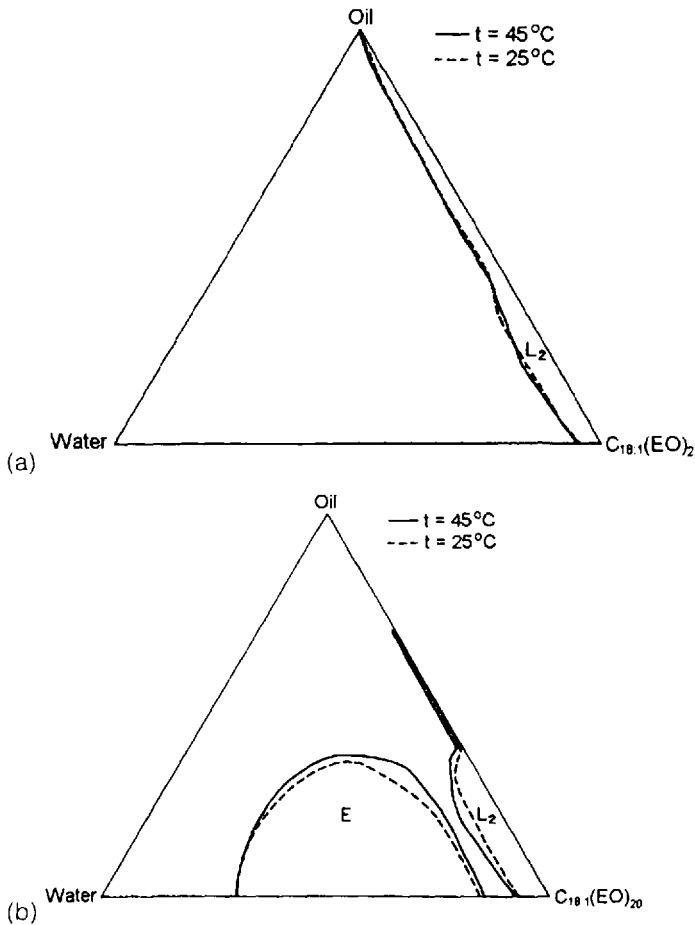


Figure 17.6 (a) Phase diagram of a paraffinic mineral oil, water, and an ethoxylated oleyl alcohol (2 EO) at 25°C and 45°C. L_2 represents the water-in-oil microemulsion phase. (b) Phase diagram obtained at 25°C and 45°C when a 20 EO ethylate of oleyl alcohol is used. E represents the area where a liquid-crystalline mesophase is obtained. (c) Phase diagram obtained at 25°C and 45°C when a mixture of 0.58/0.42 wt/wt ratio of the 2 EO ethoxylated oleyl alcohol/20 EO ethoxylated oleyl alcohol is used (HLB = 10.9). L_1 and L_2 represent o/w and w/o microemulsions. D is the liquid-crystalline region. (d) The phase diagram obtained with the same four components except with the addition of pentanol as a cosurfactant at a 1/1 wt/wt ratio with the oil. At maximum water solubilization, the pentanol is 20.4 wt/%.

volume ratio or volume occupied by the internal phase, and K is a constant dependent on the emulsifying system and relative particle size [24]. This relationship means that emulsion viscosity increases as the volume of the internal phase increases.

There are situations in which the Einstein equation is not true, such as the point of emulsion inversion. However, Pell and Holtzmann have shown that when using well-chosen emulsifiers as the internal phase approaches a theoretical limiting volume (52% for constant-volume spheres), there will be a phase inversion where the

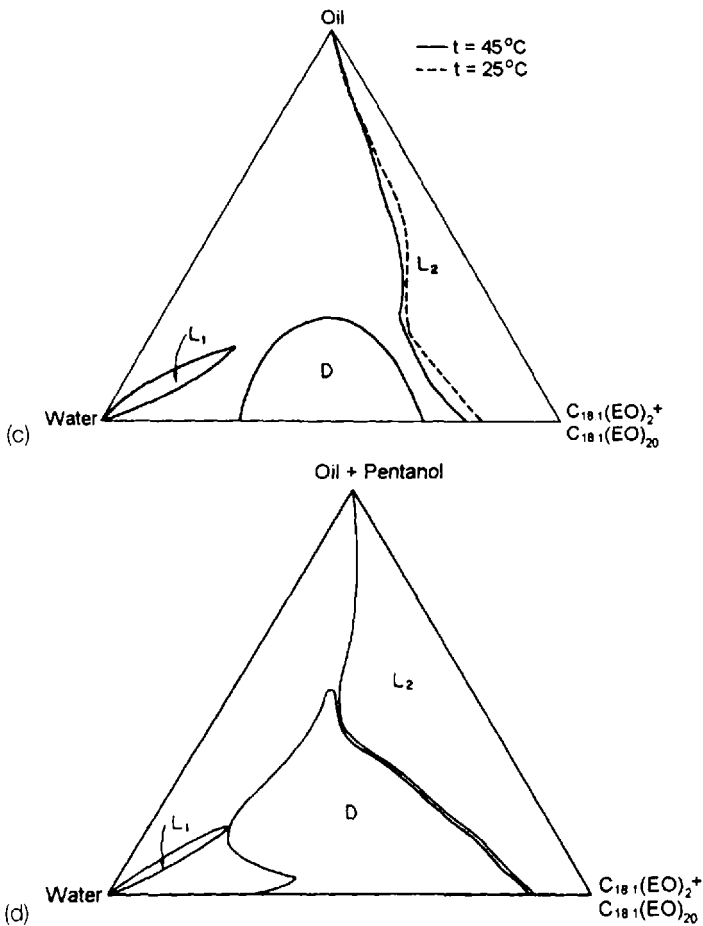


Figure 17.6 Continued.

internal phase becomes the continuous phase. This new system then follows the Einstein equation again. This is demonstrated in Table 17.8 [24]. In this example, as the water concentration (internal phase) is increased from 20% to 60%, the viscosity increases from 135 to >2000 SUS. A phase inversion occurs when water concentra-

Table 17.8 Effect of Internal-Phase Volume Ratio on Emulsion Viscosity

Emulsion	Composition (%)			Emulsion viscosity at 100°F (SUS)	Emulsion Type
	Emulsifier	Oil	Water		
A	3.0	77.0	20.0	135	W/O
B	3.0	37.0	60.0	>2000	W/O
C	3.0	17.0	80.0	95	O/W

tion is increased to 80% and the viscosity if 95 SUS. However, the oil, which is the internal phase, represents only 17% of the fluid volume.

Effect of Particle Size on Viscosity

Emulsion viscosity (η) is dependent on the diameter of the particle. Generally, emulsion viscosity increases with decreasing particle size as shown by the Sherman equation [24]:

$$\eta = X \frac{1}{d_m} + C \quad (17.5)$$

where d_m is the average particle diameter and X and C are constants. This effect is illustrated by the data in Table 17.9 [24].

Emulsion Turbidity

Emulsion turbidity is quantified by the Raleigh equation [25]:

$$\tau = \frac{32\pi^3 n^2 \Delta n^2 N V^2}{3\lambda^4} \quad (17.6)$$

where

τ = the turbidity

λ = the wavelength of light

Δn = the difference of the refractive index between the medium and scattering unit

V = the volume of the scattering unit

N = the number of scattering units per unit volume

This equation indicates that increasing turbidity will occur with increasing particle size. Therefore, macroemulsions, which exhibit larger particle sizes (V) than microemulsions, will be more turbid, as is observed. Particle sizes can be increased by increasing the oil-surfactant ratio or, in the case of nonionic surfactants, by optimizing the temperature [25]. Generally, oil solubilization in water increases significantly as the cloud point of the emulsifier is approached. The effect of temperature

Table 17.9 Effect of Internal-Phase Ratio on Particle Diameter and Emulsion Viscosity

ϕ	d_m (μ)	η (poises)
0.1809	1.59	2.45
	1.15	3.77
0.3707	2.74	3.09
	1.41	3.91
0.5704	3.61	4.83
	1.38	5.82
0.6739	3.98	6.38
	1.56	7.12
0.7280	2.71	7.58
	1.46	8.18

is most notable with nonionic emulsifiers. Typically, similar temperature effects are not observed with ionic surfactants [25].

Pell and Holtzmann showed that solution viscosity was dependent on the ratio of emulsifying agent to oil as shown in Table 17.10 [24]. In general, increasing the concentration of the emulsifier will produce a slight increase in viscosity. The emulsion viscosity increases at the point of inversion with increasing surfactant–oil ratio as indicated by the phase–volume ratio in Table 17.10 [24].

Schulman found that emulsions could be converted into microemulsions by the addition of an alcohol as a cosurfactant for an oil-in-water system emulsified by an ionic surfactant [25]. The alcohol acts as a lipophilic cosurfactant for an ionic surfactant, which is often too hydrophilic. Light-scattering experiments showed that these systems, called “Schulman’s microemulsions,” contained a range of colloidal particles from 100 to 1000 Å in diameter. Particles of approximately 100 Å are consistent with the dimensions expected for micelles. Therefore, Schulman considered a microemulsion as a “swollen” micellar solution [25].

Ease of Formation

The ease of formation of the emulsion/microemulsion systems may be analyzed using the basic solubility equation [25]:

$$\ln a_2 = \ln x_2 + \frac{V_2 \phi_1^2 B'}{RT} \quad (17.7)$$

where

a_2 = the relative activity of the solute in equilibrium with the solute in the micelle and in bulk solution

x_2 = the solubility expressed as mole fraction

V_2 = the molecular volume of the solute

ϕ_1 = the volume fraction of the solvent

B' = the energy of mixing per unit volume at infinite dilution

Because the activity of water is always considered to be approximately 1, the amount solubilized is proportional to the number and size of the micelles and to the type of hydrophilic portion of the emulsifier. The molecular volume of solubilized water is very small compared to an oil molecule and, therefore, is constant. This illustrates that the molecular volume of the solute (V_2) is important with respect to solubility.

The amount of oil solubilized in water is also proportional to the number and size of the micelles formed but not very dependent on the lipophilic groups; however,

Table 17.10 Effect of Internal-Phase Ratio on Emulsion Viscosity

Ratio of emulsifying agent	Viscosity (η) (apparent poises)	Phase-volume ratio (Φ) at inversion
1	2.7	0.594
2	5.53	0.732
3.5	12.05	0.780
5	13.15	0.723

it is dependent on the molecular volume of the oil. For W/O microemulsions, V_2 is small and solubilization is large and independent of the surfactant type. However, for O/W microemulsions, V_2 is large and variable, resulting in low solubilization of the larger oil molecules. This explains why W/O microemulsions are easier to prepare than O/W microemulsions [25].

Coalescence and Emulsion Type

The Bancroft rule states "the phase in which the stabilizing agent (emulsifier) is more soluble will be the continuous phase" [21]. In an earlier discussion, it was shown that emulsifier HLB values may be selected to favor the emulsion type (O/W or W/O). However, these are empirical rules that must be confirmed by experiment. Davies and Rideal have proposed that coalescence kinetics is responsible for emulsion stability and the type of emulsion formed in shaken systems [21]. Coalescence kinetics will be discussed further here.

For an oil-in-water emulsion, the coalescence of two oil droplets will require the displacement of water of hydration surrounding the micellized oil droplet. The total energy of displacement, $\sum E_h$. This is dependent on the number and type of hydrated groups on each molecule of the emulsifying molecule and on θ , the ratio of the surface covered [21]:

$$W_1 = \theta \sum E_h \quad (17.8)$$

A strongly hydrated emulsifying agent is required to stabilize the oil-in-water emulsion. This occurs by hydrophobic interaction with the oil to promote adsorption and by increasing θ . However, hydration of the micelle formed hinders close contact of the oil droplet surfaces. Therefore, both charge and hydration may decrease the coalescence rate (Rate 1) and two energy barriers (W_1 and W_2) act simultaneously [21]:

$$\text{Rate 1} = C_1 \exp \left(\frac{-0.24\psi_0^2 - \theta \sum E_h}{RT} \right) \quad (17.9)$$

where ψ_0 is the electrical potential on the surface of the droplet, ψ_0^2 is the repulsive potential, and C_1 is the collision factor. For oil emulsified with sodium oleate, $\psi_0 = -175$ mV, assuming one electronic charge per 45 \AA^2 [25]. This equation can be used to analyze the effects of the addition of a coemulsifier. For example, if cetyl alcohol is added to a potassium oleate stabilized oil-in-water emulsion, the value for ψ_0 would not be expected to change. However, the values for θ and E_h will be affected. In this particular system, it has been shown that Rate 1 is 10 times greater when cetyl alcohol is added as a coemulsifier than when potassium oleate is used by itself [21].

For the coalescence of two water droplets in a water-in-oil system, the rate of coalescence (Rate 2) will depend on hydrodynamic factors included in the collision factor, C_2 , on the number m of the $-\text{CH}_2-$ groups in each hydrocarbon chain, and on θ , the fraction of the surface actually covered by the emulsifier. The energy barrier for water passage over each $-\text{CH}_2-$ group is approximately 300 cal and the water must "bridge" $2m$ $-\text{CH}_2-$ groups [21]:

$$W_2 = 2m\theta \times 300 \quad (17.10)$$

$$\text{Rate 2} = C_2 \exp \left(\frac{-600m\theta}{RT} \right) \quad (17.11)$$

These equations indicate that a high fraction of surface coverage of long chains of $-\text{CH}_2-$ groups are required to stabilize a water-in-oil emulsion.

The ratio of the rates of coalescence is [21]

$$\frac{\text{Rate 2}}{\text{Rate 1}} = \frac{C_2}{C_1} \exp \left(\frac{+0.24\phi_0^2 + \theta \sum E_n - 600m\theta}{RT} \right) \quad (17.12)$$

If a mixture of oil and water and an emulsifying agent are shaken, a mixture of two systems will be formed as shown in Figs. 17.7a and 17.7b [21], one with water as the continuous phase and the other with oil as the continuous phase. The relative coalescence rates will determine which system (O/W or W/O) will be more stable [21]:

$$\text{O/W emulsion preferred if } \frac{\text{Rate 2}}{\text{Rate 1}} \geq 1 \quad (17.13)$$

$$\text{W/O emulsion preferred if } \frac{\text{Rate 2}}{\text{Rate 1}} \leq 1 \quad (17.14)$$

Generally, one emulsion form is more stable than the other only if Rate 1 or Rate 2 is smaller than about $10^{-6}C_1$ or $10^{-6}C_2$ [21].

Emulsion Stability

An O/W emulsion will break or undergo an inversion if Rate 1 (W/O) is large. The particular pathway, breakage or inversion, is dependent on the stability of the inverse system (in this case, W/O). If the inverse system is unstable and if Rate 2 (O/W) is large, the emulsion will break. However, inversion will occur if Rate 2 is small. Typically, coalescence will occur for $10^{-2}C_1$ or $10^{-2}C_2$. This is illustrated in Fig. 17.8 [21]. The emulsion will be stable for prolonged periods (months) for $10^{-5}C_1$ and $10^{-5}C_2$.

CHEMICAL AND PHYSICAL METHODS OF BREAKING AN EMULSION. Generally two or more emulsifiers are blended to obtain the desired HLB to stabilize the formation of the emulsion [26]. Such an emulsion may be broken chemically by the addition of an additive (e.g., another emulsifier) that favors the formation of the opposite type of emulsion or salt.

Physical methods of breaking an emulsion include the following [21]:

- Emulsions may be broken by centrifuging, filtration, slow stirring, and low-intensity ultrasonic vibrations.
- Generally heating an emulsion to approximately 70°C will break an emulsion.
- Passing the emulsion through an electrical field will break an O/W emulsion because the charged droplets will migrate to one of the electrodes.

2.3.4 Emulsion Inversion

There are conditions, such as varying ratios of oil–water, the addition of electrolytes, and temperature variation, under which W/O emulsions may be converted into O/W and vice versa [27,28]. This is illustrated in Fig. 17.9 [21]. The left side of Fig. 17.9 illustrates droplets of water evenly dispersed throughout the continuous oil phase. As the emulsion becomes less stable, particulate motion increases and the water

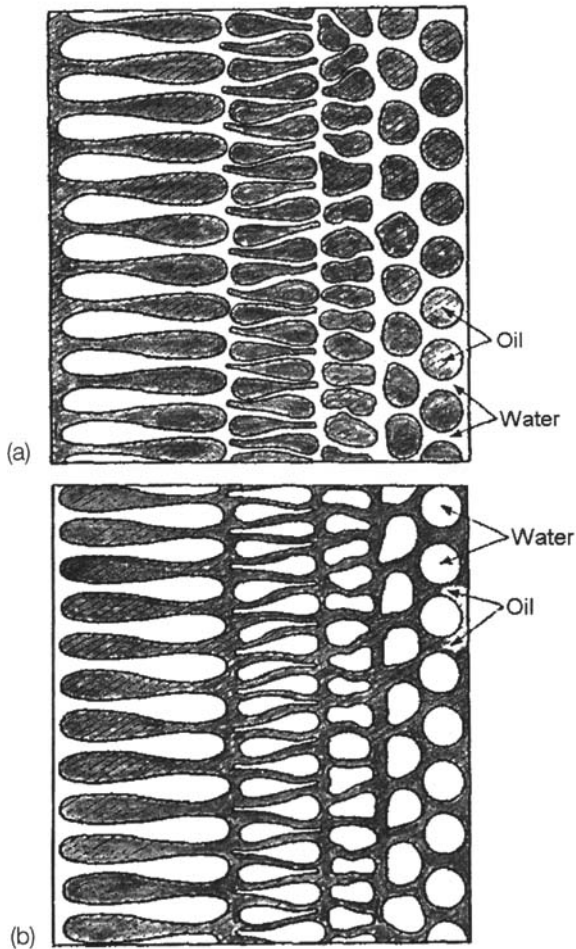


Figure 17.7 Illustration of (a) an oil-in-water emulsion and (b) an water-in-oil emulsion.

droplets become more distorted until they begin to agglomerate. This process continues until a critical point is reached and an inversion of the continuous phase occurs, as indicated in the center region of Fig. 17.9. Finally, when the phase inversion is complete, oil droplets are evenly dispersed in water, which is the continuous phase. This stepwise process is illustrated microscopically in Fig. 17.10 [28].

2.4 Emulsion Preparation

Emulsions may be made by dispersion or chemical methods [21]. Perhaps the most well-known physical method of mixing is with the use of a “colloid-mill,” which is a homogenizer. Ye has reported the use of a centrifugal pump where appropriate amounts of oil with additives, including the emulsifier, and water are pumped as separate streams through a nozzle where the mixture is mixed at a high shear rate [18]. The successful use of a mechanical stirrer to prepare an O/W hydraulic fluid emulsion where water is added slowly to the oil–additive–emulsifier mixture has also been reported [19].

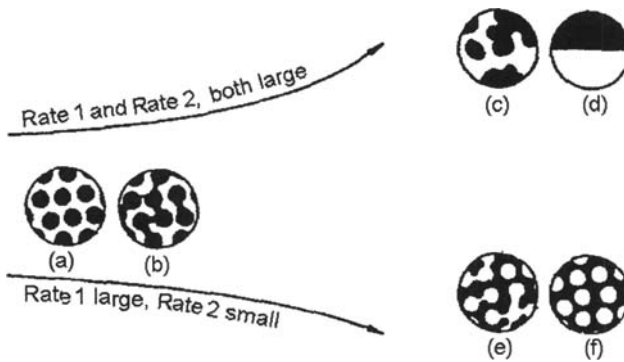


Figure 17.8 Illustration of the breaking and inversion of an emulsion; the dark area is representative of oil and the white area represents water. The O/W emulsion breaks because Rate 1 is large. Phase separation occurs if Rate 2 is large (a, b, c, and d). If Rate 2 is small, phase inversion (a, b, e, and f) occurs.

One of the most common problems encountered in mixing an emulsion is that insufficient mixing times are used [19]. Coleman showed that in one case, an emulsion began to separate after mixing with a mechanical mixer at room temperature. This was due to inadequate mixing, as indicated microscopically by nonuniform droplet formation as shown in Fig. 17.11a. This fluid was then mixed further in a homogenizer, which provided a stable emulsion with uniform droplet size, as indicated in Fig. 17.11b [19].

It is also possible to mix an emulsion by chemical condensation, also known as spontaneous emulsion, although this is not commonly done in the preparation of hydraulic fluid emulsions [21]. This form of mixing is accomplished by first mixing the oil with a water-miscible solvent such as ethyl alcohol. The alcohol–oil mixture is then poured into water, where the emulsion with approximately 1- μm droplets are formed.

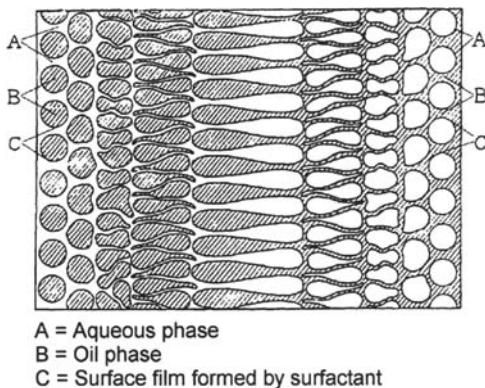


Figure 17.9 Schematic representation of a phase inversion from a O/W emulsion to a W/O emulsion.

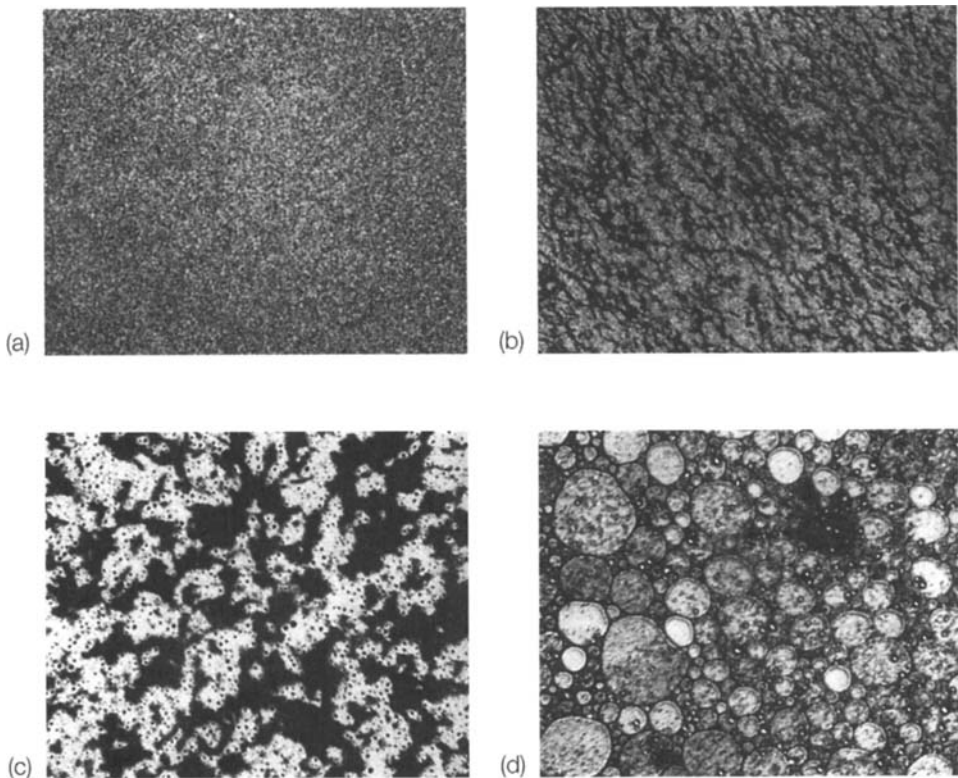


Figure 17.10 (a–d) Photomicrographs (100 \times) which show differing degrees of emulsion formation of W/O systems.

It is possible to obtain phase inversion during mixing. Figure 17.12 illustrates that there is a general correlation between the phase-inversion point (ϕ_i) during mixing of an emulsion and the magnitude of variables that may cause phase inversion, such as a variation in HLB of the emulsifier system, the viscosity of the oil, and so forth [21].

2.5 Physical Properties

2.5.1 Water Quality

Water quality can affect emulsion stability, eventually breaking the emulsion [30]. Emulsion breakdown may lead to increased pump and component wear and corrosion. Valve lockage may occur due to the presence of scums and greases. Therefore, hard water should not be used in preparing HFA or HFB fluids, particularly if ionic surfactants are used in the emulsifier system [31]. However, water hardness is not the most critical criterion because emulsion stability may be affected by ions other than those indicated by “hardness,” most typically, calcium and magnesium salts.

The British National Coal Board Standard No. 463/1981 makes the following recommendations for water quality in preparing HFA emulsions for mining applications [32]:

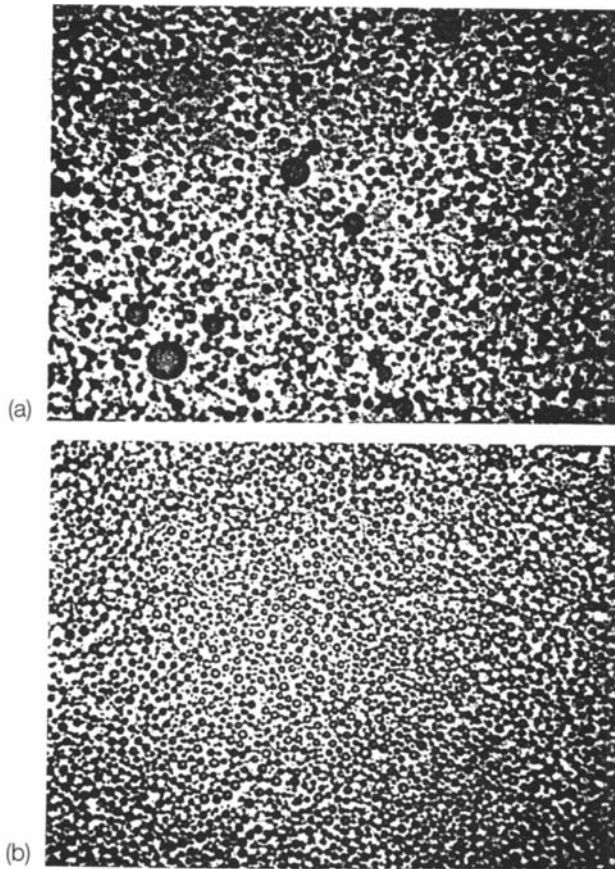


Figure 17.11 Photomicrographs ($75\times$) illustrating the effect of mixing on particle size and uniformity: (a) initial emulsion; (b) emulsion after additional mixing.

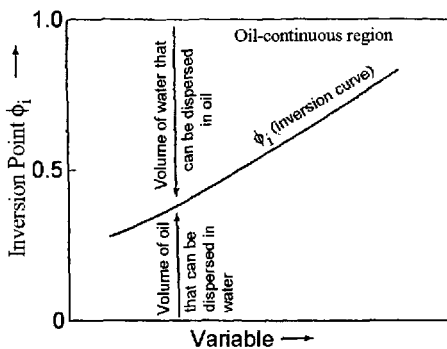


Figure 17.12 Inversion point versus composition on phase volume.

- The water is to be free from suspended contaminants.
- The pH is to be within the range 6–9.
- Total hardness for mixing with No. 18 Ordinary Emulsifying Oil up to approximately 250 mg/L CaCO₃ equivalent. Higher values may be used where tests show adequate stability.
- Total hardness for mixing No. 19 Superior Emulsifying Oil up to approximately 750 mg/L CaCO₃ equivalent. Higher values may be used where tests show adequate stability.
- Chloride and sulfate contents up to approximately 200 mg/L Cl⁻ and 400 mg/L SO₄²⁻. Higher values may be used where tests show stability and rust-preventing properties are adequate.

Tests for Emulsion Stability with Varying Water Hardness

The British Coal Board test for emulsion stability with varying water hardness is conducted by mixing 475 mL of NCB 18 or NCB 19 water, as defined in Table 17.11, with 25 mL of the soluble oil to be tested using a hypodermic syringe into a 500-mL conical flask at 20°C while mixing with a magnetic stirrer [32]. A stopper is placed on the flask and the resulting HFA emulsion is stored in an oven for 168 h at 70°C. The presence and volume of any oil that may separate or any creaming, as illustrated in Fig. 17.13, that may occur is noted. Any water separation at the bottom of the flask and the presence of any flocculation which may occur is noted.

2.5.2 Viscosity

Water Concentration

As noted in previous sections, HFA fluids contain >80% water and most typically contain approximately 95% water. These fluids, without the addition of a thickener, exhibit viscosities as low as 1–2 cSt [31,33]. HFB fluids, on the other hand, are formulated to contain approximately 40% water in order to provide the necessary fire resistance. Figure 17.14 shows that HFA and HFB fluids not only contain very different amounts of water, but increasing water concentration exhibits the opposite effect on fluid viscosity [34]. HFA fluids exhibit the expected decrease in viscosity with increasing water concentration. However, the viscosity increases dramatically with increasing water concentration for HFB fluids. Therefore, the water concentration of HFB fluids must be monitored closely during use.

Table 17.11 British Coal Board Solution of Standard Water Hardness

Test water	Total hardness		Ion concentration (ppm)				
	CaCO ₃ equivalent (ppm) ^c	°d	Ca	Mg	Na	Cl	SO ₄
NCB 18 ^a	250	14	50	30	130	200	240
NCB 19 ^b	750	42	150	90	130	200	720

^aNCB 18 water. The following salts are added to distilled water: 308 mg/L MgSO₄·7H₂O, 215 mg/L CaSO₄·2H₂O, 330 mg/L NaCl.

^bNCB 19 water. The following salts are added to distilled water: 924 mg/L MgSO₄·7H₂O, 645 mg/L CaSO₄·2H₂O, 330 mg/L NaCl.

^cEquivalents amount of hardness to calcium carbonate (CaCO₃) expressed in ppm.

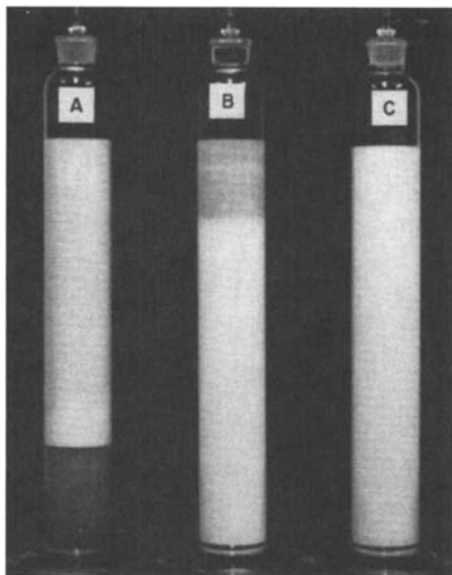


Figure 17.13 Effect of freeze–thaw cycling on three different emulsions.

Effect of Base-Oil Viscosity

The O/W emulsion viscosity is dependent on a number of variables, including water content, degree of emulsification, type and concentration of emulsifier, and base-oil viscosity [28]. Figure 17.15 shows that emulsion viscosity increases with base-oil viscosity and water content [35]. Although base-oil viscosity has some effect on the viscosity of W/O emulsions, the effect is minimal in view of the very high water concentration and the relatively low final formulated viscosities.

Effect of Shear Rate

Coleman showed that the viscosity of W/O emulsions (HFB fluids) decreased with increasing shear rate, as illustrated in Figs. 17.16a–17.16b. The amount of viscosity loss with increasing shear rate and initial fluid viscosity is illustrated in Figs. 17.16a

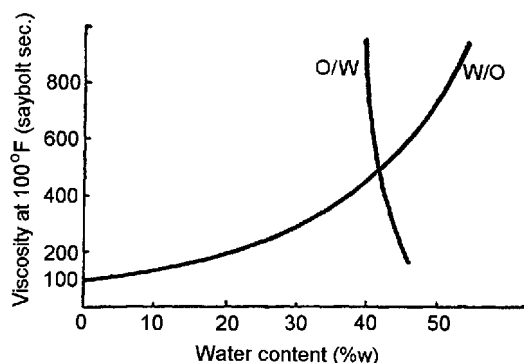


Figure 17.14 Effect of water content on O/W and W/O emulsion viscosity.

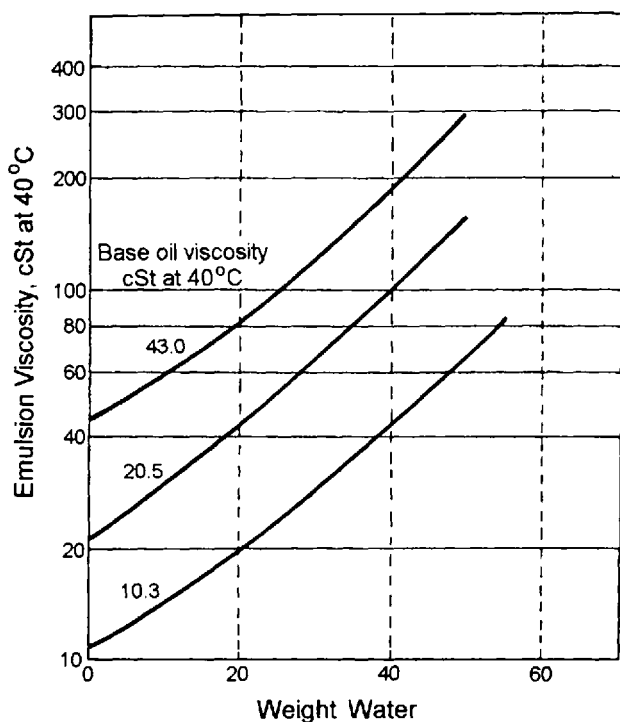


Figure 17.15 Effect of water content on W/O emulsion viscosity.

and 17.16b [19]. The viscosity loss was temporary and the fluids returned to their initial viscosity (non-Newtonian) when the high fluid shear rates were removed. Interestingly, the non-Newtonian behavior increased with increasing water content for emulsions with the same initial viscosity, as illustrated in Fig. 17.16c [19]. Because of these non-Newtonian effects, W/O emulsions were initially developed to provide a viscosity of 250 SUS (approximately 54 cSt) at 100°F when measured at a shear rate of $10,000 \text{ s}^{-1}$, a typical shear rate encountered in hydraulic pump applications. Therefore, the starting kinematic viscosity was increased to 400 SUS (approximately 86 cSt) at 100°F, which was higher than the 150–315 SUS (approximately 32–68 cSt) at 100°F typically used for petroleum-oil formulations to provide proper pump operation and lubrication [36]. This is illustrated in Fig. 17.17 [36]. Because of this higher viscosity, it was recommended that hydraulic pump suction be maintained to avoid cavitation during cold start-up [36]. Although the specific hydraulic pump requirement recommended by the manufacturer should be confirmed, the inlet vacuum values shown in Table 17.12 are typical of those often recommended [28].

The O/W emulsions (HFA-E) fluids typically do not exhibit Newtonian shear-thinning behavior (Newtonian) as was shown by Isaksson in Fig. 17.18 [37]. This is not surprising in view of the relatively low initial viscosities exhibited by these fluids. However, thickened HFA fluids, HFA-S, may be non-Newtonian, as illustrated in Fig. 17.19 [37]. The degree of non-Newtonian behavior is dependent on the molec-

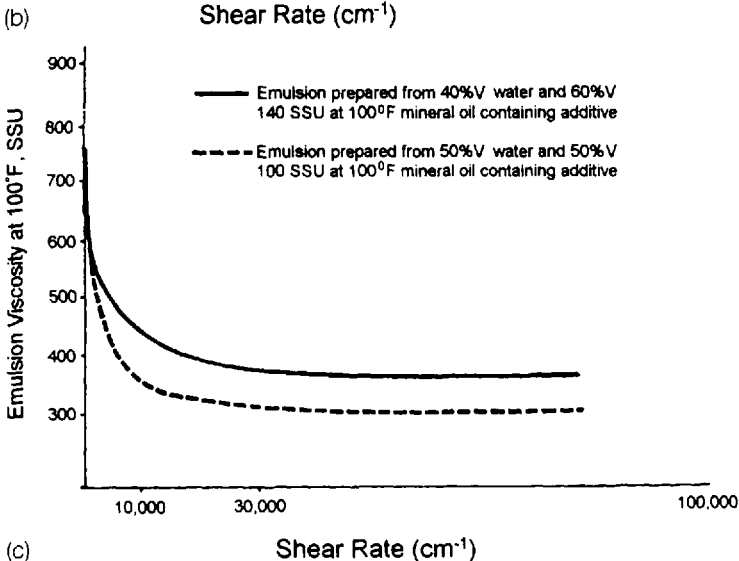
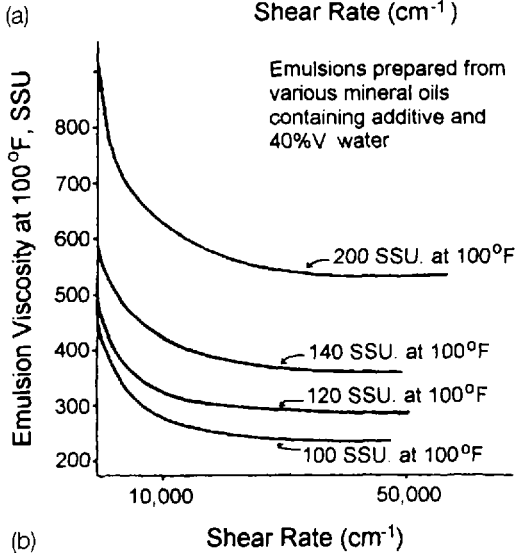
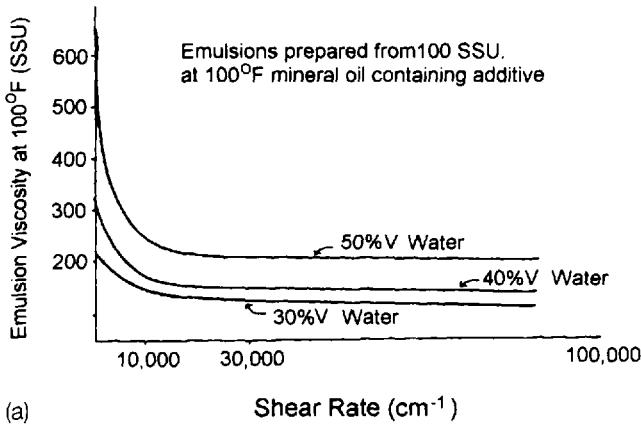


Figure 17.16 (a) Non-Newtonian (temporary) viscosity loss as a function of water content of a 100-SUS mineral oil containing an additive at 100°F. (b) Non-Newtonian behavior as a function of base-oil viscosity at 100°F. (c) Non-Newtonian viscosity properties as a function of base-oil viscosity at a constant initial viscosity.

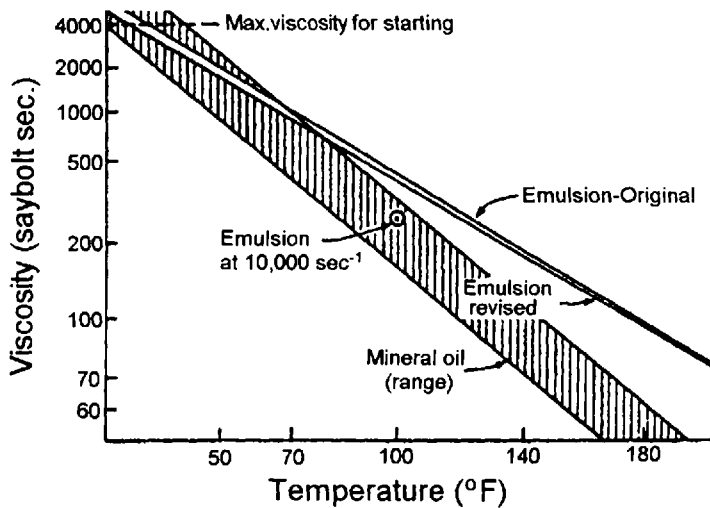


Figure 17.17 Effect of temperature on mineral oil and different emulsions at a low shear rate.

ular weight of the synthetic polymer thickener, thickener concentration, initial fluid viscosity, shear rate, and degree of associative thickening involved.

Viscosity–Temperature Behavior

Viscosity–temperature behavior is expressed numerically as the viscosity index (VI). The higher the value, the less the variation with respect to temperature. For example, a representative VI for petroleum oil is 95. A VI of 140 has been reported for an HFB fluid [38]. This means that the variation of viscosity is significantly less for an HFB fluid than for a petroleum oil, as illustrated in Fig. 17.17 [36].

Viscosity–temperature behavior is seldom reported for HFA fluids because of the already low initial viscosity. The variation in viscosity with temperature is small, as illustrated in Fig. 17.20 [39]. However, even a small viscosity change may be significantly important. A viscosity variation from 1.2 cSt at 20°C to 0.65 cSt at 50°C has been reported [40].

Figure 17.21 illustrates the discharge fluid low rate for an HFB fluid as a function of temperature [28]. This figure shows that the optimal fluid flow rate occurs between 125°F and 150°F. The fluid flow rate decreases at lower temperatures due

Table 17.12 Maximum Recommended Pump Inlet Vacuum

Pump type	Maximum intake vacuum (inches of mercury)
Vane	5
Gear	7
Piston	11

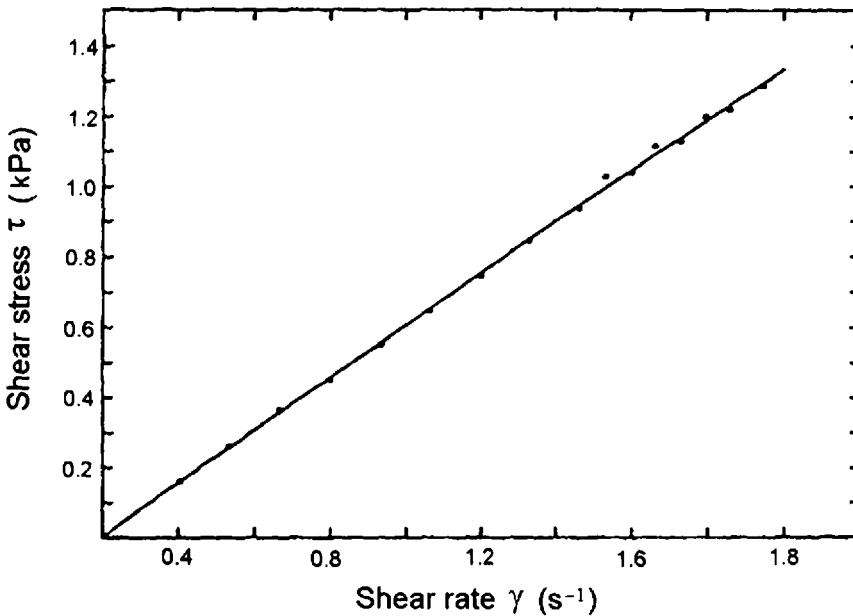


Figure 17.18 Shear stress as a function of shear rate for a water glycol at $n = 0.974$, $h_m = 22.8^\circ\text{C}$, where n is the power-law index and h_m is the measured temperature.

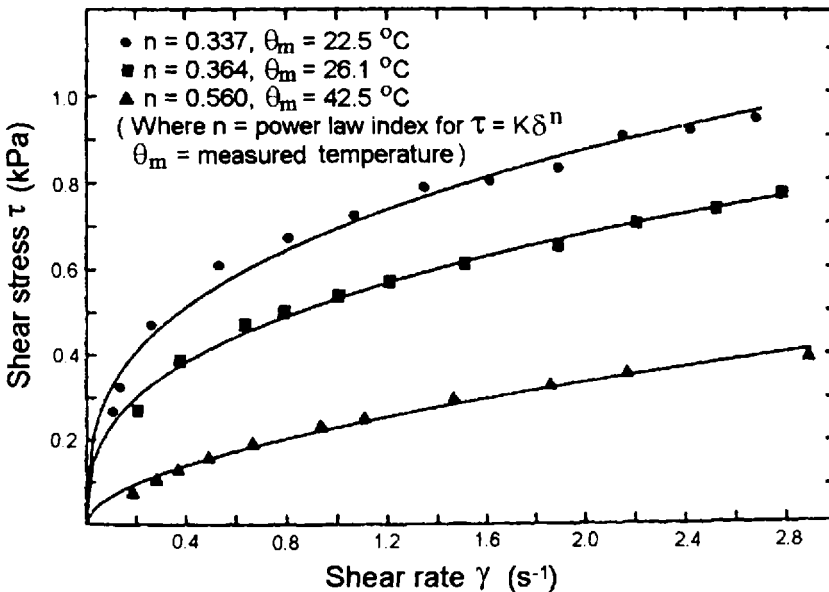


Figure 17.19 Shear stress as a function of shear rate for a HWBHF based on a water-soluble synthetic polymer.

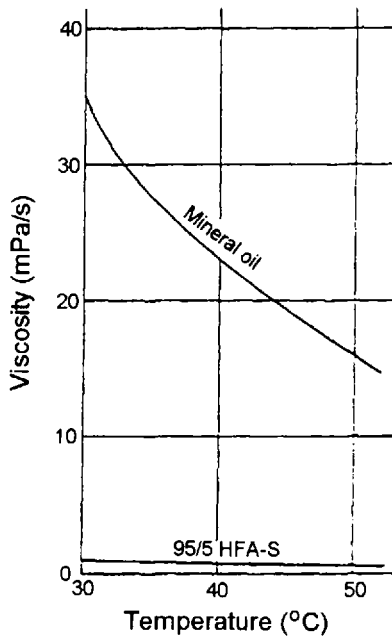


Figure 17.20 Viscosity–temperature relationship comparison of a mineral oil and an HFA hydraulic fluid.

to increasing viscosity with increasing temperature. Decreasing fluid flow rates at higher temperatures occur because of increasing leakage due to low viscosity. Most sources report 150°F as the maximum operating temperature for either HFA or HFB fluids because of greatly increasing vapor pressure and high evaporation rate [28,35,41,42]. The minimum recommended operating temperatures for these fluids are 5°C [41]. The optimal fluid temperature is 125°F [42].

Viscosity–Pressure Coefficients

The importance, calculation, and use of viscosity–pressure coefficients are described in detail in Chapter 2. The pressure–viscosity coefficients for a number of HFA fluids and an HFB fluid are provided in Table 17.13 [37,44]. The values for water and oil are provided for comparison. In general, the pressure–viscosity coefficients are dependent on the water concentration, and the values for HFA fluids are little different from water itself. Interestingly, the pressure–viscosity coefficient for the water-in-oil emulsion shown is nearly equal to the value determined for oil itself. These data suggest that the lubrication film-forming properties for the HFA fluids are very poor. However, at least within the recommended temperature range, the lubrication properties for the HFB fluid is similar to the oil from which it is formulated [43].

The viscosity–pressure coefficients are most important for the high contact pressures encountered with elasto-hydrodynamic lubrication (see Chapter 6). Although petroleum oils do exhibit some increase in viscosity at typical hydraulic system pressures (see Chapter 14), there is minimal, if any, fluid viscosity increase

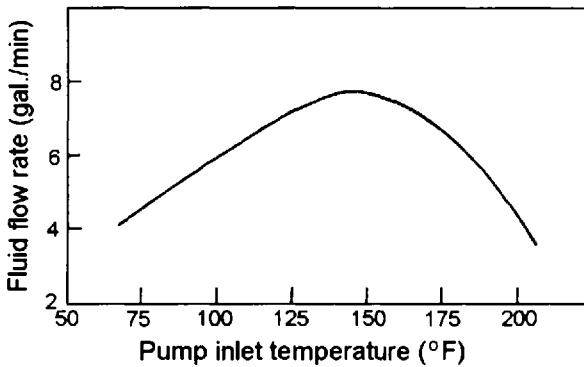


Figure 17.21 Effect of emulsion fluid temperature on the discharge flow rate for a hydraulic vane pump.

observed at most hydraulic system pressures with water-containing fluids [45,46]. This is illustrated for an HFA fluid in Fig. 17.22 [45].

Emulsion Thermal Stability

It is critically important that hydraulic fluid emulsions remain stable during use. There are various tests to evaluate emulsion thermal stability. One test is to store the emulsion at an elevated temperature (140°F) which serves as an accelerated test. The fluid being tested is observed for oil and/or water separation. This test was used to differentiate emulsion thermal stability of two fluid formulations after use (see Fig. 17.23) [36]. Interestingly, the used fluids exhibited better stability than the fresh fluid. The same accelerated test was performed on the two fluids illustrated in Fig. 17.23 without prior use. The results, shown in Fig. 17.24, illustrate the amount of improvement that can be achieved through fluid formulation [36].

Table 17.13 Viscosity–Pressure Coefficients for HFA and HFB Hydraulic Fluids*

Fluid classification	Note	Viscosity-pressure coefficient (α) $\text{mm}^2\text{N}^{-1}\text{b}$
Water	—	0.5×10^{-9}
HFA-E	Emulsion, 95% H ₂ O	1.39×10^{-9}
HFA-E	Microemulsion, 95% H ₂ O	1.87×10^{-9}
HFA-S	Synthetic polymer solution, 80% H ₂ O	3.23×10^{-9}
HFA-S	Synthetic polymer solution, 88% H ₂ O	2.62×10^{-9}
HFA-S	Synthetic polymer solution, 90% H ₂ O	7.5×10^{-9}
HFB	Water-in-oil, 40% H ₂ O	$20.7 \times 10^{-9\text{c,d}}$
	Mineral oil	$28, 26^{\text{e,f}} \times 10^{-9}$

*All values taken from Ref. 37 unless otherwise noted.

^bAll values determined at ~21–23°C unless otherwise noted.

^cValues were taken from Ref. 44.

^dThe α values were determined at 25°C.

^eThe α values were determined at 50°C.

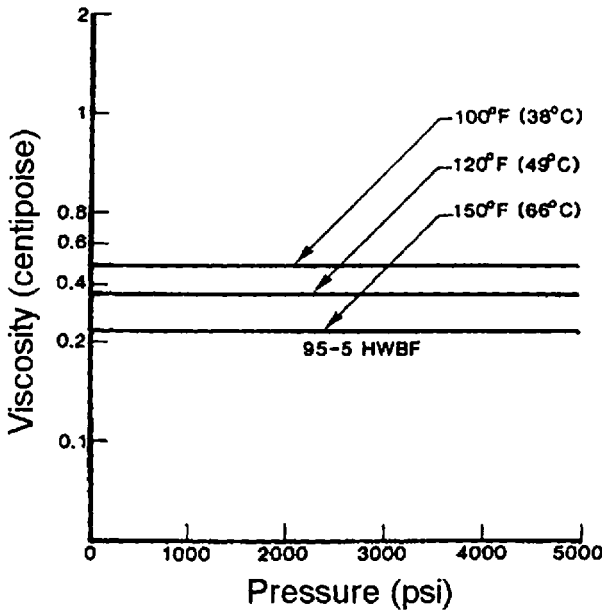


Figure 17.22 Viscosity-pressure relationship for a HWBHF at different temperatures.

Typically, the HFB hydraulic fluid emulsion is shipped to the user, where it is stored in drums until use. When stored, the fluid may encounter various (cold-hot) temperature cycles, which may affect the emulsion stability. This type of thermal stability is simulated by storing the fluid for a prescribed period of time at a cold (0°F) and hot (150°F) temperature. The results of such a test on three different emulsion formulations are illustrated in Fig. 17.13 [28].

Other tests that have been used to evaluate emulsion thermal stability include storage for specified periods of time at different temperatures [9,28,47], three cycles

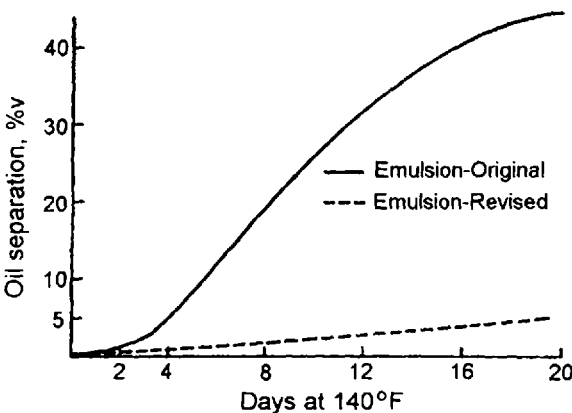


Figure 17.23 Effect of emulsion formulation on aging stability in use.

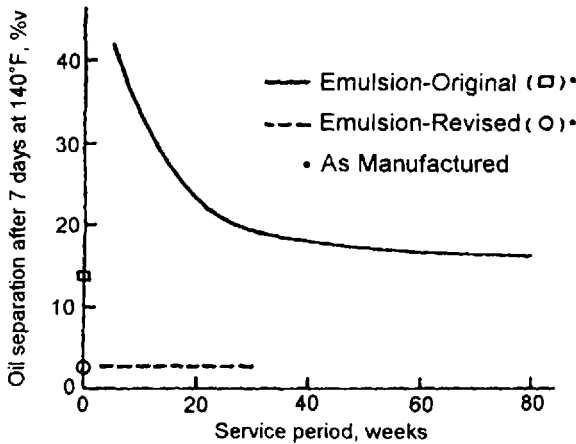


Figure 17.24 Effect of emulsion stability of fresh, as-manufactured emulsion fluids.

of freezing for 2 h then heating to 100°C [47], centrifuging [47], and attempted breaking of the emulsion after heating and remixing [47].

Foaming and Air Entrainment

Two important properties for any hydraulic fluid are low foaming and minimal air entrainment. This subject is discussed extensively in Chapter 4, including mechanisms of foaming and air entrainment, impact on fluid compressibility, and various testing procedures. Therefore, foaming and air entrainment will not be discussed in detail here, other than to discuss two generally applicable test procedures.

Although there are various tests that can be used to determine the propensity of a fluid to exhibit foaming problems in use, usually ASTM D 892 [48] or an equivalent is the test most often cited [49]. This test, which is described in detail in Chapter 4, involves bubbling air into the fluid through an air stone at a prescribed pressure and for a specific time. The amount of foam and the stability is determined.

Equally important is the evaluation of air entrainment of a hydraulic fluid. The relative amount of formation of entrained air and the failure to dissipate it leads to a number of very significant deleterious processes, such as accelerated fluid oxidation (see Chapter 14) and cavitation (see Chapters 4 and 14). Currently, the most commonly accepted test to measure air entrainment is ASTM D 3427 [50] or its equivalent [49]. This test, which is described in detail in Chapter 4, involves blowing compressed gas through the hydraulic fluid at a specified temperature, typically 25°C, 50°C, or 75°C. After the gas flow is stopped, the time required for the bubbly fluid to decrease in 0.2% volume is determined.

2.6 Chemical Properties

2.6.1 Oxidative Stability

Various tests may be used to evaluate oxidative stability of emulsion hydraulic fluids. One test, a modified ASTM D 943 Turbine Oil Stability Test (TOST), has been used to evaluate oxidative stability [51]. (This is modified by eliminating the water addition step [36].) Test results comparing two emulsion formulations (shown in Table

Table 17.14 Oxidative Stability of Emulsion Hydrolic Fluids

Fluid	Time to develop acidity of 2.0 mg KOH/g (hr)		
	1	2	Average
No. 1	450	380	415
No. 2	1010	1050	1030

Note: This test was conducted by a modified ASTM D 943 (TOST), omitting the addition of water.

17.14) illustrate that a fluid lifetime of greater than 1000 h would be expected for a well-formulated HFB fluid [36].

Another test that has been reported is the “Work Factor Test,” which is Method 345 of the Federal Specification VV-L-791, where the fluid is used to lubricate a 6-in. babbitt bearing loaded at 150 psi and rotating at 3000 rpm for 1175 h. A 4-gal reservoir is used, with the fluid maintained at 140–150°F. Water, lost by evaporation, was replaced every 4 h. Well-formulated HFB fluids should exhibit no apparent increase in acidity by this test.

2.6.2 Corrosion

There are various tests that have been used to evaluate the corrosion-inhibiting properties of HFA and HFB fluids toward ferrous and nonferrous metals. The more commonly encountered tests will be discussed in this section.

ASTM D 665 (No Added Water)—Ferrous Metals

ASTM D 665 (see Chapter 14) is modified for use with water-containing fluids by eliminating the water-addition step of the testing protocol [19,26,32,47,52,53]. This test involves immersing a cylindrical steel test specimen into 300 mL of stirred fluid (a dynamic test) at 60°C (140°F) for 24 h. The steel test specimen is inspected for the presence of rust. Modifications of this test include no stirring (a static test [19]), using a slightly higher temperature (65°C, 150) [19,26], longer immersion times (48 h [47], 7 days [26], and 1 month [19]), and partial immersion of the test specimen in order to obtain some measure of vapor-phase corrosion-inhibition properties [26,47].

Nonferrous Metals

Inhibition toward nonferrous metals, including aluminum, brass, copper, and silver, may be determined by partially immersing standard test coupons of the desired metal into the fluid contained in a beaker, as shown in Fig. 17.25 [49], or a sealed flask, as shown in Fig. 17.26 [49], without stirring, at 65°C for a period of time, typically 7 days [19,26,49]. Changes in weight of the test specimen and changes in surface condition and color of the fluid are recorded and classified as follows [49]:

0 = No effect

1 = Slight color change or oxidation of less than 20% of the surface

2 = Strong color change

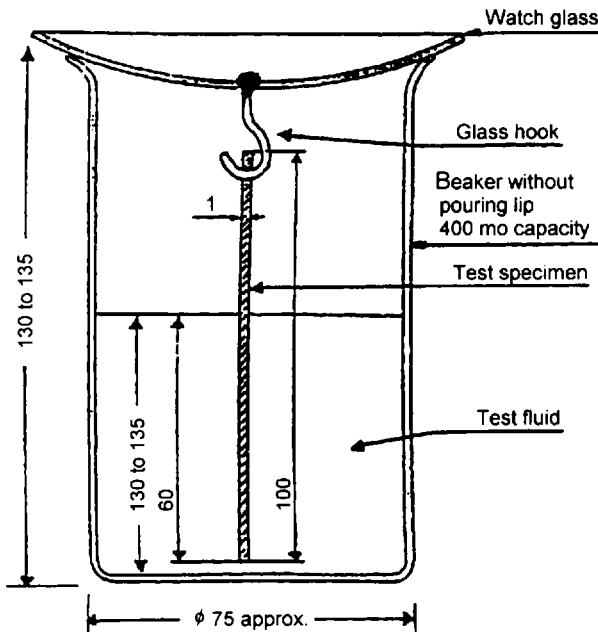


Figure 17.25 Illustration of a test apparatus for performing corrosion tests on metal test coupons.

- 3 = Deposits or oxidation of more than 20% of the surface
- 4 = Corrosion or pitting
- 5 = Other effects to be specified

Multimetal Testing

Another variation of the Nonferrous Metals Test (see previous subsection) is to immerse metal pairs, as illustrated in Fig. 17.27a. The metal pairs that are tested include the following [49,53]:

1. Steel and zinc
2. Copper and zinc
3. Aluminum and zinc
4. Steel and aluminum

The metals are mounted as illustrated in Fig. 17.27b with 1-mm plastic spacers between them. In this test, the metals are immersed into the fluid without stirring for 28 days at 35°C. At the conclusion of the test, the weight loss of the test specimens is determined and changes in surface condition and color of the fluid is recorded and classified as described in Section 2.6.2.3.

2.7 Material Compatibility

Proper material choice is critical if optimal equipment failures are to be avoided and if optimal lifetimes are to be achieved. In this section, material compatibility, including paint, metal, elastomer, and filter compatibility will be discussed. This discussion will be based on the information provided in Table 17.15 [54].

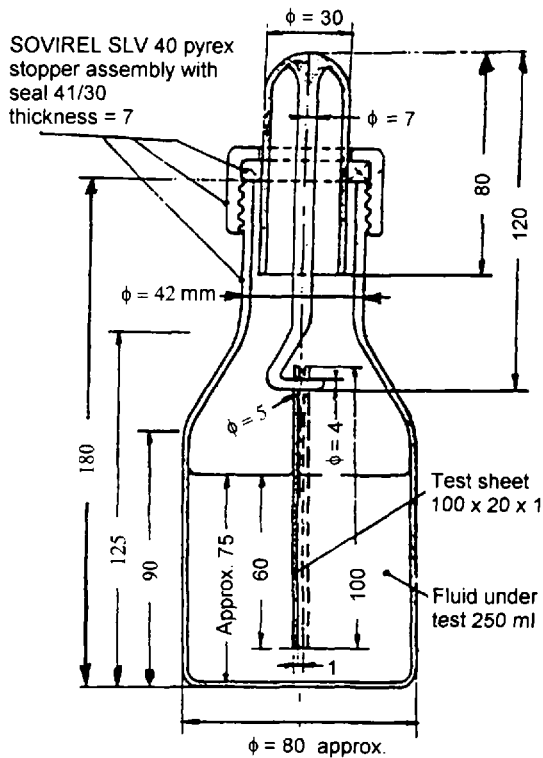


Figure 17.26 Pressure bottle assembly for corrosion tests of metal coupons.

2.7.1 Paint Compatibility

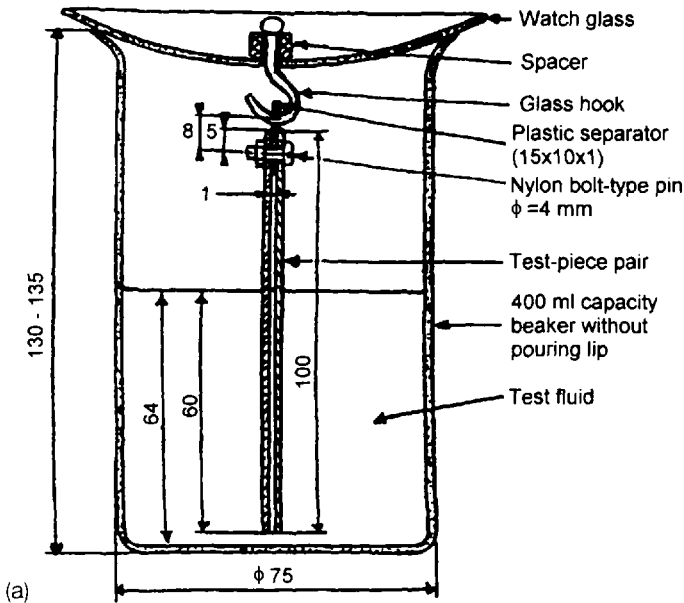
Epoxy and phenolic paints are generally suitable for emulsion hydraulic fluids [54]. However, it is prudent to verify compatibility either by testing or by contacting the paint manufacturer before painting hydraulic equipment and especially before painting the inside of a fluid reservoir.

2.7.2 Metal Compatibility

Emulsion hydraulic fluids are generally compatible with all metals except for lead and magnesium, as shown in Table 17.15.

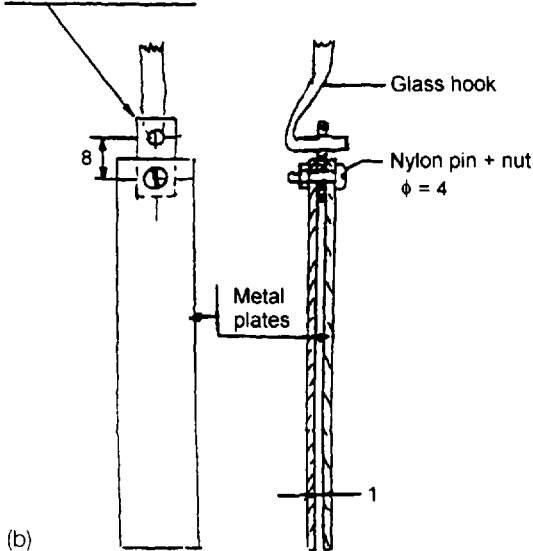
2.7.3 Plastic and Elastomer Compatibility

Table 17.15 shows that emulsion hydraulic fluids are generally compatible with most common plastics and with the BUNA-N seals typically used with mineral oil [54]. However, the designer/user is cautioned to confirm elastomer compatibility by testing (see Chapter 9) or with the seal supplier because results may vary with the elastomer supplier. For example, one source found that BUNA-N seals swelled approximately 9.6%, whereas Viton only swelled 0.7% [26]. However, another report stated that BUNA-N swelled less than 1% and the Viton seal material evaluated was not gen-



(a)

Plastic space (nylon)
20x20x1



(b)

Figure 17.27 (a) Test assembly for evaluating corrosion properties of different metal pairs. (b) Metal coupon holder assembly for testing of metal pairs.

erally compatible with emulsion hydraulic fluids [55]. Unfortunately, such compatibility variations among seal suppliers for the same nominal fluid composition is not uncommon.

As with other water-containing fluids, cork and leather should not be used as seal materials for either HFA or HFB fluids [56].

Table 17.15 Material Compatibility of Fire-Resistant Hydraulic Fluids

Material		Water-glycol	Phosphate ester	Emulsion
Paint	general industry	not suitable	not suitable	not suitable
	epoxy and phenol	suitable	suitable	suitable
Metal	steel	suitable	suitable	suitable
	bronze	low suitability	suitable	suitable
	zinc	not suitable	suitable	suitable
	cadmium	not suitable	suitable	suitable
	lead	not suitable	suitable	not suitable
	copper	suitable	suitable	suitable
	aluminum	not suitable	suitable	suitable
	anodized aluminum	suitable	suitable	suitable
Plastic	magnesium	not suitable	suitable	not suitable
	poly(methyl methacrylate)	suitable	not suitable	suitable
	poly(propylene)	suitable	not suitable	suitable
	poly(styrene)	suitable	not suitable	suitable
	epoxy	suitable	suitable	suitable
Rubber	nylon	suitable	suitable	suitable
	polychloroprene	suitable	not suitable	suitable
	butylene nitrile rubber	suitable	not suitable	suitable
	poly(butylene)	suitable	suitable	not suitable
	ethylene propylene rubber	suitable	suitable	not suitable
	polyamine ester	not suitable	low suitability	not suitable
	silicon rubber	suitable	suitable	suitable
	ethylene polytetrafluoride	suitable	suitable	suitable
Filtering medium	fluorine rubber	suitable	suitable	suitable
	celluloid (treated by phenol)	suitable	suitable	suitable

Elastomer Compatibility Testing

Seal compatibility testing strategies are provided in Chapter 9. In this chapter, some commonly encountered testing procedures will be briefly discussed.

STATIC TESTS. Static seal testing for hydraulic fluid compatibility typically involves immersion of the material of interest in a flask or bottle at 65°C [26] or 70°C [31] for extended periods of time (1–6 weeks). Dimensional change such as volume swell and changes in length are typically measured relative to the initial size of the test specimen. Test specimens vary widely from the actual seal, O-ring, or small (50 mm × 25 mm) rectangular pieces cut from a sheet of the elastomer [32].

The European standard for determination of seal compatibility with water-containing fire-resistant hydraulic fluids utilizes test specimens of uniform thickness (2 mm) that may be rectangular (50 × 235 mm) or circular (36 mm in diameter) [49]. The test materials vary with the fluid of interest and are summarized in Table 17.16 [49]. The test specimens are immersed in a sealed glass jar for 168 h at the specified test temperature provided in Table 17.16. The percentage change in volume is measured at the conclusion of the test by [49]

Table 17.16 Standard Elastomers and Test Conditions

Type of fluid	Suitable test elastomers	Test temperature (°C, ±2°C)	Test duration (± 2 h)
HFA	NBR 1*** EPDM FPM 1	60	168*
HFB	NBR 1*** FPM 1	60	168*
HFC	NBR 1 EPDM FPM 1	60	168*
HFDR	NBR 1*** FPM 1***	100	168
HFDS	FPM 1	100	168

*The test duration is 168 h, but equilibrium may be achieved in these fluids.

**FPM 1 is not suitable for use with alkyl phosphate esters.

***High swelling rates (>25%) have been observed for these combinations of materials and fluids.

$$\Delta V = \frac{(m_3 - m_4) - (m_1 - m_2)}{m_1 - m_2} \times 100 \quad (17.15)$$

where

m_1 = the initial mass of the elastomer test specimen in air

m_2 = the apparent mass of the elastomer test specimen in water

m_3 = the mass of the elastomer test specimen in air after the test is completed

m_4 = the apparent mass of the elastomer test specimen in water after the test is completed

The change in hardness is also determined according to ISO 48 [57] on the test specimens and calculated by [49]

$$\Delta H = H_2 - H_1 \quad (17.16)$$

where

H_1 = the measured hardness of the test specimen before testing

H_2 = the measured hardness of the test specimen after testing

A seal material is compatible if the following are true:

- The volume increase is less than 7% and if there is no volume contraction.
- The hardness does not increase more than 2 IRH degrees or fall by more than 7 IRH degrees with respect to the initial hardness.

COMPRESSION TESTS. Compression tests are also often used to determine the ability of the elastomer to recover to its initial dimension before the compression test. Compression set values of 50–120% are considered satisfactory [26].

LIP-SEAL TESTS. A significant problem with water-containing fluids such as hydraulic emulsions is lip-seal failure [26]. Schmiede et al. devised the test rig illustrated in Fig. 17.28 to evaluate lip-seal fluid compatibility in use. This device is

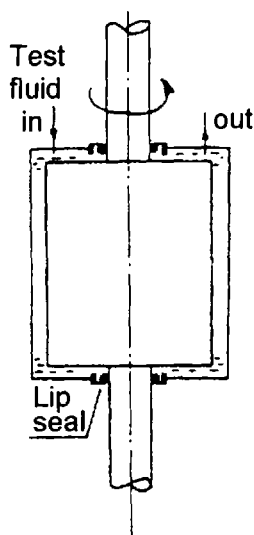


Figure 17.28 Lip-seal test rig.

a hollow vessel with a hardened, ground steel shaft supported and sealed at each end by neoprene lip seals. The device rotates at 1450 rpm and the test fluid is circulated as shown under 103 kPa (15 psi) pressure. Internal friction typically causes the fluid temperature to rise to 35°C. The test can be conducted for 1000 h without gross leakage.

2.7.4 Strainers, Filters, and Screens

Cellulosic or untreated paper filters should not be used with water-containing fluids [56,59]. However, treated cellulosic filters are reported to be suitable [54]. Filter sizes as low as 5–10 μm have been reported to be suitable for W/O emulsions [56,60]. Filter sizes as low as 3 μm have been reported for microemulsions [60].

Fine filtration should only be placed at the pressure or return side of the pump. On the suction side of the pump, only screens or filters large enough not to restrict flow should be used. Filters or strainers constructed with zinc or cadmium should only be used with fluid manufacturers approval [59].

The use of Fuller's earth (activated clay) or similar adsorbant filters should not be used because of the potential for additive removal by preferential adsorption [59].

Filtration may also be performed as a side stream. For example, a separate filter loop was installed on top of the reservoir, which was independent of the main circulation system of the hydraulic circuit [60]. This system was used when the system was down for significant periods of time.

2.8 Fluid Maintenance

It is recommended that HFA fluids be checked weekly for acidity and viscosity. Caution should be taken to prevent contamination by salt. Preferably, distilled or

deionized water should be used for makeup [54]. The use of tap water will lead to hard metal contamination and reduced emulsion stability. HFA fluids are susceptible to biological attack and should be checked periodically.

HFB fluids, as with their HFA counterparts, may lose water by evaporation. Therefore, water content must be monitored and maintained in order to maintain fire resistance. Invert emulsion (HFB) fluids should be monitored for water content (see the following subsection), viscosity, pH, particle count, and emulsion stability [54]. It is recommended that these analyses be performed biweekly [60].

Tramp oil, a common contaminant, will simply dissolve in the oil phase of the invert emulsion, generally not causing any significant effect on pump performance [61].

2.8.1 Water Analysis

Water content may be determined by distillation according to ASTM D 95 [62] after correction for the concentration of glycol, if present, which will codistill with water. The correction procedure is described in Ref. 49. Alternatively, water content may be determined by Karl Fisher analysis according to ASTM D 1744 [49,63].

Water content may be also readily determined in the plant or mine by mixing the fluid 1:1 by volume with water. A reagent is then added to assist in breaking the emulsion. The mixture is centrifuged until the water and oil separation is complete. The water content is determined by measuring the relative amount of water separated.

Another recently reported test is to use the water-analysis apparatus illustrated in Fig. 17.29 [35]. The fluid is accurately injected into the apparatus which is instrumented to measure the small, but quantitative, temperature rise which occurs when water is adsorbed by the zeolite. An added advantage of this method is that it is not affected by the presence of glycols which may be added to the fluid as a freeze point protectant. (This instrument is also reported to be applicable for use with HFC fluids [35].)

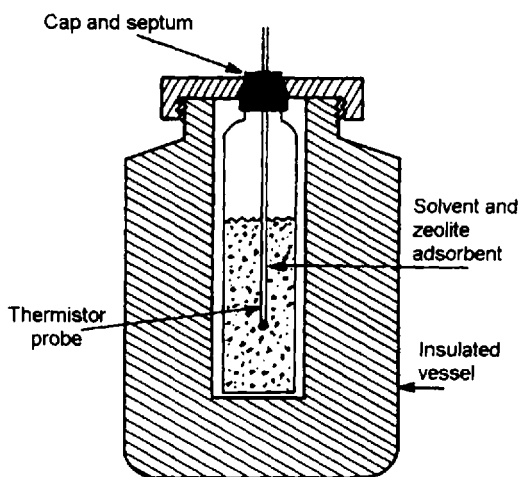


Figure 17.29 Mobil water-analysis apparatus.

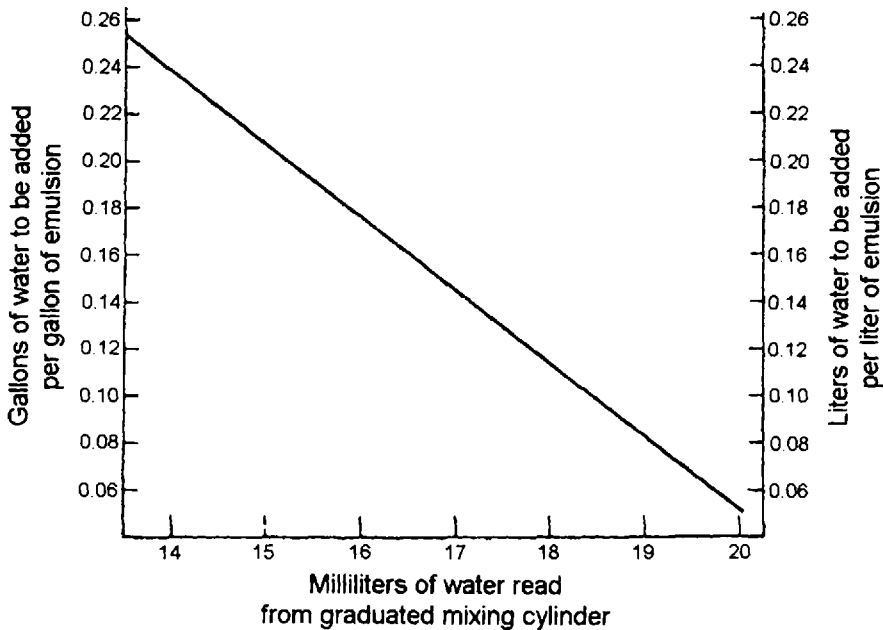


Figure 17.30 Example of a water makeup chart for a W/O emulsion.

After the water level is determined, a chart such as that shown in Fig. 17.30 is used to determine the amount of water that must be added to the system to maintain fire resistance. *Note:* The water reading chart shown in Fig. 17.30 is for illustrative purposes only and will vary with the manufacturer. Consult the fluid manufacturer for the correct chart for the fluid being used.

2.8.2 Viscosity

Kinematic fluid viscosity is determined by ASTM D 446 [64]. See Chapter 10 for details.

2.8.3 pH

The pH of a fluid is easily measured quickly and accurately with inexpensive commercially available meters by simply dipping the probe into the fluid and reading the pH value from the analog or digital output. However, these devices must be periodically calibrated according to the manufacturer's instructions.

2.8.4 Fluid Cleanliness

There are numerous excellent methods of measuring the particle count of hydraulic fluids. Particle count analysis is discussed in Chapter 3. However, in many cases, a simple "patch test" is used to quantify the presence of particulates in the fluid. For HFA and HFB fluids, the analysis may be done according to ASTM F 311 [65] or ASTM 312 [66]. For both methods, 100 mL of the fluid is drawn through a membrane filter under vacuum. The collected particles are counted and measured under a microscope [60]. Alternatively, a Millipore patch test may be used [35].

2.8.5 Emulsion Stability

Emulsion stability with respect to water hardness was discussed in a subsection of Section 2.5.1 and emulsion thermal stability was discussed in a subsection Section 2.5.2. In addition to these tests, a quick test that may be readily used in the plant is to evaluate emulsion stability. This test involves pouring drops of an emulsion into a beaker of water. A stable emulsion will form "beads" as it drops into the water and then rises to the surface. These beads will exhibit a strong tendency to resist breakage. However, if the emulsion is unstable, the drops will spread throughout the water, forming a milky white appearance. This is a pass/fail test [60].

2.8.6 Biological Stability: Biodegradation Versus Biodeterioration

Biodegradation has been defined as "the process by which a potential pollutant, such as a petroleum product, is converted by biological (usually microbiological) agents into simple, environmentally acceptable, derivatives [67]. *Biodeterioration* has been defined as the "loss of product quality or performance and could be regarded as the initial stages of biodegradation, but in the wrong place at the wrong time; that is when the petroleum product is stored or in use" [67]. Biodegradation processes are discussed in Chapter 8. Biodeterioration processes and their prevention will be discussed in this section.

Fluid Biodeterioration Processes

Emulsion biodeterioration is a water-dependent process as illustrated in Table 17.17, where the relationship between relative humidity and microbial susceptibility is shown [67]. The biodeterioration process, illustrated in Fig. 17.31 [68], involves the reaction of water with a substrate such as oil or the emulsifier in the presence of bacteria or fungi to yield a product designated as a "biomass." If this degradation process is not inhibited, enormous quantities of biomass may be present in the system

Table 17.17 Approximate Ranges of Water Activity (Relative Humidity) and Microbial Growth

Micro-organisms	Range of water activity of tolerated	
	Lower	Upper
Spoilage bacteria	0.92	0.99
Yeasts	0.86	0.98
Osmophilic yeasts	0.61	0.87
Molds	0.61	0.098
Metal working fluid examples tested		
Concentrates	0.69	0.98
Diluted fluid	0.98	0.99

Note: Reducing water activity within the range causes a decrease in growth rate, a delay in growth initiation, and a population decrease in size of final population.

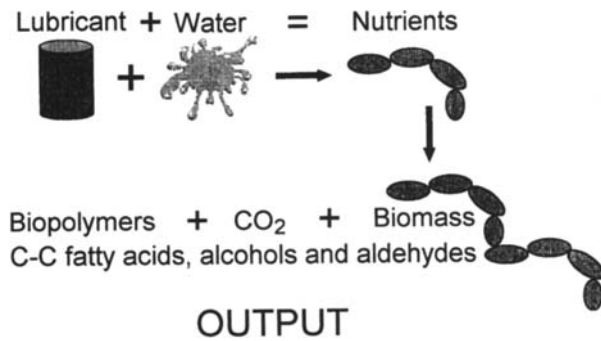


Figure 17.31 Bioconversion of lubricant components into biomass, carbon dioxide, low-molecular-weight (odorous) organic molecules, and biopolymers (slime).

in the form of sludge [69] or “microbial scums” which are composed of dead cells, gelatinous slimes, and fungal threads [30]. It has been reported that a bacterial cell may double in size and divide into two new cells every 15 min until a limiting condition is encountered [69].

In addition to solid by-products, obnoxious gases may be formed from the biodeterioration of certain additives acting as microbial nutrients such as nitrites and nitrates which are converted to ammonia and sulfur or sulfate which is converted to hydrogen sulfide (H₂S), which exhibits a characteristic “rotten egg” odor [70].

Biodeterioration processes that occur in the presence of air (oxygen) are enhanced by system agitation and are designated as “aerobic” processes. However, biodeterioration processes may also occur without air (oxygen) being present. These are called anaerobic processes, which are inhibited by system agitation [70].

In summary, the biodeterioration process leads to the following [70]:

- Progressive stepwise oxidation of the hydrocarbon and continuous reduction of pH as shown in Fig. 17.32 [69].

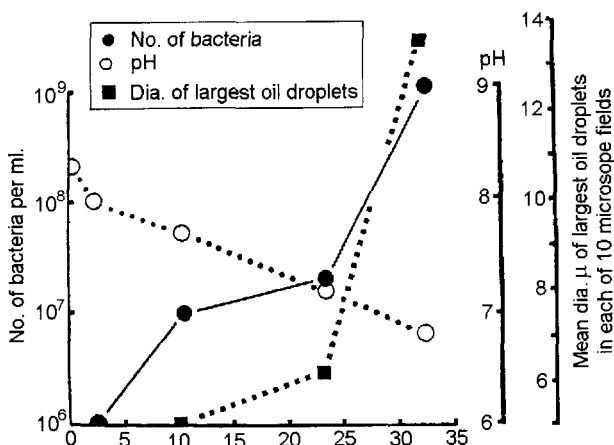


Figure 17.32 Bacterial degradation and related changes in pH and emulsion distribution.

- Saturation of unsaturated bonds.
- Degradation of lubrication-enhancing additives and corrosion inhibitors, causing greater wear and surface rusting of hydraulic system components.
- Emulsifier degradation leading to an increase in the size of the dispersed oil droplets as shown in Figs. 17.32 and 17.33 and ultimately to emulsion breakage with free oil separation [69]. Interestingly, even a doubling of droplet diameter through the degradation process will cause an eight-fold decrease in the number of droplets [69]. Therefore, it is possible to monitor the average diameter of the largest droplets as a means of predicting emulsion failure. However, this is dependent on the particular emulsion being used [69].
- Accumulation of slimes, sludges, overloading of filters, and centrifuges.
- Unpleasant odors and fluid and surface discoloration [71].

Monitoring Procedures

Any effort to control biological attack, whether bacterial or fungal, on an emulsion hydraulic fluid is necessarily dependent on adequate procedures for detecting, identifying, and quantifying the microbial species present. It is not sufficient to simply wait until slime or sludge formation is visible or noxious vapors are present. By this time, it may be too late to apply preventative or corrective procedures [68].

There are four strategies for monitoring microbial contamination: (1) gross, (2) physical, (3) chemical, and (4) microbiological [68]. Gross detection procedures include visual observation of slimes or the detection of foul odors. Physical detection procedures include the observation of haze and visible, nonmetallic particulate matter in the fluid. Chemical tests that are often used include pH, alkalinity, and corrosivity. For example, if the alkalinity of a used fluid has dropped >25%, there is a strong potential that the cause is microbial contamination.

The fourth procedure is to conduct a microbiological test. One test is to directly observe the microbial species on a glass slide under a microscope [68,69]. However, this is not a practical test, especially for industrial use.

An older test that has been successfully applied for monitoring microbial contamination of hydraulic fluids is the "Red Spot Test" [70,72,73]. This test is conducted by taking a drop of fluid using a standard wire loop placed in a nutrient medium containing tri-phenyl tetrazolium chloride. After incubation at 37°C overnight, the initially colorless droplet is reduced by the bacteria to provide a red color. The intensity of the red color is proportional to the number of organisms present. However, this test is only applicable for aerobic organisms [73].

Currently, there are three bench test procedures that may be used for monitoring resistance to microbial growth: ASTM D 3946 [74], ASTM E 686 [75], and ASTM E 979 [76]. Alternatively, a commercial dip-slide test that is coated with a microbial growth media is used. This is called a "viable titer method," in which the population densities of the microbial species are estimated after incubation for 24–72 h, as illustrated in Fig. 17.34. Viable titer procedures may not detect microbial species that do not form colonies and, therefore, may not correlate with biodeterioration processes.

There are a number of simple tests that are being developed to provide rapid and accurate bioassays of industrial fluids. These include the catalase test [68,77]

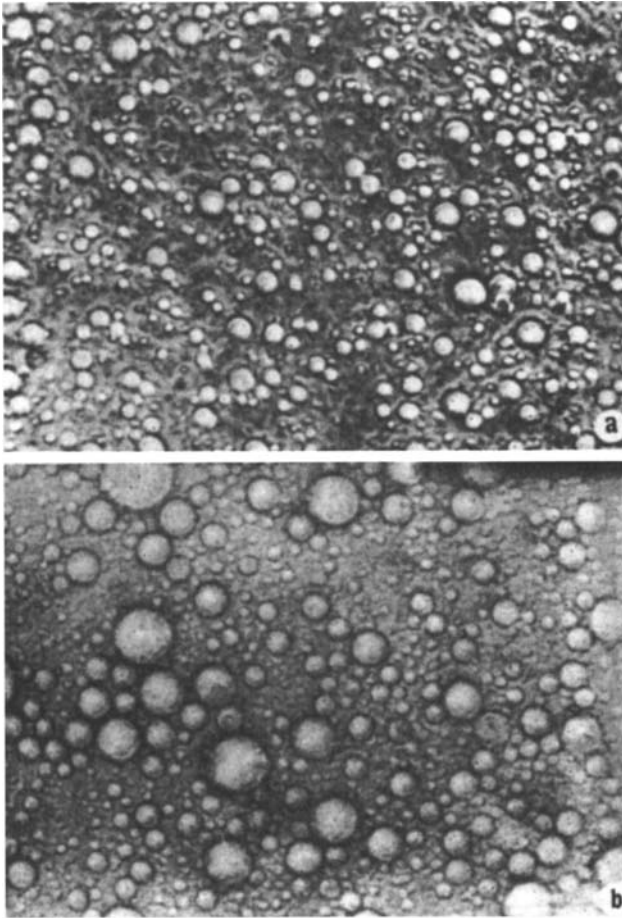


Figure 17.33 (a) Oil emulsion before biological attack. (b) Oil emulsion during attack but before complete failure has occurred. (Both photomicrographs taken at same scale.)

and the lipopolysaccharide assay [68,78]. It is beyond the scope of this text to describe the details of these test procedures.

Microbial Control Strategies

There are four strategies to provide microbial control in emulsion hydraulic fluids. These include (1) use of fluid components resistant to biological growth, (2) microbial removal or kill procedures, (3) use of biocides/biostats, and (4) shock treatments.

MICROBIAL GROWTH-RESISTANT FLUID COMPONENTS. Conversely, chemicals that undergo microbial attack easily are called “biologically soft.” Many emulsifiers are biologically soft, as are many paraffinic components of petroleum oil in the presence of sufficient amounts of water. Chemicals that are resistant to biological attack are called “biologically hard” [67]. Some components in an emulsion, such as a glycol, which may be present to provide freeze point protection, may provide resistance to biological attack [67]. In some cases, if structurally similar biologically

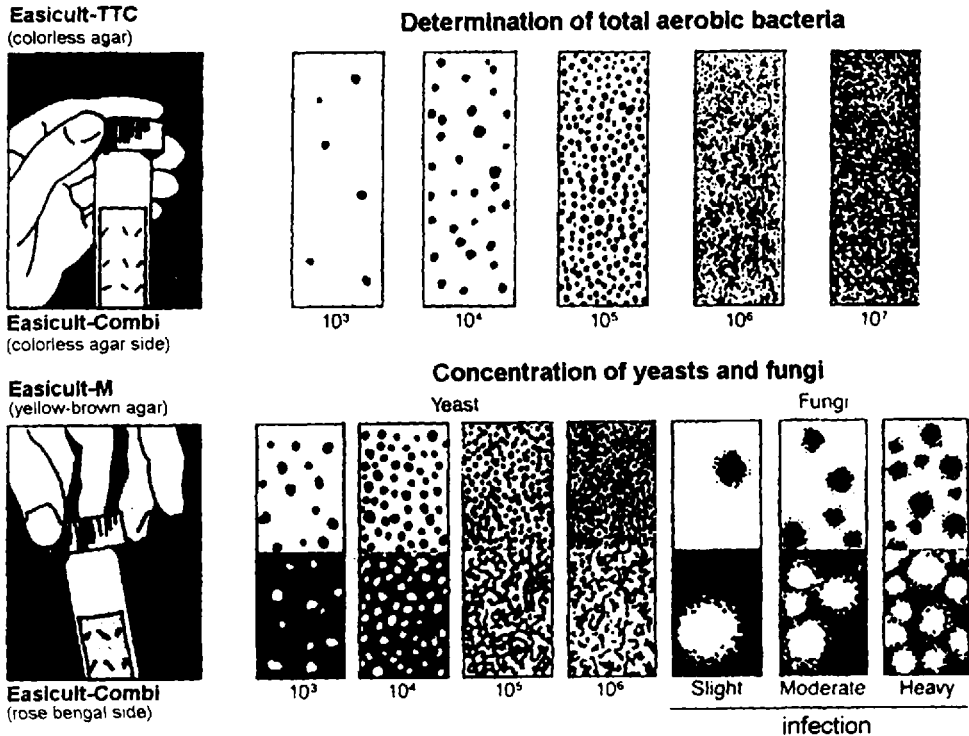


Figure 17.34 Dipstick test for bacteria and fungi detection.

hard and biologically soft components are mixed, the mixture is biodegradable by a co-oxidation process.

One emulsion formulation strategy is to use components that are biologically hard initially, especially emulsifiers [69], but become biologically soft during use or if mixed with the appropriate component to render them biologically soft after use. In addition, optimal quantities of nitrogen-, sulfur-, and phosphorus-containing additives should be used to provide satisfactory lubricity properties and corrosion inhibition while minimizing potential for biological attack [69].

MICROBIAL REMOVAL OR KILL PROCEDURES. There are a number of physical practices (filtration, heat, centrifugation) that may be used that will significantly aid in the control of biological growth, including the following [69]:

1. Elimination of contaminated fluid from the system before recharging. The amount of contaminated residual fluid and the level of contamination will determine the lifetime of the new system. Ideally, the system will be sterilized before the new charge of fluid is added [67,69].
2. Maintain as high a fluid temperature as possible while still maintaining emulsion compatibility.
3. Avoid pockets of stagnation in pipes and tanks, especially for systems susceptible to anaerobic degradation.
4. Frequent cleaning and sterilization of cooling towers.
5. Use of microbe-free fluids.

There is a theoretical relationship between kill or removal and biological growth rate. For net reduction in microbial species [7],

$$\mu < AB \quad (17.17)$$

where

μ = the specific microbial growth rate (0.693/doubling time)

A = fractional flow through the device (flow rate/volume)

B = fractional kill (removal) in the device (microbial numbers – inflow – outflow/inflow)

USE OF BIOCIDES. A *biocide* is a chemical that is used to kill biological organisms. A *biostat* may also be used; characteristically, it is less chemically reactive than a biocide and functions to prevent reproduction of biological organisms [71].

There are currently approximately 30 Environmental Protection Agency (EPA)-registered active ingredients for biocide use in lubricant applications [68]. These may be classified as (1) target microorganisms or (2) active ingredient chemistry. Targeted microorganisms include the following [68]:

- Bactericides—target bacteria and are generally ineffective against fungi
- Fungicides—target fungi (yeasts and molds) and are not very effective against bacteria
- Microbiocides—“broad spectrum” which kill both bacteria and fungi

Chemical classification is based on chemical structure (alkanes, heterocyclic, phenolic, and so forth) and is much more complicated. Because chemical classification may be confusing, it will not be discussed further here.

SHOCK TREATMENTS. One effective method of delaying the onset of biodegradation problems is to clean the system with very high concentrations (much higher concentration than typically used for preservation) of a fast-acting, broad-spectrum biocide [67]. In view of the high biocide concentrations used, health, safety, and disposal problems must be carefully considered.

A second method that may be used to perform periodically is to dose the system with very high biocide concentrations, also known as a shock treatment. Although this procedure may allow some degradation to occur, shock treatment would be used within a sufficiently short period of time to minimize any such occurrences [67].

2.9 Fire Resistance

HFB fluids are one of the most commonly used fire-resistant fluids for underground mining use [79]. HFB fluids are classified as fire resistant because of their flammability properties relative to oil. Although HFB fluids burn, they burn with smaller flames than mineral oils [35]. Spray flammability tests have shown that the spray flammability of HFB fluids occurs with long intermittent bursts [80]. Flammability in the hot-channel flammability test (see Chapter 7) exhibits a delayed ignition, then burns continuously [80].

The results of these tests showed that there is a measure of improvement in fire resistance relative to mineral oil, but they are significantly poorer than other fluids of this class. This is illustrated by comparing the “escape time” of different fire-resistant fluids. “Escape time” is defined as “the elapsed time between initial

Table 17.18 Escape Time at 1400°F
Comparison of Various Fire-Resistant Fluids

Fluid type	Typical escape times (s)
Petroleum oil	None—instant ignition
Polyol ester	2
Invert emulsion	16
Water-glycol	45
Phosphate ester	No ignition

Note: Test conducted by pouring 100 mL of fluid onto molten metal up to 1400°F.

fluid–heat contact and ignition” [80]. The escape time data for the various fire-resistant fluids shown in Table 17.18 show that although the HFB fluid evaluated was better than mineral oil, it was substantially poorer than the water–glycol and phosphate ester. It should be noted that the polyol ester evaluated was little different than petroleum oil in this test. Also, although the phosphate ester did not burn, white smoke was formed [80].

Based on similar test results, Loudon has ranked the fire resistant offered by different fluids as water–glycol > phosphate ester > invert emulsion > polyol esters > petroleum oil [81].

The fire resistance of HFB fluids (invert emulsions) is proportional to the water content of the fluid, as shown in Fig. 17.35 [4]. The water content must be maintained between 35% and 40% to maintain fire-resistance properties. If the water content is less than 35%, the fire-resistance properties are lost [4]. Law has graphically illustrated the optimization of an HFB fluid formulation with respect to base-oil viscosity, water content for fire resistance, and optimal physical properties (Fig. 17.36 [35]).

2.10 Lubrication Properties

2.10.1 Fluid Lubrication

One of the most critical functions of a hydraulic fluid, in addition to power transmission, is fluid lubrication. Some of the contacts that require lubrication include the vane and ring for vane pumps, piston slipper pads, and the brush plate for piston pumps, the gears of a gear pump, and bearing lubrication in all pumps. Invert emulsions, for example, provide lubrication challenges relative to mineral oils for which most pumps were designed. For example, the shear-thinning viscosity behavior of HFB fluids has required design changes where hydrostatic lubrication is utilized. Because both HFA and HFB fluids may be subject to metallic contact, severe wear may result. Shear thinning or insufficient fluid viscosity may also affect internal leakage and hydraulic efficiency [40]. Therefore, it is important to assess fluid lubrication properties to determine if it is appropriate to use a particular fluid with a particular pump or hydraulic component.

Fluid lubrication fundamentals are discussed in detail in Chapter 6. In this section, the application of the fundamental properties of HFA and HFB fluids, particularly with respect to hydrodynamic and elasto-hydrodynamic (EHD) lubrication,

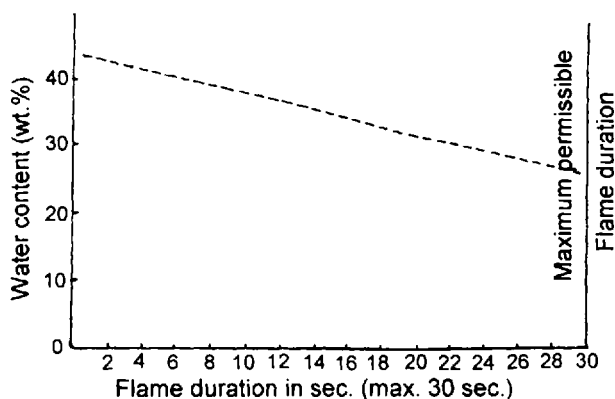


Figure 17.35 Effect of emulsion water content on fire resistance.

will be discussed. Wherever possible, distinctions between the inherently different lubrication properties of HFA and HFB fluids will be made.

Film-Thickness Studies

Hamaguchi et al. studied the EHD film-thickness properties of a paraffinic-oil (W/O) emulsion similar to an HFB hydraulic fluid [82]. The results of this study showed that the film thickness was nearly independent of water concentration up to 80% water (see Fig. 17.37), even though the fluid viscosity increased 1000% over this water concentration range, as shown in Fig. 17.38. A similar emulsion was prepared from Shell Vitrea 69 mineral oil. The film thickness versus water concentration relationship was similar to that obtained for the paraffinic oil, as shown in Fig. 17.39. The effect of base-oil viscosity W/O emulsions prepared from these oils is shown in Fig. 17.36 [35]. The EHD lubrication properties on emulsion is primarily determined by the properties of the base oil [82].

Hamaguchi et al. reported that negligible film-forming properties were observed for oil-in-water emulsions such as HFA fluids [82].

Model of Film Formation

Because the fluid films formed by both HFA and HFB fluids are heterogeneous, a two-phase model of the hydrodynamic films formed by these fluids is necessary. The model proposed by Liu et al. for a heterogeneous film formed during rolling in the "x direction" is illustrated in Fig. 17.40 [29]. For an HFB fluid, this model shows that a portion of the film consists of dispersed large water droplets which form patches of water on the contact surface. The remaining portion of the surface is covered by the continuous oil phase of the emulsion. Localized viscosity is either that of the water or that of the oil. The critical diameter defining large and small droplets is dependent on the local film thickness, water concentration in the continuous phase, and the viscosity of the continuous phase [29].

A small element ($\Delta x \Delta y$) of the film shown in Fig. 17.41 is large enough to contain a number of water patches but still small with respect to the EHD conjunction [29]. If the film thickness (h) is assumed to be constant over this element, the Reynolds equation is

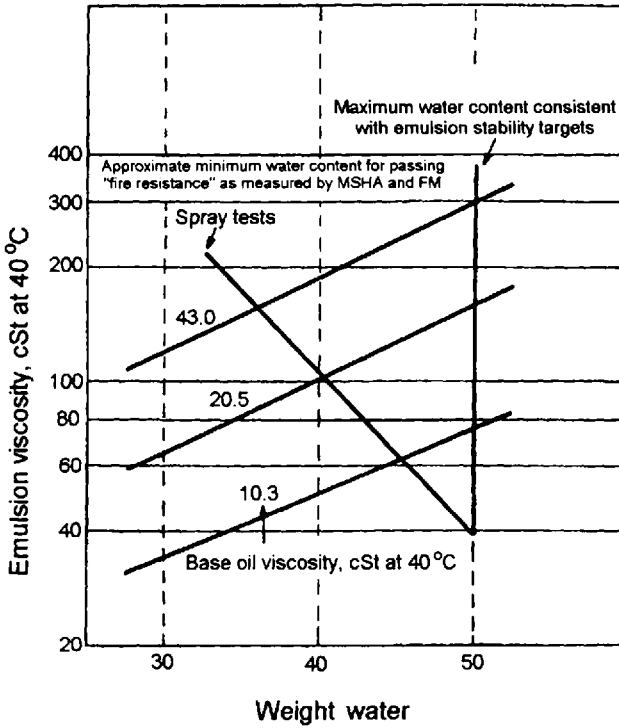


Figure 17.36 Establishment of minimum acceptable water content for an HFB emulsion hydraulic fluid.

$$\frac{\partial}{\partial x} \left(\frac{h^3}{12\eta} \frac{\partial P}{\partial x} \right) + \frac{\partial}{\partial y} \left(\frac{h^3}{12\eta} \frac{\partial P}{\partial y} \right) = 0 \tag{17.18}$$

where h is the film thickness, η is the viscosity, and P is the contact pressure [29]. After solving this equation, the equivalent viscosity of W/O emulsions relative to the viscosity of the base oil may be plotted against the total water concentration of the W/O emulsion (ϕ) and the fraction of water concentration that forms the patches

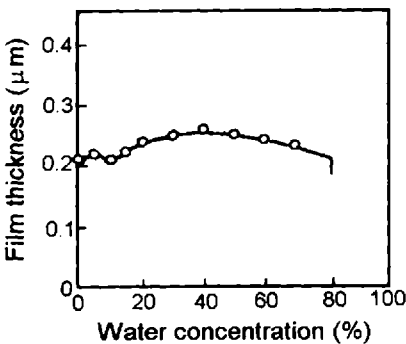


Figure 17.37 Effect of water concentration on lubricant (paraffin oil) film thickness.

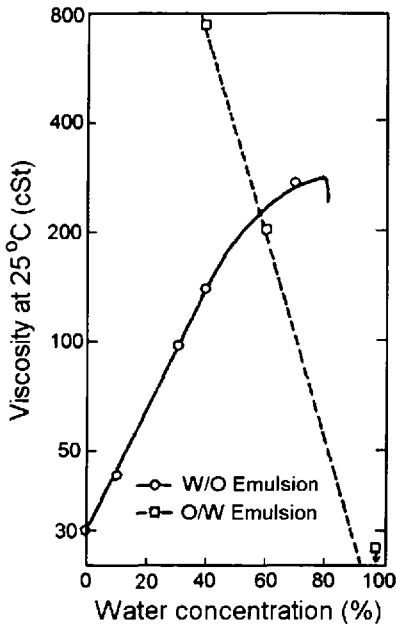


Figure 17.38 Effect of water content on O/W and W/O emulsions used for film-thickness studies.

(ξ) [29]. This relationship is shown in Fig. 17.42, where the viscosity of the base oil is assumed to be 1.0.

Figure 17.42 shows that W/O films may be either thicker or thinner than films formed with the base oil, depending on the diameter of the water droplets. This means that water droplets may be trapped within the wear contact and are restrained from escaping by the high viscosity of the oil [29].

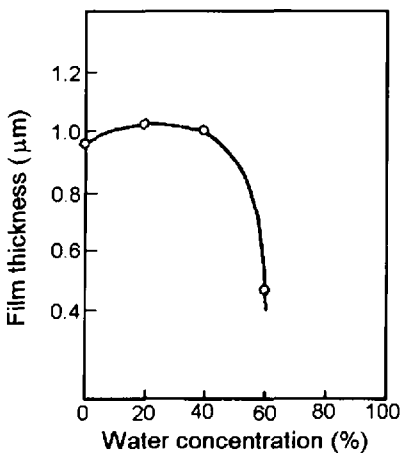


Figure 17.39 Effect of water content on lubricant (mineral oil) film thickness.

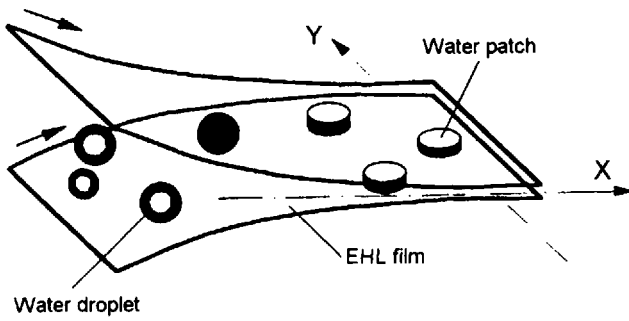


Figure 17.40 Two-phase hydrodynamic film.

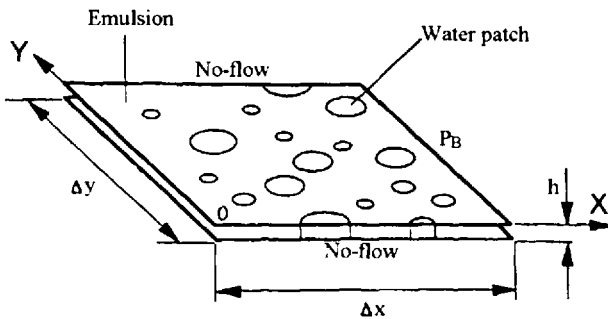


Figure 17.41 An element of the EHL film.

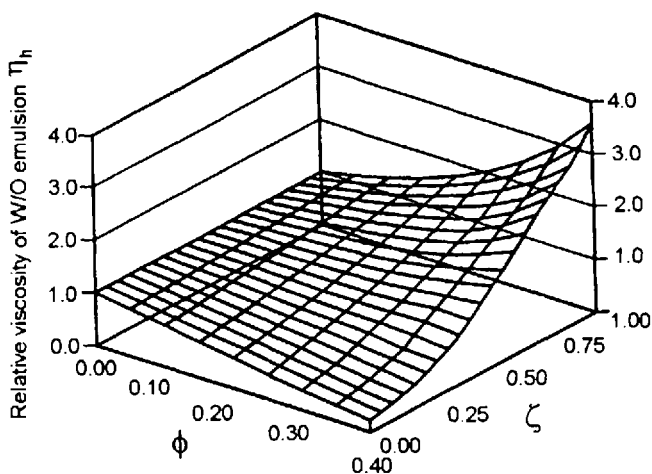


Figure 17.42 Relative viscosity (η_h) versus water concentration (ϕ) and volume fraction (ξ) of small water particles (viscosity of base oil = 1.0)

Pressure–Viscosity Effects

Although hydrodynamic fluid lubrication is primarily dependent on the bulk viscosity at the temperature of the wear contact, elasto-hydrodynamic lubrication is also dependent on the contact pressure. Therefore, the fluid film thickness at the wear contact is dependent on the viscosity–pressure coefficient. This relationship is evident from another form of the Reynolds equation [17]:

$$h_0 = K(\eta_0)^{0.7}(\alpha)^{0.5} \quad (17.19)$$

where

h_0 = the minimum film thickness

η_0 = the viscosity of the lubricant at atmospheric pressure

α = the pressure–viscosity coefficient

K = a constant

Physically, this means that fluids that exhibit higher-pressure viscosity coefficients will increase in viscosity faster with increasing contact pressure (loading). If the fluid viscosity increase with pressure is sufficient, the fluid film thickness will decrease less with increasing load, thus better inhibiting asperity contact and the formation of a higher wear boundary lubrication condition. *Note:* Pressure–viscosity coefficients are described in detail in Chapter 4 and their effect on lubrication and wear is described in Chapter 6.

In a subsection of Section 2.5.2, pressure–viscosity coefficients for a number of W/O and O/W emulsions were provided. In general, it was observed that the pressure–viscosity coefficient was dependent on the water content of the fluid. High-water-content fluids (O/W emulsions) exhibited pressure–viscosity coefficients approaching those of water, and W/O emulsions exhibited pressure–viscosity coefficients similar to those of the base oil. (A typical pressure–viscosity coefficient for a mineral oil is 17.7 GPa^{-1} [29].)

The effect of pressure–viscosity coefficient on bearing wear is modeled by the “lubricant film parameter” or lambda ratio (Λ) through the lubricant central film thickness (h'_c) and surface roughness (σ) (see Chapter 12):

$$\Lambda = \frac{h'_c}{\sigma} \quad (17.20)$$

This equation shows that wear is a function of both film thickness and surface roughness.

Fatigue Failure

Although there is a great deal of variation of fatigue wear among different fluids of the same class, there is a general trend for increasing wear with increasing water content [111]. This is especially true for HFA and HFB fluids, where the wear rate of HFA fluids is typically much greater than the wear rate for HFB fluids [17]. Spikes has suggested the following causes for greater wear of water-based hydraulic fluids relative to mineral oil [17]:

- Low EHD film thickness and lambda ratio
- Chemical promotion of crack formation and growth leading to fatigue

- Removal or prevention of protective chemical films due to low temperature of dissolution
- Increased corrosion leading to corrosive/abrasive wear

In many applications, such as rolling element bearing wear, the predominant failure mechanism is fatigue wear. Fatigue wear may be enhanced by water-based fluids because of low EHD film thickness leading to asperity contact, chemical promotion of crack growth, and pressure pulsation of water entrapped with cracks [12]. At this time, the primary mechanism of fatigue crack growth promotion is not clear but are thought to be due to hydrogen embrittlement, stress corrosion cracking, and corrosion fatigue [17].

Yardley et al. studied fatigue failures of rolling element bearings with various fire-resistant fluids [83]. Based on their studies, they proposed the following load-life relationship [29]:

$$L_{10} = \left(\frac{C}{PD} \right)^B \quad (17.21)$$

where L_{10} is the average lifetime in revolutions when 10% of the bearings will fail, C is the dynamic capacity of the bearing or "load that a bearing can carry for a life of 1 million inner-race revolutions with a 90% probability of survival" [84], P is the bearing load, and B and D are constants taken from Table 17.19. Tables such as this are used in the derating of hydraulic pumps for use with fluids other than mineral oil. However, it should be noted the C/P ratio will vary with the bearing type and material. Nevertheless, these data show that the relative order of bearing derating for use with fire-resistant fluids with respect to fatigue failures is as follows: (worst) HFA \gg HFC $>$ HFB $>$ phosphate ester \approx mineral oil.

Fluid Properties and Pump Design

As discussed previously, fluid viscosity is one of the most important variables to consider when converting a hydraulic system to a fire-resistant fluid from a mineral oil. Proper fluid viscosity is vitally important if optimal lubrication is to be maintained. However, this is a particularly critical design consideration for HFA fluids which may exhibit viscosities as low as 1 cSt compared to viscosities of up to 90

Table 17.19 Constants in the Load-Life Relationship of Four Fire-Resistant Fluids

$L_{10} = \left(\frac{C}{PD} \right)^B$			
Fluid	B	Standard error of B	D
Phosphate ester	3.19	0.54	1.05
O/W emulsion	2.64	0.37	1.71
W/O emulsion	2.25	0.21	1.25
Water-glycol	1.69	0.28	1.41

cSt and higher for HFB fluids. In this section, a selected overview of some of the important rheological properties of a hydraulic fluid on hydraulic pump operation will be provided. Most of this review is based on a series of papers providing a more complete analysis by Taylor et al. [85–88].

IMPORTANCE OF FLUID VISCOSITY. Because HFA fluids contain mostly water, they provide many operational problems in a hydraulic system, particularly with respect to leakage flow and bearing lubrication. Leakage flow across the seal lands of a pump is directly proportional to the viscosity of the fluid. This is significant because an HFA fluid may exhibit a viscosity of 1/20, or less, of a typical mineral oil. HFB fluids provide an interesting contrast because they increase in viscosity with increasing water content. (This is why it is often recommended that HDFB fluids be replaced when the water content is greater than $\pm 5\%$ of their correct operational range [58].)

Note: It is important to account for fluid density because absolute viscosity is the important design parameter for hydraulic systems; for example, compare mineral oil with a kinematic viscosity of 32 cSt and a density of 0.88. The absolute viscosity is $32 \times 0.88 = 28.2$ cP. However, an emulsion with the same kinematic viscosity except with a density of 1.27 will exhibit an absolute viscosity of $32 \times 1.27 = 40.6$ cP. Failure to provide this adjustment may lead to failure to accurately predict the transition from laminar to turbulent flow [55,86].

The effect of viscosity on flow rate is important when considering hydrostatic lubrication (e.g., flow rate through a slipper is an important contributor toward volumetric efficiency). The flow rate is a function of bearing geometry, port pressure, film thickness, and fluid viscosity as shown by

$$Q = q \frac{h^3}{\eta} P_p \quad (17.22)$$

$$q = \frac{\pi}{6} \frac{1}{\ln(D/\alpha)} \quad (17.23)$$

where

- Q = the flow rate
- h = film thickness
- P_p = port pressure
- η = the absolute oil viscosity
- D = the port diameter
- α = the pad diameter

Figure 17.43 [85] illustrates the variation of flow rate versus viscosity at different film thickness and Fig. 17.44 shows the variation of flow rate versus film thickness with varying fluid viscosity [86]. These figures show that flow rate increases with increasing film thickness and decreasing viscosity. This illustrates one of the major problems with the use of HFA fluids.

Excessive flow rates may be reduced by pump design. For example, the film thickness of a hydrostatic bearing may be reduced by decreasing the film thickness as long as the film thickness is sufficient to prevent asperity contact.

The flow rate of a hydrostatic bearing with capillary compensation is [86]

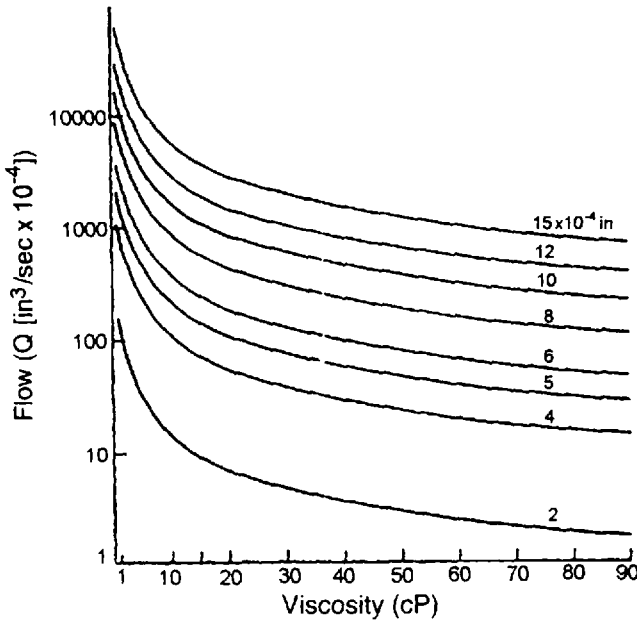


Figure 17.43 Flow rate versus fluid viscosity at different film thicknesses.

$$Q = \frac{K_c}{\eta} (P_s - P_p) \quad (17.24)$$

where P_s is the supply pressure and K_c is the capillary coefficient, which is a function of capillary diameter (d_c) and capillary length (l_c):

$$K_c = \frac{\pi d_c^4}{128 l_c} \quad (17.25)$$

Because the supply pressure and port pressure are constant, the capillary diameter can be reduced to compensate for leakage due to low viscosity. However, this is often difficult to practice because of the very small capillary diameters required [86].

The pumping power of a hydrostatic bearing is proportional to film thickness and inversely proportional to fluid viscosity, as shown by

$$H_t = \frac{\pi}{4} \frac{\eta}{h} \frac{u_0^2}{h} \cdot (D^2 - d^2) + \frac{(1 - d/D)^4 \eta}{2} \frac{u_m^2 A}{h} \quad (17.26)$$

$$u_0 = \frac{\pi D_0 \eta}{60} \quad (17.27)$$

$$u_0 = \frac{\pi D \eta}{60} \quad (17.28)$$

where

D = the port diameter

d = the pad diameter

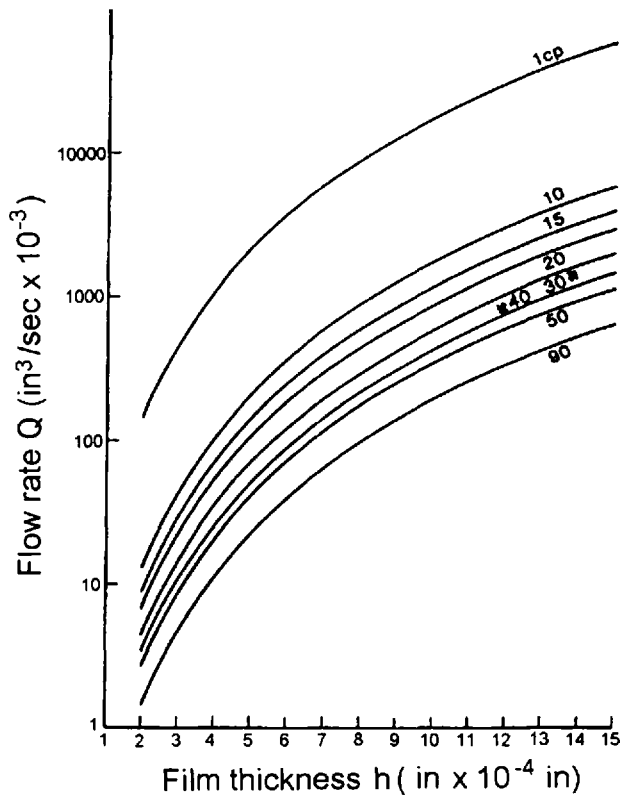


Figure 17.44 Fluid flow rate versus film thickness with ranging fluid viscosity.

D_0 = the pitch circle diameter

U_0 = the sliding velocity relative to the pitch circle diameter

U_m = the sliding velocity of the runner relative to the pad

A = the pad area [85]

This is illustrated in Fig. 17.45 [86]. When the fluid viscosity is 1 cP, the power loss increases dramatically with increasing film thickness, resulting in very large power losses. Interestingly, the optimum film thickness increases with increasing viscosity.

Figure 17.46 [86] illustrates total power loss versus viscosity. The solid line is minimum power loss and the dashed line is maximum power loss. These data show that the difference between minimum and maximum power loss is approximately 0.5–1.0 hp unless the viscosity is approximately 1 cP. This means that film thickness is critically important for HFA fluids. In general, the film thickness should be kept as thin as possible while still providing adequate lubrication for HFA fluids.

HYDRODYNAMIC BEARINGS. Hydrodynamic bearings are lubricated without external pumping equipment. This is accomplished by fluid viscosity, elliptical contact geometry (see Fig. 17.47 [85]), and the relative motion of the moving surfaces. Figure 17.48 [85] illustrates the characteristic converging geometry of a contact for hydrodynamic lubrication. As the surfaces move in relative motion, the fluid, owing to its viscosity, adheres to the surfaces and is dragged into the contact. The critical

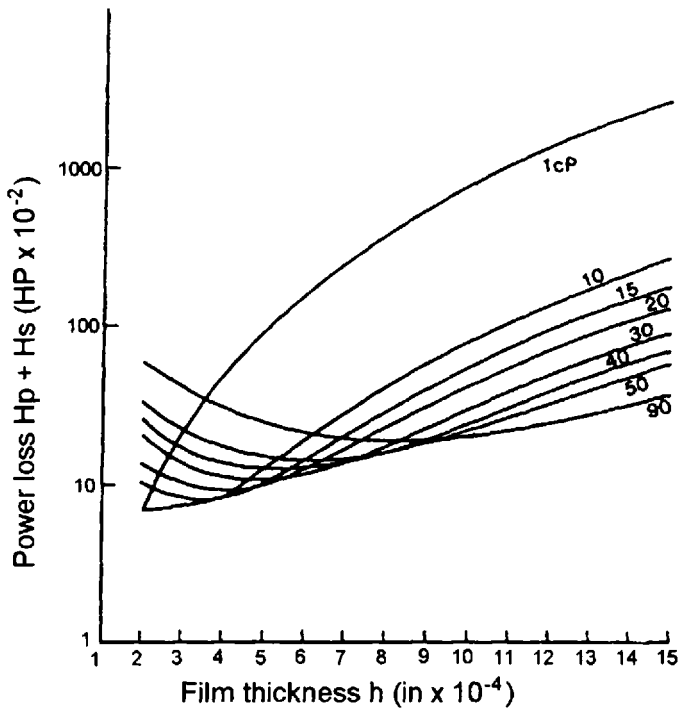


Figure 17.45 Variation of power loss with film thickness.

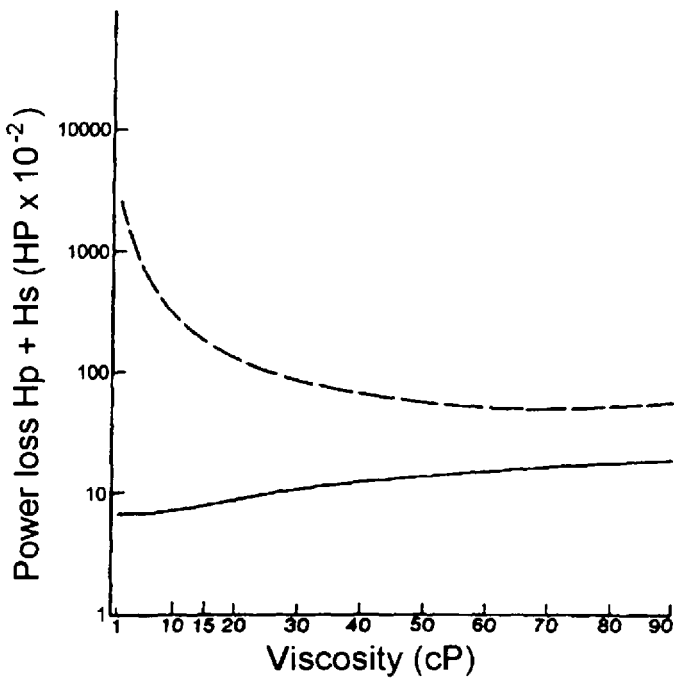


Figure 17.46 Total power loss with fluid viscosity.

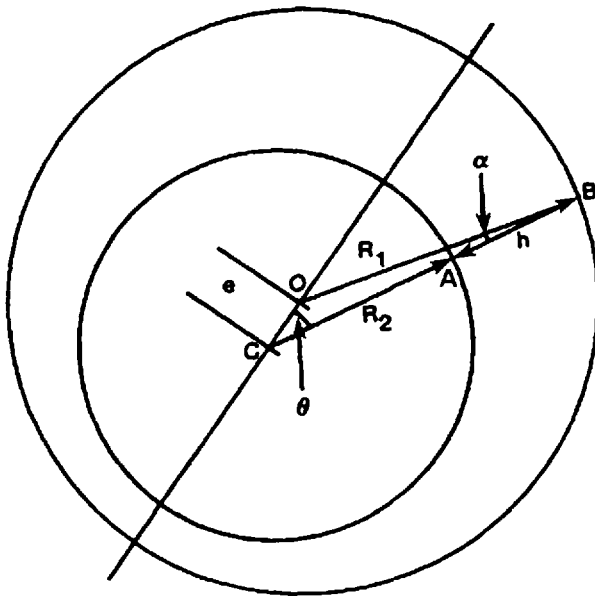


Figure 17.47 Geometry of a hydrodynamic bearing.

parameters for hydrodynamic bearings are film thickness, pressure distribution, maximum load capacity (maximum load corresponding to the minimum film thickness), flow rate, friction loss, and temperature rise [85]. The equations governing film thickness, pressure distribution, load-carrying capacity, and frictional force for hydrodynamic journal and thrust bearings are shown in Table 17.20 [85].

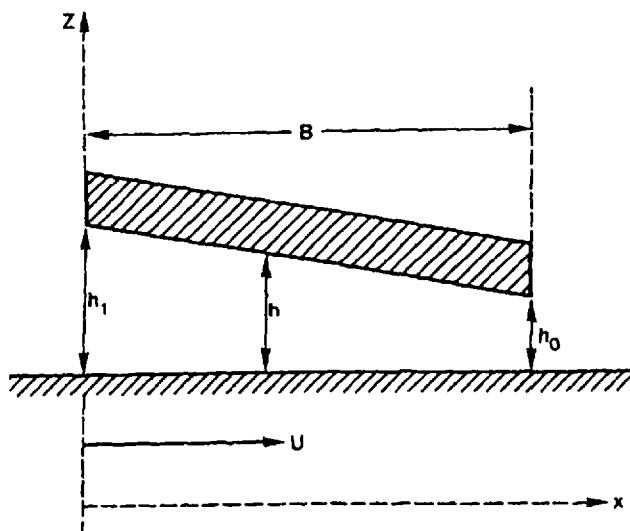


Figure 17.48 Geometry of a hydrodynamic bearing.

Table 17.20 Governing Equations for Hydrodynamic Lubrication of Hydrodynamic Journal and Thrust Bearings

Equations	Hydrodynamic journal bearing	Hydrodynamic thrust bearing
Film thickness	$h = C(1 + \varepsilon \cdot \cos \theta)$	$\frac{h}{h_0} = \left(1 + K - K \frac{x}{B}\right)$
Pressure distribution	$p = \frac{6u\eta R}{c^2} \left\{ \frac{\varepsilon \sin \theta (2 + \varepsilon \cos \theta)}{(2 + \varepsilon^2)(1 + \varepsilon \cos \theta)} \right\}$	$\frac{dp}{dx} = \frac{6u\eta h_0 \left(1 + K - K \frac{x}{B}\right) - h_0 A_0}{\left(1 + K - K \frac{x}{B}\right)^3 h_0^3}$
Load bearing capacity	$W = \omega A P_p$	$W = W^* \frac{6u\eta B^2 L}{h_0^2}$
Flow rate	—	$Q = L u h_0 \left[\frac{(1 + K)}{(2 + K)} \right]$
Friction force	$F = \frac{2\pi\eta U R L}{C}$	$F = \frac{\eta U R B}{h_0} \left\{ \frac{4 \ln(1 + K)}{K} - \frac{6}{(2 + K)} \right\}$

Note: A is the pad area; A_0 is h/h_0 ; B is the breadth of the bearing in the direction of motion; c is radial clearance; F is friction force; h is film thickness; h_0 is minimum film thickness; $K = (h_c - h_0)/h_0$; L is the bearing length; R is the journal radius; U is the velocity; ε is the eccentricity ratio; η is the oil viscosity.

One of the most important parameters for a journal bearing is the load-bearing capacity because it will determine the performance and lifetime of the bearing. The Sommerfield equation is typically used to analyze the performance of a journal bearing; it is written as [87]

$$\frac{W/L}{u\eta} \frac{C^2}{R^2} = \frac{6\pi\varepsilon}{(1 - \varepsilon^2)^{3/2}(1 + \varepsilon^2/2)} \quad (17.29)$$

where

- W = the load
- L = the bearing length
- U = the surface velocity
- C = the radial clearance
- R = bearing radius
- ε = journal eccentricity
- η = the absolute viscosity

The value on the right-hand side of this equation is called the Sommerfield number. The inverse of this relationship is called the "duty parameter." As is evident from this equation, these values provide a measure of the effect of fluid viscosity, surface speed, and load on hydrodynamic lubrication. Figure 17.49 provides a plot of the Sommerfield number versus various L/D ratios.

The load capacity of the bearing is dependent on the fluid viscosity [87]:

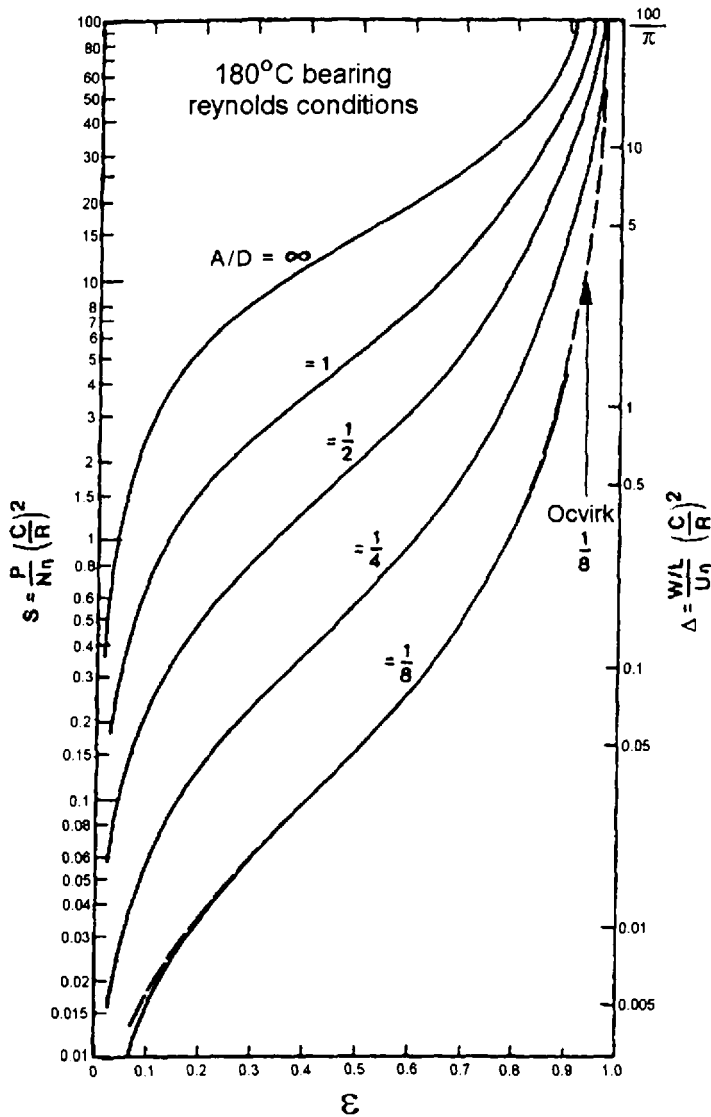


Figure 17.49 Sommerfeld number versus ϵ for various L/D ratios.

$$\frac{W}{L} = 6W^*u\eta \frac{R^2}{C^2} \tag{17.30}$$

where W^* is the nondimensional load factor equal to

$$W^* = \frac{1}{K} \left(\frac{\log \epsilon(1 + K)}{K} - \frac{2}{2 + K} \right) \tag{17.31}$$

where K is the film thickness ratio. These equations show that the load capacity of a journal bearing is dependent on fluid viscosity. Thus, if a pump is designed to

operate with a mineral oil, a low-viscosity HFA fluid will only provide a fraction of the load-bearing capacity. Therefore, the pump must be derated.

3 HYDRAULIC PUMP TESTING

Over the years, it has been found that in order to obtain a reasonably reliable assessment of the antiwear properties of a hydraulic fluid, it was necessary to perform pump tests [53,89–92]. These tests may be conducted with specialized pump tests, including gear [53,89] and piston [53,91]. One of the most common tests is ASTM D 2882 [93] and its international equivalents such as DIN 51389 [94] which are based on the Vickers V 104 van pump. Although HFB fluids may generally be tested under ASTM 2882 conditions, HFA fluids cannot. Janko reported the maximum test pressure that could be utilized was 54 bars [91].

In addition to pump tests, it is often necessary to conduct valve tests with different fluids. Such work has been described by various authors, including Kelly [40,95], and will not be detailed here.

3.1 Hydraulic Pump Derating

For various reasons presented earlier, it would not be expected that HFA and HFB fluids would be direct replacements for mineral oil as a hydraulic fluid. Therefore, these fluids, like most other fire-resistant fluids, are derated with respect to maximum pressure and speed. An example of hydraulic pump derating is provided in Table 17.21 [96]. This table illustrates that Sundstrand routinely recommends the greatest derating for use of their pumps with HFA fluids. Although not derated to as large an extent as HFA fluids, HFB fluids are derated relative to polyol esters.

In addition to fluid derating, additional recommendations are also made, such as the use of elevated and pressurized reservoirs, increased inlet size, and reduction of inlet vacuum to 2 in. Hg or greater and inlet pressurization [55,96].

The specific derating procedures vary with manufacturer and specific products and are influenced by fluid specific gravity and inlet gravity and inlet suction head [97]. Therefore, the equipment manufacturer should be consulted when the conversion from mineral oil is contemplated.

4 CONVERSION PROCEDURES

It has been suggested that the following steps be followed when converting from mineral oil to emulsion hydraulic fluids [98,99,110]:

Table 17.21 Illustration of Sundstrand Hydraulic Pump Derating for Fire-Resistant Fluids

Fluid type	Speed (% catalog)	Pressure (% catalog)	Maximum temperature (°F)
Phosphate ester	100	100	180
Polyol ester	85	85	150
Invert emulsion (60/40 oil/water)	65	70	140
Water-glycol (60/40 oil/water)	65	60	140
HWCF (95/5 water/oil)	65	40	122

1. Completely drain the system of the previous fluid. This includes reservoir, accumulator, coolers, lines, and cylinders. Low-pressure air may be used to assist in oil removal, particularly from remote parts of the system [100].
2. Disconnect, remove, and clean or replace filters and intake pipe strainers.
3. Replace seals with materials that are compatible with emulsion hydraulic fluids. Most of the materials used for petroleum oil are acceptable. In addition, silicone, teflon, Viton, Fuorel, and Kel-f are usually suitable [97]. However, all seal and gaskets materials of leather, cork, and paper must be replaced [101] .
4. Wipe reservoir dry with lint-free rags. If there is paint on the inside surfaces, remove using commercial paint remover or hot caustic. Paint removal is very important because paints typically used for oil hydraulic systems are readily attacked by water-containing fluids [100]. Residual paint residues will contaminate the fluid and interfere with the operation of hydraulic actuators.
5. Reconnect system; clean and reinstall intake strainers. Typically, inlet strainers are limited to 60 mesh or less. They may be constructed of brass or plated with copper or nickel. However, precautions should be taken to ensure that they are compatible with the emulsion fluid being used [100].
6. If a petroleum oil was used previously:
 - (a) Fill machine with light hydraulic oil
 - (b) Operate machine for 20 min
 - (c) Pump out sump; drain all accumulators, cylinders, and coolers
 - (d) Wipe reservoirs clean
7. It is recommended that the system be flushed with the emulsion hydraulic fluid itself prior to final filling [9,100,102]. The use of solvents or chemical cleaners may affect fluid emulsion stability. Although residual petroleum oil, either hydraulic oil or flushing fluid is typically compatible in an invert emulsion [9,103], the presence of residual oils may exhibit an unfavorable effect on flammability [100,102,104]. One report recommends draining mineral oil, flushing with emulsion hydraulic fluid by running for 30 min, drain flushing charge and recharging with new emulsion fluid and run for 1 week, draining and recharging with new fluid, and running normally [105].
8. Fill with emulsion hydraulic fluid.
9. Install water-compatible filter and do not place filter too close to pressure pulsation to avoid filter fatigue [106].
10. Cycle machine for 10 min.
11. Check reservoir level.
12. Check all piping for leaks, and tighten if necessary. The following guidelines with respect to piping have been recommended [107]:
 - (a) Loose, vibrating pipes are dangerous and prone to breakage. Copper pipe should only be used, if at all, for low pressure <300 psi.
 - (b) Flexible hose should be inspected very carefully and replaced if necessary. The use of a flexible hose can be avoided by the use of telescoping joints or unions that may be loosened for necessary adjustments. If a flexible hose is used, it should be enclosed in a shroud and vented to a waste pit.

- (c) Fragile piping should not be placed in an area where it can be walked on, run over, or used as a ladder. If it cannot be moved, it should be protected by adequate guards.
- (d) Avoid temporary repairs. Malleable or wrought iron fittings in high-pressure lines should be replaced immediately. Strains introduced by bending or straining pipes to make them fit may lead to subsequent rupture.
- (e) Long, overhead runs of pipe should be avoided because rupture may spray fluid over danger areas.
- (f) Pipe passageways through floors or between machines should be packed with a flexible, fire-resistant filling (ceramic) to prevent flames from spreading from one floor to another.
- (g) Be sure machines are operating properly. Rough hydraulic flow indicates improper circuit design, which may lead to subsequent leaks and breakdowns.

4.1 System Preparation

In addition to the changeover guidelines listed above, a number of additional precautions have been recommended [106]:

1. A reservoir design, preferably using stainless steel, that provides sufficiently quiet conditions so that particulate contaminants will settle into a sump for subsequent removal.
2. Owing to their reduced compressibility relative to mineral oil, emulsion hydraulic fluids are “stiffer.” These stiffer systems may produce higher-pressure ripples which may affect hydraulic components such as valves and seals. For example, if adequate design precautions are not taken, valve housings may undergo premature fatigue failures due to the high-pressure ripple effect.
3. The pump inlet should have a positive inlet pressure with minimal bends to eliminate potential cavitation. The pump inlet pressure may be increased with the use of a feed pump or by increasing fluid head at the inlet. If the inlet vacuum is too high (see Table 17.15), precautionary measures must be taken. Small improvements can be made by increasing the size of the pipe into the inlet and, if necessary, reducing the pump speed to provide lower displacement [99]. “It is absolutely necessary that suction line restrictions be reduced to allow adequate flow of the fluid to the pump under all operating conditions” [110].
4. To prevent erosion, avoid continual fluid relief over a relief valve at high pressure.
5. Avoid using aluminum components.
6. Heat exchangers may be required to prevent reservoir temperatures from exceeding the recommended maximum temperature of 150°F [100].

4.2 Pumps—Selection and Preparation

Before any conversions are made, the hydraulic pump manufacturer should be consulted with respect to recommended derating practices and potential material incom-

patibilities, such as pump seals, with the emulsion hydraulic fluid to be used [99]. In some cases, the particular pump being used may not perform satisfactorily with a fire-resistant fluid [109]. In such cases, a recommendation may be made to replace the pump with a model compatible for use with fire-resistant fluids, exhibiting higher performance and efficiency than the older model being used [97].

4.2.1 Cavitation

High inlet vacuum during normal operation may lead to cavitation. This condition may be detected by installing a vacuum gauge in the suction line immediately ahead of the pump inlet. Recommended maximum inlet vacuum conditions are provided in Table 17.12 [28,109].

If the inlet vacuum is higher than recommended, the suction-line strainer or filter may be clogged. Other causes for pump cavitation include the following [28]:

1. Screen size is too small. It should not be smaller than 60 mesh.
2. If the pump suction line is too long or too small in diameter, cavitation may result. A collapsed suction hose will also lead to cavitation. The solution is to follow the manufacturer's recommendations.
3. Elevation of the pump above the reservoir may lead to cavitation. The pump or reservoir should be moved to provide a positive fluid head at the inlet.
4. An air leak on the suction side of the pump will cause fluid aeration and increase the potential for cavitation [108].
5. Fluid foaming in the reservoir may lead to cavitation. This may be caused by improper formulation chemistry or contamination.

REFERENCES

1. J. Reichel, "Standardization Activities for Testing of Fire Resistance," in *Fire Resistance of Industrial Fluids, ASTM STP 1284*, G. E. Totten and J. Reichel, eds., 1996, American Society for Testing and Materials; Philadelphia, pp. 61–71.
2. S. P. Pollack, "Researching New Hydraulic Fluids," *Coal Age*, 1957, January, pp. 82–84.
3. K. C. Goodman, "Living with Fire-Resistant Hydraulic Fluids," Report of Denison Engineering Division, Columbus, OH, June 1965.
4. F. Townshend and P. Baker, "Factors Relating to the Selection and Use of Fire-Resistant Fluids in Hydraulic Systems," *Hydraulic Pneumatic Power*, 1974, April, pp. 134–140.
5. C. Staley, "Fire-Resistant Hydraulic Fluids—Comparisons and Applications," *Petrol. Times*, 1967, November 24, pp. 1709–1712.
6. A. E. Morris and H. Lefer, "Changing Requirements in Hydraulic Fluids," *Hydraulics Pneumatics*, 1965, February, pp. 69–74.
7. Anon., "Water-Based Fluids in Hydraulic Applications," *Ind. Lubr. Tribol.*, 1996, 48(4), pp. 39–41.
8. B. Brooke, "Development of a High-Water-Based Fluid System for a Universal Beam Rolling Mill," *Conference Proceedings: Hydraulics, Electrics and Electronics in Steel Works and Rolling Mills*, 1994, Mannesmann Rexroth GmbH; Lohr-am-Main, Germany.
9. K. J. Young and A. Kennedy, "Development of an Advanced Oil-in-Water Emulsion Hydraulic Fluid, and its Application as an Alternative Mineral Hydraulic Oil in a High Fire Risk Environment," *Lubr. Eng.*, 1993, 49(11), pp. 873–879.

10. International Standard ISO 6743/4, Lubricants, Industrial Oils and Related Products (Class L)—Classification—Part 4: Family H (Hydraulic Systems) 1982.
11. N. Garti, R. Felkenkrietz, A. Aserin, S. Ezrahi, and D. Shapira, "Hydraulic Fluids Based on Water-in-Oil Microemulsions," *Lubr. Eng.*, 1993, 49(5), pp. 404–411.
12. W. H. Millett, "Nonpetroleum Hydraulic Fluids—A Projection," *Iron Steel Eng.*, 1977, 54(5), pp. 36–39.
13. F. Günther and R.-D Henning, "Erfahrungen bei Entwicklung und Einsatz von HF-A-Flüssigkeiten," *Ölhydraulik Pneumatik*, 1978, 22(6), pp. 342–344.
14. R. C. Rasp, "Water-Based Hydraulic Fluids Containing Synthetic Components," *J. Synth. Lubric.*, 1989, 6, pp. 233–252.
15. H. A. Spikes, "Wear and Fatigue Problems in Connection with Water-Based Hydraulic Fluids," 1987, 4(2), pp. 115–135.
16. K. Janko, "A Practical Investigation of Wear in Piston Pumps Operated with HFA Fluids with Different Additives," *J. Synth. Lubr.*, 1987, 4, pp. 99–114.
17. H. A. Spikes, "Wear and Fatigue Problems in Connection with Water-Based Hydraulic Fluids," *J. Synth. Lubr.*, 1987, 4(2), pp. 115–135.
18. R. Z. Ye, "Water-Based Hydraulic Fluid Compositions and Processes," *FRH J.* 1986, 6, pp. 137–144.
19. L. E. Coleman, "Development of Fire-Resistant Emulsion Hydraulic Fluid," *J. Inst. Petrol.*, 50(492), pp. 334–344.
20. G. M. Barrow, *Physical Chemistry*, 2nd ed., 1966, McGraw-Hill; New York, p. 756.
21. J. T. Davies and E. K. Rideal, *Interfacial Phenomenon*, 1961, Academic Press; New York, pp. 359–387.
22. Anon., "Types of Fire Resistant Hydraulic Fluid," *Ind. Lubr. Tribol.*, 1992, 44(1), pp. 13–15.
23. *The ATLAS HLB System—A Time Saving Guide to Emulsifier Selection*, Atlas Chemical Industries, Inc.; Wilmington, DE.
24. E. D. Pell and R. T. Holtzmann, "Hydraulic Fluid Emulsions," in *Emulsions and Emulsion Technology—Part II*, K. J. Lissant, ed., 1974, Marcel Dekker; New York, pp. 639–699.
25. K. Shinoda and H. Kunieda, "How to Formulate Microemulsions with Less Surfactant," in *Microemulsions—Theory and Practice*, M. L. Prince, ed., 1977, Academic Press; New York, pp. 64–86.
26. J. T. Schmiede, S. Simandiri, and A. J. Clark, "The Development and Applications of an Invert Emulsion, Fire-Resistant Hydraulic Fluid," *Lubr. Eng.*, 1985, 41, pp. 463–469.
27. G. H. A. Clowes, "Protoplasmic Equilibrium," *J. Phys. Chem.*, 1916, 20, pp. 407–451.
28. Anon., "Fire Resistant Hydraulic Fluids," *Lubrication*, 1962, 48(11), pp. 161–180.
29. W. Liu, D. Dong, Y. Kimura, and K. Okada, "Elastohydrodynamic Lubrication with Water-in-Oil Emulsions," *Wear*, 1994, 179, pp. 17–21.
30. P. Deakin, "Fire Resistant Hydraulic Fluids," *Mining Technol.*, 1990, November/December, pp. 300–303.
31. G. F. Berg, "The Oil in Hydraulic Drives," *Die Technik*, 1949, 4(12), pp. 545–548.
32. British Coal Corp., *Emulsifying Oils for Dilute Emulsions for Hydraulic Purposes, N.B.C. Specification 463/1981*, 1981, British Coal Corporation, London.
33. E. Trostmann, *Water Hydraulics Control Technology*, 1996, Marcel Dekker; New York, p. 57.
34. G. T. Coker and C. E. Francis, "The Place for Emulsions as Fire-Resistant Power Transmission Fluids," *Lubr. Eng.*, 1956, 12(5), pp. 323–326.
35. D. A. Law, "The Development and Testing of an Advanced Water-in-Oil Emulsion for Underground Mine Service," ASLE Preprint, Preprint No. 80-AM-88-1, 1980.

36. C. E. Francis and R. T. Holmes, "New Developments Reflect Improved Performance," *Lubr. Eng.*, 1958, 14(9), pp. 385–390.
37. O. Isaksson, "Rheology for Water-Based Hydraulic Fluids," *Wear*, 1987, 115(1–2), pp. 3–17.
38. V. H. Schäfer, "Schwer Brennbare Flüssigkeiten für hydraulische Systeme," *Geisseri*, 1964, 51(26), pp. 817–819.
39. F. Stumpmeier, "Progressive Wasserhydraulik: Teil I: Allgemein und Pumpen/Motoren," *Ölhydraulik Pneumatik*, 1979, 23(3), pp. 185–188.
40. E. S. Kelly, "Fire Resistant Fluids: Factors Affecting Equipment and Circuit Design," 3rd International Fluid Power Symposium, 1973, Paper number F1.
41. W. Guse, "Schwerentflammbare Druckflüssigkeiten—Eigenschaften und Verwendung," *Ölhydraulik Pneumatik*, 1980, 24(6), pp. 449–454.
42. C. R. Schmitt, "Fire Resistant Hydraulic Fluids for Die Casting—Part 3," *PMM*, 1955, February, pp. 81–85.
43. R. Q. Sharpe, "Designing for Fire Resistant Hydraulic Fluids," *Product Eng.*, 1956, August, pp. 162–166.
44. G. Dalmaz, "Traction and Film Thickness Measurements of a Water Glycol and a Water-in-Oil Emulsion in Rolling-Sliding Point Contacts," *Proceed. 7th Leeds-Lyon Symp. on Tribology, Friction and Traction*, 1980, pp. 231–243.
45. R. Taylor and Y. Y. Wang, "Lubrication Regimes and Tribological Properties of Fire-Resistant Hydraulic Fluids," *Lubr. Eng.*, 1984, 40(1), pp. 44–50.
46. P. J. Law, "High Water Content Fluids—Products for the Future," in *Conference Proceedings: Hydraulics, Electrics and Electronics in Steel Works and Rolling Mills*, Mannesmann Rexroth GmbH, Lohr-am-Main, Germany.
47. L. N. Lapshina and A. A. Chesnokov, "Fire-Resistant Emulsion Fluids for Hydraulic Systems (Review)," *Chem. Technol. Fuels Oils*, 1975, 11, pp. 902–907.
48. ASTM D 892, "Standard Test Method for Foaming Characteristics of Lubricating Oils," American Society for Testing and Materials, Conshocken, PA.
49. "Requirements and Tests Applicable to Fire-Resistant Hydraulic Fluids Used for Power Transmission and Control (Hydrostatic and Hydrokinetic)," European Safety and Health Commission for the Mining and Other Extractive Industries, Doc. No. 4746/10/91 EN, Luxembourg, April 1994.
50. ASTM D 3427 - 86, "Standard Method for Gas Bubble Separation Time of Petroleum Oils," American Society for Testing and Materials, Conshocken, PA.
51. ASTM D 943 - 81, "Standard Test Method for Oxidation Characteristics of Inhibited Mineral Oils," American Society for Testing and Materials, Conshocken, PA.
52. ASTM D 665 - 92, "Standard Test Method for Rust-Preventing Characteristics of Inhibited Mineral Oil in the Presence of Water," American Society for Testing and Materials, Conshocken, PA.
53. K. J. Young, "Development and Application of Advanced Emulsion Hydraulic Fluids," SAE Technical Paper Series, Paper 951196, 1995.
54. Z. Wang, "Use and Maintenance of Fire-Resistant Hydraulic Oil," *Runhua Yu Mifeng*, 1987, 5(9), pp. 60–64.
55. R. D. Rynders, "Fire Resistant Fluids from a Component Builder's Point of View," *Nat. Conf. Ind. Hydraulics*, 1962, 16, pp. 39–46.
56. K. G. Henrikson, "Fire-Resistant Fluids and Mobile Equipment," SAE Technical Paper Series, Paper 650671, 1965.
57. ISO 48 - 1994, "Rubber vulcanized or thermoplastic determination of hardness between 10 IRHD and 100 IRHD."
58. A. P. Bell, "Fire Resistant Hydraulic Fluids of Invert Emulsion Type in Use in the Mining Industry, 1990, November/December, p. 305.

59. *Design, Operation and Maintenance of Hydraulic Equipment for Use with Fire Resistant Fluids*, National Fluid Power Association, Milwaukee, WI.
60. J. L. Borowski, "The Use of Invert Emulsion Hydraulic Fluid in a Steel Slab Caster," ASLE Preprint, Preprint No. 80-AM-88-2, 1980.
61. R. J. Foitl and W. J. Kucera, "Formation and Evaluation of Fire-Resistant Fluids," *Iron Steel Eng.*, 1964, July, pp. 117-120.
62. ASTM D 95 - 83, "Standard Method for Water in Petroleum Products and Bituminous Materials by Distillation," American Society for Testing and Materials, Conshocken, PA.
63. ASTM D 1744 - 92, "Standard Test Method for Determination of Water in Liquid Petroleum Products by Karl Fisher Reagent," American Society for Testing and Materials, Conshocken, PA.
64. ASTM D 446 - 89a, "Standard Specifications and Operating Instructions for Glass Capillary Kinematic Viscometers," American Society for Testing and Materials, Conshocken, PA.
65. ASTM F 311, "Standard Practice for Processing Aerospace Liquid Samples for Particulate Contamination Analysis using Membrane Filters," American Society for Testing and Materials, Conshocken, PA.
66. ASTM F 312, "Standard Test Methods for Microscopical Sizing and Counting Particles from Aerospace Fluids on Membrane Filters," American Society for Testing and Materials, Conshocken, PA.
67. E. C. Hill and G. C. Hill, "Biodegradable After Use But Not In Use," *Ind. Lubr. Tribol.*, 1994, 46(3), pp. 7-9.
68. F. J. Passman, "Biocide Strategies for Lubricant Rancidity and Biofouling Prevention," *Proceed. AISE 1996 Annual Convention, Assn. of Iron and Steel Engineers*, 1996, Vol. 1, pp. 413-428.
69. E. C. Hill, "The Significance and Control of Microorganisms in Rolling Mill Oils and Emulsions," *Metals Mater.*, 1967, No. 9, pp. 294-297.
70. Anon., "Microbiology of Lubricating Oils," *Process Biochem.*, 1967, May, pp. 54-56.
71. E. C. Hill, "Degradation of Oil Emulsions," *Engineering*, 1967, June, pp. 983-984.
72. E. C. Hill, I. Davies, J. A. V. Pritchard, and D. Byron, "The Estimation of Microorganisms in Petroleum Products," *J. Inst. Petrol.*, 1967, 53(524), pp. 275-279.
73. E. C. Hill, J. Graham Jones, and A. Sinclair, "Microbial Failure of a Hydraulic Oil Emulsion in a Steel Rolling Mill," *Metals Mater.*, 1967, 1(12), pp. 407-409.
74. ASTM D 3946 - 92, "Standard Test Method for Evaluating the Bacteria Resistance of Water-Dilutable Metalworking Fluids," American Society for Testing and Materials, Conshocken, PA.
75. ASTM E 686, "Standard Test Method for Evaluation of Antimicrobial Agents in Metalworking Fluids," American Society for Testing and Materials, Conshocken, PA.
76. ASTM E 979, "Standard Test Method for Evaluation of Antimicrobial Agents as Preservatives for Invert Emulsion and Other Water Containing Hydraulic Fluids," American Society for Testing and Materials, Conshocken, PA.
77. J. Gannon and E. O. Bennett, "A Rapid Technique for Determining Microbial Loads in Metalworking Fluids," *Tribology*, 1981, 14, pp. 3-6.
78. J. D. Sloyer, "Rapid Determination (60 Seconds) of Bacterial Contamination in Industrial Fluids," in *Proceedings of the AAMA Metalworking Fluids Symposium: The Industrial Metalworking Environment Assessment & Control*, 1996, American Automobile Manufacturers Association; Detroit, pp. 362-363.
79. G. M. G. Blanpain, "Fire-Resistant Hydraulic Fluids in the French Mines," *Fluid Power Equipment Mining, Quarrying, Tunneling*, 1974, February 12-13, pp. 145-155.

80. *Houghto-Safe® Fire-Resistant Fluids Handbook*, Houghton International, Valley Forge, PA.
81. B. J. Loudon, "Fire-Resistant Hydraulic Fluids," *Surface Coatings Australia*, 1989, July, pp. 23–29.
82. H. Hamaguchi, H. A. Spikes, and A. Cameron, "Elastohydrodynamic Properties of Water in Oil Emulsions," *Wear*, 1977, 43, pp. 17–24.
83. E. D. Yardley, P. Kenny, and D. A. Sutcliffe, "The Use of Rolling Fatigue Test Methods over a Range of Loading Conditions to Assess the Performance of Fire-Resistant Fluids," *Wear*, 1974, 28, pp. 29–47.
84. E. V. Zaretsky, "Current Practice," in *STLE Life Factors for Roller Bearings*, 1996, Society of Tribologists and Lubrication Engineers; Park Ridge, IL, p. 7.
85. R. Taylor and Y. Y. Wang, "The Effect of Fluid Properties on Bearing Parameters: Part 1," *FRH J.*, 1984, 4(2), pp. 161–168.
86. R. Taylor and Y. Y. Wang, "The Effect of Fluid Properties on Bearing Parameters: Part 2," *FRH J.*, 1984, 5(1), pp. 31–37.
87. R. Taylor and Y. Y. Wang, "The Effect of Fluid Properties on Bearing Parameters: Part 3," *FRH J.*, 1984, 5(1), pp. 39–44.
88. R. Taylor and Z. L. Lin, "The Application of Tribological Principals to the Design of the Valve Plate of an Axial Piston Pump: Part 3—Fire Resistant Fluid Considerations," *FRH J.*, 1984, 5(1), pp. 99–101.
89. V. W. Castleton, "Practical Considerations for Fire-Resistant Fluids," *Lubr. Eng.*, 1998, 54(2), pp. 11–17.
90. Anon., "Lubrication Engineers Take a Second Look at Fire-Resistant Fluids," *Coal Age*, 1971, July, pp. 118–119.
91. K. Janko, "A Practical Investigation of Water in Piston Pumps Operated with HFA Fluids with Different Additives," *J. Synth. Lubr.*, 1987, 4, pp. 99–114.
92. W. M. Shrey, "Evaluation of Fluids by Hydraulic Pump Tests," *Lubr. Eng.*, 1959, 15, pp. 64–67.
93. ASTM D 2882, "Standard Test Method for Indicating the Wear Characteristics of a Petroleum and Non-Petroleum Hydraulic Fluids in a Constant Volume Vane Pump," American Society for Testing and Materials, Conshocken, PA.
94. DIN 51389 - 1981, "Testing of cooling lubriants; Determination of the pH value of water-mixed cooling lubricants."
95. E. S. Kelly, "Erosive Wear of Hydraulic Valves Operating with Fire-Resistant Emulsions," *Proceedings of the 2nd Fluid Power Synposium*, 1971, The British Hydro-mechanics Research Assoc.; Guildford, UK, pp. F4-45–F4-73.
96. *Sauer Sundstrand—All Series: Fluid Quality Requirements*, Sauer Sundstrand Inc., Ames, IA.
97. G. C. Bonnell, "Fire-Resistant Fluids for Diecasting," *Foundry*, 1967, 95(5), pp. 224–229.
98. C. R. Schmitt, "Fire-Resistant Hydraulic Fluids for the Die Casting Industry," *PMM*, 1957, May, pp. 111–113.
99. C. R. Schmitt, "Fire-Resistant Hydraulic Fluids: Part 5—Change-Over Practices," *Appl. Hydraulics*, 1957, October, pp. 160–162.
100. E. J. Egan, "How to Install Fire-Resistant Hydraulic Fluids," *Iron Age*, 1956, October 11, pp. 95–97.
101. E. C. Brink, "Fire-Resistant Hydraulic Fluids," *Lubrication*, 1972, 58, October/December, pp. 77–96.
102. A. S. Morrow, H. E. Sipple, and R. T. Holmes, "Fire-Resistant Hydraulic Fluids for the Die Casting Industry: Part 1—Emulsion Types," *PMM*, 1957, January, pp. 133–144.

103. R. J. Foitl, "Formation and Evaluation of Fire-Resistant Hydraulic Fluids," *Iron Steel Eng.*, 1964, July, pp. 117–120.
104. D. Klamann, "Hydraulic Fluids," in *Lubricants and Related Properties—Synthesis, Properties, Applications, International Standards*, Verlag Chemie; Basel, pp. 306–331.
105. L. Jackson, "Fire-Resistant Hydraulic Fluids for the Die Casting Industry: Part 6—Safety & Use Factors," *PMM*, 1957, June, pp. 41–42.
106. A. Pollock, "The User's Experience of Hydraulic Systems Incorporating High Water Based Fluids," in *Conference Proceedings: Hydraulics, Electrics, and Electronics in Steel Works and Rolling Mills*, Mannesmann Rexroth GmbH; Lohr-am-Main, Germany.
107. Anon., "Are Your Hydraulic Oil Lines Fireproof?" *Mill Factory*, 1952, May, pp. 139–140.
108. Texaco, *Operation and Care of Hydraulic Machinery*, Texaco, Inc., White Plains, NY.
109. T. L. Jackson and R. C. Alston, "The Selection and Application of Fire Resistant Hydraulic Fluids," *Plant Eng.*, 1968, 12(12), pp. 743–748.
110. E. S. Kelly, "Fire Resistant Fluids: Factors Affecting Equipment and Circuit Design," *Proceedings of the 3rd Int. Fluid Power Symposium, BHRA Fluid Eng.*, 1973, pp. F1-1–F1-24.

Water–Glycol Hydraulic Fluids

GEORGE E. TOTTEN and YINGHUA SUN

Union Carbide Corporation, Tarrytown, New York

1 INTRODUCTION

Hydraulic systems use fluids for energy transmission. In 2000 B.C. the ancient Egyptians provided some of the earliest recorded uses of fluid power with their water-driven devices [1]. Hydraulic theories were developed by Pascal (1650) and Bramah (1795). However, industrial hydraulic systems were not developed in large scale until the early 1900s [1]. The most common hydraulic fluids were, and continue to be, derived from mineral oil.

In 1943, the U.S. Navy experienced numerous on-board ship and aircraft disasters resulting from hydraulic line rupture and subsequent ignition of the resulting sprays. This led to the development, by the Naval Research Laboratory, of a new class of fire-resistant hydraulic fluids known as *hydrolubes* [2–6]. Hydrolubes were defined as “polymer-thickened, corrosion-inhibited, aqueous fluids having one or more glycols as major constituents” [4]. Hydrolubes, also known as *water–glycol* hydraulic fluids, were patented in 1947 by Roberts and Fife [7]. Although the naval research and initial trials were successful, the use of HFC fluids in naval operations did not gain acceptance [8]. Early water–glycol compositions were only applicable for relatively low-pressure systems [9]. However, superior performing formulations suitable for high-pressure, ≥ 5000 psi, hydraulic pump use have been reported [10,11].

Water–glycol (W/G) hydraulic fluids, which are also designated as “HFC” fluids, are part of a larger class of fire-resistant hydraulic fluids, which include polyol ester, phosphate ester, oil-in-water (invert) emulsions, water-in-oil emulsions, and high-water-base hydraulic fluids (HWBHF). The ISO 6743/4 classification ratings for fire-resistant hydraulic fluids is provided in Table 18.1 [12,13].

Table 18.1 Fire-Resistant Hydraulic Fluid Classification According to ISO 6743/4

Category	Composition	Operational temperature
Water-based fluids		
HFAE	Oil-in-water emulsions, >80% water in final diluted fluid. (concentrate portion $\leq 20\%$)	5– $\leq 55^{\circ}\text{C}$
HFAS	Mineral-oil-free synthetic solutions, >80% water in final diluted solutions (concentrate portion $\leq 20\%$)	5– $\leq 55^{\circ}\text{C}$
HFB	Water-in-oil emulsions, 35–40% water in final diluted solution (mineral-oil portion $\leq 60\%$)	5– $\leq 60^{\circ}\text{C}$
HFC	Aqueous polymer solutions (hydrolules), water portion $\leq 35\%$ in final diluted solution	–20– $\leq 60^{\circ}\text{C}$
Water-free fluids		
HFDR	Phosphate ester fluids	–20– 70°C^a
HFDS	Chlorinated hydrocarbons	
HFDT	HFDR/HFDS blends	10– 70°C^a
HFDU	Synthetic fluids, other compositions	–35– $\leq 90^{\circ}\text{C}$

^aFor hydrodynamic couplings, the maximum temperature is 150°C .

From 1940 to 1950, a number of fires originating with mineral-oil hydraulic fluids occurred, resulting in the loss of lives and destruction of expensive equipment and buildings [14,15]. HFC fluids, originally developed and commercialized for the Navy, were well suited for use as fire-resistant hydraulic fluids for various industries where high-temperature processing was performed. High-temperature uses include heat treating [14], plastics [15], zinc and aluminum die casting [16], coal mining [13,16], iron and steelmaking [17,18], hydraulic presses [18], and machine tools for the automotive industry [18]. Over the years, various pumps have been developed for use with HFC fluids [19,20], proper operating conditions have been established [21] and fluid performance has significantly improved due to formulation improvements [22,23]. A list of illustrative hydraulic applications of different fire-resistant hydraulic fluids is provided in Table 18.2 [13].

This chapter will provide an overview of water–glycol fluid composition, physical and chemical properties, lubrication evaluation and properties, pump derating, bearing consideration, maintenance, and system conversions.

2 DISCUSSION

2.1 Water–Glycol Hydraulic Fluid Composition

Water–glycol (W/G) hydraulic fluids contain water, glycol, thickener, and an additive package [18,24–27]. The general classes and functions of W/G hydraulic fluid formulation components are summarized in Table 18.3. The additive package typically

Table 18.2 Hydraulical Equipment and Machinery Using Fire Resistant Fluids in Underground Mining

Use	Hydraulically driven machinery and equipment	Hydraulic Fluids Used					Drive	
		Water	HFA	HFC	HFD	Mineral oil	Hydrostatic	Hydrodynamic
Off-highway	Drill carriages and drills			X			X	
	Percussion drills			X			X	
	Side-tipping loaders			X			X	
	Drilling/milling-type roadheaders			X			X	
	Impac rippers			X			X	
	TBMS			X			X	
	Fluid couplings	X						X
Coal mining	Drum shearer-loaders (winches)			X	X		X	
	Pumps for powered support		X				X	
	High-pressure water inductions system	X					X	
	Fluid couplings	X						X
Infra-structure	Rope-driven transport systems		X	X		X		
	Diesel monorail locos		X			X		
	Hydraulic monorail transport units		X			X		
	Diesel locos (floorbound)					X	X	
	Chain creepers		X	X		X		
	Fluid couplings	X					X	
Other	Trackless vehicles (drive line)			X			X	X
	Small equipment ($V > 10$ L)						X	
	Electro-hydraulic control units			X				X

Table 18.3 Water–Glycol Hydraulic Fluid Composition

Component	Purpose
Water	Fire protection
Glycol	Freeze point reduction and some thickening
Thickener	Thicken the formulation and provide adequate film viscosity at the wear contact
Antiwear additives	Provide mixed-film and some boundary lubrication
Corrosion inhibitors	Vapor and liquid corrosion protection

consists of amines for corrosion inhibition, antiwear additives (typically carboxylic acids), dyes to facilitate system leak detection, antifoams to reduce foaming and air entrainment, and so forth. The most common glycols used in water–glycol hydraulic fluid formulations are ethylene glycol (I), diethylene glycol (II), and propylene glycol (III):



The most common glycol in use in the world today for water–glycol formulation is diethylene glycol [24].

The role of the glycol in reducing the freezing point of the mixture is illustrated in Fig. 18.1 [3]. Figure 18.1 shows that the minimum freezing point of the ethylene glycol (also known as “monoglycol”) is produced at -65°F when a eutectic mixture (67%/33% by volume of ethylene glycol/water) is formed. Although this composition produces the minimum freezing point, very small changes in water content produce relatively large increases in the freezing point. Similar data, in addition to other physical properties, for diethylene glycol (diglycol) and propylene glycol are found in the appendices to this volume.

There are at least two problems with using a water–glycol fluid. One is poor film thickness and the other is a poor viscosity index (VI). This problem is addressed by the use of a thickener. The thickener most often used is a poly(alkylene glycol) —PAG (IV), which is a “random” copolymer of ethylene oxide and propylene oxide [3]. Poly(alkylene glycol) polymer configurations may be branched [27] or linear, such as the linear polymer shown by (IV) [24]:



One of the first poly(alkylene glycol) thickeners reported for use in hydrolube formulation was UCON[®] Lube 75H 90,000, which is a copolymer containing 75% by weight oxyethylene units designated as $(\text{CH}_2\text{CH}_2\text{O})$ and 25% by weight of oxypropylene units, which is designated as $(\text{CH}_2\text{CH}(\text{CH}_3)\text{O})$ in (IV) [3]. The polymer exhibits a viscosity of 90,000 SUS at 100°F . The thickening and viscosity–temperature behavior of a 55 (ethylene glycol)/45 (water) mixture with varying quantities of 75H 90,000 added is shown in Table 18.4 [3]. Based on recommendations made by the Bureau of Aeronautics, the fluid–thickener combination was selected to provide a minimum viscosity of 10 cS at 130°F , maximum viscosity of 2000 cS at -40°F , and a freezing point of $\leq -50^\circ\text{F}$.

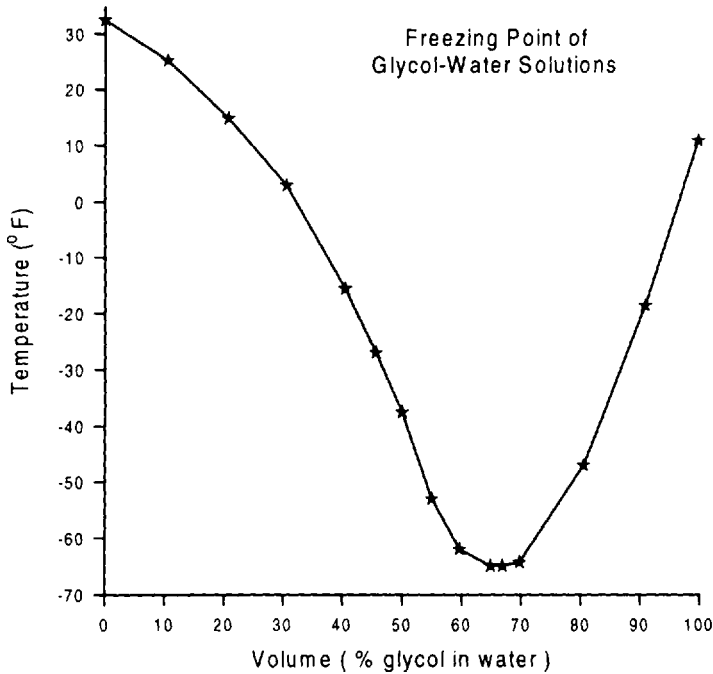


Figure 18.1 Freezing points of ethylene glycol–water mixtures.

In addition to the antiwear additives, it is important to recognize that both the water content and corrosion inhibitors that are present in a W/G hydraulic fluid may dramatically affect antiwear performance. In Fig. 18.2, it is shown that water concentrations in excess of approximately 40% will result in corresponding decreases in pump wear performance [28]. Spikes (see Fig. 18.3) has shown that fluid-film thickness decreases rapidly as water content increases, a phenomenon that will increase wear [29]. Water concentrations greater than approximately 35% are believed

Table 18.4 Viscosities of a Poly(Alkylene Glycol)-Thickened Ethylene Glycol–Water Mixture

% UCON® Lube 75H 90,000 in a 55%/45% by weight Ethylene Glycol–Water Mixture	Temperature				
	–40°F	0°F	100°F	130°F	210°F
0	134.0	25.0	2.6	1.74	0.79
5	552.1	86.9	7.0	4.53	1.93
10	1500	223.0	16.5	10.06	3.66
20	—	1007.0	60.0	35.3	13.9
30	—	3730	170	98.9	34.9
40	—	—	—	236.2	79.1
50	—	—	—	498.7	158.8

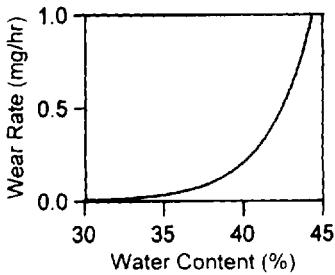


Figure 18.2 Effect of water content on ASTM D 2882 V-104 Vickers vane-pump wear for a water-glycol hydraulic fluid.

necessary to provide the desired fire safety [30,31]. For these reasons, water-glycol fluids typically contain 35–40% water.

Because W/G fluids contain water, corrosion inhibition is necessary. One corrosion-inhibitor system that may be used for water-glycol hydraulic fluids is based on an amine additive system. As originally reported by Brophy et al. [3], the concentration of the corrosion inhibitor, which may be quantitatively measured by “reserve alkalinity” determination, may also affect wear rates as shown in Fig. 18.4 [28].

2.2 Chemical and Physical Properties—General Comparison

To perform acceptably in a hydraulic system, any fire-resistant hydraulic fluid, including water-glycol fluids, must exhibit the following properties [32]:

- Good fire resistance
- Proper viscosity

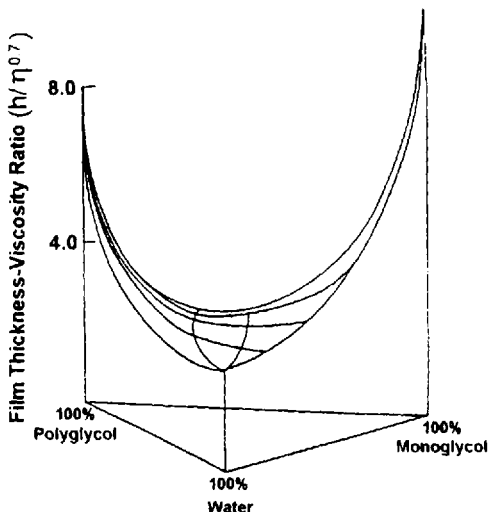


Figure 18.3 Effect of water, ethylene glycol, and poly(alkylene glycol) thickener composition on film thickness and viscosity.

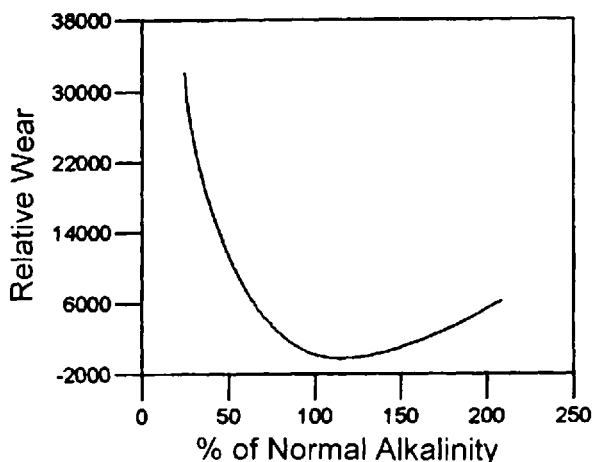


Figure 18.4 Effect of amine concentration (reserve alkalinity) on ASTM D 2882 V-104 Vickers vane-pump wear for a water-glycol hydraulic fluid.

- Good resistance to oxidation and deposit formation
- Good wear resistance
- Good resistance to rust and corrosion
- Low foaming
- Seal compatibility
- Paint compatibility

A general qualitative comparison of water-glycol hydraulic fluids to water-in-oil emulsions, phosphate esters, and an antiwear mineral oil is provided in Table 18.5 [20,33]. A more specific comparison of a water-glycol fluid to a mineral oil is provided in Table 18.6 [22]. The dependence of these properties on temperature and pressure is shown in Tables 18.7 and 18.8, respectively. *Note:* Physical property data are always dependent on the composition of the formulation being compared. Therefore, the specific data shown here should only be taken as illustrative examples. The reader should obtain the specific data of interest from the supplier of the fluid being considered.

2.2.1 Vapor Pressure

The vapor-pressure dependence on temperature is shown in Fig. 18.5. Above approximately 65°C (150°F), the vapor pressure of a water-glycol hydraulic fluid, like other water-containing fluids, rapidly increases with increasing temperature [22]. Therefore, to minimize the potential for evaporative water loss, pressurized reservoirs should be used if fluid temperatures are to exceed 65°C (150°F).

2.2.2 Viscosity

Fluid viscosity is not only an important parameter with respect to hydraulic system operation, but it is also important with respect to lubrication. Therefore, it is desirable that the hydraulic fluid viscosity exhibit as small a change in viscosity with varying temperature as possible. Figure 18.6 shows that water-glycol hydraulic fluids, as a

Table 18.5 Generic Physical Property Comparison of Different Fire-Resistant Hydraulic Fluids with an Antiwear Petroleum Oil

	Antiwear oil	Water-glycols	Water-in-oil emulsions	Phosphate esters
Properties				
Specific gravity	0.85	1.09	0.91	1.15
Flash point (°F)	420	None	None	500
Autogenous ignition temperature (°F)	650	830	830	1100+
Bulk fluid temperature limits (°F)	-20-180	0-150	15-150	20-200
Low-temperature performance	Excellent	Excellent	Good	Fair
Lubricity	Excellent	Good	Good	Excellent
Oxidation stability	Excellent	Good	Good	Excellent
Rust protection	Good	Good	Good	Fair to good
Bulk modulus	Medium	Medium	Medium	High
Foaming resistance	Excellent	Good	Excellent	Good
Air release	Good to excellent	Fair to good	Fair to good	Fair
Compatibility				
Oil-resistant paint	OK	No	OK	No
Nonferrous metals	OK	Check ^a	OK	OK
BUNA N (nitrile)	OK	OK	OK	No
Butyl	No	OK	No	OK
Neoprene	OK	OK	OK	No
Silicone	No	OK	No	OK
Viton	OK	OK	OK	OK
Paper	OK	Check	Check	Check

^aNot compatible with zinc, cadmium, lead, magnesium, and unanodized aluminum.

Table 18.6 Quantitative Comparison of Physical Properties Between a Petroleum Oil and a Water–Glycol Hydraulic Fluid

Property	Water–Glycol (41 cS at 50°C)	Petroleum oil (36 cS at 50°C)
Density (g/cm ³ at 15°C)	1.060	0.885
Vapor pressure (mbar at 50°C)	80	0.001
Vapor pressure (mbar at 70°C)	182	0.02
Air solubility % at 20°C/1030 mbars	27–30	9
Compressibility at 20°C/bar	51×10^{-6}	65×10^{-6}
Specific heat at 20°C (J/g °C)	3.3	1.8
Thermal conductivity (mW/cm °C)	3.0	1.3

Table 18.7 Dependence of Water–Glycol Fluid Physical Property on Temperature

Temperature (°F)	Viscosity (lb/ft min)	Density (lbs/ft ³)	Specific Heat (BTU/lb.)	Thermal conductivity (BTU/ft °F)	Vapor pressure (psia)
160	0.546	65.0	0.737	0.26	3.7
130	0.842	65.8	0.729	0.26	1.7
100	1.39	66.5	0.719	0.26	0.74
0	20.7	68.5	—	—	—
–30	83.5	69.1	—	—	—
–35	113	69.1	—	—	—

Table 18.8 Dependence of Water–Glycol Fluid Physical Property on Pressure

Pressure (psi)	Compressibility (psi ⁻¹ at 78°F)	Viscosity (cps)	
		100°F	150°F
1,000	3.58×10^{-6}	35	14.1
2,000	3.24×10^{-6}	36	14.3
3,000	3.14×10^{-6}	37	14.8
10,000	2.96×10^{-6}	44	18
20,000	—	56	23
30,000	—	70	28

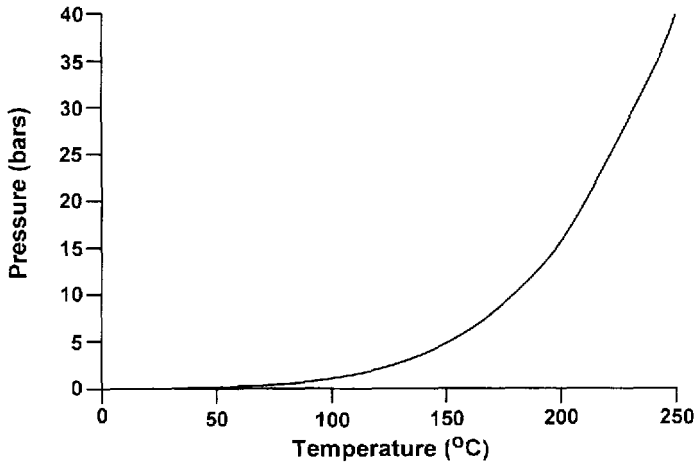


Figure 18.5 Effect of water-glycol hydraulic fluid temperature on vapor pressure.

class, exhibit significantly less variation in viscosity with respect to temperature than mineral oils, petroleum oil, and, especially, phosphate esters [34]. Figure 18.7 shows that the variation of viscosity response of water-glycols with varying temperature is similar for different viscosity grades.

The viscosity of water-glycol hydraulic fluids is dependent on water concentration, as illustrated in Fig. 18.8 [30]. Clearly if excessive water additions are made to a system containing a water-glycol, low fluid viscosities will be obtained, which may lead not only to poor hydraulic response but also poor lubrication because of

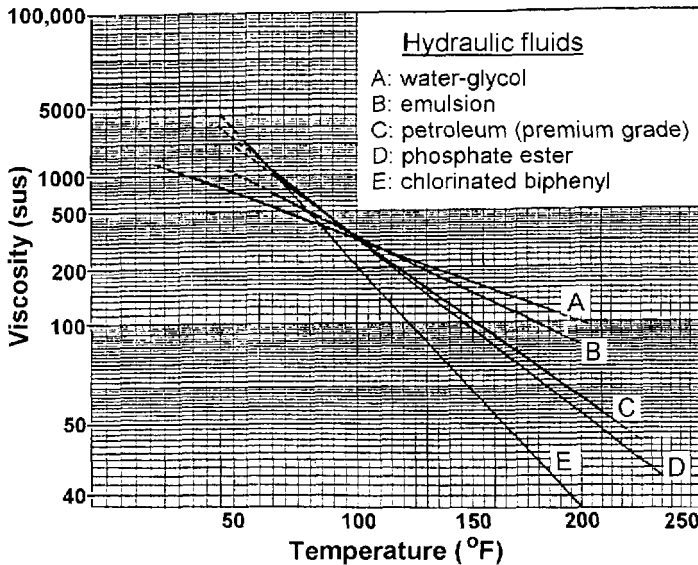


Figure 18.6 Viscosity-temperature relationships for a number of hydraulic fluids, including a water-glycol hydraulic fluid formulation.

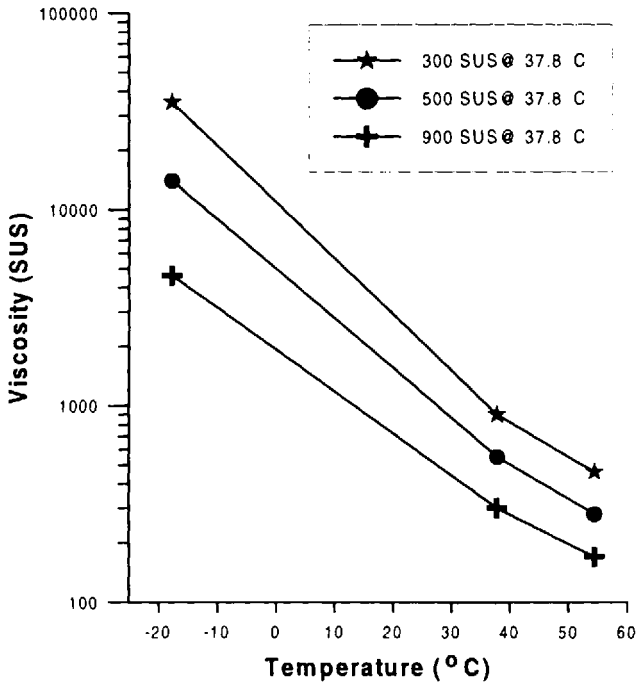


Figure 18.7 Effect of water-glycol hydraulic fluid viscosity on the viscosity-temperature relationship.

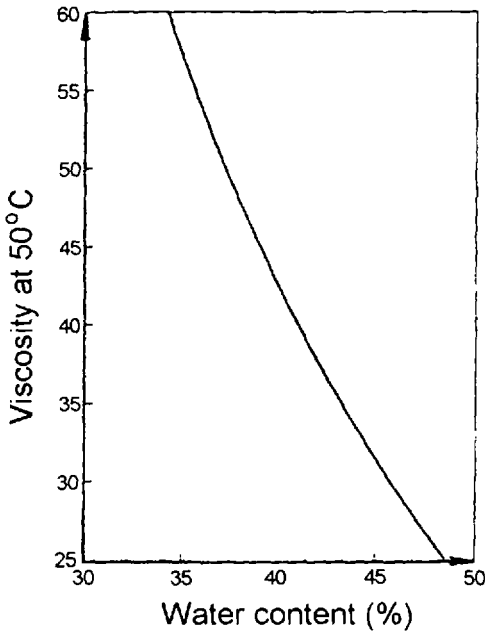


Figure 18.8 Effect of water content on water-glycol hydraulic fluid viscosity.

insufficient film thickness at the wear contact. (See Figs. 18.2 and 18.3). The loss of sufficient amounts of water by evaporation will result in excessively high viscosities and loss of fire resistance if the water concentration is less than 30–35% [30]. Although slightly different charts will be obtained for different water–glycol fluids, the overall responses will be the same. These data show why it is important to maintain the correct water concentration in use.

Generally, water–glycols are not used at temperatures above approximately 60°C [35]. However, if pressurized reservoirs are used, fluid temperatures of 60–70°C are possible [30]. Low-temperature limits vary from approximately 10°C to about –25°C, depending on the fluid [35].

2.2.3 Viscosity Stability

Newtonian Versus Non-Newtonian Behavior

Although numerous water-soluble polymers have been used as thickeners for W/G fluids, the most common thickener in use from the time of initial development (1947) [3] until the present time is poly(alkylene glycol) (PAG). PAG thickeners provide Newtonian thickening behavior, which means that the fluid does not undergo significant viscosity loss due to shear thinning (temporary or permanent) during use; therefore, fluid viscosity is independent of shear rate.

The Newtonian behavior of a recently developed W/G fluid in shear fields typically found in hydraulic pumps was recently demonstrated using high-shear capillary viscometry [36]. The results shown in Fig. 18.9 illustrate that a W/G hydraulic fluid containing a “typical” PAG polymer thickener does not undergo any significant shear-thinning behavior that would lead to hydraulic leakage and corresponding loss of pump efficiency. Similar high-shear viscometry results have been reported by Isaksson [37].

Mechanical Shear Degradation

Shear rate is defined as “the ratio of the velocity of the fluid divided by the clearance” [38]. High shear rates may be encountered in numerous areas within the hydraulic pump, such as the relief valve seat and roller bearing assemblies. Very

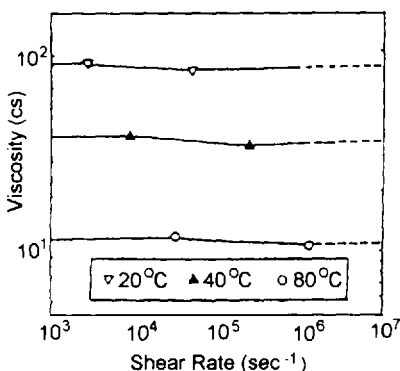


Figure 18.9 High-shear-rate viscosity profile of a water–glycol hydraulic fluid at different fluid temperatures.

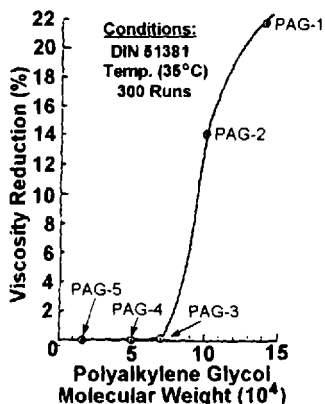


Figure 18.10 Stability of different poly(alkylene glycol) polymers to mechanodegradation.

high-shear fields, approximately 10^6 s^{-1} , have been estimated to be present in hydraulic pumps [39].

A hydraulic fluid may not only undergo viscosity losses when subjected to high shear rates due to non-Newtonian behavior, but the polymer used to thicken some non-PAG-containing W/G hydraulic fluids may actually undergo molecular degradation (mechanodegradation), resulting in *permanent* viscosity loss. Shear stability is related to the molecular weight of the thickener as illustrated in Fig. 18.10 [18].

The shear stability of PAG-thickened water–glycol hydraulic fluids is illustrated in Fig. 18.11 for a series of fluids subjected to an ultrasonic shear test [40]. In this example, it is observed that typical PAG-thickened W/G hydraulic fluids were shear stable, as evidenced by no viscosity loss in the ultrasonic shear test, which means that the polymeric thickener is not expected to produce a permanent viscosity loss in the high-shear conditions encountered during operation in the hydraulic pump.

Shear stability testing procedures are reviewed in Chapter 4. In addition to the ultrasonic shear stability test shown above, Blanpain [30] has reported that water–glycol hydraulic fluids will easily pass a Fuel Injector Shear Stability Test (FISST), ASTM D 5275 [41], or the Kurt Orbahn method [42].

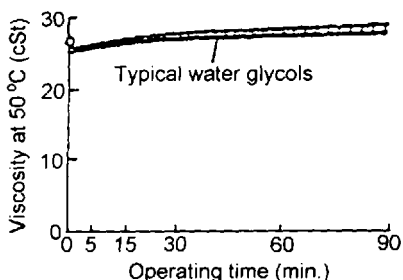


Figure 18.11 High-shear-rate stability of different water–glycol hydraulic fluids according to an ultrasonic high-shear stability test. The “typical” water–glycols were thickened with a poly(alkylene glycol) polymer. In the experiment, water–glycol was thickened with a non-PAG polymer thickener.

2.2.4 Foaming and Air Release

Although some water–glycols may exhibit longer air-release times than petroleum–oil hydraulic fluids [30,43], properly formulated fluids should exhibit comparable air-release properties to a premium petroleum oil [32]. Foaming and air-release properties and testing procedures were discussed in Chapter 4 and will not be discussed in detail here. To reduce air entrainment, reservoir capacity should be increased and a baffle placed between the suction and return lines. The fluid return line should be placed below the air–liquid surface.

2.2.5 Nitrosamine Formation

Some of the earliest corrosion inhibitors used in W/G hydraulic fluid formulation included sodium nitrite and amine nitrites [44]. The technology available at the time required the use of these particular additives in order to achieve the necessary solution, vapor, and dry-film corrosion-inhibition properties. However, recent concerns over potential nitrosamine formation [45] during use of these additives, particularly in metalworking and cosmetic formulation, led to the development of non-nitrite-containing W/G hydraulic fluids [10,11]. Nitrite-containing additives are no longer used in W/G hydraulic fluid formulations in the United States.

Currently, various amine-containing corrosion-inhibitor additives are used that provide outstanding corrosion protection in use. The vapor- and liquid-phase corrosion-inhibition properties of a typical W/G hydraulic fluid is illustrated in Fig. 18.12. These inhibitory properties are maintained during use, as long as the concentration of the corrosion inhibitor is maintained [46].

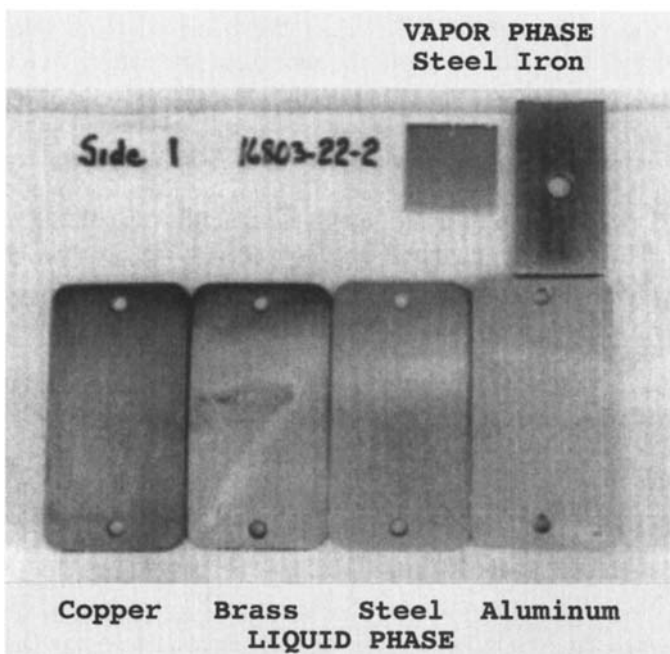


Figure 18.12 Illustration of vapor- and liquid-phase corrosion inhibition for a water–glycol hydraulic fluid obtained with an amine-containing additive.

2.2.6 Phenol Content

Increasingly stringent regulation of allowable wastes into water emitted from aluminum die-casting plants has caused the aluminum die-casting industry, a major user of fire-resistant hydraulic fluids, to limit the incoming "phenol content" of their hydraulic fluids. Hydraulic fluids are discharged from the plant as a result of fluid leakage from the hydraulic systems during use. The idea is that if there are no "phenolics" contained in the incoming fluid, then they should not be present in the waste water, as no phenolics are used in the plant.

One of the specified analytical procedures for determination of phenols and phenolic derivatives, according to the *Federal Register* (40 CFR 403 and 40 CFR 464), is the 4-aminoantipyrine (4-AAP) colorimetric titration procedure [47], which is illustrated in Fig. 18.13.

In this procedure, 4-AAP is reacted with a phenolic substrate to yield a highly colored dye which is quantitatively analyzed by visible spectroscopy at 460 nm. Because this is a colorimetric procedure, any substrate capable of reacting with 4-AAP and producing a colored product will cause an interference and produce erroneous phenol-content values. Therefore, this test has been called the "phenol-response" test in the industry, because the analysis is based on the formation of a colored dye and is not necessarily indicative of the actual phenolic content of the fluid. Although some fluid formulations do contain very low levels of "phenol response," in many cases there were no actual phenolic derivatives and false interference "phenol-response" results have been obtained. Nevertheless, it was necessary to assist the die-casting industry to comply with the federal wastewater requirements. This necessitated the development of fluids that contain no phenolics and do not produce any unacceptable "phenol-response" to the 4-AAP analysis.

2.2.7 Oxidative Stability

It is well known that a hydraulic fluid may undergo oxidation during prolonged use. Mineral oils, polyol esters, and other fluids may form sludge, resulting in poor lubrication if a sufficient amount of these oxidation by-products are present. Water-glycol hydraulic fluids, when used at temperatures less than 150°F, do not result in any sludge formation [32]. Higher temperatures (>150°F) may result in slight sludge formation, as shown in Fig. 18.14 [32,48]. However, any sludging or "gumming" that may be observed is often attributable to contamination by petroleum oils that may be present after initial system conversions or by adding the wrong fluid to the water-glycol-containing reservoir [48]. Oxidation at higher temperatures may be simply due to coevaporation of corrosion inhibitors, which may also inhibit oxidation, as will be discussed subsequently.

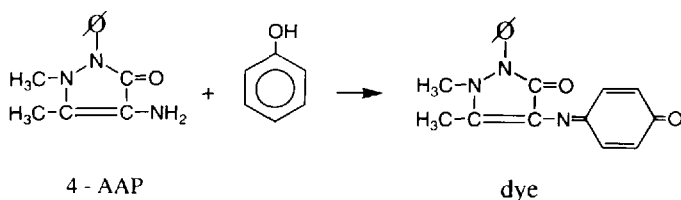


Figure 18.13 Phenol derivitization by the 4-aminoantipyrine (4-AAP) reaction.

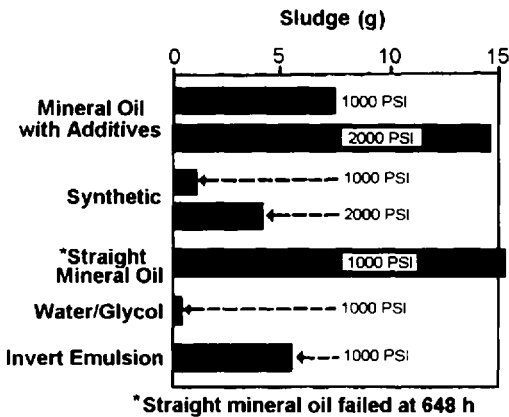


Figure 18.14 Relative propensity for sludge formation for various classes of hydraulic fluid.

Iwamiya studied the thermal stability of a PAG-thickened water–glycol hydraulic fluid at elevated temperatures in a seal tube where evaporation could not occur. The results of this study are shown in Fig. 18.15 [18]. From these results, it is apparent that fluid viscosity will decrease at points of localized high temperature. This should be contrasted to mineral oils, for which viscosity increases and sludging occur under the same conditions.

Oxidation Mechanism

Igarashi recently described some of the mechanisms encountered in the oxidation of mineral oils [49]. Oxidation of hydraulic fluids is accelerated when the fluid is abused either by overheating or by aeration. Water–glycol hydraulic fluids are also potentially susceptible to various oxidative-degradation processes if they are abused. In some cases, as with other classes of hydraulic fluids, by-products from degradation reactions may interfere with the wear-inhibiting mechanism of the additives used for fluid formulation.

FLUID DEGRADATION MECHANISM. The oxidation and thermal degradation processes for anhydrous poly(alkylene oxides) are well known and have been published previously [50]. Figure 18.16 illustrates the potential degradation processes for an uninhibited anhydrous poly(ethylene oxide) homopolymer [46]. This degra-

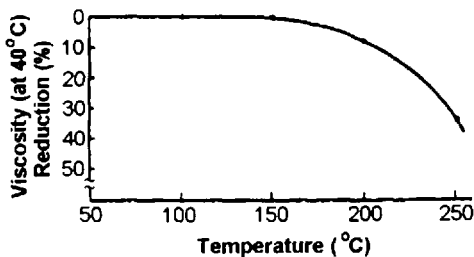


Figure 18.15 Thermal-oxidative stability of a water–glycol hydraulic fluid.

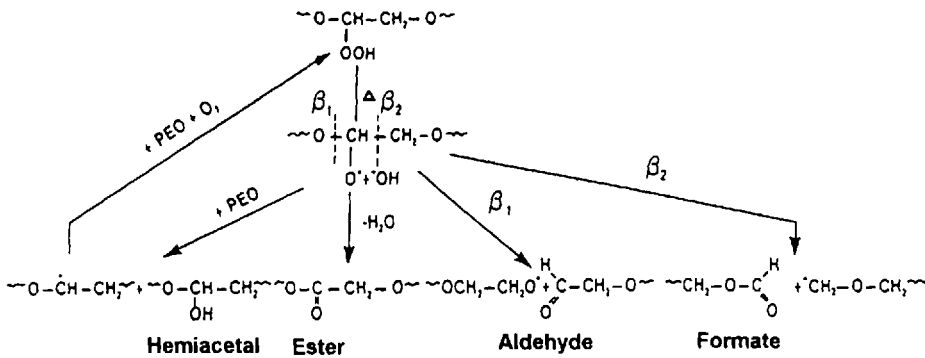


Figure 18.16 Mechanistic pathway for uncatalyzed thermal oxidation of an anhydrous poly(ethylene oxide).

ation pathway is also pertinent for diethylene glycol, which is present in most water-glycol hydraulic fluids today and is representative, although considerably less complex, to that of a poly(alkylene oxide) copolymer of ethylene and propylene oxide, which is present in most water-glycol hydraulic fluids as a thickener.

It is known that the oxidative-degradation processes illustrated in Fig. 18.16 are slower in the presence of water than in their nonaqueous state [51]. During normal use, water-glycol hydraulic fluids do not form low-molecular-weight carboxylic acid by-products, or at least not at a significant rate during the lifetime of the fluid. The corrosion literature provides at least two examples of degradation pathways that elucidate the potential oxidative-degradation mechanism for water-glycol hydraulic fluids [52,53].

The kinetics and severity of degradation of aqueous ethylene glycol coolant solutions were studied at 100°C and 180°C in solutions containing metals by Beavers (presumably in a sealed tube) [53]. The conclusions from this study were as follows:

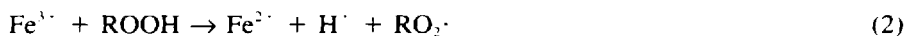
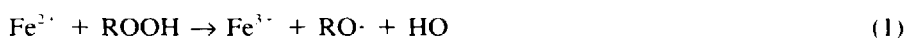
- Although degradation of aqueous ethylene glycol did not occur in the absence of metals, it was accelerated by their presence, although very slowly, even at these elevated temperatures.
- Degradation of ethylene glycol was accompanied by the generation of low-molecular-weight carboxylic acids and decreasing pH.
- Aeration only slightly accelerated the degradation process.
- The rate of degradation at 100°C and 180°C was essentially the same, which is unusual considering the temperature difference.

Subsequent work by Brown et al. showed that formic acid was one of the by-products in the oxidative degradation of aqueous ethylene glycol [52]. The rate of degradation was accelerated by the presence of copper(II) salts of these acids which arise from the corrosion of copper in the system [52]. {Earlier work by Beavers showed that iron(III) salts similarly catalyzed the degradation reaction [53].} The presence and concentration of organic acids, including formic acid, was determined by ion chromatography [54].

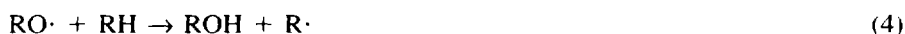
Taken together, the results reported by Brown et al. [52] and Beavers [53] suggest that water-glycol hydraulic fluids degrade by a metal-catalyzed oxidative process that is nearly independent of solution temperature but is slowly accelerated

by aeration. These observations would suggest that the degradation process would be inhibited when the system is properly protected against corrosion and that degradation would then be accelerated by any process that would cause substantial depletion of the corrosion inhibitor below a "critical" level. This is the concentration below which there is insufficient inhibitor remaining to inhibit the formation of soluble corrosion metal by-products.

These results can be explained by a previously published metal-catalyzed peroxide degradation mechanism [55,56]. It is known that metal ions such as iron(III) and copper(II) will catalyze the degradation of peroxide species (ROOH), such as those shown in Fig. 18.16, which are formed in the oxidative degradation of glycols, such as ethylene glycol, diethylene glycol, propylene glycol, and poly(alkylene glycol) copolymers [51]. In fact, this process can be catalyzed by various metal ions, including both iron(III) and copper(II):

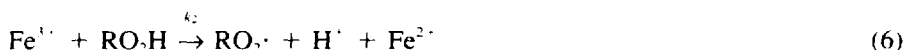


In Eqs. (1) and (2), both $\text{RO}_2\cdot$ and $\text{RO}\cdot$ are capable of undergoing further free-radical generating reactions such as



It is important to note that the presence of metal ions does not catalyze the formation of peroxide during the oxidation reaction. Instead, the metal ions catalyze the decomposition of the peroxide species after their formation by the process shown in Fig. 18.16 [46]. Of course, the peroxide intermediate may also decompose without the presence of metal ions, but this process would be much slower.

The relative kinetic reactions of these two possible degradation routes, uncatalyzed and catalyzed, can be represented as [46]



$$-\frac{d[\text{ROOH}]}{dt} = k'[\text{ROOH}] \quad (7)$$

$$= k_1[\text{ROOH}] + k_2[\text{Fe}^{3+}][\text{ROOH}] \quad (8)$$

where k' represents the overall hydroperoxide decomposition rate constant k_1 and k_2 are uncatalyzed and catalyzed hydroperoxide decomposition rate constants, respectively. Lloyd has reported that the relative rate of k_2/k_1 is approximately 100,000/1 [51].

This mechanism explains why the oxidation rate of glycols in the absence of metal ions would be expected to be relatively slow, as observed by Brown et al. and Beavers [52,53] (and other water-glycol hydraulic fluid users). This was observed in practice when various amines and amine blends were used as corrosion inhibitors for water-glycol hydraulic fluids [57]. Fluid suppliers generally recommend that the level of the corrosion inhibitor in the system be maintained by periodic monitoring and replenishment, if necessary. The only systems where fluid degradation produced

substantial quantities of formic acid were those that exhibited a corresponding loss of reserve alkalinity (amine corrosion inhibitors) [57]. Thus, the reserve alkalinity must be maintained if optimal fluid stability is to be achieved. Appropriate maintenance procedures are recommended by the fluid supplier, which will provide adequate control in operating systems.

EFFECT OF FORMIC AND ACETIC ACID ON PUMP WEAR. The effect of formic acid and reserve alkalinity on wear rate exhibited by a typical water–glycol hydraulic fluid in a hydraulic pump was studied by simply adding the desired quantity of the low-molecular-weight carboxylic acid (formic and acetic acid were used for this work) to the water–glycol fluid used in this study, using a statistically designed experimental matrix.

The reserve alkalinity, which is directly related to the concentration of the amine corrosion inhibitor present in the fluid, was determined for each fluid tested. Upon the addition of the formic or acetic acid, it was found that the reserve alkalinity decreased, which was expected. For the “high” amine-containing fluids, additional amine (in this case, morpholine) was added to bring the total reserve alkalinity of the formic-acid-spiked fluid into the recommended maintenance range. The “low” reserve alkalinity data points represent the fluids where formic acid was formed and reserve alkalinity was not maintained. The “high” reserve alkalinity data points represent fluids where reserve alkalinity was maintained, even though formic acid may be present. The experimental matrix and the data obtained from this study are summarized in Fig. 18.17 [46].

The results shown in Fig. 18.17 indicate that formic acid concentrations above 0.15% do, in fact, produce an accelerated wear rate, especially at concentrations above 0.30%, which is consistent with the results reported earlier [55]. (A typical wear rate of approximately 0.15–0.20 mg/h would be expected for this particular fluid when low-molecular-weight carboxylic acids are absent.) However, the data do show, as Brown et al.’s and Beaver’s results suggest it should, that reserve alkalinity

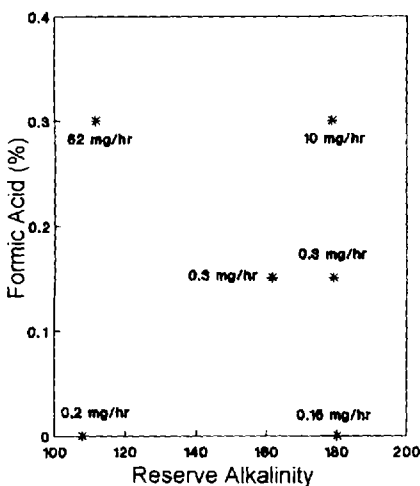


Figure 18.17 Two-dimensional experimental design matrix to illustrate the effect of formic acid and reserve alkalinity on pump wear.

must be maintained to at least minimize the wear increase caused by the presence of formic acid.

Another low-molecular-weight acid that may be formed by oxidative degradation of the glycol and poly(alkylene glycol) is acetic acid. To evaluate the effect of acetic acid on wear rate, a pump test was performed on a fluid spiked with 0.3% acetic acid without adjusting for the corresponding decrease in reserve alkalinity arising from the acid addition. The wear rate obtained was 0.31 mg/h, which is substantially lower than the corresponding value for the same concentration of formic acid addition (61.5 mg/h, Fig. 18.17).

EFFECT OF THE PRESENCE OF FORMIC ACID ON CORROSION. Formic acid probably acts to increase hydraulic pump wear by selective adsorption at the active site on steel or other metallic surface, thus blocking the necessary chemisorption of the antiwear additive. This same mechanism would be expected to produce greater corrosion for formic-acid-containing fluids. To study this effect, the relative corrosion performance of three fluids [a typical water-glycol with no formic acid added which had a reserve alkalinity (RA) = 179, a similar fluid with 0.3% formic acid added but without reserve alkalinity adjustment (RA = 108), and the same fluid with 0.3% formic acid addition but with reserve alkalinity adjustment by morpholine addition (RA = 176)]. The "200-Hour Corrosion Test" used for this work is described in Section 2.2.8. Figure 18.18 shows that the corrosion obtained with the formic-acid-spiked fluid was not significantly higher than that obtained for the unspiked fluid [46].

These observations are consistent with the corrosion results reported previously by Beavers [53]. They are also different from the relative order of pump wear rates discussed earlier. Even though formic acid may be selectively adsorbed relative to a less acidic carboxylic, also in the amine salt form, there is still sufficient protection to effectively inhibit corrosion, even though higher wear rates were obtained for this same level of formic acid. However, these results are limited and *do not* imply that sufficient corrosion protection would result at all possible formic acid concentrations.

2.2.8 Corrosion

There are numerous tests that have been used to determine the corrosion resistance offered by water-glycol hydraulic fluids. In this section, selected test procedures used to evaluate corrosion properties of water-glycol hydraulic fluids will be discussed.

Pump Testing

One of the first tests was to run a pump test using the fluid of interest and inspect the different components both visually and by weight loss to determine material compatibility (corrosion) [58–60]. Although this test procedure does provide the necessary corrosion-inhibition information, there are at least three problems. One problem is the relatively high cost of the pump, components, and energy consumed to perform the test. The second problem is that different pumps utilize different materials of construction. Therefore, more than one pump test will be required to obtain data on the range of materials of interest. This problem, however, has been addressed by mounting the test coupons of the materials of interest on a glass rack and immersing them in the 5-gal reservoir of the Vickers V-104 vane pump used to conduct the ASTM D 2882 pump test and monitoring the appearance and weight

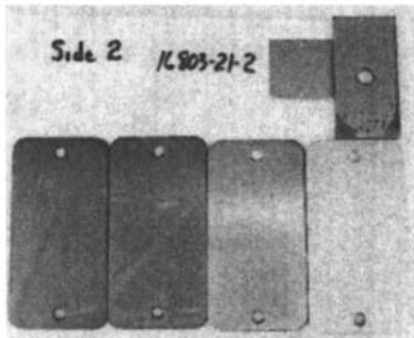
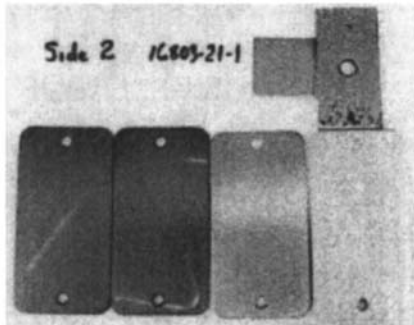
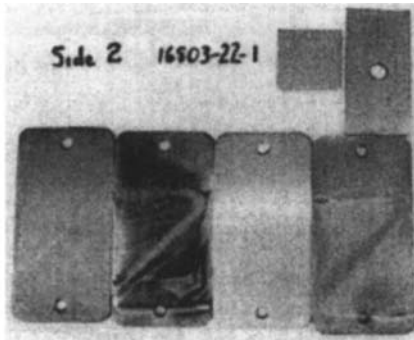


Figure 18.18 Illustration of the effect of the presence of formic acid on metal corrosion. Fluid 1 contains no additional formic acid, Fluid 2 contains % formic acid without adjusting reserve alkalinity, and Fluid 3 contains 0.3% formic acid with readjustment of reserve alkalinity to initial condition.

loss at the conclusion of the test [58–60]. The third problem is that long running times, >100–200 h, are often required to obtain the necessary long-term compatibility information. This is not an accelerated test.

Static Tests

In the static test, five metal coupons (aluminum, bronze, steel, copper, zinc, and brass) are mounted on a glass rack and placed in a 400-mL beaker as described in

Section 4.4.4.1 of Procedure B of Mil-H-19457. After static (no fluid flow) immersion using 300 mL of fluid at 130°F (or 158°F) for a testing period of 90 h or 1 week, the corrosion resistance of the coupons is rated visually and gravimetrically [58].

Blanpain has reported on the use of a similar method in which the test metals, aluminum, copper, brass, zinc, cadmium, and copper/zinc are immersed in a flask containing the water–glycol fluid of interest and the sample/fluid–containing flask is then stoppered and immersed in a liquid constant-temperature bath at 35°C. The method may also be modified to evaluate vapor-phase corrosion protection [43].

Modified Turbine-Oil Rust Test

The metal coupons are cleaned, mounted on a glass rack, and then placed into the 400-mL Berzelius beaker used for the ASTM Turbine Oil Rust Test (ASTM D 665) [61]. The test coupons are then covered with 300 mL of the fluid. The fluid is agitated by using a shortened paddle attached to the drive spindle of the test apparatus. The paddle stem is shortened to provide clearance over the glass rack, which is immersed in the beaker. The plastic cover for the beaker is used and the fluid is held at 140°F while agitating at 1000 rpm. At the conclusion of the test, the coupons are inspected visually for rusting and weighed.

In general, dynamic tests (those with agitation) provide much better correlation of corrosion results to a pump test than do static tests (no agitation) [58].

Electrochemical Methodology

There are a number of electrochemical tests that have been reported to determine corrosion-resistance potential [62]. One test that has been specifically reported for use to determine the corrosion-protection potential of water–glycol hydraulic fluids was reported by Katorgin and Romanova [63]. In this test, the rate of contact corrosion is calculated from the intensity of the electrical current between electrodes of different metals immersed into the water–glycol fluid. A schematic of the test cell is provided in Fig. 18.19 [63].

The working electrodes, which are located parallel to one another, model the materials used for the hydraulic pump of interest. The remaining surfaces of the electrode are coated with an epoxy coating. To eliminate electrical resistance, the value of the current intensity reduced to zero resistance was used for the calculations. The rate of contact corrosion is calculated from

$$V = \frac{3.627Ai}{zQ}$$

where

- V = the corrosion rate of the anode metal (mm/yr)
- A = the atomic mass of the metal (g)
- i = the current density (mA/cm²)
- z = the ionic charge on the dissolved metal
- Q = the density of the anode metal (g/cm³)
- 3.627 = the conversion factor (yr⁻¹ × mA⁻¹)

The current density is calculated from

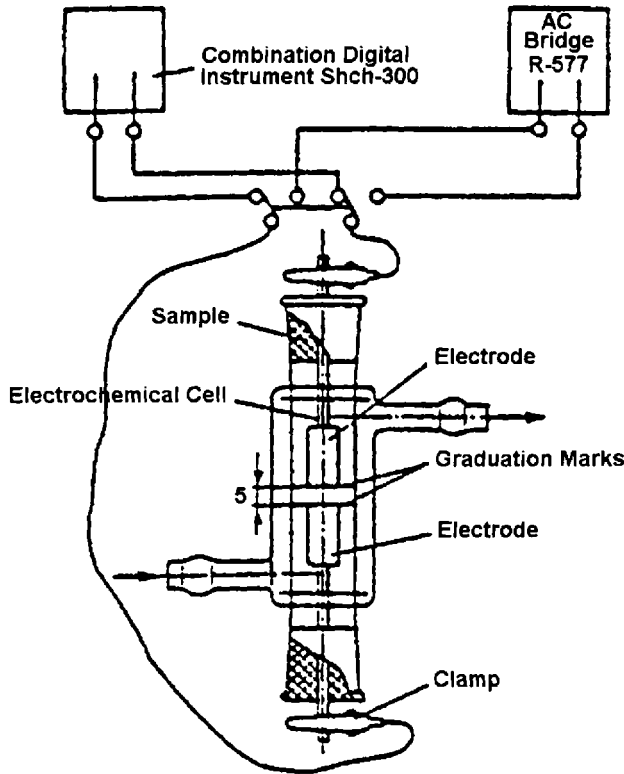


Figure 18.19 Electrolytic cell for determination of the rate of contact corrosion of metals.

$$i = \frac{I_0}{S}$$

$$I_0 = \frac{UI}{U - IR}$$

where

I_0 = the current reduced to zero resistance of the fluid (mA)

S = the electrode surface area (cm²)

U = the equilibrium value of the potential difference between the electrodes (mV)

I = the magnitude of the current between the electrodes (mA)

R = the electrical resistance of the fluid between the electrodes

“200-Hour” Accelerated Test

One of the most common tests in current use for the evaluation of liquid and vapor-phase water–glycol hydraulic fluid corrosion inhibition is the “200-Hour Corrosion Test.” (Though variations of this test are known by other acronyms, the term “200-Hour Corrosion Test” will be used here.) The “200-Hour Corrosion Test” consists of refluxing and aerating the solution to be tested continuously for 200 h and measuring the solution corrosion by weight loss of the immersed metal coupons of steel

(SAE-1010, low carbon), cast aluminum (SAE-329), copper (CA-110), and brass (SAE-70C). Vapor-phase corrosion effects are also monitored by coupons of cast iron (G-3500) and steel (SAE-1010) suspended above the solution. Figure 18.20 illustrates a typical corrosion test cell [46,56].

The corrosion test procedure follows. To the test cell with the metal specimens placed in the order shown in Fig. 18.20 was added 300 g of the water-glycol hydraulic fluid being tested. A water condenser was attached to the center ground glass connector and an air line was connected to the gas sparge tube. The total apparatus was placed into a constant-temperature bath and heated to $70 \pm 2^\circ\text{C}$ and held at this temperature for the duration of the test. A constant airflow rate of $793 \text{ cm}^3/\text{min}$ was maintained through the sparge tube throughout the duration of the test. Periodically, deionized water was added to maintain a constant fluid volume in the test cell. (The periodic water addition was required because of losses through the condenser due to evaporation.) After the 200-h duration of the test, the metal specimens were removed, dried, weighed, and photographed.

2.2.9 Compatibility

An extensive comparison of fluid compatibility for various materials including paints, metal, plastics, and elastomers is provided in Table 18.9 for petroleum oil/polyol

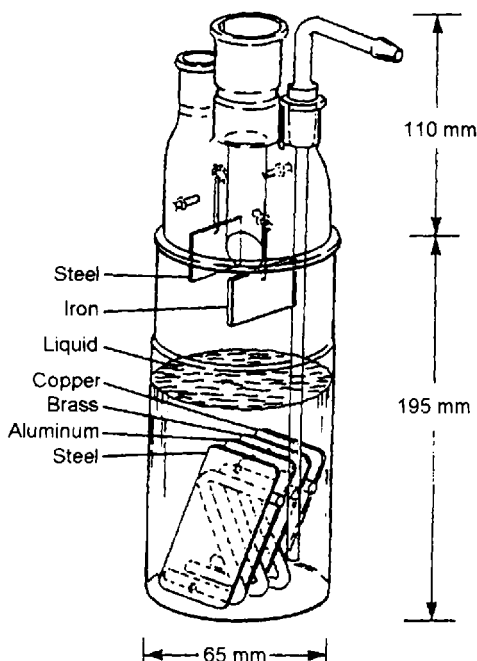


Figure 18.20 Corrosion test apparatus. This assembly is convenient for corrosion-inhibitor studies of water-glycol hydraulic fluids under laboratory conditions. Immersed metal specimens are separated by a glass "Z-bar" in the specific order shown. Vapor-space test specimens are hung from the top of the glass test cell. Fluid temperature is monitored with an immersion thermometer, air is blown into the mixture using an aeration tube, and a cold-water condenser is used to reduce fluid loss by evaporation.

Table 18.9 Comparison of Material Compatibility of Fire Resistant Fluids

Material	Oil/polyol ester	Water–glycols	Phosphate esters	Inverse emulsions
Paints, common industrial	NC	NC	NC	NC
Paints, epoxy and phenolic	C	C	C	C
Metals, ferrous	C	C	C	C
Metals, bronze	C	LC ^a	C	C
Metals, zinc	C	NC	C	C
Metals, cadmium	C	NC	C	C
Metals, lead	C	NC	C	NC
Metals, brass/copper	C	C	C	C
Metals, aluminum, unanodized	C	NC	C	C
Metals, aluminum, anodized	C	C	C	C
Metals, magnesium	C	NC	C	NC
Plastics, clear “Lucite” type	NC	C	NC	C
Plastics, acrylic	NC	C	NC	C
Plastics, styrene	NC	C	NC	C
Plastics, nylon	NC	C	C	C
Plastics, PVC	NC	C	NC	C
Leather	^b	^b	^b	^b
Rubber, neoprene	NC	C	NC	C
Rubber, BUNA N	NC	C	C	NC
Rubber, butyl	NC	C	C	NC
Rubber, ethylene propylene	NC	C	C	NC
Rubber, polyurethane	NC	NC	LC ^c	NC
Rubber, silicone	C	C	C	C
Rubber, Teflon	C	C	C	C
Rubber, Viton	C	C	C	C
Filter media, cellulosic, phenolic treated	C	C	C	C
Filter media, adsorbant (earth type)	NC	NC	NC ^d	NC

Note: C = compatible. LC = low compatibility. NC = not compatible.

^aBronze with lead content over 20% limited to 120°F.

^bLeather compatibility depends on the type of impregnation and conditions. Consult leather packing manufacturer for specific recommendations.

^cCompatibility marginally good, some sources better than others.

^dActive earth media are unsatisfactory for routine use but are acceptable for reclaiming purposes.

esters, water-glycols, phosphate esters, and inverse emulsions [64]. However, the reader is cautioned that these compatibility values are affected by numerous variables, including fluid and material chemistries. Therefore, validation of these compatibility references with the appropriate fluid and seal manufacturer is recommended.

Seal Compatibility

It is desirable that seals used in hydraulic equipment do not exhibit excessive volume swell ($>+4$ and/or -2%) in use. Similarly, Shore hardness should not exceed the ± 4 Shore hardness units. These values were established by testing the seal material at 60°C for 21 days [43]. Although natural rubber, BUNA N, neoprene, butyl, and silicone are designated as "compatible" in Table 18.9 for water-glycols, Table 18.10 illustrates that each swells to a different degree [64,65].

More detailed information on detail on seal materials, fluid compatibility, and compatibility testing are available in Chapter 11.

Metal Compatibility

Water-glycol hydraulic fluids are compatible with steel, anodized aluminum, copper, and brass as long as the corrosion inhibitor is properly maintained. The use of un-anodized aluminum is not recommended. Also, the use of aluminum as a bearing material is not recommended [66].

Zinc and cadmium are dissolved by the relatively alkaline water-glycol solution forming insoluble soap complexes with the antiwear additive [65]. Therefore, the use of galvanized-metal-, zinc- or cadmium-coated components with water-glycol hydraulic fluids is not recommended [18,65]. However, suitable alternatives include tin, nickel, or stainless steel [67].

Paint Compatibility

A problem commonly encountered in the fluid power industry is the attempted use of painted reservoirs that were previously in use with mineral oils. Water-glycol hydraulic fluids exhibit a solvent effect on these paints, thus acting as a paint remover [65]. Therefore, paint on surfaces that come into contact with the water-glycol should be removed [68]. Paints that *are not* compatible include phenolic and phthalic resin-based paints [18] and alkyd- and vinyl-based coatings. Compatible coatings are from best to worst: catalyzed phenolic $>$ catalyzed epoxy-phenolic $>$ catalyzed epoxy coatings. The user is advised to test the compatibility of any paint that he plans to

Table 18.10 "Typical" Rubber Swell Data for a Water-Glycol Hydraulic Fluid

Type of rubber	Linear swell (%) 5 days at 158°F
Natural	1.0
BUNA S	1.6
BUNA N	3.5
Neoprene	1.1–2.0
Butyl	0.0–0.8
Silicone	0.0–2.0

use. This is especially true if fluid temperatures in excess of 60°C (140°F) are to be encountered. It is now common practice to specify surfaces that will come into contact with water–glycols be unpainted [67].

2.3 Performance Testing

Perhaps the most striking feature of W/G hydraulic fluids is the progressive performance improvements that have been made since their introduction in 1947. Table 18.11 illustrates the progressive reduction in wear rates, approaching those obtained with mineral oil, achieved with W/G fluids containing >35% water from 1955 to 1974 when tested according to DIN 51,389 E [Vickers V-104C vane pump for 250 h at 10 MPa (1500 psi) and 1500 rpm] [22]. Some W/G fluids today exhibit less than 100 mg total wear over the 250-h test period [13]. Historical results cannot be reproduced, as the fluids were formulated with obsolete additives no longer available. In addition, the reported test conditions are significantly different than those reported today. For example, lower pressures and longer times and, in many cases, different pumps were used.

In another more recent study comparing the ASTM D-2882 Vickers V-104 vane-pump test, 100 h at 13.7 MPa (2000 psi) and 1200 rpm, showed that it is now possible to formulate high-performance W/G hydraulic fluids [12] that exhibit even lower wear rates than achievable with mineral oils. The reported wear rate data are provided in Table 18.12 [9].

In addition to exhibiting low wear rates, these high-performance W/G fluids may also be used at high pressures (≥ 34 MPa, 5000 psi) previously unattainable with other water-containing hydraulic fluids [9].

Cole has recently shown that W/G hydraulic fluids may be used in hydraulic equipment equipped with servo valves [69]. Although this study showed that the dynamic response was slightly reduced with W/Gs, the performance could be restored by using slightly larger piping, controls, and servo valves.

One historical area that has caused many problems in expanding the use of W/G hydraulic fluids was reduced roller bearing lifetimes obtained with these fluids due to fatigue failure [70,71]. However, more recent studies have identified improved bearing materials and designs that are more suitable for use with W/G hydraulic fluids, thus permitting their use under more stringent lubrication conditions (e.g., higher pressure and greater rpm speeds) [13].

Table 18.11 Historical Wear Rates of Water–Glycol Hydraulic Fluids (1955–1974)

Year	Total wear (mg)
1955–1965	4700–15100
1965–1970	1300–2800
1970–1974	300–1100
After 1974	Approx 100 (mineral oil) <100

Note: All tests conducted according to DIN 51,389 E using a Vickers V-104C vane pump for 250 h at 10 MPa (1500 psi) and 1500 rpm.

Table 18.12 Comparison of ASTM D-2882 Vane-Pump Test Results for Various Fire-Resistant Hydraulic Fluids and Mineral Oil

Fluid	Wear Rate (mg/h)
Typical W/G hydraulic fluid	0.65
Phosphate ester	0.05
Polyol ester	0.10
High-Performance W/G hydraulic fluid	0.10
Rust and oxidation oil	7.0
Antiwear oil	0.24
Low-wear invert emulsion	3.5
High-wear invert emulsion	10+ ^a

Note: These tests were conducted over 100 h at 13.7 MPa (2000 psi) and 1200 rpm using a Sperry-Vickers V-104 vane pump according to ASTM D-2882. The pump was equipped with a 30-L/min (8 ppm) ring. The "pass" criterion is 1.0 mg/h. ^aTest incomplete because of rotor breakage.

Water-glycol fluids may encounter mixed-elasto-hydrodynamic (EHD) and boundary lubrication regimes at some moving surfaces during operation of a hydraulic pump, including (1) the interface between the leading edge of the vanes and the cam ring of a vane pump, (2) the line contact between the mating gear teeth of a gear pump, (3) the interface between the connecting rod and piston of certain types of piston pumps, (4) the interface between the piston and swash plate of other types of axial piston pumps, and (5) the interface between rotary valve plates and housings [72].

This section will discuss the effect of interfacial film formation and film-thickness properties of water-glycol hydraulic fluids on EHD, mixed-EHD, and boundary lubrication. Also included in this discussion will be factors affecting the fatigue strength of surfaces lubricated by water-glycol hydraulic fluids.

2.3.1 Film-Forming and Lubrication Fundamentals of Water-Glycol Hydraulic Fluids

Various workers have studied the effect of the viscosity and pressure-viscosity effects on the film-thickness properties of water-glycol hydraulic fluids [73-82]. A summary of various pressure-viscosity coefficients for various fluids is provided in Table 18.13.

This study shows that the pressure-viscosity coefficient is lower for a water-glycol than for mineral oil and also lower than that exhibited by a water-in-oil emulsion (which is comparable to a mineral oil). This results in lower film thicknesses relative to mineral oil, as shown in Fig. 18.21 [79]. The pressure-viscosity coefficient (and, thus, film thickness as shown in Fig. 18.3) decreases with increasing water content, as shown in Fig. 18.22 [73,78]. Taken together, both pressure-viscosity coefficient and film thickness are dependent on the water, glycol, and thickener content of the water-glycol hydraulic fluid.

Water-glycol fluids exhibit lower pressure-viscosity coefficients and film thickness than mineral oil. Vernesnyak et al. have studied the effect of load, temperature, and speed and found that the film thickness was much greater for mineral

Table 18.13 Summary of Published Viscosity Coefficients for Various Hydraulic Fluids

Fluid	Water conc. (%)	Pressure–viscosity coefficient (GPa ⁻¹)	Ref.
Water	100	0.75	37
Water–glycol	35	4.38	37
Water–glycol	36	2.04	78
Water–glycol	41	4.5	79
Water–glycol	48	1.96	78
Water–glycol	50	4.22	37
Polyol ester	0	11.5	81
Mineral oil	0	20.4	79

oil than a water–glycol at room temperature. However, at higher temperatures (≥ 40 – 50°C), which are more representative of the actual fluid temperatures in use, the film thicknesses for water–glycol fluids may even exceed mineral-oil fluids. This was attributed to the much steeper viscosity–temperature relationship (lower VI, sometimes as low as 85–100) exhibited by mineral oils. It was concluded that the films formed for water–glycols were sufficient to provide adequate lubrication in EHD and mixed-EHD lubrication [74–76]. This is illustrated by Fig. 18.23, which shows that the effect of temperature on both fluid viscosity and the pressure–viscosity coefficient for mineral oil, phosphate ester, and a water–glycol are dependent on the use condition [83].

In another study, it was concluded that although thickened (or VI-improved) fluids may exhibit higher viscosity–pressure coefficients and therefore greater film coefficients, this advantage may be lost for non-Newtonian fluids if sufficient shear rates are encountered to cause shear thinning [37].

Wedeven et al. has shown that although a water–glycol hydraulic fluid may exhibit lower film thicknesses than a polyol ester (consistent with pressure–viscosity coefficients for these fluids), it was still possible for the water–glycol to exhibit

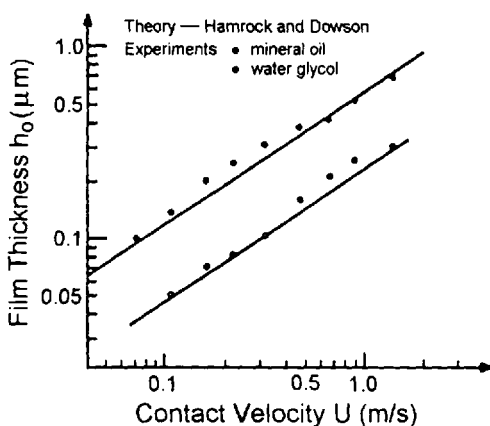


Figure 18.21 Central film thickness versus speed at a constant load of 2.6 N for a mineral oil and a water–glycol hydraulic fluid.

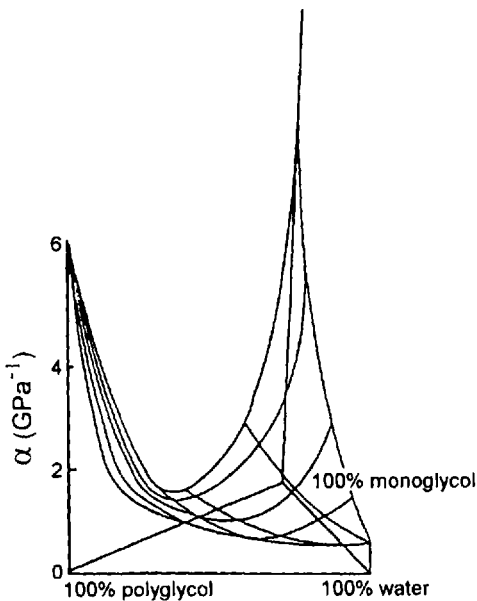


Figure 18.22 Pressure–viscosity coefficient as a function of ethylene glycol, poly(alkylene glycol), and water concentration.

significantly lower friction coefficients, as shown by Fluid No. 2 in Fig. 18.24 [81]. The differences observed in film-thickness values for different fluids is most critical as the film thickness approaches the asperity depth in the mixed friction to boundary lubrication transition.

One other caution is the source of pressure–viscosity coefficients. Many values that are reported are “effective pressure–viscosity” coefficients derived from lubrication tests using the Reynolds equation (see Chapter 2). Other data are obtained from viscometry results. However, it is common for significant differences to exist between the two sources of data, as shown in Table 18.14. Therefore, pressure–viscosity coefficient data obtained using the same methodology should be compared [81].

There are other factors that affect lubrication at the tribocontact in addition to film-thickness measurements. One especially important factor in sliding contact lubrication is additive chemistry and surface film formation. To some extent, this factor may counterbalance a less favorable pressure–viscosity coefficient and lower film thickness. The reader is directed to Chapter 2 for a more complete discussion on this topic.

As indicated in the above discussion, there are a number of ways to address potentially unfavorable film-thickness problems. Fein and Villforth provided a number of guidelines in this regard that should be followed. These are summarized in Table 18.15 [77].

2.3.2 Rolling Contact Fatigue

In the previous subsection, it was shown that water-containing lubricants such as water–glycol hydraulic fluids exhibit lower pressure–viscosity coefficients, and

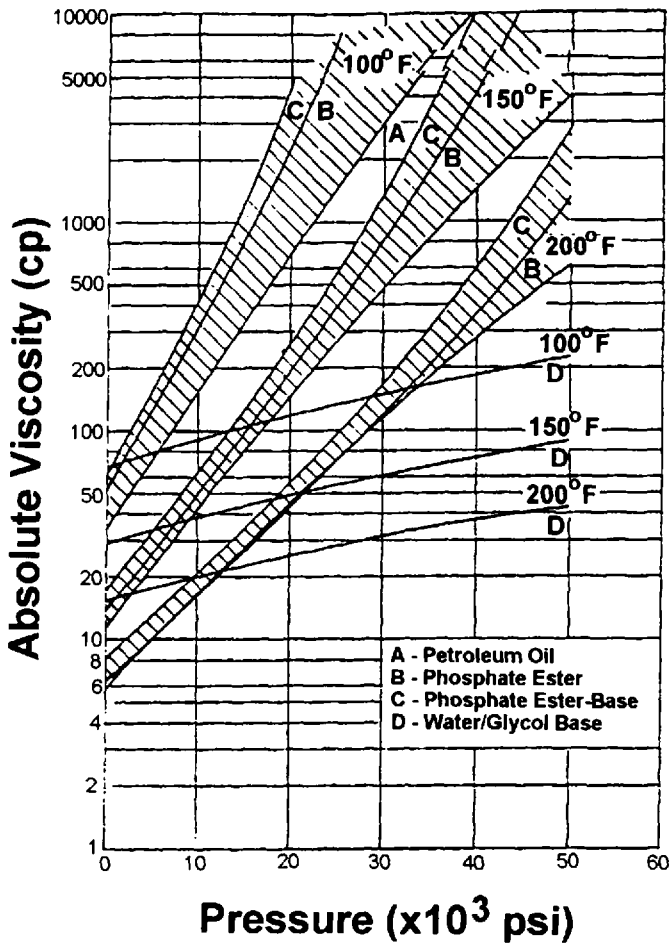


Figure 18.23 Pressure-viscosity coefficient isotherms for (A) petroleum oil, (B) phosphate ester, (C) phosphate ester blend, and (D) a water-glycol hydraulic fluid.

therefore lower film thicknesses, than mineral oil and some other synthetic fluids. One lubrication application area where this has been found to be a problem is in the lubrication of rolling element bearings. It has been shown that the bearing life is shorter using water-glycol hydraulic fluids than mineral oil [84–97]. The relative L_{10} fatigue lives of water-glycol fluids has been estimated as 0.17–0.40 of the value reported for mineral oils [100]. (The L_{10} life is the number of revolutions during which 10% of all nominally identical bearings would be expected to fail.) An example of this problem is illustrated in Fig. 18.25 [84].

It has long been known that fluid viscosity will affect bearing lifetimes [90]. The effect of water-glycol viscosity on bearing wear was studied by Sullivan and Middleton [91]. The first step in this analysis was to determine the lubrication regimes for the steel twin-disk wear contact of the Amsler test machine shown in Fig. 18.34 [91]. This was done by plotting the coefficient of friction versus “bearing number,” which is defined as

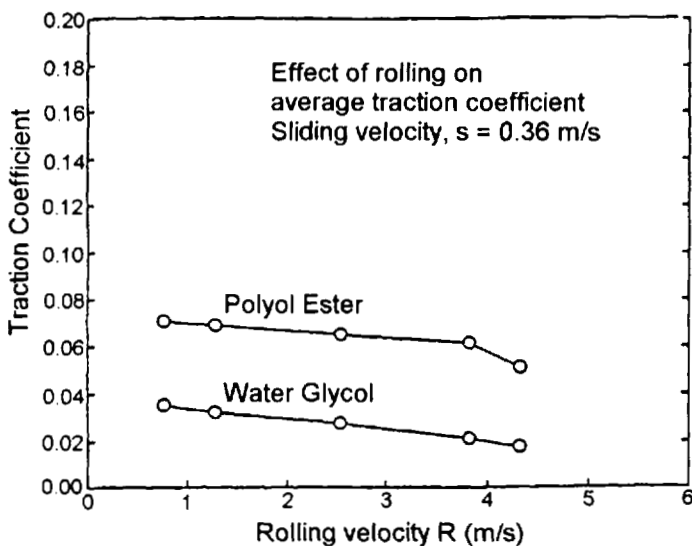


Figure 18.24 Effect of rolling velocity on average traction coefficient at a constant sliding speed of 35 cm/s for a polyol ester and a water-glycol hydraulic fluid.

$$\text{Bearing number} = \frac{\text{Viscosity } (\eta) \times \text{speed } (s)}{\text{Contact pressure } (p)}$$

This relationship, illustrated by Fig. 18.26, is the classical Stribeck curve [91]. (Interestingly, the formation of this curve required three viscosity grades of the water-glycol fluid.)

The effect of bearing number on wear is illustrated in Fig. 18.27 [91]. Similarly, the number of cycles for the first surface pit to appear was plotted versus bearing number, as shown in Fig. 18.28 [91]. These data show that wear decreases with increasing bearing number (viscosity).

Surface roughness effects may be modeled using the lambda function (Λ), which is defined as

$$\Lambda = \frac{\text{EHD film thickness } (h_0)}{\text{Composite relative roughness } (\sigma)}$$

Figure 18.29 is a plot of Λ versus the number of cycles for the first surface pit to appear [91]. These data illustrate that the surface pitting rate increases with

Table 18.14 Comparison of Pressure-Viscosity Coefficients Obtained by Viscometry and Lubrication Experiments Using the Reynolds Equation

Fluid	Capillary viscometry (GPa^{-1})	Optically measured from EHD contact (GPa^{-1})
Water-glycol	2.97	1.8
Polyol ester	11.5	7.8

Table 18.15 Guidelines for Increasing Film Thickness in Practice

Situation	Low speed	High speed
Frictional heat source	Increase viscosity; increase lubricant flow	Improve external cooling; optimize lubricant application, viscosity, and flow for minimum bearing temperature
External heat source	Increase lubricant flow; optimize viscosity for minimum bearing temperature; reduce heat from source	Increase lubricant flow; optimize viscosity for minimum bearing temperature; reduce heat from source
Low temperature	Decrease viscosity; increase temperature; increase lubricant flow to the loaded surfaces	Decrease viscosity; increase temperature; increase lubricant flow to the loaded surfaces
High bearing load	Increase viscosity	Improve external cooling; optimize lubricant flow and viscosity for minimum bearing temperature
Contamination (dirt, wear, debris, etc.)	Increase viscosity; remove and/or inhibit formation	Remove and/or inhibit formation

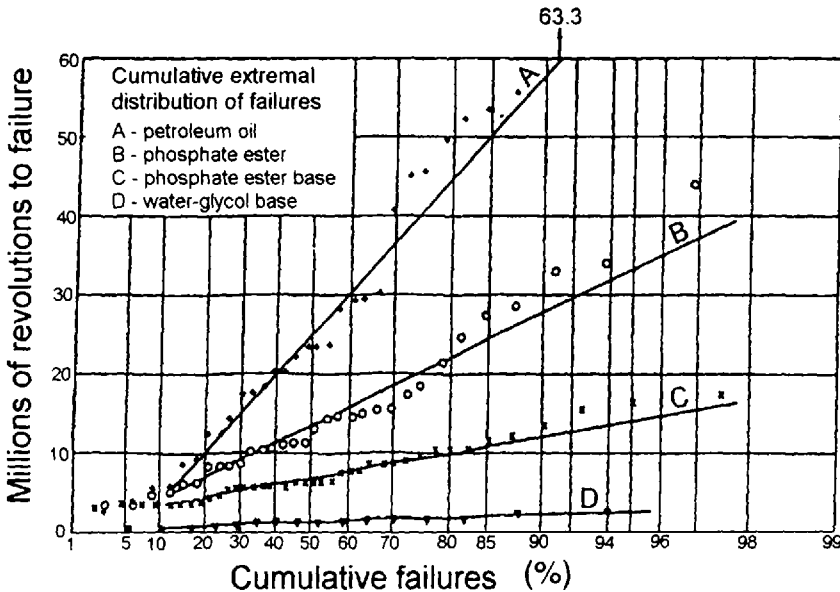


Figure 18.25 Comparison of the fatigue life of angular contact ball bearings lubricated with a petroleum oil and various fire-resistant hydraulic fluids.

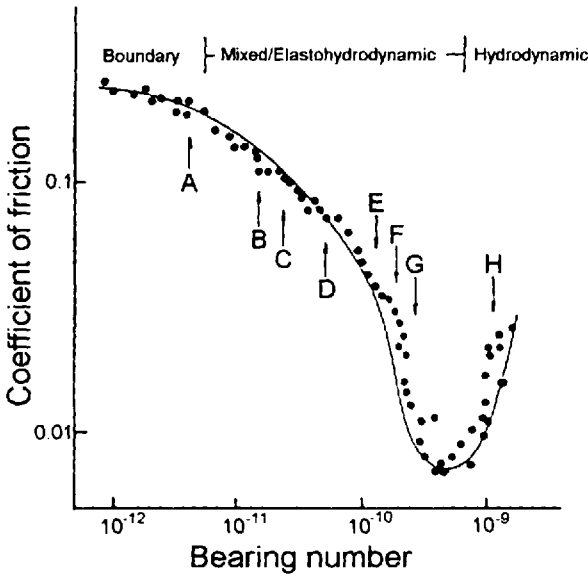


Figure 18.26 Stribeck curve generated from bearing number and coefficient of friction for a water-glycol hydraulic fluid. Three viscosity grades of the water-glycol hydraulic fluid were necessary to develop this curve.

increasing surface roughness and correlates well with the bearing number (fluid viscosity) effects shown in Fig. 18.29. In another study, it was found that bearing lifetimes was a more reliable ranking than wear measurement [101].

There have been many studies conducted in an attempt to quantify bearing lifetime for fire-resistant fluids from more established handbook values for petroleum-oil lubricants. One approach utilizes a lubricant factor (F) and the equation

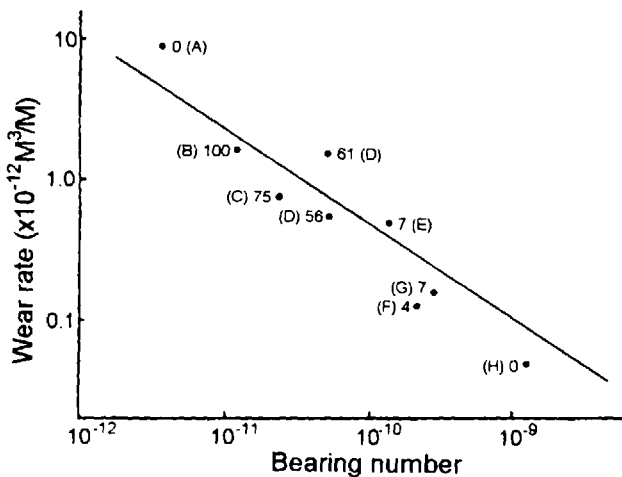


Figure 18.27 Correlation of wear rate versus bearing number for a water-glycol hydraulic fluid.

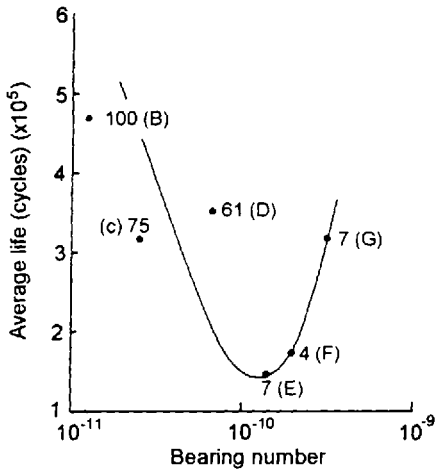


Figure 18.28 Correlation of average life cycles versus bearing number for a water-glycol hydraulic fluid.

$$F = \left(\frac{\text{Modal life for petroleum oil}}{\text{Modal life for fire-resistant fluid}} \right)^{1/3}$$

where F values of 2.6 for water-glycol fluids have been reported [83].

Another relationship developed by Kenny and co-workers is

$$L_{10} = \left(\frac{C}{KP} \right)^n \times 10^6 \text{ revolutions}$$

where C is the dynamic load rating, P is the dynamic bearing load, and n and K are constants. For a water-glycol, the values for n and K was reported to be 2.46 and 2.01, respectively [85,86,102].

There are various mechanisms that may possibly explain the observed lower fatigue strength exhibited by rolling element bearings lubricated by aqueous fluids such as a water-glycol. One possible explanation is hydrogen embrittlement [93,94]. Figure 18.30 illustrates that the fatigue life of steel balls pretreated cathodically in

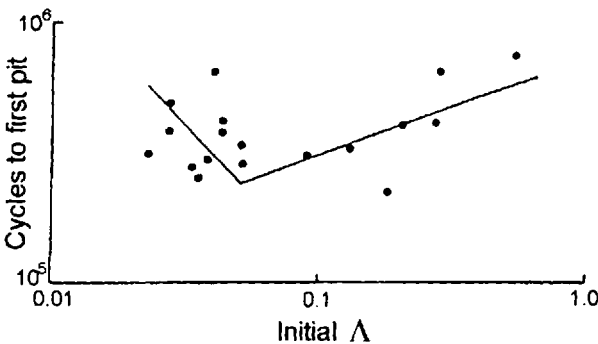


Figure 18.29 Correlation of cycles to obtain the first pit versus lambda (Λ) factor.

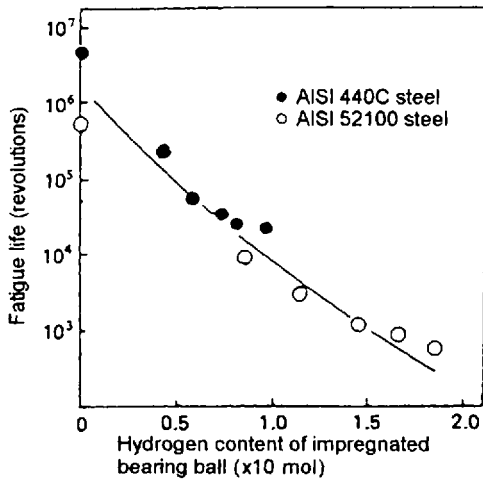


Figure 18.30 Effect of hydrogen content of impregnated ball bearings ($\times 10$ mols) on fatigue life (revolutions).

water to introduce hydrogen into the steel decreases with increasing hydrogen content in the steel [102]. These data were used to confirm a prior observation that the intergranular crack growth observed for bearings used with a water–glycol hydraulic fluid was indicative of hydrogen embrittlement (concentration of hydrogen at the grain boundaries). Interestingly, the simple exposure of steel to hydrogen gas did not induce this effect. Furthermore, in the absence of oxygen, water had little effect [102].

Sullivan and Middleton showed that surface pitting rates increased with decreasing film thicknesses. However, the probability and rate of crack initiation can be significantly reduced with the appropriate antiwear additive selection. Therefore, it would appear that crack initiation is caused by a fatigue process related to asperity interaction. The crack propagation times decreased with an increase in film thickness and were additive independent. It was suggested that crack propagation was enhanced by a hydraulic pressure wedge during system pressurization. The lower compressibility of the water–glycol fluid relative to mineral oil may enhance pressure transfer into the crack [94].

Spikes has summarized four possible reasons for poorer fatigue strength provided by water-containing fluids [102]:

1. Low EHD film thickness illustrated by lambda ratio
2. Chemical promotion of crack formation and growth
3. Removal or prevention of protective films due to low temperature or dilution
4. Increased corrosion and corrosion/abrasion wear

Commentary on Film-Thickness/Rolling Contact Fatigue Data

Shitsukawa et al. have reported that recent improvements in fatigue life have been obtained because of improvements in steel quality and surface roughness of the bearing raceways [92]. In addition, the following were reported:

- Bearing life may depend on surface roughness rather than Λ , when Λ is very small and Λ alone does not fully define a lubrication condition.
- Previous studies have drawn different conclusions regarding fatigue life and the magnitude of Λ . For example, Skurka [103] stated that bearing life is not affected whether Λ is large or small and Talian [104] reported that bearing life is always proportional to Λ .
- Test bearings have different geometry, manufacturing processes, and surface roughness. There has not been a complete series tests reported using the same bearings from the same manufacturing process (same material chemistry and properties) in which only the film thickness was varied.

Recently Yano et al. [99], using the Unisteel machine to evaluate fatigue life properties of water–glycol hydraulic fluids with subsequent pump test validation, reported that additives exhibited a “remarkable” effect on fatigue life and the effect was even more significant for fatty acid–amine pairs. One fluid exhibited a fatigue life of 48% of a mineral oil. In addition, L_{10} lives increased with decreasing water content, with the most significant improvement occurring in the range 35–40% water.

The effect of bearing material chemistry using water–glycol fluids has been reported by Reichel [98]. A piston-pump test rig, where two axial piston pumps were operated in single closed-loop system. One unit was operated as a pump, the other as a motor. Both were operated at 1500 rpm, a constant pressure of 280 bars, and at a fluid temperature of 40°C. Figure 18.31 shows that bearings exhibiting L_{10} lives of 10–90% with respect to a mineral oil were obtained. (The C/P values varied from 3.4 to 8.4.*) Of the bearing materials examined by Reichel [98], Cronidur 30, a high-nitrogen stainless steel (X 30 CrMoN₁₅), provided excellent L_{10} lifetimes obtained with eight different water–glycol formulations as shown in Fig. 18.32.

2.3.3 Fatigue Life Evaluation

In this section, a selected overview of different testing procedures that have been used to evaluate fatigue life of rolling element bearings will be discussed. In addition, actual pump tests such as the Reichel test [98], one of the oldest and most common testing methodologies used to evaluate the lifetime of an actual bearing assembly, will be discussed. One such test was described by Bietkowski, who mounted two test bearings in sealed housings on a horizontal shaft supported by two large roller bearings [101]. The bearings were loaded with hanging weights, typically 3.34 kN. The shaft was rotated at the desired speed, typically 1450 rpm for 400 h, or failure, whichever came first. The lubrication rate was approximately 2 mL/min.

In some cases, a customized machine may be built to simulate the desired lubrication conditions: both contact stress and film thickness. The contact fatigue rig used by Danner is illustrated in Figure 18.33 [107]. A 1.25-in. test specimen illustrated in Figure 18.33a contacts a 3-in.-diameter driver, as illustrated in Fig. 18.33b.

*Fatigue life L_{10} is related to the ratio of C (the load that the bearing can carry for a life of 10^6 inner-race revolutions with a 90% probability of survival or dynamic load capacity) and P (equivalent bearing load or static load) by the Lundberg–Palmgren equation

$$L_{10} = \left(\frac{C}{P} \right)^p$$

where p is the load-life exponent. See Ref. 105.



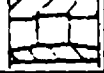

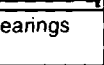
Roller bearing design	c/p	L ₁₀ h	L _{HFC}		Axial piston unit/ swivel angel
			h	%	
Conical roller bearings 	8.42	2,962	96	< 10	bent shaft design 40°
	8.42	2,200	222		
	3.0	58,575	2,000	> 4	swash plate design 14°
	3.0	58,575			
	2.9	52,231			
2.9	52,231				
Cylindrical roller bearings (without cage) 	8.38	10,100	160	1-2	swash plate design 14°
	8.38	13,000	122		
	8.90	16,000	357		
Cylindrical roller bearings 	4.14	681	122	<20	bent shaft design 28°
Bevel ball bearings 	5.4	1,732	850	<50	bent shaft design 25°
Double race ball bearings (plastic cage) 	3.4	440	1,180	>250	swash plate design 14°

Figure 18.31 Lifetime of different roller bearings in axial piston pumps using a water-glycol hydraulic fluid.

The test specimen was constructed from carburized AISI 4620 steel. The contact surfaces were ground to the approximate surface finish of the bearings being modeled. The load (0–4000 lbs.) was applied through a cantilever. The lubricant is supplied to the outlet side of the contact through a recirculating circuit with filtration. The contact temperature is measured by a thermocouple riding on an oil film on the inlet side. Rotational speeds of 100–3600 rpm were possible.

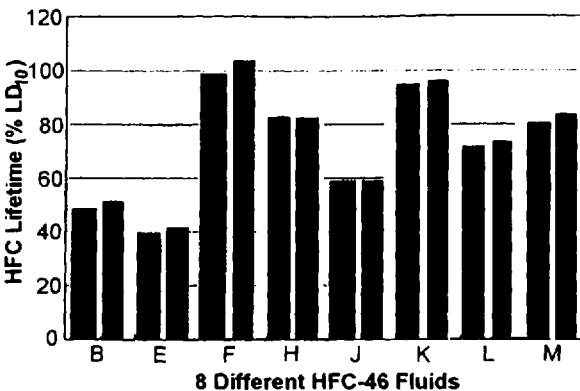


Figure 18.32 Lifetime of bevel ball bearings in an axial piston pump using a water-glycol hydraulic fluid. [Test conditions: pressure = 280 bars, rotational speed = 1500 rpm, and fluid temperature 45°C (113°F).]

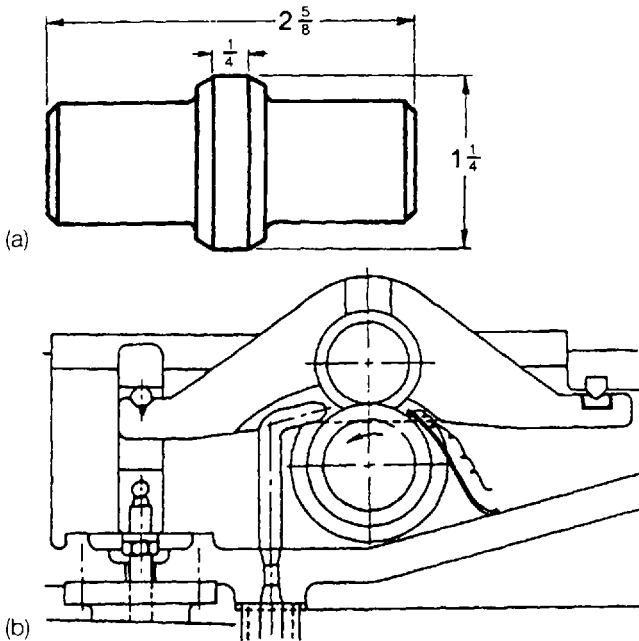


Figure 18.33 Rolling contact fatigue test rig: (a) fatigue test specimen; (b) cross section of test rig.

Sullivan and Middleton utilized an Amsler two-disk machine. The 40-mm-diameter AISI 52100 bearing steel two-disk contact is illustrated in Fig. 18.34 [94]. The driving disk had a 750 Vickers hardness (HV) and the driven disk had a HV of 250, with surface roughnesses of $0.07 \mu\text{m}$ and $0.25 \mu\text{m}$, respectively. The disks were loaded through a variable-compression spring to 900 N, which provided a Hertzian stress of 1.01 GPa. The disks were capable of being rotated independently at 20–4000 rpm with 10% slip.

Of the various bench tests that have been used, two of the most common are the 4-ball test rig [90,95] and the Unisteel test machine. In the 4-ball test, a hardened steel ball is held in a chuck at the end of a spindle which is loaded by a lever arm at 25–750 kg and rotated at a constant speed of 1500 rpm [90]. The upper ball is loaded against three balls held in a steel cavity and allowed to rotate freely, creating the desired rolling/sliding, as illustrated in Fig. 18.35.

Today, one of the most commonly used bench tests to model contact fatigue is the Unisteel Rolling Fatigue Machine illustrated in Fig. 18.36. In this test, a flat ring test piece forms the upper half of a thrust bearing assembly. This is run with the cage, half the balls, and one race from a standard production thrust bearing. The lubricant is drip-fed and the load is applied by a dead-weight lever arm. Typically, a 3.34-kN load is applied and rotated at 1500 rpm [97].

2.3.4 Hydraulic Pump Derating Practice

Most hydraulic pump companies have traditionally derated the catalog pressure ratings for their pumps for use with fire-resistant fluids. Some pump products are not

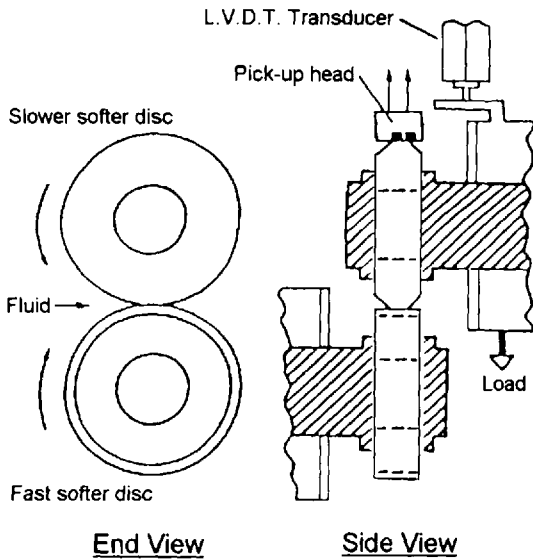


Figure 18.34 Amsler twin-disk test machine.

recommended for use with fire-resistant fluids at all. One illustration of pump de-rating is provided by Edgington for Lucas axial piston pumps, which is illustrated in Fig. 18.37 [21]. Traditionally, boosted inlet suction pressure recommended to minimize cavitation potential has also been recommended for water–glycol fluids [106]. Another illustration of this is the general derating conditions published by Sundstrand and shown in Table 18.16 [107]. Sundstrand recommends that inlet vacuum not exceed 2 in. Hg and that an elevated reservoir be used with an increased inlet line size [107].

Similarly, Racine derates their pumps for use with water–glycol hydraulic fluids and recommends that a flooded inlet be used and that the inlet vacuum not exceed 3 in. Hg and that an elevated reservoir be used. Illustrative examples to assist in calculation of the inlet vacuum are provided in Table 18.17 [108]. If the pump must be mounted on top of the reservoir, the liquid level should not be more than 12 in. below the pump. Strainers should be rated at least three times the pump outlet flow. Strainers should be no finer than 60 mesh (238 μm) [109].

In some cases, rolling element bearing lubrication problems with water–glycols can be successfully resolved by either changing the bearing design, i.e., from uncaged to caged bearings for Rexroth Hydromatik and Breuningham pumps, or by the use of bronze sleeve bearings [110].

2.4 Fluid Maintenance Procedures

2.4.1 Fluid Contamination and Performance

Hydraulic pump lubrication is not only dependent on fluid chemistry, but it is also negatively affected by liquid and solid contamination [111–117]. In water–glycol hydraulic fluids, the most common liquid contamination is usually petroleum oils.

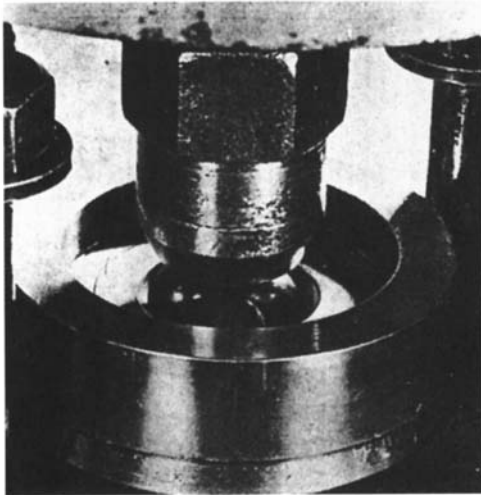
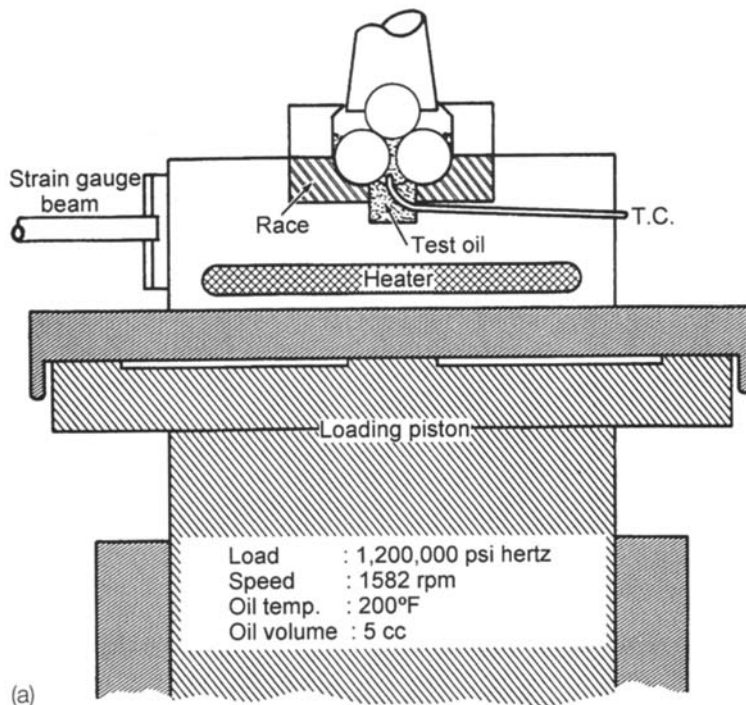


Figure 18.35 Illustration of the 4-ball test configuration.

Because water–glycols and petroleum oils are mutually insoluble, residual oil may be skimmed from the fluid reservoir, although often not before selectively extracting some additives from the fluid formulation. Although this is usually not a serious problem, every effort should be made to prevent this form of contamination. Solid contamination may have disastrous effects because solid debris, through abrasive

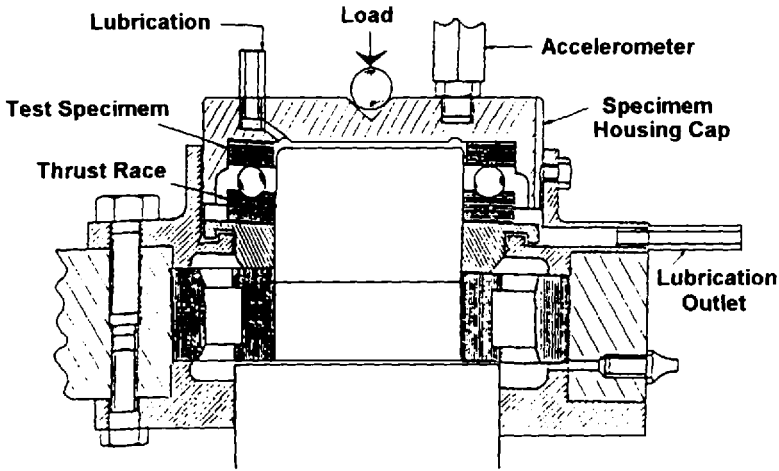


Figure 18.36 Schematic of Unisteel test machine.

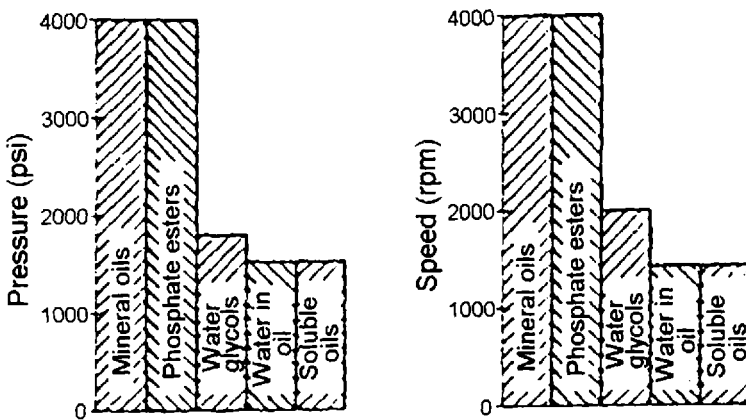


Figure 18.37 Maximum continuous operating pressures and speeds of typical Lucas axial-piston pumps using mineral oils and various fire-resistant hydraulic fluids.

Table 18.16 Modified Operating Parameters for Fire-Resistant Fluids

Fluid type	Speed (% catalog)	Pressure (% catalog)	Maximum temp. (°F)
Phosphate ester	100	100	180
Polyol ester	85	85	150
Invert emulsion (60 oil/40 water)	65	70	140
Water-glycol (60/40)	65	60	140
HWCF (95 water/5 oil)	65	40	122

Table 18.17 Calculation of the Inlet Condition

A. The pressure loss at a pump suction inlet will be caused by the following:

1. Pressure loss due to length of piping = length (ft) × graph value × flow (gal/min) × SPG
2. Pressure loss due to elbows = number × graph value × flow (gal/min) × SPG
3. Pressure loss due to bends = number × graph value × flow (gal/min) × SPG
4. Pressure loss due to suction strainers = No. of elements × graph value × flow (gal/min) × SPG
5. Pressure loss due to head or lift = ft × 0.88 × SPG

Notes: 1 ft height of a fluid with a SPG of 1 = 0.88 for other fluids in. Hg = 0.88 × SPG

If the fluid is above the pump inlet, the pressure should be subtracted from the other losses and if the fluid is below the pump inlet, the pressure is added to the other losses.

The pressure loss caused by the design of the suction system can be determined from the data given in Fig. 18.38; for example:

Fluid viscosity 200 cS at 55°C
 Flow rate 18 gal/min
 Pipe size 1.5 in. in diameter
 SPG 1.15
 Head of fluid 2 ft

3-element 0.005-in. suction strainer

1 bend and 4 ft. of pipe

From Figure 18.37:

$$\begin{aligned} \text{loss due to length of pipe} &= 4 \times 0.026 \times 18 \text{ gal/min} \times 1.5 = 2.160 \\ \text{loss due to bend} &= 1 \times 0.04 \times 18 \text{ gal/min} \times 1.15 = 0.830 \\ \text{loss due to suction strainer} &= \frac{0.35 \times 18 \text{ gal/min} \times 1.15}{3} = 2.420 \\ \text{positive head} &= 2 \times 0.88 \times 1.15 = 2.02 \end{aligned}$$

Loss at inlet

3.39 in. Hg

Note: SPG refers to specific gravity.

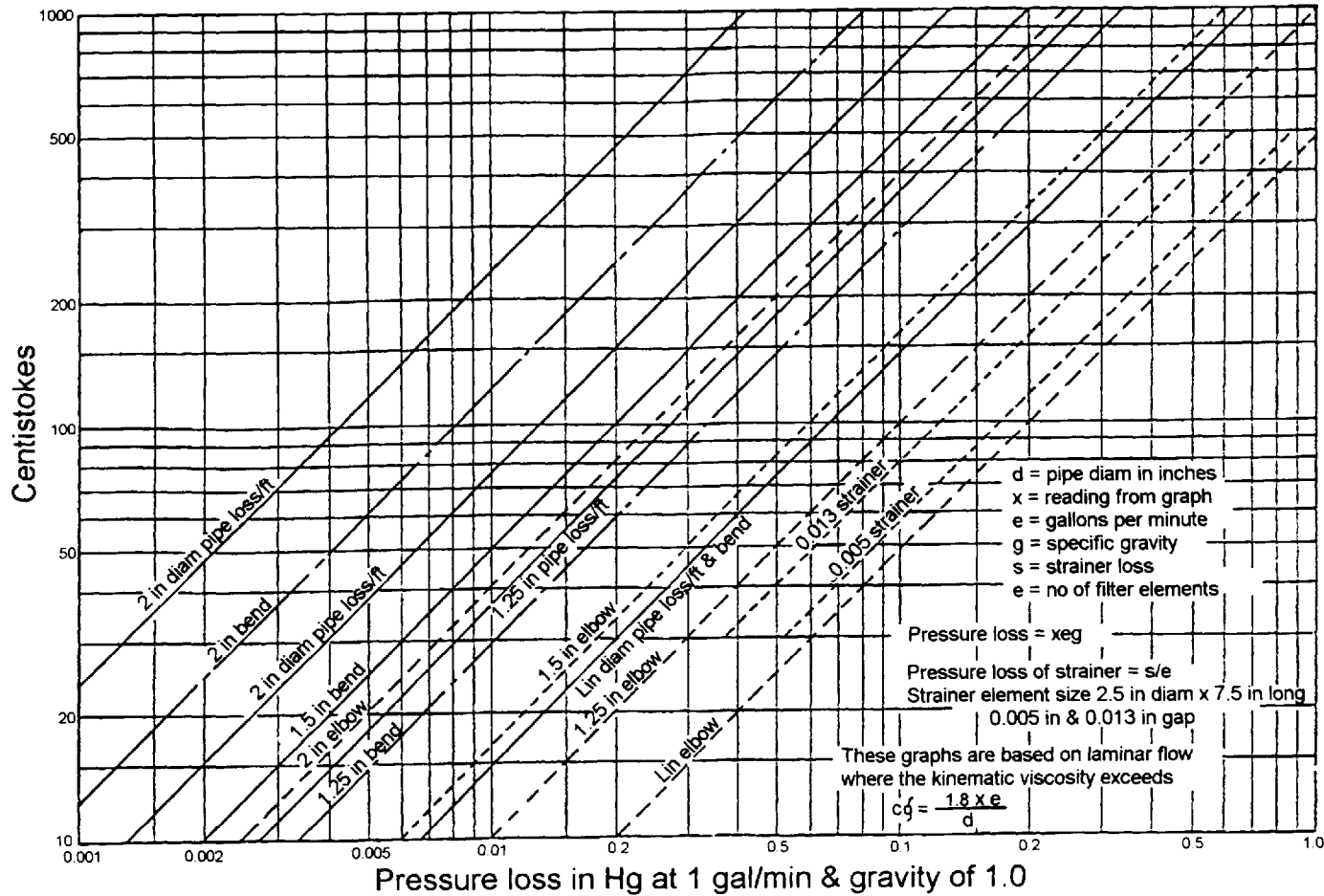


Figure 18.38 Correlation of hydraulic fluid viscosity and pressure loss in pipe elbows of different cross-section sizes.

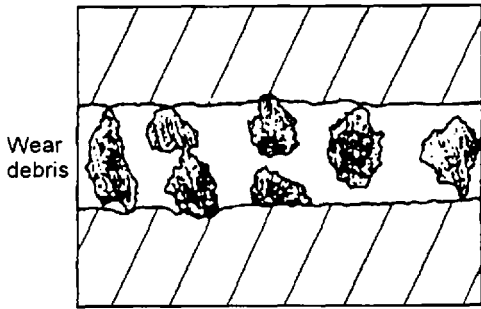


Figure 18.39 Mechanism of abrasive wear due to solid contamination.

action, will cause increased wear at the lubrication contact, as shown in Fig. 18.39 [113–116].

Any wear in hydraulic systems is deleterious because optimal pump performance is dependent on the clearances within the system. Table 18.18 provides a summary of typical clearances encountered in a hydraulic system [111].

Fitch and Hong have illustrated the relative sensitivity of vane, gear, and piston pumps to solid contamination, which is shown in Fig. 18.40 [113]. To address the problems of pump wear due to contamination, Sperry-Vickers has developed filtration recommendations based on filter β -ratios developed earlier by Fitch and others [117,118]. These recommended values are provided in Table 18.19.

These data show that no matter how good the lubrication properties, solid contamination can destroy a hydraulic system. Thus, fluid contamination must be removed using appropriate filtration if optimal performance is to be obtained.

2.4.2 W/G Fluid Analysis Procedures

The following discussion will focus on analytical procedures that may be used to monitor fluid chemistry and physical property variation. *Note:* All of the examples shown in the following discussion are for illustrative purposes only. Because these values are fluid specific, they will vary with the supplier. Therefore, the reader should

Table 18.18 Typical Hydraulic Component Clearances

Component	Clearance (μm)
Slide bearings	0.5
Vane pump (tip of vane)	0.5
Control valve	0.1–0.5
Rolling element bearing	0.1–1.0
Hydrostatic bearings	1–25
Gears	0.1–1.0
Gear pump (tooth to case)	0.5–5.0
Piston pump (piston to bore)	5–40
Servo valves	1–40

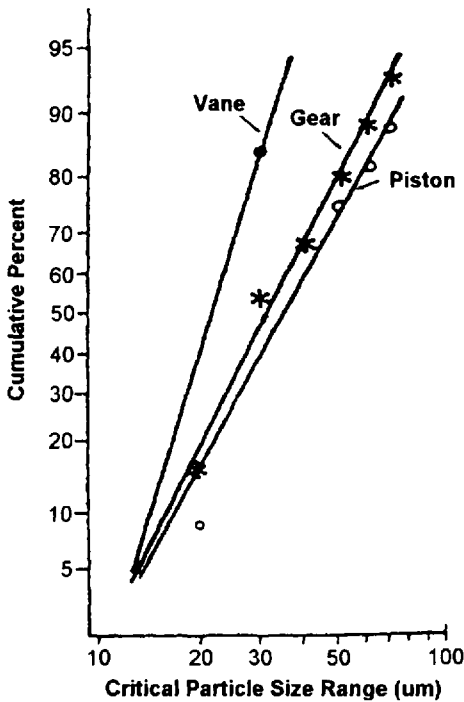


Figure 18.40 Relative sensitivity of different types of hydraulic pump to contamination.

consult with their fluid supplier to obtain the appropriate recommendations to use with these procedures.

Initial Fluid Observation

The first step of any analysis is to simply observe the sample. This is easily done by looking at the sample in a clear container such as a bottle. The sample should be clear without the presence of oil layers or solid debris. If solid debris is observed, a magnet should be used to determine if it is magnetic. Magnetic solids may be the result of either wear or corrosion. Nonmagnetic debris may be due to elastomeric seal erosion, carbonaceous deposits, or external nonmetallic contamination.

Water Content and Makeup

Antiwear properties and the fire resistance of a water-glycol hydraulic fluid is dependent on total water content. Therefore, water should not be added indiscriminately nor should wide variations in water content by evaporation during use be allowed. Water contained in a water-glycol fluid may be lost through evaporation during normal hydraulic operation. Water loss increases fluid viscosity. Therefore, water must be added back to the system to maintain fire resistance, assure proper viscosity, and, thus, system operation.

The most common methods for the determination of water content of a water-glycol hydraulic fluid are the refractive index, viscosity, distillation, and Karl Fischer analysis. Of these, the most commonly used is the refractive index. The refractive

Table 18.19 Suggested Acceptable Contamination Levels

Target contamination class to ISO code		Suggested maximum particle level		Sensitivity	Type of system	Suggested filtration rating
5 μm	15 μm	5 μm	15 μm			$\beta_x > 100$
13	9	4,000	250	Critical	Silt-sensitive control system with very high reliability; Laboratory or aerospace	3
15	11	16,000	1,000	Semicritical	High-performance servo and high-pressure long-life systems (i.e., aircraft, machine tool, etc.)	5
16	13	32,000	4,000	Important	High-quality reliable systems; general machine requirement	10
17	14	130,000	8,000	Average	General machinery and mobile systems	10
19	15	250,000	16,000	Crude	Low-pressure heavy industrial systems, or applications where long life is not critical	15–25

index is readily determined using a portable temperature-compensated refractometer that provides readings in degrees Brix.

To perform this analysis, the cover plate over the instrument prism is lifted, a drop of fluid is placed on the prism, as shown in Fig. 18.41a, and the cover plate is placed over the liquid. (*Note:* the prism should be cleaned prior to use or incorrect readings may result.) The instrument is next held toward a light source, as shown in Fig. 18.41b. The degrees Brix reading is then read from the eyepiece, as shown in Fig. 18.41c. Water content is obtained from the refractometer reading and a calibration chart such as that shown in Fig. 18.42. After the water concentration is determined, additional water should be added if necessary. Some suppliers provide "water makeup" tables such as Table 18.20 or fluid-dependent plots such as Fig. 18.43.

The principal limitation of water determination by refractive index is that the refractive index is affected by additive depletion, fluid degradation, or contaminants that may be present in the hydraulic fluid. Therefore, it is advisable to periodically cross-check water analyses obtained by refractive index by at least one other analytical method.

Water content may also be determined by viscosity measurement. One common method of viscosity measurement is to follow the ASTM D-445 procedure for kinematic viscosity [119]. The Cannon-Fenske tube used in this determination is shown in Fig. 18.44. Because viscosity is temperature dependent, it is essential that a constant-temperature bath be used for viscosity measurements. Plots of viscosity versus water content, such as Fig. 18.45, are available from the water-glycol hydraulic fluid producer. If water additions are necessary, water makeup charts such as that illustrated by Fig. 18.46 are available. Alternatively, a water "makeup" table analogous to Table 18.21 may be obtained from the W/G hydraulic fluid supplier for the specific fluid being used.

The load bearing capacity of a fluid film is dependent on fluid viscosity. Oxidative and thermal degradation processes will result in a decrease of fluid viscosity. Thus, routine viscosity measurement is one of the best methods of monitoring fluid stability. However, such comparative measurements must be made at the same total water content.

The water content may also be determined by azeotropic distillation from benzene or toluene [43]. This procedure, described in ASTM D95 [120], is relatively labor intensive and not commonly conducted on water-glycol hydraulic fluids at the present time.

The fourth, and most unambiguous, method of water determination is by Karl Fischer analysis (ASTM D-1744) [121]. The advantage of Karl Fischer analysis is that it is a direct measure of water content, whereas viscosity and refractive index are both indirect measurements that are substantially affected by either contamination (refractive index) or fluid degradation (viscosity). Figure 18.47 illustrates the level of agreement that has been obtained with known water contents and this Karl Fischer procedure.

The quality of water used for system makeup is critically important because polyvalent hard metal ions (Ca^{2+} , Mg^{2+} , Mn^{2+} , etc.) present in tap water or city water will react with the antiwear additive, usually an organic carboxylic acid salt, to form a polyelectrolyte complex (V) [122], which appears as a "white, soapy" solid [123,124]. This process must be prevented for two reasons. The first is that it will lead to continuous depletion of the critically important antiwear additive. Sec-

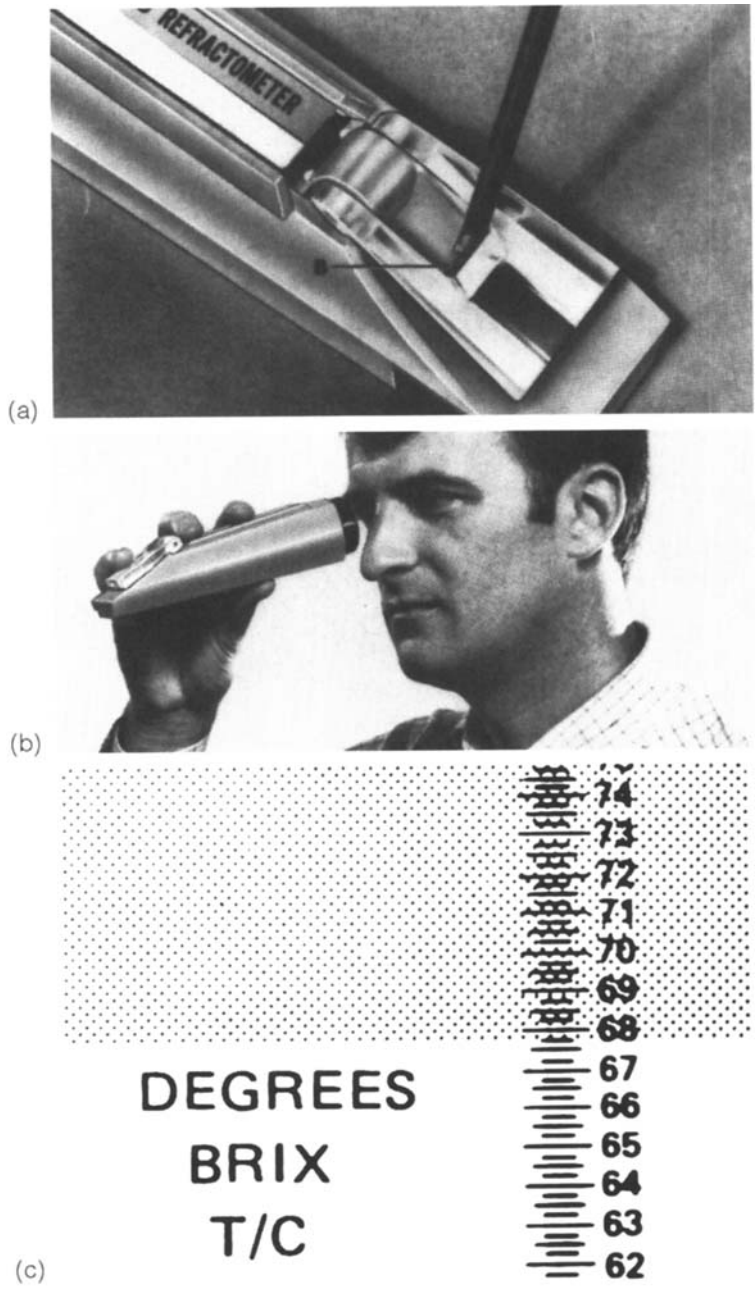


Figure 18.41 Determination of water content using a hand-held refractometer: (a) placing fluid on the prism, (b) reading the instrument, and (c) illustrative scale reading. (Courtesy of Leica, Inc.)

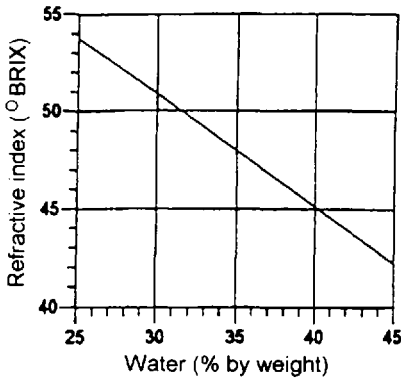


Figure 18.42 Water content versus refractive index in degrees Brix.

Table 18.20 Water Addition by Refractive Index

Water Makeup ^d	Refractive index (degrees BRIX)
None	43.75–46.00
5	46.00–47.25
10	47.25–48.75
15	48.75–50.50
20	50.50–52.50
25	52.50–54.25

^dGallons of water added to each 100 gal of W/G hydraulic fluid.

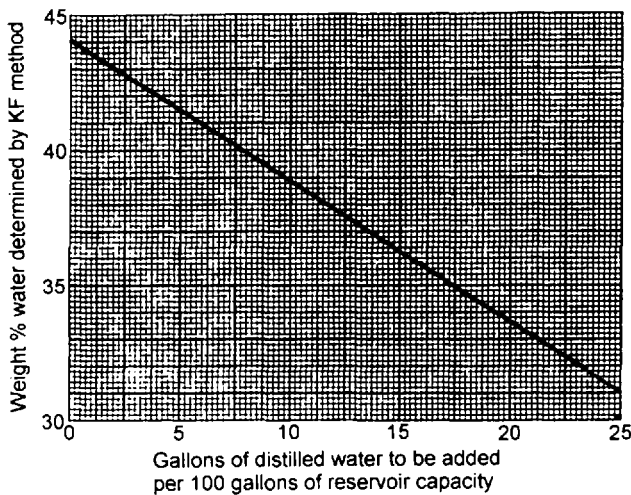


Figure 18.43 Water makeup graph.

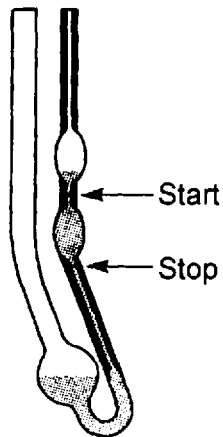
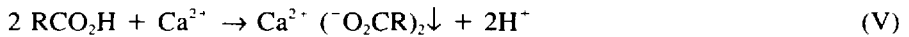


Figure 18.44 Cannon-Fenske viscometer.

ond, the presence of such precipitates, like any solid material, will increase wear and possibly plug filters:



Only distilled or deionized water, with a conductance of less than 15 $\mu\text{mho/cm}$ (a maximum total water hardness of 5 ppm has also been recommended [30,124]), should be added to a W/G hydraulic fluid system. It is recommended that total hardness of the system should not exceed 250 ppm [125]. The ionic content of water

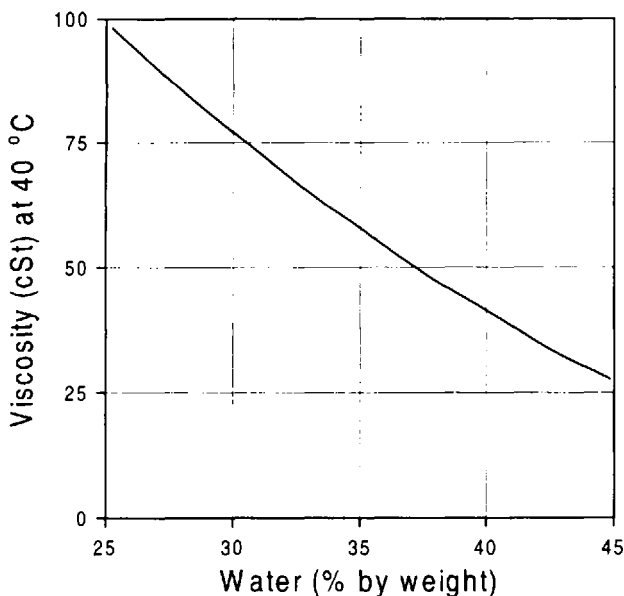


Figure 18.45 Viscosity versus water content.

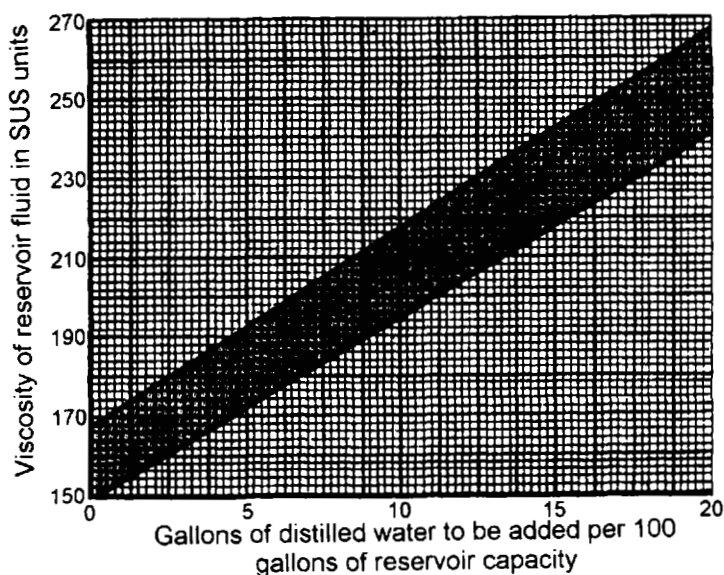


Figure 18.46 Water makeup graph based on fluid viscosity measurement.

can be monitored by conductance. It is recommended that the maximum conductance of makeup water be less than $15 \mu\text{mho/cm}$.

Reserve Alkalinity (Corrosion Inhibitor)

Amine concentration in a W/G hydraulic fluid is designated as "reserve alkalinity" and is conventionally reported as the volume in milliliters of 0.1*N* hydrochloric acid (HCl) required to titrate 100 mL of W/G fluid to pH 5.5. A typical titration plot is shown in Fig. 18.48. Two breaks in the titration curve are observed because two chemical moieties are actually being analyzed, the amine carboxylate (VI) and the excess "free" amine (VII).

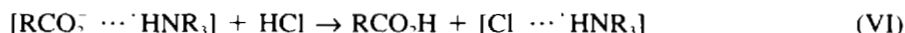


Table 18.21 Water Addition by Viscosity

Water makeup ^a	Viscosity (cSt at 40°C)
None	39–50
5	50–56
10	56–68
15	68–82
20	82–102
25	102–124

^aGallons of water added to each 100 gal of W/G hydraulic fluid.

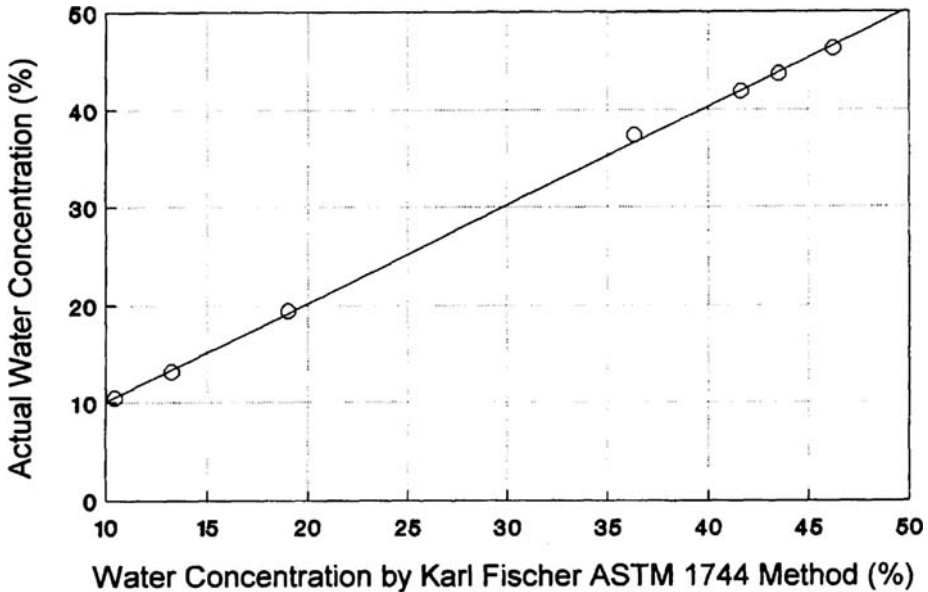


Figure 18.47 Correlation of water-glycol hydraulic fluid water content and Karl Fischer analysis (ASTM D-1744, pyridine-cellosolve method).

Thus, acid titration also provides a method for quantifying the concentration of antiwear additive.

Changes in corrosion inhibitor concentration may also be monitored by pH [123-126]. It is recommended that the pH of the W/G system be greater than 8.0 [123,124].

Fluid Degradation

The presence of formic acid is particularly deleterious because concentrations higher than 0.15% may lead to excessive wear, as discussed earlier in this chapter and shown in Fig. 18.16. Because formic acid may result in increased wear, an analysis should be conducted to detect its presence in the used fluid. The analytical procedure

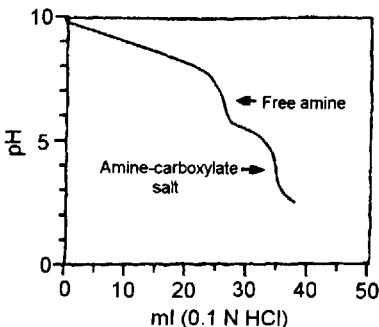


Figure 18.48 Determination of reserve alkalinity by acidic titration.

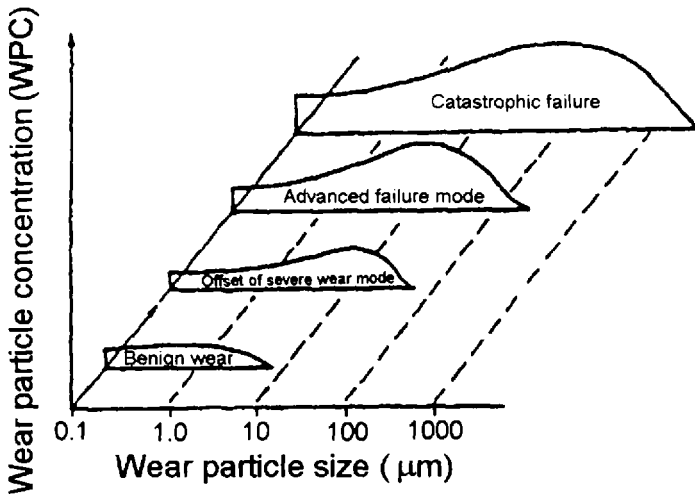


Figure 18.49 Typical progression of severe wear.

most usually performed for acid detection in aqueous solution is ion chromatography [127].

Ferrography

It has thus far been shown that hydraulic fluid quality and performance is dependent on fluid cleanliness and chemistry variation. On occasion, it is necessary to troubleshoot fluid performance in improperly operating systems. In addition, to the chemical and physical analyses described earlier, it is often of value to analyze any wear debris that may be formed. One of the principal methods of wear debris analysis is ferrography [128,129].

Ferrography may be used to determine the concentration and distribution of wear particles contained in a hydraulic fluid. This is illustrated in Fig. 18.49, which shows the progression of wear as a function of total particle concentration [130]. Generally, "benign" wear occurs when the particles are less than 15 μm . Wear particles producing catastrophic failure are typically $>200 \mu\text{m}$. Ferrography can be used to detect and characterize wear particles in this size range.

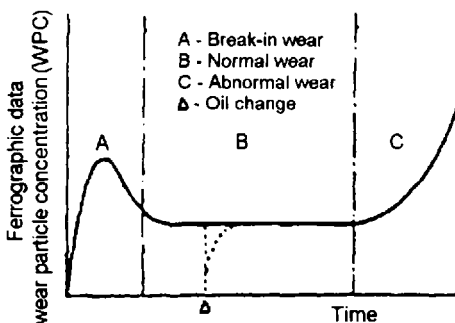


Figure 18.50 Ferrographic profile of large wear particles.

Wear particles may also be profiled over time, as shown in Fig. 18.50 [130]. Although all particles are susceptible to removal by filtration, large-particle filtration generally occurs more rapidly. Therefore, the larger particles indicated by ferrography are a good indicator of “current wear rate.”

Ferrographs can be used to elucidate the identity of wear particles. This information is available from various collections published in handbooks [131]. For example, using ferrography, it is possible to identify carbonaceous material, rust, copper, soft metal (i.e., aluminum, zinc, etc.), and severe and normal wear. Some typical ferrographs are shown in Fig. 18.51.

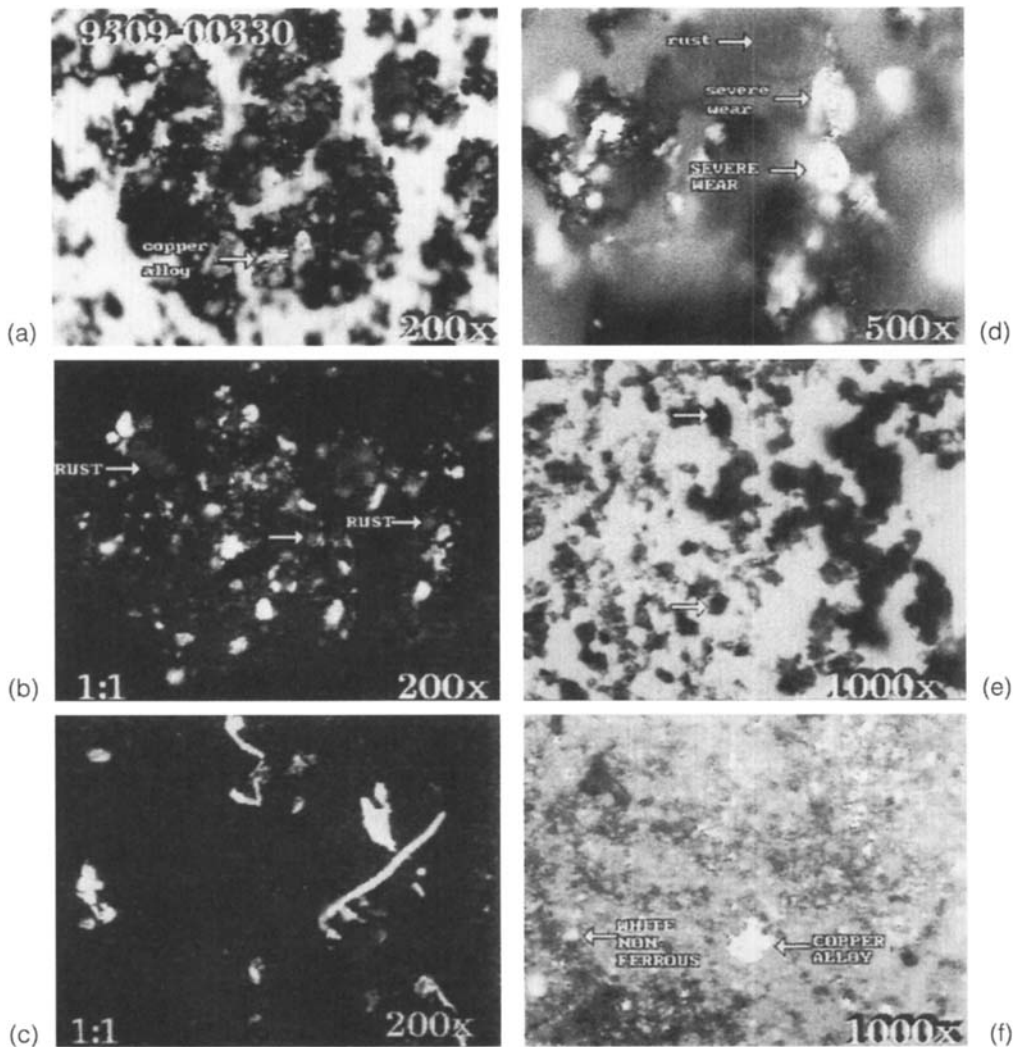


Figure 18.51 Typical ferrograms that may be obtained from ferrographic analysis: (a) copper-alloy wear debris, (b) rust contamination, (c) white nonferrous and copper-alloy debris, (d) rust and severe wear particles, (e) amorphous carbon contamination, and (f) crystalline fiber contamination. (Courtesy of Engineered Lubricants, Inc.)

2.5 Biodegradability and Toxicity

There is increasing interest in the biodegradability and toxicological issues relating to the use, incidental release, and disposal of all hydraulic fluids, including water-glycol hydraulic fluids [132]. (Further information is available regarding these are other testing requirements in Chapter 13 and will not be discussed further here.) Although relatively little information is available regarding the biodegradability and toxicology of water-glycol hydraulic fluids, one report has issued recently illustrating that one composition exhibits both outstanding high-pressure applicability and is biodegradable (85% in 28 days by the OECD 301B—modified Sturm test) [133]. Work is continuing in this area.

2.6 System Conversion Guidelines

Proper fluid conversion procedure is essential if optimal hydraulic system performance is to be achieved. In this section, conversion procedures from mineral oil and from other fire-resistant fluids will be discussed. The reader is encouraged to obtain a copy of an industry standard such as the NFPA T2.13.1 R3 standard for more comprehensive compilations of recommended procedural guidelines [134].

2.6.1 Piping Inspection and Repair

System conversion is an excellent time to perform a system inspection and repair hydraulic piping problems. The following list of inspection pointers originally written by Oilgear for oil hydraulic systems is appropriate for any hydraulic fluid system [139]:

1. Look for loose or vibrating pipes that may break due to work hardening of the metal. Copper is especially vulnerable. Because copper is only recommended for low pressure (<300 psi), it should not be used for water-glycol systems, which are typically used at pressures higher than 300 psi.
2. Flexible hose should be inspected very closely. Flexible hose is susceptible to sudden rupture or blowout at couplings and should not be used in potentially dangerous area. Flexible hose may often be avoided by telescoping joints, rotary joints, or unions, which may be loosened for repairs. If flexible hose must be used, it should be enclosed in a manner that permits venting to a sump or waste pit.
3. Fragile piping should not be placed in an area where it can be run over, walked on, or used as a ladder. It should be moved or covered with adequate protection.
4. Avoid temporary repairs. Maleable or wrought iron fittings should be replaced immediately. Avoid bending or straining pipes to "make them fit." The strain may lead to subsequent line breakage.
5. Long overhead runs of pipe should be avoided because rupture may lead to spraying of fluid over dangerous areas.
6. Pipe passageways through floors or between machines should be patched with nonflammable ceramics to prevent fluid from spreading from one floor or machine to another.
7. Be sure that machines are operating smoothly. Rough hydraulic flow may indicate improper circuit design and may result in future leaks and breakdowns in the system.

Pumps designed for oil hydraulic fluids may not have proper inlet flow conditions for the more dense water–glycol fluid. Properly sized inlet piping and minimum distance between the reservoir and inlet and maximum distance of the reservoir placement above the inlet is essential to minimize pressure drops, which may lead to fluid starvation and cavitation [135]. If, after performing the calculations shown in Table 18.17, excessive inlet vacuum conditions exist, larger inlet pipe diameter (and possibly pump speed reduction to reduce flow) may be helpful. A chart such as that provided in Fig. 18.52 can be used to determine proper pipe sizing when volume flow rate and velocity are known [135].

2.6.2 Additional Considerations

Water–glycol fluids as a class are incompatible with most paints used with hydraulic oil. Therefore, conventional paint inside of a fluid reservoir must be removed. Although it is desirable to use unpainted reservoir surfaces, there are some paints such as modified phenolic or epoxy-based paints that may be used. However, paint compatibility should be tested before use [141].

Water–glycol hydraulic fluids should be used at temperatures below 150°F; as a result, heat exchangers may be required to maintain optimum reservoir temperatures [136,137].

When switching to a water–glycol fluid, it is essential that as much residual oil as possible be removed. Low-pressure air may be used to blowout residual oil from remote parts of the system [137]. The reservoir should be wiped down to remove all traces of the residual oil [64,66,136]. If it can be utilized, steam cleaning can be effective [64,66].

Flushing fluids are not recommended because residual amounts of the fluid are almost certain to remain and disrupt the overall chemistry of the fluid. (As shown previously, maintenance of fluid composition is critically important if optimal performance is to be assured.) Instead, the water–glycol itself should be used as the flushing fluid [64,66,106,136].

The filters in the system must be compatible with the water–glycol hydraulic fluid being used. Do not use paper or treated-paper filters. Clean the filter housings and plug bypasses.

Additional cleaning guidelines are provided in Table 18.22 [138].

2.6.3 Converting from Petroleum Oil to Water–Glycol Fluids

In converting a hydraulic system from petroleum hydraulic oils to water–glycol hydraulic fluids, follow accepted engineering practices and be as thorough as possible [134]. A little extra attention at this point is necessary for safer and better performance and lower maintenance expense. The following procedure is recommended in making changeover from petroleum oils to water–glycol conversion:

1. Drain the oil from the system completely. Particular attention should be paid to the reservoir, pipe lines, cylinders, accumulators, filters, or other equipment in which oil might be trapped.
2. Clean the system of residual sludge and deposits and remove paint from the inside of the reservoir unless the paint has been tested and found to be resistant to the softening and lifting action of the hydrolube. Steam cleaning has been very effective in many instances. Carbon tetrachloride or other chlorinated metal cleaners **should not be used**.

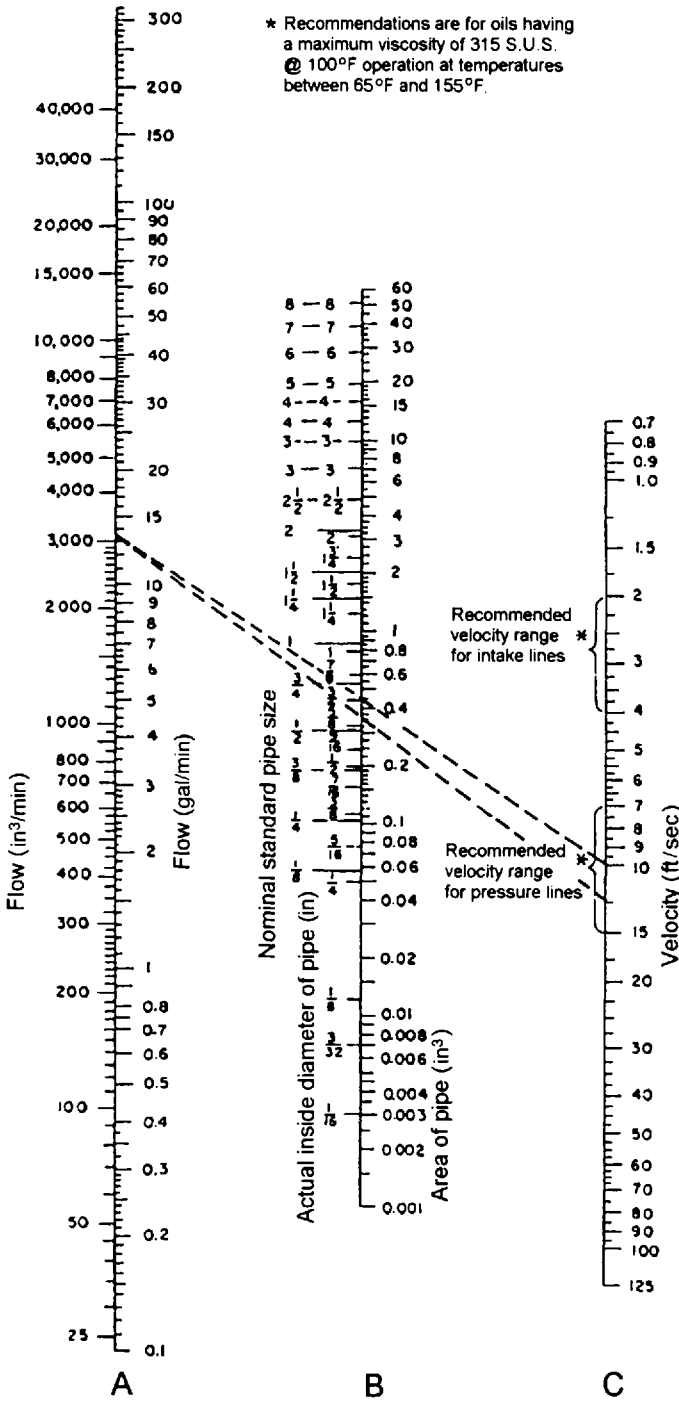


Figure 18.52 Nomogram for determination of pipe size as a function of flow volume and velocity.

Table 18.22 Conversion Guidelines from Petroleum to Water–Glycol Hydraulic Fluids

Component	Procedure
Reservoir ^a	Drain and clean; remove internal gaskets; install a 10- μ m breather
Inlet to pump	Check size of inlet pipe; supercharge or establish positive fluid head; install 60-mesh strainer four times pump capacity
Pump	Derate all pumps except piston type by 125%; drain and clean
Valves	May require change in contro orifice size; drain and clean
Fluid motors and cylinders	May require size change; drain and clean
Accumulators	Drain and clean
Piping	Use Teflon thread sealant; clean by swabbing
Filters	Change to compatible elements (do NOT use paper!); Clean housing
Coolers	Drain and clean
Start-up	Check with fluid supplier; follow his instructions
Fluid maintenance	Check water content and pH weekly at start
Component maintenance	Inspect pumps evey 500 h, until a standard maintenance program is established; each inspection may vary

^aSome designers use a closed reservoir with double-check valves to obtain supercharge pressure. Pressure is established by virtue of fluid and air expansion with temperature rise; 15–25 psi can be obtained by this method. One gravity-operated check valve in combination with a filter breather, relieves vacuum created by cooling after shutdown. A relief valve limits maximum pressure within the reservoir.

3. Disconnect the filter.
4. Flush the system with a minimum amount of the water–glycol fluid being used. Flush initially by operating at no load or at minimum operating pressure, then bring the fluid up to normal temperature and operate all parts. Many users follow the practice of operating on the flush fill for several hours to provide complete circulation and take full advantage of the solvent cleaning characteristics of the hydrolube fluid.
5. Drain the flushing charge as completely as possible, while it is still warm and without allowing it to settle. This fluid can be retained for further use after suspended solids have settled and residual petroleum oil has separated. With proper attention to removal of suspended contaminants, the flushing fluid can be used in preparing other machines for service or for makeup purposes.
6. Install a clean filter cartridge. Replace filter elements having zinc- or cadmium-plated parts with appropriate substitutes. Do not use a highly adsorptive filter medium, such as clay or Fuller's earth, because these filters may alter fluid composition by removing essential additives.
7. Examine pump parts, O-rings, and auxiliary equipment. Replace worn pump parts. Repair leaking pipe joints. Replace deteriorated gaskets, seals, and packings. Replace cork shaft seals and other water-susceptible packings and materials. Substitute waterproof materials.
8. Reconnect the system and tighten all joints and connections.
9. Fill system with proper grade of water–glycol hydraulic fluid.

10. Operate at reduced pressure to insure proper lubrication of the hydraulic pump; then bring up to standard operating conditions.

During the first few weeks of operation, filters and inlet screens may become clogged by sludge and deposits that have been loosened by the solvent action of the hydrolube. The result may be pump starvation and cavitation, noisy operation, and high pump wear. Therefore, replace filter cartridges and clean inlet screens as needed.

Even with the most careful cleaning procedures, a small amount of petroleum oil may remain in the system. Small quantities will not interfere with performance of the water-glycol fluid but will reduce the fire resistance, especially if residual oil collects in one part of the system such as the reservoir or accumulators. Hydraulic oil is lighter than the hydrolube fluids and will rise to the top of the reservoir. During the initial period of operation, periodically skim or siphon the residual oil from the surface of the fluid in the sump.

2.7 Fire Resistance

Even after 50 years of use [3,30,140], there is still no consensus on the best evaluation procedures to quantify the relative fire resistance offered by a hydraulic fluid [141]. However, Factory Mutual Corporation has recently developed a testing procedure which provides more adequate discrimination between various fire-resistant hydraulic fluids. A review of fire resistance testing procedures and the results reported to date is provided in Chapter 7. The order of fire resistance offered by various major classes of fire-resistant fluids capable of high-pressure use is water-glycol > phosphate ester > polyol ester > mineral oil.

REFERENCES

1. E. C. Brink, Jr., "Fire Resistant Hydraulic Fluids," *Lubrication*, 1972, 58, pp. 77-96.
2. W. H. Millett, "Fire Resistant Hydraulic Fluids," *Appl. Hydr.*, 1957, June, pp. 124-128.
3. J. E. Brophy, V. G. Fitzsimmons, J. G. O'Rear, T. R. Price, and W. A. Zisman, "Aqueous Nonflammable Hydraulic Fluids," *Ind. Eng. Chem.*, 1951, 43(4), pp. 884-896.
4. J. G. O'Rear, R. O. Militz, D. R. Spessard, and W. A. Zisman, "The Development of the Hydrolube Non-Flammable Hydraulic Fluids," *Naval Research Laboratory Report No. P-3020*, April 1947.
5. C. M. Murphy and W. A. Zisman, "Non-Flammable Hydraulic Fluids," *Lubr. Eng.*, 1949, October, pp. 231-235.
6. W. A. Zisman, J. K. Wolfe, H. R. Baker, and D. R. Spessard, U.S. Patent 2,602,780 (1952).
7. F. H. Roberts and H. R. Fife, U.S. Patent 2,425,755 (1947).
8. Anon., "Navy Announces Hydrolube Development," *Appl. Hydraul.*, 1948, September, p. 15.
9. G. E. Totten and G. M. Webster, "High Performance Thickened Water-Glycol Hydraulic Fluids," in *Proc. of the 46th National Conference on Fluid Power, March 23-24, 1994*, 1994, National Fluid Power Association; Milwaukee, WI, pp. 185-194.
10. W. E. F. Lewis, "Water-Based Energy Transmitting Fluid Compositions," U.S. Patent 4,434,066 (1984).
11. W. E. F. Lewis, "Energy Transmitting Fluid," U.S. Patent 4,855,070 (1989).

12. International Standard ISO 6743/4, "Lubricants, Industrial Oils and Related Products (Class L)—Classification Part 4: Family H (Hydraulic Systems), First Edition—1982-11-15.
13. J. Reichel, "Fluid Power Engineering With Fire Resistant Hydraulic Fluids—Experiences with Water-Containing Hydraulic Fluids," *Lubr. Eng.*, 1994, 50(12), pp. 947-952.
14. C. R. Schmitt, "Fire Resistant Hydraulic Fluids for Near-Surface Systems Safeguard Life and Property at No Loss in Efficiency," *Ind. Heating*, 1957, 24(9), pp. 1756-1770.
15. J. Mathe, "Fire-Resistant Hydraulic Fluids for the Plastics Industry," *SPE J.*, 1967, July, pp. 17-20.
16. C. Staley, "Fire-Resistant Hydraulic Fluids—Comparisons and Applications," *Petroleum Times*, 1967, 71(1834), pp. 1709-1714.
17. R. E. Rush, "Fire-Resistant Fluids in Basic Steelmaking—Which One?" 1980, 57(12), pp. 54-55.
18. Y. Iwamiya, "Water-Glycol Hydraulic Fluids," *Junkatsu*, 1987, 32(8), pp. 534-539.
19. C. G. Bonnell, "Fire-Resistant Fluids for Diecasting Hydraulic Systems," *Foundry*, 1967, 95(5), pp. 224-229.
20. H. L. Stewart, "Fire-Resistant Hydraulic Fluids," *Plant Eng.*, 1979, 33(4), pp. 157-160.
21. R. Edgington, "The Use of Fire-Resistant Hydraulic Fluids in Axial Piston Pumps," *Eng. Digest*, 1965, 26(11), pp. 91-92.
22. K. D. Aengeneyndt and P. Lehringer, "Schwerentflammbare Hydraulikflüssigkeiten auf Wasser-Glykol-Basis: Gestern-Heute-Morgen, Giesserei, 1978, 65(3), pp. 58-63.
23. G. E. Totten and R. J. Bishop, Jr., "Historical Overview of the Development of Water-Glycol Hydraulic Fluids," SAE Technical Paper Series, Paper 952077, 1995.
24. G. E. Totten, "Thickened Water-Glycol Hydraulic Fluids for Use at High Pressures," SAE Technical Paper Series, Paper 921738, 1992.
25. F. O. Hosterman, "A Progress Report: Nonflammable Hydraulic Fluids," *Appl. Hydraul.*, 1951, September, pp. 66-71.
26. W. H. Millet, "Nonpetroleum Hydraulic Fluids—A Projection," *Iron Steel Eng.*, 1977, 54(5), pp. 36-39.
27. R. C. Rasp, "Water-Based Hydraulic Fluids Containing Synthetic Components," *J. Synth. Lubr.*, 1989, 6(3), pp. 233-251.
28. G. E. Totten, R. J. Bishop, Jr., R. L. McDaniels, and D. A. Wachter, "Water-Glycol Hydraulic Fluid Maintenance," *Iron Steel Eng.*, 1996, October, pp. 34-38.
29. G. T. Y. Wan, P. Kenny, and H. A. Spikes, "Elastohydrodynamic Properties of Water-Based Fire-Resistant Hydraulic Fluids," *Tribol. Int.*, 1984, 17(6), pp. 309-315.
30. G. Blanpain, "The Use of Polyglycols in French Coal Mines," in *IP. Int. Symposium on Performance Testing of Hydraulic Fluids, Oct. 1978, London, England*, R. Tourret and E. P. Wright, eds., 1978, Heyden and Son; London, pp. 389-403.
31. A. J. Papay, "Hydraulics," *Chem. Ind.*, 1993, 48, pp. 427-452.
32. R. Q. Sharpe, "Designing for Fire Resistant Hydraulic Fluids," *Product Eng.*, 1956, August, pp. 162-166.
33. B. J. Loudon, "Fire-Resistant Hydraulic Fluids," *Surf. Coatings Australia*, 1989, July, pp. 23-29.
34. Anon., "Fire Resistant Hydraulic Fluids," *Lubrication*, 1962, 48(11), pp. 161-180.
35. C. Staley, "Fire Resistant Hydraulic Fluids," *Chemicals for Lubricants and Functional Fluids Symposium*, 1979.
36. G. E. Totten and G. M. Webster, "High-Performance Thickened Water-Glycol Hydraulic Fluids," in *Proc. of 46th National Conf. on Fluid Power*, National Fluid Power Association; Milwaukee, WI, 1994, pp. 185-194.

37. O. Isaksson, "Rheology for Water-Based Hydraulic Fluids," *Wear*, 1987, 115(1–2), pp. 3–17.
38. R. D. Rynders, "Fire Resistant Fluids from a Component Builder's View Point," *Natl. Conf. Ind. Hydraul.*, 1962, 16, pp. 39–46.
39. H. van Oene, "Discussion of Papers 73046 and 730487," *SAE Trans.*, 1973, pp. 1580.
40. P. P. Zaskal'ko, A. V. Mel'nikova, O. N. Diment, S. G. Titurenko, and E. V. Stepanova, "Mechanical Stability of Nonflammable Hydraulic Fluids," *Chem. Technol. Fuels Oils*, 1974, 10(3–4), pp. 307–309.
41. ASTM D 3945, "Standard Test Method for Shear Stability of Polymer-Containing Fluids Using a Diesel Injector Nozzle," American Society for Testing and Materials, Conshohocken, PA.
42. IP 294/77 Kurt Orbahn Method, "Shear Stability of Polymer-Containing Oils Using a Diesel Injector Rig."
43. G. M. G. Blanpain, "Fire-Resistant Hydraulic Fluids in the French Mines," in *Conf. Proceed. Fluid Power Equipment in Mining, Quarrying and Tunneling*, 1974, pp. 145–155.
44. W. A. Zisman, J. K. Wolfe, H. R. Baker, and D. R. Spessard, U.S. Patent 2,602,780 (1952).
45. Anon., *Minutes of Nitrosamine Task Force Meeting*, Cosmetic, Toiletry and Fragrance Association, Inc.; 1977.
46. G. E. Totten, R. J. Bishop, R. L. McDaniels, D. P. Braniff, and D. J. Irvine, "Effect of Low Molecular Weight Carboxylic Acids on Hydraulic Pump Wear," *SAE Technical Paper Series*, Paper 941751, 1994.
47. ASTM 1783, "Standard Test Method for Phenolic Compounds in Water," American Society for Testing and Materials, W. Conshohocken, PA.
48. W. M. Shrey, "Effect of Fire-Resistant Fluids on Design and Operation of Hydraulic Systems," *Iron Steel Eng.*, 1962, 39(9), pp. 191–197.
49. J. Igarashi, "Oxidative Degradation of Engine Oils," *Jpn. J. Tribol.*, 1990, 35, pp. 1095–1105.
50. L. Costa, A. M. Gad, G. Camino, G. C. Cameron, M. Y. Qureshi, "Thermal and Thermooxidative Degradation of Poly(ethylene oxide)—Metal Salt Complexes," *Macromolecules*, 1992, 25, pp. 5512–5518.
51. W. G. Lloyd, "The Influence of Transition Metal Salts in Polyglycol Autoxidations," *J. Polymer Sci., Part A*, 1963, 1, pp. 2551–2563.
52. P. W. Brown, K. G. Galuk, and W. J. Rossiter, "Characterization of Potential Thermal Degradation Products from the Reactions of Aqueous Ethylene Glycol and Propylene Glycol Solutions with Copper Metal," *Solar Energy Mater.*, 1987, 16, pp. 309–313.
53. J. A. Beavers, "The Effect of Degradation of Glycols on Corrosion of Metals Used in Non-Concentrating Solar Collectors," in *International Corrosion Forum Sponsored by the National Association of Corrosion Engineers*, paper 207.
54. W. J. Rossiter, P. W. Brown, and M. Godette, "The Determination of Acidic Degradation Products in Aqueous Ethylene Glycol and Propylene Glycol Solutions by Ion Chromatography," *Solar Energy Mater.*, 1983, 9, pp. 267–279.
55. Mannesmann Roth GmbH, "Hydraulic Power Units for Use With HFC Fluids," Mannesmann Rexroth GmbH.
56. C. W. West, "Additives for Corrosion Control," *Soap Chem. Specialties*, 1964, September/October.
57. C. W. McGary, "Degradation of Poly(ethylene)Oxide," *J. Polym. Sci.*, 1960, 46, pp. 51–57.
58. P. Rakoff, G. J. Colucci, and R. K. Smith, "Development of Fire Resistant Water Based Hydraulic Fluids," NTIS Accession No. AD-608 564, Nov. 27, 1964.

59. P. Rakoff, G. J. Colucci, and R. K. Smith, "Development of Fire Resistant Water Based Hydraulic Fluids," NTIS Accession No. AD-605 910, Sept. 28, 1964.
60. P. Rakoff, G. J. Colucci, and R. K. Smith, "Development of Fire Resistant Water Based Hydraulic Fluids," Dept. of Navy, Contract No. 90269, January 27, 1965.
61. ASTM D 665-83, "Standard Test Method for Rust-Preventing Characteristics of Inhibited Mineral Oil in the Presence of Water," American Society for Testing and Materials, Conshohocken, PA.
62. R. Baboian, ed., *Corrosion Tests and Standards*, 1995, American Society for Testing and Materials, Conshohocken, PA.
63. V. A. Katorgin and T. V. Ramanova, "Estimation of the Rate of Contact Corrosion of Metals," *Chem. Technol. Fuels Oils*, 1989, 25(1–2), pp. 113–115.
64. W. H. Millet, "Fire Resistant Hydraulic Fluids for Die Casting—Part 1, Aqueous Fluids," *Precision Metal Molding*, 1954, December, pp. 85–90.
65. W. H. Millet, "Fire-Resistant Hydraulic Fluids: Part 2—Aqueous Base Types," *Appl. Hydraul.*, 1957, June, pp. 124–128.
66. G. F. Kramer and J. Näscher, personal correspondence, Union Carbide Corporation, Tarrytown, NY, 1988.
67. H. A. Snow, "Modern Fire Resistant Hydraulic Fluids for Industrial Use," *Sci. Lubr.*, 1960, May, pp. 39–42.
68. V. G. J. Haden, "Fire-Resistant Hydraulic Fluids," *Metal Forming*, 1968, December, pp. 352–354.
69. G. V. Cole, "Investigation Into the Use of Water-Glycol as the Hydraulic Fluid in a Servo System," AERE R.11324, AERE Harwell—Engineering Projects Division, Harwell, UK, July 1984.
70. P. Kenny, J. D. Smith, and C. N. March, "The Fatigue Life of Ball Bearings When Used with Fire-Resistant Fluids," in *Inst. Petroleum Symp. on Performance Testing of Hydraulic Fluids*, 1978, paper 30.
71. D. V. Culp and R. L. Widner, "The Effect of Fire Resistant Hydraulic Fluids on Tapered Roller Bearing Fatigue Life," *SAE Technical Paper Series*, Paper 770748, 1978.
72. A. J. Zino, "What to Look for in Hydraulic Oils. VI—Lubricating Value," *Am. Machinist*, 1948, January 15, pp. 97–100.
73. H. A. Spikes, "Wear and Fatigue Problems in Connection with Water-Based Hydraulic Fluids," *J. Synth. Lubr.*, 1987, 4(2), pp. 115–135.
74. V. P. Versnyak, L. V. Zaretskaya, T. V. Imerlishvili, V. I. Kel'bas, N. V. Lukashvili, L. O. Sedova, V. M. Ryanoshapka, V. Sh. Schvartsman, and V. Kh. Shoiket, "Behavior of Water Glycol Hydraulic Fluids in EHD Contacts," *Sov. J. Friction Wear*, 1989, 10(5), pp. 120–126.
75. V. P. Versnyak, L. V. Zaretskaya, T. V. Imerlishvili, V. I. Kel'bas, N. V. Lukashvili, L. O. Sedova, V. M. Ryanoshapka, V. Sh. Schvartsman, and V. Kh. Shoiket, "Behavior of Aqueous Glycol Hydraulic Fluids in Elastohydrodynamic Contacts," *Trenie Iznos*, 1989, 10(5), pp. 919–927.
76. V. P. Versnyak, L. V. Zaretskaya, T. V. Imerlishvili, V. I. Kel'bas, N. V. Lukashvili, L. O. Sedova, V. M. Ryanoshapka, V. Sh. Schvartsman, and V. Kh. Shoiket, "Thickness of a Lubricating Film of Aqueous Glycol Fluids Under Different Friction Regimes," *Trenie Iznos*, 1991, 12(1), pp. 144–153.
77. R. S. Fein and F. J. Villforth, "Lubrication Fundamentals," *Lubrication*, 1973, 59, October–December, pp. 77–96.
78. G. T. Y. Wan and H. A. Spikes, "The Elastohydrodynamic Lubricating Properties of Water–Polyglycol Fire-Resistant Fluids," *ASLE Trans.*, 1994, 27(4), pp. 366–372.
79. G. Dalmaz and M. Godet, "Film Thickness and Effective Viscosity of Some Fire Resistant Fluids in Sliding Point Contacts," *Trans. ASME*, 1978, 100, pp. 304–308.

80. G. Dalmaz, "Traction and Film Thickness Measurements of a Water Glycol and a Water in Oil Emulsion in Rolling-Sliding Contacts," in Proc. of 7th Leeds-Lyon Symposium on Tribology, Friction and Traction, 1980, pp. 231-242.
81. L. D. Wedeven, G. E. Totten, and R. J. Bishop, "Performance Map and Film Thickness Characterization of Hydraulic Fluids," SAE Technical Paper Series, Paper 952091, 1995.
82. M. Ratoi-Salagean and H. A. Spikes, "The Lubricant Film-Forming Properties of Modern Fire Resistant Hydraulic Fluids," in *Tribology of Hydraulic Pump Testing—ASTM STP 1310*, G. E. Totten, G. H. Kling, and D. J. Smolenski, eds., 1996, American Society for Testing and Materials; Conshohocken, PA, pp. 21-37.
83. H. V. Cordiano, E. P. Cochran, and R. J. Wolfe, "A Study of Combustion Resistant Hydraulic Fluids as Ball Bearing Lubricants," *Lubr. Eng.*, 1956, July/August, pp. 261-266.
84. H. V. Cordiano, E. P. Cochran, and R. J. Wolfe, "Effect of Combustion-Resistant Hydraulic Fluids on Ball-Bearing Fatigue Life," *Trans. ASME*, 1956, 78, pp. 989-996.
85. P. Kenny, J. D. Smith, and C. N. March, "The Fatigue Life of Ball Bearings When Used with Fire-Resistant Hydraulic Fluids, in Int. Petroleum Symp. on Performance Testing of Hydraulic Fluids, 1978, paper 30.
86. E. D. Yardley, P. Kenny, and D. A. Sutcliffe, "The Use of Rolling-Fatigue Test Methods over a Range of Loading Conditions to Assess the Performance of Fire-Resistant Fluids," *Wear*, 1974, 28, pp. 29-47.
87. C. N. March, "The Evaluation of Fire-Resistant Fluids Using the Unisteel Rolling Contact Fatigue Machine," in *Rolling Contact Fatigue: Performance Testing of Lubricants*, R. Tourret and E. P. Wright, eds, 1976 Institute of Petroleum; London, pp. 217-229.
88. R. A. Hobbs, "Fatigue Lives of Ball Bearings Lubricated with Oils and Fire-Resistant Fluids," in *Elastohydrodynamic Lubrication*, Symposium Proc IME, 1972, Inst. of Mech. Eng., London, UK, pp. 1-4.
89. R. V. Culp and R. L. Widner, "The Effect of Fire Resistant Hydraulic Fluids on Tapered Roller Bearing Fatigue Life," SAE Technical Paper Series, Paper 770748, 1977.
90. F. T. Burwell and D. Scott, "Effect of Lubricant on Pitting Failure of Ball Bearings," *Engineering*, 1956, July 6, pp. 9-12.
91. J. L. Sullivan and M. R. Middleton, "The Pitting and Cracking of SAE 52100 Steel in Rolling/Sliding Contact in the Presence of an Aqueous Lubricant," *ASLE Trans.*, 1985, 28, pp. 431-438.
92. S. Shitsukawa, M. Shibata, and T. M. Johns, "Influence of Lubrication on the Fatigue Life of Ball Bearings," SAE Technical Paper Series, Paper 972710, 1997.
93. V. Riddel, P. Pacor and K. K. Appledorn, "Cavitation Erosion and Rolling Contact Fatigue," *Wear*, 1974, 27, pp. 99-108.
94. J. L. Sullivan and M. R. Middleton, "The Mechanisms Governing Crack and Pit Formation in Steel in Rolling Sliding Contact in Aqueous Lubricants," *J. Synth. Lubr.*, 1989, Vol. 6(1), pp. 17-29.
95. "The Development of Equipment and Techniques for Evaluating Effects of Oils on Bearing Fatigue Life," CRC. Project No. 413, Group on Gas Turbine Lubrication, of the Aviation Fuel, Lubricant and Equipment Research Committee of the Coordinating Research Council, Inc., May 1968.
96. C. H. Danner, "Relating Lubricant Film Thickness to Contact Fatigue," SAE Technical Paper Series, Paper 700560, 1970.
97. P. Kenny and E. D. Yardley, "The Use of the Unisteel Rolling Fatigue Machines to Compare the Lubricating Properties of Fire-Resistant Fluids," *Wear*, 1972, 20, pp. 105-121.

98. J. Reichel, "Fluid Power Engineering With Fire Resistant Hydraulic Fluids," 1994, 50(12), pp. 947–951.
99. N. Yano, T. Ohnishi, and T. Saitoh, "Improvement in Rolling Contact Fatigue Performance of Water–Glycol Hydraulic Fluids," STLE Annual Meeting in Kansas City, MO, 1996.
100. G. T. Y. Wan, P. Kenny, and H. A. Spikes, "Elastohydrodynamic Properties of Water-Based Fire-Resistant Hydraulic Fluids," Tribol. Int., 1984, 17(6), p. 309–316.
101. R. Bietowski, "Ball Bearing Lubricants—Use of Fire Resistant Hydraulic Fluids," Colliery Guardian, 1971, May, pp. 235–239.
102. R. J. Wakelin, "Life of Rolling Bearings in Contact with Fire Resistant Fluids," Final Report, M.O.D. (AS) Contract K78A/118/CB 78A, February 1975.
103. J. C. Skurka, "Elastohydrodynamic Lubrication of Roller Bearings," J Lubr., 1970, 93, pp. 281–291.
104. T. E. Talian, Y. P. Chiu, and E. Van Amerongen, "Prediction of Traction and Microgeometry Effects on Rolling Contact Fatigue Life," J Lubr. Tech., 1978, 100(1), pp. 156–166.
105. R. J. Boness, W. J. Crecelius, W. R. Ironside, C. A. Moyer, E. E. Pfaffenberger, and J. V. Poplawski, "Current Practice," in *STLE Life Factors for Rolling Bearings*, Erwin V. Zaretsky, ed., 1992, Society of Tribologists and Lubrication Engineers; Park Ridge, IL, pp. 1–45.
106. F. Townshend and P. Baker, "Factors Relating to the Selection and Use of Fire-Resistant Fluids in Hydraulic Systems," Hydraul. Pneumatic Power, 1974, April, pp. 134–140.
107. Sauer-Sundstrand, *Fluid Quality Requirements*, Rev. A, Sauer-Sundstrand Company; Ames, IA.
108. T. L. Jackson and R. C. Alston, "The Selection and Application of Fire Resistant Hydraulic Fluids," Plant Eng., 1968, 12(12), pp. 743–748.
109. Robert Bosch Group, *Fire Resistant Fluids*, Robert Bosch Group; Racine, WI.
110. C. R. Schmitt, "Fire Resistant Hydraulic Fluids for Die Casting," PMM, 1955, February, pp. 81–83.
111. A. Zingaro, "Walking the Fluid Cleanliness Tightrope," Hydraulics Pneumatics, 1994, April, 47(4), pp. 37–40.
112. A. Zingaro, "Walking the Fluid Cleanliness Tightrope [reprint]," Hydraulics Pneumatics, 1994, December, 47(12), pp. 25–26.
113. E. C. Fitch and I. T. Hong, FRH J., 1986, 6, pp. 41–51.
114. E. C. Fitch and I. T. Hong, FRH J., 1986, 6, pp. 53–61.
115. J. L. Xuan, FRH J., 1986, pp. 63–68.
116. R. F. Ou, FRH J., 1986, 6, pp. 69–75.
117. E. C. Fitch, *Fluid Contamination Control*, 1988, FES Inc.; Stillwater, OK.
118. Vickers Inc., "Contamination Control," in *Vickers Industrial Hydraulics Manual*, 3rd ed., 1992, Vickers Inc.; Maumee, OH, p. 6.22.
119. ASTM D-445, "Standard Test Method for Kinematic Viscosity of Transparent and Opaque Liquids (the Calculation of Dynamic Viscosity)," American Society for Testing and Materials, Conshohocken, PA.
120. ASTM D-1744, "Standard Test Method for Water in Liquid Petroleum Products by Karl Fischer Reagent," American Society for Testing and Materials, Conshohocken, PA.
121. ASTM D-4006, "Standard Test Method for Water in Crude Oil by Distillation," American Society for Testing and Materials, Conshohocken, PA.
122. L. Holiday (ed.), *Ionic Polymers*, 1975, John Wiley & Sons, New York.
123. P. N. Skoog, "Care and Maintenance of Water/Glycol Hydraulic Fluids," Foundry Manag. Technol., 1990, November, pp. 40–41.

124. P. N. Skoog, "The Care and Maintenance of Water Glycol Hydraulic Fluids," *Hydraulics Pneumatics*, 1991, November, pp. 41–44.
125. Oilgear Co., *High Water Content Fluid*, The Oilgear Company; Milwaukee, WI.
126. T. Murata, "Fire Resistant Working Fluids: Monitoring of Water–Glycol System Working Fluids," *Nisseki Rebyu*, 1989, 31(1), pp. 13–18.
127. W. J. Rossiter, P. W. Brown, and M. Godette, "The Determination of Acidic Degradation Products in Aqueous Ethylene Glycol and Propylene Glycol Solutions by Ion Chromatography," *Solar Energy Mater.*, 1983, 9, pp. 267–279.
128. R. K. Tessmann, "Ferrographic Measurement of Contaminant Wear in Gear Pumps," in *Proc. Natl. Conf. Fluid Power*, 1978, 32, pp. 179–183.
129. P. V. Ciekurs, S. A. Ropar, and V. T. Kelley, "Prediction of Hydraulic Pump Failures Through Wear Debris Analysis," *Naval Air Engineering Center Report*, NAEC-92-171, July 19, 1983.
130. Anon., "A Report on Ferrography and Its Application for Determining Wear Particle Equilibrium," *Technical Report*, 1998, Engineered Lubricants; Maryland Heights, MO.
131. Standard Oil, *Wear Particle Atlas—Revised*, SOHIO Predictive Maintenance Series, 1976, BP America, Inc.; Cleveland, OH.
132. P. N. Skoog, "Fire-Resistant Hydraulic Fluids in the 90's," *Die Casting Eng.*, 1989, 33(6), p. 30.
133. G. E. Totten, J. Cerf, R. J. Bishop, and G. M. Webster, "Recent Results of Biodegradability and Toxicology Studies of Water–Glycol Hydraulic Fluids," *SAE Technical Paper Series*, Paper 972744, 1997.
134. NFPA/T2.13.1 R3-1997, "Recommended Practice—Hydraulic Fluid Power—Use of fire resistant fluids in industrial systems, 4th ed., August 14, 1997.
135. C. R. Schmitt, "Changing Over to Fire-Safe Hydraulic Fluids," *Prod. Eng.*, 1956, November, pp.194–198.
136. J. R. Hemeon, "Changing to a Fire-Resistant Fluid," *Appl. Hydraul.*, 1955, July, pp. 66–68, 105.
137. E. J. Egan, "How to Install Fire-Resistant Hydraulic Fluids," *Iron Age*, 1956, October 11, pp. 95–97.
138. K. C. Goodman, *Living with Fire-Resistant Hydraulic Fluids*, 1965, Denison Hydraulics; Columbus, OH.
139. Anon., "Are Your Hydraulic Oil Lines Fireproof," *Mill Factory*, 1952, May, pp. 139–140.
140. R. A. Onions, "An Investigation into the Possibility of Using Fire-Resistant Hydraulic Fluids for the Royal Naval Systems," *Performance Testing of Hydraulic Fluids International Symposium*, R. Tourret and E. P. Wright, eds., 1979, Institute of Petroleum; London, pp. 439–458.
141. G. E. Totten and G. M. Webster, "Review of Testing Methods for Hydraulic Fluid Flammability," *SAE Technical Paper Series*, Paper 932436, 1993.
142. W. H. Millet, "Fire-Resistant Hydraulic Fluids," *Plant Eng.*, 1973, 27(23), pp. 141–143.

Polyol Ester Fluids

ROBERT A. GERE and THOMAS V. HAZELTON

Quaker Chemical Corporation, Conshohocken, Pennsylvania

1 INTRODUCTION

Fluid power engineers and users have traditionally selected hydraulic fluids based on mineral oil because they have high-performance characteristics and are economically favorable. External factors, however, often dictate an alternative selection. One major concern is the potential flammability of mineral-oil-based hydraulic fluids. Major capital and personnel losses have occurred because of hydraulic-fluid-related fires [1]. More recently, potential environmental problems associated with mineral-oil fluids have gained notoriety. These problems include low rates of biodegradability, aquatic toxicity, handling of contaminated material, and high waste-treatment costs. Long-term availability and future cost implications question further the viability of mineral-oil-based products.

A simple and attractive alternative to mineral-oil-based hydraulic fluids that addresses these problems are fluids based on polyol esters.

Esters are described as compounds produced by the reactions between organic and inorganic acids and alcohols. Naturally occurring esters (glycerides) are a major component of all fats and vegetable oils. Synthetic esters can be constructed from many organic and inorganic acids and alcohols and the choices made determine physical and chemical properties and cost of the resultant ester.

This chapter deals with hydraulic fluids based on polyol ester technology. The term "polyol ester" relates to the base stock used in the final product. Polyol ester hydraulic fluids, like most commercial hydraulic fluids, use performance-enhancement additives that can account for up to 10% of the total product. These fluids are typically prepared from long-chain carboxylic fatty acids (derived from natural fats and oils) and polyhydric alcohols that contain two or more hydroxyl groups.

Polyol-ester-based hydraulic fluids have been commercially available for about 25 years and are considered a major category of fire-resistant or *less hazardous*

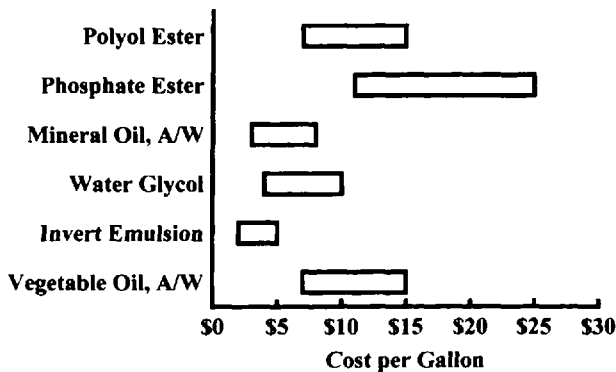


Figure 19.1 Hydraulic fluid costs.

hydraulic fluids [2,3]. They are classified as HFD-U under ISO standard 6753/H for fire-resistant hydraulic fluids. Factory Mutual Research Corporation initially listed polyol ester fluids as *less hazardous hydraulic fluids* in 1973 [4]. With the growing need for fluids that are environmentally compatible, polyol ester hydraulic fluids are finding a niche in this market because they are readily biodegradable and have low aquatic toxicity. The products exhibit excellent lubrication characteristics and have found applicability in most general-purpose power units. In 1996, approximately 3 million gallons of polyol ester hydraulic fluids were produced worldwide.

The cost of a polyol ester hydraulic fluid is approximately two to three times that of mineral-oil fluids. However, if fire resistance is required or if the fluid is used in environmentally sensitive areas, the selection of a polyol ester fluid can be a cost-effective choice. Figure 19.1 shows the relative cost of a polyol ester hydraulic fluid compared with other popularly used fluids.

In this chapter, polyol ester chemistry, the method of manufacture, and the role of performance-enhancement additives will be reviewed. Physical and chemical properties and operational characteristics such as fire resistance, environmental properties, and general compatibility with hydraulic power units will be discussed. Fluid limitations and maintenance requirements, including conversion procedures, will be described.

2 POLYOL ESTER TECHNOLOGY

2.1 Basic Chemistry

Polyol esters are members of the general ester family formed by the reaction between alcohols and inorganic or organic acids. The reaction process is generally called esterification with water formed as a by-product. Figure 19.2 is a representation of the esterification process and illustrates the large number of potential ester products possible and the route to polyol esters.

The alcohol portion of the ester can have a single functional group ($-\text{OH}$) or multiple ones (polyhydric). The structure of the compound may be an open-carbon-chain (aliphatic) or a closed-ring (aliphatic or aromatic) structure. Polyol esters typically employ open-chain alcohols. Phosphate esters are fire-resistant hydraulic fluids

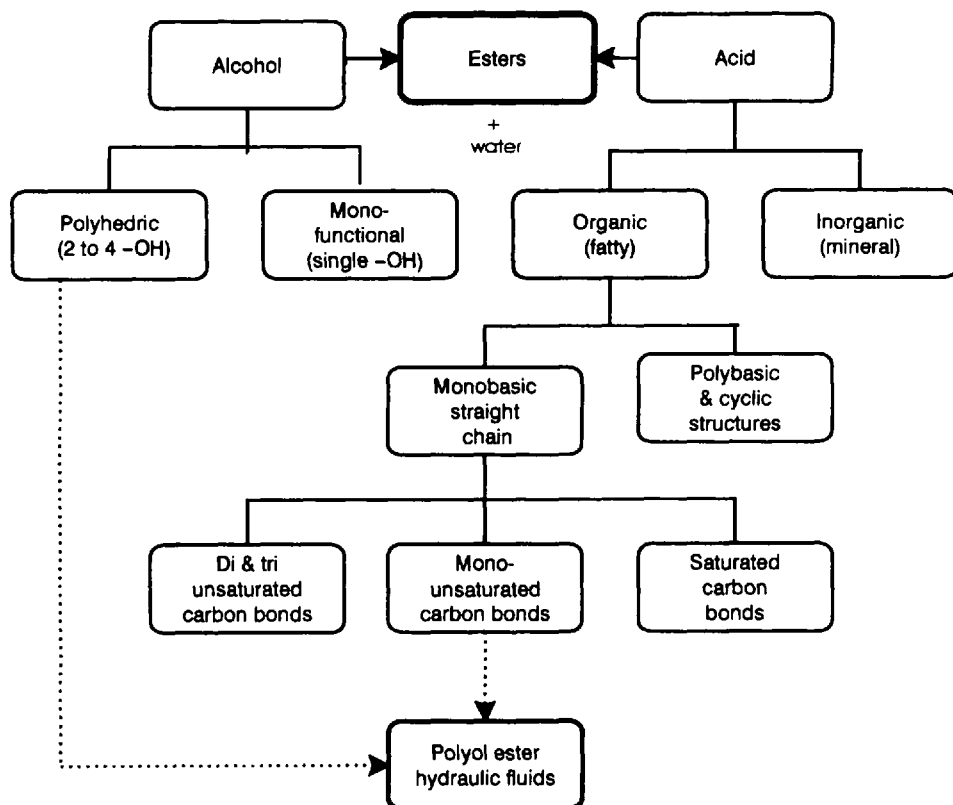


Figure 19.2 Formation of esters.

formed by a closed-ring-structure alcohol and an inorganic acid. Organic acids form the acid portion of a polyol ester.

Organic acids are generally called “fatty acids” because most organic acids are obtained from naturally occurring materials such as animal and marine fats and seed oils (e.g., rapeseed oil and sunflower oil). They are present in these sources as a glyceride and are, in fact, polyol esters. Here, the alcohol portion is glycerol, $C_3H_5(OH)_3$. Many seed-oil-based hydraulic fluids currently being marketed as “environmentally compatible lubricants” are natural glyceride polyol ester fluids. A large variety of fatty acids are recovered from these fat and seed sources, varying in carbon chain length, structure, and number of carboxyl groups [5]. Most fatty acids are of a straight-carbon-chain structure with a single carboxyl group ($-COOH$). The number of carbon elements may vary from 10 to 20+ but generally contain 14, 16, and 18. Polybasic (more than one carboxyl group) and cyclic structures are not as common. Monobasic straight-chain fatty acids also vary with respect to their level of saturation. Fatty acids that contain double bonds between carbons are said to be unsaturated. A monounsaturated acid contains one such bond. Di- and tri-unsaturated structures are also common, and although possible, more than three is unusual. Fatty acids with single carbon-to-carbon bond linkages are said to be saturated.

In a polyol ester, the fatty acid portion represents approximately 80% of the total ester because of its large size compared with most polyhydric alcohols, and two or more acid groups are used for each alcohol molecule. As a result, many properties characteristic of the acid, particularly oxidative resistance, are conferred upon the final ester.

In the commercial recovery of fatty acids, many different acids are obtained from a given glyceride source and separation of specific acids is difficult; mixtures of acids are typically realized. The level of the desired fatty acid will vary significantly based on cost and purity of the glyceride source and the efficiency of the separation processes.

The selection of a fatty acid is based on several factors, including the following:

- Higher carbon lengths produce esters with higher viscosity, flash/fire points, vapor pressure, and pour points.
- Saturated acids are more thermally stable and oxidation resistant than unsaturated acids.
- The higher the degree of unsaturation, the more unstable the ester becomes.
- Saturated acids produce esters with higher viscosities and pour points than unsaturated acids.

Polyol esters are generally prepared from monounsaturated fatty acids containing 16 and 18 carbon-length chains because they offer the best combination of physical and chemical properties. Figure 19.3 illustrates a typical reaction to form a polyol ester from glycerol and a C₁₈ monounsaturated fatty acid (oleic acid).

2.2 Polyol Ester Base Stocks

Although many aliphatic alcohols are multifunctional, the three most commonly used to produce polyol esters for hydraulic fluid service are shown in Fig. 19.4. The major difference among them is the number of hydroxyl groups. The viscosity of the polyol ester formed from these polyols is directly related to the number of hydroxyl sites and the choice is generally based on the desired ISO class of the hydraulic fluid.

To prepare polyol esters suitable for typical hydraulic fluid service, the fatty acid of choice is 18-carbon-length monobasic and monounsaturated. The chemical name for this compound is oleic acid. Selection of this fatty acid, found in abundant supply and with a relatively stable price history, is based primarily on the physical

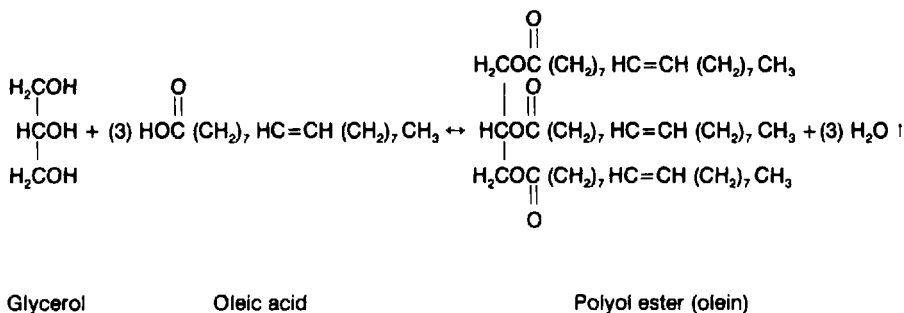
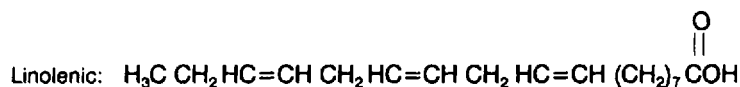
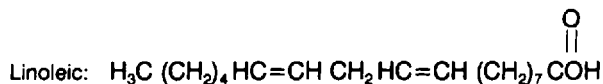
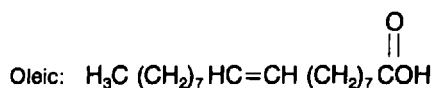
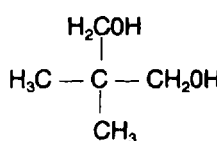


Figure 19.3 Polyol ester reaction.

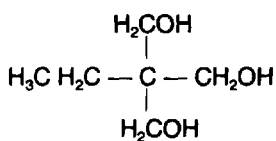
C-18 Monofunctional fatty acids



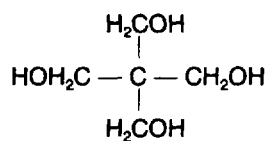
Polyhydric alcohols



Neopentyl glycol



Trimethyl propane



Pentaerythritol

Figure 19.4 Polyol Ester Starting Materials

and chemical properties of the esters formed with the polyols shown in Fig. 19.4. Figure 19.4 also shows the chemical structure for oleic acid; its reaction equation with a polyol is shown in Fig. 19.3. Oleic acid is present in virtually every natural fat and oil. Table 19.1 shows the major sources for oleic acid and the approximate distribution of the major fatty acids present. The presence of acids other than oleic acid is important because certain acids will not be readily separated in the separation processes to purify the acid. Esters formed from these acids may detract from the

Table 19.1 Oleic Acid Sources

Acid	Source (%)					
	Lard	Tallow	Palm oil	Corn oil	Soya oil	Tall oil
Oleic (C-18 ₁) ^a	43	43	37.5	26.5	22.5	59.5
Palmitic (C-16 ₀)	26	26	47	11.5	—	—
Stearic (C-18 ₀)	13.5	22.5	4	2	3	2
Linoleic (C-18 ₂)	9	1.5	—	59	54.5	37
Palmitoleic (C-16 ₁)	4	2.5	—	—	—	—
Myristic (C-12 ₀)	1.5	3	1	—	—	—
Linolenic (C-18 ₃)	—	—	—	1	8.5	—

^aDenotes length of carbon chain (C-18) and number of double bonds, 0, 1, 2, or 3 (subscript).

Source: Technical Bulletin 140A9, Henkel Corporation, Emery Group, Cincinnati, OH.

properties of the oleic acid ester. Saturated acids such as stearic and palmitic are readily separated from the unsaturated acids because of significant differences in their melting points. Separating unsaturated acids is more difficult because their melting points are similar and fractional distillation processes must be employed. This is not only a costly step but it is difficult because their vapor pressures are similar. All commercial grades of oleic acid will be approximately 75% pure, with the balance containing a variety of other fatty acids. The composition will depend on the original source.

Table 19.2 shows the nominal acid composition of oleic acid derived from three sources—beef tallow, tall oil, and a vegetable oil. The major differences in the fatty acids listed is the number of double bonds in the carbon-carbon chain. Oleic acid, with one double bond, forms a polyol ester with properties well suited to serve as a hydraulic fluid base for most fluid power applications. Esters formed from the saturated acids will have higher titer points than the oleic acid ester. This means that at low temperatures, these esters may partially desolubilize and cloud the fluid. In a severe case, these esters may coalesce and settle out of the fluid as deposits. Fatty acids with more than one double bond will form esters that are inherently more susceptible to oxidation and degradation [6]. There are also grades of products within each source category that vary in oleic acid content and undesirable acids. The compositions shown in Table 19.2 are representative and may vary between fatty acid suppliers and the level of distillation efficiencies employed.

Tallow is the preferred source for oleic acid based on cost and availability and generally contains a minimum level of undesirable other acids. Oleic acid from tallow is typically used in high-quality polyol ester hydraulic fluids. Commercial fluids are available that are based on other acid sources because of lower cost and with some sacrifice in fluid quality.

The three primary polyol ester base stocks described may be used singularly or in combination to optimize certain properties, particularly viscosity. Mixtures may also be formed in situ by combining different alcohols during the reaction. Table 19.3 reviews the structure of these three polyol esters and the nominal characteristics associated with each.

Table 19.2 Oleic Acid Composition

Acid	Source (%)		
	Tallow	Tall oil	Vegetable oil
Oleic (C-18 ₁) ^a	73	67	60
Palmitic (C-16 ₀)	5	10	3
Stearic (C-18 ₀)	—	3	2
Linoleic (C-18 ₂)	8	3	24
Palmitoleic (C-16 ₁)	6	2	—
Myristic (C-12 ₀)	4	—	—
Linolenic (C-18 ₃)	1	5	8

^aDenotes length of carbon chain (C-18) and number of double bonds, 0, 1, 2, or 3 (subscript).

Source: Technical Bulletin 140A9, Henkel Corporation, Emery Group.

Table 19.3 Polyol Ester Base Stocks

Polyol ester	Formula	Molecular weight	Flash/fire point ^a (°C)	Viscosity @ 40°C ^b (cSt)	Pour point ^c (°C)
TMPO	C ₆₃ H ₁₁₀ O ₆	962	316/354	50	-25
NPGO	C ₃₃ H ₇₆ O ₄	656	288/316	37	-20
PEO	C ₈₁ H ₁₄₀ O ₈	1240	316/354	68	-30

Note: Trimethylol propane oleate (TMPO): CH₃-CH₂-C-(CH₂-O-R)₃; neopentyl glycol oleate (NPGO): (CH₃)₂-C-(CH₂-O-R)₂; pentaerythritol oleate (PEO): C-(CH₂-O-R)₅, where R = C₁₈ oleic acid chain.

^aBased on ASTM D-92.

^bBased on ASTM D-88.

^cBased on ASTM D-97.

2.3 Manufacturing Process

2.3.1 Reactor Considerations

Polyol ester reactions are normally carried out in batch processing vessels. The following criteria are considered in the design of an appropriate reactor:

- **Capacity:** Most commercial manufacturing vessels are between 3000 and 10,000 gal. Dedicated equipment should be used whenever possible.
- **Material of Construction:** The reactor should be fabricated from stainless steel or glass-lined steel because of the corrosive nature of the raw materials at the elevated temperatures employed.
- **Heating and Cooling:** Polyol ester reactions are carried out at temperatures up to 288°C (550°F) and precise control of heating and cooling profiles is required to yield a high-quality product. Steam-heated reactors are inadequate for preparing quality esters.
- **Water Removal:** Water, the major by-product produced, must be removed continuously to force the reaction to completion. Removal of the water formed may also promote the removal of nonreacted starting materials. Provision for continuous reflux of these materials along with water removal should be provided. The reactor should have vacuum capability to help in water removal. Inert-gas sparging is also recommended to minimize the risk of oxidation to both the unreacted acid and the ester.

2.3.2 Reactants

The two reactants are oleic acid and the appropriate alcohol. Depending on the desired polyol ester, the alcohol will be either neopentyl glycol, pentaerythritol, or trimethylol propane, or a mixture of the three. The quantity of alcohol used is typically 5–15% above the stoichiometric requirement. The excess alcohol facilitates completion of the reaction; it is later stripped.

2.3.3 Reaction Catalysts

The basic polyol ester reaction can be achieved without the use of a catalyst. However, to maximize the degree of reaction completion, temperatures in excess of 260°C

(500°F) and extended reaction times must be employed. Both factors contribute to oxidative and thermal degradation, higher product viscosity because of undesirable polymerization, and incomplete utilization of the available hydroxyl sites. These all contribute to attenuation of many of the critical ester properties (e.g., flash/fire points, hydrolysis stability, and resistance to oxidation). The use of a catalyst reduces both reaction time and reaction temperature.

There are a number of potential catalysts, but the most commonly used are sulfonic acid derivatives and certain organometallic compounds. Catalysts, such as the organometallics, are generally used at concentrations less than 0.15% and may or may not be recoverable from the final product. Each type of catalyst has advantages and disadvantages and choice becomes a matter of trade-off. Benefits derived from the use of a catalyst are as follows:

- Reduced reaction temperature and reaction time
- Higher reaction efficiencies (utilization of more hydroxyl sites)
- Enhancement of most performance characteristics
- Improved product quality

In addition, the beneficial interaction between additives and the base stock increases significantly with improved quality of the base stock.

2.3.4 Manufacturing Process Cycle

The overall process is best described by reviewing the time versus temperature profile shown in Fig. 19.5. The profile is for illustrative purposes only and will vary significantly depending on equipment, batch size, and starting materials.

The major steps are as follows:

- Charge the appropriate quantities of starting materials. Because the final product will require certain physical and chemical characteristics to be within precise specifications, exact control of the starting materials is critical.

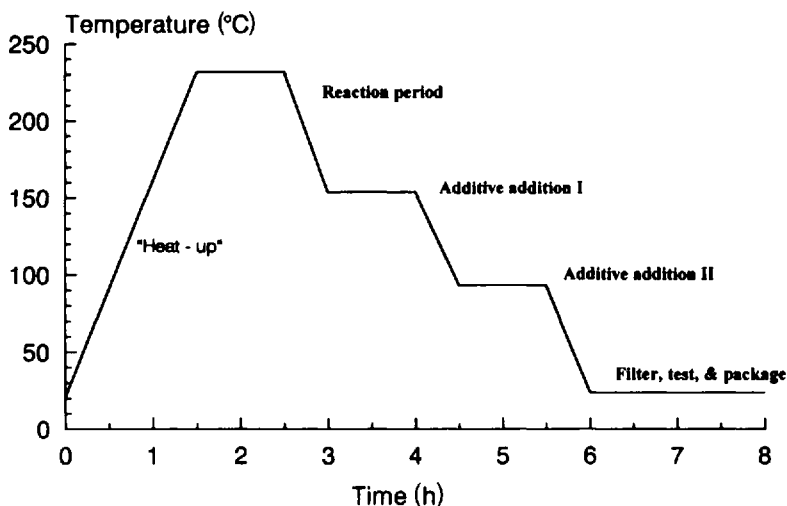


Figure 19.5 Reaction profile.

- The chemical reaction begins early in the “heat-up” cycle and, therefore, the time–temperature profile should be precise and conform to previous optimization studies. Automatic control is highly recommended.
- The length of time at the reaction temperature is critical because it must be sufficiently long to complete the reaction yet minimize oxidative and thermal degradation that may contribute to the formation of the unwanted side chemical reactions. The duration of this period is best determined by monitoring free acid and ending the reaction phase when the acid content has stabilized or stalled.
- Cooling periods should be as short as possible. Because some additives employed may have different optimum solubility temperatures and heat sensitivities, two additive addition levels are shown. Having low acid and hydroxyl numbers is important. Residual alcohol can be removed by vacuum stripping during the initial cooling period. Unreacted acids are more difficult to remove because of their low vapor pressures. Ideally, all acid should be used during the reaction phase but, if not, neutralizing with an agent such as calcium or sodium hydroxide to form an insoluble acid–salt can be effective.
- After cooling, the final steps are filtration and packaging. The product is filtered to remove residual particulates formed during the reaction (e.g., neutralization salts, scale, and undissolved additives). The filtration process is typically multistage. Gross particles are removed by simple screening. Fine filtration is accomplished by means of plate and frame filters, bag filters, cartridge media, sand filters, and so forth. Ideally, the filtering process should be done with process control monitoring to ensure that the final product is within specified cleanliness specifications. When the product is within all specifications, it may be held in intermediate bulk storage or packaged directly for delivery to the end user. All shipping containers should satisfy stringent cleanliness standards.

2.3.5 Process Control and Product Specifications

The goal of the manufacturing process is to produce a product that satisfies all fluid performance goals and conforms to a rigorous quality control standard. This can be accomplished through an in-process monitoring program that regulates the critical steps of the process and assures product compliance to final specifications. Industry-accepted statistical process control (SPC) principles should be incorporated.

Acid number history during the reaction is perhaps the most important in-process control parameter. Acid number reduction is a direct measure of reaction completion and is related to final ester quality. This parameter must be stabilized during the reaction phase of the process.

The product must satisfy all of the specifications established by the manufacturer to assure that the product will meet all required performance characteristics. Typical parameters that might be incorporated into a final product specification are as follows:

- Total acid number: <5 mg KOH/g
- Strong acid number: 0 mg KOH/g
- Hydroxyl number: <1 mg KOH/g
- Viscosity at 40°C: ISO grade \pm 10% (cSt)

- Cleanliness: NAS Class 7 (ISO 16/13)
- Moisture content: <0.05% (500 ppm)
- Color and odor: clear light amber, burnt almond
- Pour point: -26°C (

2.4 Fluid Additives

Commercial polyol ester hydraulic fluids incorporate performance-enhancement additives into the base ester to provide the requisite properties of a quality hydraulic fluid. The selection and level of these additives along with the quality of the base stock often account for the differences among fluids. The cost of additives is a major component of the product price structure.

2.4.1 Viscosity Index Improvers

Polyol esters exhibit a temperature–viscosity relationship similar to all hydraulic fluids—a tendency to have high viscosities at low temperatures and low viscosities at high temperatures. The viscosity index (VI) is a mathematical expression that describes the rate of change in viscosity as a function of temperature [7]. Viscosity index improvers are additives that reduce this rate of change to provide a more uniform viscosity over the operating temperature.

Viscosity index improvers are high-molecular-weight polymers such as polyisobutylenes, polymethacrylates, ethylene–propylene copolymers, styrene–isoprene copolymers, styrene–butadiene copolymers, and styrene–maleic ester copolymers. At low temperatures, these polymers are marginally soluble in the fluid, have a compact structure, and exert a small influence on fluid viscosity. As the fluid temperature increases, the solubility increases and the polymer uncoils or expands [8]. This decreases the mobility of the fluid and results in higher viscosity.

Figure 19.6 compares the temperature–viscosity properties of ISO Grade 46 polyol esters with and without a VI improver. The benefit derived from the additive appears small, as both fluids exhibit high viscosity indexes. The VI values with and without the additive are 200 and 170, respectively. Viscosities index values for min-

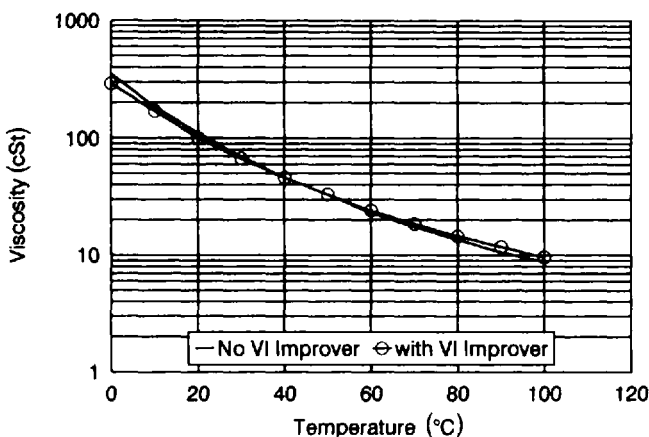


Figure 19.6 Viscosity index of polyol esters.

eral oil hydraulic fluids are typically 75–150. Figure 19.7 compares the viscosity properties of a high-VI antiwear ISO 46 Grade mineral oil ($VI \approx 95$) fluid with a polyol ester containing a VI improver ($VI \approx 230$). Viscosity differences at low temperatures are significant.

Although the value of a VI improver may be marginal with respect to increasing the viscosity index of a polyol ester, it does play a major role with respect to fire resistance. A major feature of a fire-resistant hydraulic fluid is the reduction of damage caused by spray-mist fires. Ruptures in high-pressure lines or hoses in a hydraulic system operating on mineral-oil-based fluids often create a spray mist, which if ignited, may burn throughout the spray envelope. In such a spray mist, the oil particle sizes formed are very small, depending on the operating pressure and the geometry of the rupture. Small mist particles, because of a high ratio of surface area to mass, are susceptible to ignition [9]. Thermal properties of the fluid are also important factors. This subject is discussed more fully in Section 4.2.

Fire-resistant polyol ester hydraulics fluids incorporating VI improvers influence the spray characteristics of a fluid under these conditions. The polymer acts as a binder and causes the fluid under expulsion to form large spray particles (lower surface area to mass ratio) that are more difficult to ignite.

Because VI improvers are high-molecular-weight polymers, shear stability is an important consideration in their selection. Table 19.4 illustrates the shear stability of three representative VI improvers with varying molecular weights. The polymers were incorporated into an NPG Oleate at 3% concentration. The differences between the initial molecular weight and preshear value are attributable to the breakdown caused by incorporating the polymer into the base ester. This often requires extensive mixing at an elevated temperature. Polymer B was readily solubilized, whereas polymers A and C required substantial mixing energy, resulting in molecular-weight breakdowns. Based on molecular-weight changes, polymer B would not be suitable for use as an additive because of excessive shear loss. Polymers A and C show less shear loss in this test and would be viable candidates for use in polyol ester fluids. Field experience has shown that with molecular-weight loss of this scale, compromise in fire resistance would not be expected.

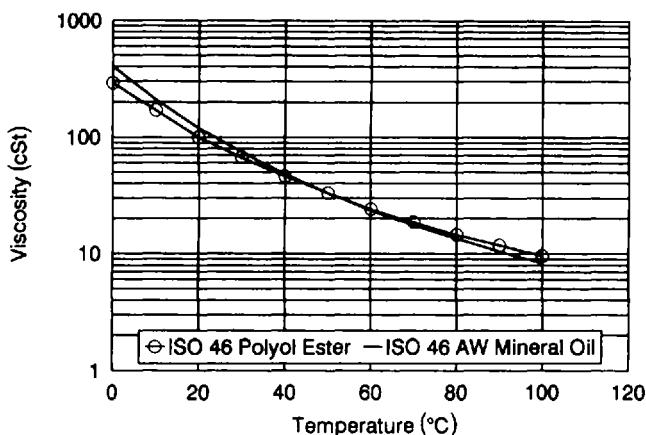


Figure 19.7 Viscosity index comparison.

Table 19.4 Shear Stability of VI Improvers

	Polymer		
	A	B	C
Molecular weight	91,750	44,200	107,000
		Preshear	
Fluid viscosity (cSt)	45.6	49.2	47.1
Molecular weight	54,200	126,100	107,000
		Postshear	
Fluid viscosity (cSt)	43.4	41.9	44.5
Molecular weight	44,200	67,100	62,500
Molecular weight loss (%)	18.5	41.3	18.7
Sonic shear index (SSI) ^a (%)	11.9	33.2	13.3

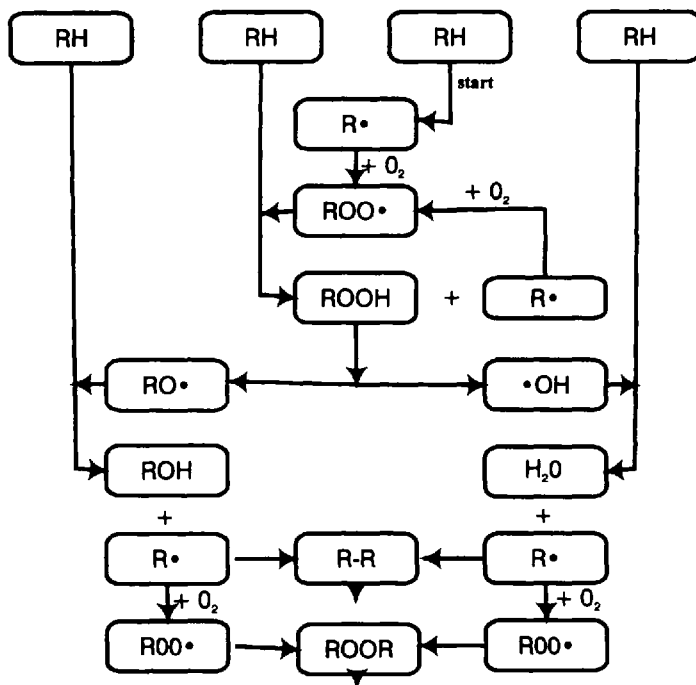
$$^a\text{SSI} = \frac{\text{Preshear viscosity} - \text{Postshear viscosity}}{\text{Preshear viscosity} - \text{Base viscosity}} \times 100.$$

2.4.2 Antioxidants

The operating environments for all hydraulic fluids, irrespective of type, are severe considering the high mechanical energy imparted, exposure to high localized temperatures, and, sometimes, sustained high bulk temperatures. Additional factors, such as air entrainment, external contaminants, and internal contaminations brought on by wear processes and corrosion, exacerbate the situation and create an atmosphere conducive to fluid degradation.

The major fluid degradation process is oxidation, particularly fluids based on hydrocarbon structures, and the subsequent formation of oxygen-containing hydrocarbons. Fluids are often differentiated by their ability to resist oxidation. Fluid oxidation results primarily in fluid viscosity increases and the generation of particulate matter and varnish. Fluid viscosity increases are caused by the solubility of high-molecular-weight polymers formed in the oxidation process; insoluble oxidative products lead to varnish and sludge. Fluid degradation of this form leads to a sluggish hydraulic system response, plugged filters and screens, and sticking valves and actuators.

Polyol ester fluids are no exception and effects from oxidation can be extreme. The mechanism of oxidation is similar to that associated with mineral-oil hydraulic fluids. The generally accepted theory on hydrocarbon oxidation is that the process is initiated by the formation of a primary alkyl radical ($R\cdot$) at the most vulnerable carbon-hydrogen bonds [10]. This radical is rapidly oxidized to its peroxide free radical ($ROO\cdot$) and initiates a chain reaction. Figure 19.8 is a flowchart outlining the steps involved in this chain reaction. The initial peroxide radicals subsequently react with additional energized hydrogens in the polyol ester molecule to form hydroperoxides ($ROOH$) and additional peroxide radicals. The process continues in a chain reaction. This phase of the autoxidation process, sometimes called an induction period, is relatively slow and innocuous to the hydraulic fluid. There is a point in



RH - alkyl group R• & ROO• - alkyl & peroxide free radicals

Figure 19.8 Polyol ester oxidation steps. RH = alkyl group; R• = alkyl free radical; ROO• = peroxide free radical.

which the hydroperoxide concentration (or concentration of oxygen into the fluid) reaches a level where other oxidative processes are initiated, ending the benign induction period. The major reaction now becomes one of molecular degradation (severing the O—O bond) of the peroxides to form new aggressive radicals (RO• and •OH). They, in turn, react with the polyol ester, which may lead to the formation of complex branched chains, polymers, acidic oxidative products, insoluble condensates, and a variety of varnish and sludgelike materials. This phase of the process can be rapid, as the rate of oxidation accelerates.

All commercial polyol ester hydraulic fluids incorporate antioxidants designed to disrupt the chain reaction and extend the induction period. One type of antioxidant “caps” the initially formed peroxide radicals and prevents subsequent chain-reaction steps. These antioxidants are hydrogen donors that recombine with the alkyl and peroxide radicals to form stable low-energy radicals that do not subsequently react with the base ester. Commonly used materials are sterically hindered phenols and, occasionally, secondary aromatic amines. There are many compounds designed for this process and the formulator must optimize his specific product with available commercial antioxidant products. The antioxidant will be gradually consumed, depending on the specific fluid and the operating conditions encountered.

Another type of antioxidant additive functions on a different mechanism and prevents decomposition of the hydroperoxides into $\text{RO}\cdot$ and $\cdot\text{OH}$ radicals. They react stoichiometrically with the hydroperoxides to form stable compounds; thioethers and phosphites represent this type of antioxidant. These materials are not regenerative and oxidation rates increase rapidly after the additive has been depleted. Antioxidants are typically formulated into the fluid at levels from 0.5% to 2%.

Beyond the role of antioxidant additives, the autoxidation process is sensitive to other factors, including the following:

- The major portion of the polyol ester molecule is derived primarily from oleic acid. Because of its original source, low levels of linoleic acid, linolenic acid, and other polyunsaturated acids are also present. The major difference between these acids is the number of double bonds in its structure. The number and position of double bonds drastically affect the rate of oxidation. Methyl groups positioned between double-bond carbon linkages are readily activated and subjected to autoxidation. The monounsaturated version (oleic) provides the greatest resistance, and linolenic (three double bonds) the most vulnerable. The relative rates of oxidation of oleic, linoleic, and linolenic acids are 6, 64, and 100 [6]. The higher-quality polyol fluids use fatty acid sources that maximize oleic acid content (see Table 19.1).
- Dissolved metal ions, particularly copper, in the polyol ester can affect the autoxidation process [8]. Divalent copper (Cu^{2+}) is the predominate form of dissolved copper and is not considered a pro-oxidant; however, if reduced to the cuprous state (Cu^{1+}), it becomes an active catalytic agent and accelerates the decomposition of the hydroperoxides into additional chain-promoting free radicals. Compounds employed as the primary antioxidant (sterically hindered phenols) are capable of acting as a reducing agent in converting Cu^{2+} to Cu^{1+} . The net effect is that the dissolved copper ions contribute to the degeneration of the antioxidant and adversely affect the life of the fluid. A chelating agent such as disalicylidene propylenediamine forms copper adducts that have no pro-oxidant characteristics. These additives, however, have no effect in slowing the rate of migration of additional copper ions into solution. Additives that promote the formation of a passivation film on nonferrous metal surfaces will reduce such migration. Examples of these materials include mercaptobenzothiazole, mercaptobenzimidazole, and aromatic triazole derivatives. These additives may also limit the corrosive effects of sulfur.

2.4.3 Corrosion Inhibitors

Corrosion inhibitors are used to reduce chemical attack on ferrous and nonferrous metal surfaces. Polyol esters are generally benign to the common materials of construction. However, once in service, several factors contribute to increases in their chemical aggressiveness. The major one is fluid oxidation and the resultant formation of potentially corrosive acids. Metal attack by these materials contributes to further fluid oxidation and continuation of the corrosion process. This process is accelerated by water contamination and high operating temperatures.

Ferrous-metal corrosion inhibitors prevent the formation of rust by forming a protective film barrier. Highly polar compounds such as sulfonic and succinic acid

derivatives and certain amides are commonly used. The dosage level in the hydraulic fluid is typically 0.25%. It should be noted that these barrier films are susceptible to mechanical wear or abrasion and the polar nature of the additive may interfere with other polar-type additives in the fluid [10]. Polyol esters are highly polar and provide a natural level of corrosion protection. Most polyol ester hydraulic fluids do not incorporate rust inhibitors.

Nonferrous inhibitors also provide protection by the formation of film barriers. Chemical compounds such as heterocyclic sulfur–nitrogen compounds, mercapto-benzothiazole, and dimercaptothiadiazole derivatives are commonly used. Dosage levels range from 0.1% to 0.5%. All polyol ester products contain nonferrous corrosion inhibitors, with a range of effectiveness among fluids from different suppliers. This effect is related to the overall efficiency of the antioxidant system and the quality of the base ester.

It is particularly important that the moisture level and total acid number (TAN) in the hydraulic fluid be monitored and controlled, as they are major influences in nonferrous-metal attack. The presence of water is detrimental because it can solubilize acid products and increase their chemical activity. If possible, moisture level should be maintained at 0.2% or less and the TAN less than 5 mg KOH/g.

2.4.4 Antiwear and Extreme-Pressure Additives

A hydraulic fluid's basic function is to transmit power, a function that is readily achieved by virtually any liquid. However, the practical application of fluid power requires the fluid to operate under high pressures in high-speed equipment. This creates the additional fluid requirement of being a lubricant that satisfies the needs of modern high-speed hydraulic pumps and motors and other system components.

Like mineral-oil base stocks, a polyol ester base provides lubrication (hydrodynamic) between sliding and rotating surfaces through a film of lubricant that separates the surfaces. Fluid viscosity is the principal fluid attribute that maintains the film and prevents wear. However, under high pressure and reduced relative speeds, the lubricating film is forced out or becomes too thin to separate the surfaces, and metal-to-metal contact occurs. Without additional protection, this contact can lead to catastrophic failures of the surfaces involved. Under these conditions, the type of lubrication changes from hydrodynamic to boundary (see Chapter 6). Polyol ester-based hydraulic fluids are formulated with antiwear additives to address this problem. Briefly, these additives are (1) adsorbed onto the metal surfaces to provide a lubricating film and (2) decomposed under the high temperatures generated by frictional heat to form reactive products that combine chemically with the metal surfaces to form a separating film. Examples of antiwear additives used include the following:

- Metal dialkyl dithiophosphates
- Metal diaryl dithiophosphates
- Alkyl phosphates
- Phosphorized fats and olefins
- Phospho-sulfurized fats and olefins
- Sulfurized fats, fat derivatives, and carboxylic acids
- Chlorinated fats, fat derivatives, and carboxylic acids
- Fatty acids, other carboxylic acids, and their metal salts

- Esters of fatty acids
- Oxidized paraffins and oils

Besides reducing metal wear, some types of antiwear agents may also function as antioxidants and corrosion preventives [11]. The fluid supplier must therefore optimize the selection of an antiwear additive with other ingredients in the additive package. Additive interactions may also synergistically enhance or antagonistically diminish certain performance characteristics [12]. Also, depending on the application, ashless (no heavy metals) additives should be used [13].

2.4.5 Combustion Inhibitors

For applications requiring the use of fire-resistant hydraulic fluids, polyol esters are finding wide acceptance. This is based in part on flash/fire points and autoignition temperatures higher than mineral-oil fluids. VI improvers augment these properties and contribute to the fluid's overall fire resistance (see Sec. 2.4.1), particularly spray-mist ignition. An acceptable level of fire resistance was established in Factory Mutual Research Corporation (FMRC) testing and polyol-ester-based fluids have been listed in the FM Approval Guide for years [4]. FMRC is changing its approval standards to one in which total heat release from a spray fire and ease of ignition will be measured and integrated into a calculated Spray Flammability Parameter (SFP) [14]. Some polyol-ester-based fluid manufacturers are developing products that will have SFP values comparable to other types of fluids with high fire resistance under the new FMRC standard.

2.4.6 Others

A variety of other additives may be incorporated into polyol-ester-based fluids to address problem areas unique to specific applications:

- **Foam inhibitors:** Entrained and dissolved gases can affect fluid performance. Entrained air is usually introduced at the low-pressure portion of the system (e.g., pump-suction piping and the fluid reservoir) and will be partially soluble at operating pressures. Residual entrained air can create a "spongy" hydraulic system operation and lead to a variety of system problems. Depressurization of the fluid releases dissolved air and may generate foam in the reservoir. These problems are properly addressed by ensuring that suction piping does not ingest air and all return lines extend well below the liquid level in the reservoir to reduce surface turbulence. Other consequences of dissolved and entrained air are increased pump wear through cavitation and fluid oxidation.

Generally, polyol-ester-based fluids do not incorporate foam inhibitors or air-release agents. For applications prone to air ingestion, their use should be a consideration. Materials commonly used are silicones (polysiloxanes or dimethylsiloxanes) and polyacrylates. These materials are used at low concentrations (1–50 ppm) and form a fine dispersion. Overdosage can result in excessive foam and loading of system filters. Foam inhibitors function by changing the surface-tension properties of the fluid and the coalescing of the small air bubbles into large ones.

- **Demulsifiers:** Water contamination can be detrimental to polyol-ester-based hydraulic fluids and should be avoided if possible. Because of the high shear

rates imposed by the hydraulic pumps, water is readily dispersed or even emulsified into the fluid. This water is not easily separated and may contribute to fluid and system degradation. One approach to reducing the effect of water is the use of additives that coalesce water droplets and ease their removal. Certain polyesters, phosphorous-containing chemicals, Ca and Mg sulfonates, and heavy-metal soaps are effective demulsifiers. Additives used for other functions in the lubricant formulation should be evaluated for potential demulsification response.

- **Dispersants:** Particulate matter contaminating the fluid often settles in dead areas of the hydraulic system and eventually builds up to a point where large aggregates may break loose and cause damage. Dispersant additives help in the suspension of insoluble products formed by fluid oxidation and corrosion. Polybutenylsuccinic acid derivatives are commonly used. The use of a dispersant will ease the removal of these particles by the hydraulic system filters.
- **Pour point depressants:** Polyol esters are primarily derived from oleic acid (Sec. 2.2). Small quantities of other fatty acids are also involved in the esterification process. These esters may have high titer and melting points and come out of solution at a higher temperature than the oleic acid ester. Pour point depressants will suppress this early precipitation and improve low-temperature flow properties. This additive technology is well established for mineral-oil fluids and has just recently been extended to vegetable oils and ester fluids. Compounds such as polymethacrylates, wax alkylated naphthalene polymers, wax alkylated phenol polymers, and chlorinated polymers are candidates for this group of additives.

2.4.7 Fluid Cost Implications

The performance improvements realized by these additives are significant and directly influence the cost of the fluid. The use of performance-enhancement additives is a value-added feature that varies widely among suppliers. It is estimated that additives account for 10–30% of the cost of the fluid. Other factors affecting the cost are raw material source and manufacturing quality standards. Each of these factors influences the final product cost and partially explains why the price of a polyol-ester-based hydraulic fluid may range from \$6.00 to \$20.00/gal.

3 SUMMARY OF PHYSICAL AND CHEMICAL PROPERTIES

Three ISO grade fluids, -46, -68, and -100, satisfy most of the industrial applications. Engineering properties specific to each ISO class are summarized in Table 19.5. Figures 19.9 and 19.10 show viscosity and specific gravity as a function of temperature, respectively. Properties that are applicable to the general class of polyol ester-based fluids are shown in Table 19.6. Besides the bulk modulus data shown in Table 19.6, Fig. 19.11 shows the compressibility (percent volume reduction) of an ISO grade 68 fluid at 20°C. Figure 19.12 shows the effect of pressure (up to 10,000 psi) on fluid viscosity at various temperatures. It should be noted that these properties represent high-quality commercial products currently available. These properties are dependent on the specific chemistry involved with a given fluid and the level and

Table 19.5 Typical Properties of ISO 46, 68, and 100 Polyol Ester Fluids

Property	ASTM method	ISO viscosity grade		
		46	68	100
Viscosity (cSt) at	D-88			
25°C (77°F)		82	100	168
40°C (104°F)		46	68	100
100°C (212°F)		9	10	13
Viscosity index	D-2270	230	235	>200
Specific gravity at	D-1298			
25°C (77°F)		0.91	0.91	0.92
50°C (122°F)		0.89	0.89	0.91
Coefficient of thermal expansion (per °F)	D-1903	4.06×10^{-4}	4.08×10^{-4}	4.17×10^{-4}
Flash point (COC) (°C)	D-92	260	260	257
(°F)		(500)	(500)	(495)
Fire point (COC) (°C)	D-92	288	293	354
(°F)		(550)	(560)	(670)
Autoignition temperature (°C) (°F)	E-659	404	404	404
		(760)	(760)	(760)

Source: Product Brochure: *Qunitolubric 822 Fire Resistant Hydraulic Fluids*, Quaker Chemical Corporation, Conshohocken, PA.

quality of the various additives used. It is recommended that specific suppliers be contacted for engineering properties that are applicable to their products.

4 RATIONALE FOR SELECTING POLYOL-ESTER-BASED HYDRAULIC FLUIDS

The vast majority of power units either in service or in the planning phase are designed assuming the use of mineral-oil hydraulic fluids. This is based on many years of experience, performance, and cost. Most hydraulic systems and components use the established properties of mineral-oil lubricants for design criteria. The decision to use an alternative hydraulic fluid, for whatever reason, requires an insight into the suitability of that fluid for all aspects of the hydraulic system. This requires analysis in areas such as the fluid's antiwear properties, metals and elastomer compatibility, temperature limits, environmental compatibility, presence of hazardous ingredients, special handling procedures, costs, and other considerations.

In existing hydraulic systems, the decision to change fluids is motivated by factors such as previously unrecognized fire hazards or new regulations regarding potential spills. These factors will dictate the use of fire-resistant fluids or ones that are environmentally compatible. Regarding new systems, the design process is simpler in that suitable components can be selected for any candidate fluid. Within these broad alternative fluid categories are additional choices that relate to the type of chemistry employed. A critical step, therefore, in the selection of a replacement fluid is an analysis of the potential impacts the fluid might have on the operation, life, maintenance, and operating cost of the system.

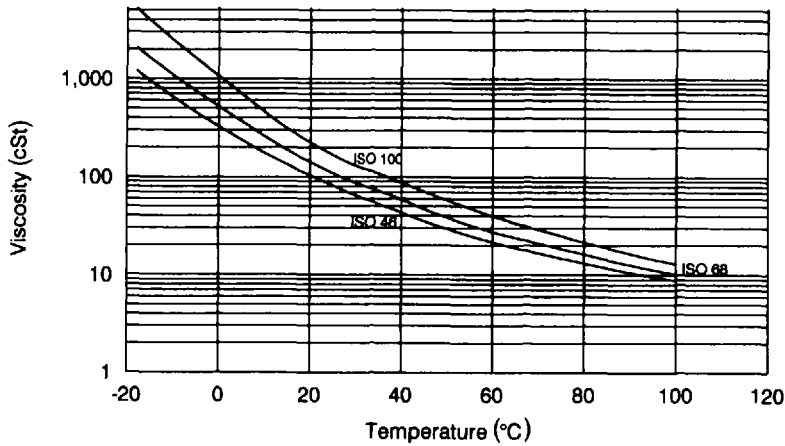


Figure 19.9 Viscosity of ISO 46, 68, and 100 polyol ester fluids.

Polyol-ester-based hydraulic fluids offer certain advantages over other fluid types and often represent a simple and economic alternative to mineral-oil-based lubricants. The factors that should be considered in selecting an alternative fluid, the advantages, and the disadvantages associated with polyol-ester-based hydraulic fluids are discussed.

4.1 Pump Testing and Lubrication Properties

The trend in fluid power technology has been continually driven toward more compact, higher-performance hydraulic systems. As a result, higher operating pressures, higher pump speeds, and more complex duty cycles have become standard with increasingly higher demands on all aspects of hydraulic fluid performance. The ability of a fluid to provide extended pump and component life expectancy is arguably its most important attribute.

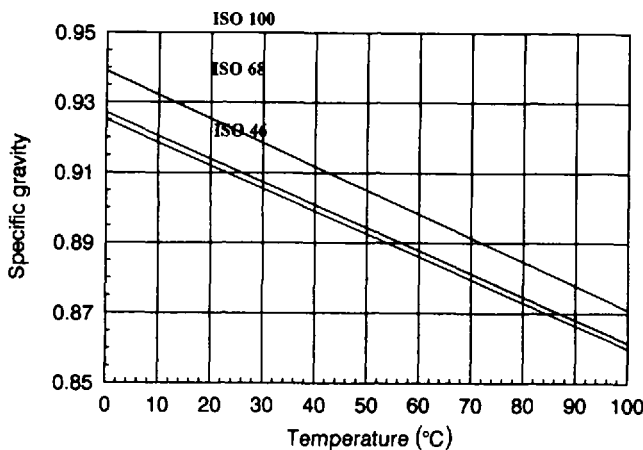
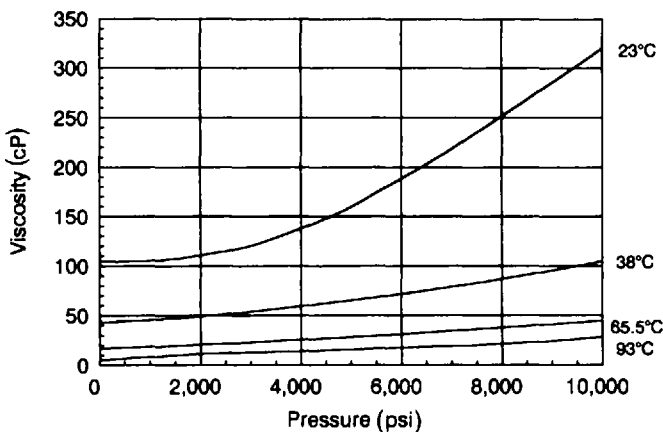


Figure 19.10 Specific gravity of ISO 46, 68, and 100 polyol ester fluids.

Table 19.6 Typical Properties—Polyol Ester Fluids

Property	ASTM method	Value
Total acid number	D-974	<2 mg KOH/g
Strong acid number	D-974	0
Vapor pressure at 20°C (68°F)		3.2×10^{-6} mm Hg
66°C (150°F)		7.5×10^{-6} mm Hg
Pour point	D-97	<-26°C (<-15°F)
Bulk modulus at 20°C (68°F) at		
207 bar (3,043 psi)		1.84×10^4 bars (27.05×10^4 psi)
345 bars (5,072 psi)		1.94×10^4 bars (28.52×10^4 psi)
89 bars (10,128 psi)		2.18×10^4 bars (32.05×10^4 psi)
Thermal conductivity at	D-2717	
19°C (66°F)		1.439 cal/h cm ² C/cm (0.0971 Btu/h/ft ² °F/ft)
71°C (160°F)		1.385 cal/h cm ² °C/cm (0.0934 Btu/h ft ² °F/ft)
Specific heat at 20°C (68°F)	D-2766	0.49 cal/g °C
Solubility in water		Negligible
Water separation	D-1401	40:35:5 (30) mL oil:water:emulsion (min.)
Foaming tendency	D-892	Pass
Dielectric breakdown voltage	D-877	30,000 V (30 kV)

Source: Product Brochure: *Quintolubric 822 Fire Resistant Hydraulic Fluids*, Quaker Chemical Corporation, Conshohocken, PA.

**Figure 19.11** Compressibility of ISO 68 polyol ester fluids.

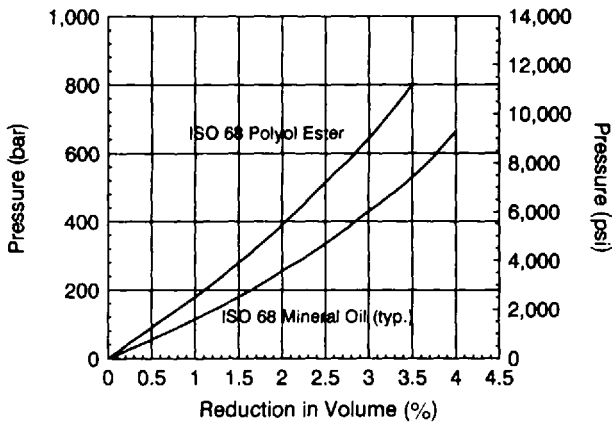


Figure 19.12 Pressure–viscosity relationship of ISO 68 polyol ester fluid.

Polyol-ester-based hydraulic fluids have shown a high level of antiwear characteristics and acceptable service in nearly all types of commercial hydraulic pumps at fully rated operating conditions. Performance history has varied because of product differences in additives and base stocks with varying specifications. Less than ideal operating conditions have also been factors.

Fluid suppliers have conducted extensive laboratory and formulation studies to maximize the lubrication and pump antiwear properties of polyol esters. Unfortunately, traditional bench-scale lubrication test procedures do not satisfactorily reflect the wear processes in a hydraulic pump [15]. One exception to this generalization is the FZG gear test (DIN 51354). It has been suggested that this test and a standard vane-pump test be used to establish minimum requirements for hydraulic fluid specifications [16]. Polyol-ester-based hydraulic fluids do very well in the FZG test (+12 stages). The major product development tool, therefore, has been small-scale pump testing as defined in ASTM D-2882-90 [15]. This method is based on the Vickers 104C/105C vane pump and the evaluation criterion is the loss in weight created by wear between the pump vanes and cam ring. It is based on the assumption that weight loss of the rotating parts is directly related to the antiwear properties of the hydraulic fluid. The wear process is accelerated by operating the pump at 2000 psi instead of the nominal design pressure of 1000 psi, thereby increasing the pressure loading of the vanes by 100%. The test has been used for many years, and although there are acknowledged reservations about the extension of results to other pump types [17], it has served as a significant test for fluid development and qualification. This test is inexpensive to run and provides rapid response. Test conditions are as follows:

- Duration: 100 h
- Operating pressure: 2000 psi
- Operating temperature: 66°C (150°F) for fluid viscosity <50 cSt (at 38°C and 79°C (175°F) for fluid viscosity >50 cSt
- Fluid volume: 3 or 15 gal
- Pump: Vickers 104C or 105C (rated at 7.5 gal/min flow at 1200 rpm, 49°C, and 1000 psi)

The test measurement is the combined loss in weight of the pump vanes and cam ring over the test period. Because of the differences in commercial polyol-ester-based hydraulic fluids, it is difficult to present precise information on the results obtained in this test. Table 19.7 illustrates representative weight losses for ISO 46, 68, and 100 fluids. Three values are given: the minimum that could be expected from a superior fluid, the maximum weight losses associated with marginal fluids that have sufficient antiwear properties to survive the test, and a value that represents the better polyol-ester-based fluids. There are no statistically significant differences in the wear characteristics among the ISO fluid classes.

Polyol-ester-based fluids have also been tested under the conditions specified in ASTM D-2882 in which the running time was significantly extended. An ISO Grade 68 fluid was tested for 8000 h and the total ring and vane weight loss was 19.1 mg. An interim weight loss measurement after 167 h was 5.1 mg.

Despite a fluid's performance as measured under ASTM D-2882, many pump manufacturers and system designers remain skeptical of a fluid's ability to perform satisfactorily, particular in pump designs other than the vane type, unless it satisfies certain test criteria specific to their equipment. Warranty considerations are a major factor for this position.

Several manufacturers conduct "in-house" tests on selected new fluids or provide specifications for an acceptable test protocol to be conducted by a fluid supplier or a third party.

Certain polyol-ester-based hydraulic fluids have been evaluated under various manufacturers' test programs and have been judged satisfactory. Individual fluid suppliers should be contacted about their status with the following established tests.

- Denison HF-O
- Vickers 35VQ25A
- Rexroth Piston Pump Test (Proposed)
- Racine Wear Test

Also refer to Chapter 10 for a more detailed description of these tests. Based on many factors, including results from the above tests and extensive field experience, many pump manufacturers have endorsed the use of polyol-ester-based hydraulic fluids. It should also be noted that some manufacturers have placed limitations on the operating conditions and certain applications when using a polyol-ester-based fluid. These limitations are often temporary, pending results over a trial period. These issues should be reviewed with the applicable original equipment manufacturer. The following pump manufacturers have endorsed the use of polyol-ester-based fluids based on the above:

Table 19.7 Polyol Ester ASTM D-2882 Pump Test Results

Fluid	Minimum wear ^a	Maximum wear ^a	Typical wear ^a
ISO 46	<10 mg	<100 mg	<20 mg
ISO 68	<10 mg	<100 mg	<20 mg
ISO 100	<10 mg	<100 mg	<20 mg

^aWeight loss of cam ring and vanes.

- Vickers, Inc.
- Parker Hannifin Corp.
- Sauer-Sunstrand
- Eaton Corp.
- Oilgear Co.

Some equipment manufacturers may be reluctant to approve or recommend the general class of polyol-ester-based fluids and may restrict approvals to specific brands.

4.2 Hydraulic System Compatibility

The possible conversion from one fluid type to another requires an analysis of the hydraulic system and an assessment of its compatibility with the new fluid. Historically, converting from a mineral-oil fluid to a fire-resistant type was viewed with skepticism. A common view was that a fluid change inevitably created hydraulic system compromises. Retrofitting seals, hoses, and elastomers with more expensive, chemical-resistant types was one concern. Derating pump speed and pressure and restricted operating temperatures were also associated with the use of fire-resistant fluids. These types of problems are not a major consequence when converting to polyol-ester-based hydraulic fluids. The major considerations are presented in the following subsections.

4.2.1 Components

The suitability of each component in the system must be established. Endorsement of the fluids by the original equipment manufacturer (OEM) is the preferred approach. Lacking this, experience with the fluid and recommendations by the fluid suppliers and the OEM become important factors. Because of the chemistry of polyol-ester-based fluids and their typical properties, few components are excluded for use. Based on experience, OEMs may express a preference for the type of fluid to be used and possibly, the supplier. These preferences may influence warranty conditions.

4.2.2 Metals

The basic metals used in hydraulic pumps, valves, and other components are generally compatible with polyol-ester-based hydraulic fluids. These metals include iron, steel, aluminum, nickel, tin, copper, magnesium, titanium, and silver. Three incompatible metals are lead, zinc, and cadmium [18]. Zinc and cadmium are occasionally used as cladding materials and should not be used in applications in which they are continuously exposed to the fluid. Reservoir coating is one example. Pipe and tube fittings are often plated with zinc or cadmium. Any corrosive attack would more than likely be cosmetic and not affect the functionalism or life expectancy of the fitting. These metals are also used as alloy constituents and could present potential problems. Lead is used in certain bronze alloys and, under continual exposure, may be leached out of the alloy. Surface pitting would be apparent. Generally, alloys with lead content less than 5% are acceptable. Sintered metal components may show the effects of lead dissolution more rapidly and should not be used.

These general compatibility comments pertain principally to the interaction between fresh fluid and the individual metals. Under service conditions, the fluid may undergo degradation through oxidation that can significantly alter its interaction

with metals. Products of fluid oxidation are generally acidic and more corrosive than the original fluid. High operating temperatures and water contamination are major factors that may initiate metal attack. Dissolved metal ions and products of metal corrosion, acting as catalysts, accelerate the oxidation process and cause additional fluid breakdowns. Polyol-ester-based fluids generally contain additives to reduce these effects. Federal Test Method Standard 791B is a useful test method for evaluating a metal's compatibility with polyol-ester-based fluids because it combines a simulated oxidation environment with metals commonly used in hydraulic systems. In this test, 1-in.-square coupons of steel, copper, aluminum, magnesium, and cadmium-plated steel are immersed in a 100-mL sample of fluid. Air, at 5 L/h, bubbles through the fluid, maintained at 250°F, for 168 h (7 days). At the end of this period, the metal specimens are inspected for visual appearance and any changes in weight determined. Additionally, the fluid is tested for changes in total acid number (TAN) and viscosity. Figure 19.13 shows representative photographs of the metal specimens with three levels of corrosive attack: mild, moderate, and heavy. Table 19.8 summarizes the weight losses associated with each level of attack.

This is a useful test for evaluating fluid additives, comparing competitive polyol-ester-based products, and evaluating the effects of service on fluids. There are commercial-grade polyol-ester-based fluids that rank in the "zero to light" category for all metals except cadmium. The cadmium specimens exhibit excessive weight losses and surface pitting.

4.2.3 Seals, Packing, and Hose Elastomers

Seals, hoses, packing, accumulator bladders, and other nonmetal components used with mineral-oil-based hydraulic fluids are usually compatible with polyol-ester-based hydraulic fluids. This can be a major factor in the conversion from a mineral-oil-based fluid to one requiring fire resistance. The OEMs responsible for the various system components should be consulted and recommendations from the fluid supplier solicited before making a final decision.

Table 19.9 lists most of the elastomers employed in hydraulic systems. Those listed as "Recommended" elastomers are suitable for service with polyol-ester-based fluids with rare exceptions. These materials have been tested for compatibility by most of the fluid suppliers and have had a successful history of usage under normal conditions. "Conditional" elastomers should be used only under certain conditions. The elastomer may undergo excessive swelling and softening because of fluid absorption and should not be used in dynamic applications. These materials may be suitable for static seal applications. However, replacement with a "Recommended" elastomer is recommended during the fluid changeover procedure or during the next regularly scheduled maintenance procedure. "Others" are elastomers that do not have an established history of service or have been proven unsatisfactory with polyol-ester-based hydraulic fluids. If there are compelling reasons to use these materials, the fluid and seal suppliers should be consulted. Compatibility testing should be conducted before use.

With all materials, the fluid operating temperature may be a major factor. Fluid and elastomer suppliers usually recommend operating temperature limits.

4.2.4 Coatings

Reservoir surfaces generally do not need protective coatings. If required, epoxy coatings and thermally cured phenolic or polyurethane paints may be used. Again, com-

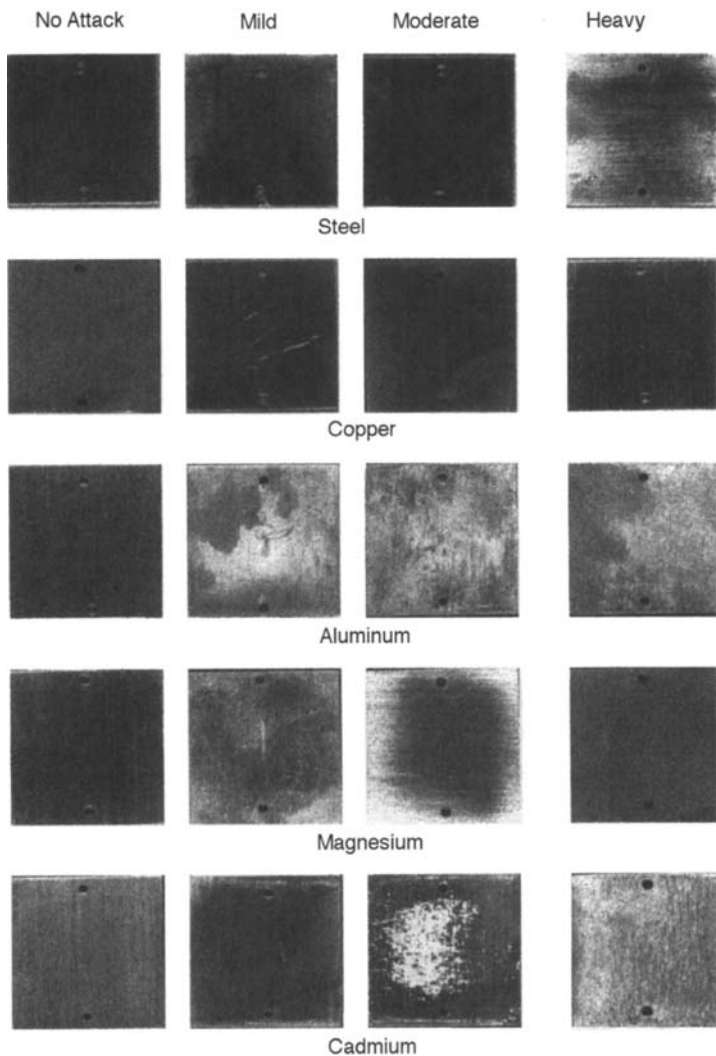


Figure 19.13 Metal corrosion—Federal Test Method No. 791B.

Table 19.8 Metal Corrosion—Federal Test Method No. 791B

Metal	Weight loss (mg/cm ²)		
	Mild	Moderate	Heavy
Steel	0 to ± 0.077	± 0.077 to ± 0.38	$> \pm 0.38$
Copper	0 to ± 0.077	± 0.077 to ± 1.16	$> \pm 1.16$
Aluminum	0 to ± 0.077	± 0.077 to ± 0.38	$> \pm 0.38$
Magnesium	0 to ± 0.077	± 0.077 to ± 0.38	$> \pm 0.38$
Cadmium	0 to 27	27 to 78	> 78

Table 19.9 Compatibility of Elastomers with Polyol Ester Fluids

Recommended for all applications	
Fluorocarbon rubber (FPM)	BUNA N/nitrile ^a
Epichlorohydrin Rubber (CO, ECO)	Polyacrylate rubber (ACM)
Fluorosilicone (FSI)	Polyurethane rubber (AU, EU)
Polytetrafluoroethylene (TFE)	
Conditional compatibility ^b	
Ethylene-propylene rubber (EPDM, EPM)	Butyl rubber (IIR)
Buna N/nitrile (NBR) ^c	Neoprene rubber (chloroprene, CR)
Others ^d	
BUNA S rubber (SBR)	Chlorosulfonated polyethylene (CSM)
Polychloroprene (CR)	Polysulfide (T)
Butadiene rubber (BR)	Chlorinated polyethylene (CM)
Ethylene acrylic	

^aCompounded with >30% nitrile copolymer.

^bShould not be used for dynamic applications; provides reduced life expectancy for static seals.

^cCompounded with <30% nitrile.

^dCheck with seal and/or fluid supplier for recommendations.

patibility tests should be done. Latex, acrylic, and alkyd paints are not suitable. These paints are often applied to exterior surfaces for cosmetic purposes and could be subjected to blistering and peeling. Stainless-steel reservoirs may be used under extreme conditions.

4.2.5 Plastics

Most thermoplastics are compatible with polyol-ester-based fluids and are suitable for components such as molded reservoirs, tubing, and fittings. Polyvinyl chloride (PVC), polyethylene, polyurethane, polypropylene, polytetrafluoroethylene (Teflon), and polyamide have been used successfully. Specific recommendations and operating limits should be solicited from both the fluid and seal suppliers. If necessary, compatibility testing should be done.

4.2.6 Filter Media

Polyol-ester-based lubricants are compatible with all commercial filter media including sintered powder, wound and woven metal, natural and synthetic fiber, and impregnated fiber. There are no restrictions on micron ratings. Adsorbent cartridge filters that incorporate Fuller's earth, activated alumina, or other exchange resins are often used with phosphate-ester-based fluids to maintain a low level of acidity [19]. This type of medium is not necessary with polyol-ester-based fluids. Water-absorbent media, however, are useful and should be employed in applications subject to water contamination.

4.3 Oxidation and Thermal Stability

The major factor in the practical life of a hydraulic fluid is its ability to resist oxidative and thermal degradation. These changes can cause a fluid to undergo sig-

nificant increases in viscosity and total acid number (TAN), generate varnish and sludge, and cause an accelerated corrosive attack on metals.

Polyol-ester-based hydraulic fluids, by nature of their chemistry, are vulnerable to oxidation because of polyunsaturation in the fatty acid portion of the ester (see Sec. 2.1). Fortunately, two factors reduce this generalization. Additive technology has progressed significantly in recent years and fluid oxidation can only be effectively reduced. In addition, base ester quality has improved since the commercial introduction of polyol-ester-based fluids, making the ester more responsive to additives and less susceptible to oxidative attack.

Most of the commonly used test procedures for measuring hydraulic fluid oxidation resistance and thermal stability have been developed for mineral-oil fluids. These include Federal Test Method Standards No. 791B and ASTM methods D-943, D-2070, D-2272, and D-4310. The two that are most applicable to polyol-ester-based fluids are the Federal Test Method 791B and the Cincinnati Milacron Thermal Stability Test (ASTM D-2070). Compared with other tests, these procedures do not incorporate water into the test. Polyol esters, like phosphate esters, are acknowledged to be more water sensitive than oil-based fluids.

The test conditions of the two methods are summarized in Table 19.10. The Federal method is directed toward measuring oxidation and incorporates an air sparge as the oxygen source. This test was briefly described in Section 4.2.3. The Cincinnati Milicron procedure, on the other hand, is directed toward the thermal stability of the fluid and is conducted at a higher temperature, 135°C (275°F) versus 121°C (250°F). Test duration and sample sizes are the same in both tests. Metal specimens are used in both tests and serve a dual purpose. Metals act as catalysts in the oxidation process and the metals listed are commonly found in hydraulic systems. Also, oxidized or thermally degraded hydraulic fluids produce corrosive by-products and accelerate metal attack. These tests offer a measure of this effect.

The evaluation criteria are similar for each test. In the Federal method, metal corrosion is judged by weight change and surface inspection. Fluid oxidation is monitored by changes in TAN and viscosity over the test period.

Table 19.10 Oxidation and Thermal Stability Test Methods

Test parameter	Federal Test Method Standard No. 791B	ASTM D-2070:Thermal Stability of Hydraulic Oils
Duration	168 h (7 days)	168 h (7 days)
Temperature	121°C (250°F)	135°C (275°F)
Airflow	3 L/h	None
Fluid sample size	200 mL	200 mL
Metals		
Steel	✓	✓
Aluminum	✓	
Magnesium	✓	
Cadmium	✓	
Copper	✓	✓
Metal configuration	2.54-cm × 2.54-cm × 8.13 mm thick	6.35-mm-diameter × 7-cm-long rod

Thermal breakdowns of a hydraulic oil generally result in the formation of particulate matter and metal corrosion. In the Cincinnati Milacron test, the sludge formed is separated by filtration, weighed, and expressed as milligram of sludge per 100 mL of fluid. The metal specimens are weighed for weight loss and assessed for surface effects (e.g., pitting, discoloration).

Results from the metal corrosion phase of the Federal test method were shown in Fig. 19.13 and Table 19.8. In addition, the changes in fluid properties, because of oxidation, are shown in Table 19.11. Again, representative numbers are shown for three levels of fluid oxidation: mild, moderate, and severe. The results shown in the "mild" category represent high-quality polyol fluids in all ISO viscosity grades.

Table 19.12 shows the results from the Cincinnati Milicron Thermal Stability test using a similar format (i.e., three levels of fluid stability). As in the Federal test method, the results shown under "mild" represent the higher grades of polyol-ester-based fluids.

One shortcoming of standard oxidation and thermal stability testing is the inability to correlate the results with field experience. Monitoring fluid conditions during extended pump testing provides added insight into a fluid's resistance to the thermal and oxidative stresses induced by such a test. Again, these effects will vary widely based on the particular polyol-ester-base fluid being evaluated.

The ISO 46 and 68 fluids have been tested under ASTM D-2882 conditions continuously for 5000 h (approximately 7 months) and monitored for TAN and viscosity change. Viscosity and TAN as a function of time are shown in Fig. 19.14. Given the severity of the test conditions and duration, the results reflect a stable fluid. These results also show the influence of fluid temperature on the condition of the fluid under high-stress conditions. The ISO 68 fluid was tested at 79°C (175°F) and the ISO 46 at 65.5°C (150°F); the higher temperature caused higher increases in acid number and viscosity because of an increased rate of fluid oxidation.

4.4 Operational Temperature Range

The liquid range of polyol-ester-based hydraulic fluids is broad, less than 0°C (32°F) and greater than 93°C (200°F); however, the practical operating range is much narrower. The recommended range is between 10°C (50°F) and 66°C (150°F). The fluid is functional beyond these limits; however, certain characteristics become compromised. At the high end, continuous exposure at elevated temperatures will cause oxidation and thermal breakdowns of the fluid. Excursions into temperatures as high as 93°C (200°F) are possible, but some fluid degradation will take place, depending on the temperature reached and the exposure time. In these instances, fluid monitoring programs should be started. At the low-temperature end, the limitation is one of equipment compatibility with the fluid viscosity at that temperature.

4.5 Fire Resistance

The major growth in the use of polyol-ester-based hydraulic fluids has been in applications with the potential for fire. A fire hazard associated with the use of mineral-oil-based hydraulic fluids is the ignition potential of spray mists. Spray particles are often formed under high-pressure expulsion of the fluid from the hydraulic system and are readily ignited; the flame is then propagated throughout the spray envelope. This relative ease of ignition is attributed to the fluid's low fire point and the small

Table 19.11 Fluid Oxidation—Federal Test Method 791B

	Degree of fluid oxidation ^a		
	Mild	Moderate	Heavy
Viscosity ^b at 40°C (cSt)			
Initial	68	68	68
Final	60–75	41–60; 75–85	<41; >85
Change ^c (%)	0–10	10–25	>25
Total acid number ^d			
Initial	2.0	2.0	2.0
Final	1.6–2.4	1.2–1.6; 2.4–2.8	<1.2 to >2.8
Change ^c (%)	0–20	20–40	>40

^aFluid oxidation rates are representative of ISO 46, 68, and 100 fluids.

^bASTM D-88.

^cFluid property changes are generally positive (+).

^dASTM D-974.

particle size of the mist. Other hazards include pool fires, ignition of oily waste material, and secondary fire damage. Polyol-ester-based fluids derive their fire resistance from a combination of factors. The flash, fire, and autoignition temperatures are relatively high compared with mineral-oil fluids (Table 19.13), and the products are formulated with modifiers that alter the spray-mist characteristics. A larger-particle-sized coarse spray is produced, which is more difficult to ignite, and the flame does not readily propagate throughout the spray [20].

Polyol-ester-based hydraulic fluids have been tested by Factory Mutual Research Corp. (FMRC) and have been listed in their Approval Guide [4] since 1973.

Table 19.12 Thermal Stability of Polyol Ester Fluids (ASTM D-2070)

	Degree of fluid degradation ^a		
	Mild	Moderate	Heavy
Viscosity ^b at 40°C (cSt)			
Initial	68	68	68
Final	60–75	48–60; 75–88	<48; >88
Change ^c (%)	0–10	>10; <30	>30
Sludge formation ^d	0–8	8–20	>20
Total acid number ^e			
Initial	2.0	2.0	2.0
Final	1.7–2.3	1.4–1.7; 2.3–2.6	<1.4; >2.6
Change ^c (%)	0–15	>15; <30	>30

^aFluid degradation rates are representative of ISO 46, 68, and 100 fluids.

^bASTM D-88.

^cFluid property changes are generally positive (+).

^dIn units of mg of sludge formed per 100 mL of sample.

^eASTM D-974.

Cincinnati Milicron Thermal Stability Test.

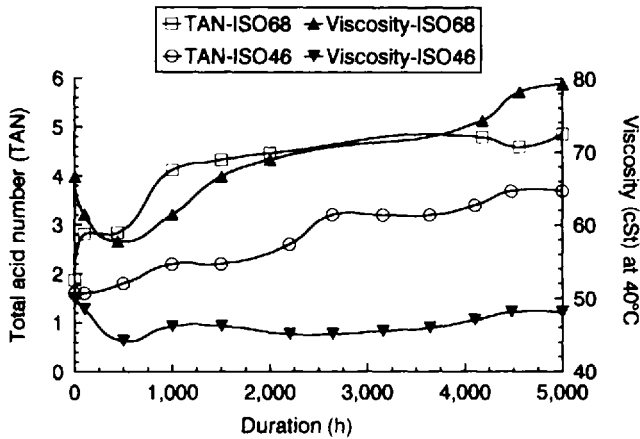


Figure 19.14 Extended pump testing of polyol ester hydraulic fluids.

The Mine Safety & Health Administration (MSHA) employs a spray-mist ignition as part of their test protocol and has approved several polyol-ester-based lubricants for mining applications [21]. FMRC has proposed a revised Approval Standard that significantly changes their test methods [22]. The new standard combines a measure of a fluid's heat release from a spray fire with an ignition threshold related to fire points. This results in a calculated Spray Flammability Parameter (SFP). Fluids are ranked as Class I, II, or III based on their SFP value, with Class I representing the highest level of fire resistance. Polyol-ester-based hydraulic fluids will be classified under both Class I and Class II.

The pros and cons of polyol-ester-based fluids as fire-resistant hydraulic fluids can be summarized as follows:

Advantages

- Within manufacturers' specifications, the fluids exhibit excellent spray-mist fire protection.
- High fire point, >288°C (550°F), and very low vapor pressure.
- When burning under continuous ignition, excessive quantities of smoke or particulate matter are not generated and are not considered toxic. Other synthetic fluid types, notably phosphate esters, under sim-

Table 19.13 Thermal Properties of Polyol Ester Fluids

	Flash point ^{a,b}	Fire point ^{a,b}	Autoignition ^{b,c}
Polyol ester	260–295°C (500–560°F)	280–350°C (536–662°F)	388–404°C (730–760°F)
Mineral oil	102–200°C (215–392°F)	110–225°C (230–437°F)	230–350°C (446–662°F)

^aASTM D-92.

^bRepresentative values.

^cASTM D-2155/E-659.

ilar conditions may significantly reduce visibility and habitability without assisted breathing equipment.

- Because of low smoke generation, radiant energy is low with reduced secondary fire damage.
- In “pool fires,” the low vapor pressure of polyol esters contributes to a longer ignition delay.

Disadvantages

- As with all hydraulic fluids, fire resistance may be dependent on fluid condition and service history. A fluid monitoring program should be started with the fluid supplier.
- The autoignition temperature (404°C, 740°F) is low compared with other non-water-containing fire-resistant fluids and may present some risk in certain applications involving molten light metals and superheated manifolds. Water-containing fluids offer other problems in these applications.

4.6 Fluid Loss and Environmental Considerations

All hydraulic systems are subject to fluid leakage caused by unpredictable component failures, routine system and fluid maintenance procedures, and other factors. In stationary systems, this leakage can be readily contained through dikes or drip pans. With mobile applications, contamination of the surroundings with hydraulic fluid is inevitable and the net effect on waste-treatment facilities, natural waterways, and the general environment must be considered. Excessive contamination could result in fines, the need to restore damaged property, increased waste-treatment costs, and higher insurance rates.

Except for vegetable-oil-based fluids, this is one area in which polyol-ester-based lubricants have clear advantages over other fluids, particularly the historic fire-resistant types. These advantages are as follows:

- **Biodegradability:** The chemical structure, similar to natural glycerides, lends itself to biodegradability. All of the test protocols under consideration by the global community for rating biodegradability rank polyol esters within proposed guidelines. For examples, CEC-L-33-T-82 is widely used to measure biodegradability rates of lubricants in water. This test measures the biological depletion rate of a hydrocarbon chain over a 21-day period. Polyoleates exhibit greater than 80% degradation [23] in this test, generally superior to most other lubricant base stocks. It should be noted that biodegradability studies generally relate to the base stock of the fluid under consideration. Additives may compromise the biodegradability of the base stock because they generally do not have comparable degradation rates. Usually, the low level of additives used reduces this concern. Nevertheless, before a specific fluid is selected or specified, the original manufacturer should be responsible for supplying biodegradability data specific to that fluid.
- **Aquatic toxicity:** The LC_{50} for a fully formulated polyol-ester-based fluid has been reported as greater than 2000 ppm under testing done according to OECD 203, “Fish Acute Toxicity Test” [24]. This characteristic, how-

ever, is also dependent on the additives used in the product and results specific to a given product should be obtained from the supplier.

- **Nonhazardous components:** Many commercial products are free of hazardous materials listed under EPA and OSHA (40 CFR and 29 CFR). State regulatory requirements should be consulted as necessary.
- **Water miscibility:** Polyol-ester-based fluids are not miscible with water and have a density less than water. This eases removal of the fluid from settling ponds and waste-treatment ponds using conventional skimming techniques. In contrast, many other fire-resistant fluids are either soluble in water (water-glycol) or heavier than water (phosphate ester) and add to waste-treatment chemical costs. The “floating” feature of a polyol-ester-based fluid also allows visual detection of leakage.
- **Incineration:** Reclaimed or recovered hydraulic fluids are often disposed of through incineration to recover their Btu content. Most polyol-ester-based fluids can also be treated in this manner. Many other fire-resistant fluids are not so easily accommodated because of water content or chemical toxicity.

4.7 Comparison of Polyol-Ester-Based Hydraulic Fluids with Other Fluids

Under certain circumstances, hydraulic fluids are a potential replacement for mineral-oil hydraulic fluids. Other fluid types can also be considered, each with certain advantages and disadvantages. Based on characteristics generally thought to be important, Table 19.14 summarizes how various fluids compare. Such a ranking can be subjective based on the particular bias of the scorer. Nevertheless, an objective rating was attempted based on a collection of experiences. It is acknowledged that one characteristic may be all-important, despite that fluid’s ranking in other categories. It is simply intended as a general guide.

4.8 Conversion Considerations and Procedures

Converting from the different types of hydraulic fluids to a polyol-ester-based hydraulic fluid is a straightforward process. Specific recommendations and suggestions

Table 19.14 Comparison of Polyol Esters with Other Fluids

Fluid property	Relative ranking ^a
Fire resistance	WaG > PhE > PoE > IvE > VgO > MnO ≈ Pao
Oxidation resistance	WaG ≈ Pao > MnO > PhE ≈ PoE > IvE > VgO
Lubrication	MnO > PhE ≈ PoE ≈ Pao ≈ VgO > WaG > IvE
Biodegradability	VgO ≈ PoE > WaG > PhE > IvE > MnO ≈ Pao
Hydrolytic stability	WaG > IvE > MnO ≈ Pao > PoE > VgO > PhE
Unit cost (\$/gal)	Pao ≈ PhE > PoE ≈ Vgo > WaG > MnO > IvE
Ease of disposal	VgO ≈ PoE > WaG > PhE ≈ IvE ≈ MnO ≈ Pao
Seal compatibility	MnO > IvE > WaG > VgO ≈ PoE ≈ Pao > PhE
Thermal stability	Pao ≈ PhE > MnO > PoE > VgO > IvE ≈ WaG

^aWaG = water-glycol; PhE = phosphate ester; IvE = invert emulsion; VgO = vegetable oil; MnO = mineral oil; Pao = polyalphaolefin; and PoE = polyol ester.

should be made by the manufacturer of the replacement fluid. These recommendations should include a detailed analysis of the hydraulic system regarding its general compatibility and any changes that should be made to adapt to the new fluid. Often, the supplier will be actively involved in the conversion. The conversion procedures are summarized in Table 19.15 and general comments on various aspects of the procedures are as follows:

- **Seal and hose compatibility:** Fluid and elastomer suppliers should verify the compatibility of a given material with a polyol-ester-based fluid. Generally, seals and hoses used with mineral-oil, vegetable-oil, synthetic ester, or invert emulsion fluids will be satisfactory. Seals and hoses used with other fluid types should be checked for their compatibility with polyol-ester-based fluids and, if necessary, replaced with suitable ones.
- **Drain and purge requirements:** For all conversions, the recommended practice is to drain the original fluid from the reservoir and lines. A polyol-ester-based fluid is generally compatible with mineral-oil- and vegetable-oil-based fluids and can be used as makeup. However, all of the benefits of the new fluid will not be fully realized, particularly fire resistance. In these applications, at least 95% of the old fluid should be removed. Polyol-ester-based fluids are also compatible with most phosphate-ester-based fluids *if* the fluid is in excellent condition (moisture <0.05% and total acid number <0.05). A polyol-ester-based fluid will chemically react with strong mineral acids in phosphate esters to form a varnishlike material that will cause valve sticking and reduced pump life. Water-based fluids must be completely removed from the system with a target efficiency of at least 97%.
- **System flushing:** For systems containing water-based fluids, a flushing fluid must be used before adding a polyol-ester-based hydraulic fluid. This fluid replaces the quantity of water-based fluid initially drained and may be an inexpensive mineral-oil- or polyol-ester-based fluid. The system is operated at reduced pressure and all functions actuated for approximately 30 cycles.

Table 19.15 Hydraulic System Conversion Practices

	Mineral oil	Water glycol	Phosphate ester	Invert emulsion	Vegetable oil	HWCF (95:5)
Compatibility						
• Seals	OK	← Verify →		← OK →		Verify
• Hoses	OK	← Verify →		← OK →		Verify
• Coatings	OK	← Verify →		← OK →		Verify
Drain fluid & purge	Not req'd	Yes	Not req'd	Yes	Not req'd	Yes
System flush	Not req'd	Yes	Yes	Yes	Not req'd	Yes
Clean components	← Yes →					
Replace filter elements	← Yes →					
System start-up	← Yes →					
Monitor fluid	← Yes →					
Monitor filters	← Yes →					

Abbreviation: HWCF, high water content fluid.

The purpose is to displace any residual fluid trapped in lines and components with a non-water-containing fluid. The contaminated flushing medium is then drained and discarded. Some fluid suppliers provide a flushing compound that will absorb or emulsify the residual water-based fluid. This fluid can be saved and reused for subsequent conversions; it may have to be processed to remove excess water according to the supplier's recommendations.

For conversions involving mineral-oil- or vegetable oil-based fluids, a flushing procedure is generally not required. In a phosphate ester conversion, the need for a flushing procedure is based on the fluid condition. If the fluid's acid level is high, flushing is necessary. For hydraulic systems that have had a history of varnish buildups, use additives that, when added to the flushing medium, will dissolve or loosen accumulated varnish. This is a recommended procedure and the material is generally available from the fluid supplier.

- **System cleanliness:** To the extent possible, residual fluid and particulate matter should be removed from system components. In particular, the reservoir should be wiped down and any deposits such as scale and other foreign matter removed from the internal surfaces. It is also recommended that heat exchangers and fluid coolers be inspected and serviced if necessary.
- **Filter elements:** After the final flushing, or just before adding the new fluid, all filter elements should be replaced. Screens should be cleaned and replaced if damaged.
- **System start-up:** Start-up procedures should follow the recommendations provided by the original equipment manufacturer. This generally involves low initial loads and operating pressures, cycling valves, and bleeding-off any entrained air.
- **Fluid monitoring:** This is the most critical phase of the conversion. Fluid samples should be obtained within 24 h of the changeover and tested for the amount of the previous fluid retained and dirt content. If water content is more than 2%, the fluid should be treated to remove water or dumped and the system recharged with fresh fluid. If dirt content is beyond the fluid suppliers specifications, replace filter elements and process the fluid through an external filter unit. A fluid change generally results in loosening and entrainment of contamination that has built up over time and will be circulated with the fluid. If the amount of retained old fluid is excessive, the fluid should be drained and recharged with fresh fluid. The fluid condition should be monitored weekly for the first month and regularly after that. The fluid supplier should provide guidelines on sampling frequency and condition criteria.
- **Filter monitoring:** For the above-cited reasons, filter elements may load up initially at a higher rate than normal and should be serviced as required.

5 FLUID MAINTENANCE

A major factor in the operation of a trouble-free fluid power system is fluid cleanliness and retention of its original properties. This section will identify problems

often encountered with polyol-ester-based fluids and present recommended practices that will maximize fluid life expectancy and retention of basic properties.

5.1 Types of Contamination

The sources of fluid contaminants are either generated from within the hydraulic system or originate from outside it. Contaminations generated within the system are wear particles and products caused by chemical attack on seals and hoses, corrosive attack, and degradation of the fluid through oxidation. Examples of external contamination are moisture or water ingested into the system, dirt, sand, and airborne process contaminants. Contaminants may also be introduced during routine fluid additions and maintenance procedures.

5.2 Fluid Variables to Monitor

All of the above-described potential contaminants may be identified through fluid monitoring programs and, usually, the cause or source readily identified and appropriate corrective actions taken. A fluid analysis program includes both physical testing and spectrochemical analysis.

The following physical variables should be monitored and compared with self-imposed standards or those recommended by the fluid supplier:

- **Kinematic viscosity at 40°C (104°F):** Viscosity monitoring is perhaps the most important measure of the fluid condition. Changes in viscosity that deviate from the manufacturer's standard suggest possible contamination from other fluids, excessive fluid oxidation, or degradation of additives. Listed are the normal viscosity ranges for the three common polyol-ester-based fluids. Any fluid with viscosity outside this range should be examined for potential problems.

ISO 46 viscosity grade: 41–51 cSt (191–237 SUS)

ISO 68 viscosity grade: 61–75 cSt (282–348 SUS)

ISO 100 viscosity grade: 90–110 cSt (418–510 SUS)

- **Water (% or ppm):** Water can be detrimental to a polyol-ester-based fluid because of its role in fluid oxidation and metal corrosion (see Secs. 2.4 and 4.3). The target for maximum water content should be 0.2% to assure minimum influence. A polyol-ester-based fluid can hold up to 2% water without short-term detrimental effects; however, this condition should not be allowed to continue without corrective action. Fluids contaminated with water can be treated with water-absorbent filter media or short-term elevations in fluid operating temperature. The important response is identification and correction of the conditions leading to the contamination.
- **Total acid number (ASTM-D974):** Increases in TAN values show fluid degradation has taken place and suggests metal corrosive attack rates may be accelerated. The allowable TAN will vary with fluids from different manufacturers; however, as a rule, the TAN should be <5mg KOH/g. A more realistic monitor should be the increase in TAN. Rate increases of 0.1 mg KOH/g per month or larger suggest potential fluid problems.
- **Particle count:** Automated optical particle counters are used for determining particle size distribution. These data can be used to establish a level of

Table 19.16 Cleanliness Codes

ISO contamination level	Maximum number of particles	
	>5 μm	>15 μm
12/8	40	2.5
13/9	80	5
14/10	160	10
15/11	320	20
16/12	640	40
17/13	1,300	80
18/14	2,500	160
19/15	5,000	320
20/16	10,000	640

contamination as defined by an ISO Solid Contamination Code [25]. In this code, the particle size distribution is defined by two ISO range numbers (e.g., 15/12). The first number represents the number of particles greater than 5 μm in size and the second number represents the number of particles greater than 15 μm . ISO range numbers correspond to the maximum number of particles per milliliter of fluid, as shown in Table 19.16. Figure 19.15 shows suggested ISO cleanliness levels for different types of components and operating pressures. Fluid contamination levels above the ranges shown may result in excessive component wear and improved filtration practices should be employed.

- **Total solids:** Gravimetric analysis is a useful test for determining the total weight of particulate matter in the fluid. In this test (ASTM D-4898), a

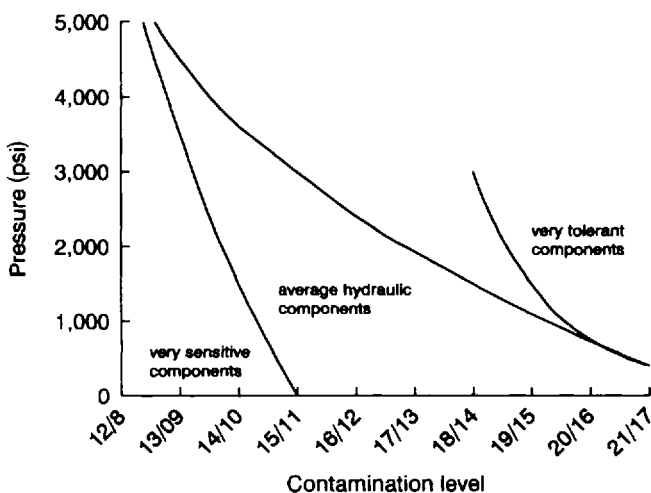


Figure 19.15 Suggested cleanliness levels. (From *Effective Contamination Control in Fluid Power Systems*, Vickers, Inc., 1980, reprinted with permission.)

known volume of the fluid is passed through a filter patch and the amount of solids retained weighed. This test is particularly useful when used with particle count data. Also, the filter patch lends itself to microscopic and photographic examination for identification of metallic and nonmetallic contaminants. Retained solids more than 1.5 mg/mL indicate a possible fluid problem.

Spectrochemical analysis is useful in that it provides evidence and identification of metals in the fluid caused by wear processes within the hydraulic system. Also, the analysis can be used to monitor the level of metal-based additives. Metals that might be present and can be identified through spectrochemical analysis include the following:

Iron	Chromium	Nickel
Aluminum	Lead	Copper
Tin	Silver	Titanium
Silicon	Boron	Sodium
Potassium	Molybdenum	Phosphorus
Zinc	Calcium	Barium
Magnesium	Antimony	Vanadium

In addition to assessing the condition of hydraulic fluids, the value of fluid analysis is to provide insight into analyzing and to determine the cause of system problems. Although certain tests can provide measurements of fluid condition, the major tool is in interpreting the overall test results and the possible interactions between different tests. Fluid analysis programs are often done in concert with the supplier, who is familiar with the allowable ranges of certain variables and is knowledgeable in the specific product chemistry. The fluid analysis program is also enhanced by knowledge of the fluid history based on previous analysis and trends in certain parameters.

5.3 Fluid Life Expectancy

The projected life of a polyol-ester-based hydraulic fluid, or any fluid, is impossible to quantify because of the many variables that might affect its potential life expectancy. The most reliable method for evaluating a fluid's potential for continued high performance is a rigorous fluid monitoring program. Fluid degradation is directly related to extreme operating temperatures and contamination with alien fluids and particulate matter.

Figure 19.16 is a general guide to the expected life expectancy of a polyol-ester-based hydraulic fluid as a function of its average operating temperature assuming no other negative variables. Because the operating temperature has such a major impact on fluid condition, continuous monitoring of heat exchangers, coolers, and fluid reservoir levels is important.

As noted in Fig. 19.16, 57°C (135°F) should be regarded as a nominal, average fluid temperature. Above that temperature, more rapid fluid degradation can be expected and, conversely, below that temperature, extended fluid life is to be expected.

5.4 Fluid Testing Program

A formal fluid sample and analysis program is recommended. This can be done with the fluid supplier but is often done independently to assure objectivity of the results

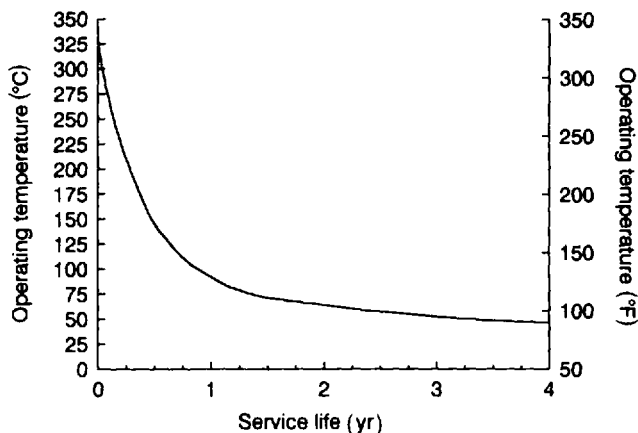


Figure 19.16 Polyol ester fluid life expectancy.

and conclusions. Because the test methodology is sophisticated and requires specialized equipment, most users will not have the resources to do “in-house” testing. Many test laboratories do have the capability and will generally supply test results within 1 week. A supplier’s response to fluid analysis should be comparable.

A fluid sample analysis program is inexpensive and often has a positive return in reduced maintenance cost, reduced unscheduled downtime, and extended fluid life. Many fluid suppliers provide fluid sample analysis as a service item or charge a nominal fee. Third-party laboratories typically do sample analysis at \$25 to \$100 per sample, depending on the scope of testing required.

The frequency of obtaining samples will vary depending on the application. Biannual sampling is adequate unless a history of system problems suggests otherwise, in which case weekly or biweekly sampling would be appropriate. For recent conversions, weekly sampling is suggested until a history of trouble-free operation has been established.

The point of fluid sampling should be selected to ensure the acquisition of representative samples. If possible, the sample valve should be upstream of the return-line filter and the valve should be of an unrestricted orifice style (ball or gate). This reduces high velocities through the valve that often separate or concentrate solids. Reservoir sampling should be a last resort, but if done, the power unit must be operating to reduce any settling effects and sampled at mid-depth of the fluid.

Maintaining a history of fluid sample reports is integral to a successful program. Trends in the various parameters are as equally important as the measurements themselves. Many fluid sample report forms incorporate a historical profile that may tabulate previous results or present them in a graph format.

5.5 Fluid Disposal Procedures

The important consideration with a polyol-ester-based hydraulic fluid spill is that the material is not regarded as hazardous by Federal Standards, although all spills to the environment are to be cleaned up. The fluid is often marketed as an environmentally safe product and is considered readily biodegradable and nontoxic to aquatic life.

This does not, however, relieve the user from exercising responsible and meaningful treatment of any materials spilled or discharged from the hydraulic system. Specific fluid hazardous material information, treatment procedures, and other safety data should be obtained from the fluid supplier before its use.

Floor spills should be treated with standard industrial absorbents and disposed of according to local, state, or federal regulations. This material is not generally considered a hazardous material. Residual spilled materials can be washed away using mild detergent and copious amounts of water.

Any significant quantity of fluid that reaches waste-treatment ponds or settling basins can be skimmed using equipment normally employed for oily wastes. The fluid recovered can be processed by waste-treatment companies or incinerated at the plant site to recover its energy value. Used fluid drained from hydraulic reservoirs can also be treated this way.

Spills from mobile equipment or at construction sites should be avoided if possible; large spills can be partially cleaned up by using absorbent materials. Minimum ground contamination will be consumed by biological processes. Ground contaminated with a polyol-ester-based fluid is not regarded as hazardous waste.

5.6 Fluid Recovery

A fluid analysis report often concludes that the fluid is no longer suitable for continued use; disposition of the contaminated fluid must be determined. Two alternatives are possible: discard the fluid or attempt to recover the fluid for continued service. Recovery is the preferred route, particularly with large fluid volume systems where the replacement cost could be significant.

A polyol-ester-based fluid can be reconditioned for additional use depending on the nature of fluid degradation and the type of application. If fluid properties such as viscosity and TAN are outside the suppliers recommended range, oxidation and shear breakdown are the probable causes and the fluid cannot be salvaged, especially when fire resistance was the reason for fluid selection. If particle count and total solids were the reasons for fluid rejection, the fluid can be cleaned by using an external filter system or upgrading the hydraulic system filters. The source of contamination should be determined and corrected. For cases where excess water was found in the fluid, vacuum flashing techniques or filtering through water-absorbing media will correct the problem. The cause for water contamination should be thoroughly investigated. Always, the advice of the supplier should be solicited.

It is not recommended that polyol-ester-based hydraulic fluids be sent to a commercial fluid recycle facility, especially when the fluid was used as a fire-resistant one. Only the original supplier can attest to the fluid meeting fire-resistant fluid industry standards.

6 SUMMARY OF APPLICATIONS

Polyol-ester-based fluids have been used in a variety of applications and are usually associated with processes that impose a potential fire hazard. More recently, the fluid has found application in environmentally sensitive areas in which biodegradability characteristics are considered highly important. A major factor in the use of polyol-ester-based fluids in diverse applications is the relative ease of replacing mineral-oil fluids with one that meets newly imposed safety and environmental requirements.

Listed are the major Standard Industrial Classifications (SIC) in which polyol-ester-based hydraulic fluids have been used. This list is representative and does not include many applications where the fluid has been successfully employed. The intent is to show the diversity of applicability for this type of fluid.

	<u>SIC No.</u>
Blast furnace and basic steel products	331
Industrial machinery and equipment	35
Iron and steel foundries	332
Motor vehicles and equipment	371
Fabricated metal products	34
Nonferrous rolling and drawing	335
Metal forging and stampings	346
Nonferrous foundries and die casting	336
Aircraft and parts	372
Heavy construction	16
Oil and gas extraction	13
Rubber and miscellaneous plastic parts	30
Electric, gas, and sanitary services	49
Lumber and wood products	24
Petroleum and coal products	29
Coal	12
Railroad equipment	374
Metal cans and shipping containers	341
Chemicals and allied products	8
Food and kindred products	20
Metal mining	10
Space propulsion units and parts	376
Water transportation	44
Pipelines except natural gas	46
Motorcycles, bicycles, and parts	375
Ship and boat building and repair	373
Paper and allied products	26
Miscellaneous primary metal products	339
Stone, clay, and glass products	32
Forestry	08
Miscellaneous amusement and recreation services	799

REFERENCES

1. G. E. Totten and G. M. Webster, "Fire Resistance Testing Procedures: A Review and Analysis," in *Fire Resistance of Industrial Fluids, ASTM 1284*, G. E. Totten and J. Reichel, eds., 1996, American Society for Testing and Materials, Philadelphia.
2. T. Evanoff, "Selection of Hydraulic Fluids for a Rolling Mill," STLE Annual Meeting, 1996.
3. R. A. Gere, T. V. Hazelton, "Rules for Choosing a Fire Resistant Hydraulic Fluid," *Hydraulic Pneumatics*, 1993, April.
4. Factory Mutual Research Corp., *Factory Mutual System Approval Guide, 1973-96*, 1996, Factory Mutual Research Corporation; Norwood, MA.
5. N. O. V. Sonntag, "Structure and Composition of Fats and Oils," in *Bailey's Industrial Oil and Fat Products, Vol. 1*, 4th ed., D. Swern, ed., 1979, John Wiley & Sons, New York.

6. N. O. V. Sonntag, "Reactions of Fats and Fatty Acids," in *Bailey's Industrial Oil and Fat Products Vol. I*, 4th ed., D. Swern, ed., 1979, John Wiley & Sons, New York.
7. E. E. Klaus and E. J. Tewksbury, "Liquid Lubricants," in *CRC Handbook of Lubrication (Theory and Practice of Tribology)*, Volume II: *Theory and Design*, E. R. Booser, ed., 1984, CRC Press; Boca Raton, FL, pp. 229–254.
8. S. Q. A. Rizvi, "Lubricant Additives and Their Functions, Lubricants and Lubrication," in *Friction, Lubrication and Wear Technology, ASM Handbook*, Peter J. Blau, volume chairman, ASM International; Metals Park, OH, 1992, pp. 98–112.
9. M. M. Khan, "Spray Flammability of Hydraulic Fluids," in *Fire Resistance of Industrial Fluids, ASTM STP 284*, 1996, American Society for Testing Materials; Philadelphia.
10. P. C. Hamblin and U. Kristen, "Ashless Antioxidants, Copper Deactivators and Corrosion Inhibitors: Their Use in Lubricating Oils," *Lubr. Sci.*, 2(4) pp. 287–318.
11. C. V. Smalheer and R. K. Smith, *Lubricant Additives, Section I: Chemistry of Additives*, 1967, The Lezius-Hiles Co.; Cleveland, OH.
12. J. A. O'Brien, "Lubricating Oil Additives," in *CRC Handbook of Lubrication (Theory and Practice of Tribology)*, Volume II: *Theory and Design*, E. R. Booser, ed., 1984, CRC Press, Inc. Boca Raton, FL, pp. 301–315.
13. W. A. Gehrmann, "Non-Zinc Hydraulic Oils: Technology, Applications, and Trends," in *International Off-Highway & Power Plant Congress & Exposition*, 1992.
14. M. M. Khan, "Spray Flammability of Hydraulic Fluids and Development of a Test Method," Technical Report FMRC J.1. OTOW3.RC, Factory Mutual Research Corp., Norwood, MA, 1991.
15. E. T. Totten, R. J. Bishop, and G. H. Kling, "Prediction of Hydraulic Fluid Performance: Bench Test Modeling," in *Proceedings of the 47th National Conference on Fluid Power*, Volume 1, 1996, NFPA; Milwaukee, WI.
16. J. Reichel, "Importance of Mechanical Tests with Hydraulic Fluids," in *Tribology of Hydraulic Pump Testing*, G. E. Totten, G. H. Kling, and D. J. Smolenski, eds., 1996, American Society for Testing and Materials; Philadelphia.
17. H. M. Melief, "Proposed Hydraulic Pump Testing for Hydraulic Fluid Qualification," in *Tribology of Hydraulic Pump Testing*, G. E. Totten, G. H. Kling, D. J. Smolenski, eds., 1996, American Society for Testing and Materials; Philadelphia.
18. The Rexroth Corporation, Information Bulletin KD012, The Rexroth Corporation, Bethlehem, PA.
19. M. P. Marino and D. G. Placek, "Synthetic Lubricants, and Applications," in *CRC Handbook of Lubrication and Tribology, Volume III: Monitoring Materials*, E. R. Booser, ed., 1984, CRC Press; Boca Raton, FL.
20. M. M. Khan, "Spray Flammability of Hydraulic Fluids," in *Fire Resistance of Industrial Fluids, ASTM STP 1284*, G. E. Totten and J. Reichel, eds., 1996, American Society for Testing Materials; Philadelphia.
21. U.S. Mine Safety and Health Administration, CFR Part 35, "Fire Resistant Fluids," 40 CFR 796.3260 Quintolubric 823–300, Report to Quaker Chemical Corporation, 1992.
22. A. V. Brandao, "Implementation of Revised Evaluations of Less Flammable Hydraulic Fluids," in *Fire Resistance of Industrial Fluids, ASTM STP 1284*, G. E. Totten and J. Reichel, eds., 1996, American Society for Testing Materials; Philadelphia.
23. International Technology Corp. "Ready Biodegradability: Modified Sturm Test, 40 CFR 796.3260 Quintolubric 822–300, Report to Quaker Chemical Corp., 1992.
24. J. McNair, "Rainbow Trout Acute Toxicity Tests, Report to Quaker Chemical Corporation, Re. Quintolubric 822–300 & EAL-224 (Mobil Oil Corporation)," Report to Academy of Natural Sciences of Philadelphia, 1993.
25. Exxon, "The ISO Cleanliness Code for Lubricating and Hydraulic Oil Systems," Exxon Marketing Technical Bulletin, No. MTB 85-15, Series RIM-4, 1985.

This page intentionally left blank

Phosphate Ester Hydraulic Fluids

W. D. PHILLIPS*

FMC Corporation (UK) Ltd., Manchester, United Kingdom

1 INTRODUCTION

The term “phosphate ester” is used to describe an enormous range of chemicals, from gases to solids, which vary considerably in their properties and applications. Depending on their composition, they may be used for many different purposes—for example, in foodstuffs, toothpaste, fertilizers, as fuel or oil additives, or as insecticides.

The presence of phosphorus in a molecule can make it less combustible; this is perhaps surprising when it is considered that elemental phosphorus is the ignitable part of a match! As a result, fire-resistant hydraulic fluids based on certain phosphate esters have now been used for over 40 years in a wide variety of industrial processes where a fire hazard exists, and they have made a significant contribution to major improvements in safe working conditions for operating personnel.

During this period, performance requirements have steadily become more severe, whereas at the same time, regulatory pressures on toxicity, environmental behavior, and disposal have also increased. The fluid suppliers have reacted to the changes by developing new products and introducing techniques for substantially extending fluid life. This has produced a very positive effect on cost/performance and a noticeable change in the perception that these products are noxious and difficult to handle.

In this chapter, the chemistry, manufacturing processes, and performance of the different types of phosphate ester in commercial use will be reviewed together with comments on their different applications. Additionally, information on in situ purification techniques, fluid maintenance, and the latest position on toxicity/ecotoxicity/fluid disposal aspects will be discussed.

**Current affiliation:* Great Lakes Chemical Corporation, Manchester, United Kingdom.

2 HISTORICAL BACKGROUND

In the field of fire-resistant hydraulic fluids, the main products in commercial use are neutral trialkyl phosphates, triaryl phosphates, and mixed alkylaryl phosphates. The chemical composition of these types of phosphate esters has been known for about 150 years [1,2], but their actual industrial use is much more recent. Tricresyl phosphate (TCP) was initially sold as a plasticizer for cellulose nitrate shortly after World War I [3] as a result of a camphor shortage. Investigations revealed that not only was the product a good plasticizer, but it also rendered the product "nonflammable" [3]. Commercial production of TCP commenced in 1919, and although its use in camphor was eventually discontinued, it subsequently found use as a "nonflammable" plasticizer in pyroxalin lacquers. In the 1930s, it was introduced into poly(vinyl chloride) formulations, a position that triaryl phosphates still hold today.

In the oil industry, triaryl phosphates were first reported as antiwear additives for mineral oils in 1940 [4] and have since become firmly established in this application, providing enhanced lubrication for a range of circulatory oils and also for selected synthetic lubricants. Subsequently, the products were also used as ignition control additives for gasoline, to avoid preignition arising from the deposition of lead salts formed by the interaction of the antiknock additive and alkyl halide scavengers. Although this application has also disappeared, as a result of concern over catalyst poisoning by phosphorus and the move away from leaded gas, there is currently a developing interest in their use as antiwear additives for fuels. This is due to the removal of sulfur-containing materials because of stricter emission regulations.

The first recorded consideration of "phosphate esters" as potential hydraulic fluids arose toward the end of World War II, following a series of fires and explosions in military hardware—particularly aircraft. The U.S. Navy instituted a study of the flammability of different liquids [5], and phosphate esters and water-glycol fluids were eventually singled out as suitable for further investigation [6]. A research program sponsored by the U.S. Navy and Air Force and carried out by the Shell Development Company subsequently focused on formulations based on blends of trialkyl phosphates and TCP [7], the trialkyl derivative being selected chiefly to reduce the density (and hence weight) of the fluid and to improve low-temperature performance. Independent of these studies, the Douglas Aircraft Company in 1946 began an intensive search for a fire-resistant hydraulic fluid for use in commercial air transports [8]. Although blends of triaryl and trialkyl phosphates were considered [9], the fluid eventually marketed was based on an alkylaryl phosphate [9–12] supplied by the Monsanto Chemical Company. The Lockheed Aircraft Corporation used trialkyl phosphates in the development of low-density hydraulic fluids [13,14] but apparently did not pursue their studies to commercialization. By the end of the 1950s, most of the passenger jet aircraft being built were operating on phosphate esters and this is still the situation over 40 years later. However, despite the appearance of several target specifications for fire-resistant hydraulic fluids for aircraft [15,16], the main military use for phosphate ester fluids has been on aircraft carriers for hydraulic lifts and so forth [17] and, for a short time, in submarines.

In the field of general industrial hydraulic fluids, density and low-temperature viscosity are normally less important than fire resistance, and although triaryl phosphates were promoted as fire-resistant fluids in the mid-1940s, they were more often

used as blending components for the even more stable (and fire-resistant) polychlorinated biphenyls (PCBs) [18]. In these formulations, phosphates were used to reduce the very high fluid density of the PCBs and therefore ease the pumping requirements.

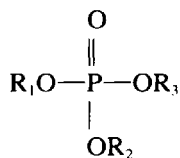
Other applications investigated included the development of hydraulic fluids for gun recoil systems and shock absorbers, which were based on a trialkyl phosphate [19].

By the early 1960s, several fluid suppliers were offering a range of phosphate esters covering different viscosity levels [20–22] in competition with the PCBs and PCB/phosphate blends [23]. Environmental concerns associated with the chlorinated products eventually resulted in their withdrawal in the 1970s. Although an attempt was made to replace them in these blends by other chlorinated aromatics, such as chlorinated benzyltoluene, use of the latter was restricted. Only in the German mining industry were such blends sold in any quantity. They were eventually banned by the European Commission in 1991 [24] because of environmental concerns similar to those associated with the PCBs.

Over the years, other attempts have been made to reduce the cost of phosphate esters—particularly the triaryl phosphates—and to improve certain physical characteristics by blending with other materials (e.g., carboxylate esters and even mineral oil). Such blends are, of course, also less fire resistant. Early developments of this type were carried out by the Cities Service Oil Co. [25]. More recently, other fluid suppliers have introduced similar products [26–29] which are attractive for those applications where the leakage rate is so high that the customer is discouraged from using a product offering the highest level of safety. As the properties of such blends are largely predictable from a knowledge of the performance of the individual components and their relative amounts, no detailed examination of these products will be made in this chapter. Instead, the focus will be on 100% phosphate-based materials, which are widely used in the most demanding applications where good fire resistance is essential.

3 STRUCTURE AND ITS INFLUENCE ON FLUID PROPERTIES

Phosphate esters are also known as esters of phosphoric acid and can be considered as having the following general structure:



For *trialkyl phosphates*, R_1 , R_2 , and R_3 are normally the same and are alkyl groups with a chain length of C_4 – C_{10} , but principally C_4 , C_8 , and C_{10} . The chain may be straight as in tri-*n*-butyl phosphate (TBP), or branched, as in tri-isobutyl phosphate (TiBP). Also used occasionally in hydraulic fluid formulations is a trialkoxyalkyl phosphate, specifically tributoxyethyl phosphate, in which case R_1 , R_2 , and R_3 in the above structure are $\text{C}_4\text{H}_9\text{OC}_2\text{H}_5$ —.

For *triaryl phosphates*, R_1 – R_3 are phenyl or substituted phenyl (e.g., methylphenyl, also known as cresyl or tolyl), dimethylphenyl (better known as xylyl), isopropylphenyl, or tertiarybutylphenyl groups. Other substituted phenyl groups,

such as nonylphenyl or cumylphenyl, have also been used in the past but are not currently available.

In addition to those triaryl phosphates where $R_1 = R_2 = R_3$, (e.g., trixylyl phosphate) there are also products where the aryl groups are different (e.g., cresyldiphenyl phosphate or xylyldiphenyl phosphate). As will be shown later, mixed aryl phosphates are now widely used as general industrial hydraulic fluids.

For mixed *alkylaryl phosphates*, the groups attached to the phosphorus are also different. The product may be a monoalkyldiaryl phosphate (e.g., octyldiphenyl phosphate) or a dialkylmonoaryl phosphate such as dibutylphenyl phosphate.

Although the phosphorus-containing nucleus of the molecule largely determines the fire resistance of the product, it is the "organic" or the hydrocarbon part of the molecule which mainly determines the variation in the physical and chemical properties, in addition to having some effect on the flammability characteristics. For example, the alkyl groups used in trialkyl or alkylaryl phosphates are either straight or branched chain. Use of the former favors viscosity-temperature properties, thermal stability, volatility, and so forth, whereas branched chains normally improve hydrolytic stability. Similarly, the properties of aryl phosphates are heavily influenced by four factors:

1. *Whether or not the aryl group is substituted.* The unsubstituted phenyl group gives the best thermal and oxidative stability but confers the worst hydrolytic stability and viscosity-temperature properties on the molecule! Triphenyl phosphate, however, is a solid at ambient temperature and therefore cannot be used alone in hydraulic applications. The general effect on phosphate performance of a single substituent on the aromatic ring is indicated in Fig. 20.1 [30]. As can be seen, if an attempt is made to improve one fluid property, this can have a detrimental effect on another aspect of behavior.

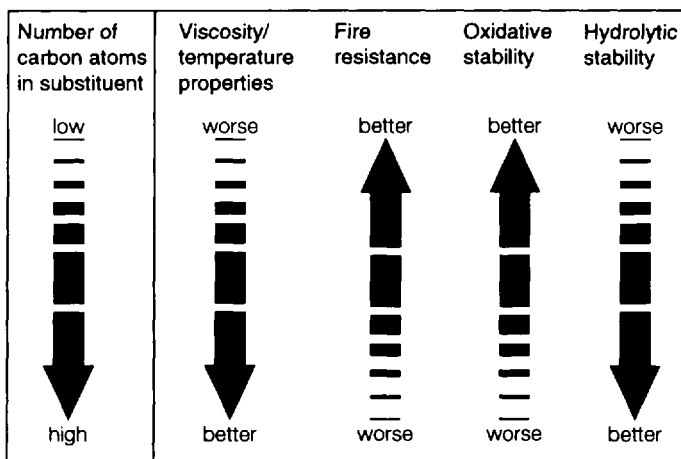


Figure 20.1 Effect of aryl group substituents on physical/chemical properties.

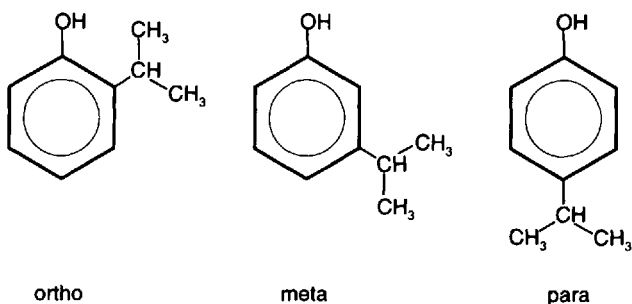


Figure 20.2 Isomeric forms of monoisopropylphenol.

2. *The structure of the substituent.* This impacts on physical properties as a result of its size (e.g., the greater the number of carbon atoms, the higher the viscosity of the fluid, provided the substituent is attached to the same place on the ring) and also on chemical properties as a consequence of its stability. Thus, the isopropylphenyl group is less oxidatively stable than the tertiary butylphenyl group.
3. *The position of the substituent on the aromatic ring.* Alkylated phenol feedstocks used in the manufacture of triaryl phosphates are available in different “isomeric” forms, where the material has the same chemical formula and molecular weight, but the substituent is attached to a different place on the aryl ring. Figure 20.2 shows the isomerism of monoisopropylphenol.

The pure phosphate esters produced from the individual isopropylphenyl isomers vary considerably in performance. Table 20.1 [30] shows the effect on viscosity and oxidation stability. The orthoisomer, which has the highest rate of change of viscosity with temperature (referred to as a

Table 20.1 Variation in Viscosity–Temperature Properties and Oxidation Stability for Isomeric Forms of Tris-isopropylphenyl Phosphate

Phosphate isomer	Viscosity (cSt)			Viscosity index	Oxidation stability ^a (% viscosity change at 37.8°C)
	99.8°C	37.8°C	0°C		
ORTHO	8.2	120	14,540	<0	4
META	5.0	34.8	508	63	800
PARA	6.3	56.7	1,450	52	2,000

^aAfter oxidation at 150°C for 7 days in the presence of metals (modified FTMS VV-L-791C, method 5308.6).

low viscosity index), has the best oxidation stability. By contrast, the para derivative has better viscosity–temperature properties (a higher viscosity index) but poor oxidation stability. These differences in behavior are due to (i) the effect of the substituent when in the ortho position on the shape and “rigidity” of the molecule and (ii) its ability when in the para position to destabilize the molecule so that less energy is required for its breakdown.

4. *The number of substituents on the aromatic ring of the alkylated phenol feedstock.* Where more than one substituent is present, the number of isomeric phosphates that can, theoretically, be components of the finished product is significantly increased. Using xylenol, for example, which has 2 methyl groups and 6 different isomeric forms, it is possible to produce over 200 isomeric phosphates. Again, the physical and chemical properties are affected, and trixylyl phosphates display higher viscosities and also better hydrolytic stability than tricresyl phosphates.

It will be appreciated from this brief explanation of the impact of ring substituents on fluid behavior that although it is possible to produce a product with, say, excellent oxidative stability or better viscosity–temperature properties, it is difficult to achieve this without some adverse impact on other fluid characteristics. A degree of compromise is, therefore, almost inevitable when designing a triaryl phosphate molecule or a fluid base stock to meet the conflicting technical requirements of a hydraulic fluid. Depending on the application, therefore, it may be appropriate to select the fluid, which is either the most hydrolytically or the most oxidatively stable.

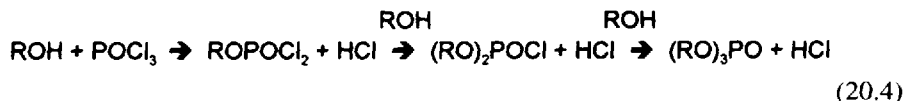
4 MANUFACTURE

Although phosphate esters can be regarded as “salts” of orthophosphoric acid, they are not currently produced from this raw material because the yields are low (~70% for triaryl phosphates) [31]. Instead phosphorus oxychloride (POCl_3) is reacted with either an alcohol (ROH), a phenol (ArOH) or an alkoxide (RONa), as indicated in the following reaction schemes:



where R represents an alkyl group and Ar an aryl group.

The above reactions pass through intermediate steps in the production of the phosphate as shown in Scheme (20.4):



The intermediate products are called phosphochloridates and it is possible to stop the reaction at each step if it is desired to produce mixed products {by using different alcohols or an alcohol and a phenoxide [Scheme (20.5)]}:



4.1 Trialkyl Phosphates

Trialkyl phosphates can be prepared by either of routes (20.1) and (20.3), although in reaction (20.1), a considerable excess of alcohol is required to drive the reaction to completion and the hydrogen chloride (HCl) by-product must be removed as rapidly as possible—usually by vacuum and/or water washing. The reaction temperature is not allowed to rise too high in order to minimize the thermal degradation of the phosphates. When the alkoxide route (20.3) is chosen, the chlorine precipitates as sodium chloride, somewhat simplifying the purification treatment. Normally, this consists of a distillation step to remove excess alcohol, an alkaline wash, and a final distillation to remove water [32]. With the alkoxide method, however, any residual sodium chloride can be removed by water washing followed by a final distillation under vacuum. If mixed alkyl phosphates are required (i.e., using more than one alcohol), they can be produced either in one step using an alcohol mix or by the reaction of the phosphochloridate intermediate with an alkoxide.

4.2 Triaryl Phosphates

Triaryl phosphates, which form the basis of the majority of hydraulic fluid formulations, are manufactured almost exclusively by reaction (20.2). Phosphorus oxychloride is added slowly to the reaction mass containing an excess of phenol in the presence of a small amount of catalyst—typically aluminum chloride or magnesium chloride—before heating slowly [32]. The hydrogen chloride is removed as it is formed, by heating under vacuum followed by absorption in water. On completion of the reaction, the product is distilled to remove most of the excess phenol(s), the catalyst residue, and traces of polyphosphates. Finally, the product is steam-stripped to remove volatiles, including residual phenol(s). Depending on the application, it may be necessary to reduce the level of acidity by subsequent alkaline washing or by a solids treatment.

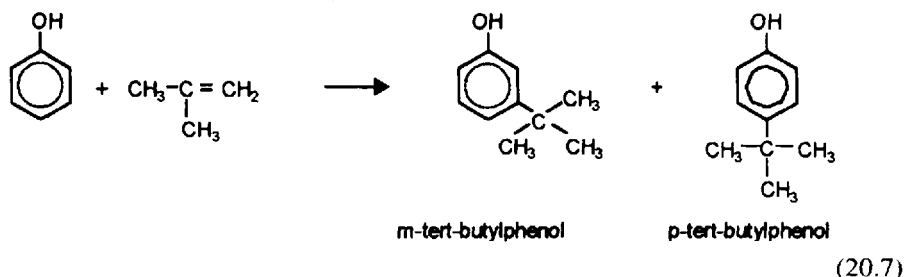
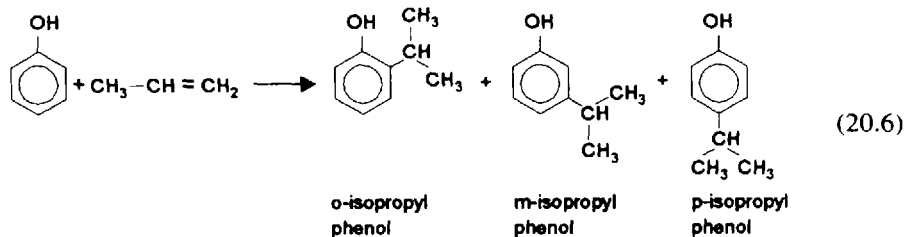
As with trialkyl phosphates, it is possible to manufacture mixed aryl phosphates as long as the reactivity of the different phenolic materials is similar. Such mixed phosphates can have improved low-temperature properties (e.g., pour point) as a result of the asymmetrical nature of the molecule, and the technique is particularly important when trying to manufacture products to meet a particular level of viscosity.

The phenolic feedstocks used for phosphate ester manufacture were originally obtained from the distillation of coal. Coal tar contained a mixture of phenol, cresols, and xylenols which was fractionated to provide the raw materials for the phosphate process. These “fractions” or “distillation cuts,” however, were still complex mixtures, often containing up to 20 different cresol, xylenol, and other alkyl phenol isomers. These mixtures were frequently referred to as “cresylic acids.”

In the 1960s, it became progressively more difficult to obtain suitable quality feedstocks from this source because of a decline in the coal distillation industry. The increasing use of natural gas for domestic heating purposes and the concurrent contraction in the steel industry led to a fall in demand for “coke,” the solid residue from the distillation of coal. As a result, many coal-tar distillers closed and the quality of available phenolic feedstocks deteriorated.

In order to assure supplies of suitable raw materials, the phosphate ester manufacturers in the late 1960s introduced feedstocks based on phenol (from petroleum

sources) which was reacted with propylene or iso-butylene to form mixtures of isopropylphenols or tertiary butyl phenols [33,34] [see reactions (20.6) and (20.7)].



No ortho derivative is normally produced when reacting phenol with isobutylene.

Depending on the reaction conditions, it is possible to control the relative amounts of the isomeric alkylated phenols to optimize the properties of the resulting phosphate. However, if the mixtures in reactions (20.6) and (20.7) are converted into phosphates, the viscosity level of the resulting liquid would be too high for most hydraulic applications. To reduce the viscosity, the alkylated phenol is mixed with a quantity of pure phenol, which enables the manufacture of fluids to meet a wide range of viscosity grades. Unfortunately, the phenol content results in the production of triphenyl phosphate, particularly in the lower-viscosity fluids (see Table 20.2) [35]. This is not very hydrolytically stable and although the stability of the mixed product is adequate for most applications where significant contact with moisture is likely, other phosphates may be preferred for more critical uses.

The TCP and TXP produced from cresylic acid or "natural" raw materials have been described as "natural" products, whereas feedstocks based on isopropylphenols and tertiary butylphenols are known as "synthetic" feedstocks (because of

Table 20.2 The Triphenyl Phosphate Content of Triaryl Phosphates

Phosphate ester	TPP content for different ISO viscosity grades (%)			
	22	32	46	68
TCP	—	0.1	—	—
TXP	—	—	None	—
IPPP	26–34	14–18	8–10	5–8
TBPP	40–48	31–40	14–21	8–12

Note: TCP = tricresyl phosphate; TXP = trixylyl phosphate; IPPP = isopropylphenyl phosphate; TBPP = tertiary butylphenyl phosphate.

their chemical synthesis) and the resulting phosphates are known as “synthetic” phosphates. Unfortunately, these terms still persist, even though the cresol and xylene feedstocks used today are obtained by the refining of petroleum (a natural product) and synthetically from phenol (cresols and xylenols), toluene (cresols), or isophorone (xylenols) [36].

It was indicated earlier that the phenolic feedstocks are frequently complex mixtures of different isomers. This, in turn, results in phosphates based on many different combinations of phenolic groups. The gas–liquid chromatograms in Fig. 20.3 show the number of major components of the three principal triaryl phosphate types and the significant differences between the products. The simplest product is a tertiary butylphenyl phosphate (TBPP) containing only about seven significant components. By comparison the isopropylphenyl phosphate (IPPP) contains about 10 major components, and trixylyl phosphate over 20 [35]. Differences in retention times for the IPPP and TBPP products indicate a broader spread of molecular weights of the component phosphates, whereas for TXP, the molecular weight range is relatively small.

4.3 Mixed Alkylaryl Phosphates

Small quantities of both alkyldiaryl- and dialkylmonoaryl phosphates are used in the production of specialty hydraulic fluids, particularly where some improvement in low-temperature properties is required with a measure of stability at high tempera-

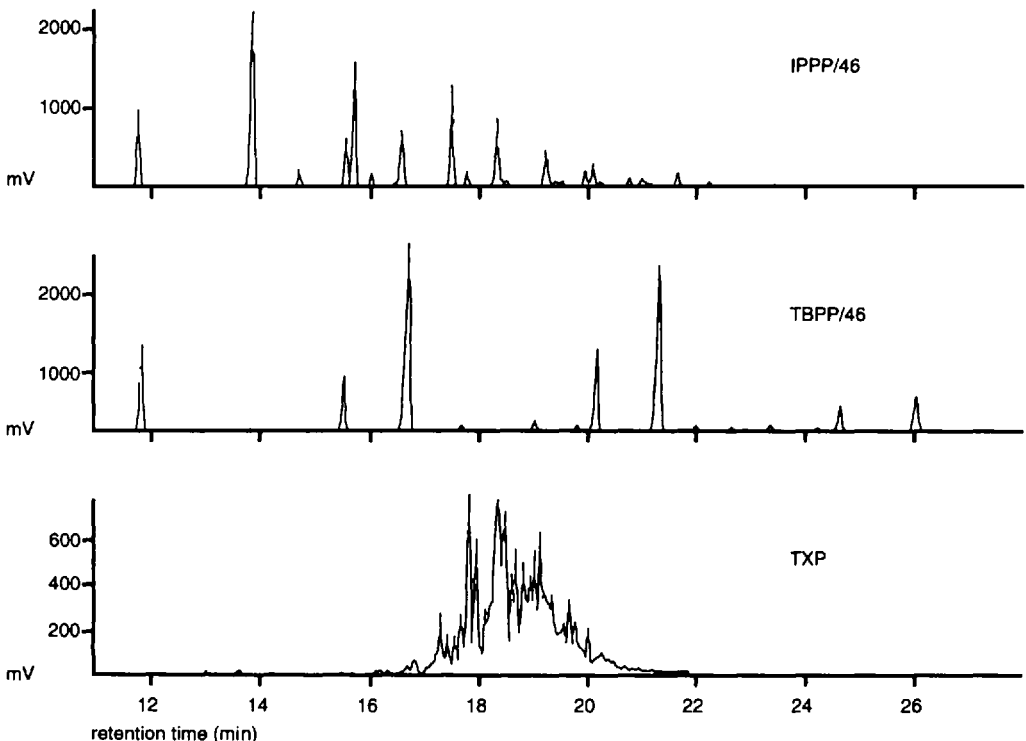
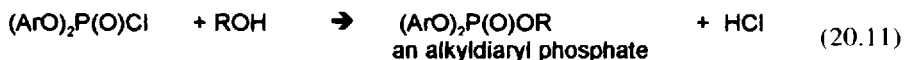
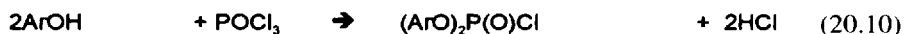
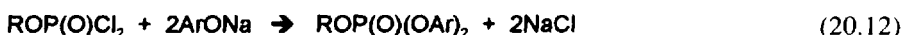


Figure 20.3 Gas–liquid chromatograms for different triaryl phosphates.

tures. These products can be most satisfactorily produced by two-stage processes from the appropriate phosphochloridate intermediate.



An alkoxide may also be used as an alternative to the use of alcohol, primarily for the preparation of alkyl-diaryl phosphates:



The purification of alkylaryl phosphates can be carried out using techniques already identified for the other two classes of phosphate esters. More detailed information on the preparation of these materials can be found in Ref. 10.

To summarize, the phosphate esters which are in commercial production and used in hydraulic fluid applications are listed in Table 20.3 together with their common abbreviations.

5 PROPERTIES OF PHOSPHATE ESTERS

In this section, the performance of phosphate esters will be examined against the principal technical requirements for hydraulic fluids (see Table 20.4). These requirements impact on both the physical and chemical properties of the fluids and will, therefore, be discussed under those headings, with the exception of fire resistance and lubrication performance, which are termed "performance properties."

5.1 Performance Properties

5.1.1 Fire Resistance

Because the fire resistance of these fluids is the principal reason for their use, it is appropriate to discuss this aspect of their behavior first. Before clarifying why phosphate esters are difficult to ignite, it is useful to recall that fire, or combustion, is essentially a vapor-phase oxidation process that requires the presence of a fuel, sufficient energy to volatilize the fuel, and oxygen. Fluid characteristics which therefore determine ignitability include vapor pressure (and, hence, viscosity, molecular weight, and heat of vaporization) and thermal/oxidation stability [37], all of which are very structure dependent. The measurement of ignition delay time (i.e., the time it takes for the fluid to ignite on a hot surface at a specific temperature) is affected by other factors, such as specific heat, thermal conductivity, and surface tension. A variety of physical and chemical properties can therefore affect the flammability characteristics. However, the term "fire resistance" should not be equated with non-flammable. If sufficient energy is injected into almost any organic molecule, it will ignite. Even water has been known to explode in contact with very hot surfaces!

At first glance, it might seem surprising that phosphate esters are much less flammable than mineral oils. Apart from a relatively high molecular weight, they only differ in terms of composition by several oxygen atoms and a phosphorus atom,

Table 20.3 Phosphate Esters Used in Hydraulic Applications

Common name	Abbreviation
Trialkyl phosphates	
Tributyl phosphate ^a	TBP
Tri-isobutyl phosphate	TiBP
Tributoxyethyl phosphate	TBEP
Trioctyl phosphate ^a	TOP
Alkylaryl phosphates	
Dibutylphenyl phosphate ^a	DBPP
Butyldiphenyl phosphate ^a	BDPP
Octyldiphenyl phosphate ^a	ODPP
Isodecyldiphenyl phosphate ^a	DDPP
Triaryl phosphates	
Triphenyl phosphate	TPP
Tricresyl phosphate	TCP
Trixylylphosphate	TXP
Cresyldiphenyl phosphate	CDP
Isopropylphenyl phosphate	IPPP ^b
Tertiary butylphenyl phosphate	TBPP ^b

^aUnless otherwise stated, the alkyl groups used in the manufacture of trialkyl phosphates and alkylaryl phosphates are of the following types: butyl is *n*-butyl, octyl is 2-ethyl-hexyl, and decyl is iso-decyl.

^bIn the subsequent tables and figures, the IPPP and TBPP abbreviations are usually followed by the ISO viscosity grade. Thus, IPPP/46 is an isopropylphenyl phosphate meeting ISO viscosity grade 46.

the latter being present in the phosphate to the extent of only a few percent (~7–12% for commercially available materials). The reason why these materials display such favorable characteristics lies, as suggested above, in a combination of their structure (and its effect on stability) and physical properties. However, whereas a low vapor pressure and generally high thermal/oxidative stability will favorably affect fire resistance, in the case of phosphate esters a further factor, the phosphorus content, plays an important role.

Table 20.4 Main Technical Requirements for Fire-Resistant Hydraulic Fluids

Fire resistance	Good resistance to shear breakdown
Low compressibility	Low foaming properties
Appropriate viscosity	Rapid air release
Adequate low-temperature behavior	Good water separation
Good lubrication performance	Noncorrosive
Adequate stability (thermal, oxidative, and hydrolytic)	Good compatibility with system materials

Irrespective of the mode of decomposition, lower-molecular-weight materials, such as alcohols, alkylphenols, and ketones, are produced during degradation, which are highly volatile and much easier to oxidize. When present in sufficient concentration (i.e., above the lower limit of flammability), they will combust and release heat.

The remainder of the molecule will contain one or more —P—O radicals, which will polymerize in a reaction that is highly endothermic (or energy absorbing) to form polyphosphates or, in an extreme case, phosphorus oxides. This reduces the total heat released and is the principal reason why phosphate esters do not propagate flame.

A high phosphorus content alone, however, is insufficient to increase the fire resistance if the breakdown products are themselves readily oxidizable! The effect of phosphorus content and other physical properties on some flammability characteristics are given in Table 20.5 [32,38,39]. Examination of the data reveals that none of the common physical properties by itself correlates satisfactorily with the listed flammability data. Some variation in these data is possible due primarily to slight differences in the composition/viscosity of the products tested, particularly the aryl phosphates.

The measurement of fire resistance in the laboratory is difficult because no single test can satisfactorily reproduce all the complex variables that together constitute the fire process [37]. The best that can usually be achieved is a comparative assessment of different fluids under the same test conditions, which may or may not represent specific industrial hazards. As a result, a large number of tests have been devised to simulate particular applications, many of which rank products in the same order and do not add to an understanding of the behavior of the material in use.

The different tests currently available for determining fire resistance can be classified according to the mode of fluid ignition (i.e., bulk fluid ignition, hot surface ignition, spray ignition, and ignition when adsorbed on a substrate) [37]. These tests essentially measure ignitability (temperature of ignition or time to ignition at a given temperature) and the tendency to propagate flame. An exception is a test which attempts to measure some intrinsic property of combustion, such as net calorific value. Unfortunately, the conditions used for measuring this property are not suitable for products that contain elements other than carbon, hydrogen, oxygen, and nitrogen [40] and can give misleading information on phosphate esters [37]. In spite of the limitations of the tests used [37], most flammability data on fluids are reported in terms of flash and fire points and autoignition temperatures. Table 20.6 [32,41–44] provides this information on commercially available fluids.

Many of the applications where phosphates are used require the better fire resistance and high-temperature stability afforded by the triaryl phosphates. As a consequence, the vast majority of fire-resistance data generated under tests more closely representing specific hazards is limited to an evaluation of these fluids.

Table 20.7 [30,32,37,41–43,45] indicates the performance of TXP and IPPP/46 fluids in the most important industry-related tests.

As will be seen from Table 20.7, the majority of tests do not discriminate between the two different triaryl phosphate esters. This is mainly due to the pass/fail requirements of specifications in which these tests appear. These tests not only fail to differentiate between triaryl phosphate esters (unless increased in severity) but also between phosphate esters and other types of fire-resistant fluids, particularly the

Table 20.5 Relationship Between Various Physical Properties and Flammability Behavior

Phosphate ester	Molecular weight	Phosphorus content (%)	Viscosity at 40°C (cSt)	Vapor pressure at 150°C (mm Hg)	Flash/fire points, open cup (°C) ISO 2592	Autoignition temperature (°C) ASTM D-2155
TBP	266	12.0	2.5	7.3	115/182	388
TOP	434	7.37	7.5	0.9	195/238	370
TPP	327	9.8	Solid	0.15	224/310	635
TXP	410	7.8	46	0.009	199/343	570

Table 20.6 Flash Point, Fire Point, and Autoignition Temperatures of Phosphate Esters

Phosphate ester	Flash point	Fire point	Autoignition temperature
	(°C) ISO 2592	(°C) ISO 2592	(°C) ASTM E-659
TBP	165	182	400 ^a
TiBP	155	170	476
TOP	190	238	370 ^a
TBEP	190	230	260 ^a
BDPP	205	246	
DBPP	171		>430
ODPP	224	238	
DDPP	240	260	
TPP	224	310	635
CDP	255	340	620
TCP	240	338	600
TXP	250	360	535
IPPP/22	255	335	570
IPPP/32	245	330	545
IPPP/46	250	335	500
IPPP/100	260	335	515
TBPP/22	240	340	590
TBPP/32	255	350	545
TBPP/46	250	350	535
TBPP/68	255	350	525
TBPP/100	255	360	520

^aASTM D-2155. This method usually gives higher values than ASTM Method E-659.

water-based products. In order to be able to rate the performance of *all* the different types of fluid under identical conditions, two new spray ignition tests have been developed: in the United States by the Factory Mutual Research Corporation [46] and detailed in a new Specification Test Standard for Flammability of Hydraulic Fluids [47], and the other in the United Kingdom by the Health and Safety Executive for inclusion in the seventh edition of the Luxembourg Report [48]. Both tests measure the heat released by a stabilized flame of the ignited fluid. Treatment of the results is slightly different in that Factory Mutual (FM) quote data in terms of a "Spray Flammability Parameter" which takes into consideration the critical heat flux for ignition, whereas the United Kingdom test [49] reports the "Ignitability Factor," which is a direct measure of the heat released.

Figures 20.4 [50] and 20.5 [47] indicate some of the results obtained to date by these new procedures and clearly show their ability to differentiate between the different types of fluid. As a result, Factory Mutual has introduced three categories of fluid performance, depending on Spray Flammability Parameter (SFP) values [47]. Aryl phosphates fall into Group 1 for the least flammable products with an SFP of $< 20 \times 10^4$, which are unable to produce a stable flame. Alkyl phosphates, however, are more flammable and fall into other categories.

Another advantage of the new tests is that they can eliminate the effects of additives (e.g., polymeric materials) which may be used to increase droplet size in

Table 20.7 Performance of Triaryl Phosphates in Hazard-Related Fire Tests

Test method	Source	Fluid type	
		TXP	IPPP/46
Bulk fluid ignition			
Oxygen Index	IEC 1144	—	23
Hot-surface ignition			
Hot Manifold Test	CETOP RP65H or VV-L-791C Method 6053	Pass	Pass
Hot Channel Test	Factory Mutual Standard 6930	Pass	Pass
Molten Metal Ignition	Rheinisch Westfälischer TÜV	16 s	16 s
Spray ignition			
The "Community of Six" Spray Test	Section 3.1.1; 7th Luxembourg Report	Fail	Fail
The "United Kingdom" Spray Test	Section 3.1.2; 7th Luxembourg Report	Pass	Pass
Heat released by a stabilized flame	Section 3.1.3; 7th Luxembourg Report	Class D	Class E
Factory Mutual Spray Test	FM Standard 6930	Pass	Pass
Wick tests			
Determination of the persistence of a flame on a wick	Section 3.2.1; 7th Luxembourg Report	Pass	Pass
Linear flame propagation rate of lubricating oils and hydraulic fluids	ASTM D5306	No ignition	No ignition
Miscellaneous tests			
Compression-Ignition Test	Section 4.5.1; MIL-H-19457D	>42:1	41:1

a spray (and therefore provide some temporary improvement to the spray ignition performance) but which have no significant effect on the flammability under other tests conditions.

5.1.2 Lubricating Properties

Hydraulic fluids are predominantly used in dynamic applications that involve continuous circulation around the system at pressures up to 350 bars. The ability to lubricate metal surfaces moving relative to one another (particularly steel on steel) as found in pumps, valves, and so forth is therefore of paramount importance. Because it also largely dictates system operating pressures and capacity, it can significantly influence the capital cost of the system. Although fluid viscosity and its change with temperature have an obvious impact on pump and valve efficiency, the ability of a fluid to lubricate satisfactorily depends mainly on its potential for forming a film between the metal surfaces that is thick enough to separate them, and the ability of that film to resist displacement under load and through relative motion of the surfaces. As in the case of fire resistance, the lubricating performance of the fluid depends on a variety of physical and chemical properties [e.g., compressibility, viscosity, specific heat and thermal conductivity (which affects the temperature of the

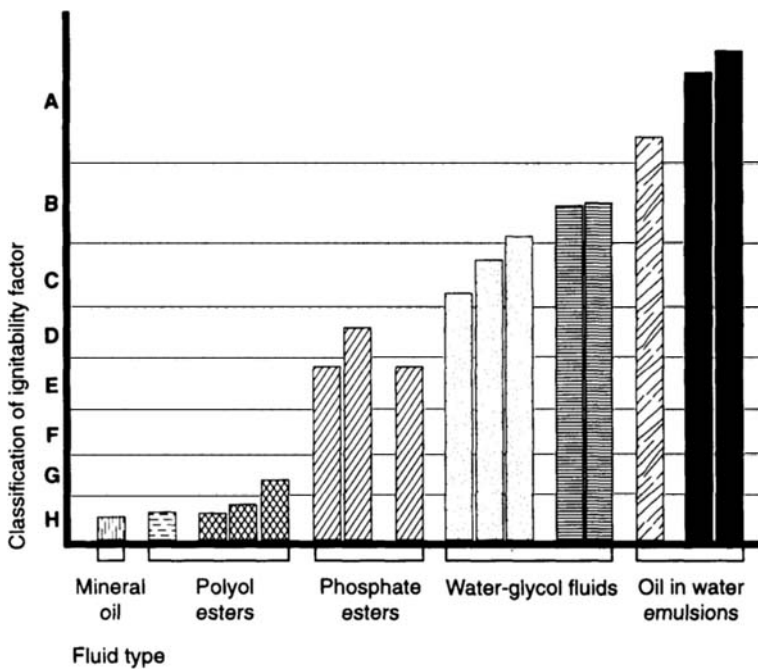


Figure 20.4 Results of a stabilized-flame heat-release spray test — 7th Luxembourg Report, Section 3.1.3.

lubricating film and hence its viscosity)], the polarity and shape of the molecule, and its thermal and hydrolytic stability.

The good antiwear properties of phosphates were referred to earlier. These are attributed to the polarity of the molecule and its acidic decomposition products, which initially form an adherent film on the metal surface, and also to the readiness of the decomposition products to react chemically with the metal surface to form iron phosphides or phosphates [4,51–53]. These are lower-melting products deformed by plastic flow and fill in the gaps between the asperities or peaks on the metal surface. Consequently, the area carrying the load is increased and the pressure/unit area ratio is reduced. This enables a higher load to be supported before breakdown of the lubricating film. In general, it can be stated that the antiwear performance of the phosphates varies with stability—particularly hydrolytic stability. The more readily the phosphate breaks down, the better the antiwear behavior. This fact may account for the variable performance of phosphate esters in some reports [54]. Although phosphates are recognized as effective antiwear agents, they have limited ability to prevent scuffing at high loads without enhancement by additives. Aryl phosphates are reported as more effective extreme-pressure agents than alkyl phosphates [55], the difference being attributed to the formation of iron phosphides by aryl phosphates and to the less effective iron phosphate by the alkyl derivatives. Table 20.8 [42,43] illustrates vane-pump wear test data on different triaryl phosphates, which confirms their good antiwear behavior; Table 20.9 [56] compares the different types of fire-resistant hydraulic fluids in terms of their pump-performance capabilities relative to mineral oil. Although the data have been provided by equip-

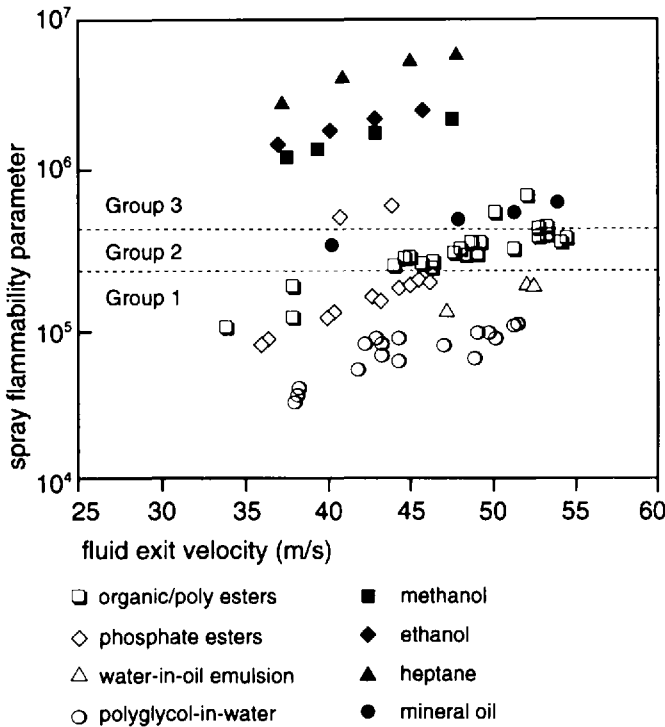


Figure 20.5 Spray flammability parameter as a function of fluid exit pressure at 6.9 mPa nozzle pressure—draft Factory Mutual Standard. (Reprinted with permission, copyright Factory Mutual Research Corporation, 1992.)

ment manufacturers, they are probably conservative estimates and, in reality, somewhat higher performance limits for the fire-resistant products may be found.

In addition to the effect on the conventional wear process, the composition of fluids can significantly impact the pitting fatigue life of ball and roller bearings. With nonaqueous fluids, the life of bearing surfaces depends mainly on the fluid-film

Table 20.8 Vickers V104C Vane-Pump Wear Test Data for Some Triaryl Phosphates at 140 Bar; Test Methods: IP281 and ASTM D-2882

Test data	Phosphate ester								
	IPPP/22		IPPP/32		IPPP/46		IPPP/68		TBPP/46
Fluid temperature (°C)	53	53	60	60	66	66	72	72	NA
Test duration (h)	100	250	100	250	250	1000	100	250	100
Ring weight loss (mg)	3.6	6.5	2.5	2.6	3.7	8.2	3.7	5.4	14.0
Vane weight loss (mg)	14.5	15.6	34.8	36.7	7.4	8.5	2.0	3.3	55.3
Total weight loss (mg)	18.1	22.1	37.3	39.3	11.1	16.7	5.7	8.7	69.3
Pump speed (rpm)	←				1440		→		1200

Table 20.9 Effect of Hydraulic Fluid Type on Pump Performance

Fluid category (ISO Standard 6743/4)	Pump type				
	Gear	Piston		Screw	Vane
		Hydrostatic bearing	Hydrodynamic bearing		
1. HFA (E and S)					
Max. continuous pressure rating (bar)	200	150 ^a	150	No known experience	Not suitable ^b
Max. continuous speed ^c (%)	100	50	50		
Bearing life ^c (%)	100	10	30		
2. HFB					
Max. continuous pressure rating (bar)	200	250	200	250	70
Max. continuous speed ^c (%)	100	100	100	100	6
Bearing life ^c (%)	100	30–70	20–40	100	100
3. HFC					
Max. continuous pressure rating (bar)	200	200	250	250	105
Max. continuous speed ^c (%)	100	100	100	100	100
Bearing life ^c (%)	100	20–60	20	100	100
4. HFD (R and U)					
Max. continuous pressure rating (bar)	250	350	350	250	140
Max. continuous speed ^c (%)	100	100	100	100	100
Bearing life ^c (%)	100	80–100	70–100	100	100
Bearing type	Plain	Roller	Roller	Roller (but no fluid contact)	Plain (sleeve)

Note: All data taken from current pump manufacturers' catalogs.

^aValues up to 300 bars are now being reported.

^bThe problems with water-based fluids in vane pumps relate to vane tip wear rather than bearing lubrication.

^cValues indicated are relative to mineral-oil performance in the same pump.

thickness and, hence, viscosity [57,58]. Phosphate esters have been found to have lives comparable with those of mineral oils of similar viscosity [57].

With water-based fluids, the water accelerates the propagation of surface cracks as well as considerably reducing the pitting life, probably by an embrittlement process [57,58].

The fatigue life of fluids is normally expressed as the L_{10} life, which is the time after which 10% of bearings would have failed. Bearing L_{10} lives characteristic of the different ISO classes of fire-resistant fluids are given in Fig. 20.6 for an axial piston pump at 1500 rpm. Again, depending on the fluid composition, pump type, and operating conditions, these values will show some variation [59,60].

The behavior of triaryl phosphate esters in gears has been studied in some detail [61,62]. The results of a comparison of the behavior of IPPP/46 and TXP on an FZG gear rig in comparison with mineral-oil show the following:

- A similar wear behavior for TXP and mineral oil (see Fig. 20.7). The inferior viscosity–temperature and viscosity–pressure characteristics of the phosphates are largely compensated for by polar effects and chemical reactivity at the metal surface. For example, the fact that an IPPP/46 fluid displays better wear characteristics than TXP [62] is probably related to its poorer hydrolytic stability. This more readily allows the production of acidic species, which subsequently react with the surface.
- Inferior frictional characteristics and, as a result, slightly higher power losses. These properties are also influenced by film thickness. Although load-dependent losses are about 20% higher for triaryl phosphates than for mineral oil, about 80% of the total losses in high-speed gears are related to no-load losses. This means, for example, that in turbine gears, the total gear losses for a phosphate would be about 4% higher than the losses for mineral oil of comparable viscosity [63].
- Inferior running-in properties. This is not surprising in view of the lack of extreme-pressure performance of this type of fluid. Mineral oil, of course, usually contains sulfur-containing impurities which assist this process. As a result, it is important to clarify the optimum conditions for running-in new gears from the manufacturer when phosphates are used.
- A better scuffing performance. In FZG tests, ISO VG 46 mineral oils (without additives) typically fail at load stages 3–5. Triaryl phosphates of similar viscosity typically fail at stages 7 and 8 [61,62]. Improving the scuffing behavior of mineral oils is, however, fairly easy; with phosphate esters, this is more difficult in view of competition between the phosphate (or its decomposition products) and the additive for the metal surface. Careful selection of the latter is necessary when upgrading the extreme-pressure performance of the phosphate.

Aluminum and its alloys are not recommended as suitable bearing materials for plain bearings in components using these fluids owing to the inability of phosphates to “wet” aluminum surfaces. Copper/lead bearings can be used, but the preferred lining material is white metal. Extended tests on TXP at bearing temperatures of 110°C and fluid inlet temperatures of 95–98°C showed no significant attack on an 80/12/5 tin/antimony/copper bearing [64].

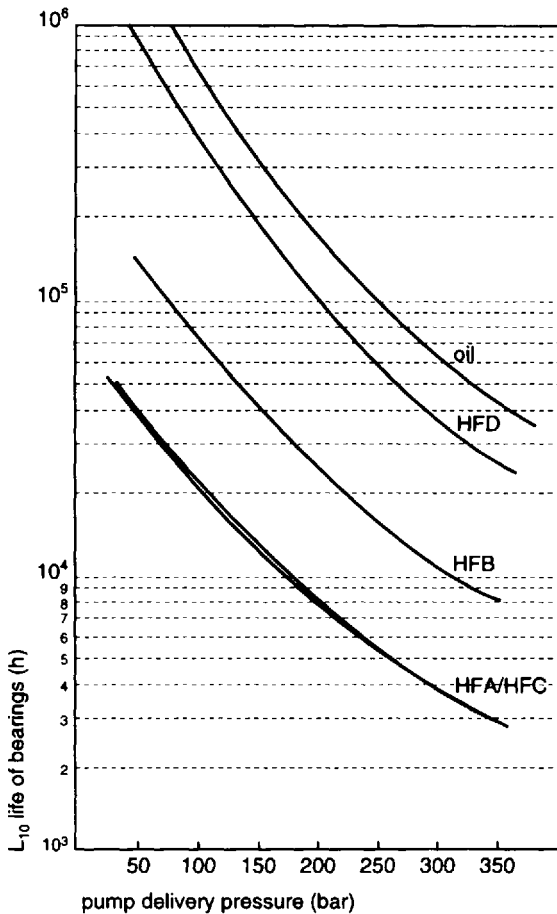


Figure 20.6 The variation in bearing L_{10} lives with pump delivery pressure for an axial piston pump operating on fire-resistant hydraulic fluids at 1500 rpm.

The scuffing resistance of alkyl or alkylaryl phosphates in gears has not been investigated in such detail. One report [65] investigated the mechanism of wear associated with this product and identified scoring as the mode of failure.

5.2 Physical Properties

5.2.1 Viscometric Properties and Low-Temperature Behavior

The viscosity of a fluid and its change with temperature and pressure significantly affects a number of aspects of fluid use and performance, such as pump efficiency. If a fluid has a very low viscosity, internal leakage and pump slippage can occur. This results in a power loss and an increase in fluid temperature. On the other hand, a high-viscosity fluid may show better internal sealing but require more power for circulation; it may display a higher pressure drop in lines and, under extreme conditions, even reduce the volume of flow to the pump, causing erratic system opera-

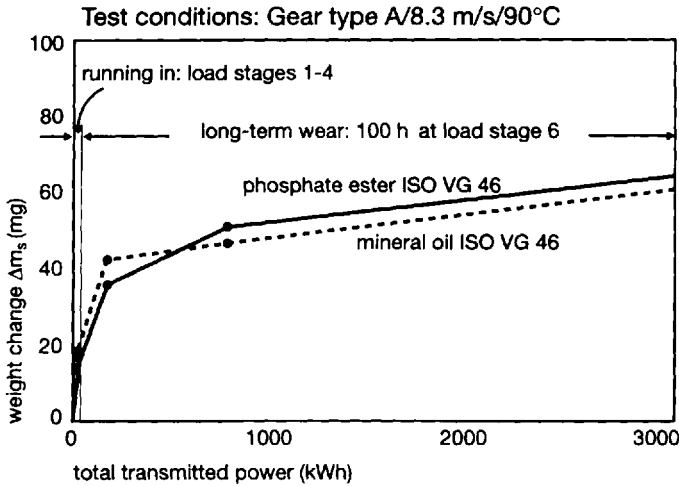


Figure 20.7 Long-term wear tests on an FZG gear machine for TXP and an ISO VG 46 mineral oil.

tion. Selection of a fluid with an appropriate viscosity for the pump design is therefore essential.

Other properties and performance parameters directly affected by viscosity include heat removal, wear properties, and air release. Obviously, secondary effects can be found on oxidation stability (and, hence, fluid life), frictional losses in bearings, cavitation, and so forth.

Depending on their chemical structure, phosphate esters are available in a wide range of viscosities, with trialkyl phosphates falling generally into ISO viscosity grades 2–7, alkylaryl phosphates in grades 10–15, and substituted aryl phosphates in grades 22–100 (Table 20.10) [10,32,38,39,41–44,66–68]. The variation in viscosity with temperature is shown in Fig. 20.8 [32] for most of the alkyl and aryl phosphates.

The rate of change of viscosity with temperature, otherwise known as viscosity index, varies considerably; trialkyl phosphates exhibit values comparable to those of paraffinic mineral oils, whereas commercial triaryl phosphate mixtures show very low values—usually between 0 and 30.

Symmetry within the molecule, steric effects, and the number of individual components assist in determining whether the product is solid or liquid and, in the latter case, its viscosity index. Triphenyl phosphate, for example, is a solid at ambient temperatures as is tris-*ortho*-isopropylphenyl phosphate. Pure tris-*para*-isopropylphenyl phosphate, by comparison, has a viscosity index of 50.

Depending on the fluid type and the pump selected for the hydraulic system, the viscosity may need to be reduced (by heating) before the pump can be operated. In the past, a critical pumping viscosity of 850 cSt maximum has sometimes been quoted and the temperature at which this is reached has been termed the critical pumping temperature [41]. Table 20.10 also indicates the critical pumping temperatures for some of the substituted aryl phosphate fluids where this aspect is more important.

Table 20.10 Typical Viscometric Properties of Phosphate Ester Fluids

Phosphate ester	Viscosity (cSt) ISO 3104						Viscosity index ISO 2909	Critical pumping temperature (°C)	Pour point (°C) ISO 3016
	0°C	20°C	37.8°C	40°C	99°C	100°C			
Trialkyl phosphates									
TBP	7	3.7	2.7	2.6	1.10	1.05	118		< -90
TiBP	10	4.9	3.1	3.0	1.12	1.10			< -90
TOP	96	40	8.0	7.9	2.20	2.20	145		-70
TBEP	80	26	6.8	6.7	2.15	2.10	90		< -70
Alkylaryl phosphates									
ODPP	66.2		9.95		2.43				-57
DDPP	89.8		12.80		2.88				-54
DBPP			4.66			1.34			< -70
Triaryl phosphates									
TPP	← Solid →								Solid, melts at 49°C
CDP	220	44	17.5		3.20				-34
TCP	1,000	80	28.3		4.00				-28
TXP	1,700	170	46.0	43	5.2	5.0			-21
IPPP/22	380	70	23.5	22	4.0	3.8	30	-8	-35
IPPP/32	990	90	35.9	32		4.7	30	0	-27
IPPP/46	1,600	155	47.0	43		5.3	15	+6	-18
IPPP/68	7,600	245	77.9	66		5.7	<0	+13	-11
IPPP/100	14,400	550	115	103		6.2	<0	+22	-5
TBPP/22	445	75		24		4.0	35		-30
TBPP/32	1,500	104	35	33	4.8	4.5	25		-26
TBPP/46	2,500	160	47	44	5.8	5.2	15		-18
TBPP/68	9,000		75	65	6.8	6.3	5		-15
TBPP/100		448	104	95	8.3	7.8	<0		-7

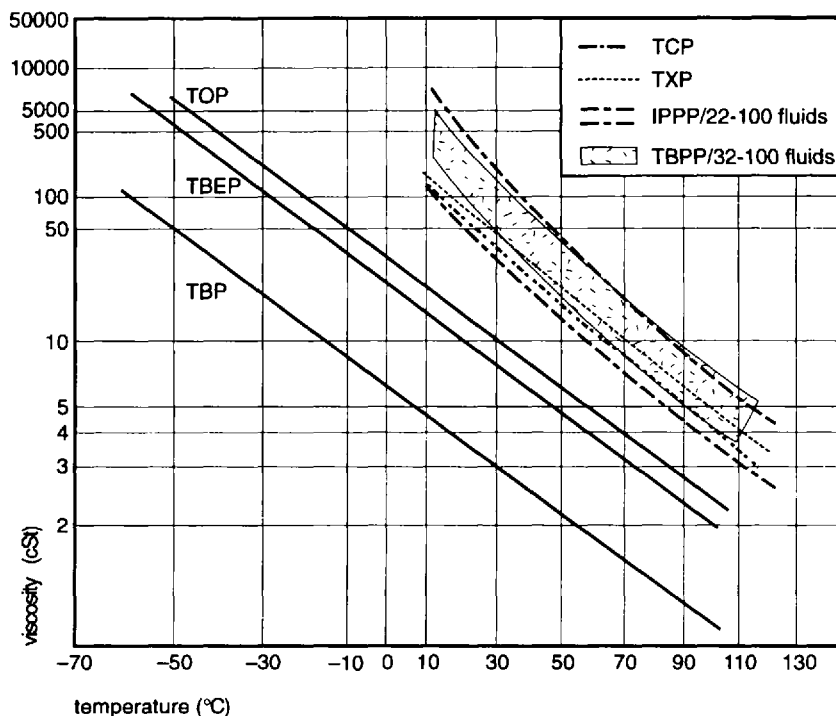


Figure 20.8 Viscosity-temperature relationships for commercial phosphate esters.

The effect of pressure on viscosity is to increase frictional losses in gears and bearings, but this can help resist the displacement of the lubricant film under load.

Figure 20.9 shows the variation in absolute viscosity of an ISO VG 46 phosphate with pressure up to ~ 800 bars and temperature up to $\sim 100^\circ\text{C}$ [42]. The data are intermediate between that of a paraffinic and a naphthenic mineral oil [68]. In the future, the viscosity at high pressures is likely to assume greater importance, as operating pressures are continually increasing.

In selecting a fluid for an application requiring a wide operating temperature range, the user has the option of taking (say) an ISO VG 46 fluid and then providing tank heating in order to minimize the effect of the poor low-temperature properties, or of selecting a product based on a thinner fluid but containing a polymeric thickener to provide an adequate working viscosity. In reality, apart from applications involving very low temperatures (where the alkyl or alkylaryl phosphates are preferred), the latter approach is not favored because (1) of concerns over the shear stability and, hence, pump performance of the thickened fluid, (2) the polymer can be removed by some types of filtration media, and (3) some thickeners can hydrolyze to give degradation products that can catalyze the hydrolysis of the phosphate ester base.

The pour points of phosphates, like their viscosities, vary considerably, depending on their structure (Table 20.10) and are generally superior to mineral oils of similar viscosity. Unlike mineral-oil-based products, however, pour point depressants are not used in commercial phosphate ester fluids as, normally, there is no need to inhibit the crystallization of a fluid component.

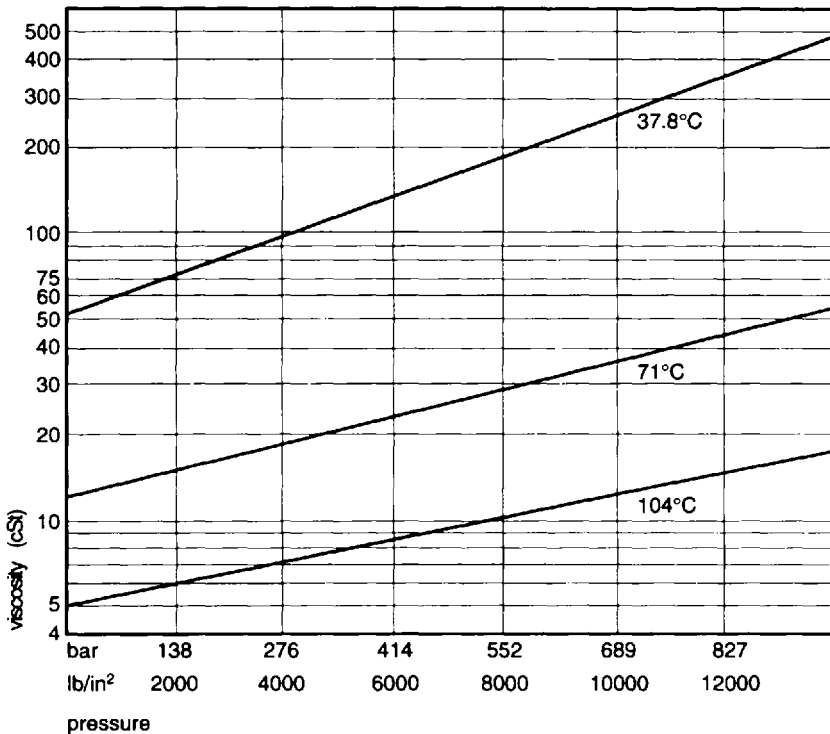


Figure 20.9 The viscosity–pressure relationship of an IPPP/46 phosphate ester.

5.2.3 Air Release, Foaming, and Demulsibility Characteristics

Air is a common “contaminant” of hydraulic fluids that is often overlooked or is thought of only in terms of its effect on compressibility. Its presence, however, can have major implications for both the performance of the fluid and the system [69–71]. Air can, of course, be present in a fluid in either the dissolved or dispersed (entrained) form. The solubility of air depends on the pressure and temperature of the fluid and is quoted in terms of an absorption coefficient (also known as the Bunsen coefficient). The higher the value, the greater the solubility of the gas.

Dissolved air normally has no effect on a fluid’s physical properties, but it is possible for dissolved air to come out of solution because of local pressure changes in the system and promote cavitation. Whereas some air bubbles may redissolve relatively quickly, others may combine to form larger bubbles, which are more difficult to solubilize and, therefore, remain as entrained air.

In contrast, dispersed or entrained air, in addition to the effect on compressibility noted earlier (and, therefore, on actuator response) will reduce the energy efficiency of the system, adversely affect lubrication performance, including the possible loss of pump suction, and increase fluid oxidation. Therefore, it is most important for entrained air to be allowed to escape or be encouraged to do so by the application of a slight vacuum to the fluid. Air, of course, should preferably not be allowed to enter the system, but as this cannot be avoided, the air content should be

minimized by a combination of good tank and pipework design and by selecting a fluid with a low air entrainment or solubility.

The air-release properties of a fluid are measured in the laboratory by first saturating the fluid with air and then measuring the time (at a constant temperature) for the air to be released to a level of 0.2% volume. Actual measurements of the air content in the system at the pump inlet are, of course, more revealing [72].

A comparison of air-release values and Bunsen coefficients for a limited range of phosphates is given in Table 20.11. The data indicate that TXP has a very low air-release value and also a low Bunsen coefficient in comparison with other phosphates and mineral oil. The figures quoted are, of course, for fresh fluids. Air entrainment is very dependent on fluid temperature and fluid viscosity—according to Stoke's Law, a thinner fluid releases air more quickly. Figure 20.10 [35] shows a typical change in air-release values with temperature for an unused natural and a synthetic phosphate.

In use, air-release values can increase as a result of fluid degradation and the generation of small amounts of surface-active materials (e.g., metal soaps). They may also be adversely affected by the presence of fine particles.

Whereas entrained air consists of bubbles separated by a thick layer of oil or fluid, foam consists of bubbles separated by a relatively thin film [70], the breakdown of which is determined by temperature and surface tension. To control the generation of foam and reduce its stability, it has been common practice for many years to incorporate small amounts of an antifoam. Most frequently, this is an organopolysiloxane (silicone), which is effective in parts per million. The effectiveness of an antifoam, however, normally depends on its insolubility in the fluid. Thus, it is necessary to produce a homogenous dispersion of the antifoam in the fluid, and with such small quantities, this is not easy to achieve. If homogeneity is not achieved, then it is possible for the antifoam to "plate out," usually on the walls of the tank. A further problem is that the addition of too much antifoam can adversely affect air entrainment [73]; therefore, a careful balance has to be maintained.

Typical foam test values for fresh phosphates are also found in Table 20.11 together with surface-tension data. The former are recorded in terms of foaming tendency and its stability at different temperatures after generating small air bubbles in the sample for a fixed period of time.

Table 20.11 Typical Air-Release and Foaming Test Values for Unused ISO VG 46 Phosphate Esters

Phosphate ester	Air-release value at 50°C (min) ISO 9120	Foaming tendency/ stability at 24°C (mL) ISO 6247	Bunsen coefficient for air at 40°C	Surface tension at 20°C (dyn/cm)
TXP	1	25/0	0.014	40
IPPP/46	5–8	40/0	0.020	33
TBPP/46	6–10	40/0	—	43
Mineral hydraulic oil (ISO VG 46)	3–5	30/0	0.085	23

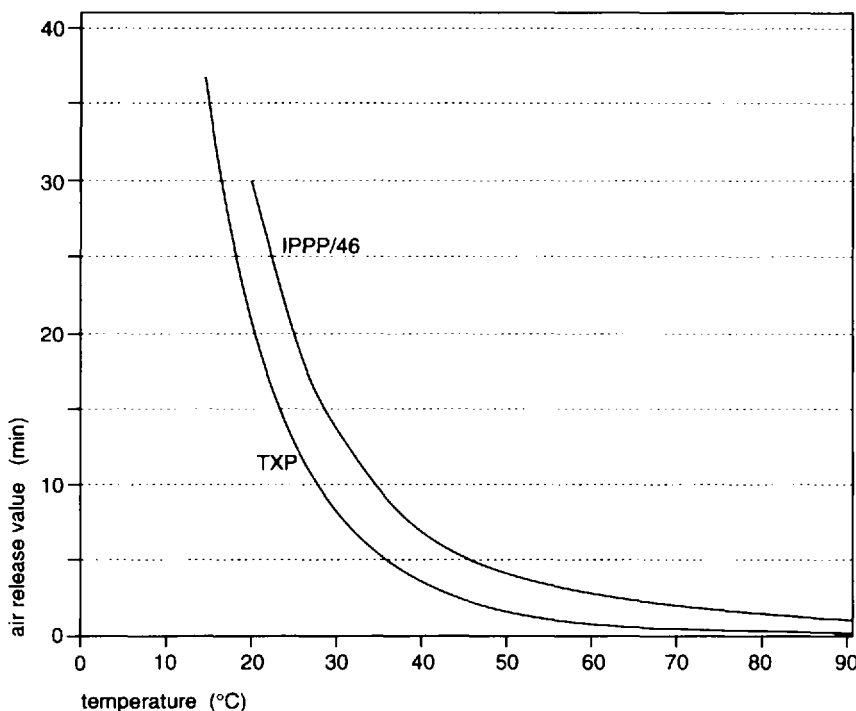


Figure 20.10 Air-release values and their variation with temperature for a natural and a synthetic triaryl phosphate.

In service, the foaming properties can deteriorate as a result of antifoam depletion or as a result of the production of surface-active species in the degradation products. The laboratory measurements are not very precise and are to be regarded more as evidence of a trend in performance, especially as tank design features heavily influence foaming behavior. In service, the presence of a stable foam needs investigation.

Demulsification or water separability characteristics is the third property in the group broadly categorized as "surface-active properties" and which are sensitive to the presence of small amounts of polar impurities or degradation products.

Mixtures of new phosphate ester and water normally separate quickly. This is advantageous for avoiding the formation of emulsions, which could cause a rapid increase in the rate of hydrolysis as well as having an adverse effect on lubrication performance. As the fluid degrades, the tendency for the water to be emulsified may increase, but this is a rare occurrence because of the small amounts of water normally present in the system.

5.2.4 Bulk Modulus and Compressibility

The bulk modulus of a fluid is defined as the ratio of pressure on the fluid to the resulting decrease in volume, and it is the reciprocal of compressibility. The ability of a fluid to resist compression is of prime importance when it is used as a hydraulic medium. Highly compressible oils result in sluggish operation, a buildup of heat,

Table 20.12 Bulk Modulus and Compressibility of an ISO VG 46 Phosphate Ester Hydraulic Fluid at 37.8°C

Pressure (bar)	Bulk modulus ($\times 10^4$)bar	Compressibility ($\times 10^{-5}$)/bar
138	1.99	5.02
344	2.12	4.71
689	2.34	4.27
1034	2.53	3.95

and significant energy losses [74,75]. Table 20.12 details the isothermal secant bulk moduli and compressibility values of an IPPP/46 triaryl phosphate ester over a wide range of pressures [41], whereas Fig. 20.11 [76] shows that phosphate esters are less compressible or “elastic” than mineral oil but more compressible than a water–glycol fluid. This property can sometimes influence the choice of fluid, as a high elasticity can adversely affect the accuracy and precise operation of equipment.

5.2.5 Vapor Pressure, Volatility, and Boiling Point

In addition to its impact on volatility and, hence, the operating temperature range of a hydraulic fluid, vapor pressure is also an important factor in determining the cavitation tendency of the fluid. Cavitation is caused by evaporation of a liquid as a result of a sudden drop in pressure followed by a subsequent condensation of the vapor as the vapor pressure falls below the boiling point. This can arise from changes in flow rate (e.g., in restrictors, pumps, and valves). Liquids that have high vapor pressures are, therefore, more likely to promote cavitation, cause damage to the

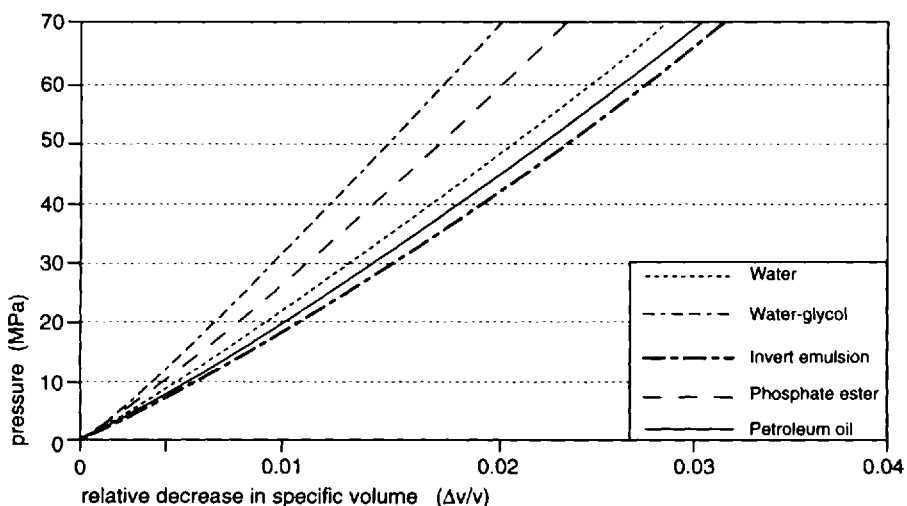


Figure 20.11 Generalized isentropic compressibility curves for various types of hydraulic fluids at 20°C. (Reprinted with permission. Copyright 1965, Institute of Petroleum.)

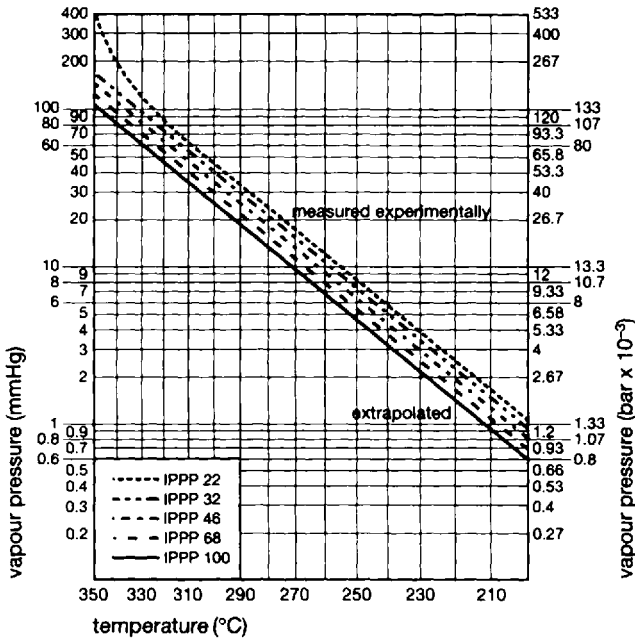


Figure 20.12 Vapor pressure characteristics of IPPP fluids.

surfaces where the bubbles collapse, and cause pressure variations in the circuit. The vapor pressure of phosphates, as expected, varies with chemical structure; the trialkyl phosphates are the most volatile, whereas the triaryl derivatives have such a low vapor pressure that determination is difficult below about 200°C. Under normal use conditions, therefore, phosphate ester fluids would be unlikely to produce a significant concentration of vapor in the operating environment.

The vapor pressure characteristics of a range of isopropylphenyl phosphates are given in Fig. 20.12 [41]. Additional data are listed in Table 20.13 [44].

Allied to vapor pressure is boiling point and Table 20.14 gives available data on a variety of products at different pressures [41,42,44,68].

5.2.6 Thermal Properties

As the fluid is circulated around the hydraulic or lubrication system, heat is generated by the compression of the fluid in the pump, at restrictions in the circuit, by frictional losses in bearings, and so forth. To avoid excess thermal stress on sensitive components (e.g., bearing surfaces), it is important that the lubricant assists with the removal of heat. The efficiency of this process depends on the flow rate, the thermal conductivity, and specific heat of the fluid or lubricant.

A comparison of the specific heat and thermal conductivity of a triaryl phosphate ester with mineral oil and other fire-resistant fluids is given in Table 20.15 [56]. The lower values for the phosphates indicate a slightly inferior cooling behavior, although this is somewhat offset by the higher density.

Specific heat (C_p) data on a range of phosphates is given in Table 20.16 [41–44,68] and shows quite a wide variation in results but no clear trend.

Table 20.13 Vapor Pressure Data for Phosphate Ester Fluids

	Vapor pressure (mm Hg)				
	10°C	70°C	110°C	210°C	310°C
Trialkyl phosphates					
TBP	1.1×10^{-3}	0.1325	1.398	91.42	
TiBP	2.4×10^{-3}	0.256	2.648	157.6	
TBEP	1.7×10^{-8}	6.2×10^{-5}	3.4×10^{-3}	4.35	472.8
TOP	7.8×10^{-5}	1.1×10^{-2}	0.1251	9.41	160.8
Alkylaryl phosphates					
DBPP	1.1×10^{-4}	0.0205	0.2698	26.17	528.2
Triaryl phosphates					
TPP	1.1×10^{-6}	4.68×10^{-4}	9.2×10^{-3}	1.8	59.9
CDP	4.2×10^{-7}	2.4×10^{-4}	5.4×10^{-3}	1.39	52.85
TCP	1.1×10^{-7}	8.62×10^{-5}	2.0×10^{-3}	0.768	35.12
TXP	2.4×10^{-9}	7.05×10^{-6}	3.6×10^{-4}	0.38	37.4
IPPP/22	4.2×10^{-10}	3.02×10^{-6}	2.4×10^{-4}	0.562	92.14
IPPP/32	1.6×10^{-8}	3.05×10^{-5}	1.0×10^{-3}	0.921	70.34
IPPP/46	2.6×10^{-9}	7.77×10^{-6}	4.0×10^{-4}	0.441	43.84
IPPP/68	3.4×10^{-8}	4.25×10^{-5}	1.0×10^{-3}	0.743	45.09
IPPP/100					33
TBPP/32	1.1×10^{-7}	1.0×10^{-4}	3.0×10^{-3}	1.12	56.15
TBPP/46	8.6×10^{-8}	7.69×10^{-5}	2.0×10^{-3}	0.831	41.25
TBPP/68				0.06	45.1
TBPP/100				0.02	31.2

The coefficient of thermal expansion for a number of phosphates between 25°C and 50°C is detailed in Table 20.17 [41,42,44], together with data on mineral oil and a polyol ester. Although there is some variation in reported data, it can be seen that values are very low and similar to those of mineral oil.

5.2.7 Electrical Properties

In order to avoid the electrochemical erosion of servo valves in steam turbine control systems, it has become common practice to specify minimum limits for the volume resistivity of both fresh and used fluid. Many turbine builders now require a minimum of 50 MΩ·m on fresh fluid (at 20°C) and 40 MΩ·m on product in service. These values are normally achieved by removing polar species such as water or acidic products from the fluid. In use, this is effectively achieved by in situ purification of the fluid with an adsorbent medium. Traditionally, fuller's earth or activated alumina have been used, but ion-exchange resins are now becoming more widely accepted.

Volume resistivity is very temperature dependent and Fig. 20.13 [35] shows the variation of \log_{10} resistivity with the reciprocal of temperature for TXP.

The reciprocal of resistivity is conductivity, and this parameter is sometimes specified as an alternative. The turbine governor application, however, is the only hydraulic or lubricant application to date requiring the measurement of electrical

Table 20.14 Boiling-Point Data for Phosphate Ester Fluids

Phosphate ester	Boiling point (°C)		
	at 760 mm Hg	at 10 mm Hg	at 4 mm Hg
Trialkyl phosphates			
TBP	284	155	139
TiBP	264	137	
Tri- <i>n</i> -propyl	252		
TOP	384	211	215
TBEP	320	220	222
Alkylaryl phosphates			
ODPP		239 (decomp)	
DDPP		245 (decomp)	
DBPP	325	185	
Triaryl phosphates			
TPP	413	254	
CDP	414	265	
TCP	427	271	
TXP	402	276	
IPPP/22	365	255	
IPPP/32	385	258	
IPPP/46	396	262	
IPPP/68	407	267	
IPPP/100	415	272	
TPBB/32	402	260	
TPBB/46	416	269	
TBPP/68	424	270	
TBPP/100	435	271	

characteristics. As trialkyl or alkylaryl phosphates are not used in this application, data on this aspect of their performance are not available.

The permittivity (or dielectric constant) of a triaryl phosphate is high (for IPPP/46 at 20°C, the value is 6.75 [35]). Because of their polar nature and sensitivity to moisture, the dissipation factors of triaryl phosphates are also high (e.g., 7% at 20°C

Table 20.15 Specific Heat and Thermal Conductivity Data on Different Fire-Resistant Hydraulic Fluids

Property	Fluid type			
	Triaryl phosphate	Water-glycol	Polyol ester	Mineral oil
Specific heat (C_p) at 25°C (J/g °C)	1.6	3.2	2.0	1.89
Thermal conductivity at 20°C (W/mK)	0.132	0.444	0.160	0.134

Table 20.16 Specific Heat of Phosphate Ester Fluids (ASTM D3947-80, Differential Scanning Calorimetry)

Phosphate ester	Specific heat (C_p) J/g °C		
	at 25°C	at 60°C	at 150°C
TBP	1.40	1.58	2.04
TiBP	—	2.23	—
TBEP	2.00	2.17	2.20
TOP	—	1.97	2.20
CDP	1.45	1.89	2.60
TCP	1.45	1.85	2.13
TXP	1.50	1.66	1.88
IPPP/22	1.50	1.93	2.33
IPPP/32	1.50	1.75	1.99
IPPP/46	1.60	1.70	1.97
IPPP/68	1.60	1.84	2.09
IPPP/100	1.60	1.85	2.10
TBPP/22	1.50	1.78	2.10
TBPP/32	1.50	1.78	1.85
TBPP/46	1.60	1.87	2.11
TBPP/68	1.06	1.69	1.86
TBPP/100	1.70	1.94	2.09

[35] for IPPP/46). Breakdown-voltage values can, depending on product purity, be ≥ 60 kV (at 20°C) [35].

5.2.8 Shear Stability

The importance of retaining the viscosity of the hydraulic fluid in service has previously been mentioned. Any significant change can, of course, affect the pump operating efficiency and should be avoided.

Table 20.17 Coefficients of Thermal Expansion for Different Phosphate Esters

Phosphate ester	Coefficient of thermal expansion ($\times 10^{-4}$ °C)
TBP	8.6
TiBP	8.7
TBEP	8.1
TOP	8.0
TCP	5.8–6.7
TXP	6.3
IPPP 22-100	6.9
TBPP 22-100	7.0
Polyol ester (ISO VG 32)	7.5
Mineral oil (ISO VG 32)	7.5

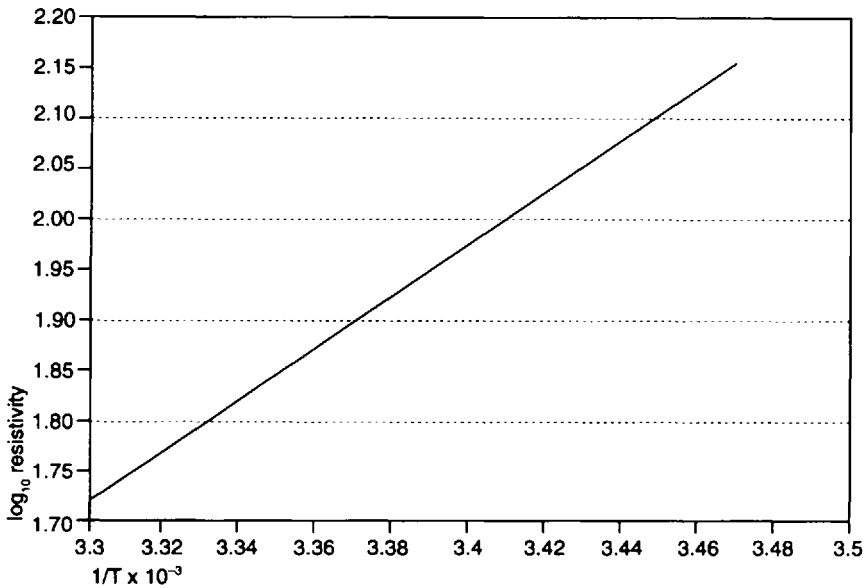


Figure 20.13 The variation in volume resistivity with temperature for TXP.

One of the principal reasons for viscosity changes in used hydraulic fluids is their breakdown on exposure to the shearing forces present in pumps, valves, bearings, and so forth, and in view of the trend toward higher system operating pressures and smaller system capacities, the use of shear-stable fluids is increasingly required.

Although the triaryl phosphates have low viscosity indices, they are seldom formulated with polymeric thickeners—largely because of the existence of products meeting all the widely used viscosity grades and because minor changes to system design (e.g., the incorporation of tank heating) can enable the disadvantage of their high viscosity at low temperatures to be overcome. Polymeric thickeners can also be hydrolytically unstable and some types are removed from solution when the fluid is treated by an adsorbent solid. Therefore, except when it is necessary to operate in very cold conditions, phosphate esters do not contain viscosity index improvers and, as a result, retain their viscosity stability over long periods of time at high pressures.

5.2.9 Miscellaneous Physical Properties

Specific Gravity

The specific gravity of phosphate esters also depends on chemical structure: The trialkyl phosphates exhibit values slightly less than one at ambient temperature, whereas the triaryl derivatives are some 10–15% higher. The effect of the high specific gravity of the latter, which is up to 30% greater than mineral oil, is to require more energy for fluid circulation. The dirt suspension capacity is also greater, resulting in cleaner systems but necessitating adequate sizing of the filters or more frequent changes, at least during commissioning and outages. Table 20.18 [38,39,41–44] lists typical specific-gravity data on a variety of phosphates at ambient temperatures. As many of the triaryl phosphates are complex mixtures, there is some var-

Table 20.18 Specific Gravity and Refractive Index Data on Phosphate Ester Fluids

Phosphate ester	Specific gravity at 20/20°C (ASTM D 1298)	Refractive index at 25°C (ASTM D 1218)
Trialkyl phosphates		
TBP	0.980	1.423
TiBP	0.965	1.417
TOP	0.920	1.444
TBEP	1.020	1.434
Alkylaryl phosphates		
ODPP	1.091	1.508
DBPP	1.069	
IDPP	1.070	1.510
DDPP	1.087	1.506
Triaryl phosphates		
TPP	1.767	—
CDP	1.195	1.561
TCP	1.140	1.552
TXP	1.132	1.553
IPPP/22	1.175	1.553
IPPP/32	1.153	1.552
IPPP/46	1.130	1.545
IPPP/68	1.121	1.547
IPPP/100	1.140	1.555
TBPP/22	1.180	1.556
TBPP/32	1.170	1.555
TBPP/46	1.155	1.551
TBPP/68	1.145	1.554
TBPP/100	1.135	1.555

iation in the data and average values are quoted. Figure 20.14 [35] indicates the variation of specific gravity with temperature of TXP.

Refractive Index

Refractive index can sometimes help in identifying a pure phosphate ester. It has also been used to provide an approximate value for the degree of contamination of a phosphate by a mineral oil, but to do this, the refractive index of both components must be known. Table 20.18 [38,39,41–44] lists the refractive indices at ambient of most phosphates in commercial use.

Solubility Data

The solubility of phosphate esters in water and mineral oil and vice versa is given in Table 20.19 [35]. The oil used in this study was a solvent-refined paraffinic-type product. Greater compatibility would be expected from oils containing a higher concentration of naphthenic or aromatic components.

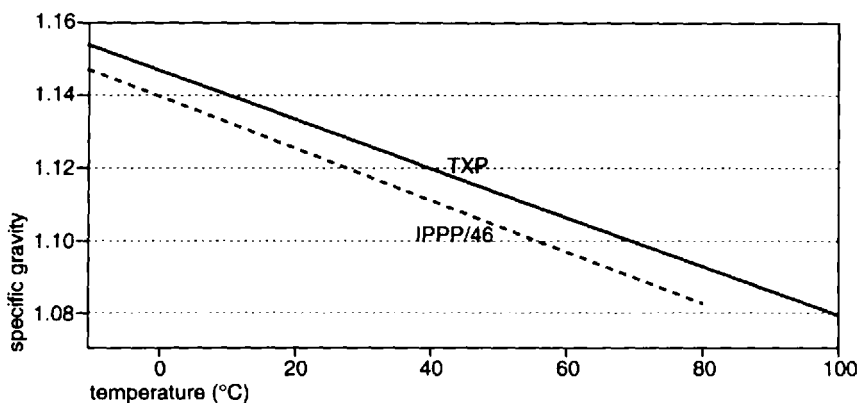


Figure 20.14 Typical specific gravity-temperature variation of TXP and IPPP/46.

5.3 Chemical Properties

5.3.1 Thermal Stability

The thermal stability of a fluid can provide an approximate guide to its upper operating temperature, but then only in terms of its ability to withstand breakdown in the absence of air or oxygen—a situation which rarely, if ever, exists in practice. In reality, the presence of a small amount of dissolved oxygen can result in degradation at lower temperatures—particularly in the presence of metals—and apparent changes in the physical/chemical properties of the fluid may be due to oxidation rather than pure thermal breakdown. Where changes in fluid vapor pressure are measured, results are influenced by the presence of volatile impurities or base-stock

Table 20.19 Solubility Data for Phosphate Esters with Mineral Oil and Water

Phosphate ester	Phosphate in water at 25°C (mg/L)	Phosphate in oil at 25°C (% v/v)	Water in phosphate at 25°C (% v/v)	Oil in phosphate at 15°C (% v/v)
TBP	280	Miscible	7	
TiBP	<1000			
TBEP	1100	7	7.3	
TOP	<1000	Miscible		
ODPP	1.9			
DBPP	96			
DDPP	0.75			
TPP	2.1		Nil (TPP is solid)	Nil (TPP is solid)
CDP	0.24			
TCP	0.36	1-2	0.2-0.3	2-4
TXP	0.11	1-2	0.2-0.3	2-4
IPPP/46	0.7	1-2	0.2-0.3	2-4
TBPP/46	2.1	1-2	0.2-0.3	2-4

components, particularly for products which are complex mixtures. Most of the tests will at best provide a ranking of different fluids rather than absolute values.

An early assessment of the thermal stability of an alkyl and an aryl phosphate was provided by Blake et al. [77] using an isoteniscope for measuring the change of vapor pressure with temperature. When a sudden change in rate occurred (or when a value of 0.014 mm Hg/s was reached), it was assumed that this was the decomposition temperature. With this technique, values of 195°C and 423°C were recorded for tri-*n*-octyl phosphate and TPP, respectively. By comparison, the decomposition temperature of a refined mineral oil was given as ~355°C. These figures compare with 485°C (for TPP) and 375–379°C for TCP reported by Raley [78], using the same technique.

More recently, Lhomme et al. [79] reported that TBP starts to decompose below its boiling point of 284°C under helium, whereas trimethyl and triethyl phosphates exhibit initial degradation at 300°C and 200°C, respectively. In contrast, TPP was very stable and only began to decompose at ~600°C and was not completely thermally degraded at 1000°C [80]!

Marino [32] reported on two studies using differential scanning calorimetry (DSC) and thermogravimetric analysis (TGA) for comparing the thermal stability of a range of phosphate esters. Table 20.20 lists these results and other data produced by these methods [44,81]. Both methods give a similar ranking of the relative sta-

Table 20.20 Thermal Stability of Phosphate Ester Fluids in an Inert Nitrogen Atmosphere

Phosphate ester	DSC initiation of decomposition (°C) (ASTM E-537)	TGA temperature required for given weight loss (°C) (ASTM D-3850)	
		5%	10%
Trialkyl phosphates			
TBP	283	169	197
TiBP	—	126	141
TOP	281	205	231
TBEP	276	157	181
Alkylaryl phosphates			
ODPP	252	226	231
DDPP	264	233	246
Triaryl phosphates			
CDP	306	236	254
TCP	333	272	306
TXP	311	276	302
IPPP/22	314	264	293
IPPP/32	311	282	307
IPPP/46	311	281	307
TBPP/22	347	274	305
TBPP/32	345	277	305
TBPP/46	338	278	306

bility of these materials. The tertiary butylated phenyl phosphates are the most stable followed by other triaryl phosphates, and, finally, by the alkyl and alkylaryl phosphates. It is to be expected that there would be no significant difference between the latter two groups: the stability of the alkyl group in the mixed alkylaryl phosphate being the weakest link in the chain. Therefore, the low TGA value for ODPP is a surprise and may be linked to product purity.

A number of studies of the pyrolysis and combustion of phosphate esters have been made, mainly to clarify if any highly toxic decomposition products were being produced. Lhomme et al. [80] examined the degradation products under helium of trimethyl, triethyl, and triphenyl phosphate and, as a result, proposed a general pyrolysis scheme (Fig. 20.15). Depending on the phosphate structure and temperature, different degradation pathways were followed. At "low" temperatures, the alkyl phosphates followed reaction (a) as a result of the cleavage of the —C—O bond and the production of olefins, monohydrogen phosphates, dihydrogen phosphates, and so forth. With increasing temperature, path (b) was followed, involving the breakage of the —P—O bond, whereas at very high temperatures, the phosphate residue forms phosphorus pentoxide (probably after passing through an intermediate phase involving the formation of polyphosphates and pyrophosphates).

With triphenyl phosphate, both reactions (a) and (b) take place simultaneously but at much higher temperatures ($>600^\circ\text{C}$).

Under oxidative conditions in excess air, the differences in stability between alkyl and aryl phosphates persist, although degradation commences at lower temperatures and appears complete (for both types) by about 900°C , based on the production of carbon dioxide (Fig. 20.16) [80].

Pyrolysis studies of IPPP/46 under a helium atmosphere have also been carried out at temperatures between 500°C and 1000°C [35]. Measurements were made of (1) the amounts of carbon monoxide and dioxide formed using nondispersive infrared analysis, (2) the organic volatiles, which were identified using gas chromatography/mass spectrometry, and (3) the amount of phosphorus pentoxide generated, which

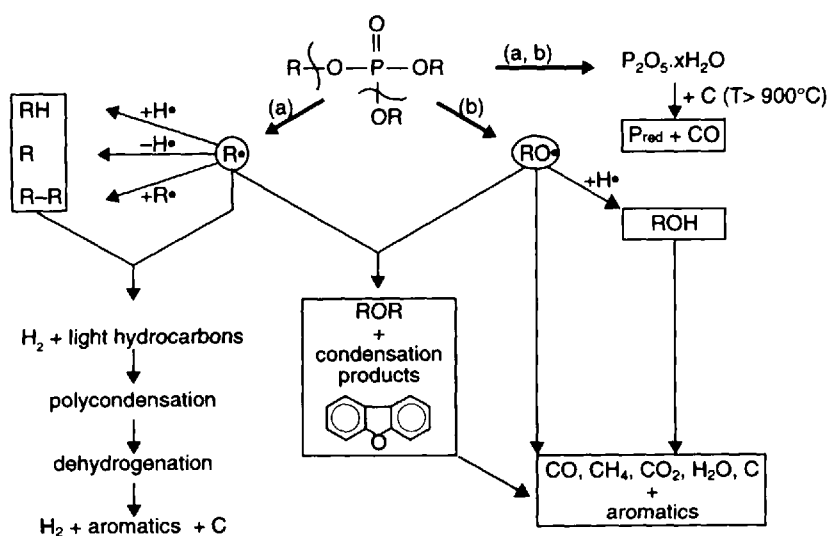


Figure 20.15 General pyrolysis scheme of phosphates.

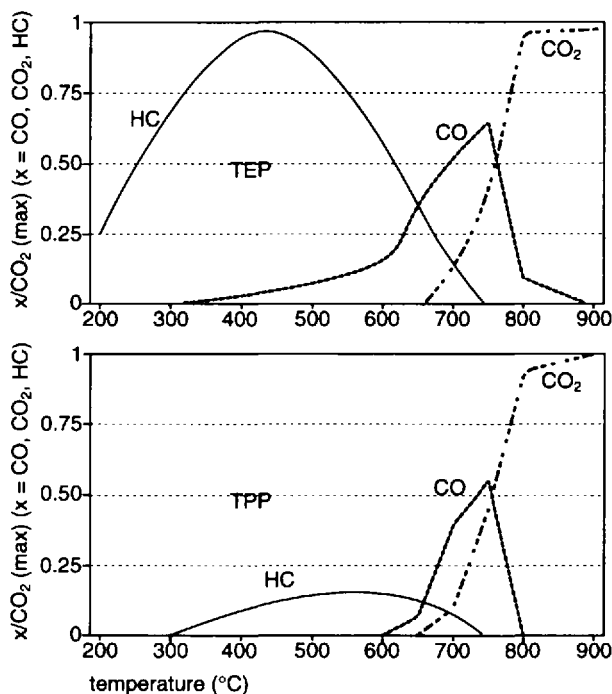


Figure 20.16 CO/CO₂ (max.), CO₂/CO₂ (max.), and hydrocarbon/CO₂ (max.) ratios as a function of temperature for triethyl phosphate (TEP) and triphenyl phosphate (TPP). (Reprinted with permission. Copyright 1984, American Chemical Society.)

was collected in aqueous potassium hydroxide and determined as orthophosphate by ion chromatography. For comparison, the same product was also examined for the production of carbon dioxide and phosphorus pentoxide under combustion conditions by passing air over the sample. Comparative results on the generation of oxides of carbon and phosphorus are given in Table 20.21; the main changes in the production of organic volatile degradation products are shown in Fig. 20.17. It can be seen that

Table 20.21 Development of Carbon Oxides and Phosphorus Pentoxide Under Pyrolysis and Combustion Conditions for an IPPP/46 Phosphate

Yield of degradation products (%)	Temperature (°C)					
	500		700		1000	
	Pyrolysis	Combustion	Pyrolysis	Combustion	Pyrolysis	Combustion
Carbon monoxide	0.63	—	0.56	0.1	1.1	11.23
Carbon dioxide	<0.001	—	<0.001	0	<0.001	49.63
Phosphorus pentoxide	<0.01	—	<0.01	0.57	<0.01	1.42

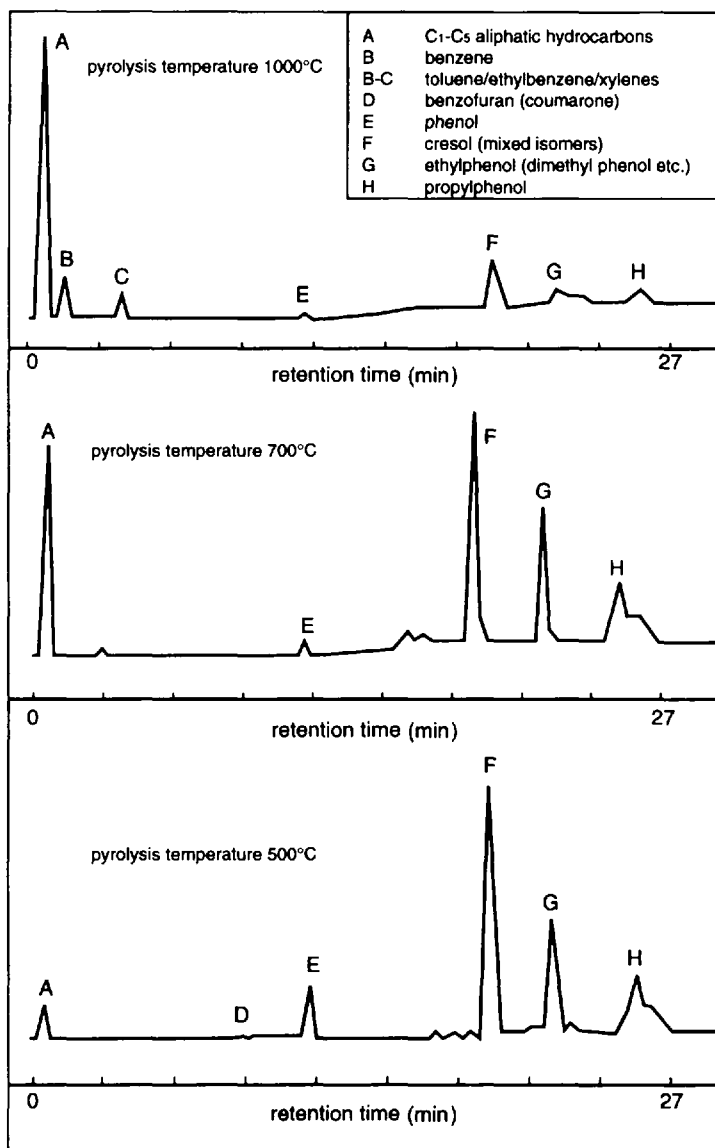


Figure 20.17 Chromatograms of pyrolysis products from IPPP/46.

virtually no degradation takes place up to 1000°C under pyrolytic conditions. Under combustion or oxidative decomposition, the product shows significant degradation at the latter temperature, but the values for phosphorus pentoxide content are lower than might be expected.

Unfortunately, neither of the above studies included an assessment of the stability of phosphates in comparison with that of other “fire-resistant” hydraulic fluids—or even with mineral oil. A highly detailed comparison of the former group was, however, made as part of an investigation into coal mine combustion products,

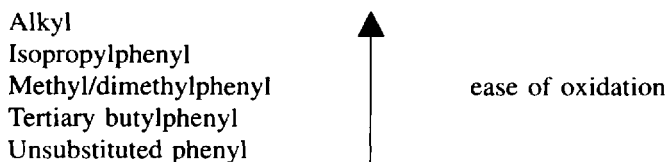
their identification and analysis by Paciorek et al. [82]. In this study, three water-glycol fluids, a water-in-oil emulsion, a synthetic organic ester fluid, and several triaryl phosphates—including a blend with mineral oil—were heated in the presence of a limited amount of air at 370°C and 420°C. This was followed by separation of all products by vacuum line fractionation and analyses of the fractions by gas chromatography/mass spectroscopy. The report concluded that at the temperatures investigated, “pure” phosphate esters “represent probably the least dangerous of all the compositions tested insofar as flammability and the overall toxicity of the degradation productions are concerned.” The authors, however, did point out that blends of phosphates and mineral oil could evolve the toxic product phosphine.

The conclusion was based on the fact that the phosphate esters showed very little decomposition under these conditions, and although phenolic species were evolved, the concentration and toxicity of these were judged to be less important than the amounts of carbon monoxide, acrolein, and so forth produced by the other fluids.

5.3.2 Oxidative Stability

Oxidation stability is an important property for fluids that are exposed to high temperatures, both from within the hydraulic system, in pumps, valves, bearings, and restrictors, and occasionally also from external heat sources (e.g., steam lines). In addition, compression of free air in the pump can cause bubble-wall temperatures to rise by several hundred degrees [83] and to exceed the thermal stability of the fluid, concurrently causing rapid oxidation. Although the temperature increase is very localized, continuous operation under these conditions can, within months, result in considerable degradation of the fluids. Such a condition is frequently the result of a combination of poor system design and high air entrainment in the fluid and confirms the need for stable products in view of the trend to smaller systems and higher operating pressures.

The initial step in the oxidation process is normally the reaction of oxygen with the alkyl groups (of alkyl phosphates) or the alkyl part of substituted aryl groups (e.g., the methyl or isopropyl groups). Where the aryl group is unsubstituted, the initial degradation arises through thermal breakdown (fission) of the P—O bond and the evidence suggests that this is also the main degradation process for the tertiary butylphenyl phosphates because of the high stability of the substituted group. The ease of oxidation of the phosphate molecule therefore varies approximately with the structure as follows:



There are many tests to evaluate and compare the oxidation stability of phosphate esters. Some of the procedures used with mineral oils [e.g., ASTM D-943 (TOST) test and the ASTM D-2272 (rotating bomb) test] are unsuitable in their existing form because they involve significant quantities of water. This causes hydrolytic breakdown to dominate over oxidative breakdown, and the test results do not necessarily reflect the ranking obtained under dry test conditions. Table 20.22

Table 20.22 Rotating Bomb Oxidation Test Results on Triaryl Phosphates; Test Method: ASTM D-2272

Phosphate ester	Time to a pressure drop of 175 kPa (25.4 psi) (min)
TXP type B (uninhibited)	600
TXP type A (inhibited)	455
TXP type A (uninhibited)	450
TBPP/46 (uninhibited)	300
TBPP/32 (uninhibited)	300
IPPP/46 (inhibited)	250

[35] shows rotating bomb oxidation stability test data on a range of phosphates with the most hydrolytically stable product exhibiting the longest test life. Furthermore, an inhibited xylyl phosphate shows no improvement over the unstabilized base.

One of the first comparisons of oxidation stability of the modern range of phosphate esters was carried out in 1979 [84] on a microoxidation tester using uninhibited fluids. Very small samples (40 μ L) were placed in a mild-steel cup and heated to temperatures of 225–270°C while a current of air was circulated over the sample. At the end of the prescribed period, the fluid was dissolved in a solvent and analyzed using gas-phase chromatography. The results are shown in Table 20.23. All of the phosphates showed good stability under these conditions, with the TBPP ester exhibiting essentially no oxidation. As expected, TBP was the least stable and little difference was seen between TCP and TXP.

A similar picture is seen in the results of DSC/TGA data (Table 20.24) [44,85] and also in DIN 51373 oxidation tests (Table 20.25) [35].

Table 20.23 Oxidative Stability of Phosphate Esters in a Microoxidation Tester; Test Conditions: Air Blown in Presence of Steel at 225°–270°C

Phosphate ester	Time (min)	Temperature (°C)	Percent of original product		
			Unoxidized	Oxidized	Evaporated
TBP	5	225	43	6	51
	10	225	19	8	73
TCP	30	225	85	1	14
	60	225	67	2	31
	30	250	57	3	40
	15	270	60	5	35
TXP	15	250	84	2	14
	30	250	65	4	31
	15	270	55	6	39
<i>r</i> -Butylphenyl-diphenyl phosphate	360	250	77	<1	22
	180	270	81	<1	15

(Reprinted with permission. Copyright, 1981, STLE, Park Ridge, Illinois.)

Table 20.24 Oxidative and Thermal Stability of Commercial Phosphate Esters by DSC (ASTM E-537) and TGA (ASTM D-3850)

Phosphate ester	DSC onset of oxidation (°C) (ASTM E-537)	TGA temperature required for given weight loss in oxygen (°C) (ASTM D-3850)		
		1 wt%	5 wt%	10 wt%
TBP	175	76	113	127
TiBP	192	84	116	130
TBEP	155	61	169	187
TOP	160	122	189	203
TPP	*	188	236	252
CDP	265	198	230	246
TCP	215	184	255	278
TXP	210	224	268	286
IPPP/22	215	200	239	263
IPPP/32	215	201	252	272
IPPP/46	210	202	265	287
IPPP/68	210	218	265	288
IPPP/100	180	224	243	258
TBPP/22	295	213	262	280
TBPP/32	295	222	268	286
TBPP/46	300	227	272	292
TBPP/68	300	230	275	293
TBPP/100	305	234	277	295
ISO VG 22 mineral oil	167	155	205	225

*Does not oxidize under these conditions.

The effect of the position of the substituent on the aryl ring was shown, with respect to isopropylphenyl phosphates, in Table 20.1. The advantages of the ortho isomer from the point of view of stability are, of course, offset by its poor viscosity index. Because commercial products contain a mixture of different isomeric products, the resultant behavior of the finished product will depend on the proportion of each isomer present.

Table 20.25 Comparison of the Oxidation Stability of Different Types of Uninhibited ISO VG 46 Triaryl Phosphate Esters; Test Method: DIN 51373—Air Blown at 120°C for 164 h in the Presence of Metals

Phosphate ester	Viscosity change at 40°C (%)	Total acidity increase (mg KOH/g)	Metal weight changes (mg)	
			Copper	Iron
TBPP/46	-0.6	+0.01	+0.1	+0.2
TXP	+3.0	+0.47	+0.2	+0.2
IPPP/46	+46.5	+8.45	-0.3	0

The isopropylphenyl phosphates and TCP/TXP are also very responsive to the addition of stabilizers, which can improve performance and significantly extend life. In contrast, the tertiary butylphenyl phosphates are not as responsive to classical antioxidants but have such good oxidation stability that this is rarely a disadvantage. A comparison of the high-temperature stability of uninhibited TBPP/32 and TBPP/46 products in comparison with various formulated conventional and highly refined mineral gas turbine oils is given in Table 20.26 [86].

Although the mineral oil products show substantial increases in viscosity and acidity as the test duration increases, there is no significant change in the viscosity of the TBPP products and only moderate increases in acidity.

One additional aspect of oxidation stability that is of concern in some applications is the deposit-forming tendency at high temperatures. This property, also known as "coking," occurs when a thin film of fluid is heated on a metal surface while exposed to air. Depending on the stability of the product, the deposit can vary from soft and carbonaceous, to a hard, brittle layer, to a lacquer. The formation of such deposits can occur on heater and valve surfaces and can reduce component efficiency. In situ conditioning, however, has been shown to control the deposit formation [87].

Table 20.27 [35] shows the variation in coking tendencies for a range of triaryl phosphates and commercial mineral gas turbine oils.

It was mentioned earlier in Section 5.1.1 that the flammability characteristics were more likely to correlate with oxidation stability than other physical properties. An examination of the ranking of ease of oxidation in this section will be seen to broadly correlate with the fire-resistance data.

5.3.3 Hydrolytic Stability

In the presence of small amounts of water, phosphate esters tend to hydrolyze [i.e., break down into their constituent acids and alcohols (or phenols)]. It is the most common form of degradation of phosphates and the one which frequently dictates their service life.

The hydrolysis reaction is not rapid at ambient temperatures but accelerates with increasing temperatures and is catalyzed by the presence of strong acids. As these are normally produced by phosphate hydrolysis, the reaction is said to be autocatalytic. Strong bases can also catalyze the reaction.

The hydrolysis of triaryl phosphates (e.g., triphenyl phosphate) takes place in steps, as indicated in Fig. 20.18. The replacement of successive aryl groups with —OH becomes increasingly difficult and the last step is not normally achieved without using very severe conditions, such as boiling with dilute acid. In view of the relatively low acidities found with these products in practice, it is extremely unlikely that under most service conditions, phosphoric acid would be generated.

The reaction scheme shown in Fig. 20.18 shows the strong acids ($\text{pH} < 7$)—also known collectively as partial phosphates—which are produced. Although these are of greatest importance in view of their reactivity, weak acids ($\text{pH} > 7$) are also formed in this process. These are phenols or alcohols, and although they are not normally thought to have a major effect on the performance of the fluid, there is some evidence to suggest they may adversely affect foaming when present in significant quantities.

Table 20.26 High-Temperature Oxidation Tests on Tertiary Butylphenyl Phosphates and Commercial Industrial Gas Turbine Lubricants; Test Method: Federal Test Method Standard VV-L-791C, Method 5308.6 at 175°C

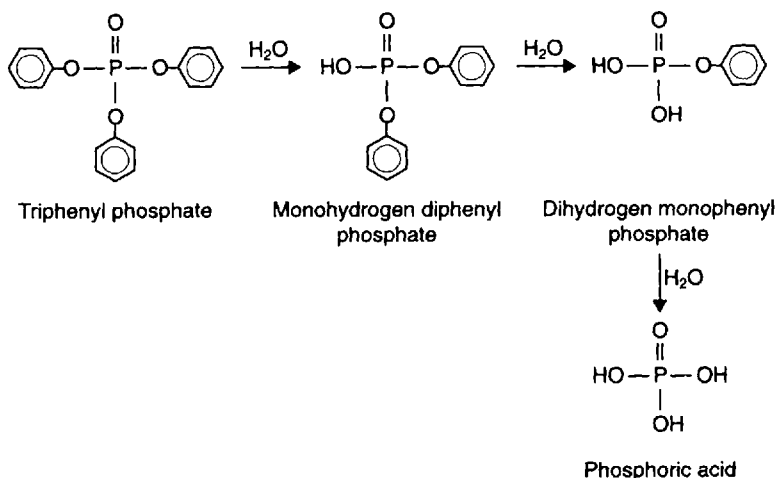
Phosphate fluid	Test duration (day)	Viscosity increase (%)	Acidity increase (mg KOH/g)	Metal weight changes (mg/cm ²)				
				Fe	Cu	Cd/Fe	Al	Mg
TBPP/32	3	3	0.11	-0.11	-0.17	-0.03	-0.07	-0.03
	6	4.4	0.37	0.02	0.04	0.02	Nil	0.02
	9	3.8	0.85	-0.01	0.1	0.03	Nil	-0.02
TBPP/46	3	6	0.27	-0.01	0.03	-0.01	-0.11	-0.02
	6	6.4	0.23	0.11	0.29	0.17	0.08	0.13
	9	7.3	1	-0.04	-0.02	0.18	-0.11	0.07
Gas turbine oil A (ISO VG 32)	3	3.6	0.44	Nil	0.02	-0.04	Nil	0.01
	6	4.2	0.8	0.03	0.04	0.02	Nil	0.03
	9	25	5.3	0.14	0.01	-0.15	0.09	0.06
Gas turbine oil B (ISO VG 46)	3	18.3	2.2	0.03	0.08	-0.1	0.05	0.06
	6	24.3	3.1	0.21	0.13	0.07	0.02	0.07
	9	49.5	5	0.56	0.04	0.97	0.32	0.33
Gas turbine oil C (ISO VG 46)	3	23.4	3	0.02	-0.03	0.05	0.03	0.02
	6	28.6	4.5	0.04	-0.1	-0.05	0.03	0.01
	9	80.6	7	0.18	-0.47	-11.7	0.05	0.04
Gas turbine oil D (ISO VG 46)	3	13.4	2	0.06	0.02	-0.04	Nil	0.01
	6	21.2	5.1	0.24	-0.13	0.02	0.52	0.35
Turbine industry limits	3	-5 to +15	2.5 max.	—	—	—	—	—
ASTM D-4293 limits	3	-5 to +15	3.0 max.	—	—	—	—	—

Table 20.27 Coking Tendency Data for Triaryl Phosphates; Test Method: Federal Test Method Standard VV-L-791C, Method 3462

Phosphate ester	Deposit formation (mg) at		
	300°C	316°C	325°C
TXP (uninhibited)	460	1820	1750
TXP (inhibited)	43	1006	1420
TBPP/32 (uninhibited)	3	16	6
TBPP/46 (uninhibited)	3	4	2
IPPP/46 (inhibited)		4	
Mineral gas turbine lubricants			
ISO VG 32	25	170	130
ISO VG 46	49	185	227

The presence of strong acids can have different effects on other aspects of fluid and system performance. Some of these are beneficial, whereas others can cause operational problems. The acids may, for example, inhibit the corrosion of ferrous metal surfaces but promote corrosion of nonferrous components; they may adversely affect the electrical properties of the fluid but assist in reducing wear. In general, the uncontrolled generation of acidic products is harmful to the life and performance of the fluid, and in certain critical applications such as the power generation industry, it is customary to remove them as they are produced by circulating the fluid through an adsorbent solid.

Because of the importance of hydrolytic stability in determining both fluid and system performance, a number of studies of the stability of phosphate esters in the presence of water have been carried out [10,32,88,89]. Hydrolytic stability tests are not the most precise, because they normally require an excess of water present to accelerate the degradation and the degree of contact between the two fluids, which

**Figure 20.18** The Hydrolysis of Triphenyl Phosphate.

determines the rate of hydrolysis, is difficult to control. A test in which the two fluids are stirred together will normally result in the generation of more acidity than one in which the two layers are not in motion. Another important variable is the initial acidity of the fluid; if this is not the same as that of other fluids being tested (within the precision of the test), then a comparison can be meaningless. Consequently, it is sometimes difficult to compare data from different sources.

The available data indicates that hydrolytic stability is very structure dependent. Triaryl phosphates are generally more stable than trialkyl phosphates, whereas increasing the length of the alkyl chain (whether or not attached to an aromatic ring) and increased branching on the alkyl chain also results in increased stability (Table 20.28) [68].

In comparing the different types of unstabilized triaryl phosphates (Table 20.29) [32], it is apparent that TXP is, by far, the most resistant to hydrolysis and this is also seen in data on formulated fluids (Table 20.30) [32]. The inferior stability of the IPPP and TBPP-based fluids is mainly due to the presence of triphenyl phosphate (see Table 20.2), which is unstable in the presence of moisture (see Table 20.31).

In addition to the effects of the different substituents on the aryl ring, the position of these substituents (or the isomer distribution) also impacts on the stability of the fluid. Table 20.31 [35] shows the effect of hydrolysis on various pure cresyl and xylyl phosphate isomers. In this test, the fluid (5 g) was maintained at 90°C for 2 weeks in the presence of 5 mL of water, after which the total increase in acidity generated was determined. As can be seen, the xylyl phosphates are generally significantly more stable than the cresyl derivatives with the exception of the *p*-cresyl phosphate isomer. Single-point determinations, however, do not necessarily reveal the whole picture and additional data would ideally be required to confirm the stability ranking.

The sensitivity of phosphates to moisture has in the past limited their use, as it significantly reduced their service life and increased the cost of using this type of fluid. In the power-generation industry, an "on-line" purification technique has been used for some years to remove acid as it is formed, thereby prolonging fluid life. However, by selecting a particular xylenol isomer distribution, products with superior hydrolytic stability can be produced [90]. Figure 20.19 [35] shows, for example, the hydrolytic stability of two synthetic phosphates, TBPP/46 and IPPP/46, in comparison with two xylyl phosphates, including one fluid, which has been specifically developed with improved stability.

Fluids based on such feedstocks have now been used successfully for extended periods as main bearing lubricants in steam turbines without the need for in situ purification.

5.3.4 Radiation Stability

Lubricants in nuclear applications must be able to withstand radiation without significant deterioration and be nonreactive toward reactor materials of construction. Past studies of resistance to radiation for both alkyl and aryl phosphates indicated that they were not very stable in such an environment [91–93] and degrade to form significant amounts of acid.

Recently, as a result of an interest in the use of triarylphosphates as reactor coolant pump lubricants, further studies were carried out in which the fluids were subjected to a gamma radiation dose of 0.6 Mrad. This level is thought to be rep-

Table 20.28 Hydrolytic Stability of Selected Phosphate Esters; Test Conditions: 24-Hour Reflux Period with Water

Phosphate ester	mL 1N. NaOH/mol
TBP	4.
TOP	0.2
TCP	1.2
<i>n</i> -Butyl diphenyl	27.8
<i>t</i> -Butyl diphenyl	7.3
<i>n</i> -Octyl diphenyl	14.6
6-Methylheptyl diphenyl	7.6
ODPP	3.6
<i>n</i> -Octyl dicresyl	4.4
2-Ethylhexyl dicresyl	1.7

(Reprinted with permission. Copyright 1954. American Chemical Society.)

representative of about 18 months' operation—the minimum acceptable life—during which time no fluid maintenance would be possible because of its location in the reactor. After this length of operation, the radiation level of the fluid should still be low enough not to require disposal as special waste. Table 20.32 shows the fluid properties before and after radiation for three uninhibited triaryl phosphate esters and one containing a stabilizer package. As can be seen, the main effect is on hydrolytic stability. Oxidation stability and physical properties are not significantly changed. The stability of the TXP sample is thought adequate for service operation.

5.3.5 Rusting and Corrosion

The rusting (of ferrous metals) and corrosion (of nonferrous components) can both take place in hydraulic systems. The former phenomenon is possible in either the liquid or vapor phase, whereas the latter normally occurs only in the liquid phase.

Table 20.29 Hydrolytic Stability of Unstabilized Phosphate Esters; Test Method: ASTM D-2619

Phosphate ester	Increase in fluid acidity (mg KOH/g)	Increase in water acidity (mg KOH)	Copper weight loss (mg/cm ²)
TCP	0.10	9.1	0.3
TXP	Nil	Nil	0.03
IPPP/46	0.01	3.63	0.15
TBPP/46	0.05	6.17	0.18
TBPP/68	0.09	8.98	0.34
TBPP/100	0.2	11.2	0.45
Standard criteria	0.2 max.	5 max.	0.3 max.

Table 20.30 Hydrolytic Stability of Formulated Phosphate Ester Hydraulic Fluids; Test Method: ASTM D-2619

Phosphate ester	Increase in fluid acidity (mg KOH/g)	Increase in water acidity (mg KOH)	Copper weight loss (mg/cm ²)
TXP	0.02	Nil	-0.008
IPPP/46	0.05	0.4	0.05
TBPP.46	0.03	2.7	0.05
Standard criteria	0.2	5	0.3

With nonaqueous fluids like phosphate esters, rusting occurs if free water is present. Water has a much higher solubility in phosphate esters than in mineral oil, with the result that levels up to ~0.25% at ambient temperatures or ~0.5% at temperatures of 50–60°C can be tolerated before rusting commences. If the temperature of the fluid cycles up and down, then it could be possible for free water to separate out at the lower temperature. Therefore, it is important to monitor the water content and check that it remains below the solubility level at the lowest temperature likely to be experienced (unless inhibitors are incorporated). High water levels, of course, reflect mechanical problems in the system and require investigation as soon as possible.

Phosphate esters are also strongly polar and form an adsorbent layer on the metal surface, which helps reduce contact with water. As a result of these properties, phosphate fluids seldom require the use of rust inhibitors, and systems containing them can be made from mild steel. As rust inhibitors can also interfere with the foaming and surface-active properties of the fluid, they should not be used unless the fluid is likely to operate very wet. Rusting can occur above the liquid layer in the tank if condensation is a regular feature and if fluid has not wetted the surface. This can be easily overcome by ensuring a flow of dry air through the tank. This

Table 20.31 Hydrolytic Stability of Different Cresyl and Xylyl Phosphate Isomers; Test Conditions: 90°C for 2 Weeks with 5 g Each of Fluid and Water

Phosphate isomer	Melting point (°C)	Total acid value increase (mg KOH/g)
Tri- <i>o</i> -cresyl	Liquid	27.2
Tri- <i>m</i> -cresyl	Liquid	34.8
Tri- <i>p</i> -cresyl	78	0.21
Tri-2,3-xylyl	60–61	0.13
Tri-2,4-xylyl	Liquid	0.74
Tri-2,5-xylyl	79–80	0.18
Tri-3,4-xylyl	71–72	0.11
Tri-3,5-xylyl	43–45	0.33
Triphenyl	49	171.3

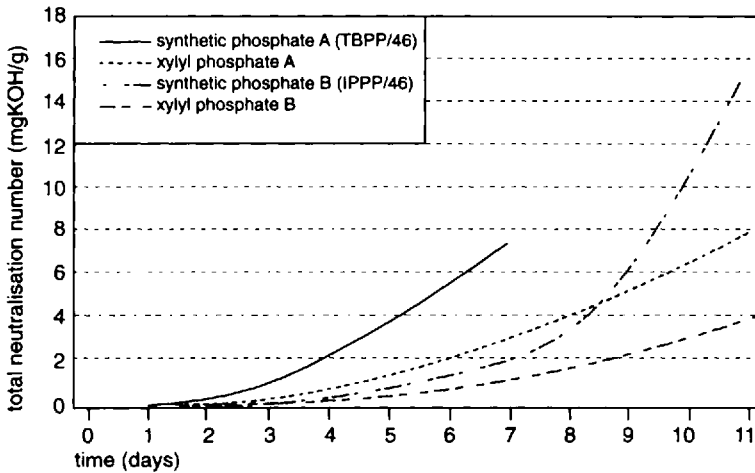


Figure 20.19 Hydrolytic stability of different phosphate esters under extended test method: ASTM D-2619.

technique can also be used to remove water from the bulk fluid should the content increase as a result, for example, of cooler leaks. If gross contamination of phosphates leads to a layer of free water on the top of the phosphate ester, it is relatively simple to remove this water by siphoning or skimming. Unlike other fluids, free water tends not to collect in other parts of the system because of the greater density of the phosphates.

The corrosion of ferrous metals is not normally a concern with phosphates and when fluid acidities are kept low (preferably <0.5 mg KOH/g), the corrosion of nonferrous metals, particularly copper, zinc, lead, and their alloys is minimized. Table 20.33 [35] indicates the performance of an IPPP/46 fluid against the corrosion requirements of the 7th Luxembourg Report and no significant weight changes are seen on any of the metals. Where the stress on the fluid is likely to lead to significant degradation, phosphate esters are generally used with either continuous or intermittent on-line conditioning involving passing the fluid through an adsorbent solid, which removes the acid.

6 COMPATIBILITY

There are several different aspects of phosphate ester compatibility which need to be considered:

- With system constructional materials, both metallic and nonmetallic
- With mineral oil, in case of contamination
- With preservative fluids used during system assembly and storage
- Between different phosphate types in the event of topping-up a “synthetic” fluid with a “natural” or vice versa
- Between phosphate esters and other types of hydraulic fluids in the event that one fluid replaces the other in the system or is used inadvertently as top-up

Table 20.32 Effect of Gamma Irradiation on Different Triaryl Phosphates

Physical property	TXP (uninhibited)	TXP (inhibited)	TBPP/46	IPPP/46
Preirradiation				
Neutralization No. (mg KOH/g)	0.03	0.03	0.01	0.01
Viscosity at 40°C (cSt)	49.68	53.58	42.01	44.56
Foam sequence 1 at 24°C (mL)	150-0	190-0	0-0	430-10
Air release (min)	2.0	7.0	9.0	3.0
Flash point (°C)	250	250	253	238
Fire point (°C)	344	352	340	328
DIN 51373—oxidation stability				
Cu weight change (mg)	-0.1	0.0	+0.1	-0.2
Fe weight change (mg)	0.0	0.0	-0.1	+0.2
Fluid final neutralization No. (mg KOH/g)	0.55	0.11	0.02	2.64
Volatiles neutralization No. (mg KOH/g)	0.07	Nil	0.03	0.90
Total neutralization No. change (mg KOH/g)	0.59	0.08	0.04	3.53
ASTM D-2619—hydrolytic stability				
Cu weight change (mg/cm ²)	Nil	Nil	-0.008	-0.27
Fluid final neutralization No. (mg KOH/g)	0.08	0.06	0.09	0.05
Neutralization No. change (mg KOH/g)	0.05	0.03	0.08	0.04
Acid content (mg KOH)	3.44	2.89	5.62	7.29
Postirradiation				
Neutralization No. (mg KOH/g)	0.19	0.17	0.15	0.13
Viscosity at 40°C (cSt)	51.31	53.52	41.86	45.08
Foam sequence 1 at 24°C (mL)	170-0	210-0	0-0	540-530
Air release (min)	2.0	4.5	6.0	7.5
Flash point (°C)	252	254	246	232
Fire point (°C)	350	356	338	328
DIN 51373—oxidation stability				
Cu weight change (mg)	-0.4	-0.3	+0.1	-0.8
Fe weight change (mg)	0.0	+0.5	0.0	+0.3
Fluid final neutralization No. (mg KOH/g)	0.92	0.23	0.18	1.76
Volatiles neutralization No. (mg KOH/g)	0.14	Nil	Nil	0.58
Total neutralization No. change (mg KOH/g)	0.87	0.06	0.03	2.21
ASTM D-2619—hydrolytic stability				
Cu weight change (mg/cm ²)	-0.015	-0.105	-0.285	-0.89
Fluid final neutralization No. (mg KOH/g)	0.39	0.32	1.76	0.36
Neutralization No. change (mg KOH/g)	0.20	0.15	1.61	0.23
Acid content (mg/KOH)	7.23	6.29	43.85	18.59

Phosphate esters are compatible with all common constructional metals, but they do not “wet” the surface of aluminum. Therefore, the bearing manufacturers should be consulted prior to the use of aluminum alloys as plain bearing materials. When used for other purposes in equipment, the aluminum surface should be hard-anodized. Phosphate esters can be used on conjunction with copper and its alloys provided that the acidity levels in service do not exceed those recommended by the equipment manufacturers.

Table 20.33 Determination of the Corrosivity of an IPPP/46 Fluid; Test Method: 7th Luxembourg Report, Section 5.9.1

Test no.	Test metal(s)	Metal weight change (mg)	Metal appearance		Test fluid appearance
			In fluid	In air	
1	Steel	+0.5	Very slight tarnish	No change	No deposits or color change
2	Copper	+0.1	No change	No change	No deposits or color change
3	Zinc	+0.1	No change	No change	No deposits or color change
4	Aluminum	+0.1	No change	No change	No deposits or color change
5	Cadmium	+0.1	No change	No change	No deposits or color change
6	Brass	+0.2	Slight tarnish	No change	No deposits or color change
7	Steel	+0.3	No change	No change	No deposits or color change
	Cadmium	+0.2	No change	No change	No deposits or color change
8	Copper	Nil	No change	No change	No deposits or color change
	Zinc	+0.2	No change	No change	No deposits or color change
9	Aluminum	+0.1	No change	No change	No deposits or color change
	Zinc	+0.4	No change	No change	No deposits or color change
10	Steel	+0.2	Very slight tarnish	No change	No deposits or color change
	Aluminum	+0.2	Very slight tarnish	No change	No deposits or color change

Note: Test conditions: (a) 250 cm³ of test fluid with 60 mm of test specimen(s) immersed in fluid; (b) temperature 35°C; (c) duration 28 days.

Bearing materials suitable for use with phosphates include white metal and copper/lead linings.

The compatibility of phosphate esters with different types of paints, packings, seals, hoses, and filtration media is given in Table 20.34 [32,94,95]. Such a table can only provide general guidance. There are, for example, a variety of different types of fluorocarbon rubber that do not all perform equally in compatibility tests and the manufacturer should be contacted for more specific recommendations.

Mineral oil has variable solubility in phosphate esters, depending on the temperature, type of oil (i.e., whether paraffinic, naphthenic or aromatic), and on the type of phosphate. Unsurprisingly, paraffinic oils have a greater solubility in trialkyl phosphate and naphthenic or aromatic hydrocarbons in triaryl phosphates. Whereas the major problem of oil contamination is a loss of fire resistance, the fluid surface-active properties can also be adversely affected. Mineral oil is difficult to remove from phosphates, and contamination may require replacement of the fluid charge.

Mineral-oil-based preservatives, which are used to prevent rust on system components during storage, can promote foaming and increase air entrainment if allowed to contaminate phosphates. If these are used, it will be advantageous to flush through a new system before filling with the operating charge. A phosphate-ester-based preservative could be advantageous if suitable facilities for storage are available at the equipment builder.

Different types of phosphate esters from different sources can normally be mixed. Indeed, mixtures of synthetic and natural triaryl phosphate fluids are in wide commercial use, as well as mixtures of trialkyl and triaryl phosphates. If there is any doubt, advice should be sought from the fluid or equipment supplier.

Table 20.34 Phosphate Ester Compatibility with Standard Constructional Materials

Material	Triaryl phosphate ester	Trialkyl phosphate ester	Alkylaryl phosphate ester
Elastomers			
Butadiene acrylonitrile (BUNA N or nitrile)	Unsatisfactory	Unsatisfactory	Unsatisfactory
Chlorosulfonated polyethylene	Unsatisfactory	Unsatisfactory	Unsatisfactory
Ethylene propylene (EPR, EPDM)	Recommended	Recommended	Recommended
Epichlorohydrin	Unsatisfactory	Unsatisfactory	Unsatisfactory
Fluorinated hydrocarbon	Recommended	Unsatisfactory	Unsatisfactory
Isobutylene isoprene (butyl rubber)	Recommended	Recommended	Recommended
Isoprene	Unsatisfactory	Unsatisfactory	Unsatisfactory
Polyacrylate	Unsatisfactory	Unsatisfactory	Unsatisfactory
Polyamide (Nylon)	Recommended	Recommended	Recommended
Polyisochloroprene (Neoprene)	Unsatisfactory	Unsatisfactory	Unsatisfactory
Polyurethane	Unsatisfactory	Unsatisfactory	Unsatisfactory
Silicone rubber	Acceptable	Acceptable	Acceptable
Styrene butadiene (BUNA S)	Unsatisfactory	Unsatisfactory	Unsatisfactory
Plastics			
ABS	Unsatisfactory	Unsatisfactory	Unsatisfactory
Acrylic	Unsatisfactory	Unsatisfactory	Unsatisfactory
Polyamide	Recommended	Recommended	Recommended
Polycarbonate	Acceptable	Acceptable	Acceptable
Polyester	Acceptable	Acceptable	Acceptable
Polyethylene	Acceptable	Acceptable	Acceptable
Polypropylene	Acceptable	Acceptable	Acceptable
Polystyrene	Unsatisfactory	Unsatisfactory	Unsatisfactory
Polysulfone	Unsatisfactory	Unsatisfactory	Unsatisfactory
Polyvinyl chloride (PVC)	Unsatisfactory	Unsatisfactory	Unsatisfactory
Polytetrafluoroethylene (PTFE [®])	Recommended	Recommended	Recommended
Paints and finishes			
Acrylic	Unsatisfactory	Unsatisfactory	Unsatisfactory
Alkyd resin (stoved)	Acceptable	Acceptable	Acceptable
Epoxy resin	Recommended	Recommended	Recommended
Latex	Unsatisfactory	Unsatisfactory	Unsatisfactory
Phenolic resins	Unsatisfactory	Unsatisfactory	Unsatisfactory
Polyurethane paint	Acceptable	Acceptable	Acceptable
Metals			
Aluminum	Acceptable	Acceptable	Acceptable
Brass	Acceptable	Acceptable	Acceptable
Bronze	Acceptable	Acceptable	Acceptable
Cadmium	Acceptable	Acceptable	Acceptable
Cast iron	Recommended	Recommended	Recommended
Copper	Acceptable	Acceptable	Acceptable
Magnesium	Acceptable	Acceptable	Acceptable

(Table continues)

Table 20.34 Continued

Material	Triaryl phosphate ester	Trialkyl phosphate ester	Alkylaryl phosphate ester
Nickel	Recommended	Recommended	Recommended
Steel (all grades)	Recommended	Recommended	Recommended
Silver	Recommended	Recommended	Recommended
Titanium	Recommended	Recommended	Recommended
Zinc	Acceptable	Acceptable	Acceptable
Filter media			
Activated clays, (e.g., fuller's earth)	Acceptable	Acceptable	Acceptable
Activated alumina	Acceptable	Acceptable	Acceptable
Activated carbon	Acceptable	Acceptable	Acceptable
Cellulose	Acceptable	Acceptable	Acceptable
Ion-exchange resins	Recommended	Recommended	Recommended

Note: Materials indicated as acceptable may be used under certain conditions and the manufacturer or fluid supplier should be consulted prior to use.

If a new phosphate fluid charge is to replace one which has been significantly degraded, then it is normally advisable to flush the system before filling with the new operating charge. This need not be carried out using the same quality of fluid required for normal use, but the flushing fluid should be clean, dry, and of relatively low acidity (a value of 0.15 mg KOH/g maximum is regarded as acceptable). Fluid suppliers should be consulted for the availability of a suitable product. Details of appropriate flushing procedures can be found in fluid suppliers' or manufacturers' literature [94,95] or in national/international use guides (Appendix 1).

With regard to the compatibility of phosphates with other hydraulic fluid types, the following general rules apply when topping-up a system or changing from one fluid to another:

- Phosphate esters should never be added to systems containing mineral oil or water-containing fluids, and vice versa. Quite apart from the immiscibility of the two fluids, it is probable that, in the former case, the phosphate will be incompatible with the seals, paints, and gaskets used in the system.
- Although phosphate esters have greater compatibility with carboxylate (polyol) esters, no addition of phosphate should be made without consulting the equipment manufacturer because of possible incompatibility with seals, paints, and so on. Adding carboxylates to phosphate fluids is unlikely to be a problem from the seal compatibility aspect, but it will reduce fire resistance and probably both oxidative and hydrolytic stability.
- When changing from one fluid type to another, particularly from aqueous to nonaqueous or vice versa, certain system modifications may be necessary and prior discussions with the equipment builders are essential.

After modification, a system flush is necessary and recommendations on suitable procedures are available in relevant national/international use guides [e.g., ISO 7745 (Appendix 1)] or in fluid manufacturers' literature [94,95].

7 HEALTH, SAFETY AND ENVIRONMENTAL BEHAVIOR

7.1 Toxicity

The toxicity profile of the commercially available phosphate esters used in hydraulic fluids is essentially benign. However, some differences in behavior between fluids do exist and these are outlined below.

Despite the positive picture available from the existing data, misconceptions regarding the health and environmental hazards of phosphate esters persist. Some of the concern is due to confusion over nomenclature as the description “phosphate esters,” in addition to generically describing the products used as hydraulic fluids and so forth, is also used (often incorrectly) in connection with pesticides, insecticides, and so on. The similarity between the terms “phosphate esters” and “phosgene” (the nerve gas) has also led to completely incorrect conclusions. It must be emphasized, therefore, that the phosphate esters used in lubricant applications are not biologically active materials. However, many years ago, TCP was responsible for causing neurotoxicity when ingested [96]. This problem arose as a result of the presence of a specific isomer, tri-*ortho*-cresyl phosphate (TOCP). Subsequent investigations of other “natural” phosphates indicated a similar but less severe behavior, and for a period, it was assumed that other phosphate isomers were also highly neurotoxic. What was not appreciated at the time, because of the lack of sophistication of the analytical techniques then available, was that these other products also contained TOCP or other isomers based on *ortho*-cresol as contaminants. It was predominantly these *ortho*-substituted components that were causing the development of neurotoxic symptoms.

Structure–activity studies for neurotoxicity have since been completed on over 70 substituted triaryl phosphates [97]. Based on these studies, it has been found that the primary structural requirement for neurotoxicity is a substituent in the *ortho* position on the phenyl ring with at least one hydrogen on the alpha carbon atom, and the neurotoxicity increases with the number of hydrogen atoms on the *ortho* substituent. As a result, industry has since taken considerable care to reduce or eliminate *o*-cresol from commercially available feedstocks. Today, TCP is derived from a feedstock with extremely low levels, whereas the synthetic triaryl phosphates are based on phenol obtained from petrochemical sources, which ensures they have a very low neurotoxic potential [98]—significantly below levels which would require labeling the materials as hazardous.

In order to assess toxicity and ecotoxicity behavior, it is, of course, necessary to have an agreed set of test methods and limits for determining acceptable performance. Unfortunately there is still no complete international agreement in the area and national requirements can differ. In Europe, however, a set of toxicity requirements are laid down in the Luxembourg Report [48], which details methods for the testing of acute toxicity in terms of the following:

- Acute oral toxicity (LD₅₀)
- Skin and eye irritation
- Toxicity of hot and cold aerosols
- Toxicity of thermal decomposition products
- Neurotoxicity (for phosphate esters)

For a product to meet the requirements, it must not only pass each individual test but also meet a maximum points rating based on its behavior in each test. Triaryl

phosphates readily meet these requirements. However, although trialkyl phosphates have not been fully evaluated, some products are known to be skin irritants.

In addition, European legislation on product labeling (Directive 93/21/EEC) [99] requires that its toxicity be assessed and the product labeled accordingly. Included in the acute tests accepted for classification purposes are the following:

- Acute oral toxicity (LD_{50})
- Skin and eye irritation
- Skin sensitization
- Mutagenicity data (Ames test)

Most of the data on triaryl phosphates given in Table 20.35 [100] have been obtained against the requirements of the Luxembourg Report. Data on the alkyl and alkylaryl products may have been produced under dissimilar test conditions and, therefore, not be strictly comparable [101–106].

It should also not be assumed that the highest LD_{50} data automatically equate with the lowest acute toxicity. In order to reduce animal tests, products, today, are evaluated at much lower dose levels than in the past. A product with a test pass at a single-dose level of 2 g/kg is now accepted as having a very low acute toxicity.

In general, the results tabulated on acute toxicity are low. The skin irritant behavior of TBP and TiBP, however, requires additional care in their handling and use. As a result, TBP and TiBP currently require a hazard warning label (based on their toxicological properties) under EU guidelines.

7.2 Ecotoxicity

The 7th Luxembourg Report also *recommends* procedures for assessing the environmental behavior of hydraulic fluids. As a minimum, it advises the production of acute fish toxicity and information on biodegradability. Methods for assessing acute daphnia toxicity, bacterial toxicity, and bioaccumulation are also indicated for possible use by competent authorities when determining their specific requirements.

Included in the recommendations is the determination of the Water Hazard Classification. This rating scheme originated from the chemical industry in Germany (where it is known as the Wassergefährdungsklasse or WGK [107]) and uses acute toxicity and ecotoxicity data to rank products in terms of their pollution potential. The categories range from 0 (no pollution potential) to 3 (severe pollution potential) and most phosphates fall into category 1 (slight potential) and are, therefore, similar to or better than mineral oil in this respect (category 1–2).

In Europe, under Directive 93/21/EEC [99], the environmental behavior of chemicals has to be assessed for labeling purposes. This takes into consideration biodegradability data on the fluid together with acute fish and daphnia or algal toxicity.

The ecotoxicity data on phosphate esters are given in Table 20.36 [103–106,108,109]. Where adequate data exist, none of the products appears to have a serious pollution potential. It should be noted that testing of products, like some of the phosphates which have a very low solubility in water, can give misleading results. Dispersants used to “solubilize” the fluids in water can, themselves, influence the data—hence, the variation in fish toxicity data on IPPP/46. It has now also been found that the Daphnia toxicity tests for insoluble products produce anomalous re-

Table 20.35 Toxicity Behavior of Phosphate Esters

Property	Fluid								
	TBP	TiBP	TBEP	TOP	ODPP	DDPP	TXP	IPP/46	TBPP/46
Acute toxicity LD ₅₀ (g/kg)	1.2	>5	>3	>5	>15	>15	>30	>20	>30
Irritancy effects									
Skin	Irritant	Irritant	None	Irritant	Slight	Moderate	None	None	None
Eye	None	None	None	None	Slight	Slight	None	None	None
Exposure to hot and cold aerosols	—	—	—	No effect	—	Moderate	No effect	No effect	No effect
Toxicity of thermal decomposition products	—	—	—	—	—	—	Moderate– reversible	Moderate– reversible	Moderate– reversible
Neurotoxicity	Negative	Negative	Negative	Negative	—	Negative	Negative >10 g/kg	Negative >25 g/kg	Negative >25 g/kg
Mutagenicity	Equivocal	—	Negative	Negative	—	Negative	Negative	Negative	Negative
EU hazard label required?	Yes	Yes	No	Yes	No	Yes	No	No	No

Table 20.36 Ecotoxicity Behavior of Phosphate Esters

Property	Fluid							
	TBP	TBEP	TOP	ODPP	DDPP	TXP	IPPP/46	TBPP/46
Biodegradability	—	Readily	Readily	Readily	—	Inherently	Readily	(Readily) ^b
Acute fish toxicity (mg/L)	Moderate–high (2.4–13)	Moderate (16–44)	Low–moderate (20–>100)	High	Moderate (7.6–18)	Low–high (0.16–>100) ^a	Low (>1,000)	(High) (1–10) ^b
Acute daphnia toxicity (mg/L)	High (2.6)	Low (>75)	Moderate (6.5–36.5)	—	High (0.48)	Moderate 3.9 ^a	Low >100	(Moderate) (>10) ^b
Algal toxicity (mg/L)	—	—	—	—	Low (71–79)	—	—	—
Bacterial toxicity (mg/L)	—	—	>100	>10,000	—	—	>100	—
WGK value (water pollution hazard)	2	1	2	2	—	1	1	(1) ^b
EU environmental label required?	No	No	No	—	—	Yes	No	No

^aValues are well above the solubility of product in water at ambient temperature.

^bValues given are based on the evidence available to date.

sults due to physical immobilization of the organisms rather than as a result of chemical "poisoning."

The low water pollution potential of phosphates has been confirmed by a U.S. industry aquatic surveillance program, which sampled river water close to sites where phosphates were manufactured or used. The results showed the absence of a significant concentration of aryl phosphates in surface water [110]. A study carried out by the Japanese authorities produced similar findings [111].

Testing continues on many of these products, particularly in view of the difficulty in evaluating products that have a very low solubility in water, and the user is advised to consult the fluid supplier for the latest health, safety, and environmental information.

7.3 Disposal of Used Phosphate Esters

One aspect of the use of phosphate esters that has become increasingly important to end users is their disposal, normally as a result of excessive degradation but also due to contamination. Depending on the extent of degradation and/or contamination, reclamation by the fluid supplier or by a specialist reclaimer may be feasible, and several alternative procedures are available. The most widely used is high-temperature incineration, either in admixture with mineral oil by an authorized waste-disposal company or, possibly, in a cement kiln. A new technique is to hydrogenate the phosphate and use the product as fuel. Landfill, although no longer environmentally favored, is still occasionally used in secure and approved sites, and phosphates are said to be beneficial in assisting the biodegradation process by acting as a nutrient for the bacteria. In all cases, the local regulations regarding disposal of chemicals must be met.

The disposal or recycling of used fluid normally requires transportation of the fluid to the disposer or reclaimer. However, strict regulations now control the labeling and transportation of waste—particularly if this involves movement across national borders and the waste is classified as hazardous. As the regulations are still evolving and vary from country to country, it is essential that the user consult an authorized waste disposal company and the fluid supplier when considering the most appropriate means of disposal.

Obviously, the quantity of phosphate fluid requiring disposal can be minimized by good maintenance and particularly by the use of in situ conditioning.

8 ADDITIVE SOLVENCY AND THE FORMULATION OF HYDRAULIC FLUIDS

The polar nature of phosphate esters makes them good solvents for most types of additives, with the possible exception of nonpolar products based on aliphatic hydrocarbons (e.g., polymeric thickeners).

In the same way that additives are used to improve the performance of mineral oil in many applications, it is also possible to improve the behavior of phosphate esters [84]. Not all additive types have a beneficial effect and their use will depend on the application. For example, polymeric thickeners and other highly polar additives, such as rust or corrosion inhibitors, can promote foaming, emulsification, and a reduction in volume resistivity, and are removed quite rapidly from solution by

some adsorbent solids used in fluid purification. The benefits of these products—in certain applications—are therefore outweighed by their disadvantages. On the other hand, the use of stabilizers (i.e., antioxidants, metal passivators and acid scavengers) can be very beneficial, particularly in applications where no on-line purification is available. Small amounts of antifoams and dyes for identification purposes may also be added to phosphate esters. Dyed fluids, however, can be more difficult to reclaim for future use because of the variety of colors produced; the dyes can also interfere with the measurement of acidity by colorimetric techniques.

9 FLUID OPERATING LIFE

The economics of using a hydraulic fluid should not only take purchase price into consideration but also other fluid-related variables, including operating life, maintenance, and disposal costs. Predicting fluid life is, however, difficult because of the use of different system designs, but the important factors that affect fluid life in service can be identified as indicated in Fig. 20.20.

9.1 System Design

Many aspects of system design can affect fluid life. These include operating pressures and temperatures, tank design and fluid circulation rate, the type and design of the pump, the routing of the pipe work, and so forth [112]. If a fluid-related problem appears, although the outward manifestation can be a change in fluid condition or performance, the actual origin of the problem is often design related.

9.2 Leakage/Top-up Rates

In heavy engineering processes, leakage rates can be high. Obviously, it can be less expensive to suffer leaks than to shut down equipment, and if a low cost fluid is being used, there is less incentive to employ good housekeeping (or adequate maintenance). In some cases, the rate of leakage is so high that the fluid is never physically replaced, the amount of top-up compensating for any fluid degradation and depletion of additives.

9.3 Fluid Type

As was indicated earlier in this chapter, the chemistry of the different fluid types available can play an important part in deciding their suitability for specific appli-

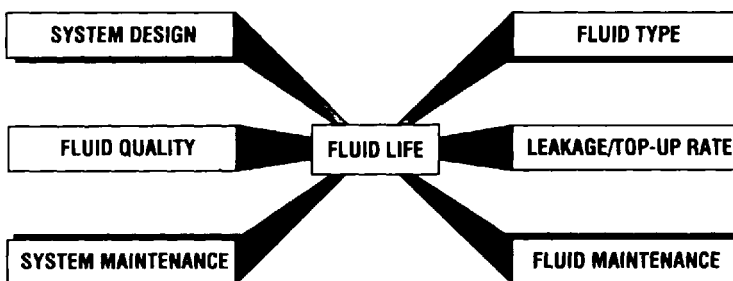


Figure 20.20 Major factors influencing fluid life.

cations. Thus, in an environment where significant water contamination is likely, a hydrolytically stable product should be used.

9.4 Fluid Quality

To control the quality of fluids used in hydraulic systems, there are national and international specifications available which specify limits on the most important fluid parameters. A list of these standards is given in Appendix 1.

9.5 System Maintenance

It is widely accepted that effective mechanical filtration significantly improves the life of system components and, in certain cases, of the fluid itself. Mention has already been made of the adverse effects of solid particles on resistivity, foaming, and demulsification. Depending on the size and hardness of the particles, the wear performance of the fluid can also be impaired. The use of filters appropriate to the degree of cleanliness required for the correct functioning of the system and to the tolerances found in system components is therefore essential.

9.6 Fluid Maintenance

In service, phosphate esters can degrade either due to contamination or through interaction with their environment (e.g., through thermal stress). In practice, there is considerable overlap between the effect of contaminants and the degradation caused by system operation. Indeed, one can lead to the other. If, for example, the phosphate is contaminated by mineral oil, the air content of the fluid is increased. This, in turn, can lead to fluid oxidation by compression of the air bubbles in the pump. Although fluid maintenance is often less for phosphate esters than for other types of fire-resistant fluids, it is still necessary to monitor and control the contamination of the fluid, whether from internal sources such as wear particles or from the external environment (moisture, dust, etc.), to ensure satisfactory operation of equipment and extend fluid life [113].

In the case of phosphate esters, considerable attention has also been given to controlling the generation of acidic degradation products, as they normally impair the performance and, hence, the life of the fluid. This aspect is discussed in greater detail in Section 11.

The most common contaminants are, of course, water, dirt, and mineral oil. Even air (certainly when in excess) can be regarded as a contaminant. Less frequently found, but still detrimental, are chlorinated solvents, as they can promote servo-valve erosion [114] when they are converted to ionic chloride and, in sufficient quantities, cause disposal problems.

The principal effects of contaminants on phosphate ester performance are shown in Fig. 20.21 [115].

10 MONITORING OF FLUID CONDITION

The following determinations are routinely carried out on phosphate ester fluids:

Viscosity change is often used as a measure of oxidative degradation. However, phosphate esters do not normally display significant viscosity changes in use.

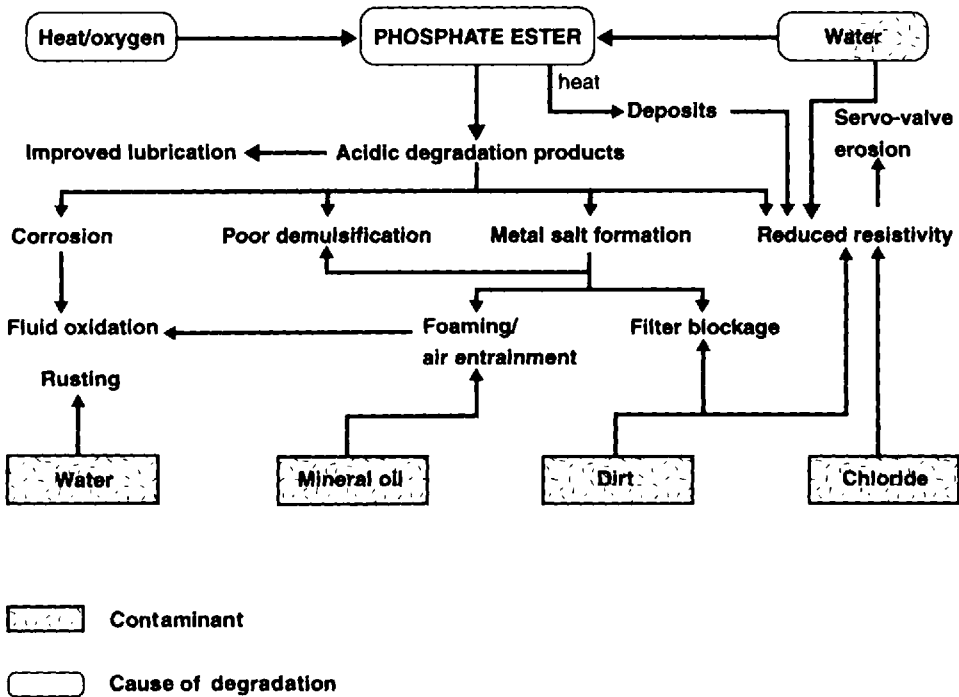


Figure 20.21 Impact of contaminants and fluid degradation products on phosphate ester performance.

If such changes are noted in a short period, they are more likely to result from contamination (e.g., with water or mineral oil).

Acidity is an indicator of both oxidative and hydrolytic breakdown. It is perhaps the single most important parameter for monitoring phosphate ester condition. A decision to replace the fluid or the conditioning media is usually made on the basis of this determination.

Water content is monitored in view of the sensitivity of esters to moisture and the subsequent development of acidity.

Particulate levels are monitored for the reasons outlined in Section 9.5.

Appearance is a simple check to see if the color is changing quickly, which may indicate excessive degradation or, if the fluid is becoming turbid, of water contamination.

These checks are required by equipment builders for general fluid applications. Additional tests, such as foaming, air release, and volume resistivity, would be required for specialist uses. The frequency of testing will depend on the severity of the operating conditions and the sophistication of the equipment (e.g., whether fine tolerance valves are used). The testing will also be more frequent during commissioning of the system or after refurbishment. In normal operation, samples of phosphate esters might be evaluated on a monthly or quarterly basis, but not all the tests would necessarily have the same frequency. A general list of methods used to assess fluid quality is given in Appendix 2. Guidance on the frequency of testing and proposed

operating limits are given in the standards listed in Appendix 1. In addition to these national/international standards, individual equipment builders frequently have their own specifications and it is important for the end user to follow the manufacturer's requirements, particularly during the warranty period.

11 CONTROL OF FLUID DEGRADATION AND PERFORMANCE

As contaminants are often responsible for initiating fluid degradation (oxidative and hydrolytic) or impairing the physical/chemical properties, which then lead to reduced performance, one method of maintaining fluid quality and extending fluid life is to remove the contaminants as soon as they enter the system. (It is, of course, preferable to avoid their entry, but this is not completely possible because of system design, and, often, inadequate maintenance). There are techniques for removing most of the common contaminants either on-line or off-line. Table 20.37 [115] lists the most widely used methods together with those recommended for removing acidic degradation products. With the exception of mechanical filtration, most of the techniques are rarely used. Only in power-generation applications with phosphate esters has there been any attempt to date to introduce on-line conditioning. The reasons for this include cost and the fact that it makes little sense in systems with high leakage rates. In the power-generation industry, however, leakage rates are more tightly controlled and the treatment significantly improves the cost-effectiveness of the fluid. Steam turbine hydraulic systems are also more likely than most to suffer from water ingress, and with this treatment, fluid life can be considerably extended. As a result

Table 20.37 Common Hydraulic Fluid Contaminants and Techniques Used for Their Removal

Contaminant	On-line removal	Off-line removal
Water	Vacuum dehydration Water-absorbing polymers Adsorbent solids Physical separation (e.g., centrifuging, siphoning) Increased bulk temperature	Vacuum dehydration
Acid	Adsorbent solids (e.g., fuller's earth, ion-exchange resins)	Water or alkali washing
Particulates	Cellulose or glass filters Adsorbent solids Electrostatic precipitation/filtration Magnetic filtration	
Chlorinated solvents	Vacuum techniques Degradation products can be removed by adsorbent solids	Distillation
Mineral oil	No suitable procedure for removing small quantities Large amounts may be removed by centrifuging	Precipitation by cooling Distillation

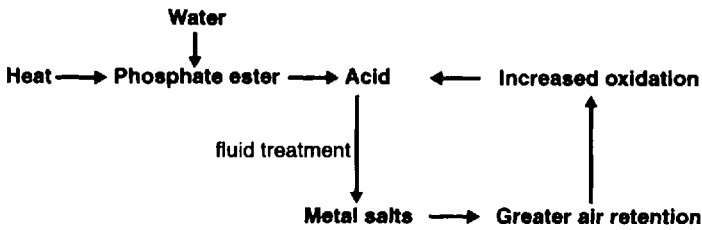


Figure 20.22 The fluid degradation cycle.

of an increasing emphasis on reducing process costs and the expense of disposing of waste fluid, a greater use of on-line conditioning in other industries seems inevitable.

The use of adsorbent solids to remove acid degradation products has not been without its problems! For many years, Fuller's earth and activated alumina have been used to remove the acid from phosphates by circulating a small quantity of fluid on a bypass loop from the main reservoir through the adsorbent solid. Unfortunately, the solids contain impurities which react with the acid degradation products to form metal soaps, which are initially soluble. These soaps, which can reach high molecular weights [115,116], adversely affect the surface-active properties of the fluid, and as a result of a deterioration in the air-release properties, fluid oxidation increases with the generation of more acid [116,117]. Thus, a cycle of degradation (Fig. 20.22) [115] begins. Under certain conditions, the soaps precipitate and form gelatinous deposits in the tank, valves, filters, and so forth. Systems that seem clean when operational can, on cooling, show evidence of deposits. These problems have more frequently been associated with the "synthetic" phosphates, probably because of their inferior hydrolytic stability.

Fortunately, new techniques for acid removal, such as the use of ion-exchange resins, are now available which do not have the above-indicated side effects [115], and where these are in use, phosphate ester life has been extended to such an extent that it approaches that of the equipment. Quite apart from the savings on the cost of replacement fluid, the difficulty (and expense) of the disposal of used material should now be almost eliminated.

12 APPLICATIONS

Phosphate ester fire-resistant hydraulic fluids are ideally suited for most industrial processes involving high temperatures, or where system designs are unsuitable for the use of water-based fluids. These applications include the following:

- | | |
|-----------------------------|--------------------------------|
| Continuous casting machines | Hydraulic mining equipment |
| Die-casting machinery | Ship control systems |
| Hydraulic presses | Gate valve activators |
| Centrifugal compressors | Steam turbine governor systems |
| Glass-working machinery | Aircraft hydraulic systems |
| Hydraulic jigs | Clay guns |
| Injection-molding machines | Ingot manipulators |
| Oven controls | Foundry equipment |

Automatic welders
 Billet loaders
 Furnace mechanisms
 Gas turbine hydraulics
 Hot-roll mills

Fork lift trucks
 Hydraulic lifts
 Aerial bucket trucks
 Fluid couplings

There are also some applications where the fluid serves as a combined hydraulic fluid and lubricant, for example, in steam and gas turbines [86].

APPENDIX 1

International Specifications and Use Guides for Fire-Resistant Hydraulic Fluids Including Phosphate Esters

Organization	Standard no.	Title
ISO	6743-4	Lubricants, industrial oils and related products (class L). Classification—Part 4: Family H (Hydraulic systems)
ISO	7745	Hydraulic Fluid Power—Fire-resistant (FR) fluids—Guidelines for use
ISO	12922	Lubricants, industrial oils and related products—fire resistant hydraulic fluids for hydraulic systems
IEC	978	Maintenance and use guide for triaryl phosphate ester turbine control fluids
IEC	1221	Petroleum products and lubricants—triaryl phosphate ester turbine control fluids (category ISO-L-TCD)—specifications
CETOP	RP 86H	Guidelines for the use of fire-resistant fluids in hydraulic systems
CETOP	RP 97H	Fluids for hydraulic transmissions—fire-resistant fluids—specifications
EC Mines Safety & Health Commission		Requirements and tests applicable to fire-resistant hydraulic fluids used for power transmission and control (hydrostatic and hydrokinetic)—seventh edition.

Additional National Specifications and Use Guides for Fire-Resistant Fluids Including Phosphate Esters

Organization	Standard no.	Title
ANSI	B93.5-1979 (R 1988)	Practice for the Use of Fire-Resistant Fluids for Industrial Hydraulic Fluid Power Systems
AAMA	525	Fire-Resistant Hydraulic Fluids
VDMA	24317	Schwerentflammbare Druckflüssigkeiten—Richtlinien

Key to Appendix 1

ISO International Standards Organization
 IEC International Electrotechnical Commission

CETOP	European Oil Hydraulics and Pneumatics Committee
ANSI	American National Standards Institute
NFPA	National Fluid Power Association (USA)
AAMA	American Automobile Manufacturers Association
VDMA	German Association of Machinery and Engineering

APPENDIX 2

Suitable Test Methods for Monitoring Phosphate Ester Quality

Fluid property	Test method
Kinematic viscosity	ISO 3104
Neutralization no.	ISO 6618/6619
Pour point	ISO 3016
Density	ISO 3675
Foaming	ISO 6247
Air release	ISO 9120
Rust prevention	ISO 7120
Corrosion protection	CETOP RP48H
Water content	ISO 760
Flash/fire points	ISO 2592
Particulate levels	ISO 4407/4406
Emulsion stability	ISO 6614
Color	ISO 2049
Volume resistivity	IEC 247
Chlorine content	Micro-coulometry
Mineral oil	Thin-layer chromatography
Metal content	ASTM D-2788 (mod)

REFERENCES

1. Williamson and Scrugham, Ann., 1854, 92, pp. 316.
2. F. Vogeli, Ann., 1849, 69, pp. 190.
3. E. G. Egan, "A Synthetic Lubricant for Hydraulic Fluid," *Lubr. Eng.*, 1947, 3, February–March, pp. 24–26.
4. O. Beeck, J. W. Givens, and E. C. Williams, *Proc. Roy. Soc.*, 1940, 177A, pp. 103–118.
5. M. V. Sullivan, J. K. Wolfe, and W. A. Zisman, "Flammability of the Higher Boiling Liquids and their Mists," *Ind. Eng. Chem.*, 1947, 39(12), pp. 1607–1614.
6. C. M. Murphy and W. A. Zisman, "Synthetic Hydraulic Fluids," *Product Eng.*, 1950, September, pp. 109–113.
7. F. J. Watson, U.S. Patent 2,549,270 (1951), U.S. Patent 2,636,861 (1953) (to Shell Development Co.).
8. D. H. Moreton, "Development and Testing of Fire-Resistant Hydraulic Fluids," *SAE Technical Paper*, Paper 490229, 1949.
9. D. H. Moreton, U.S. Patent 2,566,623 (1951), U.S. Patent 2,834,733 (1958), U.S. Patent 2,894,911 (1959) (to Douglas Aircraft Co.).
10. H. R. Gamrath, R. E. Hatton, and W. E. Weesner, "Chemical and Physical Properties of Alkyl Aryl Phosphates," *Ind. Eng. Chem.*, 1954, 46, pp. 208–212.

11. H. R. Gamrath and J. K. Craver, U.S. Patent 2,596,140 (1952), U.S. Patent 2,596,141 (1952) (to Monsanto Chemical Co.).
12. H. R. Gamrath and R. E. Hatton, U.S. Patent 2,678,329 (1954) (to Monsanto Chemical Co.).
13. W. F. Hamilton, M. F. George, and G. B. Weible, U.S. Patent 2,392,530 (1946) (to Lockheed Aircraft Co.).
14. M. F. George and P. Reedy, U.S. Patent 2,659,699 (1953) (to Lockheed Aircraft Co.).
15. U.S. Military Specifications MIL-F-7100 (1950) and MIL-H-83306 (1971).
16. U.K. Aircraft Material Specifications DTD 5507 (1956) and DTD 5526 (1962).
17. U.S. Military Specification MIL-H-19457 (Ships); originally published 1961.
18. H. R. Gamrath and R. E. Hatton, U.S. Patent 2,698,537 (1955), U.S. Patent 2,707,176 (1955) (to Monsanto Chemical Co.).
19. J. D. Morgan, U.S. Patent 2,410,608 (1946) (to Cities Service Oil Co.).
20. Stauffer Chemical Co., "Cellulube® Fire-Resistant Fluids and Lubricants," Technical Bulletin, Stauffer (now Akzo) Chemical Co., 1966.
21. E. F. Houghton & Co., "Fire-Resistant Hydraulic Fluids," Technical Bulletin, E. F. Houghton & Company, Philadelphia, PA, 1960.
22. The Geigy Co., "Fire-Resistant Hydraulic Fluids," Technical Service Bulletin, The Geigy Co., Ltd., Manchester, UK, 1962.
23. Monsanto Chemical Co., "Pydraul®150," Technical Bulletin, 1959; "Pydraul®625," Technical Bulletin, 1959; "Pydraul®AC," Technical Bulletin, 1957; "Pydraul®F-9," Technical Bulletin, 1959; Monsanto Chemical Co., St. Louis, MO.
24. European Council Directive 76/769/EEC, Eleventh Amendment, L186, 12/7/91, p. 64.
25. J. D. Morgan and R. E. Lowe, U.S. Patent 2,395,380 (1946), U.S. Patent 2,396,161 (1946); U.S. Patent 2,396,192 (1946), U.S. Patent 2,409,443 (1946); U.S. Patent 2,409,444 (1946); U.S. Patent 2,423,844 (1947) (to Cities Service Oil Co.).
26. Stauffer Chemical Co., "Fyrlube® Fire-Resistant Hydraulic Fluids," Technical Bulletin, Stauffer (now Akzo) Chemical Co., Westport, CT.
27. Stauffer Chemical Co., "Fyrtek® Fire-Resistant Hydraulic Fluid," Product Data Sheet, Stauffer (now Akzo) Chemical Co., Westport, CT.
28. E. F. Houghton & Co., "Vital® Hydraulic Fluid 29," Technical Data Sheet, E. F. Houghton & Co., Philadelphia, PA, 1971.
29. D. A. Stuart Co., "DASCO FR 300 Fire-Resistant Hydraulic Fluids," Product Data Bulletin, D. A. Stuart Co., Chicago, IL, 1970.
30. W. D. Phillips and R. Schade, "Nicht-wässrige schwerbrennbare Hydraulikflüssigkeiten," in *Hydraulikflüssigkeiten*, W. J. Bartz, ed., Expert Verlag, 1995.
31. W. H. Prah, British Patent No. 763,311 (1956).
32. M. P. Marino, "Phosphate Esters," in *Synthetic Lubricants and High-Performance Functional Fluids*, R. L. Shubkin, ed., Marcel Dekker; New York, 1992.
33. K. M. Garrett, British Patent 1,165,700 (1965) (to Bush Boake Allen Ltd.).
34. D. R. Randell and W. Pickles, British Patent 1,146,173 (1966) (to J. R. Geigy A. G.).
35. FMC Corporation (UK) Ltd., unpublished data.
36. *Chemical Economics Handbook*, SRI International, Menlo Park, CA, 1993.
37. W. D. Phillips, "Fire-Resistance Tests for Fluids and Lubricants—Their Limitations and Misapplication", ASTM STP1284 (1996).
38. FMC Corp., "Triocetyl Phosphate," Technical Data Sheet, FMC Corporation, Philadelphia, PA, 1991.
39. FMC Corp., "Tributyl Phosphate," Technical Data Sheet, FMC Corporation, Philadelphia, PA, 1987.
40. ASTM Test Method D240-92—Standard Test Method for Heat of Combustion of Liquid Hydrocarbon Fuels by Bomb Calorimeter.

41. FMC Corp., "Reolube® HYD Fluids," Technical Bulletin, FMC Corporation, Manchester, UK, 1994.
42. Akzo Chemicals, "Fyrquel® Fire-Resistant Hydraulic Fluids," Technical Bulletin, 88-151, Akzo Chemicals Inc., Chicago, IL, 1988.
43. E. F. Houghton & Co., Houghto-Safe® 1000 Series," Technical Bulletin, E. F. Houghton & Co., Philadelphia, PA, 1990.
44. D. G. Placek and M. P. Marino, "Phosphate Esters," in *STLE/CRC Tribology Data Handbook, Synthetic Oil Properties*, CRC Press; Boca Raton, FL, 1996.
45. R. Beyer and K. Bauer, "Schwerentflammbarkeit von Druckflüssigkeiten beim Kontakt mit Metallschmelzen," Sonderdruck Ölhydraulik und Pneumatik, 1988, 6.
46. M. M. Khan and A. V. Brandao, "Method for Testing the Spray Flammability of Hydraulic Fluids," SAE Technical Paper, Paper 921737, 1992.
47. Anon., "Unveiling a New Protocol for Less Flammable Hydraulic Fluids," Factory Mutual Approved Product News, 1996, pp. 6–8.
48. *Requirements and Tests Applicable to Fire-Resistant Hydraulic Fluids Used for Power Transmission and Control*, 7th ed., E.C. Safety and Health Commission for the Mining and Other Extractive Industries, Luxembourg, 1994, Doc. No. 4746/10/91EN.
49. A. J. Yule and K. Moodie, "A Method for Testing the Flammability of Sprays of Hydraulic Fluid," Fire Safety J., 1992, 18, pp. 273–302.
50. Data provided by Health and Safety Executive, Buxton, U.K. and by the Laboratoire Centrale de Houillères du Bassin de Lorraine, Marienau, France.
51. F. T. Barcroft and S. G. Daniel, "The Action of Neutral Organic Phosphates as E. P. Additives," ASME Trans., 1964, 64-Lub 22.
52. D. Godfrey, "The Lubrication Mechanism of Tricresyl Phosphate on Steel," ASLE Preprint 64 LC-1, 1964.
53. H. E. Bieber, E. E. Klaus, and E. J. Tewkesbury, "A Study of Tricresyl Phosphate as an Additive for Boundary Lubrication," ASLE Trans., 1968, 11, pp. 155–161.
54. J. M. Perez, R. C. Hansen, and E. E. Klaus, "Comparative Evaluation of Several Hydraulic Fluids in Operational Equipment. A Full-Scale Pump Stand Test and the Four Ball Wear Tester, Part II—Phosphate Esters, Glycols and Mineral Oils," Lubr. Eng., 1990, 46(4), pp. 249–255.
55. Y. Yamamoto and F. Hirano, "Scuffing Resistance of Phosphate Esters," Wear, 1978, 50, pp. 343–348.
56. W. D. Phillips, "A Comparison of Fire-Resistant Hydraulic Fluids for Hazardous Industrial Applications," Journal of Synthetic Lubrication, 1998, 14, 3, pp. 211–235.
57. R. A. Hobbs, "Fatigue Lives of Ball Bearings Lubricated with Oils and Fire-Resistant Fluids," in *Elastohydrodynamic Lubrication Symposium*, Institute of Mechanical Engineers, 1972, paper C1.
58. R. A. Hobbs and G. W. Mullett, "Effects of Some Hydraulic Fluid Lubricants on the Fatigue Lives of Roller Bearings," Proc. Inst. Mech. Eng. (1968–69), 183(Pt. 3P), pp. 23–29.
59. D. V. Culp and R. L. Widner, "The Effect of Fire-Resistant Hydraulic Fluids on Tapered Roller Bearing Fatigue Life," SAE Technical Paper, Paper 770748, 1977.
60. E. D. Yardley, P. Kenny, and D. A. Sutcliffe, "The Use of Rolling Fatigue Test Methods over a Range of Loading Conditions to Assess the Performance of Fire-Resistant Fluids," Wear, 1974, 28, pp. 29–47.
61. K. Michaelis, "Reibungs, Verschleiss und Fresshalten natürlicher Phosphatester in Zahnradgetrieben," Antriebstechnik, 1988, 27(8), pp. 43–46.
62. H. Winter and K. Michaelis, "Gutachtliche Beurteilung der Fressstragfähigkeit von Reolube® Turbofluid 46," Internal Report No. 1313, FZG Institute, München, Germany, 1983.

63. K. Michaelis, "Efficiency of Gears Lubricated with Phosphate Esters," private communication, 1995.
64. H. Peecken and Th. Niester, "Verträglichkeit des Synthetischen Schmierstoffes, Reolube® 46T mit dem Gleitlagerwerkstoff Tego V738," Internal Report 9/89 Institute für Maschinenelemente und Maschinengestaltung, Aachen, 1989.
65. V. N. Borsoff, "Wear Studies with Radioactive Gears," *Lubr. Eng.*, 1956, 12, p. 24–28.
66. Monsanto Chemical Co., "Santiciser® 141," Technical Data Sheet, Monsanto Chemical Co., St. Louis, MO.
67. Monsanto Chemical Co., "Santiciser® 148," Technical Data Sheet, Monsanto Chemical Co., St. Louis, MO.
68. H. R. Gamrath, R. E. Horton, and W. E. Weesmer, *Ind. Eng. Chem.*, 1954, 46, p. 208.
69. T. I. Fowle, "Aeration in Lubricating Oils," in *Tribology International*, 1981, 14(3), pp. 151–157.
70. Mobil Oil Co., "Foaming and Air Entrainment in Lubrication and Hydraulic Systems," Mobil Oil Co., Mobil Oil Co. Ltd., London, UK, 1971.
71. L. Döllinger and H. Vogt, "Untersuchungen zum Luftaufnahme-und-abgabeverhalten (LAAV) von Schmierölen und Hydraulikflüssigkeiten in Maschinenanlagen," *DGMK Forschungsber.*, 1981, 221.
72. W. Schöner, "Betriebliche Luftgehaltmessungen in Schmier-und-Steuerflüssigkeitsschleisläufen," *Elektrizitätswirtschaft*, 1982, 81(17/18), pp. 564–567.
73. D. R. Hatton, "Some Practical Aspects of Turbine Lubrication," *Can. Lubr. J.*, 1984, 4(1), pp. 3–8.
74. A. T. J. Hayward, "The Compressibility of Hydraulic Fluids," *J. Inst. Petrol.*, 1965, 51, pp. 35–47.
75. L. H. Smith, R. L. Peeler, and L. H. Bernd, "Hydraulic System Bulk Modulus—Its Effect on System Performance and Techniques for Physical Measurement," in 16th National Conference on Industrial Hydraulics, 1960, Vol. 14, pp. 179–197.
76. W. Scott, "The Influence of Fire-Resistant Hydraulic Fluids on System and Component Design," *Wear*, 1979, 56, pp. 105–121.
77. E. S. Blake, W. C. Hammann, J. W. Edwards, T. E. Richards, and M. R. Oak, American Chemical Society, Petroleum Chemical Division Symposium, 1960.
78. C. F. Raley, Jr., WADC Technical Report 53-337, Wright Air Development Center, Wright-Patterson Air Force Base, OH, 1955.
79. V. Lhomme, C. Bruneau, A. Brault, G. Chevalier, and N. Soyer, "Dégradation thermique du tributylphosphate et de quelques homologues," Report C. E. A., R-5095, Service de documentation du C. E. N. Saclay, Gif-sur-Yvette, France, 1981.
80. V. Lhomme, C. Bruneau, N. Soyer, and A. Brault, "Thermal Behaviour of Some Organic Phosphates," *Ind. Eng. Chem. Prod. Res. Dev.*, 1984, 23(1), pp. 98–102.
81. S. G. Shankwalkar and C. Cruz, "Thermal Degradation and Weight Loss Characteristics of Commercial Phosphate Esters," *Ind. Eng. Chem. Res.*, 1994, 33(3), pp. 740–743.
82. K. L. Paciorek, R. H. Kratzer, J. Kaufman, and J. H. Nakahara, "Coal Mine Combustion Products, Identification and Analysis," U.S. Bureau of Mines Open File Report 104-77, 1976.
83. H-J. Lohrentz, "Die Entwicklung extrem hoher Temperaturen in Hydrauliksystemen und die Einflüsse dieser Temperaturen auf die Bauteile und ihre Funktionen," *Mineralöltechnik*, 1968, 14/15.
84. L. Cho and E. E. Klaus, "Oxidative Degradation of Phosphate Esters," *ASLE Trans.*, 1979, 24(1), pp. 119–124.
85. S. G. Shankwalkar and D. G. Placek, "Oxidation and Weight Loss of Commercial Phosphate Esters," *Ind. Eng. Chem. Res.*, 1992, 31, pp. 1810–1813.

86. W. D. Phillips, "Triaryl Phosphates—the Next Generation of Lubricants for Steam and Gas Turbines," ASME Paper 94-JPGC-PWR-64, 1994.
87. J. F. Anzenberger, Sr., "Evaluation of Phosphate Ester Fluids to Determine Stability and Suitability for Continued Service in Gas Turbines," ASLE Paper 86-AM-IE-2, 1986.
88. F. H. Westheimer, "The Hydrolysis of Phosphate Esters," *Pure Appl. Chem.*, 1977, 49, pp. 1059–1067.
89. (a) M. M. Mhala and M. D. Patwardhan, "Hydrolysis of Organic Phosphates. I. Hydrolysis of p-chloro-m-tolyl Phosphate," *Indian J. Chem.*, 1968, 6(12), pp. 704–707. (b) M. M. Mhala, M. D. Patwardhan, and T. R. Kasturi, "Hydrolysis of Organic Phosphates. II. Hydrolysis of p-chloro- and p-bromophenyl Orthophosphates," *Indian J. Chem.*, 1969, 7(2), pp. 145–148. (c) M. M. Mhala, C. Holla, G. Kasturi, and K. Gupta, "Hydrolysis of Organic Phosphates. III. Hydrolysis of o-methoxy-, p-methoxy-, and p-ethoxy-phenyl Dihydrogenphosphates," *Indian J. Chem.*, 1970, 8(1), pp. 51–56. (d) M. M. Mhala, C. Holla, G. Kasturi, and K. Gupta, "Hydrolysis of Organic Phosphates. IV. Hydrolysis of di-o-methoxy-, di-p-methoxy-, and di-p-ethoxyphenyl Hydrogen Phosphates," *Indian J. Chem.*, 1970, 8(4), pp. 333–336. (e) M. M. Mhala and S. Prabha, "Hydrolysis of Organic Phosphates. V. Hydrolysis of 2, 3-dimethoxyphenyl Dihydrogen Phosphate," *Indian J. Chem.*, 1970, 8(11), pp. 972–976. (f) M. M. Mhala and S. B. Saxena, "Hydrolysis of Organic Phosphates. VI. Hydrolysis of Monoallyl Orthophosphate (Disodium Salt)," *Indian J. Chem.*, 1971, 9(2), pp. 127–130. (g) M. M. Mhala and S. B. Saxena, "Hydrolysis of Organic Phosphates. VII. Hydrolysis of Diallyl Orthophosphate (Sodium Salt)," *Indian J. Chem.*, 1972, 10(7), pp. 703–705. (h) M. M. Mhala and S. Prabha, "Hydrolysis of Organic Phosphates. VIII. Hydrolysis of 2,6-dimethoxyphenyl Hydrogen Phosphate," *Indian J. Chem.*, 1972, 10(10), pp. 1002–1005. (i) M. M. Mhala and S. Prabha, "Hydrolysis of Organic Phosphates. IX. Hydrolysis of tris(2,6-dimethoxyphenyl) Phosphate," *Indian J. Chem.*, 1972, 10(11), pp. 1073–1076. (j) M. M. Mhala and P. Nand, "Hydrolysis of Organic Phosphates: Part IX—Hydrolysis of 1-nitro-2-naphthyl- and 4-nitro-1-naphthyl-phosphate Monoesters," *Indian J. Chem.*, 1976, 14A(5), pp. 344–346.
90. G. D. Vilyanskaya, V. V. Lysko, M. S. Fragin, V. N. Kazanskii, and A. G. Vainstein, "Improving Fire Protection in Turbine Plants by Using Fire-Resistant Oils," *Therm. Eng.*, 1988, 35(4), pp. 193–195.
91. C. L. Mahoney, E. R. Barnum, W. W. Kerlin, K. J. Sax, and W. S. Saari, "Effect of Radiation on the Stability of Synthetic Lubricants," in *Proceedings Fifth World Petroleum Congress*, 1959, pp. 147–161.
92. P. E. B. Vaile, "Lubricants for Nuclear Reactors," *Proc. Inst. Mech. Eng.*, 1962, 176(2), pp. 27–59.
93. R. M. Wagner, E. M. Kinderman, and L. H. Towle, "Radiation Stability of Organophosphorus Compounds," *Ind. Eng. Chem.*, 1959, 51(1), pp. 45–46.
94. FMC Corp., "Reolube® Turbofluids—A Guide to Their Maintenance and Use," *Technical Bulletin*, FMC Corporation (U.K.) Ltd., 1995.
95. Azko Chemicals, "'Fyrquel® Compatibility Guide,'" *Technical Bulletin*, Azko Chemicals, Inc., Chicago, IL.
96. J. P. Morgan and T. C. Tulloss, "The Jake Walk Blues," *Ann Intern. Med.*, 1976, 85, pp. 804–808.
97. M. K. Johnson, "Organophosphorus Esters Causing Delayed Neurotoxic Effects: Mechanism of Action and Structure/Activity Studies," *Arch. Toxicol.*, 1975, 34, p. 259.
98. M. K. Johnson, "Organophosphates and Delayed Neuropathy—Is NTE Alive and Well?," *Toxicol. Appl. Pharmacol.*, 1990, 102, p. 385.

99. Directive 93/21/EEC, Official Journal of the European Communities, 36, No. L110A, 1993.
100. H. F. Benthe, Pharmacological/Toxicological Reports on Reolube® HYD 46 (1975), Turbofluid 46XC (1982), Reolube® MF46 (1988), University of Hamburg.
101. Society of Chemical Manufacturers, Washington, DC—Task Force on Tributyl Phosphate.
102. G. Deetman, U.S. Patent 5,464,551 (1995) (to Monsanto Co.).
103. *Joint Assessment of Commodity Chemicals, No. 21, Tri-(2-butoxyethyl)-phosphate*, European Chemical Industry—Ecology and Toxicology Centre, Brussels, 1992.
104. *Joint Assessment of Commodity Chemicals, No. 20, Tris-(2-ethylhexyl) phosphate*, European Chemical Industry—Ecology and Toxicology Centre, Brussels, 1992.
105. Bayer A. G., "Disflamoll® DPO," Safety Data Sheet, Bayer A. G., Leverkusen, Germany, 1993.
106. Monsanto Chemical Co., Santiciser® 148, Material Safety Data Sheet, Monsanto Chemical Co., St. Louis, MO, 1982.
107. "Bewertung wassergefährdender Stoffe", Beirat "Lagerung und Transport wassergefährdender Stoffe" beim Bundesminister für Umwelt, Naturschutz und Reaktorsicherheit LTWS-Schrift Nr. 10, September 1979.
108. "Determination of the Acute Toxicity of Reolube® HYD 46 to Zebra Fish," Test Report, Institut National de Recherche Chimique Appliquée, vert-le-Petit, France, 1991.
109. "Determination of the Acute Toxicity of REOLUBE® HYD 46 to Daphnia Magna," Test Report, Institut National de Recherche Chimique Appliquée, vert-le-Petit, France, 1991.
110. P. R. Michael and W. J. Adams, "Final Report of the 1982 Industry—EPA Phosphate Ester Aquatic Surveillance Program," Monsanto Chemical Co., 1983.
111. Japanese Government Agency, Chemicals in the Environment, 1985, Office of Health Studies, Japanese Government Agency.
112. J. W. G. Staniewski, "The Influence of Mechanical Design of Electro-Hydraulic Steam Turbine Control Systems on Fire-Resistant Fluid Condition," *Lubr. Eng.*, 1996, 52(3), pp. 255–258.
113. K. J. Brown, Condition Monitoring and Maintenance of Steam Turbine Generator Fire-Resistant Triaryl Phosphate Control Fluids," STLE Special Publication SP-27, Park Ridge, IL, 1989, pp. 91–96.
114. G. E. Wolfe, M. Cohen, and V. T. Dimitroff, "Ten Years Experience with Fire-Resistant Fluids in Steam Turbine Electrohydraulic Controls," *Lubr. Eng.*, 1970, 26(1), pp. 6–14.
115. W. D. Phillips and D. I. Sutton, "Improved Maintenance and Life Extension of Phosphate Esters Using Ion Exchange Treatment," in 10th International Tribology Colloquium, Technische Akademie Esslingen, 1996.
116. H. Grupp, "Aufbau von schwer entflammaren Hydraulikflüssigkeiten auf Phosphorsäureesterbasis, Erfahrungen aus dem praktischen Einsatz im Kraftwerk," *Masch. Schaden*, 1979, 52(3), pp. 73–77.
117. C. Tersiguel-Alcover, "Problems Encountered With Phosphate Esters on Hydraulic Systems of EDF Power Plants," *Proc. Int. Tribol. Congress*, 1981, 3, pp. 296–307.

This page intentionally left blank

Vegetable-Based Hydraulic Oils

LOU A. T. HONARY

University of Northern Iowa, Cedar Falls, Iowa

1 INTRODUCTION

The use of vegetable oils as fuel, lubricating fluid, and energy transfer media has been known for many years. Their usage, however, has depended on the availability of petroleum. Both World Wars, for example, saw an increased usage of vegetable oils for fuel, lubrication, and energy transfer. Similarly, the oil embargo of 1973 resulted in an increased interest in the use of vegetable-based oils as well as other alternatives such as water-based lubricants.

Concern for the environment has created a new impetus for the use of vegetable oils in industrial applications. The environment factor promises to be a more steady and persistent force in promoting the use of vegetable oils than the fluctuating availability of petroleum. Either because of imposed environmental regulations or society's desire for a more environment-friendly lubricant, the interest and increased use of vegetable-based hydraulic fluids and industrial lubricants will continue. Therefore, the engineer dealing with industrial lubricants should become familiar with vegetable oils and their characteristics related to industrial use. Because this chapter deals with *hydraulic fluids*, the emphasis will be placed on the use of vegetable oils for hydraulic systems. Furthermore, the chapter provides information on the chemistry of vegetable oils, the general performance requirement of hydraulic fluids, standard test procedures required for the oil approval, and the performance reports on some of the vegetable-based hydraulic oils. Also, issues of biodegradability and toxicity will be discussed.

2 VEGETABLE OILS

Oils and fats are important ingredients in human dietary food. Besides being an important source of food energy, they also act as carriers for soluble vitamins and

give food its necessary sensory characteristics. Plants and animals are the main sources of oils and fats. The world production of edible oils is made up of 71% vegetable oils, 26% animal fat, and 2% marine animal fats (Fig. 21.1). According to the United States Department of Agriculture (USDA) reports [1], the world production of major *oilseed* in 1994–1995 was 260.60 million metric tons (MMT). Of this, the U.S. production was reported at 79.72 MMT, or one-third of the world production. The world production of *vegetable oils* was reported at 69.04 MMT, of which 8.58 MMT was produced in the United States [2]. Soybean oil contributed one-third of the world's oilseeds, with almost one-half produced in the United States.

Vegetable oils may be classified into three categories based on their production, use, and volume: (1) major oils, (2) minor oils, and (3) nonedible oils [3]. Major oils are those known for human or animal feed consumption and often play important economic roles in the regions producing them. Table 21.1 presents major vegetable oils and their volume production. A second source (Fig. 21.2) illustrates the annual production of some of the major vegetable oils in gallons.

Oils that are known for their uses but do not match the large production magnitude of major oils are considered *minor oils*. These oils have fatty acid profiles that could make them effective for industrial uses. Table 21.2 presents a list of minor oils and some of their volumes.

The majority of oil plants are cultivated for food applications. Nevertheless, a number of nonedible oils such as linseed, castor, tung, and tall are commercially grown for their unique chemical constituents that are important for the industry (Table 21.3). They are used in nonlubricant applications such as soaps, paints, varnishes, resins, plastics, and the agrochemicals.

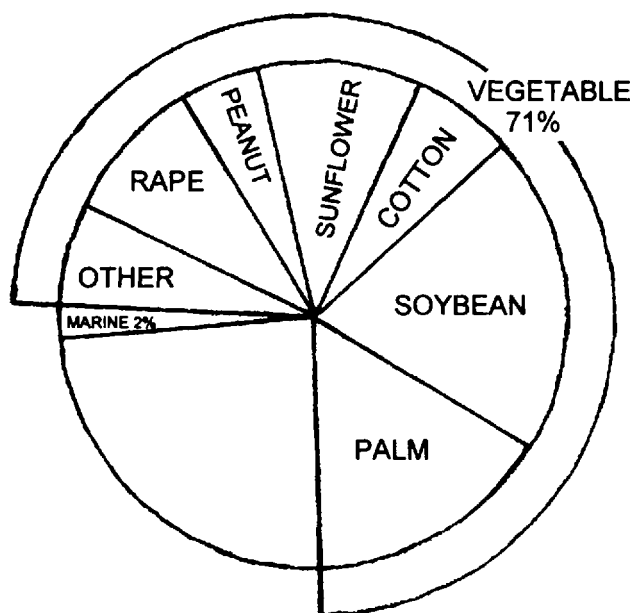


Figure 21.1 Worldwide production of edible oils and fats. (From Meike and Co., in Ref. 3.)

Table 21.1 World Production of Major Vegetable Oils

Oil	Production 1987–1988 (MMT)	% Total production	Relative rank
Soybean	15.50	29.1	1
Palm	8.52	16.0	2
Rapeseed	7.03	13.2	3
Sunflower	7.00	13.1	4
Cottonseed	3.31	6.0	5
Coconut	2.71	5.1	6
Peanut	2.69	5.0	7
Olive	1.63	3.1	8
Palm kernel	1.14	2.1	9
Corn	1.13	2.1	10
Linseed	0.65	1.2	11
Sesame	0.58	1.1	12

Source: USDA (1988).

3 CHEMISTRY OF VEGETABLE OILS

The basic units of fats and oils consist of one molecule of glycerol combined with three molecules of fatty acids such that they form either liquid (oil) or solid (fat). Because of the *three* fatty acids, the resulting molecule is called a *triglyceride*. Paterson [4] illustrates a triglyceride in Fig. 21.3.

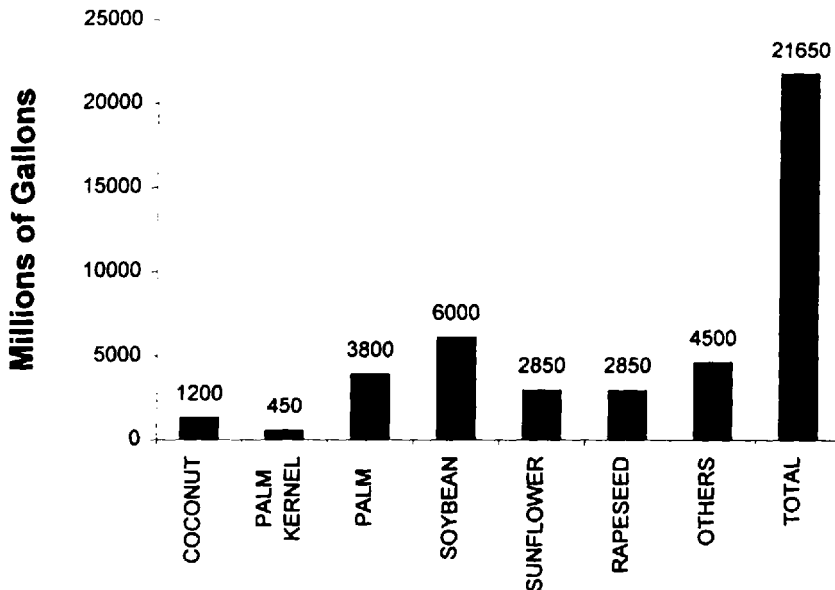


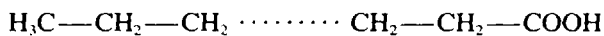
Figure 21.2 Worldwide production of vegetable oils in gallons. (From A. J. Kaufman and R. J. Ruebusch, *Inform*, 1990, 1, pp. 1034–1048.)

Table 21.2 World Production of Minor Vegetable Oils

Oil	Production 1000 metric tons
Niger	200
Olive	1,965
Mango kernel	14,635
Poppy	
Cocoa bean	2,002
Shea	
Hemp seed	25.3
Grape seed	64,770
Perilla	
Chinese V. tallow	
Ethiopian mahogany	
German sesame	
Watermelon	28,128
Avocado	1,780
Apricot	

Source: USDA (1988).

Fatty acids contain a chain of carbon atoms combined with hydrogen (forming hydrocarbon). They terminate in a carboxyl group. If the three fatty acids are alike, the molecule is a *simple* triglyceride; if they are different, it is a *mixed* triglyceride:



Fatty acids can be divided into two classes: saturated and unsaturated. Each carbon atom along the chain has the ability to hold two hydrogen atoms. The fatty acid is saturated if all hydrogen atoms are in place; in other words, when all available carbon valencies for hydrogen are satisfied. If two adjacent carbons are missing hydrogen atoms, the carbons bond *doubly* to one another, creating a point of unsaturation. If there is more than one double bond, the fatty acid is *polyunsaturated*, as compared to *monounsaturated* when there is only one double bond. The relative amounts of these fatty acids vary for the different vegetable oils. When 1 mol of the triglyceride molecule is hydrolyzed, it would give 3 mol of fatty acids and 1 mol of glycerol.

Unsaturation is inversely related to the liquidity of the oil or its melting point and directly related to its solubility and chemical reactivity. With an increase in unsaturation, the melting point goes down while solubility and chemical reactivity increase, resulting in oxidation and thermal polymerization. Saturated oils, in general, show more oxidative stability but have high melting points, like palm oil, which is solid at room temperature.

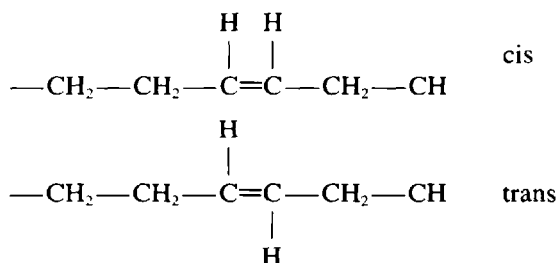
Patterson [5] indicates that unsaturation may be distributed in different ways along the chain which impacts the chemical properties of both the fatty acid and the glyceride. The distribution in a chain with a single bond may be such that the two hydrogen atoms from each side of the double bond lie on the same side of the chain.

Table 21.3 World Production of Nonedible Vegetable Oils

Oil	Major Fatty Acid
Linseed	Linolenic (57%)
Castor	Ricinolenic (89)
Neem	Oleic (49–61%)
Mahua	Oleic (43%)
Karanj/pangam	Oleic (61%)
Undi	Oleic (48–53%)
Kusum	Oleic (60%)
Khakan	Lauric (47%)
Pisa	Lauric (96%)
Kokum	Stearic (56%)
Nahor	Oleic (55–66%)
Sal	Oleic (41.4%)
Dhupa	Stearic (49%)

Source: Bhatia (1983), Pryde (1982), Weiss (1983), Bringi (1987) in Salunkhe, D.K. et al (1992): *World Oilseeds: Chemistry, Technology, and Utilization*, Van Nostrand Reinhold; New York, 1992.

This is a *cis* configuration, where the chain is shaped into a rigid arc and the hydrogen atoms are toward the outside of the arc. Alternately, the hydrogen atoms may be positioned on opposite sides of the chain. In this case the configuration is a *trans* as follows:



Whereas for a normal single-bond atom, there is complete freedom of rotation, there is rigidity at a double bond and only two fixed positions of *cis* and *trans* are possible. Because the saturated fatty acids have no double bonds to distort the chain, they pack more easily into crystal forms and, therefore, have higher melting points than unsaturated fatty acids of the same length. They are also less vulnerable to attack.

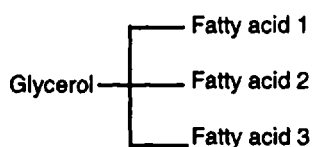


Figure 21.3 Structure of a triglyceride. (From Ref. 4.)

Table 21.4 Fatty Acids in Crude and in Partially Hydrogenated Soybean Oils

Common name	Systemic name	Symbolic notation	Formula
Saturated			
Lauric	Dodecanoic	12:0	$\text{CH}_3(\text{CH}_2)_{10}\text{COOH}$
Myristic	Tetradecanoic	14:0	$\text{CH}_3(\text{CH}_2)_{12}\text{COOH}$
Palmitic	Hexadecanoic	16:0	$\text{CH}_3(\text{CH}_2)_{14}\text{COOH}$
Stearic	Octadecanoic	18:0	$\text{CH}_3(\text{CH}_2)_{16}\text{COOH}$
Archidic	Eicosanoic	20:0	$\text{CH}_3(\text{CH}_2)_{18}\text{COOH}$
Behenic	Docosanoic	22:0	$\text{CH}_3(\text{CH}_2)_{20}\text{COOH}$
Monounsaturated			
Palmitoleic	<i>cis</i> -9- Hexadecenoic	9 <i>c</i> -16:1	$\begin{array}{c} \text{H} \quad \quad \quad \text{H} \\ \quad \quad \quad \diagdown \quad \diagup \\ \quad \quad \quad \text{C}=\text{C} \\ \quad \quad \quad \diagup \quad \diagdown \\ \text{CH}_3(\text{CH}_2)_5 \quad \quad \quad (\text{CH}_2)_7\text{COOH} \end{array}$
Oleic	<i>cis</i> -9- Octadecenoic	9 <i>c</i> -18:1	$\begin{array}{c} \text{H} \quad \quad \quad \text{H} \\ \quad \quad \quad \diagdown \quad \diagup \\ \quad \quad \quad \text{C}=\text{C} \\ \quad \quad \quad \diagup \quad \diagdown \\ \text{CH}_3(\text{CH}_2)_7 \quad \quad \quad (\text{CH}_2)_7\text{COOH} \\ \text{CH}_3(\text{CH}_2)_7 \quad \quad \quad (\text{CH}_2)_7\text{COOH} \end{array}$
Elaidic	<i>trans</i> -9- Octadecenoic	9 <i>t</i> -16:1	$\begin{array}{c} \quad \quad \quad \text{H} \quad \quad \quad \text{H} \\ \quad \quad \quad \diagdown \quad \diagup \\ \quad \quad \quad \text{C}=\text{C} \\ \quad \quad \quad \diagup \quad \diagdown \\ \text{CH}_3(\text{CH}_2)_m \quad \quad \quad (\text{CH}_2)_n\text{COOH} \end{array}$
Positional isomers	<i>trans</i> - <i>x</i> - Octadecenoic (where <i>x</i> = 2 to 16)	9 <i>t</i> -16:1	$\begin{array}{c} \text{H} \quad \quad \quad \text{H} \\ \quad \quad \quad \diagdown \quad \diagup \\ \quad \quad \quad \text{C}=\text{C} \\ \quad \quad \quad \diagup \quad \diagdown \\ \text{H} \quad \quad \quad \text{H} \\ m+n = 14 \end{array}$
	<i>cis</i> -9-Eicosenoic	9 <i>c</i> -20:1	$\begin{array}{c} \text{H} \quad \quad \quad \text{H} \\ \quad \quad \quad \diagdown \quad \diagup \\ \quad \quad \quad \text{C}=\text{C} \\ \quad \quad \quad \diagup \quad \diagdown \\ \text{CH}_3(\text{CH}_2)_9 \quad \quad \quad (\text{CH}_2)_7\text{COOH} \end{array}$

Diunsaturated

Linoleic	<i>cis</i> -9, <i>cis</i> -12-Octadecadienoic	9 <i>c</i> -, 12 <i>c</i> -18:2	$\text{CH}_3(\text{CH}_2)_3 \left[\begin{array}{c} \text{H} \quad \text{H} \\ \diagdown \quad / \\ \text{C}=\text{C} \\ / \quad \diagdown \\ \text{CH}_2 \quad \text{---} \end{array} \right]_2 (\text{CH}_2)_7\text{COOH}$
Conjugated diene	<i>cis</i> -9-Hexadecenoic Octadecadienoic	9 (10) <i>c</i> -, 11 (12) <i>c</i> -18:2 <i>m</i> = 2 or 3 usually <i>n</i> = 7 or 8 usually <i>m</i> + <i>n</i> = 10	$\text{CH}_3(\text{CH}_2)_m \left[\begin{array}{c} \text{CH}_2 \quad \text{H} \\ \diagdown \quad / \\ \text{C}=\text{C} \\ / \quad \diagdown \\ \text{H} \quad \text{---} \end{array} \right]_2 (\text{CH}_2)_n\text{COOH}$
Nonconjugatable diene	<i>cis</i> -9- <i>trans</i> -13-Octadecadienoic	9 <i>c</i> -, 13 <i>t</i> -18:2	$\text{CH}_3(\text{CH}_2)_3 \begin{array}{c} \text{H} \quad \text{H} \\ \diagdown \quad / \quad \diagdown \quad / \\ \text{C}=\text{C} \quad \text{C}=\text{C} \\ / \quad \diagdown \quad \diagdown \quad / \\ \text{H} \quad (\text{CH}_2)_2 \quad (\text{CH}_2)_7\text{COOH} \end{array}$
Triunsaturated			
Linolenic	<i>cis</i> -9-, <i>cis</i> -12-, <i>cis</i> -15- Octadecadienoic	9 <i>c</i> -, 12 <i>c</i> -15 <i>c</i> -18:3 also 18:3 w/ 3	$\text{CH}_3 \left[\begin{array}{c} \text{H} \quad \text{H} \\ \diagdown \quad / \\ \text{C}=\text{C} \\ / \quad \diagdown \\ \text{CH}_2 \quad \text{---} \end{array} \right]_3 (\text{CH}_2)_7\text{COOH}$
Tetraunsaturated			
Arachidonic	<i>cis</i> -5-, <i>cis</i> -8-, <i>cis</i> -11-, <i>cis</i> -14- Eicosatetraenoic	5 <i>c</i> -, 8 <i>c</i> -, 11 <i>c</i> -, 14 <i>c</i> -20:4	$\text{CH}_3(\text{CH}_2)_3 \left[\begin{array}{c} \text{H} \quad \text{H} \\ \diagdown \quad / \\ \text{C}=\text{C} \\ / \quad \diagdown \\ \text{CH}_2 \quad \text{---} \end{array} \right]_3 (\text{CH}_2)_7\text{COOH}$

Source: Ref. 6.

There are many factors that affect the fatty acid makeup of vegetable oils. In addition to their natural makeup, changes in environmental factors such as photo-period, light intensity and quality, and nutrition impact the properties of vegetable oils. Because the fatty acid composition of oils and fats is unique, their characteristics are different. These fatty acids are expressed in either their common names, their systemic names, by symbolic notation, or by their formula. Table 21.4 shows fatty acids in crude and partially hydrogenated soybean oils. The only process that can affect the types of fatty acid present is *partial hydrogenation*, which results in the formation of small amounts of geometrical and positional isomers of the present unsaturated acids.

4 HYDROGENATION

Most triglycerides contain both saturated and unsaturated fatty acids. Hydrogenation is a way to affect the fatty acid contents of the oils. Simply stated, hydrogenation is one way of saturating the double bonds. In the geometrical isomers, the *cis* bonds are partially converted to the *trans* form. In the positional isomers, however, the original *cis* -9 double bonds, such as the oleic acid, is converted partially to a mainly double bond at other positions in the chain [6]. Linolenic acid, which is higher in some oils such as soybean, is a polyunsaturated fatty acid that can lead to a higher degree of autoxidation, which, in turn, results in off-flavor and odor. Through partial hydrogenation, the linolenic acid can be lowered.

Direct addition of hydrogen to the double bond of an unsaturated fatty acid involves overcoming a considerable energy barrier. However, both hydrogen and unsaturated bonds are readily absorbed at the surface of a catalyst such as nickel. In this case, the energy barrier is smaller and the reaction can be much faster and energy is released. Also, the desorption of the reaction products from the surface of nickel requires overcoming a modest energy barrier before more energy is released. When hydrogenation takes place, the net energy release for a drop of one unit in iodine value is sufficient to raise the temperature of the oil by approximately 1.7°C. This, of course, depends on the specific heat of the oil, which varies with temperature. The exothermic heat of reaction has been computed as 1.7 BTU/lb. or 0.942 kcal/kg per unit drop in iodine value [7]. The degree of hydrogenation is expressed by the iodine value (I.V.). The iodine value is defined as *the number of grams of iodine absorbed under standard conditions by 100 grams of fat*; it represents the degree of unsaturation in the fatty acid chain. The saponification number, defined as *the number of milligrams of potassium hydroxide required to saponify 1 g of fat*, is a measure of the average molecular weight of fatty materials.

With partial hydrogenation, the amounts of linolenic and linoleic acid contents are reduced while increasing the amount of the *monoene* content. This not only saturates naturally occurring *cis* double bonds but also isomerizes them to a higher-melting *trans* form [8]. Partial hydrogenation can also lead to an increase in the amount of saturated fatty acid content. By increasing the extent of hydrogenation, the oil begins to change physically and turn into semisolids and solids, which are suitable for margarine and shortening uses. Soybean salad oil, for example, which is partially hydrogenated to improve its shelf life, could be used for industrial uses. However, where a lower pour point and higher degree of fluidity are desired, a partially hydrogenated oil may need to be "winterized" to reduce the amount of

solids (high-melting triglycerides). The pour point is the *lowest temperature at which fluid movement can be detected*. The cloud point is the temperature at which paraffin wax or other solids begin to crystallize when the liquid is chilled. The cloud point is usually several degrees higher than the pour point. Both values are important at low temperatures. If the ambient temperature falls below the pour point, oil will not flow through the system.

Erickson et al. [9] provides a simple description of winterization which involves chilling the fat at a prescribed rate and allowing the solid portions to crystallize. Then, through some sort of filtration, the solids can be separated. If the oil is allowed to cool too rapidly, small crystals are formed that are more difficult to filter. Filtering cold oil, which presents a higher resistance to flow, requires energy and is time-consuming, thus increasing the cost of the process.

A more descriptive explanation of the hydrogenation process is provided by Mounts [10] as the reaction of fats and oils with hydrogen gas in the presence of a catalyst. By adding hydrogen to the oil, unsaturated bonds are transformed to saturated bonds. Hydrogenation is the reaction of fats and oils with hydrogen gas in the presence of a catalyst, causing unsaturated bonds of fatty acids to be saturated. Partial hydrogenation of an oil results in the shifting of the melting point to higher temperatures and improvement in stability (in relation to oxidation and flavor deterioration). Hydrogenation can result in hardening of the oil, but when hydrogenation of an oil remains light, the oil maintains its liquidity while exhibiting increased stability at high temperatures. Hydrogenation can also result in the shifting of double bonds and twisting to produce trans fatty acids (from the cis form) with higher melting points.

Before processing, a catalyst (most often nickel) is added to the oil to increase the rate of reaction. The action of the catalyst will be decreased by the presence of free fatty acids, soap, water, sulfur, or phosphatides, so the oil must be free of these substances. The hydrogenation process is generally performed in a cylindrical pressure vessel with the capability of varying the pressure. During the process, hydrogen gas is dispersed into the oil as fine bubbles, and agitators mix the oil and gas. The oil is then cooled by coils, which are used in heating and cooling of the mixture. When hydrogenation is complete, the oil is filtered until clear.

Certain fatty acids will be hydrogenated more quickly, and each fatty acid has its own rate of reaction. Mono-, di-, and tri-unsaturated fatty acids undergo hydrogenation in sequential fashion. Varying the temperature, pressure, catalyst concentration, or agitation of the process can alter hydrogenation selectivity. Increasing the temperature decreases the selectivity of fatty acids hydrogenated, but it increases the formation of the trans form of fatty acids and increases the hydrogenation rate in general. Increasing the pressure causes decreasing selectivity of fatty acids hydrogenated and decreasing formation of trans fatty acids, but it increases the rate of hydrogenation. An increase in agitation decreases the selectivity of hydrogenation and decreases selectivity of trans fatty acid formation, but it increases the rate of hydrogenation. An increase in the concentration of the catalyst leads to increases in selectivity of fatty acid hydrogenation, trans fatty acid formation, and the rate of hydrogenation.

It is believed that flavor problems with vegetable oils are related to the linolenic acid content present. Possible remedies for this problem include using a copper catalyst during the hydrogenation process. This catalyst can produce an oil that has

a linolenic acid content of less than 1%. Copper catalysts, however, are more sensitive to deactivating substances (free fatty acids, phosphatides, etc.) and are also less active than nickel catalysts. Another option is to use a nickel–silver catalyst, which produces high linolenic selectivity during hydrogenation. Hydrogenation reactions are mostly accomplished using nickel catalysts. Copper catalysts are also used as an alternate to nickel, although copper catalysts are less active. By choice of conditions and the percentage of nickel catalyst, the unsaturated fatty acids begin a reaction sequence in which linolenic acid (18:3) is converted to linoleic (18:2), the linoleic acid is converted to oleic (18:1), and the oleic acid is converted to stearic (18:0) [11]. It should be noted that all of these conversions occur simultaneously, which means that during the conversion of linolenic acid to linoleic, the linoleic acid is also changing to oleic.

Another means of changing properties of a vegetable oil to become more comparable with those of low viscosity oils is by converting them chemically to monoesters. The process used to make this conversion involves reacting an alcohol with the vegetable oil in the presence of a catalyst. Three mono-ester molecules and a glycerol molecule are obtained from each triglyceride molecule. The glycerol, a by-product, is removed by water extraction. The final ester product is termed a methyl ester if methyl alcohol is used and an ethyl ester if ethyl alcohol is used.

5 GENETIC MODIFICATION

Interestingly, agronomists and food scientists have been investigating the genetics of the oilseeds for the development of healthier food. It is now clear that through genetic modification of the seeds, the fatty acid profile of the oil seeds can be altered. This concept eliminates the need for hydrogenation and thus reduces the cost of the base oil for use in industrial application.

Genetic modification, changing the chemical composition of the seed, has been accomplished for some of the vegetable oils, including rapeseed, sunflower, and soybean. Salunkhe et al. [12] reported on the changes in the genetic makeup of rapeseed oil starting in the late 1960s. Accordingly, prior to 1970, rapeseed oil contained 20–50% erucic acid. The first Canadian low-erucic-acid variety, containing about only 3% erucic acid, was licensed in 1968. In 1974, a yet lower acid variety containing less than 0.3% erucic acid was introduced, following the Canadian government's encouragement to switch to low-acid varieties. Canola is the Canadian version of the rapeseed with distinctly low erucic and low glucosinolate. It has a linoleic to linolenic acid ratio of 2:1. In the United States, various genetically modified seeds for canola, sunflower, and soybean are developed by major seed and chemical companies. Currently, the availability of these oils with high oleic acids of up to 80–90% and excellent oxidative stability promise to create many new opportunities for vegetable-based industrial lubricants and hydraulic fluids.

Perhaps the most promising new research advance to date is the development of new mutant lines of soybeans, which lead to new lines of soybeans. These mutant lines with *improved fatty acid profiles* of the oil can be cloned and then integrated into high-yielding elite lines by providing molecular markers. Clone genes are introduced into soybeans to create transgenic lines with increased lysine, oleic, or stearic acid contents. These are oils with a very low content of polyunsaturated fatty acids and show high oxidative stability.

Kinney [13] reported on the design of transgene constructs, which were assisted by using soybean somatic embryos in suspension culture as a model system for soybean seed transformation. The system has allowed the selection of those genes and promoters that are the most effective way of achieving the desired phenotypes in soybeans. According to Kinney, in soybeans, gene–transgene suppression is a more effective means of silencing endogenous genes than antisense. Sense suppression of genes encoding microsomal, fatty acid omega-6 desaturates, has resulted in soybean lines with over 80% oleic acid in their seed oil. This is over four times the oleic acid content of most commodity soybean oils. The high-oleic trait is reported to show stability in over at least three generations [14]. Accordingly, in one of the new lines, the oleic acid content was 81.3% and the seeds had an average of 7.6% palmitic acid, 5.9% stearic acid, 1.3% linoleic acid, and 3.1% linolenic acid.

6 FATTY ACID NAMES AND FORMULAS

Table 21.5 shows fatty acid components found in vegetable oils. The effect of each component on the oxidative stability of the oil in an industrial use is not known. However, some of the fatty acids, particularly those that are common to major oils, have been studied and their effects on the performance of the hydraulic oil are reported.

Table 21.6 shows the percentage of fatty acid components of selected vegetable oils. These percentage compositions are determined by gas–liquid chromatography and exclude acids that occur in trace amounts.

7 FATTY ACID AND OXIDATIVE STABILITY

Most studies dealing with the performance of vegetable oils in hydraulic systems use the percentage of some of the fatty acids, particularly oleic, linolenic, and euricic, as factors affecting the oil's resistance to oxidation. Canola oil, for example, is very low to trace on euricic acid (low-euricic version of rapeseed). Most specialty oils used for lubricant preparation are high in oleic and often low in linolenic acids. A vegetable oil that has poor oxidative stability, once exposed to the high pressure, high temperature, and metallic surfaces in a hydraulic system, will quickly thicken with a noticeable change in viscosity. A highly oxidized oil could begin to polymerize with layers of plastic forming on the exposed surface of the oil. Eventually, the entire body of the oil will polymerize.

Honary [15] reported that most untreated vegetable oils meet ASTM wear protection requirements of hydraulic pumps because they naturally adhere better to metal surfaces preventing boundary lubrication. In ASTM D-2882, for example, untreated crude soybean oil showed 40 mg wear. It is the lack of oxidative stability, however, that results in increased viscosity of the oil and, in extreme cases, leads to polymerization. Therefore, in studying the performance of vegetable oil in hydraulic pumps, the changes in viscosity should be carefully monitored. An increase of less than 10% in viscosity for an oil tested in an ASTM D-2271 is desirable. It is also observed that although the addition of additive packages to vegetable oils improves many of the oils' characteristics, it could negatively impact its natural lubricity. For vegetable-based hydraulic fluid, tests that are longer in duration, such as ASTM D-2271 (1000-h), are more desirable than shorter-term tests such as ASTM

Table 21.5 Fatty Acid Components Found in Vegetable Oils

Carbon atoms: double bonds	Fatty acids
C4	Butanoic (butyric)
C6	Hexanoic (caproic)
C8	Octanoic (caprylic)
C10	Decanoic (capric)
C10:1	Decenoic
C12	Lauric (dodecanoic)
C12:1	<i>cis</i> -9-Dodecenoic
C14	Myristic (tetradecanoic)
C14:1	<i>cis</i> -9-Tetradecenoic
C15	Pentadecanoic
C16	Palmitic (hexadecanoic)
C16:1	<i>cis</i> -9-Hexadecenoic
C17	Heptadecanoic
C17:1	Heptadecenoic
C18	Stearic (octadecanoic)
C18:1	Oleic (<i>cis</i> -9-octadecenoic)
C18:2	Linoleic (<i>cis</i> -9-, <i>cis</i> -12-octadecadienoic)
C18:3	Linolenic (<i>cis</i> -9-, <i>cis</i> -12-, <i>cis</i> -15-octadecatrienoic)
C18:4	<i>cis</i> -6-, <i>cis</i> -9-, <i>cis</i> -12-, <i>cis</i> -15-Octadecatetraenoic
C18:1 (OH)	Ricinoleic (12-hydroxy- <i>cis</i> -9-octadecenoic)
C18 (OH) ₂	Dihydroxystearic
C19	Nonadecanoic
C20	Eicosanoic (arachidic)
C20:1	<i>cis</i> -9-, or <i>cis</i> -11-Eicosenoic
C20:2	Eicosadienoic
C20:3	Eicosatrienoic
C20:4	Arachidonic (<i>cis</i> -5-, <i>cis</i> -8-, <i>cis</i> -11-, <i>cis</i> -14-Eicosatetraenoic)
C20:5	Eicosapentaenoic
C22	Docosanoic (behenic)
C22:1	<i>cis</i> -13-Docosenoic (euricic)
C22:2	Docosahexaenoic
C22:5	4,8,12,15,19-Docosapentaenoic
C22:6	Docosahexaenoic
C24	Tetracosanoic (lignoceric)
C24:1	Tetracosenoic

Source: Karlshamns USA, Inc., *Typical Fatty Acid Compositions of Selected Edible Fats and Oils*, Karlshamns USA, Inc., Janesville, WI (no date).

D-2882 (100-h). Increased oleic acid combined with a reduced percentage of linolenic acid, as developed through new genes, could present improved oxidative stability, as well as a reduced cost of the base oil, due to elimination of the need for chemical modification such as hydrogenation.

In the production of vegetable oils, soybean, palm, rapeseed, and sunflower oils together account for about 73% of all vegetable oils produced [16]. These oils

Table 21.6 Average Compositions for Crude and Refined Soybean Oils

Composition	Crude oil	Refined oil
Triglycerides (%)	95–97	>99
Phosphatide (%)	1.5–2.5	0.003–0.015
Unsaponifiable matters (%)	0.6	0.3
Plant sterols (%)	0.33	0.13
Tocopherols (%)	0.15–0.21	0.11–0.18
Hydrocarbon (squalene) (%)	0.014	0.01
Free fatty acids (%)	0.3–0.7	0.05
Trace metals		
Iron (ppm)	1–3	0.1–0.3
Copper (ppm)	0.03–0.05	0.02–0.06

Source: Pryde (1980) in Ref. 3.

have also been researched and used for various industrial applications, including use as hydraulic fluids.

8 BRIEF DESCRIPTION OF SELECTED VEGETABLE OILS

8.1 Soybean

There are three species of soybean (*Glycine max*): *glycine ussuriensis* (wild), *glycine max* (cultivated), and *glycine gracillis* (intermediate) [17]. It is the world's most important oil seed, with more than 50% of the world's production in the United States. Other countries producing soybeans include Canada, Argentina, Brazil, Paraguay, China, India, Indonesia, Korea, Thailand, Italy, and Romania.

8.1.1 Chemical Composition of Soybean

Salunkhe et al. [18] documented that the protein and oil makeup about 60% of the bean, and about one-third consists of carbohydrates, including polysaccharides, stachyose (3.8%), raffinose (1.1%), and sucrose (5.0%). Accordingly, phosphatides, sterols, minerals, and other constituents are also present as minor constituents. In terms of oxidative stability, soybean oil contains more than 50% polyunsaturated fatty acids and about 15% saturated fatty acids, most of which is palmitic acid [19]. The oil is usually chemically hydrogenated to improve its oxidative stability. Optimized, hydrogenated soybean oils have been developed mainly for increased shelf life in the kitchen and stability during frying. The same technology can be applied for improving the oil's stability for use in industry uses such as hydraulic fluids.

8.1.2 Lipids Content and Composition

Soybean lipids are deposited in spherosomes and can be identified by electron microscopy. The spherosomes in soybean cotyledons are interspersed between protein bodies and are about 0.2–0.5 μm in diameter. The total lipid content in soybean ranges from 18% to 23%. Soybean oil contains 88.1% neutral lipids, 9.8% phospholipids, and 1.6% glycolipids [20]. Neutral lipids primarily consist of triglycerides, accompanied by a smaller proportion of free fatty acids, sterols, and sterol esters.

The main components in neutral lipids, phospholipids, and glycolipids are palmitic, oleic, linoleic, and linolenic acids [21].

The average oil content on a moisture-free basis in soybean seed is about 20%. However, temperature has a marked effect on both polyunsaturated fatty acids and the oil content of soybean. Soybeans produced under controlled-temperature conditions showed oil contents of 23.2% at 85°F, 20.8% at 77°F, and 19.5% at 70°F [22]. Basically, growing conditions, especially temperature, have a significant impact on the fatty acid profile of the beans. In the United States, most of the soybeans grown are processed into defatted meal flakes and crude oil. The meal is used mainly for animal feed and the oil is processed as edible vegetable oil.

8.1.3 Changes Due to Processing

A bitter flavor in soybeans along with rancid odor can be sensed when soybean oil oxidizes in the presence of oxygen, metals, and temperature. Saponins are complex glycosides of triterpenoid alcohols and occur in soybean to the extent of 0.5%. Because of their polarity, saponins are insoluble in hexane and remain in defatted meal. Defatted meal contains 0.6% saponins [23].

Storage

Freshness of the vegetable-based oil is essential for use in hydraulic and other industrial applications. Soybeans are usually dried to reduce the moisture content of the beans to less than 12%. With an initial 12% moisture, soybeans will usually store without change in grade for 2 years. However, high-moisture beans (14% or more) deteriorate during storage. In the long-term storage of soybeans, the nutritive value can be lowered more than that in wheat or corn. Soybeans are easy to store and have a high bulk density. Honary [24] reported that soybean oil which showed good oxidative stability in a hydraulic system failed to perform as well when the oil was improperly stored for a period of time. Compared to their petroleum counterparts, vegetable oils require storage facilities that protect the oil from exposure to oxygen. In short, the oil should be kept fresh by storing in cold storage facilities and preferably topped off with nitrogen to prevent exposure to oxygen. The *Handbook of Soy Oil Processing and Utilization*, which is a joint publication of the American Soybean Association and American Oil Chemist Society, provides extensive coverage of the storage and transportation requirements for soybeans. Such information can be applied to most other vegetable oils as well.

8.1.4 Processing Soybean for Oil

Extracting oil requires three basic steps: (1) bean preparation, (2) oil extraction, and (3) solvent stripping and reclamation [25]. After processing, the oil may be degummed for use in food-related applications. Small on-the-farm extruder/expeller units are finding popularity among farmers wishing to extract the meal for feed purposes. These units do not use the conventional oil-extraction techniques. Instead, the bean is forced through an extruder unit, which creates high-pressure-induced temperatures. The shear and grinding process results in the rupture of the cell walls. When the cell walls, particularly the oil cell walls rupture, they release some of the natural tocopherols, which are antioxidant, as well as some of the lecithin. Honary [26] reported that crude soybean oil obtained through this process showed more oxidative stability using ASTM D-2271 (hydraulic pump test) than the crude oil

obtained through conventional hexane-extracted processing. This could be attributed to the retention of the natural antioxidant (tocopherol) in the oil by the extrusion process. The oil is then extracted from the meal by the use of an expeller, which is essentially a mechanical press. Figure 21.4 presents the extruder–expeller process in concept; Fig. 21.5 shows a unit commonly used for extruding the soybean and many other vegetable seeds. The extruded meal will need to be pressed to extract the oil.

8.1.5 Refining

Refining is a purifying treatment designed to remove free fatty acids, phosphatides and gums, coloring matter, insoluble matter, settlings, and other unsaponifiable materials from the triglycerides [27]. Accordingly, oils such as soybean are refined through chemically refining, caustic refining, and physical or steam refining. Refining removes particles, such as free fatty acids, coloring and insoluble matters, phosphatides, and so forth and is used as a purifying process. This prevents foaming, smoking, cloudiness, and so on when the oil is heated.

In the process of chemical refining, an alkali solution is used. The alkali combines with free fatty acids to form soaps that can be separated (process of saponification). Phosphatides and gums absorb the alkali and are coagulated through hydration or degradation. Coloring is degraded, absorbed by gums, or made water soluble by the alkali. The caustic process of refining involves analyzing the amount of free fatty acids and neutral oil in order to determine the amount of caustic soda to be added. The formation of different density layers occurs as one layer containing most of the oil and the other layer most of the unwanted particles. These are separated using a centrifuge.

Physical refining does not use caustic soda and does not have soapstock. Treatment with phosphoric acids removes phosphatides. This oil can then be used in steam refining. Steam refining uses a stripping steam to remove odor from the oil, and it also removes free fatty acids.

Another related refining process is known as the Zenith process. This process removes non-fatty-acid substances with concentrated phosphoric acid. The acid treatment removes calcium and magnesium from gums. Table 21.6 shows the average compositions for crude and refined soybean oils.

8.1.6 Degumming

Degumming is defined as the removal of phospholipids and other nontriglyceride materials. A by-product of degumming is lecithin, which can be used as an emulsifying agent. Treating crude soybean oil with caustic soda neutralizes free fatty acids, hydrolyzes phosphatides, and removes some colored pigments and unsaponifiable matters.

8.1.7 Bleaching

Bleaching is an important technique which uses activated earth to absorb pigments, oxidation products, phosphatides, soaps, and trace metals. Natural clays or earths (Fuller's earth), which are basically hydrated aluminum silicates are used for bleaching. The process is simple. The neutralized oil is mixed with the appropriate amount of clay, heated to the bleaching temperature, and then filtered.

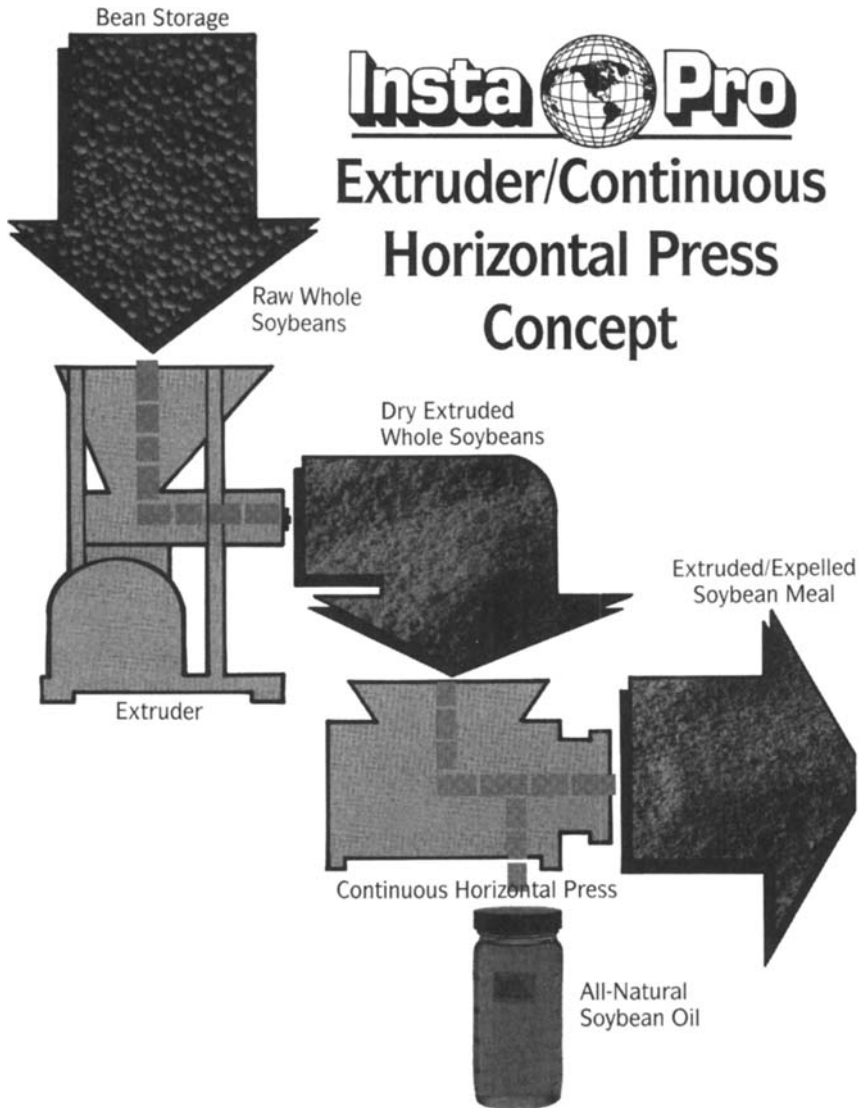
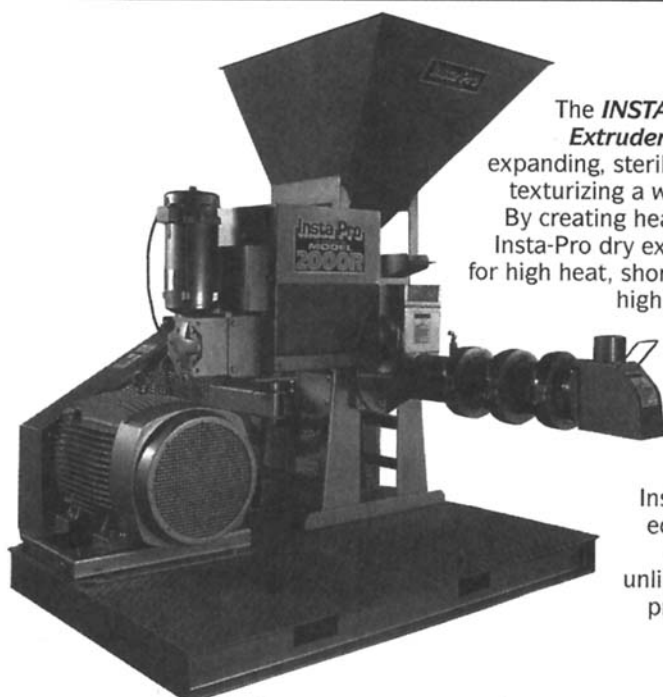


Figure 21.4 Extruder–expeller concept. (Courtesy of Insta-Pro® International, Des Moines, IA.)

8.1.8 Deodorizing

Deodorization primarily removes volatile substances and converts the oil into a bland-tasting, clear liquid [28]. Noticeable flavor and odor will have essentially disappeared when the free fatty acid content is lowered to 0.01% to 0.03% and the protein content is miniscule. The process of deodorizing involves heating, steam stripping, and cooling the oil before exposing it to the atmosphere. The high temperature is needed to remove triglycerides, which are less volatile than the flavor



The **INSTA-PRO® Model 2000R Extruder** is capable of cooking, expanding, sterilizing, dehydrating and texturizing a wide range of products. By creating heat through friction, the Insta-Pro dry extrusion process allows for high heat, short-cook time producing high quality feed and food.

Insta-Pro extrusion is an economical, easy-to-use operation which offers unlimited opportunities in processing possibilities.

Specifications:

Power Rating:	55.95 kw/75 hp
Motor RPM:	1,725
Extruder RPM:	550
Capacity/Hr.:	590-910 kg/1300-2000 lbs.
Dimensions:	(inches) 70"H x 62"W x 71"L (centimeters) 177.8 x 157.5 x 180.34
Electrical:	220/440 volts, 3-phase/60 Hz., 176/87 amps. 220/380 volts, 3-phase/50 Hz., 199/99 amps.
Weight:	1,089.6 kg/2,400 lbs.

Features:

- Over-the-top vibratory feeder, DC control side mount volumetric feeder with agitator
- Wall mount control panel
- Digital temperature indicators
- Optional stainless steel volumetric feeder
- Ridged, compact state-of-the-art construction
- Core parts interchangeable with Insta-Pro® Model 2500 extruder
- Highly cost efficient
- Versatile
- Engine driven units available

Figure 21.5 Extruder. (Courtesy of Insta-Pro® International, Des Moines, IA.)

and odor components present in the oil. These substances must be volatilized to condense and, subsequently, remove them from the oil. Stripping steam is added to increase the rate of this process. The process removes free fatty acids, but the content cannot be reduced below 0.005% because of interactions with the stripping steam. Steam distillation also may result in the conversion of up to 25% of the linolenic acid present from the cis form to the trans form due to elevated temperature and time periods.

8.1.9 Protection Against Oxidation

For edible oils, several methods are used to prevent oxidation. These methods can be applied to industrial lubricants uses as well and include (1) exclusion of air during processing, (2) cooling the deodorized oil before exposing it to the atmosphere, (3) preventing exposure of oil to air by a cover of nitrogen, and (4) addition of chemical antioxidants and metal scavengers [29]. Propyl gallate and tertiary butyl hydroquinone (TBHQ) may be added to increase oxidative stability, and *t*-butylhydroxy toluene (BHT) or *t*-butyl hydroxyanisole (BHA) may be added to increase shelf life. These additives may be used in amounts of up to 0.01% singly or 0.02% in combination. The oil is then filtered after the deodorization process has been completed to remove any solids that have formed or been introduced. After the process is completed, the free-fatty-acid content should be less than 0.03% (gram weight) and peroxide values should be zero:

Density: 0.9075

Viscosity: 30.52 cSt at 40°C (7.42 at 100°C)

Viscosity index: 224

TAN (ASTM 664): 0.10

Pour point: 16°F (−9°C)

Flash point: 597°F (314°C)

Gross heat of combustion (BTU/lb.): 16,770.

8.2 Palm Oil

Palm oil is a competitive product for use as fuel, lubricants, and other nonfood *new uses* such as palm ink. Oil palm (*Elaeis guineensis* Jacq.) is an important edible oil obtained from either palm fruit or from the palm kernel. Palm kernel is obtained as a minor product during the processing of oil palm fruit. Honary [30] reported that untreated palm olein tested in a ASTM D-2271 hydraulic pump test showed high oxidative stability as measured by changes in the oil viscosity. Palm oil contains some triglyceride species that are completely saturated. It consists of mostly monoglycerides (48–55%) and diunsaturated glycerides (30–43%) with small quantities of saturated (6–8%) and unsaturated glycerides (6–8%) [31]. The fatty acid composition of palm kernel was reported by Godin and Spensley [32] to be caprylic (3–4%), capric (3–7%), lauric (46–52%), myristic (15–17%), palmitic (6–9%), stearic (1–3%), oleic (13–19%), and linolenic (0.5–2.0%).

Maiti et al. [33] reported the fatty acid profile of palm oil to be myristic (0.5–6.0%), palmitic (35–40%), stearic (40–50%), oleic (40–50%), and linolenic (5–11%) acid contents. These values change for palm oil produced in different parts of the world and various sources. Palm olein is the liquid fraction of palm oil and is used worldwide as cooking oil. Honary [34] reported on the performance of an untreated palm olein as a hydraulic fluid with a supplier-reported fatty acid composition of lauric (0.2%), myristic (1.0%), palmitic (39.6%), stearic (4.6%), oleic (43.3%), linolenic (11%), and arachidic (0.3%). Accordingly, the oil contained 43.3% monounsaturates, 11.0% polyunsaturated, and a high level of 45.7% saturates with 0% in trans acids. This type of oil showed excellent oxidative stability in a hydraulic pump test, but had the drawback of a very high melting point of about 75°F, being solid at room temperature.

8.3 Rapeseed

Agronomically, rapeseed is good for northern climates; it thrives well in a cool, moist climate and is grown extensively in northern Europe and Canada [35]. Accordingly, the so-called zero-erucic variety contains 53% oleic acid and 11% linolenic acid. After soybean and palm, rapeseed is the largest produced vegetable oil in the world. Other countries growing rapeseed include India, China, Pakistan, and Australia. Like soybean, the meal obtained after extraction of oil is used as animal feed.

Rapeseed refers to more than one plant species and is often used to denote the seeds derived from oil-yielding members of the Brassica family, including some mustard seeds grown for edible or industrial oil [36]. *Brassica napus* and *B. campestris* are the two most important and widely grown species with summer types grown in North America and a mixture of summer and winter types grown in Europe. *B. juncea* and *B. campestris* are grown in India and the Far East. Wild populations of *B. campestris* have been reported from different regions of Europe and Asia. *B. napus*, which is derived genetically from a natural hybridization of *B. campestris* and *B. oleracea*, occurs naturally in more restricted areas, mainly Europe and North Africa.

8.3.1 Chemical Composition

Chemical composition of rapeseed varies widely depending on both genetic and environmental factors. The oil content ranges from 33.2% to 47.6% (8.5% moisture basis) and protein content from 29.5% to 57.5% (oil-free meal, 8.5% moisture basis). Rapeseeds, in general, contain about twice as much oil as soybeans, and the oil-free meal has only slightly less protein. Table 21.7 presents a comparison of proximate compositions of rapeseed and soybeans [37].

Lipids

The crude oil initially extracted from rapeseed is like other oils, made up mainly (95–98%) of triacylglycerols (triglycerides). Other constituents, present in greater or lesser amounts, include phosphatides, fatty acids, sterols, hydrocarbons, alcohols, tocopherols, lipochromes, pigments, sulfur compounds, and minerals [38].

The fatty acid composition of rapeseed oil varies from cultivar to cultivar, mainly due to wide variations in their erucic acid (C22:1) contents. Rapeseed oil and oils from other members of the Cruciferae family are unusual in that they contain substantial amounts of long-chain fatty acids (C18). The triacylglycerol composition of rapeseed oil is characterized by the occurrence of C20–C24 fatty acids almost

Table 21.7 Comparison of Proximate Compositions of Rapeseed and Soybeans

Component	Rapeseed (%)	Soybean (%)
Moisture	69	11–14
Oil content (moisture-free basis)	38–50	16–22
Protein content (moisture- and oil-free bases)	36–44	45–60
Fiber content	11–16	3.3–6.4

Source: Anjou et al. (1977), in Ref. 3.

exclusively in the 1 and 3 positions, C18 fatty acids in the 2 position, and a preference of linoleic and linolenic acids for the 2 position in zero erucic acid oils [39]. The positioning of polyunsaturated fatty acids might be of technological importance, giving a greater tendency to oxidative stability compared to soybean oil, which has a random distribution of linolenic acid. Reduction in the erucic acid (C22:1) content has resulted in a marked increase in oleic acid (C18:1), along with smaller increases in linoleic (C18:2) and linolenic (C18:3) acid contents.

Canola (*CAN*adian Oil Low Acid, which is a low erucic acid version of rapeseed) is a major base oil for industrial lubricants uses. Canola (*B. napus* L. and *B. campestris* L.) contains less than 2% erucic acid (C22:1) in its oil and less than 30 μmol of glucosinolates per gram of fat-free meal [40]. Accordingly, features that have given prominence to canola are the following: lower saturated fat than other vegetable oils (6%), which is less than safflower (10%), sunflower (11%), corn (13%), olive (14%), soybean (15%), and tropical oils (about 50%), and a high concentration of monounsaturated fat (oleic acid at 62%)—only olive oil has a higher level of oleic acid (77%). The balance of a high monounsaturated fat combined with low saturated fat results in a nutritionally healthy oil. The high oleic acid content resulting in a higher oxidative stability makes the oil suitable for industrial lubricant applications. Genetically modified, high-oleic versions of canola oil have been tested for hydraulic and other industrial lubricants uses with good results.

Properties

Rapeseed oils exhibit a saponification value of 168–192 and an iodine value of 81–112. Vaisey-Genser and Ylimaki [41] found BHA/BHT with monoglyceride citrate to be ineffective against oxidation of canola oil. A polymeric antioxidant, *anoxomer*, effectively inhibited oxidative changes in canola oil stored for 12 days at 65°C when added at levels of 2000–4000 ppm. The levels of 500 and 1000 ppm *anoxomer* delayed oxidation.

Erucic acid (C22:1) confers certain physical properties to rapeseed oil. Appleqvist [42] reported that high-erucic-acid rapeseed oils had lower specific gravities (in the range of 0.906–0.914) than low-erucic-acid oils. Their results indicate a specific gravity of 0.9171 for canola oil (0.7% erucic acid) compared to 0.9159 for the high erucic acid (23%) fully refined oil. The higher specific gravity of 0.9187 observed for soybean oils was explained by the high linoleic acid content of this oil compared to canola, a high-oleic-acid oil.

Other Lipids

The nontriacylglycerol portion of crude rapeseed oil makes up 2–3% of the total oil and consists primarily of free fatty acids, monoacylglycerols and diacylglycerols, phosphatides, glycolipids, and unsaponifiables. Free fatty acids (about 1% of the total oil) and partially esterified glycerols are related in composition to the triacylglycerol fraction [43].

8.3.2 Functional Properties

Solubility

The isoelectric pH of rapeseed protein has been reported to be lower (pH 3.5) than soybean proteins.

Water Absorption

The water-binding properties of a protein determine the extent of its interaction with water. Sosulski et al. [44] reported that rapeseed protein products had a high water absorption.

Oil Absorption

Naczka et al. [45] reported that canola meals prepared by the methanol–ammonia treatment showed higher fat absorption than laboratory-produced, hexane-extracted canola meals.

Emulsifying and Foaming Properties

Khalil [46] studied the foaming capacity of proteins of several oilseed. Foaming capacity was best for rapeseed protein, followed by soybean and sunflower seed protein. It was concluded that the foaming behavior follows a pattern paralleling pH solubility profile.

8.4 Sunflower Oil

Sunflower oil has major uses as a cooking oil and margarine. The oil has differing fatty acid composition if it is grown in northern climates as compared to southern climates. According to Erickson et al. [47], oil from northern-grown seeds has a high linoleic acid content (64%) and low linolenic acid content (<1%); whereas oil from southern-grown seeds contains a low linoleic acid content (49%) and a high oleic acid content (34% vs. 21%).

Sunflower [*Helianthus annuus* variety *macrocarpus* (DC) CkII] is known in two types: oilseed and nonoil or confectionary. The confectionary type is consumed as whole roasted seed and represents less than 10% of total sunflower production [48]. The fatty acid composition of sunflower oil is primarily palmitic (7.2%), stearic (4.1%), oleic (16.2%), and a large portion of linoleic (72.5%) [49].

Sunflower oil is extracted from the seed or kernels using similar equipment and conditions as for soybean oil. After cleaning, drying, and dehulling, the oil is extracted by either mechanical-extraction, prepress solvent-extraction, or by direct solvent-extraction methods. Other processes such as bleaching, deodorizing, and winterization are also used to prepare the oil for food uses. Sunflower oil is considered a premium oil as well as being one of the most palatable vegetable oils. Recent developments in genetic modification of the seeds have resulted in new high oleic and “ultrahigh oleic” sunflower oils with high oxidative stability. Naegley [50] and Honary [51] reported on the performance of sunflower oil for industrial applications.

Naegley [52] compared the oxidative stability of several vegetable oils including high-oleic and very high-oleic sunflower oils in the presence of oxygen (Fig. 21.6). In order to further improve the oxidative stability of sunflower oil, Naegley compared the effects of two antioxidants, tocopherol and TBHQ, on the oil using the Active Oxygen Method (AOM) (Fig. 21.7).

The physicochemical characteristics of sunflower oil were reported by Weiss (1983) in Ref. 3 as follows:

Density at 60°C:	0.894–0.899
Titer (°C):	17–20
Melting point (°C):	0

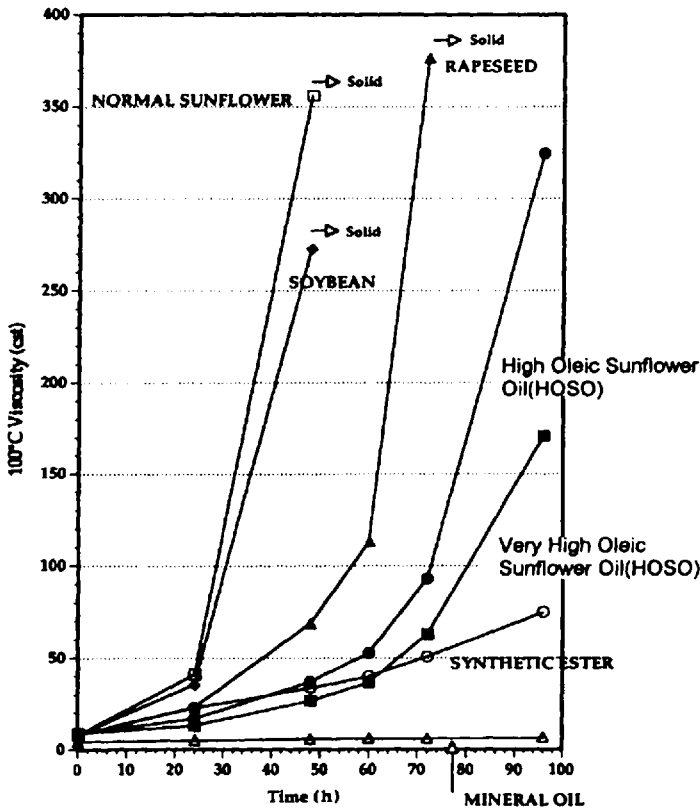


Figure 21.6 Viscosity increase of base oils in the presence of oxygen (10 L/h) at 120°C. (From Ref. 52.)

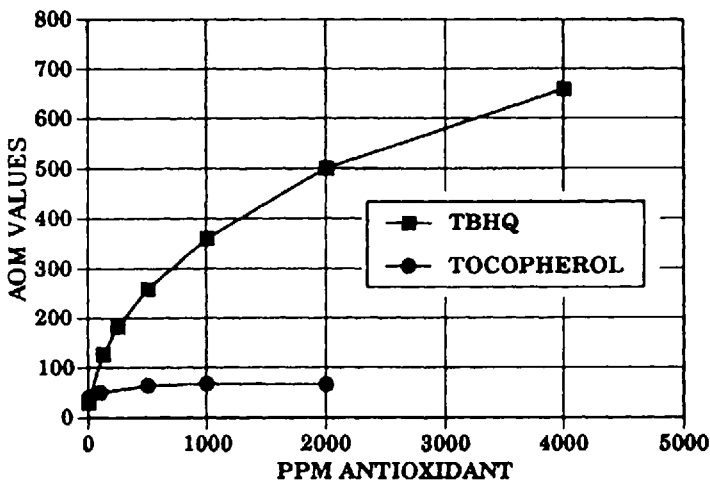


Figure 21.7 Effect of TBHQ and tocopherol on the stability of high-oleic sunflower oil (From Ref. 52.)

Smoke point (°C):	250*
Refractive index (at 25°C):	1.4597
Iodine value:	128
Saponification value:	191
Free fatty acids (%):	0.01–0.03*
Unsaponifiables (%):	0.3–0.5
AOM time (h):	10–15*

8.5 Corn

Corn is one of the major cereal grains, after wheat and rice, grown throughout the world. The oil content of the corn kernel, on a moisture-free basis, is about 5% as compared to soybean, which is about 20% [53]. New genetic research has resulted in the development of the soy called high-oil corn, which contains about 8% oil. The high-oil corn, however, can be directly utilized for commercial oil extraction. The high-oil types are generally low yielders and need to be genetically improved for better agronomical performance. The oil is concentrated in the germ and is recovered both by wet milling, in the production of starch, and by dry milling, in the production of grits, meal, and flour. More than 90% of the corn grain produced is processed and fed to animals in the Western world, whereas in Asia and Africa, almost all grain produced is utilized for human consumption by traditional processing, without separating the germ [54].

Corn is a premium oil because of its high polyunsaturated fatty acid content and its low content (<1%) of linolenic acid. Leibovitz and Ruckenstein [55] list the fatty acid composition of corn oil as follows: lauric acid (0.1%), myristic acid (0.2%), palmitic acid (11.8%), palmitoleic (trace), stearic acid (2.0%), oleic acid (24.1%), linoleic acid (61.9%), and linolenic acid (0.7%).

The physicochemical characteristics of corn oil were reported by Salunkhe et al. [56] as follows:

Specific gravity:	0.918–0.925
Density at 60°C:	0.892–0.897
Titer (°C):	18–20
Melting point (°C):	0
Refractive index (at 25°C):	1.4596
Iodine value:	103–133
Saponification value:	187–195
Free fatty acids, as oleic (%):	0.03–4
Unsaponifiables (%):	1.2–2.8

8.6 Safflower Oil

Safflower is grown in the southwest United States and has been considered for use in industrial applications. Safflower oil has a high linoleic acid content (73%) and a low linolenic acid content (<1%), therefore commanding premium prices. A high-oleic variety containing 78% oleic and 12% linoleic is available [57]. According to Salunkhe et al. [58], the ranges for five important fatty acids of high oleic safflower

*Note: For refined, bleached, and deodorized oil [Adams (1982) in Ref. 3].

Table 21.8 Fats and Oils Composition

Fatty acid component		Vegetable based								
		Canola	Castor	Coco butter	Coconut	Corn	Cotton	Crambe	Linseed	Olive
C4	Butanoic (butyric)									
C6	Hexanoic (caproic)									
C8	Octanoic (caprylic)				7.6					
C10	Decanoic (capric)				7.3					
C10:1	Decenoic									
Total C10					7.3					
C12	Lauric (dodecenoic)				48.2	0.1	0.1			
C12:1	<i>cis</i> -9-Dodecenoic									
Total C12					48.2	0.1	0.1			
C14	Myristic (tetradecenoic)			0.5	16.6	0.7	0.7			
C14:1	<i>cis</i> -9-Tetradecenoic									
Total C14				0.5	16.6		0.7			
C15	Pentadecanoic									
Total C15										
C16	Palmitic	3.2	1.2	25.0	8.0	11.5	21.6	2.0	5.5	9.0
	(hexadecanoic)									
C16:1	<i>cis</i> -9-Hexadecenoic		0.2		1.0		0.6	0.4		0.6
Total C16		3.2	1.4	25.0	9.0	11.5	22.2	2.4	5.5	9.6
C17	Heptadecanoic						0.1			
C17:1	Heptadecenoic						0.1			
Total C17							0.2			
C18	Stearic (octadecanoic)	0.9	1.0	34.5	3.8	2.2	2.6	0.4	3.5	2.7
C18:1	Oleic (<i>cis</i> -9-octadecenoic)	60.8	3.0	36.5	5.0	26.6	18.6	16.9	19.1	80.3
C18:2	Linoleic (<i>cis</i> -9-, <i>cis</i> -12-octadecatrienoic)	19.0	3.5	3.0	2.5	58.7	54.4	8.6	15.3	6.3
C18:3	Linolenic (<i>cis</i> -9-, <i>cis</i> -12-octadecadienoic)	9.1	0.2	0.5		0.8	0.7	6.4	56.6	0.7
C18:4	<i>cis</i> -6-, <i>cis</i> -9-, <i>cis</i> -12-, <i>cis</i> -15-octadecatrenoic									

C18:4(OH)	Ricinoleic (12-hydroxy- <i>cis</i> -9-octadecenoic)		89.2							
C18(OH) ₂	Dihydroxystearic		1.4							
Total C18		95.8	98.3	74.5	11.3	88.3	76.3	32.3	94.5	90.0
C19	Nonadecanoic									
Total C19										
C20	Eicossanoic (arachidic)		0.3				0.3	0.5		0.4
C20:1	<i>cis</i> -9-, or <i>cis</i> -11-Eicosenoic							3.2		
C20:2	Eicosadienoic									
C20:3	Eicosatrienoic									
C20:4	Arachidonic (<i>cis</i> -5-, <i>cis</i> -8-, <i>cis</i> -11-, <i>cis</i> -14-eicosatetraenoic)									
C20:5	Eicosapentaenoic									
Total C20			0.3				0.3	3.7		0.4
C22	Docosanoic (behenic)						0.2	2.0		
C22:1	<i>cis</i> -13-Docosenoic (erucic)	1.0						57.2		
C22:2	Docosadienoic							0.8		
C22:5	4,8,12,15,19-Docosapentaenoic									
C22:6	Docosahexaenoic									
Total C22		1.0					0.2	60.0		
C24	Tetracosanoic (lignoceric)									
C24:1	Tetracosenoic									
Total C24										
Others								1.6		
Total		100.0	100.0	100.0	100.0	100.0	100.0	100.0	100.0	100.0
Chemical Values										
Iodine value		94–126	81–91	81–91	7–12	118–128	98–118	91	155–205	80–88
SAP value of oil		186–198	176–187	177–187	250–264	187–193	189–198	169	188–196	188–196
Melting point (°C)			–20 to –10		23–26	–12 to –10	–2 to 2		–20	
Titer (of split acids) (°C)		0–2	1–3	1–3.5	20–24	14–20	30–37		19–21	17–26

Table 21.8 Continued

Fatty acid component		Vegetable based								
		Palm kernel			Palm oil					
		Palm kernel	Olein	Stearine	Palm oil	Olein	Stearine	Peanut	Rapeseed	Safflower
C4	Butanoic (butyric)									
C6	Hexanoic (caproic)		0.2	0.1						
C8	Octanoic (caprylic)	1.4	4.3	2.4						
C10	Decanoic (capric)	2.9	3.7	3.2						
C10:1	Decenoic									
Total C10		2.9	3.7	3.2						
C12	Lauric (dodecenoic)	50.9	42.6	55.2	0.3	0.2	0.7			
C12:1	<i>cis</i> -9-Dodecenoic									
Total C12		50.9	42.6	55.2	0.3	0.2	0.7			
C14	Myristic (tetradecenoic)	18.4	12.4	19.9	1.1	1.0	1.5	0.1	0.1	
C14:1	<i>cis</i> -9-Tetradecenoic									
Total C14		18.4	12.4	19.9	1.1	1.0	1.5	0.1	0.1	
C15	Pentadecanoic									
Total C15										
C16	Palmitic	8.7	8.4	8.1	42.9	39.8	55.7	11.1	4.0	6.5
	(hexadecanoic)									
C16:1	<i>cis</i> -9-Hexadecenoic				0.2	0.2		0.2	0.1	
Total C16		8.7	8.4	8.1	43.1	40.0	55.7	11.3	4.1	6.5
C17	Heptadecanoic							0.1		
C17:1	Heptadecenoic				0.1			0.1		
Total C17							0.1	0.2		
C18	Stearic (octadecanoic)	1.9	2.5	3.3	4.6	4.4	4.8	2.4	1.3	2.5
C18:1	Oleic (<i>cis</i> -9-octadecenoic)	14.6	22.3	6.9	39.3	42.5	29.5	46.7	17.6	12.5
C18:2	Linoleic (<i>cis</i> -9-, <i>cis</i> -12-octadecatrienoic)		3.4	0.8	10.7	11.2	7.2	32.0	12.7	77.5
		1.2								
C18:3	Linolenic (<i>cis</i> -9-, <i>cis</i> -12-octadecadienoic)				0.4	0.2	0.1		5.3	
C18:4	<i>cis</i> -6-, <i>cis</i> -9-, <i>cis</i> -12-, <i>cis</i> -15-octadecatrienoic									
C18:4(OH)	Ricinoleic (12-Hydroxy- <i>c</i> -9-octadecenoic)									

C18(OH), Total C18	Dihydroxystearic	17.7	28.2	11.0	55.0	58.3	41.6	81.1	36.9	92.5
C19 Total C19	Nonadecanoic									
C20	Eicossanoic (arachidic)		0.1	0.1	0.3	0.4	0.4	1.3	0.9	0.5
C20: 1	<i>cis</i> -9- or <i>cis</i> -11- Eicosenoic		0.1					1.6	10.6	0.5
C20: 2	Eicosadienoic									
C20: 3	Eicosatrienoic									
C20: 4	Arachidonic (<i>cis</i> -5-, <i>cis</i> -8-, <i>cis</i> -11-, <i>cis</i> - 14-eicosatetraenoic)									
C20: 5	Eicosapentaenoic									
Total C20			0.2	0.1	0.3	0.4	0.4	2.9	11.5	1.0
C22	Docosanoic (Behenic)				0.1	0.1	0.1	2.9	0.7	
C22: 1	<i>cis</i> -13-Docosenoic (erucic)								45.8	
C22: 2	Docosadienoic								0.1	
C22: 5	4,8,12,15,19- Docosapentaenoic									
C22: 6	Docosahexaenoic									
Total C22					0.1	0.1	0.1	2.9	46.6	
C24	Tetracosanoic (lignoceric)							1.5	0.2	
C24: 1	Tetracosenoic								0.6	
Total C24								1.5	0.8	
Others										
Total		100.0	100.0	100.0	100.0	100.0	100.0	100.0	100.0	100.0
Chemical values										
Iodine Value		14–19	23–31	6–9	50–55	56 min.	48 max.	84–100	100–110	140–150
SAP Value of oil		245–255			196–202			188–195	183–188	188–194
Melting point (°C)		24–26			27–50			–2	–7 to –10	–18 to –16
Titer (of split acids) (°C)		20–28			40–47			26–32	23–26	16–18

Table 21.8 Continued

Fatty acid component		Vegetable based			Animal based			Marine based			
		Soybean	Sunflower	Tall oil	Butter	Lard	Tallow	Yellow grease	Herring	Menhaden	Sardine
C4	Butanoic (butyric)				2.3						
C6	Hexanoic (caproic)				1.6						
C8	Octanoic (caprylic)				1.5						
C10	Decanoic (capric)				2.2						
C10:1	Decenoic				0.4						
Total C10					2.6						
C12	Lauric (dodecanoic)				2.5	0.3					
C12:1	<i>cis</i> -9-Dodecenoic				0.2						
Total C12					2.7	0.3					
C14	Myristic (tetradecanoic)	-0.1			8.2	1.7	3.0	2.6	7.6	7.3	6.0
C14:1	<i>cis</i> -9-Tetradecenoic				2.6	0.2	0.4	0.3			
Total C14		0.1			10.8	1.9	3.4	2.9	7.6	7.3	6.0
C15	Pentadecanoic					0.1		0.4	0.4		
Total C15						0.1		0.4	0.4	0.4	
C16	Palmitic (hexadecanoic)	10.5	7.0	0.2	25.8	26.2	26.3	26.3	18.3	23.6	10.0
C16:1	<i>cis</i> -9-Hexadecenoic				4.6	4.0	2.6	3.2	8.3	9.9	13.0
Total C16		10.5	7.0	0.2	30.4	30.2	28.9	29.5	26.6	33.5	23.0
C17	Heptadecanoic					0.5	0.4	0.3	0.5	0.9	
C17:1	Heptadecenoic					0.3	0.4				
Total C17						0.8	0.8	0.3	0.5	0.9	
C18	Stearic (octadecanoic)	3.2		2.2	9.1	13.5	22.4	18.4	2.2	2.6	2.0
C18:1	Oleic (<i>cis</i> -9-octadecenoic)	22.3	3.3	58.6	32.1	42.9	43.1	45.3	16.9	17.0	24.0
C18:2	Linoleic (<i>cis</i> -9-, <i>cis</i> -12-octadecatrienoic)		21.0	36.0	4.9	9.0	1.4	3.6	1.6	1.2	
C18:3	Linolenic (<i>cis</i> -9-, <i>cis</i> -12-octadecadienoic)	54.5									
		8.3	68.0		2.0	0.3			0.6		
C18:4	<i>cis</i> -6-, <i>cis</i> -9-, <i>cis</i> -12-, <i>cis</i> -15-octadecatrienoic		0.7							4.1	

C18:4(OH)	Ricinoleic (12-hydroxy- <i>cis</i> -9-octadecenoic)										
C18(OH) ₂	Dihydroxystearic										
Total C18		88.3	93.0	96.8	48.1	65.7	66.9	67.3	21.3	24.9	26.0
C19	Nonadecanoic									1.2	
Total C19										1.2	
C20	Eicossanoic (arachidic)	0.2		0.7		0.2					
C20:1	<i>cis</i> -9-, or <i>cis</i> -11-eicosenoic	0.9		0.7		0.8			9.4		
C20:2	Eicosadienoic									0.3	
C20:3	Eicosatrienoic									0.2	
C20:4	Arachidonic (<i>cis</i> -5-, <i>cis</i> -8-, <i>cis</i> -11-, <i>cis</i> -14-eicosatetraenoic)								0.4	3.4	26.0
C20:5	Eicosapentaenoic								8.6	12.0	
Total C20		1.1		1.4		1.0			18.4	15.9	26.0
C22	Docosanoic (behenic)										
C22:1	<i>cis</i> -13-Docosenoic (erucic)								11.6		
C22:2	Docosadienoic									1.7	
C22:5	4,8,12,15,19-Docosapentaenoic								1.3	9.1	19.0
C22:6	Docosahexaenoic								7.6		
Total C22									20.5	10.8	19.0
C24	Tetracosanoic (lignoceric)										
C24:1	Tetracosenoic								0.4	0.8	
Total C24									0.4	0.8	
Others				1.6					4.3	4.3	
Total		100.0	100.0	100.0	100.0	100.0	100.0	100.0	100.0	100.0	100.0
Chemical values											
Iodine value		120–141	125–136	122–142	25–42	53–57	48–52	50–65	123–142	140–188	170–193
SAP value of oil		189–195	188–194	197–200	233–240	190–202	192–202	190–202	180–192	189–193	189–193
Melting point (°C)		–23 to –20	–18 to –16		28–35	33–46	40–47				
Titer (of split acids) (°C)		20–21	16–20	4–15	33–38	32–43	40–47	39–43	23–27	27–28	31–33

Note: Typical percent composition determined by chromatography. Some values obtained from literature.

Source: Karlshamns USA, Inc., *Typical Fatty Acid Compositions of Selected Edible Fats and Oils*, Karlshamns USA, Inc., Janesville, WI (no date).

oil were palmitic acid (0.9–3.1%), stearic acid (9.4–12.0%), oleic acid (65.9–73.4%), and linoleic (65.9–73.4%).

Many other vegetable oils have been explored for industrial and hydraulic uses. Recently, due to environmental concerns, most growers groups in the United States have explored new uses of their vegetable oils. Table 21.8 presents the fatty acid profiles of several vegetable oils, including most of the aforementioned oils. These are products that are commercially available in the United States and are representative of the fatty acid compositions.

9 VEGETABLE OILS IN HYDRAULIC USE

Although all of these fatty acids play an important role in the characteristics of the oil, various research results have indicated that some are more critical if the oil is to be used as hydraulic fluid. Naegley [59] used the active oxygen method (AOM) to show how the percentage of *oleic acid* (total 18:1) relates to the oxidative stability, which is an inherent weakness of most vegetable oils (Fig. 21.8). Hydraulic and other industrial fluids must have a high degree of oxidative stability to perform in the demanding industrial applications where high pressures, high temperatures, exposure to metals, and moisture could cause the oil to oxidize. Naegley's data present only the percentage of oleic acid and their relationship to oxidative stability. Other fatty acids, too, have an impact on the oxidative stability of the vegetable oils, although to a lesser extent than oleic acid. One that is particularly observed is the percentage of linolenic acid, which, due to its unsaturated nature, plays an important role in the oxidative stability.

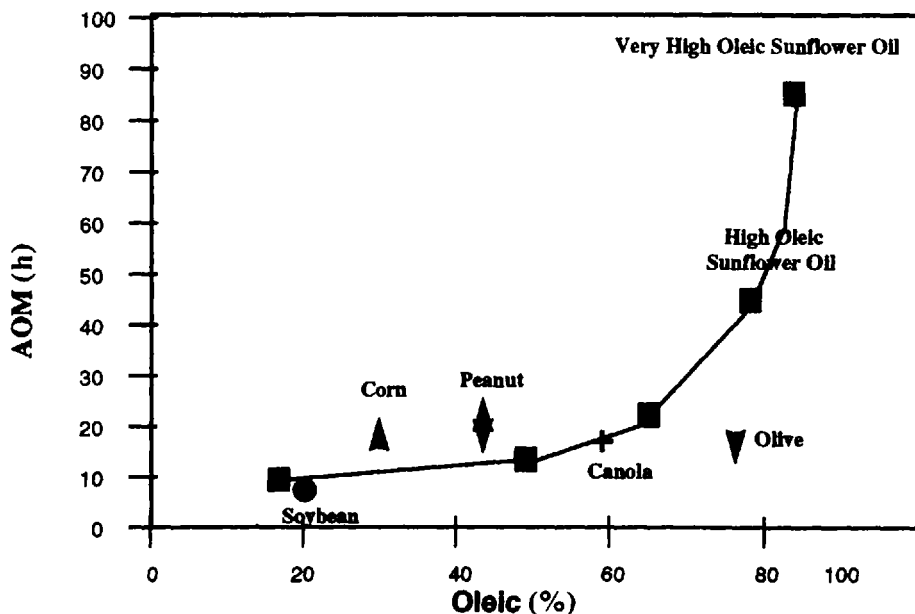


Figure 21.8 Oxidative stability versus percent oleic value. (From Ref. 52.)

Honary [60] showed that common vegetable oils in their untreated but fresh crude form pass the wear protection of the ASTM D-2882 pump test. When crude and filtered commodity soybean oil, for example, was used in the ASTM D-2882 pump test, the cam ring and vanes showed a combined wear amount of 40 mg. Figure 21.9 shows vane pump components used in the ASTM D-2882 and D-2271 tests. This is less than the typical 50-mg limit of wear expected of an oil to pass this test. The oil, however, showed a considerable amount of change in viscosity, indicating oxidation. This problem was evident in tests of hydrogenated soybean oil, as well as other vegetable oils. In fact, in some cases, it was observed that the addition of antiwear additive packages resulted in a poorer wear-protection performance for the vegetable oil than the untreated oil. This is a cause for concern regarding the suitability of some of the pump tests that have been designed for petroleum-based fluid. Untreated vegetable oils used in the ASTM D-2882 showed high levels of polymerization after use.

Figure 21.10 illustrates the hydraulic test setup for the ASTM D-2882 and D-2271. These tests require a Vickers 104-C vane pump to be operated at 13.79 ± 0.28 MPa (2000 ± 40 psig) for 100 h at an elevated temperature of $65 \pm 3^\circ\text{C}$ ($150 \pm 5^\circ\text{F}$) for the ASTM D-2882 test and 6.89 ± 0.14 MPa (1000 ± 20 psig) for 1000 h at $79 \pm 3^\circ\text{C}$ ($175 \pm 5^\circ\text{F}$) for the ASTM D-2271 test. According to Honary, most vegetable oils perform well in the ASTM D-2882, which is a 100-h test to determine wear-protection performance of antiwear hydraulic fluids. It is the changes in the viscosity of the vegetable oils that need to be the focus of most tests dealing with vegetable-based oils. The ASTM D-2271 is a 1000-h test and untreated vegetable oils show as much as 100% or more change in their viscosity by the end of this test. Furthermore, pump tests that use higher pressures than either D-2882 and D-2271 increase the viscosity change dramatically. For example, according to Honary [61], a vegetable-based tractor hydraulic fluid which showed only 7% change in viscosity

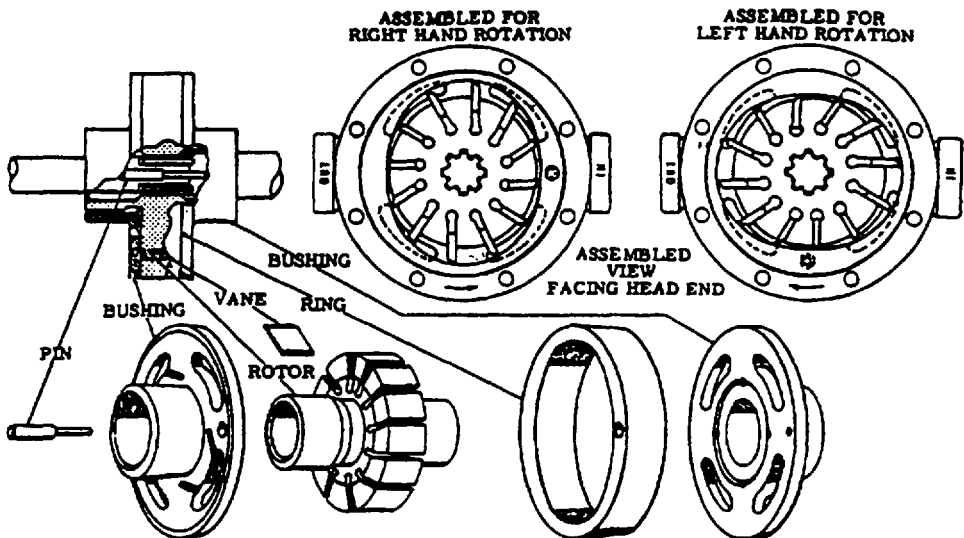


Figure 21.9 ASTM pump wear-test setup as presented by ASTM (1990).

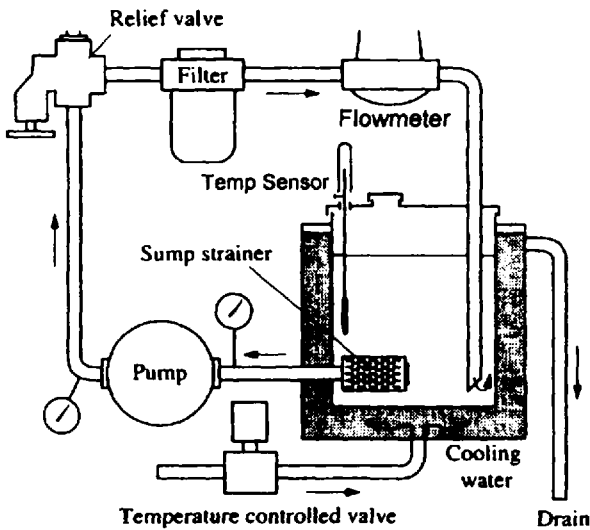


Figure 21.10 Components of the Vickers 104-C pump as presented by ASTM (1990).

in an ASTM D-2271 test, showed 67% change in viscosity when the same test was modified and run at 3000 psi, instead of the standard 1000 psi.

To test vegetable-oil performance in hydraulic pump tests, Honary [62] recommended the use of ASTM D-2271, which is a 1000-h test at a lower pressure (1000 psi) versus 2000 psi for ASTM D-882, but at a higher temperature of 79°C (175 ± 5°F) instead of 65°C (150 ± 5°F) in ASTM D-2882. The reason was to expose the oil to an extended period of time to better assess its oxidative stability as observed by increases in viscosity. Honary [63] further used hydraulic pump test results to confirm the relationship between percentages of fatty acids and changes in viscosity as a measure of oxidative stability (Table 21.9).

The three fatty acids which have the most noticeable impact on the viscosity of the oil are as expected: oleic, linoleic, and lenolenic. Figures 21.11, 21.12, and 21.13 present graphical representations of the relationships between individual fatty acid contents and changes in viscosity in the ASTM D-2271 tests.

Vegetable oils also show a dramatic change in their total acid number (TAN) when they oxidize. Oxidation of untreated vegetable oils in a hydraulic system correspond to an increase in the TAN along with rancidity odor. Vegetable-based hydraulic fluids should be tested for changes in viscosity as well as TAN, along with other properties such as cleanliness that are commonly tested on conventional hydraulic fluids. Honary [64] documented changes in the TAN of several vegetable oils in ASTM D-2271. Table 21.10 presents the results of several tests.

10 ROLE OF LUBRICANTS IN HYDRAULIC SYSTEMS

Hydraulic oil performs several major functions, including energy transfer, sealing, heat removal, removal of wear materials, friction reduction, and self-conditioning. The self-conditioning of the oil is its property to dissipate heat and entrapped air, to allow settling of suspended contaminants, and to present a certain degree of emul-

Table 21.9 Relationship Between Fatty Acid Contents and Changes in Viscosity in ASTM D-2271 (104-C), 1000 Hours at 79°C

Vegetable-oil types	Percentage of fatty acids						Δ Viscosity (cSt) in 1000-h test (% change)
	16:0 (Palmitic)	16:1 (Palmitoleic)	18:0 (Stearic)	18:1 (Oleic)	18:2 (Linoleic)	18:3 (Linolenic)	
Crude soy oil (extracted)	11	0.1	4.2	23.4	52.5	8.8	43.86 (146.6%)
Low-linolenic soy oil	9.7	0.0	4.2	32.9	50.3	2.9	39.56 (126.3%)
PHW soybean oil	9.5	—	4.0	37.5	42.31	4.75	17.83 (46.2%)
Crude soy oil (expelled)	11	0.1	4.2	23.4	52.5	8.8	34.25 (110%)
UHO sunflower oil	4.0	0.0	1.4	86.8	6.2	0.1	16.23 (40.1%)
HO sunflower	3.5	0.1	4.8	78.2	13.3	0.1	19.24 (50.03%)
HO canola oil	3.4	0.2	2.0	76.5	8.1	7.0	19.53 (51.13%)
HO canola (low linolenic)	4.0	—	3.0	76.0	11	3.0	14.08 (n/a)
Palm olein	39.6	—	4.6	43.3	—	11	12.97 (31.04%)

Note: Crude soy oil (extracted) = conventional hexane extracted soybean oil; crude soy oil (expelled) = extruded and then expelled soybean oil; PHW = partially hydrogenated winterized; UHO = ultrahigh oleic; HO = high oleic.

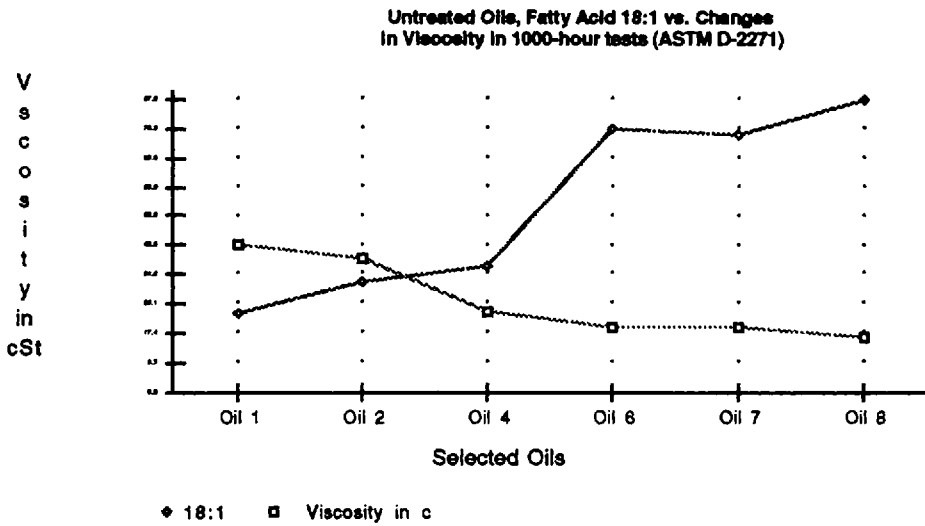


Figure 21.11 Relationship between the oleic acid content and changes in viscosity.

sification while maintaining a desired level of demulsibility. Additionally, the oil should be able to maintain its chemical properties when exposed to various chemicals in the presence of pressure-induced heat [65]. When evaluating a vegetable-based oil for hydraulic use, parameters to look for are the following:

- Viscosity of the oil according to ASTM D-445 and D-88 at specific temperatures
- Viscosity index of the oil as determined from tables in ASTM D-2270, 567, and 39B
- Oxidation stability using ASTM D-943, 942, 2893, 2272, and 2619

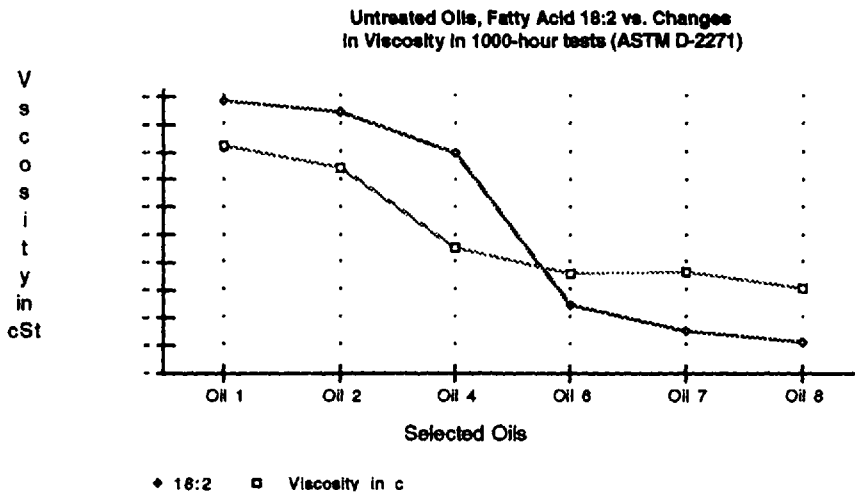


Figure 21.12 Relationship between the linoleic acid content and changes in viscosity.

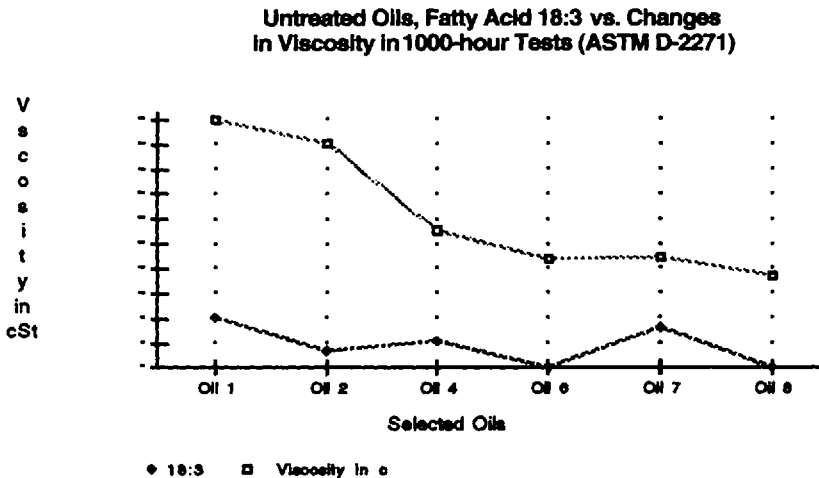


Figure 21.13 Relationship between the linolenic acid content and changes in viscosity.

- Thermal stability using ASTM standards for % viscosity increase (ASTM D-2161)
- Antifoaming properties using ASTM D-892
- Antiwear performance using ASTM D-2882 and D-2271
- Hydrolytic stability using ASTM D-2619
- Shear stability using ASTM standards
- Extreme-pressure test using ASTM D-2509, 2782, 2596, 2783, and 2672
- Load-carrying ability using ASTM standards
- Electric strength using ASTM standards
- Rust and oxidation inhibition using ASTM B-117, D-1748, D-665, D-1743
- Pour point using ASTM D-97
- Flash point using ASTM D-92
- Water emulsification ASTM D-2711 and demulsification D-1401

11 CHEMISTRY OF PETROLEUM-BASED HYDRAULIC OILS

The term “oil” is ambiguous and has several legitimate meanings. Two that are often confused are *hydrocarbon* and *triglyceride* oils. Triglyceride, which is vegetable or seed based, is *not* a hydrocarbon, which is a compound of hydrogen and carbon; rather, it is a mixture of partially oxygenated hydrocarbons [66]. Most hydraulic oils are petroleum based. Petroleum in its crude form is made up of various hydrocarbons differentiated by their molecular weight and structure. Table 21.11 presents a variety of hydrocarbons found in crude oil and their approximate boiling range and the ranges of their boiling points [67].

Figure 21.14 illustrates typical hydrocarbon configurations. In addition to the hydrocarbons, crude oils contain various other compounds, some of which are environmentally undesirable and functionally pose performance limitations. Those compounds include sulfur, nitrogen, oxygen, various metals such as vanadium and nickel, and some water and salt [68]. Comparatively, the fatty acids common in most vegetable oils are presented in Table 21.12.

Table 21.10 Relationship Between Fatty Acid Contents and Changes in TAN in ASTM D-2271 (104-C), 1000 Hour at 79°C (175 ± 5°F)

Vegetable-oil types	Percentage of fatty acids						Δ TAN (% change)
	16:0 (Palmitic)	16:1 (Palmitoleic)	18:0 (Stearic)	18:1 (Oleic)	18:2 (Linoleic)	18:3 (Linolenic)	
Crude soy oil (extracted)	11	0.1	4.2	23.4	52.5	8.8	0.17 (26.2%)
Low-linolenic soy oil	9.7	0.0	4.2	32.9	50.3	2.9	-1.39 (-70.2%)
PHW soybean oil	9.5	—	4.0	47.5	42.31	4.75	0.17 (45.9%)
Crude soy oil (expelled)	11	0.1	4.2	23.4	52.5	8.8	0.20 (40%)
UHO sunflower oil	4.0	0.0	1.4	86.8	6.2	0.1	-0.23 (-9.3%)
HO canola oil	3.4	0.2	2.0	76.5	8.1	7.0	-0.33 (-39.8%)
HO canola (low linolenic)	4.0	—	3.0	76.0	11	3.0	0.18 (58.1%)

Note: Crude soy oil (extracted) = conventional hexane extracted soybean oil; Crude soy oil (expelled) = extruded and then expelled soybean oil; PHW = partially hydrogenated winterized; UHO = ultrahigh oleic; HO = high oleic.

Table 21.11 Hydrocarbon Components and Approximate Boiling Range (in °C)

Natural gas hydrocarbons	Below -20
Gasoline components	30-200
Diesel and home heating oils	200-350
Lubricating oils and heavier fuels	Above 350

Source: Ref. 67.

Gapinski et al. [69] reported the percentages of saturates, monounsaturates, and polyunsaturates in common vegetable oils. Table 21.13 presents these percentages for 10 of the most common vegetable oils in their natural state (no hydrogenation or genetic modification).

Both petroleum and vegetable oils are subject to oxidation, particularly when used in industrial applications such as hydraulic fluid. Oxidation of hydrocarbons at low temperatures is called autoxidation. In its initial stage, it is characterized by a slow reaction with oxygen, followed by a phase of increased conversion, until the process eases continuation [70]. The degradation is driven by an autocatalytic reaction consisting of four distinct stages: (1) initiation of the radical chain reaction, (2) propagation of the radical chain reaction, (3) chain branching, and (4) termination of the radical chain reaction. This is similar to the polymerization process, which is often terminated by the introduction of impurities or elimination of the free radicals.

In vegetable oils, the fatty acid compositions play an important role in the stability of the oil. As the amount of unsaturation increases, for example, so does the relative rate of oxidation. A vegetable oil that has a high degree of polyunsaturation would tend to oxidize and polymerize when exposed to the metallic components

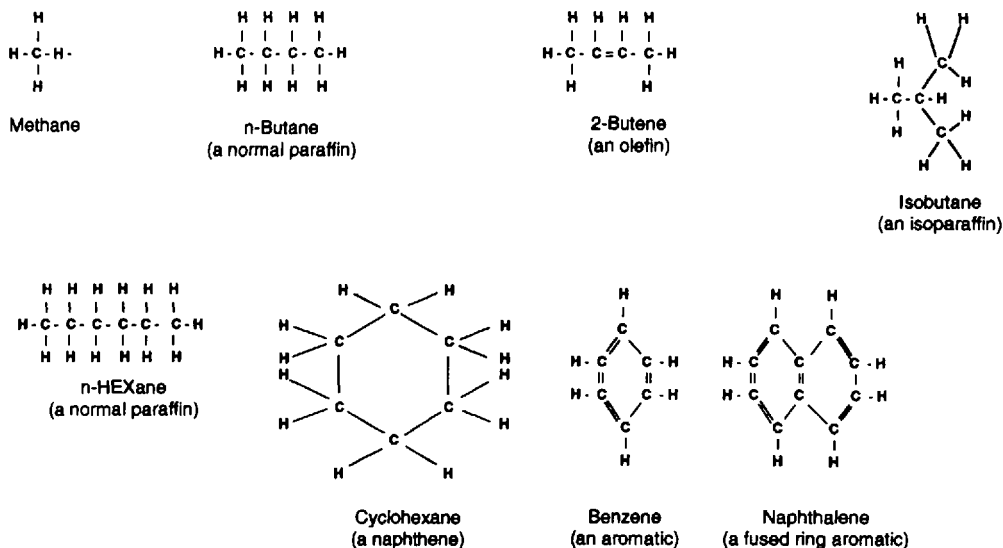


Figure 21.14 Typical hydrocarbon configurations. (From Ref. 68.)

Table 21.12 Fatty Acids Common in Most Vegetable Oils

Name	Abbrev.	Formula	Class
Palmitic	C16	$\text{CH}_3(\text{CH}_2)_{14}\text{---COOH}$	Saturated
Stearic	C18	$\text{CH}_3(\text{CH}_2)_{16}\text{---COOH}$	Saturated
Oleic	C18:1	$\text{CH}_3(\text{CH}_2)_7\text{---CH=CH---(CH}_2)_7\text{---COOH}$	Unsaturated
Linoleic	C18:2	$\text{CH}_3(\text{CH}_2)_4\text{---CH=CH---CH}_2\text{---CH=CH---(CH}_2)_7\text{---COOH}$	Polyunsaturated
Linolenic	C18:3	$\text{CH}_3\text{CH}_2\text{---CH=CH---CH}_2\text{---CH=CH---CH}_2\text{---CH=CH---(CH}_2)_7\text{---COOH}$	Polyunsaturated

Source: Kaufman in Ref. 66.

Table 21.13 Composition of Common Vegetable Oils

Oil	Monounsaturates	Polyunsaturates	Saturates
Olive	75%	11%	14%
Canola	58%	36%	6%
Peanut	48%	34%	18%
Palm	39%	10%	51%
Corn	25%	62%	13%
Soybean	24%	61%	15%
Sunflower	20%	69%	11%
Cottonseed	19%	54%	27%
Safflower	13%	78%	9%
Coconut	6%	2%	92%

Source: Ref. 69.

of the hydraulic system, in the presence of oxygen and pressure induced heat. Table 21.14 presents the relative rates of oxidation of unsaturated fatty acids [71].

The melting points of fatty acids vary due to their levels of saturation or unsaturation. As indicated earlier, the melting point of partially hydrogenated vegetable oils could be reduced by the winterization process. The melting points of individual fatty acids were reported by Swern [72]. Although the oil's melting point may differ as a whole, Table 21.15 shows the melting points of individual fatty acids.

Vegetable oils are excellent producers of energy. The potential use of vegetable oil as diesel fuel has resulted in the creation of a large body of knowledge about this area of use. The overall efficiency for sunflower oil, for example, is the highest of all the farm fuel alternatives. Studies of the use of vegetable oils as diesel fuel indicate that there are similarities between the two areas. Shultz and Morgan [73] reported that for bio-diesel fuels, different fatty acids affect the stability and melting point of an oil. Unsaturation is a desirable property for maintenance of liquidity at low temperature, but undesirable with respect to oxidative stability.

In general, vegetable oils are water insoluble. The vegetable-oil molecule has a carbon chain that is much longer than the carbon chain of a diesel fuel. Vegetable oils have 5–18% less energy content than diesel fuel. The amount of decrease in energy content compared to diesel fuel depends on the type of the vegetable oil.

Table 21.14 Relative Rates of Oxidation of Unsaturated Fatty Acids

Fatty acid	Relative oxidation rate
Stearic	0.6
Oleic	6
Linoleic	64
Linolenic	100

Source: Ref. 71.

Table 21.15 Melting Points of Selected Triglycerides

Fatty acid	Carbons	Melting point (°C)
Myristic	14 : 0	57.00
Palmitic	16 : 0	63.5
Stearic	18 : 0	73.1
Oleic	18 : 1	5.5
Linoleic	18 : 2	-13.1
Linolenic	18 : 3	-24.2

Source: Ref. 72.

An empirical equation can be used to calculate the gross heat of combustion based on the saponification value and the iodine value. Kaufman [74] presented the equation as follows:

$$\text{Heat of combustion (cal/g)} = 11,380 - (\text{Iodine value}) - 9.15(\text{Saponification value}).$$

Kaufman et al. [75] compared the fuel properties of No. 2 diesel fuel with crude (filtered) sunflower oil (Table 21.16).

Other physical property differences between vegetable oils and diesel fuel include higher specific gravities along with higher flash, cloud, and pour points for vegetable oils. High specific gravities result in greater densities and weight per unit volume. A higher flash point reduces fire hazard. Higher cloud and pour points may become a limitation for the use of vegetable oils as fuel in colder climates.

One method of changing the physical properties of the vegetable oils to be more comparable with those of diesel fuels is to *blend* the vegetable oils with diesel fuel. Vegetable oils blend well with diesel fuel and do not show tendencies to separate or settle out.

Several tests of (treated) soybean oil mixed with petroleum-based hydraulic fluid showed that vegetable oils mix well with petroleum oils. Honary [76] reported the result of ASTM D-2271 tests using a mixture of soybean-based hydraulic fluid with a typical antiwear petroleum-based hydraulic fluid. The mixture showed little increase in the viscosity of the oil. Further testing of a soybean-based hydraulic fluid in mobile equipment that had some residual petroleum-based hydraulic oil showed no adverse impact on the performance of the vegetable-based oil (Table 21.17).

11.1 Solubility

Vegetable oils are miscible with many organic solvents, particularly those that do not form hydrogen bonds (that are polar and aprotic). Several solvents have been experimented on for miscibility because of their use in the solvent-extraction process of the seed oil. Pride [77] indicates that in order to have miscibility, the oil and the solvent should have properties in the same order of magnitude. Solubility characteristics can be estimated from dielectric constants or solubility parameters as a measure of polarity. Examples of the dielectric constants of some of the common liquids are as follows: water (dielectric constant = 78.5), ethanol (dielectric constant = 24.3),

Table 21.16 Comparison of Fuel Properties of No. 2 Diesel Fuel and Sunflower Oil

Property	No. 2 diesel fuel	Sunflower oil crude/filtered
Density	847	921
Gross heating value (kJ/L)	38,400	36,600
Cetane rating	48	28
Viscosity (mm ² /s)		
0°C	6.4	188
100°C	2.4	34
Pour point (°C)	-50	-9
Cloud point (°C)	-17	-7

Source: Ref. 75.

hexane (dielectric constant = 1.89), and vegetable oils (dielectric constant = 3.0–3.2).

12 COMPATIBILITY WITH RUBBER HOSES

In general, vegetable oils are shown to be compatible with common hydraulic hoses. Several tests of compatibility were conducted to determine the interaction of various vegetable oils with rubber hoses [78]. The test procedure included exposing a segment of a hydraulic hose to a specific volume of the test oil for a period of 72 h at 100°C (212°F) and measuring the increase in the volume of the hose. This test was described by Hedges [79] for use when no information is available on the compatibility of the elastomeric material for a given fluid. Accordingly, a clean 1000-mL glass flask is filled with 700 mL of the fluid to be tested and the rubber hosing to be used is cut into a convenient segment. The chunk of rubber hosing should be measured, obtaining values for mass, width, length, and height of the sample. The volume of the sample before testing is determined by immersing it in water to determine the amount of water displaced by the sample. Observations should be made and recorded for the appearance and feel of the sample. A hot plate is set up with a thermal control device to heat the fluid to a constant temperature of 100°C. A segment of the rubber hosing is placed into the flask with the fluid, and the flask is placed on the hot plate to be heated at 100°C (212°F) for 72 h, magnetically stirring the hose. The flask may be heated for 72 continuous hours or the testing time may be broken up into convenient time periods to equal 72 h. After the test is completed, the rubber sample should be removed from the fluid and washed in soap and water. The sample should be inspected for any stickiness or visual swelling. Any change in appearance or consistency, such as wearing away of the rubber or gumminess due to chemical reaction, should be recorded. Volumetric expansion of each sample can be determined by immersing it in water and determining the amount of water displaced. Length, width, height, and mass of the sample should be measured. All measurements should be recorded and compared to the original values, and any significant differences should be noted. Honary [80] reported on the results of three tests of hose compatibility as follows:

Table 21.17 Performance of Mixtures of Soybean Hydraulic Fluid and Conventional Hydraulic Fluid in ASTM D-2271

Vegetable-oil types	Percentage of fatty acids						Δ Viscosity (in cSt) in 1000-h test (% change)
	16:0 (Palmitic)	16:1 (Palmitoleic)	18:0 (Stearic)	18:1 (Oleic)	18:2 (Linoleic)	18:3 (Linolenic)	
1. PHW soybean oil	9.5	—	4.0	47.5	42.31	4.75	17.83 (46.2%)
2. HO canola (low linolenic)	4.0	—	3.0	76.0	11	3.0	14.08 (n/a)
3. Mixture of 50–50 of oils 1 and 2 (above)							16.76 (46.5%)
4. Conventional petroleum hydraulic oil							0.67 (1.5%)
5. Soybean-based tractor hydraulic fluid (based on PHW above)							2.05 (4/6%)
6. Mixture of 50–50 of oils 4 and 5 (above)							0.67 (1.6%)

Note: PHW = partially hydrogenated winterized; HO = high oleic.

1. Rubber hosing tested at 104°C (219.2°F) for 94 h in crude soybean oil. The sample showed an increase of less than 10% for all the measurements with 0% water volume displacement (as measured). No significant signs of wear were evident on the sample. No corrosion of the rubber or burning was noted. Some swelling of the ends of the hosing was noted, but the amount was small. Compatibility with the rubber hosing does not appear to be a significant problem for the crude soybean oil.
2. Rubber hosing tested at 100°C (212°F) for 100.5 h. The expansion for all measurements was less than 10%, with 0% water volume displacement (as measured). When the rubber hosing was wiped with a paper towel, some rubber wiped off on the towel. However, it was discovered that rubber hosing which had undergone no testing performed in the same manner.
3. Rubber hosing tested in a commercially available rapeseed-based hydraulic oil containing full additive package at 103°C (217.4°F) for 78.25 h. The hose volume increase from 7.5 cm³ to 8.0 cm³, an increase of 6.25%. This expansion, although within the acceptable limits of under 10%, could be attributed to the presence of additives in the oil.

Volume expansions of 40–50% were noted when the same test was repeated for methyl esters derived from various vegetable oils. This is mainly due to the solvent properties of the esters, which when used as bio-diesel could interact with the rubber fuel lines.

13 OTHER PROPERTIES OF VEGETABLE OILS

13.1 Film Thickness

Film thickness tests of three soybean oils and a fully formulated soybean-based mobile hydraulic fluid were conducted using an optical interferometry elasto-hydrodynamic (EHD) rig [81]. Furthermore, a conventional petroleum-based mobile hydraulic fluid was tested for comparison purposes. The rig incorporated a 3/4-in. steel ball rolling against a 6-in. glass disk. The film thickness interference fringes were obtained under the following conditions:

Load (W) = 40 lb-ft (max. Hertzian pressure P_h = 153 ksi)

Temperature (T) = 40°C (104°F) and 75°C (167°F)

Rolling Speed U_m = 10, 20, and 40 in./s

Viscosity and density of the tests oils as presented in Table 21.18

Table 21.19 presents the film thicknesses of the test oils and three rolling speeds at the two temperatures. In lubricants, the measured film thickness increases with the rolling speed and decreases with the temperature. The lower thermal reduction factors (defined as $\phi = -dH/dT$) the higher resistance to film thickness variation as the temperature changes. In this case, soybean oil showed more favorable film thickness–temperature characteristics than the formulated petroleum sample. Both crude soybean oils (both were expelled oils) showed a high resistance to temperature-induced film-thickness variations. Under elasto-hydrodynamic conditions, the viscosity of lubricants tend to increase drastically with pressure. To describe such behavior, an experimental function may be used to model the *viscosity–pressure* relationship:

Table 21.18 Viscosity and Density of the Test Oils

Test oil	Viscosity (cSt) at		Density (g/cm ³)
	40°C	100°C	
Crude soybean #1	30.7	7.8	0.890
Crude soybean #2	31.1	7.4	0.885
Partially hydrogenated soybean	35.6	7.9	0.830
Formulated soybean hydraulic oil	48.1	10.5	0.897
Formulated petroleum hydraulic oil	56.9	9.4	0.874

Table 21.19 Film Thickness at Selected Temperatures and Rolling Speeds

Oil	Temperature (°C)	Rolling speed (in./s)	Film thickness (μin.)	
Crude soybean #1	40	10	3.0	
		20	3.6	
		40	6.7	
	75	10	2.1	
		20	3.1	
		40	3.8	
Crude soybean #2	40	10	3.1	
		20	5.4	
		40	6.5	
	75	10	2.2	
		20	3.0	
		40	5.8	
	Partially hydrogenated soybean	40	10	2.3
			20	4.9
			40	7.5
75		10	2.2	
		20	2.7	
		40	4.3	
Formulated soybean hydraulic oil		40	10	2.5
			20	6.5
			40	10.3
	75	10	2.4	
		20	2.7	
		40	3.3	
	Formulated petroleum hydraulic oil	40	10	2.7
			20	6.9
			40	11.8
75		10	2.2	
		20	2.3	
		40	3.1	

Source: Ref. 81.

Table 21.20 Estimated Viscosity–Pressure Coefficients

Test oil	Estimated viscosity–pressure coefficients (MPa ⁻¹)
Crude soybean #1	1.91×10^{-2}
Crude soybean #2	1.17×10^{-2}
Partially hydrogenated soybean	2.01×10^{-2}
Formulated soybean hydraulic fluid	2.71×10^{-2}
Formulated petroleum hydraulic fluid	2.64×10^{-2}

Source: Ref. 81.

$$\eta = \eta_0 e^{\alpha p}$$

where η is the viscosity at pressure p , η_0 denotes the viscosity at ambient pressure, and α is the *viscosity–pressure* coefficient. Direct measurement of α is a difficult task because high pressures of 1 GPa are required. This is not often available from the lubricant suppliers and, therefore, a safe estimated value for mineral oils was used ($\alpha = 2 \times 10^{-2}$ MPa⁻¹). This is a rather safe estimate, as the viscosity–pressure coefficients of most lubricants is around this value. Using regression from the measured film thickness, values which were shown in Table 21.19, the estimated viscosity–pressure coefficients of the test oils were determined and are presented in Table 21.20.

Finally, another property of vegetable oils reported [82] is the ultrasonic velocities in some vegetable oils. Using a simple Hartley circuit with a piezoquartz in the oscillating circuit, ultrasonics of about 7 mcycle/s were generated. To determine the ultrasonic velocities in the oils, the following procedure was used: (1) A parallel beam of monochromatic light was passed through the oil; (2) the sound waves were passed through the light, focusing onto a photographic plate; and (3) the diffraction rate of effect produced was used to calculate the sound velocities. Using this method, Table 21.21 shows the sound velocities determined for several vegetable oils. The data presented in Table 21.21 indicate that despite their higher viscosity than other organic compounds, the sound velocity is below 100 m/s observed in glycerine [83]. However, due to the fact that (1) lowering of velocity occurs in esters and (2) gly-

Table 21.21 Sound Velocities Determined for Several Vegetable Oils

Oil	Temperature (°C)	Frequency of oscillation (mcycle/s)	Sound velocity (m/s)
Olive oil	32.5	7.03	1381
Sesame oil	32.5	7.189	1432
Rapeseed oil	30.75	6.977	1450
Coconut oil	31.0	6.970	1490
Peanut oil	31.5	7.054	1562
Linseed oil	31.5	7.107	1772
Mustard oil	31.5	6.934	1825

Table 21.22 Adiabatic Compressibility of Several Vegetable Oils

Oil	Temperature (°C)	Density	Adiabatic compressibility (× 10/atm)
Olive oil	32.5	0.904	58.73
Sesame oil	32.5	0.916	53.94
Rapeseed oil	30.75	0.912	52.71
Coconut oil	31.5	0.916	49.79
Peanut oil	31.5	0.914	44.35
Linseed oil	31.5	0.922	34.97
Mustard oil	31.5	0.904	33.61

cerine having three OH groups takes three acid radicals during esterification, the observed velocities conform to previous works. The lower velocity in such high-viscosity oils give absorption coefficients very near the theoretical values.

Using the determined sound velocities and the densities of these oils, Pancholy et al. calculated the adiabatic compressibilities of the vegetable oils. Table 21.22 presents the results of their calculations. Because the chemical compositions of the oils are not definite, the values of velocities and compressibilities of these oils can be taken as representative for each case.

14 BIODEGRADABILITY

One of the most important advantages of vegetable oils for use in industrial applications is their inherent biodegradability. There are reasons, other than regulatory requirements, for users to switch to vegetable-based hydraulic fluids. These include long-term risk management, a genuine concern for the environment, and the fact that vegetable oils are renewable and often home-grown. In Europe, there have been government mandates requiring the use of "biodegradable" lubricants in some applications or regions; in the United States the future of such regulations is sketchy. Many of the standards of biodegradation, as well as definitions associated with biodegradability, are still under development. A recent survey of hydraulic fluids sold in the United States as biodegradable indicated that such claims are based on varied interpretations. With time, however, there will be more uniformity and acceptability of some of the current standards. There will be additional standards created to more directly address biodegradability of vegetable oils.

According to the California Advertising Statute, amended in 1991, a manufacturer cannot claim a product is biodegradable unless it meets the following definition:

Biodegradable means that a material has the proven capability to decompose in the most common environment where the material is disposed of within 3 years through natural biological processes into nontoxic carbonaceous soil, water, carbon, dioxide or methane [84].

Several ASTM committees have been working on developing approved definitions and standards for biodegradability, biotoxicity, and ecotoxicity. Many of the definitions that apply to vegetable oils are recently approved or are still in the approval

process. As detailed discussion of biodegradability is not in the scope of this chapter, ASTM publications should be consulted when designing hydraulic fluids for biodegradability.

Biodegradation may be defined as the process of chemical breakdown or transformation of an oil caused by organisms or their enzymes. A material may be considered completely biodegraded if it is totally utilized by micro-organisms and eventually forms carbon dioxide and water; this is called ultimate biodegradation. For an oil to be considered biodegradable, it should meet the ultimate biodegradability test. This is a test that estimates the extent to which the carbon in a material is converted to CO₂ or methane. This can be accomplished either by measuring the CO₂ or methane or by measuring the O₂ consumption and indirectly determining CO₂ consumption. A recognized test of ultimate biodegradation is the Modified Sturm Test or the OECD 301B. A recently completed standard by ASTM for ultimate biodegradation is ASTM D-5864, which is similar to the Modified Sturm Test and is especially for determining the aerobic aquatic biodegradability of all lubricants and their components. Both tests measure the evolution of CO₂ in 28 days. ASTM D-5864 is the Test Method for Determining the Aerobic Aquatic Biodegradation of Lubricants.

Primary biodegradation refers to degradation of the oil by microorganisms resulting in a change in its physical and/or chemical properties. The most common test for primary biodegradation is one designed by the Coordinating European Council for Biodegradability of Two-Stroke Cycle Engine Oils in Water, CEC L-33-A-94 (formerly CEC L-33-T-82). This test is one of the most often mentioned methods of determining and claiming biodegradability by oil manufacturers, but the test is only for determining the primary biodegradability of lubricants and does not meet the standard for (ultimate) biodegradability. In this method, infrared spectroscopy is used to measure the disappearance of certain hydrocarbons over a 2-day period, when the lubricant is mixed with inoculum-containing microorganisms.

Harold [84] reported on typical biodegradability values of common oils in the CEC L-33-T-82 (Table 21.23).

Many European test methods and standards have been adopted or redesigned in the United States. Although it is most desirable to determine the evolution of CO₂ in the test oil, easier methods have been used to measure the oxygen uptake. Com-

Table 21.23 CEC L-33-T-82 Test Results for Common Oils

Type of oil	Amount biodegraded
Mineral oil	15–35%
White oil	25–45%
Natural and vegetable oils	70–100%
PAO	5–30%
Polyether	0–25%
PIB	0–25%
Phthalate and trimellitate esters	5–80%
Polyols and Diesters	55–100%

Source: Ref. 84.

Table 21.24 Comparison of Biodegradability Test Procedures for Oil-Soluble Lubricants

Test	Aeration method	Test duration (days)	Temp. (°C)	Sample conc. (mg/L)	Inoculum (CFU)	Inoculum source	Medium	Biodegradation parameter	Pass Criteria
CEC L-33-T-82	Shaken	21	25	50	10^6	Sewage effluent	Nutrient solution	IR absorption $\text{CH}_2\text{-CH}_3$ loss	70–80% loss
Modified Sturm OECD 301 B	Blowing air	28	20–25	10–20	10^6 to 20×10^6	Sewage effluent	Nutrient solution	CO_2 released/DOC	60% CO_2 within 28 days
Modified MITI OECD 301 C	Stirring	28	20–25	100	$10^7\text{--}10^8$	Mixed sewage from 10 different plants	Nutrient solution	O_2 depletion/DOC	Biodegrade to 60% of BOD in 28 days (70% loss of parent compound)
OECD 301 C	Closed bottle	28	20	20–10	$10^4\text{--}10^6$	Mixed sewage from specified sources	Nutrient solution	O_2 depletion	60% of theoretical O_2 depletion in 28 days

Source: Ref. 84.

monly accepted tests for measuring the consumption of O₂ include the Closed Bottle Test (OECD No. 301D), the MITI test (OECD No. 301C), and the Biological Oxygen Demand (BOD) versus Chemical Oxygen Demand (COD) method. In the BOD/COD test, BOD is measured by the oxygen content in a closed bottle containing water and a contaminated substance for a 0-, 5-, 15-, and 28-day period, whereas COD involves boiling the substance with chromic plus sulfuric acid to obtain total chemical oxidation and to measure the remaining oxidant capacity of that mixture through Fe₂/Fe₃ titration. Table 21.24 presents a comparison of some of these tests for lubricants.

The following is a list of relevant standards and organizations useful for references:

- ASTM E-943, Definition of Terms Relating to Biological Effect and Environmental Fate
- ASTM E-1440, Acute Toxicity Test with the Rotifer Brachions
- ASTM D-5864, Test Method for Determining the Aerobic Aquatic Biodegradation of Lubricants
- ISO Test 9439:1990, Technical Corrigendum 1, Water Quality Method by Analysis of Released Carbon Dioxide (International Organization for Standards)
- Organization for Economic Cooperation and Development (OECD) Guidelines for Testing of Chemicals:
 - OECD 301B, CO₂ Evolution Test (the Modified Sturm Test).
 - OECD 301C, Modified MITI Test.
 - OECD 301F, Manometric Respirometry Test
 - OECD 201, Alga, Growth Inhibition Test
 - OECD 202, Daphnia sp., Acute Immobilization test and Reproduction Test
 - OECD 203, Fish, Acute Toxicity Test
 - OECD 207, Earthworm Acute Toxicity Test
 - OECD 208, Terrestrial Plants Growth Test
- US EPA Aerobic Aquatic Biodegradation Test, 40 CFR 796.3260 (EPA Publication 560/6-82-003, number CG-2000)

15 GLOSSARY

Acid Number. A measure of the amount of KOH needed to neutralize all or part of the acidity of a petroleum product.

Acid Value (Neutralization Value). The number of milligrams of potassium hydroxide required to neutralize one gram of sample.

Acute Ecotoxicity. The propensity of a material to produce adverse behavior, biochemical, or physiological effects in non-human organisms or populations in a short period of time, usually not constituting a substantial portion of the life span of the organism.

Aerobic. (1) Taking place in the presence of oxygen; (2) living or active in the presence of oxygen.

Anaerobic. (1) Taking place in the absence of oxygen; (2) living or active in the absence of oxygen.

- Bactericide.** Additive to inhibit bacterial growth in the aqueous component of fluids, preventing foul odors.
- Base Number.** The amount of acid (perchloric or hydrochloric) needed to neutralize all or part of a lubricant's basicity, expressed as KOH equivalents.
- Boiling Point.** The temperature at which a liquid substance turns into a gas or liquid. Assumed to be at standard pressure unless otherwise indicated. Sometimes present as a temperature range if an exact value is unavailable. Sometimes accompanied by a note such as dec (decomposes) or expl (explodes).
- Boundary Lubrication.** Lubrication between two rubbing surfaces without the development of a full fluid lubricating film. It occurs under high loads and requires the use of antiwear or extreme-pressure (EP) additives to prevent metal-to-metal contact.
- Caprylic Acid.** A fatty acid obtained from coconut oil for use in synthesizing dyes, drugs, perfumes, antiseptics, and fungicides.
- Carbon Chain Composition.** The carbon chain composition, based on weight percent, usually determined by gas chromatography.
- Cetane Number.** A measure of the ignition quality of a diesel fuel, as determined in a standard single cylinder test engine, which measures ignition delay compared to primary reference fuels. The higher the Cetane Number, the easier a high-speed, direct-injection engine will start and the less "white smoking" and "diesel knock" after start-up.
- Cloud Point.** The temperature at which a cloud of wax crystals appears when a lubricant or distillate fuel is cooled under standard conditions. Indicates the tendency of the material to plug filters or small orifices under cold-weather conditions.
- Color.** A means of quantifying the effect of color-bearing moieties, typically determined by percent transmission at 440/5550 nanometers (nm). Lovibond (5 $\frac{1}{2}$ -in. cell), APHA and 1963 Gardner tube.
- Demulsibility.** A measure of a fluid's ability to separate from water.
- Denatured Ethyl Alcohol.** Made by yeast fermentation of carbohydrates or by hydrolysis of ethylene for solvents, cosmetics, and as a oxygenated gasoline additive.
- Ecotoxicity.** The propensity of a material to produce adverse behavioral, biochemical, or physiological effects in nonhuman organisms or populations.
- Elasto-hydrodynamic Lubrication (EHD).** A lubricant regime characterized by high unit loads and high speeds in rolling elements where the mating parts deform elastically due to the incompressibility of the lubricant film under very high pressure.
- Emulsifier.** Additive that promotes the formation of a stable mixture, or emulsion, of oil and water.
- Evaporation Rate.** The rate of evaporation for a liquid, in unitless values relative to butyl acetate, which is assigned an evaporation rate of 1.
- Fat.** An animal- or marine-derived triglyceride.
- Fatty Acid, Food Grade (FG).** Fatty acid food-grade additives are defined by the USA Food and Drug Administration in 21 CFR, Section 172.860 which includes "... manufactured from fats and oils derived from edible sources."

- Fatty Acid. National Formulary (NF).** Includes those fatty acids exempt from the edible source requirements as defined in USP/NF 1995 edition. These fatty acids are derived from edible sources and may be used internally.
- Fatty Acid. National Formulary—External Use Only (NF-EXT).** These fatty acids are exempt from the edible source requirements as defined in USP/NF.
- Flash Point.** The temperature at which the vapor of a liquid can be made to ignite in air.
- Free Fatty Acid (as Oleic).** A method for expressing the percentage of free acids in terms of oleic. Usually, it is used to indicate the degree of refining of the glycerides.
- Furfural.** Obtained by steam distillation of acidified plant materials for polymers and foundry binders.
- Glycerine.** A by-product of splitting or saponification of fats and oils, or made by petrochemical synthesis for cosmetics, food, drugs, and polyurethane polymers.
- Glycerine, High Gravity.** A technical-grade glycerine used for industrial applications.
- Glycerine, USP.** A high quality glycerine manufactured to meet the specifications contained in the *U.S. Pharmacopoeia*, Vol. 23, 1995 edition. These products are used in demanding applications, including the cosmetics, food, and pharmaceutical industries.
- Hydrogenation.** The process of reducing unsaturation, as measured by the iodine value.
- Hydrolytic Stability.** Ability of additives and certain synthetic lubricants to resist chemical decomposition (hydrolysis) in the presence of water.
- Inoculum.** Spores, bacteria, single-celled organisms or other live materials that are introduced into a test medium.
- Iodine Value (IV).** A measure of the degree of unsaturation of a product, expressed as centigrams of iodine absorbed per gram of sample.
- Lecithin.** A by-product of soy-oil extraction used as an emulsifying agent and antioxidant in foods.
- Magnesium Stearate.** A surfactant made from tropical-oil fatty acids and inorganic materials for use in lubricant, adhesive, and detergent manufacturing.
- Melting Point.** The temperature at which a solid substance becomes a liquid, or at which a liquid substance solidifies. Assumed to be at standard pressure unless otherwise indicated. Sometimes present as a temperature range if an exact value is unavailable. Sometimes accompanied by a note such as dec (decomposes) or subl (sublimes).
- Myristic Acid.** Obtained by fractional distillation of coconut and other vegetable oils for soaps, cosmetics, and synthesis of esters for flavors and perfumes.
- Neutralization Number.** A measure of the acidity or alkalinity of an oil. The number is the mass in milligrams of the amount of acid (HCl) or base (KOH) required to neutralize one gram of oil.
- Oleic Acid.** Obtained by fractional crystallization from mixed fatty acids for candles, soaps, and synthesis of other surfactants.

- Oxidation.** Occurs when oxygen attacks petroleum fluids or vegetable oils. The process is accelerated by heat, light, metal catalysts, and the presence of water, acids, or solid contaminants. It leads to increased viscosity and deposit formations.
- Oxidation Inhibitor.** Substance added in small quantities to a lubricant product to increase its oxidation resistance, thereby lengthening its service or storage life; also called antioxidant.
- Pumpability.** The low-temperature, low shear stress–shear rate viscosity characteristics of an oil that permit satisfactory flow to and from the unit's oil pump and subsequent lubrications of moving components.
- RTECS.** A substance's identification number on the U.S. Registry of Toxic Effects of Chemical Substances, a database by the National Institute for Occupational Safety and Health (NIOSH). More information is available at the RTECS home page at NIOSH.
- Saponification Value.** Number of milligrams of potassium hydroxide necessary to convert all saponifiable constituents into potassium soap. Measures the combined and free fatty acids present and allows for the calculation of average molecular weight.
- Saturated (Hard).** Describes the intentional hydrogenation of the double bonds in a fatty acid or glyceride, resulting in less unsaturation. Measured by iodine value.
- Sebacic Acid.** Made by high-temperature cleavage of castor oil for use as an intermediate chemical in the manufacture of polymers and plasticizers.
- Specific Gravity.** The ratio of the mass of a substance to the mass of an equal volume of distilled water at 4°C. A unitless quantity.
- Stoke (St).** A unit. Kinematic measurement of a fluid's resistance to flow defined by the ratio of the fluid's dynamic viscosity to its density.
- Tall Oil (Crude).** A by-product of paper production (chemical pulping) that is refined into rosin and fatty acids.
- Tallow Fatty Acids.** Made from splitting tallow for direct use as lubricants or in greases, and for separation into pure fatty acids.
- Titer (Titre).** Solidification point of fatty acid or acids resulting from hydrolysis of the glyceride. It is a function of the chain length and the degree of saturation of the component acids and is commonly expressed in degrees centigrade, as determined by standard methods established by the American Oil Chemists' Society (AOCS).
- Viscosity Index (VI).** A measure of the oil's resistance to viscosity change at extreme temperatures. High-viscosity-index fluids tend to display less change in viscosity with temperature than low-viscosity-index fluids.
- Unsaponifiable Matter.** Measurement of the nonfatty matter present in the product, other than moisture and insolubles.
- Unsaturated (Soft).** Describes the existence of double bonds in a fatty acid or glyceride, measured by iodine value.
- Vegetable (Veg).** Describes a fatty acid source from all vegetable materials.
- Water Solubility.** An indication of the solubility in a substance, sometimes listed in relative terms (very soluble); sometimes listed quantitatively (5 mg/mL).

REFERENCES

1. United States Department of Agriculture, *Agricultural Statistics*, 1994, U.S. Government Printing Office; Washington, DC.
2. United States Department of Agriculture, *Agricultural Statistics*, 1994, U.S. Government Printing Office; Washington, DC.
3. D. K. Salunkhe, J. K. Chavan, R. N. Adsule, and S. S. Kadem, *World Oilseeds: Chemistry, Technology, and Utilization*, 1992, Van Nostrand Reinhold; New York.
4. H. B. W. Patterson, *Hydrogenation of Fats and Oils: Theory and Practice*, 1994, AOCS Press; Champaign, IL.
5. H. B. W. Patterson, *Hydrogenation of Fats and Oils: Theory and Practice*, 1994, AOCS Press; Champaign, IL.
6. D. R. Erickson, E. H. Pryde, O. L. Brekke, T. L. Mounts, and R. A. Falb, *Handbook of Soy Oil Processing and Utilization*, 1985, American Soybean Association; St. Louis, MO/AOCS Press; Champaign, IL.
7. H. B. W. Patterson, *Hydrogenation of Fats and Oils: Theory and Practice*, 1994, AOCS Press; Champaign, IL, p. 5.
8. H. J. Dutton (1966), in D. R. Erickson, E. H. Pryde, O. L. Brekke, T. L. Mounts, and R. A. Falb, *Handbook of Soy Oil Processing and Utilization*, 1985, American Soybean Association; St. Louis, MO/AOSC Press; Champaign, IL.
9. D. R. Erickson, E. H. Pryde, O. L. Brekke, T. L. Mounts, and R. A. Falb, *Handbook of Soy Oil Processing and Utilization*, 1985, American Soybean Association; St. Louis, MO/AOSC Press; Champaign, IL.
10. T. L. Mounts, in D. R. Erickson, E. H. Pryde, O. L. Brekke, T. L. Mounts, and R. A. Falb, *Handbook of Soy Oil Processing and Utilization*, 1985, American Soybean Association; St. Louis, MO/AOSC Press; Champaign, IL, p. 131.
11. T. L. Mounts, in D. R. Erickson, E. H. Pryde, O. L. Brekke, T. L. Mounts, and R. A. Falb, *Handbook of Soy Oil Processing and Utilization*, 1985, American Soybean Association; St. Louis, MO/AOSC Press; Champaign, IL, p. 132.
12. D. K. Salunkhe, J. K. Chavan, R. N. Adsule, and S. S. Kadem, *World Oilseeds: Chemistry, Technology, and Utilization*, 1992, Van Nostrand Reinhold; New York.
13. Kinney, p. 101.
14. Kinney
15. L. A. T. Honary, *Performance of Selected Vegetable Oils in ASTM Hydraulic Tests*, SAE Technical Papers, Paper 952075, 1995.
16. G. Robbelen, R. K. Downey, and A. Ashri, "Oil Crops of the World, 1989, McGraw-Hill, New York, in D. K. Salunkhe, J. K. Chavan, R. N. Adsule, and S. S. Kadem, *World Oilseeds: Chemistry, Technology, and Utilization*, 1992, Van Nostrand Reinhold; New York, p. 217.
17. W. J. Wolf and J. C. Cowan, *Soybean as a Food Source*, 1975, CRC Press; Boca Raton, FL, in D. K. Salunkhe, J. K. Chavan, R. N. Adsule, and S. S. Kadem, *World Oilseeds: Chemistry, Technology, and Utilization*, 1992, Van Nostrand Reinhold; New York.
18. D. K. Salunkhe, J. K. Chavan, R. N. Adsule, and S. S. Kadem, *World Oilseeds: Chemistry, Technology, and Utilization*, 1992, Van Nostrand Reinhold; New York.
19. A. J. Kinney, 1995.
20. D. K. Salunkhe, S. K. Sathe, and N. R. Reddy, "Legume Lipids," in *Chemistry and Biochemistry of Food Legumes*, S. K. Arora, ed., 1982, Oxford and IBH; New Delhi, p. 52, in D. K. Salunkhe, J. K. Chavan, R. N. Adsule, and S. S. Kadem, *World Oilseeds: Chemistry, Technology, and Utilization*, 1992, Van Nostrand Reinhold; New York.

21. V. G. Mahadevappa and P. L. Raina, "Nature of Some Indian Legume Lipids," *J. Agric. Food Chem.*, 26, pp. 1241–1244, in D. K. Salunkhe, J. K. Chavan, R. N. Adsule, and S. S. Kadem, *World Oilseeds: Chemistry, Technology, and Utilization*, 1992, Van Nostrand Reinhold; New York.
22. W. J. Wolf and J. C. Cowan (1975), in D. K. Salunkhe, J. K. Chavan, R. N. Adsule, and S. S. Kadem. *World Oilseeds: Chemistry, Technology, and Utilization*, 1992, Van Nostrand Reinhold; New York.
23. D. K. Salunkhe, J. K. Chavan, R. N. Adsule, and S. S. Kadem, *World Oilseeds: Chemistry, Technology, and Utilization*, 1992, Van Nostrand Reinhold; New York.
24. L. A. T. Honary, "Potential Utilization of Soybean Oil as an Industrial Hydraulic Oil," SAE Technical Papers, Paper 941760, 1994.
25. G. C. Mustakas, "Recovery of Oil from Soybeans," in *Handbook of Soy Oil Processing and Utilization*, 1980, American Soybean Association; Champaign, IL, p. 11, in D. K. Salunkhe, J. K. Chavan, R. N. Adsule, and S. S. Kadem, *World Oilseeds: Chemistry, Technology, and Utilization*, 1992, Van Nostrand Reinhold; New York.
26. L. A. T. Honary, "Performance of Selected Vegetable Oils in ASTM Hydraulic Tests," SAE Technical Papers, Paper 952075, 1995.
27. T. L. Mounts and Khym, in D. R. Erickson, E. H. Pryde, O. L. Brekke, T. L. Mounts, and R. A. Falb, *Handbook of Soy Oil Processing and Utilization*, 1985, American Soybean Association; St. Louis, MO/AOSC Press; Champaign, IL.
28. O. L. Brekke, in D. R. Erickson, E. H. Pryde, O. L. Brekke, T. L. Mounts, and R. A. Falb, *Handbook of Soy Oil Processing and Utilization*, 1985, American Soybean Association; St. Louis, MO/AOSC Press; Champaign, IL.
29. O. L. Brekke, in D. R. Erickson, E. H. Pryde, O. L. Brekke, T. L. Mounts, and R. A. Falb, *Handbook of Soy Oil Processing and Utilization*, 1985, American Soybean Association; St. Louis, MO/AOSC Press; Champaign, IL.
30. L. A. T. Honary, "Performance of Selected Vegetable Oils in ASTM Hydraulic Tests," SAE Technical Papers, Paper 952075, 1995.
31. C. W. S. Hartley, *The Oil Palm*, 1967, Longman; London, pp. 1–70, 608–692; S. Maiti, M. R. Hedge, and S. B. Chattopadhyay, *Handbook of Annual Oil Seed Crops*, 1988, Oxford and IBH; New Delhi, pp. 279–289; both in D. K. Salunkhe, J. K. Chavan, R. N. Adsule, and S. S. Kadem, *World Oilseeds: Chemistry, Technology, and Utilization*, 1992, Van Nostrand Reinhold; New York, p. 220.
32. V. J. Godin and P. C. Spensley, *T.P.I. Crop Product Digest No. 1*, 1971, Tropical Products Institute; London, in D. K. Salunkhe, J. K. Chavan, R. N. Adsule, and S. S. Kadem, *World Oilseeds: Chemistry, Technology, and Utilization*, 1992, Van Nostrand Reinhold; New York, p. 228.
33. Maiti et al. (1988), in D. K. Salunkhe, J. K. Chavan, R. N. Adsule, and S. S. Kadem, *World Oilseeds: Chemistry, Technology, and Utilization*, 1992, Van Nostrand Reinhold; New York, p. 221.
34. L. A. T. Honary, "Performance of Selected Vegetable Oils in ASTM Hydraulic Tests," SAE Technical Papers, Paper 952075, 1995.
35. E. H. Pryde, in D. R. Erickson, E. H. Pryde, O. L. Brekke, T. L. Mounts, and R. A. Falb, *Handbook of Soy Oil Processing and Utilization*, 1985, American Soybean Association; St. Louis, MO/AOSC Press; Champaign, IL.
36. L. Bengtsson, A. V. Hofsten, and B. Loof, "Botany of Rapeseed," in *Rapeseed: Cultivation, Composition, Processing and Utilization*, L. Appelqvist and R. Ohlson, eds., 1972, Elsevier; Amsterdam, pp. 36–44, in D. K. Salunkhe, J. K. Chavan, R. N. Adsule, and S. S. Kadem, *World Oilseeds: Chemistry, Technology, and Utilization*, 1992, Van Nostrand Reinhold; New York.
37. K. Anjou, B. Lonnerdal, B. Uppstrom, and P. Aman, "Composition of Seeds from Some Brassica Cultivars," *Swedish J. Agric. Res.*, 1977, 7, pp. 169–178, in D. K. Salunkhe,

- J. K. Chavan, R. N. Adsule, and S. S. Kadem, *World Oilseeds: Chemistry, Technology, and Utilization*, 1992, Van Nostrand Reinhold; New York.
38. J. K. Daun and W. Bushuk, "Rapeseed," in *Handbook of Processing and Utilization*, in *Agriculture*, 2, 2, Plant products, I. A. Wolff, ed., 1983, CRC Press; Boca Raton, FL, pp. 257–297, in D. K. Salunkhe, J. K. Chavan, R. N. Adsule, and S. S. Kadem, *World Oilseeds: Chemistry, Technology, and Utilization*, 1992, Van Nostrand Reinhold; New York.
 39. L. A. Appelqvist, "Damage Occurring During Drying Process of Oilseeds," *Svenstc. Frotidning*, 1972, 223, in D. K. Salunkhe, J. K. Chavan, R. N. Adsule, and S. S. Kadem, *World Oilseeds: Chemistry, Technology, and Utilization*, 1992, Van Nostrand Reinhold; New York, p. 63.
 40. R. J. Kemble, V. Armavil, L. Tulsieram, C. Baszczynski, B. Sys, D. Charne, J. Patel, B. Gillespie, and I. Grant, "The Use of RFLP in the Development of Specialty Oil Canolas," in *Seed Oils for the Future*, S. L. MacKenzie and D. C. Taylor, eds., 1992, AOCS Press; Champaign, IL.
 41. M. Vaisey-Genser and G. Ylimaki, "Effects of Non-absorbable Antioxidants on Canola Oil Stability to Accelerated Storage and to Frying Temperature," *Can. Inst. Food Sci. Technol. J.*, 1985, 18, pp. 67–71, in D. K. Salunkhe, J. K. Chavan, R. N. Adsule, and S. S. Kadem, *World Oilseeds: Chemistry, Technology, and Utilization*, 1992, Van Nostrand Reinhold; New York.
 42. L. Appelqvist, "Damage Occurring During Drying Process of Oilseeds," 1972, in D. K. Salunkhe, J. K. Chavan, R. N. Adsule, and S. S. Kadem, *World Oilseeds: Chemistry, Technology, and Utilization*, 1992, Van Nostrand Reinhold; New York, p. 65.
 43. D. K. Salunkhe, J. K. Chavan, R. N. Adsule, and S. S. Kadem, *World Oilseeds: Chemistry, Technology, and Utilization*, 1992, Van Nostrand Reinhold; New York.
 44. F. W. Sosulski, E. S. Humbert, K. Bui, and J. D. Jones, "Functional Properties of Rapeseed Flours, Concentrates, and Isolates," *J. Food Sci.*, 1976, 41, pp. 1349–1352, in D. K. Salunkhe, J. K. Chavan, R. N. Adsule, and S. S. Kadem, *World Oilseeds: Chemistry, Technology, and Utilization*, 1992, Van Nostrand Reinhold; New York.
 45. M. Naczki, L. L. Diosady, and L. J. Rubin, "Functional Properties of Canola Meals Produced by a Two Phase Solvent Extraction System," *J. Food Sci.*, 1985, 50, pp. 1685–1688, in D. K. Salunkhe, J. K. Chavan, R. N. Adsule, and S. S. Kadem, *World Oilseeds: Chemistry, Technology, and Utilization*, 1992, Van Nostrand Reinhold; New York.
 46. M. Khalil, "Foaming Properties of Oilseed Proteins," *Nahrung*, 1985, 29, pp. 201–207, in D. K. Salunkhe, J. K. Chavan, R. N. Adsule, and S. S. Kadem, *World Oilseeds: Chemistry, Technology, and Utilization*, 1992, Van Nostrand Reinhold; New York.
 47. D. R. Erickson, E. H. Pryde, O. L. Brekke, T. L. Mounts, and R. A. Falb, *Handbook of Soy Oil Processing and Utilization*, 1985, American Soybean Association; St. Louis, MO/AOSC Press; Champaign, IL, p. 8.
 48. D. K. Salunkhe, J. K. Chavan, R. N. Adsule, and S. S. Kadem, *World Oilseeds: Chemistry, Technology, and Utilization*, 1992, Van Nostrand Reinhold; New York.
 49. Maiti et al., "*Handbook of Annual Oilseed Crops*," 1988, in D. K. Salunkhe, J. K. Chavan, R. N. Adsule, and S. S. Kadem, *World Oilseeds: Chemistry, Technology, and Utilization*, 1992, Van Nostrand Reinhold; New York.
 50. P. C. Naegley, "Environmentally Acceptable Lubricants," in *Seed Oils for the Future*, S. L. MacKenzie and D. C. Taylor, eds., 1992, AOCS Press; Champaign, IL.
 51. L. A. T. Honary, "Performance of Selected Vegetable Oils in ASTM Hydraulic Tests," SAE Technical Papers, Paper 952075, 1995.
 52. P. C. Naegley, in *Seed Oils for the Future*, S. L. MacKenzie and D. C. Taylor, eds., 1992, AOCS Press; Champaign, IL.
 53. D. R. Erickson, E. H. Pryde, O. L. Brekke, T. L. Mounts, and R. A. Falb, *Handbook of Soy Oil Processing and Utilization*, 1985, American Soybean Association; St. Louis, MO/AOSC Press; Champaign, IL.

54. D. K. Salunkhe, J. K. Chavan, R. N. Adsule, and S. S. Kadem, *World Oilseeds: Chemistry, Technology, and Utilization*, 1992, Van Nostrand Reinhold; New York.
55. Z. Leibovitz and C. Ruckenstein, "Our Experiences in Processing Maize (Corn) Germ Oil," *J. Am. Oil Chem. Soc.*, 1983, 60, pp. 395–399, in D. K. Salunkhe, J. K. Chavan, R. N. Adsule, and S. S. Kadem, *World Oilseeds: Chemistry, Technology, and Utilization*, 1992, Van Nostrand Reinhold; New York.
56. D. K. Salunkhe, J. K. Chavan, R. N. Adsule, and S. S. Kadem, *World Oilseeds: Chemistry, Technology, and Utilization*, 1992, Van Nostrand Reinhold; New York.
57. D. R. Erickson, E. H. Pryde, O. L. Brekke, T. L. Mounts, and R. A. Falb, *Handbook of Soy Oil Processing and Utilization*, 1985, American Soybean Association; St. Louis, MO/AOSC Press; Champaign, IL, p. 8.
58. D. K. Salunkhe, J. K. Chavan, R. N. Adsule, and S. S. Kadem, *World Oilseeds: Chemistry, Technology, and Utilization*, 1992, Van Nostrand Reinhold; New York.
59. P. C. Naegley, in *Seed Oils for the Future*, S. L. MacKenzie and D. C. Taylor, eds., 1992, AOCS Press; Champaign, IL.
60. L. A. T. Honary, "Potential Utilization of Soybean Oil as an Industrial Hydraulic Oil," SAE Technical Papers, Paper 941760, 1994.
61. L. A. T. Honary, "Performance of Selected Vegetable Oils in ASTM Hydraulic Tests," SAE Technical Papers, Paper 952075, 1995.
62. L. A. T. Honary, "Potential Utilization of Soybean Oil as an Industrial Hydraulic Oil," SAE Technical Papers, Paper 941760, 1994.
63. L. A. T. Honary, "Potential Utilization of Soybean Oil as an Industrial Hydraulic Oil," SAE Technical Papers, Paper 941760, 1994; L. A. T. Honary, "Performance of Selected Vegetable Oils in ASTM Hydraulic Tests," SAE Technical Papers, Paper 952075, 1995.
64. L. A. T. Honary, "Performance of Selected Vegetable Oils in ASTM Hydraulic Tests," SAE Technical Papers, Paper 952075, 1995.
65. W. C. Gergel, S. Q. A. Rizvi, and R. C. Beercheck, *Lubrication Theory and Practice* (no date), The Lubrizol Corporation.
66. E. B. Shultz, Jr. and R. O. Morgan, *Fuels and Chemicals from Oilseeds: Technology and Policy Options*, 1984, Westview Press; Boulder, CO.
67. W. C. Gergel, S. Q. A. Rizvi, and R. C. Beercheck, *Lubrication Theory and Practice* (no date), The Lubrizol Corporation.
68. W. C. Gergel, S. Q. A. Rizvi, and R. C. Beercheck, *Lubrication Theory and Practice* (no date), The Lubrizol Corporation.
69. R. E. Gapinski, I. E. Joseph, and B. D. Layzel, "A Vegetable-Based Tractor Lubricant," SAE Technical Papers, Paper 941758, 1994.
70. M. Rasberger, "Oxidative Degradation and Stabilisation of Mineral Oil Based Lubricants," in *Chemistry and Technology of Lubricants*, R. M. Mortier and S. T. Orszulik, eds., 1992, CVH Publishers, New York.
71. Swern, in E. B. Schulz, Jr. and R. O. Morgan, *Fuels and Chemicals from Oilseeds: Technology and Policy Options*, 1984, Westview Press; Boulder, CO.
72. Swern, in E. B. Schulz, Jr. and R. O. Morgan, *Fuels and Chemicals from Oilseeds: Technology and Policy Options*, 1984, Westview Press; Boulder, CO.
73. E. B. Schulz, Jr. and R. O. Morgan, *Fuels and Chemicals from Oilseeds: Technology and Policy Options*, 1984, Westview Press; Boulder, CO.
74. Kaufman, in E. B. Schulz, Jr. and R. O. Morgan, *Fuels and Chemicals from Oilseeds: Technology and Policy Options*, 1984, Westview Press; Boulder, CO.
75. Kaufman, in E. B. Schulz, Jr. and R. O. Morgan, *Fuels and Chemicals from Oilseeds: Technology and Policy Options*, 1984, Westview Press; Boulder, CO.
76. L. A. T. Honary, "Performance of Selected Vegetable Oils in ASTM Hydraulic Tests," SAE Technical Papers, Paper 952075, 1995.

77. E. H. Pryde, in D. R. Erickson, E. H. Pryde, O. L. Brekke, T. L. Mounts, and R. A. Falb, *Handbook of Soy Oil Processing and Utilization*, 1985, American Soybean Association; St. Louis, MO/AOSC Press; Champaign, IL, p. 43.
78. L. A. T. Honary, "Potential Utilization of Soybean Oil as an Industrial Hydraulic Oil," SAE Technical Papers, Paper 941760, 1994.
79. C. S. Hedges, *Fluid Power in Plant and Field*, 1981, Womack Educational Publications; Dallas, TX, p. 136.
80. Honary, 1993.
81. X. Ai, and H. P. Nixon, "Soybean-Based Lubricant Evaluation," unpublished report, University of Northern Iowa, Ag-Based Industrial Lubricants Research Program, 1996.
82. M. Pancholy, A. Pande, and S. Parthasarathy, "Ultrasonic Velocities in Some Vegetable Oils," in *J. Sci. Ind. Res.*, 1944, 3, p. 111.
83. L. Zachooal, *J. Phys. Rad.*, 1939, 10, p. 350, in M. Pancholy et al., "Ultrasonic Velocities in Some Vegetable Oils," *J. Sci. Ind. Res.*, 1944, 3, 112.
84. S. Harold, *Biodegradability: Review of the Current Situation*, 1993, The Lubrizol Corporation, p. 4.

This page intentionally left blank

Electro-rheological Fluids

CHRISTIAN WOLFF-JESSE

Hoveloh 6a, Ascheberg, Germany

1 INTRODUCTION

The term "electro-rheological fluid" (ERF) refers to a substance whose rheological behavior can be varied by the influence of a strong electrical field. Depending on field strengths, the physical state of ERFs can be varied from a solid to a liquid within a millisecond, depending on the field strength. In hydraulics, the electro-rheological (ER) effect may be used to control pressures and volume flows in electro-rheological flow resistors and for the construction of valves of simple design, which operate without moving parts. The ER effect was discovered in 1939 by Winslow [1,2].

Electro-rheological fluids consist of a dispersion of conductive solid particles within a dielectric carrier fluid. The addition of "activators," which may be dispersed into the ERF, may be required to facilitate or reinforce the ER effect. For many years, water was considered one of the most important components for the formulation of electro-rheological fluids. However, the poor reproducibility of fluid properties and highly temperature-dependent behavior of water-containing ERFs inhibited development of electro-rheological applications. These early problems have been overcome through evolutionary technical developments which will be discussed here.

In closed systems, the ER effect can be used to dissipate energy. In open systems, actuators may be constructed which transfer hydraulic energy from pump flow into mechanical work. The development of new anhydrous ERF particles composed of soft synthetic materials to avoid the danger of abrasive effects within the hydraulic circuit has facilitated the design of hydraulic systems employing ERFs.

Electro-rheological fluids are typically used in applications that fit one of three possible operational modes: shear, flow, and squeeze modes. (These will be discussed in detail in Sec. 2.2.) In the shear mode, the electrodes are moved relative to each

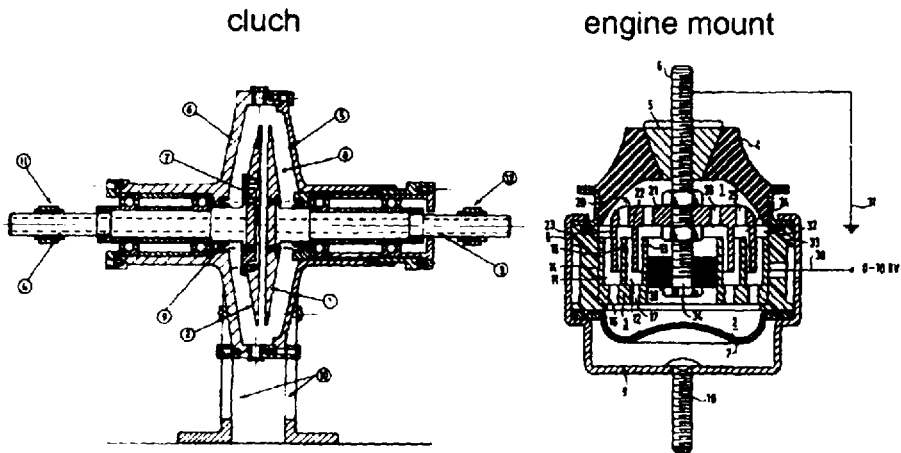


Figure 22.1 Possible methods of application of ERF in the shear mode.

other, as illustrated in Fig. 22.1. This operational mode is utilized in clutches and engine mounts [3,4].

The flow mode occurs when the ERF flows between two stationary electrodes. Possible fields of application for the flow mode include hydraulic valves, engine mounts, shock absorbers in motor vehicles and aircraft chassis, and vibration dampers for machine tools [5–9]. Figure 22.2 represents the application of ERF in the flow mode in an adaptive motor vehicle shock absorber [10].

In the squeeze mode, the electrodes are moved in the field direction relative to one another. The squeeze mode produces considerable forces with small amplitudes, such as those present in vibration dampers [11,12].

In addition to electro-rheological fluids, magneto-rheological fluids (MRFs) are also gaining ever-greater commercial acceptance. MRFs are also dispersions whose rheological properties vary in proportion to an applied magnetic field. However, because the magnetizable material in MRFs are normally metallic, these fluids are not suitable for use in hydraulic equipment because of their abrasive properties [13].

In this chapter, various aspects of ERFs will be discussed; they include the following:

- Basic properties and operational modes
- Fluid structure–property relationships
- Testing and measurement of the ER effect
- Hydraulic application behavior of ERFs
- Hardware considerations for ERF hydraulic applications

2 ELECTRO-RHEOLOGICAL FLUID FUNDAMENTALS

Even after years of intensive research, a fundamental correlation of the physico-chemical properties involved in the ER effect has not been adequately developed. Nevertheless, models and calculation formulas which are suitable for the design of electro-rheological flow resistors are available and will be presented here.

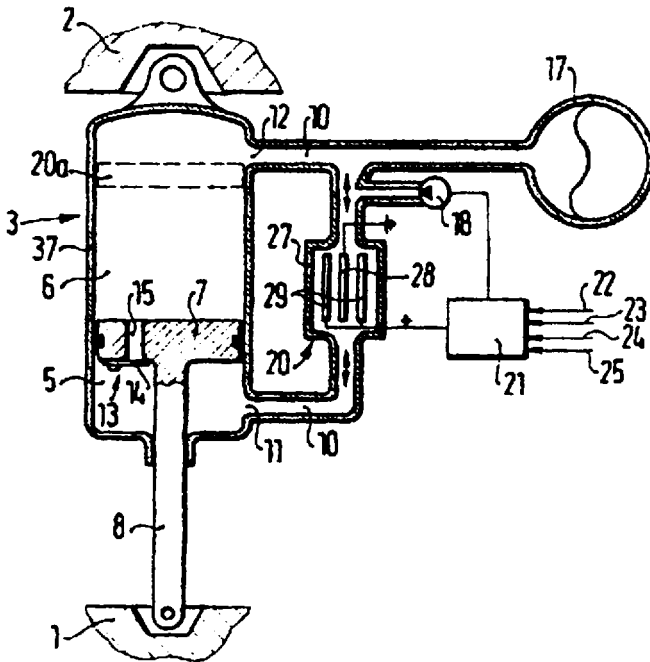


Figure 22.2 ERF vehicle shock absorber.

2.1 Electro-Rheological Theory

One important theory is the model of chain formation. If an electrical field is applied to a nonoperative ERF via two electrodes, the formation of chain structures can be observed under the microscope. As represented in Fig. 22.3, the particles at first move freely within the dispersion before the electrical field is applied. When an electrical field is applied, the particles are polarized and the dipolar particles formed attract each other. This results in the formation of long chains orientated in direction of the lines of the electric field. However, it is important to note that this effect is not due solely to dipolar attraction forces but also to the conductivity of the particles and the carrier fluid [14].

2.2 Rheological Basics

Rheology is a branch of mechanics and is concerned with the flow properties of materials. The shear gradient, D , is defined as the variation of the velocity of neighboring fluid layers in direction y of the gap height, h (see Fig. 22.4) and the following correlation is effective:

$$D = \frac{dv}{dy} \tag{22.1}$$

The interrelationship between the shear stress, τ , and the shear gradient, D , is the "flow law."

Newtonian fluids possess a linear correlation between the load D and the resulting shear stress τ . The proportionality factor is defined as dynamic viscosity η .

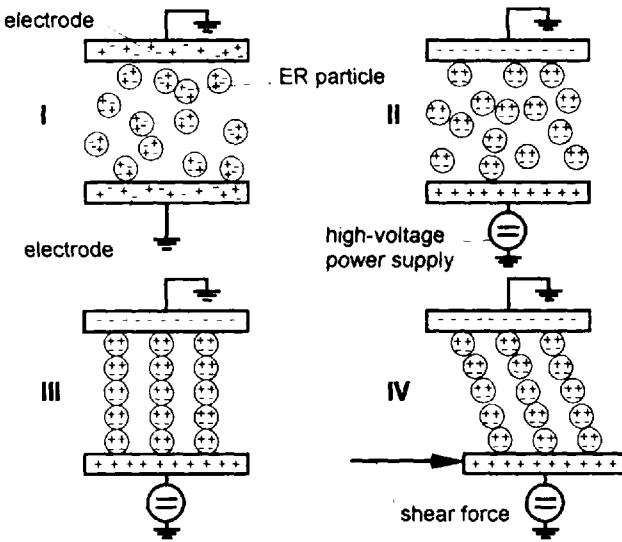


Figure 22.3 Theory of chain formation.

The slope of the straight line corresponds to dynamic viscosity η . This results in the Newtonian flow law (Newton's equation):

$$\tau = \eta D \tag{22.2}$$

Fluids which exhibit nonlinear flow behavior are non-Newtonian fluids.

Mathematical modeling of flow properties is application dependent. For example, dilatant behavior is characterized by increasing viscosity with increasing shear rate. Decreasing viscosity with increasing shear rates is characteristic of structure-viscous (thixotropic) behavior.

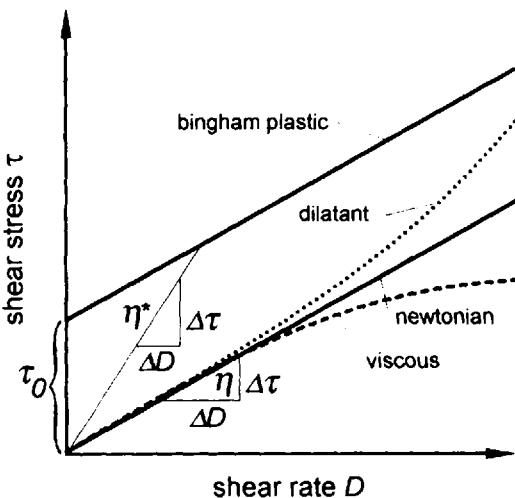


Figure 22.4 Flow curves.

The rheological behavior of an ERF in an electrical field can be modeled as a Bingham body. At lower shear stresses, these materials behave like elastic or viscoelastic solids. Above a threshold shear stress, the yield stress, the material becomes fluid. The flow law for a Bingham body is

$$\tau = \tau_0 + \eta_B D \tag{22.3}$$

with $D = 0$ for $\tau \leq \tau_0$, where η_B is the Bingham viscosity, τ_0 is the yield stress, and D is the shear gradient.

2.3 Operational Modes

As discussed earlier, the ER effect is utilized in one of three operational modes. These will be discussed in detail here.

2.3.1 Shear Mode

In the shear mode, the ERF is subjected to a stationary drag flow through a parallel gap. Assuming that the pressure is constant in the flow direction, both for Newtonian and an “ideal” ERF without field impact, the linear velocity profile within the gap is represented by Fig. 22.5.

The shear mode can be employed in applications such as variable torque transfer in clutches and breaks, the adjustment of different damping characteristics in dampers and engine mounts and the determination of flow properties in rotary viscometers. In rotary viscometers, the fluid is sheared in an annular gap and the fluid parameters are deduced from the rotational frequency of the measuring body and the torque transmitted by the fluid for the determination of the flow curve and the flow law.

2.3.2 Squeeze Mode

In the squeeze mode, the electrodes are moved but not in the direction of the electric field lines, as illustrated in Fig. 22.6. The ERF is compressed and squeezed to the edge of the gap. In a low-load electric field, the ERF behaves like an elastic solid particle. It has been shown that under these conditions, significantly higher forces can be attained with correspondingly lower deformation amplitudes.

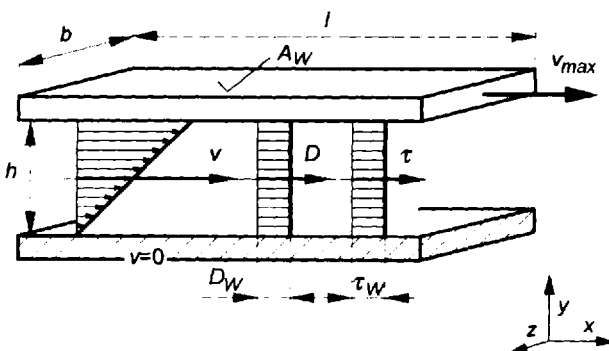


Figure 22.5 Velocity profile of a Newtonian fluid in the shear mode.

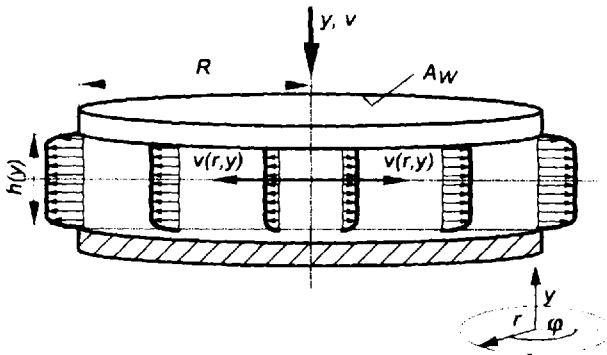


Figure 22.6 Application of the ER effect in the squeeze mode.

2.3.3 Flow Mode (Poiseuille Flow)

The flow mode most often used in ERF hydraulic circuit design is the flow mode. In the flow mode, the ERF fluid is transmitted via a stationary throttle gap due to an adjacent pressure difference. ERFs can, from a rheological perspective, be considered as plastic materials. When a sufficient electric field is applied, they exhibit a threshold flow limit. At electric fields above this limit, fluid flow begins. Fluid shear stress is dependent on the shear gradient. Without the electric field, the ERF behaves like a Newtonian fluid.

If the pressure gradient over the gap length is constant, the shear stress is linear over the gap height. The wall shear stress can be obtained from the balance of forces of pressure and friction. Generally, the following equation is applied:

$$\tau_w = \Delta p \frac{h}{2l} \quad (22.4)$$

where

- τ_w = wall shear stress
- Δp = pressure difference
- h = gap height
- l = gap length

For a Newtonian fluid, the parabolic velocity profile illustrated in Fig. 22.7 results. However, in the presence of an electric field, the ERF behaves like a Bingham body and exhibits the flow profile illustrated in Fig. 22.8. Decreasing shear stress in the direction of the gap center causes the development of the plug flow. The plug height $h(E)$ is directly dependent on the yield stress $\tau(E)$ and is modeled by Eq. (22.5):

$$h(E) = \frac{2\tau(E)l}{\Delta p} \quad (22.5)$$

The shear areas at the edge exhibit a parabolic flow profile because the flow behavior is Newtonian. The relationship between volume flow and the adjacent pressure difference Δp can be established from [15]

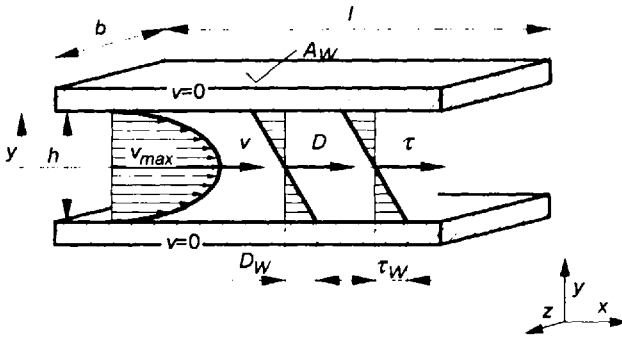


Figure 22.7 Velocity profile of a Newtonian fluid in the flow mode.

$$Q = \frac{b}{12\eta} \left(\frac{l}{\Delta p} \right)^2 \left[4[\tau(E)]^3 - 3\tau(E)h^2 \left(\frac{\Delta p}{l} \right)^2 + h^3 \left(\frac{\Delta p}{l} \right)^3 \right] \quad (22.6)$$

where

- Q = volume flow
- Δp = pressure difference
- η = dynamic at zero field
- $\tau(E)$ = the electro-rheological influenced yield stress
- h = gap height
- b = gap width
- l = gap length

The complexity of the equation makes a theoretical calculation of flow resistance very expensive. Therefore, a simplified calculation of the real flow behavior of an ERF in the flow mode was developed.

2.4 Simplified Equations to Calculate the Flow Behavior of ERF

A comparison of the pressure difference over an electrode gap is dependent on the volume flow in the flow mode and is illustrated in Fig. 22.9. The flow curve of a Bingham body, shown in Fig. 22.4, shows that the attainable pressure difference can

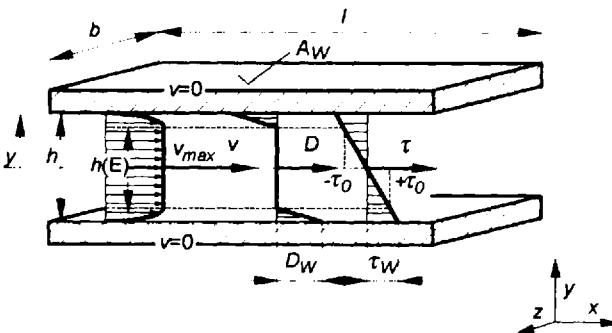


Figure 22.8 Velocity profile of a Bingham plastics in the flow mode.

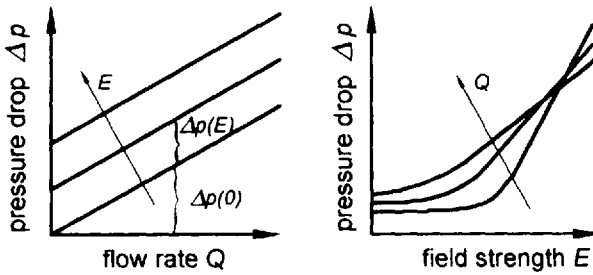


Figure 22.9 Idealized laminar flow characteristics of an ERF.

also be described as the sum of an electro-rheological yield pressure difference $\Delta p(E)$ and a Newtonian basic pressure difference $\Delta p(0)$:

$$\Delta p = \Delta p(E) + \Delta p(0) \quad (22.7)$$

If the yield pressure difference $\Delta p(E)$ depends only on the field strength and not on the shear gradient or on the volume flow, the flow pressure difference according to Eq. (22.4) is

$$\Delta p(E) = 2\tau(E) \frac{l}{h} \quad (22.8)$$

According to Eq. (22.8), the total pressure difference over an electrode gap is dependent on the yield stress and the geometrical dimensions:

$$\Delta p = 2\tau(E) \frac{l}{h} + \frac{12Q\eta l}{bh^3} \quad (22.9)$$

This equation shows that the attainable pressure difference of an electro-rheological flow resistor with a given yield stress is dependent on gap geometry, viscosity, and volume flow.

The switching ratio, G , which is the ratio of yield pressure difference $\Delta p(E)$ and initial pressure difference $\Delta p(0)$, is used in practical applications:

$$G = \frac{\Delta p(E)}{\Delta p(0)} \quad (22.10)$$

In this way, the ER effect in electro-rheological flow resistors can be quantitatively determined.

3 STRUCTURE AND PROPERTIES OF AN ER HYDRAULIC FLUID

3.1 Special Requirements of Hydraulic Fluids

The use of electro-rheological fluids in hydraulic applications requires the use of ERFs with specific physical and chemical properties because they are not only used for the control of pressures and volume flow but also for the transfer of hydrostatic power. The design and construction of the hydraulic system necessitates particular properties of the pressure medium. Therefore, physical and chemical properties of the pressure fluid must be available.

In the subsequent discussion, the fluid properties and performance data of an ERF which was investigated in detail as part of a research project at the Department of Fluidpower Transmission and Control at the Rheinisch-Westfälische Hochschule Aachen will be presented as an example [16].

3.2 General Structure of the ERF

The ERF that will be discussed here was a dispersion of conductive particles in a dielectric base fluid, or dispersent; in this case, a silicone fluid. The dispersed phase contained synthetic network-polyurethane particles. To improve serviceability, additional auxiliary dispersants and stabilizers were added to the dispersion [7,13,17,18]. Figure 22.10 illustrates the fundamental structure of the ERF [19].

The silicone fluid was a synthetically produced, clear, odorless fluid commonly used in various industrial applications. Because of their extremely low conductivity and high breakthrough resistance, silicone fluids are very suitable for use as an ERF base fluid. Another advantage is that silicone fluids are obtainable in different viscosity categories and they are mutually compatible. Therefore, ERF fluid viscosity may be varied.

To minimize flow loss in hydraulic resistors, an ERF should, if intended for use as a pressure transmission medium, exhibit a minimal viscosity. However, because low-viscosity silicone fluids are poor lubricants, antiwear additives must be added to minimize wear in the hydraulic system.

Although dispersant properties significantly affect thermal and tribological characteristics of the dispersion, the structure and the arrangement of the dispersed phase also significantly influences the electro-rheological effect. The minimal abrasiveness of soft polyurethane plastics are adequate for use in hydraulic circuits.

The polarizability of the polyurethane particles, which is required for the electro-rheological effect, is provided by the use of metal salts introduced into the polymer matrix. The quantity and the quality of the dissolved salts imparts the required electrical properties, which are dependent on polymer chemistry [17].

3.3 Properties of the ERF

An important property of pressure transmission media is the viscosity-temperature behavior. Figure 22.11 provides a comparison of the viscosity-temperature behavior

dispersed phase	continuous phase
<ul style="list-style-type: none"> ▪ crosslinked polyurethane ▪ dissolved salts ▪ volume fraction < 60% ▪ particle size app. 3-5 μm ▪ density app. 1.09 g/cm³ 	<ul style="list-style-type: none"> ▪ polydimethylsiloxane oil ▪ dispersing agents ▪ stabilizers ▪ density app. 0.92 g/cm³

Figure 22.10 General design of the ERF.

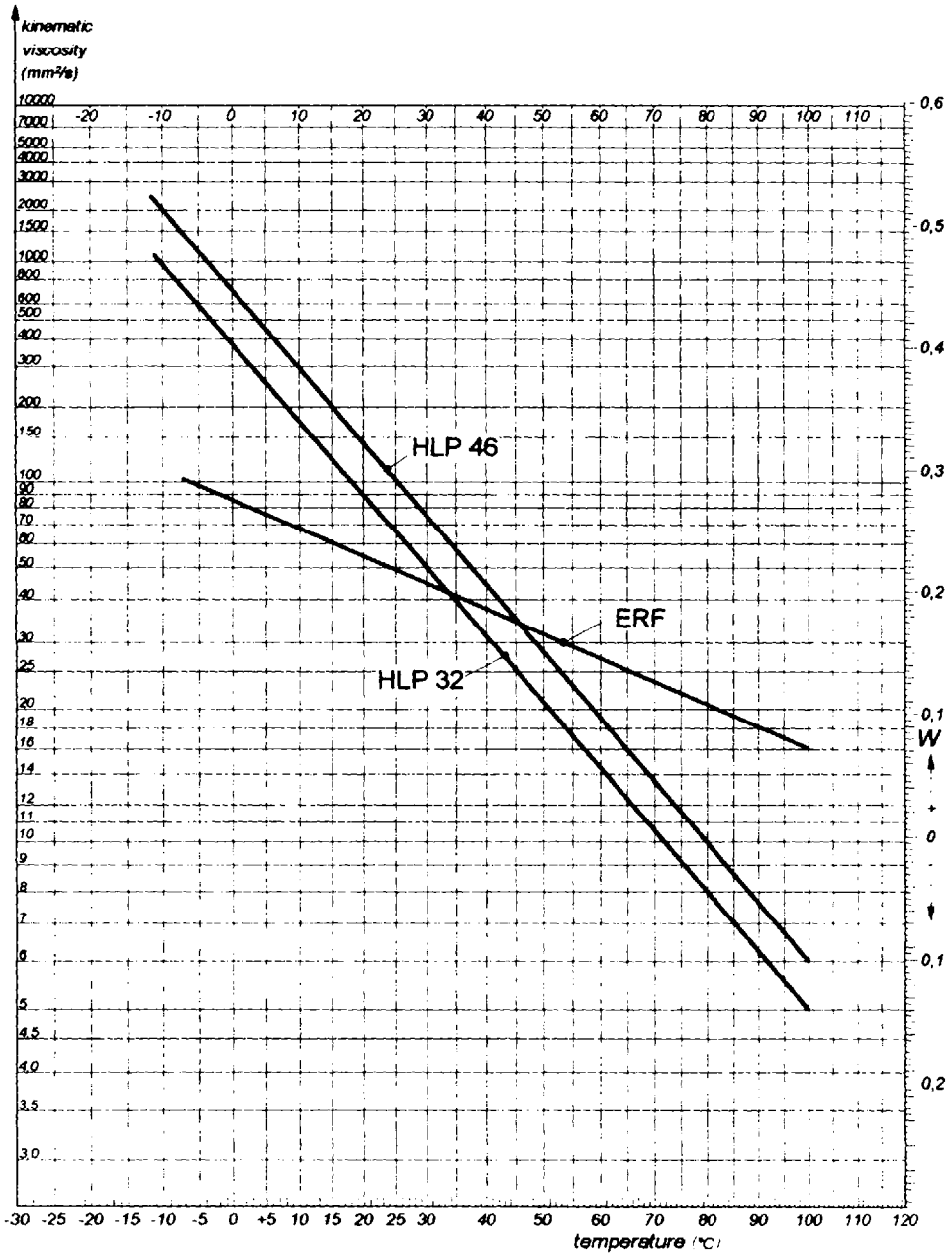


Figure 22.11 Viscosity-temperature behavior of the ERF.

of an ERF dispersion (VI 492) and ISO-VG 32 and HLP 46 mineral oils (VI 91-102). The superior viscosity–temperature behavior of the ERF becomes apparent, as it exhibits the flattest viscosity versus temperature response, which is reflected in the viscosity index (VI).

The viscosity–pressure behavior of the ERF at three different temperatures is illustrated in Fig. 22.12. The viscosity–pressure relationship at constant temperature can be approximated from

$$\eta = \eta_{\text{atm}} e^{bp} \quad (22.11)$$

where η_{atm} is the dynamic viscosity at atmosphere pressure, $b = 0.69 \times 10^{-3} \text{ bar}^{-1}$ (ERF), and $b = 1.7 \times 10^{-3} \text{ bar}^{-1}$ (mineral oil). The ERF exhibits a lower b value (pressure–viscosity coefficient) relative to the mineral oil, which means that the ERF will exhibit a lower load capacity. Lower b values indicate lower viscosity at the same pressure than a fluid with a higher b value. Because the load capacity of an oil is proportional to its viscosity under a given load, the ERF will exhibit a lower load capacity than the mineral oil. Therefore, the lower load capacity of the ERF must be accommodated in the design of highly loaded hydrodynamic mounts to minimize wear and avoid seizure.

In Fig. 22.13, the primary hydraulic characteristics of the ERF are compared with a silicon fluid. The temperature behavior of the ERF is controlled by the properties of the base oil. The low bulk modulus of the ERF will also influence the behavior of hydraulic control systems.

4 CHARACTERISTICS OF ER FLUIDS IN HYDRAULIC SYSTEMS

It has been shown that shear stress and shear gradients of ERFs, which are determined by viscometry in the shear mode, cannot be transferred into the flow mode where hydraulic systems typically operate. Therefore, experimental examinations of ERFs in a flow resistor are required to determine the ER effect. The primary factors influencing flow behavior of an ERF in a hydraulic flow resistor will be discussed in the subsequent discussion.

4.1 Test Equipment and Measuring Technique

4.1.1 Test Bench

A test bench, which was constructed mostly from conventional hydraulic components, was designed to examine flow properties of the ERF under the most realistic conditions. The hydraulic circuit diagram for the test bench is provided in Fig. 22.14. The pressure supply, which provides a constant volume flow of $Q_p = 11.41/\text{min}$, is provided by a gear pump driven by an electric motor. During testing and measurements, variable volume flow may be obtained using the flow control unit. The fluid is delivered through an electrode gap. At both the inlet and at the output, a pressure transducer is used to record the pressure difference.

A 4/3-way switch valve which controls a hydraulic cylinder was installed behind the ER flow resistor. A simple analogous electronic system switches the valve to automatically reverse the cylinder in the end positions. Behind the actuator, an adjustable pressure relief valve, to increase the system pressure to $p_{\text{PRV}} = 70$ bars, is

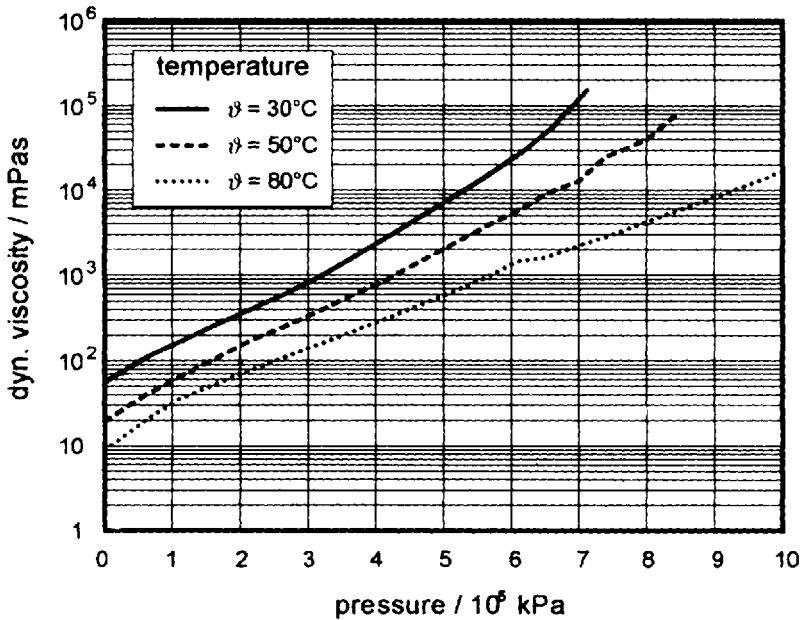


Figure 22.12 Viscosity–pressure behavior of the ERF.

introduced into the circuit. Temperature controls, such as cooler and heating devices, are positioned in front of the reservoir.

Because of the special structure of the ERF and the associated sedimentation tendency, the reservoir consists of a stainless-steel cylinder with a conical bottom, which is illustrated in Fig. 22.15. The reservoir return line is situated below the oil level, thus ensuring a favorable mixing of the ERF while minimizing the risk of foaming.

The filter element indicated in Fig. 22.14 is exclusively used for cleaning the system with pure base fluid. ERF filtration is not possible because the dispersed phase would plug the filter element within a short time.

4.1.2 Design of the ER Flow Resistor

The electro-rheological behavior of the ERF is recorded using a flow resistor, as illustrated in Fig. 22.16 in sectional view. The flow resistor was designed as an annular gap consisting of a mandrel and a sleeve. This is constructed of dynamically balanced pivoting parts, which provides the advantage of low cost. In addition, the gap dimensions can easily be adjusted by varying the sleeve and mandrel.

High voltage is applied to the outer-electrode sleeve and the inner electrode and all the other component parts are grounded. Insulation is provided at the ends of the sleeve to ensure centering of the sleeve and mandrel and to provide dimensional precision of the electrode gap. The cover and bottom of the resistor contains bolt holes where the pressure and temperature transducers are situated. The modular design of the resistor allows an easy variation of the gap geometry by making use of different sleeves and mandrels.

parameter	dimension	silicon oil	ERF
density	g / cm^3 (at 25°C)	0,92	1,04
dynamic viscosity	mPa s (at 25°C)	4,6	50
kinematic viscosity	mm^2 / s (at 25°C)	5	48
viscosity index	-	450	492
flame point	°C	120	110
ignition point	°C	400	400
thickening point	°C	- 100	- 60
neutralization number	mgKOH / g	0,00	0,25
water content	%	0,01	0.04
heat transfer	$\text{W} / \text{m K}$	0,116	useless
specific heat	$\text{J} / \text{g K}$	1,51	unknown
Bunsen number	-	0,174	unknown
steam pressure	mbar (at 25°C)	$1,93 \times 10^{-5}$	unknown
specific volume	cm^3 / g	1,09	unknown
bulk modulus	N / m^2 (at 1 bar)	$9,843 \times 10^8$	$1,597 \cdot 10^9$
dielectricity	DIN 53483 50 Hz	2,8	unknown
specifc resistor	Ω / m	$4 \cdot 10^{14}$	useless
break throw resistance	kV / cm (at 20°C)	120	useless

Figure 22.13 Listing of fluid parameters.

4.2 Influencing Parameters in Flow Mode

The impact of volume flow, temperature, and system pressure level on the ER effect will be discussed in this subsection. The dimensions of resistor used for these measurements were as follows:

- gap height (h): 0.75 mm
- gap length (l): 40 mm
- average diameter (d_m): 12.25 mm

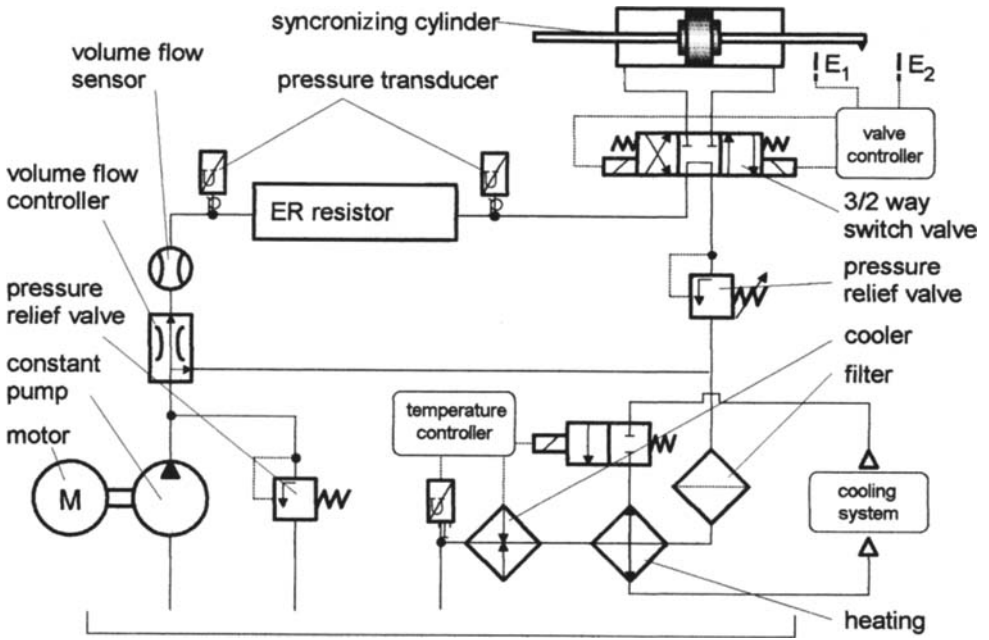


Figure 22.14 Hydraulic circuit of the load testing bench.

4.2.1 Flow Rate

Figure 22.17 illustrates the flow behavior of the ERF when subjected to an electric field. The solid line at the bottom of the figure, which describes the behavior without an applied electric field, shows the proportional flow behavior in a laminar throttle, which is typical of a Newtonian fluid. When influenced by an electrical field, the

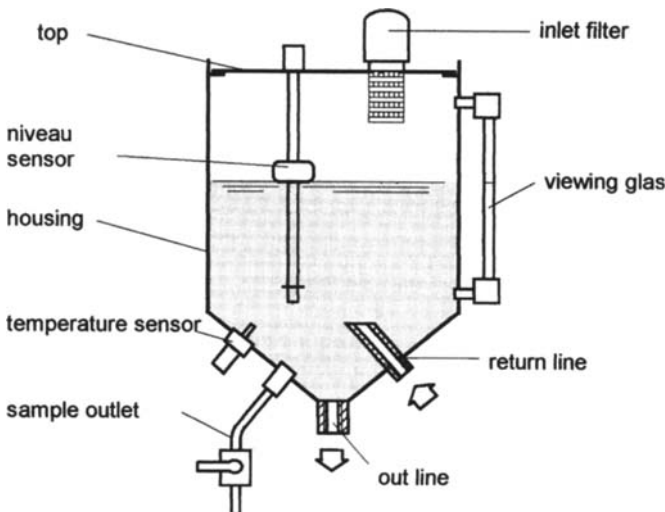


Figure 22.15 Design of the reservoir.

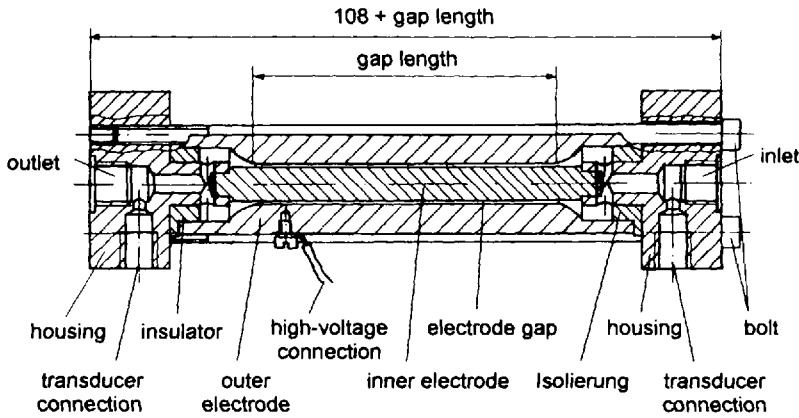


Figure 22.16 Cross section of the ER resistor.

yield pressure difference develops, which is dependent on the height of the field strength. As the pressure continues to increase, the fluid begins to flow and the volume flow increases. Interesting, the curves in Fig. 22.17 are almost parallel.

Figure 22.18 illustrates the effect of the pressure difference on field strength with respect to three different volume flows. The maximum pressure difference attainable at these gap dimensions is $\Delta p = 8$ bars. Before the application of an electric field, a small pressure difference exists with increasing volume flow. Figure 22.18 illustrates that increases in the pressure difference only occur above a limiting electric field strength, E_0 , which is dependent on volume flow. The limiting field strength increases with rising volume flow.

The correlation between the attainable pressure difference and electric current is illustrated in Fig. 22.19. At a relatively low flow rate, $Q = 2$ L/min, the correlation is nearly linear. However, the correlation is increasingly nonlinear with increasing

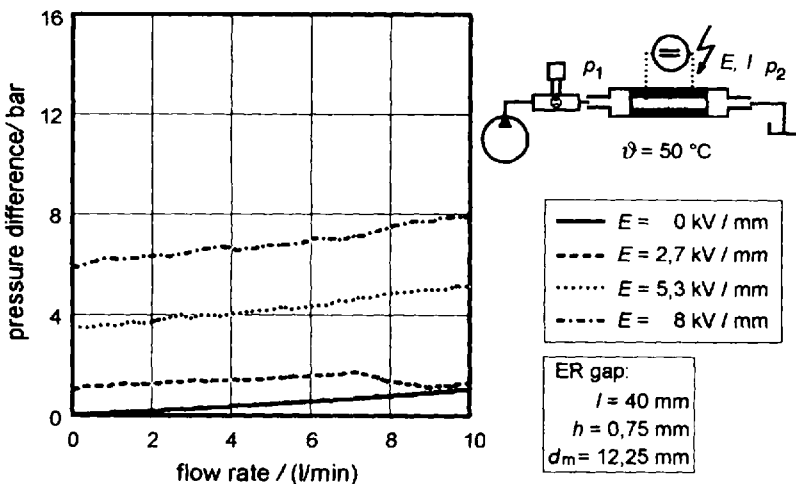


Figure 22.17 Influence of the flow rate on the pressure difference.

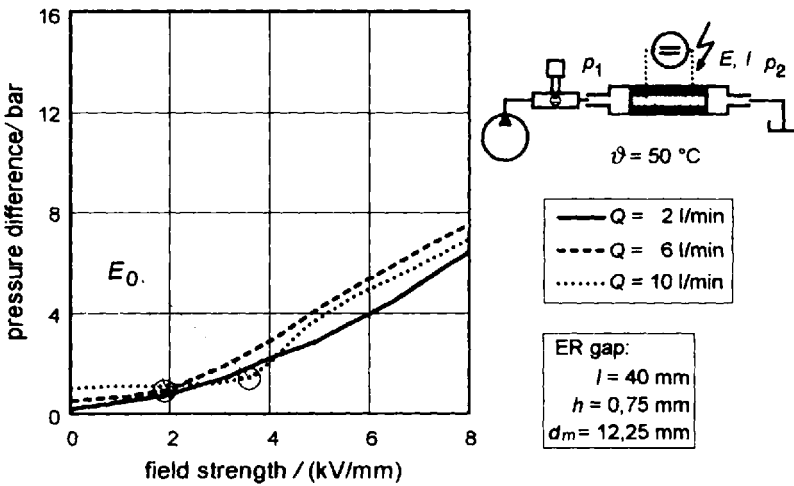


Figure 22.18 Influence of the field strength on the pressure difference.

flow rates. Generally, the increase in the pressure difference–current relationship is greater with decreasing flow rate.

These results show that the ER effect in the flow mode is dependent on the flow rate delivered through the gap. This is reasonable because the flow-rate dependence on gap geometry also influences the shear gradient in the fluid.

4.2.2 Temperature

Fluid temperature also contributes to the ER effect. Figure 22.20 illustrates the effect of the pressure difference on the electric field strength. The pressure difference $\Delta p(0)$ decreases with increasing temperature because the flow resistance decreases with decreasing viscosity. However, an increase in temperature with higher field strengths

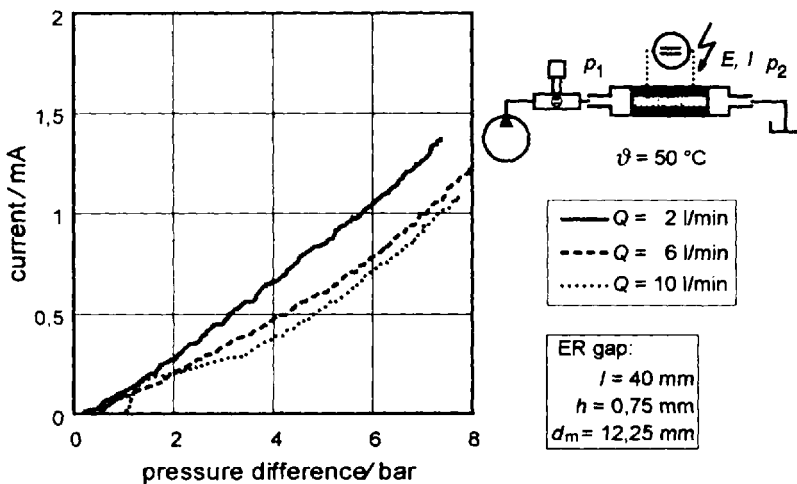


Figure 22.19 Conductivity in relation to the pressure difference.

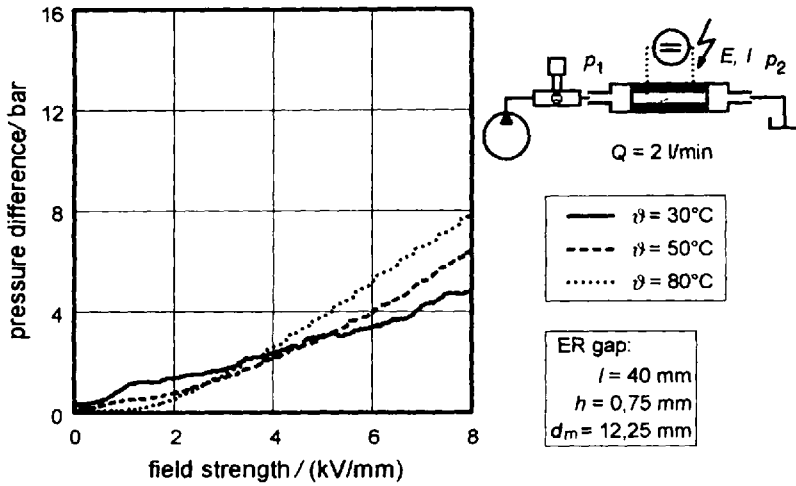


Figure 22.20 Influence of the temperature on the pressure difference.

increases the ER effect. This is indicated by the increasing slopes of the field strength–pressure difference curves.

The effect of electric current on field strength is temperature dependent. In Fig. 22.21, the current increases with increasing temperature, and at a temperature of $\vartheta = 80^\circ\text{C}$, the power limit of the voltage supply used for this work was achieved. The attainable pressure difference and switching relation was enhanced with increasing temperature, but the current flowing through the electrode gap increases at the same time.

Not only the maximum pressure difference and the switching relation but also electrical control power must be considered in the analysis of the ER effect. The

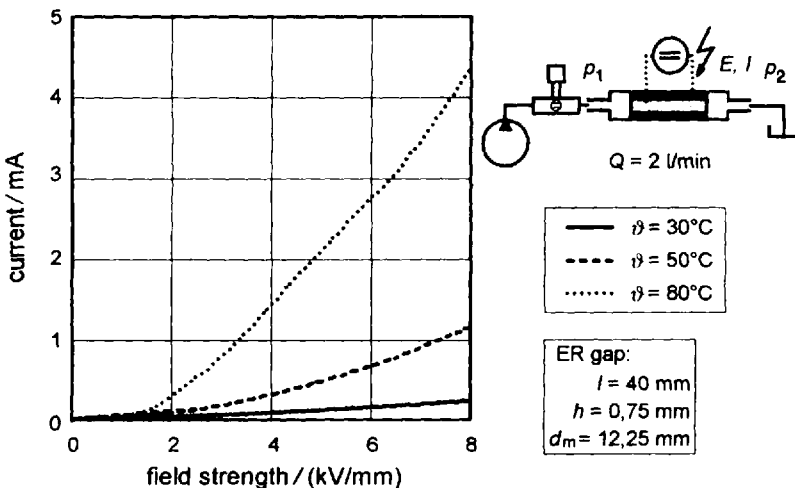


Figure 22.21 Influence of the temperature on the electrical conductivity.

importance of electrical control power of each individual ER valve must be considered during the analysis of the entire hydraulic system.

4.2.3 System Pressure Level

According to Eq. (22.9), the attainable pressure difference is primarily dependent on the geometry of the electrode gap. Thus, it is theoretically possible to produce any magnitude of pressure difference by diminishing the gap height or enlarging the gap length. However, the limits of the reduction of gap height and enlargement of gap length are both set by the practical application. Whereas a reduction of the gap height increases the risk of electrical breakthrough, an increase of the gap is limited primarily by problems arising from the construction of the circuit. However, a series circuit of several single resistors may be used to achieve pressure differences of 150 bars [16].

5 APPLICATION OF ERF IN HYDRAULIC SYSTEMS

For the commercial application of ERFs, they must be stable, both in performance and oxidatively. To prevent wear damage by the solid particles due to high shear stress which would reduce the ER effect, they must neither be abrasive nor may they be too soft. In addition to determining ERF aging stability, compatibility with conventional hydraulic components is also important in the assessment of potential applications.

To assess the applicability of the ERFs, hydraulic tests were conducted where the ERF was loaded with a system pressure of $p_L = 30$ bars and a flow rate of $Q_L = 6$ L/min in a bench test over a period of 2000 h. After 400 h of operation, the pressure-difference dependence on the field strength was determined using the measuring equipment described in Section 4.1.1.

5.1 Aging Stability

Figure 22.22 illustrates the results of the ERF endurance test. These data indicate that no substantial changes which would impair the ER effect have occurred in the

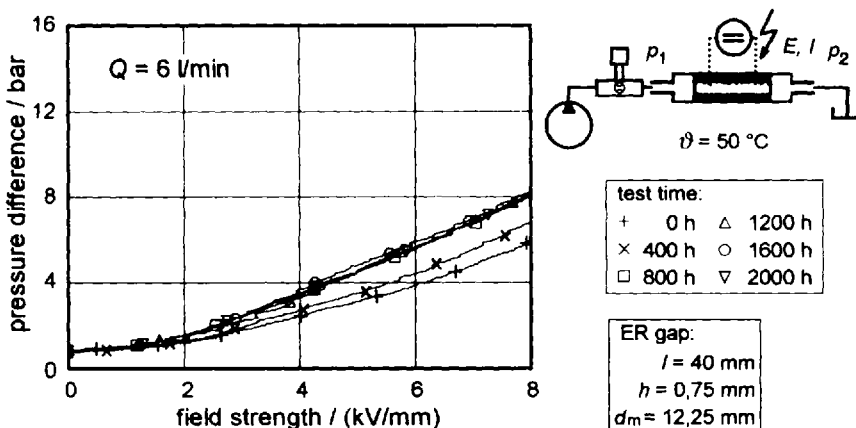


Figure 22.22 Influence of test duration on the pressure difference.

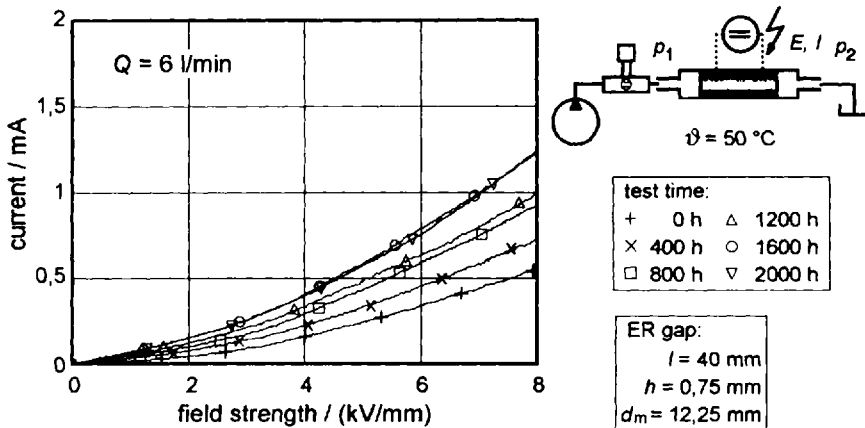


Figure 22.23 Influence of test duration on the conductivity.

fluid. It should be noted that the effect initially increases and then remains almost constant. Although the magnitude of this behavior was not always observed, generally the fluids examined fluids typically exhibited an improvement, not a deterioration of the ER effect.

Apart from the hydraulic power losses due to the pressure drop in the ER gap, electrical power consumption also plays an important role in the assessment of ERF efficiency. A correlation between the load duration and conductivity can be observed through power consumption, as illustrated in Fig. 22.23. Although the curves are subject to a certain degree of scattering, there is a clear tendency toward an increase of conductivity with prolonged load duration.

Although the reason for the increase of conductivity was not clearly evident from this work, chemical characterization work has shown that trace amounts of metal ions accumulated in the ERF. However, no metal particles attributable to abrasive wear processes was evident. The source of increase of the ferric ions in the ERF was not resolved. An accumulation of metal particles due to abrasive wear processes in the system, however, cannot be excluded because of insufficient filtration.

In addition to the detection of the electro-rheological data such as the current and the pressure difference dependence on the field strength, the impact of viscosity and density of the ERF performance was examined. No significant variations due to the continuous-load test were observed.

In summary, under the moderate conditions applied in these tests, the ERF showed an excellent aging behavior. The conductivity increase poses the only potential problem that must be considered during the application of the ERF in a hydraulic system.

5.2 Hydraulic Component Compatibility

5.2.1 Elastomer Behavior

To examine the compatibility of the ERF with different elastomers, swelling tests with different materials at ambient temperature and 74°C were conducted. After 5

days and at the end of the test, the mass, volume, and dimensions of the samples were measured and compared with the initial state. Figure 22.24 illustrates the results of these tests.

The NBR materials examined showed a marked temperature dependence with regard to variation of mass, volume, and diameter. In each case, a volume decrease and weight loss occurred. Furthermore, the variation depends on the hardness of the material. The softer the material, the greater the variation of the volume or mass. Unfortunately, material hardness variation was not determined.

The measured property variations of fluouorocarbon (FKM) lies within the range of measuring accuracy. Only an increase in diameter was observed during the tests. Therefore, this material appears to be compatible with the ERF.

Relative to the NBR materials, the variations (PTFE) and polyurethane (PU) also indicate that they are compatible with the ERF fluid. However, there is a greater tendency for swelling based on volume and mass increase data relative to FKM.

In addition to chemical compatibility, an evaluation of the sealing properties of grooved-ring sealings of different materials was also performed. This test was conducted at a chamber pressure of 30 bars over a period of 167 h. The ERF with all the rod seals exhibited moderate leakage behavior.

In summary, although NBR is generally suited as a seal material for most hydraulic fluids, a small volume and mass decrease leads to a deterioration of the sealing behavior in dynamic seals. To avoid this, FKM is compatible with ERF and should be used as dynamic seals.

5.2.2 Sedimentation Stability

The ERF is relatively resistant to sedimentation because of the minimal differences in density between the dispersed phase and the dispersant. Furthermore, the ERF exhibits excellent redispersing capacity because the particles mix almost completely when the test bench is first started. Only in areas with a low flow velocity, such as in manifolds and connecting parts and in unfavorably arranged piping, durable sedimentation of the particles is possible. If necessary, separated particles may be readily redispersed by mechanical agitation. Except for minimal loss of the ER effect, no negative effects ensued from this level of sedimentation. Sediment formation should be avoided, however, in the design of the suction conditions in the hydraulic pump inlet because of potential damage and loss of suction pressure. Also, when resistance heaters are used, there is the danger of thermal decomposition of the polyurethane particles due to overheating at the heating elements. Therefore, heating of the ERF should be avoided.

5.2.3 Wear Interaction

In addition to ERF behavior under a shear load in a hydraulic system, the influence of the fluid on the hydraulic components parts must also be evaluated to determine its applicability in hydraulic applications. In this study, gear pumps and radial piston pumps with check valve distribution were used. Although gear pumps provided trouble-free operation, there was some operational problems with the radial piston pumps early in the tests. Pump disassembly revealed that some pistons did not move freely in the cylinder bore and that the spring power was insufficient to fill the cylinder chamber. Enhancement of the piston operation prevented recurrence of these problems. These results illustrate that gear and radial piston pumps are generally ac-

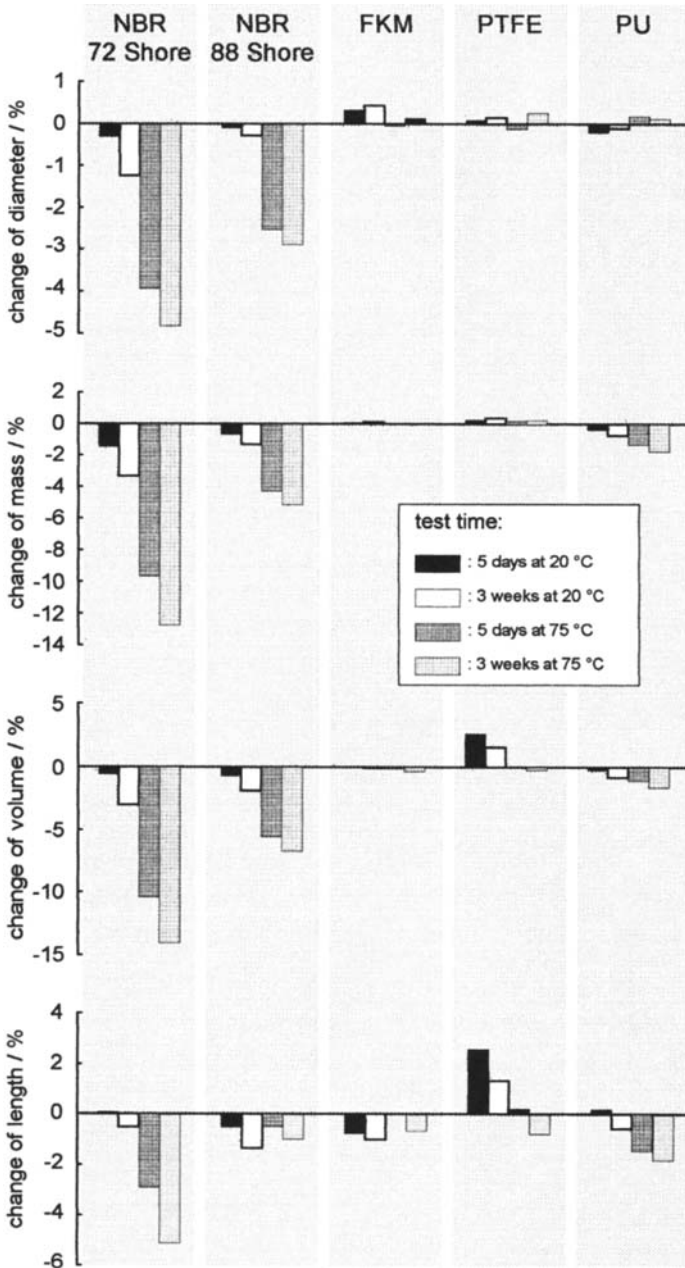


Figure 22.24 Swelling behavior of sealing materials.

ceptable for use with ERFs. Increased wear due to the dispersed particles was not observed in these studies.

Two types of valves were evaluated for use with ERFs: seated and slide valves. Pressure-relief valves, which are seated valves, did not exhibit any problems. There were occasional operational problems due to particle agglomeration with slide valves. These disturbances occurred only after long downtimes of when the test bench was not filled with ERF for a relatively long period of time. It should be noted that the hydraulic components used for the test bench were those conventionally used with mineral-oil-based hydraulic fluids.

Increased wear attributable to dispersed solid particles was not observed for the components evaluated. Because of their low contamination sensitivity, seated valves are generally more suited for use with ERFs than slide valves. Fittings and bore sizes for system components should be sufficient to avoid plugging by particles in the ERF, which would certainly lead to functional disturbances.

6 ELECTRO-RHEOLOGICAL HYDRAULIC ACTUATOR

One of the main advantages of ER technology is in the short reaction time of the ER effect. The dynamic properties of ERFs have been studied previously, both experimentally and theoretically [20,21]. In this section, a hydraulic cylinder actuator in which the ERF assumes the control function and for hydraulic power transmission is discussed. Therefore, a compact cylinder with respect to design and time behavior which differs from conventional cylinder drive systems should be developed.

6.1 Control Designs for ER Actuators

Different circuit designs may be used to control hydrostatic drives. Important factors for circuit-design selection are expected system behavior and dynamics and circuit cost. In ER technology, each electro-rheological flow resistor is equivalent to one metering edge in a valve. For example, Fig. 22.25 illustrates two circuit designs for electro-rheological control of a hydrostatic cylinder. The upper part of the figure illustrates valve control with four metering edges. In this case, two resistors are switched consecutively using the bridge circuit represented in the figure. This circuit design is recognizable by its high reinforcement of velocity and power [22]. A disadvantage is that control of the four ER flow resistors requires at least two power supply units. The lower portion of Fig. 22.25 illustrates the use of a differential cylinder that may reduce the number of necessary flow resistors required by one-half.

The disadvantage of both designs shown in Fig. 22.25 is that at least two flow resistors and two pressure supply units are required for the control. The initial pressure drop passes via the unswitched valve directly as an efficiency balance loss. In high flow rates, a deterioration of the circuit efficiency will result.

To control an actuator with only one flow resistor, the circuit variants represented in Fig. 22.26 can be used. Variants I and II permit actuator positioning by means of a constant and adjustable control resistor. Running-in of the cylinder to variant II is conducted mechanically using a spring. In variant I, running-in is performed hydraulically using the supply pressure.

Variant III presents the simplest design of a single edge control for a differential cylinder. In this case, the recoil force is provided via an external force using a spring

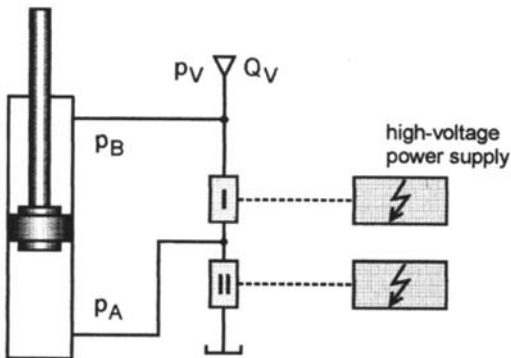
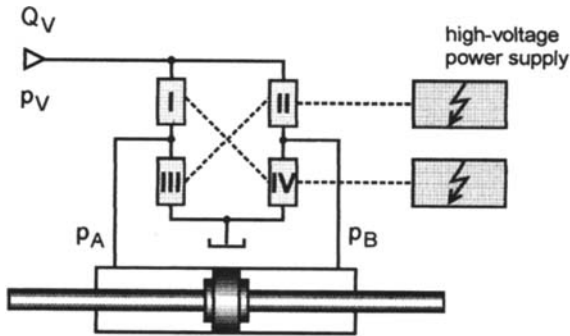


Figure 22.25 General design of a cylinder control unit with ER flow resistors.

or a load. The flow into the reservoir is controlled by an adjustable resistor. In this circuit variant, supply pressure is dependent on load pressure, and system dynamics depends on the pressure from the pressurized oil volume.

6.2 Hardware Design

6.2.1 Test Equipment

The test stand, which has been described in Section 4, provides the basis of the cylinder test stand illustrated schematically in Fig. 22.27. Besides characteristics such as pressure, flow rate, and temperature, additional variables such as stroke, velocity, and acceleration must also be recorded. A different procedure has been generally

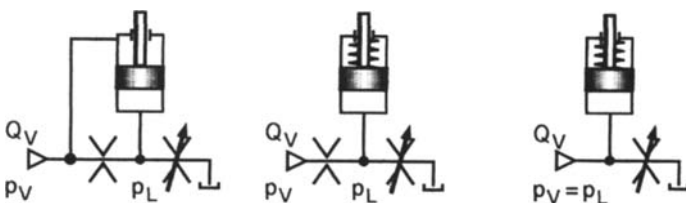


Figure 22.26 Simple circuit conceptions for cylinder actuators.

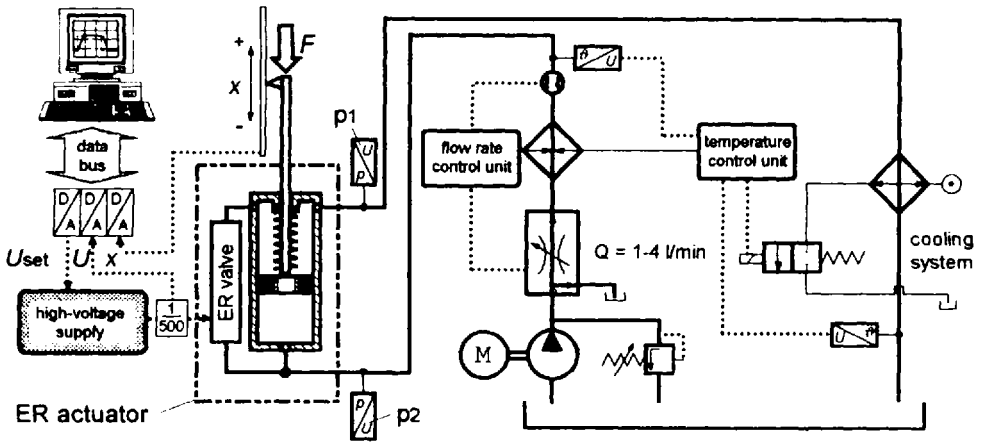


Figure 22.27 Schematic representation of the cylinder test bench.

used in practical applications because of the employment of micro-electronics. In this method, only the stroke is recorded using a transducer and it is input to the computer. Velocity and acceleration are then calculated by differentiation from the position signal.

6.2.2 Actuator Design

As illustrated in Fig. 22.28, construction consists of several nested cylinder tubes and two connection blocks. The blocks, which are attached to the front of the tubes, serve as guides for centering the tubes and are connected to each other via four

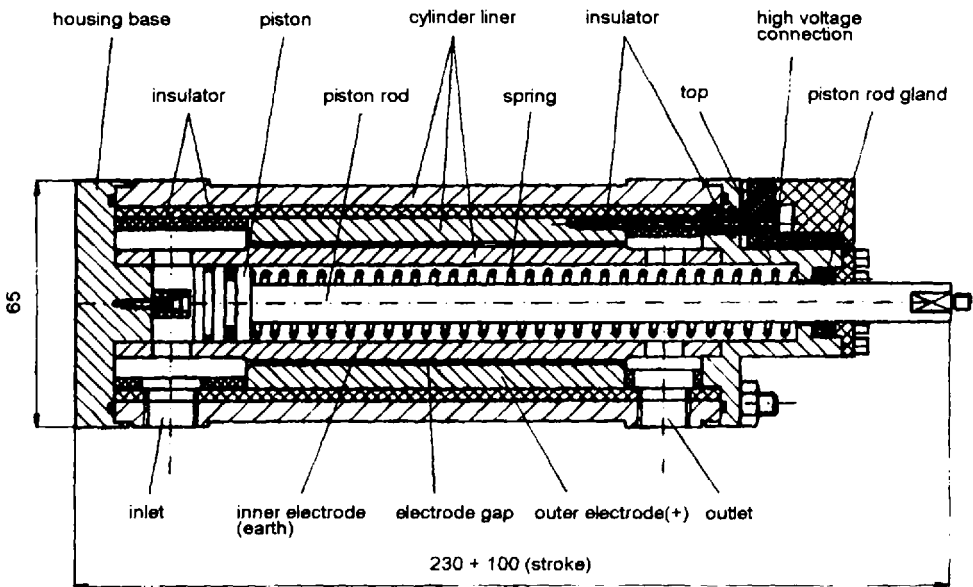


Figure 22.28 Design of the ER actuator.

preloaded threaded rods. The inner cylinder tube fulfills a double function. On the one hand, it serves as a cylinder tube and as a guide for the piston; on the other hand, it functions as a grounded inner electrode of the ER flow resistor. Another tube is arranged around the cylinder tube, forming the external ring of the electrode gap. The external electrode is contained within another tube, which is coated on the inside with synthetic material for the purpose of insulation. The connection blocks are equipped with bore holes for the hydraulic connections and for temperature and pressure transducers. The piston rod is mounted on a carriage attached to a linear guide. The carriage guide permits the actuator to be loaded by mounting a spring or by adding additional masses.

A pressure develops over the electrode gap which is dependent on field strength. As long as the pressure required for extending the piston is not attained, complete flow rate discharges via the resistor. If the pressure independent of the field strength exceeds the load pressure, the piston is accelerated and the piston rod is extended. When the valve is completely closed, the actuator reaches its maximum extending velocity. Exactly at the moment when the cylinder is totally extended, the whole flow rate discharges via the ER resistor. This ensures a pressure limit in the system. As soon as the field strength in the gap is reduced or switched off, the system pressure decreases and the piston is pushed back by the force of the preloaded spring or an external load.

6.3 System Characteristics

In addition to the compact design, another advantage of ER technology is the fact that electro-rheological resistors eliminate the need for mobile parts. Pressure development and, thus, the dynamic behavior of the valve is primarily dependent on the reaction time of the effect and the system dynamics of the hydraulic system.

6.3.1 High-Voltage Power Supply

Because of the complexity of the electro-rheological effect, voltage production and the resulting design of the high-voltage supply play an important role. With regard to dynamic behavior, where rapid reduction in the development of electrical field is observed, efficiency potential of the high-voltage supply has a fundamental impact on the ER effect. In these studies, two different high-voltage supplies differing primarily in their time behavior were used. Depending on the DC power pack, the supply voltage is divided into rectangular signals using a high-frequency transducer transformed onto the high voltage. Variation of the basic voltage is realized by the variation of the impulse width of the divided DC signal. The high voltage is subsequently rectified and smoothed using a RC filter.

This type of voltage supply has the advantage of a simple and low-cost design. A disadvantage is unfavorable time–response behavior because the basic voltage is smoothed via capacitors. When the control signal is varied in steps, low-dynamic behavior of the basic signal follows because of the high capacitive internal resistance. When the voltage is switched off, voltage reduction occurs only through Ohm's resistance of the connected load, which leads to extremely long switching-off delay times.

Compared to a single-quadrant amplifier, high-voltage amplifiers operating with two or four quadrants provide a distinctly better time–response behavior. These

amplifiers have both a source and a sink. Thus, it is possible to produce almost any dynamic behavior of the high-voltage signal. The disadvantage of these devices, however, is high cost. However, for special cases, individually tuned amplifier conceptions that will provide sufficient dynamic system behavior with a warrantable expenditure are possible.

6.3.2 Time Response Behavior of ER Resistors

Because no spool position signal is available in electro-rheological flow resistors, the time-response behavior can only be measured from the pressure signal. In this case, the actual dynamic behavior of the valve is superimposed by the system dynamics of the connected hydraulic system. For the analysis of the time-response behavior, a four-quadrant high-voltage amplifier with a rectangular voltage signal was controlled and the pressure difference and the basic voltage were recorded. The measurement results in Fig. 22.29 show that pressure development occurs simultaneously with the increase of the high voltage and achieves its final value after approximately $t = 10$ ms. When the field is switched off, no delay time of the pressure signal can be observed. The pressure variation during switching on or off can be attributed to the influence of the connected hydraulic system.

Time-response behavior becomes even more apparent when the step response is encountered. Figure 22.30 shows that the pressure increase occurs after less than 1 ms.

To characterize the time-response behavior of hydraulic valves, characteristics such as -3 dB frequency or 90° frequency is typically used. Because no spool position is available as a variable in ER valves, dynamic behavior can only be measured indirectly by the pressure difference as a variable and it be compared with the input signal. Pressure development, however, is influenced by the capacity of the oil volume pressurized between the pump and ER valve and by volume flow, which means that it is not valve dynamics but system dynamics that is recorded. Specifi-

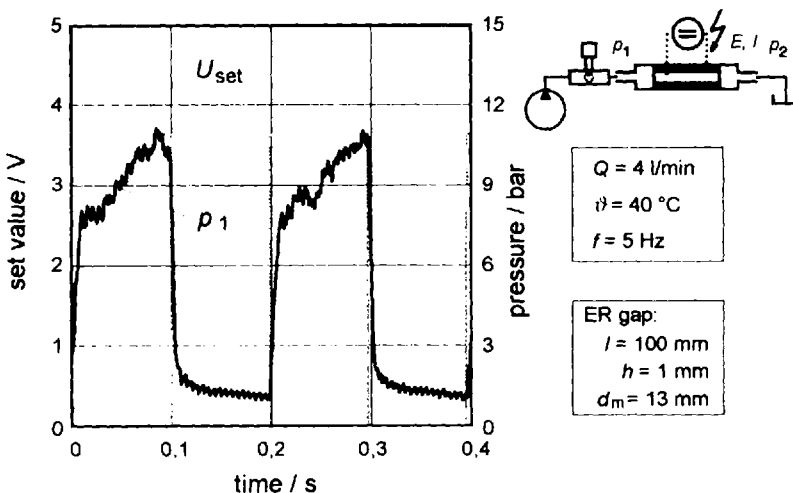


Figure 22.29 Step response behavior of the ER valve.

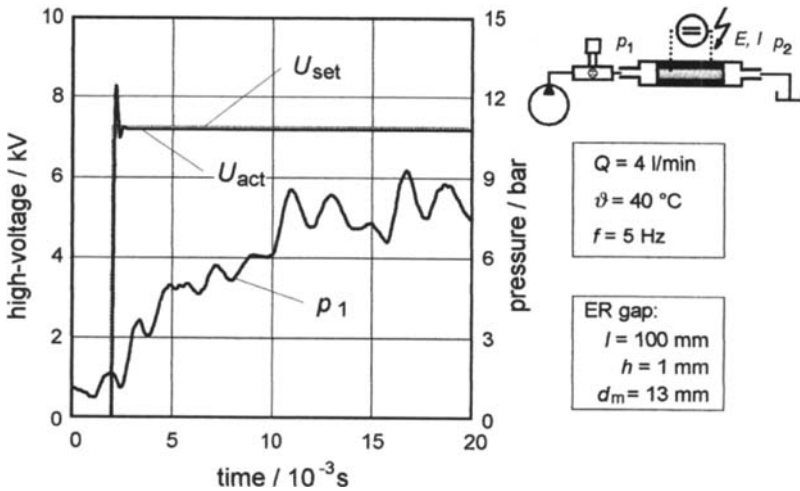


Figure 22.30 Time-response behavior of the ERF in the flow mode.

cation of characteristics such as -3 dB frequency and the 90° frequency is not possible for electro-rheological flow resistors.

6.3.3 Closed-Loop Controlled Actuator

Test-bench control and regulation are implemented using a microcomputer. This permits easy and flexible programming by control algorithms. Data exchange and control of the high-voltage supply are performed using A/DD/A converters.

In hydrostatic drives, where dynamic behavior of the control element typically exceeds that of the controlled subsystem, a three-input controller has prevailed in the market [23,24]. With the control design illustrated in Fig. 22.31, in addition to

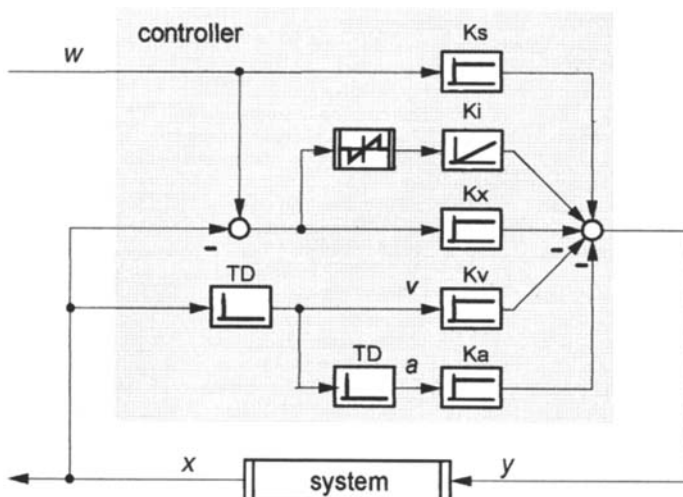


Figure 22.31 Structure of the three-input-state controller.

the control error, velocity and acceleration are loaded and applied for the calculation of the correcting variable. Therefore, theoretically, any dynamic behavior can be used for the control subsystem. For compensation of the stationary position error, an integrator is switched in parallel switching into the correcting variable [25]. Unstable control behavior due to large steps of nominal value can be avoided. To compensate for the impact of the spring force of the recoil spring, an off-set depending on the nominal value can also be switched on the control signal by means of a factor K_s . The variables, velocity and acceleration, are calculated in the computer by means of differentiation from the position signal. Therefore, special demands with regard to signal quality, solution, and precision must be made.

Figure 22.32 represents a positioning process of the actuator. A nominal step signal value with an amplitude of 50 mm was given. The actuator is loaded with a load of $m = 21$ kg. Because the behavior of the controlled subsystem depends primarily on the particular operating point, the regulator can be adjusted separately for

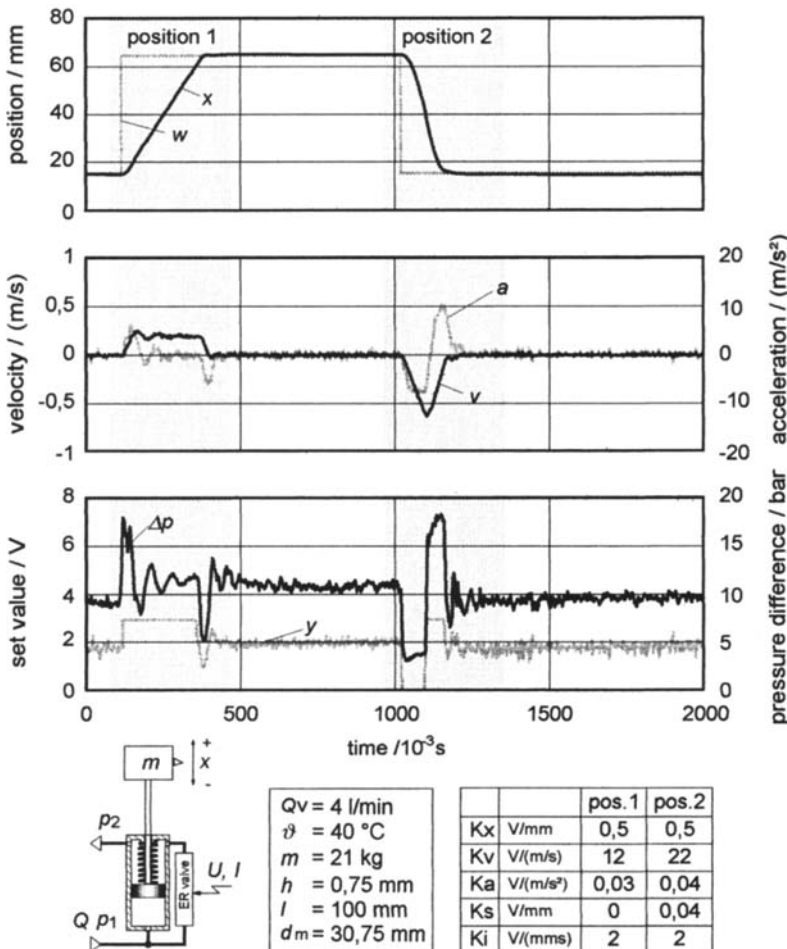


Figure 22.32 Positioning behavior of the ER actuator.

both nominal positions. The position signal in the upper portion of the figure indicates that the actuator attains the upper nominal value, overshoot-free, with excellent dynamic behavior. The maximal pump volume flow limits extending velocity to approximately 0.25 m/s. The maximal running-in velocity is almost twice as high. To reduce the motion energy, the delay time is longer and the maximal acceleration in breaking the actuator down to standstill is higher than 10 m/s^2 . In the control unit, this has been considered a form of slightly higher speed amplification in the lower nominal value. The acceleration feedback, must to be reduced to avoid high frequency vibrations in the position signal. The regulator is damped too much to permit an overshoot-free attainment of the nominal positions. The positioning accuracy is excellent and the maximum deviation in both nominal positions amounts to only $\sim 0.1 \text{ mm}$.

Studies have shown that it is possible to use electro-rheologically controlled actuators in a closed-loop control. ER technology has been used successfully in three-input control designs. When the positioning processes are run with extremely high speed, the quality of the position signal is insufficient and may cause an unstable regulator behavior. Because of the very short response times of ER valves, new control engineering methods must be applied to better utilize the possibilities of ER technology. Direct measurement of the variables using suitable transducers and the improvement of the system dynamics using a valve control with two or four metering edges could provide potential starting points. Using a separate highly dynamic control of each metering edge, new control designs are possible.

7 CONCLUSIONS

After 50 years of intensive ER technology research, commercialization of this technology has not occurred. Particularly in hydraulic systems, the use of ERF as a pressure-transfer medium has, until now, failed because of the abrasive effect of the dispersed particles and the inability to reproduce ERFs with reproducible ER properties. It was only by the development of novel, anhydrous, and nonabrasive ER fluids that new possibilities for the application of this technology has been possible.

The results of fundamental investigations with respect to the use of ERFs in hydraulic systems discussed in this chapter illustrate both the possibilities and limitations of ER technology. Recent research results have shown that in the regions of pressure and volume flow studied, ERFs exhibit sufficient shear stability toward the loads occurring in hydraulic systems. Provided that considerable dead volumes are avoided in the choice of the hydraulic component parts and in system design, the sedimentation tendency of the fluid can be controlled. The accumulation of ER particles which may damage the suction line of the pump must be avoided in reservoir design.

The hydraulic components used in testing did not show any wear or operational problems. Because of decreased lower sensitivity to solid-phase sedimentation in narrow gaps, seated valves are preferred for use with ERFs.

A cylinder actuator, which was controlled with an ER valve, was designed and constructed. As a result of the simple design of electro-rheological flow resistors, the valve function could be integrated directly into the hydraulic cylinder, permitting compact design of the actuator. A three-input control design allows the actuator to

be positioned in a closed-loop control with an excellent dynamic performance and high precision.

In conclusion, it may be said that employment of ERFs in hydraulic systems is now possible, which should lead to the commercialization of ER technology. However, these systems currently require a high-voltage supply. Large and expensive laboratory devices must be substituted by smaller, compact voltage amplifiers with a low-power consumption. The advantages of ER technology, including easy design of control elements and high system dynamics, are achieved in practical applications. This technology offers a variety of new possibilities for the future of fluid power.

REFERENCES

1. W. Winslow, "Method and Means for Translating Electrical Impulses Into Mechanical Forces," U.S. Patent 2,417,850 (1947).
2. W. Winslow, "Induced Fibration of Suspensions," *J. Appl. Phys.*, 1949, p. 20.
3. N. N., "Aktives Zweikammer-Motorlager mit hydraulischer Dämpfung," German Patent DE 35 25673 A1 (1987).
4. R. Stanway, "On the Design of Force Actuators and Sensors Using Electro-Rheological Fluids," in *Proceedings of Actuator '90*, 1990.
5. D. A. Brooks, "Design and Development of Flow Based Electro-Rheological Devices," in *Proceedings of the Conference on Electrorheological Fluids*, 1991.
6. M. Ishiyama, Application of Electrorheological Fluids for the Improvement of Dynamic Characteristics of Machine Tool Table Systems," in *Proceedings of the American Society for Precision Engineering Conference*, 1994.
7. N. N., "Aktives Zweikammer-Motorlager," German Patent EP 0 218 202 A3 (1987).
8. L. Zheng, "Behavior of Electrorheological Valves and Bridges," in *Proceedings of the Conference on Electrorheological Fluids*, 1991.
9. L. Zheng, "Electrorheologically Controlled Landing Gear," *Aerospace Eng.*, 1993, 6.
10. N. N., "Verfahren und Vorrichtung zum Steuern der Dämpferhärte eines Stoßdämpfers für Fahrzeuge," German Patent DE 34 43183 A1 (1986).
11. D. J. Jendritza, "Technischer Einsatz Neuer Aktoren," *Kontakt Studium Elektron.*, 1994, p. 484.
12. J. L. Sproston, "A Comparison of the Performance of ER Fluids in Squeeze," in *Proceedings of the Conference on ERF and MRF*, 1995.
13. K. D. Weiss, "High Strength Magneto- and Electro-rheological Fluids," in *Proceedings of the International Off-Highway & Powerplant Congress*, 1993.
14. J. N. Foulc, "Correlation Between Electrical and Rheological Properties of Electrorheological Fluids," in *Proceedings of the Conference on ERF and MRF*, 1995.
15. L. Zheng, "An Electro-Rheological Servo Positioning Control System," in *Proceedings of the Conference on Electrorheological Fluids*, 1991.
16. C. Wolff-Jesse, "Untersuchung des Einsatzes elektrorheologischer Flüssigkeiten in der Hydraulik," Dissertation RWTH, Aachen, Germany, 1996.
17. R. Bloodworth, "Electrorheological Fluids Based on Polyurethane Dispersions," in *Proceedings of the Conference on Electrorheological Fluids*, 1993.
18. "Elektroviskose Flüssigkeiten auf der Basis dispergierter Polyether," German Patent EP 0 432 601 A1 (1990).
19. W. Backé, *Grundlagen der Ölhydraulik, Lecture script*, Edition 9, Aachen, Germany, 1992.
20. D. J. Peel, "The Time Response Sequence of an Electro-Rheological Fluid," in *Proceedings of Actuator '90*, 1990.

21. E. Wendt, "Properties of a New Generation of Non-abrasive and Water-free Electro-rheological Fluids," in Proceedings of Actuator '94, 1994.
22. W. Backé, Servohydraulik, *Lecture script*, Edition 6, Aachen, Germany, 1992.
23. P. Anders, "Auswirkung der Mikroelektronik auf die Regelungskonzepte fluidtechnischer Systeme und der Einsatz von Personal Computern als Auslegungswerkzeug." Dissertation RWTH, Aachen, Germany, 1986.
24. A. Klein, "Einsatz der Fuzzy-Logik zur Adaption der Positionsregelung fluidtechnischer Zylinderantriebe," Dissertation RWTH, Aachen, Germany, 1993.
25. C. Boes, "Hydraulische Achsantriebe im digitalen Regelkreis." Dissertation RWTH, Aachen, Germany, 1995.

This page intentionally left blank

Standards for Hydraulic Fluid Testing

PAUL MICHAEL

Benz Oil, Milwaukee, Wisconsin

1 INTRODUCTION

ASTM, ISO, DIN, and other organizations develop and periodically update test methods used for predicting and preventing hydraulic fluid problems [1]. These standardized laboratory procedures evaluate either physical or performance properties of hydraulic fluids. Many of these tests measure the ability of a fluid to prevent wear or resist the detrimental effects of fluid contamination and high temperatures. Others measure simple physical characteristics of the fluid. By selecting the appropriate method, standardized tests may be used as a problem-solving tool or to predict fluid performance. In addition, standardized tests are the basis for worldwide hydraulic fluid specifications. These specifications have been developed to help users of hydraulic fluids select products that meet hydraulic equipment performance requirements. In this chapter, hydraulic fluid test methods and specifications are reviewed.

2 HIGH-TEMPERATURE TESTS

One of the most important characteristics of a hydraulic fluid is its ability to withstand high temperatures. This is because horsepower losses in hydraulic systems directly result in the transfer of heat to the fluid. The amount of energy transferred to the fluid may be calculated using horsepower and temperature rise equations (see Fig. 23.1) [2].

The majority of hydraulic fluids are hydrocarbon, specifically mineral-oil based, and are susceptible to degradation caused by heat [3]. High temperatures (in excess of 60°C) can cause hydraulic fluid to thermally degrade and oxidize [4–6]. Rate constants for oxidation of saturated hydrocarbons at 125°C are as much as 40 times higher than rate constants at 60°C [7]. Thus, fluid oxidation is highly dependent on

The following equations permit calculation of the maximum fluid temperature rise as it flows through restrictions in a hydraulic system, such as a pressure relief valve:

$$\text{Temperature increase } (^{\circ}\text{F}) = \frac{\text{heat generation rate (Btu/min)}}{\text{oil specific heat (Btu/lb/}^{\circ}\text{F)} \times \text{oil flow rate (lb/min)}}$$

$$1 \text{ hp} = 42.4 \text{ Btu/min} = 2544 \text{ Btu/hr}$$

$$\text{specific heat of oil} = 0.42 \text{ Btu/lb/}^{\circ}\text{F}$$

$$\text{oil flow rate (lb/min)} = 7.42 \times \text{oil flow rate (gpm)}$$

Example

Oil at 120 °F and 1000 psi is flowing through a pressure relief valve at 10 gpm. What is the downstream oil temperature?

Solution

First calculate the horsepower lost and convert to the heat generation rate in Btu/min:

$$\text{Horse power} = \frac{P(\text{psi}) \bullet Q(\text{gpm})}{1714} = \frac{(1000) \bullet (10)}{1714} = 5.83 \text{ hp}$$

$$\text{Btu/min} = 5.83 \times 42.4 = 247 \text{ Btu/min}$$

Next calculate the oil flow rate in lb/min and the temperature increase:

$$\text{oil flow rate} = 7.42 \times 10 = 74.2 \text{ lb/min}$$

$$\text{temperature increase} = \frac{247}{0.42 \times 74.2} = 7.9 \text{ }^{\circ}\text{F}$$

$$\text{downstream oil temperature} = 120 + 7.9 = 127.9 \text{ }^{\circ}\text{F}$$

Figure 23.1 Calculating fluid temperature rise in hydraulic systems [2].

hydraulic system operating temperatures. Thermal degradation is another common temperature-dependent fluid degradation mechanism. It occurs in the relative absence of oxygen, whereas oxidation requires the presence of oxygen. Thermal degradation and oxidation are significant to hydraulic system performance because the by-products of these reactions have poor solubility in oil and tend to agglomerate into particles of brown resinous sludge. Consequently, high-temperature degradation of hydraulic fluids results in the formation of varnishlike deposits in coolers, valves, and suction strainers [8]. An abbreviated reaction scheme for liquid-phase oxidation of hydrocarbons is shown in Fig. 23.2 [7].

One of the most common methods for measuring the ability of a fluid to resist oxidation is ASTM D-943-91, Standard Test Method for Oxidation Characteristics of Inhibited Mineral Oils [9] [also known as the Turbine Oil Oxidation Stability Test (TOST)]. In this test, 300 mL of fluid and 60 mL of distilled water are placed in a large test tube together with coils of copper and iron wire (see Fig. 23.3) [9].

Initiation	$I \text{ (initiator)} \rightarrow 2r^*$
Initiation	$r^* + RH \rightarrow R^* + rH$
Propagation	$R^* + O_2 \rightarrow ROO^*$
Propagation	$R-H + ROO^* \rightarrow ROOH + R^*$
Branching	$ROOH \rightarrow RO^* + ^*OH$
Branching	$ROOH + CH_2=CHX \rightarrow RO^* + HOCH_2C^*HX$
Branching	$2 ROOH \rightarrow ROO^* + H_2O + RO^*$
Branching	$ROOH + RH \rightarrow RO^* + H_2O + R^*$
Termination	$R^* + ROO^* \rightarrow ROOR$
Termination	$ROO^* + ROO^* \rightarrow R=O + ROH + O_2$
Termination	$R^* + R^* \rightarrow R-R$

Figure 23.2 Mechanism of liquid-phase oxidation of hydrocarbons [7].

The fluid is heated to 95°C (203°F) and oxygen is bubbled through the fluid at a controlled rate. The test is complete when the total acid number (TAN) of the fluid reaches 2.0 mg KOH/g. As can be seen from the reaction scheme in Fig. 23.2, precursors to carboxylic acids are among the chemical by-products of hydrocarbon oxidation. The amount of acidic additives and oxidation byproducts present in the fluid can be determined by titration with bases. For the D-943 test, a variation on ASTM D-664 Acid Number of Petroleum Products by Potentiometric Titration [9] is used. This method, ASTM D-3339, Test Method for Acid Number By Semi-Micro Color Indicator Titration [10], is utilized because it permits a 0.2–1.0-g sample size for total acid numbers in the 0.5–3.0 range. The number of hours to form 2.0 mg of KOH equivalents of acidic oxidation products per gram of fluid reflects the oxidation life of the fluid. Typical values for the oxidation life of various hydraulic fluids are shown in Table 23.1. In general, turbine oils provide longer oxidation life than antiwear hydraulic fluids because they do not contain zinc dithiophosphate, which is subject to hydrolysis. Ester-based fluids such as rapeseed oil are also subject to hydrolysis, which accounts for their poor performance in the D-943 test. When the D-943 test is run without water (dry method), the oxidation life of a synthetic ester can be extended by nearly a factor of 100.

The amount of sludge produced in the TOST test may be measured by ASTM D-4310 [10]. Standard Test Method for Determination of the Sludging Tendencies of Inhibited Mineral Oils. In this test, the fluid is subjected to D-943 test conditions for 1000 h. At the end of this time, the sludge produced is determined gravimetrically by filtration of the oxidation tube contents through 5- μ m-pore size cellulose acetate filter disks. To a certain extent, the D-943 and D-4310 tests evaluate different mechanisms of high-temperature degradation. In the D-943 test, the acidity is measured

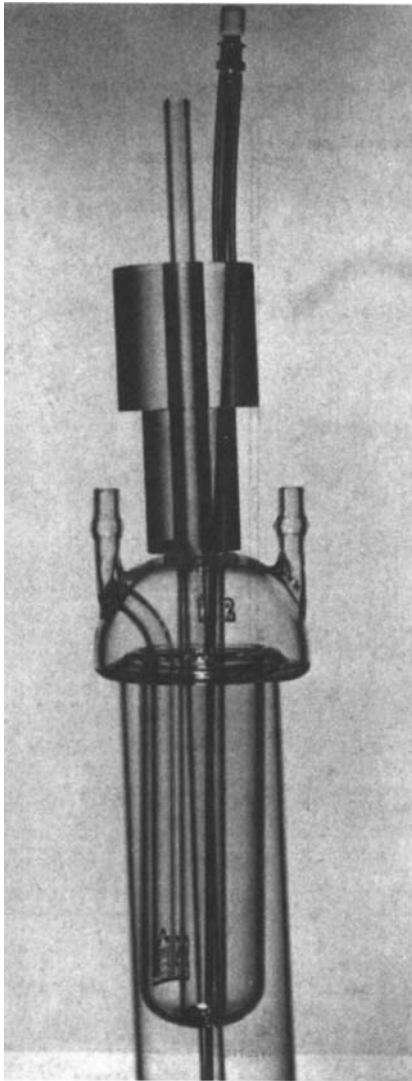


Figure 23.3 ASTM D-943, oxidation cell with sampling tube [9].

and this acidity is usually due to formation of carboxylic acids by the conventional liquid-phase oxidation mechanism shown in Fig. 23.2. Sludge formation in hydraulic oils is frequently the result of thermal degradation of the zinc dialkyldithiophosphate (ZDP) antiwear additive which may be present in the fluid. Consequently, the D4310 test is used to evaluate thermal stability of ZDP, whereas the D-943 test is used to evaluate the stability of the base oils and the effectiveness of oxidation inhibitors. Figure 23.4 is a model for the mechanism of sludge formation by zinc dialkyldithiophosphate [3].

Another test for measuring the sludging tendency of an oil is the Cincinnati Milacron Thermal Stability Test [11]; see Table 23.2 for test performance require-

Table 23.1 Typical Values for the Oxidation Life of Some Hydraulic Fluids

Fluid description	Hours to TAN of 2.0 by the D943 method
Rapeseed-based hydraulic oil ^a	28
Synthetic ester with antioxidant ^b	65
Mineral oil without additives ^c	300
Antiwear hydraulic fluids ^d	Up to 4000
Synthetic ester with antioxidant, dry method ^b	5500
Turbine oils ^d	Up to 5500

^aData from J. M. Wain, "The Development of Environmentally Acceptable Hydraulic Oil Formulations," SAE Technical Paper Series, Paper 910965, 1991.

^bData from M. Hutchings, CIBA Corp, presented at the Meeting of the NY Section of STLE, 1997.

^cData from A. Laning, personal communication, Lubrizol, 1997.

^dData from T. Warne and P. Vienna, "High Temperature Oxidation Testing of Lubricating Oils," *Lubr. Eng.*, 1984, 40, 4.

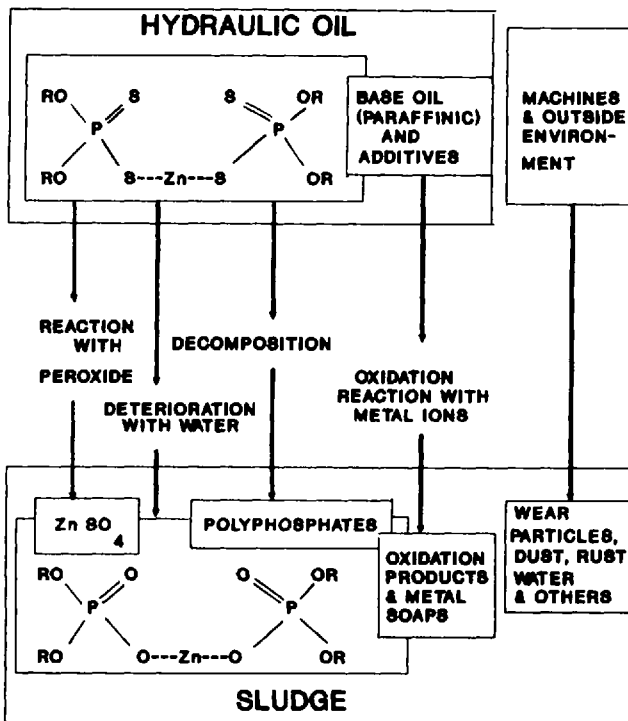


Figure 23.4 Mechanism of sludge formation by zinc dialkyldithiophosphate [3].

Table 23.2 Cincinnati Milacron
Thermal Stability Test
Performance Requirements

Condition of steel rod
Visual: No discoloration
Deposit: 3.5 mg max.
Corrosion: 1.0 mg max.
Condition of copper rod
Visual: 5 max.
Corrosion: 10.0 mg max.
Condition of fluid
Viscosity: 5% change max.
Sludge: 25 mg/100 mL max.
Total acid number: $\pm 50\%$ max.

ments. In this test, polished preweighed copper and steel rods are placed in a beaker containing 200 cm³ of oil and heated to 135°C (275°F) for 168 h. At the end of the test, the copper and steel rods are examined for discoloration due to corrosion caused by carboxylic acids and sulfur compounds formed by thermal degradation. Sludge content and viscosity increase are also measured.

The combined forces of heat and moisture may cause hydrolytic degradation of a hydraulic fluid. Hydrolytically unstable oils form acidic and insoluble contaminants, which can cause hydraulic system malfunctions similar to those produced by oxidation and thermal degradation of fluids. In addition, hydrolytic stability is a key factor in the wet filterability behavior of hydraulic oils [12]. The ASTM D-2619 Standard Test Method for Hydrolytic Stability of Hydraulic Fluids (Beverage Bottle Method) [10] is used to measure this fluid property. In this test, 75 g of fluid and 25 g of water are sealed in a beverage bottle with a copper strip present for 48 h at 93°C (200°F). At the end of the test, the oil and water layers are separated and insolubles are weighed. Viscosity and acid numbers are also determined. Based upon the Denison HF-O specification (see Sec. 7 for details), the weight loss of the copper specimen should be less than 0.209 mg and the acid number of the water phase should be less than 4.0 mg KOH/g. Because exposure to water can be expected throughout the life of a fluid, hydrolytic stability is an important design characteristic of hydraulic fluids.

3 CORROSION AND RUST TESTING

Corrosion of hydraulic system components can be caused by fluid contamination and the by-products of fluid degradation, resulting in accelerated wear, rust, valve sticking, and systemic deposits. Ferrous-metal corrosion in a hydraulic system is most often caused by water contamination, whereas copper and its alloys are particularly susceptible to attack by high-temperature fluid degradation by-products. Two strategies for dealing with water contamination in hydraulic fluids are (1) protection of the system by formulating hydraulic fluids to assure rapid separation of water contamination and (2) protection of the system by incorporating corrosion-inhibitor ad-

ditives to provide a chemical barrier to corrosion. Although both strategies are beneficial to system performance, often the best strategy is to exclude water contamination by preventing ingress through reservoir breathers, rod wiper seals, reservoir covers, and inlet line fittings [13].

The ability of fluids to prevent rusting of ferrous parts due to water contamination may be measured by ASTM D-665, Rust-Preventing Characteristics of Inhibited Mineral Oil in the Presence of Water [9]. In Part A of this test, 10% distilled water is added to oil that has been heated to 60°C (140°F). Round steel rods are polished to remove their oxide coating and immersed in the oil. The oil–water mixture is continuously stirred to avoid separation while the temperature is maintained at 60°C. At the end of 24 h, the specimens are inspected for rust (see Fig. 23.5).

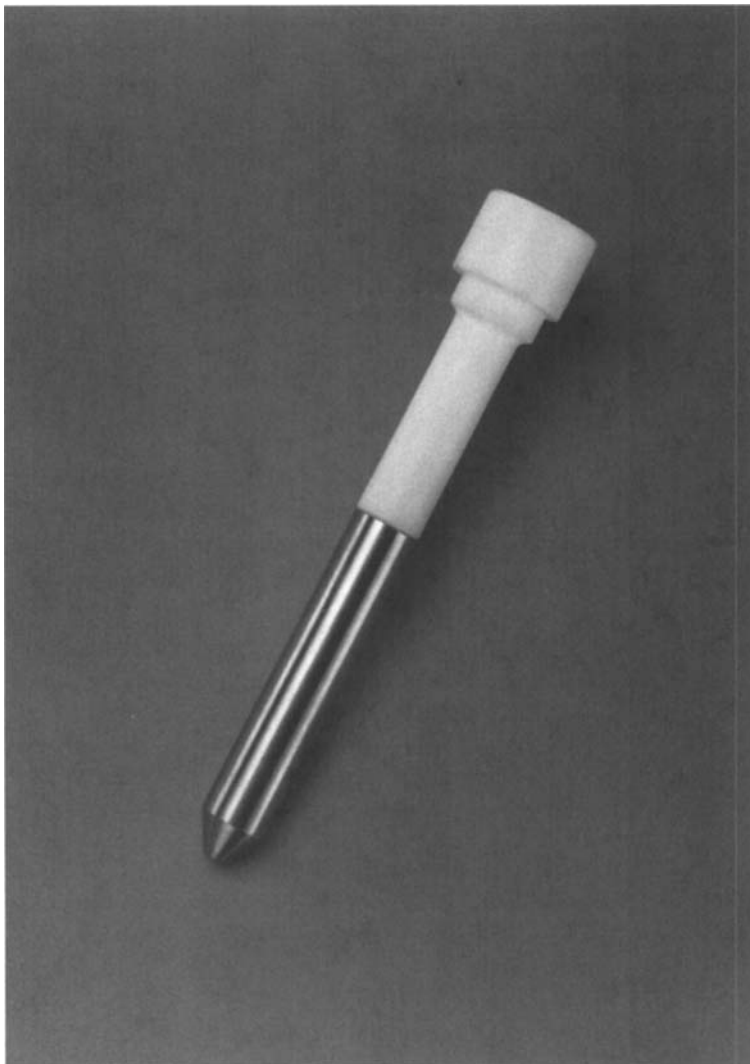


Figure 23.5 Test specimen for D-665 rust test. (Courtesy of Koehler Instrument Co.)

In Part B of the method, the same procedure is used, except synthetic seawater is substituted for distilled water. As described in Part B of the method, synthetic seawater is made by the addition of sodium chloride, magnesium chloride, calcium chloride, and several other ionic compounds to distilled water. Part B is particularly pertinent in maritime hydraulic fluid applications, where seawater contamination, rather than fresh water or condensation, is a likely source of contamination.

The speed with which water is separated from oil and the tendency of an oil to form a cuff of emulsified oil at the interface between the oil and water phases may be measured by ASTM D-1401, Standard Test Method for Water Separability of Petroleum Oils and Synthetic Fluids [9]. In this test, a 40-mL sample of oil and 40 mL of distilled water are stirred for 5 min at 54°C (130°F) in a graduated cylinder. The time required for the emulsion formed to split into water and oil phases is recorded. An oil with good demulsibility will completely separate in 30 min or less without a “cuff” of emulsified oil between the phases (see Fig. 23.6) [14].

Some hydraulic fluids, particularly those used in applications that require enhanced fire resistance, are formulated with water. Such fluids have entirely different

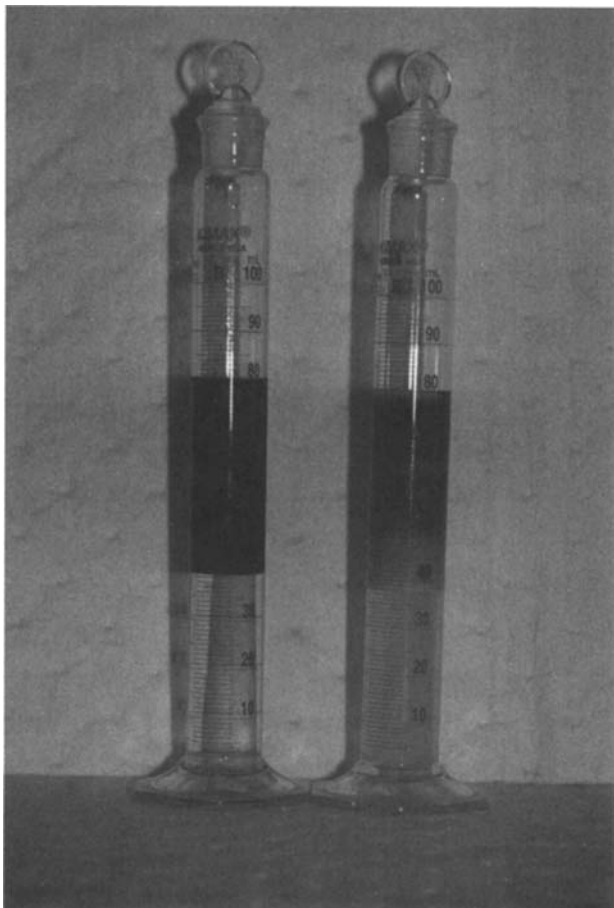


Figure 23.6 Example oil fluids with good and poor demulsibility.

corrosion-inhibition requirements. For instance, water–glycol hydraulic fluids must also prevent corrosion in the vapor phase above the liquid due to evaporation. Thus, they are formulated with a vapor-phase corrosion inhibitor. The standard test method for measuring vapor-phase corrosion inhibition of hydraulic fluids is ASTM D-5534, Test Method for Vapor-Phase Rust-Preventing Characteristics of Hydraulic Fluids [15]. In this test, a steel specimen is attached to the cover of a ASTM D-3603 test apparatus that contains hydraulic fluid maintained at a temperature of 60°C (140°F). (ASTM D 3603 is the Horizontal Disk Method for Rust-Preventing Characteristics of Steam Turbine Oils in the Presence of Water [15].) The specimen is then exposed to water and hydraulic fluid vapors for a period of 6 h. At the end of this time, the specimen is inspected for evidence of corrosion and results are reported on a pass–fail basis. This test is particularly relevant for water–glycol and invert emulsion hydraulic fluids because corrosion of the underside of reservoir covers is known to occur in systems that use these fluids.

Accelerated corrosion can occur when dissimilar metals are in electrical contact in the presence of an electrolyte (i.e., conductive solution). This corrosion mechanism, known as galvanic corrosion, has been found to be particularly relevant for certain biodegradable oils [16]. The ability of a fluid to prevent galvanic corrosion may be measured by FTM 5322.2 [17]. In this test, a brass clip is fitted to the oil-coated surface of a steel disk. The bimetallic (brass–steel) couple is then stored in approximately 50% relative humidity for 10 days. At the end of the 10-day period, the surfaces are inspected for evidence of staining as depicted in Fig. 23.7. The steel disks are rated on a pass–fail basis.

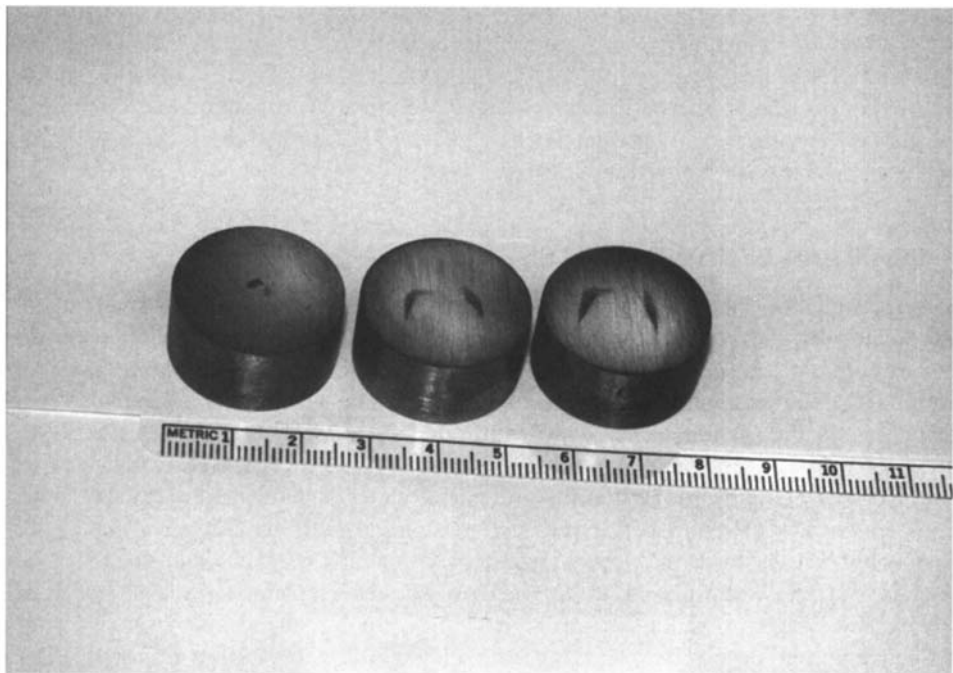


Figure 23.7 Staining on test specimens due to galvanic corrosion. (Courtesy of Benz Oil, Milwaukee, Wisconsin.)

Table 23.3 Copper Strip Classifications

Classification	Designation	Description
Freshly polished	None	
1a	Slight tarnish	Light orange, almost the same as a freshly polished strip
1b	Slight tarnish	Dark orange
2a	Moderate tarnish	Claret red
2b	Moderate tarnish	Lavender
2c	Moderate tarnish	Multicolored, lavender, blue, or silver over claret red
2d	Moderate tarnish	Silvery
2e	Moderate tarnish	Brassy
3a	Dark tarnish	Magenta overcast on brassy strip
3b	Dark tarnish	Multicolored showing red and green (peacock)
4a	Corrosion	Transparent black, dark gray, or brown
4b	Corrosion	Graphite or lustrous black
4c	Corrosion	Glossy or jet black

From Ref. 9.

Sulfur-containing additives such as sulfurized olefins, organic polysulfides, and thiocarbamates may be used as antiwear and extreme-pressure additives in hydraulic fluids, particularly farm tractor hydraulic fluids [18]. Depending on the chemical activity of these sulfur compounds, oils can exhibit varying degrees of corrosiveness to copper. The standard test method for measuring the copper-corrosion properties of an oil is ASTM D-130, Standard Test Method for Detection of Copper Corrosion from Petroleum Products by the Copper Strip Tarnish Test [9]. In this test, a polished copper strip is immersed in an oil and heated for a predefined period of time. At the end of the test, the copper strip's appearance is compared to a standard. The rating system used for the D-130 test appears in Table 23.3. Color standards are also available from ASTM* for rating these strips.

4 FOAM AND AERATION TESTS

Fluid recirculation through hydraulic systems and reservoirs may cause mechanical introduction of air into hydraulic fluids, particularly if reservoir size or design do not promote air separation. Air may be present in the fluid in one or more possible forms: dissolved air, entrained air, or foam [19]. Foam appears as a separate layer of bubbles on the surface of the liquid, entrained air appears as subsurface bubbles, and dissolved air is invisible (unless a vacuum is placed on the fluid, which causes it to come out of solution). Hydraulic fluid performance is dependent on the presence of air contamination. First, air is much more compressible than oil and, therefore, the responsiveness of a hydraulic system that contains entrained air tends to be sluggish. Second, compression of entrained air can cause cavitation, which may lead to wear and cause hydraulic systems to be noisy. Finally, an oil that produces a lot of foam may bubble out of hydraulic reservoir breathers, creating a fluid spill. Be-

*ASTM Headquarters, 1916 Race Street, Philadelphia, PA 19103.

Table 23.4 Air-Release Requirements DIN Specification 51524

Property	Spec./method	Viscosity grade				
ISO Grade	DIN 51519	15	32	46	68	100
Air release (min)	DIN 51381	5	5	10	10	14

cause of the importance of properly managing air contamination in hydraulic fluids, there are a number of standardized test methods for evaluating this feature of fluid performance.

The foaming tendency and stability of an oil may be measured by ASTM D-892 (Fig. 23.14), Standard Test Method for Foaming Characteristics of Lubricating Oils [9]. In this test, an oil sample is equilibrated at 24°C (75°F). Oil is blown with air for 5 min and allowed to settle for 10 min. The volume of foam is measured at the end of both periods. The test is repeated at 93.5°C (200°F) and again at 24°C (75°F) after the foam breaks. Various levels of foaming tendency are permitted by industry standards, but stable foam is generally not tolerated [20,21].

Not only must a hydraulic fluid resist the tendency to form stable foam, it also must allow air to rapidly rise and separate from the fluid. The Waring blender test is one test method that may be used to measure the air-release properties of fluids [22,23]. In this test, 700 mL of the fluid is stirred at an agitation rate approaching 20,000 rpm for 25 s. The fluid is then poured into a 1000-mL graduated cylinder and the rate of air-bubble loss is observed. Air-release properties of a hydraulic fluid may also be quantified by IP 313, DIN 51381, or ASTM D-3427 [10], Standard Test Method for Gas Bubble Separation Time of Petroleum Oils. In these tests, the time in minutes for finely dispersed air in oil to decrease to 0.2% under standard test conditions is measured using a density balance. Air-release times and specifications vary with oil viscosity. Table 23.4 lists DIN 51524 requirements for air-release times.

5 SHEAR STABILITY TESTS

Mobile hydraulic equipment such as excavators, cranes, and timber harvesters frequently are required to operate under extreme high- and low-temperature conditions. In order to accommodate wide-ranging environmental conditions, multigrade hydraulic fluids are often employed. These fluids typically contain viscosity-index-improving polymers such as polymethacrylate and ethylene-propylene copolymers that thicken oil at high temperatures while having little impact upon their low-temperature fluidity [18]. Conceptually, a 10W30 multigrade oil consists of a 10W base oil and sufficient polymer to thicken the oil at 100°C to a viscosity equal to that of a 30 weight oil. Multigrading benefits hydraulic performance because increasing the high-temperature viscosity of a fluid improves lubrication and the volumetric efficiency of pumps. High pressures generated in hydraulic systems subject fluids to shear rates up to 10^7 s^{-1} [24]. Not only does this hydraulic shear cause fluid temperature rise and air entrainment within a hydraulic system, shear may bring about permanent and temporary viscosity loss in hydraulic fluids (Fig. 23.8) [25]. Permanent viscosity loss results from mechanical scission of less stable polymer molecules

TEMPORARY AND PERMANENT VISCOSITY LOSSES

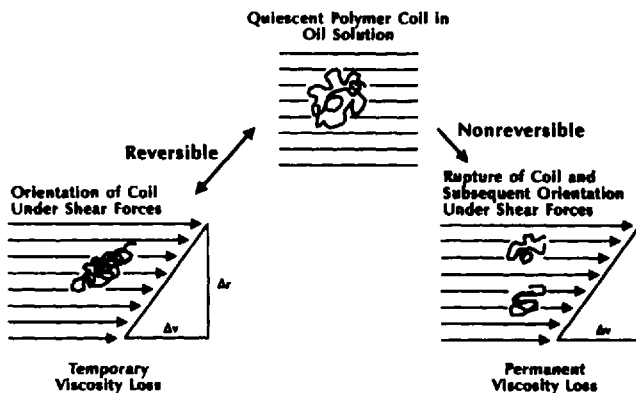


Figure 23.8 Viscosity-index-improvers are relatively large molecules that are subject to permanent and temporary viscosity loss due to mechanical shear.

in multigrade hydraulic fluids and often occurs after a relatively short period of time (<24 h of operation). The polymer (as opposed to the base oil) is susceptible to mechanical shear because it has a higher molecular weight and, therefore, a larger molecular volume. As a result, with polymer-containing multigrade hydraulic fluids, the functional viscosity of an oil may differ from that predicted from kinematic viscosity measurements of new oil [26].

Several laboratory test methods are designed to stress multigrade oils so that they produce a permanent viscosity loss such as would take place in service. The two methods most generally used are sonic shearing with a high-frequency sonic oscillator and mechanical shearing with a Bosch diesel fuel-injection pump. In ASTM D-3945, Standard Test Method for Shear Stability of Polymer-Containing Fluids Using a Diesel Injector Nozzle, the polymer-containing fluid is passed through a diesel injector nozzle at a shear rate that causes polymer molecules to degrade [15]. Under standard test conditions, the kinematic viscosity of the fluid is measured after 30–250 cycles through the injector pump in order to determine the extent of permanent viscosity loss that has taken place. In ASTM D-5621, Standard Test Method for Sonic Shear Stability of Hydraulic Fluid, the polymer-containing oil is irradiated with a sonic oscillator for 40 min and changes in kinematic viscosity are measured [15]. Based on data from Kopko and Stambaugh, the Fuel Injector Shear Stability Test lacks the necessary severity to predict permanent viscosity loss produced by hydraulic equipment [27]. However, 40 min of irradiation with a high-frequency sonic oscillator produced viscosity changes that closely correlate to that experienced in the ASTM D-2882 Vane Pump Test. Consequently, this test method has become the basis for an ASTM multigrade hydraulic fluid viscosity classification system [15].

6 IN-SERVICE FLUID MONITORING

Whereas the above-described standard performance tests are primarily used to evaluate new hydraulic fluids, there are also a number of standard analytical methods for condition monitoring of in-service hydraulic fluids. The characteristics most commonly measured are water content, particulate contamination, fluid degradation, and wear metals concentration. Through these analytical methods it is possible to check for fluid degradation and contaminants as well as to detect mechanical problems within the hydraulic system. As a result, condition monitoring of in-service hydraulic fluids can reduce equipment downtime and maintenance costs. The following section provides descriptions of common hydraulic fluid analytical methods used to detect water contamination, fluid degradation, and wear. (See Chapter 12 for a detailed discussion of particle-counting techniques.)

Various methods may be used to monitor water content of hydraulic fluids. In ASTM D-95, Standard Test Method for Water in Petroleum Products and Bituminous Materials by Distillation, the material to be tested is diluted with a water-immiscible solvent such as toluene and heated under reflux conditions [19]. The resulting distillate is condensed and separated in a trap. The amount of water present in the sample is determined by observing the volume of water that settles in the graduated section of the trap. (See Fig. 23.9.)

Centrifuge tests such as ASTM D-96, Standard Test Method for Water and Sediment in Crude Oil by Centrifuge Method, can also be used for nonemulsified or insoluble water contamination in fluids. Although distillation and centrifuge methods provide reasonably accurate results for samples that contain free-water contamination, these methods are generally not sensitive enough to quantify trace quantities of water (<1000 ppm). A more accurate method for determining trace quantities of water is the Karl Fischer test [28]. (ASTM D-1744, Standard Test Method for Determination of Water in Liquid Petroleum Products by Karl Fischer Reagent). In this test,

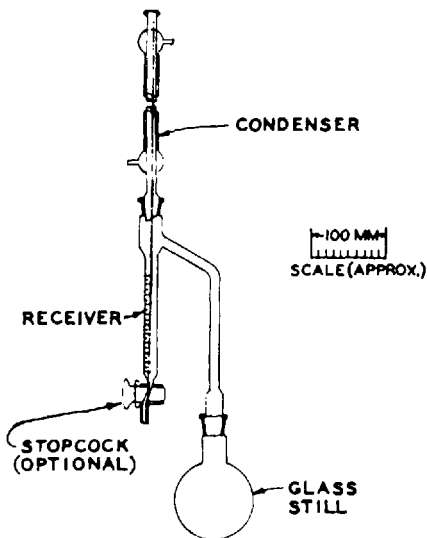


Figure 23.9 Distillation apparatus for measuring water content of petroleum products [9].

the fluid is dispersed in a solvent such as methanol and titrated with standard Karl Fisher reagent to an electrometric endpoint. The endpoint of the titration, at which free iodine is liberated, may be registered either potentiometrically or by color indication. Although this method has the capability to be more accurate than distillation or centrifuge techniques, the Karl Fisher test is not without its limitations. Zinc dialkyldithiophosphate, calcium sulfonate, magnesium sulfonate, and other oil additives react with iodine and have been known to interfere with the titration [29].

In a recent round-robin conducted by the ASTM Committee D-2 Interlab Cross-check Program [30], 62 laboratories evaluated a sample of oil that was found to contain a mean water content of 963.2 ppm. The standard deviation of the round-robin data was 739.8 ppm. Thus, discrepancies of several hundred parts per million in the comparison of Karl Fischer results among laboratories are probably to be expected. Although these results may not be considered to indicate a high level in reproducibility, the reproducibility of a sample that contains less than 1% water in the ASTM Distillation Test is on the order of 2000 ppm, whereas dissolved water often is entirely undetectable in centrifuge tests.

The use of spectrometric wear metals tests for monitoring hydraulic fluid condition is common. There are two different analytical methods for wear metals testing: emission spectroscopy and absorption spectroscopy [31]. Emission spectrometers detect light emitted by elements in a sample as the result of the sample being aspirated into a plasma of ionized gas that excites the sample to the point of atomic emission. Atomic absorption spectrometers detect light absorbed by elements in a sample as the result of the sample being aspirated into a high-energy flame. In the case of emission spectroscopy, when a substance is excited by a plasma or electrical discharge (arc or spark), the elements present emit light at wavelengths that are specific for each element. In the case of absorption spectroscopy, ground-state atoms absorb energy from an external, element-specific light source, such as a hollow-cathode lamp. The light emitted is dispersed by a grating or prism monochromator. The spectral lines produced are recorded by diode arrays and/or photomultiplier tubes linked directly to a computer-driven data processing system. Although both techniques have been used to great advantage in military, railroad, trucking, aviation, and other applications, wear metals analysis is often of limited benefit in hydraulic applications [32]. The major limiting factor of this analytical technique is that it is designed to measure ppm quantities of iron, copper, lead, chromium, tin, silicon, and other wear particles produced by bearing, compression ring, and cylinder wear in reciprocating equipment. Because it is difficult to excite large particles to the point of atomic emission or adsorption, the maximum particle size these techniques can detect is in the 2–10- μm range (Fig. 23.10). In hydraulic applications, the internal clearances of pumps and valves are in the 2–15- μm range.

Thus, particles larger than those detectable through spectrometric wear metal analysis are critical to system performance. Another reason why elemental analysis is of limited value in hydraulic applications is that it does not provide an indication of the chemical state of the element. For instance, zinc dithiophosphate is a commonly used antiwear additive that contains the elements zinc and phosphorus (as well as sulfur, carbon, hydrogen, and oxygen). If one were to measure the zinc and phosphorus contents of used and new antiwear hydraulic fluids by spectroanalysis, it is likely that the fluids would contain roughly equal levels of these elements. However, when ZDP oxidizes, it forms polyphosphates, zinc polyphosphates,

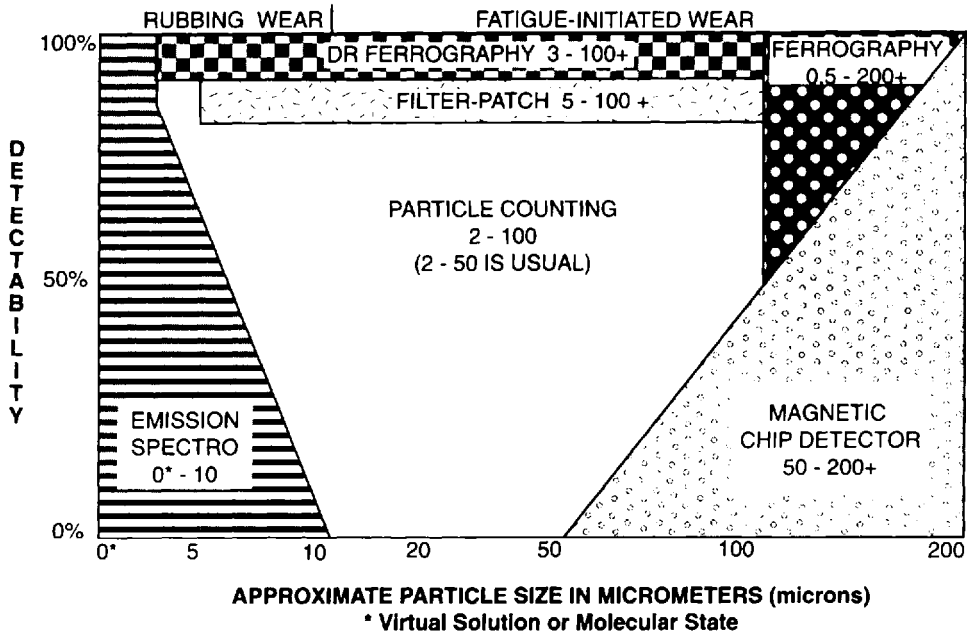


Figure 23.10 Detection limits of fluid tests based on particle size [33].

and other chemical species [33]. Although these changes have a minimal impact on the total zinc and phosphorus content of a fluid, degraded fluids have inferior oxidation stability and antiwear performance [34]. Thus, spectrometric methods cannot be used to measure additive depletion in used hydraulic fluids.

There are, however, a number of analytical methods for measuring the additive composition of fluids. Many of these methods are used as quality control tools for inspecting new fluids. For hydrocarbon-based fluids, a spectroscopic technique known as infrared analysis is widely employed. Infrared absorption results from changes in the vibrational and rotational state of a molecule [35]. In infrared (IR) analysis, cells consisting of transparent salts such as silver chloride, potassium bromide, and sodium chloride are usually filled by capillary action and irradiated by a source of infrared light and the amount of light transmitted through the sample is measured. Whereas emission and absorption spectroscopy detect elements, an IR spectroscope identifies actual chemical species. For instance, there are distinct differences between the infrared spectra of zinc dithiophosphate and its degraded polyphosphate form. Figure 23.11 [36] depicts the changes in ZDP infrared spectra that occurs when it thermally degrades. In addition to qualitative and quantitative additive measurement, comingling of fluids, water contamination, additive depletion, and oxidation can be detected by IR analysis.

Thermal degradation of hydraulic fluids in service is often both the result of and a consequence of additive depletion and oxidation of the base fluid; for instance, when the antioxidant in a conventional mineral-based hydraulic fluid becomes depleted, carboxylate compounds, including carboxylic acids, frequently appear in the

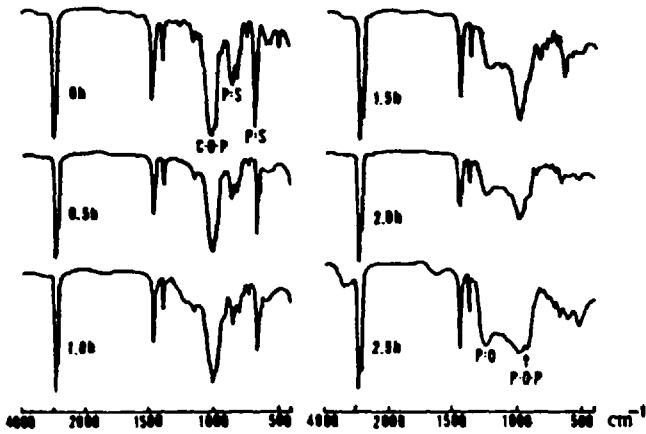


Figure 23.11 Infrared spectra of zinc dialkyldithiophosphate heated to 180°C [37].

IR spectra as shown in Fig. 23.12 [37]. These carboxylates are the result of base-oil oxidation. Although thermal degradation of mineral-oil-based hydraulic fluids is readily detectable by infrared analysis [38], IR analysis of water-containing fluids such as water-glycols is complicated by spectral interference from water itself. Nonetheless, water-glycol hydraulic fluids are susceptible to depletion of their amine-based additive system and oxidation of the glycol base fluid to form carboxylic acids [39].

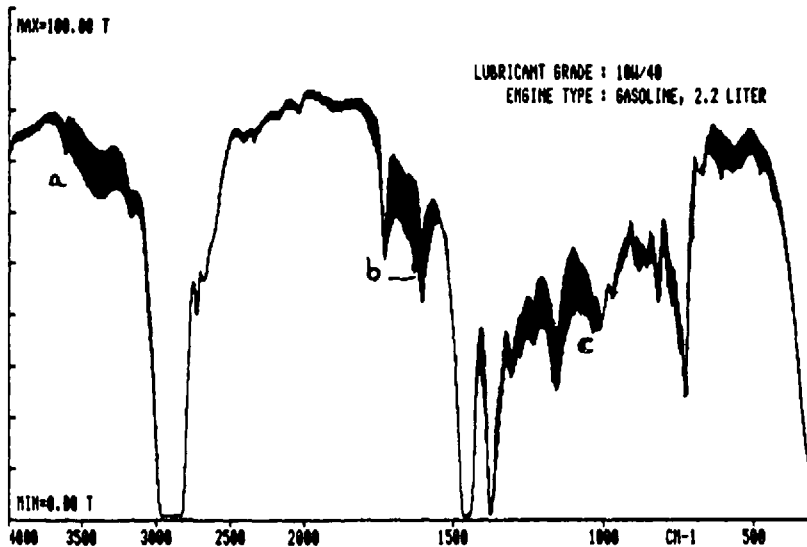


Figure 23.12 Infrared spectra of new and used oils: a indicates traces of water contamination, b indicates formation of oxidation debris (carboxylic acids), and c indicates depletion of zinc antiwear additive [38].

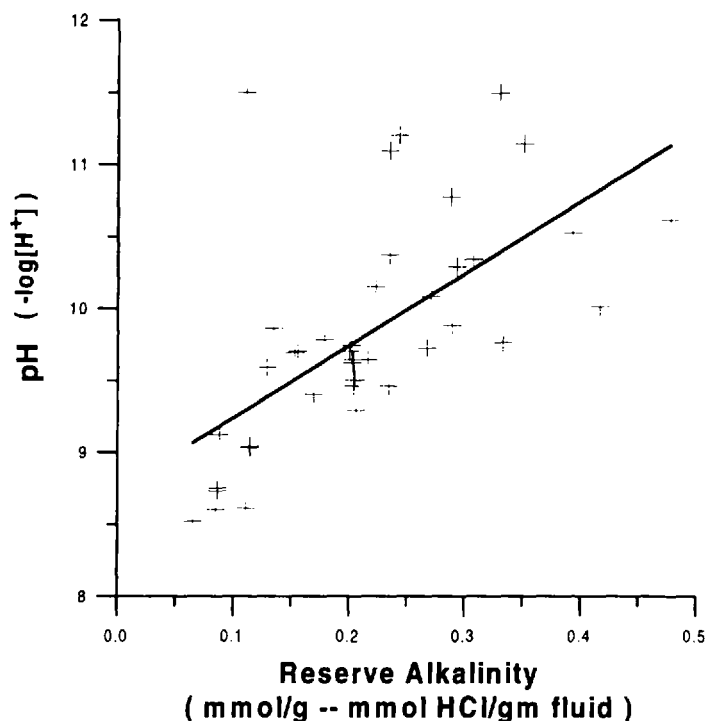


Figure 23.13 Correlation between pH and reserve alkalinity.

Formic acid, in particular, is known to have a detrimental effect on the antiwear characteristics of these fluids. In addition, depletion of corrosion inhibitors may be the result of tramp-oil contamination, hard-water contamination, and evaporation brought about by high temperatures. The additive or amine concentration of a water-glycol hydraulic fluid is designated as “reserve alkalinity.” Measuring the reserve alkalinity of a fluid is generally done by titrating a sample of the diluted fluid with 0.1*N* HCl. The results are conventionally reported as the milliliters of 0.1*N* hydrochloric acid (HCl) required to titrate 100 mL of fluid to a pH of 5.5 [40]. Another method for monitoring the condition of a water-glycol fluid is the pH test. Whereas the reserve alkalinity test is a direct measure of the free-amine content of the fluid, pH provides an indirect measurement of fluid alkalinity by determining the hydrogen ion content of the fluid. There is poor correlation between pH and reserve alkalinity (see Fig. 23.13) (G. E. Totten, unpublished data). This is because the pH of a solution depends to a greater extent on the dissociation constant than concentration [41].

7 FLUID CLASSIFICATIONS AND SPECIFICATIONS

Commercial, military, national, and international standards organizations have established classification schemes for various fluid types such as mineral oil, water-



Figure 23.14 ASTM D-892 apparatus. (Courtesy of Koehler Instrument Co.)

glycol, and biodegradable fluids. These organizations also have established performance specifications for many fluid types as well. In general, the purposes of performance standards are the following:

- Define minimum performance requirements for hydraulic fluids
- Provide fluid suppliers with performance targets
- Improve the availability of suitable hydraulic fluids
- Provide a user-friendly, internationally recognizable classification system

Many of these standards, such as the commercial standards listed in Table 23.5 and the regional standard listed in Table 23.6, rely upon the tests described earlier in this chapter to evaluate fluid suitability.

Although commercial standards provide useful selection guidelines for certain applications, oftentimes hydraulic systems use components from multiple suppliers based on different continents throughout the world. Consequently, international standards, particularly those developed by the International Standards Organization (ISO), have increasing importance in the hydraulics industry. The ISO Standard for classifying hydraulic fluids is ISO 6743-4. This classification system provides standard symbols for different fluid types, such as mineral-oil-based hydraulic fluids (Table 23.7) and fire-resistant hydraulic fluids (Table 23.8). ISO 6743-4 is currently being revised to include symbols for biodegradable hydraulic fluids (Table 23.9). Performance specifications for mineral-oil-based fluids are defined in ISO 11158.

Table 23.5 Commercial Hydraulic Fluid Specifications

Specification	Denison		Vickers		Cincinnati Milacron
	HF-0	HF-2	M-2950-S	I-286-S	P68, P-69, P-70
Pump wear tests					
Denison T-6-C	Pass				
Denison P-46	Pass	Pass			
Vickers 35VQ-25			Pass		
Vickers V-104C, mg				<50	<50
High-temp. tests					
Turbine Oil Oxidation Life ASTM D943, hours	>1000	>1000	>1000		
1000 Hour Sludge Test, mg. Insolubles, D-4310	<200	<400			
Copper wt. loss, mg	<50	<200			
Iron wt. loss, mg	<50	<100			
Hydrolytic stability TAN mg KOH/g, D2619	<4.0	<6.0			
Cincinnati Milacron Thermal Stability	Pass				Pass
Water tolerance tests					
Demulsibility D1401			Pass ^a	Pass ^a	
Rust Test D665					
Part A	Pass	Pass	Pass ^a	Pass ^a	Pass
Part B	Pass	Pass	Pass ^a	Pass ^a	
Filterability TP 02100	<600				
(a) 1.2 μm without water					
(b) 1.2 μm with water	<2 × (a)				
Miscellaneous tests					
Foam D892 at 10 min.	Nil	Nil			
Viscosity Index, min.	90	90			90

^aEvidence of satisfactory performance required, test method unspecified.

Table 23.6 DIN Standard 51524

DIN 51 524		Part 1	Part 2	Part 3
Classification		HL	HLP	HLVP
ISO grade	DIN 51 519	10-100	10-100	15-100
Viscosity index	IOS 2909	NR	NR	≥140 ^a
Flash point (°C)	DIN 51 367	Pass	Pass	Pass
Pour point (°C)	DIN 51 597	Pass	Pass	Pass
Demulsibility	DIN 51 599	Pass	Pass	Pass
Air release	DIN 51 381	Pass	Pass	Pass
Foam test	DIN 51 566	150/0-75/0-150/0	150/0-75/0-150/0	150/0-75/0-150/0
Copper corrosion	DIN 51 759	2	2	2
Steel corrosion	DIN 51 585	max. 0-A	max. 0-A	max. 0-A
Seal compatibility				
Volume change—NBR	DIN 53 521	Pass	Pass	Pass
Hardness change—NBR	DIN 53 505	Pass	Pass	Pass
FZG Test	DIN 51 354			
(a) Damage stage ^b		N/A	10	10
(b) Wear (mg/kW h)			0.27	0.27
Vickers vane pump	DIN 51 389			
(a) Wear of ring (mg), max		N/A	120	120
(b) Wear of vanes (mg), max			30	30
Oxidation Test	DIN 51 558			
TAN@1000 h		<2.0	<2.0	<2.0

^a≥120 for ISO VG 100.

^bNot required for ISO VG < 32.

Table 23.7 Comparison of Classification Symbols for Mineral-Oil-Based Hydraulic Fluids

Governing organization	ISO	AAMA	DIN	ASTM
Applicable standard	6743-4 ^a	524 ^b	51524	D6158 ^c
Hydraulic oils—mineral-oil based	H	H	H	H
Noninhibited mineral oils	HH	—	—	HH
Rust and oxidation hydraulic oils	HL	HL	HL ^d	HL
Antiwear hydraulic oils	HM	HM	HLP ^e	HM
Multigrade antiwear hydraulic oils	HV	HV	HVLP ^f	—
Antiwear hydraulic slide-way oils with antislip/stick properties	HG	—	—	—
Multigrade rust and oxidation hydraulic oils	HR	HR	—	—

^aISO 6743-4:1982, Lubricants, Industrial oils and related products (Class L)—Classification—Part 4: Family H (hydraulic systems).

^bAAMA 524, Lubricants, industrial oils, and related products Part 1, Type HF (Fire-resistant hydraulic fluids), 1996, American Automobile Manufacturers Association, Detroit, MI.

^cReference 15.

^dHL Hydraulic Oils, Minimum Requirements, DIN 51524 Part I, 1990, Deutsche Norm, Beuth Verlag GmbH, Berlin.

^eHLP Hydraulic Oils, Minimum Requirements, DIN 51524 Part II, 1990, Deutsche Norm, Beuth Verlag GmbH, Berlin.

^fHVLP Hydraulic Oils, Minimum Requirements, DIN 51524 Part III, 1990, Deutsche Norm, Beuth Verlag GmbH, Berlin.

Table 23.8 ISO Classification Symbols for Fire-Resistant Hydraulic Fluids

Governing organization	ISO ^a
Applicable standard	6743-4
Hydraulic oils—fire resistant	HF
Oil-in-water emulsion (fire resistant)	HFAE
Chemical solutions in water (fire resistant)	HFAS
Water-in-oil emulsion (fire resistant)	HFB
Water-glycol solutions (fire resistant)	HFC
Phosphate ester fluid (fire resistant)	HFDR
Chlorinated hydrocarbon fluids (fire resistant)	HFDS
Mixtures of HFDR and HFDS	HFDT
Other non-water-containing synthetic fluids	HFDU

^aISO 6743-4:1982, Lubricants, Industrial oils and related products (Class L)—Classification—Part 4: Family H (hydraulic systems).

Table 23.9 Proposed Classifications for Biodegradable Hydraulic Fluids

Governing organization	ISO
Applicable standard	6743-4 ^a
Hydraulic oils—biodegradable	HE
Triglyceride type	HETG
Polyglycol type	HEPG
Synthetic ester type	HEES
Poly alphaolefin type	HEPR

^aISO/FDIS 6743-4:1999(E), Lubricants, Industrial oils and related products (Class L)—Classification—Part 4: Family H (hydraulic systems); under preparation.

REFERENCES

1. G. W. Kushnier, "The Pacific Area Standards Congress (PASC)," *ASTM Standardization News*, 1997, October.
2. A. Esposito, *Fluid Power with Applications*, 1988, Prentice-Hall; Englewood Cliffs, NJ, p. 478.
3. D. Saxena, R. T. Mookken, S. P. Srivastava, and A. K. Bhatnagar, "An Accelerated Aging Test for AW Oils," *Lubr. Eng.*, 1993, 49, p. 10.
4. J. Igaraski, *Jpn. J. Tribol.*, 1990, 35, pp. 1095–1105.
5. X. Maleville, D. Faure, A. Legros, and J. C. Hipeaux, "Oxidation of Mineral Base Oils of Petroleum Origin: The Relationship between Chemical Composition, Thickening and Composition of Degraded Products," *Lubr. Sci.*, 1996, 9, p. 1.
6. S. Korcek and R. K. Jensen, Relationship Between Base Oil composition and Oxidation Stability at Increased Temperatures," ASLE Preprint No. 75AM-1A-1V (1975).
7. E. Denisov, *Handbook of Antioxidants*, 1995, CRC press; Boca Raton, FL, p. 19.
8. Sasaki, A Study of Hydraulic Valve Problems," *Lubr. Eng.*, 1989, 45, p. 3.

9. *Annual Book of ASTM Standards, Volume 5.01, Petroleum Products and Lubricants*, 1997, ASTM; Philadelphia.
10. *Annual Book of ASTM Standards, Volume 5.02, Petroleum Products and Lubricants*, 1997, ASTM; Philadelphia.
11. *Cincinnati Milacron Lubricants Manual*, Pub. No. 10-SP-95046, 1995, p. 2–40.
12. B. J. Lloyd, "Water Water Everywhere," *Lubes and Greases*, 1997, 3(11).
13. J. Elefthakis and D. Norvelle, "*Bird Bones and Sludge—A Complete Guide to Hydraulic System Contamination Control*", 1996, Vickers, Rochester Hills, MI, p. 9.1.
14. L. Tsong-Dsu and J. Mansfield, "Effect of Contamination on the Water Separability of Steam Turbine Oils," *Lubr. Eng.*, 1995, 51(1).
15. *Annual Book of ASTM Standards, Volume 5.03, Petroleum Products and Lubricants*, 1997, ASTM; Philadelphia.
16. I. Rhee, C. Velz, and K. Von Bernewitz, "Evaluation of Environmentally Acceptable Hydraulic Fluids," U.S. Tank—Automotive Command Technical Report No. 13640, 1995.
17. Federal Test Method Standard No. 791, *Lubricants, Liquid Fuels and Related Products; Methods of Testing*.
18. S. Q. A. Rizvi, "Lubricant Additives and Their Functions," *ASM Handbook*, 10th ed. Vol. 18, *Friction Lubrication, and Wear Technology*, 1992, ASM International; Materials Park, OH, pp. 98–112.
19. G. E. Totten, Y. H. Sun, and R. J. Bishop, "Hydraulic Fluids: Foaming, Air Entrainment and Air Release—A Review," SAE Technical Paper Series, Paper 972789, 1997.
20. *HVLP Hydraulic Oils, Minimum Requirements, DIN 51524 Part III*, 1990, Deutsche Norm, Beuth Verlag GmbH; Berlin.
21. *Denison Fluid Standard HF-O Hydraulic Fluid—For Use in Axial Piston Pumps and Vane Pumps in Severe Duty Applications*, Denison Hydraulics, Marysville, OH.
22. P. D. Claxon, "Aeration of Petroleum Based Steam Turbine Oils," *Tribology*, February, 1972, p. 8–13.
23. ASTM D3519 Standard Test Method for Foam in Aqueous Media (Blender Test), *Annual Book of ASTM Standards, Volume 5.02, Petroleum Products and Lubricants*, 1997, ASTM; Philadelphia.
24. C. Carpsjo, in *International Symposium on Performance Testing of Hydraulic Fluids*, 1978, Institute of Petroleum; London.
25. R. L. Stambaugh and R. J. Kopko, "Behavior of Non-Newtonian Lubricants in High Shear Rate Applications," SAE Trans., 1973, Paper 730487.
26. R. L. Stambaugh, R. J. Kopko, and T. F. Roland, "Hydraulic Pump Performance—A Basis for Fluid Viscosity Classification," in SAE International Off Highway Congress, 1990, Paper 901633.
27. M. D. Behrens and S. W. Rein, "An Automated Fuel Injector Shear Stability Tester," SAE Tech. Paper Series, Paper 690158, 1969.
28. P. K. B. Hodges, *Hydraulic Fluids*, 1996, John Wiley and Sons, New York, p. 116.
29. *Karl Fischer Applications*, 1992, Mettler-Toledo AG., Griefensee, Switzerland.
30. "Committee D-2 Interlaboratory Crosscheck Program," *Engine Oil Lubr.*, 1997, May, p. 164.
31. J. A. Dean, *Analytical Chemistry Handbook*, 1995, McGraw-Hill; New York.
32. J. Poley, "Oil Analysis for Monitoring Hydraulic Oil Systems. A Step-Stage Approach," *Lubr. Eng.*, 46(1), pp. 41–47.
33. R. B. Jones and R. C. Coy, "The Chemistry of Thermal Degradation of Zinc Dialkyl-dithiophosphate Additives," *ASLE Trans.*, 24(1), pp. 91–97.
34. S. M. Hsu, C. S. Ku, and P. T. Pei, "Oxidation Degradation Mechanisms of Lubricants," in *Aspects of Lubricant Oxidation*, ASTM Special Technical Publication 916, W. H. Stadtmiller and A. N. Smith, eds., 1986, ASTM; Philadelphia, pp. 27–48.

35. J. A. Dean and G. J. Shugar, *The Chemist's Ready Reference Handbook*, 1990, McGraw-Hill, New York.
36. M. Okada and M. Yamashita, "Development of an Extended-Life Hydraulic Fluid," *Lubr. Eng.*, 1987, 43(6).
37. D. L. Wooton, B. J. Lawrence, and J. G. Demrath, "Infrared Analysis of Heavy-Duty Diesel Engine Oils," SAE Tech. Paper Series, Paper 841372, 1984.
38. J. P. Coates and L. C. Setti, "Infrared Spectroscopic Methods for the Study of Lubricant Oxidation Products," *Lubr. Eng.*, 1985, 29(3).
39. G. E. Totten, R. J. Bishop, R. L. McDaniels, D. P. Braniff, and D. J. Irvine, "Effect of Low Molecular Weight Carboxylic Acids on Hydraulic Pump Wear," SAE Tech. Paper Series, Paper 941751, 1994.
40. D. A. Wachter, R. J. Bishop, R. L. McDaniels, and G. E. Totten, "Water-Glycol Hydraulic Fluid Performance Monitoring: Fluid Performance and Analysis Strategy," SAE Tech. Paper Series, Paper 952155, 1995.
41. A. K. Covington, "pH Scale for Aqueous Solutions," *Handbook of Chemistry & Physics*, 1993, CRC Press; Boca Raton, FL, pp. 8-30, 8-31.

This page intentionally left blank

Appendixes

APPENDIX 1: TEMPERATURE CONVERSION TABLE

Equivalent Temperature Readings for Fahrenheit and Celsius Scales [$^{\circ}\text{F} = (9/5)^{\circ}\text{C} + 32$;
 $^{\circ}\text{C} = (5/9)(^{\circ}\text{F} - 32)$]

$^{\circ}\text{Fahrenheit}$	$^{\circ}\text{Celsius}$	$^{\circ}\text{Fahrenheit}$	$^{\circ}\text{Celsius}$	$^{\circ}\text{Fahrenheit}$	$^{\circ}\text{Celsius}$	$^{\circ}\text{Fahrenheit}$	$^{\circ}\text{Celsius}$
-459.4	-273	-39	-39.4	-18.4	-28	2	-16.7
-436	-260	-38.2	-39	-18	-27.8	3	-16.1
-418	-250	-38	-38.9	-17	-27.2	3.2	-16
-400	-240	-37	-38.3	-16.6	-27	4	-15.6
-382	-230	-36.4	-38	-16	-26.7	5	-15
-364	-220	-36	-37.8	-15	-26.1	6	-14.4
-346	-210	-35	-37.2	-14.8	-26	6.8	-14
-328	-200	-34.6	-37	-14	-25.6	7	-13.9
-310	-190	-34	-36.7	-13	-25	8	-13.3
-292	-180	-33	-36.1	-12.0	-24.4	8.6	-13
-274	-170	-32.8	-36	-11.2	-24	9	-12.8
-256	-160	-32	-35.6	-11	-23.9	10	-12.2
-238	-150	-31	-35	-10.0	-23.3	10.4	-12
-220	-140	-30	-34.4	-9.4	-23	11	-11.7
-202	-130	-29.2	-34	-9	-22.8	12	-11.1
-184	-120	-29	-33.9	-8	-22.2	12.2	-11
-166	-110	-28	-33.3	-7.6	-22	13	-10.6
-148	-100	-27.4	-33	-7	-21.7	14	-10
-139	-95	-27	-32.8	-6	-21.1	15	-9.4
-130	-90	-26	-32.2	-5.8	-21	15.8	-9
-121	-85	-25.6	-32	-5	-20.6	16	-8.9
-112	-80	-25	-32.9	-4	-20	17	-8.3
-103	-75	-24	-31.7	-3	-19.4	17.6	-8
-94	-70	-23.8	-31.1	-2.2	-19	18	-7.8
-85	-65	-23	-30.5	-2	-18.9	19	-7.2
-76	-60	-22	-30	-1	-18.3	19.4	-7
-67	-55	-21	-29.4	-0.4	-18	20	-6.7
-58	-50	-20.2	-29	0	-17.8	21	-6.1
-49	-45	-20	-28.9	+1	-17.2	21.2	-6
-40	-40	-19	-28.3	1.4	-17	22	-5.6

Equivalent Temperature Readings for Fahrenheit and Celsius Scales (Continued)

°Fahrenheit	°Celsius	°Fahrenheit	°Celsius	°Fahrenheit	°Celsius	°Fahrenheit	°Celsius
23	-5	54	12.2	85	29.4	116.6	47
24	-4.4	55	12.8	86	30	117	47.2
24.8	-4	55.4	13	87	30.6	118	47.8
25	-3.9	56	13.3	87.8	31	118.4	48
26	-3.3	57	31.9	88	31.1	119	48.3
26.6	-3	57.2	14	89	31.7	120	48.9
27	-2.8	58	14.4	89.6	32	120.2	49
28	-2.2	59	15	90	32.2	121	49.4
28.4	-2	60	15.6	91	32.8	122	50
29	-1.7	60.8	16	91.4	33	123	50.6
30	-1.1	61	16.1	92	33.3	123.8	51
30.2	-1	62	16.7	93	33.9	124	51.1
31	-0.6	62.6	17	93.2	34	125	51.7
32	0	63	17.2	94	34.4	125.6	52
33	+0.6	64	17.8	95	35	126	52.2
33.8	1	64.4	18	96	35.6	127	52.8
34	1.1	65	18.3	96.8	36	127.4	53
35	1.7	66	18.9	97	36.1	128	53.3
35.6	2	66.2	19	98	36.7	129	53.9
36	2.2	67	19.4	98.6	37	129.2	54
37	2.8	68	20	99	37.2	130	54.4
37.4	3	69	20.6	100	37.8	131	55
38	3.3	69.8	21	100.4	38	132	55.6
39	3.9	70	21.1	101	38.3	132.8	56
39.2	4	71	21.7	102	38.9	133	56.1
40	4.4	71.6	22	102.2	39	134	56.7
41	5	72	22.2	103	39.4	134.6	57
42	5.6	73	22.8	104	40	135	57.2
42.8	6	73.4	23	105	40.6	136	57.8
43	6.1	74	23.3	105.8	41	136.4	58
44	6.7	75	23.9	106	41.1	137	58.3
44.6	7	75.2	24	107	41.7	138	58.9
45	7.2	76	24.4	107.6	42	138.2	59
46	7.8	77	25	108	42.2	139	59.4
46.4	8	78	25.6	109	42.8	140	60
47	8.3	78.8	26	109.4	43	141	60.6
48	8.9	79	26.1	110	43.3	141.8	61
48.2	9	80	26.7	111.1	43.9	142	61.1
49	9.4	80.6	27	111.2	44	143	61.7
50	10.0	81	27.2	112	44.4	143.6	62
51	10.6	82	27.8	113	45	144	62.2
51.8	11	82.4	28	114	45.6	145	62.8
52	11.1	82.9	28.3	114.8	46	145.4	63
53	11.7	84	28.9	115	46.1	146	63.3
53.6	12	84.2	29	116	46.7	147	63.9

Equivalent Temperature Readings for Fahrenheit and Celsius Scales (Continued)

°Fahrenheit	°Celsius	°Fahrenheit	°Celsius	°Fahrenheit	°Celsius	°Fahrenheit	°Celsius
147.2	64	179	81.7	210	98.9	241	116.1
148	64.4	179.6	82	210.2	99	242	116.7
149	65	180	82.2	211	99.4	242.6	117
150	65.6	181	82.8	212	100	243	117.2
150.8	66	181.4	83	213	100.6	244	117.8
151	66.1	182	83.3	213.8	101	244.4	118
152	66.7	183	83.9	214	101.1	245	118.3
152.6	67.7	183.2	84	215	101.7	246	118.9
153	67.2	184	84.4	215.6	102	246.2	119
154	67.8	185	85	216	102.2	247	119.4
154.4	68	186	85.6	217	102.8	248	120
155	68.3	186.8	86	217.4	103	249	120.6
156	68.9	187	86.1	218	103.3	249.8	121
156.2	69	188	86.7	219	103.9	250	121.1
157	69.4	188.6	87	219.2	104	251	121.7
158	70	189	87.2	220	104.4	251.6	122
159	70.6	190	87.8	221	105	252	122.4
159.8	71	190.4	88	222	105.6	253	122.8
160	71.1	191	88.3	222.8	106	253.4	123
161	71.7	192	88.9	223	106.1	254	123.3
161.1	72	192.2	89	224	106.7	255	123.9
162	72.2	193	89.4	224.6	107	255.2	124
163	72.8	194	90	225	107.2	256	124.4
163.4	73	195	90.6	226	107.8	257	125
164	73.3	195.8	91	226.4	108	258	125.5
165	73.9	196	91.1	227	108.3	258.8	126
165.2	74	197	91.7	228	108.9	259	126.1
166	74.4	197.6	92	228.2	109	260	126.7
167	75	198	92.2	229	109.4	260.6	127
168	75.6	199	92.8	230	110	261	127.2
168.8	76	199.4	93	231	110.6	262	127.8
169	76.1	200	93.3	231.8	111	262.4	128
170	76.7	201	93.9	232	111.1	263	128.3
170.6	77	201.2	94	233	111.7	264	128.9
171	77.2	202	94.4	233.6	112	264.2	129
172	77.8	203	95	234	112.3	265	129.4
172.4	78	204	95.6	235	112.8	266	130
173	78.3	204.8	96	235.4	113	267	130.6
174	78.9	205	96.1	236	113.3	267.8	131
174.2	79	206	96.7	237	113.9	268	131.3
175	79.4	206.6	97.7	237.2	114	269	131.7
176	80	207	97.2	238	114.4	269.6	132
177	80.6	208	97.8	239	115	270	132.2
177.8	81	208.4	98	240	115.6	271	132.8
178	81.1	209	98.3	240.8	116	271.4	133

Equivalent Temperature Readings for Fahrenheit and Celsius Scales (Continued)

°Fahrenheit	°Celsius	°Fahrenheit	°Celsius	°Fahrenheit	°Celsius	°Fahrenheit	°Celsius
272	133.3	300	148.9	327.2	164	355	179.4
273	133.9	300.2	149	328	164.4	356	180
273.3	134	301	149.4	329	165	357	180.6
274	134.4	302	150	330	165.6	357.8	181
275	135	303	150.6	330.8	166	358	181.1
276	135.6	303.8	151	331	166.1	359	181.6
276.8	136	304	151.1	332	166.7	359.6	182
277	136.1	305	151.7	332.6	167	360	182.2
278	136.7	305.6	152	333	167.2	361	182.8
278.6	137	306	152.2	334	167.8	361.4	183
279	137.2	307	152.8	334.4	168	362	183.3
280	137.8	307.4	153.3	335	168.3	363	183.9
280.4	138	308	153.3	336	168.9	363.2	184
281	138.3	309	153.9	336.2	169	364	184.4
282	138.9	309.2	154	337	169.4	365.6	185
282.2	139	310	154.4	338	170	366	185.6
283	139.4	311	155	339	170.6	366.8	186
284	140	312	155.6	339.8	171	367	186.1
285	140.6	312.8	156	340	171.1	368	186.7
285.8	141	313	156.1	341	171.7	368.6	187
286	141.1	314	156.7	341.6	172	369	187.2
287	141.7	314.6	157	342	172.2	370	187.8
287.6	142	315	157.2	343	172.8	370.4	188
288	142.2	316	157.8	343.4	173	371	188.3
289	142.8	316.4	158	344	173.3	372	188.9
289.4	143	317	158.3	345	173.9	372.2	189
290	143.3	318	158.9	345.2	174	373	189.4
291	143.9	318.2	159	346	174.4	374	190
291.2	144	319	159.4	347	175		
292	144.4	320	160	348	175.6		
293	145	321	160.6	348.8	176		
294	145.6	321.8	161	349	176.1		
294.8	146	322	161.1	350	176.7		
295	146.1	323	161.7	350.6	177		
296	146.7	323.6	162	351	177.2		
296.6	147	324	162.2	352	177.8		
297	147.2	325	162.8	352.4	178		
298	147.8	325.4	163	353	178.3		
298.4	148	326	163.3	354	178.9		
299	148.3	327	163.9	354.2	179		

APPENDIX 2: SI UNIT CONVERSIONS

Conversions of USCS to SI Units

Energy		
To convert from	To	Multiply by ^a
British thermal unit (ISO/TC 12)	Joule	+03 1.055 06
British thermal unit (International Steam Table)	Joule	+03 1.055 04
British thermal unit (mean)	Joule	+03 1.055 87
British thermal unit (thermochemical)	Joule	+03 1.054 350 264 488
British thermal unit (39°F)	Joule	+03 1.059 67
British thermal unit (60°F)	Joule	+03 1.054 68
Calorie (International Steam Table)		
Calorie (mean)	Joule	+00 4.190 02
Calorie (thermochemical)	Joule	+00 4.184
Calorie (15°C)	Joule	+00 4.185 80
Calorie (20°C)	Joule	+00 4.185 90
Calorie (kilogram, International Steam Table)	Joule	+00 4.1868
Calorie (kilogram, mean)	Joule	+03 4.190
Calorie (kilogram, thermochemical)	Joule	+03 4.184
Electronvolt	Joule	-19 1.602 10
Erg	Joule	-07 1.00
Foot-pound force (ft-lbf)	Joule	+00 1.355 817 9
Foot poundal	Joule	-02 4.214 011 0
Joule (International of 1948)	Joule	+00 1.000 165
Kilocalorie (International Steam Table)	Joule	+03 4.1868
Kilocalorie (mean)	Joule	+03 4.190 02
Kilocalorie (thermochemical)	Joule	+03 4.184
Kilowatt hour	Joule	+06 3.600 59
Kilowatt hour (International of 1948)	Joule	+06 3.600 59
Ton (nuclear equivalent of TNT)	Joule	+09 4.20
Watt hour	Joule	+03 3.60

Energy/area time

To convert from	To	Multiply by ^a
Btu (thermochemical)/foot ² second	Watt/meter ²	+04 1.134 8931
Btu (thermochemical)/foot ² minute	Watt/meter ²	+02 1.891 488 5
Btu (thermochemical)/foot ² hour		+00 3.152 480 8
Btu (thermochemical)/inch ² second	Watt/meter ²	+06 1.634 246 2
Calorie (thermochemical)/cm ² minute	Watt/meter ²	+02 6.973 333 3
Erg/centimeter ² second	Watt/meter ²	-03 1.00
Watt/cm ²	Watt/meter ²	+04 1.00

Conversions of USCS to SI Units (Continued)

Forcé		
To convert from	To	Multiply by ^a
Dyne	Newton	-05 1.00
Kilogram force (kgf)	Newton	+00 9.806 65
Kilopound force	Newton	+00 9.806 65
Kip	Newton	+03 4.448 221 615 260 5
lbf (pound force, avoirdupois)	Newton	+00 4.448 221 615 260 5
Ounce force (avoirdupois)	Newton	-01 2.780 138 5
Pound force lbf (avoirdupois)	Newton	+00 4.448 221 615 260 5
Pounds	Newton	-01 1.382 549 543 76
Acceleration		
To convert from	To	Multiply by ^a
Foot/second ²	Meter/second ²	-01.3048
Free fall, standard	Meter/second ²	+00 9.806 65
Gal (galileo)	Meter/second ²	-02 1.00
Inch/second ²	Meter/second ²	-02 2.54
Area		
To convert from	To	Multiply by ^a
Acre	Meter ²	+03 4.046 856 422 4
Circular mil	Meter ²	-10 5.067 074 8
Foot ²	Meter ²	-02 9.290 304
Inch ²	Meter ²	-04 6.4516
Mile ² (U.S. statute)	Meter ²	+06 2.589 988 110 336
Yard ²	Meter ²	-01 8.361 273 6
Density		
To convert from	To	Multiply by ^a
Gram/centimeter ³	Kilogram/meter ³	+03 1.00
lbm/inch ³	Kilogram/meter ³	+04 2.767 990 5
lbm/foot ³	Kilogram/meter ³	+01 1.601 846 3
Slug/foot ³	Kilogram/meter ³	+02 5.153 79

^aThe first two digits of each number represent a power of 10.

APPENDIX 3: COMMONLY USED PRESSURE CONVERSIONS; FRACTION NOTATION

Commonly Used Pressure Conversions

1 bar = 100,000 Pa	1 MPa = 10 bar
1 bar = 100 kPa	1 MPa = 1,000 kPa
1 bar = 0.1 MPa	1 MPa = 1,000,000 Pa
1 kPa = 1000 Pa	1 bar = 14.5 psi
1 kPa = 0.01 bar	100 kPa = 14.5 psi
1 kPa = 0.001 MPa	1 MPa = 14.5 psi

Examples for Using Fractions and Multiples of Base Units

Fract./Mult	Symbol	Pa	m	L	N	mW
10^{-1}	m		mm	mL		
10^{-2}	c		cm			
10^{-1}	d		dm ³	dL ³		
10	da				daN ³	
10^2	h			hL		
10^3	h	kPa	km			kW
10^6	M	MPa			MN	mW

^aUnits used in Europe.

APPENDIX 4: VOLUME AND WEIGHT EQUIVALENTS

Volume and Weight Equivalents (Example: 20 U.S. Gallons 3.7854 = 75.708 Liters)

Convert from \ Convert to	Volume and weight equivalents						Weight equivalent basis water at 60°F (15.6°C)		
	U.S. gallons	Imperial gallons	Cubic inches	Cubic feet	Liters	Cubic meters	Pounds	U.S. tons	Kilograms
U.S. gallons	1	0.8327	231	0.13368	3.7854	0.0037854	8.338	0.00417	3.782
Imperial gallons	1.20094	1	277.39	0.16054	4.546	0.004546	10.0134	0.005	4.542
Cubic inches	0.004329	0.003605	1	0.0005787	0.016387	0.000016387	0.036095	55,409	0.016372
Cubic feet	7.48052	6.229	1,728	1	28.317	0.02832	62.3714	0.03119	28.291
Liters	0.2642	0.22	61.024	0.035315	1	0.001	2.2029	0.0011	0.1
Cubic meters	264.2	220	61,024	35.315	1,000	1	2,202.65	1.10133	1,000
Pounds	0.1199	0.09987	27.71	0.016033	0.4539	0.000454	1	0.0005	0.45359
U.S. tons	239.87	199.7	55,409	32.066	907.9	0.908	2,000	1	907.2
Kilograms	0.2644	0.2202	61.08	0.03534	1	0.001	2.205	0.0011	1

Note: The capacity of a barrel varies in different industries. For instance:

- 1 bbl of beer = 31 U.S. gallons
- 1 bbl of wine = 31.5 U.S. gallons
- 1 bbl of oil = 42 U.S. gallons
- 1 bbl of whiskey = 45 U.S. gallons

Drums: The drum is not considered to be a unit of measure as is the barrel. Drums are usually built to specifications and are available in sizes from 2½ gallons to 55 gallons; the most popular sizes are the 5 gallon, 30 gallon, and 55 gallon drums.

APPENDIX 5: HEAD AND PRESSURE EQUIVALENTS

Equivalents of Head and Pressure (Example: $15 \text{ lb/ft}^2 \times 4.88241 = 73.236 \text{ kg/m}^2$)

Convert from	Convert to					Water (68°F) ^a		Mercury (32°F) ^b		Bars ^c	Mega Pascals (MPa) ^c
	lb/in. ²	lb/ft ²	Atmospheres	kg/cm ²	kg/m ²	in.	ft	in.	mm		
lb/in. ²	1	144	0.068046	0.070307	703.07	27.7276	2.3106	2.03602	51.715	0.06895	0.006895
lb/ft ²	0.0069444	1	0.00473	0.000488	4.88241	0.1926	0.01605	0.014139	0.35913	0.000479	0.0000479
Atmospheres	14.696	2,166.2	1	1.0332	10,332.27	407.484	33.957	29.921	760	1.01325	0.101325
kg/cm ²	14.2233	2,048.155	0.96784	1	10,000	394.38	32.865	28.959	735.559	0.98067	0.098067
kg/m ²	0.001422	0.204768	0.0000968	0.0001	1	0.03944	0.003287	0.002896	0.073556	0.000098	0.0000098
in. Water ^a	0.036092	5.1972	0.002454	0.00253	25.375	1	0.08333	0.07343	1.8651	0.00249	0.000249
ft Water ^a	0.432781	62.3205	0.029449	0.03043	304.275	12	1	0.88115	22.3813	0.029839	0.0029839
in. Mercury ^b	0.491154	70.7262	0.033421	0.03453	345.316	13.6185	1.1349	1	25.40005	0.033864	0.0033864
mm Mercury ^b	0.0193368	2.7845	0.0013158	0.0013595	13.59509	0.53616	0.04468	0.03937	1	0.001333	0.0001333
Bars ^c	14.5038	2,088.55	0.98692	1.01972	10,197.2	402.156	33.513	29.53	750.062	1	0.1
MPa ^c	145.038	20,885.5	9.8692	10.1972	101,972	4,021.56	335.13	295.3	7,500.62	10	1

^aWater at 68°F (20°C).

^bMercury at 32°F (0°C).

^cMPa (megaPascal) = 10 bars = 1,000,000 N/m² (Newtons/meter²).

APPENDIX 6: FLOW EQUIVALENTSFlow Equivalents—for Any Liquid (Example: 100 U.S. gal/min \times 0.0631 = 6.31 liters/sec)

Convert from \ Convert to	U.S. gal/min	Imp. gal/min	U.S. million gal/day	Cu. ft per sec (sec-ft)	Cu meters per hour	Liters per sec	Barrels (42 gal) per min	Barrels (42 gal) per day
U.S. gal/min	1	0.8327	0.00144	0.00223	0.2271	0.0631	0.0238	34.286
Imp. gal/min	1.201	1	0.00173	0.002676	0.2727	0.0758	0.02859	41.179
U.S. million gal/day	694.4	578.25	1	1.547	157.7	43.8	16.53	23,810
Cu ft/sec	448.83	373.7	0.646	1	101.9	28.32	10.686	15,388
Cu m/sec	15,852	13,200	22.83	35.35	3,600	1,000	377.4	543,462
Cu m/min	264.2	220	0.3804	0.5886	60	16.667	6.29	9,058
Cu m/hr	4.403	3.67	0.00634	0.00982	1	0.2778	0.1048	151
Liter/sec	15.85	13.2	0.0228	0.0353	3.6	1	0.3773	543.3
Liters/min	0.2642	0.22	0.00038	0.000589	0.06	0.0167	0.00629	9.058
Barrels (42 gal)/min	42	34.97	0.0605	0.0937	9.538	2.65	1	1,440
Barrels (42 gal)/day	0.0292	0.0243	0.000042	0.000065	0.00662	0.00184	0.00069	1

Note: 1 miners inch of water = 8.977 gpm (in Idaho, Kansas, Nebraska, New Mexico, N. Dakota, and Utah)
 = 11.22 gpm (in Arizona, California, Montana, Nevada and Oregon)
 = 11.69 gpm (in Colorado)

Barrel per day = 31 gal \times 0.02153 = gpm (beer)
 31.5 gal \times 0.02188 = gpm (wine)
 42 gal \times 0.02917 = gpm (oil)
 45 gal \times 0.03125 = gpm (whiskey).

APPENDIX 7: VISCOSITY CONVERSION CHARTS

Approximate Viscosity Conversions

Seconds Saybolt Universal (SSU)	Kinematic viscosity		Seconds Saybolt Furoil (SSF)	Seconds Redwood 1 Standard	Seconds Redwood 2 Admiralty	Degrees Engler	Degrees Barbey
	centistokes	ft ² /sec					
31	1.0	0.00001076	—	29	—	1.00	6,200
31.5	1.13	0.00001216	—	29.4	—	1.01	5,486
32	1.81	0.00001948	—	29.8	—	1.08	3,425
32.6	2.00	0.00002153	—	30.2	—	1.10	3,100
33	2.11	0.00002271	—	30.6	—	1.11	2,938
34	2.40	0.00002583	—	31.3	—	1.14	2,583
35	2.71	0.00002917	—	32.1	—	1.17	2,287
36	3.00	0.00003229	—	32.9	—	1.20	2,066
38	3.64	0.00003918	—	33.7	—	1.26	1,703
39.2	4.00	0.00004306	—	35.5	—	1.30	1,550
40	4.25	0.00004575	—	36.2	5.10	1.32	1,459
42	4.88	0.00005253	—	38.2	5.25	1.36	1,270
42.4	5.00	0.00005382	—	38.6	5.28	1.37	1,240
44	5.50	0.00005920	—	40.6	5.39	1.40	1,127
45.6	6.00	0.00006458	—	41.8	5.51	1.43	1,033
46	6.13	0.00006598	—	42.3	5.54	1.44	1,011
46.8	7.00	0.00007535	—	43.1	5.60	1.48	885
50	7.36	0.00007922	—	44.3	5.83	1.58	842
52.1	8.00	0.00008611	—	46.0	6.03	1.64	775
55	8.88	0.00009558	—	48.3	6.30	1.73	698
55.4	9.00	0.00009688	—	48.6	6.34	1.74	689
58.8	10.00	0.0001076	—	51.3	6.66	1.83	620
60	10.32	0.0001111	—	52.3	6.77	1.87	601
65	11.72	0.0001262	—	56.7	7.19	2.01	529
70	13.08	0.0001408	—	60.9	7.60	2.16	474
75	14.38	0.0001548	—	65.1	8.02	2.37	431
80	15.66	0.0001686	—	69.2	8.44	2.45	396
85	16.90	0.0001819	—	73.4	8.87	2.59	367
90	18.12	0.0001950	—	77.6	9.30	2.73	342
95	19.32	0.0002080	—	81.6	9.71	2.88	321
100	20.52	0.0002209	—	85.6	10.12	3.02	302
120	25.15	0.0002707	—	102	11.88	3.57	246
140	29.65	0.0003191	—	119	13.63	4.11	209
160	34.10	0.0003670	—	136	15.39	4.64	182
180	38.52	0.0004146	—	153	17.14	5.12	161
200	42.95	0.0004623	—	170	18.90	5.92	144
300	64.6	0.0006953	32.7	253	28.0	8.79	96
400	86.2	0.0009278	42.4	338	37.1	11.70	71.9
500	108.0	0.001163	52.3	423	46.2	14.60	57.4
600	129.4	0.001393	62.0	507	55.3	17.50	47.9
700	151.0	0.001625	72.0	592	64.6	20.44	41.0
800	172.6	0.001858	82.0	677	73.8	23.36	35.9
900	194.2	0.002090	92.1	762	83.0	26.28	31.9
1,000	215.8	0.002323	102.1	846	92.3	29.20	28.7
1,200	259.0	0.002788	122	1,016	111	35.1	23.9

Approximate Viscosity Conversions (Continued)

Seconds Saybolt Universal (SSU)	Kinematic viscosity		Seconds Saybolt Furoil (SSF)	Seconds Redwood 1 Standard	Seconds Redwood 2 Admiralty	Degrees Engler	Degrees Barbey
	centistokes	ft ² /sec					
1,400	302.3	0.003254	143	1,185	129	40.9	20.5
1,600	345.3	0.003717	163	1,354	148	46.7	18.0
1,800	388.5	0.004182	183	1,524	166	52.6	15.6
2,000	431.7	0.004647	204	1,693	185	58.4	14.4
2,500	539.4	0.005806	254	2,115	231	73.0	11.5
3,000	647.3	0.006967	305	2,538	277	87.6	9.6
3,500	755.2	0.008129	356	2,961	323	102	8.21
4,000	863.1	0.009290	408	3,385	369	117	7.18
4,500	970.9	0.01045	458	3,807	415	131	6.39
5,000	1,078.8	0.01161	509	4,230	461	146	5.75
6,000	1,294.6	0.01393	610	5,077	553	175	4.78
7,000	1,510.3	0.01626	712	5,922	646	204	4.11
8,000	1,726.1	0.01858	814	6,769	738	234	3.59
9,000	1,941.9	0.02092	916	7,615	830	263	3.19
10,000	2,157.6	0.02322	1,018	8,461	922	292	2.87
15,000	3,236.5	0.03438	1,526	12,692	—	438	1.92
20,000	4,315.3	0.04645	2,035	16,923	—	584	1.44

Viscosity—Unit Conversions

Multiply	By	To obtain
	Kinematic viscosity ^a	
ft ² /sec	92,903.04	Centistokes
ft ² /sec	0.092903	Sq. meters/sec
Sq. meters/sec	10.7639	ft ² /sec
Sq. meters/sec	1,000,000	Centistokes
Centistokes	0.000001	Sq. meters/sec
Centistokes	0.0000107639	ft ² /sec
	Absolute or dynamic viscosity ^b	
lbf-sec/ft ²	47,880.26	Centipoises
lbf-sec/ft ²	47.8803	Pascal-sec
Centipoises	0.000102	kg-sec/sq. meter
Centipoises	0.0000208854	lbf-sec/sq. ft*
Centipoises	0.001	Pascal-sec
Pascal-sec	0.0208854	lbf-sec/sq. ft*
Pascal-sec	1,000	Centipoises
	Absolute to kinematic viscosity	
Centipoises	1/density (g/cm ³)	Centistokes
Centipoises	0.00067197/density (lb/ft ³)	ft ² /sec
lbf-sec/ft ²	32.174/density (lb/ft ³)	ft ² /sec
kg-sec/m ²	9.80665/density (kg/m ³)	Sq. meters/sec
Pascal-sec	1000/density (g/cm ³)	Centistokes
	Kinematic to absolute viscosity	
Centistokes	Density (g/cm ³)	Centipoises
Sq. meters/sec	0.10197 × density (kg/m ³)	kg-sec/sq. meter
ft ² /sec	0.03108 × density (lb/ft ³)	lbf-sec/ft ²
ft ² /sec	1488.16 × density (lb/ft ³)	Centipoises
Centistokes	0.001 × density (g/cm ³)	Pascal-sec
Sq. meters/sec	1000 × density (g/cm ³)	Pascal-sec

^aSee previous page for conversion in SSU, Redwood, and so forth.

^bSometimes absolute viscosity is given in terms of pounds mass; in this case: centipoises × 0.000672 = lb m/ft sec.

APPENDIX 8: NUMBER OF U.S. GALLONS IN ROUND AND RECTANGULAR TANKS

Number of U.S. Gallons in Round Tanks for One Foot in Depth (1' to 23' diameter)

Diameter of tanks	No. U.S. gals	Cubic ft and area in ft ²	Diameter of tanks	No. U.S. gals	Cubic ft and area in ft ²	Diameter of tanks	No. U.S. gals	Cubic ft and area in ft ²
1'	5.87	0.785	4'-7"	123.42	16.50	12'-6"	918	122.72
1'-1"	6.89	0.922	4'-8"	127.95	17.10	12'-9"	955.09	127.68
1'-2"	8	1.069	4'-9"	132.56	17.72	13'	992.91	132.73
1'-3"	9.18	1.227	4'-10"	137.25	18.35	13'-3"	1031.50	137.89
1'-4"	10.44	1.396	4'-11"	142.05	18.99	13'-6"	1070.80	143.14
1'-5"	11.79	1.576	5'	146.88	19.63	13'-9"	1110.80	148.49
1'-6"	13.22	1.767	5'-1"	151.82	20.29	14'	1151.50	153.94
1'-7"	14.73	1.969	5'-2"	156.83	20.97	14'-3"	1193	159.48
1'-8"	16.32	2.182	5'-3"	161.93	21.65	14'-6"	1235.30	165.13
1'-9"	17.99	2.405	5'-4"	167.12	22.34	14'-9"	1278.20	170.87
1'-10"	19.75	2.640	5'-5"	172.38	23.04	15'	1321.90	176.71
1'-11"	21.58	2.885	5'-6"	177.72	23.76	15'-3"	1366.40	182.65
2'	23.50	3.142	5'-7"	183.15	24.48	15'-6"	1411.50	188.69
2'-1"	25.50	3.409	5'-8"	188.66	25.22	15'-9"	1457.40	194.83
2'-2"	27.58	3.687	5'-9"	194.25	25.97	16'	1504.10	201.06
2'-3"	29.74	3.976	5'-10"	199.92	26.73	16'-3"	1551.40	207.39
2'-4"	31.99	4.276	5'-11"	205.67	27.49	16'-6"	1599.50	213.82
2'-5"	34.31	4.587	6'	211.51	28.27	16'-9"	1648.40	220.35
2'-6"	36.72	4.909	6'-3"	229.50	30.68	17'	1697.90	226.98
2'-7"	39.21	5.241	6'-6"	248.23	33.18	17'-3"	1748.20	233.71
2'-8"	41.78	5.585	6'-9"	267.69	35.78	17'-6"	1799.30	240.53
2'-9"	44.43	5.940	7'	287.88	38.48	17'-9"	1851.10	247.45
2'-10"	47.16	6.305	7'-3"	308.81	41.28	18'	1093.60	254.47
2'-11"	49.98	6.681	7'-6"	330.48	44.18	18'-3"	1956.80	261.59
3'	52.88	7.069	7'-9"	352.88	47.17	18'-6"	2010.80	268.80
3'-1"	55.86	7.467	8'	376.01	50.27	18'-9"	2065.50	276.12
3'-2"	58.92	7.876	8'-3"	399.88	53.46	19'	2120.90	283.53
3'-3"	62.06	8.296	8'-6"	424.48	56.75	19'-3"	2177.10	291.04
3'-4"	65.28	8.727	8'-9"	449.82	60.13	19'-6"	2234	298.65
3'-5"	68.58	9.168	9'	475.89	63.62	19'-9"	2291.70	306.35
3'-6"	71.97	9.621	9'-3"	502.70	67.20	20'	2350.10	314.16
3'-7"	75.44	10.085	9'-6"	530.24	70.88	20'-3"	2409.20	322.06
3'-8"	78.99	10.559	9'-9"	558.51	74.66	20'-6"	2469.10	330.06
3'-9"	82.62	11.045	10'	587.52	78.54	20'-9"	2529.60	338.16
3'-10"	86.33	11.541	10'-3"	617.26	82.52	21'	2591	346.36
3'-11"	90.13	12.048	10'-6"	647.74	86.59	21'-3"	2653	354.66
4'	94	12.566	10'-9"	678.95	90.76	21'-6"	2715.80	363.05
4'-1"	97.96	13.095	11'	710.90	95.03	21'-9"	2779.30	371.54
4'-2"	102	13.635	11'-3"	743.58	99.40	22'	2843.60	380.13
4'-3"	106.12	14.186	11'-6"	776.99	103.87	22'-3"	2908.60	388.82
4'-4"	110.32	14.748	11'-9"	811.14	108.43	22'-6"	2974.30	397.61
4'-5"	114.61	15.321	12'	846.03	113.10	22'-9"	3040.80	406.49
4'-6"	118.97	15.90	12'-3"	881.65	117.86	23'	3108	415.48

Number of U.S. Gallons in Round Tanks for One Foot in Depth (23'-3" to 32'-9" diameter)

Diameter of tanks	No. U.S. gals	Cubic ft and area in ft ²	Diameter of tanks	No. U.S. gals	Cubic ft and area in ft ²	Diameter of tanks	No. U.S. gals	Cubic ft and area in ft ²
23'-3"	3175.90	424.56	26'-6"	4125.90	551.55	29'-9"	5199.90	695.13
23'-6"	3244.60	433.74	26'-9"	4204.10	562	30'	5287.70	706.86
23'-9"	3314	443.01	27'	4283	572	30'-3"	5376.20	718.69
24'	3384.10	452.39	27'-3"	4362.70	583.21	30'-6"	5465.40	730.62
24'-3"	3455	461.86	27'-6"	4443.10	593.96	30'-9"	5555.40	742.64
24'-6"	3526.60	471.44	27'-9"	4524.30	604.81	31'	5646.10	754.77
24'-9"	3598.90	481.11	28'	4606.20	615.75	31'-3"	5737.50	766.99
25'	3672	490.87	28'-3"	4688.80	626.80	31'-6"	5829.70	779.31
25'-3"	3745.80	500.74	28'-6"	4772.10	637.94	31'-9"	5922.60	791.73
25'-6"	3820.30	510.71	28'-9"	4856.20	649.18	32'	6016.20	804.25
25'-9"	3895.60	520.77	29'	4941	660.52	32'-3"	6110.60	816.86
26'	3971.60	530.93	29'-3"	5026.60	671.96	32'-6"	6205.70	829.58
26'-3"	4048.40	541.19	29'-6"	5112.90	683.49	32'-9"	6301.50	842.39

Number of U.S. Gallons in Rectangular Tanks for One Foot in Depth

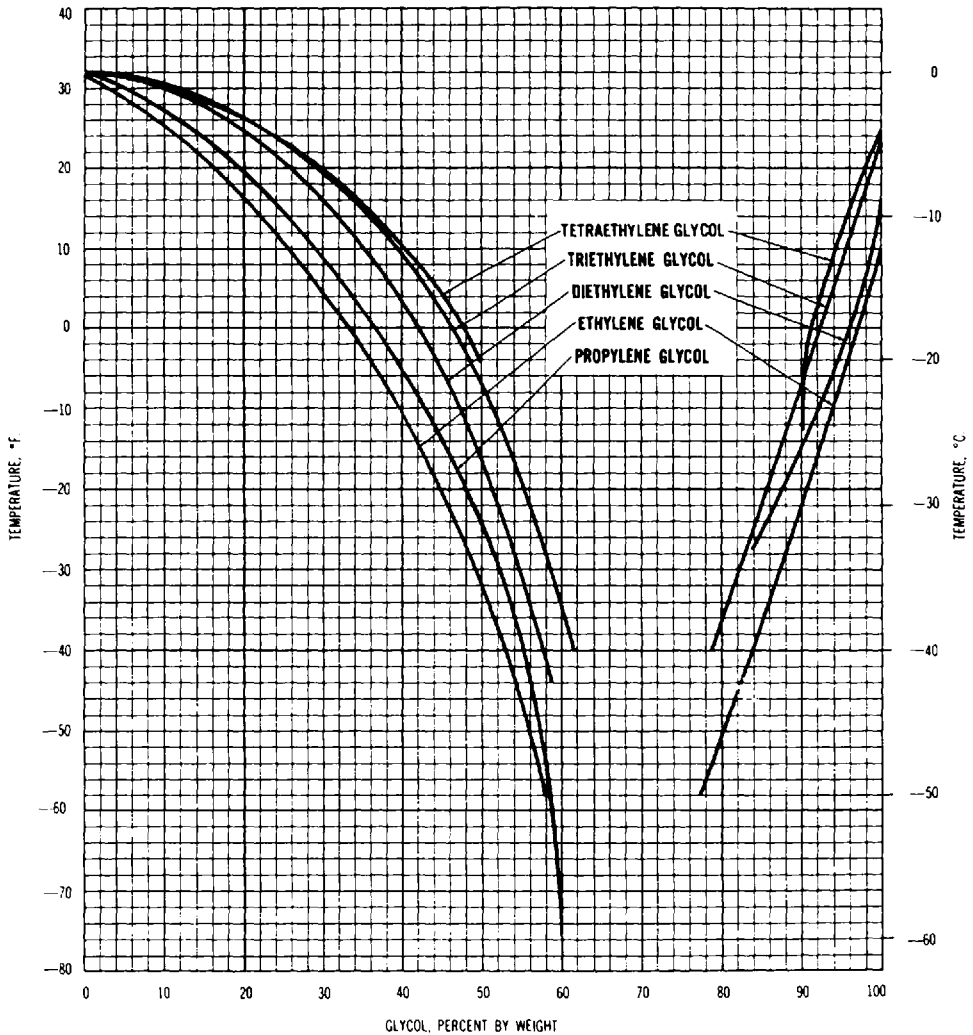
Width of tank	Length of tank																		
	3'	3'-6"	4'	4'-6"	5'	5'-6"	6'	6'-6"	7'	7'-6"	8'	8'-6"	9'	9'-6"	10'	10'-6"	11'	11'-6"	12'
2'	44.88	52.36	59.84	67.32	74.81	82.29	89.77	97.25	104.73	112.21	119.69	127.17	134.65	142.13	149.61	157.09	164.57	172.05	179.53
2'-6"	56.10	65.45	74.80	84.16	93.51	102.86	112.21	121.56	130.91	140.26	149.61	158.96	168.31	177.66	187.01	196.36	205.71	215.06	224.41
3'	67.32	78.54	89.77	100.99	112.21	123.43	134.65	145.87	157.09	168.31	179.53	190.75	201.97	213.19	224.41	235.63	246.86	258.07	269.30
3'-6"	—	91.64	104.73	117.82	130.91	144.00	157.09	170.18	183.27	196.36	209.45	222.54	235.63	248.73	261.82	274.90	288.00	301.09	314.18
4'	—	—	119.69	134.65	149.61	164.57	179.53	194.49	209.45	224.41	239.37	254.34	269.30	284.26	299.22	314.18	329.14	344.10	359.06
4'-6"	—	—	—	151.48	168.31	185.14	201.97	218.80	235.63	252.47	269.30	286.13	302.96	319.79	336.62	353.45	370.28	387.11	403.94
5'	—	—	—	—	187.01	205.71	224.47	243.11	261.82	280.52	299.22	317.92	336.62	355.32	374.03	392.72	411.43	430.13	448.83
5'-6"	—	—	—	—	—	226.28	246.86	267.43	288.00	308.57	329.14	349.71	370.85	390.85	411.43	432.00	452.57	473.14	493.71
6'	—	—	—	—	—	—	269.30	291.74	314.18	336.62	359.06	381.50	403.94	426.39	448.83	471.27	493.71	516.15	538.59
6'-6"	—	—	—	—	—	—	—	316.05	340.36	364.67	388.98	413.30	437.60	461.92	486.23	510.54	534.85	559.16	583.47
7'	—	—	—	—	—	—	—	—	366.54	392.72	418.91	445.09	471.27	497.45	523.64	549.81	575.99	602.18	628.36
7'-6"	—	—	—	—	—	—	—	—	—	420.78	448.83	476.88	504.93	532.98	561.04	589.08	617.14	645.19	673.24
8'	—	—	—	—	—	—	—	—	—	—	478.75	508.67	538.59	568.51	598.44	628.36	658.29	688.20	718.12
8'-6"	—	—	—	—	—	—	—	—	—	—	—	540.46	572.25	604.05	635.84	667.36	699.42	731.21	763.00
9'	—	—	—	—	—	—	—	—	—	—	—	—	605.92	639.58	673.25	706.90	740.56	774.23	807.89
9'-6"	—	—	—	—	—	—	—	—	—	—	—	—	—	675.11	710.65	746.17	781.71	817.24	852.77
10'	—	—	—	—	—	—	—	—	—	—	—	—	—	—	748.05	785.45	822.86	860.26	897.66
10'-6"	—	—	—	—	—	—	—	—	—	—	—	—	—	—	—	824.73	864.00	903.26	942.56
11'	—	—	—	—	—	—	—	—	—	—	—	—	—	—	—	—	905.14	946.29	987.43
11'-6"	—	—	—	—	—	—	—	—	—	—	—	—	—	—	—	—	—	989.29	1032.3
12'	—	—	—	—	—	—	—	—	—	—	—	—	—	—	—	—	—	—	1077.2

APPENDIX 9: WATER VAPOR PRESSURE CHART

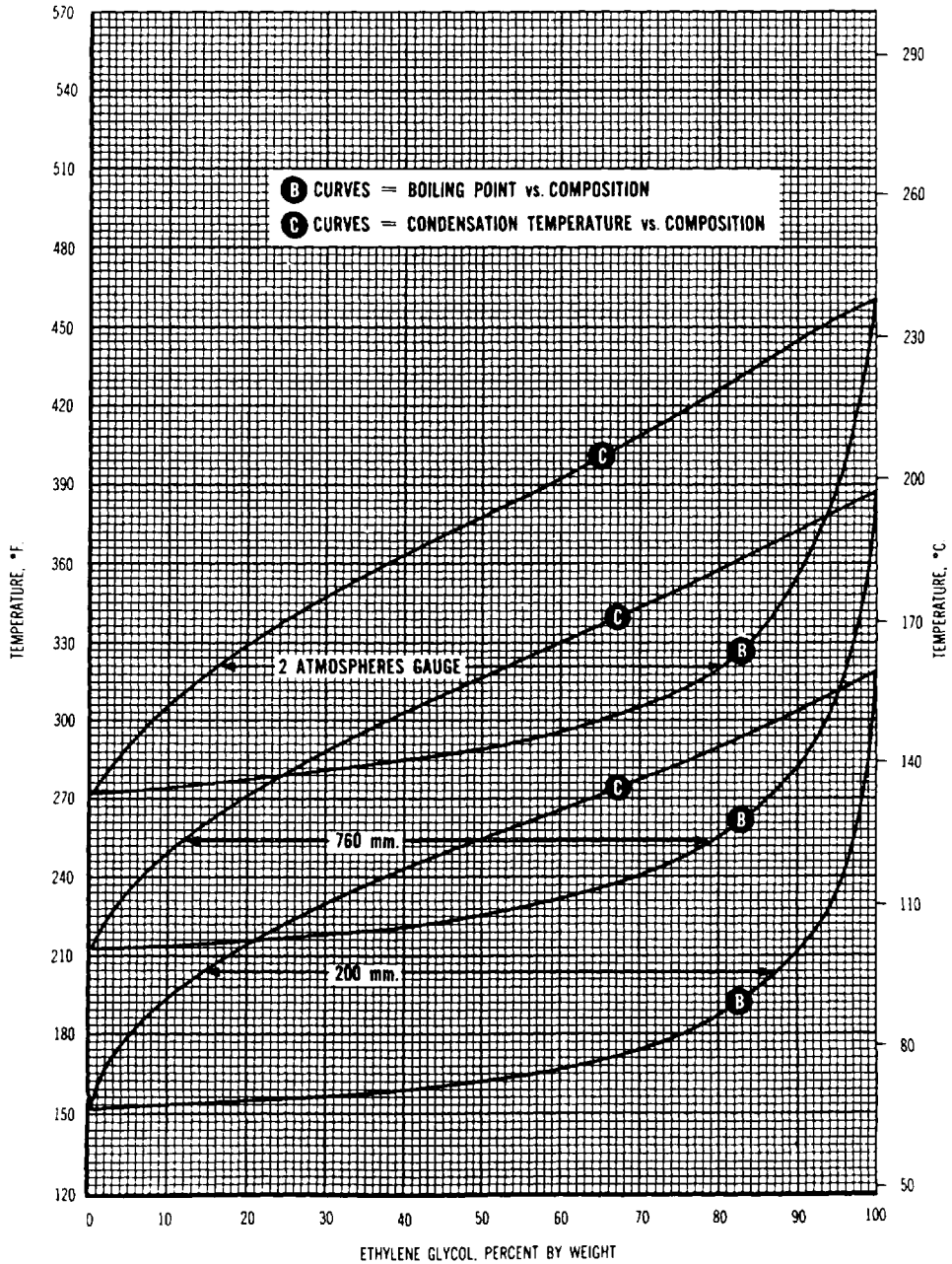
Vapor pressure				Vapor pressure				Vapor pressure				Vapor pressure			
Temp. (°C)	mm Hg	lb/in.	Head (ft)	Temp. (°C)	mm Hg	lb/in.	Head (ft)	Temp. (°C)	mm Hg	lb/in.	Head (ft)	Temp. (°C)	mm Hg	lb/in.	Head (ft)
0	4.579	0.09	0.21	26	25.209	0.49	1.15	51	97.20	1.91	4.4	76	301.4	6.00	13.9
1	4.926	0.10	0.23	27	26.739	0.53	1.22	52	102.09	2.01	4.6	77	314.1	6.15	14.2
2	5.294	0.10	0.24	28	28.349	0.56	1.3	53	107.20	2.11	4.9	78	327.3	6.42	14.8
3	5.655	0.11	0.26	29	30.043	0.59	1.35	54	112.51	2.22	5.1	79	341.0	6.68	15.5
4	6.101	0.12	0.28	30	31.284	0.62	1.4	55	118.04	2.33	5.4	80	355.1	6.92	16.1
5	6.543	0.13	0.30	31	33.695	0.66	1.5	56	123.80	2.44	5.6	81	369.7	7.25	16.8
6	7.013	0.14	0.32	32	35.663	0.70	1.6	57	129.82	2.55	5.9	82	384.9	7.55	17.5
7	7.513	0.15	0.35	33	37.729	0.74	1.7	58	136.08	2.67	6.2	83	400.6	7.85	18.2
8	8.045	0.16	0.37	34	39.898	0.78	1.8	59	142.60	2.80	6.5	84	416.8	8.16	18.9
9	8.609	0.17	0.39	35	42.175	0.83	1.9	60	149.38	2.94	6.8	85	433.6	8.50	19.6
10	9.209	0.18	0.41	36	44.563	0.88	2.0	61	156.43	3.07	7.1	86	450.9	8.83	20.4
11	9.844	0.19	0.44	37	47.067	0.93	2.1	62	163.77	3.21	7.4	87	468.7	9.15	21.2
12	10.518	0.21	0.48	38	49.692	0.98	2.3	63	171.38	3.36	7.8	88	487.1	9.55	22.1
13	11.231	0.22	0.51	39	52.442	1.03	2.4	64	179.31	3.51	8.1	89	506.1	9.92	22.9
14	11.987	0.24	0.55	40	55.324	1.09	2.5	65	187.54	3.68	8.5	90	525.8	10.3	23.8
15	12.788	0.25	0.58	41	58.34	1.15	2.7	66	196.09	3.84	8.9	91	546.1	10.7	24.8
16	13.643	0.27	0.62	42	61.50	1.21	2.8	67	204.96	4.02	9.3	92	567.0	11.1	25.6
17	14.530	0.29	0.66	43	64.80	1.27	2.9	68	214.17	4.20	9.7	93	588.6	11.6	26.8
18	15.477	0.30	0.69	44	68.26	1.34	3.1	69	223.73	4.38	10.2	94	610.9	12.0	27.7
19	16.477	0.32	0.74	45	71.88	1.41	3.3	70	233.7	4.57	10.7	95	633.9	12.4	28.6
20	17.535	0.34	0.78	46	75.65	1.49	3.5	71	243.9	4.78	11.1	96	657.6	12.9	29.8
21	18.650	0.37	0.84	47	79.60	1.57	3.7	72	254.6	5.00	11.6	97	682.1	13.4	31.0
22	19.827	0.39	0.90	48	83.71	1.65	3.8	73	265.7	5.21	12.1	98	707.3	13.9	32.1
23	21.068	0.41	0.95	49	88.02	1.73	4.0	74	277.2	5.43	12.5	99	733.2	14.3	33.0
24	22.377	0.44	1.02	50	92.51	1.82	4.2	75	289.1	5.67	13.1	100	760	14.7	34.0
25	23.756	0.47	1.08												

APPENDIX 10: PHYSICAL PROPERTIES OF ETHYLENE, DIETHYLENE, AND PROPYLENE GLYCOL

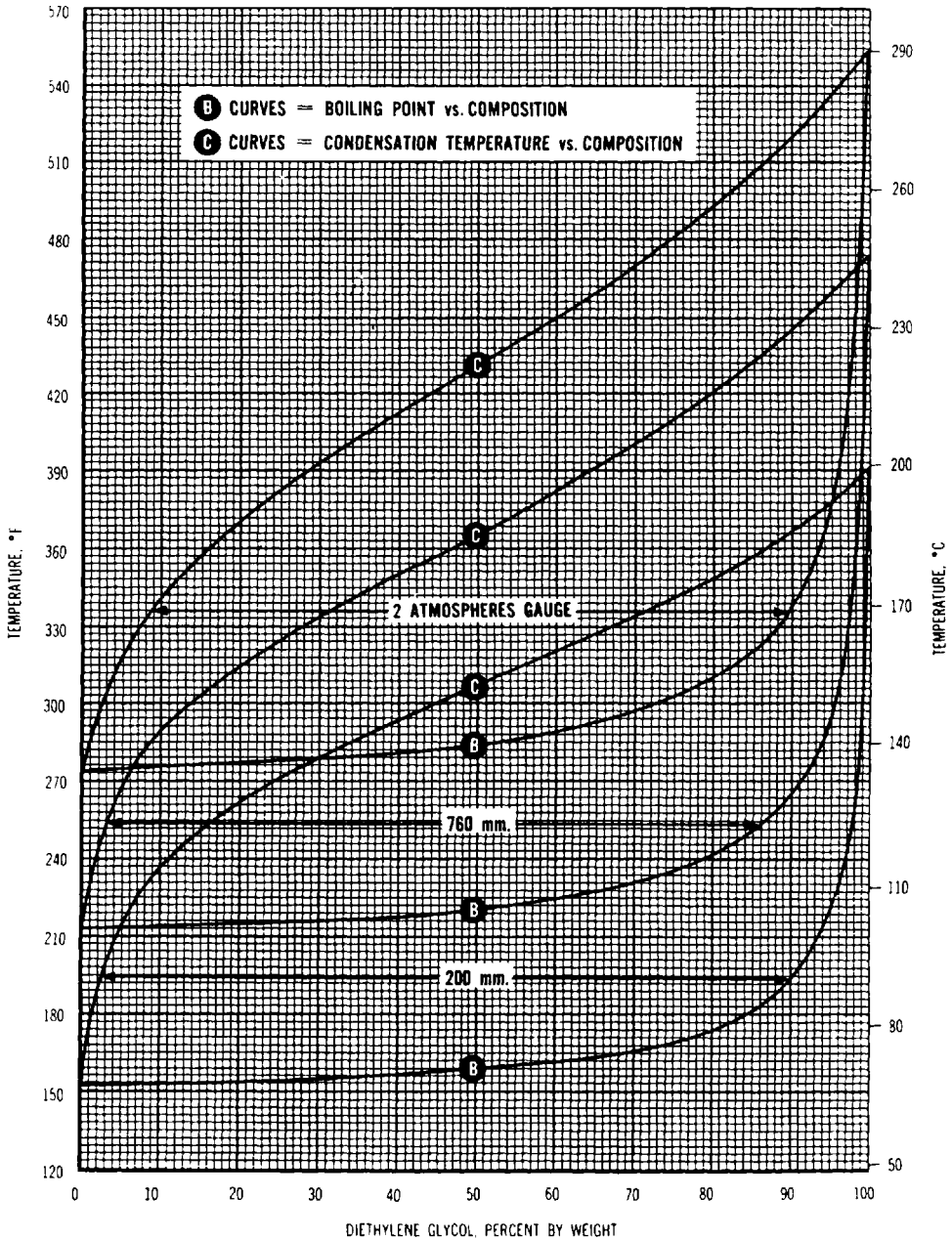
1 Freezing Points of Aqueous Glycol Solutions



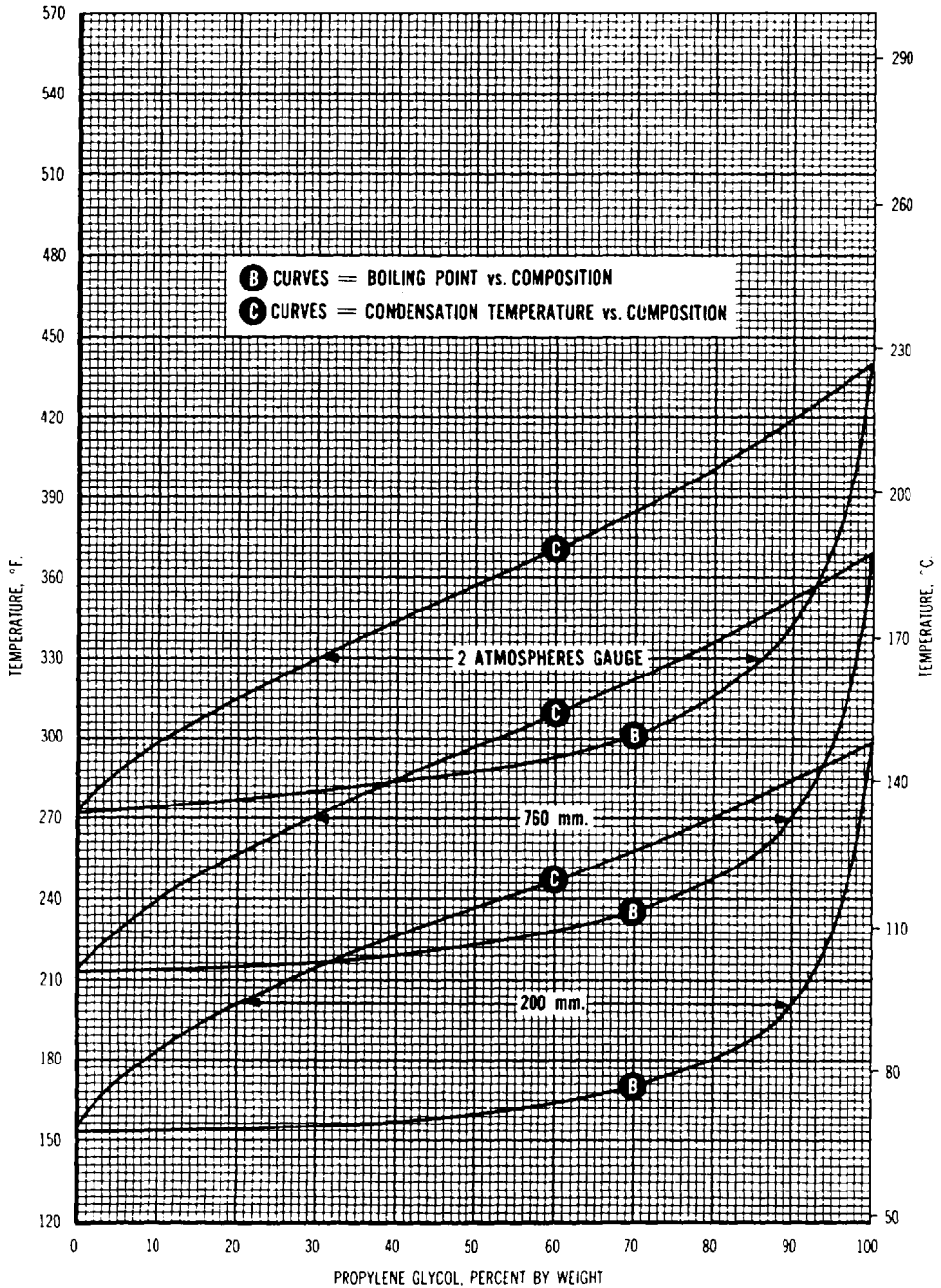
2 Boiling Points and Condensation Temperatures versus Composition of Aqueous Ethylene Glycol Solutions at Various Pressures



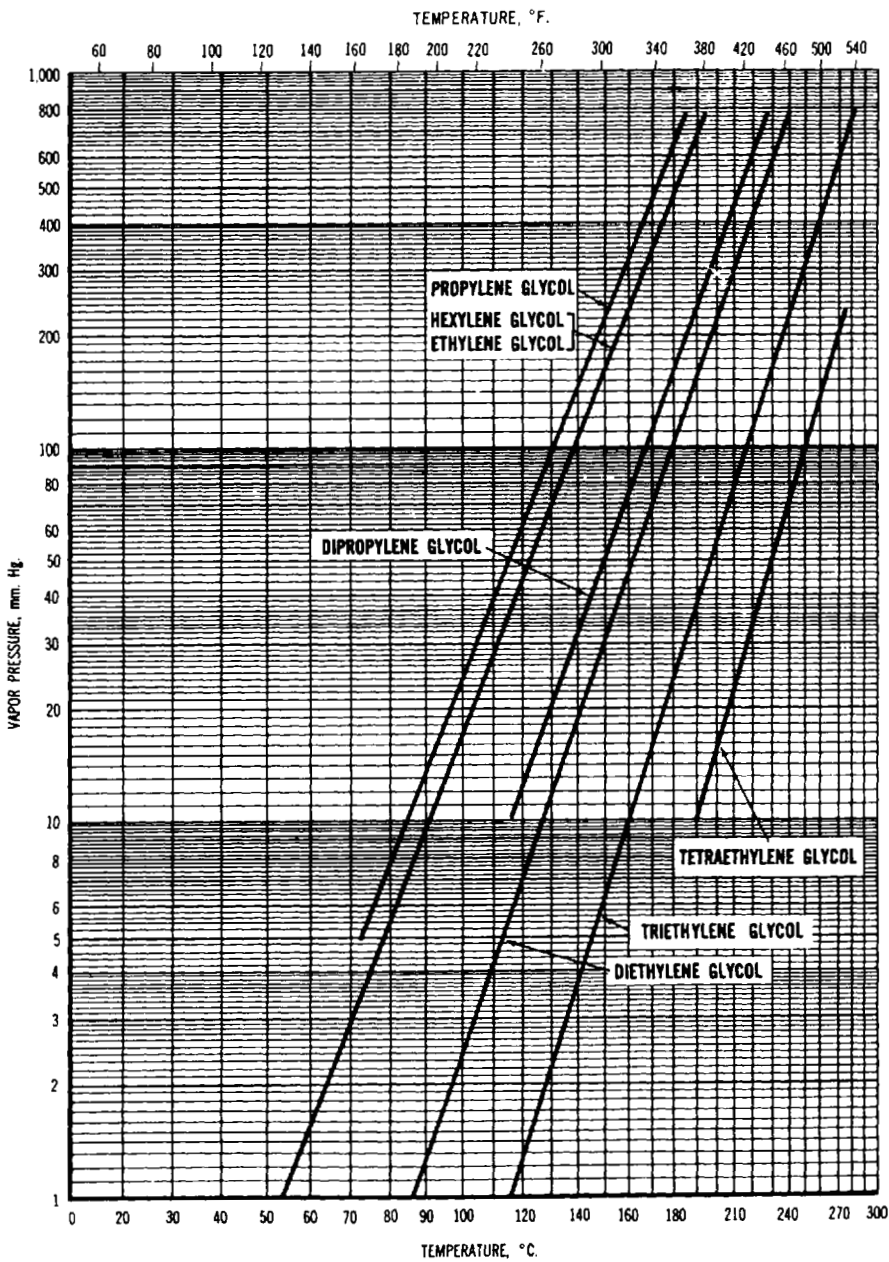
3 Boiling Points and Condensation Temperatures versus Composition of Aqueous Diethylene Glycol Solutions at Various Pressures



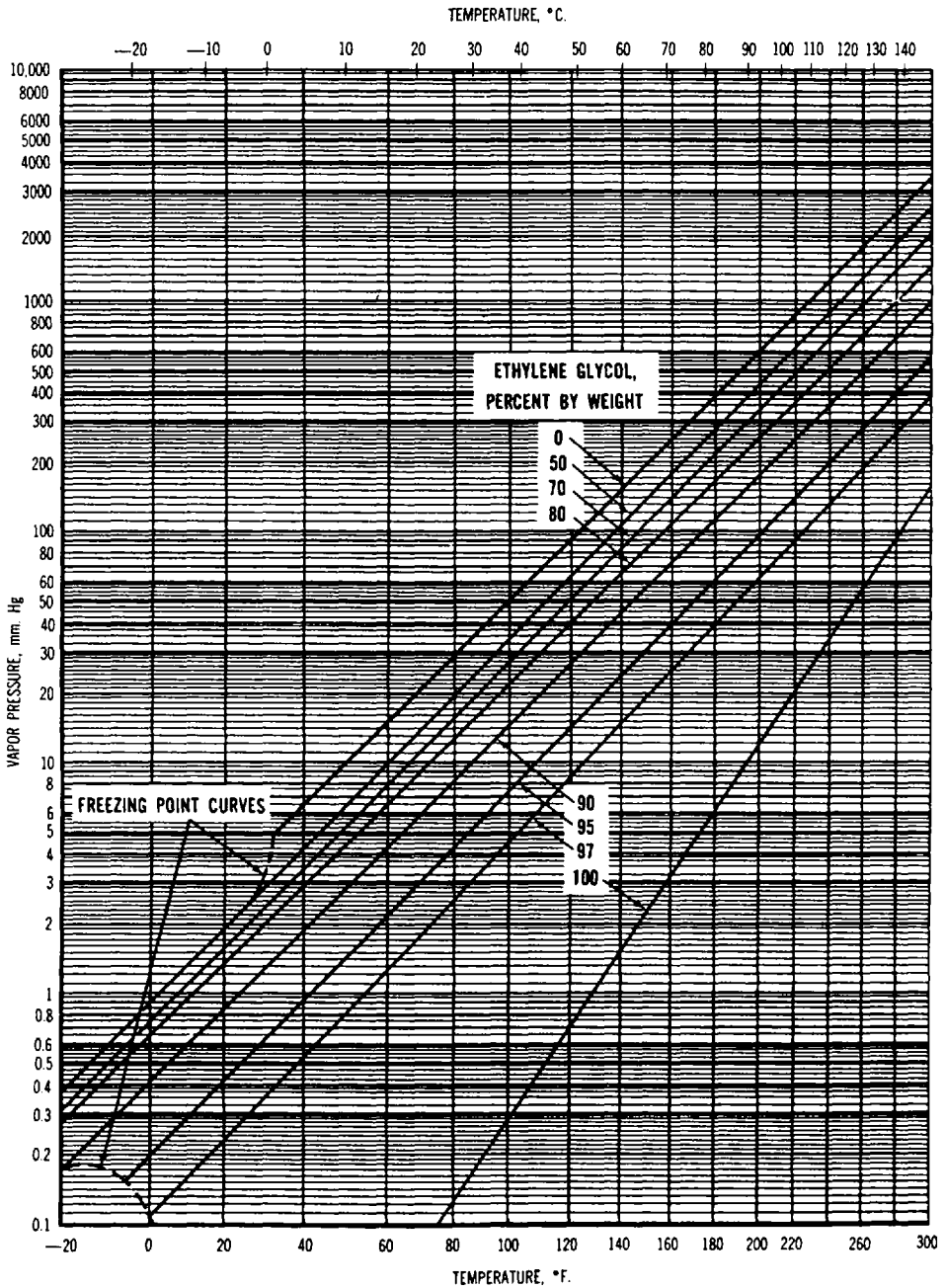
4 Boiling Points and Condensation Temperatures versus Composition of Aqueous Propylene Glycol Solutions at Various Pressures



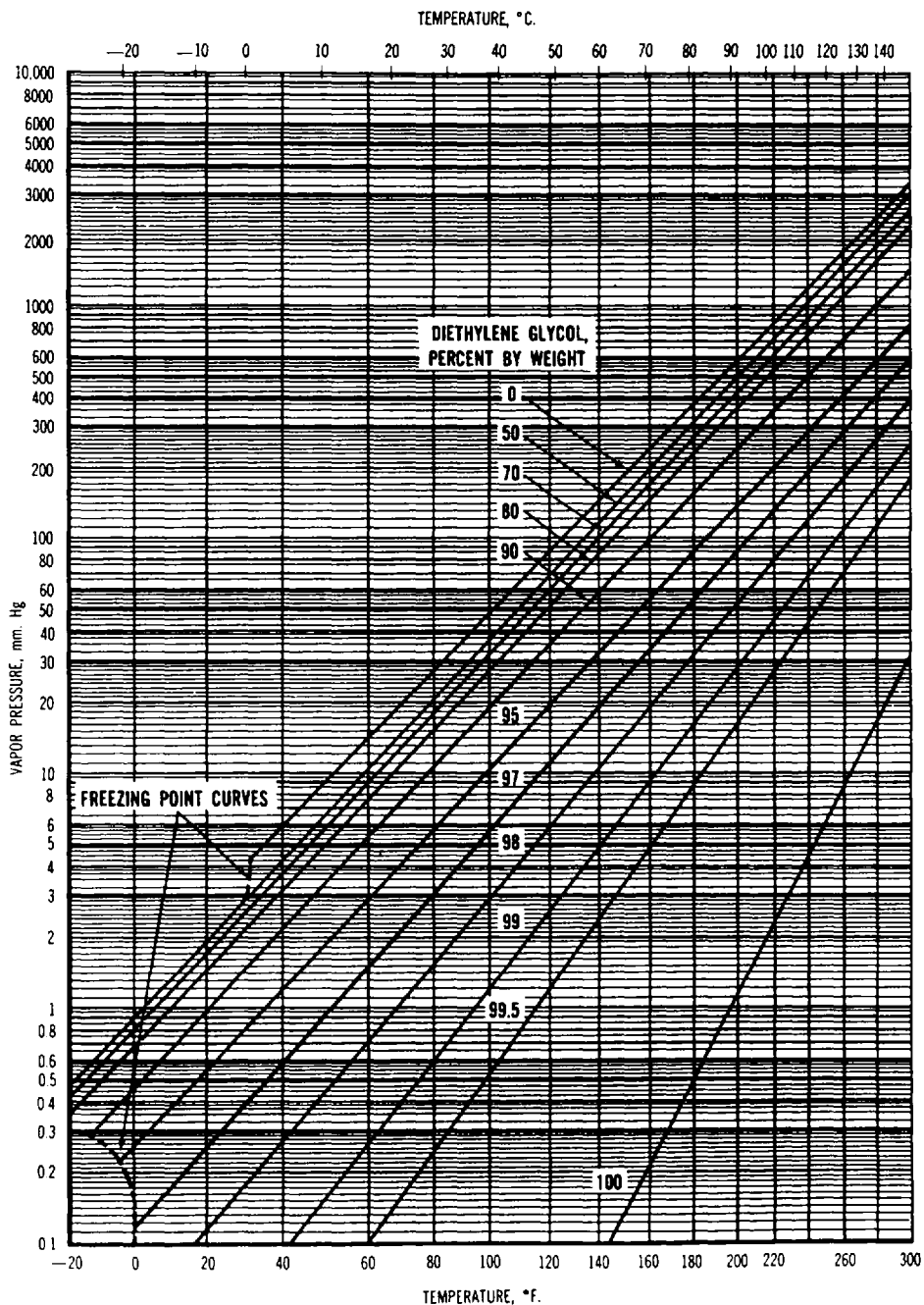
5 Vapor Pressures of Glycols at Various Temperatures (NOTE: Ethylene glycol and hexylene glycol have similar vapor pressures in this temperature range.)



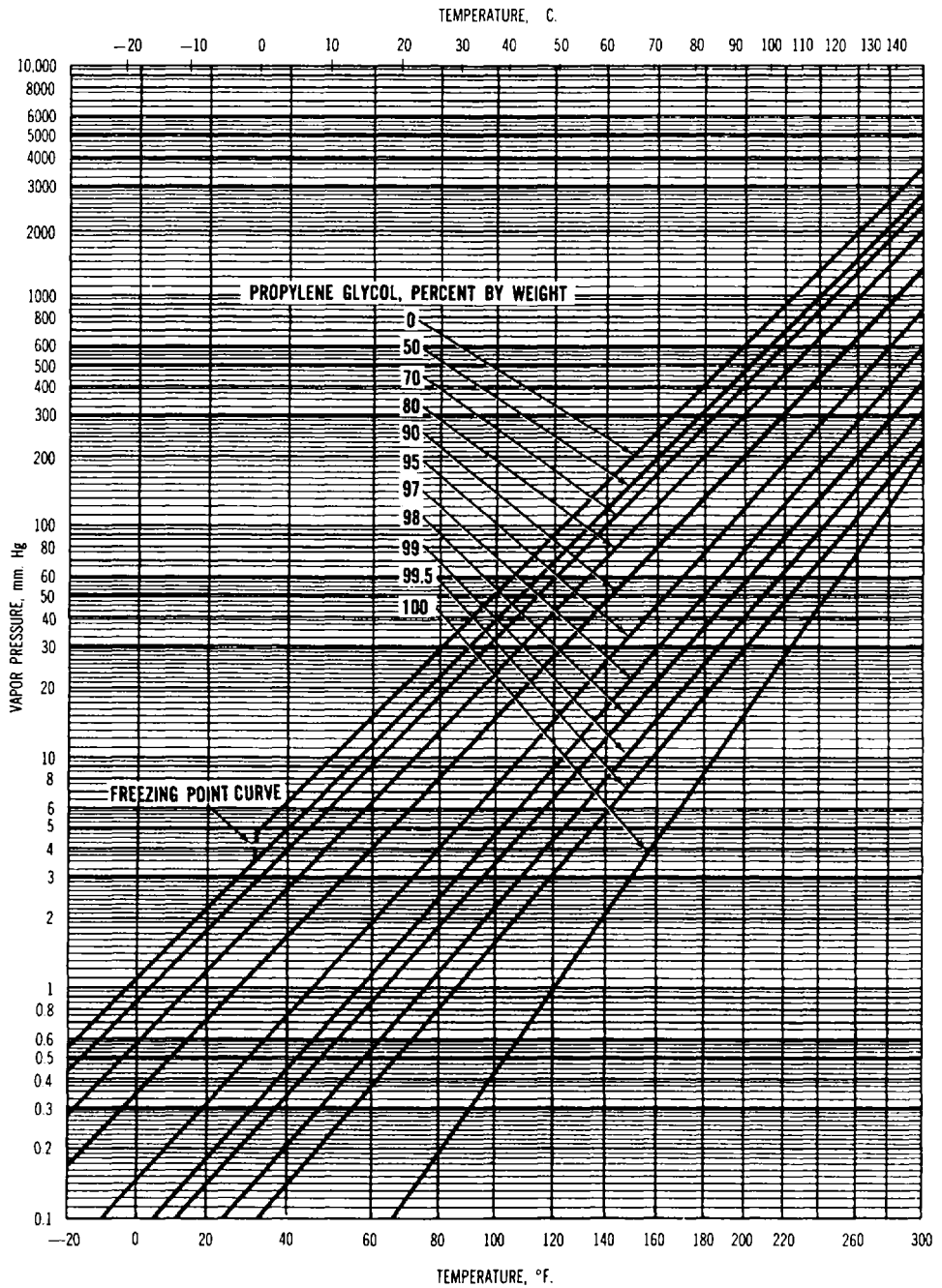
6 Vapor Pressures of Aqueous Ethylene Glycol Solutions



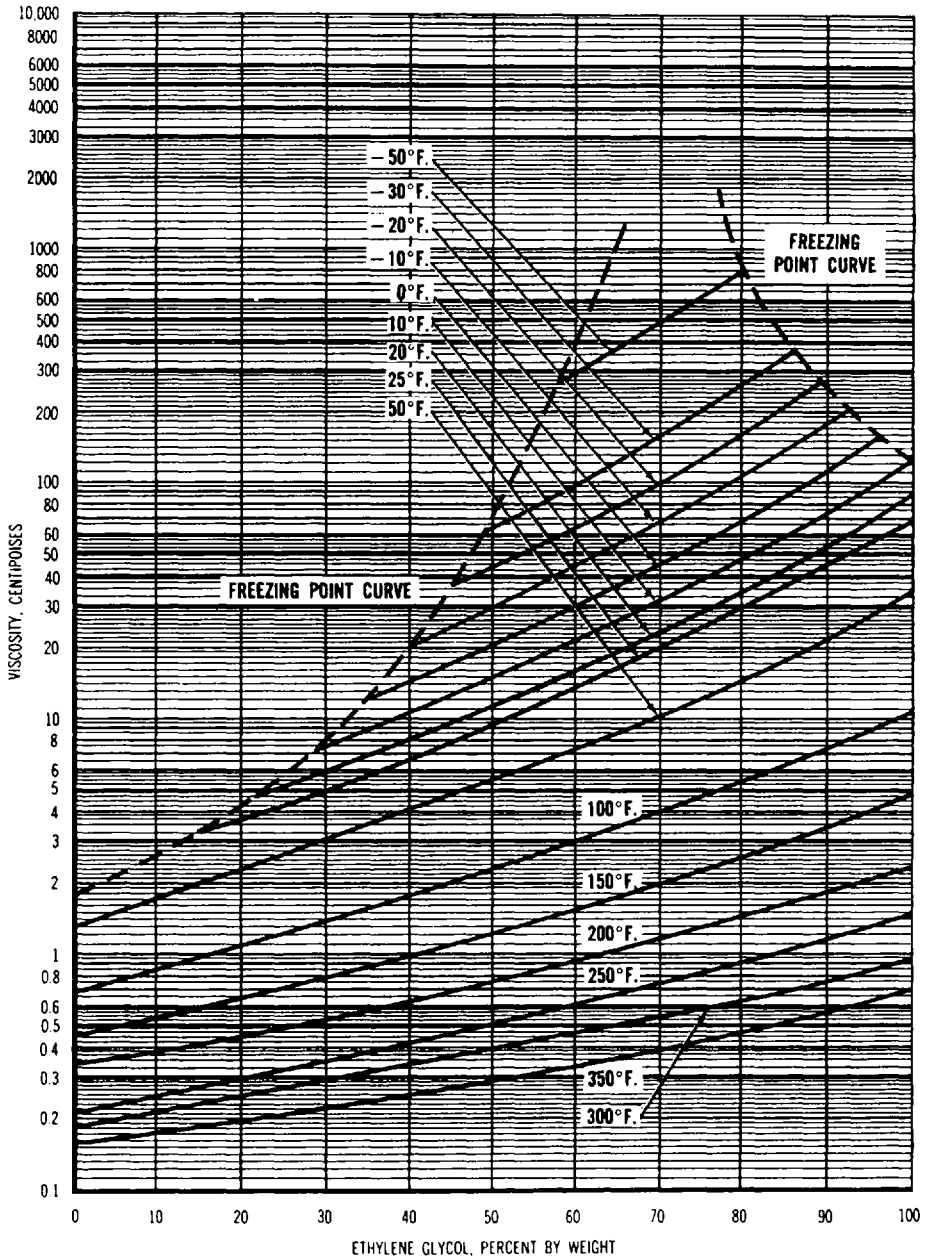
7 Vapor Pressures of Aqueous Diethylene Glycol Solutions



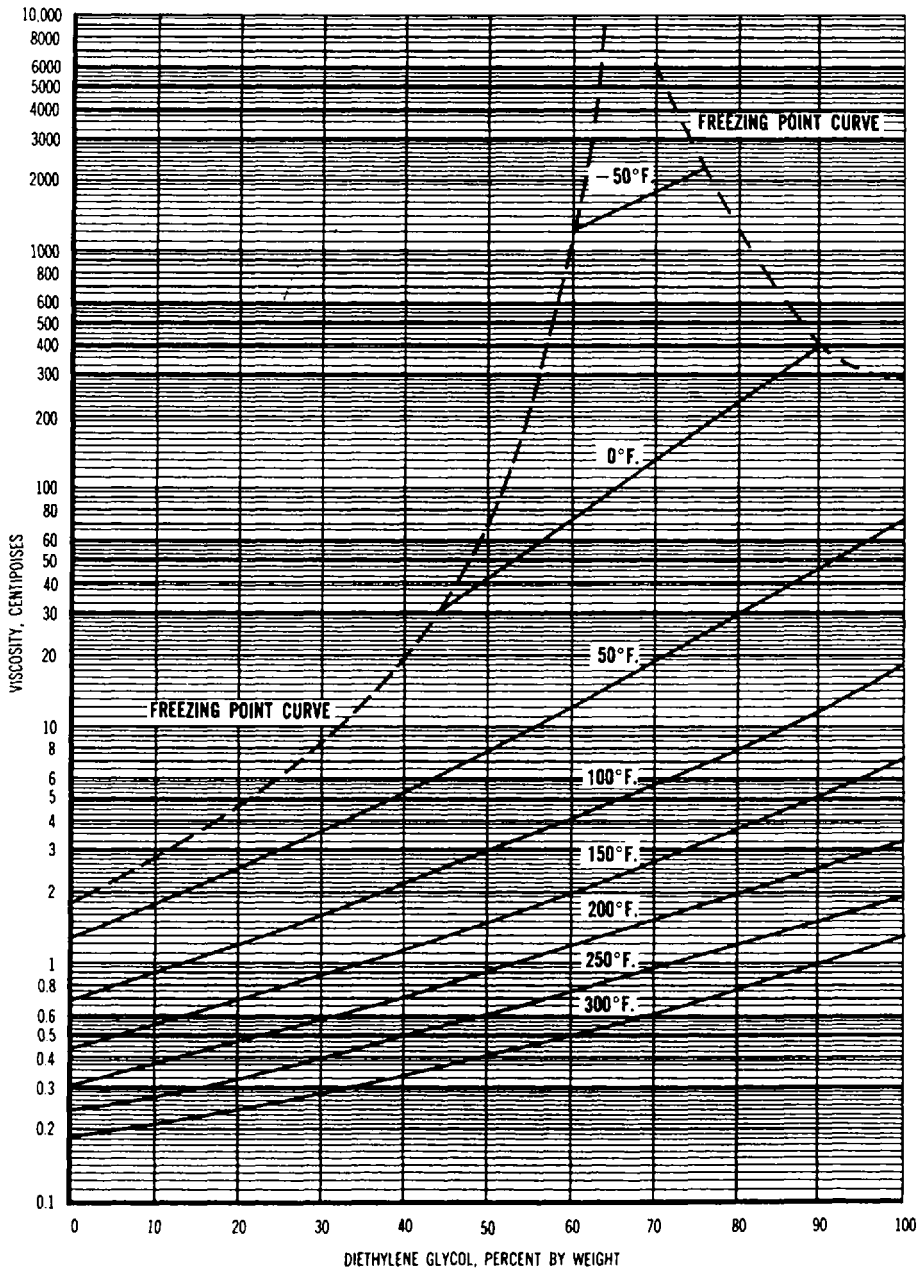
8 Vapor Pressures of Aqueous Propylene Glycol Solutions



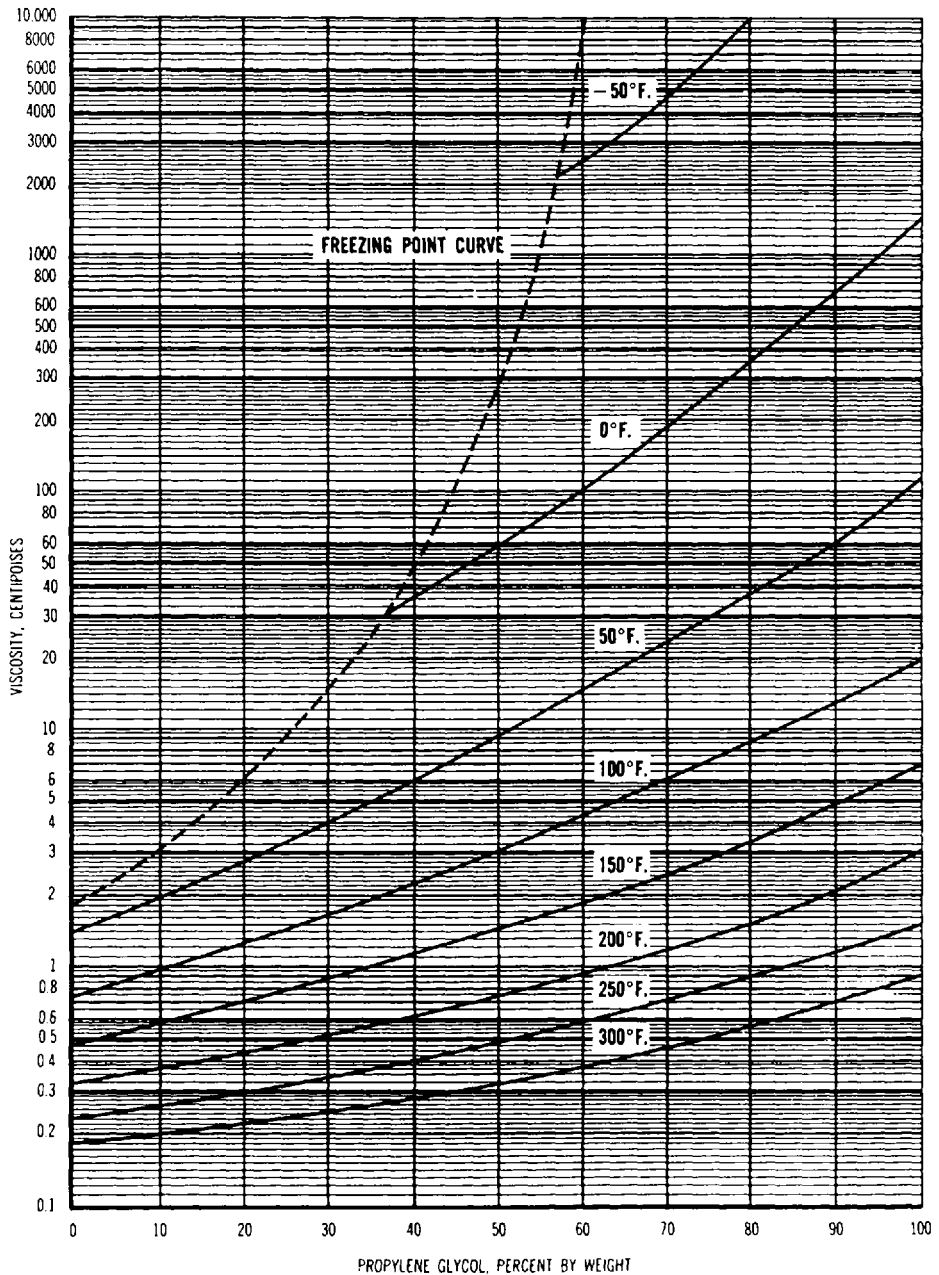
9 Viscosities of Aqueous Ethylene Glycol Solutions



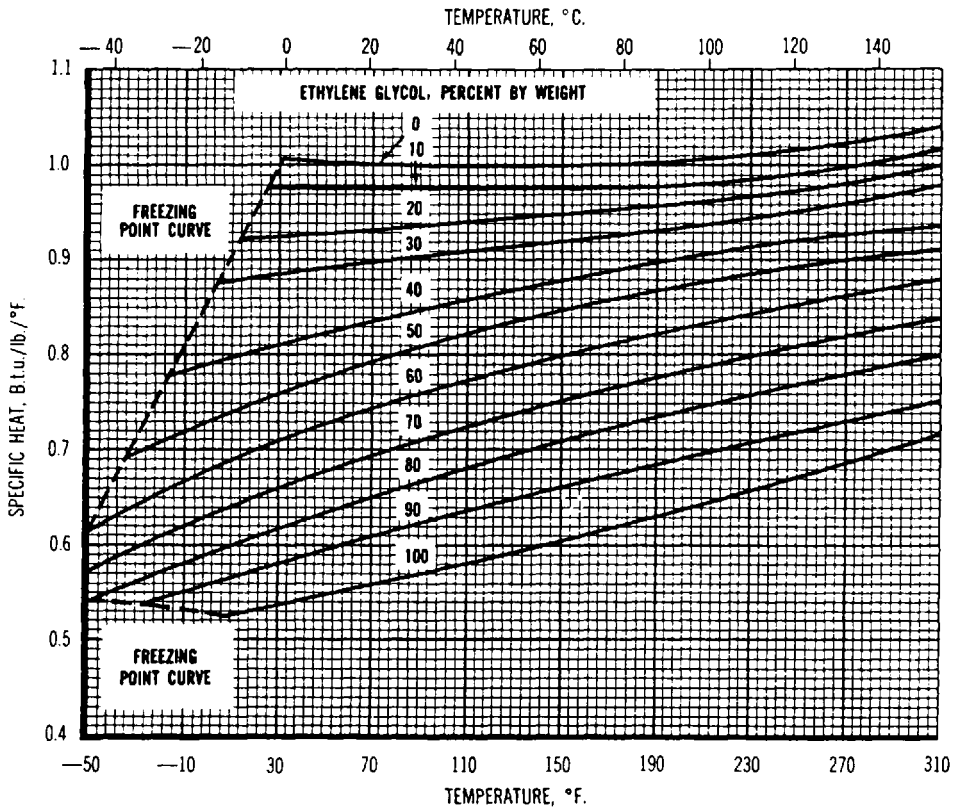
10 Viscosities of Aqueous Diethylene Glycol Solutions



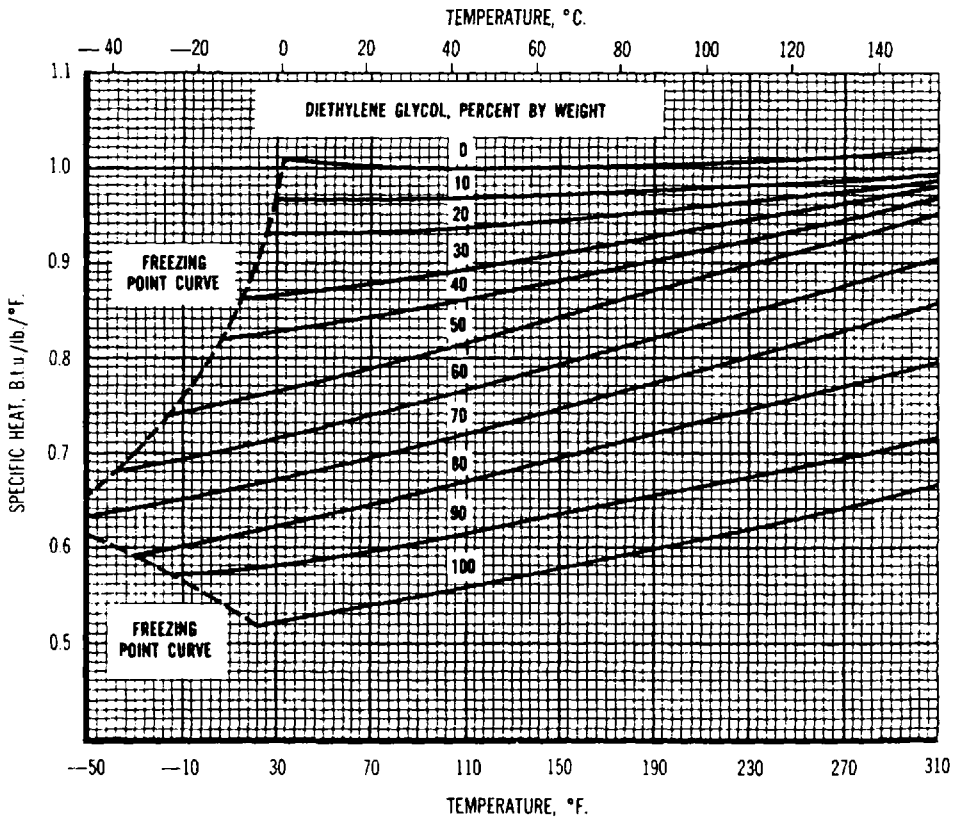
11 Viscosities of Aqueous Propylene Glycol Solutions



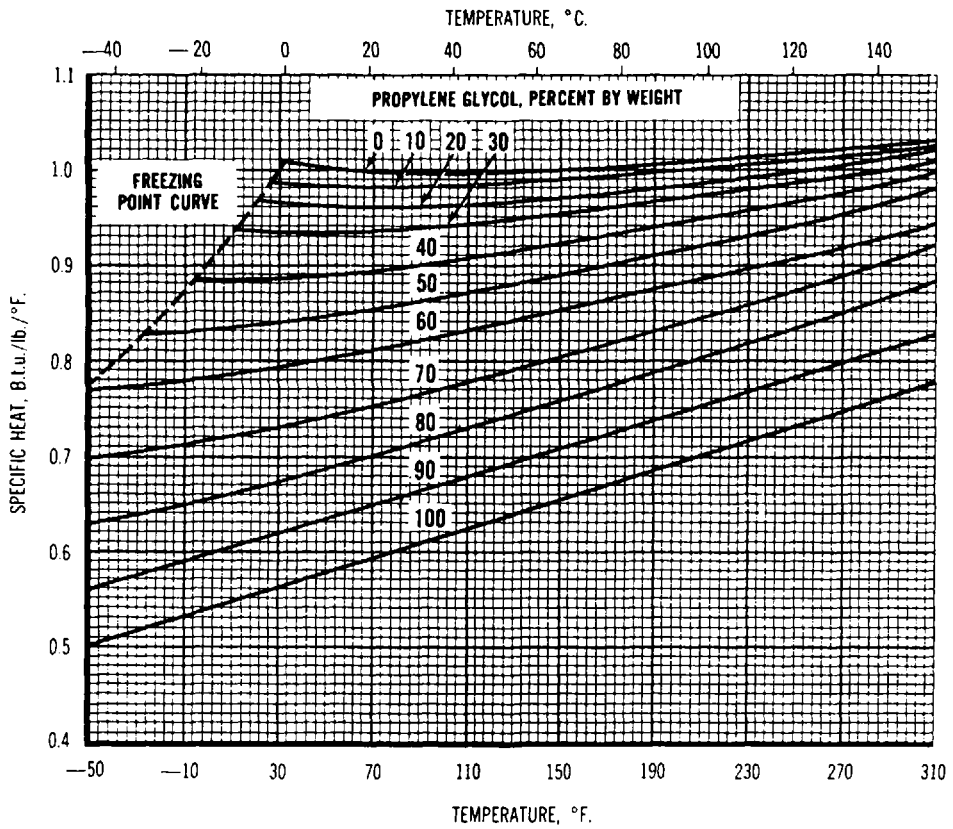
12 Specific Heats of Aqueous Ethylene Glycol Solutions



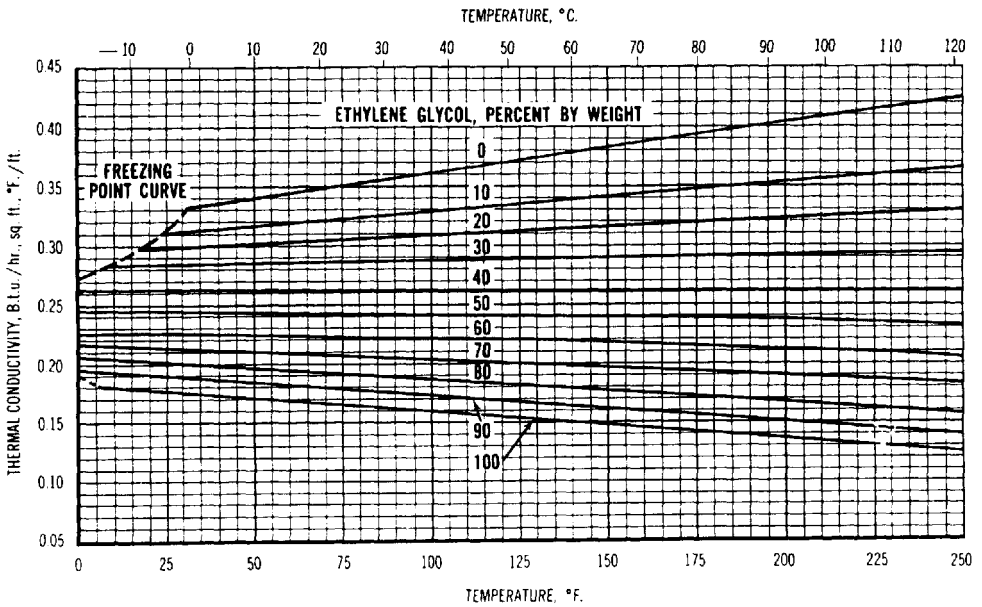
13 Specific Heats of Aqueous Diethylene Glycol Solutions



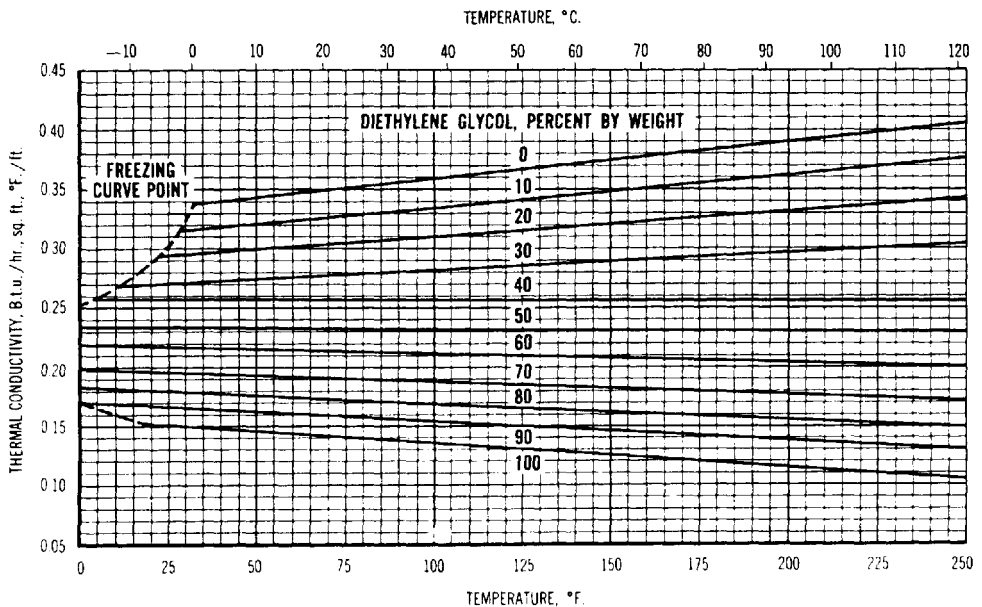
14 Specific Heats of Aqueous Propylene Glycol Solutions



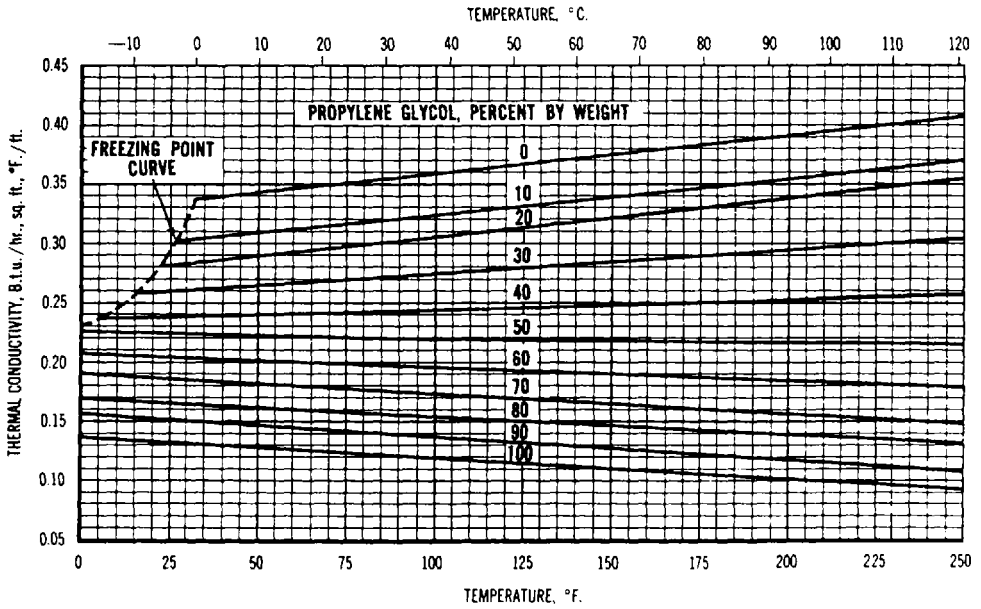
15 Thermal Conductivities of Aqueous Ethylene Glycol Solutions



16 Thermal Conductivities of Aqueous Diethylene Glycol Solutions



17 Thermal Conductivities of Aqueous Propylene Glycol Solutions



APPENDIX 11: COMMON WEAR PROBLEMS RELATED TO LUBRICANTS AND HYDRAULIC FLUIDS

Names of wear		Definition	Susceptible machine parts	Conditions promoting wear	Symptoms		
Preferred	Other				Unaided eye	Microscopically	Oil analysis
Mild adhesion	Normal	Generally, transference of material from one surface to another due to adhesion and subsequent loosening during relative motion. Mild adhesion involves transfer and loosening of surface films only	All	Moderate loads, speeds and temperatures Good, clean, dry lubricants Proper surface finish	Low rates of wear No damage Deeper original grinding marks still visible	Smooth microplateaus among original grinding marks Slight coloration due to films	1-5 ppm wear metals by emission spectroscopy Low % solids by filtration Metal salts (oxides, sulfides, phosphates, etc.) in wear fragments by x-ray diffraction
Severe adhesion	Scuffing Galling Scoring ^b	Cold welding of metal surfaces due to intimate metal-to-metal contact	Piston rings and cylinder barrels Valve train Rolling & sliding bearings Gears Cutting tools Metal seals Chains	High loads, speeds and/or temperatures Use of stainless steels or aluminum Insufficient lubricant Lack of anticuff additives No break	Rough, torn, melted or plastically deformed metal band or streaks High-temperature oxidation High friction, high rates of wear Possible seizure	Rough irregular surface Metal from one surface adhering to other surface by spot test or microprobe analysis	Large metallic wear fragments of irregular shape ^c
Abrasion	Cutting Scratching "Wire wool" damage Gouging Scoring	Cutting and deformation of material by hard particles (three-body) or hard protuberances (two-body)	All surfaces in relative motion	Hard particles contaminating oil Insufficient metal hardness Hard metal with rough surface against soft metal	Scratches or parallel furrows in the direction of motion similar to "sanding" High rates of wear	Clean furrows, burrs, chips Embedded abrasive particles In sliding bearings with soft overlay embedded particles cause polished rings	High-metal contents in oil and high silicon (>10 ppm) by emission spectroscopy High % solids by filtration Chips and burrs by ferrography
Erosion	Solid particles impact erosion	Cutting of materials by hard particles in a high-velocity fluid impinging on a surface	Journal bearings near oil holes Valves Nozzles	High-velocity gas or liquid-containing solids impinging on a surface ^d	Smooth broad grooves in direction of fluid flow Matte texture clean metal similar to sandblasting	Short V-shaped furrows by scanning electron microscopy Embedded hard particles	Elements of hard particles by emission spectrograph Chips & burrs by ferrography
Polishing	Bore polishing	Continuous removal of surface films by very fine abrasives	Cylinder bores of diesel engines Gear teeth Valve lifters	Combination of corrosive liquid and fine abrasive on oil	High wear but a bright mirror finish Wavy profile	Featureless surface except scratches at high magnification by electron microscopy	Combination of fine-metal corrosion products & fine abrasive by x-ray diffraction

Contact fatigue	Fatigue wear Frosting Surface fatigue Spalling	Metal removal by cracking and pitting, due to cyclic elastic stress during rolling and sliding	Rolling and sliding bearings Valve train parts Gears	Cyclic stress over long periods Water or dirt in oil Inclusions in steel	Cracks, pits, & spalls	Combination of cracks & pits with sharp edges Subsurface cracks by metallographic cross section Numerous metal inclusions	Particles of metal with sharp edges Metal spheres by electron microscopy
Corrosion	Chemical wear Oxidative wear Corrosive film wear	Rubbing off of corrosion products on a surface	All bearings Cylinder walls Valve train Gears Seals and chains	Corrosive environment Corrodible metals Rust-promoting conditions High temperatures	Corroded metal surface	Scale, films, pits containing corrosion products Dissolution of one phase in two-phase alloy	Detection of corrosion products of worn metal Detection of anion such as chloride by x-ray fluorescence
Fretting corrosion	False brinelling Fretting Friction oxidation	Wear between two solid surfaces experiencing oscillatory relative motion of low amplitude	Vibrating machines Bearing housing contacts Splines, keys, couplings Fasteners	Vibration causing relative motion	Corroded stained surfaces ⁴ Loose colored debris around real contact areas Rouge (Fe ₂ O ₃) colored films, debris, grease or oil for steel	Thick films of oxide of metal Red & black for steel	Identify metal oxide (α-Fe ₂ O ₃ for steel) by x-ray diffraction
Electro-corrosion	"Erosion" Electrical erosion Electrochemical wear Electrical attack	Dissolution of a metal in an electrically conductive liquid by low-amperage currents	Aircraft hydraulic valves Hydraulic pumps and motors	High-velocity liquid flow causing streaming potentials Stray currents Galvanic metal combinations	Local corroded areas Black spots such as made by a small drop of acid Corroded, worn metering edges	Corrosion pits, films, dissolution of metals	Detection of corrosion products Electrically conductive liquids ¹
Electrical discharge	Electrical pitting Sparking	Removal of metal by high-amperage electrical discharge or spark between two surfaces	Bearings in high-speed rotating machinery such as compressors, atomizers Static charge producers	High-speed rotation High-velocity two-phase fluid mixtures High-potential contacts Sparks	Metal surface appears etched In thrust bearing, sparks make tracks like an electrical engraver	Pits near edge or damage showing once molten state, such as smooth bottoms, rounded particles, gas holes Rounded particles near pits, welded to surface	Detection of large rounded particles by microscopic examination of filtrate or in ferrograph
Cavitation damage	Cavitation erosion Fluid erosion	Removal of metal by bubble implosion in a cavitating liquid	Hydraulic parts, pumps valves, gear teeth Cylinder liners, piston rings Sliding bearings	Sudden changes in liquid pressure due to changes in liquid velocity or to shape or motion of parts	Clean frosted or rough appearing metal Deep rough pits or grooves	Clean, metallic, bright, rough metal, pits Removal of softer phase from two-phase metal ¹¹	Observation of large chunks or spheres of metals in oils

Appendix 11 (Continued)

Names of wear		Prevention	
Preferred	Other	Mechanical changes	Lubricant changes
Mild adhesion	Normal'	None	None
Severe adhesion	Scuffing	Reduce load, speed, and temp	Use more viscous oil to separate surfaces
	Galling	Improve oil cooling	Use "extreme pressure" additives such as a sulfur-phosphorus or borate compound
	Scoring'	Use compatible metals	
		Apply surface coatings such as phosphating	
		Modify surface, such as ion implantation ^d	
Abrasion	Cutting	Remove abrasive by improved air & oil filtering, clean oil-handling practices, improved seals, flushing & frequent oil changes ^f	Oil free of abrasive particles
	Scratching		Use more viscous oil
	"Wire wool" damage		
	Gouging	Increase hardness of metal surfaces	
	Scoring		
Erosion	Solid particles impact erosion	Same as above	Same as above
		Reduce impact angle to less than 15°	
Polishing	Bore polishing	None	Choose less chemically active additive
			Remove corrosive contaminant
			Remove abrasive
Contact fatigue	Fatigue wear	Reduce contact pressures & frequency of cyclic stress	Use clean, dry oil
	Frosting	Use high-quality vacuum-melted steels	Use more viscous oil
	Surface fatigue	Use less abusive surface finish	Use oil with higher-pressure viscosity coefficient
	Spalling		

Corrosion	Chemical wear Oxidative wear Corrosive film wear	Use more corrosion-resistant metal (not stainless) Reduce operating temperature Eliminate corrosive material	Remove corrosive material such as too chemically active additive & contaminants Use improved corrosion inhibitor Use fresh oil
Fretting corrosion	False brinelling Fretting Friction oxidation	Reduce or stop vibration by tighter fit or higher load Improve lubrication between surfaces by rougher (than honed) surface finish	Use oil of lower viscosity Relubricate frequently ¹ Use oxidation inhibitors in oil
Electro-corrosion	"Erosion" Electrical erosion Electrochemical wear Electrical attack	Decrease liquid velocity & velocity gradients Use corrosion-resistant metals Eliminate stray currents Use nongalvanic couples	Decrease or increase electrical conductivity of lubricants or hydraulic fluids
Electrical discharge	Electrical pitting Sparking	Improve electrical insulation of bearings Degauss magnetic rotating parts Install brushes on shaft Improve machine grounding	Use of oil of higher electrical conductivity
Cavitation damage	Cavitation erosion Fluid erosion	Use hard, tough metals such as tool steel Reduce vibration, flow velocities, & pressures Avoid restriction & obstructions to liquid flow	Avoid low-vapor-pressure, aerated, wet oils Use noncorrosive oils

¹Mild adhesion is a desirable wear condition.

²Scoring is not recommended because it implies a scratch or furrow cut.

³Emission spectroscopy usually misses large (>5 μm) wear fragments.

⁴Increasing metal hardness does not reduce scuffing.

⁵The nist cinnib wear problem.

⁶Do not shot peen, bead, or sandblast any surface in a lubricated machine because abrasive cannot readily be removed properly.

⁷Sandblasting embeds sand in surfaces.

⁸An example of polishing combination in oil is active sulfur additive and Fe₂O₃ (jeweler's rouge).

⁹A new additive reduces promotion of contact fatigue by water; some extreme pressure additives are suspected of promoting contact fatigue.

¹⁰Rust (hydrated iron oxide Fe₂O₃·H₂O) is common corrosion product of ferrous metal.

¹¹Damage on one surface is mirror image of damage on other.

¹²Highly compounded oils can be electrically conductive—or electrolytes; phosphate ester hydraulic fluids are conductive.

¹³Not to be confused with pump cavitation, which is a different phenomenon.

¹⁴Corrosion and abrasive in oil increase cavitation damage.

¹⁵Graphite phase in cast-iron susceptible to removal by cavitation.

This page intentionally left blank

Index

- Abrasion wear:
 - mechanism, 621
 - ploughing, 620
 - 3-body wear, 150
 - 2-body wear, 621
- Accelerometers, 591
- Accumulators, 47
- AC Fine Test Dust, 153
- Acoustical analysis (*see* Vibrational analysis)
- Acoustic impedance, 578
- Actuators, 46
- Additives:
 - additive analysis, 768
 - additive response, 762
 - air-release agents, 818
 - antifoams, 817
 - antiwear, 762, 764, 806
 - ashless fluid technology, 766
 - base-oil effects, 761
 - boundary lubrication, 762
 - demulsifiers, 819
- [Additives]
 - detergents, 805
 - dispersants, 803
 - extreme pressure, 762, 809
 - friction modifiers, 762, 764, 819
 - function and chemical type, 763(T), 800
 - interaction, 803
 - oxidation inhibitors, 811
 - pour point depressants, 816
 - rust inhibitors, 739, 814
 - rust preventatives, 739, 814
 - viscosity index (VI) improvers, 814
 - ZDDP additives, 765, 809
- Adhesion, 367
- Adhesion wear:
 - mechanism, 625
 - microwelding, 622
 - polishing, 628
 - six laws of, 626
 - smearing, 624
 - tempering colors, 624

- Adsorption isotherms, 807
- Air entrainment:
 - bubbly oil viscometer, 243
 - dissolved air, 221
 - entrained air, 227
 - free air, 227
 - hydraulic problems, 221, 608
 - in-line analysis, 251
 - system sources, 221
 - tests, 243
 - TÜV method, 246
 - Waring blender test, 246
- Air release:
 - air dissolution, 237
 - drag coefficients, 235
 - Hadamard-Rybcznski model, 232
 - pressure, effect on, 238
 - Reynolds number, 234
 - specifications, 252
 - Stokes model, 235
 - viscosity, effect on, 238
- Aliasing, 565
- Aniline point, 715
- Antifoam, 817
 - mechanism, 231
- Antioxidants
- Antiwear additive, 798, 806, 997
- Aquatic toxicity, 442
- Ashless fluid technology, 766
- Asperities, 92, 342, 364, 365, 373

- Bankroft rule, 863
- Bearing number, 948
- Beer's Law, 768
- Bench tests:
 - Aachen sliding wear, 532
 - Cameron-Plint, 532
 - cyclic contact stress, 529
 - FZG gear, 531
 - Gamma-Falex, 527
 - Leeds testing machine, 532
 - Mizuhara and Tsuya
 - recommendations, 542
 - modified Amsler disk, 535
 - pin-on-V-block, 527
 - pump test correlations, 525
 - sequential 4-ball, 526
 - Shell 4-ball, 525, 768, 769
 - [Bench tests]
 - SRV test, 528
 - Timken test, 528
 - Unisteel rolling fatigue, 533
- Bifurcation, 375
- Bingham fluid, 321, 1157
- Biodegradability specifications, 450, 455
- Biodegradable fluids, 430
- Biodegradation:
 - aquatic biodegradability, 441
 - aquatic toxicity, 442
 - CEC-L-33-A-94, 440
 - hazard evaluation, 450
 - inherent biodegradation, 437
 - Modified Sturm, 440
 - OECD tests, 438
 - primary biodegradation, 431
 - ready biodegradation, 431
 - soil biodegradability and toxicity, 445
 - standard tests, 437
 - test strategies, 438
 - ultimate biodegradation, 431
- Boundary lubrication, 366, 376, 796
- Brinelling, 659
- Bubbly oil, 243
- Bulk modulus, 60, 252
 - adiabatic, 253
 - effect of fluid aeration, 261
 - effect of oil type, 267
 - Hayward equation, 261
 - isothermal bulk modulus, 257
 - measurement, 266
 - prediction, 264
 - secant bulk modulus, 255
 - tangent bulk modulus, 260
 - variation with pressure and temperature, 260

- Cavitation:
 - bubble-collapse mechanism, 280
 - cavitation pressure, 277
 - erosion rates, 284
 - flow losses, 272
 - gaseous, 268, 689
 - in pumps and orifices, 275
 - in spool and poppet valves, 277

- [Cavitation]
 - jet, 278
 - material effects, 281
 - test methods, 285
 - vaporous, 268, 689
 - vibrational analysis, 597
- Cavitation numbers, 269, 271, 689
- Cavitation wear:
 - fluid viscosity at onset, 608
 - Hobb's correlation, 631
- Chemical adsorption, 367
- Chemical boundary lubrication, 376
- Cincinnati Milicron Thermal Stability Test, 755, 1188
- Clearances, component, 961
- Cloud point, 322
- Coefficient of friction, 331, 374, 797
- Cole chart, 156
- Colloidal particles, 850, 861
- Combined radius of curvature, 370
- Combustion inhibitors, 998
- Compressibility (*see also* Bulk modulus):
 - adiabatic, 253
 - isentropic (mineral oil), 255
 - fire-resistant fluids, 259(T)
- Conjunction zone, 355
- Contacts classification:
 - conformal, 341
 - geometry, 341, 538
 - line contact, 371
 - lubricated, 342
 - nonconformal, 341
 - point contact, 370
 - scale, 341
- Contact-stress fatigue wear:
 - causes, 647
 - failure modes, 650
 - fatigue life, 650
- Contact stress fields, 342
- Contact surface fatigue:
 - bearing life rating, 82
- Contaminant control, 798
- Contaminant tolerance, 180
- Contamination, 24, 611
 - particulate:
 - AC Fine Test Dust, 153
 - automatic particle counting, 162
- [Contamination]
 - dynamic sampling, 160
 - fluid sampling, 157
 - gravimetric analysis, 164
 - ingression, 149
 - ISO Solid Contaminant Code, 164
 - particle distribution, 156
 - particulate load, 151
 - required cleanliness level, 160
 - shape factor, 152
 - sources, 148, 150
 - static sampling, 160
 - turbulent-flow sampling, 160
- Copper strip tarnish test, 743
- Corn oil, 1117
- Corrosion:
 - causes, 634
 - corrosion and rust testing, 740
 - electrochemical methodology, 938
 - galvanic corrosion, 635, 637, 1193
 - prevention, 636
 - pump tests for, 936
 - static tests, 937
 - turbine oil rust test, 937
 - "200-hour" accelerated test, 939
- Corrosion wear:
 - causes, 632
 - electrochemical attack, 632
 - electrochemical erosion, 638
- Critical micelle concentration, 853
- CV factor, 45
- Cylinder lunge, 60
- Cylinders, 46
- Darcy's equation, 31, 610
- DC resistivity, 294
- Decibels, 579
- Density, 287
- Design, 18
- Displacement, 20
- Dissolved oxygen effects, 768
- Ecolabeling, 428
- Efficiency:
 - mechanical, 7, 27
 - overall, 7, 27
 - volumetric, 7, 27

- Einstein equation, 858
- Elasticity modulus, 76
- Elastohydrodynamic lubrication, 796
 - conjunction zone, 355
 - minimum film thickness, 75
- Elastomer:
 - compounding, 472
 - properties, 487
- Elastomeric seals, 469, 472, 476
- Electrical conductivity, 288
- Electrical current wear, 665
- Electrochemical erosion, 638
- Electrorheological fluids:
 - actuator design, 1174, 1176, 1179
 - aging stability, 1170
 - calculation of ERF flow behavior, 1159
 - ERF flow resistor design, 1164
 - ERF properties, 1161
 - ERF structure, 1161
 - Flow rate, 1166
 - fluid fundamentals, 1154
 - fluid requirements, 1160
 - hardware design, 1175
 - influencing flow mode, 1165
 - material compatibility, 1171
 - operational modes, 1157
 - power supply, 1177
 - rheological basics, 1155
 - sedimentation stability, 1172
 - system pressure, 1170
 - temperature effects, 1168
 - test bench, 1175
 - time response behavior, 1178
 - viscosity-pressure behavior, 1163
 - wear interaction, 1172
- Ellipse parameter, 77
- Emulsions:
 - base oil viscosity, effect of, 870
 - biological stability, 888
 - cavitation, 911
 - classification, 848
 - coalescence and emulsion type, 863
 - conversion procedures, 908
 - corrosion, 879
 - ease of formation, 862
 - emulsification, 851, 856
 - emulsion inversion, 864
 - emulsion stability, 864
- [Emulsions]
 - emulsion stability test, 869, 888
 - emulsion theory, 858
 - emulsion thermal stability, 876
 - emulsion turbidity, 861
 - fatigue failure, 899
 - fire resistance, 893
 - fluid maintenance, 885
 - fluid properties and pump design, 900
 - foaming and air entrainment, 878
 - formulation, 850
 - lubrication properties, 894
 - material compatibility, 880
 - oil-in-water (o/w) emulsion, 854
 - oxidative stability, 878
 - particle size on viscosity, effect of, 861
 - phase diagram characterization, 857
 - preparation, 865
 - pressure-viscosity, effect of, 899
 - pump derating, 908
 - pump selection, 910
 - seal compatibility, 883
 - shear rate, effect of, 870
 - strainers, filters and screens, 885
 - system preparation for conversion, 910
 - viscosity-pressure coefficients, 875
 - viscosity-temperature behavior, 873
 - water-in-oil (w/o) emulsion, 854
 - water quality, effect of, 867, 869
- Entraining velocity, 386
- Environmental impact, 427
- Equivalent length, 52
- Erosion wear, 628
- Extreme pressure additive, 798, 997
- Failure analysis, 665
- Fanning's equation, 610
- Fatigue, 383
 - spalling, 383
 - pitting, 383
- Fatigue life testing:
 - Amsler two-disk machine, 955
 - bearing test rig, 953
 - Danner contact fatigue test rig, 953
 - 4-ball test, 955

- [Fatigue life testing]
 - piston pump testing, 953
 - Unisteel test, 953, 955
- Ferrography, 970
- Film thickness, 75, 358, 896
- Filterability, 738, 815, 1190
- Filters:
 - depth-type, 166
 - performance factors, 190
 - surface-type, 166
- Filter test systems:
 - drawdown, 167
 - filtration ratio, (α and β), 171
 - flow and impulse effects, 173
 - multipass, 167, 168
 - pressure-drop, 170
 - single-pass, 167
- Filtration performance, 167
 - β -ratio, 188
 - component contaminant tolerance, 180
 - dual flow, 175
 - filtration and cleanliness guidelines, 25
 - full flow, 175
 - off-line, filtration, 179
 - partial flow, 175
- Fire:
 - ignition sources, 395
 - influencing factors, 395
 - mechanisms, 394
- Flammability testing:
 - autoignition temperature, 399
 - ceramic wick test, 406
 - cone calorimeter, 405
 - flame propagation, 408
 - fluid volatility, 397
 - gunfire resistance, 403
 - heating time, 405
 - heat of combustion, 404
 - high-pressure spray, 415
 - hot channel ignition, 411
 - hot manifold, 410
 - hot surface ignition, 410
 - Houghton hot surface ignition, 410
 - linear flame propagation, 408
 - low-pressure spray, 413
 - molten metal, 410
 - open-cup flash point, 398
- [Flammability testing]
 - oxygen index, 398
 - pipe cleaner wick test, 407
 - pool fires, 404
 - rapid compression, 401
 - shock-tube ignition, 403
 - soaked-cube flammability, 408
 - spray flammability parameter, 415
 - spray ignition, 413
 - stabilized heat release, 419
- Flash temperature, 375
- Flow:
 - control, 33
 - dividers, 38
 - equations, 26
 - loss due to cavitation, 272
 - slip, 26
- Fluid aeration, 212, 221, 243
- Fluid classification, 396
- Fluid cleanliness, 158
- Fluidity, 308
- Fluid oxidation testing procedures, 752, 1152
- Fluid sampling, 157
- Flushing fluid, 782
- Flushing procedure, 782
- Foaming, 60
 - ASTM D-892, 242
 - hydraulic problems, 221
 - stability, 229
 - tests, 238
- Formic acid formation, 933, 935
- 4-AAP test, 931
- Fretting corrosion, 664
- Friction, 356, 374, 378
- Friction modifier, 798
- Fuel Injector Stability Test, 929
- Galling, 383
- Galvanic couple, 635 (*see also* Corrosion wear)
- Gas solubility:
 - Beerbower solubility parameter, 214
 - Bunsen coefficient, 219
 - Henry's Law, 213
 - Hildebrand and Scott solubility parameter, 220
 - Ostwald coefficient, 214

- Glycol, 920
- Gow-Joule effect, 506
- Hanning window, 587
- Head (NPSH), 610
- Hertzian contact, 75, 352
- HLB, 852, 855
- Horsepower, 6
- Hydraulic circuit:
 - closed-loop, 22
 - components, 47
 - half closed-loop, 23
 - open-loop, 21
 - supercharge, 22
- Hydraulic failures, fluid causes:
 - cavitation, 608
 - contamination, 611
 - fluid oxidation, 613
 - foaming and aeration, 606
 - improper viscosity, 616
 - overpressurization, 616
 - troubleshooting, 617(T)
- Hydraulic principles:
 - efficiency, 7
 - energy, 2
 - horsepower, 6
 - power, 2
 - pressure, 5
 - torque, 5
 - work, 2
- Hydrodynamic bearings, 903
- Hydrodynamic films, 344
- Hydrodynamic lubrication, 349, 796
- Hydrodynamic pressure, 348
- Hydrodynamic squeeze film, 347
- Hydrogen embrittlement, 120
- Hydrostatic bearing, 901
- Inlet:
 - friction head, 31
 - net positive suction head, 27
- In-line analysis, 157
- ISO Solid Contaminant Code, 164
- Karl Fischer analysis, 964
- Kurt Orbahn method, 929
- Lambda ratio, 389, 650, 654, 659, 899, 948
- Leakage flow, 684
- Load-life (L_{10}) relationship, 81, 900, 951, 953
- Lubricant factor, 950
- Lubricant flow number, 654
- Lubricant purity factor, 83
- Lundberg and Palmgren, 126
- Material parameter, 76
- Mechanical seals, 514
- Mechanodegradation (*see* Shear degradation)
- Meshing frequency, 592
- Micelle, 849
- Microbial control, 891
- Micro-diesel effect, 238, 745
- Micro-EHD lubrication, 362
- Microphones, 591
- Microscuffing, 383
- Mineral oil hydraulic fluid
 - classification:
 - by additives, 724
 - by ISO/6743/4, 726
 - by oil type, 724
 - by viscosity, 726
- Mineral oil hydraulic fluids:
 - additives, 759
 - air entrainment, 732
 - ASTM Rust-Preventing Characteristics Test, 741
 - chemical corrosion, 740
 - Cincinnati Millicron Test, 755, 1188
 - common pump performance tests, 772
 - compressibility and bulk modulus, 729
 - Copper Strip Tarnish Test, 743
 - corrosion and rust testing, 740, 1190
 - corrosion properties, 738
 - demulsibility, 736, 1192
 - density, 733
 - dielectric strength, 735
 - dissolved oxygen on wear, effect of, 768
 - electrical conductivity, 735

[Mineral oil hydraulic fluids]

- estimation of cavitation potential, 729
- filterability, 738, 1190
- fluid cleanliness, 781
- fluid maintenance, 775, 1197
- fluid performance tests, 774
- fluid replacement, 782
- fluid wear classification tests, 771
- foaming, 730
- foaming and air entrainment, 745, 1194
- galvanic corrosion, 1193
- gas solubility, 730
- heat capacity, 734
- Hot Panel Coking Test, 753
- infrared spectroscopy, 755
- low temperature properties, 178(T)
- lubrication performance, 768
- maximum inlet viscosity, 728
- neutralization number, 750
- oil oxidation:
 - effect of water and catalysts, 744(T)
 - mechanisms, 747, 1187
- oxidation stability, 743, 1189
- pour point, 733
- recycling and reclamation, 784
- Rotary bomb oxidation test (RBOT), 752
- seal compatibility, 735
- shear stability, 1195
- thermal conductivity, 734
- thermal expansion, 734
- Turbine Oil Stability Test (TOST), 752, 1186
- vapor phase rust, 1193
- Vickers V-104 vane pump test, 770
- viscosity, 727
- viscosity index, 728
- viscosity-pressure behavior, 728

Mineral oils:

- calculation of composition from physical properties, 712
- effect of composition on properties, 718(T)

[Mineral oils]

- Fourier transform infrared spectroscopy, 723
- gel permeation chromatography, 723
- nomenclature, 721
- nuclear magnetic resonance spectroscopy, 722
- oil composition, 711, 1129
- oil refining processes, 717
- thin-layer chromatography, 723
- Mixed film lubrication, 116, 378
- Moody diagram, 31
- Motors, 10
- Natural frequency, 54, 57, 287
- n-d-m* Method, 714
- Near-surface region, 345
- Nitrosamine formation, 930
- Optical interferometry, 359
- Overpressurization, 618
- Oxidation, 613
- Palm oil, 1112
- Particles, 149, 151, 156
- Performance characteristics, 2, 4
- Performance maps, 387, 537
- Petroleum wax structure, 723
- Phenol content, 931
- Phosphate esters:
 - additive solvency, 1081
 - air release, 1048
 - aluminum bearing materials, use of, 1043
 - boiling point, 1051
 - bulk modulus, 1050
 - compatibility, 1072
 - demulsification, 1050
 - disposal, 1081
 - ecotoxicity, 1078
 - electrical properties, 1053
 - fatigue life, 1043
 - fire resistance, 1034
 - fluid maintenance, 1083
 - foaming, 1050
 - FZG test results, 1043
 - historical development, 1026
 - hydrolytic stability, 1066

[Phosphate esters]

- low temperature viscosity
 - properties, 1044
- lubricating properties, 1039
- manufacture, 1030
- mixed alkylaryl phosphates, 1033
- oxidative stability, 1063
- pour points, 1047
- radiation stability, 1069
- refractive index, 1057
- rusting and corrosion, 1070
- shear stability, 1055
- solubility data, 1057
- specifications, 1087(T)
- specific gravity, 1056
- structure/property effects, 1027
- system design, 1082
- thermal properties, 1052
- thermal stability, 1058
- toxicity, 1077
- trialkyl phosphates, 1031
- triaryl phosphates, 1031
- vapor pressure, 1051
- viscosity-pressure effects, 1047
- viscosity properties, 1044

Pipes, hoses, and fittings:

- equivalent length values, 52
- friction losses, 31
- installation, 25
- pressure losses, 52, 960
- sizing, 49, 974

Piping inspection and repair, 972

Pitting, 383

Poisson ratio, 76, 370

Polymer chemistry, 469

Polyol esters:

- antifoams, 998
- antioxidants, 994
- antiwear additives, 997
- biodegradability and toxicity, 1013
- chemistry, 984
- combustion inhibitors, 998
- conversion procedures, 1014
- corrosion inhibitors, 996
- demulsifiers, 998
- dispersants, 999
- ester composition, 988(T)
- extreme pressure additives, 997

[Polyol esters]

- filter media, 1008
- fire resistance, 1010
- fluid maintenance, 1016
- lubrication properties, 1001
- manufacturing process, 989
- material compatibility, 1005
- oxidation and thermal stability, 1008
- physical and chemical properties, 999
- polyol ester basestocks, 986
- pour point depressants, 999
- reclamation, 1021
- shear stability, 993
- use temperature range, 1010
- viscosity index improvers, 992

Pour point, 322

Power law fluids, 199

Pressure, 5

Pressure-viscosity coefficient,

- effective, 946

Protective film, 375

Pumpability, 197

Pump derating, 908

Pump failure modes, 543, 606

Pump lubrication, 564, 602

Pumps and motors:

- displacement, 20
- efficiency, 7
- failure, causes, 606
- fluid viscosity limits, 196
- gear pumps-external, 11
- gear pumps-internal, 11
- head pressure estimation, 32
- inlet condition, 27
- lubrication, 602
- performance parameters, 4
- piston:
 - axial, 15
 - bent-axis, 15, 18
 - pressure-compensated, 17
 - radial, 15, 18
 - variable displacement, 17
- positive displacement, 3
- proof and burst pressure, 26
- sizing and selection, 21
- vane pumps-balanced, 10
- vane pumps-unbalanced, 11

Pump tests:

- Bosch cycled-pressure vane pump, 545
- Denison HFO pump test, 555
- Denison T5D-042 vane pump, 555
- evaluation of pump lubrication, 564
- fluid-specific properties, importance of, 544
- gear pump testing, 563
- Komatsu HPV35 + 35 piston pump, 559
- Manton Gaulin Model 500 piston pump, 561
- MP-1 vane pump, 545
- Rexroth A4VSO piston pump, 557
- Sundstrand Water Stability Test Procedure, 557
- Universal hydraulic pump test stand, 565
- Vickers AA65560-1SC-4 piston pump, 557
- Vickers low-volume vane pump, 549
- Vickers PV3-075-15 piston pump, 563
- Vickers 35VQ25 vane pump, 552
- Vickers 20VQ5 vane pump, 550
- Vickers V-104 vane pump, 545
- V-104 test reproducibility problems, 548
- PV-factor, 287

Raleigh equation, 861

Rapeseed oil, 1113

Rating life- L_{10} , 81

Recycling and reclamation, 784

Refractive index, 964

Relative working life, 78

Relativity permittivity, 295

Reserve alkalinity, 968

Reservoir:

- air bubble removal, 223, 226
- air entrainment, 222
- design, 53, 222
- pressurization, 224
- venting, 227

Response time, 54

Reynolds equation, 349, 896

Reynolds number, 50, 681

Rho-C values, 729

Rolling element bearings:

- abrasive wear, 90
- adhesive wear, 92
- alternative lubricant effects, 120
- bedding positions, 66
- coatings, 111
- corrosive wear, 94
- dynamic equivalent load, 82
- dynamic load rating, 81
- fatigue wear, 88
- fretting corrosion, 95
- lubrication, 113
- lubrication effectiveness, 78
- material selection, 104
- minimum oil film thickness, 75
- raceway curvature, 101
- selection, 74, 78
- size, 78
- static load rating, 78
- true brinelling, 134
- types, 67
- water contamination, 120
- wear, design effects, 97

Root-cause analysis, 669

Rotary bomb oxidation test (RBOT), 1063

Rust and oxidation (R&O) oils, 800

Rusting, 738

Safflower oil, 1117

Scuffing, 382

galling, 383

microscuffing, 383

Seal compatibility:

- compatibility testing, 482, 489
- empirical prediction methods, 480
- fluid/elastomer selection guidelines, 484
- physical property testing, 487
- Seal compatibility index, 735
- Seal compatibility testing, 482, 489, 883
- Seal life, 511

- Seal materials:
 - ethylene propylene diene (EPDM), 478
 - fluorocarbon, 479
 - nitrile materials, 476
 - urethane, 479
- Seals-failure analysis, 513
- Seal-system design, 507
- Seal technology:
 - compounding, 472
 - molding, 473
 - peroxide cure, 474
 - sulfur cure, 474
 - vulcanizing, 472
- Seal types, 495
- Shape factors, 152
- Shear degradation:
 - pump rotational speed, effect on, 210
 - stability tests, 208, 210, 1195
 - viscosity, effect on, 209
- Shear stability, 326, 815
- Shear stability index, 328, 994
- Shannon's theorem, 585
- Sherman equation, 861
- Signal analysis, 580
- Slide-to-roll ratio, 390
- Sliding velocity, 379, 387
- Snuffer fluids, 847
- Soil biodegradability, 445
- Sommerfeld number, 906
- Soybean oil, 1017
- Spalling, 383
- Spray flammability parameter, 415
- Standards, 1201
- Steady-state pipe flow, 681
- Stribeck curve, 118, 524, 536
- Stuffing boxes, 494
- Subsurface region, 345
- Surface energy, 367, 807
- Surface films, 344
- Surface roughness, 389, 950
- Surfactants, 851
- Symbols, 47
- Synthetic hydrocarbons:
 - alkyl aromatic fluids, 834
 - development history, 826
 - MIL-H-5606 fluid, 826
 - Polyalphaolefins, 827
 - Silahydrocarbon fluids, 837
 - Tempering colors, 624
 - Testing standards, 1185
 - Thermal conductivity, 287
 - Thermal correction factor, 77
 - Thickening mechanism, 319
 - Thixotropic, 1156
 - TOST test, 1063, 1186
 - Tribochemical action, 376
 - Tribocouples, 808
 - Tribological aspect numbers, 538
 - Tribology, systematic, 340
 - Triglyceride, 1097
 - Turbine oil rust test, 938
- Ultrasonic shear test, 929
- Valves:
 - check, 41
 - counterbalance, 40
 - CV factor, 45
 - directional control, 43
 - flow, 45
 - needle, 33
 - flow calculation, 35
 - pressure reducing, 40
 - pressure relief, 39
- Vapor pressure, 210
- Vegetable oils:
 - biodegradability, 1140
 - chemistry, 1097
 - classification, 1096
 - compatibility, 1135
 - compressibility, 1140
 - corn oil, 1117
 - fatty acid composition, 1100, 1106, 1118
 - film thickness, 1137
 - genetic modification, 1104
 - heat of combustion, 1134
 - hydraulic oil base stock, 1124
 - hydrogenation, 1102
 - melting point, 1134
 - nomenclature, 1143
 - oxidative stability, 1105, 1112, 1128
 - palm oil, 1112
 - rapeseed oil, 1113
 - safflower oil, 1117
 - solubility, 1134

- [Vegetable oils]
 - sound velocity, 1139
 - soybean oil, 1107
 - soybean oil processing, 1108
 - sunflower oil, 1115
 - unsaturation, 1098
 - viscosity, 1128
 - viscosity index, 1128
 - viscosity-pressure coefficient, 1139
- Velocity parameter, 76
- Vibrational analysis:
 - basic definitions, 578
 - digital processing, 583
- Vegetable oils:
 - filters, 589
 - Fourier signal analysis, 580
 - sensors, 590
 - waveform sampling, 584
- Viscosity:
 - absolute, 306
 - Bingham fluid, 321
 - Carreau model, 201
 - chain entanglement, 319
 - classification, 332, 726
 - Couette flow, 306
 - free-volume, relationship to, 318
 - kinematic viscosity, 308
 - molecular basis of, 315
 - Newtonian, 198, 307
 - Newton's Law, 305
 - Non-Newtonian, 199, 321
 - Poiseuille equation, 308
 - Poiseuille flow, 306
 - polymer thickening, 319
 - power-law fluids, 198
 - pseudoplastic, 324
 - pump viscosity limits, 196
- Viscosity Index, 309
- Viscosity-pressure relationship:
 - Appeldoorn equation, 207
 - ASTM slope, 204
 - barus equation, 204, 312
 - factors affecting, 314
 - prediction, 207(T)
 - Roeland's equation, 313
 - So and Klaus correlation, 205
 - variation with mineral oil
 - composition, 80, 203
- [Viscosity-pressure relationship]
 - viscosity-pressure coefficient, 312, 353
 - Winer α^* , 204
 - Winer α_{OT} , 204
 - Wu and Klaus correlation, 206
- Viscosity-temperature relationship:
 - Andrade equation, 201
 - Eyring and Ewell equation, 201
 - mineral oil, 79
 - temperature-viscosity coefficient, 202
 - Vogel equation, 202
 - Walther equation, 202, 309
- Viscous flow, 346
- Viscous friction, 379
- von Mises equation, 373
- Water:
 - chemical properties, 681
 - physical properties, 676
 - sea water, 675
 - tap water, 675
- Water-glycol:
 - additive precipitation, 967
 - biodegradability and toxicity, 449
 - compressibility-pressure relationship, 925(T)
 - corrosion tests, 936
 - density, 923
 - film-forming properties, 944
 - fire resistance, 976
 - fluid classification, 918
 - fluid composition, 918
 - fluid maintenance, 956
 - foaming and air release, 930
 - formic acid content, 933
 - hydrolubes, 917
 - Karl Fisher analysis, 964
 - material compatibility, 940
 - nitrosamone formation, 930
 - oxidation mechanism, 932
 - oxidative stability, 931
 - performance testing, 943
 - pH, 969
 - phenol content, 931
 - pressure-viscosity coefficients, 944

[Water-glycol]

- pump derating, 955
- reserve alkalinity, 968, 1201
- rolling contact fatigue, 946
- shear stability, 928
- specific heat, 925(T)
- system conversion, 972
- thermal conductivity, 925(T)
- “200-hour” accelerated test, 939
- vapor pressure, 923
- viscosity, 923, 928
- water content:
 - effects, 927
 - by refractive index, 962
 - by viscosity, 962

[Water-glycol]

- water quality, 964
- Water hardness, 964
- Water hydraulics:
 - actuators, 697
 - pumps, 690
 - valves, 693
- Water quality standards, 681
- Waveform processing, 584
- Wear:
 - mild wear, 382
 - polishing, 382
- Wear coefficients, 629
- Work function, 488